

EFFECTS OF EXOGENOUS CADMIUM ON ACTIVITY OF ANTIOXIDANT ENZYME, CD UPTAKE AND CHEMICAL FORMS OF RYEGRASS

QIN, Y.[#] – LI, X.[#] – XU, W.^{*} – CHAI, Y. – CHI, A. – WANG, W. – LI, T. – HUANG, C. – ZHENG, Y.

*College of Resources and Environmental Sciences, Southwest University
Chongqing 400715, P. R. China
(phone: +08-6-10-236-825-1249)*

[#]These authors should be considered co-first authors.

**Corresponding author
e-mail: xuwei_hong@163.com*

(Received 24th Jun 2017; accepted 25th Sep 2017)

Abstract. The cadmium (Cd) contamination in farmland soils in China has been becoming more and more serious because of the large amount of industrial waste residue, sewage irrigation and the unreasonable application of pesticides and fertilizers. Pot experiment was conducted to study the effects of different Cd levels (0, 75, 150, 300 and 600 mg·kg⁻¹) on dry weight, activities of antioxidant enzyme and Cd chemical forms of the two ryegrass varieties (Band and Arbde). The results showed that dry weights of shoot and plant of ryegrass (Band and Arbde) were firstly increased with the increase of Cd level, which reached the highest values respectively at 75 mg·kg⁻¹ and 150 mg·kg⁻¹, and respectively increased by 10.06% and 4.04%, 25.84% and 16.89% compared with the control. Shoot Cd concentrations of Band and Arbde were 171.827 mg·kg⁻¹ and 169.122 mg·kg⁻¹ respectively at 150 mg·kg⁻¹ Cd. The average Cd concentrations of chemical forms in shoots of the two ryegrass varieties were in order of NaCl extractable Cd (F_{NaCl}) > acetic acid extractable Cd (F_{HAC}) > water extractable Cd (F_W) > residual Cd (F_R) > HCl extractable Cd (F_{HCl}) > alcohol extractable Cd (F_E). Compared with the two ryegrass varieties, Arbde was more effective in remediation of cadmium contamination in soils due to higher plant biomass and greater Cd accumulation.

Keywords: *Cd contamination; ryegrass; activity of antioxidant enzyme; Cd uptake; Cd chemical forms*

Introduction

Cadmium (Cd) pollution in soil has become a global issue due to the emission of three types of industrial waste, i.e. mining, chemical fertilizers and pesticides used in agriculture and sewage irrigation (Ren et al., 2014; Hejazi et al., 2017). The Yangtze River Basin is located in cadmium ore resources enrichment area of China, and there were reports that Cd content in soils and agricultural products exceeds Chinese government standard (Sun et al., 2016). The soil Cd pollution around smelting plant is more serious, for example, in the investigation of the surrounding environment of a smelting plant in Northeast China, it is found that the content of Cd in collected soil samples is from 4.1 to 167.6 mg·kg⁻¹ (Chen, 2016; Hashemi, 2017). Cadmium is highly toxic to plants, water soluble and therefore promptly adsorbed in tissues and its presence greatly influences the entire plant metabolism (Li et al., 2016). Cadmium pollution has the characteristics of concealment, latency, accumulation and long term, which could access to biological body with long-term accumulation through the food chain, thus endangering human health, such as Japan's "Itai-Itai Disease" (Liu et al., 2015).

Phytoremediation as a kind of in-situ remediation technology with low cost and small environmental disturbance, is considered to be the best remediation method of heavy metal contaminated soil (Chen et al., 2015; Radan et al., 2017). At present, Cd enrich plants has been found included *Solanum nigrum* L., *Zygophyllum fabago* L., *Arabidopsis thaliana*. L., *Trifolium repens* L. and *Iris hex agona* L., etc (Chen, 2016). Unfortunately, most of the plants that were already found out to have lots of accumulation of Cd grow slowly, and have low biomass so that their restoration takes a long period, while they require grow in very restricted conditions. These conditions limit using phytoextraction technology at large scale. Ryegrass (*Lolium multiflorum* L.) is the annual or perennial herbs, and is a kind of forage grass with higher yield in gramineous plants. It has been reported that ryegrass is an ideal plant for phytoremediation of heavy metals in soils due to surviving in tailings with poor ecological environment, and fast vegetation construction and strong tiller ability, and rapidly covering the ground (Xu et al., 2007; Wu et al., 2014; Xiang, 2014). Perennial ryegrass have obvious remediation effect on Cd polluted soil (Feng et al., 2016; Sun et al., 2016; Vazdani et al., 2017). Studies on the growth and Cd uptake by ryegrass under Cd stress have been reported (Xu et al., 2007; Chen et al., 2015; Feng et al., 2016), however, there are few studies on difference of Cd resistance, Cd uptake and Cd chemical forms between ryegrass varieties. In order to further explore the effects of different Cd levels (0, 75, 150, 300 and 600 mg·kg⁻¹) on growth, activity of antioxidant enzyme and the Cd chemical forms in ryegrass, two ryegrass varieties (Band and Arbde) planted in pots containing Cd pollution and were then analyzed (Ahamed and Lognathan, 2017). This work will provide interesting data for studying on the expression difference of Cd accumulation /Cd tolerance related genes between ryegrass varieties, and breeding and cloning high biomass and high Cd-enrichment varieties in future research.

Materials and methods

Plant material, soil and Cd treatments

Two ryegrass (*Lolium multiflorum* L.) varieties (Band and Arbde) were used in the present study. The seeds were purchased from Jiangxi Scarecrow agricultural park. Purple soil based on Chinese Soil Taxonomy (CST) was collected from purple soil base of Southwestern University in Beibei region, Chongqing. The contents of organic matter, total nitrogen, alkali-degradable nitrogen, available P, available K, Cd in soil, and the soil pH were 8.87 g·kg⁻¹, 1.54 g·kg⁻¹, 74.60 mg·kg⁻¹, 65.07 mg·kg⁻¹, 38.59 mg·kg⁻¹, 0.110 mg·kg⁻¹, and 5.23, respectively.

The pot experiment was conducted with Cd concentrations of 0, 75, 150, 300 and 600 mg·kg⁻¹ (CdCl₂·2.5H₂O) from March 3, 2015 to May 5, 2015 in the greenhouse of College of Resources and Environmental Sciences at Southwest University, China. 5 kg of air-dried soil was passed through a 40-mesh screen and then treated with CdCl₂·2.5H₂O (0, 75, 150, 300 and 600 mg·kg⁻¹) solution and mixed to be homogeneously put in a plastic pot (diameter, 25 cm; height, 17 cm) and kept balance for two weeks. Thirty seedlings with the same growth potential were planted in each pot. The base fertilizer included P (NH₄H₂PO₄), K (KCl), and N (NH₄H₂PO₄ and urea) at concentrations of 100 mg·kg⁻¹, 150 mg·kg⁻¹, and 180 mg·kg⁻¹, respectively. The seedlings of ryegrasses (*Lolium multiflorum* L.) with 10 cm high were then transplanted 30 plant for each pot. The moisture content in soil was kept 60% of the maximum

moisture in the fields with deionized water. Fast- measurement of Soil Moisture (TZS-IW, Zhejiang Tuopu Instrument Co., Ltd., China) was used to determine the moisture content in soil. The experiment was performed in triplicate, and was randomized complete block arrangement. The plants were harvested on May 5, 2015, and were kept at 105 DEG C for 15 min for denaturing the enzymes, and then oven-dried at 60 DEG C until there was no further change in the weight of the sample.

Soil physical and chemical properties

Soil pH was determined by soil water ratio of 1:2.5; organic matter, total nitrogen, available nitrogen, available phosphorus and available potassium in soils were determined by conventional analysis methods (Yang et al., 2008; Issaka and Ashraf, 2017; Xiao et al., 2017).

Antioxidant enzyme activity and MDA content

Tissue samples of shoot and root in two ryegrass (*Lolium multiflorum* L.) varieties (Band and Arbde) were homogenized in ice-cold deoxygenated 20 mmol·L⁻¹ Tris-HCl buffer (pH 7.4, 1:9, W/V) and centrifuged at 3000 ×g for 10 min. Aliquots of 100 μL were used for enzyme activity measurement. The activity of catalase (CAT) was measured using a microtiter plate assay (Grant et al., 2008; Yang et al., 2017). The activity of peroxidase (POD) was determined by monitoring the increase in absorbance at 470 nm during the oxidation of guaiacol (Hemeda and Klein, 1990). The activity of superoxide dismutase (SOD) was determined by the method of Minami and Yoshikawa (1979) with 50 mmol·L⁻¹ Tris-Ca-codylic sodium salt buffer (pH 8.2) containing 0.1 mmol ·L⁻¹ EDTA.

Plant Cd fraction

The concentrations of Cd in its various chemical forms in ryegrass shoots were determined through continuous leaching method (Tessier et al., 1979). A flame atomic absorption spectrometer (Perkin SIMMA 6000 Elmer, Norwalk, USA) was used to determine Cd concentration. The detection limit was 0.005 mg·kg⁻¹. The plant reference material (GBW # 08513) provided by National Institute of Standards and Technology was adopted to monitor the quality of determination results. The recovery rates of cadmium in all plant samples were higher than 95%, and the accuracy of relative standard deviation (RSD) was less than 10%.

Soil Cd fraction

The concentrations of Cd in its various chemical forms in soil was conducted by five-step sequential extraction method proposed by Tessier et al. (1979), and the extracted Cd was determined by atomic absorption spectrophotometry (Perkin Elmer SIMMA 6000, Norwalk, USA). The detection limit was 0.005 mg·kg⁻¹. The plant reference material (GBW # 08303) provided by National Institute of Standards and Technology was adopted to monitor the quality of determination results. The recovery rates of Cd in all plant samples were higher than 95%, and the accuracy of relative standard deviation (RSD) was less than 10% (Zhao and Chen, 2017).

Statistical analysis

Three-way analysis of univariate ANOVA and correlation analysis were performed using SPSS version 21.0 package (SPSS, 2012). The effects of interaction among Cd levels on dry weight of plant, antioxidant enzyme activity, Cd concentration and Cd uptake in plant, and Cd fraction in plant and soil for different ryegrass varieties was subjected to a two-way analysis of variance (ANOVA; i.e., varieties and Cd treatments) followed by the least significant difference (LSD) test ($p < 0.05$) (Xu et al., 2010).

Results

Biomass

As shown in *Figure 1*, with the increase of Cd level in soils, shoot dry weight of Band and Arbde were increased. Highest shoot dry weight of Band was found in 75 $\text{mg}\cdot\text{kg}^{-1}$ Cd and increased by 10.06% compared with the control, while highest shoot dry weight of Arbde was observed at 150 $\text{mg}\cdot\text{kg}^{-1}$ Cd and increased by 25.84% compared with the control. At the same Cd level, shoot dry weight of Arbde was higher than that of Band.

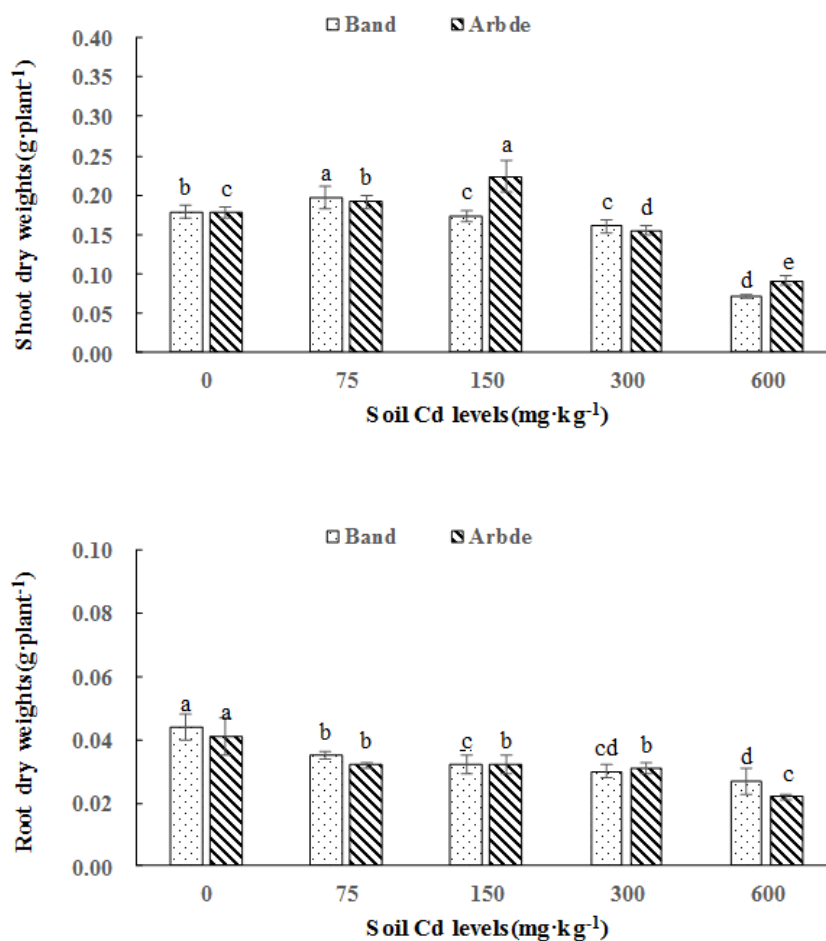


Figure 1. Effects of different Cd levels ($\text{mg}\cdot\text{kg}^{-1}$) on dry weight of ryegrass; different letters (a, b, c) indicate significant difference at $P \leq 0.05$ among different Cd levels in the same variety

Antioxidant enzyme activity

Significant difference of the activities of SOD, POD and CAT in shoots and roots of ryegrass were found between different varieties and among different Cd pollution levels ($P < 0.05$) (Figs. 2-4). As shown in Figure 2, the activity of SOD in shoots of Band significantly increased with the increase of Cd level in soil, with increases of 14.52%-68.38% compared with the control, while the activity of SOD in shoots of Arbde decreased with the increase of Cd level in soil, with the decrease of 4.17%-41.67% compared with the control. The activity of SOD in roots of the two varieties increased with the increase of Cd level in soils, and highest activities of SOD in roots of Band and Arbde were observed at the Cd level of $75 \text{ mg} \cdot \text{kg}^{-1}$ and respectively increased by 3.24% and 10.66% compared with the control.

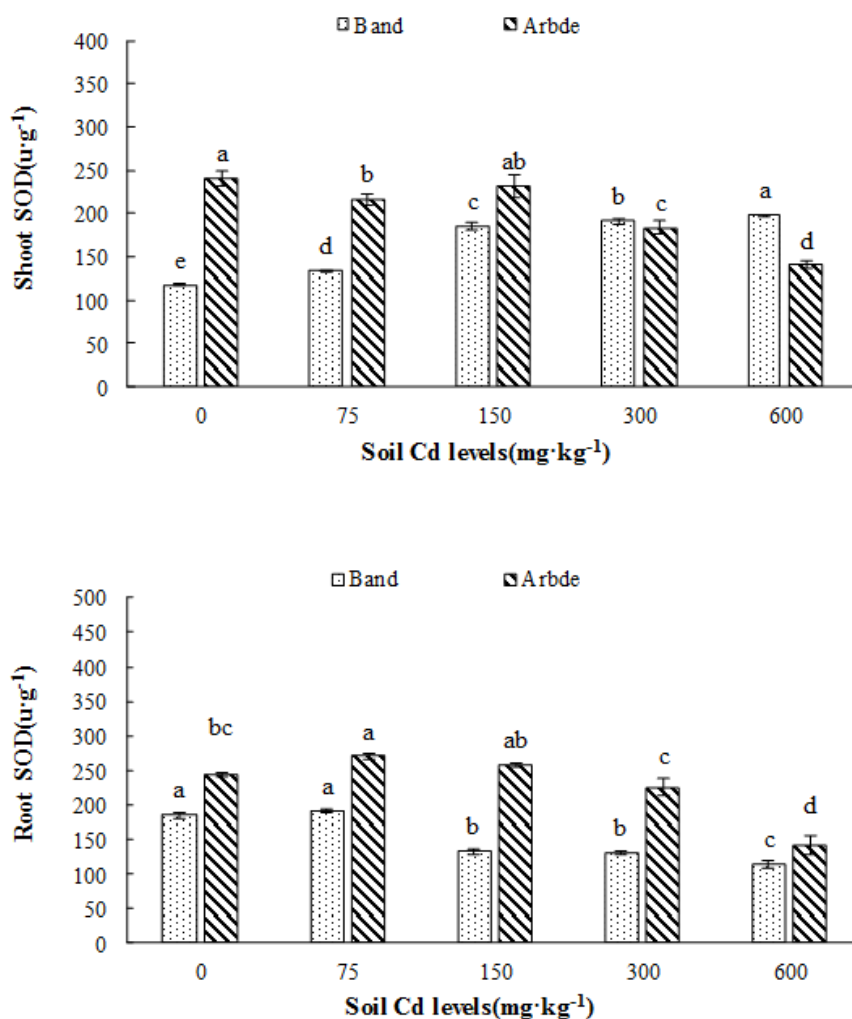


Figure 2. Effects of different cadmium levels on SOD activity in ryegrass; different letters (a, b, c) indicate significant difference at $P \leq 0.05$ among different Cd levels in the same variety

As shown in Figure 3, the activity of CAT in shoots and roots of Band and Arbde increased significantly with the increase of Cd level in soils. Highest activities of CAT

in shoots and roots were found in 150 mg·kg⁻¹ Cd, and respectively increased by 8.83% and 136.36% compared with the control. Under the same Cd level, the activity of CAT in roots of the two varieties ryegrass was lower than that in shoots.

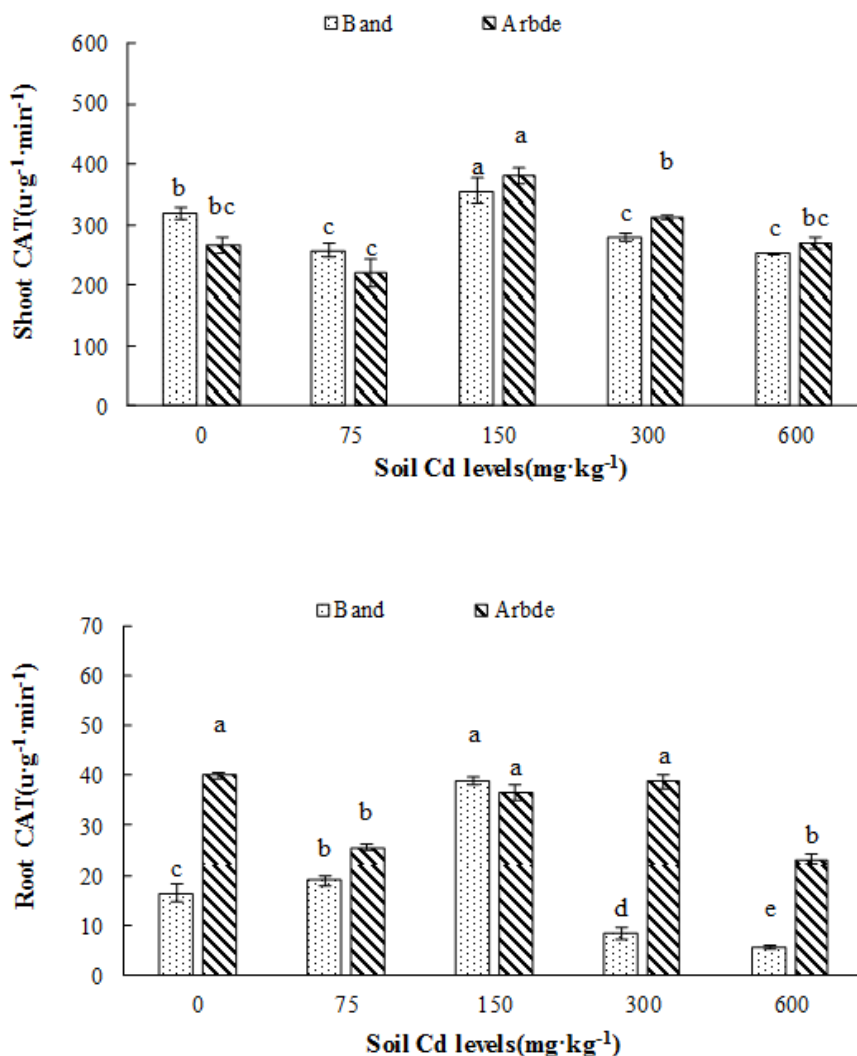


Figure 3. Effects of different cadmium levels on CAT activity in ryegrass; different letters (a, b, c) indicate significant difference at $P \leq 0.05$ among different Cd levels in the same variety

As shown in Figure 4, the activity of POD in shoots and roots of the two varieties of ryegrass increased significantly with the increase of Cd level. The activity of POD in shoots and roots of Band respectively increased by 23.50%-201.67% and 7.42%-20.01% compared with the control, respectively. The activity of POD in shoots and roots of Arbde respectively increased by 50.62%-232.06% and 4.58%-59.62% compared with the control.

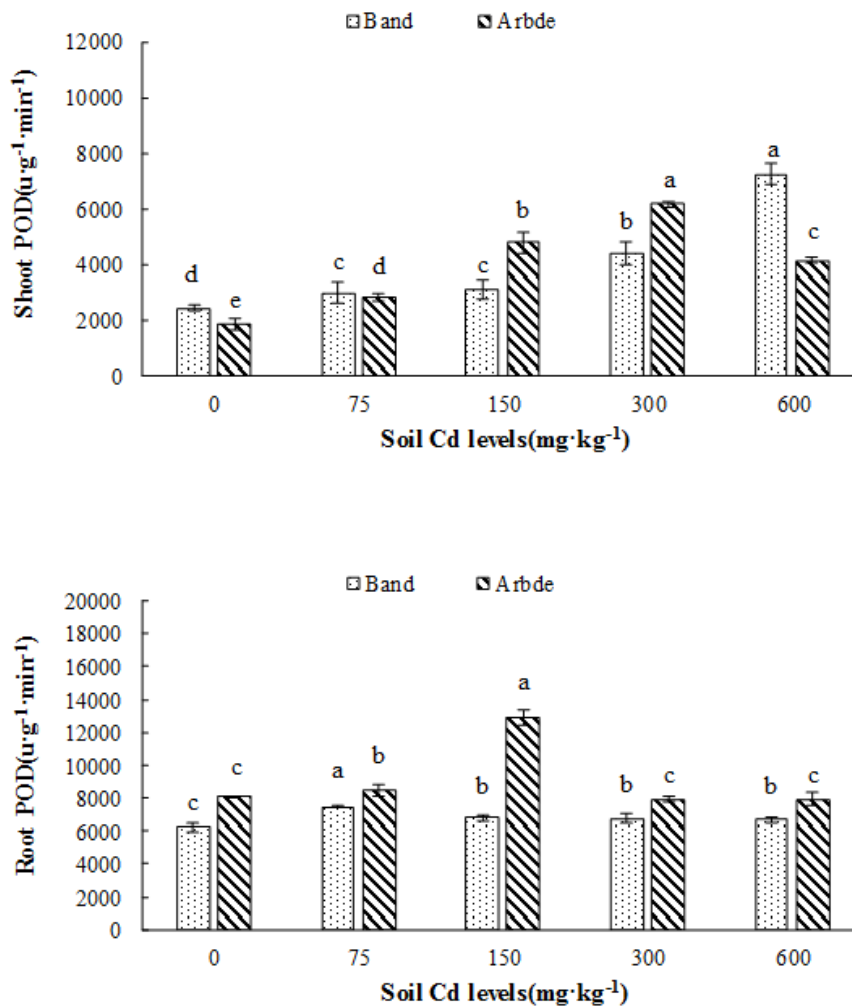


Figure 4. Effect of different cadmium levels on POD activity in ryegrass; different letters (a, b, c) indicate significant difference at $P \leq 0.05$ among different Cd levels in the same variety

MDA content

As shown in *Figure 5*, the MDA content in shoots and roots of the two varieties of ryegrass increased significantly with the increase of Cd level. Highest MDA contents in shoots and roots of Band significantly increased by 2.78% and 88.05% at 150 mg·kg⁻¹ and 75 mg·kg⁻¹ Cd respectively compared with the control. In the case of shoots and roots of Arbde, highest MDA contents in shoots and roots of Arbde significantly increased by 66.62% and 23.86% at 300 mg·kg⁻¹ and 150 mg·kg⁻¹ Cd respectively compared with the control.

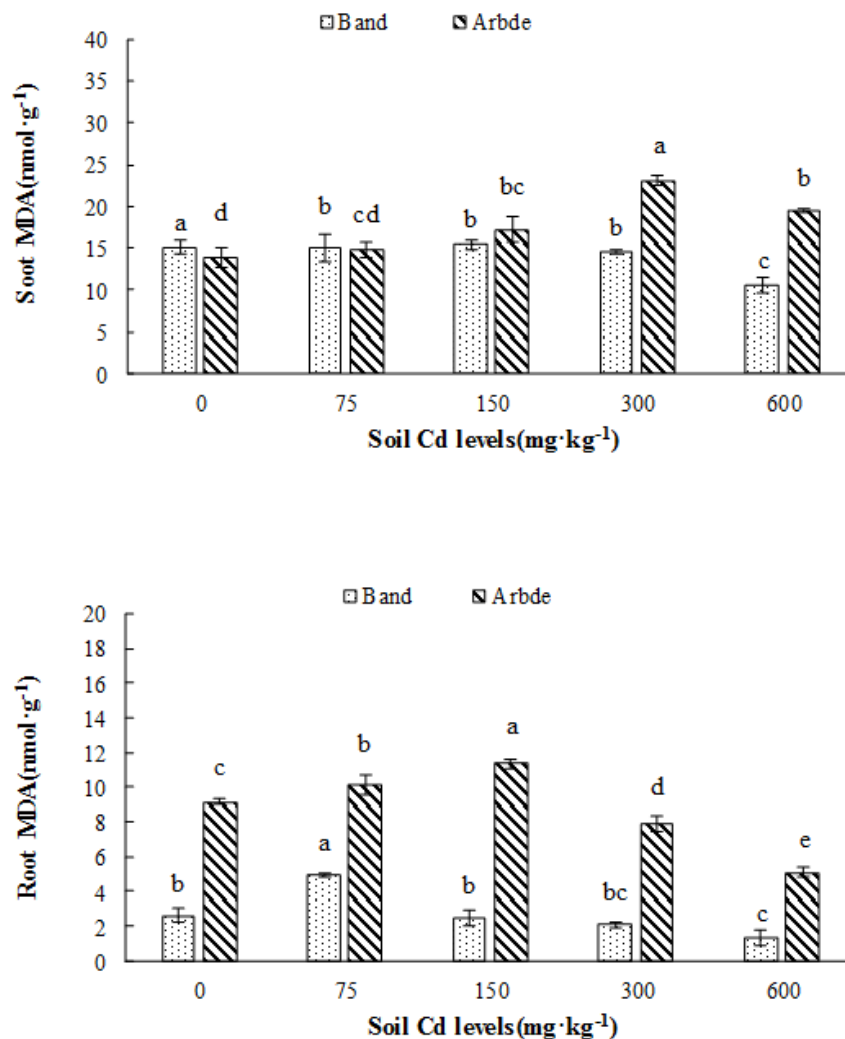


Figure 5. Effects of different cadmium levels on MDA content in ryegrass; different letters (a, b, c) indicate significant difference at $P \leq 0.05$ among different Cd levels in the same variety

Concentration of Cd in shoot and root

As shown in Figure 6, Cd concentrations in shoots and roots of the two ryegrass varieties increased significantly with the increase of Cd level ($P < 0.05$). When exposed to $150 \text{ mg} \cdot \text{kg}^{-1}$ Cd, Cd concentrations in shoots and roots of Band and Arbde were respectively as $171.827 \text{ mg} \cdot \text{kg}^{-1}$, $374.494 \text{ mg} \cdot \text{kg}^{-1}$ and $169.122 \text{ mg} \cdot \text{kg}^{-1}$, $229.676 \text{ mg} \cdot \text{kg}^{-1}$, which exceeded the critical value of cadmium hyperaccumulator ($100 \text{ mg} \cdot \text{kg}^{-1}$ Cd). At the same cadmium level, Cd concentrations in roots of the two ryegrass varieties were higher than those in shoots, and Cd concentrations in shoots and roots of Band was lower than that of Arbde.

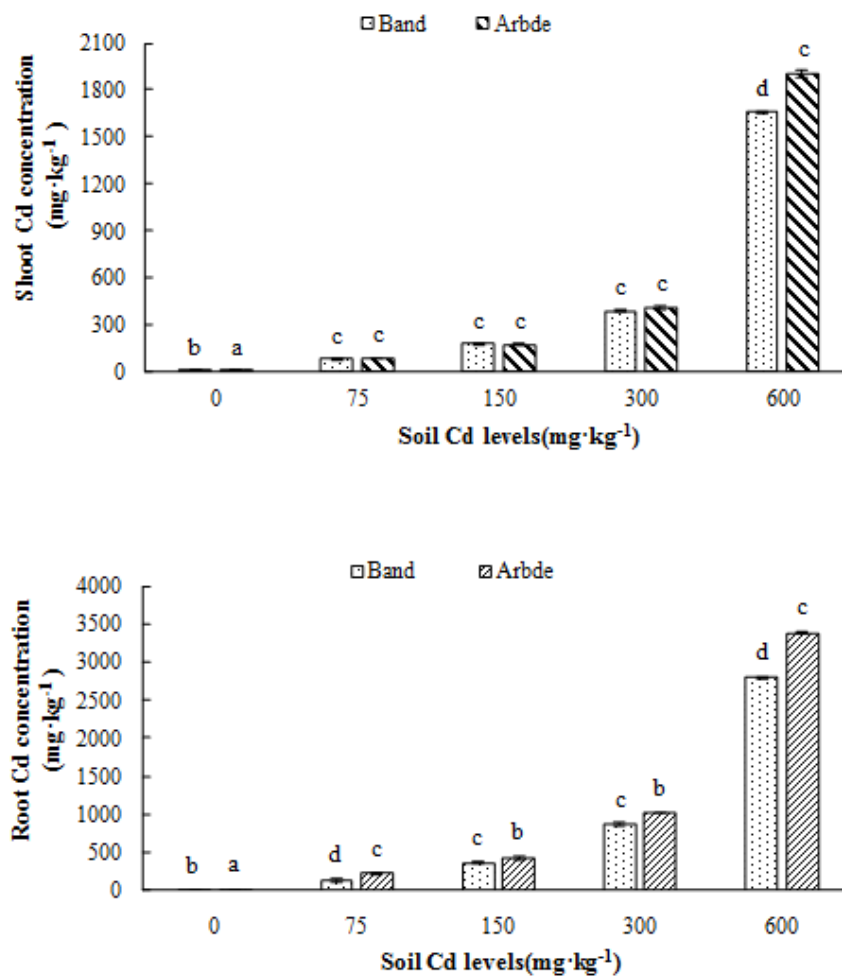


Figure 6. Effect of different Cd levels on Cd content in different parts of ryegrass; different letters (a, b, c) indicate significant difference at $P \leq 0.05$ among different Cd levels in the same variety

Cd accumulation in shoot and root

As shown in Figure 7, Cd accumulation in shoots and roots of the two ryegrass varieties increased with the increase of level of cadmium in soils, and significant differences were found between varieties and among Cd treatments ($P < 0.05$). When exposed to 75-600 mg·kg⁻¹ Cd, Cd accumulations in shoots and roots of Band were 53.84-422.93 times and 8.10-116.56 times that of the control. Highest Cd accumulation in shoots was observed at 600 mg·kg⁻¹ Cd by 118.977 ug·plants⁻¹; Cd accumulations in shoots and roots of Arbde were 25.72-304.23 times and 6.94-70.04 times that of the control. Under the same Cd level, the total amount of Cd accumulation in the plant (the sum of Cd accumulations in shoots and roots) of Arbde was greater than that of Band.

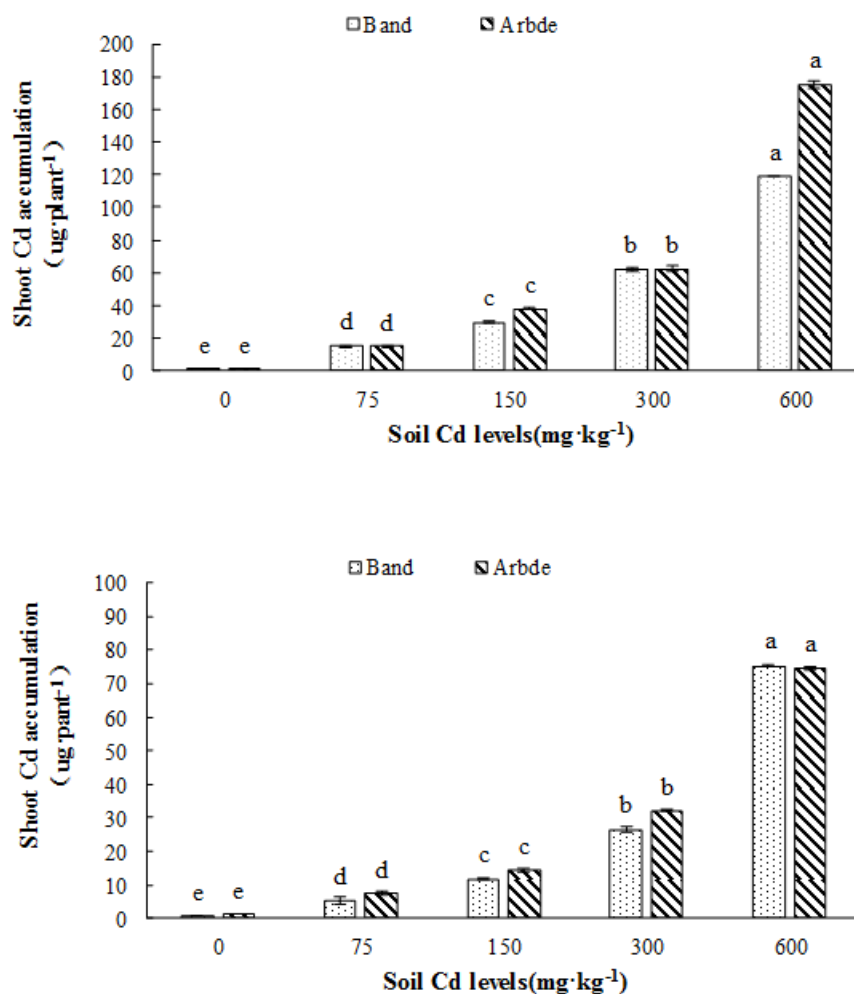


Figure 7. Effect of different cd levels on cd accumulation in different parts of ryegrass; different letters (a, b, c) indicate significant difference at $P \leq 0.05$ among different Cd levels in the same variety

Plant Cd fraction

As shown in *Figure 8*, significant differences of distribution proportion of cadmium with different forms (FDC) in shoots of the two ryegrass were found between varieties and among Cd treatments ($P < 0.05$). The concentrations of Cd chemical forms in shoots of the two ryegrass varieties were in order of sodium chloride extraction state (F_{NaCl}) > acetic acid extraction state (F_{HAc}) > ionized water extraction state (F_{W}) > residual state (F_{R}) > hydrochloric acid extraction state (F_{HCl}) > ethanol extraction state (F_{E}). F_{NaCl} , F_{HAc} and F_{W} of Band and Arbde respectively accounted for 40.7%-52.8% and 38.2%-50.0%, 19.2%-31.7% and 21.6%-36.3%, 12.5%-29.6% and 10.55%-27.17% of total amount of Cd extraction, while F_{E} with higher activity had the lowest content, and only accounted for 1.1%-3.6% and 1.4%-4.0% of total amount of Cd extraction.

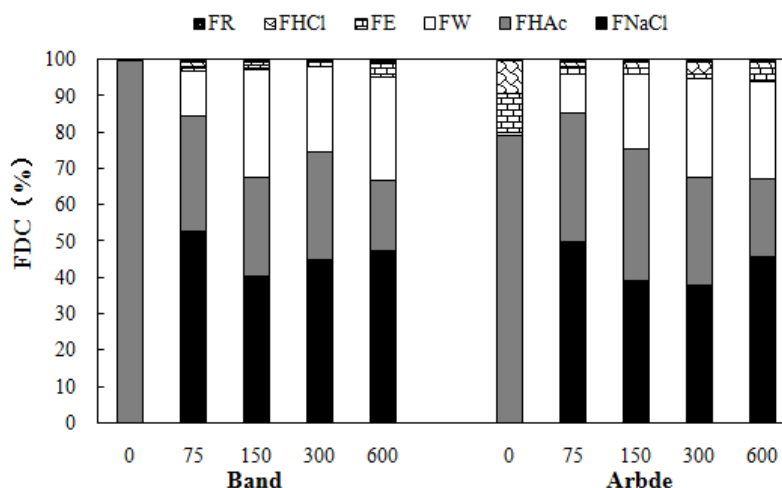


Figure 8. Effect of different Cd levels on the distribution of cadmium in ryegrass

Soil Cd fraction

The content and the distribution proportion (FDC) of Cd with different forms of the treated soils in the experiment were respectively shown in *Figure 9* and *Figure 10*. The contents of Cd with different forms (EXC-Cd, CAB-Cd, FeMn-Cd, OM-Cd and RES-Cd) in soils increased with the increase of Cd level ($P < 0.05$). The FDC of Cd with various chemical forms in soil was in order of EXC-Cd > CAB-Cd > FeMn-Cd > RES-Cd > OM-Cd. The FDC of EXC-Cd in soil of Band and Arbde were respectively as 61.42%-82.64% and 55.09%-83.23%. The FDC of OM-Cd was lowest with FDC of 0.87%-6.26%. Under the same cadmium level, soil EXC-Cd concentration of Arbde were lower than that of Band, but no significant differences were found in other soil Cd chemical forms.

Correlation between plant Cd concentration and soil Cd fraction

As shown in *Table 1*, significant correlations were observed among Cd concentration of shoots in Band and EXC-Cd, CAB-Cd, FeMn-Cd and RES-Cd in soil, whose correlation coefficients were respectively as 0.966, 0.943, 0.803 and 0.666. Moreover, significant correlations were also found among Cd concentration in roots of Band and EXC-Cd, CAB-Cd, FeMn-Cd and RES-Cd in soil, whose correlation coefficients were respectively as 0.983, 0.960, 0.838 and 0.687. As shown in *Table 2*, significant correlations were observed among Cd concentration of shoots in Arbde and CAB-Cd in soil, whose correlation coefficient was 0.847. Significant correlations were also found among Cd concentration in roots of Arbde and EXC-Cd and CAB-Cd in soil, whose correlation coefficients were respectively as 0.989 and 0.885.

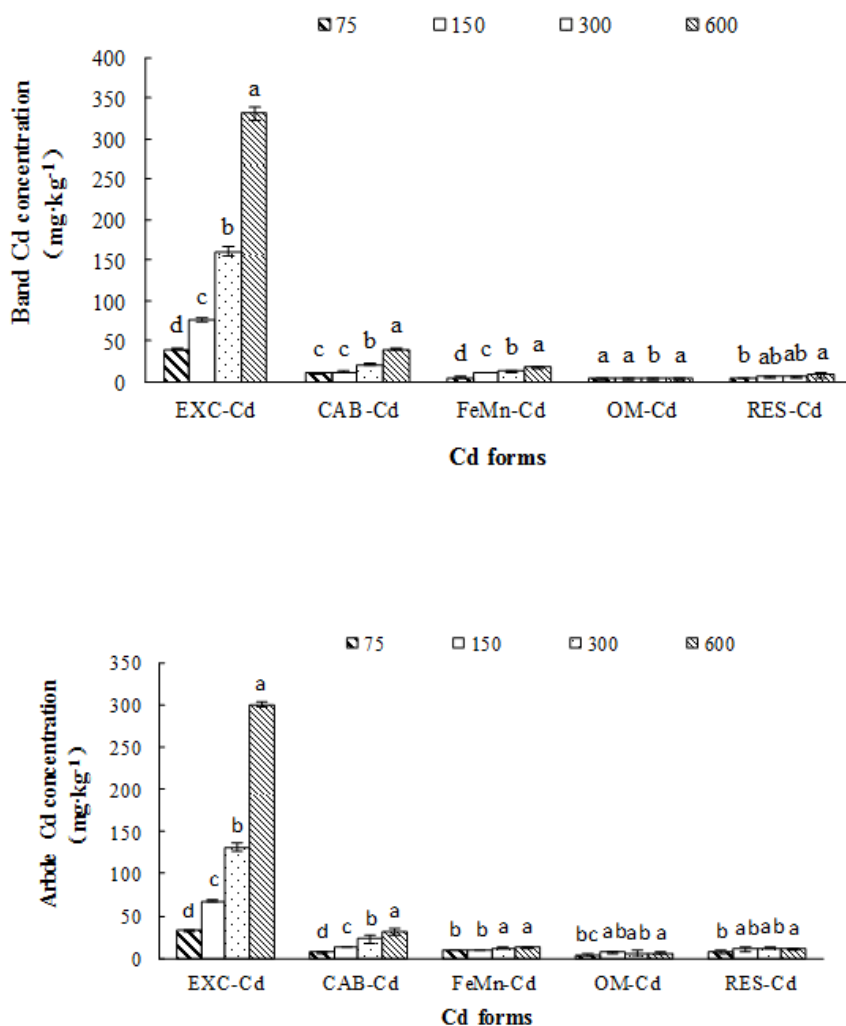


Figure 9. Effect of different Cd levels on concentration of Cd in soil; different letters (a, b, c) indicate significant difference at $P \leq 0.05$ among different Cd levels in the same variety

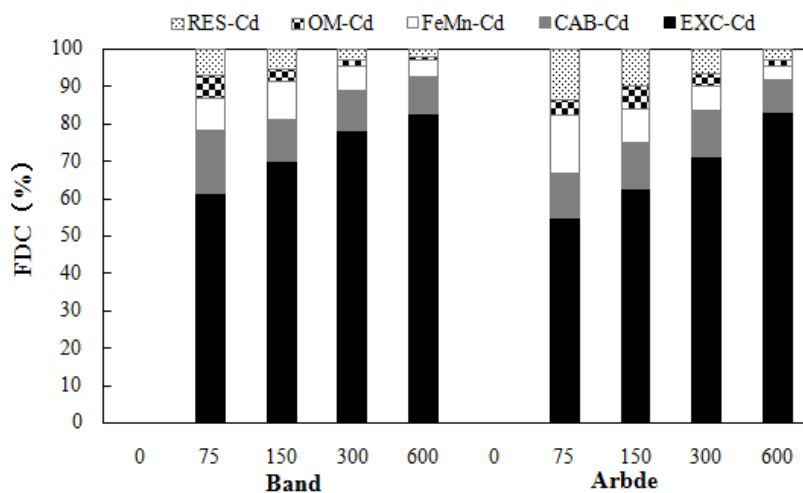


Figure 10. Effect of different Cd levels on Cd fraction distribution coefficient (FDC) in soils

Table 1. Correlation coefficient between Cd contents of Band and the concentration of Cd fractions in soil

	Shoot-Cd	Root-Cd	EXC-Cd	CAB-Cd	FeMn-Cd	OM-Cd	RES-Cd
Shoot-Cd	1						
Root-Cd	0.996**	1					
EXC-Cd	0.966*	0.983**	1				
CAB-Cd	0.943**	0.960**	0.988**	1			
FeMn-Cd	0.803**	0.838**	0.911**	0.930**	1		
OM-Cd	0.281	0.297	0.394	0.523*	0.615*	1	
RES-Cd	0.666**	0.687**	0.767**	0.812**	0.878**	0.706**	1

Table 2. Correlation coefficient between Cd contents of Arbde and the concentration of Cd fractions in soil

	Shoot-Cd	Root-Cd	EXC-Cd	CAB-Cd	FeMn-Cd	OM-Cd	RES-Cd
Shoot-Cd	1						
Root-Cd	0.996**	1					
EXC-Cd	0.973*	0.989**	1				
CAB-Cd	0.847**	0.885**	0.932**	1			
FeMn-Cd	0.555*	0.609*	0.697**	0.839**	1		
OM-Cd	0.405	0.449	0.546*	0.577*	0.698**	1	
RES-Cd	0.396	0.459	0.567*	0.730**	0.931**	0.793**	1

Discussion

Under Cd stress, plants are often shown with the toxicity symptom of Cd such as growth inhibition and so on, and the toxic effects increase with the increase of Cd level (Antoniadis et al., 2017). However, some studies have pointed out that low Cd stimulates and promotes plant growth (Shi et al., 2015). In this experiment, shoot dry weights of Arbde and Band firstly increased with the increase of Cd level in soil, and then decreased. 75 mg·kg⁻¹ Cd and 150 mg·kg⁻¹ Cd stimulate the growth of Band and Arbde, which was probably because the perennial ryegrass was likely to distribute Cd²⁺ to non metabolic active site such as vacuole, apoplast and so on in order to reduce the toxicity of Cd²⁺ to cells (Liu et al., 2013).

When exposed to Cd, large amount of reactive oxygen species and peroxides in plants are produced, such as O₂⁻, OH⁻, H₂O₂, etc., resulting in disruption of cell membrane integrity and stability, and peroxidation damage to the plant (Zhang et al., 2015). These free radicals and peroxides in plants are removed or reduced by increasing the activities of antioxidant enzymes of SOD, POD and CAT. SOD, as the first line of defense of plant antioxidants, can eliminate excess superoxide anion in cells, and POD and CAT can make H₂O₂ differentiate into non-toxic water and oxygen molecules so as to alleviate the peroxidation damage of Cd to the plant (Li et al., 2013; Wang et al., 2008). Malondialdehyde (MDA) is the product of membrane lipid peroxidation in plant cells subjected to oxidative stress under stress, which is usually regarded as physiological indexes of oxidative damage, and its content can reflect the intensity of

plant responses to stress conditions and the extent of cell membrane lipid peroxidation (Becana et al., 2000).

In the present study, the activities of SOD and POD enzymes in the two ryegrass varieties increased firstly with the increase of Cd in soil, and then decreased, which was in line with the typical defense characteristics of plants under Cd stress. This result was consistent with the result of Yang et al. (2000). The activity of CAT decreased with the increase of Cd level in soil. The reason may be that CAT is the most sensitive antioxidant enzyme to heavy metals, and its activity is firstly inhibited, causing the elimination of H₂O₂ in the body to be blocked and only to be conducted by POD, thus the activity of POD increased (Yu et al., 2010). The content of MDA increased firstly with the increase of Cd in soil, and then decreased, and can exhibit strong reactive oxygen tolerance, which was probably because the active oxygen in the body can be eliminated at high Cd stress (Xu et al., 2010).

Cadmium with strong mobility is easy to be absorbed by plants, and most plants can transfer Cd from roots to shoots (Zhang et al., 2013). In the present study, Cd concentrations in roots of the two ryegrass varieties were higher than those in shoots. It suggested that roots had stronger Cd enrichment ability, but the abilities to transfer Cd from root to shoot were weaker. This result is similar to the reports of Huang et al. (2016), Chen et al. (2014) and Sun et al. (2016). The Cd concentration in shoot of Cd hyperaccumulator with the critical content of 100 mg·kg⁻¹ was 100 times as much as common plants (Li et al., 2016). In this experiment, when exposed to high Cd (≥150 mg·kg⁻¹), Cd concentration in shoots of Band and Arbde both exceeded the critical value of hyperaccumulator, and the two ryegrass varieties with strong tolerance to Cd had no obvious toxic symptoms, which were similar to the findings of Sun et al. (2016). Under the same Cd level in soil, Cd concentration and Cd accumulation in shoots and roots of Arbde were higher than those of Band. It was suggested that Arbde was more effective in remediation of cadmium contamination in soils due to higher plant biomass and greater Cd accumulation.

There were obvious differences in Cd migration ability of different Cd chemical forms in plants, which further affects the transport and transfer of cadmium in plants and the toxicity of cadmium to plants (Li et al., 2015). In the present study, F_{NaCl} was dominant chemical form of cadmium in Band and Arbde due to Cd had a strong affinity to sulfhydryls in proteins or other organic compounds, which was consistent with the early report by Zhang et al. (2011). The F_E with higher activity in Band and Arbde only accounted for 1.1%-3.6% and 1.4%-4.0% of the total amount of Cd extraction respectively, thus greatly limiting the toxic effect of Cd on ryegrass growth.

The available cadmium in soil is one of important factors affecting Cd uptake by plants (Castaldi et al., 2005). In the experiment, the concentration of various Cd chemical forms in soils were significantly positively correlated with Cd concentrations of shoot and root in the two ryegrass varieties ($P < 0.01$) (excepted for OM-Cd), which were consistent with the study of Yang et al. (2011). EXC-Cd was dominant chemical form of cadmium in soils of the two ryegrass, and the FDC of Cd with various chemical forms in soil was in order of EXC-Cd > CAB-Cd > FeMn-Cd > RES-Cd > OM-Cd, which was consistent with the results of Chen (2016). With the increase of Cd level, the percentage of EXC-Cd accounting for the total cadmium was also increasing, which was consistent with the research results reported by Zhang et al. (2013). Cadmium concentrations of roots in the two ryegrass varieties had a very significant positive correlation with EXC-Cd, indicating the absorption of Cd concentration in roots of

ryegrass and the exchangeable cadmium content in soil, which was consistent with the results of (Yang et al., 2011). Under the same Cd level, the concentrations of EXC-Cd in soil of Band was higher than that of Arbde, corresponding to the result that Cd concentrations in shoots and roots of Arbde were higher than those of Band (excepted for shoot Cd concentration at 150 mg·kg⁻¹ Cd), which was probably caused by the difference between varieties, while the specific reasons need to be studied.

Conclusion

The shoot dry weight of the two ryegrass varieties (Band and Arbde) increased firstly and then decreased with the increase of Cd level in soil, and reached the maximum at 75 mg·kg⁻¹ and 150 mg·kg⁻¹ of Cd respectively. The activities of SOD, POD and the contents of MDA in shoots and roots of the two ryegrass varieties increased with the increase of Cd level in soil, while CAT activity decreased. The concentrations of Cd chemical forms in shoots of the two ryegrass varieties were in order of F_{NaCl} > F_{HAC} > F_w > F_R > F_{HCl} > F_E. The order of FDC of Cd in each form was described as EXC-Cd > CAB-Cd > FeMn-Cd > RES-Cd > OM-Cd. Except for OM-Cd. the concentration of various Cd chemical forms in soils were significantly positively correlated with Cd concentrations of shoot and root in the two ryegrass varieties (*P* < 0.01) (excepted for OM-Cd). Compared with the two ryegrass varieties, Arbde was more effective in remediation of cadmium contamination in soils due to stronger tolerance to Cd, higher biomass and greater Cd accumulation. Recommendations for future studies are to found the plants or varieties with high Cd-accumulation are needed to be screened out and cultured, and their genes are induced into plants with great biomass, rapid growing and strong adaptability, so that ideal Cd super-accumulation plants.

Acknowledgments. This work was supported by Fund of China Agriculture Research System (CARS-23), the National Science and Technology Pillar Program of China (No. 2007BAD87B10), Chinese Undergraduate Training Programs for Innovation and Entrepreneurship (201610635028), and Southwestern University Undergraduate Science and Technology Innovation “Guangjiong” Training Project (20150490).

REFERENCES

- [1] Ahamed, A. J., Loganathan, K. (2017): Water quality concern in the Amaravathi River Basin of Karur district: a view at heavy metal concentration and their interrelationships using geostatistical and multivariate analysis. – *Geology, Ecology, and Landscapes* 1(1): 19-36.
- [2] Antoniadis, V., Shaheen, S. M., Boersch, J., Froehne, T., Du, L. G., Rinklebe, J. (2017): Bioavailability and risk assessment of potentially toxic elements in garden edible vegetables and soils around a highly contaminated former mining area in Germany. – *J. Environ. Manage* 186: 192-200.
- [3] Becana, M. D., Dalton, D. A., Moran, J. F. (2000): Reactive oxygen species and antioxidants in legume nodules. – *Physiol. Plantarum* 109(4): 372-381.
- [4] Castaldi, P., Santona, L., Melis, P. (2005): Heavy metal immobilization by chemical amendments in a polluted soil and influence on white lupin growth. – *Chemosphere* 60(3): 365-371.
- [5] Chen, R. (2016): Mechanism and Remediation Effect of Biochar and Soil Conditioner on Cadmium Contaminated Soil. – Chongqing: Southwest University.

- [6] Chen, Y. H., Liu, X. Y., Wang, M., Wang, X. J., Yan, X. M. (2014): Cadmium tolerance, accumulation and relationship with Cd subcellular distribution in *Ricinus communis* L. Environ. – Sci-China 34(9): 2440-2446.
- [7] Chen, Y. Q., Jiang, L., Xu, W. H., Chi, S. L., Chen, X. G., Xie, W. W., Xiong, S. J., Zhang, J. Z., Xiong, Z. T. (2015): Effect of ryegrass and arbuscular mycorrhizal on Cd absorption by varieties of tomatoes and cadmium forms in soil. – Environ. Sci. 36(12): 4642-4650.
- [8] Du, P., Xue, N., Liu, L., Li, F. (2008): Distribution of Cd, Pb, Zn and Cu and their chemical speciations in soils from a peri-smelter area in northeast China. – Environ. Geol. 55(1):205-213.
- [9] Feng, P., Sun, L., Shen, X. H., Jiang, C., Li, R. L., Zeng, Z. J., Zheng, H. Y., Zhang, H., Guo, W., Han, X. D., Hong, Y. N. (2016): Response and enrichment ability of perennial ryegrass under lead and cadmium stresses. – Acta Pratacult. Sin. 25(1):153-162.
- [10] Grant, C. A., Clarke, J. M., Duguid, S., Chaney, R. L. (2008): Selection and breeding of plant cultivars to minimize cadmium accumulation. – Sci. Total Environ. 390(2-3): 301-310.
- [11] Hashemi, N. (2017): Recognizing the potential of sustainable use of pasture resources in south khorasan province with approach of carrying capacity. Environment Ecosystem Science, 1(2): 09-12.
- [12] Hejazi, S.M., Lotfi, F., Fashandi, H., Alirezazadeh, A. (2017): Serishm: an eco-friendly and biodegradable flame retardant for fabrics. Environment Ecosystem Science, 1(2): 05-08.
- [13] Huang, D. F., Xi, J. B., Zhao, Y. L., (2016): The Physiological Response of Two Varieties of *Lolium perenne* Under Cadmium Stress. – Nor. Horticult. (3): 66-68.
- [14] Issaka, S., Ashraf, M. A. (2017): Impact of soil erosion and degradation on water quality: a review. – Geology, Ecology, and Landscapes 1(1): 01-11.
- [15] Li, H. T., Dong, R. (2015): Pb & Cd absorption and accumulation characteristics, subcellular distribution and chemical forms in two types of Hemerocallis plants. – J. South Chin. Agric. Univ. 36(4): 59-64.
- [16] Li, P., Peng, X. J., Luan, Z. K., Zhao, T. K., Zhang, C. J., Liu, B. C. (2016): Effects of red mud addition on cadmium accumulation in cole (*Brassica campestris* L.) under high fertilization conditions. – J. Soil Sediment 16(8): 2097-2104.
- [17] Li, X., Yue, H., Wang, S., Huang, L. Q., Ma, J., Guo, L. P. (2013): Research of different effects on activity of plant antioxidant enzymes. – China Journal of Chinese Materia Medica 38(7): 973-978.
- [18] Liu, J. X., Xu, X. Q., Qian, Y. Q., Ju, G. S., Han, L., Sun, Z. Y. (2013): Responses of antioxidative enzymes and phytochelatin in *Lolium perenne* to Cd²⁺ stress. – Chin. J. Ecol. 32(7):1787-1793.
- [19] Liu, Y. Z., Xiao, T. F., Ning, Z. P., Jia, Y. L., Li, H. J., Yang, F., Jiang, T., Sun, M., (2013): Cadmium and selected heavy metals in soils of Jianping area in Wushan country, the three gorges region: distribution and source recognition. – Environ. Sci. 34(6):2390-2398.
- [20] Liu, Y., Xiao, T., Baveye, P. C., Zhu, J., Ning, Z., Li, H. (2015): Potential health risk in areas with high naturally-occurring cadmium background in southwestern China. – Ecotox. Environ. Safe. 112: 122-131.
- [21] Radan, A., Latifi, M., Moshtaghi, M., Ahmadi, M., Omidi, M. (2017): Determining the Sensitive Conservative Site in Koleh Ghazi National Park, Iran, In Order to Management Wildlife by Using GIS Software. Environment Ecosystem Science, 1(2): 13-15.
- [22] Reiser, R., Simmler, M., Portmann, D., Cucas, L., Schulin, R., Robinson, B. (2014): Cadmium concentrations in New Zealand pastures: relationships to soil and climate variables. – J. Environ. Qual. 43(3): 917.
- [23] Shi, C., Wang, C. L., Huang, C. F., An, S. Z. (2015): Effects of Cd stress on the growth and physiological characteristics of *Avena fatua* seedlings. – Acta Agrect. Sin. 23(3): 526-532.
- [24] Sun, Y. Y., Guan, P., He, B., Shi, J. M. (2016): Effects of Cd stress on Cd accumulation,

- physiological response and ultrastructure of *Lolium multiflorum*. – Pratacult. Sci. 33(8):1589-1597.
- [25] Tessier, A., Campbell, P. G. C., Bisson, M. (1979): Sequential extraction procedure for the speciation of particulate trace metals. – Anal. Chem. 51(7): 844-851.
- [26] Vazdani, S., Sabzghabaei, G., Dashti, S., Cheraghi, M., Alizadeh, R., Hemmati, A. (2017): Fmea Techniques Used in Environmental Risk Assessment. Environment Ecosystem Science, 1(2): 16-18.
- [27] Wang, H., Zhao, S. C., Xia, W. J., Wang, X. B., Fan, H. L., Zhou, W. (2008): Effect of cadmium stress on photosynthesis, lipid peroxidation and antioxidant enzyme activities in maize (*Zea mays* L.) seedlings. – Plant Nutrition and Fertilizing Science 14(1): 36-42.
- [28] Wu, Q. L., Wang, W. C., He, S. Y. (2014): Enhancement of GA₃ and EDTA on *Lolium perenne* to remediate Pb contaminated soil and its detoxification mechanism. – Chin. J. Appl. Ecol. 25(10): 2999-3005.
- [29] Xiang, T. (2014): Study on remedial of Cd-Contaminated soil by herbaceous flowers. – Chongqing: Chongqing University.
- [30] Xiao, H., Wang, M., Sheng, S. (2017): Spatial evolution of URNCL and response of ecological security: a case study on Foshan City. Geology, Ecology, and Landscapes, 1(3): 190-196.
- [31] Xu, W. H., Wang, H. X., Liu, H., Balwant, S. (2007): Effects of individual and combined pollution of Cd and Zn on root exudates and rhizosphere Zn and Cd fractions in ryegrass (*Loliurn perenne* L.). – Environ. Sci. 28(9): 2089-2095.
- [32] Xu, W., Kachenko, A. G., Singh, B. (2010): Effect of soil properties on arsenic hyperaccumulation in *pteris vittata* and *pityrogramma calomelanos* var. *austroamericana*. – Int. J. Phytoremediat 12(12): 174-187.
- [33] Yang, J. H., Wang, C. L., Dai, H. L. (2008): Soil agrochemical analysis and environmental monitoring. – China Land Press, Beijing.
- [34] Yang, S., Li, J., Song, Y. (2017): Application of surfactant Tween 80 to enhance Fenton oxidation of polycyclic aromatic hydrocarbons (PAHs) in soil pre-treated with Fenton reagents. Geology, Ecology, and Landscapes, 1(3): 197-204.
- [35] Yang, W. D., Chen, Y. T. (2008): Membrane leakage and antioxidant enzyme activities in roots and leaves of *salix matsudana* with cadmium stress. – Acta Botanica Boreali Occidentalia Sinica 28(11): 2623-2269.
- [36] Yang, Y., Nan, Z., Zhao, Z., Wang, Z., Wang, S., Wang, X., Jin, W., Zhao, C. (2011): Bioaccumulation and translocation of cadmium in cole (*Brassica campestris* L.) and celery (*Apium graveolens*) grown in the polluted oasis soil, Northwest of China. – J. Environ. Sci-China 23(8): 1368-1374.
- [37] Yu, K. L., Meng, Q. M., Zou, J. H. (2010): Effects of Cd²⁺ on seedling growth, chlorophyll contents and ultrastructures in maize. – Acta Agric. Boreali Sin. 25(3): 118-123.
- [38] Zhang, X. J., Liu, J. Z., Xu, W. H., Chen, G. Q., Wang, H. X., Zhang, H. B., Han, G. Q., Zeng, H. J., Lan, C. T., Xiong, Z. T., Wei, Q. S. (2011): Effect of phosphor on accumulation and chemical forms of cadmium, and physiological characterization in different varieties of *capsicum annuum* L. – Environ. Sci. 32(4): 1171-1176.
- [39] Zhang, X., Li, K. W., Chen, K. J., Liang, J., Cui, L. J. (2013): Effects of cadmium stress on seedlings growth and active ingredients in *salvia miltiorrhiza*. – Plant Sci. J. 31(6): 583-589.
- [40] Zhang, Y. P., Shen, R. G., Yao, X. Q., Chen, Y. Y. (2015): Effects of cadmium stress on antioxidant enzyme activities and photosynthesis in melon seedlings. – Chin. Agric. Bull. 31(34): 82-88.
- [41] Zhao, S., Chen, T. (2017): Design and development of national geographic condition monitoring system based on WebGIS. – Geology, Ecology, and Landscapes 1(1): 12-18.

IN VITRO CHARACTERIZATION OF BACTERIAL ENDOPHYTES FROM TOMATO (*SOLANUM LYCOPERSICUM* L.) FOR PHYTOBENEFICIAL TRAITS

IQBAL, S.¹ – HAMEED, S.¹ – SHAHID, M.^{2,1*} – HUSSAIN, K.^{1,3} – AHMAD, N.^{1,4} – NIAZ, M.⁵

¹*Microbial Physiology Lab, National Institute for Biotechnology & Genetic Engineering (NIBGE),
P.O. Box 577, Jhang Road, Faisalabad, Pakistan*

²*Department of Bioinformatics and Biotechnology, Government College University,
Faisalabad-38000, Pakistan*

³*Department of Botany, Ghazi University
Dera Ghazi Khan, Pakistan*

⁴*Department of Chemistry, Faisalabad Campus, University of Education,
Faisalabad-38000, Pakistan*

⁵*Department of Botany, Government College University,
Faisalabad-38000, Pakistan*

*Corresponding author:

e-mail: shahidmpg@yahoo.com; phone: +92-300-7919822

(Received 28th Aug 2017; accepted 18th Dec 2017)

Abstract. Bacterial endophytes, with plant beneficial traits, are being routinely isolated and investigated to address environmental impacts and low nutrient use efficiency of chemical fertilizers. The current study was framed with a hypothesis that local cultivar of tomato (*Solanum lycopersicum* L. cv. Nagina) harbors multi-trait endophytes with plant-beneficial attributes. From a collection of purified root endophytes, only two isolates viz. NgE3 and NgE4 with desired PGP traits were identified as *Bacillus subtilis* and *Paenibacillus* sp., respectively on the basis of 16S rRNA gene sequence analysis. Both the strains exhibited substantial nitrogenase activity, tricalcium phosphate-solubilizing ability and were positive for 1-aminocyclopropane-1-carboxylate (ACC) deaminase synthesis. A considerable quantity of Indole-3-acetic acid was measured only in the culture supernatant of *Paenibacillus* strain NgE4, while N-acyl homoserine lactones (AHLs) production was found positive in *Bacillus subtilis* NgE3. Both the strains also revealed considerable antifungal activity (> 70%) against at least 3 out of 5 fungal pathogens tested. The root colonization potential of *Bacillus* and *Paenibacillus* strains was confirmed by localizing the strains in the tomato root cortical cells as endophytes through transmission electron microscopy. Keeping in view very limited research reported on bacterial endophytes in Pakistan, both phytobeneficial strains are potential resources as bio-inoculants for the tomato to design greenhouse and field experiments.

Keywords: *isolation, plant-beneficial traits, 16S rRNA, transmission electron microscopy, antifungal activity*

Introduction

Maintenance of agricultural productivity for ever-increasing world population along with preservation of natural resources has become a major challenge in both developed and developing countries (Singh, 2017). Up to now, the farmer's strategy to increase crop productivity was totally based on the use of chemical fertilizer inputs; however, increasing the fertilizer inputs is no more boosting the agricultural yields in recent

decades due to their low nutrient use efficiency (Yousaf et al., 2017). Therefore, this prompts the need to characterize the plant beneficial bacteria for their ultimate field inoculation as nutrient supplying agents (Hanif et al., 2015; Pii et al., 2015; Akram et al., 2016; Mahmood et al., 2017). Such beneficial bacterial agents, often known as plant growth-promoting rhizobacteria (PGPRs), establish a strong association with rhizosphere, the soil adhering to the root surfaces (Kloepper et al., 1989). They are also found in the direct attachment to the root surfaces as rhizoplastic bacteria, and tend to pierce root epidermis and cortex as endophytes (Sylvia et al., 2005; Shaid et al., 2015).

With the advent of advanced molecular techniques, it is now possible to sequence the genomes of both bacterial and fungal endophytes without isolation and purification on culture media. Thus, the more advanced definition of endophytes is the set of microbial genomes inside the plant organs (Bulgarelli et al., 2013). Endophytes are of three types depending upon plant inhabiting life strategies (Hardoim et al., 2008). Obligate endophytes transmit via seeds and are unable to thrive outside the plants. For instance, *Xylella fastidiosa* is found in plant tissues as obligate endophyte and is capable of persisting inside the plant for long period of time (Hardoim et al., 2008). *Xylella fastidiosa* transmit through insect vectors. Facultative endophytes live freely in soil and cause infection and colonization as opportunity arrives (Hardoim et al., 2008); most endophytes known for plant growth promotion belong to this class, e.g. *Pseudomonas fluorescence* and *Azospirillum brasilense*. These endophytes enter in plants through cracks in lateral roots or wounds caused by nematodes or plant pathogens (Rosenblueth and Martínez-Romero, 2006). Many other rhizosphere competent bacterial genera are considered as endophytes at some stage of their life cycle. The third category, known as passive endophytes, is not competitive in terms of root colonization and plant growth promotion. Even though they lack the active machinery of plant infection and colonization, transmission via plant roots may occur as result of stochastic events (Verma et al., 2004; Rosenblueth and Martínez-Romero, 2006; Hardoim et al., 2008). After infection and transmission to roots, endophytes can exist both inter- and intracellularly (Hurek et al., 1994; Zakria et al., 2007). A variety of plant species bear bacterial endophytes as part of their root microbiome, with some being known to improve plant growth and productivity by exploiting a variety of mechanisms (Gaiero et al., 2013). Endophytic bacteria are also known to tolerate salt-stress and induce salinity tolerance mechanisms in plants (Damodaran et al., 2014; Yaish et al., 2015). Despite the extensive research on bacterial root endophytes to apply as inoculants for plant growth promotion (Thakore, 2006), a limited understanding exists about the drivers of endophytic communities and mechanisms involved for the success of inoculation in crop productivity. Bacterial endophytes, by synthesizing ACC deaminase enzyme, reduce ethylene concentration and help plants to thrive in adverse environmental conditions. Bacterial endophytes have also been described to produce phytohormones like indole-3-acetic acid (Hardoim et al., 2008). Moreover, different types of AHLs (C6, C8, C10, oxo-C12, 3-oxo-C6 etc.) are known to produce by endophytes for signal transduction during the association. These AHLs participate in plant signaling pathways to sense ecological dynamics (Hartmann et al., 2014).

In vitro characterization of endophytes for plant beneficial properties is the first key step towards the selection of potential bacterial inoculants and investigation of the mechanism involved in phytostimulation (Jasim et al., 2014). So far, most of the studies on bacterial endophytes from tomato were either aimed at their characterization for PGP traits (Amareesan et al., 2012) or biocontrol of phytopathogens (Munif et al., 2013;

Upreti and Thomas, 2015). The present piece of work is conducted to target multi-trait bacterial endophytes from a local tomato cultivar bearing not only PGP characteristics but also antagonism against plant pathogenic fungi. The study will go a long way in the elucidation of the role of these endophytes for vigor and yield improvement of the tomato crop. Furthermore, the baseline information of these endophytic bacterial associations of tomato will steer to more comprehensive studies in terms of exploring the biochemical and genetic basis of this association.

Materials and methods

Isolation and morphological studies

Tomato plants (cv. Nagina), grown at experimental field of Nuclear Institute of Agriculture and Biology (NIAB, 31°23'42.13 N, 73°1'37.24 E), Faisalabad, Pakistan were uprooted followed by excision of aerial parts with sterilized a knife for isolation of bacteria from endosphere portion of the plant. This cultivar is considered as salt tolerant genotype (Amjad et al., 2014a; 2014b), and thus, selected for isolation of root endophytes. The samples were carried in sterilized polythene bags (25×30 cm) to the Microbial Physiology Laboratory, National Institute for Biotechnology and Genetic Engineering (NIBGE), Faisalabad, Pakistan. Root portions were subjected to washing with tap water followed by sterile distilled water to detach adhered soil. Root surfaces were disinfected by dipping in ethanol (70%) for 1 min and sodium hypochlorite (5 % [w/v]) for another 10 min, followed by 5-6 washings with sterilized distilled water. For bacterial isolation, 1 g of macerated roots were put in 9 ml of saline solution (0.85% (w/v) NaCl) by serial dilution technique described by Somasegaran and Hoben (1994). Aliquots (100 µl) from two dilutions (10^{-4} and 10^{-6}) were spread on Luria-Bertani (LB) agar plates using a sterilized glass spreader, followed by 48 h incubation in a microbial incubator (Memmert, Germany) preset at 28 ± 2 . Bacterial colonies were selected on the basis of prolific growth and colony morphology and purified through repeated streaking. The purified isolated were maintained at LB-agar plates to carry out further experiments. Five copies of each purified isolate were preserved in 20% (v/v) glycerol at -80 °C. Various morphological characteristics like the colony and cell morphology, motility and Gram's reactions were studied under the light microscope as described by Vincent (1970).

Nitrogen fixation

Nitrogen fixation ability of isolates (NgE3 and NgE4) was assessed by acetylene reduction assay (ARA) using GC-FID as described by Hardy et al. (1968). The purified isolates were individually inoculated into 30 ml semisolid nitrogen free malate (NFM) medium (In 1 l distilled water: 5g l⁻¹ malic acid, 0.5 g l⁻¹ K₂HPO₄, 0.2 g l⁻¹ MgSO₄·7H₂O, 0.02 g l⁻¹ CaCl₂, 0.1 g l⁻¹ NaCl, 0.002 g l⁻¹ NaMoO₄·2H₂O, 5 ml 0.5% (w/v) bromothymol blue (BTB), 10 µg biotin, 0.2% (w/v) agar, pH 7 was adjusted with KOH (Okon et al., 1977), in Erlenmeyer flasks (100 ml) and allowed to grow in an orbital shaker (150 rpm, Gallenham, UK) at 28 ± 2 °C for 72 h. A well-grown culture (4 ml) was further inoculated to glass vials (12 ml) containing 4 ml NFM medium and followed by incubation at 28 ± 2 °C for 24 h. After replacing the steel caps of vials with rubber septa, air 10% (v/v) was exchanged with the same volume of acetylene gas with the help of a sterilized syringe followed by incubation at 28 ± 2 °C for 24 h. Estimation

of acetylene (C₂H₂) reduction to ethylene (C₂H₄) was made with Gas chromatograph (Thermoquest, Trace GC, Model K, Rodono Milan, Italy) fitted with a Porapak N column (2 mm × 2 m) and a flame ionization detector (FID). The operating conditions of GC were: oven temperature 80 °C, right inlet 100 °C, right detector 180 °C, hydrogen flow rate 30 ml min⁻¹, nitrogen flow rate 42 ml min⁻¹ and air flow rate was maintained at 300 ml min⁻¹. Standard ethylene (200 µl, Spancan Calibration Gas, Spantach Products, England) was injected before analyzing samples and peak area was recorded followed by same volume of each sample. Protein concentration in vial mixture was determined by the method described by Bradford (1976).

Indole-3-acetic acid (IAA) production

The isolates were inoculated into Erlenmeyer flasks (500 ml) containing 100 ml LB broth supplemented with tryptophan (100 mg l⁻¹) and subjected to incubation at 28 ± 2 °C for 48 h in an orbital shaker at 150 rpm (Gallenhamp, UK). Supernatant, collected in separate tubes after spinning at 13000 g, was acidified (pH 2.8) with HCl. Supernatant was mixed with equal volume of ethyl acetate for IAA extraction in separating funnel (Tien et al., 1979). The IAA-containing upper layer of separating funnel was collected in separate sterilized tubes followed by removal of excessive ethyl acetate under vacuum at 45 °C, using a rotary evaporator (EYELA, Tokyo, Japan). This extract was dissolved in methanol (1 ml) and filter sterilized through 0.2 µm nylon filter (Millipore, USA) prior to analyze by HPLC (λ = 260 nm) (Perkin Elmer, USA) equipped with Turbochrom software and C₁₈ column (150 mm length, 4 mm diameter and 120Å pore size) at a flow rate of 0.5 ml min⁻¹ using 30:70 (v/v) methanol:water as mobile phase.

Phosphate solubilization and detection of organic acids

Each of the purified isolates was spot-inoculated on Pikovskaya's agar (Pikovskaya, 1948) plates, incubated at 28 ± 2 °C in a microbial incubator (Mettler, Germany) and observations were taken to 168 h for halo-zone formation. For quantitative analysis of phosphate solubilization and organic acid production, 100 ml of Pikovskaya's broth was inoculated with single purified colonies of each isolate in Erlenmeyer flasks (500 ml) and incubated at 28 ± 2 °C for 240 h in an orbital shaker (Gallenhamp, UK) at 150 rpm. An aliquot of 20 ml of pure bacterial culture from each flask was harvested after 72 h, 120 h and 168 h and centrifuged at 13000 g for 10 min to collect the supernatant. The quantification of phosphate solubilization was accomplished according to phosphomolybdate blue color method (Murphy and Riley, 1962) using spectrophotometer (JENWAY6305, UK) (λ = 882 nm). For the determination of the organic acids, the cell-free supernatant of isolates was filtered through nylon filters (0.2 µm, Millipore, USA) and 20 µl was injected into HPLC (λ = 210 nm) equipped with Turbochrom software (Perkin Elmer, USA) and C₁₈ column (150 mm length, 4 mm diameter and 120Å pore size). A flow rate of 0.6 ml min⁻¹ was maintained using methanol: acetic acid (30:70 (v/v)) as a mobile phase. The standards of organic acids (gluconic, malic, lactic, acetic, citric, and tartaric acid) were commercially purchased (Sigma-Aldrich, Germany).

ACC deaminase activity

The ability of endophytes to use 1-aminocyclopropane-1-carboxylic acid (ACC) as sole nitrogen source was determined in 5 ml DF salt minimal media (Penrose and Glick,

2003) containing 3 μl of 0.5 M ACC. The cultures were incubated at 28 ± 2 °C at constant shaking (150 rpm) for 48 h. The turbidity of cultures in comparison with non-inoculated control indicated the ability to utilize ACC.

Screening for *N*-acyl homoserine lactone (AHL) production

The purified isolates (NgE3 and NgE4) were streaked onto the center of a Tryptone Yeast extract (TY) (Beringer, 1974) agar plates and were allowed to grow overnight in a microbial incubator (Memmert, Germany) preset at 28 ± 2 °C. The indicator strain *Chromobacterium violaceum* CV026 (obtained from John Innes Centre, Norwich, UK) was grown separately in LB broth at 28 ± 2 °C with constant shaking overnight up to an OD of 10^6 CFU ml^{-1} . Detection of AHLs was made by the plate overlay assay as described earlier by McLean et al. (2004). The reference strain A34 (obtained from the John Innes Centre, Norwich, UK) was used as the positive control. A34 is a *Rhizobium leguminosarum* 8401 containing *p*RLI1. Plates were incubated at 30 ± 2 °C overnight, and purple pigmentation produced by the indicator strain on the plates was an indicator of AHL production.

Antifungal activity

The antifungal activity was tested using a dual-culture assay as described by Sakthivel and Gnanamanickam (1986). A drop of the exponentially grown bacterial culture (approx. 20 μl) was spotted onto potato dextrose agar (PDA) plates close to the walls of the Petri dish on both sides and the plates were allowed to dry in laminar air flow cabinet. A 6-mm agar disk of each of three fungal species, namely, *Fusarium solani*, *F. oxysporum* and *F. moniliforme*, *Aspergillus niger* and *A. flavus* (obtained from Department of Plant Pathology, University of Agriculture, Faisalabad, Pakistan), were separately placed at the center of PDA plates. Fungal disc was grown separately over Petri plate containing PDA to serve as a control. The incubation of plates was made at 28 ± 2 °C in microbial incubator (Memmert, Germany) for 5 days to measure the inhibition of radial fungal growth between fungal and bacterial colonies.

$$\text{Inhibition (\%)} = (1 - [\text{fungal growth} / \text{Control growth}]) \times 100$$

16S rRNA gene sequencing

Total genomic DNA of isolates (NgE3 and NgE4) was isolated by the alkaline lysis method (Maniatis et al., 1982) and quantified by ultraspec™ 3100 (OD_{260, 260/280}). This DNA was used as template to amplify the 16S rRNA gene with primers fd1 and rd1 as described earlier by Weisburg et al. (1991) with slight modifications as: for 50 μL reaction in ultra-pure water, 5 μl of Taq buffer (Fermentas, USA), 3 μl of 25 mM MgCl_2 (Fermentas, USA), 5 μl of 2 mM dNTPs (Fermentas, USA), 0.5 μl of 100% DMSO, 1.5 μl each of forward and reverse primer, 0.75 μl of 5 U μl^{-1} Taq DNA polymerase (Fermentas, USA) and 40 ng of template DNA. Polymerase chain reaction (PCR) was conducted in thermal cycler (PeQLab, advanced Primus 96, Germany) with modified temperature conditions as: 30 cycles of 95 °C for 1 min, 55 °C for 30 s, and 72 °C for 1 min. The initial denaturation and final extension steps were performed at 95 °C for 5 min and 72 °C for 10 min, respectively. Amplicons were purified with QIAquick PCR purification kit (Qiagen, USA) according to manufacturer's protocol and sequenced

directly on both sides (Macrogen, Korea). The gene sequence was analyzed using sequence scanner software package. Forward and reverse sequenced strands were joined by Caps 3 assembly online software and compared with others in the GenBank database using the NCBI BLASTn tool. Final sequences were deposited in Genbank and accession numbers were obtained.

Ultrastructure studies

For ultrastructure-studies, tomato (cv. Nagina) seeds were surface sterilized by immersing them in an aqueous solution of sodium hypochlorite (5% (v/v)) for 10 min followed by 5-6 washings with sterilized distilled water. The seeds were soaked in the inoculum (1×10^8 CFU ml⁻¹) for 30 min and allowed to germinate on water-agar (1.5% (w/v)) plates. Root hairs of ten days old seedlings were cut into pieces (approximately 1-3 cm) and embedded in water-agar (1.5% (w/v)) again followed by cutting of approximately 2-3 mm small agar cubes. The cubes were put in 1.5-ml tubes in the presence of 5 % (v/v) glutaraldehyde (made in 0.2 M PIPES buffer, pH 8.0) as a fixative. After 16-18 h, the fixative was replaced with 0.2 M PIPES buffer [0.58 g NaCl, 3 g PIPES {piperazine-*N,N'* bis(2-ethanesulfonic acid)}, 1M NaOH, 0.2 g MgCl₂.6H₂O, pH 6.8] (Salema and Brandao, 1973) and samples were washed 2 × 1 h in fresh buffer. Afterwards, these samples were treated with aqueous osmium tetra oxide (0.2 % (w/v)) made in PIPES buffer solution (0.2 M, pH 6.8) for 16-18 h and washed 2 × 30 min with sterilized distilled water. After treating with aqueous uranyl acetate (5 % (w/v)) for 16-18 h, the samples were washed with sterilized distilled water for 2 × 30 min. First dehydration was carried out with absolute alcohol for 2 × 30 min and then with propylene oxide (100% (v/v)) for 1 × 30 min. Infiltration of samples was carried out with propylene oxide in ratio 1:1 for 24-48 h and then with spur-resin for further 24-72 h. The accelerator Benzyl Di-Methyl Amine (BDMA) was used in all infiltration steps. Samples were placed on flat embedding molds for polymerization for 72 h at 65-70 °C in the oven (Memmert, Germany). Polymerized resin blocks were left at room temperature for at least 24 h before cutting ultra-thin sections. Ultra-thin sections (150-200 nm) were cut on ultra-microtome (RMC-7000) and the sections were carefully placed on copper grids. The sections were double stained with uranyl acetate and lead citrate for 30 min and 10 min, respectively. The grids were washed with deionized water and observed under Transmission Electron Microscope (TEM, JEOL 1010, Japan).

Results

Morphological and physiological characterization

Isolate NgE3 was appeared with round and whitish colonies on agar medium and its cells were found as long rods under a light microscope. In addition, it showed 73.93 ± 4.23 nmol mg⁻¹ protein h⁻¹ nitrogenase activity and 4.92 ± 0.64 µg ml⁻¹ IAA production ability (Table 1). Isolate NgE3 was also found positive for AHLs production and demonstrated substantial (> 79%) inhibition of three fungal pathogens *viz.* *Fusarium oxysporum*, *Aspergillus niger* and *A. flavus*. On the other hand, isolate NgE4 had curled and off-white colonies with cell shapes appeared as short rods under a light microscope. Nitrogenase activity of NgE4 was measured as 63.00 ± 6.35 nmol mg⁻¹ protein h⁻¹. It also synthesized 1.66 ± 0.11 µg ml⁻¹ IAA in the culture medium (Table 2). In addition,

isolate NgE4 also showed biocontrol potential (> 79%) against *Fusarium solani*, *F. oxysporum* and *Aspergillus flavus* (Table 3), but was found negative for AHLs production. ACC deaminase and catalase enzyme activity was found positive in both isolates. Moreover, both the isolates were found Gram-positive showing the cell motility glass slide. Isolates NgE3 and NgE4 were unable to show the antifungal activity against a panel of fungal pathogens tested and also lacked AHL production.

Table 1. Morphological and physiological characterization of isolates NgE3 and NgE4

Isolate**	Colony morphology	Cell morphology	IAA production ($\mu\text{g ml}^{-1}$)	AHLs production
NgE3	Round and whitish	Long rods	4.92 (0.64)	+
NgE4	Curled and off-white	Short rods	1.66 (0.11)	-

**Both isolates were Gram-positive and motile. Isolates NgE3 and NgE4 were also found positive for catalase and ACC deaminase activity. Standard error of three replicates is presented in parentheses

Table 2. The antifungal activity of bacterial endophytes from the tomato against different fungal pathogens

Isolate	% inhibition				
	<i>Fusarium</i>			<i>Aspergillus</i>	
	<i>solani</i>	<i>oxysporum</i>	<i>moniliforme</i>	<i>niger</i>	<i>flavus</i>
NgE3	46 (5)*	78 (4)	51 (11)	76 (5)	79 (3)
NgE4	77 (6)	83 (6)	42 (3)	66 (10)	86 (13)

*Standard error of three replicates is presented in parentheses

Table 3. Phylogenetic identity of *16S rRNA gene sequences after BLASTn analysis*

Isolate	Sequence length (bp)	Similarity %	Closest GenBank match	Strain identified	Accession #
NgE3	1057	99	<i>Bacillus subtilis</i> subsp. <i>subtilis</i> strain DDKRC2	<i>Bacillus subtilis</i>	KC202298
NgE4	857	98	<i>Paenibacillus</i> sp. IHB B 3310	<i>Paenibacillus</i> sp.	KC202299

Relationship between phosphate solubilization and organic acid production

Isolate NgE3 solubilized $44.71 \pm 2.25 \mu\text{g ml}^{-1}$ insoluble tricalcium phosphate (TCP) after 168 h of incubation with the drop in the pH of the medium up to 5.3, which was found directly correlated ($P \leq 0.001$, $r = 0.97$) to synthesis of lactic acid in the culture medium ($21.89 \pm 1.66 \mu\text{g ml}^{-1}$). Similarly, isolate NgE4 converted $54.40 \pm 1.92 \mu\text{g ml}^{-1}$ of TCP to soluble form with the total lowering of pH up to 4.2. The amount of TCP solubilized by NgE4 was positively correlated to both gluconic acid ($P \leq 0.001$, $r = 0.99$) and lactic acid ($P \leq 0.001$, $r = 0.99$). The total amount of gluconic and lactic

acids produced by NgE4 after 168 h of incubation were measured as $19.40 \pm 0.82 \mu\text{g mL}^{-1}$ and $14.06 \pm 0.85 \mu\text{g mL}^{-1}$, respectively (Fig. 1).

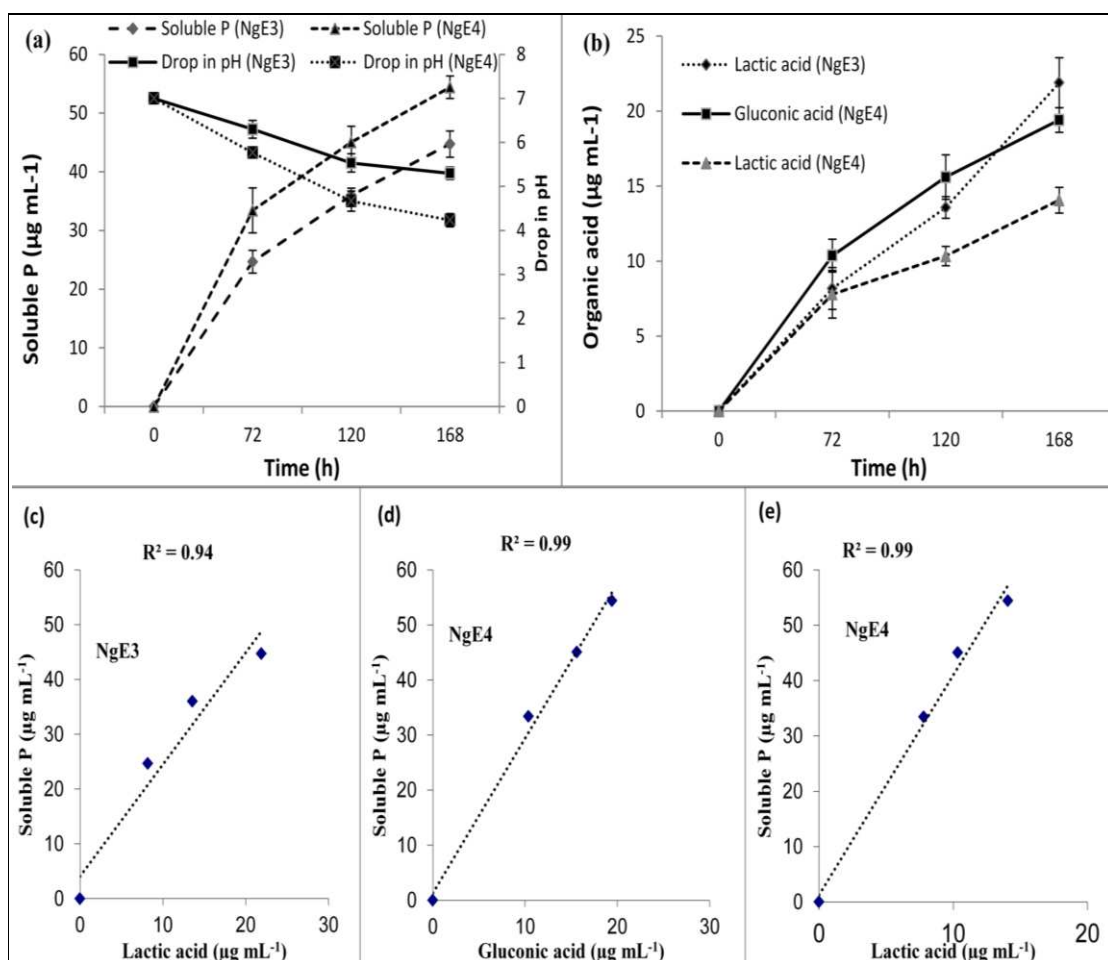


Figure 1. Phosphate solubilized by isolates NgE3 and NgE4 with respect to drop in pH of medium (a), organic acids produced by the isolates at time intervals (b) and relationship between organic acid production and phosphate solubilization as determined through regression correlation analysis (c, d, e)

Molecular identification and phylogenetic analysis

Isolate NgE3 was identified as *Bacillus subtilis* (KC202298) on the basis of 16S rRNA gene sequence analysis (Table 3). In phylogenetic tree, constructed to compare strain NgE3 with type strains of genus *Bacillus*, it clustered itself with *Bacillus subtilis* NCDO 1769^T and *Bacillus subtilis* IAM 12118^T. On the other hand, NgE4 was identified as *Paenibacillus* sp. as it demonstrated 98% 16S rRNA gene sequence similarity with more than one *Paenibacillus* spp. Phylogenetic tree showed its grouping with *P. pabuli* JCM 9074^T and *P. illinoisensis* JCM 9907^T (Fig. 2).

Ultrastructure studies for root colonization

When observed by TEM, both *Bacillus subtilis* NgE3 and *Paenibacillus* sp. NgE4 infected the tomato root hair cells under gnotobiotic conditions. The colonization

pattern of both strains apparently looked similar with the only difference in the number of bacterial cells infected the tomato root hair cells was greater in case of *Paenibacillus* sp. NgE4. Both the strains were found potential bacterial endophytes through ultrastructure TEM studies (Fig. 3).

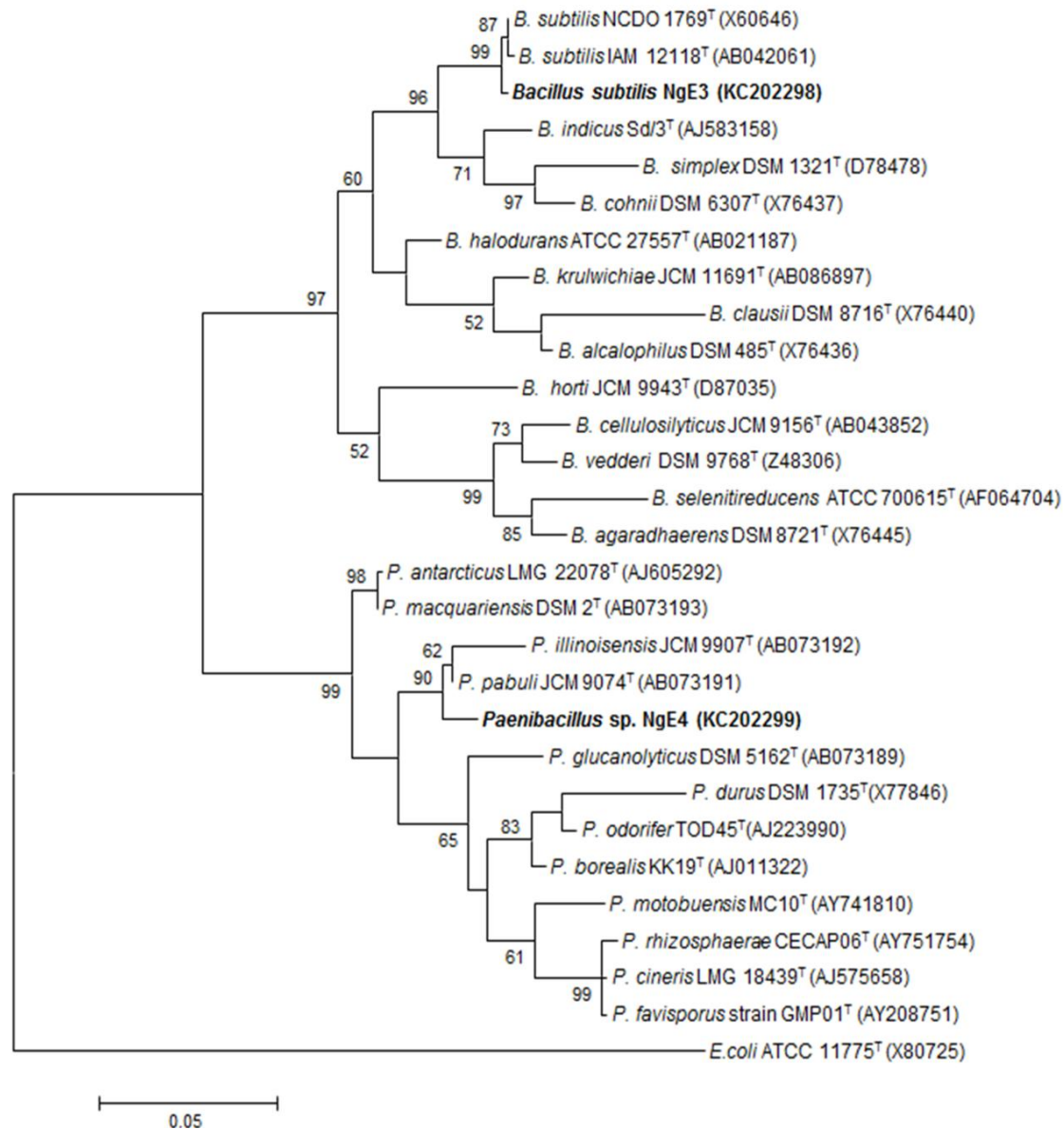


Figure 2. Phylogenetic analysis based on 16S rRNA gene sequences of strains NgE3 and NgE4 with their respective type strains. The evolutionary history was inferred using the Neighbor-Joining method. Only greater than 50% of replicate trees in which the associated taxa clustered together in the bootstrap test (1000 replicates) are shown next to the branches. The tree is drawn to scale, with branch lengths in the same units as those of the evolutionary distances used to infer the phylogenetic tree. The evolutionary distances were computed using the Maximum Composite Likelihood method and are in the units of the number of base substitutions per site. Evolutionary analyses were conducted in Phylmyl software package. *E. coli* strain ATCC 11775^T was included as an outgroup

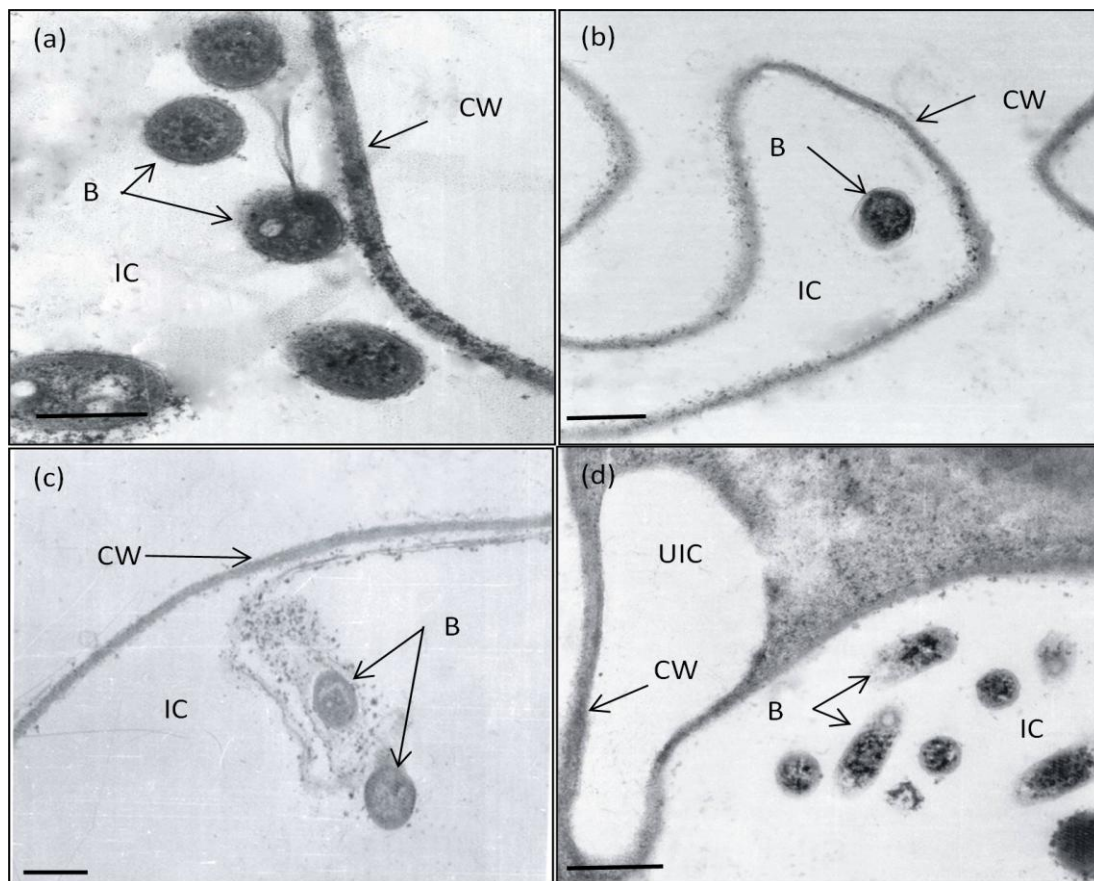


Figure 3. Tomato root endosphere colonization of strains *Bacillus subtilis* NgE3 (a, b) and *Paenibacillus* sp. NgE4 (c, d). B Bacteria, CW Cell wall, IC Infected cell, UIC Uninfected cell. Scale bar: 1 μ m

Discussion

Recently, endophytic bacteria have gained significant attention due to their interesting features related to plant growth and health issues. A very limited research is available on exploiting the potential of bacterial endophytes in Pakistan. The present study demonstrated the in vitro efficiency of *Bacillus subtilis* NgE3 and *Paenibacillus* sp. NgE4 in terms of nitrogen fixation, P-solubilization through organic acid production, synthesis of IAA, ACC deaminase activity, AHLs production and biocontrol potential. Globally, bacterial endophytes have already been reported to exhibit phytobeneficial characteristics (Gyaneshwar et al., 2001; Miliūtė and Buzaitė, 2011; Oteino et al., 2015) and stress tolerance (Khan et al., 2015).

Reduction of acetylene (C_2H_2) into ethylene (C_2H_4) is an indirect approach to authenticate the diazotrophic nature of bacteria. Conversion of a significant amount of acetylene by NgE3 and NgE4 ($73.93 \pm 4.23 \mu g ml^{-1}$ and $63.00 \pm 6.35 \mu g ml^{-1}$, respectively) into ethylene confirmed the nitrogen-fixing ability of the strains. Gyaneshwar et al. (2001) reported bacterial endophyte *Serratia marcescens* IRBG500 as diazotroph on the basis its acetylene reduction ability and *nifH* gene sequence analysis. Bacteria make inorganic soil phosphates available to plants through the secretion of organic acids in plant vicinity (Richardson et al., 2009; Shahid et al., 2015). Secretion of low molecular weight organic acids in soil by phosphate solubilizing bacteria is the major

mechanism that works through acidification of soil or media (Gyaneshwar et al., 1999; Puente et al., 2004; Khan et al., 2009). Through their hydroxyl and carboxyl groups, these organic acids play their role in detaching the cations bound to soil phosphates (Al-phosphates, Ca-phosphates and Fe-phosphates) transforming them into primary and secondary ortho-phosphates (Kpombrekou and Tabatabai, 1994). Moreover, extracellular oxidation of glucose to GA via quinoprotein glucose dehydrogenase is the most effective mineral phosphate solubilization phenotype in Gram-negative bacteria (Rodríguez et al., 2000). In our study, phosphate solubilization by strains NgE3 and NgE4 was found significantly correlated with gluconic acid ($P \leq 0.001$, $r = 0.99$) and lactic acid ($P \leq 0.001$, $r = 0.99$) (Fig 1). The amount of IAA produced by strains NgE3 and NgE4 ($4.92 \pm 0.64 \mu\text{g ml}^{-1}$ and $1.66 \pm 0.11 \mu\text{g ml}^{-1}$) is also similar to the findings of Miliūtė and Buzaitė (2011) who isolated 9 bacterial endophytes from apple tree buds and all of them were able to produce IAA in vitro. The positive reaction of both strains for ACC deaminase enzyme activity aided their significance for plant growth under stress conditions (Penrose and Glick, 2003; Glick et al., 2007; Mahmood et al., 2017). Similarly, biocontrol potential of isolates NgE3 and NgE4 against major phytopathogenic fungal strains is in agreement with the previous findings (Senthilkumar et al., 2009; Wang et al., 2013), which revealed antifungal activity of screened bacterial endophytes against many fungal pathogens including *Fusarium* and *Aspergillus* spp. *N*-acylhomoserine lactone (AHL)-based quorum sensing (QS) systems have been described in many bacterial endophytes (Liu et al., 2011), but in current study one of the two isolates NgE3 demonstrated AHLs production trait. Besides other plants, bacterial endophytes have also been isolated and characterized for plant growth-promoting attributes (Amaresan et al., 2012), biocontrol activity (Munif et al., 2013; Upreti and Thomas, 2015) and production of AHLs (Singh et al., 2015) from tomato plant.

The in vitro demonstration of plant-beneficial attributes and biocontrol efficiency led to the identification of NgE3 and NgE4 on molecular basis through the sequencing of the most accepted taxonomic marker, the 16S rRNA gene. Isolate NgE3 was identified as *Bacillus subtilis* and isolate NgE4 as *Paenibacillus* sp. with 99% and 98% sequence identity, respectively (Table 3). In the neighbor-joining phylogenetic tree, *Bacillus subtilis* NgE3 clustered itself with *Bacillus subtilis* NCDO 1769^T and *Bacillus subtilis* IAM 12118^T. On the other hand, *Paenibacillus* sp. NgE4 grouped itself with *P. pabuli* JCM 9074^T and *P. illinoisensis* JCM 9907^T (Fig. 2). Earlier, endophytes from genus *Bacillus* and *Paenibacillus* have been reported to carry plant beneficial characteristics. Malfanova et al. (2011) isolated *Bacillus subtilis* HC8 from the giant hogweed *Heracleum sosnowskyi* Manden, which significantly promoted plant growth and protected tomato against tomato foot and root rot. Many *Paenibacillus* spp. with positive effects on plant growth have been isolated by Ulrich et al. (2008) from poplar, larch and spruce. Similarly, it was concluded that inoculation of *Paenibacillus* sp. strongly affected the metabolic composition of in vitro-grown plants (Scherling et al., 2009).

Root colonization efficiency of *Bacillus subtilis* NgE3 and *Paenibacillus* sp. NgE4 was confirmed through ultra-structure studies (Fig. 3). Both strains infected tomato root hair cells. *Paenibacillus* sp. NgE4 densely colonized the endosphere of tomato root hair cells compared to *Bacillus subtilis* NgE3. Both the strains were found potential bacterial endophytes through ultrastructure TEM studies. Plant beneficial bacteria, as epiphytes and endophytes have been routinely localized in rhizosphere and endosphere with TEM and immunogold labeling techniques (Schloter et al., 1997; Hameed et al., 2005; Jeun et al., 2008; Yasmeen et al., 2012; Shahid et al., 2015).

Conclusion

The bacterial endophytes NgE3 and NgE4 had great in vitro potential for major plant beneficial traits. Prior to their addition to indigenous biofertilizer regimes, the strains might be inoculated directly to tomato plants under pot and field experiments to check their effect on plant growth and disease suppression.

Acknowledgements. Authors are thankful to Higher Education Commission (HEC), Pakistan for proving funds for this research under HEC 5000 PhD Fellowship program. We would like to express our gratitude to Mr. Javed Iqbal, Electron Microscopist, NIBGE, Faisalabad, Pakistan for his technical help in ultra-structure studies. Technical help of Microbial Physiology Laboratory staff at NIBGE is thankfully acknowledged.

REFERENCES

- [1] Akram, M. S., Shahid, M., Tariq, M., Azeem, M., Javed, M. T., Saleem, S., Riaz, S. (2016): Deciphering *Staphylococcus sciuri* mediated anti-oxidative defence mechanisms and growth modulations in salt stressed maize. – *Frontiers in Microbiology* 7: 867.
- [2] Amaresan, N., Jayakumar, V., Kumar, K., Thajuddin, N. (2012): Isolation and characterization of plant growth promoting endophytic bacteria and their effect on tomato (*Lycopersicon esculentum*) and chilli (*Capsicum annuum*) seedling growth. – *Annals of Microbiology* 62: 805-810.
- [3] Amjad, M., Akhtar, J., Anwar-ul-Haq, M., Ahmad, R., Zaid, M. (2014a): Characterization of comparative response of fifteen tomato (*Lycopersicon esculentum* Mill.) genotypes to NaCl stress. – *Journal of Agricultural Science and Technology* 16: 851-862.
- [4] Amjad, M., Akhtar, J., Anwar-Ul-Haq, M., Imran, S., Jacobsen, S. E. (2014b): Soil and foliar application of potassium enhances fruit yield and quality of tomato under salinity. – *Turkish Journal of Biology* 38: 208-218.
- [5] Beringer, J. (1974): R factor transfer in *Rhizobium leguminosarum*. – *Journal of General Microbiology* 84: 188-198.
- [6] Bradford, M. M. (1976): A rapid and sensitive method for the quantitation of microgram quantities of protein utilizing the principle of protein-dye binding. – *Annals of Biochemistry* 72: 248-254.
- [7] Bulgarelli, D., Schlaeppi, K., Spaepen, S., van Themaat, E. V. L., Schulze-Lefert, P. (2013): Structure and functions of the bacterial microbiota of plants. – *Annual Reviews of Plant Biology* 64: 807-838.
- [8] Damodaran, T., Rai, R., Jha, S., Kannan, R., Pandey, B., Sah, V., Mishra, V., Sharma, D. (2014): Rhizosphere and endophytic bacteria for induction of salt tolerance in gladiolus grown in sodic soils. – *Journal of Plant Interactions* 9: 577-584.
- [9] Gaiero, J. R., McCall, C. A., Thompson, K. A., Day, N. J., Best, A. S., Dunfield, K. E. (2013): Inside the root microbiome: bacterial root endophytes and plant growth promotion. – *American Journal of Botany* 100: 1738-1750.
- [10] Glick, B. R., Todorovic, B., Czarny, J., Cheng, Z., Duan, J., McConkey, B. (2007): Promotion of plant growth by bacterial ACC deaminase. – *Critical Reviews Plant Sciences* 26: 227-242.
- [11] Gyaneshwar, P., Parekh, L., Archana, G., Poole, P., Collins, M., Hutson, R., Kumar, G. N. (1999): Involvement of a phosphate starvation inducible glucose dehydrogenase in soil phosphate solubilization by *Enterobacter asburiae*. – *FEMS Microbiology Letters* 171: 223-229.

- [12] Gyaneshwar, P., James, E. K., Mathan, N., Reddy, P. M., Reinhold-Hurek, B., Ladha, J. K. (2001): Endophytic colonization of rice by a diazotrophic strain of *Serratia marcescens*. – Journal of Bacteriology 183: 2634-2645.
- [13] Hameed, S., Mubeen, F., Malik, K. A., Hafeez, F. Y. (2005): Nodule Co-occupancy of *Agrobacterium* and *Bradyrhizobium* with Potential Benefit to Legume Host. In: Wang, Y. P. (eds). Biological Nitrogen Fixation, Sustainable Agriculture and the Environment. Springer, Dordrecht.
- [14] Hanif, K., Hameed, S., Imran, A., Naqqash, T., Shahid, M., Van-Elsas, J. D. (2015): Isolation and characterization of a β -propeller gene containing phosphobacterium *Bacillus subtilis* strain KPS-11 for growth promotion of potato (*Solanum tuberosum* L.). – Frontiers in Microbiology 6: 1-12.
- [15] Hardoim, P. R., van Overbeek, L. S., van Elsas, J. D. (2008): Properties of bacterial endophytes and their proposed role in plant growth. – Trends in Microbiology 16: 463-471.
- [16] Hardy, R. W., Holsten, F. R. D., Jackson, E. K., Burns, R. E. (1968): The acetylene-ethylene assay for nitrogen fixation: Laboratory and field evaluation. – Plant Physiology 43: 1185-1207.
- [17] Hartmann A., Rothballer, M., Hense, B. A., Schroder, P. (2014): Bacterial quorum sensing compounds are important modulators of microbe-plant interactions. – Frontiers in Plant Science 5: 131.
- [18] Hurek, T., Reinhold-Hurek, B., Van Montagu, M., Kellenberger, E. (1994): Root colonization and systemic spreading of *Azoarcus* sp. strain BH72 in grasses. – Journal of Bacteriology 176: 1913-1923.
- [19] Jasim, B., Joseph, A. A., John, C. J., Mathew, J., Radhakrishnan, E. (2014): Isolation and characterization of plant growth promoting endophytic bacteria from the rhizome of *Zingiber officinale*. – 3 Biotechnology 4: 197-204.
- [20] Jeun, Y. C., Lee, Y. J., Kim, K. W., Kim, S. J., Lee, S. W. (2008): Ultrastructures of *Colletotrichum orbiculare* in the leaves of cucumber plants expressing induced systemic resistance mediated by *glomus intraradices* BEG110. – Mycobiology 36: 236-241.
- [21] Khan, A. A., Jilani, G., Akhtar, M. S., Naqvi, S. M. S., Rasheed, M. (2009): Phosphorus solubilizing bacteria: occurrence, mechanisms and their role in crop production. – Journal of Agricultural Biological Science 1: 48-58.
- [22] Khan, M. U., Sessitsch, A., Harris, M., Fatima, K., Imran, A., Arslan, M., Shabir, G., Khan, Q. M., Afzal, M. (2015): Cr-resistant rhizo-and endophytic bacteria associated with *Prosopis juliflora* and their potential as phytoremediation enhancing agents in metal-degraded soils. – Frontiers in Plant Sciences 5: 755.
- [23] Kloepper, J. W., Lifshitz, R., Zablutowicz, R. M. (1989): Free-living bacterial inocula for enhancing crop productivity. – Trends in Biotechnology 7: 39-44.
- [24] Kpombekou, K., Tabatabai, M. (1994): Effect of organic acids on release of phosphorus from phosphate rocks. – Soil Science 158: 442-453.
- [25] Liu, X., Jia, J., Papat, R., Ortori, C. A., Li, J., Diggle, S. P., Gao, K., Cámara, M. (2011): Characterisation of two quorum sensing systems in the endophytic *Serratia plymuthica* strain G3: differential control of motility and biofilm formation according to life-style. – BMC Microbiology 11: 26-34.
- [26] Mahmood, F., Shahid, M., Hussain, S., Shahzad, T., Tahir, M., Ijaz, M., Hussain, A., Mahmood, K., Imran, M., Babar, S. A. K. (2017): Potential plant growth promoting strain *Bacillus* sp. SR-2-1/1 decolorized azo dyes through NADH-ubiquinone oxidoreductase activity. – Bioresource Technology 235: 176-184.
- [27] Malfanova, N., Kamilova, F., Validov, S., Shcherbakov, A., Chebotar, V., Tikhonovich, I., Lugtenberg, B. (2011): Characterization of *Bacillus subtilis* HC8, a novel plant-beneficial endophytic strain from giant hogweed. – Microbial Biotechnology 4: 523-532.

- [28] Maniatis, T., Fritsch, E. F., Sambrook, J. (1982): Molecular Cloning; A Laboratory Manual, 2nd ed. – Cold Spring Harbor Laboratory, Cold Spring Harbor, NY.
- [29] McLean, R. J., Pierson, L. S., Fuqua, C. (2004): A simple screening protocol for the identification of quorum signal antagonists. – *Journal of Microbiological Methods* 58: 351-360.
- [30] Miliūtė, I., Buzaitė, O. (2011): IAA production and other plant growth promoting traits of endophytic bacteria from apple tree. – *Biologija* 57: 98-102.
- [31] Munif, A., Hallmann, J., Sikora, R. A. (2013): Isolation of root endophytic bacteria from tomato and its biocontrol activity against fungal diseases. – *Microbiology Indonesia* 6: 148-156.
- [32] Murphy, J., Riley, J. P. (1962): Modified solution method for determination of phosphate in natural water. – *Analytica Chimica Acta* 27: 31-36.
- [33] Okon, Y., Albrecht, S. L., Burriss, R. H. (1977): Methods for growing *Spirillum lipoferum* and for counting it in pure culture and in association with plants. – *Applied and Environmental Microbiology* 33: 85-88.
- [34] Oteino, N., Lally, R. D., Kiwanuka, S., Lloyd, A., Ryan, D., Germaine, K. J., Dowling, D. N. (2015): Plant growth promotion induced by phosphate solubilizing endophytic *Pseudomonas* isolates. – *Frontiers in Microbiology* 6: 1-9.
- [35] Penrose, D. M., Glick, B. R. (2003): Methods for isolating and characterizing ACC deaminase-containing plant growth-promoting rhizobacteria. – *Physiology Plantarum* 118: 10-15.
- [36] Pii, Y., Mimmo, T., Tomasi, N., Terzano, R., Cesco, S., Crecchio, C. (2015): Microbial interactions in the rhizosphere: beneficial influences of plant growth-promoting rhizobacteria on nutrient acquisition process: A review. – *Biology and Fertility of Soils* 51: 403-415.
- [37] Puente, M., Bashan, Y., Li, C., Lebsky, V. (2004): Microbial populations and activities in the rhizoplane of rock-weathering desert plants. I. Root colonization and weathering of igneous rocks. – *Plant Biology* 6: 629-642.
- [38] Richardson, A. E., Barea, J. M., McNeill, A. M., Prigent-Combaret, C. (2009): Acquisition of phosphorus and nitrogen in the rhizosphere and plant growth promotion by microorganisms. – *Plant and Soil* 321: 305-339.
- [39] Rodríguez, H., Gonzalez, T., Selman, G. (2000): Expression of a mineral phosphate solubilizing gene from *Erwinia herbicola* in two rhizobacterial strains. – *Journal of Biotechnology* 84: 155-161.
- [40] Rosenblueth, M., Martínez-Romero, E. (2006): Bacterial endophytes and their interactions with hosts. – *Molecular Plant-Microbe Interactions* 19: 827-837.
- [41] Sakthivel, N., Gnanamanickam, S. (1986): Toxicity of *Pseudomonas fluorescens* towards rice sheath-rot pathogen *Acrocyldrium oryzae*. – *Current Science* 55: 106-107.
- [42] Salema, R., Brandao, I. (1973): The use of PIPES buffer in the fixation of plant cells, for electron microscopy. – *Journal of Submicroscopic Cytology* 5: 79-96.
- [43] Scherling, C., Ulrich, K., Ewald, D., Weckwerth, W. (2009): A metabolic signature of the beneficial interaction of the endophyte *Paenibacillus* sp. isolate and in vitro-grown poplar plants revealed by metabolomics. – *Molecular Plant-Microbe Interactions* 22: 1032-1037.
- [44] Schlöter, M., Wiehe, W., Assmus, B., Steindl, H., Becke, H., Höflich, G., Hartmann, A. (1997): Root colonization of different plants by plant-growth-promoting *Rhizobium leguminosarum* bv. trifolii R39 studied with monospecific polyclonal antisera. – *Applied and Environmental Microbiology* 63: 2038-2046.
- [45] Senthilkumar, M., Swarnalakshmi, K., Govindasamy, V., Lee, Y. K., Annapurna, K. (2009): Biocontrol potential of soybean bacterial endophytes against charcoal rot fungus, *Rhizoctonia bataticola*. – *Current Microbiology* 58: 288-293.
- [46] Shahid, M., Hameed, S., Imran, A., Ali, S., van Elsas, J. D. (2012): Root colonization and growth promotion of sunflower (*Helianthus annuus* L.) by phosphate solubilizing

- Enterobacter* sp. Fs-11. – World Journal of Microbiology and Biotechnology 28: 2749-2758.
- [47] Shahid, M., Hameed, S., Tariq, M., Zafar, M., Ali, A., Ahmad, N. (2015): Characterization of mineral phosphate-solubilizing bacteria for enhanced sunflower growth and yield-attributing traits. – Annals of Microbiology 65: 1525–1536.
- [48] Singh, B. K. (2017): Creating new business, economic growth and regional prosperity through microbiome-based products in agricultural industry. – Microbial Biotechnology 10: 224-227.
- [49] Singh, R. P., Baghel, R. S., Reddy, C., Jha, B. (2015): Effect of quorum sensing signals produced by seaweed-associated bacteria on carpospore liberation from *Gracilaria dura*. – Frontiers in Plant Sciences 6: 1-13.
- [50] Somasegaran, P., Hoben, H. J. (1994): Handbook for Rhizobia: Methods in Legume-Rhizobium Technology. – Springer-Verlag, Berlin.
- [51] Sylvia, D. M., Fuhrmann, J. J., Hartel, P., Zuberer, D. A. (2005): Principles and Applications of Soil Microbiology. – Pearson, Prentice Hall, NJ.
- [52] Thakore, Y. (2006): The biopesticide market for global agricultural use. – Industrial Biotechnology 2: 194-208.
- [53] Tien, T. M., Gaskins, M. H., Hubbell, D. H. (1979): Plant growth substances produced by *Azospirillum brasilense* and their effect on the growth of pearl millet. – Applied and Environmental Microbiology 37: 1016-1024.
- [54] Ulrich, K., Stauber, T., Ewald, D. (2008): *Paenibacillus*—a predominant endophytic bacterium colonising tissue cultures of woody plants. – Plant Cell, Tissue and Organ Culture 93: 347-351.
- [55] Upreti, R., Thomas, P. (2015): Root-associated bacterial endophytes from *Ralstonia solanacearum* resistant and susceptible tomato cultivars and their pathogen antagonistic effects. – Frontiers in Microbiology 6: 1-12.
- [56] Verma, S. C., Singh, A., Chowdhury, S. P., Tripathi, A. K. (2004): Endophytic colonization ability of two deep-water rice endophytes, *Pantoea* sp. and *Ochrobactrum* sp. using green fluorescent protein reporter. – Biotechnology Letters 26: 425-429.
- [57] Vincent, J. M. (1970): A Manual for the Practical Study of the Root Nodule Bacteria. – Burgess and Son Ltd., Westerham.
- [58] Wang, K., Yan, P. S., Ding, Q. L., Wu, Q. X., Wang, Z. B., Peng, J. (2013): Diversity of culturable root-associated/endophytic bacteria and their chitinolytic and aflatoxin inhibition activity of peanut plant in China. – World Journal of Microbiology and Biotechnology 29: 1-10.
- [59] Weisburg, W. G., Barns, S. M., Pelletier, D. A., Lane, D. J. (1991): 16S ribosomal DNA amplification for phylogenetic study. – Journal of Bacteriology 173: 697-703.
- [60] Yaish, M. W., Antony, I., Glick, B. R. (2015): Isolation and characterization of endophytic plant growth-promoting bacteria from date palm tree (*Phoenix dactylifera* L.) and their potential role in salinity tolerance. – Antonie van Leeuwenhoek 107: 1519-1532.
- [61] Yasmeeen, T., Hameed, S., Tariq, M., Iqbal, J. (2012): *Vigna radiata* root associated mycorrhizae and their helping bacteria for improving crop productivity. – Pakistan Journal of Botany 44: 87-94.
- [62] Yousaf, M., Li, J., Lu, J., Ren, T., Cong, R., Fahad, S., Li, X. (2017): Effects of fertilization on crop production and nutrient-supplying capacity under rice-oilseed rape rotation system. – Scientific Reports 7: 1270.
- [63] Zakria, M., Njoloma, J., Saeki, Y., Akao, S. (2007): Colonization and nitrogen-fixing ability of *Herbaspirillum* sp. strain B501 gfp1 and assessment of its growth-promoting ability in cultivated rice. – Microbes and Environment 22: 197-206.

EVALUATION OF MODCLARK MODEL FOR SIMULATING RAINFALL-RUNOFF IN TANGRAH WATERSHED, IRAN

GHARIB, M.¹ – MOTAMEDVAZIRI, B.^{1*} – GHERMEZCHESHMEH, B.² – AHMADI, H.¹

¹*Department of Watershed Management, Science and Research Branch, Islamic Azad University, Tehran, Iran*

²*Soil Conservation and Watershed Management Institute, Agricultural Research, Education and Extension Organization (AREEO), Tehran, Iran*

**Corresponding author*

e-mail: bmvaziri@gmail.com; phone: +98-912-483-6636

(Received 1st Sep 2017; accepted 15th Jan 2018)

Abstract. Rainfall-runoff hydrological models are one of the common methods for simulating flood hydrographs. These models come in three Lumped, semi-distributed and fully distributed scale, in terms of spatial accuracy in simulation in which precision increases with increasing spatial accuracy. ModClark model is a distributed model. The purpose of this study is to evaluate the efficiency and accuracy of the ModClark model in simulating flood hydrograph in Tangrah watershed located in Iran and comparing the rainfall-runoff simulated using this model and Soil Conservation Service (SCS) model. five rainfall-runoff events were extracted at Tangrah Station. Then, the parameters of the model were calibrated based on three observed hydrographs and validated based on two observed hydrographs. Finally, to evaluate the results of simulation of flood hydrograph after optimization, the Determination Coefficient (R^2) and Root Mean Square Error (RMSE) methods were used. The results of the model evaluation showed that ModClark with an RMSE of 1.55 and with an R^2 of 0.84, is more accurated and efficient than the SCS model in simulating flood hydrograph. Considering the high accuracy of ModClark distributed model, using this hydrologic model, we can study the interaction of physiographic and climatic factors on the potential of watersheds' runoff production.

Keywords: *flood hydrographic, simulation, distributed model, ModClark*

Introduction

Runoff is one of the most important hydrological variables used in many water resources applications. Reliable prediction of the amount of runoff flowing upland to rivers is difficult and time-consuming (Kumar et al., 2010). Rainfall-runoff hydrological models for flood hydrograph simulation are suitable methods for better flood management, especially in ungauged basins. In order to estimate the flood discharge, there are various models used in simulating the watershed response against rainfall and they include a variety of lump, quasi-distributed and distributed models (Saghafian et al., 2010). Today, with access to satellite imagery and map data, it is possible to simulate the response of a watershed to a rainfall with specific characteristics with the help of distributed models. Models in which the spatial distribution of rainfall characteristics and watersheds are taken into account are known as distributed hydrological models (Saghafian et al., 2010). Planning for controlling and managing the floods, maintaining the quality and their proper utilization requires an accurate understanding of rainfall-runoff modeling. The most important challenge of the model is the selection of a particular rainfall-runoff model which can simulate a wide range of floods. Water resources experts have always sought for the equation between rainfall and runoff values in watersheds and in different time and place conditions. To date,

several rainfall-runoff models with different capabilities and complexities have been developed and used to predict floods. Several studies have been conducted on rainfall-runoff modeling. Ghitoto (1991) in his research on calculating runoff hydrograph, showed that in large basins, flood discharge generated by the SCS method is closer to the observed values. One-dimensional and two-dimensional numerical models used to predict the flood rise in the rivers were investigated by Horritt and Bates (2002). In this study, TELEMAC-2D, HEC-RAS and LISFOOD-FP models were compared in a 60-km range of the Severn River. The results showed that the HEC-RAS and TELEMAC-2D models can be calibrated by discharge, and the information of the water uplift area and flood area can be predicted. Emerson et al. (2003) developed a model for rainfall-runoff using the HEC-HMS model. From the results of the implementation of the model, the storage levels are responsible for the reduction in the amount of peak flow for the storm event. Kathol et al. (2003) in order to determine peak flow and runoff in two agricultural basins in the southeastern state of South Dakota and by using the HEC-HMS model concluded that, the value of the curve number is of high sensitivity, while the initial loss rate is less sensitive than varying the value of the objective function in the HEC-HMS model. Foody et al. (2004) used the HEC-HMS model to simulate the flood in order to identify flood-sensitive areas in an area in western Egypt which led to the identification of two sensitive areas. Knebl et al. (2005) conducted a modeling of the flood streaming in the summer of 2002 using HEC-HMS and HEC-RAS software and radar data in the San Antonio Watershed in the United States. He used the ModClark method to convert rainfall into runoff and calibrated watershed parameters manually. The results indicated that the model was a suitable tool for regional hydrological forecasting in the basin. Khosroshahi and Saghafian (2005) investigated the response of Damavand watershed sub-basins using the HEC-HMS model. In this research, the contribution of each sub-basin was calculated in peak discharge of the output flood such that no single-variable relationship exist between the flood index and other characteristics of the sub-basins, including the curve number and ground gradient. Alvankar et al. (2006) examined the effect of cell size in calculating peak flood discharge in distributed models for simulating hydrograph of the watershed of Kan. Using the SCS penetration model, Clarck's developed clustering model for Geographic Information System (GIS)-based flood simulation was developed in the Visual Basic environment. The results of this study showed that by increasing the size of cells from $30 \times 30 \text{ m}^2$ to $960 \times 960 \text{ m}^2$, the flood peak discharge decreases. Teymouri et al. (2007) simulated the peak discharge of flood hydrograph using ModClark distribution method in Kasilian watershed. The results of this study indicate the high capability of HEC-HMS model in simulating the distribution method of peak flood discharge and the relatively efficient performance of this method in the studied basin. Sarangi et al. (2008) by comparing the geomorphology methods and curve numbers in ungauged basins to calculate direct runoff hydrographs found that, the geomorphology method is more appropriate in small watersheds with similar geomorphologic features. Studies by Linde et al. (2008) showed that distributive models were better than Lumped reality models in terms of showing the reality. Zhang et al. (2008) in China used the MIKE-SHE model to quantitative runoff simulation. Calibration and validation of the model showed that this model can well handle the runoff simulation in small basins. The appropriate scale plays an important role in calibrating the model, and the estimated value for the parameters is influenced by the time and space scales of input data of the model. Paudel et al. (2009) in a research using GIS, radar data and HEC-HMS

hydrologic software compared both distributed and lump models. They used the ModClark distributed and Clark lump models and the Curve Number Method in the casualty section for transfer. The results of this study showed that the use of any distributed, lump, real or artificial rainfall data is possible to enter the model. Also, using the same Curve Number (CN) values, the ModClark method showed better results than Clark's method. Chidaz et al. (2009) used Snyder, SCS unit hydrograph and Clark methods to estimate flood hydrograph in the Kasilian Watershed. Comparison of the results of these three methods showed that SCS unit hydrograph method is more suitable for predicting flood hydrograph compared to the other two methods. Saghafian et al. (2010) used the ModClark Distributed Rainfall-Runoff Model at the sub-basin level and the HEC-RAS model for hydraulic regeneration in the main river network. The intensity of flooding for $2 \times 2 \text{ km}^2$ cell units was obtained by implementing "Unit Flood Response" method in the form of sequential removal of cells and simulation of flood hydrograph for rainfall design, and the effect of each cell on the total area outlet hydrograph was obtained. The results showed that the largest and closest sub-basins to the outlet, or the furthest and smallest, do not necessarily have the highest and lowest impact on the maximum flood discharge. In a study in India, two HEC-HMS and Water Erosion Prediction Project (WEPP) models used to simulate flow based on daily rainfall data were compared. In general, the HEC-HMS model was preferred to the WEPP model for daily flow simulation (Verma et al., 2010). Ghavidelfar et al. (2011) compared Clark lump and ModClark distributed models in the Randan watershed in Tehran province. The results showed that both models accurately simulate flood hydrograph. They argued that ModClark distributed model in the estimation of time to peak and runoff volume showed better results compared to peak discharge. Bhattacharya et al. (2012) in the article of ModClark Model investigated the development and application of the spatial distribution model of unit hydrograph. Their research results showed that the ModClark model is based on Clark's unit hydrograph method which utilizes the NEXRAD rainfall network data, and the results of the calibration has been satisfactory. Shabanlou and Rajabi (2012) compared the ModClark distributed and SCS lump models in the Karoun watershed. Using the information and GIS maps of the region and using HEC-HMS software and the HEC-GeoHMS appendix, they simulated flood water. The results demonstrate the superiority of ModClark's distributed model compared to the lump SCS model in flood hydrograph simulation. Halwatura et al. (2013) To simulate runoff in the tropical region of Attanagalu Oya from the HEC-HMS model. Their research results showed that the Snyder's unit hydrograph method is more accurate in comparison with the Clarke unit hydrograph method in flow simulation. Shabanlou (2014) in a study titled Flood Hydrograph Calculation Using Different Methods in the Karun River simulated flood hydrograph in Karoun watershed using the SCS Model with HEC-HMS Software, and compared this model with the ModClark model using GIS with the use of both distributed and lump mathematical models, and from the field data the results of the distributed model are closer to the recorded hydrograph of the basin. Sampth et al. (2015) conducted a runoff simulation in the tropical region of the Deduru Oya River Basin in Sri Lanka using the HEC-HMS model. The results of this study showed that the HEC-HMS model with an 80% efficiency coefficient is able to simulate runoff and estimate the potential of inter-basin flow in this area, and is a suitable tool for managing water resources. Studies by Jiang et al. (2015), in relation to rainfall-runoff modeling, parameter estimation and sensitivity analysis in Luanhe Province, China, showed that

the distributed model has a better performance than the Lumped model. Thomas and Roy (2016) investigated the comparison of hydrograph extraction in the Bharathapuzha River Basin. According to this study, because in most areas without statistics, the preparation and development of unit hydrograph is difficult, therefore, the incompatibility of observation simulator hydrograph can be attributed to the large area of the watershed. Saghafian et al. (2016), investigated A coupled Modclark-Curve number rainfall-runon-runoff model. In this Research, a novel rainfall-runon-runoff mathematical model is developed via Soil Conservation Service (SCS) infiltration and ModClark rainfall-runoff coupled models. After deriving model formulation, three different spatial patterns of curve number (uniform, downstream increasing, and decreasing) in conjunction with various rainfall durations and intensities were investigated under with and without runon scenarios over a V-shaped watershed. The results indicated that there was lower surface runoff volume and peak discharge in all cases when runon was accounted for. In particular, in regions with low curve number, there were major differences between the hydrographs simulated by the commonly practiced norunon model and the presented runon model. Moreover, the runon effect in case of decreasing curve number in downstream direction was more pronounced than that of the increasing case. However, this effect decreased with depth, intensity, and duration of rainfall. Rezaei et al. (2016) in their study entitled “Flood spatial variability” using the “Unit Flood Response” method in Khanmirza Basin concluded that, ModClark model simulates the peak discharge with high precision and this model has high accuracy in simulating flood hydrograph. In the sources, there are few studies on the comparison and accuracy of the ModClark model in Iran. The purpose of this study was to evaluate the efficiency and accuracy of the ModClark method in simulating flood hydrograph in Tangrah watershed located in Iran. Most important reasons of selecting Tangrah watershed for this study are the flooding potential and the high runoff production potential, the morphometric and morphological diversity of the region, the existence of an active hydrometric station in the catchment outlet, the existence of the active rexording rain gauge station inside the basin, the existence of a sufficient number of rainfall events with the presence of rainfall-runoff data in the area.

Materials and methods

Study area

Tangrah watershed with an area of 1860 km² and an average height of 1398 m is a part of the Madrasou watershed in Iran country where the runoff from the basin flows through the Dough River to the Golestan dam (*Fig. 1*). This basin is divided into two parts: mountainous and plain, with a variety of morphological, morphometric, climatic and land use variations. The type of climatic of the region is classified as semi-arid to wet (Water Research Institute, 2010). Tangrah watershed area has two hydrometric stations of Dasht and Tangrah such that, the only hydrometric station of Tangrah has limnograph and long term statistical period and the Rain gauge Station of Golestan National Park is the only station with sufficient statistics inside the basin. Therefore, the hydrometric station of Tangrah was used as the basis for comparing the hydrograph of model simulation and observation hydrograph for calibration and validation of the model. *Figure 2* shows the elevation digital model of the study area.

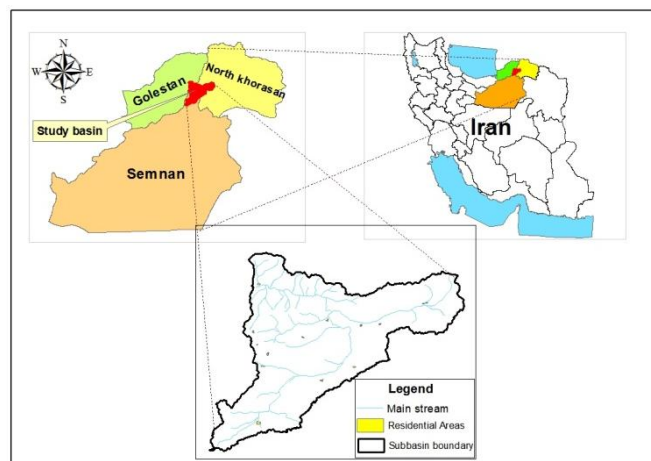


Figure 1. Position of research area (Madarsou, Tangrah watershed and Dough river)

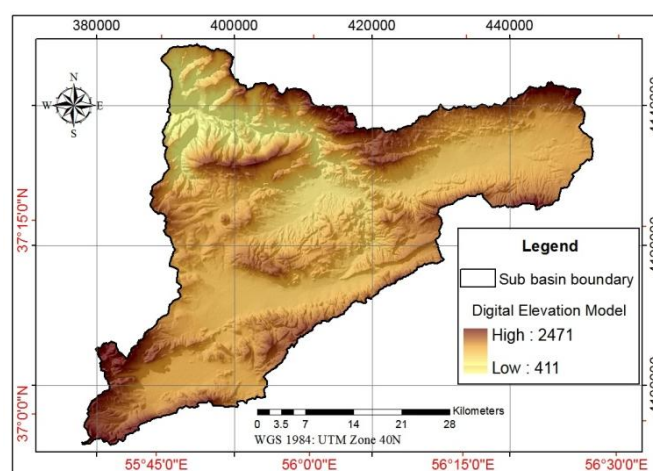


Figure 2. Elevation digital model map of Tangrah watershed

Research methodology

In this study, two methods of SCS and ModClark were evaluated. In the HEC-HMS module, various methods of runoff simulation have been modeled and recognized as valid modules. This modulus can be executed for Iran in order to simulate runoff with the ModClark method. The ModClark method is a quasi-distributed method and should be more precise than lump methods. This methodology was programmed by Alvankar (2003).

The SCS method is a unit instantaneous hydrograph. SCS unit hydrograph is a dimensionless and single-peak method. In this approach, for the conversion of rainfall into runoff using the SCS lump method, the CN value is imported into the model (US Army Engineers Group, 2000). The US Soil Conservation Agency has made it possible to access the initial values of some of the parameters considering the physiographic properties of the basin. In this connection, a relationship between concentration time and lag time has been proposed, where t_c is the concentration time and t_{lag} is lag time of the basin. One of the inputs of the HEC-HMS model in this method is the lag time parameter t_{lag} (Eq. 1).

$$t_{lag} = 0.6 t_c \quad (\text{Eq.1})$$

This model is conducted on the HEC-HMS software; this software uses a unit t-hour hydrograph and additional rainfall height at each interval, which is equivalent to the continuity of the hydrograph, to calculate the flood hydrograph.

The ModClark Distributed Hydrograph Model was developed by Peters and Easton in 1996. This developed model is a Clark rainfall-runoff model in which the spatial distribution of rainfall is taken into account. ModClark model includes time-distributed area and a linear reservoir (Paudel et al., 2009). The most important differences between these two methods are how to rout and simulate the nature of the flow reservoir. In the Clark method, all isochronous regions are modeled with a linear reservoir while in the ModClark method each of the individual isochronous regions is routed separately (Figure. 3).

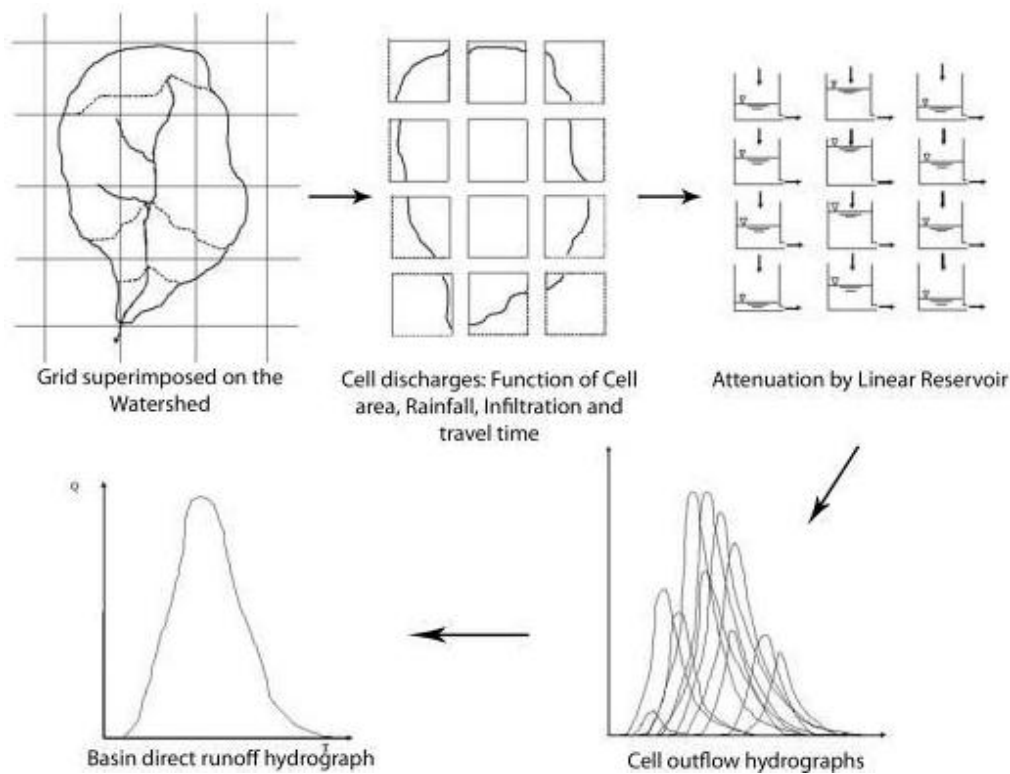


Figure 3. ModClark conceptual model (Kull and Feldman, 1998)

In this method, the travel time is calculated for all cells in a basin. The travel time of each cell to the basin outlet is proposed in relation to (Eq. 2) (Kull and Feldman, 1998).

$$T_{cell} = T_c \frac{L_{cell}}{L_{max}} \quad (\text{Eq.2})$$

where: T_{cell} is the travel time from each cell to the basin outlet, T_c is the concentration time of the basin, L_{cell} is the distance between each cell to the basin outlet and L_{max} is the maximum length of the water flow in the basin. In this method, the effective rainfall in each cell with the lag time is proportional to the length of the movement of that cell

to the outlet of the basin. In this model, it is not necessary to determine the coefficient of roughness on the ground and the depth of the subcortical flow, and the estimation of the hydrograph is conducted with the help of two main parameters, the concentration time and the Clark storage factor. Runoff height is calculated in each step using the spatial distribution map of rainfall and the CN map in each cell. Then, in the next step, the runoff depth of each cell is routed according to the time of the cell's movement to the output. In the final step, the obtained hydrograph is routed according to the relationship in the linear reservoir (Eq. 3).

$$S_{(t)} = KO_{(t)} \quad (\text{Eq.3})$$

where $S_{(t)}$ is storage at time t , $O_{(t)}$ is the output of the reservoir at time t and K is the Clark storage coefficient.

In order to simulate flood hydrograph with the aforementioned methods, topographic, land use and soil hydrological group maps were prepared in GIS environment. A map of the region's curve number was obtained by integrating the land use map with the hydrologic group of soil (Fig. 4).

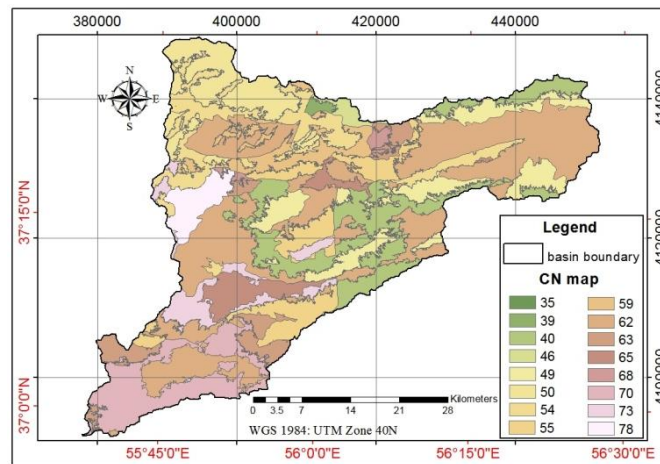


Figure 4. Map of curve number of Tangrah Watershed in moderate humidity

At this stage, after investigation of observed flood hydrographs, 5 events with available rainfalls were selected. Since the rainfall generating each flood hydrograph must be entered into the model to simulate the flood hydrograph, in order to determine the flood generating rainfall, in the history of each event, the rainfall distribution was extracted using the daily rainfall recorded at the rain gauge stations in and around the study area, using the Inverse Distance Weighted (IDW) method in the GIS environment. The time distribution of the storms was determined from the Recording rain gauge station data of the Golestan National Park. After preparing the map of the area's curve number, effective rainfall and initial loss, the SCS method was used based on the following relationships (Eqs. 4, 5 and 6):

$$S = \frac{25400}{CN} - 2540 \quad (\text{Eq.4})$$

$$P_e = \frac{(P - I_a)^2}{P - I_a + S} \quad (\text{Eq.5})$$

$$I_a = a \cdot S \quad (\text{Eq.6})$$

where P_e is the effective rainfall height in mm, P represents Rainfall height in mm, S is Maximum reservoir potential in mm, CN is the average weight curve of the basin, I_a is the initial loss in mm and a is a coefficient of 0.2.

The concentration time was calculated by using Bransby Williams method. This relationship has been recommended for basins larger than 50 square miles (Eq. 7).

$$T_c = \frac{L}{1.483} \sqrt[5]{\frac{M^2}{F}} \quad (\text{Eq.7})$$

where L is the Main waterway length (km), D represents Circle equivalent diameter (km), M^2 is the area of the basin (sq. Km), and F is the mean waterway slope (percent). The parameters required for each of these methods are presented in *Table 1* after calculating the aforementioned equations.

Finally, after providing the aforementioned information for the implementation of SCS model, basin model, meteorological model (hydrograph of each rainfall) and control characteristics (curve number, initial loss, concentration time, lag time) were defined in HEC-HMS software. After completing and entering the data, the HEC-HMS model was used for rainfall-runoff observation data and simulation hydrograph. To calibrate and validate the model, events were divided into two categories such that, three were selected for calibration and two events were selected for validation. During the model calibration process, the input parameters of the model were optimized for each event. Calibrated parameters of three events were averaged and used as input parameters for two validation events.

For simulating flood by the ModClark method, Flood module developed by Alvankar (2003) in the Visual Basic environment was used. After providing the digital data about rainfall, curve number and flow path length, Raster map of these parameters was provided in the GIS environment and then entered into the Flood model. The time distribution of rainfall was also used from the Recording rain gauge station data of Golestan National Park. To determine the movement distance of each cell to the outlet of the basin, the DEM of the basin was used and the movement distance of each cell to the basin outlet was calculated. It should be noted that the concentration time of the watershed indicates the time of water flow from the farthest cell to the outlet of the basin. Input parameters of CN index, the initial losses, concentration time and reserve coefficient were calculated. It should be noted that the reserve coefficient was used graphically (Viessman et al., 1972) and it was used as a preliminary estimation in the calibration step. The steps to implement the model are shown in *Figure 5*.

In the ModClark method, five events with rainfall/runoff data were selected for rainfall-runoff simulation.

Evaluation of the model efficiency

In this research, to evaluate the results of simulation of flood hydrograph after optimization, the determination coefficient (R^2) and Root Mean Square Error (RMSE) were used. The general formula for these two statistics is shown in the following

relationships (Eq. 8 and 9). Finally, the best simulation belongs to the rainstorm with the maximum efficiency or lower RMSE.

$$RMSE = \sqrt{\left(\frac{1}{n} \sum_{i=1}^n [(O_o) - (Q_E)]^2\right)} \quad (\text{Eq.8})$$

$$R^2 = \frac{(\sum_{i=1}^n (Q_O - Q_{Ave})(Q_E - Q_{Ave-E})^2)}{\sum_{i=1}^n (Q_O - Q_{Ave})^2 (\sum_{i=1}^n (Q_E - Q_{Ave-E})^2)} \quad (\text{Eq.9})$$

In these equations O_o and Q_E are, respectively the values of observation and simulation data (Q_o : observed discharge, Q_E : simulated discharge), Q_{Ave} : mean of observed discharge, Q_{Ave-E} : mean of simulated discharge and n the number of data. Finally, after calibrating and validating using ModClark and SCS methods, the results of the data analysis were evaluated based on the two methods of statistical analysis of the determination coefficient (R^2) and Root Mean Square Error (RMSE).

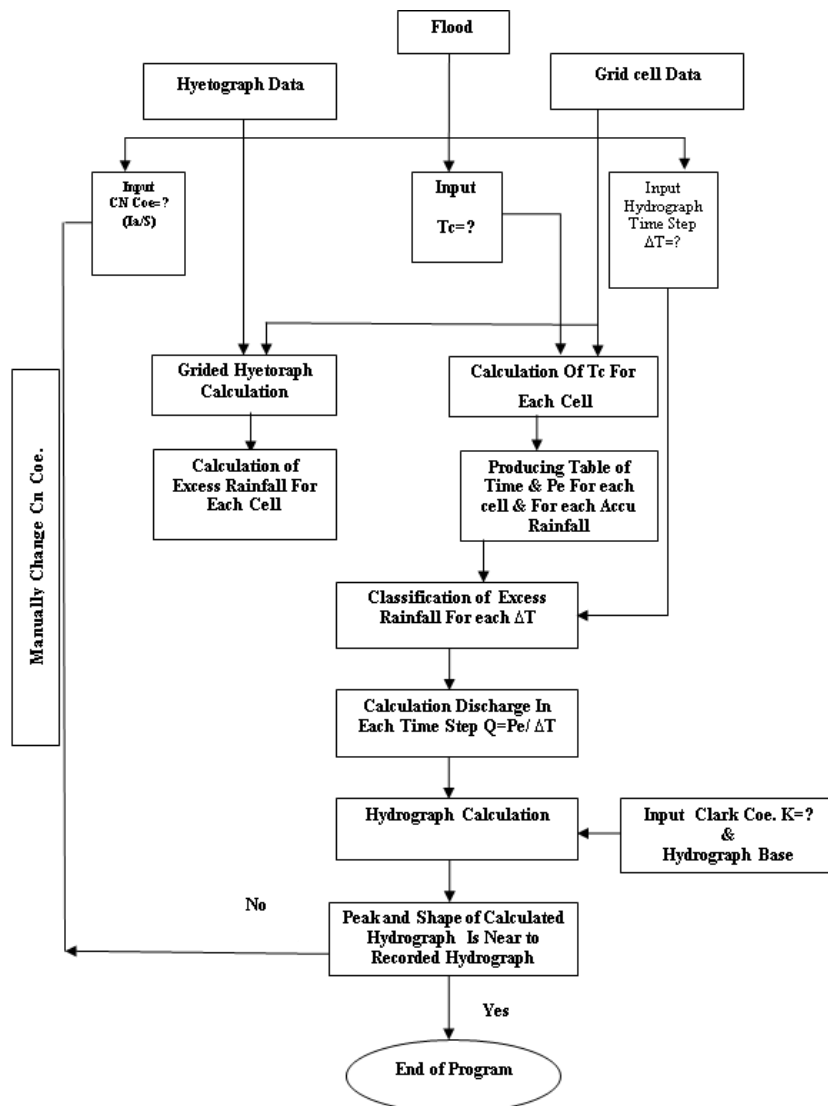


Figure 5. Flowchart of methods in the ModClark method

Results

In this study, the efficiency of the ModClark method and SCS for 5 events was compared. The SCS method was implemented in HEC-HMS software and the ModClark method in Flood software. The optimized values of the model parameters are presented in *Table 1*.

Table 1. Primary and optimized parameters in different events in the HEC-HMS software

Optimized parameter values			Initial parameter values			Subbasin	Event date
Lag time (min)	Curve number (CN)	Initial losses (mm)	Lag time (min)	Curve number (CN)	Initial losses (mm)		
1080	59.9	34	1080	59.9	34	Nardin	1999.04.08 validation
660	55.44	40.83	660	55.44	40.83	Cheshmehkhan	
623.98	81.714	37.354	540	54.69	42.08	Tangrah	
1080	77.42	14.81	1080	77.42	14.81	Nardin	2003.05.25 calibration
660	74.1	17.75	660	74.1	17.75	Cheshmehkhan	
540	73.52	18.29	540	73.52	18.29	Tangrah	
1090.2	74.354	14.938	1080	77.42	14.81	Nardin	2004.05.05 calibration
660	74.1	17.75	660	74.1	17.75	Cheshmehkhan	
346.28	61.96	10.808	540	73.52	18.29	Tangrah	
1080	59.9	34	1080	59.9	34	Nardin	2004.09.18 calibration
660	55.44	40.83	660	55.44	40.83	Cheshmehkhan	
560.85	42.916	42.703	540	54.69	42.08	Tangrah	
1080	77.42	14.81	1080	77.42	14.81	Nardin	2006.04.08 validation
660	74.1	17.75	660	74.1	17.75	Cheshmehkhan	
817.73	97.798	17.799	540	73.52	18.29	Tangrah	

With frequently running model, the hydrologic model and comparison of observed and simulated hydrographs, the hydrologic parameters of the basin varied sufficiently such that the error value obtained from the difference in the peak discharge of the observable and simulated hydrograph peak was minimized. *Table 2* shows the output results in different events in the SCS method. According to *Table 2*, in the event of 2004.5.5, the values of model R2 and RMSE in the SCS method are estimated to be 0.88 and 1.8, respectively. Based on the results of the table, the difference between peak flow and flood volume is estimated to be $4.5 \text{ m}^3 \text{ s}^{-1}$ and 760 m^3 , respectively. *Figure 6* shows the observed and simulated hydrograph using the SCS method in the events of 2003.5.25 and 2004.9.18. The parameters required for simulating of hydrograph in ModClark method shown in *Table 3* represent before and after calibration.

The results of calibration of the model and optimization of the parameters and observation of simulated and observed hydrograph changes verified that, curve number parameters, initial loss and lag time in SCS and CN coefficients, initial loss and K coefficients in the ModClark model showed the most change compared to the primary.

Table 2. Percentage of observed flood and simulation characteristics differences in calibration and validation stage in HEC-HMS software

RMSE	Determination coefficient (R ²)	Correlation coefficient (R)	Difference percentage	Difference	Simulated	Observed	Parameter	Event date
22.8	0.12	0.34	-33.30	-380.5	762.1	1142.6	Volume (1000m ³)	1999.04.08 validation
			0.2	0.1	13.5	13.4	Peak discharge (m ³ s ⁻¹)	
12.7	0.41	0.638	41.92	3111	10532.8	7421.8	Volume (1000m ³)	2003.05.25 calibration
			27.7	22.7	104.9	82.2	Peak discharge (m ³ s ⁻¹)	
1.8	0.88	0.943	0.76	13	1721.7	1708.6	Volume (1000m ³)	2004.05.05 calibration
			4.5	1.3	31.1	29.8	Peak discharge (m ³ s ⁻¹)	
5.2	3.02	-1.738	89.28	764.2	1620.1	855.9	Volume (1000m ³)	2004.09.18 calibration
			185.5	19.6	30.2	10.6	Peak discharge (m ³ s ⁻¹)	
0.8	0.86	0.93	-64.93	-158	85.3	243.3	Volume (1000m ³)	2006.04.08 validation
			-50.5	-1.3	1.2	2.5	Peak discharge (m ³ s ⁻¹)	

Table 3. Hydrological parameters of Tangrah watershed area after calibration and validation in the ModClark method

CN coefficient		Reserve coefficient (h)		Initial losses ratio (I _a /s)		Concentration time (h)		Event date
After calibration	Before calibration	After calibration	Before calibration	After calibration	Before calibration	After calibration	Before calibration	
1.1	1.2	23.2	25.93	0.15	0.2	25.93	25.93	1999.04.08
1	1.012	24.1	25.93	0.16	0.2	25.93	25.93	2003.05.25
1.21	1	24.5	25.93	0.14	0.2	25.93	25.93	2004.05.05
1.09	1	21.1	25.93	0.15	0.2	25.93	25.93	2004.09.18
1.1	1.2	23.2	25.93	0.15	0.2	25.93	25.93	2006.04.08

Table 4 shows the values of the simulation results evaluation in different methods of SCS and ModClark. Based on the results of Table 4, in the 2003.5.25 event, the RMSE in the SCS and ModClark methods have values of 12.7 and 11.77, respectively, and the R2 in the SCS and ModClark method have values of 0.41 and 0.46, respectively. According to the above two parameters, the ModClark method has been simulated more accurately than the SCS method.

Table 4. Estimates of simulation results in different ModClark and SCS methods

RMSE	R ²	Used model	Event date
22.8	0.12	SCS	1999.04.08 validation
2.81	0.74	ModClark	
12.7	0.41	SCS	2003.05.25 calibration
11.72	0.46	ModClark	
1.8	0.88	SCS	2004.05.05 calibration
9.96	0.79	ModClark	
5.2	3.02	SCS	2004.09.18 calibration
2.54	0.56	ModClark	
0.8	0.86	SCS	2006.04.08 validation
0.28	0.93	ModClark	

Figure 6 shows the observed and simulated hydrographs by the ModClark and SCS methods on 2003.5.25 (at calibration stage) and Figure 7 shows the observed and simulated hydrographs by the ModClark and SCS methods on 2006.4.8 data (in the validation step). In Table 5, the results of the evaluation of the SCS and ModClark models are presented in the flood peak estimation at the validation step.

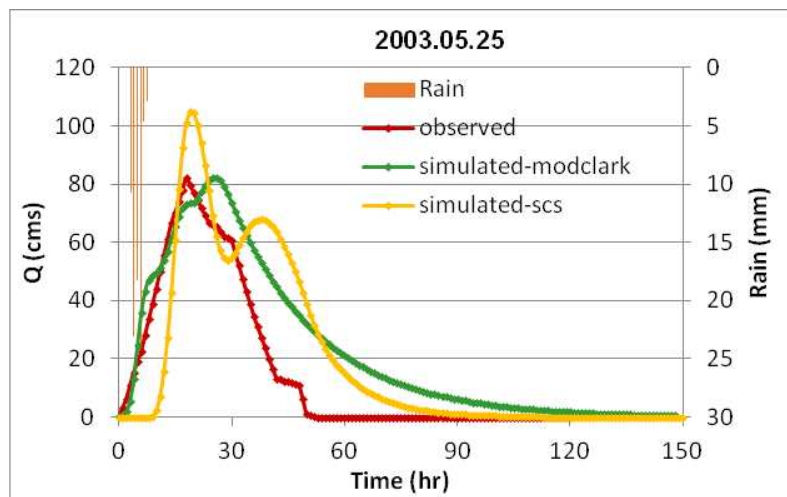


Figure 6. Observed and simulated hydrograph by ModClark and SCS methods on 2003.5.25 (calibration)

Table 5. The results of the evaluation of the SCS and ModClark models in estimating flood peak discharge at the validation step

RMSE	R ²	Used model	Event date
0.74	2.81	1999.04.08	Mod-Clark validation
0.93	0.28	2006.04.08	
0.84	1.55	Mean of Mod-Clark validation	
0.12	22.8	1999.04.08	SCS validation
0.86	0.8	2006.04.08	
0.49	11.8	Mean of SCS validation	

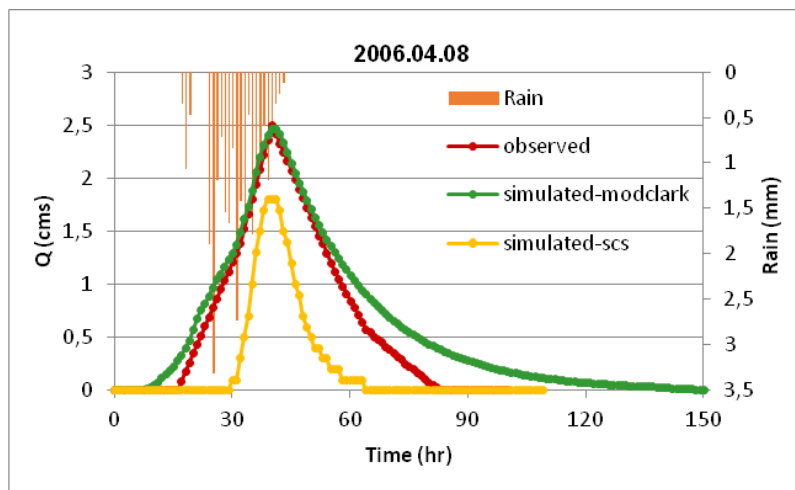


Figure 7. Observed and simulated hydrographs by ModClark and SCS methods on 2006.4.8 (validation)

Discussion and conclusion

The results of calibration and optimization of this study showed that, the ModClark method is superior to the SCS method for estimating peak flow of flood hydrograph (Table 4). In terms of peak discharge estimation, the least difference between the peak discharge of simulations and observations is associated with the ModClark method (Table 5). The survey on model parameters shows that the curve number parameter and initial losses in the SCS model (Table 1) and the parameters of curve number and initial losses and reserve coefficient in the ModClark model are highly sensitive, provided the other parameters are less sensitive than changing the value of the objective function in the above models (Table 3).

The results of comparison of discharge showed that the ModClark model in the validation step simulated the flood hydrograph with RMSE and the R² values of 1.55 and 0.84, respectively and the ModClark model has the best fitness between the observed and simulated data compared to the SCS method. Also, in terms of peak Flow estimation, the ModClark method also has a lower predictive error. This suggests that the simulation of flood hydrographs works better in the ModClark method. The reason for this is based on the concept of linear reservoir model and considering the parameter of the K Muskingum coefficient. The SCS method depends greatly on the calibration due to the dependence on the empirical relationships. So the error is very high. The lowest RMSE is associated with the ModClark method. Therefore, this method is well suited for estimating equilibrium flows. Eventually, events simulated by the ModClark method have the best fitness with real conditions (Fig. 7). The most important point in the research is that, in modest humidity conditions with CN2, better and more accurate results are obtained than wet and dry conditions. the results of this study are consistent with the results of Saghafian et al. (2010), Ghavidelfar et al. (2011), Shabanlou (2014) and Rezaei et al. (2016).

By comparing the parameters RMSE and the R² (Table 4), in both calibration and validation stages, ModClark method has lower mean squared errors and a more accurate R² than the SCS method. Given that, the more closer the root mean square error is to zero and the R², the more accurate the model is in flood hydrograph simulation. The

ModClark method has RMSE and R^2 values more accurate than the SCS method and the results of this study are consistent with the results of Knebl et al. (2005), Alvankar et al. (2006), Paudel et al. (2009), Saghafian et al. (2010), Ghavidelfar et al. (2011), Shabanlou and Rajabi (2012) and Jiang (2015) based on well suited capability of the ModClark model for estimating the flood hydrograph.

Finally, the result of this research was shown ModClark distributed model has better accuracy of SCS model, so this model can be used in determining of flooding area. Considering the high accuracy of ModClark model, using this hydrologic model, we can study the interaction of physiographic and climatic factors on the potential of watersheds' runoff production. Also the results showed that because the use of the ModClark model requires highly precise inputs, therefore; it is possible to use this method in very important tasks such as determining areas with high runoff potential in very small units. Since the SCS-CN penetration estimation method is sensitive to the depth of precipitation, it is suggested that other methods of infiltration be used. It is suggested that considering the different conditions in watersheds with various climate conditions and different geomorphology, the efficiency of ModClark model in more watersheds of the country should be considered in order to determine the applicability; and considering the high sensitivity of the model with the CN parameter, this method will be further investigated in different areas of the country. It is recommended to use other distributed models for rainfall-runoff simulating and compare with the present study.

REFERENCES

- [1] Alvankar, S. R. (2003): Distributed model of flood simulation Using GIS. – Phd dissertation on irrigation. Islamic Azad University, Science and Research Branch of Tehran (in Persian).
- [2] Alvankar, S. R., Saghafian, B., Sedghi, H. (2006): Effect of pixel size of a hydrologic model on simulation of flood peak. – Journal of Agricultural Sciences Islamic Azad University 12(2): 329-344 (in Persian).
- [3] Bhattacharya, A. K., McEnroe, B. M., Zhao, H., Kumar, D., Shinde, S. (2012): Modclark model: improvement and application. – IOSR Journal of Engineering (IOSRJEN) 2(7): 100-118.
- [4] Chidaz, A., Mohseni Saravi, M., Vafakhah, M. (2009): Evaluating the HEC-HMS model for estimating flood hydrograph in Kasilian basin. – Journal of Watershed Management Researches (Pajouhesh and Sazandegi) 84: 59-71 (in Persian).
- [5] Emerson, C. H., Welty, C., Traver, R. G. (2003): Application of HEC-HMS to model the additive effects of multiple detention basins over a range of measured storm volumes. – Civil Engineering Database. Part of World Water & Environmental Resources Congress 2003 and Related Symposia.
- [6] Foody, G. M., Ghoneim, E. M., Arnell, N. W. (2004): Predicting locations sensitive to flash flooding in an arid environment. – Journal of Hydrology 292(1-4): 48-58. DOI: 10.1016/j.jhydrol.2003.12.045.
- [7] Ghavidelfar, S. Alvandkar, S. R., Razmkhah, A. (2011): Comparison of the lumped and quasi-disributed Clark runoff models in simulating flood hydrographs on a semi-arid watershed. – Water Resources Management 25(6): 1775-1790. DOI: 10.1007/s11269-011-9774-5.
- [8] Ghitoto, R. D. (1991): Runoff hydrograph computation method. – A designer course at Clarion Palaz Hotel.

- [9] Halwatura, D., Najim, M. M. M. (2013): Application of the HEC-HMS model for runoff simulation in a tropical catchment. – *Environmental Modelling & Software* (46): 155-162. DOI: 10.1016/J.envsoft.2013.03.006.
- [10] Horritt M. S., Bates, P. D. (2002): Evaluation of 1D and 2D numerical models for predicting river flood inundation. – *Journal of Hydrology* 268: 87-99.
- [11] Jiang, Y., Liu, C. M., Li, X. Y, Liu, L. F., Wang, H. R. (2015): Rainfall-runoff modeling, parameter estimation and sensitivity analysis in a semiarid catchment. – *Environmental Modelling & Software* (67): 72-88. DOI: 10.1016/J.envsoft.2015.01.008.
- [12] Kathol, J. P., Werner, H. D., Trooien, T. P. (2003): Predicting Runoff for Frequency based storm Using a Prediction Runoff Model. – A.S.A.E., South Dakota, U.S.A.
- [13] Knebl, M. R., Yang, Z. L., Hutchison, K., Maidment, D. R. (2005): Regional Scale flood modeling using NEXRAD, rainfall, GIS, and HEC-HMS\RAS: a case study for the San Antonio River basin summer 2002 storm event. – *Journal of Environmental Management* 75: 325-336. DOI: 10.1016/j.jenvman.2004.11.024.
- [14] Kull, D. W., Feldman, A. D. (1998): Evaluation of Clark's unit graph method to spatially distributed runoff. – *Journal of Hydrologic Engineering ASCE* 3(1): 9-19.
- [15] Kumar, P. S., Ratna, K. B. M. J., Praveen, T. V., Venkata, K. V. (2010): Analysis of the runoff for watershed using SCS-CN method and geographic information systems. – *International Journal of Engineering Science and Technology* 2: 3947-3654.
- [16] Linde, A. H. te, Aerts, J. C. J. H., Hurkmans, R. T. W. L., Eberle, M. (2008): Comparing model performance of two rainfall-runoff models in the Rhine basin using different atmospheric forcing data sets, hydrology and earth system sciences. – 12(2008): 943-957.
- [17] Paudel, M., Nelson, E. J., Scharffenberg, W. (2009): Comparison of lumped and quasi-distributed Clark runoff models using the SCS curve number equation. – *Journal of Hydrology Engineering ASCE* 34(3): 1098-1106. DOI: 10.1061/ASCE_HE.1943-5584.0000100.
- [18] Peters, L., Easton, D. (1996): Runoff simulation using radar rainfall data. – *Water Resource Bulletin AWRA* 32(4): 753-760.
- [19] Rezaei, M., Vafakhah M., Ghermezcheshmeh, B. (2016): Spatial variability using a flood response method in Khanmiriza watershed. – *Scientific-Research Journal of Engineering and Watershed Management* 8(1): 150-139 (in Persian).
- [20] Roy, A., Thomas, R. (2016): A comparative study on the derivation of unit hydrograph for Bharathapuzha River Basin. – *Procedia Technology, International Conference on Emerging Trends in Engineering, Science and Thechnology (ICETEST-2015)* 24: 62-69.
- [21] Saghafian, B., Khosroshahi, M. (2005): Unit response approach for priority determination of flood source areas. – *Journal of Hydrologic Engineering ASCE* 10(4): 270-277. DOI: 10.1061/(ASCE)1084-0699.
- [22] Saghafian, B., Ghermezcheshmeh, B., Kheirkhah, M. M. (2010): Iso-flood severity mapping: a new tools for distributed flood source identification. – *Natural Hazards* 55(2): 557-570. DOI: 10.1007/s11069-010-9547-0.
- [23] Saghafian, B., Noroozpour, S., Kiani, M., Rafieei Nasab, A. (2016): A coupled Modclark-curve number rainfall-runon-runoff model. – *Arabian Journal of Geosciences* 9(4): 277. DOI: 10.1007/s12517-015-2295-4.
- [24] Sampth, D. S., Weerakoon, S. B., Herath, S. (2015): HEC-HMS model for runoff simulation in a tropical catchment with intra-basin divisions. Case study of the Deduru Oya River Basin, Sri Lanka. – *Engineer* 48(1): 1-9.
- [25] Sarangi, A., Singh, D. K., Singh, A. K. (2008): Evaluation of curve number and geomorphology-based models for surface runoff prediction from ungauged watersheds. – *Current Science* 94(12): 1620-1626.
- [26] Shabanlou, S. (2014): Calculation of flood hydrograph for karun basin by different methods. – *Agricultural Communications* 2(2): 54-61.

- [27] Shabanlou, S., Rajabi, A. (2012): Comparison of estimated flood hydrographs using lumped and distributed models. – *Journal of Environmental Research and Development* 7(1): 79-87.
- [28] Teymouri, M., Habibnejad, R. M., Ghanbarpour, M. R., Abbasi, A. A. (2007): Simulation of peak discharge of flood hydrograph using ModClark distribution method. – *Journal of Agricultural Science and Natural Resources of Khazar* 1(5): 29-42 (in Persian).
- [29] US Army Corps of Engineers (2000): Hydrologic modeling system. HEC-HMS: Technical Reference Manuals. – Hydrologic Engineers Center, Davis, CA, USA.
- [30] Verma, A. K., Jha, M. K., Mahana, R. K. (2010): Evaluation of HEC-HMS and WEPP for simulating watershed runoff using remote sensing and geographical information system. – *Paddy and Water Environment* 8: 131-144. DOI: 10.1007/s10333-009-0192-8.
- [31] Viessman, W., Harbaugh, T. E., Knapp, J. (1972): *Introduction to Hydrology*. – Intext Ed. Pub., New York.
- [32] Water Research Institute. (2010): Project Reports of Gorganroud Flood Warning System. – Water Resources Department, Tehran.
- [33] Zhang, Z., Wang S. W., Sun, G., Steven, G. M., Zhang, H., Jianlao, M., Eduard, K., Strauss, P. (2008): Evaluation of the MIKE SHE Model for application in the Loess Plateau China. – *American Water Resources Association* 44(5): 1108-1120.

COMPARING PHENOTYPIC VARIATION OF ROOT TRAITS IN THAI RICE (*ORYZA SATIVA* L.) ACROSS GROWING SYSTEMS

SAENGWILAI, P.^{1,2*} – KLINSAWANG, S.¹ – SANGACHART, M.¹ – BUCKSCH, A.^{3,4,5}

¹*Department of Biology, Faculty of Science, Mahidol University
Bangkok 10400, Thailand*

²*Center of Excellence on Environmental Health and Toxicology (EHT)
Bangkok, Thailand*

³*Department of Plant Biology, University of Georgia
Athens, GA, 30602, USA*

⁴*Warnell School of Forestry and Natural Resources, University of Georgia
Athens, GA, 30602, USA*

⁵*Institute of Bioinformatics, University of Georgia
Athens, GA, 30602, USA*

**Corresponding author*

e-mail: patompong.sae@mahidol.edu; phone: +66-9-1725-4817

(Received 8th Sep 2017; accepted 15th Jan 2018)

Abstract. Root systems have long been neglected in plant breeding due to their inaccessibility and the laborious nature of root studies. Over the past years, root scientists developed the classification system, methodologies and growing systems for high throughput measurements of root traits. We compared root traits obtained with three growing systems for eleven Thai rice varieties. We found considerable differences in the variation of root traits between the laboratory system with paper roll-up, a pot system in the greenhouse and a field system. The variation of root traits ranged from 1.31 folds in root cortical aerenchyma (RCA) to 4.20 folds in crown root growth angle in a roll-up system. Varieties also differed in root plasticity among the three growing environments. Principal components analysis indicated that root anatomical traits contributed 55% to the observed variation in the field. Hierarchical cluster analysis revealed that upland varieties clustered in a steep-angled group while lowland varieties clustered in a shallow-angled group. The observed clustering could be linked to the amount of RCA. Our results suggest that optimization of root growth angle could be an important strategy for improved adaptation of rice plants growing in flooded and non-flooded areas. We propose Thai rice varieties as donors in root trait driven breeding programs to enhance water and nutrient uptake.

Keywords: *breeding, RCA, root system, varieties*

Introduction

Rice (*Oryza sativa*) is a staple crop for over 3.5 billion people (IRRI et al., 2010) and an economic driver for many countries in south and southeast Asia. A prime example of the economic importance of rice is Thailand (Wailes and Chavez, 2012) with 25 million tons produced on paddy fields in 2016. Rice production depends on high water availability and highly fertile soils; however, one-third of the global rice production area is planted in nutrient deficient soils (Haefele et al., 2014). In addition, ongoing climate change and a predicted fertilizer shortage limit resource availability for rice production (Haefele et al., 2006). This scenario poses significant economic challenges to large- and small-scale rice farmers. Improved rice varieties with

enhanced capability of water and nutrient uptake efficiency are one of the solutions to drought and nutrient limited growth conditions.

Root systems play important roles in water and nutrient acquisition of a plant as well as anchorage to support the plant structure. Continuous shoot improvements of the last decades neglected the phenotypic variation of root architectural, morphological, and anatomical traits despite the widely available genetic resources. The key to understand the potential of root phenotypes lies in the understanding of root structure and function relative to its developmental processes on architectural and anatomical scale (Lynch, 2007; Lynch, 2014). Rice root architecture consists of five root types including the embryonic and the postembryonic roots such as the radicle, the embryonic crown roots, the postembryonic crown roots, the large lateral roots, and the small lateral roots (Rebouillat et al., 2008). Variation in root architecture has been shown to positively influence soil exploration and acquisition of water and nutrients in nutrient limited and drought conditions. For instance, rice promotes deep rooting which enhances growth and yield under drought (Uga et al., 2013) similar to well-known observations in maize under drought and low nitrogen conditions (Hund et al., 2009; Saengwilai et al., 2014b; Trachsel et al., 2013). Under phosphorus (P) stress, root traits that describe shallow foraging strategies increase the acquisition of immobile P in the topsoil, e.g. shallow rooting angle and high lateral branching density (Lynch and Brown, 2001; Zhu and Lynch, 2004).

Root hairs constitute the finest architectural level. They are tip-growing extensions from root epidermal cells (Datta et al., 2011). Root hair development is not purely dependent on the genotype, but also depends on environmental factors such as soil texture, type and level of nutrients in soils (Gilroy and Jones, 2000). The ability to adapt to different environmental conditions is measurable as surface area of root hairs that increases the contact with the soil. As a consequence, more surface contact with the soil increases efficiency of nutrient uptake capacity (Gilroy and Jones, 2000; Miguel et al., 2015).

Rice root anatomy summarizes the internal organization of cell and tissue types. The components of the internal arrangement are root epidermis, exodermis, sclerenchyma layer, cortex, endodermis, pericycle, cortical aerenchyma and xylem and phloem vessels. Anatomical traits have been hypothesized to deliver major improvements in crop production through improving resource capture, transport, and utilization (Lynch, 2014; Postma and Lynch, 2010). For example, smaller diameter of xylem vessels improved water use efficiency by conserving water resources for grain filling in wheat (Richards and Passioura, 1989). Another example is reduced cortical cell file number and increased cortical cell size, which led to reduced root respiration and increased rooting depth in maize. As a consequence, improved water acquisition and greater yield under drought was observed (Chimungu et al., 2014a; 2014b). The formation of root cortical aerenchyma (RCA) improves crop growth and productivity under drought and suboptimal nitrogen conditions in maize (Saengwilai et al., 2014a; Zhu et al., 2010).

Root traits have been studied in various growing systems. Among culturing approaches, a roll-up or cigar-roll and a greenhouse pot system have been commonly used for phenotyping roots of several crop species. The roll-up system allows for a rapid, low cost, and non-destructive evaluation of root traits in young seedlings. In addition, the roll-up system is capable to observe delicate traits such as root hair length and density (Zhu et al., 2005). A pot system using soil permits a more realistic condition for root growth in a controlled environment and is widely used for genetics and

physiological studies in rice (Vejchasarn et al., 2016). In the field, shovelomics, a manual high throughput approach, facilitates the evaluation of mature root architecture (Trachsel et al., 2011). Although studies have demonstrated significant correlations of root traits in different culture systems (Tuberosa et al., 2002), such comparisons in rice are still scarce. To assist breeding efforts towards improved drought tolerance and higher yield under nutrient limited growth conditions, a better understanding of root traits among rice varieties in different growing systems is much needed. In our study, we aim to 1) investigate phenotypic variation of root architectural and anatomical traits in eleven Thai rice varieties with low-cost phenotyping technologies and to 2) examine correlations among root traits and growing conditions.

Materials and methods

Plant materials

Rice (*Oryza sativa* L.) is a member of Poaceae family and the common cultivated varieties are annual plants that grow up to two meters tall. Rice cultivation occurs in different types of managed ecosystems such as irrigated, rainfed upland, rainfed lowland, flood-prone systems. In our study, eleven Thai rice varieties were selected because of their popularity among Thai farmers, variation in growing system, and potential as donors in rice breeding program. The varieties include photoperiod sensitive lowland varieties (Khao Dawk Mali 105 (KDML105), Niaw San-pah-tawng, RD13), photoperiod insensitive lowland varieties (RD1, Phitsanulok 2, RD7 and RD31), photoperiod sensitive upland varieties (Goo Meuang Luang, Nam Roo and Leum Pua) and photoperiod insensitive upland varieties (R258). Seeds were obtained from the Rice Department of the Ministry of Agriculture and Cooperatives of Thailand.

Growth conditions

Roll-up system

The laboratory experiment was carried out at the Phayathai campus of Mahidol University, Bangkok, Thailand (13°45'54.3"N 100°31'35.4"E). Seeds were surface sterilized in 10% NaOCl for 1 min. The seeds were put in a rolled germination paper (Anchor Paper Company, St. Paul, MN, USA) soaked with 0.5 millimolars (mM) CaSO₄ and placed in darkness at 28 degree Celsius (°C) in a germination chamber for two days then exposed to supplement lights and harvested at 7 days after germinating.

Greenhouse pot system

The greenhouse experiment was carried out at the Salaya campus of Mahidol University, Nakhon Pathom, Thailand (13°47'40.2"N 100°19'26.7"E). Seeds of lowland rice varieties including KDML105, Phitsanulok 2, RD13, RD31, and RD7 were surface-sterilized in 10% NaOCl for 1 min. The seeds were pre-germinated in rolled germination papers (Anchor Paper Company, St. Paul, MN, USA) soaked with 0.5 mM CaSO₄ and placed in the darkness at 28°C for two days. At planting, the plants were transferred to 10 Liter (L) pots with growth media consisting of a mixture (volume based) of 50% medium size (0.3 to 0.5 Milliliters (mm)) commercial grade sand, 35% horticultural vermiculite, 15% Perlite. One day before planting, the pots were saturated with 3 liters of a nutrient solution adjusted to pH 6. The nutrient solution contained (in

μM): NO_3 (7000), NH_4 (1000), P (1000), K (3000), Ca (2000), SO_4 (500), Mg (500), Cl (25), B (12.5), Mn (1), Zn (1), Cu (0.25), Mo (0.25) and FeDTPA (100). Each pot received three seedlings and after 4 days, the plants were thinned to one plant per pot. Plants were watered with 75 ml of deionized water every other day until harvest.

Field study

The field experiment was carried out on a research farm in the Tha Yang district located in the Petchaburi province of western Thailand ($12^\circ56'37.3''\text{N}$ $99^\circ55'24.1''\text{E}$) (Fig. 1). The soil in Tha Yang is classified as loamy sand which are derived from residuum on hill slopes with a layer of angular rock fragments occurring within 50 cm of the surface. The average ambient temperature during the study was $27\pm 2^\circ\text{C}$ and the relative humidity was 90%. The five lowland rice varieties were selected for this experiment. The trial was arranged in a randomized complete block design (RCBD) with three replications. The seeds were sown in wet seed beds for 30 days and then transplanted into the field. Each variety was planted in three-row plots. Each plot consisted of 12 plants. Row width was 12 centimeters (cm), and the distance within a row was 12 cm. Water was maintained in the rice field to suppress weed growth during the growing season. In the trial, soil nutrient levels were adjusted to meet the requirements for rice production as determined by soil tests at the beginning of the growing seasons. The trial was managed according to typical farmer practice.

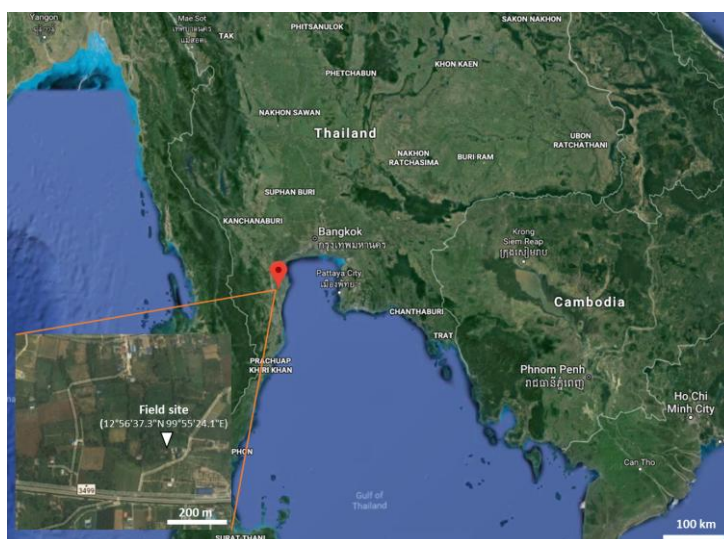


Figure 1. A satellite image of the field experimental site in Tha Yang district, Petchaburi province, Thailand (modified from Map data ©2018 Google)

Shoot and root analyses

Prior to root excavation, shoot characteristics including tiller numbers and height were assessed. Root excavation was carried with the shovelomics protocol described in Trachsel et al. (2010) and Vejchasarn et al. (2016). Root crowns were collected by excavating a 15-cm radius around the stem to a depth of at least 15 cm. The majority of soil was removed by carefully shaking the root system. The remaining soil was removed by soaking the roots in diluted commercial detergent for 8-12 hours. In a final step we rinsed the soaked root systems with water using a low pressure garden hose. A Four-

centimeter root segment was collected at 8 cm from the base of the representative nodal roots for morphological and anatomical analyses. The samples were stored in 75% EtOH at 4°C until processing and analysis.

Root architectural analysis

For the roll-up system, root architectural traits were manually evaluated by counting numbers of roots, and by measurements obtained with a ruler. Root architectural traits including crown root growth angle, crown root number, lateral root branching and lateral root length were evaluated using a modified Shovelomics protocol for the pot and field experiment. Our protocol evaluated crown root growth angle with a scoring board and manually counted the number of crown roots. We quantified lateral root branching as a count of lateral roots in a two-centimeter segment starting at 8 cm offset of the root base. Lateral root length was measured with a ruler. Shoots and roots were dried at 60°C for 72 h prior to weight determination. The measurements were carried out with 4 replications and 4 sub-replications per sample.

Root morphological analysis

Root hair evaluation was carried out as described by Vejchasarn et al. (2016). Primary root or crown root samples were stained with 0.5% of toluidine blue for 45 s before the images of the root hairs were taken. We used the imaging system MVX10 of the Macro Zoom to obtain root hair images. Root hair length was measured in the obtained images with Image-J version 1.46 (Abràmoff et al., 2004) and root hair density was measured by counting the number of root hairs in the one-millimeter root segment.

Root anatomical analysis

Root segments were selected from the middle of the crown root samples and preserved in 75% EtOH at 4°C until processing and analysis. Root cross-sections were obtained by free hand-sectioning using Teflon-coated double-edged stainless-steel blades. The root sections were examined with a light microscope at 2.8x magnification. Three sections were selected to be imaged as representative sub-samples. Root anatomical traits were quantified using the semi-automated image analysis program *RootScan* (Burton et al., 2012). All together eight root anatomical traits were evaluated in this study (*Table 1*).

Table 1. Abbreviations and descriptions of traits measured in this study

Trait	Description	Trait	Description
TRL	Total root length, cm	TSA	Total stele area, mm ²
RW	Root weight, g	AA	Aerenchyma area, mm ²
LB	Lateral root branching on radicle	perAA	Percent of cortex as aerenchyma, %
LL	Lateral root length on radicle	MXVA	Metaxylem vessel area, mm ²
CA	Crown root angle	CCFN	Cortical cell file number
CB	Crown root branching	CCC	Cortical cell count
CN	Crown root number	RHL	Root hair length, mm
RXSA	Root cross sectional area, mm ²	RHD	Root hair density
TCA	Total cortical area, mm ²	SW	Shoot weight, g

Statistical analysis

Statistical analysis was performed using R version 2.15.1. Linear mixed effect models were fit using the *lme* function from the package *nlme* (Pinheiro et al., 2012). ANOVA was used to compare varieties as well as upland and lowland characteristics. The protected least significant difference post hoc ($\alpha = 0.05$) was used for multiple comparison tests. Correlations and a principal component analysis were performed on mean values of the measurements taken per genotype.

Results

Natural variation among root traits and growing systems

Significant phenotypic variation between the selected varieties was observed in all experiments for anatomical and architectural traits. In the roll-up system, varieties significantly differed in their shoot and root traits (Table 2).

Table 2. Summary of phenotypic variation of root traits (Table 1) showing mean, range, and significant level among 11 commercial and traditional varieties of Thai rice in the roll-up system

Variety	TRL	RW	CA	CN	LB	LL	RHD	RHL
Goo Meuang Luang	20.05 a	0.06 cd	55.63 a	5.31 bcd	17.58 a	0.74 ab	31.54 ab	0.19 ab
KDML105	17.56 ab	0.04 f	28.46 e	4.31 e	16.11 ab	0.57 cb	34.01 a	0.18 a
Leum Pua	18.29 ab	0.07 b	14.06 f	4.31 e	16.33 ab	0.36 ef	31.61 ab	0.16 ef
Nam Roo	16.89 ab	0.07 b	28.67 cd	5.33 bcd	17.63 a	0.44 def	31.70 ab	0.19 ab
Niaw San-pah-tawng	12.99 b	0.06 bc	21.47 d	5.53 bcd	10.67 b	0.32 f	34.86 a	0.21 a
Phitsanulok 2	14.99 ab	0.05 e	34.67 c	5.80 bc	15.67 ab	0.47 de	26.27 b	0.18 bc
R258	13.57 ab	0.09 a	59.00 a	5.10 cde	15.13 ab	0.31 f	29.07 ab	0.19 ab
RD1	15.97 ab	0.07 b	36.67 bc	6.50 ab	14.80 ab	0.60 bcd	28.00 ab	0.14 f
RD13	15.46 ab	0.04 f	50.00 ab	4.71 de	15.75 ab	0.39 ef	30.73 ab	0.16 de
RD31	17.27 ab	0.05 f	22.00 cd	6.83 a	16.37 a	0.61 bc	28.84 ab	0.17 cd
RD7	17.84 ab	0.04 f	28.06 cd	6.33 ab	15.56 ab	0.80 a	30.56 ab	0.19 bc
Range	1.41x	2.12x	4.20x	1.58x	1.65x	2.58x	1.33x	1.50x
Significance	*	*	*	*	*	**	**	*
Variety	RSXA	TCA	TSA	AA	perAA	MXVA	CCFN	SW
Goo Meuang Luang	0.17 bcde	0.15 bcdef	0.015 bcd	0.043 cde	28.19 b	0.0006 e	8.67 ab	2.16 b
KDML105	0.16 cde	0.15 cdef	0.012 def	0.050 cde	33.24 ab	0.0007 cde	7.33 b	4.14 b
Leum Pua	0.26 a	0.24 a	0.024 a	0.081 a	34.02 ab	0.0015 a	9.33 ab	2.44 b
Nam Roo	0.20 bc	0.18 bc	0.019 bc	0.059 bcd	32.28 ab	0.0012 bc	9.00 ab	3.66 b
Niaw San-pah-tawng	0.18 bcd	0.17 bcd	0.014 cde	0.060 bc	36.09 a	0.0010 bcd	9.33 ab	8.03 a
Phitsanulok 2	0.15 de	0.14 def	0.011 def	0.040 de	29.16 b	0.0006 de	9.67 ab	1.88 b
R258	0.18 bcd	0.16 bcde	0.019 bc	0.047 cde	30.76 ab	0.0012 b	9.33 ab	2.52 b
RD1	0.16 cde	0.15 cdef	0.012 def	0.049 cde	32.82 ab	0.0006 e	9.00 ab	2.11 b
RD13	0.18 bcd	0.17 bcd	0.015 bcd	0.060 bc	35.40 a	0.0008 cde	9.33 ab	1.92 b
RD31	0.13 e	0.2 f	0.010 f	0.038 e	32.03 ab	0.0005 e	9.33 ab	3.12 b
RD7	0.21 b	0.19 b	0.017 bc	0.069 ac	36.88 a	0.001 bc	10.00 a	4.12 b
Range	2.05x	2.02x	2.40x	2.14x	1.31x	2.9x	1.36x	4.27x
Significance	**	**	**	**	**	**	**	*

*, ** and *** denote significances at 0.05, 0.01 and 0.001. Different letters represent significant difference. Maximum and minimum values are highlighted in dark and light color, respectively. The reported range value denotes to the x-fold difference between maximum and minimum values for each trait

The range of shoot dry weight (SW) was substantial, showing a 4.27-fold increase between smallest and largest average value per genotype. The identified extremal varieties are Niaw San-pah-tawng and Phitsanulok 2. For architectural root traits, a remarkable 4.20-fold increase between extrema was observed for the crown root angle (CA). The extremal variation for anatomical traits was 1.31-fold in the percentage of aerenchyma (perAA). Generally, the ranges of the variation in anatomical root traits were higher than those of root architectural traits. Leum Pua, a traditional upland variety, had largest cross-sectional area (RXSA) of 0.26 mm² on average with high aerenchyma area (AA) of 0.081 mm² on average. In contrast, the lowland variety RD 31 had the smallest RXSA roots (0.13 mm² on average) with smaller AA (0.038 mm² on average) compared to upland varieties.

In the pot system, five lowland varieties including KDML105, Phitsanulok 2, RD13, RD31, and RD7 were selected for this set of experiment to compare traits among varieties grown under optimal growth conditions. We found that varieties significantly differed in their shoot and root traits except for root hair density (RHD) and cortical cell file number (CCFN) (Table 3). Among those with significant differences, the variation of root traits ranged from 1.25-fold in total root length (TRL) to 2.28-fold in lateral root branching of the crown root (CB). KDML105 was most outstanding in its anatomical traits showing the thickest roots with large metaxylem vessel area (MXVA) and highest aerenchyma formation (AA and perAA). Phitsanulok 2 had the lowest AA, perAA and smallest MXVA. The ranking for anatomical traits of these two varieties were consistent across growing systems (Table 2 and 3). Unfortunately, the root segments of RD13 dried out during the storage process and could not be evaluated.

Table 3. Summary of phenotypic variation of root traits (Table 1) showing mean, range, and significant level among 5 lowland rice varieties in the pot system

Variety	SW	TRL	CA	CN	LB	LL	RHD	RHL
KDML105	27.27 ab	45.50 b	40.00 a	271.33 bc	41.00a	4.79 ab	17.50	0.09 b
Phitsanulok2	24.35 b	42.88 bc	37.50 ab	263.00 c	27.38 b	4.99 ab	22.33	0.18 a
RD31	30.39 ab	50.10 a	37.50 ab	334.00 ab	19.25 c	3.91 b	33.00	0.10 b
RD7	28.51 ab	42.75 bc	32.50 b	369.00 a	24.88 bc	5.73 a	22.50	0.10 b
RD13	35.54 a	40.00 c	27.50 b	408.00 a	18.00 c	5.53 ab		
Range	1.46x	1.25x	1.45x	1.55x	2.28x	1.47x	1.89x	2.00x
Significance	*	*	*	*	*	**	NS	*
Variety	RXSA	TCA	TSA	AA	perAA	MXVA	CCFN	CCC
KDML105	0.79 a	0.74 a	0.06 a	0.42 a	56.19 a	0.005 a	10.83	550.00 ab
Phitsanulok2	0.57 b	0.35 b	0.05 a	0.19 b	37.70 b	0.003 b	10.89	671.80 a
RD31	0.52 b	0.48 b	0.04 b	0.27 b	54.19 a	0.004 b	10.33	459.40 b
RD7	0.54 b	0.49 b	0.04 b	0.27 b	53.31 a	0.004 b	10.89	530.70 ab
Range	1.52x	2.11x	1.50 x	2.21x	1.49x	1.67x	1.05x	1.46x
Significance	**	**	**	**	**	**	NS	*

*, ** and *** denote significances at 0.05, 0.01 and 0.001. NS means no significant difference. Different letters represent significant difference. Maximum and minimum values are highlighted in dark and light color, respectively. The reported range value denotes to the x-fold difference between maximum and minimum values for each trait

The five varieties grown in the pot system were also evaluated in the field at 60 days after transplanting. We found that varieties significantly differed in their shoot and root traits except for RHD, perAA and grain yield (Table 4). Among those with significant genotypic differences, the variation of root traits ranged from 1.39-fold in CB to 2.14-fold in AA. Despite considerable variation in AA, perAA appeared to be high and not significantly different among varieties. Among all varieties, the photoperiod-sensitive lowland variety, RD13, showed consistently shallower root systems with the largest number of crown roots (CN) in the pot system and in the field. Additionally, Phitsanulok 2 maintained its ranking as having low AA with relatively small MXVA (Table 3 and 4).

Table 4. Summary of phenotypic variation of root traits (Table 1) showing mean, range, and significant level among 5 lowland rice varieties grown in the field

Variety	SW	TN	CA	CB	CN	RHL	RHD	Grain (g/plant)
KDML105	13.91 a	5.56 a	23.89 b	2.74 ab	205.30 a	0.09 ab	12.78 a	-
Phitsanulok 2	6.66 c	4.56 ab	35.83 b	3.04 a	154.00 b	0.08 b	8.67 a	1.98 a
RD13	13.51 a	4.56 ab	25.83 a	2.74 ab	228.40 a	0.09 ab	13.56 a	-
RD31	6.00 c	3.89 b	31.39 ab	2.41 ab	134.40 b	0.07 b	9.38 a	1.74 a
RD7	9.61 b	4.89 ab	29.44 ab	2.19 b	211.30 a	0.11 a	9.67 a	2.52 a
Range	2.32x	1.43x	1.50x	1.39x	1.70x	1.57x	1.56x	1.45x
Significance	***	**	**	*	**	**	NS	NS
Variety	RXSA	TCA	TSA	AA	perAA	MXVA	CCFN	CCC
KDML105	0.93 b	0.90 a	0.03 a	0.53 b	58.11 a	0.0031 a	11.80 a	212.57 b
Phitsanulok 2	0.68 b	0.65 b	0.02 ab	0.37 b	57.55 a	0.0021 b	9.13 ab	146.13 c
RD13	1.43 a	1.40 a	0.03 a	0.79 a	55.85 a	0.0032 a	9.67 a	331.17 a
RD31	0.68 b	0.65 b	0.02 ab	0.38 b	57.55 a	0.0020 b	6.22 b	160.00 bc
RD7	0.71 b	0.69 b	0.02 b	0.38 b	53.04 a	0.0021 b	9.89 a	195.50 bc
Range	2.10x	2.15x	1.5x	2.14x	1.10x	1.52x	1.90x	2.27x
Significance	**	**	**	**	NS	*	**	***

*, ** and *** denote significances at 0.05, 0.01 and 0.001. NS means no significant difference. Different letters represent significant difference. Maximum and minimum values are highlighted in dark and light color, respectively. The reported range value denotes to the x-fold difference between maximum and minimum values for each trait

Correlation analysis

Correlation analysis was performed for root traits in the roll-up, pot, and field system. In the roll-up system, anatomical traits showed strong positive correlations with correlation coefficient values (r) ranging from 0.70 to 1.00 (Table 5). Smaller correlation values were observed for perAA which was only positively correlated with aerenchyma area (r = 0.70; p < 0.05) and cortical cell file number (CCFN). The crown root number (CN) observed in the roll-up system showed a marginally negative correlation with total stele area (TSA) and metaxylem vessel area (MXVA) (r = -0.53; p < 0.1). However, this relationship disappeared in plants grown in the pots and in the field (Table 5).

Table 5. Correlation matrix among root traits of 11 commercial and traditional Thai rice varieties grown in the roll-up system and five lowland varieties grown in the pot and the field system

Roll-up system	RXSA	TCA	TSA	AA	perAA	MXVA	CCFN	CCC	CA	CN	PB
TCA	1.00***										
TSA	0.93***	0.91***									
AA	0.94***	0.95***	0.79**								
perAA	0.41	0.44	0.33	0.70*							
MXVA	0.90***	0.88***	0.94***	0.81**	0.36						
CCFN	0.23	0.23	0.22	0.25	0.21	0.26					
CCC	0.88***	0.89***	0.70*	0.88***	0.47	0.68*	0.31				
CA	-0.25	-0.27	-0.10	-0.40	-0.44	-0.22	0.11	-0.18			
CN	-0.51	-0.5	-0.53	-0.41	0.19	-0.53	0.48	-0.38	-0.11		
PB	0.56	0.18	0.16	-0.1	-0.49	-0.11	-0.22	-0.10	0.21	-0.21	
RHL	0.17	-0.2	0.12	-0.23	-0.17	0.13	0.07	-0.22	0.13	-0.10	-0.30
Pot system	CN	CA	LB	LL	RXSA	TSA	AA	MXVA	TCA	perAA	CA
CA	0.91*										
LB	-0.73	0.68									
LL	0.44	-0.67	0.11								
RXSA	-0.58	0.66	0.97*	0.10							
TSA	-0.90	0.58	0.80	-0.22	0.70						
AA	0.19	0.45	0.75	0.12	0.86	0.24					
MXVA	-0.33	0.59	0.85	0.16	0.94	0.42	0.98*				
TCA	-0.11	0.41	0.74	0.09	0.84	0.21	1.000***	0.97*			
perAA	0.49	0.11	0.17	0.17	0.33	-0.44	0.77	0.62	0.79		
CCFN	-2.38	0.28	0.56	0.87	0.37	0.67	0.10	0.18	0.11	-0.36	
Field system	RXSA	TCA	TSA	AA	perAA	MXVA	CCFN	CCC	RHL	CA	CB
TCA	1.00***										
TSA	0.47	0.45									
AA	1.00***	1.00***	0.51								
perAA	0.18	0.04	0.79	0.11							
MXVA	0.85	0.85*	0.77	0.87*	0.25						
CCFN	0.34	0.34	0.35	0.35	-0.06	0.66					
CCC	0.98**	0.98**	0.31	0.97**	-0.24	0.79	0.35				
RHL	0.14	0.11	0.42	0.15	0.14	0.28	0.34	0.13			
CA	-0.65	-0.65	-0.53	-0.67	-0.01	-0.78	-0.59	-0.70	-0.73		
CB	0.25	0.24	0.59	0.26	0.67	0.44	0.25	-0.12	-0.40	0.18	
CN	0.71	0.71	0.10	0.70	-0.51	0.69	0.75	0.80	0.22	-0.75	-0.11

*, ** and *** denote significances at 0.05, 0.01 and 0.001

In pots, perAA and CCFN were not correlated with any other root traits (Table 5). We collected crown root traits for mature rice plants at 60 days after transplanting and found that crown root growth angle (CA) was negatively correlated with CN ($r = -0.91$; $p < 0.05$). Our observation suggests that varieties with fewer crown roots were steeper

than varieties with more crown root number. Moreover, we found that lateral root branching was positively correlated with root cross sectional area (RXSA) or root size ($r = -0.97$; $p < 0.05$). Hence, the larger the root segments the more lateral root density can be observed. Similar results were found in the field where anatomical traits were positively correlated among each other except for aerenchyma and CCFN traits (Table 5). However, the relationship between CA and CN was negative but not significant. In addition, correlation analysis was performed for the five low-land varieties grown in all three systems (Table 6). We found strong but marginally significant relationships between the experimental systems. Root anatomical traits including RXSA, TCA, and AA were correlated between traits measured in the pot and the field ($r = 0.95$; $p < 0.1$). In addition, root hair density (RHD) was correlated between the roll-up system and the field ($r = 0.90$, $p < 0.1$).

Table 6. Correlation coefficient and *p* values for Spearman-rank correlation analysis between root traits measured in the roll-up, the pot, and in the field of 5 Thai rice varieties

Trait	Description	Roll-up:Pot	Pot:Field	Field:Roll-up
RSXA	Root cross sectional area, mm ²	0.80	0.95*	0.67
TCA	Total cortical area, mm ²	0.60	0.95*	0.67
TSA	Total stele area, mm ²	-0.20	0.77	0.29
AA	Aerenchyma area, mm ²	0.60	0.95*	0.41
perAA	Percentage of cortex as aerenchyma, %	0.40	0.63	-0.67
MXVA	Metaxylem vessel area, mm ²	-0.40	0.32	0.56
CCFN	Cortical cell file number	-0.40	0.00	-0.21
CCC	Cortical cell count	-0.20	-0.40	0.30
RHL	Root hair length, mm	-0.32	-0.60	0.50
RHD	Root hair density	-0.40	-0.40	0.90*
CA	Crown root angle	-0.82	-0.05	0.30
CB	Crown root branching	-0.10	0.31	0.05
CN	Crown root number	0.10	0.70	-0.50

*denotes significances at $P < 0.1$

Principal component analysis

Principal component analysis (PCA) was performed separately on the mean values of root traits for the plants grown in the roll-up, the pot, and the field system. Based on the variable loadings, principal component 1 was predominantly composed of anatomical traits. Biplots of the first and second components showed similar trends in trait structure in all growing systems (Fig. 2). perAA and CCFN were independent from other anatomical traits. The results from correlation analysis show the same independence.

Hierarchical cluster analysis

Hierarchical cluster analysis was performed for the root traits measured in the roll-up experiment. Certain traits had more pronounced influences and determined cluster membership. Strongly clustered traits included metaxylem vessel area, percentage of aerenchyma, root growth angle, and lateral root branching (Fig. 3). Leum Pua variety was distinguished from other rice varieties by its large diameter xylem vessel (0.0015

mm²). Other than Leum Pua variety, the varieties with low perAA were clustered by crown root growth angle. The crown root growth angle further clustered upland and lowland varieties. A shallow angle classified lowland rice varieties and a steep angle identifies to upland varieties (Fig. 3).

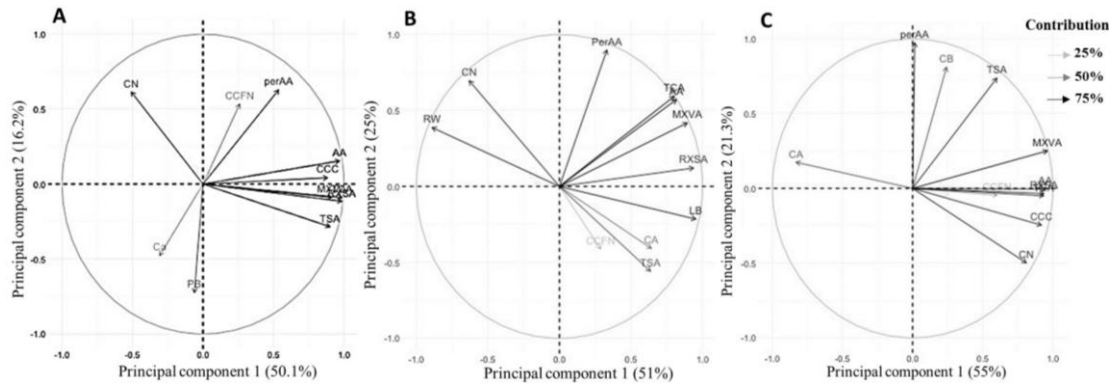


Figure 2. Biplots of principal components analysis for root traits in (A) 11 commercial and traditional varieties grown in the roll-up system (B) 5 lowland varieties grown in the pot system and (C) in the field system

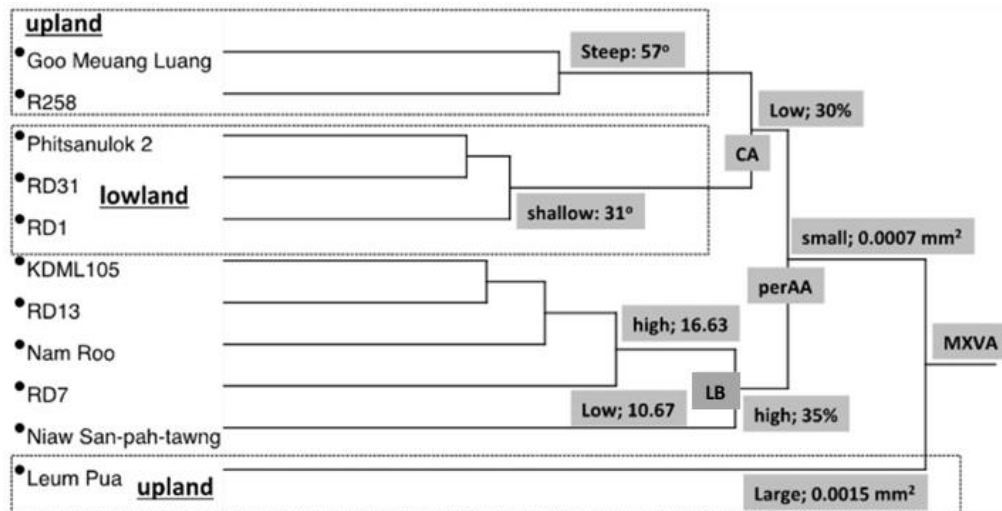


Figure 3. Hierarchical clustering analysis with the Ward cluster method. Root anatomical, morphological and architectural traits of 11 Thai rice varieties grown in the roll-up system are shown. Mean values of the traits are denoted within gray boxes per cluster group. See Table 1 for abbreviations and descriptions of root traits

Discussion

We observed large phenotypic variation for anatomical and architectural root traits in popular Thai rice varieties. The variation was investigated for eleven traditional and commercial Thai rice varieties in the roll-up system and for five lowland rice varieties in the pot and the field system. We found that the variation of root traits ranged from 1.31-fold in root cortical aerenchyma (RCA) to 4.20-fold in crown root growth angle in the roll-up system (Table 2). The major contribution of the variation within a root

system came from anatomical traits. We found evidence for this contribution in the results of the principal component analysis in which anatomical traits clustered into one group and contributed the major portion to the first principle component (*Fig. 2*). Similar trends were found in root systems of other monocots such as the *Zea* species (Burton et al., 2013). Anatomical variation related to differences in performance and stress response in many crop species, including maize (Saengwilai et al., 2014a), common bean (Peña-Valdivia et al., 2010) and rice (Henry et al., 2012). Variation in the number and diameter of xylem vessels is known to strongly affect axial water conductance and potentially enhance water use efficiency under terminal drought (Lynch et al., 2014). In wheat, it has been shown that narrow xylem vessels enhance wheat adaptation under drought and has been used in wheat breeding programs to improve drought tolerance (Richards and Passioura, 1989). In case of rice, the reverse was proposed, namely that less axial resistance in roots would favor water acquisition from deeper soil layers (Yambao et al., 1992). In our study, we found that variation in the size of metaxylem vessel was substantial. The results from hierarchical clustering analysis indicate that metaxylem vessel area in our data set was the first major factor differentiating rice varieties into different groups (*Fig. 3*). Among the varieties, Leum Pua, an upland variety, had two-fold larger metaxylem vessel area than the average of the rest of the data set in the roll-up system. Other upland varieties such as Goo Meuang Luang and R258 appeared to have small metaxylem area; however, these varieties have steep root system which could enhance deep soil exploration in the upland environments. We suggest that root growth angle might be important strategy for adaptation to stress environments.

We suggest that deep rooting may be associated with the adaptation under drought conditions by drought avoidance. Several root traits have been shown to contribute to deep rooting such as high root cortical aerenchyma (Saengwilai et al., 2014a), reduced crown root number (Saengwilai et al., 2014b), and low lateral root branching (Zhan et al., 2015). In rice, expression of *DEEPER ROOTING 1* gene (*DRO1*) causing a steeper root growth angle that results in an overall deeper root system with increased yield in drying soils (Uga et al., 2013). In our study, we found that upland varieties such as Goo Meuang Luang and R258 had steep root growth angle of more than 50 degree from horizon whereas lowland varieties had much shallower growth angle in the roll-up system. The five low land varieties planted in the pot and field system maintained their shallow root growth angle. Similar to the results reported in other monocot studies (Trachsel et al., 2013; Uga et al., 2013), we propose that root growth angle could be a promising trait for plant breeding programs that can be screened already at the seedling stage.

While many of the traits measured in cross-sections were found to be highly correlated with one another, we observed that the percentage of aerenchyma and root hair length was independent from some anatomical root traits and whole root characteristics. These results suggest that these traits are feasible for rice breeding program because breeders could pyramid aerenchyma and root hair length with other root and shoot traits without complications. Correlations greater than 0.95 were observed between cortical components such as RXSA, TCA, and AA. Strong positive correlations may mean that these traits share measurement elements, and offer overlapping information. In particular, metaxylem vessel area was positively correlated to total stele area. It has been reported that stele and xylem might be controlled by various genetic factors and correlation between the total stele area and metaxylem

vessel area can be attributed either to a tight linkage of the QTLs for traits or to pleiotropy of one QTL (Uga et al., 2008). Our results suggest that the efficiency of root phenotyping can be improved by eliminating such redundant traits and/or replacing redundant traits with traits that correlate weakly with other parameters.

Traits correlation between the three experimental systems was weak. We expected weak correlations because plants in each system correspond to different ages, developmental stages, and different environments. Overall, the demonstrated strong variations in root traits suggest ample opportunities for plant breeders to develop new varieties by using existing Thai germplasm. Varieties such as KDML 105 have high market values and therefore they are popular among Thai farmers. Hence, it is possible to maximize water and nutrient use efficiency by considering root traits in irrigation and fertilizer regimes.

Conclusion

Characterization of the structural and functional diversity of root traits is an important step for plant breeding. Breeders may be reluctant to utilize exotic donors in their programs because of the risk to lose important traits for enhanced environmental adaptation. However, our results suggested that traits of Thai rice roots vary considerably and hold an unused potential for plant breeding programs. We see ample opportunity for introgression of our investigated traits into elite rice varieties by using Thai germplasms as parents. We recommend that upland varieties particularly Goo Meuang Luang and R258 could be used as donors for steep root angle which could enhance drought tolerance while Leum Pua, a traditional variety, could serve as a donor for enhanced water acquisition by increasing metaxylem area. Further experiments of the physiological utility of rice root traits in edaphic stresses are required to pinpoint more beneficial root traits and to identify new rice ideotypes. The future challenge is to identify molecular markers associated with variation of root traits to enhance efficiency and effectiveness of plant breeding programs.

Acknowledgement. We thank members of MUSC Root lab, Phytoremediation research and Root Laboratory, Faculty of Science, Mahidol University for their assistance throughout the project. This research project is supported by Mahidol University.

REFERENCES

- [1] Abramoff, M. D., Magalhães, P. J., Ram S. J. (2004): Image processing with Image – J. Biophotonics International 11: 36-42.
- [2] Burton, A. L., Brown, K. M., Lynch, J. P. (2013): Phenotypic diversity of root anatomical and architectural traits in *Zea* species. – Crop Science 53: 1042-1055.
- [3] Chimungu, J. G., Brown, K. M., Lynch, J. P. (2014a): Reduced root cortical cell file number improves drought tolerance in maize. – Plant Physiology 166: 1943-1955.
- [4] Chimungu, J. G., Brown, K. M., Lynch J. P. (2014b): Large root cortical cell size improves drought tolerance in maize. – Plant Physiology 166: 2166-2178.
- [5] Datta, S., Kim, C. M., Pernas, M., Pires, N. D., Proust, H., Tam, T., Vijayakumar, P., Dolan, L. (2011): Root hairs: development, growth and evolution at the plant-soil interface. – Plant and Soil 346: 1-14.

- [6] Gilroy, S., Jones, D. L. (2000): Through form to function: root hair development and nutrient uptake. – Trends in Plant Science 1385: 56-60.
- [7] Haefele, S. M., Naklang, K., Harnpichitvitaya, D. (2006): Factors affecting rice yield and fertilizer response in rainfed lowlands of northeast Thailand. – Field Crops Research 98: 39-51.
- [8] Haefele, S. M., Nelson, A., Hijmans, R. J. (2014): Soil quality and constraints in global rice production. – Geoderma 235-236: 250-259.
- [9] Henry, A., Cal, A. J., Batoto, T. C. (2012): Root attributes affecting water uptake of rice (*Oryza sativa*) under drought. – Journal of Experimental Botany 63: 4751-4763.
- [10] Hund, A., Trachsel, S., Stamp, P. (2009): Growth of axile and lateral roots of maize: I development of a phenotyping platform. – Plant and Soil 325: 335-349.
- [11] IRRI, AfricaRice, CIAT (2010): Global Rice Science Partnership (GRiSP). – International Rice Research Institute, Los Baños, Philippines; Africa Rice Center, Cotonou, Benin; and International Center for Tropical Agriculture, Cali, Colombia.
- [12] Lynch, J. P. (2007): Roots of the second green revolution. – Australian Journal of Botany 55: 493-512.
- [13] Lynch, J. P. (2014): Root phenes that reduce the metabolic costs of soil exploration: opportunities for 21st century agriculture. – Plant Cell and Environment 38: 1775-1784.
- [14] Lynch, J. P., Brown, K. M. (2001): Topsoil foraging – an architectural adaptation of plants to low phosphorus availability. – Plant and Soil 237: 225-237.
- [15] Miguel, M. A., Postma, J. A., Lynch, J. P. (2015): Phene synergism between root hair length and basal root growth angle for phosphorus acquisition. – Plant Physiology 167: 1430-1439.
- [16] Peña-Valdivia, C. B., Sánchez-Urdaneta, A. B., Rangel, J. M., Muñoz, J. J., García-Nava, R., Velázquez, R. C. (2010): Anatomical root variations in response to water deficit: wild and domesticated common bean (*Phaseolus vulgaris* L.). – Biological Research 43: 417-27.
- [17] Pinheiro, L., Bates, D., DebRoy, S., Sarkar, D. (2012): The nlme package; linear and nonlinear mixed effects models. R Version 3.
- [18] Postma, J. A., Lynch, J. P. (2010): Theoretical evidence for the functional benefit of root cortical aerenchyma in soils with low phosphorus availability. – Annals of Botany 107: 829-841.
- [19] Rebouillat, J., Dievart, A., Verdeil, J. L., Escoute, J., Giese, G., Breitler, J. C., Gantet, P., Espeout, S., Guiderdoni, E., Périn, C. (2008): Molecular genetics of rice root development. – Rice 2: 15-34.
- [20] Richards, R. A., Passioura, J. B., (1989): A breeding program to reduce the diameter of the major xylem vessel in the seminal roots of wheat and its effect on grain yield in rain-fed environments. – Australian Journal of Agricultural Research 40: 943-950.
- [21] Saengwilai, P., Nord, E., Chimungu, J., Brown, K. M., Lynch, J. P. (2014a): Root cortical aerenchyma enhances nitrogen acquisition from low nitrogen soils in maize (*Zea mays* L.). – Plant Physiology 166: 726-735.
- [22] Saengwilai, P., Tian, X., Lynch, J. P. (2014b): Low crown root number enhances nitrogen acquisition from low-nitrogen soils in maize. – Plant Physiology 166: 581-589.
- [23] Trachsel, S., Kaepler, S. M., Brown, K. M., Lynch, J. P. (2010): Shovelomics: high throughput phenotyping of maize (*Zea mays* L.) root architecture in the field. – Plant and Soil 341: 75-87.
- [24] Trachsel, S., Kaepler, S. M., Brown, K. M., Lynch, J. P. (2013): Maize root growth angles become steeper under low N conditions. – Field Crops Research 140: 18-31.
- [25] Tuberosa, R., Sanguineti, M. C., Landi, P., Giuliani, M. M., Salvi, S., Conti, S. (2002): Identification of QTLs for root characteristics in maize grown in hydroponics and analysis of their overlap with QTLs for grain yield in the field at two water regimes. – Plant Molecular Biology 48: 697-712.

- [26] Uga, Y., Okuno, K., Yano, M. (2008): QTLs underlying natural variation in stele and xylem structures of rice root. – *Breeding Science* 58: 7-14.
- [27] Uga, Y., Sugimoto, K., Ogawa, S., Rane, J., Ishitani, M., Hara, N., Kitomi, Y., Inukai, Y., Ono, K., Kanno, N., Inoue, H., Takehisa, H., Motoyama, R., Nagamura, Y., Wu, J., Matsumoto, T., Takai, T., Okuno, K., Yano, M. (2013): Control of root system architecture by DEEPER ROOTING 1 increases rice yield under drought conditions. – *Nature Genetics* 45: 1097-102.
- [28] Vejchasarn, P., Lynch, J. P., Brown, K. M. (2016) Genetic variability in phosphorus response of rice root phenotypes. – *Rice* 9: 1-29.
- [29] Wailes, E. J., Chavez, E. C. (2012): ADB Sustainable Development Working Paper Series ASEAN and Global Rice Situation and Outlook. – Asian Development Bank, Manila, Philippines.
- [30] Yambao, E. B., Ingram, K. T., Real, J. G. (1992): Root xylem influence on the water relations and drought resistance of rice. – *Journal of Experimental Botany* 43: 925-932.
- [31] Zhan, A., Schneider, H., Lynch, J. P. (2015): Reduced lateral root branching density improves drought tolerance in maize. – *Plant Physiology* 168: 1603-1615.
- [32] Zhu, J., Lynch, J. P. (2004): The contribution of lateral rooting to phosphorus acquisition efficiency in maize (*Zea mays*) seedlings. – *Functional Plant Biology* 31: 949-958.
- [33] Zhu, J., Kaepler, S., Lynch, J. P. (2005): Mapping of QTL controlling root hair length in maize (*Zea mays* L.) under phosphorus deficiency. – *Plant and Soil* 270: 299-310.
- [34] Zhu, J., Brown, K. M., Lynch, J. P. (2010): Root cortical aerenchyma improves the drought tolerance of maize (*Zea mays* L.). – *Plant Cell and Environment* 33: 740-749.

EFFECTS OF EDAPHIC AND PHYSIOGNOMIC FACTORS ON SPECIES DIVERSITY, DISTRIBUTION AND COMPOSITION IN RESERVED FOREST OF SATHAN GALI (MANSEHRA), PAKISTAN

KHAN, K. R.^{1,2*} – ISHTIAQ, M.^{3*} – IQBAL, Z.¹ – ALAM, J.¹ – BHATTI, K. H.⁴ – SHAH, A. H.² – FAROOQ, M.² – ALI, N.¹ – MUSHTAQ, W.³ – MEHMOOD, A.¹ – MAJID, A.¹

¹*Department of Botany, Hazara University, Mansehra-21300, Pakistan*

²*Department of Botany, Government Post-Graduate College, Mansehra-21300, Pakistan*

³*Department of Botany, (Bhimber Campus), Mirpur University of Science & Technology (MUST), Mirpur-10250 (AJK), Pakistan*

⁴*Department of Botany, University of Gujrat, Gujrat, Pakistan*

**Corresponding authors*

e-mail: drishtiaqajk@gmail.com; khalid_botnist@yahoo.com

(Received 13th Sep 2017; accepted 11th Jan 2018)

Abstract. Forests have pivotal role in life sustenance of indigenous people of the area and economy of any country at mass level. Forest health, diversity and richness depends various environmental parameters. In this study, impact of edaphic and physiographic factors on plant communities of reserved forest of Sathan Gali (Mansehra), Pakistan is analyzed. Quantitative and qualitative characteristics of plant species were studied dividing the area into 13 stands on physiognomic features. In this analysis 136 plant species of 58 families were classified into four prominent plant communities through TWINSpan approach. The family index depicted that Asteraceae was dominant among 58 families. Biological spectrum (BS) expressed Therophytes as the dominant plants with 27.34% species, while leaf size spectrum (LSS) classification showed Mesophytes having 25.83% species contribution. Importance value index (IVI) analysis proved that *Pinus wallichiana* had highest value (351.69) followed by *Fragaria nubicola* (62.88). In analysis, maximum species diversity (MSD) was found in *Pinus-Pteris-Sarcococca* community (0.102) while species richness (SR) was in *Pinus-Digitalia-Sarcococca* community (1.87) whereas maximum species maturity (MSM) was found in *Pinus-Cedrus-Viburnum* community (65.74). In two statistical analyses; it was found that DCA ordination of reserved forest indicated that the maximum gradient length was 3.32 for axis 1 and 2.57 for axis II while CCA ordination revealed that the maximum eigenvalue was 0.49 for axis 1 and 0.40 for axis II. Among environmental variables the maximum positive strength and impact on composition of community was recorded for altitude and phosphorous (P) while maximum negative strength was recorded for barometric pressure and temperature.

Keywords: *therophytes, biological spectrum, mesophytes, species richness, DCA*

Introduction

Plants are very integral part of biosphere and ecosystem for life sustenance on the earth. Plants have diverse occurrence on earth and among these rich areas of diverse types of plants is named as forest. The forests are rich source of plant biodiversity of any country. Without healthy forests economy and environment of any country cannot be sustainable. Furthermore, forests are playing major role in provision of all necessities of life for many communities around the globe. Forests health and pattern of richness depends on many biotic and abiotic factors and later one have silent role on it. Phytosociology is the study of characteristics, classifications, relationships, and

distribution of plant communities in forest or other plant rich zones (Mueller-Dombois and Ellenberg, 1974). The historical background of phytosociology can be traced back to Swiss botanist Josias Braun Blanquet (1884-1980) who is considered the founder of the phytosociology. In the 20th century great efforts were made in the field of ecology and phytosociology. Braun Blanquet defined the plant association as a stable plant group in equilibrium with the surrounding environment characterized by certain dominant species illuminating a particular ecology. These leading species represent the major trends in the local vegetation allowing the ecologists to identify, distinguish and discuss dynamics of the community (Leveque, 2001). In the last few decades' scope of phytosociology became wider and investigates number of quantitative, qualitative and synthetic characteristics of plant communities e.g. density, dominance, abundance, floristic composition, vegetation structure, physiognomy, development and exchange multilateral relations of plants to one another and to the environmental variables and the classification of communities (Rieley and Page, 1990).

The existence of distinct forest types is exploratory of diversity in climatic and edaphic factors. Vegetation is the mainly physical representation of the environment (Kent, 2012). Any type of changes in habitats are first observed in the vegetation and forests are indicators of it. Vegetation is the result of the habitat, environmental conditions and existing biodiversity. Such study provides information about recognition and definition of different vegetation types and plant communities, identifying relationship between plant species distribution and environmental control. It also provides basis for prediction of possible future climatic changes (Kent and Coker, 1994) and on basis of which we may plan recommendations and practical steps to cope hazardous changes in environment.

Ecological diversity is considered to be a measure of the health of an ecosystem (McGardy-Steed and Morin, 2000). Variation in species diversity along environmental gradient is a major topic of ecological investigation in latest years (Currie and Francis, 2004). Monitoring of vegetation is an easy way for understanding the climatic conditions of an area (Niemi and Donald, 2004). With climate change, phytosociological studies will become more important because in most cases, only vegetation data is available to use for making comparisons. Phytosociological studies visualize the existing vegetation structure, species diversity, soil plant relationship and generate data on seasonal and temporal variations in available nutrients (Mueller-Dombois and Ellenberg, 1974). Plant communities as concrete definable units of vegetation that can be recognized and are apparent to the eye. Plant communities are often named after species that contribute to their unique structure or composition. The altitude, latitude, slope angle, aspect and humidity play an important role in formation and composition of plant community (Currie and Francis, 2004; Shaheen et al., 2012).

Species diversity is measured mathematically by indices and provides information about species richness, consistency and community composition as well as rarity or commonness of a species (Whittaker, 1977). Maturity index indicates about the ongoing climax trend as well as successional variations in a given community under the impact of ecological conditions and through this index we can find out the best suitable and favorable altitudinal zones for the plants (Rodolfo and Sermolli, 1948). Modern software packages have made the phytosociological studies more meaningful and predictable. A growing number of studies have used software packages. Peer et al. (2007) applied TWINSpan and recognized 11 plant communities in Hindu Kush Mountains. Hussain et al. (2008) conducted study on species composition and

community structure of 23 forest stands in Kumaon Himalaya. Out of which, they reported 19 tree communities and 17 ground vegetation communities. The distribution of tree species on DCA axis 1 showed influence of altitudinal gradient while the second axis of DCA indicated canopy cover and shrub diversity. Haq et al. (2015) and Mehmood et al. (2015) also evaluated similar approaches for the recognition plant communities.

The present study was designed with the objectives to investigate and correlate the vegetation of an unexplored Sathan Gali (Study area) with edaphic and physiographic factors and to classify the vegetation structure into plant communities with its ecological characteristics. It will be helpful for the conservation and sustainable utilization of plant resources of the area and also for further ecological investigations.

Materials and methods

Study area

Sathan Gali lies in District Mansehra of Khyber Pakhtoonkhawa (KPK), Pakistan. The study area is situated from 34.36132 to 34.36650 North latitudes and 073. 11 067 to 073. 12488 East longitudes. Mansehra District of KPK consists of three tehsils; Mansehra, Oghi, and Balakot. Mansehra makes its boundary on the North to Kohistan and Battagram Districts, on the East surrounding by Muzaffarabad district of Azad Jammu and Kashmir, on the South to Abbottabad and Haripur districts and on the West to Shangla and Buner Districts (Fiaz, 2012) as these areas are shown in *Figures 1* and *2*.

Climate of area

The area receives heavy rain fall in Winter and Monsoon. The temperature of the area remains pleasant throughout the year except May and June. Snow often occurs in these forests particularly near its upper limits during the months of December to February. This heavy snow causes physical damage to the vegetation. As trees are over laden with snow and when wind blow most of the trees break. In May and June, the temperature is high as compared to rest of the months (Khan et al., 2016).

Edaphology

The rocks are gneiss, gneissose, schists, granitoid gneisses, mica schist and shales. Soil possesses higher moisture retaining capacity under the vegetation cover and acidic in nature. As agriculture land is inadequate and the peoples thus try to bring every available bit of land under cultivation in order to fight against the hunger. Terraces on hills slopes are constructed for cropping but they are not effective and durable. The soils from such slopes get washed away within two to three years and barren bed rocks left behind (Saddozai, 1996).

Soil analysis

Soil samples, down to a depth of 30cm, were collected from each stand. These soil sample were analyzed for percentage of sand, silt and clay), total organic matter (OM. %), pH, electrical conductivity in the Baffa laboratory (Allen et al., 1986).

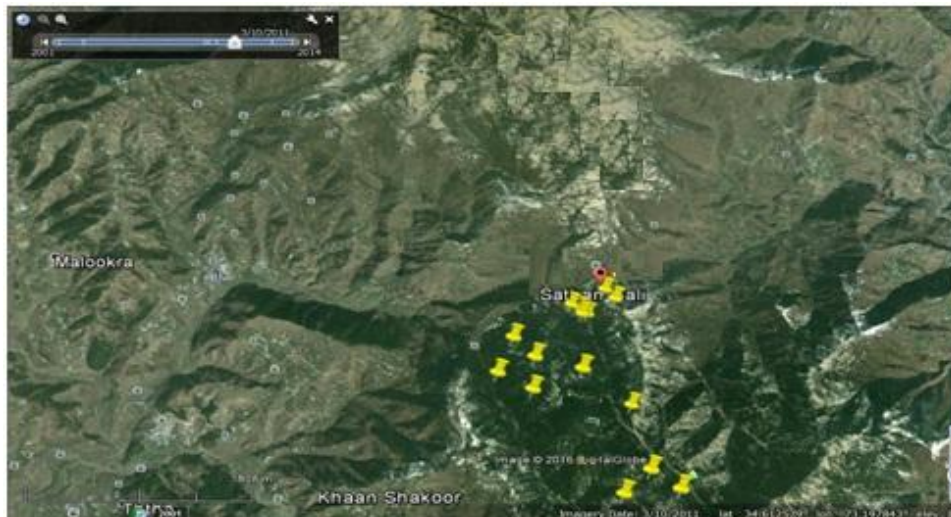


Figure 1. Map of the study area highlighting the stands selected for study in reserved forest



Figure 2. Scenic view of reserved forest

Field studies

The detailed field surveys have been carried out to study the phytosociological attributes of Sathan Gali (Reserved forest), Mansehra, Pakistan at regular intervals of different seasons, during 2013-2015. The whole area was divided into 13 stands on the basis of physiognomy of vegetation. Quadrature method was used for sampling the vegetation. The size of quadrate was $10 \times 2 \text{ m}^2$ for trees $5 \times 2 \text{ m}^2$ for shrubs and $1 \times 1 \text{ m}^2$ for herbs, respectively (Malik, 1986). The number of quadrates for trees, shrubs and herbs were 5, 10 and 20 respectively. Both systematic and random quadrants that give better results were used. The distance between two adjacent stands was approximately 100m. The phytosociological attributes density, relative density, frequency, relative frequency, canopy cover, relative canopy cover, species diversity, species richness,

species maturity and importance values index (IVI) were calculated. Trees with less than 1.5m were considered as shrub. Coverage of shrubs and herbs was calculated after coverage classes Daubenmire (1959). Collected plant specimens of each species were dried, poisoned and mounted on standard herbarium sheets. The collected specimens were identified with the help of Flora of Pakistan (Nasir and Ali, 1971-1994; Ali and Qaisar, 1995-2004) and voucher specimens were deposited in the Herbarium of Hazara University Mansehra, KPK, Pakistan (HUP).

Data analysis

TWINSPAN was used for the classification of species and samples at the same time which is based on dividing reciprocal averaging ordination space. Detrended Correspondence Analysis (DCA) analysis was done to evaluate similarities/differences between the species and samples. A Canonical Correspondence Analysis (CAA) is an ordination to determine and analyze the correlation between species and environmental variables. The life form classes and leaf spectra of all plant species were determined and classified following after Raunkiaer (1934) and Mueller-Dombois and Ellenberg (1974). The recorded data was analyzed through CANOCO and PC-ORD softwares (Haq et al., 2015).

Results

Forest being important part of ecosystem of KPK and provides a major part of livelihood for indigenous and rural people. These forest also provide medicines, shelter, fuel resources, fodder and aesthetic values to communities. Reserved forests of Sathan Gali (Mansehra) are first time explored to know impact of edaphic and physiognomic factors on the plants and their communities structure. The study was based on comprehensive and planned field visits in year 2015-16. The analysis of area revealed that many plant species are over exploited and many parts of forests are being deteriorating due to dominant species loss. The study area was divided into 13 stands. The study generated list of 136 species which belonged to 58 families. The dominant family was Asteraceae in the area. The collected ecological data was subjected to multivariate analysis and *TWINSPAN* which produced following communities as described here below. The research work and its analysis showed that reserved forest of Sathan Gali was under stress and many factors were effecting the plants' communities. The data obtained from 13 stands of Reserved Forest were analyzed by *TWINSPAN* classification protocol. It divided the obtained results into four different plant communities which were *Pinus-Pteris-Sarcococca* Community, *Cedrus-Fragaria-Pteris* Community, *Pinus-Cedrus-Viburnum* Community and *Pinus-Digitaria-Sarcococca* Community (Fig. 3).

Communities' description of Sathan Gali reserved forest

Pinus-Pteris-Sarcococca (PPS) community

Pinus wallichiana-Pteris vitata-Sarcococca saligna community was recorded at an elevation of 1900-2100 m in stands 9 and 10. The co-ordinates range was 34.36413 to 34.36449 N and 73.19157 to 73.19423 E. The steepness of slope was 40-70° on East aspect. This community consisted of 28 plant species. The dominant plant of this community was *Pinus wallichiana* with IVI value of 87.88. *Pteris vitata* and

Sarcococca salignawere co-dominants with IVI value of 13.57 and 5.25, respectively. Therophytes were dominant by contributing 9 species followed by Geophytes and Nanophanerophytes 5 species by each (Fig. 5). Leaf size spectra was dominant by Nanophyll 10 plant species followed by Microphyll by 9 plant species (Fig. 4).

Soil of this community was sandy clay loam with acidic pH, nitrogen 0.41%, potassium 135ppm, phosphorus 7.9 and electrical conductivity 2.4. Organic matter (OM) was less in this community. This describes that PPS community plant taxa prefer acidic and low OM soils, so these dominant in the stands.

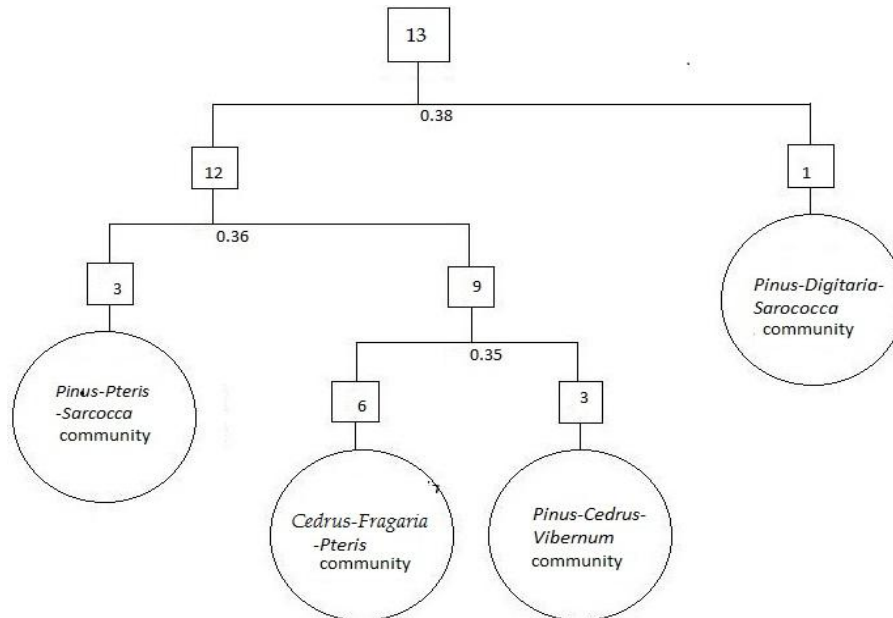


Figure 3. TWINSpan classification of vegetation of reserved forest

Cedrus-Fragaria-Pteris (CFP) community

Cedrus deodara-Fragaria nubicola-Pteris vitata community was reported at an elevation of 6400 to 7300 ft in stand 1,3,4,8,12 and 13. These stands were located at West, North and South aspects. The co-ordinates range was between 34.36132 to 34.36650 N and 073.12206 to 073, 12488 E with 40-65° steepness of slope. It was dominated by *Cedrus deodora* with IVI value of 166.05. *Fragaria nubicola* and *Pteris vatata* were co-dominant with IVI of 46.38 and 29.28, respectively. A total of 62 plant species in this community were recorded. Among biological spectrum (BS) Geophytes were dominant by contributing 16 plant species followed by Therophytes 14 species, Hemicytphytes 12 plant species (Fig. 5). A leaf size spectrum was dominant by Microphyll with 23 species followed by Mesophyll 17 and Nanophanerophytes by 7 species (Fig. 4).

Soil of this community was sandy loam with acidic pH, percentage of organic matter was high, and contents of nitrogen, potassium and phosphorous were between in ranges of 0.03-1.3%, 105-135 ppm and 5-8, respectively. The electrical conductivity was 0.01-1.2. It shows that CFP community was more dominant in soils of sandy-loamy with high OM range. This makes differ from above PPS community.

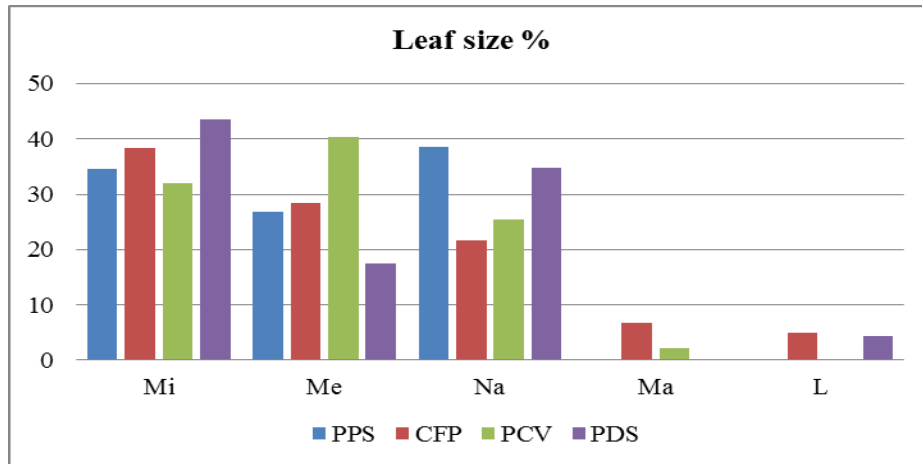


Figure 4. Leaf size of reserved forest plant communities

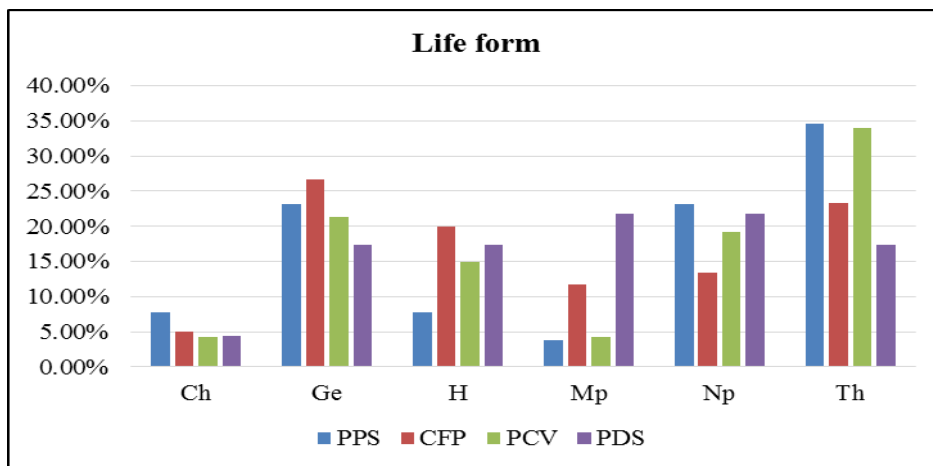


Figure 5. Life form of reserved forest plant communities

Pinus-Cedrus-Viburnum (PCV) community

At an elevation of 6300-6900 ft *Pinus wallichiana-Cedrus deodara-Viburnum cotonifolium* community was harbored at Northern aspect with 50-60° slope of steepness. The co-ordinates range was 34.36432 to 34.36582 N and 073. 11067 to 073. 11741E. *Pinus wallichiana* was dominant with importance value index of 101.74. *Cedrus deodara* and *Viburnum* was co-dominant species with IVI of 29 and 14.94, respectively. A total of 51 plant species were recorded in this community. Therophytes were dominant life form of the vegetation with addition of 16 plant species followed by Geophytes and Nanophanerophytes (Fig. 5). Among leaf size Mesophylls were dominant by contributing 19 species followed by Microphylls 15 plant species (Fig. 4).

Soil of this community was found sandy-clay-loam. The loam soil of this community had acidic pH, less organic matter, potassium, phosphorus and nitrogen were 120-130 ppm, 4-8 and 0.21-0.57%, respectively. The electrical conductivity was 0.01-1.1. This analysis of community soil and plants types depicts that loamy soil with less OM contents having N contents of 120-130 ppm prefer to support plants of genera *Pinus*, *Cedrus* and *Viburnum*. So the community PCV is dominating in this belt of forest.

Pinus-Digitaria-Sarcococca (PDS) community

At an elevation of 3700 ft in stand 11, *Pinus wallichiana*- *Digitaria nodosa*-*Sarcococca saligna* community was reported. The range of co-ordinates for this community was 34.36132 N and 73.11791 E. This community was recorded at Southern aspect at 50° slope of steepness. The total numbers of plant species recorded for this community were 24. *Pinus wallichiana* was dominant with IVI 44.96. *Digitaria nodosa* and *Sarcococca saligna* were co-dominant with IVI value of 10 and 6, respectively. Biological spectrum was dominated by Nanophanerophytes having 5 species followed by Hemicryptophytes and Geophytes by 5 plant species each (Fig. 5). A leaf size spectrum was dominant by Microphyll with 10 plant species followed by 5 species of Nanophanerophytes (Figs. 4 and 6).

Soil in this community was sandy loam with high acidic pH 7.5, organic matter percentage was low. The contents of nitrogen, potassium, phosphorous were 0.052%, 125% ppm, and 3.2 respectively. The electrical conductivity was 1.4. The soil composition and elevation determines the constitution of plants in PDS community. These plants would like to climate of low OM and acidic soil.

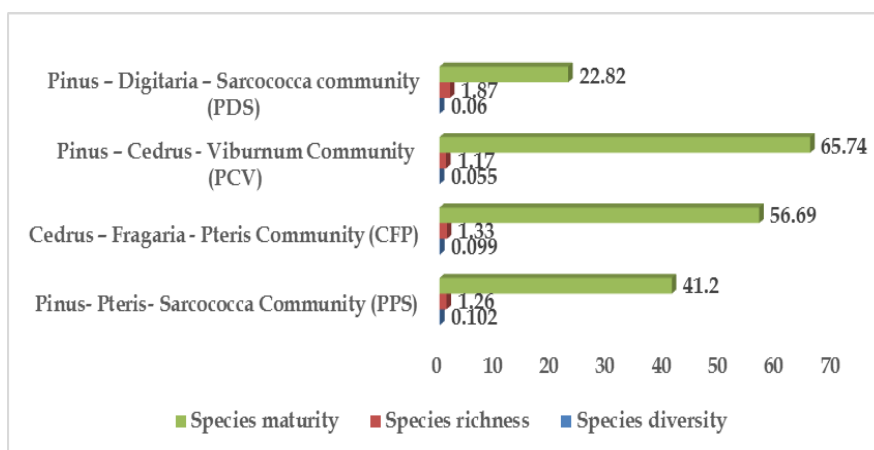


Figure 6. Graphical representation of different components of plant species diversity

Detrended correspondence analysis (DCA)

The total species surveyed were 136 belonging to 58 families. These data of Reserved Forest's species were subjected to Detrended Correspondence Analysis which indicated that total variation was 3.28. The response data was compositional having a gradient length of 3.3 SD unit long. The DCA ordination showed that the maximum gradient length was 3.32 for axis 1 and 2.57 for axis II. The maximum Eigenvalue was 0.49 for axis 1 and 0.34 for axis II.

The DCA ordination of the species showed that different species clustered in ordination space on the basis of similarities in habitat and species composition. The species clusters including *Vaccaria* sp., *Rhamnus virgata*, *Ajuga* sp., *Taxus wallichiana* were positively correlated with each other. These species were negatively correlated with *Viola* sp., *Bupleurum lanceolatum*, *Ajuga bracteosa*, *Rumex nepalensis* and *Isodon rugosus*. The species which were positively correlated with each other and negatively correlated with the above species were *Juglans regia*, *Pinus roxburghii*, *Alnus nitida* and *Viburnum cotinifolium*. The species which were on the top of ordination space

included *Rumex dentatus*, *Clinopodium vulgare*, *Indigofera heterantha*, *Solanum surattense* and *Saromatium venosum*. The species which were near average position which included *Paeonia emodi*, *Fragaria nubicola*, *Myrsine africana* and *Impatiens bicolor* were positively correlated with each other.

DCA ordination of stand also showed that stand of different communities clustered in ordination space almost similar fashion. It was found that *Pinus-Digitaria-Sarcococca* community showed different behavior and was away from other communities on axis I. This community distance occurrence is also confirmed by TWINSpan classification (Figs. 7 and 8). The other communities like *Pinus-Pteris-Sarcococca* Community was at the top of ordination space while remaining *Pinus-Cedrus-Viburnum* Community and *Cedrus-Fragaria-Pteris* Community were in the center (Fig. 8).

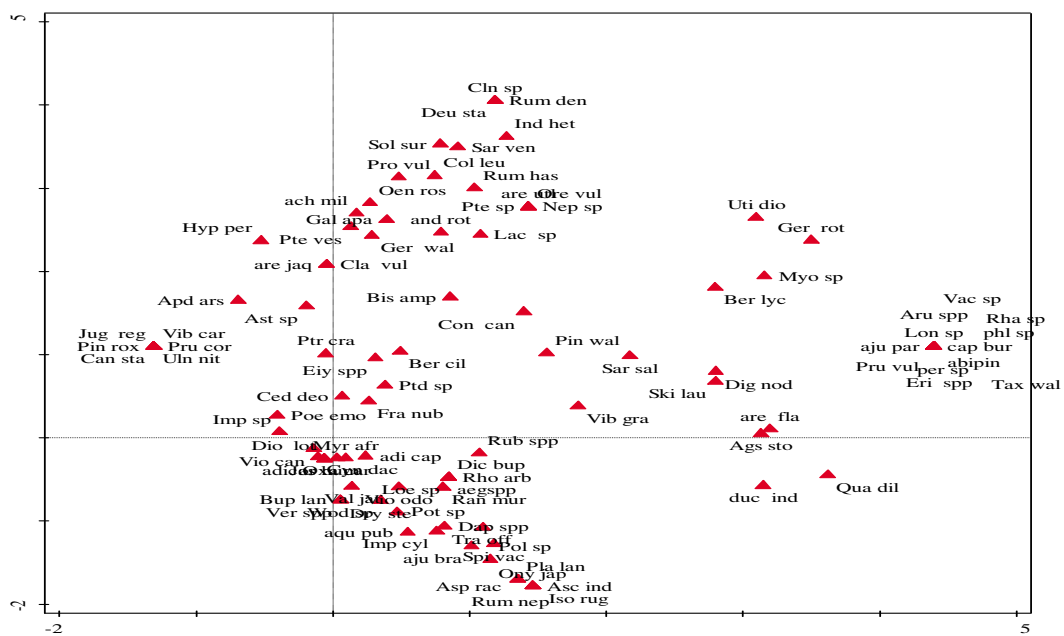


Figure 7. DCA ordination of plant species of reserved forest

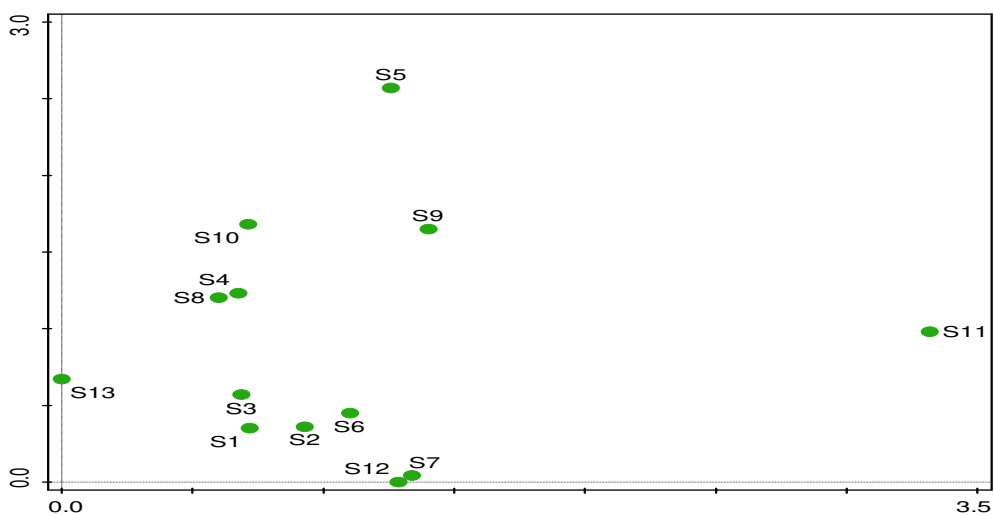


Figure 8. DCA ordination of stands of vegetation of reserved forest

Canonical correspondence analysis (CCA)

The collected data of reserved forest of Sathan Gali was further analyzed by using other statistical method named Canonical Correspondence Analysis. CCA ordination showed that total variation was 3.28, explanatory variable account for 100% while adjusted explained variation was 0%. The maximum eigenvalue was 0.49 for axis 1 and 0.40 for axis II. The explained variation for axis I was 14.88 and 27.32 for axis II. The pseudo canonical correlation for all axis was 1 and occurrence value was 274. The permutation test result showed that pseudo F less than 0.1 and P = 1. The CCA ordination of species showed that different species were sensitive with environmental variable and clustered in ordination space at different locations.

Impact of edaphic factors on plant communities' structure

The species which were sensitive with altitude, air moisture, aspect, wind pressure and potassium were *Arisaema flavum*, *Quercus dilatata*, *Duchesnea indica*, *Aegopodium burtii*, *Taxus wallichiana*, *Abies pindrow*, *Geranium rotundifolium*. *Urtica dioeca* and *Sarcococca saligna* taxa were positively correlated with electrical conductivity (EC) of soil. Some species were positively correlated with nitrogen conc., longitude, latitude and organic matter which included *Paeonia emodi*, *Hypericum perforatum*, *Viburnum grandiflorum*, *Juglans regia*. The taxa *Pteris* sp. and *Geranium wallichinum* were positively correlated with phosphorus contents and its availability to the plants.

Impact of climatic factors on plant communities' structure

The species which were highly sensitive to temperature were *Solanum surratense*, *Saromatium venosum*, *Indigofera hetrentha* and *Rumex hastatus*. The CCA ordination of environmental variables showed that the altitude and aspects were negatively correlated with temperature, slope, angle and phosphorus (*Fig. 10*). Similarly nitrogen, latitude and organic matter were negatively correlated with electrical conductivity and pH. The maximum gradient strength was recorded for pH, aspect, nitrogen and latitude. The minimum strength was recorded for potassium followed by slope angle and air moisture. The maximum stands of communities were near average position while *Pinus-Digitaria-Sarcococca* Community was away from average position contributing 25 species (*Fig. 9*), which showed that this community was rich in floristic composition and habitat type from rest of the associations (*Fig.10*).

The results depict that edaphic and environmental factors are key constraints on forest plant composition and their proliferation in an area. Various climatic and soil composition do impose impact on types of dominant taxa in the study area of reserved forest of Sathan Gali in Mansehra of KPK. The characteristics of plants communities of different locations were presented in *Figure 6* and it depicts the structure, richness, diversity and maturity of analyzed strands.

Discussion

Geographic analysis of study area

Pakistan being the part of western Himalaya harbors rich floral diversity owing to important geographical position. The study area (reserved forest of Sathan Gali) lies in

the western Himalayas shows rich floristic diversity. A total of 127 plants species belonging to 58 families were recorded from Reserved forest of Sathan Gali. According to plant habit, herbaceous growth form with 73.64 % species was the most dominant one. Our findings are in congruent with previous works of many researchers conducted in allied and neighboring regions of the country (Ijaz, 2014; 2015; Khattak et al., 2015; Khan et al., 2015a, b; Shah et al., 2015; Ahmad et al., 2016; Rahman et al., 2016a, b).

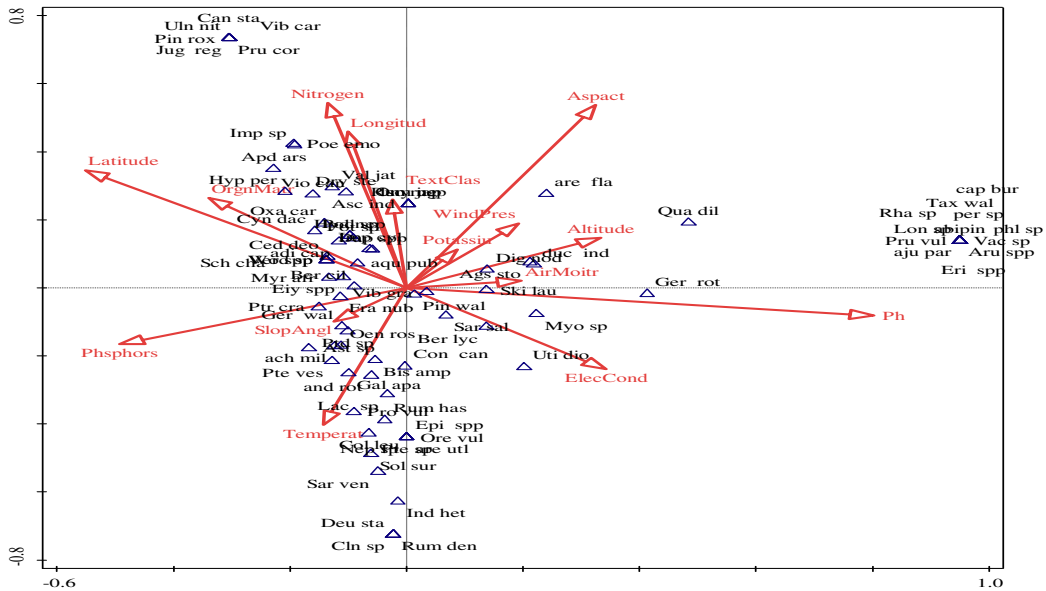


Figure 9. CCA ordination of plant species of reserved forest

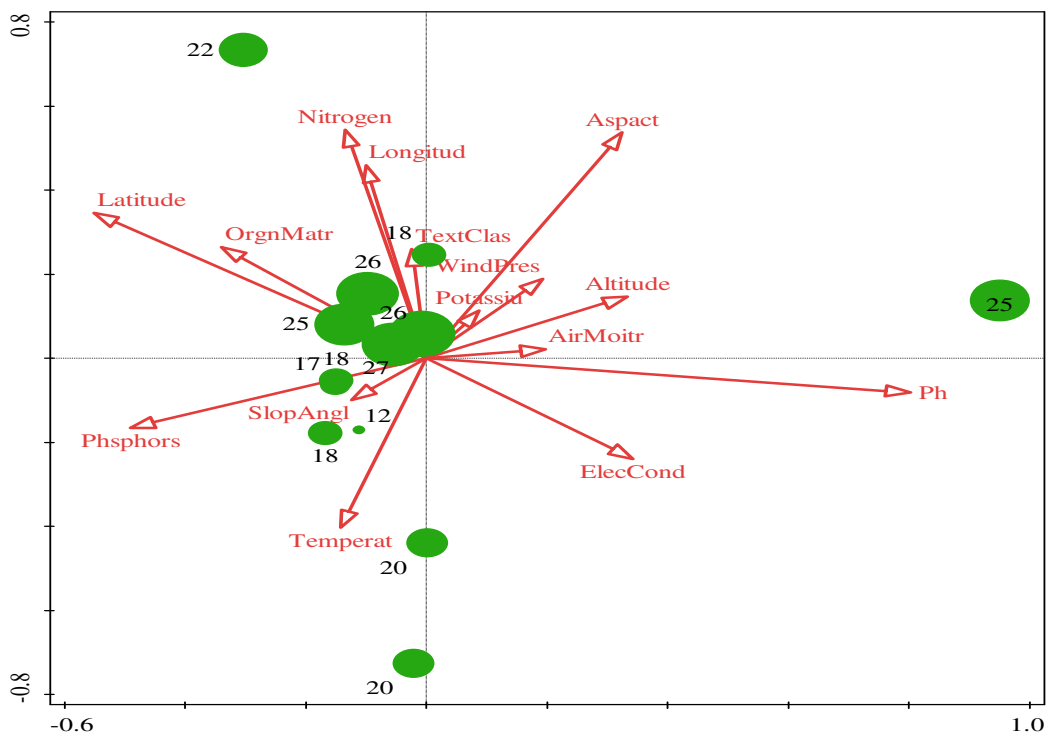


Figure. 10. CCA ordination of stands of reserved forest

Phytosociological analysis

Phytosociology is the study of plant communities and their inter-relationship and interaction with environment. While a community is grouping of plant population formed in one habitat type in specific area, display mutual competition and dependence. The existence and establishment of plant communities indicates the plant type and habitat condition under which they develop (Malik, 1986). The analysis of the study area showed that dominant family was found to be Asteraceae followed by Labiateae (10 species), Poaceae and Rosaceae (8 plant species) each, Polygonaceae and Pteridaceae by 5 species each. The past work of Stewart (1972) depicted that these families are dominantly occurring in Pakistan and Azad Jammu and Kashmir. The work of other ecologists described that Himalayan and other areas like Sathan Gali forest do had more or less same list of families as we had listed in the research (Iqbal et al., 2015; Ijaz et al., 2016).

There is natural principle that edaphic and physiognomic parameters do exert their pivotal impacts on type of plants in an area, their correlation with other plants-making communities. In the field analysis of Sathan Gali forest, it was found that key types of four communities were found. Their composition was variable with factors of environmental such as altitude, latitude, temperature, precipitation, humidity and soil type. Similar ideas were described by Berg et al. (2000) and he said that precipitation and elevation strongly influence the floristic composition among different forests of an area. The floristic diversity, richness and maturity are also correlated with variation in altitude (Shaheen et al., 2016; Adam and Mamat, 2005). The life span of plants and their intercorrelation do become changed with alteration in edaphic factors and time elapsed and similar findings were reported by Madsen and Ilgaard in 2008 & Titshall et al., 2000.

Community analysis in study area by TWINSpan

This research produced list of 131 plants species belonging to 58 families from the study area. The data collected from 13 stands of 455 quadrats resulted in a total of 4 different plant communities recognized by TWINSpan viz (1) *Pinus-Pteris-Sarcococca* Community (PPS); (2) *Cedrus-Fragaria-Pteris* Community (CFP); (3) *Pinus-Cedrus-Viburnum* Community (PCV) and (4) *Pinus-Digitaria-Sarcococca* Community (PDS). These communities' occurrence and congruence was interdependent on altitude, precipitation, latitude, soil structure, minerals contents in soil as shown in the results section above. Similar studies were conducted by Haq on subtropical forests of Nandiar Khuwar catchment district Battagram, Khyber Pakhtunkhwa, Pakistan and he found edaphic and climatic factors had strong influence on types of communities and their richness (Haq et al., 2015).

Community analysis in study area by DCA & CCA

In constrained DCA ordination of reserved forest of Sathan Gali indicated that the total variation in the species data was 3.28. The DCA ordination of the species showed that different species clustered in ordination space on the basis of similarities in habitat and species composition. CCA showed percentage variance of 10.16%, 15.98% and 21.01% for axis I, II and III, respectively. This result showed that there is strong association of species and habitat types with environmental variables. CCA technique is used to find out the relationship between environmental variable and vegetation. This

CCA analysis has also been used to determine the vegetation-environmental relationship (Mehmood et al., 2015). It is therefore important to correlate the vegetation structure of the area with environmental variables for a proper understanding of the of plant species distribution mechanism in an area (Eriksson and Bergstrom, 2005). The first two axis explain 45% of total variation so our analysis indicate significant results. The length of arrow showed the magnitude of particular factor's effect on plant species distribution.

Mehmood et al. (2015) and Haq et al. (2015) reported that the distribution of plant is greatly affected by variation in altitude in the areas adjacent to study field. Zhang et al. (2006) also showed that altitude is an important factor for plant distribution. Due to change in altitude the temperature declines and humidity increases which favors the plant of higher elevation. Our findings are also in accordance with Shaheen et al. (2011) who reported that altitude is a main parameter for distribution of species in Bagh, AJK. These results showed that a specific environmental variable has a great impact on species distribution in different vegetation zones of the study area (Haq et al., 2015).

The life form of plants is an adaptive response to environment and provides an ecological classification that may be indicative of habitat conditions (Archibold, 1995). Occurrence of similar biological spectrum in different regions indicates similar climatic conditions. The present findings as described in the result section were in agreement with Shaheen et al. (2016), who had reported Therophytes as the leading life form in Havelian, Abbottabad, Pakistan.

Leaf spectra (LS) are characteristic of the existing environmental and habitat conditions of any area and our classes on basis of LS are also in-line with past work of Hussain et al. (2015). Leaf size spectrum (LSS) analysis showed that the study area was dominated by microphylls contributing 68 (40.47%) species, followed by Mesophylls containing 45 (26.78%) species and these types of classes were also mentioned by Malik et al. (2007) where he found that microphyllous and nanophyllous were the dominant leaf size from Kotli Azad Kashmir and Waziristan and these clustering was totally based edaphic and climatic factors (Siddiqui et al., 2014). So, on basis this research findings, indigenous people of the Sathan Gali and relevant departments can use this research information for propagation of the most prevalent species of the plants as this area's soil and climate will prefer to assist such taxa to grow and compete with already plants' communities. These forests can be made rich and diverse by using the preservation and conservation strategies implemented after due re-forestation process.

Conclusion

It is concluded that phytosociological analysis of any area is the best method to find the appropriate species for growing or cultivation on it. The findings of the work on Sathan Gali reserved forest showed that *Pinus wallichian*, *Taxus wallichiana*, *Pinus roxburghii*, *Alnus nitida* *Quercus dilatata*, *Juglans regia*, *Abies pindrow*, *Arisaema flavum*, *Duchesnea indica*, *Aegopodium burttii*, *Rumex dentatus*, *Clinopodium vulgare*, *Indigofera heterantha*, *Solanum surattense*, *Saromatium venosum*, *Paeonia emodi*, *Fragaria nubicola*. *Myrsine Africana*, *Impatiens bicolor* *Bupleurum lanceolatum*, *Ajuga bracteosa*, *Rumex nepalnsis* and *Isodon rugosus* were prominent plants of the area. These are providing key resources as food, fodder, sheltering, hedging, furniture, medicines, aesthetics and commercial purposes i.e. livelihood for the indigenous and neighboring areas of Sathan Gali reserved forest of Mansehra, Pakistan. It was

concluded that mainly edaphic factors and environmental characteristics are limiting constraints for the forest diversity, richness and maturity. The controlling and modification of these analyzed parameters may assist in rich and gloomed forest growth having dynamic communities' structure.

REFERENCES

- [1] Adam, J. H., Mamat, Z. (2005): Floristic composition and structural composition of lime stone forests at three different elevations in Bau, Kuching and Saravak, Malaysia. – *J. Biol. Sci.* 5(4): 478-485.
- [2] Ahmad, Z., Khan, S. M., Ali, S., Rahman, I. U., Ara, H., Noreen, I., Khan, A. (2016): Indicator species analyses of weed communities of maize crop in district Mardan, Pakistan. – *Pak. J. Weed Sci. Res.* 22(2): 227-238.
- [3] Ali, S. I., Qaisar, M. (1995-2004): *Flora of Pakistan*. – Pakistan Agriculture Research Council, Islamabad.
- [4] Allen, S. E., Grimshaw, H. M., Parkinson, J. A., Quamby, C., Roberts, J. D. (1986): *Chemical Analysis*. – In: Moore, P. D., Chapman, S. B. (eds.) *Methods in Plant Ecology*. (2nd ed.). Blackwell Scientific Publications, Oxford.
- [5] Archibold, O. W. (1995): *Ecology of World Vegetation*. – Chapman & Hall, London.
- [6] Berg, V. D., Eduardo, G., Oliveira-Filho, T. A. (2000): Floristic composition and phytosociological structure of a riparian forest in Itutinga, State of Minas Gerais, Brazil and comparisons with other areas. – *Rev. Bras. Bot.* 23(3): 231-253.
- [7] Currie, D. J, Francis, A. P. (2004): Regional versus climate effect on taxon richness in angiosperms; reply to Qian and Ricklefs. – *American Naturalist* 163: 780-785.
- [8] Daubenmire, R. F. (1959): A canopy coverage method of vegetation analysis. – *North West Sci.* 33: 43-46.
- [9] Eriksson B. K., Bergström, L. (2005): Local distribution patterns of macroalgae in relation to environmental variables in the northern Baltic Proper. – *Estuar. Coast. Shelf Sci.* 62: 109-117.
- [10] Fiaz, M. (2012): *Species Diversity of Basidiomycetes of District Mansehra*. – PhD Thesis, Hazara University Mansehra, KPK, Pakistan.
- [11] Haq, F., Ahmad, H., Iqbal, Z. (2015): Vegetation description and phytoclimatic gradients of subtropical forests of Nandiar Khuwar Catchment District Battagram. – *Pak. J. Bot.* 47(4): 1399-1405.
- [12] Hussain, F., Shah, S. M. Badshah, L., Durrani, M. J. (2015): Diversity and ecological characteristics of flora of Mastuj Valley, district Chitral, Hindukush range, Pakistan. – *Pak. J. Bot.* 47(2): 495-510.
- [13] Hussain, M. S., Sultana, A., Khan, J. A., Khan, A. (2008): Species composition and community structure of forest stands in Kumaon Himalaya, Uttarakhand, India. – *Tropical Ecology* 49(2): 167-181.
- [14] Ijaz, F. (2014): *Biodiversity and traditional uses of plants of Sarban Hills, Abbottabad*. – M. Phil. Thesis, Hazara University Mansehra, KP, Pakistan.
- [15] Ijaz, F., Iqbal, Z., Alam, J., Khan, S. M., Afzal, A., Rahman, I. U., Islam, M., Sohail, M. (2015): Ethnomedicinal study upon folk recipes against various human diseases in Sarban Hills, Abbottabad, Pakistan. – *World J. Zoology* 10(1): 41-46.
- [16] Ijaz, F., Iqbal, Z., Rahman, I. U., Khan, A., Shah, S. M., Khan, G. M., Afzal, A. (2016): Investigation of traditional medicinal floral knowledge of Sarban Hills, Abbottabad, KP, Pakistan. – *J. Z.* 179: 208-233.
- [17] Iqbal, M., Khan, S., Khan, M. A., Rahman, I. U., Abbas, Z. (2015): Exploration and inventorying of weeds in wheat crop of the district Malakand, Pakistan. – *Pak. J. Weed Sci. Res.* 21(3): 435-452.

- [18] Kent, M., Coker, P. (1994): *Vegetation Description and Analysis. A Practical Approach.* – John Wiley and Sons, Chichester.
- [19] Khan, K. U., Shah, M., Ahmad, H., Ashraf, M., Rahman, I. U., Iqbal, Z., Khan, S. M., Majid, A. (2015a): Investigation of traditional veterinary phytomedicines used in Deosai Plateau, Pakistan. – *Global Vet.* 15(4): 381-388.
- [20] Khan, S. M., Din, N. U., Sohail, I. U., Rahman, F., Ijaz, Z., Ali, Z. (2015b): Ethnobotanical study of some medicinal plants of Tehsil Kabal, District Swat, KP, Pakistan. – *Med. Aromat. Plants* 4(3): 189.
- [21] Khattak, N. S., Nouroz, F., Rahman, I. U., Noreen, S. (2015): Ethnoveterinary uses of medicinal plants of district Karak, Pakistan. – *Journal of Ethnopharmacol.* 171: 273-279.
- [22] Leveque, C. M. (2001): *Les parcs culturels: presentation d'une initiative europeenne.* – In: Sagnes, J. (ed.) *Deux siecles de Tourisme en France.* Presses Universitaires de Perpignan, Perpignan.
- [23] Madsen, J. E., Iigaard, I. B. (2008): Floristic composition, structure and dynamics of an upper montane rain forest in Southern Ecuador. – *Nordic J. Bot.* 14(4): 403-423.
- [24] Malik, N. Z., Arshad, M., Mirza, N. S. (2007): Phytosociological Attributes of Different Plant Communities of Pir Chinasi Hills of Azad Jammu and Kashmir. – *International Journal of Agriculture & Biology* 9(4): 569-574.
- [25] Malik, Z. H. (1986): Phytosociological study on the vegetation of Kotli Hills. – M. Phil Thesis, University of Peshawar.
- [26] McGrady-Steed, J., Morin, P. J. (2000): Biodiversity, density compensation and the dynamics of populations and functional groups. – *Ecology* 81: 361-373.
- [27] Mehmood, A., Khan, S. M., Shah, A. H., Ahmad, H. (2015): First floristic exploration of the District Torghar, Khyber Pakhtunkhwa, Pakistan. – *Pak. J. Bot.* 47(SI): 57-70.
- [28] Mueller-Dombois, D., Ellenberg, H. (1974): *Aims and Methods of Vegetation Ecology.* – Wiley and Sons, New York.
- [29] Nasir, E., Ali, S. I. (1971-1994): *Flora of Pakistan.* – Pakistan Agriculture Research Council, Islamabad.
- [30] Niemi, G. J., Donald, M. E. (2004): Application of ecological indicators. – *Annual Review of Ecology, Evolution and Systematics* 35(57): 89-111.
- [31] Peer, T., Gruber, J. P., Millingard, A., Hussain, F. (2007): Phytosociology, structure and diversity of the steppes vegetation in the mountains of Northern Pakistan. – *Phytocoenologia* 37: 1-65.
- [32] Rahman, I. U., Ijaz, F., Afzal, A., Iqbal, Z., Ali, N., Khan, S. M. (2016a): Contributions to the phytotherapies of digestive disorders. Traditional knowledge and cultural drivers of Manoor Valley, Northern Pakistan. – *J. Ethnopharmacol.* 192: 30-52.
- [33] Rahman, I. U., Ijaz, F., Afzal, A., Iqbal, Z., Ali, N., Afzal, M., Khan, M. A., Muhammad, S., Qadir, G., Asif, M. (2016b): A novel survey of the ethno medicinal knowledge of dental problems in Manoor Valley (Northern Himalaya). – *Pakistan. J. Ethnopharmacol.* 194: 877-894. DOI: <http://dx.doi.org/10.1016/j.jep.2016.10.068>.
- [34] Raunkiaer, C. (1934): *The Life Forms of Plants and Statistical Plant Geography.* – Oxford University Press, London.
- [35] Rieley, J., Page, S. (1990): *Ecology of Plant Communities: A phytosociological Account of the British Vegetation.* – John Wiley and Sons, Inc., New York.
- [36] Rodolfo, E., Pichi, S. (1948): An index for establishing the degree of maturity in plant communities. – *Journal of Ecology* 36(1): 85-90.
- [37] Shah, A. H., Khan, S. M., Shah, A. H., Mehmood, A., Rahman, I. U., Ahmad, H. (2015): Cultural uses of plants among Basikhel Tribe of District Tor Ghar, Khyber Pakhtunkhwa, Pakistan. – *Pak. J. Bot.* 47(SI): 23-41.
- [38] Shaheen, H., Shinwari, Z. K. (2012): Phytodiversity and endemic richness of Karambar lake vegetation from Chitral, Hindukush-Himalayas. – *Pak. J. Bot.* 44(1): 15-20.

- [39] Shaheen, H., Qureshi, R. A., Shinwari, Z. K. (2011): Structural diversity, vegetation dynamics and anthropogenic impact on lesser Himalayan subtropical forests of Bagh District, Kashmir. – Pak. J. Bot. 43(4): 1861-1866.
- [40] Shaheen, S., Iqbal, Z., Ijaz, F., Alam, J., Rahman, I. U. (2016): Floristic composition, biological spectrum and phenology of Tehsil Havelian, District Abbottabad, Pakistan. – Pak. J. Bot. 48(5): 1849-1859.
- [41] Siddiqui, M. F., Shaukat, S. S., Ahmed, M., Khan, I. A., Khan, N. (2014): Foliar and soil nutrient distribution in conifer dominated forests of moist temperate areas of Himalayan and Hindukush region of Pakistan: a multivariate approach. – Pak. J. Bot. 46(5): 1811-1827.
- [42] Titshall, L. W., O'Connor, T. G., Morris, C. D. (2000): Effect of long-term exclusion of fire and herbivory on the soils and vegetation of sour grassland. – African Journal of Range and Forage Science 17: 70-80.
- [43] Whittaker, R. H. (1977): Evolution of species diversity in land plant communities. – Evolutionary Biology 10: 1-67.
- [44] Zhang, X. P., Wang, M. B., Shi, B. (2006): Quantitative classification and ordination of forest communities in Pangquangou National Nature Reserve. – Acta Ecologica Sin. 26(3): 754-761.

MAXIMUM ENTROPY MODELING OF FARMLAND DAMAGE CAUSED BY THE WILD BOAR (*SUS SCROFA*)

LEE, W.-S.¹ – KIM, S.-O.² – KIM, Y.³ – KIM, J.-H.² – JANG, G.-S.^{2*}

¹*Department of Landscape Architecture, Daegu University
201, Daegudae-ro, Gyeongsan-si, Gyeongsangbuk-do 38453, Republic of Korea
(phone: +82-10-2895-9858)*

²*Department of Life Sciences, Yeungnam University
280, Daehakro, Gyeongsan 38541 Republic of Korea
(phone: +82-53-810-2371; fax: +82-53-810-4618)*

³*Department of Statistics, Kyungpook National University
80, Daehakro, Bukgu, Daegu 41566, Republic of Korea
(phone: +82-10-4750-9794)*

**Corresponding author
e-mail: sunside@ynu.ac.kr*

(Received 17th Sep 2017; accepted 15th Jan 2018)

Abstract. Farmland damage caused by wild boars was modeled by the Maxent model using the field-inspecting data surveyed in Gyeongnam Province of South Korea during 2012 and 2013. A total of 3,854 cases (2,286 in 2012 and 1,568 in 2013) were chosen for the model after the field inspection. The Maxent model obtained quite high AUCs exceeding 0.8, indicating that the probability derived from the model had high accuracy. The variable ‘distance from forest boundary (d_forest)’ revealed a higher probability for damaged areas located closer to forest boundaries. The areas damaged by wild boars were also located much closer to agricultural areas, including paddies and fields. Overall, areas located within 500 m of other agricultural areas showed a higher likelihood of damage by wild boars. Based on the predictions in Maxent, damage to farmland caused by wild boars was more closely related to distance from its habitat (i.e., forest) and use of land as food resources (i.e., rice paddies and fields) than topographical factors such as elevation and slope.

Keywords: *spatial modeling, presence-only data, Maxent, machine-learning modeling*

Introduction

The “Injurious Animal Destruction” program introduced during the Japanese occupation of the Korean peninsula and the Korean War (1950-1953) resulted in loss of many top predators including tigers, wolves and leopards from South Korea (Kim et al., 2011; Lee et al., 2012). Owing to the loss of top predators, wild boar populations have increased explosively in South Korea. A combination of factors have led to the rapid increase of wild boars, including changes in agricultural practices, lack of predators, reduced hunting pressure, and climate changes (Massei and Genov, 2004).

Wild boars can have a variety of impacts on the environment within and/or around their habitat, such as causing damage to agricultural land (Herrero et al., 2006) and pastures (Alexiou, 1983), as well as impacts on forest regeneration (Groot Bruinderink and Hazebroek, 1996) and predation (Pavlov et al., 1981), consumption of forest fruits (Herrero et al., 2006), and consumption of carrion (Herrero and Fernández de Luco, 2003). As there has been intensive land use and anthropogenic activities around forest patches because of insufficient land for cultivation during the last few decades in South

Korea, the edge areas inside and outside forest patches have been rapidly exchanged for agricultural lands, including rice paddies and fields. In general, regions near forest patch boundaries are known act as buffer zones between the inside forest and human-based land uses outside the forest. These areas accommodate a variety of living things including insects, herbs and other animals. However, wild boars living inside the forest don't seem to realize the condition of the area nearby the forest after there being the land use change. Therefore, there have been conflicts between wild boars trying to obtain food and farmers who want to keep their farms free from damage. This phenomenon happened in South Korea corresponded to the opinion proposed by Peracino and Bassano (1995), and now farmland damage caused by wild boars has been a great public concern in South Korea.

As damage to farmland caused by wild boars has become a social and public concerns, the Korean government revised the act on the prevention of and countermeasures against agricultural and fisheries disasters and its enforcement regulation to include inspection of farmland damaged by harmful wild animals such as wild boars and record the information in a register at every town hall for providing a subsidy to the damage (national legislation data infrastructure center; <http://www.law.go.kr>). For this reason, the database of farmland damage kept in each city hall has much high accuracy in terms of the location of damage caused by wild boars; therefore, it can be applied for analysis of spatial patterns and characteristics of farmland damage caused by wild boars.

Information regarding farmland damage caused by wild boars can be transformed into a binary type of response variable for spatial modeling. At this time, various forms of regression analyses can be applied to predicting and modeling the farmland damage caused by wild boars. Recently, generalized linear models (GLM; McCullagh and Nelder, 1989; Friston et al., 1995), generalized additive models (GAM; Guisan et al., 2002) and maximum entropy (Maxent; Phillips et al., 2006) have been becoming increasingly popular for prediction of species distribution (Scott et al., 2002). The Maxent model, which is derived from a branch of statistics referred to as machine learning (Yackulic et al., 2013), is a general-purpose method for making predictions or inferences from incomplete information (Phillips et al., 2006). Although the Maxent model can be applied using presence/absence data, it is well known to produce much higher confidence in the presence-only model (Yackulic et al., 2013). Thus, the data describing damage caused by wild boars can be applied in Maxent to precisely predict the probability of damage caused by wild boars. Therefore, this study initiated a new approach to investigate the farmland damage caused by wild boars using field-survey data. In this study, farmland damaged by wild boars were applied as presence-only data in a maximum entropy model (Maxent) to estimate the spatial patterns and sensitivity of wild boars in farmland. The results presented herein will be useful to managing the wild boar population on the Korean peninsula and provide ideas to facilitate co-existence of wild boars and humans.

Materials and methods

Study species (wild boar) and data sources

The wild boar is a large mammal that has one of the broadest geographic distributions, and can occupy a wide range of environments, including semi-deserts, wetlands, high mountain environments, and forests. Although the wild boar is a

generalist omnivore that can feed on a wide variety of foods for which the availability in space and time is not constant (Herrero et al., 2006), this study focused on farmlands that were near forests and sensitive to damage caused by wild boars.

Data describing damage caused to farmland by wild boars was collected in Gyeongnam Province (area = 10,537.32 km²), which is located in southeastern South Korea. The damage data has higher confidence because it was recorded in the register after inspection of individual fields for damage caused by wild boars. A total of 2,286 cases in 2012 and 1,568 in 2013 were recorded in the register within Gyeongnam Province. The spatial location was digitalized into the spatial point (shape file), and used as presence only data for the response variable in this study (Fig. 1). The results of inspections revealed rice paddy fields were most preferred by wild boars (993 in 2012; 710 in 2013), followed by dry fields (721 in 2012; 501 in 2013).

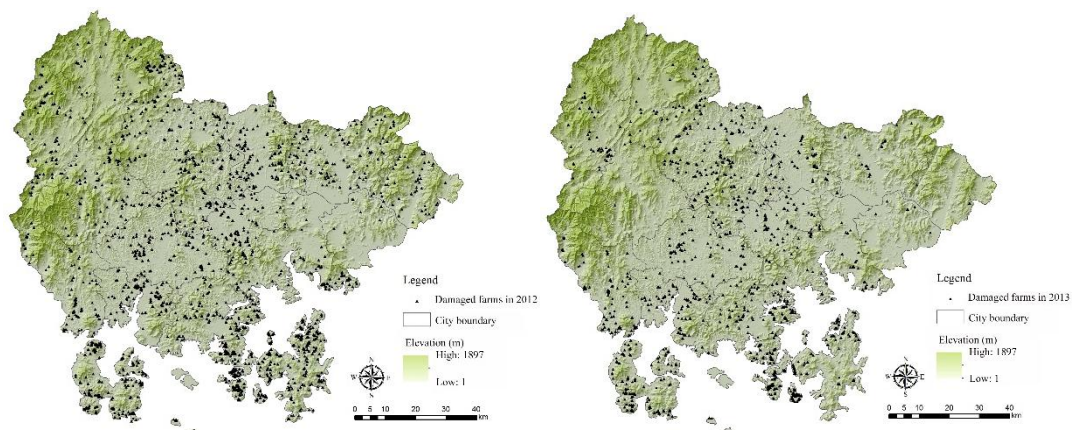


Figure 1. Distribution of farmland damaged by wild boars

Environmental variables for explaining the farmland damage by wild boars

Nine independent variables for explaining farmland damage caused by wild boars were selected based on topographical and environmental conditions around accessibility to land uses by a wild boar (Table 1).

Topographical factors could be major indicators to explain wildlife habitat (Guisan and Zimmermann, 2000) because there can be environmental variability and strong local gradients of insulation depending on topography such as elevation and surface orientation (slope, aspect and hillshade) (Fu and Rich, 2002; Kim et al., 1998; Seo et al., 2000; Polfus et al., 2011). Elevation, slope and aspect have commonly been used for modeling species distribution because different levels of solar energy could be radiated according to these topographic conditions, resulting in generation of different habitat conditions. In this study, environmental variables related to topographic factors (elevation, slope, aspect and hillshade) were obtained from a digital topographic map drawn on a scale of 1 to 5,000 (NGII, National Geographic Information Institute, Suwon, South Korea).

In general, forests are recognized as resources consisting of a variety of ecological benefits including production of food and cover (McCollin, 1998), and habitat components (Olson et al., 2004). Wild boars, which are known to have home ranges of 1.1 to 3.9 km² (Boitani et al., 1994), are known to rest in forested habitats during

daytime, while they forage for food in farmlands at night, which is when they cause damage (Schley et al., 2008; Lee and Lee, 2014).

Table 1. Estimates of parameters applied in the model

Section	Acronym	Parameter	Type	Source	References
Topography	Elevation	Elevation	Continuous	DEM	Kim et al.(1998); Seo et al.(2000)
	Slope	Slope	Continuous	DEM	Kim et al.(1998); Seo et al.(2000); Fu and Rich (2002)
	Aspect	Aspect	Continuous	DEM	Kim et al.(1998); Seo et al.(2000);); Fu and Rich (2002)
	Hillshade	Hill shade	Continuous	DEM	Kim et al.(1998); Seo et al.(2000); Fu and Rich (2002); Polfus et al., 2011
Accessibility	D_stream	Distance to stream	Continuous	Land cover map	Kim et al.(2012); Song and Kim (2012)
	D_forest	Distance to forest (outside)	Continuous	Forest map	Kim et al.(1998); Seo et al.(2000); McCollin (1998)
	D_paddy	Distance to paddy	Continuous	Forest map	Kim et al.(1998); Seo et al.(2000)
	D_field	Distance to field	Continuous	Land cover map	Kim et al.(2012); Song and Kim (2012)
	D_road	Distance to roads	Continuous	Topographic map	Kim et al.(2012); Song and Kim (2012)

Therefore, the spatial proximity from natural resources could be a criterion to measure the maximum range from which wild boars try to obtain food on farmlands, and one of the references to inspect which areas would be sensitive to damage caused by wild boars (Kim et al., 2012; Song and Kim, 2012). The spatial proximity from artificial land uses (e.g., roads, buildings and other pavements) has frequently been referred to estimate the sensitivity of wild boar's responses to artificial impacts such as noise (Kim et al., 2012; Song and Kim, 2012). This study adopted the distance from roads as an explanatory variable for the model. The road data, which included all roads except for highways and unpaved roads under 3 m in width, were extracted from the digital topographic map drawn on a scale of 1 to 5,000 (NGII).

Prior to model building we assessed the strength of Pearson's correlation coefficients between pairs of variables: if variables were highly correlated ($r > 0.7$) then one of the variables was removed from the set (referring to Gormley et al., 2011). A final set of nine candidate variables remained for model building.

Model building and evaluation in Maxent

The damage information, which was registered in city halls, was gathered in 2012 and 2013. This information was used as presence-only data in the Maxent model, which is a machine learning approach based on maximum entropy (Phillips et al., 2006). Maxent has been known to perform as well as, or better than, other methods for modeling presence-only data (Elith et al., 2006). In the present study, Maxent used the presence-only data to randomly select 10,000 points ('pseudo-absence'), which were combined with topographical and environmental covariates to construct an index of habitat suitability based on a 30-m spatial pixel ranging from 0 (least suitable habitat) to 1 (most suitable habitat). The Maxent model was also run 100 times with 0.01 in the convergence threshold, which was defined as the maximum percentage of pixels with cluster assignments that can go unchanged between iterations. Additionally, 25% of the presence data were withheld to be used as training data to evaluate the model's performance.

Model performance was assessed by determining how well the model discriminates between unsuitable and suitable areas over a range of thresholds (Fielding and Bell, 1997). A receiver operating characteristic (ROC) curve, which compares the model sensitivity (true positives) against 1-specificity (false positives) over the entire range of thresholds, was plotted to assess performance of the Maxent model. Because we only have occurrence data and no absence data, the "fractional predicted area" (the fraction of the total study area predicted present) was used instead of the more standard commission rate (fraction of absences predicted present) (Phillips et al., 2006). Additionally, the area under the ROC curve (AUC) was used to guarantee the probability that a randomly selected presence site will be ranked as more suitable than a randomly chosen pseudo-absence site for presence-only modeling (Gormley et al., 2011). An AUC of 0.5 indicates that the model performs no better than random, whereas an AUC of 1 means a model with perfect discrimination and a model with an AUC > 0.7 is considered to provide a confident result in general (Swets, 1988). An additional measure of model performance is the regularized training gain ('Gain'), which describes how much better the Maxent distribution fits the presence data compared to a uniform distribution (Gormley et al., 2011).

Results

Maxent model using data describing farmland damage by wild boar

Three variables (distance to roads, hillshade and aspect) were consistently removed in both years because of the lower % contribution (<1%) in the preliminary Maxent modeling, and six biophysical factors were used as covariates to explain the presence of damage by wild boars. The AUC (0.834 for 2012; 0.867 for 2013; 0.816 for both) and gain (0.774 for 2012; 0.9757 for 2013; 0.6736 for both) values indicate that the Maxent models with six variables explain the farmland damage by wild boars well. The plots (*Fig 3a, 3b*) of false negative rate and fractional predicted area (FPA) show little overlap which is meaning the usefulness of the Maxent models in this study. *Table 2* shows that the variables *d_forest* and *d_field* made a relatively higher percent contribution to the Maxent model and three variables (*d_forest*, *d_field* and *d_paddy*) made an approximately 90% relative contribution to the Maxent model. These three variables were also shown to contain a substantial amount of information that was not

contained in the other variables. Conversely, three other variables (slope, elevation and d_stream) achieved relatively lower percent contribution (<4%) to the model for both years (Fig. 3), and achieved little gain when used alone. The results obtained when omitting each variable while including all others showed that no one variable contained a substantial amount of information that was not contained in the other variables. Therefore, the probability of presence increased with increasing d_forest, d_field and d_paddy.

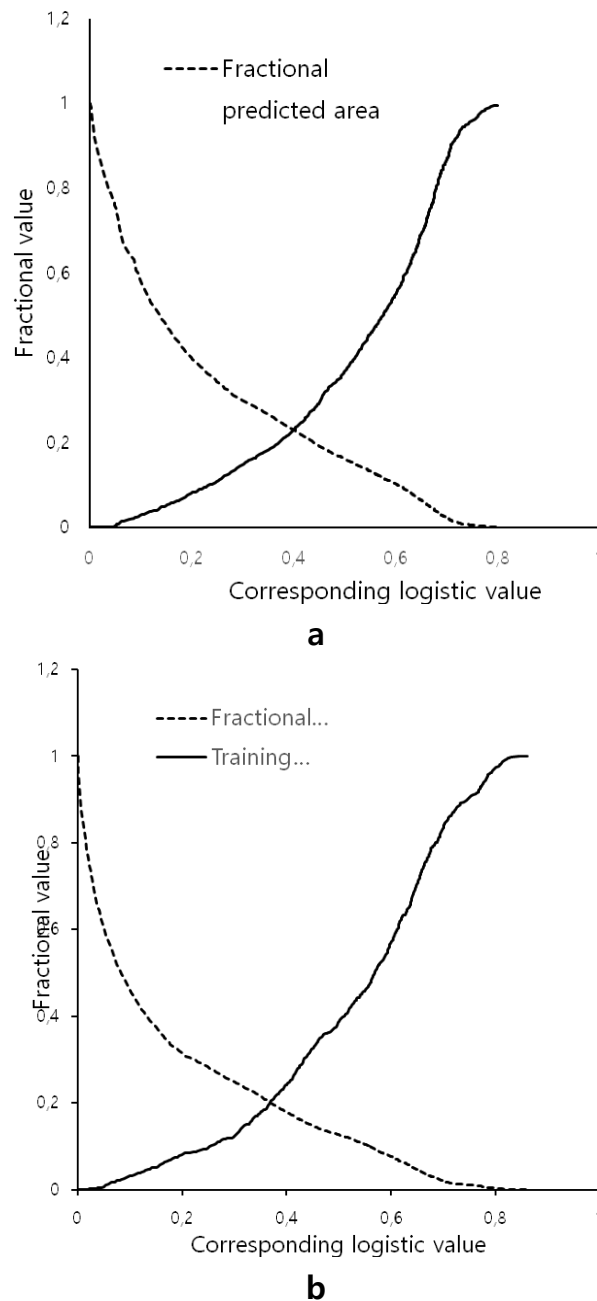


Figure 2. Performance of the Maxent model of farmland damage caused by wild boars in Gyeongnam Province. (a) False negative error rate (solid line) and FPA (dashed line) based on all threshold values in 2012. (b) False negative error rate (solid line) and FPA (dashed line) based on all threshold values in 2013

Partial response curves in the Maxent model

Six pairs of partial response curves for 2012, 2013 and both years showed very consistent curvatures for the damage probability by wild boars depending on changes of each factor (Figs. 4, 5, 6). The variable d_forest was explaining that there was a higher probability for the damage area to be located close to forest boundaries. Most areas with higher damage probability were found within 500 m of the forest boundaries, whereas the probability was much lower close to zero at the outside area exceeding the 500 m distance from forest boundaries. The damage probability was also found to be dependent on elevation with the inverse correlation. Specifically, the damage probability decreased as the elevation increased, and finally there was little probability as it exceeded 800 m in elevation. The inclination of the farmland damage on elevation is not completely irrelevant to the distribution of farmlands per elevation in South Korea. The damage probability did not seem to be dependent on the distance to water resources. The probability was almost higher than 0.5 in general (Figs. 4d, 5d, 6d), although there were slight biases in the probability. The areas damaged by wild boars were located much closer to agricultural areas, including paddies (Fig. 4e, 5e, 6e) and fields (Figs. 4f, 5f, 6f). There was also higher probability of damage by wild boars in the areas distributed within 500 m of other agricultural areas.

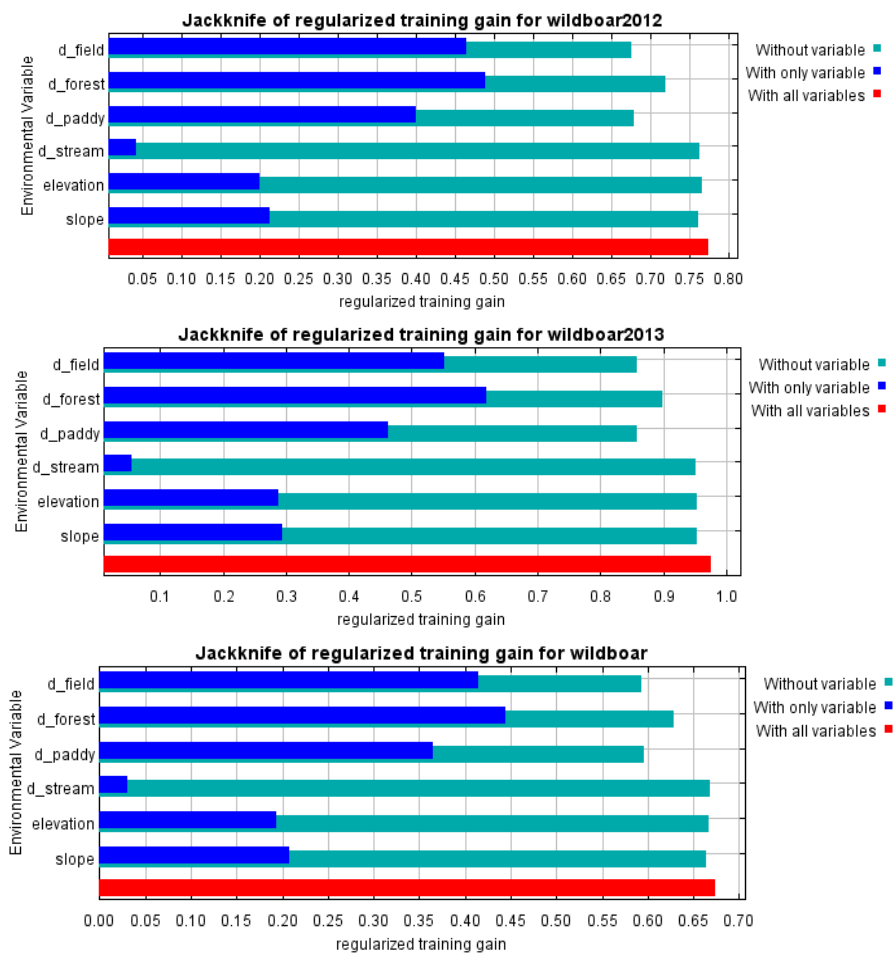


Figure 3. Jackknife regularized training gain, with only that variable and without variable from a model

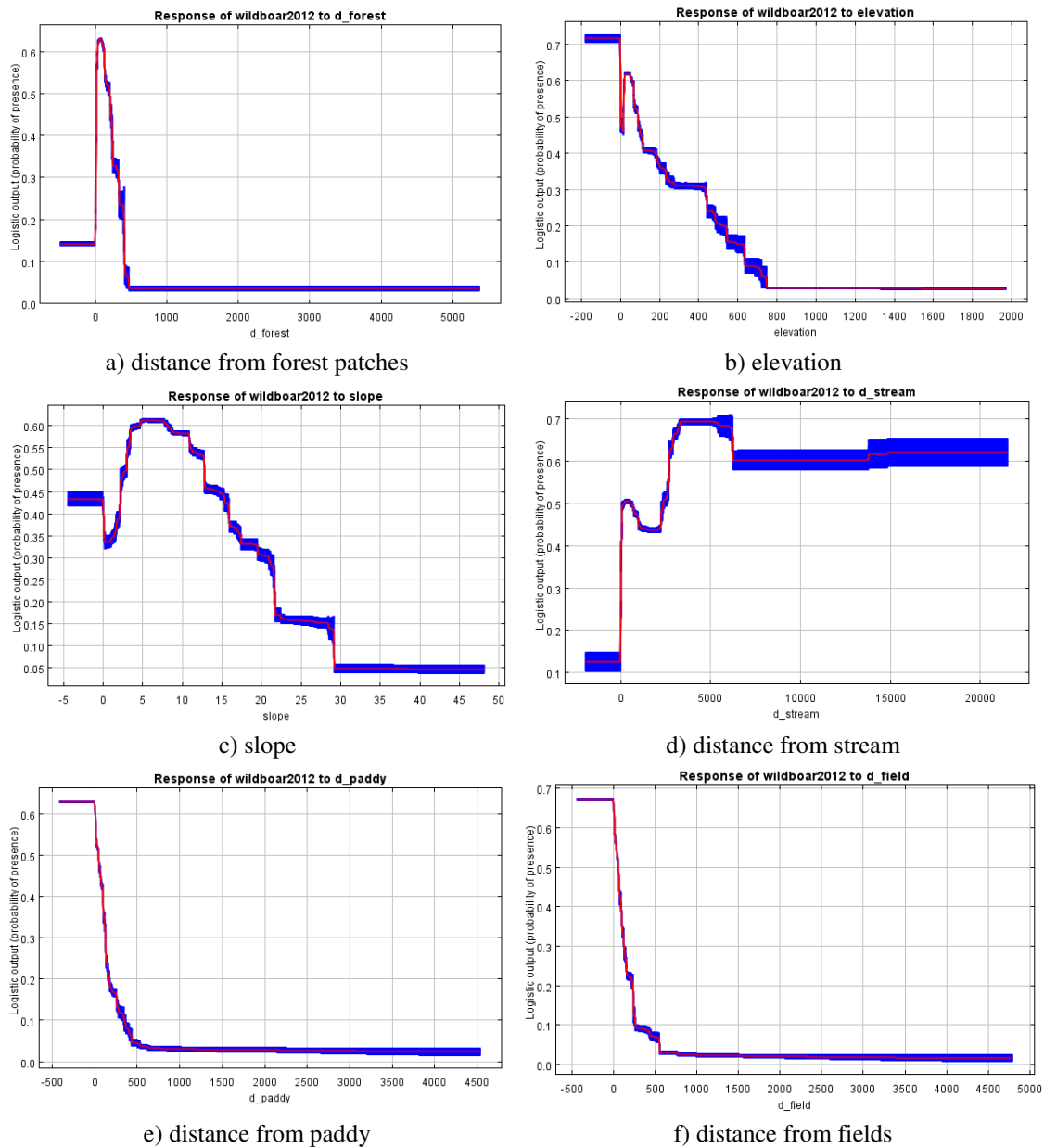
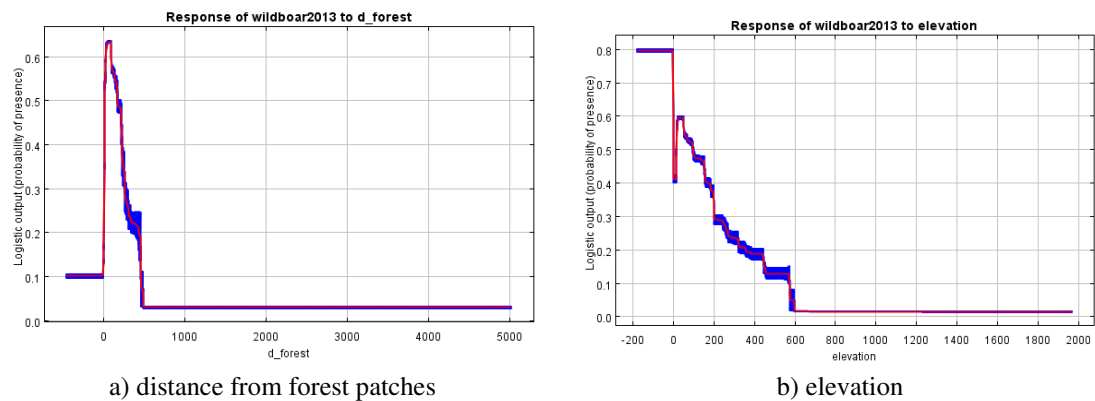


Figure 4. Partial response curve for 2012



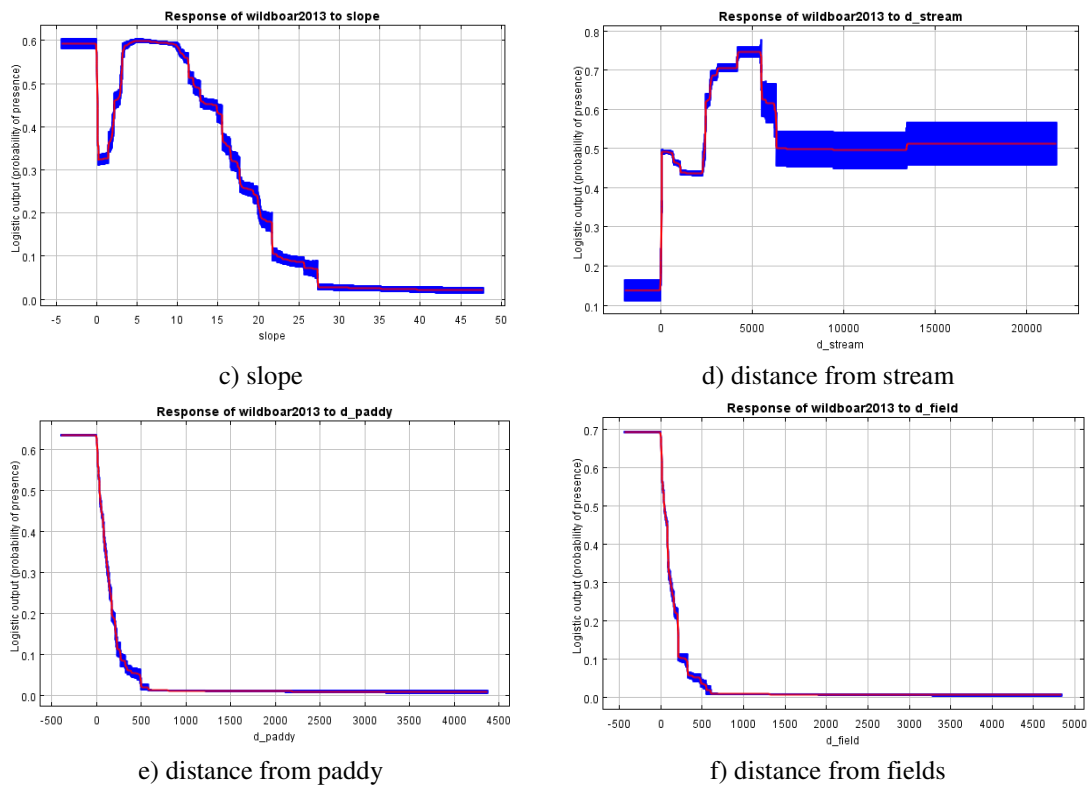


Figure 5. Partial response curve for 2013

Predicting farmland damage by wild boars using the Maxent model

There was a strong positive correlation ($r = 0.9814$) between predictions for 2012 and 2013 (Fig. 7a, b). Specifically, cells with a higher damage probability index in 2012 had higher damage probabilities in 2013. In both years, prediction maps consistently indicated that areas with the highest probability of damage by wild boars were located close to forest boundaries. Although there were several large plains of relatively higher damage probability around the Nam and Nakdong rivers (e.g., Changyeong, Hama and Jinju), farmlands of higher damage potential seemed to be evenly distributed across the province. Furthermore, the probability of damage by wild boar was higher in areas near forest boundaries within some islands (e.g., the Geoje and Namhae islands) (Figs. 7a, b, c).

There was also a regional increase in damage probability between 2012 and 2013, especially for northwestern (e.g., Geochang, Hapcheon and Hamyang) and western (e.g., Hadong and Sancheong) areas with mountainous topography (Fig. 7d). Specifically, these areas had relatively higher damage probabilities in 2012 than 2013. Moreover, Geochang (180.22 km²), Hamyang (128.94 km²) and Hapcheon (117.51 km²) showed higher damage probability in 2012 than in 2013 (Table 3). Eastern mountainous areas (e.g., eastern Miryang) and some areas in north and south Geoje also showed much higher probability in 2012 than in 2013. None of the other areas was showing that there was a considerably large area getting a probability biased in each year. As shown in Table 2, the area of damage probability in 2012 was higher than in 2013 (1301.49 km²; 12.35%), while the area of damage probability in 2013 was higher than in 2012 (827.25 km²; 7.85%).

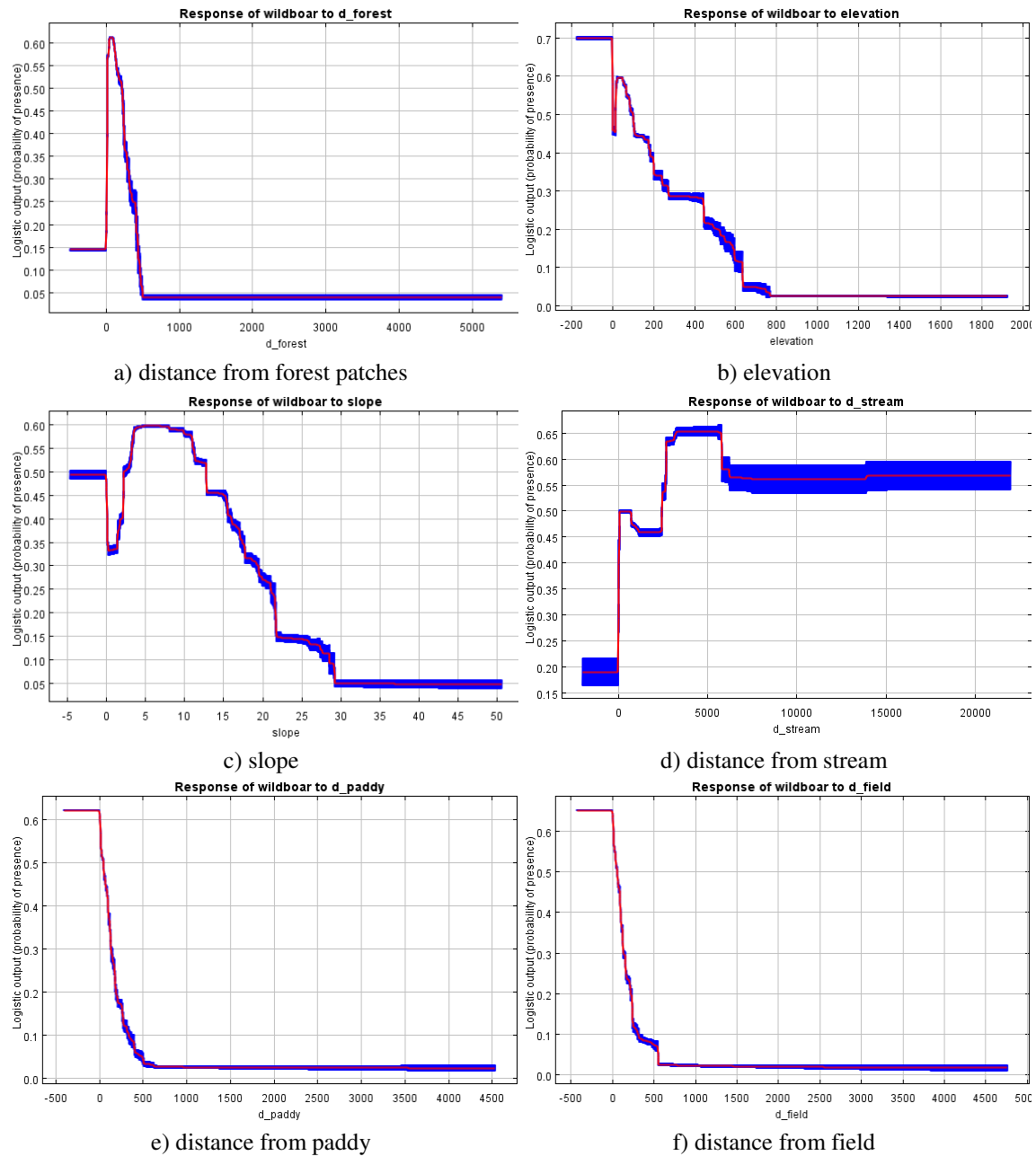


Figure 6. Partial response curve for both years

Table 2. Relative contribution of variables to the Maxent model of farmland damage caused by wild boars in Gyeongnam, South Korea

Variable	2012	2013	Both 2012 and 2013
d_forest	35.8	43.0	40.4
d_field	38.7	33.9	37.9
d_paddy	18.7	13.4	16.5
elevation	1.3	4.0	1.6
d_stream	2.9	3.8	1.6
slope	2.6	2.0	2.0

Discussion

Maxent model and its accuracy using the presence-only data

We used the presence-only data describing farmland damage by wild boars in 2012 and 2013 to estimate the damage probability; therefore, most common areas were predicted to have similar damage probability in both years. We first used the correlation coefficient and % contribution to obtain the covariates that best explained the Maxent model so that six variables were finally selected for the model in both years after three variables were consistently removed. Three AUCs over 0.8 indicated that the Maxent models applied to estimate the damage probability had high accuracy, and the prediction maps derived from the models commonly showed the probability of damage by wild boars across the province. Based on the contribution to the model, three variables (d_forest, d_field and d_paddy) made higher contributions, while the other three variables made relatively lower contributions (*Table 2*). These findings indicate that the farmland damage caused by wild boars was mostly related to the distance from their habitats (i.e., forest) and land uses (i.e., rice paddy and field) rather than topographical factors such as elevation and slope. Two other variables (d_paddy and d_field) did not make a higher contribution than the variable d_forest; however, these two variables had relatively lower regularized gain without each variable based on the Jackknife test (*Fig. 3*), indicating there might be a higher loss of information estimated without each variable than others in the model. Water resources, one of major habitat components influencing wildlife, were not found to be a primary factor influencing farmland damage caused by wild boars (*Table 2; Fig. 3*).

Characteristics of farmland damage caused by wild boars through partial response curves

There are several reasons for frequent farmland damage caused by wild boars near forest boundaries. Fundamentally, the higher density of dominant plant species within the interior forest could suppress the growth of understory vegetation by intercepting direct sunlight. This oligotrophic condition under the crown of the dominant species within the interior forest can cause a deficit of food resources for wild boars so that they are obliged to leave the interior to find new food resources. In addition, forest patches in South Korea have been suffering from severe deforestation during the last few decades (Kwon et al., 2016). Especially, forest edge and ecotone forest have been intensively deforested and transformed into other anthropogenic land uses such as residential areas and farmland. Ecotones, which were first mentioned by Clements (1904) are defined as zonation in a habitat that obviously separates two different series of zones (Myster, 2012). Shifts in forest-grassland ecotones and their transformation imply a change of biodiversity, as well as primary and secondary productivity in there (Smith et al., 1997). Subsequent to damage to the forest edge observed in this study, wild boars lost their food and cover resources within forests. As a result, they tried to find other food resources outside the forests (*Figs. 4a, 5a, 6a*) including rice (*Figs. 4e, 5e, 6e*) and other crops (*Figs. 4f, 5f, 6f*). These findings are in accordance with the finding that wild boar most preferred rice paddies, followed by dry fields. Rapid increases in the wild boar population led to a new conflict factor between residents and wild boars in South Korea. This phenomenon was caused by the loss of top predators as mentioned by Kim et al. (2011).

Damage prediction and its bias in 2012 and 2013

The farmland damage caused by wild boars was spread across the province. The damage was found to be most frequently within Tongyeong (302 cases in 2012, 273 cases in 2013), Geoje (238 cases in 2012, 90 cases in 2013), Namhae (204 cases in 2012, 168 cases in 2013) and Hapcheon (179 cases in 2012, 171 cases in 2013). Several factors were analyzed to determine the reason for the biased frequency of farmland damage among cities in the province (Table 3). The different ratios in the size of forest and agricultural area per city did not influence the bias of frequency of farmland damage caused by wild boars. The three cities most influenced by damage (Tongyeong, Geoje, and Namhae) were islands; however, there was no evidence to differentiate the higher damage frequency in these islands from the relatively lower frequency in other cities. Only what we have paid attention to is that the ratio of coniferous trees to others was so higher in these islands (Table 4). Coniferous trees such as *Pinus thunbergii* have long occupied seaside areas including these three islands because of their endurance against salt stress. The allelopathic effects of pine trees tend to exclude other species from their community (Table 4). This mechanism could strengthen the oligotrophic condition in interior forests in these islands, which could drive wild boars to find alternative food resources outside a forest. Moreover, a considerable area in the four cities mentioned above have been established as a national park in South Korea, including three island cities protected as oceanic national parks and a mountainous national park of about 70 km² that shares its area with Hapcheon. In the region outside the protection area, there have been regular hunting fields operated by each city hall for regulating the number of wild boars. The number of wild boars has been sporadically regulated by operating hunting fields in every year, therefore, there might be doubt that the protection area can afford to accommodate relatively higher density of wild boars than other outside area so that farmlands nearby the protection area seemed more sensitive to damage by wild boars than in other regions.

Table 3. Data describing farmland damage caused by wild boars

Cities	Total area (TA) (km ²)	Forest area (FA) (km ²)	Farmland area (FLA) (km ²)	FA/TA	FLA/TA	FLA/FA	Damage frequency in 2012	Damage frequency in 2013
Chanwon	747	430	118	57.51%	15.76%	27.40%	103	68
Jinju	713	418	141	58.61%	19.84%	33.86%	115	85
Tongyeong	239	155	49	64.97%	20.46%	31.49%	302	273
Sacheon	399	231	87	58.03%	21.72%	37.43%	116	90
Gimhae	463	237	99	51.09%	21.26%	41.62%	14	7
Miryang	799	519	165	64.93%	20.70%	31.88%	112	19
Geoje	402	283	66	70.48%	16.36%	23.22%	238	90
Yongsan	485	362	46	74.63%	9.51%	12.74%	59	2
Uiryeong	483	331	90	68.57%	18.69%	27.26%	136	133
Haman	417	212	118	50.86%	28.38%	55.80%	99	61

Changyeong	533	285	147	53.55%	27.56%	51.48%	132	64
Goseong	518	339	111	65.46%	21.43%	32.74%	145	135
Namhae	358	240	78	67.08%	21.91%	32.67%	204	168
Hadong	676	489	112	72.32%	16.52%	22.84%	86	130
Sancheong	795	618	97	77.81%	12.18%	15.65%	135	2
Hamyang	725	562	101	77.42%	13.86%	17.91%	83	54
Geochang	803	609	120	75.86%	14.96%	19.72%	28	16
Hapcheon	984	710	150	72.22%	15.25%	21.11%	179	171

Table 4. Dominant plant species and area per city

Cities	Total	Conifer (%)	Broad leaf (ha)	Mixed (ha)	Others (ha)
Changwon	42,968.99	15,383.95 (36)	5,341.88	22,232.95	10.22
Jinju	41,785.79	18,130.36 (43)	5,013.23	18,458.49	183.71
Tongyeong	15,542.25	11,182.00 (72)	437.46	3,922.79	-
Sacheon	23,130.13	10,548.60 (46)	2,498.19	9,918.65	164.69
Gimhae	23,675.28	8,512.61 (36)	3,953.39	11,168.23	41.06
Myrang	51,853.49	24,451.74 (47)	14,203.96	13,138.48	59.31
Geoje	28,335.29	12,566.58 (44)	4,957.47	10,701.35	109.90
Yangsan	36,223.15	7,450.41 (21)	19,022.67	9,691.97	58.10
Uiryeong	33,110.40	17,003.56 (51)	3,476.97	12,526.98	102.89
Haman	21,189.52	11,609.69 (55)	1,365.15	8,188.89	25.79
Changyeong	28,529.70	20,435.58 (72)	1,163.21	6,929.92	0.99
Goseong	33,888.65	20,314.60 (60)	3,054.70	10,459.09	60.26
Namhae	23,984.83	15,017.27 (63)	1,751.34	7,210.92	5.30
Hadong	48,851.59	18,161.36 (37)	15,318.61	14,717.24	654.37
Sancheog	61,844.62	29,131.06 (47)	23,179.32	9,195.35	338.90
Hamyang	56,165.10	30,794.38 (55)	17,428.49	7,917.56	24.67
Geochang	60,928.35	25,042.58 (41)	9,073.14	26,810.63	2.00
Hapcheon	71,028.71	29,443.23 (41)	8,585.18	32,815.41	184.89

The reason for the regional bias between 2012 and 2013 may have been a difference in the number of acorns dropped in the autumn between the two years. According to field sampling conducted during the last several years (from 2010 to 2015), there has been biased acorn fall between odd and even years, with odd years showing relatively low

acorn fall in autumn, while there was large acorn fall in the even years that might have provided sufficient food to support wild boars through the upcoming winter, spring and summer. Indeed, the large acorn fall in the autumn of 2012 might have allowed the wild boars to survive in the forest through the warmer seasons in 2013, which could have led to a lower frequency of farmland damage caused by the wild boar in 2013 (Fig. 7).

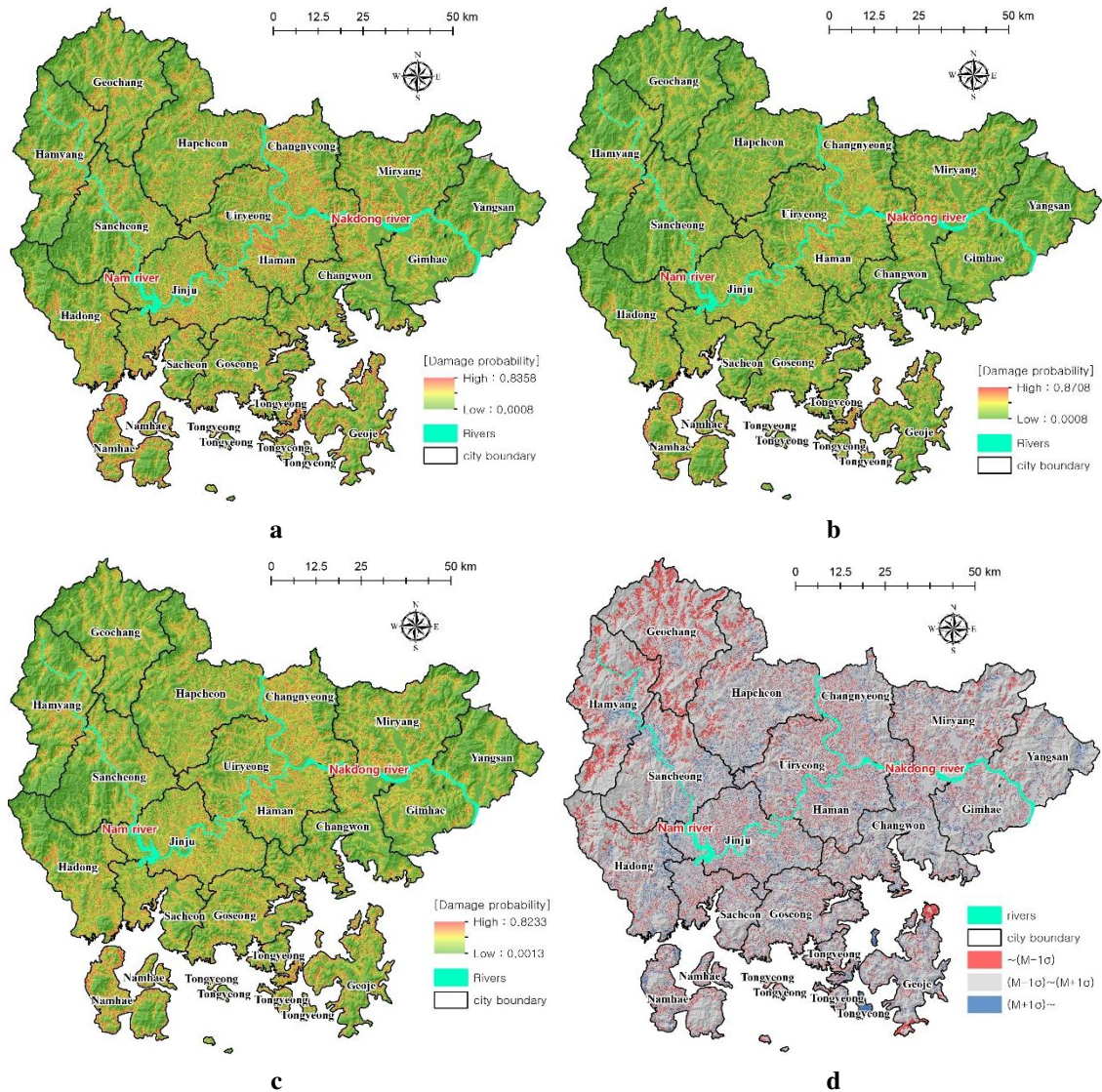


Figure 7. Predictions of farmland damage by wild boar using the Maxent model. (a) Prediction map for 2012. (b) Prediction map for 2013. (c) Prediction map for both years. (d) Difference in damage probability between 2012 and 2013 (M : mean, σ : Stdev.). The map was the prediction map in 2013 subtracted from the one in 2012

Conclusion

Sudden increase of wild boar population and the side effect on ecosystems and farmlands have emerged as a big concern in the South Korean society. Based on the Maxent modeling with AUC over 0.8, farmlands nearby forest boundaries were known to have the higher sensitivity to the farmland damage by wild boars rather than other

farms. It was assumed that indiscreet and unilateral development of forest edge areas, which has done during the last several decades, was responsible for abrupt and nationwide occurrence of farmland damages by wild boars over recent years.

According to the statistics and modelings on the farmland damage by wild boars, farmlands with root crops (i.e., potato and sweet potato) and rice close to forest boundaries were verified as the top priority targets to wild boars. This means that wild boars have not been recognizing the reduction of their habitat and/or the loss of common land between people and them in their forest territory. Ignorance of wild boars on the human occupation in farmlands would be finally sustainable cause of conflict between farmers and wild boars.

Recommendations

Modeling the damage sensitivity by wild boars nearby forest patches would be a good reference to understand wild life animals which have been making intensive interactions with people. As a large area of natural resource has been modified and/or changed into anthropocentric land uses, the conflict between people and wild life would much frequently happen from now on. Therefore, modeling and estimating process for understanding the behavior of wild life animals would be a mandatory progress, and it is the time to get the further study on the coexistence with wild life animals in natural resources.

Acknowledgement. This research was supported by Yeungnam University Research Grants in 2016.

REFERENCES

- [1] Alexiou, P. N. (1983): Effect of feral pigs (*Sus scrofa*) on subalpine vegetation at Smokers Gap, ACT. – Proceedings of the Ecological Society of Australia 12: 135-142.
- [2] Boitani, L., Mattei, L., Nonis, D., Corsi, F. (1994): Spatial and activity patterns of wild boars in Tuscany, Italy. – Journal of Mammalogy 75(3): 600-612.
- [3] Clements, F. E. (1904): Development and Structure of Vegetation. Report of the Botanical Survey of Nebraska. – The Woodruff-Collins Printing Company, Lincoln.
- [4] Elith, J., Graham, C. H., Anderson, R. P., Dudik, M., Ferrier, S., Guisan, A., Hijmans, R. J., Huettmann, F., Leathwick, J. R., Lehmann, A., Li, J., Lohmann, L. G., Loiselle, B. A., Manion, G., Moritz, C., Nakamura, M., Nakazawa, Y., Overton, J. M., Peterson, A. T., Phillips, S. J., Richardson, K., Scachetti-Pereira, R., Schapire, R. E., Soberón, J., Williams, S., Wisz, M. S., Zimmermann, N. E. (2006): Novel methods improve prediction of species' distributions from occurrence data. – Ecography 29(2): 129-151.
- [5] Fielding, A. H., Bell, J. F. (1997): A review of methods for the assessment of prediction errors in conservation presence/absence models. – Environmental Conservation 24(1): 38-49.
- [6] Friston, K. J., Holmes, A. P., Worsley, K. J., Poline, J. B., Frith, C. D., Frackowiak, R. S. J. (1995): Statistical parametric maps in functional imaging: A general linear approach. – Human Brain Mapping 2(4): 189-210.
- [7] Fu, P., Rich, P. M. (2002): A geometric solar radiation model with applications in agriculture and forestry. – Computers and Electronics in Agriculture 37(1-3): 25-35.
- [8] Gormley, A. M., Forsyth, D. M., Griffioen, P., Lindeman, M., Ramsey, D. S. L., Scroggie, M. P., Woodford, L. (2011): Using presence-only and presence-absence data to

- estimate the current and potential distributions of established invasive species. – *Journal of Applied Ecology* 48(1): 25-34.
- [9] Groot Bruinderink, G. W. T. A., Hazebroek, E. (1996): Wild boar (*Sus scrofa scrofa* L.) rooting and forest regeneration on podzolic soils in the Netherlands. – *Forest Ecology and Management* 88(1-2): 71-80.
- [10] Guisan, A., Zimmermann, N. E. (2000): Predictive habitat distribution models in ecology. – *Ecological Modeling* 135(2-3): 147-186.
- [11] Guisan, A., Edwards, T. C., Hastie, T. (2002): Generalized linear and generalized additive models in studies of species distributions: setting the scene. – *Ecological Modeling* 157(2-3): 89-100.
- [12] Herrero, J., Fernández de Luco, D. (2003): Wild boars in Uruguay: scavengers or predators? – *Mammalia* 67(4): 485–492.
- [13] Herrero, J., García-Serrano, A., Couto, S., Ortuño, V. M., García-González, R. (2006): Diet of wild boar *Sus scrofa* L. and crop damage in an intensive agroecosystem. – *European Journal of Wildlife Research* 52(4): 245-250.
- [14] Kim, J. Y., Seo, C. W., Kwon, H. S., Ryu, J. E., Kim, M. J. (2012): A study on the species distribution modeling using national ecosystem survey data. – *Environmental Impact Assessment* 21(4): 593-607.
- [15] Kim, W. J., Park, C. H., Kim, W. M. (1998): Development of habitat suitability analysis models for wild boar (*Sus scrofa*): A case study of Mt. Sulak and Mt. Jumbong. – *Journal of Korean Society for Geospatial Information System* 16(4): 59-64.
- [16] Kim, Y. K., Hong, Y. J., Min, M. S., Kim, K. S., Kim, Y. J., Voloshina, I., Myslenkov, A., Smith, G. J. D., Cuong, N. D., Tho, H. H., Han, S. H., Yang, D. H., Kim, C. B., Lee, H. (2011): Genetic status of asiatic black bear (*Ursus thibetanus*) reintroduced into South Korea Based on mitochondrial DNA and microsatellite loci analysis. – *Journal of Heredity* 102(2): 165-174.
- [17] Kwon, H. S., Kim, B. J., Jang, G. S. (2016): Modelling the spatial distribution of wildlife animals using presence and absence data. – *Contemporary Problems of Ecology* 9(5): 515-528.
- [18] Lee, M. Y., Hyun, J. Y., Lee, S. J., An, J., Lee, E., Min, M. S., Kimura, J., Kawada, S., Kurihara, N., Luo, S. J., O'Brien, S. J., Johnson, W. E., Lee, H. (2012): Subspecific status of the Korean tiger inferred by the ancient DNA analysis. – *Animal Systematics, Evolution and Diversity* 28(1): 48-53.
- [19] Lee, S. M., Lee, W. S. (2014): Diet of the wild boar (*Sus scrofa*) in agricultural land of Geochang, Gyeongnam Province, Korea. – *The Korea Forest Society* 103(2): 307-312 (in Korean with English abstract).
- [20] Massei, G., Genov, P. V. (2004): The environmental impact of wild boar. – *Galemys* 16: 135-145.
- [21] McCollin, D. (1998): Forest edges and habitat selection in birds: a functional approach. – *Ecography* 21(3): 247-260.
- [22] McCullagh, P., Nelder, J. A. (1989): *Generalized Linear Models*. – Chapman & Hall, London.
- [23] Myser, R. W. (2012): *Ecotones between Forest and Grassland* – Springer, New York.
- [24] Olson, G. S., Glenn, E. M., Anthony, R. G., Forsman, E. D., Reid, J. A., Loschl, P. J., Ripple, W. J. (2004): Modeling demographic performance of northern spotted owls relative to forest habitat in Oregon. – *Journal of Wildlife Management* 68(4): 1039-1053.
- [25] Pavlov, P. M., Hone, J., Kilgour, R. J., Pedersen, H. (1981): Predation by feral pigs on Merino lambs at Nyngan, New South Wales. – *Australian Journal of Experimental Agriculture and Animal Husbandry* 21: 570–574.
- [26] Peracino, V., Bassano, B. (1995): The wild boar (*Sus scrofa*) in the Gran Paradiso National Park (Italy): presence and distribution. – *Journal of Mountain Ecology* 3: 145-146.

- [27] Phillips, S. J., Anderson, R. P., Schapire, R. E. (2006): Maximum entropy modeling of species geographic distributions. – *Ecological Modelling* 190(3-4): 231-259.
- [28] Polpus, J. L., Hebblewhite, M., Heinemeyer, K. (2011): Identifying indirect habitat loss and avoidance of human infrastructure by northern mountain woodland caribou. – *Biological Conservation* 144(11): 2637-2646.
- [29] Schley, L., Dufrene, M., Kier, A., Frantz, A. C. (2008): Patterns of crop damage by wild boar (*Sus scrofa*) in Luxembourg over a 10-year period. – *European Journal of Wildlife Research* 54(4): 589-599.
- [30] Scott, J. M., Heglund, P. J., Samson, F., Haufler, J., Morrison, M., Raphael, M., Wall, B. (2002): *Predicting Species Occurrences: Issues of Accuracy and Scale*. – Island Press, Covelo.
- [31] Seo, C. W., Park, C. H. (2000): Wild Boar (*Sus scrofa coreanus* Heude) habitat modeling using GIS and logistic regression. – *Korean Journal of Geographic Information System* 6(2): 247-256.
- [32] Smith, T. B. Wayne, R. K., Girman, D. J., Bruford, M. W. (1997): A role for ecotones in generating rainforest biodiversity. – *Science* 276: 1855–1857.
- [33] Song, W. K., Kim, E. Y. (2012): A comparison of machine learning species distribution methods for habitat analysis of the Korea water deer (*Hydropotes inermis argyropus*). – *Korean Journal of Remote Sensing* 28(1): 171-180.
- [34] Swets, J. A. (1988): Measuring the accuracy of diagnostic systems. – *Science* 240(4857): 1285-1293.
- [35] Yackulic, C. B., Chandler, R., Zipkin, E. F., Royle, J. A., Nichols, J. D., Grant, E. H. C., Veran, S. (2013): Presence-only modelling using MAXENT: When can we trust the inferences? – *Methods in Ecology and Evolution* 4(3): 236-243.

EXPLORING NATURAL VARIATION OF ROOT ARCHITECTURAL TRAITS IN SEEDLINGS OF MAIZE HYBRID AND INBRED LINES FROM THAILAND

SALUNGYU, J.¹ – KENGGANNA, J.¹ – LAVOY, W.¹ – SAENGWILAI, P.^{1,2*}

¹*Department of Biology, Faculty of Science, Mahidol University
Bangkok 10400, Thailand*

²*Center of Excellence on Environmental Health and Toxicology (EHT), Faculty of Science,
Mahidol University, Bangkok 10400, Thailand*

**Corresponding author
e-mail: patompong.sae@mahidol.edu*

(Received 18th Sep 2017; accepted 12th Jan 2018)

Abstract. Root architectural traits refer to a spatial configuration of the root system providing a critical role in soil resource acquisition. In past decades, several lines of evidence have shown that maize possesses large phenotypic variations, including root architecture closely relating to physiological utility. Thailand has developed a unique maize germplasm over the years; however, root traits have often been neglected and have yet to be explored. In this present study, we examined natural variation of root architectural traits of twenty-eight inbred and hybrid lines at the seedling stage using a well-established roll-up culture system. We found that variation in root traits ranged from 4.22-fold in primary roots to 13.14-fold in seminal root length, while shoot mass presented the highest phenotypic variation among traits (23.42-fold). Most root architectural traits of maize hybrid lines were significantly higher than the inbred lines, particularly, seminal root length, which was 34.30% greater than that of inbred lines. In addition, we found that root traits, like other agronomic traits, express heterosis. Our findings suggest ample opportunity for incorporating root traits in maize breeding program in Thailand.

Keywords: *maize, hybrid, breeding, seminal roots, roll-up*

Introduction

Maize (*Zea mays* L.) is the world's most widely grown crop and is used as a staple food source, especially in Latin America and Africa. It has been estimated that within a decade, the global demand for maize will surpass other cereal crops (Ranum et al., 2014; Reynolds et al., 2015). This poses a challenge to maize breeders and farmers who must increase maize production. While developing nations are struggling with limited resources and inadequate accessibility to technologies, rich nations have applied excessive amount of fertilizers leading to substantial pollution of air and water resources (Tilman et al., 2002). In Thailand, maize is one of five prominent crops grown in the highlands. The Thai government has long supported the expansion of maize farming areas and the improvement of varieties to withstand various environmental conditions (Ekasingh et al., 2014). The 3 most popular hybrid maize varieties cultured in Thailand are Nakhon Sawan 3, NSX 052014 and NSX 111044 (Butthong et al., 2014). These genotypes produce high yields and are able to tolerate drought conditions (Butthong et al., 2014). Nevertheless, Thai maize production was reduced by 17.69% in the past decade (Pipitkul et al., 2015). The reductions in maize yield is primarily attributed to drought (Pipitkul et al., 2015). Not only is the increase in maize production

necessary, but it will require substantial changes in agronomic practices and methods for crop improvement.

Plant root system plays important role in plant growth, resource allocation, and acquisition of water and nutrients from soil. Therefore, improving plant roots could lead to increased crop productivity (Lynch, 2007). The maize root system consists of two components: the embryonic and post embryonic root system. The embryonic root system is formed during embryogenesis and it is composed of a primary root and a variable number of seminal roots. The postembryonic root system is formed during postembryonic development and it is composed of shoot borne roots and lateral roots that originate in the pericycle of other root types. Shoot borne roots formed below the soil level are referred to as crown roots, while those formed aboveground are designated as brace roots (Bennetzen et al., 2009). Identification of relevant root traits is essential for plant breeders in crop improvement programs. The goals of root breeding are to help soil exploration and effective use of water and nutrients, while also maintaining growth and crop productivity. Lynch (2013) proposed an ideotype of maize root systems for higher acquisition of water and nitrogen called “Steep, Cheap, and Deep”. A primary root with a large diameter and few long lateral roots was proposed as ideal characteristics for deeper rooting and greater access to water and nitrate residing deep in the soil strata under drought and low nitrogen conditions (Lynch, 2013). Crown root system with a low amount of crown root and few long lateral roots is suggested as the primary trait for enhancing water acquisition. Moreover, seminal roots with shallow root angles, a small diameter, high lateral root density and long root hairs are suitable for phosphorus and potassium uptake, while long and low lateral root density are optimal for nitrogen and water acquisition (Postma et al., 2014). Anatomical traits also play important roles in improving water and nitrogen use efficiency in maize. Root cortical aerenchyma (RCA), tissues with large intercellular spaces, reduces root respiration and allows deeper rooting in the subsoil (Zhu et al., 2010). Several studies confirmed that high RCA maize varieties are able to tolerate and improve their growth under stressful conditions such as low nitrogen soil and drought (Zhu et al., 2010; Saengwilai et al., 2014a).

For crop selection and plant breeding purposes, the evaluation of root traits of a large number of mature plants in the field may not always be practical. Since seedlings with beneficial root traits could subsequently develop a more vigorous root system, resulting in more biomass and yield (Bocev, 1963), researchers are turning toward identification of root characteristics in plant seedlings that are associated with adaptation of mature plants in the field. For examples, Thomas et al. (2016) demonstrated that *Brassica napus* with long primary root length identified in 2-week-old seedlings in a pouch system was correlated with shoot mass ($r = 0.49$, $p < 0.001$) and yield ($r = 0.50$, $p < 0.01$) of plants in the field (Thomas et al., 2016). In maize, Tuberosa et al. (2002) showed that there were significant negative correlations between seminal root weight and primary root diameter of 21-day-old seedlings grown in hydroponics and grain yield in mature plants in the field under drought conditions (Tuberosa et al., 2002). In addition, root traits measured at the seedling stage such as primary root length, number of crown roots, number of seminal roots, number of lateral roots, fresh root weight, and dry root weight were shown to have high heritability under normal and drought conditions and thus seedling root traits can be improved through selection and breeding (Qayyum et al., 2012).

Maize breeders often develop hybrids to benefit from heterosis, which is defined as the superior performance of an F1 hybrid compared with the performance of the inbred parents (Hoecker et al., 2006; Bennetzen et al., 2009). The phenomenon of heterosis in maize has been well described not only for shoot traits and yield, but also for root traits including primary root length, primary root width, lateral root density and longitudinal size of cortical cell (Hoecker et al., 2006). For example, F1 hybrids developed from a cross between UH250xUH301 had 110% greater lateral root density compared to their parents at 5 days after germination (DAG) while seminal root number of hybrids were 55.56% greater than the parents at 14 DAG (Hoecker et al., 2006). To benefit from heterosis, breeders combine the heterotic groups while inbred lines are kept and selected separately within these groups. In Thailand, there is a lack of knowledge on root traits of inbred and hybrid maize lines currently used in the breeding program, therefore, the information of phenotypic variation and heterosis of root traits are required for the development of breeding program targeting root traits. In this study, we aimed (1) to explore phenotypic variation of root architectural traits among twenty-eight Thai maize lines during seedling stage. We also (2) compared root architectural traits between Thai maize inbred and hybrid lines, and (3) investigated possible correlations among root architectural traits.

Materials and methods

Plant materials

Twenty-eight Thai maize lines were used to perform the experiment. These lines consisted of 6 inbred lines from the National Research Centre of Millet and Corn (Suwan Farm), and 12 inbred and 10 hybrid lines from Nakhon Sawan Field Crops Research Center (NSFCRC). Among the hybrid lines, NS2 is derived from a cross between Tak Fa 1 and 2 while NS3 is from Tak Fa1 and 3 (*Table 1*).

Roll-up paper culture system

The roll-up paper culture system was prepared according to the protocol described by Zhu et al. (2006). Specifically, seeds were sterilized in 10% (v/v) NaOCl for 1 min followed by soaking with distilled water. The experiment was a randomized complete block design with four replicates. In each replicate, five seeds of uniform size for each maize line were selected and were wrapped in brown germination paper as a cigar roll. The roll-up papers were soaked vertically with 0.5 mM CaSO₄ in beakers and placed in darkness at 28±1°C for 3 days (Saengwilai et al., 2014b). The seedlings were then grown under a photoperiod of 12/12 h with photosynthetically active radiation of 200 μmol photo m⁻²s⁻¹. Roots and shoots were evaluated at 7 days after germinating.

Root trait measurement

At harvest, two plants per line in each replication were selected and then shoots were separated from the roots. To evaluate root architectural traits including primary root length, seminal root number and seminal root length, the roots were scanned by using Epson Perfection V800 Photo Color Scanner (Epson America, Inc. Company). The root images were analyzed by ImageJ program (Schindelin et al., 2013). Lateral root numbers were counted using ImageJ program, while lateral root density was determined by calculating lateral root number per 1 centimetre of primary root length. Moreover,

both shoots and roots from each line were dried at 60 °C for 48 h and then weighed by microbalance.

Statistical analysis

Statistical analyses were performed using package R, version 3.4.1 (R Core Team, 2017). One and Two-way ANOVA was used to evaluate phenotypic differences within the inbred and hybrid lines and between these two groups for all traits. Tukey's Honest Significant Difference (HSD) test ($\alpha = 0.05$) was used for multiple comparison tests. A correlation analysis was performed on corresponding traits using the mean values of the traits. A principal component analysis (PCA) was performed within each group. The first two components were characterized based on variable eigenvalues and on vector clustering within plots of components 1 and 2.

Results

Phenotypic variation of Thai maize root traits in seedling stage

Twenty-eight Thai maize lines were planted in a roll-up system to investigate root architectural traits during the seedling stage (*Fig. 1*). Maize lines were grouped based on individual descent, composing of 18 inbred and 10 hybrid lines. The range of all of the values was examined to determine the variation of each root architectural trait. Significant variations of root architectural traits are presented in *Table 1*. Among root traits, primary root length had the lowest range of variation, while seminal root length had the greatest variation. However, when comparing ranges among all traits, shoot mass had the highest phenotypic variation of 23.42-fold difference.

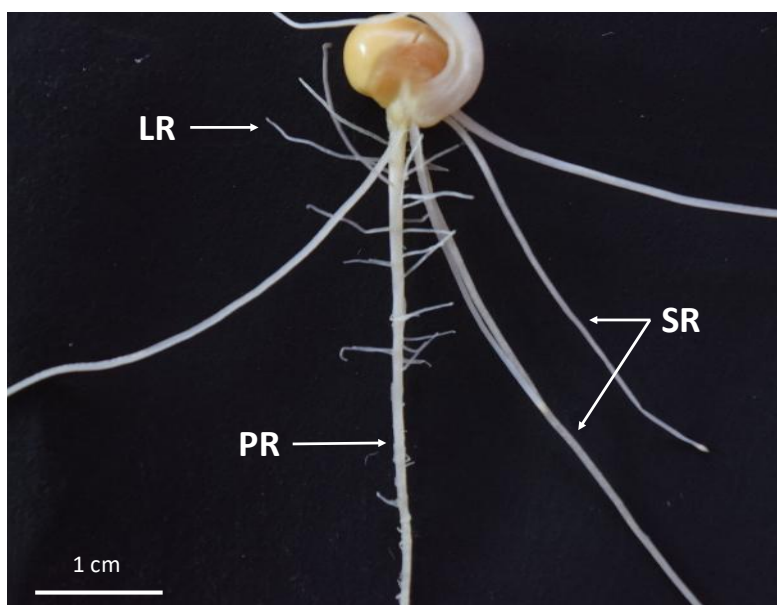


Figure 1. Root system of a 7-day-old maize seedling showing a primary root (PR), seminal roots (SR), and lateral roots (LR)

SW14D-C5 1039-60 Ki60 appeared to have higher overall values of root architectural traits such as total seminal root number and lateral root density among inbred lines

(Table 1). This line also had the greatest shoot mass and dry mass compared to other inbred lines. Among hybrid lines, NSX 102005 had the highest primary root length (21.74 ± 0.62 cm), while NSX 042022 had the highest total seminal root number (5.38 ± 0.18), lateral root density (5.92 ± 0.58 roots/1 cm of primary root) and shoot mass (0.077 ± 0.040 g). Comparing root traits of NS3 with its parents Tak Fa 1 and Tak Fa 3, we found that most of root architectural traits express heterosis except root mass which was not significant among the lines (Table 1).

Table 1. Phenotypic variation of Thai maize root traits in seedling stage. Root traits including PRL; Primary root length (cm), TSN; Total seminal root number (roots), SRL; Seminal root length (cm) and LRD; Lateral root density (roots per 1 cm of primary root) were quantified. SM; Shoot mass (g) and Root mass (g) were also investigated

Lines	Root traits						Type
	PRL	TSN	SRL	LRD	RM	SM	
SW14D-C5 1039-3 Ki3	16.96 ±0.89	3.13 ±0.40	8.90 ±0.39	1.71 ±0.26	0.15 ±12.07	0.026 ±0.002	Inbred
SW14D-C5 1039-11 Ki11	12.80 ±1.17	3.38 ±0.46	8.89 ±0.84	3.25 ±0.38	0.15 ±12.34	0.032 ±0.003	Inbred
SW14D-C5 1039-21 Ki21	17.66 ±0.89	3.50 ±0.19	15.05 ±0.96	4.13 ±0.89	0.23 ±9.13	0.031 ±0.002	Inbred
SW14D-C5 1039-48 Ki48	20.26 ±0.70	4.88 ±0.23	14.89 ±0.59	3.25 ±0.33	0.16 ±11.38	0.030 ±0.002	Inbred
SW15D-B5 1006-20 Ki53	17.59 ±0.70	3.38 ±0.32	8.82 ±0.67	4.67 ±0.58	0.24 ±9.05	0.026 ±0.001	Inbred
SW14D-C5 1039-60 Ki60	17.75 ±1.40	5.13 ±0.35	13.95 ±0.87	6.08 ±0.29	0.25 ±8.76	0.037 ±0.002	Inbred
Nei 452006	17.21 ±1.00	4.25 ±0.25	10.71 ±0.86	5.29 ±0.39	0.15 ±12.00	0.030 ±0.001	Inbred
Nei 452007-1	15.91 ±0.85	3.75 ±0.37	11.73 ±0.83	4.58 ±0.80	0.13 ±13.48	0.025 ±0.002	Inbred
Nei 452009	15.04 ±0.72	3.63 ±0.32	9.29 ±0.79	3.21 ±0.42	0.14 ±9.60	0.035 ±0.003	Inbred
Nei 462013	15.14 ±1.44	3.88 ±0.30	9.59 ±1.28	0.79 ±0.21	0.18 ±10.76	0.026 ±0.001	Inbred
Nei 532005	16.78 ±1.35	3.00 ±0.33	7.51 ±0.51	2.92 ±0.61	0.17 ±10.93	0.025 ±0.002	Inbred
Nei 542011	16.35 ±0.85	1.88 ±0.35	8.18 ±1.62	3.79 ±0.19	0.17 ±11.29	0.024 ±0.002	Inbred
Nei 542014	15.15 ±0.30	3.00 ±0	11.93 ±0.86	4.17 ±0.57	0.14 ±12.55	0.027 ±0.001	Inbred
Nei 542017	15.14 ±1.25	3.38 ±0.32	13.56 ±0.55	6.08 ±0.30	0.14 ±12.72	0.025 ±0.001	Inbred
Nei 542019	15.87 ±1.50	3.13 ±0.23	13.86 ±0.89	3.92 ±0.68	0.13 ±13.15	0.023 ±0.001	Inbred
Tak Fa 1	17.52 ±0.85	4.00 ±0.27	12.33 ±0.87	5.33 ±0.41	0.15 ±12.28	0.031 ±0.002	Inbred
Tak Fa 2	14.41 ±0.89	1.25 ±0.53	5.66 ±1.50	3.29 ±0.65	0.14 ±12.80	0.019 ±0.003	Inbred
Tak Fa 3	13.78 ±1.49	4.63 ±0.32	9.76 ±1.24	2.58 ±0.43	0.15 ±11.98	0.034 ±0.002	Inbred
NSX 042007	21.11 ±0.50	5.00 ±0.46	16.76 ±0.85	4.63 ±0.30	0.14 ±12.84	0.036 ±0.002	Hybrid
NSX 042022	20.48 ±0.51	5.38 ±0.18	15.96 ±0.71	5.92 ±0.58	0.13 ±13.07	0.077 ±0.040	Hybrid
NSX 052014	21.22 ±0.77	5.38 ±0.26	18.33 ±0.93	3.38 ±0.15	0.21 ±9.78	0.046 ±0.002	Hybrid
NSX 102005	21.74 ±0.62	4.75 ±0.41	17.51 ±1.2	5.92 ±0.25	0.16 ±11.71	0.041 ±0.004	Hybrid
NSX 112011	13.78 ±0.47	4.71 ±0.89	11.97 ±0.82	2.13 ±0.43	0.17 ±8.50	0.027 ±0	Hybrid
NSK 112014	21.29 ±0.34	5.13 ±0.23	17.40 ±0.84	4.83 ±0.60	0.19 ±10.4	0.050 ±0.002	Hybrid
NSX 112017	20.84 ±0.58	4.50 ±0.19	17.49 ±1.00	5.92 ±0.42	0.14 ±12.83	0.032 ±0.002	Hybrid
NSX 112019	21.69 ±0.39	4.75 ±0.25	20.54 ±0.45	4.83 ±0.36	0.11 ±14.78	0.037 ±0.001	Hybrid
NS 2	21.25 ±0.75	4.00 ±0.45	9.99 ±3.79	3.83 ±1.50	0.18 ±8.08	0.022 ±0.014	Hybrid
NS 3	22.29 ±0.67	5.25 ±0.37	18.03 ±1.22	5.50 ±0.39	0.14 ±12.64	0.050 ±0.001	Hybrid
Mean	17.71	4	12.93	4.2	0.16	0.03	
Standard error	0.25	0.092	0.315	0.124	0.002	0.001	
Range	4.22	9	13.14	9	3.65	23.42	
F-value of variability	9.198***	8.793***	13.170***	8.256***	6.319***	2.100**	
Degree of freedom	27	27	27	27	27	27	
Mean square	63.42	8.641	116.49	15.04	0.005	0.001	

***, **, * indicated significant level at $p < 0.001$, $p < 0.01$, $p < 0.05$. All traits varied significantly within each population

Comparing root and shoot traits between maize inbred and hybrid lines

We found that root traits of hybrid lines are significantly different from those of inbred lines (Fig. 2). Primary root length of hybrid lines was 22.18% greater than that of inbred lines. This trend remained consistent with seminal root traits, lateral root traits and shoot mass. Hybrid lines had greater seminal root length and seminal root number by 34.30% and 28.56% respectively compared to inbred lines. Lateral root density of maize hybrid lines was 21.20% higher when compared with inbred lines. In addition, shoot mass of hybrid lines was greater than inbred lines by 33.65%. Interestingly, an average root mass of hybrid lines was not significantly different from inbred varieties.

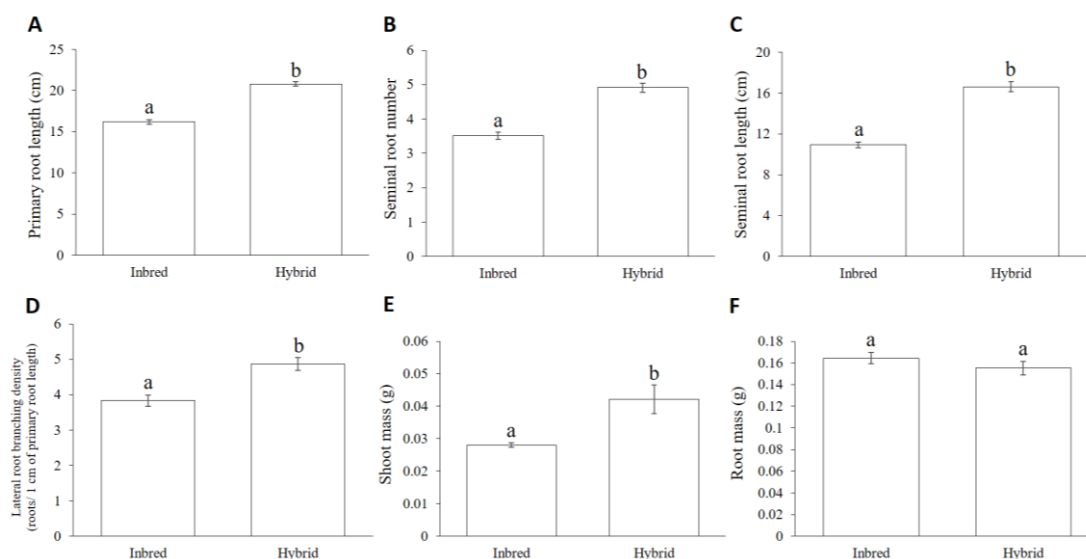


Figure 2. Phenotypic variation of Thai maize root traits in seedling stage comparing between inbred and hybrid lines using Tukey's HSD. Root traits including PRL; Primary root length, TSN; Total seminal root number, SRL; Seminal root length and LRD; Lateral root density were quantified. SM; Shoot mass and Root mass were also investigated. The data shown are means of four replicates \pm SE. Different letters represent significant differences ($P < 0.05$). All traits varied significantly within each group

Correlations among root traits and principal component analysis

We further investigated correlations among traits. We found that primary root length was highly correlated with seminal and lateral root traits. As shown in Table 2, primary root length correlated with seminal root length ($r^2 = 0.74$). Additionally, primary root length had a significant positive correlation with shoot mass ($r^2 = 0.52$). Within the seminal root class, seminal root length correlated with total seminal root number ($r^2 = 0.47$) and lateral root density on seminal roots ($r^2 = 0.42$). Interestingly, seminal root length highly correlated with shoot mass ($r^2 = 0.58$).

Principal component analysis (PCA) of root architectural traits and root biomass were performed separately on Thai maize inbred and hybrid lines. For inbred lines, principal component 1 (PC1) and PC2 contributed 67.3% of the total variation in plant traits (Fig. 3A). While, the first two components of hybrid lines accounted for 74.7% of the total variation (Fig. 3B). Root architectural traits, such as primary root length, seminal root length, seminal root number, and lateral root density of inbred lines

strongly associated with PC1. Similarly, primary root length, seminal root length, and lateral root density of hybrid lines were also heavily involved in PC1 (Fig. 3B). Seminal root length appeared to be a major contributor to PC1 in both inbred and hybrid group. While, seminal root number was a major contributor to PC2 in hybrid lines, and root mass contributing heavily to PC2 among maize inbred lines.

Table 2. Correlation of root and physiological traits of seedling among 28 Thai maize lines at 7 DAP in roll-up system. PRL; Primary root length, TSN; Total seminal root number, SRL; Seminal root length and LRD; Lateral root density, SM; Shoot mass and Root mass were also investigated

TSN	0.43***				
SRL	0.74***	0.47***			
LRD	0.39***	0.22**	0.42***		
SM	0.52***	0.48***	0.58***	0.30**	
RM	-0.074	-0.04	-0.13	-0.16*	-0.019
	PRL	TSN	SRL	LRD	SM

***, **, * indicated significant level at $p < 0.001$, $p < 0.01$, $p < 0.05$ as Spearman's principle correlation. All traits varied significantly within each population

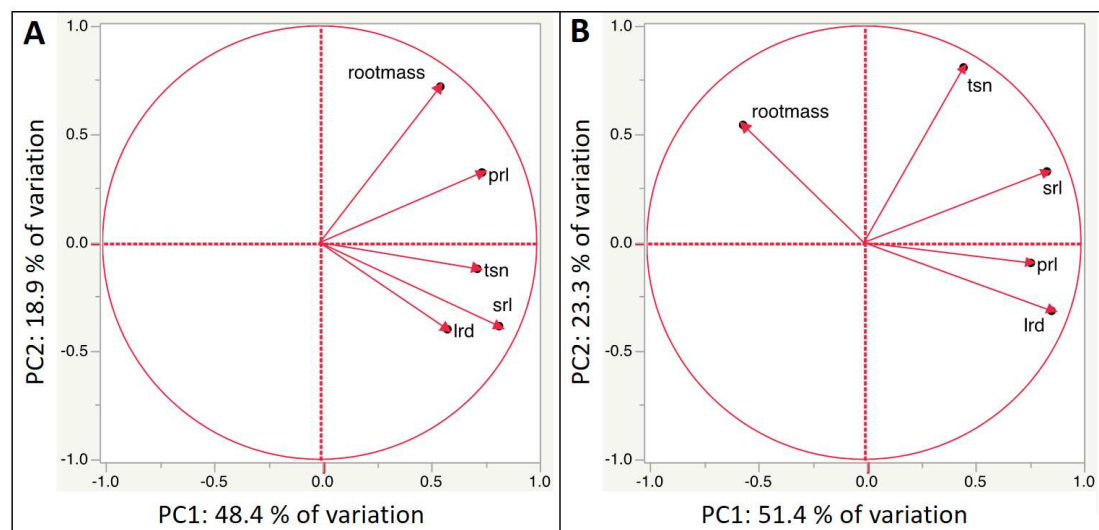


Figure 3. Biplots of principal component 1 and 2 of root architectural traits and root biomass in Thai maize inbred (A) and hybrid lines (B). The x and y axes are components 1 and 2, respectively. Axis labels include the percentage of variation explained by each of these two components

Discussion

From the beginning of maize domestication shoot traits have been the main focus for crop improvement. The below-ground part, roots, have often been neglected or indirectly selected despite their importance for water and nutrient acquisition. During the past decades, several lines of evidence have shown that variation in root traits largely influences adaptation of maize in the field. (Hufford et al., 2012; York et al., 2015). Therefore, root traits have increasingly become a target for maize improvement

worldwide. The results of the present study show that Thai maize lines exhibit a large natural variation of root traits relating to their abilities in water and nutrient uptake.

Root system of plant seedlings play an important role in plant establishment and thus influence the likelihood of survival to reproduction (Tuberosa et al., 2009). The variation of root number, length, and branching of seedling roots have been shown to be associated with maize adaptation to edaphic stresses. In our study, we found that maize lines were significantly different in their root traits, particularly, seminal roots. The range of seminal root length found among hybrid Thai maize lines (9.9-20.5) fell within the same range as those from seventy-five B73×Gaspé Flint introgression library (8.8-29.3) grown in the same roll up system (Salvi et al., 2016). Interestingly, Thai maize had greater range of seminal root number (4.0-5.4) compared to the 75 hybrid lines (0.2-3.7) studied by Salvi et al. (2016). Seminal root traits can vary depending on genetic background of each line (Hochholdinger et al., 2004a; Hochholdinger et al., 2004b; Hochholdinger et al., 2005). Environmental factors may increase seminal root number especially when nutrient limitation such as phosphorus occurs (Zhu et al., 2006). Having high plasticity in both length and number in response to the environment, seminal roots play a large role in soil exploration, and therefore, are critical for plant's establishment and could serve as a great target trait for maize improvement (Richards, 2006; Zhu et al., 2006; Lynch, 2013).

Correlation analysis indicated that most root traits positively correlated amongst each other, with root mass as an exception only significantly correlating with lateral root density. Previous studies have already shown that an enlarged root system through the alteration of root length, density and root mass is beneficial for nitrogen and water acquisition (Ehdaie et al., 2010; Palta et al., 2011). Root mass is an integrated trait which reflects plant's carbon investment to the whole root structure. In terms of carbon investment, having a large root mass may be detrimental to plants under drought or suboptimal nutrient conditions. The competition between roots and shoots for photosynthates may result in overall reduction in growth rate and yield. The formation of large root systems incurs a high carbon cost. To survive in a depriving environment, genotypes with root traits enhancing soil exploration with minimal carbon investment are the most competitive (Lynch, 2005). Among maize root architectural traits, lateral roots are considered carbon efficient because they are smaller in diameter, have lower carbon investment than main axis roots, and are crucial for nutrient exploration in both topsoil and subsoil layers (Lynch, 2013). We found that plants with low root weight tended to have dense lateral root density such as Nei 452007-1 and Nei 542017. Compared to primary and seminal roots which are axial roots determined by genetic inheritance, lateral roots are the only root class that can be formed at the pericycle layer in every root class, and respond to unfavourable environments such as phosphorus deficiency (Lynch et al., 2005; Bennetzen et al., 2009). Therefore, carbon resources of the plant might be translocated to optimize nutrient acquisition by altering their lateral root numbers.

We found that hybrid maize had greater root length and number than inbred maize. This is consistent with other studies (Hoecker et al., 2006; Chairi et al., 2016). With a detailed observation, we found that root traits, like other agronomic traits, express heterosis as evidenced by the observation of root traits of NS3 and its parents, Tak Fa 1 and Tak Fa 3. Heterosis refers to the performance of the hybrid F1 generation that exhibits phenotypic traits above the average of the two parents in regards to viability, development, and production (Tollenaar et al., 2004; Chairi et al., 2016). Heterosis of

hybrid lines has been shown to improve agronomic traits of maize (Springer et al., 2007; Garcia et al., 2008; Liu et al., 2013; Thiemann et al., 2014). For example, F1 hybrids developed from a cross between B73 and Mo17, had greater ear length, height, seed weight (g/ear), and 11 DAP seedling biomass by 48.3%, 21.8%, 101.7%, and 69.0% respectively (Auger et al., 2005). Additionally, the B73xMo17 hybrids further demonstrated heterosis with an increase of yields (mg/ha) by 64.7% (Zanoni et al., 1989). However, the quantitative measurements of heterosis varies significantly among traits and hybrid lines (Springer et al., 2007). Several studies have been carried out in order to attempt to explain the promising genetic principle of heterosis. The high vigor of hybrids over inbred lines has been shown to be contributed by many genes (Birchler et al., 2003; 2006; Hoecker et al., 2006; Liu et al., 2013). Among different root traits, root mass of NS3 did not show heterosis and was not significantly different from those of its parents. This result suggests despite being highly genetically dependant, breeding techniques that target root mass may be more complicated than initially thought. More research on heterosis of root traits is needed in order to successfully implement root traits of hybrid lines in a plant breeding program.

In the past decade, root traits of seedlings have been subjected to quantitative trait loci (QTL) studies and several significant QTL have been identified. For examples, Zhu et al. (2006) reported several QTLs for seminal root length and number of maize seedlings of the IBM population under high and low phosphorus conditions. The identified QTLs were on chromosomes 1, 2, 3 under high phosphorus and on chromosomes 1, 2, 6 under phosphorus deficiency (Zhu et al., 2006). Furthermore, Burton et al. (2014) reported 15 QTLs controlling length of multiple root classes, diameter and number of seminal roots, and dry weight of embryonic and nodal root systems of 28-day-old maize seedlings (Burton et al., 2014). The identification of QTLs associated with seedling root traits makes it possible to target root traits by marker assisted selection during breeding (Tuberosa et al., 2002; Hochholdinger et al., 2004b; Hochholdinger et al., 2008).

Conclusions

It has been shown that variation of root traits in maize influences water and nutrient acquisition under fertile and resource-limiting conditions (Chimungu et al., 2014a; 2014b; Saengwilai et al., 2014a; 2014b; Gao et al., 2016). This study demonstrates that Thai maize possesses phenotypic differences in root architectural traits and reveal potential donors for plant breeding targeting root traits such as SW14D-C5 1039-48 Ki48 for long primary and seminal root length and Nei 542017 for increased lateral root density. Since evaluation of root traits from mature field-grown plants are often laborious, time-consuming and destructive, screening for root traits in plant seedlings provides a more feasible option for breeders because a large number of genotypes can be evaluated in a relatively short period of time. Further studies are underway to investigate levels of plasticity among root traits in response to environmental stresses and transitioning of root traits from seedlings in the roll-up system to the field.

Acknowledgements. We thank Dr. Sansern Jampatong from National Research Centre of Millet and Corn (Suwan Farm) and and Mr. Suriphat Thaitad from Nakhon Sawan Field Crops Research Center (NSFCRC) for Thai maize lines seed supply and advice. This research project is supported by Mahidol University.

REFERENCES

- [1] Auger, D. L., Gray, A. D., Ream, T. S., Kato, A., Coe, E. H., Birchler, J. A. (2005): Non additive gene expression in diploid and triploid hybrids of maize. – *Genetics* 169: 389–397.
- [2] Bennetzen, J., Hake, S., Hochholdinger, F. (2009): *Handbook of Maize: Its Biology*. – Springer Science, New York.
- [3] Birchler, J. A., Auger, D. L., Riddle, N. C. (2003): In search of the molecular basis of heterosis. – *The Plant Cell* 15(10): 2236–2239.
- [4] Birchler, J. A., Yao, H., Chudalayandi, S. (2006): Unraveling the genetic basis of hybrid vigor. – *Proceedings of the National Academy of Sciences of the United States of America* 103(35): 12957–12958.
- [5] Bocev, B. (1963): Maize selection at an initial phase of development. – *Crop Science* 1(54): 179–182.
- [6] Burton, A. L., Johnson, J. M., Foerster, J. M., Hirsch, C. N., Buell, C. R., Hanlon, M. T., Kaeppler, S. M., Brown, K. M., Lynch, J. P. (2014): QTL mapping and phenotypic variation for root architectural traits in maize (*Zea mays* L.). – *Theoretical and Applied Genetics* 127(11): 2293–2311.
- [7] Butthong, T., Thaitad, S., Krutloima, P., Wongsupthai, S., Chaitawon, C., Tiampeng, P., Malipan, A., Seangkao, S., Praphet, A., Kanlayasillapin, P., Seangsoda, P. (2014): Regional yield trial: promising drought tolerance hybrid maize (early maturity). – Annual Report 13-24, Department of Agriculture, Ministry of Agriculture and Cooperatives, Thailand.
- [8] Chairi, F., Elazab, A., Sanchez-Bragado, R., Araus, J. L., Serret, M. D. (2016): Heterosis for water status in maize seedlings. – *Agricultural Water Management* 164: 100–109.
- [9] Chimungu, J. G., Brown, K. M., Lynch, J. P. (2014a): Large root cortical cell size improves drought. – *Plant Physiology* 166: 2166–2178.
- [10] Chimungu, J. G., Brown, K. M., Lynch, J. P. (2014b): Reduced root cortical cell file number improves drought tolerance in maize. – *Plant Physiology* 166(4): 1943–1955.
- [11] Ehdaie, B., Merhaut, D. J., Ahmadian, S., Hoops, A. C., Khuong, T., Layne, A. P., Waines, J. G. (2010): Root system size influences water-nutrient uptake and nitrate leaching potential in wheat. – *Journal of Agronomy and Crop Science* 196(6): 455–466.
- [12] Ekasingh, B., Gypmantasiri, P., Thong-Ngam, K., Grudloyma, P. (2014): Maize in Thailand: Production Systems, Constraints, and Research Priorities –Mexico, D.F. CIMMYT.
- [13] Gao, Y., Lynch, J. P. (2016): Reduced crown root number improves water acquisition under water deficit stress in maize (*Zea mays* L.). – *Journal of Experimental Botany* 67(15): 76–81.
- [14] Garcia, A. A. F., Wang, S., Melchinger, A. E., Zeng, Z.-B. (2008): Quantitative trait loci mapping and the genetic basis of heterosis in maize and rice. – *Genetics* 180(3): 1707–1724.
- [15] Hochholdinger, F., Park, W. J., Sauer, M., Woll, K. (2004a): From weeds to crops: genetic analysis of root development in cereals. – *Trends in Plant Science* 9(1): 42–48.
- [16] Hochholdinger, F., Woll, K., Sauer, M., Dembinsky, D. (2004b): Genetic dissection of root formation in maize (*Zea mays*) reveals root-type specific developmental programmes. – *Annals of Botany* 93(4): 359–368.
- [17] Hochholdinger, F., Woll, K., Sauer, M., Feix, G. (2005): Functional genomic tools in support of the genetic analysis of root development in maize (*Zea mays* L.). – *Maydica* 50: 437–442.
- [18] Hochholdinger, F., Wen, T. J., Zimmermann, R., Chimot-Marolle, P., Da Costa E Silva, O., Bruce, W., Lamkey, K. R., Wienand, U., Schnable, P. S. (2008): The maize (*Zea mays* L.) roothairless3 gene encodes a putative GPI-anchored, monocot-specific, COBRA-like protein that significantly affects grain yield. – *Plant Journal* 54(5): 888–898.

- [19] Hoecker, N., Keller, B., Piepho, H.-P., Hochholdinger, F. (2006): Manifestation of heterosis during early maize (*Zea mays* L.) root development. – *Theoretical and Applied Genetics* 112(3): 421–429.
- [20] Hufford, M. B., Xu, X., van Heerwaarden, J., Pyhäjärvi, T., Chia, J.-M., Cartwright, R. A., Elshire, R. J., Glaubitz, J. C., Guill, K. E., Kaeppeler, S. M., Lai, J., Morrell, P. L., Shannon, L. M., Song, C., Springer, N. M., Swanson-Wagner, R. A., Tiffin, P., Wang, J., Zhang, G., Doebley, J., McMullen, M. D., Ware, D., Buckler, E. S., Yang, S., Ross-Ibarra, J. (2012): Comparative population genomics of maize domestication and improvement. – *Nature Genetics* 44(7): 808–811.
- [21] Liu, X., Zhang, S., Shan, L. (2013): Heterosis for water uptake by maize (*Zea mays* L.) roots under water deficit: responses at cellular, single-root and whole-root system levels. – *Journal of Arid Land* 5(2): 255–265.
- [22] Lynch, J. P. (2005): *Root Architecture and Nutrient Acquisition*. – BassiriRad, H. *Nutrient Acquisition by Plants*. Springer-Verlag, Berlin/Heidelberg.
- [23] Lynch, J. P. (2007): Roots of the second green revolution. – *Australian Journal of Botany* 55: 493–512.
- [24] Lynch, J. P. (2013): Steep, cheap and deep: an ideotype to optimize water and N acquisition by maize root systems. – *Annals of Botany* 112(2): 347–357.
- [25] Lynch, J. P., Ho, M. D. (2005): Rhizoeconomics: Carbon costs of phosphorus acquisition. – *Plant and Soil* 269(1–2): 45–56.
- [26] Palta, J. A., Chen, X., Milroy, S. P., Rebetzke, G. J., Dreccer, M. F., Watt, M. (2011): Large root systems: are they useful in adapting wheat to dry environments? – *Functional Plant Biology* 38: 347–354.
- [27] Pipitkul, P., Chanakai, S., Kerdpol, P., Limsawad, Y., Wongvidecha, K., Vachrangkool, T., Suton, N., Rakdech, R., Techakampolsarakij, P., Malaikritsanachalee, K., Changsi, S., Gawga, S., Pitaksanakul, S., Jeengao, N. (2015): *Agricultural Statistic of Thailand, 2015* – Buddhapress, Bangkok.
- [28] Postma, J. A., Dathe, A., Lynch, J. P., Science, P., Pennsylvania, J. A. P. (2014): The optimal lateral root branching density for maize depends on nitrogen and phosphorus. – *Plant Physiology* 166(2): 590–602.
- [29] Qayyum, A., Ahmad, S., Liaqat, S., Malik, W., Noor, E., Muhammad, H. (2012): Screening for drought tolerance in maize (*Zea mays* L.) hybrids at an early seedling stage. – *African Journal of Agricultural Research* 7(24): 3594–3603.
- [30] R Core Team (2017): *R: A language and environment for statistical computing*. – R Foundation for Statistical Computing, Vienna, Austria. <http://www.r-project.org/>. (accessed: 3 July 2017).
- [31] Ranum, P., Peña-Rosas, J. P., Garcia-Casal, M. N. (2014): Global maize production, utilization, and consumption. – *Annals of the New York Academy of Sciences* 1312(1): 105–112.
- [32] Reynolds, T. W., Waddington, S. R., Anderson, C. L., Chew, A., True, Z., Cullen, A. (2015): Environmental impacts and constraints associated with the production of major food crops in Sub-Saharan Africa and South Asia. – *Food Security* 7(4): 795–822.
- [33] Richards, R. A. (2006): Physiological traits used in the breeding of new cultivars for water-scarce environments. – *Agricultural Water Management* 80: 197–211.
- [34] Saengwilai, P., Nord, E. A., Chimungu, J. G., Brown, K. M., Lynch, J. P. (2014a): Root cortical aerenchyma enhances nitrogen acquisition from low-nitrogen soils in maize. – *Plant Physiology* 166(2): 726–735.
- [35] Saengwilai, P., Tian, X., Lynch, J. P. (2014b): Low crown root number enhances nitrogen acquisition from low-nitrogen soils in maize. – *Plant Physiology* 166(2): 581–589.
- [36] Salvi, S., Giuliani, S., Ricciolini, C., Carraro, N., Maccaferri, M., Presterl, T., Ouzunova, M., Tuberosa, R. (2016): Two major quantitative trait loci controlling the number of seminal roots in maize co-map with the root developmental genes *rtcs* and *rum1*. – *Journal of Experimental Botany* 67(4): 1149–1159.

- [37] Schindelin, J., Arganda-Carreras, I., Frise, E., Kaynig, V., Longair, M., Pietzsch, T., Preibisch, S., Rueden, C., Saalfeld, S., Schmid, B., Tinevez, J.-Y., White, D. J., Hartenstein, V., Eliceiri, K., Tomancak, P., Cardona, A. (2013): Fiji-an open source platform for biological image analysis. – *Natural Methods* 9(7): 1–15.
- [38] Springer, N. M., Stupar, R. M. (2007): Allelic variation and heterosis in maize: how do two halves make more than a whole? – *Genome research* 17(3): 264–275.
- [39] Thiemann, A., Fu, J., Seifert, F., Grant-Downton, R. T., Schrag, T. A., Pospisil, H., Frisch, M., Melchinger, A. E., Scholten, S. (2014): Genome-wide meta-analysis of maize heterosis reveals the potential role of additive gene expression at pericentromeric loci. – *BMC Plant Biology* 14: 88.
- [40] Thomas, C. L., Graham, N. S., Hayden, R., Meacham, M. C., Neugebauer, K., Nightingale, M., Dupuy, L. X., Hammond, J. P., White, P. J., Broadley, M. R. (2016): High-throughput phenotyping (HTP) identifies seedling root traits linked to variation in seed yield and nutrient capture in field-grown oilseed rape (*Brassica napus* L.). – *Annals of Botany* 118(4): 655–665.
- [41] Tilman, D., Cassman, K. G., Matson, P. A., Naylor, R., Polasky, S. (2002): Agricultural sustainability and intensive production practices. – *Nature* 418: 671–677.
- [42] Tollenaar, M., Ahmadzadeh, A., Lee, E. A. (2004): Physiological basis of heterosis for grain yield in maize. – *Crop Science* 44(6): 2086–2094.
- [43] Tuberosa, R., Salvi, S. (2009): QTL for Agronomic Traits in Maize Production. – In: Bennetzen, J., Hake, S. (eds.) *Handbook of Maize: Its Biology*. Springer New York.
- [44] Tuberosa, R., Sanguineti, M. C., Landi, P., Giuliani, M. M., Salvi, S., Conti, S. (2002): Identification of QTLs for root characteristics in maize grown in hydroponics and analysis of their overlap with QTLs for grain yield in the field at two water regimes. – *Plant Molecular Biology* 48: 697–712.
- [45] York, L. M., Galindo-Castañeda, T., Schussler, J. R., Lynch, J. P. (2015): Evolution of US maize (*Zea mays* L.) root architectural and anatomical phenes over the past 100 years corresponds to increased tolerance of nitrogen stress. – *Journal of Experimental Botany* 66(8): 2347–2358.
- [46] Zanoni, U., Dudley, J. W. (1989): Comparison of different methods of identifying inbreds useful for improving elite maize hybrids. – *Crop Science* 29(3): 577.
- [47] Zhu, J., Mickelson, S. M., Kaeppler, S. M., Lynch, J. P. (2006): Detection of quantitative trait loci for seminal root traits in maize (*Zea mays* L.) seedlings grown under differential phosphorus levels. – *Theoretical and Applied Genetics* 113(1): 1–10.
- [48] Zhu, J., Brown, K. M., Lynch, J. P. (2010): Root cortical aerenchyma improves the drought tolerance of maize (*Zea mays* L.). – *Plant, Cell & Environment* 33(5): 740–749.

ASSESSMENT OF THE WEED INCIDENCE AND WEED SEED BANK OF CROPS UNDER DIFFERENT PEDOLOGICAL TRAITS

SKUODIENĖ, R. * – REPŠIENĖ, R. – KARČAUSKIENĖ, D. – ŠIAUDINIS, G.

*Vėžaičiai Branch of the Lithuanian Research Centre for Agriculture and Forestry
Gargždų 29, 96216 Vėžaičiai, Klaipėda distr., Lithuania*

**Corresponding author*

e-mail: regina.skuodiene@vezaiciai.lzi.lt; phone: +370-46-458-233

(Received 27th Sep 2017; accepted 15th Jan 2018)

Abstract. Weed community variations result from an interaction of different cropping and pedo-climatic aspects. The aim of the study was to investigate changes of the weed incidence in limed and unlimed soils of different texture in the Western Lithuania. Soil acidity decrease from pH 4.2-5.8 to 5.1-6.4 resulted in total weed number decrease: in sandy soils it decreased by 46.7%, in sandy loam soils - by 34.3% and in loam soils - by 24.0%. However, due to better nutrient and growth conditions, the weed mass was 11.1-72.6% greater in limed soil. The annual weeds were spread much more in a sandy soil (94.1% of the total weed number), while the perennial weeds - in a loam soil (51.2%). In sandy soils of all surveyed sites, most weeds were monocotyledonous (on the average 64.8%), while in sandy loam and loam soils – dicotyledonous (70.6%). The number of observed weed species was greater in sandy loam and loam soils both in crops and in the soil seed bank. Weed species diversity of the soil seed bank was particularly influenced by crop type and the crop preceding in the rotation. The most frequent weed species sequences in crops and soil seed bank matched by 67%.

Keywords: *agrobiological composition of weeds, most frequent weed species, soil contamination with weed seeds, soil texture, soil pH*

Introduction

Agricultural plants' productivity depends on geographical situation, soil, level of agriculture and agroclimatic conditions (Čiuberkis and Vilkonis, 2013). Weed growth is determined by many factors in addition to the soil's physical and chemical properties. These include field cropping history, proximity of sources of infestation, the weed seed population present or supplied to a field, water supply, and growing season conditions. The effects of soil structure, water-holding capacity, and nutrient level are more important than soil type (Zimdahl, 2007). Soil and crop management practices can directly influence the environment of seeds in the soil weed seed bank and can thus be used to manage seed longevity and germination behaviour of weed seeds (Hossain and Begum, 2015).

According to Radosevich et al. (2007), many weed species have patchy distributions in arable fields that can be strongly affected by their environments, in particular the soil. Weed community is changing depending on edaphic and climatic conditions (Walter et al., 2002) as well as the application of crop management measures (Kutyna and Mlynkowiak, 2014). For example, reduced soil tillage, and in some cases spring ploughing gave significantly higher aggregate stability than autumn ploughing, thus providing protection against erosion. However, decreasing tillage intensity increased the amounts of weeds, particularly of *Poa annua* on silt soil (Seehusen et al., 2017). It was established in other surveys, that soil management practices, such as soil tillage and crop rotation explain the majority of weed community variation across different soil typologies (Fried et al., 2008). Vidotto et al. (2016) indicates, that soil texture has

significant influence on weed specific composition. Monocotyledonous weeds are spreading more rapidly in alkaline sandy soil (with high pH) while dicotyledonous - in alkaline loam soil. Other researches suggest, that significant interactions occurred between weed species and soil texture, weed species and planting depth and soil texture and planting depth. For all weed species and soil textures, emergence decreased as planting depth increased with the greatest percent emergence at the soil surface (Hoyle et al., 2013).

Physical properties of the soil have a strong effect on buried-seed ecology and consequently on seed bank dynamics in the agroecosystem. Germination inhibition due to burial depth was found to be directly proportional to clay content and inversely proportional to sand content (Benvenuti, 2003).

Weediness evaluation in Lithuania was started in 1957. Herbicides were not widely used at that time. In winter crops there had been 348-609 unit m⁻² of weeds and in spring crops - 291-591 unit m⁻² of weeds. Perennial weeds were especially spread. After about 25 years, the weediness decreased by 60-80%. The annual dicotyledonous weeds became dominant. At present time, however, a problem of the annual monocotyledonous weeds becomes apparent (Auškalnienė et al., 2011). Recently, more and more farmers move to extensive farming using small amounts of herbicides or no herbicides at all.

Bathygleyic Distric Glossic Retisol (RT) (WRB, 2014) prevailing in the West Lithuania are acid, low in organic matter and contain high level of toxic Al (Repsiene and Karcauskiene, 2016). According to these observations, we hypothesised that choosing different soil management practice (crop rotation, soil tillage, fertilisation) it is possible to affect not only chemical but also physical characteristics of the soil both in positive and negative ways. Given that management practices, the soil texture and pH status of soils can have a major impact on the weed flora, we utilised data from a field experiment to test the effects of soil acidity factors on the weed properties.

The aim of the study was to investigate changes of the weed incidence in limed and unlimed soils of different texture in the Western Lithuania.

Materials and methods

Experimental site

Experiments were carried out during the period 2012-2015 in different sites of the Western Lithuania, varying in their relief and soil characteristics.

The first experimental site was a coastal area of the Seaside Lowland in the Nemunas delta (*Fig. 1*). The geographical location of the site is Latitude 55°19 N and Longitude 21°35 E. The soil was *Bathihypogleyi-Dystri-Haplic Arenosols (ARh-dy-gld-w)* (WRB, 2014) with a texture of sand.

The second experimental site was the Western Plateau of Žemaičiai Highland (*Fig. 1*). The geographical location of the site is Latitude 55°37 N and Longitude 21°57 E. The soil was *Bathygleyic Distric Glossic Retisol (RT)* (WRB, 2014) with a texture of sandy loam.

The third experimental site was the Western Plateau of Žemaičiai Highland (*Fig. 1*). The geographical location of the site is Latitude 55°32 N and Longitude 21°54 E. The soil was *Hapli-Endohypogleyic Luvisol (LVg-n-w-ha)* (WRB, 2014) with a texture of loam.

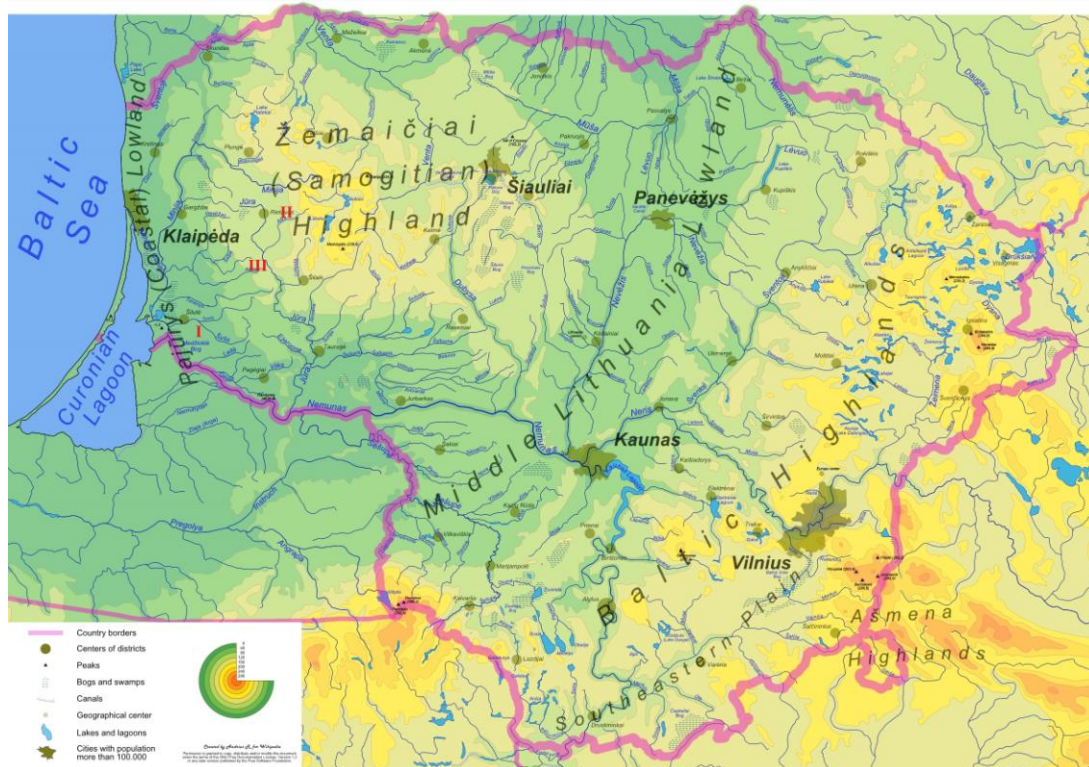


Figure 1. The locations of research area: I – first experimental site, II – second experimental site, III – third experimental site

These fields were chosen because they had a known history of weed infestation due to extensive farming mode. Soil properties were also considered in the study for each site; in particular, soil reaction (pH) and texture (relative proportions of sand, silt and clay) (Table 1).

Experimental design

Field experiments in all surveyed sites were conducted according to the same scheme: 1) unlimed soil; 2) limed soil.

The experiment was established in four replications. The treatments were assigned randomly. The trial field area was $5.0 \text{ m} \times 9.5 \text{ m} = 47.5 \text{ m}^2$.

Liming was conducted with liming material – ground chalk containing 97.8% of CaCO_3 . The soil was limed once in 2011 before the trial arrangement. Liming material was scattered and incorporated with a cultivator at a depth of 0-15 cm.

Sandy soil was limed with 4.5 t ha^{-1} of CaCO_3 , sandy loam soil – with 7.0 t ha^{-1} of CaCO_3 and loam soil – with 6.0 t ha^{-1} of CaCO_3 . The quantities of liming material were calculated according to approved recommendations, soil type and texture and pH value.

Plant growing technology (soil tillage, fertilisation, plant care) was used in different experimental sites. Crop rotation (cereal and row crops) of the first surveyed site was as follows: winter triticale, potatoes, winter wheat, peas. Crop rotation (cereal and row crops) of the second surveyed site was as follows: spring rape, maize, maize, barley + undersowing (perennial grasses). Crop rotation (cereal crops) of the third surveyed site was as follows: spring wheat, winter rye, spring wheat, winter wheat.

Table 1. Sites characteristics, Western Lithuania

Indices	Experimental site		
	I	II	III
Pedological indices			
Soil type	Arenosols	Retisol	Luvisol
Soil texture	Sand	Sandy loam	Loam
Sand, %	93.8±7.55	65.1±5.20	50.4±4.35
Silt, %	3.6±0.25	24.7±1.95	30.7±2.45
Clay, %	2.6±0.20	10.2±0.80	18.9±1.15
pH _{KCl} (unlimed soil)	4.91±0.13	4.20±0.26	5.79±0.22
pH _{KCl} (limed soil)	5.93±0.35	5.08±0.17	6.45±0.17
Mobile Al mg kg ⁻¹ (in unlimed soil)	3.88± 2.22	31.64±13.12	0.00
Mobile P ₂ O ₅ mg kg ⁻¹	114.5±6.36	225.0±38.59	60.0±45.25
Mobile K ₂ O mg kg ⁻¹	74.0±19.8	115.5±16.26	81.5±17.68
Humus, %	1.66±0.16	2.51±0.16	2.95±0.18
Climatic indices (SRC)			
Total annual precipitation, mm	801	816	816
Annual mean temperature, °C	7.4	6.3	6.3
Growing season's total precipitation, mm	508	495	495
Growing season's mean air temperature, °C	12.9	11.9	11.9

Note: SRC – The standard rate of climate

Methods of analysis

Agrochemical characteristics of the soil were determined from the soil samples taken from 0-20 cm layer before establishing the experiment: soil pH_{KCl} was measured according to potentiometric method determined in 1M KCl (soil – solution ratio 1:2.5 (ISO 10390:2005), available P₂O₅ and K₂O – using Egner-Riehm-Domingo (A-L) method (LVP D-07:2012). Mobile Al was determined according ISO11260 and ISO14254 Sokolov method. Humus was determined according Tiurin method (ISO 10694:1995). Soil texture was determined according to the composition of three fractions: sand, silt and clay. Analysis was accomplished using Kaczynski method and modified according to FAO (ISO 11277:2009).

Weed record was performed in stationary areas 0.25 m² in size in six positions of every plot during crop maturity phase. The weeds were eradicated and their specific composition and dry matter mass were determined. Weed number was recalculated to weeds per m² and mass – g m⁻².

Soil contamination with weed seeds was investigated in the depths of 0-10 cm and 10-20 cm. Soil samples were collected using an agrochemical drill during crop maturity phase. The soil was dried out. One hundred gram (100 g) dry soil sample was weighed and wet-sieved through a 0.25 mm sieve until all contents of the soil were washed out. Remained mineral part of the soil was separated from the organic part and weed seeds using the saturated salt solution. Weed seed number (A) was recalculated to thousands of unit m⁻² using the following Equation 1:

$$A = n \cdot h \cdot p \cdot 100 \quad (\text{Eq.1})$$

where,

A = weed seed number (unit m^2),

n = seed number in a sample (unit),

h = depth of the soil (cm),

p = soil density ($g\ cm^{-3}$).

Agrometeorological conditions

Meteorological conditions in 2012-2015 were diverse. Climatic conditions of the first experimental site were evaluated according to the data of Šilutė meteorological station (Fig. 2). During the vegetation period in 2012 and later in the year, the amount of precipitation was greater by 12.2 and 12.7% compared to the long-term mean (Table 1). During the vegetation period in 2013, 2014, 2015 and later in the year, the amount of precipitation was smaller compared to the long-term mean by, respectively: 16.5; 40.2; 40.0 and 15.0; 32.8; 15.7%. The month of July in 2014 and the months of August and October in 2015 were especially dry.

The average air temperature during the vegetation period in 2013 and 2014 was greater than the long-term mean by, respectively, 0.7 and 1.1°C, and the average temperature of the year in 2013, 2014 and 2015 were greater by, respectively, 0.5; 1.2 and 1.3°C.

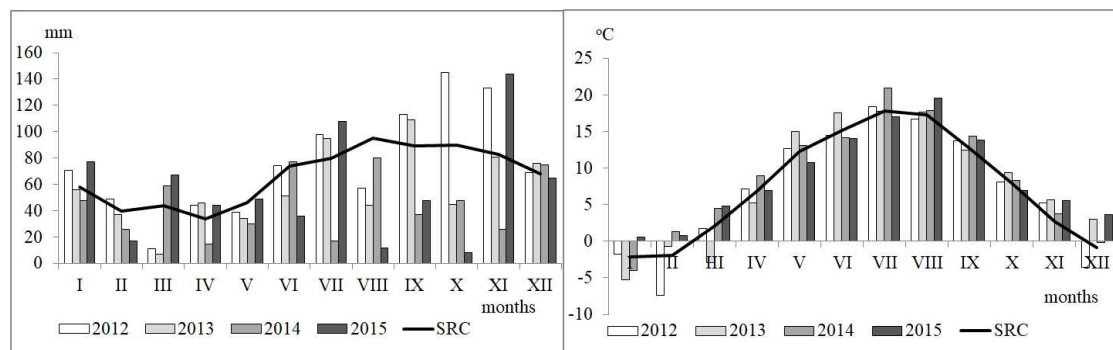


Figure 2. The average daily air temperature (°C) and precipitation (mm) during the study period (2012-2015). Data from the Šilutė (first experimental site) Meteorological Station. Note: SRC – The standard rate of climate

Climatic conditions of the second and third experimental sites were evaluated according to the data of Laukuva meteorological station (Fig. 3). The weather in 2012 was more humid: the amount of precipitation during the vegetation period was greater by 10.9% and later in the year it was greater by 4.5% compared to the long-term mean. The amount of precipitation in 2013, 2014 and 2015 during the vegetation period and later in the year was smaller compared to the long-term mean by, respectively, 5.1; 10.9; 29.1 and 11.4; 15.3; 8.2%. The months of August and October in 2015 were especially dry.

The average air temperature during the vegetation period was greater than the long-term mean in 2012, 2013 and 2014 by, respectively, 1.2; 0.7 and 1.1°C, and the average temperature of the year was greater in 2013, 2014 and 2015 by, respectively, 1.0, 1.2 and 1.3°C.

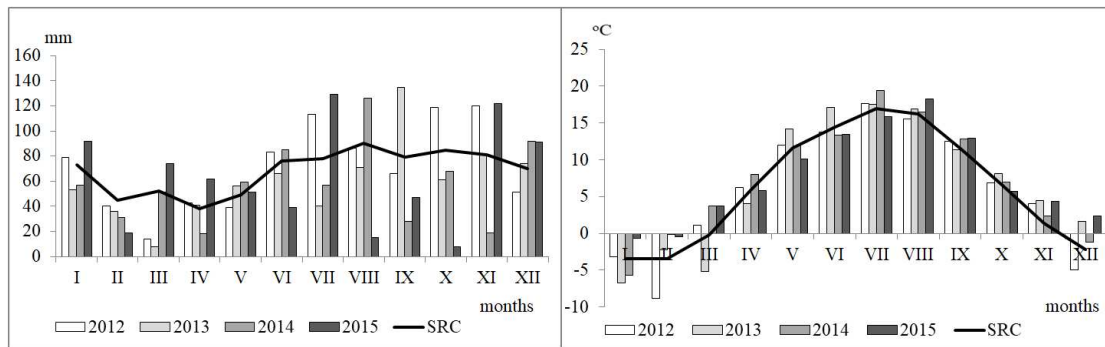


Figure 3. The average daily air temperature (°C) and precipitation (mm) during the study period (2012-2015). Data from the Laukuva (second and third experimental sites) Meteorological Station. Note: SRC – The standard rate of climate

Statistical analysis

Significance of the differences between the means was determined according to the Fisher's protected least significant difference (LSD) at 0.05 probability level. The data were processed using software ANOVA (Clewer and Scarisbrick, 2001). Data of weed density and mass were transformed according to the recommended procedures, using Equation 2:

$$Y = \sqrt{x+1} \quad (\text{Eq.2})$$

where x is the primary data, Y is transformed data of weed density and mass, however, means on the original scales are reported (Onofri et al., 2010).

Correlation-regression analysis was also performed. The symbols used in the paper are: *significant at $P < 0.05$, and **significant at $P < 0.01$, ns - not significant.

Results and discussion

Weed community diversity

Anthropogenic activity has the impact on biodiversity changes. Weed community diversity is affected by crop rotation, fertilization, technologies application (especially the use of herbicides) (Andreasen and Streibig, 2011). Crop weed infestations mainly depend on weed species which dominate the weed flora at different soil acidity and nutrient content in soil (Skuodienė and Repšienė, 2009; Karcaukiene et al., 2016).

Crop weediness and soil contamination with weed seeds depended on applied crop management measures and crop condition. In experimental areas, different in edaphic (environmental) conditions, 41 weed species were found. Independently from different soil pH, the number of weed species in sandy loam and loam soils was greater by 1.5 and 3.0 times compared to a sandy soil. (Table 2). All weed species (in surveyed sites) were determined to belong to 16 families from *Magnoliophyta* division and one family from *Equisetophyta* division. Number of observed weed species was great in loam soils. A number of factors may contribute to this effect: extensive farming mode, even in wheat mono-cropping.

Independently from different soil texture, a positive liming effect on crop weediness was estimated in all surveyed sites. The greater competitive ability of crops of the rotation resulted in general decrease of crop weediness. The number of weeds per square metre and their dry matter mass in many ways were significantly lower compared to unlimed plots (Table 2). In unlimed sandy soil, on the average, 65.3 units of weeds per square metre were estimated, in sandy loam soil – 14.0 units and in loam soil – 166.3 units of weeds. In limed sandy soil the weed number was lower by 46.7%, in sandy loam soil – by 34.3% and in loam soil it was lower by 24.0% compared to unlimed plots.

Due to better nutrition and growth conditions in limed soil, a tendency of weed mass increase was observed. In a sandy soil the weed mass was greater by 65.3%, in a sandy loam soil – by 72.6% and in a loam soil it was greater by 11.1% compared to unlimed plots. Under the similar environmental conditions in a sandy loam soil with pH 5.2, the weed number was 86.9 units per square metre and their mass – 54.7 g. (Skuodiene et al., 2016).

A similar tendency was established estimating a mass of the single weed. Literature indicates, that dry matter mass of the single weed depended on favourable nutrition and meteorological conditions, fertilisation and cultured plants' competition as well as the competitive ability that were formed by preceding crops (Arlauskienė and Maikštėnienė, 2005). A mass of the single weed depended on soil edaphic conditions and weediness intensity. Together with decrease of weed number ($r = -0.405^*$) and increase of their mass ($r = 0.432^*$), the mass of a single weed was increasing. The greatest mass was in crops in a sandy loam soil, respectively: 3.9 g in unlimed soil and 10.4 g in limed soil. Due to continuous cropping for several years, the lowest (1.0-1.6 g) mass of a single weed was estimated in crops of high weediness. In general, the average mass of a single weed was determined by a total number of weeds, development stage of individual weed species and weed mass.

Table 2. Agrobiological composition of weeds

Weeds indices	Experimental site					
	I (Sand)		II (Sandy loam)		III (Loam)	
	Unlimed soil	Limed soil	Unlimed soil	Limed soil	Unlimed soil	Limed soil
Number of weed species	9	7	12	12	23	25
Weed number, plants m ⁻²	65.3	34.8*	14.0	9.2*	166.3	126.4
Weed DM mass, g m ⁻²	49.0	81.0*	55.4	95.6*	69.2	76.9
Mass of a single weed, g	1.04	2.81*	3.96	10.39**	1.00	1.63
Annual dicotyledonous, %	22.4	36.2	37.1	73.8	43.5	58.8
Annual monocotyledonous, %	69.0	60.6	10.0	0.0	0.0	0.2
Perennial dicotyledonous, %	8.2	3.2	9.3	9.8	26.9	23.2
Perennial monocotyledonous, %	0.0	0.0	33.6	8.2	28.5	16.8

* and ** - the least significant at $P < 0.05$ and $P < 0.01$, respectively

The annual weeds spread in cereal and row crops rotation, respectively: in a sandy soil – 94.1%, in a sandy loam soil – 60.4% of the total weed number. Perennial weeds,

in the rotation with nearly the same crop species grown for every year, had formed 51.2% of the total weed amount.

In sandy soils the most weeds of all investigated crops were monocotyledonous (on the average 64.8%) and in sandy loam and loam soils – dicotyledonous (70.6%).

Crop weediness depended on edaphic conditions of the area. It is stated, that linear correlation analysis identified some significant relationships between the pedological parameters pH, sand, silt and clay and some weed indices (Vidotto et al., 2016). Correlation analysis showed that soil texture had significant impact on weed number and agrobiological distribution and soil pH was significant for a mass of the single weed (Table 3).

Table 3. Linear correlation coefficients (*r*) of the relationships among some pedological parameters and weed indices

Characters	pH	Sand	Silt	Clay
Weed number, plants m ⁻²	ns	-0.396*	0.401*	0.387*
Mass of a single weed, g	-0.455*	ns	ns	ns
Annual dicotyledonous, %	0.385*	0.532**	0.579**	0.499**
Annual monocotyledonous, %	-0.380*	-0.901**	-0.853**	-0.899**
Perennial dicotyledonous, %	0.474**	-0.676**	0.630**	0.691**
Perennial monocotyledonous, %	ns	-0.725**	0.701**	0.698**

* and ** - the least significant at $P < 0.05$ and $P < 0.01$, respectively; ns - not significant

Weed seed bank

The seed bank is an indicator of past and present weed populations. It is also the main source of arable weed propagules and can have severe and long-lasting effects on crop yields (Sosnoskie et al., 2006). There are enormous numbers of viable weed seeds in the soil. According to the average data, there are 17.0 to 38.8 thousands of weed seeds per square metre in the soil seed bank (Table 4). During the research, 35 weed species were found in the soil seed bank. The number of weed species in sandy loam and loam soils was greater by 1.4 times compared to a sandy soil.

The total amount of weed seeds in limed sandy loam soil was significantly lower compared to unlimed soil of the same texture. In limed sandy soil the number of weeds was lower by 15.5% and in a sandy loam soil it was lower by 39.5% compared to unlimed plots. There were no significant differences in a loam soil. It is likely that no significant differences were obtained because cereals had been continuously cropped for several years. Soil contamination with weed seeds depends on crop condition and the application of crop management measures and corresponds to patterns that the amount of weed seeds in the soil depends on plants that were grown before and agrotechnique that was used (especially the use of herbicides) (Menalled et al., 2001; Sadrabadi Haghghi et al., 2013; Woźniak and Soroka, 2015).

Seeds are dispersed both horizontally and vertically in the soil profile. Benvenuti (2007) indicates that the vertical position of the seed was dependent on soil texture. Data of our research showed that weed seed number in the upper (0-10 cm) and the deeper (10-20 cm) layers of the soil differed (Table 4). The soil texture had the impact on weed seed distribution in different soil layers. In light-textured soil (I experiment) in the depth of 0-10 cm, the number of weed seeds was lower than in the depth of 10-20

cm (47.7% of the total weed amount). In a sandy loam soil of the II experiment in 0-10 cm layer there were 51% of weed seeds while in a loam soil – 59.2%. Gselman and Kramberger (2004) and Janicka (2006) indicate that the greatest seed reserves were in the surface layer of the soil (0-5 cm).

Table 4. Weed seed bank in the topsoil

Seed bank indices	Experimental site					
	I (Sand)		II (Sandy loam)		III (Loam)	
	Unlimed soil	Limed soil	Unlimed soil	Limed soil	Unlimed soil	Limed soil
Number of weed species	13	10	19	15	20	13
Seeds, unit m ⁻² 0-20 cm	38837	32808	28177	17046*	26532	28109
Seeds, unit m ⁻² 0-10 cm	18515	15677	15270	8165*	14731	17685
Seeds, unit m ⁻² 10-20 cm	20322	17131	12907	9241	11801	10425

* and ** - the least significant at $P < 0.05$ and $P < 0.01$, respectively

Although, during the investigation, 41 weed species were found in crops and 35 species in the seed bank, only a few of species were spread. In crops, 11 species were present on more than 20%, 5 species – on more than 50% and 2 species – on more than 70% of the surveyed sites (Table 5). In the soil seed bank, 12 species were present on more than 20%, 6 species – on more than 50% and 4 species on more than 70% of the surveyed sites.

Independently from the soil texture, all surveyed sites were mostly contaminated with seeds of *Chenopodium album* L., *Fallopia convolvulus* L., *Persicaria lapathifolia* L. Weed species diversity of the soil seed bank was particularly influenced by crop type and the crop preceding in the rotation. The most frequent weed species sequences in crops and soil seed bank matched by 67%. According to other surveys conducted in sandy loam soils, the weed species in crops and soil seed bank matched by 27-40% (Skuodienė et al., 2013).

The most frequent weed species in crops and soil seed bank were as follows:

Sandy soil (I experiment). *Echinochloa crus-galli* (L.) P.Beauv., *Fallopia convolvulus* L., *Sonchus arvensis* L., *Spergula arvensis* L., *Persicaria lapathifolia* L. – the light-demanding but shade-tolerant weeds dominated. *Spergula arvensis* L., *Fallopia convolvulus* L. and *Echinochloa crus-galli* (L.) P.Beauv. formed the greatest part of the soil seed bank.

Sandy loam soil (II experiment). *Elytrigia repens* L., *Persicaria lapathifolia* L., *Fallopia convolvulus* L., *Chenopodium album* L., *Polygonum aviculare* L. – the weeds preferring fertile soils dominated. *Chenopodium album* L., *Fallopia convolvulus* L. and *Persicaria lapathifolia* L. formed the greatest part of the soil seed bank.

Loam soil (III experiment). *Galeopsis tetrahit* L., *Tripleurospermum perforatum* (Merat.) M.Lainz, *Persicaria lapathifolia* L., *Sonchus arvensis* L., *Elytrigia repens* L. – the hardy-annual, over-wintering and perennial weeds dominated. *Fallopia convolvulus* L., *Tripleurospermum perforatum* (Merat.) M.Lainz, *Chenopodium album* L., *Persicaria lapathifolia* L. and *Viola arvensis* Murray formed the greatest part of the soil seed bank.

Table 5. Frequency of encounters for the most diffused weed species across all surveyed sites

Aboveground		Seed bank	
Species	Encounter frequency (%)	Species	Encounter frequency (%)
<i>Persicaria lapathifolia</i> L.	100	<i>Chenopodium album</i> L.	96
<i>Fallopia convolvulus</i> L.	80	<i>Fallopia convolvulus</i> L.	96
<i>Sonchus arvensis</i> L.	70	<i>Persicaria lapathifolia</i> L.	92
<i>Viola arvensis</i> Murray.	70	<i>Viola arvensis</i> Murray.	75
<i>Elytrigia repens</i> L.	60	<i>Echinochloa crus-galli</i> (L.) P.Beauv.	54
<i>Polygonum aviculare</i> L.	50	<i>Spergula arvensis</i> L.	54
<i>Spergula arvensis</i> L.	50	<i>Scleranthus annuus</i> L.	42
<i>Echinochloa crus-galli</i> (L.) P.Beauv.	40	<i>Galeopsis tetrahit</i> L.	42
<i>Galeopsis tetrahit</i> L.	40	<i>Rumex acetosella</i> L.	38
<i>Gnaphalium uliginosum</i> L.	40	<i>Stellaria media</i> (L.) Vill.	33
<i>Equisetum arvense</i> L.	40	<i>Tripleurospermum perforatum</i> (Merat.) M.Lainz	29
<i>Chenopodium album</i> L.	20	<i>Sonchus arvensis</i> L.	25

Conclusions

Weed community variation and soil contamination with weed seeds resulted from different soil pH, pedological aspects and cropping management. Together with decreasing soil acidity from pH 4.2-5.8 to pH 5.1-6.4, the total number of weeds decreased by 24.0-46.7%. However, due to better nutrient and growth conditions, the weed mass was 11.1-72.6% greater in limed soil.

The mass of a single weed was determined by a total number of weeds, development stage of individual weed species and weed mass. The mass of a single weed increased, together with a decrease of weed number ($r = -0.405^*$) and increase of their mass ($r = 0.432^*$). The greatest mass of a single weed was in crops of the least weediness, respectively: 3.9 g in unlimed soil and 10.4 g in limed soil. The least mass (1.0-1.6 g) of a single weed was determined in crops where the weed number was the greatest.

The annual weeds were spread much more in a sandy soil (94.1% of the total weed number), while the perennial weeds – in a loam soil (51.2%).

In sandy soils of all surveyed sites, most weeds were monocotyledonous (on the average 64.8%), while in sandy loam and loam soils – dicotyledonous (70.6%).

There were 17.0 to 38.8 thousands of weed seeds per square metre in the soil seed bank. The smallest amount of weed seeds was found in a sandy loam soil, while in a sandy soil it was the greatest. The soil texture had the impact on weed seed distribution in different soil layers. In sandy soil in the depth of 0-10 cm, the number of weed seeds was 47.7% of the total weed amount, in a sandy loam soil – 51%, in a loam soil – 59.2%.

The number of observed weed species was greater in sandy loam and loam soils both in crops and in the soil seed bank. The most frequent weed species sequences in crops and soil seed bank matched by 67%. Soil was mostly contaminated with seeds of *Chenopodium album* L., *Fallopia convolvulus* L. and *Persicaria lapathifolia* L.

Effective control of the weediness is possible only when the optimal pH reaction of the soil is maintained and the proper crop rotation is applied. Under the changing climatic conditions weediness management is going to be even more difficult, therefore the scientific researches will have to be oriented to ecophysiological investigations of weeds.

Acknowledgments. The paper presents research findings, obtained through the long-term research programme “Productivity and sustainability of agricultural and forest soils” implemented by Lithuanian Research Centre for Agriculture and Forestry.

REFERENCES

- [1] Arlauskienė, A., Maikštėnienė, S. (2005): The effect of legume preceding crop biomass on weed infestation in cereals. – *Vagos* 66(19): 7-16.
- [2] Auškalnienė, O., Pšibišauskienė, G., Auškalnis, A., Lazauskas, S., Povilaitis, V., Sakalauskiene, S., Sakalauskaitė, J., Duchovskis, P., Raudonius, S. (2011): Changes of segetal flora in Lithuania over the last decades. – *Trends of Rural Development in the Knowledge Society* 2: 217-222.
- [3] Benvenuti, S. (2003): Soil texture involvement in germination and emergence of buried weed seeds. – *Agronomy Journal* 95: 191-198.
- [4] Benvenuti, S. (2007): Natural weed seed burial: effect of soil texture, rain and seed characteristics. – *Seed Science Research* 17(3): 211-219.
- [5] Čiuberkis, S., Vilkonis, K. K. (2013): Weeds in agro-ecosystems of Lithuania. – AB Spauda, Vilnius (in Lithuanian).
- [6] Clewer, A. G., Scarisbrick, D. H. (2001): Practical statistics and experimental design for plant and crop science. – Wiley and Sons, Chichester.
- [7] Fried, G., Norton, L. R., Reboud, X. (2008): Environmental and management factors determining weed species composition and diversity in France. – *Agriculture, Ecosystems and Environment* 128: 68-76.
- [8] Gselman, A., Kramberger, B. (2004): Longevity and vertical distribution of dandelion (*Taraxacum officinale* F. Weber.) seeds in meadow soil. – *Grassland Science in Europe* 9: 252-254.
- [9] Hossain, M. M., Begum, M. (2015): Soil weed seed bank: Importance and management for sustainable crop production - A Review. – *Journal of the Bangladesh Agricultural University* 13(2): 221-228.
- [10] Hoyle, J. A., McElroy, J. S., Guertal, E. A. (2013): Soil texture and planting depth affect large crabgrass (*Digitaria sanguinalis*), Virginia buttonweed (*Diodia virginiana*), and cock's-comb kyllinga (*Kyllinga squamulata*) emergence. – *HortScience* 48(5): 633-636.
- [11] Janicka, M. (2006): Species composition of the soil seed bank in comparison with the floristic composition of meadow sward. – *Grassland Science in Europe* 11: 200-202.
- [12] Karcauskiene, D., Ciuberkis, S., Raudonius, S. (2016): Changes of weed infestation under long-term effect of different soil pH levels and amount of phosphorus:potassium. – *Acta Agriculturae Scandinavica, Section B - Soil & Plant Science* 66(8): 688-697.
- [13] Kutyna, I., Młynkowiak, E. (2014): The influence of differentiated natural and agrotechnical ecological conditions on the number of species in segetal communities and their mean number in the phytosociological releve. – *Folia Pomeranae Universitatis Technologiae Stetinensis Agric., Aliment., Pisc., Zootech.* 312(31): 69-96.
- [14] Menalled, F. D., Gross, K. L., Hammond, M. (2001): Weed aboveground and seedbank community responses to agricultural management systems. – *Ecological Applications* 11(6): 1586-1601.
- [15] Onofri, A., Carbonell, E. A., Piepho, H. P., Mortimer, A. M., Cousens, R. D. (2010): Current statistical issues in weed research. – *Weed Research* 50: 5-24.

- [16] Radosevich, S. R., Holt, J. S., Ghersa, C. M. (2007): *Ecology of Weeds and Invasive Plants: Relationship to Agriculture and Natural Resource Management* (3ed.). – John Wiley and Sons, New York.
- [17] Repsiene, R., Karcauskiene, D. (2016): Changes in the chemical properties of acid soil and aggregate stability in the whole profile under longterm management history. – *Acta Agriculturae Scandinavica, Section B - Soil & Plant Science* 66(8): 671-676.
- [18] Sadrabadi Haghighi, R., Critchley, N., Leifert, C., Eyre, M., Cooper, J. (2013): Individual and interactive effects of crop type and management on weed and seed bank composition in an organic rotation. – *International Journal of Plant Production* 7(2): 243-268.
- [19] Seehusen, T., Hofgaard, S., Tørresen, K. S., Riley, H. (2017): Residue cover, soil structure, weed infestation and spring cereal yields as affected by tillage and straw management on three soils in Norway. – *Acta Agriculturae Scandinavica, Section B - Soil and Plant Science* 67(2): 93-109.
- [20] Skuodienė, R., Repšienė, R. (2009): The effects of organic fertilisers and liming on segetal flora in a sustainable crop rotation on acid soil. – *Zemdirbyste-Agriculture* 96(4): 154-169.
- [21] Skuodienė, R., Karčauskienė, D., Čiuberkis, S., Repšienė, R., Ambrazaitienė, D. (2013): The influence of primary soil tillage on soil weed seedbank and weed incidence in cereal-grass crop rotation. – *Zemdirbyste-Agriculture* 100(1): 25-32.
- [22] Skuodienė, R., Karčauskienė, D., Repšienė, R. (2016): The influence of primary soil tillage, deep loosening and organic fertilizers on weed incidence in crops. – *Zemdirbyste-Agriculture* 103(2): 135-142.
- [23] Sosnoskie, L. M., Herms, C. P., Cardina, J. (2006): Weed seed bank community composition in a 35-yr-old tillage and rotation experiment. – *Weed Science* 54: 263-273.
- [24] Vidotto, F., Fogliatto, S., Milan, M., Ferrero, A. (2016): Weed communities in Italian maize fields as affected by pedo-climatic traits and sowing time. – *European Journal Agronomy* 74: 38-46.
- [25] Walter, A. M., Christensen, S., Simmelsgaard, S. F. (2002): Spatial correlation between weed species densities and soil properties. – *Weed Research* 42: 26-38.
- [26] Woźniak, A., Soroka, M. (2015): Biodiversity of weeds in pea cultivated in various tillage system. – *Romanian Agricultural Research* 32: 231-237.
- [27] WRB. (2014): *World reference base for soil resources 2014. International soil classification system for naming soils and creating legends for soil maps.* – World Soil Resources Reports No. 106. FAO, Rome.
- [28] Zimdahl, R. L. (2007): *Fundamentals of Weed Science.* – Academic Press, San Diego, CA.

INFLUENCE OF LONG-TERM CHICKEN MANURE APPLICATION ON THE CONCENTRATION OF SOIL TETRACYCLINE ANTIBIOTICS AND RESISTANT BACTERIA VARIATIONS

WANG, W. Z. – CHI, S. L. – XU, W. H.* – ZHANG, C. L.

*College of Resources and Environmental Sciences, Southwest University
400715 Chongqing, P. R. China*

**Corresponding author
e-mail: xuwei_hong@163.com*

(Received 3rd Oct 2017; accepted 29th Jan 2018)

Abstract. A fixed field experiment was carried out to investigate the influence of different amounts of cured and fresh chicken manure (low chicken manure: 300 kg·667 m⁻², high chicken manure: 600 kg·667 m⁻²) on the concentration of tetracyclines (TCs); number of microbes, including antibiotic resistant bacteria; organic matter content; and enzyme activity in soil. Results show that after a one-year application of chicken manure, the quantity of soil bacteria was 3.2-4.3 times that of the control soil. The quantity of soil bacteria and actinomycetes in cured chicken manure (CCM) treatments was significantly higher than in fresh chicken manure (FCM) treatments by 17.0%-33.9% and 201.2%-271.2%, respectively. The application of low cured chicken manure (L-CCM) significantly reduced the number of fungus, which was 83.8% lower than the control. The application of CCM significantly increased the activities of soil urease and catalase by 81.9%-103.0% and 7.9%-17.9%, respectively, compared to the control. After applying chicken manure in soil where *Ipomoea aquatic* Forsk was planted, the soil antibiotic residues increased by 3.6%-27.5%. When applying chicken manure to soil where *Lactuca sativa* L. or *Brassica juncea* var. *gemmifera* was planted, the soil antibiotic residues decreased by 19.4%-52.2% and 22.6%-26.6%, respectively. After one year, the antibiotic residues in soil treated with FCM and CCM were higher than the control level by 176.5%-217.9% and 168.5%-191.5%, respectively. The number of resistant bacteria in CCM treatments was significantly higher than that in FCM treatments and in the control. The number of resistant bacteria in the L-CCM treatment was the highest, wherein the quantity of resistant bacteria to oxytetracycline, tetracycline and chlortetracycline was higher than that in other treatments by 11.6%-339.6%, 127.0%-635.4% and 32.2%-130.9%, respectively. The drowned planting mode may worsen soil tetracycline antibiotic residues, when compared to drought planting. Long-term application of FCM may cause residue and accumulation of tetracycline antibiotics in soil; hence the hazard to the environment is worthy of further study.

Keywords: *chicken manure, tetracycline antibiotics, resistant bacteria, soil enzyme activity, planting mode*

Introduction

In recent years, the adsorption, migration, and conversion of novel organic pollutant antibiotics in soil-water-plant have become an area of intense research. Antibiotics are widely used to reduce disease in the livestock and poultry industries. In 2010, the annual administration of antibiotics in the livestock and poultry industry reached approximately 63,151 tons, and it is expected to increase by 67% by 2030 (Boeckel et al., 2015). China accounts for 60%-65% of the world's total antibiotic use (Tasho and Cho, 2016). Furthermore, production of livestock and poultry manure from large-scale farms in China can reach 2.1 billion tons, 80% of which are directly applied to farmland without comprehensive treatment (Sun et al., 2017). In eastern China, the concentration of antibiotic residues in livestock and poultry manure can be as high as 1420 mg·kg⁻¹

(Chen et al., 2012). Tetracycline antibiotics are one of most widely used classes of antibiotics in the world, and include tetracycline (TC), oxytetracycline (OTC) and chlortetracycline (CTC). Liguoro et al. (2003) detected OTC in livestock and poultry manure at concentrations up to $871.7 \text{ mg}\cdot\text{kg}^{-1}$ and $115.5 \text{ mg}\cdot\text{kg}^{-1}$, respectively, and CTC in a pig manure treatment pond was detected at concentrations up to $1.0 \text{ mg}\cdot\text{kg}^{-1}$. Hamscher et al. (2002) detected TC and CTC in livestock manure at $4.0 \text{ mg}\cdot\text{kg}^{-1}$ and $0.1 \text{ mg}\cdot\text{kg}^{-1}$, respectively.

Farmland is a main site where antibiotics are spread. Livestock and poultry manure are applied to farmlands as organic fertilizer, which is one of the main mechanisms in which antibiotics enter the soil (Kemper, 2008). Tetracycline antibiotics are recalcitrant and easily accumulate in soils, thereby posing potential threats to the environment and human health (Pan and Chu, 2017). Hamscher et al. (2002) studied the concentration of antibiotic residues in soils that received long-term application of livestock and poultry manure. They found that the average TC concentration was $86.2 \text{ }\mu\text{g}\cdot\text{kg}^{-1}$ in 0-10 cm soil, $198.7 \text{ }\mu\text{g}\cdot\text{kg}^{-1}$ in 10-20 cm soil, and $171.7 \text{ }\mu\text{g}\cdot\text{kg}^{-1}$ in 20-30 cm soil. After application of livestock and poultry manure, the highest concentrations of OTC, TC and CTC in surface soil (0-30 cm) were $27 \text{ }\mu\text{g}\cdot\text{kg}^{-1}$, $443 \text{ }\mu\text{g}\cdot\text{kg}^{-1}$, $93 \text{ }\mu\text{g}\cdot\text{kg}^{-1}$, respectively. Of the 14 sampling points, TC concentrations exceeded the emission reference value ($100 \text{ }\mu\text{g}\cdot\text{kg}^{-1}$) prescribed by the European Medicine Agency at 3 points (Sarmah et al., 2006). A study investigating the soil antibiotic content in northern Zhejiang, China, found that the average residual OTC, TC and CTC in manure-treated topsoil was 38-fold, 13-fold and 12-fold more or higher than without application of livestock and poultry manure in farmland (Zhang et al., 2008).

After entering into the environment, manure-associated antibiotics are highly recalcitrant. Moreover, even extremely low concentrations of antibiotics can significantly affect microbial activity (Tasho and Cho, 2016). Yang et al. (2010) found that the growth of most predominant bacteria in the wheat root system was fully suppressed in soils with OTC and TC concentrations of $0.05 \text{ mg}\cdot\text{L}^{-1}$ and $0.5 \text{ mg}\cdot\text{L}^{-1}$, respectively. Many antibiotic resistant bacteria have been detected and separated from soil (Brandt et al., 2009). The antibiotic resistant bacteria, which are generated by residual antibiotics in livestock manure, may enter plant systems via the root, and then enter into the human body via the food chain; thus leading to drug resistance in humans (Zhang et al., 2012). This will bring serious threats to human health. If antibiotic-resistance continues to grow, numerous human and animal diseases will be untreatable (Hu et al., 2015; Tasho and Cho, 2016). It is of great importance to investigate the influence of different fertilization methods and manure types on the environmental deposition of antibiotics (Pruden et al., 2013). Furthermore, drought and drowned cultivation may effect on the decomposition of antibiotics (Hu et al., 2015). Therefore, a fixed field experiment was carried out to analyze tetracycline residues and the variation in antibiotic resistant bacteria after one-year of application using different types and amounts of chicken manure. Furthermore, the influence of different planting modes (drought planting mode and drowned planting mode) on tetracycline residues was investigated.

Materials and method

Three vegetables (*Ipomoea aquatic* Forsk (drowned cultivation mode), *Lactuca sativa* L. and *Brassica juncea* var. *gemmifera* Lee et Lin (drought cultivation mode))

were used in the present study. A fixed field experiment was conducted from March, 2015 to March, 2016 in the Shengde Village, Sansheng Town, Beibei District of Chongqing (29°56'16"N, 106°38'16"E). The contents of organic matter, total nitrogen, alkali-degradable nitrogen, available K, available P and the soil pH were 53.4 g·kg⁻¹, 1.04 g·kg⁻¹, 120.8 mg·kg⁻¹, 90.5 mg·kg⁻¹, 75.0 mg·kg⁻¹, and 4.52, respectively. The average concentrations of quartz, montmorillonite, kaolinite and illite accounted for 14.12%, 16.82%, 7.14% and 61.91% of the total soil clay minerals in the 0-20 cm depth, respectively. Chicken manure was collected from a large chicken farm near the fixed field experimental site. The content of TC, OTC and CTC in fresh chicken manure (FCM) was 1021.64, 272.03 and 13937.18 µg·kg⁻¹, respectively; the content of TC, OTC and CTC in cured chicken manure (CCM) was 18.37, 29.96 and 69.03 µg·kg⁻¹, respectively.

Five plot experiments were conducted without chicken manure (CK), low-fresh chicken manure (L-FCM; 300 kg·667m⁻²), high-fresh chicken manure (H-FCM; 600 kg·667m⁻²), low-cured chicken manure (L-CCM; 300 kg·667m⁻²), and high-cured chicken manure (H-CCM; 600 kg·667m⁻²). The area of each square test plot was 6 m². The experiment was performed in triplicate, and arranged randomly. Before planting, chicken manure was applied according to the predetermined amount. Farmland irrigation and pest control in the experimental field were carried out according to the regular practices of peasant households. Before applying the chicken manure and when harvesting the vegetables, topsoil samples (0-15 cm) were randomly collected from different points using a soil auger sterilized with 70% ethanol. Soil samples were put in an icebox and then taken back to the laboratory. A portion of the soil samples were stored at 4°C. Refrigerated samples were used to test the antibiotic content, soil microorganism abundance, antibiotic resistant bacteria abundance and soil enzyme activity. The remaining portion was air-dried and then used to test the organic content.

Determination of organic matter and enzyme activity in soil

The organic content in the soil was measured as described by Nelson and Sommers (1982). Soil catalase activity was measured by the permanganate titration method and expressed as the 0.1 N KMnO₄ amount (mL) per gram of soil and 20 min (He et al., 2015). Urease activity was measured by indophenol blue colorimetry and expressed as the NH₃-N amount (µg) per gram of soil (He et al., 2015).

Quantification of microorganisms and antibiotic resistant bacteria in soil

Bacteria were cultured in beef extract water peptone agar medium. Fungi were cultured in Martin-Bengal red medium. Actinomycetes were cultured in improved Gause No.1 medium. All microbes were quantified as per the colony forming unit method (Negreanu et al., 2012). The quantity of antibiotic resistant bacteria was measured as described by Negreanu et al. (2012).

Analysis of tetracycline antibiotics in soil and manure

Tetracyclines in the soil and in livestock and poultry manure were extracted and measured as described by Jacobsen et al. (2004). Measurements were conducted using a high performance liquid chromatograph (HPLC, Shimadzu, Japan) equipped with SPD-20A UV-detector. The chromatographic column (Inertsil ODS-3; 4.6×150 mm, 5 µm) was run at a mobile phase flow rate of 1 mL·min⁻¹, injection volume of 10 µL, UV

detection wavelength of 355 nm, and a sampling time of 25 min. The average recovery rates of OTC (58.3%), TC (57.1%) and CTC (87.4%) were measured by the addition standard method. All variable coefficients were under 11.04%.

Statistical analysis

The data were subjected to three-way univariate ANOVA using SPSS version 21.0 (IBM Corp., Armonk, NY, USA). Parameters for soil organic content, enzyme activity, soil resistant bacteria and soil-associated tetracycline residues were analyzed. Additionally, the correlation between the application amount of chicken manure and tetracycline residues was determined. Prior to ANOVA, normal probability and residual plots were constructed for each dataset and examined for unequal variance and deviations from normality among the residuals. All data fulfilled the conditions for equal variance and normality. Means were considered statistically significant at $P \leq 0.05$ using Fisher's least significant difference test.

Results and analysis

Soil organic content and enzyme activity

After application of chicken manure, the content of organic matter in the soil increased by 1.0%-3.2% when compared with the control (*Table 1*). No significant difference in soil organic matter content was found among treatments. Soil catalase activity in FCM and CCM treatments significantly increased by 84.3%-91.5% and 81.9%-102.9%, respectively, compared to the control (*Table 1*). Soil catalase activity in the H-CCM treatment ($600 \text{ kg} \cdot 667 \text{ m}^{-2}$) was 11.7% higher than that in the L-CCM treatment ($300 \text{ kg} \cdot 667 \text{ m}^{-2}$). Compared with the control, soil urease activity in the H-FCM treatment ($600 \text{ kg} \cdot 667 \text{ m}^{-2}$) decreased by 34.2%. Soil urease activity in the H-CCM treatment was 17.9%, 18.3% and 79.1% higher than the control treatment, L-FCM treatment ($300 \text{ kg} \cdot 667 \text{ m}^{-2}$) and H-FCM treatment, respectively.

Table 1. Effects of different chicken manure on the contents of organic matter, enzyme activities and microbial quantity in soil after one year

Treatment	Organic matter/ $\text{g} \cdot \text{kg}^{-1}$	Catalase activity/ $\text{ml} \cdot \text{h}^{-1} \cdot \text{g}^{-1}$	Soil urease activity/ $\mu\text{g} \cdot \text{g}^{-1}$	Bacteria $\times 10^6$ /CFU $\cdot \text{g}^{-1}$	Actinomycetes $\times 10^5$ /CFU $\cdot \text{g}^{-1}$	Fungi $\times 10^4$ /CFU $\cdot \text{g}^{-1}$
CK	54.39 \pm 3.84a	0.57 \pm 0.06c	0.26 \pm 0.04a	7.22 \pm 0.10c	5.87 \pm 0.26b	23.44 \pm 3.70a
L-FCM	55.20 \pm 4.39a	1.08 \pm 0.06ab	0.26 \pm 0.06a	23.02 \pm 2.56b	2.81 \pm 0.26c	10.23 \pm 2.56b
H-FCM	56.11 \pm 4.59a	1.04 \pm 0.02ab	0.17 \pm 0.02b	23.13 \pm 4.41b	2.23 \pm 0.60c	6.87 \pm 1.49bc
L-CCM	54.94 \pm 4.05a	1.02 \pm 0.03b	0.28 \pm 0.03a	30.81 \pm 2.57a	8.47 \pm 1.56a	3.80 \pm 1.29c
H-CCM	55.34 \pm 4.37a	1.11 \pm 0.01a	0.30 \pm 0.05a	27.06 \pm 1.51ab	8.29 \pm 0.55a	22.69 \pm 3.02a

Different letters (a, b, c) indicate significant difference at $P \leq 0.05$ among different treatments

The abundance of soil microorganisms was as follows: bacteria > actinomycetes > fungi (*Table 1*). Application of chicken manure significantly increased the quantity of bacteria, which was 3.2-4.3 times that in the control. The bacterial abundance in the L-CCM treatment was significantly larger than that in L-FCM treatment, with increases of 17.0%-33.9%. The number of actinomycetes in the CCM treatments significantly increased by 41.3%-44.4%, compared with the control.

However, the abundance of actinomycetes in the FCM treatments was lower than in the control, with reductions of 52.1%-61.9%. The actinomycetes abundance in CCM treatments with identical application amounts was 201.2%-271.2% higher than in FCM treatments. The application of chicken manure reduced the abundance of fungi in the soil with L-CCM treatments by 62.9%, compared with that in L-FCM treatments.

Quantity of antibiotic resistant bacteria in the soil

The abundance of soil antibiotic resistant bacteria in the same treatments was as follows: Anti-OTC > Anti-TC > Anti-CTC (Fig. 1a). The quantity of resistant bacteria treated with chicken manure was higher than that in control soil, with the CCM treatments being significantly higher than the FCM treatments. The highest abundance of resistant bacteria was found in the L-CCM treatment, wherein the number of Anti-OTC, Anti-TC and Anti-CTC in the soil was 11.6%-339.6%, 127.0%-635.4% and 32.2%-130.9% higher, respectively, than in the other treatments.

Application of chicken manure increased the proportion of resistant bacteria in the soil (Fig. 1b). The proportions of Anti-TC treated with chicken manure were significantly higher than the control by 42.9%-102.2%.

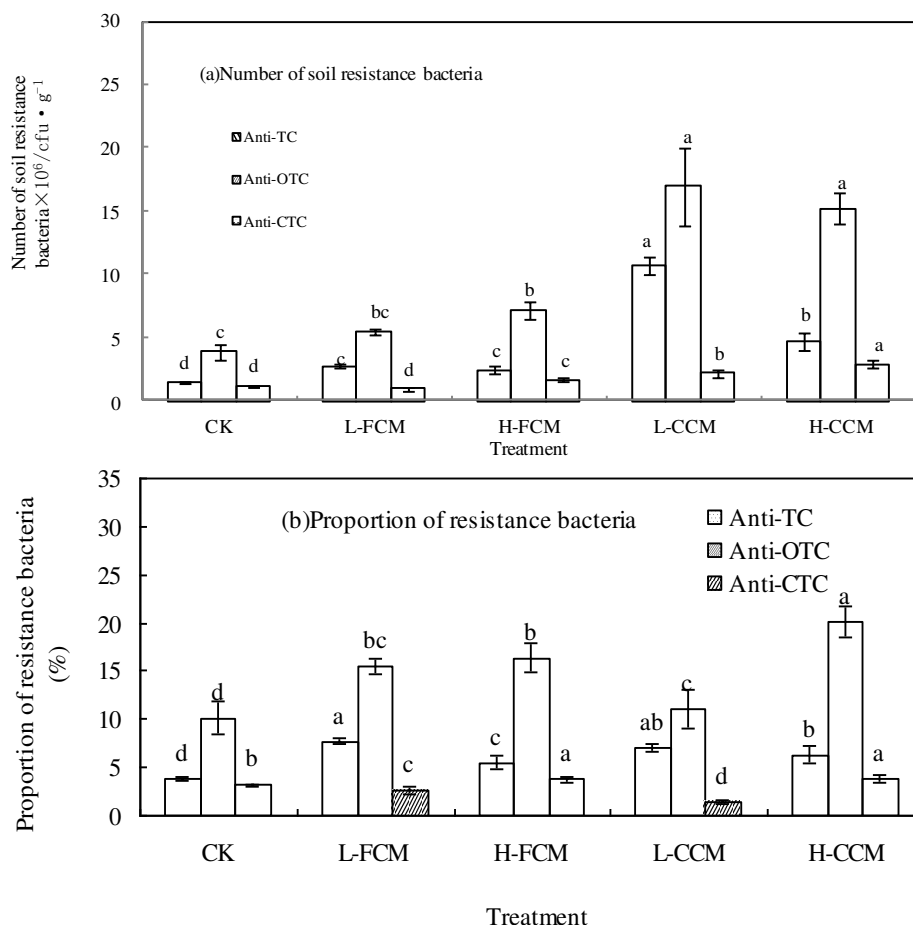


Figure 1. Effects of different chicken manure treatments on the amount and proportion of soil tetracycline resistant bacteria. Anti-TC: Tetracycline resistant bacteria; Anti-OTC: Oxytetracycline resistant bacteria; Anti-CTC: Chlortetracycline resistant bacteria; Different letters (a, b, c) indicate significant difference at $P \leq 0.05$ among different treatments

The proportions of Anti-OTC in FCM treatments and H-CCM treatments were also significantly higher than that in the control. The proportions of Anti-CTC in H-FCM treatments and CCM treatments were higher than that in the control, while the proportion of Anti-CTC in the L-CCM treatments was lower than that in control by 54.8%.

Variation of tetracycline antibiotic residues in soil

The total amount of soil tetracycline after harvesting *Ipomoea aquatica* Forsk in the L-FCM, H-FCM, L-CCM and H-CCM treatments increased by 7.3%, 27.5%, 19.4% and 3.6%, respectively, compared with that before planting (Fig. 2a).

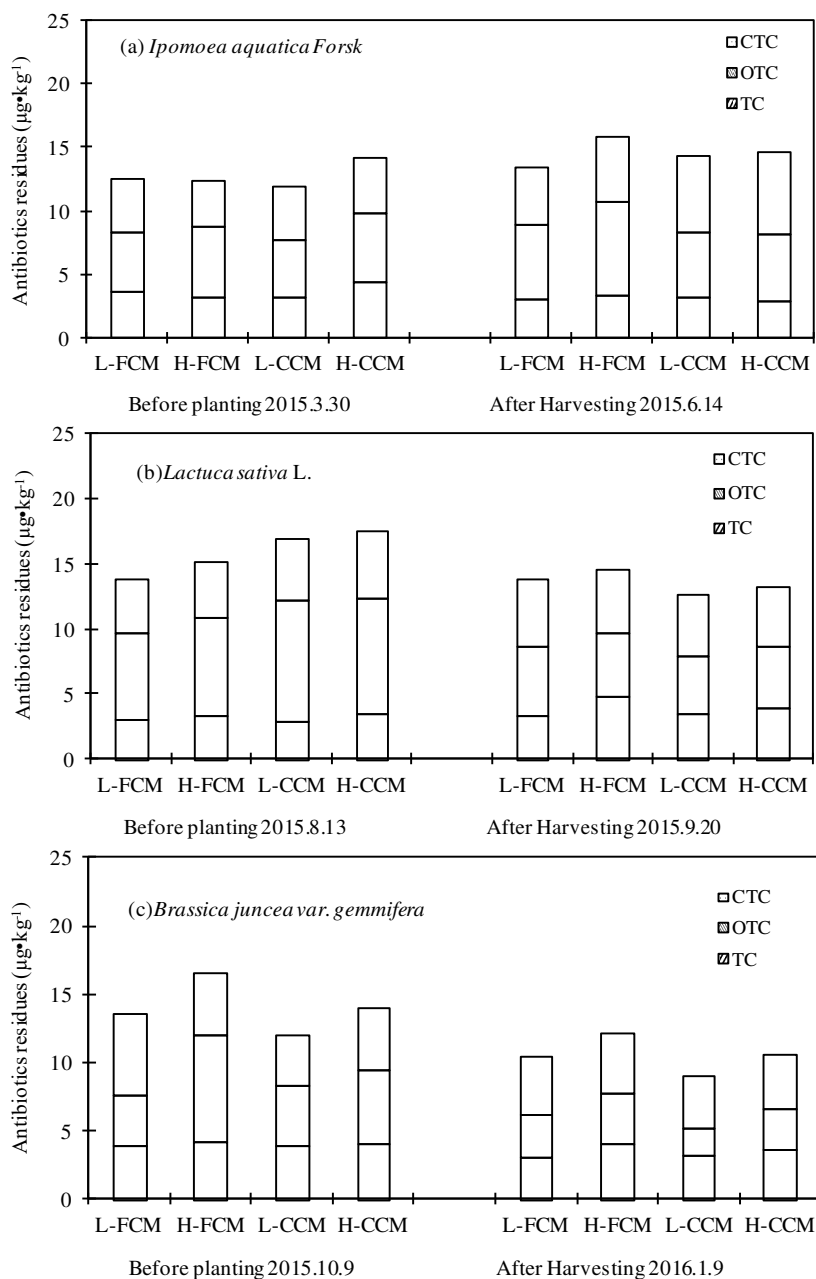


Figure 2. The concentration changes of tetracycline antibiotics in soil during the application of chicken manure in different vegetable crop cropping patterns

The highest amount of soil tetracycline was found in the H-FCM treatment. The OTC amount in the L-FCM and H-FCM treatments increased by 25.2% and 32.8%, respectively. The amount of CTC in soils treated with chicken manure generally increased, with the highest CTC content observed for the H-CCM treatment, which increased by 52.2% compared with that before planting *Ipomoea aquatica* Forsk.

The total amount of soil tetracycline decreased after harvesting *Lactuca sativa* L. compared with before planting (Fig. 2b). The total amount of antibiotics after harvesting *Lactuca sativa* L. in the L-CCM and H-CCM treatments decreased by 33.6% and 32.7%, respectively. Furthermore, the OTC content in H-CCM and L-CCM treatments decreased by 47.3% and 52.2%, respectively, compared with that before planting *Lactuca sativa* L.

The total amount of soil tetracycline in the L-FCM, H-FCM, L-CCM and H-CCM treatments after harvesting *Brassica juncea* var. *gemmifera* decreased by 22.6%, 26.6%, 24.9% and 24.2%, respectively, compared with before planting. Moreover, the soil OTC contents decreased by 14.7%, 52.1%, 55.5% and 45.1%, (Fig. 2c).

The total amounts of soil tetracycline after one year of treatment with L-FCM, H-FCM, L-CCM and H-CCM increased by 176.5%, 217.9%, 168.5% and 191.5%, respectively, compared to the control (Fig. 3). The highest total amount of soil tetracycline ($13.069 \mu\text{g}\cdot\text{kg}^{-1}$) was found in the H-FCM treatment. Soil tetracycline residues in high chicken manure treatments ($600 \text{ kg}\cdot 667\text{m}^{-2}$) were higher than that in the low chicken manure treatments ($300 \text{ kg}\cdot 667\text{m}^{-2}$) by 8.5%-15.0%, and approximately twice that of the control. The antibiotic residues in the FCM treatments were higher than that in the CCM treatments by 3.0%~9.1%. In general, the TC residues in the soils treated with L-CCM was the lowest, while that with H-FCM was the highest.

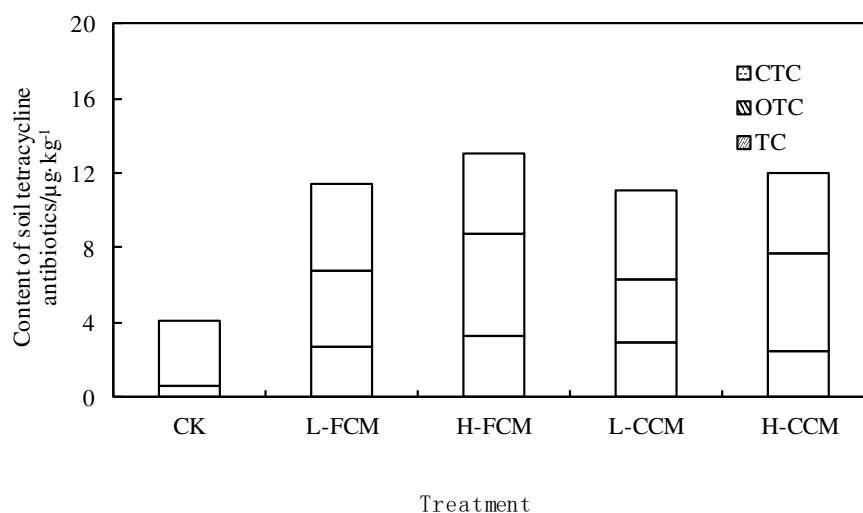


Figure 3. The amount of soil tetracycline antibiotics in the chicken manure treatments after one year

The application amount of chicken manure significantly and positively correlates with the total amount of soil tetracycline ($r = 0.880$), wherein the TC and OTC residues are positively correlated with the application amount of chicken manure ($r = 0.648$, $P < 0.05$; $r = 0.936$, $P < 0.01$). Conversely, the CTC residue does not correlate with the chicken manure application amount (Table 2).

Table 2. The correlations of chicken manure application amount and soil tetracycline antibiotic residues

	Application amount of chicken manure	Soil TC	Soil OTC	Soil CTC	ΣTCs
Application amount of chicken manure	1				
Soil TC	0.648*	1			
Soil OTC	0.936**	0.714*	1		
Soil CTC	0.323	0.716*	0.458	1	
ΣTCs	0.880**	0.874**	0.959**	0.645*	1

* or ** indicates significant difference of the correlations of chicken manure application amount and soil tetracycline antibiotic residues at $P \leq 0.05$ or $P \leq 0.01$ level. ΣTCs indicates the total amount of the three tetracycline antibiotics

Discussion

With the application of organic manure fertilizers, antibiotics enter and then accumulate in soil. Antibiotic residues in soil are largely determined by the soil characteristics, such as pH, organic matter content and mineral composition. Soil mineral and organic matter fractions could be the primary antibiotic adsorption sites (Qiu et al., 2004). In the present study, no significant difference in soil organic contents was found between different treatments after one year of applying different chicken manures. This may be because the difference in chicken manure application amounts among treatments was not significant or because the test period was only one year; therefore, further long-term in-situ monitoring may be required.

Soil microorganisms and enzymes are important components of soil biochemical characteristics, which play important roles in nutrient transformation and organic matter decomposition (Zhang et al., 2012). Soil enzymes are important components of the soil ecosystem and a key index for evaluating ecological environment and fertility of the soil (Yao et al., 2010). In the present study, the application of chicken manure significantly increased catalase activity in the soil; however, no significant difference in soil catalase activity was found between the FCM and CCM treatments. This result is similar to that of Yao et al. (2010). In this study, soil urease activity after application of FCM was lower than after application of CCM. The reasons may be because FCM normally results in strong acidity (pH 3.6-4.7), which is far from the suitable pH value of urease (6.5-7.0) (Dodd et al., 1987). In addition, FCM is generally in an organic or slowly-released state that cannot be absorbed and used by plants, leading to slow fertilizer efficiency, which affects urease activity (Liu et al., 2003). Application of CCM increases soil urease activity, which is consistent with results published by Jin et al. (2013). In the present study, the quantity of soil bacteria in the CCM treatments was larger than that in FCM treatments. This may be caused by the strong acidity and slowly-released nutrients from FCM, which affects the urease activity, thus resulting in a decreased bacterial abundance.

The quantity of soil bacteria in the high chicken manure treatments ($600 \text{ kg} \cdot 667 \text{ m}^{-2}$) was generally lower than that in the low chicken manure treatments ($300 \text{ kg} \cdot 667 \text{ m}^{-2}$). This indicates that the application amount of organic fertilizer affects the quantity of soil bacteria. The application of CCM caused a significant increase in the quantity of actinomycetes, while FCM limited the quantity of actinomycetes. The number of soil

fungi decreased after the application of chicken manure. This result further confirms that appropriate application of CCM is beneficial for the growth of bacteria and actinomycetes in soil, and it also limits the growth of soil fungi and reduces harm to plants. These results are in agreement with those published by Yang et al. (2007).

The application of chicken manure increased the number of resistant bacteria, wherein the CCM treatment increased this subpopulation more than FCM did. This may be because the antibiotic degradation products in CCM have a larger influence on soil resistant bacteria. In the present study, compared to the control, appropriate application of CCM reduced the proportion of Anti-OTC, which is consistent with the research results of Zhang et al. (2012). The quantity and proportions of Anti-CTC in the soil after application of different chicken manures, and the proportion of soil Anti-CTC in high chicken manure treatments, was larger than that in low chicken manure treatments. This is probably because the high application amount of chicken manure ($600 \text{ kg} \cdot 667 \text{ m}^{-2}$) improves the soil physicochemical properties and changes its adsorption capacity for CTC (Pils and Laird, 2007). In the present study, the application of CCM greatly reduced the number and proportion of resistant bacteria, while the application of FCM increased these values, which is similar to the results reported by Yang et al. (2014).

During the yearlong application of chicken manure, three crops (*Ipomoea aquatica* Forsk, *Lactuca sativa* L. and *Brassica juncea* var. *gemmifera*.) were planted using two different cultivation modes (drowned and drought cultivation). The soil antibiotic residues after harvesting *Ipomoea aquatica* Forsk in drowned cultivation mode increased, while the residues after harvesting *Lactuca sativa* L. and *Brassica juncea* var. *gemmifera* in drought planting mode decreased. This may be because, in drought cultivation using *Lactuca sativa* L. and *Brassica juncea* var. *gemmifera*, the water downwardly infiltrated and evaporated, then the antibiotics also downwardly infiltrated under the plough layer, or the soil physicochemical property changed due to lack of water; therefore the antibiotic residues in plough layer soil decreased (Du and Liu, 2011; Hu et al., 2015). After application of chicken manure for one year, the soil antibiotic residues significantly increased, wherein the residue in the FCM-treated soil was higher than that in the CCM-treated soil. The reasons may be because the FCM is acidic. With the increase of soil pH and ion strength, the absorption capacity of the soil for tetracycline decreased (Gündoğan et al., 2004). The antibiotic residues in high chicken manure treatments ($600 \text{ kg} \cdot 667 \text{ m}^{-2}$) were higher than that in low chicken manure treatments ($300 \text{ kg} \cdot 667 \text{ m}^{-2}$), which is similar to the results reported by Zhang et al. (2015). The total antibiotic content in the soil was significantly positively correlated with the application amount of chicken manure. This result further confirms that the higher the amount of manure application are, the higher the soil antibiotic residues. However, the soil CTC content was not correlated with the application amount of manure, possibly because the soil CTC content is correlated with the type of manure or soil background value; however, these results should be validated by further long-term studies.

Conclusion

After one year, soil catalase activity increased in chicken manure-treated soils. Soil urease activity increased in CCM treatments. The quantity of bacteria and actinomycetes significantly increased in L-CCM treatments, while the number of fungi significantly decreased. The application of CCM significantly increased the quantity of actinomycetes, while the application of L-CCM significantly reduced the proportion of

antibiotic resistant bacteria. The antibiotic residues in CCM-treated soil were lower than that in FCM-treated soil. The antibiotic residues in high chicken manure treatments ($600 \text{ kg} \cdot 667 \text{ m}^{-2}$) were higher than that in low chicken manure treatments ($300 \text{ kg} \cdot 667 \text{ m}^{-2}$). The cultivation mode also affected antibiotic residues in soil, wherein the drowned cultivation mode may worsen the tetracycline antibiotics residues in the soil. Long-term application of FCM may cause residue and accumulation of tetracycline antibiotics in soil and harm to the ecological environment.

Acknowledgements. This work was supported by Fund of China Agriculture Research System (CARS-23) and the National Science and Technology Pillar Program of China (No. 2007BAD87B10).

REFERENCES

- [1] Boeckel, T. P. V., Brower, C., Gilbert, M., Grenfell, B. T., Levin, S. A., Robinson, T. P., Teillant, A., Laxminarayan, A. (2015): Global trends in antimicrobial use in food animals. – *Proceedings of the National Academy of Sciences of the United States of America* 112(18): 5649-5654.
- [2] Brandt, K. K., Sjøholm, O. R., Krogh, K. A., Halling-Sørensen, B., Nybroe, O. (2009): Increased pollution-induced bacterial community tolerance to sulfadiazine in soil hotspots amended with artificial root exudates. – *Environmental Science & Technology* 43(8): 2963-2968.
- [3] Chen, Y. S., Zhang, H. B., Luo, Y. M., Song, J. (2012): Occurrence and assessment of veterinary antibiotics in swine manures: A case study in East China. – *Chinese Science Bulletin* 57(6): 606-614.
- [4] Dodd, J. C., Burton, C. C., Burns, R. G., Jeffries, P. (1987): Phosphatase activity associated with the roots and the rhizosphere of plants infected with vesicular-arbuscular mycorrhizal fungi. – *New Phytologist* 107(1): 163-172.
- [5] Du, L. F., Liu, W. K. (2011): Occurrence, fate, and ecotoxicity of antibiotics in agroecosystems. A review. – *Agronomy for Sustainable Development* 32: 309-327.
- [6] Gündoğan, R., Acemioğlu, B., Alma, M. H. (2004): Copper (II) adsorption from aqueous solution by herbaceous peat. – *Journal of Colloid & Interface Science* 269(2): 303-309.
- [7] Hamscher, G., Sczesny, S., Höper, H., Nau, H. (2002): Determination of persistent tetracycline residues in soil fertilized with liquid manure by high-performance liquid chromatography with electrospray ionization tandem mass spectrometry. – *Analytical Chemistry* 74(7): 1509.
- [8] He, F., Wang, H., Chen, Q., Yang, B., Gao, Y., Wang, L. (2015): Short-term response of soil enzyme activity and soil respiration to repeated carbon nanotubes exposure. – *Soil Sediment Contam.* 24: 250-261.
- [9] Hu, J., Wan, W. N., Mao, D. Q., Wang, C., Mu, Q. H., Qin, S. Y., Luo, Y. (2015): Occurrence and distribution of sulfonamides, tetracyclines, quinolones, macrolides, and nitrofurans in livestock manure and amended soils of Northern China. – *Environmental Science and Pollution Research* 22: 4545-4554.
- [10] Jacobsen, A. M., Halling-Sørensen, B., Ingerslev, F. (2004): Simultaneous extraction of tetracycline, macrolide and sulfonamide antibiotics from agricultural soils using pressurised liquid extraction, followed by solid-phase extraction and liquid chromatography–tandem mass spectrometry. – *Journal of Chromatography A* 1038(1-2): 157-170.
- [11] Jin, L. J., Shen, L., Liu, Y. R., Li, P., Wang, J. G. (2013): Effect of chicken manure and tetracycline on soil urease and phosphatase activity. – *Journal of Agro-Environment Science* 32(5): 986-990.

- [12] Kemper, N. (2008): Veterinary antibiotics in the aquatic and terrestrial environment. – *Ecological Indicators* 8(1): 1-13.
- [13] Liguoro, M. D., Cibin, V., Capolongo, F., Halling-Sørensen, B., Montesissa, C. (2003): Use of oxytetracycline and tylosin in intensive calf farming: evaluation of transfer to manure and soil. – *Chemosphere* 52(1): 203-212.
- [14] Liu, G. S., Xu, D. M., Xu, Z. J., Wang, H. Y., Liu, W. P. (2003): Relationship between hydrolase activity in soils and soil properties in Zhejiang province. – *Acta Pedologica Sinica* 40(5): 756-762.
- [15] Negreanu, Y., Pasternak, Z., Jurkevitch, E., Cytryn, E. (2012): Impact of treated wastewater irrigation on antibiotic resistance in agricultural soils. – *Environmental Science & Technology* 46(9): 4800-4808.
- [16] Nelson, R. E., Sommers L. E. (1982): *Methods of Soil Analysis. Part 2: Chemical and Microbiological Properties* (second ed.). – American Society of Agronomy, Madison, WI.
- [17] Pan, M., Chu, L. M. (2017): Fate of antibiotics in soil and their uptake by edible crops. – *Science of the Total Environment* 599–600: 500-512.
- [18] Pils, J. R. V., Laird D. A. (2007): Sorption of tetracycline and chlortetracycline on K- and Ca-saturated soil clays, humic substances, and clay-humic complexes. – *Environmental Science & Technology* 41(6): 1928-1933.
- [19] Pruden, A., Larsson, D. G., Amezcua, A., Collignon, P., Brandt, K. K., Graham, D. W., Lazorchak, J. M., Suzuki, S., Silley, P., Snape, J. R., Topp, E., Zhang, T., Zhu, Y. G. (2013): Management options for reducing the release of antibiotics and antibiotic resistance genes to the environment. – *Environmental Health Perspectives* 121(8): 878-885.
- [20] Sarmah, A. K., Meyer, M. T., Boxall, A. B. (2006): A global perspective on the use, sales, exposure pathways, occurrence, fate and effects of veterinary antibiotics (VAs) in the environment. – *Chemosphere* 65(5): 725.
- [21] Sun, W., Qian, X., Gu J., Wang, X. J., Zhang, L., Guo, A. Y. (2017): Mechanisms and effects of arsanilic acid on antibiotic resistance genes and microbial communities during pig manure digestion. – *Bioresource Technology* 234: 217-223.
- [22] Tasho, R. P., Cho, J. Y. (2016): Veterinary antibiotics in animal waste, its distribution in soil and uptake by plants: A review. – *Science of the Total Environment* 563-564: 366-376.
- [23] Yang, Y. H., Yang, L. P., Zhao, Z. X., Wu T. (2007): Effect of differ kinds of organic manure and application time on micro-organism in flued-cured tobacco planting soil. – *Chinese Agricultural Science Bulletin* 23(1): 292-295.
- [24] Yang, Q. X., Zhang, J., Zhu, F. K., Yu, N. (2010): Sensitivity to veterinary antibiotics of dominant bacteria in wheat rhizosphere. – *Environmental Science and Technology* 32(2): 85-89.
- [25] Yang, Q. X., Ren, S. W., Niu, T. Q., Guo, Y. H., Qi, S. Y., Han, X. K., Liu D., Pan F. (2014): Distribution of antibiotic-resistant bacteria in chicken manure and manure-fertilized vegetables. – *Environmental Science and Pollution Research* 21: 1231-1241.
- [26] Yao, J. H., Niu, D. K., Li, Z. J., Liang, Y. C., Zhang, S. Q. (2010): Effects of antibiotics oxytetracycline on soil enzyme activities and microbial biomass in wheat rhizosphere. – *Scientia Agricultura Sinica* 43(4): 721-728.
- [27] Zhang, H. M., Zhang, M. K., Gu, G. P. (2008): Residues of tetracyclines in livestock and poultry manures and agricultural soils from North Zhejiang Province. – *Journal of Ecology and Rural Environment* 24(3): 69-73.
- [28] Zhang, H., Zhang, L. L., Wang, J., Zhu, K. F., Wang, H. T., Yang, Q. X. (2012): Influence of oxytetracycline exposure on antibiotic resistant bacteria and enzyme activities in wheat rhizosphere soil. – *Acta Ecologica Sinica* 32(2): 508-516.
- [29] Zhang, M. K., Gu, G. P., Bao, C. Y. (2015): Degradation characteristics of veterinary antibiotics in soils and its relationship with soil properties. – *Chinese Agricultural Science Bulletin* 31(31): 228-236.

GERMINATION TRAITS OF ADRIATIC LIZARD ORCHID (*HIMANTOGLOSSUM ADRIATICUM*) IN HUNGARY

GILIÁN, L. D.^{1,2*} – BÓDIS, J.¹ – ESZÉKI, E.³ – ILLYÉS, Z.⁴ – BIRÓ, É.¹ – NAGY, J. GY.²

¹*Department of Plant Sciences and Biotechnology, Georgikon Faculty, University of Pannonia
H-8360 Keszthely, Festetics u. 7., Hungary
(phone: +36-83-545-095; fax: +36-83-545-058)*

²*Doctoral School of Biological Sciences, Institute of Botany and Ecophysiology
Szent István University
H-2100 Gödöllő, Páter Károly utca 1., Hungary
(phone: +36-28-522-000; fax: +36-28/410-804)*

³*Botanical Garden of Eötvös Loránd University
H-1083 Budapest, Illés u. 25., Hungary
(phone: +36-1-210-1074; fax: +36-1-314-0535)*

⁴*Mindszenty Ifjúsági Ház
H-8900 Zalaegerszeg-Botfa, Várberki u. 13., Hungary
(phone: +36-30-954-7755)*

**Corresponding author
e-mail: lilla.gilian@gmail.com*

(Received 10th Oct 2017; accepted 5th Feb 2018)

Abstract: The germination of the orchids is the most sensitive period of their life. In case of the extremely rare *Himantoglossum adriaticum* in Hungary, no such information has been published yet. Our aim is to present the results of the in situ and the ex situ germination of *H. adriaticum* seeds originate in West Hungary. There were 10-10 seed packets sowed 10-20 cm far-, and 3-3 as control 10 m away from the living mother plants on the natural habitats of Keszthelyi-hills and of Sümeg-Tapolca region. The success of germination was significantly higher close to the mother plant than in the control packets either 8 or 11 months after sowing on both places and was a bit better in Keszthely than on Sümeg-Tapolca region. Parallely with it we sowed the seeds of same origin into six flasks, onto Fast medium in the orchid laboratory of Eötvös Loránd University's Botanical Garden in Budapest. During this ex situ germination, the first protocorm was appeared 9 months after sowing. The germination was outstanding only in one flask. Our results show, that the germination in the natural habitat was much higher than in vitro on the generally used artificial media.

Keywords: *Orchidaceae, field research, in situ propagation, ex situ propagation, in vitro, micropropagation, flask, Fast-media*

Introduction

Nowadays, because of the environment-forming activity of people, the number and the area of natural habitats are decreasing all over the world. As we face the sixth great extinction event in the history of life on earth (Canadell and Noble, 2001), an increasing attention is being paid to biodiversity conservation (Swarts and Dixon, 2009).

The family *Orchidaceae*, with its more than 25,000 species, is the largest in the plant kingdom (Mabberley, 1997; Cribb et al., 2003). One-third of the orchids are terrestrials, and yet almost half of the extinct embryophytes according to The World Conservation Union (IUCN, 1999) are terrestrial herbaceous perennials. Terrestrial orchids thus

represent a life-form class likely to experience a greater extinction risk as a result of the multiplicity of threatening processes, particularly under current climatic change scenarios (Swarts and Dixon, 2009).

Fragmentation of habitats, removal of key species critical to the continued existence of ecosystems, increased susceptibility to fire threats, pollinator decline and introduction of feral animals are also documented to result in drastic losses in orchid populations and diversity (Sosa and Platas, 1998; Coates and Dixon, 2007). Historically, collection of wild orchids has threatened many species with extinction (Cribb et al., 2003). Koopowitz et al. (2003) described a ‘golden age’ of plant collecting from the mid-1800s until the onset of the First World War. As a consequence, many orchids are recognized as endangered and vulnerable species (Shirokov et al., 2016). Based on Molnár V. et al. (2015), pollination crisis has not affected Hungarian orchids yet (at least in terms of reproductive success).

In the case of terrestrial orchids, for example, range and abundance may be driven by factors pertaining to the underground and above-ground life history phases of species (Woolcock and Woolcock, 1984; Clements, 1988; Dixon, 1989). The first need, represented in the underground phase, is a mycorrhizal association with a fungal endophyte (Warcup, 1971; Ramsay et al., 1986; Rasmussen, 2002). The second is effective pollination/fertilization in the above-ground phase (Stoutamire, 1983; Roberts, 2003). The great taxonomic diversity of *Orchidaceae* is often attributed to specialization of these two requirements (Swarts and Dixon, 2009).

Despite the orchids worldwide dispersion and extreme plasticity, the majority of these species are of key conservation importance (Jacquemyn et al., 2005; Kull and Hutchings, 2006; Swarts and Dixon, 2009). Protecting orchids, first of all we have to ensure them their suitable habitats. The specialist species with small area are much more vulnerable of the rapidly changing environmental conditions, than the widespread, generalist species. Causes of their decline are complex, but – independently of the conservation status – the long-term persistence of plant populations in every case partly depends on seed production (Biró et al., 2014) and their viability. Based on these facts, it is necessary to explore the reproductive capacity (viability) and the possibility of propagation of these species.

As for the in situ germination researches, it has been about 20 years since seed packets were first employed successfully to explore orchid germination and seedling development (Rasmussen and Whigham, 1993; Masuhara and Katsuya, 1994; Van der Kinderen, 1995; Zelmer et al., 1996). Because orchid seeds are minute, the first life stages of seedlings previously defied observation, but now experimental sowing in the field constitutes a useful routine procedure for identifying germination requirements (Rasmussen et al., 2015). The germination of terrestrial orchids is the most sensitive period of their life, because of their seed structure and their mycorrhizal fungus relationships. Under natural conditions, seeds of most terrestrial orchid species will germinate only in association with a compatible mycorrhizal fungus (Warcup, 1981; Ramsay et al., 1986; Arditti et al., 1990). Due to limited food reserves, orchid seeds have a complete dependency on nutrients supplied by the mycorrhizal association during early germination and seedling establishment phases (Rasmussen, 1995), although some species may substitute or acquire new mycorrhizal associates depending upon plant maturity (Bidartondo and Read, 2008).

For some protected plants the artificial germination (ex situ, in vitro), the grow-up and the replantation to their natural habitat has become inevitable. As regards artificial

seed germination, orchids can be classified into three categories (Arditti, 1967; 1979; Arditti and Ernst, 1984). Terrestrial, temperate zone orchids are more difficult to germinate aymbiotically (Arditti, 1982) than the tropical ones. By ex situ, in vitro germination, it is very important, that the core must be unripe on the plant when we collect the seeds, because the seeds are only sterile until the cores are closed (Fast, 1980). In this case, seeds can be used without disinfection (Richter, 1982). After sowing, the seeds get a cold treatment called “chilling time”, because it increases the degree of germination (De Pauw and Remphrey, 1993). According to Miyoshi and Mii (1988) a 12-week-long chilling time seems the most effective for the seeds.

As for our target species, *Himantoglossum adriaticum* H. Baumann has a central submediterranean distribution, currently known to occur in Austria, Bosnia-Herzegovina, Croatia, Czech Republic, Hungary, Italy, Slovakia, Slovenia (Fig. 1). The Czech Republic is at the boarder of the distribution (Dostalova et al., 2011; Pecoraro et al., 2013; Rybka et al., 2005; Bernhardt, 2011). Red Data Books of many countries contains this species (Conti et al., 1997; Király, 2007; Maglocky and Feráková, 1993; Grulich, 2012). The conservation status of *H. adriaticum* is Critically Endangered in the Czech Republic and in Slovakia, Endangered in Austria and in Hungary, Vulnerable in Slovenia and Near Threatened in Croatia (Dostalova et al., 2011). Additionally, *H. adriaticum* is suffering ongoing population declines and is listed in the Annex II of Council Directive 92/43/EEC (the ‘Habitats Directive’).

The reproductive success of *Himantoglossum adriaticum* is generally low. The flowers have been observed to be pollinated by the following bee species: *Andrena haemorrhoea*, *A. carbonaria*, *A. nigroaenea*, *A. potentillae*, *Apis mellifera* (Claessens and Kleynen, 2011), *Colletes similis* (Vöth, 1990; Sulyok et al., 1998), *Bombus spp.* (Teschner, 1980), *Osmia caerulea*, *Lasioglossum (Evylaeus) morio*, *Lasioglossum (Evylaeus) lucidulum*, *Megachile melanopyga* (Bódis, 2010). Previously published fruit set data varied between 4.5 and 44% in Austria (Vöth, 1990), and between 5.4% and 23.3% in Hungary (Bódis and Molnár, 2009).

In case of any germination traits of *Himantoglossum adriaticum*, there is no information has been published yet. Our aim is to present the peculiarity of germination of *H. adriaticum*, either in laboratory (ex situ, in vitro) or under field conditions (in situ).

Materials and methods

Himantoglossum adriaticum

The *Himantoglossum adriaticum* – called “Adriatic lizard orchid” – is an Adriatic-Mediterranean, in Hungary is a collin-submontane species (Bódis et al., 2011). The characteristic habitat of the species is full sun to mid-shade and dry calcareous substrates. It prefers poor grassland, banks, thickets, woodland edges and open woodlands, up to 1600 m of altitude above sea level (Delforge, 2006). It often occurs in secondary habitats such as road sides, vineyards and abandoned mines (Dostalova et al., 2011).

In Hungary it has known only 5 populations: in the Keszthely Hills, in the Sümegeg-Tapolca Region, in the Bakony Hills, in the Kőszeg Mountains and in the Sopron Mountains (Fig. 1). The decrease of the historically known presence of the species is 35% (Bódis et al., 2011).

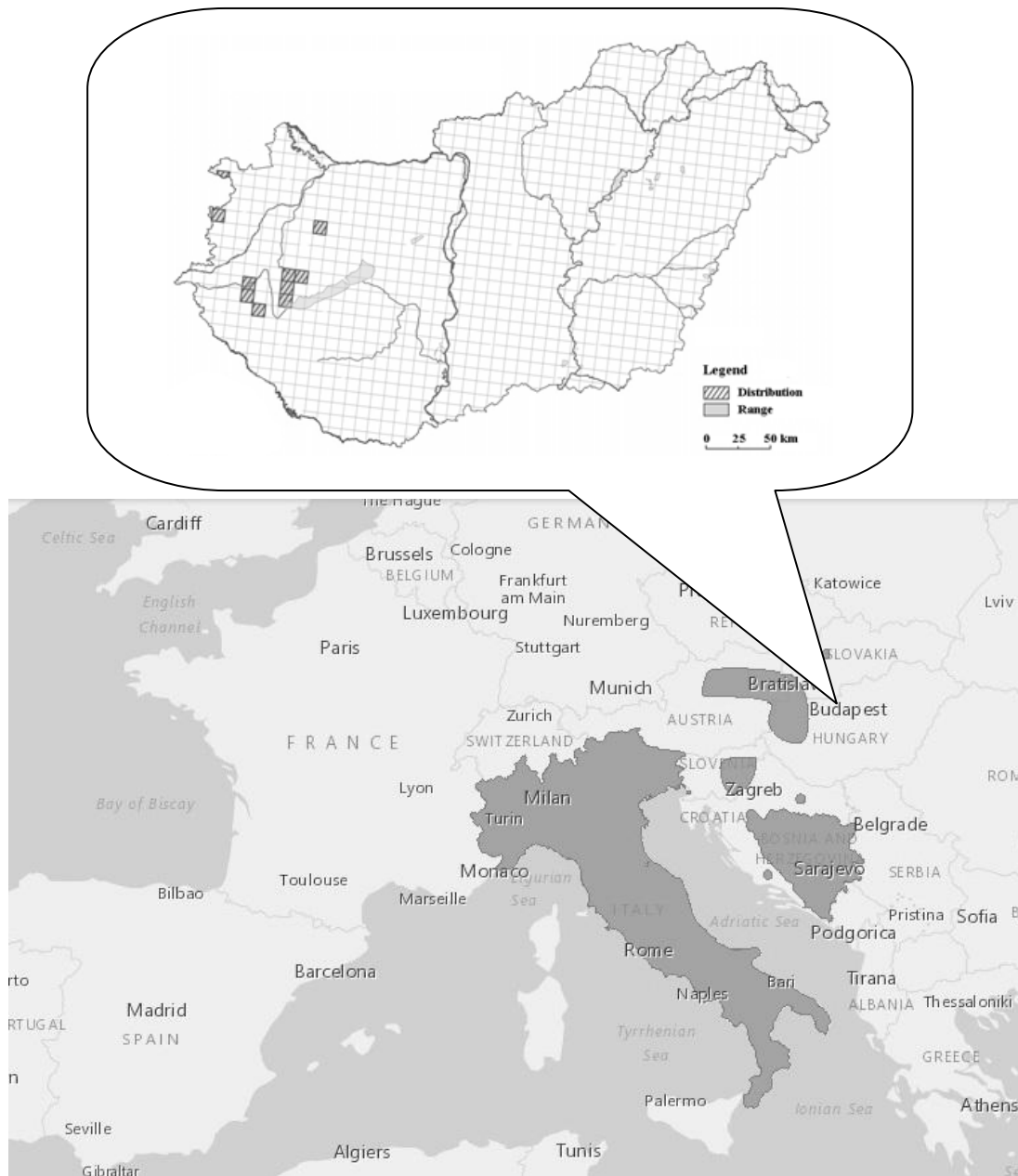


Figure 1. Map of the *H. adriaticum* populations in Europe, and highlighted in Hungary.
(Source: Europe map: The IUCN Red List of threatened species.
<http://maps.iucnredlist.org/map.html?id=162219>. Hungary map: Ministry of Agriculture,
Department of Nature Conservation, modified by the authors)

As for the relationship with mycorrhizal fungus, to get to know the mycorrhizal partner of this species, we need molecular taxonomic researches, for which roots or protocorms with initial shooting can be used. In Hungary, no one published experiments to get to know this. Based on Pecoraro et al. (2013) the international database (GenBank) contains, that they isolated *Tulasnellaceae* family from Italian *H. adriaticum* roots. We made an experiment to isolate the specific mycorrhizal fungal symbionts of the species in the study areas from protocorms, but those results have not been published yet.

Origin of seeds

The *H. adriaticum* seeds were sown, originated from the Hungarian natural habitats (Keszthely Hills (K), Sümeg-Tapolca Region (ST), Bakony Mountains (B3, B13, B15) and Kőszeg Mountains (KO)) and from the Croatian Istrian Peninsula (U), as a comparison. The capsules were ripe, dried, but they had not opened yet. The seeds were stored in a refrigerator for 15 days until use.

It was important to examine whether there is a significant difference between the germination of the seeds from different places. To do this we used the data of the variability testing, and we made variance analysis and significant difference calculations with Microsoft Excel 2013 computer program. In the variance analysis, the null hypothesis says that there is no significant difference between the habitats in the point of the germination averages. If the p-value > 0.05 the null hypothesis can be accepted. The result was also confirmed with the significant difference calculations (SD5%).

Treatments and viability testing of seeds

To get to know the theoretical viability of the seeds we used triphenyltetrazolium chloride (TTC). The more seeds are painted red, the higher viability rate they have. This method of Van Waes and Debergh (1986a, b) has become widely used for viability studies.

Before the painting with TTC, in order to crack the seed coat (because of the seeds of orchids are too small to scarify them with a scalpel to let the liquid reach the embryo) we tried 7 pretreatments: we let 100-100 seeds (from a mixture of the seeds from all habitats) in 0.5%; 1%; 2% and 4% sodium hypochlorite, in calcium hypochlorite, in sulphuric acid, and made a mechanical pericarp damage.

In the course of sodium-hypochlorite treatment, we let the seeds in 0.5%; 1%; 2% and 4% sodium-hypochlorite for 10 min.

In the course of calcium-hypochlorite treatment, we dissolved 10 g calcium-hypochlorite in 90 cm³ distilled water, and after 10 min we put the seeds into the mixture for 10 min.

In the course of the acidic treatment, we put the seeds into 1% sodium-hypochlorite for 10 min and after that into 2% H₂SO₄ for further 10 min.

In the course of the mechanical pretreatment, we used quartz sand. We put the seeds and quartz sand into a test tube and shake them for 50 s on a test tube shaker. As we tested before, this time was enough to crack the seed coat without making destruction.

After the pretreatments we flush the seeds with distilled water for 3 times, then used the TTC method. We made a tincture from 1 g TTC and 100 cm³ distilled water, the seeds were put into this, and were laid in a full dark place for 5 days on 30°C temperature.

From these 7 kinds of pretreatments, we used that in our further experiment, which gave the best result. From all habitat we used 100-100 seeds in 10-10 test tube, and made the TTC viability-test after doing the best pretreatment on them. According to this we determined the viability of the seeds.

Study area of the in situ germination

The first study area of *H. adriaticum* was in Keszthely Hills, in western Hungary, at the boundary of the village Gyenesdiás and Keszthely town. The orchid population was found by I. Szabó, on both sides of the Pilikán-Szoroshad minor road, in dolomite

grassland (*Chrysopogono-Caricetum humilis*), on the edge of the forest (Szabó, 1987). In the study area calciphilous oak woodland (dominated by *Quercus petraea*), shrub woodland and Black pine (*Pinus nigra*) plantation form a vegetation mosaic with dolomite grassland. Habitats are disturbed, the vegetation is degraded (owing to mainly human activities). *H. adriaticum* grows in the grassland near the road and on the edge of the expanding shrubs and trees (*Origanetalia vulgaris*) (Bódis and Molnár, 2009).

The second study area was the Sümeg-Tapolca Region. The largest Hungarian population is located next to the Sümeg and Nyirád roads, 4 and 2 km along (Sulyok et al., 1998). The specimens appear lonely or in small groups especially in the mowed road curbs (degraded *Festuco-Brometea*). Today the plants are located on the area of the Nyirád road, where grasslands and grassy shrubs were connected to the road fifty years ago. There are higher number of specimens in the “forest road” between Sümeg and Tapolca, especially in the yard of the Forester’s House of Úrbér, on the lawn and in the road curbs. Many small vegetative individuals grow under Common Dogwood (*Cornus sanguinea*) and Blackthorn (*Prunus spinosa*) bushes. The flowering specimens are typically found in the shrub-grass meadows, and located along the road, in multifarious exposures and habitats. In addition to the fact that this is the largest population, diverse micro-habitats (which are independent from each other) facilitate the long-lasting survival (Bódis and Molnár, 2009).

As for the climate, the study areas are about 30 km away from each other, and both are in moderately warm-moderately dry climate. In the experimental areas, the annual average temperature is between 10 and 11°C and the annual precipitation amount is 650-750 mm.

2014 was a very rainy year, so the annual precipitation amount was above the average. The Walter-Lieth climate diagrams (*Fig. 2 a* and *b*) were made from the data were got online through MetNet and were drawn in RStudio program by us. They represent the climate of the two study areas in 2014. The diagrams show that the end of the winter, the spring and the summer, and the first two months in the autumn were subhumid and superhumid. In June, there was only few rain, so the germination could not be started. The extra rain in July, August and September were important for start up the germination in the seed baits.

The soil pH are 7.3-7.9 on the Hungarian habitats of *H. adriaticum* according to Molnár V. (2011).

Research process of in situ germination

Seed packets were constructed from 40x60mm rectangles of heat-sealed nylon mesh (Illyés, 2011) and about 300-500 seeds of *H. adriaticum* were placed in each. The pore size of the mesh (85 µm and 100 µm) was chosen to retain the seeds without impending fungal growth. The mesh was folded once and clipped into plastic glassless slide mounts (Rasmussen and Whigham, 1993).

Seed pockets were positioned vertically in top-soil (approx. depth 5 cm) at 6-6 places in the Keszthely Hills and Sümeg-Tapolca Region in October 2013 (*Table 1*). 10-10 seed baits were positioned about 10-20 cm of a living plant and 6-6 seed baits about 10 m away of the living plants, as a control, where neither adult nor germinating plants were found. Seed baits were excavated at two occasions: in June 2014 and in September 2014. For the first time, we wanted to know whether the germination started. For the second time we can noticed various stages of germination (*Figs. 3* and *4*), so it was important to classify them by stages (*Table 2*).

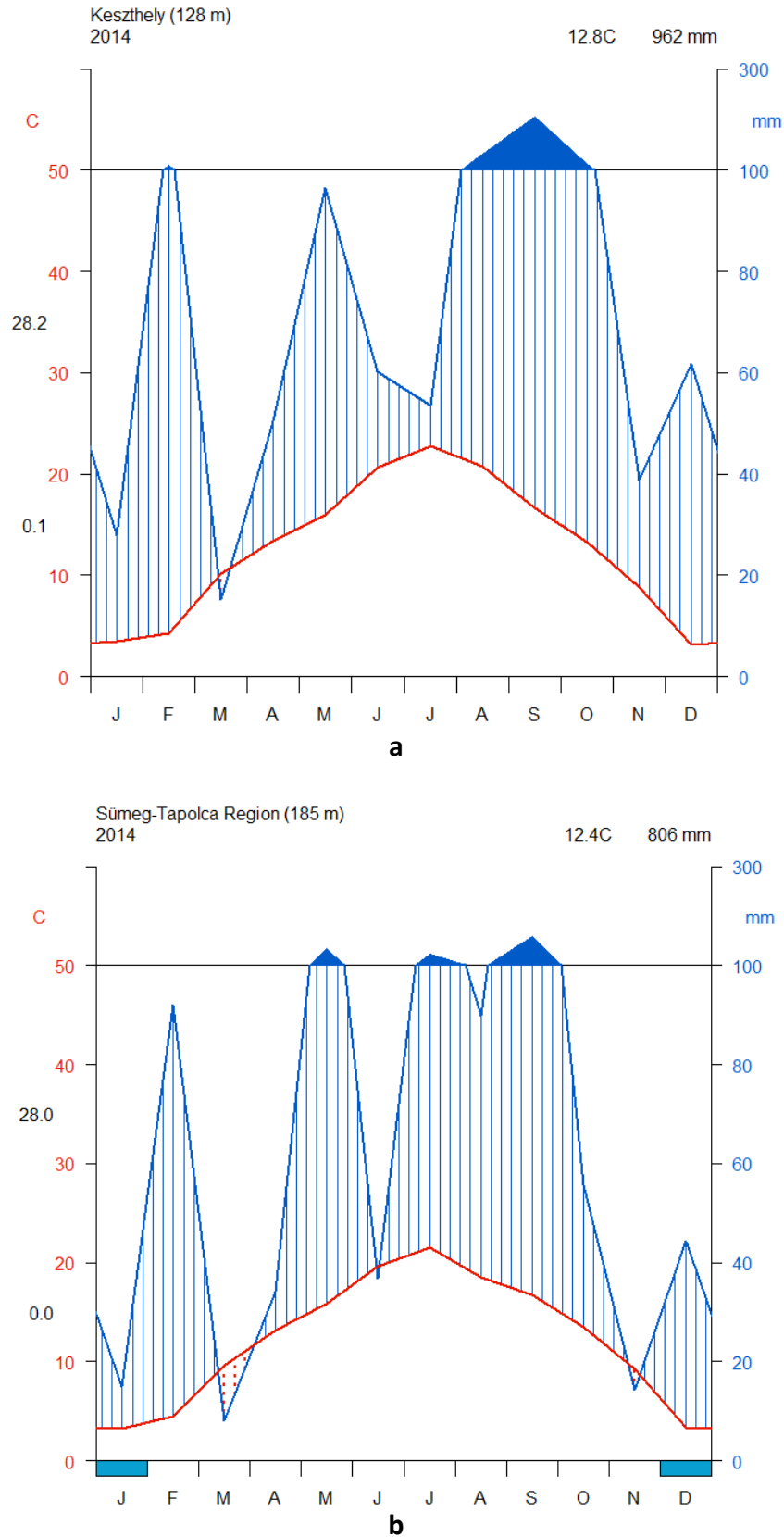


Figure 2. a: Walter-Lieth climate diagram of Keszthely for 2014. b: Walter-Lieth climate diagram of Sümeg-Tapolca Region for 2014

Table 1. GPS datas of in situ seed baits that were placed into the field

Date of placement	Place	GPS coordinates of baits placed next to a living plant	GPS coordinates of controll baits
12.10.2013.	Keszthely 1	46°47'33.1" 17°16'34.1"	46°47'32.8" 17°16'34.1"
	Keszthely 2	46°47'40.8" 17°16'38.8"	46°47'40.8" 17°16'38.7"
	Keszthely 3	46°47'43.1" 17°16'40.1"	46°47'43.4" 17°16'39.4"
	Keszthely 4	46°47'33.2" 17°16'36.4"	46°47'33.0" 17°16'36.3"
	Keszthely 5	46°47'53.3" 17°16'51.9"	46°47'53.6" 17°16'52.4"
	Keszthely 6	46°48'04.1" 17°16'57.5"	46°48'04.0" 17°16'58.4"
01.10.2013.	Sümeg-Tapolca 1	46°57'28.8" 17°20'49.2"	46°57'28.5" 17°20'50.3"
	Sümeg-Tapolca 2	46°57'29.7" 17°20'49.4"	46°57'29.5" 17°20'50.4"
	Sümeg-Tapolca 3	46°57'25.4" 17°21'10.2"	46°57'27.5" 17°21'09.7"
	Sümeg-Tapolca 4	46°57'22.7" 17°21'16.4"	46°57'22.7" 17°21'16.8"
	Sümeg-Tapolca 5	46°57'08.8" 17°21'58.1"	46°57'08.9" 17°21'57.7"
	Sümeg-Tapolca 6	46°56'43.5" 17°22'24.1"	46°56'43.4" 17°22'23.8"

Table 2. Protocorms classified by stages at in situ germination

Stages	Short explanation
0.	The protocorm visibly swollen in the seed coat, but it still did not break it through
1.	The protocorm broke through the seed coat but the seed coat is still visible on it
2.	The seed coat is no more visible and we can see the rhizoid hairs
3.	The size of the protocorms is few mm and they are perceptible to the eye and we can see the shoot initiation

Research process of ex situ (in vitro) germination

The ex situ germination was carried out in the laboratory of the Eötvös Loránd University's Botanical Garden on September 2013. We made the pretreatment, which was equivalence also the necessary sterilization, and the sowing in laminar flow with sterile instruments. The seeds were sown on modified "Fast" media, because it gives the best germination results of Hungarian terrestrial orchids (R. Eszéki, Szendrák, 1992). We summarized the recipe of modified "Fast" media in *Table 3*.

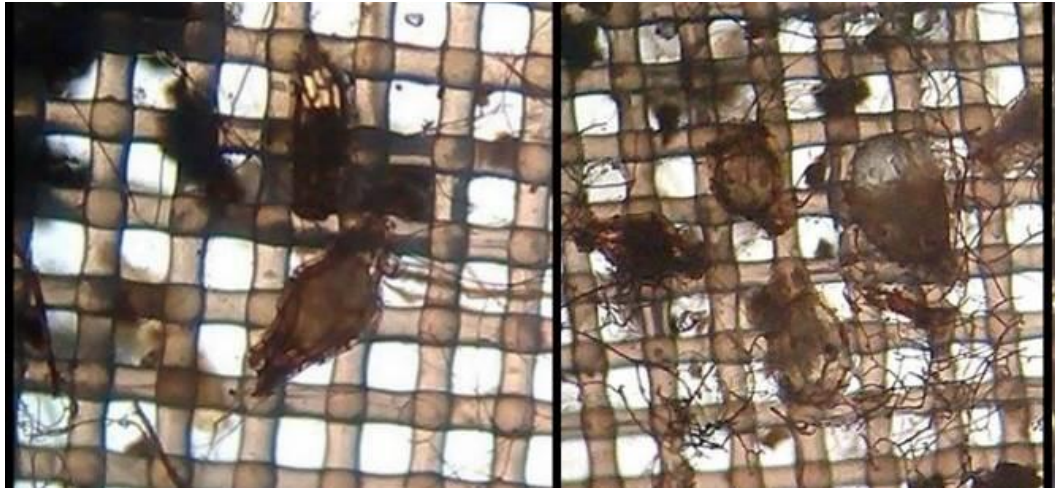


Figure 3. In situ stage 0 and stage 1

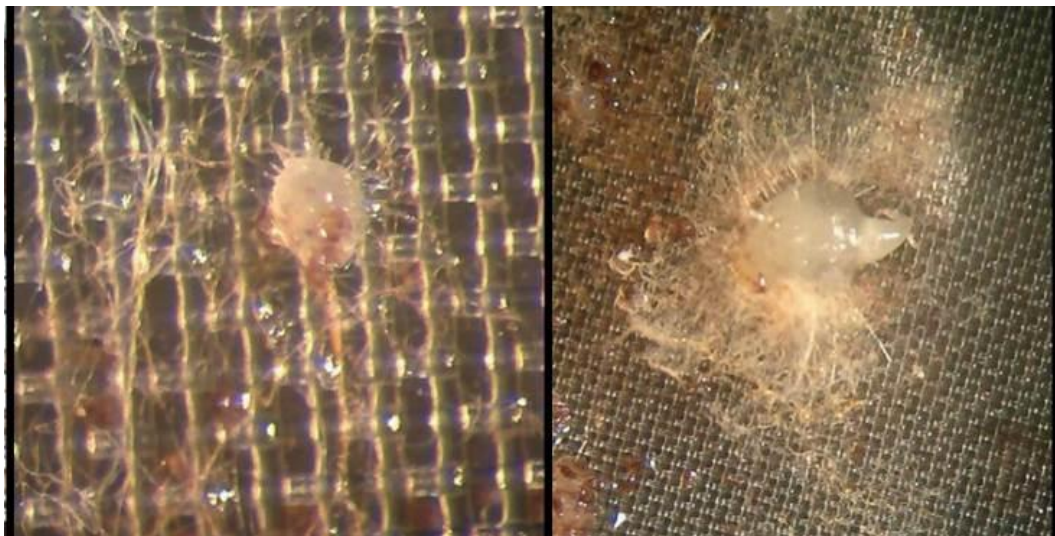


Figure 4. In situ stage 2 and stage 3

Table 3. The recipe of modified “Fast” media

Ingredients (1200ml)	Quantity
Ph:5.5	
Ca (NO ₃) ₂ X 4H ₂ O	100 mg
NH ₄ NO ₃	200 mg
KH ₂ PO ₄	100 mg
KCl	200 mg
MgSO ₄ X 7H ₂ O	100 mg
Fe-chelate	30 mg
Heller-mikro	1 ml
Saccharose	14 g
Fructose	6 g
Pepton	1 g
Polivitaplex	250 mg
Inozit	100 mg
Agar	10 g

Before sowing, we made a pretreatment: we dissolved 10 g calcium-hypochlorite in 90 cm³ distilled water, then gave some drop of Tween to the mixture and let it clear. Then we put the seeds into test tubes and pour the filtrate on them for 10 min. After that, in the sterile box, we sowed the seeds from the test tubes onto the modified Fast media with a sterile scalpel. We covered the flasks with foil three times, then covered them with aluminium foil. The first week was an incubation time, we monitored if it stayed sterile or not. After the incubation time we put the flasks into fridge (4°C) for 3 months. Then, we put them into a dark box on room temperature (24°C) until the first protocorms appeared. After the first protocorms appearance we checked the flasks monthly.

Results

Viability testing

In the variance analysis, the p-value was higher than 0.05 (*Table 4*), so the null hypothesis could be accepted.

Table 4. Results of the variance analysis

VARIANCE ANALYSIS						
<i>Source of variation</i>	<i>SS</i>	<i>df</i>	<i>MS</i>	<i>F</i>	<i>p-value</i>	<i>F crit.</i>
Between groups	115	3	38.33333	1.721987	0.179812	2.866266
Within groups	801.4	36	22.26111			
Total	916.4	39				

Based on the results, we can state that there is no significant difference between the seed's average of germination, so it does not cause any problems during the experiments that the seeds originated from different habitats. Thus, the seeds can be used separately from each habitat, or a mixture can be made from the seeds of all of the habitats, it has no effect on the results.

From the pretreatments the mechanical pericarp fracture gave the best results (*Table 5*), so we made the testing with this method. The germination of the seeds after the ten times repetitions of viability testing was 17.7% on average.

In situ germination

We summarized the results of the in situ germination 8 and 11 month after sowing.

The in situ germination was 0.094% in the Keszthely Hills 8 months after sowing. 10-20 cm from the living plants this rate increased to 0.1%. The germination in the control packets was 0.08%. 11 months after sowing, the germination increased to 42%, included the "Stage 0" protocorms too. Next to the living plants, the germination was 50.3%. In the control packets this value was 19.4%.

On the Sümeg-Tapolca Region, the in situ germination was 0.11% 8 months after sowing. 10-20 cm from the living plants the germination was 0.13%. In the control packets we have not found any protocorms. 11 months after sowing, the germination of the seeds was 34.7%. Next to the living plants, this value increased to 39.9%. The germination was 3.5% in the control packets.

Table 5. Percentage of seeds were painted red by TTC

Pretreatments, length of time		Seeds were painted red (%)
1.	Sodium-hypochlorite, 10 min, 0.5%	21
2.	Sodium-hypochlorite, 10 min, 1%	17.5
3.	Sodium-hypochlorite, 10 min, 2%	17
4.	Sodium-hypochlorite, 10 min, 4%	19
5.	10 g sodium-hypochlorite/90 cm ³ H ₂ O, 10 min	16
6.	1% sodium-hypochlorite, 10 min, after then 2% H ₂ SO ₄ , 10 min	13
7.	Mechanical pericarp fracture 50 s	35

Ex situ germination

After the sowing, none of the flasks became infected. During the ex situ germination, the first protocorm was appeared 9 months after sowing. The germination was outstanding only in one flask (from the Bakony mts.), marked “B13”. The germination of this flask was 1.3% 13 months after sowing. In the other flasks, there was maximum 1-2 protocorms. After the first protocorm’s appearance, we checked the flasks monthly. We summarized these results in *Table 6*. In October 2014, 13 months after sowing, we checked every flask and kept a record of the protocorms and seedlings according to stages we found in them (*Figs. 5, 6 and 7*). In *Table 7*, a short explanation can be found about the protocorms and seedlings by stages. The results of protocorms and seedlings were found in the flasks 13 months after sowing are summarized in *Table 8*.

After the first protocorm’s appearance, we put the flasks onto natural light. Newer protocorms appeared which started to grow faster than the protocorms appeared in the dark. The new protocorms became larger and more powerful in a month.

18 months after sowing, the protocorms appeared on natural light have grown to a powerful 6-11-cm big seedling.

Table 6. Protocorms founded in flasks monthly (B – Bakony mts, ST – Sümeg-Tapolca Region, KO – Kőszeg mts, U – Istrian Peninsula)

Time of checking	B3	B13	B15	ST	KO	U
2014.06.04	2	30	0	1	0	0
2014.07.11	2	46	0	1	0	0
2014.08.11	3	74	2	2	0	2
2014.09.09	3	87	1	2	0	3
2014.10.04	3	104	1	2	1	3

Table 7. Protocorms and seedlings by stages, short explanation

Stages	Short explanation
Stage 1.	The white protocorm with rhizoid hair appears
Stage 2.	The shoot initiation appears on the white protocorm
Stage 3.	One-leaved-staged green seedling appears on the white protokorm. <1cm
Stage 4.	Green, two-leaved-staged seedling. ~1 cm
Stage 5.	Green, two-leaved-staged seedling. ~2 cm
Stage 6.	Green, two-leaved-staged seedling. ~3 cm
Stage 7.	Green, two-leaved-staged seedling. >5 cm

Table 8. Protocorms and seedlings by stages in flasks, 13 months after sowing (*S* = Seeds were sown onto the media in one flask, *St* = Stage, *T* = total, *GR* = germination rate)

Flask code	S (pcs)	13 months after sowing onto “Fast” media								
		St 1 (pcs)	St 2 (pcs)	St 3 (pcs)	St 4 (pcs)	St 5 (pcs)	St 6 (pcs)	St 7 (pcs)	T (pcs)	GR (%)
B3	9216	0	0	0	0	1	1	1	3	0.03
B13	8100	10	8	10	20	22	24	10	104	1.3
B15	12224	1	0	0	0	0	0	0	1	0.008
ST	9960	0	1	0	1	0	0	0	2	0.02
KO	11300	0	1	0	0	0	0	0	1	0.009
U	10184	0	0	3	0	0	0	0	3	0.03

Discussion

During the viability test, after the pretreatments, if the TTC gets into the seed coat, it colours the seeds to red. This is only a theoretical ratio, it is not suitable to determine the true germination rate. This result is not comparable with the results of the in situ germination rate, because the microflora in the soil is like to digest the outer husk down from the embryo. We cannot reach artificially as good results as it can with this natural way of “pretreatment”. The theoretical germination rate we get during viability tests is smaller (17.7% on average) than the measured germination rates (42%) on their natural habitat (in situ), but much higher, than the ex situ germination in flasks (0.18%). So, the seed’s reddish discoloration (formazan formation) during the TTC test was not necessarily a warrant for the seeds high germination.



Figure 5. Ex situ stage 1 and stage 2-3

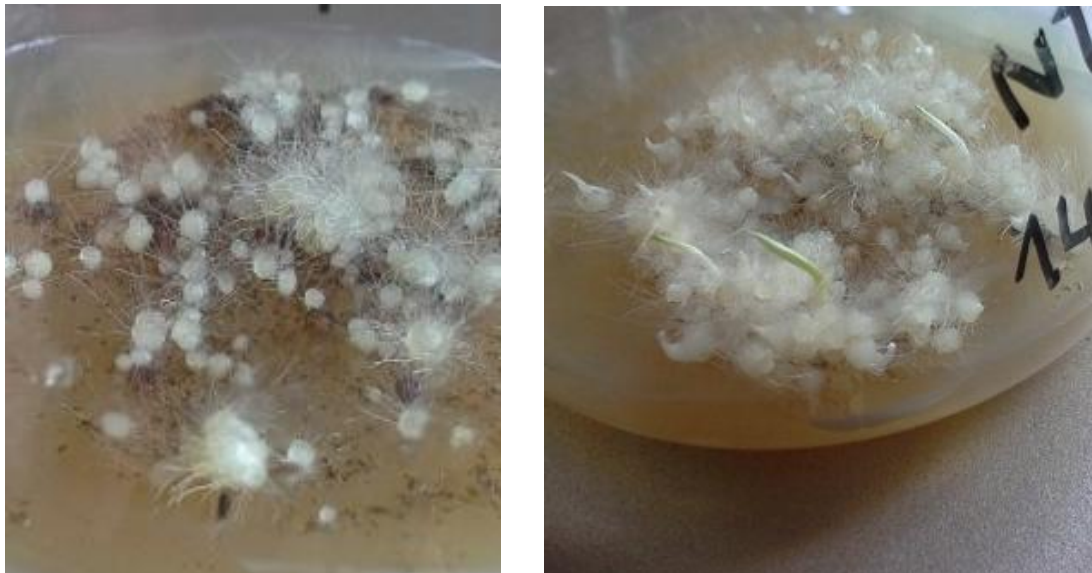


Figure 6. *Ex situ* stage 4 and stages 5-6

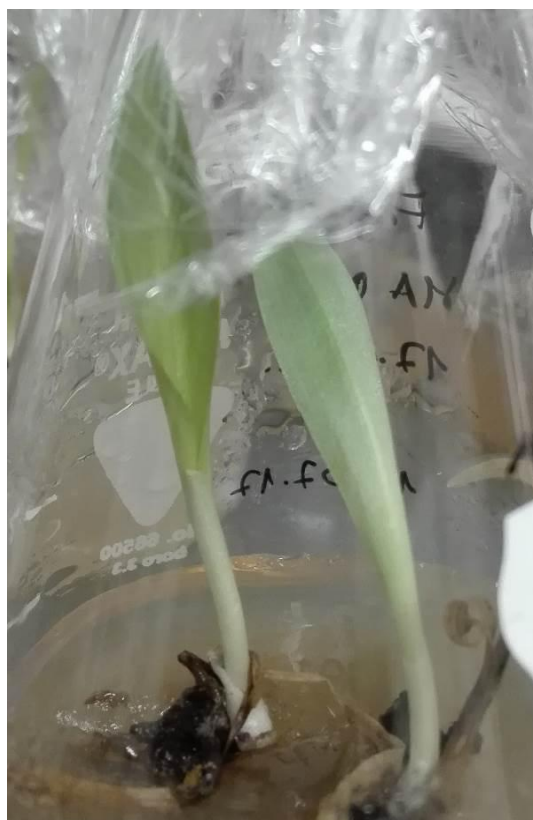


Figure 7. *Ex situ* stage 7

If we see the in situ germination's results, it is perceptible, that between the sown in October and the excavation in June, the 8 months were not enough for most of the seeds to germinate, but between the two excavations in June and September, in that 3 months the germination was started.

If we see the in situ germination's results, it is perceptible, that between the sown in October and the excavation in June, the 8 months were not enough for most of the seeds to germinate, but between the two excavations in June and September, in that 3 months the germination was started.

Consequently, the seeds needed 8-11 months after sowing to start to germinate on their natural habitats. It is very important to note, that into this result, we also calculated the protocorms in stage 0 and 1, so the "near-germination" seeds too. In these stages, the seeds do not need symbiotic fungal relationships, so these are not "real" protocorms, but very important data to see, how many seeds are viable, how many has the option, that meeting with the right fungi, the shoot initiation starts to grow, and it became a real seedling.

According to our microscopic observation, the symbiosis of the fungi and the orchid protocorm starts between the first and second stage: after when the white protocorm with rhizoid hair appears but before when the shoot initiation appears on this white protocorm.

Comparing the in situ and the ex situ germination, the seeds of *H. adriaticum* started to germinate 9-11 months after sowing in a high volume, so the seeds were in a resting period till then, but kept their ability of germination.

Conclusion

Our research shows, that the germination rate of *H. adriaticum* seeds is reassuringly high in its natural habitats, so this phase of the plants life is probably not a key element of the species endangerment. Meeting with the fungal partner, which pushes the germination on and starts the embryo's growth, is a much rarer event. Our next step is to determine the specific mycorrhizal fungal symbionts of the species in the Hungarian habitats both from protocorms and roots, so that we could compare the results. We can declare that the seeds from the Hungarian habitats are able to germinate artificially. According to the in vitro germination, the species can be germinated on modified "Fast" media (pH 5.5). Based on Molnár V. (2011) about the soil pH on the natural habitats of the species, we think that *H. adriaticum* seeds could achieve higher germination rates with higher media pH. So, the next step in our research will be to measure the soil pH on their natural habitats, and saw the seeds onto media with multifarious pH, from which we can ascertain that our speculation is true or not.

Acknowledgements. Thanks to Mrs. Nóra Baranyai for the help in the statistical analysis. Thank you for referees for the detailed and helpful comments, remarks and suggestions they gave us.

REFERENCES

- [1] Arditti, J. (1967): Factors affecting the germination of orchid seed. – Bot. Rev. 33: 1-97.
- [2] Arditti, J. (1979): Aspects of the physiology of orchids. – Advances Bot. Res. 7: 241-665.
- [3] Arditti, J. (1982): Orchid Seed Germination and Seedling Culture - A Manual. – In: Arditti, J. (ed.): Orchid Biology: Reviews and Perspectives, III. Cornell University Press, Ithaca.
- [4] Arditti, J., Ernst, R. (1984): Physiology of Germinating Orchid Seeds. – In: Arditti, J. (ed.) Orchid Biology: Reviews and Perspectives, III. Cornell University Press, Ithaca.

- [5] Arditti J., Ernst, R., Wing Yam, T., Glabe, C. (1990): The contribution of orchid mycorrhizal fungi to seed germination: a speculative review. – *Lindleyana* 5: 249-255.
- [6] Bernhardt, K. G. (2011): *Himantoglossum adriaticum*. – IUCN 2013. IUCN Red List of Threatened Species. Version 2013.2. www.iucnredlist.org.
- [7] Bidartondo, M. I., Read, D. J. (2008): Fungal specificity bottlenecks during orchid germination and development. – *Mol. Ecol. Aug.* 17(16): 3707-16.
- [8] Biró, É., Bódis, J., Nagy, T., Tökölyi, T., Molnár V., A. (2014): Honeybee (*Apis mellifera*) mediated increased reproductive success of a rare deceptive orchid. – *Applied Ecology and Environmental Research* 13(1): 181-192.
- [9] Bódis, J. (2010): *Himantoglossum adriaticum* populációk dinamikája: demográfiai és életmenet jellemzők [Variation of demography and life history characteristics in *Himantoglossum adriaticum* populations] (in Hungarian). – PhD Thesis. Biológiai Doktoriskola, Pécsi Tudományegyetem, Pécs.
- [10] Bódis, J., Molnár, E. (2009): Long-term monitoring of *Himantoglossum adriaticum* H. Baumann population in Keszthely Hills, Hungary. – *Natura Somogyiensis* 15: 27-40.
- [11] Bódis, J., Sramkó, G., Óvári, M., Molnár V., A. (2011): The Lifestyle and Stock Dynamics of European Orchids. – In: Molnár V., A. (ed.) *Atlas of Orchids in Hungary*. Kossuth Kiadó, Budapest.
- [12] Canadell, J., Noble, I. (2001): Challenges of a changing earth. – *Trends in Ecology and Evolution* 16: 664-666.
- [13] Claessens, J., Kleynen, J. (2011): The flower of the European orchid. Form and function. – Claessens & Kleynen, Geulle.
- [14] Clements, M. A. (1988): Orchid mycorrhizal associations. – *Lindleyana* 3: 73-86
- [15] Coates, D. J., Dixon K. W. (2007): Current perspectives in plant conservation biology. – *Australian Journal of Botany* 55: 187-193.
- [16] Conti, F., Manzi, A., Pedrotti F. (1997): *Liste rosse regionali delle piante d'Italia*. – WWF/Società Botanica Italiana, Camerino.
- [17] Cribb, P. J., Kell, S. P., Dixon, K. W., Barrett, R. L. (2003): *Orchid Conservation: A Global Perspective*. – In: Dixon, K. W., Kell, S. P., Barrett, R. L., Cribb, P. J. (eds.) *Orchid Conservation*. Natural History Publications, Kota Kinabalu.
- [18] De Pauw, M. A., Remphrey, W. R. (1993): In vitro germination of three *Cypripedium* species in relation to time of seed collection, media, and cold treatment. – *Canadian Journal of Botany* 71: 879-885.
- [19] Delforge, P. (2006): *Orchids of Europe, North Africa and Middle East*. – A&C Black, London.
- [20] Dixon, K. W. (1989): Seed Propagation of Ground Orchids. – In: Dixon, K. W., Buirchell, B. J., Collins, M. J. (eds.) *Orchids of Western Australia*. 2nd edn. Native Orchid Study and Conservation Group Inc, Victoria Park.
- [21] Dostalova, A., Montagnani, C., Hodálová, I., Jogan, N., Király, G., Ferakova, V., Bernhardt, K. G. (2011): *Himantoglossum adriaticum*. – The IUCN Red List of Threatened Species 2011: e.T162219A5559772.
- [22] Fast, G. (1980): Vermehrung und Anzucht. – In: Fast, G. (ed.) *Orchideenkultur, Botanische Grundlagen, Kulturverfahren, Pflanzenbeschreibungen*. Eugen Ulmer Verlag, Stuttgart.
- [23] Grulich, V. (2012): Red List of vascular plants of the Czech Republic. – *Preslia* 84: 631-645.
- [24] Illyés, Z. (2011): Orchid Type Mycorrhiza. – In: Molnár V., A. (ed.) *Atlas of Orchids in Hungary*. – Kossuth Kiadó, Budapest.
- [25] IUCN (1999): IUCN guidelines for the prevention of biodiversity loss due to biological invasion. – *Species* 31-32: 28-42.
- [26] Jacquemyn, H., Brys, R., Hermy, M., Willems, J. H. (2005): Does nectar reward affect rarity and extinction probabilities of orchid species? An assessment using historical records from Belgium and the Netherlands. – *Biological Conservation* 121(2): 257-263.

- [27] Király, G. (ed.) (2007): Red list of the vascular flora of Hungary (in Hungarian). – Private edition, Sopron.
- [28] Koopowitz, H., Lavarack, P. S., Dixon, K. W. (2003): The Nature of Threats to Orchid Conservation. – In: Dixon, K. W., Kell, S. P., Barrett, R. L., Cribb, P. J. (eds.) Orchid Conservation. Natural History Publications, Kota Kinabalu.
- [29] Kull, T., Hutchings, M. J. (2006): A comparative analysis of decline in the distribution ranges of orchid species in Estonia and the United Kingdom. – *Biological Conservation* 129: 31-39.
- [30] Mabberley, D. J. (1997): *The Plant Book*. – Cambridge University Press, Cambridge.
- [31] Maglocky, S., Feráková, V. (1993): Red list of ferns and flowering plants (Pteridophyta and Spermatophyta) of the flora of Slovakia (the second draft). – *Biologia* 48(4): 361-385.
- [32] Masuhara, G., Katsuya, K. (1994): *In situ* and *in vitro* specificity between *Rhizoctonia* spp. and *Spiranthes sinensis* (Persoon) Ames var. *amoena* (M.Bieberstein) Hara. – *New Phytologist* 127: 711-718.
- [33] Miyoshi, K., Mii, M. (1988): Ultrasonic treatment for enhancing seed germination of terrestrial orchid, *Calanthe discolor*, in asymbiotic culture. – *Scientia Horticulturae* 35: 127-130.
- [34] Molnár V., A. (ed.) (2011): *Atlas of Orchids in Hungary*. – Kossuth Kiadó, Budapest.
- [35] Molnár V., A., Löki, V., Takács, A., Schmidt, J., Tökölyi, J., Bódis, J., Sramkó, G. (2015): The reproductive success of Hungarian orchids has not changed in the last century. – *Applied Ecology and Environmental Research* 13(4): 1097-1108.
- [36] Pecoraro, L., Girlanda, M., Kull, T., Perini, C., Perotto, S. (2013): Fungi from the roots of the terrestrial photosynthetic orchid *Himantoglossum adriaticum*. – *Plant Ecology and Evolution* 146(2): 145-152.
- [37] R. Eszéki, E., Szendrák, E. (1992): Experiments to propagate native hardy orchids (Orchidaceae) in the ELTE Botanical Garden. – 20th Cong. Hung. Biol. Soc. 1992, Kecskemét.
- [38] Ramsay, R. R., Sivasithamparam, K., Dixon, K. W. (1986): Patterns of infection and endophytes associated with Western Australian orchids. – *Lindleyana* 1: 203-214.
- [39] Rasmussen, H. N. (1995): *Terrestrial orchids, from seed to mycotrophic plant*. – Cambridge University Press, Cambridge.
- [40] Rasmussen, H. N. (2002): Recent developments in the study of orchid mycorrhiza. – *Plant and Soil* 244: 149-163.
- [41] Rasmussen, H. N., Whigham, D. F. (1993): Seed ecology of dust seeds *in situ*: A new study technique and its application in terrestrial ecology. – *American Journal of Botany* 80: 1374-1378.
- [42] Rasmussen, H. N., Dixon, K. W., Jersáková, J., Těšitelová, T. (2015): Germination and seedling establishment in orchids: a complex of requirements. – *Annals of Botany* 116(3): 391-402.
- [43] Richter, W. (1982): *Orchideen: Pflegen, Vermehren, Züchten*. – Neumann, Radebeul.
- [44] Roberts, D. L. (2003): Pollination biology: the role of sexual reproduction in orchid conservation. – In: Dixon, K. W., Kell, S. P., Barrett, R. L., Cribb, P. J. (eds.) *Orchid conservation*. Natural History Publications, Kota Kinabalu.
- [45] Rybka, V., Rybková, R., Pohlová, R. (2005): Plants of the Natura 2000 Network in the Czech Republic. – *Sagittaria*, Praha.
- [46] Shirokov, A. I., Syrova, V. V., Kryukov, L. A., Shtarkman, N. N., Shestakova, A. A. (2016): Reintroduction of *Dactylorhiza incarnata* into the natural habitats of the European Russia. – *Applied Ecology and Environmental Research* 15(1): 445-455.
- [47] Sosa, V., Platas, T. (1998): Extinction and persistence of rare orchids in Veracruz, Mexico. – *Conservation Biology* 12: 451-455.
- [48] Stoutamire, W. P. (1983): Wasp-pollinated species of *Caladenia* (Orchidaceae) in south-western Australia. – *Australian Journal of Botany* 31: 383-394.

- [49] Sulyok, J., Vidéki, R., Molnár V., A. (1998): Data for the knowledge of *Himantoglossum* species in Hungary (in Hungarian) – *Kitaibelia* 3(2): 223-229.
- [50] Swarts, N. D., Dixon, K. W. (2009): Terrestrial orchid conservation in the age of extinction. – *Annals of Botany* 104: 543-556.
- [51] Szabó, I. (1987): A Keszthelyi-hegység növényvilágának kutatása. [Research of the flora of the Keszthely Hills] (in Hungarian). – *A Bakony Természettudományi Múzeum Közleményei* 6: 77-98.
- [52] Teschner, W. (1980): Sippendifferenzierung und Bestäubung bei *Himantoglossum* Koch. – *Jahresberichte des Naturwissenschaftlichen Vereins Wuppertal* 33: 104-116.
- [53] Van der Kinderen, G. (1995): A method for the study of field germinated seeds of terrestrial orchids. – *Lindleyana* 10: 68-73.
- [54] Van Waes, J. M., Debergh, P. C. (1986a). Adaptation of the tetrazolium method for testing the seed viability, and scanning electron microscopy study of some Western European orchids. – *Physiology of Plants* 66: 435-442.
- [55] Van Waes, J. M., Debergh, P. C. (1986b). In vitro germination of some Western European orchids. – *Physiology of Plants* 67: 253-261.
- [56] Vöth, W. (1990): Effective und potentielle Bestäuber von *Himantoglossum*. – *Mittlungblatt AHO Baden-Württemberg* 22: 337-351.
- [57] Warcup, J. H. (1971): Specificity of mycorrhizal association in some Australian terrestrial orchids. – *New Phytologist* 70: 41-46.
- [58] Warcup, J. H. (1981): The mycorrhizal relationships of Australian orchids. – *New Phytologist* 87: 371-381.
- [59] Woolcock, C. E., Woolcock, D. T. (1984): Australian terrestrial orchids. – Melbourne: Thomas Nelson.
- [60] Zelmer, C. D., Cuthbertson, L., Currah, R. S. (1996): Fungi associated with terrestrial orchid mycorrhizas, seeds and protocorms. – *Mycoscience* 37: 439-446.
- [61] Website of MetNet: Climatic data for making the Walter-Lieth diagrams. – <https://www.metnet.hu/napi-adatok?sub=2&order=1>.

RELATIONSHIP BETWEEN OPTICAL MICROSCOPIC STRUCTURE AND PHYSICAL CHARACTERIZATION OF ORGANIC WASTES ORIGINATED PEAT SUBSTITUTES

DEDE, O. H. * – OZTEKIN, M. H.

*Department of Environmental Engineering, Engineering Faculty, Sakarya University
54187 Sakarya, Turkey
(ohdede@sakarya.edu.tr, +90-264-295-5761; hazeloztekn@gmail.com, +90-544-270-0643)*

**Corresponding author
e-mail: ohdede@sakarya.edu.tr, phone: +90-264-295-5761; fax: +90-264-346-0633*

(Received 20th Oct 2017; accepted 12th Feb 2018)

Abstract. The aim of the study was to determine relationship between the microscopic structure and physical characterization of organic wastes which have a potential as a substrate occurred during the agricultural and industrial activities. The microscopic structure of the samples was observed using scanning electron microscope (SEM). Physical properties were specified according to EU standards using the methods from the existing literature. According to the results of this study the organic waste samples show difference in decomposing depending on their surface and internal structure. Micro pores are prevailing in the waste with higher decomposing rate (HH, SMC, MWC), while the waste with lower decomposing rate (TW, MS, RH) has higher content of macro pores. When the pore diameter of the samples increases, their porosity and air capacity raise as well, but their water holding capacity decreases. Best results were determined at hazelnut husk and the insufficient results were obtained at rice hull. Comparing the physical properties obtained with the desired ideal values for the growing medium indicates that hazelnut husk, sawdust, spend mushroom compost and municipal solid waste compost can be used as pure and that other organic wastes can be used in the mixtures as growth medium components.
Keywords: *soiless growing media, potting media, internal structure, physical properties, waste reclamation*

Introduction

Serious problems are experienced in the management and disposal of organic wastes, as significant types of waste both in the rural and urban areas, due to their various types and high amounts. On the other hand, agricultural wastes generated particularly in rural areas are released into forests and stream beds or tried to be disposed by burning. This in turn causes the contamination of water resources, air pollution, release of pathogen microorganisms and odor problems. (Dede et al., 2006). Yet, with their high organic matter and plant nutrient content these wastes can be utilized in vegetative production, the most ecologic and sustainable method of disposal. The literature includes many studies demonstrating that agricultural-based organic wastes can be successfully utilized in vegetative production, where it is reported that their utilization as growth medium particularly in the cultivation of potted ornamental plants would constitute a significant alternative to natural soil and peat (Apaolaza et al., 2005; Rigane et al., 2011; Belda et al., 2013).

The basic properties sought in growth media to be used in the cultivation of potted ornamental plants are high stability in order to allow the roots to anchor and support the plant, good hydraulic properties in order to supply water to the plant, the ability to supply the roots with the needed air and containing various plant nutrients (Tariq et al., 2012). Considering the fact that plant nutrient content can be improved by means of

simple applications such as using natural or artificial fertilizers, the suitability of the physical and hydrophysical properties of organic materials would be determinative in its stability as growth medium (Abad et al., 2001; Yahya et al., 2010).

Generally, growing mediums are classified according to their hydraulic properties. In this classification, growing media is divided into four types (Yahya et al., 2010). Type 1: aerated growing media with high water availability and high water buffering capacity, Type 2: less aerated growing media with average to high water availability, Type 3: highly aerated growing media with low water availability, and Type 4: growing media with low water availability but a very low water buffering capacity.

On the other hand, the physical and hydraulic properties of the materials used as growing media can often be controlled by particle size distribution. However, in some cases different physical and hydraulic properties can be seen in growing media with similar particle size distributions (Abad et al., 2001; Ozdemir et al., 2015). This can be attributed to differences in surface and interior structures of the growing media.

This study aims to explain the effects of surface and internal structure of organic wastes on physical and hydraulic properties and to determine the usability of organic wastes examined as growing media.

Materials and methods

Organic wastes sampling

Organic waste samples that could be used as a growing media analyzed in this study have been collected from different regions of Turkey. In the selection of organic wastes we have taken into account if the waste has been created in great amounts directly during agricultural production or as a result of processing of agricultural products, if other purpose cannot be found for it and if it has a specific decomposing stability. As a result of these criteria it has been decided that Hazelnut Husk (HH), Maize straw (MS), Pine Bark (PB), Tea waste (TW), Saw dust (WW), Rice Hull (RH), Spent Mushroom Compost (SMC), Municipal waste compost (from Istanbul municipal composting facility) (MWC) will be used in this study. From the collected samples hazelnut husk and maize straw were processed by a shredder machine, while for the other samples it was not deemed necessary. Also, by comparing the analyzed samples to Sphagnum peat and to the characteristics considered ideal for growing media by the written literature we tried to specify the possibility of its use as a growing media.

Scanning electron microscope (SEM) analysis

The surface and internal structure of the samples were observed using scanning electron microscope (SEM) (JEOL – JSM - 6060 LV Model). SEM images of the samples were taken at 1000x – 3000x magnifications for analysis. The samples were sputtered a film of gold, about 5 nm thick, to enhance their conductivity before characterization by means of SEM.

Cold stage has been applied in order to prevent the samples from changing their shape as a result of high vacuum in SEM. On the other hand, in order to be certain that the structure of the sample was not damaged three replicates of each material have been made during the preparation of samples and the images obtained from them have been compared to each other (Fornes et al., 2007; Guo and Liu, 2007; Masaphy et al., 2009).

Physical and physicochemical properties

In order to put forth the characterization of the waste samples used in the study, physical and physicochemical properties were specified according to European Union standards using the methods from the existing literature.

Particle size distribution in the samples was found by drying them on 35 °C and putting them in the electromagnetic digital vibrating sieve set (CISA model 002) that used a series of different sieves with 16, 8, 4, 2, 1, 0.5, 0.25 and 0.125 mm gaps and by measuring peaces remaining in each sieve after 10 min of sieving. The index of particle sizes CI (Coarseness index), geometric average of particle diameters (d_g) and geometric deviations (σ_g) were calculated using the obtained results and below-mentioned equations (Eqs. 1, 2, 3 and 4). Pieces larger than 1 mm were taken into account while calculating CI (Abad et al., 2005; Richards et al., 1986).

$$CI = \sum \%P_i; i > 1\text{mm} \quad (\text{Eq.1})$$

$$d_g = \exp(a) \quad (\text{Eq.2})$$

$$a = \sum_i m_i \ln d_i \quad (\text{Eq.3})$$

$$\sigma_g = \exp \sqrt{\sum_i m_i (\ln d_i)^2 - a^2} \quad (\text{Eq.4})$$

m_i = weight of particles put in the sieve,
 d_i = average diameter of two consecutive sieves.

In accordance with the EU standards specific weights of samples were determined by using % of organic matter and % of the ash content (mineral matter). Volume weights, in accordance with the EU standards, were found by measuring the dry weight of samples in a known volume after it has been kept under 10 cm suction pressure in a water column. Total porosity was calculated using the % rate of pore volume within the mass of the certain weight of samples (Volume-Weight). The air capacity was found by measuring the loss that resulted from the water saturation of the samples and their drainage under 10 cm pressure.

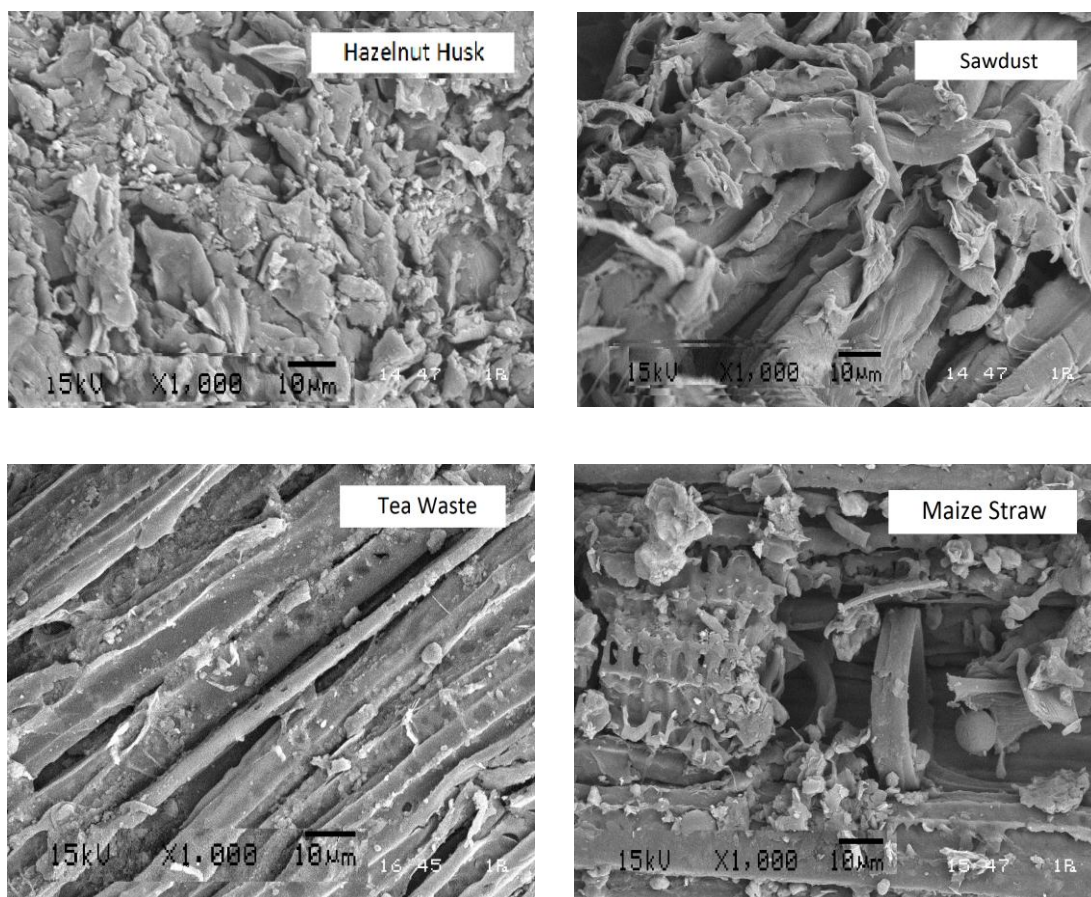
Volumetric shrinkage of organic waste samples was found by drying the samples on 105 °C and expressing in percents the volume loss caused by the drying process. Water holding capacity was measured by submerging the samples in water, holding them under 10 cm pressure and then determining the amount of water left in the samples. Wettability, in accordance with Australian Standard (2003), was determined by measuring the amount of time needed for the dried samples to absorb 10 ml of pure water.

Water suspension method was used in order to determine pH value and electrical conductivity of the selected organic waste. pH was determined, in accordance with the EU standards, by putting the material prepared in 1:5 ratio into pure water suspension and measuring its pH with a glass electrode pH-meter (European Standard, Une-En 13037). Total organic matter content was calculated in percents by heating the dried (105 °C) sample in a furnace on 550 °C for 4 h (Benito et al., 2006).

All data was analyzed statistically using analysis of variance (F-test) at $P \leq 0.05$ and means of the treatments were compared by the Least Significant Difference (LSD) at $P = 0.05$.

Results and discussion

It is known that the analysis of the pore structure provides important information about growing media, its hydraulic characteristics, air capacity and degradation level (Marianthi et al., 2006). This is why SEM analysis was used in this study to facilitate understanding of hydraulic and physical characteristics of the samples by examining surface and internal structure of the organic waste samples whose potential to be used as a growing media is being investigated. The results are presented in *Figure 1*. Since SEM figures examined both surface and internal structure they can be divided into two groups. The samples with advanced decomposing formed the first group; spend mushroom compost, municipal waste compost and peat. They possess a very small number of macro pores and a homogeneous spread of micro pores. Hazelnut husk samples, despite having low decomposition rate, resemble this group very much. The second group we will introduce includes slow decomposing samples such as maize straw, rice hull, tea waste and saw dust whose structure, especially the internal one, is full of macro pores.



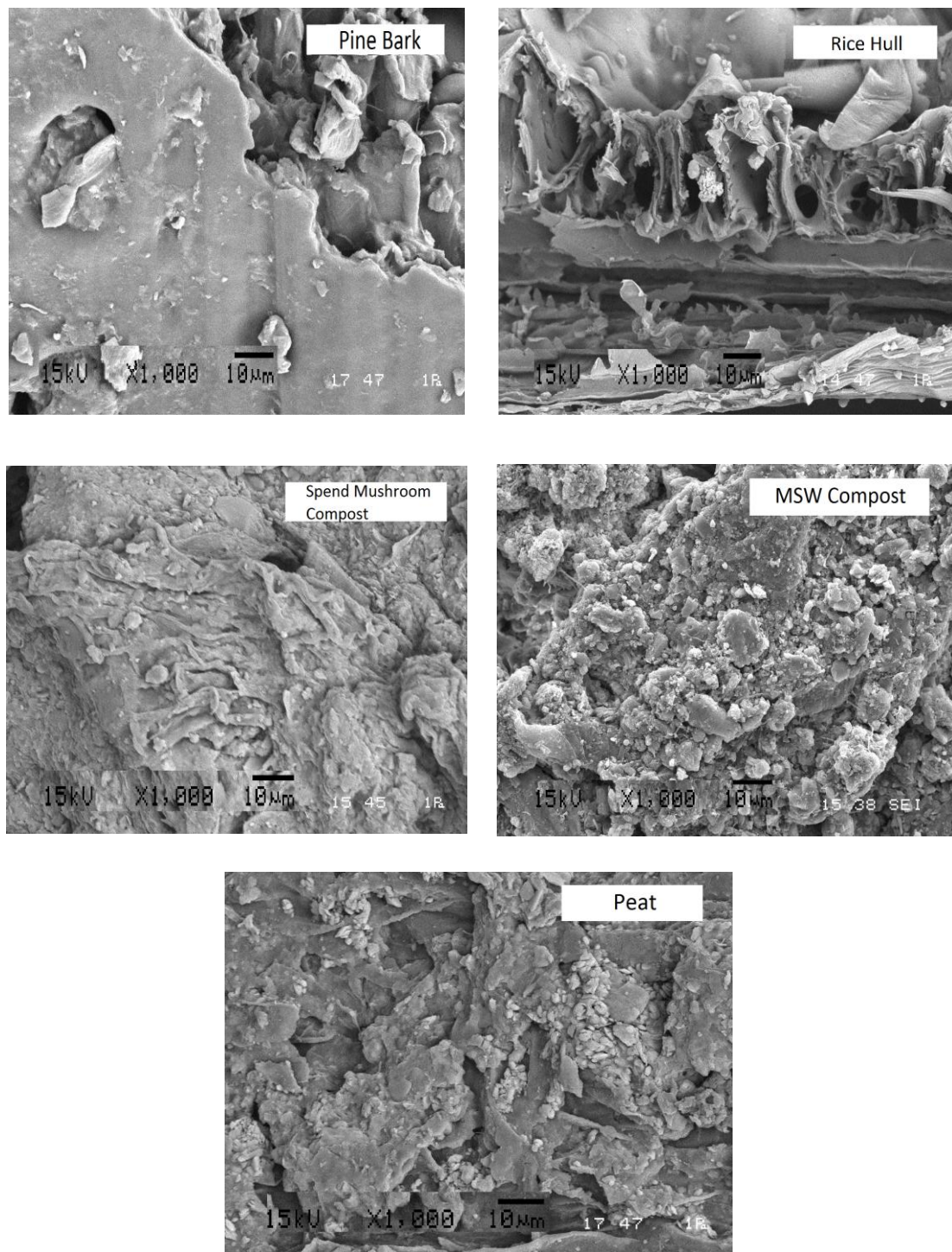
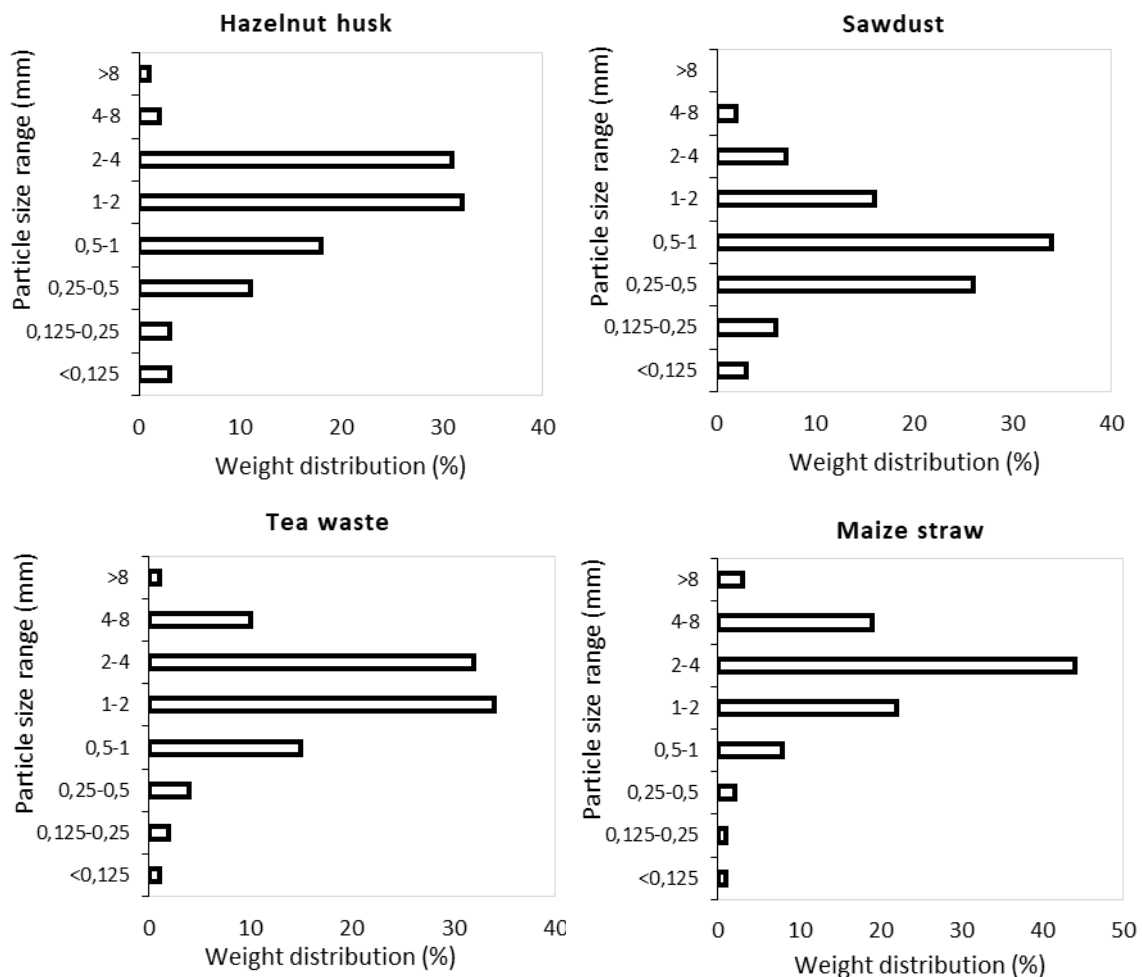


Figure 1. Scanning electron microscope (SEM) micrographs of the surface and interval structure of the organic waste samples, MSV compost and peat

Even though it is also connected to porosity and particle size distribution, the difference in two groups' hydraulic properties can be clearly understood from their surface and internal characteristics. When the pore diameter of the samples increases,

their gravitational water drainage and air capacity raises as well, but its water holding capacity decreases. Contrary to that, when the pore diameter of the samples decreases, its water holding capacity goes up, while the air capacity goes down (Fornes et al., 2003). Applying composting that would significantly increase decomposition rate of wastes such as maize straw, tea waste and rice hull, would be suitable for its use as a growing media because it would change the surface and internal structure of the waste and thus improve its hydraulic properties.

Even though we can use SEM figures to obtain information important for understanding the hydraulic properties of the samples through analyzing its surface and internal structure, the analysis of particle size distribution can help us understand the differences of the physical characteristics of samples that share similar structure (Ozdemir et al., 2015). By analyzing organic waste samples' particle sizes we can see that maize straw and rice hull (2-4 mm) are mostly composed of bigger particles, while municipal waste, pine bark and saw dust (0.5-2 mm) are mostly composed of smaller particles. However, tea waste, hazelnut husk, waste mushroom compost and peat samples' particle size distribution tends to stay within 1-4 mm, thus we can say that they are composed of a homogeneous mixture of big, middle sized and small particles (Fig. 2).



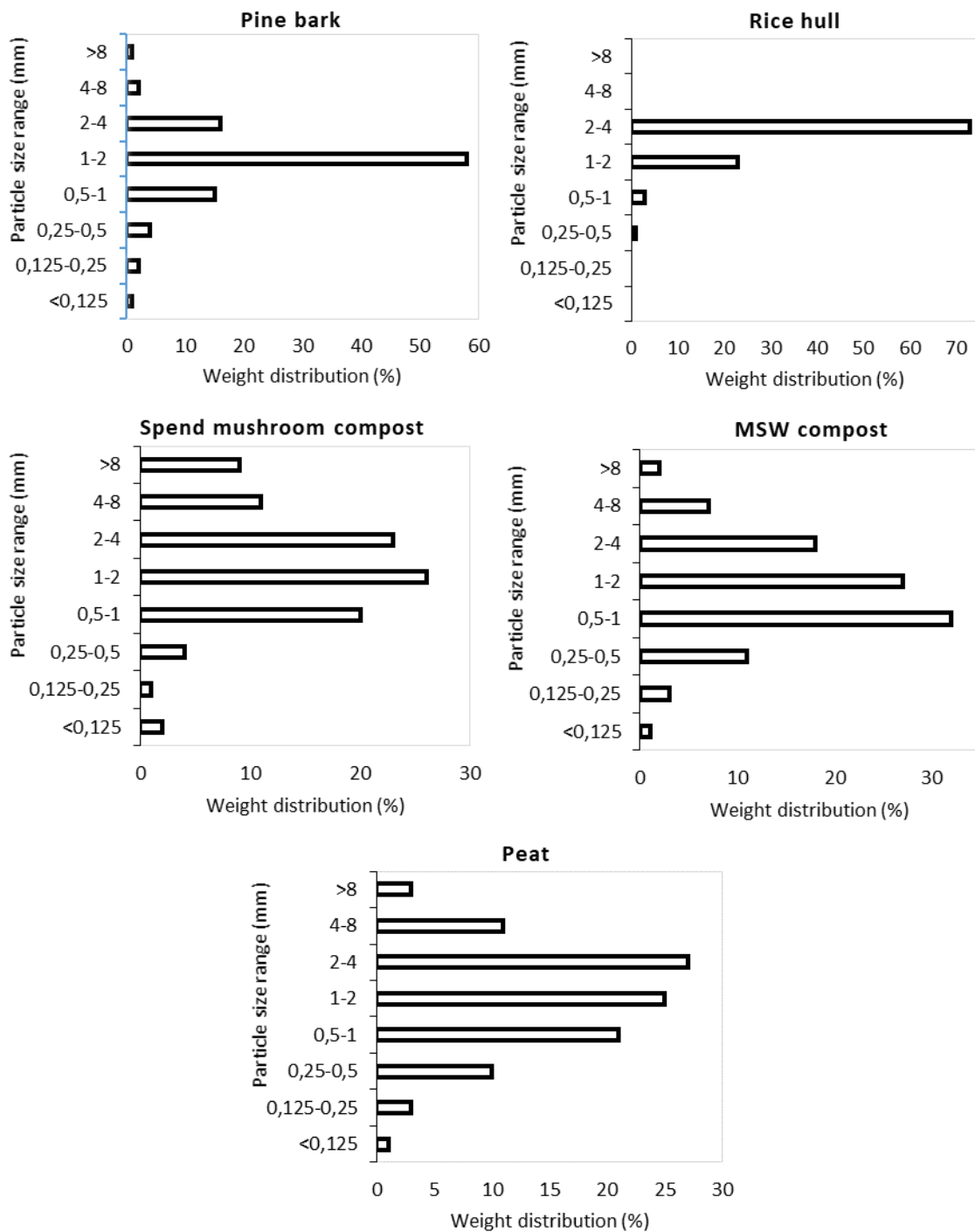


Figure 2. Particles size distribution of organic waste samples, MSW compost and peat

According to the calculations of organic waste samples' index of particle sizes (CI), geometric average and the standard deviation of geometric average while taking into account particles bigger than 1mm when calculating, the rice hull has the highest CI value of 96, while saw dust has the lowest CI value of 25 (Table 1). Hazelnut husk (66) and peat (66.67) were found to have similar results when calculating index of particle sizes.

When the values of particle size distribution on Shape 1 and CI, Dg, σ_g values in *Table 1* are analyzed together, we can say that maize straw and spend mushroom compost need to be subjected to additional fragmentation of large particles, while rice hull, compost and saw dust can be used in a mixture with growing media with large particles. Hazelnut husk and peat can be used as a growing media without adding anything (Abad et al., 2003).

Table 1. Particle size index (CI), geometric average of sample particle size, standard deviation of geometric average calculated from particle size distribution in organic waste samples, MSW compost and peat

Samples	CI (%V/V)	Dg	σ_g
Hazelnut husk	66 e*	1.269 g	2.625 c
Sawdust	25 g	0.698 i	2.342 e
Tea waste	77 c	1.733 d	2.316 f
Maize straw	88 b	2.462 a	2.284 g
Pine bark	78 c	1.392 f	2.013 h
Rice hull	96 a	2.404 b	1.496 i
Spend Mushroom Compost	73 d	1.841 c	2.846 a
MSW compost	54 f	1.226 h	2.529 d
Peat	66.6 e	1.542 e	2.707 b

*Data followed by the same letter are not different at $p = 0.05$

The results of other physical properties analyzed in this study are presented in *Tables 2* and *3*. According to these results municipal waste compost has the highest volume weight (0.649 g/cm^3) and specific weight (2.089 g/cm^3), while the lowest values of volume weight (0.05 g/cm^3) and specific weight (1.474 g/cm^3) were found in maize straw. While composting municipal solid waste, even if waste decomposing process is applied, it will be mixed with a significant amount of inorganic waste. This situation increases volume weight and specific weight of MSW compost. Maize straw has the highest porosity value (96.56%), while the lowest porosity value (71.55%) was determined in peat. The highest air capacity was observed in tea waste (76.73%) while the lowest is observed in municipal waste compost (23.1%). The volume change of growing media after drying, expressed as shrinkage value, is most pronounced in peat with 31.99%, while it is least pronounced in saw dust with 15.27%. Up to 30% of shrinkage in pot plant growing media is tolerated (Abad et al., 2001). Since shrinkage means the reaction of the material filled in the pot to getting compact, as well (Hicklenton et al., 2001), in comparison with the peat, all samples can be said to be durable to getting compact (*Table 2*). At the same time, when analyzing shrinkage results, a significant decrease in volume is observed after drying rice hull and spend mushroom compost.

Seeing as growing media is used for plant production, among its most important properties are water holding capacity and wettability. According to the results shown in *Table 3*, all the samples' water holding capacity values differ slightly comparing to the desired ideal value, while the wettability values are found to be within the ideal value span. The highest water holding capacity value is 458 ml/l and it is found in peat, while the lowest water holding capacity is 89 ml/l and it is found in rice hull sample. The

samples with particle size distribution and porosity values similar to peat such as tea waste and spend mushroom compost are found to have low water holding capacity comparing to peat. The reason for this is thought to be the difference in pore size distribution of the analyzed samples (Paredes et al., 1999).

Table 2. Physical properties of organic waste samples, MSW compost and peat

Samples	Bulk density (g/cm ³)	Particular density (g/cm ³)	Porosity (% V/V)	Air capacity (% V/V)	Shrinkage (% V/V)
Hazelnut husk	0.169 c*	1.489 f	88.91 d	55.12 d	16.12 h
Sawdust	0.172 c	1.508 e	88.72 d	50.71 e	15.27 i
Tea waste	0.076 e	1.502 e	94.21 b	76.73 b	17.21 g
Maize straw	0.050 f	1.474 f	96.56 a	76.09 b	21.13 e
Pine bark	0.177 c	1.489 f	88.21 e	56.42 c	18.82 f
Rice hull	0.099 d	1.524 d	93.47 c	84.53 a	24.99 c
Spend mushroom compost	0.178 c	1.614 c	89.02 d	44.45 f	25.55 b
MSW compost	0.649 a	2.089 a	68.92 g	23.11 g	21.93 d
Peat	0.458 b	1.856 b	73.28 f	27.72 h	31.99 a
Ideal values	< 0.40	1.4-2.0	> 80	20-30	< 30

*Data followed by the same letter are not different at p = 0.05

Table 3. Hydraulic properties of organic waste samples, MSW compost and peat

Samples	Water holding capacity (ml/l)	Wettability (min)
Hazelnut husk	335 d*	1.52 d
Sawdust	379 c	1.38 e
Tea waste	182 g	< 1 g
Maize straw	205 f	< 1 g
Pine bark	320 e	1.32 f
Rice hull	89 h	< 1 g
Spend mushroom compost	446 b	2.59 c
MSW compost	456 a	3.46 a
Peat	458 a	3.28 b
Ideal values	600-1000	< 5

*Data followed by the same letter are not different at p = 0.05

The highest value of wettability is found in MSW compost (3.46 min) and the lowest is < 1 min and was observed in maize straw, tea waste and rice hull samples. However, this is due to the high porosity values of these samples which obstructs the samples from holding water and causes them to be drained fast. Organic substances are believed to have enhanced wettability due to increased porosity (Beardsell and Nichols, 1982). This is why we could say that maize straw, tea waste and rice hull samples' water holding capacity could not be determined and that their wetting period is much longer than the ideal values needed for growing media.

Physiochemical properties of the organic waste samples researched for their potential to be used as a growing media are presented in *Table 4*. According to these results, the

highest pH value is 7.57 and is found in rice hull, while the lowest pH value is 4.82 and is found in hazelnut husk.

Table 4. Chemical properties of organic waste samples, MSW compost and peat

Samples	pH	EC (mS/cm)	Organic matter content (%)
Hazelnut husk	4.82 g*	2.975 b	94.22 b
Sawdust	6.47 e	0.202 i	91.49 d
Tea waste	5.52 f	0.532 g	92.42 c
Maize straw	7.15 c	0.582 f	96.37 a
Pine bark	5.47 f	0.762 e	94.39 b
Rice hull	7.57 a	0.315 h	89.24 e
Spend mushroom compost	7.3 b	1.68 d	77.65 f
MSW compost	7.3 b	2.887 c	32.38 h
Peat	6.92 f	3.46 a	51.7 g
Ideal values	5.2-6.3	0.75-3.49	> 85

*Data followed by the same letter are not different at $p = 0.05$

At the same time, from all the samples taken, only pine bark and tea waste have pH values within the ideal value range. On the other hand, the highest EC value is 4.1 mS/cm found in raw peat. The lowest EC value is 1.68 seen in spend mushroom compost. According to the results of organic matter analysis, the highest value is 96.87% in maize straw, while the lowest organic matter value is 32.38% in municipal waste compost. Also, sample with the lowest organic matter value, that is municipal waste compost, together with spend mushroom compost (77.65%) and peat (51.7%) were found to have organic matter value below the ideal value range.

Conclusion

It is determined by this study that the physical and hydraulic properties of the growth media obtained from organic wastes vary with the particle size distribution as well as the surface and interior structures of the organic wastes used. However the results obtained from examined samples has shown that hazelnut husk, sawdust, spend mushroom compost and MSW compost from among the samples examined can be used purely, and that other organic wastes can be used in the mixtures which will be prepared as growth medium components. But because of the low water holding capacities and water redrawing difficulties during the use of the growth mediums consisted of those wastes, it is important to make a good watering program and not to allow drying. It is considered that especially the wastes of corn straw and rice hull can be useful in improving the significant physical properties – such as porosity, air capacity and water holding capacity – of plant growth mediums which will be prepared.

REFERENCES

- [1] Abad, M., Fornes, F., Carrion, C., Noguera, V. (2005): Physical properties of various coconut coir dusts compared to peat. – Hortscience 40: 2138-2144.

- [2] Abad, M., Noguera, P., Bures, S. (2001): National inventory of organic wastes for use as growing media for ornamental potted plant production: case study in Spain. – *Bioresource Technology* 77: 197-200.
- [3] Abad, M., Noguera, P., Puchades, R., Maquieira, A., Noguera, V. (2003): Physico-chemical and chemical properties of some coconut coir dusts for use as a peat substitute for containerised ornamental plants. – *Bioresource Technology* 82: 241-245.
- [4] Apaolaza, L. H., Gasco, A. M., Gasco, J. M., Guerrero, F. (2005): Reuse of waste materials as growing media for ornamental plants. – *Bioresource Technology* 96: 125-131.
- [5] Australian Standard (2003): Potting Mixes, AS 3743-1993. – Standards Australia International, Sydney.
- [6] Beardsell, D. V., Nichols, D. G. (1982): Wettability properties of dried out nursery container media. – *Sci. Horticul.* 17: 49-59.
- [7] Belda, R. M., Mendoza Hernández, D., Fornes, F. (2013): Nutrient rich compost versus nutrient poor vermicompost as growth media for ornamental plant production. – *J. Plant Nutr. Soil Sci.* 176: 827–835.
- [8] Benito, M., Masaguer, A., Moliner, A., De Antonio, R. (2006): Chemical and physical properties of pruning waste compost and their seasonal variability. – *Bioresource Technology* 97: 2071-2076.
- [9] Dede, O. H., Koseoglu, G., Ozdemir, S., Celebi, A. (2006): Effects of organic wastes substrates on the growth of impatiens. – *Turkish Journal of Agriculture and Forestry* 30: 375-381.
- [10] European Standard 13037. (1999): Determination of pH. In: *Soil Improvers and Growing Media*. European Committee for Standardization, Brussels.
- [11] Fornes, F., Belda, R. M., Abad, M., Noguera, P., Puchades, R., Maquieira, A., Noguera, V. (2003): The microstructure of coconut coir dusts for use as alternatives to peat in soilless growing media. – *Australian Journal of Experimental Agriculture* 43: 1171-1179.
- [12] Fornes, F., Belda, R. M., Carrion, C., Noguera, V., Garcia-Agustin, P., Abad, M. (2007): Pre-conditioning ornamental plants to drought by means of saline water irrigation as related to salinity tolerance. – *Scientia Horticulturae* 113: 52-59.
- [13] Guo, Z., Liu, W. (2007): Biomimic from the superhydrophobic plant leaves in nature: Binary structure and unitary structure. – *Plant Science* 172: 1103-1112.
- [14] Hicklenton, P. R., Rodd, V., Warman, P. R. (2001): The effectiveness and consistency of source-separated municipal solid waste and bark composts as components of container growing media. – *Scientia Horticulturae* 91: 365-378.
- [15] Marianthi, T. (2006): Kenaf (*Hibiscus cannabinus* L.) core and rice hulls as components of container media for growing *Pinus halepensis* M. Seedlings. – *Bioresource Technology* 97: 1631-1639.
- [16] Masaphy, S., Zabari, L., Pastrana, J., Dultz, S. (2009): Role of fungal mycelium in the formation of carbonate concretions in growing media—an investigation by SEM and synchrotron-based X-ray tomographic microscopy. – *Geomicrobiology Journal* 26: 442-450.
- [17] Ozdemir, S., Dede, O., Celebi, A. (2015): Improvement of the wettability properties of compost using seaweed. – *Compost Science and Utilization* 23: 87-93.
- [18] Paredes, C., Cegarra, J., Roig, A., Sfinchez-Monedero, M. A., Bernal M. P. (1999): Characterization of olive mill wastewater (alpechin) and its sludge for agricultural purposes. – *Bioresource Technology* 67: 111-115.
- [19] Richards, D., Lane, M., Beardsell, D. V. (1986): The influence of particle-size distribution in pinebark:sand:brown coal potting mixes on water supply, aeration and plant growth. – *Scientia Hort.* 29: 1-14.
- [20] Rigane, M. K., Michel, J. M., Medhioub, K., Morel, P. (2011): Evaluation of compost maturity, hydrophysical and physicochemical properties: indicators for use as a component of growing media. – *Compost Science & Utilization* 19: 226-234.

- [21] Tariq, U., Rehman, S., Khan, M. A., Younis, A., Yaseen, M., Ahsan, M. (2012): Agricultural and municipal waste as potting media components for the growth and flowering of *Dahlia hortensis* 'Figaro'. – *Turk J Bot* 36: 378-385.
- [22] Yahya, A., Sye, C. P., Ishola, T. A., Suryanto, H. (2010): Effect of adding palm oil mill decanter cake slurry with regular turning operation on the composting process and quality of compost from oil palm empty fruit bunches. – *Bioresource Technology* 101: 8736-874.

DETERMINATION OF YIELD AND QUALITY CHARACTERISTICS OF SOME ALFALFA (*Medicago sativa* L.) CULTIVARS IN THE EAST ANATOLIA REGION OF TURKEY AND CORRELATION ANALYSIS BETWEEN THESE PROPERTIES

CACAN, E.^{1*} – KOKTEN, K.² – KAPLAN, M.³

¹*Department of Crop and Animal Production, Vocational School of Genc, University of Bingol, Bingol, Turkey*

²*Department of Field Crops, Faculty of Agriculture, University of Bingol, Bingol, Turkey*

³*Department of Field Crops, Faculty of Agriculture, University of Erciyes, Kayseri, Turkey*

**Corresponding author*

e-mail: erdalcacan@gmail.com; phone: +90-505-844-5280; fax: +90-426-411-2083

(Received 31st Oct 2017; accepted 12th Feb 2018)

Abstract. This study was conducted to determine yield and some quality features of some alfalfa cultivars for three years between 2014 and 2016 in the East Anatolian Region of Turkey and correlation analysis between these properties. In this study, sixteen different alfalfa cultivars (Verdor, Magna-601, Magnum-V, Basbag, Elci, Kayseri, Nimet, Savas, Omerbey, Ozpinar, Alsancak, Gea, Verko, Sunter, Bilensoy-80 and Gozlu-1) were used. Experiments were conducted in the randomized block design with three replications. According to the results of this study significant differences were determined in terms of plant height, green herbage yield, dry herbage yield, crude protein ratio, crude protein yield, acid detergent fiber (ADF), neutral detergent fiber (NDF), digestible dry matter (DDM), dry matter intake (DMI) and relative feed value (RFV) of alfalfa cultivars. In alfalfa cultivars, the highest green plant height, green herbage yield, dry herbage yield, crude protein yield and relative feed value were determined in Gea (54.7 cm, 3591 kg da⁻¹, 1227 kg da⁻¹, 301 kg da⁻¹ and 262.1, respectively). The highest crude protein ratio was determined in Magnum-V (25.9%). The least ADF contents were obtained from Gea (18.7%) and the least NDF contents were obtained from Gea, Sunter, Nimet and Ozpinar (27.1%, 27.4%, 27.5% and 27.7%, respectively). The highest digestible dry matter was determined in Gea (74.4%). The highest dry matter intake was obtained from Gea, Sunter, Nimet and Ozpinar (4.53%, 4.52%, 4.48% and 4.45%, respectively). Also, significant correlations were found between the traits studied. As a result, Gea variety with high dry herbage and crude protein yield, low ADF-NDF ratios and high relative feed value was recommended for alfalfa culture in similar ecologies. Outside Gea; it seems that Bilensoy-80, Magna-601, Magnum-V, Omerbey, Sunter, Verdor and Verko cultivars gave results above averages and were remarkable in terms of yield and quality.

Keywords: *crude protein, hay yield, lucerne, relative feed value, Eastern Anatolia Region, ADF, NDF*

Introduction

Alfalfa (*Medicago sativa* L.) is one of the most important forage plants in the world, which has a very broad adaptability to different climatic conditions (Moreira and Fageria, 2010). Alfalfa, due to its superior forage qualities and high yields, is called “Queen of the forages” in Turkey and many countries of the world (Yuksel et al., 2016).

Feeds play a great role in animal nutrition. They provide fiber, minerals, protein and energy (Kamalak and Canobolat, 2010; Kiraz, 2011). Alfalfa, which has high protein

content, is also a very rich source of nutrients in terms of mineral substances and many vitamins (Geren et al., 2009). Alfalfa hay has significantly high digestibility coefficients for crude fiber, organic matter, crude protein and fat compared to grasses (Sommer et al., 2005).

Alfalfa is the most widely cultivated forage crop in the world and in Turkey. There is still a need to increase alfalfa cultivated lands to make livestock activities more productive and profitable. Increasing alfalfa cultivated lands and use of high-yield and quality alfalfa cultivars with a high adaptation capacity to regional conditions over currently cultivated lands are quite significant issues. Therefore, scientific research should be conducted to identify such high-yield and quality genotypes with high adaptation capacities and research outcomes should be put into practice. With the selection of proper genotypes, farmers and producers will get higher yields per unit area and will have high quality products.

Annual green and dry herbage yields per decare are the most significant yield parameters of alfalfa. Alfalfa herbage quality is designated by crude protein (CP), acid detergent fiber (ADF) and neutral detergent fiber (NDF). ADF and NDF values represent the compounds constituting cell membrane and low values are desired for roughage quality. Low ADF and NDF values result in high digestible dry matter (DDM), dry matter intake (DMI) and relative feed value (RFV). The ratios of these parameters directly influence roughage quality (Kaplan et al., 2016).

Genotypes have quite diverse nutritional compositions, thus nutritional composition of different species should be investigated (Ulger and Kaplan, 2016). Especially ADF, NDF, crude protein and crude ash contents should be investigated to assess the nutritional composition of feedstuffs (Uke et al., 2017).

To determine these parameters, several studies has carried out in different regions of Turkey (Kusvuran et al., 2005; Demiroglu et al., 2008; Basbag, 2009; Avci et al., 2010; Saruhan and Kusvuran, 2011; Yuksel et al., 2016).

Therefore the present study was conducted to determine yield and quality parameters of sixteen alfalfa cultivars in East Anatolia Region ecological conditions, to reveal the correlation between yield and quality parameters of these cultivars and ultimately to identify the most appropriate cultivar.

Materials and methods

Study area

The study was conducted in the province of Bingol. Bingol province is located in the Eastern Anatolia Region of Turkey. The Bingol province has a surface area of 8253 km² and an average elevation of 1150 m. Total area of 8253 km² consists of 27.92% forest, 10.25% afforestation area, 7.28% agricultural land, 51.0% pasture, 2.2% meadow and 1.3% other areas. Located in the Upper Euphrates section of the Eastern Anatolia Region, Bingol is located between 41° 20' - 39° 56' east longitudes and 39° 31' - 36° 28' north latitudes (Anonymous, 2018). Bingol land is very mountainous. Steppe vegetation is seen where the forests are destroyed. The most cultivated crops in agricultural land are field crops. In field crops, most wheat and alfalfa cultivation is done.

Experiments were conducted over the experimental fields of Bingol University under irrigated conditions for three years (2014-2016). This area is 15 km away from the center of Bingol province with an average elevation of 1092 m. The study area is located between 38.81589° north latitudes and 40.53866° east longitudes (*Fig. 1*).



Figure 1. Photographs of study area

Experimental material

This study on the adaptation of alfalfa cultivars is done for the first time in Bingol province. Bingol province is located at the transition point between Southeastern Anatolia Region and Eastern Anatolia Region. Partly cold, partly under the influence of hot climate is located. For this reason, while choosing alfalfa cultivars for adaptation study, it has been taken care to use cultivars belonging to both hot and cold regions. Another reason for the select of these alfalfa cultivars are they are widely grown in Turkey.

A total of sixteen alfalfa cultivars (Verdor, Magna-601, Magnum-V, Basbag, Elci, Kayseri, Nimet, Savas, Omerbey, Ozpinar, Alsancak, Gea, Verko, Sunter, Bilensoy-80 and Gozlu-1) were used as the plant material of the experiments. These varieties were obtained from various institutions and organizations in Turkey.

Treatments

Field experiments were conducted over deep-tilled cultivated and harrowed lands. Experiments were set on 5th of May 2014 in randomized blocks design with 3 replications. Plots were 5 m long. Sowing was performed with the aid of hand marker. Each plot had 6 rows 20 cm apart. Sowing was implemented as to have 3 kg seeds per decare. Before sowing, 4 kg nitrogen (N) and 10 kg phosphorus (P_2O_5) were applied to experimental plots. Sprinklers were used for irrigations. Irrigation intervals were 7-12 days and irrigation duration was 8 h.

Climate data

Climate data for Bingol province were supplied from General Directorate of Meteorology (*Table 1*). Long-term (2000-2015) monthly average temperature was 12.3 °C, total annual precipitation was 917.8 mm and average relative humidity was 56.6%. For the experimental years of 2014, 2015 and 2016 monthly average temperature (13.7 °C, 13.7 °C and 12.8 °C) and relative humidity (51.9%, 52.7% and 56.6%) values were close to long-term averages. However, precipitations of experimental years (757.7 mm, 801.8 mm and 832.5 mm) were lower than the long-term averages. In the months when precipitation was insufficient, irrigation was done every 7-12 days.

Table 1. Monthly average climate data of Bingol for 2014-2016 and long years (2000-2015)

Months	Average temperature (°C)				Total precipitation (mm)				Relative humidity (%)			
	2014	2015	2016	Long years	2014	2015	2016	Long years	2014	2015	2016	Long years
January	-0.4	-1.8	-2.8	-2.5	143.1	148.2	235.1	154.0	71.3	74.7	75.3	73.3
February	2.0	1.9	2.4	-0.9	82.3	115.8	86.3	137.7	57.7	73.8	73.7	72.2
March	8.6	5.4	7.0	4.9	83.5	154.4	125.5	124.1	62.9	65.9	60.4	64.2
April	13.2	10.9	13.9	10.9	41.6	66.7	45.5	103.8	53.3	58.7	48.4	61.2
May	17.2	16.6	16.3	16.2	63.2	21.2	62.2	66.8	52.1	52.0	57.4	55.8
June	22.3	22.9	22.2	22.6	25.9	8.1	34.6	18.4	36.9	37.0	43.6	42.5
July	27.8	27.9	26.9	27.0	4.0	0.0	3.5	7.3	26.3	26.8	33.4	36.7
August	28.0	27.5	28.0	26.8	0.9	0.6	0.0	5.4	24.0	29.7	28.0	36.8
September	21.3	23.4	19.9	21.3	63.7	0.8	29.1	16.4	36.2	30.2	40.3	42.2
October	13.7	14.3	15.2	14.2	87.3	220.9	4.4	70.3	62.3	68.3	43.0	58.9
November	6.3	14.4	6.4	6.5	99.0	18.9	53.7	91.8	64.3	56.4	47.9	64.7
December	4.6	1.3	-2.2	0.2	63.2	46.2	152.6	121.8	75.7	58.6	73.4	70.7
Total/Ave.	13.7	13.7	12.8	12.3	757.7	801.8	832.5	917.8	51.9	52.7	52.1	56.6

Source: General Directorate of Meteorology (Bingol)

Soil structure

Bingol province agricultural soils are generally clay-loam texture, neutral or near neutral in reaction (pH), without salt, low and moderate level calcareous, low organic matter, the amount of phosphorus is insufficient and the amount of potassium is sufficient (Ates and Turan, 2015).

Soil samples were taken from 10 different locations of experimental fields from 0-30 cm depths. Samples were analyzed at Soil-Plant Analyses Laboratory of Bingol University Agricultural Faculty. Analysis results were assessed through the limiting values specified in Sezen (1995) and Karaman (2012). Experimental soils had loamy texture (43.31% saturation). Soils were slightly acidic (pH of 6.37), unsaline (0.0066%), poor in organic matter (1.26%), lime (0.15%) and potassium (24.45 kg da⁻¹) and medium in phosphorus (7.91 kg da⁻¹).

Plant harvesting

Since weeds, disease and harmful were not seen in the research area, no medication was applied. In the study, harvesting was carried out in the period when plants were 10% flowering (Manga et al., 2003).

Plant heights were measured over randomly selected 10 plants of each plot as the height from the soil surface to upper most bud. Average of 10 plants was considered as the plant height. The harvested herbage from each plot was weighed to get green herbage yields. Then, plot herbage yields were converted into yields per decare. From each green herbage harvest, 0.5 kg was dried at 70 °C for 48 h. Dried samples were weighed to get dry herbage yields of the plots. Then, these values were also converted into dry herbage

yields per decare. Experiments were conducted for 3 years. Two cuts were performed in the first year and five cuts were performed in the second and third year.

Plant analysis

Crude protein, ADF (Acid Detergent Fiber) and NDF (Neutral Detergent Fiber) analyses were performed at laboratories of Dicle University Scientific and Technological Research Center with NIRS (Near Infrared Spectroscopy - Foss Model 6500) analysis device. With ADF and NDF ratios, digestible dry matter ($DDM = 88.9 - (0.779 \times \%ADF)$), dry matter intake ($DMI = 120/\%NDF$) and relative feed value ($RFV = (DDM \times DMI)/1.29$) was calculated (Morrison, 2003).

Statistical analysis

Experimental data were subjected to ANOVA with JMP statistical software. Means were compared with HSD test. Correlation coefficients were calculated to determine the relationships among investigated traits (Kalayci, 2005).

Results

Green herbage and dry herbage yields ($kg\ da^{-1}$)

Green herbage and dry herbage yields of sixteen alfalfa cultivars are provided in Table 2. The differences in green herbage and dry herbage yields of the cultivars and the years were found to be significant ($P < 0.01$).

Table 2. Green and dry herbage yields of alfalfa cultivars

No	Cultivar	Green herbage yield ($kg\ da^{-1}$)				Dry herbage yield ($kg\ da^{-1}$)			
		2014	2015	2016	Mean	2014	2015	2016	Mean
1	Alsancak	1502.8	3249.7	3536.3	2762.9 e**	539.8	1153.2	1362.6	1018.5 cd**
2	Basbag	1736.6	3450.0	3382.5	2856.3 de	524.1	1255.0	1340.0	1039.7 b-d
3	Bilensoy-80	1608.9	3778.6	3646.9	3011.5 c-e	550.1	1363.9	1489.0	1134.3 a-c
4	Elci	1518.5	3507.6	3689.1	2905.1 de	542.5	1350.5	1497.3	1130.1 a-c
5	Gea	1712.0	4382.6	4678.4	3591.0 a	572.7	1533.1	1576.2	1227.3 a
6	Gozlu-1	1186.9	3688.9	3330.1	2735.3 e	381.1	1252.3	1138.9	924.1 d
7	Kayseri	1322.0	3911.4	3522.8	2918.7 de	451.8	1390.9	1424.2	1089.0 a-d
8	Magna-601	1712.1	4573.3	4380.7	3555.4 ab	495.9	1633.4	1476.0	1201.8 ab
9	Magnum-V	1468.3	4022.2	4411.0	3300.5 a-d	480.6	1430.1	1472.2	1127.6 a-c
10	Nimet	1717.3	3336.0	4171.8	3075.0 b-e	563.9	1228.2	1371.7	1054.6 b-d
11	Omerbey	1571.5	4273.8	4428.9	3424.7 a-c	538.0	1507.1	1555.5	1200.2 ab
12	Ozpinar	1822.0	3249.5	3669.3	2913.6 de	597.5	1148.8	1439.5	1061.9 a-d
13	Savas	1506.2	3498.9	3722.9	2909.3 de	515.8	1198.1	1273.8	995.9 cd
14	Sunter	1455.4	4125.1	4286.7	3289.1 a-d	506.7	1454.9	1437.1	1132.9 a-c
15	Verdor	1740.1	3831.7	4229.9	3267.2 a-d	544.0	1379.4	1515.0	1146.1 a-c
16	Verko	1698.4	3882.2	3977.9	3186.2 a-e	544.6	1470.7	1454.2	1156.5 a-c
Mean		1579.9 C**	3797.6 A	3941.6 A	3106.4	521.8 C**	1359.4 B	1426.4 A	1102.5
**Significant at $P < 0.01$, CV: 9.76%						**Significant at $P < 0.01$, CV: 9.14%			

The greatest green herbage yield was obtained from Gea cultivar and the cultivars Magna-601, Omerbey, Magnum-V, Sunter, Verdor and Verko were also placed in the same statistical group. The lowest green herbage yield was obtained from Gozlu-1 and Alsancak cultivars. Considering the green herbage yields of the years, the greatest value was obtained in 2015 and 2016 the lowest value was obtained in 2014. Three-year average green herbage yield was calculated as 3106.4 kg da⁻¹.

The greatest dry herbage yield was obtained from Gea cultivar and the cultivars Magna-601, Omerbey, Verko, Verdor, Sunter, Ozpinar, Magnum-V, Kayseri, Elci and Bilensoy-80 were also placed in the same statistical group. The lowest dry herbage yield was obtained from Gozlu-1 cultivar. Considering the dry herbage yields of the years, the greatest value was obtained in 2016 and the lowest value was obtained in 2014. Three-year average dry herbage yield was calculated as 1102.5 kg da⁻¹.

Dry herbage yield and averages obtained from the cultivars used in the research are given in *Figure 2*. It is seen that Bilensoy-80, Elci, Gea, Magna-601, Magnum-V, Omerbey, Sunter, Verdor and Verko cultivars gave results above the averages in terms of dry herbage yield.

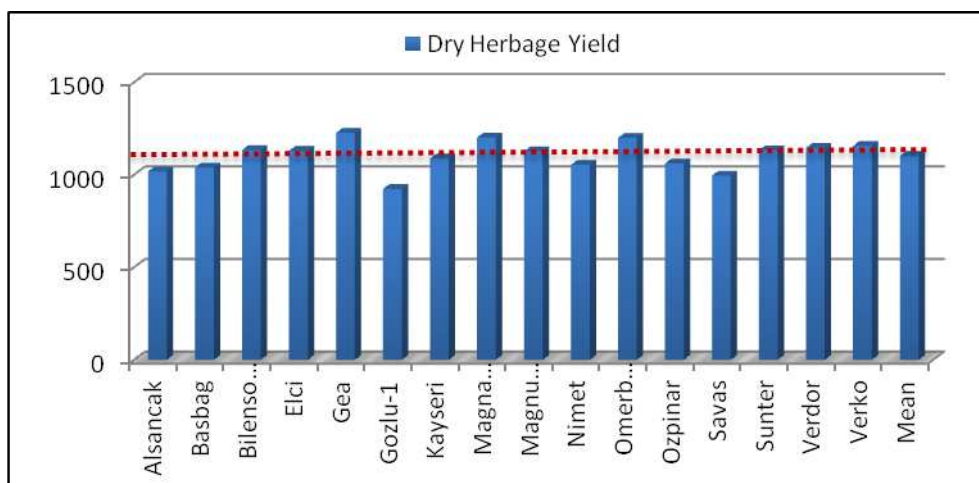


Figure 2. Dry herbage yield of alfalfa cultivars

Crude protein ratio (%) and crude protein yields (kg da⁻¹)

Crude protein ratios and crude protein yields of sixteen alfalfa cultivars are provided in *Table 3*. While the differences in crude protein ratios of the cultivars were found to be significant at 5% level, the differences in crude protein ratio of the years, crude protein yields and crude protein yield of the years were found to be significant at 1% level.

The greatest crude protein content was obtained from Magnum-V cultivar and the lowest protein content was obtained from Elci and Basbag cultivars. With regard to crude protein contents of the years, the greatest value was observed in 2014 and the lowest value was seen in 2016. Three-year average crude protein content was calculated as 25.0%.

While the greatest crude protein yield was obtained from Gea cultivar and the lowest crude protein yield was obtained from Gozlu-1 cultivar. Considering the crude protein yields of the years, the greatest values were observed in 2016 and 2015 and the lowest

value was seen in 2014. Three-year average crude protein yield of the cultivars was calculated as 266.2 kg da⁻¹.

Table 3. Crude protein ratios and yields of different alfalfa cultivars

No	Cultivars	Crude protein ratios (%)				Crude protein yields (kg da ⁻¹)			
		2014	2015	2016	Mean	2014	2015	2016	Mean
1	Alsancak	28.2	23.8	21.4	24.5 ab*	152.3	292.1	274.2	239.5 cd**
2	Basbag	26.8	23.1	22.1	24.0 b	140.5	295.7	289.5	241.9 cd
3	Bilensoy-80	29.2	24.2	22.7	25.4 ab	160.9	337.6	328.6	275.7 a-c
4	Elci	26.3	23.2	22.3	23.9 b	142.0	333.3	313.5	262.9 a-c
5	Gea	27.7	25.4	22.5	25.2 ab	158.7	355.0	389.5	301.1 a
6	Gozlu-1	28.4	23.7	22.0	24.7 ab	108.1	252.0	297.1	219.1 d
7	Kayseri	28.7	24.1	22.7	25.2 ab	129.8	323.3	335.3	262.8 a-c
8	Magna-601	27.0	24.6	23.3	25.0 ab	133.9	343.5	401.1	292.8 ab
9	Magnum-V	29.2	24.0	24.5	25.9 a	140.2	360.8	342.7	281.2 a-c
10	Nimet	29.9	23.9	22.8	25.6 ab	168.9	313.2	294.0	258.7 a-d
11	Omerbey	28.9	24.1	23.0	25.4 ab	155.9	358.8	363.3	292.7 ab
12	Ozpinar	28.1	24.0	22.3	24.8 ab	167.4	320.6	275.6	254.5 b-d
13	Savas	27.5	24.1	23.5	25.0 ab	141.4	298.8	288.2	242.8 cd
14	Sunter	28.8	24.3	22.9	25.4 ab	146.1	329.7	353.7	276.5 a-c
15	Verdor	27.1	23.5	23.5	24.7 ab	146.9	357.1	323.3	275.8 a-c
16	Verko	27.9	24.3	22.9	25.0 ab	151.9	333.5	357.1	280.9 a-c
Mean		28.1 A**	24.0 B	22.8 C	25.0	146.6 B**	325.3 A	326.7 A	266.2

*Significant at P < 0.05; **Significant at P < 0.01, CV: 4.42% **Significant at P < 0.01, CV: 9.96%

Crude protein yield and averages obtained from the cultivars used in the research are given in *Figure 3*. Bilensoy-80, Gea, Magna-601, Magnum-V, Omerbey, Sunter, Verdor and Verko cultivars gave results above the averages in terms of crude protein yield.

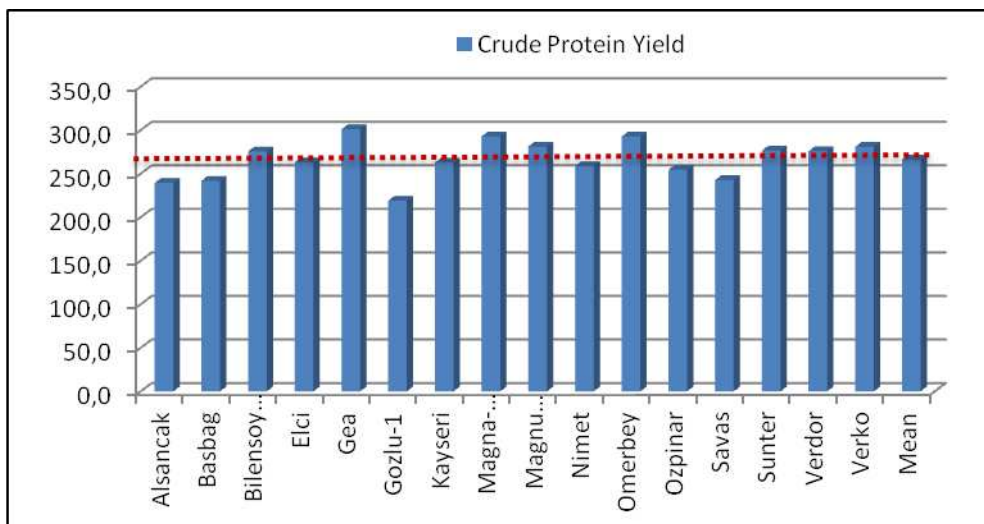


Figure 3. Crude protein yield of alfalfa cultivars

Acid detergent fiber (ADF) and neutral detergent fiber (NDF) ratios (%)

Acid detergent fiber (ADF) and neutral detergent fiber (NDF) ratios of sixteen alfalfa cultivars are provided in *Table 4*. The differences in ADF and NDF of both the cultivars and the years were found to be significant at 1% level.

Table 4. ADF and NDF ratios of alfalfa cultivars

No	Cultivars	ADF (%)				NDF (%)			
		2014	2015	2016	Mean	2014	2015	2016	Mean
1	Alsancak	18.5	19.1	22.2	20.0 a-c**	23.7	28.3	33.8	28.6 ab**
2	Basbag	18.2	22.9	22.7	21.2 a-c	27.9	27.7	34.9	30.2 ab
3	Bilensoy-80	17.9	18.9	22.2	19.7 a-c	25.3	27.8	34.4	29.2 ab
4	Elci	20.0	26.5	22.5	23.0 a	30.7	31.2	34.7	32.2 a
5	Gea	15.8	18.9	21.3	18.7 c	23.6	24.8	32.8	27.1 b
6	Gozlu-1	19.5	20.9	23.2	21.2 a-c	24.7	29.4	35.8	30.0 ab
7	Kayseri	18.9	19.7	21.6	20.1 a-c	23.9	29.4	33.8	29.0 ab
8	Magna-601	19.0	22.7	22.3	21.3 a-c	26.5	28.4	34.1	29.7 ab
9	Magnum-V	19.9	21.1	20.5	20.5 a-c	24.2	29.6	32.5	28.8 ab
10	Nimet	16.5	19.0	21.9	19.1 bc	23.5	25.3	33.7	27.5 b
11	Omerbey	18.2	19.8	22.7	20.2 a-c	24.5	28.0	35.0	29.2 ab
12	Ozpinar	18.5	19.3	21.4	19.7 a-c	23.3	26.7	33.1	27.7 b
13	Savas	18.7	26.1	23.3	22.7 ab	31.4	28.3	36.0	31.9 a
14	Sunter	17.7	17.7	21.4	18.9 bc	22.2	27.0	33.1	27.4 b
15	Verdor	18.7	21.2	20.6	20.2 a-c	25.5	27.9	32.1	28.5 ab
16	Verko	18.3	19.0	21.3	19.5 a-c	24.0	27.5	33.6	28.4 ab
Mean		18.4 C**	20.8 B	21.9 A	20.4	25.3 C**	28.0 B	34.0 A	29.1
**Significant at P < 0.01, CV: 11.22%						**Significant at P < 0.01, CV: 8.42%			

While the lowest ADF ratios were observed in Gea cultivar and the greatest ADF ratios were observed in Elci cultivar. Considering the ADF ratios of the years, the greatest value was observed in 2016 and the lowest value was observed in 2014. Three-year average ADF ratio of the cultivars was calculated as 20.4%.

The lowest NDF ratio was observed in Gea, Nimet, Ozpinar and Sunter cultivars. The greatest NDF ratio was observed in Elci and Savas cultivars. Considering the NDF ratios of the years, the lowest value was observed in 2014 and the greatest value was seen in 2016. Three-year average NDF ratio of the cultivars was calculated as 29.1%.

Digestible dry matter (%) and dry matter intake (%)

Digestible dry matter (DDM) and dry matter intake (DMI) ratios of different alfalfa cultivars are provided in *Table 5*. The differences in DDM and DMI of both the cultivars and the years were found to be significant at 1% level.

The greatest DDM ratios were observed in Gea cultivar and the lowest DDM ratios were observed in Elci cultivar. Considering the DDM ratios of the years, the greatest value was observed in 2014 and the lowest value was seen in 2016. Three-year average DDM ratio of the cultivars was calculated as 73.0%.

The greatest DMI ratios were observed in Gea, Sunter, Ozpinar and Nimet cultivars. The lowest DMI ratio was observed in Elci and Savas cultivars. Considering the DMI ratios of the years, the greatest value was observed in 2014 and the lowest value was seen in 2016. Three-year average DMI ratio of the cultivars was calculated as 4.23%.

Table 5. DDM and DMI values of alfalfa cultivars

No	Cultivars	DDM (%)				DMI (%)			
		2014	2015	2016	Mean	2014	2015	2016	Mean
1	Alsancak	74.5	74.0	71.6	73.4 a-c**	5.16	4.30	3.56	4.34 ab**
2	Basbag	74.7	71.1	71.2	72.4 a-c	4.31	4.33	3.45	4.03 ab
3	Bilensoy-80	74.9	74.2	71.6	73.6 a-c	4.75	4.35	3.49	4.20 ab
4	Elci	73.3	68.2	71.4	71.0 c	4.18	3.84	3.46	3.83 b
5	Gea	76.6	74.2	72.3	74.4 a	5.08	4.86	3.66	4.53 a
6	Gozlu-1	73.7	72.7	70.8	72.4 a-c	4.87	4.08	3.37	4.11 ab
7	Kayseri	74.1	73.5	72.1	73.2 a-c	5.04	4.09	3.56	4.23 ab
8	Magna-601	74.1	71.2	71.6	72.3 a-c	4.53	4.23	3.53	4.09 ab
9	Magnum-V	73.4	72.5	72.9	72.9 a-c	4.97	4.05	3.69	4.24 ab
10	Nimet	76.0	74.1	71.9	74.0 ab	5.12	4.76	3.56	4.48 a
11	Omerbey	74.7	73.5	71.2	73.2 a-c	4.92	4.29	3.43	4.21 ab
12	Ozpinar	74.5	73.9	72.2	73.5 a-c	5.21	4.50	3.64	4.45 a
13	Savas	74.4	68.6	70.8	71.2 bc	3.86	4.30	3.34	3.83 b
14	Sunter	75.1	75.1	72.2	74.1 ab	5.44	4.50	3.63	4.52 a
15	Verdor	74.3	72.4	72.8	73.2 a-c	4.75	4.29	3.76	4.27 ab
16	Verko	74.7	74.1	72.3	73.7 a-c	5.04	4.36	3.58	4.33 ab
Mean		74.6 A**	72.7 B	71.8 C	73.0	4.83 A**	4.32 B	3.54 C	4.23
**Significant at P < 0.01, CV: 2.44%						**Significant at P < 0.01, CV: 8.82%			

Relative feed value and plant heights (cm)

Relative feed values (RFV) and plant heights of different alfalfa cultivars are provided in *Table 6*. The differences in RFV and plant heights of both the cultivars and the years were found to be significant at 1% level.

The greatest RFV was observed in Gea cultivar and the lowest RFV was observed in Elci and Savas cultivars. Considering the RFV of the years, the greatest value was observed in 2014 and the lowest value was seen in 2016. Three-year average RFV of the cultivars was calculated as 240.1.

The greatest plant height was observed in Gea cultivar and the lowest value was observed in Savas cultivar. Considering the average plant heights of the year, the greatest value was observed in 2016 and the least value was seen in 2014. Three-year average plant height was calculated as 50.6 cm.

Relative feed values and averages obtained from the cultivars used in the research are given in *Figure 4*. Alsancak, Gea, Kayseri, Nimet, Ozpinar, Sunter, Verdor and Verko cultivars gave results above the averages in terms of relative feed value.

Table 6. RFV and plant heights of alfalfa cultivars

No	Cultivars	RFV				Plant heights (cm)			
		2014	2015	2016	Mean	2014	2015	2016	Mean
1	Alsancak	297.6	246.0	197.6	247.1 ab**	38.2	54.4	57.9	50.1 a-c**
2	Basbag	249.6	238.6	190.6	226.3 bc	39.3	46.7	55.9	47.3 cd
3	Bilensoy-80	276.1	250.1	193.9	240.0 a-c	42.3	53.3	58.4	51.3 a-c
4	Elci	237.0	203.7	191.5	210.7 c	43.7	52.1	58.3	51.4 a-c
5	Gea	301.5	279.7	205.0	262.1 a	41.7	59.8	62.7	54.7 a
6	Gozlu-1	278.4	229.9	185.6	231.3 a-c	43.7	51.9	59.8	51.8 a-c
7	Kayseri	289.8	233.1	198.9	240.6 a-c	43.2	57.5	61.4	54.0 ab
8	Magna-601	260.1	233.3	195.9	229.8 a-c	43.2	51.9	57.5	50.8 a-c
9	Magnum-V	282.6	227.6	208.7	239.6 a-c	47.2	45.5	52.4	48.4 c
10	Nimet	301.7	273.6	198.5	257.9 ab	38.8	53.1	52.5	48.1 c
11	Omerbey	285.1	244.6	189.6	239.8 a-c	40.8	49.4	56.5	48.9 bc
12	Ozpinar	300.3	257.3	204.3	254.0 ab	42.5	52.4	57.9	50.9 a-c
13	Savas	222.5	229.0	183.2	211.6 c	36.2	39.1	50.4	41.9 d
14	Sunter	316.4	261.5	203.1	260.3 ab	43.1	57.1	62.4	54.2 ab
15	Verdor	273.6	240.9	212.3	242.3 a-c	45.3	55.1	58.4	52.9 a-c
16	Verko	291.6	250.7	200.5	247.6 ab	42.6	55.0	61.0	52.9 a-c
Mean		279.0 A**	243.7 B	197.4 C	240.1	42.0 C**	52.1 B	57.7 A	50.6
**Significant at P < 0.01, CV: 8.96%						**Significant at P < 0.01, CV: 6.77%			

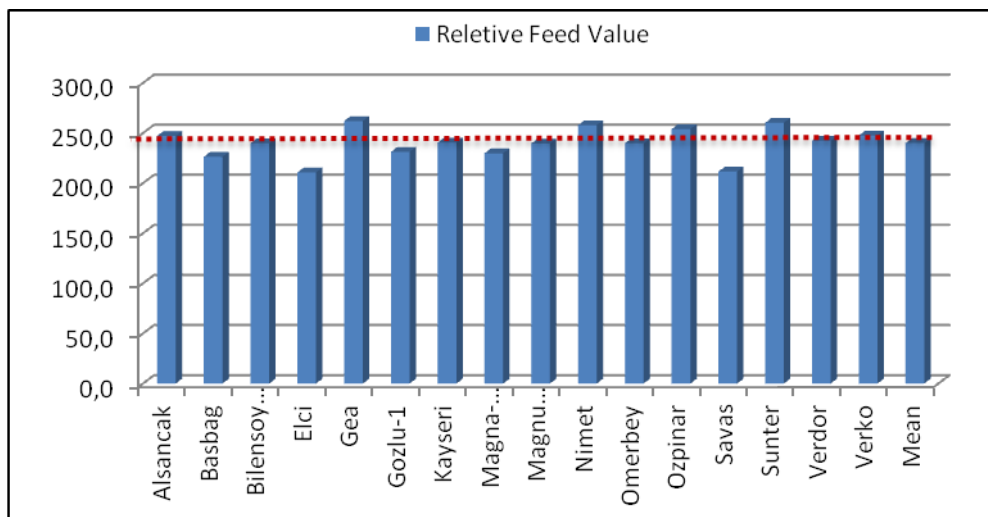


Figure 4. Relative feed value of alfalfa cultivars

Correlations among investigated traits

Correlation coefficients among investigated traits of sixteen alfalfa cultivars are provided in Table 7. Plant height had highly significant positive correlations with green herbage yield, dry herbage yield, crude protein yield, ADF and NDF ratio and had highly significant negative correlations with crude protein ratio, DDM, DMI and RFV.

Table 7. Correlations coefficients among investigated traits⁺

	GHY	DHY	CPR	CPY	ADF	NDF	DDM	DMI	RFV
PH	0.774**	0.794**	-0.751**	0.758**	0.318**	0.595**	-0.318**	-0.609**	-0.606**
GHY		0.972**	-0.805**	0.947**	0.409**	0.575**	-0.409**	-0.620**	-0.634**
DHY			-0.831**	0.945**	0.434**	0.592**	-0.434**	-0.632**	-0.649**
CPR				-0.771**	-0.515**	-0.809**	0.515**	0.827**	0.837**
CPY					0.402**	0.521**	-0.402**	-0.563**	-0.581**
ADF						0.508**	-1.000**	-0.496**	-0.618**
NDF							-0.508**	-0.986**	-0.977**
DDM								0.496**	0.618**
DMI									0.989**

+ Correlations coefficients for 2014, 2015 and 2016, **significant at P < 0.01

PH = Plant Height, GHY = Green Herbage Yield, DHY = Dry Herbage Yield, CPR = Crude Protein Ratio, CPY = Crude Protein Yield, ADF = Acid Detergent Fiber, NDF = Neutral Detergent Fiber, DDM=Digestible Dry Matter, DMI=Dry Matter Intake, RFV=Relative Feed Value

Green herbage yield had highly significant positive correlations with dry herbage yield, crude protein yield, ADF and NDF, and had significant negative correlations with crude protein ratio, DDM, DMI and RFV. Dry herbage yield had highly significant positive correlations with crude protein yield, ADF and NDF, and had highly significant negative correlations with crude protein ratio, DDM, DMI and RFV. Crude protein ratio had highly significant positive correlations with DDM, DMI and RFV, and had highly significant negative correlations with crude protein yield, ADF and NDF. Crude protein yield had highly significant positive correlations with ADF and NDF, and had highly significant negative correlations with DDM, DMI and RFV.

ADF had highly significant positive correlations with NDF, and had highly significant negative correlations with DDM, DMI and RFV. NDF had highly significant negative correlations with DDM, DMI and RFV. DDM had highly significant positive correlations with DMI and RFV and there were highly significant correlations between DMI and RFV.

Discussion

Precipitation and temperature may result in significant differences in yields of the years (Luo et al., 2016). Regional climate, soil conditions, plant genetics, sowing time and cultural practices significantly influence dry matter yield and green herbage yields (Seydosoglu, 2014). Green herbage yields were reported as between 931-11843 kg da⁻¹ (Seker, 2003; Kusvuran et al., 2005; Kir and Soya, 2006) and dry herbage yields were reported as 225-3287 kg da⁻¹ (Sengul et al., 2003; Seker, 2003; Kusvuran et al., 2005; Kir and Soya, 2006; Demiroglu et al., 2008; Avci et al., 2010; Saruhan and Kusvuran, 2011) for alfalfa genotypes. Green and dry herbage yields varied based on number of cuts, ecological conditions, genetics structure and thus different values were reported in different studies.

Ball et al. (2001) indicated that variations dry matter and protein contents mostly resulted from genetic differences and that these parameters commonly varied based on leaf and shoot ratios, ripening period, temperature and fertilization practices. Crude protein ratios were reported as between 15.95-28.09% (Sengul et al., 2003; Kir and

Soya, 2006; Basbag et al., 2009; Canbolat and Karaman, 2009; Avci et al., 2010; Kiraz, 2011; Saruhan and Kusvuran, 2011; Cacan et al., 2015). Crude protein yields were reported as between 34-321 kg da⁻¹ (Sengul et al., 2003; Kir and Soya, 2006). Present crude protein ratios and crude protein yields were slightly higher than those earlier findings. Higher crude protein ratios are due to differences in the varieties used. The difference in crude protein yields is due to differences in hay yields of alfalfa varieties. With regard to crude protein content, all cultivars were placed in the best quality group (Rohweder et al., 1978).

ADF and NDF ratios are significant quality indicators of forage crops (Aydin et al., 2010) and such ratios should be low in quality forage since they obstruct the digestibility and consequently decrease the quality of forage. Since high ADF and NDF ratios have negative effects on feed intake and digestibility, the feeds with ideal ADF and NDF values are usually preferred (Kiraz, 2011). ADF ratios of some alfalfa clones were reported as between 16.8-41.0%, NDF ratios as between 20.3-49.0% (Basbag et al., 2009; Canbolat and Karaman, 2009; Avci et al., 2010; Kiraz, 2011; Cacan et al., 2015), DDM ratios as between 56.9.0-75.8%, DMI ratios as between 2.46-5.90% (Basbag et al., 2009; Canbolat and Karaman, 2009; Avci et al., 2010; Kiraz, 2011; Cacan et al., 2015) and RFV as between 127.0-347 (Basbag et al., 2009; Canbolat and Karaman, 2009; Kiraz, 2011; Cacan et al., 2015). With regard to ADF and NDF ratios, all cultivars were placed in the best quality group (Rohweder et al., 1978).

As the plant ages, the proportion of ADF and NDF compounds forming the cell wall also increases (Uke et al., 2017). Therefore, the rates of ADF and NDF are steadily increasing in 2015 and 2016. This situation, directly affects the DDM, DMI and RFV rates, which tend to be lower as years go by. Also, according to the quality standards reported by Lacefield (1988), in terms of crude protein (above 19%), ADF (below 31%), NDF (below 40%), DDM (above 65%), DMI (above 3%) and RFV (above 151) values, alfalfa cultivars appear to be in group "prime".

In previous studies, plant heights were reported as between 49.7-86.8 cm (Seker, 2003; Kusvuran et al., 2005; Kir and Soya, 2006; Demiroglu et al., 2008; Basbag, 2009; Yesil and Sengul 2009; Saruhan and Kusvuran, 2011). Since Bingol province has a colder ecology, present findings were slightly lower than those earlier findings. As the years progress, the height of the plant seems to increase. This situation parallels directly with the increase of herb yields over the years.

Conclusion

The results revealed that the greatest plant height, green herbage and dry herbage yield was obtained from Gea cultivar, the greatest crude protein ratio was obtained from Magnum-V cultivar, the greatest crude protein yield from Gea cultivar, the lowest ADF ratio from Gea cultivar, the lowest NDF ratio from Gea, Nimet, Ozpinar and Sunter cultivars, the greatest DDM from Gea cultivar, the greatest DMI from Gea, Nimet, Ozpinar and Sunter cultivars and the greatest RFV from Gea cultivar.

The most important yield parameter in alfalfa cultivation is dry herbage yield. Therefore, the cultivars with high dry herbage yields should be selected in cultural practices. It is also critical that the herbage should also have a high protein yield, low ADF and NDF ratios and high digestibility. Considering all these values, Gea cultivar with high dry herbage and crude protein yield, low ADF-NDF ratios and high relative feed value was recommended for alfalfa culture. Outside Gea; it seems that Bilensoy-

80, Magna-601, Magnum-V, Omerbey, Sunter, Verdor and Verko cultivars gave results above averages and were remarkable in terms of yield and quality.

In addition, significant correlations were found between yield and quality attributes in the study. As the years progress, the dry herbage yield and crude protein yield obtained from alfalfa cultivars is increasing and the relative feed value is decreasing as it is inversely proportional to this.

Acknowledgments. This study was supported by Scientific Research Projects Department of Bingol University (BAP-554-179-2014).

REFERENCES

- [1] Anonymous (2018): Geographical structure. – Republic of Turkey Bingol Governorship. <http://www.bingol.gov.tr>.
- [2] Ates, K., Turan, V. (2015): Some soil characteristics and the fertility status of agricultural soils in Bingöl central district. – Turk J Agric Res 2:108-113.
- [3] Avci, M., Çınar, S., Yucel, C., Inal, I. (2010): Evaluation of some alfalfa (*Medicago sativa* L.) lines for herbage yield and forage quality. – Journal of Food, Agriculture & Environment 8(3&4): 545-549.
- [4] Aydin, N., Mut, Z., Mut, H., Ayan, I. (2010): Effect of autumn and spring sowing dates on hay yield and quality of oat (*Avena sativa* L.) genotypes. – Journal of Animal and Veterinary Advances 9(10): 1539-1545.
- [5] Ball, D. M., Collins, M., Lacefield, G. D., Martin, N. P., Mertens, D. A., Olson, K. E., Putnam, D. H., Undersander, D. J., Wolf, M. W. (2001): Understanding Forage Quality. – American Farm Bureau Federation, Park Ridge, IL.
- [6] Basbag, M. (2009): Determination of seed yields of some alfalfa (*Medicago sativa* L.) cultivars in Diyarbakir ecological conditions. – J Agric Fac HR U 13(1): 43-49.
- [7] Basbag, M., Demirel, R., Avci, M. (2009): Determination of some agronomical and quality properties of wild alfalfa (*Medicago sativa* L.) clones in Turkey. – Journal of Food, Agriculture & Environment 7(2): 357-359.
- [8] Cacan, E., Aydin, A., Basbag, M. (2015): Determination of quality features of some legume forage crops in Bingol University campus. – Turkish Journal of Agricultural and Natural Sciences 2(1): 105-111.
- [9] Canbolat, O., Karaman, S. (2009): Comparison of in vitro gas production, organic matter digestibility, relative feed value and metabolizable energy contents of some legume forages. – Journal of Agricultural Sciences 15(2): 188-195.
- [10] Demiroglu, G., Geren, H., Avcioglu, R. (2008): Adaptation of different alfalfa (*Medicago sativa* L.) genotypes under Aegean Region conditions. – Ege Üniv Ziraat Fak Derg 45(1): 1-10.
- [11] Geren, H., Kir, B., Demiroglu, G., Kavut, Y. T. (2009): Effects of different soil textures on the yield and chemical composition of alfalfa (*Medicago sativa* L.) cultivars under Mediterranean climate conditions. – Asian Journal of Chemistry 21(7): 5517-5522.
- [12] Kalayci, M. (2005): Use JUMP with Examples and Anova Models for Agricultural Research. – Anatolia Agricultural Research Institute Directorate, Erzurun.
- [13] Kamalak, A., Canbolat, O. (2010): Determination of nutritive value of wild narrow-leaved clover (*Trifolium angustifolium*) hay harvested at three maturity stages using chemical composition and in vitro gas production. – Tropical Grasslands 44(2): 128-133.
- [14] Kaplan, M., Baran, O., Unlukara, A., Kale, H., Arslan, M., Kara, K., Buyukkilic, S. B., Konca, Y., Ulas, A. (2016): The effects of different nitrogen doses and irrigation levels on yield, nutritive value, fermentation and gas production of corn silage. – Turkish Journal of Field Crops 21(1): 101-109.

- [15] Karaman, M. R. (2012): Plant Nutrition. – Dumat Press, Ankara.
- [16] Kir, B., Soya, H. (2006): The investigation on quality characteristics with seed and hay yields in some alfalfa cultivars. – Ph. D. Thesis, Field Crops Department, University of Ege, İzmir.
- [17] Kiraz, A. B. (2011): Determination of relative feed value of some legume hays harvested at flowering stage. – Asian Journal of Animal and Veterinary Advances 6(5): 525-530.
- [18] Kusvuran, A., Tansi, V., Saglamtimur, T. (2005): Determination of adaptation of alfalfa (*Medicago sativa* L.) and some grasses under the irrigated conditions of Turkish Republic of Northern Cyprus. – Turkey VI. Field Crops Congress, 5-9 September, Volume-II, p. 1181-1186, Antalya.
- [19] Lacefield, G. D. (1988): Alfalfa Hay Quality Makes the Difference. – University of Kentucky Department of Agronomy, Agriculture and Natural Resources, Lexington, KY.
- [20] Luo, K., Jahufer, M. Z. Z., Wu, F., Di, H., Zhang, D., Meng, X., Wang, Y. (2016): Genotypic variation in a breeding population of yellow sweet clover (*Melilotus officinalis*). – Frontiers in Plant Science 7: 1-10.
- [21] Manga, I., Acar, Z., Ayan, I. (2003): Leguminous Forage Crops. Textbook No. 7. – Faculty of Agriculture, Ondokuz Mayıs University, Samsun, Turkey.
- [22] Moreira, A., Fageria, N. K. (2010): Liming influence on soil chemical properties, nutritional status and yield of alfalfa grown in acid soil. – R Bas Ci Solo 34: 1231-1239.
- [23] Morrison, J. (2003): Hay and Pasture Management. – In: University of Illinois at Urbana-Champaign (ed.) Illinois Agronomy Handbook. University of Illinois, Urbana-Champaign.
- [24] Rohweder, D. A., Barnes, R. F., Jorgensen, N. (1978): Proposed hay grading standards based on laboratory analyses for evaluating quality. – Journal of Animal Science 47: 747-759. <http://jas.fass.org/cgi/reprint/47/3/747>.
- [25] Saruhan, V., Kusvuran, A. (2011): Determination of yield performances of some lucerne cultivars and genotypes under the Southeastern Anatolia Region conditions. – Ege Üniv Ziraat Fak Derg 48(2): 133-140.
- [26] Sezen, Y. (1995): Fertilizers and Fertilization. – Agriculture Faculty, Ataturk University, Erzurum.
- [27] Seker, H. (2003): Adaptation and yield trial of some new alfalfa cultivars to Erzurum ecological condition. – Ataturk Univ J of Agricultural Faculty 34(3): 217-221.
- [28] Sengul, S., Tahtacioglu, L., Mermer, A. (2003): Determination of suitable alfalfa (*Medicago sativa* L.) cultivars and lines for Eastern Anatolia Region. – Ataturk Univ J of Agricultural Faculty 34(4): 321-325.
- [29] Seydosoglu S. (2014): Researches on determination yield and yield components of some common vetch (*Vicia sativa* L.) genotypes in ecological conditions of Diyarbakır. – Turkish Journal of Agricultural Research 1: 117-127.
- [30] Sommer, A., Vodnansky, M., Petrikovic, P., Pozgaj, R. (2005): Influence of lucerne and meadow hay quality on the digestibility of nutrients in the roe deer. – Czech J Anim Sci 50(2): 74-80.
- [31] Uke, O., Kale, H., Kaplan, M., Kamalak, A. (2017): Effects of maturity stages on hay yield and quality, gas and methane production of quinoa (*Chenopodium quinoa* Willd.). – KSU J Nat Sci 20(1): 42-46.
- [32] Ulger, I., Kaplan, M. (2016): Variations in potential nutritive value, gas and methane production of local sainfoin (*Onobrychis sativa*) population. – Alinteri 31(2): 42-47.
- [33] Yesil, M., Sengul, S. (2009): A study on determining some of the morphological characteristics of alfalfa ecotypes collected from various region of Turkey. – Alinteri Journal of Agricultural Sciences 16(B): 1-6.
- [34] Yuksel, O., Albayrak, S., Turk, M., Sevimay, C. S. (2016): Dry matter yields and some quality features of alfalfa (*Medicago sativa* L.) cultivars under two different locations on Turkey. – Suleyman Demirel University Journal of Natural and Applied Sciences 20(2): 155-160.

IRRIGATION POND STRATIFICATION STRUCTURE DETERMINATION AND TEMPERATURE - DISSOLVED OXYGEN MODELING USING CE-QUAL-W2

HASANOĞLU, E.¹ – GÖNCÜ, S.^{2*}

¹*Department of Environmental Engineering, The Graduate School of Science, Anadolu University
Eskisehir, Turkey*

²*Department of Environmental Engineering, Faculty of Engineering, Anadolu University
Eskisehir, Turkey*

**Corresponding author
e-mail: sgoncu@anadolu.edu.tr*

(Received 30th Oct 2017; accepted 12th Feb 2018)

Abstract. Thermal stratification experienced in irrigation ponds leads to intensification of agricultural pollution events due to hypolimnetic oxygen depletion. In this study, stratification in a small pond in western Turkey was investigated. Pond bathymetry was determined with a combination of an Acoustic Doppler Current Profiler (ADCP) equipment measurement and field study using Real Time Kinematic GPS (RTK GPS) equipment. The Relative Thermal Resistance to Mixing (RTRM) index and 2-dimensional hydrologic model CE-QUAL-W2 was utilized to characterize the stratification structure. Based on these monitoring results, the temperature profile was constructed. The pond volume was found to be occupied by 60% with the epilimnion, 20% metalimnion and 20% hypolimnion. The model was calibrated with monitoring data from 2013 and validated with data from 2014. It was determined that the pond was monomictic. The pond was modeled with CE-QUAL-W2 and the dates of stratification, the temperature and dissolved oxygen profiles were simulated with absolute mean errors of 0.77 °C for temperature and 1.09 mgO₂/L for dissolved oxygen. Different irrigation and meteorological scenarios were examined to predict pond volumes and temperatures till 2020. As a result of scenario implementations, drip irrigation practices were found to be the best management application for the sustainable management of the pond.

Keywords: *2D modeling, relative thermal resistance to mixing (RTRM), thermal stratification, forecasting, scenario implementation*

Introduction

Temperature is one of the most important physical property of water bodies as it affects density, vapor pressure, viscosity, dissolved oxygen concentration and chemical and biological reaction kinetics. Heating of natural bodies by solar radiation and atmospheric temperatures from the surface down to the deeper parts results in different water densities at different depths and hence to thermal stratification (Chapra, 1997). Stratification can affect many important water quality parameters adversely, foremost the dissolved oxygen. Stratification prevents the transfer of oxygen to the hypolimnion layer. Moreover, due to anoxic conditions prevailing in the deeper layers, the solubility of phosphorus and iron increase and especially phosphorus is released to the water column in overturning periods, thus leading to algal blooms (Salonen et al., 1999). Decreased oxygen levels due to stratification also affect fish populations and diversity adversely. Therefore, stratification is a phenomenon that needs careful consideration in the study of standing water bodies.

There are several studies concerning stratification in water bodies which are directed to different aims using a variety of methods. A major portion of these studies is related to the determination of the stratification structure, its evolution and assessment (Birge, 1910; Kindle, 1929; Lap et al., 2009). Some studies are concerned with the relationship of the geological properties of the region with stratification (Chapman et al., 1998). Other deal with the effects of surface heat exchange and wind parameters on stratification (Churchill and Kerfoot, 2007). Studies about the timing of stratification and the determination of the lake number which is used to identify the different layers are also widespread (Elci, 2008; Song et al., 2013; Branco and Torgersen, 2009). In Turkey, there are studies about the relationship of stratification with water quality parameters (Elci, 2008; Gunduz et al., 1998; Erturk et al., 2008; Caliskan and Elci, 2009; Alpaslan et al., 2012). Reservoirs are multi-purpose deep waterbodies and water temperature and dissolved oxygen status are very important. Due to improper practices, climate change effects and drought conditions may result in reduced hypolimnetic volumes, anoxic conditions and algal blooms. (Hudson and Vandergucht, 2015). Zhang et al. (2015) stated that dissolved oxygen profiles are directly linked with the water temperature depth profiles in reservoirs. Also increases in the daily mean air temperatures may cause a decrease of the oxycline depth, respectively expediting oxygen stratification and diminishing water quality.

The literature also contains studies concerning the modeling of stratification coupled with water quality. The foundation for such studies were one-dimensional models of stratification (Babajimopoulos and Papadopoulos, 1986; Rice et al., 1989; Bell et al., 2006; Spigel et al., 2005; Dueri et al., 2009). 2-D mathematical models were employed to more accurately represent the thermal stratification structure. 3-D models based on 3-D hydrodynamical formulations were also attempted (Hassan et al., 1998; Li et al., 2010; Bocaniov et al., 2014). Because reservoirs usually have a deep water column, thermal stratification and dissolved oxygen conditions are more common than in shallow lakes. For this reason, reservoir thermal and oxygen stratification structures were modeled in different studies (Kuo et al., 2006; Bonnet and Poulin, 2004; Lindim et al., 2011; Kerimoglu and Rinke, 2013)

Studies conducted using CE-QUAL-W2 are widespread in literature. Cole (2000) reviewed temperature models of reservoirs with CE-QUAL-W2 and presented results of these studies. Besides modeling temperature and water quality parameters, they also created several scenarios on how to increase the trophic status of the reservoir from eutrophic to oligotrophic. Berger et al. (2005) modeled temperature in Lake Laurance and presented aspects of hydrodynamical and temperature calibration. They also created scenarios to determine how the outflow temperatures changed accordingly. Kim and Kim (2006) modeled temperature changes in Lake Soyang with CE-QUAL-W2 model. Data from 1996 was used for calibration and data from the 1995-2005 period for validation. Kuo et al. (2006) repeated their studies for the Te-Chi ve Tseng-Wen reservoirs with CE-QUAL-W2 to improve the trophic status. Williams (2007) modeled Lake Powell with CE-QUAL-W2 water temperature and water quality parameters. Stansbury et al. (2008) modeled Lake Ogallala with respect to dissolved oxygen again with CE-QUAL-W2 to determine its sources and consumes. Batick (2011) reviewed the general features of the model, its development and input parameters, using it for the modeling of the Cheatham Reservoir temperature and dissolved oxygen profiles.

The aim of this study is to investigate the stratification structure of a relatively clean surface water body (Borabey Pond) and to determine how dissolved oxygen

concentrations change spatially within the water body. The CE-QUAL-W2 model was implemented, with the meteorological conditions an inflow and outflow quantities as driving forces, to characterize mass transfer in the ponds thermal stratification structure and modeling of the dissolved oxygen concentration. Furthermore, scenarios were developed to forecast how the pond temperature will behave in the future in response to changing pond volumes as a result of management practices and climatic influences.

Study site

The Borabey Pond is situated to the north of Eskişehir, in Northwestern Inner Anatolia, Turkey. It is located in the foothills of the Bozdağ mountain at an altitude of 924 m (the maximum water level of the pond). The earthen dam of the reservoir was constructed in 1991-1992 to serve irrigation needs of a 2.48 km² farming area (Hasanoğlu, 2012). The location of the pond is given in *Figure 1*.

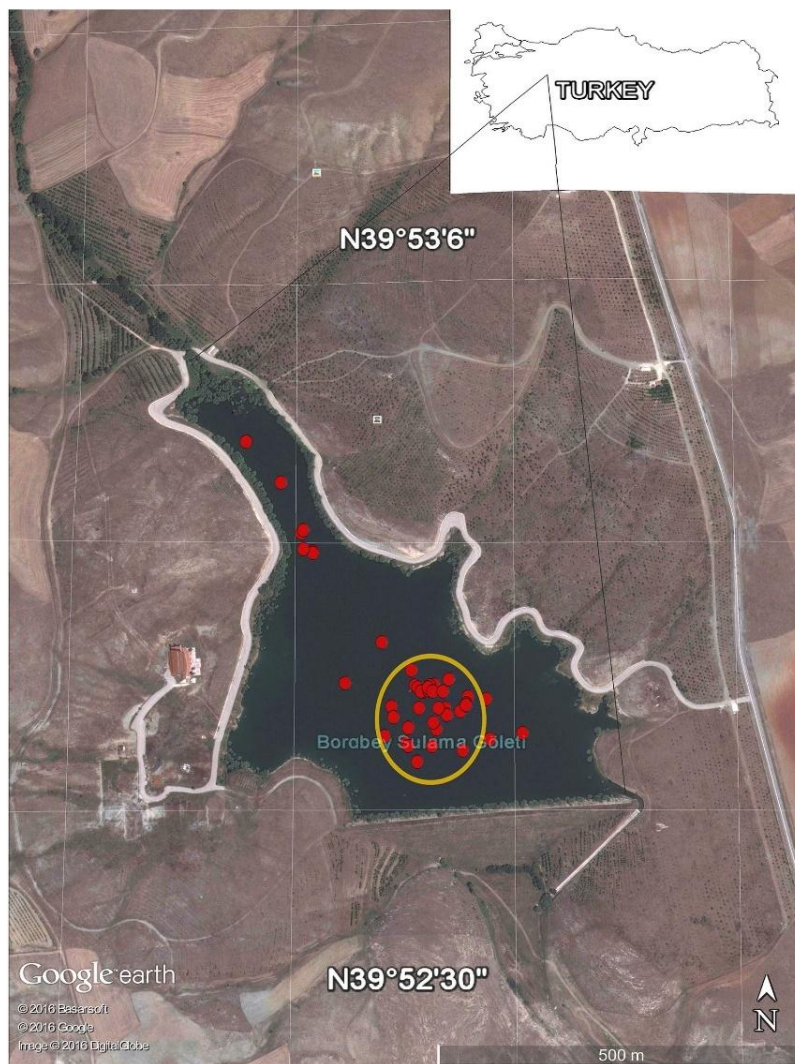


Figure 1. Borabey Pond location in Turkey and measurement locations (red dots) during in 2013 and 2014

The watershed area is 8583 km². The pond is 200 m wide and 620 m long on average with a maximum width of 350 m. The mean depth is 8.5 m with a maximum value of 18.8 m. The water level of the pond shows fluctuations due to changes in water inputs and irrigation withdrawals. The minimum talveg elevation is 906 m above mean sea level and the maximum water level is held fixed at 924 m via an outlet weir at this elevation. The water source feeding the pond is a small creek which carries water in the rainy season and dries up in summer. A pipe at 906.62 m within the pond near the dam is used to release irrigation water to ditches downstream. The volume of the pond at maximum level amounts to 1.6 million m³.

Materials and methods

Meteorological and limnological observations

The modeling period was chosen as the years of 2013 and 2014 and meteorological data related to this period was obtained from a weather station (Davis Vantage Pro 2) located at the shore of the pond. The meteorological time series at 15-min intervals comprise of air temperature, dew point temperature, wind velocity, wind direction, precipitation amount and solar radiation. Precipitation ranged within this period from a low of 2 mm in July 2013 to a high of 97 mm in October 2013. Temperatures changed between -10.8 °C in December 2013 to 36.1 °C in August 2014. Due to the presence of missing values in February 2013, the model was run beginning in the 56th day of 2013.

The pond stratifies in summer and overturns in spring and fall. In this respect the pond is a monomictic water body. The epilimnion occurs at a mean depth of 7 m. Periodic water temperature and dissolved oxygen measurements were conducted in the Borabey Pond to determine the stratification structure and to calibrate and validate the CE-QUAL-W2 model. The vertical temperature profile was determined with the vertical profiler (Casaway-CTD) equipment while the dissolved oxygen measurements were conducted using multi parameter meter (HACH HQ40d) with a LOD probe. The measurements were taken at 1 m depth intervals and 46 temperature and 41 dissolved oxygen profiles were generated. The measurements were primarily concentrated in the deeper zones of the pond.

Statistics about temperature, dissolved oxygen measurements and water density results as derived from measurements are displayed in *Table 1*. The locations of the measurement points are shown in *Figure 1*.

The bathymetry of the pond was determined with Sontek M9 Acoustic Doppler Current Profiler. Because the pond shows varying densities along the depth, a correction for this feature was applied using density results from Castaway CTD observations (Göncü et al., 2014). The resulting bathymetric map is presented in *Figure 2*. The measurements were processed with ArcGIS 10 to create the contours in *Figure 2*. ArcGIS was also employed to determine the surface area and volume of the pond at various depths.

The watershed of the pond is shown in *Figure 3* with the subwatersheds. The areas and other relevant data were provided by the ArcGIS software and ArcHydro module. Subwatershed No.1 did not feed the pond in the 2013-2014 period as its waters were derived to another pond nearby. Subwatersheds No.2 and No.3 also could not feed the pond as the creeks emptying them were diverted for irrigation purposes. Thus, within the simulation period only the remaining 3.24 km² of the watershed provided the pond with water.

Table 1. Descriptive statistics about dissolved oxygen, temperature observations and derived water density results

Observation start date: 26.02.2013			
Observation end date: 25.11.2014			
	Dissolved oxygen mg/L	Temperature °C	Density kg/m³
n	556	1757	601
Min	0.05	2.58	997.48
P10	0.25	6.29	997.99
P25	4.63	8.80	998.83
P50	7.83	12.29	999.77
P75	9.39	18.68	1000.08
P90	11.07	21.87	1000.15
Max	11.92	23.93	1008.45
Std. dev.	3.62	5.78	1.35

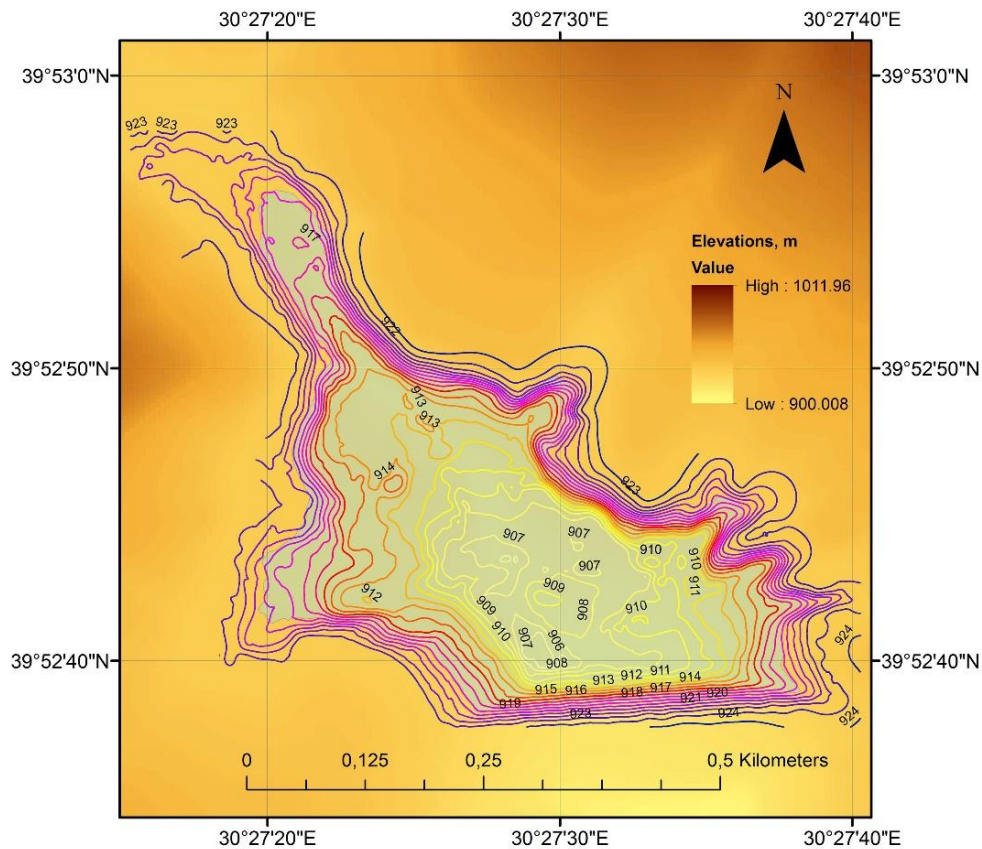


Figure 2. Borabey Pond bathymetric map

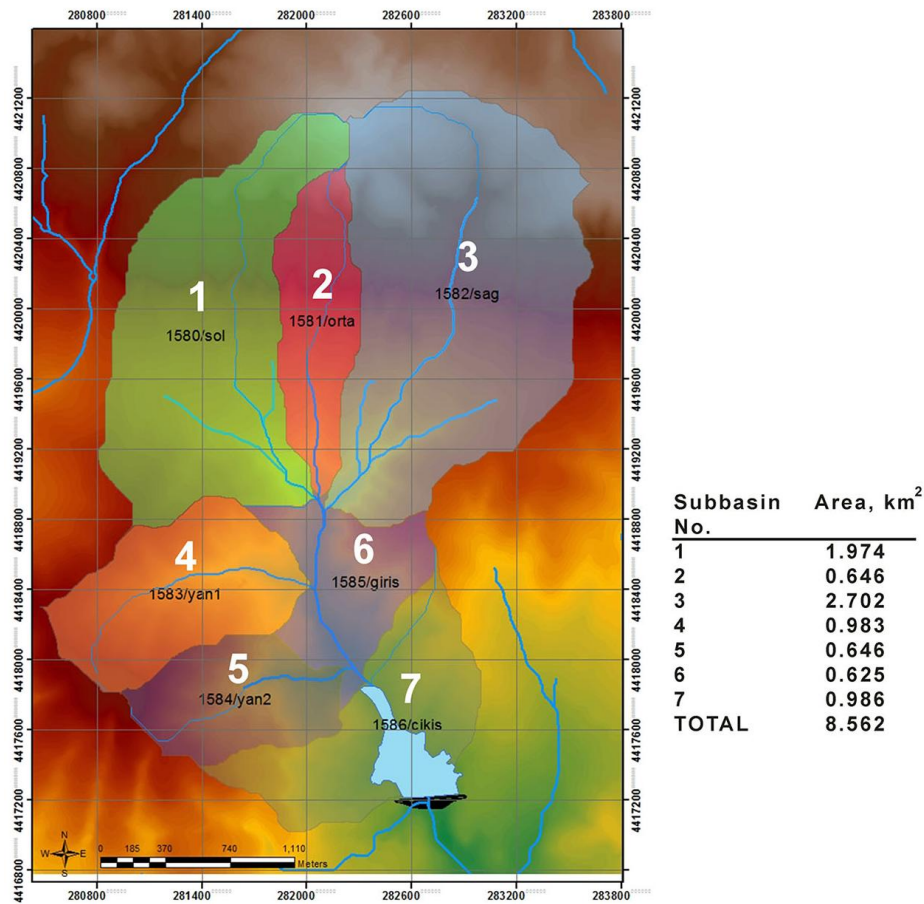


Figure 3. Borabey Pond watershed and subwatersheds

Determination of RTRM index

The strength of the thermal stratification is obtained from the RTRM (Relative Thermal Resistance to Mixing) index which is determined for consecutive depths. This index was first introduced by Birge (1910). Becker et al. (2009), Branco et al. (2009) and Alpaslan et al. (2012) named the index RWCS (Relative Water Column Stability) and used it as such.

The index is determined by Equation 1 (Chimney et al., 2006).

$$\psi = \frac{\rho_{z_2} - \rho_{z_1}}{\rho_4 - \rho_5} \quad (\text{Eq.1})$$

Ψ stands for the RTRM index and is a dimensionless quantity. ρ_{z_1} and ρ_{z_2} are the water densities at the respective depths z_1 and z_2 and are given in kg/m^3 . ρ_4 and ρ_5 are the water densities at 4 and 5 °C, respectively (Chimney et al., 2006). The index is determined at 1-m intervals. Values larger than 20 generally indicate the upper and lower boundaries of the metalimnion. A cumulative RTRM index indicates the total resistance of the thermal stratification to mixing (Kortmann et al., 1982).

Figure 4 displays the cumulative RTRM values at the deepest zone of the Borabey Pond at monthly intervals during the 2013-2014 period calculated from density

observations made by Castaway CTD. The figure displays clearly the monomictic stratification pattern. The volumes of the epilimnion, metalimnion and hypolimnion during stratification as obtained from the bathymetric calculations.

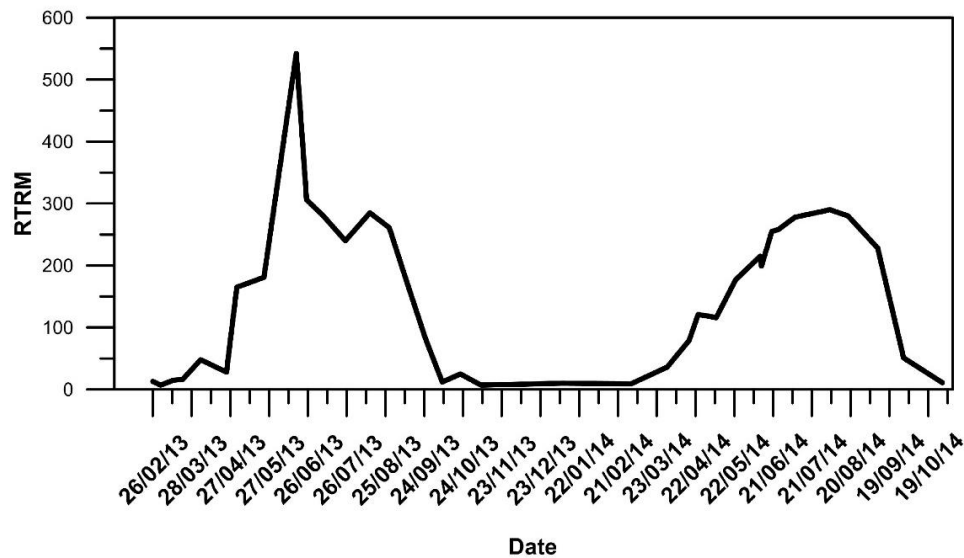


Figure 4. Borabey Pond RTRM profile

Dissolved oxygen and temperature modeling

CE-QUAL-W2 is a 2-D (in the longitudinal and vertical dimensions) hydrodynamical and water quality model. As it inherently assumes homogeneous longitudinal cross-sections, it is more appropriate for long and narrow water bodies. The model can be applied to streams, lakes, watersheds, estuaries and combinations of these systems (Cole and Wells, 2013).

The CE-QUAL-W2 model can estimate water elevations, velocities, temperatures and water quality concentrations. Quality constituents can be added or removed from the model and combinations can also be handled. The model manages complex systems comprising of different stream branches. The minimum data requirements are bathymetry, inflows and outflows, meteorological time series and initial conditions (Batick, 2011).

Temperature, as it is a primary factor for hydrodynamical and water quality simulations, is required and cannot be left out. Water quality constituents include inorganic solids, phytoplankton and epiphyton groups, CBOD, organic and nutrients like phosphorus and nitrogen species (Batick, 2011). The model was tested in many reservoirs for its capability of adequately representing the thermal stratification pattern and simulating water quality and is widely used today (Cole and Tillman, 1999; Deliman and Gerald, 2002; Bowen and Hieronymus, 2003; Colarusso et al., 2003; Kim and Kim, 2006; Ha and Lee, 2007; Diogo et al., 2008; Zhang et al., 2008; Bonalumi et al., 2012).

From the bathymetric data of the Borabey Pond the grid structure was obtained with the use of the ArcGIS software. The finite difference grid structure is displayed in Figure 5. Six segments were distinguished in the longitudinal direction with the corresponding number of layers. Using the elevation-surface, area-volume relationships,

the average width of every layer was obtained. A total of 80 layers each with a uniform depth of 1 m was created and the correspondence of the grid structure with the actual bathymetry was tested with the Nash-Sutcliffe efficiency index (NSE). An index of 0.99 was obtained for surface areas and 0.97 for volumes, thus indicating a very good grid representation of the bathymetry.

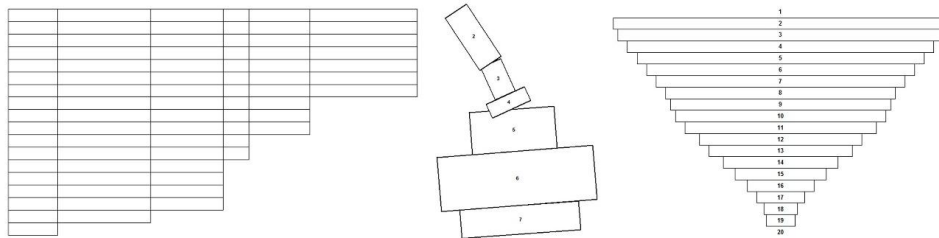


Figure 5. The finite difference grid structure of the Borabey Pond bathymetry

Therefore, inflow water quantities were estimated by comparing the watershed area with the watershed area of a 5 km distant pond (The Keskin Pond) which shows similar hydrological characteristics. So discharge values obtained for the Keskin Pond were transferred to the Borabey Pond by the method of watershed drainage-area ratios (Dayyani et al., 2003). So, for the year of 2013 and 2014, derived flow values were constructed. The actual flow values for 2013 for the Borabey Pond were found to be in good agreement with the corresponding derived flow values.

For the outflow quantities from the pond, the irrigation withdrawals were used. The irrigation withdrawal quantities were not of daily resolution. To refine the resolution to daily values, the crop patterns downstream of the pond were compared to the patterns in the region and correlations were established between the amounts of water used for irrigation in the region and regional crop patterns to be used to estimate the daily amount withdrawn from the pond taking into consideration the watershed areal differences, too.

As the input creek temperatures, the water temperatures measured at the place where the creek enter the lake were utilized. From the temperature profiles obtained by the CASTAWAY CDT profiler equipment, spline smoothing was used to find daily temperatures. As the outlet water temperature, the temperature obtained from the profiles at the depth of the outlet structure were utilized.

The water levels in the pond were measured at discrete times at a water level gage during the 2013 and 2014 period. The interpolation to daily values was obtained by Akima Spline Interpolation with the HydroClimATe software.

All meteorological time series (air temperature, dew point temperature, wind velocity, wind direction, precipitation and solar radiation) were obtained from the station at the pond with the exception of cloudiness for which the time series were obtained from the Eskisehir Anadolu Airport Meteorological Station LTBY which is 9 km distant to the Borabey Pond.

Kaya (2013) measured, on a monthly basis, water quality parameters at the pond. These included phosphate, ammonia, nitrite and nitrate. Algae concentrations were calculated from Chlorophyll-a with a numerical approach. Labile and refractory dissolved organic matter (L-DOM and R-DOM) and labile and refractory particulate organic matter (L-POM and R-POM) were obtained from total organic carbon and algae

concentrations (Cole and Tillman, 1999). February 26, 2013 was fixed as the starting day of simulations and 15-min intervals were used in correspondence with meteorological time series intervals.

Model calibration and validation

Data in the simulation year 2013 were used for calibration and data in 2014 for validation. In the calibration of CE-QUAL-W2 model the water elevation is a key parameter as it affects all the subsequent calculations. Therefore, the agreement between observed and simulated water level is checked first. The levels are calibrated by incrementally increasing or decreasing the input volumes (Devonis, 2011). The initial agreement is displayed in *Figure 6*. The disagreement in 2014 was corrected with calibration. The water level observations were obtained from readings at an established gauging station in the pond. An NSE index of 0.97 was obtained after calibration.

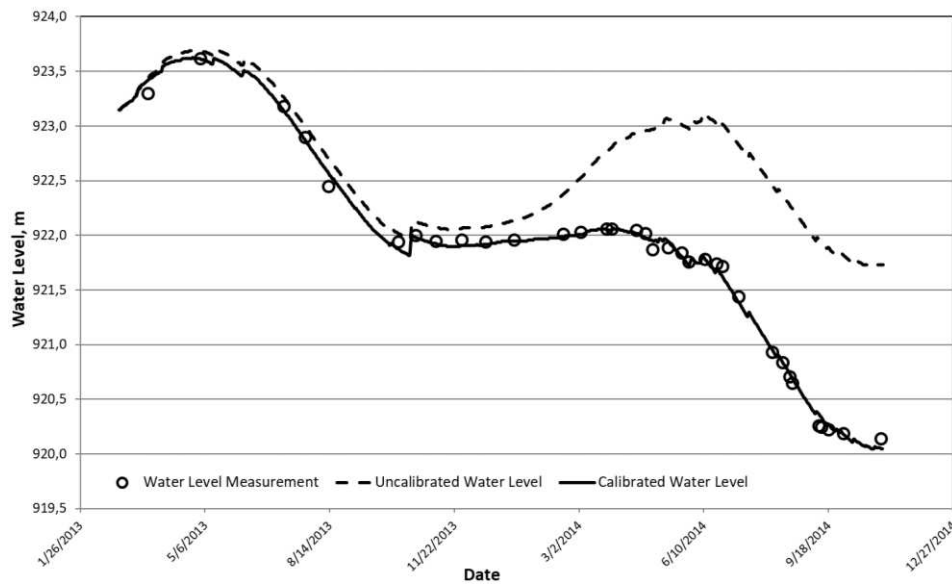


Figure 6. The Borabey Pond water level with and without calibration between 2013 and 2014

For the calibration of temperature, a sensitivity analysis for 8 parameters was conducted. Default values were used as initial values and these were varied by $\pm 5\%$, $\pm 10\%$ and $\pm 15\%$. The model was thus run 56 times and absolute mean errors were calculated between modeled and observed temperatures. *Table 2* displays the results of the sensitivity runs. From these, it was found that the most sensitive parameters were EXH2O, BETA, AFW, BFW and CFW as *Table 3*. The model was calibrated using these parameters.

The change of solar radiation with depth is given in *Equation 2*:

$$H_s(z) = (1 - \beta) H_0 e^{-\eta z} \quad (\text{Eq.2})$$

Here $H_s(z)$ is the solar radiation at depth z , β the ratio of radiation absorbed by the water surface (BETA in CE-QUAL-W2), H_0 the incident radiation on the surface and η

the light extinction coefficient (EXH2O). As BETA and EXH2O affect the heat transfer in water bodies, they were calibrated together.

Table 2. Sensitivity analysis results for temperature calibration parameters

Variable	Description	Unit		-15%	-10%	-5%	Initial value	+5%	+10%	+15%
BETA	Solar radiation absorbed in surface layer	-	Value	0.38	0.41	0.43	0.45	0.47	0.50	0.52
			AME	0.68	0.69	0.70	0.70	0.71	0.74	0.76
EXH2O	Extinction coefficient for pure water	m ⁻¹	Value	0.38	0.41	0.43	0.45	0.47	0.50	0.52
			AME	0.72	0.69	0.69	0.70	0.73	0.78	0.82
AX	Longitudinal eddy viscosity	m ² s ⁻¹	Value	0.0327	0.0347	0.0366	0.0385	0.0404	0.0424	0.0443
			AME	0.70	0.70	0.70	0.70	0.70	0.70	0.70
DX	Longitudinal eddy diffusivity	m ² s ⁻¹	Value	0.0327	0.0347	0.0366	0.0385	0.0404	0.0424	0.0443
			AME	0.70	0.70	0.70	0.70	0.70	0.70	0.70
CBHE	Sediment heat exchange coefficient	Wm ⁻² s ⁻¹	Value	0.26	0.27	0.29	0.30	0.32	0.33	0.35
			AME	0.71	0.70	0.70	0.70	0.70	0.70	0.70
AFW	a coefficient in the wind speed formulation	Wm ⁻² mmHg ⁻¹	Value	7.82	8.28	8.74	9.20	9.66	10.12	10.58
			AME	0.70	0.68	0.68	0.70	0.74	0.79	0.85
BFW	b coefficient in the wind speed formulation	Wm ⁻² mmHg ⁻¹ (ms ⁻¹)-cfw	Value	0.39	0.41	0.44	0.46	0.48	0.51	0.53
			AME	0.68	0.69	0.69	0.70	0.71	0.73	0.74
CFW	c coefficient in the wind speed formulation	-	Value	1.70	1.80	1.90	2.00	2.10	2.20	2.30
			AME	0.68	0.68	0.68	0.70	0.74	0.80	0.89

Table 3. Effects of parameter perturbation on model

	Parameter perturbation		
	± 5%	± 10%	± 15%
BETA	0.71	3.57	5.71
EXH2O	2.86	6.43	7.14
AX	0.00	0.00	0.00
DX	0.00	0.00	0.00
CBHE	0.00	0.00	-0.71
AFW	4.29	7.86	10.71
BFW	1.43	2.86	4.29
CFW	4.29	8.57	15.00

During calibration, EXH2O and BETA were varied concurrently and the least AME was observed at an EXH2O value of 0.49 m^{-1} and a BETA value of 0.29. AME was reduced from $0.70 \text{ }^\circ\text{C}$ to $0.68 \text{ }^\circ\text{C}$ in this process. It was observed that BETA and EXH2O reduced AME while the others increased it. In literature an AME range of $0.3\text{-}0.9 \text{ }^\circ\text{C}$ is considered an adequate range and when the calibration was stopped the AME was within this range and thus deemed adequate (Cole, 2000).

In dissolved oxygen calibration, the first step is the determination of sediment oxygen demand (SOD) which varies between $0.1\text{-}1 \text{ gO}_2/\text{m}^2.\text{day}$ (Cole and Wells, 2013). The zeroth order SOD reaction rate was calibrated as $1 \text{ gO}_2/\text{m}^2.\text{day}$ which gives the minimum AME. This value lead to an AME of $1.12 \text{ mgO}_2/\text{L}$ in observation and simulation comparisons.

There are different equations in the CE_QUAL-W2 manual which can be used to calculate the relationship of the oxygen reaeration with wind velocity (Cole and Wells, 2013). These equations were tried and the equation which gives the minimum AME value ($1.18 \text{ mgO}_2/\text{L}$) was chosen. In literature, AME values ranged between 0.58 and $1.25 \text{ mgO}_2/\text{L}$. Thus the AME was deemed to be adequate. After calibration, the model was run for the complete 2013-2014 period and the results for 2014 were used for validation.

The validation results for 2014 show an AME of $0.86 \text{ }^\circ\text{C}$ for temperature and $1.18 \text{ mgO}_2/\text{L}$ for dissolved oxygen. When the two-year period was considered, the AME for temperature dropped to $0.77 \text{ }^\circ\text{C}$ and $1.09 \text{ mgO}_2/\text{L}$ for dissolved oxygen.

Results and discussion

The comparison of model results and observations for temperature profiles at the sixth segment are displayed in *Figure 7*. As the correspondence of the two curves in each profile shows, the model is capable of adequately representing the beginning and ending times of stratification and the vertical profiles.

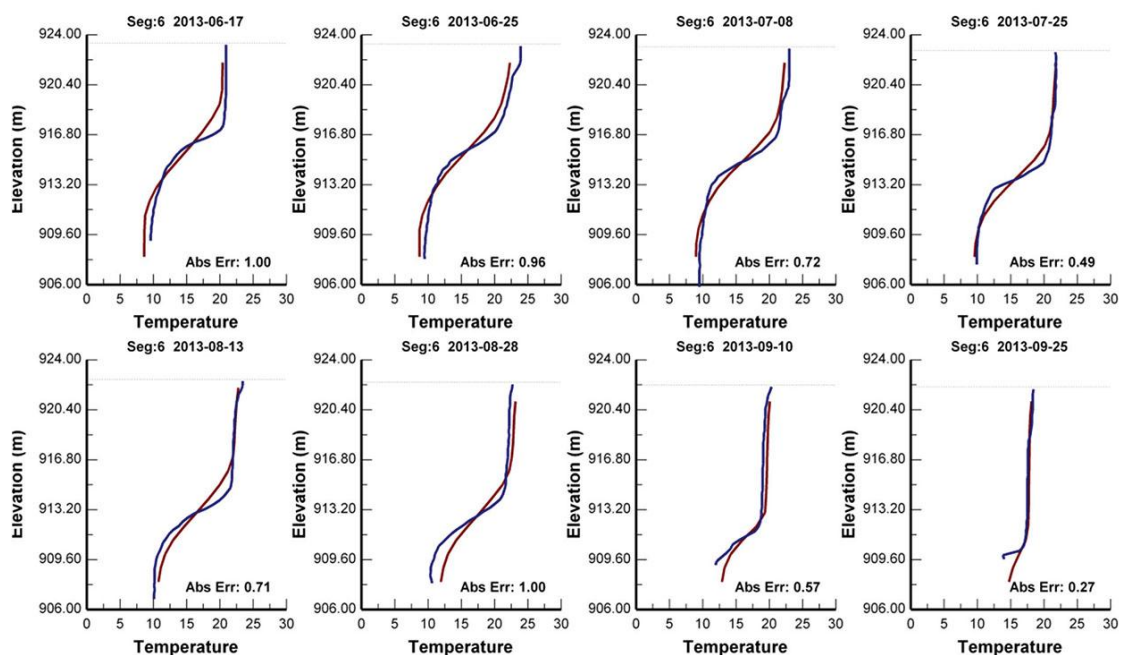


Figure 7. Observation and model results for temperature

The thermocline in the summer stratification begins, on the average, at 6 m below water surface and reaches around 10 m. The change in water temperature in this region amounts to 5 °C. The fall overturn is observed at the end of September (Figs. 7 and 8).

The temperature profile also affects the distribution of the water quality constituents in the water body. Due to the inhibition of oxygen transfer from the atmosphere by the onset of stratification, the dissolved oxygen levels in the hypolimnion begin to decrease, enhanced by oxidation of organic matter and nitrification.

Figure 8 shows the comparison of the vertical temperature profiles of both simulation and observations. Figure 9 displays the same for dissolved oxygen. As the figure implies, very low dissolved oxygen levels occur during stratification periods, as expected, while in between (in the mixing period between fall 2013 and spring 2014) the oxygen levels do not change appreciably in the vertical direction.

When the temperature and dissolved oxygen observations, calculated RTRM values and model simulations are considered together, it is seen that the stratification sets on at the end of April 2013 and continues till the end of August. In 2014 it begins in mid April and ends likewise at the end of August. According to the RTRM results, the total resistance to mixing is higher in 2013 than in 2014.

The absolute mean error (AME) between the temperature and dissolved oxygen observations and modeled results obtained by the modeling study of the Borabey Pond using the CE-QUAL-W2 model is on the average 0.77 °C for temperature and 1.09 mgO₂/L for dissolved oxygen. These are reasonable values as indicated in literature where ranges for temperature and dissolved oxygen are between 0.4-0.9 °C and 0.55-1.25 mgO₂/L, respectively (Cole and Wells, 2013).

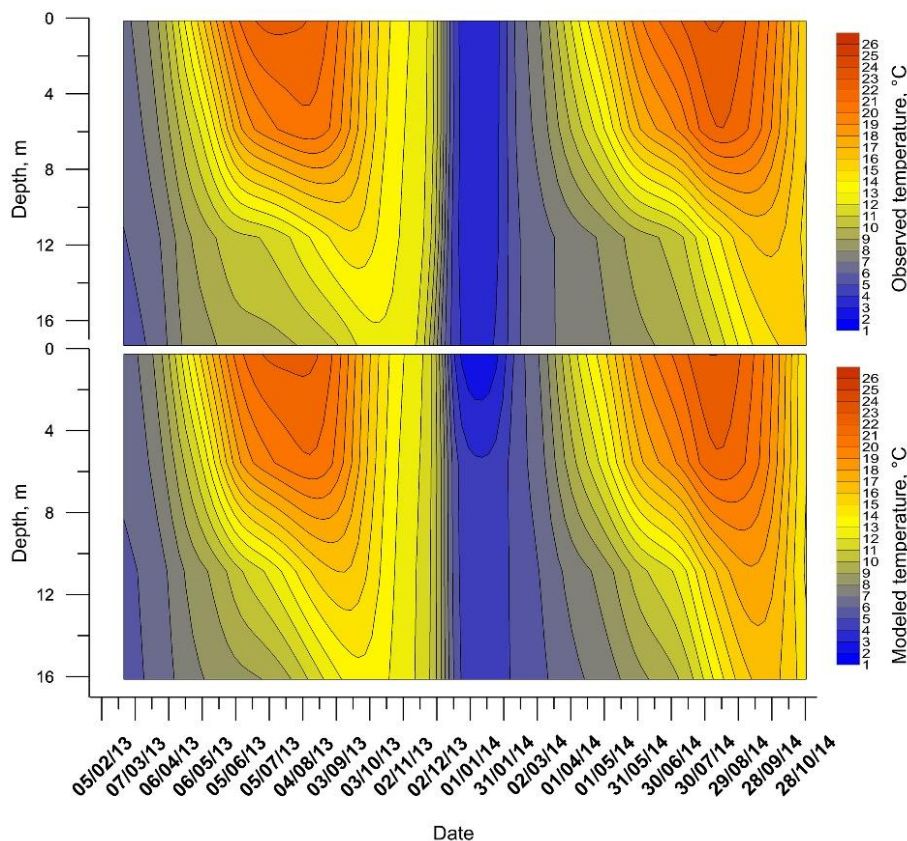


Figure 8. Temperature isopleths according to time (observation and model results)

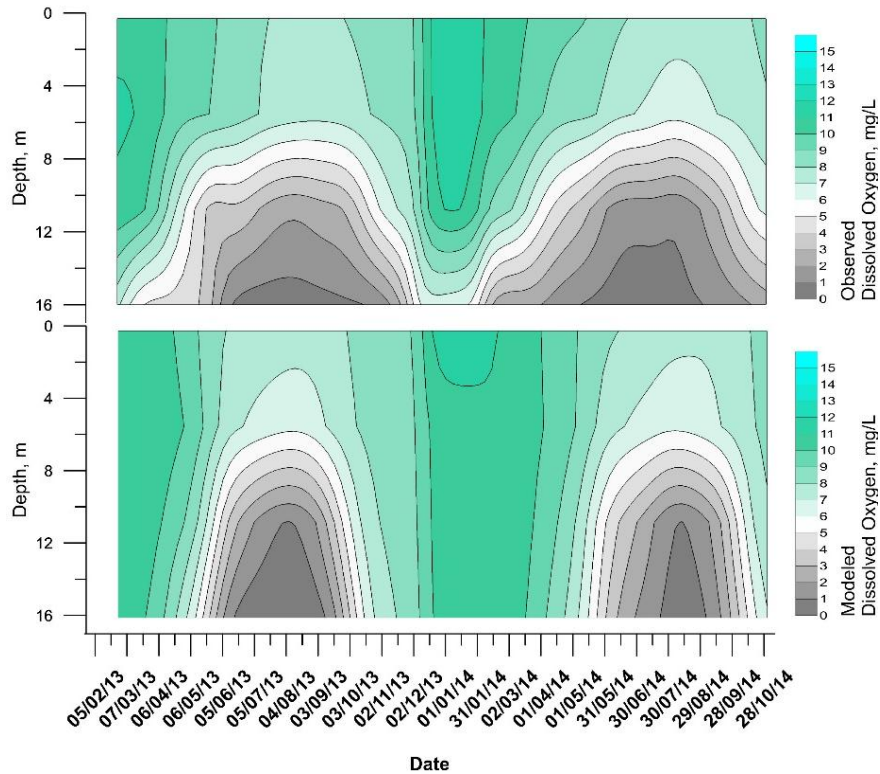


Figure 9. Dissolved oxygen isopleths according to time (observation and model results)

When the observations and simulations were compared for temperature, it was seen that CE-QUAL-W2 modeled the temperature profiles quite consistently together with the beginning and ending dates of stratification. For dissolved oxygen, the observations and simulations agreed especially during the stratification period and also the depths at which the dissolved oxygen levels begin to drop are established. However, the beginning and ending dates of changes in oxygen levels due to stratification were not captured adequately.

Figure 10 displays RTRM profiles, simulated temperature, and dissolved profiles together for a specific date (July 23, 2013). At this date the AME for temperature was 0.56 C and 1.5 mgO₂/L for dissolved oxygen. Based on the RTRM values the metalimnion began 8 m below the surface. The temperature and dissolved oxygen profiles also showed correspondingly the commencement of the metalimnion. Below 10 m, RTRM became less than 20 and the hypolimnion began and the profiles tended to flatten as expected.

In both 2013 and 2014, during the stratification periods, the pond volume was occupied by the hypolimnion, metalimnion and epilimnion by 20%, 20% and 60%, respectively as shown in Table 4. These volumes were calculated with the utilization of the water level – surface area – volume relationships after the determination of the depths of the respective layers using the RTRM values for the days in which observations were carried out.

This volumetric distribution is valid if yearly average volumes are taken into consideration. When the stratification structure was examined, it was observed that the thermal stratification commenced in the spring months with the increase in air temperatures and the hypolimnion zone was relatively larger from May onwards

(Fig. 12). Then the hypolimnion column decreased and was destroyed with the onset of increasing wind velocities in autumn. In winter, lower temperatures were encountered in the upper layers and higher temperatures at lower layers. A surficial stratification was also observed in the winter months which however was insignificant as RTRM calculations showed.

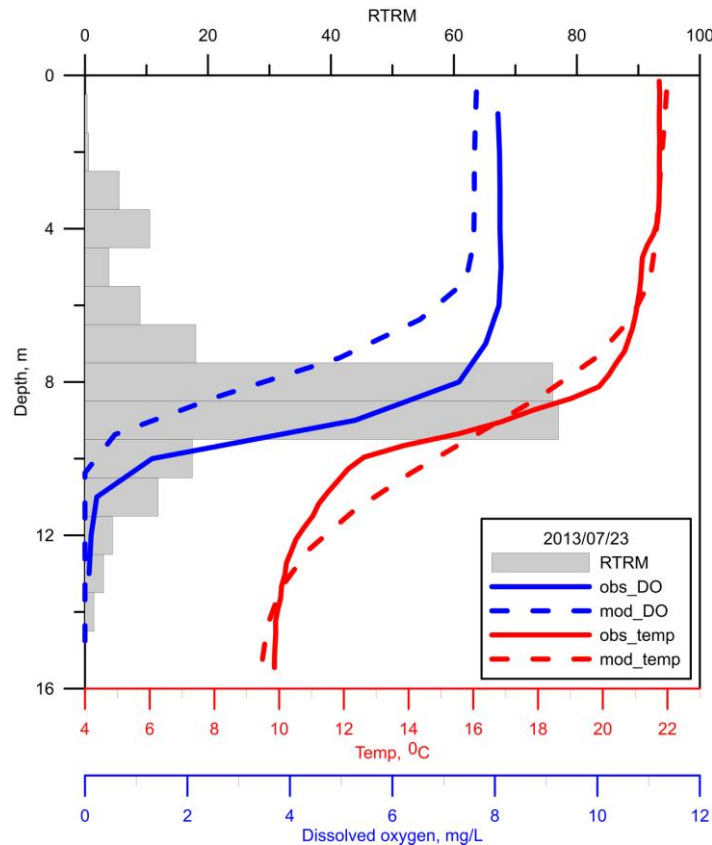


Figure 10. July 23th 2013 observation, model and RTRM results

Table 4. Thermal stratification volumes in 2013 and 2014

	Volume of zones		Percentage of zones	
	2013	2014	2013	2014
Epilimnion, m ³	697226	645403	55	61
Metalimnion, m ³	311529	234742	24	23
Hypolimnion, m ³	270180	162288	21	16
TOTAL, m ³	1278935	1046434	100	100

Scenarios

Six scenarios were created to determine how the volume of the pond will change in the future in response to irrigation practice changes. Consequently CE-QUAL-W2 was used to predict the response of temperature to these volume changes.

The Borabey Pond outlet flow changes in accordance to changes in the use of the water downstream. The fields below the dam outlet are sprinkler irrigated. In the scenarios created, an alternative drip irrigation method was implemented. Shifting from spray to drip irrigation leads to an average of 50% reduction in irrigation volumes (Güngör and Göncü, 2013). This amount of reduction was incorporated into the scenarios for drip irrigation.

The inflow into the pond changes according to meteorological forcing and seasonal variations. Another factor is the derivation of upstream water to the nearby Keskin Pond. In the scenarios, the input volumes into the pond change according to whether the year is wet or dry. It was observed before, that there was much less inflow in 2014 compared to 2013. Thus 2014 was considered a dry year and 2013 a wet year. Wet (W) and Dry (D) year sequences were created using the input volumes in the corresponding 2013 and 2014 years.

Table 5 displays the scenarios with the corresponding season types (W, D) and irrigation practices (Spr. for sprinkler irrigation and Drp. for drip irrigation).

Table 5. Scenarios

Scenario 1	Years							
	2013	2014	2015	2016	2017	2018	2019	2020
Season type	W	D	D	D	D	D	D	D
Irrigation method	Spr.	Spr.	Spr.	Spr.	Spr.	Spr.	Spr.	Spr.
Scenario 2	Years							
	2013	2014	2015	2016	2017	2018	2019	2020
Season type	W	D	D	D	D	D	D	D
Irrigation method	Spr.	Spr.	Drp.	Drp.	Drp.	Drp.	Drp.	Drp.
Scenario 3	Years							
	2013	2014	2015	2016	2017	2018	2019	2020
Season type	W	D	W	W	W	W	W	W
Irrigation method	Spr.	Spr.	Spr.	Spr.	Spr.	Spr.	Spr.	Spr.
Scenario 4	Years							
	2013	2014	2015	2016	2017	2018	2019	2020
Season type	W	D	W	D	W	D	W	D
Irrigation method	Spr.	Spr.	Spr.	Spr.	Spr.	Spr.	Spr.	Spr.
Scenario 5	Years							
	2013	2014	2015	2016	2017	2018	2019	2020
Season type	W	D	W	D	W	D	W	D
Irrigation method	Spr.	Spr.	Drp.	Drp.	Drp.	Drp.	Drp.	Drp.
Scenario 6	Years							
	2013	2014	2015	2016	2017	2018	2019	2020
Season type	W	D	W	W	W	W	W	W
Irrigation method	Spr.	Spr.	Drp.	Drp.	Drp.	Drp.	Drp.	Drp.

The model was implemented for each scenario with the inputs as given in Table 5 and run from 2014 to 2020. Figure 11 displays how the pond volume changed with respect to scenarios.

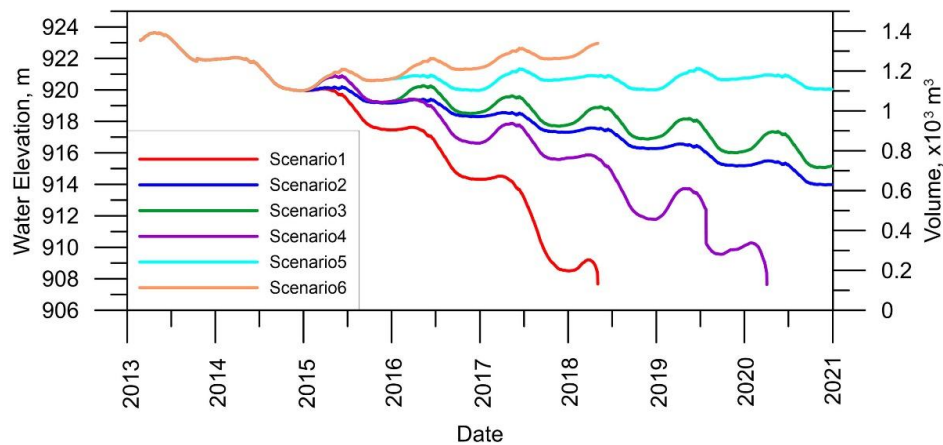


Figure 11. Pond volume and water level change with respect to scenarios

With the exception of scenarios 5 and 6, decreases in pond volumes were observed. Only scenario 6 predicted increases in pond volume. Scenario 6 combined wet periods with drip irrigation which led to water savings over a large volume. For scenarios 1 and 4 which combine sprinkler irrigation with dry periods/wet-dry sequences the pond became almost dry.

Table 6 presents the outlet temperature changes in the pond according to scenarios. For every scenario except the last one, temperature increases were predicted. Figure 12 displays the evolution of temperature for every scenario and corresponding linear trends.

Table 6. Outlet water temperature according to scenarios

Scenarios	Total temperature change (°C) in years	Temperature change (°C)/year
1	5.34 °C in 4.9 years	1.08
2	6.05 °C in 7.9 years	0.86
3	5.35 °C in 7.9 years	0.68
4	3.34 °C in 7.1 years	0.47
5	0.21 °C in 7.8 years	0.03
6	-2.18 °C in 5.2 years	-0.42

The model simulations showed that the stratification pattern changed with decreasing pond volume. In the first scenario, temperature fluctuations change from a range of 4-14 °C to a range of 4-23 °C. The linear change was observed as 0.82 °C/year. As the stratification pattern was destroyed due to decreasing volume, the pond temperature became more affected by atmospheric conditions. The same was observed for scenario 4, especially when the water depth dropped to around 7 m.

On the other hand, though the periodic fluctuation range showed increases, scenarios 2 and 3 did not show the effects of atmospheric influences as the water depth did not fall below 7 m. In scenario 5, there was a very small linear trend and the fluctuation range did not change with time. In the last scenario, the water temperatures dropped and the fluctuation range decreased in accordance with volume increases.

These findings imply that, if it is planned to obtain benefits from the Borabey Pond for future years, the water withdrawals need to be reduced. Effective reductions can be achieved by shifting to drip irrigation practices. However, even this may not be sufficient to maintain desired water levels (Scenario 2). The transfer of water from the Borabey watershed to the Keskin Pond must be stopped, at least for some months in a dry year. Otherwise, a dry-up period of the pond in a dry weather sequence seems inevitable.

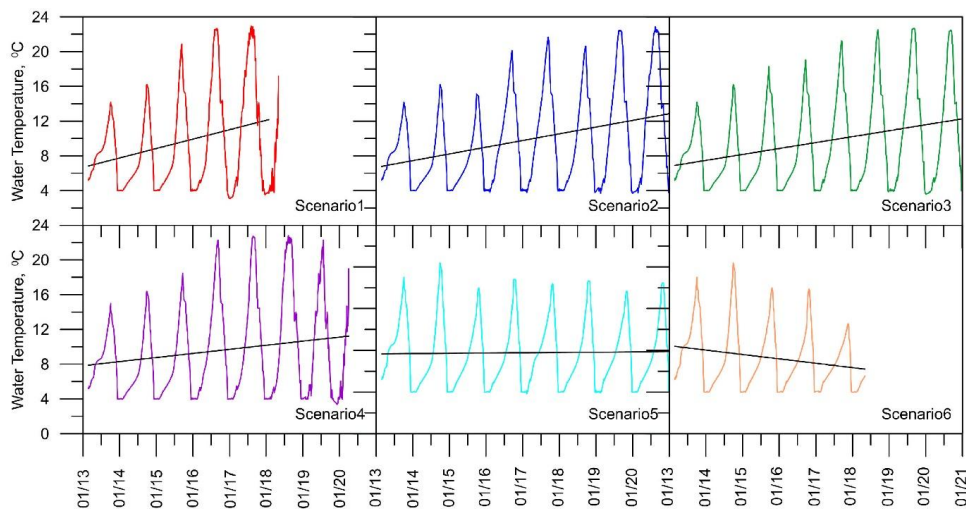


Figure 12. Evolution of temperature for every scenario and corresponding linear trends

Conclusions and recommendations

In this modeling study, some problems were encountered which are prone to affect model results. The input and output flows were not measured, but estimated based on assumptions. This created uncertainties on the primary model inputs. The input and output volumes which were estimated can also be more accurately found out using a comprehensive watershed model. When such less biased results become available in the future, the accuracy of this study can be assessed by changing the relevant pond input and output values. Moreover, long-term constituent concentrations in the quality constituents other than dissolved oxygen averages of observations were utilized for the inflow concentrations and initial pond concentrations. These concentrations, especially those that affect the oxygen depletion dynamics, need to be monitored more closely.

In the simulation of water temperature, the constituent concentrations affect the absorption of light with depth and directly influence the light extinction coefficient (EXH₂O). If constituent concentrations cannot be adequately modeled due to uncertainties in the inputs, the light extinction coefficient will show uncertainties, to which will increase errors in the temperature simulations. In order to reduce errors due to constituent concentrations the absorption coefficients due to inorganic suspended solids (EXSS), organic suspended solids (EXOM) and algae (EXA) were set to zero and the light extinction coefficient was made depended only on water absorption of light.

The AME in temperature simulation was observed to be 0.77 °C if the light extinction coefficient was only dependent on water absorption, but to rise to 1.12 °C when the effects of the water quality constituents were taken into account. This stresses

the importance of correctly representing the amounts of constituents related to carbon and of algae and protozoa in the water body.

In the modeling of the dissolved oxygen levels, all the mathematical relationships about the reaeration process were examined and it was found out that the different relationships created different AME values. During the calibration period the AME changed between 1.018 and 1.298 mg/L due to the different relationships. This shows that the different mathematical formulations simulate the real world differently and this fact should be taken into account during the modeling. More studies about the applicability of a particular formulation to a particular environmental setting are needed for better modeling of the behavior of dissolved oxygen during stratification.

Acknowledgements. The authors thank to Anadolu University, Scientific Research Project Funding (AU BAP) for their financial support [Project number: 1208F129].

REFERENCES

- [1] Alpaslan, K., Sesli, A., Tepe, R., Ozbey, N., Birici, N., Seker, T., Kocer, M. A. T. (2012): Vertical and seasonal changes of water quality in Keban Dam Reservoir. – *Journal of FisheriesSciences.com* 6(3): 252-262.
- [2] Babajimopoulos, C., Papadopoulos, F. (1986): Mathematical prediction of thermal stratification of Lake Ostrovo (Vegoritis), Greece. – *Water Resources Research* 22(11): 1590-1596.
- [3] Batick, B. M. (2011): Modeling Temperature and Dissolved Oxygen in the Cheatham Reservoir with CE-QUAL-W2. – Unpublished MSc Thesis, Vanderbilt University, Nashville.
- [4] Becker, V., Huszar, V. L. M., Crossetti, L. O. (2009): Responses of phytoplankton functional groups to the mixing regime in a deep subtropical reservoir. – *Hydrobiologia* 628(1): 137-151.
- [5] Bell, V. A., George, D. G., Moore, R. J., Parker, J. (2006): Using a 1-D mixing model to simulate the vertical flux of heat and oxygen in a lake subject to episodic mixing. – *Ecological Modelling* 190(1-2): 41-54.
- [6] Berger, C. J., Wells, S. A., Annear, R., (2005): Laurence Lake Temperature Model. – Maseeh College of Engineering and Computer Science Department of Civil and Environmental Engineering, Portland State University, Portland, Oregon.
- [7] Birge, E. (1910): An unregarded factor in lakes temperatures. – *Trans. Wis. Acad. Sci. Arts Lett* 16: 989-1004.
- [8] Bocaniov, S. A., Ullmann, C., Rinke, K., Lamb, K. G., Boehrer, B. (2014): Internal waves and mixing in a stratified reservoir: Insights from three-dimensional modeling. – *Limnologia - Ecology and Management of Inland Waters* 49: 52-67.
- [9] Bonalumi, M., Anselmetti, F. S., Wuest, A., Schmid, M. (2012): Modeling of temperature and turbidity in a natural lake and a reservoir connected by pumped-storage operations. – *Water Resources Research* 48: 1-18.
- [10] Bonnet, M. P., Poulin, M. (2004): DyLEM-1D: a 1D physical and biochemical model for planktonic succession, nutrients and dissolved oxygen cycling: Application to a hyper-eutrophic reservoir. – *Ecological Modelling* 180(2): 317-344.
- [11] Bowen, J. D., Hieronymus, J. W. (2003): A CE-QUAL-W2 model of Neuse Estuary for total maximum daily load development. – *Journal of Water Resources Planning and Management-Asce* 129(4): 283-294.
- [12] Branco, B. F., Torgersen, T. (2009): Predicting the onset of thermal stratification in shallow inland waterbodies. – *Aquatic Sciences* 71(1): 65-79.

- [13] Branco, C. W. C., Kozłowsky-Suzuki, B., Sousa-Filho, I. F., Guarino, A. W. S., Rocha, R. J. (2009): Impact of climate on the vertical water column structure of Lajes Reservoir (Brazil): A tropical reservoir case. – *Lakes & Reservoirs: Research & Management* 14(3): 175-191.
- [14] Caliskan, A., Elci, S. (2009): Effects of selective withdrawal on hydrodynamics of a stratified reservoir. – *Water Resources Management* 23(7): 1257-1273.
- [15] Chapman, L. J., Chapman, C. A., Crisman, T. L., Nordlie, F. G. (1998): Dissolved oxygen and thermal regimes of a Ugandan crater lake. – *Hydrobiologia* 385: 201-211.
- [16] Chapra, S. C. (1997): *Surface Water-Quality Modeling*. – McGraw-Hill, New York.
- [17] Chimney, M. J., Wenkert, L., Pietro, K. C. (2006): Patterns of vertical stratification in a subtropical constructed wetland in south Florida (USA). – *Ecological Engineering* 27(4): 322-330.
- [18] Churchill, J. H., Kerfoot, W. C. (2007): The impact of surface heat flux and wind on thermal stratification in Portage Lake, Michigan. – *Journal of Great Lakes Research* 33(1): 143-155.
- [19] Colarusso, L. A., Chermak, J. A., Priscu, J. C., Miller, F. K. (2003): Modeling pit lake water column stability using Ce-Qual-W2. – *Tailings and Mine Waste* 03: 213-222.
- [20] Cole, T. M. (2000): Reservoir thermal modeling using CE-QUAL-W2. – *Development and Application of Computer Techniques to Environmental Studies* VII(4): 237-246.
- [21] Cole, T. M., Tillman, D. H., (1999): *Water Quality Modeling of Lake Monroe Using CE-QUAL-W2*. – US Army Corps of Engineers Waterways Experiment Station, Louisville.
- [22] Cole, T. M., Wells, S. A. (2013): *CE-QUAL-W2: A two-dimensional, laterally averaged, hydrodynamic and water quality model, version 3.7*. – Unpublished Thesis, Portland State University, Portland.
- [23] Dayyani, S., Mohammadi, K., Najib, H. R. (2003): River flow estimation for ungauged stations using GIS model. – *Seventh International Water Technology Conference Egypt* 1-3 April 2003.
- [24] Deliman, P. N., Gerald, J. A. (2002): Application of the two-dimensional hydrothermal and water quality model, CE-QUAL-W2, to the Chesapeake Bay - Conowingo Reservoir. – *Lake and Reservoir Management* 18(1): 10-19.
- [25] Devonis, C. S. (2011): *Wachusett Reservoir Contaminant Spill Modeling Using CE-QUAL W2*. – Unpublished Thesis, University of Massachusetts, Amherst.
- [26] Diogo, P. A., Fonseca, M., Coelho, P. S., Mateus, N. S., Almeida, M. C., Rodrigues, A. C. (2008): Reservoir phosphorous sources evaluation and water quality modeling in a transboundary watershed. – *Desalination* 226(1-3): 200-214.
- [27] Dueri, S., Castro-Jimenez, J., Zaldivar, J. M. (2009): Modelling the influence of thermal stratification and complete mixing on the distribution and fluxes of polychlorinated biphenyls in the water column of Ispra Bay (Lake Maggiore). – *Chemosphere* 75(9): 1266-72.
- [28] Elci, S. (2008): Effects of thermal stratification and mixing on reservoir water quality. – *Limnology* 9(2): 135-142.
- [29] Erturk, A., Ekdal, A., Gurel, M., Zorlutuna, Y., Tavsan, C., Seker, D. Z., Tanik, A., Ozturk, I. (2008): Application of Water Quality Modelling as a Decision Support System Tool for Planned Buyuk Melen Reservoir and its Watershed. – In: Gönenç, I. E., Vadineanu, A., Wolflin, J. P., Russo, R. C. (eds.) *Sustainable Use and Development of Watersheds*. Springer, Dordrecht.
- [30] Göncü, S., Avdan, U., Yiğit Avdan, Z., Albek, E., (2014): Monitoring the Porsuk Reservoir Dissolved Oxygen Concentration Based on Stratification and Investigation of a Suitable Hypolimnetic Aeration Method Intended to Increase the Lake Assimilation Capacity. – 1208F129, Eskisehir-TURKEY, Anadolu University Research Project.
- [31] Gunduz, O., Soyupak, S., Yurteri, C. (1998): Development of water quality management strategies for the proposed Isikli reservoir. – *Water Science and Technology* 37(2): 369-376.

- [32] Güngör, Ö., Göncü, S. (2013): Application of the soil and water assessment tool model on the Lower Porsuk Stream Watershed. – *Hydrological Processes* 27(3): 453-466.
- [33] Ha, S. R., Lee, J. Y. (2007): Application of CE-QUAL-W2 Model to Eutrophication Simulation in Daecheong Reservoir Stratified by Turbidity Storms. – In: Sengupta, M., Dalwani, R. (eds.) *Proceedings of Taal2007: The 12th World Lake Conference*, Jaipur, India.
- [34] Hasanoğlu, E. (2012): Investigation of Thermal Stratification Structure and Dissolved Oxygen Profiles in Borabey Pond. – Unpublished MSc Thesis, Anadolu University, Eskişehir.
- [35] Hassan, H., Aramaki, T., Hanaki, K., Matsuo, T., Wilby, R. (1998): Lake stratification and temperature profiles simulated using downscaled GCM output. – *Water Science and Technology* 38(11): 217-226.
- [36] Hudson, J. J., Vandergucht, D. M. (2015): Spatial and temporal patterns in physical properties and dissolved oxygen in Lake Diefenbaker, a large reservoir on the Canadian Prairies. – *Journal of Great Lakes Research* 41: 22-33.
- [37] Kaya, M. (2013): Interaction of Water Quality with Basin Components in Small Water Bodies. – Unpublished MSc Thesis, Anadolu University, Eskişehir.
- [38] Kerimoglu, O., Rinke, K. (2013): Stratification dynamics in a shallow reservoir under different hydro-meteorological scenarios and operational strategies. – *Water Resources Research* 49: 7518-7527.
- [39] Kim, Y., Kim, B. (2006): Application of a 2-dimensional water quality model (CE-QUAL-W2) to the turbidity interflow in a deep reservoir (Lake Soyang, Korea). – *Lake and Reservoir Management* 22(3): 213-222.
- [40] Kindle, E. M. (1929): A Comparative study of different types of thermal stratification in lakes and their influence on the formation of Marl. – *The Journal of Geology* 37(2): 150-157.
- [41] Kortmann, R. W., Henry, D. D., Kuether, A., Kaufman, S. (1982): Epilimnetic nutrient loading by metalimnetic erosion and resultant algal responses in Lake Waramaug, Connecticut. – *Hydrobiologia* 91(1): 501-510.
- [42] Kuo, J. T., Lung, W. S., Yang, C. P., Liu, W. C., Yang, M. D., Tang, T. S. (2006): Eutrophication modelling of reservoirs in Taiwan. – *Environmental Modelling & Software* 21(6): 829-844.
- [43] Lap, B. Q., Tuan, N. V., Hamagami, K., Iguchi, S., Mori, K., Hirai, Y. (2009): Formation and disappearance of thermal stratification in a small shallow lake. – *Journal of the Faculty of Agriculture Kyushu University* 54(1): 251-259.
- [44] Li, Y. P., Acharya, K., Chen, D., Stone, M. (2010): Modeling water ages and thermal structure of Lake Mead under changing water levels. – *Lake and Reservoir Management* 26(4): 258-272.
- [45] Lindim, C., Pinho, J. L., Vieira, J. M. P. (2011): Analysis of spatial and temporal patterns in a large reservoir using water quality and hydrodynamic modeling. – *Ecological Modelling* 222(14): 2485-2494.
- [46] Rice, D. A., Tsay, T. K., Effler, S. W., Driscoll, C. T. (1989): Modeling thermal stratification in transparent Adirondack Lake. – *Journal of Water Resources Planning and Management-Asce* 115(4): 440-456.
- [47] Salonen, K., Sarvala, J., Jarvinen, M., Langenberg, V., Nuottajarvi, M., Vuorio, K., Chitamwebwa, D. B. R. (1999): Phytoplankton in Lake Tanganyika - vertical and horizontal distribution of in vivo fluorescence. – *Hydrobiologia* 407: 89-103.
- [48] Song, K., Xenopoulos, M. A., Buttle, J. M., Marsalek, J., Wagner, N. D., Pick, F. R., Frost, P. C. (2013): Thermal stratification patterns in urban ponds and their relationships with vertical nutrient gradients. – *J Environ Manag* 127: 317-323.
- [49] Spigel, R. H., Howard-Williams, C., Gibbs, M., Stephens, S., Waugh, B. (2005): Field calibration of a formula for entrance mixing of river inflows to lakes: Lake Taupo, North

- Island, New Zealand. – *New Zealand Journal of Marine and Freshwater Research* 39(4): 785-802.
- [50] Stansbury, J., Kozimor, L., Admiraal, D., Dove, E. (2008): Water quality modeling of the effects of macrophytes on dissolved oxygen in a shallow tailwater reservoir. – *Lake and Reservoir Management* 24(4): 339-348.
- [51] Williams, N. T. (2007): Modeling Dissolved Oxygen in Lake Powell. – Unpublished Thesis, Brigham Young University, Provo, UT.
- [52] Zhang, H., Culver, D. A., Boegman, L. (2008): A two-dimensional ecological model of Lake Erie: Application to estimate dreissenid impacts on large lake plankton populations. – *Ecological Modelling* 214(2-4): 219-241.
- [53] Zhang, Y., Wu, Z., Liu, M., He, J., Shi, K., Zhou, Y., Wang, M., Liu, X. (2015): Dissolved oxygen stratification and response to thermal structure and long-term climate change in a large and deep subtropical reservoir (Lake Qiandaohu, China). – *Water Research* 75: 249-258.

EVALUATION OF THE SIGNIFICANCE OF LINEAR NON-FOREST WOODY VEGETATION IN THE DEVELOPMENT OF AN ECOLOGICAL NETWORK

DIVIAKOVÁ, A. – KOČICKÁ, E. – BELČÁKOVÁ, I.* – BELÁŇOVÁ, E.

*UNESCO-Chair on Sustainable Development and Ecological Awareness, Faculty of Ecology and Environmental Sciences, Technical University in Zvolen
T. G. Masaryka 24, 960 53 Zvolen, Slovakia
(phone: +421-45-5206-329)*

**Corresponding author
e-mail: belcakova@tuzvo.sk; phone: +421-45-5206-329*

(Received 25th Jul 2017; accepted 18th Dec 2017)

Abstract. Non-Forest Woody Vegetation (NFWV) is a very important element of a human environment as well as landscape-ecological stability; it fulfils many major functions. The linear formations of NFWV as elements of ecological networks have a direct impact on the potential of a landscape. International policies and programs constitute a foundation for developing national programs of ecological networks, an example of which is the so-called Territorial System of Ecological Stability (TSES) in Slovakia. Within the existing methodology concept of TSES, however, the issue of NFWV is significantly understated, particularly in evaluations of its features, its functional significance from various points of view, and its measures intended to bring about ecological stability. The aim of this contribution is to present results from a study focused on evaluating the landscape-ecological and biotic significance of linear formations of NFWV based on detailed field research. The model territory is located in central Slovakia in the southeastern part of the Štiavnické vrchy Mountains, near the village of Žibritov.

Keywords: *habitat, landscape-ecological stability, functions of vegetation, phytocoenological survey, zoological survey, local level*

Introduction

The establishment of ecological networks is currently one of the main objectives of landscape ecology and the protection of the nature and landscapes. These objectives are set out in important international documents such as Agenda 21, the UN Convention on Biological Diversity, the Pan-European Biological and Landscape Diversity Strategy, European Ecological Network (EECONET) under the European program of International Union for Conservation of Nature (IUCN), and the European Landscape Convention. The principles of NATURA 2000 also articulate a need to preserve networks of significant ecosystems. International policies and programs constitute a foundation for developing national programs of ecological networks, an example of which is the so-called Territorial System of Ecological Stability (hereinafter referred to as TSES) in Slovakia (Miklós et al., 2011).

From theoretical and methodological perspectives, TSES is a modern concept of nature conservation and biodiversity that stands on the principles of the protection of natural conditions and life forms, i.e., the protection of geobiodiversity. The whole system can be seen as a network of ecologically significant segments of a landscape, which is efficiently distributed on the basis of functional and spatial criteria, covering biotic, hydrological, soil and relief conditions. It consists of biocentres (providing a food chain and conditions for reproduction, rest and shelter), biocorridors, and buffer

zones (providing for the overcoming of barriers that isolate them from each other, the exchange of genetic information and the migration of ecosystems, as well as the interaction of different ecosystems with different levels of stability).

Currently, TSES can be considered the most remarkable and noticeable success in the enforcement of ecological principles in the legislation of decisive planning processes. It is therefore undeniably important in the responsible assessment of vegetation, both in detail and according to clearly defined criteria. In the concepts of the existing TSES methodologies, however, the issue of NFWV is significantly understated, particularly evaluations of its features, its functional significance from various points of view, and its measures intended to bring about ecological stability.

NFWV is defined as a permanent stand of a wood species, including a herbaceous layer, which is not a forest, agricultural crops, or part of the greenery of an urban residential area or other urban development in a landscape (Bulír, 1981; Mareček, 2005). It includes both natural elements of vegetation growing in a spontaneous way and artificially created vegetation formations (Bulír, 1987; Machovec, 1994).

Linear formations of NFWV as elements of ecological networks fulfil a number of important functions and have a direct impact on the potential of a landscape. It is therefore undeniably important to assess such vegetation responsibly, both in detail and according to clearly defined criteria. As mentioned above, linear formations of NFWV can mostly be a part of biocorridors. A biocorridor is a dynamic element that is interlinked with biocentres and, as such, it can create a mutually dependent territorial system. The functionality of a biocorridor is determined by many of its features: its length, width, connectivity, shape of edges, number of gaps, etc. At a local level, biocorridors are mostly represented by important linear elements (Löw et al., 1995).

Forman and Godron (1986) divide corridors according to several criteria: their structure (linear and strip), origin (remnant, along cultivated and regenerated watercourses), or their connectivity. Löw et al. (1995) classify corridors, e.g., by the origin and development of ecosystems, their functionality, biocenosis diversity, connectivity (continuous and discontinuous), and the similarity of connected biocentres (contrast, modal).

More and more authors point to the necessity of maintaining the connectivity of lines within overall landscape management. For example, according to Smith and Hellmund (1993), greenways or wildlife corridors should be seen as elements of the integral strategies of landscape management necessary to maintain the values of a natural environment. In a similar way, Hudgens and Haddad (2003) stress the complexity of the research issues and functionality of corridors; they think viewpoints on biocorridors should be much more panoramic due to their cumulative effects. Linear elements are important landscape elements that enable the movement of species between fragmented habitats (Forman and Baudry, 1984; Saunders and Hobbs, 1991; Opdam et al., 1995; Bennet, 1999). The movement of various plant and animal species along corridors has been monitored by many authors (Hobs, 1992; Mann and Plummer, 1995; Rosenberg et al., 1997). NFWV affect biodiversity since they can be habitats, refuges, corridors or barriers. These functions are essential for many plants and animals that would otherwise not be able to survive in an agricultural landscape (Burel, 1996). In linear biotic formations, predators may prevent pest outbreaks, e.g., invasions of voles (Delattre et al., 1999).

The significance of the width of linear NFWV formations for many groups of invertebrates has been documented in the literature on the subject (Hinsley and Belami,

2000). Wider vegetation strips promote heterogeneity of microhabitats and diversity of food and other parameters, which facilitate the diversity of invertebrate communities.

Furthermore, as many writers claim, the interconnectivity of NFWV formations is an important attribute affecting their colonization by invertebrates (Baudry, 1988), especially less mobile ones (Cameron et al., 1980). However, identification of the most important attributes of NFWV formations that influence the abundance and diversity of birds is quite complicated. There are numerous studies which assert that the abundance of bird species rises with the increasing size of NFWV lines (with regard to their width and length) (Arnold, 1983; Osborne, 1984; Shalaway, 1985; Green et al., 1994; MacDonald and Johnson, 1995).

Most cases reveal a correlation between the width of NFWV formations and the diversity of bird communities, whereas their height or any other dimension does not seem to be as significant (Hinsley et al., 1999). According to the available data (Hinsley and Belami, 2000), an important factor affecting the structuring of bird communities in NFWV formations is the composition and the height of the forest layer (high NFWV strips with a lot of trees appear to be very attractive to forest bird species).

Another important parameter for all groups of animals is the linkage between NFWV formations and forest habitats (Cameron et al., 1980). The significance of such connectivity was mentioned above. Such a linkage to forest habitats can also encourage the movement of typical forest animal species into the NFWV habitats. On the other hand, the spatial interconnection between multiple linear formations of NFWV allows for communication among individual habitats and provides shelter in the event of migration (e.g., Johnson and Beck, 1988).

We investigated the linear formations of NFWV in an agricultural landscape in the region of Krupina (Slovakia), one of the major wine and fruit-growing regions in Slovakia, which has a typical landscape structure, i.e., vineyards, orchards and lines of trees planted between meadows and arable land.

The verification and supplementation of these actions were carried out on the basis of detailed field research, followed by determining and evaluating the landscape-ecological and biotic significance of linear formations of NFWV (acting as biocorridors and interactive elements).

The landscape-ecological and biotic significance of linear formations of NFWV as biocorridors or interacting objects on a local level of TSES were evaluated.

Methods

Based on the results of our landscape-ecological syntheses, the inventory and mapping of linear formations of NFWV; zoological research; and interpretations of the production, structural, status and ecosozological features of the vegetation; and subsequently on the basis of selected natural hazards, we determined the significance of the linear formations of NFWV, i.e., the conservation of nature, landscape-ecological, biotic (significance of the habitat) and anti-erosion formations. The assessments resulted in specific proposals for the model territory; i.e., TSES elements, proposals for the protection of vegetation, and proposed guidelines for the development of a TSES project.

The focus of the work consisted of the application of theoretical and methodological approaches in the field of landscape ecology, the protection of nature and landscapes, geographic information systems, geobotany, and remote sensing.

The model territory is located in central Slovakia in the southeastern part of the Štiavnické vrchy Mountains, near the village of Žibritov (latitude 48°23'26.98"N, longitude 18°59'3.21"E). The highest point of the territory is Buzalkov Hill (711 m a. s. l.); the lowest point is where the Bebrava River leaves the territory (377 m a. s. l.); the vertical distance is therefore 334 m.

Most of the model territory is made up of strongly rugged hills, with a smaller part made up of very strongly rugged uplands. On average there are less than 50 summer days per year (Mind'áš and Škvarenina, 2002). The prevailing type of runoff regime is rain-snow, with the highest level of watercourses in March (February to April), the second highest in the late autumn and early winter, and the lowest water levels in September (Šimo and Zatl'ko, 2002). The area is dominated by eutric cambisols, typical acid cambisols and luvic cambisols on mineral-rich weathered vulcanites and cambisols on volcanic rocks on steep 12-25° slopes (Čurlík and Šály, 2002). The area is represented by medium heavy soils (clay) and medium heavy- to- lighter soils (sandy loam). The designated area has the character of an agricultural landscape with prevailing permanent grasslands and a varying proportion of NFWV. The area is interesting due to its rich network of linear vegetation elements on borders where regionally rare species of old fruit trees can be found (*Fig. 1*).

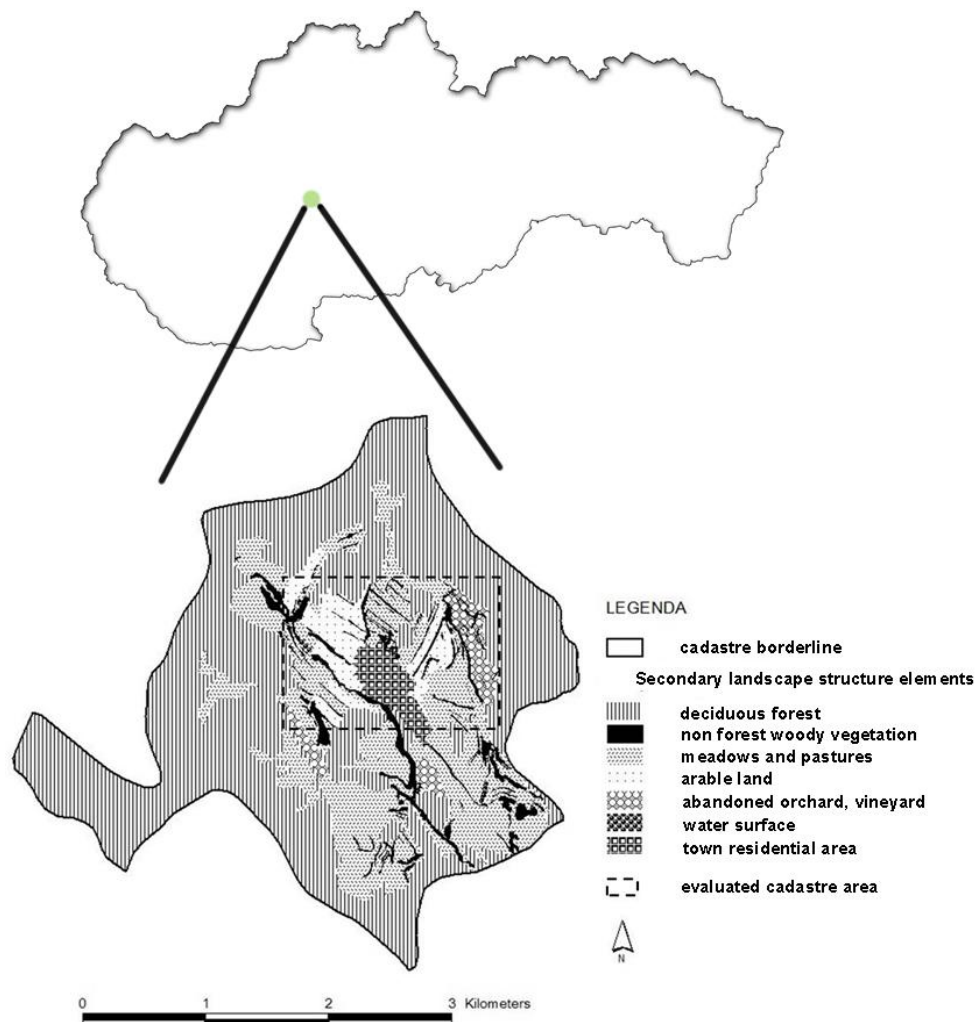


Figure 1. Location of Žibritov study area (AUT)

Phytocoenological survey of linear formations of NFWV

During the fieldwork, 38 phytosociological entries at 38 sites and 38 inventories of plant species were made for a total of 76 entries. Selected characteristics (ecological analyses of communities, structural characteristics, status characteristics, ecosozological characteristics, production features and then nature conservation, landscape ecological and anti-erosion significance) were assessed in only 38 linear formations where phytosociological entries were made; the biotic significance (significance of a habitat) was evaluated in 20 linear formations (Fig. 2), particularly in those lines where a zoological survey was conducted. NFWV was mapped within the current landscape structure and by a field inventory of the plant species based on the methods of the Zurich-Montpellier school.

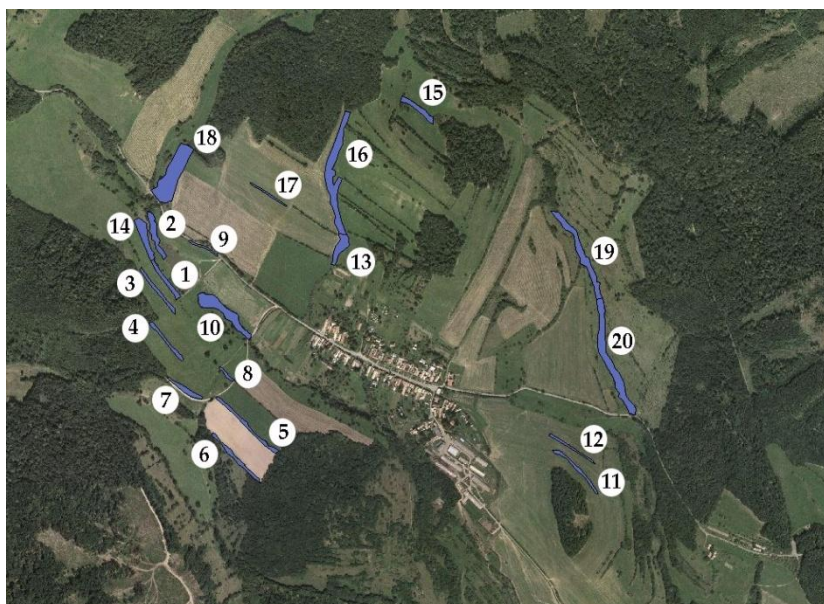


Figure 2. Sites evaluated (AUT)

Zoological survey of the NFWV linear formations

A basic zoological survey was conducted on 20 randomly selected linear formations of the NFWV of the study area where the following model animal groups were monitored: selected groups of animals living in the upper soil layer or on its surface (Opiliones, Chilopoda, Diplopoda), birds, and small terrestrial mammals. They were chosen in order to characterize the richness of the animal species with different relations to the particular mesohabitats of the NFWV formations. Trapping of epigeic macrofauna was carried out using pitfall traps that were placed in the landscape (Stašiov, 2006). The relation of birds to the NFWV formations was determined based on visual observations, vocal performances, and other signs of residence (e.g., hollowed-out tree trunks and old nests). Throughout the fieldwork period we recorded the appearance of larger mammals in the FWV formations observed (visually and through signs of their residence).

Based on the results of both the phytocoenological and the zoological surveys we determined selected structural, state, ecosozological and production characteristics of the vegetation, which have been used for landscape-ecological interpretation.

Numerical methods and multidimensional analysis of phytocoenological and zoological data

The impact of the variables of the environment on the composition of the species of the NFWV formations as well as the impact of the NFWV characteristics on the composition of the species of the model of fauna groups were observed using direct gradient analysis (RDA). The CAP and CANOCO software packages were used for the statistical data processing (Ter Braak and Šmilauer, 1998).

Landscape-ecological significance of the vegetation

The landscape-ecological significance (V_{ke}) was determined on the basis of the following criteria (Jurko, 1990): hemeroby level (H), threat (O), regional rarity (V_r), diversity (D), feeding potential (P_k), melliferous potential (P_m) and stability (S_{pa}). Each criterion was rated on a 10-point scale with increasing values (*Table 1*).

Table 1. Values of selected criteria for determining the landscape-ecological significance of vegetation

Value	H - Degree of hemeroby (%)	O - Threat to habitats (as per the Slovak system of habitats and their significance)	V_r - Regional rarity (index value)	D - Diversity (Shannon index value)	P_k - Feeding potential (%)	P_m - Melliferous potential	Degree of ecological stability S_{pa}
10. Extremely high	Natural T < 2	16 and more	27 and more	> 4.2	91 and more	181-200	10. Extremely high stability
9. Very high	T: 3-5	12.6-15	23-26	4.0-4.1	81-90	161-180	9. Very high stability
8. High to very high	Almost natural T: 6-10, N < 3	10.1-12.5	20-22	3.8-3.9	71-80	141-160	8. High to very high stability
7. High	T: 11-15, N < 7	7.6-10%	17-19	3.6-3.7	61-70	121-140	7. High stability
6. Medium to high	Semi-natural T: 16-20, N: 8-12	6.1-7.5	14-16	3.4-3.5	51-60	101-120	6. Medium to high stability
5. Medium	T: 21-25, N < 13-18	4.6-6	11-13	3.2-3.3	41-50	81-100	5. Medium stability
4. Low to medium	Cultivated T: 26-35, N: 19-22	3.1-4.5	8 - 10	3.0-3.1	31-40	61-80	4. Low to medium stability
3. Low	Artificial T > 36, N: 23-35	1.6-3	5-7	2.8-2.9	21-30	41-60	3. Low stability
2. Very low	N > 36	0-1.5	2-4	2.6-2.7	11-20	21-40	2. Very low stability
1. Extremely low	Devastated	0	1 or less	< 2.6	0-10	0-20	Extremely low stability

The final value of the landscape-ecological significance was calculated using *Equation 1*:

$$V_{ke} = \frac{(H + O + V_r + D + P_k + P_m) * S_{pa}}{100} \quad (\text{Eq.1})$$

The final value was classified on an 8-point scale: 1. extremely low (< 0.4), 2. very low (0.4-1), 3. low (1-2), 4. low to medium 4 (2-2.5), 5. medium (2.5-3), 6. high (3-3.5), 7. very high (3.5-4), 8. extremely high (> 4).

The biotic significance (the significance of the habitats) V_{bio} was assessed in the first 20 linear formations (as the zoological survey was carried out only at the first 20 sites), according to the criteria defined by the results from the field survey and the modified methodology by Sláviková (1987). The following criteria were involved: the value of the Shannon diversity index of plant (H_{D1}) and animal (H_{D2}) communities, the minimum width of a formation, adjacent habitats, line connectivity with other formations, and stratification. Values of 1-3 were attached to the criteria (*Table 2*).

The final value of the biotic significance of the assessed lines was the sum of the points for particular characteristics; it was classified on a 3-point scale V_{bio} : 1 - high (15-16p), 2 - medium (13-14p), and 3 - low (10-12p).

Table 2. Values of selected criteria for determining the biotic significance of vegetation

Value	H_{D1} - Diversity (value of Shannon index of plant communities)	H_{D2} - Diversity (value of Shannon index of animal communities)	Min. width (m)	Surrounding habitats	Connectivity	Stratification
3 - High	3.9-4.2	2.5-2.2	15 and more	Meadow vegetation	Water habitats	3 layers
2 - Medium	3.5-3.8	2.1-1.8	10-14	Arable land	Habitats connected with a forest or other NFWV	2 layers
1 - Low	3.1-3.4	1.7-1.4	9 and less	Roads	Isolated habitats without water	1 layer

TSES elements and nature and landscape protection

After the assessment of the qualitative and quantitative characteristics of the evaluated lines, the formations were proposed as TSES elements; i.e., as part of local biocorridors or interactive elements, or they were proposed for nature protection.

Results

Evaluation of the NFWV linear formations based on the phytocoenological survey

Based on the physiognomy, composition of species, and ecotopes of the following types of habitats, linear formations of NFWV were specified in the territory observed (*Table 3*):

Table 3. The habitat types

Code	Habitats (site)
V1-V4	Hygrophilous habitats of submontane alder floodplain forests (<i>Alnion incanae</i>) Pawlowski et al. 1928, <i>Alnenion glutinoso-incanae</i> Oberd. 1953: <i>Aegopodio-Alnetum</i> - <i>riparian vegetation</i> (sites No. 2, 10, 19, 20)
L1-L4	Fragments of Carpathian oak-hornbeam forests (zv. <i>Carpinion</i> Issler 1931, <i>Carici pilosae-Carpinion betuli</i> J. et M. Michalko: <i>Quercopetreae-Carpinetum</i> Soó et Pócs 1957) – fragments of forest vegetation (Site Nos.13, 14, 16, 18)
KL	Blackthorn hazel shrubbery called Berberidion Br.-Bl. 1950, <i>Populo-Coryletum</i> Br.-Bl. 1950) (Site No.15)
Ra1-Ra8, Rb1	Avenues (bocages) - linear woody, mostly three-layer formations of small dimensions, surrounded by grasslands or arable land in balks where the tree layer is represented by human-planted species (<i>Pyrus domestica</i> , <i>Malus domestica</i> , <i>Juglans regia</i> , <i>Prunus domestica</i>); these are thus anthropogenically determined biocorridors (Ra Site Nos. 1, 3, 4, 5, 6, 8, 11, 12). They occur mostly in meadows, but also on arable land along roads. They adjoin forest stands, other formations of NFWV, or are completely isolated. Avenues with the occurrence of synanthropic species and avenues with intergrowing species of surrounding forest stands and with the occurrence of synanthropic species are in Rb site No. 17
C1, C2	Continuous accompanying tree-lines along a third class road running across the centre of the study area or along an unpaved field road. This concerns Site Nos. 7 and 9

Evaluation of habitats based on ecological and location features

The environmental characteristics and quantitative features of the NFWV lines assessed are documented in *Tables 4* and *5*.

Table 4. Environmental characteristics and quantitative features of the NFWV lines assessed

Variable/Site	1	2	3	4	5	6	7	8	9	10	11	12	13	14	15	16	17	18	19	20
Minimum width (m)	10	9	8	7	7	6	6	7	4	15	7	5	11	14	15	15	5	47	14	15
Maximum width (m)	18	21	11	13	14	19	16	10	7	50	13	9	35	32	22	41	7	70	33	30
Area (m ²)	531	477	531	518	531	510	528	509	508	480	480	480	540	531	530	550	540	526	530	530
Length (m)	147	161	174	159	258	215	127	62	105	217	201	178	104	140	122	400	139	20	323	390
Geological substrate	4	4	1	1	1,3	1,3	3	3	1	4	1	1	1	3	2	1,2	1,5	1	3	3,4
Soil type	1	2	1	1	1	1	1	1	1	2	1	1	1	1	1	1	1	1	1	1
Soil depth	2	5	2	2	2	2	2	4	4	5	2	2	2	2	5	2	2	1	5	5
Soil group	1	2	1	1	1	1	1	1	1	2	1	1	1	1	2	1	1	1	2	2
Slope inclination	5	2	5	4	4	4	4	4	3	2	4	4	4	4	4	4	4	4	4	4
Altitude (m a. s. l.)	531	477	531	518	531	510	528	509	508	480	480	480	540	531	530	550	540	526	530	530
Landforms	6	8	6	6	2	6	2	6	6	8	6	6	6	6	4	3	6	3	4	4
Orientation to cardinal points	2	4	2	2	2	2	4	2	5	4	2	2	6	3	4	5	6	7	4	4
Surrounding biotopes	1	1	1	1	2	3	5	1	5	4	1	1	2	1	1	2	6	5	1	1
Connectivity	2	2	3	1	1	1	1	2	2	3	3	3	2	2	3	1	3	1	2	2
Cover of layer E ₃ (%)	40	100	50	80	60	65	65	60	70	100	50	40	60	70	60	60	35	80	100	100
Cover of layer E ₂ (%)	80	75	80	50	75	90	85	50	70	50	70	80	90	90	85	90	95	65	35	25
Crown cover E ₃	5	1	4	4	3	3	3	4	3	1	3	5	3	2	3	3	5	1	1	1
Crown cover E ₂	4	2	2	3	2	3	3	2	1	3	3	3	1	1	1	2	2	4	5	5

Table 5. Explanations for Table 4

Code	Environmental characteristics
Geological substrate	
1	Unspecified pyroxene andesite
2	Pyroxene andesite (augite-hypersthene)
3	Deluvial sediments - polygenetic slope loam
4	Fluvial floodplain sediments: mostly loam and sandy loam
5	Deluvial-fluvial hillwash loam, sandy loam
Soil type	
1	Cambisol
2	Luvisol
Soil depth (cm)	
1	Very shallow (15)
2	Shallow (15-30)
3	Moderately deep (30-60)
4	Deep (60-100)
5	Very deep (100-200)
Soil group (granularity)	
1	Silty - loam
2	Silty - clayey - loam
Slope orientation (°)	
2	1-3
3	3-7
4	7-12
5	12-17
Landform	
2	Plateau
3	Dome-shaped peak
4	Ridge
6	Transport slope
8	Slope plateau
Orientation to cardinal points	
2	NE
3	E
4	SE
5	S
6	SW
7	W
Surrounding biotopes	
1	Meadow
2	Meadow and large block fields
3	Forest and large block fields
4	Meadow and small-scale and narrow-strip fields
5	Meadow and road
6	Large block fields

Connectivity	
1	To forest
2	To other NFWV types
3	Isolated
Crown cover of E ₃ , E ₂	
1	Dense to continuous - crowns of neighbouring trees (shrubs) overlap and touch, they affect each other
2	Loose - tree (shrubs) crowns touch; or there is a gap of an average crown size of the wood species typical of a given formation
3	Interrupted to gapped - a gap of an average crown size of the wood species typical of a given formation, to a gap of 5 m
4	% of the interlocking parts is less than or equal to the gapped parts of a formation
5	Sparse trees and shrubs

No neophytes were present in the linear formations evaluated or their surroundings. The occurrence of therophytes was also relatively low, i.e., about 3.56%. The final assessment states that almost all the habitats mapped showed near-natural hemeroby levels; they recorded average values of 9, 8 in the evaluation of landscape-ecological significance. Protected, endangered or rare species were not observed. According to aspects of regional rarity, common taxa represented the largest group (abundant). Uncommon taxa are species scattered in the study area and are habitat-bound (e.g., *Sorbus torminalis*, *Quercus cerris*, *Pyrus pyraster*, *Bryonia dioica*, *Poa palustris*, etc.) or species in less well-known sites and less widespread species. Rare species include domesticated wood species, which in the area of Žibřítov have their northernmost sites (*Malus domestica*, *Pyrus domestica*, *Mespilus germanica*, *Cerasus sp.*, etc.) and are evaluated in terms of their historically determined occurrence; then there are species that occur sporadically in the southeastern and southern parts of the Štiavnické vrchy mountains, in the oak-hornbeam forests (e.g., *Carduus nutans*).

The final values of regional rarity ranged from 3.4 to 26.0. Formations with the highest values were avenues (Site Nos. 6, 11 and 12). On the other hand, low or very low values (3.4, 8) were assigned to avenues with synanthropic species, blackthorn shrubbery with synanthropic species and fragments of forest stands (e.g., Site Nos. 13 and 16). The other sites showed medium- to- high degrees of regional rarity.

Species with low feeding potential represent the largest group in the habitats evaluated. These include hygrophilous, synanthropic and forest species such as *Artemisia vulgaris*, *Aruncus sylvestris*, *Barbarea vulgaris*, *Centaurea phrygia*, *Juncus conglomeratus*, etc. Species with medium and excellent feeding potential had the lowest representation (*Festuca pratensis*, *Lolium perenne*, *Poa palustris*, *Trifolium repens*, *Poa pratensis* etc.). Five percent (5%) of the species were inappropriate or even very harmful for use as food (*Colchicum autumnale*, *Euphorbia cyparissias*, *Pteridium aquilinum*, etc.).

Very low levels of feeding potential (29-30) were observed in fragments of some forest ecosystems (Site Nos. 14, 16 and 18) and narrow tree-lines occurring mostly along roads (e.g., Site Nos. 8 and 14). Avenues or avenues with intergrowing species of surrounding forest stands reached an average value (46-48), which was the highest among all the sites evaluated (e.g., Site Nos. 1, 6, 17). The other sites have low-to-medium levels of feeding potential.

An overall assessment of the melliferous potential shows that the sites evaluated have great potential, i.e., they have a high percentage of species with reserves of nectar and pollen. The highest melliferous potential with very high values, i.e., above 150%, was observed at Site Nos. 1 and 7. These are avenues with intergrowing forest species. Medium-to-high values of melliferous potential (106-110%) were assigned to linear fragments of forest stands (Site Nos. 13 and 18) as well as some alleys (e.g., Site No. 17). The other sites assessed showed high or high-to-very high values of melliferous potential.

Each type of habitat was assigned the following degree of ecological stability (Table 6).

Table 6. *The ecological stability of the types of habitat*

Code	Degree of ecological stability (Site)
10	Extremely high stability – original habitats without human intervention, value was not assigned
9	Very high stability – submontane alder floodplain forests (Site Nos. 2, 10, 19 and 20)
8	High-to-very-high stability – fragments of oak-hornbeam forests (Site Nos. 13, 14, 16, 18)
7	High stability – blackthorn hazel shrubbery (Site No. 15)
6	Medium-to-high stability – avenues with intergrowing species of surrounding forest stands (Site Nos. 1, 3, 4, 5, 6, 7, 8, 11 and 12)
5	Medium stability – avenues along roads (Site No. 9)
4	Low-to-medium stability – avenues with intergrowing species of surrounding forest stands and with synanthropic species (Site No. 17)

The values of the Shannon diversity index H ranged from 3.2 to 4.1. A lower degree of diversity was observed in riparian vegetation along the left-bank tributary of the Bebrava River (Sites 19 and 20) with formations made of grazed permanent grasslands, avenues with synanthropic species in balks, on arable land (Site No. 17), and fragments of forest stands (Site Nos. 13, 14 and 18).

Conversely, the highest degree of diversity was found to be in avenues with intergrowing forest species (e.g., Site Nos. 1, 3, 4) that occurred in the north-western part of the study area, mostly on twice-mown meadows (lowland hay meadows, *Arrhenatherion elatioris*, Koch, 1926). The other sites showed medium to medium-high biodiversity.

The defined criteria utilised to evaluate the importance of NFWV in our research is documented in Table 7.

Evaluation of the impact of environmental variables on types of vegetation

The variables tested (15 variables) amounted to 39.9% of the total variability in the specific data. The variables with a demonstrable impact were types of soil, minimum width, altitude, orientation to the cardinal points, geological substrate, and cover of E₂ and E₃ layers (Fig. 3).

For other variables (the area, length, maximum width, type of soil, depth of soil, land forms, skeletalness, connectivity, slope inclination), the probability of error was quite high. The variable soil type has the most variability in this case, i.e., 11.3%. Riparian vegetation (Site Nos. 2, 10, 19 and 20) and blackthorn hazel shrubbery (Site No. 15) had a positive correlation with the soil texture. Only these sites were covered with silty-

clayey-loam soil; the other sites were covered with silty-loam soil. In the lines mentioned wet habitats most commonly occurred.

Table 7. Defined criteria utilised in the evaluation of the landscape ecological and biotic importance of the NFWV

Criteria/site	1	2	3	4	5	6	7	8	9	10	11	12	13	14	15	16	17	18	19	20
H (% presence of terophytes)	4.1	10	1.8	3.1	0.7	1.2	3	4.5	7.8	7.9	7	5.6	0.8	1.6	1.1	4.1	1.8	1.7	1.3	2
V_r	13	20	15	20	22	26	22	19	23	22	26	26	3.4	11	12	8	25	13	15	9.1
H_{D1}	4	3.7	4.1	4	4	3.8	3.8	3.8	3.6	3.5	3.7	3.4	3.3	3.3	3.9	3.3	3.3	3.3	3.2	3.4
H_{D2}	2.5	2.3	2.4	2.5	2.2	2.2	2.2	1.5	2.2	2.1	2.3	2.2	2.3	2.2	2.1	2.1	2	2.1	2.1	1.7
P_k	48	28	41	45	36	48	35	30	33	37	37	40	34	29	40	30	46	20	29	27
P_m	167	124	147	130	143	132	156	123	144	140	128	128	110	128	132	153	106	107	149	140
S_{pa}	6	9	6	6	6	6	5	6	5	9	6	6	8	8	7	8	4	8	9	9

Explanations: H – hemeroby gradient, V_r – regional rarity, H_{D1} – Shannon index of diversity of vegetation communities, H_{D2} – Shannon index of diversity of animal communities, P_k – feeding potential, P_m – melliferous potential, S_{pa} – stability status

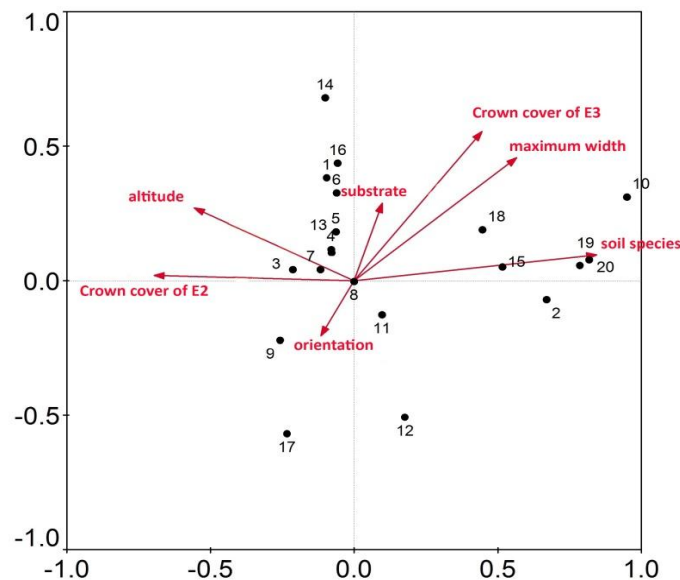


Figure 3. RDA ordination diagram (ordination of phytocoenological entries and environmental characteristics (AUT))

The cover of the E₃ layer represented 9.6% of the total variability of the data and positively correlated with Site No. 21. It was a fragment of oak-hornbeam forests, with an E₃ cover layer of 100% and dense- to-continuous crown cover. With an increasing cover of the E₃ layer, the cover of species in layers E₂ and E₁ decreases.

Another significant variable was the minimum width, which represented 5.2% of the total variability. Site No. 18, which was a fragment of oak-hornbeam forests and a strip with the greatest width of 47 m, had a positive correlation with a minimum width. The abundance of species in each layer increases with the increasing width of the lines evaluated. The other significant variables represented less than 5% of the total variability of the data.

Evaluation of the linear formations of NFWV based on the zoological survey

The zoological survey of the macroedaphone in twenty formations of NFWV found 15 taxa of *Opiliones*, 15 taxa of *Millipedes*, and 19 taxa of *Centipedes*). From afaunistic point of view, the most important are the finds of *Dicranolas mascabrum* and *Lamyces fulvicornis*, which are rare species, and *Egeanus convexus* and *Zacheus crista*, which are on the red list of rare and endangered species.

When evaluating the impact of environmental variables on the structure of communities of the selected groups of macroedaphone, the only significant variable was the “minimum width” structural feature (Fig.4).

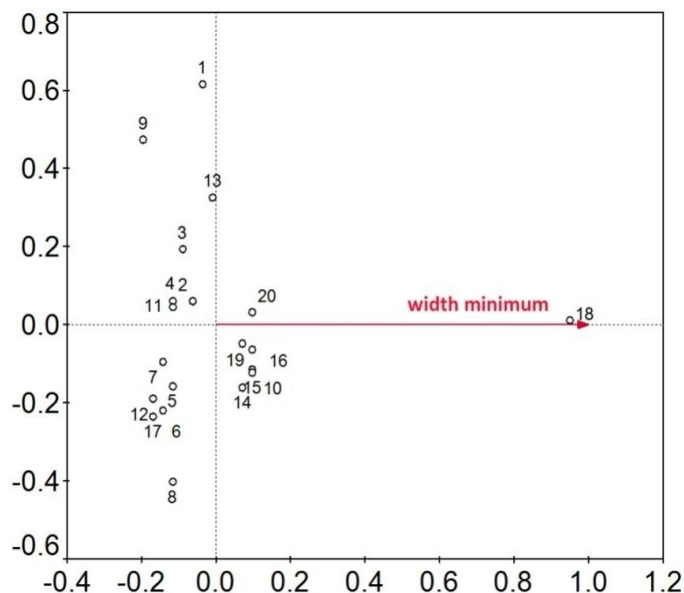


Figure 4. Evaluation of the impact of environmental variables on the structure of communities of the selected groups of macroedaphone (AUT)

The most favourable formations in the study area appear to be habitats with the greatest width.

We determined that there are 37 bird species in the NFWV formations observed. The area was dominated by species typical of an open landscape with the occurrence of NFWV and species typical of forest habitats or synanthropic bird species.

Based on the data on the presence of species, a classification of the habitats observed was made in terms of their significance and suitability as representatives of avifauna. Three main groups of habitats (categories) can be defined in the study area:

- Habitats of NFWV with water: in terms of birds, they are the most important and most valuable biocorridors. The highest number of bird species live here and in the greatest abundance (Site Nos. 2, 10, 19, 20).
- Habitats of NFWV that adjoin forests (or link forest stands) represent an intermediate stage between 1 and 3 (Site Nos. 4, 5, 6, 7, 13, 16 and 18).
- Habitats without water that do not adjoin forests: the lowest number of bird species live here and are in the lowest abundance as well (Sites Nos. 1, 3, 8, 11, 12, 14 and 17).

In the evaluation of the significance of the characteristics of the NFWV formations studied, the following significant environmental variables for bird communities were determined: connectivity (a link with another NFWV formation or forest habitat), the nature of the surrounding habitats, the E₂ cover layer, and orientation to the cardinal points (Fig. 5).

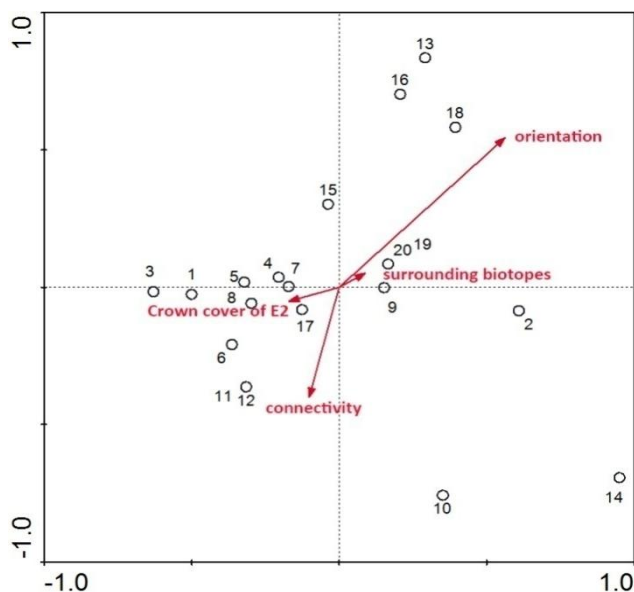


Figure 5. Evaluation of the significance of the environmental characteristics and features of the NFWV formations for bird communities

The formations observed have six (6) species of small mammals that are typical of submontane and alpine communities of shrubs and forests. The overall abundance of this group of animals was very low; therefore, the data on their occurrence were not subject to further analysis.

Evaluation of the landscape-ecological and biotic significance of the vegetation

An overall assessment of the landscape-ecological significance of the vegetation shows that most of the sites evaluated recorded low- to- medium values ranging from 2.0 to 2.5. These are mainly avenues, avenues with intergrowing species of the surrounding forest stands that occur in meadows with a high regional rarity index, a high diversity index, high values of melliferous potential and a moderate level of feeding potential. There are also fragments of forest stands and blackthorn hazel shrubbery with a high degree of hemeroby and stability.

The riparian vegetation had the highest V_{ke} values, ranging from 2.61 to 3.06 (Site Nos. 2, 10, 19 and 20). This concerns natural riparian vegetation, i.e., alder floodplain forests with a very high degree of stability, hemeroby and diversity, high values of melliferous potential and medium values of feeding potential.

Conversely, Site Nos. 7, 8, 9 and 17 had low-to-very low values of landscape-ecological significance (1.36-1.98). These are avenues and blackthorn shrubbery that mostly grow on arable land with an increased occurrence of synanthropic species, low diversity and stability.

The assessment of the biotic significance of the vegetation shows that the highest values of the significance of habitats (15-16b) were assigned to riparian vegetation (Site Nos. 2, 10 and 19), tree lines occurring in the vicinity of water areas that adjoin forests (Site Nos. 1 and 4) and blackthorn hazel shrubbery (Site No. 15). Site Nos. 7, 8, 9, 12 and 17 had the lowest values (10-12b). These are avenues along roads that are completely isolated or occurring in meadows and on arable land. The other sites, which were mostly avenues adjoining forest stands or another NFWV formation, belong to moderately significant habitats (13-14b), i.e., Site Nos. 3, 5, 6, 11, 13, 14, 16, 18 and 20. *Figure 6* shows the values of the landscape-ecological and biotic significance of each site.

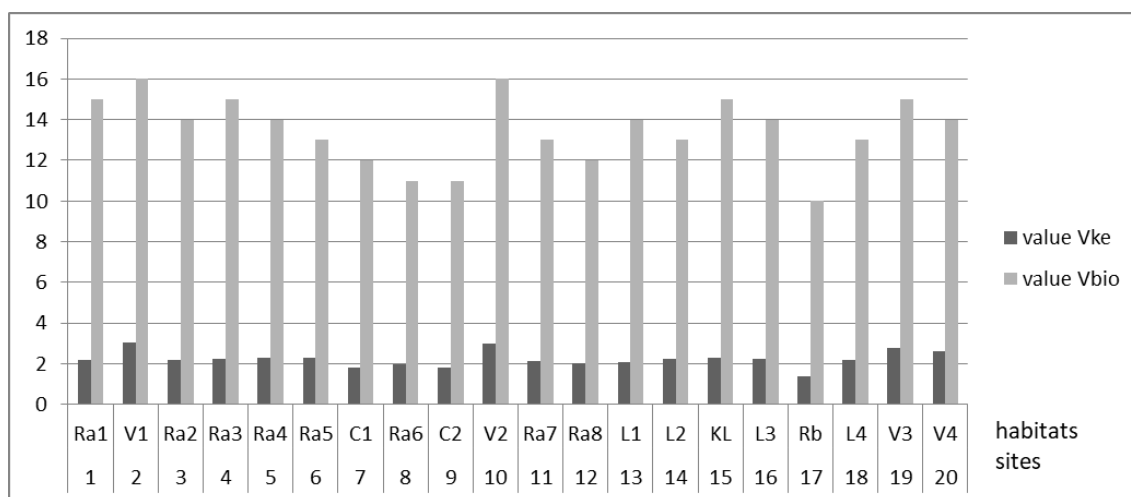


Figure 6. Landscape-ecological and biotic significance of the assessed sites (AUT)

The overall assessment of the landscape-ecological and biotic (significance of the habitat) importance of the linear formations examined reveals that the most valuable habitats include riparian vegetation - sub-mountain alder floodplain forests (Site Nos. 2, 10, 19 and 20), which function as a part of local biocorridors since they meet the criteria (quantitative and qualitative) to be designated as such. These valuable lines of extraordinary biodiversity have medium-to-high landscape-ecological significance, so the significance values are lower from the point of view of nature protection (the evaluations did not consider protection of habitats, only the protection of individual species). They are habitats with an extremely high degree of ecological stability, hemeroby, diversity, and feeding and melliferous potential, and with a relatively low number of regionally rare species. From a zoological perspective, they represent the most valuable habitats for members of avifauna (most abundantly inhabited by bird species) and higher vertebrates. These habitats are also important from the point of view of the group of macroedaphones.

The fragments of oak-hornbeam Carpathian forests (Site Nos. 13, 16 and 18) are essential in terms of their significance for erosion control and exhibited a medium-to-low value of landscape-ecological significance, with a low-to-very low value of significance for nature protection (again, the assessment did not take the protection of habitats into account); in terms of their biotic significance (significance of a habitat), they are also considered valuable. They occur on slopes on arable land, where the

erosive rate of soil removal (according to the erosion models) exceeds the limit values for a certain depth of soil. They are also valuable in terms of the fauna studied. They satisfy the quantitative criteria of a local biocorridor (except for Site No. 14) and can function as the elements of a local TSES as well as a part of the local biocorridors.

This habitat is linked with a forest ecosystem, which is surrounded by meadow communities with a high degree of ecological stability, and a diversity index as well as feeding or melliferous potential (Site No. 15). The site also fulfils the criteria of a local biocorridor and thus can be a part of a local TSES and a local biocorridor.

The other vegetation lines assessed, i.e., mostly regionally valuable tree-lines and blackthorn shrubbery, were assigned medium- to- low significance values. Some of the lines evaluated are linked to forest stands or other linear NFWV formations (Site Nos. 1, 4, 5, 6 and 7) surrounded by meadow cover.

Many of these lines occur on slopes and arable land, where the erosive soil removal rate (according to the erosion models) exceeds the limit values for a certain soil depth and are mostly isolated (Site Nos. 3, 8, 9, 11, 12 and 17).

However, they do not meet the qualitative criteria for the delineation of local corridors (a minimum length of less than 15 m). In a local TSES, they can function as interactive elements, which are necessary or important when performing an anti-erosion function.

Discussion

The structure of the landscape of the model territory is remarkable for its ecologically significant linear biotic elements with trees representing local TSES elements, i.e., biocorridors, interaction points, and anti-erosion elements. It is largely influenced by fruit growing and a viniculture, which was introduced into this territory from the region of Krupina. The whole Krupina region ranks among the most productive fruit-growing and viniculture regions due to its natural predispositions and favourable slope orientation (south, south-west or west) (Jančová, 1986). The most important fruit species include plums, pears, apples and especially cherries. So far, nine cherry, 14 plum, seven pear, and 18 apple varieties have been recorded in the territory (Vachold, 1998; Ištvanová, 2012). In the old orchards and avenues, species still grow which are typical of a wine-growing region, e.g., *Sorbus domestica*, *Morus nigra*, *Mespilus germanica* and *Castanea sativa*. Species such as *Castanea sativa* or *Mespilus germanica* reach their northern distribution limit in the former district of Zvolen and climb to an altitude of 450 m a. s. l. (Benčat', 1982). The occurrence of *Mespilus germanica* in the study areas was documented at an altitude of 530 m a. s. l. (Site No. 19). Many writers have pointed out the need to protect old fruit trees in the region because of their importance, status and functions (Jančová, 1998; Brodianska, 1999).

A bocage, a landscape with a network of tree lines which act as elements that fulfill a range of diverse functions, has been developing and changing over many centuries and is considered today as a sustainable landscape element; and thus a special system of management should be adopted in these cases (Matějka, 2010).

The range of changes in the properties and functions of linear formations should be discussed on the European and international levels. They should function as an impetus for preserving measures to identify rare or threatened parts of a landscape. This is a major task for scientists, policymakers, and planners (Baudry et al., 2000).

The determinations of the landscape-ecological and biotic (significance of a habitat) significance were based on a multi-criteria evaluation, which enables a prompt comparison of the results of individual habitats, although it may seem that it results in a simplification of the results, a loss of information, and neglect of the relations between the variables and the final value. Therefore, it is crucial to interpret the results even further (Špulerová, 2004). The topic of the multi-criteria evaluation of NFWV has been studied by many writers (Sláviková, 1987; Jurko, 1990; Halada, 1998; Špulerová, 2004, etc.). Landscape-ecological significance (V_{ke}) was defined by applying seven (7) criteria (Jurko, 1990), which reflect the values of the habitats concerned. It can be assumed that the feeding potential might have influenced the final values of V_{ke} . The same can be claimed regarding the melliferous potential. It is highly likely that stability is a very important factor affecting the final value V_{ke} .

Based on the aforementioned results and the conclusions reached by other writers, the biotic habitat significance V_{bio} was evaluated by applying the following criteria: diversity of plant and animal species, minimum width, surrounding habitats, layering, and connectivity with other formations. The diversity values for animal and plant species did not differ considerably within the study area, but in the case of a 3-point scale, they might have affect the final value V_{bio} . The vertical stratification, however, did not influence the final value as all the lines assessed included all the vegetation layers. It is highly likely that the results were most significantly affected by the minimum width, surrounding habitats, and connectivity with other formations.

In the study area, the incidence and cover of the vegetation species in the linear formations of NFWV were influenced not only by the environmental properties (soil type, altitude, orientation, geological substrate), but also by the data from the phytocoenological surveys such as the minimum length of the line and the E_2 and E_3 covers.

Several other writers have arrived at the same results (e.g., Royand Blois, 2008) and argue that the incidence of species, abundance and diversity of plant species of linear corridors increases with their width, overlapping of their main vegetation layer, and dependence on the soil properties. Špulerová (2004) claims that the richness and coverage of plant species depend on the type of soil, inclination and the cover of E_1 , E_2 , E_3 layers.

In the case of NFWV in the cadastre of Žibřitov, the key factors for the structure of the animal species inhabiting the territory are the width of the line and the connectivity and character of any adjacent habitats. This has been confirmed by RDA analyses of bird communities and selected groups of macroedaphones as well as field observations of higher vertebrates. Signs of the presence of these animals have been detected almost exclusively in formations which were linked with surrounding forest habitats or which created a network of NFWV formations.

Conclusions

NFWV is a very important element of a landscape. In almost every area-based territorial plan, in studies of TSES at different hierarchical levels, in rural development and village renewal plans, and in hydro-ecological plans, it is recommended to maintain and restore NFWV and the ecological stability of an agricultural landscape through the protection and restoration of the network of eco-stabilizing elements. When designing plantings or modifications to existing vegetation, it is essential to consider the functions of vegetation. Without that consideration, landscaping alterations would not be comprehensive.

The nature conservation, anti-erosion, biotic and landscape-ecological significance of vegetation has a vital impact on the overall ecological assessment of an area, which is particularly used for judging the ecological stability of a landscape. To achieve stability, the appropriate representation and distribution of cultural and natural communities is of great importance.

An assessment of the current ecological (health) condition of a landscape is mostly aimed at the elements of the primary and secondary landscape structure, which includes NFWV. In most cases, it involves a determination of the ecological stability, diversity, loads, balance, capacity and potential of vegetation. It also exploits interpretations of the formations of vegetation, their productive properties, functional characteristics and other special-purpose classifications of the biota. The interpretation is predominantly aimed at indicators such as the dynamics and degree of changes in the vegetation, the diversity of the vegetation, the vegetation cover, the degree of the synanthropy of the vegetation, the functional value of the vegetation, and the special-purpose characteristics of the vegetation, e.g., a determination of the importance of a particular function of the current vegetation, the classification of vegetation complexes in terms of their ability to perform certain functions on agricultural land, etc., the vertical and horizontal stability of the landscape, and the aesthetic effect as well as the perception of the landscape (Ružička, 2000). Such representations allow not only for an assessment of the current ecological state of a landscape, but also provide important arguments for the protection of the NFWV elements, which perform significant functions in the landscape and directly influence its potential.

These evaluations of vegetation, however, are not present in the methodologies of the terrestrial systems of ecological stability. Therefore, we decided to address this issue, so the output of the study presented is a proposal for monitoring the qualitative and quantitative properties of NFWV in the field mapping for TSES projects, as well as a proposal for the interpretations of the structural, ecological-habitat characteristics and special-purpose properties of vegetation, which could be further used in the projecting of TSES.

The results of the research, mapping and evaluation of the linear formations of NFWV can be summarized as follows:

- Riparian vegetation in alder floodplain forests had high values of landscape-ecological and biotic significance in the model territory. They perform a full range of hydrological, climatic and refugial functions along with water management functions. Furthermore, fragments of Carpathian oak-hornbeam forests, blackthorn hazel shrubbery, blackthorn shrubbery and tree lines function as important ecostabilising elements in the countryside.
- The diversity of the structure and habitats of the landscape in the area of the Štiavnické vrchy mountains is affected by changes in land use caused by agriculture. The decline in the traditional uses and management of the land has significantly altered the physiognomic and ecological character of the landscape's structure (Jančová, 1998).
- In the model territory of the cadastre of Žibritov, which is a small picturesque village situated in a natural environment, some changes have taken place, although they are not dramatic ones. Although a network of regionally rare vegetation lines has been preserved here, they require special attention. They include tree lines with the presence of old fruit trees, which are the most important habitats for nature conservation. These habitats typically have a high

diversity of species, perform compensatory (counterbalance the negative impact of human activity), utility and anti-erosion functions, and serve as a habitat for various plant and animal species by facilitating their migration and distribution. They provide shelter, a resting place and sources of food.

The results of the particular research demonstrate that the most valuable habitats include tree lines with mature fruit trees and exotic tree species. However, these habitats are threatened by the decline of older individuals; their health condition is affected by the occurrence of mistletoe; incidents of chlorosis and defoliation were detected. A lot of older varieties of tree species have properties superior to newer varieties (resistance to frost, animal pests or fungi). Fruit trees are beneficial elements. Moreover, they also fulfil aesthetic and recreational functions (the colour of their blossoms in the spring, the colour of their fruit in the autumn, relaxation). These functions, however, may pose problems because a habitat also provides a refuge for endangered plant and animal species. Unfortunately, many of the aforementioned old fruit species and rare varieties are withered, invaded by mistletoe, and are slowly dying off. Therefore, the implementation of a proposal for management and protection procedures might promote the cultural and ecological legacy of these rare tree lines.

According to the information available, there is a programme in progress called "Saving and preserving the gene pool of old and regional tree varieties in the region of Krupina". Therefore, we suggest including the territory studied in this programme, conducting a detailed inventory survey, and mapping the old varieties of fruit trees. Also, unwanted elements should be isolated, and we propose further management measures and monitoring.

Thorough research of NFWV and the consequently reliable interpretations of vegetation are a prerequisite for a highly successful development of TSES projects and other landscape-ecological documents and materials.

Acknowledgements. This paper was supported by the VEGA scientific grant agency, project No. 1/0096/16 and the KEGA cultural and educational grant agency, project No. 13TUZ-4/2016.

REFERENCES

- [1] Arnold, G. W. (1983): The influence of ditch and hedgerow structure, length of hedgerows, and area of woodland and garden on bird numbers on farmland. – *Journal of Applied Ecology* 20: 731–750.
- [2] Baudry, J. (1988): Hedgerows and Hedgerow Networks as Wildlife Habitat in Agricultural Landscapes. – In: Park, J. R. (ed.) *Environmental Management in Agriculture*. Belhaven Press, London.
- [3] Baudry, J., Bunce, R. G. H., Burel, F. (2000): Hedgerows: An international perspective on their origin, function and management. – *Journal of Environmental Management* 60: 7–22.
- [4] Benčat', F. (1982): Atlas rozšírenia cudzokrajných drevín na Slovensku a rajonizácia ich pestovania. Textová a mapová časť. – VEDA, Slovak Academy of Sciences, Bratislava.
- [5] Bennett, A. F. (1999): Linkages in the Landscape: The Role of Corridors and Connectivity in Wildlife Conservation. – IUCN, Gland, Switzerland and Cambridge.
- [6] Brodianska, M. (1999): Krajinný ráz a ekozozologický význam podhoria CHKO Štiavnické vrchy v k.ú. Krupina. – Ph.D thesis. Technical University in Zvolen, Zvolen.

- [7] Bulíř, P. (1981): Rekonstrukce a zakládání rozptýlené zeleně v zemědělské krajině. – In: Štěpán, J. (ed.) *Ekologie krajiny. Acta ecologica naturae ac regionis*. Spoluvydavatel Terplan - Státní ústav pro územní plánování. Ministerstvo výstavby a techniky ČSR, Praha.
- [8] Bulíř, P. (1987): Inventarizace, evidence a pasportizace rozptýlené zeleně. – OBIS Výzkumný a šlechtitelský ústav okrasného zahradnictví, Průhonice.
- [9] Burel, F. (1996): Hedgerows and their role in agricultural landscapes. – *Critical Review in Plant Sciences* 15:169–190.
- [10] Cameron, R. A. D., Down, K., Pannett, D. J. (1980): Historical and environmental influences on hedgerow snail faunas. – *Biological Journal of the Linnean Society* 13: 75–87.
- [11] Čurlík, J., Šály, R. (2002): Typy pôd. – In: Miklós, L., Hrnčiarová, T. et al. (eds.) *Atlas krajiny SR. MZP SR, Bratislava, Esprit, s.r.o., Banská Štiavnica*.
- [12] Delattre, P., De Sousa, B., Fichet-Calvet, E., Qu'ér'e, J. P., Giraudoux, P. (1999): Vole outbreaks in a landscape context: evidence from a 6-year study of *Microtus arvalis*. – *Landscape Ecology* 14: 401–412.
- [13] Forman, R. T. T., Baudry, J. (1984): Hedgerows and hedgerow networks in landscape ecology. – *Environmental Management* 8: 495–510.
- [14] Forman, R. T. T., Godron, M. (1986): *Landscape Ecology*. – John Wiley, New York.
- [15] Green, R. E., Osborne, P. E., Sears, E. J. (1994): The distribution of passerine birds in hedgerows during the breeding season in relation to characteristics of the hedgerow and adjacent farmland. – *Journal of Applied Ecology* 31: 677–692.
- [16] Halada, L. (1998): *Krajinnoekologické hodnotenie vegetácie*. – Ph.D Thesis. Institute of Landscape Ecology, Slovak Academy of Sciences, Nitra.
- [17] Hinsley, S. A., Bellamy, P. E. (2000): The influence of hedge structure, management and landscape context on the value of hedgerows to birds: A review. – *Journal of Environmental Management* 60: 33–49.
- [18] Hinsley, S. A., Bellamy, P. E., Sparks, T. H., Rothery, P. (1999): A Field Comparison of Habitat Characteristics and Diversity of Birds, Butterflies and Plants between Game and Nongame Areas. – In: Firbank, L. G. (ed.) *Lowland Game Shooting Study*. ITE, Cumbria.
- [19] Hobbs, R. J. (1992): The role of corridors in conservation: solution or bandwagon? – *Trends in Ecology and Evolution* 7: 389–392.
- [20] Hudgens, B. R., Haddad, N. M. (2003): Predicting which species will benefit from corridors in fragmented landscapes from population growth model. – *The American Naturalist* 161(5): 808–820.
- [21] Ištvanová, Z. (2012): *Význam ovocných drevín v k.ú. Žibritov pre biodiverzitu krajiny a zachovanie starých a krajových odrôd*. – Ph. D Thesis. Technical University in Zvolen, Zvolen.
- [22] Jančová, G. (1986): Zachovajme krajinný charakter podhoria Štiavnických vrchoch. – *Chránené územia Slovenska* 7: 46–48.
- [23] Jančová G. (1998): Krajinná štruktúra CHKO Štiavnické vrchy v katastrálnom území Krupina a Žibritov. – *Enviromagazín* 3(1): 14–15.
- [24] Johnson, R. J., Beck, M. M. (1988): Influences of shelterbelts on wildlife management and biology. – *Agriculture, Ecosystems and Environment* 22/23: 301–335.
- [25] Jurko, A. (1990): *Ekologické a socioekonomické hodnotenie vegetácie*. – *Príroda*, Bratislava.
- [26] Löw, J., et al. (1995): Rukověť projektanta místního územního system ekologické stability. – *Veronika*, Brno.
- [27] MacDonald, D. W., Johnson, P. J. (1995): The relationship between bird distribution and the botanical and structural characteristics of hedges. – *Journal of Applied Ecology* 32: 492–505.

- [28] Machovec, J. (1994): Rozptýlená zeleň v krajine. – Vysoká škola zemědělská v Brně, Brno.
- [29] Mann, C. C., Plummer, M. L. (1995): Are wildlife corridors the right path? – *Science* 270: 1428–1430.
- [30] Mareček, J. (2005): Krajinářská architektura venkovských sídel. – ČZU, Praha.
- [31] Matějka, K. (2010): Ecotonal elements with woody species stand in the Bohemian forest landscape, their occurrence and classification. – *Studia Oecologica* 4: 15–28.
- [32] Miklós, L., Diviaková, A., Izakovičová, Z. (2011): Ekologické siete a územné systémy ekologickej stability. – Technical University in Zvolen, Zvolen.
- [33] Mind'áš, J., Škvarenina, J. (2002): Výskyt hmieľ. – In: Miklós, L., Hrnčiarová T. et al. (eds.) *Atlas krajiny SR. MŽP SR, Bratislava, Esprit, s.r.o., Banská Štiavnica.*
- [34] Opdam, P., Foppen, R., Reijnen, R., Schotman, A. (1995): The landscape ecological approach in bird conservation: integrating the metapopulation concept into spatial planning. – *Ibis* 137: 139–146.
- [35] Osborne, P. (1984): Bird numbers and habitat characteristics in farmland hedgerows. – *Journal of Applied Ecology* 21: 63–82.
- [36] Rosenberg, D. K., Noon, B. R., Meslow, E. C. (1997): Biological corridors: form, function and efficacy. – *BioScience* 47: 677–687.
- [37] Roy, V., Blois, S. (2008): Evaluating hedgerow corridors for the conservation of native forest herb diversity. – *Biological Conservation* 141: 298–307.
- [38] Ružička, M. (2000): Krajinnoekologické plánovanie LANDEP. (Systémový prístup v krajinnej ekológii). – *Biosféra, Zv. 1, Bratislava.*
- [39] Saunders, D. A., Hobbs, R. J. (eds.) (1991): *Nature Conservation 2: The Role of Corridors.* – Surrey Beatty and Sons, London.
- [40] Shalaway, S. D. (1985): Fencerow management for nesting birds in Michigan. – *Wildlife Society Bulletin* 13: 302–306.
- [41] Sláviková, D. (1987): Ochrana rozptýlenej zelene v krajine. – ÚV Slovenského zväzu ochrancov prírody a krajiny, Bratislava.
- [42] Smith, D., Hellmund, P. C. (ed.) (1993): *Ecology of Greenways, Design and Function of Linear Conservation Areas.* – University of Minnesota Press, USA.
- [43] Stašiov, S. (2006): Ekológia pôdnych organizmov (metódy výskumu mezo- až megazooedafónu). – Technical University in Zvolen, Zvolen.
- [44] Šimo, E., Zaľko, M. (2002): Typy režimu odtoku. – In: Miklós, L., Hrnčiarová, T. et al. (eds.) *Atlas krajiny SR. MŽP SR, Bratislava, Esprit s.r.o., Banská Štiavnica.*
- [45] Špulerová, J. (2004): Hodnotenie nelesnej drevinno-bylinnej vegetácie pre potreby krajinnoekologického plánovania. – PhD Thesis. Institute of Landscape Ecology, Slovak Academy of Sciences, Bratislava.
- [46] Ter Braak, C. J. F., Šmilauer, P. (1998): *CANOCO reference manual and users guide to CANOCO for Windows. Software for canonical community ordination (version 4).* – Centre of Biometry, Wageningen.
- [47] Vachold, J. (1998): *Správa o stave genofondu starých domácich odrôd ovocia.* – Manuscript, Banská Štiavnica.

PHYSIOLOGICAL, BIOCHEMICAL AND PHYLOGENETIC CHARACTERIZATION OF EXTREMELY HALOPHILIC BACTERIA ISOLATED FROM KHEWRA MINE, PAKISTAN

LEENA, M. C. – AAMER, A. S. – ABDUL, H. – FARIHA, H.*

*Department of Microbiology, Quaid-i-Azam University
Islamabad 44000, Pakistan*

**Corresponding author*

e-mail: farihasan@yahoo.com; phone: +92-51-9064-3065

(Received 3rd Aug 2017; accepted 30th Nov 2017)

Abstract. Microflora entrapped in the salt deposits of Khewra salt mine, Pakistan has adapted to extreme conditions and nutrient scarcity to survive. Due to assumption that halophilic archaea dominate hypersaline environments, bacteria have often remained unexplored. The reports on extremely halophilic bacteria indigenous to Khewra mine are quite limited resulting in largely unexplored biodiversity of the salt mine. Here we attempted to fill that gap by isolating eight halophilic bacteria, out of which four extremely halophilic bacteria were selected for physiological, biochemical and molecular characterization. The phylogenetic characterization inferred through comparative partial 16S rRNA sequences identified these strains as HSL1-*Oceanobacillus onchorhynchi* subsp. *Incaldanensis*, HSL4-*Staphylococcus lentus*, HSL6-*Bacillus endophyticus* and HSL7-*Bacillus aquimaris*. These isolates could tolerate a wide range of temperatures (15–45°C), pH (5–9) and survived up to 16% NaCl concentration. This tolerance is due to the stability of their enzymes. Enzyme assays revealed a substantial amount of production of protease, amylase, lipase, xylanase, urease, gelatinase, cellulose, and DNase. Conclusively, isolation and characterization of the extremely halophilic bacteria from Khewra mine indicated their important ecological role and contribution towards the microbial diversity. The ability to produce extreme-enzymes also established the potential of the isolates as valuable resources for significant biotechnological applications.

Keywords: *halophiles, halophilic bacteria, halo-enzymes, phylogeny, hypersaline environments*

Introduction

Extremophiles are those organisms that can survive in intense environments. Such environments include high and low extremes of temperature, pH, pressure, nutrients, water content, salt content, heavy metal toxicity, organic solvent toxicity, and radiations. Prokaryotes usually dominate the regions concentrated with salts. Habitats such as soda lakes, brines and coastal lagoons are inhabited by fewer life forms but have a significant presence of halophiles. The careful study of halophiles evolutionary patterns also helps to understand, the evolution of the environment.

Halophiles are classified as slightly (0.2–5%), moderately (5–16%) and extremely (16–30%) halophilic species depending upon their growth response to NaCl concentration (Kushner, 1978). Halotolerant bacteria are non-halophilic microorganisms that can tolerate high salt concentrations, i.e., above 15% of NaCl, and can also survive without NaCl (Kushner, 1985; Oren, 2008). Halophilic adaptation to high salinity and in some cases extreme temperatures and radiation is due to the evolution of their biochemical and physiological functions. The protein chemistry of halo-enzymes enables them to exhibit unique attributes, which equip them to thrive in variable habitats (Burg, 2003). Extremophiles selectively thrive under harsh environmental conditions by developing unique adaptive strategies including synthesis of bioactive compounds such

as compatible solutes, bacteriorhodopsins, extreme-enzymes, and bio-surfactants (Donio et al., 2013). In accordance with BCC reports of 2011, the enzyme industry, especially when it comes to commercial programs, experienced an increase of US\$ 3.3 million from the previous year. This kind of demand from the customers motivates the search for enzymes that can withstand the extreme hostile conditions of the industrial procedures. Currently, the efficiency of most of the enzymes decreases when met with the extreme temperature and acidity (Cojoc et al., 2009; Kakhki et al., 2011). Halophiles have been continuously found with an unrivaled capacity to synthesize bioactive secondary metabolites with potent biological activities, which establish their remarkable potential in commercial applications (Vahed et al., 2011).

Pakistan is unique in its biodiversity and blessed with diverse extreme environments. Remote areas of Pakistan are endowed with many thermal springs, salt mines, and many glacial areas. Khewra salt mine, Pakistan is considered as the largest salt mine in the world based on area, second only to Wieliczka Salt mine in Poland (Sameeni, 2009). Geologists placed the age of Khewra mine to 600 million years. Paleontologists and stratigraphic constraints suggested that the tectonic movements due to conventional currents generated by the core of the earth commenced the formation of rift basins along the middle eastern side of Gondwanaland in the latest Precambrian. The continental drift theory suggests that Indo-Pak made its incredible journey away from Antarctica towards Asia approximately 180 million years ago, covering a distance of about 5500 miles (Redfern, 2001). During this time, marine deposits swept across the Middle East in the late lower and middle Cambrian period (Husseini and Husseini, 1990). Consequently, evaporates started precipitating salt; forming salt deposits in the form of Khewra salt mine. However, the microflora of these areas is yet to be uncovered and those species, which have been isolated, are yet to be validated by the ecological ministry of Pakistan. A few reports have been presented on halophilic diversity from salt ranges of Khewra, which were mostly focused on the isolation of moderately halophilic bacteria such as *Halomonas magadiensis*, *Virgibacillus* species (Akhtar et al., 2008).

Objective

Interest in the extremophile diversity has grown over the last decade as it may support the theory that such extreme conditions have been present on the primitive earth. A similar logical argument underlies the search for life forms outside the planet earth (Akhtar et al., 2008). The chronological history of biodiversity of microbes entrapped in the rock salt deposits of Khewra mine over a period of millions of years suggested them to have conserved DNA bases as of their ancestors. It is generally assumed that hypersaline environments are dominated by halophilic archaea, whereas bacteria have often been considered not relevant to high saline environments and hence ignored. A diversity of halophilic bacteria could enlighten us about their role in the maintenance of such high saline environments. Also, the adaptations of halophilic bacteria to harsh conditions can help us understand about their resemblance with the organisms which were prevalent on the primitive earth. These interesting questions clearly justify the motivation of current exploration of isolating and characterizing extremely halophilic bacteria from the ancient rock salt deposits of Khewra salt mine and screening their highly stable enzymes for potential commercial applications.

Hence, this presentation reports on novel studies performed on extremely halophilic bacteria from the rock salt deposits, and saline soils of Khewra. These studies include a

screening of bacteria for valuable commercial halo-enzymes, development of growth patterns of bacteria with respect to different physiological parameters, and to track the evolutionary pattern of these bacteria based on their phylogenetic resemblance with their ancestors.

Materials and methods

Site description

In South Asia, the Khewra salt mines are the oldest salt mines situated at the foothills of the Salt Range about 288 m above the sea level from where salt has been mined since 320 BC. The crystals are colored light pink with variations of white and red famously referred to as Himalayan pink salt. It is considered to be 98% pure. Salt and brine samples were collected from the Khewra salt mine. Location coordinates were noted by GPS tracker as 32°39' 0"N, 73°1' 0"E (Fig. 1). The pH (measured by pH strips) and temperature (measured by a laboratory thermometer) of the brine were first noted at the sampling site, and later pH was measured under laboratory conditions by a pH meter (Sartorius professional meter PP15). The pH of the brine was 7.1 and temperature was 25°C at the time of sampling. The salinity of brine was measured by using a hand-held refractometer as 30‰, and the Total Dissolved Solids were calculated as 32%.

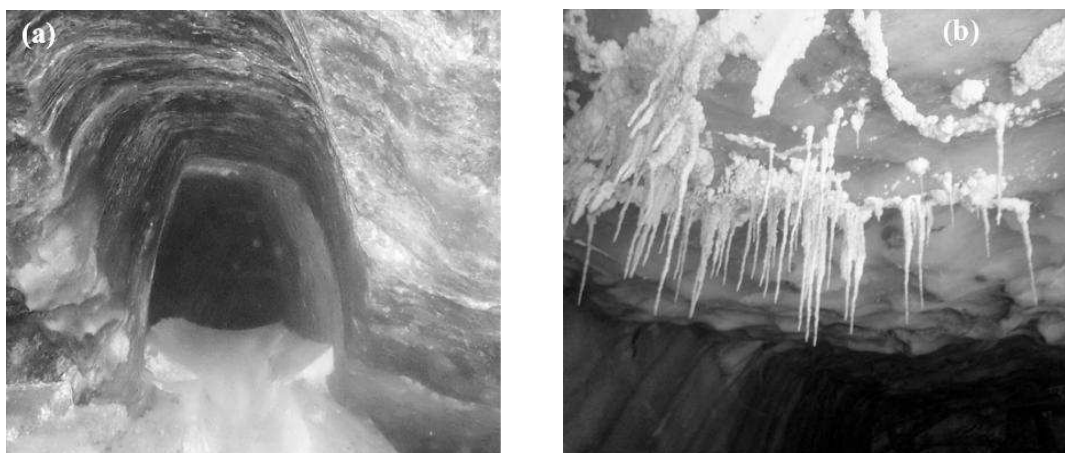


Figure 1. Selected photos from Khewra salt mine. a) Khewra's red Himalayan rock salt. b) Salt deposits in Khewra Mine

Analysis of brine obtained from Khewra mine

The analysis of sulfates, chlorides, phosphates and bicarbonates in brine was done using Spectroquant (Pharo 100 Spectroquant® Merck, Germany) using respective protocols from Standard Methods for the Examination of Water and Wastewater by (APHA), American Public Health Association (Table 2).

Isolation of extremely halophilic bacteria

Isolation was done from both brine and salt samples using serial dilution method up to 15 folds of dilution. The samples were inoculated on nutrient agar plates with 3% NaCl concentration using Spread plate method. After 48–72 h of incubation, individual

colonies were picked out and purified using three rounds of streaking on a nutrient agar plate.

Media and culturing

Most of the reagents and chemicals used in this study were of analytical grade and obtained from BDH (Dorset, England), Sigma- Aldrich (St. Louis, MA, USA), E Merck (Darmstadt, Germany), Difco Laboratories (Detroit, USA), AVACADO research chemicals Ltd (London, UK). Eight distinct colonies names as (HSL1, HSL2, HSL3, HSL4, HSL5, HSL6, HSL7, and HSL8) from salt and water samples collected from Khewra salt mine, were isolated for the present study. The bacterial cultures were maintained on a nutrient agar medium, containing 16% NaCl. Extremely halophilic were screened out by sub-culturing on the nutrient agar plates with varying salt concentrations, ranging from 3 to 22% and incubated for 24–72 h. Out of eight, four extreme halophilic strains (HSL1, HSL4, HSL6, and HSL7) that grew above 16% NaCl concentration were selected for further research.

Morphological and biochemical studies of halophilic strains

The bacterial colonies were distinguished on the basis of size, pigmentation, form, margin and elevation. These were also characterized on the basis of Gram's staining, cell morphology, and motility under a microscope. Four selected bacterial strains were characterized biochemically according to Bergey's Manual of Determinative Bacteriology by Holt et al., 1994. Following basic tests were performed: Triple sugar iron (TSI) test, Catalase test, SIM (Sulfide, Indole, Motility) test, H₂S test, Citrate utilization test, Oxidase test, and Urease test.

Physiological properties of halophilic bacteria

Growth optimization was carried out at various temperatures and pH, i.e., 15–50°C and pH 4.0–9.0, respectively. The growth was observed both qualitatively (nutrient agar plates) and quantitatively (nutrient broth) over the period of seven days. By taking OD at 650 nm at regular time intervals, we monitored the growth at regular time intervals quantitatively using Agilent 8453 UV-visible Spectrophotometer. All the optimization experiments were done in triplicates, and the average value of each reading was plotted for accuracy with error bars indicating standard deviation. All data is presented as a standard error of the mean. The growth patterns of strains were also tested on varying salinity by growing them on nutrient agar plates having various salt ranges (0–22%). Also, the growth of strains on salts other than NaCl was studied by growing them on plates of nutrient agar supplemented with 3% of each salt for 24–48 h. The salts used were KCl, CaCO₃, NH₄Cl, MgSO₄, and BaCl₂.

Screening of enzyme activity

To establish the potential of these strains in industrial applications, these strains were screened for the production of amylase, protease, lipase, DNase, cellulase, and gelatinase. Nutrient agar plates containing 1.5% of starch, casein, tween 80 and cellulose as substrates were separately streaked with halophilic strains to determine the production of amylase, protease, and lipase and cellulase activity respectively. DNase agar medium was used for DNase test. Zones of hydrolysis around colonies indicated a

positive activity of DNase and lipase enzymes. Iodine solution (2%) was poured on starch plates for 5 min. Clear halos indicated positive results. Cellulose plates were first stained with 0.5% Congo red for 5 min and then de-stained with 1M NaCl. Clear halos indicated cellulase activity. Protease activity was determined by pouring glacial acetic acid on the streaked plates followed by the production of clear zones. For gelatinase production, strains were inoculated in media having following composition (g/L): peptone 5, beef extract 3, gelatin 120, NaCl 5. Liquefaction of gelatin indicated a positive result.

Enzyme assays

To further understand the specific activity of amylase and protease, enzyme assays were performed. The proteolytic activity was measured by following the technique developed by Kunitz (1965) where production of extracellular protease can be determined by observing the split contents of casein dissolved in 5% TCA solution. Controls were prepared in the same way except that 2.25 ml TCA was added before incubation. The specific activity of protease was determined by measuring the amount of tyrosine released per ml/min under the conditions of the assay at OD₂₈₀ nm. Lipase assay was performed as described by Lesuisse et al. (1993) and the specific activity was taken at OD₄₂₀ nm. Amylase assay was performed as described by Bernfeld (1955) with specific activity measured at OD₅₄₀ nm of glucose released per ml/min under the assay conditions.

Genomic DNA extraction and PCR

For molecular characterization, first, the genomic DNA was extracted using ethanol precipitation method (Delbes et al., 2000), with slight modification. The genomic DNA is confirmed by gel electrophoresis by running it on 1% gel in 0.5 X TBE buffer. Gel images were observed by Bio-Rad gel documentation system. Using the universal primers 8F-5'AGAGTTTGATCCTGGCTCAG and 1492R-5'AAGTCGTAACAAGGTAACC, 1500bp regions of 16S rRNA gene of the extracted DNA was amplified. The PCR products were then sent to Macrogen, Inc., Seoul, Korea for sequencing.

Phylogenetic analysis using 16S rRNA

Sequenced 16S rRNA genes data was assembled manually (<http://www.ncbi.nlm.nih.gov/blast/bl2seq/wblast2.cgi>) utilizing Blast 2 sequences (Tatusova and Madden, 1999). To determine sequence of a clone, the sequences of both the strands were separately compiled and then aligned to each other with their complementary region. A consensus sequence was originated by aligning multiple sequences of every clone belonging to the same component of individual isolates by using ClustalW (Thompson et al., 1994). The sequences of genomic components were aligned in ClustalW Sequence Alignment program using IUB matrix for DNA alignments in the Molecular Evolutionary Genetics Analysis Program (MEGA) version 6. Neighbor-Joining (NJ) analysis was carried out using Maximum Composite-likelihood model with uniform rates among the sites; the 1000 bootstrap replicates were used to evaluate the significance of generated tree.

Results

Morphological and biochemical characterization

Four extreme halophilic strains (HSL1, HSL4, HSL6, and HSL7) were characterized. Based on colony morphology, Gram staining and Biochemical tests, following basic identification were achieved. HSL1 strain was gram-negative rods with creamy, waxy colony and hard texture. This colony was flat with undulated margins. HSL1 strain was motile. It showed positive results for catalase and oxidase and negative results for urease and indole production. This strain was able to ferment glucose. HSL4 strain was gram-positive cocci in the form of tetrads having whitish, smooth and entire colony with slightly raised surface and round margins. This strain was motile, catalase positive, oxidase, urease, and indole negative. It was able to ferment lactose. HSL6 strain was gram-positive rods displaying beige color colony having irregular, lobate margins and hard, flat surface. This strain was non-motile, indole, catalase and urease negative. It was oxidase positive and able to ferment glucose. HSL7 strain is gram-positive rods having smooth, orange colored, having round margins. The colony displayed convex elevation. This strain was motile, catalase positive, urease, oxidase and indole negative and able to ferment lactose (*Table 1*).

Table 1. Characteristics of the sampling site

Characteristics	Isolates			
	HSL1	HSL4	HSL6	HSL7
Form	Irregular, waxy, hard	Entire, smooth, mucoid	Irregular, hard	Smooth, mucoid, hard
Elevations	Flat	Slightly raised	Flat	Convex
Margins	Undulate	Mucoid	Lobate	Round
Cell shape	Rods	Cocci	Rods	Rods
Gram stain	Negative	Positive	Positive	Positive
Catalase	+	+	-	+
Oxidase	+	-	+	-
Motility	+	+	-	+
Citrate utilization	-	-	+	-
Urease test	-	-	-	-
Lactose fermentation	+	+	-	+
Protease	-	+	-	+
Amylase	-	-	+	+
DNase	-	-	-	+
Gelatinase	-	+	-	-
Lipase	-	-	-	-
Cellulase	-	-	-	-

Qualitative screening for enzyme activity

HSL1 did not hydrolyze starch, gelatin, cellulose, and casein and also shows negative results for and Tween 80 and DNase. HSL4 did not hydrolyze starch (amylase), gelatin

(gelatinase) and is negative for DNase and Tween 80 (lipase). But it showed positive results for (protease) casein and (cellulase) cellulose hydrolysis. HSL6 showed negative results for gelatin, casein and cellulose hydrolysis and is also negative for DNase and Tween 80. It only showed a positive result for amylase production. HSL7 displayed positive results for amylase, protease, DNase, but showed negative results for Tween 80, cellulose and gelatin hydrolysis (*Table 1*).

Physiological analysis of growth of halophilic bacteria

HSL4 showed maximum tolerance at 22% NaCl followed by HSL1, HSL7, and HSL6 at 16% salt concentration. Isolate HSL6, however, showed slight growth at 16% and the rest of the strains showed no growth above 16% NaCl. The strains HSL1, HSL4, HSL6, and HSL7, showed significant growth on the salts of chlorides, sulfates, and carbonates displaying their tolerance for all of these salts, besides NaCl (*Table 2*).

Table 2. Morphological and biochemical characteristics of isolated strains along with physicochemical features of sampling site and samples

	Samples	Temperature	pH	Salinity (refractometer)
Khewra salt mine (32°39'0"N,73°1' 0"E)	Brine, salt	25°C	7.2	30%
Concentration of salts in brine (mg/l)	Sulfates	Chlorides	Bicarbonates	Phosphates
	9400	2202.42	200	0.15

Optimization of growth

Effect of pH on growth of bacteria

Quantitative and qualitative analysis of the effect of pH on growth of strains after 24 h, depicted that isolate HSL1 tolerated and survived at pH ranging from 5 to 9 but showed maximum growth at pH 7. Isolate HSL4 tolerated pH ranging from 5–9 but showed maximum growth at pH 7. Isolate HSL6 tolerated at pH 5–9 but showed maximum growth at pH 6. Isolate HSL7 showed maximum growth at pH 8 but were not able to tolerate pH 5–9 (*Fig. 2*).

Effect of temperature on growth of bacteria

Quantitative and qualitative observations of the growth of strains at different temperatures were performed for 4 days. Isolate HSL1 can tolerate and survive at 15–45°C but showed maximum activity at 35°C. Significant growth was observed at 15°C and 45°C after 2–3 days. Isolate HSL4 survived at temperature 15–45°C but showed maximum activity at 35°C. Significant growth at all temperatures can be observed after 2–3 days. Isolate HSL6 survived at temperature 15–50°C but showed maximum activity at 25°C. A significant amount of growth at all temperatures can be observed after 2–3 days but growth decreases at 50°C after 3 days. Isolate HSL7 showed maximum growth at the temperature range of 15 to 45°C but showed maximum activity at 35°C. Significant growth at all temperatures was observed after 2–3 days (*Fig. 3*).

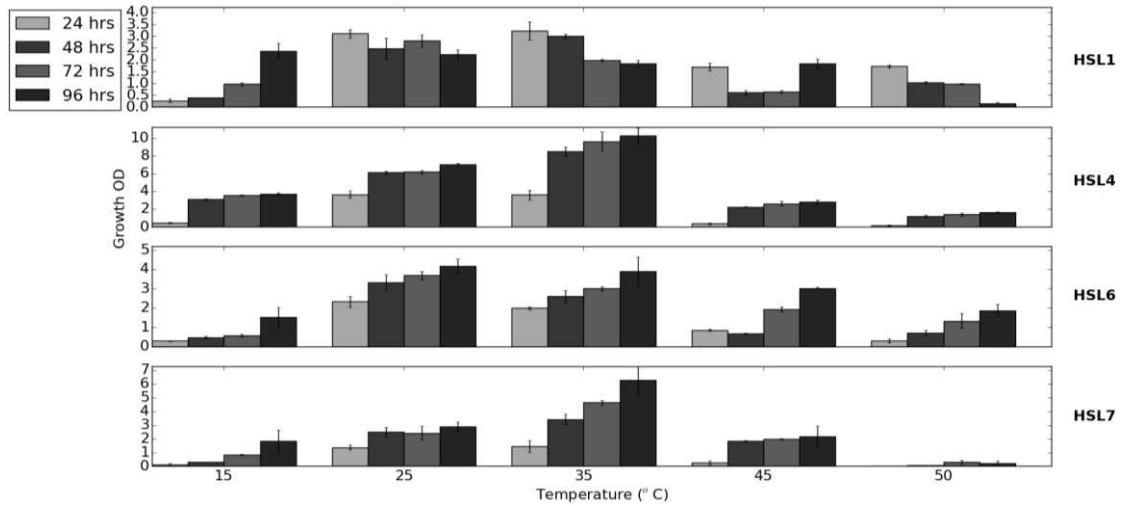


Figure 2. Effect of pH on growth of bacteria

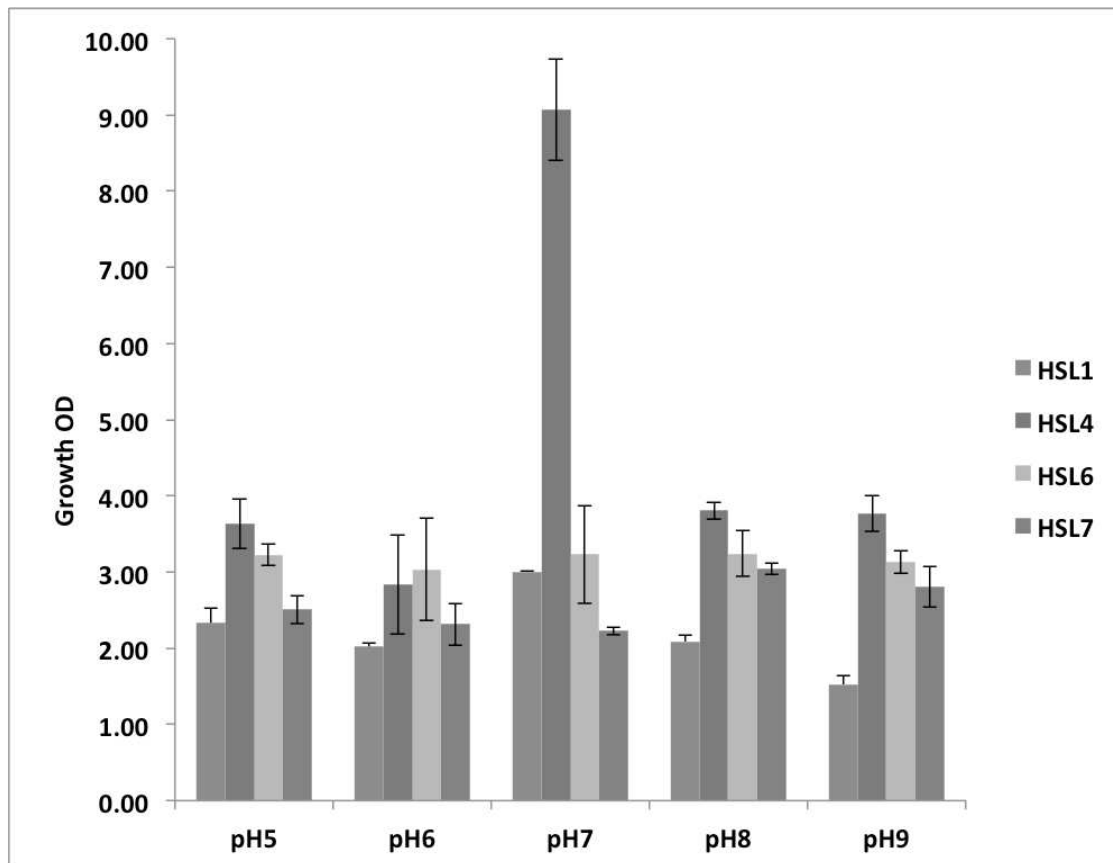


Figure 3. Effect of temperature on growth of bacteria

Quantitative analysis of industrially important enzymes

Enzyme assays for lipase, protease and amylase were performed to quantitatively measure enzyme activity produced by extremely halophilic bacteria.

Lipase

As no clear zone was observed around the cultures grown on a media supplemented with Tween 80, it was assumed that the isolates did not hydrolyze Tween 80. It is then also confirmed by the quantitative assay. Isolates HSL1, HSL4, HSL6, and HSL7 did not produce lipase enzyme.

Protease

Isolates HSL4 and HSL7 showed positive results for the production of protease. The specific activity of the enzyme measured by determining the concentration of tyrosine released per ml per min under the assay conditions. It was observed that the production of protease increased with time for three days (Fig. 4a).

Amylase

The positive results for amylase production were shown by isolate HSL6 and HSL7 qualitatively. Specific activity is determined by measuring the amount of glucose released under the reaction conditions per ml per min (Fig. 4b).

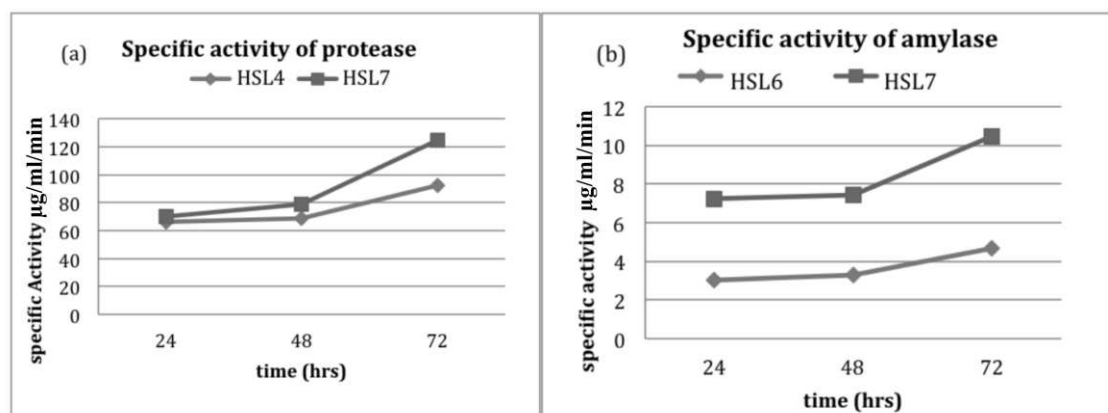


Figure 4. a) Specific activity of amylase. b) Specific activity of protease

Molecular characterization

The genomic DNA is isolated by a method by Delbes and coworkers (2000). The isolated DNA is confirmed by analyzing DNA with gel electrophoresis with 1% Gel in 0.5 X TBE buffer. Gel images were observed by Bio-Rad gel documentation system.

16S rRNA sequencing and phylogenetic tree

According to the BLAST results, HSL1, HSL4, HSL6, and HSL7 showed 99% identity with *Oceanobacillus onchorhynchi subsp. Incaldanensis*, *Staphylococcus lentus*, *Bacillus endophyticus* and *Bacillus aquimaris* respectively. The partial 16S rRNA were submitted to NCBI. The accession numbers obtained of these strains are the following. KP866216 for HSL1, KP866217 for HSL4, KP866218 for HSL4 and KP866219 for HSL7. The phylogenetic tree reflects the relationship between the halophilic bacterial isolates inferred from the 16S rRNA gene sequence. The bootstrap value is shown at the

nodes of the phylogenetic tree and is expressed as the percentage of 1000 replications (Fig. 5).

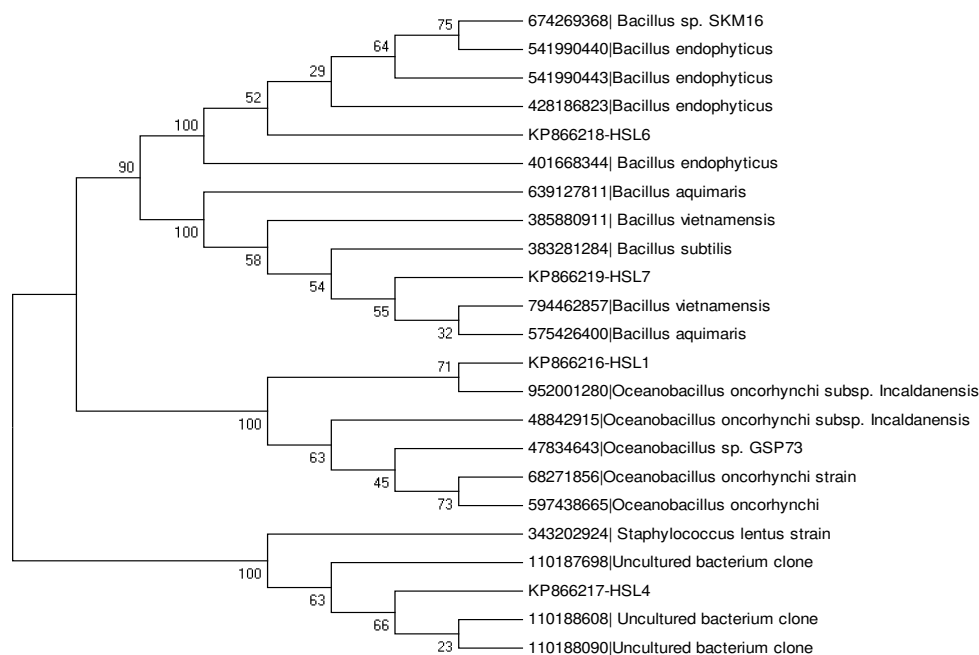


Figure 5. Phylogenetic tree showing the interrelationships between halophilic bacteria and reflecting their evolutionary pattern. The bootstrap value generated as percentage of 1000 replications is shown at the nodes

Discussion

The present research is focused on the screening and profiling of extremely halophilic bacteria indigenous to Khewra salt range. The isolated bacteria were characterized biochemically and molecularly using 16S rRNA molecular techniques. Furthermore, their different physiological features and their potential biotechnological applications have also been analyzed in this study.

This is the first report that analyzed the tolerance of extremely halophilic bacteria, from Khewra mine, against the salts other than NaCl. The salts used were KCl, CaCO₃, NH₄Cl, MgSO₄, and BaCl₂. The media supplemented with 3% of these salts were used to investigate the tolerance of isolates against these salts. The presence of Na⁺; K⁺; Mg²⁺; and SO₄²⁻ had been reported previously in the rock salt deposits of Khewra salt mine (Sharif et al., 2007). The analysis of brine samples from Khewra also revealed the presence of SO₄²⁻, PO₄³⁻, Cl⁻ and CO₃²⁻. The values of Na⁺; K⁺; Ca²⁺; Mg²⁺; Cl⁻ and SO₄²⁻ ions in Khewra were comparable to the values investigated in other salt environments as well (Grant et al., 1998). The growth of the isolates in the presence of all these salts highlighted their role in the cycling of various nutrient components. Furthermore, this could lead to valuable insights on the possible ecological role of these extreme halophilic bacteria as they survive under the ecological constraints of the closed environment of Khewra salt mine.

The media used for culturing was nutrient agar, which is rich in nutrients, thus making it suitable for the growth of diversified microbes. The results of the basic characterization highlights diversified colonial morphologies. Both gram-positive and

gram-negative extremely halophilic bacteria were observed. However, Gram staining procedure may not be very reliable and may prove unsatisfactory in several cases (Duckworth et al., 1996), which could be true for this report as well. One of the isolate HSL1 is a gram-negative rod and shows 99% resemblance of its 16S rRNA sequence with *Oceanobacillus onchorhynchi subsp. Incaldanensis*, which was originally reported as Gram-positive rods (Romano et al., 2006). However, colony morphology and biochemical characteristics were found to be similar since both strains displayed beige or off-white colonies. Both were motile and could grow at 20% of NaCl concentration. Both showed negative results for, amylase, urease and protease production and positive results for oxidase and catalase reactions. Lipase production of *Oceanobacillus onchorhynchi subsp. Incaldanensis* has not been reported. HSL1 strain showed negative results for lipase production or hydrolysis of Tween 80. The major difference between the two strains was in the pH tolerance of these species. Where *Oceanobacillus onchorhynchi subsp. Incaldanensis* could only survive at pH 6–9 (Optimum pH 9.0), strain HSL1 could grow at pH ranging from 5 to 9 with optimum growth at pH 7. The temperature range for *Oceanobacillus onchorhynchi subsp. Incaldanensis* was reported between 10 and 40°C but HSL1 can survive even at 45°C (Romano et al., 2006). The difference of Gram-staining and physiological attributes between *Oceanobacillus onchorhynchi subsp. Incaldanensis* and HSL1 allowed us to tentatively assume that HSL1 might be a different strain of the same species.

Isolate HSL4 showed 99% resemblance of its 16S rRNA sequence with *Staphylococcus lentus*. According to our study, the basic identification features of the two strains were quite similar morphologically. However, the biochemical and physiological parameters of HSL4 and *Staphylococcus lentus* showed some variations. HSL4 was extremely halophilic and could grow at NaCl concentration up to 22% whereas *Staphylococcus lentus* has been reported as moderately halophilic. The temperature stability of the two strains was also different, as HSL4 could tolerate temperatures ranging from 15 to 45°C, whereas *Staphylococcus lentus* showed no growth at 15°C and 45°C (Schleifer et al., 1983). Biochemical tests also showed considerable variations. *Staphylococcus lentus* was positive for oxidase, gelatinase, and DNase tests, whereas HSL4 was negative for all these tests. It can be deduced from the above results that HSL4 strain resembled very closely to *Staphylococcus lentus* on the basis 16S rRNA sequence. However, HSL4 strain was quite distinct from *Staphylococcus lentus* on the basis of physiology and biochemical characteristics, therefore rendering HSL4 a different strain of *Staphylococci* genus having more diverse range for growth as described for other strains of *Staphylococci* (Graham and Wilkinson, 1992; Morikawa et al., 2010).

HSL6 was also identified as a gram-positive bacillus and showed 99% sequence similarity with *Bacillus endophyticus* discovered by Reva and coworkers (2002). The morphology and biochemical characteristics of the HSL6 were found to be quite similar to *Bacillus endophyticus*. The difference between the two could be found in their ability to hydrolyze starch. *Bacillus endophyticus* was reported to show a negative result for amylase production (Reva et al., 2002), whereas strain HSL6 was able to produce a substantial amount of amylase. Conclusively, strain HSL6 was identified as *Bacillus endophyticus*.

Strain HSL7 showed a maximum resemblance of its 16S rRNA with two species. *Bacillus subtilis* (99%) and *Bacillus aquimaris* (99%). However, based on the colony morphology, physiology, and biochemical characteristics, *Bacillus subtilis* was

completely ruled out. HSL7 strain shared most of its characteristics with *Bacillus aquimaris*. Both were gram-positive rods, motile and had orange mucoid, circular colonies. This strain was positive for the production of protease, amylase, and catalase and negative for urease, gelatinase, and oxidase and indole production. All these characteristics were also true for *Bacillus aquimaris* which was isolated from the tidal flat of Yellow sea, Korea (Yoon et al., 2003). However, the physiological attributes of HSL7 strain and *Bacillus aquimaris* were slightly different. Though both were extremely halophilic and could survive at NaCl concentration up to 18%, they also showed variations in physiology. HSL7 grew best at pH 8 and survived at pH ranging from 5 to 9. The growth of HSL7 was also observed at 45°C temperature. Contrary to this, *Bacillus aquimaris* was reported to have an optimum growth at pH 7 and could not survive at pH 5 or 9. It also showed no growth at temperature 45°C. These differences in the growth pattern of HSL7 and *Bacillus aquimaris* might have arisen due to their adaptations to various habitats from which they had been isolated. Due to maximum similarities between the HSL1 and *Bacillus aquimaris* strains, HSL7 was identified as *Bacillus aquimaris*.

In the present study HSL1-*Oceanobacillus onchorhynchi* subsp. *Incaldanensis*, HSL4-*Staphylococcus lentus*, HSL6-*Bacillus endophyticus* and HSL7-*Bacillus aquimaris* were found to be efficient producers of commercially important enzymes with tremendous potential for commercial exploitation. Their wide range of tolerance to salt, temperature, and pH is because of the stability of their enzymes making them very useful in industry. Enzymes assays revealed, a substantial amount of enzyme production from these strains such as protease, amylase, lipase, xylanase, urease, gelatinase, cellulase and DNase.

Conclusion

Conclusively, this report filled a gap in addressing the prokaryotic halophilic diversity by isolation of the extremely halophilic bacteria from the salt mines of Khewra, Pakistan. The rich diversity of *Bacillus* in the salt deposits is consistent with the other reports of halophiles from salt mines around the globe, and highlight their extensive role in maintaining the ecosystem (Rohban et al., 2009; Roohi et al., 2014). Moreover, some reports suggested *Bacillus* species to be ideal for the production of industrially important enzymes due to the short duration of fermentation cycle, accelerated growth rates and capability to produce extracellular enzymes (Schallmey et al., 2004). Since most strains studied in this research are bacilli, the enzymes produced from these species can be expected to have significant potential ensuring high yield, increased stability and reliability; thus, making these enzymes commercially very important. The isolates revealed unique biotechnological applications by producing a substantial amount of amylase and protease as well as screening positive for xylanase, urease, gelatinase, cellulase, and DNase. The isolated bacteria are poly-extremophile with an ability to survive in a wide range of pH, temperature, and salinity.

Future Prospects

Khewra salt mine has proven to be a vital ecological niche supporting the survival of a diverse range of microorganisms, and little is known about extreme-enzymes produced by rock salt microbiota. To answer the fascinating question of their adaptations leading to their long-term survival within the salt crystals, diversity analysis

should be conducted by combining the culture-dependent and culture-independent techniques using sophisticated technologies such as Next-Generation Sequencing. This would aid in understanding the entire community profile and the interactions among the community in the hypersaline environment. Such insights would lead to possible exploitation of early evolutionary and extraterrestrial life and environment (Bowers et al., 2009). To further exploit the stability of halo-enzymes for production in commercial applications, more investigations should be directed towards the characterization of the enzymes at multiple concentrations of salinities, temperature, and pH. Future studies should also be directed towards the corresponding encoding genes for adaptations in high salinity, to further analyze the use of these extreme-enzymes in large-scale industrial processes.

REFERENCES

- [1] Akhtar, N., Ghauri, M. A., Iqbal, A., Anwar, M. A., Akhtar, K. (2008): Biodiversity and phylogenetic analysis of culturable bacteria indigenous to Khewra salt mine of Pakistan and their industrial importance. – *Braz J Microbiol* 39: 143-150.
- [2] Bowers, K. J., Mesbah, N. M., Wiegel, J. (2009): Biodiversity of poly-extremophilic bacteria: Does combining the extremes of high salt, alkaline pH and elevated temperature approach a physico-chemical boundary for life. – *Saline Syst* 5: 9-17
- [3] Burg, B. (2003): Extremophiles as a source for novel enzymes. – *Curr Opin Microbiol* 6: 213-218.
- [4] Cojoc, R., Merciu, S., Popescu, G., Dumitru, L., Kamekura, M., Enache, M. (2009): Extracellular hydrolytic enzymes of halophilic bacteria isolated from a subterranean rock salt crystal. – *Rom Biotechnol Lett* 14: 4658-4664.
- [5] Donio, M. B. S., Ronica, F. A., Viji, V. T., Velmurugan, S., Jenifer, J. S. C. A., Michaelbabu, M. V., Prasenjit, D. P., Citarasu, T. (2013): *Halomonas* sp. BS4. A biosurfactant producing halophilic bacterium isolated from solar salt works in India and their biomedical importance. – *Springerplus* 2: 149
- [6] Delbes, C., Moletta, R., Godon, J. J. (2000): Monitoring of activity dynamics of an anaerobic digester bacterial community using 16S rRNA PCR-Single-Strand Conformation Polymorphism analysis (SSCP). – *Environ Microbiol* 5: 506-515.
- [7] Duckworth, A. W., Grant, W. D., Jones, B. E., Steenbergen, R. V. (1996): Phylogenetic diversity of soda lake alkaliphiles. – *FEMS Microbiol Ecol* 19: 181-191.
- [8] Graham, J. E., Wilkinson, B. J. (1992): *Staphylococcus aureus* osmoregulation: roles for choline, glycine betaine, proline, and taurine. – *J Bacteriol* 174: 2711-2716.
- [9] Grant, W. D., Gemmell, R. T., Mcgenity, T. J. (1998): Halophiles. – In: Horikoshi, K., Grant, W. D. (eds.) *Extremophiles*, pp. 93-132. Wiley-Liss, New York.
- [10] Holt, J. G., Krieg, N. R., Sneath, P. H., Staley, J. T., Williams, S. T. (1994): *Bergey's Manual of Determinative Bacteriology*, pp. 39-63. – Williams and Wilkins, Baltimore.
- [11] Hussein, M. I., Hussein, S. I. (1990): Origin of the Infracambrian salt basins of the Middle East. – *Geological Society, London, Special Publications* 50(1): 279-292.
- [12] Kunitz, N. (1965): *Methods of Enzymatic Analysis* (2nd ed). – Verlag Chem, pp. 807-814. Academic Press, New York, London.
- [13] Kushner, D. J. (1978): Life in High Salt and Solute Concentrations. – In: Kushner, D. J. (ed.) *Microbial Life in Extreme Environments*, pp. 317-368. Academic Press, London.
- [14] Kushner, D. J. (1985): The *Halobacteriaceae*. – In: Woese, C. R., Wolfe, R. S. (eds.) *The Bacteria*. Vol. 8, pp. 171-214. Academic Press, Orlando.
- [15] Lesuisse, E., Schanck, K., Colson, C. (1993): Purification and preliminary characterization of the extracellular lipase of *Bacillus subtilis* 168, an extremely basic pH tolerant enzyme. – *Eur J Biochem* 216: 155-160.

- [16] Kakhki, A. M., Amoozegar, M. A., Khaledi, E. M. (2011): Diversity of hydrolytic enzymes in haloarchaeal strains isolated from Salt Lake. – *Int J Environ Sci Technol* 8(4): 705-714.
- [17] Morikawa, K., Ohniwa, R. L., Ohta, T., Tanaka, Y., Takeyasu, K., Msadek, T. (2010): Adaptation beyond the stress response: Cell structure dynamics and population heterogeneity in *Staphylococcus aureus*. – *Microb Environ* 25: 75-82.
- [18] Oren, A. (2008): Microbial life at high salt concentrations: phylogenetic and metabolic diversity. – *Saline Systems* 4: 2.
- [19] Redfern, R. (2001): *Origins: The Evolution of Continents, Oceans, and Life*. – University of Oklahoma Press, Norman.
- [20] Reva, O. N., Smirnov, V. V., Pettersson, B., Priest, F. G. (2002): *Bacillus endophyticus* sp. nov., isolated from the inner tissues of cotton plants (*Gossypium* sp.). – *Int J Sys Evo Microbiol* 52(1): 101-107.
- [21] Rohban, R., Amoozegar, M. A., Ventosa, A. (2009): Screening and isolation of halophilic bacteria producing extracellular hydrolyses from Howz Soltan Lake, Iran. – *Ind J Microbiol Biotechnol* 36: 333-340.
- [22] Roohi, A., Ahmed, I., Paek, J., Sin, Y., Abbas, S., Jamil, M., Chang, Y. H. (2014): *Bacillus pakistanensis* sp. nov., a halotolerant bacterium isolated from salt mines of the Karak Area in Pakistan. – *Antonie Leeuwenhoek* 105:1163–1172.
- [23] Romano, I., Lama, L., Nicolaus, B. (2006): *Oceanobacillus oncorhynchi* subsp. *incaldanensis* subsp. nov., an alkalitolerant halophile isolated from an algal mat collected from a sulfurous spring in Campania (Italy), and emended description of *Oceanobacillus oncorhynchi*. – *Int J Sys Evo Microbiol* 56: 805-810.
- [24] Sameeni, S. J. (2009): The Salt Range: Pakistan's Unique Field Museum of Geology and Paleontology. – In: Lipps, J. H., Granier, B. R. C. (eds.) *PaleoParks - The Protection and Conservation of Fossil Sites Worldwide, Book 3, Chapter 6. Carnets de Géologie/Notebooks on Geology*, Brest.
- [25] Schallmeyer, M., Singh, A., Ward, O. P. (2004): Developments in the use of *Bacillus* species for industrial production. – *Can J Microbiol* 50(1): 1-17.
- [26] Schleifer, K. H., Geyer, U., Kilpper-Bälz, B.R., Devriese, L. A. (1983): Elevation of *Staphylococcus sciuri* subsp. *lentus* to species status: *Staphylococcus lentus* (Kloos et al.) comb. nov. – *Syst Appl Microbiol* 4: 382-387.
- [27] Tatusova, T. A., Madden, T. L. (1999): BLAST 2 Sequences, a new tool for comparing protein and nucleotide sequences. – *FEMS Microbiol Lett* 174: 247-250
- [28] Thompson, J. D., Higgins, D. G., Gibson, T. J. (1994): CLUSTAL W: improving the sensitivity of progressive multiple sequence alignment through sequence weighting, position-specific gap penalties and weight matrix choice. – *Nucleic Acids Res* 22(22): 4673-4680.
- [29] Vahed, Z. S., Forouhandeh, H., Hassanzadeh, S., Klenk, H., Hejazi, M. A., Hejazi, M. S. (2011): Isolation and characterization of halophilic bacteria from Urmia Lake in Iran. – *Mikrobiologija* 80(6): 826-33.
- [30] Yoon, J., Kim, I., Kang, K. H. (2003): *Bacillus marisflavi* sp. nov. and *Bacillus aquimaris* sp. nov., isolated from sea water of a tidal flat of the Yellow Sea in Korea. – *Int J Sys Evo Microbiol* 53: 1297-1303.
- [31] Bernfeld, P. (1955): Amylases, alpha and beta. – *Meth Enzymo* 1: 149-158.

QUALITATIVE ANALYSIS OF NATURAL TERROIR UNITS. CASE STUDY: MODRA WINE RAYON (SLOVAKIA)

KARLÍK, L.^{1*} – †LAUKO, V.¹ – FALĽAN, V.² – MATEČNÝ, I.²

¹*Department of Regional Geography, Planning and Environment, Faculty of Natural Sciences, Comenius University in Bratislava
Ilkovičova 6, Mlynská Dolina, 842 15 Bratislava 4, Slovakia
(phone: +421-908-081-951; fax: +421-2-6542-9064)*

²*Department of Physical Geography and Geoecology, Faculty of Natural Sciences, Comenius University in Bratislava
Ilkovičova 6, Mlynská Dolina, 842 15 Bratislava 4, Slovakia
(phone: +421-2-6029-6518)*

**Corresponding author
e-mail: karlik3@uniba.sk*

(Received 9th Aug 2017; accepted 5th Feb 2018)

Abstract. The importance of the terroir concept is rapidly increasing not only because consumer interest in the origin of the product, but also because of winemaker's interest in qualitatively high and unique wine production. The main aim of the article is to present a methodological framework of Natural terroir units (NTU's) for countries which still do not have applied French appellation system. The study depicts a logical framework consisting of natural terroir factors selection, followed by data reclassification, encoding and the final data composition and utilization. In this work, we identified and described 182 regional types in 362 NTU's in the Modra wine rayon. In the final stage were selected the most valuable vineyard sites for Green Veltliner using NTU coding system. The findings were subsequently compared to results which were obtained by decades lasting empirical observations in the study area conducted by enologist and winemakers. Most of the selected NTU's matched to empirical study results. Identification is proven in the GIS environment; this is considered the most useful instrument because of its ability to manipulate spatial data and perform spatial analysis.

Keywords: *coding system, empirical validation, vineyards, GIS, map composition*

Introduction

Wine character differs from continent to continent, country to country, region to region, even vineyard to vineyard, and of course from producer to producer. These differences are affected by countless variables inherited from natural conditions, processing techniques, cultivar selection, tradition and human factors which are difficult to define. The specific natural and human aspects form unique areas called terroir, and their possible combinations imprint persistent and invariable specificity on the product. Therefore, understanding terroir carries explicit regional recognition for every product, and generates not only opportunity, but more importantly, product demand and its propagation in the market place.

Terroir is the complex of geographical conditions which give wine its specific taste and distinguishes it from others. The term "terroir" is recognized and revered throughout the viticulture world because it embraces the influence of natural landscape properties; including geology, soil, topography and climate. It determines the most suitable wine variety for each particular site, and also the technical processes of wine makers; including the use of autochthonous microorganisms during fermentation (Van

Leeuwen et al., 2004). No other agricultural product has such a strong relationship with the soil as wine (Van Leeuwen, 2010). For instance, top-rated Cabernet Sauvignon wines in Catalonia came from soil with a more limited water regime, and its success was most likely due to accumulation of the phenolic compounds responsible for wine color and taste (Ubalde et al., 2010). Climate there affected almost all variables of grape composition – berry weight, grape-ripening speed and wine composition. Terroir labelled wines generally have greater demand than non-terroir varieties because consumers are interested in place of origin, and they want information before they buy. Terroir-identified products also carry a guarantee of quality under strict control of national authorities. According to California Wine Industry (2016), the Slovak Republic produced 376,270 hl of wine in 2016. Although this quantity is negligible compared to the largest producers from France (46,701,000 hl), Italy (44,739,000 hl), Spain (38,200,400 hl). Slovakia cannot be considered a “small wine country”; judging on its world-competition wine results (Ďurčová, 2013, 2014).

At the highest level, the total vine-growing area in Slovakia is subdivided into 6 vineyard regions (*Fig. 1*). There is then the lower level of 40 wine rayons (zones) created by 511 vine-growing settlements (ÚKSUP, 2015). The traditional labelling system used here is a tribute to the historical influence of the prior German population. This system concentrated on sugar content and thus distinguished between wine categories. However, updated legislative framework (NRSR, 2009) has determined that sugar content is not the only relevant characteristic of wine quality, and European Union influence has seen Slovak viticulture approach French wine categorization. This categorization accounts for the precise grape origin; especially in which vineyard the grape ripened and what conditions were uniquely characteristic of this particular allotment.

This principle has been applied traditionally in France for centuries, and it clearly indicates which vineyards are qualitatively the best. At this stage, no final appellation system is legislated for Slovakia, so labelling may be based on either place of origin or on wine attributes.

Complete use of French labelling and abandonment of the German system has received threats concerning recognition of the place of origin. There are only several products labelled under the French principle in Slovakia, and while these products are registered in the DSC (Districtus Slovakia Controlatus) appellation system which is similar to the French AOC (Appellation d'origine contrôlée), geographic conditions are not appropriately indicated in the DSC. Accurate mapping of agricultural landscapes including vineyards and their potential evaluation is often performed in geographic information systems (Irimia and Patriche, 2010; Irimia et al., 2012; Masný and Zaušková, 2015; Incze and Novák, 2016). However, there is a lack of terroir research providing understanding of Slovak viticulture areas. Wine regions have very good soils, the climate and ecological conditions to equal well-known European vineyards, but many have been transformed into building areas, and also abandoned (Pospíšilová et al., 2005a). Modern GIS technology and remote sensing present new opportunities in terroir mapping (Johnson et al., 2012), and positive results and technological progress have encouraged increased interest in terroir study and identification in many wine-producing countries.

From above mentioned, we can postulate our hypothesis which assumes that, there are homogenous natural spatial units in viticultural landscape which have impact on wine character.

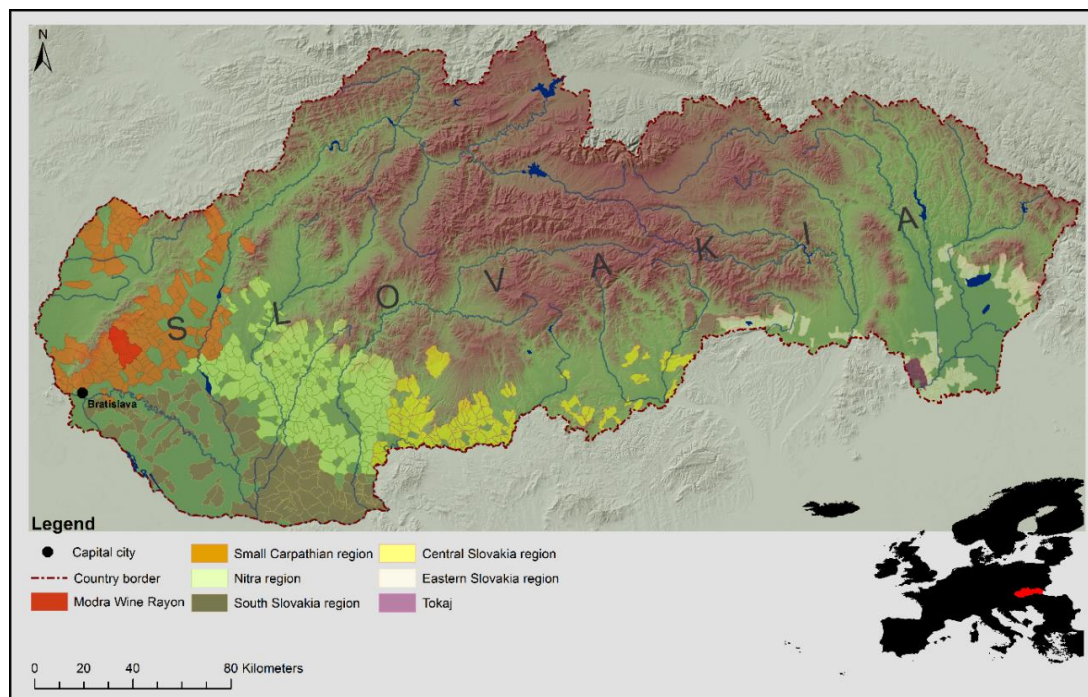


Figure 1. Map with the location of the Modra wine rayon relative to other major grape growing regions in Slovakia (NRSR, 2009)

The importance of terroir unit identification comes from resolution of OIV – Office International de la Vigne et du Vin – concerning the identification of terroir in all countries where wine is produced. Carey et al., 2002 argue that, terroir research provides producers better understanding of their vineyards and improves their quality. An NTU map is more useful than a soil map because it relates all the natural factors influencing wine production. The aim of presented study is to create methodological approach to identify NTU as the basis for complex terroir. The secondary aim of this study is to highlight the application of these units in further geographical/geocological research and to perform validation of the delimited NTU's with empirical research executed in the study area in last decades.

Different authors identify natural terroir elements differently and give unequal weight to certain aspects (Carey et al., 2002; Vadour, 2002; Pospíšilová et al., 2005a; Tomasi et al., 2013). Most work has been performed in GIS; enabling working with more spatial variables, assessment of viticulture potential and landscape suitability and identification of homogenous production zones. For example the following authors employed GIS in their terroir work; (a) (Boyer and Wolf, 1998, 2000) used GIS to study viticulture potential, and they applied combined geographical information for vineyard suitability in Virginia USA; (b) Jones et al. (2004) analyzed terroir potential in the Umpqua Valley in Oregon; (c) Jones (2006) assessed viticulture potential in the Oregon Rogue River area; (d) Chen (2011) used complex analysis of nine variables to determine terroir suitability in Nebraska; (e) (Magarey et al., 1998; Jones and Duff, 2003) predicted potential in new areas of existing viticultural regions and (f) Imre and Mauk (2003) characterized terroir in New Zealand.

Both regional characterization and suitability modelling are limited by data availability and scale (Vadour, 2002; Van Leeuwen et al., 2004). This especially applies

to the Slovak Republic and several other post-communist countries which have potential to develop their viticulture due to global climate change. *Table 1* shows overview of the used natural factors in selected terroir studies.

Table 1. Overview of the selected natural factors in recent studies. Highlighted available factors were used in our study

Author	Selected natural factors
Bonfrante et al. (2011)	Elevation, slope, geological unit, soil texture , CaCO ₃ , pH, soil organic matter, available water capacity,
Carey et al. (2008)	Landform, aspect, elevation , soil type, geological unit
Falt'an et al. (2016)	Landform, soil substrate (geological unit) , slope angle , soil type, pH, carbonates (%), nitrogen (%)
Falt'an et al. (2017)	Landform, soil substrate (geological unit) , soil type, slope, solar radiation , aspect
Irimia et al. (2012)	Slope, aspect , annual average temperature, the hottest month average temperature, growing degree days, solar insolation , average rainfall for the period from 1st April to 30 September, soil texture , humus content, the length of bioactive period
Jones et al. (2004)	Elevation, slope , aspect, drainage, available water capacity, soil depth , pH, growing degree days
Sarmiento et al. (2006)	Elevation, slope , aspect

Climatic data is especially important in cultivar selection because each cultivar needs specific total temperature to complete its vegetation cycle (Huglin, 1986; Carey, 2005). Hence, planting late-ripening cultivars in colder regions precludes it from finishing its vegetation cycle. The lower temperature limit for viticulture without winter protection is considered to be -1°C of the coldest month's mean temperature (Gladstones, 2000). In contrast, faster ripening cultivars in warmer regions lose production quality because of over-growth. The generally accepted temperature for grapevine requisites is 10°C and above; where the vegetation cycle responsible for further production commences (Homolová and Kropáč, 1993). This 10°C is therefore often used in calculations evaluating viticulture regions in climatic indexes such as Huglin and "growing-degree-days".

Geology affects the bouquet and taste of wine, and although bedrock generally asserts less impact on wine and its quality than topographic, soil and climatic components (Hugett, 2005). While bedrock influence occurs in shallow sandy soils (Záruba and Homolová, 1985) and affects older plants more; with their deeper root system giving essential nutrients more frequently than the soil layer, some authors are adamant that geology should be considered separately from soil.

Humid soils and excessive irrigation can yield a relatively small undeveloped root system; with excess water precluding a vigorous root system and reducing the capacity to store starch in subsequent seasons (Atkinson, 2011). However, soil does affect wine character and quality, and it is extremely difficult to separate it from the geological effect emanating from bedrock. The following elements are most frequently assessed in terroir: soil chemistry, temperature, texture, depth and water status.

Topography has both direct and indirect effects on environmental parameters such as mesoclimate and soil. However, its great importance in terroir studies is apparent when

a relatively small change in topographic conditions can imprint significant change in wine specificity (Bryan, 2003).

Elevation is by far the most influential topographic characteristic in Slovak viticulture. Annual air temperatures depend mainly on elevation; and Slovakia has the desirable 8°C at less than 200 m elevation required for good grapevines. Production is also possible in 9°C average temperature and up to 300 m, and vines can still flourish at 10°C and up to 350 m. While lower-situated areas are at risk of inversion freezing, locations above 350 m are too cold for production (Záruba and Homolová, 1985).

Slope is important in terroir studies because grape growing is restricted unless certain slope conditions are met. Although flat surfaces provide easy work conditions, they are prone to freezing in temperature inversion and therefore not the best option. Producers report that the most suitable slopes range from 5 to 15%; with 25% the critical value precluding best practice (Jones et al., 2004).

Southern, south-eastern and south-western oriented surfaces in northern hemisphere are the most suitable for grape production. Heliophytes, such as grapevines, thrive in these orientations when exposed to high irradiation in the vegetation period. Slovakia does not have surplus irradiation to cause plant damage; therefore northern, north-eastern and north-western aspects here are certainly excluded for premier wines, and used only for fast-ripening and resistant cultivars (Braun and Vanek, 2003).

Material and methods

Study area

Slovakia is situated in Central Europe with total area of 49,036 km². The Republic's northern and central parts are mountainous and follow the Carpathian range, while important lowland agricultural areas are typical in the south and east. These latter localities deliver the entire wine production described in *Figure 1*.

The 113.74 km² study area is approximately 30 kilometers north-east of Bratislava and includes the wine settlements of Modra, Dubová, Vištuk, Vinosady and Šenkvice. Prevailing south-east relief is formed by the Danube plains which pass into the highlands of the Malé Karpaty Mts. in the north-west. Slovak Republic viticulture zoning places this rayon in the Small Carpathian Region (Malokarpatská vinohradnícka oblasť).

For the Modra wine rayon are typical cool climate conditions. *Table 2* depicts basic spatial statistic of local climate which is frequently used for viticultural regions assessment.

Table 2. Spatial statistics for climate variables averaged over the mapped agricultural area of Modra wine rayon Súľovský (2017)

Variable	Mean	Max	Min	Range
Growing season average temperature (GST, °C units)	16.33	16.38	16.23	0.15
Huglin index (HI, °C units)	1895.86	1929.38	1870.89	58.49
Minimal air temperature in January (°C)	-19.38	-20.50	-19.11	1.39
Mean air temperature in January (°C)	-0.65	-1.16	-0.38	0.68
Growing season precipitation (mm)	407.07	454.10	386.42	67.68

The central Modra wine rayon contains significant elevation contrast between the Malé Karpaty Mts. and the Danube plain. The lowest 145 m area is near the water surface in the southern rayon portion and the 709 m Veľká homoľa hill is in the northwest. Slope impact has previously been described, and this 564 m difference in 12 km affects annual air temperature, rainfall and incoming potential global solar radiation. The southern region inclines only 5%, but the rayon slope is more than 20% at the foot of the Malé Karpaty Mts. and the greatest slopes are in the mountainous areas where watercourses cross the terrain (*Fig. 2*). In these localities is sum of the potential global solar irradiation highest (*Fig. 3*).

Biotite granite dominates the central rayon area at the foot of the Malé Karpaty Mts. The mountains then provide large areas of proluvial sediments, loamy to sandy gravels and alluvial materials; creating the alluvial cones typical of relief in the Modra rayon (*Fig. 4*). Nearby water flows are several fluvial sediment types with unsorted loams, sandy sediments and loamy-sands. Meanwhile, the southern rayon contains various aeolian and aeolian-delluvial sediments in loess and loess loams. While the prevailing soil type here is Cambisol, the lightest sandy and loamy-sandy soils in the central rayon are mostly related to granite (*Fig. 5*). Approximately 50% of the study area has loamy soils with 35 to 45% humus horizon fractions less than 0.01 mm. Slightly lighter soils with more sand content are in the rayon south-west; mainly in flat areas. The heaviest soils are the clay-loams azonally near water flows and surfaces (VÚPOP, 2015) and the most skeletal granite soils, at 20-25% in the surface horizon and over 50% sub-surface, are only in two small localities on the central rayon eastern and western borders. The moderate 20-25% soils are most common in both layers in the entire non-forested area at the foot of the Malé Karpaty Mts. Soils with the lowest skeleton content of 5 to 25% in the surface horizon and 10 to 25% in the subsurface flank the moderate skeletal soils. These granite remnants form a transition from moderate skeletal soils to the non-skeletal soils present on the Danube plain aeolian sediments in the rayon's south.

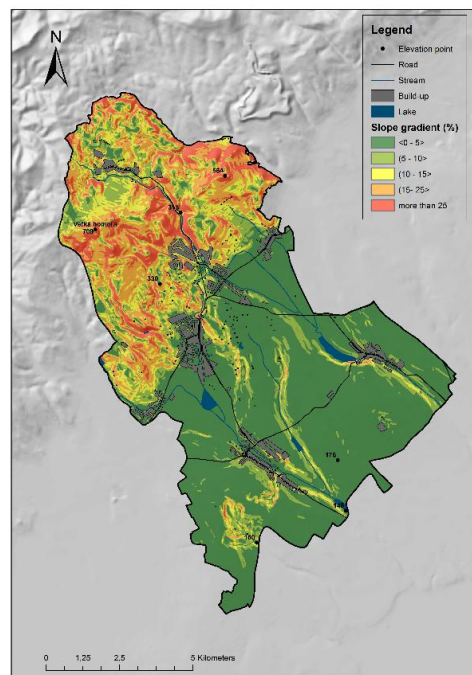


Figure 2. Map showing the slope of the Modra wine rayon

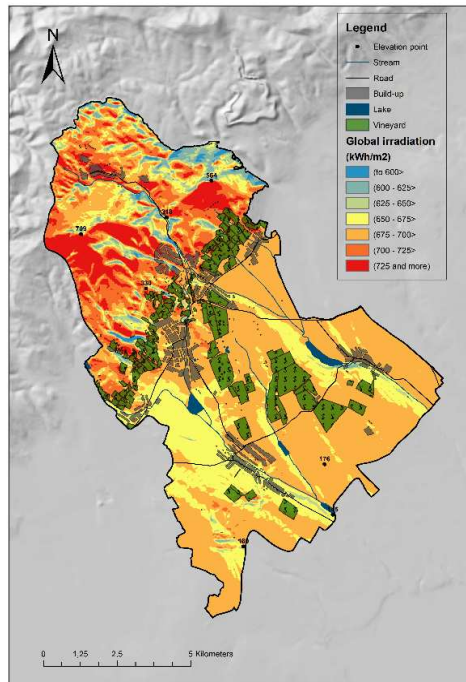


Figure 3. Map showing the slope and potential global irradiation gradient of the Modra wine rayon

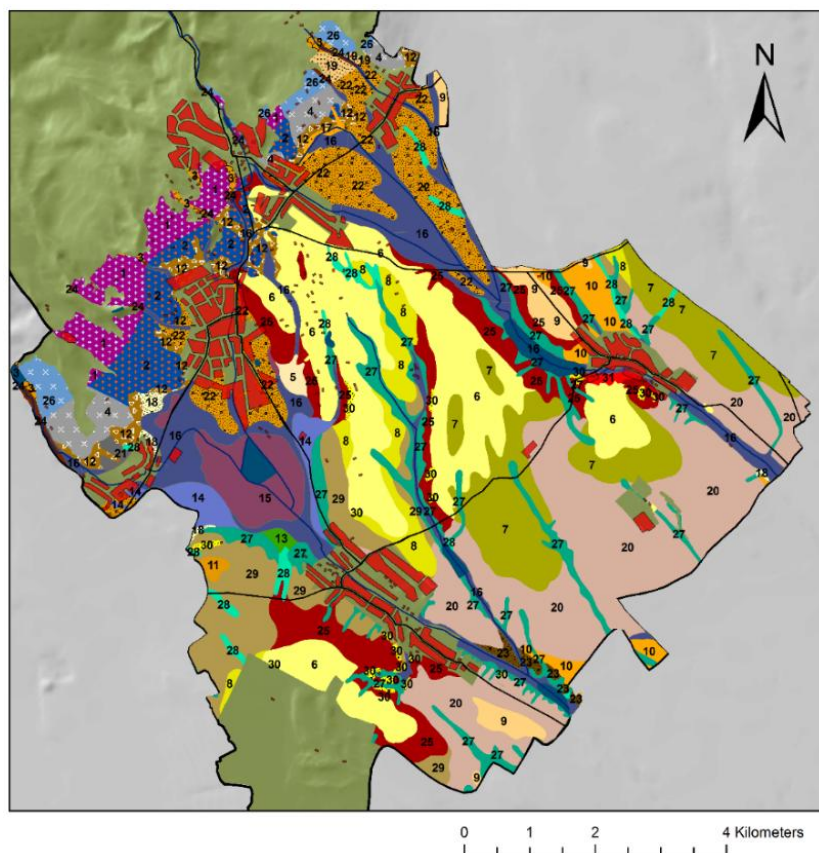


Figure 4. The map showing geological variability in the Modra wine rayon with codes (legend) of geological units included in Table 3 (ŠGÚDŠ, 2013)

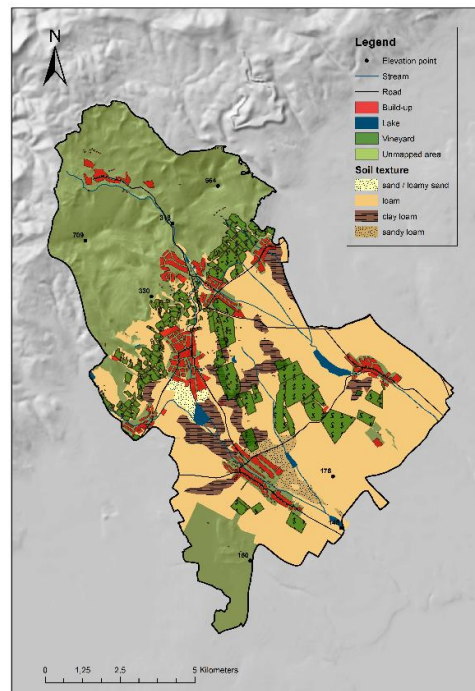


Figure 5. Soil texture in the Modra wine rayon (VÚPOP, 2015)

The following three soil types are present between the surface and the 50% skeleton content depth: (1) the deepest are at 60 cm in the lowest flat localities on quarternary Aeolian sediment; (2) soils at 30 to 60 cm are on alluvium and deluvium cones and (3) shallow soils cover some of the rockiest areas (Fig. 6).

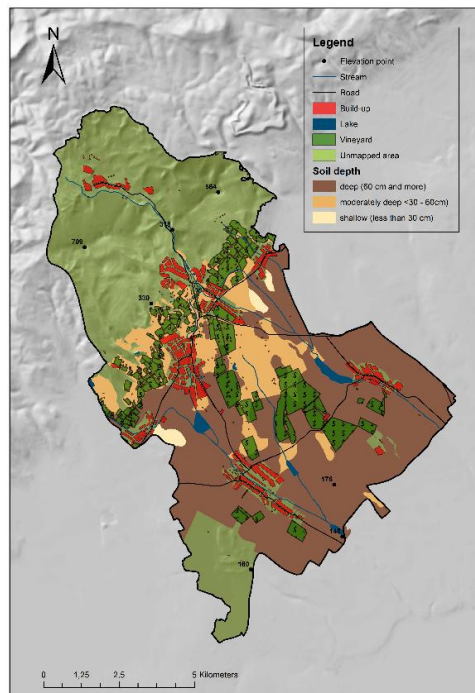


Figure 6. Soil depth in the Modra wine rayon (VÚPOP, 2015)

Analysis of data

Agricultural land was chosen for Natural Terroir Units (NTU's) identification because forests and built up areas have no current viticulture potential and from this reason they were masked out. Elevation, Slope, Potential global solar irradiation in vegetation period, Soil texture, Soil skeleton, Soil depth and Geological units were selected and logically reclassified (encoded) in regard to qualitatively high grape production and its limitations using Spatial Analyst tool Reclassify. This tool assign to the initial values new user defined values. All of the new values were ascending ordered for purpose of preservation of logical frame for further analyses and practical usage. Potential global solar irradiation for the vegetation period and slope were derived from digital elevation model (DEM) in ArcGIS 10.1.

Encoding logic and raster interval selection is discussed below in the text. Subsequently, ArcGIS 10.1 spatial analyst tool Combine was used for the final map composition, whereby composition of the analytical maps of natural characteristics identified potential NTU's. Raster output was in next stage converted into vector format using Raster to Polygon conversion tool in ArcGIS 10.1. Final raster composition resulted in over 2,500 created NTU's of which all polygons smaller than 3 ha were removed by clustering with the neighboring NTU's having largest area. It is important to note here, that most of the clustered features were only small sliver polygons which were product of raster composition. This step was carried out using Generalization tool Eliminate in ArcGIS 10.1. Subsequently it was assigned specific key to every NTU of eight digits; with geological conditions comprising the final two digits (*Fig. 7*). Geology affects bouquet and gives the wine a more specific character than the other elements, and two code digits were necessary to differentiate over nine classes in the geologically complex Modra wine rayon. *Figure 8* depicts the NTU map created by overlapping the seven independent environmental factors. Physical-geographical data were verified by field investigation in an integrative geo-ecological approach in the 2015/16 growing seasons (Minár et al., 2001), and vineyard research points were located in individual NTU centroids (*Fig. 9*).

Encoded elevations

Elevation values correlate strongly with climate characteristics in study area, so it was more important to encode elevation information in NTU, rather than some other climate aspects. *Table 3* has elevation reclassified into the following three intervals; (a) less than 200 m is numbered 1 in the first code position, because this has relatively high risk of ground frost during vegetation; (b) 200 to 300 m is numbered 2 as it is optimal for rainfall, temperature and ground freezing risk and (c) all higher areas are numbered 3 because higher rainfalls and lower temperatures make these areas least optimal for growth (Homolová and Kropáč, 1993; *Table 4*).

Encoded slopes

Slope is encoded twice; once in the second position as a discrete characteristic, and again as potential global irradiation input. Slope in the former case is subdivided into 4 classes placed in position 3; (a) flat areas with less than 5% slope are numbered 1 and (b) ideal slope 5.1 to 15% is numbered 2 (Jones et al., 2004; Sarmiento et al., 2006); and these classes led to the delimitation of all intervals (*Table 4*).

1	2	3	4	5	6	7 & 8
•Elevation	•Slope	•Solar irradiation	•Soil texture	•Soil depth	•Soil skeleton	•Geological unit

Figure 7. Final composition of the coding system for NTU natural characteristics

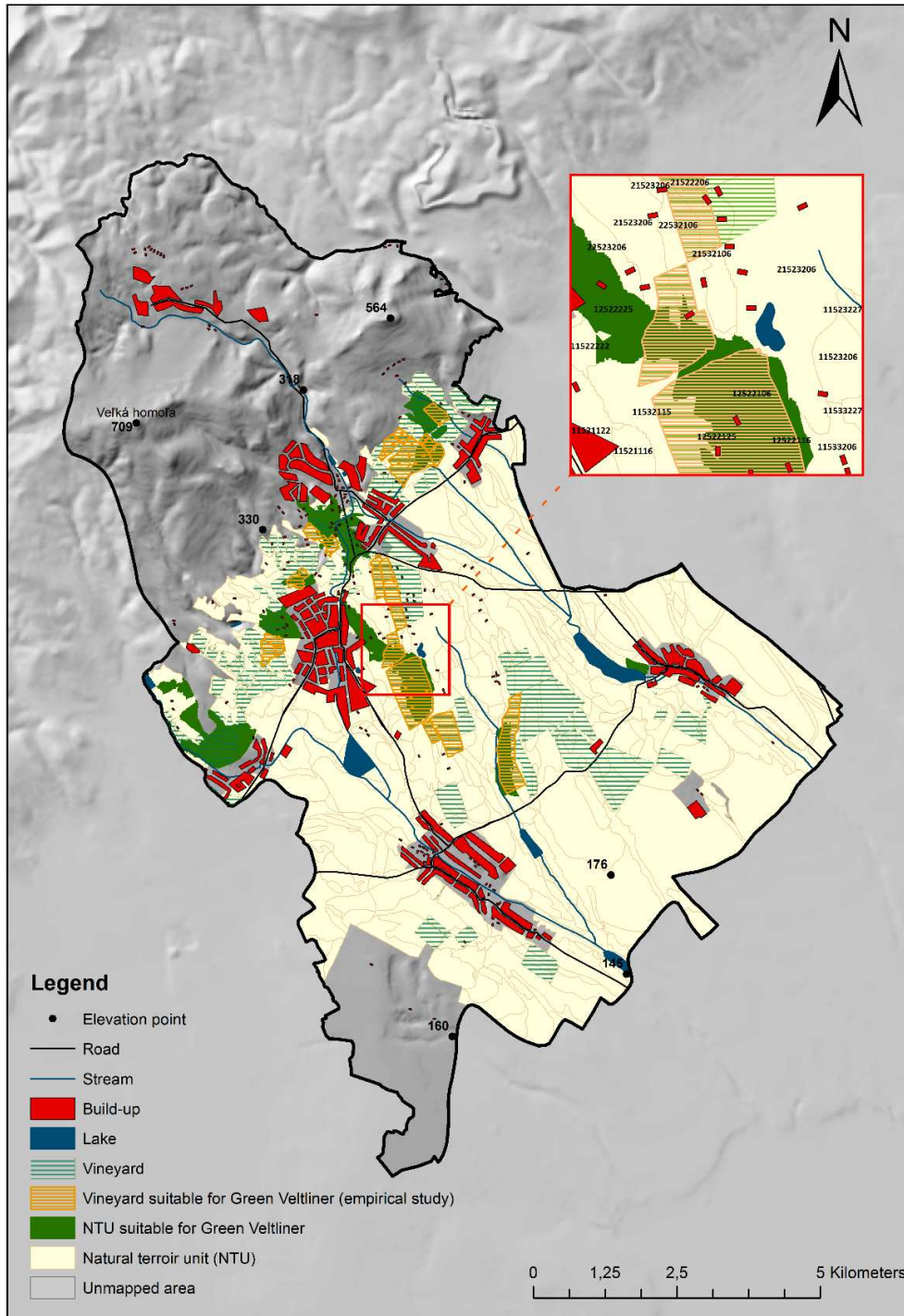


Figure 8. The delimited NTUs of the Modra wine rayon and the most suitable NTUs for Green Veltliner production



Figure 9. Soil pits localization based on NTU map

Table 3. The illustration of the NTU attribute table that implies values of individual codes of the natural characteristics

NTU	Elevation	Slope	Irradiation	Texture	Depth	Skeleton	Geology
33723226	3	3	7	2	3	2	26
32622203	3	2	6	2	2	2	03
23613226	2	3	6	1	3	2	26
23623204	2	3	6	2	3	2	04
22523212	2	2	5	2	3	2	12
22622222	2	2	6	2	2	2	02
22622219	2	2	6	2	2	2	19
22522226	2	2	5	2	2	2	26
22522222	2	2	5	2	2	2	22

Table 4. NTU code system

Elevation (m)	Code	Geological unit	Code
Less than 200	1xxxxxxx	Biotite granite	xxxxxxx1
201 to 300	2xxxxxxx	Tonalite	xxxxxxx2
More than 301	3xxxxxxx	Deluvium – mostly loamy and loamy–rocky	xxxxxxx3
Slope (%)	Code	Phyllite “Harmonia series”	xxxxxxx4
Less than 5	x1xxxxxx	Loamy and sandy gravels, sands and gravels in floodplain in alluvial cones	xxxxxxx5
5.1 to 15	x2xxxxxx	Loamy to sandy weathered gravels and rocky fragments in alluvial cones	xxxxxxx6
15.1 to 25	x3xxxxxx	Loamy to sandy weathered gravels and rocky fragments in alluvial cones with loess surface	xxxxxxx7
More than 25	x4xxxxxx	Loamy to sandy weathered gravels and rocky fragments in alluvial cones with loess loam surface	xxxxxxx8
Potential global irradiation (kWh/m²)	Code	Loamy to sandy-loamy gravels with rocky fragments in alluvial cones	xxxxxxx9
Less than 600	xx1xxxxx	Loamy to sandy-loamy gravels with rocky fragments in alluvial cones with loess loam surface	xxxxxxx10
(600 to 625>	xx2xxxxx	Loamy to sandy-loamy gravels with rocky fragments in alluvial cones with loess surface	xxxxxxx11
(625 to 650>	xx3xxxxx	Loamy-rocky deluviums and rubbles	xxxxxxx12
(650 to 675>	xx4xxxxx	Loams, sandy-loams to loamy-sands in dejection cones	xxxxxxx13
(675 to 700>	xx5xxxxx	Loams, sandy-loams to loamy gravels with rocky fragments in floodplain alluvial cones	xxxxxxx14
(700 to 725>	xx6xxxxx	Peat soils	xxxxxxx15
More than 725	xx7xxxxx	Non sorted loams, sandy loams, loamy sands to gravels of valley rivers and flows	xxxxxxx16
Soil texture	Code	Sandy loams to loamy sands with rocky fragments	xxxxxxx17
Sand / loamy sand	xxx1xxxx	Sandy loams with gravels	xxxxxxx18
Loam	xxx2xxxx	Sandy gravels (alluvial cones)	xxxxxxx19
Clay loam	xxx3xxxx	Loess	xxxxxxx20
Sandy loam	xxx4xxxx	Silts, clays, sands, gravels	xxxxxxx21
Soil skeleton	Code	Mostly loamy and sandy gravels, sands and sandy loams with rocky fragments in aluvial cones	xxxxxxx22
Without skeleton	xxxx1xxx	Mostly loamy and sandy gravels, sands and sandy loams with rocky fragments in aluvial cones with loess surface	xxxxxxx23
Slightly skeletal	xxxx2xxx	Mostly loamy sediments, non sorted	xxxxxxx24
Moderate skeletal	xxxx3xxx	Resedimented loamy and sandy-loamy gravels of deluviums	xxxxxxx25
Highly skeletal	xxxx4xxx	Seritic-chloritic siliceous phyllite with biotite	xxxxxxx26
Soil depth	Code	Proluvial-deluvial loams, sandy and clay loam with rocky fragments	xxxxxxx27
Deep	xxxxx1xx	Proluvial-deuvial loams, sandy loams with graels, gravels	xxxxxxx28
Moderately deep	xxxxx2xx	Loess loams with loess and soliflued bedrock sediments	xxxxxxx29
Shallow	xxxxx3xx	Gravels, sands, sandstones, lignits, coal clays	xxxxxxx30
		Different rocks on upheavals	xxxxxxx31

Encoded potential global solar irradiation

In Slovak Republic conditions, it is paramount for grapevines to reach the maximum total solar energy during vegetation. Higher solar irradiation in Italy, Spain and Portugal can promote leaf-burn, but this is extremely unlikely in Slovakia. *Table 3* depicts Modra potential global solar irradiation classified in 7 categories; and this element takes the third encoded position. Higher irradiation values enhance production.

Encoded soil properties

Soil has such a strong place in terroir studies that we encoded three soil characteristics. From original map legends, we designated (a) texture in the fourth encoded position, with four possible categories; (b) skeleton has the fifth position, with skeletal lack signified by the number 1 and (c) depth has the sixth position with three categories; from deep soils numbered 1 to shallow with 3 (*Table 4*).

Encoded geological unit

In the Modra wine rayon there is a very complex geological composition defined by 31 classes (*Table 4*). We decided to retain original geologic map legend, because here applies the same as in soil mapping dataset of Slovak republic and at any time can be these data generalized using by suitable regionalization procedures. *Table 3* depicts selection from NTU attribute table.

Results and discussion

NTU map creation and its strengths

The final composition of our analytical maps covered 362 discrete areas classified into 182 regional types (*Fig. 8*). These quasi homogenous areas which differ minimally in one of the seven coded characteristics are Natural Terroir Units (NTU's). High natural condition complexity in the Modra rayon demanded this number of areas; but appropriate encoding enabled easy research use. Our composite NTU maps characterize the viticulture area and grape production better than the following individual maps; (a) climatic maps provide single information on rainfall, annual temperature and wind direction and (b) soil map content is very important; but this product of bedrock, climatic conditions, topographic parameters and many other factors has complex character in the natural terroir. For example; solar irradiation is an absolute limiting threshold in grape production, but it is not directly incorporated in the soil and soil properties. These factors led to NTU map construction which provided a complex view of the natural conditions in our vineyards.

The value and strength of our NTU identification methodology primarily lie in its easy and effective reproduction in global wine-producing regions. Identification data are easy to obtain and comparison between regions is therefore simple. The density and size of the created regions reflect overall environmental heterogeneity; where small thick regions possess greater natural condition heterogeneity and areas less dense and smaller in size signify homogenous natural conditions. Here, we identify and isolate the homogenous areas in this complex mosaic because these are the production sites of authentic wines with specific sensoric characteristics.

Our methodology drafts an innovative approach for complex terroir terrain research at the plot level (*Fig. 9*). The NTU map reveals the homogenous areas forming the basic natural elements of complex terroir; both depiction of the natural terroir units and solution to “place of origin” identification. However, these NTUs and their borders must be subsequently refined and modified in the terrain. Two or more NTU are sometimes recognized within a delimited vineyard. These differences should lead to different wine styles if the grapes were separately processed by the same procedures. The NTU map provides reasonable possibility for further spatial reorganization of the vineyard system, and enables dissolution of heterogeneous vineyards into homogenous subdivisions. These then become areas for authentic wines production with strictly given homogenous natural conditions stored in the appellation system; and precisely such areas are planned for development in the Slovak Republic to replace German wine classification. Initial geographic information used in terroir potential studies is usually reclassified or replaced by ranked values; thus limiting combined consideration of the climate, soil and topographic aspects (Boyer and Wolf, 1998; Sarmiento et al., 2006).

Our methodology, however, maintains initial landscape information and includes more natural elements; and this complexity proves valuable for further use. Terroir-potential maps of viticulture areas solely classify them into suitable or unsuitable. This categorization not only overshadows, but it also hides, most of the complex information gathered on the viticultural landscape. Therefore, our method of NTU map construction preserves the vast and valuable information for grape growers lost in previous methods. While South African research (Carey et al., 2002) was on smaller scale, our NTU map contains the most detailed soil, geological and topographical available data. This has application advantages including; (a) generalization according to user need and (b) the basis for further terrain research where the geographer can rapidly detect prospective soil pits as further research localities. In addition to the complexity of our NTU map, the spatial data in the specific 8 digit code also provides evidence of the importance of our methodology. This code enables creation of regional and national databases essential for wine producers intending to plant new vineyards. These databases will (a) extract the most influential natural conditions affecting production quality; (b) be easily updated and (c) code system extension will be continuously ongoing from detailed field terroir research. Thus, producers in touch with environmental needs of the desired cultivar will select NTUs with the highest production potential. While unselected units may also be suitable, these localities can be retained for additional cultivars. We have decided to choose the Green Veltliner sample because it is the most widespread cultivar in the Modra wine rayon. Its popularity illustrates selection of the most valuable production areas identified in natural terroir units.

Green Veltliner encoding

Ampelographic literature cites that the Green Veltliner cultivar provides the best wines on sloping terrain (Pospíšilová et al., 2005a). The following encoding was adopted; (a) we chose number 2 in our second slope-code position; ranging from 5.1 to 15% slope; (b) this variety is resistant to freezing, so we chose 1 and 2 in the first code position because it is located in the lowest situated rayon areas often subject to spring frost; (c) it prefers sunny locations; so it is in the sunniest 6 and 7 codes in the 3rd position (d) deep and moderately deep soils are best for this variety, so 1 and 2

were selected in the 5th code position. Shallow soils were not considered because Kraus (1967) confirms these are absolutely unsuitable for qualitative high Green Veltliner production; (e) there is no evidence that skeletal soils are unsuitable for this cultivar. Although they are harder to process, uniform nutrient distribution results in increased overall quality, and the skeleton ensures very suitable surroundings from the thermal and water regime (Kraus, 1967); (f) we retained the last two code digits for geological conditions. Here, organic soils were ineligible for selection because nutrient distribution and water regime render them unproductive (Kraus, 1967).

The remaining geological classes have only informal character; with potential effect on bouquet and wine character. They qualitatively affect production, but have non-assessable production limitation. NTU were subsequently selected from an attribute table using SQL code; and 26 of the 362 areas were selected as the most valuable for Green Veltliner production. These were verified (*Fig. 8*) by comparing results from decades long-term empirical tests by the globally recognized breeder and enologist Dorota Pospíšilová, Ph.D. and colleagues (Pospíšilová et al., 2005b). These authors drafted the most bonity vineyards in Modra, and the most valuable varieties for each plot. Only the western portion of the Modra wine rayon remains unvalidated because this area was not covered in the research.

Conclusion

Detailed field research is important in viticulture studies, and this enabled us to identify natural terroir spatial characteristics based on NTU delimitation. This identification provided the following important findings; (a) the enhanced GIS emergence in geographical research; where GIS technology enabled varietal selection in our terroir studies through analyzing topographic, topo-climatic, soil and geological conditions (b) GIS technology combined, reclassified and verified our spatial information; (c) NTU identification delivered important information on the Modra wine rayon; with methodology applicable to every viticulture area (d) this latter knowledge highlights the advantageous application of similar units with similar conditions in further complex terroir research. The high NTU number clearly indicates that Modra wine rayon natural conditions are heterogeneous and quite complex. The complexed 362 unique areas were classified into 182 classes of natural terroir units. *Comparison* of the study results to empirical research conducted in the Modra wine rayon confirmed our hypothesis that, there exist selected site units (NTU's) which provide valuable environment for qualitatively high wine production considering to other non-selected areas. To identify complex terroir units, it is paramount to know the natural conditions which will be registered in the central appellation system; and our NTUs should be applied as complex terroir units in further research. Slovakia is working on new terroir-based classification system. This applied research output can contribute for further development of terroir classification of Slovak viticulture. Output natural terroir units are able to be processed in the next step using PCA analysis and further clustering in order to get homogenous areas in every surveyed area. But our work is aimed to uncover basic viticultural spatial units (NTU's) and therefore they were not used other multivariate statistics methods. The authors wished to generate a foundation for future terrain including lab analysis of soil samples from NTU's centroids with aim to create management vineyard zonation reflecting its terroir.

Acknowledgements. The authors thank the wine-growers in the Modra wine rayon for their support, and especially Ing. Dorota Pospíšilová, PhD. for her valuable information and recommendations on methodology verification. This work was created in projects supported by the Scientific Grant Agency of the Ministry of Education of the Slovak Republic and Slovak Academy of Science under VEGA grants 1/0540/16 and 1/0421/16 and under Comenius University Grant n. 398/2016 and under APPV Grant No. 15-0597 “ Use of geoeological data in the implemenatation of precision agriculture.”

REFERENCES

- [1] Atkinson, J. (2011): Terroir and the Côte de Nuits. – *Journal of Wine Research* 22: 35-41.
- [2] Bonfrante, A., Basile, A., Langella, G., Manna, P., Terribile, F. (2011): A physically oriented approach to analysis and mapping of terroirs. – *Geoderma* 167-168: 103-117.
- [3] Boyer, J., Wolf, T. K. (1998): GIS and GPS indentify viticultural potential. – *American Journal of Enology and Viticulture* 49: 449.
- [4] Boyer, J., Wolf, T. K. (2000): GIS and GPS aid the exploration of Viticultural potential in Virginia. – *Vineyard and Winery Management* 6: 48-54.
- [5] Braun, J., Vanek, G. (2003): Pestujeme vinič (in Slovak). – *Nezávislosť*, Bratislava.
- [6] Bryan, B. A. (2003): Physical environmental modeling, visualization and query for supporting landscape planning decisions. – *Landscape and Urban Planning* 65: 237-259.
- [7] California Wine Industry (2016): World Wine Production by Country 2011-2014. – California Wine Industry, San Francisco.
- [8] Carey, V. A., Archer, E., Saayman, D. (2002): Natural terroir units: What are they? How can they help the wine farmer? – *WineLand* 2: 86-88.
- [9] Carey, V. A. (2005): The use of viticultural terroir units for demarcation of geogrpahical indications for wine production in Stellenbosh and surrounds. – Ph.D. Thesis, Department of Viticulture and Oenology, Stellenbosh University, Stellenbosh.
- [10] Carey, V. A., Archer, E., Barbeau, G., Saayman, D. (2008): Viticultural terroirs in Stellenbosch, South Africa. II. The interaction of Cabernet Sauvignon and Sauvignon Blanc with environment. – *Journal International des Sciences de la Vigne et du Vin* 42: 185-201.
- [11] Chen, T. (2011): Using a geographic information system to define regions of grape cultivar suitability in Nebraska. – Master Thesis, Department of Agriculture, University of Nebraska, Lincoln.
- [12] Ďurčová, E. (2013): Slovenské vína na seba v Paríži upútali pozornosť vinárskeho sveta (in Slovak). – *Vinič a víno* 2: 58-59.
- [13] Ďurčová, E. (2014): Naše vína šíria vo svete dobré správy o Slovensku (in Slovak). – *Vinič a víno* 3: 94-96.
- [14] Faltán, V., Pírová, L., Petrovič, F. (2016): Detailed mapping of geocomplexes in the vineyard landscape. – *Folia Oecologica* 43: 138-146.
- [15] Faltán, V., Krajčírovičová, L., Petrovič, F., Khun, M. (2017): Detailed geoeological research of terroir with the focus on georelief and soil – a case study of Krátke Kesy vineyards. – *Ekológia* 36: 214-225.
- [16] Gladstones, J. (2000): Past and future climatic indices for viticulture. – *Australian & New Zealand Wine Industry Journal* 15: 67-73.
- [17] Homolová, E., Kropáč, A. (1993): Základy vinohradníctva a zeleninárstva (in Slovak). – *Príroda*, Bratislava.
- [18] Hugett, J. M. (2005): Geology and Wine: a review. – *Proceedings of the Geologist Association* 117: 239-247.
- [19] Huglin, P. (1978): New assessment mode of the helio-thermal conditions in vineyards. – *Comptes Rendus de l'Académie d'Agriculture de France* 64: 1117-1126.
- [20] Huglin, P., Schneider, Ch. (1986): *Biology and Ecology of Grape*. – Lavoisier, Paris.

- [21] Imre, S., Mauk, P. (2003): Geology and Wine 12: New Zealand terroir. – *Geoscience Canada* 36: 145-159.
- [22] Incze, J., Novák, J. T. (2016): Identification of extent, topographic characteristics and land abandonment process of vineyard terraces in the Tokaj-Hegyalja wine region between 1784 and 2010. – *Journal of Maps* 12: 507-513.
- [23] Irimia, L., Patriche, C. V. (2010): Evaluating the ecological suitability of the vineyards by using Geographic Information Systems (GIS). – *Cercetări Agronomice în Moldova* 1: 49-58.
- [24] Irimia, L., Patriche, C. V., Quenol, H. (2012): Mapping viticultural potential in temperate climate areas. Case study: Bucium vineyard (Romania). – *Cercetări Agronomice în Moldova* 2: 75-84.
- [25] Irimia, L., Patriche, C. V., Quenol, H. (2013): Viticultural potential assessment and natural terroir units delineation using environmental criteria specific to Romanian viticulture. Case study: Urlați wine-growing center, Dealul Mare vineyard. – *Soil Forming Factors & Processes from the Temperate Zone* 12: 34-37.
- [26] Johnson, L., Nemani, R., Hornbuckle, J., Bastiaanssen, W., Thoreson, B., Tisseyre, B., Pierce, L. (2012): Remote Sensing for Viticultural Research and Production. – In: Dougherty, P. (ed.) *Geography of Wine*. Springer, New York.
- [27] Jones, G. V. (2006): Climate and Terroir: Impacts of Climate Variability and Change of Wine. – In: Macqueen, R. W., Meinerd, L. D. (eds.) *Fine Wine and Terroir – The Geoscience Perspective*. Geoscience Canada Reprint Series Number 9, Geological Association of Canada, St. John's.
- [28] Jones, G. V., Duff, A. (2003): The climate and landscape potential for quality wine production in the Snake River Valley AVA. – Open report to the Idaho Wine Commission.
- [29] Jones, G. V., Snead, N., Nelson, P. (2004): Geology and wine 8. Modeling viticultural landscapes: A GIS analysis of the terroir potential in the Umpqua Valley of Oregon. – *Geoscience Canada* 31: 167-181.
- [30] Kraus, V. (1967): *Vinohradnictví – biologické základy agrotechniky révy vinné* (in Czech). – Státní Pedagogické Nakladatelství, Praha.
- [31] Magarey, R., Seem, R., De Gloria, S. (1998): Prediction of vineyard site suitability. – *Grape Res News* 9: 1-2.
- [32] Masný, M., Zaušková, L. (2015): Multi-temporal analysis of an agricultural landscape transformation and abandonment (Ľubietová, Central Slovakia). – *Open Geosciences* 7: 888-896.
- [33] Minár, J. (2003): Detailed physical-geographical (geoecological) research and mapping in the landscape ecology. – *Ekológia* 22: 141-149.
- [34] NRSR (National Council of the Slovak Republic) (2009): Act 313/2009 about viticulture and winemaking.
- [35] Pospíšilová, D., Sekera, D., Ruman, T. (2005a): *Ampelografia Slovenska* (in Slovak). – VŠSVVM, Modra.
- [36] Pospíšilová, D., Sekera, D., Šimora, R. (2005b): *Vypracovanie zonalizácie viniča obce Modra* (in Slovak). – Viticultural Breeding Research Institute, Modra.
- [37] Sarmiento, E., Weber, E., Hasenack, H., Tonietto, J., Mandelli, F. (2006): Topographic modeling with GIS at Serra Gaúcha, Brazil: elements to study viticultural terroir. – *Proceedings of the Terroir Viticoles Congrès International* 6: 365-372.
- [38] ŠGÚDŠ (2013): *Geological Map of the Slovak Republic (1:10 000)*. – ŠGÚDŠ, Bratislava.
- [39] Súľovský, M. (2017): *Detailný geoekologický výskum stanovištných podmienok vinohradov v Malokarpatskej vinohradníckej oblasti* (in Slovak). – Ph.D. Thesis, Department of Physical Geography Faculty of Natural Sciences, Comenius University, Bratislava.
- [40] Tomasi, D., Gaiotti, F., Jones, G. V. (2013): *The Power of Terroir: the Case Study of Prosecco Wine*. – Springer, Amsterdam.

- [41] Ubalde, J., Sort, X, Zayas, A., Poch, R. (2010): Effect of soil and climatic conditions on grape ripening and wine quality of Cabernet Sauvignon. – *Journal of Wine Research* 21: 1-17.
- [42] ÚKSUP (2015): *Vineyard Register*. – ÚKSUP, Bratislava.
- [43] Vadour, E. (2002): The quality of grapes and wine in relation to geography: notions of terroir at various scales. – *Journal of Wine Research* 13: 117-141.
- [44] Van Leeuwen, C. (2010): *Soils and Terroir Expression in Wines*. – In: Landa, E. R., Feller, Ch. (eds.) *Soil and Culture*, Springer, Dordrecht.
- [45] Van Leeuwen, C., Friant, P., Choné, X., Tregoat, O., Koundouras, S., Doubourdieu, D. (2004): Influence of climate, soil, and cultivar in terroir. – *American Journal of Enology and Viticulture* 55: 207-217.
- [46] VÚPOP (2015): *Rated Soil Ecological Units – Maps (BPEJ)* – VÚPOP, Bratislava.
- [47] Záruba, F., Homolová, L. (1985): *Vinohradníctvo (in Slovak)*. – *Príroda*, Bratislava.

PREDICTING SUITABLE DISTRIBUTION FOR AN ENDEMIC, RARE AND THREATENED SPECIES (GREY-SHANKED DOUC LANGUR, *PYGATHRIX CINEREA* NADLER, 1997) USING MAXENT MODEL

TRAN, V. D.^{1*} – VU, T. T.¹ – TRAN, Q. B.² – NGUYEN, T. H.³ – TA, T. N.¹ – HA, T. M.⁴ – NGUYEN, H. V.⁵

¹*Department of Wildlife, Faculty of Forest Resource and Environment Management, Vietnam National University of Forestry
Xuan Mai, Chuong My, Ha Noi, Vietnam*

²*Department of Environment Management, Faculty of Forest Resource and Environment Management, Vietnam National University of Forestry,
Xuan Mai, Chuong My, Ha Noi, Vietnam*

³*Faculty of Forest Science and Forest Ecology, Georg-August-Universität
Göttingen, Germany*

⁴*Vietnamese Academy of Forest Science
Duc Thang, Bac Tu Liem, Ha Noi, Vietnam*

⁵*Institute for Forest Ecology and Environment, Vietnam Forestry University
Xuan Mai, Chuong My, Hanoi, Vietnam*

**Corresponding author*

e-mail: dungtv@vfu.edu.vn; phone: +84-964-500-491

(Received 4th Oct 2017; accepted 5th Feb 2018)

Abstract. Species distributional data has very important roles in management and conservation of wildlife, especially for rare species. In this study, we used the MaxEnt model to predict the potential distribution of the grey-shanked douc langur (*Pygathrix cinerea* Nadler, 1997) which is endemic to Vietnam and listed as one of the most endangered primate species in the world. We collected 158 independent localities and 16 environmental variables from different sources were used for analysis. The projection habitat suitability shows that the suitable areas are approximately from 14°N-16°N. The precipitation of driest month (bio14) had the highest percentage contribution to the model output with 27.7%. The total suitable area is 16,680.52 km². The areas of high and very high suitability account for 19%, and 2% respectively. The potential distribution area of the species is not much found in the existing protected area. Priorities for conservation and survey efforts should be given to the forested areas in Quang Ngai (Ba To district), Kon Tum (Kon Plong district), Binh Dinh (An Lao district), Gia Lai (K 'Bang district) and Quang Nam provinces. Conservation efforts should also be prioritized for areas beyond the boundary of protected areas, especially for areas that have been proposed as biodiversity corridors.

Keywords: *douc langur, ecological niche modelling, maximum entropy, species distribution models, suitable habitat*

Introduction

Lacking species distributional data has caused many difficulties in management and conservation of wildlife (Nazeri et al., 2012), especially rare species. Understanding the most basic requirements of living habitats and distribution of each species is a top priority for conservation programs and action plans. Species distribution modelling using an ecological niche model is an instrument that can be used to help us understand

more about the distribution of species (Phillips et al., 2006; Nazeri et al., 2012). However, modelling the potential distribution or suitable habitat of a species requires a wide variety of complex data coming from environmental studies, natural resources studies, biodiversity assessment and detailed studies of species (Franklin and Miller, 2009; Sarma et al., 2015).

Ecological Niche Modelings (ENMs) is a method using occurrence data of species associated with environmental data, thereby creating models generate geographic areas which match with the ecological requirements of that species. ENMs is often used for the following purposes: (1) assessing/ estimating suitable habitat for species; (2) assessing changes in species distribution over time based on scenarios of changes in environmental conditions; (3) assessing ecological niches or ecological requirements of species (Warren and Seifert, 2011). The accuracy of the predicted results depends on a number of factors such as the complexity and accuracy of the models, the environmental data layers, and the species distribution data (Raxworthy et al., 2007). The study area is divided into different grid cells (pixel). Variables are used to generate a value of the environment at each grid cells, and algorithms are used to identify the degree of suitable or inappropriate of grid cells for the species (Raxworthy et al., 2007; Hirzel et al., 2002).

Grey-shanked douc langur (GSDL; *Fig. 1*) (*Pygathrix cinerea* Nadler, 1997) is one of three species in the genus *Pygathrix* that were recorded in Vietnam. *P. cinerea* was first described as a subspecies of *P. nemaus* (Nadler, 1997). However, later genetic work suggested the divergence at the species level (Roos and Nadler, 2001). The current GSDL's populations are found in fragmented habitat in Central Vietnam, between 13°30'N and 16°N. It has been recorded in five provinces: Quang Nam, Quang Ngai, Kon Tum, Gia Lai and Binh Dinh of Vietnam (Ha, 2000; 2004; Nadler et al., 2003; Nguyen et al., 2010; Nadler and Brockman, 2014). Most recently, the population of *P. cinerea* was estimated to be 600-700 individuals (Nadler, 2010). Hunting and habitat loss are serious threats to the population of the *P. cinerea* (Vu et al., 2008; Nguyen et al., 2012).



Figure 1. Grey-shanked douc langur (*Pygathrix cinerea*). (Source: Kon Ka Kinh National Park)

GSDL is listed as “Critically Endangered” in the Vietnam Red Data Book (Ministry of Science and Technology and Vietnam Academy of Science and Technology, 2007) and the IUCN Red List of Threatened Species since 2008 (Vu et al., 2008) because the population was declining at over 80% in the entire distribution range due to several threats. The decline is predicted to continue at the same rate or slightly higher in the next 30-36 years (approximately three generations) (Vu et al., 2008). In addition, grey-shanked douc is one of top 25 endangered primate species in the world (Schwitzer et al., 2014).

Few studies of grey-shanked douc langur have been so far conducted. These studies focused on investigating the presence (Ha, 2000; Nadler et al., 2003; Minh et al., 2005; Nguyen et al., 2010), or surveying for population size, density (Ha, 2003; 2004; 2007; Nguyen et al., 2007), and ecological characteristics such as food selection, and behavioural ecology (Ha, 2003; 2004; 2007; Nadler et al., 2003; Nguyen et al., 2012). These studies have provided useful information on the ecological characteristics of this species. Recently, new populations of GSDL are still being discovered (FFI, 2016), therefore, investigating the presence of the species in the areas that have not been surveyed before is necessary. Bett et al. (2012) modelled the distribution of the three species in the *Pygathrix* genus, however, vegetation and terrain-related variables were not used. Variables related to vegetation and terrain have been shown to be important in modelling the distribution of mammal species (Cork and Catling, 1996), especially for *Pygathrix* because these species only feeds on plants and move predominately in canopy. The terrain in the region where *Pygathrix* has been recorded and surrounding region is remarkably diverse, the elevation range from 0 m asl up to 2600 m asl (Nadler and Brockman, 2014). More importantly, the vegetation also changes significantly with the elevation gradient as well as longitudinal and longitudinal gradients. Remarkably, vegetation is divided into two forest types, including dry forest and evergreen forest. This difference is believed to influence the distribution of the species. Bett et al. (2012) did not rank the site with varying suitability that is unusually needed for prioritizing sites for conservation activities. A distributional map that is modelled using climatic variables together with terrain and vegetation variables will be helpful in guiding the survey and conservation efforts for GSDL.

Materials and methods

Study area

The study area ranges from nearly 13°N to 16°N, including parts of South Central Coastal region and Central Highland region of Vietnam. This area is separated from northern Vietnam by the Hai Van Pass and southern Vietnam by Ba-Da Rang river. The topography of this area is very complex. Mount Ngoc Linh on the northwestern Kon Tum Massif is the highest peak in the central of Vietnam (2598 m). The coastal lowlands and southern part have a drier, semi-arid climate with annual averaged rainfall below 750 mm. The climate is less seasonal with averaged temperature ranging from 24 °C to 29 °C throughout the year. The interior lowlands and foothills are wetter than the coastal area, with rainfalls from 1500-2000 mm per year. This area also has two distinct seasons including wet and dry seasons. The mountainous area of Annamite range is cooler and wetter than the lowland. Rainfall recorded at elevations above 1000 m is usually more than 2000 mm and increases with altitude. The vegetation and habitats of this area are also diverse. Under 800 m, the evergreen broadleaf forest is

dominated by tropical plant families such as Fagaceae and Magnoliaceae. As elevation increases the climate becomes cooler and wetter, mixed evergreen broadleaf forests and coniferous forests become dominated. Semi-evergreen forest and deciduous forest are dominating habitats in the south of Kon Tum Plateau (Sterling et al., 2006).

Occurrence data

We collected a total of 158 independent localities that recorded the occurrence of GSDL through previously published studies, including Tran and Hoang (2015); Ha (2000; 2003; 2004; 2007); Minh et al. (2005); Nadler (1997); Nadler et al. (2003); Nguyen et al. (2010) and aggregated data in Bett et al. (2012).

Environmental variables

To predict the appropriate distribution of GSDL, we collected and analyzed 25 environmental variables from different sources (*Table 1*). They were selected based on relationships between the variables and the ecological features of the species. These variables are often used in simulating the distribution of many species (Peterson et al., 2007; Kurmar and Stohlgren, 2009). Of the selected environmental variables, there were 19 climate variables and 3 topographical variables including altitude, slope, and slope direction. Vegetation-related variables included land cover, Normalized Difference Vegetation Index (NDVI), and percentage of tree cover. Climate variables consisting of 19 different map layers were downloaded from Woldclim (www.worldclim.com). These included 11 temperature variables and 8 precipitation related variables (Hijmans et al., 2005). Topographic map which was processed using the signal from The Shuttle Radar Topography Mission (SRTM) had 90 m × 90 m resolution (downloaded from <http://srtm.csi.cgiar.org>). Slope and aspect data layer were calculated from the elevation map layer on ArcMap 10.1 (ESRI) software. The land cover map that was made using data from the MODIS image that was downloaded from http://landcover.usgs.gov/global_climatology.php (Broxton et al., 2014). The vegetation variable was categorized with assigned values ranging from 1 to 16. The resolution of vegetation layer was 500 × 500 m. The normalized difference vegetation index (NDVI) for Asia was downloaded from <https://earthexplorer.usgs.gov/> with 250 × 250 m resolution. All NDVI layers of all months in 2013 were used to calculate the average NDVI layer of the year using ArcMap 10.1 software (ESRI). Percentage of tree cover is calculated based on canopy coverage. It is extracted from MODIS image with 500 m × 500 m resolution (downloaded from <http://www.iscgm.org/gm/glcnm.html>). In addition, the value 254 showed water surface and 255 meant no data area.

In order to eliminate highly correlated variables, data from 2000 randomly selected points in the region was exported to Excel for calculating the correlation coefficient. The Pearson correlation coefficient was used to calculate the correlation between pairs of variables. With pairs of variables having a coefficient of $|r| > 0.85$ would retain only one variable for subsequent calculations. Finally, we selected 16 variables out of 25 variables for use in running the final model. The variables used are shown in *Table 1*.

Prediction of distribution using MaxEnt

Although there exist a variety of computer programs for modelling species distribution, in this study, the MaxEnt model was applied due to the following reasons: 1) MaxEnt outperforms other methods based on more accurate predictions; 2) The

software is easy to use and suitable for small sample sizes (Peterson et al., 2007; Baldwin, 2009; Merow et al., 2013). In addition, MaxEnt is free software and can be downloaded from: http://biodiversityinformatics.amnh.org/open_source/maxent/ (Phillips et al., 2017).

Table 1. Environmental data variables were used in the model. (Bold variables were used in the final model prediction.)

Variables	Source	Data type
BIO1 = annual mean temperature	Worldclim	Continuous
BIO2 = mean diurnal range (mean of monthly = max temp - min temp)		
BIO3 = isothermality (BIO2/BIO7) (* 100)		
BIO4 = temperature seasonality (standard deviation *100)		
BIO5 = max temperature of warmest month		
BIO6 = min temperature of coldest month		
BIO7 = temperature annual range (BIO5-BIO6)		
BIO8 = mean temperature of wettest quarter		
BIO9 = mean temperature of driest quarter		
BIO10 = mean temperature of warmest quarter		
BIO11 = mean temperature of coldest quarter		
BIO12 = annual precipitation		
BIO13 = precipitation of wettest month		
BIO14 = precipitation of driest month		
BIO15 = precipitation seasonality (coefficient of variation)		
BIO16 = precipitation of wettest quarter		
BIO17 = precipitation of driest quarter		
BIO18 = precipitation of warmest quarter		
BIO19 = precipitation of coldest quarter		
LcType = land cover	landcover.usgs.gov	Categorical
TreeCover = percent tree coverage	iscgm.org	Categorical
NDVI	earthexplorer.usgs.gov	Continuous
Elevation	srtm.csi.cgiar.org	Continuous
Aspect	Calculated from SRTM in ArcMap	Continuous
Slope (%)	Calculated from SRTM in ArcMap	Continuous

All data layers of the environmental variables were converted to raster and resampled to a resolution of 90 × 90 m. Data was then transformed to ASCII data (*.asc) using ArcMap 10.1 (ESRI)

MaxEnt is the software that uses predictive methods to simulate the potential distribution of species from existing information (Phillips et al., 2006). Species occurrence data is used as input (called occurrence data), along with the use of environmental condition variables (such as temperature, rainfall, etc.) to interpolate for each grid cell. At present, the model is very popular for ecological niche modelling (distribution) of species. Several studies have used MaxEnt for distribution modelling of mammal species (Syfert et al., 2014) and (Nazeri et al., 2012). Particularly, the model have also been used to predict the distribution of primate species, for example: Hoo'clock gibbon (Sarma et al., 2015), Loris species in the genus *Nycticebus* (Thorn et al., 2009), Loris family (Kumara et al., 2009), and *Pygathrix* genus (Bett et al., 2012).

In this study, the following indexes were used: percentage of random sample to test = 20%, regularization multiplier = 0.2, maximum iteration = 1000, convergence threshold = 0.001, maximum number of background points = 10,000. These values have also been widely used in other studies (Nazeri et al., 2012; Sarma et al., 2015; Onojeghuo et al., 2015). Of 158 presence data points, 127 points were used as a training sample, and 31 points as reference data for validation.

The area under the response curve (AUC), with values ranging from 0 to 1 was used under application of the Receiver Operator Characteristic model (ROC) to determine model suitability (Phillips, 2006; Nazeri et al., 2012). In this context, AUC values > 0.75 (larger values meaning higher model suitability) allowed usage of the model for species distribution (Elith, 2000; Nazeri et al., 2015). When the AUC = 1, the predictive ability of the model is considered perfect. If the AUC < 0.5, the model does not have the ability to predict (Phillips, 2006; Bett et al., 2012).

The background points chosen can strongly affect model outcome because of the geographic extent of any MaxEnt model. In this study, to avoid overestimating a lack of niche overlap we selected the study area encompassed the entire Indochinese peninsula. Running model in this entire area allowed us to determine the other suitable areas of *P. cinerea* extended beyond the current range in Central of Vietnam.

In order to assess variable importance, the Jackknife method (Pearson et al., 2007) was applied, where MaxEnt eliminated unsuitable variables, followed by model creation based upon the remaining suitable variables. Therewith, influences of model variables upon the general species model is shown (Phillips, 2006).

MaxEnt generated a map layer showing levels of suitability to GSDL with value ranging from 0 to 1 for each pixel, whereas greater pixel values represented higher prediction suitability. The files were generated in ASCII (*.asc) format and converted into raster format (*.tif) with ArcMap 10.1. In this study, the value of “equal training sensitivity and specificity” was used to classify suitable (> 0.2) and unsuitable areas (0-0.2). Then, suitable habitats were divided into 4 categories: Very high potential (> 0.8), High potential (0.6-0.8), Medium potential (0.4-0.6), Low potential (0.2-0.4).

Results

Discrimination capacity of the model ranged at $AUC_{train} = 0.987$ and $AUC_{test} = 0.987$. Total area with high suitability was 367.7 km² and low suitability about 7067.7 km² (Figs. 2 and 3).

Potential distribution area as well as contribution of each environmental variable (temp.; precip, etc) were modeled. The biggest contribution (27.7%) resulted from precipitation of the driest month (bio14) followed by temperature annual range (bio7)

(18.3%). Temperature seasonality (bio4) and land cover (LCtype) ranged at 10.7% and 9.7%, respectively (Table 2). Percentage contributions of Bio 1, Bio19, slope, NDVI, and aspect were small (< 1.0%).

Table 2. Analysis of variable contribution

No	Variable	Percentage contribution (%)	No	Variable	Percentage contribution (%)
1	Bio14	27.7	9	Bio18	3.6
2	Bio7	18.3	10	TreeCover	2.7
3	Bio4	10.7	11	Bio2	1.4
4	LcType	9.7	12	Bio1	0.6
5	Bio3	8.6	13	Slope	0.1
6	Bio15	6.1	14	Bio19	0.1
7	Bio12	6.0	15	NDVI	0.1
8	Elevation	4.2	16	Aspect	0

The suitability of each variable for distribution areas of GSDL is shown in response curves (Appendix 1). For climatic variables, the results show that the potential distribution of GSDL concentrates in the areas where precipitation in the driest month ranges from 30 to 35 mm and annual rainfall from 2000 to 2300 mm. The difference between the hottest month and the coldest month is best suited at around 16°C and average annual temperature at 19-24 °C. Regarding vegetation it was found that GSDL preferred evergreen broadleaf forest (LCtype 2) over any other forest types. Suitable topographic elevations for GSDL ranged at [500,1400] m asl. Areas most suitable in this regard ranged at [1000,1400] m asl.

The Jackknife test in MaxEnt model shows that precipitation of driest month (bio14) and temperature annual range (bio7) are the most important variables if they are simulated in isolation to other variables. Omitting of annual precipitation (bio 12) and percentage of tree cover (TreeCover) resulted in reduced gain level of the model (Appendix 2).

Discussion

The map in Figure 2 graphically shows the expansion of suitable distribution area of GSDL ranging from 14 to 16° North. The potential distribution lies within the boundaries of 5 provinces including Quang Nam, Quang Ngai, Kon Tum, Gia Lai and Binh Dinh. This modelling result fits the known distribution of the species (Ha, 2000; 2004; Nadler et al., 2003; Nguyen et al., 2010; Nadler and Brockman, 2014) and aligns with IUCN's distribution map, which indicates the models reliability. Our finding is also consistent with the previous study of Bett et al. (2012). However, Bett et al. (2012) only used climate-related variables. In our study, the vegetation-related variables (land cover, NDVI, and percentage of tree cover) and topographic variables (elevation, aspect, and slope) were added. In fact, these variables affect the predicted range of the species, thus increasing model precision through presence of more variables (Wilson et al., 2013). Therefore, potential distribution modelled for GSDL is narrowed down and becomes more fragmented.

The model is divided into areas of varying suitability degrees, with suitable area for GSDL being mainly concentrated in the intersectional area between the south central coast and central highland and in the eastern and southern slope of Kon Tum Mountain (Fig. 2). These areas are wetter and receive more rain than western parts (Sterling et al., 2006). In addition, they still remain good natural broad-leaved forest habitats. Areas of highest suitability are mainly concentrated in the borders of Quang Ngai (Ba To district), Kon Tum (Kon Plong district), Binh Dinh (An Lao district) and Gia Lai (K 'Bang district) provinces; and in Kon Ka Kinh National Park, Kon Cha Rang Nature Reserve, An Toan Nature Reserve. Other high suitable areas lie among Nam Tra My, Bac Tra My, Hiep Duc, Phuoc Son, and Nam Giang districts of Quang Nam province. Thereby, the suitable areas for GSDL are mainly concentrated in the eastern and southern slope of Kon Tum Mountain.

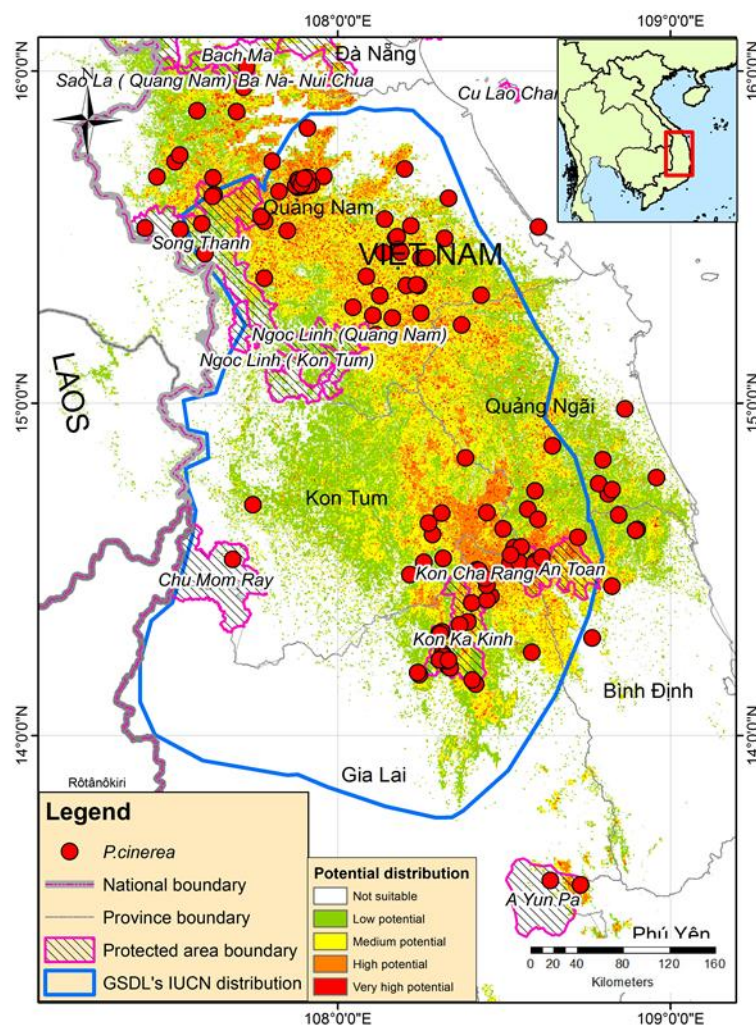


Figure 2. Prediction of areas potentially suitable for distribution of *P. cinerea* within protected area as well as occurrence data (red dots)

The total suitable area for GSDL at 16,680.52 km². The low suitable areas account for about 42% of the total area. Of this, area with medium, high and very high suitability account for 37%; 19% and 2% respectively (Fig. 3). The total area of

GSDL's distribution within the boundaries of existing protected area system only ranges at 1680.37 km² (about 10% of the total suitable area as the model predicted). Therefore, the current network of Vietnam's protected area occupies a small part of suitable habitat of GSDL, especially regarding areas of high and very high suitability. This result also indicates that more survey efforts to further to the north of the current distribution range of GSDL need to be considered for discovering new populations. The establishment of new protected areas for the conservation of wildlife and habitat protection is very important and urgent.

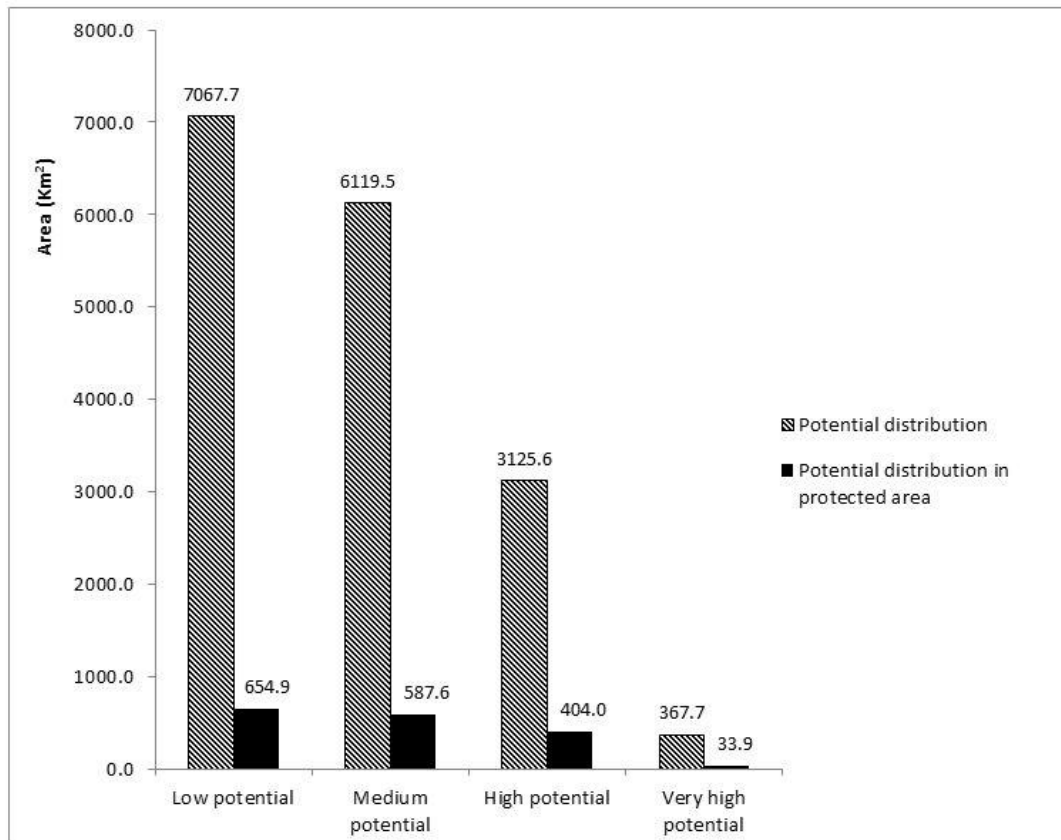


Figure 3. Potential distribution area of GSDL with low, medium, high, and very high suitability

By now, many species are threatened with extinction and face habitat loss. Habitat loss and a number of the individuals remaining are two greatest concerns for species conservation (Nazeri et al., 2012). In the case of rare primate species like GSDL, the greatest threats are habitat loss and hunting (Vu et al., 2008; Nguyen et al., 2012). The GSDL's potential distribution which is not included in the existing protected areas can cause severe impacts to the species population in the future. However, the establishments of protected areas only proceeds with long-term the national planning, which might interfere with economic development. Conservation outside the protected areas is critically important for GSDL.

The potential distribution area of GSDL is not much found within the existing protected areas but coincides with many proposed biodiversity corridors. For example, the area between Kon Ka Kinh National Park and Kon Cha Rang Nature Reserve is highly suitable for GSDL. It lies within the proposed corridor connecting Kon Ka

Kinh NP and Kon Cha Rang Nature Reserve covering an area of about 108,607 km². The objective of this corridor is to support and manage the biodiversity of the adjunction area (Breese, 2009). The area also coincides with a biodiversity corridor for adaptation and mitigation of climate change proposed by Vu (2014) with a length of about 20 km covering an area of about 95,116 km². In addition, potential distribution areas of GSDL are also located in many other proposed biodiversity corridors such as Kon Cha Rang-Ngoc Linh, Ngoc Linh-Ngoc Linh, Ngoc Linh-Song Thanh, and Song Thanh-Sao La. These areas are quite large. Most of them are natural forest which is similar to the habitats found in protected forests. Therefore, the feasibility for establishment of biodiversity corridor is very high (Vu, 2014). Biodiversity corridor establishment is urgently needed to improve the protection of GSDL throughout its entire distribution range.

Modelling of GSDL's potential distribution area has been applied based on ecological factors including climate, topography, and vegetation related variables in connection with occurrence data. In particular, environmental factors have a complex impact on the distribution of primates (Kamilar, 2009). Previous studies have also shown that the distribution of animals is highly dependent on the environment (Zonneveld et al., 2009) and that abiotic factors have different effects on the distribution of primates at different regions (Vidal-Garcia and Serio-Silva, 2011). Furthermore, climate biology features are also thought to affect the distribution of species in *Pygathrix* ssp. (Bett et al., 2012). The use of climate variables is an effective way of identifying geographical distributions of species (Sarmar et al., 2015). In the predictive distribution model of GSDL, precipitation of the driest month (bio14) has the highest effect of all parameters. This is in line with the findings of (Bett et al., 2012). In the South Central and Central Highland regions of Vietnam, climate features vary immensely. Differences in climatic conditions are due to a large variation in altitude, surrounding terrain and ridge direction (Sterling et al., 2006). In particular, a high mountain present between Da Nang city and Thua Thien Hue province creates the climatic difference between South-Central Coast and the Northern Central Coast regions which might be a major barrier for further expansion of GSDL to the North.

The high level of impact from climate variables within the model is a hint for future impacts of climate change on GSDL populations, potentially causing distribution shifts northward shifts distribution, or in areas of higher altitude. Influence upon the future distribution can occur either in trends or shrinks (Root and Schneider, 2002). Therefore, more in-depth studies on the future impacts of climate change on species distribution are necessary. In addition to direct effects, climate change might indirectly affect the distribution of GSDL by influencing growth and distribution of flora consumed by the animals (Vidal-Garcia and Serio Silva, 2011; Sarma et al., 2015). The indirect effects of climatic factors might be critical as the species do predominately feeds on plants like GSDL. Another our study showed that the distribution of grey-shanked douc langur was predicted to decrease dramatically under the effects of climate change. Furthermore, the projections indicate that a larger suitable area will be disappeared, particularly high and very high suitable areas (Tran et al., 2018).

The influence of vegetation-related variables (land cover, percentage of tree cover, NDVI) within the model is not negligible. The predicted distribution shows that GSDL tend to be distributed in the evergreen broadleaved forest more than in any other forest types. Distribution is mainly limited to areas with percentage of tree cover of 60% or higher. This result is consistent with previously published studies on the ecology of

GSDL (Ha, 2004; 2009; Nadler, 2014). GSDL prefer forest with high dense canopy cover and complex vertical structures that provides many types of fruits and seeds for feeding (Ha, 2009; Nguyen et al., 2012).

The potential distribution map of GSDL will be an important basis for the implementation of conservation programs for the species in the Central Highland and South Central Coast. Priority should be given to Kon Ka Kinh, Kon Cha Rang, and An Toan Nature Reserves, as well as the northern part of Song Thanh Nature Reserve because much of highly suitable area lies within these protected areas. Conservation outside the protected areas is also very important for GSDL because both modelling and field surveys have found the habitat outside the protected areas hold significant populations. Additionally, more surveying efforts should also be given to the area on the northern part of the distribution range and along the border between Kon Tum, Quang Nam, and Quang Ngai provinces.

Conclusion

The projection of MaxEnt model shows that the suitable area for GSDL is approximately from 14°N-16°N. It lies within the boundaries of 5 provinces including Quang Nam, Quang Ngai, Kon Tum, Gia Lai and Binh Dinh. The precipitation of driest month (bio14) had the highest impact with 27.7%. Then, the temperature annual range (bio7) was the second one with 18.3%. The total suitable area of GSDL is 16,680.52 km². The least suitable area accounts for about 42% of the total area. The area of medium suitability is about 37%. The areas of high and very high suitability account for 19%, and 2%, respectively. The potential distribution area of the species is not much found in the existing protected areas. Priorities for conservation and survey efforts should be given to the forested areas in Quang Ngai (Ba To district), Kon Tum (Kon Plong district), Binh Dinh (An Lao district) and Gia Lai (K 'Bang district) provinces; and in Kon Ka Kinh National Park, Kon Cha Rang Nature Reserve, An Toan Nature Reserve. Another important areas lies among Nam Tra My, Bac Tra My, Hiep Duc, Phuoc Son, and Nam Giang districts of Quang Nam province. Conservation efforts should also be prioritized for areas beyond the boundary of protected areas, especially for areas that have been proposed as biodiversity corridor. In the next studies, we need to collect more occurrence data of GSDL in the field. In addition, we should add environmental variable such as the impacts of human or road systems in the study area to run the model. It allows MaxEnt model to increase the accuracy of the distribution. Furthermore, we should implement the deep studies about the impact of climate change on the distribution of GSDL by using the climate change scenarios in the future.

Acknowledgements. We are grateful to Ms. Pham Thi Nhung, Ms. Nguyen Thi Huyen Chung and Ms. Tran Thi Phuong Hoa (Vietnam National University of Forestry) for supporting the data collection.

REFERENCES

- [1] Baldwin, R. A. (2009): Use of maximum entropy modeling in wildlife research. – *Entropy* 11: 854-866.
- [2] Bett, N. N., Blair, M. E., Sterling, E. J. (2012): Ecological niche conservatism in Doucs (Genus *Pygathrix*). – *Int J Primatol* 33: 972-988.

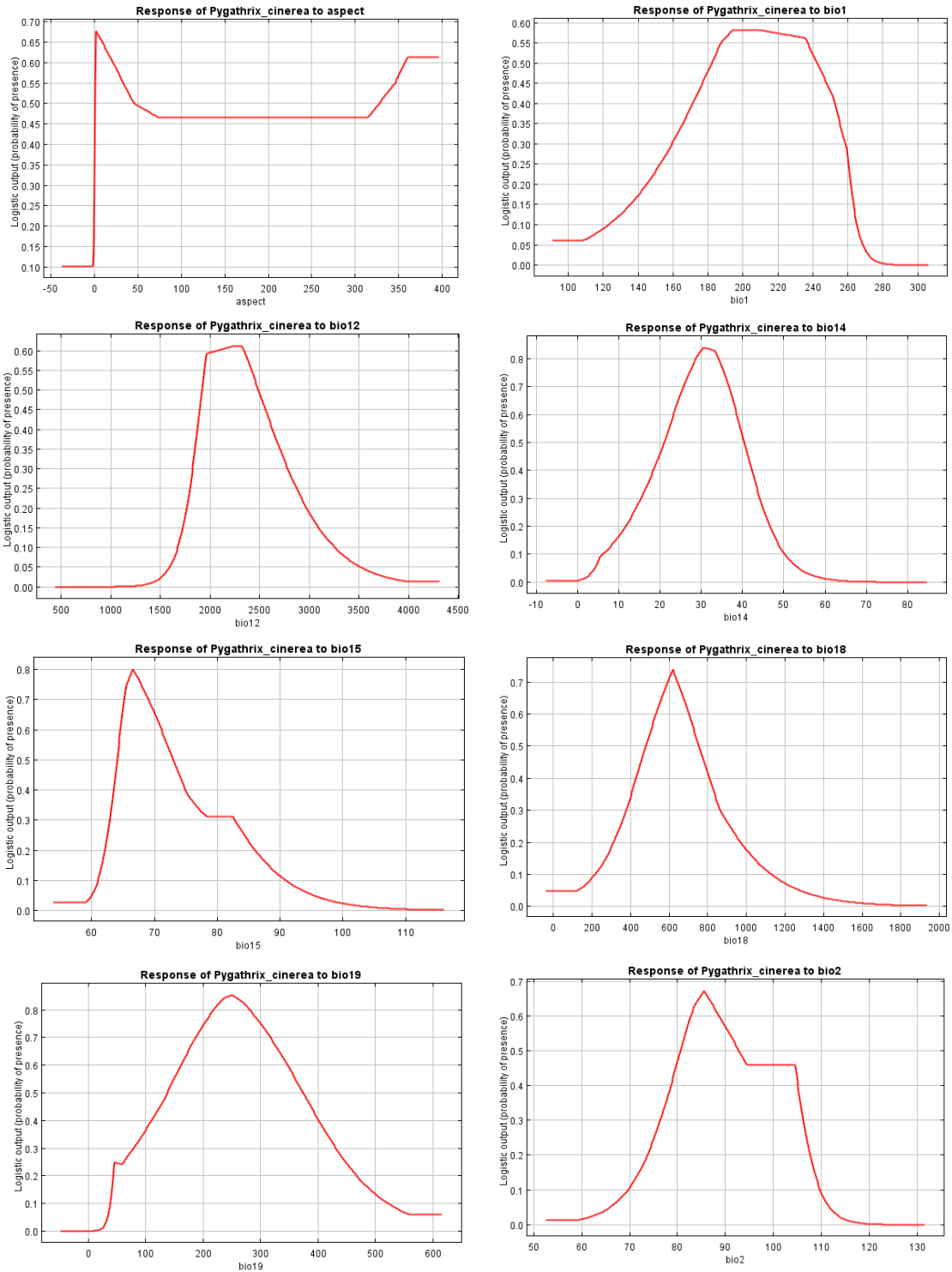
- [3] Breese, J. (2009): Making the Link: The Connection and Sustainable Management of Kon Ka Kinh National Park and Kon Chu Rang Natural Reserves. Final Report. – UNDP, Hanoi, Vietnam.
- [4] Broxton, P. D., Zeng, X., Sulla-Menashe, D., Troch, P. A. (2014): A global land cover climatology using MODIS data. – J Appl Meteor Climatol 53: 1593 -1605. doi: <http://dx.doi.org/10.1175/JAMC-D-13-0270.1>.
- [5] Cork, S. J., Catling, P. C. (1996): Modelling distributions of arboreal and ground-dwelling mammals in relation to climate, nutrients, plant chemical defenses and vegetation structure in the eucalypt forests of south eastern Australia. – Forest Ecol Manag 85: 163-175.
- [6] Elith, J. (2000): Quantitative Methods for Modeling Species Habitat: Comparative Performance and an Application to Australian Plants. – In: Ferson, S., Burgman, M. (eds.) Quantitative Methods for Conservation Biology. Springer, New York.
- [7] FFI (2016): Vietnamese primatologists discover 500 grey-shanked douc langurs. – <http://vietnamnews.vn/society/283188/vietnamese-primatologists-discover-500-grey-shanked-douc-langurs.html#74IQzgohrb3y68Yy.99>. Accessed 8 May 2017.
- [8] Franklin, J., Miller, J. A. (2009): Mapping Species Distributions – Spatial Inference and Prediction. – Cambridge University Press, New York.
- [9] Ha, T. L. (2000): Records of Grey-shanked Douc Langur (*Pygathrix cinerea*) in the Central Highlands of Vietnam. Report. – Frankfurt Zoological Society-Vietnam Primate Conservation Programme. Frankfurt Zoological Society, Hanoi.
- [10] Ha, T. L. (2003): A preliminary Survey of Distribution and Population of Grey-Shanked Douc Monkeys (*Pygathrix cinerea*) in Vietnam. – Oxford Brookes University, Oxford.
- [11] Ha, T. L. (2004): Distribution and Status of the Grey-Shanked Douc (*Pygathrix cinerea*) in Vietnam. – In: Nadler T, Streicher U., Ha, T. L. (eds.) Conservation of Primates in Vietnam. Frankfurt Zoological Society, Hanoi.
- [12] Ha, T. L. (2007): Distribution, population and conservation status of the grey-shanked douc (*Pygathrix cinerea*) in Gia Lai Province, Central Highlands of Vietnam. – Vietnamese J Primatol 1: 55-60.
- [13] Hijmans, R. J., Cameron, S. E., Parra, J. L., Jones, P. G., Jarvis, A. (2005): Very high resolution interpolated climate surfaces for global land areas. – Int J Climatol 25: 1965-1978.
- [14] Hirzel, A. H., Hausser, J., Chessel, D., Perrin, N. (2002): Ecological niche factor analysis: how to compute habitat-suitability maps without absence data. – Ecology 87: 2027-2036.
- [15] Kamilar, J. M. (2009): Environmental and geographic correlates of the taxonomic structure of primate communities. – Am J Phys Anthropol 139: 382-393.
- [16] Kumar, S., Stohlgren, T. J. (2009): Maxent modeling for predicting suitable habitat for threatened and endangered tree *Canacomyrica monticola* in New Caledonia. – J Ecol Nat Environ 1: 094-098.
- [17] Kumara, H. N., Irfan-Ullah, M., Kumar, S. (2009): Mapping potential distribution of slender loris subspecies in peninsular India. – Endanger Species Res 7: 29-38.
- [18] Merow, C., Smith, M. J., Silander, J. A. Jr. (2013): A practical guide to MaxEnt for modeling species' distributions: what it does, and why inputs and settings matter. – Ecography 36: 1058-1069. doi: 10.1111/j.1600-0587.2013.07872.x.
- [19] Minh, H., Khanh, T. V., Thuong, H. V., Long, B. (2005): Primate Conservation in Quang Nam Province, Central Vietnam. – WWF Indochina and Quang Nam Forest Protection Department, Vietnam.
- [20] Ministry of Science and Technology and Vietnam Academy of Science and Technology (2007): Vietnam's Red Data Book, Part I. – Animals, Natural Science and Technology Publishing Company, Hanoi.
- [21] Nadler, T. (1997): A new subspecies of douc langur, *Pygathrix nemaesus cinereus* ssp. nov. – Zoologischer Garten (NF) 67: 165-176.

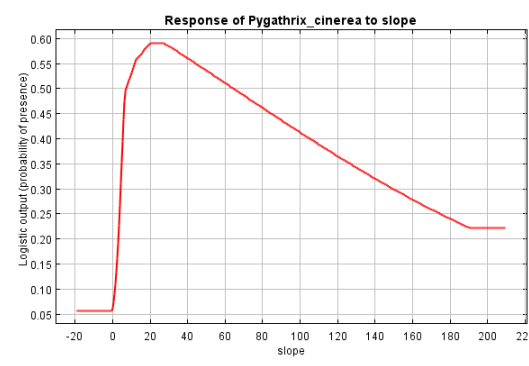
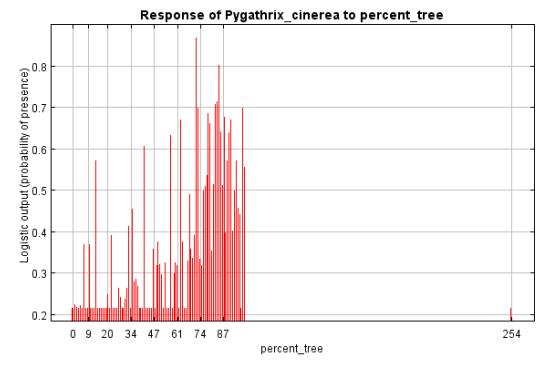
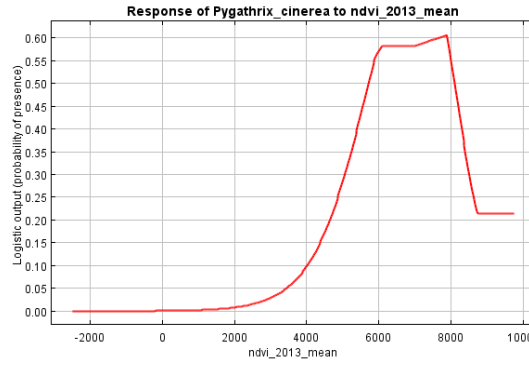
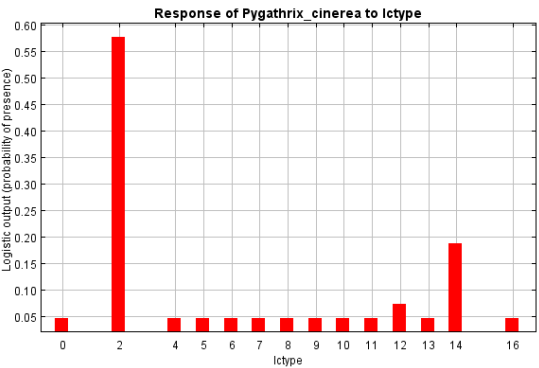
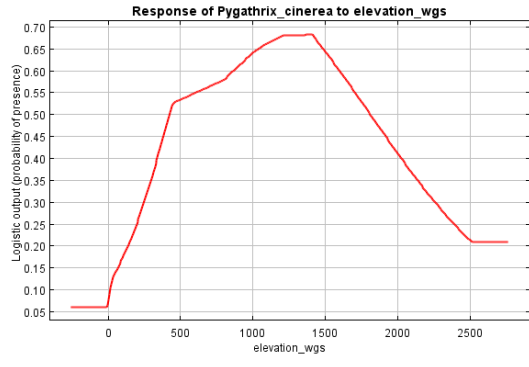
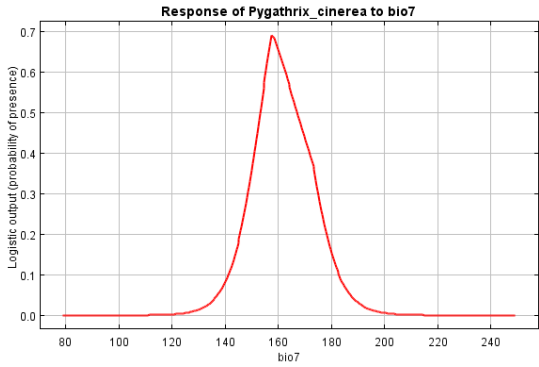
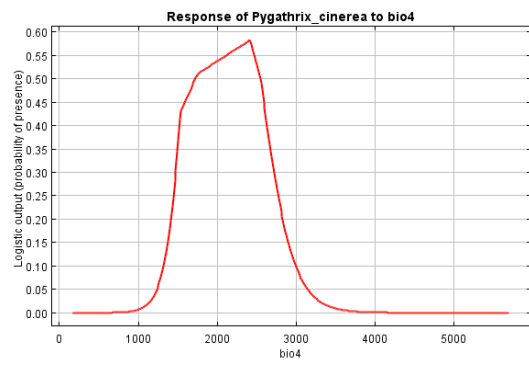
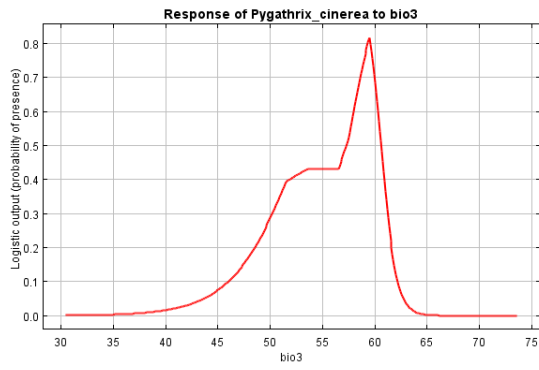
- [22] Nadler, T. (2010): Status of Vietnamese Primates – Complements and Revisions. – In: Nadler, T., Rawson, B. M., Van, N. T. (eds.) Conservation of Primates in Indochina. Frankfurt Zoological Society and Conservation International, Hanoi.
- [23] Nadler, T., Brockman, D. (2014): Primates of Vietnam. – Endangered Primate Rescue Center, Cuc Phuong National Park, Ninh Binh.
- [24] Nadler, T., Momberg, F., Dang, N. X., Lormee, N. (2003): Vietnam Primate Conservation Status Review 2002. – Fauna and Flora International and Frankfurt Zoological Society, Hanoi.
- [25] Nazeri, M., Jusoff, K., Madani, N., Mahmud, A. R., Bahman, A. R., Kumar, L. (2012): Predictive Modeling and Mapping of Malayan Sun Bear (*Helarctos malayanus*) Distribution Using Maximum Entropy. – PLoS ONE 7: e8104. doi:10.1371/journal.pone.0048104.
- [26] Nguyen, T. T., Le, V. K., Le, K. Q. (2010): New data on the distribution of grey-shanked douc langurs (*Pygathrix cinerea*) in Quang Ngai Province, Vietnam. – In: Nadler, T., Rawson, B. M., Van, N. T. (eds.) Conservation of Primates in Indochina. Frankfurt Zoological Society and Conservation International, Hanoi.
- [27] Nguyen, T. T., Ha, T. L., Bui, V. T., Tran, H. V., Nguyen, A. T. (2012): The feeding behavior and phytochemical food content of grey-shanked douc langur (*Pygathrix cinerea*) at Kon Ka Kinh National Park, Vietnam. – Vietnamese J Primatol 2: 25-35.
- [28] Onojeghuo, A. O., Blackburn, A. G., Okeke, F., Onojeghuo, A. R. (2015): Habitat Suitability Modeling of Endangered Primates in Nigeria: Integrating Satellite Remote Sensing and Spatial Modeling Techniques. – Journal of Geoscience and Environment Protection 3: 23-38.
- [29] Pearson, R. G., Raxworthy, C. J., Nakamura, M., Peterson, A. T. (2007): Predicting species' distributions from small numbers of occurrence records: A test case using cryptic geckos in Madagascar. – J Biogeogr 34: 102-117.
- [30] Peterson, A. T., Papes, M., Eaton, M. (2007): Transferability and model evolution in ecological niche modeling: a comparison of GARP and MAXENT. – Ecography 30: 550-560.
- [31] Phillips, S. J. (2006): A Brief Tutorial on Maxent. – AT&T Research, Florham Park, New Jersey. <http://www.cs.princeton.edu/~schapire/maxent/tutorial/-tutorial.doc>. Accessed 28 December 2016.
- [32] Phillips, S. J., Anderson, R. P., Schapire, R. E. (2006): Maximum entropy modeling of species geographic distributions. – Ecol Model 190: 231-259.
- [33] Phillips, S. J., Dudík, M., Schapire, R. E. (2017): [Internet] Maxent software for modeling species niches and distributions (Version 3.4.1). – http://biodiversityinformatics.amnh.org/open_source/maxent/. Accessed 4 October 2017.
- [34] Raxworthy, C. J., Ingram, C. M., Rabibisoa, N., Pearson, R. G. (2007): Application of ecological niche modeling for species delimitation: A review and empirical evaluation using day Geckos (*Phelsuma*) from Madagascar. – Syst Biol 56: 907-923. doi:10.1080/10635150701775111.
- [35] Roos, C., Nadler, T. (2001): Molecular evolution of the Douc Langurs. – Zool Garten N F 7: 11-6.
- [36] Root, T. L., Schneider, S. H. (2002): Climate Change: Overview and Implications for Wildlife. – In: Schneider, S. H., Root, T. L. (eds.) Wildlife Responses to Climate Change: North American Case Studies. Island Press, Washington D. C.
- [37] Sarma, K., Kumar, A., Krishna, M., Medhi, M., Tripathi, O. P. (2015): Predicting suitable habitats for the Vulnerable Eastern Hoolock Gibbon *Hoolock leuconedys*, in India using the MaxEnt model. – Folia Primatol 86: 387-397. doi: 10.1159/000381952.
- [38] Schwitzer, C., Mittermeier, R. A., Rylands, A. B., Taylor, L. A., Chiozza, F., Williamson, E. A., Wallis, J., Clark, F. E. (eds.) (2014): Primates in Peril: The World's 25 Most Endangered Primates 2012-2014. – IUCN SSC Primate Specialist Group, International

- Primatological Society, Conservation International, and Bristol Zoological Society, Arlington, VA.
- [39] Sterling, E. J., Hurley, M. M., Le, M. D. (2006): A Natural History of Vietnam. – Yale University Express, New Haven.
- [40] Syfert, M. M., Joppa, L., Smith, M. J., Coomes, D. A., Bachman, S. P., Brummitt, N. A. (2014): Using distribution models to inform IUCN Red List assessments. – *Biol Conserv* 177: 174-184.
- [41] Thorn, J. S., Nijman, V., Smith, D., Nekaris, K. A. I. (2009): Ecological niche modeling as a technique for assessing threats and setting conservation priorities for Asian slow lorises (Primates: Nycticebus). – *Divers Distrib* 15: 289-298.
- [42] Tran, V. B., Hoang, M. D. (2015): First records of primate species of A Yun Pa proposed nature reserve. – *Proceeding of the Sixth National Workshop on Ecology and Biological Resources, Hanoi, Vietnam.*
- [43] Tran, V. D., Tran, T. P. H., Ta, T. N., Vu, T. T. (2018): Assessing impact of future climate change on the distribution of Gray-shanked douc (*Pygathrix cinerea*) using ecological niche modelling. – In press.
- [44] Vidal-Garcia, F., Serio-Silva, J. C. (2011): Potential distribution of Mexican primates: Modeling the ecological niche with the maximum entropy algorithm. – *Primates* 52: 261-270.
- [45] Vu, N. T., Lippold, L., Nadler, T., Timmins, R. J. (2008): *Pygathrix cinerea*. – The IUCN Red List of Threatened Species 2008: e.T39827A10273229. <http://dx.doi.org/10.2305/IUCN.UK.2008.RLTS.T39827A10273229.en>. Accessed 27 December 2016.
- [46] Vu, T. T. (2014): Proposing green corridors to conserve biodiversity of southern Vietnam in the context of climate change. – *Journal of Forest and Environment* 65: 24-31.
- [47] Warren, D. L., Seifert, S. N. (2011): Ecological niche modeling in MaxEnt: the importance of model complexity and the performance of model selection criteria. – *Ecol Appl* 21: 335-342.
- [48] Wilson, J. W., Sexton, J. O., Jobe, R. T., Haddad, N. M. (2013): The relative contribution of terrain, land cover, and vegetation structure indices to species distribution models. – *Biol Conserv* 164: 170-176.
- [49] Zonneveld, M. V., Koskela, J., Vinceti, B., Jarvis, A. (2009): Impact of climate change on the distribution of tropical pines in Southeast Asia. – *Unasylva Journal* 60: 24-29.

Appendix 1

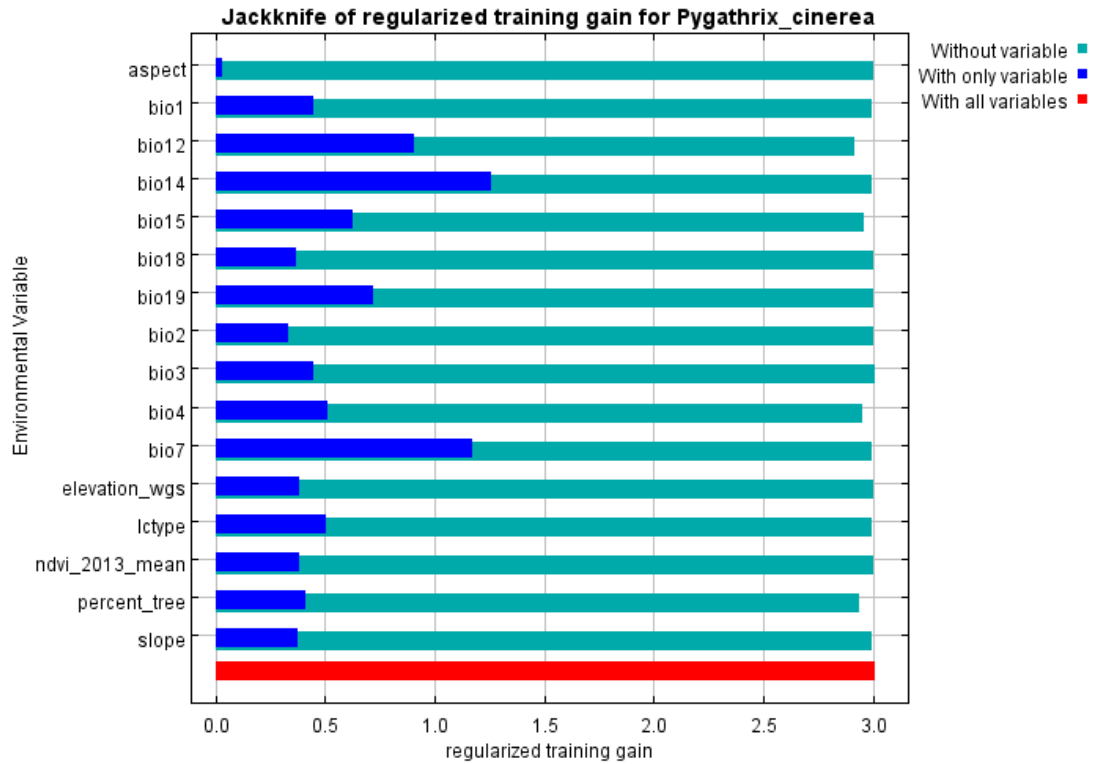
Variable response curves for the predictors of *Pygathrix cinerea* by the MaxEnt model





Appendix 2

Results of jackknife test of relative variable importance of predictor variable for *Pygathrix cinerea*



THE EFFICIENCY OF BIOLOGICAL CONTROL TREATMENTS OF CODLING MOTH (*CYDIA POMONELLA* L.) ON THREE DIFFERENT APPLE VARIETIES

TOMAŠ, V.^{1*} – ŠIMIĆ, D.¹ – MIHALJEVIĆ, I.¹ – DUGALIĆ, K.² – VILJEVAC VULETIĆ, M.¹ – VUKOVIĆ, D.¹ – ZDUNIĆ, Z.¹ – BARIĆ, B.³ – BRMEŽ, M.⁴

¹*Agricultural Institute Osijek
Južno predgrađe 17, 31103 Osijek, Croatia
(phone: +385-31-515-539; fax: +385-31-515-539)*

²*Food and Rural Affairs, Croatian Center for Agriculture
Svetošimunska cesta 25, 10000 Zagreb, Croatia
(phone: +385-1-462-9240; fax: +385-1-462-9241)*

³*Faculty of Agriculture, University of Zagreb
Svetošimunska cesta 25, 10000 Zagreb, Croatia
(phone: +385-1-239-3777; fax: +385-1-231-5300)*

⁴*Faculty of Agriculture in Osijek, J. J. Strossmayer University of Osijek
Vladimira Preloga 1, 31000 Osijek, Croatia
(phone: +385-31-554-801; fax: +385-31-554-853)*

**Corresponding author
e-mail: vesna.tomas@poljinis.hr; phone: +385-31-515-539; fax: +385-31-515-539)*

(Received 10th Oct 2017; accepted 12th Feb 2018)

Abstract. Codling moth (*Cydia pomonella* L.) is one of the most important apple pests which population is steadily growing. The aim of this study, conducted in Eastern Croatia, was to determine the efficiency of two biological preparations CpGV and kaolin clay compared with pyrethroids and control treatment. The preparations used in treatments were: 1) *Cydia pomonella* granulovirus (CpGV), 2) deltamethrin, beta cyfluthrin and alpha-cipemetrina, 3) kaolin, 4) control treatment, applying in two different methods of time control, on the three apple varieties ‘Melrose’, ‘Jonagored’ and ‘Golden Delicious’ clone B. The efficiency of the treatment 1 (CpGV) ranged from 78% to 95%, of treatment 2 (pyrethroids) from 96% to 97%, and treatment 3 (kaolin) – between 21.5 and 57%. There was significant negative correlation between yield and damage ($r = -0.56$). Two methods of determining time control did not differ significantly. Variety ‘Melrose’ had the highest number of fruits damage in all three years and ‘Golden Delicious’ clon B the lowest number which can be related to the codling moth caterpillar affinity to a certain variety. It is very important to make the best choice of preparations in control and at the same time be sure of their positive effect on the environment and human health.

Keywords: *CpGV, kaolin, pyrethroid, time of control, variety*

Introduction

The apple is a fruit species with the highest number of control treatments in the world (Blommers, 1994). In Croatia, the total number of apple control treatments are around 15 and 25 against all diseases and pests, while the number of control treatment of codling moth ranges from 6 to 8 treatments during one growing season. Despite ecological concern about the harmful pesticides effects on the environment, control of phytophagous species is mostly based on the use of chemical control (Choinard et al., 2016; Iraqui and Hmimina, 2016; Tamošiūnas et al., 2014). In the orchard with use of insecticides with

broad spectrum of action, the result is absence of useful entomofauna diversity (Ismail and Albittar, 2016; Blommers et al., 1987) which contributes to the reduction of natural phytogamous population with no harmful effects on the environment. Biological control incorporates various approaches called integrated pest management which combines a variety of pest control methods (Mahr et al., 2008). The biological control methods imply use of pheromones and mating disruption (Ciglar, 1998; Maceljski, 2002), natural predators and parasitoids (Lacey and Unruh, 2005) as well as use of biological control agents (CpGV - *Cydia pomonella* granulovirus and EpNS - entomopathogenic nematodes). *Cydia pomonella* granulovirus (CpGV) was used for 30 years in the most European countries (Sauer et al., 2017) while in Croatia it was registered in 2011 when it is commercial use started. Microbial agent (CpGV) belongs to genus *Granulovirus*, family *Baculoviridae* (Crook, 1991). It is highly pathogenic for codling moth and for some related moth species (Luque et al., 2001) but harmless for nontarget organisms (Stara and Kocourek, 2003).

The research hypothesis was that biological preparation on the basis of baculovirus would provide satisfactory fruit quality (codling moth damage less than 1%) as well as more ecologically acceptance than chemical preparations (pyrethroid treatment) while kaolin treatment would have less fruit damage than the control treatment. The second hypothesis was that monitoring of codling moth life stage in insect cage would be more accurate in determining the time control than the flight monitoring on pheromone traps. The third hypothesis was existence of codling moth affinity according to certain varieties. According to hypothesis the first aim of this study was to examine the efficiency of biological products in Eastern Croatia on the basis of CpGV and kaolin clay as well as efficiency of plant protection products from group of synthetic pyrethroids compared with control treatment. The efficiency of treatment is manifested through two characteristics: fruit damage from codling moth (% damage), which is a direct indicator, and fruit yield. The second aim of this research was to determine the time of application using two methods: monitoring developmental codling moth stages in insect cage and using pheromone traps for codling moth and summing the effective temperatures. The third aim was to determine the affinity of codling moth to the tested varieties.

Materials and methods

Study sites

The experiment was performed at the orchard of Agricultural Institute Osijek, Eastern Croatia (45°31'44,56" N, 18°45' 44,88" E) during 2012–2014 in four different control treatments of codling moth (*Cydia pomonella* L.). In 2012 climatic conditions were less favourable for the apple production, because of period of negative temperatures down to -6 °C during the phenological stage of development BBCH 5–59 when apple was in stage of floral balloons. Low temperatures caused a decrease in the apple yield for 50% in 2012. During 2013 and 2014 there were not similar extremes that could negative effect on the apple production. Climate data for this research was collected by weather stations which was located in the experimental orchard (Figs. 1, 2 and 3).

The treatments

Treatment 1 was based on biological product baculovirus (Granupom), used in a dose of 150 ml/ha/1 m height, with the addition of 300 g sugar. Treatment 2 was based

on the group of synthetic pyrethroids- beta-ciflutrin (Beta Baythroid EC 025) in a dose of 500 ml ha⁻¹, deltametrin (Rotor 1.25 EC) in dose of 600 ml ha⁻¹ and alfa-cipemetrin (Fastac 10 SC) in dose of 250 ml ha⁻¹. Chemical preparations from group of synthetic pyrethroids were involved in this research because of expected good results in efficiency in codling moth control as well as comparisons with the efficiency of biological products. Treatment 3 was based on the kaolin clay (Cutisan) 15 kg ha⁻¹ according to manufacturer's recommendations for codling moth control. Treatment 4 was control or untreated plot. The experiment included three apple varieties 'Golden Delicious' clone B, 'Jonagored' and 'Melrose'. Growing form of trees was spindly bush. Experimental orchard was planted in 2005 on the vegetative rootstock MM106. Experimental orchard was on 0.4 ha and divided into four equal parts, which represents different codling moths control treatments. Each part, from each other was separated with protective zone of three trees. Experimental orchard was also divided through the whole length in two equal parts, left and right side with 60 trees in each side. Every side of the same control treatment represents different method of time control. Every block of four experimental parts in orchard contained 5 experimental trees in the row of each variety, in total there were three rows with all three varieties with 15 trees per time of control, 30 trees per treatment, 120 trees in all four treatments. In the left part of experimental orchard (which contained 60 experimental fruit trees per one method of time control), treatments were done on the basis of monitoring imago flight by pheromone traps (critical number (threshold) was 3–5 adults per trap in one day or in several days) and after catching critical number per trap started with summarizing effective temperature till sum of 90 °C (which represents time of hatching larvae-L1. In the other part of the experimental orchard (which contained another 60 experimental fruit trees), the treatments were done on the basis of controlling the pest biology in insect cage for first generation combined with Wildbolz method (Wildbolz, 1962) for other generations. This method is based on the regular summarizing the effective temperature starting from January 1. Caterpillar hatching started at sum 90 °C of effective temperatures. At the 100 °C of effective temperatures codling moth flight started. The effective sum of 610 °C is necessary for ending period of one codling moth generation. During the fruit harvest every experimental tree was harvested separately, fruits were placed in labelled boxes and 100 apples were randomly allocated from each tree according to EPPO standards (2004) for visual control of damage. A 1500 apples were examined per time of control on three varieties, 3000 fruits were examined per treatment in left and in right side of experimental orchard which represents different time of control. In total there were examined 12000 apples in all four treatments and in two different methods of time control. After visual inspection of 100 apples the damage based on the number of incoming and outgoing tunnels and wholes from caterpillars of codling moth was determined.

Statistical analysis

Statistical analysis was performed using R software (R core team, 2013). *Anova* function from *car* package was used for factorial analysis of variance with four sources of variation: time of control, codling moth treatment, variety and replication. *Agricolae* package was used to calculate Tukey's honest significant difference (HSD) test at $P < 0.05$ level (HSD_{0.05}).

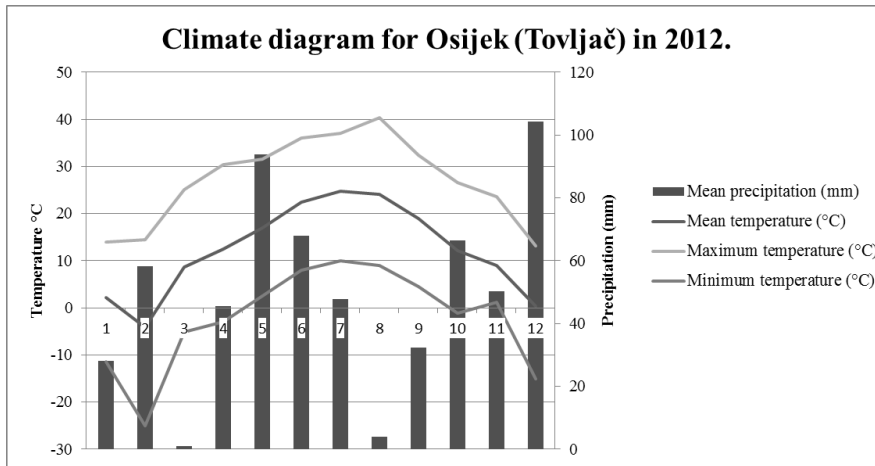


Figure 1. The monthly meteorological data for experimental orchard during 2012

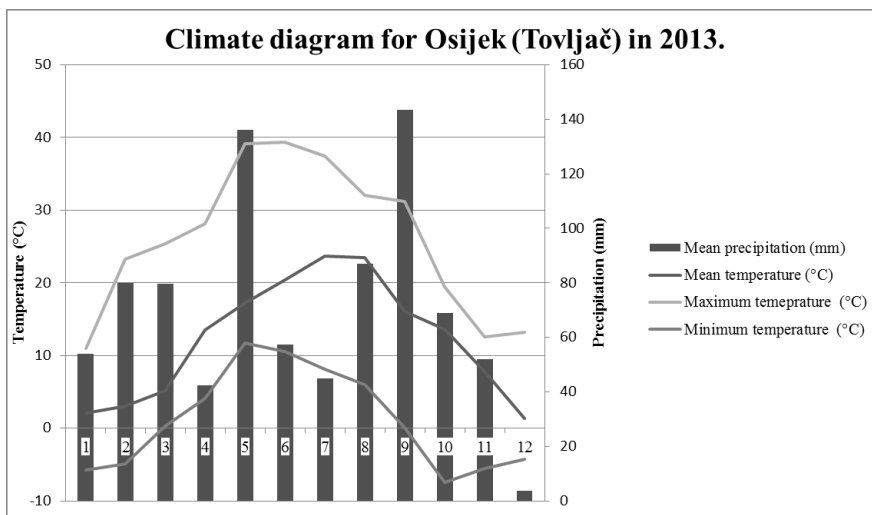


Figure 2. The monthly meteorological data for experimental orchard during 2013

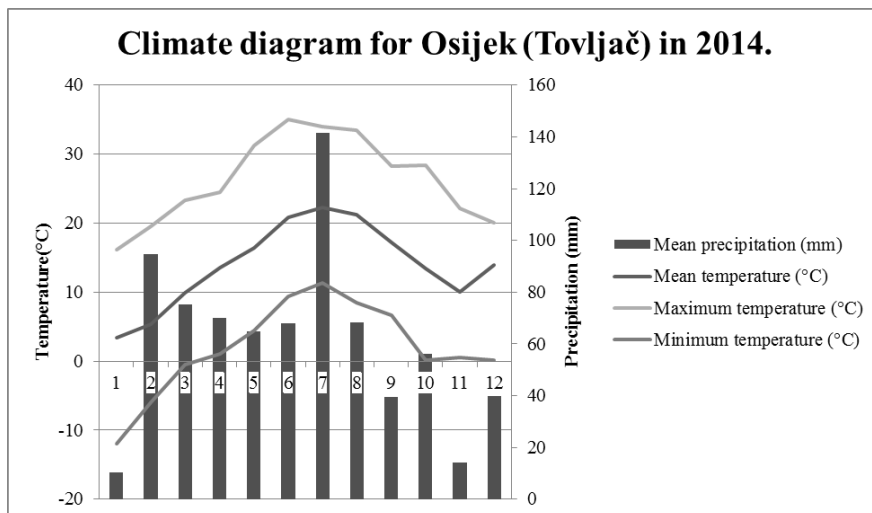


Figure 3. The monthly meteorological data for experimental orchard during 2014

Results

Analysis of variance (ANOVA) revealed consistent non-significant effects of replication, time of control and interactions with time of control over the three years for both traits (Table 1). The effects of codling moth treatment and variety were mostly highly significant. The only significant interaction in the analysis was detected between codling moth treatment and variety for yield in 2013.

Table 1. Results of F-test from ANOVA for fruit yield and damage caused by codling moth (transformed data) in a three-factor design experiment conducted in Eastern Croatia over three years

Source of variation	df	Yield (kg)			Damage (%-transformed)		
		2012	2013	2014	2012	2013	2014
Replication (R)	4	1.2	2.6	0.2	1.1	0.6	0.2
Time of control (T)	1	0.1	2.8	0.01	0.6	1.5	3.0
Codling moth treatment (C)	3	39.1**	3.4*	22.0**	574.9**	1118.0**	318.6**
Variety (V)	2	4.0*	6.2**	43.5**	5.8**	5.5**	5.7**
T × C	3	0.7	1.5	2.1	0.01	0.04	0.1
T × V	2	0.3	2.3	0.1	0.04	0.01	0.4
C × V	6	1.4	3.9**	1.8	1.5	1.2	1.3
T × C × V	6	0.8	1.4	0.6	0.1	0.04	0.5

df – degrees of freedom, ** – significant at the 0.05 and 0.01 probability levels, respectively

The separate analysis over three years are shown in Figure 4. demonstrating different mean values for fruit yield and damage across the codling moth treatment and variety. The pyrethroid treatment performed consistently the best results in comparison with baculovirus treatment and kaolin in all three tested years. Moreover, the differences between pyrethroid and baculovirus treatments were significant in all three varieties in 2012 and 2014. The highest yield (71.35 kg) in 2013 and the lowest percentage of fruit damage (1%) had variety ‘Golden Delicious’ clone B in the same treatment.

Combined ANOVA showed that fruit yield and damage differed significantly among treatments in all three years. The interactions between three codling moth damages and yield were significant in all three years of investigation. There were negative relations between the two traits with different association strengths across the three years (Fig. 5). The strongest association was in 2012 when the highest mean values for damage and the lowest mean values for yield were observed.

In the three-year field experiment, the highest average efficiency had treatment 2 with pyrethroids (96.6%), followed by treatment 1 with CpGV (85.86%) and the lowest efficiency had treatment 3 with kaolin (45.16%). The efficiency of pyrethroids was stable across the years (Table 2).

Discussion

Difference in yield between varieties among different treatments was expected because fruitfulness is not only result of intensity of pest infestation but genetic characteristics of each variety among other different but very important factors, such as

fertilization, growth form, pruning, climate condition. In 2012, average yield of all three varieties were 19.11 kg which can be explained by the influence of frost and low temperatures during beginning of apple flowering in this year (Fig. 4).

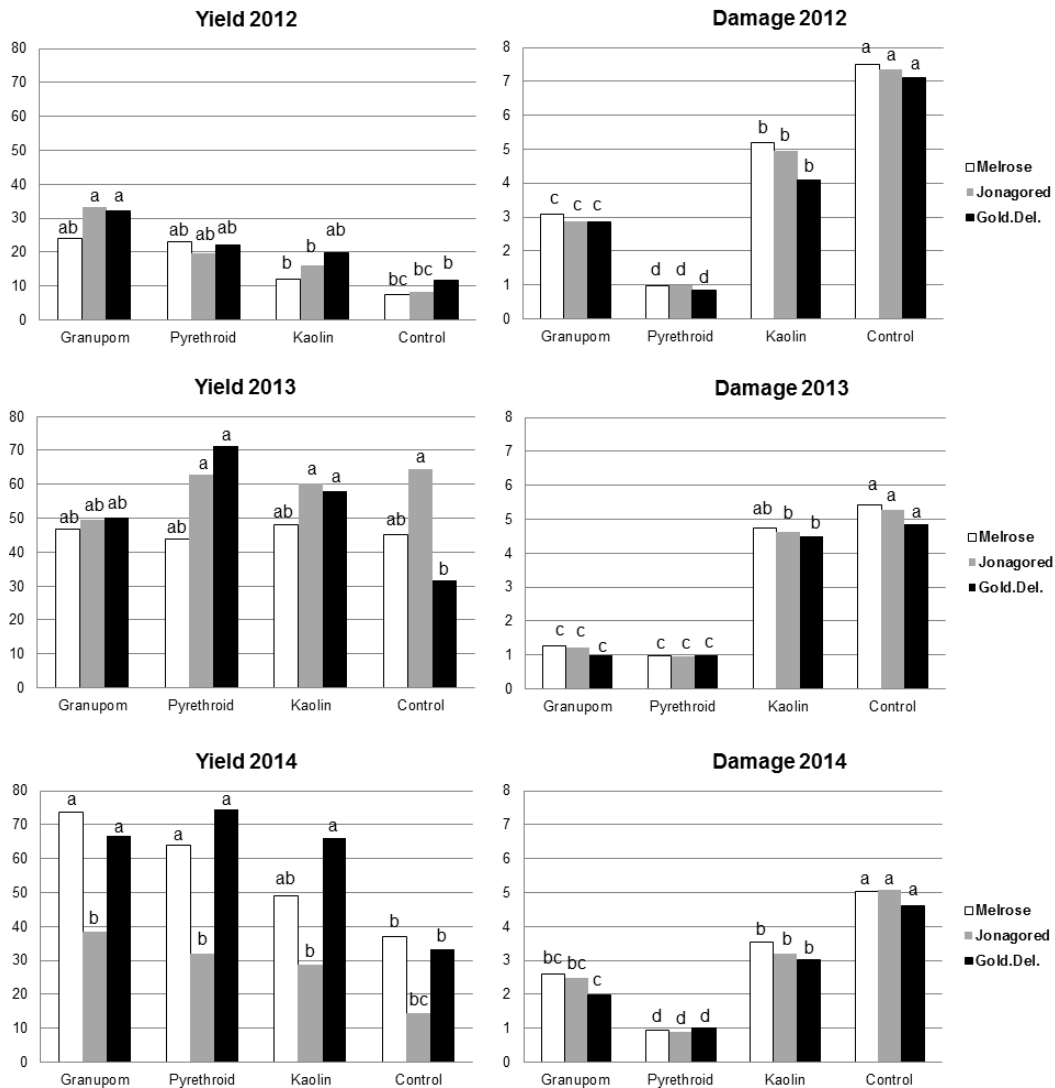


Figure 4. Mean values for fruit yield (kg) and fruit damage (%-transformed) in three apple varieties across three codling moth treatments and control averaged over two methods of time control of codling moth. Means with the same letters are not significantly different according to the Tukey's $HSD_{0.05}$

Table 2. Efficiency of applied treatments in the control of codling moth in 2012, 2013 and 2014 at locality Agricultural institute Osijek in Eastern Croatia

Treatment	Efficiency %			
	2012	2013	2014	Average
1 (CpGV)	84.60	95	78	85.86
2 (pyrethroids)	97	97	96	96.6
3 (kaolin)	57	21.5	57	45.16
4 (control)	—	—	—	—

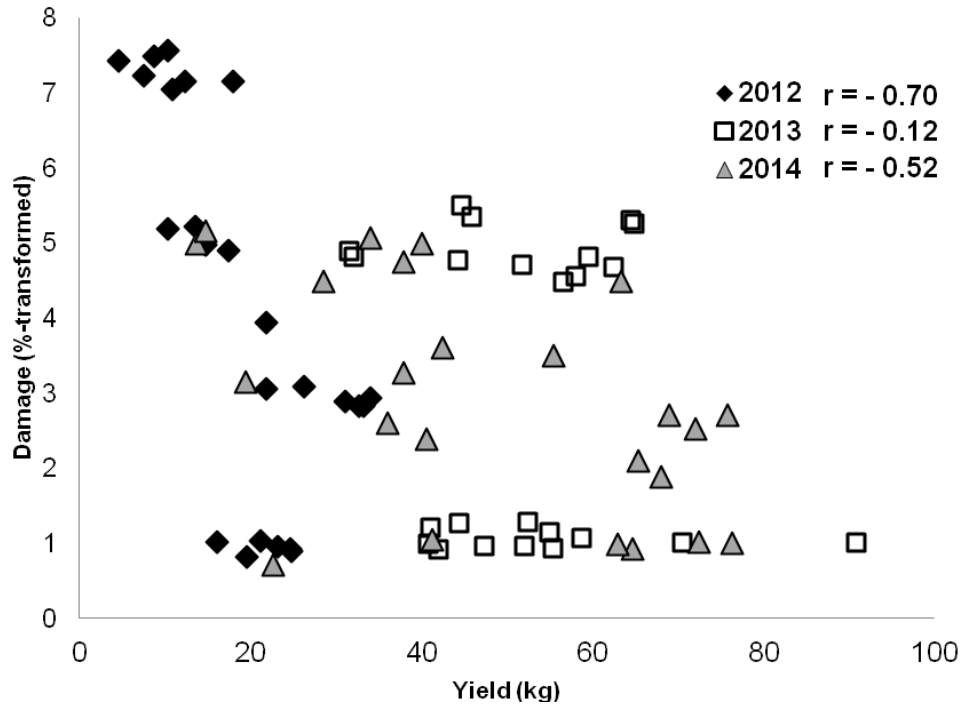


Figure 5. Relations between fruit yield and codling moth damage across the three years including all times of control, moth treatments and varieties. Note: Correlation coefficients (r) between the traits are indicated for specific year

A research in America showed that differences in annual fruit yield among three different production systems were inconsistent (Reganold et al., 2001). In this research damage on the apples from the codling moth was different between treatments and in the years of study. The higher percentage (more than 1%) of fruit damage in treatment 1 (CpGV), occurred due to short period of residual control which requires more frequent applications because of its sensitivity to solar radiation and its incapability to be exposure to UV radiation and extreme high temperatures (Arthurs and Lacey, 2004; Lacey and Arthurs, 2005). Baculovirus can persist for long periods in water and in the soil when is protected from sunlight and extreme high temperatures (Hajek et al., 2017). According to Wearing (1993), this virus has slow action and less efficiency in preventing codling moth damage. Results of early field efficiency trials showed that applications of CpGV are comparable to applications of chemical insecticides in their ability to control codling moth apple damage (Huber and Dickler, 1977; Mantinger et al., 1992). The best results with lowest percent of apple damage were in treatment 2 (pyrethroids). Conventional production in apple orchard results with little damage at harvest period (Suckling et al., 1999) but frequent insecticide applications are harmful to human health, the environment and beneficial organisms (Pajač et al., 2011). The most similar results in fruit damage with control had treatment 3 which included use of kaolin clay as shown in Fig. 5. According to Unruh et al. (2000), reduced number of codling moth damage was noticed on the apple fruits with kaolin film in compare with the control results. Kaolin clay particles do not kill pests but repellent them or act as barrier (Glenn, 2016; Glenn et al., 2002; Showler and Sétamou, 2004; Lapointe, 2000). Unruh et al. (2000) stressed that film of kaolin clay particles on fruits are very good protection against pest but only when their population is very low.

In this study, a highly significant negative correlation between yield and fruit damage was recorded. A study in the US also showed that fruit damage of codling moth was negatively correlated with yields so that in years of low crop damage percentage was relatively high, while in years of high yield percentage of damage was relatively low (Clark and Gage, 1997). This occurred because the same population of codling moth, in the years of smaller yield, had a smaller amount of available food. Combined analysis of variance showed highly significant differences between the years of research, considering the yield and apple fruit damage from codling moth. Less significance occurred in the source variation treatment \times time of control \times variety. This indicates that climate has great impact on the yield and fruit damage, and that the year is the most critical factor in production of apples. In the same conditions of apple production, using the same treatments, time of control and varieties, characteristic of yield has very low repeatability. Correlation between yield and fruit damage was negative and significant ($P < 0.01$), and increasing damage on the apples from codling moth reduces yield.

Results of conducted research in treatment 1 (CpGV) were similar to the results of efficiency from Czech Republic which varied from 75.5 to 96% (Stara and Kocourek, 2003). In Germany, the efficiency of CpGV was 70% (Kienzle et al., 2002). The reason for reduced efficiency could be because of use CpGV preparations for many years (Arthurs et al., 2004).

Treatment 2 (pyrethroids) efficiency varied from 96 to 97% while results of cypermethrin efficiency from Serbia varied from 92.2 to 97.6% (Miletić et al., 2011). Pyrethroids still have good efficiency but they also have broad spectrum of impact on beneficial insect so it is reason of limited number of applications during year season in integrated production.

The efficiency of treatment 3 (kaolin clay), varied between 21.5 and 57%. The average efficiency in three years amounted to 45.16%. This preparation is primarily used in orchards as protection from strong direct sunlight and to prevent the fruit surface sunburn (Glenn et al., 2002). In this study was shown that kaolin have effect on minimizing damage on the fruits from codling moth in comparison to control as confirmed by other studies (Showler, 2003; Knight et al., 2000; Unruh et al., 2000). Due to a low efficiency below 60%, and its main effect in the prevention sunburns, should be included in the program of controlling first generation of codling moth (Knight et al., 2000) as well as additional product in an integrated control production. Statistical analysis did not confirm significant difference among different methods of calculating time control of *Cydia pomonella* and yield as well as fruit damage. It seems that both methods of calculating time control are based on monitoring of codling moth biology getting therefore equal results. The different number of fruit damages between varieties within the same treatment gives the conclusion of bigger or less attraction of codling moth caterpillar for certain variety. The similar conclusion was made according to other authors (Hussain et al., 2014; Wenninger and Landolt, 2011; Landolt and Guédot, 2008). Biological control can be effective, economical and safe and it should be more widely used than it is today (Mahret et al., 2008).

Conclusions

1. The *Cydia pomonella* granulovirus (CpGV) based preparation had a lower average efficiency, 88.86%, compared to the preparations from the group of synthetic pyrethroids and was with 4.88% average fruit damage in the treatment. The kaolin

preparation had an average efficiency of 45.16% with 17.99% average fruit damage. Both preparations should be used in codling moth control program because of their positive impact on environment and human health. 2. Efficiency of two methods of determining control time did not differ significantly. Both methods showed equally good results.

3. Varieties in the study showed statistically significant differences in yield and fruit damage in all years of study. 'Melrose' had the highest number of fruits damage in all three years which can be related to the codling moth caterpillar affinity to a certain variety, than came 'Jonagored' and least attracti was 'Golden Delicious' clone B. It can be concluded that the affinity of codling moth to apple fruit is stronger when fruit surface has dominant red coloration and in this case further investigation is required.

REFERENCES

- [1] Arthurs, S., Lacey, L. A. (2004): Field evaluation of commercial formulations of the codling moth granulovirus: persistence of activity and success of seasonal applications against natural infestations of codling moth in Pacific Northwest apple orchards. – *Biological Control* 31(3): 388-397.
- [2] Blommers, L. H. M. (1994): Integrated pest management in European apple orchards. – *Annual Review of Entomology* 39: 213-241.
- [3] Blommers, L., Vaal, F., Freriks, J., Helsen, H. (1987): Three years of specific control of summer fruit tortix and codling moth on apple in the Netherlands. – *Journal of Applied Entomology* 104: 353-371.
- [4] Chouinard, G., Firllej, A., Cormier, D. (2016): Going beyond sprays and killing agents: Exclusion, sterilization and disruption for insect pest control in pome and stone fruit orchards. – *Scientia Horticulturae* 208: 13-27.
- [5] Ciglar, I. (1998): Integrirana zaštita voćnjaka i vinograda - [Integrated Pest Management in Orchards and Vineyards]. – Zrinski, Čakovec, Croatia.
- [6] Clark, M. S, Gage, S. H. (1997): Relationship between fruit yield and damage by codling moth and plum curculio in a biologically-managed apple orchard. *The Great Lakes Entomologist* 30(4): 161-168.
- [7] Crook, N. E. (1991): Baculoviridae: Subgroup B. Comparative Aspects of Granulosis Viruses. – In: Kurstak, E. (ed.) *Viruses of Invertebrates*, pp. 73-110. Marcel Dekker, New York.
- [8] EPPO Standards (2004): Efficacy evaluation of plant protection product – insecticides and acaricides. Efficacy evaluation of insecticides. *Cydia pomonella*. – *Bulletin OEPP/EPPO Bulletin* 3: 4-6.
- [9] Glenn, D. M. (2016): Effect of highly processed calcined kaolin residues on apple productivity and quality. – *Scientia Horticulturae* 201: 101-108.
- [10] Glenn, D. M., Prado, E., Erez, A., Puterka, G. J. (2002): A reflective, processed – kaolin particle film affects fruit temperature, radiation and solar injury in apple. – *Journal of the American Society for Horticultural Science* 127: 188-193.
- [11] Hajek, A. E., Shapiro-Ilan, D. I. (2017): *Ecology of Invertebrate Diseases*. – Wiley, New York.
- [12] Huber, J., Dickler, E. (1977): Codling moth granulosis virus: Its efficiency in the field in comparison with organophosphorus insecticides. – *Journal of Economic Entomology* 70: 557-561.
- [13] Hussain, B., Ahmad, B., Bilal, S. (2014): Monitoring and mass trapping of the codling moth, *Cydia pomonella*, by the use of pheromone baited traps in Kargil, Ladakh, India. – *International Journal of Fruit Science* 00: 1-9.

- [14] Iraqui, S. E., Hmimina, M. (2016): Assessment of control strategies against *Cydia pomonella* (L.) in Morocco. – *Journal of Plant Protection Research* 56(1): 82-88.
- [15] Ismail, M., Albitar, L. (2016): Mortality factors affecting immature stages of codling moth *Cydia pomonella* (Lepidoptera; Tortricidae), and the impact of parasitoid complex. – *Biocontrol Science and Technology* 26(1): 72-85.
- [16] Kienzle, J., Schulz, C., Zebitz, C. P. W., Huber, J. (2002): Persistence of the biological effect of codling moth granulovirus in the orchard preliminary field trials, p. 244. – 10th International Conference on Cultivation Technique and Phytopathological Problems in Organic Fruit-Growing and Viticulture 2002. Weinsberg, Germany.
- [17] Knight, A. L., Unruh, T. R., Christanson, B. A., Puterka, G. J., Glenn, D. M. (2000): Effects of kaolin based particle film on the oblique banded leafroller (Lepidoptera: Tortricidae). – *Journal of Economic Entomology* 93(3): 744-749.
- [18] Lacey, L. A., Arthurs, S. P. (2005): New method for testing solar sensitivity of commercial formulations of the granulovirus of codling moth (*Cydia pomonella*, Tortricidae; Lepidoptera). – *Journal of Invertebrate Pathology* 90: 85-90.
- [19] Lacey, L. A., Unruh, T. R. (2005): Biological control of codling moth (*Cydia pomonella*, Lepidoptera; Tortricidae) and its role in integrated pest management, with emphasis on entomopathogens. – *Vedalia* 12(1): 33-60.
- [20] Landolt, P. J., Guèdot, C. (2008): Field attraction of codling moths (Lepidoptera: Tortricidae) to apple and pear fruit and quantitation of kairomones from attractive fruit. – *Annals of the Entomological Society of America* 101(3): 675-681.
- [21] Lapointe, S. L. (2000): Particle film deters oviposition by *Diaprepes abbreviatus* (Coleoptera): Curculionidae. – *Journal of Economic Entomology* 93(5): 1459-1463.
- [22] Luque, T., Finch, R., Crook, N., O'Reilly, D. R., Winstanley, D. (2001): The complete sequence of the *Cydia pomonella* granulovirus genome. – *Journal of General Virology* 82: 2531-2547.
- [23] Maceljčki, M. (1999): Poljoprivredna entomologija [Agricultural Entomology]. – Zrinski, Čakovec, Croatia.
- [24] Mahr, D. L., Whitaker, P., Ridgway, N. M. (2008): Biological Control of Insects and Mites: An Introduction to Beneficial Natural Enemies and Their Use in Pest Management. – Extension Biological Control Programs, University of Wisconsin, Madison.
- [25] Mantinger, H., Boshari, S., Paoli, N. (1992): Bekämpfung des Apfelwicklers mit Granulovirus. – *Obstbau-Weinbau* 9: 253-255.
- [26] Miletić, N., Tamaš, N., Graora, D. (2011): The control of codling moth (*Cydia pomonella* L.) in apple trees. – *Zemdirbyste-Agriculture* 98(2): 213-218.
- [27] Pajač, I., Pejić, I., Barić, B. (2011): Codling moth, *Cydia pomonella* (Lepidoptera; Tortricidae) – Major pest in apple production: an overview of its biology, resistance, genetic structure and control strategies. – *Agriculturae Conspectus Scientificus* 76(2): 87-92.
- [28] R Core Team. (2012): R: A Language and Environment for Statistical Computing. – R Foundation for Statistical Computing, Vienna, Austria. <http://www.R-project.org/>.
- [29] Reganold, J. P., Glover, J. D., Andrews, P. K., Hinman, H. R. (2001): Differences in annual fruit yield were inconsistent among the three production systems but cumulative yields were similar for all three systems. – *Nature* 410: 926-930.
- [30] Sauer, A.J., Fritsch, E., Undorf-Spalin, K., Nguyen, P., Marec, F., Heckel, D.G., Jehle, J.A. (2017): Novel resistance to *Cydia pomonella* granulovirus (CpGV) in codling moth shows autosomal and dominant inheritance and confers cross-resistance to different CpGV genome groups. *PLOS ONE* 12(6); e0179157.doi: 10.1371/journal.pone.0179157
- [31] Showler, A. T. (2003): Effects of kaolin particle film on beet armyworm, *Spodoptera exigua* (Hubner) (Lepidoptera: Noctuidae), oviposition, larva feeding and development on cotton, *Gossypium hirsutum* L. – *Agriculture, Ecosystems and Environment* 95: 265-271.

- [32] Showler, A. T., Sétamou, M. (2004): Effects of kaolin particle film on selected arthropod populations in cotton in the lower Rio Grande Valley of Texas. – *Southwestern Entomologist* 29: 137-146.
- [33] Stara, J., Kocourek, F. (2003): Evaluation of efficacy of *Cydia pomonella* granulovirus (CpGV) to control the codling moth (*Cydia pomonella* L.) in field trials. – *Plant Protection Science* 39(4): 117-125.
- [34] Suckling, D. M., Walker, J. T. S., Wearing, C. H. (1999): Ecological impact of three pest management systems in New Zealand apple orchards. – *Agriculture, Ecosystems and Environment* 73(2): 129-140.
- [35] Tamošiūnas, R., Valiuškaitė, A., Survilienė, E., Duchovskienė, L., Rasiukevičiūtė, N. (2014): Variety-specific population density and infestation levels of apple sawfly (*Hoplocampa testudinea* Klug) in two differently managed apple orchards in Lithuania. – *Zemdirbyste-Agriculture* 101(2): 205-214.
- [36] Unruh, T. R., Knight, A. L., Upton, J., Glenn, D. M., Puterka, G. J. (2000): Particle films for suppression of the codling moth (Lepidoptera: Tortricidae) in apple and pear orchards. – *Journal of Economic Entomology* 93(3): 737-743.
- [37] Wearing, C. H. (1993): Control of codling moth with commercial preparation of codling moth granulosus virus, pp. 146-151. – *Proceedings of the 46th New Zealand Plant Protection Conference*.
- [38] Wenninger, E. J., Landolt, P. J. (2011): Apple and sugar feeding in adult codling moths, *Cydia pomonella*: Effects on longevity, fecundity and egg fertility. – *Journal of Insect Science* 11(1): 161.
- [39] Wildbolz, T. (1962): Über die Möglichkeit der Prognose und der Befallsüberwachung und über Toleranzgrenzen bei der integrierten Schädlingsbekämpfung im Obstbau. – *Entomophaga* 7: 273-278 (in German).

FIRST RECORD OF *OXYCARENUS LAVATERAE* (FABRICIUS, 1787) (HETEROPTERA, LYGAEIDAE) IN TURKEY

ARSLANGÜNDOĐDU, Z.* – HIZAL, E. – ACER, S.

*Department of Forest Entomology and Protection, Faculty of Forestry, University of Istanbul
Istanbul, Turkey*

**Corresponding author
e-mail: zeynel@istanbul.edu.tr*

(Received 7th Nov 2017; accepted 20th Feb 2018)

Abstract. In autumn of 2017, *Oxycarenus lavaterae* (Hemiptera: Heteroptera: Oxycarenidae) was observed on linden trees (*Tilia tomentosa*) in a park in Sariyer, Istanbul, northwestern Turkey. This is the first record of this species from Turkey.

Keywords: Hemiptera, Oxycarenidae, *Tilia tomentosa*, invasive, Istanbul

Introduction

Oxycarenus lavaterae (Fabricius, 1787) (Heteroptera: Lygaeidae: Oxycarenidae) is widely distributed in Western Mediterranean region of Europe (Péricart, 1998, 2001). It occurs from northwest Africa to Portugal, southern Spain, southern France, southern Germany, Italy, Slovenia and Croatia (Velimirovic et al., 1992; Kalushkov, 2000; Rabitsch and Adlbauer, 2001; Wermelinger et al., 2005). During the last 20 years, *O. lavaterae* continued to spread eastwards into the Balkan Peninsula and northwards to the central Europe (*Figure 1*) (Velimirovic et al., 1992; Kondorosy, 1995; Bianchi and Stehlik, 1999; Protic and Stojanovic, 2001; Rabitsch and Adlbauer, 2001; Deckert, 2004; Wermelinger et al., 2005; Kment, 2009; Kment et al., 2006; Rabitsch, 2008, 2010; Hebda and Olbrycht, 2016). *O. lavaterae* spread to the east of Mediterranean area and can be found in Saudi-Arabia and Yemen as well as in tropical Africa to South Africa (Rabitsch and Adlbauer, 2001). Mass increase of *O. lavaterae* was previously observed and reported from and near Italy. Already in 1906 an exceptional infestation took place near the Lago Maggiore, Varese. In the same area, similarly Péricart (1998), and Dioli (1993) reported a massive increase of the population of the bug.

Oxycarenus lavaterae is a phytophagous insect native to the Western Mediterranean. The species has several known host plants, most of them belonging to Malvales. The species associated are members of plant family Malvaceae and Tiliaceae. *Oxycarenus lavaterae* sucks on green plant parts (e.g. leaves and unhindered shoots). In infested areas, most records originate from planted *Tilia cordata* trees in suburban and urban habitats (Rabitsch, 2008). When appearing in abundance, these bugs can cause damage in weakening linden trees, hence they are considered as insects with an economic importance (Velimirovic et al., 1992; Wachmann et al., 2007).

Depending on the temperature, multiple generations are produced each year. In their natural distribution area in Southern Europe, three to four generations are observed (Wermelinger et al., 2005; Kalushkov et al., 2007a; Simov et al., 2012; Nedvěd et al., 2014). They are encountered frequently on single trees and collect in masses on linden trees in autumn and spring (Wermelinger et al., 2005; Kalushkov, 2000). The bug winters in the form of larger or smaller agglomerations. They typically take shelter in

sun exposed bark cracks on trunk and branches, and overwinter as adult; however, rarely few larvae are noticed (Bărbuceanu and Nicolaescu, 2012). Most animals are likely to endure winter in the rind of old linden trees, and therefore the mortality rate is high due decrease of shelter for the winter.

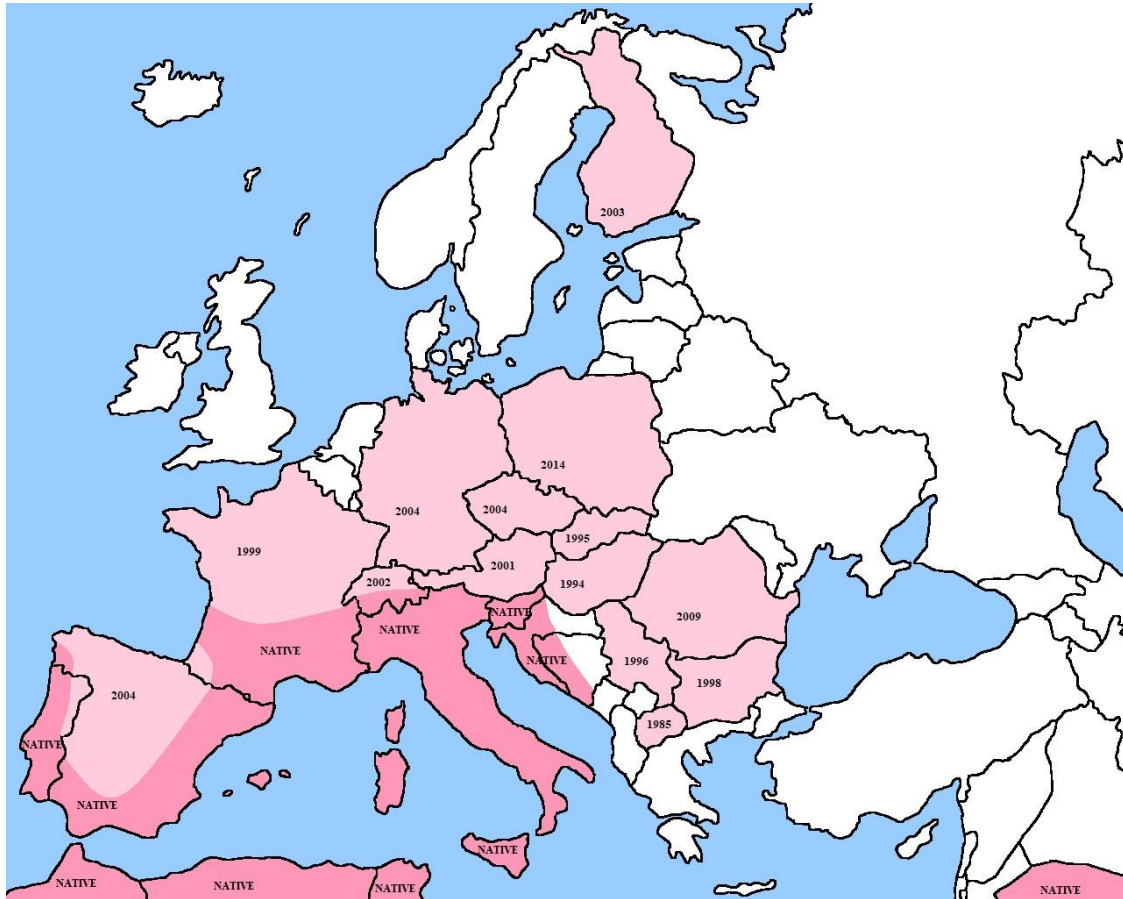


Figure 1. Distribution of *O. lavaterae* (Fabricius, 1787)

Material and methods

Our sampling area was located in “15 Temmuz Hatıra Ormanı” located in Garipce, Sariyer Istanbul, (41° 12' S, 29° 5' W), northwestern Turkey. The park mostly consists of shrubs, pseudo shrubs and *Pinus nigra* trees. Very recently (May 2017), 250 sycamore and 82 linden trees (*Tilia tomentosa*) were planted. These trees were imported from Italy and Spain. Several dead linden trees were noticed by the park superintendent. Site was visited in September-October 2017. Insect colonies, which consisted of nymphs and adult insects, were located on trunks of several linden trees. Samples were collected in plastic containers with the help of thin brushes and transferred to laboratory for identification. Samples were examined with Leica stereomicroscope and photographs were taken. Body lengths were measure from the tip of the anterior to the posterior edge of the dorsal plater under the stereomicroscope. Insects were identified using online identification keys and literature (e.g. Péricart, 1998; Costas et al., 1997). Representative samples were preserved as biological museum materials in the insect collection of the Istanbul University Forest Entomology and Protection.

Results and discussion

The insect was identified as *Oxycarenus lavaterae*. It was found on in the field studies carried out in September-October 2017, the insects were identified on four of the trees and they were found to be in adult stage mostly as nymphs (*Figure 2*). The morphological description and size were similar to the reports. Our specimens' size were between 4.5–5.4 mm in adult females, of 4.2–5 mm in males. Nymphen stages have monochrome red hind whips. The nymphs can be easily recognized by their black head, black wing bads and the red-coloured abdomen. Adult animals show the typical red-black drawing on the wings, which is similar to that of the fire bug or the cinnamon bug. The front wings are colourless and transparent and reach the top of the abdomen or are a little longer. The head, antennae, the throat (Pronotum) and the sign (Scutellum) of the bug are coloured black. The hemipedema (hemielytren) are red to reddish brown and the wing membrane is bright.



Figure 2. *Oxycarenus lavaterae* a) Top view. b) Bottom view. c) On the linden tree as a group

Several plant species were reported as host of the *O. lavaterae* in which all life stages were encountered (*Table 1*). In the park, we only encountered the insect on *Tilia tomentosa*, a host that is widely reported (*Table 1*).

Four species of the genus *Oxycarenus* Fiber, 1837 in Turkey is known including *Oxycarenus hyalinipennis* (Costa, 1847) (Lodos et al., 1999; ađatay, 1985; nder et al., 2006; Őerban, 2010; Kckbasmacı and Kıyak, 2015; Yazıcı et al., 2015); *Oxycarenus longiceps* Wagner, 1954 (Lodos et al., 1999; ađatay, 1985; nder et al., 2006; Kckbasmacı and Kıyak, 2015); *Oxycarenus modestus* (Fallén, 1829) (Lodos et al., 1999; nder et al., 2006); and *Oxycarenus pallens* (Herrich-Schäffer, 1850) (nder

and Adıgüzel, 1979; Lodos et al., 1999; Çağatay, 1985; Kıyak et al., 2004; Önder et al., 2006; Matocq and Özgen, 2010; Yazıcı et al., 2015; Fent and Dursun, 2016). To our knowledge, *O. lavaterae* was never reported from Turkey.

Table 1. Known host plants of the *Oxycarenus lavaterae*

Plants		References
Scientific name	Common name	
<i>Alcea</i> sp., <i>Alcea rosea</i>	Hollyhock	Stichel, 1958; Péricart, 1998; Wermelinger et al., 2005; Kment et al., 2006; Rabitsch, 2008
<i>Althaea</i> sp.		Velimirovic et al., 1992; Wachmann et al., 2007
<i>Althaea officinalis</i>	Marsh mallow	Callot, 2016
<i>Citrus</i> sp.		Wermelinger et al., 2005
<i>Citrus sinensis</i> var. <i>clemenules</i>	Sweet orange	Ribes et al., 2004
<i>Corylus</i> sp.		Kalushkov, 2000; Rabitsch and Adlbauer, 2001
<i>Corylus avellana</i>	Corkscrew hazel	Frey-Gessner, 1863, 1865; Péricart, 1998; Wermelinger et al., 2005; Kment et al., 2006; Rabitsch, 2008
<i>Cynara scolymus</i>	Globe artichoke	Stichel, 1958; Rabitsch and Adlbauer, 2001
<i>Geranium</i> sp.		Stichel, 1958; Rabitsch and Adlbauer, 2001
<i>Geranium sanguineum</i>	Bloody cranesbill	Otto, 1996
<i>Geranium sylvaticum</i>	Wood cranesbill	Otto, 1996
<i>Gossypium</i> sp.		Ciampolini and Tremtera, 1987; Ferrer, 1996; Alvorado et al., 1998; Wermelinger et al., 2005
<i>Helianthus annuus</i>	Sunflower	Kalushkov and Nedvěď, 2010
<i>Hibiscus</i> sp.		Stichel, 1958; Velimirovic et al., 1992; Wachmann et al., 2007; Callot, 2016
<i>Hibiscus syriacus</i>	Rose of Sharon	Kalushkov and Nedvěď, 2010
<i>Lagunaria patersonii</i>	Primrose tree	Péricart, 1998; Wermelinger et al., 2005; Kment et al., 2006; Rabitsch, 2008; Borges et al., 2013
<i>Lavatera</i> sp.		Velimirovic et al., 1992; Kalushkov, 2000; Rabitsch and Adlbauer, 2001; Wachmann et al., 2007
<i>Lavatera cretica</i>	Cornish mallow	Cuesta Segura et al., 2010
<i>Lavatera olbia</i>	Tree mallow	Péricart, 1998; Wermelinger et al., 2005; Kment et al., 2006; Rabitsch, 2008
<i>Malva</i> sp., <i>Malva sylvestris</i>	Common mallow	Ciampolini and Tremtera, 1987; Ferrer, 1996; Alvorado et al., 1998
<i>Platanus acerifolia</i>	London plane	Hebda and Olbrycht, 2016
<i>Populus</i> sp.		Goula et al., 1999; Rabitsch and Adlbauer, 2001
<i>Prunus</i> sp.		Ciampolini and Tremtera, 1987; Ferrer, 1996; Alvorado et al., 1998; Wermelinger et al., 2005
<i>Sterculia</i> sp.		Ciampolini and Trematerra, 1986
<i>Tilia</i> sp.		Velimirovic et al., 1992; Kalushkov, 2000; Rabitsch and Adlbauer, 2001; Wachmann et al., 2007
<i>Tilia cordata</i>	Little-leaf linden	Velimirovic et al., 1992; Kalushkov et al., 2007a/b; Kalushkov and Nedvěď, 2010; Seward et al., 2017; Simov et al., 2012
<i>Tilia platyphyllos</i>	Broad-leaved linden	Schneider and Dorow, 2016; Seward et al., 2017
<i>Tilia parvifolia</i>	Small-leaved linden	Kalushkov et al., 2007a/b
<i>Tilia rubra</i>	Large-leaved linden	Kalushkov et al., 2007a/b
<i>Tilia tomentosa</i> (= <i>Tilia argentea</i>)	Silver linden	Kalushkov et al., 2007a/b; Kalushkov and Nedvěď, 2010; Simov et al., 2012
<i>Triticum vulgare</i>	Wheat	Kalushkov and Nedvěď, 2010
<i>Vitis</i> sp.		Ciampolini and Tremtera, 1987; Ferrer, 1996; Alvorado et al., 1998; Wermelinger et al., 2005

O. lavaterae was reported from Bulgaria in 1998 and subsequent spread appears to be towards western European countries. Because it was encountered for the first time on imported trees, it is highly likely that they have not spread into Turkey. *Oxycarenus lavaterae* are invasive insects (Kalushkov and Nedvĕd, 2010; Putschkov, 2013; Nedvĕd et al., 2014; Hebda and Olbrycht, 2016). In particular, on weakened trees these bugs can be found in massive groups and cause the death. The four infested trees died and were removed from the park in an effort to eradicate the insects. Even though *O. lavaterae* is not very harmful (Reynaud, 2000; Ribes et al., 2004; Simov et al., 2012), they have the potential to spread to many parts of Turkey because linden trees are commonly planted in parks and recreational areas in Turkey.

REFERENCES

- [1] Alvorado, M., Duran, J. M., Serrano, A., de la Rosa, A., Ortiz, E. (1998): Contribucion al conocimiento de las chinches (Heteroptera) fitofagas del algod6n en Andalucia Occidental. – Boletin de Sanidad Vegetal Plagas 28: 817-828.
- [2] Bărbuceanu, D., Nicolaescu, D. P. (2012): Pest of ornamental trees and shrubs in the parks of Pitesti and methods of fighting them. – Current Trends in Natural Sciences 1(1): 2-5.
- [3] Bianchi, Z., Stehlik, J. L. (1999): *Oxycarenus lavaterae* (Fabricius, 1787) in Slovakia (Heteroptera: Lygaeidae). – Acta Musei Moraviae, Scientiae Biologicae 84: 203-204.
- [4] Borges, P. A. V., Reut, M., da Ponte, N. B., Quartau, J. A., Fletcher, M., Sousa, A. B., Pollet, M., Soares, A. O., Marcelino, J. A. P., Rego, C., Cardoso, P. (2013): New records of exotic spiders and insects to the Azores, and new data on recently introduced species. – Arquipelago: Life and Marine Sciences 30: 57-70.
- [5] Callot, H. (2016): Quelques observations de pullulations d'Hétéroptères. – Bulletin De La Société Entomologique De Mulhouse en Alsace 72(1): 6-14.
- [6] Ciampolini, M., Tremtera, P. (1987): Biological studies on *Oxycarenus lavaterae* (F.) (Heteroptera, Lygaeidae). – Bollettino di Zoologia Agraria e di Bachicoltura, Serie II, 19: 187-197.
- [7] Costas, M., Vázquez, M. A., López, T. (1997): Sobre las especies del género *Oxycarenus* Fieber, 1837 (Heteroptera, Lygaeidae) de la Península Ibérica. – Zool. baetica 8: 5-17.
- [8] Cuesta Segura, D., Baena Ruiz, M., Mifsud, D. (2010): New records of terrestrial bugs from the Maltese Islands with an updated list of Maltese Heteroptera (Insecta: Hemiptera). – Bulletin of the Entomological Society of Malta 3: 19-39.
- [9] Çağatay (Aysev), N. (1985): Türkiye Oxycareninae (Heteroptera-Lygaeidae) Alt Familyasının Taksonomisi ve Erkek Genital Organının Önemi Üzerine Çalışmalar. – Bitki Koruma Bülteni 25(1-2): 18-29.
- [10] Deckert, J. (2004): Zum Vorkommen von Oxycareninae (Heteroptera, Lygaeidae) in Berlin und Brandenburg. – Insecta (Berlin) 9: 67-75.
- [11] Dioli, P. (1993): Eterotteri insubrici ed eterotteri xerotermitici nei territori perilacustri della Lombardia e del Ticino (Hemiptera, Heteroptera). – Memorie Soc. Ticinese Sci. Nat. 4: 81-86.
- [12] Fent, M., Dursun, A. (2016): Beiträge zur Lygaeidae-Fauna (Hemiptera: Heteroptera) des Westlichen Schwarzmeer-Gebietes in der Türkei. – Heteropteron 47: 30-36.
- [13] Ferrer, M. M. (1996): La nueva plaga del melocoton precoz en las Islas canarias: Danos, reconocimiento y control. – Phytoma Espana 79: 27-32.
- [14] Frey-Gessner, E. (1863): Zusammenstellung der durch Meyer-Dür im Frühling im Tessin und Anfang Sommer 1863 im Ober-Engadin beobachteten und gesammelten Hemiptern und Orthoptern. – Mitteilungen der Schweizerischen Entomologischen Gesellschaft 1: 150-154.

- [15] Frey-Gessner, E. (1865): Verzeichnis schweizerischer Insekten (Fortsetzung aus Heft 7). – Mitteilungen der Schweizerischen Entomologischen Gesellschaft 1: 304-310.
- [16] Goula, M., Espinosa, M., Eritja, R., Aranda, C. 1999: *Oxycarenus lavaterae* (Fabricius, 1787) en Cornelia de Llobregat (Barcelona, Espana) (Heteroptera, Lygaeidae). – Bulletin de la Société entomologique de France 104(1): 39-43.
- [17] Hebda, G., Olbrycht, T. (2016): *Oxycarenus lavaterae* (Fabricius, 1787) (Hemiptera: Heteroptera: Oxycarenidae) – a new species to the fauna of Poland. – Poznań Entomological News 35(3): 133-136.
- [18] Kalushkov, P. (2000): Observations on the biology of *Oxycarenus lavaterae* (Fabricius) (Heteroptera: Lygaeidae), a new Mediterranean species in the Bulgarian fauna. – Acta Zoologica Bulgarica 52: 13-15.
- [19] Kalushkov, P., Nedvěd, O. (2010): Suitability of Food Plants for *Oxycarenus lavaterae* (Heteroptera: Lygaeidae), a Mediterranean Bug Invasive in Central and South-East Europe. – Comptes rendus de l'Academie bulgare des Sciences Tome 63(2): 271-276.
- [20] Kalushkov, P., Simov, N., Tzankova, R. (2007a): Biology and Acclimatization of *Oxycarenus lavaterae* (Heteroptera: Lygaeidae) a New Invasive Mediterranean Species in Bulgarian Fauna. – In: Ninov, N. (ed.) Proceedings of the International Conference 'Alien Arthropods in South East Europe – Crossroad of Three Continents', pp. 44-47. University of Forestry, Sofia.
- [21] Kalushkov P., Simov, N., Tzankova, R. (2007b): Laboratory and field investigation on the biology of *Oxycarenus lavaterae* (Fabricius) (Heteroptera: Lygaeidae) in Bulgaria. – Acta Zoologica Bulgarica 59(2): 217-219.
- [22] Kıyak, S., Öz Saraç, Ö., Salur, A. (2004): Additional Notes on the Heteroptera fauna of Nevşehir province (Turkey). – Gazi Univ J Sci 17: 21-29.
- [23] Kment, P. (2009): *Oxycarenus lavaterae*, an expansive species new to Romania (Hemiptera: Heteroptera: Oxycarenidae). – Acta Musei Moraviae, Scientiae Biologicae 94: 23-25.
- [24] Kment, P., Vahala, O., Hradil, K. (2006): First records of *Oxycarenus lavaterae* (Fabricius, 1787) (Heteroptera: Oxycarenidae) from the Czech Republic with review of its distribution and biology. – Klapalekiana 42: 97-127.
- [25] Kondorosy, E. (1995): *Oxycarenus lavaterae* a new lygaeid species in the Hungarian bug fauna (Heteroptera: Lygaeidae). – Folia Entomologica Hungarica 56: 237-238 (in Hungarian, English abstr.).
- [26] Küçükbasmacı, İ., Kıyak, S. (2015): A study on the fauna of Heteroptera of Ilgaz Mountains (Kastamonu, Çankırı) with a new record for Turkey. – Nevşehir Bilim ve Teknoloji Dergisi 4(1): 1-33.
- [27] Lodos, N., Önder, F., Pehlivan, E., Atalay, R., Erkin, E., Karsavuran, Y., Tezcan, S., Aksoy, S. (1999): Faunistic studies on Lygaeidae (Heteroptera) of Western Black Sea, Central Anatolia and Mediterranean regions of Turkey, pp. ix + 58. – Ege University, İzmir.
- [28] Matocq, A., Özgen, İ. (2010): Preliminary list of Heteroptera collected in Mardin and Siirt Provinces from South-Eastern Anatolia of Turkey (Hemiptera). – Mun. Ent. Zool. 5: 1011-1019.
- [29] Nedvěd, O., Chehlarov E., Kalushkov P. (2014): Life history of the invasive bug *Oxycarenus lavaterae* (Heteroptera: Oxycarenidae) in Bulgaria. – Acta Zoologica Bulgarica 66(2): 203-208.
- [30] Otto, A. (1996): Die Wanzenfauna montaner Magerwiesen und Grünbrachen im Kanton Tessin (Insecta: Heteroptera). Eine faunistisch-ökologische Untersuchung. – Diss. ETH Zurich, Nr. 11457.
- [31] Önder, F., Adıgüzel, N. (1979): Some Heteroptera collected by light trap in Diyarbakır (Turkey). – Türkiye Bitki Koruma Dergisi 3(1): 25-34.
- [32] Önder, F., Karsavuran, Y., Tezcan, S., Fent, M. (2006): Türkiye Heteroptera (Insecta) Katalođu. (Heteroptera (Insecta) Catalogue of Turkey). – Meta Basım Matbaacılık, İzmir.

- [33] Péricart, J. (1998): Hémiptères Lygaeidae euro-méditerranéens. Vol. 2. Faune de France, 84B, i-iii. – FFSSN, Paris.
- [34] Péricart J. (2001): Family Lygaeidae Schilling, 1829 – Seed Bugs. – In: Aukema B, Rieger, C (eds.) Catalogue of the Heteroptera of the Palaearctic Region, pp. 35-220. The Netherlands Entomological Society, Wageningen.
- [35] Protic, L., Stojanovic, A. (2001): *Oxycarenus lavaterae* (Fabricius, 1787) (Heteroptera: Lygaeidae) another new species in the entomofauna of Serbia. – Protection of Nature (Beograd) 52: 61-63 (in Serbian, English summary).
- [36] Putchkov, P. V. (2013): Invasive true bugs (Heteroptera) established in Europe. – Український Ентомологічний Журнал (Ukrainian Entomological Magazine) 2(7): 11-28.
- [37] Rabitsch, W. (2008): Alien true bugs of Europe (Insecta: Hemiptera: Heteroptera). – Zootaxa 1827: 1-44.
- [38] Rabitsch, W. (2010): True Bugs (Hemiptera, Heteroptera). – In: Roques, A., Kenis, M., Lees, D., Lopez-Vaamonde, C., Rabitsch, W., Rasplus, J. Y., Roy D. (eds). Alien Terrestrial Arthropods of Europe, pp. 407-433, Chapter 9.1. BioRisk 4. Pensoft Publishers, Sofia.
- [39] Rabitsch, W., Adlbauer, K. (2001): Erstnachweis und bekannte Verbreitung von *Oxycarenus lavaterae* (Fabricius, 1787) in Österreich (Heteroptera: Lygaeidae). – Beiträge zur Entomofauna 2: 49-54.
- [40] Reynaud, P. (2000): Bug *Oxycarenus lavaterae* responsible for extraordinary infestations in Paris. – Phytoma, La défense des végétaux 528: 30-33 (in French).
- [41] Ribes, J., Piñol, J., Espadaler, X., Cañellas, N. (2004): Heterópteros de un cultivo ecológico de cítricos de Tarragona (Cataluña, NE España) (Hemiptera: Heteroptera). – Orsis 19: 21-35.
- [42] Schneider, A., Dorow, W. H. O. (2016): Erstnachweis von *Oxycarenus lavaterae* (Fabricius, 1787) für Hessen. – Heteropteron 45: 23-24.
- [43] Seward, E. A., Votýpka, J., Kment, P., Lukeš, J., Kelly, S. (2017): Description of *Phytomonas oxycareni* n. sp. from the Salivary Glands of *Oxycarenus lavaterae*. – Protist 168: 71-79.
- [44] Simov, N., Langourov, M., Grozeva, S., Gradinarov, D. (2012): New and interesting records of alien and native true bugs (Hemiptera: Heteroptera) from Bulgaria. – Acta Zoologica Bulgarica 64(3): 241-252.
- [45] Stichel, W. (1958): Illustrierte Bestimmungstabelle der Wanzen. II. Europa, pp. 97-224. Hemiptera-Heteroptera Europae 4. – Stichel, Berlin-Hermsdorf.
- [46] Şerban, C. (2010): Faunistic data on some true bugs species (Insecta: Heteroptera) from West Turkey. [Results of the “Taurus”–2005 and “Focida”–2006 expeditions]. – Travaux du Muséum National d’Histoire Naturelle (Grigore Antipa) 53: 171-180.
- [47] Velimirovic, V., Durovic, Z., Raicevic, M. (1992): Bug *Oxycarenus lavaterae* Fabricius (Lygaeidae, Heteroptera) new pest on lindens in Southern part of Montenegro. – Zastita Bilja 43: 69-72.
- [48] Wachman, E., Melber, A., Deckert, J. (2007): Wanzen. Band 3. Pentatomomorpha I. Aradida, Lygaeidae, Piesmatidae, Berytidae, Pyrrhocoridae, Alydidae, Coreidae, Rhopalidae, Stenocephalidae. Die Tierwelt Deutschlands, 78. Teil. – Goecke & Evers, Keltern.
- [49] Wermelinger, B., Wyniger, D., Forster, B. (2005): Massenaufreten und erster Nachweis von *Oxycarenus lavaterae* (F.) (Heteroptera: Lygaeidae) auf der Schweizer Alpennordseite. – Mitteilungen der Schweizerischen Entomologischen Gesellschaft 78: 311-316.
- [50] Yazıcı, G., Yıldırım, E., Moulet, P. (2015): Contribution to the knowledge of the Lygaeoidea (Hemiptera, Heteroptera) fauna of Turkey. – Linzer boil. Beitr. 47(1): 969-990.

HORIZONTAL FLUX OF SUSPENDED PARTICLES SAMPLING BY BIG SPRING NUMBER EIGHT (BSNE) SAMPLER IN LAKE URMIA AREA

ZABIHI, F.¹ – ESFANDIARI, M.¹ – DALALIAN, M. R.^{2*} – MOEINI, A.¹

¹*Department of Soil, Science and Research Branch, Islamic Azad University
Tehran, Iran*

(phone: +98-914-104-5508; +98-912-947-6853; fax: +98-21-2240-3348)

²*Department of Soil Science, Tabriz Branch, Islamic Azad University
Tabriz, Iran*

**Corresponding author*

e-mail: mdalalian@iaut.ac.ir; phone: +98-912-520-2818

(Received 14th Aug 2017; accepted 15th Jan 2018)

Abstract. Lake Urmia has become one of the key dust sources in northwestern of Iran due to a sharp drop in its water level that caused an increasing dried land around the lake area. There has not been any studied concerning of how much dust is emitted and transported in this area. The aim of this research study was to measure the amount of dust suspended particles flux in the lake area. To implement this objective, 56 aeolian dust samplers were mounted at 0.15, 0.5, 1 and 2 m heights in 14 different poles and the suspended particles flux was measured during one year period. The data showed that the flux in March, June, and October accounted for 53% of the annual total. The suspended particles flux decrease rapidly with increasing height of soil surface. The obtained data showed that the suspended particles flux is strongly correlated with the amount of monthly precipitation and mean wind velocity but there was no significant relationship between monthly suspended particles flux and speed of the strongest wind. The result also showed that the wind direction did not influence flux. Different heights of the soil surface, sampling times and sampling sites had significant ($P \leq 0.01$) effects on flux.

Keywords: *dust center, height of soil surface, sampling site, sampling time, wind erosion, wind speed*

Introduction

According to FAO report, approximately 430 million ha of drylands, which comprise 40% of earth's surface are susceptible to wind erosion. Many studies have estimated the amount of global wind erosion and dust transport. However, because the wind not only mobilizes dust but also transport coarser soil particles (sand), therefore the estimation of the total amount of wind erosion especially amount of dust is uncertain. The rate of global dust emission is reported in a range of 5×10^{11} to 33.2×10^{11} kg.yr⁻¹. The studies of dust sources that were concluded by global-scale high-resolution satellite imagery, showed that natural dust sources do account for about 75% of dust emission and the remaining 25% of emission were attributed to anthropogenic sources. The fraction of dust sources is highly variable (FAO, 2015).

The Lake Urmia which is located in northwestern of Iran is one of the main sources of aeolian dust in Iran. This lake has shown a sharp drop in water level due to decreasing in rainfall precipitation and excessive water intake, especially for agricultural consumption. The human factors such as the construction of numerous dams on the rivers that lead to the lake and the drill of multiple unauthorized wells are considered for water decline. According to the reports, during the last 20 years (1995 to 2015), the water level of the Lake Urmia has fallen by 8 meters (Tajrish, 2016). The

area of Lake Urmia is 5822 km². According to official reports, more than 80% of it was dried in 2013. This means that about 4657 km² area is converted into drylands (Asghai Zamani, 2013). Unfortunately, the trend has been continued and this area is highly exposed to wind erosion and susceptible to generate dust particles with a diameter less than 0.1 mm. Therefore, the Lake Urmia is considered to be a key source area for dust storms in N.W. of Iran.

The strong dust transport that occurs during dust storms often creates a serious hazard for human (Dong et al., 2010). If the dust transportation continues and after passing some distance and settles into the ground surfaces, the salinity of these particles may cause to increase the salinity of agricultural lands in the region. The results of the chemical soil test in the area showed that the salinity of the investigated soil was very high (EC = 143.1 Ds.m⁻¹ and SAR = 80.5).

On the other hand, drying of the Lake Urmia caused the reflection of solar radiation to increase. The Albedo coefficient of drylands around the lake was 5.2 times more from 2007 to 2013. The diseases that caused by frequent exposure to ultraviolet radiation include cancer, eye injuries (black eyes, cataracts, burns, blindness, and luminosity) and dermatological injuries (Tajrishi, 2016). Also, it has been reported that if the amount of suspended particles in the air exceeds the limit of (15 × 10⁻⁸ kg.m⁻³), it will cause respiratory illnesses. These factors threaten the lives of more than 7 million people in the region.

Even though, many types of research have designated to transform and provide guidance to water level restoration, but there is no information on the amount of suspended particle caused by wind erosion in the drylands area of the Lake Urmia. Government officials especially Urmia Lake Restoration Program just paying attention to restore the water level to this lake.

In studies of aeolian dust, the most important parameter is the amount of dust transported in the air (i.e., the horizontal dust flux) (Dong et al., 2010). Hence in order to provide suggestions and solutions for dealing with wind erosion especially suspended particles in the air, we need to know the amount of suspended particle flux and their transportation mechanism of how it is changing at different heights of soil surface at different sampling times and different sampling distance sites.

To support such goals, we need to accurately install the instrument to trap the suspended particles. The wind tunnels designed to study wind erosion limit the maximum height of studied particles (normally the height of particles being tested should not exceed ¼ to 1/3 the height of the tunnel). Thus, to translate wind tunnel soil losses to equivalent losses from a field is difficult. Also, wind tunnels do not study erosion events for long-term (Fryrear et al., 1988).

Using the samplers to study the suspended particles has started since 1957 and has been changed a lot to increase the efficiency of samplers. The last and most advanced sampler for suspended particles gathering is BSNE (Big Spring Number Eight) sampler that was made by Donald Fryrear in Big Spring-Texas for the first time in 1986. More important properties of this sampler include (a) its ability to orientate into erosive winds; (b) the possibility to collect samples from different heights at the same location; (c) the least need to servicing and controlling for long collection periods; (d) its ability to earn data of vertical and horizontal distribution; (e) its construction is simple and it is durable (Fryrear, 1986). Studies that compare this sampler with other samplers have shown that this sampler is the most efficient and recommended sampler for field

measurements (Goossens and Offer, 2000; Shannak et al., 2014; Goossens and Buck, 2012; Dong et al., 2010).

The objective of this research study was to investigate and presents results for the amount of horizontal suspended particles flux and its variation with different heights, sampling time and sampling site based on continuous sample collection and detail observation from March 2016 until February 2017 for assessing wind erosion in the studied area.

Materials and methods

Location

In this study, one of the dust centers that located in the southeastern zone of Lake Urmia was selected (*Fig. 1 C*). This area was exposed to wind erosion and it was a suitable place to study wind erosion and the flux of suspended particles. Lack of insignificance of earth's slope gradient, shortage of plant cover and having high wind speed and low rainfall (the average 11 years of meteorological information of a studied region in duration from 2000 to 2011 that were obtained from Tabriz weather station has been shown in *Table 1*) are parameters used to select location sites.

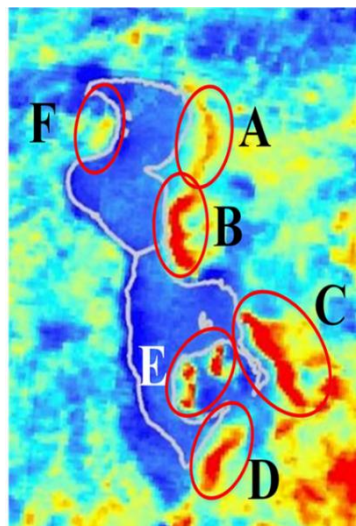


Figure 1. Plan of dust centers around Lake Urmia (recognized by BTM methods - one of the recognition methods based on Brightness temperature difference) (Tajrishi, 2016)

Table 1. The average 11 years of meteorological information of studied zone (from 2000 to 2011)

Months	Jan.	Feb.	Mar.	Apr.	May	Jun.	Jul.	Aug.	Sep.	Oct.	Nov.	Dec.
Mean wind velocity (m.s ⁻¹)	0.99	1.89	5.17	2.7	2.44	5.03	5.11	3.96	1.54	1.81	1.52	0.95
Speed of strongest wind (m.s ⁻¹)	30	30	45	25	30	38	28	45	80	40	30	25
Total amount of rainfall (mm)	24.21	20.95	3.9	53.41	27.29	1.86	2.41	2.19	27.06	12	20.55	23.9

Geographical location of the studied region was 45° 51' 0.771" eastern longitude and 37° 47' 0.675" northern latitude with semi-arid and cold climate. This zone was located at 30 km distance from the Tabriz-Azarshahr road and western south of East-Azarbayjan province- Khasselou village. Topsoil samples that were taken from the zoned area had 28% sand, 40% silt, and 32% clay. The bulk density of soil was 1.34 gr.cm⁻³ and soil texture was clay loam (Table 2).

Table 2. Results of chemical and physical analysis of the initial soil

Depth (cm)	Sand%	Silt%	Clay%	Soil texture	ρb (gr.cm ⁻³)	ECe (dS.m ⁻¹)	pH	%T.N.V	%OC	SAR
0-10	28	40	32	C-L	1.34	143.1	7.84	16.25	0.45	80.5
10-20	25	42	33	C-L	1.35	142.1	7.95	16.21	0.4	79.5
20-30	20	45	35	C-L	1.32	140	8	16.22	0.39	79

Field instrument

In this study, the modified BSNE samplers with opening 20 mm wide and 50 mm height were used. The 18 mesh stainless screen in the opening of sampler for dust entering and the 120 mesh stainless steel screen on the top of the sampler was used which allowed the air to exit while the airborne material remained in the sampler tray. 4 samplers were installed on the same mounting pole (a ½" steel pipe with an outside diameter of 1.8 cm) at 0.15, 0.5, 1 and 2 m heights of the soil surface (Fryrear et al., 1991). An 18 × 20 cm sheet provided as sampler tail that accompanied by a rubber retainer in lower of each sampler that allowed to rotate and orient according to wind direction (Figs. 2 and 3). 14 poles were installed in a circular pattern (Fig. 4) inside 3.2 ha area. This pattern permitted field erosion data collection regardless of the wind direction and provided a range of field lengths with a minimum number of sampler locations (Fryrear et al., 1991).

Samples gathering and analytical methods

Totally, 56 samplers were installed in the above-mentioned pattern. After 30 days of installing, the tray of each sampler was evacuated and gathered particles were dried at 105°C and transported to the laboratory for physical testing. This gathering was continued monthly in 12 interval periods (from March 2016 until February 2017).

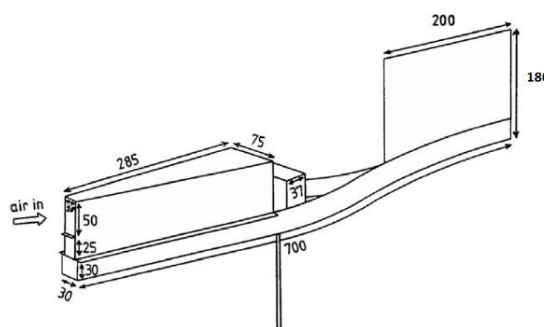


Figure 2. BSNE sampler- (all dimensions are in mm)



Figure 3. Samplers that were made and installed

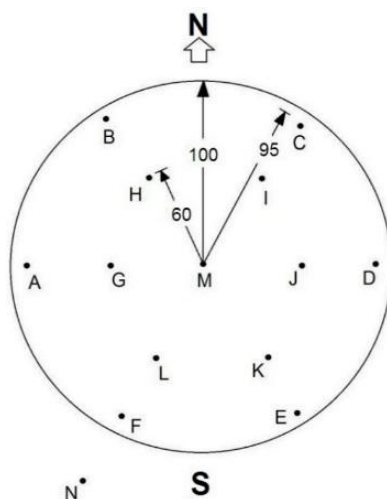


Figure 4. The installation pattern of 14 poles

To determine the horizontal flux of suspension particles, sample weight of suspended gathered particles calculated via particle size distribution curve (particles were sieved via series with 18, 30, 60, 100, 200, 270 and 400 meshes that corresponds to 1, 0.595, 0.25, 0.149, 0.074, 0.053 and 0.037 mm in diameters respectively). Horizontal flux was calculated by the formula in *Equation 1* (Wang et al., 2004):

$$F = \frac{W}{S.T} \quad (\text{Eq.1})$$

where F = horizontal flux of suspension particles ($\text{kg} \cdot \text{m}^{-2} \cdot \text{mon}^{-1}$), W = weight of suspension particles sampled by sampler (kg), S = area of sampler opening (m^2) and T = time (mon).

According to Goossens and Buck (2012) findings, there was no relation between the efficiency of BSNE sampler and wind velocity. Therefore the sampling efficiency of the sampler was supposed to be constant of wind velocity and they used *Equation 2* for efficiency estimating of suspended particles.

$$y = -0.0047x^2 + 1.2145x + 6.1302 \quad (\text{Eq.2})$$

This equation showed that there was a strong relationship between the sampling efficiency (y in percent) with the particles diameter (x in micron); ($r^2 = 0.9969$).

This equation was constant for particles larger than 10^{-4} m (0.1 mm) (the upper boundary of suspended particles). In this study the equation 2 for efficiency estimating of made samplers was used.

To study the effect of sampling time (during the research period from March 2016 until February 2017) and height of soil surfaces (0.15, 0.5, 1 and 2 m) on suspended particles flux, the data of calculated flux in different times and different heights of soil surface were analyzed. Factorial experiment on the basis of completely randomized design with 14 replication was carried out. Also, to study the effect of sampling time and sampler's distance from each other (14 sites of installation of the poles) on suspended particles flux, the data of calculated flux in different times and different sites were analyzed. Factorial experiment on the basis of completely randomized design with 4 replication was carried out. Comparison of means by Duncan multiple range test at 1% probability level was carried out. Before data analyzing, the normality test of variables was carried out. Data analysis was done using SPSS-16 software and the graphs and tables were drew by Excel software.

The data of meteorological information of studied zone during research period were obtained from Tabriz weather station (*Table 3*). As seen in the table the range of mean wind velocity varied from 3.3 to 8.1 $\text{m} \cdot \text{s}^{-1}$. The maximum speed of strongest wind was 20 $\text{m} \cdot \text{s}^{-1}$ in November. The minimum horizontal vision varied from 0.02 km in January 2017 to 7 km in August 2016. The highest rainfall was 68.6 mm in April 2017, and the lowest was 0 mm in August 2016. This report showed that the highest and lowest amount of rainfall in the months exactly corresponds to the average 11 years of meteorological data gathering (*Table 2*).

Results and discussion

Variation in horizontal flux with height

The variation of horizontal suspended particle's flux with a height of soil surface (the flux profile) is expressed by a power law (*Eq. 3*).

$$f(z) = az^b \quad (\text{Eq.3})$$

where $f(z)$ is the horizontal suspended particle's flux ($\text{kg} \cdot \text{m}^{-2} \cdot \text{mon}^{-1}$) at height z (m) and a , b are regression coefficients.

Table 3. Meteorological information of studied zone during research period (March 2016-February 2017)

Date	Minimum surface temperature (°C)	Air temperature (°C)			Relative air moisture (%)			Mean wind velocity (m.s ⁻¹)	Speed of strongest wind (m.s ⁻¹)	Direction of strongest wind	Total of rainfall (mm)	Maximum of daily rainfall (mm)	Horizontal vision (km)	
		Min	Max	Mean	Min	Max	Mean						Min	Max
Mar-16	-1.2	-3.2	19.2	7.9	21	97	57.5	8.7	15	360	1.5	10	2.5	25
Apr-16	0.1	-3.8	20.4	9.1	20	98	62.5	4.4	19	330	46.6	23.3	0.3	30
May-16	5.1	2.4	28.6	16.2	13	96	54	6.8	16	340	26.1	18.7	2.3	30
Jun-16	9.21	10	32.2	20.5	11	94	44.5	7.5	19	210	1.1	12.8	2	25
Jul-16	16.1	15.6	38.4	26.2	8	84	38.8	5.6	16	070	3.3	2.5	5	25
Aug-16	18.5	17	39.4	28.6	7	68	31.8	6.1	13	060	1.8	-	7	20
Sep-16	12.6	11	37.4	24.5	8	80	34.8	7.1	17	350	1.7	4.1	4	27
Oct-16	3.7	1.8	28.8	16	9	90	39.9	7.7	18	350	1.3	0.7	2.5	35
Nov-16	-0.4	-4.2	20.8	8.6	21	97	61.8	5.4	10	230	26.4	8.4	0.5	30
Dec-16	-8.9	-14.4	11.6	-0.6	17	96	61.2	4.8	6	350	23	10.5	0.15	30
Jan-17	-13.8	-18	5.4	-5.5	50	97	76.3	3.3	6	300	24.6	8.1	0.02	12
Feb-17	-9	-16	6.7	-3.2	38	95	67.8	4.3	12	150	22.4	2.1	0.3	30

Figure 5 shows the variation in horizontal flux collected by the BSNE sampler as a function of the height of soil surface for every month during the duration of the research period. In all cases, the horizontal suspended particle's flux decreases with increasing height of soil surface.

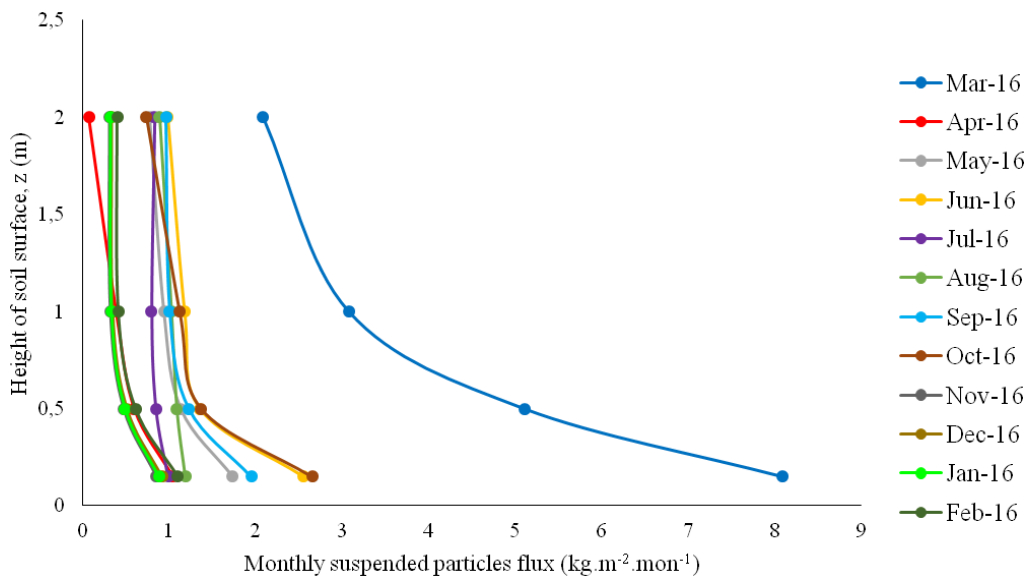


Figure 5. Vertical profile of suspended particles flux (from Mar. 2016 until Feb. 2017)

Previous researchers had shown the variation in Aeolian sediment flux as a function of height that were focused on saltation. The Aeolian saltation flux decayed with height exponentially, but Dong and et al. (2010) and Fryrear and Saleh (1993) based on another author's reports explained that power function could better describe this variation. They noticed that the flux of suspended sediments decayed relatively gently with height compared with the saltation flux. Fryrear (1987) and Zobeck and Fryrear

(1986) used a power function for Aeolian sediment flux at height as low as 0.15 m. Vories and Fryrear (1988) recommended only applying a power function to the height of 0.5 m and above because more of the particles below 0.5 m were saltation. Dong and et al. (2010) concluded that the Aeolian sediment flux at height below 5 m decays more rapidly than above 5 m with increasing height of soil surface, also the flux data above 5 m showed wider scattering than those at lower heights, but the overall variation with height can nonetheless be reasonably well explained using a power function.

By summing up the monthly suspended particles flux for each height reveals that the variation of the annual flux as a function of height can also be explained well by using a power function ($r^2 = 0.9981$) (Eq. 4 and Fig. 6).

$$F(z) = 447.5z^{-2.523} \quad (\text{Eq.4})$$

where $F(z)$ is the annual sediment flux ($\text{kg}\cdot\text{m}^{-2}\cdot\text{mon}^{-1}$) at height z (m).

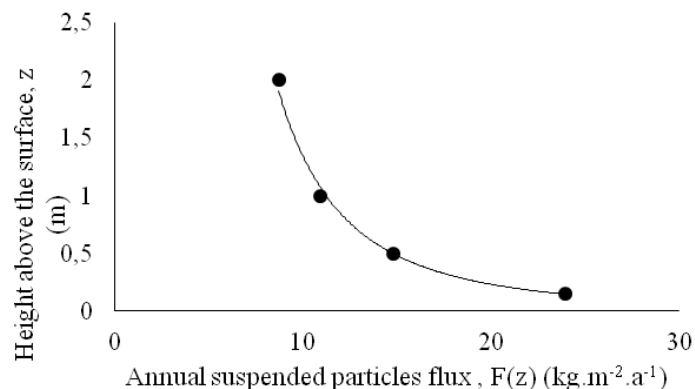


Figure 6. Variation in annual suspended particle's flux), $F(z)$, as a function of height (z)

Results of the regression analysis between the fluxes of suspended particles as a function of the height of soil surface had been shown in Table 4.

Table 4. Results of the regression analysis between the flux of suspended particles as a function of height

Month	a	b	r^2
Mar. 2016	8.2427	-1.852	0.9812
Apr. 2016	0.2555	-0.887	0.8282
May 2016	0.8287	-3.207	0.9952
June 2016	1.5311	-2.595	0.9535
July 2016	0.137	-10.15	0.7465
Aug. 2016	0.8835	-8.737	0.9241
Sept. 2016	1.2509	-3.317	0.94
Oct. 2016	1.0936	-2.055	0.989
Nov. 2016	0.099	-2.288	0.9475
Dec. 2016	0.1177	-2.288	0.9475
Jan. 2017	0.1072	-2.288	0.9475
Feb. 2017	0.1786	-2.288	0.9475

The cumulative percentage of the annual suspended particles flux as a function of the height of soil surface (*Fig. 7*) derived from *Equation 4* shows that 80% of flux was transported below 80 cm and 90% below 120 cm of the surface. This suggests that the majority of suspended particles flux moves below 1 m height of soil surface and will settle back to the ground in a short distance and that only a small fraction will be transported over long distances. These results are according to Dong et al. (2010).

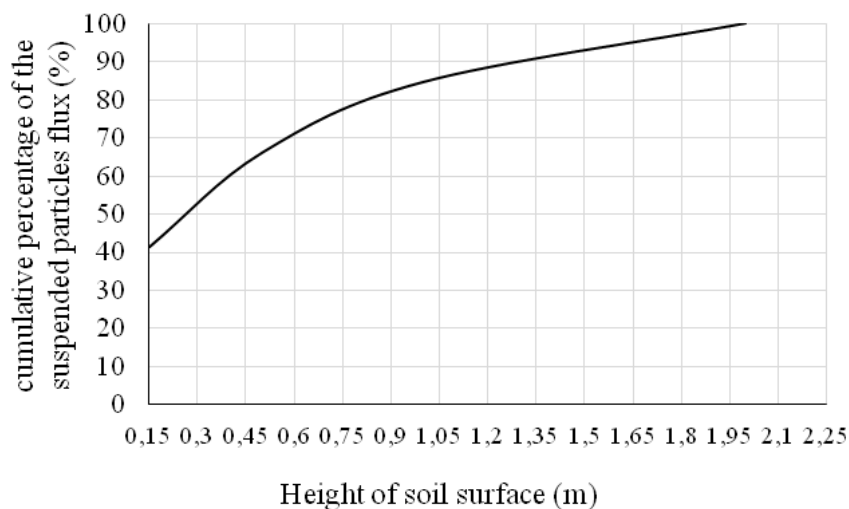


Figure 7. Plot of cumulative percentage of the annual flux of suspended particles as a function of height

Variation in monthly suspended particles flux

If the variation in suspended particles flux with height for a given month can be established, the monthly total suspended particles flux can be calculated as follows (*Eq. 5*):

$$F_i = \int_0^{\infty} f_i(z) dz \quad (\text{Eq.5})$$

where F_i is the total suspended particles flux passing through a unit width in a month I and $f_i(z)$ is the function for month i . In theory, $f_i(z)$ can be considered as equivalent to the regression function in *Equation 3* that we obtained earlier. The annual suspended particles flux fitted *Equation 4* with smaller errors. Dong et al. (2010) concluded that the monthly total suspended particles flux can be estimated by *Equation 6*.

$$F_i = \frac{F_{iob}}{F_{ob}} \int_0^{\infty} F(z) dz \quad (\text{Eq.6})$$

where F_{iob} is the observed total suspended particles flux in the month I that is obtained by summing the monthly suspended particles flux collected at all 4 heights, and F_{ob} is the observed annual total suspended particles flux obtained by summing the annual

suspended particles flux at all 4 heights. $F(z)$ is the function of the variation in annual suspended particles with height (Eq. 4). Hence Equation 7 can be used to estimate the monthly total suspended particles flux.

$$F_i \approx \frac{F_{iob}}{F_{ob}} \int_0^z F(z) dz = \frac{F_{iob}}{F_{ob}} \int_0^\infty 447.5z^{-2.523} dz = -\frac{F_{iob}}{F_{ob}} 293.83z^{-1.523} \quad (\text{Eq.7})$$

Figure 8 shows the relationship between the total monthly suspended particles flux and the main meteorological parameters at the study site during research period (from Mar. 2016 until Feb. 2017). Correlation coefficients between monthly suspended particles flux (F) and monthly precipitation (P), speed of the strongest wind (SW) and monthly mean wind velocity (MW) showed that the monthly suspended particles flux is strongly correlated with the monthly precipitation and monthly mean wind velocity, but there was no significant relationship between monthly suspended particles flux and speed of the strongest wind (Table 5). This can be explained by the fact that when the monthly precipitation is low, the soil surface is arid and prone to the emission of suspended particles into the air.

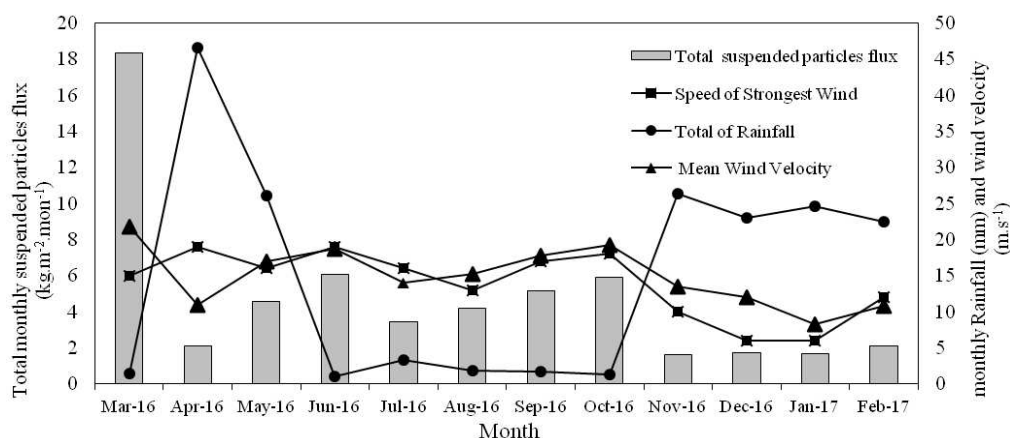


Figure 8. Variation of monthly suspended particles flux (grey bars) and its relationship with the main meteorological parameters at the study site

Table 5. Correlation coefficients between monthly suspended particles flux and main meteorological parameters during research period

	F	MW	SW	P
F	1	0.609*	0.516 ^{ns}	-0.779**
MW		1	0.818**	-0.698*
SW			1	-0.509 ^{ns}
P				1

ns, * and ** are insignificant, significant at $P \leq 0.05$ and $P \leq 0.01$

Aeolian transport mainly occurs in March, June, and October in the Lake Urmia area. These months account for 53% of the total annual suspended particles flux (Fig. 9). March has the greatest Aeolian transport.

The comparison between suspended particles flux and the average 11 years of meteorological data (from 2000 until 2011) at the studied area (Fig. 10 and Table 6) shows that there is a correlation between the monthly precipitation and monthly suspended particles flux, too.

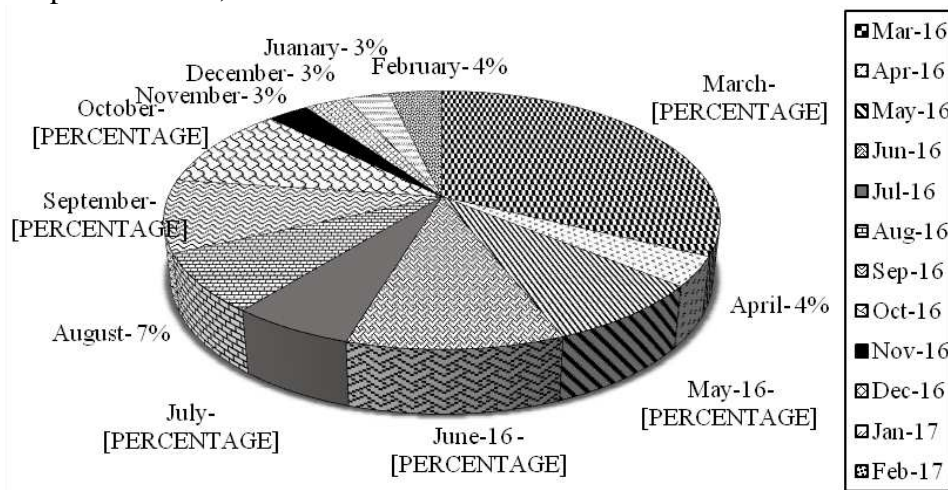


Figure 9. Share of each month of the total annual suspended particles flux

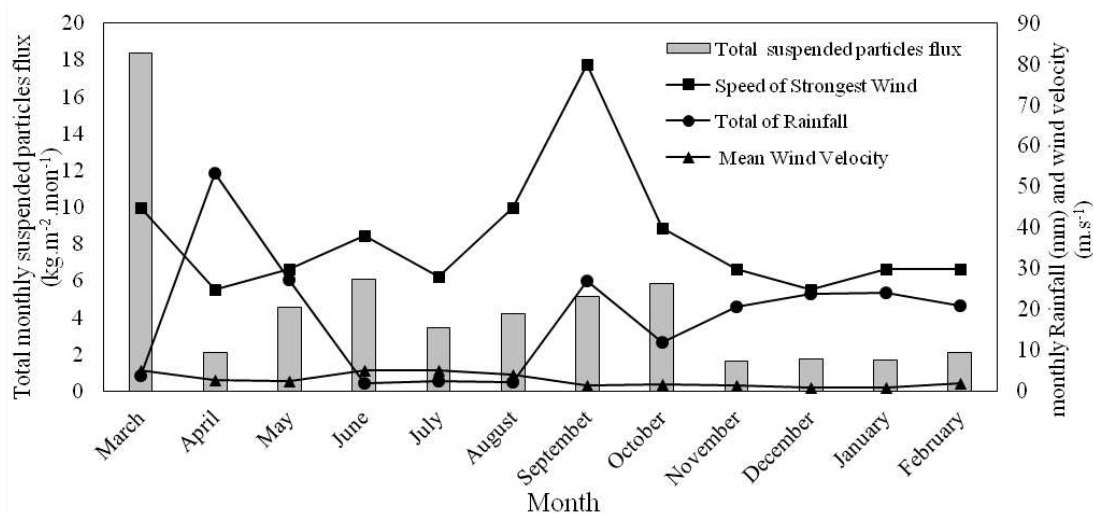


Figure 10. Variation of monthly suspended particles flux (grey bars) and its relationship with the average 11 years of meteorological data (from 2000 until 2011) in the studied area

Table 6. Correlation coefficients between monthly suspended particles flux and the average 11 years of meteorological data (from 2000 until 2011)

	F	MW	SW	P
F	1	0.581*	0.349 ^{ns}	-0.608*
MW		1	0.024 ^{ns}	-0.44 ^{ns}
SW			1	-0.153 ^{ns}
P				1

ns, * and ** are insignificant, significant at $P \leq 0.05$ and $P \leq 0.01$

The effects of height of soil surface, sampling time and sampling site on the suspended particle's flux

To study the effects of sampling time during research period (from March 2016 until February 2017) and height of soil surfaces (0.15, 0.5, 1 and 2 m) on suspended particles flux, the data of suspended particles flux in different times and heights were analyzed. The results of variance analysis (mean and corresponding effects) (Table 7) showed that corresponding effect of sampling time and height of soil surface on suspended particles flux were significant ($P \leq 0.01$).

Table 7. Mean squares of sampling time and height of soil surface effects on suspended particles flux

Source	Df	Mean squares
The height of soil surface	3	0.265**
Sampling time	11	0.377**
Height of soil surface × sampling time	33	0.035**
Error	624	0.007
CV%		45.42

ns, * and ** are insignificant, significant at $P \leq 0.05$ and $P \leq 0.01$

The mean comparison results of the corresponding effect of sampling time and height of soil surface on suspended particles flux (Fig. 11) showed that when the height of soil surface increased, the suspended particles flux decreased. This was accordance with results of Dong et al. (2010) and Zobeck and Fryrear (1986) studies.

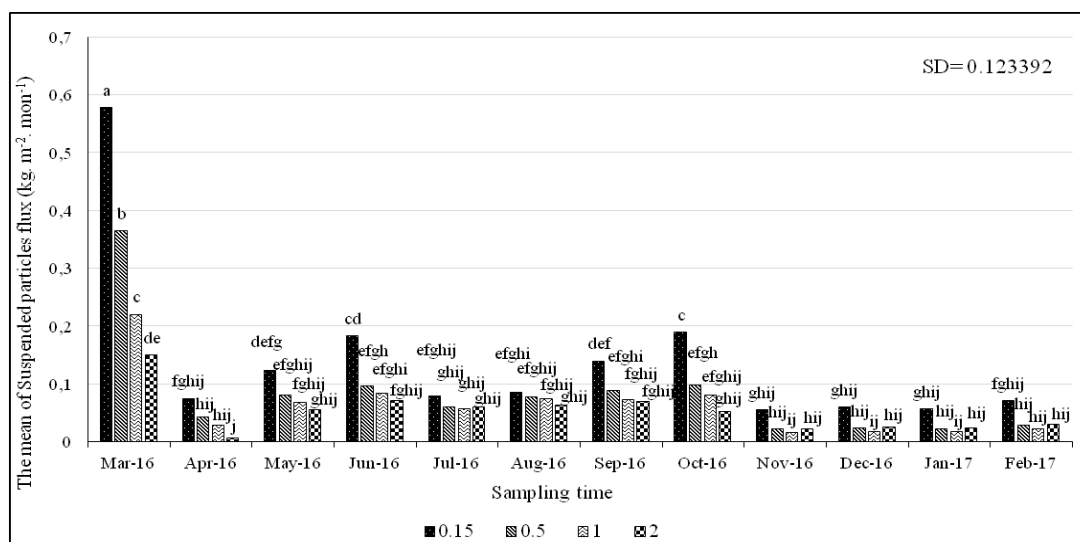


Figure 11. Mean comparison of the corresponding effect of sampling time and sampling height of soil surface on suspended particles flux

To study the effects of sampling time during research period (from March 2016 until February 2017) and sampling site (sampler's distance from each other by 14 poles that were installed in different sites) on suspended particles flux, data of calculated flux in

different times and sites were analyzed. The results of variance analysis (*Table 8*) showed that the mean effects of sampling time and sampling site on suspended particles flux were significant ($P \leq 0.01$), but the corresponding effect of sampling time and sampling site was insignificant.

Table 8. Mean squares of sampling time and sampling site effects on suspended particles flux

Source	df	Mean squares
Sampling time	11	0.378**
Sampling site	13	0.019**
Sampling site × sampling time	143	0.01 ^{ns}
Error	504	0.009
CV%		45.65

ns, * and ** are insignificant, significant at $P \leq 0.05$ and $P \leq 0.01$

The mean comparison result of the main effect of sampling time on suspended particles flux (*Fig. 12*) showed that there was a significant difference ($P \leq 0.01$) between different times of sampling. The greatest mean of suspended particles flux was in March 2016. According to (*Fig. 8*), the amount of precipitation was low and wind velocity was high in this month. Actually, there was an inverse correlation between suspended particles flux and total monthly rainfall.

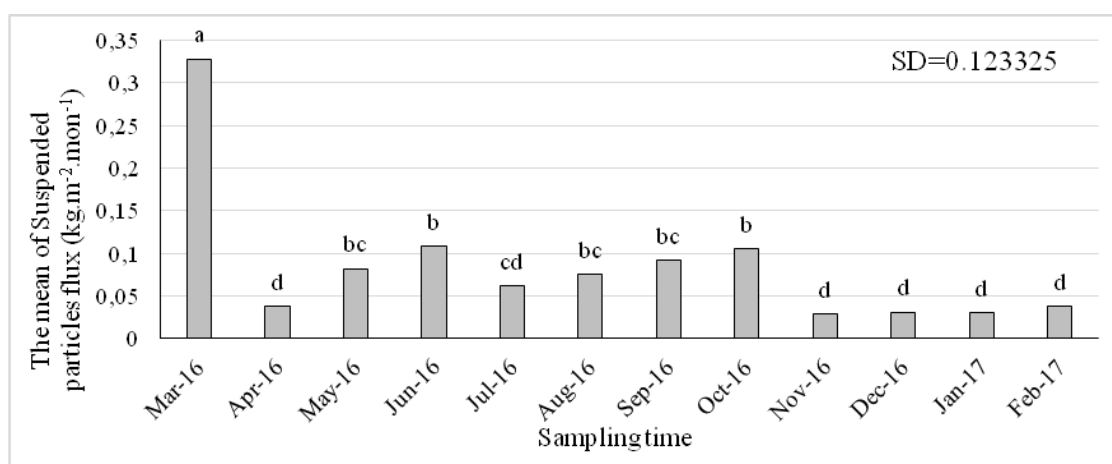


Figure 12. Mean comparison of the main effect of sampling time on suspended particles flux

The mean comparison result of the main effect of sampling site on suspended particles flux (*Fig. 13*) showed that there was significant difference ($P \leq 0.01$) between different sampling sites, but just in one site (I-pole), differences were significant compared to other sites, and it was ignored, suggesting that the sampling site did not influence flux. Therefore, the 14 poles were installed in a circular pattern in different directions (*Fig. 4*). This can be inferred as the wind direction did not influence on suspended particles flux.

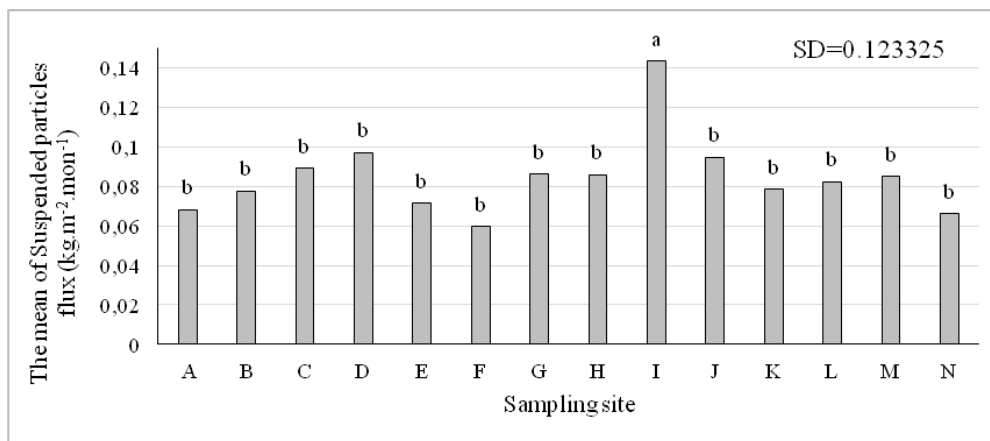


Figure13. Mean comparison of the main effect of sampling site on suspended particles flux

Conclusions

In this research study, we measured the horizontal flux of suspended particles for the one-year duration in surrounding dry lands of lake Urmia which is one of the main aeolian dust deposit in N.W.of Iran. The results of our study showed that the strongest aeolian transport dust occurs in March, June, and October. These months had the lowest amount of precipitation.

The horizontal suspended particles flux showed that it had a strong correlation with the amount of monthly precipitation and monthly mean wind velocity but there was no significant relationship between monthly suspended particles flux and speed of the strongest wind during the time of the study. The result also showed that the wind direction did not influence on suspended particles flux. Hence, due to a shortage of rainfall and the lack of soil surface covering in March, the amount of suspended particles flux was greatest in this month. Parameters such as different height of the soil surface, different sampling times and different sampling sites had a significant effect ($P \leq 0.01$) on suspended particles flux.

Several authors have proposed a power decay law to describe the variation in suspended flux with height, and we used that approach to provide a good fit for the observed data in this study.

Finally, our finding showed that the majority of suspended flux transported below 1 m height of soil surface will settle back to the ground in a short distance. This finding can help us in implementing the prevention programs such as windbreaker building. The design of the height and distance of windbreakers are important for their efficiency usage.

To confront wind erosion by mechanical means, the windbreaker is one of the direct methods of prevention. Other mechanical methods are mulching and plowing the land in opposite direction of the dominant slope. Indirect methods are planting the native plant vegetation that grows in the region. Usually, these are the halophytic vegetation. Protecting grassland from degradation and rehabilitating the dried-up terminal lake will be important steps in reducing and preventing future dust storm.

For future studies, we suggest that the suspended particles flux be examined as toxin materials in surrounding lake Urmia area. We recommend that trace toxic elements and other elements such as Na, Ca, K, Mg, Al and heavy metals such as Fe, Mn, Si be measured for purpose of health considerations, because the area is designated as one of the locations that are susceptible to hazards of dust pollution.

REFERENCES

- [1] Asghai Zamani, A. (2013): Evaluation of Urmia lake level changes as profound environmental challenges facing the North West of Iran. – *Geographic Space* 13(41): 77-91.
- [2] Dong, Z., Man, D., Luo, W., Qian, G., Wang, J., Zhao, M., Liu, S., Zhu, G., Zhu, S. (2010): Horizontal aeolian sediment flux in the Minqin area, a major source of Chinese dust storms. – *Geomorphology* 116: 58-66.
- [3] FAO (Food and Agriculture Organization of the United Nations) (2015): Status of the World's Soil Resources, Main Report - Chapter6 - Global Soil Status, Processes, and Trends. – Food and Agriculture Organization of the United Nations and Intergovernmental Technical Panel on Soils, Rome.
- [4] Fryrear, D. W. (1986): A field dust sampler. – *Journal of Soil and Water Conservation* 41(2): 117-120.
- [5] Fryrear, D. W. (1987): Aerosol Measurements from 31 Dust Storm. – In: Ariman, T., Veziroglu, T. N. (eds.) *Particulate and Multiphase Proceeding, 2. Contamination Analysis and Control*. Hemisphere Publishing Corporation, New York.
- [6] Fryrear, D. W., Stout, J. E., Gillette, D. A. (1988): Instrumentation for wind erosion. – *Proc. Wind Erosion Conference*, Lubbock, TX.
- [7] Fryrear, D. W., Saleh, A. (1993): Field wind erosion: vertical distribution. – *Soil Science* 155(4): 294-300.
- [8] Fryrear, D. W., Stout, J. E., Hagen, L. J., Vories, E. D. (1991): Wind erosion: Field measurement and analysis. – *American Society of Agricultural Engineers* 34(1): 155-160.
- [9] Goossens, D., Buck, B. J. (2012): Can BSNE (Big Spring Number Eight) samplers be used to measure PM10, respirable dust, PM2.5, and PM1.0. – *Aeolian Research* 5: 43-49.
- [10] Goossens, D., Offer, Z. Y. (2000): Wind tunnel and field calibration of six Aeolian dust samplers. – *Atmospheric Environment* 34: 1043-1057.
- [11] Shannak, B., Corsmeier, U., Kottmeier, C., Al-azab, T. (2014): Wind tunnel study of twelve dust samples with large particle size. – *Atmospheric Environment* 98: 442-453.
- [12] Tajrishi, M. M. (2016): The revival of Urmia Lake, Challenges, and necessities. – *The International Conference on Geographic and Environmental Impacts of Urmia Lake Conditions*, The University of Tabriz, Iran, November.
- [13] Vories, E. D., Fryrear, D. W. (1988): Field measurements of wind erosion. – *1988 Wind Erosion Conference Proceedings*, Lubbock, Texas.
- [14] Wang, G., Wanquan, T., Mingyuan, D. (2004): Flux and composition of wind-eroded dust from different landscapes of an arid inland river basin in north-western China. – *Journal of Arid Environments* 58: 373-385.
- [15] Zobeck, T. M., Fryrear, D. W. (1986): Chemical and Physical Characteristics of windblown sediments. I. Quantities and Physical Characteristics. – *American Society of Agricultural Engineers* 29(4): 1032-1036.

FACTORS INFLUENCING DIETARY CHOICES OF IMMIGRANTS UPON RESETTLEMENT IN HOST COUNTRIES – A SCOPING REVIEW

DWEBA, T. P. – OGUTTU, W. J. – MBAJIORGU, C. A.*

*Department of Agriculture and Animal Health, University of South Africa
Florida Science Campus, Johannesburg, P. O. BOX 392, UNISA 0003, South Africa*

**Corresponding author
e-mail: mbajica@unisa.ac.za*

(Received 6th Sep 2017; accepted 20th Dec 2017)

Abstract. The adverse effects of migration on eating habits are well documented. Accessing healthy, culturally appropriate food is essential for achieving food security and overall health. However, less is known about the factors that affect post-immigration dietary choices. This scoping review assesses current findings regarding factors determining dietary choices. Electronic databases of papers published between 2005 and 2015 were used to retrieve and review papers for this review. Titles were reviewed by three reviewers to select papers that met the inclusion criterion set for this paper. A total of 50 papers were eventually selected and included in the review. Based on the work done in South Africa and internationally, various factors that affect dietary choices of immigrants were identified and include: climate change related factors, socio-economic factors, difficulty in navigating the new shopping environment, immigrant's perceptions towards host country's food, language barriers, failure to access traditional ingredients, safety of food sold in the ethnic markets, pressure from children to adopt host country's food and role of religion in determining immigrant's food choices in host countries. Findings of this study demonstrate that there are major research gaps on dietary patterns of sub-Saharan African immigrants, and identifies research priorities in this field.

Keywords: *ethnic food markets, traditional food ingredients, food safety, food insecurity, food accessibility*

Introduction

According to the 1996 World Food Summit “Food security is a condition that exists when all people, at all times, have physical and economic access to sufficient, safe, and nutritious food to meet their dietary needs and food preferences for an active and healthy life” (FAO, 2006). This therefore means that accessing healthy, culturally appropriate food is essential for food security to be realized by any immigrant (Jacobus and Jalali, 2011; Vahabi and Damba, 2013) hence migrating into a new country with different food culture, poses dietary challenges.

Loss of food products and food consumption patterns is one of the major challenges faced by immigrants upon resettlement in host countries (Njomo, 2013). This is attributed to the fact that apart from its nutritious role, food has religious, cultural and social roles among native people. As a result, in different countries, there are distinct variations in what is considered edible (Hadley et al., 2010; Dharod et al., 2011; Garnweidner et al., 2012; Mannion et al., 2014).

The challenges encountered often result in adopting unhealthy eating habits and subsequent decline in nutritional health of the immigrants (Renzaho and Burns, 2006; Satia, 2010; Kiptinness and Dharod, 2011; Okafor et al., 2014; Terragni et al., 2014). The unhealthy eating habits are known to lead to the loss of what is known as “Healthy Immigrant Effect” (HIE) (Sanou et al., 2014), a term that refers to a phenomenon in

which immigrants are habitually healthier than the natives of the host country. This is because immigrants are forced to undergo high dietary acculturation; whereby they adopt eating habits of their host country. The result, is a rapid decline in the HIE upon settlement in the host countries. Several authors have shown that acculturation whenever it occurs, is associated with adopting unhealthy eating habits (Renzaho and Burns, 2006; Satia, 2010; Kiptinness and Dharod, 2011; Okafor et al., 2014; Terragni et al., 2014). This is because the resulting dietary changes are habitually associated with high intake of fat, salt and refined cereals (Dharod et al., 2011). This places immigrants at an increased risk of developing chronic diseases of the lifestyle (Deng et al., 2013; Sanou et al., 2014).

While dietary acculturation among immigrants upon resettlement in host countries is common, generally immigrants prefer to maintain their original food culture (Kiptinness and Dharod, 2011; Vue et al., 2011; Garnweidner et al., 2012; Lesser et al., 2014; Lindsay et al., 2014). As a result, majority of immigrants tend to develop bicultural eating patterns (Vue et al., 2011; Garnweidner et al., 2012).

Given the issues raised in the paragraph above, it is evident that immigrants moving to new countries do face unique dietary challenges which have potential to impact on their health and wellbeing while in their new home. In light of this, the question that arises is what determines immigrants' dietary choices upon settlement, and what dietary related challenges do they encounter in the host countries?

Recent immigration trends indicate that majority of African international migration takes place within the continent. It is reported that about 70% of all international migrations are intra-regional (Ratha and Shaw, 2007; Adepoju, 2008; Njomo, 2012). The number of immigrants from Sub-Saharan Africa to South Africa has been on the increase due to unstable economic conditions, soaring ethnic conflicts, and volatile political situations in most African countries (Adepoju, 2008; Njomo, 2013; Statistics South Africa, 2013). Besides war and harsh economic conditions prevailing in a number of African countries, climate change, which results into environmental effects such as loss of arable land, negative impact on the ecosystem and loss of natural environments, which, societies depend on, plays an important role in migration of people from one country to another (McMichael, 2012).

Official reports based on the 2011 census, suggested that there are approximately 2.2 million recorded immigrants in South Africa (Wilkinson, 2015; Chiumia, 2016); however this number could be more due to illegal immigrants and the fact that figures suggest that the number of permits that are issued are increasing every year (Statistics South Africa, 2014b). A major part (70%) of these immigrants are from African countries (Wilkinson, 2015). Immigrants living in South Africa are predominantly from Zimbabwe (42.6%), the Democratic Republic of Congo (12.9%), Nigeria (10.3%), and Lesotho (4.7%). The remaining 29.5% are from Rwanda, Burundi, Cameroon, Kenya, Tanzania, Uganda, Eritrea, Ethiopia, Somalia, Cote D'Ivoire, Gabon, Ghana, Niger, Sierra Leone, Togo, Angola, Botswana, Lesotho, Malawi, Mozambique, Namibia and Zambia (South African Press Association, 2014). According to Njomo (2013): these immigrants come to South Africa in search of better living conditions.

Despite these statistics, little is known about sub-Saharan African intra-regional immigrant dietary patterns, challenges and nutritional health. Therefore, the aim of this review was to highlight challenges faced by immigrants in accessing healthy, culturally appropriate food, and the possible impact this may have on the immigrants' dietary patterns upon resettlement in host countries. This review also identified

knowledge gaps and research priorities related to sub-Saharan African immigrant's dietary patterns who have migrated within the continent. Although this paper covers factors affecting a range of immigrants, a special emphasis is placed on sub-Saharan immigrants. Furthermore research gaps and priorities identified are specific to sub-Saharan immigrants in South Africa.

Methodology

A scoping review was undertaken to explore studies that had been undertaken on food related challenges experienced by immigrants upon resettlement in their host countries. In line with the objectives of a scoping review discussed by Arksey and O'Malley (2005) there was no consideration to study designs or quality of the studies. This review was undertaken to evaluate the type and extent of the research that has been undertaken, to summarize research findings and identify research gaps.

Different sources such as electronic databases and reference lists were utilised to identify relevant studies. Only studies published from January 2005 to April 2015 were included in this review. Research conducted prior to this date was deemed unlikely to reflect current research trends. Secondly, only studies published in English were considered due to costs involved in translation. The first step involved identification of all relevant articles using key words. This process yielded a large number of irrelevant articles. An initial screening yielded 2,720 articles. Papers that did not meet the inclusion criterion were discarded. An inclusion criterion was then refined to narrow down the number of articles. This inclusion criterion included papers related to factors determining dietary choices of sub-Saharan immigrants.

Titles were screened by three reviewers for relevance and those titles that did not fit the criterion were discarded. Copies of full articles that appeared to meet the set criteria were downloaded and saved in Mendeley. Copies of full articles that were not accessible were also excluded. After reviewing titles only 108 articles were retained. The abstracts for these papers were then reviewed, and out of the 105 articles that were retrieved from the electronic searches, 24 papers were selected for the review. From the 24 articles that were identified, reference lists were then utilised to identify further studies. Furthermore, papers citing any of the selected papers were also reviewed for relevance. Although the main focus of the review was sub-Saharan immigrants, at this stage in cases whereby there was paucity of studies; relevant citing papers including other immigrant groups were also included. From this process, 11 articles from the references and 15 citing articles were selected for inclusion. In total 50 papers were retrieved and included in the review. The process and results of the retrieval are summarized in *Figure 1*.

Each article was reviewed extensively and relevant information was recorded using Microsoft Excel. This included information on the study population, sample size, study area, and major findings (*Appendix*). The information was then analysed by the three authors using a narrative synthesis. The information was then organised thematically into eight factors affecting dietary choices. These factors include climate change barriers, socio-economic status, difficulty in navigating the environment, perceptions towards the host country's food, language barriers, accessibility of traditional food ingredients, safety of the food from the ethnic markets, pressure from children to adopt host country's food culture, and religious factors.

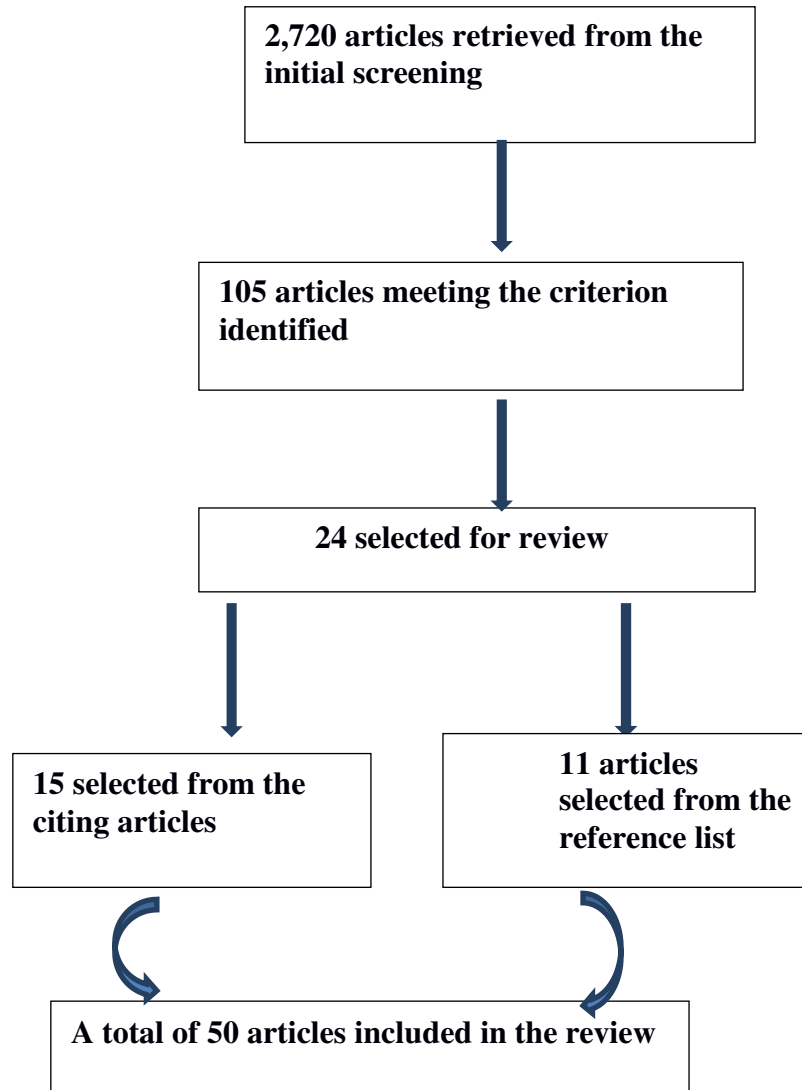


Figure 1. The methodological framework of how literature used in this paper was selected

Climate change related barriers

Apart from being the causal effect of migration, climate change can also be the driver of many food related challenges that immigrants encounter in host countries or destinations (McMichael et al., 2012; McMichael, 2015). Climate change driven migration is usually abrupt, therefore its aftermaths are comparable to those of refugees, as the affected usually have limited choice of their destination; with some ending up in developing countries that have limited resources (McMichael et al., 2012). In cases where climate change related migration results in large-scale population displacements, people often end up in settlements that are crowded, poorly ventilated, and with poor sanitation, resulting in adverse food related challenges (McMichael et al., 2012; Pendleton et al., 2014).

Firstly, as mentioned above, overpopulation that results from climate change driven migration leads to loss of arable land and natural environments that societies depend on for their well-being, thus affecting agricultural productivity not only for the immigrants but for native communities as well (McMichael et al., 2012). As the population grows;

forests, swamps, lakes and other habitats are cleared for residential areas, causing loss of biodiversity thus affecting lives and livelihoods of those that are directly dependent on healthy ecosystems (Berjak et al., 2011). Inadequate arable land combined with loss of biodiversity in turn forces immigrants who mostly originate from rural areas to depend mainly on shops for access of food, making them vulnerable to price fluctuations.

Secondly, conditions alluded to in the previous section can result into outbreaks of disease such as cholera, typhoid hepatitis A, measles, respiratory diseases, diarrheal diseases and malaria (McMichael et al., 2012). Apart from putting pressure on the health system that is already under siege due to overcrowding, such diseases decrease productivity and earning capacity thus negatively affecting economic resources for accessing food (WHO, 2013).

Socio-economic causes

According to Hadley et al. (2010) and Sanou et al. (2014), socio-economic status of immigrants is major mediating factor to food insecurity. This is associated with lower incomes and low employment levels (Hadley et al., 2010; Vahabi and Damba, 2013; Anderson et al., 2014). This phenomenon is even higher amongst refugees as they are characterized with lack of formal education, language barriers, and lower employment levels (Hadley et al., 2010; Kiptinness and Dharod, 2011; Anderson et al., 2014). Lack of education makes it difficult for immigrants to find employment thus limiting their financial resources and hence the vulnerability to food insecurity (Kiptinness and Dharod, 2011; Vahabi and Damba, 2013; Anderson et al., 2014). For example in a study by Kiptinness and Dharod (2010) conducted in United States amongst Bhutanese refugees, about 64% (n = 9) of the participants had no formal education. As a result only 14% (n = 2) of them were able to get part-time or fulltime employment. Hadley et al. (2010) who studied Somali refugees also found similar results. The majority of the households of the Somali refugees that participated in their study had lower monthly household incomes. Vahabi and Damba (2013) also came to the same conclusion, stating that the majority of Latin American immigrants in their study had low income due to difficulties in finding decent jobs. Anderson et al. (2014) observed that about 71% (n = 35) who had experienced food insecurity were of a low education and income status. The latter study by Anderson et al. (2014) was conducted amongst Sudanese refugees. In study done in Ghana, more than half of the Liberian refugees (51.9%; n =124) based in Buduburam, were not employed (Ross, 2016).

In literature low employment levels of immigrants has been associated with inability to speak the host country's official language (Shackelford, 2010; Vahabi and Damba, 2013; Anderson et al., 2014). It is reported that those that have language difficulties face increased and long-term disadvantages due to limited employment prospects. This is despite their education level (Shackelford, 2010). According to Vahambi and Damba (2013), language difficulties were a major hindrance to employment amongst Latin American immigrants. This is despite the fact that majority were well educated and had extensive work experience. Majority of these immigrants were either unemployed or holding low-paying or seasonal jobs. This phenomenon is consistent with findings of a study by Anderson et al. (2014), which showed that language barriers had a bearing on low employment levels among immigrants. It is reported that the low employment

levels is aggravated by the imposed employment restrictions on foreign nationals (Shackelford, 2010).

Several authors suggest that food insecurity is highly prevalent amongst immigrants especially sub-Saharan immigrants (Dharod et al., 2011; Jacobus and Jalali, 2011; Anderson et al., 2014). The situation is worse for the newly settled immigrants and refugees (Hadley et al., 2010). In a study conducted in Midwestern United States amongst refugees by Hadley et al. (2010), 78% (n = 218) of the respondents revealed that they had experienced food insecurity. The refugees in the study by Hadley et al. (2010) came from countries like Sierra Leone, Liberia, Somali, Ghana, Somali, Togo and Meskhetian Turk. Dharod et al. (2011) also confirmed these results in a pilot study conducted amongst Somali refugees living in United States. These authors reported that 72% (n = 25) of the study population were food insecure. Another study conducted amongst African Immigrants in Lewiston also revealed major challenges with regards to food access (Jacobus and Jalali, 2011). According to Vahambi and Damba (2013) a low socio-economic status impacts on a household's ability to access adequate food by altering quality and quantity of food purchases (Vahabi and Damba, 2013).

Furthermore, several researchers (Dharod et al., 2013; Anderson et al., 2014; Sanou et al., 2014) show that households of low socio-economic status tend to adopt unhealthy dietary transitions. An illustrated example is the observation by Anderson et al. (2014) on Sudanese in United States who replaced high-cost and micro-nutrient dense food items with cheaper energy-dense, processed food and snacks. This form of dietary change is unhealthy because it lacks dietary diversity and results in excessive consumption of energy and unhealthy fats. These inappropriate dietary changes are associated with weight gain, development of type 2 diabetes, cardiovascular diseases and other nutrition related problems (Schönfeldt and Hall, 2012).

Studies indicate that due to the high levels of food insecurity within the immigrant communities, majority of immigrants end up depending on social support programmes (Dharod et al., 2011, 2013; Jacobus and Jalali, 2011; Anderson et al., 2014). These food assistance programs vary from one area to the other. Some offer money to unemployed immigrants, while others offer food items (Vahabi et al., 2011). However, it has been shown that social support programmes are not able to solve the problem of food insecurity among immigrants (Dharod et al., 2011; Vahabi et al., 2011; Anderson et al., 2014). For example, Dharod et al. (2011) showed that 55% (n = 19) of the households that received social support once a month, reported that the benefit lasted for less than a month, which renders them vulnerable to food insecurity. Vahambi and Damba (2013), who showed that the majority of respondents who received money from the state welfare programme could not meet their household food costs, confirmed this. Furthermore, Anderson et al. (2014) reported that social support programmes were insufficient, by noting that recipients were unable to cover their food and housing costs. In fact, according to some authors, the prevalence of food insecurity tends to be higher among the beneficiaries of social support programmes (Dharod et al., 2011; Vahabi et al., 2011; Vahabi and Damba, 2013).

Studies that have been conducted in United States and Canada indicate that, food assistance programs lack cultural sensitivity (Jacobus and Jalali, 2011; Vahabi et al., 2011; Vahabi and Damba, 2013). This lack of cultural sensitivity often leads to food banks and shelters supplying immigrants with limited and culturally inappropriate foods (Vahabi et al., 2011). For example, research has shown that immigrants often complained that food banks supplied them with unfamiliar foods (Vahabi et al., 2011;

Vahabi and Damba, 2013). These unfamiliar foods included canned and dried foods which immigrants were unable to prepare, as opposed to fresh foods to which immigrants are accustomed. Provision of culturally inappropriate food was also reported in shelters and soup kitchens (Jacobus and Jalali, 2011; Vahabi et al., 2011). As a result, majority of these programs failed to alleviate food insecurity amongst immigrants (Vahabi et al., 2011).

The findings presented here are strong evidence that socio-economic status of immigrants, which steadily decreases upon settlement in host countries, does negatively affect their food security status. The number of sub-Saharan immigrants in South Africa has been increasing over the years (Statistics South Africa, 2014a). For example, the 2011 census revealed that, 5.7% of the South African born population is foreign-born (Statistics South Africa, 2013). In addition to this, 6,801 permanent residence permits were approved in 2013, compared to 1,283 that were approved in 2012. Although the number for temporal residence has been fluctuating, over 100,000 permits per year were approved in 2011, 2012 and 2013 (Statistics South Africa, 2014b). This notwithstanding, there is no evidence of studies that have assessed the socio-economic and food security status of the growing population of immigrants in South Africa.

Although there is paucity of studies on sub-Saharan immigrants' socio-economic status in South Africa, studies conducted in other parts of the world suggest that the general trend is for immigrants to be of a low socio-economic status. Results of similar studies conducted on the African continent seem to suggest the same socio-economic trends. For example, Liberian immigrants residing in Ghana were unemployed and fell into the category of low or middle income earners (Ross et al., 2016). In South Africa, apart from the negative impact of the low economic status of immigrants on their food security status the situation could also negatively affect the health of immigrants. This could in turn place tremendous pressure on the South African public health system. To help mitigate this emerging burden, evidence based studies are required.

Difficulty in navigating the new food environment

Several challenges in navigating the new food environment have been widely documented in the literature as risk factors to food insecurity and unhealthy eating habits among immigrants (Hadley et al., 2010; Kiptinness et al., 2011; Dharod et al., 2011; Mannion et al., 2014; Terragni et al., 2014). The challenges of navigating the new food environment that have been recorded in various literature include unfamiliar food purchasing environment, unfamiliar food items, and cooking practices. This group of factors that are classified as non-income related factors, aggravate food insecurity among immigrants who by virtue of low household incomes are prone to food insecurity (Hadley et al., 2010; Dharod et al., 2011; Mannion et al., 2014; Terragni et al., 2014).

Unfamiliar shopping environment has also been identified as one of the causes of shopping difficulties amongst immigrants upon resettlement. Large supermarkets are reportedly one of the most prominent overwhelming features that immigrants are confronted with upon immigration (Hadley et al., 2010; Kiptinness et al., 2011; Terragni et al., 2014; Wilson and Renzaho, 2014). This is attributed to the fact that most immigrants are accustomed to small shops and open markets back in their countries of origin. In such environments, immigrants find it difficult to locate and identify items thus curtailing their shopping capabilities (Hadley et al., 2010; Njomo, 2012; Terragni et al., 2014).

Furthermore, most large supermarkets sell mainly frozen and processed foods, as opposed to fresh foods that most immigrants are familiar with (Hadley et al., 2010; Terragni et al., 2014). This becomes a challenge because most immigrants do not know how to incorporate these foods in their meals. Additionally supermarkets found in host countries are characterised by food that is packaged and wrapped, which makes it difficult to identify the food items (Terragni et al., 2014; Wilson and Renzaho, 2014). This coupled with language barriers, leads to most food items being excluded as it forces immigrants to stick to their traditional foods and thus restricting the variety of food being consumed (Hadley et al., 2010).

Some researchers (Hadley et al., 2010; Kiptinness and Dharod, 2011; Dharod et al., 2013; Terragni et al., 2014; Wilson and Renzaho, 2014) argue that even in countries where the large supermarkets do stock ethnic foods, majority of immigrants still prefer to buy from the small ethnic retailers. This is could be due to the overwhelming environment in the supermarkets or due to cultural familiarity, familiarity with the language and trust as small ethnic shops are usually owned by fellow countrymen (Dharod et al., 2013). Additionally the ethnic shops offer more than just ethnic foods, they act as social centres where immigrants can meet friends and socialize, cultural consultants, and information sharing centres (Jacobus and Jalali, 2011; Njomo, 2013). However, this is contrary to what was observed in South Africa, where Njomo (2013) observed that majority of sub-Saharan African immigrants who participated preferred to buy their ethnic foods from the mainstream supermarkets. In fact, these respondents indicated that they regularly patronise major supermarket chains such as Shoprite, Pick n Pay, Checkers, Spar and Woolworths to source food. The above observation is attributed to the belief that supermarkets tend to sell cheaper, offer a wide variety and good quality products. Given that this observation was made in only study that was limited in scope, the view that immigrants prefer mainstream supermarkets over ethnic food retailers deserves further investigation to ascertain if it is the general trend.

Unfamiliar food items have also been identified as further barriers to accessing adequate food amongst immigrants in host countries. The problem here is lack of knowledge on how to prepare and include these new foods in their diets (Hadley et al., 2010; Mannion et al., 2014; Sanou et al., 2014; Terragni et al., 2014). For example, in South Africa it has been reported that sub-Saharan immigrants often complain that food sold in the large supermarkets is not familiar and is new especially to those that have just relocated (Njomo, 2012). Of the 281 immigrants surveyed by Hadley et al. (2010); 40% (n = 111) indicated that they were not familiar with food sold in the shops, and 63% (n = 169) indicated they did not know how to prepare it. This is complicated by the fact that in most cases immigrant women associate the term “safe” food with known foods (Mannion et al., 2014). Based on the experiences of Sudanese refugee women, navigating a new food environment, Mannion et al. (2014) suggests that immigrant women are often reluctant to try new foods due to lack of trust, knowledge, and not knowing how these foods are prepared. In the study by Mannion et al. (2014), a nutrition resource that was developed to assist Sudanese women with the selection of healthy foods, failed because apart from using a foreign language it also contained mainly food items that were unfamiliar to the group. This suggests that generally new foods create distrust and uncertainty about safety of foods. This uncertainty and mistrust reduces the number of food items available to immigrants especially when familiar food is not available (Terragni et al., 2014).

Immigrant's perceptions towards host country's food

Immigrants' perceptions towards host country's food culture has been observed to play a major role in determining the adoption of the food culture of the host country. According to Garnweidner et al. (2012), immigrants tend to compare their original food culture to that of the host country and make clear differentiation between them. Consequently terms such as "our food" when referring to their original food and "their food" when referring to host country's food are often used. Based on their cultural and religious beliefs they then decide if the food is culturally appropriate or inappropriate. From available literature it seems that reasons for negative perceptions vary from one person to the other. In previous studies by Garnweidner et al. (2012) and Vahabi and Damba (2013), negative perceptions were caused by differences in taste while according to Mannion (2014), they were caused by distrust of the new food. However, despite the reasons, negative perceptions lead to rejection of the host country's food culture (Vahabi and Damba, 2013; Garnweidner et al., 2012).

A typical example of this is illustrated by a study that was conducted amongst Hmong women residing in United State that reported that most immigrants' mothers perceived host country's food to be unhealthy and less filling (Vue et al., 2011). A study conducted in Norway amongst African and Asian immigrants also showed that the immigrants had negative perceptions of the host country's food culture. The study showed that the host country's food was perceived as tasteless, not filling and lacking nutrients. Because of these negative perceptions, the host country's food was sometimes not considered as food by immigrants but as snack (Vue et al., 2011; Garnweidner et al., 2012). The negative perceptions were also observed by Vahabi and Damba (2013), in a study that was conducted in Canada amongst Spanish/Portuguese immigrants who indicated that the quality, taste and smell was different from what they were used to. Furthermore, immigrants in the study by Vahabi and Damba (2013) believed that Canadian food posed health hazards especially to children. They also complained of the poor nutritional value, high fat and salt content of the food. As a result, Canadian food was deemed culturally inappropriate. Based on these findings it is apparent that, how immigrants perceive the host nation's food is one of the major barriers to food acquisition amongst immigrants. Therefore, in the absence of original food ingredients, this has the potential to impact on the food security of the immigrant community.

Mannion et al. (2014) also observed the same phenomenon in their study, and indicated that Sudanese refugees residing in Canada excluded most food items from their diets because they associated host country's food with obesity due to its perceived high fat content. Probably unbeknown to them, the fear of obesity has a scientific basis related to the fact that it is associated with the development of non-communicable diseases (NCDs) such as cancers, cardiovascular diseases, chronic respiratory diseases and diabetes. NCDs increase health care costs, depletes household resources, slows down poverty reduction initiatives (Schönfeldt and Hall, 2012; WHO, 2014) and results into premature deaths (WHO, 2014). In 1990, NCDs were responsible for 27% of the total death rate. This rate is expected to escalate to 50% in developing countries by 2020 (Schönfeldt and Hall, 2012). It is further reported that NCDs were the leading cause of deaths globally, accounting for 68% of the world's 56 million deaths in 2012 (WHO, 2014).

Apart from social assistance programs lacking in cultural sensitivity as discussed earlier, negative perceptions to these programmes also affect nutrition education and health promotion programs (Garnweidner et al., 2012). For example, as was alluded

to in the previous section; a nutrition resource, which was meant to be a nutrition education resource tool for immigrants proved ineffective. One of the reasons for the failure of this nutrition resource tool was the fact that Canadian foods that were used as examples were considered to be unhealthy by immigrants. Vue et al. (2011) and Garnweidner et al. (2012) argue that nutrition messages become ineffective when they are not customized and are culturally insensitive. Cultural sensitivity is described as the ability to acknowledge the differences that exist within cultures by tailoring and respecting these when encountering diverse groups and individuals (Garnweidner et al., 2012).

Therefore, negative perceptions could have serious implications on immigrants being food secure especially where there is scarcity or difficulty in accessing their original food in the host countries. This emerged in a study that was conducted amongst Sudanese refugees residing in United States, whereby a large proportion of those that experienced higher levels of household food insecurity preferred traditional food (Anderson et al., 2014). This means that health practitioners need to be cognisant of immigrant's food culture and incorporate this knowledge when designing and implementing nutrition programs. This will enable health care professionals to design tailor made communication messages that take into account background, religious beliefs and context (Garnweidner et al., 2012). In countries like South Africa where immigrant's dietary patterns have not been established (Njomo, 2012), future studies on immigrant's food culture are necessary. Such studies should look at immigrant's perceptions towards host country's food culture. In addition to learning the immigrant's perspectives; ethnic food markets and restaurants can be used as case studies to learn and understand immigrants' food culture.

Language barrier

Inability to speak the host country's official language has been associated with food insecurity amongst immigrants in previous studies (Hadley et al., 2010; Vahabi et al., 2011; Vahabi and Damba, 2013; Anderson et al., 2014). Studies show that, immigrants that experience language barrier experience high levels of food insecurity (Hadley et al., 2010; Vahabi and Damba, 2013). Studies also reveal that language difficulties directly affect immigrant's ability to access food by restricting shopping choices (Vahabi and Damba, 2013), their ability to read labels (Hadley et al., 2010) and benefit from promotional information such as discounts and coupons (Vahabi et al., 2011; Vahabi and Damba, 2013).

According to (Vahabi and Damba, 2013) not being proficiency in English restricted the number of shops immigrants utilised to buy their groceries. Results of the study by Vahabi and Damba (2013) indicated that respondents avoided small convenience stores due to language difficulties. Instead, they preferred large chain stores where they could search for food items independently without seeking assistance from shopkeepers. This could have negative implications for food security in cases where chain stores are located far away from residential areas. This is because proximity to the food source is a major determinant to food access (Jacobus and Jalali, 2011). In fact long distances to grocery shops is known to increase transportation costs and in this way negatively impacts on immigrants ability to access food (Vahabi and Damba, 2013).

Language barrier also results inability to read food items, nutritional labels, and selection of appropriate food to purchase (Hadley et al., 2010; Vahabi et al., 2011;

Vahabi and Damba, 2013). For example, studies conducted amongst Latin Americans in Toronto, Canada, found that they struggled to understand ingredients and nutritional composition of foods, making it difficult to make healthy choices. The result could be restricted food choices and a decrease in the variety of foods consumed especially when access to traditional foods is limited. A similar study conducted in Canada amongst Sudanese women, confirmed these findings, revealing that difficulties in language impeded on their ability to recognise food (Mannion et al., 2014). This was further confirmed in a study conducted in Norway where women from South Asian, African, and Middle Eastern Countries found it difficult to read packaging information or ask for help from shop assistants (Terragni et al., 2014).

Failure to access traditional ingredients in the host countries

Available evidence suggests most immigrants prefer to maintain their traditional diets. However, they are unable to do so due to unavailability and inaccessibility of traditional ingredients (Renzaho and Burns, 2006; Garnweidner et al., 2012; Njomo, 2013; Vahabi and Damba, 2013; Sanou et al., 2014; Terragni et al., 2014). This in addition to the factors mentioned above has the potential to negatively affect the food security and nutritional status of immigrants. It forces them to replace their diets with unhealthy food items (Kiptinness and Dharod, 2011).

The unavailability of immigrant's food especially from the mainstream supermarkets has been reported in several host countries including South Africa, Canada, and North America (Deng et al., 2013; Dharod et al., 2013; Njomo, 2013; Vahabi and Damba, 2013). In South Africa, the unavailability of ethnic food ingredients has led to the emergence of ethnic shops and restaurants in main city centres around the country. However, these ethnic food shops are unable to stock sufficient amounts and a variety of foods (Njomo, 2013).

In South Africa, information on ethnic markets is scanty. Only one study could be sourced, and the study in question was limited in scope as it considered only immigrants in Cape Town. In view of this, studies in other provinces especially Gauteng which is home to the largest number of sub-Saharan immigrants in South Africa are needed. The authors are of view that such studies should assess the availability and accessibility of ethnic foods for the sub-Saharan immigrant community that is resident in South Africa.

Accessibility of traditional food ingredients is further exacerbated by the high prices of these foods in the host countries (Jacobus and Jalali, 2011; Deng et al., 2013; Njomo, 2013; Popovic-Lipovac and Strasser, 2015). The majority of immigrants, who participated in the study by Njomo (2013), indicated that ethnic foods for sub-Saharan immigrants living in South Africa are very expensive as compared to countries like Canada and America. The cause of the high prices is the unavailability of these traditional food ingredients from the major grocery stores (Njomo, 2013; Vahabi and Damba, 2013) and high export prices (Jacobus and Jalali, 2011; Njomo, 2012). This is a serious problem when one considers the fact that the majority of immigrants are often characterized by low incomes due to low employment levels. As a result the majority of immigrants tend to resort to consumptions of high-calorie, low-nutrient dense food (Kiptinness and Dharod, 2011; Vahabi and Damba, 2013). This trend is associated with weight gain and development of chronic diseases of the lifestyle (Kiptinness and Dharod, 2011; Popovic-Lipovac and Strasser, 2015). In view of this, there is a need to increase the availability and accessibility of immigrant's original

food ingredients in host countries. However, to achieve maximum availability and accessibility of food by immigrants in question, there is a need for clear understanding of the food culture of immigrants. This will help stakeholders understand food preferences immigrants and how they would like to see the foods presented. This can be achieved through encouraging ethnic food business owners to form cooperatives or groups so that they can have greater buying power and be able to negotiate with the big suppliers (Jacobus and Jalali, 2011). Through cooperative buying these small businesses can also buy in bulk and pull resources together to curb transportation costs. They can also through cooperatives negotiate with local farmers to produce some of their food in the host country.

Safety of food sold in the ethnic markets

Food safety refers to a series of activities that are undertaken to prevent foodborne illnesses by ensuring safe handling, preparation and storage of food. Worldwide failure to comply with acceptable food safety standards is reportedly responsible for an estimated 2.2 million deaths annually especially within the poor communities (WHO, 2013). Furtherance to this, the effects of foodborne illnesses do not only threaten the life of individuals concerned, but also have adverse economic consequences on communities, businesses and countries. They negatively affect the health care systems, tourism, productivity and livelihood (WHO, 2013; Grace et al., 2015a).

Review of literature indicates that food safety is a growing concern within the ethnic food industry (Rudder, 2006; Roberts et al., 2011; Njomo, 2012, 2013; Stenger et al., 2014). In United States and Europe alone the outbreaks related to ethnic food increased from 3% to 11% between 1990 to 2000 (Quinlan, 2013). This is attributed to poor hygienic practices (Grace et al., 2015b; Harris et al., 2015); poor quality of food (Rudder, 2006; Njomo, 2012, 2013), and failure to comply with food safety regulations (Roberts et al., 2011; Harris et al., 2015).

Good employee hygienic food handling practices are critical in preventing cross contamination of food, equipment and utensils (Harris et al., 2015). However, many studies show that employees in the ethnic food restaurants (Rudder, 2006; Roberts et al., 2011; Grace et al., 2015b; Harris et al., 2015) tend not follow critical good hygienic practices. For example a study conducted in Greater Manchester by Rudder (2006), found that majority of ethnic retailers failed to meet the minimum standard of food hygiene and lacked the necessary knowledge required to implement effective food safety measures. In fact, majority of ethnic retailers that were studied were considered a high risk and therefore suspected to be the cause for food borne illnesses such as *Escherichia Coli*. Roberts et al. (2011) also observed that a number of violations in the ethnic food restaurants were directly related to poor employee hygienic practices.

According to Quinlan (2013), dirty floors, work surfaces, equipment; and lack of disinfectants were among the top hygienic concerns within the ethnic food restaurants in a study that was conducted in the UK. Poor hygienic practices have been associated with cultural food handling methods and beliefs, which are often in contrary with the food safety guidelines. This is due to lack of knowledge and skills to implement effective monitoring systems for personal hygiene and food handling practices (Harris, 2015). Grace et al. (2015b) are of the view that ethnic food restaurant operators and employees often lack information with regards to good hygiene practices and basic resources such as tap water, power supply and waste disposal facilities.

The quality of food sold by ethnic retailers has been identified as being of poor quality from a food safety perspective (Rudder, 2006; Njomo, 2012, 2013). For example, food safety has been mentioned as being problematic amongst Hispanic families residing in United States. It has also, been shown that immigrants who attempt to maintain their original food culture experience a high number of food borne illnesses incidences (Stenger et al., 2014). This has been shown to be true especially where the majority of these immigrants preferred and obtained their food from ethnic food retailers even where ethnic foods are available in the mainstream supermarkets.

In South Africa majority (55%; n = 225) of sub-Saharan immigrants that participated in a study that was conducted in the Western Cape, complained about the poor quality of food sold by ethnic retailers (Njomo, 2012). Njomo (2013) goes on to suggest that food at these shops was often decomposed, smelt and taste bad. Ethnic retailers interviewed by Njomo (2013) in Cape Town attributed the poor quality of food to poor preservation methods used to preserve the food in question, the duration it takes, lack of skills and resources to transport ethnic foods from supplying countries to South Africa. This could also be because the value chain within the ethnic food retailers in South Africa is already complex and extended. It is known that complex value chains make food vulnerable to contamination (Oguttu et al., 2014). This coupled with poor resources that are a characteristic of the informal sector like ethnic markets, could compromise food quality even further. Of noteworthy though, is that there is paucity of studies that have assessed the microbiological quality of foods in the ethnic markets and restaurants (Roberts et al., 2011) especially in South Africa.

Available research suggests that majority of the ethnic food markets, and restaurants fail to comply with food safety regulations (Rudder, 2006; Roberts et al., 2011; Harris et al., 2015). For example in a study by Rudder (2006), a number of the ethnic retailers failed to meet the minimum standards of food legislation which stated that food premises should have soap, proper drying methods and a basin. In addition, majority of the structures in which these businesses operated were in breach of the legislation for structures selling food. They had damaged equipment, poor ventilation, broken floors and ceiling.

Failure to adhere to regulatory requirements was observed in studies conducted in the United States by Roberts et al. (2011) and Harris et al. (2015), which analysed inspection health reports. Even within the ethnic markets, variations in adherence to regulatory requirements have been observed. For example, Roberts (2011) observed that independent ethnic markets had more critical and non-critical violations recorded, as compared to chain-ethnic restaurants and non-ethnic restaurants. Moreover, Harris et al. (2015) concluded that failure by ethnic restaurants to comply with the food legislation as stipulated by the United States' Food and Drug Administration is a national issue. Non-compliance was attributed to cultural differences, and inability of restaurant operators to comprehend government regulations (Roberts et al., 2011; Harris et al., 2015). Poor communication of food safety regulations due to language barriers has also been blamed for non-compliance of ethnic food markets and restaurants (Rudder, 2006; Roberts et al., 2011). Language barriers makes it difficult to train the actors within the sector (Rudder, 2006). These findings suggest that there is a need for cultural appropriate training material (Harris et al., 2015). Moreover, to address the language barrier the training material should be made available in the native language of the owner of the ethnic restaurant (Roberts et al., 2011).

Based on the preceding section, it is clear that food safety is a major problem within the ethnic food markets. However, since food safety concerns associated with ethnic markets have not been documented, studies to ascertain if there are any food safety concerns in the ethnic retail industry, especially in a country like South Africa where this industry is still in its infancy and remains the only source of ethnic foods for sub-Saharan immigrants are needed. Furthermore, a study that looks at food safety within the ethnic retail sector would act as a preventative measure of food borne illnesses within this growing section of the South African population. This could thus reduce the resources that would be required to treat the outbreak of illnesses if the matter is not given the attention. Moreover, future research on food safety knowledge amongst the ethnic restaurant and ethnic food markets managers will enable the authorities to develop appropriate training manuals.

Pressure from children to adopt host country's food

Pressure from children to adopt host country's food has been described as one of the challenges immigrant mothers experience upon resettlement. This is because, when children of immigrants get exposed to the host country's food culture during the school going age, they tend to adopt the eating habits of the host country (Vue et al., 2011; Mannion et al., 2014; Terragni et al., 2014; Wilson and Renzaho, 2014). According to Vue et al. (2011) and Dharod et al. (2013) children are usually easily acculturated than their parents due to peer pressure, media and environment. The result is that most children immigrants tend to prefer the host country's food over the traditional food of the countries their parents came from (Vue et al., 2011; Dharod et al., 2013; Mannion et al., 2014). This causes frustration amongst mothers who lack knowledge and do not trust the food culture of the host country.

Terragni et al. (2014) observed that the cause of the easy acculturation among children of immigrants, is children become reluctant to take food to school that is different from what the rest of the children bring in their lunch boxes. This is a problematic, because as mentioned above the immigrant mothers lack knowledge and do not trust host country's food culture. Subsequently most mothers are often conflicted between the desires to indulge children's preferences versus that of wanting to uphold traditional eating patterns (Mannion et al., 2014).

The other problem associated with the pressure from children to adopt the host country's food is related to convenience. For example, in the study done in Australia by Wilson and Renzaho (2014), the refusal of children to eat their traditional food was associated with the inconvenience of carrying the food to school that required reheating. The problem that arises from this, is that parents often choose unhealthy foods as a response to the demands of their children (Vue et al., 2011). This could be associated with not being familiar with the host country's food culture discussed in earlier sections in this paper. Dharod et al. (2013) supports this view by noting that such children tend to prefer fast foods as opposed to the traditional ethnic foods that the parents want them to eat or take to school. This could have dire consequences for dietary changes and malnutrition. In view of this, there is a need to investigate whether this is true for the immigrants from sub-Saharan Africa living in South Africa.

Role of religion in determining immigrant's food choices in host countries

Religious beliefs play a major role in shaping the dietary patterns of people. Certain religious affiliations often result into what is known as food avoidance, a situation whereby members are prohibited from consuming certain foods. Generally, food avoidances are either temporal or permanent. However, those that are due to religious affiliations tend to be permanent because the foods in question are regarded as being impure or hold a sentimental value. The two most known religions that endorse permanent food prohibitions are Muslims and Hindus (Hartog, 2006). Fundamentally, food avoidances define what food is and what is acceptable to consume. According to Jacobus and Jalali (2011) food avoidances are the reason why immigrants could experience food insecurity despite the availability of the traditional ingredients in host countries (Jacobus and Jalali, 2011).

For example, in the case of Muslims who have to eat halal food, they are frequently not sure if the food they are buying is actually halal or not, which forces them to restrict their food baskets to fewer food items (Garnweidner et al., 2012; Terragni et al., 2014). This lack of trust causes Muslim immigrants to exclude all foods affected by religious rules from their diets (Garnweidner et al., 2012; Terragni et al., 2014). This phenomenon of religiously "safe" food was also highlighted in a study that was conducted amongst the African immigrant population residing in Lewiston. Due to issues related to trust, most respondents in the study preferred small ethnic markets run by fellow compatriots. Apart from exclusion of pork, meat for Muslims has to be slaughtered in a certain manner by trained Muslim men (Jacobus and Jalali, 2011; Harrow, 2013). Furthermore separate utensils have to be used for Halal otherwise if contaminated it becomes Haram (Harrow, 2013). Haram refers to all the food that is forbidden according Islamic food laws and customs. However, the availability of these special personnel is usually a problem in host countries. As a result, halal products have to be imported from abroad. This in turn inflates the costs of such foods thus limiting the availability and access of halal products due to imports costs and lack of competition. Additionally, it has been reported that most Muslims also prefer to source imported products such as rice, spices, dried fruits and condiments from these halal speciality shops just to ensure that they are not haram (Jacobus and Jalali, 2011).

Similar to Islamic religion, Hindus have numerous permanent food avoidances (Hartog et al., 2006; Harrow, 2013). However contrary to Islamic belief, Hindus avoid certain food not because they are considered unclean but due to respect (Hartog et al., 2006; Harrow, 2013). A typical example of this is a cow which is highly respected in Hindu culture. Therefore, Hindus do not kill cows for food and they avoid all beef or beef products (Hartog et al., 2006; Harrow, 2013). Other food avoidances include alcohol and all animal products including rennet, eggs or gelatine of animal origin. Furthermore, due to the avoidance of beef and beef related products prevention of cross contamination during food preparation, cooking utensils becomes very crucial. Therefore any such any food suspected of having been contaminated is completely avoided. Similarly like when preparing food for Muslims, separate utensils and food preparation areas should be used when cooking food for Hindus. Consequently, fear of cross-contamination has been cited as a the main reason why majority of Hindus avoid eating from public places. Furthermore, there are certain rituals that need to be adhered to when preparing, cooking and serving food to Hindus (Harrow, 2013). Therefore cynicism alluded to in the preceding section could result especially when food is sold by

people outside this religious group. Consequently, this could have food inaccessibility implications and adverse effect food security.

Based on this review it is apparent that religious beliefs are one of the barriers to accessing sufficient food amongst immigrants especially if religious beliefs of the host country differ vastly from their own country of origin. In South Africa for example majority (85, 5%) of the population are Christians, with only 2% and 1% of the population affiliated to Muslims and Hindus religions respectively (Statistics South Africa, 2014a). This could have a negative impact on the availability and accessibility of appropriate food for people belonging to these groups. Consequently, it could have adverse implications on the health of immigrants belonging to these religious groups as it limits food choices resulting into monotonous diets. The most notable fact about this is the exclusion of meat by most immigrant's due to the fear of eating food that is religiously unacceptable (Terragni et al., 2014). Consuming a limited variety of food is associated with malnutrition. Exclusion of meat without proper replacement could result into nutrient deficiencies such as protein, iron and vitamin A deficiencies (Schönfeldt and Hall, 2012). In South Africa, there is a need for studies that assess the impact of religious reasons on immigrant's ability to access food, in particular how pre-migration religious beliefs influence food choices among immigrants upon resettlement.

Conclusion and recommendations

This review highlights several factors that limit dietary choices of immigrants upon resettlement in new countries. These include climate change, socio-economic status, new shopping environment, negative perceptions towards host country's food, acculturation with ease by their children to the host country's food, and language barriers. This review also identifies several factors that impede access to culturally acceptable foods by immigrants. These factors include inaccessibility, and poor quality of ethnic foods and religious factors. These are unique factors that play a major role in determining the household food security of immigrants upon resettlement. Limited understanding of these factors by the host country's authorities hampers efforts to protect immigrants from food insecurity, and places immigrants at the risk of developing lifestyle diseases, which in turn could put tremendous pressure on the public health systems of the host countries. This could also jeopardize global efforts to contain Non Communicable Diseases (NCD) by 2025, as stipulated in the Global Status Report on Non Communicable Diseases of 2014 (WHO, 2014).

The present study revealed that there is scantiness of dietary related studies on Sub-Saharan African immigrants migrating within the continent. This is despite the fact that majority of migration in Sub-Saharan Africa takes place within the continent. Available Studies have been limited to countries like Canada and United States.

Moreover, statistics indicate that the number of Sub-Saharan immigrants living in South Africa is on the increase. In view of this, research is needed to establish dietary patterns of these immigrants and the challenges they face in terms of accessing their foods. An understanding of immigrant's dietary patterns and challenges could assist the health professionals and policy makers to design tailor made nutrition programs and provide maximum nutritional health equity. This will not only improve their health status, but also has potential to reduce the burden on the health care system that could ensue if this matter is was left unattended. Available evidence suggests that though

ethnic markets are the only source of ethnic foods for Sub-Saharan immigrants living in South Africa, there is paucity of studies on ethnic food markets.

Despite diverse food patterns within the sub-Saharan region, ethnic food preferences, and the availability and accessibility of ethnic food to immigrants within the continent has not been fully investigated. Therefore, further studies are also required to establish availability and accessibility of immigrant's ethnic / traditional food in South Africa.

Additionally, studies to verify the prevalence of food related challenges and factors that impede on sub-Saharan immigrants accessing their traditional food in South Africa are needed. These studies should also establish the relationship between these factors and food insecurity within the immigrant population. In South Africa, though food insecurity studies have not traditionally been tracked by citizenship status, there is an urgent need for evidence-based research on prevalence, causes and potential consequences of food insecurity among all sectors of the South African population including immigrants.

Further research on food safety from the ethnic food markets is another area that merits consideration and further research.

REFERENCES

- [1] Adepoju, A. (2008): Current African Issues – Migration in sub-Saharan Africa. – The Nordic Africa Institute, Uppsala.
- [2] Anderson, L., Hadzibegovic, D. S., Moseley, J. M., Sellen, D. W. (2014): Household food insecurity shows associations with food intake, social support utilization and dietary change among refugee adult caregivers resettled in the United States. – *Ecology of Food and Nutrition* 53(3): 312–32.
- [3] Arksey, H., O'Malley, L. (2005): Scoping studies: towards a methodological framework. – *International Journal of Social Research Methodology: Theory and Practice* 8(1): 19–32.
- [4] Berjak, P., Bartles, P., Benson, E. E., Harding, K., Mycock, D. J., Pammenter, N. W., Sershen, Wesley-Smith, J. (2011): Cryoconservation of South African plant genetic diversity. – *In Vitro Cellular & Developmental Biology-Plant* 47(1): 65–81. <https://link.springer.com/content/pdf/10.1007%2Fs11627-010-9317-4.pdf>
- [5] Deng, F., Zhang, A., Chan, C. (2013): Acculturation, dietary acceptability, and diabetes management among Chinese in North America. – *Frontiers in Endocrinology* 4(108): 1–7.
- [6] Dharod, J. M., Croom, J., Sady, C. G., Morrell, D. (2011): Dietary intake, food security, and acculturation among Somali refugees in the United States: results of a pilot study. – *Journal of Immigrant & Refugee Studies* 9: 82–97.
- [7] Dharod, J. M., Xin, H., Morrison, S. D., Young, A., Nsonwu, M. (2013): Lifestyle and food-related challenges refugee groups face upon resettlement: do we have to move beyond job and language training programs? – *Journal of Hunger & Environmental Nutrition* 8(2): 187–199.
- [8] FAO (2006): Policy Brief. Issue 2: Food Security. FAO, Rome. – [http://www.fao.org/forestry/\(1312\)8-0e6f36f27e0091055bec28ebe830f46b3.pdf](http://www.fao.org/forestry/(1312)8-0e6f36f27e0091055bec28ebe830f46b3.pdf) [2004, May 15].
- [9] Garnweidner, L. M., Terragni, L., Pettersen, K. S., Mosdøl, A. (2012): Perceptions of the host country's food culture among female immigrants from Africa and Asia: aspects relevant for cultural sensitivity in nutrition communication. – *Journal of Nutrition Education and Behavior* 44(4): 335–42.

- [10] Grace, D., Roesel, K., Kohei, M., Kurwijila, L., Saskia, H., Girma, Z., Matusse, H. (2015a): Introduction. – In: Roesel, K., Grace, D. (eds.) *Food Safety and Informal Markets. Animal Products in Sub-Saharan Africa*. 1st ed. Routledge, Abington.
- [11] Grace, D., Makita, K., Kang’ethe E., Bonfoh, B., Roesel, K. (2015b): Taking Food Safety to Informal Markets. – In: Roesel, K., Grace, D. (eds.) *Food Safety and Informal Markets. Animal Products in Sub-Saharan Africa*. 1st ed., pp. 11–22. Routledge, Abington.
- [12] Hadley, C., Patil, C. L., Nahayo, D. (2010): Difficulty in the food environment and the experience of food insecurity among refugees resettled in the United States. – *Ecology of Food and Nutrition* 49(5): 390–407.
- [13] Harris, K. J., Murphy, K. S., DiPietro, R. B., Rivera, G. L. (2015): Food safety inspections results: A comparison of ethnic-operated restaurants to non-ethnic-operated restaurants. – *International Journal of Hospitality Management* 46: 190–199.
- [14] Harrow, M. (2013): *Working Effectively with Minority Ethnic Food Businesses: Resource Handbook*. – YFA Consultancy and Food Standards Agency, London.
- [15] Hartog, A. P. den, Staveren, W. A. van, Brouwer, I. D. (2006): *Food Habits and Consumption Patterns in Developing Countries*. – Wageningen Academic Publishers, Wageningen, The Netherlands.
- [16] Jacobus, M. V., Jalali, R. (2011): Challenges to food access among Lewiston’s African immigrants. – *Maine Policy Review* 20 (1): 151–158.
- [17] Kiptinness, C., Dharod, J. M. (2011): Bhutanese refugees in the United States: Their dietary habits and food shopping practices upon resettlement. – *Journal of Hunger & Environmental Nutrition* 6 (1): 75–85.
- [18] Lesser, I., Gasevic, D., Lear, S. (2014): The association between acculturation and dietary patterns of South Asian immigrants. – *Plos One* 9(2): 1–6.
- [19] Lindsay, K. L., Gibney, E. R., McNulty, B. A., McAuliffe, F. M. (2014): Pregnant immigrant Nigerian women: an exploration of dietary intakes. – *Public Health* 128(7): 647–53.
- [20] Mannion, C., Raffin-Bouchal, S., Henshaw, C. J. (2014): Navigating a strange and complex environment: experiences of Sudanese refugee women using a new nutrition resource. – *International Journal of Women’s Health* 6: 411–22.
- [21] McMichael, C., Barnett, J., McMichael, A. J. (2012): An II wind? Climate change, migration and health. – *Environmental Health Perspectives* 120(5): 645–654. [https://www.ncbi.nlm.nih.gov/pmc/articles/PMC\(3346\)786/pdf/ehp.1104375.pdf](https://www.ncbi.nlm.nih.gov/pmc/articles/PMC(3346)786/pdf/ehp.1104375.pdf).
- [22] McMichael, C. (2015): Climate change-related migration and infectious disease. – *Virulence* 6(6): 548–553. <http://www.tandfonline.com/doi/pdf/10.1080/21505594.2015.1021539?needAccess=true>.
- [23] Njomo, L. M. (2012): Satisfying the indigenous food needs of sub-Saharan African immigrants in South Africa: A food consumption behaviour model for South Africa’s leading supermarket chains. – *African Journal of Business Management* 6(25): (7557)–7568.
- [24] Njomo, L. M. (2013): Examining the impacts of ethnic grocery shops on the food consumption behaviour of sub-Saharan African immigrants in South Africa. – *Universal Journal of Education and General Studies* 2(4): 142–149.
- [25] Oguttu, J. W., McCrindle, C. M. E., Makita, K., Grace, D. (2014): Investigation of the food value chain of ready-to-eat chicken and the associated risk for staphylococcal food poisoning in Tshwane Metropole, South Africa. – *Food Control* 45: 87–94.
- [26] Okafor, M., Carter-Pokras, O., Zhan, M. (2014): Greater Dietary acculturation (dietary change) is associated with poorer current self-rated health among African immigrant adults. – *Journal of Nutrition Education and Behavior* 46(4): 226–235.
- [27] Pendleton, W., Crush, J., Nickanor, N. (2014): Migrant Windhoek: Rural-Urban Migration and Food Security in Namibia. – *Urban Forum* 25(2): 191–205. <http://doi.org/10.1007/s12132-014-9220-x>

- [28] Popovic-Lipovac, A., Strasser, B. (2015): A review on changes in food habits among immigrant women and implications for health. – *Journal of Immigrant and Minority Health/Center for Minority Public Health* 17: 582–590.
- [29] Quinlan, J. J. (2013): Foodborne illness incidence rates and food safety risks for populations of low socioeconomic status and minority race/ethnicity: a review of the literature. – *International Journal of Environmental Research and Public Health* 10(8): 3634–3652.
- [30] Ratha, D., Shaw, W. (2007): *South-South Migration and Remittances*. (World Bank Working Paper No. 102). – World Bank, Washington DC, USA.
- [31] Renzaho, A. M. N., Burns, C. (2006): Post-migration food habits of sub-Saharan African migrants in Victoria: A cross-sectional study. – *Nutrition Dietetics* 63(2): 91–102.
- [32] Roberts, K., Kwon, J., Shanklin, C., Liu, P., Yen, W.-S. (2011): Food safety practices lacking in independent ethnic restaurants. – *Journal of Culinary Science & Technology* 9(1): 1–16.
- [33] Ross, W. L., Gallego, D. F., Pérez, R., Amber, E., Fiedler, H., Lartey, A., Sandow, A. (2016): Dietary patterns in Liberian refugees in Buduburam, Ghana. – *Maternal & Child Nutrition* 2016(June): 1–10.
- [34] Rudder, A. (2006): Food safety and the risk assessment of ethnic minority food retail businesses. – *Food Control* 17(3): 189–196.
- [35] Sanou, D., O'Reilly, E., Ngnie-Teta, I., Batal, M., Mondain, N., Andrew, C., Newbold, B. K., Bourgeault, I. L. (2014): Acculturation and nutritional health of immigrants in Canada: a scoping review. – *Journal of Immigrant and Minority Health/Center for Minority Public Health* 16(1): 24–34.
- [36] Satia, J. (2010): Dietary acculturation and the nutrition transition: an overview. – *Applied Physiology, Nutrition, and Metabolism = Physiologie appliquée, nutrition et métabolisme* 35(2): 219–23.
- [37] Schönfeldt, H. C., Hall, N. (2012): Red Meat in Nutrition and Health: Communicating Current Science about Red Meat as Part of a Healthy South African Diet. – *Institute of Food, Nutrition and Well-Being, Pretoria*.
- [38] Shackelford, E. (2010): Issue Brief : Immigration and Socioeconomic Status. https://academiccommons.columbia.edu/download/.../shackelford_issue_brief.pdf
- [39] Statistics South Africa. (2013): Discussion Document. Documented Immigrants in South Africa (2011). – Statistics South Africa, Pretoria.
- [40] Statistics South Africa (2014a): General Household Survey 2013. Statistical Release P0318. – Statistics South Africa, Pretoria.
- [41] Statistics South Africa (2014b): Documented Immigrants in South Africa, 2013. – Statistics South Africa, Pretoria.
- [42] Stenger, K. M., Ritter-Gooder, P. K., Perry, C., Albrecht, J. A. (2014): A mixed methods study of food safety knowledge, practices and beliefs in Hispanic families with young children. – *Appetite* 83: 194–201.
- [43] Terragni, L., Garnweidner, L. M., Pettersen, K. S., Mosdøl, A. (2014): Migration as a turning point in food habits: the early phase of dietary acculturation among women from South Asian, African, and Middle Eastern Countries living in Norway. – *Ecology of Food and Nutrition* 53(3): 273–91.
- [44] Vahabi, M., Damba, C. (2013): Perceived barriers in accessing food among recent Latin American immigrants in Toronto. – *International Journal for Equity in Health* 12(1): 1.
- [45] Vahabi, M., Damba, C., Rocha, C., Montoya, E. C. (2011): Food insecurity among Latin American recent immigrants in Toronto. – *Journal of Immigrant and Minority Health* 13(5): 929–939.
- [46] Vue, W., Wolff, C., Goto, K. (2011): Hmong food helps us remember who we are: perspectives of food culture and health among Hmong women with young children. – *Journal of Nutrition Education and Behavior* 43(3): 199–204.

- [47] WHO (2013): Advancing Food Safety Initiatives Strategic Plan for Food Safety 2013-2022. – World Health Organization, Geneva.
- [48] WHO (2014): Global Status Report On Noncommunicable Diseases 2014. World Health Organization, Geneva.
http://apps.who.int/iris/bitstream/10665/148114/1/9789241564854_eng.pdf?ua=1
- [49] Wilkinson, K. (2015): Do five million immigrants live in SA. – Mail & Guardian, 6 May.
<https://mg.co.za/article/2015-05-06-do-5-million-immigrants-live-in-sa>
- [50] Wilson, A., Renzaho, A. (2014): Intergenerational differences in acculturation experiences, food beliefs and perceived health risks among refugees from the Horn of Africa in Melbourne, Australia. – Public Health Nutrition (4): 1–13.

APPENDIX

Appendix 1. Summary of sample size and study areas of studies included in the review

Article	Study population	Sample size	Study area
1. Adepoju, 2008	Sub-Saharan immigrants: This is not a research article, but a review of the migration trends in sub-Saharan Africa	Not applicable	Not applicable
2. Anderson et al., 2014	Sudanese	49	Atlanta, United States
3. Arksey and O'Malley, 2005	Article about the methodology on scoping studies	Not applicable	Not applicable
4. Berjak et al., 2011	Review article about studies conducted on conservation of plant genetic diversity	Not applicable	South Africa
5. Deng et al., 2013	Chinese immigrants		North America
6. Dharod et al., 2011	Somali refugees	35	United States
7. Dharod et al., 2013	Refugees (country of origin not specified)	13	United States
8. FAO, 2006			
9. Garnweigner et al., 2012	African and Asian immigrants	21	Oslo, Norway
10. Grace et al., 2015a	Introduction to a book about informal markets	Not applicable	Studies conducted in sub-Saharan African countries
11. Grace et al., 2015b	A chapter in a book on informal markets	Not applicable	Studies conducted in sub-Saharan African countries
12. Hadley et al., 2012	Refugees including countries/ethnicities such as Sierra Leone, Liberia, Ghana, Somalia, Togo, and Meskhetian Turk	281	United States
13. Harris et al., 2015	Reviewed data on number of inspections and violations at ethnic and non-ethnic restaurants	34,259 restaurants	United States
14. Harrow, 2013	Not a research article but a handbook that assisted in defining some of the terminologies used in the manuscript		United Kingdom
15. Hartog et al., 2006	Not a research article but a handbook that assisted in defining some of the terminologies used in the manuscript		
16. Jacobus and Jalali, 2011	African immigrants	9 (in depth interviews)	Lewiston
17. Kiptinness and Dharod, 2011	Bhutanese refugees	14	United states
18. Lesser et al., 2014	South Asian immigrants	207	Canada
19. Lindsay et al., 2014	Nigerian pregnant women	52	Dublin, Ireland
20. Mannion et al., 2014	Sudanese refugee women	8	Calgary, Canada

21. McMichael et al., 2012	Review of previous studies on refugees, people on resettlement schemes and those who migrate to urban areas	Not applicable	Not specified.
22. McMichael C., 2015	Review	Not applicable	Drawing examples from Bangladesh, China, the Horn of Africa and the Greater Mekong Sub region
23. Njomo, 2012	Sub-Saharan immigrants	409	Cape Town, South Africa
24. Njomo, 2013	Sub-Saharan immigrants	409	Cape Town, South Africa
25. Oguttu et al., 2014	Informal food markets	100 food samples	Tshwane Metropole, South Africa
26. Okafor et al., 2014	African immigrants	763	United States
27. Pendleton et al., 2014	Rural-urban immigrants	144	Windhoek, Namibia
28. Popovic-Lipovac et al., 2015	Review article	179 articles	Studies conducted in Canada, USA, UK, Sweden, Germany and Netherlands
29. Quinlan, 2013	Review article on food safety risks for minority and low socioeconomic status population	Not specified	Studies conducted in United States and Europe
30. Ratha and Shaw, 2007	South-South Migration	Data from 167.6 million immigrants across the globe	Global trends
31. Renzaho and Burns, 2006	Sub-Saharan African migrants	139 households	Victoria
32. Roberts et al., 2011	Ethnic and non-ethnic restaurants	924 restaurants	Kansas, United States
33. Ross et al., 2016	Liberian refugees and Ghanians	480	Buduburam, Ghana
34. Rudder, 2006	Ethnic restaurants	40 ethnic restaurants	Borough of Bolton, Greater Manchester.
35. Sanou et al., 2014	A review	49 articles	Canada
36. Satia, 2010	A review	28 articles	North America
37. Schönfeldt and Hall, 2012	A book on Red Meat in Nutrition and Health	Not applicable	South Africa
38. Shackelford, 2010	Policy brief not a research article		United States
39. Statistics South Africa, 2013	Discussion document Documented immigrants	Not applicable	South Africa
40. Statistics South Africa, 2014a	General Household Survey	Not applicable	South Africa
41. Statistics South Africa, 2014b	Discussion document Documented immigrants	Not applicable	South Africa
42. Stenger et al., 2014	Hispanic families	52	Midwestern state

43. Terragni et al., 2014	Women from South Asia, African, and Middle East	21	Norway
44. Vahabi and Damba, 2013	Latin American immigrants	70	Toronto
45. Vahabi et al., 2011	Latin American immigrants	70	Toronto
46. Vue et al., 2011	Hmong women	15	California
47. WHO, 2013	Not a research article but a strategic plan about advancing food safety initiatives	Not applicable	Not applicable
48. WHO, 2014	Not a research article but a global status on the Noncommunicable diseases	Not applicable	Not applicable
49. Wilkinson, 2015	Newspaper article based on immigrants, living South Africa Johannesburg		
50. Wilson and Renzaho, 2014	Horn of Africa immigrants	40	Melbourne, Australia

A MULTI-OBJECTIVE APPROACH FOR LAND CONSERVATION CAPABILITY EVALUATION USING MULTI-CRITERION EVALUATION MODELS

RAHDARI, V.^{1,2*} – SOFFIANIAN, A. R.¹ – POURMANAFI, S.¹ – GHAIUMI, M. H.³ – MOSADEGHI, R.⁴ – AMIRI, F.⁵

¹*Natural Resource Faculty, Isfahan University of Technology
Isfahan, Iran*

²*Natural Resource Faculty, Zabol University
Zabol, Iran*

³*Soil & Geomorphology Department, Iranian Soil and Water Research Institute
Isfahan Branch, Iran*

⁴*Griffith Centre for Coastal Management, Griffith University
Queensland 4222, Australia*

⁵*Natural Resource Faculty, Islamic Azad University
Bushehr Branch, Iran*

**Corresponding author*

e-mail: v.rahdari@gmail.com; phone: +98-915-341-0168

(Received 21st Sep 2017; accepted 15th Jan 2018)

Abstract. In order to protect ecosystem functions and structures, it is essential to identify areas with high conservation potentials. The present study investigates the use of Multi-Criteria Evaluation (MCE) Models and effects of trade-off levels on the results of land conservation capability in the Pelasjan sub-basin, western part of the Gavkhooni watershed and Gavkhooni wetland water source in central Iran. Delphi survey method was used to gather, condense and use experts' knowledge in determining and ranking the evaluation criteria. Analytic Hierarchy Process (AHP) was then used to estimate the criteria weights. Subsequently, to create a single ranked map of potential conservation area, a weighted linear combination (WLC) model and ordered weighted averaging (OWA) model with medium risk and trade-off were used. Conservation capability maps, were then classified into 6 classes based on conservation capability values ranges. The comparison analysis has shown that designed OWA model with lower trade-off level leads to relate areas as very high and high capability classes. Models accuracy assessments have shown that OWA model was more accurate and realistic, but with regard to Plasjan's importance as a habitat for fauna and flora, producing water, and high quality soil and biodiversity, it is highly necessary to consider WLC results.

Keywords: *AHP, fuzzy, Gavkhooni wetland, OWA, Plasjan sub-basin, trade-off, WLC*

Introduction

For effective land conservation, suitable areas should be determined by considering multiple factors including ecological and natural systems, social and economic criteria and existing land uses (Bryan et al., 2009; Alexander and Sahotra, 2006; Mousavi et al., 2015; Farrashi et al., 2016). This complexity has triggered considerable interest in applying quantitative methods such as Multi-criteria decision-making (MCDM) techniques to these problems (Ananda and Herath, 2009; Chen et al., 2010; Mosadeghi, 2013).

MCDM techniques combined with GIS have been successfully applied in a number of land capability analyses, environmental planning and management studies. Using spatial MCDM techniques can improve the transparency and analytic rigor of the land capability analysis including land conservation allocation (Jiang and Eastman, 2000; Malczewski, 2006b; Mosadeghi et al., 2015; Villacreses et al., 2017). Multi-criteria evaluation (MCE) is a subdivision of MCDM, which can use and combine different criteria to evaluate land capabilities for each land use. In MCE models, the weights and relative importance of different criteria are considered unequal. Different MCE techniques use different algorithms to assign weight at either the cardinal or ordinal level of measurement (Hajkowitz and Collins, 2007; Mosadeghi, 2013). For the purpose of this study, Analytical Hierarchical Process (AHP) is used to rank the importance of each capability criterion. The AHP was used due to the following benefits: (1) it is well-known and well-reviewed in the literature; (2) it includes an efficient criterion weighting process of pair-wise comparison; (3) it incorporates hierarchical description of criterion which keeps the number pair-wised comparison manageable; and (4) its use is facilitated by available software (Satty, 1994; Norris and Marshal, 1995; Kristof, 2005; Chakhar and Mousseau, 2008; Ho, 2008; Drobne and Liseč, 2009; Moeinaddini et al., 2010; Hajehforooshnia et al., 2011; Mosadeghi, 2013; Sánchez et al., 2013; Mosadeghi et al., 2015; Farashi et al., 2016; Allaouia et al., 2018).

The study also explores the use of two different MCE operators, weighted linear combination (WLC) and ordered weighted averaging (OWA) in producing the final suitability maps.

In MCE model, a criterion with a higher weight can compensate for the weakness of other criteria with lower weights in a spatial position. In MCE process, trade-off is related to capability of compensating for the weakness of a criterion with other criteria. With increasing amount of trade-off in MCE model, more areas will be considered as high capability areas whose amounts of risk and trade-off would be determined by decision-makers. Weighted linear combination (WLC) and ordered weighted averaging (OWA) are two useful methods for land capability evaluation (Seok, 2008; Chen and Paydar, 2012; Mokarram and Hojati, 2017; Villacreses et al., 2017). OWA is a combined technique in which users can control risk and trade-off levels by considering objects and land condition (Parhizkar, 2011; Mousavia et al., 2014). OWA uses a class of multi-criteria operators and involves two sets of weights: Original criteria weights and ordered weights (Malcezewski, 2006; Makropoulos; 2006; Boroushaki and Malczewski, 2008; Chen and Paydar, 2012; Chen et al., 2013; Sánchez et al., 2013; Zavadskas et al., 2015; Mokarram and Hojati, 2017; Villacreses et al., 2017). The former are assigned to a given criterion for all locations in a study area to indicate their relative importance (Seok, 2008; Ali Yahyai et al., 2012; Chen and Paydar, 2012; Allaouia et al., 2018). For calculating the ordered weights, at first layers would be ordered by paying attention to their original weights in an increasing trend and then ordered weights would be assigned with values between (1) and (0). If (1) is assigned to the first criterion with the lowest original weight and (0) is assigned to other layers, the model has no risk and trade-off; and if 1 is assigned to the last criterion with the highest original weight and 0 is assigned to other layers, the model has the highest risk and no trade-off. When numbers between (0) and (1) are assigned to all criteria, the model has a range of risk and trade-off (Malcezewski, 2006; Sánchez-Lozano et al., 2013; Mokarram and Hojati, 2017).

Therefore, it is possible to control the risk and trade-off in OWA model through a set of ordered weights for each criterion at every location (pixel) (Malczewski, 2006b; Ahn, 2008; Boroushaki and Malczewski, 2008; Chen and Paydar, 2012; Chen et al., 2013; Mosavi and Yazdani, 2014; Allaouia et al., 2018; Mokarram and Hojati, 2017). Decision area is triangular, which in fact, any assignment of ordered weights results in a decision rule that falls somewhere in a triangular decision strategy space defined by the dimensions of risk and trade-off (Drobne and Liseć, 2009; Mokarram and Hojati, 2017). WLC is an MCE method with the highest trade-off and medium risk (Malczewski, 2006b; Ahn, 2008; Boroushaki and Malczewski, 2008; Drobne and Liseć, 2009; Moeinaddini et al., 2010; Ali Yahyai et al., 2012; Allaouia et al., 2018; Mokarram and Hojati, 2017). *Figure 1* shows decision area triangles.

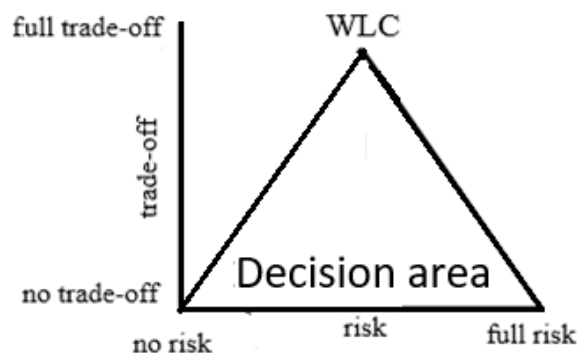


Figure 1. Decision area, risk and trade-off (Mokarram and Hojati, 2017)

In most studies, effects of trade-off were not considered and also were mostly focused on ecological parameters. In this study, for producing proper conservation capability models, we considered a set of ecological, social and economic criteria. The objective of this study is to produce land conservation capability models with WLC and OWA methods and to investigate trade-off effects on multi-criteria land evaluation results. In this case, we used different levels of trade-off using WLC and OWA models to produce conservation capability models for Gavkhooni wetland water source (Pelasjan sub-basin).

Materials and methods

The study area

The study area was Pelasjan sub-basin including the western part of the Gavkhooni watershed located in central Iran covering approximately 412,999 ha. The Zayandehrood is the major river in Gavkhooni watershed to which Pelasjan sub-basin gives the highest portion of water. The Gavkhooni wetland is located in the eastern part of Gavkhooni watershed and is the terminal basin of the Zayandehrood River. Pelasjan sub-basin's average temperature is 8-13 °C with 400-1250 mm precipitation. Agricultural activities and animal husbandry are the main activities of people living in these areas. *Figure 2* shows the location of the Zayandehrood River Basin and Pelasjan sub-basin in the western part of the Gavkhooni wetland in Iran.

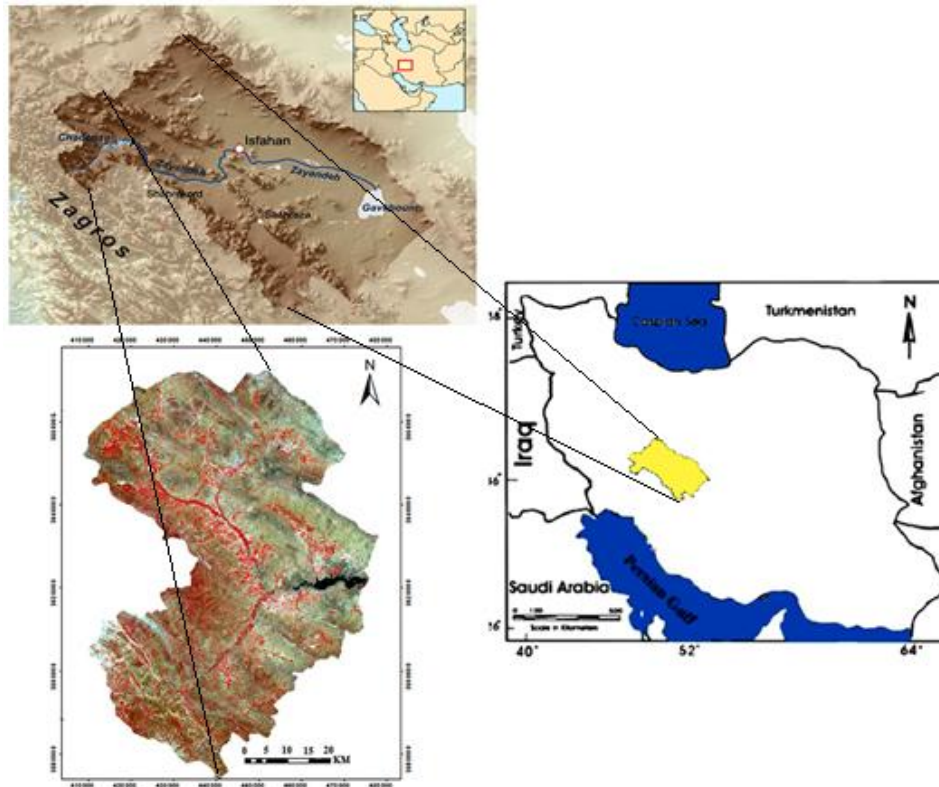


Figure 2. Pelasjan sub-basin located in the western part of Gavkhooni wetland

Data selection

For data selection, at first, literatures about different aspects of conservation were reviewed. Then, with 21 questionnaires, expert opinions were given using Delphi method in 3 steps, and appropriate data were determined. Experts were selected based on their experience and knowledge in biodiversity, hydrology and soil. For producing an LULC map, Landsat 8 and OLI sensor images for June 2016 were prepared. Other layers were selected from the Isfahan University of Technology archives produced in 2016. With regard to the literature review and expert’s knowledge, a study’s hierarchy scheme was designed (Fig. 3).

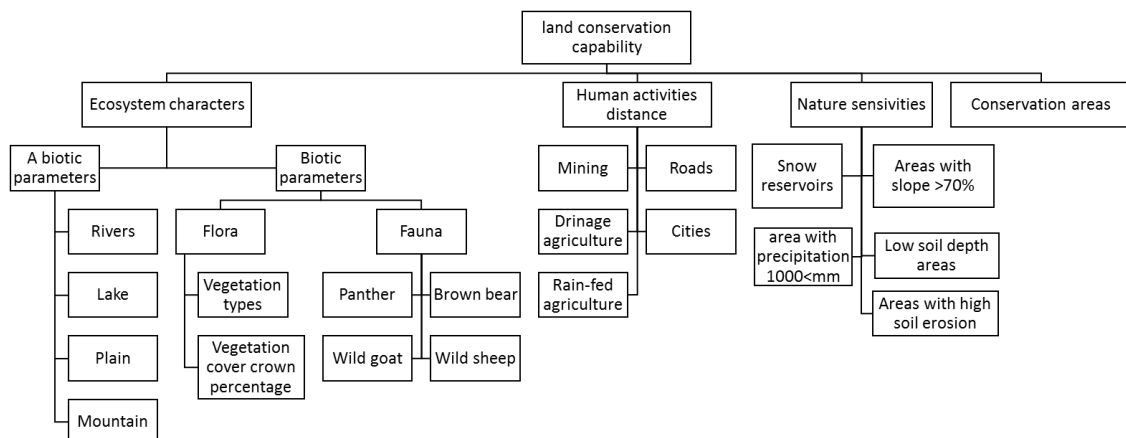


Figure 3. Hierarchical system designed for study

Field sampling

According to the phenology of natural vegetation in rangelands and agricultural crops, plant field sampling was conducted in June 2016, and 210 samples of LULC were recorded using GPS. The collected samples were used for producing LULC maps and accuracy assessment.

Data pre-processing

Atmospheric and radiometric corrections were performed on satellite images with FLASH method. All criteria geo-referencing was controlled using 25 control points with the nearest neighbor method.

Developing LULC maps

To produce an LULC map, OLI sensor images were classified using the hybrid classification method (Estman, 2001) on each image. The LULC map was produced in 8 classes. Conservation area borders were added as the eighth class. The accuracy of LULC map was determined by calculating the kappa index and overall accuracy. Then, the layers of LULC map were utilized in capability models evaluation.

Criteria standardization

By paying attention to literature review and expert knowledge, all criteria were standardized between zero and 255, and constraints were standardized using the Boolean method (Malczewski, 2004; Mirghaed et al., 2014). Appropriate Fuzzy functions and their thresholds were determined for each criterion with literature review and expert knowledge.

Criteria's weights calculating

AHP method was applied to calculate the criteria weights. For this purpose, criteria, sub-criteria and indices were compared in a pairwise method provided by experts in the research questionnaire, and the final weights were calculated according to a hierarchical structure in expert choice softer version 11 (Fig. 3). In this way, the accuracy of pairwise comparisons was determined by calculating the coefficient of consistency, and questionnaires that had more than 0.1 errors were returned to the interviewers to be improved. Finally, the weights of all considered criteria, sub-criteria, indices and sub-indices were calculated.

Layers combination using WLC and OWA methods

To combine the individual suitability layers for each criterion, two combination operators, WLC and OWA methods, were used according to Figure 3. The layers, from the lowest branches were combined by applying their weights in each branch based on Equation 1 (Malczewski, 2006b; Ahn, 2008; Boroushaki and Malczewski, 2008; Dorbne and Lisec, 2009; Koravand, 2015; Farashi et al., 2016; Mokarram and Hojati, 2017):

$$S = \sum_{i=1 \text{ to } n} W_i X_i \prod C_i \quad (\text{Eq.1})$$

S = capability degree
 W_i = each criterion weight
 X_i = fuzzy value of i parameter
 \prod = multiplication sign
 C_i = Boolean constraint

In OWA model, layers were ordered by considering their original weights in an increasing trend. Ordered weights were calculated as *Equation 2* according to risk and trade-off level (Dorbne and Liseć, 2009; Mokarram and Hojati, 2017).

$$W_i = \left(\frac{1}{n} \right) \alpha \quad (\text{Eq.2})$$

The layers, from the lowest branches were combined by applying their weights in each branch based on *Equation 3* (Malczewski, 2006b; Dorbne and Liseć, 2009; Parhizkar, 2011; Mokarram and Hojati, 2017).

$$OWI_i = \sum_{j=1}^n \left(\frac{w_i v_j}{\sum_{i=1}^n w_i v_j} \right) Z_{ij} \quad (\text{Eq.3})$$

V_j = ordered criterion weight
 W_i = ordinary criterion weight
 Z_{ij} = sorted criteria

According to the input data (criterion weights and criterion map layers), the OWA combination operator associates with the i-th location (e.g., raster or point) a set of ordered weights. α risk and trade-off level, n rank of each criterion and $\alpha = 0.5$ (Moosavi and Yazdani, 2014; Morshedi and Kooravand, 2015). In the WLC and OWA models, all standardized Boolean constraints were done.

In this study, decision area is a right triangle on the left of the main decision-making triangle, which designed OWA decision area, is Trapezius in WLC decision area, and the area of designed OWA model in the study is less than the WLC model.

Figure 4 shows the decision area in this study.

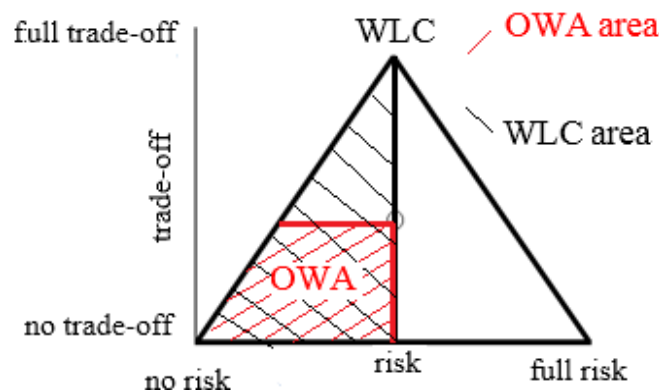


Figure 4. Decision area in this study

Conservation capability model classification

Each model was classified into 6 classes with calculating standard deviation and its average according to *Table 1*.

Table 1. Definition capability class range

Conservation capability's class	Range	Conservation capability's class	Range
Without capability	0	With medium capability	$\bar{X} - Sx < X < \bar{X}$
With very low capability	$0 < X < \bar{X} - 1.5 * (Sx)$	With high capability	$\bar{X} < X < \bar{X} + Sx$
With low capability	$\bar{X} - 1.5 * (Sx) < x < \bar{X} - Sx$	With very high capability	$\bar{X} + Sx < X < \bar{X} + 1.5 Sx$

\bar{X} = Average, Sx = standard deviation

Models accuracy assessment

For models accuracy assessment, it is supposed that the criterion conservation capability with the highest weigh should have more correlation with the final model result. Therefore, the ecosystems characterizing a criterion which has the highest weight among all criteria was selected, and because it is produced via combination of two sub-criteria, fauna distribution with the highest weight was selected for the assessment of WLC and OWA criterion models. Fauna distribution was divided into 6 class-like models, and in each class, samples were selected and were comprised with final WLC and OWA conservation capability models in IDRISI-Terset software, and total accuracy coefficient was calculated in sampled areas with 125400 (30 × 30) pixels from conservation capability classes for conservation capability models via *Equation 4* (Estma, 2001).

$$\text{Overall accuracy} = \frac{\text{Accurated classified pixels}}{\text{Total pixels}} \quad (\text{Eq.4})$$

Results

LULC map of the area was prepared using Landsat satellite images, OLI sensor, and by applying a hybrid image classification method with overall accuracy of 92% and the kappa coefficient of 0.88 in 8 classes plus conservation area border (*Fig. 5*). All layers were standardized using proper Fuzzy functions between 0 and 255. Criteria's weights were calculated using the AHP method. *Table 2* shows all used layers' weights and Fuzzy functions.

After calculating original and ordered weights, all layers were combined by applying WLC and OWA models. *Figures 6* and *7* show the classified conservation capability maps produced with WLC and OWA methods, respectively, in *Table 1*. *Table 3* presents the area of each conservation capability class as hectare and a percentage of the study area.

In model's results, each class of current LULC in very high and high conservation capability was determined. *Figures 8* and *9* show the conversion capability of LULC with very high and high conservation capability classes, respectively.

Table 2. Conservation layers' weights and fuzzy functions

	Criteria weighting	Sub-criteria	Sub-criteria weight	Indices	Indices weights	Sub-indices	Sub-indices weights	Appropriate fuzzy function
Ecosystems characteristics	0.33	Biotic elements	0.55	Flora	0.41	Vegetation types	0.67	User defined
						Cover crown percentage	0.33	
				Fauna distribution	0.59	Panther	0.27	Decreasing sigmoid
						Brown bear	0.32	
						Wild sheep	0.21	
		Abiotic elements	0.45	Rivers	0.33	Decreasing sigmoid		
				Lakes	0.29			
				Plains	0.13			
				Mountains	0.25			
		Human activities distance	0.16	Mining	0.21	Increasing sigmoid		
Roads	0.14							
Cities	0.23							
Drainage agriculture	0.12							
Rain-fed agriculture	0.1							
Nature sensitivities	0.31	Slope >70%	0.38	User defined				
		Areas with high soil erosion	0.32	User defined				
		Snow reservoirs	0.1	Decreasing sigmoid				
		Areas with low soil depth	0.2	User defined				
Under conservation area	0.2						Decreasing sigmoid	

Table 3. Conservation capability area with MCE methods (hectare)

	Conservation capability class	WLC area	WLC percentage	OWA area	OWA percentage
1	Very high	14722	3.52	9772	2.39
2	High	79871	19.11	60686	14.87
3	Moderate	204296	48.89	157976	38.73
4	Low	85011	20.34	142297	34.87
5	Very low	919	0.22	4188	1.03
6	Without capability	33105	7.92	33105	8.11

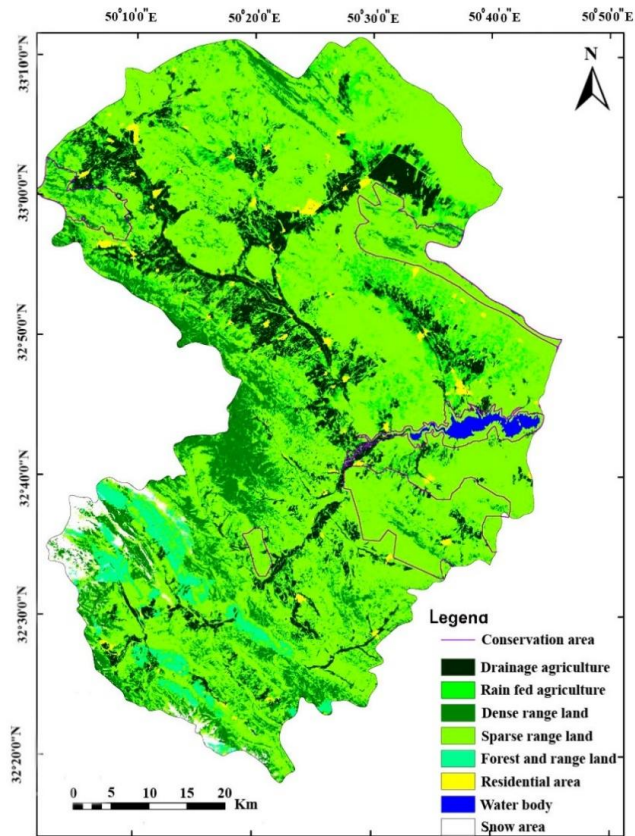


Figure 5. LULC map using OLI image in 2015

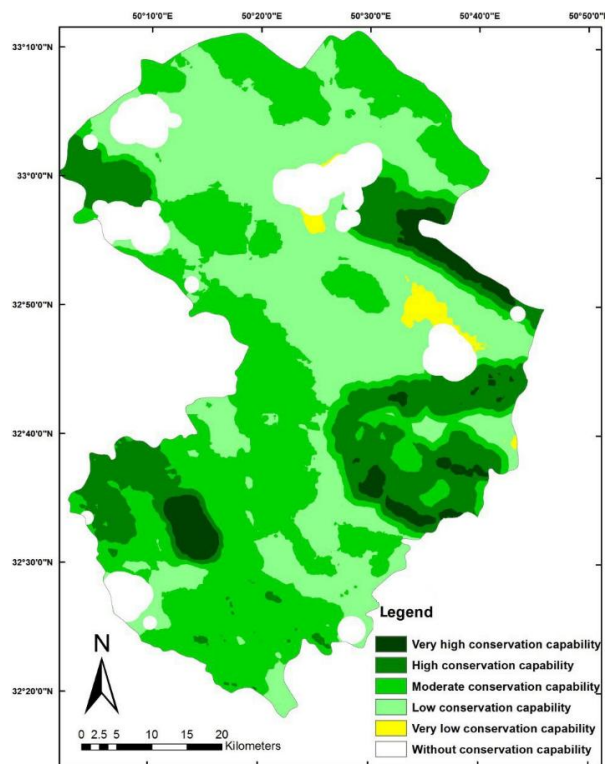


Figure 6. Land capability map with WLC

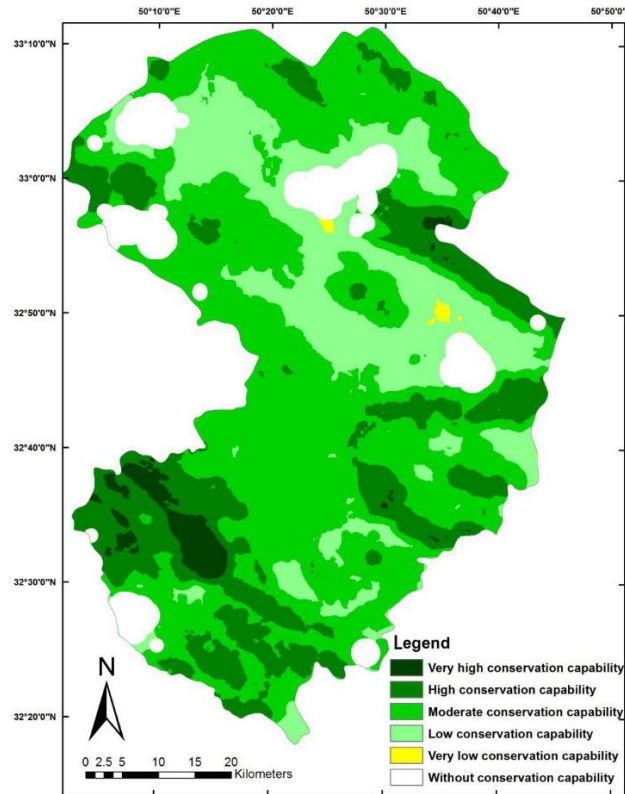


Figure 7. Land capability map with OWA

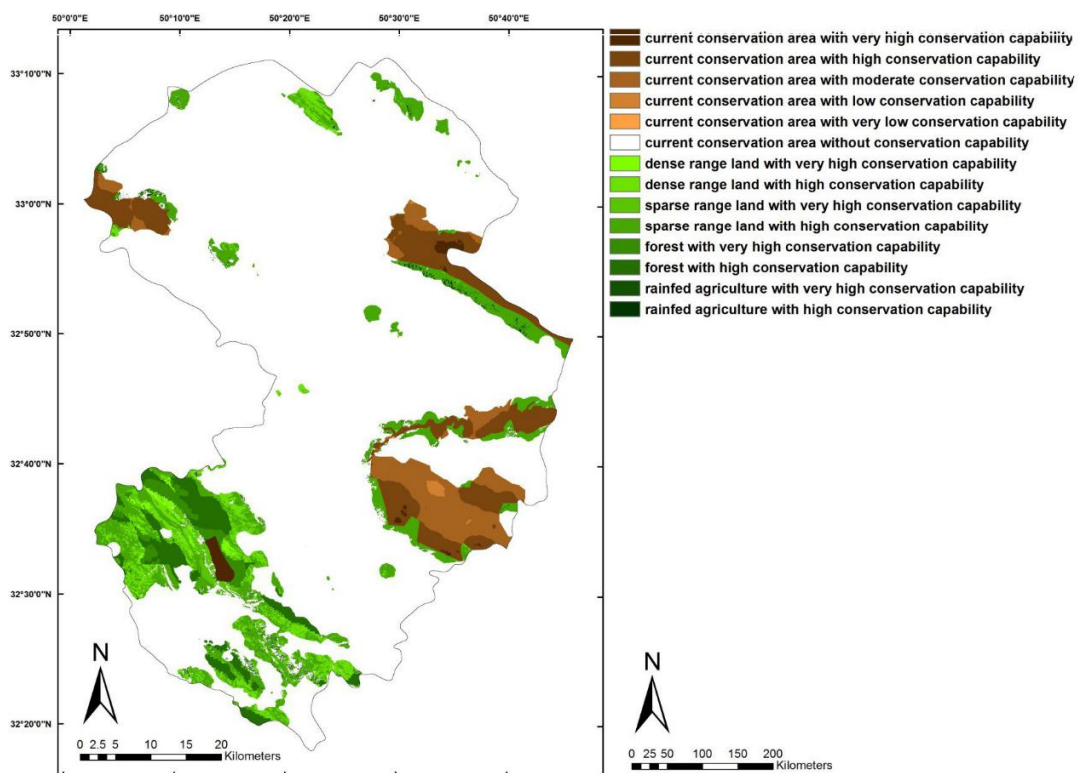


Figure 8. LULC in very high and high conservation capability classes in WLC

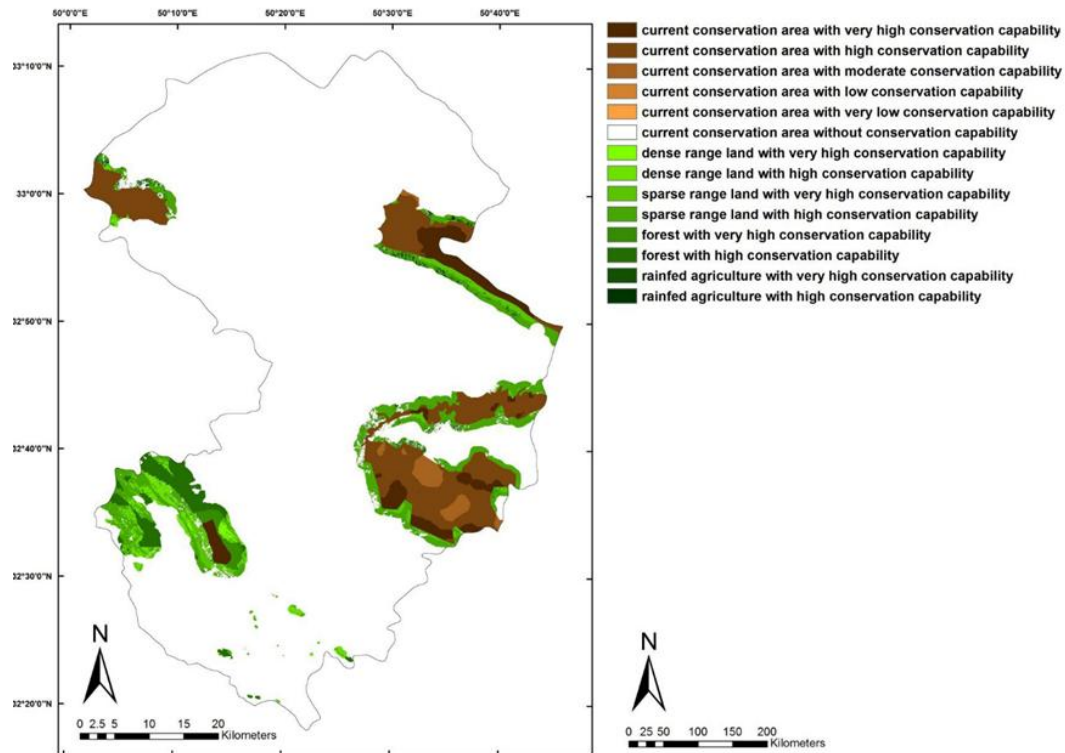


Figure 9. LULC in very high and high conservation capability classes in OWA

Table 4 shows the results of overlaying map of LULC on the conservation capability maps with very high and high classes. In this table, the elements of column represent each LULC class area with very high and high conservation capability with different methods. In this table, LULC classes areas are shown by conservation region and without conservation region. In this case, it becomes clear which LULC are in conservation region.

Table 4 shows which LULCs are proper for selecting as new conservation areas or completing current under conservation areas.

Accuracy assessment of WLC and OWA models has shown that OWA model with an overall accuracy of 0.85 has more accuracy than WLC model with a total accuracy of 0.72.

Discussion

In most studies on conservation capability evaluation, researchers have focused on biodiversity elements; and as a result, they have considered a few aspects of conservation (Allahyari et al., 2010). In this study, because of valuable habitats for terrestrial and aquatic animals and the importance of Pelasjan sub-basin in Gavkhooni watershed, as the main source of water for international Gavkhooni wetland, different aspects of conservation such as dispersion of endangered animals like brown bear, panther, wild goat and sheep, flora, and areas with high precipitation were considered in an attempt to prevent from any change in their natural conditions. Moreover, land conservation capability was evaluated by using WLC and OWA combination methods. By considering the same risk level in two models, the effects of trade-off levels were

investigated on evaluation results (Malczewski, 2006b; Boroushaki and Malczewski, 2008; Chen and Paydar, 2012; Chen et al., 2013; Sánchez et al., 2013; Zavadskas et al., 2015; Mokarram and Hojati, 2017; Villacreses et al., 2017). Layers weights were prepared using AHP method making it possible to compare relative layers' importance and consistency of pairwise comparison, which made the accuracy of pairwise comparisons possible (Jayanath and Herath, 2009; Hasanzadeh et al., 2013; Maddahi et al., 2014). *Table 3* and *Figures 6* and *7* show that higher conservation capability areas are in the WLC model because of the higher trade-off level compared to designing OWA model.

Table 4. LULC area and overlaying on land capability map results area (hectare)

	Conservation area	Dense range land	Sparse range land	Forest	Irrigated agriculture	Rain-fed agriculture	Residential area	Water body	Snow reservoir
LULC class without conservation areas	0	48830	256291	11102	58029	25684	4269	2654	0
LULC class with conservation areas	41661	44788	225185	10345	56096	24626	4155	0	6114
WLC with very high capability	8905	1240	2354	3750	0	63	0	2654	5520
WLC with high capability	28176	10169	29306	9238	0	1392	0	0	594
OWA with very high capability	4037	391	3546	1470	0	94	0	2234	4890
OWA with high capability	25194	7902	20806	5773	0	1245	0	220	1224

Some similarity was expected between categories of a criteria's conservation capability and final conservation capability maps because by decreasing the original weights, the effects of trade-off increase. In order to assess the conservation capability maps, fauna sub-criterion with the highest weight in the ecosystem criterion, which has the highest weight among all criteria, was selected (Feizizadeha et al., 2014; Morshedi and Koravand, 2015).

Comparisons between fauna distribution sub-criterion and the final map of conservation capability produced by medium risk and trade-off in OWA and high trade-off in WLC models, have shown that because of lower trade-off level in OWA, its result is more similar to the real conditions (fauna distribution). On the other hand, OWA model has considered less area in the first two classes with the highest conservation capability in comparison to WLC results (*Table 3*). (Malczewski, 2006a; Hajehforooshnia et al., 2011; Farashi and Shariatic, 2013; Sánchez et al., 2013; Feizizadeha et al., 2014; Morshedi and Koravand, 2015; Farashi et al., 2016).

In *Table 4*, because some criteria such as irrigated agriculture and residential area (Urban) were constraints and they were used with Boolean logic on land capability maps, they had no capability for conservation.

Table 4 and *Figures 8* and *9* show that some parts of the current conservation areas do not have very high and high capability for conserving due to their proximity to urban areas, mines, or irrigated and rain-fed agriculture.

Accuracy assessment results have shown that designed OWA model in this study with medium risk and trade-off is more accurate than WLC model with the highest risk and trade-off model. Therefore, more trade-off level in WLC models led to lower conservation value in fauna distribution criterion in a pixel to compensate via other criteria, which have more conservation value in that pixel.

Conclusion

The results of this research indicate that applications of MCE in GIS are multifunctional and can incorporate different levels of complexity of the decision problem. In this case, the choice of ordinary and ranked weights has played a crucial role. It is obvious that decision-makers with a preference for a subjective scale may not arrive at the same weights for the factor criteria. Therefore, experts and stakeholders must be selected carefully. This may lead to different results for suitability maps and can affect the final decision with regard to the overall objective. In AHP method, this can be reduced using calculating consistency coefficient. However, it must be noted that the presented methods are only tools to aid decision-makers; they are not the decisions themselves. For the final point, although OWA model is more similar to each main criterion conservation capability classes, it is suggested that in sensitive areas, especially in watershed water resources like Plasjan sub-basin, because of their important functions in a watershed, there is an increase the risk and trade-off to consider more areas as proper conservation areas. Then, WLC conservation capability evaluation model was suggested in these sensitive areas. As a water reservoir and biodiversity conservation, Pelasjan sub-basin has a very important role in the Gavekhooni basin in the center of Iran. Then, it is highly necessary to consider more areas for conserving its functions and structures; in this research, WLC model results with more trade-off level are more acceptable.

For future studies, we recommend that the effects of weights' uncertainty on land capability evaluation be analyzed.

REFERENCES

- [1] Ahn, B. S. (2008): Preference relation approach for obtaining OWA operators weights. – *International Journal of Approximate Reasoning* 47: 166–178.
- [2] Alexander, M. A., Sahotra, S. (2006): Incorporating multiple criteria into the design of conservation area networks: a mini review with recommendations. – *Diversity and Distributions* 12: 125–137.
- [3] Ali Yahyai, S., Charabi, Y., Gastli, A., Al badi, A. (2012): Wind farm land suitability indexing using multi-criteria analysis. – *Renewable Energy* 44: 80–87.
- [4] Allahyari, F., Danehkar, A., Sharifipor, R. (2010): Determining conservation area using ulti criteria spatial evaluation. – *Journal of Environmental Geology* 13(4): 65–78 (in Persian).
- [5] Allaouia, H., Guoa, Y., Choudhary, A., Bloemhof, J. (2018): Sustainable agro-food supply chain design using two-stage hybrid multi-objective decision-making approach. – *Computers & Operations Research* 89: 369–384.

- [6] Ananda, J., Herath, G., (2009): A critical review of multi-criteria decision making methods with special reference to forest management and planning. – *Ecological economics* 68(10): 2535–2548.
- [7] Boroushaki, S., Malczewski, J. (2008): Implementing an extension of the analytical hierarchy process using ordered weighted averaging operators with fuzzy quantifiers in ArcGIS. – *Computers & Geosciences* 34: 399–410.
- [8] Bryan, B. A., Grandgirard, A., Ward, J. R., (2009): Managing natural capital and ecosystem services: Identifying strategic regional priorities in the South Australian Murray-Darling Basin. – *CSIRO Water for a Healthy Country National Research Flagship*.
- [9] Chakhar, S., Mousseau, V. (2008): Spatial Multi Criteria Decision Making. – In: Shekhar, S., Xiong, H. (eds.) *Encyclopedia of GIS*, pp. 747–753. – Springer, New York.
- [10] Chen, Y., Paydar, Z. (2012): Evaluation of potential irrigation expansion using a spatial fuzzy multi-criteria decision framework. – *Environmental Modelling & Software* 38: 147–157.
- [11] Chen, Y., Yu, J., Khan, S. (2013): The spatial framework for weight sensitivity analysis in AHP-based multi-criteria decision making. – *Environmental Modelling & Software* 48: 129–140.
- [12] Cheng, C. H., Wang, G. W., Wu, M. C. (2009): OWA-weighted based clustering method for classification problem. – *Expert Systems with Applications* 36: 4988–4995.
- [13] Drobne, S., Lisec, A. (2009): Multi-attribute decision analysis in GIS: weighted linear combination and ordered weighted averaging. – *Informatica* 33: 459–474.
- [14] Estman, J. R. (2001): *Guide to GIS and Image Processing Volume. Release 2.* – Clark University, USA.
- [15] Farashi, A., Naderi, M., Parvin, N. (2016): Identifying a preservation zone using multi criteria decision analysis. – *Animal Biodiversity and Conservation* 39(1): 29–36.
- [16] Feizizadeha, B., Shadman, M., Jankowskic, P., Blaschke, T. (2014): A GIS-based extended fuzzy multi-criteria evaluation for landslide susceptibility mapping. – *Computers & Geosciences* 73: 208–221.
- [17] Hajehforooshnia, S., Soffianian, A., Mahiny, S., Fakheran, S. (2011): Multi objective land allocation (MOLA) for zoning Ghamishloo wildlife sanctuary in Iran. – *Journal for Natural Conservation* 19: 254–262.
- [18] Hajkowicz, S., Collins, K. (2007): A review of multiple criteria analysis for water resource planning and management. – *Water Resource Management* 21(9): 1553–1566.
- [19] Hasanzadeh, M., Danehkar, A., Azizi, M. (2013): The application of analytical network process to environmental prioritizing criteria for coastal oil jetties site selection in Persian Gulf coasts (Iran). – *Ocean Coast. Manag.* 73: 136–144.
- [20] Jayanath, A., Herath, A., G. (2009): Critical review of multi-criteria decision making methods with special reference to forest management and planning. – *Ecological Economics* 68: 2535–2548.
- [21] Jiang, H., Eastman, J. R. (2000): Application of fuzzy measures in multi-criteria evaluation in GIS. – *International Journal of Geographical Information Systems* 14(2): 173–184.
- [22] Kristof, G. M., (2005): *Planning Business Improvement Using Analytic Hierarchy Process and Design structure Matrix.* – Master Thesis, Montana State University, Bozeman.
- [23] Maddahi, Z., Jalalian, A., Zarkesh, M. M. K., Honarjo, N. (2014): Land suitability analysis for rice cultivation using multi criteria evaluation approach and GIS. – *European Journal of Experimental Biology* 4(3): 639–648.
- [24] Makropoulos, C. K., Butler, D. (2006): Spatial ordered weighted averaging: incorporating spatially variable attitude towards risk in spatial multi-criteria decision-making. – *Environmental Modelling & Software* 21(1): 69–84.

- [25] Malczewski, J. (2004): GIS-based land-use suitability analysis: a critical overview. – *Progress in Planning* 62(1): 3–65.
- [26] Malczewski, J. (2006): Ordered weighted averaging with fuzzy quantifier GIS-based multi-criteria evaluation for land-use suitability analysis. – *International Journal for Applied Earth Observation and Geoinformation* 8: 270–277.
- [27] Malczewski, J. (2006): GIS-based multi criteria decision analysis: a survey of the literature. – *International Journal of Geographical Information Science* 20(7): 703–726.
- [28] Mirghaed, F. A., Sori, B., Pirbavaghar, M. (2014): Using fuzzy simple additive weight (FSAW) for land evaluation in order to determining area with conservation capability in parcel A, Gheshlagh dam basin. – *Journal of Environmental Science and Technology* 16: 273–280 (in Persian).
- [29] Moeinaddini, M., Khorasani, N., Danehkar, A., Darvishsefat, A. A., Zienalyan, M. (2010): Siting MSW landfill using weighted linear combination and analytical hierarchy process (AHP) methodology in GIS environment (case study: Karaj). – *Waste Manag.* 30(5): 912e920.
- [30] Mokarram, M., Hojati, M. (2017): Using ordered weight averaging (OWA) aggregation for multi-criteria soil fertility evaluation by GIS (case study: southeast Iran). – *Computers and Electronics in Agriculture* 44(132): 1–13.
- [31] Morshedi, J., Koravand, A. (2015): Suitable lands site selection for amygdalus scoparia implant using GIS technology and AHP method in Mordghafar watershed Izae township. – *Journal of Wetland Eco-Biology* 7(26): 69–86 (in Persian).
- [32] Mosadeghi, R. (2013): A Spatial Multi-Criteria Decision Making Model of Coastal Land Use Planning. – PhD Thesis, Griffith School of Environment, Griffith University, Australia.
- [33] Mosadeghi, R., Warnken, J., Tomlinson, R., Mirfenderesk, H. (2015). Comparison of Fuzzy-AHP and AHP in a spatial multi-criteria decision making model for urban land-use planning, *Computers. – Environment and Urban Systems* 49: 54–65.
- [34] Mousavi, M., Yazdani, C. R. (2014): Land use suitability analysis using AHP-OWA for Tabriz city. – *Journal of Geography and Urban Planning Resource* 3: 361–381(in Persian).
- [35] Mousavi, S. H., Danehkar, A., Shokric, M. R., Poorbagherd, H., Azhdarie, D. (2015): Site selection for artificial reefs using a new combine Multi-Criteria Decision-Making (MCDM) tools for coral reefs in the Kish Island – Persian Gulf. – *Ocean & Coastal Management* 111: 92–102.
- [36] Norris, G. A., Marshall, H. E. (1995): Multiattribute Decision Analysis Method for Evaluating Buildings and Building Systems. – Building and Fire Research Laboratory. US National Institute of Standards and Technology, Gaithersburg, MD 20899.
- [37] Parhizkar, A., Ghaffari, A. (2011): GIS and Multi Criteria Decision Analysis. – Samt Press, Tehran (in Persian).
- [38] Sánchez-Lozano, J. M., Teruel-Solano, J., Soto-Elvira, P. L., García-Cascales, M. S. (2013): Geographical Information Systems (GIS) and Multi-Criteria Decision Making (MCDM) methods for the evaluation of solar farms locations: Case study in south-eastern Spain. – *Renewable and Sustainable Energy Reviews* 24: 544–55.
- [39] Satty, L. (1994): *The Analytic Hierarchy Process*. 1st edition. – McGraw-Hill, New York, USA.
- [40] Seok, A. B. (2008): Preference relation approach for obtaining OWA operators weights. – *International Journal of Approximate Reasoning* 47: 166–178.
- [41] Villacreses, G., Gaona, G., Martínez-Gomez, J., Juan Jijon, D. (2017): Wind farms suitability location using geographical information system (GIS), based on multi-criteria decision making (MCDM) methods: The case of continental Ecuador. – *Renewable Energy* 109: 275–286.
- [42] Zavadskas, E. K., Turskis, Z., Bagocius, V. (2015): Multi-criteria selection of a deep-water port in the Eastern Baltic Sea. – *Applied Soft Computing* 26: 180–192.

ASSESSMENT OF GENETIC VARIATION IN TURKISH LOCAL MAIZE GENOTYPES USING MULTIVARIATE DISCRIMINANT ANALYSIS

ÖNER, F.

*Department of Field Crops, Agricultural Faculty, Ordu University
52200 Ordu, Turkey*

(e-mail: fatihoner38@gmail.com; phone: +90-452-226-5200; fax: +90-452-234-6632)

(Received 21st Sep 2017; accepted 20th Feb 2018)

Abstract. The objective of study was to assess genetic variations among tassel and ear traits of Turkish local maize (*Zea mays* L.) genotypes. Seventy-nine maize germplasms consisting of three races (flint, pop and dent) from northern part of Turkey were evaluated for 16 traits (6-ear and 10-tassel) by using multivariate analysis. ANOVA revealed significant differences in ear and tassel traits. The highest positive correlations were observed between ear length and number of kernels per ear ($r = 0.75$, $p < 0.01$); between tassel length and number of kernels per ear ($r = 0.75$, $p < 0.01$). The highest negative correlations were observed between mean node distance and tassel diameter ($r = -0.30$, $p < 0.01$). Six ear traits revealed that number of ears and ear diameter multivariate correlations covered 91.6% and ear diameter, alone, 47.6% of total variation among accessions. Eight tassel traits were revealed that tassel length and tassel diameter multivariate correlation covered 88.8% and tassel diameter alone 85.1% of total variation. Totally, sixteen ear and tassel traits revealed that tassel diameter and number of flowers per main branch multivariate correlation covered 94.8% and number of flowers per main branch alone 86.8% of total variation. The races are separated into the groups, densely. Although tassel traits displayed low eigenvalue accounting for 56.8% of total variance between races, ear traits displayed very high eigenvalue accounting for 94.6% of total variance. Combined ear and tassel traits had higher eigenvalue accounting for 74.6% of total variance. Results indicated that the first and the second principal component were belonging to ear and tassel traits for Turkish maize races, respectively. The broad trait variation in maize germplasm implies large opportunities for genetic improvement of northern Turkish maize accessions.

Keywords: *corn accessions, morphological traits, diversity, kernel, correlation*

Introduction

Traditional cultivars and primitive landraces of maize (*Zea mays* L.) are invaluable treasure for humankind (Kumari et al., 2016). Turkish maize germplasm was broadly collected by Harlan (1951) in 1948. Ilarslan et al. (2001, 2002) studied these germplasm and classified their races using isozyme and multivariate analysis on agronomic and morphologic traits. They studied on three races as pop, flint and dent maize collected within the period of 1948-1952 from the whole Turkey and used 25 characters as leaf, ear, tassel and kernel traits for classification. With the study of 19 isozyme systems, they indicated that there were large genetic variation among these accessions and races without any specific clustering pattern (Ilarslan et al., 2001). In the same accessions, genetic variability was identified using multivariate analysis. Discriminant analysis showed a high eigenvalue accounting for 66.59% of total variance between races in the first canonical variable and 33.41% of total variance between races in the second canonical variable (Ilarslan et al., 2002). In most studies, it has been emphasized that phenotypic and phenological information based on morphological descriptors continues to be the first step to increase their use in corn breeding for the evaluation, identification and classification of germplasm collections (Sharma et al., 2010; Kumar et al., 2015;

Asare et al., 2016; N'Da et al., 2015; Twumasi et al., 2017). Morphological traits and ear properties can need for future breeding progress (Badu-Apraku et al. 2014). The most commonly used parameters in the genetic diversity of corn plant are related to tassel characteristics, ear and grain characteristics (Rahman et al., 2015). The assessment of morphological characters in germplasm is important for an accurate measurement of the differences between populations for their breeding potential (Orr and Sundberg, 1994). Ear morphology also was suggested to be very useful descriptor for race classification with high heritability (Ortiz and Sevilla, 1997; Brandolini and Brandolini, 2001; Abu-Alrub et al., 2004; Sofi, 2007; Iqbal et al., 2015). Ear diameter and ratio of ear length to diameter are the most useful descriptors for maize races (Abu-Alrub et al., 2004). The classification of maize accessions is a useful approach with good descriptors for maize breeding.

Northern part of Turkey, particularly, Black Sea region carries 56% of corn plantation of Turkey. Mostly, flint type maize is cultivated for animal and human consumption. The germplasm collected from the northern part of Turkey also needs a classification in terms of pop, flint and dent maize races. It was suggested that in Turkey, like other crop species, maize has a heterogeneous mixture which were studied by Anderson and Brown (1953) and Ilarslan et al. (2001, 2002). The cultivation of maize probably originated in Central America and spread to Europe via Spain, Portugal trade routes through the Ottoman traders to central Europe and the Balkans (Pavlicic and Trifunovic, 1967; Abu-Alrub et al., 2004). The spread of maize has been rapid from European regions of the Ottoman Empire by Turkish traders after its introduction in Europe (Kün, 1994; Brandolini and Brandolini, 2001). The introduction of maize to Turkey was around 1600s through Egypt and Syria. On the other hand, large-scale introduction of maize accessions was done by Turkish Agricultural Institutes after 1920s (Kün, 1994). However, there are no studies investigating the genetic variations among the maize accessions and races of the northern part of Turkey.

The objective of this research was; firstly, to assess genetic variation in tassel and ear traits as a descriptor among flint, dent and pop maize races collected from the northern part of Turkish maize varieties and second, to assess the separate effects of traits for classification in these accessions using multivariate analysis.

Material and methods

Plant material

Maize

Maize or corn is an annual outcrossing cereal in the Poaceae (Gramineae) family, reproducing excessively by seed. It is considered as one of the most productive crop species, and also the most studied and characterized crop plant. Maize is a monoecious plant growing up 4 m tall and forms a seasonal root systems bearing a single erect stem or stalk, made up of nodes and internodes. The leaves are arranged in two opposing rows along the stalk. The mature plant can have up to approximately 30 leaves, each consists of a sheath surrounding the stalk and an expanded blade. The corn plant produces a branched inflorescence of male flowers, the tassel and an axillary female inflorescences forming a cylindrical cob, the ears. The cobs have 16-30 rows of spikelets which develop into “kernels” when the seeds mature and long protruding styles, the corn silks. Mature kernels are typically white or yellow, but may also range

in color from red to purple. Maize is one of the major source of starch worldwide and the kernel texture, shape and size is dependent on sugar and starch content, which differs with each variety.

Several maize types can be discerned on the basis of kernel and endosperm structure and composition. The general characteristics of the maize varieties used in this study are given below.

Dent corn: It has a large notch or depression in the kernel, when mature. Dent corn is the most commonly grown for grain and silage. Hard endosperm is present on the sides and base of the kernel, with the remainder of the kernel filled with soft starch. When the kernel starts drying, the soft starch at the top of the kernel shrinks, forming the depression or notch which it is named.

Flint corn (crusty corn): Flint corn kernels, with a very tough crust, are characterized by their hard endosperm around a small soft center. Flint maize is predominantly grown for food use.

Popcorn: It is characterized by a high proportion of hard endosperm, which is much higher than in any other kernel. The explosive capacity of the kernel, when subjected to heat, is a distinctive attribute of popcorn as well. Popcorn, produced on a small scale compared to other types, is used for making popcorn and consumed as a snack-food.

Samples

Seventy-nine maize accessions (59 flint, 16 pop and 4 dent race accessions) were collected from different locations and altitudes of northern part of Turkey (41.21°N, 36.11°S; *Fig. 1*) between the years 2010-2014. Characteristics of samples are given in *Table 1*.



Figure 1. Origin of the accessions used in this study

Collected maize accessions were evaluated in the field during summer of 2015 at the Faculty Farm of Ordu University, Ordu-Turkey (elevation: 24 m). The accessions were planted on May 15 as single-row-plots (30 plants per row in a randomized block design). The measurements were done on randomly selected 6 individuals from each row with the exception of the edge rows. Rows spacing was 0.70 m and on-row plant spacing was 0.20 m. Variety classification was carried out for sixteen traits by the

most heritable and discriminate agronomic and morphologic variables reported by several researchers (Twumasi et al., 2017; Suryanarayana et al., 2017; Sofi, 2007; Sanchez-Gonzales et al., 1992; Revilla and Tray, 1995). These variables were utilized also by Ilarslan et al. (2002) in 32 Turkish accessions. The traits were expressed in millimeters and numbers (*Table 2*). The data were standardized by calculating means and standard deviations for each trait across 79 accessions in accordance with Sneath and Sokal (1973).

Statistical analysis I

Mean values and standard errors were calculated and standardized for either tassel and ear traits or both of them to compare the effect of analysis. Data correlation matrix was constructed from the mean values and used in the multivariate discriminant function analysis to classify 65 Turkish maize accessions. Principal components were calculated from the matrix of correlations. The grouping in the collection, the clustering by un-weighted pair group method of arithmetic average (UPMGA) was computed using Euclidean dissimilarity (*Table 1*). The multivariate discriminant function analysis was performed using the statistical software Numerical Taxonomy and Multivariate Analysis System Version 2.1 (NTSYS-pc, Rohlf, 1993).

Table 1. Accession number, location of accessions, kernel type, and altitude of maize accessions

No.	Access. no.	Location of accessions	Kernel type	Altitude	No.	Access. no.	Location of accessions	Kernel type	Altitude
		Black Sea Region							
1	3	Samsun	F	32	45	70	Samsun	F	46
2	4	Samsun	F	45	46	71	Samsun	F	47
3	8	Samsun	F	30	47	72	Samsun	F	51
4	12	Samsun	F	48	48	73	Samsun	F	52
5	16	Samsun	F	23	49	74	Samsun	F	55
6	17	Samsun	F	55	50	75	Ordu	F	234
7	29	Tokat	F	520	51	76	Samsun	D	55
8	28	Tokat	F	618	52	77	Ordu	D	229
9	27	Tokat	F	581	53	78	Ordu	D	244
10	25	Trabzon	F	420	54	79	Samsun	D	50
11	23	Trabzon	F	250	55	80	Zonguldak	F	500
12	22	Rize	F	280	56	81	Zonguldak	F	521
13	20	Samsun	F	35	57	84	Artvin	F	1500
14	21	Rize	F	678	58	54	Samsun	F	55
15	19	Samsun	F	39	59	48	Giresun	F	1000
16	31	Çorum	F	467	60	53	Trabzon	F	155
17	32	Ordu	F	125	61	82	Karabük	P	800
18	41	Karabük	F	345	62	83	Karabük	P	800
19	86	Samsun	F	605	63	6	Samsun	P	67
20	87	Giresun	F	818	64	11	Samsun	P	56
21	88	Samsun	F	35	65	14	Samsun	P	34
22	89	Samsun	F	35	66	15	Samsun	P	34

23	90	Samsun	F	35	67	26	Tokat	P	903
24	43	Artvin	F	1210	68	24	Trabzon	P	874
25	46	Ordu	F	365	69	30	Çorum	P	250
26	49	Samsun	F	68	70	47	Trabzon	P	200
27	50	Karabük	F	350		Marmara			
28	51	Samsun	F	35		Region			
29	52	Samsun	F	44	71	35	Çanakkale	F	600
30	55	Trabzon	F	235	72	36	Çanakkale	F	600
31	56	Ordu	F	130	73	39	Çanakkale	P	600
32	57	Samsun	F	46	74	40	Çanakkale	F	345
33	58	Samsun Samsun	F	43	75	37	Çanakkale	P	600
34	59	Samsun	F	120	76	38	Çanakkale	P	600
35	60	Trabzon	F	112	77	42	Bursa	P	450
36	61	Trabzon Samsun	F	150	78	34	Çanakkale	P	678
37	62	Trabzon	F	165		East			
38	63	Samsun	F	29		Anatolia			
39	64	Samsun	F	163		Region			
40	65	Samsun	F	45	79	85	Bingöl	P	800
41	66	Ordu	F	54					
42	67	Samsun	F	47					
43	68		F	243					
44	69		F	39					

Table 2. Ear and tassel trait means and standard deviation for maize races; flint, pop and dent

Trait/Varieties	Flint(59) mean±SD	Pop(16) mean±SD	Dent(4) mean±SD	F ¹
<i>Ear Traits</i>				
Ear number (number) EN	1.13±0.21	1.10±0.10	1.12±0.19	**
Ear diameter (cm) ED	20.79±3.10	18.01±2.30	20.24±3.09	**
Ear length (cm) EL	16.10±3.77	14.25±2.55	18.00±3.55	*
Ear row number (number) ER	11.11±2.82	14.37±2.55	11.79±3.01	**
Ear kernel number (number) EK	29.61±7.41	33.31±8.70	30.63±7.90	-
Ear height (cm) EH	88.71±35.60	81.87±29.31	131.25±27.8	**
<i>Tassel Traits</i>				
Tassel length (cm) TL	38.457±7.518	36.00±4.83	46.75±4.72	**
Number of branch (number) NB	14.64±4.59	17.06±5.01	15.29±4.67	-
Tassel weight (g) TW	16.52±9.26	16.96±7.72	17.01±9.40	-
Number of flower (number) NF	720±371.05	848.6±228.3	751.2±343.7	**
Tassel diameter (cm) TD	4.66±0.68	4.63±0.84	4.69±0.71	**
Main branch flower number (number) NBFM	131.55±42.47	165.43±54.0	138.02±45.8	**
Branch length (cm) BL	19.14±4.54	17.44±2.88	18.90±4.29	**
Number of flower per branch NFB	48.50±11.40	52.87±10.46	49.11±11.50	**
First branch angle (degree) FNA	64.57±9.70	62.62±6.90	64.24±9.14	**
Mean distance between nodes MDB	0.79±0.20	0.71±0.18	0.77±0.21	*

*p < 0.05, **p < 0.01

Results and discussion

Analysis of maize races

The ear and tassel traits of maize races, except for number of kernels per ear, tassel weight and number of branch per tassel, revealed significant relationships. Particularly, studied traits showed significantly different values in different races (*Table 2*).

Some results were related to Turkish accessions collected from the whole Turkey studied by Ilarslan et al. (2002), because they are highly heritable traits (Sanchez-Gonzales, 1989; Sanchez-Gonzales et al., 1993; Revilla and Tracy, 1995; Iqbal et al., 2015). The high variance within varieties indicates that accessions have already been utilized by farmers for many years. Most of the accessions came from the coastal regions where growing seasons are longer than inland regions. The preference of flint and pop maize races comes from the intense use of them for either human or animal food in the coastal region and timely-earning for other alternative plants for winter.

The correlation between inter and intra-ear and tassel traits was significant. For example, positive correlations were observed among number of ear, ear diameter, number of kernels per ear, ear height, tassel length, number of flower per tassel, tassel diameter, number of flower per main branch, branch angel. The highest positive correlations were observed between ear length and number of kernels per ear; between tassel length and number of ears. The highest negative correlations were observed between mean node distance and tassel diameter (*Table 3*).

Table 3. Correlation coefficients between ear and tassel traits

	EN	ED	EL	ER	EK	EH	TL	NB	TW	NF	TD	NBFM	BL	NFB	FNA
ED	0.42**	1.00													
EL	-0.12	0.24*	1.00												
ER	0.44**	0.41**	0.11	1.00											
EK	-0.07	0.08	0.75**	0.24*	1.00										
EH	0.35**	0.27**	0.36**	0.06	0.21*	1.00									
TL	0.75**	0.47**	0.11	0.37**	0.02	0.53**	1.00								
NB	0.11	-0.07	-0.01	0.08	0.11	0.06	0.01	1.00							
TW	0.13	-0.12	-0.04	-0.09	0.08	0.36**	0.21*	0.15	1.00						
NF	0.49**	0.24*	0.06	0.33**	0.11	0.22*	0.50**	0.32**	0.43**	1.00					
TD	-0.25*	0.10	0.31**	-0.04	0.22*	0.10	-0.09	0.23*	-0.15	-0.06	1.00				
NBFM	0.24*	0.43**	0.24*	0.20*	-0.01	0.36**	0.46**	-0.07	-0.08	0.14	0.35**	1.00			
BL	0.52**	0.13	-0.28**	0.22*	-0.08	0.07	0.36**	0.01	0.26**	0.47**	-0.38**	-0.11	1.00		
NFB	0.06	0.09	-0.53	0.12	-0.05	-0.16	-0.02	0.03	0.00	0.22*	-0.10	-0.14	0.21*	1.00	
FNA	0.56**	0.35**	0.12	0.39**	0.17	0.25*	0.56**	0.03	0.25*	0.46**	-0.16	0.13	0.34**	0.26**	1.00
MDB	-0.03	-0.08	-0.09	-0.44	0.04	-0.20*	-0.22*	-0.04	-0.08	-0.18	-0.28*	-0.30**	0.01	-0.16	0.05

* $p < 0.05$, ** $p < 0.01$

Turkish farmers usually grow the plants with the seeds selected from previous plants with better growth forms, morphologic and agronomic characteristics. Used seeds by farmers in the following year are limited to randomly bulked seed collections of previous year. Maize is an out-breeder and there is no isolation distance for maize plantations. Flint and pop maize plants are grown as mixed in the same fields in most of the farms.

On the other hand, exchange of seeds between villages is limited with the easy and cheap facilities within the village. The seeds used in this study were collected from high and low altitude farms. However, low altitude farm owners prefer hybrid plants which can allow gene flow between growth plantations until 200 m in plain areas (Luna et al., 2001).

The Fisher's linear discriminant functions and Classification Function Coefficients showed that the most important ear traits were number of ears, ear diameter, number of kernels per ear and ear height while tassel traits were tassel length, tassel diameter, number of flowers per main branch, branch angle, and mean node distance, respectively (Table 4). The most preferable traits were found to be number of ears and tassel length.

Table 4. Eigenvalue, multivariate correlation of ear and tassel traits for races

Function	Eigenvalue (ear)	% of variance	Cumulative %	Canonical correlation	Eigenvalue (tassel)	% of variance	Cumulative %	Canonical correlation
1	5.179	94.6	94.6	0.916	3.444	56.8	56.8	0.880
2	0.294	5.4	100.0	0.476	2.617	43.2	100.0	0.851

Six ear traits revealed that first two multivariate correlations covered 91.6% and second, 47.6% of total variation, and eight tassel traits were revealed that first two multivariate correlations covered 88.8% and second, 85.1% of total variation among accessions.

The first multivariate discriminant function (Fig. 2a and b) had high eigenvalue with 94.6% of total variance between varieties for ear trait and 56.8% of total variance between varieties for tassel trait belonged to flint and pop maize accessions while the second multivariate variable belonged to flint and dent maize accessions for ear traits (Table 5).

Table 5. Classification of function coefficients for ear traits

Ear traits	Races			Tassel traits	Races		
	1	2	3		1	2	3
EN	0.071	0.124	0.122	TL	0.062	0.095	0.092
ED	0.064	0.076	0.091	TD	0.062	0.046	0.070
EK	0.071	0.096	0.095	NBFM	0.023	0.019	0.107
EH	0.024	0.018	0.045	FNA	0.080	0.105	0.097
-	-	-	-	NBF	0.030	0.044	-0.006
(Constant)	-59.488	-117.143	-137.964	(Constant)	-75.475	-111.050	-153.13

These results showed that north Turkish maize accessions were classified for their racial characteristics which were grouped as flint, pop and dent maize accessions from the angle of race with tassel and ear traits by multivariate discriminant function analysis. In previous studies, it was revealed (Ilarslan et al., 2002) that the results were quite similar each other for classification of maize varieties. On the other hand, significant relationships were not observed between pop and flint maize varieties studied by enzyme polymorphism (Ilarslan et al., 2001) but, the same study suggested that there can be a gene flow between flint and pop maize varieties. Grobman et al.

(1961) and Iqbal et al. (2015) studied maize accessions assigned to the races on the basis of ear traits as descriptor. In both study, tassel and ear traits were used as a descriptor of maize accessions.

The cross sections of centroid of multivariate discriminant function in *Figure 2a* and *b* showed the center of accessions that display a good value for races. In *Figure 2a*, the distribution of accessions for ear traits showed a grouping but not dense, whereas tassel traits showed more clear distributions of accessions (*Fig. 2b*).

Figure 2a gives information on the classification of accessions that seem to be mixture of different races between dent and pop type maize accessions analyzed by ear traits. Whereas *Figure 2b* looks like that there was a mixture of between flint and pop maize varieties. These two results explain that the importance of trait used in the analysis was not because of pollen exchanges.

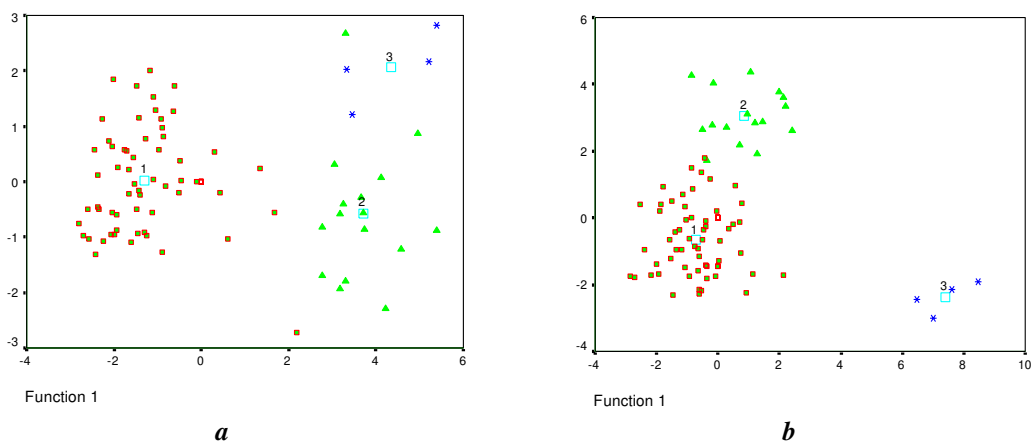


Figure 2. The grouping of Turkish maize accessions based on multivariate discriminant function analysis for (a) ear and (b) tassel traits. Maize varieties were displayed as F(1), P(2), and D(3)

Classification of germplasms

The Fisher's linear discriminant functions and Classification Function Coefficients showed that the most important traits in the classification were tassel diameter, number of flowers per main branch, branch angel, number of ears and number of kernels per ear, respectively. Their Classification Function Coefficients are given based on races in *Table 6*. The most preferable trait was found to be tassel diameter for further studies.

Table 6. Classification of function coefficients for ear and tassel traits

	Races		
	1	2	3
TD	0.048	0.025	0.050
NBFM	0.063	0.083	0.175
FNA	0.103	0.140	0.133
NBF	0.023	0.034	-0.014
EN	0.098	0.159	0.177
ER	0.092	0.137	0.127
(Constant)	-112.232	-203.531	-263.767

Totally, sixteen ear and tassel traits were subjected to multivariate discriminant function analysis and the results revealed that first two multivariate correlations covered 94.8% and second, 86.8% of total variation among accessions. The first multivariate discriminant function (*Fig. 2*) had high eigenvalue (74.6% of total variance between varieties) belonged to flint and pop maize accessions while the second multivariate variable belonged to flint and dent maize accessions (*Table 7*).

Table 7. Eigenvalue, multivariate correlation of ear and tassel traits for races

Function	Eigenvalue	% of variance	Cumulative %	Canonical correlation
1	8.795	74.6	74.6	0.948
2	2.992	25.4	100.0	0.866

These results showed that north Turkish maize accessions can be classified for their racial characteristics grouping as flint, pop and dent maize accessions from the angle of seed collection and ear traits by multivariate discriminant function analysis. The cross sections of centroid of multivariate discriminant function are shown in *Figure 3*.

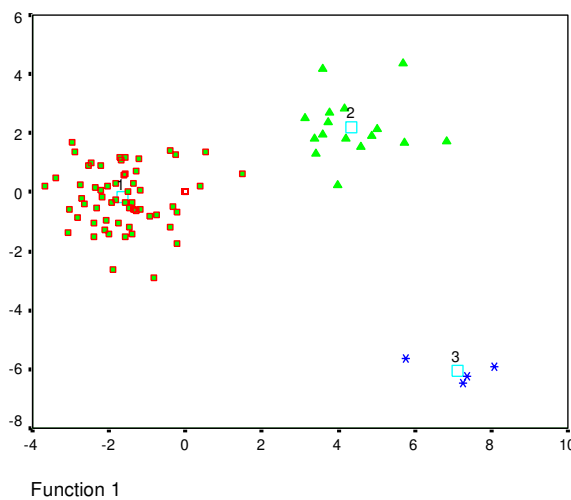


Figure 3. The grouping of Turkish maize accessions based on multivariate discriminant function analysis for ear and tassel traits. Maize varieties were displayed as F(1), P(2) and D(3)

Previous studies revealed that the results were quite similar each other for classification of maize varieties (Ilarslan et al., 2002). On the other hand, any relationships were not observed between pop and flint maize varieties studied by enzyme polymorphism and the accessions were not classified in cluster analysis with respect to location, many small clusters formed (Ilarslan et al., 2001) but, the same study suggested that there can be a gene flow between flint and pop maize varieties. In this study, there was a good clustering between accessions for maize races. It was observed that the selection and amount of descriptor were important for classification of germplasm. The dendrogram classified the accessions based on their races as seen in *Figure 4*.

The clustering did not show any grouping for location. The classification of accessions implies that the accessions were conserved by the farmers in the growth plantations. It should be kept in mind that most of the accessions belonged to flint type.

Tassel traits with high heritability can be used as descriptors (Ortiz et al., 1997; Iqbal et al., 2015). Also, ear traits are important for classification and characterization of germplasms. The study showed that maize accessions collected from north of Turkey in 2010-2014 maintain considerable genetic variation in ear and tassel traits at the level of either varieties. Turkish seed collections are available in NCRPIS, Ames, USA collected in 1948-1952, which is set up test plantations to increase the seeds and maintain the genetic resources for further exploration in maize breeding programs. Ilarslan et al. (2002) studied on these accessions (32 accessions) for the genetic composition of maize genetic resources of Turkey. When Turkish accessions between 1948-1952 and 2015 were compared, it seems that there was a higher variation between research years (68% for 1948-1952 and 74.6% for 2015). The reason of this may come from the study area which is the northern part of Turkey and most of the genotypes belonged to flint type accessions (59). In addition to this suggestion, introduction of high yield genetic lines may increase the genetic variation.

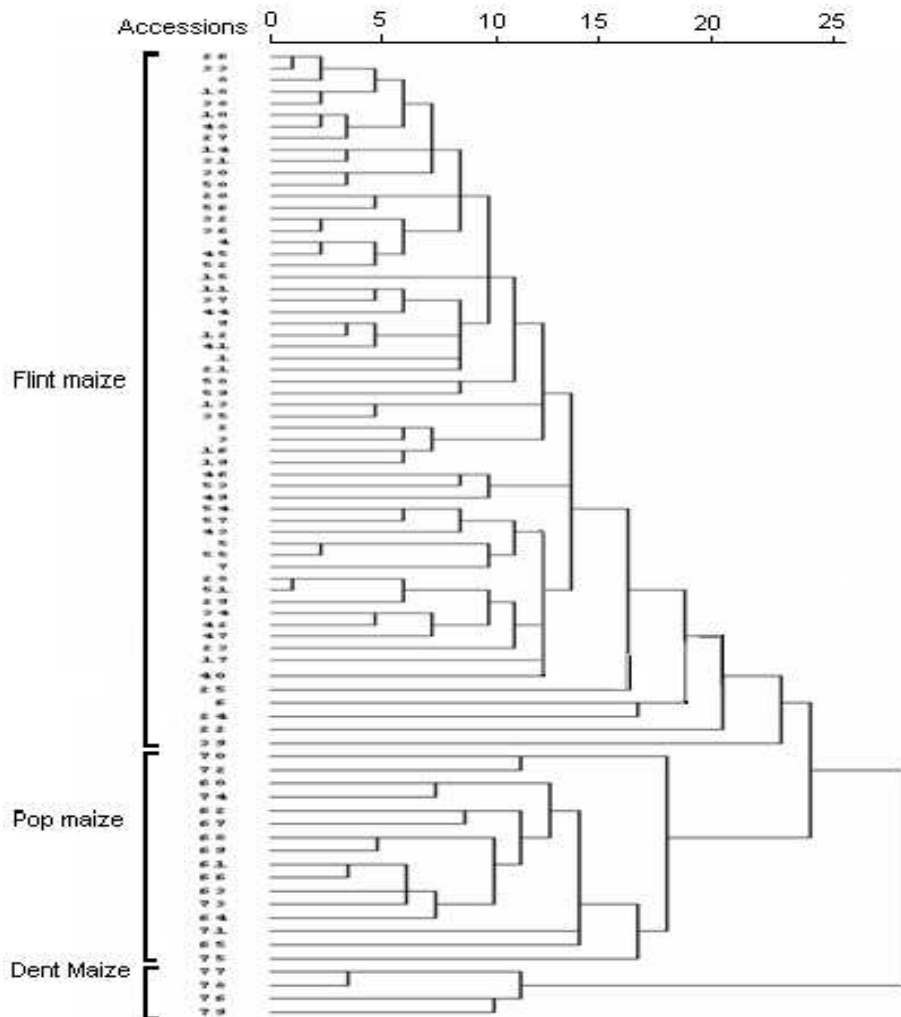


Figure 4. The clustering by unweighted pair group method of arithmetic average showing the clusters of Turkish accessions of maize collected the north of Turkey

Conclusions

This study displays an informative knowledge of populations between years and preferable traits for selection to understand the background of accessions of following generations with high adaptive capacity for the region and selection effect of farmers for conservation of maize genetic resources. However, the application of analysis showed a value related to the number of trait. The increasing number of heritable traits gives more effective classification of genotypes. As seen in *Figure 3*, the races were separated into the groups, densely. In conclusion, ear traits are the best descriptors for classification of germplasm and tassel traits are not reliable descriptors alone. Likewise, there were not any overlapping accessions among the races. It was considered that the selection and amount of descriptor are important for classification of germplasm. The broad trait variation in the maize germplasm implies large opportunities for genetic improvement of northern Turkish maize accessions.

REFERENCES

- [1] Abu-Alrub, I., Christiansen, S., Madsen, Sevilla, R., Ortiz, R. (2004): Assessing tassel, kernel and ear variation in Peruvian highland maize. – *Plant Genetic Resources Newsletter* 137: 34-41.
- [2] Anderson, E., Brown, W. L. (1953): The popcorns of Turkey. – *Annals of the Missouri Botanical Garden* 40: 33-49.
- [3] Asare, S., Tetteh, A. Y., Twumasi, P., Adabe, K. B., Akromah, R. A. (2016): Genetic diversity in lowland, midaltitude and highland African maize landraces by morphological trait evaluation. – *African Journal of Plant Science* 10(11): 246-257.
- [4] Badu-Apraku, B., Fakorede, M. A. B., Oyekunle, M. (2014): Agronomic traits associated with genetic gains in maize yield during three breeding eras in West Africa. – *Maydica* 59: 49-57.
- [5] Brandolini, A., Brandolini, A. (2001): Classification of Italian maize (*Zea mays* L.) germplasm. – *Plant Genetic Resources Newsletter* 126: 1-11.
- [6] Grobman, A., Salhuana, W., Sevilla, R., Mangelsdorf, E. (1961): Races of Maize in Peru; Their Origin, Evolution and Classification. – National Academy of Science-National Research Council (Pub. 915), Washington DC.
- [7] Harlan, J. R. (1951): Anatomy of gene centers. – *The American Naturalist* 85(821): 97-103.
- [8] Ilarslan, R., Kaya, Z., Kandemir, I., Bretting, P. K. (2001): Genetic variability among Turkish pop, flint and dent maize (*Zea mays* L. spp. mays) varieties: Morphological and agronomical traits. – *Euphytica* 128: 173-182.
- [9] Ilarslan, R., Kaya, Z., Kandemir, I., Bretting, P. K. (2002): Genetic variability among Turkish pop, flint and dent maize (*Zea mays* L. spp. mays) varieties: Enzyme polymorphism. – *Euphytica* 122: 171-179.
- [10] Iqbal, J., ShinWari, Z. K., Rabbani, M. A. (2015): Maize (*Zea mays* L.) germplasm agromorphological characterization based on descriptive, cluster and principal component analysis. – *Pakistan Journal of Botany* 47(SI): 255-264.
- [11] Kumar, A., Kumari, J., Rana, J. C., Chaudhary, D. P., Kumar, R., Singh, H., Singh, T. P., Dutta, M. (2015) Diversity among maize landraces in North West Himalayan region of India assessed by agro-morphological and quality traits. – *Indian Journal of Genetics and Plant Breeding* 75(2): 188-195.
- [12] Kumari, J., Kumar, A., Bhatt, K. C., Mishra, A. K., Singh, T. P. (2016): Characterization of maize collections from Nagalng State of North Eastern Himalayan Region. – *Plant Gene and Trait* 7(12): 1-7.

- [13] Kün, E. (1994): Tahillar II (Sıcak İklim Tahillari). – Ankara Üniversitesi Ziraat Fakültesi yayinlari 1360: 141-206.
- [14] Luna, S. V., Figueroa, J. M., Baltazar, B. M., Gomez, L. R., Townsend, R., Schoper, J. B. (2001): Maize pollen longevity and distance isolation requirements for effective pollen control. – *Crop Science* 41: 1551-1557.
- [15] N'Da, H. A., Akanvou, L., Bi-Zoro, A. I., Kouakou, C. K. (2015): Phenotypic diversity of farmer's maize (*Zea mays* L) varieties in Cote d'Ivoire. – *Maydica* 60(13): 1-7.
- [16] Orr, A., Sundberg, M. D. (1994): Inflorescence development in a perennial teosinte: *Zea perennis* (Poaceae). – *American Journal of Botany* 81: 598-608.
- [17] Ortiz, R., Sevilla, R. (1997): Quantitative descriptors for classification and characterization of highland Peruvian maize. – *Plant Genetic Resources Newsletter* 110: 49-52.
- [18] Pavlicic, J., Trifunovic, V. (1967): A study of some important ecological corn types in Yugoslavia and their classification. – *Journal of Scientific Agricultural Research* 19: 42-62.
- [19] Rahman, S., Mia, M. M., Quddus, T., Hassan, L., Haque, A. M. (2015): Assessing genetic diversity of maize (*Zea mays* L.) genotypes for agronomic traits. – *Research in Agriculture, Livestock and Fisheries* 2(1): 53-61.
- [20] Revilla, P., Tracy, J. (1995): Morphological characterization and classification of open-pollinated sweet maize cultivars. – *Journal of American Society, Horticultural Science* 120: 112-118.
- [21] Rohlf, F. J. (1993): NTSYS-pc. Numerical Analysis and Multivariate Analysis System Version 1.7. – Applied Biostatistics, Inc., New York, USA.
- [22] Sanchez-Gonzalez, J. J. (1989): Relationships among the Mexican Varieties of Maize. – Ph. D. Dissertation, North Carolina State University, Raleigh.
- [23] Sanchez-Gonzalez, J. J., Goodman, M. M. (1992): Relationships among the Mexican and some north American and south American varieties of maize. – *Maydica* 37: 41-51.
- [24] Sanchez-Gonzalez, J. J., Goodman, M. M., Rawlings, J. O. (1993): Appropriate characters for racial classification in maize. – *Economic Botany* 47: 44-59.
- [25] Sharma, L., Prasanna, B. M., Ramesh, B. (2010): Analysis of phenotypic and microsatellite-based diversity of maize landraces in India, especially from the North East Himalayan region. – *Genetica* 138(6): 619-631.
- [26] Sneath, P., Sokal, R. R. (1973): Numerical Taxonomy. – W. H. Freeman and Company, San Francisco.
- [27] Sofi, A. P. (2007): Genetic Analysis of tassel and ear characters in maize (*Zea mays* L.) using triple test cross. – *Asian Journal of Plant Sciences* 6(5): 881-883.
- [28] Suryanarayana, L., Sekhar, M. R., Babu, D. R., Ramana, A. V., Rao, V. S. (2017): Cluster and principal component analysis in maize. – *International Journal of Current Microbiology and Applied Sciences* 6(7): 354-359.
- [29] Twumasi, P., Tetteh, A. Y., Adabe, K. B., Asare, S., Akromah, R. A. (2017): Morphological diversity and relationships among the IPGRI maize (*Zea mays* L.) landraces held in IITA. – *Maydica* 2017 62(35): 1-9.

GIS-BASED DETECTION AND QUANTIFICATION OF PATCH-BOUNDARY PATTERNS FOR IDENTIFYING LANDSCAPE MOSAICS

HARDT, E.^{1,2*} – DE PABLO, C. L.³ – DE AGAR, P. M.³ – DOS SANTOS, R. F.^{2,4} – PEREIRA-SILVA, E. F.^{4,5}

¹*Department of Environmental Sciences, Federal University of São Paulo
Rua São Nicolau, 210, 09913-030 Diadema, Brazil
(phone: +55-11-4044-0500 ramal 3470)*

²*Laboratory of Environmental Planning, Campinas State University
Campinas, Brazil*

³*Department of Ecology, Complutense University of Madrid
Madrid, Spain*

⁴*Department of Ecology, University of São Paulo
São Paulo, Brazil*

⁵*Center of Natural and Human Sciences, Federal University of ABC
São Bernardo do Campo, Brazil*

**Corresponding author
e-mail: elisa.hardt@unifesp.br*

(Received 24th Sep 2017; accepted 5th Feb 2018)

Abstract. The study of boundaries between patches allows us to understand the complexity of landscape interactions, especially those involved in the anthropic use of natural resources, which is a common source of environmental problems when harnessing landscape services. The study of the relationships between those two elements makes it possible to identify distinct homogeneous environmental areas in which the same ecological interactions occur. These areas are the mosaics that make up a landscape. This paper presents a GIS-based procedure to identify and quantify the boundaries of land use/cover patches and to record those data in matrices of patches by boundaries. These matrices, by means of a multivariate analysis, allow us to recognize landscape mosaics. This semi-automated procedure contributes to making the concept of landscape mosaics operative and enabling its application to landscape management. To exemplify its possibilities, we tested three alternatives for quantifying boundary measures: presence/absence, frequency and length. They each describe interactions with different details and provide different nuances in interpretations of landscape organization. In the study case, the frequency data provided a more easily understandable interpretation of the mosaic identification and characterization of landscape heterogeneity because these data are less conditioned by the spatial distribution, size or length of rare boundaries. Irrespective of the boundary measure used, a large central mosaic is always identified, highlighting the influence of landscape homogeneity and fragmentation on mosaic identification and the robustness of the tested procedure.

Keywords: *landscape ecology, landscape evaluation, landscape model, land use and cover, spatial analysis*

Introduction

Landscape ecology provides a suitable set of concepts and knowledge for studying the ecological functioning of landscape pattern and its relationship with human society (Wiens et al., 2007; Kirchoff et al., 2013; Bastian et al., 2015). Landscape pattern is the central topic in landscape ecology, as it is both consequence and cause of

ecological functioning (Forman and Godron, 1981; Turner, 1989) on which the supply of environmental services is based (MEA, 2005; TEEB, 2010). The study of landscape pattern, being directly related to functioning, is therefore crucial in ecosystem services conservation planning and management (Forman, 1990; De Groot et al., 2010; Frank et al., 2012; Maes et al., 2013; Martín de Agar et al., 2016).

Landscape pattern is usually studied as spatial distributions of patches and boundaries (Forman and Godron, 1981; Urban et al., 1987). The relationships between the two allow us to understand and interpret the ecological functioning of landscapes (Turner, 1989; Forman, 1990; Cantwell and Forman, 1993; Cadenasso et al., 2003; Roldán et al., 2003; Hersperger, 2006). Landscape spatial heterogeneity based on the joint spatial pattern of these elements is referred to as landscape mosaics (Forman, 1995; Roldán et al., 2003; Hersperger, 2006). This is a central issue in ecology and has special scientific relevance because it permits understandings of how patches and boundaries interact with each other to define zones with similar ecological interactions. These zones are the basis of ecological planning and service assessments (Martín de Agar et al., 2016).

Mosaics are defined as sets of patches with a similar pattern of boundaries (Roldán et al., 2003). Accordingly, a landscape comprises different mosaics (Roldán et al., 2006; De Pablo et al., 2012), on which patches have homogeneous ecological functioning, and the boundaries denote places where this functioning change, including the type, direction and magnitude of interactions taking place among the former (Margalef, 1979; Wiens et al., 1985; Gosz, 1991; Wiens, 2002; Cadenasso et al., 2003; Peters et al., 2006). Such mosaic-based studies of landscape integrate information provided by patches, boundaries and the relationships between them (Roldán et al., 2003; Peters et al., 2006). The usefulness of this approach has been demonstrated from both academic (Roldán et al., 2006; De Pablo et al., 2010) and applied perspectives (Hardt et al., 2013; Bertolo et al., 2015; Martín de Agar et al., 2016). Studies have been undertaken on the complexity of interactions between natural resources and anthropic uses in the Atlantic Forest in São Paulo, Brazil (Hardt et al., 2013; Bertolo et al., 2015), and in a traditional mountainous agrarian, livestock and forestry cultural landscape in Madrid, Spain (Roldán et al., 2006; De Pablo et al., 2010; Martín de Agar et al., 2016). Numerous techniques have been developed to identify boundaries from spatial data (Jacquez et al., 2000, 2008; Fagan et al., 2003; Fortin and Dale, 2005; Banerjee et al., 2015). At present, many landscape studies, especially those with applied objectives, are based on land cover or land use maps. On those maps, it is easy to recognize the boundaries from the edges between patches (Rescia et al., 1997; Metzger and Müller, 1996; Roldán et al., 2003). However, to identify and map a mosaic as a set of patches with similar boundaries, additional techniques are needed to determine the spatial interactions between the two. It is also necessary to build a matrix of patches by boundaries in order to collect the spatial relationships between both, on which mosaics recognition is based.

The goal of this paper is to develop a Geographical Information System (GIS) procedure for identifying and recording boundaries of individual landscape patches and for building matrices of patches \times boundaries. This paper details this GIS procedure coupled to the multivariate analysis needed to identify and map landscape mosaics that synthesize the spatial heterogeneity. A case study in an Atlantic Forest area is used to illustrate the results obtained in each procedure stage. The procedure is based on that of Roldán et al. (2003) that worked with a non-automated technique and was applied by

Hardt et al. (2013) to landscape management. The novelty of this paper is the semi-automatic recording of boundary measures (presence/absence, frequencies and lengths) for each patch obtained from raster or vector land use/cover maps.

It is primarily a technical issue, but the developed tool provides a basis for facilitating the use of current techniques for mosaic recognition in landscape studies. It is an innovative application of a remote sensing methodology to tackle a common Brazilian environmental problem: the increase in tropical forest interaction complexity with anthropic uses. This understanding aids, for example, in the conservation, planning and management of natural resources in regions that face complex environmental issues.

Although the procedure described above has already been applied in some studies (Hardt et al., 2013; Bertolo et al., 2015; Martín de Agar et al., 2016), this is the first time that the unpublished developed procedure is presented step by step for easy application to other landscapes, thus allowing the landscape mosaic identification technique to be well known by scientists, planners and managers involved in nature conservancy.

Materials and methods

The case study

The methodological procedure was originally developed for a case study in an Atlantic Forest landscape in Serra do Japi, State of São Paulo, Brazil (*Appendix A*). The mountainous area is covered by a semi-deciduous forest, Red-Yellow Latosols (Oxisols) predominate, and the climate is seasonal, with a hot and rainy season and a dry and cold season (Morelato, 1992).

Methodological procedure

The procedure developed for identifying and mapping boundaries and mosaics consists of three stages that are described in detail in the next subsections.

Stage 1 – Identifying boundaries

Boundaries were recognized using ArcGIS on a land use/cover map created by photointerpretation of orthophotos from 2005 (scale 1:25,000). The procedure consists of identifying the common edges between adjoining patches. Different pairs of adjacent land use/cover identify the differing boundaries, which are each stored in separate layers. Using the land use/cover layers in a polygon vector format as inputs, the layers of the patch edges are generated by just dilating the polygons of land use/cover (*Fig. 1-I; Tables 1A-I and B-I*).

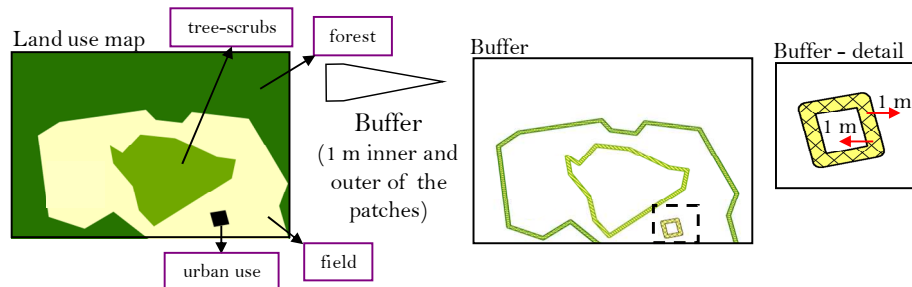
There are two alternatives depending on whether these layers will be stored in raster or vector format. For the former, the layers of the edges are converted to raster format and are then reclassified as prime numbers (*Fig. 1-II; Table 1A-II*). Subsequently, all possible pairs of layers that represent the different land uses/covers are multiplied (*Fig. 1-III; Table 1A-III*). Because these are codified as prime numbers, the result of each multiplication is unique, and each multiplication represents a single type of boundary among the existing uses in the study area. All layers obtained by multiplication are then added to generate a raster layer with all boundaries.

To draw a boundary map in vector format, the boundary layers of all possible pairs of land uses/covers, as obtained in *Table 1B-II*, are directly overlaid. The denomination of the boundaries is then included, and the data are merged into a single file (*Table 1B-III*).

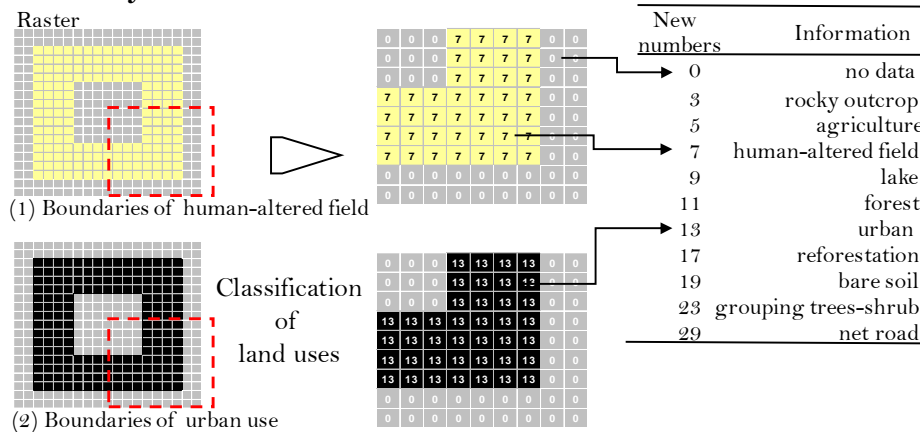
Stage 2 – Drawing up patches × boundaries matrices

In this stage, the types of boundaries for each patch of land use/cover are identified and organized in a matrix using the same procedure for both raster and vector formats. Boundary type is recorded as i) presence-absence, which represents whether a boundary type is or is not present, ii) frequency, which is the number of segments of a boundary type and iii) length, which is the sum of the segment lengths of a boundary type.

I. Buffer Wizard



II. Reclassify



III. Raster calculator

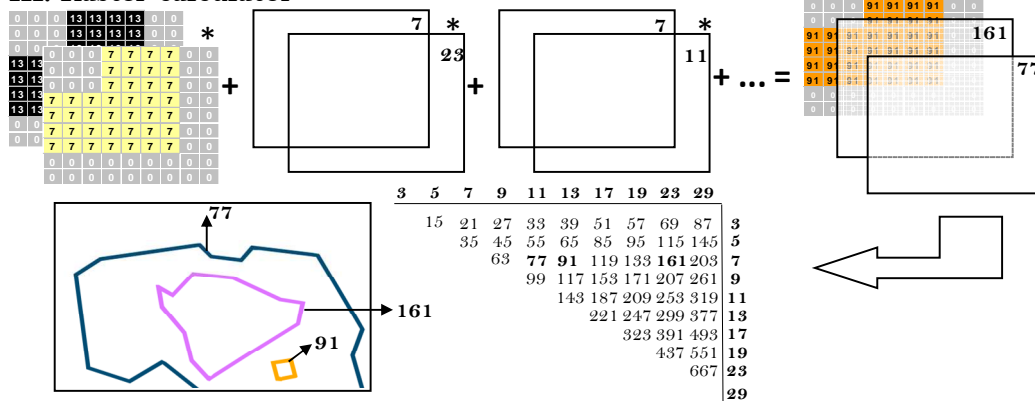


Figure 1. Boundary detection for land use/cover layers in raster format

Table 1. Stage i) Identification and characterization of boundaries using ArcGis® 10.3

A) For boundary mapping in raster format																	
Action	Commands																
I. Create layers of patch edges for each land use/ cover type using polygon internal and external dilation (Fig. 1.I Buffer Wizard). This action allows adjacent patches to be superposed in the next step.	⇒ in ArcMap: Customize > Commands > Categories: Tools > Commands: Buffer wizard [select a “use type layer” > Next > Distance units are: meters > At a specific distance: 1 meters > Next > Dissolve barriers between buffers: No > Create buffer so they are inside and outside the polygon(s) > In a new layer, specify output shapefile > Finish] ⇒ Repeat this procedure for all use types ¹																
II. Identification of edge types between patches using codes classify of layers into prime numbers (Fig. 1.II Reclassify). ²	⇒ in ArcToolbox: Spatial Analyst Tools > Reclass > Reclassify [select a “buffer output” as Input raster > Reclass field: select Value > Classify > New values: input the new number and 0 to NoData > Name the Output raster > OK] ⇒ Repeat this procedure for all use types ¹																
III. Multiplication of pairs of layers reclassified by superposition and the sum of all the resulting layers (Fig. 1.III Raster Calculator). The calculation allows the type of boundary between patches to be described because the multiplication of prime numbers always results in unique combinations.	⇒ in ArcToolbox: Spatial Analyst Tools Map Algebra > Raster Calculator [create an expression like this ([layer_use1] * [layer_use2]) + ([layer_use1] * [layer_use3]) +...+ ([layer_use n-1] * [layer_use n]) > Name output raster as “boundary map” > Evaluate] ⇒ Exclude the combinations that are different from expected																
B) For boundary mapping in vector format																	
Action	Commands																
I. Same as for the raster technique (Fig. 1.I).	Same as for the raster technique																
II. Superposition of all pairs of boundary layers between land use/ cover patches generated in the previous stage for the identification of boundaries. Ex. of land use/ cover combinations:	⇒ in ArcToolbox: Analysis Tools > Overlay > Intersect [Input features: add 2 types of “buffer output” > Name the output feature class > OK] ⇒ Repeat this tool for all combinations of buffer layers ¹																
<table border="1"> <thead> <tr> <th>uses</th> <th>urban</th> <th>field</th> <th>forest</th> </tr> </thead> <tbody> <tr> <td>urban</td> <td>-</td> <td>urb-fie</td> <td>urb-for</td> </tr> <tr> <td>field</td> <td>-</td> <td>-</td> <td>fie-for</td> </tr> <tr> <td>forest</td> <td>-</td> <td>-</td> <td>-</td> </tr> </tbody> </table>	uses	urban	field	forest	urban	-	urb-fie	urb-for	field	-	-	fie-for	forest	-	-	-	
uses	urban	field	forest														
urban	-	urb-fie	urb-for														
field	-	-	fie-for														
forest	-	-	-														
III. Denomination of boundary types for each resulting layer in the previous step to merge them in a single file.	⇒ in ArcMap: Open Attribute Table of a “buffer intersect output” > Table Options > Add Field [Name the new field as “boundary” > Type: text] > Editor > Start Editing > Attribute table [include the boundary type in the new field > Explode Multi-part feature > Save edits] ⇒ Repeat this procedure for all boundary types ¹ ⇒ In ArcToolbox: Data Management Tools > General > Merge [Input as Dataset all “buffer intersect output” > name the output dataset as “boundary map” > Field map: keep the new field only > OK]																

¹Batch automation or the “Line Window” command can be used to speed up the repetition process

²It precedes the conversion of original vector buffer layers into raster format

The proceeding starts by including in each layer the fields in which the boundary presence-absence, frequency or length will be registered (*Table 2-I*). The new file must be superposed with the land use/cover map, and the boundaries can be identified (*Table 2-II*). Attention should be given to deleting any superposition that exceeds a two-by-two combination.

In the next step, the matrix of patches × boundaries is reorganized (*Table 2-III*) to calculate the presence-absence, frequency or length of all the boundaries of each patch (*Table 2-IV*).

Stage 3 – Identifying and mapping mosaics

This stage begins by using the multivariate analysis of the patches × boundaries matrix to identify the landscape mosaics. The matrix is exported to statistical software such as SPSS (*Table 3-I*) and submitted to multivariate ordination and clustering analyses (*Table 3-II*) based on the method developed by Roldán et al. (2003, 2006).

Table 2. Stage ii) Development of patch × boundary matrices using ArcGis® 10.3

Action	Commands
I. Preparation of boundary layers for subsequent boundary measure registration.	⇒ in ArcMap: Open Attribute Table of “ <i>boundary map</i> ” > Table Options > Add Field [Name the new field > Type: long integer] > Editor > Start Editing > Attribute table [a) For the presence/absence frequency: attribute value (1) for the new field created as “ <i>count</i> ”; b) For the length: right click on the new field created as “ <i>length</i> ” < Field Calculator > “ <i>length</i> ” = [Area]/2 > Save edits]
II. Superposition of the land use/cover map with the boundary map for the identification of the boundary types × land use/cover patch.	⇒ in ArcToolbox: Analysis Tools > Overlay > Spatial Join [Target features: “ <i>use map</i> ” > Join features: “ <i>boundary map</i> ” > Name the output feature class > Join operation: join one to many > Field map of join features: “ <i>use map</i> ” (ID, use type); “ <i>boundary map</i> ” (boundary, count, length) > OK]
Example of a table created in this stage:	⇒ In ArcMap - correction of superposition errors: Start Editing > Selection > Select by Attributes [Layer: “ <i>spatial join output</i> ” > Method: Create a new selection > “use type” = “ <i>use1</i> ” > Ok] > Selection > Select by Attributes [Layer: “ <i>spatial join output</i> ” > Method: Remove from current selection > (“ <i>boundary</i> ” = “ <i>boundary1</i> ” OR “ <i>boundary</i> ” = “ <i>boundary2</i> ” ... “ <i>boundary</i> ” = all combinations types for “ <i>use1</i> ”)] > Press Delete
	⇒ Repeat this correction for all use types*

<p>III. Reorganization of the boundaries table by land use/cover patches.</p> <p>Example of tables created in this step:</p> <p>a) For the presence/absence and frequency</p> <table border="1"> <thead> <tr> <th>ID</th> <th>use</th> <th>boundary</th> <th>join count</th> <th>URB-FIE</th> <th>URB-FOR</th> <th>URB-LAK</th> <th>...</th> </tr> </thead> <tbody> <tr> <td>1</td> <td>urban</td> <td>URB-FIE</td> <td>1</td> <td>1</td> <td>0</td> <td>0</td> <td></td> </tr> <tr> <td>1</td> <td>urban</td> <td>URB-FOR</td> <td>1</td> <td>0</td> <td>1</td> <td>0</td> <td></td> </tr> <tr> <td>1</td> <td>urban</td> <td>URB-LAK</td> <td>1</td> <td>0</td> <td>0</td> <td>1</td> <td></td> </tr> <tr> <td>n</td> <td>...</td> <td></td> <td></td> <td></td> <td></td> <td></td> <td></td> </tr> </tbody> </table> <p>b) For the length</p> <table border="1"> <thead> <tr> <th>ID</th> <th>use</th> <th>boundary</th> <th>length</th> <th>URB-FIE</th> <th>URB-FOR</th> <th>URB-LAK</th> <th>...</th> </tr> </thead> <tbody> <tr> <td>1</td> <td>urban</td> <td>URB-FIE</td> <td>10</td> <td>10</td> <td>0</td> <td>0</td> <td></td> </tr> <tr> <td>1</td> <td>urban</td> <td>URB-FOR</td> <td>22</td> <td>0</td> <td>22</td> <td>0</td> <td></td> </tr> <tr> <td>1</td> <td>urban</td> <td>URB-LAK</td> <td>9</td> <td>0</td> <td>0</td> <td>9</td> <td></td> </tr> <tr> <td>n</td> <td>...</td> <td></td> <td></td> <td></td> <td></td> <td></td> <td></td> </tr> </tbody> </table>	ID	use	boundary	join count	URB-FIE	URB-FOR	URB-LAK	...	1	urban	URB-FIE	1	1	0	0		1	urban	URB-FOR	1	0	1	0		1	urban	URB-LAK	1	0	0	1		n	...							ID	use	boundary	length	URB-FIE	URB-FOR	URB-LAK	...	1	urban	URB-FIE	10	10	0	0		1	urban	URB-FOR	22	0	22	0		1	urban	URB-LAK	9	0	0	9		n	...							<p>⇒ in ArcToolbox: Data Management Tools > Table > Pivot Table [Input table: “<i>spatial join output</i>” > Input fields: all attribute fields > Pivot field: “<i>boundary</i>” > Value field:</p> <p>a) For the presence/absence and frequency: select the “<i>count</i>” field;</p> <p>b) For the length: select the “<i>length</i>” field</p> <p>> Name the output table > OK]</p>
ID	use	boundary	join count	URB-FIE	URB-FOR	URB-LAK	...																																																																										
1	urban	URB-FIE	1	1	0	0																																																																											
1	urban	URB-FOR	1	0	1	0																																																																											
1	urban	URB-LAK	1	0	0	1																																																																											
n	...																																																																																
ID	use	boundary	length	URB-FIE	URB-FOR	URB-LAK	...																																																																										
1	urban	URB-FIE	10	10	0	0																																																																											
1	urban	URB-FOR	22	0	22	0																																																																											
1	urban	URB-LAK	9	0	0	9																																																																											
n	...																																																																																
<p>IV. Summary of boundary attributes by patch ID.</p> <p>Examples of patch × boundary matrices:</p> <p>a) For presence/absence</p> <table border="1"> <thead> <tr> <th>ID</th> <th>use</th> <th>MAX_{URB-FIE}</th> <th>MAX_{URB-FOR}</th> <th>...</th> </tr> </thead> <tbody> <tr> <td>1</td> <td>urban</td> <td>1</td> <td>1</td> <td></td> </tr> <tr> <td>2</td> <td>field</td> <td>1</td> <td>0</td> <td></td> </tr> <tr> <td>3</td> <td>forest</td> <td>0</td> <td>1</td> <td></td> </tr> <tr> <td>n</td> <td>...</td> <td></td> <td></td> <td></td> </tr> </tbody> </table> <p>b) For frequency</p> <table border="1"> <thead> <tr> <th>ID</th> <th>use</th> <th>SUM_{URB-FIE}</th> <th>SUM_{URB-FOR}</th> <th>...</th> </tr> </thead> <tbody> <tr> <td>1</td> <td>urban</td> <td>5</td> <td>3</td> <td></td> </tr> <tr> <td>2</td> <td>field</td> <td>1</td> <td>0</td> <td></td> </tr> <tr> <td>3</td> <td>forest</td> <td>0</td> <td>11</td> <td></td> </tr> <tr> <td>n</td> <td>...</td> <td></td> <td></td> <td></td> </tr> </tbody> </table> <p>c) For length</p> <table border="1"> <thead> <tr> <th>ID</th> <th>use</th> <th>SUM_{URB-FIE}</th> <th>SUM_{URB-FOR}</th> <th>...</th> </tr> </thead> <tbody> <tr> <td>1</td> <td>urban</td> <td>10</td> <td>22</td> <td></td> </tr> <tr> <td>2</td> <td>field</td> <td>18</td> <td>0</td> <td></td> </tr> <tr> <td>3</td> <td>forest</td> <td>0</td> <td>4</td> <td></td> </tr> <tr> <td>n</td> <td>...</td> <td></td> <td></td> <td></td> </tr> </tbody> </table>	ID	use	MAX _{URB-FIE}	MAX _{URB-FOR}	...	1	urban	1	1		2	field	1	0		3	forest	0	1		n	...				ID	use	SUM _{URB-FIE}	SUM _{URB-FOR}	...	1	urban	5	3		2	field	1	0		3	forest	0	11		n	...				ID	use	SUM _{URB-FIE}	SUM _{URB-FOR}	...	1	urban	10	22		2	field	18	0		3	forest	0	4		n	...				<p>⇒ in ArcToolbox: Analysis tools > Statistics > Summary Statistics [Input table: select a “<i>pivot table output</i>” > Name the output table > Statistics field(s): include all boundary types) > Statistic type:</p> <p>a) For presence/absence: MAX - for value field (1) > Case field: ID</p> <p>b) For frequency: SUM - for value field (1) > Case field: ID</p> <p>c) For length: SUM - for value field “<i>length</i>” > Case field: ID</p> <p>> OK]</p>					
ID	use	MAX _{URB-FIE}	MAX _{URB-FOR}	...																																																																													
1	urban	1	1																																																																														
2	field	1	0																																																																														
3	forest	0	1																																																																														
n	...																																																																																
ID	use	SUM _{URB-FIE}	SUM _{URB-FOR}	...																																																																													
1	urban	5	3																																																																														
2	field	1	0																																																																														
3	forest	0	11																																																																														
n	...																																																																																
ID	use	SUM _{URB-FIE}	SUM _{URB-FOR}	...																																																																													
1	urban	10	22																																																																														
2	field	18	0																																																																														
3	forest	0	4																																																																														
n	...																																																																																

Patches with similar coordinates on the ordination axes have similar boundary pattern and consequently may be regarded as belonging to the same mosaic. To better identify these groups, patches are also clustered according to their coordinates on the ordination axes (Roldán et al., 2003). Each of the identified clusters corresponds to a mosaic. The mosaic to which each patch corresponds is recorded in a table. The table is

incorporated into ArcGis® to map the mosaics (*Table 3-III*). This step is performed by joining the table with the land use/cover map in accordance with the patch number register (ID). This allows the mosaics to be mapped, as presented in Hardt et al. (2013).

Table 3. Stage iii) Identification and mapping of landscape mosaics

Action	Commands
I. Export the table of patches × boundaries from ArcGIS® to statistical software.	⇒ in any Statistical software: Open the *.dbf corresponding to the <i>output table</i> obtained in the last step of stage ii). For example, SPSS software opens directly the *.dbf file generated by ArcGis® 10.3.
II. Mosaics identification: a) DCA analysis of the patches × boundaries table; b) Cluster analysis of the patches according to their scores on the DCA axes.	⇒ in the statistical software selected: Start from one of the boundary measures recorded in <i>the output table</i> and subject the selection (patches selected boundary measure) to the DCA and cluster analysis. See Roldán et al. (2003, 2006) for details. The final step is to build a table of patches × cluster number. This <i>new table</i> contains the number of the cluster or mosaic corresponding to each patch.
III. Mosaic mapping in ArcGIS® by joining the land use/cover map with the cluster table created in the last step, followed by a new representation of the patches using cluster numbers that identify the mosaics.	⇒ in ArcMap: Insert the <i>new table</i> of patches × cluster number > Add Data [" <i>new table</i> " > Add > Save] > mosaic mapping by right clicking on the <i>land use/cover map</i> > Joins and Relates > Join [Join attributes from a table > Field layer join based on: " <i>ID</i> " > Table to join: " <i>new table</i> " > Field table join on: " <i>ID</i> " > OK] > attribute the mosaic's symbology by right clicking on the <i>land use/cover map</i> > Properties > Symbology [Categories > Value Field: " <i>cluster number</i> " > Add all values > OK].

The instructions shown in *Tables 1* and *2* refer to ArcGis®, but the sequence of operations may also be implemented in another GIS using the tools corresponding to each of the operations described in detail.

Example of the methodological procedure

The validity of the method for the three types of boundary measures was tested for a case study in Serra do Japi (São Paulo, Brazil) by comparing the mosaics' complexity results with the local reality aided by the statistical analysis described below. This study case used part of a database developed to describe the utility of landscape mosaics for decision making for Atlantic Forest conservation. Additional details of this analysis can be found in Hardt et al. (2013).

The land use/cover map (*Appendix A*) shows the spatial distribution of 3,979 patches corresponding to ten land uses/covers (*Appendix B*) that have 30,057 boundaries of 37 distinct types. Three matrices of patches × boundaries were calculated using of presence/absence, frequency or length boundary data for each patch.

Each matrix was subjected to a Detrended Correspondence Analysis (DCA; Hill, 1981) using PC-Ord[®] 4.0 software. The scattergrams of the boundaries and patches according to axes 1-2 and 2-3 of the three DCA are shown in *Fig. 2*. The patches were then clustered according to their coordinates on the first three axes of the DCA using a free trial version of XlStat[®]. The clustering was performed by applying Ward's method as the amalgamation algorithm and Euclidean distance as the measure of similarity (*Fig. 3*).

The group similarity cut-off level in the dendrograms was standardized at 95%. The clusters were characterized according to their boundaries by means of Chi-square analyses for the presence/absence data and Student's t-test for the frequency and length data. Finally, the patch clusters were incorporated into the ArcGis[®] database for mapping the mosaics. Thus, three landscape mosaic maps of the Serra do Japi were drawn (*Fig. 3*).

The distribution of boundaries and patches in the ordination scattergrams indicates that boundary frequency is the boundary measure that most clearly displays the boundary distribution variability in the sets of patches (*Fig. 2c*). For the presence/absence (*Fig. 2a*) and length (*Fig. 2d*) data, the distribution of these two elements was strongly conditioned by a single type of boundary (between outcrop – AFL – and forest – BOS – represented by the AFL-BOS code) with a small number of occurrences in the landscape. This makes the scattering of data in the space defined by the first ordination axis more compact (*Figs. 2a* and *d*), with many of the patches having very similar coordinates. This hinders the interpretation of the variability of boundaries and the recognition of groups of patches, on which the identification of the mosaics is based (Roldán et al., 2003, 2006). It does not occur when frequencies are studied because the frequencies of this boundary do not greatly limit the dispersion of data (*Fig. 2c*).

To corroborate this result, new scattergrams were drawn by removing the patches with higher coordinates on axis 1, that is, those with positions that were highly dependent on the AFL-BOS boundary. A wider distribution of patches and boundaries was obtained for the presence/absence data (*Fig. 2b*), but most of them continued to have very close coordinates.

The scattergram of the length matrix (*Fig. 2e*) shows sets of patches arranged in rows. This indicates that these sets responded to variations in the lengths of one or a few boundaries, which is related to the particular structure of the study area, in which there are large forest patches that are located at high altitudes and are surrounded by small fragments of other anthropic uses (*Appendix A*). Therefore, the forest patches have more variable perimeter lengths than other land uses/covers. This increases the possibility that forest patches will have boundaries with varied lengths, from very short to very long.

Boundaries that characterize the selected clusters, i.e., the identified mosaics, are also included in the dendrograms obtained from patch clustering (*Fig. 3*). Both the presence/absence (*Fig. 3a*) and length (*Fig. 3c*) data produced dendrograms with a cluster that remained undivided from the first division. In these cases, this cluster is characterized by the AFL-BOS boundary. The dendrogram obtained from the frequency data (*Fig. 3b*) had a better organized set and sub-set structure because no clusters remained undivided from the first division. These results agree with those obtained from the ordination scattergrams because the boundary frequency data provided a more easily understandable interpretation and did not uniquely depend on the spatial distribution or length of just one boundary.

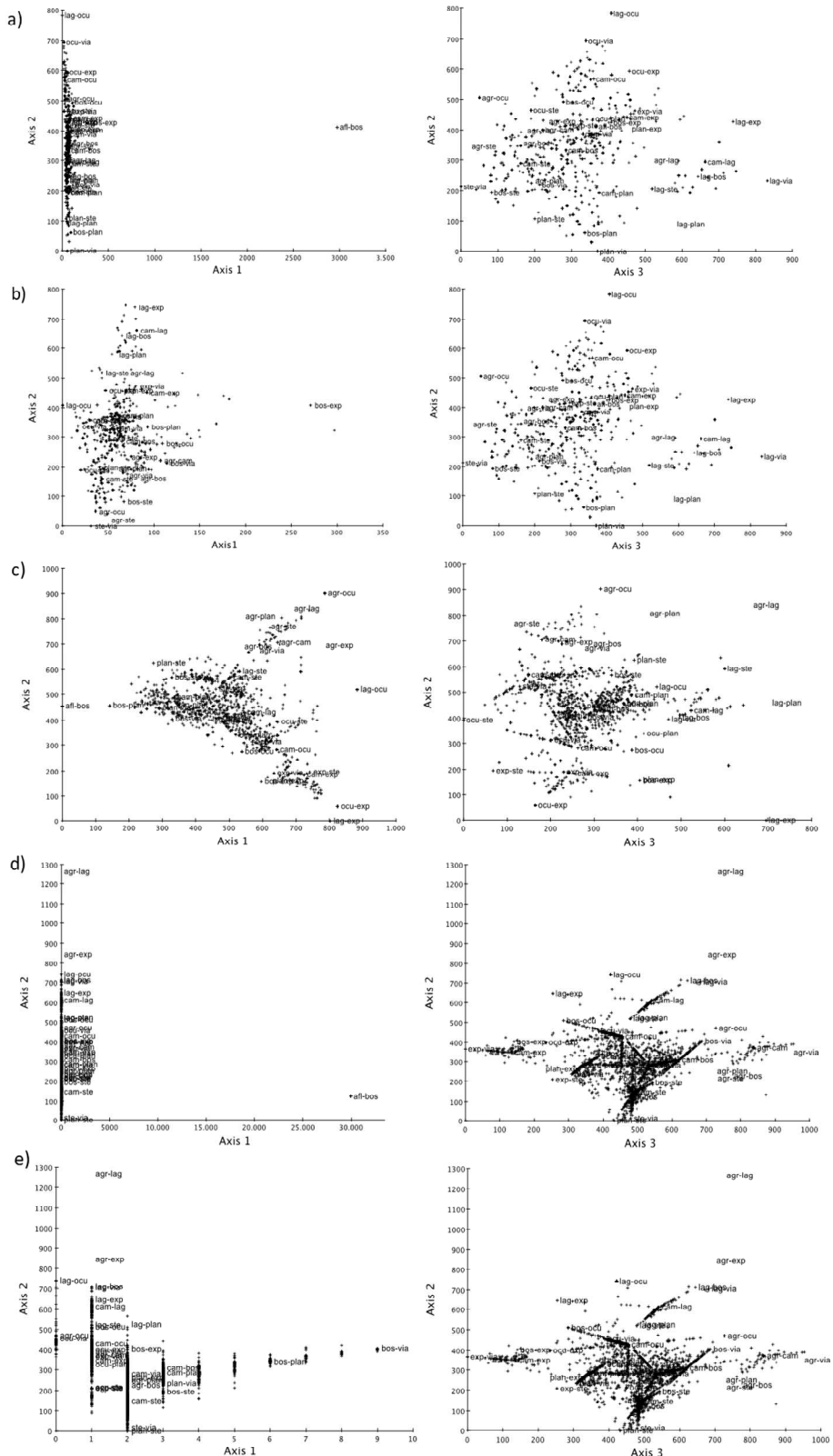


Figure 2. Results of the DCA ordination of patch \times boundary matrices. Scattergrams for axes 1 and 2 and axes 2 and 3 of a) the presence/absence matrix, b) the presence/absence matrix without outliers, c) the frequency matrix, d) the length matrix, and e) the length matrix without outliers. Patches are represented by crosses, and boundaries are represented by abbreviations of the land use/cover codes, which are presented in Appendix B

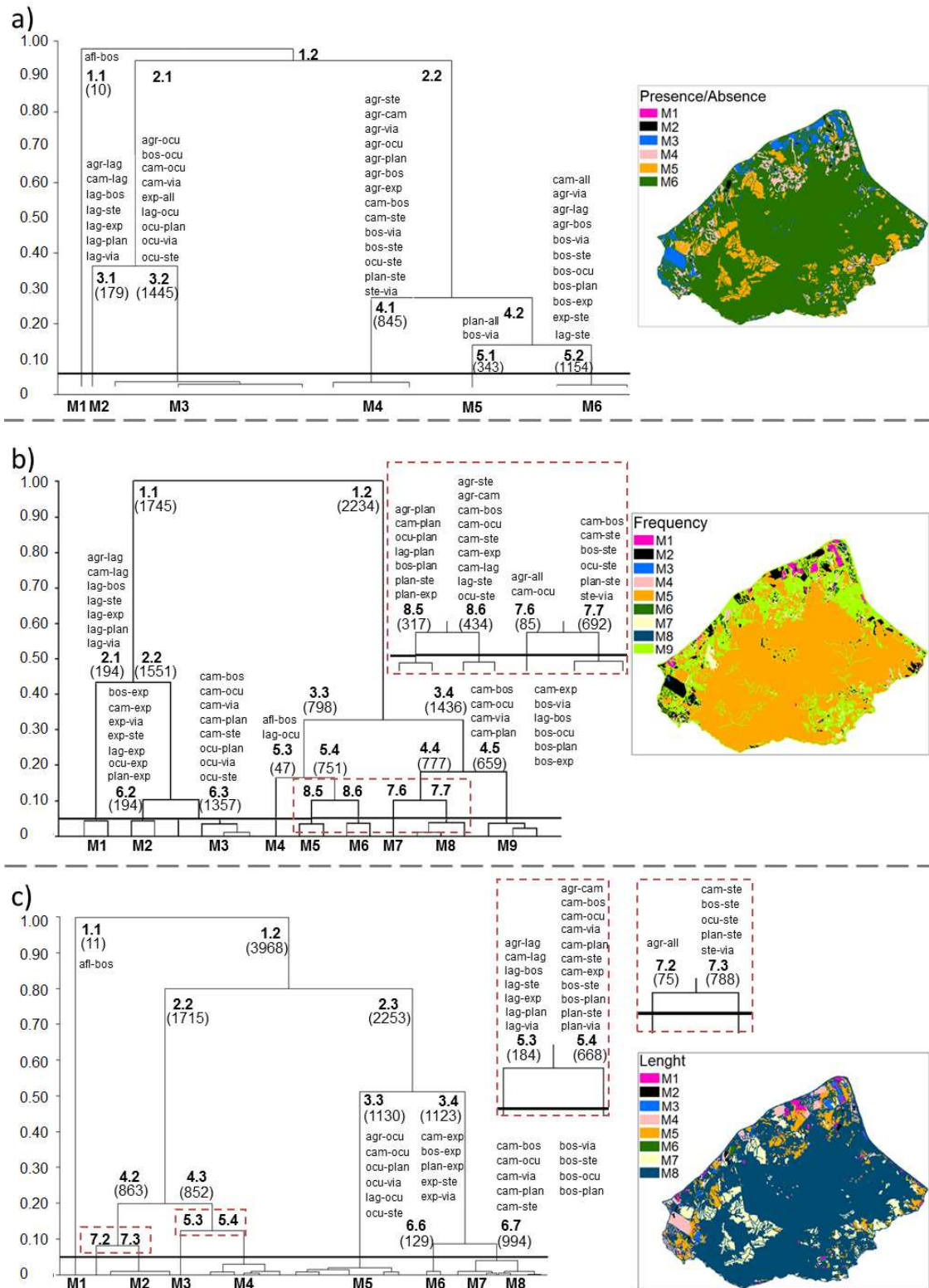


Figure 3. Clustering results of patches in mosaics (I) and the corresponding mosaic map (II) obtained from data on boundary presence/absence (a), frequency (b) and length (c)

A large central mosaic and a more heterogeneous peripheral landscape is identified in all the mosaic maps, irrespective of the boundary measure used (Fig. 3). These

results agree with that reported by Hardt et al. (2013) on the landscape spatial structure in the same study area. This indicates that the differences in the results obtained using the three boundary measures depend on the different landscape details highlighted by each measure.

In summary, in this example, boundary frequency is the boundary measure that most clearly allows us to identify mosaic-patch sets with a similar boundary pattern (Figs. 2c and 3b). The frequency distribution of boundaries did not seem to be highly conditioned by the low frequencies of some of them, which were present only in some patches, as seemed to be case for the presence/absence measure. In addition, the sizes of the patches were less important for the frequency measure because that variable had a lower variation rank than the length measure.

Discussion

Building matrices of patches \times boundaries has been the constraining factor in landscape mosaic mapping. Methodological procedures like the one described, which is the only one known by the authors, allows these matrices to be easily drawn up, thus contributing to operationalizing the concept of landscape mosaics and making its application in landscape management possible (Hardt et al., 2013; Bertolo et al., 2015; Martín de Agar et al., 2016). The procedure has also the advantage of using standard GIS and statistical software.

The procedure developed permits input land use/cover maps in both raster and vector formats to be used. It works practically without limitation to large datasets, depending only on the software used and on the available memory and system cache of the user's computer. The implementation of this concept has previously been limited by the difficulty when working with large territories, which probably explains the small number of studies on the complexity of landscape interactions based on mosaics (Cantwell and Forman, 1993; Roldán-Martín et al., 2003, 2006; Hersperger, 2006) and their use in environmental planning and management (Hardt et al., 2013; Bertolo et al., 2013).

Each boundary measure provides a particular interpretation of landscape organization, and researchers must therefore evaluate the measures that best meet their objectives. In the example, the mosaics identified using boundary presence/absence was not the most revealing of the landscape variability. The qualitative aspect seems to be a large constraint, as the occurrence of a low presence boundary conditioned the results by impeding the easy observation of other patterns.

In our example, when mosaics are characterized by boundary length, the information provided was apparently influenced in both qualitative aspects as related to very low frequency boundaries (Fig. 2d) and patch size (Fig. 2e). This is the case of large forest patches having boundaries of all lengths. They condition the patch arrangement "in lines" (Fig. 2e), depending mainly on the differences in the lengths of the boundaries and less on their natures. The large forest patches conditioned the dispersion of the others in the DCA, primarily because of they may have boundaries of different lengths, which condition the identification of mosaics.

Boundary identification is closely related to the degree of landscape fragmentation and connectivity (Metzger and Muller, 1996; Rescia et al., 1997; Collinge and Forman, 1998; Trani and Giles, 1999; Zeng and Ben Wu, 2005). However, when a landscape becomes more fragmented, the boundary frequencies tends to provide information about

the fragmentation pattern that cannot be derived from length (Zeng and Ben Wu, 2005). Boundary frequency enable reporting stages prior to the rupture of the landscape based on the identification of patch perforations (Forman, 1995). Because of that ability, mosaics identified by frequency boundaries are apparently important in assessing the history of fragmentation pressures, understanding rupture dynamics over time and even indicating probable future scenarios (Hardt et al., 2013).

In our example, the relative similarities among the three mosaic maps (*Fig. 3*) could have been due to landscape homogeneity (Corbacho et al., 2000) explained by the small fragmentation in the central area and the large fragmentation in the peripheral areas.

Measures of boundaries such as frequency and length respond to spatial pattern in landscape heterogeneity (Metzger and Muller, 1996) and are particularly sensitive to environmental changes (Fortin et al., 2000). In that sense, mosaic landscape organization models should reflect depth spatial heterogeneity in such a way that they clearly show patterns of ecological interactions and landscape complexity (Lovett et al., 2005; Roldán-Martín et al., 2006; Hardt et al., 2013).

There are other models that describe the influences of spatial pattern on ecological processes and their changes over time, including the well-known patch-corridor-matrix model (Forman, 1995). However, that model is limited in its ability to detect landscape spatial heterogeneity, which can lead to errors in decision-making for landscape management (Hardt et al., 2013)

The described method has many possible practical outputs that could assist decision making in landscape management, for example, comparisons between mosaics built from historical maps, which record landscape changes, highlight driving forces and change vectors. These affect land cover/use and boundaries. New mosaics can appear as the result of changes in boundaries as well as land cover/uses, as reported by Hardt et al. (2013). For that reason, this analysis permits future scenarios to be proposed for nature conservation that have different degrees of human interference, keeping in mind that in landscapes with less complex spatial interactions and mosaics with simpler boundary structures, management is easier. Mosaics can also be used to identify priority areas for conservation according to the types and complexities of neighborhood spatial relationships, including the definition of appropriate management actions in accordance with them.

Due to their capabilities, mosaics can be used as units of landscape organization (Wiens, 1999; Hersperger, 2006) to identify territories that differ in structure, function, and forest conservation status (Hardt et al., 2013). In this way, mosaics can be a key tool to identify action zones for environmental planning and management, where planners and decision makers need to analyze the consequences on ecosystem service provision, especially in regions that face complex environmental issues and where natural resources share space with anthropic uses.

Conclusions

The methodological procedure contributes to making the concept of landscape mosaics more operative and applicable for environmental planners.

The procedure works with any size area, with large data sets and in automated processes. However, the usefulness of the different boundary measures should be assessed in accordance with landscape characteristics and study purpose.

The case study highlights the influence of landscape homogeneity and fragmentation on the similarities among mosaics that are obtained by different boundary attributes. It also differentiated boundary frequency as the attribute that can be used to more easily identify and interpret mosaics due to its capacity to interpret the dynamics of landscape rupture patterns.

Acknowledgements. This work was supported by the FAPESP-BR [grant number 06/55385-0; 08/01505-0, the CAPES-BR and Fundación Carolina-ES [grant number BEX 3967/10-7], the Santander/UCM-ES group [grant mobility 2011] and the Ministry of Science and Innovation-ES [grant MA-2012].

REFERENCES

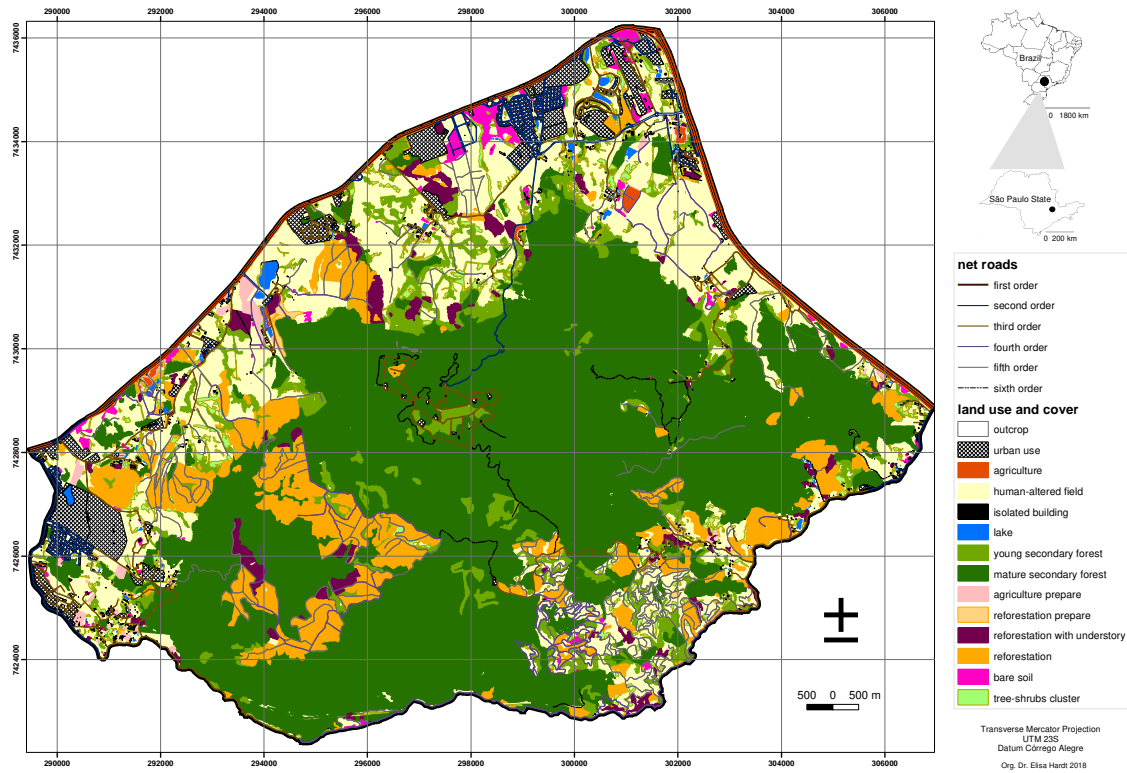
- [1] Banerjee, S., Carlin, B. P., Gelfand, A. E. (2015): Hierarchical Modelling and Analysis for Spatial Data. – CRC Press/Chapman & Hall, Boca Raton.
- [2] Bastian, O., Grunewald, K., Khoroshev, A. V. (2015): The significance of geosystem and landscape concepts for the assessment of ecosystem services: exemplified in a case study in Russia. – *Landscape Ecology* 30: 1145-1164.
- [3] Bertolo, L. S., Santos, R. F., Martín de Agar, P., De Pablo, C. T. L. (2015): Land-use changes assessed by overlay or mosaic methods: which method is best for management planning? – *Ecological Indicators* 55: 32-43.
- [4] Cadenasso, M. L., Pickett S. T. A., Weathers, K. C., Jones, C. G. (2003): A framework for a theory of ecological boundaries. – *BioScience* 53: 750-758.
- [5] Cantwell, M. D., Forman, R. T. T. (1993): Landscape graphs: ecological modeling with graph theory to detect configurations common to diverse landscapes. – *Landscape Ecology* 8(4): 239-255.
- [6] Collinge, S. K., Forman, R. T. T. (1998): A conceptual model of land conversion processes: predictions and evidence from a field experiment with grassland insects. – *Oikos* 82: 66-84.
- [7] Corbacho, P. P., Zárata, A., Rebollo, J. C, De Pablo, C. L. (2000): Landscape Homogenisation and Fragmentation: Changes in the Spatial Organisation of the Madrid Landscape (Spain). – In: Brandt, J. B., Tress, B., Tress, G. (eds.) Multifunctional Landscapes: Interdisciplinary Approaches to Landscape Research and Management. Conference on Multifunctional Landscapes. Centre for Landscape Research, Roskilde.
- [8] De Groot, R. S., Alkemade R., Braat L., Hein L., Willemen L. (2010): Challenges in integrating the concept of ecosystem services and values in landscape planning, management and decision making. – *Ecological Complexity* 7: 260-272.
- [9] De Pablo, C. L., Roldán, M. J., Martín de Agar, P. (2012): Magnitude and significance in landscape change. – *Landscape Research* 37(5): 571-589.
- [10] Fagan, W. F., Fortin, M. J., Soykan, C. (2003): Integrating edge detection and dynamic modeling in quantitative analyses of ecological boundaries. – *Bioscience* 53: 730-738.
- [11] Forman, R. T. T. (1990): Ecological Sustainable Landscapes: the Role of Spatial Configuration. – In: Zonneveld, I. S., Forman, R.T.T. (eds.) Changing Landscapes: An Ecological Perspective. Springer-Verlag, New York.
- [12] Forman, R. T. T. (1995): Land mosaics: The Ecology of Landscapes and Regions. – Cambridge University Press, Cambridge.
- [13] Forman, R. T., Godron, M. (1981): Patches and structural components for a landscape ecology. – *BioScience* 31(10): 733-740.
- [14] Fortin, M. J., Dale, M. R. T. (2005): Spatial Analysis: A Guide for Ecologists. – Cambridge University Press, Cambridge.

- [15] Fortin M. J., Olson R. J., Ferson S., Iverson L., Hunsaker C., Edwards G., Levine D., Butera K., Klemas V. (2000): Issues related to the detection of boundaries. – *Landscape Ecology* 15: 453-466.
- [16] Frank, S., Fürst, C., Koschke, L., Makeschin, F. (2012): A contribution towards a transfer of the ecosystem service concept to landscape planning using landscape metrics. – *Ecological Indicators* 21: 30-38.
- [17] Gosz, J. R. (1991): Fundamental Ecological Characteristics of Landscape Boundaries. – In: Holland, M. M., Risser, P. G., Naiman, R. J. (eds.) *Ecotones: The role of Landscape Boundaries in the Management and Restoration of Changing Environments*. Chapman & Hall, New York.
- [18] Hardt, E., Dos Santos, R. F., De Pablo, C. L., Martín de Agar, P., Pereira-Silva, E. F. L. (2013): Utility of landscape mosaics and boundaries in forest conservation decision making in the Atlantic Forest of Brazil. – *Landscape Ecology* 28(3): 385-399.
- [19] Hersperger, A. M. (2006): Spatial adjacencies and interactions: neighbourhood mosaics for landscape ecological planning. – *Landscape and Urban Planning* 77: 227-239.
- [20] Jacquez, G. M., Maruca, S., Fortin, M. J. (2000): From Fields to Objects: a review of geographic boundary analysis. – *Journal of Geographical Systems* 2: 221-241.
- [21] Jacquez, G. M., Fortin, M. J., Goovaerts, P. (2008): Preface to the special issue on spatial statistics for boundary and patch analysis. – *Environmental and Ecological Statistics* 15: 365-367.
- [22] Kirchoff, T., Trepl, L., Vicenzotti, V. (2013): What is Landscape Ecology? An analysis and evaluation of six different conceptions. – *Landscape Research* 38(1): 33-51.
- [23] Lovett, G. M., Jones, C. G., Turner, M. G., Weathers, K. C. (2005): *Ecosystem Function in Heterogeneous Landscapes*. – Springer, New York.
- [24] Maes, J., Teller A., Erhard M. et al. (2013): *Mapping and Assessment of Ecosystems and their Services: an Analytical Framework for Ecosystem Assessments under Action 5 of the EU Biodiversity Strategy to 2020*. – Publications Office of the European Union, Luxembourg.
- [25] Margalef, R. (1979): The organization of space. – *Oikos* 33: 152-159.
- [26] Martín de Agar, P., Ortega, M., De Pablo, C. L. (2016): A procedure of landscape services assessment based on mosaics of patches and boundaries. – *Journal of Environmental Management* 180: 214-227.
- [27] Metzger, J. P., Müller, E. (1996): Characterizing the complexity of landscape boundaries by remote sensing. – *Landscape Ecology* 11: 65-77.
- [28] MEA, Millennium Ecosystem Assessment (2005): *Ecosystems and Human Well-Being: Synthesis*. – Island Press, Washington.
- [29] Peters, D. P. C., Gosz, J. R., Pockman, W. T., Small, E. E., et al. (2006): Integrating patch and boundary dynamics to understand and predict biotic transitions at multiple scales. – *Landscape Ecology* 21: 19-33.
- [30] Morellato, L. P. C. (1992): *História natural da Serra do Japi: ecologia e preservação de uma área florestal no sudeste do Brasil (Natural History of the Serra do Japi: Ecology and Preservation of a Forest Area in Southeastern Brazil)*. – Editora da Unicamp, Campinas.
- [31] Rescia, A. J., Schmitz, M. F., Martín de Agar, P., De Pablo, C. L., Pineda F. D. (1997): A fragmented landscape in northern Spain analyzed at different spatial scales: implications for management. – *Journal of Vegetation Science* 8: 343-352.
- [32] Roldán, M. J. R., De Pablo, C. T. L., Martín de Agar, P. (2003): *Landscape Mosaics Recognition and Changes Over Time: A Methodological Approach*. – In: Mander, U., Antrop, M. (eds.) *Multifunctional Landscapes: Continuity and Change*. Wit Press, Boston.
- [33] Roldán, M. J. R., De Pablo C. T. L., Martín de Agar, P. (2006): Landscape changes over time: comparison of land uses, boundaries and mosaics. – *Landscape Ecology* 21: 1075-1088.

- [34] TEEB (2010): The Economics of Ecosystems and Biodiversity Ecological and Economic Foundations. – Pushpam Kumar, Earthscan, London and Washington.
- [35] Trani, M. K., Giles Jr., R. H. (1999): An analysis of deforestation: metrics used to describe pattern change. – *Forest Ecology and Management* 114: 459-470.
- [36] Turner, M. G. (1989): Landscape ecology: the effect of pattern on process. – *Annual Review of Ecology, Evolution, and Systematics* 20: 171-179.
- [37] Urban, D. L., O'Neill, R. V., Shugart, H. H. (1987): Landscape ecology. – *BioScience* 37: 119-127.
- [38] Wiens J. A. (1999): The Science and Practice Landscape Ecology. – In: Klopatek, M., Gardner, R. H. (eds.) *Landscape Ecological Analysis: Issues and Applications*. Springer, New York.
- [39] Wiens, J. A. (2002): Riverine landscapes: taking landscape ecology into the water. – *Freshwater Biology* 47: 501-515.
- [40] Wiens, J. A., Crawford, C. S., Gosz, J. R. (1985): Boundary dynamics: a conceptual framework for studying landscape ecosystems. – *Oikos* 45: 421-427.
- [41] Wiens, J. A, Moss, M. R., Turner, M. G., Mladenoff, D. (2007): *Foundation papers in landscape ecology*. – Columbia University Press, New Work.
- [42] Zeng, H., Ben Wu. X. (2005): Utilities of edge-based metrics for studying landscape fragmentation. – *Computers, Environment and Urban Systems* 29: 159-178.

APPENDIX

Appendix A. Land use/cover map of Serra do Japi, Brazil. Created in ArcGIS® by visual interpretation of aerial orthophotos from 2005. Land uses/covers are described in Appendix B



Appendix B. Description and codes of the land use/cover categories identified in Serra do Japi, Brazil

Category	Code	Criterion of classification
Rocky outcrop	AFL	Natural open habitat with low vegetation cover
Agriculture	AGR	Annual or perennial croplands
Human-altered field	CAM	Pasturelands, abandoned areas (old areas of agriculture and silviculture), yards, lawns, and wasteland or unused lands
Bare soil	EXP	Rural or urban areas without vegetation
Forest	BOS	Semi-deciduous seasonal forests
Lake	LAG	Natural lakes and reservoirs
Net road	VIA	Trails, tracks and roads
Reforestation	PLAN	Plantations of <i>Eucalyptus</i> spp., <i>Pinus</i> spp. or <i>Araucaria</i> spp.
Grouping of trees/shrub	STE	Patches and corridors of trees and shrubs, natural or human-modified, without forest structure
Urban	OCU	Urban nuclei and isolated residential, commercial or industrial buildings

DIFFERENT SEEDLING RAISING METHODS AFFECT CHARACTERISTICS OF MACHINE-TRANSPLANTED RICE SEEDLINGS

CHENG, S. R.^{1,2†} – ASHRAF, U.^{1,3†} – ZHANG, T. T.^{1,2†} – MO, Z. W.^{1,2} – KONG, L. L.¹ – MAI, Y. X.¹ – HUANG, H. L.¹ – TANG, X. R.^{1,2*}

¹*Department of Crop Science and Technology, College of Agriculture, South China Agricultural University, Guangzhou, Guangdong 510642, China*

²*Scientific Observing and Experimental Station of Crop Cultivation in South China, Ministry of Agriculture of the P. R. China, Guangzhou, Guangdong 510642, China*

³*Department of Agronomy, University of Agriculture Faisalabad 38040, Pakistan*

[†]*These authors have contributed equally to this work.*

**Corresponding author*

e-mail: tangxr@scau.edu.cn; phone/fax: +86-20-8528-0204-618

(Received 4th Oct 2017; accepted 12th Feb 2018)

Abstract. Present study was aimed to select the suitable seedling raising method with high seedling quality for the machine-transplanted rice. The seeds of two rice cultivars i.e., *Xiangyaxiangzhan* and *Wufengyou 615* were grown under four different seedling-raising methods i.e., the traditional seedling-raising method (TWSM), the dry seedbed nursery raising method (DSBM), the wet seedbed raising method (WSBM), and the substrate seedbed nursery raising method (SSBM). Results showed that the highest seed germination and seedling establishment rates were recorded in SSBM followed by DSBM, and TWSM. Rice seedlings grown in SSBM have maximum seedling length, longer leaves and leaf sheath as well as dry biomass than other establishment methods. Further, number of roots, root length, root surface area and root diameter were also found significantly ($P \leq 0.05$) higher than those seedlings which were established by normal farmer practice (TWSM). Additionally, higher proline, protein and soluble sugars contents and SPAD values (an indicator of chlorophyll contents) were also recorded in SSBM. Hence, SSBM would result in improved rice seedlings, compared to those under traditional nursery, dry bed nurse and wet bed nursery.

Keywords: *physiological character, root growth, rice nursery, seed germination, seedling-raising methods*

Introduction

Rice (*Oryza sativa*) is the most important cereal crop that feeds more than half of the world's population (Ruiz-Sánchez et al., 2010; Abid et al., 2015; Kargbo et al., 2016). Rice ranks first among the cereal crops in China and it has been cultivated for more than 7000 years ago, feeding more than 65% of the population of China as a staple food (Ivanic and Martin, 2008). In China, rice covers an area of 30.14 million hectare with an annual production of 204.24 million tons. Hence, rice production in China contributes to food security not only for China but also for the rest of the world (Yao et al., 2007; Ashraf et al., 2015).

Seedling transplanting has many advantages over direct seeding; however, manual transplantation of rice nursery is time consuming and slow process (Ehsanullah et al., 2014) as compared with mechanical transplantation. The

development of modern, large-scale, professional and commercial production of rice through mechanized planting plays a critical role to ensure efficient transplanting and maintaining rice productivity (Zhu et al., 2007). Presently, mechanized rice transplanting technology has been successfully adopted in Europe, America, Japan and many other developed countries, whilst in China, the mechanized transplanting is still not widely adopted. Recently, a report stated that mechanized rice transplantation was about 34% at the end of 2014 in China (Yang et al., 2003; Li, 2015).

Healthy and well-nourished seedlings with uniform growth (grown on PVC trays to load to the machine for transplanting) are the prerequisites for uniform transplantation in the field and these seedlings must meet certain technical standards in the system of mechanical transplanting of rice seedlings (Biswas et al., 2000). To develop standard seedlings, as required by the mechanized transplantation, the compatibility among seedlings cultivation/growing method, machine operational system, quality of the rice seedlings must be considered (Zhang and Gong, 2014). Conventional nursery raising is often practiced in paddy soils which is often silty in nature (Mishra and Salokhe, 2008; Li et al., 2014) which makes the manual transplantation difficult. Thus, rather growing rice nursery in the fields, nursery raising in PVC trays and/or in nursery mat is conducive for machine transplanting. Hence, for mechanized transplanting rice technology, indoor seedling/nursery raising on artificial media can also be practiced other than outdoor nursery (that may be threatened by environmental extremities). For indoor nursery raising, seedling growing medium may largely affect the growth and development of rice seedlings. Present study thus focused to test the effect of different nursery management methods on germination, morphological growth and physiological characters of rice seedlings with the aim to determine the best possible nursery raising method for machine-transplanted rice seedlings.

Materials and methods

Experimental site

The seedlings were raised in green house located at Experimental Research Farm, College of Agriculture, South China Agricultural University, Guangzhou, China (23°09' N, 113°22' E and 11 m above the sea level) during 2015. The region has subtropical monsoonal type of climate normally with yearly average temperature ranges ranged from 21 to 29 °C and 70-80% relative humidity and high rainfall during May-July (Li et al., 2016; Mo et al., 2016). Moreover, the average temperature, rainfall, and relative humidity for experimental period was remained 28 °C, 19.17 mm and 79.60%, respectively.

Plant material and treatment description

Seeds of two local and widely cultivated rice cultivars i.e., *Xiangyaxiangzhan* and *Wufengyou 615*, were collected from the College of Agriculture, South China Agricultural University, Guangzhou, China. Prior to sowing, seeds of both rice cultivars were soaked in water for 48 h in dark chamber at room temperature. Seeds were sown in four different methods i.e., (i) traditional seedling-raising method in

which the seeds were directly sowed on the wet seedbed (TWSM) (taken as control), (ii) the dry seedbed raising method in which the seeds were sown in PVC trays covered with air dried soil collected from paddy fields, and applied with distilled water (DSBM), (iii) the wet seedbed raising method in which the seeds were sown in PVC trays covered with well cultivated puddled soil, collected from paddy fields (WSBM), and (iv) the substrate seedbed raising method in which seeds were sown in PVC trays covered with a substrate (agricultural organic waste product including rice husk, obtained from Lianyungang Heroda Fertilizer Technology Co., Ltd, China) and sprayed with distilled water (SSBM). The dimensions of PVC trays used for nursery rising was 58.5 cm × 28.5 cm. The seeding density of both *Xiangyaxiangzhan* and *Wufengyou 615* were 10000-12000 per m².

Determination of seed germination rate and seedling establishment percentage

To determine seed germination rate and seedling establishment percentage, seedlings from an area of 15 cm × 15 cm area from each establishment method were carefully uprooted (about 60 seedlings) at 15 days after sowing (DAS), washed thoroughly with tap water and then with distilled water and the seedlings were graded in to: a) full mature seedlings, and b) young seedlings (one-half of the height of the full mature seedlings). The number of full mature seedlings, young seedlings and non-germinated seeds were counted. The seed germination rate and seedling establishment percentage was recorded as:

Rice germination rate (%) = (number of full mature seedlings + number of young seedlings) / (total germinated and un-germinated seeds) × 100

Percentage of seedling establishment (%) = (Number of full mature seedlings / total number of germinated and un-germinated seeds) × 100

Morpho-physiological characteristics of rice seedlings

The seedlings of both rice cultivars at 10, 15 and 20 DAS were sampled for morpho-physiological parameters while for the estimation of physio-biochemical traits, the seedlings were separated into roots and shoots and stored at -80 °C.

Seedling length, first leaf sheath length, length of first and second leaves was measured with a measuring ruler. Seedling fresh and dry biomass (seedlings were placed in oven at 80 °C till constant weight) per 100 seedlings were recorded by an electric balance (Sartorius, Japan). The number of primary and secondary roots was counted manually whereas root length, root surface area and root diameter of 4 well mature seedlings were recorded by a root scanner (WinRHIZO, ProLA2400, Canada) according to Oršanić et al. (2011).

SPAD values of seeding

SPAD values characterized as chlorophyll contents, were recorded from 10 seedlings of each treatment with a SPAD meter 'SPAD-502' (Konica Minolta, Japan) according Asai et al. (2009) which provided a precise, rapid and non-destructive estimation of leaf chlorophyll contents.

Estimation of proline, protein and soluble sugar

The proline content was determined according to Celik and Atak (2012). Fresh leaf samples (0.3 g) were homogenized with 4 mL of 3% sulfosalicylic acid and heated at 100 °C for 10 min. After cooling, 2 mL of filtrate, 2 mL of acid ninhydrin, and 2 mL of glacial acetic acid was taken in a test tube and boiled in water bath at 100 °C for 30 min. The reaction was terminated on ice, and the reaction mixture was then extracted with 4 mL of toluene. The solution was vortex mixed and 3 mL of the upper toluene extract was centrifuged at 4000 g for 5 min. The absorbance was read at 520 nm. Protein content was assayed using the coomassie brilliant blue G-250 (CBB-G) method as described by Aminian et al. (2013) and the absorbance was read at 595 nm. The soluble sugar contents of the rice leaves were estimated by the method of Karim et al. (2012) with minor modifications. Leaves (0.2 g) were ground with liquid nitrogen to a fine powder and then added 15 mL of distilled water to heat at 100 °C for 20 min. After cooling, 0.1 mL of filtrate and 5 mL of enthroned sulfuric acid solution were mixed and then heated at 100 °C for 10 min and the absorbance was recorded at 620 nm.

Experimental design and data analysis

Treatments were arranged according to completely randomized design (CRD) with three replications. The data were analyzed by an analysis of variance (ANOVA) technique with statistical software Statistix 8.0 (Analytical, Tallahassee, Florida, USA) while the differences among means were separated by least significant difference (LSD) test at the 5% significance level. The Sigma Plot 12.5 (Systat Software Inc., San Jose, CA, USA) was used to make the figures.

Results

Germination and seedling establishment

The highest germination rate and the percentage of seedling establishment were observed in SSBM treatment for both cultivars (*Fig. 1*). DSBM and SSBM significantly increased germination rate for *Xiangyaxiangzhan* by 9.69% and 10.53%, respectively, and for *Wufengyou 615* by 3.66% and 3.85%, respectively. However, WSBM treatment obviously reduced germination rate by 4.40% and 3.77% for *Xiangyaxiangzhan* and *Wufengyou 615*, respectively (*Fig. 1 A, B*). Seedling establishment was substantially increased in SSBM by 23.66% and 13.52% for *Xiangyaxiangzhan* and *Wufengyou615*, respectively. For *Xiangyaxiangzhan*, DSBM treatment significantly increased seedling establishment percentage but WSBM treatment show opposite trend. For *Wufengyou 615*, DSBM and WSBM did not affect the seedling establishment percentage significantly (*Fig. 1 C, D*).

Morphological growth

Different seedling establishment methods substantially affected morphological characters of both rice cultivars. For *Xiangyaxiangzhan*, seedling length, length of first leaf sheet, length of first and second leaf as well as dry biomass were recorded maximum in SSBM and the values were 0.40, 22.01, 66.81, 27.93, 45.37% and 14.49, 13.65, 77.37, 28.41, 26.00%, and 5.64, 0.72, 65.96, 19.77, 12.39%, higher than TWSM at 10 15 and 20 DAS, respectively (*Tables 1 and 2*).

Table 1. The seedling length and shoot dry weight of rice seedlings in response to different seedling raising methods

Cultivar	Treatment	Seedling length (cm)			Shoot dry weight (mg)		
		10 DAS	15 DAS	20 DAS	10 DAS	15 DAS	20 DAS
Xiangyaxiangzhan	TWSM	17.37 a	19.67 ab	21.82 a	10.80b	15.00b	23.40bc
	DSBM	16.52 a	19.76 ab	22.67 a	11.90b	21.00a	21.80c
	WSBM	17.39 a	18.03 b	19.36 b	10.90b	13.40b	25.20ab
	SSBM	17.44 a	22.52 a	23.05 a	15.70a	18.90a	26.30a
Wufengyou 615	TWSM	23.23 a	24.07 a	29.42 a	22.00a	26.90a	47.30a
	DSBM	18.96 b	19.99 b	23.30 c	13.70b	18.00b	33.10b
	WSBM	18.58 b	19.94 b	22.70 c	12.40b	17.00b	32.10b
	SSBM	19.06 b	23.24 a	25.03 b	20.00a	27.00a	47.40a

Different lowercase letters followed by the mean of different treatments in the same column within one variety indicate significant difference at $P < 0.05$ level. TWSM: traditional seedling-raising method, DSBM: dry seedbed nursery raising method, WSBM: wet seedbed raising method, and SSBM: substrate seedbed nursery raising method

Table 2. Effects of different seedling raising methods on leaf and leaf sheath length

Cultivar	Treatment	First leaf sheath length (cm)			First leaf length (cm)			Second leaf length (cm)		
		10 DAS	15 DAS	20 DAS	10 DAS	15 DAS	20 DAS	10 DAS	15 DAS	20 DAS
Xiangyaxiangzhan	TWSM	3.18 b	3.59 b	4.19 a	2.35b	2.43b	2.82b	9.20b	9.47c	10.42c
	DSBM	3.62 a	4.08 a	4.13 a	3.23ab	3.33ab	3.68ab	9.47b	11.23ab	11.64ab
	WSBM	3.22 b	3.36 b	3.58 a	3.06ab	3.22b	3.51ab	10.53ab	10.53bc	11.17bc
	SSBM	3.88 a	3.90 ab	4.16 a	3.92a	4.31a	4.68a	11.77a	12.16a	12.48a
Wufengyou 615	TWSM	3.43 a	3.72 a	4.34 a	2.70a	2.88ab	3.57b	7.43b	9.83ab	10.28b
	DSBM	3.33 ab	3.72 a	4.16 ab	2.66a	2.91ab	3.40b	9.00a	9.18b	10.34b
	WSBM	2.94 b	3.34 a	3.58 b	2.31b	2.43b	2.76b	6.06c	9.00b	9.44c
	SSBM	3.09 ab	3.66 a	4.35 a	2.72a	3.01a	4.43a	8.39ab	10.81a	13.61a

Different lowercase letters follow by the mean of different treatments in the same column within one variety indicate significant difference at $P < 0.05$ level. TWSM: traditional seedling-raising method, DSBM: dry seedbed nursery raising method, WSBM: wet seedbed raising method, and SSBM: substrate seedbed nursery raising method

For *Wufengyou 615*, seedling length was considerably reduced under all seedling establishment methods at all sampling intervals, compared with TWSM. Moreover, SSBM was found statistically at par ($P > 0.05$) with TWSM and/or higher than other seedling establishment methods regarding length of first leaf sheet (at all sampling intervals), first leaf length (at 10 and 15 DAS). The second leaf length were recorded maximum in DSBM at 10 DAS while at 15 and 20 DAS, the second leaf length was highest in SSBM. The dry biomass were also remained maximum in SSBM (higher than other two seedling establishment methods) but statistically similar ($P > 0.05$) with TWSM at 10, 15 and 20 DAS. Overall, the morphological parameters were increased with an increase in seedling age (from 10 to 20 DAS) in both *Xiangyaxiangzhan* and *Wufengyou 615*.

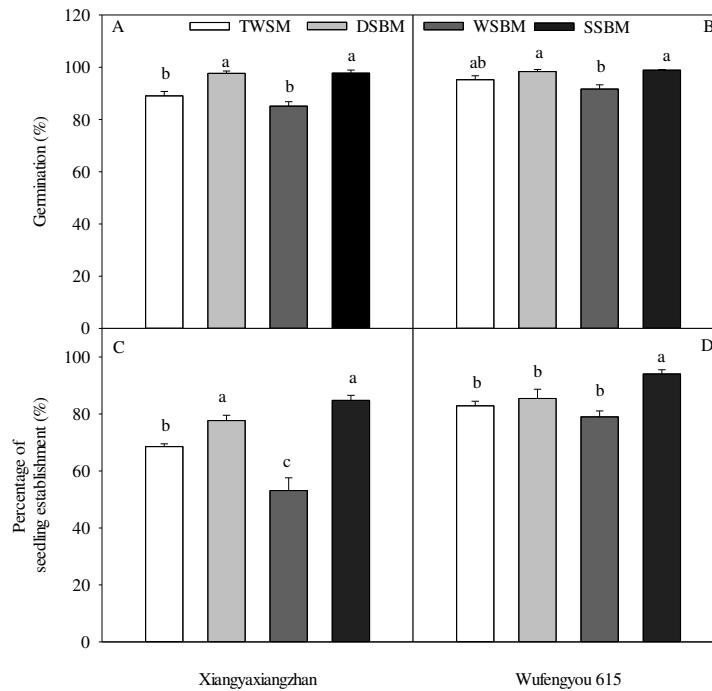


Figure 1. The seed germination rate and percentage of seedling establishment in response to the different seedling raising methods for Xiangyaxiangzhan (A, C) and Wufengyou 615 (B, D). Different lowercase letters followed by the mean of different treatments within one variety indicate significant difference at $P < 0.05$ level. TWSM: traditional seedling-raising method, DSBM: dry seedbed nursery raising method, WSBM: wet seedbed raising method, and SSBM: substrate seedbed nursery raising method

Furthermore, differential responses of both rice cultivars regarding root morphological characters were noted under different seedling establishment methods. For example, root numbers, root length, root surface area and root diameter were higher in modified seedling establishment methods than TWSM whilst SSBM proved better than other methods (Table 3). For Xiangyaxiangzhan 44.41, 36.42, 19.81, 18.75 and 3.37, 13.52, 19.01, 33.33%, and 19.15, 23.24, 13.94, 85.71% higher root numbers, root length, root surface area and root diameter were recorded in SSBM at 10, 15 and 20 DAS, respectively. Similarly, for Wufengyou 615, 42.51, and 18.63, 19.81 % higher root numbers 31.95, 32.26, and 23.25% higher root length, 44.33, 45.99 and 40.83% higher root surface area, 9.68, 112.00 and 65.43% higher root diameter were recorded at 10, 15 and 20 DAS, respectively.

Table 3. Effects of different seedling raising methods on the morphological indexes of root

Cultivar	Treatment	Number of root			Number of the white root			Root length(cm)			Diameter (mm)		
		10 DAS	15 DAS	20 DAS	10 DAS	15 DAS	20 DAS	10 DAS	15 DAS	20 DAS	10 DAS	15 DAS	20 DAS
Xiangyaxiangzhan	TWSM	9.12c	14.83a	14.83b	1.86b	2.84c	2.77c	64.55b	84.00b	157.21b	0.32a	0.33a	0.42b
	DSBM	11.81ab	14.19ab	14.50b	10.37a	11.28b	11.90b	73.79b	93.06ab	178.42ab	0.32a	0.38a	0.47b
	WSBM	11.07bc	12.50b	13.00b	1.93b	2.89c	2.45c	69.59b	92.13ab	178.8ab	0.31a	0.35a	0.62ab
	SSBM	13.17a	15.33a	17.67a	11.89a	13.73a	15.38a	88.06a	95.36a	193.75a	0.38a	0.44a	0.78a

Wufengyou 615	TWSM	12.28b	15.67bc	16.00bc	2.67c	3.31c	3.82b	61.29b	74.05c	184.53c	0.31a	0.25b	0.81c
	DSBM	13.06b	16.33b	17.00b	11.84b	12.44b	15.25a	82.45a	83.95b	207.48ab	0.33a	0.46a	1.16b
	WSBM	13.33b	13.77c	15.00c	2.84c	3.29c	4.33b	71.05ab	91.14ab	203.09bc	0.30a	0.51a	1.16b
	SSBM	17.50a	18.59a	19.17a	13.48a	16.23a	16.27a	80.87a	97.94a	227.43a	0.34a	0.53a	1.34a

Different lowercase letters follow by the mean of different treatments in the same column within one variety indicate significant difference at $P < 0.05$ level. TWSM: traditional seedling-raising method, DSBM: dry seedbed nursery raising method, WSBM: wet seedbed raising method, and SSBM: substrate seedbed nursery raising method

Physiological characters and SPAD values

Seedling raising methods variably affected physiological characters i.e., leaf proline, protein and soluble sugar contents as well as leaf chlorophyll contents (in terms of SPAD) values of both rice cultivars. Leaf proline contents were improved significantly ($P < 0.05$) in rice seedlings raised by SSBM method (except at 15 DAS in *Xiangyaxiangzhan*) than other raising method including TWSM at all sampling stages in both rice cultivars (Fig. 2).

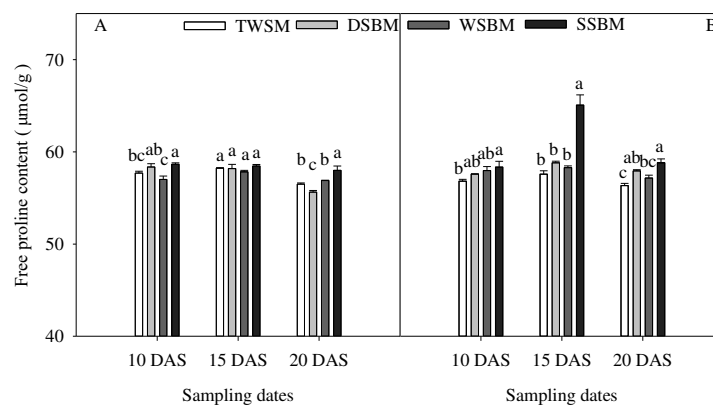


Figure 2. Effects of different seedling raising methods on proline content in leaves of seedlings for two cultivars (A: *Xiangyaxiangzhan*; B: *Wufengyou 615*). Different lowercase letters followed by the mean of different treatments within one variety indicate significant difference at $P < 0.05$ level. TWSM: traditional seedling-raising method, DSBM: dry seedbed nursery raising method, WSBM: wet seedbed raising method, and SSBM: substrate seedbed nursery raising method

The leaf protein contents were remained highest in the seedlings raised by SSBM method which was remained statistically similar ($P > 0.05$) with WSBM and TWSM and minimum were recorded in DSBM at 10 DAS. At 15 DAS, maximum protein contents were recorded in the leaves of *Wufengyou 615* established by DSBM followed by TWSM, SSBM while minimum in WSBM (Fig. 3). Further, at 20 DAS, the leaf proline contents were remained statistically similar ($P > 0.05$) for all seedling establishment methods. The SSBM resulted in higher soluble sugar contents for both rice cultivars at 10 and 15 DAS, however, at 20 DAS; the maximum soluble sugars were recorded in TWSM whilst minimum in WSBM and DSBM in *Xiangyaxiangzhan*

and *Wufengyou 615*, respectively (Fig. 4). Overall, the soluble sugar contents were increased with increase in seedling age from 10 to 20 DAS for *Xiangyaxiangzhan*, and increased from 10 to 15 DAS and then reduced to 20 DAS in *Wufengyou 615*. Furthermore, all seedling raising methods remained statistically similar ($P > 0.05$) for leaf protein contents for *Xiangyaxiangzhan* at all sampling stages, while affected differently at 10 and 15 DAS for *Wufengyou 615* (Fig. 3). Regarding SPAD values, maximum values were recorded at SSBM at all sampling stages and the values of percentage increase were 15.21, 17.56, and 24.12% in *Xiangyaxiangzhan* at 10, 15 and 20 DAS (Fig. 5). For *Wufengyou 615*, highest SPAD values were recorded in the seedlings raised by SSBM method at all sampling stages and the values were significantly higher than other seedling raising methods and TWSM.

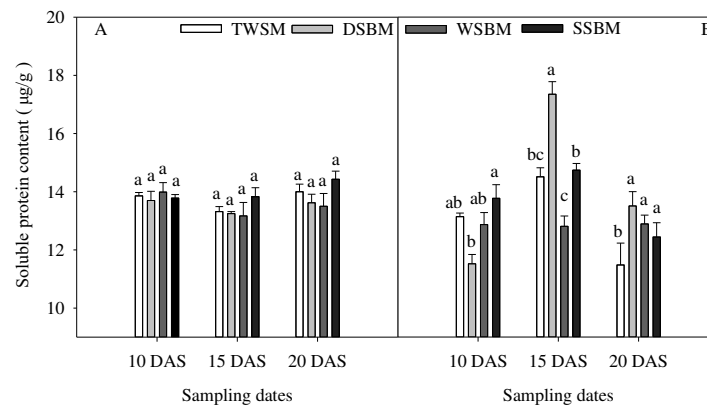


Figure 3. Effects of different seedling raising methods on soluble protein content in leaves of seedlings for two cultivars (A: *Xiangyaxiangzhan*; B: *Wufengyou 615*). Different lowercase letters followed by the mean of different treatments in the same column within one variety indicate significant difference at $P < 0.05$ level. TWSM: traditional seedling-raising method, DSBM: dry seedbed nursery raising method, WSBM: wet seedbed raising method, and SSBM: substrate seedbed nursery raising method

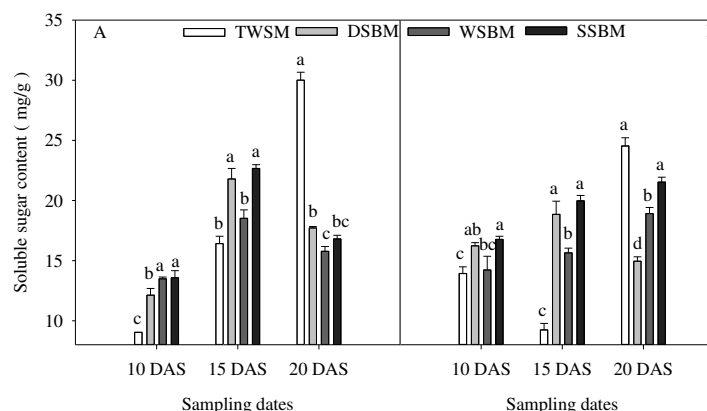


Figure 4. Effects of different seedling raising methods on soluble sugar content of seedling for two cultivars (A: *Xiangyaxiangzhan*; B: *Wufengyou 615*). Different lowercase letters followed by the mean of different treatments within one variety indicate significant difference at $P < 0.05$ level. TWSM: traditional seedling-raising method, DSBM: dry seedbed nursery raising method, WSBM: wet seedbed raising method, and SSBM: substrate seedbed nursery raising method

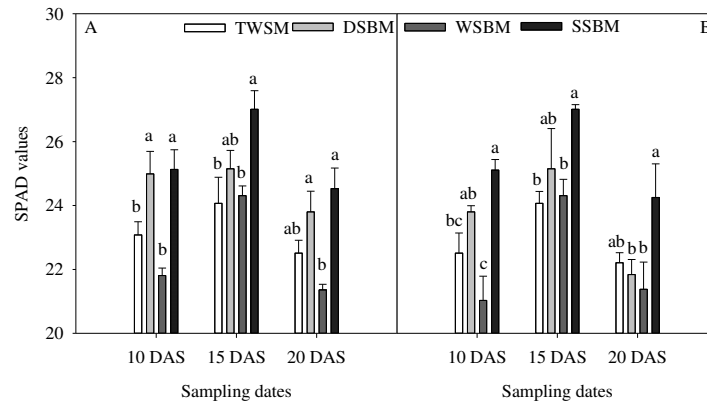


Figure 5. Effects of different seedling raising methods on SPAD values of seeding for two cultivars (A: Xiangyaxiangzhan; B: Wufengyou 615). Different lowercase letters followed by the mean of different treatments within one variety indicate significant difference at $P < 0.05$ level. TWSM: traditional seedling-raising method, DSBM: dry seedbed nursery raising method, WSBM: wet seedbed raising method, and SSBM: substrate seedbed nursery raising method

Correlation analysis

There was no significant correlation between shoot dry weight at 10 DAS and seedling establishment for *Wufengyou 615* (Fig. 6 A). Only *Xiangyaxiangzhan* presented a high positive correlation between shoot dry weight at 10 DAS and seedling establishment ($r = 0.6686$, $P < 0.05$), indicating same effects of different seedling raising methods on the shoot dry weight and seedling establishment for this variety. There was however a high ($P < 0.05$) positive correlation between shoot dry weight at 15 DAS and seedling establishment for both cultivars (Fig. 6 B) where the correlation coefficients (r) are 0.5792 ($P < 0.05$) for *Wufengyou 615* and 0.7849 ($P < 0.01$) for *Xiangyaxiangzhan*. This result suggests that the increased percentage of seedling establishment is closely linked to shoot dry weight. Further, shoot dry weight at 15 DAS was positively associated with leaf sheath length at all sampling dates, but the significance was only recorded for *Wufengyou 615* and 20 DAS in *Xiangyaxiangzhan* (Fig. 6 C, D, E). In addition, the positive associations were also recorded for the percentage of seedling establishment with germination rate, SPAD values at 15 DAS, number of roots and white roots at all dates for the two cultivars (Fig. 7).

Discussion

Rice seed germination and seedling growth is affected by the seed viability and vigour, nature of the growing medium, water application and the various other external factors. These external factors might be promoting or inhibitory and the effects of these factors on the rice nursery and/or seedling growth vary overtime. In this study, highest germination rate and seedling establishment in SSBM may possibly due to fertile growing medium of amorphous nature (non-compacted) with significant amount of organic matter. Our results are in concomitant with the findings of Mishra and Salokhe (2008), who found in reduced soil environments (under aerobic conditions), the coleoptile of the rice seeds were poorly developed

than flooded soil. Further, type of growing media and growing environments determine the quality of the seedlings growing in it for nursery raising (Wilson, 2001; Agbo and Omaliko, 2006), which have significant impacts on its later growth and performance in the field after transplanting (Baiyeri, 2006). Hence, higher seed germination and seedling establishment in SSBM indicates their relations with the type of growing medium.

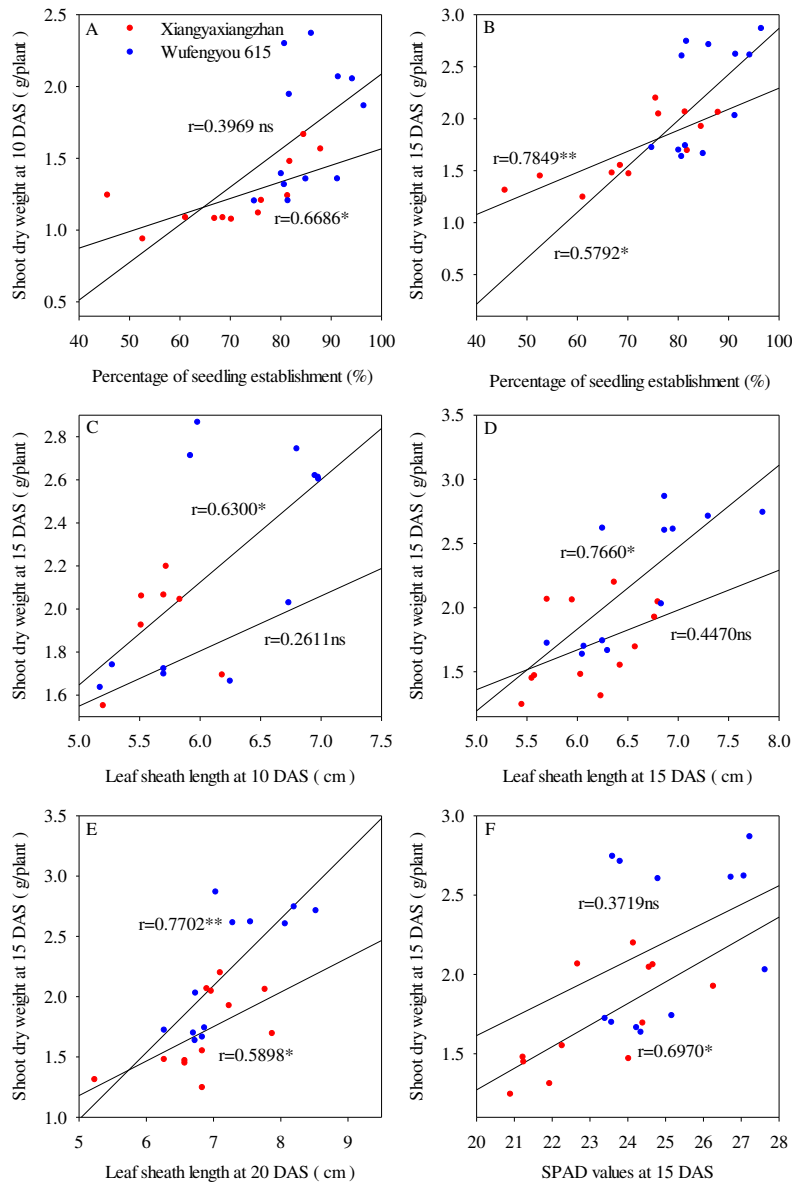


Figure 6. Correlation analyses between (A) shoot dry weight at 10 DAS and percentage of seedling establishment, (B) percentage of seedling establishment and shoot dry weight at 15 DAS, (C) shoot dry weight at 15 DAS and leaf sheath at 10 DAS, (D) shoot dry weight at 15 DAS and leaf sheath length at 15 DAS, (E) shoot dry weight at 15 DAS and leaf sheath length at 20 DAS, (F) shoot dry weight at 15 DAS and SPAD values at 15 DAS for Xiangyaxiangzhan and Wufengyou 615, respectively. ns: non-significant at $P < 0.05$ level; *: significant at $P < 0.05$ levels; **: significant at $P < 0.01$ levels

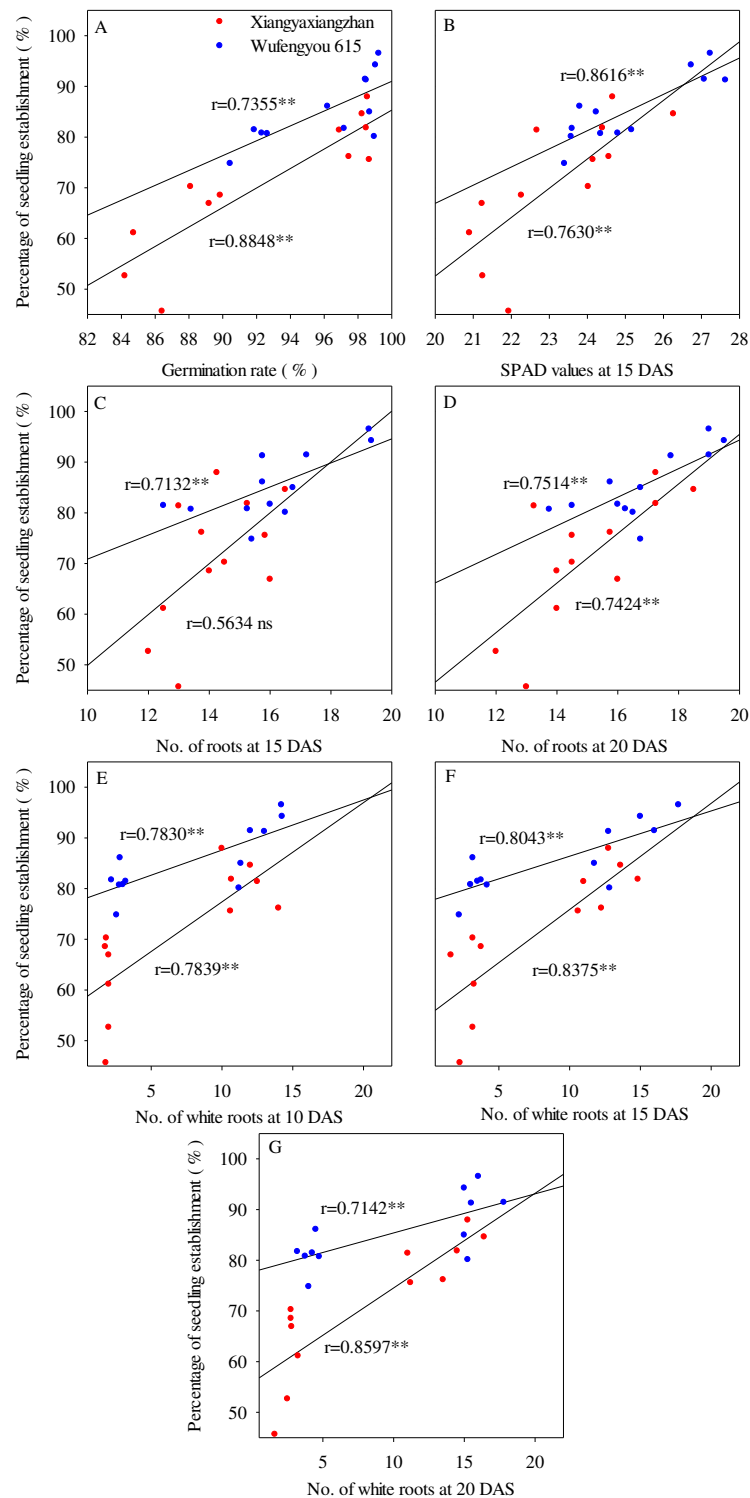


Figure 7. Correlation analyses between (A) percentage of seedling establishment and germination rate, (B) percentage of seedling establishment and SPAD values at 15 DAS, (C) percentage of seedling establishment and the No. of roots at 15 DAS, (D) percentage of seedling establishment and No. of roots at 20 DAS, (E) percentage of seedling establishment and the No. of white roots at 10 DAS, (F) percentage of seedling establishment and the No. of white roots at 15 DAS, and (G) percentage of seedling establishment and the No. of white roots at 20 DAS for Xiangyaxiangzhan and Wufengyou 615, respectively. ns: non-significant at $P < 0.05$ level; **: significant at $P < 0.01$ levels

Different seedling establishment methods substantially affected morphological characters of both rice cultivars. Development of shoot and leaves along with the growth of roots is prerequisite or transitory phase for rice seeds from heterotrophic to autotrophic level (Sasaki, 2004). Our results revealed that nursery management practices and type of nursery growing medium influenced growth and development of rice seedlings. Better root growth with higher root surface area in SSBM mimics in shoot growth with seedling length, leaf length and dry biomass. Ros et al. (2003) argued that rice seedlings establishment and their consequent growth not only related to above-ground morphological characters but also on the root growth and development. Raising healthy and well-established seedlings with well-flourished and healthy root system or simply, the morphogenesis of rice seedlings might have strong associations with nature and type of seedbed and/or growing media, number of seeds per area and soil conditions (Yamauchi and Biswas, 1997). Hence, root elongation under modified nursery raising methods, especially SSBM, showed that use of substrate (organic in nature) of rice seedlings favors root formation and seedling development. Furthermore, Subedi et al. (2013) also stated that nursery management practices considerably influence seedling characteristics of low land rice, whereas Panda et al. (1991) reported that seedlings raised in nutritious seed-bed would result in healthy and vigorous seedlings and performs better in the field conditions.

Moreover, seedling raising methods variably affected physiological characters i.e., leaf proline, protein and soluble sugar contents and leaf chlorophyll contents (in terms of SPAD) values of both rice cultivars. Overall, seedlings grown by substrate method also performed physiologically better than other nursery establishment methods, while all other modified seedling raising methods also proved better than TWSM (normally practiced by the farmers). Previously, Thakur et al. (2010) also reported rice establishment method induced regulations in physiological characters of rice seedlings. Higher chlorophyll contents in the leaves would lead to increased photosynthesis, hence improved seedling growth. Dark green leaves with higher SPAD values were observed in modified seedling establishment methods than TWSM. These findings are in accordance with Harper et al. (2004) and Thakur et al. (2010). Overall, the results of this study depicted that improved seedling establishment methods with better growing medium may induce multiple, positive and significant changes in morphogenesis, phenotype and growth of rice seedlings, however, evoking these changes and responses of rice nursery to the specific seed establishment methods yet need to be studied and their performance in the field conditions as well. Hence, keeping in view this point, field based evaluation of rice nursery managed by different rice nursery establishment methods would thus be focused in our subsequent experiments to draw a most comprehensive inference.

Conclusion

In sum, different seedling raising methods significantly affect rice seedling growth and seedling establishment. Among modified rice seedling raising methods, SSBM proved better for both *Xiangyaxiangzhan* and *Wufengyou 615* rice cultivars. Along with morphological growth, significant improvements were also observed in physiological characteristics of the seedlings of both rice cultivars. Hence, addition of organic manure contained material in the growing media of rice nursery may improve morpho-physiological features of rice seedlings for the purpose of better stand establishment in the paddy fields.

Acknowledgements. Founding provides by Agricultural research project of Guangdong Province (2011AO20202001), and Agricultural standardization project in Guangdong Province (4100F10003) is highly acknowledged.

REFERENCES

- [1] Abid, M., Khan, I., Mahmood, F., Aahraf, U., Imran, M., Anjum, S. A. (2015): Response of hybrid rice to various transplanting dates and nitrogen application rates. – *Philippine Agric Scientist* 98(1): 98-104.
- [2] Agbo, C. U., Omaliko, C. M. (2006): Initiation and growth of shoots of *Gongronema latifolia* benth. Stem cuttings in different rooting media. – *African J Biotechnol* 5(5): 425-428.
- [3] Aminian, M., Nabatchian, F., Vaisi-raygan, A., Torabi, M. (2013): Mechanism of Coomassie Brilliant Blue G-250 binding to cetyltrimethylammonium bromide: an interference with the Bradford assay. – *Anal Biochem* 434(2): 287-291.
- [4] Asai, H., Samson, B. K., Stephan, H. M., Songyikhangsuthor, K., Homma, K., Kiyono, Y., Inoue, Y., Shairaiwa, T., Horie, T. (2009): Biochar amendment techniques for upland rice production in Northern Laos: 1. Soil physical properties, leaf SPAD and grain yield. – *Field Crops Research* 111(1): 81-84.
- [5] Ashraf, U., Kanu, A. S., Mo, Z. W., Hussain, S., Anjum, S. A., Khan, I., Abbas, R. N., Tang, X. R. (2015): Lead toxicity in rice: effects, mechanisms, and mitigation strategies—a mini review. – *Environ Sci Pollut Res* 22(23): 18318-18332.
- [6] Baiyeri, K. P. (2006): Seedling emergence and growth of pawpaw (*Carica papaya*) grown under different coloured shade polyethylene. – *International Agrophysics* 20(2): 77-84.
- [7] Biswas, J. C., Ladha, J. K., Dazzo, F. B., Yanni, Y. G., Rolfe, B. G. (2000): Rhizobial inoculation influences seedling vigor and yield of rice. – *Agronomy Journal* 92(5): 880-886.
- [8] Celik, O., Atak, C. (2012): The effect of salt stress on antioxidative enzymes and proline content of two Turkish tobacco varieties. – *Turkish Journal of Biology* 36: 339-356.
- [9] Ehsanullah, Anjum, S. A., Ashraf, U., Rafiq, H., Tanveer, M., Khan, I. (2014): Effect of sowing dates and weed control methods on weed infestation, growth and yield of direct-seeded rice. – *Philippine Agric Scientist* 97(3): 307-312.
- [10] Harper, A. L., Von Gesjen, S. E., Linford, A. S., Peterson, M. P., Faircloth, R. S., Thissen, M. M., Brusslan, J. A. (2004): Chlorophyllide a oxygenase mRNA and protein levels correlate with the chlorophyll a/b ratio in *Arabidopsis thaliana*. – *Photosynthesis Research* 79(2): 149-159.
- [11] Ivanic, M., Martin, W. (2008): Implications of higher global food prices for poverty in low-income countries. – *Agricultural economics* 39: 405-416.
- [12] Kargbo, M. B., Pan, S. G., Mo, Z. W., Wang, Z. M., Luo, X. W., Tian, H., Hossain, M. F., Ashraf, U., Tang, X. R. (2016): Physiological basis of improved performance of super rice (*Oryza sativa*) to deep placed fertilizer with precision hill-drilling machine. – *Int J Agric Biol* 18: 797-804.
- [13] Karim, M. A., Komdo, T., Ueda, K., Higuchi, H., Nawata, E. (2012): Effect of NaCl treatment on growth and some physiological characteristics of a salt-tolerant soybean genotype AGS 313 bred in Bangladesh. – *Tropical Agri Develop* 56(4): 139-142.
- [14] Li, M. J., Aahraf, U., Tian, H., Mo, Z. W., Pan, S. G., Anjum, S. A., Tang, X. R. (2016): Manganese-induced regulations in growth, yield formation, quality characters, rice aroma and enzyme involved in 2-acetyl-1-pyrroline biosynthesis in fragrant rice. – *Plant Physiol Biochem* 103: 167-175.
- [15] Li, Q. D. (2015): Level of rice planting mechanization over 38%. – *Agriculture Machinery Technology Extension* 1: 12 (in Chinese).

- [16] Li, Y. X., Xing, X. M., Li, G. H. (2014): Study of the Quality and Growth Characteristics in Field About water Volume of Machine Transplanting Seedling. – 2014 National Youth Symposium on the Cultivation and Physiology of Crops: Yangzhou, Jiangsu, China (in Chinese).
- [17] Mishra, A., Salokhe, V. M. (2008): Seedling characteristics and the early growth of transplanted rice under different water regimes. – *Exp Agri* 44(03): 365-383.
- [18] Mo, Z. W., Li, W., Pan, S. G., Fitzgerald, T. L., Xiao, F., Tang, Y. J., Tang, X. R. (2015): Shading during the grain filling period increases 2-acetyl-1-pyrroline content in fragrant rice. – *Rice* 8(9): 1-10.
- [19] Oršanić, M., Drvodelić, D., Ugarković, D. (2011): Ecological and Biological Properties of Holm Oak (*Quercus ilex* L.) on the Island of Rab. – *Croatian J Forest Eng* 32(1): 41-42.
- [20] Panda, M. M., Reddy, M. D., Sharma, As. R. (1991): Yield performance of rainfed lowland rice as affected by nursery fertilization under conditions of intermediate deep water (15–50 cm) and flash floods. – *Plant and Soil* 132(1): 65-71.
- [21] Ros, C., Bell, R. W., White, P. F. (2003): Seedling vigour and the early growth of transplanted rice (*Oryza sativa*). – *Plant and Soil* 252(2): 325-337.
- [22] Ruiz-Sánchez, M., Aroca, R., Muñoz, Y., Polon, R., Ruiz-lozano, J. M. (2010): The arbuscular mycorrhizal symbiosis enhances the photosynthetic efficiency and the ant oxidative response of rice plants subjected to drought stress. – *Journal of Plant Physiology* 167(11): 862-869.
- [23] Sasaki, R. (2004): Characteristics and seedling establishment of rice nursling seedlings. – *Japan Agricultural Research Quarterly* 38(1): 7-13.
- [24] Subedi, R. (2013): Nursery management influences yield and yield attributes of rainfed lowland rice. – *Journal of Sustainable Society* 2(4): 86-91.
- [25] Thakur, A. K., Uphoff, N., Antony, E. (2010): An assessment of physiological effects of system of rice intensification (SRI) practices compared with recommended rice cultivation practices in India. – *Experimental Agriculture* 46(01): 77-98.
- [26] Wilson, S. B, Stoffella, P. J, Graetz, D. A. (2001): Use of compost as a media amendment for containerized production of two subtropical perennials. – *Journal of Environmental Horticulture* 19(1): 37-42.
- [27] Yamauchi, M., Biswas, J. K. (1997): Rice cultivar difference in seedling establishment in flooded soil. – *Plant and Soil* 189(1): 145-153.
- [28] Yang, M. J., Yang, L., Li, Q. D. (2003): Agricultural mechanization system of rice production of Japan and proposal for China. – *Transactions of the CSAE* 19(5): 77-82.
- [29] Yao, F., Xu, Y., Lin, E., Yokozawa, M., Zhang, J. (2007): Assessing the impacts of climate change on rice yields in the main rice areas of China. – *Climatic Change* 80(3-4): 395-409.
- [30] Zhang, H. C, Gong, J. L. (2014): Research status and development discussion on high-yielding agronomy of mechanized planting rice in China. – *Scientia Agricultura Sinica* 47(7): 1273-1289 (in Chinese).
- [31] Zhu, D. F, Chen, H. Z, Xu, Y. C. (2007): Countermeasure and perspective of mechanization of rice planting in China. – *Northern Rice* 05: 13-18 (in Chinese).

WEED INFESTATION AND BIODIVERSITY OF WINTER WHEAT UNDER THE EFFECT OF LONG-TERM CROP ROTATION

NIKOLIĆ, LJ.^{1*} – ŠEREMEŠIĆ, S.¹ – MILOŠEV, D.¹ – ĐALOVIĆ, I.² – LATKOVIĆ, D.¹

¹*Faculty of Agriculture, University of Novi Sad
Trg D. Obradovića 8, Novi Sad, Serbia
(phone: +381-21-485-3500; fax: +381-21-459-761)*

²*Institute of Field and Vegetable Crops
Maksima Gorkog 30, Novi Sad, Serbia
(phone: +381-21-489-8100; fax: +381-21-662-1212)*

**Corresponding author
e-mail: ljiljana.nikolic@polj.uns.ac.rs
(phone: +381-21-485-3453; fax: +381-21-454-442)*

(Received 6th Oct 2017; accepted 12th Feb 2018)

Abstract. The paper presents the study of the floristic composition of weeds and weed infestation in winter wheat in long-term crop rotations at the experimental station near Novi Sad (Serbia). During the study period, a total of 48 weed species were determined, out of which 33 were determined in each study year. In two study years, there were 18 common species, while 15 species determined in 1991 were not found 19 years later. On the other hand, the study in 2010 recorded 15 new species that had not been previously found. The greatest floristic diversity (20 species) was found on fertilized four-year rotation in 1991 and unfertilized two-year rotation in 2010. The lowest diversity was recorded in 2010 on fertilized four-year rotation (9 species) and fertilized three-year rotation (10 species). The highest weed infestation was recorded in 1991 on unfertilized two-year rotation (2963 plants m⁻²) and unfertilized three-year rotation (2126 plants m⁻²), which is statistically significant compared to other variants. The lowest average weed infestation was observed in 2010 on fertilized three-year rotation (40 plants m⁻²) and fertilized four-year rotation (53 plants m⁻²). Long-term crop rotations have a significant effect on the floristic composition and structure of weeds in winter wheat.

Keywords: *weed, invasive plants, winter wheat, crop rotation*

Introduction

Weeds, as highly adaptable plants, impede the implementation of planned cultivation practices in agricultural production. Therefore, finding adequate measures of weed control is a complex problem that requires a holistic approach (Avola et al., 2008). Weed control is a continuous process which includes a number of interrelated activities, the duration of which exceeds a single vegetation period. Preceding crops and the timing of tillage significantly affect the presence of weeds. In addition to common cultivation practices and applying agricultural chemicals, crop rotation has an important role in agricultural production because alternation of different crops has a beneficial effect on reducing weeds and establishing balance within an agroecosystem (Barberi et al., 1997; Suarez et al., 2001; Derksen et al., 2002; Anderson, 2005; Wozniak and Soroka, 2015). Balance in agroecosystems and in biodiversity directly affects sustainability of their structures and function (Oljača et al., 2014), which is one of the most important goals of contemporary agriculture.

In order to provide the necessary “biological minimum” for achieving high and stable yields in crop production, it is very important to ensure proper alternation of

crops, taking into account self-tolerance and mutual tolerance of crops. Crop rotation is therefore given a great importance, also because it reduces the occurrence of plant diseases, pests and weeds (Molnar, 2003).

Due to significant effects of the year of growing (temporal effect) and the cultivation practice, it is very difficult to determine the cumulative contribution of crop rotation in weed control. Also, since in multi-year crop rotations phenological phases of cultivated crops and weeds overlap, these rotations reduce weed seedbank in the soil, which is particularly reflected in weed reduction in a subsequent period (Andersson and Milberg, 1998; Teasdale et al., 2004).

In a long-term period, properly set crop rotations may have positive environmental impact on biodiversity conservation of the weed flora, as agricultural land is a typical habitat for certain segetal weeds, the survival of which is becoming more endangered, due to intensive agricultural practices (Hulina, 2005; Šilc, 2005). In order to identify the changes in weed flora, it is essential to study long-term crop rotations. Therefore, this research was based on the data obtained from the experiments established 70-40 years ago, in which we could determine the cumulative effects of crop rotation. The aim of this paper was to analyze the floristic composition and the intensity of weed infestation in winter wheat grown in different crop rotation and fertilization treatments over a period of nineteen years. The obtained results can be as a good basis for monitoring biodiversity of weeds in different crop rotations, but can also indicate the most favorable crop rotation treatment for weed reduction.

Materials and methods

Weed survey and data collection

In order to study long-term effects of different crop rotation and fertilization treatments on weed infestation of winter wheat crops, floristic surveys were conducted in 1991 and 2010 in field trials “Plodoredi” of the Institute of Field and Vegetable Crops in Novi Sad (Serbia) at the experimental station Rimski Šančevi (45.19°N, 19.50°E).

The weed flora was studied on the following variants of the experiment: unfertilized two-year and three-year rotations (MW and MWSo), established in 1946/47, two-year, three-year and four-year rotations with application of mineral fertilizers (MW-N, MWSo-N and MWSoSb-N), established in 1969/70, four-year rotation with application of mineral fertilizers (MFW), established in 1950/51, and monoculture of wheat with applied mineral fertilizers (W-N), established in 1969/70.

The study was conducted on the Chernozem soil, which belongs to automorphic soil types, class A-C (humus-accumulative soils, the subtype of chernozem on loess and loess-like sediments, the carbonate chernozem variety, medium depth) (Škorić et al., 1986). The basic chemical soil properties are shown in *Table 1*. The method used for the analysis of organic matter content in soil samples is Tyrin’s titrimetric method, in which a soil sample is oxidised with 0.2M potassium dichromate with sulphuric acid and heated to the boiling point for 5 minutes DM 8/1-3-017. Soil pH reaction was determined in a suspension with H₂O and 1 M KCl (ratio of 1:2.5, w/v), using a Metrel MA3657 pH-meter, while the content of CaCO₃ was determined volumetrically, by Scheibler’s calcimeter; (Soil Survey Staff, 1993). Total nitrogen contents were determined with a CHNS analyzer (Elementar Vario EL, Germany). Determination of readily available phosphorus was performed by AL method (extraction with ammonium

lactate) with spectrophotometric determination. Determination of readily available potassium was performed by AL method (extraction with ammonium lactate) followed by flame photometric determination.

The meteorological conditions, i.e. medium monthly temperatures and precipitations in two investigated years (1990/91 and 2009/10), according to meteorological station Rimski Šančevi, are shown in *Figure 1*.

The intensity of weed infestation was determined by the quantitative method of squares, i.e. by counting the number of weeds per 1 m².

Weed sampling was done in relation to the phenological development of winter wheat according to decimal BBCH (Biologische Bundesanstalt, Bundessortenamt und Chemische Industrie) scale. The plants in all treatments of crop rotation were counted three times during the winter wheat growing season at beginnings of the development stages BBCH 30, BBCH 53, BBCH 85, with 3 replications.

Weed species were determined according to Josifović (1970-1986) and Tutin et al. (1964-1980). The data were statistically accessed using the statistical software Statistica 12.

Table 1. Basic chemical soil properties on the experimental field (mean values± SD)

Year	pH		CaCO ₃ %	Organic matter %	Total N %	Al-P ₂ O ₅ mg/100g	Al-K ₂ O mg/100g
	in KCl	in H ₂ O					
1991	7.42±0.06	7.91±0.07	3.5±1.91	2.52±0.28	0.17±0.02	61.01±46.18	38.83±15.98
2010	7.52±0.10	8.1±0.12	5.64±4.23	2.7±0.38	0.2±0.02	65.93±61.50	37.56±12.98

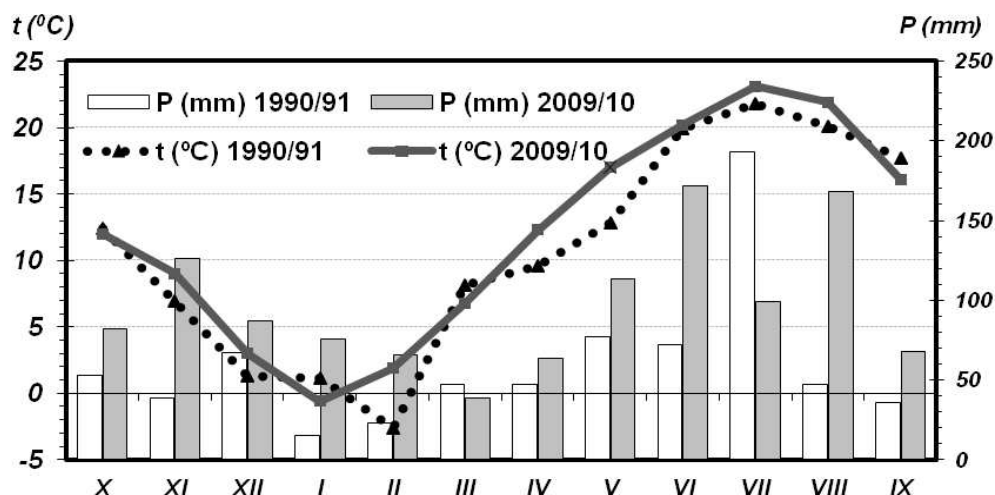


Figure 1. Medium monthly temperatures and precipitations in two production years (1990/91 and 2009/10)

Treatments in the experiment

The study included the following treatments: fertilized monoculture (100% winter wheat) – W-N, fertilized two-year crop rotation (50% maize and 50% winter wheat) – MW-N, fertilized three-year crop rotation (33.33% maize, 33.33% soybean and 33.33% winter wheat) – MWS_o-N, fertilized four-year crop rotation (25% maize, 50% winter

wheat and 25% field peas) – MFW-N, fertilized four-year crop rotation (33.33% maize, 33.33% winter wheat, 16.16% soybean and 16.16% sugar beet) – MWSoSb-N, unfertilized two-year crop rotation (50% maize and 50% winter wheat) – MW and unfertilized three-year rotation (33.33% maize, 33.33% soybean and 33.33% winter wheat) – MWSo. The fertilized treatments included mineral nitrogen (N) fertilizers at 100 kg ha⁻¹ rate for winter wheat (50 kg ha⁻¹ in autumn and 50 kg ha⁻¹ in spring). Phosphorus (P) and potassium (K) fertilization was based on soil analyses and was applied in autumn. Unfertilized two-year rotation (MW) and three-year rotation (MWSo) had not received any fertilization since 1946-1947, while crop residue incorporation started in 1986-1987. Cultivation of winter wheat was based on conventional tillage including moldboard plowing and seed bed preparation with a Kongskilde germinator. The sowing took place in October at a seeding rate of 250 kg ha⁻¹. Weed control in winter wheat started in 2000 with active matter 2.4D and iodosulfuron-methyl-sodium + amidosulfuron. Control of *Sorghum halepense* (L.) Pers. and other grass weeds was carried out by glyphosate each year in August after winter wheat harvest.

Results

Composition of weed species

The floristic composition of weeds and the intensity of weed infestation in winter wheat in different crop rotation treatments on the experimental field of the Institute of Field and Vegetable Crops (Serbia) in 1991 and 2010 are presented in *Table 2*.

In the floristic composition of the cropping systems in two study years there were a total of 48 plant species, out of which 33 species were determined in each study year. In two study years, 18 common species were identified, while 15 species were present only in the first study year and were not found 19 years later (marked with * in the table). On the other hand, the study in 2010 recorded 15 new species that had not been previously found (marked with ** in the table) (*Table 2*).

In all crop rotation treatments in 1991, the following weed species were constantly present: *Polygonum convolvulus*, *Convolvulus arvensis*, *Lamium purpureum*, *Polygonum aviculare*, *Polygonum lapathifolium* and *Stellaria media*. On the other hand, in the more recent study conducted in 2010, which included all wheat-based cropping systems, only three weed species were determined: *Polygonum convolvulus*, *Consolida regalis* and *Veronica hederifolia*. The species which was continuously present in both study years in all crop rotation treatments is *Polygonum convolvulus* (*Table 2*).

This paper analyzes floristic composition of weeds in different winter wheat systems of crop rotation and fertilization. The greatest floristic diversity (20 species) was found on fertilized four-year crop rotation (MWSoSb-N) in 1991 and unfertilized two-year rotation (MW) in 2010. Although floristic diversity in these two crop rotations was higher, it had no significant impact on the intensity of weed infestation in these crop rotations, which was 102 and 125 plants m⁻², respectively. The floristic diversity was the lowest in 2010 on fertilized four-year rotation - MWSoSb-N (9 species), on which the intensity of weed infestation was also low, and on fertilized three-year rotation – MWSo-N (10 species), which had the lowest intensity of weed infestation (*Table 2*; *Fig. 2* and *3*). Accordingly, it can be concluded that in all experiment wheat-based treatments, with the exception of unfertilized two-year rotation, there was a trend of a moderate decrease of floristic diversity over the period of 19 years (*Table 2*; *Fig. 2*).

Table 2. Average infestation in wheat in different treatments of crop rotation 1991 and 2010 (no. ind. m⁻²)

EPPO Code	Plant species	Crop rotation													
		W-N		MW-N		MW		MWSO-N		MWSO		MFW-N		MWSOSb-N	
		1991	2010	1991	2010	1991	2010	1991	2010	1991	2010	1991	2010	1991	2010
ADOAE	<i>Adonis aestivalis</i> L.**		0.44												0.44
AGRRE	<i>Agropyrum repens</i> (L.) Beauv.*			1.67											
AMBEL	<i>Ambrosia artemisiifolia</i> L.						29.55				77.77	0.11	2.66	0.08	
ANGRV	<i>Anagallis arvensis</i> L.			0.67		809.33	0.44			708				0.33	
ANGCO	<i>Anagallis femina</i> Mill.**						0.44								
POLCO	<i>Polygonum convolvulus</i> (L.) Dum.	40	59.11	98.67	25.66	310.33	2.22	33	5.33	109	2.22	42.66	15	30.42	6.21
CAPBP	<i>Capsella bursa-pastoris</i> (L.) Med.		31.11	1	0.44		0.44			18		0.11	1.77	0.08	
CUCLA	<i>Caucalis daucoides</i> L.*	1		1											
CENCY•	<i>Centaurea cyanus</i> L.		1.77		0.88							1.66			
CHEAL	<i>Chenopodium album</i> L.	10.33	0.44	9.33			0.44	50.33	4.88			13.11	10.21	26.58	9.33
CHEHY	<i>Chenopodium hybridum</i> L.**		0.44		1.33				1.77				3.1		0.44
CIRAR	<i>Cirsium arvense</i> (L.) Scop.	0.33					2.22							0.08	
CNSRE•	<i>Consolida regalis</i> S.F. Gray.		110.64	3	45.77	66.67	3.10		15.99		0.44		11.55		8.44
CONAR	<i>Convolvulus arvensis</i> L.	8.67		4.33		24		1	0.44	45.33		8.89		8.08	
DATST	<i>Datura stramonium</i> L.**								0.88						2.66
EQUAR	<i>Equisetum arvense</i> L.*			0.33		45.33						0.22			
ERICA	<i>Erigeron canadensis</i> L.*					274.67				108				2.25	
EPHCY	<i>Euphorbia cyparissias</i> L.*			0.33											
EPHHE	<i>Euphorbia helioscopia</i> L.**						11.55				12.44				
FUMOF•	<i>Fumaria officinalis</i> L.	16		0.33	0.44					6.66		4.78		0.08	
GAETE	<i>Galeopsis tetrahit</i> L.		0.11		0.44	376				213.33					
GALAP	<i>Galium aparine</i> L.	8.33	13.77	3.67	17.33		4					0.11		0.17	
HELTU	<i>Helianthus tuberosus</i> L.**								4.88				3.11		

LAMAM•	<i>Lamium amplexicaule</i> L.**		0.44		1.33							2.66		
LAMPU	<i>Lamium purpureum</i> L.*	4.67		0.33		20		0.33		188.66		9		0.33
LHTTU•	<i>Lathyrus tuberosus</i> L.**				1.33		1.33				1.77			
LITAR	<i>Lithospermum arvense</i> (L.) Vahl.	1.33	0.88	1.67	0.88	210.67							0.44	0.33
MEDLU	<i>Medicago lupulina</i> L.**						1.33							
OXAST	<i>Oxalis stricta</i> L.**						7.1							
PAPRH•	<i>Papaver rhoeas</i> L.**		14.88		1.33									
POAAN	<i>Poa annua</i> L.*									2.66				
POLAV	<i>Polygonum aviculare</i> L.	13.33		8.67		28.67	2.66	1.33		58	5.33	0.11		12.58 0.88
POLLA	<i>Polygonum lapathifolium</i> L.*	7.75		13.67		19.67		1.33		19		23.78		8.33
RANAR•	<i>Ranunculus arvensis</i> L.**						0.64							
RHIAG	<i>Rhinanthus major</i> Ehrh.*									122.66				
SAMEB	<i>Sambucus ebulus</i> L.*							2.66						0.33
SETVI	<i>Setaria viridis</i> (L.) Beauv.*					148				124				
SINAR	<i>Sinapis arvensis</i> L.		0.44			5.33	44			16	72.74		9.77	
SOLNI	<i>Solanum nigrum</i> L.**				0.88		1.77		0.44		1.33			
SONOL	<i>Sonchus oleraceus</i> (L.) Gou.*					5.33								
SORHA	<i>Sorghum halepense</i> (L.) Pers.**						10.22		3.55		7.55			0.44
STAAN	<i>Stachys annua</i> L.**										1.33			
STEME	<i>Stellaria media</i> (L.) Vill.	30		33.67		320	0.88	5.33		156.66	15.55	85.44		8.42
TAROF	<i>Taraxacum officinale</i> Weber.*	3.33				32		17.66		130.66				2.83
TRFRE	<i>Trifolium repens</i> L.*					85.33				8				0.42
VERHE	<i>Veronica hederifolia</i> L.	0.33	256		87.55		0.44		1.77		0.44	3.11	40.88	23.99
VICVI	<i>Vicia vilosa</i> Roth.*					178.67		0.33		91.33		0.66		0.08
VIOAR•	<i>Viola arvensis</i> Murr.	14		1.67	0.44	2.67		1.66						0.33
Total number of plant species		15	14	18	15	19	20	12	10	18	12	15	11	20 9
Average number of ind. m⁻²		159	491	184	186	2963	125	115	40	2126	199	194	101	102 53

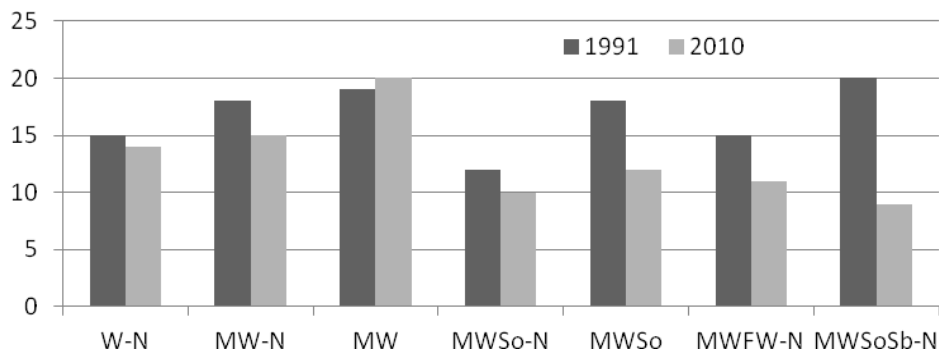


Figure 2. Number of weed species in different treatments of crop rotation

Weed infestation in winter wheat

With regard to the intensity of infestation, extremely high weed infestation was recorded in 1991 on unfertilized two-year and three-year rotations – 2963 and 2126 plants m^{-2} , respectively. The difference between weed infestation in these two treatments and other crop rotation treatments is statistically significant or highly significant (*Tables 2 and 3; Fig. 3*). Such high levels of weed infestation on unfertilized rotations could be accounted for by a high number of weeds in the seedling stage in the very first stages of wheat vegetative growth, by the preceding crop (maize, soybean), which was favorable for weed infestation, and by the absence of fertilization, which in these treatments provided for better competitiveness of weeds compared to winter wheat. The lowest average weed infestation in winter wheat crops was recorded in the second study year, 19 later, on fertilized three-year rotation and four-year rotation (MWSOsb-N), on which there were 40 and 53 plants m^{-2} , respectively (*Table 2; Fig. 3*).

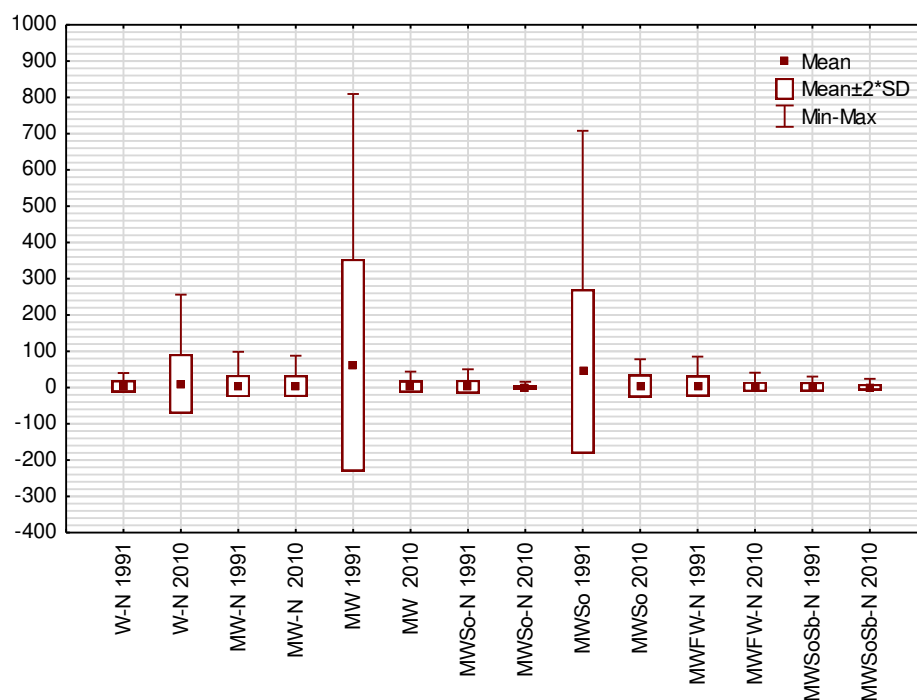


Figure 3. Weed infestation in winter wheat in different treatments of crop rotation (no. ind. m^{-2})

Trends in changes of weed infestation

Table 4 shows the changes in the average weed infestation observed over time between certain crop rotation systems. It can be observed that over the period of 19 years in winter wheat monoculture there was a prominent trend of increasing weed infestation by even 68%, while on fertilized two-year rotation there was a relatively unchanged level of weed infestation with only a minor increase of 1%, which could be accounted for by the cumulative effect of crop rotation on the number of weeds. However, in other crop rotation treatments there was a prominent trend of reducing weed infestation after the period of 19 years.

Weed species significant for biodiversity

This study determined the presence of a number of invasive species, including *Ambrosia artemisiifolia*, *Helianthus tuberosus*, *Datura stramonium*, *Erigeron canadensis* and *Sorghum halepense* (Table 2). These species were more prominent only in the treatments of unfertilized two-year and three-year crop rotations, which could be affected also by the preceding crop, among which these weeds usually proliferate. *Ambrosia artemisiifolia* is of particular interest as it is invasive both at the local and global level (DAISIE – Delivering Alien Invasive Species Inventories for Europe, EPPO – European and Mediterranean Plant Protection Organization, GISD – Global Invasive Species Database), while *Helianthus tuberosus* is invasive at the European level (DAISIE, EPPO). The other three species (*D. stramonium*, *E. canadensis* and *S. halepense*) are on the list of invasive weeds in Serbia (Lazarevic et al., 2012). It is encouraging that the invasive species in the studied crop rotations were not too numerous and did not contribute substantially to the overall weed infestation of winter wheat in the study period, with the exception of *E. canadensis* in 1991 on unfertilized two-year rotation (274.67 plants m⁻²) and unfertilized three-year rotation (108 plants m⁻²) and *A. artemisiifolia* (77.77 plants m⁻²) only in 2010 on unfertilized three-year rotation.

With regard to biodiversity conservation, on the other hand, it is necessary to stress the presence of threatened weeds according to Hulina (2005) (Table 2, marked with •). From the category of endangered weed species, there was *F. officinalis*, which in the studied crop rotation treatments decreased in number in the second study year by 80%. From the category of vulnerable weed species, there were seven species, three of which (*C. cyanus*, *C. regalis* and *V. arvensis*) were present in both study periods, while four species (*L. amplexicaule*, *L. tuberosus*, *P. rhoeas* and *R. arvensis*) appeared only in 2010. The presence of *V. arvensis* from the category of vulnerable species also declined by 80% over the period of 19 years. The treatment of fertilized two-year rotation proved to be favorable for survival of the endangered species *F. officinalis* and the vulnerable species *V. arvensis*.

Discussion

The composition of weed flora in a certain crop is determined by the existing environmental conditions as well as applied cultural practices. This study was conducted in the winter wheat to determine the presence of different weed species in the same treatments of crop rotation for two study periods. Based on the comparative analysis of the soil properties from 1991 and 2010 (Table 1), the most significant

change was recorded for the organic matter content (Seremesic et al., 2017). This change can be accounted for by introduction of more productive varieties and hybrids and by plowing in of plant residues. The cumulative effect of crop rotation had an impact on the observed soil properties, which indirectly had an impact also on the floristic composition and structure of the weeds. Despite certain differences between the studied years in terms of meteorological indicators (*Fig. 1*) and application of herbicides in the entire studied area (from 2000), the presence of different species, i.e. disappearance of certain species and appearance of new ones could be attributed to the effects of crop rotation on weed flora diversity, which is consistent with the results of previous research (Andersson and Milberg, 1998; Suarez et al., 2001; Derksen et al., 2002; Moss et al., 2004; Anderson, 2005; Kovačević et al., 2007; De Mol et al., 2015).

In the first study year, seven species were constantly present in all treatments of crop rotation (*Polygonum convolvulus*, *Convolvulus arvensis*, *Lamium purpureum*, *Polygonum aviculare*, *Polygonum lapathifolium* and *Stellaria media*), while 19 years later only three weed species were constantly present in all crop rotations (*Polygonum convolvulus*, *Consolida regalis* and *Veronica hederifolia*). The only constantly present species in both study years in all crop rotations was *Polygonum convolvulus* (*Table 2*). These weed species were found to have the greatest impact on the increasing intensity of weed infestation in certain experiment treatments. All these species, except for *Convolvulus arvensis* which belongs to geophytes, are therophytes, the predominance of which in cropland indicates instability of the weed community because of applied agricultural practices (Kovačević, 2007; Milošev et al., 2009; Nikolić et al., 2012).

Biodiversity of an ecosystem is a reflection of the existing conditions in it and its balance. Although contemporary crop production leads to uniformity of agroecosystems at all levels, it should be noted that different crop production systems do not equally affect the level of biodiversity. There is an increasing trend of using crop production systems that favor increasing biodiversity as a necessary prerequisite in raising productivity and protecting agroecosystems, while special role in these systems is given to crop rotation, through which biodiversity is increased over time (Oljača, 2013). The system of crop rotation generates special environmental conditions that do not aim to reduce weed flora diversity, but rather to prevent excessive occurrence of certain weed species that could cause considerable yield loss to a particular crop (Barberi et al., 1997; Wozniak and Soroka, 2015). Accordingly, this paper analyzes also the floristic composition of weeds in winter wheat cultivated in different systems of crop rotation and fertilization. The greatest floristic diversity (20 species) was found on fertilized four-year crop rotation (MWSoSb-N) in 1991 and unfertilized two-year rotation (MW) in 2010 (*Table 2*). Although these two crop rotation treatments had higher floristic diversity, it had no significant impact on the intensity of weed infestation of these crop rotations, which was 102 and 125 plants m⁻², respectively, according to the results of previous research (Nikolić et al., 2016).

It can be concluded that in our agroecological conditions, three-year crop rotation with the use mineral fertilizers proved to be the most beneficial for reduction of weeds. Milošev et al. (2014) identified three-year wheat-based rotation as the most favorable also in terms of the optimal use of production conditions and the lowest negative impact on the environment. The analysis of weed infestation in two study years indicates that the differences were statistically highly significant ($p = 0.00^{**}$), which also demonstrates the positive effects of long-term crop rotation on weed reduction in winter wheat.

Table 3. The significance of differences in the number of weed individuals per m² between different treatments of crop rotation

	W-N		MW-N		MW		MWSO-N		MWSO		MFW-N		MWSOSb-N		
	1991	2010	1991	2010	1991	2010	1991	2010	1991	2010	1991	2010	1991	2010	
W-N	1991				0.0068**			0.0413*	0.0138*						
	2010				0.0207*										
MW-N	1991				0.0075**				0.0156*						
	2010				0.0076**				0.0157*						
MW	1991	0.0068**	0.0207*	0.0075**	0.0076**		0.0062**	0.0061**	0.0048**		0.0079**	0.0077**	0.0058**	0.0058**	0.005**
	2010					0.0062**				0.0123*					
MWSO-N	1991					0.0061**				0.0119*					
	2010	0.0413*				0.0048**				0.009**					
MWSO	1991	0.0138*		0.0156*	0.0157*		0.0123*	0.0119*	0.009**		0.0165*	0.016*	0.0113*	0.0113*	0.0094**
	2010					0.0165**									
MFW	1991					0.0077**				0.016*					
	2010					0.0058**				0.0113*					
MWSOSb-N	1991					0.0058**				0.0113*					
	2010					0.0050**				0.0094**					

Legend: Values marked with asterisks are significantly at $p < 0.05$ (*) and $p < 0.01$ (**) levels, empty – non significant

Table 4. Review of weed infestation of wheat and trend of changes

Crop rotation	Year		Trend of changes (no. ind. m ⁻²)	Trend of changes (%)
	1991	2010		
	Average (no. ind. m ⁻²)	Average (no. ind. m ⁻²)		
W-N	159	491	+ 332	+ 68
MW-N	184	186	+ 2	+ 1
MW	2963	125	- 2838	- 96
MWSO-N	115	40	- 75	- 65
MWSO	2126	199	- 1927	- 91
MFW	194	101	- 93	- 48
MWSOSb-N	102	53	- 49	- 48

In all other crop rotations (except for the monoculture and fertilized two-year rotation) during the 19-year period there was a strong trend of weed reduction, which is in accordance with a number of other studies (Andersson and Milberg, 1998; Smith and Gross, 2007). The results show that the intensity of weed infestation was reduced by 48% on fertilized four-year rotation (MWSoSb-N) and fertilized four-year rotation (MFW –N), by 65% on fertilized three-year rotation and even by 91% on unfertilized three-year rotation and 96% on unfertilized two-year rotation (*Table 4*).

The presence of invasive species in a certain area indicates the onset of secondary succession influenced by various factors, including ecological factors (climatic, edaphic, etc.), applied cultivation practices, the type of crops, the preceding crop, the historical factor, etc. (Czárán and Bartha, 1990; Pickett et al., 2001). Studying the interaction between individual factors and occurrence of invasive species is very complex and it is not included in this research, which is only to determine the presence of these species. In the contemporary floristic research of agroecosystems, it is of great importance to monitor occurrence and expansion of invasive plant species (Ziska et al., 2011; Chikuruwo et al., 2017). Although invasive plant species were not present in large numbers in the second study period, it is necessary to monitor their presence and abundance because of potential threats to biodiversity and functioning of ecosystems in case of their unexpected spreading (Chytrý et al., 2005; Pink and Pal, 2009; Kenis et al., 2012).

Due to the application of total herbicides after the winter wheat harvest, most of the invasive weeds were successfully controlled, and it can be assumed that the presence of maize and soyabean in the unfertilized treatments had greater impact than the presence of winter wheat on the number of weeds. In drier years the number of invasive weeds can be expected to increase. The study years in this research, on the other hand, were considered as normal production years in terms of temperature and precipitation. When assessing the occurrence of certain weed species, however, the priority should be given to environmental factors (geographical location, climate and soil type), then to crop management factors, and only then to the factor of “the year” (Hallgren et al., 1999; De Mol et al., 2015).

On the other hand, besides monitoring the presence of invasive weed species because of their importance for biodiversity conservation of agroecosystems according to the action plan (The 2001 Biodiversity Action Plan for Agriculture /COM/2001/0162), it is important also to determine the presence of the weed species (*Table 2*, marked with •) that, according to Hulina (2005), are already categorized as endangered or vulnerable in the neighboring region of Croatia, according to the categories of IUCN Red List (Walter and Giller, 1998).

Although one endangered species (*F. officinalis*) and one vulnerable species (*V. arvensis*) showed a decreasing trend, after the 19-year period no species from these categories disappeared. Moreover, after the period of 19 years four new species from the category of vulnerable species appeared (*L. amplexicaule*, *L. tuberosus*, *P. rhoeas* and *R. arvensis*). It can be concluded that the wheat crop grown in crop rotations provides for the survival of these weed species, which in very similar neighboring agroecosystems have already been identified as endangered and vulnerable, as survival of these species is the most certain in conditions of the agroecosystems.

In the long term, diversity of crops in crop rotations without external chemical inputs results in changes of soil properties (Van Eerd et al., 2013) that do not lead to increasing of weeds, nor to the development of weed communities that are difficult to control (Smith and Gross, 2007). Use of crop rotation is also justified in terms of environmental

protection and sustainability of agroecosystems, since it leads to reduced use of chemical substances. Intensive application of pesticides has resulted in high levels of pesticide residues in the soil and groundwater and has reduced beneficial insects and fauna. People have become concerned about pesticide residues entering food chains and affecting human health. Short rotations, especially monocultures, have increased soil erosion and reduced biological diversity (Molnar, 2003).

Conclusions

Based on the results obtained in this study carried out over the period of 19 years, it can be concluded that cultivation of winter wheat in long-term crop rotations has a significant effect on the floristic composition and structure of weeds, without causing significant development of invasive plant species (*Table 2*). Also, there was a marked trend of decreasing wheat infestation in crop rotations (*Table 4*), which is of particular importance from the aspect of sustainable and environmentally friendly agriculture. A good indicator of this trend is the treatment of wheat monoculture, where despite the application of herbicides, after nineteen years there was a marked trend of increasing weed infestation compared to other treatments of crop rotation in the same agroecological conditions.

In the continuation of the research, it is planned to further analyze the ecological indices of weed species taking into account the meteorological and soil conditions of the studied area, in order to provide a more comprehensive understanding of the trend of succession changes of the weed flora in the conditions of long-term crop rotation.

Acknowledgement. We are grateful to the Institute of Field and Vegetable Crops in Novi Sad for allowing us to work in their fields “Plodoredi”.

REFERENCES

- [1] Anderson, L. R. (2005): A multi-tactic approach to manage weed population dynamics in crop rotation. – *Agronomy Journal* 97: 1579-1583.
- [2] Andersson, N. T., Milberg, P. (1998): Weed flora and the relative importance of site, crop, crop rotation, and nitrogen. – *Weed Science* 46(1): 30-38.
- [3] Avola, G., Tuttobene, R., Gresta, F., Abbate, V. (2008): Weed control strategies for grain legumes. – *Agronomy of Sustainable Development* 28(3): 389-395.
- [4] Barberi, P., Silvestri, N., Bonari, E. (1997): Weed communities of winter wheat as influenced by input level and rotation. – *Weed Research* 37: 301-313.
- [5] Chikuruwo, C., Masocha, M., Murwira, A., Ndaimani, H. (2017): Predicting the suitable habitat of the invasive *Xanthium strumarium* in southeastern Zimbabwe. – *Applied Ecology and Environmental Research* 15(1): 17-32.
- [6] Chytrý, M., Pyšek, P., Tichý, L., Knollová, I., Danihelka, J. (2005): Invasions by alien plants in the Czech Republic, a quantitative assessment across habitats. – *Preslia* 77: 339-354.
- [7] Czárán, T., Bartha, S. (1990): The Effect of Spatial Pattern on Community Dynamics: A Comparison of Simulated and Field Data. – In: Grabherr, G., Mucina, L., Dale, M. B., Ter Braak, C. J. F. (eds.) *Progress in Theoretical Vegetation Science. Advances in Vegetation Science*, Vol. 11, pp. 229-239. Springer, Dordrecht.
- [8] De Mol, F., Von Redwitz, C., Geroeitt, B. (2015): Weed species composition of maize fields in Germany is influenced by site and crop sequence. – *Weed Research* 55: 574-585.

- [9] Derksen, A. D., Andersen, L. R., Blackshaw, E. R., Maxwell, B. (2002): Weed dynamics and management strategies for cropping systems in the Northern Great Plains. – *Agronomy Journal* 94: 174-185.
- [10] Hallgren, E., Palmer, M., Milberg, P. (1999): Data diving with cross-validation: an investigation of broad-scale gradients in Swedish weed communities. – *Journal of Ecology* 87: 1037-1051.
- [11] Hulina, N. (2005): List of threatened weeds in continental part of Croatia and their possible conservation. – *Agriculturae Conspectus Scientificus* 70(2): 37-42.
- [12] Josifović, M. (ed.) (1970-1986): *Flora Republike Srbije, I-X*. – SANU, Beograd.
- [13] Kenis, M., Bache, S., Baker, R. H. A., Branquart, E., Brunel, S., Holt, J. et al. (2012): New protocols to assess the environmental impact of pests in the EPPO decision-support scheme for pest risk analysis. – *Bulletin OEPP/EPPO* 42(1): 21-27.
- [14] Kovačević, D., Dolijanović, Ž., Milić, V. (2007): The influence of the soil treatment system on wheat's weed /Uticaj sistema obrade zemljišta na korovsku sinuziju ozime pšenice. – *Journal of Scientific Agricultural Research* 68(243): 85-94 (in Serbian with English abstract).
- [15] Lazarević, P., Stojanović, V., Jelić, I., Perić, R., Krsteski, B., Ajtić, R. et al. (2012): Preliminary list of invasive species in the Republic of Serbia/Preliminarni spisak invazivnih vrsta u republici Srbiji sa opštim merama kontrole i suzbijanja kao potpora budućim zakonskim aktima. – *Protection of nature* 62(1): 5-31 (in Serbian with English abstract).
- [16] Milošev, D., Šeremešić, S., Nikolić, Lj., Knežević, A., Đalović, I., Vuga-Janjatov, V. (2009): Floristic composition and structure of weed flora in long-term winter wheat cropping systems. – *Herbologia* 10(1): 31-41.
- [17] Milošev, D., Šeremešić, S., Đalović, I., Pejić, B., Ćirić, V. (2014): Assessing the agro-ecosystem performance in a long-term winter wheat cropping. – *Contemporary Agriculture* 63(4-5): 494-500.
- [18] Molnar, I. (2003): Cropping systems in Eastern Europe, past, present and future. – *Journal of Crop Production* 9: 623-647.
- [19] Moss, R. S., Storkey, J., Cussans, W. J., Perryman, A. M. S., Hewitt, V. M. (2004): Symposium the broadbalk long-term experiment at Rothamsted, what has it told us about weeds? – *Weed Science* 52: 864-873.
- [20] Nikolić, Lj., Milošev, D., Šeremešić, S., Latković, D., Červenski, J. (2012): Diversity of weed flora in conventional and organic agriculture. – *Acta Herbologica* 21(1): 13-20 (in Serbian with English abstract).
- [21] Nikolić, Lj., Šeremešić, S., Milošev, D., Đalović, I. (2016): Weed Infestation of Wheat and Maize in Crop Rotations/Zakorovljenost pšenice i kukuruza u uslovima plodoreda. Paper presented at the 10th Weed Science Congress, 21-23 September, Vrdnik, Serbia. – In: Janjić, V. (ed.) *Proceedings of 10th Weed Science Congress* (pp. 50). Serbian Weed Science Society, Beograd, Serbia (in Serbian with English abstract).
- [22] Oljača, S., Kovačević, D., Dolijanović, Ž., Milić, V. (2014): Organic Agriculture in Terms of Sustainable Development of Serbia. – Paper presented at the Fifth International Scientific Agricultural Symposium „Agrosym 2014, 6-9 October, Jahorina, Bosnia and Herzegovina (in Serbian with English abstract).
- [23] Pickett, S. T. A., Cadenasso, M. L., Bartha, S. (2001): Implications from the Buell-Small Succession Study for vegetation restoration. – *Applied Vegetation Science* 4(1): 41-52.
- [24] Pinke, G., Pál, R. (2009): Floristic composition and conservation value of the stubble-field weed community, dominated by *Stachys annua* in western Hungary. – *Biologia* 64(2): 279-291.
- [25] Seremesic, S., Ćirić, V., Milošev, D., Vasin, J., Djalovic, I. (2017): Changes in soil carbon stock under the wheat-based cropping systems at Vojvodina province of Serbia. – *Archives of Agronomy and Soil Science* 63(3): 388-402.

- [26] Šilc, U. (2005): Weed vegetation of the northern part of Ljubljansko polje. – *Hacquetia* 4(2): 161-171.
- [27] Škorić, A., Filipovski, G., Ćirić, M. (1985): Klasifikacija zemljišta Jugoslavije. Akademija nauke i umetnosti BiH. – Posebna izdanja, knjiga LXXVIII, Sarajevo, SR Jugoslavija.
- [28] Smith, R. G., Gross, L. K. (2007): Assembly of weed communities along a crop diversity gradient. – *Journal of Applied Ecology* 44(5): 1046-1056.
- [29] Suarez, A. S., De la Fuente, B. E., Ghersa, M. C., Leon, J. C. R. (2001): Weed community as an indicator of summer crop yield and site quality. – *Agronomy Journal* 93: 524-530.
- [30] Teasdale, R. J., Mangum, W. R., Radhakrishnan, J., Cavigelli, A. M. (2004): Weed seedbank dynamics in three organic farming crop rotations. – *Agronomy Journal* 96: 1429-1435.
- [31] Tutin, G., Heywood, V. H., Burges, N. A., Valentine, D. H., Walters, S. M., Webb, D. A. (eds.) (1964-1980): *Flora Europea*, 1-5. – University Press, Cambridge.
- [32] Van Eerd, L. L., Congreves, A. K., Hayes, A., Verhallen, A., Hooker, C. D. (2014): Long-term tillage and crop rotation effects on soil quality, organic carbon, and total nitrogen. – *Canadian Journal of Soil Science* 94(3): 303-315.
- [33] Ziska, H. L., Blumenthal, M. D., Runion, G. B., Hunt, Jr. R., Diaz-Soltero, H. (2011): Invasive species and climate change: an agronomic perspective. – *Climate Change* 105: 13-42.
- [34] Woźniak, A., Soroka, M. (2015): Structure of weed communities occurring in crop rotation and monoculture of cereals. – *International Journal of Plant Production* 9(3): 487-506.
- [35] Walter, K. S., Giller, H. J. (eds.) (1998. 1997): *IUCN Red List of Threatened Plants*. Compiled by World Conservation Monitoring Centre. IUCN – The Conservation Union, Gland, Switzerland and Cambridge, UK.

MODELING OF NITROGEN TRANSPORT IN VARIABLY SATURATED SOILS

KARRA, R. – MASLOUHI, A.* – BAMBA, Y. O.

*Laboratory for Natural Resources and Environment, Department of Physics, Faculty of Sciences, Ibn Tofail University
B.P. 242, 14000 Kenitra, Morocco
(phone: +212-5-3732-9200; fax: +212-5-3737-4052)*

**Corresponding author
e-mail: maslouhi_a@yahoo.com*

(Received 12th Oct 2017; accepted 12th Feb 2018)

Abstract. Nitrate contamination in irrigation groundwater is a serious worldwide problem. The aim of this paper is to focus on the mathematical modeling of the water flow and the reactive solute in porous media. In this approach, a mathematical model based on a single flow equation is developed; which can be used for both unsaturated and saturated zones regarded as a single continuum. The model is based on the finite element method using the *Freefem++* code and generates a solution for two-dimensional water flow and solute transport equations. The self-adaptive meshing capability of the code has confirmed that the capillary fringe is a zone with complicated physical processes. The nitrogen transformations in the soil were simplified using parameters that can be calculated from easily measured chemical soil properties or obtained from the literature. This study shows the interest of modeling various chemical, physical and biological processes that influence the fate of nitrogen in the agricultural soils for evaluating the groundwater contamination by nitrates. The nitrogen simulation shows that in the saturated zone, the flow is mostly loaded by the nitrate and the ammonium nitrogen has an insignificant effect on the solute transport in the aquifer. The validity of the model is proved by a good-fit between computed and observed data measurements in the laboratory-scale physical model. In general, the numerical model constitutes a rapid tool to predict with an excellent precision the water flow and the reactive solute evolution in groundwater.

Keywords: *FreeFem++, mesh adaptation, nitrate, pollution, porous media, simulation, water*

Introduction

Groundwater contamination by nitrates in Mnasra aquifer has generated widespread interest in the last few years (Saâdi et al., 1999; Ibnoussina et al., 2006), due to concerns raised by the increasing level of degradation of water quality and the related toxicological consequences of nitrates for human health (Bryan, 2011). With the intensification and modernization of agriculture, the amounts of nitrogen fertilizers are constantly increasing (Manzoni and Porporato, 2009; Shekofteh et al., 2013). Contamination of groundwater and surface water by excess nitrates resulting from increasing urbanization and intensified agricultural activities is a global concern (Deb et al., 2016). The Gharb water table, whose concentrations exceed the 200 mg/l in many wells, is beyond the allowed limit of 50 mg/l established by the World Health Organization (Saâdi and Maslouhi, 2003). Indeed, the massive use of nitrogen fertilizers has been implicated in the release of greenhouse gases into the atmosphere. In France (large agriculture producer), the average values of agricultural nitrogen balances show an excess of 1.5 to 2 million tons of nitrogen.

If nitrogen migrates to bodies of water or lakes, it can cause algal blooms, oxygen deprivation for many species of fish in aquatic systems. In Italy, agriculture accounts for

68% of the nitrogen supply in the Po river. Lake Victoria has experienced increased eutrophication over the last 50 years, at which high concentrations of nitrate is considered a major contributing factor (Bryan, 2011). Wastewater infiltration basins in the Reedy Creek Improvement District present a significant risk of aquifer contamination due to the nitrate concentration of the water applied to the basin.

Excessive concentrations of nitrate in drinking water cause methaemoglobinemia, a blood disorder that mainly affects infants under 6 months of age (“blue baby” syndrome). Consumption of nitrate-polluted water has also been implicated circumstantially in the increased risk of gastrointestinal cancer in adults. The potential impact of contamination by fertilizers and pesticides on water supply led to the development of models to simulate the soil and plant system.

Saâdi and Maslouhi (2003) developed a mechanistic model to predict the water runoff and transformations of nitrogen in the unsaturated soil in the agricultural area of Mnasra. Therefore, the knowledge of the hydraulic soil properties is essential for the assessment of the hydrological processes (Bagarello and Iovino, 2012; Moret-Fernández et al., 2015).

Water flow and nitrogen transport in a porous unsaturated-saturated medium constitute a difficult phenomena to study (i.e. Nonlinear Differential Equations). Conventional models often use the coupled unsaturated-saturated flow process. Groundwater flow in the saturated zone is described by a horizontal flow, whereas the flow in the unsaturated zone is considered vertical. The unknown, *a priori*, position of the water table makes the coupled problem difficult to solve (Maslouhi et al., 2009). Study of water flow and solute transport in the unsaturated and saturated zones has often been carried out by using distinct mathematical models, which are applied separately in each zone (Dupuy et al., 1997; Lindström et al., 2010). This kind of approach is based on a technique of artificial coupling, connecting the two zones, which often generates numerical disturbances at the unsaturated-saturated interface (i.e. the water table).

Diaw et al. (2001) performed a study of one-dimensional water flow through the unsaturated-saturated zone. However, Vachaud et al. (1973) first investigated the two-dimensional steady state flow through the unsaturated-saturated zones. In this approach, a mathematical model based on a single flow equation was developed. It can be used for both unsaturated and saturated zones, regarded as a single continuum. The purpose of this study is to calibrate and verify the developed model with the measurements obtained from soil tank experiment; and to simulate the water flow and nitrogen transport in the porous medium. This numerical simulation studies the unsteady-state pressure distributions and nitrogen concentrations for variably-saturated soil.

The transport of mineral substances like nitrate nitrogen $NO_3^- - N$ and ammonia nitrogen $NH_4^+ - N$, is described by the convection-dispersion equation (Saâdi et al., 1999; Filipović et al., 2014). Several mathematical models with different degree of nonlinearity and different level of complexity describe the process of mineralization that occurs at the soil surface, affected by physical and biological interaction (Maggi et al., 2008; Manzoni and Porporato, 2009). The process of mineralization and nitrification in the unsaturated zone are described here by a simplified first order kinetics (Butturini et al., 2000; Saâdi and Maslouhi, 2003). The Hénin-Dupuis model allows the description of the process of mineralization. It is a mono-compartmental model with the benefit of using a simple formula (ordinary differential equation). Its parameters are affected by climatic conditions, soil characteristics and management practices (Ibnoussina et al.,

2006). The adsorption of ammonium NH_4^+ ions in the soil is described by a linear isothermal equilibrium and the contribution of fertilizer is described by a condition of mass flow at the surface (Bechtold et al., 2006; Deb et al., 2016). In this case, the used models have the advantage of using a reduced number of parameters for the model calibration. Furthermore, the parameters are calculated from easily measured chemical soil properties or obtained from the literature. Riparian areas can reduce nitrogen inputs to aquatic systems through plant uptake and microbial denitrification. For example, denitrification “hot spots” can be found along root canals where moisture and organic matter content are high or in anaerobic locations. In a field case, the nitrate concentration would not be well simulated by the model in riparian zones or areas with high denitrification (Maggi et al., 2008). Indeed, this process can lead to a real transformation of nitrogen to gaseous forms (up to 5%). In laboratory experiment, denitrification was assumed negligible.

The model also presents the flexibility to integrate other physico-chemical processes. Numerical modeling is based on a finite element computer *Freefem++* code (Hecht, 2012). This code was adapted to the equations used in this study, namely: the Richards equation to study the water flow in the unsaturated-saturated domain and the transport equation, of the advection-diffusion type for the study of nitrogen transfer in two compartments of the porous media. The advantage of using this code is the self-adaptive mesh generation; it improves the accuracy of the automatically refined domain (Belhamadia et al., 2014). Therefore, the information in the vicinity of the singular areas is more accurate (infiltration area, free surface, capillary fringe) while saving on computation and simulation time. The memory and space gain is significant when the simulations are realized on a large scale domain (Hecht, 2012). *Freefem++* also takes advantage of the multi-core processor structure and parallel computing. The numerical model was validated using experimental data performed at the scale model, and allowed to predict with high accuracy the position of the free surface of the water table and the advancement of a reactive solute in the two compartments. The results of this study can be helpful to prevent the nitrogen pollution, ensure the safety of water table supply, the sustainability of water resources and an auxiliary instrument for decision making in water management.

Materials and methods

Study domain

In the laboratory experiments, a slab of soil with a length of 600 cm, 200 cm of depth and 30 cm of width was used. A rainfall simulator was designed as a source of flow in an infiltration band of 100 cm. To impose a constant hydraulic head in the outlet, a reservoir was attached to the slab. In the xOz coordinate system, the Ox axis correspond to the surface of the ground, the Oz axis being vertically downward and the origin O being in the infiltration band center. The problem is assumed as a plane one with a symmetry about the Oz axis; the problems of transfers can be studied only in the half of the system. Assuming a horizontal water table established on a thickness e above an impermeable bottom at a depth of e_0 . A constant infiltration flow of q_0 is applied to the surface of the ground. Furthermore, the reservoir is assumed between two parallel trenches of the same length as the slab, where the piezometric level is maintained at a constant depth e_0 . A Mariotte bottle system was used to keep a constant inlet flux and

an electric pump to maintain water table level in the outlet. *Figure 1* shows the geometry of the studied system. The flow domain boundaries are:

- A portion of the upper horizontal surface (ground surface) on which is applied a constant flux $q_0 = 15 \text{ cm/h}$, causing infiltration. The infiltration band will simulate a canal of irrigation or an artificial catchment basin. The value of q_0 is chosen to be smaller than the saturated hydraulic conductivity of this soil.
- A nozzle rainfall simulator is used. It is delimited by a steel rectangle of 5 cm height. The water table level in the outlet is imposed to H_0 .

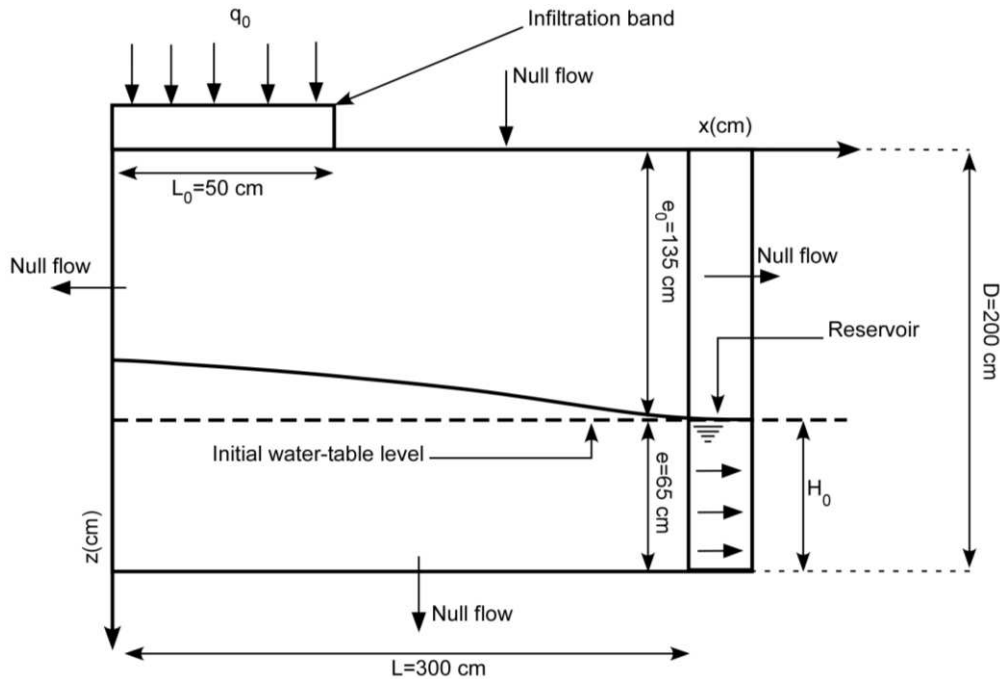


Figure 1. Schematic representation of the flow domain

The sample soil was taken from a field in the Mnasra zone. The soil used is a fine sand of fairly regular grain-size distribution. Soil hydraulic characteristics and properties are listed in *Table 1*. In order to avoid nitrogen contamination, the chosen field has not been fertilized or manured for at least 12 months.

Two approaches can be used for in situ hydrodynamic soil characterization. The direct method based on experimental measures combined with infiltration models or the inverse method that identifies the hydrodynamic parameters from measurements. The inverse method is not covered by this study. In the direct method, several experimental techniques are required to determine the parameters. As part of this experiment, a disk infiltrometer is used to measure the soil hydraulic properties near saturation. Its advantage lies in its in situ use, its rapid implementation and the numerous studies on it (Moret-Fernández et al., 2015; Rezaei et al., 2016). It allows a potential range between [0-200 mm], the potential range, although reduced, integrates the possible flow configurations between the relative water content and saturated water content. It gives a specific advantage compared to other devices for soil hydraulic conductivity measurements, such as the Guelph Permeameter and Compact Constant Head Permeameter *CCHP* (Cheng et al., 2011; Reynolds and Jeffrey, 2012).

Hydrodynamic characterization

Several empirical models are used to relate the water content, pressure head and hydraulic conductivity; their parameters specify different types of soils. The most common of these forms are the Brooks–Corey (1964) and Genuchten (1980), although many more have been presented in the literature over the past two decades.

The Mualem (1976) and Genuchten (1980) model is widely used to describe the relationship between the pressure head and water content, as shown in *Equation 1*:

$$\frac{\theta(h) - \theta_r}{\theta_s - \theta_r} = \left[1 + (\alpha h)^n \right]^{-m} \quad (\text{Eq.1})$$

θ is the volumetric water content (L^3L^{-3}), h is the pressure head (L), θ_s is the saturation water content scale parameter, which is called the volumetric water content at natural saturation (L^3L^{-3}). θ_r is the residual water content (L^3L^{-3}). $\alpha(L^{-1})$, $n(-)$, $m(-)$ are shape parameters related to the pore size distribution. They are subjected to the constraint of $m = 1 - k_m/n$, where k_m is an integer value initially introduced by van Genuchten to calculate closed-form analytical expressions for the hydraulic conductivity function when substituted in the predictive conductivity model of Mualem.

The Brooks-Corey hydraulic model is also widely accepted, the unsaturated hydraulic conductivity function is based on *Equation 2*:

$$K(h) = K_s \left(\frac{\theta - \theta_r}{\theta_s - \theta_r} \right)^\eta \quad \text{for } h < h_e \quad (\text{Eq.2})$$

with: $\eta = 2/\lambda + 3$.

K is the hydraulic conductivity (LT^{-1}), h_e is the air entry pressure and λ is a positive pore size distribution index, being small for clay soils and large for sandy soils.

According to Bagarello and Iovino (2012), only the combination of van Genuchten water retention equation (*Eq. 1*) $h(\theta)$, based on Burdine theory (i.e. $k_m = 2$) together with the Brooks and Corey conductivity equation (*Eq. 2*) stays valid for a large type of soils encountered in practice without becoming inconsistent with the general water infiltration theory. This is due to the rather limiting constraint which exists for the shape parameter m when using Mualem theory (i.e. $k_m = 1$): $0.15 \leq m \leq 10$.

Moreover, to get the curves $K(h)$ and $\theta(h)$, the models of van Genuchten and Brooks-Corey are adjusted on the points of experimental measures. To minimize the error between the simulated and observed values, the adjustment is performed according to the Levenberg-Marquardt algorithm (Rezaei et al., 2016). The Levenberg-Marquardt method is a standard technique for solving nonlinear least squares problems. *Equation 3* is the appropriate form of the objective function Φ :

$$\min \Phi(h, (\theta, K)) = \frac{\sum_{i=1}^r [\theta_{\text{mes}}(h_i) - \theta_{\text{fit}}(h_i)]^2 + \sum_{i=1}^r [\ln(K_{\text{mes}}(h_i)) - \ln(K_{\text{fit}}(h_i))]^2}{r, \sigma_s^2} \quad (\text{Eq.3})$$

where θ_{mes} and θ_{fit} are the measured and predicted water content, K_{mes} and K_{fit} are the measured and predicted hydraulic conductivity, σ_s^2 are variations of the measured data and r is the number of observations.

Thus, by undertaking several tests at different pressure heads, the $h(\theta)$ and $K(h)$ curves were obtained (Fig. 2).

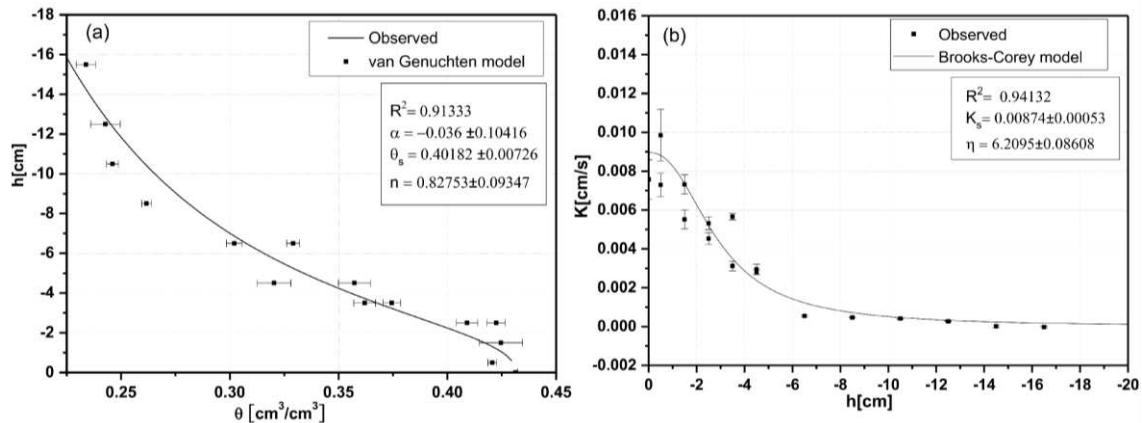


Figure 2. Suction and hydraulic conductivity curves for the studied soil

The combination of van Genuchten and Brooks-Corey models give excellent agreement between measured and calculated (fitted) values with $R^2 = 0.94$ for $K(h)$ and $R^2 = 0.91$ for $h(\theta)$.

Water flow in unsaturated-saturated porous media

The 2D equation of flow in the case of the unsaturated zone is obtained by combining the generalized Darcy equation, which expresses the law of flows proportionality, to the mass balance equation. The unsaturated and saturated zones can be considered as a single continuum domain. Equation 4 is used in the two zones has the form of the Richards equation:

$$C(h) \frac{\partial h}{\partial t} = \frac{\partial}{\partial x} \left(K(h) \frac{\partial h}{\partial x} \right) + \frac{\partial}{\partial z} \left(K(h) \left(\frac{\partial h}{\partial z} - 1 \right) \right) - S \quad (\text{Eq.4})$$

with $C(h) = \partial\theta/\partial h$ is the specific moisture capacity (L^{-1}), t is the time (T), S is a sink/source term (T^{-1}) and z is the depth (L).

-In the case of the vadose zone:

The sink term does not apply, so the classical Richards equation for the unsaturated zone becomes (Eq. 5):

$$C(h) \frac{\partial h}{\partial t} = \nabla (K(h) \nabla (h - z)) \quad (\text{Eq.5})$$

-In the case of the saturated zone:

$C = S_s$ is the specific storativity of a porous medium and $K(h) = K_s$ is the saturated hydraulic conductivity (LT^{-1}).

Thus, the diffusivity equation characterizing the transient state flow in a saturated zone as described in *Equation 6*:

$$S \frac{\partial h}{\partial t} = \frac{\partial^2 h}{\partial x^2} + \frac{\partial^2 h}{\partial z^2} \quad (\text{Eq.6})$$

with: $S = \frac{S_s}{K_s}$ the total storativity of the porous medium.

At the soil surface, *Equation 5* can be subject either to a flux boundary condition (Neumann, *Eq. 7*) or a pressure head boundary condition (Dirichlet, *Eq. 8*):

$$q_1 = q(0, t) = -K(h) \left(\frac{\partial h}{\partial z} \Big|_{z \rightarrow 0^+} - 1 \right) \quad (\text{Eq.7})$$

$$h(0, t) = h_1 \quad (\text{Eq.8})$$

where: q_1 and h_1 are respectively the Darcian water flux or water flux density (LT^{-1}) and the pressure head at the soil surface. At natural field conditions, they can have either positive or negative values. q_1 is given by *Equation 9*:

$$q_1 = \frac{P}{\Delta t} \quad (\text{Eq.9})$$

where: P is rainfall and/or irrigation (L), during the time increment Δt (T).

Nitrogen transport equation

The transport of mineral nitrogen in unsaturated soil is described by the 2D convection-dispersion equation in its most general form (Filipović et al., 2014) as shown in *Equation 10*:

$$\begin{aligned} \frac{\partial(\rho_d S_i)}{\partial t} + \frac{\partial(\theta C_i)}{\partial t} = \frac{\partial}{\partial x} \left(\theta D_{ap} \frac{\partial C_i}{\partial x} \right) - \frac{\partial(Q_x C_i)}{\partial x} \\ + \frac{\partial}{\partial z} \left(\theta D_{ap} \frac{\partial C_i}{\partial z} \right) - \frac{\partial(Q_z C_i)}{\partial z} + \sum_j T_{i,j} (C_i, S_i) \end{aligned} \quad (\text{Eq.10})$$

where $C_i(ML^{-3})$ and $S_i(MM^{-1})$ are the concentrations of the element (i) associated with liquid and solid phases respectively, ρ_d is the density of the dry soil (ML^{-3}), $T_{i,j}$ is the rate of loss or creation of the element (i)($ML^{-3}T^{-1}$), the index (j) is associated to the various reactions which the element (i) in the soil can undergo, D_{ap} is the apparent diffusion-dispersion coefficient of the element (i)(L^2T^{-1}) with $D_{ap} = \xi_i Q / \theta + D_{0,i}$ where ξ_i and $D_{0,i}$ are respectively the dispersivity (L) and molecular diffusion (L^2T^{-1}) of the element (i) in the soil. Q_x and Q_z are the Darcy flow (MT^{-1}) to x and z directions respectively. Knowledge of water content, and water flux density is obtained from solutions of the Richards equation. When dealing with nitrogen transport and

transformations in an unsaturated soil, the chemical species (*i*) are the nitrate nitrogen NO_3^- and ammonium nitrogen NH_4^+ (Hanson et al., 2006).

Nitrification and soil organic nitrogen mineralization processes are modeled using first-order rate kinetics as described by Saâdi et al. (1999) and Maggi et al. (2008). The latter process is described by the Hénin-Dupuis's simple model in *Equation 11* (Saâdi and Maslouhi, 2003):

$$\frac{dN_{org}}{dt} = -k_{min} (N_{org} - N_{\infty}) \quad (\text{Eq.11})$$

where N_{org} is the instantaneous soil organic nitrogen (ML^{-2}), N_{∞} is the organic nitrogen supplied to the ploughed layer such as roots and straw. k_{min} is the first order rate conditional constant (T^{-1}) which is specific to the climate and crops developed in each region.

The nitrification process is modeled as stated by several authors (e.g. Butturini et al., 2000; Shekofteh et al., 2013) in *Equation 12*:

$$\frac{dC_{NO_3^-}}{dt} = k_{nit} C_{NH_4^+} \quad (\text{Eq.12})$$

where k_{nit} is the first order rate conditional constant (T^{-1}), which can easily be found in literature (Ibnoussina et al., 2006).

The ammonium nitrogen NH_4^+ adsorption by negatively charged clay particles and organic colloids in the soil is described by a linear equilibrium isotherm *Equation 13* (Deb et al., 2016):

$$S_{NH_4^+} = K_d C_{NH_4^+} \quad (\text{Eq.13})$$

where: K_d is the partitioning coefficient between soil solid and liquid phases (L^3M^{-1}). A good approximation for the K_d is gotten, using the cation exchange capacity (*CEC*) as the unique input parameter (Lindström et al., 2010). The parameters k_{min} , K_d , k_{nit} , λ are taken, as described in *Table 1*.

Equation of nitrogen transport in the water table

The water table is characterized by saturated water content θ_s and a saturated hydraulic conductivity K_s . The NO_3^- ions will behave as tracers and will be easily led to the water table. The strong absorption and rapid nitrification of ions NH_4^+ to ions NO_3^- make their probability to reach the water table insignificant. Given all these conditions, the nitrate nitrogen transport equation in the water table is given by *Equation 14*:

$$\begin{aligned} (\theta_s + \rho_d K_d) \frac{\partial (C_{NO_3^-})}{\partial t} = & \frac{\partial}{\partial x} \left(\theta_s D_{ap} \frac{\partial C_{NO_3^-}}{\partial x} \right) - \frac{\partial (Q_x C_{NO_3^-})}{\partial x} \\ & + \frac{\partial}{\partial z} \left(\theta_s D_{ap} \frac{\partial C_{NO_3^-}}{\partial z} \right) - \frac{\partial (Q_z C_{NO_3^-})}{\partial z} + K_{nit} \theta_s C_{NH_4^+} \end{aligned} \quad (\text{Eq.14})$$

where: $C_{NO_3^-}$ and $C_{NH_4^+}$ are the nitrate nitrogen and ammonium nitrogen concentrations.

At the lower boundary condition ($x = X_{\max}$) and ($z = Z_{\max}$) no boundary flux condition was used, which is equivalent to Equation 15:

$$\frac{\partial C_i}{\partial x} \Big|_x = 0 \quad \text{and} \quad \frac{\partial C_i}{\partial z} \Big|_z = 0 \quad (\text{Eq.15})$$

Table 1. Soil hydraulic and transport parameters of the study domain

Parameters description	Value
Saturated hydraulic conductivity K_s (cm^2/s)	0.00874
Pressure head scale parameter α (m^{-1})	-36
Saturated volumetric water content θ_s ($m^3 m^{-3}$)	0.4
Shape parameter m (-)	0.827
Shape parameter η (-)	6.2
Specific storage S_s (cm^{-1})	4.6×10^{-5}
Effective porosity ω (-)	0.38
Molecular diffusion in the soil D_0 ($m^2 d^{-1}$)	6.24×10^{-5}
Soil dispersivity λ (cm)	2
Mineralization potential rate k_{min} (d^{-1})	3.32×10^{-4}
Nitrification potential rate k_{nit} (d^{-1})	0.24
Cation exchange capacity CEC (g^{-1})	100
Solid/liquid partitioning coefficient K_d ($m^3 kg^{-1}$)	6×10^{-3}

Numerical model

The flow and reactive transport equations, subject to their initial and boundary conditions, were solved by applying the finite element method. The *Freefem++* code was adapted to the problem needs (Hecht, 2012), namely: Richards equation to study the water flow in the unsaturated zone (Eqs. 5 and 6), the diffusivity equation for the groundwater flow and the transport equation of advection–dispersion type to study the nitrogen transfer in the unsaturated–saturated zone (Eq. 10). The nodes are placed to the basin boundary at regular intervals (e.g. 20 nodes for a boundary of 200 cm). The finite element grid is then automatically obtained, based on the Delaunay-Voronoi algorithm. The *UMFPACK* solver is used. The generated mesh can be automatically adapted to sensitive zones like infiltration band and the capillary fringe. A polynomial space of 0-degrees for the flux and 1-degrees for the pressure, hydraulic head and concentration are used. The simulation was run with a time step of 2 min with a total time of 120 h. Once the pressure head h is computed in the unsaturated zone, θ and q are calculated. The water content θ is used to calculate the rates of the biochemical nitrogen kinetics. Subsequently, the systems of equations describing the mass transport of NH_4^+ and NO_3^- are composed and the amounts of mineralization and nitrification rates are evaluated to the NH_4^+ system. Finally, the NH_4^+ transport system for the ammonium concentrations and the NO_3^- transport system are solved.

Results

Model validation

For the validation, the numerical simulations of the water table profiles are compared with experimental measurements obtained from a laboratory scale with piezometers for different times of recharge. The model was also validated using experimental data taken from the Vachaud's experiment (Vachaud et al., 1973). The above calculations were performed using the mean K_s -value (Fig. 2). Figure 3 shows a rather good agreement between the positions of measured and calculated water table profiles during the recharge periods at 3 h and 8 h.

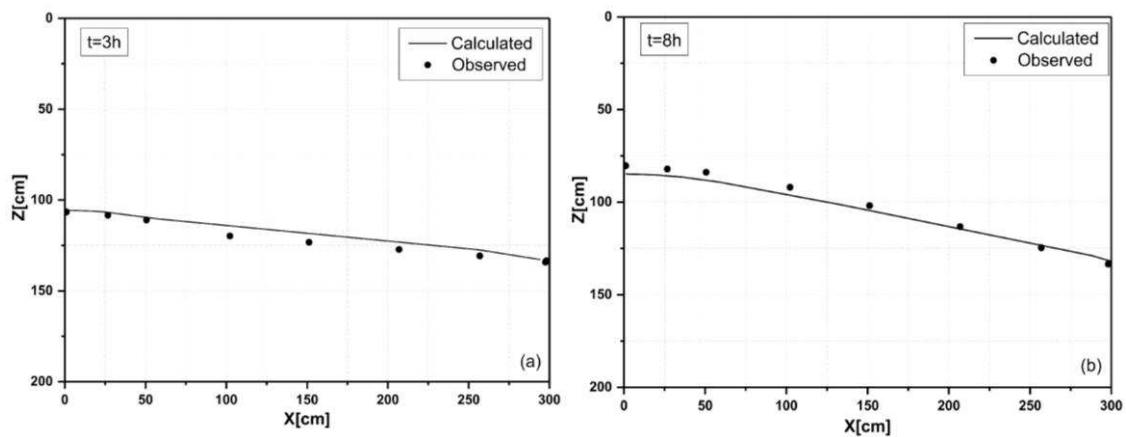


Figure 3. Comparison between computed and observed water table position at 3 h and 8 h (steady state condition)

When the wet front from the surface soil reaches the water table, the free surface starts rising. From that moment, the water table stabilizes over time to a maximum position. The aquifer is hydrostatically balanced and therefore the flow entering through the infiltration band becomes equal to that exiting through the outlet of the aquifer.

There is an important flow in the saturated portion of the soil above the free surface with values identical to those obtained under the free surface. It is interesting to note that capillary flow induces a significant vertical upward flow component in the unsaturated zone located above the free surface. The deformation of the flow lines has substantially a vertical component within the band of horizontal infiltration and below the free surface.

The model was validated on measures of nitrate concentrations drained by leaching at the outlet of the aquifer (Fig. 4). The experimental measurement and model simulation have a good agreement.

Mesh adaptation

Using *Freefem++* code allows the resolution of equations characterizing transport phenomenon in a variably-saturated soils. The mesh refinement is carried out automatically during the recharge in areas that may be considered to be mathematical singularities such as: the infiltration band and the capillary fringe. This procedure improves significantly the quality of the results (Hecht, 2012). Figure 5 shows the areas affected by the auto-adaptive mesh refinement after the refinement procedure.

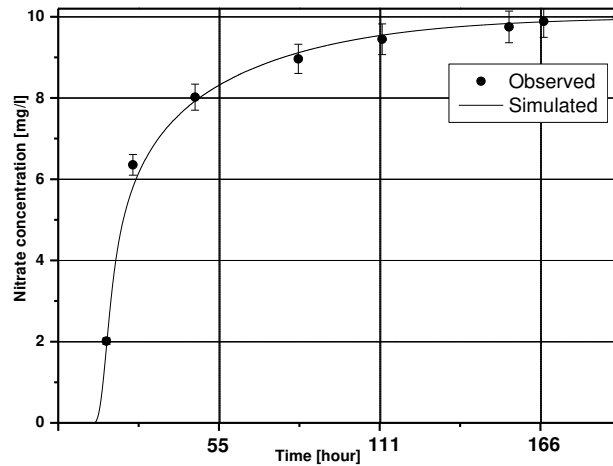


Figure 4. Measured and calculated quantities of leached nitrate at the outlet of the aquifer

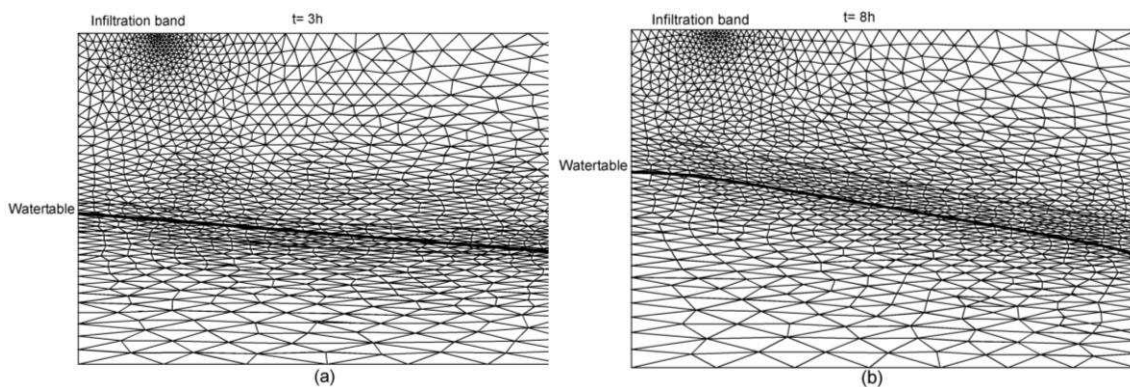


Figure 5. Self-adaptive mesh generated at the wet front and the capillary fringe at 3 h and 8 h (the steady state)

Classically, the numerical solution is checked with the exact analytical solution. However, in this case the gain for using the anisotropic mesh adaptation technique is evaluated by comparing numerical solutions denoted by V_m^h , with the reference solution, V_m^{ref} at steady state (Belhamadia et al., 2014), the following error is presented in *Equations 16* and *17*:

$$E_2 = \frac{\|V_m^h - V_m^{ref}\|_2}{\|V_m^{ref}\|_2} \quad (\text{Eq.16})$$

with:

$$\|V_m^h - V_m^{ref}\|_2 = \left(h^2 \sum_{i=1}^m |V_m^{h,i} - V_m^{ref,i}|^2 \right)^{\frac{1}{2}} \quad (\text{Eq.17})$$

Mesh adaptation has the ability to capture much more detail with more accuracy and a high order of convergence. It allows the generation of the optimum mesh size for a

given accuracy with gains in *CPU* time, memory and storage space. An extremely fine mesh is chosen as a referential mesh. The errors are in the L_2 norm. The results in the uniform and adaptive mesh are described in *Table 2*.

Table 2. Comparison of the error E_2 at $t = 8$ h, number of dof (degrees of freedom) and number of triangles obtained with standard meshes and the adapted meshes (Freefem++)

Meshes	Standard meshes			Adapted <i>ff++</i> meshes
	(a)	(b)	(c)	(d)
Nb of dof	426	10028	39220	1238
Nb of triangles	770	19654	77638	2348
Error	0.674	0.163	0.096	0.114
Total CPU time	25.527 s	303.178 s	1014.16 s	47.639 s

It takes nearly 20 times for a very fine structured mesh to reach an error equal to that of the adapted mesh. On the other hand, a low structured mesh has a substantial error. The small error reflects the advantage of using the mesh adaptation. As can be seen, the adapted mesh has a reasonable *CPU* time and a low computational cost. Even that the structured mesh (b) takes more time and computation, it is not as close to observations as the adapted mesh (d).

Discussion

Accuracy-uncertainty

The accuracy of the model was evaluated by calculating the root mean squared error (*RMSE*; Hill and Tiedeman, 2007). To construct the *RMSE*, we first need to determine the residuals. The residuals are the difference between the measured water table profiles and the predicted values at steady state and then use the *RMSE* as a measure of the spread of the Z values about the predicted Z value. Low *RMSE* values indicate little difference between the predicted and observed variables, and thus indicate a more accurate model.

The *RMSE* of the model was then normalized (*NRMSE*) to the range of the parameter measurements. Normalizing the *RMSE* provided a context for the accuracy of the model given these ranges. *NRMSE* was on a scale of 0–1, and gives the overall error of the model.

The statistical methods also included a calculation of the index of agreement (*Skill*). A skill parameter developed by Willmott and recently used in different modeling studies (Moriassi et al., 2007), was also considered to estimate the accuracy of the model. This parameter allows to take into account modeled and observed deviations around the observed mean to estimate the performance of the simulation. The value of (*Skill*) reflects the degree to which the calculated variation accurately estimates the measured variation. Perfect agreement between model and observations corresponds to a skill parameter of 1. MS Excel was used for statistical calculations. *Equations 18, 19* and *20* present respectively the statistical indicators (*RMSE*), (*NRMSE*) and (*Skill*) defined as follows:

$$RMSE = \sqrt{\left[\frac{\sum_{i=1}^p (Z_{meas,i} - Z_{pred,i})^2}{p} \right]} \quad (\text{Eq.18})$$

$$NRMSE = \left[\frac{RMSE}{\bar{Z}_{meas}} \right] \quad (\text{Eq.19})$$

$$Skill = 1 - \frac{\sum_{i=1}^p (|Z_{pred,i} - Z_{meas,i}|)^2}{\sum_{i=1}^p (|Z_{pred,i} - \bar{Z}_{meas}| + |Z_{meas,i} - \bar{Z}_{meas}|)^2} \quad (\text{Eq.20})$$

where $Z_{meas,i}$ is the measured value and $Z_{pred,i}$ is the calculated value of water table level at x . \bar{Z}_{meas} is the mean measured by the water table level and p number of measures.

As listed in *Table 3*, the *RMSE* values (2.78 and 3.28 cm) indicate the low discrepancy between observed and calculated values. The *skill* indicator close to 1 shows the good performance of the model. The uncertainty of the model prediction has been estimated, the results demonstrate the good performance of the model and confirms the water table level prediction.

Table 3. Statistical indicators of the hydrodynamic model performance

Statistical indicators	RMSE (cm)	NRMSE (-)	Skill (-)
Validation (at 3 h)	2.78	0.02	0.98
Validation (at 8 h)	3.28	0.03	0.97

Sensitivity analysis

Mathematical models are developed to approximate engineering, physical, environmental, social, and economic phenomena of various complexities. Sensitivity analyses (*SA*) determine parameters that are most influential on the model output. In this case, a sensitivity analysis was performed with respect to the soil shape parameters (m and η) and scale parameters (θ_s , α and K_s). These parameters were varied by $P_0 - \delta \times P_0$ and $P_0 + \delta \times P_0$, where $P_0 = (m, \eta, \theta_s, \alpha \text{ and } K_s)$, $\delta = 20\%$, compared to their experimental values. The deviation of the simulated water table level relative to the measured is then quantified. *Figure 6a, b* shows the results of the sensitivity analysis for the water table. It can be shown that the model is more sensitive to the hydraulic conductivity K_s than all other parameters (see *Fig. 6*).

This result shows that the hydraulic conductivity K_s must be measured with the most precise way possible. A small error in K_s can lead to a great water table level error as demonstrated in the sensitivity analysis. *Figure 6c, d* shows the simulated k_{min} and N_{org} sensitivity for different times.

The variation of α and n is not enough significant, so the three curves (simulated, +20% and -20%) are matching. The parameters k_{min} and N_{org} has a little effect (only near the surface) on the sensitivity of the results. However, for an agricultural field with a higher soil organic nitrogen the results will probably be more sensitive to k_{min} changes.

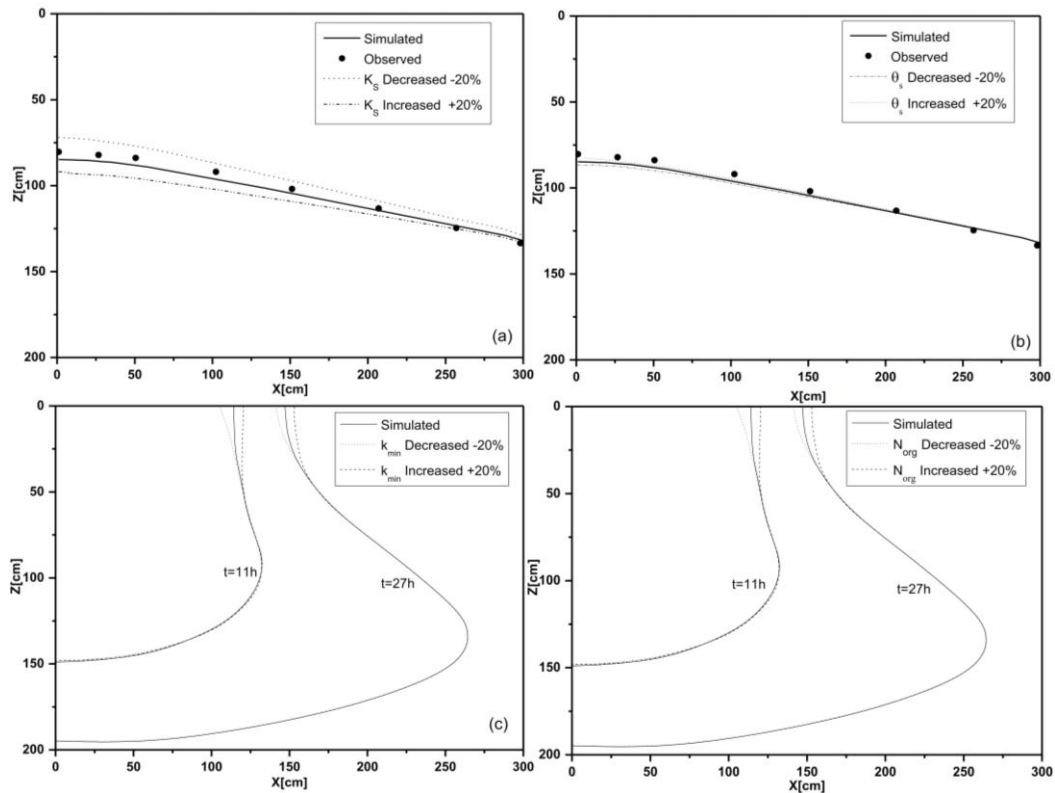


Figure 6. Sensitivity analysis of the water table position relative to K_s and θ_s ; k_{min} and N_{org} mineralization sensitivity

Nitrate transport simulation

In Hénin-Dupuis model, k_{min} can take different values depending on the climate of the study area and the type of culture that is practiced. In the case of this study, the nitrate transport was tested in a laboratory scale model under controlled conditions (low organic matter and constant temperature).

Figure 7 shows the spatial distribution of simulated nitrate concentration $C_{NO_3^-}$ at different times. The transport simulation was run with a time step of 2 min with a total time of 120 h. The leaching of nitrate is done with a relative delay to the flow, because of the flux imposed on the infiltration band during the recharge of the groundwater. The nitrate concentrations are important in the soil near the surface because of the application of nitrogen on the surface 10 mg/l. These concentrations decrease with depth and their presence in the root zone is very important due to the mineralization of organic nitrogen in this layer and the rapid nitrification of NH_4^+ ions. These concentrations continue to decrease in the saturated zone and to be driven by the movement of the aquifer from the surface of soil to the outlet. The NO_3^- ions which behave as tracers are very mobile. They move easily in soil and appear in all depths of the basin with different concentrations, in accordance with literature (e.g., see Allred et al., 2007; Shekofteh et al., 2013).

Nitrogen dynamics

In this study, the effect of denitrification was omitted. Denitrification in soils requires a large population of denitrifying bacteria, electron donor compounds and

anaerobic condition. Riparian areas can reduce nitrogen inputs to aquatic systems through plant uptake and microbial denitrification. For example, denitrification can be found along root canals where moisture and organic matter content are high or in anaerobic locations (Bechtold et al., 2006). In a field case, the nitrate concentration would not be well simulated by the model in riparian zones or areas with high denitrification. Indeed, this process can lead to a real transformation of nitrogen to gaseous forms (Maggi et al., 2008).

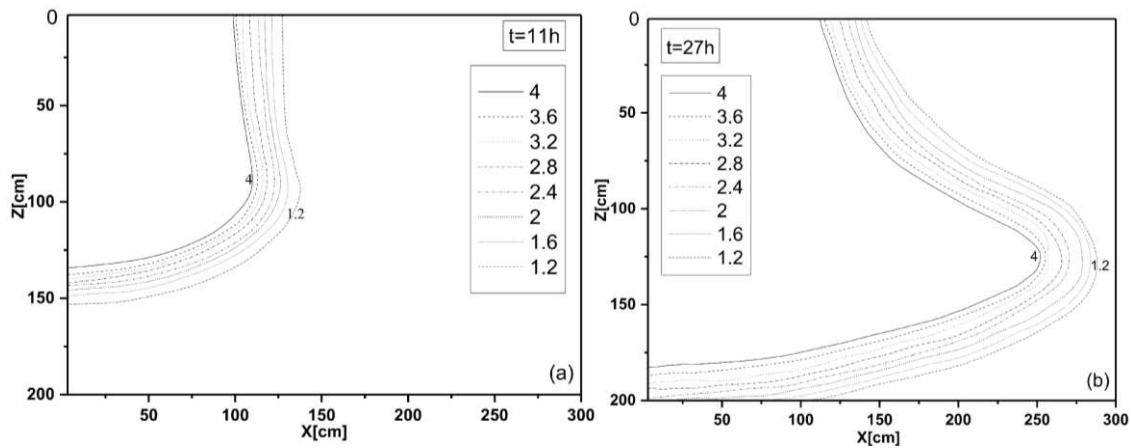


Figure 7. Spatial distribution of nitrate $C_{NO_3^-}$ concentrations(mg/l) at 11 h and 27 h

It is well established that bacterial activity controls the turnover rates of nitrogen mineralization. Indeed, several studies have shown that the mineralization of nitrogen varies linearly with temperature and soil pH, two parameters that directly influence bacterial activity and population. Differences in mineralization dynamics between soils with identical characteristics suggest a difference in the microbial communities that populate them (Bechtold et al., 2006; Manzoni and Porporato, 2009). Soils containing high organic matter and bacterial activity generate a strong mineralization that does not affect the model but only the kinetics of transformation. The transport models require a global vision to fully evaluate the role of microbes in nitrogen dynamics.

Ammonification and nitrification were the primary processes affecting nitrogen in the unsaturated zone. Nitrification decrease in the unsaturated zone. In agreement with the experience of Hanson and Šimůnek in 2006 and its conclusion, the ammonium remained concentrated in the surface due to rapid nitrification. Ammonium was limited to upper place of the unsaturated zone with almost no presence near the water table. In contrast to ammonium, nitrate spread continuously downwards during the 5-day simulation period, as nitrate is not adsorbed and denitrification is negligible (Hanson et al., 2006). Thus, more than 97% of the nitrogen load discharged in effluent was transported to the water table, mostly as nitrate, due to the low level of organic matter in the soil and the small scale of our basin (Filipović et al., 2014; Maggi et al., 2008). However, as shown by Sâadi et al. (2003), The ammonium peaks at the soil surface disappear completely for depths far from the surface. Their probability of reaching the aquifer is nil. The high adsorption and rapid nitrification of NH_4^+ ions near the surface are the main reasons for this. Hence, at agriculture sites constrained to similar conditions as in this study, most of the nitrate mass that leaches under the root zone will

eventually reach groundwater. These results, obtained with the single-compartment model (Hénin-Dupuis), coincides with the results of the multi-compartment models (Manzoni and Porporato, 2009).

Different parameters can influence nitrate transport. The distribution coefficient K_d is a constant that relates the sorbed nitrate concentration to the aqueous concentration. K_d is strongly dependent on the amount of organic matter. Thus, an increase in K_d will increase the amount of nitrate sorbed to the soil, resulting in less concentration reaching the groundwater. The experience of Ibnoussina et al. (2006) shows that the clay soil is characterized by a low nitrate transport. The nitrification rate constants were lower for the clay column than for the sand column.

Other Results of this study suggest that saturated hydraulic conductivity K_s (related to pore size) may partly account for higher nitrate concentrations (Shekofteh et al., 2013). The thickness of the unsaturated zone also influence the nitrate transport. The deeper is the water table, the less is the nitrate contamination. The dispersion D_{ap} also decreased with increasing water content, it suggest a more significant transport effect on the unsaturated zone than the saturated zone.

Conclusion

The present study focused on: (1) The development of a new mathematical formulation for water flow and nitrate transport prediction in unsaturated-saturated zones which are regarded as a single continuum, (2) A numerical model (i.e. *Freefem++* code) was used to study the water flow and nitrogen dynamics in the porous media. The self-adaptive mesh generation gives the numerical approach the capacity and efficiency to study singular areas with reduced CPU from ~303 s to ~47 s. In addition, the advantage of the numerical model required a few variables, making the parameterization simpler. The obtained results from the model show a good-fit with laboratory observations data. On the other hand, the statistical indicators confirm the model accuracy. The sensitivity test shows that the hydraulic conductivity is more sensitive than water content (i.e. In hydraulic model); for transport model the k_{min} and N_{org} parameters are sensitive in the root zone (0-50 cm).

Finally, It can be concluded that the developed model is a rigorous, practical and a useful forecasting tool, which can be used to simulate the transport of nitrogen in groundwater systems. It can also be used to design remedial systems such as bioremediation trenches. The approach used is simple and adaptable and thus can be applied to a real landscape scale situation. This implies that in a next step the model should be extended to a large field with seasonal periods and variably irrigation cycles.

REFERENCES

- [1] Allred, B. J., Bigham, J. M., Brown, G. O. (2007): The impact of clay mineralogy on nitrate mobility under unsaturated flow conditions. – *Vadose Zone Journal* 6(2): 221-232.
- [2] Bagarello, V., Iovino, M. (2012): Testing the BEST procedure to estimate the soil water retention curve. – *Geoderma* 187-188: 67-76.
- [3] Bechtold, J. S., Naiman, R. J. (2006): Soil texture and nitrogen mineralization potential across a riparian toposequence in a semi-arid savanna. – *Soil Biology and Biochemistry* 38(6): 1325-1333.

- [4] Belhamadia, Y., Fortin, A., Bourgault, Y. (2014): On the performance of anisotropic mesh adaptation for scroll wave turbulence dynamics in reaction–diffusion systems. – *Journal of Computational and Applied Mathematics* 271: 233-46.
- [5] Bryan, N. S., Loscalzo, J. (2011): Nitrite and Nitrate in Human Health and Disease, pp 263-278. – In: Bendich, A. (ser. ed.) *Nitrite and Nitrate in Cancer*. Springer-Humana Press, New York.
- [6] Butturini, A., Battin, T. J., Sabater, F. (2000): Nitrification in stream sediment biofilms: the role of ammonium concentration and DOC quality. – *Water Res.* 34(2): 629-639.
- [7] Brooks, R. H., Corey, A. T. (1964): Hydraulic properties of porous media and their relation to drainage design. – *Transactions of the Asae* 7: 26-28.
- [8] Cheng, Q., Chen, X., Chen, X., Zhang, Z., Ling, M. (2011): Water infiltration underneath single-ring permeameters and hydraulic conductivity determination. – *Journal of Hydrology* 398: 135-143.
- [9] Deb, S. K., Sharma, P., Shukla, M. K., Ashigh, J., Šimůnek, J. (2016): Numerical evaluation of nitrate distributions in the onion root zone under conventional furrow fertigation. – *Journal of Hydrologic Engineering* 21(2): 05015026.
- [10] Diaw, E. B., Lehmann, F., Ackerer, P. (2001): One-dimensional simulation of solute transfer in saturated-unsaturated porous media using the discontinuous finite elements method. – *Journal of Contaminant Hydrology* 51: 197-213.
- [11] Dupuy, A., Razack, M., Banton, O. (1997): Contamination nitraté des eaux souterraines d'un Bassin versant agricole hétérogène-2: Evolution des concentrations dans la nappe. – *Revue des sciences de l'eau* 10(2): 185-198.
- [12] Filipović, V., Toor, G. S., Ondrašek, G., Kodešová, R. (2014): Modeling water flow and nitrate–nitrogen transport on golf course under turfgrass. – *Journal of Soils and Sediments* 15(8): 1847-59.
- [13] Hanson, B. R., Šimůnek, J., Hopmans, J. W. (2006): Evaluation of urea–ammonium–nitrate fertigation with drip irrigation using numerical modeling. – *Agricultural water management* 86(1): 102-113.
- [14] Hecht, F. (2012): New development in FreeFem++. – *Journal of Numerical Mathematics* 20: 251-265.
- [15] Hill, M. C., Tiedeman, C. R. (2006): *Effective Groundwater Model Calibration: with Analysis of Data, Sensitivities, Predictions, and Uncertainty*. – John Wiley & Sons, Hoboken, NJ.
- [16] Ibnoussina, M. H., El Haroui, M., Maslouhi, A. (2006): Expérimentation et modélisation de la lixiviation de l'azote nitrique dans un sol sableux. – *Comptes Rendus Geoscience* 338: 787-794.
- [17] Lindström, G., Pers, C., Rosberg, J., Strömqvist, J., Arheimer, B. (2010): Development and testing of the HYPE (Hydrological Predictions for the Environment) water quality model for different spatial scales. – *Hydrology Research* 41(3-4): 29.
- [18] Maggi, F., Gu, C., Riley, W. J., Hornberger, G. M., Venterea, R. T., Xu, T., Spycher, N., Steefel, C., Miller, N. L., Oldenburg, C. M. (2008): A mechanistic treatment of the dominant soil nitrogen cycling processes: Model development, testing, and application. – *Journal of Geophysical Research: Biogeosciences* 113: G02016.
- [19] Manzoni, S., Porporato, A. (2009): Soil carbon and nitrogen mineralization: theory and models across scales. – *Soil Biology and Biochemistry* 4: 1355-1379.
- [20] Maslouhi, A., Lemacha, H., Razack, M. (2009): Modelling of water flow and solute transport in saturated-unsaturated media using a self adapting mesh. – *IAHS Publication P 331*: 480-487.
- [21] Moret-Fernández, D., González-Cebollada, C., Latorre, B., Pérez, V. (2015): A modified hood infiltrometer to estimate the soil hydraulic properties from the transient water flow measurements. – *Journal of Hydrology* 530: 554-560.

- [22] Moriasi, D. N., Arnold, J. G., Van Liew, M. W., Bingner, R. L., Harmel, R. D., Veith, T. L. (2007): Model evaluation guidelines for systematic quantification of accuracy in watershed simulations. – Transactions of the ASABE 50(3): 885-900.
- [23] Mualem, Y. (1976): A new model for predicting the hydraulic conductivity of unsaturated porous media. – Water Resources Research 12: 513-522.
- [24] Reynolds, W. D., Jeffrey, K. L. (2012): A drive point application of the Guelph Permeameter method for coarse-textured soils. – Geoderma 187: 59-66.
- [25] Rezaei, M., Seuntjens, P., Shahidi, R., Joris, I., Boëne, W., Al-Barri, B., Cornelis, W. (2016): The relevance of in-situ and laboratory characterization of sandy soil hydraulic properties for soil water simulations. – Journal of Hydrology 534: 251-265.
- [26] Saâdi, Z., Maslouhi, A. (2003): Modeling nitrogen dynamics in unsaturated soils for evaluating nitrate contamination of the Mnasra groundwater. – Advances in Environmental Research 7: 803-823.
- [27] Saâdi, Z., Maslouhi, A., Zéraouli, M., Gaudet, J. P. (1999): Analyse et modélisation des variations saisonnières des concentrations en nitrates dans les eaux souterraines de la nappe Mnasra, Maroc. – Comptes Rendus de l'Académie des Sciences II A 329(8): 579-585.
- [28] Shekofteh, H., Afyuni, M., Hajabbasi, M. A., Iversen, B. V., Nezamabadi-Pour, H., Abassi, F., Sheikholeslam, F., Shirani, H. (2013): Modeling of nitrate leaching from a potato field using HYDRUS-2D. – Communications in Soil Science and Plant Analysis 44: 2917-2931.
- [29] Van Genuchten, M. T. (1980): A closed-form equation for predicting the hydraulic conductivity of unsaturated soils. – Soil Science Society of America Journal 44(5): 892-898.
- [30] Vachaud, G., Vauclin, M., Khanji, D. (1973): Étude expérimentale des transferts bidimensionnels dans la zone non saturée application à l'étude du drainage d'une nappe à surface libre. – La Houille Blanche 65-74.

A HEIGHT-DIAMETER MODEL FOR BRUTIAN PINE (*PINUS BRUTIA* TEN.) PLANTATIONS IN SOUTHWESTERN TURKEY

ÇATAL, Y.* – CARUS, S.

*Department of Forest Engineering, Faculty of Forestry, Süleyman Demirel University
Isparta, Turkey*

**Corresponding author
e-mail: yilmazcatal@sdu.edu.tr*

(Received 13th Nov 2017; accepted 20th Feb 2018)

Abstract. In this study, models for the tree total height have been developed for brutian pine (*Pinus brutia* Ten.) stands in southwestern Turkey. For this purpose, 52 sample plots were measured. A total of 36 models that estimate the relationship between height and diameter in terms of stand variables (i.e. basal area, quadratic mean diameter, maximum diameter, dominant diameter, dominant height, arithmetic mean height, age, number of trees per hectare and site index), were fitted to correspond to 766 trees for non-linear regression procedures. Comparison of the models was carried out by using mean absolute error (MAE), maximum absolute error (MaxAE), root mean square error (RMSE), correlation coefficients (R), mean error (Bias) and the Akaike's information criterion (AIC). The most successful model among the 36 height-diameter models used was the Cox II_a model. This model was followed by Cox II_b and Sharma & Parton, respectively. As a result, the suggested model improves the accuracy of height prediction, ensures compatibility among the various estimates in a growth and yield model, and maintains projections within reasonable biological limits. Examples of applications of the selected generalized diameter-height models to the forest management are presented, namely how to use it to complete missing information from forest inventory and also showing how such an equation can be incorporated in a stand-level decision support system that aims to optimize the forest management for the maximization of wood volume production in southwestern Turkey brutian pine stands.

Keywords: *generalized height-diameter models, stand age, stand density, site index*

Introduction

All models are an abstraction of reality that attempt to conceptualize key relationships of a system. Models can be both quantitative and conceptual in nature, but all models are integrators of multiple fields of knowledge. Forest growth and yield models are no different (Weiskittel et al., 2011). Total height is less frequently used in the development of forest models than diameter, as it is difficult and costly to measure, and consequently inaccurate measurements are often made (Sharma and Parton, 2007). When actual height measurements are not available, height-diameter functions can also be used to indirectly predict height growth (Larsen and Hann, 1987).

The relationship between tree height and diameter is one of the most important elements of forest structure. Many growth and yield models require height and diameter as basic input variables, with all or part of the tree height predicted from measured diameters (Wykoff et al., 1982; Huang et al., 2000).

Height-diameter relationships are applied to even-aged stands and can be fitted to linear functions, such as second-order polynomial equations, or more usually, to non-linear models (Colbert et al., 2002; Soares and Tomé, 2002; Castedo Dorado et al., 2006; Lootens et al., 2007). Model selecting a functional form for the height–diameter relationship, the following mathematical properties should be considered: (i) monotonic ascent, (ii) inflection point and (iii) horizontal asymptote (Lei and Parresol,

2001). The number of parameters and their biological interpretation (e.g., asymptote, maximum or minimum growth rate) and satisfactory predictions of the height-diameter relationships are also important features (Peng, 1999).

A generalized height-diameter function estimates the specific relationship between individual tree heights and diameters using stand variables such as basal area per hectare, quadratic mean diameter, stands age, number of trees. The reason for using them is to avoid having to establish individual height-diameter relationships for every stand (Curtis, 1967). A wide variety of both local and generalized height-diameter models are available in the forestry literature (Huang et al., 2000; Soares and Tomé, 2002; López Sánchez et al., 2003; Temesgen and Gadow, 2004). Because of different geographical conditions in Turkey, the variety of tree species, habitat and stand structures is very high. However, equations reveal height-diameter relations for a limited number of different tree species and natural stands have been developed in Turkey (Sönmez, 2008; Mısır, 2010; Çatal, 2012; Diamantopoulou and Özçelik, 2012; Özçelik and Çapar, 2014). Generalized diameter-height models should be created to deal with pure brutian pine (*Pinus brutia* Ten.) plantation which was established 50 years ago. However, height-diameter models for brutian pine plantations are not yet available in Turkey.

Ecologically and economically, it is one of the most important forest tree species in Turkey. Brutian pine accounts for 25.1% of Turkey's total forest area, where it covers 5.6 million hectares. The species is considered fast growing and drought-tolerant with desirable wood characteristics. It is also widely used in reforestation and afforestation in Turkey (Anonymous, 2015). The aim of this study is to find an equation from selected generalized height-diameter models that could be used to predict the diameter-height relationship in artificial brutian pine stands in southwestern Turkey, by considering a number of stand variables (e.g., dominant diameter, dominant height, age, density, site index, etc.). The models divided into three groups and compare the models in three groups. These groups were the following i) diameter measurements, knowledge of stand age and number of trees per hectare, ii) measurements of diameter and height of sample trees, and ii) addition of measurements of stand age to the second group.

Materials and methods

Data used

Brutian pine is a characteristic species of the eastern Mediterranean and commonly found in fire-related ecosystems of the eastern Mediterranean region. It usually grows in pure stands and is valuable for its timber products as well as for soil stabilization and wildlife habitats. In Turkey, brutian pine forms extensive forests, especially in regions where the Mediterranean climate prevails.

This research was carried out in the region of southwestern Turkey, located, 50 km to the east of Burdur (*Fig. 1*).

The 650 ha study area is situated at 37°38'06'' N lat., 30°32'37'' E long., average slope 15°, predominantly north-facing aspect, 1,150 m asl. The soil is generally shallow or medium-deep, and stony, with a predominantly clay texture. Brutian pine plantations were established in 1974 using a spacing of 3 × 2 m.

Tree heights and diameters were measured in 52 sample plots established in pure and, even-aged artificial brutian pine stands in southwestern Turkey region. The plots were square or rectangular with areas varying between 400 and 1600 m². The number of

trees per plot ranges between 32 and 115 depending on stocking. The sample plots were installed in order to provide the greatest variety of combinations of stand age, stand density degree and site index. In each sample plot, diameters at breast height of all trees were crosswise measured, using Haglöf calipers, to the nearest millimetre. Heights were measured using a Silva hypsometer to the nearest 0.1 m. In each sample plot 10-20 sample trees with different diameters and heights were chosen. Sample trees should not have any crown or stem damage.

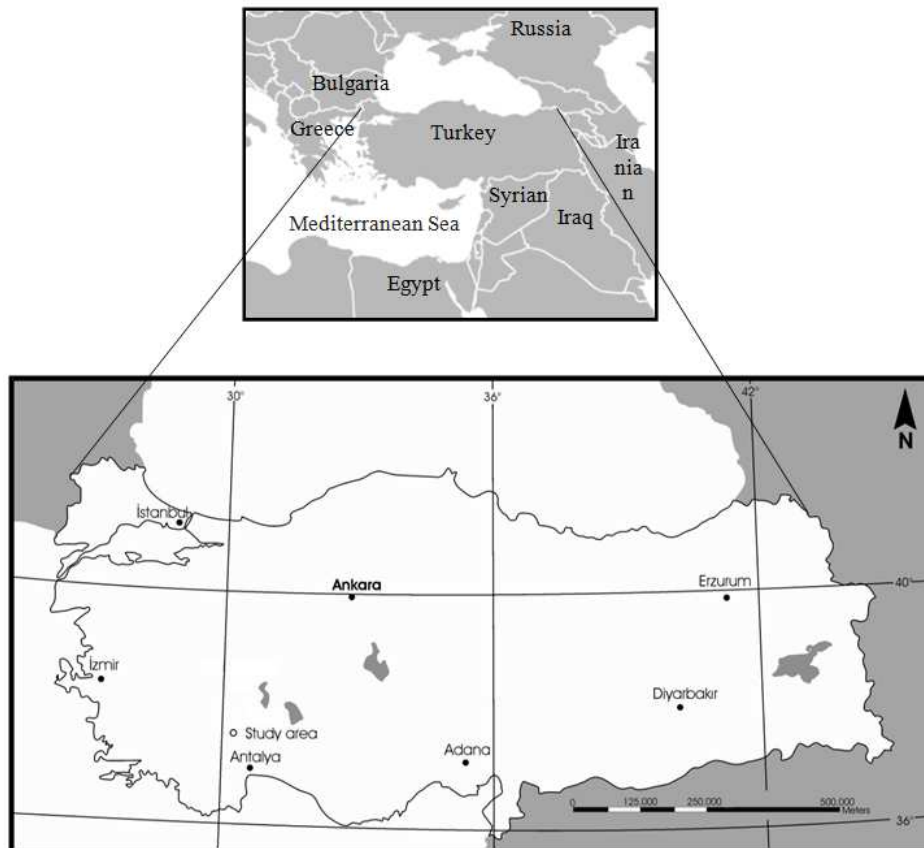


Figure 1. Location of sample plots in Turkey

In addition the following stand variables were calculated based on the data collected in the plots: stand basal area, quadratic mean diameter, maximum diameter, dominant diameter, dominant height, stand mean height, stand age (it was calculated from the year of planting), stand density and site index, defined as stand dominant height at 30 years of age and determined from the site index curves available for this species in the region (Usta, 1991).

Models analysed

A large number of generalized height-diameter models have been discussed in the forestry literature, many of which been developed for modelling the relationship between tree height and diameter at breast height by additional stand and site variables. In the present study, we have considered the most commonly used 36 generalized height-diameter equations (*Table 1*).

Table 1. Generalized height-diameter models evaluated

The first group model (Group model 1)	Author (s)	Model
$h = 1.30 e^{(a_0 + a_1 \frac{1}{d} + a_2 \frac{1}{t} + a_3 \frac{1}{d_g t})}$	Curtis (1967)	1
$h = e^{(a_0 + a_1 \ln d_g + a_2 \ln N + a_3 \sqrt{d})}$	Cox I (1994)	2
$h = 1.30 + 10^{(a_0 + a_1 \frac{1}{d} + a_2 \frac{1}{\sqrt{t}} + a_3 \frac{1}{d\sqrt{t}} + a_4 \frac{\log N}{\sqrt{t}})}$	Clutter and Allison (1974)	3
The second group model (Group model 2)	Author (s)	Model
$h = 1.30 + \left[a_0 \left(\frac{1}{d} - \frac{1}{D_0} \right) + \left(\frac{1}{H_0 - 1.3} \right)^{1/3} \right]^{-3}$	Mónnes (1982)	4
$h = 1.30 + (H_0 - 1.3) \left(\frac{d}{D_0} \right)^{a_0}$	Canadas et al. I (1999)	5
$h = 1.30 + \frac{d}{\frac{D_0}{H_0 - 1.3} + a_0 (D_0 - d)}$	Canadas et al. II (1999)	6
$h = 1.30 + (H_0 - 1.3) \frac{1 - e^{a_0 d}}{1 - e^{a_0 D_0}}$	Canadas et al. III (1999)	7
$h = 1.30 + \left[a_0 \left(\frac{1}{d} - \frac{1}{D_0} \right) + \left(\frac{1}{H_0 - 1.3} \right)^{1/2} \right]^{-2}$	Canadas et al. IV (1999)	8
$h = 1.30 + (H_0 - 1.3) e^{a_0 \left(1 - \frac{d}{d_g} \right) + a_1 \left(\frac{1}{d_g} - \frac{1}{d} \right)}$	Gaffrey (1988)	9
$h = 1.30 + (H_0 - 1.3) \left[1 + a_0 (H_0 - 1.3) \left(\frac{1}{d} - \frac{1}{D_0} \right) \right]^{-1}$	Prodan (1968)	10
$h = 1.30 + H_0 (1 + a_0 + a_1 H_0 + a_2 d_g) e^{a_3 H_0} \left(1 - e^{a_4 \frac{d}{H_0}} \right)$	Soares and Tome (2002)	11
$h = 1.30 + (H_m - 1.3) e^{a_0 \left(1 - \frac{d}{d_g} \right)} e^{a_1 \left(\frac{d}{d_g} - \frac{1}{d} \right)}$	Sloboda et al. (1993)	12
$h = H_0 (1 + a_0 e^{a_1 H_0}) \left(1 - e^{-\frac{a_2 d}{H_0}} \right)$	Harrison et al. (1986)	13
$h = 1.30 + \frac{a_0 H_0^{a_1} (H_0 - 1.3)}{\left(\frac{D_0 - d}{d} \right)^{a_2}}$	Castedo Dorado et al. (2001)	14
$h = a_0 H_0 \left(1 - e^{-\frac{a_1 d}{d_g}} \right)^{a_2}$	Pienaar et al. _a (1990)	15
$h = a_0 H_0 \left(1 - e^{-\frac{a_1 d}{D_0}} \right)^{a_2}$	Pienaar et al. _b (1990)	16
$h = 1.30 + (H_m - 1.3) e^{a_0 \left(1 - \frac{d}{D_0} \right)} e^{a_1 \left(\frac{d}{D_0} - \frac{1}{d} \right)}$	Sloboda et al. (1993)	17
$h = 1.30 + a_0 H_0^{a_1} d^{a_2 H_0^{a_3}}$	Hui and Gadov (1993)	18

$h = 1.30 + (a_0 + a_1 H_0 - a_2 d_g) e^{\left(\frac{a_3}{d}\right)}$	Mirkovich (1958)	19
$h = 1.30 + (a_0 + a_1 G + a_2 H_0) e^{\left(a_3 \frac{1}{d}\right)}$	Ademe et al. (2008)	20
$h = 1.30 + (a_0 + a_1 H_0 - a_2 d_g) e^{\left(\frac{a_3}{\sqrt{d}}\right)}$	Schröder and Álvarez González I (2001)	21
$h = H_m \left[a_0 + a_1 H_m + a_2 \frac{H_m}{d_g} + a_3 d + a_4 \frac{N}{d_g (H_m d_g)} \right]$	Cox III _a (1994)	22
$h = 1.30 + (a_0 + a_1 H_0 - a_2 d_g + a_3 G) e^{\left(\frac{-a_4}{\sqrt{d}}\right)}$	Schröder and Álvarez González II (2001)	23
$h = a_0 + a_1 H_m + a_2 d_g^{0.95} + a_3 e^{-0.08d} + a_4 H_m^3 e^{-0.08d} + a_5 d_g^3 e^{-0.08d}$	Cox II _a (1994)	24
$h = a_0 + a_1 H_m + a_2 d_g + a_3 e^{a_4 d} + a_5 H_m^{a_6} e^{a_4 d} + a_7 d_g^{a_8} e^{a_4 d}$	Cox II _b (1994)	25
$h = 1.30 + a_0 G^{a_1} (1 - e^{(-a_2 N^{a_3} d)})$	Sharma and Zhang (2004)	26
$h = 1.30 + a_0 H_0^{a_1} (1 - e^{(-a_2 \left(\frac{N}{G}\right)^{a_3} d)})^{a_4}$	Sharma and Parton (2007)	27
$h = 1.30 + a_0 H_0^{a_1} (1 - e^{(-a_2 D_0^{a_3} d)})^{a_4}$	Richards (1959)	28
$h = 1.30 + a_0 (H_0 - 1.30)^{a_1} e^{(-a_2 d^{-a_3} + a_4 G)}$	Budhathoki et al. (2008)	29
$h = \left[1.30^{a_0} + (H_0^{a_0} - 1.30^{a_0}) * \frac{1 - e^{-a_1 d}}{1 - e^{-a_1 D_0}} \right]^{a_0}$	Castedo Dorado et al. (2001)	30
The third group model (Group model 3)	Author (s)	Model
$h = H_0 e^{\left(a_0 + a_1 H_0 + a_2 \frac{N}{1000} + a_3 t\right) \left(\frac{1}{d} - \frac{1}{D_0}\right)}$	Tome (1989)	31
$h = e^{\left(a_0 + a_1 SI + a_2 \frac{N}{1000} + a_3 \frac{1}{t} + a_4 \frac{1}{d}\right)}$	Bennet and Clutter (1968)	32
$h = 1.30 + \frac{H_0}{e^{a_0 + \left(\frac{1}{d} - \frac{1}{D_{\max}}\right) (a_1 + a_2 \ln N + a_3 \frac{1}{t} + a_4 \ln H_0)}}$	Lenhart (1968)	33
$h = a_0 H_0^{a_1} 10^{\left(\frac{a_2}{t} + \left(\frac{1}{d} - \frac{1}{D_{\max}}\right) (a_3 + a_4 \frac{\log N}{t})\right)}$	Amateis et al. (1995)	34
$h = e^{\left(a_0 + a_1 \ln H_0 + a_2 \frac{1}{t} + a_3 \frac{\ln N}{d} + a_4 \frac{1}{dt} + a_5 \frac{1}{d}\right)}$	Burkhart and Strub (1974)	35
$h = a_0 H_0^{a_1} G^{a_2} N^{a_3} e^{\left(\frac{a_4}{t} + \frac{a_5}{d}\right)}$	Pascoa (1987)	36

The terminology used in the up models is as follows: d = diameter at breast height over bark (cm), t = age of stand, d_g = quadratic mean diameter of stand (cm), G = basal area of stand (m²/ha), D_{max} = maximum diameter of stand (cm), D₀ = dominant diameter of stand (cm), H_m = mean height of stand (m), H₀ = dominant height of stand (m), N = number of trees in stand (stems/ha), SI = site index (m), log = common logarithm (base 10), ln = natural logarithm (base e = 2,718), a₀, a₁... = regression coefficients

The models were classified in three groups according to the sampling effort (Sanchez et al., 2003). These groups; i) *low sampling effort models*; including measurements of diameter and knowledge of stand age, ii) *medium sampling effort models*, including measurements of diameter and heights of sample tree, iii) *high sampling effort models*, including knowledge or measurements of stand age as well.

Statistical analysis

In this study the models described above are non-linear; therefore model fitting was carried out with non-linear regression (NLIN) procedure of SPSS statistical analysis software package. The initial values of parameters were obtained by starting the iterative procedure also used by other authors in similar studies (Castedo Dorado et al., 2006; Özçelik and Çapar, 2014; Ahmadi et al., 2016).

Comparison of estimation of models was based on graphical and numerical analysis of residuals and six goodness of fit statistics: mean absolute error (MAE), which expresses the average of absolute errors between forecast and actual value; maximum absolute error (MaxAE), which maximum absolute value for prediction values; root mean square error (RMSE), which analyses the precision of estimations; correlation coefficients (R), which reflect the total variability that is explained by the model considering the total number of parameters to be estimated; mean error (Bias), which average error for estimated values, and the Akaike's information criterion (AIC), which is an index that is used to select the best model. These evaluation statistics are defined as (Eqs. 1-6):

Mean absolute error:

$$MAE = \frac{\sum_{i=1}^n |h_i - \hat{h}_i|}{n} \quad (\text{Eq.1})$$

Maximum absolute error:

$$MaxAE = \text{Max}(|h_i - \hat{h}_i|) \quad (\text{Eq.2})$$

Root mean square error:

$$RMSE = \sqrt{\frac{\sum_{i=1}^n (h_i - \hat{h}_i)^2}{n - k}} \quad (\text{Eq.3})$$

Correlation coefficients:

$$R = \frac{\sum_{i=1}^n (h_i - \bar{h}_i) * (\hat{h}_i - \bar{\hat{h}}_i)}{\sqrt{\sum_{i=1}^n (h_i - \bar{h}_i)^2} * \sqrt{\sum_{i=1}^n (\hat{h}_i - \bar{\hat{h}}_i)^2}} \quad (\text{Eq.4})$$

Mean error:

$$Bias = \frac{\sum_{i=1}^n (h_i - \hat{h}_i)}{n} \quad (\text{Eq.5})$$

Akaike’s information criterion:

$$AIC = n * \ln(RMSE) + 2 * p \quad (\text{Eq.6})$$

where h_i = observed height, \hat{h}_i redicted height, \bar{h}_i ean of observed heights, n = number of observations in dataset and k = number of estimated parameters.

Results and discussion

Data summary

Approximately 80% (42 sample plots) of sample plots data were used to develop model and remaining 20% (10 sample plots) were used to test developed models. The dataset for test of developed models was intended to obtain a measure of the adequacy of the calibration from different sampling stands. Since the data set is large enough, this proportions used is unlikely to reduce the precision of the parameter estimates compared with those obtained with the model built from the entire dataset in forestry research or data mining (Soares and Tomé, 2002; Castedo Dorado et al., 2006). The mean, minimum and maximum values and standard deviations of stand variables are shown in *Table 2*.

Table 2. Characteristics of the fitting and evaluation data set

Variables	Fitting data set (n = 794)				Evaluation data set (n = 241)			
	Mean	Minimum	Maximum	Standard deviation	Mean	Minimum	Maximum	Standard deviation
d (cm)	21.2	12.1	34.7	3.2	21.5	11.0	33.5	3.6
h (m)	9.9	5.9	19.0	1.8	10.5	5.5	16.0	2.0
A (yr)	36	32	41	2.5	37	32	41	2.8
dg (cm)	20.9	18.1	25.3	1.6	21.3	18.0	26.3	2.0
G (m ² ha ⁻¹)	27.6	17.1	42.5	4.6	28.7	20.6	46.4	6.0
N (trees ha ⁻¹)	814	448	1136	136	805	624	1104	140.8
H _o (m)	10.6	8.0	17.2	1.6	11.6	9.4	15.3	2.0
D _o (cm)	25.1	21.9	30.9	1.9	25.6	21.0	31.2	2.4
D _{max} (cm)	27.3	23.7	34.7	2.3	27.3	22.3	34.6	2.9
H _m (m)	9.8	7.5	15.3	1.4	10.5	8.4	13.5	1.5
SI (m)	9.5	7.5	15.7	1.4	10.3	8.9	13.6	1.7

The terminology used in the table is as follows: d = diameter at breast height over bark (cm), A = age of stand (yr), d_g = quadratic mean diameter of stand (cm), G = basal area of stand (m²/ha), D_{max} = maximum diameter of stand (cm), D_o = dominant diameter of stand (cm), h = height of trees (m), H_m = mean height of stand (m), H_o = dominant height of stand (m), N = number of trees in stand (trees/ha), SI = site index (m), n = number of sampling trees

Relationship between height and diameter for data fitting model, validation model and all data are shown in *Figure 2*.

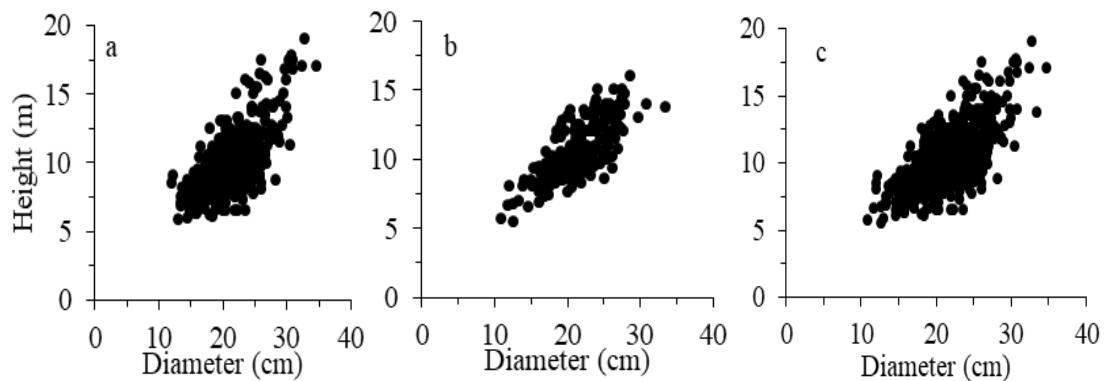


Figure 2. Relationship between diameter and height for data fitting model (a), data validation model (b) and all data (c)

Model fitting

Modelling for biological systems sense is an important tool. Modelling is the process of defining a system's change with equations (Weiskittel et al., 2011). It is therefore important to accurately determine the components of system during modelling and to select the correct equation to describe this system. In our study, it was tried to explain the change of tree height in relation with diameter at breast height according to the regression models in southwestern Turkey. The parameter values for all equations are included in *Table 3*.

The model parameters for all the tested models were found to be significant at the significance level of 0.001. In order to find out which model was more successful in explaining height-diameter relation, a ranking was made for all models according to the specified criteria and the results were shown below. In this ranking method, numerical values were given starting from the smallest MAE, MaxAE, RMSE, ME, AIC ones and for the R value, starting with the highest one. When the ranking values obtained for each model were collected, the model with the smallest value was considered as the best one (*Table 4*).

In this study were found to be similar with the model results of the previous studies (Sanchez et al., 2003; Castedo Dorado et al., 2006). In terms of group averages, the third group of equations was found to be more successful. But, the most successful model among the 36 height-diameter models used was the Cox II_a model, followed by Cox II_b and Sharma and Parton, respectively. Curtis, Gaffrey & Sharma and Zhang models have been not suitable for this region.

The results of fitting and cross-validation for the models of group 1 were the poorest. In this respect, a number of studies showed that adding stand variables to the height-diameter equation and using the generalized height-diameter models increased the precision (Sharma and Parton, 2007; Krisnawati et al., 2010; Temesgen et al., 2014). These stand variables mentioned in the literature are dominant height, stand basal area, maximum diameter, stand age, number of trees per hectare, stand density. The statistics and coefficients according to the studied model were found to be similar to the results of the previous model studies (Larsen and Hann, 1987; Colbert et al., 2002). The inclusion

of basal area and d_g into the base height-diameter function increased the accuracy of prediction (Temesgen and Gadaw, 2004).

Table 3. Parameters of non-linear regression models

Model no	Parameters								
	a_0	a_1	a_2	a_3	a_4	a_5	a_6	a_7	a_8
1	1.716443	-5.306083	-15.181403	-0.022643	-	-	-	-	-
2	-4.159129	0.960891	0.338363	0.275196	-	-	-	-	-
3	3.834179	-41.321130	-19.480656	207.082437	1.393833	-	-	-	-
4	1.846925	-	-	-	-	-	-	-	-
5	0.526950	-	-	-	-	-	-	-	-
6	-0.048474	-	-	-	-	-	-	-	-
7	-0.053122	-	-	-	-	-	-	-	-
8	1.924790	-	-	-	-	-	-	-	-
9	-0.005893	10.695102	-	-	-	-	-	-	-
10	0.283957	-	-	-	-	-	-	-	-
11	-353.995785	7.157280	5.451819	0.129807	0.000621	-	-	-	-
12	-1.851475	-0.989978	-	-	-	-	-	-	-
13	0.106958	1.500000	0.468510	-	-	-	-	-	-
14	0.966326	-0.051939	0.037236	-	-	-	-	-	-
15	1.165160	2.226022	1.982192	-	-	-	-	-	-
16	1.298927	1.668149	1.167713	-	-	-	-	-	-
17	-22.383484	-6.374520	-	-	-	-	-	-	-
18	6.314068	-0.311706	0.424369	0.074948	-	-	-	-	-
19	7.913832	1.473407	0.358958	-13.137764	-	-	-	-	-
20	2.261735	-0.016805	1.239617	-11.641012	-	-	-	-	-
21	15.323304	2.724760	0.677738	-5.761236	-	-	-	-	-
22	0.468122	-0.045892	0.929943	0.025909	0.471646	-	-	-	-
23	15.386189	2.750300	0.674077	-0.015238	5.759656	-	-	-	-
24	1.651100	1.043897	0.073152	-5.834839	-0.000625	-0.001224	-	-	-
25	-122.918442	0.975019	-0.790733	121.929973	0.001889	5×10^{-9}	6.477289	0.813999	0.894380
26	3.178352	0.562636	0.115088	-0.223862	-	-	-	-	-
27	1.122581	0.988632	0.026346	-0.374752	1.972110	-	-	-	-
28	1.072885	1.031935	1.141993	-0.850653	1.487636	-	-	-	-
29	0.016350	0.770381	-3.156851	-0.121544	-0.001077	-	-	-	-
30	-0.000691	0.114182	-	-	-	-	-	-	-
31	-2.608873	-0.804187	0.196157	0.037243	-	-	-	-	-
32	2.494066	0.060584	0.101072	-13.008971	-10.368192	-	-	-	-
33	0.073700	33.485427	-3.034925	-11.024664	-0.154562	-	-	-	-
34	1.224536	0.926236	0.319181	-7.179243	29.976501	-	-	-	-
35	0.542895	0.804716	13.096415	1.259923	-162.752624	-14.715665	-	-	-
36	1.150484	0.893337	-0.206565	0.188713	0.415724	-11.460517	-	-	-

a_0, a_1, \dots = regression coefficients

The values of statistics of the models included in group model 2 show that the second modification of Cox II_a is the equation that most accurately estimates height. The best equation was found in the second group because of a low variation in stand age. When the stand age variation was high, the group model 2 was more successful than group model 3.

The models of Cox II_b and Sharma & Parton also fit well to the data in *Table 4*. The advantage of these models was that they were functions of simple equation, although the bias and MSE were slightly higher than those of the modified versions of the Cox II_a model.

Table 4. Performance criteria for generalized height-diameter models for the fitting data

Model no	Performance criteria						
	MAE	MaxAE	RMSE	R	ME	AIC	Rank
1	1.23352 (36)	4.70653 (35)	1.54613 (36)	0.51256 (36)	-0.91648 (36)	353.990 (36)	36
2	0.90645 (34)	3.97724 (33)	1.15783 (33)	0.76586 (33)	0.00338 (16)	124.359 (33)	30
3	0.86868 (32)	5.37752 (36)	1.16102 (34)	0.76472 (34)	0.00182 (14)	128.543 (35)	32
4	0.61337 (17)	2.90029 (19)	0.78395 (15)	0.89985 (15)	0.08043 (29)	-191.270 (13)	20
5	0.61940 (21)	2.94987 (24)	0.79151 (19)	0.89780 (20)	0.09082 (35)	-183.647 (17)	24
6	0.63727 (26)	2.98865 (26)	0.81630 (25)	0.89090 (25)	0.15062 (31)	-159.161 (24)	27
7	0.61708 (19)	2.90005 (18)	0.78865 (17)	0.89858 (17)	0.08608 (30)	-186.522 (15)	21
8	0.61260 (15)	2.91290 (22)	0.78312 (14)	0.90007 (14)	0.07878 (28)	-192.109 (12)	17
9	0.89279 (33)	3.73911 (30)	1.11244 (32)	0.78572 (32)	-0.07513 (34)	88.605 (32)	35
10	0.85097 (31)	3.96399 (32)	1.09746 (31)	0.79191 (31)	-0.53040 (33)	75.841 (31)	33
11	0.68984 (28)	3.03966 (28)	0.88701 (28)	0.87043 (27)	0.05039 (25)	-85.200 (28)	28
12	0.56765 (3)	2.65307 (9)	0.71431 (2)	0.91773 (3)	0.05888 (26)	-263.132 (2)	6
13	0.63052 (23)	2.79037 (16)	0.80420 (22)	0.89458 (22)	-0.00365 (17)	-167.018 (22)	23
14	0.73644 (30)	3.66945 (29)	0.94454 (29)	0.85117 (29)	0.00550 (19)	-39.304 (30)	29
15	0.61041 (13)	2.75054 (12)	0.78863 (16)	0.89886 (16)	0.02120 (24)	-182.542 (18)	14
16	0.60687 (11)	2.93672 (23)	0.77907 (11)	0.90143 (11)	0.01516 (23)	-192.226 (10)	12
17	0.73333 (29)	4.35856 (34)	0.94479 (30)	0.85088 (30)	0.44719 (32)	-41.093 (29)	31
18	0.68532 (27)	2.88025 (17)	0.88680 (27)	0.87032 (28)	-0.00723 (20)	-87.388 (27)	26
19	0.59900 (6)	2.58431 (5)	0.77400 (7)	0.90290 (7)	0.00023 (3)	-195.410 (5)	4
20	0.62974 (22)	2.69422 (10)	0.80497 (23)	0.89451 (23)	0.00021 (1)	-164.259 (23)	15
21	0.59904 (7)	2.62233 (8)	0.77492 (8)	0.90266 (9)	-0.00045 (6)	-194.466 (8)	7
22	0.57292 (4)	2.60799 (7)	0.72224 (4)	0.91615 (4)	0.00141 (13)	-248.366 (3)	5
23	0.59916 (8)	2.60273 (6)	0.77526 (9)	0.90270 (8)	-0.00046 (7)	-192.118 (11)	8
24	0.56047 (1)	2.36446 (1)	0.70628 (1)	0.92008 (1)	-0.00044 (5)	-264.108 (1)	1
25	0.56484 (2)	2.49484 (2)	0.71598 (3)	0.91810 (2)	-0.00281 (15)	-247.278 (4)	2
26	0.91127 (35)	3.89076 (31)	1.16327 (35)	0.76332 (35)	0.00788 (21)	128.081 (34)	34
27	0.59885 (5)	2.55334 (4)	0.77289 (5)	0.70332 (5)	0.00037 (4)	-194.549 (6)	3
28	0.60058 (9)	2.95984 (25)	0.77290 (6)	0.90332 (6)	-0.00022 (2)	-194.539 (7)	9
29	0.63466 (24)	2.73507 (11)	0.80966 (24)	0.89335 (24)	0.00127 (11)	-157.646 (25)	22
30	0.60831 (12)	2.90991 (21)	0.78097 (12)	0.90079 (12)	0.01201 (22)	-192.292 (9)	11
31	0.61129 (14)	2.90111 (20)	0.78283 (13)	0.90055 (13)	0.06951 (27)	-186.403 (16)	16
32	0.63609 (25)	3.01366 (27)	0.81981 (26)	0.89049 (26)	-0.00138 (12)	-147.754 (26)	25
33	0.61363 (18)	2.78609 (15)	0.79100 (18)	0.89848 (18)	-0.00409 (18)	-176.159 (19)	19
34	0.61299 (16)	2.75859 (13)	0.79161 (20)	0.89832 (19)	0.00094 (9)	-175.547 (20)	13
35	0.61730 (20)	2.78036 (14)	0.79496 (21)	0.89754 (21)	0.00069 (8)	-170.194 (21)	18
36	0.60169 (10)	2.50238 (3)	0.77717 (10)	0.90232 (10)	0.00118 (10)	-188.160 (14)	10

MAE = mean absolute error, MaxAE = maximum absolute error, RMSE = root mean square error, R = correlation coefficients, Bias = mean error, AIC = Akaike's information criterion and rank = numerical values in ranking method

Errors of actual heights versus heights predicted in the fitting phase of the Cox II_a, Cox II_b and Sharma & Parton models are shown in *Figure 3*. There was no reason to reject the hypotheses of normality, homogeneity of variance and independence of residuals.

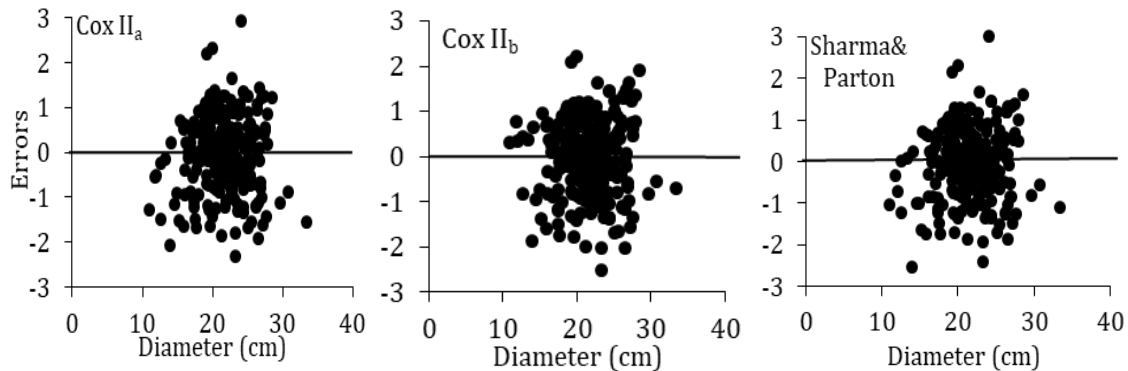


Figure 3. Errors actual heights versus predicted values in the fitting phase for the of Cox II_a, Cox II_b, Sharma & Parton models

In general, it was found that the error amounts show an increase in successful models due to the increase in height values (Ahmadi et al., 2013; Özçelik and Çapar, 2014). The amount of error in our work did not increase, but decreased because this forest is plantation and trees have got similar height. It can be said that the variation with respect to the error distributions obtained with the generalized height-diameter models is relatively constant (from -2 m to +2 m).

In this study, when it was decided whether a model is successful, it is required that the amount of error was small, and that it has a certain and constant variance in the errors were obtained. Tree height changed from 5.9 to 19.0 m in this study (in *Table 2*). In predicted of a tree height error about 2 meter was small. Cox II_a, Cox II_b, and Sharma & Parton models were found successful in this respect.

In describing the diameter-height relationship, group 3 models including the stand age was more successful (Sánchez et al., 2003). However, results of group 2 models were found as the best models because of data were taken from artificial stands in this study.

Cox II_a, Cox II_b, and Sharma & Parton models could offer a balance between the accuracy of model and sampling effort, because the value of stand age was not including for plantation in Group 2 models.

Observed heights versus the predicted heights in the cross-validation of this model are shown in *Figure 4*. The performance criterion to evaluate the behaviour of model was the determination coefficient of the straight line fitted between the observed and predicted heights. *Figure 4* shows no tendency toward the overestimation or underestimation of height values.

For the tested models, the results obtained using the independent data set is given in *Figure 4*. The most similar results of Cox II_a, Cox II_b and Sharma & Parton models are shown in *Figure 4*. Relatively similar results were obtained for same models (Sánchez et al., 2003). The overlap ratio of the predicted height values with the measured height values does not increase as the height value increases.

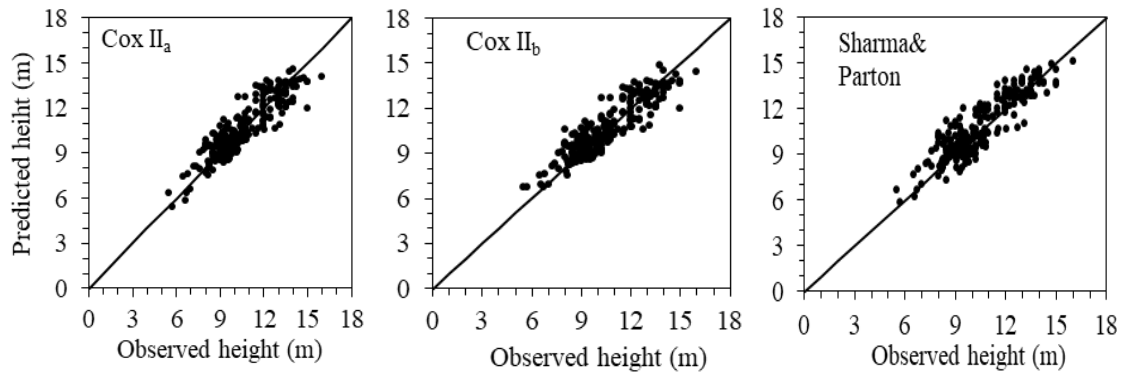


Figure 4. Observed heights versus predicted heights in the cross-validation for the Cox II_a, Cox II_b and Sharma & Parton models

As can be seen from Table 5, the tested height-diameter models were not very different from the model development data.

Table 5. Criterion values for successful models with independent data set

Model no	Performance criteria						
	MAE	MaxAE	RMSE	R	ME	AIC	Rank
24	0.68882 (3)	3.00290 (5)	0.87938 (2)	0.89799 (3)	-0.04821 (1)	-18.9777 (2)	2
25	0.67832 (1)	2.99999 (4)	0.00113 (3)	0.89895 (2)	-0.05729 (3)	-12.4986 (4)	3
27	0.71003 (5)	2.73425 (2)	0.91893 (5)	0.88752 (5)	-0.19489 (5)	-10.3754 (5)	5
19	0.70434 (4)	2.66425 (1)	0.90841 (4)	0.88974 (4)	-0.19010 (4)	-15.1503 (3)	4
22	0.68160 (2)	2.93107 (3)	0.87081 (1)	0.89963 (1)	-0.05696 (2)	-23.3373 (1)	1

MAE = mean absolute error, MaxAE = maximum absolute error, RMSE = root mean square error, R = correlation coefficients, Bias = mean error, AIC = Akaike's information criterion and rank = numerical values in ranking method

Finally, the most successful models were used for all sample plot data. Regression coefficients and statistics of these models are shown in Table 6. These parameters can use to estimate of diameter-height relationship for artificial brutian pine in southwestern Turkey.

Table 6. Regression coefficients and statistics obtained for the d-h models using the entire data set

Model no	Parameters								
	a ₀	a ₁	a ₂	a ₃	a ₄	a ₅	a ₆	a ₇	a ₈
24	4.527680	1.217846	-0.178316	-9.800583	-0.003507	-0.000524	-	-	-
25	-122.56039	0.983721	-0.711003	121.203832	0.002021	4.8x10 ⁻⁵¹	42.055083	0.903834	0.812250
27	1.426453	0.909989	0.028413	-0.304526	1.710843	-	-	-	-
19	8.405537	1.393674	0.322209	-13.749983	1.970000	-	-	-	-
22	0.431054	-0.045442	0.957580	0.025728	0.006561	-	-	-	-

a₀, a₁... = regression coefficients

Conclusions

In this study, 36 height-diameter models were calibrated and tested for brutian pine plantations in southwestern Turkey. The best predictions of height were obtained by the Cox II_a model, which used diameter (d), quadratic mean diameter (d_g), and stand mean height (H_m) as independent variables. In this model, provides little effort has been made to model the height-diameter relationship in uneven-aged stands with generalized height-diameter functions. In addition, group 2 models should be used instead of group 3 models in the artificial stands.

The inclusion of stand mean height or of stand dominant height as an independent variable in the height-diameter equations seems to be necessary in order to achieve acceptable predictions. This requires the measurement of at least one sample of heights for the practical application of the equation. The inclusion of d_g into the base height-diameter model increased the accuracy of prediction.

As a result, examples of applications of the selected generalized height-diameter models to the forest management are presented, namely how to use it to complete missing information from forest inventory and also showing how such an equation can be incorporated in a stand-level decision support system that aims to optimize the forest management for the maximization of wood volume production in southwestern Turkey brutian pine stands.

REFERENCES

- [1] Ademe, P., Del Rio, M., Canellas, I. (2008): A mixed nonlinear height-diameter model for hyreanean oak (*Quercus pyrenaica* Willd.). – For. Ecol. Manage. 256(1-2): 88-98.
- [2] Ahmadi, K., Alavi, S. J., Kouchaksaraei, M. T., Aestern, W. (2013): Non-linear height-diameter model for oriental beech (*Fagus orientalis* Lipsky) in the Hyrcanian forests. – Iran. Biotechnol. Agron. Soc. Environ. 17: 431-440.
- [3] Amateis, R. L., Burkhart, H. E., Zhang, S. (1995): TRULOB: Tree Register Updating for Loblolly Pine (An Individual Tree Growth and Yield Model for Managed Loblolly Pine Plantations). Coop. Rep. 83. – Virginia Polytechnic Institute and State University, Loblolly Pine Growth and Yield Cooperative, Blacksburg, VA, USA.
- [4] Anonymous (2015): Forest Resources. – Directorate of Forests, Ankara, Turkey.
- [5] Bennett, F. A., Clutter, J. L. (1968): Multiple-Product Yield Estimates for Unthinned Slash Pine Plantations-Pulpwood, Sawtimber, Gum. USDA For. Serv. Res. Pap. SE-35. – Southeast. Forest Exp. Stn., Asheville, NC.
- [6] Budhathoki, C. B., Lynch, T. B., Guldin, J. M. (2008): A mixed-effects model for dbh-height relationship of shortleaf pine (*Pinus echinata* Mill.). – South. J. Appl. For. 32: 5-11.
- [7] Burkhart, H. E., Strub, M. R. (1974): A Model for Simulation of Planted Loblolly Pine Stands. – In: Fries, J. (ed.) Growth Models for Tree and Stand Simulation. Research Note 30, pp.128-135, Royal College of Forestry, Stockholm, Sweden.
- [8] Cañadas, N., García, C., Montero, G. (1999): Relación altura-diámetro para *Pinus pinea* L. en el Sistema Central. – Congreso de Ordenación y Gestión Sostenible de Montes, Santiago de Compostela, 4-9 octubre. Tomo I, pp. 139-153.
- [9] Castedo Dorado, F., Ruiz, A. D., Álvarez González, J. G. (2001): Modelización de la relación altura-diámetro para *Pinus pinaster* Ait. en Galicia mediante la función de densidad bivalente SBB. – Investigación Agraria, Sistemas y Recursos Forestales 10: 111-126.

- [10] Castedo Dorado, F., Dieguez Aranda, U., Barrio Anta, M., Sanchez Rodriguez, M., Gadow, K. (2006): A generalized height-diameter model including random components for radiata pine plantations in Northwestern Spain. – For. Ecol. Manage. 229: 202-213.
- [11] Çatal, Y. (2012): Height-diameter model for black locust, Anatolian black pine and Taurus cedar tree species in Lakes Region. – SDU J. Faculty For. 13: 92-96.
- [12] Clutter, J. L., Allison, B. J. (1974): A Growth and Yield Model for *Pinus radiata* in New Zealand. In: Fries, J. (ed.) Growth Models for Tree and Stand Simulation, pp. 136-160. Research Note 30. – Royal College of Forestry, Stockholm, Sweden.
- [13] Colbert, K. C., Larsen, D. R., Lootens, J. R. (2002): Height-diameter equations for thirteen mid-western bottomland hardwood species. – North. J. App. For. 19: 171-176.
- [14] Cox, F. (1994): Modelos parametrizados de altura. Informe de convenio de investigación interempresas. – INFORA, Santiago.
- [15] Curtis, R. O. (1967): Height-diameter and height-diameter-age equations for second-growth Douglas-fir. – For. Sci. 13: 365-375.
- [16] Diamantopoulou, M. J., Özçelik, R. (2012): Evaluation of different modelling approaches for total tree-height estimation in Mediterranean region of Turkey. – Forest Systems 21: 383-397.
- [17] Gaffrey, D. (1988): Forstamts-und bestandesindividuelles Sortimentierungsprogramm als Mittel zur Planung, Aushaltung und Simulation. – Diplomarbeit Forstliche Fakultät, Universität Göttingen, Germany.
- [18] Harrison, W. C., Burk, T. E., Beck, D. E. (1986): Individual tree basal area increment and total height equations for Appalachian mixed hardwoods after thinning. – South. J. Appl. For. 10: 99-104.
- [19] Huang, S., Price, D., Titus, S. J. (2000): Development of ecoregion-based height-diameter models for white spruce in boreal forests. – For. Ecol. Manage. 129: 125-141.
- [20] Hui, G., Gadow, K. v. (1993): Zur Entwicklung von Einheitshöhenkurven am Beispiel der Baumart *Cunninghamia lanceolata*. – Allg. Forst. Lagdztg. 164: 218-220.
- [21] Krisnawati, H., Wang, Y., Ades, P. K. (2010): Generalized height-diameter model for *Acacia mangium* Willd. plantations in South Sumatra. – J. For. Res. 7: 1-19.
- [22] Larsen, D. R., Hann, D. W. (1987): Height-Diameter Equations for Seventeen Tree Species in Southwest Oregon. Research Paper No 49. – Oregon State University Forest Research Laboratory, Corvallis, OR, USA.
- [23] Lei, Y., Parresol, B. R. (2001): Remarks on Height-Diameter Modelling. Research Note SRS-10. – USDA Forest Service, Southern Research Station, Asheville, NC, USA.
- [24] Lenhart, J. D. (1968): Yield of Old-Field Loblolly Pine Plantations in the Georgia Piedmont. – Ph. D. Thesis, Univ. Ga., Athens, Greece.
- [25] Lootens, J. R., Larsen, D. R., Shifley, S. R. (2007): Height-diameter equations for 12 upland species in the Missouri Ozark Highlands. – North. J. Appl. For. 24: 149-152.
- [26] López Sánchez, C. A., Varela, J. G., Castedo Dorado, F., Alboreca, A. R., Soalleiro, R. R., Álvarez González, J. G., Rodríguez, F. S. (2003): A height-diameter model for *Pinus radiata* D. Don in Galicia (Northwest Spain). – Ann. For. Sci. 60: 237-245.
- [27] Mirkovich, J. L. (1958): Normale visinske krive za chrast kitnak i bukvu v NR Srbiji. – Glasnik sumarskog fakulteta 13, Zagreb.
- [28] Mısır, N. (2010): Generalized height-diameter models for *Populus tremula* L. stands. – Afr. J. Bio. 92: 4348-4355.
- [29] Mønness, E. N. (1982): Diameter distributions and height curves in evenaged stands of *Pinus sylvestris* L. Medd. No. – Inst. Skogforsk 36: 1-43.
- [30] Özçelik, R., Çapar, C. (2014): Developing generalized height-diameter models for natural Brutian pine stands in Antalya district. – SDU J. Faculty For. 15: 44-52.
- [31] Pascoa, F. (1987): Estrutura, crescimento e produção em povoamentos de pinheiro bravo. Um modelo de simulação. – Ph.D. Thesis, Universidade Técnica de Lisboa, Lisbon, Portugal.

- [32] Peng, C. (1999): Nonlinear Height-Diameter Models for Nine Tree Species in Ontario Boreal Forests. Forest Research Report No. 155. – Ontario Forest Research Institute, Ontario, Canada.
- [33] Pienaar, L. V., Harrison, W. M., Reheney, J. W. (1990): PMRC Yield Prediction System for Slash Pine Plantations in the Atlantic Coast Flatwoods. – PRMC Technical Report 1990-3, Athens, Greece.
- [34] Prodan, M. (1968): Forest Biometrics. – Pergamon Press, Oxford, UK.
- [35] Richards, F. J. (1959): A flexible growth function for empirical use. – J. Exp. Biol. 10: 290-300.
- [36] Sanchez, C. A. L., Varela, J. G., Dorado, F. C., Alboreca, A. R., Soalleiro, R. R., Gonzalez, J. G. A., Rodriguez, F. S. (2003): A height-diameter model for *Pinus radiata* D. Don in Galicia (North-west Spain). – Ann. For. Sci. 60: 237-245.
- [37] Schröder, J., Álvarez González, J. G. (2001): Developing a generalized diameter-height model for maritime pine in Northwestern Spain. – Forstwissenschaftliches Centralblatt 120: 18-23.
- [38] Sharma, M., Parton, J. (2007): Height-diameter equations for boreal tree species in Ontario using a mixed effects modelling approach. – For. Ecol. Manage. 249: 187-198.
- [39] Sharma, M., Zhang, S. Y. (2004): Height-diameter models using stand characteristics for *Pinus banksiana* and *Picea mariana*. – Scan. J. For. Res. 19: 442-451.
- [40] Sloboda, V. B., Gaffrey, D., Matsumura, N. (1993): Regionale und lokale Systeme von Höhenkurven für gleichaltrige Waldbestände. – Allg. Forst. Jagdztg. 164: 225-228.
- [41] Soares, P., Tomé, M. (2002): Height-diameter model equation for first rotation eucalypt plantations in Portugal. – For. Ecol. Manage. 166: 99-109.
- [42] Sönmez, T. (2008): Generalized height-diameter models for *Picea orientalis* L. – J. Environ. Biol. 30: 767-772.
- [43] Temesgen, H., Gadow, K. V. (2004): Generalized height-diameter models-an application for major tree species in complex stands of interior British Columbia. – Eur. J. Forest Res. 123: 45-51.
- [44] Temesgen, H., Zhang, C. H, Zhao, X. H. (2014): Modelling tree height-diameter relationships in multi-species and multi-layered forests: A large observational study from Northeast China. – For. Ecol. Manage. 316: 78-89.
- [45] Tomé, M. 1989. Modelação do crescimento da árvore individual em povoamentos de *Eucalyptus globulus* Labill. (1ª rotação) na região centro de Portugal. – Ph.D. Thesis, Instituto Superior de Agronomia, Universidade Técnica de Lisboa, Lisbon, Portugal.
- [46] Usta, H. Z. (1991): A Study on the Yield of *Pinus brutia* Ten. Plantations. – Turkish Forest Research Institute Publications, Ankara, Turkey.
- [47] Weiskittel, A. R., Hann, D. W., Kershaw J. A., Vanclay J. K. (2011): Forest Growth and Yield Modeling. – Wiley-Blackwell Press, Chichester, UK.
- [48] Wykoff, W. R., Crookston, C. L., Stage, A. R. (1982): User's Guide to the Stand Prognosis Model. General Technical Report. INT-133. – USDA Forest Service, Utah, USA.

INFLUENCE OF SCENIC ROAD CORRIDOR ON PLANT DIVERSITY IN KUNYU MOUNTAIN, CHINA

YIN, X. D.^{1,2} – GAO, Y.^{1,3*} – LIU, J.⁴ – ZHAO, W. G.³

¹*Shandong Provincial Key Laboratory of Water and Soil Conservation and Environmental Protection, College of Resources and Environment, Linyi University
Linyi 276005, China*

²*Linyi NO.1 High School of Shandong Province
Linyi 276000, China
(e-mail: yinxiaodi0717@126.com)*

³*Linyi Scientific Exploration Laboratory
Linyi 276037, China
(e-mail: 1396870345@qq.com)*

⁴*College of Biological Sciences and Biotechnology, Beijing Forestry University
Beijing 100083, China
(e-mail: liujian20170703@163.com)*

**Corresponding author
e-mail: gaoyuan1182@tom.com, gaoy@lyu.edu.cn*

(Received 18th Nov 2017; accepted 12th Feb 2018)

Abstract. The edge effect of forest communities in Kunyu Mountain Nature Reserve of China due to two small-scale roads was studied. By setting 3 groups of sample plots: sample plot beside 2.5 m road corridor, sample plot beside 5.0 m road corridor and sample plot in wildwood area, forest investigation was carried out using typical sampling method to evaluate and reveal the influence of edge effect (caused by 2.5 m and 5.0 m scenic road corridor) on the community structure, species composition and diversity of plants in Kunyu mountain national nature reserve. Results show (1) that compared with wildwood area, the average *DBH* (diameter at breast height) of tree layer at 2.5 m and 5.0 m scenic road corridor in Kunyu mountain national nature reserve decreases with the increase of width of road corridor. In shrub layer, edge effect is balanced by increasing the number of low-diameter shrubs while decreasing the number of high-diameter shrubs. It is worth noting that the edge effect of 2.5 m scenic road corridor is significantly higher than that of 5.0 m scenic road corridor. (2) In tree layer, the four indexes all showed as follows: sample plot near 5.0 m scenic road corridor was significantly higher than the sample plot near 2.5 m scenic road corridor and wildwood area. In shrub layer, the four indexes abovementioned can be ranked as sample plot near 5.0 m scenic road corridor>sample plot near 2.5 m scenic road corridor>wildwood area. In herb layer, the 4 indexes are ranked as sample plot near 5.0 m scenic road corridor>wildwood area>sample plot near 2.5 m scenic road corridor. Main conclusion: The 2.5 m scenic road corridor exerts an inhibition effect on the species composition and diversity of plants in Kunyu mountain national nature reserve, however, 5.0 m scenic road corridor has a promoting effect.

Keywords: *channel corridor, edge effect, species composition, plant diversity, Kunyu Mountain National Nature Reserve*

Introduction

Frequent human activities lead to habitat fragmentation and loss of species diversity. Under such background, continuous natural habitat is gradually replaced by fragmented forest patches and the forest edge area is gradually increased (Lian and Yu, 2000; Velázquez et al., 2017). Corridor refers to linear or banded landscape element

which is different from surrounding landscape matrix (Zhu et al., 2005; Naidoo et al., 2018). Corridor can lead to change of ecological factors, thus making system components and behaviors (i.e. Population density, productivity and diversity, etc.) different from that inside of system (Wang and Ma, 1985; Chen et al., 2004). Road exists as corridor of landscape. The introduction of road enhances the fragmentation degree of landscape and the influencing area of edge effect (Zhou et al., 2009). Studies show that the edge effect of corridor causes the inhomogeneous distribution of species composition and diversity between inside and outside of plants community; The positive and negative edge effects are correlated with the area, shape, forming age, connectivity of forest patches as well as the property of neighboring patches. Therefore, research results on the positive and negative corridor edge effects are quite different (Sun et al., 2008; Wu et al., 2011; Liu et al., 2012). In fragmented forest patches, environmental factors such as solar irradiance, humidity and soil are normally in graded distribution from forest edge to inner forest. Therefore, the distance between inner patch to forest edge is correlated with corridor edge effect. The species composition, community structure and diversity also vary from forest edge to inner forest (Ma et al., 2008; Su et al., 2014). Since different plants have different sensitivities to habitat fragmentation, they have different strategies to get adapted to environmental change. For example, sensitive vs. tolerant species, trees vs. shrubs, shade-tolerance species vs. shade-intolerance species, evergreen species vs. deciduous species, they have different responses to edge effect; therefore, research results on corridor edge effect are different (Tian et al., 2011).

Studying the edge-induced community-based effects helps to understand the ecosystem changes caused by the road network, which may break the ecosystem integrity through the marginal effects of microclimates (García et al., 2007). The study of action characters of edge effect of scenic road corridor can provide data reference and theoretical basis for biodiversity conservation, balance of travel activities, and construction planning of future scenic road. In this paper, based on scenic road corridor of Kunyu mountain nature reserve as research objects, the property and action characters of edge effect of scenic road corridor were analyzed, in the hope of figuring out how the edge effect of scenic road corridor (2.5 m and 5.0 m) will affect the plants community structure, species composition and diversity.

Materials and methods

Profile of research area

Kunyu mountain national nature reserve locates at eastern shandong province, China, with geographical coordinates of 37°16'–37°25' N, 121°42'–121°50' E. It is the native place of Chinese red pine (*Pinus densiflora*) and the world's largest distribution of red pine (*Pinus densiflora*) forest, the best protected natural distribution center. It is one of the most biodiversity-rich regions in the world at the same latitude. It is the only place in the world to study the location of forest ecosystems for the project “Natural Control of Forest Pests”. Kunyu mountain national nature reserve covers area of 48 km², with the main peak-Taibo Peak reaching an altitude of 923 m. The soil of Kunyu mountain nature reserve is mainly brown soil, which has a sandy texture, in acidic to slightly acidic condition. The climate here belongs to warm temperate continental monsoon climate, with four distinctive seasons, abundant sunlight, annual mean temperature at 11.9 °C and annual rainfall of 985 mm. Kunyu mountain national nature reserve is national forest park

and national 4A tourist scenic area. The forest coverage rate is about 92%, mainly consisting of red pine (*Pinus densiflora*), black pine (*Pinus thunbergii*), oak (*Quercus acutissima*) and locust (*Robinia pseudoacacia*) (Du et al., 2007).

Research method

Field investigation

Through reviewing literatures, inquiring forest management department and field investigation, forest investigation was carried out using typical sampling method (Fang et al., 2004; Fang et al., 2009). The investigation results show that the plant community was in natural growth and succession condition, i.e. indicating half-mature forest. The sample plot dimension was 20 m × 30 m. Three different sample plots were set, including sample plot near 2.5 m scenic road corridor, sample plot near 5.0 m scenic road corridor and sample plot at wildwood area. Five repeated investigations were conducted in each sample plot.

Investigations of plant species diversity were carried out in tree layer, shrub layer and herb layer. The research areas included one tree layer of 20 m × 30 m, 1 shrub layer of 10 m × 10 m and 4 herb layers of 1 m × 1 m. In tree layer, the species, number and *DBH* values of all trees with *DBH* ≥ 5 cm were measured; In shrub layer, the species, number and *DBH* values of all trees with *DBH* < 5 cm were measured. In herb layer, the species, number and heights of all herbs were measured (Fang et al., 2004; Fang et al., 2009; Wei et al., 2017).

Data analysis

Plant species diversity was analyzed and measured using general-purpose indexes (Leinster and Cobbold, 2012; Wei et al., 2017), including species richness index (*S*; Eq. 1), Shannon–Wiener diversity index (*H*; Eq. 2), Simpson diversity index (*P*; Eq. 3) and Pielou evenness index (*E*; Eq. 4).

$$S = \text{the number of plant species in sample plot} \quad (\text{Eq.1})$$

$$H = -\sum_{i=1}^s (P_i \times \ln P_i) \quad (\text{Eq.2})$$

$$P = 1 - \sum_{i=1}^s (P_i \times P_i) \quad (\text{Eq.3})$$

$$E = H / \ln S \quad (\text{Eq.4})$$

P_i refers to the ratio between importance value of the *i*-th species and total importance value in sample plot. The importance value of tree layer or shrub layer = (relative dominance + relative density + relative frequency) / 3, the importance value of herb layer = (relative dominance + relative density + relative frequency) / 3.

In the data analysis process, SPSS 17.0 software (Chinese version) and method of one-way analysis of variance and significance test was used.

Results

Species composition of tree layer

As shown in *Table 1*, the number of plant species in tree layer can be ranked as sample plot near 5.0 m scenic road corridor>wildwood area>sample plot near 2.5 m scenic road corridor; the number of plants in tree layer can be ranked as sample plot near 2.5 m scenic road corridor>wildwood area>sample plot near 5.0 m scenic road corridor; the mean DBH of plants in tree layer can be ranked as wildwood area>sample plot near 2.5 m scenic road corridor>sample plot near 5.0 m scenic road corridor.

Table 1. Species, individual number and mean DBH of trees in wildwood area, sample plot near 5.0 m scenic road corridor and sample plot near 2.5 m scenic road corridor

Tree name	Wildwood area		Sample plot near 2.5 m scenic road corridor		Sample plot near 5.0 m scenic road corridor	
	Plants number	Average DBH/cm	Plants number	Average DBH/cm	Plants number	Average DBH/cm
<i>Pinus densiflora</i>	201	10.06	338	10.57	109	11.83
<i>Quercus variabilis</i>	174	10.26	253	10.52	80	10.05
<i>Pinus thunbergii</i>	45	12.27			33	13.45
<i>Quercus mongolica</i>	37	15.08	14	13.79	27	10.74
<i>Quercus hopeiensis</i>	20	6.55				
<i>Quercus fangshanensis</i>	12	13.75	1	10.00	7	10.00
<i>Albizia kalkora</i>	8	5.00	11	10.18	22	8.36
<i>Quercus acutissima</i>	5	5.80			30	6.50
<i>Sorbus alnifolia</i>	4	5.00			4	10.25
<i>Cerasus serrulata</i>	2	5.55				
<i>Pistacia chinensis</i>	1	5.00	24	6.62	2	8.00
<i>Lauraceae. obtusifolia</i>	1	5.00			17	5.35
<i>Salix matsudana</i>	1	5.00			3	7.00
<i>Malus baccata</i>	1	5.00			1	5.00
<i>Diospyros lotus</i>			2	6.50	1	6.00
<i>Robinia pseudoacacia</i>			1	15.00	5	7.40
<i>Rhus chinensis</i>					56	7.21
<i>Larix kaempferi</i>					21	15.26
<i>Ailanthus altissima</i>					8	9.00
<i>Symplocos paniculata</i>					4	5.00
<i>Alnus Sibirica</i>					3	9.33
<i>Catalpa bungei</i>					2	20.00
<i>Celtis koraiensis</i>					1	5.00
<i>Pterocarya stenoptera</i>					1	5.00
<i>Hovenia acerba</i>					1	16.00
<i>Fraxinus rhynchophylla</i>					1	5.00
<i>Cerasus serrulata</i> var. <i>pubescens</i>					1	8.00
<i>Amorpha fruticosa</i>					1	5.00
Total	512	10.67	644	10.46	441	10.18

Species composition of shrub layer

As shown in Table 2, the number of plant species in shrub layer can be ranked as sample plot near 5.0 m scenic road corridor > wildwood area > sample plot near 2.5 m scenic road corridor; the individual number of low-DBH shrubs can be ranked as sample plot near 2.5 m scenic road corridor > sample plot near 5.0 m scenic road corridor > wildwood area; the individual number of high-DBH shrubs can be ranked as wildwood area > sample plot near 5.0 m scenic road corridor > sample plot near 2.5 m scenic road corridor.

Table 2. Species, individual number of shrubs in wildwood area, sample plot near 2.5 m scenic road corridor and sample plot near 5.0 m scenic road corridor

Shrub name	Wildwood area		Sample plot near 2.5 m scenic road corridor		Sample plot near 5.0 m scenic road corridor	
	DBH < 2.5 cm	2.5 cm ≤ DBH < 5 cm	DBH < 2.5 cm	2.5 cm ≤ DBH < 5 cm	DBH < 2.5 cm	2.5 cm ≤ DBH < 5 cm
<i>Indigofera kirilowii</i>	147		372		89	
<i>Quercus variabilis</i>	154	43	209	56	81	19
<i>Quercus mongolica</i>	97	14	106	5	29	3
<i>Cerasus glandulosa</i>	37		106	1	71	1
<i>Rhus chinensis</i>	16		29	1	147	20
<i>Lauraceae. obtusiloba</i>	12	1			104	44
<i>Quercus hopeiensis</i>	96	47				
<i>Leptopus chinensis</i>	22		100	17	2	
<i>Pinus densiflora</i>	22	25	37	36	6	3
<i>Lespedeza bicolor</i>	34		65		21	
<i>Albizia kalkora</i>	37	9	21	1	43	7
<i>Kalopanax septemlobus</i>	17				80	6
<i>Quercus acutissima</i>	21	5	4	1	39	21
<i>Euonymus phellomanus</i>	52	6	19	1	7	
<i>Grewia biloba</i>	1		68		13	
<i>Symplocos paniculata</i>	12	1	11	4	29	12
<i>Diospyros lotus</i>	5		5	1	54	
<i>Robinia pseudoacacia</i>	15		27	1	17	2
<i>Ailanthus altissima</i>	18		6		35	1
<i>Pinus thunbergii</i>	26	13			11	6
<i>Zanthoxylum schinifolium</i>	32		13		5	
<i>Euonymus alatus</i>	8		13		14	3
<i>Celastrus orbiculatus</i>	8		22			
<i>Ligustrum sinense</i>	2		7		17	2
<i>Pistacia chinensis</i>	14	2	9	1		
<i>Amorpha fruticosa</i>	4		9		10	
<i>Quercus fangshanensis</i>	8	2	2	1	4	2
<i>Cerasus serrulata</i> var. <i>pubescens</i>	6				8	
<i>Rosa multiflora</i>			7		7	

<i>Sorbus alnifolia</i>	9	1			3	1
<i>Celastrus flagellaris</i>	3				9	
<i>Ulmus pumila</i>			6	5		
<i>Fraxinus rhynchophylla</i>	4		5			1
<i>Ulmus macrocarpa</i>					8	
<i>Ampelopsis humulifolia</i>			3		3	
<i>Hibiscus syriacus</i>					4	
<i>Catalpa bungei</i>					4	
<i>Deutzia grandiflora</i>			3			
<i>Salix matsudana</i>	1	1				1
<i>Hovenia dulcis</i>					1	1
<i>Vitis amurensis</i>					2	
<i>Cerasus serrulata</i>	2					
<i>Celtis koraiensis</i>			1			
<i>Pterocarya stenoptera</i>						1
<i>Malus baccata</i>			1			
<i>Ziziphus jujuba</i> var. <i>spinosa</i>			1			
Total	936	170	1292	133	983	157

Species diversity

As shown in *Figure 1A1–1A3*, the species richness index, Shannon–Wiener diversity index and Simpson diversity index of plants in tree layer can be ranked as sample plot near 5.0 m scenic road corridor>wildwood area>sample plot near 2.5 m scenic road corridor ($P < 0.05$). However, the Pielou evenness index is ranked as sample plot near 5.0 m scenic road corridor>sample plot near 2.5 m scenic road corridor>wildwood area ($P < 0.05$), as shown in *Figure 1A4*.

The species richness index, Shannon–Wiener diversity index, Simpson diversity index and Pielou evenness index of plant community in shrub layer are ranked as sample plot near 5.0 m scenic road corridor>sample plot near 2.5 m scenic road corridor>wildwood area (see *Fig. 1B1–1B4*).

The species richness index, Shannon–Wiener diversity index, Simpson diversity index and Pielou evenness index of plant community in herb layer are ranked as sample plot near 5.0 m scenic road corridor>wildwood area>sample plot near 2.5 m scenic road corridor (see *Fig. 1C1–1C4*).

Discussion

According to the investigation in Kunyu mountain national nature reserve of China, it can be known that compared with wildwood area, the mean DBH of tree layer decreases with the increase of width of scenic road corridor. The edge effect of shrub layer can be balanced by increasing the individual number of low-DBH shrubs and decreasing the number of high-DBH shrubs. Moreover, the edge effect of 2.5 m scenic road corridor than that of 5.0 m scenic road corridor.

In tree layer, the four indexes all showed as follows: sample plot near 5.0 m scenic road corridor was significantly higher than the sample plot near 2.5 m scenic road corridor and wildwood area.

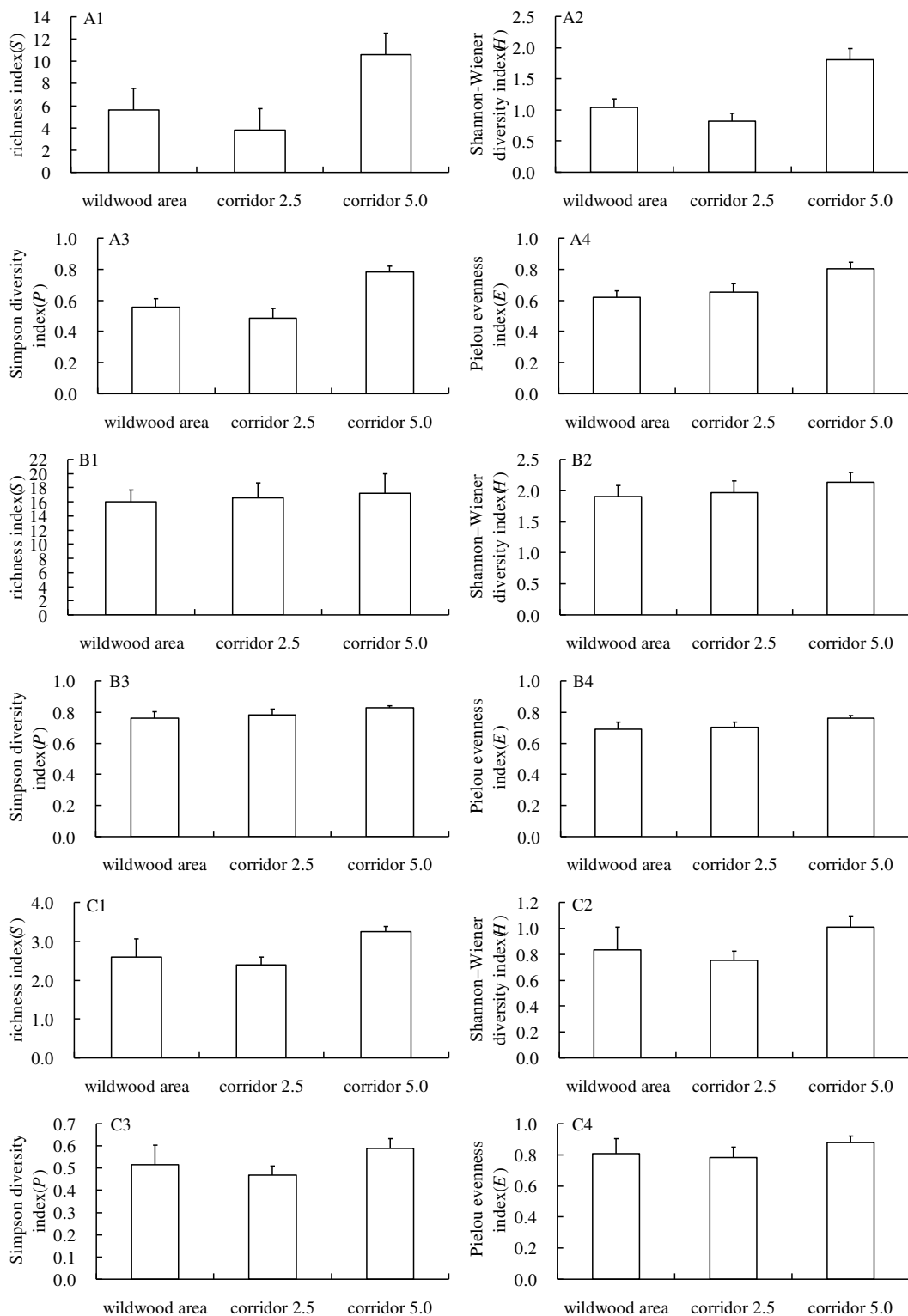


Figure 1. The richness index (1), Shannon-Wiener diversity index (2), Simpson diversity index (3) and Pielou evenness index (4) for the tree layer (A), shrub layer (B) and herb layer in wildwood area, sample plot near 2.5 m scenic road corridor and sample plot near 5.0 m scenic road corridor in Kunyu Mountain (average + standard error). Corridor 2.5: sample plot near 2.5 m scenic road corridor; corridor 5.0: sample plot near 5.0 m scenic road corridor

In shrub layer, the four indexes abovementioned can be ranked as sample plot near 5.0 m scenic road corridor>sample plot near 2.5 m scenic road corridor>wildwood area. In herb layer, the four indexes can be ranked as sample plot near 5.0 m scenic road corridor>wildwood area>sample plot near 2.5 m scenic road corridor. This study shows that the upper trees in forest plant community of Kunyu Mountain are less sensitive to edge effect compared with understory plants, which is inconsistent with the results of study on *Cryptomeria fortunei* plantation in Zhougong mountain of Western Sichuan province (Wang et al., 2016).

Researches have shown that edge effect influences the richness and density of evergreen broad-leaf forest (Li et al., 2008), and forest edge effect is positive for extrinsic plant seed invasion (Lin and Cao, 2009). The influence of forest road on species diversity index only reaches into the plant community which is 5 m near road (Watkins et al., 2003), while a narrow corridor (< 4 m) will cause decrease of *Pinus koraiensis* growth level (Wang et al., 2003).

Conclusion

This study shows that two scenic road corridors (2.5 m and 5.0 m) have opposite effects on forest plant community in Kunyu Mountain of China. The 2.5 m scenic road corridor exerts an inhibition effect on the species composition and diversity of plants in Kunyu mountain national nature reserve, however, 5.0 m scenic road corridor has a promoting effect. We suggest that we can continue to study the two road corridors in Kunyu Mountain, especially the corridor width to study the physiological and biochemical indexes such as growth, development and reproduction of plants.

Acknowledgements. Funded by the Fund of Shandong Provincial Key Laboratory of Water and Soil Conservation and Environmental Protection, Linyi University, No STKF201603.

REFERENCES

- [1] Chen, L. D., Xu, J. Y., Fu, B. J., Lu, Y. H. (2004): Quantitative assessment of patch edge effects and its ecological implications. – *Acta Ecologica Sinica* 24: 1827-1832 [in Chinese].
- [2] Du, N., Wang, Q., Guo, W. H., Wang, R. Q. (2007): Ecological characteristics of typical plant communities in Kunyu Mountain. – *Chinese Journal of Ecology* 26: 151-158 [in Chinese].
- [3] Fang, J. Y., Shen, Z. H., Tang, Z. Y., Wang, Z. H. (2004): The protocol for the survey plan for plant species diversity of China's Mountains. – *Biodiversity Science* 12: 5-9 [in Chinese].
- [4] Fang, J. Y., Wang, X. P., Shen, Z. H., Tang, Z. Y., He, J. S., Yu, D., Jiang, Y., Wang, Z. H., Zheng, C. Y., Zhu, J. L., Guo, Z. D. (2009): Methods and protocols for plant community inventory. – *Biodiversity Science* 17: 533-548 [in Chinese].
- [5] García, J. D. D., Arévalo, J. R., Fernández-Palacios, J. M. (2007): Road edge effect on the abundance of the lizard *Gallotia galloti*, (Sauria: Lacertidae) in two Canary Islands forests. – *Biodiversity and Conservation* 16: 2949-2963.
- [6] Leinster, T., Cobbold, C. A. (2012): Measuring diversity: the importance of species similarity. – *Ecology* 93: 477-489.

- [7] Li, M. H., Song, R. S., Jiang, Y. F., Zhao, G. F., Fu, H. L., Zheng, Y. M., Yu, M. J. (2008): Plant diversity in the six evergreen broad-leaved forest fragments in East China. – Chinese Journal of Ecology 28: 1137-1146 [in Chinese].
- [8] Lian, Z. M., Yu, G. Z. (2000): Edge effect and biodiversity. – Biodiversity Science 8: 120-125 [in Chinese].
- [9] Lin, L. X., Cao, M. (2009): Edge effects on soil seed banks and understory vegetation in subtropical and tropical forests in Yunnan, SW China. – Forest Ecology and Management 257: 1344-1352.
- [10] Liu, Y. G., Wang, Q., Wang, J. (2012): Landscape pattern and patch stability in Jiuzhaigou Nature Reserve. – Journal of Northeast Forestry University 40(4): 31-33 [in Chinese].
- [11] Ma, W. Z., Liu, W. Y., Yang, L. P., Yang, G. P. (2008): Edge effects on epiphytes in montane moist evergreen broad-leaved forest. – Biodiversity Science 16: 245-254 [in Chinese].
- [12] Naidoo, R., Kilian, J. W., Preez, P. D., Beytell, P., Aschenborn, O., Taylor, R. D., Stuart-Hill, G. (2018): Evaluating the effectiveness of local- and regional-scale wildlife corridors using quantitative metrics of functional connectivity. – Biological Conservation 217: 96-103.
- [13] Su, X. F., Yuan, J. F., Hu, Z. G., Xu, G. F., Yu, M. J. (2014): Edge effect of the plant community structure on land-bridge islands in the Thousand Island Lake. – Chinese Journal of Applied Ecology 25: 77-84 [in Chinese].
- [14] Sun, Q., Lu, J. B., Wu, J. G., Zhang, F. F. (2008): Effects of island area on plant species distribution and conservation implications in the Thousand Island Lake region. – Biodiversity Science 16: 1-7 [in Chinese].
- [15] Tian, C., Yang, X. B., Liu, Y. (2011): Edge effect and its impacts on forest ecosystem: A review. – Chinese Journal of Applied Ecology 22: 2184-2192 [in Chinese].
- [16] Velázquez, J., Gutiérrez, J., Hernando, A., García-Abril, A. (2017): Evaluating landscape connectivity in fragmented habitats: Cantabrian capercaillie (*Tetrao urogallus cantabricus*) in northern Spain. – Forest Ecology and Management 389: 59-67.
- [17] Wang, D. Y., Hao, J. F., Li, Y., Qi, J. Q., Pei, Z. L., Huang, Y. J., Jiang, Q., Chen, Y. (2016): Examination of edge effects in a *Cryptomeria fortunei* plantation in Zhougong Mountain, western Sichuan. – Biodiversity Science 24: 940-947 [in Chinese].
- [18] Wang, R. S., Ma, S. J. (1985): Edge effect and its application in economic ecology. – Chinese Journal of Ecology 4(2): 38-42 [in Chinese].
- [19] Wang, W. J., Zu, Y. G., Yang, F. J., Wang, H. M., Wang, F. (2003): Photosynthetic ecophysiological study on the growth of Korean pine (*Pinus koraiensis*) afforested by the edge-effect belt method. – Chinese Journal of Ecology 23: 2318-2326 [in Chinese].
- [20] Watkins, R. Z., Chen, J. Q., Pickens, J., Brososfske, K. D. (2003): Effects of forest roads on understory plants in a managed hardwood landscape. – Conservation Biology 17: 411-419.
- [21] Wei, J. J., Gao, Y., Zhao, W. G., Liu, J. (2017): Hillside topographic pattern of shrub and herb diversity of forest in Mount tai of China. – Journal of Environmental Protection and Ecology 18: 571-580.
- [22] Wu, Y. N., Tao, J. P., Xi, W. M., Zhao, K., Hao, J. H. (2011): The edge effects on tree-liana relationship in a secondary natural forest in Bawangling Nature Reserve, Hainan Island, China. – Acta Ecologica Sinica 31: 3054-3059 [in Chinese].
- [23] Zhou, T., Peng, S. L., Lin, Z. G. (2009): Edge effect of road in Dinghushan forests. – Chinese Journal of Ecology 28: 433-437 [in Chinese].
- [24] Zhu, Q., Yu, K. J., Li, D. H. (2005): The width of ecological corridor in landscape planning. – Acta Ecologica Sinica 25: 2406-2412 [in Chinese].

A GENERAL EMPIRICAL MODEL FOR ESTIMATION OF SOLAR RADIATION IN YANGTZE RIVER BASIN

CHEN, J. L.^{1*} – HE, L.² – WEN, Z. F.¹ – LV, M. Q.¹ – YI, X. X.¹ – WU, S. J.¹

¹*Chongqing Institute of Green and Intelligent Technology, Chinese Academy of Sciences
400714 Chongqing, China
(phone: +86-23-6593-5555; fax: +86-23-6593-5000)*

²*Key Laboratory of Poyang Lake Wetland and Watershed Research, Ministry of Education
330000 Nanchang, China
(phone: +86-23-6593-5555; fax: +86-23-6593-5000)*

**Corresponding author
e-mail: chenjilong@cigit.ac.cn
(phone: +86-23-6593-5912; fax: +86-23-6593-5000)*

(Received 18th Nov 2017; accepted 12th Feb 2018)

Abstract: Solar radiation is the principal and fundamental energy for many physical, chemical and biological processes. Estimation of solar radiation by Ångström-Prescott (A-P) model from sunshine duration is common employed. In this paper, the original linear A-P model and four commonly used modification models (quadratic, cubic, power and logarithmic functions) are comparatively studied. It is found that the linear, second and cubic models give very similar goodness of fit, and the linear model is recommended due to its greater simplicity and convenience. The A-P model parameter a, sum a + b correlate most significantly with altitude. Based on these correlations, the deterministic equations of parameters a and b are proposed. Consequently, the A-P model with the estimated parameters by deterministic equations is used to estimate solar radiation, and it gives good performance with the RMSE < 1.7 MJ m⁻², RRMSE < 20% and R² > 0.89. It is therefore recommended to use these equations to determine the A-P parameters in Yangtze River basin in China, and it is believed particularly useful for the site where lacks of the measured solar radiation data for calibration.

Keywords: *empirical model, meteorological variable, Ångström-Prescott equation, sunshine duration, geographical information*

Introduction

Solar radiation arriving on the earth's surface plays an important role in most land surface processes including physical, biological and chemical processes, e.g., hydrological cycling, vegetation growth, climate and weather change (Liu et al., 2017). It is also one of the key input variables in crop growth, and hydrological and climate models. And the importance of global solar radiation in ecology, agriculture, environment and the associated researches has been well documented (Yorukoglu and Celik, 2006; Chen et al., 2011). However, it is not widely measured due to the cost and difficulty of maintenance and calibration of the measurement equipment (Chen et al., 2013). Only a few meteorological stations measure global solar radiation. For example, in the USA, less than 1% of meteorological stations are recording solar radiation (Thorton and Running, 1999). In China, more than 2000 stations have record of meteorological data, only 98 stations are recording solar radiation (Chen et al., 2004). The ratio of stations recording solar radiation to those recording temperature is about 1:500 around the world (Thorton and Running, 1999). By contrast, other routinely measured data, such as air temperature, sunshine duration, are easily available.

Therefore, developing method based on those readily available meteorological data for accurately estimating solar radiation has been the focus of many studies.

Major methods including satellite-derived (Frulla et al., 1988; Chen et al., 2014), stochastic algorithm (Richardson, 1981; Hansen, 1999), empirical relationship (Chen and Li, 2013; Chen et al., 2015), interpolation (Chen et al., 2012) and learning machine method (Chen et al., 2011) have been developed for the purpose. The satellite-derived method is promising for estimating solar radiation data over large regions, but it is relatively new and may suffer from the shortage of the historical meteorological data (Abraha and Savage, 2008). Stochastic weather generators are useful to generate daily simulations from data averages (Wilks and Wilby, 1999). However, the generated data cannot be used for model validation for a particular period of time as the data may not match the actual weather at a particular time. Spatial interpolation technique can predict values at unknown locations and create surface from the surrounding measured points. The main problem, however, is the lack of sufficient stations of solar radiation measurements (Chen and Li, 2014).

The empirical relationship using the easily available meteorological data, such as sunshine duration, maximum and minimum temperatures, is attractive for its simplicity, efficiency and lower data requirement. And the well-known sunshine-based Ångström- Prescott (A-P) model (Chen and Li, 2013; Chen et al., 2015) and the temperature-based Hargreaves and Samani model (1982), Bristow and Campbell model (1984) are widely used in the world. It is generally recognized that the A-P model performs much better than other temperature-based models (Iziomon et al., 2002; Podesta et al., 2004; Trnka et al., 2005).

The A-P model was proposed by Ångström (Chen et al., 2015) in 1924 and further modified by Prescott (Chen and Li, 2013) in 1940. The original form of the model is (Eq. 1):

$$R_s = \left(a + b \frac{H}{H_0}\right) R_a \quad (\text{Eq.1})$$

where R_s is monthly mean daily global radiation ($\text{MJ m}^{-2} \text{d}^{-1}$), R_a is monthly mean daily extra-terrestrial solar radiation ($\text{MJ m}^{-2} \text{d}^{-1}$), H is monthly mean daily actual sunshine hours (h), H_0 is monthly mean daily potential sunshine hours (h), a and b are empirical parameters which are calibrated from the long-term measured solar radiation data. The A-P model is widely used for its simplicity and significant performance. One of the principal limitations is that it requires calibration using local measured solar radiation data and it is therefore open to question how transferable these calibration values are to other locations (Miller et al., 2008). Ångström suggested values of 0.2, and 0.5, and Prescott 0.22, and 0.54 for the empirical parameters a , and b , respectively (Chen and Li, 2013). Page gave the corresponding values of 0.23, and 0.48, which was believed to be applicable anywhere in the world (Page, 1961). FAO 56 recommended the values of 0.25, and 0.50 for parameters a , and b for the sites where no solar radiation data is available, respectively (Allen et al., 1998). Lots of literature reported the calibrated the A-P model parameters for different places, and showed that they varied from location to location; furthermore, they were related to the geographic elements (Bandyopadhyay et al., 2008; Liu et al., 2009), indicating that the fixed parameters are not appropriate for all the sites where no solar radiation data is available in a large area. Only a few works

discussed and gave the determination equations for the A-P model parameters relating to the geographic elements (Bandyopadhyay et al., 2008).

Therefore, the current study is carried out to develop a general empirical model for estimation of solar radiation in Yangtze River basin, which plays significant role in water supply for agriculture industry for China, and hence the eco-environmental models and crop growth simulation are widely studied. However, only a few meteorological stations provide solar radiation recorders. Therefore, solar radiation estimation is of vital importance and significance. While only a few works were reported for this region. Chen et al. (2004) developed an empirical model at 10 located in Yangtze River basin. While this new model was reported to give similar performance with the A-P model (Wu et al., 2007). Therefore, the objectives of the current study are (1) to calibrate the A-P model parameters in the Yangtze River basin; (2) to investigate and relationship between A-P model parameters and geographic elements; and (3) to recommend determination equations of A-P model parameters for the sites where no measured solar radiation data is available for calibration in study area.

Materials and method

Data set

The current study focuses on the Yangtze River basin (*Fig. 1*). The Yangtze River is 6300 km long with a basin area of $180 \times 10^4 \text{ km}^2$. It is characterized by abundant water resources, and thus plays significant role in water supply for agriculture industry, because economy of much of the Yangtze River basin is focused largely on agricultural production. It is one of the major grain production areas of China and hence the eco-environmental models and crop growth simulation are widely studied. A large part of the Yangtze River basin is subtropical monsoon climate. Average annual precipitation in the basin varies from 270-500 mm in the west to 1600-1900 mm in the southeast. Average annual sunshine hours range from 1000 to 2500 h.

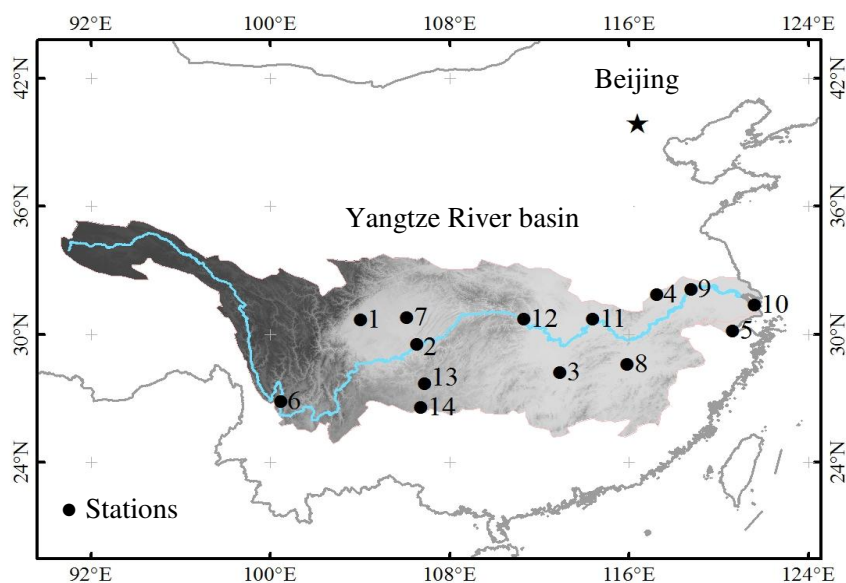


Figure 1. Location of the study meteorological stations in the Yangtze River basin (stations are numbered in compliance with Table 1)

A total of 14 stations with long-term available records of solar radiation were used in the present study. The mapping of stations roughly range from 26° to 34° latitude North, from 97° to 121° longitude East, and from 3 to 3394 m altitude. *Table 1* shows the temporal period and the geographical information of the meteorological stations. The monthly mean daily global radiation data were obtained from the National Meteorological Information Center (NMIC), China Meteorological Administration (CMA). The period of records range from 6 to 30 years covering the period between 1961 and 2000. Quality control tests were conducted by the suppliers. A year with more than 5 days of missing or faulty data in the same month was discarded (e.g., the year of 1992 for Nanchang and the year of 1984 for Wuhan). For each station, two data sets were created. About 70% of the total records were used for calibrating the parameters, and the remainder for evaluating the model (*Table 1*).

Table 1. Detailed information of the studied 14 stations in the Yangtze River basin

Station ID	Station name	Latitude (N)	Longitude (E)	Altitude (m)	Calibration period	Validation period
1	Chengdu	30.67	104.02	506	1973-1992	1993-2000
2	Chongqing	29.58	106.47	259	1973-1992	1993-2000
3	Changsha	28.22	112.92	68	1987-1996	1997-2000
4	Hefei	31.87	117.23	28	1978-1992	1993-2000
5	Hangzhou	30.23	120.17	42	1973-1992	1993-2000
6	Lijiang	26.83	100.47	2394	1977-1992	1993-2000
7	Nanchong	30.78	106.10	309	1874-1985	1986-1990
8	Nanchang	28.60	115.92	47	1973-1991	1993-2000
9	Nanjing	32.00	118.80	9	1973-1992	1993-2000
10	Shanghai	31.17	121.43	3	1961-1983	1983-1990
11	Wuhan	30.62	114.13	23	1973-1983 1985-1992	1993-2000
12	Yichang	30.70	111.30	133	1973-1992	1993-2000
13	Zunyi	27.7	106.88	844	1973-1984	1985-1990
14	Guiyang	26.58	106.72	1074	1973-1992	1993-2000

Models and calibration

The extra-terrestrial solar radiation (R_a) and potential sunshine duration (H_o) are calculated using the equations (Eqs. 2-6) detailed by Allen et al., (1998).

$$R_a = 37.6d(\omega \sin \phi \sin \delta + \cos \phi \cos \delta \sin \omega) \quad (\text{Eq.2})$$

$$d = 1 + 0.033 \cos\left(\frac{2\pi}{365}n\right) \quad (\text{Eq.3})$$

$$\delta = 0.4093 \sin\left(\frac{2\pi}{365}n - 1.39\right) \quad (\text{Eq.4})$$

$$\omega = \arccos(-\tan \phi \tan \delta) \quad (\text{Eq.5})$$

$$H_o = 24\omega / \pi \quad (\text{Eq.6})$$

where d is the relative distance between the sun and the earth, ω is sunset hour angle (rad), φ is latitude (rad), δ is solar declination angle (rad), n is the number of the day of year starting from the first of January. The A-P model parameters a and b are calibrated by least square linear regression between R_s/R_a and H/H_o for the calibration period for each station (Table 1).

Performance criteria

To assess the performance of models, root mean square error (RMSE), relative root mean square Error (RRMSE), The relative percentage error (e%), coefficient of variation (CV) and coefficient of determination (R^2) are determined. The metric CV calculated as ratio of standard deviation to arithmetic mean is adopted to measure the variation of the parameter, and R^2 is adopted to measure the correlation between the observed and predicted values. The former three indicators are calculated by Equations 7-9.

$$RMSE = \sqrt{\frac{\sum_{i=1}^n (y_i - \hat{y}_i)^2}{n}} \quad (\text{Eq.7})$$

$$RRMSE = \frac{1}{\bar{y}} \sqrt{\frac{\sum_{i=1}^n (y_i - \hat{y}_i)^2}{n}} \quad (\text{Eq.8})$$

$$e = \frac{100(\hat{y}_i - y_i)}{y_i} \quad (\text{Eq.9})$$

where n , y , \hat{y} and \bar{y} represent the number of testing data, the observation value, the predicted value and the average value of the observation, respectively. Lower values of RMSE, RRMSE, and absolute e% indicate a better estimation accuracy of the model.

Results and discussion

Variation of A-P model parameters

The calibrated A-P model parameters a and b are summarized in Table 2. Parameter a vary from 0.103 in Hefei to 0.225 in Lijiang (averaged 0.137, SD = 0.031), b vary from 0.550 in Chengdu to 0.621 in Changsha (averaged 0.579, SD = 0.017), and R^2 vary from 0.718 to 0.915 (averaged 0.831, SD = 0.062). Obviously, parameter b is more stable with the lowest SD (0.017) and CV (2.858%) in the present study area, while parameter a show a higher variation with the CV of 22.534%.

The values of R^2 indicate that the linear function gave goodness of fit on the calibration data; however, some researchers studied and proposed several types of regression models on the corresponding calibration data at specific sites, such as, quadratic (Ogelman et al., 1984; Akinoglu and Ecevit, 1990), cubic (Bahel et al., 1987; Ertekin and Yaldiz, 2000), and logarithmic models (Newland, 1988; Ampratwum and

Dorvlo, 1999). *Table 2* presents the coefficient of determination of quadratic, cubic, logarithmic and power functions. All the regression equations give goodness of fit on the calibration data, with the values of $R^2 > 0.7$. The linear A-P, quadratic and cubic models return quite similar values of R^2 within the same station, and the cubic model is the best with the highest values of R^2 . However, it is noted that it is only slightly better. The logarithmic and power function even gives the worse fit than the simple linear A-P model. Therefore, there is no reason to choose a complex function to gain probably negligible accuracy at the cost of losing the simplicity and convenience of the simple A-P model (Liu et al., 2009).

Table 2. The calibrated parameters of linear model and coefficient of determination of quadratic, cubic, logarithmic and power functions at 14 stations in the study area

Stations	Linear model				Quadratic	Cubic	Logarithmic	Power function
	a	b	a + b	R ²	R ²	R ²	R ²	R ²
Chengdu	0.164	0.55	0.714	0.747	0.757	0.758	0.732	0.744
Chongqing	0.119	0.585	0.703	0.867	0.878	0.878	0.781	0.792
Changsha	0.125	0.621	0.746	0.867	0.875	0.875	0.827	0.815
Hefei	0.103	0.59	0.693	0.773	0.777	0.777	0.765	0.720
Hangzhou	0.127	0.568	0.694	0.718	0.786	0.787	0.750	0.768
Lijiang	0.225	0.576	0.801	0.873	0.874	0.875	0.831	0.946
Nanchong	0.155	0.583	0.738	0.872	0.872	0.873	0.765	0.845
Nanchang	0.12	0.579	0.7	0.915	0.921	0.920	0.886	0.920
Nanjing	0.13	0.578	0.709	0.781	0.783	0.784	0.744	0.788
Shanghai	0.158	0.565	0.723	0.872	0.873	0.872	0.849	0.860
Wuhan	0.11	0.564	0.674	0.771	0.772	0.773	0.746	0.737
Yichang	0.12	0.594	0.713	0.811	0.813	0.816	0.751	0.779
Zunyi	0.131	0.58	0.711	0.895	0.918	0.918	0.781	0.807
Guiyang	0.133	0.582	0.714	0.87	0.873	0.874	0.797	0.832
Minimum	0.103	0.55	0.674	0.718	0.757	0.758	0.732	0.720
Maximum	0.225	0.621	0.801	0.915	0.921	0.920	0.886	0.946
Mean	0.137	0.579	0.717	0.831	0.841	0.841	0.786	0.811
SD	0.031	0.017	0.03	0.062	0.057	0.056	0.046	0.066
CV	22.53%	2.86%	4.25%	7.46%	6.76%	6.71%	5.85%	8.11%

Relationship between the parameters and geographical information

Generally, the A-P model parameters vary from station to station as shown in *Table 2*. To find out the relationship between the parameters and station geographical information, the correlation analysis is carried out and a summary is presented in *Table 3*.

Parameters *a*, *b*, the sum *a + b* show very weak correlation with latitude ($p > 0.05$). While parameter *a*, and the sum *a + b* are correlated most significantly with altitude ($r = 0.786$, $p = 0.0009$, and $r = 0.746$, $p = 0.0022$, respectively), and less significantly with longitude ($r = -0.532$, $p = 0.0403$, and $r = -0.535$, $p = 0.0486$, respectively), one probable explanation is in that the significantly correlation between the altitude and longitude of the study area ($r = 0.933$, $p = 0.00254 < 0.001$).

Table 3. Correlation coefficients between A-P model parameters and geographical information

Geographical information	a	b	a + b
Latitude	-0.346	0.246	0.485
Longitude	-0.532*	-0.009	-0.535*
Altitude	0.786**	0.096	0.746**

*Significant at 0.05 significance level

**Significant at 0.01 significance level

Parameter a represents the overall atmospheric transmission for total cloud conditions, and the sum $a + b$ denotes the overall atmospheric transmission under clear sky conditions (Podesta et al., 2004). The correlations indicate a general increasing trend for a and the sum $a + b$ as the altitude increasing from east to west in the study area, indicating that the highland western area tends to have more clear days than the lowland eastern area, this maybe the effect of reduced air mass and shorter path length at the high altitude (Liu et al., 2009).

Estimating A-P model parameters using the geographical information

The significant correlations are important in increasing the availability of A-P model parameters without the need for calibration. Parameters a , and sum $a + b$ correlate most significantly with altitude (Table 3), based on these correlations, we propose equations relating A-P model parameters to the most dominant factor (altitude). The regression functions between parameters a , sum $a + b$ and altitude are given below (Eqs. 10-11), respectively.

$$a = 4 \times 10^{-5} \text{ Altitude} + 0.1221 \quad (\text{Eq.10})$$

$$\text{sum} = 3 \times 10^{-5} \text{ Altitude} + 0.7025 \quad (\text{Eq.11})$$

where *altitude* is the elevation of the station in m, *sum* is the sum of parameter a and b . Consequently, the determination equation (Eq. 12) of parameter b is calculated by subtracting Equation10 from Equation11:

$$b = -10^{-5} \text{ Altitude} + 0.5804 \quad (\text{Eq.12})$$

The A-P model parameters estimated by the corresponding model and the performances are listed in Table 4. Overall, all the models give good performances with $\text{RMSE} \leq 0.02$ and $\text{RRMSE} < 14\%$; better performances are found in estimation of sum $a + b$ and b , with the absolute $e\% < 6\%$, and $< 7\%$, RMSE of 0.020, and 0.017, RRMSE of 2.76%, and 2.92%, respectively; while the RMSE of 0.019 and RRMSE of 13.54% in estimation of parameter a . Obviously, the mean of estimated parameters a , b , and sum $a + b$ are nearly identical to those of calibrated parameters (Tables 4 and 2), with the slightly differences of 0.001, 0.003, and 0.002, respectively. The estimated parameter a are much lower than the suggested values by Ångström and Prescott (Chen and Li, 2013), Page (1961) and FAO (Allen et al., 1998), while parameter b are larger.

Table 4. The estimated A-P model parameters at 14 stations in the study area

Stations	a	e%	b	e%	a + b	e%
Chengdu	0.142	-13.05	0.575	4.65	0.718	0.59
Chongqing	0.132	11.78	0.578	-1.18	0.710	1.01
Changsha	0.125	-0.38	0.580	-6.63	0.705	-5.58
Hefei	0.123	19.75	0.580	-1.61	0.703	1.57
Hangzhou	0.124	-2.15	0.580	2.20	0.704	1.41
Lijiang	0.218	-3.26	0.556	-3.41	0.774	-3.37
Nanchong	0.134	-13.25	0.577	-0.94	0.712	-3.53
Nanchang	0.124	2.97	0.580	0.13	0.704	0.62
Nanjing	0.122	-6.09	0.580	0.35	0.703	-0.84
Shanghai	0.122	-22.79	0.580	2.77	0.703	-2.82
Wuhan	0.123	11.63	0.580	2.92	0.703	4.35
Yichang	0.127	6.36	0.579	-2.45	0.706	-0.97
Zunyi	0.156	18.98	0.572	-1.42	0.728	2.34
Guiyang	0.165	24.57	0.570	-2.09	0.735	2.86
Mean	0.138	2.505	0.576	-0.479	0.715	-0.170
RMSE	0.019	–	0.017	–	0.020	–
RRMSE	13.54%	–	2.92%	–	2.76%	–

Estimating solar radiation using the estimated parameters

The A-P model with the parameters *a* determined by Equation 10, and *b* by Equation 12 is consequently used to estimate solar radiation and the performance is presented in Figure 2. Overall, it gives good estimation performance with RMSE < 1.7 MJ m⁻² (averaged 1.182 MJ m⁻²), RRMSE < 20% (averaged 11.48%) and R² > 0.89 (averaged 0.940). There is a substantially good agreement between estimated and observed values as shown in Figure 2, where the points tend to line up around the 1:1 line, indicating that the observed solar radiation are close to the estimated.

Yangtze River basin is one of the major grain production areas of China and hence the eco-environmental models and crop growth simulation are widely studied. Therefore, solar radiation estimation using these measured meteorological variables is of vital importance and significance. Some works have reported the validation of the existing solar radiation in Yangtze River basin. Chen et al. (2004) introduced a new model using ambient temperature and A-P model at 10 sites in Yangtze River basin. While the new model was reported to give similar fit with A-P model at Nanchang station (Wu et al., 2007). In another work, Chen et al. (2006) modified the A-P model at 10 sites in Yangtze River basin. Comparing our general model with their site-specific models, the model give similar performance at most sties in Yangtze River basin, suggesting that the general model have great potential practical applications in agriculture, environment and ecology.

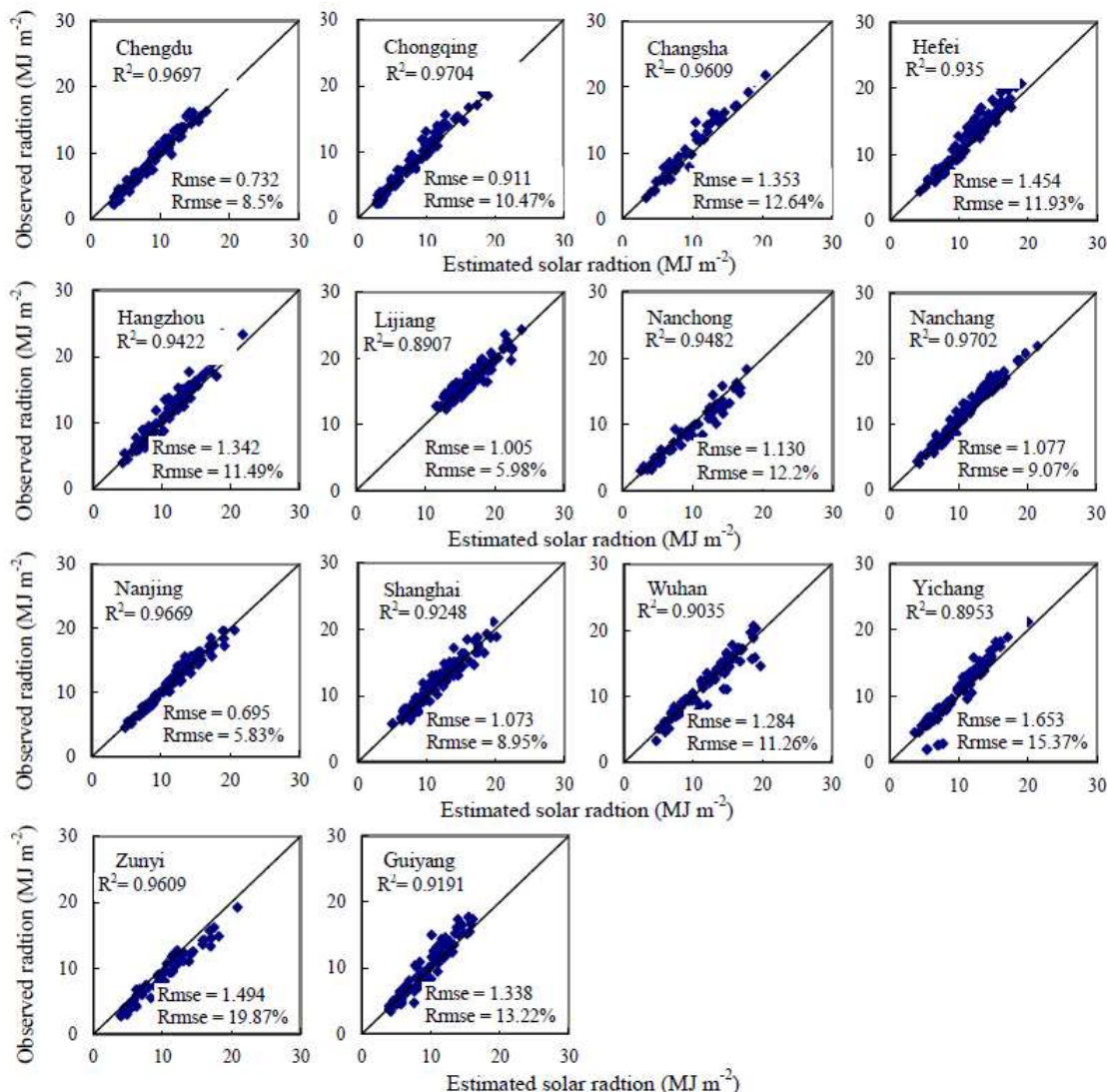


Figure 2. Scatter plots of the observed vs. estimated radiation at 14 stations in Yangtze River basin

Conclusion

Solar radiation is an essential and important variable to many simulation models. Ångström-Prescott model is widely used to estimate solar radiation when it is not readily available. The commonly used modifications to the Ångström-Prescott model, including the linear, second and cubic regression equations, give very similar goodness of fit and accuracy. Therefore, the simple Ångström-Prescott model is recommended in Yangtze River basin in China, due to its greater simplicity and convenience. Parameter a , sum $a + b$ correlate significantly with altitude. The deterministic equations for parameters a and b are given, and good estimation accuracy are obtained. Consequently, the Ångström-Prescott model with the parameters by corresponding deterministic equations is evaluated. Overall, it gives good estimation performance according to the performance indicators of root mean square error, relative root mean square error, coefficient of determination. Therefore, it is recommended to use these equations to determine the corresponding parameters in Yangtze River basin in China, and it is

believed particularly useful for the site where no observation of solar radiation data is available for calibration. Besides sunshine duration, air temperature, relative humidity, precipitation and atmospheric pressure are also routinely measured. Many works have shown that models using these meteorological variables in combination with sunshine duration significantly outperformed models using sunshine duration alone (Trabea and Shaltout, 2000; Liu et al., 2012). Thus, future work will investigate the potential of models using more combination of meteorological variables to increase the reliability of the general model.

Acknowledgements. The work was supported by Youth Innovation Promotion Association (Chen jilong), National Natural Science Foundation of China (41401051), STS project (KFJ-SW-ST-180) Chongqing Science and Technology project (KJ-2017026, cstc2015jcyjA00007), Fuling Science and Technology project (2016ABB1040), Opening Fund of Key Laboratory of Poyang Lake Wetland and Watershed Research, Ministry of Education (WE2016002, ZK2015001). We thank the National Meteorological Information Center, China Meteorological Administration for providing the long-term data records.

REFERENCES

- [1] Abraha, M. G., Savage, M. J. (2008): Comparison of estimates of daily solar radiation from air temperature range for application in crop simulations. – *Agricultural and Forest Meteorology* 148: 401-416.
- [2] Akinoglu, B. G. Ecevit, A. (1990): Construction of a quadratic model using modified Ångström coefficients to estimate global solar radiation. – *Solar Energy* 45(2): 85-92.
- [3] Allen, R. G., Pereira, L. S., Raes, D., Smith, M. (1998): Crop evapotranspiration. Guidelines for computing crop water requirements. – FAO Irrigation and Drainage paper 56, Rome.
- [4] Ampratwum, D. B., Dorvlo, A. S. S. (1999): Estimation of solar radiation from the number of sunshine hours. – *Applied Energy* 63(3): 161-167.
- [5] Bahel, V., Bakhsh, H., Srinivasan, R. (1987): A correlation for estimation of global solar radiation. – *Energy* 12(2): 131-135.
- [6] Bandyopadhyay, A., Bhadra, A., Raghuwanshi, N. S, Singh, R. (2008): Estimation of monthly solar radiation from measured air temperature extremes. – *Agricultural and Forest Meteorology* 148(11): 1707-1718.
- [7] Bristow, K. L. Campbell, G. S. (1984): On the relationship between incoming solar radiation and daily maximum and minimum temperature. – *Agricultural and Forest Meteorology* 31(2): 159-166.
- [8] Chen, D. L, Yu, Q., Wu, D. R, Haginoya, S. (2012): Observation and calculation of the solar radiation on the Tibetan Plateau. – *Energy Conversion and Management* 57: 23-32.
- [9] Chen, J. L., Li, G. S. (2013): Estimation of monthly average daily solar radiation from measured meteorological data in Yangtze River Basin in China. – *International Journal of Climatology* 33: 487-498.
- [10] Chen, J.L., Li, G.S., Wu, S.J. (2013): Assessing the potential of support vector machine for estimating daily solar radiation using sunshine duration. – *Energy Convers Manage* 75: 311-318.
- [11] Chen, J. L., Li, G. S. (2014): Evaluation of support vector machine for estimation of solar radiation from measured meteorological variables. – *Theoretical and Applied Climatology* 115: 627-638.
- [12] Chen, J. L., Liu, H. B., Wu, W., Xie, D. T. (2011): Estimation of monthly solar radiation from measured temperatures using support vector machines - A case study. – *Renewable Energy* 36(1): 413-420.

- [13] Chen, J. L., Xiao, B. B., Chen, C. D., Wen, Z. F., Jiang, Y., Lv, M. Q., Li, G. S. (2014): Estimation of monthly-mean global solar radiation using MODIS atmospheric product over China. – *Journal of Atmospheric and Solar-terrestrial Physics* 110: 63-80.
- [14] Chen, J. L., Xiao, B. B., Chen, C. D., Wen, Z. F., Jiang, Y., Lv, M. Q., Wu, S. J., Li, G. S. (2015): Estimation of solar radiation using two-step method in Yangtze River basin in China. – *MAUSAM* 66(2): 225-236.
- [15] Chen, R. S., Ersi, K., Yang, J. P., Lu, S. H., Zhao, W. Z. (2004): Validation of five global radiation models with measured daily data in China. – *Energy Conversion and Management* 45: 1759-1769.
- [16] Chen, R. S., Ersi, K., Ji, X. B., Yang, J. P., Zhao, W. Z. (2006): Trends of the global radiation and sunshine hours in 1961-1998 and their relationships in China. – *Energy Conversion and Management* 47: 2859-2866.
- [17] Ertekin, C., Yaldiz, O. (2000): Comparison of some existing models for estimating global solar radiation for Antalya (Turkey). – *Energy Conversion and Management* 41(4): 30-31.
- [18] Frulla, L. A., Gagliardini, D. A., Grossi, G. H., Lopardo, R., Tarpley, J. D. (1988): Incident solar radiation on Argentina from the geostationary satellite GOES: comparison with ground measurements. – *Solar Energy* 41(1): 61-69.
- [19] Hansen, J. W. (1999): Stochastic daily solar irradiance for biological modeling applications. – *Agricultural and Forest Meteorology* 94(1): 53-63.
- [20] Hargreaves, G. H., Samani, Z. A. (1982): Estimating potential evapotranspiration. – *J. Irrig. Drain. Engrg. ASCE* 108: 225-230.
- [21] Iziomon, M. G., Mayer, H. (2002): Assessment of some global solar radiation parameterizations. – *Journal of Atmospheric and Solar-Terrestrial Physics* 64(15): 1631-1643.
- [22] Liu, J. D., Pan, T., Chen, D. L., Zhou, X. J., Yu, Q., Flerchinger, G. N., Liu, D. L., Zou, X. T., Linderholm, H. W., Du, J., Wu, D. R. (2017): An improved Ångström-type model for estimating solar radiation over the Tibetan Plateau. – *Energies* 10(7): 892-901.
- [23] Liu, X. Y., Mei, X. R., Li, Y. Z., Zhang, Q., Wang, Q. S. (2009): Calibration of the Ångström-Prescott coefficients (a, b) under different time scales and their impacts in estimating global solar radiation in the Yellow River basin. – *Agricultural and Forest Meteorology* 149(3): 697-710.
- [24] Miller, D. G., Rivington, M., Matthews, K. B., Buchan, K., Bellocchi, G. (2008): Testing the spatial applicability of the Johnson-Woodward method for estimating solar radiation from sunshine duration data. – *Agricultural and Forest Meteorology* 148(3): 466-480.
- [25] Newland, F. J. (1988): A study of solar radiation models for the coastal region of South China. – *Solar Energy* 43(4): 227-235.
- [26] Ögelman, H., Ecevit, A., Tasdemiroglu, E. (1984): A new method for estimating solar radiation from bright sunshine data. – *Solar Energy* 33(6): 619-625.
- [27] Page, J. K. (1961): The estimation of monthly mean values of daily total short wave radiation on vertical and inclined surface from sunshine records for latitudes 40N-40S. – *Proceedings of UN Conference on New Sources of Energy* 4: 378-90.
- [28] Podestá, G. P., Núñez, L., Villanueva, C. A., Skansi, M. A. (2004): Estimating daily solar radiation in the Argentine Pampas. – *Agricultural and Forest Meteorology* 123(1): 41-53.
- [29] Richardson, C. W. (1981): Stochastic simulation of daily precipitation, temperature, and solar radiation. – *Water Resources Research* 17(1): 182-190.
- [30] Thornton, P. E., Running, S. W. (1999): An improved algorithm for estimating daily solar radiation from measurements of temperature, humidity, and precipitation. – *Agricultural and Forest Meteorology* 93(4): 211-228.
- [31] Trabea, A. A., Shaltout, M. A. M. (2000): Correlation of global solar radiation with meteorological parameters over Egypt. – *Renewable Energy* 21: 297-308.

- [32] Trnka, M., Zalud, Z., Eitzinger, J., Dubrovský, M. (2005): Global solar radiation in Central European lowlands estimated by various empirical formulae. – *Agricultural and Forest Meteorology* 131(1): 54-76.
- [33] Wilks, D. S., Wilby, R. L. (1999): The weather generation game: a review of stochastic weather models. – *Progress in Physical Geography* 23: 329-357.
- [34] Wu, G. F., Liu, Y. L., Wang, T. J. (2007): Global solar radiation with measured meteorological data. - A case study in Nanchang station, China. – *Energy Conversion and Management* 48: 2447-2452.
- [35] Yorukoglu, M., Celik, A. N. (2006): A critical review on the estimation of daily global solar radiation from sunshine duration. – *Energy Conversion and Management* 47(15): 2441-2150.

THE CONSEQUENCES OF GLOBAL WARMING DUE TO ICE-ALBEDO FEEDBACK AND GREENHOUSE EFFECT IN AN ENERGY BALANCE DAISYWORLD MODEL

RUEANGPHANKUN, T.¹ – SUKAWAT, D.² – YOMSATIEANKUL, W.^{1*}

¹*Department of Mathematics, Faculty of Science,
King Mongkut's University of Technology Thonburi (KMUTT)
126 Pracha Uthit Road, Bang Mod, Thung Khru, Bangkok 10140, Thailand*

²*The Joint Graduate School of Energy and Environment,
King Mongkut's University of Technology Thonburi (KMUTT)
126 Pracha Uthit Road, Bang Mod, Thung Khru, Bangkok 10140, Thailand*

**Corresponding author
e-mail: warisa.yom@mail.kmutt.ac.th*

(Received 16th Nov 2017; accepted 27th Feb 2018)

Abstract. The detrimental effects of global warming on vegetation have been mathematically modelled with the application of Daisyworld. Daisyworld models explain the interaction between life and the physical environment. Daisyworld helps to describe the adaptive mechanisms for two plant species of daisy populations; namely black and white daisies. An environmental condition that affects the daisy growth rate is the Earth's surface temperature. This study aims to modify the Daisyworld equations by incorporating global warming factors into the model. The factors include ice-albedo feedback and greenhouse gases. Three different scenarios are examined, the ice-albedo feedback, greenhouse gases and a combination of ice-albedo feedback and greenhouse gases. In addition, greenhouse gases are considered with the differentiations of CO₂. The numerical results compare the relationship between the planet temperature and fractional area of black and white daisies on the Earth's surface among the three scenarios. Under the scenario of applying both ice-albedo feedback and greenhouse gases, the results illustrate that as the Earth's average temperature increases, the plant species become more vulnerable to extinction.

Keywords: *Daisyworld, global warming, ice-albedo feedback, greenhouse gases, CO₂, daisy extinction, planet temperature*

Introduction

The current state of the Earth's climate has changed dramatically because of global warming (Viola, 2010). Global warming refers to the increase of temperature of the Earth, having adverse effects on both societies and the ecosystem. The main cause of this phenomenon is human induced. Especially the release of greenhouse gases into the atmosphere through the burning of fossil fuels such as coal, oil and natural gas for energy production. This, coupled with large-scale deforestation, creates the greenhouse effect. Greenhouse gases absorb heat energy reflected from the Earth back into the atmosphere storing some heat within the Earth's atmosphere. The major greenhouse gases are water vapour, carbon dioxide (CO₂), methane (CH₄), nitrous oxide (N₂O), chlorofluorocarbons (CFCs), and sulfur hexafluoride (SF₆). These gases originate from processes conducted at industrial factories, electrical industry and the transportation sector. The effect of global warming leads to the melting of icebergs, rising sea level and more frequent/violent meteorological events (Viola, 2010; Wang and Chameides, 2005).

As mentioned above, greenhouse gases are influential factors on global warming. Of the many different greenhouse gases, a large focus has been placed on CO₂. Since the industrial revolution, the amount of CO₂ in the atmosphere has significantly increased (NOAA Climate.gov, 2017). An extensive amount of fossil fuels has been burned each decade following the industrial revolution. The overall affect is copious amounts of CO₂ being released into the Earth's atmosphere. Before the industrial revolution, the atmospheric concentration of CO₂ was about 280 ppm. When a continual observation began at Mauna Loa in 1958, CO₂ concentration was roughly 316 ppm. In 2013, the daily average concentration of CO₂ measured at Mauna Loa surpassed 400 ppm. Since then, the monthly average of carbon dioxide levels has periodically exceeded 400 ppm, as shown in *Figure 1* (NOAA Climate.gov, 2017).

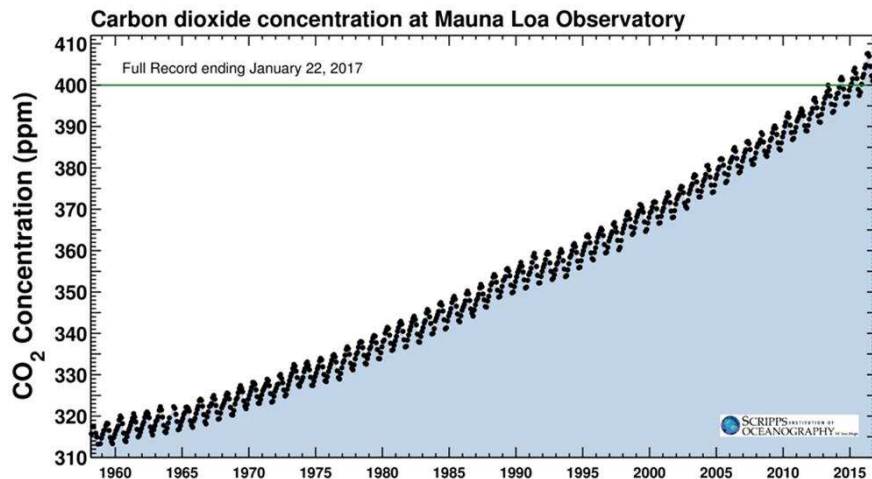


Figure 1. Concentrations of carbon dioxide in Earth's atmosphere have risen rapidly since measurements began nearly 60 years ago, climbing from 316 parts per million (ppm) in 1958 to more than 400 ppm today. SCRIPPS INSTITUTION OF OCEANOGRAPHY (Jones, 2017)

Furthermore, another factor which affects the global temperature change is ice-albedo feedback. The factor describes the climatic process of changing ice coverage. The occurrence of this phenomenon is due to ice having a higher albedo than either land or water surfaces. This means that it reflects more of the solar radiation, lessens the effect caused by surface warming, refrigerates the surface temperature and induces the formation of ice. Hence, as global ice cover decreases due to ice melting, the reflectivity of Earth's surface decreases accordingly. The more incoming solar radiation absorbed by the surface, the more the surface temperature increases, causing ice to melt and escalating the average temperature of the Earth (McGehee and Widiasih, 2012).

Global warming attributes to the rise of the average temperature of the Earth's atmosphere through many factors (Viola, 2010; Wang and Chameides, 2005). Using the mathematical model Daisyworld, factors ascribed to the global warming phenomenon can be studied within a planetary system. This model is a tool in describing and analyzing the fundamental processes of the global climate and terrestrial biosphere. A zero-dimensional Daisyworld model (known as the original model) was presented by Watson and Lovelock in 1983. The model proposes that the planet behaves as a self-regulating super-organism, in which the biotic and abiotic environment interact and adapt to potential changes to continue their existence (Barnsley, 2007; Dyke, 2008).

Watson and Lovelock first presented Daisyworld in 1983 as an imaginary planet illuminated by the distant sun. The imaginary planet size is defined to represent the size of Earth. The atmospheric greenhouse gases are assumed to remain constant; therefore, the greenhouse effect of the planet does not change. The results have summarized that the planet is warmed by radiation from the sun. Moreover, it has been described as a consequence of life in a changing environment on the planet, concluding that the environment is related to life. Hence, life and environment are studied as two components in a coupled system. The environment is expressed by the global and local temperature of the planet. In which temperature depends on the albedo of the planet surface and the amount of incident luminosity from the sun. The albedo is the fraction of the solar radiation which reflects from the surface of the planet back to space. While the solar luminosity is the total output power of the sun radiating back to space. The changing of solar luminosity acts as an external factor in the Daisyworld model. In this regard, life is represented by two inhabitants of daisy population, consisting of the black and the white daisy. The black daisies reflect less light but absorb more solar radiation than the bare ground. In contrast, the white daisies reflect lighter but absorb less solar radiation than the bare ground. The growth rate of the black and white daisies depends on local temperature. The Daisyworld model also covers bare ground (Barnsley, 2007; Watson and Lovelock, 1983; Adams et al., 2003).

There are several studies that have researched the extensions of the zero-dimensional Daisyworld model by Watson and Lovelock (1983). Saunders (1994) shows how regulation can arise without natural selection through the application of the Daisyworld model. Lenton and Lovelock (2000) suggested that constraints on adaptation are an important part of a self-regulating planetary system. Cohen and Rich (2000) introduced interspecific competition into the growth equations of Daisyworld, which explains the interaction between the daisy populations. Boyle et al. (2011) proposed the impact on environmental variables and the physiological effects of symbiosis, which promotes homeostasis of the planet. Weaver and Dyke (2012) explain the original model of environmental self-regulation, which changes in insolation, and self-organisation of life as an important separation of timescales. Zeng et al. (1990) studied life and environment, investigating interactions to evaluate the existence of periodic and chaotic properties of the model. Rueangphankun et al. (2016a) describes the interaction between life and environment in the Daisyworld model, considering both snow and green daisies within the model. Nevison et al. (1999) modified the original model by the addition of a differential equation for temperature. This lead to periodic shifts of temperature within the model. Salazar and Poveda (2009) extended the model of Nevison et al. (1999) by incorporating the hydrological cycle and clouds as model parameters. Rueangphankun et al. (2016b) studied the numerical simulation of global environment in different scenarios of solar luminosity. Furthermore, there are also some researchers who modified the Daisyworld model of Watson and Lovelock (1983) to one-dimensional and two-dimensional aspects (Adams et al., 2003; Ackland et al., 2003; Biton and Gildor, 2012; Punithan et al., 2012).

The following studies describe how the Daisyworld model considers the greenhouse gas effect on the average temperature of Earth's atmosphere. Svirezhev and Bloh (1998) introduced a zero-dimensional climate-vegetation model containing a global carbon cycle and suggesting a new model by adding the hydrological cycle. The model describes the interaction between climate and biosphere parameters. Viola et al. (2013) explains global warming by adding greenhouse gases in the analysis, and considers

climate variability using a sinusoidal variation of solar luminosity. Paiva et al. (2014) propose a model describing global warming with the inclusion of greenhouse gas emission and absorption rates. Alberti et al. (2015) examined a modified version of the Daisyworld model which includes spatial dependency, variable heat diffusivity and the greenhouse effect by means of a grayness function.

However, there have been few studies using the Daisyworld model to describe the effects of ice-albedo feedback on global temperature. Although the ice-albedo feedback has not been applied to the Daisyworld model, there are still researchers interested in this topic. Fraedrich (1979) shows an analysis of qualitative aspects of the global climate system with ice-albedo feedback and the greenhouse effect. Winton (2008) evaluates the potential of the sea ice-albedo feedback and nonlinearity of Arctic climate change. McGehee and Widiasih (2012) investigate an approximation of Budyko's ice-albedo feedback model and give a simple explanation for the invariant manifold.

The objective of this study aims to modify the Daisyworld model based on the idea of how global warming is influenced by ice-albedo feedback and the greenhouse gases. In this study, the interaction between the organisms and the physical environment of the planet under the influence of global warming factors is investigated. The environment is represented by the temperature of the planet, and the organisms are represented by the black and the white daisies populations. As previously mentioned, the Daisyworld model has not been used to establish a relationship between ice-albedo feedback and global warming. Researchers have mainly focused on using Daisyworld to establish a relationship between greenhouse gases and global warming. The model in this paper is divided into three different scenarios. Each scenario considers the exclusion and inclusion of organisms. In the first scenario, a model using only ice-albedo feedback is built, as it has been linked to global warming. The second scenario focuses on the relationship between CO₂ emissions and global warming. For this particular scenario, the quantification of CO₂ levels in the atmosphere is divided into three mathematical expressions: constant value, linear increase and a sine function variation over a linear increase. The final scenario incorporates both the ice-albedo feedback and CO₂ levels into the Daisyworld model. The temperature results of the planet from the three different model scenarios are compared.

This article is managed as follows: Section 2 explains the Daisyworld model. In Section 3 describes the modified Daisyworld model of a scenario only using the ice-albedo feedback, a scenario only using CO₂ levels and a scenario with both ice-albedo feedback and CO₂. In Section 4, the results and discussion of this work are illustrated. Lastly, Section 5 presents conclusions.

Daisyworld model

The original Daisyworld model represents life by daisy populations. The planet is populated by both a black and white daisy species. The daisy population is related to the change of area within the planet. The area of change is dependent on the growth and decay of each daisy species. This change in area influences the covered and uncovered areas (*Fig. 2*). The model represents both the growth and decay of each species population. Thus, the area changes of both daisy species can be defined by the following differential equations (*Eqs. 1 and 2*; Barnsley, 2007; Watson and Lovelock, 1983):

$$\frac{d\alpha_b}{dt} = \alpha_b (\alpha_g \beta_b - \gamma) \quad (\text{Eq.1})$$

$$\frac{d\alpha_w}{dt} = \alpha_w (\alpha_g \beta_w - \gamma) \quad (\text{Eq.2})$$

where α_b and α_w are the areas covered by the black and white daisies, respectively. β_b and β_w are the growth rates per unit time and unit area of the black and white daisies, respectively, γ is the death rate per unit time of the daisies. The variable α_g is the area of bare ground in an original model represented by (Eq. 3):

$$\alpha_g = 1 - \alpha_b - \alpha_w \quad (\text{Eq.3})$$

Hence, the total area covered by the bare ground and both types of daisies is equal to 1, as follows (Eq. 4; Watson and Lovelock, 1983):

$$\alpha_g + \alpha_b + \alpha_w = 1 \quad (\text{Eq.4})$$

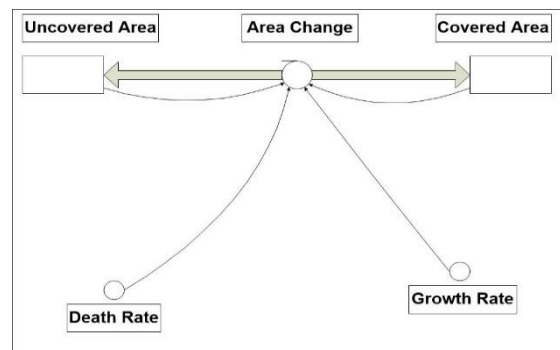


Figure 2. Basic growth model used in Daisyworld

The growth rates of the black and white daisies are assumed to be a parabolic function of local temperature (Fig. 3), as follows (Eqs. 5 and 6; Watson and Lovelock, 1983):

$$\beta_b = 1 - C(\delta - T_b)^2 \quad (\text{Eq.5})$$

$$\beta_w = 1 - C(\delta - T_w)^2 \quad (\text{Eq.6})$$

where T_b and T_w are the local temperatures over the areas covered by the black and white daisy species, respectively. C is equal to $1/(17.5)^2$ while the optimal growth temperature, δ , is equal to 22.5 °C. The parabolic function is zero when the local temperature is equal to 5 °C and 40 °C (Fig. 3). This means the daisy population stops growing and has a maximum value of one when the local temperature equals 22.5 °C. According to these results, the optimal temperature for daisy population growth is 22.5 °C.

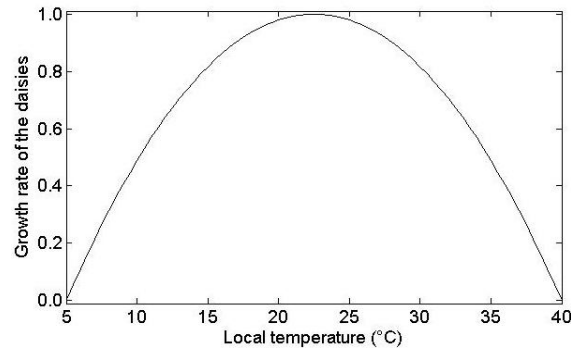


Figure 3. Relationship between the growth rate of the daisies and local temperature of each species

The local temperature of an area covered by either species of the daisies can be expressed as (Eqs. 7 and 8; Watson and Lovelock, 1983):

$$T_b^4 = q(A_l - A_b) + T^4 \quad (\text{Eq.7})$$

$$T_w^4 = q(A_l - A_w) + T^4 \quad (\text{Eq.8})$$

where A_l , A_b and A_w are the albedos of land, the black and the white daisies, respectively, q , a positive constant, expresses the degree to which solar energy, after having been absorbed by the planet, T is the temperature of the planet in Daisyworld. From Equations 7 and 8, the local temperature for black and white daisy species can be simplified with little error. Using a linear approximation from Taylor's theorem, Equations 7 and 8 can be expressed as (Eq. 9 and 10; Watson and Lovelock, 1983):

$$T_b = q'(A_l - A_b) + T \quad (\text{Eq.9})$$

$$T_w = q'(A_l - A_w) + T \quad (\text{Eq.10})$$

where $q' = q/4T^3$. The error introduced by this approximation is normally less than 2 °C for the temperature of interest. The albedo of the original Daisyworld varies as a function of the fraction of land or the planet surface covered by bare ground, the black and the white daisies, as well as their respective albedo values (Barnsley, 2007). All of the albedo values are between 0 and 1. An albedo of 0 is a perfect absorber of light while 1 is a perfect reflector of light. The albedo of land, A_l , of the original model can be defined as follows (Eq. 11; Watson and Lovelock, 1983):

$$A_l = \alpha_g A_g + \alpha_b A_b + \alpha_w A_w \quad (\text{Eq.11})$$

And $A_b < A_g < A_w$, where A_g is the albedo of bare ground. Watson and Lovelock (1983) described the temperature of Daisyworld by absorption and emission of radiation on the planet. It can be defined as follows (Eq. 12):

$$e_{sa} \sigma T^4 = SL(1 - A_l) \quad (\text{Eq.12})$$

where e_{sa} is the effective emissivity, S is the solar flux constant, L is the solar luminosity and σ is the Stefan-Boltzmann constant. Emissivity is a dimensionless number that ranges from 0 to 1. The original model of Watson and Lovelock (1983) defined $e_{sa} = 1$. Nevison et al. (1999) have replaced Equation 12 with an ODE for the planet temperature, T , which allows T to be represented in an unsteady state. The ODE can be written as (Eq. 13):

$$c \frac{dT}{dt} = SL(1 - A_l) - e_{sa} \sigma T^4 \quad (\text{Eq.13})$$

where c is the average heat capacity of the planet. The result of the Daisyworld model of Nevison et al. (1999) in Equation 13 causes self-sustained temperature oscillations that are closely coupled to oscillations in both species of daisy populations (Fig. 4).

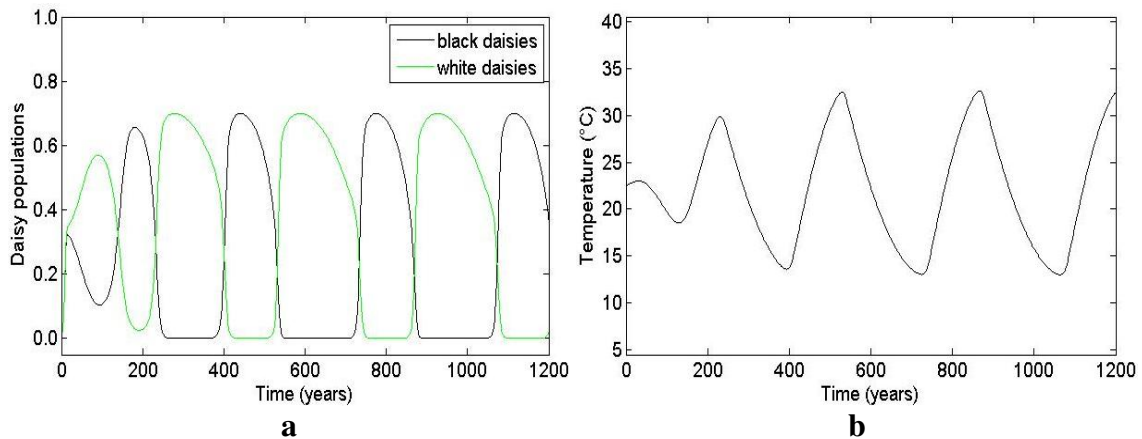


Figure 4. The Daisyworld model response (Nevison et al., 1999). (a) Area fraction of the black and the white daisies; (b) temperature of Daisyworld

A modified Daisyworld model

A modified Daisyworld model is developed by adding ice-albedo feedback and greenhouse gases into the Daisyworld model. There are three different scenarios including ice-albedo feedback, greenhouse gases and a combination of ice-albedo feedback and greenhouse gases. The detail of a modified Daisyworld model is shown in the following sections.

A modified Daisyworld model with ice-albedo feedback

The ice-albedo feedback scenario was applied to the Daisyworld model. In the model, the surface of the planet is divided into two parts, a fraction of land consisting of bare ground/ black and white daisies and a fraction of melting ice. Both fractions are represented by f and $1 - f$, respectively. The model assumes that each daisy species cannot grow in a fraction of melting ice. Thus, the total area covered by the bare ground and both species of daisy from Equation 4 can be rewritten as Equation 14 and a fraction of melting ice, a_m , can be defined as Equation 15, respectively.

$$\alpha_g + \alpha_b + \alpha_w = f \quad (\text{Eq.14})$$

$$\alpha_m = 1 - f \quad (\text{Eq.15})$$

Therefore, the albedo of the planet in this situation depends on the fractions of land and melting ice, as defined by (Eq. 16):

$$A_{l,m} = fA_l + (1-f)A_m \quad (\text{Eq.16})$$

Where A_l follows Equation 11 and $A_m = a - bT^2$ is an ice-albedo feedback introduced to link variations in the planets temperature, a and $b = 10^{-5} \text{ K}^{-2}$ represent the magnitudes of the ice-albedo feedback parameters. Therefore, the ODE in Equation 13 becomes (Eq. 17):

$$\frac{dT}{dt} = \frac{1}{c} [SL(1 - A_{l,m}) - e_{sa}\sigma T^4] \quad (\text{Eq.17})$$

In this situation, the effective emissivity is defined by $e_{sa} = e_s - e_a$, where e_s is surface emissivity and e_a is the atmospheric emittance (Fraedrich, 1979). In this work, it is defined as $a = 1.4$ and $e_{sa} = 0.8$.

A modified Daisyworld model with greenhouse effect

This section presents greenhouse effect as a temperature dependent feedback for atmospheric emittance, e_a , is expressed as (Eq. 18):

$$e_a = e_c + kT^2 \quad (\text{Eq.18})$$

where $e_c = 0.0235\ln(\text{CO}_2) + c_t$ (Bryson and Dittberner, 1976) is formulation for carbon dioxide emittance in the atmosphere, (CO_2 in ppm) and k is the greenhouse effect coefficient. In this condition, Equation 18 is added into the basic ODE in Equation 13 and there is no ice albedo feedback which leads to (Eq. 19):

$$\frac{dT}{dt} = \frac{1}{c} [SL(1 - A_l) - e_{sc}\sigma T^4 + k\sigma T^6] \quad (\text{Eq.19})$$

where $e_{sc} = e_s - e_c$ (Fraedrich, 1979). Here, $k = 7 \times 10^{-7} \text{ K}^{-2}$ and $c_t = 0$. For the greenhouse gas effect, CO_2 is divided into three situations; constant value, linear increase and a sine function variation over a linear increase.

Constant CO₂

In the first incident with greenhouse effect, CO_2 in the planet's atmosphere is assumed to remain constant. Thus, a constant value situation is considered as (Eq. 20):

$$\text{CO}_2 = 400 \text{ ppm} \quad (\text{Eq.20})$$

Linear increase of CO₂

According to (Kahn, 2017), human activities have committed a massive amount of CO₂ to the atmosphere. It has driven CO₂ levels to record highs year after year. He found that globally averaged concentrations of CO₂ have a rate of increasing about 3 ppm per year from 2015 to present. To represent annual rates of CO₂ increases in the atmosphere, linear increasing function is defined as 3 ppm per year for indicating the behavior of CO₂ (Fig. 5a). The equation can be expressed as (Eq. 21):

$$\text{CO}_2 = 400 + 3t \text{ ppm} \quad (\text{Eq.21})$$

A sine function variation over a linear increase of CO₂

Under this event, the fluctuation of atmospheric CO₂ will not increase at a linear rate but have a tendency to increase continuously (Fig. 5b). The sine function has been incorporated into Equation 21. Therefore, the instantiation of sine function variation over a linear increase is determined as (Eq. 22):

$$\text{CO}_2 = (400 + 3t) + (A \sin Bt) \text{ ppm} \quad (\text{Eq.22})$$

where the value of *A* and *B* refer to amplitude and time, respectively.

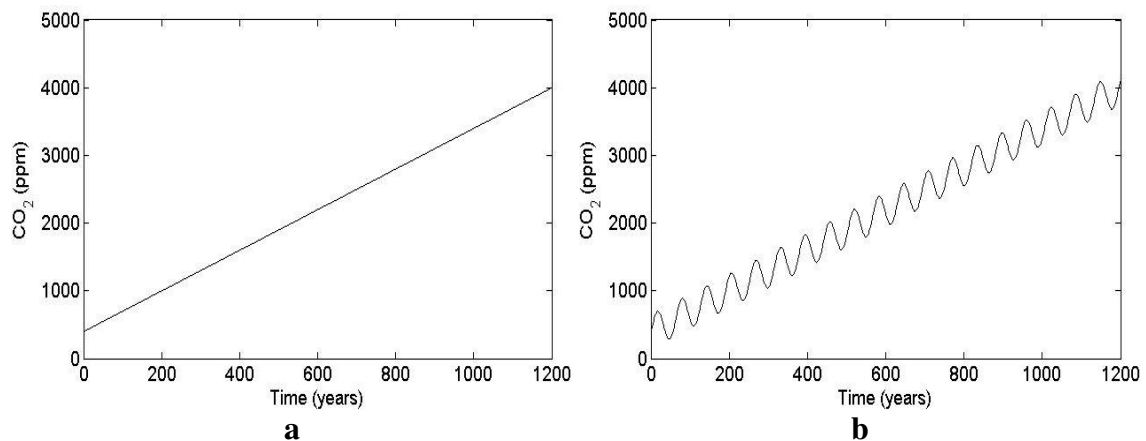


Figure 5. A different of increasing of the CO₂ concentration in the atmosphere. (a) Linear increase; (b) a sine function variation over a linear increase

A modified Daisyworld model with ice-albedo feedback and greenhouse effect

The final model scenario suggests a combination of ice-albedo feedback and CO₂ levels. According to Equation 13, the following equation can be expressed as (Eq. 23; Fraedrich, 1979):

$$\frac{dT}{dt} = \frac{1}{c} [SL(1 - A_{i,m}) - e_{sc} \sigma T^4 + k \sigma T^6] \quad (\text{Eq.23})$$

Results and discussion

Euler's method is used to connect with an iterative process to simulate three different scenarios: ice-albedo feedback; CO₂ levels; and a combination of ice-albedo feedback and CO₂ levels. Each of the above scenarios are considered as including or excluding organisms. The CO₂ levels are divided into three parts: constant value, linear increase and a sine function variation over a linear increase. The values of the parameters for each modelled scenario is shown in *Table 1*.

Table 1. Parameter values of Daisyworld model

Symbol	Parameter value	Unit	Source of information
A_g	0.5	Dimensionless	(Watson and Lovelock, 1983)
A_b	0.25	Dimensionless	(Watson and Lovelock, 1983)
A_w	0.75	Dimensionless	(Watson and Lovelock, 1983)
γ	0.3	Dimensionless	(Watson and Lovelock, 1983)
q'	20	K	(Watson and Lovelock, 1983)
σ	1789	$\text{erg} \cdot \text{cm}^{-2} \cdot \text{yr}^{-1} \cdot \text{K}^{-4}$	(Nevison et al., 1999)
S	2.89×10^{13}	$\text{erg} \cdot \text{cm}^{-2} \cdot \text{yr}^{-1}$	(Nevison et al., 1999)
L	1	dimensionless	(Watson and Lovelock, 1983)
c	3×10^{13}	$\text{erg} \cdot \text{cm}^{-2} \cdot \text{K}^{-1}$	(Nevison et al., 1999)
q	2.06×10^9	K^4	(Paiva et al., 2014)

Ice-albedo feedback

In the situation of ice-albedo feedback, the consequences of the model including and excluding the daisies represents the temperature of the planet including and excluding organisms. *Figure 6* displays the temperature of the planet excluding the daisies. The resulting plot for a planet without organisms indicates that the planet's temperature begins at 22.5 °C and increases rapidly to 105 °C under a timeframe of 600 years. After 600 years, the temperature of the planet only slightly varies. After reaching 110 °C at 800 years, the planet's temperature no longer changes. The model including black and white daisy species (i.e. organisms) was initially set to $f = 0.9$. Whereby the value of f represents the fraction of bare surface and daisy species coverage (*Fig. 7*). The fraction that equals 0.1 represents the melting of ice, $1-f$, as a result of ice-albedo feedback. Also, *Figure 7a* presents the fractional areas covered by the black and the white daisy species on the planet. While *Figure 7b* represents the temperature of Daisyworld due to ice-albedo feedback and the interaction between two species of daisy populations as in *Figure 7a*. The interaction confines the temperature values within a reasonable range for life continuation. The increase of the white daisies is more evident as the planet's average temperature decreases. The increase of black daisies is more evident as the average temperature of the planet increases. The modelled results of $f = 0.9$ for average planet temperature ranged between a minimum value of 17.5 °C and a maximum value of 26.5 °C.

The Daisyworld model was also set to $f = 0.8$ for the representation of bare surface along with black and white daisy species (*Fig. 8*). *Figure 8a* illustrates the change in

black and white daisy populations overtime, while *Figure 8b* shows the temperature of the planet over the same temporal scale. The results show that the planet's maximum temperature value was 25 °C during the first two decades and then falls to a minimum value of 18.5 °C in the following 580 years. After 200 years, there is only a minute change in the planet's temperature. The fraction of light area for each daisy population begins at 0.01 (*Fig. 8a*). In a short period of time white daisies are shown to grow almost instantaneously. At around 0.7, the growth of white daisies becomes stagnant. During the growth of white daisies, black daisy population dramatically decreases. Eventually becoming stagnant along with the white daisy population.

Figures 9-11 illustrate models representing ice-albedo feedback with different fractional values; $f = 0.7$, 0.6 and 0.5, respectively. The consequence for $f = 0.7$ in *Figure 9* elucidates that the initial temperature of the planet is 22.5 °C. The temperature increases to 25 °C and subsequently declines to a steady state of 21 °C at 400 years. Similar to the previous model where ice-albedo feedback is set at $f = 0.8$, the white daisy population under $f = 0.7$ grows increasingly fast, from 0.01 – 0.7, over a short period of time (*Fig. 9*). The population growth for white daisies becomes stagnant, hovering around 0.7 after 50 years. Similarly, the black daisy population decreases quickly, from 0.3 to 0.0, over a short period of time. The population eventually dies out after 50 years. There is a similar outcome to the model representing ice-albedo feedback at a value of $f = 0.6$. A sharp increase is illustrated by the white daisy population under a short period of time, while there is a sharp decrease in black daisy population over a short period of time. Both populations taper off into a steady state of no growth after 50 years (*Fig. 10*). The model representing an ice-albedo feedback of $f = 0.5$ illustrates that the average temperature of the planet continuously increases from 22.5 °C to 36.5 °C over 1200 years (*Fig. 11b*). While the temperature gradually increases, the white daisy population increases sharply over the first 50 years of the simulation. After 50 years, the white daisies tend to decrease continuously. The black daisy population decreases from 0.3 to 0.0 over the first 50 years of the simulation (*Fig. 11a*).

Finally, *Figure 12* illustrates an event of ice-albedo feedback with a fractional value of $f = 0.4$. The results show that the average temperature continuously increases from 22.5 °C to more than 40 °C, over the first 400 years. Under this scenario, the balance between both daisy populations and the plant's temperature illustrates inconsistent results. The decline of growth in the white daisy population occurs under a shorter period of time (~400 years). While the decline of black daisy population is similar to the former simulations (*Fig. 12a*). Eventually, the black daisies become extinct in a short period, and the white daisies go extinct after 380 years.

Under the Daisyworld simulation excluding organisms, the average temperature of the planet increases continuously, eventually leveling out around 600 years. If the Earth's temperature ever reached the values simulated in the first model, the daisies would not survive. Contrary to the simulation with organisms, the planet's average temperature rises at a slower rate with the presence of black and white daisy populations. Black and white daisy populations alter the planet's surface temperature. However, when the fraction of land decreases along with the fraction of melting ice, there is a noticeable increase in the planet's average temperature. Moreover, the excessive increase of the planet's temperature is due to the decrease of the fraction of land, inducing the extinction of life. Hence, ice-albedo feedback is an important factor to engender global warming.

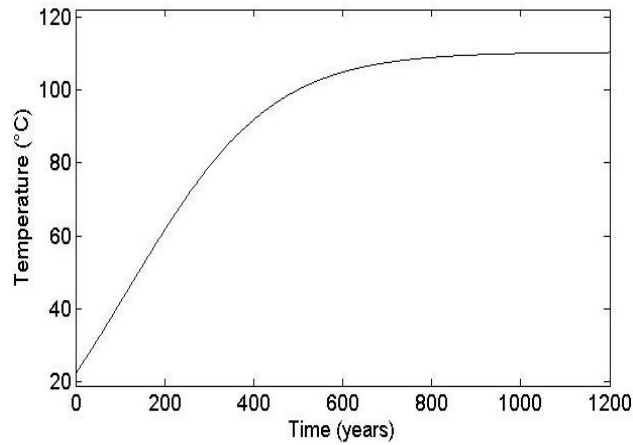


Figure 6. Temperature of the planet without organisms for ice-albedo feedback

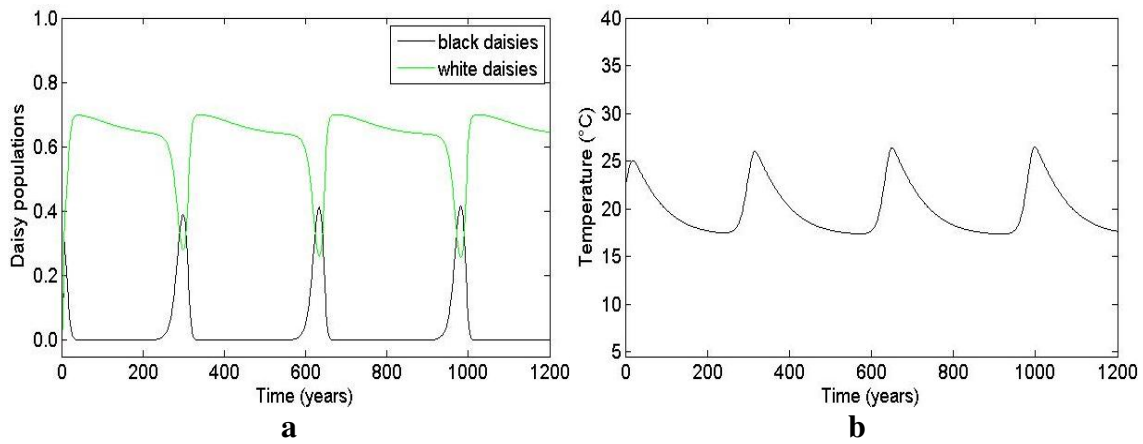


Figure 7. Model including organisms for ice-albedo feedback where $f = 0.9$. (a) Area fraction of the black and the white daisies; (b) temperature of Daisyworld

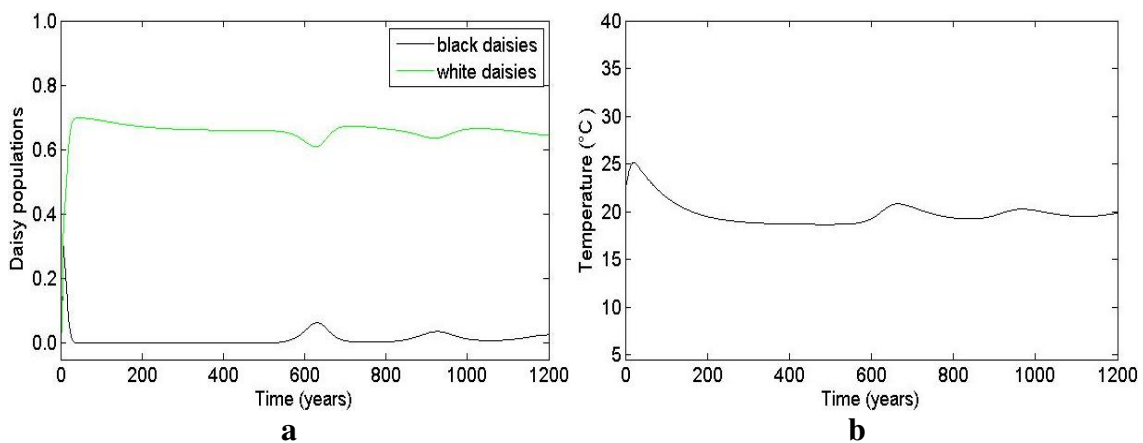


Figure 8. Model including organisms for ice-albedo feedback where $f = 0.8$. (a) Area fraction of the black and the white daisies; (b) temperature of Daisyworld

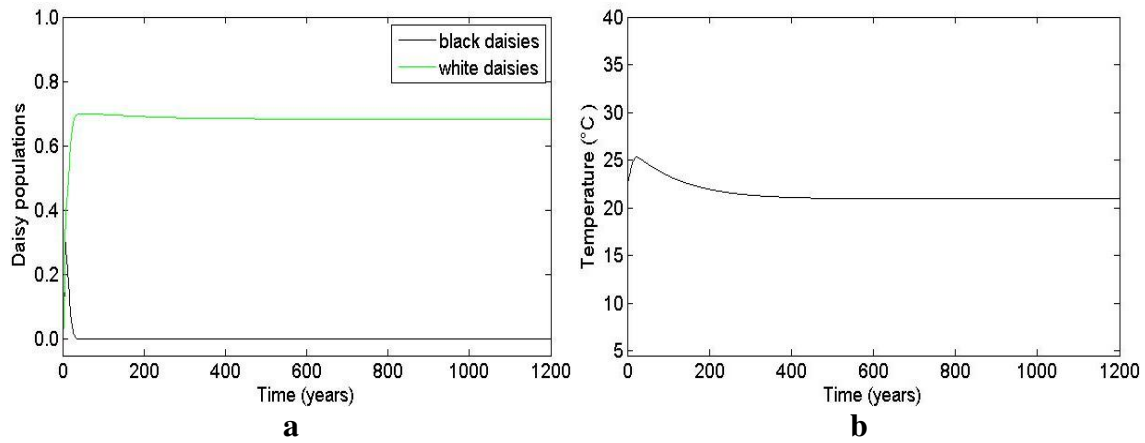


Figure 9. Model including organisms for ice-albedo feedback where $f = 0.7$. (a) Area fraction of the black and the white daisies; (b) temperature of Daisyworld

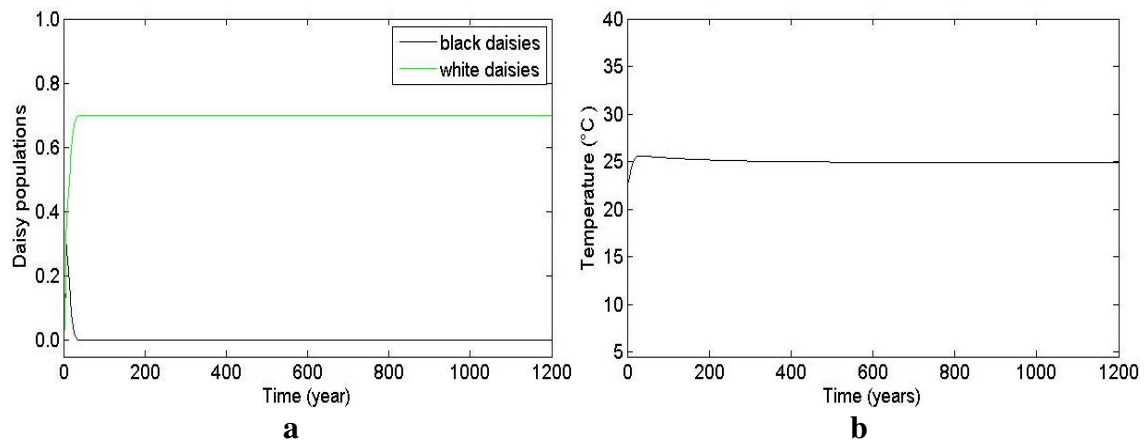


Figure 10. Model including organisms for ice-albedo feedback where $f = 0.6$. (a) Area fraction of the black and the white daisies; (b) temperature of Daisyworld

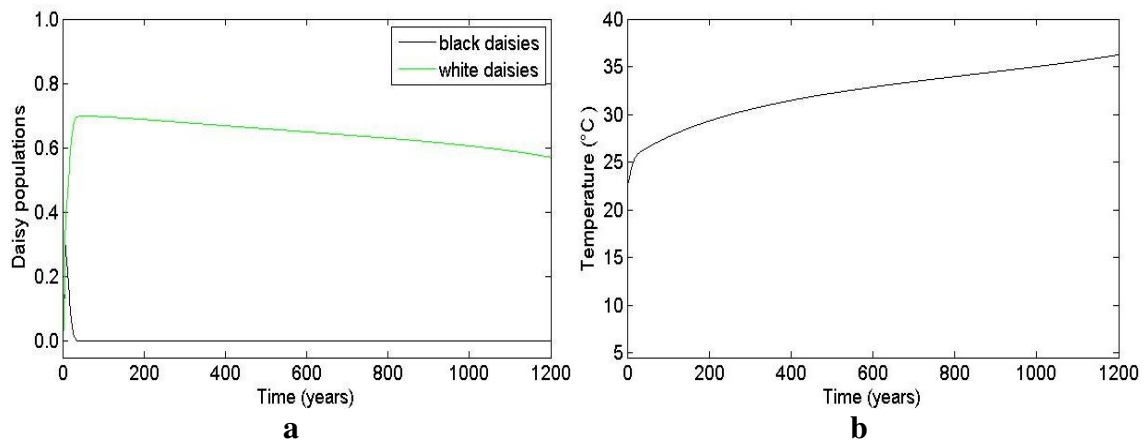


Figure 11. Model including organisms for ice-albedo feedback where $f = 0.5$. (a) Area fraction of the black and the white daisies; (b) temperature of Daisyworld

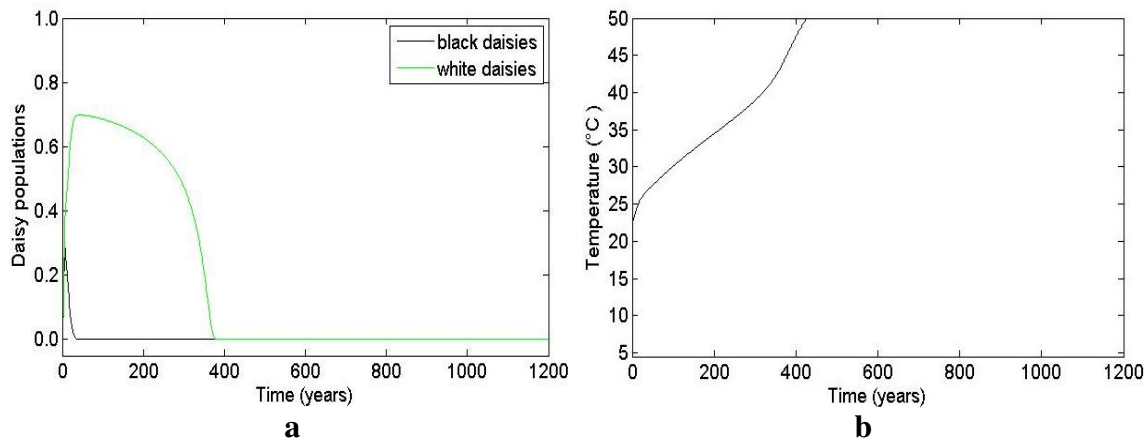


Figure 12. Model including organisms for ice-albedo feedback where $f = 0.4$. (a) Area fraction of the black and the white daisies; (b) temperature of Daisyworld

Greenhouse effect

Greenhouse gases are represented as CO_2 for the simulation of greenhouse effect on the planet's average temperature. The model in this section both incorporates the inclusion and exclusion of organisms. Firstly, the comparison of the planet's average temperature with respect to the absence of organisms and the effect of CO_2 levels in the planet's atmosphere have been simulated (Fig. 13). Figures 13a, b and c present three mathematical expressions for determining the planet's average temperature under the effects of CO_2 : a constant value, linear increase and sine function variation over a linear increase. Each simulation begins with an average temperature of 22.5 °C, gradually increasing overtime (Fig. 13). Under the scenario where CO_2 is modelled with a constant value, the average temperature increases sharply within the first 250 years. Eventually leveling out at 45 °C (Fig. 13a). For scenario two, representing a linear increase, the average temperature sharply increases within the first 250 years. The temperature slightly increases and eventually levels off around 50 °C over the following 950 years (Fig. 13b). Under the last scenario, representing a sine function over a linear increase, the results illustrate similarities with the second scenario. However, the variability in CO_2 for scenario three creates an instability in the rise of temperature. Over the first 200 years, the temperature sharply rises to 45 °C. Afterwards, the temperature gradually rises to 50 °C over the following 1000 years (Fig. 13c). After comparing all three mathematical expressions for CO_2 levels, it is found that the average global temperature in Figures 13b and c are higher than in Figure 13a.

A scenario in which organisms are present within the CO_2 model have been simulated (Fig. 14). The simulated results illustrate that both black and white daisy populations fluctuate under the shifts in average planet temperature (Fig. 14a, b). The fluctuation of black and white daisy populations is similar to the results in Figure 7. The varied species of daisy react to the differences in temperature. As temperature rises, black daisy population increases. As temperatures decrease, white daisy population increases. Since the white daisies have a high albedo, the average temperature of the planet decreases. Thus, giving rise to the black daisy population. Black daisies have a lower albedo; the average temperature of the planet increases. As the average temperature of the planet decreases, there is an increase in white daisy population.

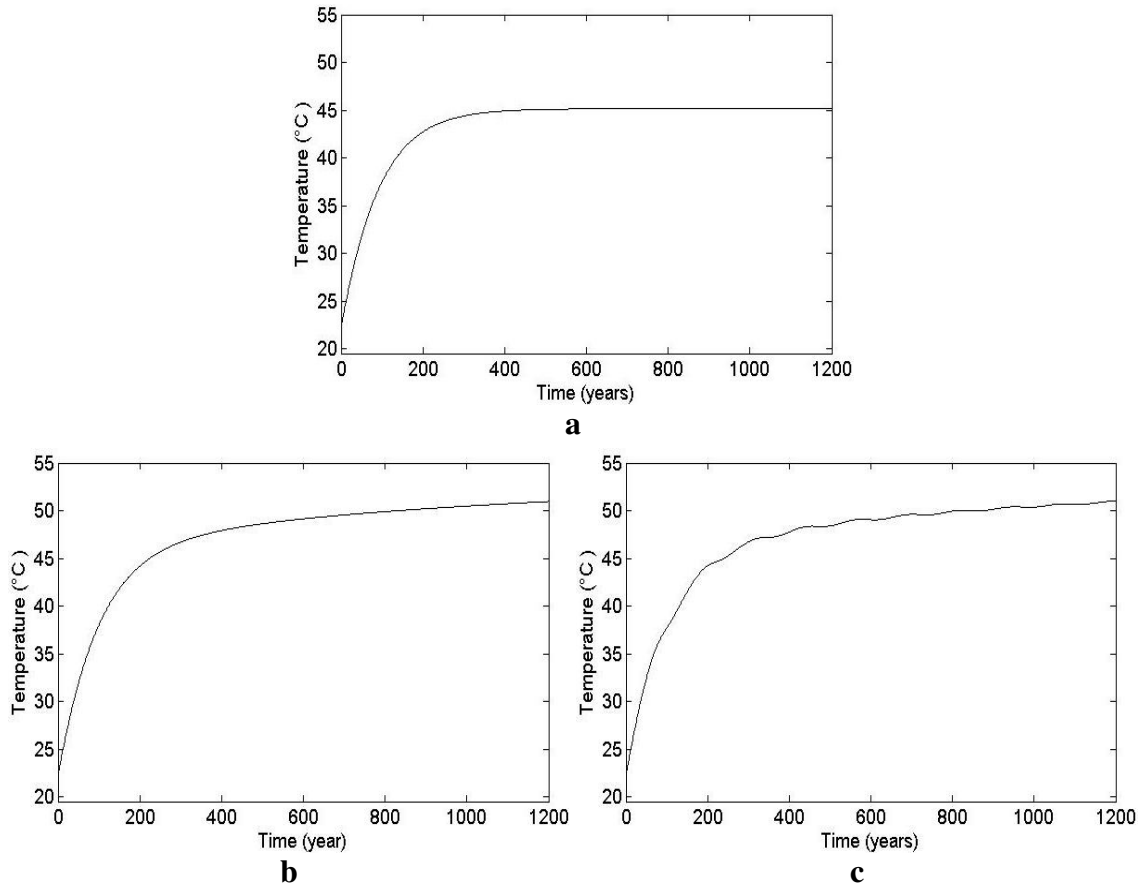


Figure 13. Temperature of the planet without organisms for greenhouse effect with different CO_2 values. (a) Constant value; (b) linear increase; (c) a sine function variation over a linear increase

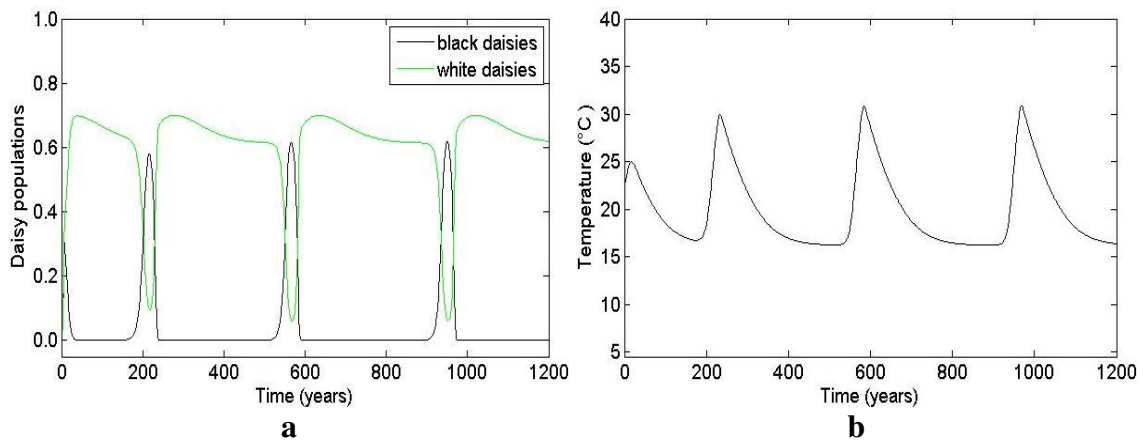


Figure 14. Model including organisms for greenhouse effect with constant CO_2 . (a) Area fraction of the black and the white daisies; (b) temperature of Daisyworld

The maximum average temperature of the planet was 30 °C, while the average minimum temperature was 16 °C. Modelling CO_2 in a linear increase fashion (Fig. 15)

corresponds with an increase in white daisy population and a decrease in black daisy population. The average temperature of the planet has a maximum value of 26 °C and a minimum value of 17 °C in the first 400 years. After 400 years, the effect of CO₂ levels influences the differences in average temperature by 2 °C. The maximum average temperature during this timeframe is 21 °C while the minimum average temperature is 19 °C. Under these conditions, the white daisy population proliferates while the black daisy population struggles to increase at any rate (*Fig. 15*). Overtime and due to the slow rise in CO₂ levels, the black daisy population will become extinct. The final CO₂ scenario presents a model of CO₂ levels fitted to a sine function variation over a linear increase (*Fig. 16*). The outcome of results illustrates a resemblance to the second scenario, in that the variation of daisy population and average temperature are similar over the temporal scale. Although, the average maximum temperature for the first 400 years is 27.5 °C, higher than the results of the second CO₂ scenario (*Fig. 16*).

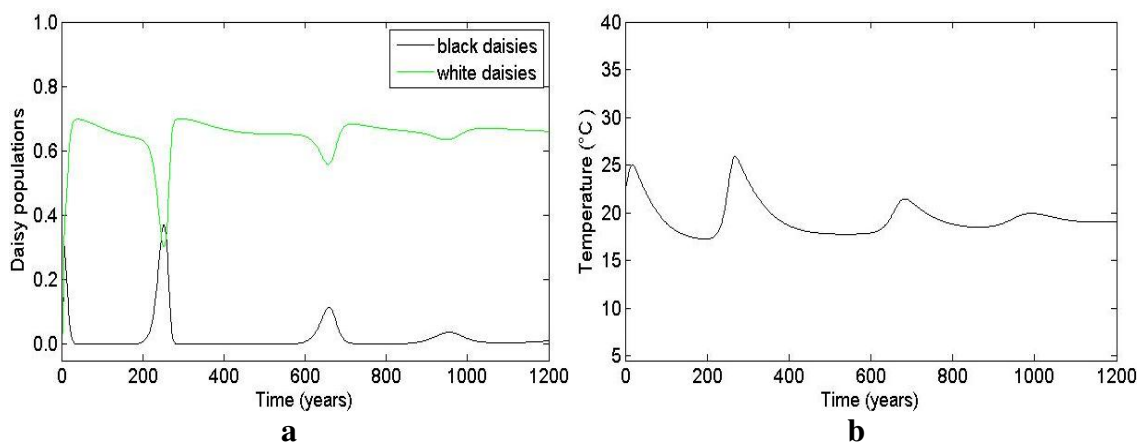


Figure 15. Model including organisms for greenhouse effect with linear increase of CO₂. (a) Area fraction of the black and the white daisies; (b) temperature of Daisyworld

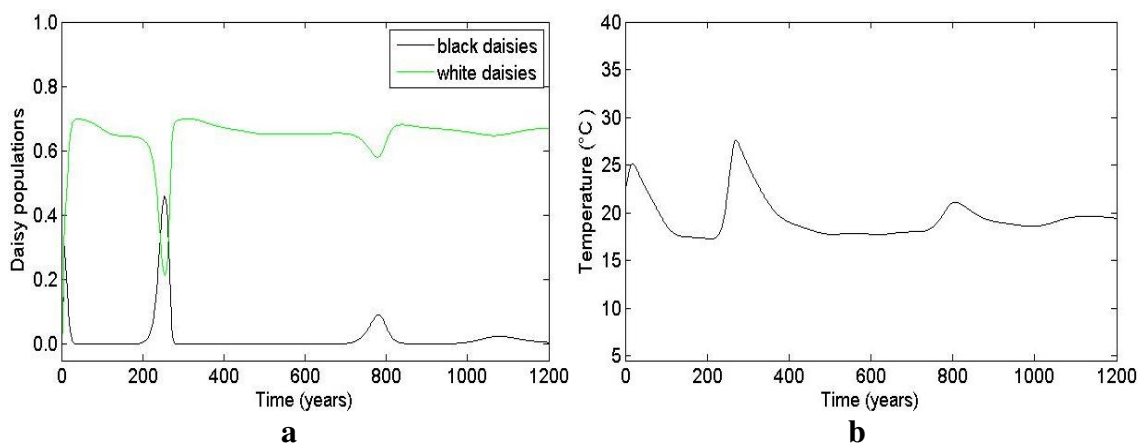


Figure 16. Model including organisms for greenhouse effect with a sine function variation over a linear increase of CO₂. (a) Area fraction of the black and the white daisies; (b) temperature of Daisyworld

Under the scenario where there are no organisms present on the planet and CO₂ is subjected to three different mathematical expressions, the average temperature sharply increases for the first 200 years and steady increases thereafter for the following 1000 years. It is evident that under the three expressions, CO₂ influences the rise in average temperature of the planet. When the planet is inhabited by white and black daisies, the different species influence the fluctuation of the planet's average temperature. The average temperatures are influenced by the adjustments of each species. However, the influence of CO₂ also impacts the average temperature overtime. Thus, forcing one species to become extinct while the other proliferates. The species in this situation is the white daisy. The white daisy can tolerate higher temperatures. While the black daisy species has a higher tolerance for lower temperature environments.

Ice-albedo feedback and greenhouse effect

The final scenario proposes an incident where the combination of ice-albedo feedback and greenhouse effect (CO₂ levels) are simulated within the model. As in the previous scenario, CO₂ levels are projected under the three mathematical expressions; constant value, linear increase and a sine function variation over a linear increase. The first model considers the average temperature of the planet without the existence of organisms. The initial average temperature of the planet is recorded at 22.5 °C for all three mathematical expressions. The average temperature under the first mathematical expression gradually rises to 132 °C, at which the temperature reaches a steady state after 1060 years (*Fig. 17a*). The average temperature of the second and third mathematical expression levels out at 160 °C after 1200 years (*Fig. 17b, c*). The characteristic of average temperature for the three mathematical expressions in this scenario are very similar to that of the scenario representing just CO₂ levels and excluding the presence of organisms.

The second model considers an instance where organisms are present on the planet with the impact of both ice-albedo feedback and CO₂ levels. Under the condition where $f = 0.9$ and CO₂ levels are under a constant mathematical expression, white daisy population proliferates within the first 20 years. The population then levels out for the next 580 years (*Fig. 18a*). The black daisies become extinct within the first 20 years of the simulation. The average temperature is initially recorded at 22.5 °C but sharply increases to 28.5 °C within the first 20 years. After which the average temperature levels out at 30.5 °C for the remainder of the simulation timeframe (*Fig. 18b*). Where $f = 0.8$ and CO₂ levels are under a constant mathematical expression, the planet's average temperature exceeds 40 °C within the first 150 years (*Fig. 19b*). The sharp increase in temperature under a short period of time results in both the black and white daisy species to become extinct within 125 years. Albeit the white daisy population outlasts the black daisy population by roughly 100 years (*Fig. 19a*).

The linear increase mathematical expression was applied to the CO₂ levels in combination with ice-albedo feedback at $f = 0.9$ and 0.8. Where $f = 0.9$ there is an initial sharp increase of average temperature in the first 20 years. The average temperature then gradually rises to a maximum of 50 °C over the next 560 years (*Fig. 20b*). The initial sharp increase in temperature results in the black daisy becoming extinct after 25 years. While the white daisy species slowly dies out and eventually becomes extinct after 550 years (*Fig. 20a*). Similarly, the mathematical expression of a linear increase for CO₂ levels illustrated temperatures exceeding 40 °C in just under 110 years (*Fig. 21b*). The subsequent effects resulted in the black daisy becoming

extinct after 25 years, while white daisy became extinct after 125 years (*Fig. 21a*). The white daisies existence is longer when $f = 0.9$ is applied to linear increase. The black daisy species does not fare well in either of the scenarios, becoming extinct within 25 years in both models.

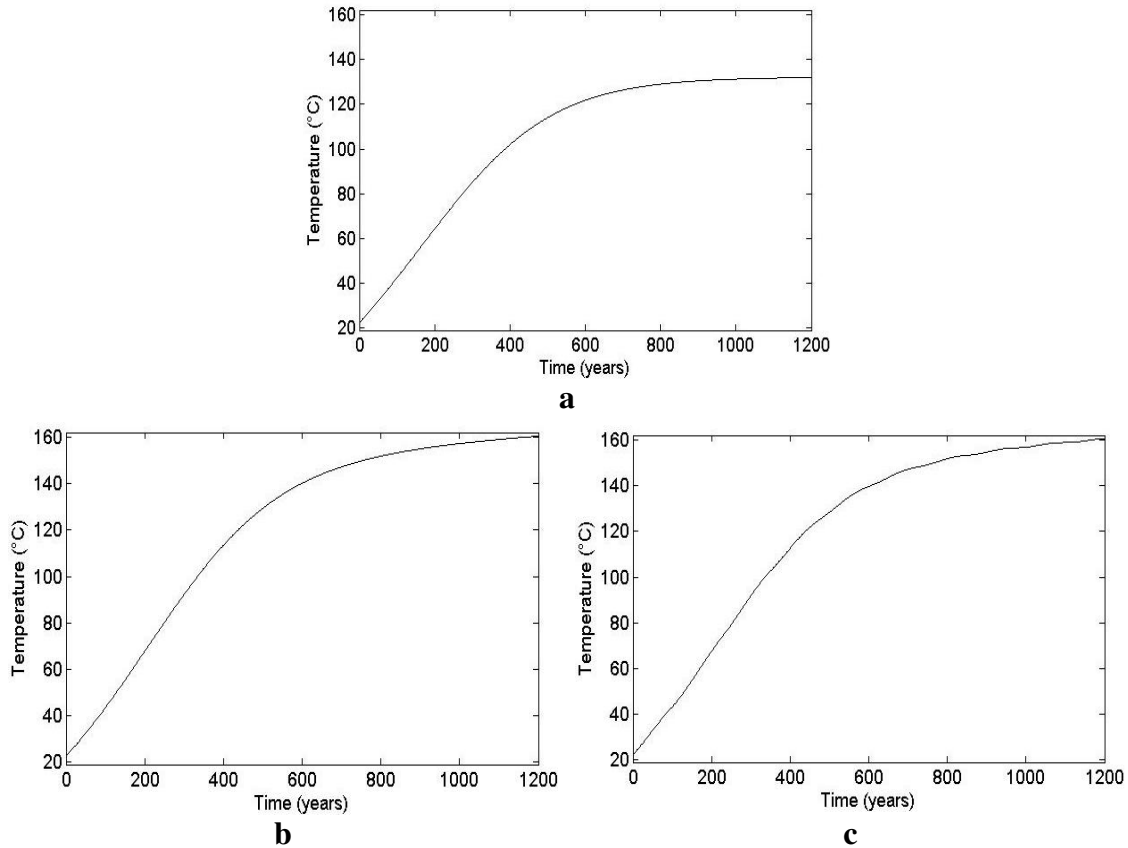


Figure 17. Temperature of the planet without organisms for both ice-albedo feedback and greenhouse effect with different CO_2 . (a) Constant value; (b) linear increase; (c) a sine function variation over a linear increase

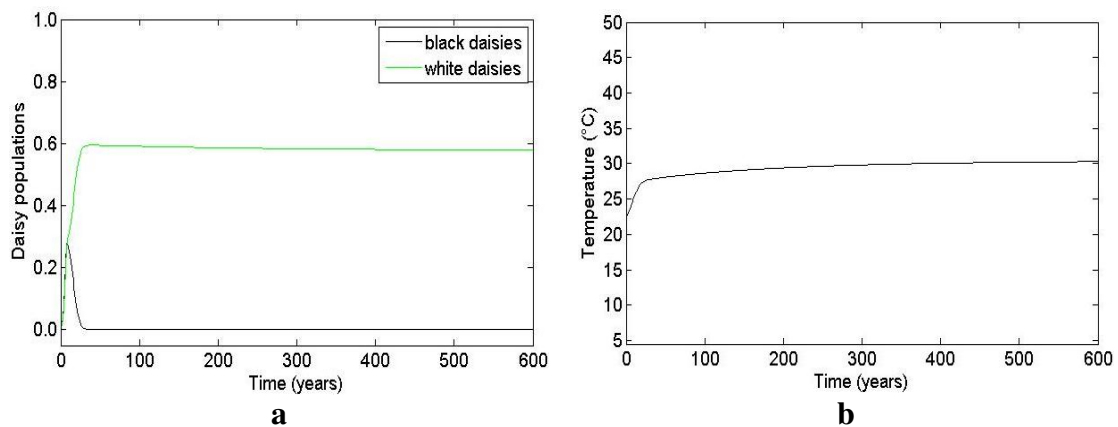


Figure 18. Model including organisms for both ice-albedo feedback and greenhouse effect where $f = 0.9$ and constant CO_2 . (a) Area fraction of the black and the white daisies; (b) temperature of Daisyworld

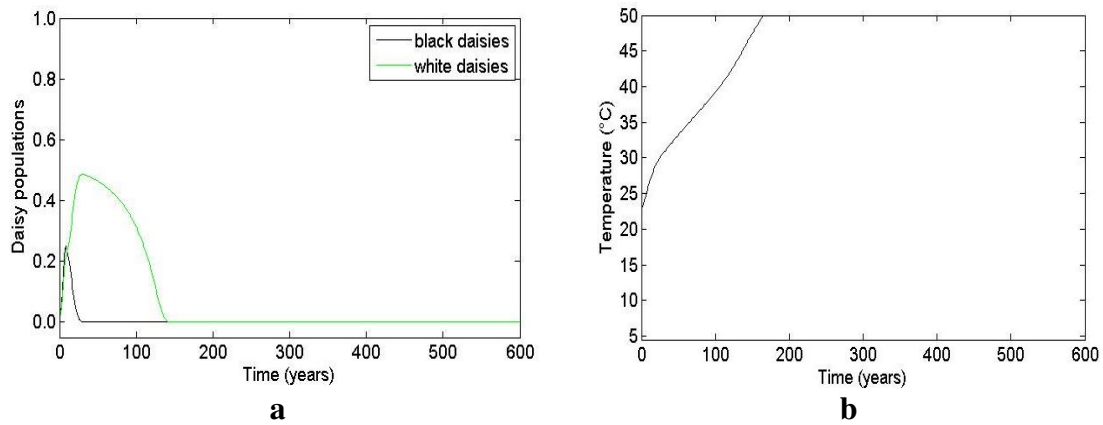


Figure 19. Model including organisms for both ice-albedo feedback and greenhouse effect where $f = 0.8$ and constant CO_2 . (a) Area fraction of the black and the white daisies; (b) temperature of Daisyworld

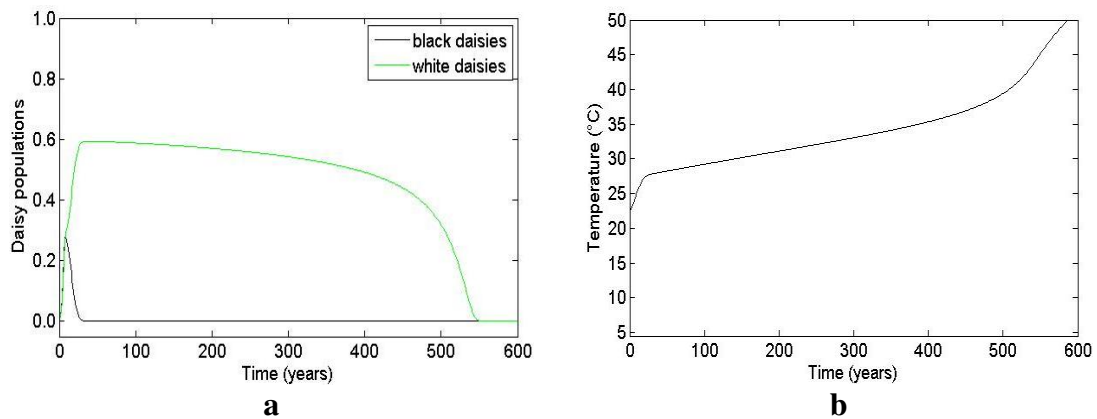


Figure 20. Model including organisms for both ice-albedo feedback and greenhouse effect where $f = 0.9$ and linear increase of CO_2 . (a) Area fraction of the black and the white daisies; (b) temperature of Daisyworld

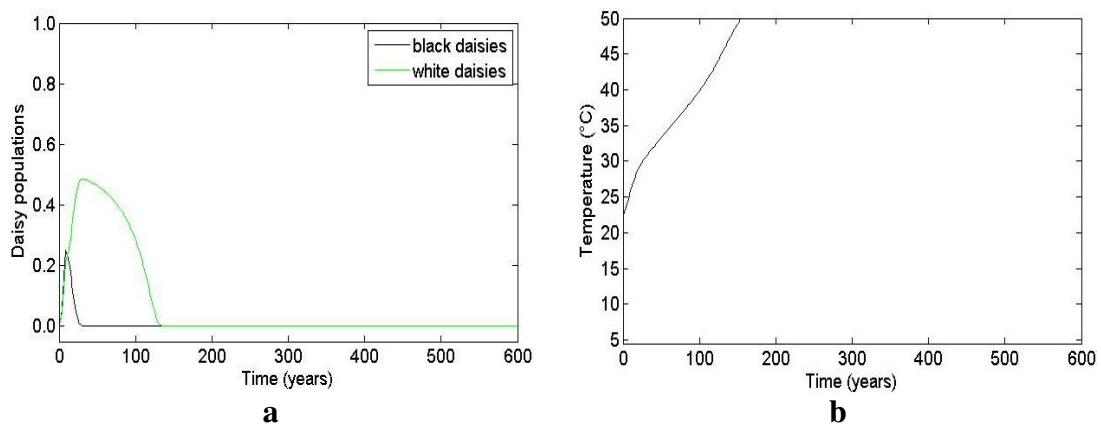


Figure 21. Model including organisms for both ice-albedo feedback and greenhouse effect where $f = 0.8$ and linear increase of CO_2 . (a) Area fraction of the black and the white daisies; (b) temperature of Daisyworld

The final scenario introduces a sine function over a linear increase for modelling CO₂ levels. Two experiment cases of $f = 0.9$ and 0.8 are applied. The results illustrate similar outcomes with the previous linear function scenario. The shape of each graph is near identical to *Figures 20 and 21*. Where $f = 0.9$ the temperature has an initial sharp increase and gradually rises to 50 °C over the next 550 years (*Fig. 22b*). Black daisies become extinct after just 25 years, while white daisies become extinct after 550 years (*Fig. 22a*). The results for $f = 0.8$ are closely related to the linear function results for $f = 0.8$ (*Fig. 23a, b*).

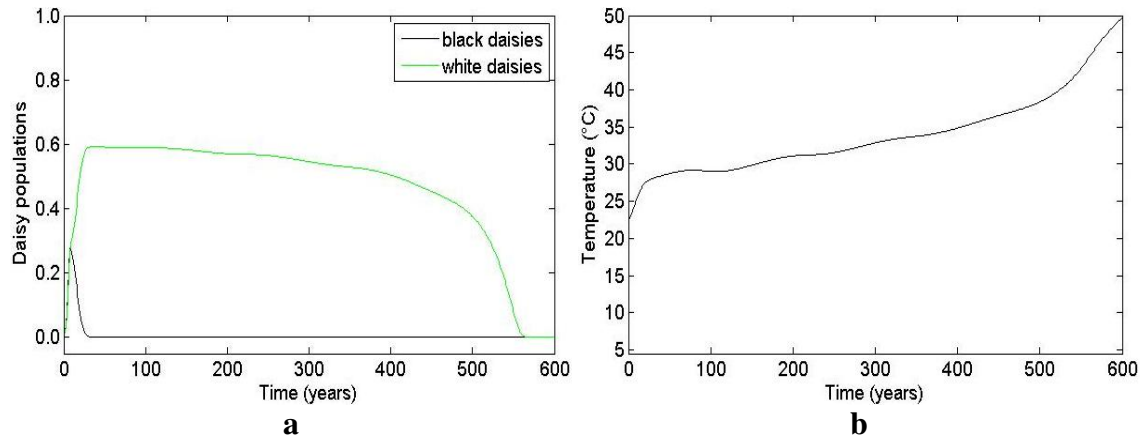


Figure 22. Model including organisms for both ice-albedo feedback and greenhouse effect where $f = 0.9$ and a sine function variation over a linear increase of CO₂. (a) Area fraction of the black and the white daisies; (b) temperature of Daisyworld

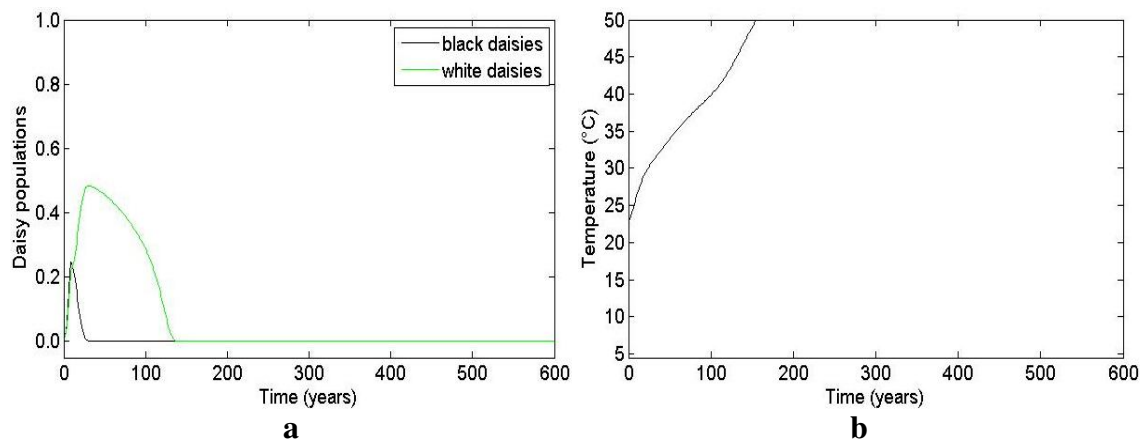


Figure 23. Model including organisms for both ice-albedo feedback and greenhouse effect where $f = 0.8$ and a sine function variation over a linear increase of CO₂. (a) Area fraction of the black and the white daisies; (b) temperature of Daisyworld

The scenarios modelled in this section focused on the impact of ice-albedo feedback and CO₂ levels. Two different factors are also incorporated into the model, one representing a planet without organisms and another representing the planet with organisms. The model illustrated that the planet's average temperature gradually rose for all three CO₂ mathematical expressions and without the presence of organisms. Each

model exceeded livable temperatures, making the planet uninhabitable for organisms. The scenario incorporating organisms also resulted in situations where both the black and white daisy species became extinct overtime. Each species attempted to adapt to the average temperature but overtime each was unsuccessful and had eventually died out. When the fraction of land, consisting of both daisy species and bare ground, was decreased in the model the melting of ice area increased. This resulted in the rise of the planet's average temperature. Ultimately resulting in the extinction of both species. The two mathematical expressions of CO₂ levels having the greatest impact on rising average temperatures and species extinction were linear increase and sine function over linear increase.

The comparison of all three scenarios in case of with and without the daisies is presented. Under the model without the daisies, the results of a scenarios with ice-albedo feedback; and a combination of ice-albedo feedback and CO₂ levels illustrate that the average temperature overtime becomes very high compared with a scenario of CO₂ levels. All three scenarios, exceeding the point at which the daisies would survive. Under the model with the daisies, the results of all three scenarios show that there is an imbalance between daisy populations and the environment. When compare the interaction between the planet temperature and fractional area of black and white daisies on the Earth's surface among the three scenarios, the results illustrate that as the Earth's average temperature increases, the daisy species become more vulnerable to extinction when apply a combination of ice-albedo feedback and CO₂ levels.

Conclusions

The Daisyworld model, developed by Nevison et al. (1999), introduces environmental processes and factors impacting daisy populations within a simulated planet. The model can be applied to evaluate the status of the Earth and to illustrate the projection of average global temperatures. This study has focused on the impacts of global warming. The specifically model scenarios based on the impact factors of ice-albedo feedback and CO₂ levels (greenhouse gas representation) are built. The two factors implemented in this study have been modified from the energy balance equation employed in the Daisyworld model. There are three scenarios describing the trend of average global temperature. Firstly, the ice-albedo feedback excluding and including organisms are modelled. The results indicated that without daisies, the average temperature continuously rose over the simulation duration. While the model with daisies illustrated less of an increase in average temperature. This is due to the fact that white daisy population growth reduces the planet's average temperature. Secondly, a scenario on the effects of CO₂ levels based on three mathematical expressions is developed. Under constant CO₂ levels without organisms, the average temperature reached a steady state, lower than the ice-albedo feedback. CO₂ levels increase the planet's average temperature continuously the other two mathematical expressions. Under the models with daisies and the two expressions linear increase and sine function over a linear increase, the black and white daisy species fluctuated between dominance. The results from these two models illustrates that species type can affect the overall average temperature of the planet. However, it was evident that the species which could adapt to high temperature was the white daisy. The results illustrated that black daisy population were at risk of extinction due to higher average temperatures for linear expression and sine over a linear function expression. The final scenario incorporated

both the ice-albedo feedback and CO₂ levels excluding and including organisms. The results illustrated similarities with the second scenario. Under the model without organisms, all three results illustrate that the average temperature overtime becomes very high. Exceeding the point at which organisms would survive. Under the model with organisms, the results illustrate that there is an imbalance between daisy populations and the environment. In all three situations the daisy species eventually become extinct from the increase in average temperature. The key factor for indicating rise in average global temperature for this study was the ice-albedo feedback. As the fraction of land decreases the ice melting area increases. The combination of both ice-albedo feedback and CO₂ levels have shown to increase the average global temperature. The results have illustrated factors which affect the rise in average global temperatures under the application of the Daisyworld model. The correspondence between the results of this study and situations of the world is driven firstly by the increasing of the amount of CO₂ in the atmosphere. As a result, the average temperature increases continuously. Secondly, the rise in the temperature is accelerated by the ice-albedo feedback. However, only two global warming factors which are ice-albedo feedback and CO₂ levels are considered in this study. Various factors such as water vapor, CH₄, N₂O, CFCs and SF₆ should be investigated in future study. Moreover, further experiment cases should be performed on how the Daisyworld model responds to other species of the daisies.

Acknowledgements. The authors thank the Department of Mathematics, Faculty of Science, King Mongkut's University of Technology Thonburi for grant and the research facilities.

REFERENCES

- [1] Ackland, G. J., Clark, M. A., Lenton, T. M. (2003): Catastrophic desert formation in Daisyworld. – *Journal of Theoretical Biology* 223: 39-44.
- [2] Adams, B., Carr, J., Lenton, T. M., White, A. (2003): One-dimensional Daisyworld: Spatial interactions and pattern formation. – *Journal of Theoretical Biology* 223: 505-513.
- [3] Alberti, T., Primavera, L., Vecchio, A., Lepreti, F., Carbone, V. (2015): Spatial interactions in a modified Daisyworld model: Heat diffusivity and greenhouse effects. – *Physical Review E* 92: 052717(1)-052717(11).
- [4] Barnsley, M. J. (2007): *Environmental Modeling: A Practical Introduction*, 1st ed., pp. 251-286. – Taylor & Francis, Boca Raton.
- [5] Biton, E., Gildor, H. (2012): The seasonal effect in one-dimensional Daisyworld. – *Journal of Theoretical Biology* 314: 145-156.
- [6] Boyle, R. A., Lenton, T. M., Watson, A. J. (2011): Symbiotic physiology promotes homeostasis in Daisyworld. – *Journal of Theoretical Biology* 274: 170-182.
- [7] Bryson, R. A., Dittberner, G. J. (1976): A non-equilibrium model of hemispheric mean surface temperature. – *Journal of the Atmospheric Sciences* 33: 2094-2106.
- [8] Cohen, J. E., Rich, A. D. (2000): Interspecific competition affects temperature stability in Daisyworld. – *Tellus* 52B: 980-984.
- [9] Dyke, J. G. (2008): Entropy production in an energy balance Daisyworld model. – *Artificial Life* XI: 189-196.
- [10] Fraedrich, K. (1979): Catastrophes and resilience of a zero-dimensional climate system with ice-albedo and greenhouse feedback. – *Quart. J. R. Met. Soc.* 105: 147-167.

- [11] Jones, N. (2017): How the world passed a carbon threshold and why it matters. – <https://e360.yale.edu/features/how-the-world-passed-a-carbon-threshold-400ppm-and-why-it-matters>.
- [12] Kahn, B. (2017): Carbon dioxide is rising at record rates. – <http://www.climatecentral.org/news/carbon-dioxide-record-rates-21242>.
- [13] Lenton, T. M., Lovelock, J. E. (2000): Daisyworld is Darwinian: Constraints on adaptation are important for planetary self-regulation. – *Journal of Theoretical Biology* 206: 109-114.
- [14] McGehee, R., Widiasih, E. (2012): A simplification of Budyko's ice-albedo feedback model. – <http://www.math.umn.edu/~McGeheeWidiasihPreprint2012March.pdf>.
- [15] Nevison, C., Gupta, V., Klinger, L. (1999): Self-sustained temperature oscillations on Daisyworld. – *Tellus* 51B: 806-814.
- [16] NOAA Climate.gov (2017): Climate change: Atmospheric carbon dioxide. – <https://www.climate.gov/news-features/understanding-climate/climate-change-atmospheric-carbon-dioxide>.
- [17] Paiva, S. L. D., Savi, M. A., Viola, F. M., Leiroz, A. J. K. (2014): Global warming description using Daisyworld model with greenhouse gases. – *Biosystems* 125: 1-15.
- [18] Punithan, D., Kim, D., McKay, R. (2012): Spatio-temporal dynamics and quantification of Daisyworld in two-dimensional coupled map lattices. – *Ecological Complexity* 12: 43-57.
- [19] Rueangphankun, T., Sukawat, D., Yomsatieankul, W. (2016a): Interaction between life and environment in a zero-dimensional Daisyworld model. – *Proceedings of the 7th RMUTP International Conference on Science, Technology and Innovation for Sustainable Development: Challenges towards the Green Innovative Society*, Bangkok, Thailand, pp. 34-37.
- [20] Rueangphankun, T., Sukawat, D., Yomsatieankul, W. (2016b): Numerical simulations of global environment using an energy balance Daisyworld model with the variations of solar luminosity. – *Proceedings of the 3rd International Conference on Civil, Biological and Environmental Engineering (CBEE-2016)*, Phuket, Thailand, pp. 125-130.
- [21] Salazar, J. F., Poveda, G. (2009): Role of a simplified hydrological cycle and clouds in regulating the climate-biota system of Daisyworld. – *Tellus* 61B: 483-497.
- [22] Saunders, P. T. (1994): Evolution without natural selection: Further implications of the Daisyworld parable. – *Journal of Theoretical Biology* 166: 365-373.
- [23] Svirezhev, Y. M., Von Bloh, W. (1998): A zero-dimensional climate-vegetation model containing global carbon and hydrological cycle. – *Ecological Modelling* 106: 119-127.
- [24] Viola, F. M., Paiva, S. L. D., Savi, M. A. (2010): Analysis of the global warming dynamics from temperature time series. – *Ecological Modelling* 221: 1964-1978.
- [25] Viola, F. M., Savi, M. A., Paiva, S. L. D., Brasil, A. C. P. Jr. (2013): Nonlinear dynamics and chaos of the Daisyworld employed for global warming description. – *Applied Ecology and Environmental Research* 11(3): 463-490.
- [26] Wang, J., Chameides, B. (2005): *Global Warming's Increasingly Visible Impacts*, 1st ed. pp. 13-22. – Environmental Defense, Los Angeles, USA.
- [27] Watson, A. J., Lovelock, J. E. (1983): Biological homeostasis of the global environment: the parable of Daisyworld. – *Tellus* 35B: 284-289.
- [28] Weaver, I. S., Dyke, J. G. (2012): The importance of timescales for the emergence of environmental self-regulation. – *Journal of Theoretical Biology* 313: 172-180.
- [29] Winton, M. (2008): Sea Ice-Albedo Feedback and Nonlinear Arctic Climate Change. – In: DeWeaver, E. T., Bitz, C. M., Tremblay, L. B. (eds.) *Arctic Sea Ice Decline: Observations, Projections, Mechanisms, and Implications*, pp. 111-131. Geophysical Monograph Series 180. American Geophysical Union, Washington, DC.
- [30] Zeng, X., Pielke, R. A., Eykholt, R. (1990): Chaos in Daisyworld. – *Tellus* 42B: 309-318.

DETERMINATION AND ANALYSIS OF KINETIC PARAMETERS OF HETEROTROPHIC BACTERIA IN MATHEMATICAL SIMULATION

LV, W. L.^{1,2,3} – GOU, S. Z.⁴ – CHEN, Y. W.^{1,2,3} – SUN, Y. F.^{1,2} – GAO, X. D.^{1,2} – TAN, Z. L.^{1,2} – LI, X. D.^{1,2*}

¹*Key Laboratory of Environmental and Applied Microbiology, Chengdu Institute of Biology, Chinese Academy of Sciences
No. 9 The 4th Section of South Renmin Road, 610041 Chengdu, China
(phone: +86-28-8289-0289; fax: +86-28-8289-0288)*

²*Environmental Microbiology Key Laboratory of Sichuan Province, Chengdu Institute of Biology, Chinese Academy of Sciences
No. 9 The 4th Section of South Renmin Road, 610041 Chengdu, China
(phone: +86-28-8289-0289; fax: 028-8289-0288)*

³*University of Chinese Academy of Sciences
No. 19(A) Yuquan Road, Shijingshan District, 100049 Beijing, China
(phone: +86-10-8825-6030; fax: +86-10-8825-6006)*

⁴*Chengdu Vocational & Technical College of Industry
No. 818 Daan Road, 610218 Chengdu, China
(phone: +86-28-6445-8874; fax: +86-28-6445-8861)*

**Corresponding author
e-mail: lixd@cib.ac.cn; phone: +86-28-8289-0289; fax: +86-28-8289-0288*

(Received 25th Aug 2017; accepted 14th Dec 2017)

Abstract. This paper studied the Anaerobic-Anoxic-Oxic (A₂/O) process of a city sewage treatment plant in Sichuan Province, China. We established a mathematical model of sewage treatment plant. The yield coefficient of heterotrophic bacteria (YH) in A₂/O process was 0.65; maximum specific growth rate (uH) of 8.6 d⁻¹; attenuation coefficient (bH) of 3.5 d⁻¹. Compared with the recommended values reported in the literature, the results showed that the yield coefficient of heterotrophic bacteria measured by this method was consistent with the recommended value and the maximum specific growth rate and attenuation coefficient were higher than the recommended value. Different water qualities of different processes and heterotrophic bacteria in the activity are not the same. So the determination of the results will be different. Using the Electrolytic Respirometer developed by Bioscience Incorporation (BI-2000), the microbial oxygen uptake rate (OUR) curve is more accurate, the sampling frequency is higher, the sampling point is more, the judgment of the logarithmic period is more accurate, the test result is more reliable and the sewage treatment plant of the upgrade and simulation to optimize the operation to provide a theoretical basis.

Keywords: anaerobic-anoxic-oxic, kinetic parameters (YH, uH, bH), mathematical simulation, OUR curve

Introduction

A₂/O Activated Sludge Process for the degradation of organic pollutants mainly rely on heterotrophic bacteria, the degradation process of activated sludge system mainly includes microbial decomposition of organic pollutants, microbial anabolism, self-decomposition and heterotrophic microbes as the main microorganisms in the activated sludge system. In the mathematical model of sewage treatment, these processes can describe by the kinetic parameters such as the yield coefficient of heterotrophic bacteria,

the growth rate and the attenuation is coefficient. Therefore, it is very important to determine the kinetic parameters of heterotrophic bacteria. As a method recommended by International Water Association (IWA), respiration measurement has applied successfully to the determination of stoichiometry and kinetic parameters of wastewater (Smriga et al., 2016) and for the determination of Chemical Oxygen Demand (COD) components (Wu et al., 2016).

At present, in most models such as Active Sludge Model 1 (ASM1), Active Sludge Model 2d (ASM2d) in the dynamic parameters of the recommended value and the recommended value has determined by the founder of the model software, according to their region of water quality and used Sewage treatment process to determine the results obtained. Due to differences in Chinese diet and differences in sewage treatment methods lead to differences in water quality components and microbial biochemical reaction environment. So the recommended value in the general model in China's application there is a certain irrational (Wu et al., 2016).

In this experiment, the A_2/O process of a city sewage of treatment plant in Sichuan Province is used as the research object, by using an electrolyte respirator BI-2000. It is determined the wastewater treatment plant yield coefficient A_2/O process in heterotrophic bacteria and the maximum growth of the attenuation coefficient Rate, which provides a basis for the determination and simulation of A_2/O process model parameters.

Materials and methods

The experiment was conducted using the Electrolytic Respirometer (BI-2000) developed by Bioscience Incorporation, USA (*Fig. 1*).



Figure 1. BI-2000 electrolytic respirometer

Because the electrolyte breathing apparatus has a higher test accuracy and test frequency -0.05 h can get a Biochemical Oxygen Demand (BOD). In addition, by improving the test frequencies in a more abundant data based on the first-order dynamic equation fitting and we make the test results obtained more accurate. Electrolyte respirator is mainly composed of 1 L reactor, electrolysis unit, CO₂ trap and related software. It is shown in *Figure 2* (Karanasios et al., 2016). The determination principle of “how much oxygen consumption, how much oxygen”, the electrolyte breathing apparatus can accurately measure the oxygen consumption of microorganisms. The specific steps are used to take the appropriate volume of activated sludge and raw water mixed in a 1L sealed reactor, the occurrence of biochemical reactions, consumption of oxygen and produce CO₂, CO₂ is loaded with 45% KOH solution of the CO₂ trap to absorb the pressure drop in the reactor. The pressure sensor detects this pressure change and turns on the power of the electrolysis unit, which produces oxygen to supplement the oxygen consumed by the reaction process and maintains the pressure balance inside and outside the reactor (Yang et al., 2016). The computer calculates the oxygen production of the electrolysis unit based on the amount of current and the turn-on time during the reaction, thereby obtaining the amount of oxygen consumed by the microorganisms in the test.

The solutions to configure in the test were 1 mol/L H₂SO₄ solution (electrolytic solution), 45% KOH solution (CO₂ absorption solution). Before the test, first open the constant temperature water tank and magnetic stirrer preheat 2 h. The reactor containing the reaction mixture, the nitrification inhibitor ATU and the magnetic stirring rotor is then preheated for a period to ensure that the temperature difference between outside and the inside of the reactor is uniform (Yuan et al., 2016). Then a CO₂ trap equipped with a KOH solution and a reactor equipped with dilute sulfuric acid Liquid electrolysis unit assembled, connected to the line, and began to record data.

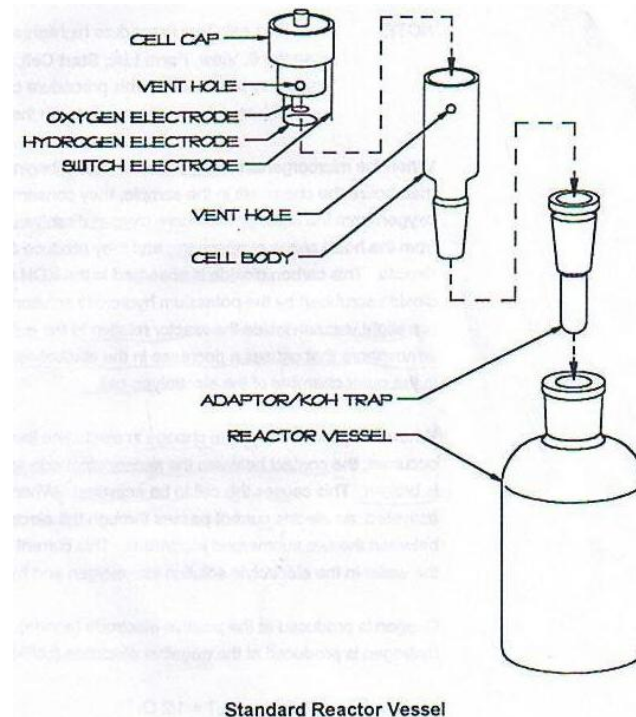


Figure 2. BI-2000 electrolyte breathing apparatus device map

Results

Heterotrophic decay coefficient b_H determination

There are two main recognized microbial attenuation theory: one is the traditional attenuation theory; the other is the theory of death regeneration.

Traditional attenuation theory thinks that the process of microbial attenuation in the process will use their internal storage of energy substances for breathing. After the death of microorganisms, the formation of cell residues (X_p). It does not take into account the decomposition of cells after death produced by other microorganisms' matrix Slowly biodegradable COD (X_s) (Xu et al., 2017). The Microbial growth and decay process will breathe oxygen consumption. When microorganisms consume Readily Biodegradable COD (S_s) and Slowly biodegradable COD (X_s), there is only the decay process that is microbial endogenous breathing consumption of oxygen.

The death regeneration theory suggests that the microbial attenuating part of the cell residue X_p , X_p is a particulate non-biodegradable organic matter and can be used no longer. The amount of microbial reduce is another part of the decomposition produces slow biodegradable organic matter X_s , X_s is hydrolyzed to produce new microorganisms for the growth of other microorganisms that is regeneration. When the matrix has consumed completely, the S_s formed by the hydrolysis of the attenuated product X_s become the matrix of the remaining microbial growth (Dorado et al., 2015). At the time the oxygen consumed is only caused by the S_s produced by this partial hydrolysis that is only depends on the growth of the heterotrophic bacteria.

The mathematical expression of death regeneration theory is as follows.

In the theory of death regeneration, the microorganisms are decomposed to form X_s ; X_s hydrolyze to produce S_s for the growth of other microorganisms. Therefore, in the batch reactor, without the carbon source, microbial concentration change has expressed by *Equation 1* (Domingo et al., 2017).

$$\frac{dX_H}{dt} = -b_H \cdot X_H + \frac{S_s}{K_s + S_s} \cdot u_H \cdot X_H \quad (\text{Eq. 1})$$

The process of hydrolysis of X_s is relatively slow so the hydrolysis process is a velocity limiting process. When no carbon source added, S_s has obtained by hydrolysis of X_s and expressed by *Equation 2*.

$$\frac{dS_s}{dt} = \frac{dX_s}{dt} = b_H(1 - f_p)X_H \quad (\text{Eq. 2})$$

The ratio of the activated biomass to the cell residue X_p in the f_p -death regeneration mode is about 0.08 (Liu et al., 2017; Piseiro et al., 2017). If the S_s produced by the hydrolysis of X_s and the S_s consumed by the microorganisms are equal (*Eqs. 3-6*).

$$\frac{dS_s \text{Consumption}}{dt} = \frac{dX_s \text{Produce}}{dt} \quad (\text{Eq. 3})$$

$$-\frac{dS_s \text{Consumption}}{dt} = \frac{1}{Y_H} \cdot \frac{S_s}{K_s + S_s} u_H \cdot X_H \quad (\text{Eq. 4})$$

$$b_H(1 - f_p)X_H = \frac{1}{Y_H} \frac{S_S}{K_S + S_S} \bullet u_H \bullet X_H \quad (\text{Eq. 5})$$

$$b_H(1 - f_p)Y_H \bullet X_H = \frac{S_S}{K_S + S_S} \bullet u_H \bullet X_H \quad (\text{Eq. 6})$$

Equation 6 into Equation 1 gets Equation 7.

$$\frac{dX_H}{dt} = b_H[Y_H(1 - f_p) - 1] \bullet X_H \quad (\text{Eq. 7})$$

When the $t = 0$, $X_H = X_H(0)$ and Equation 7 are integral, the microbial concentration of the t moment can be obtained (Eq. 8).

$$X_H(t) = X_H(0)e^{-b_H[1 - Y_H(1 - f_p)]t} \quad (\text{Eq. 8})$$

The mathematical expression of the traditional attenuation model is as follows.

The traditional decay theory does not take into account the microbial decay after the decomposition of the formation of other microbial growth of the matrix of this process, the rate of heterotrophic bacteria decay (Eq. 9).

$$\frac{dX_H}{dt} = -b'_H \bullet X_H \quad (\text{Eq. 9})$$

In Equation 9, b'_H is the attenuation coefficient from the traditional theory, to score it (Eq. 10).

$$X_H(t) = X_H(0)e^{-b'_H \bullet t} \quad (\text{Eq. 10})$$

Contrast Equations 8 and 10 available (Eq. 11):

$$b_H = b'_H / (1 - Y_H(1 - f_p)) \quad (\text{Eq. 11})$$

According to the description of the traditional attenuation theory, the dissipation rate of dissolved oxygen in relation to the attenuation of heterotrophic bacteria is as follows (Eq. 12).

$$r(t) = \frac{dS_{O_2}}{dt} = -(1 - f'_p) \frac{dX_H}{dt} = -(1 - f'_p)b'_H \bullet X_H \quad (\text{Eq. 12})$$

Equation 10 into Equation 12 (Eq. 13):

$$r(t) = \frac{dS_{O_2}}{dt} = -(1 - f'_p)b'_H \bullet X_H(0)e^{-b'_H t} \quad (\text{Eq. 13})$$

Take the logarithm of the above formula here (Eq. 14):

$$\ln r(t) = \ln[(1 - f'_{p})b'_{H}X_{H}(0)] - b'_{H} \bullet t \quad (\text{Eq. 14})$$

It can be seen from the above formula that the natural logarithm of the dissolved sludge consumption rate with the activated sludge and the slope of the time-dependent curve of the activated sludge measured in the absence of a carbon source, which are the conventional attenuation coefficient (Mozumder et al., 2015; Wang et al., 2016). Hence, the first measurement the value of b_H and Y_H , Value get b_H by calculated the formula.

Take the end of the mixture full of aeration in the aerobic tank of A_2/O process, during the demonized water washed 3 times, standing for 30 min, drained the supernatant; take the treated sludge into the breathing apparatus (Leyva-Díaz et al., 2015; Mampaey et al., 2013). To avoid nitrification affect the consumption of heterotrophic bacteria, add ATU (0.02 g/L propylene thiourea), inhibit the activities of autotrophic bacteria and then add de-ionized water, began to measure the depletion of heterotrophic oxygen consumption curve.

According to Equation 14, use $\ln(\text{OUR})$ and time t to make a map, the slope of the straight line is the attenuation coefficient of the heterotrophic bacteria u'_H . Under the same conditions, the average value has determined by Equation 11 bacteria attenuation coefficient u_H .

Under the same test conditions, the results of the four tests were as in Figure 3, the attenuation coefficient of the death regeneration model was 3.12 d⁻¹, 4.2 d⁻¹, 3.11 d⁻¹, 3.58 d⁻¹ 3.5 d⁻¹ (Liu et al., 2017; Guimerà et al., 2016). Compared with the recommended value of the model, the analysis may be due to the differences in water quality and process differences.

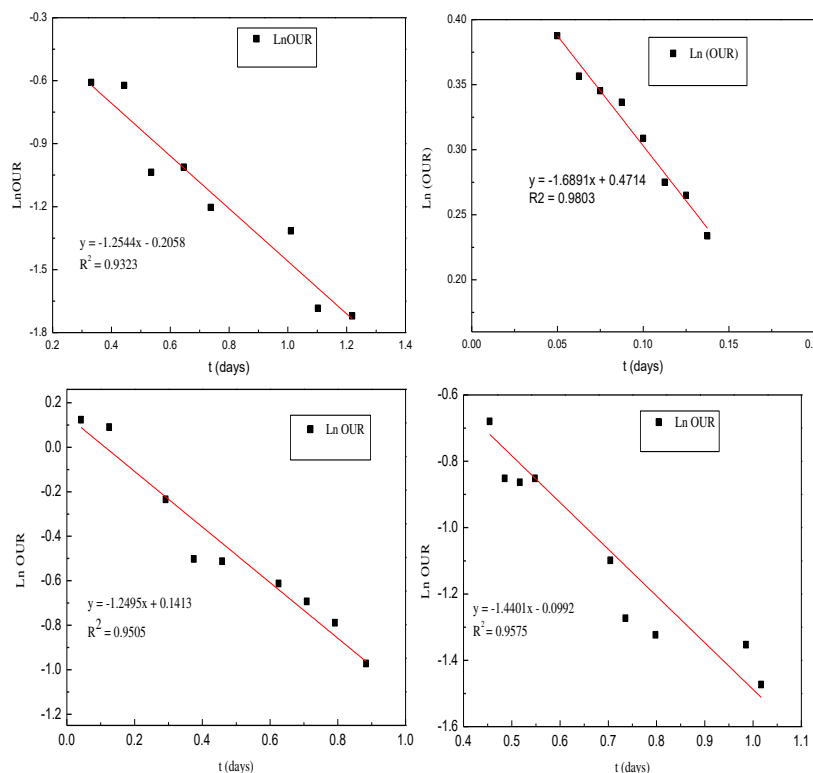


Figure 3. Determination of the traditional attenuation coefficient

From *Figure 3* we can see that $\ln(\text{OUR})$ is linearly fitted with time t and the slope is the traditional attenuation coefficient. From the above equations (*Eqs. 2-11*; Peng et al., 2017; Domingo-Félez C et al., 2017), we can see that the relationship between b_H and the b_H is $b_H = b'_H / (1 - Y_H(1 - f_p))$ and calculated according to this relationship get attenuation coefficient b_H , the results show in *Table 1*.

Table 1. Determination of attenuation coefficient of heterotrophic bacteria b_H

Number	$b'_H/d-1$	$b_H/d-1$	Recommended value
1	1.25	3.12	0.62
2	1.69	4.20	
3	1.25	3.11	
4	1.44	3.58	
Average value	1.41	3.50	

Determination of yield coefficient of heterotrophic bacteria

The heterotrophic yield coefficient (Y_H) is a relatively important stoichiometric factor. It not only affects the estimation of sludge yield and oxygen demand but also for certain wastewater components (e.g., biodegradable organic components S_S and slow Speed biodegradable components X_S , etc.) and kinetic parameters (heterotrophic bacteria than the growth rate, attenuation coefficient) have an impact. Thus, Y_H is a very critical stoichiometric parameter and Y_H inaccurate results in errors in the calculation of other component parameters (Zięba and Janiak, 2017). Therefore, Y_H is a more critical parameter, the need for accurate determination (Qin et al., 2016). At present, the more mature method is intermittent activated sludge method and breathing measurement method.

According to the definition of Y_H that is in the activated sludge system, part of the soluble organic matter consumed in the sewage is used for the respiration of microorganisms, converted into CO_2 and H_2O and the other part is absorbed into the new cells by organic matter (Peng et al., 2017). As long as the intermittent measurement of microbial COD is in the closed system, the amount of soluble organic matter reduction, and the ratio is Y_H (*Eqs. 18 and 19*).

$$Y_H = \frac{\Delta \text{COD}_{\text{Cell}}}{\Delta \text{COD}_{\text{Soluble}}} = \frac{\Delta \text{COD} - \int r(t) dt}{\Delta \text{COD}} \quad (\text{Eq. 18})$$

$$\Delta \text{COD} = \text{COD}_1 - \text{COD}_2 \quad (\text{Eq. 19})$$

In the above formula: COD_1 is the initial COD in the mixture, COD_2 is the COD in the mixed solution; ΔCOD is the COD (mg/L) degradation of the microorganisms in the mixed solution; the oxygen consumed by the microorganism as the energy the amount.

Take the A_2/O process aerobic tank at the end of the activated sludge, full aeration has repeated washing with distilled water, put away the supernatant, the depletion of activated sludge in the residual dissolved COD. Dosing nitrification inhibitor (0.2 mg/L) and part of the raw water to mix well, we take appropriate amount of mixed sample flocculation process for COD determination, the results recorded as COD_1 . Then we can

use BI-2000 for microbial oxygen consumption rate determination. Test for 1 day to read the BI-2000 electrolyte breathing apparatus on the oxygen consumption ($\int r(t)dt$) and then take the appropriate amount of the product flocculation COD measured as COD_2 . Then Y_H is calculated as follows.

$$Y_H = \frac{\Delta COD_{Cell}}{\Delta COD_{Soluble}} = \frac{\Delta COD - \int r(t)dt}{\Delta COD}$$

$$\Delta COD = COD_1 - COD_2$$

From *Table 2* we can see that the yield coefficient of heterotrophic bacteria was 0.65, which was lower than the recommended value, 0.67 was 0.02. It indicated that the activity of A_2/O activated sludge was slightly lower and the biodegradation. The same pollutants are under the premise of its less mud production.

Table 2. Heterotrophic bacteria yield coefficient Y_H determination results

Number	Y_H	Recommended value
1	0.67	0.67
2	0.66	
3	0.61	
4	0.66	
Average value	0.65	

Determination of maximum specific growth rate of heterotrophic bacteria

The oxygen consumption rate at any time in the batch reactor under the conditions of dissolved oxygen and sufficient substrate can be expressed as follows (*Eq. 20*).

$$OUR(t) = \frac{1 - Y_H}{Y_H} u_H X_H(t) + (1 - f_p) b_H X_H(t) \quad (\text{Eq. 20})$$

It can be seen that $\ln(OUR)$ depends on $X_H(t)$ that is the concentration of heterotrophic bacteria in the reactor at time t , the change of heterotrophic concentration can be expressed as follows (*Eq. 21*).

$$\frac{dX_H(t)}{dt} = (u_H - b_H) X_H(t) \quad (\text{Eq. 21})$$

Score the above formula (*Eq. 22*).

$$X_H(t) = X_H(0) e^{(u_H - b_H)t} \quad (\text{Eq. 22})$$

Equation 22 takes into *Equation 20* (*Eq. 23*).

$$\ln OUR(t) = \ln[(1 - Y_H)/Y_H \bullet u_H + (1 - f_p) \bullet b_H] X_H(0) + (u_H - b_H) \bullet t \quad (\text{Eq. 23})$$

The above formula shows that with Ln(OUR) as the ordinate and time t as the abscissa plot, the resulting slope is (u_H-b_H) and u_H can be obtained under the premise that b_H has been measured.

Take the sewage treatment plant A₂/O process in the aerobic pool of mixed liquid fully aeration, during the time washed mud 3 times use of deionized water, standing to abandon the supernatant so that the sludge in the endogenous breathing level. Take the same amount of sewage from the inlet of the biochemical section of the sewage treatment plant to add to the endogenous respiration sludge after the above treatment (Liu et al., 2016). To avoid nitrification affect the consumption of heterotrophic bacteria, add nitrification inhibitor (propylene thiourea) 0.2 mg/L to inhibit the activities of autotrophic bacteria, with BI-2000 Electrolytic Respiration Tester measured OUR curve, and then ln OUR on t mapping, linear slope of u_H-b_H, U_H has been measured under the premise of b_H being measured.

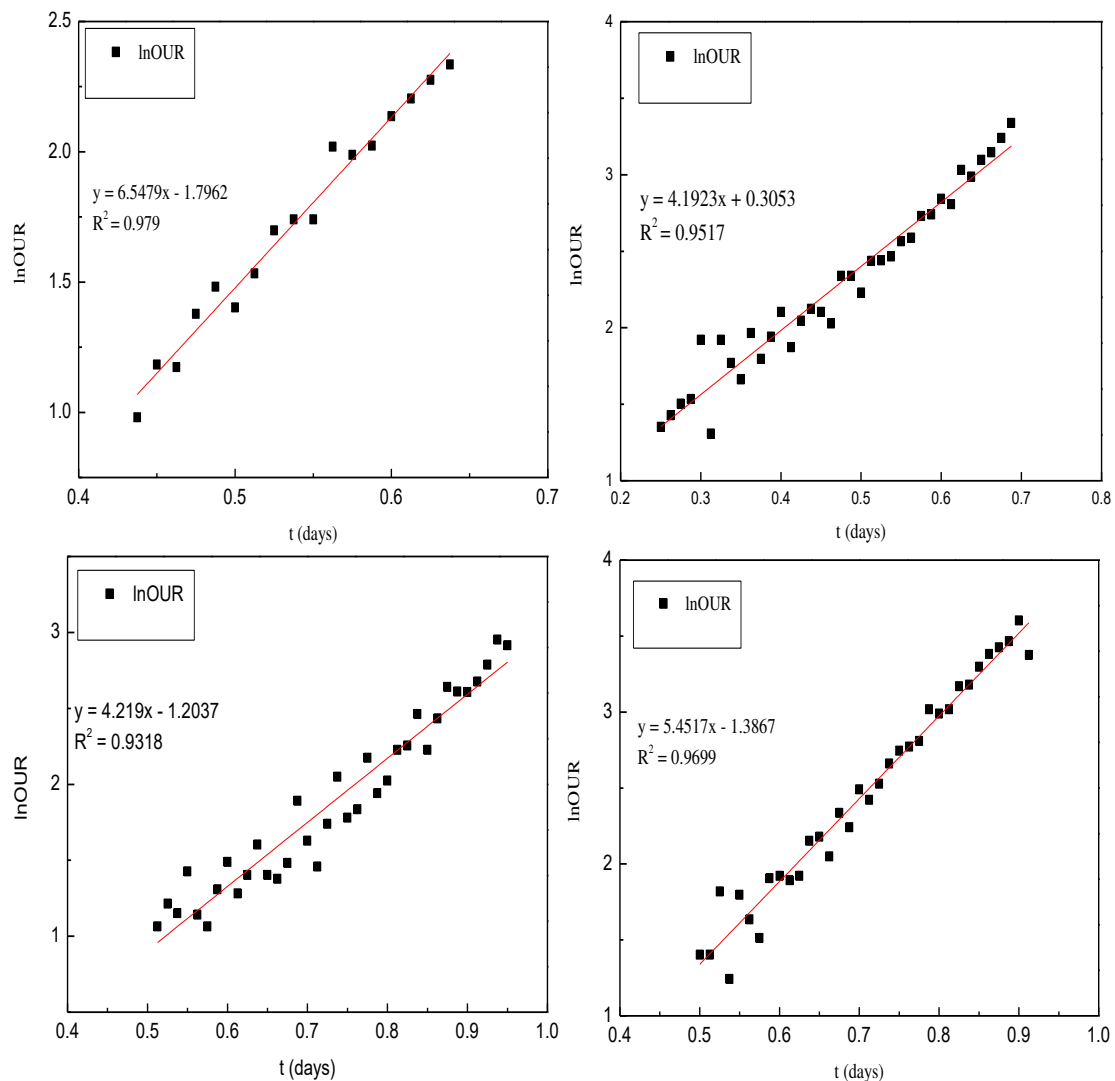


Figure 4. Maximum growth rate of heterotrophic bacteria u_H measurement curve

From *Figure 4* we can see that $\ln(\text{OUR})$ is linearly fitted with time and the fitting degree is better. It shows that the method has some rationality. From the above equations (*Eqs. 2-18*), the maximum rate of growth is calculated from the slope as shown in the following table.

Table 3. Determination of the maximum specific growth rate of heterotrophic bacteria μ_H

Number	μ_H -bH	μ_H	Recommended value
1	6.55	10.05	6.1
2	4.19	7.69	
3	4.22	7.72	
4	5.45	8.95	
Average value	5.10	8.60	

From *Table 3* it can be seen that the results of the maximum specific growth rate of heterotrophic bacteria show that the use of BI-2000 electrolyte respiration rate analyzer, the range is large and the range is roughly 7.72 d⁻¹-10.05 d⁻¹, the average is 8.6 d⁻¹ compared with ASM1 model. It indicated that in the sewage treatment plant A₂/O process the activity of microorganisms faster than the proliferation rate.

Discussion

(1) The factors influencing the stoichiometric parameters of heterotrophic bacteria were sludge load ratio and temperature. The sludge load is too high and the sludge concentration in the reactor is small. After the reaction, some sludge sticks to the head of the aeration and the wall of the bottle so that the measured Cell COD increase is too small; resulting in YH value is too small. When the sludge load is too low, the dissolved COD in the reactor has been consumed at the end of the reaction. At this time, the sludge may be in the endogenous respiration stage and does not reflect the actual sludge growth, so the measured YH value will be small.

(2) The biomechanical parameters and stoichiometric parameters of microbes have measured by BI-2000 microbiological respirometer. However, the attenuation coefficient and maximum specific growth rate of the measured heterotrophic bacteria were larger than those of the recommended value were. The uses of this method for microbial dynamics parameters and stoichiometric parameters have some limitations. In addition, the test process did not explore the sludge load ratio and temperature on the determination of the results so this is the future use of the method of the workers Provide the direction of research.

Conclusions

Study the mixture in the A₂/O process system by BI-2000 Electrolyte Respiration Tester. The YH was 0.65, the μ_H was 8.6 d⁻¹ and the bH was 3.5 d⁻¹. Experiments show that there are some differences in the relevant kinetic parameters of heterotrophic bacteria in different areas and different processes. It is suggested that in the future mathematical model construction, the measured value should be adopted when the experimental conditions permit. In addition, the kinetic parameters of sewage in

different areas will vary greatly, especially in different catering countries. When choosing references, try to refer to relevant experimental results in this area.

Acknowledgements. This work was supported by Science and Technology Service Network Initiative, Chinese Academy of Science (KFJ-SW-STS-175) and West light project of Chinese Academy of Science (Y5C5021100), and Youth Innovation Promotion Association CAS (2016331).

REFERENCES

- [1] Domingo-Félez C, Calderó-Pascual M, Sin G, et al. (2017): Calibration of the NDHA model to describe N₂O dynamics from respirometric assays[J]. – arXiv preprint arXiv:1705.05962.
- [2] Domingo-Félez, C., Pellicer-Nácher, C., Petersen, M. S., Jensen, M. M., Plósz, B. G., Smets, B. F. (2017): Heterotrophs are key contributors to nitrous oxide production in activated sludge under low C-to-N ratios during nitrification—Batch experiments and modeling. – *Biotechnology and Bioengineering* 114(1): 132-140.
- [3] Dorado, A. D., Dumont, E., Muñoz, R., Quijano, G. (2015): A novel mathematical approach for the understanding and optimization of two-phase partitioning bioreactors devoted to air pollution control. – *Chemical Engineering Journal* 263: 239-248.
- [4] Guimerà, X., Dorado, A. D., Bonsfills, A., Gabriel, G., Gabriel, D., Gamisans, X. (2016): Dynamic characterization of external and internal mass transport in heterotrophic biofilms from microsensors measurements. – *Water Research* 102: 551-560.
- [5] Karanasios, K. A., Vasiliadou, I. A., Tekerlekopoulou, A. G., Akkratos, C. S., Pavlou, S., Vayenas, D. V. (2016): Effect of C/N ratio and support material on heterotrophic denitrification of potable water in bio-filters using sugar as carbon source. – *International Biodeterioration & Biodegradation* 111: 62-73.
- [6] Leyva-Díaz, J. C., González-Martínez, A., González-López, J., Muñío, M. M., Poyatos, J. M. (2015): Kinetic modeling and microbiological study of two-step nitrification in a membrane bioreactor and hybrid moving bed biofilm reactor—membrane bioreactor for wastewater treatment. – *Chemical Engineering Journal* 259: 692-702.
- [7] Liu, H., Chen, N., Feng, C., Tong, S., Li, R. (2017): Impact of electro-stimulation on denitrifying bacterial growth and analysis of bacterial growth kinetics using a modified Gompertz model in a bio-electrochemical denitrification reactor. – *Bioresource Technology* 232: 344-353.
- [8] Liu, T., Ma, B., Chen, X., Ni, B. J., Peng, Y., Guo, J. (2017): Evaluation of mainstream nitrogen removal by Simultaneous Partial Nitrification, Anammox and Denitrification (SNAD) process in a granule-based reactor. – *Chemical Engineering Journal* 306: 973-981.
- [9] Liu, Y., Peng, L., Ngo, H. H., Guo, W., Wang, D., Pan, Y., et al. (2016): Evaluation of nitrous oxide emission from sulfide-and sulfur-based autotrophic denitrification processes. – *Environmental Science & Technology* 50(17): 9407-9415.
- [10] Mampaey, K. E., Beuckels, B., Kampschreur, M. J., Kleerebezem, R., Van Loosdrecht, M. C. M., Volcke, E. I. P. (2013): Modelling nitrous and nitric oxide emissions by autotrophic ammonia-oxidizing bacteria. – *Environmental Technology* 34(12): 1555-1566.
- [11] Mozumder, M. S. I., Garcia-Gonzalez, L., De Wever, H., Volcke, E. I. (2015): Effect of sodium accumulation on heterotrophic growth and polyhydroxybutyrate (PHB) production by *Cupriavidus necator*. – *Bioresource Technology* 191: 213-218.
- [12] Peng, L., Liu, Y., Sun, J., Wang, D., Dai, X., Ni, B. J. (2017): Enhancing immobilization of arsenic in groundwater: A model-based evaluation. – *Journal of Cleaner Production* 166: 449-457.

- [13] Peng, L., Sun, J., Liu, Y., Dai, X., Ni, B. J. (2017): Nitrous oxide production in a granule-based partial nitrification reactor: a model-based evaluation. – *Scientific Reports* 7: 45609. DOI: 10.1038/srep45609.
- [14] Piseiro, J., Galvão, A., Pinheiro, H. M., Ferreira, F., Matos, J. (2017): Determining stoichiometric parameters of detached biomass from a HSSF-CW using respirometry. – *Ecological Engineering* 98: 388-393.
- [15] Qin, W., Li, W., Zhang, D., Huang, X., Song, Y. (2016): Ammonium reduction kinetics in drinking water by newly isolated *Acinetobacter* sp. HITLi 7 at low temperatures. – *Desalination and Water Treatment* 57(24): 11275-11282.
- [16] Smruga, S., Fernandez, V. I., Mitchell, J. G., Stocker, R. (2016): Chemotaxis toward phytoplankton drives organic matter partitioning among marine bacteria. – *Proceedings of the National Academy of Sciences* 113(6): 1576-1581.
- [17] Wang, Q., Ni, B. J., Lemaire, R., Hao, X., Yuan, Z. (2016): Modeling of nitrous oxide production from nitrification reactors treating real anaerobic digestion liquor. – *Scientific Reports* 6: 25336. DOI: 10.1038/srep25336.
- [18] Wu, J., He, C., van Loosdrecht, M. C., Pérez, J. (2016): Selection of ammonium oxidizing bacteria (AOB) over nitrite oxidizing bacteria (NOB) based on conversion rates. – *Chemical Engineering Journal* 304: 953-961.
- [19] Wu, X., Yang, Y., Wu, G., Mao, J., Zhou, T. (2016): Simulation and optimization of a coking wastewater biological treatment process by activated sludge models (ASM). – *Journal of Environmental Management* 165: 235-242.
- [20] Xu, X. J., Chen, C., Wang, A. J., Ni, B. J., Guo, W. Q., Yuan, Y., et al. (2017): Mathematical modeling of simultaneous carbon-nitrogen-sulfur removal from industrial wastewater. – *Journal of Hazardous Materials* 321: 371-381.
- [21] Yang, S. S., Pang, J. W., Guo, W. Q., Yang, X. Y., Wu, Z. Y., Ren, N. Q., Zhao, Z. Q. (2017): Biological phosphorus removal in an extended ASM2 model: Roles of extracellular polymeric substances and kinetic modeling. – *Bioresource Technology* 232: 412-416.
- [22] Yuan, J., Dong, W., Sun, F., Li, P., Zhao, K. (2016): An ecological vegetation-activated sludge process (V-ASP) for decentralized wastewater treatment: system development, treatment performance, and mathematical modeling. – *Environmental Science and Pollution Research* 23(10): 10234-10246.
- [23] Zięba, B., Janiak, K. (2017): Encouraging “K” Strategy Nitrifiers over “r” Strategists in Bioaugmentation Reactor. – In: Kaźmierczak, B., Kutyłowska, M., Piekarska, K., Trusz-Zdybek, A. (eds.) *E3S Web of Conferences* (Vol. 17, p. 00101). EDP Sciences, Boguszów-Gorce.

CONTRIBUTION OF EAR AND FLAG LEAF TO GRAIN FILLING OF WHEAT IN RESPONSE TO NITROGEN UNDER LATE-SEASON WATER DEFICIT

ZAVIEH, L. M.¹ – HADI, H.^{2*} – SHISHVAN, M. T.³ – REZAEI, M.⁴

¹*Department of Agronomy, Faculty of Agriculture, Urmia University, Urmia, Iran
(tel: +98-44-3367-1651; e-mail: leylamavadat@yahoo.com)*

²*Department of Agronomy, Faculty of Agriculture, Urmia University, Urmia, Iran
(tel: +98-44-3277-9558; mobile: +98-91-4322-4159; e-mail: h.hadi@urmia.ac.ir)*

³*Department of Agronomy, Faculty of Agriculture, Urmia University, Urmia, Iran
(tel: +98-44-3277-9558; mobile: +98-91-4341-9825; e-mail: Tajbakhsh@gmail.com)*

⁴*Seed and Plant Improvement Research Department, West Azarbaijan Agricultural and Natural Resources Research and Education Center, AREEO, Urmia, Iran
(mobile: +98-91-4346-1364; fax: +98-44-3262-2221; e-mail: rezaei54@yahoo.com)*

**Corresponding author
e-mail: h.hadi@urmia.ac.ir*

(Received 15th Sep 2017; accepted 20th Feb 2018)

Abstract. In a two-year field experiment, the assessment of leaves and ears photosynthetic contribution to grain filling in winter wheat genotypes was made under nitrogen fertilizer application and water deficit condition. A split plot factorial experiment was conducted based on randomized complete block design with three replications during 2014 and 2015 growing seasons. Treatments were irrigation levels including full irrigation (I₁) as control and irrigation withholding at heading stages (I₂), nitrogen (120 kg.ha⁻¹) splitting method into different phenological stages including 20 kg.ha⁻¹ at sowing and 100 kg.ha⁻¹ at mid-tillering stage (N₁), 20 kg.ha⁻¹ at sowing, 50 kg.ha⁻¹ at mid-tillering and 50 kg.ha⁻¹ at stem elongation stage (N₂) and 20 kg.ha⁻¹ at sowing, 50 kg.ha⁻¹ at mid-tillering and 50 kg.ha⁻¹ at 50% of heading stage (N₃) and four winter bread wheat genotypes including zarrin, Pishgam, Orum, and Mihan. Results showed that water deficit stress decreased the photosynthetic contribution of the flag leaf, ear and leaves below the flag leaf to grain filling, 1000-grain weight, number of grains per ear and seed yield of wheat. Furthermore, ear photosynthetic contribution (EPC) was higher compared to the flag leaf (FLPC) and leaves below the flag leaf (OLPC) to grain filling. Higher grain yield of Mihan and Pishgam genotypes can be associated with more grains per ear, 1000-grain weight and higher photosynthetic contribution of flag leaf and ear to grain filling. Such genotypic and environmentally driven differences were associated with changes in most of the traits. According to the results, partitioning of N fertilizer application to different phenological times can be a proper tool for increasing wheat yield under water deficit condition on different genotypes.

Keywords: grain yield, leaves below flag leaf, nitrogen splitting, phenological stages, water limitation

Introduction

Wheat is considered as the most important crop grown in the semi-arid regions where water deficit stress seems to be one of the most limiting factors for agricultural products (Maccaferri et al., 2011). That is to say, such a strategic crop usually suffers from water deficit stress during grain-filling period affecting the yield of the plant. According to Maccaferri et al. (2011), the reaction and response of plants to water deficit are evaluated based on genetic, biochemical, and morpho-physiological features of a plant.

The variations in the crop on the water uptake capacity during or shortly before the post-anthesis phase can have major effects on grain yield because growing grain number and grain weight are set during this stage.

Final grain weight is in relation to the duration of grain filling period and rate, and the respective interaction in-between (Sadras and Egli, 2008). In C3 cereals, such as wheat and barley, grain filling process is determined by current photosynthesis of the upper parts of the plant, i.e. both the flag leaf and the ear (Tambussi et al., 2007) and by redistribution of assimilates stored in the stem (Ehdaie et al., 2008). Further, the leaf photosynthesis value is affected by the position of the leaf on the plant. The flag leaf and the second leaf are the most active leaves in the photosynthesis rate in the wheat (Olszewski et al., 2008). According to Maydup et al. (2010) ear, photosynthesis plays a key role in the grain yield of wheat under both stress and non-stress conditions.

N in the plant is in the structure of the protein and nucleic acids, which are the most important building and information substances of every cell. In addition, N is also found in chlorophyll enabling the plant to transfer energy from sunlight through the process of photosynthesis. So, the value of N supply to the plant will influence the amount of protein, amino acids, protoplasm, and chlorophyll formed. Moreover, it influences cell size, leaf area, and photosynthetic activity (Uribebarrea et al., 2009; Diacono et al., 2013). Dordas et al. (2008) reported that higher rates of N increase photosynthetic processes, leaf area production, leaf area duration as well as grain filling period. Lawrence et al. (2008) also reported that the reduction in photosynthesis caused by drought occurs more in the lower leaves than in the upper ones, and this reduction also was reported to be lower in the ear compared to the leaves. In the same line, under low nitrogen supply, plants use photosynthesis to maintain life functions which are not related to the yield-forming process. Under high nitrogen supply, the photosynthetic activity of ears causes the grain yield to increase (Olszewski et al., 2008). Soleymani fard and Sidat (2011) suggested that yield and yield components of safflower are increased by increasing the rate of applied nitrogen.

A better understanding of growth parameters may of help in programs the objective of which is to improve the grain yield under water limitation. Determination of response of wheat to N application is very important to maximize yield and economic profitability of wheat production in a particular environment. Considering the abovementioned facts, the present study was undertaken to know the effects of nitrogen rates on growth parameters and yield quantity of wheat under drought stress.

Material and methods

The field experiment was conducted as split factorial plot based on randomized complete block design with three replications during 2013-2014 and 2014-2015 growing seasons in the agriculture research station of Miandoab in West Azarbayjan province, Iran. The area is located at (46°6' N latitude and 36° 58' E longitude; alt. 1143 m, Miandoab, West Azarbaijan Province, Iran). Climatically, the area is placed in a semi-arid temperate zone with a pretty cold winter and a hot summer. The mean temperature and precipitation wheat growing season in 2014-2015 are presented in *Figure 1*.

In the field of the present study, each plot was included 6 rows with 4-m long. Besides, plots and blocks were separated by 3 m unplanted distances. The wheat cultivars were sown with a density of 400 seeds per m². Regarding the treatments, irrigation levels were set as the variables of the investigation where Full Irrigation (I1) was considered as

control while Irrigation Withholding during heading stages (I2), in main plots and the time of the application of nitrogen fertilizer and varieties were allocated to subplots as the treatments. Based on the results of the meteorological station located at the site of the experiment and collecting the meteorological data, amount of water were determined according to evaporation from class A pan and, using relevant calculations, the water volume required for irrigation was determined. To irrigate the volume of irrigation water in the plots, a pressure meter and pressurized water pipes were used to maintain the water volume consumed per plot in accordance with the evaporation rate of 100 mm evaporation from class A pan. Thus, the volume of water consumed for each round was about 650 m³/ha. Furthermore, Nitrogen fertilizer, 120 kg in total, was applied in three different arrangements as follow: 20 kg.ha⁻¹ nitrogen fertilizer in sowing and 100 kg.ha⁻¹ at mid-tillering stage (N1), 20 kg.ha⁻¹ nitrogen fertilizer in sowing, 50 kg.ha⁻¹ at mid-tillering and 50 kg.ha⁻¹ at stem elongation stage (N2), and 20 kg.ha⁻¹ nitrogen fertilizer in sowing, 50 kg.ha⁻¹ at mid-tillering and 50 kg.ha⁻¹ at 50% of heading stage (N3). In regard to the type of the varieties, four genotypes of winter bread wheat, Zarrin, Pishgam, Orum, and Mihan were utilized in the study.

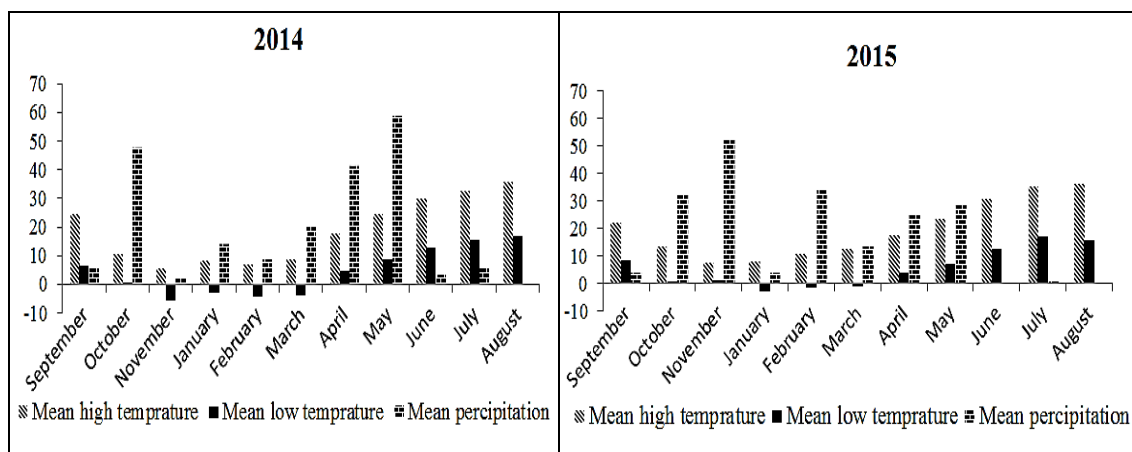


Figure 1. Mean temperature and precipitation wheat growing season at 2014-2015

Irrigation, weeding, and all other agronomic practices except those under study were kept consistent and uniform for all treatments. The soil samples were taken from the 30 cm depth of surface soil with soil auger 20 days before the beginning of the experiment in both formerly mentioned growing seasons. Moreover, the physicochemical properties of the soil samples have analyzed the result of which are presented in *Table 1*.

Table 1. Soil physico-chemical properties at depth of 0-30 cm

K available (p.p.m)	P available (p.p.m)	N total (%)	O.C. (%)	Texture	pH	Depth of sampling (cm)	Year
255	8.05	0.13	0.78	Silty-loam	8	0-30	2014
180	8.4	0.9	0.61	Silty-loam	9	0-30	2015

Some physiological traits were determined for the measurement of growth parameters. In the first sampling procedures, ten samples were taken at flowering stages in both time periods. In order to determine the weight of spike, peduncle, and internode, the samples were dried in an oven for 48 h at 80 °C. Then, the samples were treated for determining the phenotypic manipulations components. This was followed by the removal of all the leaves below the flag leaf, the flag leaf, and half of the spike. At the maturity stage, both labeled plants and 10 other randomly selected plants were harvested to determine the yield components and traits such as total dry matter, ear weight, grain weight per ear, and grain number per ear, 1000-grain weight and seed yield. Then the photosynthetic contributions of different plant parts (ear, flag leaf and leaves below the flag leaf) to grain filling in bread wheat genotypes were calculated as follows:

$$\text{EPC} = (\text{ear weight in flowering} - (\text{ear weight in physiological maturity} - \text{ear grain weight})) / \text{grain yield}$$

$$\text{FLPC} = (\text{ear grain weight} - \text{ear grain weight in flag leaf removal plant}) / \text{grain yield}$$

$$\text{OLPC} = (\text{ear grain weight} - \text{ear grain weight in other leaf removal plant}) / \text{grain yield}$$

where EPC, FLPC, and BFLPC refer to photosynthetic contributions of the ear, flag leaf and leaves below the flag leaf to grain filling, respectively.

The analysis of variance for the collected data was calculated applying SAS software a the main effects and interactions were tested using the Duncan's multiple range tests ($p \leq 0.05$).

Results and discussion

The results obtained from the combined (two-year data) analysis of variance, showed a significant effect of the interaction $I \times N \times G$ on photosynthetic contribution of the flag-leaf to grain filling, photosynthetic contribution of the ear to grain filling and number of grains per-ear in wheat plants in the field condition (*Table 2*). It was also revealed that the interaction of $Y \times I \times N \times G$ significantly affects the photosynthetic contribution of the leaves below the flag-leaf to grain filling and 1000-grain weight (*Table 2*). The photosynthetic contribution of the ear to grain filling was affected by the interaction of $Y \times I \times N$ (*Table 2*). Furthermore, the number of grains per ear and grain yield also were affected by the interaction of $Y \times I \times G$ (*Table 2*). The findings also showed that the number of grains per ear can be affected by the interaction of $Y \times N \times G$ (*Table 2*).

Photosynthetic contribution of the flag leaf to grain filling

As Amiri et al. (2013) stated in their article, due to the proximity of Flag-leaf to the spike, and the longer green life of it, the photosynthetic contribution of the flag-leaf is one of the most important sources for higher grain yield production during grain filling period. In this study, the highest photosynthetic contribution of the flag-leaf to grain filling (18.48%) was observed in Pishgaam genotype G2 (I1N2G2) under normal irrigation condition as I1 and the application of N2 (*Table 3*). The lowest value (10.22%) was obtained at I2N3G1 (*Table 3*).

Our results also showed that among the studied genotypes, Pishgaam genotype had the highest contribution of the flag-leaf to grain filling. Such results suggested that the flag-leaf contribution depends not only on sink strength but also on genotypic variations. In this line, the increase in the assimilate production was linked to the long green life of flag-leaf. N₂ fertilizer treatments increased the photosynthetic contribution of the flag-leaf compared to the other nitrogen treatments. Low photosynthesis under water deficit stress was reported to be the result of lower chlorophyll synthesis and higher chlorophyll breakdown (Osman, 2014). Chlorophyll loss can also be due to damage to mesophyll chloroplasts leading to a lower photosynthetic rate (Wang and Xiao, 2009). The importance of the flag leaf in determining the mean grain weight, at mid-tillering and stem elongation of the plant is well-known. Sanjeri et al. (2008) showed that in water deficit condition, chlorophyll content of wheat genotypes decrease and this reduction is significant among genotypes.

Table 2. Summary of the analysis of variance for all the analyzed parameters

Source of variation	Df	Mean square					
		Photosynthetic contribution of the flag leaf to grain filling	Photosynthetic contribution of the leaves below the flag leaf to grain filling	Photosynthetic contribution of the ear to grain filling	1000-grain weight	Number of grains per ear	Grain yield
Year (Y)	1	71.30*	752.03**	1428.21*	25.84ns	1936.000*	21834592.56**
Replication/year	4	22.38	3.18	220.20	60.31	204.97	1693022.33
Irrigation (I)	1	0.001 ns	64.34**	173.27ns	770.06**	26.69 ns	151850167.56**
I × Y	1	56.163*	148.88**	461.10ns	189.06 ns	38.02 ns	72061706.174**
Error a	4	8.45	2.65	153.20	13.292	116.52	43517.13
Nitrogen (N)	2	58.31**	4.33 ns	1.83 ns	69.71**	521.69**	5594760.43**
Y × N	2	18.20ns	61.10**	6.96 ns	60.007*	40.58 ns	164618.77 ns
I × N	2	36.96*	0.60 ns	24.45 ns	5.81 ns	57.69 ns	960658.56ns
Y × I × N	2	3.31 ns	42.97*	115.12*	30.271ns	44.19 ns	60796.75ns
Genotype (G)	3	97.49**	33.07*	113.34*	215.80**	150.74ns	44327283.563**
Y × G	3	67.30**	37.92*	13.71 ns	34.35*	436.88**	2116660.50**
I × G	3	8.46 ns	19.51ns	6.62 ns	19.87ns	51.65 ns	1299497.581*
Y × I × G	3	20.98ns	11.67ns	34.45 ns	8.17 ns	232.17*	7220776.007**
N × G	6	10.13 ns	14.20ns	80.92*	38.87**	22.04 ns	908637.41*
Y × N × G	6	4.81 ns	27.08*	28.70 ns	3.55 ns	144.47*	255124.24 ns
I × N × G	6	28.92*	0.20 ns	71.51*	8.65 ns	189.60*	162713.22 ns
Y × I × N × G	6	16.38ns	49.71**	21.10 ns	43.24**	28.00 ns	138935.28 ns
Error b	88	10.82	11.44	46.29	12.54	64.87	426042.78
C.V.		14.55	13.22	14.28	9.95	13.55	9.73

ns: not significant at $P \leq 0.05$; *: significant at $P \leq 0.05$; **: significant at $P \leq 0.01$

Photosynthetic contribution of the ear to grain filling

In the present study, in terms of grain filling, in all wheat genotypes, treatments, the time of nitrogen fertilizer application, and water deficit conditions, the photosynthetic contribution of the ear was better than the flag-leaf. The highest photosynthetic

contribution of the ear to grain filling (35.08%) was observed in normal irrigation as I1, application of N3, and Mihan genotype as G4 (I1N3G4) (Table 3). The lowest value (21.52%) of the photosynthetic contribution of the ear to grain filling was obtained at I2N2G2 (Table 3).

Table 3. Comparison of means for the experimental factors including genotypes and nitrogen application on photosynthetic contribution of the ear and flag leaf to grain filling

Treatment		Photosynthetic contribution of the flag leaf to grain filling(%)				Photosynthetic contribution of the ear to grain filling (%)			
Water limitation	Nitrogen application	G1	G2	G3	G4	G1	G2	G3	G4
I1	N1	11.23cde	12.28b-e	11.56cde	13.12b-e	27.73a-d	25.21b-d	33.71ab	27.48a-d
	N2	13.22b-e	18.48a	12.40b-e	18.44a	28.18a-d	27.04a-d	30.73a-d	28.64a-d
	N3	10.44e	12.21b-e	13.57b-e	14.08b-e	23.99cd	32.32abc	29.25a-d	35.08a
I2	N1	12.74b-e	16.68ab	11.28cde	13.51b-e	26.33a-d	29.19a-d	26.43a-d	26.98a-d
	N2	11.13cde	15.34a-d	15.48a-d	12.87b-e	24.88bcd	21.52d	30.70a-d	31.72abc
	N3	10.22b-e	14.49a-e	11.06de	15.71abc	23.23cd	29.83a-d	26.50a-d	25.72a-d

Means in each column followed by similar letter(s) are not significantly different at 5% probability level, using Duncan's Multiple Range Test

I1 and I2 indicate normal irrigation and irrigation withholding in heading stages. N1, N2 and N3 indicate (20 kg.ha⁻¹ nitrogen fertilizer in sowing and 100 kg.ha⁻¹ at mid tillering stage), (20 kg.ha⁻¹ nitrogen fertilizer in sowing, 50 kg.ha⁻¹ at mid tillering and 50 kg.ha⁻¹ at stem elongation stage) and (20 kg.ha⁻¹ nitrogen fertilizer in sowing, 50 kg.ha⁻¹ at mid tillering and 50 kg.ha⁻¹ at 50% of heading stage) respectively
 G1, G2, G3 and G4 indicate Zarrin, Peshgam, Orum and Mihan genotypes respectively

According to the findings of the present investigation, the photosynthetic contribution of the ear to grain filling varied from 21% to 35%. Nonetheless, under water deficit conditions, the photosynthetic contribution of the ear in all genotypes was not significant (Table 5). According to a comparable study run by Mydup et al. (2010), the ear photosynthetic may act as a buffer in preventing serious damages under water deficit condition. Probably this can mainly be attributed to high durability of ear photosynthesis and the close relationship between grain and the ear. Considering the fact that ear benefits from a long-term spike photosynthetic activity with awn, the photosynthetic contribution of the ear is greater (Amiri et al., 2013). The decreased photosynthesis of the plant under water-stressed could be explained by the stomatal closure, which reduces CO₂ diffusion. Abebe et al. (2003) indicated that an early decrease in the photosynthesis during drought season is due to an increase in stomatal resistance. The Study conducted in the years 2014-2015, showed that maximum photosynthetic contribution of the ear (32.50 g) was obtained in Y2I2N2 (Table 4), whereas the minimum value (20.33 g) was observed in Y1I2N3 (Table 6). In 2015, due largely to a good agronomical condition, the photosynthetic contribution of the ear to grain filling increased up to 58%, which was higher considering the application of N3I2 in the same year (Table 4). These results indicated that the ear, as a photosynthetic organ, is better adapted than the flag-leaf to environmental factors. Even under good agronomical conditions, the ear may be more important than the flag-leaf during grain filling (Tambussi et al., 2007).

Table 4. Comparison of means for the experimental factors including genotypes and water limitation on photosynthetic contribution of the ear to grain filling of wheat under water limitation in two years, 2014-2015

Treatment		Photosynthetic contribution of the ear to grain filling (%)		
Year	Water limitation	N ₁	N ₂	N ₃
Y ₁ = 2014	I ₁	25.02bcd	28.42abc	29.82abc
	I ₂	23.70cd	21.91d	20.33d
Y ₂ = 2015	I ₁	32.05a	28.87abc	30.50ab
	I ₂	30.77ab	32.50a	32.31a

Means in each column followed by similar letter(s) are not significantly different at 5% probability level, using Duncan's Multiple Range Test

I₁ and I₂ indicate normal irrigation and irrigation withholding in heading stages. N₁, N₂ and N₃ indicate (20 kg.ha⁻¹ nitrogen fertilizer in sowing and 100 kg.ha⁻¹ at mid tillering stage), (20 kg.ha⁻¹ nitrogen fertilizer in sowing, 50 kg.ha⁻¹ at mid tillering and 50 kg.ha⁻¹ at stem elongation stage) and (20 kg.ha⁻¹ nitrogen fertilizer in sowing, 50 kg.ha⁻¹ at mid tillering and 50 kg.ha⁻¹ at 50% of heading stage) respectively

The photosynthetic contribution of the leaves below the flag leaf to grain filling

It was well-established that the flag leaf and the ear are not the only sources of assimilates to grain filling (Tambussi et al., 2007). This study reported that the photosynthetic contribution of the ear was greater than that of the flag leaf and the leaves below the flag leaf. Owing to a good environmental condition in 2014 compared to the same period in 2015, among all genotypes, the photosynthetic contribution of the leaves below the flag leaf to grain filling was higher, and the photosynthetic contribution of the other leaves to grain filling was lower in Mihan genotype largely due to the lower height of the plants (Table 5). Indeed, the effect of the photosynthetic contribution to grain filling of flag leaf is an important parameter to assess rather than the leaves below flag leaf. The results showed that the maximum photosynthetic contribution of the leaves below the flag leaf to grain filling (19.45%) was obtained in Y1I2N2G1 (Table 5). But the lowest value (3.25%) was observed in Y2I2N3G4 (Table 5).

1000-kernel weight

Grain yield in wheat is the result of the number of grains per ear and grain weight (Ahmad et al., 1988). Some studies in 2013-2014 showed that a maximum of 1000-grain weight (53.33 g) was obtained in Y1I1N3G4 and Y1I1N2G4 (Table 5). But the minimum value (33.33 g) was observed in Y1I2N3G1 (Table 5). Mihan and Pishgaam genotypes were higher 1000-kernel weight under water deficit condition. In 2014 under water deficit condition, 1000-kernel weight decreased about 22% in I1N3G4 compared to I2N3G4 (Table 5). It seems that the environmental factors have a high influence on the 1000-kernel weight, and this trait, especially in 2015, is significantly affected by water deficit and nitrogen fertilizer division. These results are in line with the results of the study practiced by Ahmadi et al. (2006). Akinirinde (2006) and Alam et al. (2007) reported that the increase in 1000-kernel weight resulted from the increase in the photosynthesis. In the present study, the photosynthetic contribution of the leaves, flag leaf, and ear during grain filling period could correlate with grain yield. Azarpanah et al.

(2013) stated that the reduction of crop yield is related to the reduction of rate and amount of photosynthesis and thousand seeds weight.

Table 5. Comparison of means for the experimental factors including genotypes and nitrogen application on thousand grain weight and photosynthetic contribution of the leaves below the flag leaf to grain filling of wheat under water limitation in two years, 2014-2015

Year	Treatment		1000-grain weight (g)				Photosynthetic contribution of the leaves below the flag leaf to grain filling (%)			
	Water limitation	Nitrogen application	G ₁	G ₂	G ₃	G ₄	G ₁	G ₂	G ₃	G ₄
Y ₁ =2014	I ₁	N ₁	41.67f-n	45.33c-k	48.33a-g	48.67a-f	14.56a-g	17.59abc	13.14a-j	10.59c-l
		N ₂	44d-l	51.67abc	49.33a-d	53.33a	14.90a-e	14.67a-f	14.65a-f	14.51a-g
		N ₃	45.33c-k	53.00ab	47.00a-i	53.33a	18.19ab	16.80a-d	10.24d-m	13.47a-j
	I ₂	N ₁	35.67no	41.67f-n	41.33g-n	39.00k-o	8.007f-n	11.43c-l	6.81j-n	8.99e-n
		N ₂	41.67f-n	43.67d-l	42.67d-m	45.67c-k	19.45a	10.87c-l	13.33a-j	7.50h-n
		N ₃	33.33o	46.67a-j	45.33c-k	41.33g-n	14.70a-h	12.23b-k	11.89b-l	8.61e-n
Y ₂ =2015	I ₁	N ₁	42.00e-n	44.67c-l	49.00a-e	47.00a-i	7.13i-n	7.12i-n	5.90k-n	11.60b-l
		N ₂	46.67a-j	43.33d-m	43.33d-m	46.00b-k	12.46b-k	7.41h-n	5.76k-n	7.72g-n
		N ₃	36.33mno	47.67a-h	48.67a-f	48.67a-f	3.96mn	7.81f-n	10.15d-m	7.34h-n
	I ₂	N ₁	43.33d-m	39.67j-o	43.67d-l	40.33i-n	10.82c-l	11.42c-l	13.93a-i	7.83f-n
		N ₂	37.67l-o	40.67h-n	44.67c-l	43.00d-m	5.26lmn	9.03e-n	5.70k-n	9.90e-n
		N ₃	43.00d-m	46.67a-j	45.67c-k	47.00a-i	7.02j-n	8.39e-n	10.19d-m	3.25n

Means in each column followed by similar letter(s) are not significantly different at 5% probability level, using Duncan's Multiple Range Test

I₁ and I₂ indicate normal irrigation and irrigation withholding in heading stages. N₁, N₂ and N₃ indicate (20 kg.ha⁻¹ nitrogen fertilizer in sowing and 100 kg.ha⁻¹ at mid tillering stage), (20 kg.ha⁻¹ nitrogen fertilizer in sowing, 50 kg.ha⁻¹ at mid tillering and 50 kg.ha⁻¹ at stem elongation stage) and (20 kg.ha⁻¹ nitrogen fertilizer in sowing, 50 kg.ha⁻¹ at mid tillering and 50 kg.ha⁻¹ at 50% of heading stage) respectively. G₁, G₂, G₃ and G₄ indicate Zarrin, Peshgam, Orum and Mihan genotypes respectively

The number of grains ear

The number of grain ears is an important factor that affects the grain yield in wheat (Wei-Wei et al., 2012). The comparison of the effects of the interaction means of rates and time of N application and genotypes on the number of grains per ear in 2014 and 2015 indicated that the highest value (73.67) belonged to Y2N2G4, and the minimum number of grains per ear (45.50) was recorded at Y1N3G3 (Table 6). The highest number of grains per ear (66.83) was recorded at limited irrigation, application of N2 and Orum genotype (I2N2G3), and the lowest values of this trait (50.83) were recorded at I2N3G1 treatments (Table 7). The maximum number of grains per ear (70.11) was recorded at Orum genotype in normal irrigation condition in 2015 as Y2I1G3, and the minimum of this trait was recorded at Orum genotype and water limitation in 2014 as Y1I2G3 treatment (Table 8).

This reduction was probably due to the reduction of the numbers of the endosperm cells leading to the reduction of sink strength. This, in turn, could confer a critical survival advantage for few versus many seeds in terminal drought environments by reducing sink numbers at a key point in development and thus secure a sufficient sucrose supply for maturation of a few remaining seeds as observed under irrigation conditions. This is supported by a previous report showing that 180 kg.ha⁻¹ urea increased significantly the number of grains per head in safflower (Seyed Sharifi, 2011).

Dawadi and Sah (2012) suggested that a decrease in the number of grains per ear under lower N fertilizer application at stem elongation might be attributed to the poor development of sinks and the reduction of photosynthates translocation. In this study, high N rates increased the photosynthesis and delayed the appearance of phenological stages. It seems that high N rate can be one of the reasons of increasing the number of grains per ear row. Similar results have been reported by Alam and Haidar (2006). Increase in the number of grains per ear at higher N rates might be due to the lower competition for the nutrients allow the plants to accumulate more biomass with higher capacity to convert more photosynthesis into sinks (Zeidan et al., 2006). Uribelarrea et al. (2009) suggested that the effect of N stress on stem elongation on grain number occurs indirectly through its effect on photosynthesis and also on phenology stages. Seyed Sharifi (2011) suggested that increasing the number of grains may be due to the delay of the duration of the vegetative and reproductive period and lengthening of grain filling duration.

Table 6. Comparison of means for the experimental factors including genotypes and nitrogen application on number of grains per ear of wheat in two years, 2014-2015

Treatment		Number of grains per ear			
Year	Nitrogen application	G ₁	G ₂	G ₃	G ₄
Y ₁ = 2014	N ₁	51.67efg	55.00c-g	51.50fg	53.50d-g
	N ₂	66.17abc	62.83a-e	55.00c-g	58.17c-f
	N ₃	54.00d-g	55.00c-g	45.50g	61.00b-f
Y ₂ = 2015	N ₁	58.67c-f	60.83b-f	64.17a-d	64.33a-d
	N ₂	55.50c-g	63.00bcd	71.67ab	73.67a
	N ₃	58.67c-f	59.33c-f	64.50a-d	63.00a-d

Means in each column followed by similar letter(s) are not significantly different at 5% probability level, using Duncan's Multiple Range Test

N₁, N₂ and N₃ indicate (20 kg.ha⁻¹ nitrogen fertilizer in sowing and 100 kg.ha⁻¹ at mid tillering stage), (20 kg.ha⁻¹ nitrogen fertilizer in sowing, 50 kg.ha⁻¹ at mid tillering and 50 kg.ha⁻¹ at stem elongation stage) and (20 kg.ha⁻¹ nitrogen fertilizer in sowing, 50 kg.ha⁻¹ at mid tillering and 50 kg.ha⁻¹ at 50% of heading stage) respectively

G₁, G₂, G₃ and G₄ indicate Zarrin, Peshgam, Orum and Mihan genotypes respectively

Grain yield

Grain yield is a function of interaction amongst various yield components affected differently by the growing conditions and crop management practices (Cheema et al., 2010). The data presented in *Table 8* shows that the interactions of the studied experimental factors (year, irrigation, and genotype) had significant effects on grain yield of wheat. The highest figure for grain yield (9020 kg/ha) was observed in 2014, normal irrigation (I1) and Mihan genotype (G4) (*Table 8*). Whereas the lowest figure regarding of the abovementioned trait (3277 kg.ha⁻¹) was obtained in Y2I2G3 (*Table 8*). The seed yield decreased in water deficit condition except for the Y1I2G3 treatment (*Table 8*). It is assumed that the obtained reasons are as the result of lower current photosynthesis, stomata conduction, and assimilation in water deficit condition.

Table 7. Comparison of means for the experimental factors including genotypes and nitrogen application on number of grains per ear of wheat under water limitation

Treatment		Number of grains per ear			
Water limitation	Nitrogen application	G ₁	G ₂	G ₃	G ₄
I ₁	N ₁	51.50c	58.17abc	59.67abc	57.50abc
	N ₂	64.33ab	65.00ab	59.83abc	66.33a
	N ₃	61.83abc	52.33c	55.83abc	66.17a
I ₂	N ₁	58.83abc	57.67abc	56.00abc	60.33abc
	N ₂	57.33abc	60.83abc	66.83a	65.50ab
	N ₃	50.83c	62.00abc	54.17bc	57.83abc

I₁ and I₂ indicate normal irrigation and irrigation withholding in heading stages

Means in each column followed by similar letter(s) are not significantly different at 5% probability level, using Duncan's Multiple Range Test

N₁, N₂ and N₃ indicate (20 kg.ha⁻¹ nitrogen fertilizer in sowing and 100 kg.ha⁻¹ at mid tillering stage), (20 kg.ha⁻¹ nitrogen fertilizer in sowing, 50 kg.ha⁻¹ at mid tillering and 50 kg.ha⁻¹ at stem elongation stage) and (20 kg.ha⁻¹ nitrogen fertilizer in sowing, 50 kg.ha⁻¹ at mid tillering and 50 kg.ha⁻¹ at 50% of heading stage) respectively

G₁, G₂, G₃ and G₄ indicate Zarrin, Peshgam, Orum and Mihan genotypes respectively

Table 8. Comparison of means for the interaction of factors including genotype, water limitation and year on number of grains per ear and grain yield of wheat

Treatment		Number of grains per ear				Grain yield (kg/ha)			
Year	Water limitation	G ₁	G ₂	G ₃	G ₄	G ₁	G ₂	G ₃	G ₄
Y ₁ =2014	I ₁	57.56cdf	58.78b-e	54.56def	59.67b-e	6143fg	8537ab	5969g	9020a
	I ₂	57.00c-e	56.44cde	46.78f	55.44cde	5180h	7471e	6634f	7828cde
Y ₂ =2015	I ₁	60.89b-e	58.22cde	70.11a	67.00ab	7680de	8294bcd	7775de	8464abc
	I ₂	54.33ef	63.89abc	63.44a-d	67.00ab	3409i	5794g	3277i	5857g

Means in each column followed by similar letter(s) are not significantly different at 5% probability level, using Duncan's Multiple Range Test

I₁ and I₂ indicate normal irrigation and irrigation withholding at heading stages. G₁, G₂, G₃ and G₄ indicate refer to Zarrin, Pishgam, Orum and Mihan genotypes, respectively

Mihan and Pishgam genotypes had the highest seed yield in contrast to Zarrin genotype showing the lowest seed yield. The high seed yield can be associated with grains per ear, 1000-grain weight, and high photosynthetic contribution of flag leaf and ear to grain filling. These factors indicate that these genotypes are more tolerant of drought stress than the others. Yield reduction was significant in 2015 under water deficit condition resulting in a decrease of 57% in seed yield in Y2I1G3 compared to Y2I2G3 (Table 8). Results also showed that in normal irrigation (I1), wheat genotypes as Y1G4 had 7% more grain yield than Y2G4 (Table 8). However, the available literature has classically considered the flag leaf, leaf below the flag leaf and the ear

(Tambussi et al., 2007) as the main photosynthetic contributors during grain filling. Water deficit stress affects plant metabolism leading to a decrease in plant growth and grain yield. In the grains of the crops, both current assimilations were transferred directly to grains and remobilization of assimilates were stored in vegetative plant parts contributing to grain yield (Arduini et al., 2006).

Conclusion

In this research, Mihan and Pysgham cultivars with the highest seed weight and the transfer of more photosynthetic materials from flag leaf and spike had the highest seed yield in in water deficit conditions. According to the results, the application of N fertilizer in different doses and times, on different genotypes can be a proper tool for increasing wheat yield under water deficit condition.

REFERENCES

- [1] Abebe, T., Guenzi, A. C., Martin, B., Cushman, J. C. (2003): Tolerance of mannitol-accumulating transgenic wheat to water stress and salinity. – *Plant Physiology* 131: 1748-1755.
- [2] Ahmad, N., Basra, S., Qureshi, R., Ahmad, S. (1988): Grain development in wheat as affected by different nitrogen levels under warm dry conditions. – *Pakistan Journal of Agricultural Science* 25: 225-231.
- [3] Ahmadi, A., Isvand, H., Postini, K. (2006): Intraction of drought stress and nitrogen application timing on yield and physiological traits in winter wheat. – *Iranian Journal of Field Crop Science* 37: 113-123.
- [4] Akinrinde, E. A. (2006): Growth regulator and nitrogen fertilization effects on performance and nitrogen-use efficiency of tall and dwarf varieties of rice (*Oryza sativa* L.). – *Biotechnology* 5: 268-276.
- [5] Alam, M., Haider, S. (2006): Growth attributes of barley (*Hordeum vulgare* L.) cultivars in relation to different doses of nitrogen fertilizer. – *Journal of Life and Earth Science* 1: 77-82.
- [6] Alam, M., Jahan, M., Ali, M., Ashraf, M., Islam, M. (2007): Effect of vermicompost and chemical fertilizers on growth, yield and yield components of potato in barind soils of Bangladesh. – *Journal of Applied Sciences Research* 3: 1879-1888.
- [7] Amiri, R., Bahraminejad, S., Jalali-Honarmand, S. (2013): Effect of terminal drought stress on grain yield and some morphological traits in 80 bread wheat genotypes. – *International Journal of Agriculture and Crop Sciences* 5: 1145.
- [8] Arduini, I., Masoni, A., Ercoli, L., Mariotti, M. (2006): Grain yield, and dry matter and nitrogen accumulation and remobilization in durum wheat as affected by variety and seeding rate. – *European Journal of Agronomy* 25: 309-318.
- [9] Azarpanah, A., Alizadeh, O., Dehghanzadeh, H., Zare, M. (2013): The effect of irrigation levels in various growth stages on morphological characteristics and yield components of *Zea mays* L. – *Technical Journal of Engineering and Applied Sciences* 3: 1447-1459.
- [10] Cheema, M., Farhad, W., Saleem, M., Khan, H., Munir, A., Wahid, M., Rasul, F., Hammad, H., Cheema, M., Farhad, W. (2010): Nitrogen management strategies for sustainable maize production. – *Crop Environment* 1: 49-52.
- [11] Dawadi, D., Sah, S. (2012): Growth and yield of hybrid maize (*Zea mays* L.) in relation to planting density and nitrogen levels during winter season in Nepal. – *Tropical Agricultural Research* 23(3): 218-227.
- [12] Diacono, M., Rubino, P., Montemurro, F. (2013): Precision nitrogen management of wheat. A review. – *Agronomy for Sustainable Development* 33: 219-241.

- [13] Dordas, C. A., Sioulas, C. (2008): Safflower yield, chlorophyll content, photosynthesis, and water use efficiency response to nitrogen fertilization under rainfed conditions. – *Industrial Crops and Products* 27: 75-85.
- [14] Ehdaie, B., Alloush, G., Waines, J. (2008): Genotypic variation in linear rate of grain growth and contribution of stem reserves to grain yield in wheat. – *Field Crops Research* 106: 34-43.
- [15] Lawrence, J. R., Ketterings, Q., Cherney, J. (2008): Effect of nitrogen application on yield and quality of silage corn after forage legume-grass. – *Agronomy journal* 100: 73-79.
- [16] Maccaferri, M., Sanguineti, M. C., Demontis, A., El-Ahmed, A., Garcia Del Moral, L., Maalouf, F., Nachit, M., Nserallah, N., Ouabbou, H., Rhouma, S. (2011): Association mapping in durum wheat grown across a broad range of water regimes. – *Journal of Experimental Botany* 62: 409-438.
- [17] Maydup, M. L., Antonietta, M., Guiamet, J., Graciano, C., López, J. R., Tambussi, E. A. (2010): The contribution of ear photosynthesis to grain filling in bread wheat (*Triticum aestivum* L.). – *Field Crops Research* 119: 48-58.
- [18] Olszewski, J., Pszczółkowska, A., Kulik, T., Fordoński, G., Płodzień, K., Okorski, A., Wasielewska, J. (2008): Rate of photosynthesis and transpiration of winter wheat leaves and ears under water deficit conditions. – *Polish Journal of Natural Sciences* 23: 326-335.
- [19] Osman, A. R. (2014): Improving some quantitative and qualitative characteristics of *Solidago canadensis* 'Tara' using cycocel and planting density under drip irrigation and lighting systems. – *Life Science Journal* 11: 110-118.
- [20] Sadras, V. O., Egli, D. (2008): Seed size variation in grain crops: allometric relationships between rate and duration of seed growth. – *Crop Science* 48: 408-416.
- [21] Sanjari, A., Yazdan Sepas, A. (2008): Stem reservation genetic variation of bread wheat genotypes under drought stress condition after anthesis stage. – *Iranian Journal of Crop Sciences* 29: 181-191.
- [22] Seyed Sharifi, R., Khavazi, K. (2011): Effects of seed priming with Plant Growth Promoting Rhizobacteria (PGPR) on yield and yield attribute of maize (*Zea mays* L.) hybrids. – *Journal of Food, Agriculture and Environment* 9: 496-500.
- [23] Soleymanifard, A., Sidat, S. (2011): Effect of inoculation with biofertilizer in different nitrogen levels on yield and yields components of safflower under dry land conditions. – *American-Eurasian Journal Agriculture and Environment Science* 11: 473-477.
- [24] Tambussi, E. A., Bort, J., Guiamet, J. J., Nogués, S., Araus, J. L. (2007): The photosynthetic role of ears in C3 cereals: metabolism, water use efficiency and contribution to grain yield. – *Critical Reviews in Plant Sciences* 26: 1-16.
- [25] Uribelarrea, M., Crafts-Brandner, S. J., Below, F. E. (2009): Physiological N response of field-grown maize hybrids (*Zea mays* L.) with divergent yield potential and grain protein concentration. – *Plant and soil* 316: 151.
- [26] Wang, H., Xiao, L. (2009): Effects of chlorocholine chloride on phytohormones and photosynthetic characteristics in potato (*Solanum tuberosum* L.). – *Journal of Plant Growth Regulation* 28: 21.
- [27] Wei-Wei, M., Dong, W., Zhen-Wen, Y. (2012): Effects of nitrogen fertilizer on activities of nitrogen metabolism related enzymes and grain Protein quality of wheat. – *Plant Nutr. Fert. Sci.* 18(1): 10-17.
- [28] Zeidan, M., Amany, A., El-Kramany, M. (2006): Effect of N-fertilizer and plant density on yield and quality of maize in sandy soil. – *Research Journal of Agriculture and Biology Science* 2: 156-161.

APPENDIX

Appendix 1. Study site. The pollination stage in wheats are shown. In this stage samples were treated for determining the phenotypic manipulations components, e.g. all the leaves below the flag leaf, flag leaf and half of the spike were removed in samples



Appendix 2. Experimental design: a split plot based randomized complete block design with three replications

I2	Mihan	Orum	Orum	Orum	Pesh	Pesh	Pesh	Pesh	Pesh	Zrrin	Pesh	Zrrin
	Orum	Pesh	Zrrin	Zrrin	Mihan	Mihan	Mihan	Mihan	Mihan	Orum	Mihan	Orum
	Pesh	Zrrin	Pesh	Pesh	Zrrin	Zrrin	Zrrin	Zrrin	Zrrin	Mihan	Zrrin	Mihan
	Zrrin	Mihan	Mihan	Mihan	Orum	Orum	Orum	Orum	Orum	Pesh	Orum	Pesh
I1	Mihan	Orum	Orum	Orum	Pesh	Pesh	Pesh	Pesh	Pesh	Zrrin	Pesh	Zrrin
	Orum	Pesh	Zrrin	Zrrin	Mihan	Mihan	Mihan	Mihan	Mihan	Orum	Mihan	Orum
	Pesh	Zrrin	Pesh	Pesh	Zrrin	Zrrin	Zrrin	Zrrin	Zrrin	Mihan	Zrrin	Mihan
	Zrrin	Mihan	Mihan	Mihan	Orum	Orum	Orum	Orum	Orum	Pesh	Orum	Pesh
F1	F2	F3	F4	F2	F4	F1	F3	F3	F1	F4	F2	
R1				R2				R3				

I1 and I2 indicate normal irrigation and irrigation withholding in heading stages. N1, N2 and N3 indicate (20 kg.ha⁻¹ nitrogen fertilizer in sowing and 100 kg.ha⁻¹ at mid tillering stage), (20 kg.ha⁻¹ nitrogen fertilizer in sowing, 50 kg.ha⁻¹ at mid tillering and 50 kg.ha⁻¹ at stem elongation stage) and (20 kg.ha⁻¹ nitrogen fertilizer in sowing, 50 kg.ha⁻¹ at mid tillering and 50 kg.ha⁻¹ at 50% of heading stage) respectively

Zrrin, Peshgam, Orum and Mihan genotypes respectively

THE NEGATIVE EFFECT OF ARSENIC IN AGRICULTURE: IRRIGATION WATER, SOIL AND CROPS, STATE OF THE ART

SALDAÑA-ROBLES, A.¹ – ABRAHAM-JUÁREZ, M.R.^{2*} – SALDAÑA-ROBLES, A. L.¹ –
SALDAÑA-ROBLES, N.¹ – OZUNA, C.² – GUTIÉRREZ-CHÁVEZ, A. J.³

¹*Department of Agricultural Engineering, Division of Life Sciences, University of Guanajuato
Ex Hacienda El Copal, Km. 9. Carretera Irapuato-Silao, C.P. 36500. Irapuato, Gto., México*

²*Department of Food Engineering, Division of Life Sciences, University of Guanajuato
Ex Hacienda El Copal, Km. 9. Carretera Irapuato-Silao, C.P. 36500. Irapuato, Gto., México*

³*Department of Veterinary and Zootechny, Division of Life Sciences, University of Guanajuato
Ex Hacienda El Copal, Km. 9. Carretera Irapuato-Silao, C.P. 36500. Irapuato, Gto., México*

**Corresponding author*

e-mail: abrahamjrma@gmail.com

(Received 21st Sep 2017; accepted 5th Feb 2018)

Abstract. The existence of high content of arsenic exceeding international regulations established for irrigation water can be the main factor for the relationship of arsenic content found in soil and crops of many countries around the world such as Bangladesh, Mexico and Spain. The drinking water is not the only source of consumption of arsenic in human diet. Irrigating agricultural fields with arsenic contaminated water produces accumulation of arsenic in soil and subsequently an increases of arsenic concentration in crops. Concentration of arsenic in crops depends of many factors, for example, type of crop, arsenic concentration of soil and water, soil type, among others. In this paper, data from several studies are presented to show that arsenic in irrigation water tends to accumulate in agricultural soil and through several mechanisms is absorbed by crops. The problem of arsenic in agriculture requires more research that allows to know the actual situation and to propose solutions in order to solve some cases and avoid others.

Keywords: *accumulation, concentration, absorption, agriculture, impact*

Introduction

Arsenic excess present in groundwater may be a natural contaminant and it is currently a problem that impacts many sites around the world, for example India, Spain, Nicaragua, Peru, Argentina, Mexico and Chile are among the countries where have detected concentration above of 10 µg L⁻¹ of this pollutant (*Figure 1*), this concentration exceeds the permissible limit according to World Health Organization (WHO, 2003). In India, natural sources of arsenic from aquifer rocks has been reported to add arsenic to underground water (Ranhman et al., 2007), the same for Argentina (Hopenhayn et al., 1996), while in Mexico a large part comes from mining (Ongley et al., 2007). The problem of arsenic of natural origin, added to that generated by copper mining, is also critical in northern Chile (Arica), at communities that are facing water shortages at the same time (Carbonell et al., 1995).

Irrigation water is not an exception to the above described and is compromised by contamination of arsenic in surface water bodies at many countries (Azcue and Nriagu, 1994; Chen et al., 1994; Das et al., 1995; Nickson et al., 2000; Schreiber et al., 2000; Smedley et al., 2002; Mishra and Mahato, 2016; Yazdani et al., 2016; Rosas et al., 2016; Núñez et al., 2016). Concentration of arsenic in irrigation water is accumulated in

soil, showing greater accumulation at top layers of soil and it is found in soluble form. Finally, arsenic in soil and water reaches plants (Pandey and Singh, 2015; Kramar et al., 2015; Dixit et al., 2016; Dousova et al., 2016; Ma et al., 2016).

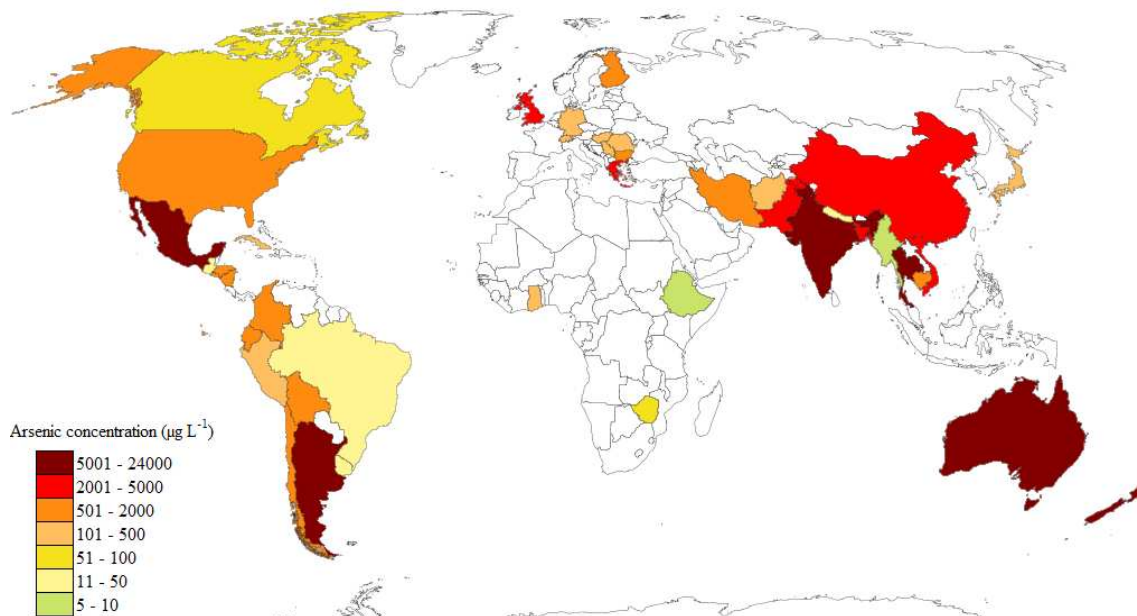


Figure 1. Arsenic concentration in groundwater around the world (elaborated with data from Rasheed et al., 2016)

Accumulated arsenic in plants affect the growing mechanisms and hence the yield of crops, as well as the accumulation of arsenic in crops may impact on health of living beings (Rosas et al., 2016). A specific case of the arsenic effect, is the 50% yield reduction when having an arsenic concentration of 43.8 mg L^{-1} in radish and 4.5 mg L^{-1} in tomato (Carbonell et al., 1995). Due to the high toxicity and bioavailability of arsenic, it is necessary to conduct research in various subjects to help tackle the problem comprehensively, for example, knowing the mechanisms by which this element moves through the system water-soil-plant, concentrations affecting yield of crops and health of living beings, geographical distribution of an index for bioavailability and propose solutions economically and technically viable.

Therefore, this article presents the state of the art about the effect of arsenic contamination in agricultural soil and water, absorption of the most common arsenic species in some parts of crops, effects on productivity of some crops and solutions proposed to the problem.

Fundamentals

Arsenic in water

Arsenic contamination of drinking water is a serious and widespread problem that threatens human health and the environment. The World Health Organization (WHO) recommends a maximum quantity of arsenic of $10 \mu\text{g L}^{-1}$ in drinking water.

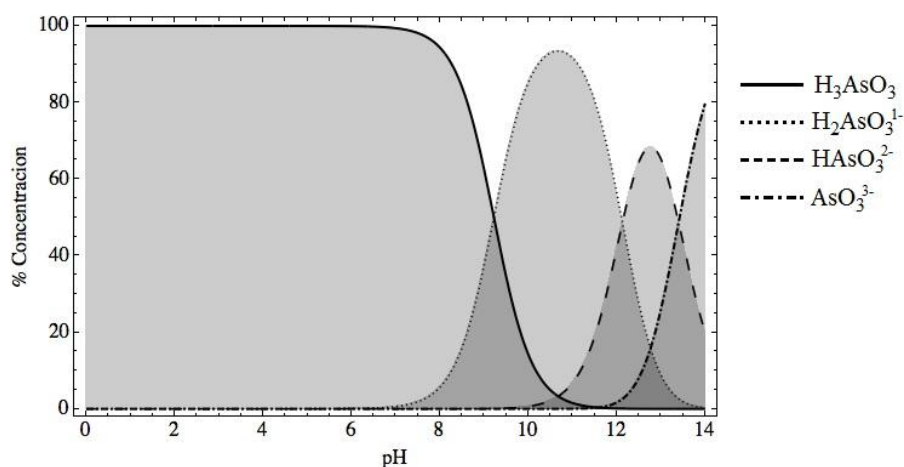
In water with dissolved oxygen concentrations below 0.8 mg L^{-1} is more common to find arsenic (III) than arsenic (V). H_2As_4^- and $\text{H}_2\text{AsO}_4^{2-}$ species may dominate under oxidizing conditions, however, the oxidation of arsenic (III) is often slow and persists under conditions of oxygenation, the *Table 1* shows some properties of Arsenic III and V. On the other hand, greater sorption of arsenic (V) of the form H_3AsO_3 could increase the rate of dissolution of arsenic (III) / arsenic (V) in surface water bodies (Boyle et al., 1998).

Table 1. Properties of Arsenic III and V

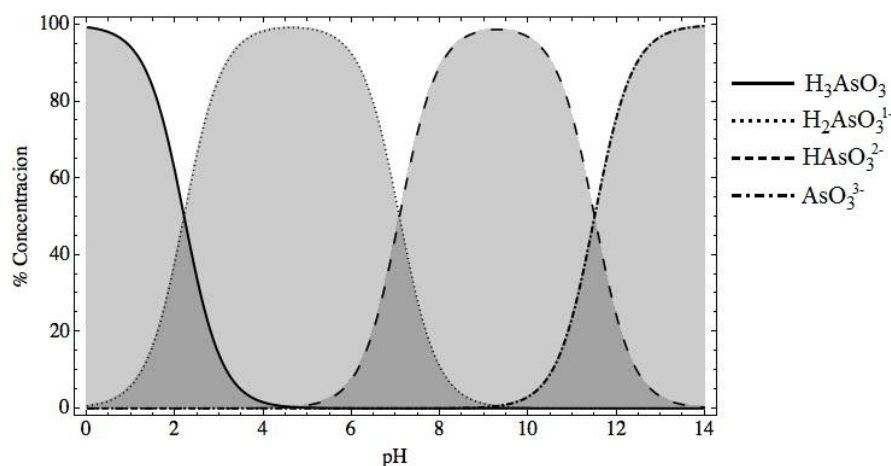
Properties	Valence state		Reference
	As III	As V	
Coordination number	Sixfold	Fourfold	Klein, 2002
Radius (Å)	0.58	0.34	Klein, 2002
Density (g cm^{-3}), 25 °C and 1 bar	5.75 (rhombohedral form)	5.75 (rhombohedral form)	Lide, 2007
Electronegativity	2.0	2.2	Langmuir, 1997
First ionization potential (eV)	9.7886	9.7886	Lide, 2007

The adsorption of arsenic depends on the species in which it is located, and represents the dominant mechanism that controls the transport of arsenic in many water systems. Hydroxides of iron, aluminum, magnesium and clay minerals are commonly associated with solid aquifers, which show that these species are important absorbents of arsenic. The amount of arsenic absorbed is influenced by the chemistry of the aqueous phase, including arsenic speciation, the presence and concentration of different ions of competition for arsenic and pH.

Chemical and physical conditions of the aqueous phase of water affect arsenic chemical behavior in the water-soil-plant system, i.e. in a water system with neutral pH conditions, inorganic arsenic (III) is an uncharged molecule H_3AsO_3 , which improves mobility, as it does not adsorb strongly enough to the surface of minerals. In contrast to the anions of arsenic (V) that are strongly adsorbed by minerals under conditions of neutral pH (Smedley et al., 2005), i.e. in moderate reduction, trivalent arsenite is stable and increases adsorption with increasing pH, on the other hand under oxidizing conditions, arsenate is stable and the absorption decreases with increasing pH. A pH diagram of aqueous arsenic species is shown in *Figure 2*.



(A)



(B)

Figure 2. pH diagram of aqueous arsenic species: (A) III. (B) V.

Another factor that influences the transport of arsenic in water, like adsorption, is organic matter. Organic matter is composed of a wide variety of organic compounds, some of the most important due to interaction with arsenic are the humic substances. Humic substances affect mobility and balance of the sorption of arsenic (Grafe et al., 2002; Redman et al., 2002; Lin et al., 2003; Ko et al., 2004; Sjöblom et al., 2004; Warwick et al., 2005; Buschmann et al., 2006), since this can be absorbed by organic material and compete for adsorption sites on mineral surfaces (Haw et al., 2004). Due to the arsenic concentration in water, the agricultural soils are contaminated, and even accumulating more arsenic after each crop cycle, which is a topic explored in more detail in the next section.

Arsenic in soil

The soil is an important natural resource, but also an important media of accumulation, transformation and migration of arsenic. The main factors influencing the concentration of arsenic in soil are the parent rocks (Tanaka, 1988) and human activities, which may come from industrial waste and/or agricultural use of arsenical pesticides. The average range of the natural content of arsenic in soils around the world is from 0.1 to 40 mg kg⁻¹ with an average of 6 mg kg⁻¹ (Vinogradov, 1959; Backer and Chesnin, 1975, Bowen, 1979, Zou, 1986; Boyle et al., 1998). Little quantities of arsenic are also accumulated in soil by fertilizers, irrigation, emissions from burning fossil fuels, industrial waste and sludge with high concentration of arsenic (Nasier et al., 1977).

Agricultural practices with chemicals, historically used, contributes to the accumulation of arsenic. Some combinations of pesticides and chemical fertilizers were widely applied over long periods of time in the past (Carbonell, 1995).

Arsenic in soil is mainly found as inorganic species although the organic arsenic is also found in organic matter of some soils, since some reducing bacteria catalyze and improve the rate of oxidation of certain arsenious minerals (Mihaljevic et al., 2004), thus converting inorganic arsenic into organophosphorus compounds. Typically, arsenic (V) is dominant with values of electric potential (Eh) around 200 mV and pH conditions of 5-8 (Henke, 2009).

Togashi et al. (2000) argue that climate, erosion and sedimentation are responsible for the enrichment of arsenic in soil. The temperature, humidity, precipitation and evaporation

are important as they contribute to the oxidation of arsenic sulfide minerals. In particular, for warm and humid climates, excessive rainfall causes intensive biological activity, thus creating reduction conditions on the surface and underground, which prevents the oxidation of sulfur. The soil surface under high temperatures and moisture can promote the oxidation of arsenic sulfide minerals, releasing arsenic into the environment (Williams, 2001).

Soil texture is another important characteristic that affects the chemistry of arsenic. Fine clay minerals tend to adsorb and trap arsenic more effectively than sandy soils (Scazzola et al., 2004). In many soils and sediments, the mobility of arsenic (V) is limited by adsorption to clay minerals, organic matter or iron oxides (Inskeep et al., 2002).

Soil organic matter is generally composed of a wide variety of compounds, that including, carboxylic acids, carbohydrates, phenols, amino acids and humic substances (Drever, 1997; Wang and Mulligan, 2006; Fakour and Lin 2014). Organic matter affects the mobility and bioavailability of arsenic in soils and sediments by the same mechanisms that water sorption (Sjöblom et al., 2004; Warwick et al., 2005; Buschmann et al., 2006). Most of the components of organic matter are found in an oxidation state under conditions of alkaline and neutral pH, which implies that compete with oxy-anions of arsenic to be adsorbed by hydroxides or oxy-hydroxides on the surface of minerals (Wilkin and Ford, 2006). Then the effect of arsenic contamination in agricultural soil and water, affects crops, decreasing the crop yield and in this way enters to the food chain.

Arsenic in agriculture

Soil and plant

There are many studies about the mobilization and accumulation of arsenic in soil, as well as the effect of oxalic, citric and malic acids on this mobilization. These acids were tested in terms of mobilizing arsenic that was bound to iron components. The results showed that the arsenic mobility increases as dose of oxalic acid increases. In other hand, it was observed that there was a close relationship between the mobilized iron and the mobilized arsenic, in fact the iron plays an important role for arsenic mobilization (Onireti and Lin, 2016), while the results of Dousova et al. (2016) showed that chemical composition (Fe, OM content) played a minor role, being important just in the kinetics of surface processes.

In the West of England, retention of arsenic was examined for forest soils rich in organic matter and spatial and temporal patterns of arsenic dissolved concentrations were analyzed. Concentration of arsenic was found to change as a function of soil depth, and the results revealed the highest arsenic concentration of 28.3 mg kg⁻¹ at the topsoil layer (0.07 m), and below 0.13 m, concentration fluctuated around 9 mg kg⁻¹. On the other hand, the study demonstrated that those soils were contaminated with anthropogenic arsenic derivatives and that organic matter plays an important role in the dynamics of arsenic (Rothwell et al., 2009). Arsenic reported, in previous publications, that major contamination of soil occurs in the upper layer of soil, which is at 0.50 m depth, where contamination occurs due to irrigation with contaminated water.

A study in Portugal (Marques et al., 2009) found that the soil on the slopes of a river presented a higher concentration of arsenic, at the closest points to a sewage canal. In addition, the highest concentrations of arsenic were found at the top layers of soil, similar to the results reported by Rothwell et al. (2009). Marques et al. (2009) found that the closer the ground to channel water, the higher concentration of arsenic. Moreover, these authors

reported that in Blackberry (*R. ulmifolius*), arsenic concentration ranged between 277 and 1721 mg kg⁻¹ at the root, from 30 to 110 mg kg⁻¹ at the stem from 60 to 265 mg kg⁻¹ at the leaf. Also they found that extractable percentage of arsenic per plant is 0.7% with respect to the total concentration of metalloid in the soil. On the other hand, arsenic concentration in Blackberry plants are higher compared with results of other studies (Ma et al., 2001). However, the absorption of arsenic in the system of plant-soil is also related by the presence of different metals and anions that compete for adsorption sites with arsenic. Several authors (Azcue and Nriagu, 1994; Cardwell et al., 2002; Marques et al., 2007) have found a clear pattern of increased concentration of arsenic present in aquatic macrophytes as Zinc concentration increases, indicating an interaction between different metals or anions.

Stoltz and Greger (2002) found that some tests showed a high correlation between the concentration of arsenic among varieties of cotton (*Eriophorum angustifolium* and *E. scheuchzeri Honckenya Hoppe*) and arsenic concentration in agricultural soil, and reported maximum concentrations of 8.4 mg kg⁻¹ in soil and 276 mg kg⁻¹ in root, like Marques et al. (2009). Also, Stoltz and Greger (2002) found that concentrations of arsenic in root is higher than the arsenic content in the aerial part. The correlation of the concentration of arsenic in plant root and the concentration of arsenic in soil was positive and significant, while for leaf and stem was generally not significant.

Studies have demonstrated that Arsenic (V) uses the same pathway than phosphate to be absorbed by the root of rice from soil, it is due to the chemical analogy of phosphate (Abedin et al., 2002; Lee et al., 2016), in Table 2, a summary plant species and the main uptake mechanism is presented. The main form of arsenic in aerobic soils is arsenic (V), this form presents many chemical similarities of phosphate and get in to plant root tissue through the mechanism of phosphate transporters. Some studies reported that the high affinity phosphate transporters AtPht1;1 and AtPht1;4 facilitate the acquisition of phosphate and arsenic (V) (Shin et al., 2004; Remy et al., 2012; Ye et al., 2015; Punshon et al., 2017). Absorption of arsenic/phosphate take place through the same plasma membrane in plants of *Holcus lanatus* and *Hordeum vulgare*, these mechanism presents a higher affinity for phosphate than arsenic (V).

Table 2. Transport mechanism in selected plant species. For a more complete review of uptake mechanism, see Farok et al., 2016

Plant species	Arsenic species	Uptake and transporter name	Reference
Xenopus Laevis oocyte	MMA	OsNIP2;1 gene	Li et al., 2009.
Rice and Castor Bean	DMA	Translocated from roots to shoots, takes place via both the xylem and the phloem	Carey et al., 2011; Ye et al., 2010.
Rice	DMAA and MMAA	Glycerol transport pathway	Rahman et al. 2011.
Rice	As ^V	Uptake and translocation root to shoot	Kamiya et al. 2013.
Arabidopsis thaliana	As ^V	Phosphate transporters	Shin et al., 2004.
Pteris vittata	As ^V	Transport	DiTusa et al., 2016.
Arabidopsis	As ^{III}	PC complex transport	Song et al., 2010.
Arabidopsis	As ^{III}	Phloem translocation	Duan et al., 2016.
Barley	As ^{III}	Transport	Katsuhara et al., 2014.
Pteris vittata	As ^{III}	Uptake	He et al., 2016.

Due to high concentrations of arsenic that crops are capable to accumulate and as a consequence entering into the food chain, several remediation/removal methods of arsenic from water and soil have been proposed.

Removal of arsenic in soil

There are several options to eliminate or reduce arsenic concentration of agricultural soil; the principals can be suggested such as adsorption, precipitation, inverse osmosis and phytoremediation. The phytoremediation of contaminated soils with arsenic has been considered feasible and environmentally friendly technique (Ma et al., 2001; Azizur and Hasegawa 2011; Ye et al., 2011). The effectiveness of phytoremediation is determined by two factors: first, identification of hyperaccumulators of arsenic, and second, by the knowledge of factors that maximize the accumulation of it.

Another study, in southeastern France (Chaney et al., 2007) found that it is possible to clean the agricultural land used for growing rice, from inorganic compounds by combining a high intake and translocation of contaminants to the harvestable biomass. In addition, phytoremediation showed that the root of plants such as amaranth (*Amaranthus blitoides*), bermuda grass (*Cynodon dactylon*), chicory (*Cichorium intybus*) and milk thistle (*Sylibum marianum*) can absorb metals especially plumb and copper (Marmioli et al., 2005; Del Río Celestino et al., 2006; Vazquez et al., 2006; Yoon et al., 2006), so the root exudative may cause precipitation or mobilization of the metal. For example, the mobility of arsenic in soils and sediments of northern Argentina is highly controlled by precipitation processes, dilution and/or sorption of the surface of metal particles (Smedley and Kinniburgh, 2002), and the final arsenic disposition is affected by organic matter (Bauer and Blodau, 2006; Buschmann et al., 2006). By the study of these mechanisms, it becomes technically feasible to devise methods to control the mobility of arsenic in soils and then propose an effective remediation for soils contaminated with arsenic.

Shrivastava et al. (2006) reported that *P. Biaurita*, *L. P. quadriaurita* Retz and *P. ryukyuensis* Tagawa are hyperaccumulators fern of arsenic and all these may be used in phytoremediation of sites contaminated by arsenic. Other arsenic hyperaccumulators as *Pteris viatta* and *Ptyrogramma calomelanos* (Francesconi et al., 2002), also *P. Longifolia* and *P. Umbrosa* (Zhao et al., 2002) were already validated.

A decade ago, biomass resulting from plants accumulating As by phytoremediation process was thought as a drawback for its application, because the biomass was usually either disposed at regulated landfills or incinerated (Chaney et al., 2007). Current research is working to find new recovery methods of As from hyperaccumulator plants. In fact, *Pteris vittata* is a good example of phytoremediation, since it takes up As and rapidly translocates it into the fronds (Danh et al., 2014). Thus, recent research is testing As removal from *P. vittata* by different methods (da Silva et al., 2018). After extracting As, next step is to use it in the industry of wood preservation chemicals, insecticides and poison for pests.

Arsenic contamination in agricultural irrigation water produces an accumulative effect on soils and crop, so many studies have been developed on these topics and the next section explores it.

Water and plant

The arsenic in soil and water is taken by crop plants up and that is how this arsenic is present in food (Punshon et al., 2017). The relationship between arsenic concentration of water and arsenic concentration absorbed by plants is influenced by parameters such

as pH, temperature, soil type and kind of plant, so Carbonell et al. (1995) remarked the need to study the interactions of arsenic through water-plant.

Dahal et al. (2008) monitored the influence of arsenic in irrigation water and alkaline soils on onion, cauliflower, rice and potato, directly in field. They found arsenic concentrations to range from 0.005 to 1.014 mg L⁻¹ for irrigation water, from 6.1 to 16.7 mg kg⁻¹ for soil; and for crops mentioned above it was found that arsenic concentration changed from high to low accumulation in different parts of plants as follows: roots > shoots > leaves > edible.

Arsenic concentration in soil is determined by its mineralogical and chemical properties as well as the amount of arsenic contained in the irrigation water. In particular, an increment of arsenic in grain is more sensible to the arsenic concentration in soil than in water (Mukherjee et al., 2017).

In cases of sprinkler irrigation Soybean as affected by high concentrations of arsenic and fluoride in irrigation water under controlled conditions, arsenic and fluoride are accumulated in soil. Moreover, as the concentration increases over 0.6 mg L⁻¹ of arsenic and 25 mg L⁻¹ of fluoride, it is observed a bioaccumulation and a biomass reduction of plant (Bustingorri and Lavado, 2014).

The arsenic contained in the irrigation water, is bioaccumulated in crops, which form part of the diet in some countries, and in this way reaches humans beings. As a consequence, this bioaccumulation of arsenic has affected negatively the human health (Mayorga et al., 2013).

Hu et al. (2015) found that by minimizing the amount of arsenic in irrigation water diminishes the amount of arsenic in rice. In fact, Newbigging et al. (2015) proposed that this is the best option, since the arsenic intake by rice is difficult to control.

The main source of arsenic in agriculture is contaminated irrigation water, thus irrigation technologies with high efficient use of water may help to solve the problem in the best sustainable way by reestablishing the levels of water in aquifers, since arsenic comes from deep groundwaters. In the meantime, studies about the removal of arsenic from water are being done due to the significant effect that arsenic in water have on crops and soil, which is the subject of next subsection.

Removal of arsenic in water

In Latin America, some people have severe health problems caused by consuming water with high content of arsenic, because of this; different arsenic removal methods have been applied to drinking water (Camacho et al., 2011). Conventional technologies such as oxidation, coagulation/co-precipitation, adsorption, reverse osmosis, ion exchange, are used to remove arsenic from water but they are expensive techniques. For this reason, more economical and decentralized methods have emerged such as natural adsorbents, sunlight or biological treatments as essential methods to reduce contamination of arsenic for low-income areas and remote regions of Latin America (Litte et al., 2010). Several adsorbents have been used to remove arsenic from water. In general, the adsorbents can be grouped into two types, namely, adsorbents with iron content (IC) and adsorbents without iron content (WIC). The adsorbents without Fe content include, Chitosan/Cu(OH)₂ and Chitosan/CuO, which were used for arsenic (V) removal from aqueous solution. A recent research results showed that sorption uptake was highly dependent on pH, temperature, initial arsenic (V) concentration and sorbent dosage (Elwakeel and Guibal, 2015). Seawater neutralized red mud (BauxsolTM technology) was used for arsenic (V) removal. Bauxsol has the potential for removing

arsenic (V) (Genc et al., 2003). The Zirconium loaded activated carbon (Zr-AC) was used for arsenic removal and it allows high flows with a remarkable adsorption capacity (Daus et al., 2004). Manna et al. (2010) investigated removal of arsenic from contaminated groundwater using a new method that works with distillation membranes in direct contact with solar membrane. This system produces almost 100% water free from arsenic. The solar distillation membrane has a high potential to remove arsenic in contaminated groundwater.

The aluminum sulfate was used to remove the arsenic from water by precipitation – co-precipitation (Meltem and Pala, 2010). In this study, a statistical design of experiments Bahnken box was done and also response surface methodology to investigate the effects of the most significant operating variables. Aluminum sulfate was found to be an effective and safe coagulant for drinking water due to the dose required of it. The optimal pH range for maximum removal of arsenate was from 6 to 8. At low concentration of arsenate, removal efficiency obtained was high using elevated doses of aluminum sulphate, whereas under high initial concentrations of arsenate, a high removal efficiency was performed with low doses of the coagulant.

Another solution is the use of adsorbent media. Adsorbents with Fe content includes, Green synthesis of $\alpha\text{Fe}_2\text{O}_3$ nanoparticles, this adsorbent shown that is affected by temperature and pH and its adsorption capacity was 38.48 mg g^{-1} indicating a good potential for the adsorption of arsenic (V) (Mukherjee et al., 2016). Alginate beds impregnated of hydrous iron oxide presented an effective removal, the adsorption efficiency for both arsenic species increased as iron loading is augmented (Sigdel et al., 2016). Moreover, Sánchez et al. (2016) studied the adsorption capacity of arsenic on a mixed oxides produced from thermal treatment of hydrotalcite-like compound's, these authors report more than 98% removal for initial concentrations below $250 \mu\text{g L}^{-1}$. The iron-aluminum hydroxide coated onto macroporous supports was proved for arsenic removal and it was compared with Granular Ferric Hydroxide (GEH), Kumar et al. (2016) show that the iron-aluminum hydroxide coated onto macroporous supports is capable to treat seven times more volume of water than GEH. The adsorption capacity of different adsorbents is related to other ions present in water, such as, phosphate, sulfate, carbonate, fluorides and humic and fulvic acids. Saldaña-Robles et al. (2017) evaluated GEH in presence of humic substances to study the adsorption capacity of arsenic (V) onto GEH. The results showed that humics and fulvic acids enhance the mobilization of arsenic (V), reducing the removal efficiency of adsorbent.

Other synthesized materials with iron such as diatom- FeO_x (Thakkar et al., 2015) and Zr- β - FeOOH (Sun et al., 2012) showed adsorption capacities for arsenite and arsenate. While, the first adsorbed 10 mg g^{-1} of arsenite and 12.5 mg g^{-1} of arsenate, the second adsorbed 60 mg g^{-1} and 120 mg g^{-1} , respectively. On the other hand, δ - FeOOH showed an adsorption capacity for arsenate of 37.3 mg g^{-1} (Faria et al., 2014). The iron coated sand (Thirunavukkarasu et al., 2002), the CFe (Gutiérrez et al., 2013), CarFe (Gutiérrez et al., 2013), NADMCF (Malana et al., 2011), BNNT (Chen et al., 2011), IOCS-2 (Thirunavukkarasu et al., 2002), kaolinite (Ladeira and Ciminelli, 2004), GAC-Fe (0.05 M) (Gu et al., 2005) and nanostructures akaganeite (Deliyanni et al., 2003) have shown potential capacity for arsenic adsorption. In the case of IC adsorbents, the adsorption is compatible with a multilayer adsorption for CFe, CarFe, NADMCF and BNNT in agreement with the Freundlich model for adsorption capacity ranging from 0.99 to 2.59 mg g^{-1} . IOCS-2, Kaolinite, GAC-Fe, GAC-Fe- O_2 and Nanostructures akaganeite show an adsorption mainly monolayer with adsorption capacity ranging 0.008 to 2.96 mg g^{-1} .

The accumulative effect caused by arsenic in agricultural soil and water on crops has been studied by several authors. This is mainly due to the environmental importance and the negative effects in the food chain and so for human health. Some arsenic effects on human health could be related by the type (inorganic or organic) and concentration of trivalent (As^{+3} , MMA^{+3} and DMA^{+3}) or pentavalent arsenic forms (As^{+5} , MMA^{+5} and DMA^{+5}). In this sense, As^{+3} and As^{+5} are considered more toxic than methylated organic (MMA^{+5} and DMA^{+5}) forms (Rasheed et al., 2016). Different organs in the human body can be affected by long term arsenic exposure provoking skin lesions, different types of cancer, diabetes, lung disease, neurotoxicity, among others (Carlin et al., 2014). According to Abdul et al. (2015), the effects of arsenic exposure may be classified into four stages: preclinical, clinical, internal complications and malignancy stages. There are many examples of arsenic human exposure. In Taiwan, residents were chronically exposed to high levels of arsenic due to drinking water and presented Black Foot Disease (Chen et al., 1985; Tseng, 1977). Hindmarsh et al. (1977) reported Peripheral neuropathy after long-term exposure to inorganic arsenic in drinking water. A recent case occurred in West Bengal, a state of India, a large population is still exposed to arsenic contamination which is acquired from drinking water, and which results in consequent escalation in the number of chronic arenicolids (Pal et al., 2015).

Arsenic in crops

The ratio of the concentration of arsenic and crops is a topic of general interest, as the plant is the media by which the arsenic reaches living beings. Furthermore, the effect that arsenic has on crop yield impacts the economy of the agricultural sector.

Several authors have studied the arsenic accumulation in wheat. The results showed that arsenic in wheat grains mainly exist as inorganic form (Shi et al., 2013; Brackhage et al., 2014). On the other hand, the results obtained by Shi et al. (2015) showed that the accumulation of arsenic and translocation were a significant difference among wheat cultivars studied.

Rice consumption is the main source of exposure to organic arsenic for people in Asia. Therefore, recent studies have been conducted on the accumulation and speciation of arsenic in different rice varieties. Lu et al. (2010) studied Indica and a hybrid of Indica and found that arsenic content in different parts of plants increased in the next order: grain <shell <stem <roots. The concentration of arsenic in the grain of both varieties was significantly different and correlated with concentration of phosphorus being higher for Indica than the hybrid of Indica. Also, inorganic arsenic was found to be the dominant specie present in grains of rice for all of analyzed species.

In Poland, studies were conducted comparing the concentration and speciation of arsenic incorporated into plants of white mustard (*Sinapis alba*), which took place in the presence of various arsenic compounds and found that mustard has the capacity to absorb different arsenic forms. The samples of mustard were grown in different solutions containing arsenic (III), arsenic (V), methylarsonic acid (MMA) or dimethylarsonic acid (DMA). The translocation factor reported by authors was high (0.70) when DMA was added to the nutrient solution (Lukasz et al., 2010).

Vamerali et al. (2009) found that the concentration of trace elements (As, Co, Cu, Pb and Zn) is higher in roots of poplar (*Populus*) and willow (*Salix*) than in the aerial shoot. Moreover, this accumulation is more pronounced in thin roots. In different species used for this study, a pronounced aging of thick roots was found.

Ruiz et al. (2008) found a concentration of 1750 mg kg^{-1} of arsenic in plant samples at sites with arsenic contaminated soil that presented a concentration range of arsenic from 1.14 to 98.5 mg kg^{-1} (dry weight), while in other plants that grow in sites with the same geological characteristics presented a concentration range from 0.06 to 0.58 mg kg^{-1} . On the other hand, the arsenite and arsenate were found in all plant samples and in some plant species was found organic arsenic as MMA, DMA and trimethylarsine oxide. The importance of know the arsenic present in water produce diferent effects in human healths

Conclusions

The presence of high concentrations of arsenic in the agricultural system of water-soil-crop has led to a serious problem. Therefore, to dimension and solve this problem, considerable research is being done around the world. In general terms, there are two sources of arsenic in agriculture, namely, arsenic coming from deep wells from sites that due to its geological characteristics contain heavy metals and arsenic coming from agrochemicals and industrial wastes. The contaminated water used in agriculture for irrigation is moving arsenic to soil and crops, which is currently the major source of this element in agriculture.

The arsenic adsorbed by crops from contaminated water depends on several factors such as pH, temperature, oxidation state of arsenic, type of soil and crop. However, it is required to study the interaction among arsenic, organic matter, metals, pH and its relationship with the mobility and adsorption in plant. It is known that bioaccumulation of arsenic in some crops leads to biomass and yield reduction. Usually, in crop plants, it is found that arsenic concentration is the highest at the root, followed by stem, leaf and the lowest concentration is found in grain or fruit. It is lacking in the technical literature a differentiation of the arsenic effects on plant depending on the way it is exposed to arsenic, either by soil or water. In the other hand, the interaction of arsenic and nutrients intake by plant and the intake mechanisms as well as the transport of arsenic in several plant structures is up to day not completely understood.

Additionally, the agricultural soil is accumulating arsenic from contaminated irrigation water. The bioaccumulation and adsorption of arsenic in soil is affected by its properties such as the content of oxalic, citric and malic acids. In the other hand, organic matter plays an important role in the dynamics of arsenic in soil, since the greater arsenic concentrations are found in surface layers (about 0.50 m deep) in cases where the arsenic contamination is due to irrigation. In addition, the adsorption of arsenic is related to the presence of ions and metals that competes by the adsorption sites of arsenic in soil.

Since cutting off the main source of arsenic may be the solution to the problem of arsenic in agriculture, reestablishing the water levels of groundwater and aquifers by good irrigation practices and efficient irrigation technologies can be considered the best sustainable solution. In the meantime, removal technologies of arsenic from water and soil may help. Thus, removal technologies of arsenic in soil such as inverse osmosis, precipitation, adsorption and phytoremediation are proposed. Among of them, phytoremediation is more environmental friendly and is easier to implement than its counterparts. However its effectivity relies in characteristics of the arsenic hyperaccumulator plant. Therefore, finding better hyperaccumulators is still an active area of research. Remediation technologies including oxidation, coagulation/

coprecipitation, adsorption, reverse osmosis and ion exchange are proposed for cleaning drinking water. However, these technologies are either too expensive to be incorporated in agricultural daily practices due to the huge water volumes required in agriculture. To the best acknowledge of the authors, it is still required to propose a remediation technology cheaper than existing ones and able to remove arsenic from water volumes required in the agriculture.

Acknowledgements. A. Saldaña-Robles would like to express her gratitude to the National Council of Science and Technology (CONACyT), for financial support provided.

REFERENCES

- [1] Abdul, K. S. M., Jayasinghe, S. S., Chandana, E. P., Jayasumana, C., De Silva, P. M. C. (2015): Arsenic and human health effects: A review. – *Environmental toxicology and pharmacology* 40(3): 828-846.
- [2] Abedin, M. J., Feldmann, J., Meharg, A. A. (2002): Uptake kinetics of arsenic species in rice plants. – *Plant Physiology* 128: 1120-1128.
- [3] Azcue, J. M., Nriagu, J.O. (1994): *Arsenic: Historical perspectives*. – Wiley & Sons, New York, USA.
- [4] Azizur, R. M., Hasegawa, H. (2011): Aquatic arsenic: Phytoremediation using floating macrophytes. – *Chemosphere* 83: 633-646.
- [5] Backer, D.E., Chesnin, L. (1975): Chemical monitoring of soils for environment quality and animal and human health. – *Advances in Agronomy* 27: 305-74.
- [6] Bauer, M., Blodau, C. (2006): Mobilisation of arsenic by dissolved organic matter from iron oxides, soils and sediments. – *Science Total Environment* 354: 179-90.
- [7] Bowen, H. J. M. (1979): *Elemental Chemistry of the Elements*. – Academic press, London and New York.
- [8] Boyle, D. R., Turner, R. J., Hall, G. E. M. (1998): Anomalous arsenic concentrations in groundwaters of an island community, Bowen Island, British Columbia. – *Environmental Geochemistry and Health* 20: 199-212.
- [9] Brackhage, C., Huang, J.H., Schaller, J., Elzinga, E. J., Dudel, E. G. (2014): Readily available phosphorous and nitrogen counteract for arsenic uptake and distribution in wheat (*Triticum aestivum* L.). – *Scientific Report* 1: 1-7.
- [10] Buschmann, J., Kappeler, A., Lindauer, U., Kistler, D., Berg, M., Sigg, L. (2006): Arsenite and arsenate binding to dissolved humic acids: influence of pH, type of humic acid and aluminium. – *Environmental Science Technology* 40: 6015-20.
- [11] Bustingorri, C., Lavado, R. S. (2014): Soybean as affected by high concentrations of arsenic and fluoride in irrigation water in controlled conditions. – *Agricultural water management* 144: 134-139.
- [12] Camacho, L. M., Gutiérrez, M., Alarcón, M. T., Villalba, M. L., Deng, S. (2011): Occurrence and treatment of arsenic in groundwater and soil in northern Mexico and southwestern USA. – *Chemosphere* 83: 211 - 225.
- [13] Carbonell, B. A. A., Burló, C. F. M., Mataix, B. J. J. (1995): *Arsénico en el Sistema Agua Planta*. – España, Universidad de Alicante.
- [14] Cardwell, A. J., Hawker, D. W., Greenway, M. (2002): Metal Accumulation in Aquatic Macrophytes from Southeast Queensland. – *Chemosphere* 48: 653-63.
- [15] Carey, A. M., Norton, G. J., Deacon, C., Scheckel, K. G., Lombi, E., Punshon, T., Gueriot, M. L., Lanzirotti, A., Newville, M., Choi, Y., Price, A. H., Meharg, A. A. (2011): Phloem transport of arsenic species from flag leaf to grain during grain filling. – *New Phytologist* 192: 87–98.

- [16] Carlin, D. J., Naujokas, M. F., Bradham, K. D., Cowden, J., Heacock, M., Henry, H. F., Waalkes, M. P. (2016): Arsenic and environmental health: state of the science and future research opportunities. – *Environmental health perspectives* 124(7): 890-899 .
- [17] Chaney, R. L., Angle, J. S., Broadhurst, C. L., Peters, C. A., Tappero, R. V., Sparks, D. L. (2007): Improved Understanding of Hyperaccumulation Yields Commercial Phytoextraction and Phytomining Technologies. – *Journal of Environmental Quality* 36: 1429-1443.
- [18] Chen, C. J., Chuang, Y. C., Lin, T. M., & Wu, H. Y. (1985): Malignant neoplasms among residents of a blackfoot disease-endemic area in Taiwan: high-arsenic artesian well water and cancers. – *Cancer research* 45: 5895-5899.
- [19] Chen, R., Zhi, C., Yang, H., Bando, Y., Zhang, Z., Sugiur, N., Golberg, D. (2011): Arsenic (V) adsorption on Fe₃O₄ nanoparticle-coated boron nitride nanotubes. – *Journal of Colloid Interface Science* 359: 261-268.
- [20] Chen, S. L., Dzung, S. R., Yang, M. H., Chlu, K. H., Shieh, G. M., Wai, C. M. (1994): Arsenic species in groundwaters of the Blackfoot Disease Area, Taiwan. – *Environmental Science and Technology* 28: 877-881.
- [21] Da Silva, E. B., de Oliveira, L. M., Wilkie, A. C., Liu, Y., Ma, L. Q. (2018): Arsenic removal from As-hyperaccumulator *Pteris vittata* biomass: Coupling extraction with precipitation. – *Chemosphere* 193: 288-294.
- [22] Dahal, B. M., Fuerhacker, M., Mentler, A., Karki, K. B., Shrestha, R. R., Blum, W. E. H. (2008): Arsenic contamination of soils and agricultural plants through irrigation water in Nepal. – *Environmental Pollution* 155: 157-63.
- [23] Danh, L.T., Truong, P., Mammucari, R., Foster, N. (2014): A critical review of the arsenic uptake mechanisms and phytoremediation potential of *Pteris vittata*. – *Int. J. Phytoremediation* 16: 429-453.
- [24] Das, D., Chatterjee, A., Mandal, B. K., Samanta, G., Chakraborti, D., Chanda, B. (1995): Arsenic in ground-water in 6 districts of West Bengal, India - the biggest arsenic calamity in the world. – *Analyst* 120: 917-24.
- [25] Daus, B., Rainer, W., Holger, W. (2004): Sorption materials for arsenic removal from water: a comparative study. – *Water Research* 38: 2948-2954.
- [26] Del Rio, C. M., R., Front, R., Moreno, R., A. De Haro, B. (2006): Uptake of Lead and Zinc by Wild Plants Growing on Contaminated Soils. – *Industrial Crops and Products* 24: 230-237.
- [27] Deliyanni, E. A., Bakoyannakis, D. N., Zouboulis, A. I., Matis, K. A. (2003): Sorption of As (V) ions by alaganeite-type nanocrystals. – *Chemosphere* 50: 155–163.
- [28] DiTusa, S.F., Fontenot, E. B., Wallace, R. W., Silvers, M. A., Steele, N. T., Elnagar, A. H., Dearman, K. M., Smith, A. P. (2016): A member of the phosphate transporter 1 (Pht1) family from the arsenic-hyperaccumulating fern *Pteris vittata* is a high- affinity arsenate transporter. – *New Phytologist* 209: 762–772.
- [29] Dixit, G., Singh, A. P., Kumar, A., Mishra, S., Dwivedi S., Kumar, S., Trivedi, P. K., Pandey, V., Tripathi, R. D. (2016): Reduced arsenic accumulation in rice (*Oryza sativa* L.) shoot involves sulfur mediated improved thiol metabolism, antioxidant system and altered arsenic transporters. – *Plant Physiology and Biochemistry* 99: 86-96.
- [30] Dousova, B., Buzek, F., Lhotka, M., Krejcova, S., Boubinova, R. (2016): Leaching effect on arsenic mobility in agricultural soils. – *Journal of Hazardous Materials* 307: 231-239.
- [31] Drever, J. I. (1997): *The Geochemistry of Natural Waters: Surface and Groundwater Environments*. – Prentice Hall, New York, USA.
- [32] Duan, G. L., Hu, Y., Schneider, S., McDermott, J., Chen, J., Sauer, N., Rosen, B. P., Daus, B., Liu, Z., Zhu, Y. G. (2016): Inositol transporters AtINT2 and AtINT4 regulate arsenic accumulation in *Arabidopsis* seeds. – *Nature Plants* 2 1:1-6.
- [33] Elwakeel, K. Z., Guibal, E. (2015): Arsenic (V) sorption using chitosan/Cu(OH)₂ and chitosan/CuO composite sorbents. – *Carbohydrate Polymers* 134: 190-204.

- [34] Fakour, H., Lin, T. F. (2014): Experimental determination and modeling of arsenic complexation with humic and fulvic acids. – *Journal of Hazardous Materials* 279: 569-578.
- [35] Faria, M., Rosemberg, R. S., Bomfeti, C. A., Monteiro, D. S., Barbosa, F., Oliveira, L. C. A., Rodriguez, M., Pereira, M. C., Rodrigues, J. L. (2014): Arsenic removal from contaminated water by ultrafine δ -FeOOH adsorbents. – *Chemical Engineering Journal* 237: 47-54.
- [36] Farooq, M. A., Islam, F., Ali, B., Najeeb, U., Mao, B., Gill, R. A., Zhou, W. (2016): Arsenic toxicity in plants: Cellular and molecular mechanisms of its transport and metabolism. – *Environmental and Experimental Botany* 132: 42-52.
- [37] Francesconi, K., Visoottiviseth, P., Sridockhan, W., Goessler, W. (2002): Arsenic Species in an Hyperaccumulating Fern, *Pityrogramma calomelanos*: A potential phytoremediator. – *Science Total Environmental* 284: 27-35.
- [38] Genc, H., Tjell, J. C., Mcconchie, D., Schuiling, O. (2003): Adsorption of arsenate from water using neutralized red mud. – *Journal of Colloid Interface Science* 264: 327–334.
- [39] Grafe, M., Eick, M. J., Grossl, P. R., Saunders, A. M. (2002): Adsorption of Arsenate and Arsenite of Ferrihydrite in the Presence and Absence of Dissolved Organic Carbon. – *Journal of Environmental Quality* 31: 1115-1123.
- [40] Gu, Z., Fang, J., Deng, B. (2005): Preparation and evaluation of GAC-based iron-containing adsorbents for arsenic removal. – *Environmental Science Technology* 39: 3833–3843.
- [41] Gutierrez, O. E., García, G., Ordoñez, E., Olguin, M. T., Cabral, P. A. (2013): Synthesis, characterization and adsorptive properties of carbon with iron nanoparticles and iron carbide for the removal of As (V) from water. – *Journal of Environmental Management* 114: 1- 7.
- [42] Haw, T. L., Wang, M. C., Gwo, C. L. (2004): Complexation of arsenate with humic substance in water extract of compost. – *Chemosphere* 56: 1105–1112.
- [43] He, Z., Yan, H., Chen, Y., Shen, H., Xu, W., Zhang, H., Shi, L., Zhu, Y.G., Ma, M. (2016): An aquaporin PvTIP4;1 from *Pteris vittata* may mediate arsenite uptake. – *New Phytologist* 209: 746–761.
- [44] Henke, K. R. (2009): Arsenic: environmental chemistry, health threats, and waste treatment. – Wiley, U.K.
- [45] Hindmarsh, J. T., McLetchle, O. R., Heffernan, L. P., Hayne, O. A., Ellenberger, H. A., McCurdy, R. F., Thiebaut, H. J. (1977): Electromyographic abnormalities in chronic environmental arsenicalism. – *Journal of Analytical Toxicology* 1(6): 270-276.
- [46] Hopenhayn, C., Biggs, M. L., Fuchs, A., Bergoglio, R., Tello, E. E., Nicolli, H., Smith, A. (1996): Bladder cancer mortality associated with arsenic in drinking water in Argentina. – *Epidemiology* 7: 117–124.
- [47] Hu, P., Ouyang, Y., Wu, Y., Shen, L., Luo, Y., Christie, P. (2015): Effects of water management on arsenic and cadmium speciation and accumulation in an upland rice cultivar. – *Journal of Environmental Sciences* 27: 225–231.
- [48] Inskip, W. P., Mcdermott, T. R., Fendorf, S. (2002): Arsenic (V)/(III) cycling in soil and natural waters: chemical and microbiological processes. – *Environmental Chemistry of Arsenic* 183.
- [49] Kamiya, T., Islam, M. R., Duan, G. L., Uruguchi, S., Fujiwara, T. (2013): Phosphate deficiency signaling pathway is a target of arsenate and phosphate transporter OsPT1 is involved in As accumulation in shoots of rice. – *Soil Science and Plant Nutrition* 59: 580–590.
- [50] Katsuhara, M., Sasano, S., Horie, T., Matsumoto, T., Rhee, J., Shibusaka, M. (2014): Functional and molecular characteristics of rice and barley NIP aquaporins transporting water: hydrogen peroxide and arsenite. – *Plant Biotechnology Journal* 31: 213–219.
- [51] Klein, C. (2002): The 22nd Edition of the Manual of Mineral Science (after James D. Dana). – John Wiley & Sons, Inc., New York, p. 641.

- [52] Ko, I., Kim, J. Y., Kim, K. W. (2004): Arsenic speciation and sorption kinetics in the As-hematite-humic acid system. – *Colloids and Surfaces A-Physicochemical and Engineering Aspects* 234: 43-50.
- [53] Kramar, U., Norra, S., Berner, Z., Kiczka, M., Chandrasekharam, D. (2015): On the distribution and speciation of arsenic in the soil-plant-system of a rice field in West-Bengal, India: A μ -synchrotron techniques based case study. – *Applied Geochemistry* 77: 4-14.
- [54] Kumar, P. S., Quiroga, F. P., Sjöstedt, C., Önnby, L. (2016): Arsenic adsorption by iron–aluminium hydroxide coated onto macroporous supports: Insights from X-ray absorption spectroscopy and comparison with granular ferric hydroxides. – *Journal of Hazardous Materials* 302: 166-174.
- [55] Ladeira, A. C. Q., Ciminelli, V. S. T. (2004): Adsorption and desorption of arsenic on an oxisol and its constituents. – *Water Research* 38: 2087–2094.
- [56] Langmuir, D. (1997): *Aqueous Environmental Geochemistry*. – Prentice Hall, Upper Saddle River, NJ, p. 600.
- [57] Lee, C. H., Wu, C. H., Syu, C. H., Jiang, P. Y., Huang, C. C., & Lee, D. Y. (2016): Effects of phosphorous application on arsenic toxicity to and uptake by rice seedlings in As-contaminated paddy soils. – *Geoderma* 270: 60-67.
- [58] Lee, C. H., Wu, C. H., Syu, C. H., Jiang, P. Y., Huang, C. C., Lee, D. Y. (2016): Effects of phosphorous application on arsenic toxicity to and uptake by rice seedlings in As-contaminated paddy soils. – *Geoderma* 270: 60-67.
- [59] Li, R. Y., Ago, Y., Liu, W. J., Mitani, N., Feldmann, J., McGrath, S. P., Zhao, F. J. (2009): The rice aquaporin Lsi1 mediates uptake of methylated arsenic species. – *Plant Physiology* 150: 2071–2080.
- [60] Lide, D. R. (ed.) (2007): *CRC Handbook of Chemistry and Physics*, 88th edn. – CRC Press, Boca Raton, FL.
- [61] Lin, Z., Puls, R. W. (2003): Potential indicators for the assessment of arsenic natural attenuation in the subsurface. – *Advances in environmental research* 7: 825-834.
- [62] Litte, M. I., Morgada, M. E., Bundschuh, J. (2010): Possible treatments for arsenic removal in Latin American waters for human consumption. – *Environmental Pollution* 158: 1105-1118.
- [63] Lu, Y., Dong, F., Deacon, C., Chen, H., Raab, A., Meharg, A. A. (2010): Arsenic accumulation and phosphorus status in two rice (*Oryza sativa* L.) cultivars surveyed from fields in South China. – *Environmental Pollution* 158: 1536-41.
- [64] Lukasz, J., Kowalska, J., Koszykowska, M., Golimowski, J. (2010): Studies on the uptake of different arsenic forms and the influence of sample pretreatment on arsenic speciation in White mustard (*Sinapis alba*). – *Environmental Pollution* 94: 125-129.
- [65] Ma, J., Mi, Y., Li, Q., Chen, L., Du, L., He, L., Lei, M. (2016): Reduction, methylation, and translocation of arsenic in *Panax notoginseng* grown under field conditions in arsenic-contaminated soils. – *Science of the Total Environment* 550: 893-899.
- [66] Ma, L. Q., Komart, K. M., Tu, C., Zhang, W., Cai, Y., Kennelly, E. D. (2001): A Fern that Hyperaccumulates Arsenic. – *Nature* 409: 579.
- [67] Malana, M. A., Qureshi, R. B., Ashiq, M. N. (2011): Adsorption studies of arsenic on nano aluminium doped manganese copper ferrite polymer (MA, VA, AA) composite: Kinetics and mechanism. – *Chemical Engineering Journal* 172: 721 – 727.
- [68] Manna, A. K., Sen, M., Martin, A. R., Pal, P. (2010): Removal of arsenic from contaminated ground water by solar-driven membrane distillation. – *Environmental Pollution* 158: 805-811.
- [69] Marmiroli, M., Antonioli, G., Maestri, E., Marmiroli, N. (2005): Evidence of the Involvement of Plant ligno-cellulosic Structure in the Sequestration of Pb, an X-Ray an X-ray spectroscopy- based Analysis. – *Journal of Environmental Pollution* 134: 217-227.

- [70] Marques, A. P., Moreira, H., Rangel, A. O., Castro, P. M. L. (2009): Arsenic, Lead and Nickel accumulation in *Rubus ulmifolius* growing in contaminated soil in Portugal. – *Journal of Hazardous Materials* 165: 174-179.
- [71] Marques, A. P., Rangel, A. O. S. S., Castro, P. M. L. (2007): Zn Accumulation in Plant Species indigenous to a Portuguese Polluted cite: relation with Soil Contamination. – *Journal of Environmental Quality* 36: 646-53.
- [72] Mayorga, P., Moyano, A., Anawar, H. M., Garcia, S. A. (2013): Uptake and accumulation of arsenic in different organs of carrot irrigated with As-rich water. – *CLEAN–Soil, Air, Water* 41(6): 587–592.
- [73] Meltem, B. B., Pala, A. (2010): A statistical experiment design approach for arsenic removal by coagulation process using aluminum sulfate. – *Desalination* 254: 42-48.
- [74] Mihaljević, M., Sisr, L., Ettler, V. (2004): Oxidation of As-bearing gold ore- a comparison of batch and column experiments. – *Journal of Geochemical Exploration* 81: 59-70.
- [75] Mishra, T., Mahato, D. K. (2016): A comparative study on enhanced arsenic (V) and arsenic(III) removal by iron oxide and manganese oxide pillared clays from ground water. – *Journal of Environmental Chemical Engineering* 4: 1224-1230.
- [76] Mukherjee, A., Kundu, M., Basu, B., Sinha, B., Chatterjee, Das Bairagya, M., Singh, U. K., Sarkar, S. (2017): Arsenic load in rice ecosystem and its mitigation through deficit irrigation. – *Journal of Environmental Management* 197: 89-95.
- [77] Mukherjee, D., Ghosh, S., Majumdar, S., Annapurna, K. (2016): Green synthesis of α -Fe₂O₃ nanoparticles for arsenic (V) remediation with a novel aspect for sludge management. – *Journal of Environmental Chemical Engineering* 4: 639-650.
- [78] Nasier, E. B., Hansi, K., Cord, T. (1977): Effect of waste water, sewage sludge and refuse compost on accumulation and movement of arsenic and selenium in cultivated soil. – *Landbauforsch Volkenrode* 27: 105-110.
- [79] Newbigging, A. M., Paliwoda, R. E., Le, X. C. (2015): Rice: reducing arsenic content by controlling water irrigation. – *Journal of Environmental Sciences* 30: 129-131.
- [80] Nickson, R. T., McArthur, J., Ravenscroft, P., Burgess, W. G., Ahmed, K. M. (2000): Mechanisms of arsenic release to groundwater, Bangladesh and West Bengal. – *Applied Geochemistry* 15: 403-413.
- [81] Núñez, C., Arancibia, V., Gómez, M. (2016): Determination of arsenic in the presence of copper by adsorptive stripping voltammetry using pyrrolidine dithiocarbamate or diethyl dithiophosphate as chelating-adsorbent agents. Effect of CPB on the sensitivity of the method. – *Microchemical Journal* 126: 70-75.
- [82] Ongley, L. K., Sherman, L., Armienta, A., Concilio, A., Salinas, C. F. (2007): Arsenic in the soils of Zimapán, Mexico. – *Environmental pollution* 145(3): 793-799.
- [83] Onireti, O., Lin, C. (2016): Mobilization of soil-borne arsenic by three common organic acids: Dosage and time effects. – *Chemosphere* 147: 352-360.
- [84] Pal, A., Sen, S., Basuthakur, S., Tripathi, S. K. (2015): Chronic arsenicosis with varied pulmonary involvement–A case series. – *Egyptian Journal of Chest Diseases and Tuberculosis* 64(1): 287-289.
- [85] Pandey, V. C., Singh, N. (2015): Aromatic plants versus arsenic hazards in soils. – *Journal of Geochemical Exploration* 157: 77-80.
- [86] Punshon, T., Jackson, B. P., Meharg, A. A., Warczack, T., Scheckel, K., Guerinot, M. L. (2017): Understanding arsenic dynamics in agronomic systems to predict and prevent uptake by crop plants. – *Science of The Total Environment* 581: 209-220.
- [87] Rahman, M. A., Hasegawa, H., Rahman, M. M., Rahman, M. A., Miah, M. A. M. (2007): Accumulation of arsenic in tissues of rice plant (*Oryza sativa* L.) and its distribution in fractions of rice grain. – *Chemosphere* 69(6): 942-948.
- [88] Rahman, M. A., Kadohashi, K., Maki, T., Hasegawa, H. (2011): Transport of DMAA and MMAA into rice (*Oryza sativa* L.) roots. – *Environmental and Experimental Botany* 72: 41-46.

- [89] Rasheed, H., Slack, R., Kay, P. (2016): Human health risk assessment for arsenic: A critical review. – *Critical Reviews in Environmental Science and Technology* 46: 1529-1583.
- [90] Rasheed, H., Slack, R., Kay, P. (2016): Human health risk assessment for arsenic: a critical review. – *Critical Reviews in Environmental Science and Technology* 46: 1529-1583.
- [91] Redman, A. D., Macalady, D. L., Ahmann, D. (2002): Natural organic matter affects arsenic speciation and sorption onto hematite. – *Environmental Science and Technology* 36: 2889-2896.
- [92] Remy, E., Cabrito, T. R., Batista, R. A., Teixeira, M. C., SáCorreia, I., Duque, P. (2012): The Pht1; 9 and Pht1; 8 transporters mediate inorganic phosphate acquisition by the *Arabidopsis thaliana* root during phosphorus starvation. – *New Phytologist* 195: 356–371.
- [93] Rosas, C. J., Portugal, L., Ferrer, L., Hinojosa R. L., Guzmán M. J. L., Hernández, R. A., Cerdà, V. (2016): An evaluation of the bioaccessibility of arsenic in corn and rice samples based on cloud point extraction and hydride generation coupled to atomic fluorescence spectrometry. – *Food Chemistry* 204: 475-482.
- [94] Rothwell, J. J., Taylor, K. G., Ander, E. L., Evans, M. G., Daniels, S. M., Allott, T. E. H. (2009): Arsenic retention and release in ombrotrophic peatlands. – *Science of the Total Environment* 407: 1405-1417.
- [95] Ruiz, C. M. J., López, S. J. F., Schmeisser, E., Goessler, W., Francesconi, K. A., Rubio, R. (2008): Arsenic speciation in plants growing in arsenic-contaminated sites. – *Chemosphere* 71: 1522-1530.
- [96] Saldaña-Robles, A., Saldaña-Robles, N., Saldaña-Robles, A. L., Damian-Ascencio, C., Rangel-Hernández, V. H., & Guerra-Sanchez, R. (2017): Arsenic removal from aqueous solutions and the impact of humic and fulvic acids. – *Journal of Cleaner Production* 159: 425-431.
- [97] Sánchez, C. M., Galicia, A. J. A., Santamaría, J. D., Hernández, M. L. E. (2016): Evaluation of the mixed oxides produced from hydrotalcite-like compound's thermal treatment in arsenic uptake. – *Applied Clay Science* 121–122: 146-153.
- [98] Scazzola, R., Mattducci, G., Guerzoni, S. (2004): Evaluation of trace metal fluxes to soils in hinterland of Porto. – *Pollution* 153: 195-203.
- [99] Schreiber, M. E., Simo, J. A., Freiberg, P. G. (2000): Stratigraphic and geochemical controls on naturally occurring in groundwater, eastern Wisconsin, USA. – *Hydrology Journal* 8: 161-176.
- [100] Shi, G. L., Lou, L. Q., Zhang, S., Xia, X. W., Cai, Q. S. (2013): Arsenic copper and zinc contamination in soil and wheat during coal mining, with assessment of health risks for the inhabitants of Huaibei, China. – *Environmental Science Pollution Research* 20: 8435–8445.
- [101] Shi, G. L., Zhu, S., Meng, J. R., Qian, M., Yang, N., Lou, L. Q., Cai, Q. S. (2015): Variation in arsenic accumulation and translocation among wheat cultivars: The relationship between arsenic accumulation, efflux by wheat roots and arsenate tolerance of wheat seedlings. – *Journal of Hazardous Materials* 289: 190-196.
- [102] Shin, H., Shin, H. S., Dewbre, G. R., Harrison, M. J. (2004): Phosphate transport in *Arabidopsis*: Pht1;1 and Pht1;4 play a major role in phosphate acquisition from both low- and high-phosphate environments. – *Plant Journal* 39: 629–642.
- [103] Sigdel, A., Park, J., Kwak, H., Park, P. K. (2016): Arsenic removal from aqueous solutions by adsorption onto hydrous iron oxide-impregnated alginate beads. – *Journal of Industrial and Engineering Chemistry* 35: 277-286.
- [104] Sjöblom, A., Hakansson, K., Allard, B. (2004): River water metal speciation in a mining region - the influence of wetlands, liming, tributaries and groundwater. – *Water Air and Soil Pollution* 152: 173-194.
- [105] Smedley, P. L., Kinniburgh, D. G. (2002): A review of the source, behaviour and distribution of arsenic in natural waters. – *Applied Geochemistry* 17: 517-568.

- [106] Smedley, P. L., Kinniburgh, D. G., Macdonald, D. M. J. (2005): Arsenic associations in sediments from the loess aquifer of La Pampa, Argentina. – *Applied Geochemistry* 20: 989-1016.
- [107] Smedley, P. L., Nicolli, H. B., Macdonald, D. M. J., Barros, A. J., Tullio, J. O. (2002): Hydrogeochemistry of arsenic and other inorganic constituents in ground water from La Pampa, Argentina. – *Applied Geochemistry* 17: 259-284.
- [108] Song, W. Y., Park, J., Mendoza C. D. G., Suter G. M., Shim, D., Hörtensteiner, S., Geisler, M., Weder, B., Rea, P. A., Rentsch, D. (2010): Arsenic tolerance in *Arabidopsis* is mediated by two ABCC-type phytochelatin transporters. – *Proceedings of the National Academy Sciences of the United States of America* 107: 21187–21192.
- [109] Srivastava, M., Ma, L. Q., Santos, J. A. (2006): Three new arsenic hyperaccumulating ferns. – *Science Total Environmental* 364: 24-31.
- [110] Stoltz, E., Greger, M. (2002): Accumulation properties of As, Cd, Cu, Pb and Zn by four wetland plant species growing on submerged mine tailings. – *Environmental and Experimental Botany* 47: 271–280.
- [111] Sun, X., Hu, C., Qu, J. (2012): Preparation and evaluation of Zr- β -FeOOH for efficient arsenic removal. – *Journal of Environmental Sciences* 25: 815-822.
- [112] Tanaka, T. (1988): Distribution of Arsenic in the natural environment with emphasis on rock and soil. – *Applied Organometallic Chemistry* 2: 283-295.
- [113] Thakkar, M., Randhawa, V., Mitra, S., Wei, L. (2015): Synthesis of diatom-FeOx composite for removing trace arsenic to meet drinking water standards. – *Journal of Colloid and Interface Science* 457: 169-173.
- [114] Thirunavukkarasu, O. S., Viraraghavan, T., Subramanian, K. S., Tanjore, S. (2002): Organic arsenic removal from drinking water. – *Urban Water* 4: 415–421.
- [115] Togashi, S., Imai, N., Okuyama, Kusunose, S. (2000): Young upper crustal chemical composition of the orogenic Japan. – *Geochemistry, Geophysics, Geosystems* 1: 1-34.
- [116] Tseng, W. P. (1977): Effects and dose-response relationships of skin cancer and blackfoot disease with arsenic. – *Environmental health perspectives* 19: 109-119.
- [117] Vamerali, T., Bandiera, M., Coletto, L., Zanetti, F., Dickinson, N. M., Mosca, G. (2009): Phytoremediation Trials on metal- and arsenic- contaminated Pyrite Wastes (Torviscosa, Italy). – *Environmental Pollution* 157: 887-94.
- [118] Vazquez, S., Agha, R., Granado, A., Sarro, M. J., Esteban, E., Penalosa, J. M., Carena, R. O. (2006): Use of White lupin Plant for Phytostabilization of Cd and As polluted Acid Soil. – *Water, Air and Soil Pollution* 177: 349-65.
- [119] Vinogradov, A. P. (1959): *The Geochemistry of Rare and Dispersed Chemical Elements in Soils*. – Consultants Bureau, Enterprises, New York.
- [120] Wang, S., Mulligan, C. N. (2006): Effect of natural organic matter on arsenic release from soils and sediments into groundwater. – *Environmental Geochemistry and Health* 28: 197-214.
- [121] Warwick, P., Inam, E., Evans, N. (2005): Arsenic's interaction with humic acid. – *Environmental Chemistry* 2: 119-124.
- [122] WHO. *Environmental Health Criteria* – 224. (2003): Arsenic and arsenic compounds. – World Health Organization, Geneva.
- [123] Wilkin, R. T., Ford, R. G. (2006): Arsenic solid-phase partitioning in reducing sediments of a contaminated wetland. – *Chemical Geology* 228: 156-174.
- [124] Williams, M. (2001): Arsenic in mine waters: international study. – *Environmental Geology* 40: 267-278.
- [125] Yazdani, M. R., Tuutijärvi, T., Bhatnagar, A., Vahala, R. (2016): Adsorptive removal of arsenic(V) from aqueous phase by feldspars: Kinetics, mechanism, and thermodynamic aspects of adsorption. – *Journal of Molecular Liquids* 214: 149-156.
- [126] Ye, W. L., Wood, B. A., Stroud, J. L., Andralojc, P. J., Raab, A., McGrath, S. P., Feldmann, J., Zhao, F. J. (2010): Arsenic speciation in phloem and xylem exudates of castor bean. – *Plant Physiology* 154: 1505–1513.

- [127] Ye, W., Khan, M. A., Mcgrath, S. P., Zhao, F. J. (2011): Phytoremediation of arsenic contaminated paddy soils with *Pteris vittata* markedly reduces arsenic uptake by rice. – *Environmental Pollution* 159: 3739-3743.
- [128] Ye, Y., Yuan, J., Chang, X., Yang, M., Zhang, L., Lu, K., Lian, X. (2015): The Phosphate Transporter Gene *OsPht1;4* Is Involved in Phosphate Homeostasis in Rice. – *PLoS ONE* 10(5): 1-15.
- [129] Yoon, J. K., Cao, X. D., Zhou, Q. X., Ma, L. Q. (2006): Accumulation of Pb, Cu and Zn in Native Plants Growing on a Contaminated Florida Cite. – *Science of the Total Environment* 268: 456-464.
- [130] Zhao, F. J., Dunham, S. J., Mcgrath, S. P. (2002): Arsenic hyperaccumulation by Diferent Fern species. – *New Phytologist* 156: 27-31.
- [131] Zou, B. J. (1986): Adsorption and relase of arsenic in soil. – *Huanjing Huaxue* 14: 8-13.

DIETARY MANIPULATION TO INCREASE THE CONCENTRATION OF N-3 FATTY ACIDS IN MILK FAT

SULI, A.^{1*} – GARIPOGLU, A. V.² – CSAPO, J.³ – BERI, B.³ – VARGANE, V. E.⁴ – MIKONE, J. E.¹

¹*Institute of Animal Sciences and Wildlife Management, Faculty of Agriculture, University of Szeged, 15 Andrassy Rd., Hodmezovasarhely 6800, Hungary*

²*Department of Animal Science, Faculty of Agriculture, Ondokuz Mayıs University, Atakum, Kurupelit Kampüsü, Samsun 55100, Turkey*

³*Faculty of Agriculture and Food Sciences and Environmental Management, University of Debrecen, 138 Boszormenyi Rd., Debrecen 4032, Hungary*

⁴*Faculty of Agriculture and Environmental Sciences, Institute of Physiology, Biochemistry and Animal Health, University of Kaposvar, 40 Guba S. Rd., Kaposvar 7400, Hungary*

**Corresponding author*

e-mail: suli@mgk.u-szeged.hu; phone: +36-70-604-3922

(Received 27th Sep 2017; accepted 11th Jan 2018)

Abstract. Linseed is an excellent source of PUFA, especially linolenic acid (18:3n-3), but it is not commonly used in dairy diet in Hungary. Aim of this study was to investigate the effect of the supplemented whole linseed on fatty acid profile of milk fat, with particular reference to health promoting components (α -linolenic acid). A total of thirty multiparous Holstein cows were used in two dairy farms to determine the effect of feeding whole linseed rich in linolenic (C18:3) fatty acids on fatty acid composition of milk fat. The experiment was conducted on two large-scale dairy farms located in Hajdú-Bihar County (referred to as farm “A” and “B”). Fifteen multiparous Holstein-Friesian (165 average days in milk) on farm A and fifteen multiparous Holstein-Friesian (200 average days in milk) on farm B were randomly allocated to treatment groups to investigate the effect of whole linseed supplementation on the composition of fatty acids of milk fat. The group on farm A and B fed TMR based maize silage without whole linseed during the control-period. In the experimental-period the cows received the same TMR on both farms, but it was supplemented with 2.60% DM of whole linseed on farm A, and 2.16% DM of whole linseed on farm B. The experimental period was four weeks in both farms. The supplementation of whole linseed had no effect ($P > 0.05$) on the short chain saturated fatty acid (SFA), and most of the medium chain saturated fatty acid. During the trial the oleic acid (18:1c) content in milk fat significantly increased (21.33% at the start, 24.71% after 2 weeks and 22.51% after 4 weeks on farm B, respectively). The proportion of α -linolenic acid (18:3n-3) increased ($P > 0.05$) during the experimental period compared to the control period (0.23% at the start, 0.58% after 2 weeks and 0.59% after 4 weeks on farm B). The concentration of long-chain polyunsaturated fatty acids (eicosapentaenoic acid and docosapentaenoic acid) significantly increased in milk fat after 4 weeks on both farms. The n-6/n-3 ratio narrowed from 13.52:1 to 3.83:1 and 3.69:1 on farm B, respectively, but this result was not significant. This study concluded that dietary supplementation of whole linseed decreased the proportion of some SFA and increased the proportion of some MUFA and PUFA.

Keywords: *dairy cattle, whole linseed, milk fatty acid composition, α -linolenic acid*

Introduction

Nowadays, the food is not just a nutrition source in the human diet; rather a value-added product having additional features. The relationship between dietary fat intake and the incidence of lifestyle diseases, particularly coronary heart disease, is well established and has contributed to the development of specific government health

recommendations for food components, especially fats (Simopoulos, 2001). As consumer expectations regarding milk and dairy products have changed in Hungary, they suffer from a negative health image (related to the nature of their lipid fraction). The predominant fatty acids in milk are short-, and medium-chain saturated fatty acids (mainly 12:0, 14:0 and 16:0). In Hungary, just like in most European countries, preserved (fermented) forages and a variety of roughages provide the basis of ruminant feed. The fatty acid (FA) composition of cow's milk has become less favourable to human health due to changed feeding and management practices, notably higher proportions of concentrates and silages in diets with less grazing (Elgersma et al., 2006). Although there are differences in the fatty acid composition of milk fat from cows consuming warm season pasture species compared with milk from cows consuming a total mixed ration (White et al., 2001), there are several other factors influencing the behaviour of the animal on rangeland, for example weather (Halasz et al., 2016), and through this the choice of pasture species.

The new economic conditions of dairy production, especially in the EU, have resulted in pressure to limit milk fat content and optimize its fatty acid composition (Demeyer and Doreau, 1999).

The positive influence of n-3 polyunsaturated fatty acids (PUFA) on cardiovascular illnesses suggests that it would be of benefit to increase such fatty acids in milk (Kinsella, 1991). Essential fatty acids, both n-6 (linoleic acid) and n-3 (α -linolenic acid) have been part of our diet since the very beginning of human life. A balanced intake of both n-6 and n-3 fatty acids is essential for health. This ratio should decrease from the current 20-30/1 to less than 4/1 to reduce the potential risk coronary heart disease (Simopoulos, 1999). Extensive research has been conducted in order to modify the fatty acid composition of milk fat to reach the expectations towards functional foods. Optimal supplementing of dairy cows' ration increases the proportion of polyunsaturated fatty acids (PUFA) and decreases the proportion of saturated fatty acids (SFA) in milk fat. Feeding oilseeds to lactating dairy cows is just one of the several methods to change the proportion of fatty acid composition of milk fat (Petit, 2003).

Linseed is an excellent source of PUFA, especially α -linolenic acid (18:3n-3), but it is not commonly used in dairy diet in Hungary. Moreover, feeding whole oilseeds would be a less expensive option compared with treating oilseeds with casein and formaldehyde as the latter requires more specialized equipment (Petit, 2003). Feeding of protected flaxseed oil or whole linseed to dairy cows could increase the n-3 fatty acid content in milk fat (Moallem, 2009).

Animal products with increased contents of n-3 fatty acid might help to solve of low n-3 fatty acid consumption of the Hungarian population (Perédi, 2002). A number of studies consider the use of oilseeds and/or their by-products and other high PUFA-containing lipids as perspective method in animal nutrition (Murphy et al., 1995a, b; Petit, 2002; Livingstone et al., 2015; Poti et al., 2015; Caroprese et al., 2017).

We hypothesized that the fatty acid composition of milk fat can be improved when the animals are fed with above 2% DM whole linseed supplemented diet.

The objective of this study was to investigate the possible changes in the fatty acid composition of milk fat by feeding whole linseed to dairy cows.

Material and methods

The experiment was conducted in two large-scale dairy farms located in Hajdú-Bihar County, Hungary. Hereafter, these farms will be referred to as “A” and “B”. Fifteen multiparous (seven cows in second parity and eight cows in third parity) Holstein-Friesian (165 average days in milk) on farm A and fifteen multiparous (six cows in second parity and nine cows in third parity) Holstein-Friesian (200 average days in milk) on farm B were randomly allocated to treatment groups. The average daily milk yield level in the treatment group was 40 kg-s on farm A and it was 38 kg-s on farm B. During the control-period the cows were fed TMR (total mixed ration) based maize silage without whole linseed three times a day. In the experimental period the cows were fed TMR based maize silage with additional whole linseed three times a day. As *Table 1* shows the whole linseed supplementation of the daily ration was 2.60% DM that equals 1.5 kg/day/cow on farm A and on farm B the whole linseed supplementation was 2.16% DM of the daily ration that equals 1.0 kg/day/cow. The maize silage based rations had similar net energy content (*Table 1*). The experimental period was four weeks. During this time, milk samples were taken three times from each cow: at the start of the experiment, after two weeks and after four weeks. Sampling was scheduled according to the milking order every time. Samples were taken at the same milking period. Individual milk samples were collected twice a day during the experimental period. Milk samples were frozen and stored until further analysis.

Table 1. *Ingredient composition and chemical composition of TMR (% of DM basis)*

Ingredients	TMR (farm A)	TMR (farm B)
Corn silage	41.45	44.64
Lucerne haylage	11.05	6.69
Lucerne hay	7.60	8.92
Meadow hay	1.03	3.32
Brewer's grains	7.60	-
Italian ryegrass silage	11.05	-
Concentrate	17.62	35.27
Whole linseed	2.60	2.16
Crude protein	16.66	16.66
Crude fat	5.36	4.42
NE _l ¹	179.54	177.30

¹Net energy for lactation (MJ)

The fatty acid composition of the milk fat was determined after precolumn derivatization in the form of fatty acid methyl esters by gascromatography (Varga-Visi and Csapó, 2002).

SPSS for Windows for 22.0 programme was used for the statistical analysis. The data were analyzed by the method of variance (One-way ANOVA). Levene-test was applied to examine homogeneity. Tamhane test (in case of heterogeneity) and the LSD test (in case of homogeneity) were used to compare the group-pairs.

The linear model can be written:

$$\chi_{ij} = \mu + \hat{a}_i + e_{ij},$$

where:

χ_{ij} : is dependable variable (fatty acids),

μ : overall mean of the observation,

\hat{a}_i : effect of treatment factors,

e_{ij} : random element.

Table 2 shows the fatty acid composition of whole linseed and TMR (farm A and B).

Table 2. Fatty acid composition of whole linseed and TMR (A and B farm)

Fatty acids (%) ¹	Whole linseed	TMR (A farm)	TMR (B farm)
14:0 ²	0.07	0.39	0.33
15:0 ³	0.02	0.07	0.05
16:0 ⁴	5.47	20.07	18.1
17:0 ⁵	0.08	0.17	0.12
18:0 ⁶	3.01	6.50	6.19
20:0 ⁷	0.12	0.88	1.66
22:0 ⁸	0.12	0.28	0.60
24:0 ⁹	0.09	0.28	0.60
16:1 ¹⁰	0.05	0.16	0.18
20:1 ¹¹	0.16	0.32	0.55
18:1n-9 ¹²	18.53	20.3	22.16
18:2n-6 ¹³	14.96	33.70	36.30
C20:2 ¹⁴	0.06	-	-
18:3n-3 ¹⁵	55.98	19.21	7.12
18:3n-6 ¹⁶	0.21	0.18	0.10
C20:3n-6 ¹⁷	0.04	-	-
C20:4n-6 ¹⁸	0.02	-	-
C20:5 ¹⁹	0.07	-	-

¹Fatty acid methyl-esters relative % by weight; ²miristic acid; ³pentadecylic acid; ⁴palmitic acid; ⁵margaric acid; ⁶stearic acid; ⁷arachidic acid; ⁸behenic acid; ⁹lignoceric acid; ¹⁰palmitoleic acid; ¹¹eicosenoic acid; ¹²oleic acid; ¹³linoleic acid; ¹⁴eicosadienoic acid; ¹⁵ α -linolenic acid; ¹⁶ γ -linolenic acid, ¹⁷eicosatrienoic acid; ¹⁸arachidonic acid; ¹⁹eicosapentaenoic acid

Results

Most milk fatty acid proportions of milk samples produced at A and B farms were affected by diets. Table 3 shows the changes in the SFA (saturated fatty acid) composition of milk fat in the experiment period on farm A.

Contents of short (6:0, 8:0), medium (10:0, 11:0 and 14:0) and long chain fatty acids (15:0, 17:0, 18:0, 20:0, 21:0 and 24:0) were not different after two or four weeks. The contents of 12:0, 16:0, 22:0 and total SFA decreased during the experiment. The 13:0 content increased at the end of the experiment.

The whole linseed supplement affected several MUFA (monounsaturated fatty acid) and PUFA (polyunsaturated fatty acid) contents of milk fat (Table 4.) Feeding whole

linseed increased the contents of some MUFA (14:1, 18:1 and, 20:1). The total proportion of MUFA increased after two weeks. The proportions of 18:2c9,t11, 18:3n-6, 18:3n-3, 20:5 and 22:5n-3 increased by the end of experiment. Increasing concentrations of 18:2c9,t11 and 18:3n-3 were pronounced after two weeks by the end of the experiment.

Table 3. The effect of whole linseed on the SFA contents of milk fat (farm A)

Fatty acids (%) ¹	At the start	After 2 weeks	After 4 weeks	P
6:0 ²	0.60 ± 0.07	0.61 ± 0.03	0.57 ± 0.02	ns
8:0 ³	0.56 ± 0.07	0.52 ± 0.04	0.55 ± 0.06	ns
10:0 ⁴	1.91 ± 0.41	1.57 ± 0.28	1.82 ± 0.34	ns
11:0 ⁵	0.17 ± 0.03	0.16 ± 0.02	0.19 ± 0.03	ns
12:0 ⁶	2.92 ^a ± 0.66	2.29 ^b ± 0.43	2.79 ^{ab} ± 0.63	<0.05
13:0 ⁷	0.14 ^{ab} ± 0.03	0.12 ^b ± 0.02	0.16 ^a ± 0.03	<0.05
14:0 ⁸	11.33 ± 1.21	10.27 ± 1.37	11.61 ± 1.36	ns
15:0 ⁹	1.06 ± 0.16	1.04 ± 0.12	1.18 ± 0.19	ns
16:0 ¹⁰	37.55 ^a ± 3.30	31.95 ^b ± 2.77	33.13 ^b ± 2.09	<0.05
17:0 ¹¹	0.69 ± 0.08	0.66 ± 0.06	0.72 ± 0.06	ns
18:0 ¹²	13.31 ± 1.40	14.09 ± 1.49	12.56 ± 2.01	ns
20:0 ¹³	0.19 ± 0.03	0.17 ± 0.01	0.18 ± 0.03	ns
21:0 ¹⁴	0.03 ± 0.01	0.03 ± 0.01	0.03 ± 0.01	ns
22:0 ¹⁵	0.09 ^a ± 0.01	0.07 ^b ± 0.01	0.07 ^b ± 0.01	<0.05
24:0 ¹⁶	0.05 ± 0.01	0.04 ± 0.01	0.04 ± 0.01	ns
ΣSFA ¹⁷	70.60 ^a ± 3.95	63.59 ^b ± 4.10	65.60 ^b ± 3.71	<0.05

¹Fatty acid methyl-esters relative % by weight; ²caproic acid; ³caprylic acid; ⁴capric acid; ⁵undecylenic acid; ⁶lauric acid; ⁷tridecylic acid; ⁸myristic acid; ⁹pentadecylic acid; ¹⁰palmitic acid; ¹¹margaric acid; ¹²stearic acid; ¹³arachidic acid; ¹⁴heneicosylic acid; ¹⁵behenic acid; ¹⁶lignoceric acid; ¹⁷Σsaturated fatty acid. The averages marked with different letters within the same lines are significantly different from each other at P < 0.05

Table 4. The effect of whole linseed on the MUFA and the PUFA contents of milk fat (farm A)

Fatty acids (%) ¹	At the start	After 2 weeks	After 4 weeks	P
14:1 ²	0.73 ^b ± 0.15	0.82 ^{ab} ± 0.15	0.99 ^a ± 0.22	<0.05
16:1 ³	1.40 ± 0.32	1.51 ± 0.25	1.57 ± 0.36	ns
18:1t ⁴	1.41 ± 0.48	1.60 ± 0.41	1.28 ± 0.35	ns
18:1c ⁵	20.77 ^b ± 2.76	27.08 ^a ± 3.37	25.50 ^a ± 2.91	<0.05
20:1 ⁶	0.04 ^b ± 0.01	0.05 ^a ± 0.01	0.05 ^a ± 0.01	<0.05
ΣMUFA ⁷	24.53 ^b ± 8.19	31.28 ^a ± 10.07	29.61 ^a ± 10.13	<0.05
18:2 ⁸	2.70 ± 0.49	2.56 ± 0.43	2.43 ± 0.35	ns
18:2c9t11 ⁹	0.30 ^c ± 0.04	0.46 ^a ± 0.07	0.38 ^b ± 0.06	<0.05
18:3n-6 ¹⁰	0.04 ^b ± 0.01	0.04 ^b ± 0.01	0.06 ^a ± 0.01	<0.05
18:3n-3 ¹¹	0.34 ^c ± 0.05	0.60 ^a ± 0.01	0.42 ^b ± 0.06	<0.05
20:2 ¹²	0.02 ± 0.005	0.02 ± 0.01	0.02 ± 0.007	ns
20:3 ¹³	0.14 ^a ± 0.04	0.08 ^b ± 0.02	0.10 ^{ab} ± 0.05	<0.05
20:4n-6 ¹⁴	0.20 ^a ± 0.04	0.16 ^b ± 0.02	0.16 ^b ± 0.02	<0.05

20:5n-3 ¹⁵	0.03 ^b ± 0.07	0.04 ^a ± 0.008	0.04 ^a ± 0.008	<0.05
22:5n-3 ¹⁶	0.07 ^b ± 0.01	0.07 ^b ± 0.01	0.08 ^a ± 0.008	<0.05
ΣPUFA ¹⁷	3.82 ^{ab} ± 1.35	4.02 ^a ± 1.37	3.65 ^{ab} ± 1.26	<0.05
Σn-6	3.08	2.84	2.75	ns
Σn-3	0.44	0.71	0.54	ns
n-6/n-3	7.00	4.00	5.09	ns

¹Fatty acid methyl-esters relative % by weight; ²myristoleic acid; ³palmitoleic acid; ⁴elaidic acid; ⁵oleic acid; ⁶eicosenoic acid; ⁷Σmonounsaturated acid; ⁸linoleic acid; ⁹conjugated linoleic acid; ¹⁰γ-linolenic acid; ¹¹α-linolenic acid; ¹²eicosadienoic acid; ¹³eicosatrienoic acid; ¹⁴arachidonic acid; ¹⁵eicosapentaenoic acid; ¹⁶docosapentaenoic acid; ¹⁷Σpolyunsaturated fatty acid

The averages marked with different letters within the same lines are significantly different from each other at P < 0.05

Our study showed that the whole linseed supplementation decreased the n-6 fatty acid contents and increased the n-3 fatty acid contents, however the n-6/n-3 ratio narrowed, but this result was not significant.

Table 5 shows the SFA contents of milk samples produced on farm B. Whole linseed had no effect on proportions of 6:0, 8:0, 10:0, 11:0, 14:0, and 24:0. The proportions of 12:0, 13:0, 15:0 and 17:0 decreased after two weeks. The 16:0 increased by the end of the experiment. During of the experiment no proven changes were observed in the total SFA contents of milk samples.

Table 5. The effect of whole linseed on the SFA contents of milk fat (farm B)

Fatty acids (%) ¹	At the start	After 2 weeks	After 4 weeks	P
6:0 ²	0.62 ± 0.11	0.67 ± 0.06	0.67 ± 0.08	ns
8:0 ³	0.60 ± 0.13	0.59 ± 0.08	0.59 ± 0.08	ns
10:0 ⁴	2.21 ± 0.61	1.87 ± 0.35	1.98 ± 0.40	ns
11:0 ⁵	0.25 ± 0.08	0.20 ± 0.04	0.22 ± 0.06	ns
12:0 ⁶	3.45 ^a ± 0.98	2.75 ^b ± 0.54	2.94 ^b ± 0.62	<0.05
13:0 ⁷	0.25 ^a ± 0.09	0.13 ^b ± 0.03	0.15 ^b ± 0.04	<0.05
14:0 ⁸	11.54 ± 1.29	11.19 ± 1.00	11.76 ± 1.06	ns
15:0 ⁹	1.56 ^a ± 0.46	0.98 ^b ± 0.11	1.05 ^b ± 0.15	<0.05
16:0 ¹⁰	36.51 ^{ab} ± 2.88	34.18 ^b ± 3.06	37.45 ^a ± 3.57	<0.05
17:0 ¹¹	0.77 ^a ± 0.10	0.61 ^b ± 0.06	0.59 ^b ± 0.06	<0.05
18:0 ¹²	10.13 ^b ± 2.17	12.79 ^a ± 1.83	10.78 ^{ab} ± 3.09	<0.05
20:0 ¹³	0.13 ^{ab} ± 0.03	0.15 ^a ± 0.02	0.12 ^b ± 0.04	<0.05
21:0 ¹⁴	0.03 ^a ± 0.01	0.03 ^a ± 0.01	0.02 ^b ± 0.01	<0.05
22:0 ¹⁵	0.06 ^{ab} ± 0.02	0.07 ^a ± 0.01	0.05 ^b ± 0.01	<0.05
24:0 ¹⁶	0.04 ± 0.01	0.06 ± 0.06	0.04 ± 0.06	ns
ΣSFA ¹⁷	68.14 ± 9.56	66.28 ± 9.17	68.56 ± 9.39	ns

¹Fatty acid methyl-esters relative % by weight; ²caproic acid; ³caprycil acid; ⁴capric acid; ⁵undecylenic acid; ⁶lauric acid; ⁷tridecylic acid; ⁸myristic acid; ⁹pentadecylic acid; ¹⁰palmitic acid; ¹¹margaric acid; ¹²stearic acid; ¹³arachidic acid; ¹⁴heneicosylic acid; ¹⁵behenic acid; ¹⁶lignoceric acid; ¹⁷Σsaturated fatty acid
The averages marked with different letters within the same lines are significantly different from each other at P < 0.05

The whole linseed supplement decreased the concentrations of some MUFA (18:11, 20:1) and PUFA (18:2, 18:3n-6, 20:3, 20:4) during the experiment (*Table 6.*). The proportion of long-chain PUFA, such as 18:1c, 18:3n-3, 20:5 and 22:5n-3 were higher in the milk fat during the experiment. The whole linseed supplement had no effect on total MUFA, however the total proportion of PUFA decreased after four weeks.

In the present study, the whole linseed supplementation decreased the n-6 fatty acid contents and increased the n-3 fatty acids contents, however the n-6/n-3 ratio was favourable, but this result was not significant.

Table 6. The effect of whole linseed on the MUFA and the PUFA contents of milk fat (farm B)

Fatty acids (%) ¹	At the start	After 2 weeks	After 4 weeks	P
14:1 ²	0.85 ± 0.27	0.88 ± 0.24	0.97 ± 0.33	ns
16:1 ³	1.78 ± 0.37	1.52 ± 0.38	1.82 ± 0.55	ns
18:1t ⁴	2.39 ^a ± 0.96	1.57 ^b ± 0.23	1.40 ^b ± 0.28	<0.05
18:1c ⁵	21.33 ^b ± 3.36	24.71 ^a ± 2.96	22.51 ^{ab} ± 2.88	<0.05
20:1 ⁶	0.05 ^a ± 0.01	0.05 ^a ± 0.01	0.04 ^b ± 0.004	<0.05
ΣMUFA ⁷	26.60 ± 8.33	28.89 ± 9.77	26.75 ± 8.76	ns
18:2 ⁸	3.19 ^a ± 0.28	2.36 ^b ± 0.25	2.28 ^b ± 0.22	<0.05
18:2c9t1 ⁹	0.45 ± 0.08	0.48 ± 0.06	0.45 ± 0.11	ns
18:3n-6 ¹⁰	0.4 ^a ± 0.01	0.03 ^b ± 0.006	0.03 ^b ± 0.006	<0.05
18:3n-3 ¹¹	0.23 ^b ± 0.02	0.58 ^a ± 0.07	0.59 ^a ± 0.11	<0.05
20:2 ¹²	0.02 ± 0.01	0.02 ± 0.01	0.03 ± 0.04	ns
20:3 ¹³	0.13 ^a ± 0.03	0.08 ^b ± 0.02	0.07 ^b ± 0.02	<0.05
20:4n-6 ¹⁴	0.20 ^a ± 0.03	0.14 ^b ± 0.02	0.13 ^b ± 0.02	<0.05
20:5n-3 ¹⁵	0.01 ^b ± 0.005	0.03 ^a ± 0.01	0.03 ^a ± 0.01	<0.05
22:5n-3 ¹⁶	0.05 ^b ± 0.01	0.07 ^a ± 0.01	0.06 ^{ab} ± 0.01	<0.05
ΣPUFA ¹⁷	4.33 ^a ± 1.56	3.79 ^b ± 1.28	3.69 ^b ± 1.25	<0.05
Σn-6	3.92	2.61	2.51	ns
Σn-3	0.29	0.68	0.68	ns
n-6/n-3	13.52	3.83	3.69	ns

¹Fatty acid methyl-esters relative % by weight; ²myristoleic acid; ³palmitoleic acid; ⁴elaidic acid; ⁵oleic acid; ⁶eicosenoic acid; ⁷Σmonounsaturated acid; ⁸linoleic acid; ⁹conjugated linoleic acid; ¹⁰γ-linolenic acid; ¹¹α-linolenic acid; ¹²eicosadienoic acid; ¹³eicosatrienoic acid; ¹⁴arachidonic acid; ¹⁵eicosapentaenoic acid; ¹⁶docosapentaenoic acid; ¹⁷Σpolyunsaturated fatty acid

The averages marked with different letters within the same lines are significantly different from each other at P < 0.05

Discussion

One of numerous possible ways to increase the proportion of PUFA and decrease the proportion of SFA of milk fat is to use linseed. According to Ferlay et al. (2013) and Hurtaud et al. (2010) the extruded linseed in increasing amount of supplementation is suitable to increase the content of n-3 series FA in milk fat, while in Saliba et al.'s (2014) opinion the linseed oil can enhance the content of α-linolenic acid of milk fat. Lerch et al. (2015) found that extruded linseed supplementation increased the PUFA content of milk fat, and did not induce oxidised off-flavours in milk or cheese.

In contrast, according to Kennelly (1996) feeding PUFA, which is protected against ruminal biohydrogenation, increases their proportion in milk. The hard seedcoat of whole linseed may effectively protect alpha-linoleic acid from ruminal biohydrogenation (Givens et al., 2009; Oba et al., 2009).

In our experiment, the dietary application had a significant impact on the proportion of several milk fatty acids on both farms. Whole linseed had influences on SFA, MUFA acid content of milk fat different levels. In general, on both farms, the dietary supplementation of whole linseed depressed ($P < 0.05$) several medium-chain SFA and increased ($P < 0.05$) some long-chain PUFA, especially alpha-linolenic acid in milk fat. Content of short-chain fatty acids in milk fat was not affected by dietary supplementation of whole linseed at each of farms.

Our results showed that the decreasing proportion of several saturated fatty acids were in correspondence with other research data (Precht and Molkentin, 2000; Chilliard et al., 2001). The decreasing tendency of SFA content – explained in the literature by de novo milk fat synthesis remission – was found in some researches, in which different protected fats and oil seeds were used (Dhiman et al., 1999; Precht and Molkentin, 2000; Chilliard et al., 2001; Petit and Gagnon, 2009).

The 18:1 (oleic acid) content increased on both farms. This finding is in line with the report of Ward et al. (2002), who found similar tendency with different oilseeds.

Reviewing data of MUFA and PUFA from whole linseed feed supplement we found that, in accordance with our theory, the biggest differences were observed in the proportion of α -linoleic acid on both farms. The proportion of α -linoleic acid doubled during the experiment on both farms. Our results are in accordance with those of Gandra et al. (2016).

Others reported an increase in the concentration of very long-chain polyunsaturated fatty acids like 20:5n-3 and 22:5n-3, as a result of feeding different forms of linseed (Hagemester et al., 2001). In our experiment, concentrations of 20:5n-3 and 22:5n-3 were increased by whole linseed supplementation.

Despite the increase in the proportion of health-promoting milk fatty acids such as 18:3n-3 as a result of whole linseed supplementation, the levels of these fatty acids remained under 1% of total milk fatty acids. These findings suggest extensive ruminal biohydrogenation of dietary PUFA. In our experiment feeding whole linseed resulted in a bigger n-3 ratio in milk fat on both farms, the ratio of n-6/n-3 narrowed during the experiment on both farms, but these results were not significant. This agrees with Petit (2002) who reported a decrease in the n-6 to n-3 fatty acid ratio when cows were fed whole linseed compared with micronized soybeans or calcium salts of palm oil.

Conclusions

Nutrition can be regarded as one of the most important source of variation composition of milk fat. The fatty acid composition of oilseeds such as full fat linseed is considered desirable for human health and thus their inclusion in the diet of dairy cattle is important as a means of achieving a more desirable fatty acid profile in milk fat. The results of the present study demonstrated that oilseeds, especially whole linseed, are easy to fit into feeding systems of intensive dairies in Hungary, too. Feeding dairy cows a diet with whole linseed decreased the proportion of several SFA and increased the proportion of some MUFA and PUFA, especially C18:3n-3. The 2.60% whole linseed supplementation of the daily ration narrowed the n-6/n-3 ratio on farm A, while the

2.16% whole linseed supplementation of the daily ration narrowed it on farm B, but these results were not significant. More research is needed on dairy farms in Hungary to use other supplements to increase the n-3 concentration in milk fat because of the composition of milk fat is important for dairy industry and human health and it is related to milk quality.

REFERENCES

- [1] Caroprese, M., Mancinoc, R., Ciliberti, M. G., DiLuccia, A., LaGatta, B., Albenzio, M. (2017): Fatty acid profile and coagulating ability of milk from Jersey and Friesian cows fed whole flaxseed. – *Journal of Dairy Research* 84(1): 14-22.
- [2] Chilliard, Y., Ferlay, A., Doreau, A. (2001): Effect of different types of forages, animal fat or marine oils in cow's diet on milk fat secretion and composition, especially conjugated linoleic acid (CLA) and polyunsaturated fatty acid. – *Livestock Production Science* 70(1-2): 31-48.
- [3] Demeyer, D., Doreau, M. (1999): Targets and procedures for alter in ruminant meat and milk lipids. – *Proceedings of Nutrition Society* 58(3): 593-607.
- [4] Dhiman, T. R., Anand, G. R., Satter, L. D., Pariza, M. W. (1999): Conjugated linoleic acid content of milk from cows fed different diets. – *Journal of Dairy Science* 82(10): 2146-2146.
- [5] Elgersma, A., Tamminga, S., Ellen, G. (2006): Modifying milk composition through forage. – *Animal Feed Science Technology* 131(3-4): 207-225.
- [6] Ferlay, A., Doreau, M., Martin, C., Chilliard, Y. (2013): Effect of incremental amounts of extruded linseed on the milk fatty acid composition of dairy cows receiving hay or corn silage. – *Journal of Dairy Science* 96(10): 6577-6595.
- [7] Gandra, J. R., Mingoti, R. D., Barletta, R. V., Takiya, C. S., Verdurico, L. C., Freitas, J. E., Paiva, P. G., Jesus, E. F., Calomeni, G. D., Renno, F. P. (2016): Effect of flaxseed, raw soybeans and calcium salts of fatty acids on apparent total tract digestibility, energy balance and milk fatty acid profile of transition cows. – *Animal* 10(8): 1303-1310.
- [8] Givens, D. I., Kliem, K. E., Humphries, D. J., Shingfield, K. J. (2009): Effect of replacing calcium salts of palm oil distillate with rapeseed oil, milled or whole rapeseeds on milk fatty acid composition in cows fed maize silage-based diets. – *Animal* 3(7): 1067-1074.
- [9] Hagemester, H., Franzen, M., Barth, C. A., Precht, D. (2001): α -linolenic acid transfer into milk fat and its elongation by cows. – *European Journal of Lipid Science Technology* 93(10): 387-391.
- [10] Halasz, A., Nagy, G., Tasi, J., Bajnok, M., Mikone, J. E. (2016): Weather regulated cattle behaviour on rangeland. – *Applied Ecology and Environmental Research* 14(4): 149-158.
- [11] Hurtaud, C., Faucon, F., Couvreur, S., Payraud, J.-L. (2010): Linear relationship between increasing amounts of extruded linseed in dairy cow diet and milk fatty acid composition and butter properties. – *Journal of Dairy Science* 93(4): 1429-1443.
- [12] Kennelly, J. J. (1996): The fatty acid composition of milk fat as influenced by feeding oilseed. – *Animal Feed Science and Technology* 60(3-4): 137-152.
- [13] Kinsella, J. E. (1991): α -Linolenic Acid Functions and Effects on Linoleic Acid Metabolism and Eicosanoid-Mediated Reactions. – In: Kinsella, J. E. (ed.) *Advances in Food and Nutrition Research*. Academic Press, Cambridge.
- [14] Lerch, S., Ferlay, A., Graulet, B., Cirié, C., Verdier-Metz, I., Montel, M. C., Chilliard, Y., Martin, B. (2015): Extruded linseeds, vitamin E and plant extracts in corn silage-based diets of dairy cows: Effect on sensory properties of raw milk and uncooked pressed cheese. – *International Dairy Journal*. 51: 65-74.
- [15] Livingstone, K. M., Humphries, D. J., Kliem, K. E., Givens, D. I., Reynolds, C. K. (2015): Effects of forage type and extruded linseed supplementation on methane

- production and milk fatty acid composition of lactating dairy cows. – *Journal of Dairy Science* 98(6): 4000-4011.
- [16] Moallem, U. (2009): The effects of extruded flaxseed supplementation to high-yielding dairy cows on milk production and milk fatty acid composition. – *Animal Feed Science and Technology* 152(3-4): 232-242.
- [17] Murphy, J. J., Conolly, J. F., Mcneil, G. P. (1995a): Effects on milk fat composition and cow performance of feeding concentrates containing full fat rapeseed and maize distillers grains on grass-silage based diets. – *Livestock Production Science* 44(1): 1-11.
- [18] Murphy, J. J., Conolly, J. F., Mcneil, G. P. (1995b): Effects of performance and milk fat composition of feeding full fat soyabeans and rapeseeds to dairy cows at pasture. – *Livestock Production Science* 44(1): 13-25.
- [19] Oba, M., Thangavelu, G., Dehghan-Banadaky, M., Ambrose, D. J. (2009): Unprocessed whole flaxseed is as effective as dry-rolled flaxseed at increasing α -linolenic concentration in milk of dairy cows. – *Livestock Science* 122(1): 73-76.
- [20] Peredi, J. (2002): A hazai lakosság alacsony n-3 zsírsavelláótságának javítási lehetőségei. – *Olaj, Szappan, Kozmetika* 51(2): 45-49.
- [21] Petit, H. V. (2002): Digestion, milk production, milk composition and blood composition of dairy cows fed whole flaxseed. – *Journal of Dairy Science* 85(6): 1482-1490.
- [22] Petit, H. V. (2003): Digestion, milk production, milk composition and blood composition of dairy cows fed formaldehyde treated flaxseed or sunflower seed. – *Journal of Dairy Science* 86(8): 2637-2646.
- [23] Petit, H. V., Gagnon, N. (2009): Milk concentrations of the mammalian lignans enterolactone and enterodiol, milk production and whole tract digestibility of dairy cows fed diets containing different concentrations of flaxseed meal. – *Animal Feed Science and Technology* 152(1-2): 103-111.
- [24] Poti, P., Pajor, F., Bodnar, A., Penksza, K., Koles, P. (2015): Effect of micro-alga supplementation on goat and cow milk fatty acid composition. – *Chilean Journal of Agricultural Research* 75(2): 259-263.
- [25] Precht, D., Molkentin, J. (2000): Frequency distributions of onjugated linoleic acid and trans fatty acid content in European bovine milk fats. – *Milchwissenschaft* 55(12): 687-691.
- [26] Saliba, L., Gervais, R., Lebeuf, Y., Vuilleumard, J.-C., Fortin, J., Chouinard, P. Y. (2014): Effect of feeding linseed oil in diets differing in forage to concentrate ratio: 2. Milk lactone profile. – *Journal of Dairy Research*. 81(1): 91-97.
- [27] Simopoulos, A. P. (1999): Essential fatty acids in health and chronic disease. – *The American Journal of Clinical Nutrition* 70(3): 560-569.
- [28] Simopoulos, A. P. (2001): n-3 fatty acids and human health: Defining strategies for public policy. – *Lipids* 36(1): S83-S89.
- [29] Varga-Visi, E., Csapó, J. (2002): Illózsírsavak, zsírsavak és koleszterin tartalom meghatározása gázkromatográffal a Kaposvári Egyetem Állattudományi Karának Kémiai Intézetében. – In: Varga-Visi, E., Csapó, J. (eds.) *Proceedings of Scientific Meeting of the Chemical Institutes. University of West Hungary, Sopron.*
- [30] Ward, A. T., Wittenberg, K. M., Przybylski, R. (2002): Bovine milk fatty acid profiles produced by feeding diets containing solin, flay and canola. – *Journal of Dairy Science* 85(5): 1191-1196.
- [31] White, S. L., Bertrand, J. A., Wade, M. R., Washburn, S. P., Green, J. T., Jenkins, T. C. (2001): Comparison of fatty acid content of milk from Jersey and Holstein cows consuming pasture or total mixed ration. – *Journal of Dairy Science* 84(10): 2294-2301.

CARBON SEQUESTRATION AND SPATIAL DIFFERENTIATION CHARACTERISTICS OF URBAN FOREST IN CHINA

LI, F. X.^{1,2*} – SHI, H.¹ – ZHAO, J. S.³ – FENG, X. G.² – LI, M.²

¹*School of Environmental and Municipal Engineering, Xi'an University of Architecture and Technology, Xi'an 710055, Shaanxi, China*
(H. Shi: e-mail: 497394178@qq.com; phone: +86-137-7216-2185; fax: +86-29-8220-5813)

²*School of Architecture, Xi'an University of Architecture and Technology*
Xi'an 710055, Shaanxi, China
(X. G. Feng: e-mail: 1010425832@qq.com; phone: +86-137-5988-6561; fax: +86-29-8220-5813;
M. Li: e-mail: 475983882@qq.com; phone: +86-135-7212-2767; fax: +86-29-8220-5813)

³*School of Land and Resources Engineering, Kunming University of Science and Technology*
Kunming 650093, Yunnan, China
(J. S. Zhao: e-mail: 1429620189@qq.com; phone: +86-137-0844-1869; fax: +86-871-6821-6333)

**Corresponding author*

F. X. Li: e-mail: lifengxiasky@163.com; phone: +86-159-2956-6258; fax: +86-29-8220-5813

(Received 30th Sep 2017; accepted 20th Feb 2018)

Abstract. Based on large-scale data measured in quadrats, and using remote sensing images, the author analyzed the spatial differentiation characteristics of carbon storage and carbon density of forest vegetation in the north foot of the Qinling Mountains in China, by combining an allometric growth model with spatial analysis using a Geographic Information System. The results showed that the average carbon density of forest vegetation in the main urban area in Xi'an occurred in the order: cultural and educational green space > scenic-area green space > road green space > industrial green space > residential green space. The average carbon density of arbor forest was 6.308 kg/m². The carbon storage capacity varied in the order: green land in cultural and educational districts > scenic-area green space > road green space > residential green space > industrial green space. The total amount of carbon storage in the arbor forest was 519,180 t C. The spatial distribution pattern of carbon density in the arbor layer in the Xi'an administrative region was not balanced, showing high value in a southern suburb and low value in a northern suburb. Increasing forest vegetation, improving the quality of the forest structure, and increasing the three-dimensional green quantity of urban forest are effective ways to improve urban environments and to enhance carbon sequestration by forests.

Keywords: forest vegetation, carbon storage, carbon density, spatial differentiation, 3S technology

Introduction

Forests are the main terrestrial ecosystem on Earth, accounting for 77% of the carbon stored globally as terrestrial vegetation. Urban vegetation is an important component of urban ecosystems, providing important ecological services (Niemelä et al., 2010; Coley et al., 1997) such as helping to regulate climate change and maintain the global carbon balance (Beer et al., 2010; Bonan, 2008; Bousquet et al., 2000). Therefore, accurately evaluating carbon sequestration by forests is significant to better management of the carbon cycle and can simultaneously provide a scientific basis for improving the ability to cope with global climate change.

There have been many international studies estimating carbon sequestration and carbon storage by forest vegetation (Dixon et al., 1994; Fang et al., 2001; Janssens et al., 2003; Jo and McPherson, 1995; McPherson, 1998; Nowak, 1993; Nowak and

Crane, 2002; Pacala et al., 2001; Piao et al., 2005). Nowak researched California urban tree carbon storage and found that in Auckland (with tree coverage of 21%); trees could store 11.0 tons of carbon per hectare (Nowak, 1993). McPherson's research in Sacramento showed that six million urban trees stored eight million tons of CO₂, with an average CO₂ sequestration of 31 tons per hectare and 0.92 tons per hectare per year (McPherson, 1998). Jo and McPherson researched the carbon sequestration of two residential areas in northern Chicago, and found that the carbon sequestration capacity of arbors and shrubs was 1.03-4.42 kg/m², and that the carbon sequestration of each residential area was 513.5-3249.5 kg (Jo and McPherson, 1995). Based on the urban green coverage, Nowak and Crane researched the carbon storage of 10 cities in the United States. The results showed that urban trees stored about 700 million tons of carbon per year, the annual carbon sequestration capacity was 22.8 million tons, and the average carbon sequestration capacity of urban trees was 25.1 tons per hectare. However, the urban vegetation carbon sequestration capacity was significantly different between cities (Nowak and Crane, 2002). Scholars have researched the carbon storage of forest vegetation in Liaoning Province, Hunan Province, Shaanxi Province, Sichuan Province, and Guangzhou City (Dongsheng et al., 1998; Huang, et al., 2000; Liu et al., 2000; Ma et al., 2012; Liu, et al., 2016; Wang et al., 2001; Zhen, et al., 2014), revealing the amount of carbon storage in the aboveground part of forest vegetation in China. However, inconsistent research methods resulted in large differences in research results, so there was still substantial uncertainty. Carbon sequestration by urban vegetation is mainly studied through ground investigation and estimation via remote sensing (Yan et al., 2016). China's forest vegetation types are diverse and complex. In general, there are few data in this field; therefore, it is necessary to select appropriate research methods to estimate the carbon storage of forest vegetation in provinces and cities accurately, to improve credibility and accurately quantify carbon sequestration by forest vegetation (Fang, 2000; Tans et al., 1990; Houghton et al., 1994; Siegenthaler and Sarmiento, 1993).

The ecological environment on the northern foot of the Qinling Mountains is fragile, and the forest vegetation has distinct regional characteristics and specialties. However, at present, estimates of the carbon storage by forest vegetation on the north foot of the Qinling Mountains are rare. For this reason, we used high-resolution remote sensing image data covering a wide range of quadrats to analyze the spatial differentiation of the carbon storage and density of the Xi'an forest vegetation in a semi-humid region on the northern foot of the Qinling Mountains to try to explore its drivers. This was done using GIS technology, to provide a scientific basis for research on the carbon-storage of forest ecosystems at national level, to provide a scientific basis for improving the ability of those in cities to cope with global climate change, and to evaluate and plan urban green space ecosystem services to achieve sustainable urban development.

Materials and methods

Overview of research areas

Xi'an City on the north foot of the Qinling Mountains is a city typical of semi-humid areas in China. It is located in the eastern part of northwest China and on the central part of the Guanzhong Plain. The geographical coordinates are 33° 42' to 34° 45' N, and 107° 40' to 109° 49' E. The area is subject to a warm-temperate semi-

humid continental monsoon climate. The average elevation is 424 m, the average annual temperature is 13.3 °C, the average precipitation is 604.2 mm, and the average humidity is 69.6%. Its jurisdiction districts include Beilin, Yanta, Xincheng, Weiyang, Lianhu, Baqiao, Chang'an, Lintong, Yanliang, and Gaoling; and include the counties of Huxian, Lantian, and Zhouzhi. These ten districts and three counties cover an area of 10,108 km². The main urban areas are in Beilin District, Yanta District, Xincheng District, Weiyang District, Lianhu District, and Baqiao District (urban area of 822.28 km²). The geographical location and administrative map of the research area is shown in *Figure 1*. The green space rate, green coverage rate, and per capita public green area of Xi'an are currently 31%, 39.82%, and 7.59 m², respectively. The basic characteristics of the vegetation are rich diversity and a number of floral preserves in which there are many tectonic residual plants. The arbor forest area in the main urban area in Xi'an is 75,959,475.45 m².

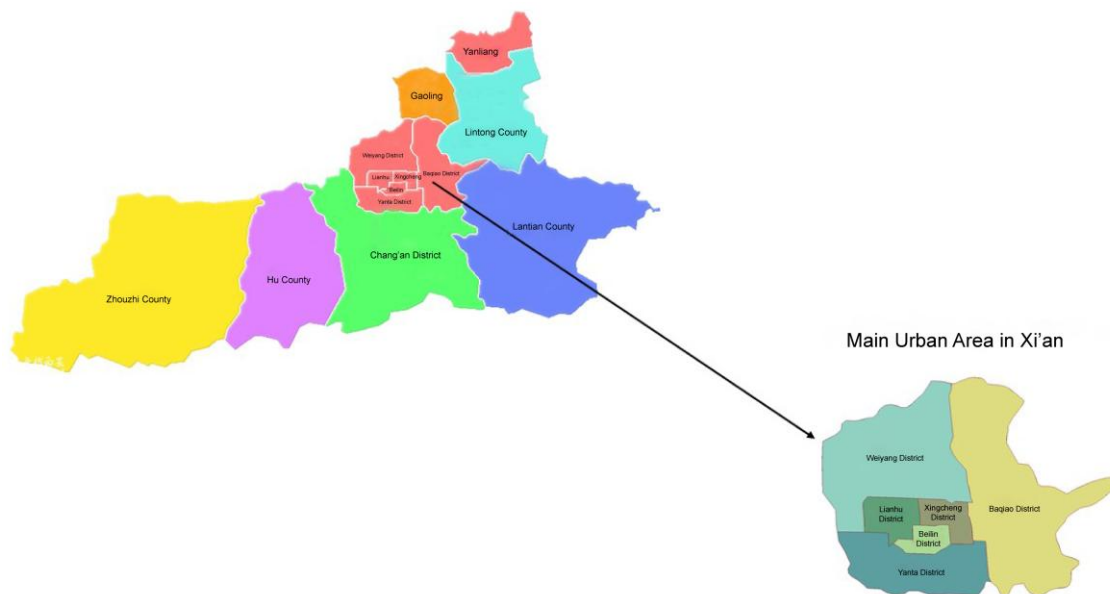


Figure 1. Geographic location and scope of the research area

Data source and quadrat setting

The basic information used in this research includes QuickBird high-resolution remote sensing image data, Landsat 8 data of Xi'an in July 2015, and Xi'an administrative map data from large-scale quadrats. Supported by 3S (Geographic Information System, Remote Sensing, and Global Positioning System) technology combined with field investigation, the author classified land use with the remote sensing software Ecognition, and extracted urban green information for Xi'an. Then the author divided the green space into road green space, residential green space, scenic-area green space, cultural and educational green space, and industrial green space (*Fig. 2*) using the GIS software ARCGIS. Because the arbor forest is the main contributor to carbon storage by forest vegetation, this paper mainly researched the carbon storage of arbor forest in the main urban areas of Xi'an.

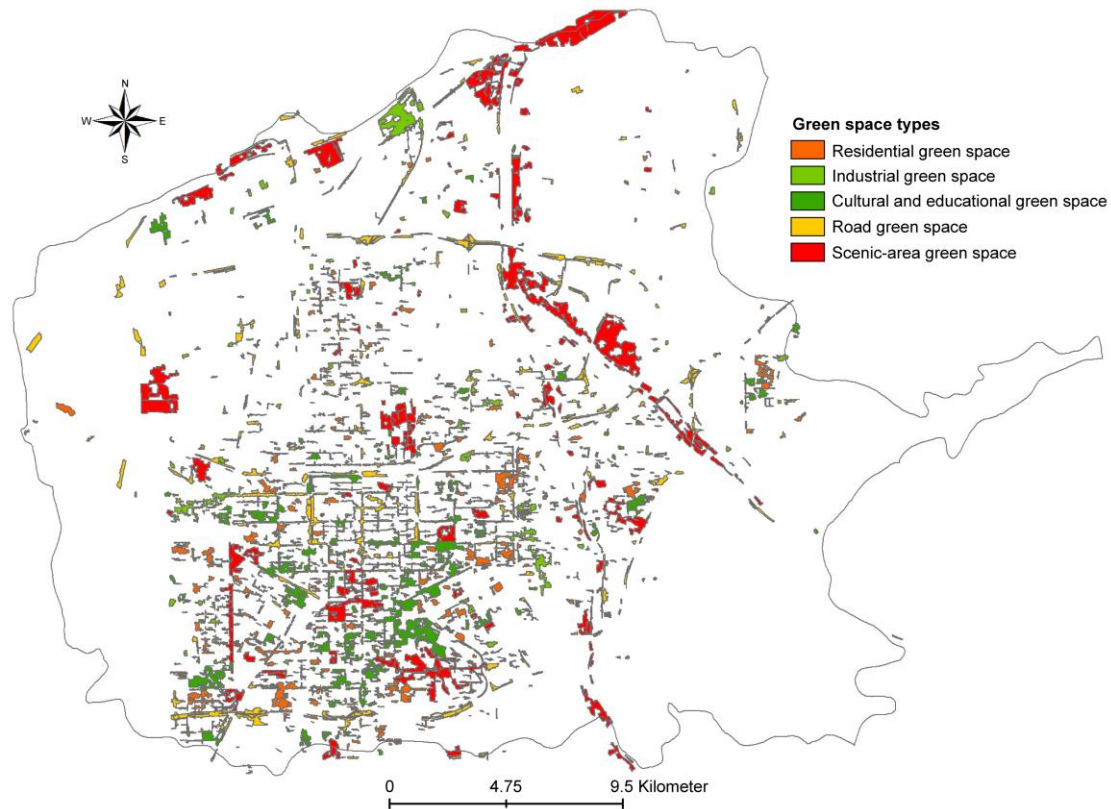


Figure 2. Classification map of urban green space in Xi'an

According to the distribution characteristics of urban plants and the actual situation of parks, roads, residential areas, cultural and educational areas, and industrial areas, the location of field investigations and the number of quadrats were determined. The size of the park quadrats was set to 20×20 m, and the distance between two adjacent quadrats was not less than 150 m, with a total of 40 quadrats from 20 parks including Xingqinggong Park, City Sports Park, and Fengqing Park being surveyed. For the setting of road quadrats, based on the length of roads and the configuration of the vegetation, the author investigated the specific situations of trees on roads (100×10 m) with a total of 140 quadrats on 113 roads (e.g., Friendship Road, Taiyi Road, and Wenjing Road) being investigated (*Fig. 3*). For the setting of residential quadrats, each quadrat contained a residential building and its surrounding street trees and green belt, and the area of a quadrat plot was determined based on actual situations, with a total of 23 quadrats in 23 residential areas being investigated (including Dongfang Yayuan, Dingxin Garden, and Hairong Yango) (*Fig. 4*). The school quadrat was set to 20×20 m (same method as for the park quadrats) with a total of 31 quadrats at 18 schools being investigated (including Xi'an University of Architecture and Technology, Xi'an Physical Education University, and Xi'an Jiaotong University). The industrial quadrats were set to 20×20 m in a total of six industrial areas (e.g., PetroChina Changqing Oilfield Company, China Typical Industries Group Co., Ltd, Xi'an Electromechanical Vehicle Parts Factory). The author investigated the type, quantity, and growth condition of trees with diameter at breast height (DBH) over 5 cm, and measured the height (H, height from the ground to the top of the canopy) and DBH (D, the diameter of trunk at 1.3 m above the ground) of each tree. There were 240 quadrats.

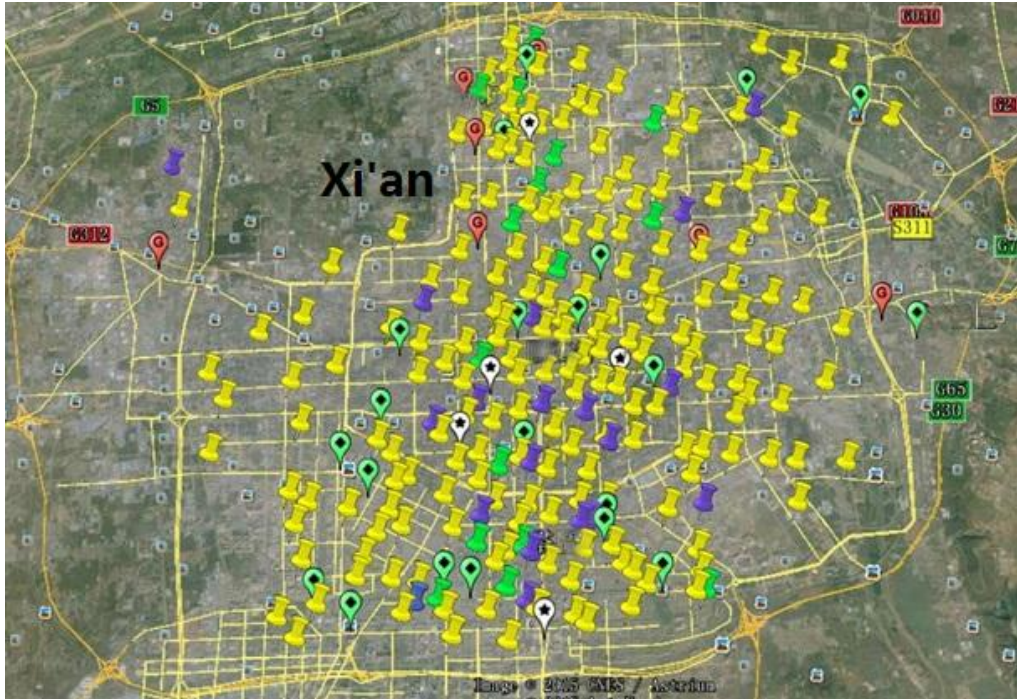


Figure 3. Sample layout map



Figure 4. Examples of some of the residential areas investigated

Estimation of forest vegetation biomass

Vegetation biomass is the unit of vegetation carbon storage. The current methods for estimating forest vegetation biomass include the variable biomass expansion factor method, the volume-derived method (i.e., the regression model of biomass and volume), the allometry equation, and remote sensing inversion. Of these, the biomass expansion factor (BEF) and the stand volume (x) establish a power exponential function relation and a reciprocal function relation, respectively, as shown in *Equations 1, 2, and 3*:

$$BEF = ax^{-b} \quad (\text{Eq.1})$$

$$BEF = a + \frac{b}{x} \quad (\text{Eq.2})$$

where a and b are constants. The regression model was established by applying the volume-derived method:

$$Y = aV + b \quad (\text{Eq.3})$$

where Y is the biomass density, V is the stand volume density, and a and b are constants. In this research, according to the measured data from field sampling quadrats, the allometry equation of urban greening tree species was adopted to calculate the vegetation biomass. The allometry equation of urban greening tree species is shown in *Table 1*, where B, D, and H represent biomass, diameter at breast height, and plant height, respectively. For tree species without corresponding models, parameters of similar species of trees were used instead, according to the actual situation in each region.

Table 1. Allometry equations of greening tree species

No.	Greening tree species	Calculation formula
1	<i>Cinnamomum camphora</i>	$B=0.937+0.037D^2H$
2	<i>Populus simonii</i>	$B=0.015(D^2H)^{1.032}$
3	<i>Styphnolobium japonicum</i>	$B=0.714+0.03D^2H$
4	<i>Ligustrum lucidum</i>	$B=0.907+0.010D^2H$
5	<i>Metasequoia glyptostroboides</i>	$B=\text{Exp}[-0.8168+2.1549\lg D]$
6	<i>Pinus massoniana</i>	$B=0.1309D^{2.4367}$
7	<i>Salix sp.</i>	$B=0.178D^{2.581}$
8	<i>Sapindus mukorossi</i>	$B=-3.672+0.4815D^2$
9	<i>Ginkgo biloba</i>	$B=-0.684+0.090D^2H$
10	<i>Cedrus deodara</i>	$B=1.26(0.3721D^{1.2928}+0.2805D^{1.3313})$
11	<i>Koelreuteria paniculata</i>	$B=0.915+0.100D^2H$
12	<i>Broussonetia papyrifera</i>	$B=1.7579(D^2H)^{1.5784}$
13	<i>Lagerstroemia indica</i>	$B=0.895+0.035D^2H$
14	<i>Platanus acerifolia</i>	$B=0.0690(D^2H)^{0.9133}$
15	<i>Cupressaceae</i>	$B=0.000030507+0.000033947D^2H+0.00012531(D^2H)^{0.733}$
16	<i>Liquidambar formosana</i>	$B=0.043(D^2H)^{0.994}$
17	<i>Ulmus pumila</i>	$B=0.1458(D^2H)^{0.8191}$
18	<i>Eucommia ulmoides</i>	$B=1.687+0.046D^2H$
19	<i>Paulownia tomentosa</i>	$B=0.077180D^{-2.27598}$
20	Hardwoods	$B=\text{Exp}(-3.5618+2.6645\ln D)$
21	Softwood	$B=\text{Exp}(-2.2796+2.2874\ln D)$

Estimation of carbon storage and carbon density of forest vegetation

Based on the high-resolution satellite remote sensing image data for Xi'an, for this paper, we combined field investigation information and data from 3S technology. The forest vegetation biomass, which was calculated using the allometry equation of

greening-tree species, was multiplied by carbon content to estimate urban forest carbon storage, as shown in *Equation 4*:

$$C = B_t \times C_c \quad (\text{Eq.4})$$

where C is the forest vegetation carbon storage, B_t is the total biomass, and C_c is the forest vegetation carbon content. The author adopted the value of 0.5 used internationally (Ge et al., 2013). Carbon density refers to carbon storage per unit area. The carbon storage and carbon density of road green space, residential green space, scenic-area green space, cultural and educational green space, and industrial green space were analyzed quantitatively. Combined with definitions of the different types of green areas, ARCGIS was used to map the spatial distribution of carbon density and carbon storage of forest vegetation in Xi'an and to analyze spatial differentiation characteristics of forest vegetation carbon storage and carbon density in the main urban area in Xi'an.

Results

Carbon storage analysis of arbor forest in Xi'an

According to the measured carbon storage per unit area of road green space, residential green space, scenic-area green space, cultural and educational green space, and industrial green space, and the green area determined by ARCGIS, the carbon storage of the forest vegetation of the main urban area in Xi'an was calculated and is shown in *Table 2*.

Table 2. Carbon storage in the main urban area in Xi'an

No.	Type	Quadrat number	Average carbon density (kg/m ²)	Area (m ²)	Carbon storage (kg)
1	Green space along roads	140	4.76	15,633,211.593	74,414,087.18
2	Residential green space	23	2.93	11,766,371.832	34,475,469.47
3	Scenic-area green space	40	6.41	28,449,692.827	182,362,531.02
4	Cultural and educational green space	31	14.24	14,816,815.179	210,991,448.15
5	Industrial green space	6	3.20	5,293,384.019	16,938,828.86
6	Total number	240			519,182,364.68

It can be seen from *Table 2* that the order of average carbon density of the arbor layer in the main urban area in Xi'an was as follows: cultural and educational green space > scenic-area green space > road green space > industrial green space > and residential green space. The average carbon density of the main urban area in Xi'an was 6.308 kg/m², higher than the average level of carbon density in Shaanxi Province. The carbon storage in the arbor layer of the main urban area in Xi'an occurred in the order: cultural and educational green space > scenic-area green space > road green space > residential green space > and industrial green space, and the green storage in the green space of cultural and educational districts was 210,990 t C, a contribution of 40.6% to carbon sequestration of the arbor layer in main urban area of Xi'an. The carbon storage of scenic-area green space contributed 35.1% to carbon sequestration of arbor layer in the whole city. Carbon storage in road green space accounted for 14.3% of the total arbor

trees in the whole city; while the carbon storage in residential green space accounted for 6.6% of the main urban area in Xi'an. The carbon storage in industrial green space accounted for 3.3% of the main urban area in Xi'an only; the total carbon storage of the main urban area in Xi'an was 519,180 t C.

The research showed that the arbor forest in cultural and educational areas and scenic areas in Xi'an played a leading role in carbon sequestration by forest vegetation in the main urban area in Xi'an; the road forest made a general contribution to carbon sequestration function of the arbor layer in the main urban area in Xi'an. However, the arbor forest in residential and industrial areas made little contribution to carbon sequestration by forest vegetation. It can be seen that in the future, we should improve green space quality in residential areas, and follow the principle "people-oriented, ecology first". In residential landscape planning and design, we should pay attention to plant configuration, and try to choose appropriate local tree species, so as to improve the quantity of three-dimensional greenery and its ecological service functions, as well as to improve the residents' quality of life and happiness index. Simultaneously, when constructing industrial green space, we should arrange arbor-shrub-grass multi-layer garden plants with strong ecological function, especially vegetation to retain dust and absorb SO₂. The objective is to increase the quantity of three-dimensional greenery and improve the ecological efficiency of green spaces. This should effectively improve the environmental quality of industrial areas.

Carbon density analysis of forest vegetation in Xi'an

The standard deviation (2.12) determined according to classical statistics was confirmed as the classification criteria of carbon density in forest vegetation in Xi'an. Moreover, the spatial distribution of carbon density of forest vegetation in Xi'an was drawn using ARCGIS software, as shown in *Figure 5*.

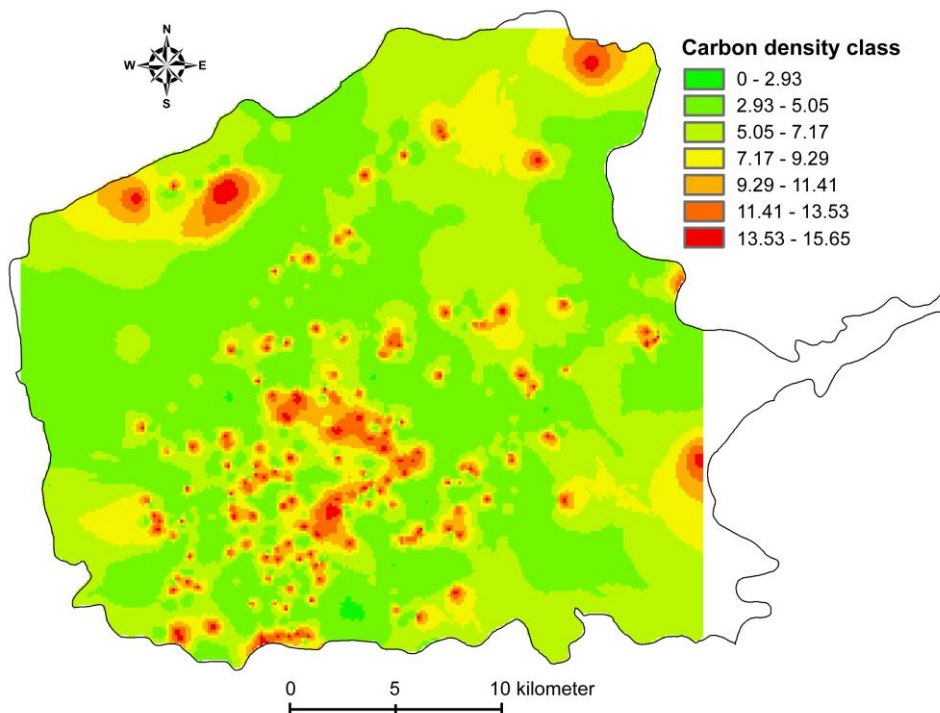


Figure 5. Spatial distribution of carbon density of arbor forest in Xi'an

It can be seen from *Figure 5* that areas with high carbon density of urban forest in Xi'an were mainly concentrated in the southern suburb of Xi'an. Individual parks and communities had high carbon density in the eastern and northern suburbs, but the overall level was general; the carbon density level in the western suburb was the lowest. In short, the carbon density of arbor forest in the main urban area of Xi'an showed the characteristics of high value in the southern suburb and low value in the northern suburb. This was closely related to the irrational distribution of green space, especially the unbalanced distribution of park green space. The distribution of park green space in the southern suburb was reasonable, with the eastern suburb was second. In contrast, the park green space in the western and northern suburbs had many defects. In addition, the cultural and educational areas in the southern suburb had more green space (six times that of the northern suburb and three times that of the western suburb); therefore, Xi'an should take great efforts to increase afforestation, especially in the eastern, western, and northern suburbs. For this, the government should strengthen the construction of large green corridors and accelerate the construction of a Xingfu forest belt along Xingfu Road, increase the quantity of three-dimensional urban green space, and strive to make Xi'an a forest city.

According to analysis of ARCGIS, the carbon density of arbor forest in the main urban area of Xi'an (0-2.93) accounted for 0.2%, and 43.6% was between 2.93-5.05, 36.0% between 5.05-7.17, 11.8% between 7.17-9.29, 4.9% between 9.29-11.41, 2.9% between 11.41-13.53, and 0.7% between 13.53-15.65. The research showed that the carbon density within the arbor forest in Xi'an was mainly concentrated in the range 2.93-7.17 kg/m².

Analysis on carbon storage and carbon density of arbor forest in each Xi'an administrative region

Spatial analysis on carbon storage and carbon density of arbor forest in each administrative region

Based on the data about carbon storage and carbon density in the arbor layer in six administrative regions of the main urban area in Xi'an, and by applying the analysis software ARCGIS10.2, the author carried out geographic space analysis on carbon storage and carbon density of arbor forest in the main urban area (Beilin District, Yanta District, Xincheng District, Lianhu District, Baqiao District, and Weiyang District). Also obtained was the spatial distribution of the carbon storage and carbon density in the arbor layer in each Xi'an administrative region (*Fig. 6*).

It can be seen from *Figure 6* that the distribution of carbon density in the arbor layer in each Xi'an administrative region was characterized by high carbon density in the southern suburbs and low carbon density in the northern suburbs. The order of average carbon density in the arbor forest in each administrative region was Beilin District > Xincheng District > Lianhu District > Yanta District > Baqiao District > Weiyang District. The distribution of carbon storage in the arbor layer in each Xi'an administrative region is characterized by high carbon storage in the southern suburbs and low carbon density in the western suburbs. The order of average carbon storage in the arbor forest in each administrative region was Yanta District > Beilin District > Weiyang District > Baqiao District > Lianhu District > Xincheng District. The research showed that Beilin District had superior carbon storage and carbon density because of substantial development, well-developed economy, and concentration of schools

(especially colleges and universities) in Beilin District. The carbon storage in arbor forest of Lianhu District in the western suburbs and Xincheng District in the eastern suburbs was relatively low. The carbon density in the Weiyang District in the northern suburbs was also low, and needs to be improved further. It can be seen from *Table 3* that in the six administrative regions, the area of Beilin District is the smallest and the population density is the highest. At the same time, its average carbon density is the highest (8.39 kg/m²), which indicated that the age of the forest and area of forest land are factors that directly affect carbon density and carbon storage. In contrast, population density and human disturbance are indirect factors that affect carbon density and carbon storage. The ratio of area of land to carbon storage is 1/1.18 in Xincheng District, 1/4.92 in Beilin District, 1/1.15 in Lianhu District, 1/0.32 in Baqiao District, 1/0.41 in Weiyang District, and 1/1.13 in Yanta District. It can be seen that Baqiao District and Weiyang District need to increase the area of green space on the existing land area, especially the area of arbor forest.

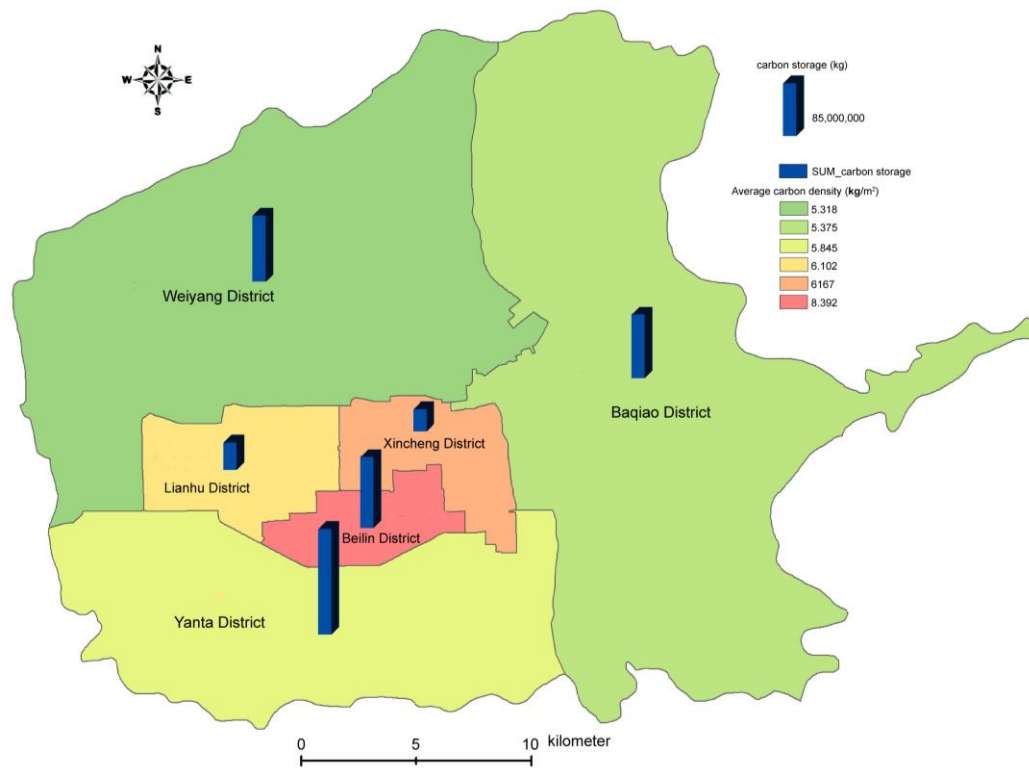


Figure 6. Spatial distribution of carbon storage and carbon density of arbor forest in each Xi'an administrative region

Spatial analysis on carbon storage and carbon density of arbor forest in different functional areas of each administrative region

By applying ARCGIS software, the author showed the spatial distribution of carbon storage and carbon density in five types of green space in six Xi'an administrative regions, including road green space, residential area, scenic area-green space, cultural and educational green space, and industrial green space, as shown in *Figures 7* and *8*. The detailed information about the spatial distribution of carbon density of each type of green space in each Xi'an administrative region is shown in *Table 3*.

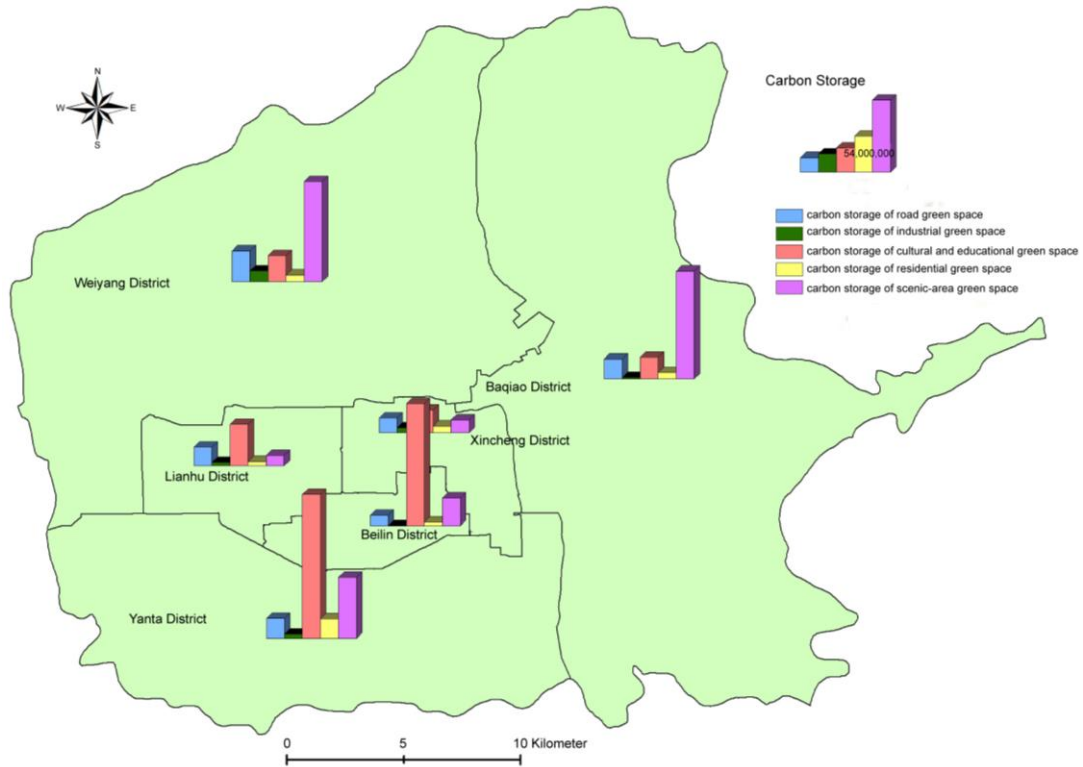


Figure 7. Spatial distribution of carbon storage of green space in each Xi'an Administrative region

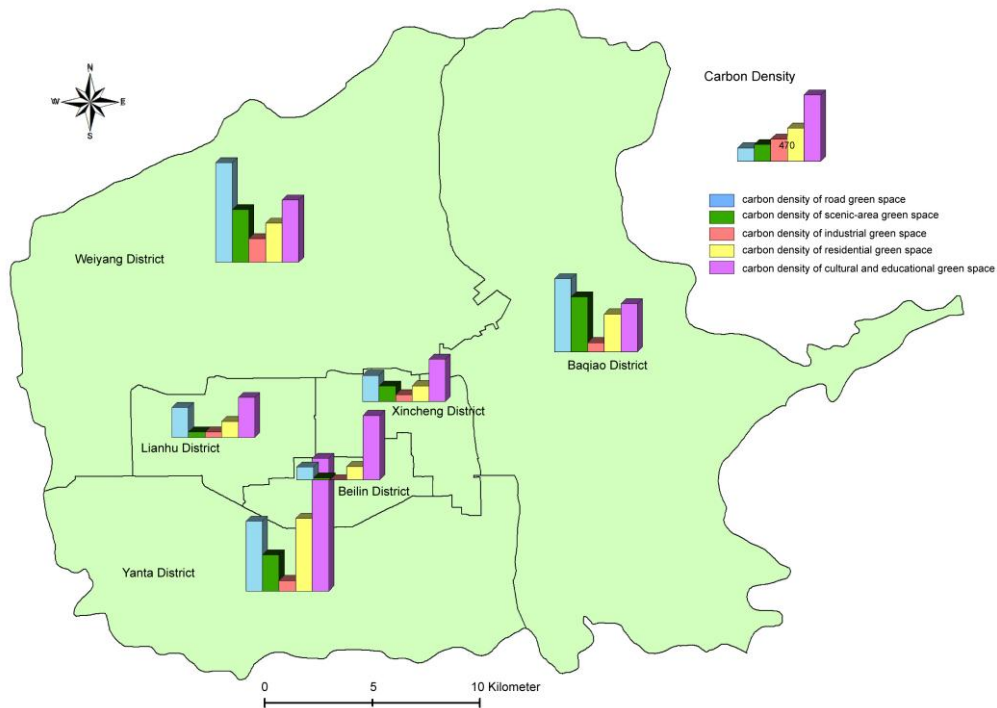


Figure 8. Spatial distribution of carbon density of green space in each Xi'an Administrative region

Table 3. Carbon storage of green space types in Xi'an administrative region

Administrative region	Road green space			Residential green space			Scenic-area green space			Cultural and educational green space			Industrial green space		
	Area (m ²)	Carbon storage (kg)	Carbon density (kg/m ²)	Area (m ²)	Carbon storage (kg)	Carbon density (kg/m ²)	Area (m ²)	Carbon storage (kg)	Carbon density (kg/m ²)	Area (m ²)	Carbon storage (kg)	Carbon density (kg/m ²)	Area (m ²)	Carbon storage (kg)	Carbon density (kg/m ²)
Xincheng District	57250.01	10627891.08	185.64	45232.66	5036204.27	111.34	88306.90	9622811.15	108.97	56963.12	17034250.39	299.04	79003.43	3792164.62	48.00
Beilin District	87835.39	7943832.77	90.44	29274.09	2744738.47	93.76	1623101.0	20808151.18	12.82	200469.20	91349788.07	455.68	0.00	0.00	0.00
Lianhu District	65773.95	14088780.57	214.20	27305.66	3120217.72	114.27	203859.80	7840447.57	38.46	108262.10	30833048.35	284.80	63920.84	2454560.27	38.40
Baqiao District	29080.89	15088328.73	518.84	18368.02	4951283.56	269.56	206459.70	80727810.54	391.01	47549.84	16250633.65	341.76	16383.51	1100971.57	67.20
Weiyang District	32352.99	22792033.26	704.48	17804.33	4903667.32	275.42	201518.0	74920380.11	371.78	43961.57	19406395.88	441.44	47578.50	7917063.03	166.40
Yanta District	30095.94	14898694.69	495.04	28548.67	14638333.0	512.75	177780.0	45582801.39	256.40	114551.90	107660462.11	939.84	40400.94	2973509.11	73.60

It can be seen in *Figures 7 and 8* and *Table 3* that the carbon storage capacity of each type of green space occurred in the order cultural and educational green space > road green space > scenic-area green space > residential green space > industrial green space in Xincheng District. In Beilin District, the order was cultural and educational green space > scenic-area green space > road green space > residential green space > industrial green space. The order was cultural and educational green space > road green space > scenic-area green space > residential green space > industrial green space in Lianhu District; but scenic-area green space > cultural and educational green space > road green space > residential green space > industrial green space in Baqiao District. For Weiyang District, the order was scenic-area green space > road green space > cultural and educational green space > industrial green space > residential green space; and cultural and educational green space > scenic-area green space > road green space > residential green space > industrial green space in Yanta District.

The carbon density of each green space type occurred in the order cultural and educational green space > road green space > residential green space > scenic-area green space > industrial green space in Xincheng District; cultural and educational green space > residential green space > road green space > scenic-area green space > industrial green space in Beilin District, and cultural and educational green space > road green space > residential green space > scenic-area green space > industrial green space in Lianhu District. For Baqiao District the order was road green space > scenic-area green space > cultural and educational green space > residential green space > industrial green space; while in Weiyang District it was road green space > cultural and educational green space > scenic-area green space > residential green space > industrial green space; and finally, in Yanta District, the order was cultural and educational green space > residential green space > road green space > scenic-area green space > industrial green space.

The research showed that the spatial distribution of carbon storage and carbon density of arbor forest in Xi'an is not balanced; it is high in the southern suburbs and low in the northern suburbs. The greatest contribution rate of carbon storage occurred in the cultural and educational green space in Yanta District, followed by the cultural and educational green space in Beilin District, scenic-area green space in Baqiao District, and scenic-area green space in Weiyang District, respectively. The least contribution rate of carbon storage was in residential green space in Weiyang District, in which the construction of residential green space should be increased.

Discussion

In the twentieth century, the urbanization process has been accelerated, the urban population in the world has increased by 10 times, and the proportion of urban population has risen from 14% to 50%. It is estimated that by 2030, more than 60% of the world's population will live in cities. As of 2010, the proportion of urban population in China reached 49.68% and the spatial expansion of the area used for urban and town land use will increasingly become the main feature of land use change in China in the next few decades (Minghong et al., 2004). This rapid expansion of cities, and the evolution of land use patterns, will have a profound impact on conditions for urban plants, further affecting their distribution pattern, species composition, and diversity. The temporal and spatial evolution of land use has been

characterized by rapid and intense expansion of land under construction and the occupation of a large amount of arable land.

At present, more than 50% of the world population lives in cities, and the cities that account for 2% of the land area now emit 78% of the greenhouse gases (Grimm, et al., 2000). The amount of CO₂ produced in urban regions is believed to be greater, accounting for 96% to 98% of total emissions (IPCC, 2000). The urban expansion in Xi'an was quite rapid, more than 10% of the annual growth rate. At present, the area of current urban regions is over 1,000 km², and the rapid development of urbanization has brought severe challenges to the urban ecological environment. These have restricted improvements of quality of life for residents and of further development of urbanization. What is more, urban heat island effect, environmental pollution, greenhouse effects, traffic jams, and other ecological and environmental problems are constant. Forest carbon sequestration plays an important role in mitigating global climate change. Carbon sequestration is of great importance in reducing the greenhouse gas concentration in the atmosphere and slowing global warming. Therefore, urban ecosystems play important roles in the global carbon cycle.

At present, there are still large uncertainties in the estimation of soil carbon sequestration and vegetation carbon sequestration, especially the carbon sequestration by scrub-grassland and trees that are outside of forests. In addition, the R&D on the atmosphere inversion model that accords with China's actual situation can not only simulate the amount and distribution of carbon sequestration, but can also predict future carbon sequestration scientifically (Fang et al., 2007).

Human activity is an important factor affecting the spatial distribution of the quantity and density of carbon stored in forest vegetation. At the same time, plant abundance, evenness, and diversity are drivers of carbon storage in forest vegetation. The carbon stored in the Xi'an forest vegetation plays an important role in regional carbon balance and cycle. Furthermore, the carbon stored in the arbor forest in Xi'an is almost proportional to the diameter at breast height (D) and the height (H) of the trees; therefore, the carbon density of forest in Xi'an is closely related to the age of the forest.

The quantity and density of the carbon stored in the Xi'an forest vegetation are relatively low because it has a relatively large proportion of young and middle-aged forests. There is great potential for carbon sequestration in the Xi'an forest vegetation in the future. Carbon storage in forest vegetation is the basis for measuring the ecological benefits of forests and a key indicator with which to measure ecological construction. The quality of the forest structure in Xi'an needs to be improved further, and the protection of urban species diversity strengthened, so that the ecosystem services of the forest city can be expanded to its fullest.

Conclusion

Through investigation of 240 quadrats from 113 roads, 20 parks, 23 residential quarters, 18 schools, and 6 industrial zones in Xi'an, 68 tree species were found in the main urban area in Xi'an. The predominant tree species were *Platanus orientalis*, *Styphnolobium japonicum* (L.) Schott (Chinese scholar tree), and *Ligustrum lucidum*. The entire group of trees belonged to 36 families and 63 genera; and accounted for 64.57% of the total vegetation. The ratio of evergreen tree species to deciduous tree species was 2:9, of which deciduous tree species mainly included 50 species

(including the Chinese scholar tree and the ginkgo (*Ginkgo biloba*) belonging to 30 families and 44 genera, and accounting for 81.22%. Evergreen tree species included 18 species (including *Cedrus deodara*, *Magnolia grandiflora*, and *Ligustrum lucidum*) belonging to 11 families and 19 genera, and accounting for 18.78%. In general, there was a smaller number of evergreen plants in Xi'an and the proportion was not balanced. Based on the high-resolution satellite remote-sensing image data, by combining with 3S technology (GIS, RS, and GPS) and applying measurements from actual quadrats, the author carried out accurate estimation of carbon density and total carbon storage by forest vegetation in the main urban area of Xi'an. Then, the author carried out quantitative analysis of the spatial distribution of carbon storage and carbon density in arbor forest in the main urban area of Xi'an using the analysis software ARCGIS10.2. This was used to analyze the spatial distribution of carbon storage and carbon density in the arbor layer in each Xi'an administrative region. From the research results discussed data, the findings are as follows.

(1) The average carbon density in the arbor layer of each type of green space in the main urban area of Xi'an occurred in the order cultural and educational green space > scenic-area green space > road green space > industrial green space > residential green space; and the average carbon density in the arbor layer in the main urban area of Xi'an was 6.308 kg/m², which is higher than that in Shaanxi Province. The average carbon storage in the arbor layer of each green space type in the main urban area of Xi'an occurred in the order cultural and educational green space > scenic-area green space > road green space > residential green space > industrial green space. The carbon storage in the cultural and educational green space was 210,990 t C, accounting for 40.6% of the arbor layer carbon sequestration in the main urban area. The carbon storage in scenic-area green space contributed 35.1% to the carbon sequestration of the arbor layer in the whole city. The carbon storage in the road green space accounted for 14.3% of total carbon storage of the arbor layer in the whole city and the carbon storage in the residential green space accounted for 6.6% of total carbon storage of arbor in the whole city. Carbon storage in the industrial green space accounted for only 3.3% of total carbon storage of the arbor layer in the whole city. The total amount of carbon storage in the arbor layer in the main Xi'an urban area was 519,180 t C.

(2) The distribution of carbon density of arbor layer in each Xi'an administrative region is characterized by high carbon density in the southern suburbs and low carbon density in the northern suburbs, and the average carbon density of arbor forest in each administrative region was in the order Beilin District > Xincheng District > Lianhu District > Yanta District > Baqiao District > Weiyang District. The distribution of carbon storage in the arbor layer in each Xi'an administrative region is characterized by high carbon storage in the southern suburbs and low carbon density in the western suburbs, and the average carbon storage in arbor forest in each administrative region was in the order Yanta District > Beilin District > Weiyang District > Baqiao District > Lianhu District > Xincheng District.

(3) The carbon storage capacity of each type of green space was in the order cultural and educational green space > road green space > scenic-area green space > residential green space > industrial green space in Xincheng District; cultural and educational green space > scenic-area green space > road green space > residential green space > industrial green space in Beilin District; cultural and educational green space > road green space > scenic-area green space > residential green space > industrial green space in Lianhu District; scenic-area green space > cultural and educational green space >

road green space > residential green space > industrial green space in Baqiao District; scenic-area green space > road green space > cultural and educational green space > industrial green space > residential green space in Weiyang District, and cultural and educational green space > scenic-area green space > road green space > residential green space > industrial green space for Yanta District.

(4) The carbon density of each type of green space occurred in the order cultural and educational green space > road green space > residential green space > scenic-area green space > industrial green space in Xincheng District; cultural and educational green space > residential green space > road green space > scenic-area green space > industrial green space in Beilin District; cultural and educational green space > road green space > residential green space > scenic-area green space > industrial green space in Lianhu District; road green space > scenic-area green space > cultural and educational green space > residential green space > industrial green space in Baqiao District; road green space > cultural and educational green space > scenic-area green space > residential green space > industrial green space in Weiyang District; and cultural and educational green space > residential green space > road green space > scenic-area green space > industrial green space in Yanta District.

(5) The greatest contribution rate of carbon storage occurred in the order cultural and educational green space in Yanta District, followed by cultural and educational green space in Beilin District, scenic-area green space in Baqiao District, and scenic-area green space in Weiyang District. The least contribution rate of carbon storage was by residential green space in Weiyang District. In general, the spatial distribution of carbon storage and carbon density in Xi'an is not balanced: high in the southern suburbs and low in the northern suburbs.

In summary, the forest vegetation in Xi'an has great potential for carbon sequestration. The results showed that the average carbon density of arbor trees in the main urban area of Xi'an was 6.308 kg/m^2 , which is higher than the average carbon density in Shaanxi Province (3.092 kg/m^2). Moreover, the arbor forest of Xi'an makes a great contribution to the forest carbon sequestration in Shaanxi Province, playing a key role in whole-province forest sequestration. Because of the characteristics of the geographical environment in Xi'an, the fragile ecological environment and serious soil erosion, an effective approach would be to increase forest vegetation, improve the quality of forest structure, increase the quantity of three-dimensional greenery, and manage forest vegetation with attention to detail, to improve the urban environment and enhance forest carbon sequestration. This would improve the ability of the urban forest to fulfill its ecological service functions. In the future, based on the remote sensing image data and use of large-scale quadrats, the existing database will be updated via GIS, and an inversion model suitable for the actual situation in each region will provide a direction for developing more accurate assessment of regional forest carbon sequestration.

Acknowledgements. The research was funded by the National Natural Science Foundation of China (51608419) and the Shaanxi Provincial Natural Science Foundation (2014JZ011).

REFERENCES

- [1] Beer, C., Reichstein, M., Tomelleri, E., Jung, M., Carvalhais, N., Rödenbeck, C., Arain, M. A., Baldocchi, D., Bonan, G. B., Bondeau, A., Cescatti, A., Lasslop, G., Lindroth, A., Lomas, M., Luysaert, S., Margolis, H., Oleson, K. W., Rouspard, O., Veenendaal, E., Viovy, N., Williams, C., Woodward, F. I., Papale, D. (2010): Terrestrial gross carbon dioxide uptake: global distribution and covariation with climate. – *Science* 329: 834-838.
- [2] Bonan, G. B. (2008): Forests and climate change: forcings, feedbacks, and the climate benefits of forests. – *Science* 320: 1444-1449.
- [3] Bousquet, P., Peylin, P., Ciais, P., Le Quéré, C., Friedlingstein, P., Tans, P. P. (2000): Regional changes in carbon dioxide fluxes of land and oceans since 1980. – *Science* 290: 1342-1346.
- [4] Coley, R. L., Sullivan, W. C., Kuo, F. E. (1997): Where does community grow? The social context created by nature in urban public housing. – *Environment & Behavior* 29: 468-494.
- [5] Dixon, R. K., Solomon, A. M., Brown, S., Houghton, R. A., Trexler, M. C., Wisniewski, J. (1994): Carbon pools and flux of global forest ecosystems. – *Science* 262: 185-190.
- [6] Dongsheng, G., Yujuan, C., Fenfang, H. (1998): The storage and distribution of carbon in urban vegetation and its role in balance of carbon and oxygen in Guangzhou 1998. – *China Environmental Science* 18: 437-441.
- [7] Fang, J. Y. (2000): Forest biomass carbon pool of the middle and high latitudes in North Hemisphere is probably much smaller than present estimates. – *Acta Phytoecologica Sinica* 24: 635-638.
- [8] Fang, J. Y., Guo, Z. D., Pu, S. L., Chen, A. P. (2007): Estimation of carbon sequestration of terrestrial vegetation in China from 1981-2000. – *Science in China (Series-D: Earth Sciences)* 37: 804-812.
- [9] Fang, J. Y., Chen, A. P., Peng, C. H., Zhao, S., Ci, L. (2001): Changes in forest biomass carbon storage in China between 1949 and 1998. – *Science* 292: 2320-2322.
- [10] Ge, Z., Zhou, D., He, Y., Chen, P., Guan, Q. (2013): Current status of arborous carbon storage in urban green space of Xuzhou City. – *China Forestry Science and Technology* 27: 30-34.
- [11] Grimm, N. B., Grove, J. M., Pickett, S. T. A., Redman, C. L. (2000): Integrated approaches to long-term studies of urban ecological systems. – *BioScience* 50: 571-584.
- [12] Houghton, J. T., Meira Filho, L. G., Bruce, J., Lee, H., Callander, B. A., Haites, E., Harris, N., Maskell, K. (eds.) (1994): *Climate Change 1994: Radiative Forcing of Climate Change and an Evaluation of the IPCC IS92 Emission Scenarios*. – Cambridge University Press, Cambridge, UK.
- [13] Huang, C. D., Zhang, J., Yang, W. Q., Tang, X., Zhang, G. Q. (2009): Spatial differentiation characteristics of forest vegetation carbon stock in Sichuan Province. – *Acta Ecologica Sinica* 29: 5115-5121.
- [14] Intergovernmental Panel on Climate Change (IPCC) (2000): *Emission Scenarios*. – In: Nakicenovic, N., Swart, R. (eds.) *Special Report on Emission Scenarios*. Cambridge University Press, Cambridge, UK.
- [15] Janssens, I. A., Freibauer, A., Ciais, P., Smith, P., Nabuurs, G. J., Folberth, G., Schlamadinger, B., Hutjes, R. W. A., Ceulemans, R., Schulze, E. D., Valentini, R., Dolman, A. J. (2003): Europe's terrestrial bio-sphere absorbs 7 to 12% of European anthropogenic CO₂ emission. – *Science* 300: 1538-1542.
- [16] Jo, H. K., McPherson, G. E. (1995): Carbon storage and flux in urban residential green space. – *Journal of Environmental Management* 45: 109-133.
- [17] Liu, G., Fu, B., Fang, J. (2000): Carbon dynamics of Chinese forests and its contribution to global carbon balance. – *Acta Ecologica Sinica* 20: 733-740.

- [18] Liu, Z., Li, B., Fang, X., Xiang, W., Tian, D., Yan, W., Lei, P. (2016): Dynamic characteristics of forest carbon storage and carbon density in Hunan Province. – *Acta Ecologica Sinica* 36: 6897-6908.
- [19] Ma, Q., Liu, K., Zhang, H. (2012): Carbon storage by forest vegetation and its spatial distribution in Shaanxi. – *Resources Science* 34: 1781-1789.
- [20] Mcpherson, E. G. (1998): Atmospheric carbon dioxide reduction by Sacramento's urban forest. – *Journal of Arboriculture* 24: 215-223.
- [21] Minghong, T., Xiubin, L., Changhe, L. (2004): Expansion of construction land in China's Large and medium-sized cities in the 1990s and its occupation of cultivated land. – *Science in China (Series-D: Earth Sciences)* 34: 1157-1165.
- [22] Niemelä, J., Saarela, S. R., Söderman, T., Kopperoinen, L., Yli-Pelkonen, V., Väire, S., Kotze, D. J. Soderman, T. (2010): Using the ecosystem services approach for better planning and conservation of urban green spaces: a Finland case study. – *Biodiversity and Conservation* 19: 3225-3243.
- [23] Nowak, D. J. (1993): Atmospheric carbon reduction by urban tree. – *Environmental Management* 37: 207-217.
- [24] Nowak, D. J., Crane, D. E. (2002): Carbon storage and sequestration by urban trees in the USA. – *Environmental Pollution* 116: 381-389.
- [25] Pacala, S. W., Hurtt, G. C., Baker, D., Peylin, P., Houghton, R. A., Birdsey, R. A., Heath, L., Sundquist, E. T., Stallard, R. F., Ciais, P., Moorcroft, P., Caspersen, J. P., Shevliakova, E., Moore, B., Kohlmaier, G., Holland, E., Gloor, M., Harmon, M. E., Fan, S. M., Sarmiento, J. L., Goodale, C. L., Schimel, D., Field, C. B. (2001): Consistent land-and atmosphere-based US carbon sink estimates. – *Science* 292: 2316-2320.
- [26] Piao, S. L., Fang, J. Y., Zhu, B., Tan, K. (2005): Forest biomass carbon stocks in China over the past 2 decades: estimation based on integrated inventory and satellite data. – *Journal of Geophysical Research* 110: G01006.
- [27] Siegenthaler, U., Sarmiento, J. L. (1993): Atmospheric dioxide and the ocean. – *Nature* 365: 119-125.
- [28] Tans, P. P., Fung, I. Y., Takahashi, T. (1990): Observational constraints on the global atmospheric CO₂ budget. – *Science* 247: 1431-1438.
- [29] Wang, X., Feng, Z., Ouyang, Z. (2001): Vegetation carbon storage and density of forest ecosystems in China. – *Chinese Journal of Applied Ecology* 12: 13-16.
- [30] Yan, S., Ying, G., Hexian, J., Yuan, R., Zelong, Q., Zhiyi, B., Jie, C. (2016): Progress in studies on carbon sequestration of urban vegetation. – *Scientia Silvae Sinicae* 52: 122-129.
- [31] Zhen, W., Huangmei, M., Zhai, Y., Chen, K., Gong, Y. Z. (2014): Variation of forest vegetation carbon storage and carbon sequestration rate in Liaoning Province, Northeast China. – *Chinese Journal of Applied Ecology* 25: 1259-1265.

THE SYNTHESIS OF PLANT GROWTH STIMULATORS BY PHYTOPATHOGENIC BACTERIA AS FACTOR OF PATHOGENICITY

DANKEVYCH, L.¹ – LEONOVA, N.¹ – DRAGOVOZ, I.¹ – PATYKA, V.¹ – KALINICHENKO, A.^{2,3} –
WŁODARCZYK, P.^{2*} – WŁODARCZYK, B.²

¹*Zabolotny Institute of Microbiology and Virology, National Academy of Sciences of Ukraine
154 Acad. Zabolotny str., Kyiv 03143, Ukraine*

²*Department of Process Engineering, Faculty of Natural Sciences and Technology,
University of Opole
Dmowskiego str. 7-9, 45-365 Opole, Poland*

³*Faculty of Economics and Management, Poltava State Agrarian Academy
Skovorody str. 1/3, Poltava 36003, Ukraine*

**Corresponding author*

e-mail: pawel.wlodarczyk@uni.opole.pl; phone: +48-77-401-6706

(Received 30th Sep 2017; accepted 12th Feb 2018)

Abstract. The environmental changes significantly influence the microorganisms and affect their properties, leading them to take uncharacteristic ecological niches. This study has focused on the ability of phytopathogenic bacteria that belongs to the genera *Pseudomonas*, *Curtobacterium*, *Ralstonia*, *Pantoea* and *Xanthomonas*, which are able to cause various diseases of legumes, to produce extracellular phytohormones with stimulatory action in vitro. The qualitative and quantitative composition of extracellular auxins and cytokinins has been determined by spectrodensitometric thin-layer chromatography. This research revealed that the synthesis of plant growth promoting phytohormones that are agents of different plant bacterial disease, play an important role in their pathogenicity and ecological plasticity. In particular, it has been established that the level of auxins synthesis by the studied bacteria, which cause diseases of legumes, correlates directly with their pathogenic properties. Also, a clear connection between the pathways of interaction with plant and the amount and spectrum of synthesized auxins and cytokinins has been revealed.

Keywords: *phytohormones, phytopathogenic bacteria, pathogens spreading, auxin, cytokinin, bacterial infection*

Introduction

It is known that the environmental changes associated with anthropogenic factor significantly affect both macro and microorganisms. Some researchers have shown that a change in the ecological conditions of microorganisms' existence leads to changes in their properties, allowing them to expand their area of presence. This tendency involves phytopathogenic bacteria. Pathogenic bacteria of polyphagous and monophagous nature expand the number of plant species that they affect. On the other hand, the bacteria, previously considered as opportunistic, increase their level of aggressiveness (Patyka and Pasichnyk, 2014; Zakharova et al., 2015; Patyka et al., 2015). Such changes of phytopathogen's properties occur due to accepting of new mechanisms of virulence, or to improvement of the ways of disease development.

Phytohormones play the regulatory role not only in the key physiological processes of plants, but they are involved also in plant–microbe interactions (Cui et al., 2009;

Boivin et al., 2016). Five main classes of compounds with phytohormonal activity can be distinguished, such as: auxins, cytokinins, gibberellins, ethylene and abscisic acid. Auxins, cytokinins and gibberellins have a stimulating effect on the key processes of plant ontogenesis, while ethylene and abscisic acid are hormones with inhibiting and anti-stress action. Auxins and cytokinins play an important role in the process of growth and development of plants as well as in their interactions with bacteria, including pathogens. Auxins are derivatives of indole compounds, the most known of which is indole-3-acetic acid (IAA). This compound is produced by plants and microorganisms *de novo* from tryptophan through many pathways (Woodward and Bartel, 2005; Spaepen et al., 2007). Synthesis of auxins and cytokinins as mechanisms to infect plant tissues is quite common in phytopathogenic bacteria. This process is thoroughly investigated in tumor-inducing species, in particular, *Agrobacterium tumefaciens*. In these bacteria the genes responsible for synthesis of cytokinins are transferred by bacterial Ti-plasmids, which are integrated into genome of plants (Jameson, 2000). The similar genes were found in cells of other phytopathogenic bacteria (Kakimoto, 2003; Frébort et al., 2011). But, besides the tumor- and gall-inducing species, other phytopathogenic bacteria, which cause necrosis, chlorosis, wilts or rots of plants, are also able to synthesize auxins and cytokinins (Jameson, 2000). Information about the role of auxins and cytokinins in plant–pathogen interaction is constantly supplemented with new data (Jin et al., 2003; Navarro et al., 2006; Chen et al., 2007; Ding et al., 2008).

Today, there are following concepts of the influence of auxins on disease development: first, exogenous auxins can weaken stiffness of the plant cell wall – a natural barrier against pathogens (Darley et al., 2001). They stimulate fast growth of plant organs by increasing the size of cells by stretching (“acid growth”). At the initial stage of infection process, pathogens synthesize IAA to stimulate the formation of enzymes of “acid growth” by a plant that induces hydrolysis of polysaccharides of the cell wall. Moreover, disaccharides and monosaccharides, which were released during this process, can serve as an ideal power source for pathogens for their survival and further spread (Lindow and Brandl, 2003). Second, exogenous auxins participate in the work of stomata, ensuring the pathways for invasion of some phytopathogens in plant tissues (Nico-Liu et al., 2006; Gottig et al., 2009). Finally, IAA-signaling can be antagonistic to the SAR-pathway (systemic acquired resistance) of formation of plant resistance to diseases (Chen et al., 2007; Pfeilmeier et al., 2016).

Synthesis of cytokinins as a mechanism for successful invasion into plant tissues is widespread among galls-forming bacteria, which usually have plasmid location of genes responsible for their synthesis. But physiological expedience of these hormones synthesis by non-tumors inducing species of phytopathogenic bacteria is not fully clear (Jameson, 2000).

The complete analysis of synthesis of plants growth promoting phytohormones by pathogenic bacteria, which cause various plant diseases, or differ by virulence properties, is rare. The present study is the first report about quantitative and qualitative analysis of extracellular auxins and cytokinins, synthesized by different species of bacteria pathogenic to legumes *in vitro*. This study can provide a new perspective on better understanding the compound role that stimulates plants’ growth and influences virulence of pathogens, plant infections and development of various diseases types. Also this research will hopefully improve the knowledge about different interactions between pathogen and plant.

Materials and methods

The subject of our research is the ability of various types of pathogenic bacteria for legume cultures to synthesize a wide range of extracellular auxins and cytokines. Objects of investigation were strains of phytopathogenic bacteria specified in *Table 1*. Strain *P. savastanoi* pv. *savastanoi* 9174^T, which is able to induce formation of tumors in plants was included in the study as a control.

Table 1. The strains of pathogenic for legumes bacteria used in research

Species, pathovar, strain	Place isolating, a year, the plant host
" <i>Pseudomonas lupini</i> " 8531, 8532, 8533, 8534, 8535	Ukraine, 1963-1971 years, lupine
" <i>Pseudomonas lupini</i> " 17, 6, 22	Ukraine, 2002-2003 years, lupine
" <i>Pseudomonas xanthochlora</i> " 8540	Ukraine, 1963-1971 years, lupine
" <i>Pseudomonas xanthochlora</i> " 3L, 9L	Ukraine, 2006-2007 years, lupine
<i>Pseudomonas syringae</i> pv. <i>syringae</i> * UCM B-1027 ^T (NCPPB 281, ICMP 3023 typical strain)	UK, 1950 year, lilac
<i>Pseudomonas savastanoi</i> pv. <i>phaseolicola</i> UCM B-1123 ^T (**NCPPB 52, ***ICMP 2740 pathotype strain)	Canada - ****, beans
<i>Pseudomonas syringae</i> pv. <i>pisi</i> 9177 ^T (ICMP 2452, NCPPB 2585 pathotype strain)	New Zealand, 1969 year, peas
<i>Pseudomonas savastanoi</i> pv. <i>savastanoi</i> 9174 ^T (NCPPB 639, ICMP 4352 pathotype strain)	Yugoslavia, 1959 year, oil
<i>Pseudomonas marginalis</i> pv. <i>marginalis</i> 9175 ^T (NCPPB 667, ICMP 3553 typical strain)	Belgium, chicory
<i>Pseudomonas savastanoi</i> pv. <i>glycinea</i> 8571 (NCPPB 1139)	Zimbabwe, soybeans
<i>Curtobacterium flaccumfaciens</i> pv. <i>flaccumfaciens</i> 6564	Ukraine, 1952 year, beans
<i>Ralstonia solanacearum</i> UCM B-1109 ^T (NCPPB 325, ICMP 5712 typical strain)	USA, 1953 year, tomato
<i>Pantoea agglomerans</i> 8490	Romania, 1970 year, oats
<i>Pseudomonas syringae</i> pv. <i>tabaci</i> 225	Ukraine, 1946 year, tobacco
<i>Xanthomonas axonopodis</i> pv. <i>glycines</i> 8609	Ukraine, 1960 year, soybean

Notes: 1.*UCM – Ukrainian Collection of Microorganisms; 2.**NCPPB National Collection of Plant Pathogenic Bacteria, UK; 3.***ICMP – International Collection of Microorganisms from Plants, New Zealand; 4.**** – data available

Phytopathogenic bacteria of the genera: *Pseudomonas*, *Curtobacterium*, *Ralstonia*, *Pantoea* were cultured in the mineral Omelyansky medium (H₂O distilled – 1l.; K₂HPO₄ – 1.0 g; (NH₄)₂HPO₄ – 1.0 g; MgSO₄ – 0.5 g; CaCl₂ – 0.1 g; NaCl and FeSO₄ – trace amounts) for 24-48 h in 750 ml flasks on a shaker (220 rev min⁻¹) at 26-28 °C. Bacteria of the genus *Xanthomonas* were cultured in similar conditions in the synthetic Lich (Lili) medium (H₂O distilled – 1.0 l; casein – 2.0 g; fumaric acid – 1.3 g; K₂HPO₄ – 1.0 g; MgSO₄·7 H₂O – 0.5 g; Na₂CO₃ – 1.1 g; Fe₂(SO₄)₃ – 0.2 mg; ZnSO₄ – 0.2 mg; MgSO₄ – 0.1 mg; glucose – 15 g). To determine the spectrum of exogenous auxins the culture medium was added with 0.1% tryptophan.

In order to separate the biomass, the culture fluids of bacteria were centrifuged for 20 min at 9000 rev min⁻¹ and at 4 °C. The cells of bacteria were washed three times. The supernatants were used for further investigation to extract phytohormonal

compounds. The sediment of cells was suspended in distilled water and then dried at 103-105 °C in a desiccator, until constant weight. The amount of absolutely dry biomass (ADB) of microorganisms was determined gravimetrically. Determination of qualitative and quantitative composition of phytohormones in the culture fluids of phytopathogenic bacteria was performed by spectrodensitometric thin-layer chromatography (Pant and Agrawal, 2014; Leonova, 2015). Extracellular auxins and cytokinins were isolated from the supernatants of phytopathogenic bacteria by extraction of phytohormones with acetic acid ethyl ether at pH 3.0 and with n-butanol at pH 8.0. The obtained extracts were evaporated under vacuum at 40-45 °C. The dry sediment was dissolved in ethanol. Ethanol extracts of the supernatants of the studied bacteria were used for accumulative thin-layer chromatography. Quantitative determination of auxins and cytokinins was performed by using a Sorbfil scanning spectrodensitometer. In the research the synthetic standards of phytohormones were used, produced by companies *Sigma-Aldrich* and *Acros Organic*.

All experiments were performed in 6 iterations. The results obtained were processed statistically using computer program *Excel* from licensed *Microsoft Office 2010*. In the table and the figures the average values and standard errors ($M \pm m$) are presented. Values of $P < 0.05$ were considered to be significant.

Results and discussion

It has been shown that legumes pathogenic bacteria are able to produce a wide range of both auxins and cytokinins (*Fig. 1*).

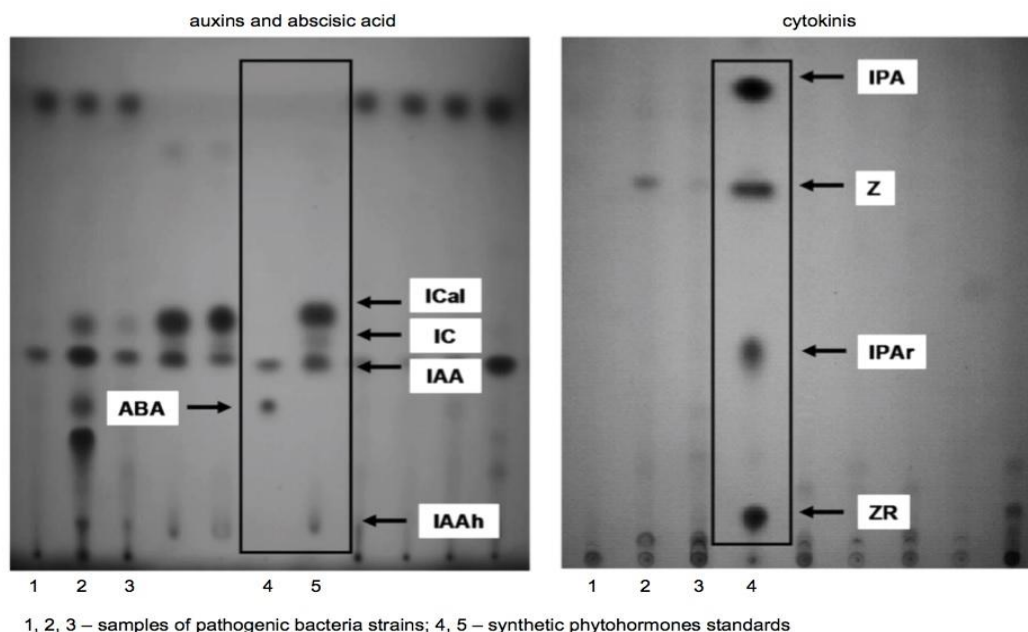


Figure 1. Detection of auxins, abscisic acid and cytokinins by TLC produced by phytopathogenic bacteria in thin layers of silicon oxide and aluminum oxide (Merck, UV_{254}): IAA – Indole-3-acetic acid; ICal – Indole-3-carboxaldehyde; IC – Indole-3-carbinol; ABA – abscisic acid; IAAh – Indole-3-acetic hydrazide; IPA – N^6 -(2-Isopentenyl)adenine; Z – zeatin; IPAr – N^6 -(2-Isopentenyl)adenosine; ZR – trans-Zeatin-riboside

The results show that the level of auxin synthesis by legumes pathogenic bacteria correlates directly with their pathogenic properties. Thus, the pathogens, which can affect a wide range of plants (polyphagous) – *P. syringae* pv. *syringae* B-1027^T, *P. marginalis* pv. *marginalis* 9175^T and *P. savastanoi* pv. *savastanoi* 9174^T synthesize higher levels of auxins (from 1987.91 to 1362.46 $\mu\text{g g}^{-1}$ ADB) compared with the phytopathogenic bacteria that cause disease in only one host plant (monophagous) – *P. savastanoi* pv. *phaseolicola* B-1123^T, *P. syringae* pv. *pisi* 9177^T (from 825.87 to 1267.5 $\mu\text{g g}^{-1}$ ADB) (Table 2).

Table 2. Analysis of extracellular auxins and cytokinins synthesis by pathogenic for legumes bacterial strains of the genus *Pseudomonas* with their pathogenic properties

Strains	Amount of phytohormones, $\mu\text{g/g}$ of absolutely dry biomass (ADB)		Pathogenic properties
	Auxins	Cytokinins	
<i>P. syringae</i> pv. <i>phaseolicola</i> UCM B-1123 ^T	1267.5	66.13	Monophagous, bean angular leaf spot
<i>P. syringae</i> pv. <i>pisi</i> 9177 ^T	825.87	92.03	Monophagous, pea bacterial blight
<i>P. syringae</i> pv. <i>syringae</i> UCM B-1027 ^T	1987.91	76.4	Polyphagous, cause different types of plant's disease belongs to more than 50 species
<i>P. marginalis</i> pv. <i>marginalis</i> 9175 ^T	1362.46	170.90	Polyphagous, cause disease of many plants species
<i>P. savastanoi</i> pv. <i>savastanoi</i> 9174 ^T (1 day cultivation)	344.67	331.97	Monophagous, causes tumours of plants which belongs to family <i>Oleaceae</i>

Furthermore, synthesis of auxins by tumor-inducing strain *P. savastanoi* pv. *savastanoi* 9174^T occurs gradually, respectively: 344.67 $\mu\text{g g}^{-1}$ ADB – the first day of culturing and 1893.24 $\mu\text{g g}^{-1}$ ADB – the second day of cultivation. This probably confirms the fact that the gradual synthesis of auxins causes stage-by-stage changes in hormonal regulation of plants, which ultimately leads to a gradual damage of plant tissue structure (Biovin et al., 2016; Jameson, 2000). Instead, already on the first day of cultivation, *P. syringae* pv. *syringae* B-1027^T, *P. marginalis* pv. *marginalis* 9175^T, significant amounts of auxins were synthesized, which indicates the possibility of using this indole compounds as the key virulence factors that quickly unbalance the hormonal regulation system of plants (Biovin et al., 2016; Jameson, 2000). Also, it should be noted that both polyphagous and monophagous differ in the spectrum of synthesized auxins (Fig. 2).

The representatives of pathovars of *phaseolicola*, *pisi*, *syringae*, included in the research, synthesize medium amounts of both IAA and indole-3-carboxylic acids, and indole-3-acetic acid hydrazide (from 41.5–58.3 to 39.71–53.1% of the total amount of auxins). Strain *P. savastanoi* pv. *savastanoi* 9174^T synthesizes almost equal numbers of both IAA and indole-3-carboxylic acids, and indole-3-carboxy-aldehyde (56.05 and 42.5% of the total amount of auxins). However almost 100% of auxins, synthesized by strain *P. marginalis* pv. *marginalis* 9175^T, accounted for IAA and indole-3-carboxylic acid (Fig. 2). No dependency was found between the number and range of synthesized

cytokinins and the pathogenic properties of polyphagous *P. syringae* pv. *syringae* B-1027^T, *P. marginalis* pv. *marginalis* 9175^T, as well as monophagous *P. syringae* pv. *phaseolicola* B-1123^T, *P. syringae* pv. *pisi* 9177^T (Fig. 3).

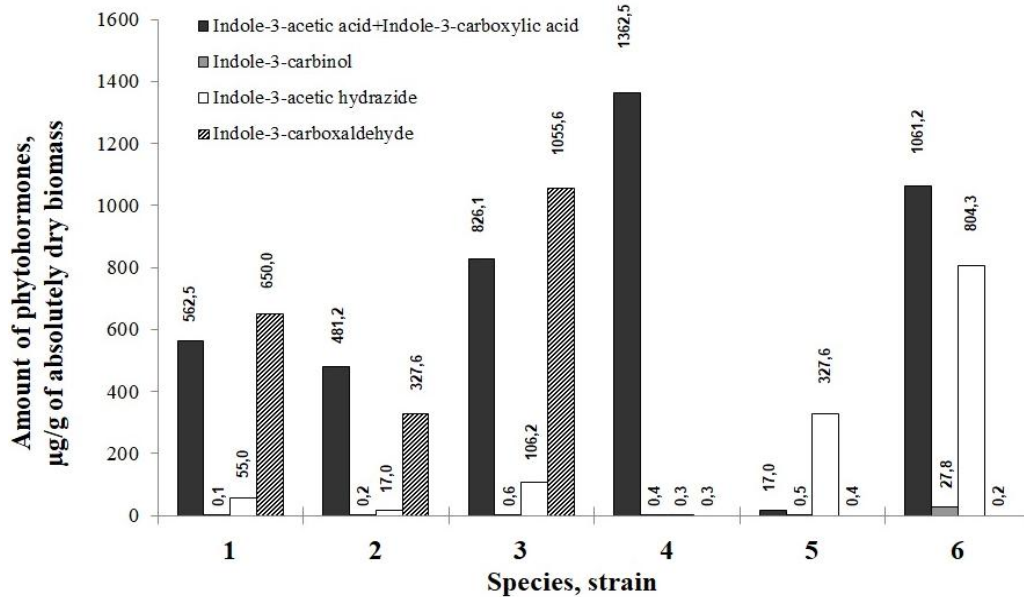


Figure 2. Synthesis of extracellular auxins by pathogenic for legume representatives of genus *Pseudomonas*: 1 – *P. syringae* pv. *phaseolicola* UCM B-1123^T, 2 – *P. syringae* pv. *pisi* 9177^T, 3 – *P. syringae* pv. *syringae* UCM B-1027^T, 4 – *P. marginalis* pv. *marginalis* 9175^T, 5 – *P. savastanoi* pv. *savastanoi* 9174^T (1 day cultivation), 6 – *P. savastanoi* pv. *savastanoi* 9174^T (2 days cultivation). Here and after: $M \pm m$, $n = 6$; $P < 0.05$ vs. control

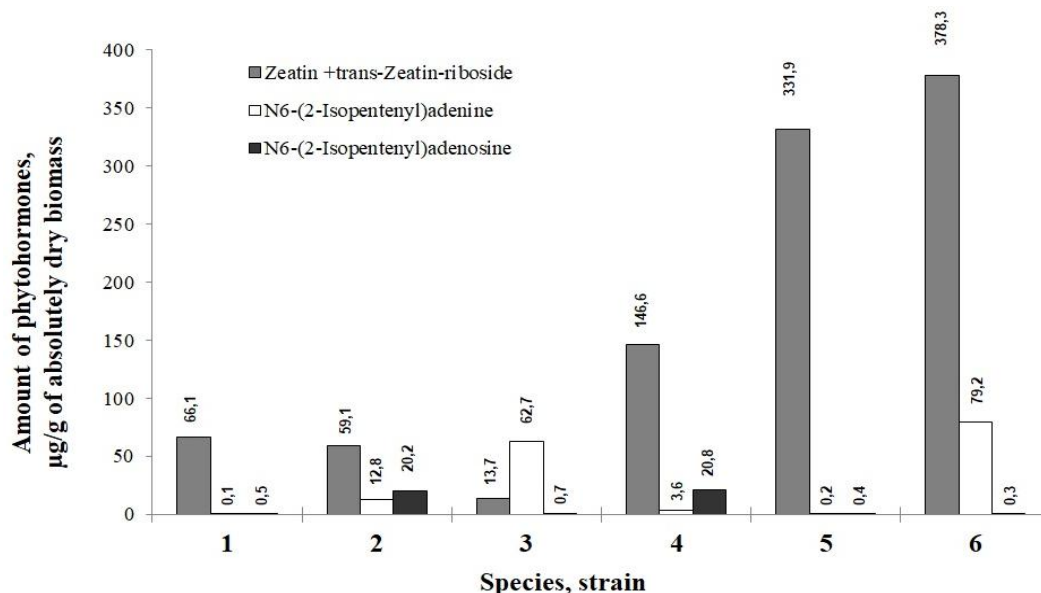


Figure 3. Synthesis of extracellular cytokinins by pathogenic for legume representatives of genus *Pseudomonas*: 1 – *P. syringae* pv. *phaseolicola* UCM B-1123^T, 2 – *P. syringae* pv. *pisi* 9177^T, 3 – *P. syringae* pv. *syringae* UCM B-1027^T, 4 – *P. marginalis* pv. *marginalis* 9175^T, 5 – *P. savastanoi* pv. *savastanoi* 9174^T (1 day cultivation), 6 – *P. savastanoi* pv. *savastanoi* 9174^T (2 days cultivation)

The highest levels of cytokinin synthesis were observed in tumor-inducing strain *P. savastanoi* pv. *savastanoi* 9174^T, both on the first and on the second day of culturing (331.97-457.51 µg g⁻¹ ADB). Also, it should be noted that this strain is able to synthesize the largest amount of such forms of cytokinins as zeatin and zeatin-riboside (Fig. 3).

During the research, on the example of two pathogens of bacterial diseases of lupine: “*Pseudomonas lupini*” (brown bacterial spot) and “*Pseudomonas xanthochlora*” (wet watery rot), a direct correlation between the level of aggressiveness of a strain on plants and the amount of synthesized auxins has been revealed (Table 3).

Table 3. Comparative characteristics of the amounts of extracellular auxins and cytokinins what synthesized by not valid taxa of pathogenic bacteria of the genus *Pseudomonas* with their level of aggressiveness on the zoned lupine’s varieties

Strains	Amount of phytohormones, µg/g of absolutely dry biomass (ADB)		Intermediate aggressive strains on host plants, scores
	Auxins	Cytokinins	
<i>P. syringae</i> (“ <i>P. lupine</i> ”) 8531	1554.82	Not determined	6.6±0.23
<i>P. syringae</i> (“ <i>P. lupine</i> ”) 8532	586.36	94.52	5.6±0.10
<i>P. syringae</i> (“ <i>P. lupine</i> ”) 8533	562.83	Not determined	4.4±0.19
<i>P. syringae</i> (“ <i>P. lupine</i> ”) 8534	914.05		4.4±0.12
<i>P. syringae</i> (“ <i>P. lupine</i> ”) 8535	1168.08		4.5±0.25
<i>P. syringae</i> (“ <i>P. lupine</i> ”) 6	2124.89	102.23	8.5±0.40
<i>P. syringae</i> (“ <i>P. lupine</i> ”) 17	2074.77	Not determined	8.2±0.50
<i>P. syringae</i> (“ <i>P. lupine</i> ”) 22	98.46	4.56	2.0±0.10
“ <i>P. xanthochlora</i> ” 8540	1207.68	27.66	7.7±0.25
“ <i>P. xanthochlora</i> ” 3L	1201.22	23.26	7.0±0.1
“ <i>P. xanthochlora</i> ” 9L	391.99	tr.	2.0±0.5

Note: “tr.” - found trace amounts

In particular, low aggressive strains of *Pseudomonas xanthochlora* produced amounts of auxins 3 times or more smaller than the highly aggressive strains. A similar regularity can be observed for *Pseudomonas lupini*. Thus, low aggressive strain “*Pseudomonas lupini*” 22 synthesizes the amount of auxins 21 or more times less than highly aggressive strains *Pseudomonas lupini* 6 and 17. However, in the medium aggressive and low aggressive collection strains of *Pseudomonas lupini*, this correlation between the level of aggressiveness and the total amount of synthesized auxins is not observed so clearly (Table 3). No direct connection between the range of indole compounds and aggressiveness of the strains has been found. Also, it should be noted that more than 90% of all auxins synthesized by low aggressive strain *Pseudomonas xanthochlora* 9L accounted for IAA, which re-affirms the primary role of the compound in initiation and development of microbe–plant interaction (Fig. 4). In addition, it was established that there is a correlation between the level of aggressiveness of a strain and the amount of synthesized cytokinins. Thus, the

smallest amounts of these compounds are synthesized by low aggressive strains *Pseudomonas xanthochlora* 9L and *Pseudomonas lupini* 22 (from trace amounts to 4.56 $\mu\text{g g}^{-1}$ ADB). Also, it should be noted that in all of the investigated strains the level of zeatin and its transport form zeatin-riboside makes the highest percentage of the pool of synthesized cytokinins (Fig. 5).

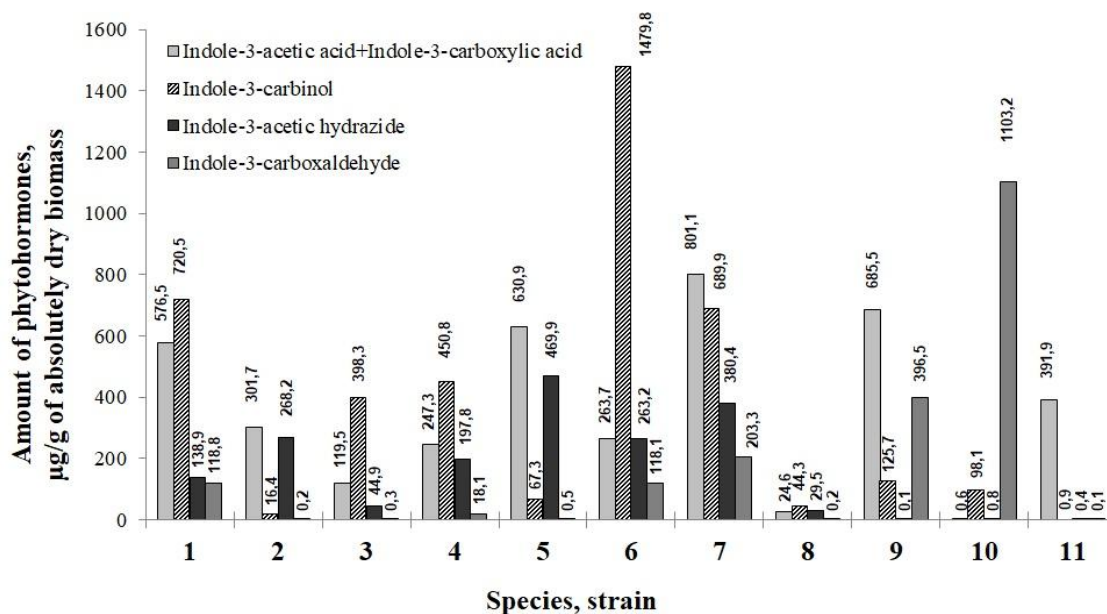


Figure 4. Synthesis of extracellular auxins by pathogenic for lupine representatives of genus *Pseudomonas*: (A) – 1, 2, 3, 4, 5, 6, 7, 8 – “*P. lupini*” 8531, 8532, 8533, 8534, 8535, 6, 17, 22 and 9, 10, 11 – “*P. xanthochlora*” 8540, 3L, 9L

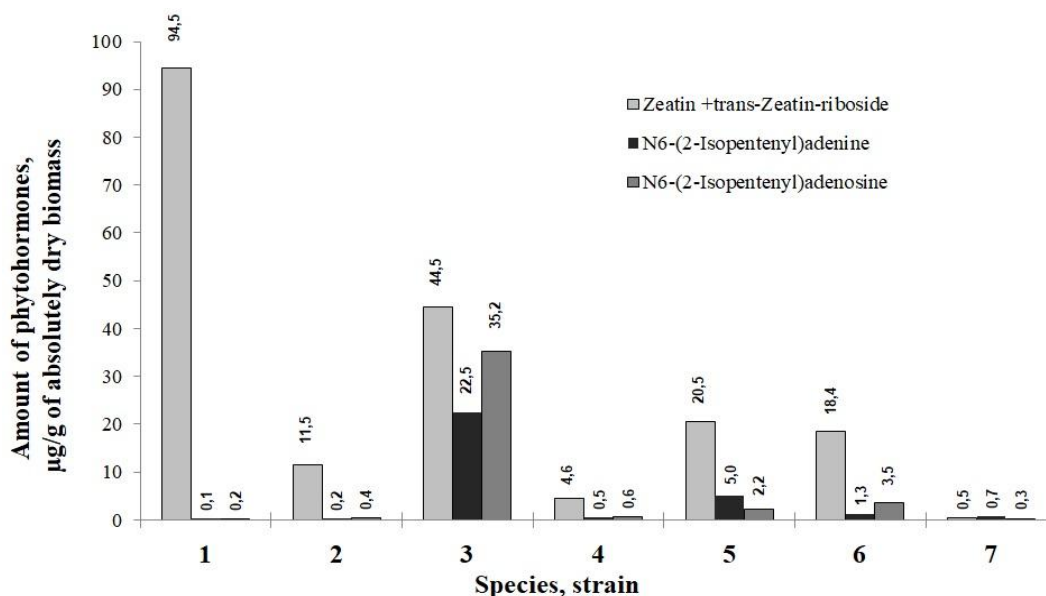


Figure 5. Synthesis of extracellular cytokinin by pathogenic for lupine representatives of genus *Pseudomonas*: 1, 2, 3, 4 – “*P. lupini*” 8532, 8535, 6, 22 and 5, 6, 7 – “*P. xanthochlora*” 8540, 3L, 9L

We have studied an ability to synthesize extracellular auxins and cytokinins by pathogens of various types of bacterial diseases of soybean. It has been established that an amount of synthesized auxins and their range depends on the pathogen's properties and the features of its interaction with a plant. Polyphagous *R. solanacearum* UCM B-1109^T, *P. syringae* pv. *tabaci* 225, *C. flaccumfaciens* pv. *flaccumfaciens* 6564 produce large amounts of auxins (from 1512.29 up to 948.8 $\mu\text{g}\cdot\text{g}^{-1}$ ADB) (Table 4) Monophagous *X. axonopodis* pv. *glycines* 8609 and *P. savastanoi* pv. *glycinea* 8571 synthesize more smaller amounts of auxins (from 445.09 to 147.38 $\mu\text{g}\cdot\text{g}^{-1}$ ADB). The highest levels of synthesis of these indole compounds were observed in strains *R. solanacearum* UCM B-1109^T (1256.81 $\mu\text{g}\cdot\text{g}^{-1}$ ADB), *P. agglomerans* 8490 (1327.0 $\mu\text{g}\cdot\text{g}^{-1}$ ADB) and *C. flaccumfaciens* pv. *flaccumfaciens* 6564 (1512.29 $\mu\text{g}\cdot\text{g}^{-1}$ ADB).

Table 4. Comparative analysis of extracellular auxins and cytokinins synthesis by agents of soybean's bacterial diseases with their pathogenic properties

Strains	Amount of phytohormones, $\mu\text{g/g}$ of absolutely dry biomass (ADB)		Pathogenic properties
	Auxins	Cytokinins	
<i>C. flaccumfaciens</i> pv. <i>flaccumfaciens</i> 6564	573.29	50.81	Polyphagous, bacterial tan spot of soybean and bacterial wilt of bean
<i>R. solanacearum</i> UCM B-1109 ^T	1256.81	222.1	Polyphagous, bacterial wilting of many plants
<i>P. agglomerans</i> 8490	1327.0	323.51	Polyphagous, disease like bacterial stem stripe and wet spottiness a of various crops
<i>P. syringae</i> pv. <i>tabaci</i> 225	510.18	194.00	Polyphagous, wildfire of soybean and tobacco
<i>P. savastanoi</i> pv. <i>glycinea</i> 8571	445.09	75.30	Monophagous, angular leaf spot of soybean
<i>X. axonopodis</i> pv. <i>glycines</i> 8609	586.0	102.27	Monophagous, soybean bacterial pustule

Pathogens of bacterial diseases of soybean differ not only by quantitative, but also by the spectrum of synthesized auxins. In particular, the highest levels of IAA and indole-3-carboxylic acid synthesis were found in both monophagous *X. axonopodis* pv. *glycines* 8609 (near 100% of the total amount of auxins) and polyphagous *C. flaccumfaciens* pv. *flaccumfaciens* (over 90%). Also, it should be noted that high level of production of both IAA and indole-3-carboxylic acid was found in *P. agglomerans* 8490 (over 50%). However, low levels of synthesis of IAA and indole-3-carboxylic acid were observed in both monophagous *P. savastanoi* pv. *glycinea* 8571 (about 48%) and polyphagous *P. syringae* pv. *tabaci* 225 (about 28%) and *R. solanacearum* UCM B-1109^T (over 29%) (Fig. 6).

In the investigation of cytokinin activity of strains – pathogens of soybean bacterial diseases, we have shown that the high level of synthesis of cytokinins is observed in polyphagous *R. solanacearum* UCM B-1109^T (222.1 $\mu\text{g}\cdot\text{g}^{-1}$ ADB) and *P. agglomerans* 8490 (323.51 $\mu\text{g}\cdot\text{g}^{-1}$ ADB) (Table 4). Also, it should be noted that both *R. solanacearum*

UCM B-1109^T and *P. agglomerans* 8490 synthesize rather large amounts of a transport form of zeatin – zeatin-riboside (65.17–32.46% of the total amount of cytokinins respectively) (Fig. 6). Instead, the other studied strains have lower levels of synthesis of exogenous cytokinins (from 194.00 to 50.81 µg·g⁻¹ ADB) compared with the above-mentioned strains. In addition, *P. syringae* pv. *tabaci* 225, *C. flaccumfaciens* pv. *flaccumfaciens* 6564 and *X. axonopodis* pv. *glycines* 8609 are also able to synthesize significant amounts of zeatin–riboside (from 22.04 to 51.14%) (Fig. 7).

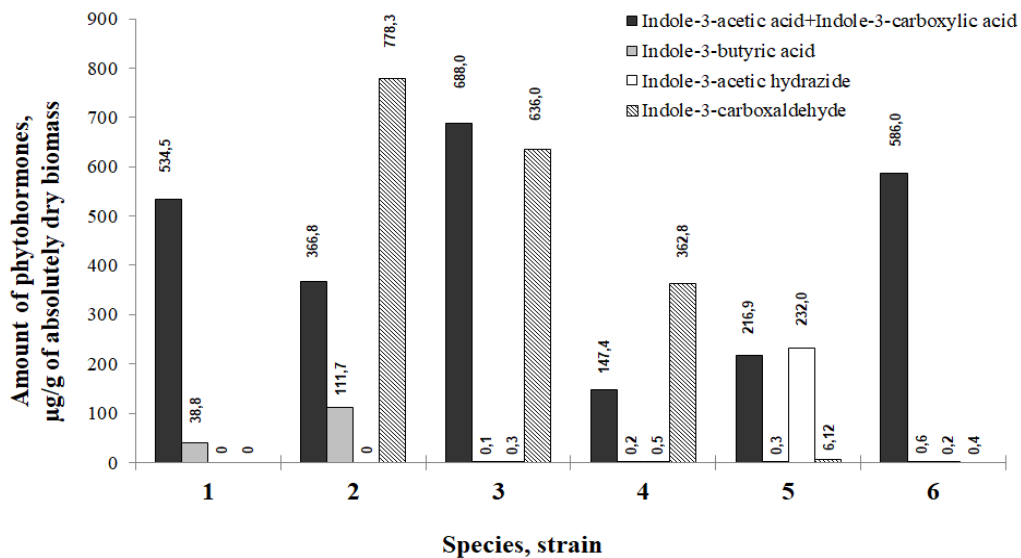


Figure 6. Synthesis of extracellular auxins by pathogenic for soybean bacteria: 1 – *Curtobacterium flaccumfaciens* pv. *flaccumfaciens* 6564, 2 – *Ralstonia solanacearum* UCM B-1109^T, 3 – *Pantoea agglomerans* 8490, 4 – *Pseudomonas syringae* pv. *tabaci* 225, 5 – *Pseudomonas savastanoi* pv. *glycinea* 8571, 6 – *Xanthomonas axonopodis* pv. *glycines* 8609

Discussion

It has been shown that the polyphagous and strains with a high level of aggressiveness synthesize much higher levels of auxins, compared with the monophagous and strains with a low level of aggressiveness. This fact does not contradict the literature data. In particular, certain researchers had shown that spontaneous mutant *Pseudomonas fluorescens* HP72 synthesizes only a small amount of IAA and has a low ability to colonize roots of bent grass (Biovin et al., 2016). The strain of *Erwinia chrysanthemi*, which is mutant by the synthesis of IAA, has very low levels of synthesis of pectate lyase that worsens local maceration of plant's tissues (Yang et al., 2007).

It has been established that an amount of synthesized auxins and their range depends on the biology of a pathogen and the features of its interaction with a plant. In particular, strains *P. syringae* pv. *syringae* B-1027^T, *P. savastanoi* pv. *phaseolicola* B-1123^T, *P. syringae* pv. *pisi* 9177^T, *P. savastanoi* pv. *glycinea* 8571, *P. syringae* pv. *tabaci* 225 and *R. solanacearum* B1109^T synthesize low and medium amounts of both IAA and indole-3-carboxylic acids. It is known that representatives of pathovars of *glycinea*, *phaseolicola*, *pisi*, *syringae*, *tabaci* are able to synthesize specific pathogenicity factors, in particular, toxins, synthesis of which may correlate with production of IAA. Thus, it was shown that strains of *P. syringae* pv. *syringae*, mutant

relating to IAA synthesis, significantly reduced production of syringomycin and, consequently, the virulence (Hwang et al., 2005). In addition, researchers have shown that synthesis of IAA by *R. solanacearum* and *P. syringae* is directly related to HRP-gene-encoded type III secretion system (Type III secretion systems (T3SSs)), which is directly transcribed into effector proteins (hairpins) in the host plant cells and it is the key to development of infection process and disease symptoms (Jin et al., 2003; Fouts et al., 2002). Probably, rather high level of synthesis of auxins, in particular, IAA, by *P. agglomerans* 8490 is related to the ability of this species to colonize all components of phyllosphere, because the interaction with a plant is a characteristic feature of the biology of this species. Also, it is known that *P. agglomerans* are able to synthesize IAA in three ways (Spaepen et al., 2007). It appears that the presented above facts fully explain the research results. The auxins for these strains play a role of signaling molecules that start a cascade of other pathogenicity reactions rather than the role of key factors of virulence, probably. However, in strains *P. marginalis* pv. *marginalis* 9175^T, *X. axonopodis* pv. *glycines* 8609 and *C. flaccumfaciens* pv. *flaccumfaciens* 6564 synthesis of the mentioned above indole compounds plays the crucial role in mechanisms of their interaction with a plant (the increased permeability of the plant cell wall, disturbance in stomata work, inhibition of responses of plant protection, etc.), because, according to the literature, information about them having specific pathogenicity factors and their relationship to synthesis of auxins is almost absent.

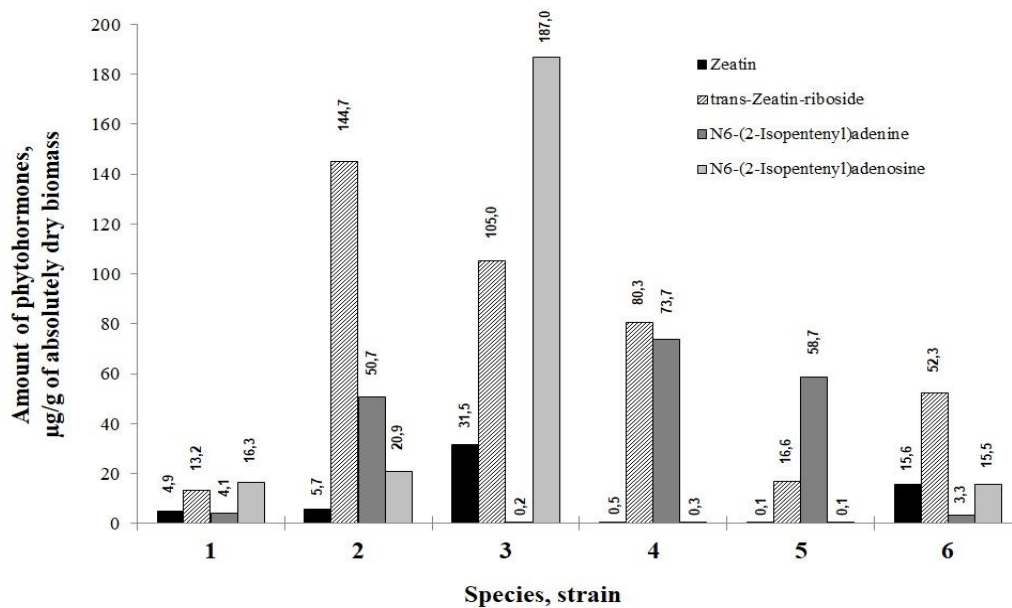


Figure 7. Synthesis of extracellular cytokinins by pathogenic for soybean bacteria: 1 – *Curtobacterium flaccumfaciens* pv. *flaccumfaciens* 6564, 2 – *Ralstonia solanacearum* UCM B-1109^T, 3 – *Pantoea agglomerans* 8490, 4 – *Pseudomonas syringae* pv. *tabaci* 225, 5 – *Pseudomonas savastanoi* pv. *glycinea* 8571, 6 – *Xanthomonas axonopodis* pv. *glycines* 8609

According to the literature, bacteria synthesize cytokinins, using them primarily as a chemical signal to interact with plant or as a mechanism for successful invasion into plant tissues (Giron et al., 2013). Using the example of *R. solanacearum*, a connection between auxin and cytokinin signaling and plant roots susceptibility to this pathogen has been revealed (Kakimoto, 2003; Giron et al., 2013). The high level of synthesis of

cytokinins by *P. agglomerans* 8490 is likely to be connected with peculiarities of the biology of this species. Moreover, as in the case of tumor-inducing species, in representatives of species *P. agglomerans* and *R. solanacearum* the genes *trm/tzs*, responsible for synthesis of auxins and cytokinins, are localized in plasmids. Therefore, the number of their copies is much larger, compared to the species with nucleoid location of the similar genes (Kakimoto, 2003).

Conclusion

It has been determined that the level of synthesized auxins produced by the studied bacteria correlates directly with their pathogenic properties. A connection between the ways of plants' infection and the amount and spectrum of synthesized auxins and cytokinins has been established. In particular, certain types of phytopathogenic bacteria, in which formation of specific pathogenicity factors (toxins, enzymes) is connected to production of auxins, synthesize low and medium amounts of indole-3-acetic acid and indole-3-carboxylic acid. For these pathogens, these compounds probably act as signaling molecules, triggering reactions of other mechanisms of pathogenesis. However, the other species, for which there is not any known connection of synthesis of specific pathogenicity factors with auxin signaling, are able to synthesize significant amounts of mentioned above indole compounds, which probably play a crucial role in their interaction with the plant.

Our investigation of quality and quantity phytohormones compositions synthesized by different pathogenic for plants bacteria will improve the understanding of pathogen-plant interactions and, thus, will create preconditions for developing strategies to prevent the pathogens spreading.

REFERENCES

- [1] Boivin, S., Fonouni-Farde, C., Frugie, F. (2016): How auxin and cytokinin phytohormones modulate root microbe interactions. – *Front. Plant Sci.* 7: 1–12.
- [2] Chen, Z., Agnew, J. L., Cohen, J. D., He, P., Shan, L., Sheen, J., Kunkel, B. N. (2007): *Pseudomonas syringae* type III effector AvrRpt2 alters *Arabidopsis thaliana* auxin physiology. – *Proceedings of the National Academy of Sciences of the United States of America* 104(50): 20131–20136.
- [3] Cui, H., Xiang, T., Zhou, J-M. (2009): Plant immunity: a lesson from pathogenic bacterial effector proteins. – *Cellular Microbiology* 11(10): 1453–1461.
- [4] Darley, C. P., Forrester, A. M., McQueen-Mason, S. J. (2001): The molecular basis of plant cell wall extension. – *Plant Mol. Biol.* 47: 179–195.
- [5] Ding, X., Cao, Y., Huang, L., Zhao, J., Xu, C., Li, X., Wang, Sh. (2008): Activation of the indole-3-acetic acid-amido synthetase GH3-8 suppresses expansin expression and promotes salicylate- and jasmonate-independent basal immunity in rice. – *Plant Cell* 20(1): 228–240.
- [6] Fouts, D. E., Abramovitch, R. B., Alfano, J. R., Baldo, A. M., Buell, C. R., Cartinhour, S., Chatterjee, A. K., D'Ascenzo, M., Gwinn, M. L., Lazarowitz, S. G., Lin, N. C., Martin, G. B., Rehm, A. H., Schneider, D. J., Dijk, K., Tang, X., Collmer, A. (2002): Genomewide identification of *Pseudomonas syringae* pv. tomato DC3000 promoters controlled by the HrpL alternative sigma factor. – *Proceedings of the National Academy of Sciences of the United States of America* 99(4): 2275–2280.

- [7] Frébort, I., Kowalska, M., Hluska, T., Frébortová, J., Galuszka, P. (2011): Evolution of cytokinin biosynthesis and degradation. – *J. Exp. Bot.* 62(8): 2431–2452.
- [8] Giron, D., Frago, E., Glevarec, G., Pieterse, C. M. J., Dicke, M. (2013): Plant-Microbe-Insect Interactions. Cytokinins as key regulators in plant–microbe–insect interactions: connecting plant growth and defence. – *Functional Ecology* 27: 599–609.
- [9] Gottig, N., Garavaglia, B. S., Garofalo, C. G., Orellano, E. G., Ottado, J. A. (2009): A filamentous hemagglutinin-like protein of *Xanthomonas axonopodis* pv. *citri*, the phytopathogen responsible for citrus canker, is involved in bacterial virulence. – *PLoS ONE Journal* 4(2): e4358.
- [10] Hwang, M. S. H., Morgan, R. L., Sarkar, S. F., Wang, P. W., Guttman, D. S. (2005): Phylogenetic characterization of virulence and resistance phenotypes of *Pseudomonas syringae*. – *Appl. Environ. Microbiol.* 71(9): 5182–5191.
- [11] Jameson, P. E. (2000): Cytokinins and auxins in plant–pathogen interactions – an overview. – *Plant Growth Regul.* 32: 369–380.
- [12] Jin, Q. L., Thilmony, R., Zwiesler-Vollick, J., He, S. Y. (2003): Type III protein secretion in *Pseudomonas syringae*. – *Microbes and Infection Journal* 5(4): 301–310.
- [13] Kakimoto, T. (2003): Biosynthesis of cytokinins. – *J. Plant Res.* 116(3): 233–239.
- [14] Leonova, N. O. (2015): Abscisic acid and ethylene production by biotechnological strains of *Bradyrhizobium japonicum*. – *Biotechnologia Acta* 8(5): 64–70.
- [15] Lindow, S. E., Brandl, M. T. (2003): Microbiology of the phyllosphere. – *Appl. Environ. Microbiol.* 69(4): 1875–1883.
- [16] Navarro, L., Dunoyer, P., Jay, F., Arnold, B., Dharmasiri, N., Estelle, M., Voinnet, O., Jones, J. D. (2006): A plant miRNA contributes to antibacterial resistance by repressing auxin signaling. – *Science* 312(5772): 436–439.
- [17] Nico-Liu, D. O., Ronald, P. C., Bogdanove, A. J. (2006): *Xanthomonas oryzae* pathovars: model pathogens of a model crop. – *Molecular Plant Pathology* 7(5): 303–324.
- [18] Pant, G., Agrawal, P. K. (2014): Isolation and characterization of indole acetic acid production plant growth promoting rhizobacteria from rhizospheric soil of *Withania somnifera*. – *Journal of Biological and Scientific Opinion* 2(6): 373–383.
- [19] Patyka, V. P., Pasichnyk, L. A. (2014): Phytopathogenic bacteria in the system of modern agriculture. – *Mikrobiology Zhurnal* 76(1): 21–26.
- [20] Patyka, W., Gnatiuk, T., Zhytkevych, N., Kalinichenko, A., Frączek, K. (2015): Occurrence of the pathogenic bacteria *Pantoea agglomerans* in soybean cultivation. – *Progress in Plant Protection* 55(3): 281–285.
- [21] Pfeilmeier, S., Cally, D., Malone, J. G. (2016): Bacterial pathogenesis of plants: future challenges from a microbial perspective. – *Molecular Plant Pathology* 17(8): 1298–1313.
- [22] Spaepen, S., Vanderleyden, J., Remans, R. (2007): Indole-3-acetic acid in microbial and microorganism – plant signaling. – *FEMS Microbiology Reviews* 31(4): 425–448.
- [23] Woodward, A. W., Bartel, B. (2005): Auxin: regulation, action and interaction. – *Ann. Bot.* 95(5): 707–735.
- [24] Yang, S., Zhang, Q., Guo, J., Charkowski, A. O., Glick, B. R., Ibekwe, A. M., Cooksey, D. A., Yang, Ch.-H. (2007): Global effect of indole-3-acetic acid biosynthesis on multiple virulence factors of *Erwinia chrysanthemi* 3937. – *Appl. Environ. Microbiol.* 73(4): 1079–1088.
- [25] Zakharova, O., Kalinichenko, A., Dankevich, L., Patyka, V. (2015): Rapeseeds bacterial diseases and their REP-PCR analysis. – *Journal of Pure and Applied Microbiology* 9(1): 205–210.

A COMPARATIVE STUDY ON THE EFFECTS OF DIFFERENT CONVENTIONAL, ORGANIC AND BIO-FERTILIZERS ON BROCCOLI YIELD AND QUALITY

ALTUNTAŞ, Ö.

*Department of Horticulture, Faculty of Agriculture, Inonu University, Malatya, Turkey
(e-mail: ozlem.altuntas@inonu.edu.tr; phone: +90-541-896-4029)*

(Received 10th Oct 2017; accepted 27th Feb 2018)

Abstract. In this study, we evaluated the effects of fertilizers of different origin on broccoli yield and some characteristics. For this purpose, 9 different fertilizers were used. The different fertilizers used in the study were; NT; Control (No Treatment), FM; Farm Manure (approximate 2-4% N) CF; Chemical Fertilizer (46% N, 46% P₂O₅, 51% K₂SO₄), HA; Humic Acid, AA; Amino Acid, HFA; Humic and Fulvic Acid, ALG; Microalga, ART; *Arthrobacter sp.*, BAS; *Bacillus subtilis* strain QST 713. During the vegetation period, the plant growth parameters were measured twice in the growth season. The first measurement was performed after 40 days of planting, while the second was done after 70 days. Two plants were harvested from each replication in order to determine the plant growth parameters of shoot fresh weight, root fresh weight, plant height, root length, shoot and root dry weight and the number of the leaves. At the end of the experiment, mineral contents of leaves, total yield and ascorbic acid contents of broccoli heads were determined. As a result, it was determined that some organic fertilizers and biofertilizers increased the yield, various plant growth parameters, nutrient uptake of broccoli and ascorbic acid contents of broccoli heads at a significant level.

Keywords: *organic farming, eco-friendly, broccoli, biofertilizer, yield, quality, nutrient elements*

Introduction

Many agricultural soil types lack at least one essential nutrient element that is necessary for plants. Soil degradation can occur due to acidity, alkalinity, salinity, anthropogenic processes and erosion. Maximum nutrient and yield are only possible by adding fertilizers to the soil in agriculture. In general terms, less efficiency counts for chemical fertilizers causing that only a small part of the fertilizer is used by plants (Arisha and Bardisi, 1999). In previous studies conducted on the efficiency of the fertilizers revealed that the efficiency was less than 50% in N, less than 10% in P, and around 40% for K in mineral fertilizers. These values are even lower in manure. When plants absorb the nutrients in an efficient manner, the costs of inputs are reduced and loss of nutrients is decreased in the ecosystem (Baligar et al., 2001).

One way to optimize the efficiency of fertilizers is managing the fertilizers in an efficient manner, which means applying them at the right time, rate and place. This is true both for conventional and organic agriculture. Optimal crop productivity and optimal nutrient use efficiency must be in balance (Roberts, 2008). Applying agricultural activities for the purpose of obtaining high yield and quality requires chemical fertilizers be applied in a frequent manner. This causes extra costs and environmental problems. The biogeochemical cycle is a complex system and is frequently influenced in a negative manner when chemical fertilizers are used too often to promote soil fertility and crop yield. For instance, applying fertilizers gives rise to leaching and nutrient runoff (especially P, and N). This has causes that there appeared an environmental degradation. Therefore, organic agriculture has attracted attention more in recent years (Esitken et al., 2005).

When chemical fertilizers are not used in an efficient manner, one possible way to reduce negative effects is inoculation with Plant Growth Promoting Rhizobacteria (PGPR), which have useful effects on plant growth. For this reason, these bacteria may be used for agricultural activities as bio-fertilizers (Baligar et al., 2001). Some bacteria species were tested, and it was concluded that they were useful for plant yield, growth and quality improvement. These bacteria can enhance yield of organic systems and help control pollution. Faster breakdown of organic substance, improved nutrient availability and soil characteristics are among the positive effects of biofertilizers. It is possible to explain these positive effects by metabolite release, which enhances growth. Although full mechanism has not been fully resolved, PGPR acts in the following mechanisms; producing plant growth hormones (like auxin, cytokinin, gibberellin); ethylene production inhibition; fixation of symbiotic N₂; inorganic phosphate solubilization; organic phosphate and/or other nutrients mineralization; acting as an antagonist to phytopathogenic microorganisms (by siderophores production); antibiotic, enzyme and fungi compound synthesis; and competition with detrimental microorganisms (Mellada et al., 2007).

Broccoli (*Brassica oleracea* L. var. *italica*) is considered as a Brassicaceae family member. It is a wild form belonging to this family, and is spread in the Mediterranean region (Decoteau, 2000) Broccoli is an important vegetable because of its high nutritional as well as commercial value (Yoldas et al., 2008). In general, more than necessary inorganic fertilizers are given to vegetables for the purpose of achieving higher yields and maximum growth value (Badr and Fekry, 1998; Arisha and Bardisi, 1999; Dauda et al., 2009) On the other hand, using inorganic fertilizers solely can lead to several problems for human health and the environment (Arisha and Bardisi, 1999). For the purpose of improving soil structure (Dauda et al., 2009), and microbial biomass an alternative to mineral fertilizers is organic manure (Naeem et al., 2006). For this reason, using locally produced manure in agricultural activities might increase crop yield, and thus, less chemical fertilizers will be used. Nowadays, consumers prefer organic foods than ever because there is a widespread belief that organic foods are healthier and more environmental-friendly. However, an important drawback of organic agriculture is the fact that most organic fertilizers have low nutrient contents (Mengel and Kirkby, 1987) which mostly depends on the source and moisture content. Another problem is the difficulties to assess the value of organic fertilizers by using direct total quantity of plant nutrients analysis. For this reason, further studies are necessary to define the availability of the nutrient elements and the efficiency of many organic fertilizers. During the decomposition of organic materials, a slow and variable release of nutrients occurs. By increasing the mineral and organic fertilizer efficiency, it is possible to use biofertilizers to increase soil productivity and plant growth in sustainable agriculture activities (Arisha and Bardisi, 1999). For this reason, the study was designed to examine the effects of organic fertilizers that have different contents on plant growth parameters, nutrient uptake, and yield of broccoli in comparison with mineral fertilizer application under field conditions.

Materials and methods

Plant material

Broccoli 'Marathon F1' (*Brassica oleracea* L. var. *italica*) plant (middle season variety) was used as plant material in the present study.

Experimental design

The study was designed and applied in high plastic tunnels at Cukurova University, Karaisali Vocational School, Adana, which is located in the southern part of Turkey. The study was applied in 2011 and 2012 growth period. In the first year, broccoli was grown in the southern region in a limited time period, which is between September and February. In the second year of the study, the application was made in the same period. *Table 1* shows some of the physical and chemical characteristics of the soil in the study area. According to soil analysis; phosphorus content is low, potassium, magnesium, calcium is high, zinc is medium, and other micro elements are sufficient.

Table 1. Analysis results of the soil used in the study

Nutrient	Concentration	Unit
Phosphorus (P)	107	kg/ha
Potassium (K)	768	kg/ha
Magnesium (Mg)	2630	kg/ha
Calcium (Ca)	20600	kg/ha
Sulphur (S)	94	kg/ha
Boron (B)	3	kg/ha
Zinc (Zn)	7	kg/ha
Manganese (Mn)	189	kg/ha
Iron (Fe)	153	kg/ha
Copper (Cu)	6	kg/ha
Salt	0.8	mmhos/cm
Organic Matter	2.34	%
Lime	28.4	%
pH	7.6	-

Broccoli (Marathon F1 cultivar) was planted in high plastic tunnels in the 3rd week of September (in the 1st year on 22.09.2011; and in the 2nd year on 19.09.2012). The selected variety is a high value for marketing that can be adapted to different climatic conditions including extreme winter colds, harvested in 75 days after planting and has a strong plant structure. It can be harvested all season. A distance of 0.80 m was given between the seedlings with an intrarow spacing of 0.60 m. A randomized complete block design was used in the study area with three replications. There were 10 plants in each plot. The applications were as follows; **NT**; Control (No Treatment), **FM**; Farm Manure (approximate 2-4% N) **CF**; Chemical Fertilizer (46% N, 46% P₂O₅, 51% K₂SO₄), **HA**; Humic Acid (Humic A), **AA**; Amino Acid (Patrone), **HFA**; Humic and Fulvic Acid (Ekoflora), **ALG**; Microalga (Allgrow), **ART**; *Arthrobacter sp.* (Roa Natura), **BAS**; *Bacillus subtilis* strain QST 713 (Serenade ASO). *Table 2* shows the doses applied in each treatment.

Treatments time

Organic and biofertilizer doses were added to the soil 3 times; 1st time: Before planting. 2nd time: 30 days after planting. 3rd time: 60 days after planting.

Table 2. Organic and bio fertilizer contents and application doses

Treatments	Ingredients	Doses
NT	Control (No Treatment)	-
FM	Farm Manure (approximate 2-4% N)	3 ton da ⁻¹
CF	Chemical Fertilizer; 46% N, 46% P ₂ O ₅ , 51% K ₂ SO ₄	20 kg N da ⁻¹ , 15 kg P ₂ O ₅ da ⁻¹ , 25 kg P ₂ O ₅ da ⁻¹
HA	Humic Acid 50%, Amino Acid 10%, N 16%, K ₂ O 1%, P ₂ O ₅ 2%, Humidity 1%, pH 3-5.	5 kg da ⁻¹
AA	Free Amino Acid, 45.43%, 10.21% Organic N	3 kg da ⁻¹
HFA	Humic + Fulvic acid 28.2%, K ₂ O 2%, P ₂ O ₅ 2%, MgO ₂ 1.1%, Fe ₂ O ₃ 0.24%, Zinc 129 ppm, Manganese 90 ppm, pH 6-8	150 kg da ⁻¹
ALG	Algae, 660 ppm N, 27 ppm NA, 5.6 ppm F, 184 ppm P 17 ppm Mn, 15 ppm Ca, 722 ppm K, 0.49 ppm Co, 0.89 ppmV, 3.7 ppmCu, 8.5 ppm Zn, 0.28 ppm Mo, 310 ppm S, 44 ppm B, 21 ppm	2 l da ⁻¹
ART	<i>Arthrobacter sp.</i>	2 l da ⁻¹
BAS	<i>Bacillus subtilis</i> strain QST 713	1 l da ⁻¹

Plant growth parameters

Plant growth parameters were measured twice in the growth season; 1st time: 40 days after planting (10 days after 1st fertilizer application). 2nd time: 70 days after planting (10 days after 2nd fertilizer application). Two plants were harvested from each replication. The parameters like growth variables (fresh weight of the shoot, fresh weight of the root, height of the plant, length of the root, dry weight of the shoot, dry weight of the root, and the number of the leaves) were recorded. Roots and shoots were separated from the surface of the soil. Plant roots were cleaned of soil with water. For the purpose of determining the dry matter amount, shoots (including the leaves and the stem) and root samples were dried at 70 °C in an oven until the humidity was evaporated.

Physical properties and the yield of the broccoli heads

The broccoli that was not mature and marketable were harvested between December and February in both years. Heads with stems were cut into 15 cm pieces. The yield per decare was computed. To define the physical properties (for example, the weight of the head), 15 broccoli heads (per treatment – 3 replicates of 5 heads) were measured. The heads were sampled from each application. The weight of the heads was computed as the mean value of 15 heads. In order to measure the head diameter, the widest part of the head was used.

Determination of mineral contents in leaves

For the purpose of determining the relation between the broccoli nutrient content and soil nutrient pools, the measurements were made when the heading process started (Jones, 1981; Mengel and Kirkby, 1987). In this respect, during the heading process,

leave samples were taken (five of the youngest leaves). These samples were then dried at oven at 70 °C for 48 h. After the drying process, they were weighed. Then they were placed in ash at 550 °C for nearly 10 h. The ash was dissolved in 3.3% HCL. Atomic Absorption Spectrometry was used to determine the K, Ca, Mg, Fe, Mn, Zn, Cu concentrations in the leaves. The nitrogen amount of the leaves was determined by using the Kjeldahl method.

Vitamin C analysis

The head samples were taken in the 4th harvest to analyze the Vitamin C content. 5 g of broccoli head was homogenized with 50 ml meta-phosphoric acid (HPO₃) solution and then filtered to analyze Vitamin C. After this process, 10 ml filtrate was titrated by using 2.6 dichlorophenolindophenol solution to obtain a pale pink color. Vitamin C content was computed after 2.6 dichlorophenolindophenol solution was calibrated by using L-Ascorbic Acid (Ugla, 2004).

Data analysis

The experiment was repeated in 2 years. For the purpose of analyzing the data, the IBM SPSS Statistics 20 Software was used. The mean values for each parameter were compared by a multiple comparison Duncan test to investigate the grouping (at $P = 0.05$). No significant interactions were detected by year. For this reason, the data were pooled.

Results and discussion

As a result of the study, it was determined that some organic fertilizers and biofertilizers increase the yield, various plant growth parameters, and nutrient intake of broccoli at a significant level. (Naeem et al., 2006) conducted a study and reported the following positive outcomes of the Plant Growth Promoting Rhizobacterias; fixation of nitrogen, reducing ethylene levels by ACC Deaminase enzyme activity, siderophores and phytohormones production (like oxins), pathogen resistance induction and nutrient solubilization. The growth and development of plants may be influenced by Plant Growth Promoting Rhizobacterias in two ways, either directly or indirectly. Direct effects are as follows; production of ACC deaminase for the purpose of reducing the ethylene levels in the plant roots (Dey et al., 2004) production of plant growth regulators like Indole Acetic Acid (IAA) gibberellic acid (Narula et al., 2006) cytokinins (Dey et al., 2004) and ethylene, (Ortiz-Castro et al., 2008) asymbiotic nitrogen fixation exhibition of antagonistic activity against phytopathogenic microorganisms by producing siderophores (b-1.3-glucanase, chitinases, antibiotics, fluorescent pigment and cyanide) and solubilization of mineral phosphates and other nutrient elements (Dauda et al., 2009). There are more than one mechanism used by PGPR for the purpose of improving plant growth. According to several studies, stimulation of plant growth is the clear result of multiple mechanisms, which might be activated simultaneously (Martinez-Viveros et al., 2010). Indirect stimulation is related with biocontrol – including production of antibiotics, chelation of available Fe in the rhizosphere, extracellular enzyme synthesis for the purpose of hydrolyzing the fungal cell wall and competition for niches in the rhizosphere (Ugla, 2004). Blue green algae are the diverse group of photosynthetic prokaryotes, which are known to fix

atmospheric nitrogen and to convert insoluble phosphorus into soluble form (Irisarri et al., 2001). Cyanobacteria play an important role in maintenance and build-up of soil fertility, consequently increasing rice growth and yield as a natural biofertilizer (Song et al., 2005) The acts of these algae include: (1) Increase in soil pores with having filamentous structure and production of adhesive substances. (2) Excretion of growth-promoting substances such as hormones (auxin, gibberellin), vitamins, amino acids (Roger and Reynaud, 1982; Rodriguez et al., 1982). (3) Increase in water-holding capacity through their jelly structure. (4) Increase in soil biomass after their death and decomposition. (5) Decrease in soil salinity. (6) Preventing weeds growth. (7) Increase in soil phosphate by excretion of organic acids (Wilson, 2006). After water, nitrogen is the second limiting factor for plant growth in many fields and deficiency of this element is met by fertilizers (Malik et al., 2001).

Humic substances, play a vital role in soil fertility and plant nutrition. Plants grown on soils which contain adequate humin, humic adds, and fulvic adds are less subject to stress, are healthier, produce higher yields; and the nutritional quality of harvested foods and feeds are superior. The value of humic substances in soil fertility and plant nutrition relates to the many functions these complex organic compounds perform as a part of the life cycle on earth. The life death cycle involves a recycling of the carbon containing structural components of plants and animals through the soil and air and back into the living plant. As a result humic acids function as important ion exchange and metal complexing (chelating) systems. Because of the relatively small size of fulvic acid molecules they can readily enter plant roots, stems, and leaves. As they enter these plant parts they carry trace minerals from plant surfaces into plant tissues. Fulvic acids are key ingredients of high quality foliar fertilizers. Plant grow is influenced indirectly and directly by humic substances. Positive correlations between the humus content of the soil, plant yields and product quality have been published in many different scientific journals (Petit, 2004).

Root length, fresh and dry root weight

The results of these parameters are given in *Tables 3* and *4*. When the root development parameters were analyzed, it was determined that the farm manure and organic fertilizers were more effective in the root length. In the first measurement date, in the root length rank, the *Arthrobacter sp.*(ART), which is one of the biofertilizers, came after HFA and AA, which are organic fertilizers, and after FM, which is a farm fertilizer (*Table 3*). In the second measurement date, the longest root was measured in *Arthrobacter sp.* (ART) application, and HFA, FM, AA, BAS followed it respectively. When the fresh and dry weight of the roots were analyzed, it was determined that biofertilizers are more influential unlike the organic fertilizers in root length. It was determined that eave-formation is more intense and this is reflected to fresh and dry root weight (*Table 4*). Especially the biofertilizers that include algae (ALG) and *Bacillus subtilis* (BAS) were determined to be the highest ones in terms of dry root weight in both measurement dates. Chemical fertilizer application (CF) and Control (NT) groups were left behind in root development.

It was determined that biofertilizer treatment improves the radical system in broccoli. Dry root weight and root length were detected to be increased at a significant level in the plants which received bio fertilizers (47% *Arthrobacter sp.* (ART), and 30% *Bacillus subtilis* (BAS), respectively) when compared with the Control Group (NT). Plant nutrient facilitation may be the mechanism with which biofertilizer improves the

crop yield and head size, because the nutritional plant status is improved with the increased availability of nutrients in the rhizosphere (Bar-Ness et al., 1992) According to the findings, inoculants may be used to allow reduction in the current high fertilizer rates and to eliminate relevant problems (Shaharoon et al., 2008; Dauda et al., 2009) without compromising the productivity of the plants.

Fresh and dry weight of shoot

In terms of the fresh weight of the shoot, although the biofertilizer that included *Bacillus subtilis* (BAS) had the highest value in both measurement dates in terms of dry weight of the shoot, (AA), which was rich in amino acid content and organic N content among the organic fertilizers, was detected to be ahead of the biofertilizers in both measurement dates. (ALG) biofertilizer, which contained algae + macro and micro elements, followed this application (Tables 3 and 4). The applications that had better root development rather than root length, and therefore higher root weights, affected the development of the shoot in a positive manner. In general, in both measurement dates, it was determined that the fresh and dry weight of the shoot was increased by biofertilizer applications. It is possible to claim that biofertilizers play active roles in the root development of the plants, and depending on this, in nutrient intake, and therefore, in the development of broccoli (Tables 3 and 4).

Plant height and number of the leaves

When the results obtained about the plant height were analyzed, it was determined that organic fertilizers came to the forefront in the first measurement date AA, HFA, HA, respectively. Organic fertilizer applications were followed by chemical fertilizer application (CF) with algae + macro and micro element (ALG) and *Bacillus subtilis*-containing (BAS) biofertilizers (Table 3).

Table 3. In the first measurement date, the effects of various organic and biofertilizers on plant growth parameters of broccoli

Treatments	Plant height (cm)	Leaf number (number/plant)	Root length (cm)	Root fresh weight (g)	Shoot fresh weight (g)	Root dry weight (g)	Shoot dry weight (g)
NT	28.21 b	16.5	20.46 b	45.48 c	600.45	8.65	54.15 c
FM	28.41 b	18.2	29.43 a	64.43 ab	705.12	12.65	70.54 bc
CF	30.17 ab	19.0	23.29 b	45.48 c	795.32	12.45	95.45 b
HA	32.37 ab	24.3	25.18 b	65.68 ab	880.41	15.65	79.23 bc
AA	35.34 a	25.2	30.15 a	69.52 a	884.65	15.45	164.95 a
HFA	35.12 a	24.2	31.11 a	75.41 a	800.64	15.75	72.42 bc
ALG	29.49 ab	22.3	24.48 b	60.65 b	765.41	13.65	110.65 ab
ART	28.61 b	18.5	27.61 a	75.23 a	845.14	17.45	98.45 b
BAS	29.23 ab	19.5	26.49 b	67.43 ab	970.25	18.45	103.35 ab

In the second measurement date, the bio fertilizers that contained microorganism showed positive effects on plant height, and the gap between the applications with

significant differences in the first measurement were closed. In the second measurement date, the lowest value in terms of plant height, which were close to each other, was measured in the control application (Table 4). No clear differences were detected in terms of the number of the leaves between the applications in the first measurement date. The highest number of leaves were determined in the organic fertilizer applications AA, HA, HFA, respectively. This was followed by the biofertilizer that had algae in it ALG (Table 3). However, in the second measurement date, AA application surpassed the other applications at a significant level and was followed by microorganism applications ALG, ART, BAS, respectively (Table 4).

Table 4. In the second measurement date, the effects of various organic and biofertilizers on plant growth parameters of broccoli

Treatments	Plant height (cm)	Leaf number (number/plant)	Root length (cm)	Root fresh weight (g)	Shoot fresh weight (g)	Root dry weight (g)	Shoot dry weight (g)
NT	40.45	24.25 c	32.18 b	125.45 d	1380.45 d	15.6 b	125.50 b
FM	45.25	27.25 bc	40.45 a	125.62 d	1560.12 d	24.81 a	185.85 ab
CF	45.45	29.20 bc	36.48 b	135.36 c	1915.58 c	24.70 a	183.27 ab
HA	45.25	31.25 b	33.58 b	135.35 c	1948.52 c	25.35 a	210.65 a
AA	47.65	42.00 a	40.35 a	145.42 b	2245.12 b	25.65 a	330.42 a
HFA	46.40	31.50 b	41.24 a	136.65 c	2485.04 a	26.54 a	230.32 a
ALG	48.45	33.30 b	39.45 ab	141.15 b	2460.15 a	28.41 a	240.52 a
ART	47.85	33.00 b	46.24 a	138.48 b	2345.65 ab	29.71 a	220.05 a
BAS	46.45	32.50 b	39.48 ab	164.18 a	2565.36 a	29.85 a	195.05 a

The plant nutrient element content in the leaves

When the results on the plant nutrient element in the leaves were analyzed it was determined that AA, which was rich in terms of amino acid content and organic N content as an organic fertilizer; ALG, which included algae + micro and macro elements as a biofertilizer; and BAS, which included *Bacillus subtilis* ranked the first (Figs. 1 and 2). In terms of macro elements, the highest nitrogen amount in the leaves was found in *Arthrobacter sp.* (ART) application, and the highest calcium amount was found in farm fertilizer (FM) application. AA application ranked the third in terms of Nitrogen amount, and ALG ranked the second in terms of calcium amount (Fig. 1). It was determined that broccoli plant made use of organic fertilizers in AA application in the most efficient way, and biofertilizers helped nutrient intake. This affected the head quality and yield in broccoli in a direct manner. It was determined that the control application (NT) was in the lowest level in terms of nutrient element (Figs. 1 and 2). Aside from the control application (NT), the lowest nutrient element contents were detected in farm fertilizer application (FM) in terms of N, Mg and Mn contents; the lowest K and Zn contents were determined in F8 application, the lowest Ca and Cu contents were determined in Chemical Fertilizer (CF) application; and the lowest Fe content was detected in HA application, which was rich in terms of humic acid (Figs. 1 and 2).

Humic acid can influence mineral nutrient intake of plants in a positive way. For this, the permeability of the membranes must be increased in the root cells. Humic elements affect the plant growth in an indirect and direct manner. It was reported in previous studies that there is a positive correlation between the humus content and plant yield. Among the direct effects, there are the changes in plant metabolism after the intake of organic macromolecules (like humic acids and fulvic acids). After the compounds enter the cells of the plant, some biochemical changes happen in the membranes and in some cytoplasmic components of plant cells. Humic substances mediate the intake of major plant nutrients. The intake of major plant nutrients improves plant growth as a stimulative effect of humic substances; nitrogen (N) phosphorus (P), and potassium (K). If humic substances exist in the soil in sufficient amounts, the necessity for N, P, and K fertilizer applications decrease. The growth of plant roots is affected by humic substances. When the soil receives humic acid and/or fulvic acid, root initiation and increased root growth occur. In this way, humic and fulvic acids are considered as root simulators. The key role of PGPR may be described as plant hormone secreting activities. In previously conducted studies, it was reported that auxin-producing rhizobacteria affected root development and had a strong growth-promoting activity (Probanza et al., 1996) However, it was also reported that *Bacillus* OSU-142 is important on N₂-fixation on sugar beet and barley, (Cakmakci et al., 2001; Sahin et al., 2004) tomatoes and pepper and apricot (Esitken et al., 2003) in field studies.

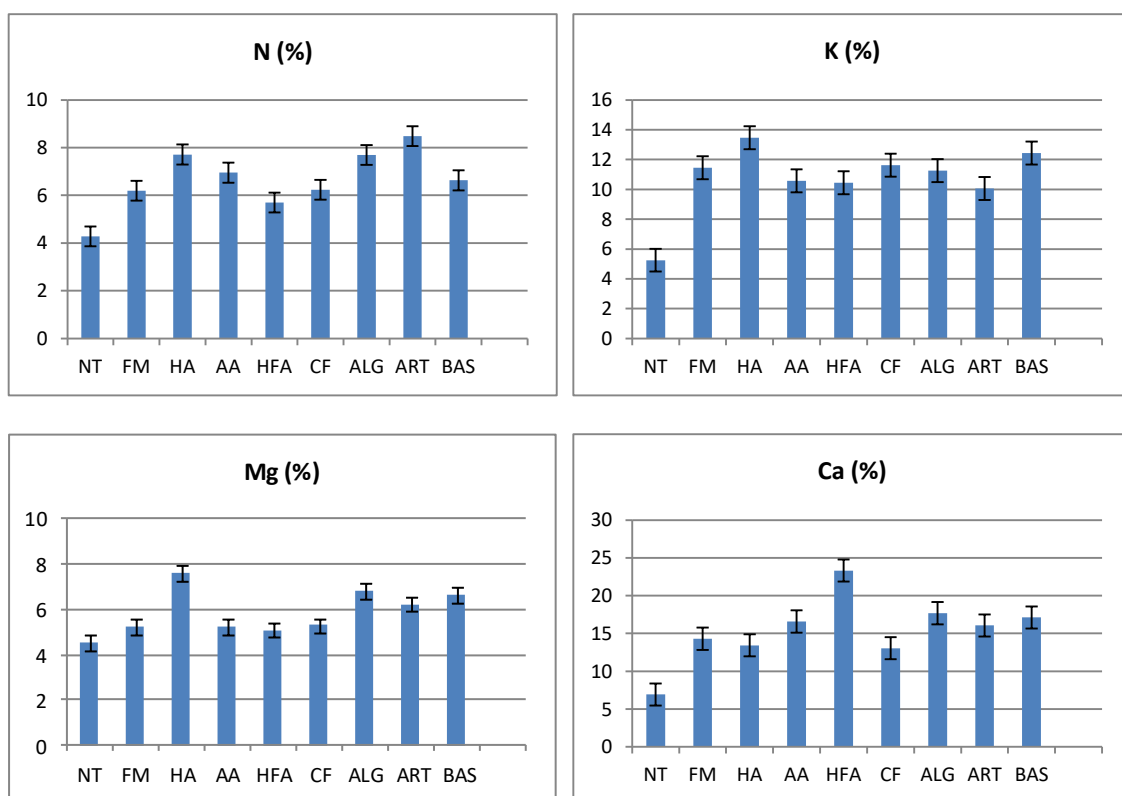


Figure 1. The effects of different organic and biofertilizers on macro nutrient element contents of broccoli leaves

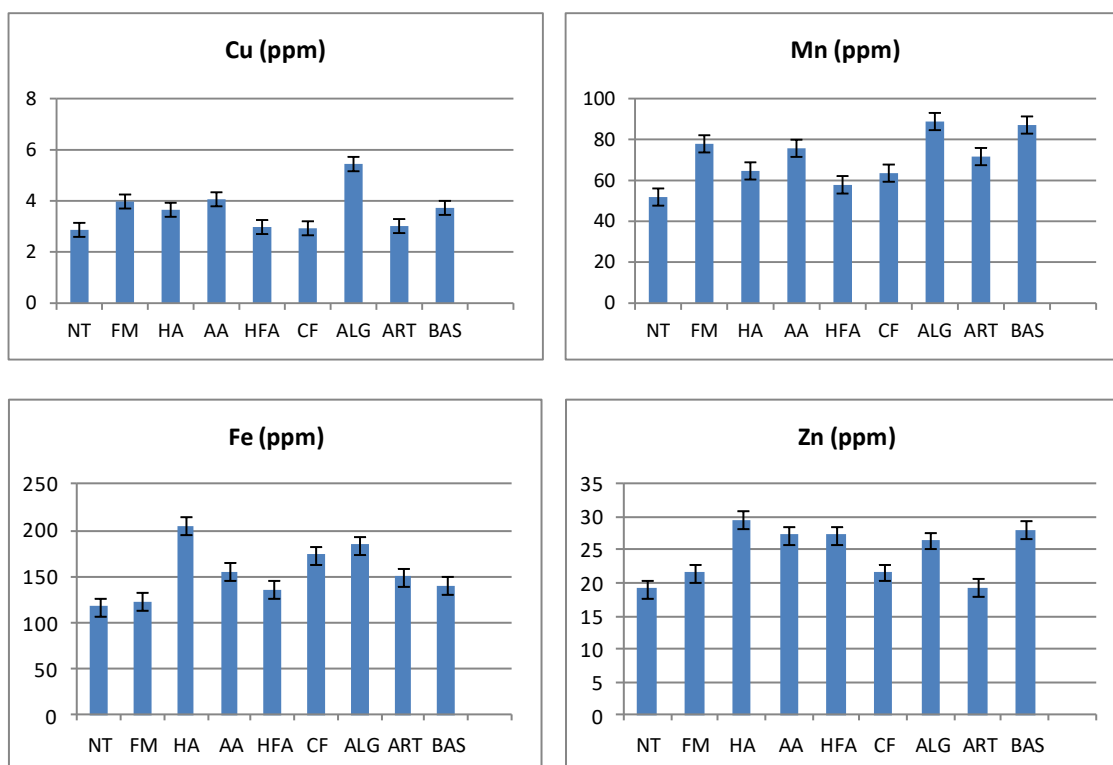


Figure 2. The effects of different organic and biofertilizers on the micro nutrient element contents of broccoli leaves

Broccoli head quality

It was determined in diameter and weight measurements of the heads of broccoli that biofertilizer applications gave better results (Table 5). The best result in terms of head diameter was determined at a statistically significant level in BAS, which included *Bacillus subtilis*, and the best results in terms of head weight were received at a statistically significant level in ALG application, which included algae + macro and micro elements. *Arthrobacter sp.* (ART), which was another biofertilizer application, followed these. Biofertilizers were more effective than the organic fertilizers in terms of main head diameter and weight. As a result of Vitamin C analyses in the heads of broccoli, it was determined that both the biofertilizers and organic fertilizers were found to be different from the control application at a significant level, and the results were close to each other aside from the control application. In terms of head quality, typical changes were detected in our results in all treatments in broccoli ripening, in other words, the head diameter increased (Elkoca et al., 2008) Although different fertilizers were given, the plants in the study showed higher Ascorbic acid values. BAS treatment was found to have the highest Ascorbic acid content when compared with other treatments (Table 5). Lai et al. (2008) indicated that yield (mean floret weight), total phenolic and flavonoid content in broccoli shows significant year on year variation, but is not significantly different in organic compared to conventional production systems.

Table 5. The effect of biofertilizer and organic fertilizer applications on diameter, weight and Vitamin C content in the heads of broccoli

Treatments	Total yield (kg/da) (main head + lateral heads)	Main head diameter (cm)	Main head weight (g)	Ascorbic acid (mg 100 g ⁻¹)
NT	691.25 c	9.00 d	162.50 g	90.03 b
FM	1254.32 b	12.50 abc	205.00 efg	95.25 a
CF	1155.75 b	10.25 cd	272.50 de	95.41 a
HA	1057.08 b	11.50 bcd	205.00 efg	95.51 a
AA	1340.62 ab	11.50 bcd	233.75 def	95.66 a
HFA	1307.5 ab	11.00 bcd	266.00 de	95.56 a
ALG	1458.33 a	13.00 ab	452.50 a	96.63 a
ART	1348.25 ab	13.00 ab	301.25 cd	96.41 a
BAS	1445.68 a	14.50 a	378.75 b	96.66 a

Total yield

Together with the main and side-heads, in terms of yield values in biofertilizer applications, ALG application, which included algae + macro and micro elements, and BAS, which included *Bacillus subtilis*, were found to be different from all other applications at a statistically significant level. These applications were followed by *Arthrobacter sp.* (ART), and AA and HFA applications which were among organic fertilizer applications. It was determined that the yield in broccoli plants was higher in biofertilizers than in organic fertilizers, chemical fertilizers and control (Table 5; Figure 3). The yield and plant growth improvement effects of bacteria, which were used in the present study, may be explained with the N₂-fixing and P-solubilizing capacity of bacteria. Positive influences of biofertilizers on yield and growth parameters (like apricot, tomatoes, sugar beet, and barley) are explained with N₂-fixation ability, phosphate-solubilizing capacity, indole acetic acid, and antimicrobial substance production (Esitken et al., 2005; Rodrigues et al., 2006; Wilson, 2006; Malik et al., 2001). In general, the improvements in macro/micronutrient contents were more emphasized in PGPR treatments. However, mineral fertilizer and control also resulted in significant nutrient increases in terms of plant leaf. It is expected that the improvement in mineral intake by plants results in and increased accumulation of minerals in the leaves of plants. Using N₂-fixing and P-solubilizing PGPR in chickpea (Pettit, 2004) barley (Rodriguez et al., 2006) tomato (Caballero-Mellado et al., 2007) lettuce (Barnes et al., 1992) stimulated macro- and micronutrient intake like N, P, K, Ca, Mg, Fe, Mn, Zn, and Cu, which show consistency with our results. (Valverde et al., 2013) belong to the results showed that application of biofertilizers combination of *Azospirillum* + *Azotobacter* (50% of each) through root dipping method during transplanting is beneficial for yield enhancement as well as for the improvement of functional biomolecules present in broccoli. According to (Singh et al., 2014; Choudhary and Paliwal, 2017) study revealed that the integration of bio-organics and mineral nutrients had shown a marked effect in enhancing yield as well as productivity of broccoli with maximum net returns. On the basis of results, it could be concluded that

the application of vermicompost @ 2.5 t ha⁻¹ + FYM @ 5 t ha⁻¹ + Azospirillum + PSB along with S @ 40 kg ha⁻¹ + Zn @ 5 kg ha⁻¹ + Boron @ 1.5 kg ha⁻¹ were best for higher yield with maximum profit and had recommended for commercial production of broccoli.

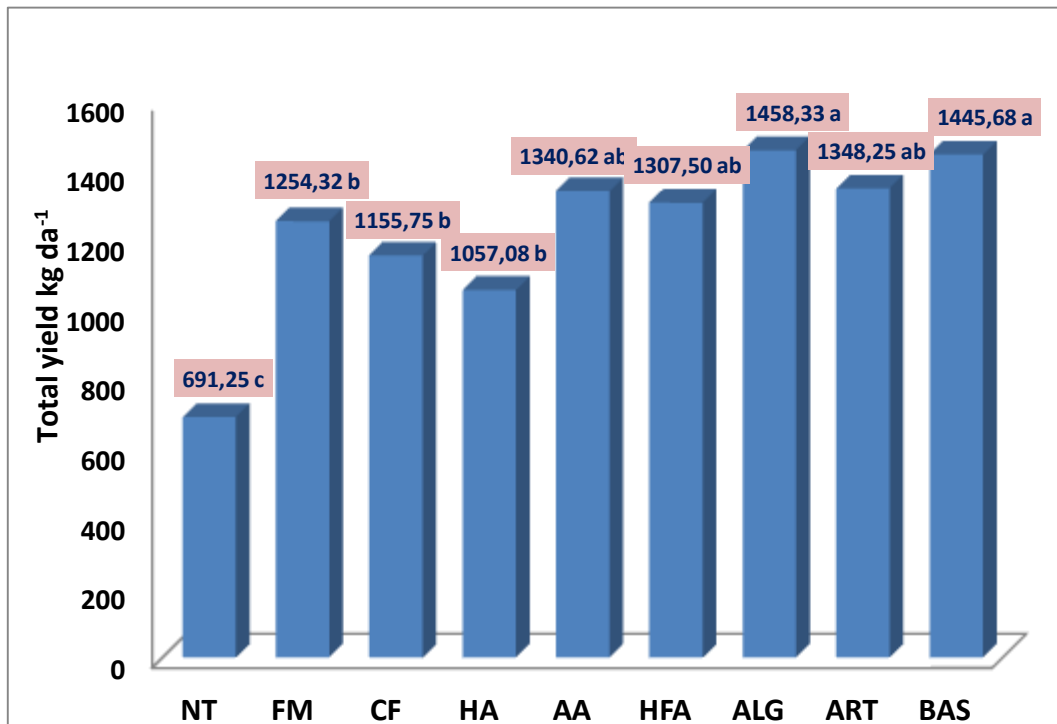


Figure 3. Effects of different organic and biofertilizers on the total yield of broccoli

Conclusion

As a conclusion, biofertilizers gave better results in broccoli cultivation than organic fertilizers, farm fertilizers and chemical fertilizers under plastic tunnels. If the biological activity is high in the soil, the nutrient intake, plant growth, yield and head quality are also high. An increase at a rate of 50% was determined in the yield with biofertilizers when compared with the control (ALG 53%, BAS 52%, ART 49%), and 20% increase was determined when compared with chemical fertilizer (ALG 21%, BAS 20%, ART 14%).

An increase at a rate of 47-48% (AA, HFA) was determined in the yield with organic fertilizers when compared with the control application; and at a rate of 14-12% when compared with chemical fertilizers (AA, HFA).

In organic agriculture; plant nutrition and plant protection are two important issues. In this research, plant nutrition sources of broccoli cultivation, which is a vegetable with both health and commercial preservation, are emphasized. While farmland is a traditional organic resource, it has always been sought to find the desired amount and the efficiency and quality of other resources due to transportation difficulty. In future studies, the impact of new organic resources can be examined.

REFERENCES

- [1] Arisha, H. M., Bardisi, A. (1999): Effect of nitrogen fertilization and plant spacing on growth, yield and pod quality of common bean under sandy soil conditions. – *Zagazig Journal of Agricultural Research* 26(2): 407-419.
- [2] Badr, L. A. A., Fekry, W. A. (1998): Effect of intercropping and doses of fertilization on growth and productivity of taro and cucumber plants. 1-vegetative growth and chemical constituents of foliage. – *Zagazig Journal of Agricultural Research* 25(2): 1087-1111.
- [3] Baligar, V. C., Fageria, N. K., He, Z. L. (2001): Nutrient use efficiency in plants. – *Communications in Soil Science and Plant Analysis* 32(7-8): 921-50. DOI:10.1081/CSS-100104098.
- [4] Bar-Ness, E., Hadar, Y., Chen, Y., Römheld, V., Marschner, H. (1992): Short-term effects of rhizosphere microorganisms on Fe uptake from microbial siderophores by maize and oat. – *Plant Physiology* 100(1): 451-456. <https://doi.org/10.1104/pp.100.1.451>.
- [5] Caballero-Mellado, J., Onofre-Lemus, J., Estrada-De Los Santos, P., Martínez-Aguilar, L. (2007): The tomato rhizosphere, an environment rich in nitrogen-fixing Burkholderia species with capabilities of interest for agriculture and bioremediation. – *Applied and Environmental Microbiology* 73(16): 5308-5319. <https://doi.org/10.1128/AEM.00324-07>.
- [6] Choudhary, S., Paliwal, R. (2017): Effect of bio-organics and mineral nutrients on yield, quality and economics of sprouting broccoli (*Brassica oleracea* var. *italica*). – *International Journal of Current Microbiology Applied Sciences* 6(12): 742-749.
- [7] Çakmakçı, R., Kantar, F., Sahin, F. (2001): Effect of N₂-fixing bacterial inoculations on yield of sugar beet and barley. – *Journal of Plant Nutrition and Soil Science* 164(5): 527-531.
- [8] Dauda, S. N., Ajayi, F. A., Ndor, E. (2009): Growth and yield of water melon (*Citrullus lanatus*) as affected by poultry manure application. – *Electronic Journal of Environmental, Agricultural and Food Chemistry* 8(4): 305-311.
- [9] Dey, R., Pal, K. K., Bhatt, D. M., Chauhan, S. M. (2004): Growth promotion and yield enhancement of peanut (*Arachis hypogaea* L.) by application of plant growth-promoting rhizobacteria. – *Microbiological Research* 159(4): 371-394.
- [10] Elkoca, E., Kantar, F., Sahin, F. (2008): Influence of nitrogen fixing and phosphorus solubilizing bacteria on the nodulation, plant growth, and yield of chickpea. – *Journal of Plant Nutrition* 31(1): 157-171. <https://doi.org/10.1080/01904160701742097>.
- [11] Esitken, A., Ercisli, S., Eken, C. (2005): Effects of mycorrhiza isolates on symbiotic germination of terrestrial orchids (*Orchis palustris* Jacq. and *Serapias vomeracea* subsp. *vomeracea* (Burm.f.) briq.) in Turkey. – *Symbiosis* 38(1): 59-68.
- [12] Karlidag, H., Esitken, A., Turan, M., Sahin, F. (2007): Effects of root inoculation of plant growth promoting rhizobacteria (PGPR) on yield, growth and nutrient element contents of leaves of apple. – *Scientia Horticulturae* 114(1): 16-20. <https://doi.org/10.1016/j.scienta.2007.04.013>.
- [13] Irisarri, P., Gonnet, S., Monza, J. (2001): Cyanobacteria in Uruguayan rice fields: Diversity, nitrogen fixing ability and tolerance to herbicides and combined nitrogen. – *Journal of Biotechnology* 91(1-2): 95-103. [https://doi.org/10.1016/S0168-1656\(01\)00334-0](https://doi.org/10.1016/S0168-1656(01)00334-0).
- [14] Jones, C. A. (1981): Proposed modifications of the diagnosis and recommendation integrated system (dris) for interpreting plant analyses. – *Communications in Soil Science and Plant Analysis* 12(8): 785-794. <https://doi.org/10.1080/00103628109367194>.
- [15] Lai, W. A., Rekha, P. D., Arun, A. B., Young, C. C. (2008): Effect of mineral fertilizer, pig manure, and *Azospirillum rugosum* on growth and nutrient contents of *Lactuca sativa* L. – *Biology and Fertility of Soils* 45(2): 155-164. <https://doi.org/10.1007/s00374-008-0313-3>.
- [16] Malik, F. R., Ahmed, S., Rizki, Y. M. (2001): Utilization of lignocellulosic waste for the preparation of nitrogenous biofertilizer. – *Pakistan Journal of Biological Sciences* 4(4): 1217-1220.

- [17] Martínez-Viveros, O., Jorquera, M., Crowley, D., Gajardo, G., Mora, M. (2010): Mechanisms and practical considerations involved in plant growth promotion by rhizobacteria. – *Journal of Soil Science and Plant Nutrition* 10(3): 293-319. <https://doi.org/10.4067/S0718-95162010000100006>.
- [18] Mengel, K., Kirkby, E. A. (1987): *Principles of Plant Nutrition*. – International Potash Institute, Bern, Switzerland.
- [19] Naeem, M., Iqbal, J., Bakhsh, M. A. A. (2006): Comparative study of inorganic fertilizers and organic manures on yield and yield components of mungbean (*Vigna radiata* L.). – *Journal of Agriculture and Social Sciences* 2(4): 227-229.
- [20] Narula, N., Deubel, A., Gans, W., Behl, R. K., Merbach, W. (2006): Paranodules and colonization of wheat roots by phytohormone producing bacteria in soil. – *Plant, Soil and Environment* 52(3): 119-129.
- [21] Ortiz-Castro, R., Valencia-Cantero, E., López-Bucio, J. (2008): Plant growth promotion by *Bacillus megaterium* involves cytokinin signaling. – *Plant Signaling and Behavior* 3(4): 263-265. <https://doi.org/10.4161/psb.3.4.5204>.
- [22] Robert E, P. (2014): Organic matter, humus, humate, humic acid, fulvic acid and humin: their importance in soil fertility and plant health. – *Igarss* 2014(1): 1-5. <https://doi.org/10.1007/s13398-014-0173-7.2>.
- [23] Probanza, A., Lucas, J. A., Acero, N., Gutierrez Mañero, F. J. (1996): The influence of native rhizobacteria on european alder (*Alnus glutinosa* (L.) Gaertn.) growth. – *Plant and Soil* 182(1): 59-66. <https://doi.org/10.1007/bf00010995>.
- [24] Roberts, T. L. (2008): Improving nutrient use efficiency. – *Turkish Journal of Agriculture and Forestry* 32(3): 177-182.
- [25] Rodríguez, A. A., Stella, A. M., Storni, M. M., Zulpa, G., Zaccaro, M. C. (2006): Effects of cyanobacterial extracellular products and gibberellic acid on salinity tolerance in *Oryza sativa* L. – *Saline Systems* 2(1): 1-7. <https://doi.org/10.1186/1746-1448-2-7>.
- [26] Roger, P. A., Reynaud, P. A. (1982): *Free-Living Blue-Green Algae in Tropical Soils*. – Martinus Nijhoff Publisher, La Hague.
- [27] Şahin, F., Çakmakçı, R., Kantar, F. (2004): Sugar beet and barley yields in relation to inoculation with N 2-fixing and phosphate solubilizing bacteria. – *Plant and Soil* 265(1-2): 123-129. <https://doi.org/10.1007/s11104-005-0334-8>.
- [28] Shaharoon, B., Naveed, M., Arshad, M., Zahir, Z. A. (2008): Fertilizer-dependent efficiency of Pseudomonads for improving growth, yield, and nutrient use efficiency of wheat (*Triticum aestivum* L.). – *Applied Microbiology and Biotechnology* 79(1): 147-155. <https://doi.org/10.1007/s00253-008-1419-0>.
- [29] Singh, A., Maji, S., Kumar, S. (2014): Effect of biofertilizers on yield and biomolecules of anti-cancerous vegetable broccoli. – *International Journal of Bio-Resource and Stress Management* 5(2): 262-268.
- [30] Song, T., Martensson, L., Eriksson, T., Zheng, W., Rasmussen, U. (2005): Biodiversity and seasonal variation of the cyanobacterial assemblage in a rice paddy field in Fujian, China. – *The Federation of European Materials Societies Microbiology Ecology* 54(4): 131-140.
- [31] Uggl, M. (2004): *Domestication of Wild Roses for Fruit Production*. – Doctoral Thesis, Swedish University of Agricultural Sciences, Alnarp, Sweden.
- [32] Valverde, J., Reilly, K., Villacreces, S., Gaffney, M., Grant, J., Brunton, N. (2015): Variation in bioactive content in broccoli (*Brassica oleracea* var. *italica*) grown under conventional and organic production systems. – *Journal of the Science of Food and Agriculture* 95(6): 1163-1171. <https://doi.org/10.1002/jsfa.6804>.
- [33] Wilson, L. T. (2006): Cyanobacteria: a potential nitrogen source in rice fields. – *Texas Rice* 6(1): 9-10.
- [34] Yoldas, F., Ceylan, S., Yagmur, B., Mordogan, N. (2008): Effects of nitrogen fertilizer on yield quality and nutrient content in broccoli. – *Journal of Plant Nutrition* 31(7): 1333-1343. <https://doi.org/10.1080/01904160802135118>.

EFFECTS OF ROOT HAIR LENGTH ON POTASSIUM ACQUISITION IN RICE (*ORYZA SATIVA* L.)

KLINSAWANG, S.¹ – SUMRANWANICH, T.¹ – WANNARO, A.¹ – SAENGWILAI, P.^{1,2*}

¹*Department of Biology, Faculty of Science, Mahidol University
Rama VI Road, Bangkok 10400, Thailand*

²*Center of Excellence on Environmental Health and Toxicology (EHT)
Bangkok, Thailand*

**Corresponding author
e-mail: patompong.sae@mahidol.edu
(phone: +66-9-1725-4817)*

(Received 12th Oct 2017; accepted 20th Feb 2018)

Abstract. Potassium (K) deficiency limits rice production worldwide. It has been shown that variation in root traits, such as root hair length, influences ion uptake in many plant species. In this study, we explored natural variation of root hair length of twelve rice varieties in a roll-up system. We found a large phenotypic variation for root hair traits ranging from 0.14 to 0.21 mm. Niaw San-pah-tawng and most upland varieties had long root hairs while lowland varieties had short root hairs. Six lowland varieties contrasting in root hair length were planted in pots under high and low K concentrations. K stress was found to decrease average biomass by 60.93% and K tissue content by 66%. Root to shoot ratio was not affected by K stress. Correlation analysis indicated that long root hair was associated with reduced percentage of leaf senescence, enhanced plant biomass, and improved tissue K content under low K condition. Our results suggest that long root hair could be a useful trait for plant breeding to improve K acquisition in rice.

Keywords: *breeding, nutrient uptake, roll up system, root traits, Thai rice*

Introduction

Potassium (K) is an essential element for plant growth and yield. It has various essential functions including osmoregulation, cellular pH regulation, cellular ion balance, translocation of assimilates, and activation of plant enzymes (Dobermann et al., 2000). Rice requires at least 14.5 kg of K to produce one ton of rice grain and exceeds 200 kg total K uptake for grain yields greater than 8 t ha⁻¹ (Dobermann et al., 1998; Witt et al., 1999). However, soil in major rice producing regions, such as in Cambodia, Vietnam, Laos, and the Northeast of Thailand are highly weathered acidic soils with low CEC and K reserves. Other regions, such as India and the Philippines, have soils in which K uptake is inhibited due to the presence of large amounts of 2:1 layer clay minerals with high K fixation capacity (Dobermann et al., 2000). These K deficient soil conditions could result in an 80% reduction of rice grain quality and yield (Slaton et al., 1995; Salim, 2002). Thus, K deficiency has become one of the major concerns for rice production (Yang et al., 2003).

With increased global rice demand, a large amount of K fertilizer is required to sustain rice yield. It is predicted that the global demand for potash would increase by 2.6% between 2014 to 2018, particularly in sub-Saharan Africa and Asia (FAO, 2015). Although the loss of K to the environment is not much of environmental concern compared to nitrogen, excessive application of K fertilizers to paddy fields could result in stagnant yield, decreased efficiency, and leaching of solution and exchangeable K (Islam

et al., 2016). As an effect, the selection and development of K-efficient rice varieties is necessary to reduce K application rate and improve yield.

Plant root is a major organ for nutrient uptake. It has been shown that variation of root traits is associated with improved nutrient efficiency and crop production in infertile environments (Lynch, 2007). In rice, Jia et al. (2008) reported that root morphology parameters including root length, surface area, volume and count of lateral roots, as well as fine (diameter < 0.2 mm) and thick (diameter > 0.2 mm) roots are involved in K uptake and the translocation of K to shoots in hydroponics. They found that K-efficient genotypes increased fine root number by 25% when grown at moderate K deficient levels compared to optimal K conditions. Additionally, the K efficient genotypes had 1.3 times greater surface area, 1.4 times higher volume, and 1.5 times more root number than the inefficient rice genotypes. Among different root types, unicellular extensions of epidermal cells, or root hairs, are known to be important for water and nutrient uptake (Bates and Lynch, 2001), rhizosheath formation, and penetration of hard soil (Brown et al., 2012; Haling et al., 2013; Lynch et al., 2014). Root hair cells develop from specialized cells called trichoblasts. In many monocots including rice, trichoblasts are morphologically different from other epidermal cells before root hair initiation and alternate with atrichoblasts along longitudinal epidermal cell files (Datta et al., 2011). Genotypic variation for root hair traits is evident in several crop species including wheat (Gahoonia et al., 1997), barley (Gahoonia et al., 2004), white clover (Caradus, 1981), bean (Yan et al., 1995), turf grass (Green et al., 1991), soybean (Wang et al., 2004), maize (Zhu et al., 2004) and rice (Nestler et al., 2016). Several plant species increase root hair length and density in response to suboptimal nutrient availability particularly under low P conditions (Ma et al., 2001; Müller et al., 2004). In most cases, plants with long root hairs are able to acquire more P and are better adapted in low P soils than those with short root hairs (Gahoonia et al., 2004).

Similar to phosphorus, K is relatively immobile in soil. Therefore, lengthening root hairs could possibly enhance K acquisition by increasing soil exploration volume and radius in the K depletion zone (Jungk, 2001; Rengel et al., 2008). Høgh-Jensen and Pedersen (2003) demonstrated that low K treatment affected the root morphology in pea, red clover, lucerne, barley, rye, perennial ryegrass, and oilseed rape. They found that crops altered root hair length in response to low K availability, and thereby maintained the uptake from sparingly soluble K sources. Furthermore, Gahoonia et al. (2006 and 2007) found that chickpea and lentil genotypes with prolific root hair formation had higher K shoot concentration than genotypes with shorter and less dense root hairs.

Compared to other crop species, rice root hairs and their effects for K uptake have been rarely investigated. In this study, we observed phenotypic variation in root hair length in twelve upland and lowland rice varieties and examined the effects of root hairs for potassium acquisition from low K soils in rice. We hypothesized that a large phenotypic variation of root hair length exist among Thai rice and rice varieties with long root hair length would acquire more K and have higher shoot mass than short haired varieties in low K conditions.

Materials and methods

Plant materials

Rice (*Oryza sativa* L.) is a member of Poaceae family. It is an annual species but may grow more than once per year under suitable conditions. Rice has round,

hollow, jointed culms, with rather flat, sessile leaf blades, and a terminal panicle (Chang and Bardenas, 1965). Rice cultivation occurs in different types of managed ecosystems such as irrigated, rainfed upland, rainfed lowland, flood-prone systems. In this study, twelve Thai rice varieties were selected to represent varieties commonly grown in an upland (non-flooded) and lowland (flooded) system. The varieties include photoperiod sensitive lowland varieties (Khao Dawk Mali 105 (KDML105), Niaw San-pah-tawng, RD13), photoperiod insensitive lowland varieties (Phitsanulok 2, Suphan Buri 1, RD1, RD7 and RD31), photoperiod sensitive upland varieties (Goo Meuang Luang, Nam Roo and Leum Pua) and photoperiod insensitive upland varieties (R258). Seeds were obtained from the Rice Department of the Ministry of Agriculture and Cooperatives of Thailand.

Growth conditions

Roll-up system

Seeds of the twelve rice varieties were surface sterilized for 1 min in 10% NaOCl and washed three times in deionized water before germination. The experiment was arranged in a randomized complete block design with three replications. In each replicate, ten seeds per variety were randomly selected and wrapped in brown germination paper in the form of a cigar roll. The rolls were then soaked in a 0.5 mM CaSO₄·2H₂O solution. Seedlings were germinated in darkness at 28 ± 1 °C in a chamber for 3 days, then placed under a photoperiod of 14:10 h supplemented with photosynthetically active radiation at 0.18 mmol photons m⁻² s⁻¹. Seven days after germination, primary roots of three seedlings for each replication were harvested and preserved in 75% ethanol.

Greenhouse system

Six lowland rice varieties including Phitsanulok 2, RD7, Niaw San-pah-tawng, Suphan Buri 1, RD1, and RD13 were planted in greenhouse pots to examine the effect of root hair length on potassium acquisition. Plants were grown in the greenhouse located on the campus of Mahidol University, Thailand 13°45'55.4"N 100°31'34.4"E. The average ambient temperature during the study was 28.5 ± 1.2 °C. The seeds of six selected lowland rice varieties were germinated in sand media for 15 days, then the seedlings were transplanted into pots 25 cm in diameter and 23 cm in height. The growth medium consisted of a mixture (volume based) of 10% clay soil and 90% acid washed sand. One day before planting, the pots were saturated with 2 L of modified Yoshida solution (Yoshida et al., 1976) adjusted to pH 5. The nutrient solution for the high K treatment consisted of 1.5 mM NH₄NO₃, 0.3 mM NaH₂PO₄·H₂O, 0.5 mM K₂SO₄, 1 mM CaCl₂·2H₂O, 1.5 mM MgSO₄·7H₂O, 0.00007 mM (NH₄)₆Mo₇O₂₄·4H₂O, 0.02 mM H₃BO₃, 0.00015 mM ZnSO₄·7H₂O, 0.0002 mM CuSO₄·5H₂O, 0.035 mM FeCl₃·6H₂O, 0.07 mM C₆H₈O₇·H₂O, 0.0625 mM H₂SO₄, 0.009 mM MnSO₄·H₂O. Initially, the low K treatment received 90% less K than the high K treatment. After the initial treatment, K was completely withdrawn from the nutrient solution. CaSO₄ was used to substitute for sulfate in the low K treatments. Plants were fertigated every other day with 100 ml of deionized water alternating with nutrient solutions. The experiment was arranged in a randomized complete block design with four replications. Blue and yellow sticky

insect traps were placed around and above the planting areas for pest control. No pesticide was applied. The plants were harvested 2 months after being transplanted.

Shoot and root harvest

At harvest, shoot height, tiller number, and the percentage of leaf senescence were measured prior to root harvest. The root system was carefully removed from the growth media and washed with tap water. Root traits including crown root number and maximum rooting depth were evaluated (Vejchasarn et al., 2016). Crown root number was manually counted. Rooting depth was determined by measuring the length of the root system after being excavated from the pot. Three crown roots for each variety replication were separated and preserved in 75% EtOH for root hair analysis. Finally, the plant shoot and root were dried at 60 °C for 3 days before assessing the dry weight.

Root hair measurement

Three representative root segments were selected from primary and crown roots of an individual plant. The roots were stained with 0.05% toluidine blue and carefully rinsed in deionized water prior to root hair examination. Root hairs were stained pinkish-blue whereas root surface remained unstained allowing for a clear observation of root hairs. For determination of root hair length, the stained roots were observed at 40× magnification under a Macro zoom imaging system (MVX10) consisting of a dissecting microscope equipped with a camera (Olympus, Tokyo, Japan). A section of the root with consistent fully elongated hairs was selected for image capture. Root hair length was quantified using a line tool in ImageJ version 1.47 (Abràmoff et al., 2004). Five representative hairs per image were selected for length measurement. Root hair length was calculated by comparing the number of pixels of a root hair to the number of pixels per mm obtained from an image of a micrometer scale taken at the same magnification (650 pixels mm⁻¹).

Potassium analysis

Dried plant samples were first grounded with a mortar. Then, five hundred milligrams of fine samples were processed through acid digestion in an opened container as described by Simmons et al. (2015). Samples were heated at 100 °C for 30 min in a block heater with 6 ml of 2:1 (HNO₃:HClO₄). The temperature was then increased to 150 °C until the solution became yellow and transparent. Once the solution changed color, 1 mL hydrochloric acid was added and the temperature was increased to 160 °C for 30 min. After, the samples were cooled, filtered with Whatman No.42 filtered paper, and adjusted to 25 mL with 1% HNO₃. The potassium concentration of the samples were then determined using the Flame Atomic Absorption Spectrophotometer (Perkin Elmer) (Simmons et al., 2015).

Statistical analysis

Statistical analyses were performed using R version 3.1.3. Linear mixed effect models were developed using the lmer function from the package lme4 (Bates et al., 2014). Correlation analyses were performed on individual plant data as well as the mean values of the measurements taken per genotype for percentage of biomass and K content reduction.

Results

Natural variation in root hair length among lowland and upland rice varieties

There was significant phenotypic variation in root hair length among 12 Thai rice varieties grown in the roll-up system (Fig. 1). Root hair length in lowland rice varieties ranged from 0.14 to 0.21 mm and upland rice varieties ranged from 0.16 to 0.19 mm (Fig. 1). Niaw San-pah-tawng, R258, and Goo Meuang Luang had the longest root hairs while RD1, Suphan Buri 1, and Leum Pua had the shortest root hairs.

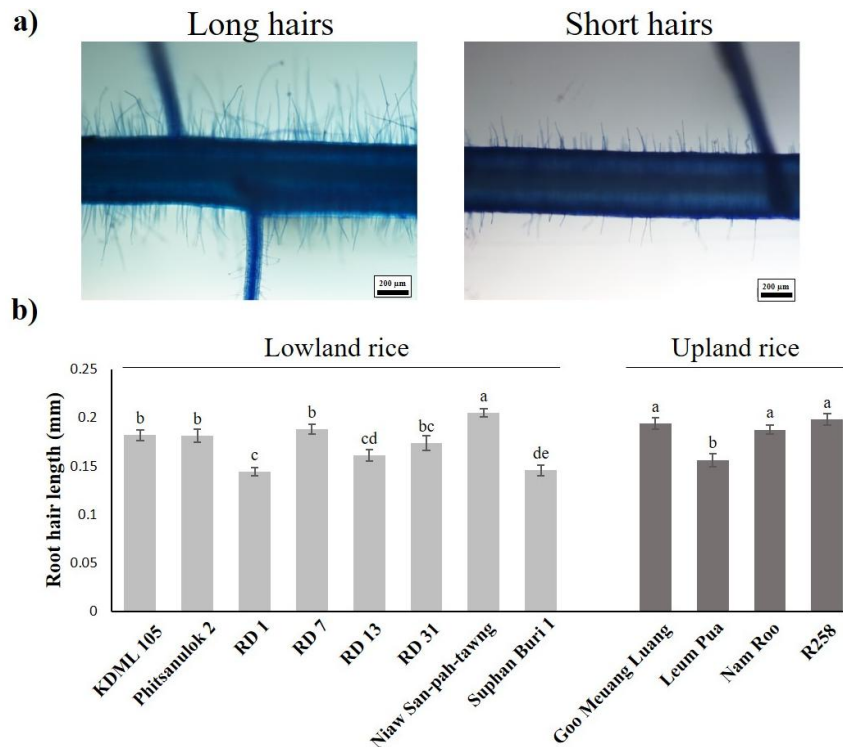


Figure 1. Root hair length among rice varieties a) images of long and short root hairs observed in this study b) variation of root hair length among lowland and upland rice. Plants were harvested at 7 days after planting in a roll up system. Different letters indicate significant difference at $p < 0.05$

Effects of low K availability on root hair length, plant growth, and tissue K content

Low K availability did not affect the average root hair length, tiller number, percentage of leaf senescence, crown root number, rooting depth, and root to shoot ratio (Table 1). However, shoot, root, and total dry weight was significantly reduced by 49%, 27% and 42%, respectively. In addition, tissue K content in shoot, root, and whole plants were reduced by 37%, 28% and 33%, respectively (Table 1). We found that root hair length was consistent among varieties and did not significantly respond to K stresses (Fig. 2a). Among the varieties, Phitsanulok 2 had long root hair while RD7 and RD13 had short root hair length in both treatments. Under high K availability, total dry weight was similar among varieties except for RD7 which had slightly lower biomass than the others (Fig. 2c). The plant's K contents were significantly different among varieties (Fig. 2b). In addition, total dry weight and plant's K content of all 6 varieties were substantially reduced under low K conditions (Fig. 2b and c).

Table 1. Effects of suboptimal potassium conditions on an average plant growth and K content. NS, non-statistical significant at $p < 0.05$

Parameter	High K	Low K	Significance
Root hair length, mm	0.139±0.01	0.137±0.01	NS
Tiller number	8.70±0.68	6.91±0.76	NS
Leaf senescence, %	25.36±1.94	35.66±4.99	NS
Crown root number	68.55±17.99	63.04±19.99	NS
Lateral root branching	12.15±0.65	11.51±0.62	NS
Rooting depth, cm	28.89±1.86	24.30±1.78	NS
Shoot dry weight, g	13.00±0.37	6.37±0.61	$p < 0.001$
Root dry weight, g	7.86±0.19	2.11±0.31	$p < 0.001$
Total dry weight, g	20.02±0.74	8.47±0.87	$p < 0.001$
Shoot K content, mg plant ⁻¹	44.44±3.36	16.29±2.09	$p < 0.001$
Root K content, mg plant ⁻¹	29.74±2.66	8.31±1.27	$p < 0.001$
Total K content, mg plant ⁻¹	74.17±4.80	24.61±3.26	$p < 0.001$
Root to shoot ratio	0.35±0.02	0.31±0.03	NS

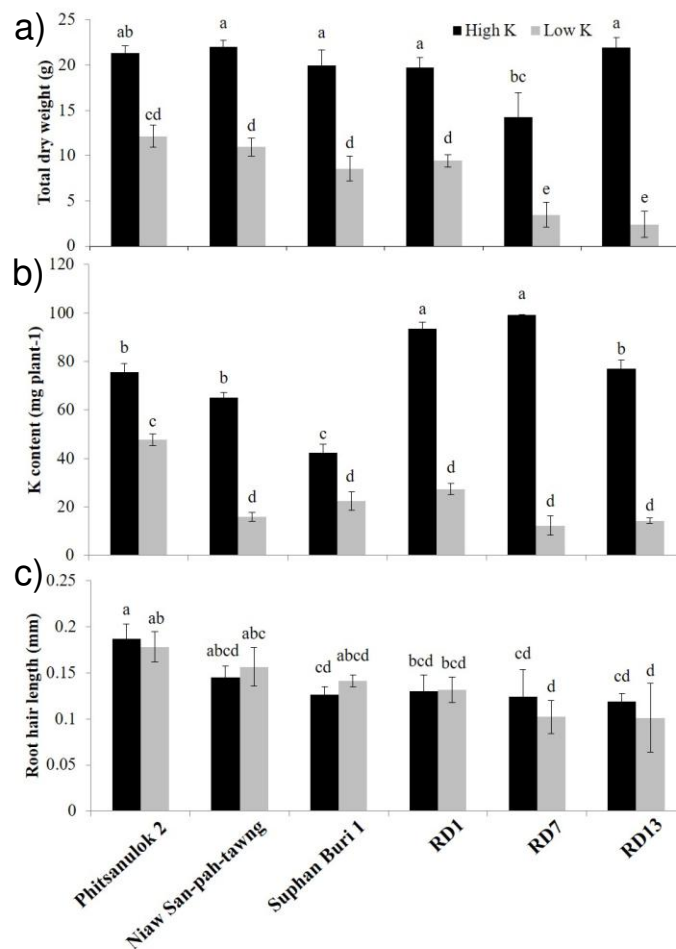


Figure 2. Bar graphs showing a) total dry weight b) potassium content and c) root hair length of six lowland rice varieties under low and optimal K conditions. Plants were harvested 2 months after planting. Different letters indicate significant difference at $p < 0.05$

Correlation analysis

Correlation analysis between root hair length, shoot, and root traits indicate that root hair length was negatively correlated with the percentage of leaf senescence ($r = -0.74$), positively correlated with plant growth ($r = 0.62$) and K accumulation ($r = 0.61$) under low K conditions (Table 2). There was no significant correlation between root hair length, crown root number, lateral root branching, and rooting depth under both high and low K conditions suggesting that root hair length is independent from these root traits (Table 2). In addition, increased root hair length was associated with high relative biomass ($r = 0.93$, $p < 0.01$) and K content ($r = 0.81$, $p < 0.05$) when compared between low K and optimal K conditions (Fig. 3).

Table 2. Correlation coefficient between root hair length and shoot and root parameters under high and low K conditions measured in pot of 6 Thai rice varieties. *, **, *** denote significance at $p < 0.05$, $p < 0.01$, and $p < 0.001$, respectively

Parameter	High K	Low K
Tiller number	0.48*	0.69**
Leaf senescence, %	-0.22	-0.74***
Crown root number	0.33	0.41
Lateral root branching	0.12	0.33
Rooting depth, cm	0.34	0.63
Shoot dry weight, g	0.25	0.59**
Root dry weight, g	0.29	0.55**
Total dry weight, g	0.42	0.62**
Shoot K content, mg plant ⁻¹	0.51*	0.59**
Root K content, mg plant ⁻¹	0.01	0.60**
Total K content, mg plant ⁻¹	0.36	0.61**
Root to shoot ratio	0.37	0.44*

Discussion

In this study, a large phenotypic variation of root hair length was found for twelve Thai rice varieties in a roll-up system (Fig. 1). Root hair length ranged between 0.14 to 0.21 mm, a typical range reported by other studies (Fig. 1). Compared to other crop species, such as wheat and maize (Zhu et al., 2005; Delhaize et al., 2015), rice root hair length has a much shorter range. Among rice varieties, we found that majority of upland varieties had long root hairs. This is not surprising because soils in upland fields are largely affected by suboptimal nutrient availability as nutrients often react with ions, such as iron, aluminum, and calcium found in soil, which leads to the formation of low mobile complexes when compared to those in rain-fed lowlands (Holford, 1997). Therefore, long root hairs found in these varieties could be one of the adaptive strategies for growing in such an environment.

It has been shown that several plant species increase root hair length in response to low K availability (Hogh-Jensen and Pedersen, 2003). In this study, we found that root hair length of all six rice varieties was not affected by suboptimal K conditions and plasticity for root hair length is not a universal trait but rather species- and genotype-specific. Additionally, long root hair was found to be associated with increased biomass and K content under low K conditions. In paddy environments, the depletion of readily

available K and exchangeable K in the rhizosphere could extend over 10 mm from the root surface at both the low and adequate K conditions (Yang et al., 2005). The results were consistent with Shi et al. (2004) research in which they reported the same range of the depletion zone of extractable K around the root (10 cm) in several plant species. Considering the effective the diffusion coefficient of K in soil which is approximately two orders of magnitude higher than that of P, the depletion zone of K around the root should be much smaller than that of P. Interestingly, Shi et al. (2004) found that the depletion range was even wider than that of the available P in the same experiment, thus, the depletion zone around a root is not only influenced by the effective diffusion of the nutrients but also the demand of the plants and possibly the concentrations of the nutrients in the soil. Our results support the hypothesis that long root hair may improve K acquisition in low K soils by increasing root surface area and decreasing the distance to the source of K, which enhances the volume of soil exploration beyond the K depletion zone.

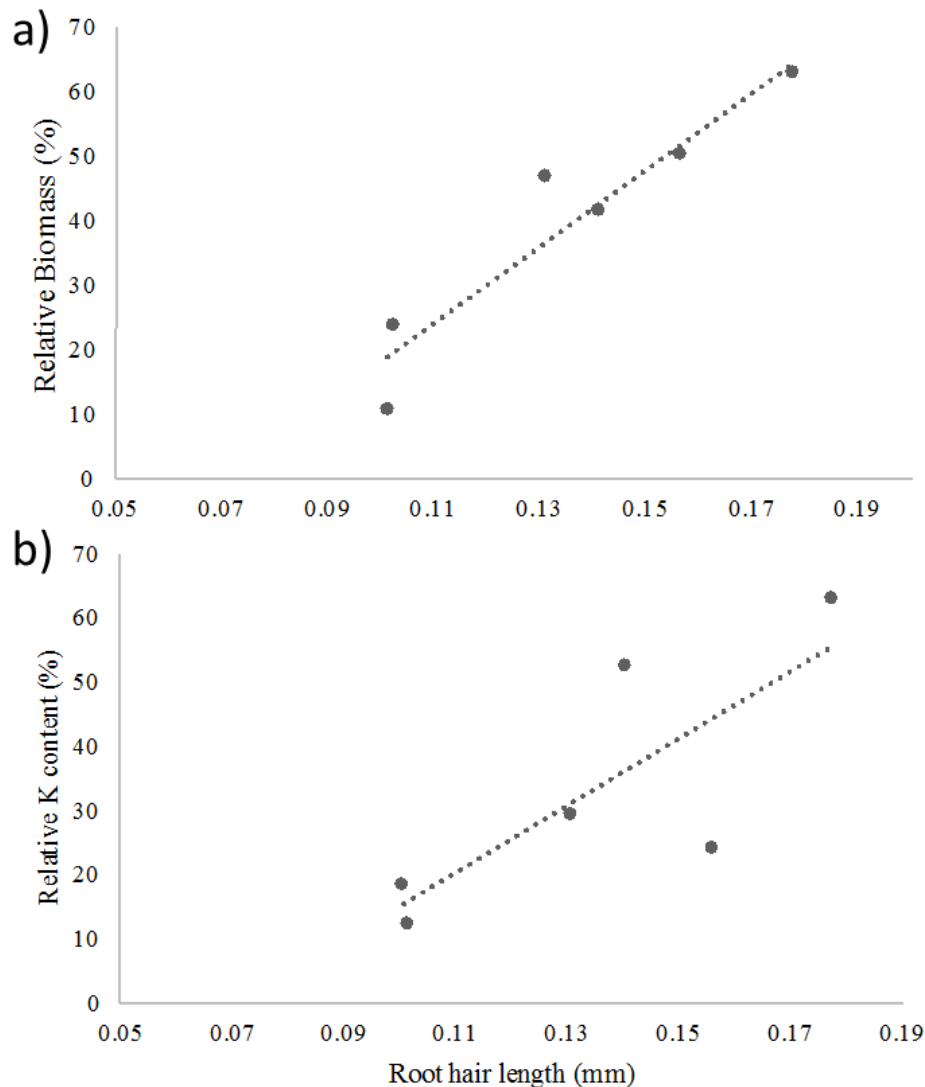


Figure 3. Correlation analysis between root hair length and relative a) biomass ($r = 0.93$, $p < 0.01$) and b) K content ($r = 0.81$, $p < 0.05$) compared between low K and optimal K conditions

A high root to shoot ratio is characteristically associated with plants growing in infertile soils (Wang and Yang, 2003). In this study, we found that root to shoot ratio was not significantly affected by low K availability. It has been suggested that root growth in potassium-deficient plants was more carbon limited when compared to plants with other deficiencies such as phosphorus and nitrogen. Limited carbon is largely due to a strong reduction in photosynthesis and the lack of an adaptive response in carbon allocation between roots and shoots. Thus, plants in K deficient conditions do not allocate more carbon to the root system (Postma et al., 2011; Miguel et al., 2015).

Several lines of evidence suggest that root traits, such as root number and root branching, influence K uptake (Yang et al., 2003). In our study, the selected rice varieties had comparable root number and branching (Fig. 4). In addition, we found that K stress did not affect average values of these root traits. Therefore, we conclude that the enhanced K uptake in the low K environment was attributable to the benefit of long root hair length.

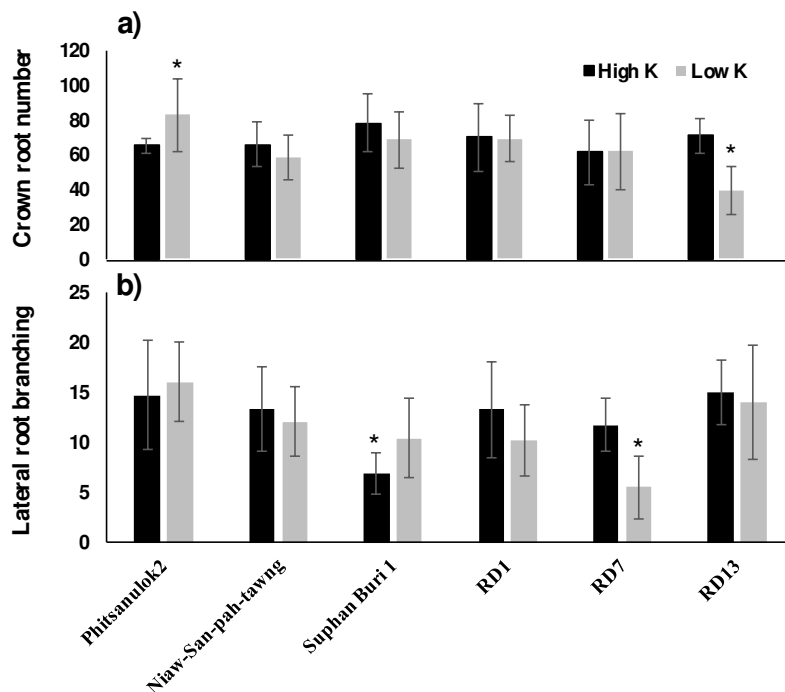


Figure 4. Bar graphs showing a) crown root number and b) lateral root number of six lowland rice varieties under low and optimal K conditions. Plants were harvested at 2 months after planting. * indicates significant difference at $p < 0.05$

Genetic studies in crop species including maize (Zhu et al., 2005), wheat (Horn et al., 2016), and common bean (Yan et al., 2004) indicate that root hair length is a complex quantitative trait and is controlled by a number of quantitative trait loci (QTLs). In rice, QTLs associated with variation of root hair length have not yet been identified. However molecular studies have shown that root hair elongation in rice is largely controlled by *OsAPY* gene encoding an enzyme apyrase, which catalyses the hydrolysis of phosphoanhydride bonds of nucleoside tri- and di-phosphates into mono-phosphates (Yuo et al., 2009). The development of molecular markers associated with root hair traits in rice is currently carried out to enhance efficiency of rice breeding program.

Conclusions

Our study shows that phenotypic variation in root hair length exists among upland and lowland Thai rice varieties. In addition, long root hair was associated with enhanced plant biomass and improved tissue K content under low K conditions. Further experiments in farmers' fields are underway to validate the physiological utility of root hair length for K acquisition in agronomic settings. For breeding perspectives, we see ample opportunity for using rice in Thai germplasms, particularly, Niaw San-pah-tawng and Pitsanulok2 which consistently had long root hairs across the growing systems, as donors for long root hairs. Furthermore, the development of high-throughput phenotyping approaches and molecular markers associated with long root hairs will help enhance efficiency and effectiveness of breeding programs targeting root hair length in rice.

Acknowledgements. This research project is supported by Mahidol University.

REFERENCES

- [1] Abramoff, M. D., Magalhães, P. J., Ram, S. J. (2004): Image processing with ImageJ. – *Biophotonics International* 11: 36–42.
- [2] Bates, D., Mächler, M., Bolker, B., Walker, S. (2014): Fitting linear mixed-effects models using lme4. – *Journal of Statistical Software* 67: 1–48.
- [3] Bates, T. R., Lynch, J. P. (2001): Root hairs confer a competitive advantage under low phosphorus availability. – *Plant and Soil* 236: 243–250.
- [4] Brown, L. K., George, T. S., Thompson, J. A., Wright, G., Lyon, J., Dupuy, L., Hubbard, S. F., White, P. J. (2012): What are the implications of variation in root hair length on tolerance to phosphorus deficiency in combination with water stress in barley (*Hordeum vulgare*)? – *Annals of Botany* 110: 319–328.
- [5] Caradus, J. R. (1981): Effect of root hair length on white clover growth over a range of soil phosphorus levels. – *New Zealand Journal of Agricultural Research* 24: 353–358.
- [6] Chang, T. T., Bardenas, E. A. (1965): The Morphology and Varietal Characteristics of the Rice Plant. Technical Bulletin, pp. 3–4. – IRRI, Los Banos.
- [7] Datta, S., Kim, C. M., Pernas, M., Pires, N. D., Proust, H., Tam, T., Vijayakumar, P., Dolan, L. (2011): Root hairs: development, growth and evolution at the plant-soil interface. – *Plant and Soil* 346: 1–14.
- [8] Delhaize, E., Rathjen, T. M., Cavanagh, C. R. (2015): The genetics of rhizosheath size in a multiparent mapping population of wheat. – *Journal of Experimental Botany* 66: 4527–4536.
- [9] Dobermann, A., Fairhurst, T. (2000): Rice: Nutrient Disorders & Nutrient Management. Handbook Series, Potash & Phosphate Institute (PPI). – Potash & Phosphate Institute of Canada (PPIC), Norcross and International Rice Research Institute, Los Banos.
- [10] Dobermann, A., Cassman, K. G., Mamaril, C. P., Sheehy, J. E. (1998): Management of phosphorus, potassium, and sulfur in intensive, irrigated lowland rice. – *Field Crops Research* 56: 113–138.
- [11] FAO (2015): “World Fertilizer Trends and Outlook to 2018.” – Food and Agriculture Organization of the United Nations (FAO), Rome.
- [12] Gahoonia, T. S., Nielsen, N. E. (2004): Barley genotypes with long root hairs sustain high grain yields in low-P field. – *Plant and Soil* 262: 55–62.
- [13] Gahoonia, T. S., Care, D., Nielsen, N. E. (1997): Root hairs and phosphorus acquisition of wheat and barley cultivars. – *Plant and Soil* 191: 181–188.

- [14] Gahoonia, T. S., Ali, O., Sarker, A. (2006): Genetic variation in root traits and nutrient acquisition of lentil genotypes. – *Journal of Plant Nutrition* 29: 643–655.
- [15] Gahoonia, T. S., Ali, R., Malhotra, R. S. (2007): Variation in root morphological and physiological traits and nutrient uptake of chickpea genotypes. – *Journal of Plant Nutrition* 30: 829–841.
- [16] Green, R. L., Beard, J. B., Oprisko, M. J. (1991): Root hairs and root lengths in nine warm-season turfgrass genotypes. – *Journal of the American Society for Horticultural Science* 116: 965–969.
- [17] Haling, R. E., Brown, L. K., Bengough, A. G., Young, I. M., Hallett, P. D., White, P. J., George, T. S. (2013): Root hairs improve root penetration, root – soil contact, and phosphorus acquisition in soils of different strength. – *Journal of Experimental Botany* 64: 3711–3721.
- [18] Hofer, R. M. (1991): Root Hairs. – In: Waisel, Y., Eshel, A., Kafkafi, U. (eds.) *Plant Roots – The Hidden Half*, pp. 129–148. Marcel Dekker, New York.
- [19] Høgh-Jensen, H., Pedersen, M. B. (2003): Morphological plasticity by crop plants and their potassium use efficiency. – *Journal of Plant Nutrition* 26: 969–984.
- [20] Horn, R., Wingen, L. U., Snape, J. W., Dolan, L. (2016): Mapping of quantitative trait loci for root hair length in wheat identifies loci that co-locate with loci for yield components. – *Journal of Experimental Botany* 67: 4535–4543.
- [21] Islam, A., Saha, P. K., Biswas, J. C., Saleque, M. A. (2016): Potassium fertilization in intensive wetland rice system : yield, potassium use efficiency and soil potassium status. – *International Journal of Agricultural Papers* 1: 7–21.
- [22] Jia, Y., Yang, X., Feng, Y., Jilani, G. (2008): Differential response of root morphology to potassium deficient stress among rice genotypes varying in potassium efficiency. – *Journal of Zhejiang University Science* 9: 427–434.
- [23] Jungk, A. (2001): Root hairs and the acquisition of plant nutrients from soil. – *Journal of Plant Nutrition and Soil Science* 164: 121–129.
- [24] Lynch, J. P. (2007): Roots of the second green revolution. – *Australian Journal of Botany* 55: 493–512.
- [25] Lynch, J. P., Brown, K. M. (2001): Topsoil foraging – an architectural adaptation of plants to low phosphorus availability. – *Plant Soil* 237: 225–237.
- [26] Lynch, J. P., Chimungu, J. G., Brown, K. M. (2014): Root anatomical phenes associated with water acquisition from drying soil : targets for crop improvement. – *Journal of Experimental Botany* 65: 6155–6166.
- [27] Ma, Z., Bielenberg, D. G., Brown, K. M., Lynch, J. P. (2001): Regulation of root hair density by phosphorus availability in *Arabidopsis thaliana*. – *Plant, Cell and Environment* 24: 459–467.
- [28] Miguel, M. A., Postma, J. A., Lynch, J. P. (2015): Phene synergism between root hair length and basal root growth angle for phosphorus acquisition. – *Plant Physiology* 175: 1430–1439.
- [29] Müller, M., Schmidt, W. (2004): Environmentally induced plasticity of root hair development in *Arabidopsis*. – *Plant Physiology* 134: 409–419.
- [30] Nestler, J., Keyes, S. D., Wissuwa, M. (2016): Root hair formation in rice (*Oryza sativa* L.) differs between root types and is altered in artificial growth conditions. – *Journal of Experimental Botany* 67: 3699–3708.
- [31] Postma, J. A., Lynch, J. P. (2011): Root cortical aerenchyma enhances the growth of maize on soils with suboptimal availability of nitrogen, phosphorus, and potassium. – *Plant Physiology* 156: 1190–1201.

- [32] Rengel, Z., Damon, P. M. (2008): Crops and genotypes differ in efficiency of potassium uptake and use. – *Physiologia Plantarum* 133: 624–636.
- [33] Salim, M. (2002): Effects of K nutrition on growth, biomass and chemical composition of rice plants and host-insect interaction. – *Pakistan Journal of Agricultural Research* 17: 14–21.
- [34] Shi, W., Wang, X., Yan, W. (2004): Distribution patterns of available P and K in rape rhizosphere in relation to genotypic difference. – *Plant and Soil* 261: 11–16.
- [35] Simmons, R. W., Chaney, R. L., Angle, J. S., Kruatrachue, M., Klinphoklap, S., Reeves, R. D., Bellamy, P. (2015): Towards practical cadmium phytoextraction with *N. occaea* *Caerulescens*. – *International Journal of Phytoremediation* 17: 191–199.
- [36] Slaton, N. A., Cartwright, R. D., Wilson, C. E. (1995): Potassium deficiency and plant diseases observed in rice fields. – *Better Crops*: 12–14.
- [37] Suzuki, N., Taketa, S., Ichii, M. (2003): Morphological and physiological characteristics of a root-hairless mutant in rice (*Oryza sativa* L.). – *Plant Soil* 101: 9–17.
- [38] Vejchasarn, P., Lynch, J. P., Brown, K. M. (2016): Genetic variability in phosphorus responses of rice root phenotypes. – *Rice* 9: 29.
- [39] Wang, L., Liao, H., Yan, X., Zhuang, B., Dong, Y. (2004): Genetic variability for root hair traits as related to phosphorus status in soybean. – *Plant and Soil* 261: 77–84.
- [40] Witt, C., Dobermann, A., Abdurachman, S., Gines, H., Guanghuo, W., Nagarajan, R., Satawatananont, S., Son, T. T., Tan, P. S., Simbahan, G. (1999): Internal nutrient efficiencies of irrigated lowland rice in tropical and subtropical Asia. – *Field Crops Research* 63: 113–138.
- [41] Yan, X., Beebe, S. E., Lynch, J. P. (1995): Genetic variation for phosphorus efficiency of common bean in contrasting soil types: II. Yield response. – *Crop Science* 35: 1094–1099.
- [42] Yan, X., Liao, H., Beebe, S. E., Blair, M. W., Lynch, J. (2004): QTL mapping of root hair and acid exudation traits and their relationship to phosphorus uptake in common bean. – *Plant and Soil* 265: 17–29.
- [43] Yang, X. E., Liu, J. X., Wang, W. M., Li, H., Luo, A. C., Ye, Z. Q., Yang, Y. (2003): Genotypic differences and some associated plant traits in potassium internal use efficiency of lowland rice (*Oryza sativa* L.). – *Nutrient Cycling in Agroecosystems* 67: 273–282.
- [44] Yang, X. E., Li, H., Kirk, G. J. D. (2005): Room - induced changes of potassium in the rhizosphere of low land rice. – *Communications in Soil Science and Plant Analysis* 36: 1947–1963.
- [45] Yoshida, S., Forno, D. A., Cock, J. H., Gomez, K. A. (1976): Laboratory Manual for Physiological Studies of Rice, pp. 61–67. – International Rice Research Institute, Philippines.
- [46] Yu, Z., Kang, B., He, X., Lv, S., Bai, Y., Ding, W., Chen, M., Cho, H. T., Wu, P. (2011): Root hair-specific expansins modulate root hair elongation in rice. – *The Plant Journal* 66: 725–734.
- [47] Yuo, T., Toyota, M., Ichii, M., Taketa, S. (2009): Molecular cloning of a root hairless gene *rth1* in rice. – *Breeding Science* 59: 13–20.
- [48] Zhu, J., Lynch, J. P. (2004): The contribution of lateral rooting to phosphorus acquisition efficiency in maize (*Zea mays*) seedlings. – *Functional Plant Biology* 31: 949–958.
- [49] Zhu, J., Kaeppler, S. M., Lynch, J. P. (2005): Mapping of QTL controlling root hair length in maize (*Zea mays* L.) under phosphorus deficiency. – *Plant and Soil* 270: 299–310.

HOW SPECIES DIVERSITY COULD REDUCE THE PREVALENCE OF INFECTIOUS DISEASES

COLLINS, O. C. – DUFFY, K. J.*

*Institute of Systems Science, Durban University of Technology
Durban 4000, South Africa
(phone: +27-31-373-6733)*

**Corresponding author
e-mail: kevind@dut.ac.za; phone+27-31-373-6733*

(Received 13th Nov 2017; accepted 27th Feb 2018)

Abstract. Understanding the benefits of biodiversity conservation is essential for developing policies that can enhance the environment and hence the well-being of humans as well. We formulate a consumer-resources model for a terrestrial ecosystem that incorporates resource diversity in the form of multiple species of resources (for example trees, grasses or both) and the consumers of those resources. This model is used to explore a potential benefit of maintaining ecosystem biodiversity, namely reducing the spread of infectious diseases. The important mathematical features of the model are derived, analysed and used to investigate our hypothesis that increasing species diversity in the resources can reduce diseases in those resources. The results of the analyses and numerical simulations suggest that indeed increasing resource diversity can lead to a decrease in infectious diseases. Of more interest, we show how increased diversity can result in eradication of disease in cases where disease persistence would normally be predicted.

Keywords: *consumer-resource model, ecosystem epidemiology dynamics, stability analysis, bifurcation, biodiversity*

Introduction

The economic and environmental benefits of biodiversity are well known (Pimentel et al., 1997). Primarily, ecosystems that are species-rich are more resilient and stabilize productivity over time (Naeem, 2009; Patz et al., 2005; Naeem and Li, 1997; Bai et al., 2004; Hautier et al., 2015). Recently, Isbell et al. (2015) showed how biodiversity increases the resistance of ecosystem productivity to a broad range of climate events.

The effects of biodiversity on human well-being are multifaceted. For example, the links between biodiversity and employment have been established Nunes et al. (2011). In health, ecosystem biodiversity plays a crucial role in regulating the transmission of many infectious diseases among human populations (WHO, 2016; Patz et al., 2005). Further evidence from the literature suggests that biodiversity conservation could promote human and wildlife health (Ostfeld and Keesing, 2012). Statistics have shown that about sixty percent of emerging infectious diseases that affect humans originate in animals and more than two-thirds of these originate in wildlife Patz et al. (2005). Meanwhile, according to the World Health Organization (WHO, 2016) zoonoses still constitute significant public health problems.

The occurrence of infectious diseases in ecosystems could be one of the factors affecting their productivity. The epidemiology of ecosystems have been investigated theoretically using a number of different approaches (Kooi et al., 2011; Auger et al., 2009; Das et al., 2011; Tewa et al., 2013) and it has been shown that maintaining biodiversity can affect disease transmission (Ezenwa et al., 2006; Haas et al., 2011;

Johnson et al., 2013; Ostfeld and Keesing, 2012). For instance: Haas et al. (2011) demonstrated that forest species diversity reduces disease risk in a generalist plant pathogen invasion. LoGiudice et al. (2003) show that the preservation of vertebrate biodiversity and community composition can reduce the incidence of Lyme disease. Johnson et al. (2013) show that maintaining biodiversity can reduce disease transmission using integrate high-resolution field data with multi-scale experiments. Ostfeld et al. (2000) examine the function of biodiversity in the ecology of vector-borne zoonotic diseases. Particularly, they show that high species diversity can lead to a reduction in infection prevalence and disease risk in vertebrate communities under certain conditions. Keesing et al. (2010) argue based on current evidence that preserving intact ecosystems and their endemic biodiversity should generally reduce the prevalence of infectious diseases.

The dynamics of mixed resource ecosystems are complex and understanding the dynamics of such ecosystems is important for proper management and preservation. Mathematical models are one of the tools that can aid this process through exploring the possible dynamics of the systems. Nakazawa et al. (2012) developed a mathematical model analysis for plant disease dynamics co-mediated by herbivory. Their results from an eco-epidemiological perspective demonstrate that integration of tripartite interactions among host plant, plant pathogens and herbivour vectors is helpful for successful control of plant diseases. Here, we consider a more complex mathematical model to investigate the impact of resource species diversity on the spread of diseases in a mixed resource terrestrial ecosystem and illustrate the mechanisms whereby species diversity could lead to a reduction in diseases. Thus, the primary aim here is to explain theoretically how species diversity could reduce certain infectious diseases in mixed resource terrestrial ecosystems.

Methods

Consumer-resource model

In this study we explore variations in biodiversity in terms of plant species richness. We develop a simple model of plant resources with animal consumers. The model is similar to that in Rosenzweig and MacArthur (1963) but here we extend it by introducing infection together with multiple resources that a consumer (or group of similar consumers) feed on. We assume that each type of resource is made up of two classes: a susceptible group S_i and an infected group I_i such that $S_i + I_i = N_i$ (all mathematical symbols used in this paper are listed with their meanings in *Appendix 3* at the end). Each susceptible group S_i grow logistically and decrease as a result of infections or removal by the consumers (Kooi et al., 2011; Rosenzweig and MacArthur, 1963). The infected group increases when the susceptible S_i become infected and decreases through death or feeding by the consumers (Nakazawa et al., 2012). Transmission of disease from the infected group (plants) I_i to susceptible plants S_i can be through indirect mode of transmission (Campbell, 1996). This is a situation when the pathogens causing the disease are carried independently by natural agencies like wind, water, animals, insects, mites, nematodes, birds etc. from the infected to susceptible plants. For instance, bacteria and fungi can be spread by water or wind. On the other hand, one of the most common vectors of viruses are insects. So for this study, infectious diseases of an ecosystem that can be transmitted by any of these indirect mode of transmission are considered. Thus, it is assumed that the pathogen density,

denoted by P , grow through the infected resources at rates v_i and die at a rate ξ , and is how S_i and I_i interact. Resource consumption is modelled by hyperbolic response functions (Turchin, 2003). Based on these assumptions, we obtain the model (Eq. 1)

$$\begin{aligned}
 \frac{dN_1}{dt} &= N_1 r_1 \left(1 - \frac{N_1}{K_1} \right) - \frac{\alpha_1 N_1 Y}{\beta_1 + N_1} - \gamma_1 I_1, \\
 \frac{dS_1}{dt} &= N_1 r_1 \left(1 - \frac{N_1}{K_1} \right) - \frac{\alpha_1 S_1 Y}{\beta_1 + N_1} - \sigma_1 S_1 P + \gamma_1 I_1, \\
 \frac{dI_1}{dt} &= \sigma_1 S_1 P - \frac{\alpha_1 I_1 Y}{\beta_1 + N_1} - (\gamma_1 + \mu_1) I_1, \\
 &\dots \\
 &\dots \\
 &\dots \\
 \frac{dN_n}{dt} &= N_n r_n \left(1 - \frac{N_n}{K_n} \right) - \frac{\alpha_n N_n Y}{\beta_n + N_n} - \gamma_n I_n, \\
 \frac{dS_n}{dt} &= N_n r_n \left(1 - \frac{N_n}{K_n} \right) - \frac{\alpha_n S_n Y}{\beta_n + N_n} - \sigma_n S_n P + \gamma_n I_n, \\
 \frac{dI_n}{dt} &= \sigma_n S_n P - \frac{\alpha_n I_n Y}{\beta_n + N_n} - (\gamma_n + \mu_n) I_n, \\
 &\dots \\
 \frac{dP}{dt} &= \sum_{i=1}^n v_i I_i - \xi P, \\
 \frac{dY}{dt} &= \sum_{i=1}^n \frac{c_i \alpha_i N_i Y}{\beta_i + N_i} - \tau Y,
 \end{aligned}
 \tag{Eq.1}$$

Note that n is the number of resources and $\sum_{i=1}^n S_i = S$, $\sum_{i=1}^n I_i = I$ with the total density $N = S + I$. The meaning of variables and parameters are given in *Table 1*. We assume that infections are not transmitted from resources to consumer and that consumers interact with all resources uniformly. We do not consider equations for $\frac{dS_i}{dt}$ in our mathematical analyses, as S_i can be easily determined from the already determined N_i and I_i . Note, increasing resource diversity for this model system is achieved by increasing n . All variables are in the units of biomass (g/m^2). Also, as the aim is to test the effects of resource diversity on the dynamics, the consumers are treated as one total biomass.

Consumer-resource model for one resource

To analyse the model, we start with the case where there is only one resource. For this homogenous case we drop the subscripts as there is only one resource (i.e. $\sum_{i=1}^1 S_i = S$, $\sum_{i=1}^1 I_i = I$ with the total density $N = S + I$ as before). We now obtain *Equation 2*:

$$\begin{aligned}
 \frac{dN}{dt} &= Nr \left(1 - \frac{N}{K} \right) - \frac{\alpha NY}{\beta + N} - \gamma I, \\
 \frac{dI}{dt} &= \sigma SP - \frac{\alpha IY}{\beta + N} - (\gamma + \mu)I, \\
 \frac{dP}{dt} &= \nu I - \xi P, \\
 \frac{dY}{dt} &= \frac{c\alpha NY}{\beta + N} - \tau Y,
 \end{aligned}
 \tag{Eq.2}$$

where variables and parameters have the same meanings as the corresponding ones defined in *Table 1*.

Table 1. Variables and parameters for model Equation 1

Variables	Meaning	Units
S_i	Density of susceptible resources i	g/m^2
I_i	Density of infected resources i	g/m^2
N_i	Total density of resources i , $S_i + I_i$	g/m^2
Y	Density of consumer	g/m^2
P	Measure of foliar diseases pathogen	g/m^2
Parameters	Meaning	Units
r_i	Growth rate of resources i	/year
K_i	Carrying capacity of resources i	g/m^2
α_i	N_i removal by Y_i	/year
β_i	N_i when α_i is half	g/m^2
c	Conversion of S_i or I_i into Y	Dimensionless
τ	Reduction of Y due to other factors	/year
σ_i	Exposure of S_i to P	/year
μ_i	Death rate of I_i	/year
γ_i	Recovery rate of I_i	/year
ν_i	Growth rate of P (from infected I_i)	/year
ξ	Death rate of P	/year

Consumer-resource model with increased species diversity, $n = 2$

Next we increased the resource diversity by setting $n = 2$ in model Equation 1 to obtain Equation 3:

$$\begin{aligned}
 \frac{dN_1}{dt} &= N_1 r_1 \left(1 - \frac{N_1}{K_1} \right) - \frac{\alpha_1 N_1 Y}{\beta_1 + N_1} - \gamma_1 I_1, \\
 \frac{dI_1}{dt} &= \sigma_1 S_1 P - \frac{\alpha_1 I_1 Y}{\beta_1 + N_1} - (\gamma_1 + \mu_1) I_1, \\
 \frac{dN_2}{dt} &= N_2 r_2 \left(1 - \frac{N_2}{K_2} \right) - \frac{\alpha_2 N_2 Y}{\beta_2 + N_2} - \gamma_2 I_2, \\
 \frac{dI_2}{dt} &= \sigma_2 S_2 P - \frac{\alpha_2 I_2 Y}{\beta_2 + N_2} - (\gamma_2 + \mu_2) I_2, \\
 \frac{dP}{dt} &= \sum_{i=1}^2 \nu_i I_i - \xi P, \\
 \frac{dY}{dt} &= \sum_{i=1}^2 \frac{c_i \alpha_i N_i Y}{\beta_i + N_i} - \tau Y,
 \end{aligned}
 \tag{Eq.3}$$

a scenario where there are two distinct resources that the consumers can feed on.

Threshold quantities used

The basic reproduction number denoted by R_0 in epidemiology is a threshold quantity that gives a condition under which a disease can be eradicated or persist in the population (van den Driessche and Watmough, 2002; Tien and Earn, 2010). For $R_0 < 1$ a disease can be eradicated but when $R_0 > 1$ a disease persists. So, to ensure disease eradication mechanisms (natural or otherwise) are required that ensure the basic reproduction number is below unity. Epidemiologically, the basic reproduction number can also be used as a measure of the number of secondary infections in the system. For example, the basic reproduction number R_0 for *Equation 2*, using the next generation matrix method (van den Driessche and Watmough, 2002), is (*Eq. 4*):

$$R_0 = \frac{\sigma \nu K}{\xi(\mu + \gamma)}
 \tag{Eq.4}$$

The consumption number denoted by C_0 for a consumer-resource system model is a threshold quantity (similar to the basic reproduction number) that gives a condition under which the consumers will survive or not in the system (Collins and Duffy, 2016a). Here, when $C_0 < 1$ consumers do not survive and when $C_0 > 1$ consumers survive. So, coexistence of consumer and resources in the system requires that the consumption number is above unity. For example, the consumption number for *Equation 2* can be calculated using the approach in Collins and Duffy (2016a) given by (*Eq. 5*):

$$C_0 = \frac{c \alpha K}{\tau(\beta + K)}
 \tag{Eq.5}$$

Mathematically, these two threshold quantities give conditions under which the equilibrium points of the system are stable and enable a qualitative analysis of the models.

Numerical simulations

Numerical simulations are used to support our analytical predictions. In particular, the impact of resource diversity on the dynamics of infected resource biomass is considered. The parameter values used for the numerical simulations are given in Table 2.

Table 2. Parameter values used for model simulations with their source

Variables/parameters	Value	Unit	Source
r	0.014	/day	Duffy (2001)
K	500	g/m^2	Owen-Smith (2004); Duffy (2001)
α	0.025	/day	Duffy (2001)
β	40	g/m^2	Duffy (2001)
c	0.75	Dimensionless	Owen-Smith (2004); Duffy (2001)
τ	0.0175	/day	Estimate
σ	0.01	/year	Estimate
γ	0.8	/year	Estimate
μ	0.002	/year	Estimate
ν	0.0275	/year	Estimate
ζ	0.033	/year	Estimate

We are interested in comparing the results of the models with increasing diversity and so to ensure these models are comparable we equal their biomasses by making:

$$r_1 = r_2 = r, \alpha_1 = \alpha_2 = \alpha, K_1 = K_2 = K/2, \mu_1 = \mu_2 = \mu, \gamma_1 = \gamma_2 = \gamma, \sigma_1 = \sigma_2 = \sigma.$$

Based on these assumptions, the basic reproduction number of Equation 1 for $n = 1$, $n = 2$ and $n = 3$ becomes equal. So to determine the impact of resource diversity on the spread of disease, we compare the dynamics of the models numerically under these assumptions.

These models are used to investigate the effect of increasing resource diversity. In most epidemiological modelling studies a fundamental result is that when the basic reproduction number is less than unity the infected populations dies out and when the basic reproduction number is greater than unity the disease persists (Castillo-Chavez et al., 2002; van den Driessche and Watmough, 2002; Tien and Earn, 2010). Ecologically, when the consumption number is less than unity, consumers will not survive and when the consumption number is greater than unity, consumers survive (Collins and Duffy, 2016a). So, the basic reproduction number and consumption number are bifurcation quantities. Thus, to investigate these scenarios numerically we consider parameter values such that the basic reproduction number and consumption number are less than and/or greater than unity. These various values of basic reproduction number and

consumption number are obtained by varying the most sensitive parameter while the others are kept fixed. We vary τ to obtain various value of C_0 since it is the most sensitive parameter for C_0 and we vary σ to obtain various value of R_0 since it is the most sensitive parameter for R_0 .

Analyses and results

Qualitative analyses

The system with $n = 1$ (Eq. 2) has many equilibrium points but we present only the ones crucial for our analyses, given by:

$$\begin{aligned} E_1 &= (N^*, I^*, P^*, Y^*) = (0, 0, 0, 0), \\ E_2 &= (N^*, I^*, P^*, Y^*) = (K, 0, 0, 0), \\ E_3 &= (N^*, I^*, P^*, Y^*) = \left(\frac{\tau\beta}{c\alpha - \tau}, 0, \frac{r}{\alpha} \left(1 - \frac{N^*}{K} \right) (\beta + N^*), 0 \right), \quad \text{if } C_0 \geq 1. \end{aligned}$$

Note that $E_3 = E_2$ if $C_0 = 1$. This suggests that C_0 and R_0 are bifurcation quantities. The short- and long-term dynamics of Equation 2 can be described by the stability about the equilibrium points Liao and Wang (2011). Thus, the stability results of the model are summarized in the following theorem.

Theorem 1

- (i) The trivial equilibrium point E_1 is unstable.
- (ii) The equilibrium point E_2 is stable if $C_0 < 1$ and $R_0 < 1$.
- (iii) For $C_0 > 1$, the equilibrium point E_3 is stable irrespective the value of R_0 .

The proof of Theorem 1 is given in *Appendix I*.

Ecologically, based on this formulation of the system dynamics, Theorem 1 implies the following for $n = 1$: (i) resources, consumers and pathogens cannot all go extinct (ii) consumers, infected resources and pathogens can be eradicated when $C_0 < 1$ and $R_0 < 1$. (iii) for $C_0 > 1$, infected resources can be eradicated irrespective the value of R_0 (i.e. for $R_0 < 1$ or $R_0 > 1$). Ecologically, co-existence of resources and consumers can occur in a system only when $C_0 > 1$. Thus, the consumption number C_0 and the basic reproduction number R_0 are important bifurcation quantities in the dynamical system analyses of Equation 2.

We present a qualitative analyse of the model for $n = 2$ (Eq. 3). Again, the system has many equilibrium points, but we analyse further the crucial ones representing disease eradication:

$$\begin{aligned} E_1 &= (N_1^*, I_1^*, N_2^*, I_2^*, P^*, Y^*) = (0, 0, 0, 0, 0, 0), \\ E_2 &= (N_1^*, I_1^*, N_2^*, I_2^*, P^*, Y^*) = (K_1, 0, K_2, 0, 0, 0), \\ E_3 &= (N_1^*, I_1^*, N_2^*, I_2^*, P^*, Y^*) = (N_1^*, 0, N_2^*, 0, 0, Y^*), \end{aligned}$$

where N_1^* and N_2^* are such that $\frac{\alpha_1 N_1^*}{\beta_1 + N_1^*} + \frac{\alpha_2 N_2^*}{\beta_2 + N_2^*} = \frac{\tau}{c}$ and $Y^* = \frac{r_1}{\alpha_1} \left(1 - \frac{N_1^*}{K_1}\right) (\beta_1 + N_1^*)$ or $Y^* = \frac{r_2}{\alpha_2} \left(1 - \frac{N_2^*}{K_2}\right) (\beta_2 + N_2^*)$.

The basic reproduction number for $n = 2$ is calculated, again using the next generation matrix method (see *Appendix 2*) as (Eq. 6)

$$\bar{R}_0 = \frac{R_{11} + R_{22} + \sqrt{(R_{11} + R_{22})^2 + 4(R_{12}R_{21} - R_{11}R_{22})}}{2}, \quad (\text{Eq.6})$$

where $R_{11} = \frac{\sigma_1 \nu_1 K_1}{\xi(\mu_1 + \gamma_1)}$, $R_{12} = \frac{\sigma_1 \nu_2 K_1}{\xi(\mu_2 + \gamma_2)}$, $R_{21} = \frac{\sigma_2 \nu_1 K_2}{\xi(\mu_1 + \gamma_1)}$, $R_{22} = \frac{\sigma_2 \nu_2 K_2}{\xi(\mu_2 + \gamma_2)}$.

Since $R_{12}R_{21} = R_{11}R_{22}$, the basic reproduction number R_0 can be simplified as (Eq. 7)

$$\bar{R}_0 = R_{11} + R_{22}. \quad (\text{Eq.7})$$

Mathematically, the quantities R_{11} and R_{22} can be regarded as the basic reproduction numbers associated with resources 1 and 2 respectively.

The consumption number (threshold quantity) denoted by \bar{C}_0 for $n = 2$ can be calculated using the approach in Collins and Duffy (2016a) and is given by (Eq. 8)

$$\bar{C}_0 = C_1 + C_2, \quad (\text{Eq.8})$$

where $C_1 = \frac{c\alpha_1 K_1}{\tau(\beta_1 + K_1)}$ and $C_2 = \frac{c\alpha_2 K_2}{\tau(\beta_2 + K_2)}$ are consumption numbers associated with resources 1 and 2 respectively.

Now again the dynamical system analyses are carried out utilizing the concept of the basic reproduction number R_0 together with the consumption number \bar{C}_0 where necessary. The dynamics of *Equation 3* can be summarized in the following stability results given in the theorem below.

Theorem 2

- (i) The trivial equilibrium points E1 is unstable.
- (ii) The equilibrium point E₂ is stable if $\bar{C}_0 < 1$ and $\bar{R}_0 < 1$.
- (iii) For $\bar{C}_0 > 1$, the equilibrium point E₃ is stable irrespective the value of \bar{R}_0 .

The proof of Theorem 2 (i) and (ii) can be established using the approach used in the proof of Theorem 1. For (iii), the proof of the special case of equivalent parameter values (see above) is also easily established. For the general case, the ensuing equations

are too complicated to solve. However, all numerical simulations performed by us support this proposition in general.

Comparing the consumption numbers of the models for $n = 1$ and $n = 2$, using the assumptions of equal biomasses, the consumption number for $n = 2$ is always greater than the consumption number for $n = 1$. This can be illustrated mathematically as follows:

$$\begin{aligned} \bar{C}_0 &= C_1 + C_2 \\ &= \frac{c\alpha_1 K_1}{\tau(\beta_1 + K_1)} + \frac{c\alpha_2 K_2}{\tau(\beta_2 + K_2)} \\ &= \frac{c\alpha K}{\tau(\beta + K/2)} \\ &> \frac{c\alpha K}{\tau(\beta + K)} = C_0 \end{aligned}$$

Thus (Eq. 9),

$$\bar{C}_0 > C_0 \quad (\text{Eq.9})$$

Similarly, we can show that this result also holds for any number of species n . So, larger values of n result in larger values of the consumption number. Thus, an increase in resource diversity n will lead to an increase in the consumption number. It can be shown that for $n = 1$ increasing the consumption number can result in a decrease in the infected biomass. Here increasing diversity is shown to result in an increase in the value of the consumption number. Thus, based on these results, increasing resource diversity as given here should lead to a decrease in the infected biomass in general. This possibility is explored numerically in the next section.

Numerical simulation results

The results of our numerical simulations are given in *Figure 1*, using the parameter values in *Table 2*. For *Figure 1* we set $\tau = 0.032$ which correspond to $C_0 = 0.5425 < 1$ and different basic reproduction numbers are calculated by varying σ ($R_0 = 0.5143, 0.9772, 2.5717, 5.1434$ using $\sigma = 0.001, 0.0019, 0.005, 0.01$ respectively).

From *Figure 1 a* and *b* the biomass of the infected resources decrease when $n = 1$ and $n = 2$, for $R_0 < 1$. For the case when $n = 2$, the infected biomass decreases faster. In *Figure 1 c* and *d* when $R_0 > 1$, the biomass of infected resources increases for both $n = 1$ and $n = 2$, but increases faster for $n = 1$. When $n = 3$ these results change fundamentally (*Fig. 1c* and *d*) in that even for $R_0 > 1$ the infected biomass is eradicated (note that the oscillation in the figure eventually dampen to zero). Increasing the consumption number to $C_0 > 1$ by varying τ strengthens this result in that now for $n = 2$ the infected biomass is eradicated as well (not shown).

Analyses of the general consumer-resource model, Equation 1

In this section, we show how some of the results of the previous sections can be extended to the general case.

The consumption number (threshold quantity) denoted by C_0 for the general model *Equation 1* can be calculated using the approach in Collins and Duffy (2016a) and is given by (*Eq. 10*)

$$\bar{C}_0 = \sum_{i=1}^n C_i, \quad (\text{Eq.10})$$

where $C_i = \frac{c\alpha_i K_i}{\tau(\beta_i + K_i)}$ is the consumption number associated with resource i .

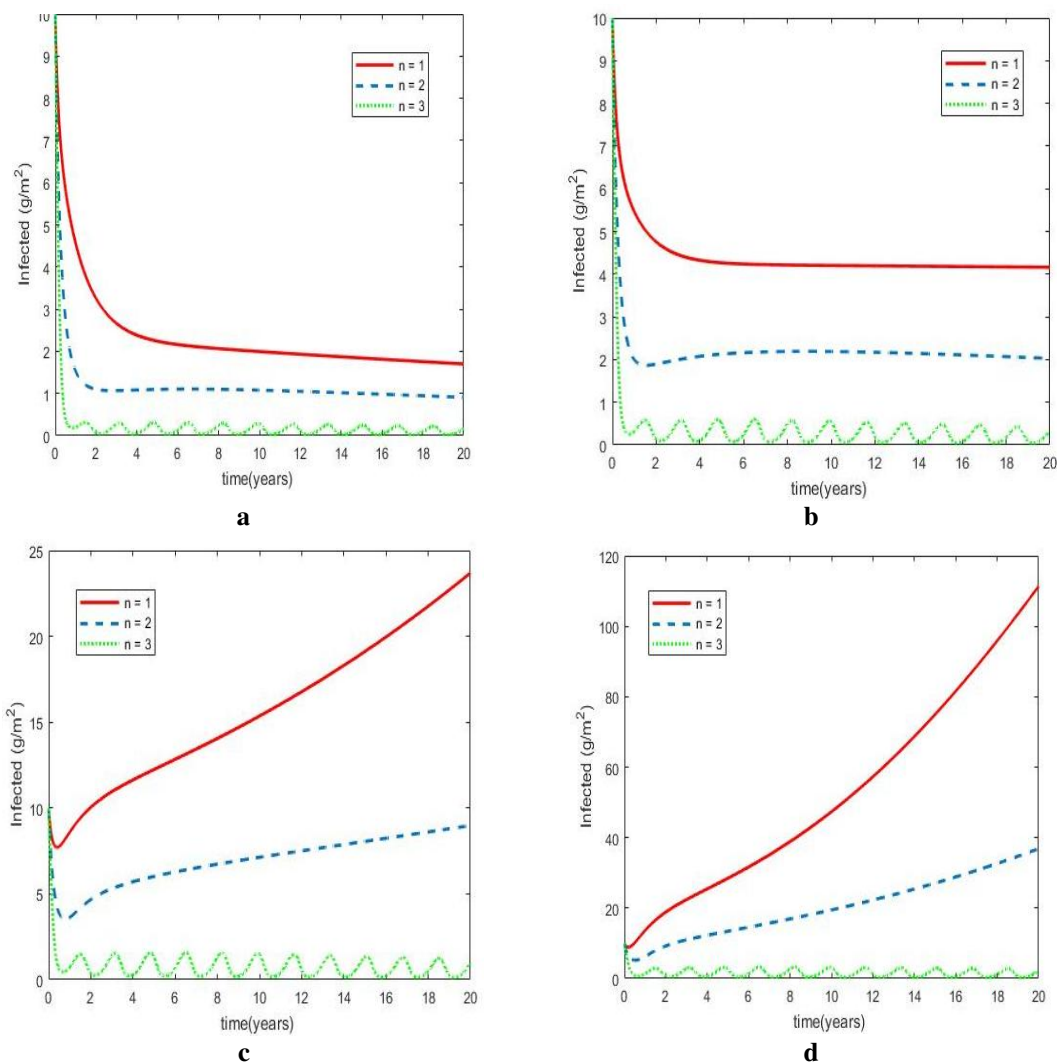


Figure 1. Plot illustrating the possible difference on the dynamics of model *Equation 1* for $n = 1, n = 2$ and $n = 3$ for $C_0 = 0.5425 < 1$ and for various values of R_0 : (a) $R_0 = 0.5143$ (b) $R_0 = 0.9772$ (c) $R_0 = 2.5717$ (d) $R_0 = 5.1434$ (see text for details)

The basic reproduction number of the more general model *Equation 1* can also be determined using the next generation matrix (see *Appendix 2*). The basic reproduction number R_0 for this general case is difficult to calculate analytically. However, if we

make the same assumptions used in the numerical simulations but for any n , the basic reproduction number R_0 becomes (Eq. 11)

$$\bar{R}_0 = \sum_{i=1}^n R_{ii} \quad (\text{Eq.11})$$

It is easy to see that for this general model, the basic reproduction number is also uniform irrespective of n (magnitude of resource diversity) under the same assumptions for equal biomass as in the cases of $n = 1$, $n = 2$ and $n = 3$. By similar reasoning, the larger the value of n , the larger the consumption number.

Discussion

A growing understanding of the benefits of biodiversity conservation is important for improved policies toward enhancing human well-being. In this study, we explored one of a potential benefit of ecosystem biodiversity where there are infectious diseases. By formulating and analysing an appropriate mathematical consumer-resource model that takes resource diversity into consideration, we were able to show how resource diversity could limit the spread of infectious diseases. Our results are based on qualitative analyses supported by numerical simulations.

A general consumer-resource model with n multiple types of resources representing resource diversity with these resources exposed to infectious disease was developed. Our analyses consider cases with $n = 1$ and $n > 1$ (i.e. a situation where there is only one type of resource and situations with more resources). The important mathematical features of the models such as the basic reproduction number and consumption number were obtained and used to investigate the dynamics. The results of the dynamical system analyses of these models using these concepts agree in general with results in epidemiology and consumer-resource system (Castillo-Chavez et al., 2002; van den Driessche and Watmough, 2002; Tien and Earn, 2010; Collins and Duffy, 2016a, b). In particular, we use these threshold quantities to consider the effects of diversity on the spread of disease. In all the cases considered increasing resource diversity reduced infected resources.

Our numerical results for $n = 1$ and $n = 2$, where $R_0 < 1$ agree with a fundamental result in epidemiological modelling that when the basic reproduction number is less than one infected populations die out (Castillo-Chavez et al., 2002; van den Driessche and Watmough, 2002; Tien and Earn, 2010). However, for the case when $n = 2$ we shown that the infected biomass decreases faster. Where $R_0 > 1$, the biomass of infected resources increase as expected. However, we show that it increased faster for $n = 1$ compared to $n = 2$. When $n = 3$ these results change fundamentally in that even for $R_0 > 1$ the infected biomass is eradicated. Increasing the consumption number to $C_0 > 1$ by varying τ strengthens this result in that then even for $n = 2$ the infected biomass can be eradicated. Overall, these results support our analytical predictions that increasing resource diversity leads to a decrease in the biomass of infected resources. However, the most interesting result is that, for a case when infected plants are expected to persist, increased diversity results in infected resources dying out. To reiterate, we show cases where even for $R_0 > 1$ then infected resources are eliminated for $C_0 > 1$ large enough.

For the general model (Eq. 1), conditions are shown, under the assumption of equal biomass, where an increase in resource diversity n will lead to an increase in the

consumption number. It is expected that the dynamics of this general model will also be governed by its corresponding basic reproduction number and consumption number (Heesterbeek and Roberts, 2007; Roberts and Heesterbeek, 2003; Collins and Duffy, 2016b). Consequently, our earlier findings that increasing diversity could lead to a decrease in the spread of infectious disease should also hold for this general model.

The models suggested here have many simplifying assumptions. However, as a first step they represent a method to compare ecosystems with different levels of diversity (here plant species richness). It is shown how increasing diversity in this system can help in reducing infectious disease in the system. Thus, increasing resource diversity through biodiversity conservation could promote healthier systems. This possibility could be important for both the environmental and agricultural future of the planet.

Conclusions

Biodiversity conservation has been shown to reduce the spread of some diseases in various ways (Haas et al., 2011; LoGiudice et al., 2003; Johnson et al., 2013; Ostfeld et al., 2000; Keesing et al., 2010). This study aimed to explain theoretically how biodiversity, through resource diversity, could lead to reduction in the spread of infectious diseases in a mixed resource ecosystem and the results are in the main consistent with this literature. As such, models of this kind with more and more detailed information can be considered to explain other aspects of system dynamics. Our model illustration here that resource diversity can lead to disease eradication is, as far as we know, new. Thus, this study complements results in this area and at the same time points to further research.

Acknowledgements. This work is based on research supported in part by the National Research Foundation of South Africa (Grant Numbers 98892 and 85494).

REFERENCES

- [1] Auger, P., Mchich, R., Chowdhury, T., Sallet, G., Tchuenta, M., Chattopadhyay, J. (2009): Effects of a disease affecting a predator on the dynamics of a predator–prey system. – *Journal of Theoretical Biology* 258(3): 344-351.
- [2] Bai, Y., Han, X., Wu, J., Chen, Z., Li, L. (2004): Ecosystem stability and compensatory effects in the Inner Mongolia grassland. – *Nature* 431: 181-184.
- [3] Campbell, R. N. (1996): Fungal transmission of plant viruses. – *Annual Review of Phytopathology* 34(1): 87 -108.
- [4] Castillo-Chavez, C., Feng, Z., Huang, W. (2002): On the Computation of R_0 and Its Role on Global Stability. – In: Bies, D., Blower, S., Driessche, P. van d., Kirschner, D., Yakubu, A.-A. (eds.) *Mathematical Approaches for Emerging and Re-emerging Infectious Diseases: An Introduction*. IMA Vol. 125. Springer-Verlag, New York.
- [5] Collins, O. C., Duffy, K. J. (2016a): Consumption threshold used to investigate stability and ecological dominance in consumer-resource dynamics. – *Ecological Modelling* 319: 155-162.
- [6] Collins, O. C., Duffy, K. J. (2016b): Understanding multiple species ecosystem dynamics using a consumer resource model. – *Natural Resource Modeling* 29(1): 145-158.
- [7] Duffy, K. J. (2011): Simulations to investigate animal movement effects on population dynamics. – *Natural Resource Modeling* 24(1): 48-60.

- [8] Ezenwa, V. O., Godsey, M. S., King, R. J., Guptill, S. C. (2006): Avian diversity and West Nile virus: testing associations between biodiversity and infectious disease risk. – *Proceedings of the Royal Society of London B: Biological Sciences* 273(1582): 109-117.
- [9] Haas, S. E., Hooten, M. B., Rizzo, D. M., Meentemeyer, R. K. (2011): Forest species diversity reduces disease risk in a generalist plant pathogen invasion. – *Ecology Letters* 14(11): 1108-1116.
- [10] Hautier, Y., Tilman, D., Isbell, F., Seabloom, E. W., Borer, E. T., Reich, P. B. (2015): Anthropogenic environmental changes affect ecosystem stability via biodiversity. – *Science* 348(6232): 336-340.
- [11] Heesterbeek, J. A. P., Roberts, M. G. (2007): The type-reproduction number T in models for infectious disease control. – *Mathematical Biosciences* 206(1): 3-10.
- [12] Isbell, F., Craven, D., Connolly, J., Loreau, M., Schmid, B., Beierkuhnlein, C., Bezemer, T. M., Bonin, C., Bruelheide, H., De Luca, E., Ebeling, A. (2015): Biodiversity increases the resistance of ecosystem productivity to climate extremes. – *Nature* 526(7574): 574-577.
- [13] Johnson, P. T., Preston, D. L., Hoverman, J. T., Richgels, K. L. (2013): Biodiversity decreases disease through predictable changes in host community competence. – *Nature* 494(7436): 230-233.
- [14] Keesing, F., Belden, L. K., Daszak, P., Dobson, A., Harvell, C. D., Holt, R. D., Hudson, P., Jolles, A., Jones, K. E., Mitchell, C. E., Myers, S. S. (2010): Impacts of biodiversity on the emergence and transmission of infectious diseases. – *Nature* 468(7324): 647-652.
- [15] Kooi, B. W., van Voorn, G. A., pada Das, K. (2011): Stabilization and complex dynamics in a predator–prey model with predator suffering from an infectious disease. – *Ecological Complexity* 8(1): 113-122.
- [16] Liao, S., Wang, J. (2011): Stability analysis and application of a mathematical cholera model. – *Mathematical Biosciences and Engineering* 8(3): 733-752.
- [17] LoGiudice, K., Ostfeld, R. S., Schmidt, K. A., Keesing, F. (2003): The ecology of infectious disease: effects of host diversity and community composition on Lyme disease risk. – *Proceedings of the National Academy of Sciences* 100(2): 567-571.
- [18] Naeem, S. (ed.) (2009): *Biodiversity, Ecosystem Functioning, and Human Wellbeing: An Ecological and Economic Perspective*. – Oxford University Press, Oxford.
- [19] Naeem, S., Li, S. (1997): Biodiversity enhances ecosystem reliability. – *Nature* 390(6659): 507-509.
- [20] Nakazawa, T., Yamanaka, T., Urano, S. (2012): Model analysis for plant disease dynamics co-mediated by herbivory and herbivore-borne phytopathogens. – *Biology Letters* 8(4): 685-688.
- [21] Nunes, P. A. L. D., Ding, H., Boteler, B., ten Brink, P., Cottee-Jones, E., Davis, M., Ghermandi, A., Kaphengst, T., Lago, M., McConville, A. J., Naumann, S., Pieterse, M., Rayment, M., Varma, A. (2011): *The Social Dimension of Biodiversity Policy: Final Report for the European Commission, DG Environment under Contract: ENV.G.1/FRA/2006/0073 2nd*, pp. vii-205. – Venice/Brussels, February 2011.
- [22] Ostfeld, R. S., Keesing, F. (2000): Biodiversity series: the function of biodiversity in the ecology of vector-borne zoonotic diseases. – *Canadian Journal of Zoology* 78(12): 2061-2078.
- [23] Ostfeld, R. S., Keesing, F. (2012): Effects of host diversity on infectious disease. – *Annual Review of Ecology, Evolution, and Systematics* 43: 157-182.
- [24] Owen-Smith, N. (2004): Functional heterogeneity in resources within landscapes and herbivore population dynamics. – *Landscape Ecology* 19(7): 761-771.
- [25] Pada Das, K., Kundu, K., Chattopadhyay, J. (2011): A predator–prey mathematical model with both the populations affected by diseases. – *Ecological Complexity* 8(1): 68-80.
- [26] Patz, J. A., Confalonieri, U. E. C., Amerasinghe, F. P., Chua, K. B., Daszak, P., Hyatt, A. D., Molyneux, D., Thomson, M., Yameogo, L., Lazaro, M. M., Vasconcelos, P., Rubio-Palis, Y., Campbell-Lendrum, D., Jaenisch, T., Mahamat, H., Mutero, C., Waltner-

- Toews, D., Whiteman, C. (2005): Human Health: Ecosystem Regulation of Infectious Diseases. – In: Hassan, R., Scholes, R., Ash, N. (eds.) Ecosystems and Human Well-Being. Current State and Trends, Vol. 1. The Millennium Ecosystem Assessment, Chap. 14, pp. 391-415. Island Press, Washington, DC.
- [27] Pimentel, D., Wilson, C., McCullum, C., Huang, R., Dwen, P., Flack, J., Tran, Q., Saltman, T., Cliff, B. (1997): Economic and environmental benefits of biodiversity. – *BioScience* 47(11): 747-757.
- [28] Roberts, M. G., Heesterbeek, J. A. P. (2003): A new method for estimating the effort required to control an infectious disease. – *Proceedings of the Royal Society of London B: Biological Sciences* 270(1522): 1359-1364.
- [29] Rosenzweig, M. L., MacArthur, R. H. (1963): Graphical representation and stability conditions of predator-prey interactions. – *The American Naturalist* 97(895): 209-223.
- [30] Tewa, J. J., Djeumen, V. Y., Bowong, S. (2013): Predator–prey model with Holling response function of type II and SIS infectious disease. – *Applied Mathematical Modelling* 37(7): 4825-4841.
- [31] Tien, J. H., Earn, D. J. (2010): Multiple transmission pathways and disease dynamics in a waterborne pathogen model. – *Bulletin of Mathematical Biology* 72(6): 1506-1533.
- [32] Turchin, P. (2003): *Complex Population Dynamics: A Theoretical/Empirical Synthesis* (Vol. 35). – Princeton University Press, Princeton, NJ.
- [33] Van den Driessche, P., Watmough, J. (2002): Reproduction numbers and sub-threshold endemic equilibria for compartmental models of disease transmission. – *Mathematical Biosciences* 180(1): 29-48.
- [34] World Health Organization (WHO) (2016): Zoonoses and the Human-Animal-Ecosystems Interface. – <http://www.who.int/zoonoses/en/> (May 2016).

Appendix 1

Proof of Theorem 1

The proof of Theorem 1 is given as follows:

- (i) The Jacobian of *Equation 2* evaluated at the trivial equilibrium point E_1 has the following eigenvalues:

$$\lambda_1 = r, \lambda_2 = -(\mu + \gamma), \lambda_3 = -\xi, \lambda_4 = -\tau.$$

Thus, E_1 is unstable since $\lambda_1 = r > 0$.

- (ii) The Jacobian of *Equation 2* evaluated at the equilibrium point E_2 has the following eigenvalues:

$$\lambda_1 = -r, \lambda_2 = \tau(C_0 - 1), \lambda_{3,4} = \frac{-(\gamma + \mu + \xi) \pm \sqrt{(\gamma + \mu + \xi)^2 + 4\xi(\gamma + \mu)(R_0 - 1)}}{2}.$$

Clearly, $\lambda_2 < 0 \Leftrightarrow C_0 < 1$ and $\lambda_{3,4} < 0 \Leftrightarrow R_0 < 1$. Thus the equilibrium point E_1 is stable if $C_0 < 1$ and $R_0 < 1$.

- (iii) The Jacobian of model *Equation 2* evaluated at the equilibrium point E_3 has the following eigenvalues:

$$\lambda_{1,2} = \frac{-(a_{22} + \xi) \pm \sqrt{(a_{22} + \xi)^2 - 4(a_{22}\xi - a_{23}\nu)}}{2}, \lambda_{3,4} = \frac{-a_{11} \pm \sqrt{a_{11}^2 - 4a_{14}a_{41}}}{2},$$

where $a_{11} = \frac{rN^*}{K(\beta + N^*)}(\beta + 2N^* - K)$, $a_{22} = \gamma + \mu + \frac{\alpha Y^*}{\beta + N^*}$, $a_{23} = \sigma N^*$,

$a_{14} = \frac{\alpha N^*}{\beta + N^*}$ and $a_{41} = \frac{\alpha c \beta N^*}{(\beta + N^*)^2}$. We observe that $\lambda_{1,2} < 0 \Leftrightarrow a_{22}\xi - a_{23}\nu > 0$. By elementary algebraic calculations we have that $a_{22}\xi - a_{23}\nu > 0$. Next, $\lambda_{3,4} < 0 \Leftrightarrow a_{11} < 0$. Similarly, we can show by elementary algebraic calculations that $a_{11} < 0 \Leftrightarrow C_0 > 0$. Thus, for $C_0 > 1$, the equilibrium point E_3 is stable irrespective the value of R_0 .

Appendix 2

Calculations of the basic reproduction number

For $n = 2$

The basic reproduction number for $n = 2$ is calculated, again using the next generation matrix approach of van den Driessche and Watmough (2002). The associated next generation matrices are given by

$$F = \begin{pmatrix} 0 & 0 & K_1\sigma_1 \\ 0 & 0 & K_2\sigma_2 \\ 0 & 0 & 0 \end{pmatrix}, V = \begin{pmatrix} \mu_1 + \gamma_1 & 0 & 0 \\ 0 & \mu_2 + \gamma_2 & 0 \\ -\nu_1 & -\nu_2 & \xi \end{pmatrix}$$

with

$$FV^{-1} = \begin{pmatrix} R_{11} & R_{12} & \frac{K_1\sigma_1}{\xi} \\ R_{21} & R_{22} & \frac{K_2\sigma_2}{\xi} \\ 0 & 0 & 0 \end{pmatrix},$$

where $R_{11} = \frac{\sigma_1\nu_1K_1}{\xi(\mu_1 + \gamma_1)}$, $R_{12} = \frac{\sigma_1\nu_2K_1}{\xi(\mu_2 + \gamma_2)}$, $R_{21} = \frac{\sigma_2\nu_1K_2}{\xi(\mu_2 + \gamma_2)}$, $R_{22} = \frac{\sigma_2\nu_2K_2}{\xi(\mu_2 + \gamma_2)}$.

The basic reproduction number R_0 for model *Equation 3* is now given by the dominant eigenvalue of the next generation matrix FV^{-1} and is

$$\bar{R}_0 = \frac{R_{11} + R_{22} + \sqrt{(R_{11} + R_{22})^2 + 4(R_{12}R_{21} - R_{11}R_{22})}}{2}.$$

For the general model, *Equation 1*

The basic reproduction number of the more general model *Equation 1* can also be determined using the next generation matrix approach of van den Driessche and Watmough (2002). The associated next generation matrices are given by

$$F = \begin{pmatrix} 0 & 0 & \dots & 0 & K_1\sigma_1 \\ 0 & 0 & \dots & 0 & K_2\sigma_2 \\ \cdot & & & & \\ \cdot & & & & \\ 0 & 0 & \dots & 0 & K_n\sigma_n \\ 0 & 0 & \dots & 0 & 0 \end{pmatrix}, V = \begin{pmatrix} \gamma_1 + \mu_1 & 0 & 0 & 0 & \dots & 0 \\ 0 & \gamma_2 + \mu_2 & 0 & 0 & \dots & 0 \\ \cdot & & & & & \\ \cdot & & & & & \\ 0 & 0 & \dots & 0 & \gamma_n + \mu_n & 0 \\ -\nu_1 & -\nu_2 & -\nu_3 & \dots & -\nu_n & \xi \end{pmatrix},$$

$$\text{with } FV^{-1} = \begin{pmatrix} R_{11} & R_{12} & \dots & R_{1n} & \frac{K_1\sigma_1}{\xi} \\ R_{21} & R_{22} & \dots & R_{2n} & \frac{K_2\sigma_2}{\xi} \\ \cdot & & & & \\ \cdot & & & & \\ R_{n1} & R_{n2} & \dots & R_{nn} & \frac{K_n\sigma_n}{\xi} \\ 0 & 0 & \dots & 0 & 0 \end{pmatrix},$$

where $R_{ij} = \frac{\sigma_i \nu_j K_i}{\xi(\mu_j + \gamma_j)}$. The basic reproduction number R_0 is as in the previous cases $n = 2$

or $n = 1$ is the dominant eigenvalue of FV^{-1} . For this general case, the dominant eigenvalues are difficult to calculate analytically. However, if we take the same assumptions used in the numerical simulation but for any n , the basic reproduction number R_0 becomes

$$\bar{R}_0 = \sum_{i=1}^n R_{ii} .$$

Appendix 3

List of all symbols used

Variables	Meaning	Units
S_i	Density of susceptible resources i	g/m^2
S	Total density of susceptible resource	g/m^2
I_i	Density of infected resources i	g/m^2
I	Total density of infected resource	g/m^2
N_i	Total density of resources i , $S_i + I_i$	g/m^2
N	Total density resource, $S + I$	g/m^2
Y	Density of consumer	g/m^2
P	Measure of foliar diseases pathogen	g/m^2
Parameters	Meaning	Units
r_i	Growth rate of resources i	/year
K_i	Carrying capacity of resources i	g/m^2
α_i	N_i removal by Y_i	/year
β_i	N_i when α_i is half	g/m^2
c	Conversion of S_i or I_i into Y	Dimensionless
τ	Reduction of Y due to other factors	/year
σ_i	Exposure of S_i to P	/year
μ_i	Death rate of I_i	/year
γ_i	Recovery rate of I_i	/year
ν_i	Growth rate of P (from infected I_i)	/year
ζ	Death rate of P	/year
Other mathematical symbols	Meaning	
E_j	Equilibrium points j	
S^*	Equilibrium point value for S	
S_i^*	Equilibrium point value for S_i	
I^*	Equilibrium point value for I	
I_i^*	Equilibrium point value for I_i	
N^*	Equilibrium point value for N	
N_i^*	Equilibrium point value for N_i	
C_0	Consumption number	
C_i	Consumption number associated with resource i	
\bar{C}_0	Consumption number for $n > 1$	
R_0	Reproduction number	
\bar{R}_0	Reproduction number for $n > 1$	
λ_j	Eigenvalue j	

Symbols that do not appear in this list are used only to simplify the writing of equations and are defined in the text.

CARBON FOOTPRINTS OF RUBBER PRODUCTS SUPPLY CHAINS (FRESH LATEX TO RUBBER GLOVE)

USUBHARATANA, P. – PHUNGRASSAMI, H.*

*Excellence Center of EcoEnergy, Chemical Engineering Department, Faculty of Engineering,
Thammasat University
Pathumthani, Thailand
(phone: +66-2-564-3001; fax: +66-2-564-3010)*

**Corresponding author
e-mail: pharnpon@engr.tu.ac.th*

(Received 16th Nov 2017; accepted 20th Feb 2018)

Abstract. Carbon footprint emissions related to the natural latex supply chain including farm cultivation, concentrated latex production and rubber glove processing were investigated. Data were collected from 656 rubber plantations covering six provinces in the northeast, east, and south of Thailand and three concentrated latex production plants including one rubber glove processing factory. Different allocation methods were considered to compare the carbon footprint results including mass allocation, economic allocation and allocation by dry rubber content (DRC). Calculation methods were based on life cycle assessment (LCA) and ISO14067. Results indicated that farm size had no impact on the carbon footprint of fresh latex, with the carbon footprint of fertilizer application at planting estimated at more than 90% of the total contribution. For concentrated latex production, almost 70% of the carbon footprint originates from rubber cultivation. Total carbon footprint emission of 200 pieces of rubber glove was about 42 kg CO₂-eq, allocated by mass during cultivation and by DRC in concentrated latex processing, with less than 1% from rubber plantations and concentrated latex processing. Allocation methods for the carbon footprint of rubber gloves do not affect the final result but have a great impact on the upstream process.

Keywords: *allocation, concentrated latex, global warming, life cycle assessment, rubber glove*

Introduction

Rubber products are derived from field latex collected from rubber trees. This field latex is converted into five primary forms as concentrated latex, air dried sheet, crepe rubber, Standard Thai Rubber (STR) and ribbed smoke sheet. These forms are used as raw material for manufacturing tires, rubber gloves, condoms, rubber hose and other rubber products. Ribbed smoke sheet and STR are usually used in the production of tires, while concentrated latex is used extensively for the manufacture of dipped products such as rubber gloves and condoms. Most rubber tree plantations are located in Southeast Asia and Thailand, Indonesia and Malaysia have suitable climates. In 2014, total global production of natural rubber was about 13 million tons. Data from the Food and Agricultural Organization of the United Nations (FAO) in 2014, showed Asia as the largest rubber producer (11.9 million tons) following by America and Africa with the same production (0.67 million tons) with the remainder from Oceania (FAOSTAT, 2017). In 2010, Thailand produced 3 million tons of rubber, accounting for 35% of the global output and this figure increased by 49% to 4.5 million tons in 2014 (FAOSTAT, 2017). However, Thai rubber output dropped in 2016 due to climate change and a sharp reduction in the rubber price. The climate fluctuation causes increasing annual rainfall (Ruangsri et al., 2015). Rainfall is a main climatic factor that influences on latex yield, an increase of rainfall can cause a loss of crop due to rainfall interference with tapping (Sdoodee and Rongsawat, 2012). Southern Thailand is a major rubber-producing area

representing 70% of the country's total output which is decreasing. Around 15% of the total output is produced in northeast Thailand where production is expected to gradually increase as the government supporting rubber plantations in new areas (OAE, 2016a). Production of latex in Indonesia and Malaysia in 2014 was 3.1 million tons and 0.6 million tons respectively (FAOSTAT, 2017). All these countries are leading rubber producers; however, each has its own distinct manufacturing process. Malaysia and Indonesia focus on block rubber export, while Thailand exports concentrated latex and rubber sheet. The total value of concentrated latex in 2016 was 1,000 million USD with rubber sheet at 777 million USD (RIU, 2017). The total value of rubber gloves in 2014 was 1,105 million USD and 98% of production was exported (OIE, 2014). Thus, the industry is a key foreign exchange earner for Thailand.

Global industry and waste including wastewater greenhouse gas (GHG) emissions grew from 10.37 Gt CO₂-eq in 1990 to 13.04 Gt CO₂-eq in 2005 to 15.44 Gt CO₂-eq in 2010 (Fischedick et al., 2014). Presently, increasing attempts to reduce environmental pollution and achieve the goal of sustainable agricultural products have focused on organic farming with synthetic fertilizer and pesticide reduction (Abeliotis et al., 2013). Limiting the use of nitrogen (N) fertilizers will reduce GHG emissions which impact on global warming (Yan et al., 2015; Adewale et al., 2016). However, to achieve real sustainability, rubber cultivation supply chains and processing methods must all be considered to understand all aspects of the product life cycle.

The rubber industry is also monitored for environmental cleanliness. Rubber products exported to the international market require paperwork regarding sustainable production (Jawit et al., 2015). Rubber tree plantations impact on the environment through several steps, starting from land cultivation for seeding, preliminary treatment and use of pesticides and herbicides, including fertilizers (Phungrassami and Usubharatana, 2015). In the process of concentrated latex production, one environmental consideration is water pollution with the main sources of rubber wastewater as skim, latex or washing in various processes (Mohammad et al., 2010). During the final production process, fuel-wood (old rubber-wood) combustion in burners without proper pollution control devices may cause high contamination from smoke in the workplace (Choosong et al., 2010).

Interest in environmental issues has risen significantly over the past decades, and the Thai Government and business owners have become aware of pollution impacts on global warming. Thailand launched the National Master Plan on Climate Change (2010-2019) to increase pollution awareness by the population (Kabiri, 2016). The Thailand Climate Change Master Plan was also recently implemented (2012-2050) with the objectives to improve economics, society and the environment, and cut GHG emissions by 2050 without impeding the country's gross domestic products.

Global GHG emissions generated from industry are comprised of direct energy and heat of emissions from production of electric and indirect CO₂ emission related CO₂ emissions precesss CO₂ industry, non CO₂ GHG emissions and direct emissions for waste or wastewater (Fischedick et al., 2014). All the stages in the manufacturing processes of rubber products, it consumes a high quantity of energy, water and other natural resources (Dayaratne and Gunawardana, 2015). Therefore, an environmental baseline survey is necessary to establish policy and action plans to reduce GHG emissions. The assessment tool for the relative impact of production systems occurring throughout the whole product life cycle is life cycle assessment (LCA) (Sparrevik et al., 2015). Both input and output data in a selected system boundary of a product are

evaluated by environmental impact assessment throughout their entire life cycle. Setting LCA objectives has an influence on delimitation and result of assessment. Several LCA studies focused on the ecological footprints of ribbed smoked sheet (RSS), ribbed smoked sheet bale (RSSB) and concentrated latex (Musikavong and Sheewala, 2017). Phungrassami and Usubharatana (2015) collected data on planting rubber trees and assessed the environmental impacts of rubber wood production in Thailand. Dayaratne and Gunawardana (2015) studied carbon footprint (CF) emissions from small and medium enterprises (SMEs) manufacturing rubber bands in Sri Lanka with a focus on energy-efficiency but did not refer to the primary products such as the carbon footprints of fresh latex and concentrated latex. Maulina et al. (2015) applied the LCA and eco-efficiency to investigate the environmental impact of crumb rubber. Lin et al. (2017) studied the LCA of rubber tires with the aim of reducing their carbon footprint by replacing carbon black with graphene. Jawjit et al. (2015) conducted a life cycle assessment of concentrated latex production in Thailand; however, the scope of their study followed a gate-to-gate approach considering concentrated latex processing only, not the upstream processes which occurred at the rubber plantation. Jawjit et al. (2010) assessed GHG emissions from concentrated latex, block rubber (STR20) and the RSS sector in the rubber industry. Their results indicated that GHG emissions from fresh latex amounted to 0.2 tons CO₂-eq/ton fresh latex (excluding land conversion) and 144 kg CO₂-eq/ton concentrated latex (considering only gate-to-gate factory). However, their paper contained no reference to the allocation of fresh latex and rubber wood which are joint-products of rubber plantations. Ounsaneha and Rattanapan (2016) studied the eco-efficiency of rubber gloves. The scope of their study was limited to a gate-to-gate approach to define the performance and environmental hotspots of the process. Results revealed that electricity usage and chemical consumption were the most significant environmental problems; however, life cycle assessment was not applied.

From the literature reviews, a full analysis of rubber glove production starting from the rubber plantation through to glove processing has rarely been reported, with most authors adopting only a gate-to-gate approach. Limited information exists regarding the carbon footprint emission allocation of the rubber supply chain.

An environmental impact assessment of products in this study focused on the CF of manufacturing rubber products such as concentrated latex as an intermediate product and rubber gloves as the final product. The CF was used to develop an environmental inventory and impact assessment based on life cycle methodology for three products as fresh latex, concentrated rubber and rubber gloves. The specific objectives were to (1) establish an inventory for CF analysis of selected products, (2) assess the CF of different farm sizes through to rubber gloves manufacture, (3) identify environmental hotspots in the selected product system boundary, and (4) consider rubber products allocation. Results will be beneficial for environmentally concerned, policy makers and other primary rubber product users who form the majority of Thailand's rubber product exports.

This paper begins with an introduction, background and rationale. Section 2 describes the principles and framework for life cycle assessment (LCA) including planting rubber trees, processing field latex into concentrated latex, and producing rubber gloves. Section 3 discusses the results of the assessment by testing three areas as GHG emissions from plantations and GHG emissions from concentrated latex production and rubber glove manufacturing. Conclusions are drawn in section 4.

Materials and methods

There is potential to decrease the global warming effect of primary rubber production through to the final product. Policy-makers and environmentally concerned customers must understand the importance of conducting CF assessments to collect benchmark information. The CF of the whole process from planting rubber trees to processing concentrated latex and manufacturing rubber gloves was investigated. A cradle to grave approach was followed to estimate GHG emissions associated with material inputs, energy, and activities during the product chain within the product system boundary. The method for LCA consideration was based on ISO14040 (2006) including ISO/TS14067 (2013) guidelines consisting of four steps as (1) goal and scope definition, (2) inventory analysis, (3) impact assessment and (4) interpretation.

Goal and scope

The goal and scope definition provides the goal of the study and description of the product system, including the functional unit and system boundary (Wang et al., 2010). The goal of the study defined the life cycle inventory and CF of two different rubber products manufactured in Thailand as latex primary product (concentrated latex) and the final product (rubber gloves); planting details were also considered. Moreover, environmental hotspots of selected products in each system boundary were identified and analyzed. The functional unit and system boundary settings were defined and related data were provided. In addition, the co-product allocations in the life cycle assessments of plantations as field latex, rubber waste and rubber wood were assessed.

A functional unit is defined and used to establish a basis for comparison of alternative products or services (ISO14044, 2006). Meier et al. (2015) examined the LCA of agricultural products and determined that most authors defined functional unit per product unit in accordance with Jawjit et al. (2010) as the default unit of weight. The functional unit in the agricultural sector can be defined by both area (expressing the intensity of the production system) and product (quantitative measure of efficiency) (Holka et al., 2016). Three processes were identified as rubber tree cultivation, processing concentrated latex and manufacturing rubber gloves. Therefore, the functional unit was set in terms of mass of fresh latex (g CO₂-eq/kg fresh latex), mass of concentrated latex (kg CO₂-eq/ton concentrated latex) and a box of rubber gloves (kg CO₂-eq/200 pieces size L weight 56 g per two pieces).

The system boundary for carbon footprint assessment of selected products manufactured in Thailand was considered as “cradle to farm gate” for rubber tree cultivation, “cradle to factory gate” for concentrated latex and “cradle to grave” for rubber gloves (*Fig. 1*).

The first process analyzed was rubber tree cultivation. The system boundaries included inputs and emissions, i.e. fertilizers and emissions due to use of N-fertilizer, diesel and GHG emissions due to fuel combustion, with pesticides also taken into account. However, impacts due to the life cycle of equipment and other infrastructure were not considered. The second process related to concentrated latex processing. All energy consumption used in production including electricity and diesel, utilities such as water and chemicals and especially preservatives for natural rubber latex were considered. The third process was rubber glove processing which considered and water consumption including several chemicals. Disposal of wastes as discarded gloves and packaging was also taken into account.

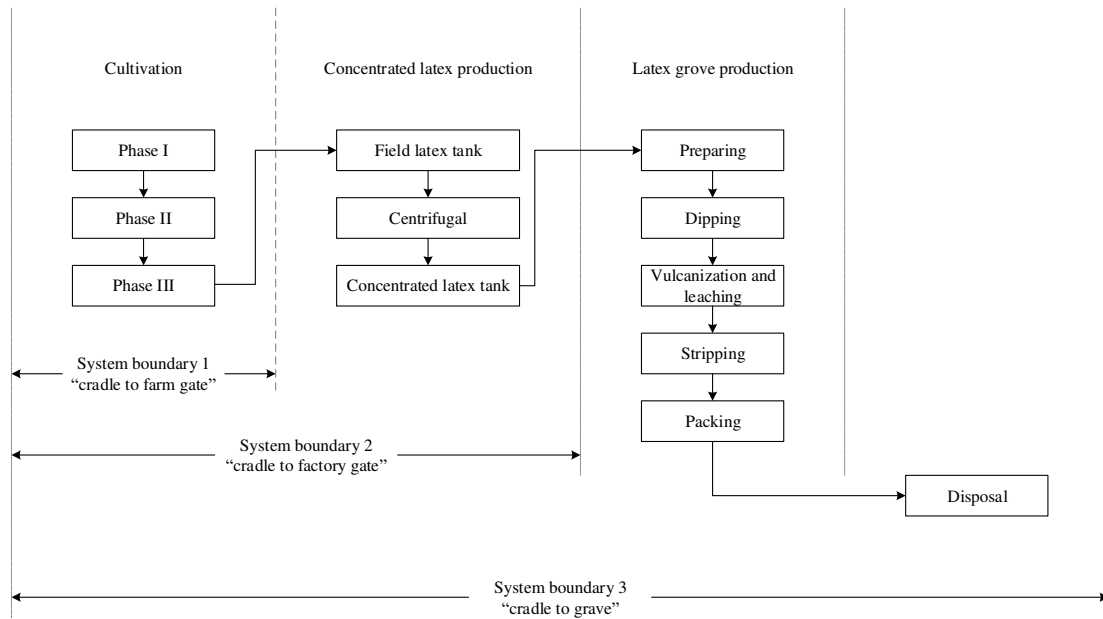


Figure 1. System boundary for the carbon footprint of selected products *i* at each level

Life cycle inventory

Cultivation

For the period of 2014-2016, a simple random sample of 656 farmers was conducted in six Thai Provinces including Chanthaburi, Rayong, Bueng Kan, Udon Thani, Nakhon Si Thammarat and Surat Thani. Bueng Kan and Udon Thani located in the northeast which is the highland area. Both two provinces are considered as the new area of rubber plantation. Chanthaburi and Rayong located in the east which is near the coast. The rest provinces located in the southern part of Thailand which also is near the coast. Rubber tree plantations in Thailand are divided based on size into three types as small-sized farms (less than 8 ha), medium-sized farms (8-40 ha) and large-sized farms (more than 40 ha) (Rubber Replanting Aid Fund Act, 1960). The planting process is divided into three major phases; preparing and cultivating the area, growing and maintaining rubber trees before the tapping period (1-8 years) and maintaining rubber trees during the tapping period (9-25 years). For phrase I, the amount of diesel and fertilizer as 3-6-8, 15-15-15 or 0-3-0 (N-P-K ratio) are used for land preparation based on the needs. In phase II, both organic and chemical fertilizer as 18-8-8, 15-15-15, 20-8-20, 25-7-7 are added to the soil. Sometimes, glyphosate or paraquat herbicides are also added. In phrase III, large amounts of fertilizer in different formulas as 16-8-8, 15-15-15, 15-7-18, 25-7-7 are required. Chemical fertilizers used in the GHG emission assessment were defined as nitrogen (N), P₂O₅ and K₂O equivalent. The products were classified into three main groups as fresh rubber, rubber residue and para-rubber wood. Although ISO14044 (2006) suggests avoiding the allocation, the products become the raw materials for concentrated latex, Thai standard rubber and rubber wood furniture. Therefore, mass allocation of environmental burdens was conducted for each product with allocation ratios as para-rubber wood 63.48%, fresh latex 35.65% and rubber residue 0.87% (Phungrassami and Usubharatana, 2015).

Concentrated latex production

Fresh latex obtained on tapping has about 30-35% dry rubber content (DRC) with the remainder as non-rubber solids and water which is delivered for concentration to the latex factory. The definition of concentrated latex is a liquid containing at least 60% DRC. Different methods are used to concentrate the including evaporation using heat to remove the water with the product called evaporation latex, creaming by adding a creaming agent when the product is called creamed latex, or a centrifugal method with the product called centrifuged latex. The centrifugal method is used in most concentrated latex factories in Thailand. The stability of fresh latex is preserved and enhanced by adding ammonia and TMTD/ZnO (tetramethyl thiuram disulfide/zinc oxide) and then it is passed through a sieve into the gutter and kept suitable for spinning by adding ammonia (>4%). For fresh latex with high magnesium content, diammonium hydrogen phosphate (DAP) is added to precipitate the magnesium. Thereafter, the fresh latex is placed into a high speed Centrifuge Separator Machine to remove the water. A 60% concentrated latex and skim latex are obtained using this process. Preservatives are added to supplement the concentrated latex. High Ammonia (HA) latex is preserved with 0.7 %wt. ammonia and Low Ammonia (LA) latex concentrate is preserved with 0.2 %wt ammonia. For skim latex containing less than 8% rubber content, NH₃ is released to air, H₂SO₄ is added and its form is changed into coagulum, crepe, and finally into crumbs.

Rubber glove production

The raw materials for rubber glove production are concentrated latex 60% DRC and a chemical latex stabilizer like potassium hydroxyl, including a chemical vulcanizing system like zinc oxide (ZnO). The concentrated latex is mixed with various compounding chemicals based on need, then brought to forming process with dipping technique, which is the main production process followed by Thailand's rubber glove manufacturers (Ounsaneha and Rattanapan, 2016). In this process, a mold is dipped in a cleaning tank which has three steps as acid clean the tank to remove mold residues, water rinse the tank to remove the acid from the previous step and alkali clean the tank to dissolve proteins and fats. Then, the mold is dipped in a tank containing calcium nitrate and calcium carbonate as a coagulant. Next, the mold is dipped into a latex dipping tank at high temperature to enhance the coagulation efficiency of the latex and to easily roll the edges of the rubber gloves. Then, the rubber gloves with the rolled edges are re-heated until vulcanization and the mold is removed. The gloves are then dried with liquid petroleum gas (LPG). The final process consists of inspection and finishing.

Impact assessment

This stage consists of classification, characterization (mandatory phase) and normalization, weighting (option phases) (ISO14040, 2006). Only mandatory phases were conducted in this study. The effect of global warming was taken as mid-point characterization factors and calculated using the International Panel of Climate Change (IPCC) methodology following AR4 (Solomon et al., 2007). Global warming potential (GWP) activities in the system boundary were estimated from *Equation 1*:

$$CF = \sum_{i=1}^n A_i \times EF_i \quad (\text{Eq.1})$$

where CF represents the total of the GHG emissions from all activities in the system boundary in kg CO₂-eq, A represents the ith activity data presented in the form of amount of environmental load such as electricity in kWh, diesel in kg, chemicals in kg, and EF_i is the GHG emission factor of the ith input in kg CO₂-eq/unit such as electricity in kg CO₂-eq/kWh. The main database used was Ecoinvent (2010) in the libraries of Simapro where materials or energy for production of one unit of a product is stored. However, in the case that materials or energy production were available in Thailand, the database managed by National Metal and Materials Technology Center, Thailand (2014) was used to reflect the actual results.

In the case of planting, direct N₂O emissions from N fertilizer utilization were estimated from *Equation 2*:

$$CF_{N_2O} = A_F \times 0.01 \times \frac{44}{28} \times 298 \quad (\text{Eq.2})$$

where CF_{N₂O} represents the direct N₂O emissions converted to CO₂ equivalent from application of N-fertilizer in kg CO₂-eq, A_F is the amount of N-fertilizer applied in the cultivation process in kg N-fertilizer, 0.01 is the emission factor for N₂O from N inputs, kg N₂O-N (kg N input)⁻¹, 44/28 is the conversion factor of N₂ to N₂O, and 298 is the relative potential of global warming in a 100-year horizon (Solomon et al., 2007). Therefore, output units for the selected products CF are kg CO₂-eq/kg product or ton of product.

Allocation scenario analysis

Further analysis of allocation methods for the CF results of the product chain was applied using hypothetical simulations. Base case assessment considered the allocation method and mass allocation was applied in planting with DRC allocation applied in concentrated latex production. Three groups of scenarios were modeled. Each model altered when comparing the base case scenarios of rubber glove' life cycle to estimate the overall environmental impact of rubber glove. The scenarios were split into multiple parts as scenario 1 which considered economic allocation in planting and DRC allocation in concentrated latex production. Scenario 2 considered mass allocation in both planting and DRC allocation in concentrated latex production and scenario 3 considered economic allocation in planting and mass allocation in concentrated latex production.

Results and discussion

Greenhouse gas emissions at plantation

A survey of Thai rubber farmers during 2014-2016 gave 381 small farmers (total area 819 ha), 253 medium farmers (total area 2,512 ha) and 22 large farmers (total area 1,007 ha) accounting for 0.14% of the total rubber wood plantation area in Thailand (total Thai plantation area was 3,138,169 ha in 2016). Most of surveyed farmers

cultivated clone RRIM600 which is highly susceptible to diseases and economic incentive to develop new rubber tree clones (Pethin et al., 2015). Details of the plantations are shown in *Table 1*. Small farms accounted for 19%, medium farms 58% and large farms 23% of the total cultivated area. The amount of fresh latex varied with farm size; however, overall yield was 1,725-3,193.75 kg/ha (a factor of 2). In addition, results revealed that farm size did not reflect yield performance management, and a large farm could have less yield than a small farm. However, larger farms had higher weighted average yields, except in Nakhon Si Thammarat where the weighted average yield of medium farms was lower than small farms. Thailand's weighted average yield in 2016 was 1,500 kg/ha (OAE, 2016b).

Table 1. Some characteristics of rubber plantation

Farm characteristics	Chanthaburi Farm size			Rayong Farm size		
	Small	Medium	Large	Small	Medium	Large
No. of farms	60	30	2	61	32	1
Total area (ha)	128	286	88	134	321	43
Yield (kg/ha/y)						
- Range	1,125-3,750	1,325-3,494	2,588-3,000	1,056-3,831	1,275-3,581	3,194
- Weighted average	2,038	2,456	2,775	2,375	2,413	3,194
Diesel (kg/ha)						
- Range	0-16	0-16	16	0-16	0-16	16
- Weighted average	10	10	16	15	15	16
Synthetic fertilizer (ha/kg)						
- Range	938-28,688	2,250-31,563	10,544-13,500	0-24,125	2,500-19,063	13,750
- Weighted average	13,219	14,631	11,888	11,163	11,763	13,750
Organic fertilizer (ha/kg)						
- Range	0-46,875	0-33,075	0	0-45,000	0-31,875	0
- Weighted average	3,031	5,750	0	6,856	2,575	0
Chemicals (ha/kg)						
- Range	0-469	0-625	313	0-750	0-438	269
- Weighted average	138	156	313	106	106	269
Farm characteristics	Bueng Kan Farm size			Udon Thani Farm size		
	Small	Medium	Large	Small	Medium	Large
No. of farms	53	30	1	61	29	2
Total area (ha)	101	289	64	170	261	96
Yield (y/ha/kg)						
- Range	900-2,769	1,350-3,038	2,700	781-2,406	1,125-3,038	2,113
- Weighted average	1,850	2,013	2,700	1,725	2,031	2,113
Diesel (ha/kg)						
- Range	23	23	31	23	23	31
- Weighted average	23	23	31	23	23	31
Synthetic fertilizer (kg/ha)						
- Range	2,344-28,500	7,875-42,563	18,256	1,688-34,719	13,281-34,094	19,844-21,388
- Weighted average	14,588	16,438	18,256	16,713	23,844	20,619
Organic fertilizer (kg/ha)						
- Range	0-47,500	0-106,250	37,150	0-56,406	0-17,813	0
- Weighted average	3,319	4,700	37,150	3,538	1,531	0
Chemicals (kg/ha)						
- Range	0-194	0-194	156	0-469	0-625	313
- Weighted average	69	63	156	138	156	313

Farm characteristics	Nakhon Si Thammarat Farm size			Suratthani Farm size		
	Small	Medium	Large	Small	Medium	Large
No .of farms	75	56	5	71	76	11
Total area (ah)	140	565	242	146	791	472
Yield (y/ha/kg)						
- Range	700-3,450	344-3,781	1,538-2,963	531-4,831	613-4,331	581-2,638
- Weighted average	2,013	1,944	2,131	1,838	1,900	2,031
Diesel (kg/ha)						
- Range	0-8	0-16	8-16	0-8	0-16	0-8
- Weighted average	8	10	16	1	9	8
Synthetic fertilizer (kg/ha)						
- Range	6,275-26,894	2,406-28,500	10,781-14,150	6,031-51,681	1,488-27,763	7,713-18,875
- Weighted average	13,381	13,525	13,044	13,613	10,681	13,238
Organic fertilizer (kg/ha)						
- Range	0-13,088	0-16,875	0-4,375	0-33,750	0-12,719	0
- Weighted average	550	569	725	763	625	0
Chemicals (kg/ha)						
- Range	0-394	0-781	0-156	0-394	0-338	0-406
- Weighted average	88	113	100	75	25	144

The plantation inventory mainly concerned fertilizer application conducted in three stages as the cultivating stage, pre-tapping stage (1-7 years) and post-tapping stage (8-25 years). Both synthetic and organic fertilizers were used but synthetic fertilizer application tended to be higher than organic fertilizer. Average application of synthetic fertilizer ranged from 10,681-23,844 kg/ha and Udon Thani applied more synthetic fertilizer than the other provinces. Average application of organic fertilizer ranged from 0 to 37,150 kg/ha.

Two sources of GHG emissions were considered as fertilizer production and nitrogen-based fertilizer. GHG emissions from fertilizer production (defined here as indirect emissions) were estimated from the amount of chemical fertilizer used multiplied by emissions factors based on the Thailand database. GHG emissions from nitrogen-based fertilizers were estimated from the quantity of nitrogen added to the soil by using *Equation 2*. An amount of 0.01% of nitrogen was converted to N₂O (defined here as direct emissions). *Table 2* shows that levels of N from synthetic fertilizer applications were higher than from organic fertilizer. Total N fertilizer application rates ranged from 2,024 to 5,793 kg N/ha (a factor of three) or 80.96 to 231.72 kg N/ha/y. Comparison to the N-fertilizer requirement of rubber plant in Nigeria and Thailand, the N-fertilizer recommendation were 112 kg N/ha for first year (Orimoloye et al., 2010) and 70 kg N/ha (Jawjit et al., 2010), respectively. However, the fertilizer application depends on plant nutrient status in soil and plant of each area (Dumrongrak, 2010).

Diesel fuel consumption of vehicles for planting was estimated from cycles of vehicle usage with two sources of GHG emissions as diesel production (defined here as indirect emissions) and fuel combustion (defined here as direct emissions).

Together with the allocations mentioned above, fertilizer application, diesel fuel consumption and pesticide use allocated to co-products like rubber wood and rubber waste were all considered in the summary of GHG emissions from fresh latex production. GHG emissions of fresh latex after the allocation were between 55.6-168.9 g CO₂-eq/kg fresh latex (*Table 3*). The weighted average of small farms was 93 g CO₂-eq/kg fresh latex, medium farms 94 g CO₂-eq/kg fresh latex and large farms 98 g

CO₂-eq/kg fresh latex, with total weighted average 95.26 g CO₂-eq/kg fresh latex. The GHG emissions were quite similar and did not depend on farm size. The greatest contribution was from fertilizer application (both synthetic and organic) at more than 90%. GHG emissions from diesel fuel and pesticide were lower compared to fertilizer (Table 4). The average GHG emissions from fertilizer was 91.34 g CO₂-eq/kg fresh latex, which closed to 89.40 g CO₂-eq/kg fresh latex (Soratana et al., 2017). The average distance of plant material delivery was 50 km and the GHG emission from delivery was less than 1 g CO₂-eq/kg fresh latex. Besides fertilizer application, yield is one of the GHG emission factors. Average global fresh latex production is 1,194 kg/ha (FAOSTAT, 2017). In this study, the yield was about 1.4-2.7 times higher than the global average. Factors for GHG emission include both N fertilizer application and yield. Fertilizer application was applied varies from farm to farm and did not reflect increased yields. The different rate of fertilizer application is not clear even the same clone and cultivation area, which is the same discussion as Yuttitham et al. (2011) studied on the GHG emission of sugarcane in Thailand. However, there are recommendation of optimum level of fertilizer application based on soil condition, by Department of Agriculture, Thai farmer usually apply fertilizer more than that level. The excess amount not only unaffected to yield, but also sometime decrease the productivity. Therefore, from this study the proportional of yield and amount of fertilizer applied is absent.

Table 2. Use of fertilizers

Fertilizer	Chanthaburi Farm size			Rayong Farm size			Bueng Kan Farm size		
	Small	Medium	Large	Small	Medium	Large	Small	Medium	Large
Synthetic (ha/kg)									
- N	2,322	2,976	2,132	1,903	1,958	3,119	2,463	3,363	3,878
- P	1,557	1,385	1,419	1,108	1,215	744	1,327	1,285	1,828
- K	2,701	2,081	1,774	1,923	1,933	2,525	2,226	2,734	4,446
Organic (kg/ha)									
- N	61	144	-	405	85	-	111	82	496
- P	51	85	-	174	46	-	64	78	617
- K	35	84	-	207	39	-	65	48	375
Fertilizer	Udon Thani Farm size			Nakhon Si Thammarat Farm size			Suratthani Farm size		
	Small	Medium	Large	Small	Medium	Large	Small	Medium	Large
Synthetic (kg/ha)									
- N	3,281	4,697	5,793	2,248	2,484	2,171	2,399	2,063	2,685
- P	1,637	4,335	1,208	1,329	1,371	1,016	1,435	1,077	1,334
- K	2,706	4,359	3,476	1,992	2,122	1,782	1,997	1,498	1,818
Organic (kg/ha)									
- N	86.	27	-	10	15	13	24.31	10.88	-
- P	63	25	-	9	10	12	14.44	10.31	-
- K	50	15	-	6	9	7	14.25	6.31	-

Table 3. GHG emissions of latex cultivation process (g CO₂-eq/kg fresh latex)

Cultivation stage	Chanthaburi Farm size			Rayong Farm size			Bueng Kan Farm size		
	Small	Medium	Large	Small	Medium	Large	Small	Medium	Large
Pre farming	0.16	0.11	0.13	0.16	0.18	0.41	0.35	0.30	0.29
Before tapping	18.80	18.90	13.70	16.10	13.70	18.90	21.00	21.80	30.60
During tapping	69.70	74.60	41.80	51.20	46.00	61.80	73.70	90.20	92.40
Total	88.66	93.61	55.63	67.46	59.88	81.11	95.05	112.30	126.29
Cultivation stage	Udon Thani Farm size			Nakhon Si Thammarat Farm size			Suratthani Farm size		
	Small	Medium	Large	Small	Medium	Large	Small	Medium	Large
Pre farming	0.28	0.25	0.32	0.19	0.29	0.31	0.07	0.21	0.14
Before tapping	30.10	27.70	28.40	20.10	23.20	18.20	20.40	17.00	14.80
During tapping	101.30	86.20	140.20	71.20	90.00	68.50	73.60	57.40	70.80
Total	131.68	114.15	168.92	91.49	113.49	87.01	94.07	74.61	85.74

Table 4. GHG emissions from fertilizer, diesel and herbicide and insecticide (g CO₂-eq/kg fresh latex)

	Chanthaburi province Farm size			Rayong Farm size			Bueng Kan Farm size		
	Small	Medium	Large	Small	Medium	Large	Small	Medium	Large
GHG from fertilizer									
Direct emission	32.60	40.60	21.50	26.90	23.10	36.70	37.60	47.00	46.50
Indirect emission	54.00	51.10	30.60	39.10	34.90	43.90	53.60	61.80	73.70
GHG from diesel									
Direct emission	0.00	0.00	0.10	0.10	0.10	0.10	0.20	0.20	0.20
Indirect emission	0.00	0.00	<0.10	<0.10	<0.10	<0.10	<0.10	<0.10	<0.10
GHG from herbicide and insecticide	2.10	1.90	3.40	1.40	1.80	0.40	3.70	3.30	5.90
	Udon Thani province Farm size			Nakhon Si Thammarat Farm size			Suratthani Farm size		
	Small	Medium	Large	Small	Medium	Large	Small	Medium	Large
GHG from fertilizer									
Direct emission	53.70	62.70	76.70	35.50	45.00	34.60	37.60	30.80	34.90
Indirect emission	73.10	46.40	84.40	51.10	63.10	46.60	52.70	40.00	43.90
GHG from diesel									
Direct emission	0.20	0.20	0.20	0.00	0.10	0.20	0.00	0.00	0.00
Indirect emission	<0.10	<0.10	<0.10	0.00	<0.10	<0.10	0.00	0.00	0.00
GHG from herbicide and insecticide	4.70	4.90	7.60	4.90	5.30	5.60	3.80	3.80	6.90

Results were compared with findings by Jawjit et al. (2010) GHG emissions of rubber plantations in Thailand, with yield estimated at 5.64 tons of fresh latex per ha/year. GHG emissions were estimated at 0.2 tons CO₂-eq/ton fresh latex, which was almost twice the average found here. The difference probably results from the fact that they did not allocate fresh latex and rubber wood; therefore, it is possible that the study was performed without any allocations. If assume that both studies used the same ratio, then GHG emissions in Jawjit et al. (2010) study would be 70 g CO₂-eq/kg fresh latex which was similar to findings.

Greenhouse gas emissions of concentrated latex production

Primary data were collected from three concentrated latex factories through observations and on-site interviews. All of those factories are located in the south. The annual average production of those factories were in range of 13-18 million kilograms. The questionnaire began with the production process, yield, and amount of materials such as fresh latex, ammonia, water and chemicals including electric energy and fuel consumption (*Table 5*). Data were derived from DRC allocation between the chosen products, scrap and skim latex which ranged from 80-90%. *Table 5* shows the capacity of concentrated high ammonia (HA) latex production at 21,000 ton/y. One ton of concentrated latex production required 1.95-2.31 tons of fresh latex, lower than recorded by Jawjit et al. (2015) at 2.5 tons. Main factors related to production are electricity, water and chemicals. Electricity consumption in each plant was 41.19-77.84 kWh/ton concentrated latex and the centrifuge process required the greatest amount of electricity accounting for 94-97% of total consumption. Water use in concentrated latex ranged from 1,999-4,715 L. Most water was required for the centrifuge process and used for cleaning the centrifugal machines and tanks at 43-92% of total water use. Water was used for preparing materials in plant A more than plants B and C. The use of ammonia ranged from 15.7-14.9 kg/ton concentrated latex.

Table 5. Some inventory data collected from three concentrated latex factories

Activities data	Unit	Factory A	Factory B	Factory C	Weighted average
Fresh latex	kg	2070	1950	2310	2085.47
Electricity	kWh	52.61	41.19	77.59	55.30
Diesel	kg	0.17	0.66	0.13	0.30
Water	kg	3489.07	1999.98	4715.15	3322.56
Ammonia	kg	15.42	15.70	14.9	15.39
Tetramethyl thiuram disulfide (TMTD)	kg	0.58	0.46	0.81	0.59
Zinc oxide (ZnO)	kg	0.58	0.46	0.81	0.59
Diammonium hydrogen phosphate (DAP)	kg	1.80	1.59	2.18	1.82
Lauric acid	kg	0.58	0.45	0.82	0.59

Unit: amounts per 1 ton of concentrated latex produced

Gate-to-gate GHG emissions were calculated for in materials delivery, fresh latex preparation, the centrifuge process and fresh latex preservation. Results showed that GHG emissions from the production process were 88.73-100.73 kg CO₂-eq/ton

concentrated latex (Table 6). The highest GHG emissions were from chemical production accounting for 43-54%. Ammonia contributed 36-46% of GHG emission, while energy use (both diesel and electricity) was responsible for 32-39%. Remaining usage was from waster production and wastewater treatment at about 9-17%, with the highest as from the centrifuge process (27-43%). After calculating the weighted average of concentrated latex production, GHG emissions were equivalent to 92.74 kg CO₂-eq/ton concentrated latex. Jawjit et al. (2010) analyzed Thailand's GHG emissions at 144 kg CO₂-eq/ton concentrated latex with hotspots mainly dependent on electricity and ammonia use.

Table 6. GHG emissions of the production of 1 ton concentrated latex (kg CO₂-eq)

Factory	Total	Production and use of energy		Production of chemicals						Others	
		[1]	[2]	[3]	[4]	[5]	[6]	[7]	[8]	[9]	[10]
Factory A	91.73	28.79	0.57	39.17	1.45	1.46	4.50	0.23	0.02	0.44	15.10
Factory B	88.76	22.73	10.54	40.83	1.18	1.19	4.13	0.18	0.00	0.68	7.30
Factory C	100.73	39.21	0.48	36.18	1.92	1.87	2.80	0.31	0.36	0.00	17.60
Weighted Average	92.74	29.22	3.35	39.02	1.47	1.48	4.05	0.23	0.08	0.42	13.43

Remark: [1]: Electricity, [2]: Diesel, [3]: Ammonia, [4]: TMTD, [5]: ZnO, [6]: DAP, [7]: Lauric acid, [8]: Other chemicals, [9]: Water, [10]: Wastewater

When considering cradle-to-gate GHG emissions beginning with growing rubber trees in section 3.1 and concentrated latex production as mentioned above, total GHG emissions were 291.40 kg CO₂-eq/ton concentrate latex. Cultivation was highest contributor to GHG emissions at 68%. In more detail, production and use of fertilizer were highest sources of GHG emissions and accounted for 60%, while electricity and diesel fuel accounted for 10%, with chemicals accounting for 15%. In comparison, Jawjit et al. (2010) calculated GHG emissions at 0.54 tons CO₂-eq/ton concentrated latex, almost 50% lower than our calculated impacts. The difference can be explained by the allocation of para cultivation. Jawjit et al. (2010) did not refer to the allocation or the proportion of fresh latex and rubber wood, including the allocation method in the concentrated latex production. If co-product allocation is not taken into account and environmental load of the product not reduced, then the environmental impact may be artificially increased.

Greenhouse gas emissions of rubber glove production

Primary data were conducted through on-site interviews with one participating latex glove industry which located in the southern part of Thailand. One hundred pairs of rubber gloves (set as the functional unit) were manufactured; however, an overview of GHG emissions was presented here, since inventory data were confidential company information. GHG emission of rubber glove production was considered by a gate-to-grave approach with a functional unit. Manufacturing 100 pairs of rubber gloves required 5 kg concentrated latex and their GHG emission was estimated at 42.06 kg CO₂-eq/100 pairs. As shown in Figure 2, %GHG emissions contribution implied that

packaging and used gloves disposal contributed 46% and 93% of that was from burning the gloves (estimated under Thailand Product Categories Rule of rubber gloves describing that rubber gloves for medical use must be burnt after use), with 37% from the energy sector as electricity and fuel divided into two parts as the dipping and drying process (55%) and chemical production (10%).

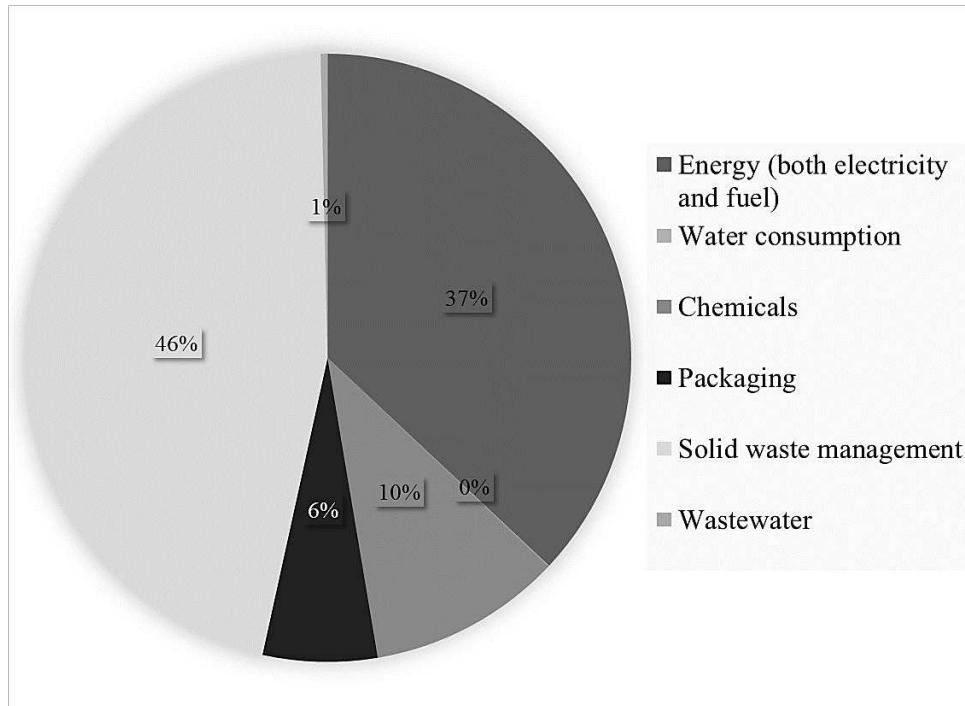


Figure 2. GHG emission percentage contribution of rubber glove production

The overall results obtained were based on the final functional unit (product of 200 pieces large size rubber gloves). Overall GHG emissions were 42.07 kg CO₂-eq, considered as cradle-to-grave. To facilitate the analysis, disaggregating GHG emissions results were divided according to each phase. *Figure 3* presents a clear understanding of the different points of each process. Considering only the planting process, fertilizer application was the main contributor to GHG emissions, while harvesting natural latex was the largest emission source when focusing on concentrated latex. Meanwhile, glove processing was the most crucial contributor to global warming impact at 52%, following by solid waste management at 46%. Production of fresh and concentrated latex gave less than 1% contribution.

Effect of allocation on the carbon footprint of rubber gloves

Determining the appropriate allocation model from the results above (base scenario) was divided into planting process based on mass-based allocation of fresh latex and rubber wood, concentrated latex production based on DRC allocation of concentrated latex and skim latex and rubber glove production based on mass-based allocation. The effects of different allocation methods were studied by defining the following scenarios: scenario 1 was economic allocation in the planting process and DRC allocation in concentrated latex production, scenario 2 was mass allocation in the planting process

and mass allocation in concentrated latex production and scenario 3 was economic allocation in the planting process and mass allocation in concentrated latex production (Table 7).

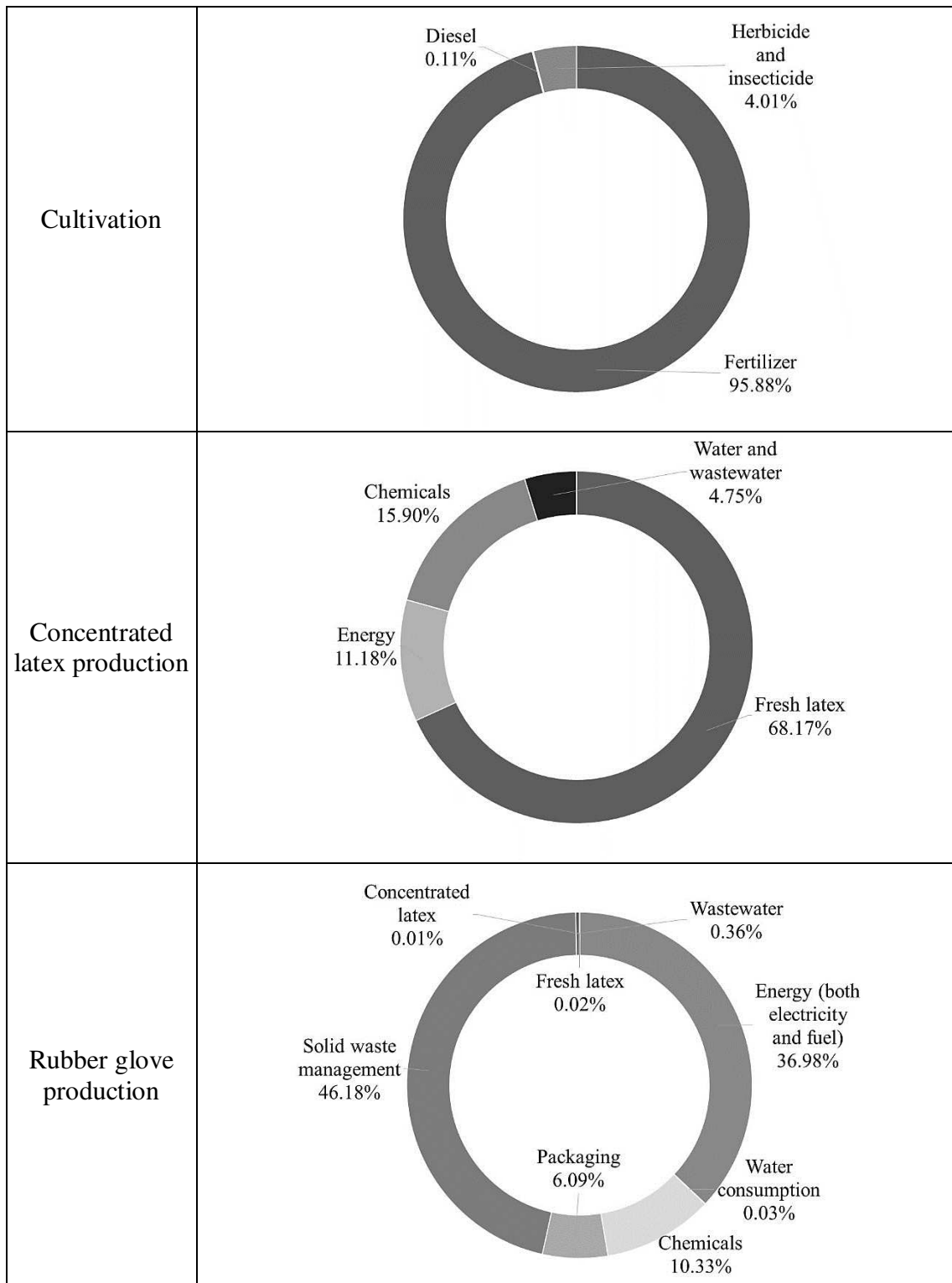


Figure 3. Carbon footprint contribution results disaggregated by the rubber glove production chain

Table 7. Allocation method for each scenario

	Cultivation	Concentrated latex production	Rubber glove production
Base scenario	Mass allocation	DRC allocation	Mass allocation
Scenario 1	Economic allocation	DRC allocation	Mass allocation
Scenario 2	Mass allocation	Mass allocation	Mass allocation
Scenario 3	Economic allocation	Mass allocation	Mass allocation

Considering the economic allocation in the planting process determined that prices of fresh latex fluctuated over time. The average price over the past three years was 1.47 USD per kilogram (~34 Baht per 1 USD) (Rubber Authority of Thailand, 2016). Price of rubber waste is similar to or 15% lower than fresh latex, while the average price of 10-inch rubber wood is about 0.067 USD per kilogram (Rubber Authority of Thailand, 2012). Therefore, the average percentage allocation of fresh latex accounted for 91%. When considering mass allocation in concentrated latex production, the amount of latex concentrated by centrifuge machinery accounted for approximately 43%. After applying mass allocation, GHG emissions from concentrated latex decreased when compared to the base scenario.

Table 8 presents two methods of allocation which led to totally different results when focusing only on the planting process. Economic allocation resulted in fresh latex providing more environmental load than rubber wood; GHG emissions became higher and percentage change was equivalent to 152.16. When focusing on concentrated latex as an intermediate product, different allocation methods led to a percentage change of -48.78 to 14.26%; however, when focusing on the final product (rubber glove), percentage change became less (-0.017 to 0.005) with no significant difference. Thus, it was very important to consider GHG emissions of rubber wood products and allocation during the upstream process became less when the supply chain length increased.

Table 8. Comparison of GHG emission for different scenarios of allocation methods

	Cultivation		Concentrated latex production		Rubber glove production	
	g CO₂-eq/kg fresh latex	% change	kg CO₂-eq/ton concentrated latex	%change	kg CO₂-eq/200 pieces	% change
Base scenario	95.26		291.40		42.07	
Scenario 1	240.20	+152.16	332.94	+14.26	42.08	0.0+1
Scenario 2	95.26	0	149.26	-48.78	42.07	0.0-2
Scenario 3	240.20	+152.16	294.20	+0.96	42.07	+0.00

Scenario 1 = economic, DRC; Scenario 2 = mass, mass; Scenario 3 = economic, mass

Conclusion

Rubber and rubber products are used globally. A cradle-to-gate GHG emission assessment was carried out through an LCA perspective for fresh latex cultivation, concentrated latex production, and a cradle-to-graves GHG emission assessment for rubber gloves production. The main purpose was to evaluate and identify hotspots of these productions.

Results gave 95.26 g CO₂-eq/kg fresh latex. Farm size was not an obvious indicator of farm management performance and hotspots were mainly from fertilizers, accounting for 96%. Average GHG emission from concentrated latex was 291.40 kg CO₂-eq/ton concentrate latex, with hotspots from utilization of fertilizers in fresh latex production, accounting for 68%. GHG emissions from rubber gloves was 42.07 kg CO₂-eq/200 pieces of rubber glove with hotspots from burning wastes and glove production generated by electric power accounting for 83%.

Other allocation methods differed for economic and mass allocation at each stage of the product life cycle. Allocation had a great impact on GHG emissions during cultivation and processing of concentrated latex but little effect on rubber glove production. Defining the allocation method for rubber products has a huge effect on GHG emissions in the upstream processes and these effects are reduced when supply chains become longer.

Acknowledgements. This research was partially supported by The Thailand Research Fund (TRF): RDG5750105 and RDG5850113.

REFERENCES

- [1] Abeliotis, K., Detsis, V., Papia, C. (2013): Life cycle assessment of bean production in the Prespa National Park, Greece. – *Journal of Cleaner Production* 41: 89-96.
- [2] Adewale, C., Higgins, S., Granatstein, D., Stockle, C. O., Carlson, B. R., Zaher, U. E., Carpenter-Boggs, L. (2016): Identifying hotspots in the carbon footprint of a small scale organic vegetable farm. – *Agricultural Systems* 149: 112-121.
- [3] Choosong, T., Chomane, J., Tekasakul, P., Tekasakul, S., Otani, Y., Hata, M., Furuuchi, M (2010): Workplace environment and personal exposure of PM and PAHs to workers in natural rubber sheet factories contaminated by wood burning smoke. – *Aerosol and Air Quality Research* 10: 8-21.
- [4] Dayaratne, S. P., Gunawardana, K. D. (2015): Carbon footprint reduction :a critical study of rubber production in small and medium scale enterprises in Sri Lanka. – *Journal of Cleaner Production* 103: 87-103.
- [5] Dumrongrak, I. (2010): Fertilizer management for sustainable rubber plantation. – *Journal of Yala Rajabhat University* 5(2): 183-199.
- [6] Ecoinvent Centre (2010): Ecoinvent database ver2.2 categories for processes. – Ecoinvent Centre. Swiss Centre for Life Cycle Inventories. Zurich. Switzerland.
- [7] FAOSTAT (2017): Food and Agriculture Organization of the United Nations. – <http://www.fao.org/faostat/en/#data>. Accessed January 2017.
- [8] Fichedick, M., Roy, J., Abdel-Aziz, A., Acquaye, A., Allwood, J. M., Ceron, J. P., Geng, Y., Kheshgi, H., Lanza, A., Perczyk, D., Price, L., Santalla, E., Sheinbaum, C., Tanaka, K. (2014): Industry. – In: Metz, B., Davidson, O. R., Bosch, P. R., Dave, R., Meyer, L. A. (eds.) *Climate Change 2014: Mitigation of Climate Change. Contribution of Working Group III to the Fifth Assessment Report of the Intergovernmental Panel on Climate Change*. Cambridge University Press, Cambridge, UK and New York, USA.
- [9] Holka, M., Jankowiak, J., Bienkowski, J. F., Dabrowicz, R. (2016): Life cycle assessment (LCA) of winter wheat in an intensive crop production system in Wielkopolska region (Poland). – *Applied Ecology and Environmental Research* 14(3): 535-545.
- [10] ISO14040 (2006): International Organization for Standardization, ISO14040:2006 Environmental Management-Life Cycle Assessment-Principles and Framework. – ISO, Geneva, Switzerland.

- [11] ISO14044 (2006): International Organization for Standardization, ISO14044:2006 Environmental Management-Life Cycle Assessment-Requirements and Guidelines. – ISO, Geneva, Switzerland.
- [12] ISO/TS14067 (2013): International Organization for Standardization, ISO/TS14067 Greenhouse Gases-Carbon Footprint of Products-Requirements and Guidelines for Quantification and Communication. – ISO, Geneva, Switzerland.
- [13] Jawjit, W., Kroeze, C., Rattanapan, S. (2010): Greenhouse gas emissions from rubber industry in Thailand. – *Journal of Cleaner Production* 18: 403-411.
- [14] Jawjit, W., Pavasant, P., Kroeze, C. (2015): Evaluating environmental performance of concentrated latex production in Thailand. – *Journal of Cleaner Production* 98: 84-91.
- [15] Kabiri, N. (2016): Public participation, land use and climate change governance in Thailand. – *Land Use Policy* 52: 511-517.
- [16] Lin, T. H., Chien, Y. S., Chiu, W. M. (2017): Rubber tire life cycle assessment and the effect of reducing carbon footprint by replacing carbon black with graphene. – *International Journal of Green Energy* 14(1): 97-104.
- [17] Maulina, S., Sulaiman, N. M. N., Mahmood, N. Z. (2015): Enhancement of eco-efficiency through life cycle assessment in crumb rubber processing. – *Procedia Social and Behavioral Sciences* 195: 2475-2484.
- [18] Meier, M. S., Stoessel, F., Jungbluth, N., Juraske, R., Schader, C., Stolze, M. (2015): Environmental impacts of organic and conventional agricultural products-Are the differences captured by life cycle assessment? – *Journal of Environmental Management* 149: 193-208.
- [19] Mohammad, M., Che-man, H., Hassan, M. A., Yee, P. L. (2010): Treatment of wastewater from rubber industry in Malaysia. – *African Journal of Biotechnology* 9(38): 6233-6243.
- [20] Musikavong, C., Gheewala, S. H (2017): Assessing ecological footprints of products from the rubber industry and palm oil mills in Thailand. – *Journal of Cleaner Production* 142: 1148-1157.
- [21] National Metal and Materials Technology Center (2014): Thai National Life Cycle Inventory Database. – MTEC, Pathum Thani, Thailand.
- [22] OAE (2016a): Office of Agricultural Economics, Agricultural Statistic of Thailand. – http://www.oae.go.th/ewt_news.php?nid=13577. Accessed January 2017.
- [23] OAE (2016b): Office of Agricultural Economics. Ministry of Agriculture and Cooperatives. – <http://www.oae.go.th/download/forecast/forecastofmarch59.pdf>. Accessed January 2017.
- [24] OIE (2014): Office of Industrial Economics. – <http://rubber.oie.go.th>. Accessed January 2017.
- [25] Orimoloye, J.R., Ugwa, I.K., Idoko, S.O. (2010): Soil management strategies for rubber cultivation in an undulating topography of Northern Cross River State. – *Journal of Soil Science and Environmental Management* 1(2): 34-39.
- [26] Ounsaneha, W., Rattanapan, C. (2016): Defining the eco-efficiency of rubber glove products manufactured from concentrated latex in Thailand. – *Environmental Progress & Sustainable Energy* 35(3): 802-808.
- [27] Pethin, D., Nakkanong, K., Nualsri, C. (2015): Performance and genetic assessment of rubber tree clones in Southern Thailand. – *Scientia Agricola* 72(4): 306-313.
- [28] Phungrassami, H., Usubharatana, P. (2015): Life cycle assessment and eco-efficiency of para-rubber wood production in Thailand. – *Polish Journal of Environmental Studies* 24(5): 2113-2126.
- [29] RIU (2017): Rubber Intelligence Unit, Office of Industrial Economics, Natural Rubber Export Statistic. – <http://rubber.oir.go.th>. Accessed January 2017.

- [30] Ruangsri, K., Makkaew, K., Sdoodee, S. (2015): The impact of rainfall fluctuation on days and rubber productivity in Songkhla province. – *International Journal of Agricultural Technology* 11(1): 181-191.
- [31] Rubber Authority of Thailand (2012): Price of parawood. – <http://www.rubber.co.th/rubber2012/web/service9.php>. Accessed March 2017.
- [32] Rubber Authority of Thailand (2016): Price of latex and rubber product. – http://www.rubber.co.th/rubber/2012rubberprice_yr.php. Accessed March 2017.
- [33] Rubber Replanting Aid Fund Act (1960): Rubber Replanting Aid Fund Act B.E. 2503. 1960. – http://www.raot.co.th/raot_en/ewt_w3c/ewt_dl_link.php?nid=1184. Accessed February 2017.
- [34] Sdoodee, S., Rongsawat, S. (2012): Impact of climate change on smallholders' rubber production in Songkhla province, Southern Thailand. – The 2012 International and National Conference for the Sustainable Community Development of “Local Community: The Foundation of Development in the ASEAN Economic Community (AEC)” February 16-19, 2012, Khon Kaen, Thailand.
- [35] Solomon, S., Qin, D., Manning, M., Chen, Z., Marquis, M., Averyt, K. B., Tignor, M., Miller, H. L. (eds.) (2007): Intergovernmental Panel on Climate Change (IPCC). *Climate Change 2007: The Physical Basis. Contribution of Working Group I to the Fourth Assessment Report of the Intergovernmental Panel on Climate Change*. – Cambridge University Press, Cambridge, UK and New York.
- [36] Soratana, K., Rasutis, D., Azarabadi, H., Eranki, P. L., Landis, A. E. (2017): Guayule as an alternative source of natural rubber: a comparative life cycle assessment with Hevea and synthetic rubber. – *Journal of Cleaner Production* 159: 271-280.
- [37] Sparrevik, M., Field, J. L., Maratinsen, V., Breedveld, G. D., Cornelissen, G. (2015): Life cycle assessment to evaluate the environmental impact of biochar implementation in conservation agriculture in Zambia. – *Environmental Science & Technology* 47: 1206-1215.
- [38] Wang, M., Xia, X., Zhang, Q., Liu, L. (2010): Life cycle assessment of a rice production system in Taihu region, China. – *International Journal of Sustainable Development & World Ecology* 17(2): 157-161.
- [39] Yan, M., Cheng, K., Lue, T., Yan, Y., Pan, G., Rees, R. M. (2015): Carbon footprint of grain crop production in China-based on farm survey data. – *Journal of Cleaner Production* 104: 130-138.
- [40] Yuttitham, M., Gheewala, S. H., Chidthaisong, A. (2011): Carbon footprint of sugar produced from sugarcane in eastern Thailand. – *Journal of Cleaner Production* 19(17-18): 2119-2127.

EVALUATION OF THE TRANSPIRATION CHARACTER OF *JUNIPERUS MACROCARPA* AS AN INVASIVE SPECIES IN WESTERN CRETE, GREECE

ELHAG, M.* – BAHRAWI, J.

*Department of Hydrology and Water Resources Management, Faculty of Meteorology,
Environment & Arid Land Agriculture, King Abdulaziz University
Jeddah 21589, Kingdom of Saudi Arabia*

**Corresponding author
e-mail: melhag@kau.edu.sa*

(Received 20th Nov 2017; accepted 20th Feb 2018)

Abstract. This study aimed at determining the transpiration characters of *Juniperus macrocarpa* in a close to 40-year-old even-aged stand categorized into three classes based on canopy size, over a two-year period (2011-2012). The site is located in Palaiochora, 77 km south of Chania, on the southwest coast of Crete. Sap flow techniques (Granier-type) were used to determine water use. Annual trends in sap flow were generally bell-shaped, and varying significantly between seasons and canopy classes. Winter sap flow was minimal but trees were active when temperatures were above freezing point and trees depended on deep water (below 60 cm) for transpiration. Rates increased from 1.46 Ld⁻¹ in winter to 3.32 Ld⁻¹ in the spring, irrespective of tree canopy class, because of improvement in weather conditions. Maximum transpiration rates were observed during the growing season with an average of 134.42 Ld⁻¹ for dominant trees and 8.68 Ld⁻¹ for suppressed ones. The daily variations in photosynthetically active radiation, vapor pressure deficit, air temperature, and surface soil water were the principal drivers for transpiration during the growing season. The findings have shown that climate in Crete does not limit the expansion of *J. macrocarpa* and that this expansion will have potentially significant impacts on the ecohydrology of the system.

Keywords: *Juniperus macrocarpa*, sap flow, semi-arid ecosystems, soil water content, transpiration rates

Introduction

Invasive woody species encroachment into semi-arid grasslands has been attributed to the introduction of livestock, fire suppression (Van Auken, 2000), changes in climate (Reich et al., 2001), increases in atmospheric CO₂ concentration (Bradley and Fleishman, 2008) landscape fragmentation (Briggs et al., 2007), reduction in wood harvest rates by native Americans (Fredrickson et al., 2006), dispersal by humans and birds, and natural expansion of the species (Van Haverbeke and Read, 1976). Generally, Junipers are widely distributed across the northern Mediterranean region, some taxa's are grown natively and few are considered to be invasive to the designated study area (Farjon, 2005; Adams, 2014).

Juniperus macrocarpa as an evergreen coniferous species has a predominantly large potential for accommodating precipitation. This is due to the evergreen nature of the species, the relatively large surface leaf area, and considerable intrusion by the understory litters. Water losses estimation from the collective intrusion of juniper canopies and underlying litter layers may reach 70 to 80% depending on the species and site conditions (Thurow and Hester, 1997). Owens et al. (2006) reported that 47% of precipitation intrusion by the Ashe juniper (*Juniperus ashei*) canopy and understory litters. The authors estimated that for a densely covered Ashe juniper forest, closely to

250 mm precipitation would be intervened annually. Owens and Ansley (1997) resolved that the potential transpiration rate of a mature Ashe juniper may reach to 125 L of water per day, which would be equivalent to 300 to 450 mm water annually on a landscape scale, depending on the forest dense cover (Elhag and Bahrawi, 2017a).

Other studies on water use by *Juniperus* species have shown that stand level transpiration rates range from 0.23 to 1.13 mm day⁻¹ in Utah juniper (*Juniperus osteosperma*) in Arizona and New Mexico, 1.21 mm in alligator juniper (*J. daydepeana*) in Arizona, and 1.90 mm day⁻¹ in Ashe juniper (*J. ashei*) in Texas. These comparatively low transpiration rates reflect juniper's conservative water use which allows it to survive in dry areas (Heilman et al., 2009).

Although several studies have examined the water use in *Juniperus* species, very few have been conducted on *J. macrocarpa* especially in semi-arid plains (Van Auken and Mckinley, 2008), where soil water has been testified to be the key limiting factor for plant growth (Chaves et al., 2003; Duursma et al., 2008). Meanwhile, the relative grasses and woody species abundance in semi-arid ecosystems determines the vegetation type (Darrouzet-Nardi et al., 2006; Bradley and Fleishman, 2008).

Moreover, scenarios of future climate change predict increasing air temperatures with increases in water vapor pressure deficits (VPD) experienced by plants (Harmsen et al., 2009). The frequency, intensity, timing, and distribution of precipitation will also be altered (Stocker, 2014). Such vicissitudes will influence vegetation function (especially water vapor flux) and will alter the consequences of the climate and vegetation interaction. Consequently, it is imperative to comprehend the means underlying the plant function and climate interactions in term of efficient water resources management and vegetation (Porporato et al., 2004; Elhag and Bahrawi, 2016).

The heat dissipation method (Granier, 1987) which is designed to measure tree sap flow is the most frequently utilized practices in ecophysiological and forest hydrological studies for whole-tree water use in xylem sap flow determination due to its plainness, a high degree of precision and consistency (Lu et al., 2000).

The adopted technique is based on two probes. The first probe is the heated probe and the second is the reference probe made of stainless steel needle. The basic principle of the two probes is to sense the temperature difference generated between the two thermo-couple copper wired probes. Therefore, both probes are literally implanted into the stem 10-15 cm apart from each other (Granier, 1987; Lu et al., 2000).

The current research hypothesis assumes that is that *Juniperus macrocarpa* is responsible for the shifts of the groundwater content in the study area. Therefore, Juniper transpiration rates are subjected for comprehensive investigation in the designated study area. The goal of the study is to estimate the whole-tree water use in term of transpiration of the woody species *Juniperus macrocarpa* in semi-arid ecosystems of western Crete and the transpiration rate significances on the water balance, soil water availability, and consequently groundwater recharge in the ecosystem.

Materials and methods

Study species

Juniperus macrocarpa is a dispersal shrub up to 6 m height; once in a while it may reaches up to 15 m height. Leaves are lanceolate in principle up to 20 mm long and up

to 4 mm wide. The stomatal structure is a dual band split by a midrib on the inward surface (Farjon, 2005). The seeds are berry-like in cones forms with a waxy covering and usually scattered (Adams, 2014). The dust cones are yellow, reaches to 3 mm long, and shedding off its duct shortly after winter (Muñoz-Reinoso, 2004).

Study area

The study area located in the South West of Crete and covers an area of about 4317.21 ha, 35° 25'51" N and 35° 09'47" N latitudes, 24° 32'07" E and 24° 54'42" E longitudes (Fig. 1). The recognized stand history and the relatively unvarying age of the *Juniperus macrocarpa* grown in the study area make it distinctively accommodated to address the issue of tree expansion in the arid ecosystems. The climate is recognized as semi-arid continental, mean annual precipitation is close to 750 mm, falling mainly in the winter season. The mean maximum temperature in July of 35.3 °C, while the mean minimum temperature in January of -3.8 °C, with the Mean annual temperature of 18 °C. Soils are loamy clay which is covered mostly by pastoral forest areas of maquis vegetation (Christodoulakis, 1996; Georghiou and Delipetrou, 2010).



Figure 1. Location of the study area

Experimental design

The site selected for the study is a stand of *J. macrocarpa* with a dense canopy. The stand is characterized by slope gradient of 27 °C and slope aspect of West with slope position of West to Southwest. A 50-m × 50-m area was fenced and basic inventory measurements were conducted. Tree density was recorded as 520 trees ha⁻¹. Moreover, 22 trees were selected for sap flow measurement. All the trees were even-aged around 40 years old. Three different classes were selected based on the canopy and growth of the trees (Hegazy and Elhag, 2006). The range of the tree height and the diameter at breast height (DBH) for each class is demonstrated in Table 1. Soil moisture determination was carried out using ML2 Theta Probe installed at a different soil depth

of 20, 40 and 60 cm, respectively. Collected data stored in 15 seconds interval using CR10X, Campbell Scientific Inc., UT data logger.

Table 1. The tree DBH and the tree height range from the selected stand

Tree classes	Tree DBH (cm)			Tree height (m)		
	Max.	Min.	Avg.	Max.	Min.	Avg.
Dominant	18.74	16.14	17.44	9.09	7.89	8.49
Co-dominant	14.35	11.35	12.85	7.66	6.26	6.96
Suppressed	10.2	6.8	8.5	5.9	4.3	5.1

Sap flow and sapwood measurements

The quantification of the *J. macrocarpa* transpiration rate was carried out following Granier (1987). Based on the heat differences between the heated probe (implanted in the tree trunk) and the referenced probe (2 cm apart) at time t the temperature difference ΔT_M ($^{\circ}\text{C}$) were constantly recorded for sap flux estimation. Based on the experiential association of Granier (1987), the density of the sap flux was conducted in term of J_s , $\text{g m}^{-2} \text{ s}^{-1}$ as follows (Eq. 1):

$$J_s = 119 \left(\frac{\Delta T_M - \Delta T}{\Delta T} \right)^{1.231} \quad (\text{Eq.1})$$

Clearwater et al. (1999) suggested an empirical correction for sap flux estimation when the sap wood depth is less than 2 cm (Eq. 2):

$$J_s = 119 \left(\frac{\Delta T_M - \frac{\Delta T - b\Delta T_M}{a}}{\Delta T - b\Delta T_M} \right)^{1.231} \quad (\text{Eq.2})$$

where

a is the probe proportion in sapwood

b is the probe proportion in the heartwood, where $b = 1 - a$.

Transpiration rates determination in term of (L day^{-1}) was conducted as a multiplication of the sapwood area by J_s . Annual transpiration rate of *J. macrocarpa* canopies in terms of (E_c , mm yr^{-1}) was conducted by multiplying J_s with sapwood area (A_s) per unit ground area (A_G) following Oren et al. (1998; Eq. 3):

$$E_c = J_s \frac{A_s}{A_G} \quad (\text{Eq.3})$$

The determination of the evaporative fraction is based on the energy balance conducted from meteorological stations (Su et al., 2001; Elhag, 2016). Consequently, the net radiation “ Rn ” is estimated by Equation 4:

$$Rn = G0 + H + \lambda \cdot E \quad (\text{Eq.4})$$

where

Rn is net radiation (watt/m^2),

G_0 is soil heat flux (watt/m²),
 H is turbulent heat flux (watt/m²),
 λE is turbulent latent heat flux (watt/m²),
 λ is latent heat of vaporization (watt/m²), and
 E is actual evaporation (mm/day).

Therefore, the daily evapotranspiration E_{daily} is exercised following Elhag and Bahrawi (2017b) as (Eq. 5):

$$E_{daily} = \Lambda_0^{24} \times 8.64 \times 10^7 \times \frac{Rn - G_0}{\lambda \rho \omega} \quad (\text{Eq.5})$$

where

Λ_0^{24} is daily evaporative fraction

$\rho \omega$ density of water measured in kilograms per cubic meter.

Statistical analysis

Initially, a various relapse approach was utilized where every single ecological variable was plotted in a stepwise and covariates relapse. The choice strategy preutilized to distinguish the factors which clarified the main changeability in sap stream. The various relapse approaches were first performed on the whole informational index and afterward performed inside each season. Second, a blended model investigation was consequently performed where the trees were plotted as an irregular impact taking into consideration the changes in the covariance structure. The model was kept running on the general information at to start with, at that point taking a gander at singular months lastly at various seasons.

Results

Trends in air temperature were reliable with the archived metrological data (22-year average), with the maximum temperature recorded in August (> 32 °C), and minimum temperature recorded in January (< -6 °C). Recorded precipitation data in 2011 was significantly exceeding the average (780 mm), while that of 2012 was average (590 mm).

The seasonal soil volumetric water content was highly variable at the 20 cm depth, reflecting recent precipitation events. In contrast, the water content at the 40 and 60 cm depths was less responsive to precipitation events. The site received a total of 229.8 mmol m⁻² s⁻¹ of photosynthetically active radiation in 2011 and 213.9 mmol m⁻² s⁻¹ in 2012. The cloudier days observed throughout the growing spell of 2012 could be recognized as a lower Photosynthetically Active Radiation (PAR) in 2012 relative to 2011 as is shown in *Figure 2*.

Annual transpiration trends were generally bell-shaped (*Fig. 3*). Transpiration rates varied significantly between seasons represented as Day of the Year (DOY). Maximum transpiration rates were observed during the growing season with an average of 134.42 Ld⁻¹ for dominant trees and 8.68 Ld⁻¹ for suppressed ones. The highest daily rates for the largest tree measured was more than 30-fold that of the smallest tree. This was probably a result of the greater leaf area (green canopy), vigor, and exposure to radiation in larger trees relative to the suppressed ones (*Tables 2 and 3*).

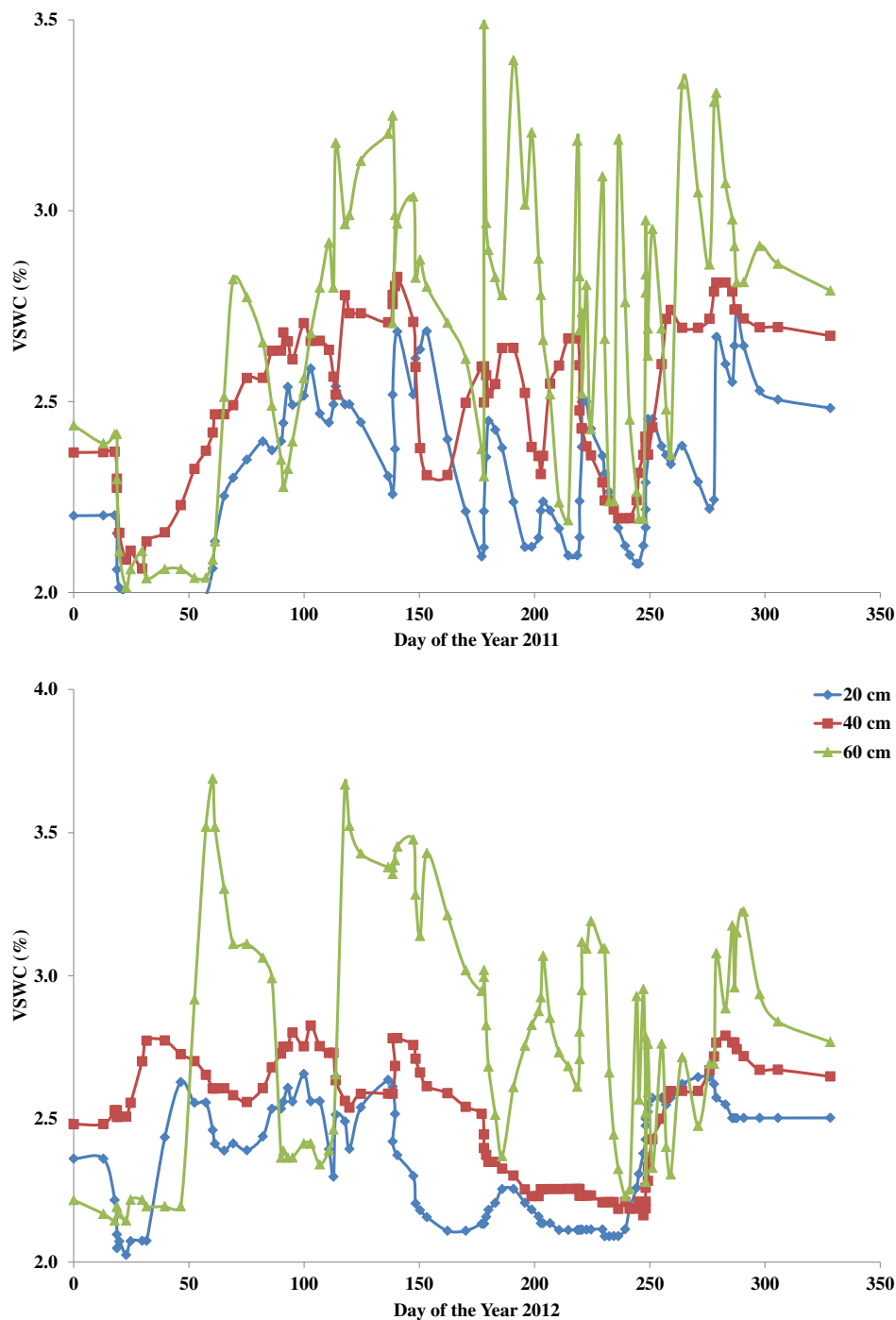


Figure 2. The daily average of soil volumetric water content (VSWC) in different depths

Table 2. Descriptive data of sap flow in $L day^{-1}$

Season	Mean	Std. error
Winter	1.46 d	0.10
Spring	3.32 cd	0.20
Summer	16.62 a	0.31
Autumn	10.77 b	0.43

Table 3. Tree class description in the designated study area

Canopy class	Average DBH (cm)	Average tree height (m)	Average height of life branches from the ground (m)	Average green canopy (%)
Dominant	17.44	8.49	1.91	75.51
Co-dominant	12.85	6.96	1.78	73.68
Suppressed	8.5	5.1	3.2	10.57

The fall season commenced at the beginning of September and ended in November. The fall was characterized by wet conditions, accompanied by a sharp decrease in PAR and air temperatures, and the resulting transpiration rates (*Fig. 3*).

With the onset of the spring season, the average daily air temperatures increased from 12 °C to 26.3 °C (in both years), and light levels increased significantly from 119 $\mu\text{mol m}^{-2} \text{s}^{-1}$ to 1298 $\mu\text{mol m}^{-2} \text{s}^{-1}$ in 2011 and 50.9 $\mu\text{mol m}^{-2} \text{s}^{-1}$ to 1301 $\mu\text{mol m}^{-2} \text{s}^{-1}$ in 2012. These higher PAR levels and warmer temperatures, in conjunction with increased cell and photosynthetic activities, resulted in increased transpiration rates. The transpiration rate increased from $1.55 \pm 0.08 \text{ Ld}^{-1}$ in the winter period to $3.29 \pm 0.15 \text{ Ld}^{-1}$ in the spring, irrespective of tree canopy class.

Variations in air temperature and light levels were shown to have the greatest influence on the transpiration of *J. macrocarpa*. Soil water content limitation varied with depth and depended on the season. *Figure 4* shows the daily maximum and average sap flow in correspondence to the minimum and maximum air temperatures.

Sap flow tendencies were commonly plotted as bell-shaped curves over the daily sampling time of 24 h, with the peak sap flow occurring near noon in spring and summer and around 1400 h in the fall. Significant diurnal variability in sap flow rates was observed and was related to variations in air temperature. In the fall, sap flow for dominant, co-dominant and suppressed trees increased from 0800 to 1400 h, peaked just after 1400 h and then began decreasing after 1600 h (*Fig. 5*).

Table 4 indicates that photosynthetic active radiation, precipitation, and VPD had the greatest influence on the transpiration rates of *Juniperus macrocarpa*. Analysis of variance for the measured environmental factors influencing tree transpiration rates is presented in *Table 4*. On an annual basis, all measured environmental parameters had significant impacts on tree level transpiration rates with the exception of volumetric soil water content at 40 and 60 cm depths, which were expected since water was not a limiting factor in 2011 and 2012. To understand the relative importance of a specific environmental parameter to the seasonal trend of tree-level transpiration rates, the data were grouped into four seasons.

In winter, which included December through to the end of February, least and mean air temperatures, rainfall, photosynthetic active radiation, average relative humidity, and deep soil water (60 cm) had a significant effect on the transpiration of the trees (*Table 4*). Air temperatures fluctuated between 3.2 °C (min temperature) and 16.8 °C (max temperature) during this period, and positive transpiration rates were observed at air temperatures greater than 14 °C.

The summer season started in May and ended in August. Daily average air temperatures and PAR reached their maximum of around 40 °C and 1488 $\mu\text{mol m}^{-2} \text{s}^{-1}$ in 2011 and 30 °C and 1398 $\mu\text{mol m}^{-2} \text{s}^{-1}$ in 2012.

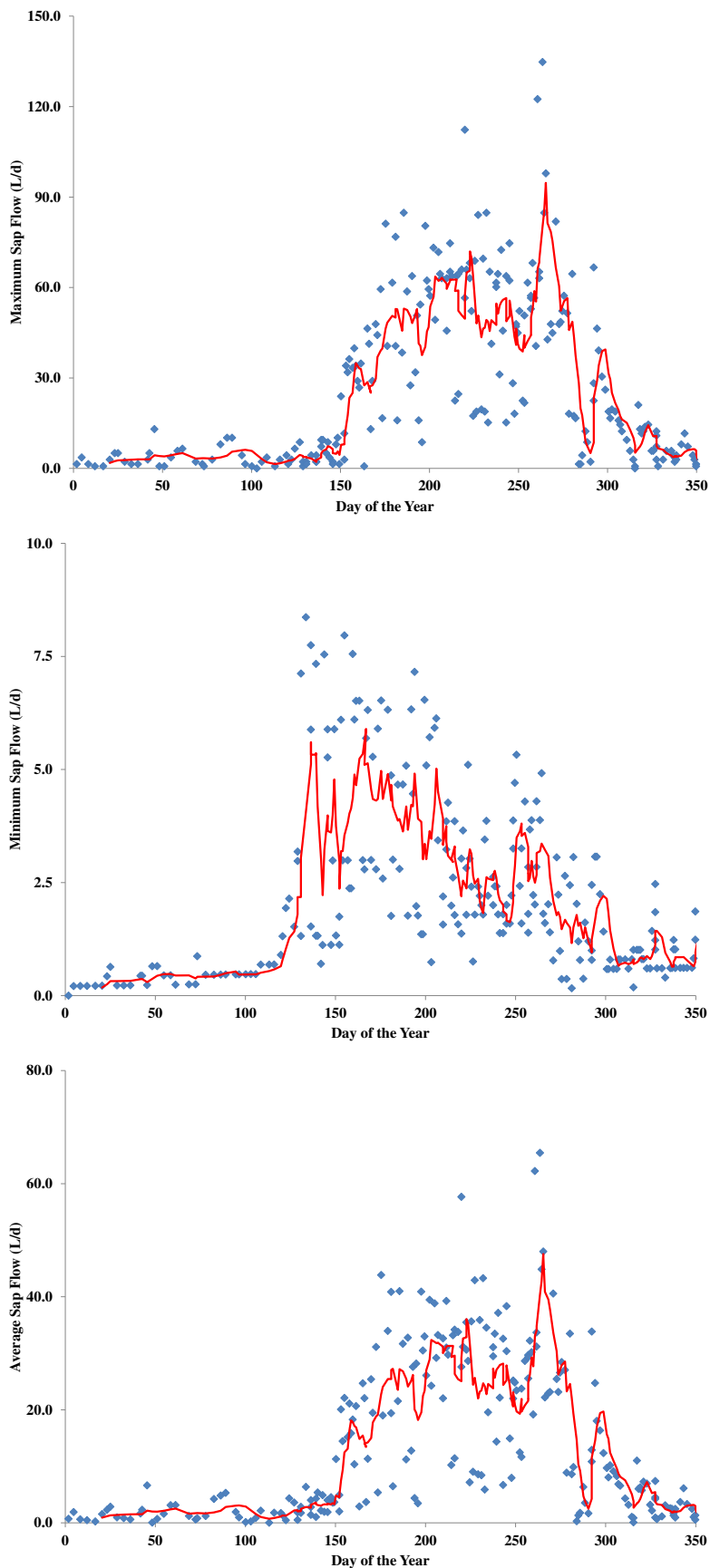


Figure 3. Maximum, mean and minimum sap flow recorded for evenly aged *J. macrocarpa*

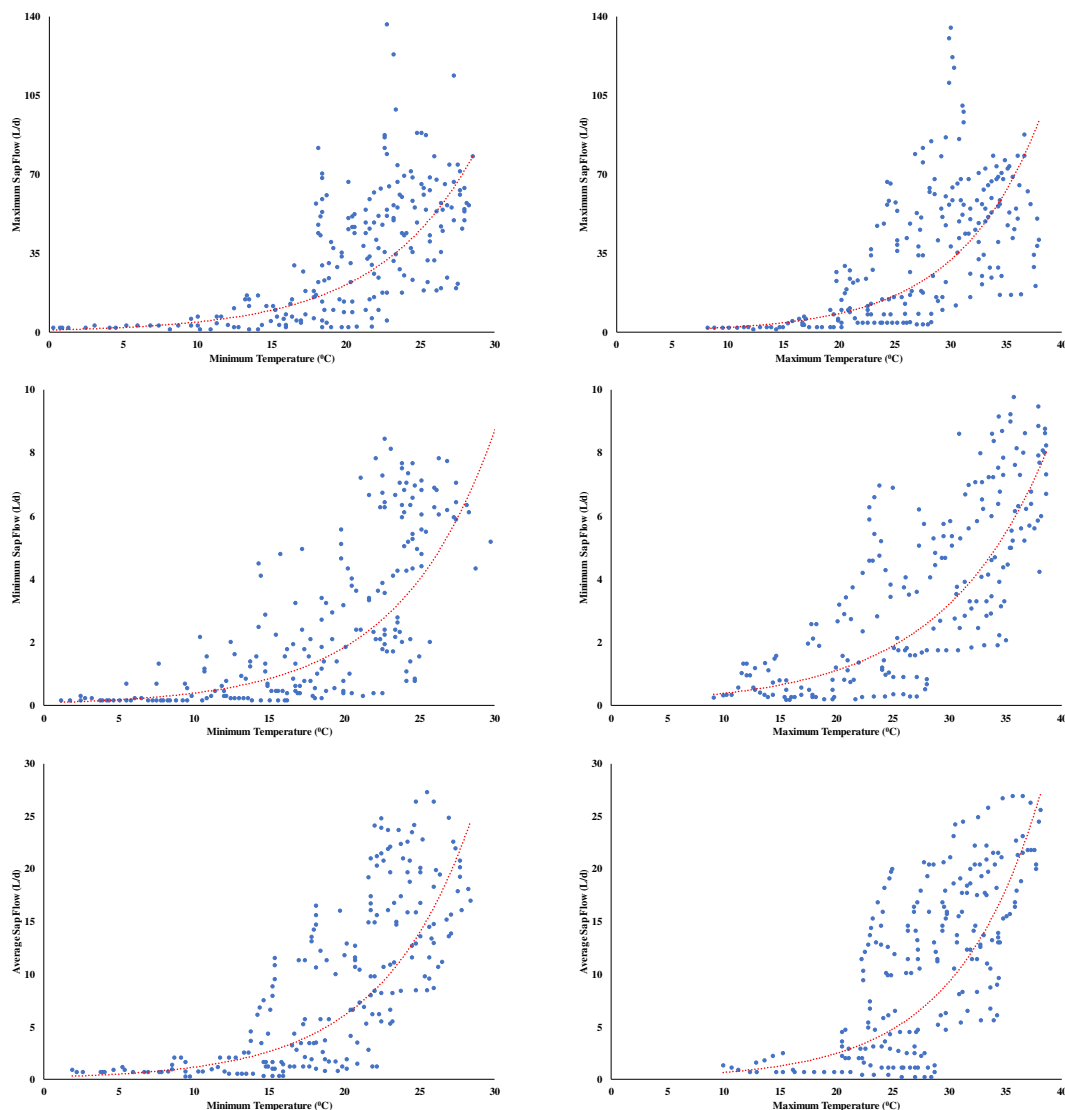


Figure 4. Daily sap flow behavior as a function of minimum air temperature (TA_{min}) and maximum air temperature (TA_{max}) within the designated study area

Daily, whole-tree transpiration (sap flow estimations) reacted significantly to the sunlight. Daytime sap flow as a rainfall and soil water content function was not substantial. However, within-day variability is highly connected to light levels (PAR). *Figure 5* shows how sensitive the flow to sudden changes is in light (example: a cloud passing). When PAR showed an increase, or decrease, the sap flow increased or decreased instantly.

Discussion

The values obtained are comparable to the water use values measured on other *Juniperus* sp. (*Table 1*). Transpiration rates of *Juniperus macrocarpa* trees in the designated study area varied among canopy classes, with highest values observed in the dominant canopy, followed by the co-dominant and finally the suppressed canopy. This

is in covenant with the outcomes of Granier et al. (1996), Andrade et al. (1998) and Meinzer et al. (2001), who reported that canopy status (dominant, co-dominant, and suppressed) is the key feature defining sap flow rates. According to Lassoie et al. (1983), photosynthetically active radiation is the most important environmental factor regulating photosynthesis in understory eastern red cedar. Hence, transpiration in understory eastern red cedar (for the suppressed stands) is in great part light-limited throughout the 5-month period when fully expanded overstory leaves are present.

Table 4. Rehashed measure examinations of fluctuation by year, season and month for sap stream as a component of every day mean temperature (°C), vapor pressure deficit (VPD), photosynthetic active radiation (PAR), precipitation (mm), daily average soil temperature (°C) and diameter at breast height (DBH)

		Air Temp. (°C)	VPD (kPa)	PAR (mmol m ⁻² s ⁻¹)	Precip. (mm)	SM Temp. (°C)	DBH (cm)
Year	2011/2012	***	***	**	***	***	*
Season	Summer	***	*	**	-	-	*
	Fall	-	-	*	**	-	*
	Winter	*	-	*	**	-	-
	Spring	*	*	*	**	-	-
Month	August	**	-	*	*	-	*
	September	-	-	*	-	-	*
	October	*	*	*	-	-	-
	November	-	-	-	-	-	-
	December	-	-	-	-	***	-
	January	*	-	*	*	-	-
	February	-	-	-	***	-	-
	March	-	-	*	*	-	-
	April	*	-	-	**	-	-
	May	-	-	-	-	*	-
	June	*	-	-	**	*	*
July	-	-	***	-	-	*	

Only significant interactions are displayed

Transpiration declined in fall and winter but continued progressive when temperatures were > 0 °C. Results were in agreement to those observed by Briggs et al. (2002) and explained by the fact that *Juniperus macrocarpa* trees maintain positive photosynthesis and stomatal conductance at temperatures above 0 °C and they efficiently utilize water from the deeper rescinded soil horizons (Brümmer et al., 2012). This might contribute to the accumulation of biomass and might result in decreased soil water content, which otherwise will be used to recharge the groundwater in grassland-dominated areas. Transpiration rates increased with the improvement in weather conditions, reaching their maximum during the growing season. The absence of a drought period during our study (2011-2012) did not show the response of *Juniperus macrocarpa* to drought stress.

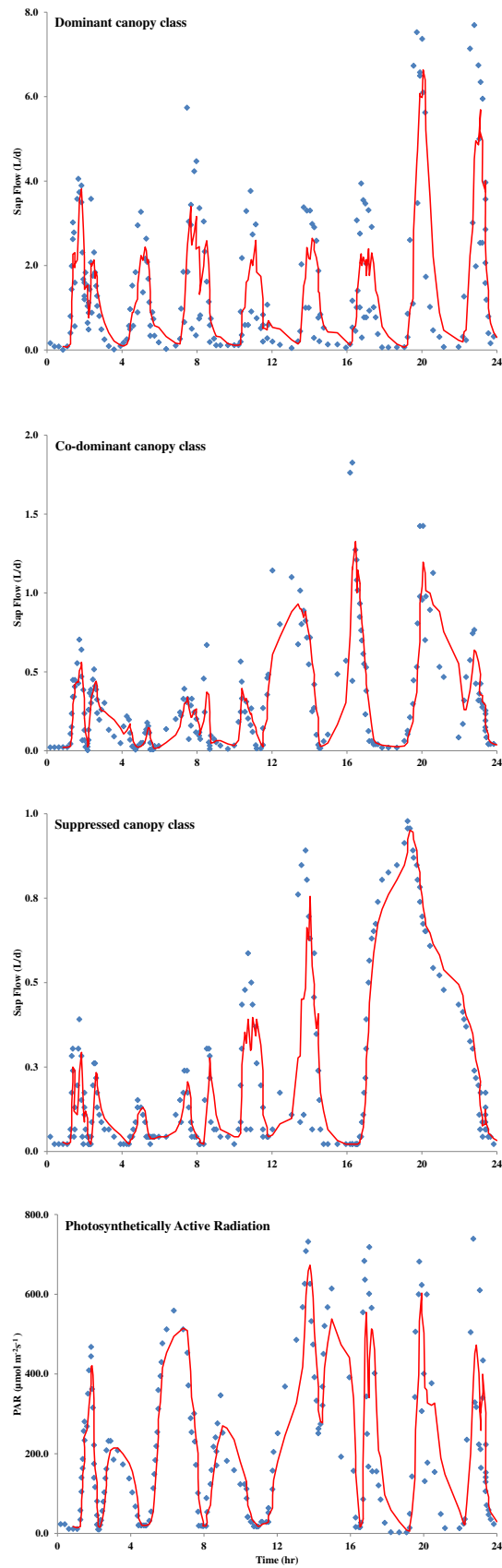


Figure 5. The daily curves of Sap flow (Lh^{-1}) and PAR for the three canopy classes of *J. macrocarpa*

However, according to Brümmer et al. (2012), even under drought stress, *Juniperus macrocarpa* has the capacity to preserve stomatal opening at low water potentials, and utilize deeper soil water. The annual transpiration rate per unit ground area (mm yr^{-1}) was estimated for 2011 through scaling up mean flux density by multiplying it by sapwood area per unit ground area (Oren et al., 1998). Results showed that trees utilized on average between 0.18 and 1.79 mm d^{-1} and averaged 376 mm yr^{-1} , which represented 52% of the annual precipitation, leading to drier soils under forested cover compared to open grasslands. In winter, fall and early spring, while grasses are dormant, trees were effectively consuming water that otherwise would go to charge the groundwater (Briggs et al., 2002).

Leaf water deficit, transpiration and stomatal opening all reflect increase in soil moisture suction but that, during the day, they are affected also by other factors which obscure the direct effect of soil moisture (Rutter and Sands, 1958). The logistic relation is the competition that limits in some cases the grass-land from maintaining its healthy growth and from another aspect grass-land may limit the expansion of the forests due to the allelopathic effect (Hegazy et al., 2004). Therefore, low soil moisture content has an insignificant role in the trees expansion which is also confirmed by the survival of *J. macrocarpa* in low soil water content (Seim et al., 2016).

Conclusion

Results indicated that diurnal air temperatures determined the overall stomatal status, whereas inconstant light levels accounted for stomatal activities during the daylight, thus regulating the jeopardy of severe water discrepancies. Transpiration character of the studied species followed the bell-shaped curve with exposure sensitivity. Moreover, the phenological classes of *Juniperus macrocarpa* did not considerably affect the transpiration character. Soil moisture, while very important, did not seem to limit the expansion of the tree under investigation, unlike what has been observed in the seven years prior to this study. Therefore, this species can continue invading and displace the dominant native grasses and potentially affect the groundwater recharge as well as the surrounding grassland. In conclusion, appropriate management must be designed to control *Juniperus macrocarpa* expansion, and more realistic and attainable goals and management regimes for the current site conditions should be adopted to minimize the impacts of this continuous invasion of *Juniperus macrocarpa* on long-term ecosystem processes especially the surrounding grassland and services including groundwater.

Acknowledgement. This work was supported by the Deanship of Scientific Research (DSR) at King Abdulaziz University, Jeddah, under grant No. (114-155-1438D). The authors, therefore, gratefully acknowledge the DSR technical and financial support.

REFERENCES

- [1] Adams, R. P. (2014): Junipers of the World: The Genus *Juniperus*. – Trafford Publishing, Bloomington.
- [2] Andrade, J. L., Meinzer, F. C., Goldstein, G., Holbrook, N. M., Cavelier, J., Jackson, P., Silvera, K. (1998): Regulation of water flux through trunks, branches, and leaves in trees of a lowland tropical forest. – *Oecologia* 115: 463-71.

- [3] Bradley, B. A., Fleishman, E. (2008): Relationships between expanding pinyon–juniper cover and topography in the central Great Basin, Nevada. – *Journal of Biogeography* 35: 951-64.
- [4] Briggs, J. M., Knapp, A. K., Brock, B. L. (2002): Expansion of woody plants in tallgrass prairie: a fifteen-year study of fire and fire-grazing interactions. – *The American Midland Naturalist* 147: 287-94.
- [5] Briggs, J. M., Schaafsma, H., Trenkov, D. (2007): Woody vegetation expansion in a desert grassland: Prehistoric human impact? – *Journal of arid environments* 69: 458-72.
- [6] Brümmer, C., Black, T. A., Jassal, R. S., Grant, N. J., Spittlehouse, D. L., Chen, B., Nestic, Z., Amiro, B. D., Arain, M. A., Barr, A. G. (2012): How climate and vegetation type influence evapotranspiration and water use efficiency in Canadian forest, peatland and grassland ecosystems. – *Agricultural and Forest Meteorology* 153: 14-30.
- [7] Chaves, M. M., Maroco, J. P., Pereira, J. S. (2003): Understanding plant responses to drought—from genes to the whole plant. – *Functional Plant Biology* 30: 239-64.
- [8] Christodoulakis, D. (1996): The phytogeographical distribution patterns of the flora of Ikaria (E Aegean, Greece) within the E Mediterranean. – *Flora* 191: 393-99.
- [9] Clearwater, M. J., Meinzer, F. C., Andrade, J. L., Goldstein, G., Holbrook, N. M. (1999): Potential errors in measurement of nonuniform sap flow using heat dissipation probes. – *Tree Physiology* 19: 681-87.
- [10] Darrouzet-Nardi, A., D’Antonio, C. M., Dawson, T. E. (2006): Depth of water acquisition by invading shrubs and resident herbs in a Sierra Nevada meadow. – *Plant and Soil* 285: 31-43.
- [11] Duursma, R. A., Kolari, P., Perämäki, M., Nikinmaa, E., Hari, P., Delzon, S., Loustau, D., Ilvesniemi, H., Pumpanen, J., Mäkelä, A. (2008): Predicting the decline in daily maximum transpiration rate of two pine stands during drought based on constant minimum leaf water potential and plant hydraulic conductance. – *Tree Physiology* 28: 265-76.
- [12] Elhag, M. (2016): Inconsistencies of SEBS model output based on the model inputs: Global sensitivity contemplations. – *Journal of the Indian Society of Remote Sensing* 44: 435-42.
- [13] Elhag, M., Bahrawi, J. (2016): Deliberation of hilly areas for water harvesting application in western Crete, Greece. – *Global Nest Journal* 18: 621-29.
- [14] Elhag, M., Bahrawi, J. A. (2017a): Consideration of Soil Water Consumption of *Juniperus Macrocarpa* in Semi-Arid Ecosystem in Western Crete, Greece, pp. 1-6. – 15th International Conference on Environmental Science and Technology, Rhodes, Greece.
- [15] Elhag, M., Bahrawi, J. A. (2017b): Realization of daily evapotranspiration in arid ecosystems based on remote sensing techniques. – *Geoscientific Instrumentation, Methods and Data Systems* 6: 141.
- [16] Farjon, A. (2005): *A Monograph of Cupressaceae and Sciadopitys*. – Royal Botanic Gardens, Kew, Richmond, Surrey, UK.
- [17] Fredrickson, E. L., Estell, R., Laliberte, A., Anderson, D. (2006): Mesquite recruitment in the Chihuahuan Desert: historic and prehistoric patterns with long-term impacts. – *Journal of Arid Environments* 65: 285-95.
- [18] Georghiou, K., Delipetrou, P. (2010): Patterns and traits of the endemic plants of Greece. – *Botanical Journal of the Linnean Society* 162: 130-422.
- [19] Granier, A. (1987): Evaluation of transpiration in a Douglas-fir stand by means of sap flow measurements. – *Tree Physiology* 3: 309-20.
- [20] Granier, A., Huc, R., Barigah, S. (1996): Transpiration of natural rain forest and its dependence on climatic factors. – *Agricultural and Forest Meteorology* 78: 19-29.
- [21] Harmsen, E. W., Miller, N. L., Schlegel, N. J., Gonzalez, J. (2009): Seasonal climate change impacts on evapotranspiration, precipitation deficit and crop yield in Puerto Rico. – *Agricultural Water Management* 96: 1085-95.

- [22] Hegazy, A., Elhag, M. (2006): Considerations of demography and life table analysis for conservation of *Acacia tortilis* in South Sinai. – *World Applied Sciences Journal* 1: 97-106.
- [23] Hegazy, A., Fahmy, G., Ali, M., Gomaa, N. (2004): Vegetation diversity in natural and agro-ecosystems of arid lands. – *Community Ecology* 5: 163-76.
- [24] Heilman, J., McInnes, K., Kjelgaard, J., Owens, M. K., Schwinning, S. (2009): Energy balance and water use in a subtropical karst woodland on the Edwards Plateau, Texas. – *Journal of Hydrology* 373: 426-35.
- [25] Lassoie, J. P., Dougherty, P. M., Reich, P. B., Hinckley, T. M., Metcalf, C. M., Dina, S. J. (1983): Ecophysiological investigations of understory eastern redcedar in central Missouri. – *Ecology* 64: 1355-66.
- [26] Lu, P., Müller, W. J., Chacko, E. K. (2000): Spatial variations in xylem sap flux density in the trunk of orchard-grown, mature mango trees under changing soil water conditions. – *Tree Physiology* 20: 683-92.
- [27] Meinzer, F., Goldstein, G., Andrade, J. (2001): Regulation of water flux through tropical forest canopy trees: do universal rules apply? – *Tree Physiology* 21: 19-26.
- [28] Muñoz-Reinoso, J. C. (2004): Diversity of maritime juniper woodlands. – *Forest Ecology and Management* 192: 267-76.
- [29] Oren, R., Ewers, B. E., Todd, P., Phillips, N., Katul, G. (1998): Water balance delineates the soil layer in which moisture affects canopy conductance. – *Ecological Applications* 8: 990-1002.
- [30] Owens, K., Ansley, J. (1997): Ecophysiology and Growth of Ashe and Redberry Juniper. *Juniper Symposium*, pp. 19-31. – Texas A&M University, San Angelo, TX.
- [31] Owens, M. K., Lyons, R. K., Alejandro, C. L. (2006): Rainfall partitioning within semiarid juniper communities: effects of event size and canopy cover. – *Hydrological Processes* 20: 3179-89.
- [32] Porporato, A., Daly, E., Rodriguez-Iturbe, I. (2004): Soil water balance and ecosystem response to climate change. – *The American Naturalist* 164: 625-32.
- [33] Rutter, A., Sands, K. (1958): The relation of leaf water deficit to soil moisture tension in *Pinus sylvestris* L. – *New Phytologist* 57: 50-65.
- [34] Seim, A., Tulyaganov, T., Omurova, G., Nikolylai, L., Botman, E., Linderholm, H. W. (2016): Dendroclimatological potential of three juniper species from the Turkestan range, northwestern Pamir-Alay Mountains, Uzbekistan. – *Trees* 30: 733-48.
- [35] Stocker, T. (2014): *Climate Change (2013): The Physical Science Basis. Working Group I Contribution to the Fifth Assessment Report of the Intergovernmental Panel on Climate Change.* – Cambridge University Press, Cambridge.
- [36] Su, Z., Schmugge, T., Kustas, W., Massman, W. (2001): An evaluation of two models for estimation of the roughness height for heat transfer between the land surface and the atmosphere. – *Journal of Applied Meteorology* 40: 1933-51.
- [37] Thurow, T. L., Hester, J. W. (1997): How an Increase or Reduction in Juniper Cover Alters Rangeland Hydrology. *Juniper Symposium Proceedings*, pp. 9-22. – Texas A&M University, San Angelo, Texas, USA.
- [38] Van Auken, O. (2000): Characteristics of intercanopy bare patches in *Juniperus* woodlands of the southern Edwards Plateau, Texas. – *The Southwestern Naturalist* 45(2): 95-110.
- [39] Van Auken, O., Mckinley, D. C. (2008): *Structure and Composition of Juniperus Communities and Factors That Control Them. Western North American Juniperus Communities.* – Springer, New York.
- [40] Van Haverbeke, D. F., Read, R. A. (1976): *Genetics of Eastern Redcedar.* – Forest Service Research Paper WO-32. USDA, Washington.

GENETIC VARIATION OF YELLOW BARBELL (*CARASOBARBUS LUTEUS* (HECKEL, 1843)) FROM FOUR POPULATIONS USING MITOCHONDRIAL DNA COI GENE SEQUENCES

PARMAKSIZ, A.* – ESKİCİ, H. K.

*Harran University, Faculty of Science-Literature, Department of Biology, Şanlıurfa, Turkey
(phone: +90-414-318-3562; fax: +90-414-318-3541)*

**Corresponding author
e-mail: aprmksz@gmail.com*

(Received 22nd Nov 2017; accepted 27th Feb 2018)

Abstract. The aim of this study is to determine genetic variation of *C. luteus* populations by conducting gene sequence analysis of mtDNA COI locus. Total DNA of 48 individuals from 4 populations in total was isolated using a commercial kit. Sequence analysis was conducted through 3500 XL Genetic Analyzer device following the amplification of target mtDNA locus via Polymerase Chain Reaction (PCR). With sequence analysis of mtDNA COI locus, 9 polymorphic sites and 4 haplotypes were determined. Haplotype and nucleotide diversity were calculated between 0.409 - 0.535 and 0.00089 - 0.00534, respectively. Pairwise F_{ST} results ranged between -0.16880 and 0.33181, values of Diyarbakır population were found to be statistically significant compared to all of the other populations. Totally 4 haplotypes were detected in Median-Joining Network haplotype network. Tajima's D and Fu' Fs tests values were statistically insignificant for all populations ($p > 0.05$). All results obtained in this study are the data that were extracted for *C. luteus* species for the first time. Haplotypes determined for mtDNA COI 625 locus are new results for the literature, generated a critical data set in terms of genetic diversity of this species.

Keywords: *population genetic, haplotype, polymorphism, Euphrates River, Tigris River*

Introduction

Carasobarbus luteus (Heckel, 1843) is an endemic species from the family Cyprinidae possessing a wide distribution in Euphrates and Tigris River, natural and artificial lakes across Mesopotamia (Kuru, 1979; Ünlü, 1991; Gökçek and Akyurt, 2008; Coad, 2010). The body is covered with large, rounded scales. The length and weight varies between 9-35 cm, 20-350 grams, respectively. The color is brownish yellow on the back and yellowish or yellowish white on the sides. The mouth is terminal or semi-terminal and has a pair of short mustaches. Since the meat is delicious, it is used as food by local people (Bilici, 2013). This species is also of economic importance due to high demand as food (Borkenhagen et al., 2011; Bilici et al., 2016).

Certain studies such as reproductive biology (Ahmed et al., 1984, Bilici et al., 2016), feeding condition (Naama and Muhsen, 1986), gonad development (Bartel et al., 1996), observations of reproductive organs and tissues (Rahemo and Al-Shatter, 2012), some biological characteristics (Al-Hazzaa, 2005; Asmaa et al., 2013; Baboli et al., 2013; Eydzadeh, 2014), spermatologic characteristics (Aral et al., 2014), characteristics of age and growth (Gökçek and Akyurt, 2008), content of digestive system (Çelik and Saler, 2016) were conducted on this species.

The genetic variation and population structure of the commercially important species should be studied for the management and conservation purposes (Ward, 2000; Ortega et al., 2006). However, there has not been any study about genetic variation of the species *C. luteus* thriving in rivers systems of Euphrates and Tigris.

In recent years, developments in sequencing techniques have made mtDNA studies popular (Liu and Zhou, 2016). If compared to nuclear markers, mtDNA markers are more sensitive to the effects of genetic drift (Filipova et al., 2011).

Because of maternal inheritance and fast evolutionary rate, it has become an important tool of comparative genomics and plays an important role in molecular diversity study and population genetic structure (Near et al., 2003; Cardenas et al., 2009; Xu et al., 2011).

COI is a protein-coding gene in mtDNA owing to fast evolution, easy amplification and sequencing, it has shown precious knowledge and largely used as genetic marker for population genetic studies (Near et al., 2003; Hu et al., 2008; Cardenas et al., 2009; Xu et al., 2011).

The aim of this study is to determine the genetic variations in populations of *C. luteus*, naturally thriving in Euphrates and Tigris Rivers, by conducting sequence analysis for mtDNA COI locus.

Materials and Methods

Study area, Sample collection and DNA extraction

Euphrates-Tigris river system, large river system of southwestern Asia and it comprises the Euphrates and Tigris rivers, which follow approximately parallel courses by way of the heart of the Middle East (Britannica, 2018). The two rivers have their resources in 50 miles of each other in eastern Turkey and tour southeast through northern Syria and Iraq to the head of the Persian Gulf (Britannica, 2018). Besides, Euphrates and Tigris river systems have a great deal of important capacity and potential for fish biodiversity and fishery. The localities of Euphrates River (Adiyaman and Hilvan) and Tigris River (Diyarbakır and Bismil) System were found to be appropriate for sampling because of the number of populations, the availability of land conditions, the availability of sufficient number of fishermen and the proximity to the city center.

Fish samples, including 48 individuals from 4 populations in total, 2 populations in Euphrates River (Adiyaman and Hilvan) and 2 populations in Tigris River (Diyarbakır and Bismil), were caught by fishing (*Figure 1*) between January 2013 and December 2013. Number of localities and samples were given in *Table 2*.

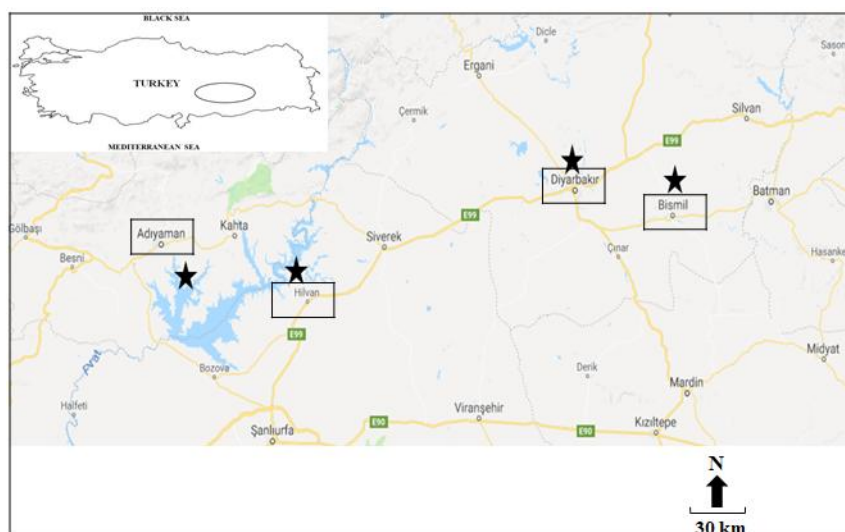


Figure 1. Location of study area

1 g specimen was dissected from muscle tissue on the base of pectoral fin of fish samples, conserved in micro centrifuge tubes with 1,5 ml volume containing 95% ethanol at +4 °C until DNA isolation. Total DNA isolation was performed using GeneJET Genomic DNA Purification Kit (ThermoScientific). 2 µl of isolated DNA samples was taken to run in 0.8% agarose gel at 120 Volts for 30 minutes, then viewed.

PCR amplification and sequencing

Primers used for amplification of mtDNA COI locus in the study by Darabi (2014) COI-625F (5'-TCA-ACC-AAC-CAC-AAA-GAC-ATT-GGC-AC-3') and COI-625R (5'-GAC-TTC-TGG-GTG-GCC-AAA-GAA-TCA-3') were used in the present study.

All PCR reactions were performed at a total volume of 25 µl containing 0.5 mM of each primer, 0.2 mM of each dNTP, 1x PCR buffer, 2.5 mM MgCl₂, 1 unit Taq polymerase and approximately 90 ng of template DNA. The PCR amplification was carried out in a BIO-RAD T100™ Thermal Cycler under the following conditions: 3 min initial denaturation at 95 °C, and 35 cycles of 30 s at 95°C for denaturation, 30 s at 62°C for annealing, and 45 s at 72 °C for extension, and a final extension at 72 °C for 10 min. A total of 3 µl of each PCR product was checked on 2% agarose gel electrophoresis with a Ladder (GeneRuler™ 100 bp DNA Ladder, ready-to-use, Fermentas) and the most specific products were selected for sequencing. Amplified PCR products were purified using the Favor/Prep gel/PCR purification mini kit (Favorgen, Vienna, Austria). Sequencing was done with an automated DNA sequencer 3500 XL Genetic Analyser (Thermo Fisher Scientific).

Sequence analysis

The raw data of mtDNA COI sequences obtained from commercial company were evaluated and converted into FASTA format by ChromasPro v 2.0.1 software (<http://www.technelysium.com.au/ChromasPro.html>). Resulting sequences of all individuals in FASTA format were aligned using BioEdit software version 7.2.5 program (Hall, 2013). The number of polymorphic sites and haplotypes, diversity of haplotypes and nucleotides, Tajima D and Fu's Fs statistics were calculated for populations using DnaSP version 5.10.01 program (Rozas et al., 2003). The phylogenetic relationship between haplotypes was identified by Network version 4.6 software (<http://www.fluxus-engineering.com>, Rohlf, 1999).

Results

Genetic variation

An average of 620 bp fragments of mtDNA COI 625 locus from 48 *C. luteus* specimens were sequenced; totally 9 variable sites and 4 haplotypes were detected. Nucleotide variations of this region are shown in *Table 1*.

As seen in *Table 2*, H1 is the haplotype which is commonly seen in all of the populations. Haplotype H2 is found in all of the populations except Diyarbakır. Haplotype H3, on the other hand, is observed only in Bismil population, H4 only in populations of Tigris River. Bismil population alone includes all of the 4 haplotypes. Nucleotide composition of this site which is approximately 620 bp is cytosine (C), thymine (T), adenine (A) and guanine (G), 26.94%, 29.35%, 26.94%, and 77% respectively. Haplotype and nucleotide diversity were calculated in a range of 0.409 -

0.535 and 0.00089 - 0.00534, respectively. Hilvan population was the one with the lowest results for haplotype diversity and values determined for other populations were similar. Adıyaman population was determined to have the highest nucleotide variation, Diyarbakır population had the lowest.

Table 1. Haplotypes and nucleotide variations of mtDNA COI 625

Haplotypes	236	257	263	275	344	362	491	504	587
H1	T	T	C	C	G	C	G	T	G
H2	C	C	T	T	.	T	.	C	.
H3	A	.	A	.	.
H4	A

Table 2. *C. luteus* sample site, size and their genetic diversity inferred from mtDNA COI gene sequence (*n* = number of individuals, *Nh*: number of haplotypes, *Hd*: haplotype diversity, π : nucleotide diversity)

River System	Locality	n	Nh	Haplotype frequency	Hd	π	Tajima's D	Fu's Fs
Euphrates River	Adıyaman	6	2	H1 (0.66) H2 (0.34)	0.533	0.00534	1.24649	4.184
Euphrates River	Hilvan	12	2	H1 (0.75) H2 (0.25)	0.409	0.00410	0.89777	5.083
Tigris River	Bismil	22	4	H1 (0.68) H2 (0.14) H3 (0.04) H4 (0.14)	0.519	0.00319	-0.75999	1.799
Tigris River	Diyarbakır	8	2	H1 (0.37) H4 (0.63)	0.535	0.00089	1.16650	0.866

Population genetic structure

As seen in Table 3, Pairwise F_{ST} values range between -0.16880 and 0.33181. Despite values between populations of Adıyaman, Hilvan and Bismil were statistically insignificant, values of Diyarbakır population yielded as statistically significant compared to all of the other populations.

Table 3. Pairwise F_{ST} values (below diagonal) and *p* values (above diagonal) between four populations of *C. luteus*

Locality	Adıyaman	Hilvan	Bismil	Diyarbakır
Adıyaman	0.00000	0.99967±0.0000	0.45818±0.0089	0.01421±0.0023
Hilvan	-0.12296	0.00000	0.49686±0.0092	0.04992±0.0034
Bismil	0.01223	-0.16880	0.00000	0.04661±0.0034
Diyarbakır	0.33181*	0.25595*	0.12370*	0.00000

* $p < 0.05$

The analysis of molecular variance of population structure revealed that percentage of variation between groups was 7.37 %, among populations within groups 1.28% and within population 91.35%. Fixation index was calculated as 0.08646 (Table 4).

Table 4. Analysis of molecular variance (AMOVA) of four populations of *C. luteus* based on mtDNA COI gene sequences

Source of variation	df	Sum of squares	Variance components	Percentage of variation	Fixation Indices	p-value
Among groups	1	2.958	0.07958 Va	7.37		
Among populations within groups	2	2.246	0.01381 Vb	1.28		
Within populations	44	43.420	0.98683 Vc	91.35	F_{st} : 0.08646	0.11535±0.00860
Total	47	48.625	1.08022			



Figure 2. Median-joining network showing relations among 4 haplotypes of four *C. luteus* population

In Median-Joining Network haplotype network created for 48 *C. luteus* samples analyzed, totally 4 haplotypes were determined, resulting network shows presence of a central haplotype (H1) which indicates an evolutionary connection. In addition, it is possible to speculate that all of the other haplotypes are connected with haplotype H1 (Figure 2).

Neutrality tests

Neutrality tests (Tajima's D and Fu' Fs tests) were applied for each population. It was determined that while Tajima's D values were negative for Bismil population, they were positive for other population, were statistically insignificant for all of the populations ($p > 0.05$). Fu' Fs tests values were calculated to be positive and were statistically insignificant for all of the populations ($p > 0.05$) (Table 2).

Discussion

In this study, genetic variation of populations was researched via sequence analysis of mtDNA COI 625 locus in 48 *C. luteus* samples from totally 4 populations in Euphrates and Tigris Rivers. 9 polymorphic sites and 4 haplotypes were determined for this studied locus. H1 was the most frequently observed haplotype for 31 individuals in total, it is possible to say that H1 is ancestry because it is common for all of the populations. In addition, haplotype H2 is also represented in other 3 populations except Diyarbakır population. Haplotype H3 was seen in only 1 individual from Bismil

population. Haplotype H4 was represented by 3 individuals from Bismil, 5 individuals from Diyarbakır as well. Haplotypes H3 and H4 are unique to Tigris River. Haplotype diversity between studied populations was calculated to be considerably similar except Hilvan population. Even though it has the highest haplotype diversity (0.535), Diyarbakır population has the lowest nucleotide variation (0.00089). Mean haplotype diversity and nucleotide diversity were determined to be 0.538 and 0.00345, respectively.

In a study by Parmaksız and Ekşi (2017) which was conducted on populations of *Capoetta trutta* in habiting in the same systems, using the same primers, haplotype diversity was determined as 0.642, nucleotide diversity as 0.00138. Despite the fact that haplotype variation was lower in this study, nucleotide variation was found to be higher.

Environmental heterogeneity and large population sizes might support the maintenance of high haplotype diversity within populations (Nei, 1987; Avise, 1998). The nucleotide diversity (π) value indicates the mean number of differences among all pairs of haplotypes in each population (Saraswat et al., 2014). So, π values are a susceptible index of the genetic diversity for a population (Nei and Li, 1979). Low nucleotide diversity and high haplotype diversity in fish presumably underwent population expansion after a period of low-effective population size (Saraswat et al., 2014). Low nucleotide diversity values are also indicative of low population diversity and genetic diversity is effected by many factors, such as habitation, bottleneck effects and anthropogenic activity (Ma et al., 2010, Fennando et al., 2000). Because the four localities where samples of our study were taken from were close to residential areas, this fish species is caught by fishermen and local people. These caught fish are both consumed by local people and sold to neighboring provinces. As the rate of fishing is high, genetic diversity of *C. luteus* populations has been decreasing.

In Median Joining network analysis, haplotype H1 is in the center of the network and dominant, all other haplotypes were consisted of haplotype H1 (Figure 2). The fact that this haplotype is found all of the haplotypes and dominant indicates that this one is ancestral haplotype.

Inter-population pair wise F_{ST} values varied between -0.16880 and 0.33181 (Table 3). Though differences between Bismil populations were insignificant, differences between Diyarbakır and all of the other populations were determined to be statistically significant.

In this study, AMOVA analysis conducted based upon the haplotype frequencies indicated that percentage of variation between groups was 7.37%, among population within groups 1.28% and within population 91.35% (Table 4). The mean fixation index was calculated as 0.08646.

In their study, Parmaksız and Ekşi (2017) calculated within population and among population within groups genetic variation as 90.14% and 9.86%, respectively; mean fixation index as 0.09865. The current study is compatible with results of this study. Low inter-population genetic variance is an indicator for that there has been a high gene flow between these populations or these populations were the ones isolated from each other last. Tigris River rises in Turkey and flows in to Persian Gulf in Shatt al-Arab passing through lands of Iraq (Zeybek et al., 2016). It can be said that there was a gene exchange between populations of this fish species because of the union before dams had been constructed on these river systems.

Tajima's D values in the populations; were positive for populations of Adıyaman, Hilvan, Diyarbakır, negative for Bismil population and all of the resulting values did not

yield statistically significant ($p > 0.05$). Fu's F_s values, on the other hand, were positive for all of the populations and were not statistically significant as well ($p > 0.05$). Mean Tajima's D value was determined to be 0.05729 and Fu's F_s value was 3.351.

Parmaksız and Ekşi (2017), in their study, calculated mean Tajima's D and Fu's F_s values as -1.08945 and -2.946, respectively and both of the values were they were negative while they were positive in the current study.

Tajima's D is used to measure the distinctness between the number of segregating sites and the pair wise genetic distance (Li et al., 2015). A positive Tajima's D and Fu's F_s Test signifies low levels of both low and high frequency polymorphisms, indicating a decrease in population size (Hu et al., 2016).

When neutrality tests in this study were considered, while there was a decrease in populations of Adıyaman, Hilvan and Diyarbakır population, a decrease was not observed for Bismil population. In addition, the fact that all 4 haplotypes were seen in Bismil population indicates that the populations has not decreased. The reason why the number of haplotypes in Bismil locality is high might be due to the presence of a large number of streams. Furthermore, the H3 haplotype is still present in the population of Bismil, but it might end up in other localities.

All of the results obtained via this study are the data of *C. luteus* obtained for the first time. Haplotypes determined for mtDNA COI 625 locus were new results for literature, created a significant data set in terms of genetic variation of this species (Table 5).

Table 5. Total haplotypes of *C. luteus* in the present study and Gen Bank

Haplotype	Gen Bank Data
H1	The current study
H2	The current study
H3	The current study
H4	The current study
H5	KM590426.1
H6	KM590425.1
H7	KM590424.1

Conclusions

Carasobarbus luteus (Heckel, 1843) has a wide distribution and the most common species in both Euphrates and Tigris basins (Kuru, 1979; Ünlü, 1991; Coad, 2010). This species is endemic and the most economically important and abundant species in the region (Bilici et al., 2017). The population of this species have been influenced by pollution, destruction of habitat and especially over fishing exploitation.

In this study, the sampling localities were only four localities. Moreover, the outcome based on COI gene presented only a portion of the entire genome here that could be only a partial solution for population genetic of the species (Gruenthal et al. 2007). Further study based on nuclear markers, mtDNA markers (cyt-b, D-loop) and a wide range sampling collection is needed to extend and corroborate the present population genetic structure.

Acknowledgements. This study was funded by Harran University Research Fund (Project No:16040).

REFERENCES

- [1] Ahmed, H. A., Al-Mukhtar, M. A., Al-Adhub, H. Y. (1984): The reproductive biology of *Carasobarbus luteus* (Pisces Cyprinidae) in Al-Hammar Marsh, Iraq. – *Cybium* 18 (4): 69-80.
- [2] Al-Hazaa, R. (2005): Some biological aspects of the himri barbel, *Barbus luteus* in the intermediate reaches of the Euphrates River. – *Turk. J. Zool.* 29(4): 311-315.
- [3] Aral, F., Doğu, Z., Şahinöz, E. (2014): Comparison of spermatological characteristics in *Carasobarbus luteus* (Heckel, 1843) and *Carassius carassius* living in Atatürk Dam Lake. – *Turk. J. Agric. Food Sci. Technol.* 2 (4): 185-189.
- [4] Asmaa, S. I., Taha, Y. A., Nada, A. A. (2013): Study of sexual dimorphism in Iraqi fresh water fish *B. luteus*. – *J. of Genet. and Envir. Res. Cons.* 1(1): 12-19.
- [5] Avise, J. (1998): *Phylogeography*. – Cambridge, MA. Harvard University Press., 102 pp.
- [6] Baboli, M., Nejad, M. (2013): Condition factor, diet and gonado somatik index of *C.luteus* (Heckel, 1843) in Karkheh River, Iran. – *J. Bio. &Env. Sci.* 3(1): 83-87.
- [7] Bartel, R., Bieniarz, K., Epler, P., Kime, D. E., Popek, W., Sokolowska-Mikolajczyk, M. (1996): Gonadal development and spawning of *Barbus sharpei*, *Barbus luteus* and Mugil fish in fresh and saltwater lakes in Iraq. – *Arch. Polish Fish.* 4 (1): 113-124.
- [8] Bilici, S. (2013): The investigations on the biology of *Carasobarbus luteus*, *Capoeta trutta* and *Garra variabilis* species Living in Tigris River. PhD thesis – Institute of Natural And Applied Sciences University of Dicle.
- [9] Bilici, S., Ünlü, E., Çiçek, T., Satici, Ö. (2016): The reproductive biology of *Carasobarbus luteus* and *Capoeta trutta* in the Tigris River, Turkey. – *Cybium* 40 (2): 147-153.
- [10] Bilici, S., Cicek, T., Ünlü, E. (2017): Observation on the age, growth and somatic condition of *Carasobarbus luteus* (Heckel, 1843) and *Capoeta trutta* (Heckel, 1843) (Cyprinidae) in the Tigris River, Turkey. – *Iranian Journal of Fisheries Sciences* 16 (1):170-187.
- [11] Borkenhagen, K., Esmaeili, H. R., Mohsenzadeh, S., Shahryari, F., Gholamifard, G. (2011): The molecular systematics of the *Carasobarbus* species from Iran and adjacent areas, with comments on *Carasobarbus albus* (Heckel, 1843). – *Environ. Biol. Fish.* 91: 327-335.
- [12] Britannica. (2018): Tigris-Euphrates river system. Britannica. Accessed February 08. <https://www.britannica.com/place/Tigris-Euphrates-river-system>
- [13] Cardenas, L., Silva, A., Magoulas, A., Cabezas, J., Poulin, E., Ojeda, F. (2009): Genetic population structure in the Chilean jack mackerel, *Trachurus murphyi* (Nichols) across the Southeastern Pacific Ocean. – *Fish Res.* 100:109-115.
- [14] Coad, B. W. (2010): *Freshwater Fishes of Iraq*. – Sofia-Moscow. Pensoft Publishers, 294 pp.
- [15] Çelik, B., Saler, S. (2016): Atatürk Baraj Gölü'nde Yaşayan Bizir, *Carasobarbus luteus* (Heckel, 1843)'un Sindirim Sistemi İçeriği. – *Journal of Limnology and Freshwater Fisheries Research* 2 (2): 83-93.
- [16] Darabi, A. R., Kashan, N., Fayazi, J., Aminafshar, M., Chamani, M. (2014): Investigation of phylogenetic relationship among two *Barbus* species (Cyprinidae) populations with mitochondrial DNA using PCR sequencing. – *IJBPAS*, 4 (2): 302-311.
- [17] Eydizadeh, A. (2014): Some biological aspect of *Carasobarbus luteus* in Hoor Al-azim wetland. – *Sci. J. Biol. Sci.* 3 (3):29-36.
- [18] Fennando, P., Pfrender, M. E., Encalada, S. E., Lande, R. (2000): Mitochondrial DNA variation, phylogeography and population structure of the Asian elephant. – *Heredity* 84:362-72.
- [19] Filipova, L., Lieb, D. A., Grandjean, F., Petrussek, A. (2011): Haplotype variation in the spiny-cheek crayfish *Orconectes limosus*: colonization of Europe and genetic diversity of native stocks. – *J. N. Am. Benthol. Soc.* 30: 871-881.

- [20] Gruenthal, K. M., Acheson, L. K., Burton, R. S. (2007): Genetic structure of natural populations of California red abalone (*Haliotis rufescens*) using multiple genetic markers. – *Mar Biol.* 152:1237–1248.
- [21] Gökçek, K. Akyurt, I. (2008): Age and Growth Characteristics of Himri Barbel (*Barbus luteus* Heckel, 1843 in Orontes River, Turkey. – *Turk J. Zool.* 32: 461-467.
- [22] Hall, T. A. (2013): BioEdit v 7.2.3. – Biological sequence alignment editor for Win 95/98/NT/2K/XP7.
- [23] Hu, J., Zhang, J., Nardi, F., Zhang, R. J. (2008): Population genetic structure of the melon fly, *Bactrocera cucurbitae* (Diptera: Tephritidae), from China and Southeast Asia. – *Genetica* 134: 319-324.
- [24] Hu, Y. D., Pang, H. Z., Li, D. S., Ling, S. S., Lan, D., Wanga, Y., Zhu, Y., Li, D. Y., Rong-Ping, W., Zhang, H. M., Wang, C. D. (2016): Analysis of the cytochrome c oxidase subunit 1 (COX1) gene reveals the unique evolution of the giant panda. – *Gene* 592: 303-307.
- [25] Kuru, M. (1979): The fresh water fish of South-eastern Turkey-2 (Euphrates-Tigris sisteme). – *Hacettepe Bull. Nat. Sci. Eng.* 7-8: 105-114.
- [26] Li, W., Chen, X., Xu, Q., Zhu, J., Dai, X., Xu, L. (2015): Genetic Population Structure of *Thunnus albacares* in the Central Pacific Ocean Based on mtDNA COI Gene Sequences. – *Biochem. Genet.* 53: 8–22. <http://dx.doi.org/10.1007/s10528-015-9666-0>.
- [27] Liu, G., Zhou, L. (2016): Population genetic structure and molecular diversity of the red swamp crayfish in China based on mtDNA COI gene sequences, – *Mitochondrial DNA Part A*, <http://dx.doi.org/10.1080/24701394.2016.1199022>.
- [28] Ma, C., Cheng, Q., Zhang, Q., Zhuang, P., Zhao, Y. (2010): Genetic variation of *Coilia ectenes* (Clupeiformes: Engraulidae) revealed by the complete cytochrome b sequences of mitochondrial DNA. – *J. Exp. Mar. Bio. Ecol.* 385:14–19.
- [29] Naama, A. K., Muhsen, K. A. (1986): Feeding periodicities of the mugilid *Liza abu* (Heckel) and cyprinid *Carasobarbus luteus* (Heckel) from Al-Hammar Marsh, southern Iraq. – *Indian J. Fish.* 33: 347-350.
- [30] Near, T. J., Pesavento, J., Cheng, C. (2003): Mitochondrial DNA, morphology, and phylogenetic relationships of Antarctic icefishes (Notothenioidei: Channichthyidae). – *Mol. Phylogenet. Evol.* 28: 87-98.
- [31] Nei, M., Li, W. (1979): Mathematical model for studying genetic variation in terms of restriction endonucleases. – *Proc. Nat. Acad. Sci.* 76: 5269-73.
- [32] Nei, M. (1987): *Molecular evolutionary genetics*. – New York, Columbia University Press., 512 pp.
- [33] Ortega-Villaizan Romo, M., Suzuki, S., Nakajima, M., Taniguchi, N. (2006): Genetic evolution of inter individual relatedness for broodstock management of the rare species barfin flounder *Verasper moseri* using microsatellite DNA markers. – *Fisheries Sci.* 72: 33-39.
- [34] Parmaksız, A., Ekşi, E. (2017): Genetic diversity of the cyprinid fish *Capoeta trutta* (Heckel, 1843) populations from Euphrates and Tigris rivers in Turkey based on mtDNA COI sequences. – *Indian J. Fish.* 64 (1): 18-22. <http://dx.doi.org/10.21077/ijf.2017.64.1.62396-03>.
- [35] Rahemo, Z. I., Al-Shatter, N. M. (2012): Observations on reproductive organs and tissues of two freshwater Cyprinid fishes. – *Trends Fish. Res.* 1 (2): 42-48.
- [36] Rohl, A. (1999): NETWORK: A program package for calculating phylogenetic network. Version 2.0b. Available from: <http://www.fluxus-engineering.com>.
- [37] Rozas, J., Sanchez-DelBarrio, J. C., Messeguer, X., Rozas, R. (2003): DnaSP DNA polymorphism analyses by the coalescent and other methods. – *Bioinformatics.* 19: 2496-2497.
- [38] Saraswat, D., Lakra, W. S., Nautiyal, P., Goswami, M., Shyamakant, K., Malakar, A. (2014): Genetic characterization of *Clupisoma garua* (Hamilton 1822) from six Indian

- populations using mtDNA cytochrome b gene. – *Mitochondrial DNA*, 25 (1): 70-77. <http://dx.doi.org/10.3109/19401736.2013.782014>
- [39] Ünlü, E. (1991): A study on the biological characteristics of *Capoeta trutta* (Heckel, 1843) living in the Tigris River, Turkey. – *Turk. J. Zool.* 15: 22-38.
- [40] Ward, R. D. (2000): Genetics in fisheries management. – *Hydrobiologia* 420:191-201.
- [41] Xu, Z. H., Chen, J. L., Cheng, D. F., Liu, Y., Eric, F. (2011): Genetic variation among the geographic population of the Grain Aphid, *Sitobion avenae* (Hemiptera: Aphididae) in China inferred from mitochondrial COI gene sequence. – *Agr. Sci. China.* 10: 1041-1048.
- [42] Zeybek, M., Ahiska, S., Yıldız, S. (2016): A preliminary taxonomical investigation on the Oligochaeta (Annelida) fauna of Tigris River (Turkey). – *Ege Journal of Fisheries and Aquatic Sciences* 33 (1): 47-53. <http://dx.doi.org/10.12714/egejfas.2016.33.1.08>.

EVALUATION OF MIXTURES OF YELLOW LUPINE (*LUPINUS LUTEUS* L.) WITH SPRING CEREALS GROWN FOR SEEDS

KSIĘŻAK, J. – STANIAK, M.* – BOJARSZCZUK, J.

*Department of Forage Crop Production, Institute of Soil Science and Plant Cultivation – State Research Institute, Czartoryskich 8, 24-100 Pulawy, Poland
(phone: +48-81-478-6790; fax: +48-81-478-6900)*

**Corresponding author
e-mail: staniakm@iung.pulawy.pl*

(Received 27th Sep 2017; accepted 27th Feb 2018)

Abstract. Cultivation of legume-cereals mixtures is considered a good agricultural practice in many European countries, especially in organic and low-input farming systems. The aim of the study was to determine the productivity of mixtures of yellow lupine (*Lupinus luteus* L.) with spring cereals, depending on the species of grain component and its percentage in mixture. Field experiments were carried out in the years of 2011-2013 at the Agricultural Experimental Station Grabów in Poland, using the system of random sub-blocks, with a control treatment, in four replications. The study included three species of cereals: wheat (*Triticum aestivum* L.), barley (*Hordeum vulgare* L.), and triticale (*Triticosecale* Wittm. ex A. Camus), as well as three percentages of lupine in the weight of sown seeds: 40, 60, 80%. The experiment was conducted on the soil of good wheat complex, class IIIa. The studies showed that the highest yield was obtained from the mixture of yellow lupine with wheat. Increasing the percentage of lupine seeds resulted in lower mixture yields, regardless of cereal species. Lupine grown in mixtures with cereals formed less pods, seeds per pod and per plant and produced a lower seed weight compared with their counterparts grown in pure stands. Legumes grown in mixture with cereals favorably affected morphological characteristics of cereals, contributing to their higher tillering and producing a higher number of grains per plant. The grain of cereals grown in mixtures with lupine had higher contents of total protein and crude fibre than the grain of cereals grown in pure stands.

Keywords: *legume, share of components, yield, structure of yield, chemical composition*

Introduction

Growing legume-cereal mixtures for grain is one of the ways of obtaining concentrated feed both in organic and in integrated production systems (Watson et al., 2002). Such sowings allow for a rational use of environmental resources, positively affect soil environment and provide a strong competition for weeds (Tofinga and Snaydon, 1992; Cremer et al., 1996; Büyükburç and Karadağ, 2002; Hauggaard-Nielsen and Jensen, 2004; Lithourgidis et al., 2006; Hauggaard-Nielsen et al., 2008; Corre-Hellou et al., 2011). Yielding and crop quality of legume-cereal mixtures largely depends on the selection of components and their participation. Generally, yield of mixture seeds decreases with increasing percentage of legumes at sowing, but interspecies interactions are largely determined by the characteristics of the components, which may, change during plant growth under the influence of variable habitat factors (Rudnicki and Kotwica, 2006). Cultivation of mixed crops increases the content of crude protein in the yield of the seeds mixture, but it is also related to selection and participation of the individual components (Staniak et al., 2014). Creating favorable conditions for cereals and legumes in mixture stands and reducing a competition between them during the period of vegetation are important agri-ecological and agri-technological issues.

Species grown in mixed crops should have similar soil and climatic requirements, a similar maturation date and a similar height. A good component for mixtures with spring cereals is yellow lupine, which is characterized by a high protein content (over 40%) rich in lysine and crude fat (over 50%), which significantly increases the nutritional value of feed from such mixtures. In addition, it has low water and soil requirements thanks to a well-developed root system. According to Rudnicki and Kotwica (2006), on light soils, yellow lupine is a much better component for mixtures than blue lupine. The level of mixtures yielding and the share of seeds of individual components in the yield, and thus the value of fodder, depends not only on the selection of species, but also on their share in sown mixture.

The aim of the study was to determine the productivity and quality of mixtures of yellow lupine (*Lupinus luteus* L.) with spring cereals, depending on the species of grain component and its percentage in the weight of sown seeds.

Review of literature

Mixtures of spring cereals with legumes are considered good agricultural practice, especially in organic and low-input farming system (Hassen et al., 2017). Cultivation of mixtures contributes to the complementary use of habitat resources and compensatory growth of individual plant species, causing an increased productivity and greater stability of yield (Niggli et al., 2008; Doré et al., 2011). Cereals sown with legumes are a strong competitor to the legume which causes that the share of legume seeds in the mixture yield is often variable and low. Increasing the percentage of legume seeds in the sowing norm increases their share in the yield, but the yield of grain cereals and the total yield of mixtures generally decreases (Rudnicki and Wenda-Piesik, 2007). The competitiveness of the plants in legume-cereals mixtures for the access to environmental resources intensifies in the conditions of reduced soil moisture (Gałęzewski, 2006). Under these conditions, many authors observed increased fallout of lupine plants from the stand. Also, these plants formed a low number of pods, which resulted in low legume yields (Kotwica and Rudnicki, 2003).

The yield and stability of the mixtures are therefore determined by the cereals, and to a lower extent – by legumes, but when determining the quality of the mixtures, the share of legume seeds in the mixture yield is crucial. One of the most important criteria for grain quality evaluation is concentration of crude protein. The seeds of legumes are significantly different from the grains of cereals. They contain large amounts of total protein and crude fibre and considerably higher amount of minerals compared to the cereals (Johnston et al., 1978; Staniak et al., 2012). According to Księżak and Staniak (2013) increasing the share of blue lupine in two-species mixtures with barley, wheat and triticale resulted in an increase in the total protein content in the yield of mixtures seeds, and the concentration of crude fibre and crude fat has been also increased. The same relationships have been found in the studies on mixtures of wheat and spring barley with peas (Pozdisek et al., 2011).

Materials and methods

Location of the experiment

Field experiments with the mixtures of yellow lupine (*Lupinus luteus* L.) with spring cereals were carried out in the years of 2011-2013 at the Agricultural Experimental Station

Grabów [51°21'18"N 21°40'09"E] in Poland, using the system of random sub-blocks, with a control treatment, in four replications. The plot size for the harvest was 27.0 m². The experiment was conducted on the silty soil developed on the light loam, good wheat complex, class IIIa. The content (mg kg⁻¹) of available phosphorus was from 13.3 to 16.0, potassium – from 8.1 to 8.4, magnesium – from 3.9 to 4.1, while pH was close to neutral (6.4-6.6).

Plant materials

The first factor was a species of spring cereals: wheat (*Triticum aestivum* L.), barley (*Hordeum vulgare* L.), triticale (*Triticosecale* Wittm. ex A. Camus), and the secondary factor was the percentage of yellow lupine in the sown mixture: 40, 60 and 80%. The density of components in pure sowing for which the density of plants in the mixtures was calculated was: lupine (variety Mister) – 100 plants·m⁻², barley (variety Skarb) – 300 plants·m⁻², wheat (variety Bamberka) and triticale (variety Nagano) – 500 plants m⁻².

Agrotechniques

Winter plowing was carried out to a depth of 25 cm, in the spring a cultivator and passive agricultural set (drag, spring-tine harrow, land roller) was used. The following mineral fertilizer doses were used (kg·ha⁻¹): P–19.6, K–45.6 and N–40. The sowing was carried out from 11 to 23 April with the usage of Amazone grain drill. Before the sowing, the seeds were treated with a seed dressing Funaben T. Basagran 1.25 dm³·ha⁻¹ or Stomp 330 EC at a dose of 3.5 dm³·ha⁻¹; it was used to remove weeds from the mixture. Harvest of mixtures was carried out in the period from 8 to 23 August with the usage of Sedmaster plot harvester.

Measurement and testing methods

Before the harvest, a number of pods and seeds per pod, and a number and weight of seeds per plant were determined in 10 randomly selected plants of lupine per each sub-plot. While in cereals, a number and weight of grains per plant, a number of grains per ear, the height of culms and a number of productive culms were specified. After the harvest, the seed yield of lupine-cereal mixture and thousand seed weight of its components were determined. The percentage of seeds of both species in the mixture was marked after the separation of the yield from the entire plot. The contents of total protein and crude fibre in cereal grains and yellow lupine seeds were also determined.

The impact of the examined experimental factors on the determined characteristics were assessed using the analysis of variance, the half-intervals of confidence being determined by Tukey's test at the significance level of $\alpha = 0.05$. The results were statistical analysis of variance using Statistica v.10.0 program.

Results and discussion

Weather conditions had a significant impact on the yield of cereals and yellow lupine in pure stands, while the yield of mixtures additionally depended on the selection and percentage of the components. The highest seed yields, especially of yellow lupine, were obtained in 2013, when the sum of precipitation during the period from April to August amounted to about 400 mm. There was a favorable distribution of rainfall in

June, a small amount of precipitation in July and August and the largest relative air humidity during flowering of plants (*Table 1*). That year also saw a slightly higher average air temperature during the growing season, compared with the mean from a multi-year period. In 2012, a small amount of rainfall in the third decade of June and the first decade of July caused strong inhibition of the growth and development of yellow lupine, and consequently, a very low yield of seeds. Rojek (1989) pointed out large water requirements and sensitivity of yellow lupine, especially in the period from flowering until the end of pod formation. Gałęzewski (2006) stated that competition for water of lupine and oats is stronger when they are grown in mixtures compared to pure stands. According to Podleśny and Podleśna (2010) mixtures of blue lupine with barley are less sensitive to droughts than lupine grown in pure stands. Also Księżak and Magnuszewska (1999) confirmed that under reduced soil moisture, growing legume-cereal mixtures provides a greater stability and higher level of yielding than the cultivation of these plants in pure stands. In 2011, with not very favorable weather conditions, the obtained seed yields were by about 25% lower compared to the yields of 2013. July and early August of that year saw a large amount of precipitation, which caused the strong lodging of plants, extended the period of plant maturing, impeded harvesting and caused higher seed shedding.

Table 1. Course of weather conditions during the vegetation periods

Months	Mean monthly of temperature (°C)				Sum of monthly precipitation (mm)			
	2011	2012	2013	Average of multi-year period	2011	2012	2013	Average of multi-year period
April	10.3	9.6	8.3	7.7	35.9	37.8	29.9	39
May	13.9	15.3	15.3	13.4	74.5	36.5	112	57
June	18.5	17.7	18.6	16.7	52.4	54.3	116.3	71
July	18.4	20.9	19.7	18.3	298.8	81.6	20.8	84
August	18.8	18.8	19.2	17.3	35.6	64.2	11.6	75

The yields of cereals grown in pure stands were similar and significantly higher than the yields of lupine grown in pure stands (*Table 2*). Among the studied mixtures, the highest seed yields were obtained from stands of lupine with wheat compared with mixtures with barley and triticale; they were higher by approximately 10 and 7% (average for three years) (*Table 3*). The yield of spring cereals mixed with yellow lupine, especially with the 80% share of this species, was generally lower than the yield of cereals grown in pure stands. Rudnicki and Gałęzewski (2007b) showed that the yields of oats-yellow lupine mixtures were lower than the yields of oats in pure stands, and that they depended mainly on the yield of oats. Different results were presented by Rudnicki and Kotwica (2006), who recorded higher yields of spring cereals mixed with lupines (yellow and blue) compared with the yields of these components in pure sowings. These authors also indicated that yellow lupine was a more favorable component for mixtures with these cereals than blue lupine.

Table 2. Seeds yield of yellow lupine and spring cereals grown in pure sowing ($t\cdot ha^{-1}$)

Cereal species	2011	2012	2013	Mean
Barley	3.18 b*	3.59 bc	4.18 b	3.61
Wheat	3.29 b	3.40 b	4.44 c	3.71
Triticale	3.36 b	3.72 c	4.13 b	3.73
Lupine	1.56 a	0.90 a	2.20 a	1.55

*Values in the same column followed by a different letter are significantly different ($p < 0.05$)

Table 3. Seeds yield of yellow lupine-cereal mixtures depending on cereal species and percentage of lupine ($t\cdot ha^{-1}$)

Years	Lupine percentage (%)	Barley	Wheat	Triticale
2011	40	2.95 b*	3.58 c	3.14 c
	60	2.94 b	3.33 b	2.93 b
	80	2.24 a	3.17 a	2.64 a
	Mean	2.71	3.36	2.90
2012	40	3.33 c	3.92 c	3.30 b
	60	3.12 b	3.42 b	3.13 b
	80	2.65 a	3.00 a	2.94 a
	Mean	3.03	3.45	3.12
2013	40	4.03 c	3.99 c	4.06 c
	60	3.78 b	3.67 b	3.64 b
	80	3.37 a	3.32 a	3.41 a
	Mean	3.73	3.66	3.70

*Values in the same column followed by a different letter are significantly different ($p < 0.05$)

The seeds yield of yellow lupine and its percentage in mixtures with cereals varied depending on weather conditions during the growing season, a species of cereal component in the mixture, and its percentage in the weight of sown seeds. The seeds yield of legumes in the mixtures with any cereal in the first and second year of the experiment was significantly lower compared to pure stands (on average by 50% in the first and 41% in the second year), while in the third year, it was higher only in mixtures with wheat (by about 36%) (Table 4). Increasing the percentage of lupine in the weight of sown seeds caused an increase in its percentage in the mixture yield, but only in the third year, with favorable moisture conditions. Its percentage in the yield was similar to the number of sown seeds. In the studies of Rudnicki and Gałęzewski (2007a), the yield of lupine seeds in mixtures with cereals was several times lower than in pure stands. At the same time, it significantly varied during individual years of the study. Increasing the sowing rate of lupine seeds in the mixtures caused an increase in the percentage of its seeds in mixture yield, but at the same time, this percentage was negatively correlated with the mixture yield. According to numerous authors, legume-cereal mixtures yield best when legume seeds constitute from 30 to 50% of seeds at the sowing (Jaranowski, 1997; Szczukowski, 1989). Książak (2006) obtained significantly higher yields of mixtures of peas with spring wheat at 30% share of legume seeds at sowing. The yields

decreased together with increasing the percentage of peas up to 40 and 50%. Książak and Magnuszewska (1999) however, did not record any effect of increasing the percentage of pea at sowing on the seed yield of pea-wheat mixtures grown conventionally. According to the literature data, triticale is the least competitive spring cereal against lupine (Kotwica and Rudnicki, 2003, 2004).

Table 4. Yield of lupine seeds and percentage of lupine seeds in yield of mixtures with cereals depending on cereal species and percentage of lupine

Years	Lupine percentage (%)	Yield of lupine seeds (t·ha ⁻¹)			Percentage of lupine seeds (%)		
		Barley	Wheat	Triticale	Barley	Wheat	Triticale
2011	40	0.49 a*	0.67 a	0.57 a	16.6	18.5	17.5
	60	0.75 b	0.84 b	0.84 b	24.9	25.0	26.7
	80	0.76 b	1.13 c	0.93 c	32.1	34.3	33.4
	Mean	0.67	0.88	0.78	24.5	25.9	25.9
2012	40	0.10 a	0.13 a	0.11 a	3.0	3.2	3.2
	60	0.21 b	0.24 b	0.22 b	6.8	7.1	6.8
	80	0.22 b	0.29 b	0.23 b	8.2	9.6	9.4
	Mean	0.18	0.22	0.19	6.0	6.6	6.5
2013	40	1.57 a	2.81 a	1.66 a	39.3	70.5	40.9
	60	1.84 b	3.08 b	1.69 a	49.4	83.8	46.1
	80	1.93 b	3.12 b	2.09 b	57.5	93.8	61.1
	Mean	1.78	3.00	1.81	48.7	82.7	49.4

*Values in the same column followed by a different letter are significantly different ($p < 0.05$)

The lowest number of pods per plant and seeds per pod, both in pure stands and in mixtures, was produced by lupine plants grown in 2012, while the highest - in 2013, the year with favorable weather conditions (*Table 5*). The most seeds per pods were set by lupine grown in the mixture with triticale, while the least - in the stand with wheat. A species of cereal had a relatively small effect on the number and weight of seeds per plant, although in all the years of the research, smaller values of these characteristics were recorded for lupine grown in a mixture with wheat compared to the stands with barley and triticale (*Table 6*). In the first two years of the experiment, lupine in mixtures set a lower number of pods and seeds, and produced a lower seed weight per plant than in pure stand. These values considerably increased in the third year of the study, regardless of the used cereal species. In 2011 and 2012, increasing the percentage of lupine in the mixture positively affected the number of pods, seeds, and seed weight per plant, while in the third year, there was a decrease in the number of pods. According to Rudnicki and Gałęzewski (2007a), all the features of yellow lupine in mixtures (except for height) were much less developed than in the cultivation in pure stands. Lupine grown in pure stand and in mixtures in 2013 had the highest weight of thousand seeds, regardless of the species of a cereal component of the mixture (*Table 7*). Moreover, lupine has larger seeds when grown in a mixture with triticale than the lupine grown with other cereal species. Increasing the percentage of lupine in the mixture with barley and wheat reduced the size of seeds, while triticale had a much lower influence on this feature.

Table 5. Number of yellow lupine pods per plants and seeds per pod depending on cereal species and percentage of lupine in mixture

Years	Lupine percentage (%)	Number of pods per plants (unit)			Number of seeds per pod (unit)		
2011	100	5.15 b*			3.67 b		
2012	100	1.74 a			2.52 a		
2013	100	6.37 b			3.53 b		
		Barley	Wheat	Triticale	Barley	Wheat	Triticale
2011	40	2.90 a	1.17 a	2.45 a	2.84 a	2.24 a	3.14 a
	60	3.20 b	2.10 b	2.45 a	2.85 a	2.22 a	3.18 a
	80	3.65 c	3.10 c	2.55 a	3.12 b	2.21 a	3.39 b
	Mean	3.25	2.12	2.48	2.94	2.22	3.24
2012	40	0.53 a	0.48 a	0.66 a	2.19 a	2.14 a	2.15 a
	60	0.62 a	0.66 b	0.94 b	2.26 a	2.10 a	2.50 b
	80	0.95 b	0.87 c	1.04 b	2.43 b	2.33 b	2.45 b
	Mean	0.70	0.67	0.88	2.29	2.19	2.37
2013	40	8.17 c	8.83 c	7.96 c	3.66 a	3.70 b	3.74 b
	60	7.30 b	7.80 b	7.27 b	3.58 a	3.60 b	3.57 a
	80	6.40 a	7.30 a	7.17 a	3.71 b	3.45 a	3.62 a
	Mean	7.29	7.98	7.47	3.65	3.58	3.64

*Values in the same column followed by a different letter are significantly different ($p < 0.05$)

Table 6. Number and weight of yellow lupine seeds on plant depending on cereal species and percentage of lupine in mixture

Years	Lupine percentage (%)	Number of seeds (unit)			Weight of seeds (g)		
2011	100	19.00 b*			2.38 b		
2012	100	4.38 a			0.53 a		
2013	100	22.47 b			3.13 c		
		Barley	Wheat	Triticale	Barley	Wheat	Triticale
2011	40	8.20 a	2.50 a	7.70 a	0.98 a	0.30 a	0.89 a
	60	9.21 a	4.80 b	7.85 a	1.12 a	0.62 b	0.94 a
	80	11.55 b	6.80 c	8.65 b	1.32 b	0.78 c	1.02 b
	Mean	9.65	4.70	8.06	1.14	0.57	0.95
2012	40	1.16 a	1.03 a	1.43 a	0.14 a	0.12 a	0.18 a
	60	1.40 a	1.39 a	2.35 b	0.16 a	0.17 a	0.29 b
	80	2.31 b	2.03 b	2.56 b	0.26 b	0.25 b	0.31 b
	Mean	1.62	1.48	2.11	0.19	0.18	0.26
2013	40	29.83 c	32.60 c	29.70 b	3.70 b	3.94 c	3.70 b
	60	26.10 b	28.03 b	25.95 a	3.06 a	3.31 b	3.24 a
	80	23.73 a	25.17 a	25.96 a	2.88 a	2.44 a	3.37 a
	Mean	26.55	28.60	27.20	3.21	3.23	3.44

*Values in the same column followed by a different letter are significantly different ($p < 0.05$)

Table 7. Weight of thousand seeds of yellow lupine depending on cereal species and percentage of lupine in mixture

Years	Lupine percentage (%)	Weight of 1000 seeds (g)		
2011	100	126.0		
2012	100	121.9		
2013	100	142.3		
		Barley	Wheat	Triticale
2011	40	119.4 a	121.1 a	113.7 a
	60	118.9 a	122.9 a	114.4 a
	80	117.8 a	119.1 a	111.7 a
	Mean	118.7	121.0	113.3
2012	40	117.5 b	118.9 a	122.0 a
	60	114.4 a	121.4 b	122.4 a
	80	113.4 a	125.0 c	122.3 a
	Mean	115.1	121.8	122.2
2013	40	125.6 b	122.8 a	127.4 a
	60	120.0 a	119.4 b	125.2 a
	80	121.7 a	117.5 b	130.1 b
	Mean	122.4	119.9	127.6

*Values in the same column followed by a different letter are significantly different ($p < 0.05$)

Growing yellow lupine in mixtures with cereals, as well as increasing its percentage had a beneficial effect on the number and weight of grains per plant (*Table 8*). In all years of the study, the smallest seed weight in the mixtures was recorded for wheat, while significantly largest, for barley. All species of cereals, grown both in mixtures and in pure stands, produced the smallest weight and number of grains per plant in 2012. Cereals in mixtures tillered slightly better than those grown in pure stands, and the tillering of cereals was positively affected by increasing the percentage of lupine in sowing. Barley grown in mixtures formed a similar number of grains per ear as barley grown in pure stand, while wheat and triticale - slightly higher (*Table 9*). Both, weather during the growing season and the share of components in the mixture, had little impact on the development of this feature, as well as on the height of culms (*Table 10*). The percentage of lupine in the mixture also had a relatively small effect on the thousand grains weight of cereals. Only in 2011, wheat and triticale reacted positively to increasing the percentage of legumes in the mixture. According to Rudnicki and Gałzewski (2007b), the reaction of oats to sowing in the mixture with lupine was relatively weak, and the composition of the mixture affected only productive tillering, and grain yielding of oats. Rudnicki and Kotwica (2007) reported that yellow lupine generally shows little competitive potential against oats, but increasing its percentage in the stand caused an increase in its competitive strength against that cereal.

Table 8. Number and weight of cereals grain per plant depending on cereal species and percentage of lupine in mixture

Years	Lupine percentage (%)	Weight of grain per plant (g)			Number of grain per plant (unit)		
		Barley	Wheat	Triticale	Barley	Wheat	Triticale
2011	0	3.30 b*	2.16 b	2.93 b	72.8 b	61.4 b	69.3 c
2012	0	2.63 a	1.46 a	1.58 a	60.8 a	46.0 a	43.7 a
2013	0	2.96 a	1.58 a	2.23 a	61.2 a	47.4 a	56.8 b
2011	40	3.77 a	1.97 a	2.83 a	73.2 a	54.8 a	66.3 a
	60	4.12 b	3.61 b	3.10 b	81.6 b	94.3 b	73.8 b
	80	4.43 b	4.14 c	3.38 c	83.0 b	100.4 c	76.4 b
	Mean	4.11	3.24	3.10	79.3	83.2	72.2
2012	40	2.37 a	1.87 a	1.86 a	54.5 a	60.1 a	52.0 a
	60	2.95 b	2.03 ab	1.94 a	70.0 b	64.8 b	52.8 a
	80	3.14 b	2.28 b	1.91 a	72.6 b	70.5 c	51.9 a
	Mean	2.82	2.06	1.90	65.7	65.2	52.2
2013	40	2.84 a	2.46 a	2.93 a	64.8 a	73.5 a	74.8 a
	60	3.00 a	2.50 a	3.19 b	69.8 b	74.3 a	81.9 b
	80	2.96 a	2.65 a	3.41 c	67.4 b	77.6 b	89.1 c
	Mean	2.93	2.54	3.18	67.3	75.1	81.9

*Values in the same column followed by a different letter are significantly different ($p < 0.05$)

Table 9. Number of grain per ear and thousand grain weight of cereals depending on cereal species and percentage of lupine in mixture

Years	Lupine percentage (%)	Number of grain per ear (unit)			Wight of 1000 grains (g)		
		Barley	Wheat	Triticale	Barley	Wheat	Triticale
2011	0	16.1 a*	30.4 b	33.5 c	48.2 b	35.2 b	42.3 c
2012	0	16.6 a	26.7 a	24.7 a	43.2 a	31.8 a	36.1 a
2013	0	16.1 a	27.9 a	28.4 b	48.4 b	33.4 ab	39.3 b
2011	40	17.0 a	31.1 a	34.6 a	52.0 a	35.6 a	42.6 a
	60	18.1 a	33.9 b	34.2 a	51.4 a	38.1 b	42.0 a
	80	17.1 a	32.6 ab	35.5 a	52.8 a	40.8 b	44.3 b
	Mean	17.4	32.5	34.8	52.1	38.2	42.9
2012	40	16.0 a	30.1 a	28.9 a	43.4 a	31.1 a	35.8 a
	60	16.8 a	31.0 a	28.7 a	42.2 a	31.4 a	36.7 a
	80	16.5 a	32.4 a	27.5 a	43.3 a	32.4 a	36.8 a
	Mean	16.4	31.2	28.4	42.9	31.5	36.4
2013	40	17.1 b	31.0 a	29.7 a	44.9 a	33.4 a	39.1 a
	60	16.9 b	32.3 a	31.2 a	43.1 a	33.6 a	39.0 a
	80	15.2 a	33.3 a	33.4 b	43.9 a	34.1 a	38.3 a
	Mean	16.4	32.2	31.4	44.0	33.7	38.8

*Values in the same column followed by a different letter are significantly different ($p < 0.05$)

Table 10. The height of cereals culm in mixture with lupine and number of shoot production

Years	Lupine percentage (%)	Height of cereals (cm)			Number of shoot production (unit)		
		Barley	Wheat	Triticale	Barley	Wheat	Triticale
2011	0	57	69	75	4.55	1.95	2.15
2012	0	58	64	75	3.67	1.73	1.87
2013	0	61	64	78	3.80	1.70	2.00
2011	40	57	68	77	4.1	1.70	1.87
	60	57	70	76	4.5	1.90	1.90
	80	58	70	75	4.6	1.90	2.10
	Mean	57 a	69 b	76 b	4.40 b	1.83 a	1.95 a
2012	40	57	62	76	3.40	2.00	1.80
	60	59	63	77	4.17	2.09	1.84
	80	61	62	74	4.37	2.17	1.89
	Mean	59 a	62 a	76 b	3.98 b	2.09 a	1.84 a
2013	40	71	69	78	3.80	2.37	2.52
	60	72	69	79	4.12	2.30	2.63
	80	73	70	80	4.43	2.33	2.67
	Mean	72 a	69 a	79 b	4.12 b	2.33 a	2.61 a

*Values in the same rows followed by a different letter are significantly different ($p < 0.05$)

The grain of spring cereal grown in mixtures with yellow lupine contained more total protein than when it is grown in pure stands (Table 11).

Table 11. Contents of total protein (%) in seeds depending on cereal species and percentage of lupine in mixture

Specification	Cereal			Mean	Lupine			Mean
	2011	2012	2013		2011	2012	2013	
Lupine	-	-	-	-	36.8	40.8	43.4	40.3
Barley – PS*	11.3	11.6	9.9	11.0	-	-	-	-
Mixtures								
40%	11.9	12.5	11.6	12.0	36.6	40.5	43.4	40.2
60%	11.8	12.4	11.8	12.0	36.9	40.2	43.6	40.3
80%	13.5	13.9	12.2	13.2	36.8	39.7	44.4	40.3
Wheat – PS	13.2	13.1	13.2	13.2	-	-	-	-
Mixtures								
40%	13.6	13.7	13.4	13.6	36.9	40.9	43.1	40.3
60%	14.1	14.1	13.5	13.9	36.1	40.1	43.5	39.9
80%	14.2	14.6	13.5	14.1	36.2	40.2	43.8	40.1
Triticale – PS	12.8	13.2	12.7	12.9	-	-	-	-
Mixtures								
40%	13.4	14.1	13.3	13.6	36.2	41.8	43.5	40.5
60%	13.8	14.2	14.0	14.0	36.2	41.2	43.5	40.3
80%	13.4	13.9	14.2	13.8	36.1	41.6	43.7	40.5

*PS – pure sowing

In the year with lower rainfall (2012), cereal grains accumulated slightly more protein than in other years. There was also an increase in the amount of this component in cereal grains in the mixtures with a higher percentage of lupine. Grains of wheat and triticale contained a similar amount of protein, but it was larger than in grains of barley. Cereals only slightly affected the accumulation of total protein by lupine seeds (a similar content); weather conditions were more important. In 2011 lupine seeds contained much less protein. The grains of cereals, grown in mixtures with lupine, contained more crude fibre than the ones from cereals grown in pure stand, while cereals did not affect the accumulation of this component by lupine seeds (*Table 12*). Cereals generally accumulated more crude fibre in 2013, while in the years of 2011 and 2012 there was a tendency to store more fibre in cereal grains with a higher percentage of yellow lupine in mixture. Legume seeds, in turn, contained significantly less crude fibre in dry year of 2012 compared to other years of vegetation.

Table 12. Concentrations of crude fibre (%) in seeds depending on cereal species and percentage of lupine in mixture

Specification	Cereal			Mean	Lupine			Mean
	2011	2012	2013		2011	2012	2013	
Lupine	-	-	-	-	12.9	12.4	12.8	12.7
Barley – PS*	3.57	3.52	4.67	3.92	-	-	-	-
Mixtures								
40%	3.47	3.80	4.80	4.02	13.4	12.3	13.1	12.9
60%	3.61	3.87	4.60	4.03	13.3	12.1	12.3	12.6
80%	3.55	3.96	4.75	4.09	12.4	12.2	13.2	12.6
Wheat – PS	2.25	2.25	2.52	2.34	-	-	-	-
Mixtures								
40%	2.22	2.22	2.74	2.39	13.2	12.4	13.4	13.0
60%	2.34	2.34	2.70	2.46	13.0	12.2	13.2	12.8
80%	2.38	2.58	2.64	2.53	12.8	12.8	13.1	12.9
Triticale – PS	2.19	2.20	2.59	2.33	-	-	-	-
Mixtures								
40%	2.39	2.50	2.74	2.54	13.1	12.5	12.8	12.8
60%	2.31	2.50	2.80	2.54	12.9	12.3	13.2	12.8
80%	2.48	2.45	2.77	2.57	13.0	12.2	13.3	12.8

*PS – pure sowing

Conclusions

1. Yields of the mixtures of spring cereals with yellow lupine, especially with the 80% share of legumes, were lower than that of the cereals grown in pure stands.
2. The yellow lupine-wheat mixture yielded better than that with barley and triticale, regardless of the percentage of components.
3. Increasing the percentage of lupine seeds at sowing resulted in a significant decrease in the level of mixture yields, regardless of the species of cereal.

4. The percentage of lupine seeds in mixture yields was much lower than at the sowing, regardless of the species of cereal, while its average percentage in the yield of the mixture with wheat was much larger than with barley and triticale.

5. Yellow lupine grown in a mixture set a lower number of pods, seeds per pod and per plant, and produced a lower seeds weight compared to the plants grown in pure stands.

6. Growing yellow lupine in a mixture with spring cereals positively affected morphological characteristics of cereals. Increasing the percentage of legume seeds at the sowing caused a better tillering of cereals and producing a higher number and weight of grains per plant.

7. The grain of cereals grown in mixtures with lupine had a higher content of total protein and crude fibre than when they were grown in pure stands. There was no significant impact of the cereal plant on the content of total protein and crude fibre in legume seeds. Weather conditions, especially humidity had a greater impact on the chemical composition of legume seeds.

8. Future research aimed at selection of compatible species and varieties, appropriate plant geometry and temporal arrangement of the various components of mixture under different locations and soil conditions could enhance adoption of legume-cereal mixtures in Europe.

Acknowledgements. This work was supported by the Ministry of Agriculture and Rural Development of Poland under multi-annual program “Improving domestic sources of vegetable protein, their production, trading and use in animal feed”.

REFERENCES

- [1] Büyükburç, U., Karadağ, Y. (2002): The amount of NO-N transferred to soil by legumes, forage and seed yield, and the forage quality of annual legume/triticale mixtures. – Turkish Journal of Agriculture and Forestry 26(5): 281–288.
- [2] Corre-Hellou, G., Dibet, A., Hauggaard-Nielsen, H., Crozat, Y., Gooding, M., Ambus, P., Dahlmann, C., Von Fragstein, P., Pristeri, A., Montie, M., Jensen, E. S. (2011): The competitive ability of pea–barley intercrops against weeds and the interactions with crop productivity and soil N availability. – Field Crops Research 122(3): 264–272.
- [3] Cremer, N. G., Bennett, M. A., Stinner, B. R., Cardina, J., Regnier, E. E. (1996): Mechanism of weed suppression in cover crop-based production systems. – Horticultural Science 31(3): 410–413.
- [4] Doré, T., Makowski, D., Malézieux, E., Munier-Jolain, N., Tchamitchian, M., Tittone, P. (2011): Facing up to the paradigm of ecological intensification in agronomy: Revisiting methods, concepts and knowledge. – European Journal of Agronomy 34(4): 197–210.
- [5] Gałęzewski, L. (2006): Response of yellow lupine on soil moisture in sole crop and in intercrop with oat. – Roczniki AR Poznań 66: 55–65.
- [6] Hassen, A., Talore, D. G., Tesfamariam, E. H., Friend, M. A., Mpanza, T. D. E. (2017): Potential use of forage-legume intercropping technologies to adopt to climate-change impacts on mixed crop-livestock systems in Africa: a review. – Regional Environmental Change 17(6): 1713-1724. DOI: 10.1007/s10113-017-1131-7.
- [7] Hauggaard-Nielsen, H., Jensen, E. S. (2004): Weed management in grain legumes using an intercropping approach. – In: Jacobsen, S.-E., Jensen, C. R., Porter, J. R. (eds.) Book of Proceedings. VIII ESA Congress, European Agriculture in a Global Context, 11–15

- July, 2004, Copenhagen, Denmark, pp. 605–606. Royal Veterinary & Agricultural University, Taastrup.
- [8] Hauggaard-Nielsen, H., Jørgensen, B., Kinane, J., Jensen, E. S. (2008): Grain legume–cereal intercropping: the practical application of diversity, competition and facilitation in arable and organic cropping systems. – *Renewable Agriculture and Food Systems* 23: 3–12.
- [9] Jaranowski, J. K. (1997): New genotype of *Pisum* sp. derived from hybridization of mutants and cultivates. – *Genetica Polonica* 18(4): 337–355.
- [10] Johnston, H. W., Sanderson, J. B., Macleod, J. A. (1978): Cropping mixtures of field peas and cereals in Prince Edward Island. – *Canadian Journal of Plant Science* 58: 421–426.
- [11] Kotwica, K., Rudnicki, F. (2003): Mixtures of spring cereals with legumes on light soil. – *Zeszyty Problemowe Postępów Nauk Rolniczych* 495: 163–170.
- [12] Kotwica, K., Rudnicki, F. (2004): Production effects of growing spring cereal and cereal-and-legume mixtures on good rye complex soil. – *Acta Scientiarum Polonorum Sectio Agriculture* 3(1): 149–156.
- [13] Księżak, J. (2006): Evaluation yields of mixtures pea with spring wheat depending on nitrogen doses. – *Fragmenta Agronomica* 3: 80–93.
- [14] Księżak, J., Magnuszewska, K. (1999): Yielding of pea and cereals mixtures in selected country region. – *Fragmenta Agronomica* 3: 89–96.
- [15] Księżak, J., Staniak, M. (2013): Evaluation of mixtures of blue lupine (*Lupinus angustifolius* L.) with spring cereals grown for seeds in organic farming system. – *Journal of Food Agriculture and Environment* 11(3/4): 1670–1676.
- [16] Lithourgidis, A. S., Vasilakoglou, I. B., Dhima, K. V., Dordas, C. A., Yiakoulaki, M. D. (2006): Forage yield and quality of common vetch mixtures with oat and triticale in two seeding ratios. – *Field Crops Research* 99(2/3): 106–113.
- [17] Niggli, U., Slab, A., Schmid, O., Halberg, N., Schlüter, M. (2008): Vision for an Organic Food and Farming Research Agenda to 2025. Report. – IFOAM EU Group, Brussels and ISOFAR, Bonn.
- [18] Podleśny, J., Podleśna, A. (2010): Effect of drought stress on blue lupine yield grown in pure stand and in mixture with barley. – *Proceedings: The Economic Importance and Biology of Crop Yields Mixed*, 3–5 March, 2010, Poznań, Poland, pp. 68–69.
- [19] Pozdisek, J., Henriksen, B., Løes, A. K., Ponizil, A. (2011): Utilizing legume-cereal intercropping for increasing self-sufficiency on organic farms in feed for monogastric animals. – *Agronomy Research* 9(1/2): 343–356.
- [20] Rojek, S. (1989): Water Requirements of Papilionaceous Plants.. In: Dzieżyc, I. (ed.) *Water Requirements of Crop*. – PWN, Warsaw, Poland.
- [21] Rudnicki, F., Gałęzewski, L. (2007a): Response of oat and yellow lupine to their various participation in intercropping and their productivity in intercrops, part I. Reaction of oat and yellow lupine to intercropping. – *Zeszyty Problemowe Postępów Nauk Rolniczych* 516: 161–170.
- [22] Rudnicki, F., Gałęzewski, L. (2007b): Response of oat and yellow lupine to their various participation in intercropping and their productivity in intercrops, part II. Yielding of intercrops. – *Zeszyty Problemowe Postępów Nauk Rolniczych* 516: 171–179.
- [23] Rudnicki, F., Kotwica, K. (2006): Productivity of lupine-cereal intercrops on rye very good soil complex. – *Proceedings: The Economic Importance and Biology of Crop Yields Mixed*, 11–12 May, 2006, Poznań, Poland, pp. 62–63.
- [24] Rudnicki, F., Kotwica, K. (2007): Competitive interactions between spring cereals and lupin in mixtures and mixture growing production effects on very good rye complex soil. – *Fragmenta Agronomica* 4(96): 145–152.
- [25] Rudnicki, F., Wenda-Piesik, A. (2007): Productivity of pea-cereal intercrops on good rye soil complex. – *Zeszyty Problemowe Postępów Nauk Rolniczych* 516: 181–193.

- [26] Staniak, M., Księżak, J., Bojarszczuk, J. (2012): Estimation of productivity and nutritive value of pea-barley mixtures in organic farming. – *Journal of Food Agriculture and Environment* 10(2): 318–323.
- [27] Staniak, M., Księżak, J., Bojarszczuk, J. (2014): Mixtures of Legumes with Cereals as a Source of Feed for Animals. – In: Pilipavicius, V. (ed.) *Organic Agriculture towards Sustainability*. INTECH, Rijeka, Croatia.
- [28] Szczukowski, S. (1989): Yields and quality of field pea reproduction in mixtures with cereals and in pure cultures. – *Acta Academiae Agriculturae sectio Technicae* 47: 3–41.
- [29] Tofinga, M. T., Snaydon, R. W. (1992): The root of cereals and peas when grown in pure stands and mixtures. – *Plant and Soil* 142: 281–285.
- [30] Watson, C. A., Atkinson, D., Gosling, P., Jackson, L. R., Rayns, F. W. (2002): Managing soil fertility in organic farming system. – *Soil Use and Management* 18: 239–247.

DISTRIBUTION AND SOURCES OF POLYCYCLIC AROMATIC HYDROCARBONS IN MARINE SEDIMENTS OF AREAS AFFECTED BY OIL SPILLS IN BEIBU GULF, CHINA

LU, Z. Q.^{1,2} – KANG, B.¹ – MA, L.^{3*} – ZHAO, X.¹

¹*College of Fisheries, Jimei University, Xiamen 361021, China*

²*Fujian Provincial Key Laboratory of Marine Fishery Resources and Eco-Environment
Xiamen 361021, China*

³*The Third Institute of Oceanography, State Oceanic Administration (SOA)
Xiamen 361005, China*

**Corresponding author*

e-mail: mali@tio.org.cn; phone: +86-59-2219-5335; fax: +86-59-2219-5335

(Received 18th Oct 2017; accepted 12th Feb 2018)

Abstract. Polycyclic aromatic hydrocarbons (PAHs) were analyzed in marine sediments sampled from an area affected by oil spills in Beibu Gulf, China, in order to determine the distribution and potential sources of these PAHs. The total PAHs concentrations presented a range from 11.30 to 141.56 ng/g with a mean value of 42.12 ng/g, which were relatively low compared to other bays around the world. The four-ring PAHs predominated in most sediment samples, accounting for an average of 41.25%. Principal component analyses (PCA) with multiple linear regression analysis (MLR) and positive matrix factorization (PMF) were used for PAHs source apportionment. The two receptor models both gave good correlation coefficients between predicted and observed PAHs concentrations ($R^2 = 0.9982$ to 0.9987). Three and five factors were obtained from PCA-MLR and PMF, respectively. One factor was identified by PCA as contributions from mixed sources of fuel combustion and coke production (51.44%). This factor was differentiated into two factors by PMF as contributions from fuel combustion (20.43%) and coke production (28.99%). Another PCA factor was attributed to combined coal combustion and crude oil pollution (35.23%). PMF also differentiated the factor into two factors, the percentages contributions of which were 23.10% and 13.27%, respectively. Both models gave comparable contributions from wood combustion (13.34% and 14.20%, respectively).

Keywords: PAHs, marine sediments, principal component analyses, positive matrix factorization, Beibu Gulf

Introduction

Beibu Gulf, a shallow marginal sea located in the northwestern South China Sea, has an area of 129,300 km² and an average depth of 38 m. Beibu Gulf is a natural semi-enclosed bay, surrounded by three provinces of China (Guangdong, Hainan and Guangxi) and Vietnam (Zhang et al., 2014; Gu et al., 2015). With the establishment of the Beibu Gulf Economic Rim and ASEAN-China Free Trade Area (ACFTA), Beibu Gulf has now become an essential economic development area in China. On the other hand, the accelerated industrialization and rapid population growth also consequently leads to increasing pollution in this coastal area (Xia et al., 2011), involving heavy metal (Xia et al., 2011; Gan et al., 2013; Gu et al., 2015) and organic pollutants (Zhang et al., 2014; Li et al., 2014, 2015; Kaiser et al., 2016; Ma et al., 2017).

One of the earliest offshore oil fields in China is located in the southwestern Weizhou Island of Beibu Gulf, and petroleum exploration has been conducted extensively in this shallow shelf sea area since the 1970s (Zhang et al., 2015). About

132.5 km long oil and gas pipelines are laid undersea. The main production facilities including platforms and wells produce a total of approximately 16,000 barrels of crude oil per day (Oil and Gas Journal News, 2016). With the rapid economic growth and the expansion of oil exploration in this area, the risk of oil spills during oil exploitation, storage, transportation, and maritime accidents is increasingly high. According to Bulletin of Marine Environmental Status of Guangxi, the oil spill accidents have occurred approximately every year in Beibu Gulf (The Oceanic Administration of Guangxi, 2008-2014). In August 2008, an oil pipeline undersea in Weizhou oil field was broken and more than 1000 t of crude oil were spilled. Almost 2.5 km shoreline of Beibu Gulf was contaminated by the leakage of crude oil.

Studies have shown that many components of crude oil have long persistence in marine sediments, such as polycyclic aromatic hydrocarbons (PAHs) (Short et al., 2004; Liu et al., 2013). PAHs are defined as a group of aromatic hydrocarbons with two or more aromatic rings in linear, angular or clustered arrangements, most of which are toxic, carcinogenic and mutagenic. Therefore, the United States Environmental Protection Agency (USEPA) classified 16 PAHs as priority pollutants in the early 1980s (Ramdine et al., 2012). PAHs are common in the marine environment and originate from different emission sources, some of them natural, but mostly related to anthropogenic activities such as fuel combustion, offshore production and oil spills (Cortazar et al., 2008; Fasano et al., 2016). Generally, the source of PAHs can be categorized as petrogenic, pyrogenic or diagenetic (Fang et al., 2007; Pongpiachan et al., 2015). So far, to our best knowledge, no or few studies have examined the impact of oil resource exploration and exploitation on the PAHs levels in marine sediments of Beibu Gulf.

The objective of the current study was to investigate the occurrence, distribution, and composition of 16 priority PAHs in surface marine sediments of Beibu Gulf, and to quantitatively identify the potential sources of these PAHs using PCA-MLR and PMF models. Results from these two receptor models were assessed and compared to improve source apportionment of PAHs.

Materials and methods

Sample collection

The sampling campaign was carried out in a series of sites of Beibu Gulf (*Fig. 1*). The sampling sites were designated as such to cover the oil spill influence areas. Surface sediments were collected using a stainless steel grab sampler and wrapped immediately into aluminum foil and then stored at -20 °C until laboratory analysis.

PAHs analysis

All the sediment samples were freeze-dried for 24 h in a vacuum freeze drier (Topcon Co., USA) and ground to a fine powder (about 60 mesh). Approximately 5 g of sample were extracted with a mixture of n-hexane : acetone (1:1) in a microwave extraction system (CEM Co., USA) by a method developed and verified by the authors (Zhang et al., 2004; Lu et al., 2005). The extract was collected and transferred to a 250 ml Erlenmeyer flask. After mixed with 1 g of activated copper powder to remove sulfides, the extract was filtered through a funnel filled with anhydrous sodium sulfate (dried at 440 °C for 4 h), and then reduced to 2 ml by rotary evaporation. The

concentrated extracts flowed through a glass column filled from top to bottom with 9 g neutral aluminum oxide, 18 g silica gel and 2 g anhydrous sodium sulfate. The column was then eluted with 150 ml mixture of n-hexane : pentane (1:1). The eluent was reduced by rotary evaporation to a final volume of 2 ml and sealed in an amber vial for later GC-MS analysis.

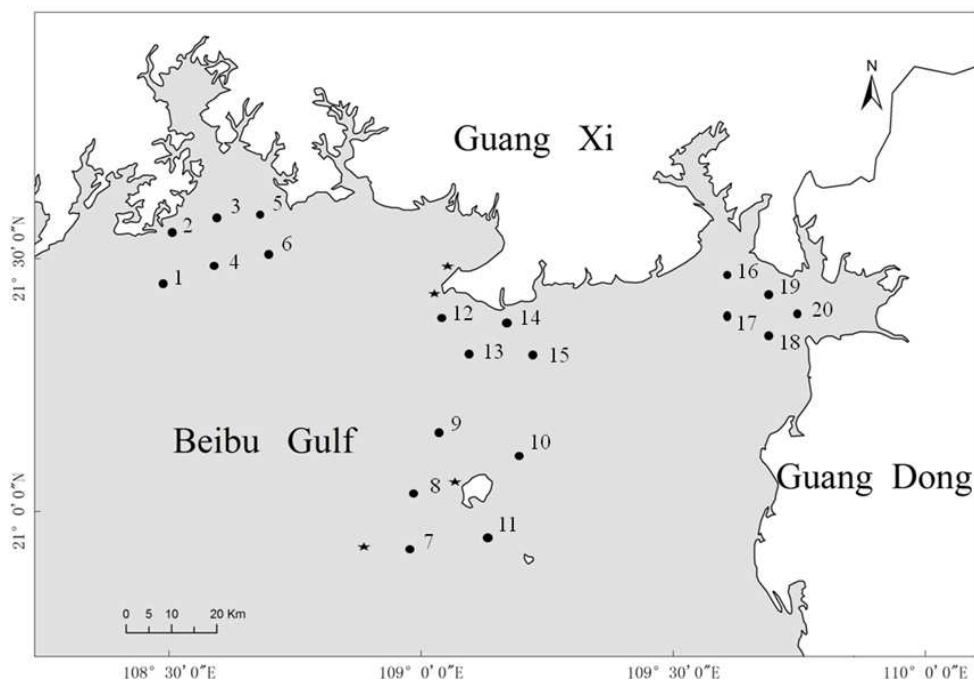


Figure 1. Sampling sites of marine sediments in Beibu Gulf. The black stars indicate the places where oil spill ever occurred during 2008-2014

The PAHs analysis was conducted by a Hewlett-Packard 6890N/5973 gas chromatography coupled with a mass spectrometer (GC/MS). The instrument was operated in selected ion monitoring mode and a 30 m × 0.25 mm (i.d.) HP-5MS capillary column was used (Agilent Co., USA). The column temperature was programmed from an initial 60 to 150 °C at 15 °C /min, from 150 to 220 °C at 5 °C /min, from 220 to 300 °C at 10 °C /min. The final temperature was held for 10 min. 16 PAHs concentrations were determined in all sediment samples including naphthalene (Nap), acenaphthylene (Acpy), acenaphthene (Acp), fluorine (Flu), phenanthrene (Phe), anthracene (Ant), fluoranthene (Flt), pyrene (Pyr), benzo(a)anthracene (BaA), chrysene (Chr), benzo(b)fluoranthene (BbF), benzo(k)fluoranthene (BkF), benzo(a)pyrene (BaP), indeno[1,2,3,cd]pyrene (IcdP), dibenzo(ah)anthracene (DahA), and benzo(ghi)perylene (BghiP).

The standard mixture of 16 PAHs, deuterated PAH surrogate (acenaphthene-d₁₀, phenanthrene-d₁₀, chrysene-d₁₂ and perylene-d₁₂) and internal standard (pyrene-d₁₀) were all obtained from Supelco, Inc. (Supelco, USA). In this study, method blanks, spiked blanks and sample duplicates were all routinely run with field samples. Mean recoveries of acenaphthene-d₁₀, phenanthrene-d₁₀, chrysene-d₁₂ and perylene-d₁₂ were 89.6±9.5%, 97.6±8.7%, 90.3±8.1% and 92.1±7.9%, respectively. The recoveries of spiked samples ranged from 83.8% to 103.9%. All reported concentrations were given on a dry weight basis and calibrated using surrogate recoveries.

Source appointment models

PCA-MLR and PMF, conventional factor analysis receptor models, were both used for source identification of PAHs in sediments by several investigators (Sofowote et al., 2008; Cao et al., 2011; Zhang, 2012; Feng et al., 2014). Before the run of model with the original data, the undetectable values were replaced with random numbers between zero and the limit of detection (Zhang et al., 2008; Liu et al., 2009).

In PCA-MLR model, factor loading and score matrices are calculated by input a set of PAHs concentrations data. The equation (Eq. 1) is given below:

$$X = T \times L \quad (\text{Eq.1})$$

where X is the PAHs concentration matrix, T represents the factor score matrix and L represents the factor loading matrix (Zhang et al., 2012). The resulting factor loading matrix can be used to identify the possible source categories. MLR was performed on the factor scores of PCAs for each sample to calculate the percent contribution of the major sources (Larsen and Baker, 2003; Sofowote et al., 2008). The PAH concentrations were Kaiser-normalized and varimax rotation was used as the referred transformation so that loadings values could be clustered around 1 and 0, making them more physically interpretable. PCA-MLR was performed in this study using SPSS 22.0 software for windows (SPSS Inc., Chicago, IL, USA).

PMF is also a multivariate factor analysis method that calculates source profile and contribution (Paatero, 1997; Zhang et al., 2012). The purpose of the PMF model is to factor the initial $n \times m$ data matrix X (n : number of samples; m : number of species) into the left and right factor matrices G ($n \times p$) and F ($p \times m$), as well as the 'residual matrix' E ($n \times m$) firstly, as follows (Eq. 2):

$$X = GF + E \quad (\text{Eq.2})$$

In this equation, G is the source contribution matrix, F is the source profile matrix and E is the residual error matrix of the elements e_{ij} . Elements of the residual matrix are defined as:

$$e_{ij} = x_{ij} - \sum_{k=1}^p g_{ik} f_{kj} \quad (\text{Eq.3})$$

$$Q = \sum_{i=1}^n \sum_{j=1}^m \left(\frac{e_{ij}}{s_{ij}} \right)^2 \quad (\text{Eq.4})$$

where g_{ik} is the k_{th} source's contribution to sample i , and f_{kj} is the j_{th} element's concentration in source k , s_{ij} represents the uncertainty in the j_{th} species for sample i (Eq.3).

Next, an uncertainty estimate and the residual matrix elements are used to calculate a minimum Q value (Eq.4). The convergent run with the Q value closest to the target Q value was used as the base run. Then 100 bootstrap runs were performed to assess the uncertainty of the factor loadings and factor scores in the base run. PMF analysis in this study was run with the US EPA PMF 3.0 model (US EPA, 2014).

Results and discussion

PAHs concentrations and composition

The total PAHs concentration in marine sediments from Beibu Gulf presented a range of values from 11.30 to 141.56 ng/g, with a mean of 42.12 ng/g (Table 1). Flu was not detected in all samples. The composition patterns of PAHs were shown in Figure 2. The concentration of PAHs in sediment samples was in the range from 3.97 to 15.56 ng/g for 2-ring PAHs, from 1.68 to 20.75 ng/g for 3-ring PAHs, from 4.34 to 62.92 ng/g for 4-ring PAHs, from 0.26 to 23.21 ng/g for 5-ring PAHs, and from 0.46 to 22.81 ng/g for 6-ring PAHs. The mean concentrations were 6.61 ng/g for 2-ring PAHs, 6.49 ng/g for 3-ring PAHs, 17.35 ng/g for 4-ring PAHs, 6.01 ng/g for 5-ring PAHs, and 5.66 ng/g for 6-ring PAHs. 4-ring PAHs were abundant at most sampling sites, accounting for 41.25% of PAHs in marine sediments.

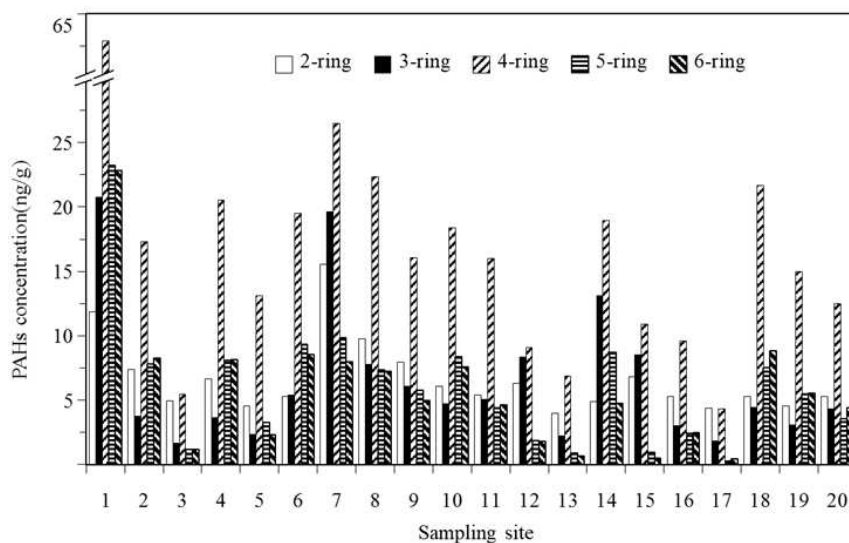


Figure 2. Concentration of 2-, 3-, 4-, 5-, 6-ring PAHs in marine sediments of Beibu Gulf

A preliminary comparison with published data conducted in other bays in China and around the world showed that PAHs concentrations in the marine sediments from Beibu Gulf were at the lower end of the global range. The mean concentration of total PAHs was comparable to the levels in Qinzhou Bay (Li et al., 2015), South China Sea (Liu et al., 2012; Kaiser et al., 2016), the Gulf of Thailand (Boonyatumanond et al., 2006) and Chesapeake Bay (Foster and Wright, 1988), and was lower than those in most other bays in China and around the world. There was no evidence that the PAH levels were significantly increased by oil spill accidents in this area. It could be seen from Figure 3 that a positive relationship was found between total PAH concentrations and total organic carbon (TOC) content ($r = 0.644$). The similar correlations had been reported by many researchers, and indicated that TOC was a crucial factor for determining the sorption and sequestration of PAHs on sediment (Wang et al., 2001; Sun et al., 2009; Huang et al., 2012). The low concentrations of PAHs in sediments might also be due to low TOC contents (0.17-1.23%, mean 0.56%). It was believed that the environmental fate and behavior of hydrophobic organic compounds was ultimately determined by the physico-chemical properties of each compound and sediment.

Table 1. Concentrations of individual PAHs (ng/g) and TOC (%) in marine sediments of Beibu Gulf

Site	Nap	Acpy	Acp	Phe	Ant	Flt	Pyr	BaA	Chr	BbF	BkF	BaP	IcdP	DahA	BghiP	ΣPAHs	TOC
1	11.87	0.35	ND	19.99	0.41	31.85	20.74	7.99	2.34	9.65	5.91	3.60	10.33	4.06	12.48	141.56	1.14
2	7.36	0.20	ND	3.23	0.33	6.50	6.51	2.99	1.28	4.86	ND	1.68	3.73	1.26	4.50	44.44	0.47
3	4.94	0.12	ND	1.44	0.11	1.70	2.78	0.78	0.21	0.48	0.38	0.29	0.49	ND	0.72	14.43	0.36
4	6.62	0.18	ND	3.14	0.35	8.99	7.21	3.23	1.09	3.80	1.59	1.52	3.77	1.17	4.41	47.06	0.62
5	4.55	0.12	ND	2.06	0.18	5.55	4.91	1.88	0.75	1.47	1.00	0.82	0.91	ND	1.43	25.62	0.60
6	5.31	0.16	ND	4.91	0.36	8.36	6.81	3.23	1.09	4.30	2.27	1.57	3.82	1.20	4.74	48.12	0.51
7	15.56	0.67	2.94	15.45	0.55	8.96	13.16	3.42	0.97	4.52	3.02	1.12	3.76	1.17	4.24	79.49	0.92
8	9.76	0.31	ND	6.99	0.46	8.96	9.73	2.95	0.73	4.04	2.36	0.94	3.17	ND	4.05	54.45	0.79
9	7.96	0.22	ND	5.58	0.29	6.14	7.37	1.99	0.54	2.59	1.91	0.64	2.22	0.61	2.78	40.84	0.52
10	6.29	0.38	ND	7.50	0.46	2.50	5.13	1.04	0.45	0.74	0.62	0.49	0.74	ND	1.03	27.37	0.27
11	3.97	0.16	ND	1.95	0.14	1.82	4.31	0.55	0.21	0.21	0.46	0.21	0.27	ND	0.42	14.68	0.16
12	5.39	0.23	ND	4.40	0.40	7.68	5.44	2.30	0.59	2.53	1.26	0.64	2.02	ND	2.63	35.50	0.78
13	4.89	0.43	2.67	9.27	0.76	7.90	5.16	3.73	2.18	3.18	1.92	2.25	2.25	1.36	2.53	50.47	0.29
14	6.07	0.23	ND	4.02	0.46	8.03	5.51	4.10	0.77	3.75	2.23	0.95	3.56	1.42	4.03	45.12	0.85
15	6.81	0.13	ND	8.37	ND	3.36	6.93	0.49	0.10	ND	0.94	ND	ND	ND	0.49	27.63	0.27
16	5.31	0.19	ND	2.62	0.22	3.81	4.04	1.27	0.49	1.13	0.69	0.59	1.07	ND	1.40	22.83	0.25
17	4.39	0.12	ND	1.67	0.06	1.56	2.33	0.32	0.13	0.16	ND	0.10	0.15	ND	0.31	11.30	0.17
18	5.28	0.20	ND	3.96	0.28	10.11	7.82	2.84	0.92	2.90	2.16	1.43	4.18	1.05	4.67	47.79	0.46
19	4.58	0.21	ND	2.67	0.20	6.84	5.58	1.88	0.66	2.24	1.39	0.99	2.50	0.86	3.05	33.63	1.23
20	5.29	0.20	ND	3.90	0.23	4.39	5.73	1.86	0.50	1.38	0.94	0.74	1.98	0.52	2.44	30.09	0.48

* ND: not detected (below the detection limit)

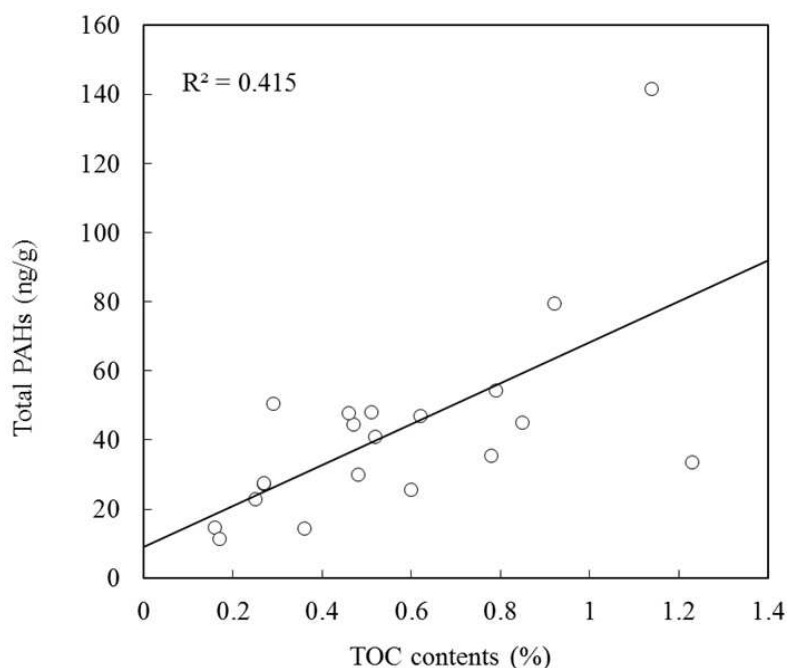


Figure 3. Relation between total PAHs concentrations and TOC contents in marine sediments of Beibu Gulf

Sources identification by isomer ratios

Each source generated a characteristic PAH pattern, therefore, analysis of the composition of these mixtures allows assessment of PAH origins (Oros and Ross, 2005). Diagnostic ratios provided only qualitative information about the contribution of various sources with regards to PAH contaminations (Wang et al., 2010). In the present study, the isomer ratios of Flt/(Flt+Pyr) and BaA/(BaA+Chr) were calculated to classify the possible sources of PAHs. For Flt/(Flt+Pyr) and BaA/(BaA+Chr), the ratios below 0.4 and 0.2 suggest petrogenic origins, whereas the ratios above 0.5 and 0.35 indicate combustion origins (Yunker et al., 2002; Tobiszewski and Namieśnik, 2012). The ratio of Flt/(Flt+Pyr) ranged from 0.30 to 0.61 and the ratio of BaA/(BaA+Chr) ranged from 0.63 to 0.84 (Fig. 4). The plot of the two ratios suggested primary contributions from mixed combustion sources. In general, a quantitative proportion of sources of PAHs cannot be given by molecular diagnostic ratios. Therefore, two mathematical models will be used for PAH source appointment in the following sections.

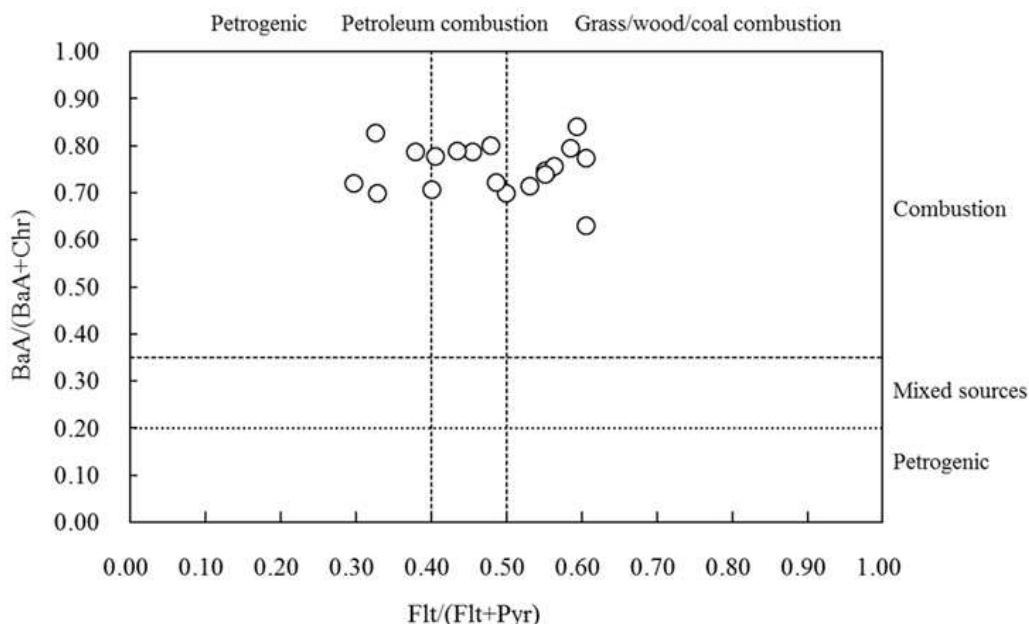


Figure 4. Source analysis of PAHs through plot for the ratios of Flt/(Flt+Pyr) vs. BaA/(BaA+Chr)

Source apportionments by PCA-MLR

In most cases, it was necessary for the control of PAH contamination to obtain more detailed information about the source apportionment (Li et al., 2012). PCA with MLR was considered to be a more suitable tool for further determining the possible PAH sources apportionment, where the model used the linear transformation to choose principal components and represented the total variability of the original PAHs data in a minimum number of factors. (Larsen and Baker, 2003; Sofowote et al., 2008; Li et al., 2012). In this study, PCA resulted in three factors accounting for 93.8% of the total variability. The rotated component matrix of PAHs in marine sediments from Beibu Gulf was presented in Table 2.

The first factor, responsible for 54.0% of the total variance, was heavily weighted by high-ring PAHs including BaP, BghiP, IcdP, BaA, DahA, Flt, BbF, Chr and BkF. IcdP and BghiP were related to the diesel and gasoline engines emission, respectively (Liao et al., 2011). Preponderance of BaP, BaA, BbF, BkF and Chr had been related to coke production emissions (Zhang et al., 2012). So, Factor 1 appeared to be related to a combined source of fuel (gasoline and diesel) combustion and coke production. The second factor, contributing to 20.7% of the total variability, was predominately composed of Nap, Phe and Pyr. Nap constituted a significant fraction of crude oils and petroleum products (Yang, 2000). Phe and Pyr were predominant in coal combustion generated PAHs. Thus, it was tentatively inferred that this factor reflected the complex origins of coal combustion and crude oil pollution. The third factor, accounting for 19.1% of the total variation, was highly loaded on Acpy, Acp and Ant. Acpy and Ant predominated PAH compounds emitted during wood combustion (Khalili et al., 1995).

Table 2. The rotated component matrix of PAHs in marine sediments of Beibu Gulf

	Component ^a		
	PC1	PC2	PC3
Nap	0.255	0.870	0.322
Acpy	0.127	0.543	0.803
Acp	-0.044	0.225	0.911
Phe	0.477	0.727	0.377
Ant	0.411	0.032	0.833
Flt	0.898	0.402	0.007
Pyr	0.677	0.719	0.084
Chr	0.853	-0.001	0.478
BaA	0.921	0.267	0.232
BbF	0.892	0.337	0.180
BkF	0.756	0.538	0.156
BaP	0.939	0.079	0.284
IcdP	0.922	0.350	0.049
DahA	0.912	0.249	0.132
BghiP	0.923	0.365	0.012
Percent of variance	54.03%	20.72%	19.08%

^a Rotation method: Varimax with Kaiser normalization

^b Loading values exceeding 0.7 are highlighted in bold face

Hence, Factor 3 was reflective of PAH source from wood combustion.

MLR analysis of the PCA factor score was performed to obtain the mass distribution of the three sources to the total PAH load in each sediment samples. The coefficients (B_i) of three factor scores were determined by the MLR analysis with a stipulated minimum 95% confidence limit. The MLR equation (*Eq.5*) for determining the standard deviate of the SumPAH values was:

$$\hat{Z}_{\text{SumPAH}} = 0.806t_1 + 0.552t_2 + 0.209t_3 \quad (\text{Eq.5})$$

The percentage contributions to the mean of the three factors could be calculated as follows (Eq.6):

$$i(\%) = 100 \times (B_i / \sum B_i) \quad (\text{Eq.6})$$

The percentages contributions were 51.44% for t_1 (attributed to mixed source of fuel combustion and coke production), 35.23% for t_2 (coal combustion and crude oil pollution), and 13.34% for t_3 (wood combustion), respectively. According to the isomer ratios analysis above, a combined combustion source was the primary source of the PAHs in most of samples. Thus, the two analyses of PAH sources were in good agreement.

Source apportionments by PMF

The five factors solution provided the most reasonable explanation of the source profile. The PMF model generated the following equation (Eq.7):

$$Y_{\text{SumPAH}} = 9.401G_1 + 5.782G_2 + 11.753G_3 + 8.317G_4 + 5.394G_5 \quad (\text{Eq.7})$$

The PMF factor profiles (F matrix) of PAHs from Beibu Gulf marine sediments were listed in *Table 3*. Factor 1 accounted for 23.10% of all factors contribution, and was heavily loaded on Phe and Pyr, also received moderate loading from Flt. Phe, Flt and Pyr were predominant in coal combustion signals. So Factor 1 was interpreted as reflecting the contribution of coal combustion. Factor 2 was dominated by Acpy, Acp and Ant. Acpy and Ant was the dominant PAHs in the wood combustion. Thus, Factor 2 notionally reflected wood combustion. The percentage contribution of this factor was 14.20%. Factor 3 accounted for 28.99% of all factors contribution, was highly loaded on Flt, Chr, BaA, BkF, BaP and DahA. Preponderance of BaP, BaA, BbF, BkF and Chr had been related to coke oven emissions. Thus, Factor 3 was identified as a coke production source. Factor 4 was classified as fuel combustion emission based on loadings of BkF, IcdP and BghiP. The higher level of BkF relative to other PAHs was indicative of diesel engine emission; IcdP and BghiP had also been related to diesel and gasoline engine emissions (Liu et al., 2009). Therefore, Factor 4 was selected to represent the fuel combustion, and the percentage contribution was 20.43%. Factor 5 was only highly loaded on Nap and percentage contribution was 13.27%. Nap was believed as a major fraction of crude oils and suggested that this factor was indicative of crude oil pollution.

Comparison of two receptor models

There was an excellent correlation between measured and predicted total PAHs values by the receptor models ($R^2 = 0.9982$ to 0.9987), indicating that most predicted total PAH concentrations were close to the measured concentrations (*Fig. 5*). These two factor analysis methods were very effective for quantifying source contributions and differentiating the source profiles. Before running the analysis, no information about the number, characteristics or types of sources impacting the environment was needed to input the models.

Table 3. PMF factor profiles of PAHs in marine sediments from Beibu Gulf

Compound	Factor 1	Factor 2	Factor 3	Factor 4	Factor 5
Nap	2.364	1.245	0.000	0.132	2.863
Acpy	0.063	0.107	0.006	0.000	0.037
Acp	0.037	0.495	0.000	0.000	0.000
Phe	2.610	1.650	1.264	0.000	0.125
Ant	0.005	0.184	0.047	0.000	0.047
Flt	1.342	0.183	3.231	1.318	1.125
Pyr	2.791	0.108	1.251	0.517	2.213
Chr	0.000	0.235	0.293	0.195	0.006
BaA	0.000	0.525	0.912	0.801	0.133
BbF	0.030	0.399	0.926	1.299	0.069
BkF	0.336	0.211	0.642	0.175	0.189
BaP	0.037	0.154	0.395	0.365	0.000
IcdP	0.207	0.041	1.004	1.208	0.094
DahA	0.091	0.085	0.410	0.271	0.000
BghiP	0.312	0.000	1.195	1.354	0.238
Estimated source	coke	Wood	Coal	fuel	oil
Percentage contribution	28.99%	14.20%	23.10%	20.43%	13.27%

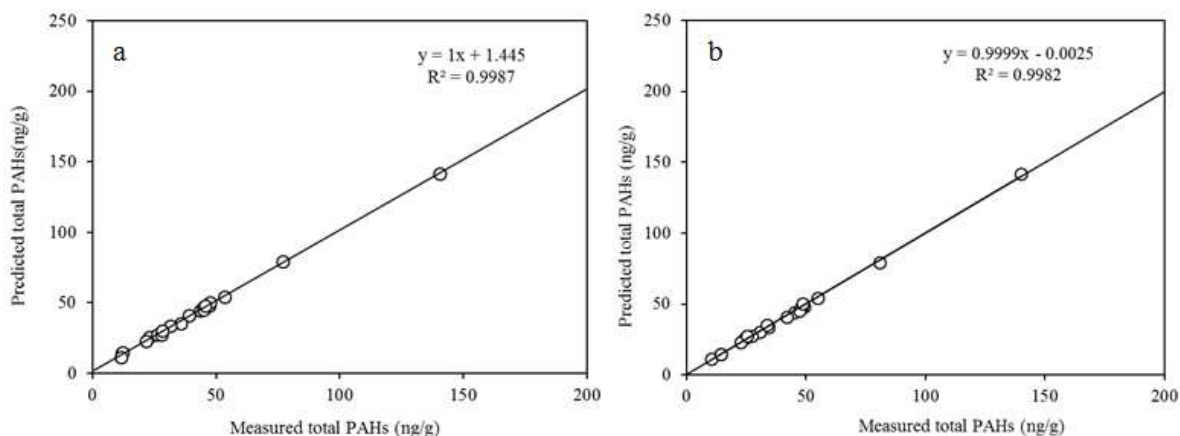


Figure 5. Correlation between measured and predicted total PAHs values by PMF (a) and PCA-MLR (b)

Furthermore, both receptor models gave comparable results for PAH source contributions. The analysis results of PMF for source apportionment were more comprehensive and interpretable than PCA-MLR. Comparable mean contributions from wood combustion sources to marine sediments of Beibu Gulf were obtained from PCA-MLR and PMF (13.34% vs 14.20%). The PAH contribution attributed to a mixed combustion source classified by PCA-MLR (51.44%) was close to the sum of coke

production and fuel combustion (49.42%), which were differentiated as two separate factors by PMF (28.99% and 20.43%, respectively). The second PCA factor (35.23%) was attributed to a mixed source of coal combustion and crude oil pollution, which was also distinguished by PMF (23.10% and 13.27%, respectively).

Conclusions

Marine sediments of Beibu Gulf contained low levels of anthropogenic PAHs compared to other bays worldwide. This indicated that PAHs in sediment resulted from historical accumulation of these compounds and were not significantly increased by oil spill accidents. The results from two receptor models (PCA-MLR and PMF) were compared to quantitatively identify that PAH sources were mainly originated from coke production (28.99%), coal, fuel and wood combustion (23.10%, 20.43% and 13.34–14.20%) as well as crude oil pollution (13.27%). Results obtained in this study could be helpful to evaluate PAH contamination levels in surface sediments of Beibu Gulf, and to provide useful information for protecting marine resources and human health in this region. Further assessment of the potential ecological risks associated with PAHs in seawater, sediments and marine organisms is necessary. Long-term monitoring should be undertaken in order to detect new contamination from the oil exploration and exploitation activities in this area.

Acknowledgements. This work was supported by the Nature Science Foundation of Fujian (No. 2015J01169), the commonweal project from the State Oceanic Administration of China (No.201505027) and the open project from Fujian Provincial Key Laboratory of Marine Fishery Resources and Eco-environment.

REFERENCES

- [1] Boonyatumanond, R., Wattayakorn, G., Togo, A., Takada, H. (2006): Distribution and origins of polycyclic aromatic hydrocarbons (PAHs) in riverine, estuarine, and marine sediments in Thailand. – *Marine Pollution Bulletin* 52(8): 942–956.
- [2] Cao, Q., Wang, H., Chen, G. (2011): Source apportionment of PAHs using two mathematical models for mangrove sediments in Shantou coastal zone, China. – *Estuaries and Coasts* 34(5): 950–960.
- [3] Cortazar, E., Bartolomé, L., Arrasate, S., Usobiaga, A., Raposo, J. C., Zuloaga, O., Etxebarria, N. (2008): Distribution and bioaccumulation of PAHs in the UNESCO protected natural reserve of Urdaibai, Bay of Biscay. – *Chemosphere* 72(10): 1467–1474.
- [4] Fang, M. D., Hsieh, P. C., Ko, F. C., Baker, J. E., Lee, C. L. (2007): Sources and distribution of polycyclic aromatic hydrocarbons in the sediments of Kaoping river and submarine canyon system, Taiwan. – *Marine Pollution Bulletin* 54(8): 1179–1189.
- [5] Fasano, E., Yebra-Pimentel, I., Martínez-Carballo, E., Simal-Gándara, J. (2016): Profiling, distribution and levels of carcinogenic polycyclic aromatic hydrocarbons in traditional smoked plant and animal foods. – *Food Control* 59: 581–590.
- [6] Feng, J., Li, X., Guo, W., Liu, S., Ren, X., Sun, J. (2014): Potential source apportionment of polycyclic aromatic hydrocarbons in surface sediments from the middle and lower reaches of the Yellow River, China. – *Environmental Science and Pollution Research* 21(19): 11447–11456.

- [7] Foster, G. D., Wright, D. A. (1988): Unsubstituted polynuclear aromatic hydrocarbons in sediments, clams, and clam worms from Chesapeake Bay. – *Marine Pollution Bulletin* 19(9): 459–465.
- [8] Gan, H., Lin, J., Liang, K., Xia, Z. (2013): Selected trace metals (As, Cd and Hg) distribution and contamination in the coastal wetland sediment of the northern Beibu Gulf, South China Sea. – *Marine Pollution Bulletin* 66(1): 252–258.
- [9] Gu, Y. G., Lin, Q., Yu, Z. L., Wang, X. N., Ke, C. L., Ning, J. J. (2015): Speciation and risk of heavy metals in sediments and human health implications of heavy metals in edible nekton in Beibu Gulf, China: A case study of Qinzhou Bay. – *Marine Pollution Bulletin* 101(2): 852–859.
- [10] Huang, W., Wang, Z., Yan, W. (2012): Distribution and sources of polycyclic aromatic hydrocarbons (PAHs) in sediments from Zhanjiang Bay and Leizhou Bay, South China. – *Marine Pollution Bulletin* 64(9): 1962–1969.
- [11] Kaiser, D., Schulz-Bull, D. E., Waniek, J. J. (2016): Profiles and inventories of organic pollutants in sediments from the central Beibu Gulf and its coastal mangroves. – *Chemosphere* 153: 39–47.
- [12] Khalili, N. R., Scheff, P. A., Holsen, T. M. (1995): PAH source fingerprints for coke ovens, diesel and, gasoline engines, highway tunnels, and wood combustion emissions. – *Atmospheric Environment* 29(4): 533–542.
- [13] Larsen, R. K., Baker, J. E. (2003): Source apportionment of polycyclic aromatic hydrocarbons in the urban atmosphere: a comparison of three methods. – *Environmental Science & Technology* 37(9): 1873–1881.
- [14] Li, B., Feng, C., Li, X., Chen, Y., Niu, J., Shen, Z. (2012): Spatial distribution and source apportionment of PAHs in surficial sediments of the Yangtze Estuary, China. – *Marine Pollution Bulletin* 64(3): 636–643.
- [15] Li, P., Wang, Y., Huang, W., Yao, H., Xue, B., Xu, Y. (2014): Sixty-year sedimentary record of DDTs, HCHs, CHLs and endosulfan from emerging development gulfs: a case study in the Beibu Gulf, South China Sea. – *Bulletin of Environmental Contamination and Toxicology* 92(1): 23–29.
- [16] Li, P., Xue, R., Wang, Y., Zhang, R., Zhang, G. (2015): Influence of anthropogenic activities on PAHs in sediments in a significant gulf of low-latitude developing regions, the Beibu Gulf, South China Sea: distribution, sources, inventory and probability risk. – *Marine Pollution Bulletin* 90(1): 218–226.
- [17] Liao, S. L., Lang, Y. H., Wang, Y. S. (2011): Distribution and sources of PAHs in soil from Liaohe Estuarine Wetland. – *Environmental Science* 32(4): 1094–1100 (in Chinese).
- [18] Liu, L. Y., Wang, J. Z., Wei, G. L., Guan, Y. F., Zeng, E. Y. (2012): Polycyclic aromatic hydrocarbons (PAHs) in continental shelf sediment of China: implications for anthropogenic influences on coastal marine environment. – *Environmental Pollution* 167: 155–162.
- [19] Liu, X., Jia, H., Wang, L., Qi, H., Ma, W., Hong, W., Guo, J., Yang, M., Sun, Ye., Li, Y. F. (2013): Characterization of polycyclic aromatic hydrocarbons in concurrently monitored surface seawater and sediment along Dalian coast after oil spill. – *Ecotoxicology and Environmental Safety* 90: 151–156.
- [20] Liu, Y., Chen, L., Huang, Q. H., Li, W. Y., Tang, Y. J., Zhao, J. F. (2009): Source apportionment of polycyclic aromatic hydrocarbons (PAHs) in surface sediments of the Huangpu River, Shanghai, China. – *Science of the Total Environment* 407(8): 2931–2938.
- [21] Lu, Z. Q., Zheng, W. J., Ma, L. (2005): Bioconcentration of polycyclic aromatic hydrocarbons in roots of three mangrove species in Jiulong River Estuary. – *Journal of Environmental Sciences* 17(2): 285–289.
- [22] Ma, L., Lu, Z. Q., Zhang, Y. B., Yang, S. Y. (2017): Distribution and sources apportionment of polycyclic aromatic hydrocarbons in the edible bivalves and

- sipunculida from coastal areas of Beibu Gulf, China. – *Applied Ecology & Environmental Research* 15(3): 1211–1225.
- [23] Oil and Gas Journal News. (2016): CNOOC begins production from two more Beibu Gulf fields. – <http://www.ogj.com/articles/2016/02/cnooc-begins-production-from-two-more-beibu-gulf-fields.html>.
- [24] Oros, D. R., Ross, J. R. (2005): Polycyclic aromatic hydrocarbons in bivalves from the San Francisco estuary: spatial distributions, temporal trends, and sources (1993–2001). – *Marine Environmental Research* 60(4): 466–488.
- [25] Paatero, P. (1997): Least squares formulation of robust non-negative factor analysis. – *Chemometrics and Intelligent Laboratory Systems* 37(1): 23–35.
- [26] Pongpiachan, S., Hattayanone, M., Choochuay, C., Mekmok, R., Wuttijak, N., Ketranakul, A. (2015): Enhanced PM₁₀ bounded PAHs from shipping emissions. – *Atmospheric Environment* 108: 13–19.
- [27] Ramdine, G., Fichet, D., Louis, M., Lemoine, S. (2012): Polycyclic aromatic hydrocarbons (PAHs) in surface sediment and oysters from mangrove of Guadeloupe: Levels, bioavailability, and effects. – *Ecotoxicology and Environmental Safety* 79: 80–89.
- [28] Short, J. W., Lindeberg, M. R., Harris, P. M., Maselko, J. M., Pella, J. J., Rice, S. D. (2004): Estimate of oil persisting on the beaches of Prince William Sound 12 years after the Exxon Valdez oil spill. – *Environmental Science & Technology* 38(1): 19–25.
- [29] Sofowote, U. M., McCarry, B. E., Marvin, C. H. (2008): Source apportionment of PAH in Hamilton Harbour suspended sediments: comparison of two factor analysis methods. – *Environmental Science & Technology* 42(16): 6007–6014.
- [30] Sun, J. H., Wang, G. L., Chai, Y., Zhang, G., Li, J., Feng, J. (2009): Distribution of polycyclic aromatic hydrocarbons (PAHs) in Henan reach of the Yellow River, Middle China. – *Ecotoxicology and Environmental Safety* 72(5): 1614–1624.
- [31] The Oceanic Administration of Guangxi. (2008–2014): Bulletin of Marine Environmental Status of Guangxi (2008–2014). – http://www.gxoa.gov.cn/gxhyj_haiyanggongbao.
- [32] Tobiszewski, M., Namieśnik, J. (2012): PAH diagnostic ratios for the identification of pollution emission sources. – *Environmental Pollution* 162: 110–119.
- [33] US EPA (2014): EPA positive matrix factorization (PMF) 5.0 fundamentals & user guide. – <https://www.epa.gov/air-research/epa-positive-matrix-factorization-50-fundamentals-and-user-guide>.
- [34] Wang, H. S., Cheng, Z., Liang, P., Shao, D. D., Kang, Y., Wu, S. C., Wong, C. K. C., Wong, M. H. (2010): Characterization of PAHs in surface sediments of aquaculture farms around the Pearl River Delta. – *Ecotoxicology and Environmental Safety* 73(5): 900–906.
- [35] Wang, X. C., Zhang, Y. X., Chen, R. F. (2001): Distribution and partitioning of polycyclic aromatic hydrocarbons (PAHs) in different size fractions in sediments from Boston Harbor, United States. – *Marine Pollution Bulletin* 42: 1139–1149.
- [36] Xia, P., Meng, X. W., Yin, P., Cao, Z. M., Wang, X. Q. (2011): Eighty-year sedimentary record of heavy metal inputs in the intertidal sediments from the Nanliu River estuary, Beibu Gulf of South China Sea. – *Environmental Pollution* 159: 92–99.
- [37] Yang, G. P. (2000): Polycyclic aromatic hydrocarbons in the sediments of the South China Sea. – *Environmental Pollution* 108(2): 163–171.
- [38] Yunker, M. B., Macdonald, R. W., Vingarzan, R., Mitchell, R. H., Goyette, D., Sylvestre, S. (2002): PAHs in the Fraser River basin: a critical appraisal of PAH ratios as indicators of PAH source and composition. – *Organic Geochemistry* 33(4): 489–515.
- [39] Zhang, G., Jin, L., Lan, L., Zhao, Z. (2015): Analysis of the orderly distribution of oil and gas fields in China based on the theory of co-control of source and heat. – *Natural Gas Industry B* 2(1): 49–76.
- [40] Zhang, J., Cai, L., Yuan, D., Chen, M. (2004): Distribution and sources of polynuclear aromatic hydrocarbons in mangrove surficial sediments of Deep Bay, China. – *Marine Pollution Bulletin* 49(5): 479–486.

- [41] Zhang, J., Li, Y., Wang, Y., Zhang, Y., Zhang, D., Zhang, R., Zhang, G. (2014): Spatial distribution and ecological risk of polychlorinated biphenyls in sediments from Qinzhou Bay, Beibu Gulf of South China. – *Marine Pollution Bulletin* 80(1): 338–343.
- [42] Zhang, W., Zhang, S., Wan, C., Yue, D., Ye, Y., Wang, X. (2008): Source diagnostics of polycyclic aromatic hydrocarbons in urban road runoff, dust, rain and canopy throughfall. – *Environmental Pollution* 153(3): 594–601.
- [43] Zhang, Y., Guo, C. S., Xu, J., Tian, Y. Z., Shi, G. L., Feng, Y. C. (2012): Potential source contributions and risk assessment of PAHs in sediments from Taihu Lake, China: comparison of three receptor models. – *Water Research* 46(9): 3065–3073.

EFFECTS OF HYDROPHILIC POLYMERS ON SOIL WATER, WHEAT PLANT AND MICROORGANISMS

KHODADADI DEHKORDI, D.

*Department of Water Engineering and Sciences, Ahvaz Branch,
Islamic Azad University, Ahvaz, Iran*
e-mail: davood_kh70@yahoo.com; dkhodadadi@iauahvaz.ac.ir; phone: +989163033474

(Received 5th Nov 2017; accepted 12th Feb 2018)

Abstract. In this study, two types of superabsorbent polymers, Super-AB-A-200 (A-200) and Super-AB-A-300 (A-300), at 180 kg ha⁻¹ were applied by scattering and mass treatments in an experimental farm to assess their influences on spring wheat growth (Chamran variety) and on the physical characteristics and microbial plenty of soil in Shush region, Iran. The following treatments were used in this study: the control treatment (CT, without SAPs), A-200 with mass application (A-200-M), A-300 with mass application (A-300-M), A-200 with scattered application (A-200-S), and A-300 with scattered application (A-300-S). Approximately 0.3 m³ of irrigation water was supplied for every subplot. The results indicated that superabsorbent polymers significantly enhanced the soil water content in the three growth stages compared with the control. The use of superabsorbent polymers did not have obvious opposite influences on the soil microbial colony and might even increase soil microbial movement.

Keywords: *soil hygroscopic moisture, superabsorbent polymer, soil water content, wheat plant, water-holding capacity*

Abbreviations: AW: Available water-holding; CT: Control treatment; CEC: Cation exchange capacity; DOC: Dissolved organic carbon; MBC: Microbial biomass carbon; OMC: Organic matter carbon; A-200: Super-AB-A-200; A-300: Super-AB-A-300; SAP: Superabsorbent polymer; SWSA: Soil water-stable aggregates; SHM: Soil hygroscopic moisture; SMR: Soil microbic respiration; SWC: Soil water content; WC: Water-holding capacity; WSA: Water-stable aggregates; RG: 16S rRNA gene

Introduction

Numerous countries worldwide do not have enough water resources to meet their actual environmental, urban, and agricultural requirements (Bouwer, 2002). Iran receives a nonuniform distribution of rainfall every year and has limited water resources. Therefore, it is a dry country, and it always faces water shortage problems. A new technique for managing soil water is to use superabsorbent polymer (SAP) as a water reservoir for preventing water loss and increasing irrigation efficiency (Seyed Doraji et al., 2010). SAP acts as a soil reformer and decreases soil water loss and increases crop yield. SAP can take up large amounts of water and aquatic solutions and increase the soil water-holding capacity (WC) (Khadem et al., 2010). SAP has a positive impact on water and nutrient retention in the soil. It postpones the time required to reach a permanent wilting point and prolongs plant survival under water stress conditions (Orikiriza et al., 2009). Yang et al. (2014) showed that adding a hydrophilic polymer to soil led to a significant increase in soil WC compared to controls. Yadollahi et al. (2012) showed that Super-AB-A-200 and organic matters could increase soil water retention significantly. Khodadadi Dehkordi (2017) reported that Super-AB-A-200 polymer could store water and nutrients in the sandy soil and release them under drought stress conditions. Besides, it could improve sandy soils and increase water-holding capacity. Previous studies on superabsorbent polymers have investigated their influences on the chemical and physical characteristics of soil

(Zhang and Miller, 1996); however, few have assessed the effects of hydrophilic polymers on microorganisms in soil and moisture available to plants under natural conditions. This study aimed to evaluate variations in the physical properties and microbial movement of soil after applying superabsorbent polymers in the field during the growth of the Chamran wheat variety.

Materials and methods

Experimental farm and treatments

The farm experiments were performed in Shush, Khuzestan province, Iran. This region has a semiarid climate and mean annual precipitation of 213 mm (*Table 1*). The soil texture was sandy loam. It had an organic matter carbon (OMC) of 0.5%, pH of 7, and cation exchange capacity (CEC) of 11.8 cmol kg; it was classified as Alfisols in the USA soil taxonomy. The experimental farm was divided into five plots. One plot was determined as the control treatment (CT) (without SAPs), and various hydrophilic polymer treatments were randomly applied in the other plots. For creating replicates, each plot (4 m × 4 m) was divided into six equal subplots. Therefore, 30 subplots were evaluated in total. Chamran wheat variety that was native to and a special variety from Shush was used for cultivation in three growing seasons. Chamran is an early-ripening and spring variety of wheat (*Triticum aestivum* L.). The hydrophilic polymers used in this study were Super-AB-A-200 (A-200) and Super-AB-A-300 (A-300) (*Tables 2 and 3*) (both manufactured by Rahab Resin Co., product license held by Iran Polymer and Petrochemical Institute) (Rahab Resin Co, 2016). These hydrophilic polymers are granular, and they are a tripolymer of acrylamide, acrylic acid, and acrylate potassium. These polymers are inexpensive, and they are easier to obtain than other types of hydrophilic polymers in Iran. The following treatments were used in this study: the control treatment (CT, without SAPs), A-200 with mass application (A-200-M), A-300 with mass application (A-300-M), A-200 with scattered application (A-200-S), and A-300 with scattered application (A-300-S). The experimental design is indicated in *Figure 1*. Approximately 0.3 m³ of irrigation water was supplied for every subplot; this is similar to the regional irrigation strategy. The irrigation water for the CT was pure and did not contain a superabsorbent. For mass application in every subplot, a depth of 1.5 cm from the soil surface was gathered and blended with hydrophilic polymers and distributed equally at a superabsorbent polymer density of 180 kg ha⁻¹. Next, 0.3 m³ of irrigation water was supplied for each subplot. For scattered application in every subplot, 0.3 m³ of irrigation water and a blend of hydrophilic polymers was sprayed onto the soil surface. The wheat variety was planted on November 22, 2013-2014-2015. Hydrophilic polymers were applied to the soil on December 27, 2013-2014-2015, when the crops became strong enough and started to grow. Soil samples were gathered at three crucial stages: stem elongation stage (sampled on January 1, 2014-2015-2016), heading stage (February 27, 2014-2015-2016), and dough stage (March 25, 2014-2015-2016). By using a core sampler, the soil samples were gathered at a depth of 0–12 cm and a space of 1–6 cm from the wheat plants. Six subsamples from each subplot were blended to prepare a compound sample. For analyzing the soil water-stable aggregates (SWSA) and other physical (maintained at 2°C) and microbial (maintained at -24°C) characteristics of soil, the samples were passed through 8 and 2 mm screens, respectively. After harvesting, the plant shoot length in the three phases and the dry weight of wheat grains were determined.

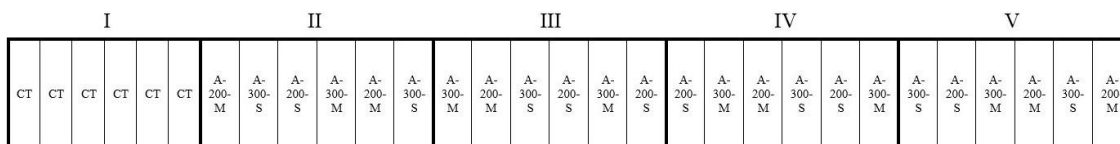


Figure 1. The experimental design of this study

Table 1. Some weather parameters of Shush city

Month	Average of min temperature (°C)	Average of max temperature (°C)	Average of temperature (°C)	Average of min humidity (%)	Average of max humidity (%)	Sum of rainfall (mm)	Sum of sunshine hours
October	20.0	40.2	29.8	17.7	58.3	0	287.60
November	14.4	29.3	20.3	37.1	75.7	25.8	178.60
December	5.2	21.9	13.1	35.5	81.2	0	260.36
January	6.4	21.8	13.4	43.6	83.5	12.5	178.60
February	6.1	20.9	13.1	40.4	78.2	28.4	174.27
March	9.0	24.3	16.0	30.3	70.1	29	210.10
April	15.3	32.4	23.2	33.1	80.0	5.5	215.07
May	21.7	40.9	29.9	28.7	65.0	2.5	246.78
June	24.8	46.3	35.0	19.0	49.0	0	300.38
July	26.6	48.1	36.7	20.6	52.6	0	356.47
August	27.4	49.7	38.0	21.5	54.8	0	352.20
September	23.3	45.5	33.7	24.3	68.1	0	332.60

Table 2. The characteristics of Super-AB-A-200 polymer

Characteristics	Super-AB-A-200 polymer
Shape	granular
Density	1.4-1.5 (gr.cm ⁻³)
Size of particles	50-150 (µm)
Maximum stability in soil	7 (year)
Practical capacity of water uptake	220 (g.g ⁻¹)

Table 3. The characteristics of Super-AB-A-300 polymer

Characteristics	Super-AB-A-300 polymer
Shape	granular
Density	1.4-1.5 (gr.cm ⁻³)
Size of particles	30-100 (µm)
Maximum stability in soil	5 (year)
Practical capacity of water uptake	600 (g.g ⁻¹)

Determination of SWSA

Soil aggregates of various sizes (<0.25, 0.25–0.5, 0.5–1, 1–2, 2–5, and >5 mm) were separated using the wet sifting procedure according to the Elliot method (Elliot, 1986;

Li et al., 2014). At room temperature and before the start of sifting, a 105 g sample was immersed into water on the largest sieve (2 mm) for 6 min. In a sedimentation cylinder and under water, the soils were sifted by mildly moving the screen vertically through water 60 times in 2.5 min. In all cases, the improvements from wet sifting were >99% by weight. The sum portion of the fraction weights was used for explaining the weight of every SWSA.

Evaluation of soil available water-holding (AW) and soil hygroscopic moisture (SHM)

First, a 30 mL beaker including 15 g of desiccated soil was placed in a dryer, and its bottom was saturated with K₂SO₄ solution. The dryer temperature was kept constant at 20°C. After water uptake for 7 days, the beaker was removed, weighed, and returned to the dryer. This process was repeated many times until the beaker weight with soil became stable. Then, the beaker (including the soil sample) was placed in an oven at 105°C for 1 day. The water content process was used to measure the SHM. The AW can be evaluated for the plant by using the SHM and soil water content (SWC) by Equation 1 (Li et al., 2014; Gupta and Larson, 1979):

$$AW = SWC - [2 \times SHM] \quad (\text{Eq.1})$$

Evaluation of soil DNA extraction and real-time PCR of bacterial plenty

Nucleic acids were obtained from 0.6 g of soil using a MoBio UltraClean™ soil DNA isolation kit according to the manufacture's instruction with a slight adjustment (He et al., 2007). The DNA obtained was saved at -24°C before usage. The bacterial plenty was assessed using the real-time PCR procedure with a focus on the 16S rRNA gene (RG) in an iCycler iQ5 thermocycler (He et al., 2007). Real-time PCR was performed using a 25 µL reaction volume including 12.5 µL of 2 × Premix Ex Taq, 100 nM of each primer, 120 nM of the probe, and 1 µL of the tenfold-diluted DNA template (1–10 ng) (Li et al., 2014). The elaboration conditions were as follows: 97°C for 12 s, 40 cycles at 97°C for 17 s, and 60 s at 58°C.

Analysis of soil microbial biomass carbon (MBC)

The chloroform fumigation extraction procedure was used for measuring the soil microbial biomass (Vance et al., 1987). In this method, each fresh soil sample was divided into 10 parts. Five of these parts (each including 15 g of dried soil) were placed into 100 mL bottles, and chloroform fumigation was carried out with adding of ethanol-free chloroform (15 µLg⁻¹ of dried soil). Then, the soils were blended completely inside the bottle. The soils were fumigated excessively with chloroform for 1 day at 35°C in dryers. When fumigant of the soils were removed, they were extracted with 45 mL of 0.5 M K₂SO₄ for 35 min. The other five nonfumigated soils were obtained similarly at the start of fumigation. The MBC was assessed as the difference in K₂SO₄-extractable dissolved organic carbon (DOC) between the fumigated and nonfumigated soils using the following extractability correction factor: K_C = 0.5 for DOC (Li et al., 2014; Jonasson et al., 1996; Rinnan et al., 2008). Then, the extracted DOC was measured using a total DOC analyzer.

Measurement of soil microbial respiration (SMR)

The soil respiration was determined using the procedure explained by Chen et al. (2000). Fresh soil (equivalent to 25 g dry weight) was placed in a sealed 500 mL bottle and settled at 20°C for 1 day. The CO₂ arising from the soil was captured in 0.2 M NaOH and assessed by titration with 0.2 M HCl to the phenolphthalein end point after adding 2 M BaCl₂. Several controls (i.e., soil-free bottle) were exposed to the same situation and applied as blanks. The derived CO₂ value was measured from the difference in molarity between NaOH from the samples and blanks.

Data analysis

The data analysis was carried out with using SPSS 21.0 software. Analysis of variance (ANOVA) was used to check the differences among the treatments used. $P < 0.05$ was considered statistically significant.

Results

Plant characteristics

Spring wheat plants grew rapidly from the stem elongation to the heading stage and quickly from the heading to the dough stage. The plant shoot lengths indicated significant differences among the three phases; however, the influence of hydrophilic polymers was minimal (Fig. 2). Only A-300-M significantly enhanced the total dry weight of wheat grain ($P < 0.05$) (Fig. 3).

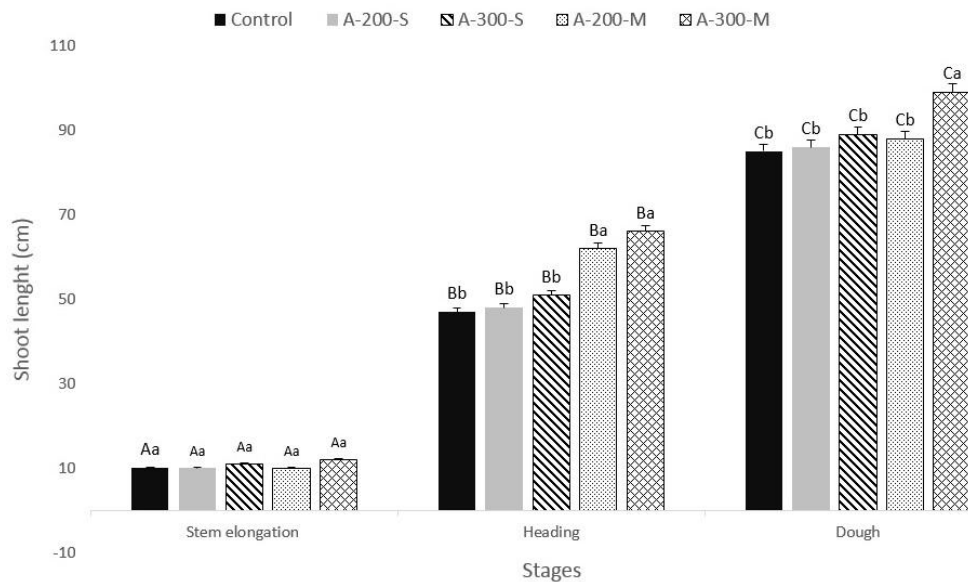


Figure 2. The shoot length of Chamran variety plants in varied stages and under varied hydrophilic polymer treatments. Varied capital letters indicate significant differences between stages for the same SAP treatment ($P < 0.05$). Varied lowercase letters indicate significant differences between hydrophilic polymer treatments in the same wheat growth stage ($P < 0.05$). Bars show the standard errors

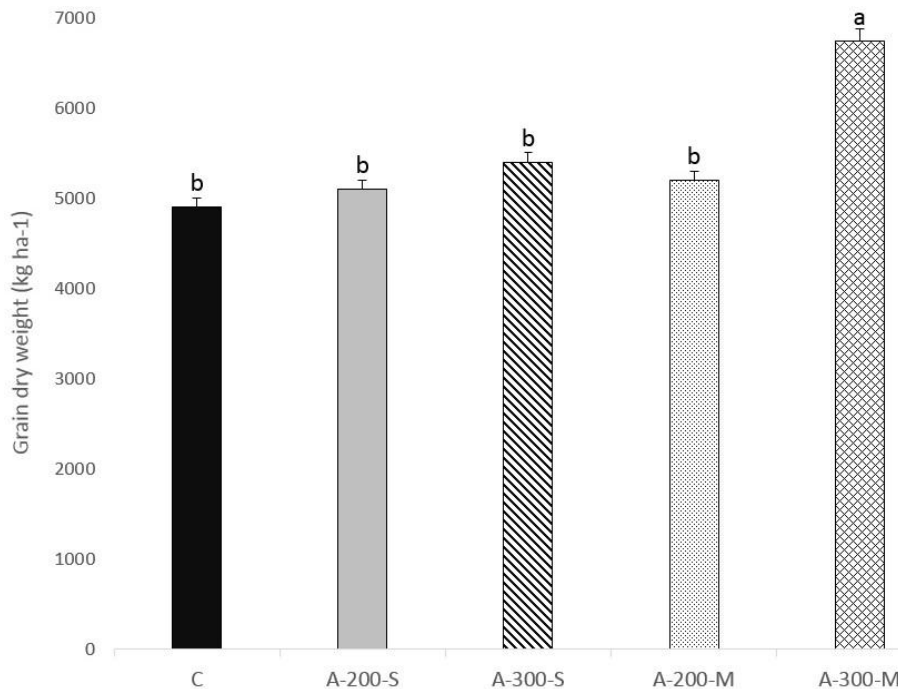


Figure 3. The grain dry weight of Chamran variety plants in varied stages and under varied hydrophilic polymer treatments. Bars show the standard errors. Bars with varied letters show significant differences at $p < 0.05$

SWSA

Table 4 shows the variation of SWSA over all Chamran variety growths and between treatments. The soil particle sizes showed significant differences among the three phases ($P < 0.05$). SAP application significantly enhanced the macro soil aggregates (size > 0.25 mm) compared with CTs in the heading and dough phases, whereas the differences among the two hydrophilic polymer treatments were not significant.

AW, SHM, and SWC

SWC varied by hydrophilic polymer treatment and growth stage (Fig. 4), whereas SHM only varied by hydrophilic polymer treatment (Fig. 5). In the stem elongation, heading, and dough stages, all superabsorbent treatments significantly enhanced SWC compared with CTs ($P < 0.05$). Furthermore, there were significant differences in SWC between the superabsorbent treatments, particularly in the heading and dough stages. The influences of mass treatments were greater than those of scattering treatments. Similarly, in the three phases, all superabsorbent treatments significantly enhanced SHM compared with CTs ($P < 0.05$). However, differences were not seen in SHM when using hydrophilic polymers. Figure 6 reveals the clear influences on AW in the first two Chamran variety growth phases and between the hydrophilic polymer treatments. The amounts of AW in the dough phase were negative; therefore, soil water could not be used completely by wheat plants in this phase. This decrease in AW during Chamran variety growth was very identical to that seen in SWC. Furthermore, the mass treatments of hydrophilic polymers were more efficient in water holding than scattering treatments.

Table 4. Water-stable soil aggregate composition at different stages and under different treatments

Application method	SWSA content (%)					
	<0.25 mm	0.25–0.5 mm	0.5–1 mm	1–2 mm	2–5 mm	>5 mm
Stem elongation stage						
C	52.0 Aa	17.1 Aa	11.2 Aa	8.5 Aa	9.1 Aa	9.7 Aa
A-200-S	45.2 Aa	18.3 Ba	12.5 Ba	9.4 Ba	10.4 Ba	11.3 Ba
A-300-S	47.3 Aa	18.2 Ba	12.2 Ba	9.6 Ba	10.6 Ba	11.6 Ba
A-200-M	45.8 Aa	18.1 Ba	12.3 Ba	9.3 Ba	10.2 Ba	11.3 Ba
A-300-M	49.7 Aa	19.4 Ba	12.8 Ba	10.1 Ba	11.2 Ba	12.4 Ba
Heading stage						
C	51.2 Aa	17.2 Ab	11.5 Ab	8.4 Ab	9.5 Ab	9.8 Ab
A-200-S	34.2 Bb	22.3 Aa	21.3 Aa	12.5 Aa	13.6 Aa	14.4 Aa
A-300-S	35.3 Bb	23.5 Aa	22.6 Aa	12.7 Aa	13.7 Aa	14.6 Aa
A-200-M	35.6 Bb	22.1 Aa	21.2 Aa	12.3 Aa	13.5 Aa	14.1 Aa
A-300-M	37.4 Bb	24.6 Aa	23.6 Aa	13.5 Aa	14.4 Aa	15.3 Aa
Dough stage						
C	50.6 Aa	17.4 Ab	11.7 Ab	8.3 Ab	9.8 Ab	9.9 Ab
A-200-S	32.4 Bb	22.6 Aa	21.4 Aa	12.6 Aa	13.5 Aa	14.3 Aa
A-300-S	33.5 Bb	23.7 Aa	22.7 Aa	12.8 Aa	13.7 Aa	14.6 Aa
A-200-M	33.4 Bb	22.3 Aa	21.4 Aa	12.5 Aa	13.4 Aa	14.2 Aa
A-300-M	35.6 Bb	24.8 Aa	23.8 Aa	13.6 Aa	14.5 Aa	15.4 Aa

Different capital letters indicate significant differences between different stages for the same hydrophilic polymer treatment ($P < 0.05$). Varied lowercase letters indicate significant differences between different hydrophilic polymer treatments in the same growth stage ($P < 0.05$)

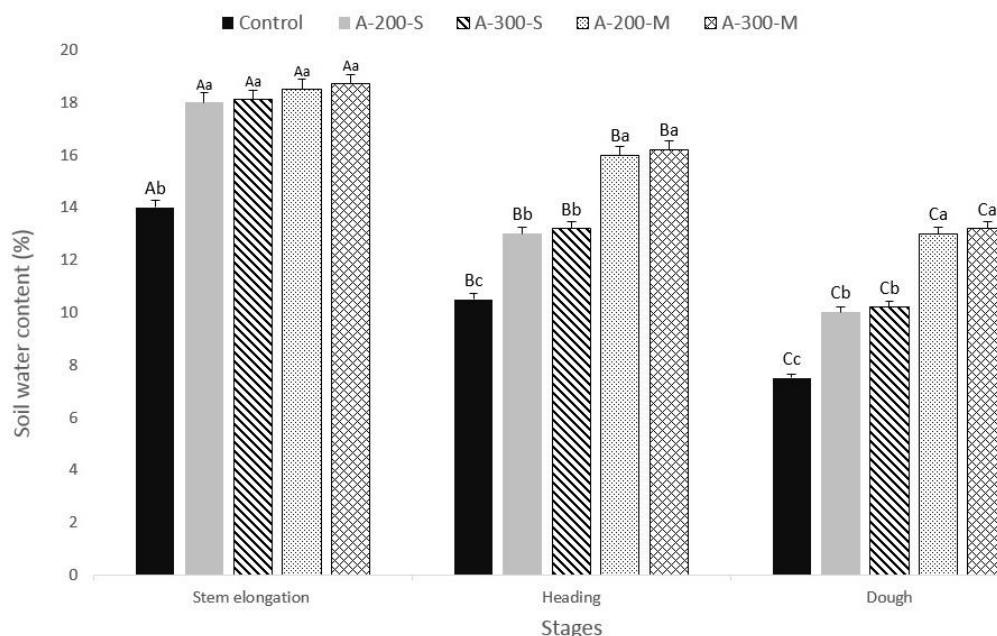


Figure 4. Soil water content (SWC) in varied stages and under varied hydrophilic polymer treatments. Different capital letters indicate significant differences between stages for the same SAP treatment ($P < 0.05$). Varied lowercase letters indicate significant differences between hydrophilic polymer treatments in the same wheat growth stage ($P < 0.05$). Bars show the standard errors

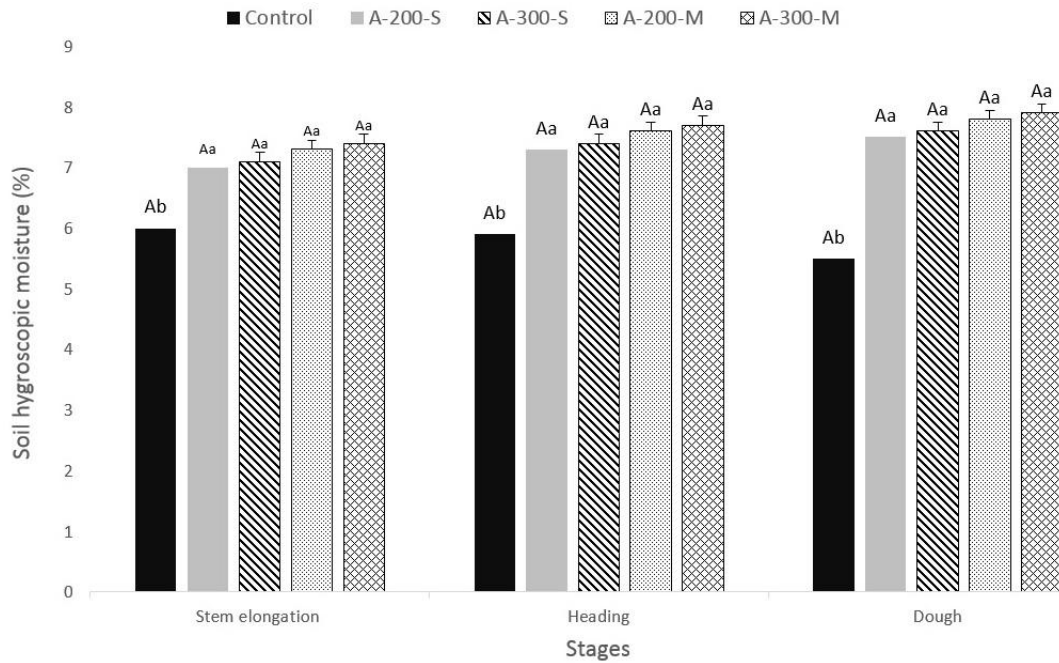


Figure 5. Soil hygroscopic moisture (SHM) in varied stages and under varied hydrophilic polymer treatments. Different capital letters indicate significant differences between stages for the same SAP treatment ($P < 0.05$). Varied lowercase letters indicate significant differences between hydrophilic polymer treatments in the same wheat growth stage ($P < 0.05$). Bars show the standard errors

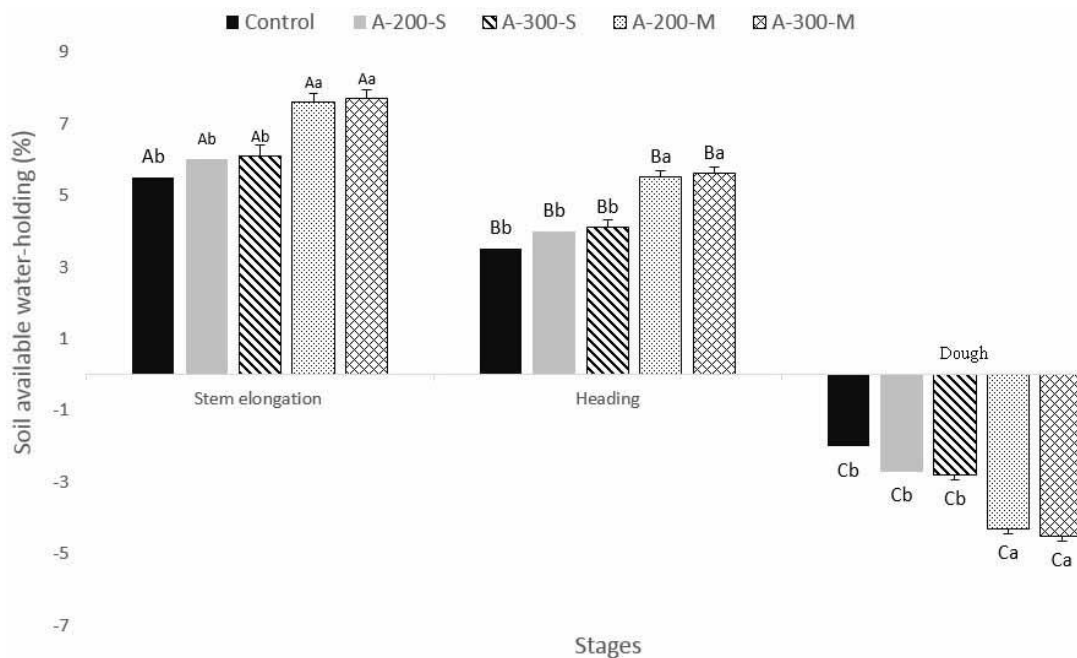


Figure 6. Soil available water-holding (AW) in varied stages and under varied hydrophilic polymer treatments. Different capital letters indicate significant differences between stages for the same SAP treatment ($P < 0.05$). Varied lowercase letters indicate significant differences between hydrophilic polymer treatments in the same wheat growth stage ($P < 0.05$). Bars show the standard errors

Bacterial plenty in soil

The bacterial plenty, measured by the number of RG copies per gram of desiccated soil, differed between the Chamran variety growth phases and hydrophilic polymer treatments (Fig. 7). In the stem elongation stage, the mass treatments significantly enhanced the bacterial RG copy numbers compared with scattering treatment and CTs. In both the heading and the dough stages, the bacterial RG copy numbers in all hydrophilic polymer treatments were significantly greater than those in the two CTs, respectively (Fig. 7). Throughout the three growth phases, the highest number of bacterial RG copies were seen in the heading phase in all treatments ($P < 0.05$).

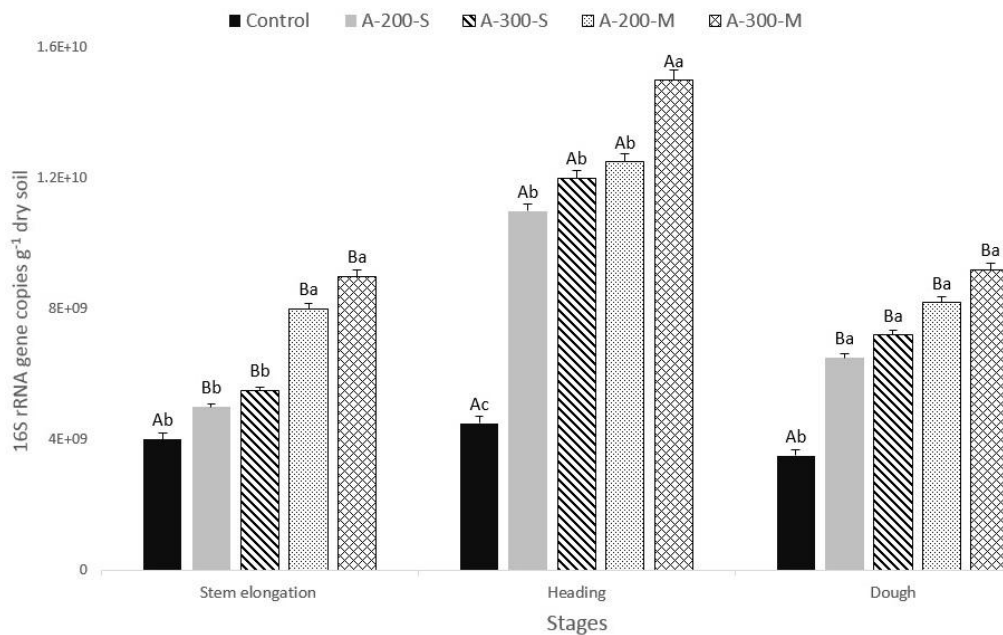


Figure 7. Abundance of bacteria in varied stages and under varied hydrophilic polymer treatments. Different capital letters indicate significant differences between stages for the same SAP treatment ($P < 0.05$). Varied lowercase letters indicate significant differences between hydrophilic polymer treatments in the same wheat growth stage ($P < 0.05$). Bars show the standard errors

SMR and Soil MBC

There were significant differences in microbial movement between the different phases ($P < 0.05$) (Figs. 8 and 9). Microbial movement, defined by SMR and MBC, was the greatest in the heading stage, indicating a trend comparable to that of bacterial plenty. Meanwhile, A-300 treatments stimulated microbial movement significantly, as was most evident in the stem elongation and heading stages, indicating that A-300 treatments were more beneficial for microbial movement than CTs or A-200 treatments.

Discussion

Influence of hydrophilic polymers on soil water and wheat growth

The results indicated that adding superabsorbent polymers could improve the soil WC and enable the soil to retain more water.

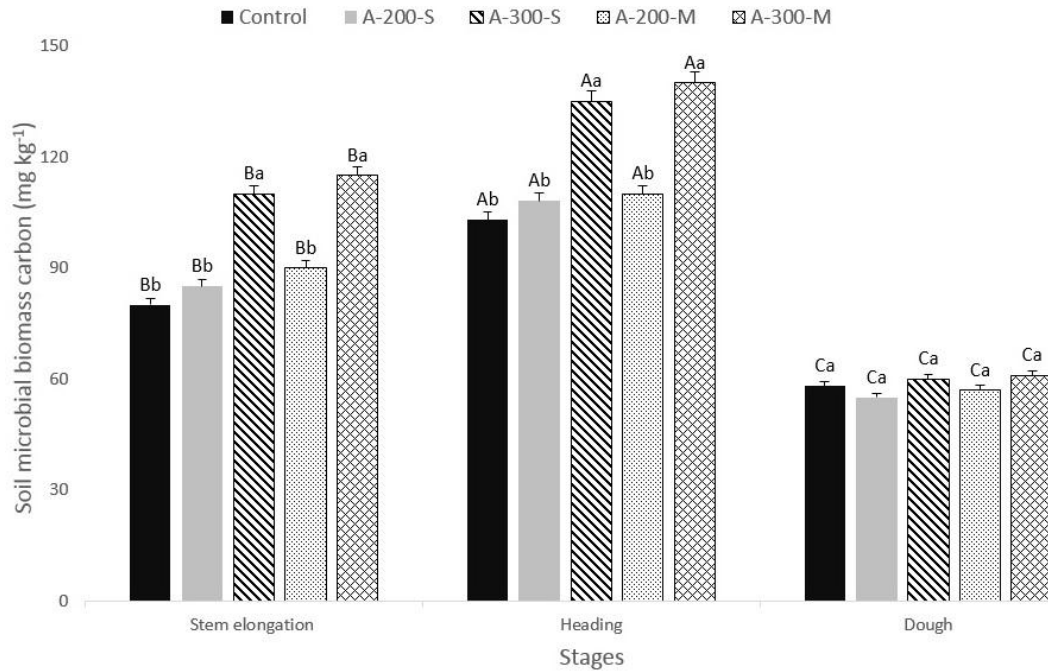


Figure 8. Soil microbial biomass carbon (MBC) in varied stages and under varied hydrophilic polymer treatments. Different capital letters indicate significant differences between stages for the same SAP treatment ($P < 0.05$). Varied lowercase letters indicate significant differences between hydrophilic polymer treatments in the same wheat growth stage ($P < 0.05$). Bars show the standard errors

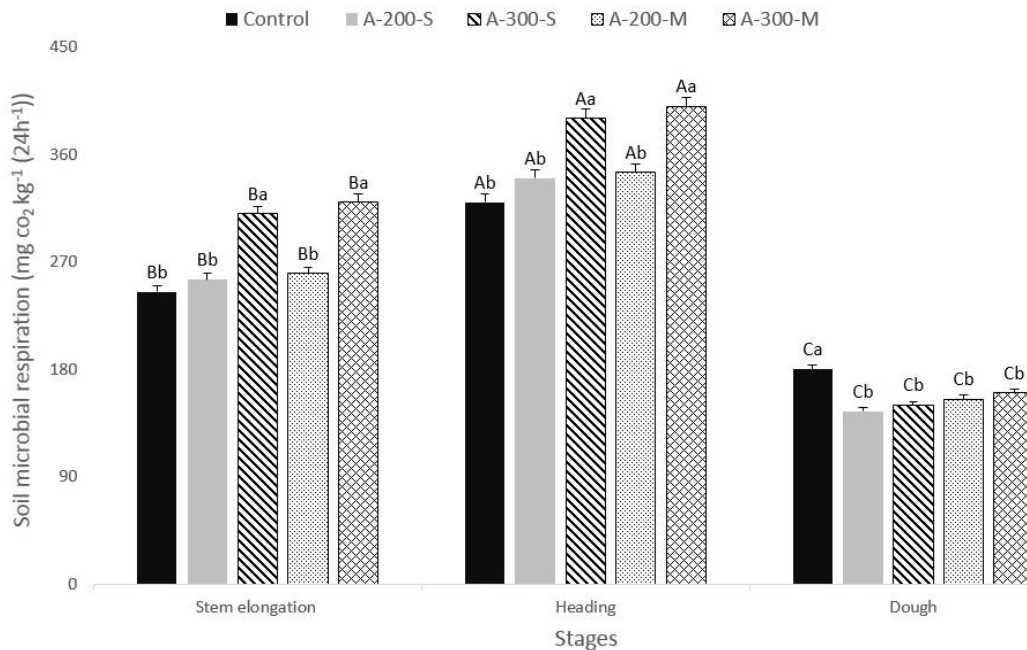


Figure 9. Soil microbial respiration (SMR) in varied stages and under varied hydrophilic polymer treatments. Different capital letters indicate significant differences between stages for the same SAP treatment ($P < 0.05$). Varied lowercase letters indicate significant differences between hydrophilic polymer treatments in the same wheat growth stage ($P < 0.05$). Bars show the standard errors

Furthermore, superabsorbent polymers greatly influenced SHM; SHM was fixed by soil particles and might not be applied by wheat plants. The fact that hydrophilic polymers enhanced SWC but not the soil-available water content suggested that the benefits of hydrophilic polymers to wheat plant growth could be limited. This fact agreed with the finding that there were nearly no significant differences in grain dry weight (except A-300-M treatment) or Chamran variety shoot length between all treatments. However, this finding differed from those of former studies with varied conditions, indicating that hydrophilic polymers could amend crop growth significantly (Yazdani et al., 2007; Islam et al., 2011).

Influence of hydrophilic polymers on SWSA

In the stem elongation stage, hydrophilic polymer treatment had no influence on large or small aggregates. However, in the heading and dough stages, A-200 and A-300 treatments raised more large aggregates related to CTs. Ajwa and Trout (2006) reported that hydrophilic polymers could be firmly adsorbed onto the soil particle surface, thereby stopping dispersion. However, the first sampling was conducted only 5 days after the use of hydrophilic polymers, and therefore, there could have been insufficient time for the hydrophilic polymer to connect perfectly with the soil particle surface. In the heading and dough stages, some part of the superabsorbent polymers would have gently infiltrated the aggregates pores (Lu and Wu, 2003) and protected or enhanced soil aggregation and pore continuation (Li et al., 2014; Ajwa and Trout, 2006; Keren and Ben-Hur, 1997).

Influence of hydrophilic polymers on bacterial plenty

The RG can present taxonomic information about the compound of bacterial colonies (Satoshi et al., 2009). RGs obtained under natural conditions have recently been used to gain insights into and understand the purposes of soil-borne microbial variations (Tiedje et al., 1999; Torsvik and Ovreas, 2002; Rodriguez-Valera, 2004; Schloss and Handelsman, 2004; Li et al., 2014). The addition of hydrophilic polymers significantly enhanced bacterial plenty from the first to the second phases of Chamran variety growth, indicating that bacterial growth had been increased. Furthermore, more RG copies were identified in the heading phase than in the other phases. This result indicates that bacterial reproduction increased upon adding hydrophilic polymers under natural conditions, particularly in the heading stage. Substrates achieved from plant, both those that were actively seeped and those that were inactively scattered, could provide most of the energy and food for soil-borne microbial colonies (Marschner et al., 2004; Li et al., 2014). Therefore, when the plants were growing quickly, they might produce more substrates, resulting in the levels of soil microbic movement being the greatest in the heading stage.

Influence of hydrophilic polymers on soil microbial movements

A significant enhancement in SMR and MBC was seen in the A-300 treatments (A-300-M and A-300-S) in the stem elongation and heading stages (Figs. 8 and 9), especially in the heading stage. A-300-M had a stronger influence on MBC than A-300-S. High microbial movement and biomass often result in high nutrient access (Tu et al., 2003; Zaman et al., 1999) and may, in turn, result in high plant production (Tu et al., 2006; Li et al., 2014); this could explain the greater wheat yield obtained by the A-300-

M treatment compared to the other treatments. The significant reduction in SMR and MBC in the dough phase could be caused by the variations in colony size and construction that could result from variations in the input of metabolizable DOC from plant (Gomez et al., 2006) and soil residues arising from plant growth effects (Patra et al., 2006; Li et al., 2014). In this phase, hydrophilic polymers might have been decomposed incompletely or completely, resulting in lower amounts of SMR and MBC. This influence was most evident in the A-300 treatments, which significantly stimulated the microbial movements in the heading stage, thereby expediting the disintegration of soil organic matter. Therefore, the SMR decreased more clearly in the dough phase compared with that in the CT because the microorganisms did not have enough substrates available. The result indicates that this decrease in SMR was not related to the opposite influence of SAPs. These findings show that the use of SAPs did not reveal any opposite influences on wheat plant growth and the physical or microbial characteristics of soil. Soil is a complicated ecosystem that is influenced by numerous factors, making it difficult to evaluate environmental influences methodically and extensively when chemical additives are applied to the soil. Nonetheless, it is crucial to find an estimation frame and make suitable adaptations to it over time.

Conclusions

The results indicate that the use of hydrophilic polymers could amend the physical characteristics of soil and may help in managing water loss. At a density of 180 kg ha⁻¹, hydrophilic polymers greatly increased the uptake of water and the presence of WSA. SAPs did not have obvious opposite effects on the soil microbial colony and might even increase it. The influences of hydrophilic polymers also depended on the processes used in the field, as only the mass application of A-300 improved the yield. No direct relations were found between the SWC and the plant characteristics. Finally, it is recommended to use other types of hydrophilic polymers on the other soil types for managing water loss. Besides, it is recommended to use other plants and other growth stages for soil sampling.

REFERENCES

- [1] Ajwa, H. A., Trout, T. J. (2006): Polyacrylamide and water quality effects on infiltration in sandy loam soils. – *Soil Sci. Soc. Am. J.* 70: 643–650.
- [2] Bower, H. (2002): Integrated water management for the 21st century: Problems and solutions. – *J. Irrig. Drain. Eng.* 128: 193–202.
- [3] Chen, C., Condon, L. M., Davis, M., Sherlock, R. R. (2000): Effects of afforestation on phosphorus dynamics and biological properties in a New Zealand grassland soil. – *Plant Soil* 220: 151–163.
- [4] Elliot, E. T. (1986): Aggregate structure and carbon, nitrogen, and phosphorus in native and cultivated soils. – *Soil Sci. Soc. Am. J.* 50: 627–633.
- [5] Gupta, S. C., Larson, W. E. (1979): Estimating soil water retention characteristics from particle size distribution, organic matter percent and bulk density. – *Water Resour. Res.* 15: 1633–1635.
- [6] Gomez, E., Ferreras, L., Toresani, S. (2006): Soil bacterial functional diversity as influenced by organic amendment application. – *Bioresour. Technol.* 97: 1484–1489.
- [7] He, J. Z., Shen, J. P., Zhang, L. M., Zhu, Y. G., Zheng, Y. M., Xu, M. G., Di, H. J. (2007): Quantitative analyses of the abundance and composition of ammonia-oxidizing

- bacteria and ammonia-oxidizing archaea of a Chinese upland red soil under long-term fertilization practices. – *Environ. Microbiol.* 9: 2364–2374.
- [8] Islam, M. R., Hu, Y., Mao, S., Jia, P., Eneji, A. E., Xue, X. (2011): Effects of water-saving superabsorbent polymer on antioxidant enzyme activities and lipid peroxidation in corn (*Zeamays* L.) under drought stress. – *J. Sci. Food Agric.* 91: 813–819.
- [9] Jonasson, S., Michelsen, A., Schmidt, I. K., Nielsen, E. V. (1996): Microbial biomass C N and P in two arctic soils and responses to addition of NPK fertilizer and sugar: implications for plant nutrient uptake. – *Oecologia* 106: 507–515.
- [10] Keren, R., Ben-Hur, M. (1997): Polymer effects on water infiltration and soil aggregation. – *Soil Sci. Soc. Am. J.* 61: 565–570.
- [11] Khadem, S. A., Galavi, M., Ramrodi, M., Mousavi, S. R., Roustafar, M. J., Rezvani-Moghaddam, P. (2010): Effect of animal manure and superabsorbent polymer on corn leaf relative water content, cell membrane stability and leaf chlorophyll content under dry condition. – *Australian Journal of Crop Science* 4: 242–247.
- [12] Khodadadi Dehkordi, D. (2017): Effect of superabsorbent polymer on salt and drought resistance of *Eucalyptus globulus*. – *Applied Ecology and Environmental Research* 15: 1791–1802.
- [13] Li, X., He, J., Hughes, J., Liu, Y., Zheng, Y. (2014): Effects of super-absorbent polymers on a soil–wheat (*Triticum aestivum* L.) system in the field. – *Applied Soil Ecology* 73: 58–63.
- [14] Lu, J. H., Wu, L. S. (2003): Polyacrylamide distribution in columns of organic matter removed soils following surface application. – *J. Environ. Qual.* 32: 674–680.
- [15] Marschner, P., Crowley, D., Yang, C. H. (2004): Development of specific rhizosphere bacterial communities in relation to plant species, nutrition and soil type. – *Plant Soil* 261: 199–208.
- [16] Orikiriza, L. J. B., Agaba, H., Tweheyo, M., Eilu, G., Kabasa, J. D., Huttermann, A. (2009): Amending soils with hydrogels increases the biomass of nine tree species under non-water stress conditions. – *Clean Soil Air Water* 37: 615–620.
- [17] Patra, A. K., Abbadie, L., Clays-Josserand, A., Degrange, V., Grayston, S. J. (2006): Effects of management regime and plant species on the enzyme activity and genetic structure of N-fixing, denitrifying and nitrifying bacterial communities in grass-land soils. – *Environ. Microbiol.* 8: 1005–1016.
- [18] Rahab Resin Co. (2016): Rahab Resin Company. – http://www.bizearch.com/company/Rahab_Resin_Co_280864.htm. Access date: 9 October 2016.
- [19] Rinnan, R., Michelsen, A., Jonasson, S. (2008): Effects of litter addition and warming on soil carbon, nutrient pools and microbial communities in a subarctic heath ecosystem. – *Appl. Soil Ecol.* 39: 271–281.
- [20] Rodriguez-Valera, F. (2004): Environmental genomics, the big picture? – *FEMS Microbiol. Lett.* 231: 153–158.
- [21] Satoshi, I., Michihiro, Y., Mami, K. (2009): Microbial populations responsive to denitrification-inducing conditions in rice paddy soil, as revealed by comparative 16S rRNA gene analysis. – *Appl. Environ. Microbiol.* 75: 7070–7078.
- [22] Schloss, P. D., Handelsman, J. (2004): Status of the microbial census. – *Microbiol. Mol. Biol. Rev.* 68: 686–691.
- [23] Seyed Doraji, S., Golchin, A., Ahmadi, S. (2010): The effects of different levels of a Superabsorbent polymer and soil salinity on water holding capacity with three textures of sandy, loamy and clay. – *Journal of Water and Soil* 24: 306–316 (in Persian).
- [24] Tiedje, J. M., Asuming-Brempong, S., Nusslein, K., Marsh, T. L., Flynn, S. J. (1999): Opening the black box of soil microbial diversity. – *Appl. Soil Ecol.* 13: 109–122.
- [25] Torsvik, V., Ovreas, L. (2002): Microbial diversity and function in soil: from genes to ecosystems. – *Curr. Opin. Microbiol.* 5: 240–245.

- [26] Tu, C., Koenning, S. R., Hu, S. (2003): Root-parasitic nematodes enhance soil microbial activities and nitrogen mineralization. – *Microbial. Ecol.* 46: 134–144.
- [27] Tu, C., Koenning, S. R., Hu, S. (2006): Soil microbial biomass and activity in organic tomato farming systems: effects of organic inputs and straw mulching. – *Soil Biol. Biochem.* 38: 247–255.
- [28] Vance, E. D., Brookes, P. C., Jenkinson, D. S. (1987): An extraction method for measuring microbial biomass C. – *Soil Biol. Biochem.* 22: 703–707.
- [29] Yang, L., Yang, Y., Chen, Z., Guo, C., Li, S. (2014): Influence of super absorbent polymer on soil water retention, seed germination and plant survivals for rocky slopes eco-engineering. – *Ecological Engineering* 62: 27–32.
- [30] Yadollahi, A., Teimoori, N., Abdoosi, V., Sarikhani-Khorami, S. (2012): Impact evaluation of Superabsorbent and organic matters in retention of water and establishment of Almond gardens in rainfed conditions. – *Journal of Water Research in Agriculture* 26: 95–106 (in Persian).
- [31] Yazdani, F., Allahdadi, I., Akbari, G. A. (2007): Impact of superabsorbent polymer on yield and growth analysis of soybean (*Glycine max* L.) under drought stress condition. – *Pak. J. Biol. Sci.* 10: 4190–4196.
- [32] Zaman, M., Di, H. J., Cameron, K. C. (1999): A field study of gross rates of N mineralization and nitrification and their relationships to microbial biomass and enzyme activities in soils treated with dairy effluent and ammonium fertilizer. – *Soil Use Manage.* 15: 188–194.
- [33] Zhang, X. C., Miller, W. P. (1996): Polyacrylamide effect on infiltration and erosion in furrows. – *Soil Sci. Soc. Am. J.* 60: 866–872.

COMPARATIVE ANALYSIS OF VEGETATION FROM ERODED AND NON-ERODED AREAS, A CASE STUDY FROM KASHMIR HIMALAYAS, PAKISTAN

DAR, M. E. U. I.^{1*} – GILLANI, N.¹ – SHAHEEN, H.¹ – FIRDOUS, S. S.¹ – AHMAD, S.² – KHAN, M. Q.¹ – HUSSAIN, M. A.³ – HABIB, T.¹ – MALIK, N. Z.⁴ – ULLAH, T. S.¹ – RAFIQUE, S.¹ – AZIZ, S.¹ – KHAN, W. A.¹ – HUSSAIN, K.¹

¹*Department of Botany, University of Azad Jammu and Kashmir
Muzaffarabad 13100, Pakistan*

²*Environmental Sciences, Department COMSATS Institute of Information Technology
Vehari Campus, Pakistan*

³*Department of Biotechnology, Mirpur University of Science and Technology (MUST)
Mirpur 10250, (AJK), Pakistan*

⁴*Department of Botany, Mirpur University of Science and Technology (MUST)
Bhimber, (AJK), Pakistan*

**Corresponding author
e-mail: ejazdar1@gmail.com*

(Received 15th Nov 2017; accepted 7th Mar 2018)

Abstract. Soil erosion negatively affects vegetation that brings deteriorating changes in the structure and composition of plant communities. Present study investigated the impact of soil erosion on vegetation along Jhelum valley road District Muzaffarabad, Azad Jammu and Kashmir. Phytosociological attributes were measured by using quadrat method. Geographical characters of each site were recorded including slope, aspect and elevation of eroded sites. Five sites were selected three were disturbed and two were used as control sites for general comparison. At disturbed sites Average Shannon diversity was 2.47; Simpson diversity was 0.94; Species richness was 1.75; Evenness was 0.7. At control sites. Average Shannon diversity was 2.95; Simpson diversity was 0.97; Species richness was 2.02; Evenness was 0.72. Maximum similarity was 66.13 recorded between Control site 1 and Control site 2 while minimum similarity was 22.98 recorded between disturbed site 1 and Control site 1. There was a general trend of low diversity of trees and shrubs at disturbed sites as compared to control sites. Therophytes were dominant at disturbed site and regeneration pattern was high at disturbed sites. A total of 99 plants representing 91 genera belonging to 45 families were recorded from investigated area. The dominant family was Poaceae followed by Asteraceae, Lamiaceae and Rosaceae. At disturbed sites Shannon diversity was 2.47; Simpson diversity was 0.94; Species richness was 1.75; Evenness was 0.7. At control sites Shannon diversity was 2.95; Simpson diversity was 0.97; Species richness was 2.02; Evenness was 0.72. At control sites, more diversity and richness was observed as compared to disturbed sites.

Keywords: *soil erosion, vegetation disturbance, vegetation regime, roadside vegetation pattern, Himalayas, anthropogenic impacts*

Introduction

The process of detachment of soil particles from soil surface and their deposition elsewhere is known as soil erosion. It reduces the productivity of soil in several ways; it decreases the water holding capacity, reduces the efficiency of plant nutrients, damage seedlings, decrease plant rooting depth, increase runoff and reduces its infiltration rates (Pimentel, 2006). Soil erosion has major effects on species composition, seed density and distribution of soil seed bank (Blaikie, 2016; Cheng et al., 2006). Soil erosion

occurs when the soil is left exposed to rain energy. Raindrops hit bare soil with great energy and easily displace the soil particles from the surface. In this way raindrops remove a thin layer of soil from land surface and generate sheet erosion (Oldeman, 1997). Rainfall energy is the cause of erosion from bare land, occurring when the soil lacks protective vegetation cover. The main cause for erosion is due to deforestation, improper treatment of catchment and other anthropogenic activities (Mahabaleshwara and Nagabhushan, 2014).

During erosion process organic matter and essential plant nutrients are detached and soil depth is reduced. These changes not only reduce vegetative growth but also reduce the presence of precious biota and overall biodiversity and soil loss (Pimentel et al., 1995). Eroded soil carries away very important plant nutrients such as nitrogen, phosphorous, potassium and calcium. Typically, eroded soil contains about 3 times more nutrients than are left in the remaining soil (Lieskovský and Kenderessy, 2014; Pimentel, 2006). Vegetation or plant cover reduces the soil erosion, its effectiveness depending upon the height and continuity of canopy, density of ground cover and root density. Forests are most effective in reducing erosion because of their canopy and dense grass (Zuazo and Pleguezuelo, 2009). The Plant cover protects soil against erosion by reducing water runoff (Puigdefábregas, 2005; Rey, 2003). Soil erosion is a physical stress affecting vegetation development and also is controlled by the response of vegetation (Shihong et al., 2003). Soil erosion can reduce soil water holding capacity and nutrients availability to inhibit the vegetation regeneration and succession and decrease vegetation cover and species richness at any disturbed site (Guerrero-Campo and Montserrat-Martí, 2004). Soil erosion is not only a negative factor on vegetation, but it is also the driving force of vegetation development and succession at any disturbed site. Effect of soil erosion on vegetation begins at the formation and development of seed and runs through the whole process of plant growth through effects on seed availability, seed redistribution, seed germination. Seeds are the foundation stone of vegetation processes of colonization Different erosion environment has showed that soil erosion is main cause of reduced cover, decrease species richness and slowed succession (Guerrero-Campo and Montserrat-Martí, 2000; Zhou et al., 2016).

The vegetation of Himalayas is highly disturbed by landslides and erosion and this phenomenon is mostly linked with diverse human activities, such as the construction of roads and buildings and removal of forests. An overall erosion impact from earthquakes is comparatively minimal mainly because these events are relatively rare. Natural phenomenon that caused erosion such as exceptional rains, earthquakes and glacial lake outburst flooding in the high Himalayas are common (Shrestha, 1997). The objective of the current study were to assess the impact of soil erosion on vegetation degradation in the investigated area, to investigate the causes of soil erosion and effects of environmental factors influencing the vegetation and compare the species diversity on eroded and control sites.

Material and Methods

This study was conducted to study impact of erosion along roadsides. Study area lies in district Muzaffarabad, the capital of the state of Azad Jammu and Kashmir situated between 34.24° latitude and 73.22° longitude in north-east of Pakistan (*Fig. 1*). The climate of the area falls under sub-tropical and humid type and varies considerably. The maximum temperature of the area recorded in the summer is 40.0 to 47.5°C and

minimum is 28.0 to 37.5°C respectively. The maximum temperature of the area recorded in the winter is 15.0 to 21.5°C and minimum is -3.0 to -1.0°C. The average annual precipitation of the district is 1511 mm. Maximum rain fall recorded in the month of July as 288.03mm whereas minimum rainfall recorded in the month of October as 36.21mm. Average relative humidity value with maximum value 76.81% and minimum value is 44.57% (PAK-MET, 2012).

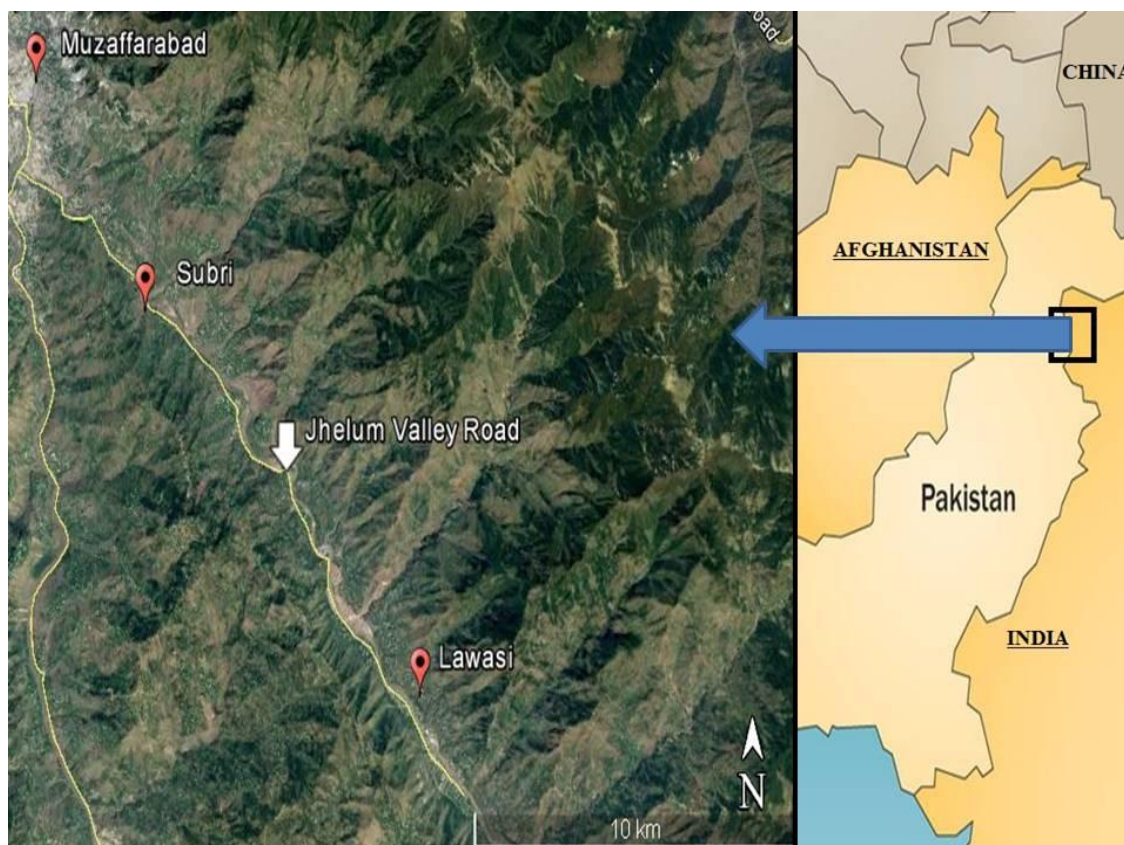


Figure 1. Map of Study area and satellite imagery of the sampling sites

This study was designed to assess vegetation cover of 3 disturbed sites and two undisturbed sites were selected nearby the disturbed site to act as control sites for comparative analysis. Quadrat method was used for vegetation sampling. The vegetation was sampled in three layers i.e., trees, shrubs and herbs. Quadrat size used for trees layer was 10×10, for shrubs layer 5×5 and 1×1 for herb layer (Fosaa, 2004). The diversity index for all the three layers tree, shrub and herb at each site was computed by Shannon-Wiener information index and dominance by Simpson's index (Ahmed et al., 2006). The vegetation data was quantitatively analyzed for abundance, density, cover and frequency. Altitude, latitude and longitude of each selected sites were recorded by using a Garmin 200 global positioning system (GPS). The Multivariate ordination techniques were applied for statistical analysis of the results. Data was subjected to PCA and Cluster analysis (Ter Braak and Smilauer, 2002).

Results

A total of 99 species representing 91 genera belonging to 45 families were recorded. The major contributors of local flora included *Poaceae* with 11 species, followed by *Asteraceae* with 9 species, *Lamiaceae* with 6 species, *Rosaceae* had 5 species. *Cyperaceae* and *Fabaceae* with 4 species each, *Amaranthaceae*, *Verbeneceae*, *Euphorbiaceae*, *Malvaceae* and *Polygonaceae*, *Pteridaceae* with 3 species whereas *Apocynaceae*, *Brassicaceae*, *Oleaceae*, *Salicaceae*, *Lythraceae*, *Anacardiaceae*, *Solanaceae* and *Rhamaceae* were represented by 2 species. The remaining families had single representative (Table 2). At disturbed sites the dominant species according to their Importance value were *Arundo donax* (12.22) and *Justicia adhatoda* (10.94), *Aristida purpurea* (7.01), *Xanthium strumarium* (7.01), *Euphorbia hirta* (9.08) (Table 1). At control sites the dominant species were *Pinus roxburgii* (2.79), *Ficus palmata* (2.00), *Indigofera heterantha* (3.13), *Zanthoxylum armatum* (2.15), *Conyza bonariensis* (8.12) and *Cynodon dactylon* (7.72). Therophytes were the dominant life form class having a percentage of 29.2% and Microphylls with a percentage of 35.3. At disturbed sites average Shannon diversity was 2.47; Simpson diversity was 0.94; species richness was 1.75; evenness was 0.7. At control sites average Shannon diversity was 2.95; Simpson diversity was 0.97; species richness was 2.02; evenness was 0.72. Maximum similarity was 66.13 recorded between control site 1 and control site 2 while minimum similarity was 22.98 recorded between disturbed site 1 and control site 1 (Table 3).

Aristida- Themeda- Cyperus Community was located in Subri at an altitude of 815 m and was classified as a disturbed site having a total of 22 species. The slope of the stand was about 30⁰ to 60⁰ (class 2). The site was located at east facing aspect. The dominant species were *Aristida purpurea* having IVI value of 35.08 followed by *Themeda anathera* having IVI value of 32.62 and *Cyperus exaltatus* having IVI value of 26.15. The codominant species was *Arundo donax* having IVI values of 23.75. Simpson and Shannon diversity values of community were 0.91 and 2.19 respectively, species richness; 1.20, species evenness; 0.70 and maturity index was 41.81 (Table 2). In the community 5 seedlings of *Alianthus altissima* and 1 seedling of *Pistacia integerrima*, 1 seedling of *Dalbergia sissoo* and 1 seedling of *Mallotus philippensis* were recorded.

Table 1. Importance Value Index (IVI) recorded from the investigated area

No.	Botanical name	Site 1	Site 2	Site 3	Site 4	Site 5	Av. IVI
1	<i>Acacia arabica</i>	0	0	0	5.54	3.124	1.73
2	<i>Achyranthes aspera</i>	0	0	0	5.18	0	1.03
3	<i>Adiantum venustum</i>	0	0	7.9	0	5.861	2.75
4	<i>Adiantum caudatum</i>	0	0	8.2	0	0	1.64
5	<i>Ajuga bracteosa</i>	0	3.25	10.31	1.58	0	3.02
6	<i>Alianthus altissima</i>	0	0	0	3.68	6.283	1.99
7	<i>Amaranthus viridis</i>	0	0	4.8	4.13	2.959	2.37
8	<i>Aristida purpurea</i>	35.08	0	0	0	0	7.01
9	<i>Arundo donax</i>	23.75	29.74	0	7.62	0	12.22
10	<i>Avena sativa</i>	0	0	0	7.66	1.58	1.84
11	<i>Bauhinia variegata</i>	0	0	0	3.6	0	0.72
12	<i>Berberis lycium</i>	0	0	0	4.37	7.767	2.42
13	<i>Bidens pilosa</i>	12.41	7.02	5.97	0	7.046	6.48
14	<i>Callicarpa macrophylla</i>	0	8.39	0	0	0	1.67

15	<i>Calotropis gigantea</i>	0	0	3.86	0	0	0.77
16	<i>Cannabis sativa</i>	0	0	2.3	0	6.584	1.77
17	<i>Capsella-bursa pastoris</i>	0	0	0	3.16	3.823	1.39
18	<i>Carissa opaca</i>	0	0	6.24	3.25	0	1.95
19	<i>Celtis eriocarpa</i>	0	0	0	1.28	0	0.25
20	<i>Chenopodium album</i>	0	6	3.33	5.61	7.198	4.42
21	<i>Cichorium intybus</i>	0	4.85	2.06	2.79	2.198	2.37
22	<i>Cirsium arvense</i>	0	7.09	0	1.8	3.132	2.40
23	<i>Conyza bonariensis</i>	8.47	6.17	6.87	11.6	7.523	8.12
24	<i>Cynodon dactylon</i>	0	13.79	6.07	4.28	14.472	7.72
25	<i>Cynoglossum lanceolatum</i>	5.66	4.85	2.3	4.13	6.254	4.63
26	<i>Cyperus exaltatus</i>	26.15	6.68	0	0	0	6.56
27	<i>Cyperus rotundus</i>	18.47	0	0	0	0	3.69
28	<i>Dalbergia sissoo</i>	0	0	0	2.91	0	0.58
29	<i>Desmodium elegans</i>	0	0	0	6.04	3.186	1.84
30	<i>Dichanthium annulatum</i>	0	3.42	6.2	5.29	0	2.98
31	<i>Diospyros lotus</i>	0	0	0	1.51	0	0.30
32	<i>Dodonaea viscosa</i>	11.33	15.49	6.79	0	11.242	8.97
33	<i>Duchesnea indica</i>	0	7.53	0	5.49	13.535	5.31
34	<i>Echinochloa colona</i>	0	0	0	4.8	0	0.96
35	<i>Elaeagnus umbellata</i>	0	0	0	4.5	0	0.9
36	<i>Eleocharis indica</i>	0	4.51	0	0	0	0.90
37	<i>Equisetum debile</i>	0	0	0	0	3.286	0.65
38	<i>Erioscirpus comosus</i>	0	6.34	0	0	0	1.26
39	<i>Euphorbia hirta</i>	0	6.85	13.22	0	2.497	4.51
40	<i>Euphorbia prostrata</i>	6.3	7.26	1.92	2.94	3.943	4.41
41	<i>Ficus palmata</i>	0	0	0	2.73	7.299	2.00
42	<i>Grewia villosa</i>	0	0	0	2.86	4.676	1.50
43	<i>Heteropogon controtus</i>	8.09	0	0	0	0	1.61
44	<i>Hibiscus rosa sinensis</i>	0	7.67	0	0	0	1.53
45	<i>Indigofera heterantha</i>	0	0	0	12.51	3.179	3.13
46	<i>Ipomoea eriocarpa</i>	0	4	0	0	0	0.8
47	<i>Jasminum officinale</i>	0	0	3.86	3.53	0	1.47
48	<i>Justicia adhatoda</i>	0	0	45.39	0	9.322	10.94
49	<i>Lantana camara</i>	0	0	10.07	0	0	2.01
50	<i>Lepidium bidentatum</i>	0	0	2.53	0	0	0.50
51	<i>Mallotus philippensis.</i>	0	0	0	5.46	1.559	1.40
52	<i>Malvastrum corommandelianum</i>	0	0	7.01	5.01	6.155	3.63
53	<i>Maytenus royleanus</i>	0	0	13	7.2	6.448	5.32
54	<i>Melia azedarach</i>	0	0	0	3.56	5.48	1.80
55	<i>Mentha royleana</i>	0	4.51	0	4.28	2.812	2.32
56	<i>Micromeria biflora</i>	0	0	9.98	3.59	6.9	4.09
57	<i>Morus alba</i>	0	0	0	3.33	3.146	1.29
58	<i>Myrsine africana</i>	0	0	0	5.5	0	1.1
59	<i>Nepeta erecta</i>	0	6.68	5.13	3.42	8.06	4.65
60	<i>Oenothera rosea</i>	9.72	4.85	2.3	3.04	7.142	5.41

61	<i>Olea ferrugenia</i>	0	0	0	2.65	3.339	1.19
62	<i>Otostegia limbata</i>	0	0	7.73	0	0	1.54
63	<i>Oxalis corniculata</i>	0	10.08	9.65	7.03	10.934	5.57
64	<i>Parthenium hysterophorus</i>	0	15.6	2.96	6.99	3.579	5.82
65	<i>Persicaria barbata</i>	0	6.34	0	5.01	3.106	2.89
66	<i>Phlomis tuberosa</i>	0	6.04	0	0	0	1.20
67	<i>Phyllanthus fraternus</i>	0	6.68	4.47	1.93	0	2.61
68	<i>Pinus roxburghii</i>	0	0	0	9.11	4.876	2.79
69	<i>Pistacia integerrima</i>	0	0	0	0	3.88	0.77
70	<i>Plantago lanceolata</i>	0	0	0	2.31	0	0.46
71	<i>Populus alba</i>	0	0	0	3.83	3.995	1.56
72	<i>Pteris cretica</i>	6.72	0	0	0	2.344	1.81
73	<i>Punica granatum</i>	17.24	0	7.26	5.86	6.053	7.28
74	<i>Pyrus pashia</i>	0	0	0	3.15	3.558	1.34
75	<i>Rhus cotinus</i>	16.74	0	3.39	5.7	0	5.16
76	<i>Rosa macrophylla</i>	0	15.83	0	3.74	0	3.91
77	<i>Rubus ellipticus</i>	0	7.67	0	5.95	0	2.72
78	<i>Rubus fruticosus</i>	10.79	0	0	12.21	3.326	5.26
79	<i>Rumex hastatus</i>	10.79	0	0	0	1.726	2.50
80	<i>Rumex nepalensis</i>	0	4.92	0	3.16	4.865	2.59
81	<i>Saccharum spontaneum</i>	0	0	0	0	4.892	0.97
82	<i>Salix alba</i>	0	0	0	1.88	4.505	1.27
83	<i>Setaria pumila</i>	0	5.19	3.89	5.89	6.048	3.02
84	<i>Solanum nigrum</i>	0	5.83	2.16	0	2.05	2.00
85	<i>Solanum virginianum</i>	0	0	1.92	0	0	0.38
86	<i>Sonchus asper</i>	6.3	0	1.26	3.27	0	2.25
87	<i>Sorghum halepense</i>	0	0	0	0	3.572	0.71
88	<i>Stellaria media</i>	0	0	4.27	0	0	0.85
89	<i>Tagetes minuta</i>	0	4.17	10.38	0	0	2.91
90	<i>Taraxacum officinale</i>	0	0	2.3	1.8	4.432	1.70
91	<i>Themeda anathera</i>	32.62	0	3.89	0	0	7.30
92	<i>Trifolium repens</i>	0	5.36	0	6.4	0	2.35
93	<i>Verbascum thapsus</i>	0	4.34	1.03	0	0.787	1.23
94	<i>Verbena tenuisecta</i>	0	0	4.1	4.17	1.946	2.04
95	<i>Woodfordia fruticosa</i>	0	0	6.71	0	0	1.34
96	<i>Xanthium strumarium</i>	7.19	24.76	9.89	0	3.602	9.08
97	<i>Zanthoxylum armatum</i>	0	0	7.26	3.5	0	2.15
98	<i>Ziziphus jujuba</i>	10.79	0	0	3.04	2.666	3.29
99	<i>Ziziphus oxyhylla</i>	0	0	7.26	4.24	2.519	2.80

Arundo-Xanthium-Rosa Community was located in Subri at an altitudinal range of 732m and was classified as a disturbed site comprising 37 species. The slope of the stand was about 0° to 30° (class 1). The site was located at west facing aspect. The dominant species of the stand were *Arundo donax* having IVI value of 29.74 followed by *Xanthium strumarium* having IVI value of 24.76, *Rosa macrophylla* having IVI

value of 15.83. The co dominant species were *Dodonaea viscosa* and *Parthenium hysterophorus* having IVI value of 15.49 and 15.6 respectively. Average value of diversity recorded were 0.96 and 2.47, species richness; 1.61, species evenness; 0.68 and maturity index was 33.78 (Table 1) In the stand one seedling of *Populus alba* and *Dalbergia sissoo* and 2 seedlings of, *Morus alba* and *Acacia arabica* were recorded.

Justicia-Euphorbia-Maytenus Community was located in Lawasi at an altitudinal range of 740m and was classified as a disturbed site. It was. The latitude and longitude of the area were 34°22'501" N and 73°29'769" E comprises of 46 species. The slope of the stand was about 30° to 60° (class 2). The site was located at west facing aspect. The dominant species of the community were *Justicia adhatoda* having IVI value of 45.39 followed by *Euphorbia hirta* having IVI value of 13.22 and *Maytenus royleana* having IVI value of 13. The co dominant species were *Tagetes minuta*, *Ajuga bracteosa* and *Lantana camara* having IVI value of 10.38, 10.31 and 10.07 respectively. Average values of diversity index recorded in the community were Simpson's and Shannon diversity; 0.97 and 2.76 respectively, species richness; 2.46, species evenness; 0.72 and maturity index value was 32.39 (Table 1). Single seedling of *Melia azedarach*, *Grewia villosa*, *Dalbergia sissoo*, *Mallotus philippensis*, *Olea ferruginea*, *Celtis eriocarpa*, *Bauhinia variegata* were recorded in the area.

Indigofera-Rubus-Conyza Community was located in Sundgran at an altitudinal range of 760 m. and was classified as a control site. The latitude and longitude of the area were 34° 19'907" N and 073°30'299" E. Community comprises of 65 species. The slope of the stand was 0° to 30° (class 1). The site was located at east facing aspect. The dominant species of the stand was *Indigofera heterantha* having IVI value of 12.51 followed by *Rubus fruticosus* having IVI value of 12.21 and *Conyza bonariensis* having IVI value of 11.6. The co dominant species were *Pinus roxburgii* and *Avena sativa* having IVI values of 9.11 and 7.66 respectively. Average values of diversity index recorded for communities were 0.98 and 3.02, species richness; 2.06, species evenness; 0.74; and maturity index was 30.64 (Table 2).

Table 2. Phytosociological parameters recorded from the investigated area

Community	No. of species	Simpson diversity	Shannon diversity	Richness	Evenness	Maturity
Disturbed site 1	22	0.91	2.19	1.20	0.70	41.81
Disturbed site 2	37	0.96	2.47	1.61	0.68	33.78
Disturbed site 3	46	0.97	2.76	2.46	0.72	32.39
Average		0.94	2.47	1.75	0.7	35.99
Control site 1	65	0.98	3.02	2.06	0.74	30.64
Control site 2	59	0.97	2.88	1.98	0.70	39.41
Average		0.97	2.95	2.02	0.72	35.02
Average		0.95	2.71	1.88	0.71	35.50

Cynodon-Duchesnea-Zanthoxylum Community was located in Garhi dupata at an altitudinal range of 1199m and was classified as a control site. The latitude and longitude of the site were 34°15'867" and 73°34'650" respectively. Community comprises of 59 species. The slope of the stand was about 0° to 30° (class 1). The site was located at south facing aspect. The dominant species were *Cynodon dactylon* having IVI value of 14.472 followed by *Duchesnea indica* having IVI value of 13.535,

Zanthoxylum armatum having IVI value of 11.608. The co dominant species were *Dodonaea viscosa* and *Oxalis corniculata* having IVI value of 11.242 and 10.932 respectively. Average values of diversity recorded for community were 0.97 and 2.88, species richness; 1.98, species evenness; 0.70 and maturity index value was 39.41 (Table 2).

Table 3. Index of Similarity and Dissimilarity between the study sites

Community	Disturbed site1	Disturbed site 2	Disturbed site 3	Control site 1	Control site 2	
Disturbed site 1	×	30.50	32.35	22.98	27.16	I.Ss
Disturbed site 2	69.5	×	50.60	45.09	45.03	
Disturbed site 3	67.65	49.4	×	43.24	45.71	
Control site 1	77.02	54.91	56.76	×	66.12	
Control site 2	72.84	54.97	54.29	33.88	×	
		I.Ds				

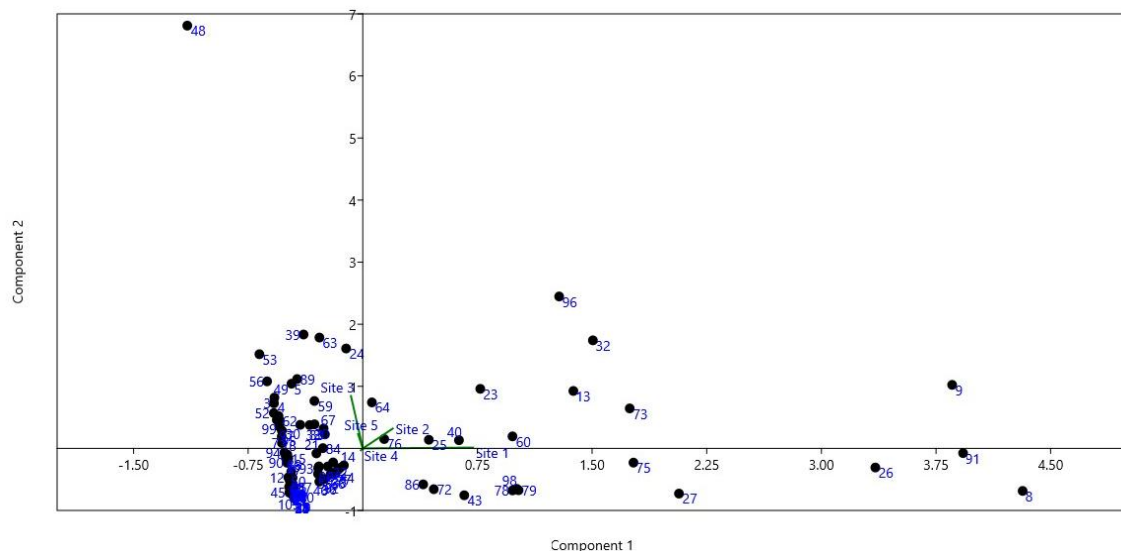


Figure 2. PCA Bi plot of the studied communities from the study site (For corresponding numbers please see Table 1)

PCA biplot showed representative species of the area separated away along the X-axis i.e. *Arundo donax*, *Aristida purpurea* representing their ultra-dominance in studied sites. *Euphorbia hirta*, *Heteropogon controtus*, *Matyenus royleana*, *Cynodon dactylon* were significantly correlated with the disturbed sites. *Justicia adhatoda* was significantly correlated with site 3 (Fig. 2). Cluster analysis grouped the data of disturbed and undisturbed sites in to the associations based on species correlation and dominance in communities. Cluster analysis had shown 5 associations of all communities (Fig. 3).

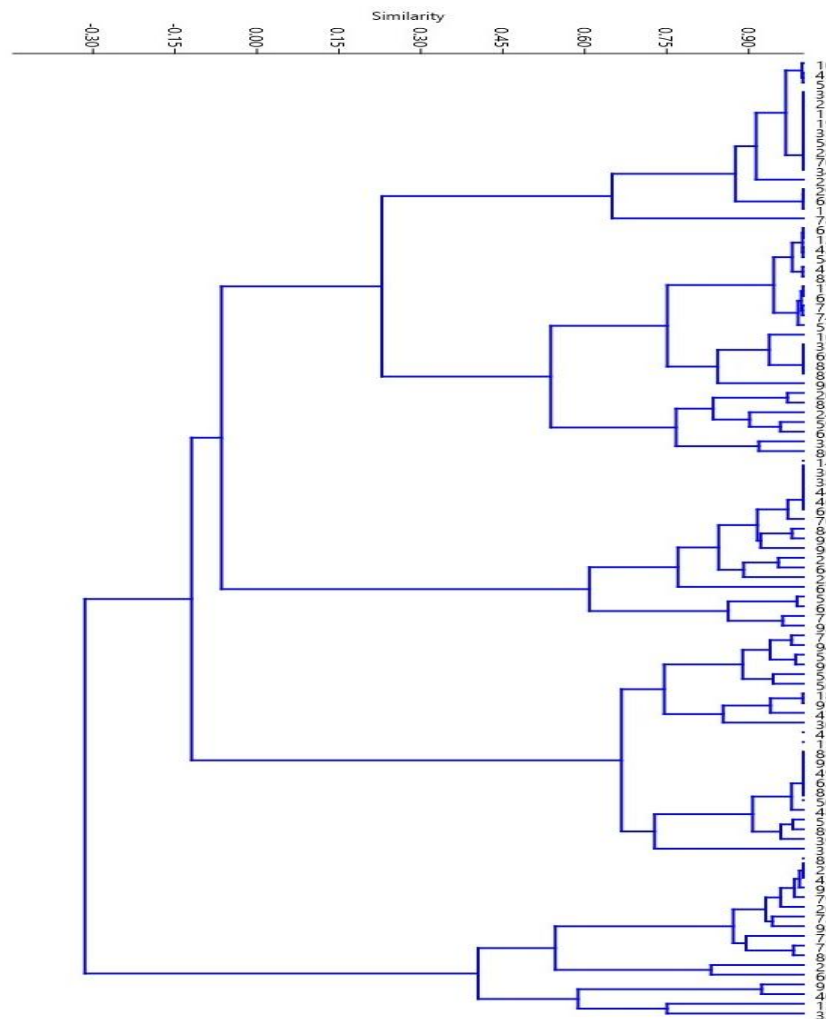


Figure 3. Dendrogram showing Cluster Analysis of the studied communities (For corresponding numbers please see Table 1)

Discussion

The study revealed that different factors affecting the vegetation of area like grazing, trampling, road construction, browsing and erosion. Soil erosion affecting vegetation development and also controlled by the response of vegetation (Shihong et al., 2003). Productivity of soil loss due to erosion because the top soil is removed, root depth reduced and plant nutrients like potassium, nitrogen, calcium are removed. When nutrients are removed by erosion then plant growth is stunted and overall productivity of soil decline. Due to erosion cover reduced, species richness decreased and succession slow down. Slope had negative impact on plant density and diversity, with increase in the degree of slope the recorded density and diversity was low in the area. At disturbed site 1 plant density and diversity low due to slope. Similar conclusion suggested by Walker et al. (2013) stating that slope and vegetation negatively relate to each other the less the slope the greater the density and diversity. On a steep slope erosion increase because the vegetation cover of annual plant decreases (Koulouri and Giourga, 2007). Aspect may also influence on soil erosion. On investigated area both aspects have same species so no clear differences were recorded. A slower recovery of vegetation and

higher erosion rates are expected in southern and western than in northern and eastern direction. As a result, southern exposed slopes usually have a lower vegetation cover than northern exposed slopes (Zuazo and Pleguezuelo, 2009). Species diversity was negatively related to the soil erosion. Average Shannon diversity index recorded was 2.71 and Average Simpson diversity recorded was 0.95. At disturbed sites Shannon and Simpson diversity was low as compared to control sites. Higher diversity value shown by control sites (2.95) which is indicator of low disturbance and low diversity recorded at disturbed sites (2.47) showing more disturbances. Similar results drawn by Luo (1996) in Hetian Fujian that at disturbed sites diversity index low because vegetation cover low on eroded site and at control sites Shannon diversity index high due to increased number of species and also natural invasion increased. At disturbed sites average species richness was low (1.75) and at control sites average species richness was high (2.02). Similar results drawn by Uniyal et al. (2010) in Gharwal Himalaya that at disturbed sites richness was low due to high erosion intensity and other anthropogenic activities while at control site species richness was high which indicates the opening of canopies that favors the growth of plant species which gives overall stability to the communities. Results showed that at disturbed site 3 species richness increased as (2.46) due to invasion of non-native flora. Eroded site break the dominance of native species that creates a condition for fast growing invasive species to attain dominance (Tang et al., 2011). Species richness and diversity was low at site 1 with increasing altitude. Sher and Khan (2007) reported the similar findings that at high altitude cover remain low and species richness and diversity decreased with increased of altitude due to trampling, grazing and soil erosion in the area. The decrease in diversity and species richness at high altitude is due to the reduced growing season, low temperature and low productivity (Diemer and Körner, 1998). Average specie evenness recorded was 0.7. Specie evenness fluctuates between stands differently might be due to disturbance in the area (Fosaa, 2004). Higher species number was found at low disturbed areas and low species number was found at highly disturbed area (Erenso et al., 2014). High dissimilarity was recorded between control and disturbed sites (77.02). High dissimilarity is due to difference in level of disturbance, microclimatic condition and altitudinal range (Javed et al., 2006). Therophytes were the dominant life form which is the indicator of the subtropical zone; it was followed by Nanophanerophytes, Megaphanerophytes, Hemicryptophytes, Chamaephytes, Geophytes, Phanerophytes and Lianas. Life form classes are indicators of micro as well as macro habitat of the species (Guo et al., 2009). Therophytes are experts of occupying vacant niches as a result of disturbances (Pyšek et al., 2005). Leaf size classes showed that vegetation of the investigated area was dominated by Microphyll, indicating the impact of xeric conditions decreasing the leaf size (Kar et al., 2010). Low maturity index of plant communities showed unbalanced and heterogenous nature of local flora. This effect is also enhanced by anthropogenic disturbances or natural disturbances which inhibit the establishment of vegetation to reach a climax stage (Saxena and Singh, 1984). The vegetation attributes of both control and disturbed sites showed impacts overall disturbance in whole investigated area.

Regeneration capacity was also examined on investigated sites. High regeneration was reported at disturbed sites while on control sites no seedlings were found. At disturbed sites adjacent to control sites, the dominant trees were *Pinus roxburgii* and *Ficus palmata*. Joshi (1990) also reported the presence of *Pinus roxburghii* at the disturbed sites adjacent to control sites. Climatic factors and biotic interference also

influence the regeneration of different species (Sen et al., 2008). Dominant grass species recorded from disturbed sites were *Aristida purpurea*, *Arundo donax*, *Cynodon dactylon*, *Themeda anathera*. These species help to stabilize the disturbed sites due to their dense cover. Vegetation restoration plays an important role for degraded ecosystem rehabilitation. Recovery after disturbance indirectly controls the soil erosion rates (Fenli et al., 2002). The establishment of grass species play a significant role in ecological restoration which have been successfully grown on degraded land (Török et al., 2008). Revegetation on eroded sites improves the soil aggregate stability by accelerating vegetation development (Burri et al., 2009).

Conclusion

Current investigation showed that *Arundo donax* and *Justicia adhatoda* were dominant species at site adjacent to control sites. *Ajuga bracteosa*, *Arundo donax*, *Cichorium intybus*, *Cirsium arvense*, *Conyza bonariensis*, *Cynodon dactylon*, *Cynoglossum lanceolatum*, *Dichanthium annulatum*, *Duchesnea indica*, *Euphorbia prostrata*, *Nepeta erecta*, *Oenothera rosea*, *Oxalis corniculata*, *Parthenium hysterophorus*, *Persicaria barbata* and *Rosa macrophylla* were common to both disturbed and undisturbed sites. Undisturbed sites had lower number of herb species as compared to disturbed sites. At disturbed sites, more shrubs and herbs were recorded due to open canopy as more light reached at forest floor allowing more species to grow.

REFERENCES

- [1] Ahmed, M., Husain, T., Sheikh, A., Hussain, S. S., Siddiqui, M. F. (2006): Phytosociology and structure of Himalayan forests from different climatic zones of Pakistan. – Pakistan Journal of Botany 38 (2): 361-383.
- [2] Blaikie, P. (2016): The political economy of soil erosion in developing countries: Routledge.
- [3] Burri, K., Graf, F., Böll, A. (2009): Revegetation measures improve soil aggregate stability: a case study of a landslide area in Central Switzerland. – Forest Snow and Landscape Research 82 (1): 45-60.
- [4] Cheng, J., Wan, H., Hu, X. (2006): Soil seed bank and meadow renewal in the grassland on Loess Plateau. – Acta Pedologica Sinica 43: 679-683.
- [5] Diemer, M., Körner, C. (1998): Transient enhancement of carbon uptake in an alpine grassland ecosystem under elevated CO₂. – Arctic and Alpine Research 30 (4): 381-387.
- [6] Erenso, F., Maryo, M., Abebe, W. (2014): Floristic composition, diversity and vegetation structure of woody plant communities in Boda dry evergreen Montane Forest, West Showa, Ethiopia. – International Journal of Biodiversity and Conservation 6 (5): 382-391.
- [7] Fenli, Z., Keli, T., Cheng-e, Z., Xiubin, H. (2002): Vegetation destruction and restoration effects on soil erosion process on the loess plateau. – Paper presented at the 12 th International Soil Conservation Organization Conference (ISCO), Beijing, China.
- [8] Fosaa, A. M. (2004): Biodiversity patterns of vascular plant species in mountain vegetation in the Faroe Islands. – Diversity and Distributions 10 (3): 217-223.
- [9] Guerrero-Campo, J., Montserrat-Martí, G. (2004): Comparison of floristic changes on vegetation affected by different levels of soil erosion in Miocene clays and Eocene marls from Northeast Spain. – Plant Ecology 173 (1): 83-93.
- [10] Guerrero-Campo, J., Montserrat-Martí, G. (2000): Effects of soil erosion on the floristic composition of plant communities on marl in northeast Spain. – Journal of Vegetation Science 11 (3): 329-336.

- [11] Guo, Q., Wang, X., Bar, G., Kang, Y., Hong, M., Pei, S., Zhang, F. (2009): Life form spectra, leaf character, and hierarchical-synusia structure of vascular plants in *Thuja sutchuehensis* community. – *Ying yong sheng tai xue bao= The journal of applied ecology* 20 (9): 2057-2062.
- [12] Javed, H. I., Naz, N., Hameed, M. (2006): Ecology of birds of Kuppi plantation, Faisalabad, Pakistan. – *I. Phyto-sociology. Rec. Zool. Surv. Pakistan* 17: 21-36.
- [13] Joshi, M. (1990): A study on soil and vegetation changes after landslide in Kumaun Himalaya. – *Proceedings of the Indian National Science Academy B* 56: 351-359.
- [14] Kar, P., Biswal, A., Barik, K. (2010): Floristic composition and biological spectrum of a grassland community of Rangamatia in the district of Mayurbhanj, Odisha. – *J. Curr. Sci.* 15 (2): 465-469.
- [15] Koulouri, M., Giourga, C. (2007): Land abandonment and slope gradient as key factors of soil erosion in Mediterranean terraced lands. – *Catena* 69 (3): 274-281.
- [16] Lieskovský, J., Kenderessy, P. (2014): Modelling the effect of vegetation cover and different tillage practices on soil erosion in vineyards: a case study in Vráble (Slovakia) using WATEM/SEDEM. – *Land Degradation & Development* 25 (3): 288-296.
- [17] Luo, X. S. (1996): The study on species diversity of vegetation community in soil erosion area of Hetian, Fujian. – *Soil and Water Conservation* 3: 48-50.
- [18] Mahabaleshwara, H., Nagabhushan, H. (2014): A study on soil erosion and its impacts on floods and sedimentation. – *International Journal of Research in Engineering and Technology* 3 (3): 443-451.
- [19] Oldeman, L. (1997): Soil Degradation: A Threat to Food Security? – Paper presented at the International Conference on Time Ecology: "Time for Soil Culture-Temporal Perspectives on Sustainable Use of Soil", April 6-9, 1997, Tutzing.
- [20] PAK-MET. (2012): The normals of climatic data of Azad Jammu and Kashmir. – Pakistan meteorological Department Government of Pakistan Islamabad, Pakistan. .
- [21] Pimentel, D. (2006): Soil erosion: a food and environmental threat. – *Environment, Development and Sustainability* 8 (1): 119-137.
- [22] Pimentel, D., Harvey, C., Resosudarmo, P., Sinclair, K., Kurz, D., McNair, M., Crist, S., Shpritz, L., Fitton, L., Saffouri, R. (1995): Environmental and economic costs of soil erosion and conservation benefits. – *Science* 267 (5201): 117-1123.
- [23] Puigdefábregas, J. (2005): The role of vegetation patterns in structuring runoff and sediment fluxes in drylands. – *Earth Surface Processes and Landforms* 30 (2): 133-147.
- [24] Pyšek, P., Jarošík, V., Kropáč, Z., Chytrý, M., Wild, J., Tichý, L. (2005): Effects of abiotic factors on species richness and cover in Central European weed communities. – *Agriculture, ecosystems & environment* 109 (1-2): 1-8.
- [25] Rey, F. (2003): Influence of vegetation distribution on sediment yield in forested marly gullies. – *Catena* 50 (2-4): 549-562.
- [26] Saxena, A., Singh, J. (1984): Tree population structure of certain Himalayan forests and implications concerning the future composition. – *Vegetation* 58: 61-69: bibliography.
- [27] Sen, A., Johri, T., Bisht, N. (2008): Analysis of the effects of anthropogenic interferences on tree species composition in the forests of Dadra and Nagar Haveli, India. – *Current Science* 95 (1): 50-58.
- [28] Sher, Z., Khan, Z. (2007): Floristic composition, life form and leaf spectra of the vegetation of Chagharzai Valley, District Buner. – *Pakistan Journal of Plant Sciences* 13(1): 57-66.
- [29] Shihong, L., Wusheng, X., Xiankun, L., Runqin, T. (2003): A review of vegetation restoration in eroded area of red soil. – *Guangxi Zhiwu* 23 (1): 83-89.
- [30] Shrestha, D. P. (1997): Assessment of soil erosion in the Nepalese Himalaya: a case study in Likhu Khola Valley, Middle Mountain Region. – *Land Husbandry* 2(1): 59-80.
- [31] Tang, C., Zhu, J., Ding, J., Cui, X. F., Chen, L., Zhang, J. S. (2011): Catastrophic debris flows triggered by a 14 August 2010 rainfall at the epicenter of the Wenchuan earthquake. – *Landslides* 8 (4): 485-497.

- [32] Ter Braak, C. J., Smilauer, P. (2002): CANOCO reference manual and CanoDraw for Windows user's guide: software for canonical community ordination (version 4.5): www.canoco.com.
- [33] Török, P., Matus, G., Papp, M., Tóthmérész, B. (2008): Secondary succession of overgrazed Pannonian sandy grasslands. – *Preslia* 80 (1): 73-85.
- [34] Uniyal, P., Pokhriyal, P., Dasgupta, S., Bhatt, D., Todaria, N. (2010): Plant diversity in two forest types along the disturbance gradient in Dewalgarh Watershed, Garhwal Himalaya. – *Current Science* 98 (7): 938-943.
- [35] Walker, L. R., Shiels, A. B., Bellingham, P. J., Sparrow, A. D., Fetcher, N., Landau, F. H., Lodge, D. J. (2013): Changes in abiotic influences on seed plants and ferns during 18 years of primary succession on Puerto Rican landslides. – *Journal of Ecology* 101 (3): 650-661.
- [36] Zhou, J., Fu, B., Gao, G., Lü, Y., Liu, Y., Lü, N., Wang, S. (2016): Effects of precipitation and restoration vegetation on soil erosion in a semi-arid environment in the Loess Plateau, China. – *Catena* 137: 1-11.
- [37] Zuazo, V. c. H. D., Pleguezuelo, C. R. o. R. (2009): Soil-erosion and runoff prevention by plant covers. A review. – In: Lichtfouse, E., Navarrete, M., Debacke, P., Souchere, V., Alberola, C. (eds.) *Sustainable agriculture*. Springer: (pp. 785-811)

SLUG CONTROL IN LEAFY VEGETABLE USING NEMATODE *PHASMARHABDITIS HERMAPHRODITA* (SCHNEIDER)

GRUBIŠIĆ, D.^{1*} – GOTLIN ČULJAK, T.¹ – MEŠIĆ, A.¹ – JURAN, I.¹ – LOPARIĆ, A.¹ –
STARČEVIĆ, D.¹ – BRMEŽ, M.² – BENKOVIĆ LAČIĆ, T.³

¹University of Zagreb, Faculty of Agriculture, Department of Agricultural Zoology
Svetošimunska 25, 10000 Zagreb, Croatia (e-mail: djelinic@agr.hr; phone: +385-1-2393-967)

²J. J. Strossmayer University of Osijek, Faculty of Agriculture in Osijek, 31000 Osijek, Croatia
(e-mail: mbrmez@pfos.hr; phone: +385-31-554-909)

³College of Slavonski Brod, Dr. Mile Budaka 1, 35000 Slavonski Brod, Croatia
(e-mail: Teuta.Benkovic.Lacic@vusb.hr; phone: +385-35-492-630)

*Corresponding author

e-mail: djelinic@agr.hr; phone: +385-1-2393-967

(Received 6th Dec 2017; accepted 27th Feb 2018)

Abstract. Vegetable crops, more than other agricultural crops, are exposed to great damages caused by slugs. Current control methods rely on chemical molluscicides that are often ineffective and harmful to non-target organisms, specially Carabids. Parasitic nematode *Phasmarhabditis hermaphrodita* (Schneider) parasites many slugs and snails and has been formulated as biological molluscicide. In this investigation, effectiveness of *P. hermaphrodita* applied in recommended and half the recommended dose in slug control in greenhouse lettuce and cabbage was evaluated and compared with metaldehyde and methiocarb pellets. Tested molluscicides did not stop feeding of *Arion lusitanicus* Mabilie and did not achieve long term protection from slug damage. The use of standard dose of *P. hermaphrodita* in lettuce and cabbage provided satisfactory protection from slugs to harvest. Half recommended dose of *P. hermaphrodita* showed lower level of protection compared with recommended dose. Repeated applications of half recommended dose of *P. hermaphrodita* could boost molluscicidal effect to the level of the efficacy reached by standard dose, so it could find their place in practice. Effective control of *A. lusitanicus* using parasitic nematodes provides great opportunity to replace chemical molluscicides in organic production and to reduce their negative side effect to non-target organisms and the environment.

Keywords: *Arion lusitanicus*, cabbage, lettuce, molluscicides, parasitic nematodes

Introduction

Slugs are serious pests in many crops all over the world (Godan, 1979; Port and Port, 1986; South, 1992) and present one of the most significant threats to sustainable agriculture (Barker, 2002). Their significance as pests is especially evident in vegetable growing. Leafy vegetables such as lettuce and brassica crops are particularly threatened. Slugs feed on plants but they also contaminate it with mucus and faeces (Port and Ester, 2002). In recent years, the slug species *Arion lusitanicus* Mabilie has become a serious pest throughout Central, Northern and Eastern Europe (De Winter, 1989; Fechter and Falkner, 1990; von Proschwitz, 1997; Briner and Frank, 1998; Turner et al., 1998). In Croatia, *A. lusitanicus* is the most common and the most damaging slug species in vegetable growing (Fischer et al., 1999; Grubišić et al., 2013). Current control methods rely on chemical molluscicides formulated into baited pellets that are often ineffective and can harm non-target organisms. Molluscicides contain metaldehyde or carbamates as active ingredient (Garthwaite and Thomas, 1996; Henderson and Triebkorn, 2002).

In organic agriculture, the use of slug pellets containing metaldehyde or carbamates is restricted or not allowed. The European Union has banned methiocarb slug pellets since 19 September 2014. The other major slug pellet product metaldehyde has come under pressure after the product has been found in watercourses. A new molluscicide based on iron phosphate has been recently registered in many European countries (Speiser and Kistler, 2002; Rae et al., 2009) and shows promise for slug control, particularly in organic agriculture (Iglesias et al., 2001). Tighter controls over metaldehyde-based slug pellets are likely in high-risk water catchment areas to try and cut pesticide levels in drinking water, which will leave only iron phosphate pellets as an alternative. In the meantime, it was evidenced that high doses of iron phosphate increase mortality and reduce surface activity of earthworms (Langan and Shaw, 2006). Therefore, the new solutions for slug control must be investigated. In 1994, the nematode *Phasmarhabdita hermaphrodita* (Schneider) has been commercialized as a biocontrol agent for slug control (Glen et al., 1996). The nematodes are mass produced in liquid medium in fermenters of up to 20 000 L, in monoxenic association with *Moraxella osloensis* Bøvre & Henriksen (Rae et al., 2007). This nematode species is used as an inundative biological control agent lethal to many slug species (Wilson et al., 1993; Glen et al., 1996; Speiser et al., 2001; Iglesias and Speiser, 2001; Grewal et al., 2003) although not all of them were killed at a similar rate, what indicated their different sensitivity to the nematode. It was noticed that sensitivity to *P. hermaphrodita* decreases with increasing of body size in large slug specimens of the family Arionidae (Glen et al., 1996; Speiser et al., 2001; Grimm, 2002; Grewal et al., 2003). Also some authors reported that *P. hermaphrodita* causes significant reduction in the plant damage by inhibiting slugs feeding, without causing their death (Glen et al., 1996; Grimm 2002; Rae et al., 2009). Nematode *P. hermaphrodita* has been used to reduce slug damage in a number of agriculture crops (Rae et al., 2007) and has been successfully used in some vegetable crops like cabbage (Grubišić et al., 2003), asparagus (Ester et al., 2003a), Brussels sprouts (Ester et al., 2003b) and Chinese cabbage (Kozłowski et al., 2014). In UK, commercial growers routinely use *P. hermaphrodita* to reduce slug damage in asparagus, lettuce, Brussels sprouts, cabbage and celery (Rae et al., 2007). Biological products based on nematode *P. hermaphrodita* are more expensive than chemical molluscicides and are not available on some markets and to all vegetable producers. Some investigations were aimed in reducing treatment cost through the reducing numbers of nematodes applied, repeated applications of low doses (Ester et al., 2003a,b; Rae et al., 2006, 2009), application of the recommended rate of nematodes in bands or around individual plants (Rae et al., 2009) and immersion of plant roots (Kozłowski et al., 2014). A significant fact like is that *P. hermaphrodita* may survive approximately six weeks in soil (Kozłowska et al., 2014) or up to 99 days (Vernavá et al., 2004) indicates that it is not necessary to apply the product multiple times, what could bring significant reduction in costs of protecting plants by use of *P. hermaphrodita* based products. The aim of this study was to investigate the possibility of reducing the recommended dose of *P. hermaphrodita*, by using it in combination with metaldehyde and in half recommended dose, in control of slug species *A. lusitanicus* in cabbage and lettuce crops. Also the aim was to check the efficiency of chemical molluscicides in control of *A. lusitanicus*, considering the dissatisfaction of producers with their effectiveness in practice and their limited use in organic production.

Materials and methods

Greenhouse experiment was performed on a commercial lettuce farm at Petina near Zagreb Croatia from October 6 to November 9 2009. Investigation in cabbage was conducted in greenhouse at Čehi near Zagreb Croatia from March 30 to May 5 2010. In both locations prevail alluvial carbonate loamy soil. Mean daily temperature evidenced at Petina, while conducting experiment in lettuce, was 9.3 °C and the mean soil temperature at 10 cm depth was 11.8 °C. Mean daily temperature evidenced at Čehi was 13.4 °C, while the mean soil temperature at 10 cm depth was also 13.4 °C. Lettuce (variety Lollo Bionda) and cabbage (variety Jetma F₁) transplants were planted in rows 30 cm apart. The slug species determined in greenhouse lettuce and cabbage was *A. lusitanicus* (Fig. 1). There were six treatments: (1) untreated control; (2) metaldehyde pellets (5% a.i., recommended rate); (3) methiocarb pellets (4% a.i., recommended rate); (4) *P. hermaphrodita* (30 nematodes per cm², recommended rate); (5) *P. hermaphrodita* (15 nematodes per cm², half the recommended rate) and (6) metaldehyde pellets (half the recommended rate) + *P. hermaphrodita* (half the recommended rate). There were four replicates (2 x 2 m) of each treatment arranged in a randomised block design. In experiment, commercial formulation of *P. hermaphrodita* known as Phasmarhabditis - System (Biobest N.V., Belgium) was used. The nematodes were stirred in watering can full of water and applied over the soil surface using a watering can fitted with a rose (Fig. 2. and Fig. 3). Pellets of molluscicides were broadcasted by hand. Slug damage in lettuce experiment (Table 1) was assessed visually by estimating the percentage of leaf area eaten by slugs 2, 7, 13, 19 and 33 days after treatment and in cabbage experiment 7, 10, 17, 23, 31 and 38 days after treatment (Table 2). All data were subjected to ANOVA and Duncan's New MRT (P=.05). Different intervals in estimating the slug damage were due to different speed of development of the lettuce and cabbage plants in different periods of the year. Also lettuce transplants were more sensitive and gentle so estimating started earlier. In cabbage, estimating lasted longer because of longer period since picking time.



Figure 1. Slug species *Arion lusitanicus* in lettuce



Figure 2. Application of *P. hermaphrodita* in lettuce



Figure 3. Application of *P. hermaphrodita* in cabbage

Results

In greenhouse experiment conducted in lettuce for 33 days (*Table 1*), from the second day onwards, damages evidenced on all treatments were significantly less than on the untreated control, indicated good slug control. Up to day 7 all treatments were equally successful. On day 13 better protection than on the other treatments was provided by metaldehyde pellets applied in recommended dose. Methiocarb pellets were less effective than metaldehyde, what was also confirmed on the last day of assessment. On day 13 recommended dose of *P. hermaphrodita* differed from the other treatments, provided the lowest level of slug control, but from day 19 to day 33 reduction in slug feeding was noticed. On day 33 the level of protection provided by recommended dose of *P. hermaphrodita* was higher than of other treatments. Since day 19 until the end of the experiment, damages on half recommended doses of *P. hermaphrodita* have been in progress.

Table 1. Slug damage (in %) after chemical and biological molluscicides use in lettuce greenhouse experiment

No. of treatment	Treatment	Days after treatment				
		2	7	13	19	33
1	Untreated	65.25 a*	47.00a	50.75a	64.75a	43.00a
2	Metaldehyde	2.00 b	1.75b	4.75c	4.50b	4.00bc
3	<i>P. hermaphrodita</i> ½ dose	3.75 b	2.25b	10.00bc	3.25b	4.00bc
4	<i>P. hermaphrodita</i> ½ dose + ½ dose metaldehyde	1.5 b	2.00b	6.25bc	3.00b	4.00bc
5	<i>P. hermaphrodita</i> recommended dose	3.25 b	1.75b	12.25b	4.50b	3.50c
6	Methiocarb	0.3 b	2.00b	7.25bc	6.00b	5.00b
	LSD P = 5%	5.484	3.677	5.836	5.164	1.263

*means followed by same letter are not significantly different according to Duncan's multiple range test (P=.05)

In the experiment in cabbage (Table 2), all treatments were significantly different from the control, and of equal efficacy in slug control, from the first week to day 23 after treatment. On day 23 metaldehyde showed significantly lower efficacy than other treatments. Towards the end of the experiment (day 38), leaf damages started to increase and the best efficacy in slug control was obtained by the recommended dose of *P. hermaphrodita*. Treatments 2, 3 and 4 did not differ significantly. Methiocarb was significantly less effective than recommended dose of *P. hermaphrodita* and, according to estimated slug damage, though not statistically, less effective than metaldehyde.

Mean percentage of slug damage in lettuce experiment evidenced on all treatments was 4,1% and in cabbage experiment was 17,5%. Considering assessed 43% damage on control plots in lettuce and 43,15 % in cabbage, all treatments significantly reduced slug damage, although they did not stop slug feeding.

Table 2. Slug damage (in %) after chemical and biological molluscicides use in cabbage greenhouse experiment

No. of treatment	Treatment	Days after treatment					
		7	10	17	23	31	38
1	Untreated	27,89a	48,2a	50,52a	20,97a	16,52a	43,15a
2	Metaldehyde	0,5b	2,25b	1,92b	19,24a	12,77ab	15,44bc
3	<i>P. hermaphrodita</i> ½ dose	1,71b	3,36b	3,23b	3,39b	4,71c	20,81bc
4	<i>P. hermaphrodita</i> ½ dose + ½ dose metaldehyde	1,22b	2,22b	2,08b	9,04b	8,52bc	18,52bc
5	<i>P. hermaphrodita</i> recommended dose	0,68b	1,75b	2,17b	4,36b	3,78c	7,22c
6	Methiocarb	3,11b	2,67b	2,33b	9,86b	6,99c	25,37b
LSD P = 5%		3,689	5,513	5,008	8,203	5,125	14,464

*means followed by same letter are not significantly different according to Duncan's multiple range test (P=.05)

Discussion

Slug species *A. lusitanicus* is very hard to control, what has been observed by many vegetable producers (Grubišić et al., 2013). In the experiments in lettuce (lasting for 33 days) and in cabbage (lasting for 38 days) slug feeding was evidenced on all treatments and on every assessment day. In experiment conducted under laboratory conditions in Croatia (Grubišić et al., 2013) adult specimens of *A. lusitanicus* infected by *P. hermaphrodita* died within 3 to 30 days. Death of infected slugs within 4 to 20 days, depending on temperature and abundances of the nematodes, have also been reported by Glen et al. (2000) and Grewal et al. (2001, 2003). At the treatments metaldehyde and methiocarb slugs were dying in the period of 9 to 24 days (Grubišić et al., 2013). Food consumption was reduced on both chemical (methiocarb and metaldehyde) and biological (*P. hermaphrodita*) treatments but the most of adult specimens of *A. lusitanicus* continued to feed with different extent until death (Grubišić et al., 2013) what could explain slug damages evidenced in lettuce and cabbage by the end of field experiments. Some previous investigations (Speiser et al., 2001; Grimm, 2002) also pointed at the negative effect of slug size on the efficacy of *P. hermaphrodita* as the reason of unsatisfactory pest control.

Mean percentage of slug damage in lettuce experiment evidenced on treatments 2, 3, 4, 5 and 6 the last day of assessment was 4,1%, so all treatments significantly reduced slug damage in relation to untreated control. Considering slug pest species *A. lusitanicus* and assessed 43% slug damage on control plots, even higher damages were expected on tested treatments. On day 13 and 19, mean percentage of slug damage on treatment with recommended rate of *P. hermaphrodita* was higher than on half the recommended rate (treatments 5 and 6), though not statistically. Considering results that *D. reticulatum* and *A. ater* actively avoid areas of soil where *P. hermaphrodita* is present at densities of 38 and 120 cm⁻² (Wilson et al., 1999), and a density of 38 cm⁻² is close to the recommended rate of *P. hermaphrodita* (30 cm⁻²), it is possible that at the plots where recommended rate of nematodes were applied, slugs were more of the time at the soil surface thus causing more damage to lettuce. Additionally, larger specimens noticed in lettuce crop usually stay on the soil surface (Frank, 1998) so it could be difficult for nematodes, which were applied on and live in soil to infect them. Many trials (Ester et al., 2003a,b; Grewal et al., 2001; Rae et al., 2009) have shown that repeated applications of low rate of *P. hermaphrodita* provided a significant reduction to slug damage, even as well as metaldehyde pellets. By the end of lettuce experiment (on day 33) equable results were evidenced with only one application of half recommended rate of *P. hermaphrodita* and metaldehyde. On day 33 recommended rate of *P. hermaphrodita* expressed better control of slugs in lettuce than the other treatments and significantly better than methiocarb. Treatment with *P. hermaphrodita* was also superior to methiocarb treatment in several experiments reported by Wilson et al. (1994a,b) and Glen et al. (1996). Repeated application of half recommended rate of *P. hermaphrodita* could boost molluscicidal effect to the level of the efficacy reached by recommended rate of *P. hermaphrodita* at the end of the experiment.

In cabbage experiment recommended rate of *P. hermaphrodita* protected plants from slug damage effectively to day 38. In previous investigations in cabbage crop in Croatia (Grubišić et al., 2003) recommended rate of *P. hermaphrodita* also provided satisfactory protection for 30 days after application, until picking time. Up to day 31 in cabbage experiment, half the recommended dose of *P. hermaphrodita* showed statistically equable results as standard dose of *P. hermaphrodita*, while on day 38 damages on treatment with half recommended dose of *P. hermaphrodita* increased. These results indicate that three to four weeks, after the first application of half the recommended rate, it should be applied again if vegetable is grown for a such a long period. Considering the results obtained by Ester et al. (2003a,b), Grewal et al. (2001), Rae et al. (2009) and the results achieved at the end of both experiments in lettuce and cabbage, the need of repeated application of half the recommended *P. hermaphrodita* rate, about three to four weeks after the first application, in order to maintain the level of efficacy to harvest, should be considered. Vernaváet al. (2004) found that nematodes were still in the soil 99 days after application of biological product based on *P. hermaphrodita*, but the height of nematodes population could be questionable.

Conclusion

All treatments, chemical (based on metaldehyde and methiocarb) and biological (based on parasitic nematode *P. hermaphrodita*), in both experiments significantly reduced slug damage in relation to untreated control. According to estimated slug damage on the last day of assessment in both experiments, though not always

statistically, recommended dose of *P. hermaphrodita* expressed better control of slugs than the other treatments. In practice, in some cases, higher yields or products of higher quality, means a lot to the producers, even the results were not statistically approved. Based on the results achieved in lettuce and cabbage experiment, it was noticed that the height of nematodes population could determine the effectiveness of nematodes in slug control, so re-application of half recommended doses of *P. hermaphrodita*, about three to four weeks after the first application, could be justified. This approach should be tested in further investigations. Re-treatments of chemical molluscicides, due to loss of efficacy, are not allowed because of the waiting period (21 days) and the proximity of harvest. Biological control of slugs using *P. hermaphrodita* should be tested in other vegetable crops in greenhouses but also in the field. The achieved results would be of great importance especially in organic vegetable growing and under the circumstances of the fewer number of limacides on the market.

Acknowledgements. This work was funded by a VIP research project VIII-5-20/08 of Ministry of Agriculture, Fisheries and Rural Development and Ura-dva d.o.o. We thank Leko M d.o.o. for import of *Phasmarhabditis* - System (Biobest N.V., Belgium).

REFERENCES

- [1] Barker, G.M. (2002): Molluscs as Crop Pests. – CABI Publishing. Wallingford, Oxon OX 10 8DE, UK, 468 pp.
- [2] Briner, T., Frank T. (1998): Egg laying activity of the slug *Arion lusitanicus* Mabilie in Switzerland. – Journal of Conchology 36: 9-15.
- [3] De Winter, A.J. (1989): *Arion lusitanicus* Mabilie in Nederland (Gastropoda: Pulmonata: Arionidae). – Basteria 53: 49-51.
- [4] Ester, A., Rozen, K. van, Molendijk, L.P.G. (2003a): Field experiments using rhabditid nematode *Phasmarhabditis hermaphrodita* or salt as control measures against slugs in green asparagus. – Crop Protection 22: 689-695.
- [5] Ester, A., Huiting, H.F., Molendijk, L.P.G., Vlaswinkel, M.E.T. (2003b): The rhabditid nematode *Phasmarhabditis hermaphrodita* Schneider as a potential biological control agent to control field slugs *Deroceras reticulatum* (Müller) in Brussel sprouts. – In: Slugs and Snails: Agricultural, Veterinary and Environmental Perspectives, BCPC Symposium Proceedings No 80. British Crop Protection Council, Alton, Hants, UK: 313-318.
- [6] Fischer, W., Reischütz, A., Reischütz, P.L. (1999): Die Spanische Wegschnecke in Kroatien. – Club Conchylia Informationen 31 (3/4): 15-17.
- [7] Frank, T. (1998): The role of different slug species in damage to oilseed rape bordering on sown wildflower strips. - Annals of applied Biology 133: 483-493.
- [8] Fechter, R., Falkner, G. (1990): Weichtiere. – Steinbachs Naturführer, Mosaik Verlag, München, Germany, 287 p.p.
- [9] Glen, D.M., Wilson, M.J., Hughes, L., Cargeeg Hajjar, A. (1996): Exploring and exploiting the potential of the Rhabditidae nematode *Phasmarhabditis hermaphrodita* as a biocontrol agent for slugs. – In: Henderson, I.F. (ed): Slug & Snail Pests in Agriculture. British Crop Protection Council, Farnham, UK: 271-280.
- [10] Glen, D.M., Wilson, M.J., Brain, P., Stroud, G. (2000): Feeding activity and survival of slugs, *Deroceras reticulatum*, exposed to the rhabditid nematode, *Phasmarhabditis hermaphrodita*: a model of dose response. – Biological Control 17: 73-81.
- [11] Garthwaite, D.G., Thomas, M.R. (1996): The usage of molluscicides in agriculture and horticulture in Great Britain over the last 30 years. – In: Henderson, I.F. (ed): Slug & Snail Pests in Agriculture. British Crop Protection Council, Farnham, UK: 39-46.

- [12] Godan, D. (1979): Schadschnecken und ihre Bekämpfung. – Ulmer, Stuttgart, Germany, 467 p.p.
- [13] Grewal, P.S., Grewal, S.K., Taylor, R.A., Hammond, R.B. (2001): Application of molluscicidal nematodes to slug shelters: a novel approach to economic biological control of slugs. – *Biological Control* 22: 72-80.
- [14] Grewal, S.K., Grewal, P.S., Hammond, R.B. (2003): Susceptibility of north American native and non-native slugs (Mollusca: Gastropoda) to *Phasmarhabditis hermaphrodita* (Nematoda: Rhabditidae). – *Biocontrol Science and Technology* 13: 119-125.
- [15] Grimm, B. (2002): Effect of the nematode *Phasmarhabditis hermaphrodita* on young stages of the pest slug *Arion lusitanicus*. – *Journal of Molluscan Studies* 68: 25-28.
- [16] Grubišić, D., Oštrec, Lj., Dušak, I. (2003): Biological control of slugs in vegetable crops in Croatia. – In: *Slugs and Snails: Agricultural, Veterinary and Environmental Perspectives*, BCPC Symposium Proceedings No 80. British Crop Protection Council, Alton, Hants, UK: 115-120.
- [17] Grubišić, D., Hamel, T., Gotlin Čuljak, T., Loparić, A., Brmež M. (2013): Feeding activity and survival of slug *Arion lusitanicus* (Gastropoda: Arionidae) exposed to the rhabditid nematode, *Phasmarhabditis hermaphrodita* (Nematoda: Rhabditidae). – *Insect pathogens and entomoparasitic nematodes IOBC – WPRS Bulletin* 90: 297-300.
- [18] Grubišić, D., Hamel, T., Gotlin Čuljak, T., Loparić, A., Brmež, M. (2013): Feeding activity and survival of slug *Arion lusitanicus* (Gastropoda: Arionidae) exposed to the rhabditid nematode, *Phasmarhabditis hermaphrodita* (Nematoda: Rhabditidae). – *IOBC-WPRS Bulletin, Proceedings of the Meeting “Biological control - its unique role in organic and integrated production” / Jehle, Johannes A., Bažok, Renata, Crickmore, Neil, Lopez-Ferber, Miguel, Glazer, Itamar, Quesada-Moraga, Enrique, Traugott, Michael. (ur.). Darmstadt : IOBC , 2013. 297-300 (ISBN: 978-92-9067-268-5).*
- [19] Henderson, I.F., Triebkorn, R. (2002): Chemical control of terrestrial gastropods. – In: *Barker, G.M. (ed.) Molluscs as Crop Pests*. CABI Publishing, Wallingford, Oxon OX 10 8DE, UK: 1-31.
- [20] Iglesias, J., Castillejo, J., Castro, R. (2001): Mini – plot field experiments on slug control using biological and chemical control agents. – *Annals of Applied Biology* 139: 285-292.
- [21] Iglesias, J., Speiser, B. (2001): Consumption rate and susceptibility to parasitic nematodes and chemical molluscicides of the pest slug *Arion hortensis* s.s. and *Arion distinctus*. – *Journal of Pesticide Science* 74: 159-166.
- [22] Kozłowska, M., Jaskulska, M., Łacka, A., Kozłowski, R.J. (2014): Analysis of studies of the effectiveness of a biological method of protection for organic crops. – *Biometrical letters*, 51 (1): 45-56.
- [23] Kozłowski, J., Jaskulska, M., Kozłowska, M. (2014): Evaluation of effectiveness of iron phosphate and parasitic nematode *Phasmarhabditis hermaphrodita* in reducing plant damage caused by the slug *Arion vulgaris* Moquin – Tandon, 1885. – *Folia Malacologica* 22 (4): 293-300.
- [24] Langan, M.A., Shaw, E.M. (2006): Response of the earthworm *Lumbricus terrestris* (L.) to iron phosphate and metaldehyde slug pellet formulations. – *Applied Soil Ecology* 34: 184-189.
- [25] Port, C.M., Port, G.R. (1986): The biology and behaviour of slugs in relation to crop damage and control. – *Agricultural Zoology Reviews* 1: 255-299.
- [26] Port, G., Ester, A. (2002): *Gastropods as Pests in Vegetable and Ornamental Crops in Western Europe*. – In: *Barker, G.M. (ed.) Molluscs as Crop Pests*. CABI Publishing, Wallingford, Oxon OX 10 8DE, UK: 337-351.
- [27] von Proschwitz, T. (1997): *Arion lusitanicus* Mabille and *A. rufus* (L.) in Sweden: A comparison of occurrence, spread and naturalization of two alien slug species. – *Heldia* 4: 137-138.

- [28] Rae, R.G., Robertson, J.F., Wilson, M.J. (2006): The chemotactic response of *Phasmarhabditis hermaphrodita* (Nematoda: Rhabditidae) to cues of *Deroceras reticulatum*. – *Nematology* 8: 197-200.
- [29] Rae, R., Verdun, C., Grewal, P.S., Robertson, J.F., Wilson, M. (2007): Biological control of terrestrial molluscs using *Phasmarhabditis hermaphrodita* – progress and prospects. – *Pest Management Science* 63: 1153-1164.
- [30] Rae, R.G., Robertson, J.F., Wilson, M.J. (2009): Optimization of biological (*Phasmarhabditis hermaphrodita*) and chemical (iron phosphate and metaldehyde) slug control. – *Crop Protection* 28: 765-773.
- [31] South, A. (1992): *Terrestrial Slugs. Biology, Ecology, Control.* – Chapman & Hall, London, UK, 428 p.p.
- [32] Speiser, B., Zaller, J.G., Newdecker, A. (2001): Size-specific susceptibility of the pest slugs *Deroceras reticulatum* and *Arion lusitanicus* to the nematode biocontrol agent *Phasmarhabditis hermaphrodita*. – *Biocontrol* 46: 311-320.
- [33] Speiser, B., Kistler, C. (2002): Field test with a molluscicide containing iron phosphate. – *Crop Protection* 21: 389-394.
- [34] Turner, H., Kuiper, J.G.J., Thew, N., Bernasconi, R., Rüetschi, J., Wüthrich, M., Gosteli, M. (1998): *Atlas der Molluscen der Schweiz und Liechtensteins.* – Fauna Helvetica, CSCF, Neuchâtel, Switzerland, 527 p.p.
- [35] Vernavá, M.N., Phillips-Aalten, P.M., Hughes, L.A., Rowcliffe, H., Wiltshire, C.W., Glen, D.M. (2004): Influences of preceding cover crops on slug damage and biological control using *Phasmarhabditis hermaphrodita*. – *Annals of Applied Biology* 145: 279-284.
- [36] Wilson, M.J., Glen, D.M., George, S.K. (1993): The rhabditid nematode *Phasmarhabditis hermaphrodita* as a potential biological control agent for slugs. – *Biocontrol Science and Technology* 3: 503-511.
- [37] Wilson, M.J., Glen, D.M., George, S.K., Pearce, J.D., Wiltshire, C.W. (1994a): Biological control of slugs in winter wheat using the rhabditid nematode *Phasmarhabditis hermaphrodita*. – *Annals of Applied Biology* 125: 377-390.
- [38] Wilson, M.J., Glen, D.M., Wiltshire, C.W., George, S.K. (1994b): Mini-plot field experiments using rhabditid nematode *Phasmarhabditis hermaphrodita* for biocontrol of slugs. – *Biocontrol Science and Technology* 4: 103-113.
- [39] Wilson, M.J., Hughes, L.A., Jefferies, D., Glen, D. M. (1999): Slugs (*Deroceras reticulatum* and *Arion ater* agg.) avoid soil treated with the rhabditid nematode *Phasmarhabditis hermaphrodita*. – *Biological Control* 16: 170-176.

CO₂ EFFECTS ON LARVAL DEVELOPMENT AND GENETICS OF MEALWORM BEETLE, *TENEBRIO MOLITOR* L. (COLEOPTERA: TENEBRIONIDAE) IN TWO DIFFERENT CO₂ SYSTEMS

NUR HASYIMAH, R.^{1,2} – NOR ATIKAH, A. R.¹ – HALIM, M.¹ – MUHAIMIN, A. M. D.¹ – NIZAM, M. S.³ – HANAFIAH, M. M.¹ – YAAKOP, S.^{1*}

¹*School of Environmental and Natural Resource Sciences, Faculty of Science and Technology, Universiti Kebangsaan Malaysia, 43650 Bangi, Selangor, Malaysia*

²*Faculty of Applied Science, Universiti Teknologi MARA, 40450 Shah Alam, Selangor, Malaysia*

³*Institute of Climate Change, Universiti Kebangsaan Malaysia, 43650 Bangi, Selangor, Malaysia*

*Corresponding author
e-mail: salmah78@ukm.edu.my

(Received 9th Dec 2017; accepted 7th Mar 2018)

Abstract. *Tenebrio molitor* has never been used as a model species for studying global warming effects. The objectives of this study were to measure the larval development and genetics of *T. molitor* under a free air CO₂ enrichment (FACE) system, open roof ventilation greenhouse system (ORVS) and a rearing room system (RR). The correlation coefficient analysis showed that the head width: body length was the best character to measure the development (0.465, 0.940 and 0.893) in all systems. Our results show that there were no significant changes in the larvae samples under RR condition, however, slight and moderate changes were observed under FACE and ORVS. Neighbour-joining analysis using cytochrome c oxidase subunit I sequence revealed the genetic data parallel with the results of the correlation coefficient. The FACE F1 progeny showed the slowest development (0.080±0.018 mm) during 0-14 days of larval development, while the most rapid before pupation occurred in the ORVS F1 (0.1205±0.0028 mm). No significant differences were noted between the systems for 0-14 days and before pupation, except for RR F1 vs ORVS F1 and ORVS F1 vs FACE F1 ($p = 0.000$, $p = 0.002$). These data can be used to clarify the changes in *T. molitor* due to global warming effects, as CO₂ could be one of the factors affecting the larval development.

Keywords: correlation, Tenebrionidae, global warming, FACE, development growth, DNA, neighbour-joining

Introduction

Tenebrio molitor L. (Coleoptera: Tenebrionidae), also known as yellow mealworm, has a high reproductive capacity and the capability to sense and avoid toxic fungi-colonised diets (Morales-Ramos et al., 2011). This insect is also viewed as a major insect pest because it attacks several classes of stored grains, milled cereals, meat scraps, dead insects, flour and is even found feeding on sparrow droppings (Ye et al., 2001). Traditionally, *T. molitor* larvae have also been used as a food source for pets, including reptiles, fish, and birds, because the larvae are a rich source of protein, vitamins, essential amino acids, minerals and essential fatty acids (Tang et al., 2012).

The increment of CO₂ concentration affects the performance of insect behavior, life history, and population abundance. Williams et al. (2003) showed that long-term exposure for an increment of 3.5 °C on *Lymantria dispar* shortened the insect development by reached pupation earlier. Consumption rates for *Octotoma scabripennis*

were higher than *O. Championi* when given CO₂-grown foliage under lower temperature (Johns et al., 2003). Research done by Chen et al. (2005) revealed that fecundity of *Aphis gossypii* was increased through successive generation with increasing of CO₂ concentration.

Based on the review by Epenhuijsen et al. (2002), mortality rate shown by *Tribolium castaneum* (Herbst) (Coleoptera: Tenebrionidae) increased rapidly as the concentration of CO₂ increased from 60 to 90% at elevated temperatures between 38-42 °C. Furthermore, the developmental delay of cowpea bruchids was more severe under 2% O₂ + 18% CO₂ compared to 10% O₂ + 10% CO₂ (Cheng et al., 2012). Insect herbivore which consumed plant lowered nutritional quality as food will cause a reduction in their performance, including by reducing their growth rates and prolonging their development time (Goverde and Erhardt, 2003). Indirectly, the mortality imposed by natural enemies increase (Stiling et al., 2003), finally reducing the abundance, diversity, and richness of herbivore if compared to ambient CO₂ environments (Cornelissen, 2011).

Evaluation and monitoring of insects morphological changes can be carried out through the morphometric analysis. For example, the measurement process on the capsule head size was conducted after the discovery of the sub-fossil weevil in that area. As a result, based on measurements and analysis performed, the sub-fossil remains belong to the Ectemnorhinus group of weevils. A total of 15 characters of weevil species have been measured and used as references for further systematic and population studies including total body length (TL), pronotum breadth (PB), femur length (FL), etc. (Janse van Rensburg, 2006). Based on the morphological and morphometric studies on insect herbivores by Stiling and Cornelissen (2007), it shows that their development time increase about 13.87%, while their relative growth rate and pupal weight are significantly decreased about 8.3% and 5.03% after being exposed to the elevated atmospheric CO₂.

One of the statistical methods used to show the relationship and the association between two variables is the analysis of Pearson's correlation coefficient or simply referred as the correlation coefficient (Camargo et al., 2011). A study done by Loudon (1989) shows that a weak positive correlation was detected between tracheal sizes within individual larvae after correcting for larval size, which treated with a different level of oxygen separately ($r = 0.53$). Other study conducted on homopterous insects also indicates that relationship between wingbeat frequencies with wing loading to be significantly correlated only in insects weighing more than 0.03 g. The lack of correlation between these two parameters in small insects with less than 0.03 g maybe due to different flying strategies (Byrne et al., 1988). So, in the present study, the similar analysis can be used to identify whether different CO₂ level affects the characters of *T. molitor* larvae.

According to Brown et al. (2003), *Tribolium castaneum* is destined to become one of the three most important insect model systems as its genetics has convenient genetic setup. Several studies were conducted to create evolutionary trends from the family Tenebrionidae, but no phylogenetically informative molecular data are available for this genus (Mestrovic et al., 2006). Sequence analysis has been performed for a 642 bp fragment of the most conserved part of the mitochondrial cytochrome c oxidase subunit I (*COI*) gene in eight species of *Tribolium*, as well as in two outgroup species, *Pimelia elevata* and *T. molitor* (Mestrovic et al., 2006).

Some studies were done on other insects as subjects or model species predict similar results in *T. molitor*. Therefore, the aims of the present study were to (1) determine the correlation and differences between morphological characters of *T. molitor* larvae, due to changes in CO₂ concentration in three different systems, and (2) determine the genetic changes in *T. molitor* larvae from FACE, ORVS and RR (as a control) populations.

Materials and methods

The study was conducted at two enriched-CO₂ systems, including; FACE (N 02°55.331', E 101°46.965') and ORVS (N 02°55.145', E 101°46.465'), which was located at Universiti Kebangsaan Malaysia (UKM).

Rearing room system (RR)

The RR system was set up as a control room for observation of *T. molitor* during this experiment. The rearing room is a closed room which is free from insecticide and chemical contamination and is designed for rearing purposes. This room is specifically used to deter other animals from approaching the sample and to reduce any large impacts due to external temperatures and humidity. Larval and adult mortality might be caused by the temperatures higher than room temperature (Singh, 1982). The room size is 214 × 166 inch and samples were placed on the bench size 134 × 36 × 34 inch. The CO₂ concentration in this system can reach about 441-553 ppm.

Free air CO₂ enrichment system (FACE)

The FACE system is a new system which provides an environment with a high CO₂ level. It enables the design of a model to show how ecosystem respond to proliferating CO₂ in the Earth's atmosphere (Norby and Zak, 2011). The components of the FACE system include a smart control panel, a control system (valve 1, valve 2, valve 3 and buzzer), sensors (temperature, humidity, carbon dioxide and wind speed), a server, internet connection, PC application and mobile application. This system is operated by support from Xbee wireless sensors on four EZ sensor nodes and one wind speed (WS) sensor node. All four EZ sensor nodes contain built-in temperature, humidity, and carbon dioxide sensors, while the WS sensor node has wind speed meter. Sensor data were sent to the server immediately after receipt by Sensor Control Programmable (SCP) using gsm/gprs communication. Android and desktop applications were used to view the data stored on a cloud server database.

Carbon dioxide emissions were controlled by opening and closing a pipe valve at 1 h intervals when the wind speed is below 15 km/h. Four carbon dioxide tanks were used to supply carbon dioxide and were changed for every 43 days. Valve 1 was opened for 5 min at the Real Time Clock (RTC) hour. Later, valve 2 was opened for 5 min after 10 min at the RTC hour and valve 3 was opened after 20 min at the RTC hour for 5 min. During the process of carbon dioxide gas emission, the buzzer was on, the date and time on the LCD were adjusted using the menu and keypad, and sensor data were sent to the server, together with a timestamp. The original CO₂ concentration that has been released into the FACE system in the range of 800-950 ppm. FACE system of UKM shows in *Figure 1b*.

Open roof ventilation greenhouse system (ORVS)

The ORVS system (Fig. 1a), had an average temperature of 34 °C and 63% humidity. The light intensity was 94-95% higher than the ambient level. CO₂ was provided by continuous spraying of pure carbon dioxide automatically from 9 am to 11 am for 2 h every day and was stopped once the concentration of CO₂ reached about 800-950 ppm. It was provided via a CO₂ cylinder connected to the air delivery system of the open roof ventilation and air blower. The CO₂ concentration in the chamber was monitored and managed with a CO₂ analyzer. After 2 h, the CO₂ concentration in the chamber and in ambient air was almost the same. The ORVS was automatically controlled by a system set up by the Climate Change Institute (IPI), UKM.



Figure 1. Elevated CO₂ systems (a) open roof ventilation greenhouse system; and (b) free air CO₂ enrichment system

Figure 2 shows the arrangement of the samples in ORVS and FACE during the process of rearing and monitoring.



Figure 2. Experimental design of *T. molitor* study in (a) open roof ventilation greenhouse system, and (b) free air CO₂ enrichment system

Sample identification and preparation

Samples of *T. molitor* larvae were obtained from a local supplier from Bandar Baru Bangi, Selangor, Malaysia. The species identification was confirmed morphologically using the species key by Bousquet (1990).

Rearing process of Tenebrio molitor

Tenebrio molitor larvae were reared in the Cytogenetic 2 Laboratory, Universiti Kebangsaan Malaysia (UKM), from October 2015 until November 2015. The larvae samples were placed in 40 × 28 × 24 cm plastic aquariums and fed with oats and cucumbers as a food source during the rearing process (Siemianowska et al., 2013). Some parameters, including temperature, humidity, and CO₂ concentration were recorded. The samples were observed and monitored until the emergence of the *T. molitor* adults.

Isolation of samples of Tenebrio molitor adults

The emerged *T. molitor* adults were collected from the rearing process and were separated into 30 of 19 × 14 × 12 cm aquariums. Forty randomly picked individuals were put into each aquarium, together with a 4 cm height of sawdust at the bottom and a 4 cm height of sifted soil. Ten aquariums were placed in each of the three systems (Free Air CO₂ Enrichment System (FACE), Open Roof Ventilation System (ORVS) and Rearing Room System (RR)). Larvae were collected two weeks later (14 days) and before pupation.

CO₂ treatment at different systems

The data for CO₂ from each system, as well as other parameters, including valve number, temperature, and humidity, were recorded at every sampling time (every 2 weeks).

Monitoring of Tenebrio molitor adult (parent) to larval stage (F1)

Samples of adult *T. molitor* were observed once a week until the first group of larvae emerged. The survival of each individual from each aquarium was monitored and recorded (Crawley, 2007). The mortality rate of adults was also recorded by collecting the dead *T. molitor* individuals during the observation.

Sampling of Tenebrio molitor larvae and adults

Aquariums containing *T. molitor* samples exposed to high CO₂ concentration were randomly collected every week. A forcep was used to collect the dead adult bodies and live larvae, which were placed into small containers and sorted according to the aquarium. The randomly picked larval samples consisted of about 40-60 individuals per session, depending on the larval size. Dead *T. molitor* adults were brought to the laboratory and recorded.

Morphometric measurement of Tenebrio molitor

Fifty larvae were picked randomly from each system and were used for morphometric measurements. The images of larvae and adults were captured and measured with a microscope (Dinolite 1.2). The characters of the larvae including the head width (HW), head length (HL), body width (BW) and body length (BL) were measured in millimeter. Generally, the width of the head capsule was measured because it exhibits distinct variations between larval stages (Hsia and Kao, 1987).

DNA isolation, PCR amplification, DNA purification sequencing analyses

DNA was extracted from larvae from each treatment using a NucleoSpin® DNA Insect kit. The kit combines enzymatic lysis by utilizing mechanical disruption of cell walls with the NucleoSpin® Bead Tubes (Macherey-Nagel, 2016). The list of isolated samples, type of treatment and age of *Tenebrio molitor* larvae used for genetic study using cytochrome c oxidase subunit I (COI) and phylogenetic analyses were summarised in *Table 1*. A pair of primers designed by Folmer et al. (1994) [LCO1490 5'-GGT CAA CAA ATC ATA AAG ATA TTG G-3 (Forward) and HCO2198 5'-TAA ACT TCA GGG TGA CCA AAA AAT CA-3 (Reverse)] was used to amplify the COI by singleplex PCR using a MyGene MG96G Asthermalcycler.

The PCR conditions were as follows: 95 °C for 3 min as the pre-denaturation, followed by denaturation with 95 °C for 1 min, an annealing process of about 1 min, elongation and final elongation at 72 °C for 10 min 30 sec. The whole PCR process consisted of 35 cycles over 150 min. The PCR products were electrophoresed on a 1.5% agarose gel and the bands corresponding to the target PCR products were purified using the Geneaid Purification Kit. All PCR products were sent to the sequencing service company, First Base Sdn. Bhd., Petaling Jaya, Selangor.

Table 1. List of samples, type of treatment and age of *T. molitor* larvae used for genetic study and phylogenetic analyses

No.	Code	System	Age (day)	Accession No
1	5RRF1	RR	71-84	MF155950
2	6RRF1	RR	71-84	MF155953
3	1ORVSF1	ORVS	85-98	MF155951
4	2ORVSF1	ORVS	85-98	MF155952
5	7ORVSF1	ORVS	85-98	MF155954
6	8ORVSF1	ORVS	85-98	MF155955
7	9ORVSF1	ORVS	85-98	MF155956
8	13ORVSF1	ORVS	85-98	MF155959
9	4FACEF1	FACE	43-56	MF155949
10	11FACEF1	FACE	43-56	MF155957
11	12FACEF1	FACE	43-56	MF155958
12	14FACEF1	FACE	43-56	MF155960
13	15FACEF1	FACE	43-56	MF155961
14	16FACEF1	FACE	43-56	MF155962

RR = rearing room; FACE = free air CO₂ enrichment; ORVS = open roof ventilation greenhouse

Pairwise alignment, basic local alignment search tool analysis (BLAST) and neighbour joining analysis

All the sequence-based samples from the FACE, ORVS and RR systems were aligned using Clustal W to determine the similarity of characters between sequences (Thompson et al., 1994). The pairwise alignment results were optimized by manually editing these sequences using MEGA7. A BLAST search showed a maximum hit for the respective species only, as available in GenBank

(<http://www.ncbi.nlm.nih.gov/genbank>). The phylogenetic tree was constructed using Neighbour Joining (NJ) using PAUP 4.0 and the Kimura-2 parameter.

Analysis

Correlation and regression analysis for all parameters (characters) in all systems were performed using Excel 2013 and SPSS version 19 software. *T*-tests and standard errors were analyzed using Minitab 17 software.

Environmental parameters control

Free air CO₂ enrichment (FACE) system

FACE system is an open system that has been created to conduct research on the effects of elevated atmospheric CO₂ concentrations, especially on plants. However, the system has been built by maintaining its environmental parameters including temperature, humidity, and wind, etc., which may reduce the effects of the CO₂ (McLeod and Long, 1999). According to Ainsworth and Long (2005), FACE system is the best system to carry out studies related to the elevated atmospheric CO₂ level in plants and ecosystems. This is due to its characteristics as an open system without barrier, which provides or mimics the natural environment except for the concentration of CO₂.

Therefore, the results obtained from the experiments are very accurate and less bias. Based on previous studies, there are some data related to CO₂ concentration levels were recorded in the FACE systems, which is in the range between 475-600 ppm (Ainsworth and Long, 2005), 550-600 ppm (Long et al., 2006) and 550-580 ppm (Norby and Zak, 2011). These concentrations are at the similar rate as enrich-CO₂ recorded during these sampling activities. The CO₂ gas injection and release processes in the FACE system are conducted every 10 s by the two sets of the four tubes, where the process is strongly influenced by wind speed (m/s) (Okada et al., 2001).

Open roof ventilation greenhouse system (ORVS)

In contrast to FACE systems, an open roof ventilation greenhouse (ORVS) is a closed system with movable shade or open roof vents which are controlled by a computer system and a good PPF sensor (Albright et al., 2000). Abiotic factors including temperature (°C), humidity (%) and CO₂ concentration (ppm) do not significantly affect the performance of the system against wind speeds (Boulard and Draoui, 1995). The monitoring process is carried out inside and outside the greenhouse on humidity and temperature, where both parameters were measured using Psychrometers. The ventilation process has to be carried out by the greenhouse during a large proportion of the daytime to regulate the temperature (Boulard and Draoui, 1995) and also to ensure that the humidity can be reduced (Harmanto, 2006).

When relative humidity inside the greenhouse exceeded 85%, 25% of the overall roof size was opened to lower the humidity rate (Sanchez-Guerrero et al., 2005). The gas tracer was supplied during closed vent with a concentration greater than 200 ppm. To ensure that the gas is mixed in the air uniformly, the vent is left closed for a while after the gas is released in the greenhouse (Kittas et al., 2005). In order to maintain the level of CO₂ inside and outside the greenhouse during the process of ventilation, the CO₂ was injected continuously and maintained at a concentration about 700-

800 mmol⁻¹, where it usually conducted when the vent roof of the greenhouse is closed in the early morning and the late afternoon (Nederhoff, 1994).

Based on the information above, FACE system and ORVS are able to maintain and control other parameters such as temperature and humidity, and provide ambient conditions except for elevated CO₂ during the experiment. It is able to directly observe the effect of CO₂ concentration towards *T. molitor* larvae caused by different CO₂ concentration without affected by other environmental parameters in both systems.

Results

Correlation coefficient and significant studies on control and treated Tenebrio molitor larvae

Correlation coefficient analysis shows the association between characters of *T. molitor* larvae from all systems (Table 2).

Table 2. Correlation coefficients among *Tenebrio molitor* larvae (F1) characters in FACE (i), RR (ii) and ORVS (iii)

Characters/System	FACE	RR	ORVS
HW vs HL	-0.018	0.961**	-0.21
HW vs BL	0.465**	0.940**	0.893**
HW vs BW	0.239**	0.956**	0.795**
HL vs BL	0.001	0.924**	0.001**
HL vs BW	-0.02	0.929**	-0.23
BL vs BW	0.328**	0.979**	0.684**

* and **: significant at the 0.05 and 0.01 level of probability, respectively

HW = head width (mm); HL = head length (mm); BW = body width (mm); BL = body length (mm); RR = rearing room system; FACE = free air CO₂ enrichment system; ORVS = open roof ventilation greenhouse system

A weak positive linear and highly significant correlation was evident between HW and BW ($r = 0.239$, $p = 0.000 < 0.01$) and BL ($r = 0.465$, $p = 0.000 < 0.01$), and between BL and BW ($r = 0.328$, $p = 0.000 < 0.01$). A correlation similarity was also found among characters in the ORVS F1 and FACE F1, where a negative correlation was found between HL and HW ($r = -0.018$, $p = 0.794 > 0.01$) and BW ($r = -0.020$, $p = 0.772 > 0.01$) (Table 2i).

The data on correlation coefficients between various parameters of RR larvae were presented in Table 2ii. All characters demonstrated strong positive linear correlations with significance at the 99% confidence level. The highest r value was between BL and BW ($r = 0.979$, $p = 0.000 < 0.01$), while the lowest r value was found between HL and BL ($r = 0.924$, $p = 0.000 < 0.01$). No negative correlation was found in any characters of the RR F1 larvae.

A strong positive linear correlation was noted between HW and BL ($r = 0.893$, $p = 0.000 < 0.01$), a moderate positive linear correlation with BW ($r = 0.795$, $p = 0.000 < 0.01$) and a moderate positive linear correlation between BL and BW ($r = 0.684$, $p = 0.000 < 0.01$). The result is accurate with a 99% confidence level for a significant correlation shown for all characters. A negative correlation was obtained

between HL and HW ($r = -0.21$, $p = 0.679 > 0.01$) and BW ($r = -0.23$, $p = 0.660 > 0.01$) (Table 2iii).

Developmental size of *Tenebrio molitor* samples from FACE, ORVS, and RR systems

The developmental size (HW/BL) of *T. molitor* larvae was measured at 0-14 days among the three systems. Figure 3 shows that FACE F1 had the lowest mean development (0.080 ± 0.018 mm), while ORVS F1, at 0.1293 ± 0.032 mm, had the highest. The descriptive error bars in a graph of experimental biology were used to determine whether the error of a reported measurement fits within the normal range. The type of error bar can be used to determine the significant differences among samples (Cumming et al., 2007). Figure 3 shows significant differences in the development of *T. molitor* larvae among systems (Table 3).

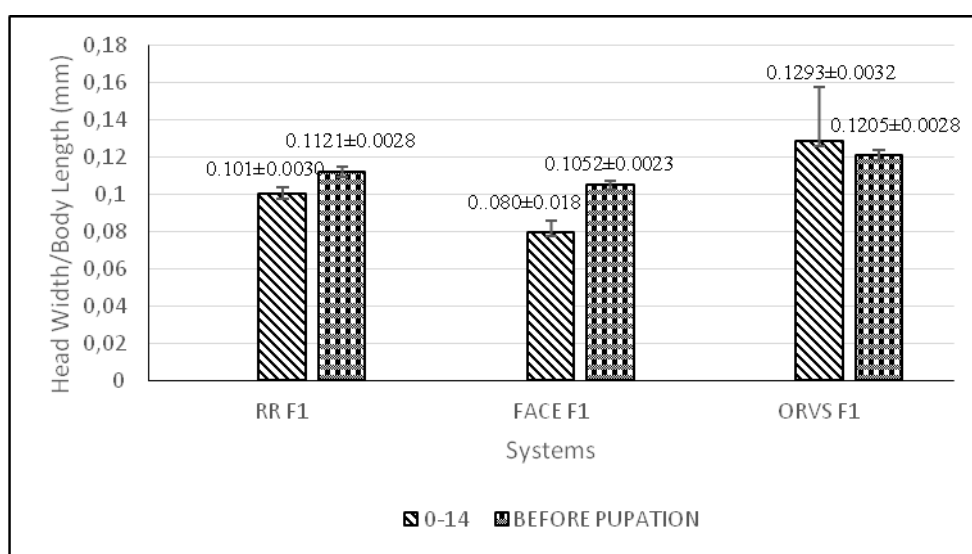


Figure 3. Developmental size of *Tenebrio molitor* larvae at 0-14 days and different days before pupation from three different systems. (RR = rearing room; FACE = free air CO₂ enrichment; ORVS = open roof ventilation greenhouse system)

The data on development size of *T. molitor* larvae before they get pupated was depicted in Figure 3. The highest mean developmental size of larvae was recorded in the ORVS F1 (0.1205 ± 0.0028 mm), followed by RR F1 (0.1121 ± 0.0028 mm) and FACE F1 (0.1052 ± 0.0023 mm). Overall, the size development of larvae before pupation at RR F1 and FACE F1 increase, while in ORVS F1 larvae showed a decrease compared to 0-14 days.

The larval development of *T. molitor* samples showed significant differences between the RR F1 vs ORVS F1 (0-14 days) only with $p = 0.000$ ($p > 0.05$). Comparison of RR F1 vs FACE F1 ($p > 0.05$, 0.078) and ORVS F1 vs FACE F1 ($p > 0.05$, 0.059) at 0-14 days revealed no significant difference based on the t-test analysis. Therefore, the t-test showed no statistically significant difference between RR F1 vs ORVS F1 ($p > 0.05$, 0.493) or RR F1 vs FACE F1 ($p > 0.05$, 0.565) before pupation, while the difference between ORVS F1 vs FACE F1 was statistically significant ($p < 0.05$, 0.002) (Table 3).

Table 3. Significant differences in *Tenebrio molitor* development (at 0-14 days and before pupation)

System/Significant difference	RR F1 vs FACE F1	RR F1 vs ORVS F1	ORVS F1 vs FACE F1
0-14 days	0.078	0.000	0.059
Before pupation	0.565	0.493	0.002

RR = rearing room; FACE = free air CO₂ enrichment system; ORVS = open roof ventilation greenhouse system

Genetic changes in *Tenebrio molitor*

Tenebrio molitor DNA samples were amplified using PCR to determine the sequence changes after treatment with CO₂. Phylogeny is a relationship classification between two species that can be represented as a phylogenetic tree (Rizzo and Rouchka, 2007). Neighbour-joining (NJ) trees were created from DNA sequencing analyzed by First Base Sdn. Bhd.

Figure 4 indicates the similarity of DNA sequences from *T. molitor* induced with high CO₂. Two clades are evident: both CLADE A and CLADE B, with 96% bootstrap values, respectively. The samples of ORVS F1 larvae induced with CO₂ were separated from the RR F1 samples (which served as a control), except for some samples of FACE F1 which found in both clades. The RR F1 was included in one subclade, with a 97% bootstrap value, with *Tenebrio obscurus* and *Tenebrio opacus* samples as outgroups. In summary, the genetic data parallel with the results of the correlation coefficient.

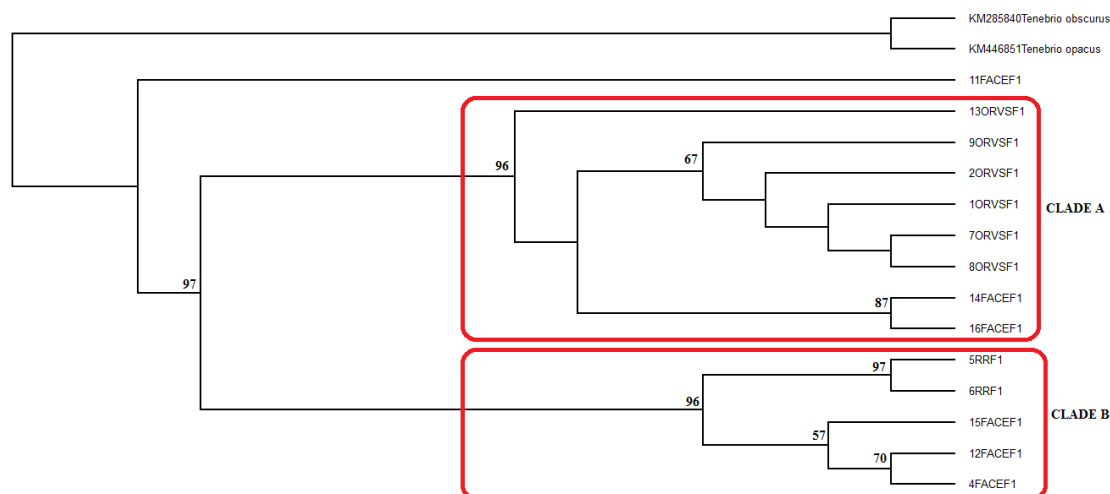


Figure 4. Neighbour joining (NJ) tree of *Tenebrio molitor* derived from NJ analyses with bootstrap values above nodes (1000 replications). (RR = rearing room; FACE = free air CO₂ enrichment system; ORVS = open roof ventilation greenhouse system)

The sequence extraction revealed 11 FACE F1 with higher nucleotide dissimilarity from the other samples when outgroups were excluded. Certain sites, including 103 (C, T), 111 (A, G), 381 (A, G), 432 (A, G), 436 (T, C), 582 (C, T), 639 (A, G) and 642 (A, G), showed a division into two types of nucleotides in almost equal quantities (Table 4).

Table 4. Sites with nucleotide changes excluding outgroup sequences

Plate no.	Nucleotide sites							
1	19	21	22	30	43	44	51	60
2	103	111	112					
3	201	237						
4	249	297	301					
5	329	330	357	381				
6	412	426	432	436	438	444	477	
7	489	495	501	519	540	558	561	
8	582	633	636	639	642	652		
9	683	685	686	687	688			

*Excluding outgroup sequences

Discussion

Larval development was measured in this experiment as a parameter to investigate the effects of exposure to elevated CO₂ on insect species, specifically in terms of prolongation of development time and changes in their growth rate (Goverde and Erhardt, 2003), longevity (Werner et al., 2006; Coll and Hughes, 2008), body size (Roth and Lindroth, 1995), adult weight (Coll and Hughes, 2008), mortality (Epenhuijsen et al., 2002), and hatch rate or pre-oviposition time (Peltonen et al., 2006; Coll and Hughes, 2008). Morphological parts were assessed as these are more conspicuous than physiological aspects, therefore more easily measured. These developmental time changes, lower survivorship, reduced adult weight, etc. are not observed only in this insect, but are seen in herbivores as well. For example, *Helicoverpa armigera*, which consumes the fruits of many crop plants, undergoes extensive mortality and delays in development time in response to high CO₂. Hence, the larvae are smaller when feeding on plants grown in elevated CO₂ than in ambient air. This response is due to the reduction in N content of the plants, which directly affects their quality, even though plant size is significantly larger when compared to plants grown at ambient CO₂ (Coll and Hughes, 2008).

The developmental results presented here were further strengthened by *t*-tests conducted on larval development between RR F1 vs ORVS F1 (0-14 days) and ORVS F1 vs FACE F1 (before pupation). Significant difference was found, with $p = 0.000$ (0-14 days) and $p = 0.002$ (before pupation). This finding indicates that increases in CO₂ above ambient levels have caused significant effects on *T. molitor* development, especially in the ORVS F1. It can be observed from the comparison of larval development, where the development of ORVS F1 only shows a significant difference when compared to other systems.

Elevated CO₂ concentration also affects the development and growth of insects indirectly, such as through their diet. *Myzus persicae* is herbivore insect species that use pepper plants as a source of food. Based on previous research, the fitness level of *M. persicae* was decreased when feeding on the pepper plants grown under higher CO₂ concentrations. Similar results were recorded on species of Brassicaceae (Oehme et al., 2011) such as *Brevicoryne brassicae* on Brussels sprout (Ryan et al., 2014), and *Acyrtosiphon pisum* on the broad bean (Ryan et al., 2014). Other than that, elevated CO₂ also affects their morphology and physiology by reducing fertility and producing a

fewer number of offspring, as well as increasing chewing insects development duration (Dáder et al., 2016).

Different results are shown between RR F1 vs FACE F1 where there was no significant difference in 0-14 days or before pupation. It is due to the relatively long duration of exposure to high CO₂ concentrations by *T. molitor* larvae in the ORVS resulting in faster interruption of its development. Indirectly, the development time and r_m of the grain aphid, *Sitobion avenae* were not affected when feeding on winter wheat which has been exposed to high CO₂ concentration of 700 ppm (Awmack et al., 1996). According to Zalucki et al. (2002), insect larval stages are suitable to be used as a subject study because it is very sensitive to any parameter changes in the environment. Limited information on the direct responses of insects to controlled atmosphere treatments has been recorded especially on their physiological and biochemical parts (Zhou et al., 2001), developmental time and consumption of herbivores (Yin et al., 2010).

However, even though no radical CO₂ effect was observed, high CO₂ exposure still affected the various larval parameters and thus reflected in correlation results, as evident by the negative correlation of HL with HW and with BW in both ORVS F1 and FACE F1 larvae. However, the exposure of the next generations of *T. molitor* to increased CO₂ concentrations is expected to increase the possibility of effects on species development, especially changes in their morphological and molecular parts. A study was done by Yin et al. (2010) on cotton bollworm, *Helicoverpa armigera* Hubner (Lepidoptera: Noctuidae) larvae for first and second successive generations when they were fed on an artificial diet or C4 plants (maize) grown under two levels of CO₂. It has resulted in prolongs larval duration, lower fecundity and reduced r_m of cotton bollworms. Furthermore, it also increased the consumption rates of the individual, decreased the total consumption of their first generation populations but increased it in the second generation.

The *T. molitor* larvae from the FACE, RR and ORVS systems showed positive correlations among several characters except for the correlation coefficient between HL vs HW, and HL vs BW, which were negatively correlated. Comparison of the correlation coefficient data, using the RR system as a control with ambient CO₂ concentration revealed a strong positive linear correlation for larval development between all characters at the 99% confidence level. Consequently, larvae exposed to higher CO₂ concentration above ambient levels in the ORVS and FACE systems showed moderate, weak and negative correlations between characters.

According to Loudon (1988), the final size of the larvae should be highly correlated with the size of pupae and the adult size in most insects. A high degree of correlation was observed for *T. molitor*, where the weight of a starved adult is highly correlated with pupal weight ($r^2 = 0.85$, $n = 50$), and pupal weight is highly correlated with final larval weight ($r^2 = 0.91$, $n = 20$). The development of larvae was measured using the BL (mm) and HW (mm) of larvae collected from each system. Generally, the head width capsule was measured because it displays different variations between larval stages (Hsia and Kao, 1987). Panzavolta (2007) used the data of head capsule width and BL to determine instar separation rules, which were analyzed using the Hcap computer program. Developmental studies of insects have also been related to body size evolution, which response to changes in the environmental conditions. For example, environmental parameters such as temperature may affect the development of insects by

changes from their original size at ambient temperature to a smaller size at higher temperatures (Yamada and Ikeda, 2000).

Overall, the developmental size of larvae from all systems showed a growing pattern, except for ORVS F1. The ORVS F1 showed a decrease in the growth rate, with a size difference of about 0.0088 mm. The FACE F1 larvae had the smallest development size at the first 14 days and showed growths in the size of 0.0252 mm. Samples from the RR F1 (0.0111 mm) also showed an increase in the growth rate and final size. These findings support the hypothesis that CO₂ concentration is able to inhibit larval growth (cited). However, further experiments using prolonged exposures of the gas on the next generations of larvae are needed to show a more pronounced effect.

Previous study done by Harrison et al. (2006) showed that hypoxia or low oxygen levels affected the development of *T. molitor*. Ambient P_{O₂} (AP_{O₂}) values of 10 kPa or below resulted in a decrease in the species size. The body size of living organisms may be reduced under hypoxic conditions as these conditions signal the deterioration of environmental conditions and require rapid maturity and small body size for ecological success. High CO₂ concentrations can also affect insect respiration; for example, *Cryptolestes turcicus* shows increased phosphine consumption when the CO₂ level is increased (Ren et al., 1994).

In the present study, *T. molitor* showed a longer development time following exposure to high concentrations of CO₂, especially in the ORVS system, where development took 62 to 69 days longer than for the RR F1. Similar results were obtained from a study on cowpea bruchids by Cheng et al. (2012). Low CO₂ concentration exposure (10% O₂ + 10% CO₂) caused less developmental delay than was observed at a higher CO₂ level (2% O₂ + 18% CO₂). Recently, strong evidence was reported showing that high levels of O₂ have no effect on large insects, as oxygen delivery does not become more challenging in larger insects. A longer delay in the development time of cowpea bruchids is expected with a longer exposure of CO₂. However, opposite results were reported for *Anagasta kuehniella* in which development from the egg-to-adult period was not influenced by CO₂ (Junior and Parra, 2013).

Apart from CO₂, other parameters should also be studied to determine their direct impact on the development of *T. molitor*. For example, the temperature in the ORVS and FACE exceeded the optimal temperature suitable for *T. molitor* reproduction. According to Fiore (1960), the reproduction of *T. molitor* is very appropriate at their optimal temperature of about 25-27.5 °C. The total developmental time for this species is 80.0-83.7 days (Park et al., 2012). At a temperature of 25 °C, a decrease in humidity had no effect on adults, larvae or pupae of *T. molitor*, but it increased mortality at 10 °C (Punzo and Mutchmor, 1980). Other insects, such as the peach fruit moth, *Carposina sasakii*, show temperature dependence in their development processes. The development time of *C. sasakii* eggs was increased by decreasing the temperature below 32 °C, whereas the developmental rates of both larvae (< 28 °C) and pupae (< 32 °C) were faster at the optimum temperature (Kim et al., 2001).

Neighbour-joining (NJ) analysis applied in PAUP 4.0 was used to investigate the associations among taxa in the profiles according to Kumar et al. (2001). The subsequent classification of 'test' taxa is also important because of its strong track record in large species assemblage analysis (Kumar and Gadagkar, 2000). This method has the extra benefit of generating results faster than alternatives (Hebert et al., 2003). The *COI* gene is one of the most preferred for evolutionary time depth studies because of the ability to conserve protein-coding genes in the animal mitochondrial genome

(Brown, 1985). Moreover, the *COI* primer is very important in the studies of systematics metazoan invertebrates, including acoelomates and pseudocoelomates (Folmer et al., 1994).

Nucleotide changes in DNA sequences were used to create a NJ tree (Fig. 4). The NJ analysis using *COI* sequences revealed ORVS F1 and RR F1 formed in different clades (A and B), with FACE F1 located in both clades. The results showed that the nucleotides in the DNA sequences of *T. molitor* larvae changed after exposure to CO₂ concentrations higher than ambient. The most significant changes were observed in ORVS F1 larvae due to the closed system state, which allowed CO₂ gases to surround the insects and resulted in a higher exposure to CO₂ in the larvae of *T. molitor* than was experienced in the FACE (open) system.

A further difference between the FACE system and ORVS is that the FACE system has been built to expose plants to increments of atmospheric CO₂ with minimal alterations of the natural environment in which the plants are naturally growing. Even so, short-term fluctuations in CO₂ concentration and a substantial infrastructure presence are problems inherent with the FACE system. The FACE system also experiences some experimental restrictions, including the unavoidable presence of CO₂ concentration gradients along the wind direction (Miglietta et al., 2001). The instability displayed by this system, therefore, becomes a factor in the reduction of CO₂ impacts on the sample. For this reason, the system itself could be a major factor affecting the distribution of FACE samples, including the appearance of FACE F1 in both Clade A and Clade B in the NJ tree.

CO₂ effects on *T. molitor* larvae in the FACE system were found in both clades of the NJ Tree. This result can be related to the location of the FACE system itself in the forest area. A forest habitat with a large number of plant species that use CO₂ in photosynthesis will reduce the CO₂ levels in FACE system and automatically decrease the exposure of CO₂ by *T. molitor* larvae. A FACE system built in a field area, as described by Scherber et al. (2013), might be more suitable for use in conducting research on the impact of CO₂ on insects. Less absorption of CO₂ by plants will increase the chances that the larvae will be exposed to higher concentrations of CO₂.

Conclusion

High levels of CO₂ in the environment have the ability to affect the development and life cycle of *Tenebrio molitor*. Increments in CO₂ cause a reduction in larval development and change the nucleotides in the DNA sequences of the mitochondrial COI gene. A strong positive correlation coefficient was shown in samples from the rearing room system (RR F1), and moderate or weak positive linear correlation coefficients in larvae from the FACE system (FACE F1) and the ORVS (ORVS F1) (significant at the 99% confidence level). A negative correlation coefficient was found for head length with a head width and body width in both the ORVS and FACE system. These results confirm that the *T. molitor* is able to survive by changing its genetic sequences and that it can adapt to climate changes through evolution. The results of this study clearly show a direct relationship between elevated CO₂ and the decrease in larval developmental size, the analysis demonstrated the occurrence of nucleotide changes in certain individuals of *T. molitor* in response to increased CO₂. The CO₂ concentration can therefore be seen to affect the morphology of *T. molitor*, even though the changes are not drastic and take more than one generation. Further study should be conducted in

the future to increase our understanding of the direct impacts of climate change, including the increase of greenhouse gases, on animals and plants, and specifically on humans. As a suggestion, the next experiments should be conducted to determine the implications of elevated CO₂ towards *T. molitor* development on different generations.

Acknowledgements. The authors would like to express their special gratitude to Mrs Nur Izzah Jamil from Universiti Teknologi Mara (UiTM) for handling SPSS workshop. Special thanks to Climate Change Institute (IPI) grant, ZF-2015-025 and GUP-2016-022. Special appreciation to Universiti Kebangsaan Malaysia (UKM) and Universiti Teknologi Mara (UiTM) for providing study facilities and scholarship.

Conflict of interest. The author confirms that this article content has no conflict of interest.

REFERENCES

- [1] Ainsworth, E. A., Long, S. P. (2005): What have we learned from 15 years of free-air CO₂ enrichment (FACE)? A meta-analytic review of the responses of photosynthesis, canopy properties and plant production to rising CO₂. – *New Phytologist* 165: 351-372.
- [2] Albright, L. D., Both, A. J., Chiu, A. (2000): Controlling greenhouse light to a consistent daily integral. – *Trans. of the ASAE* 43(2): 421-431.
- [3] Awmack, C. S., Harrington, R., Leather, S. R., Lawton, J. H. (1996): The impacts of elevated CO₂ on aphid-plant interactions. – *Aspects Appl. Biol.* 45: 317-332.
- [4] Boulard, T., Draoui, B. (1995): Natural ventilation of a greenhouse with continuous roof vents: measurements and data analysis. – *J. Agric. Engng Res.* 61: 27-36.
- [5] Bousquet, Y. (1990): Beetles Associated with Stored Products in Canada: An Identification Guide. – Research Branch Agriculture Canada, Ottawa, Canada.
- [6] Brown, S. J., Denell, R. E., Beeman, R. W. (2003): Beetling around the genome. – *Genet. Res.* 82: 155-161. <https://doi.org/10.1017/S0016672303006451>.
- [7] Brown, W. M. (1985): The Mitochondrial Genome of Animals. – In: MacIntyre, R. J. (ed.) *Molecular Evolutionary Genetics*, pp. 95-130. Plenum Press, New York.
- [8] Byrne, D. N., Buchmann, S. L., Spangler, H. G. (1988): Relationship between wing loading, wingbeat frequency and body mass in Homopterous insects. – *J. Exp. Biol.* 135: 9-23.
- [9] Camargo, M. G. G., Souza, R. M., Reys, P., Morellato, L. P. C. (2011): Effects of environmental conditions associated to the cardinal orientation on the reproductive phenology of the cerrado savanna tree *Xylopia aromatica* (Annonaceae). – *An Acad Bras Cienc* 83: 1007-1019.
- [10] Chen, F., Ge, F., Parajulee, M. N. (2005): Impact of elevated CO₂ on tri-trophic interaction of *Gossypium hirsutum*, *Aphis gossypii*, and *Leis axyridis*. – *Environmental Entomology* 34(1): 37-46.
- [11] Cheng, W., Lei, J., Ahn, J. E., Liu, T. X., Zhu-Salzman, K. (2012): Effects of decreased O₂ and elevated CO₂ on survival, development, and gene expression in cowpea bruchids. – *Journal of Insect Physiology* 58: 792-800. <https://doi.org/10.1016/j.jinsphys.2012.02.005>.
- [12] Coll, M., Hughes, L. (2008): Effects of elevated CO₂ on an insect omnivore: A test for nutritional effects mediated by host plants and prey. – *Agriculture, Ecosystem & Environment* 123: 271-279. <https://doi.org/10.1016/j.agee.2007.06.003>.
- [13] Cornelissen, T. (2011): Climate change and its effects on terrestrial insects and herbivory patterns. – *Neotropical Entomology* 40(2): 155-163.
- [14] Crawley, M. J. (2007): *The R Book*. – John Wiley & Sons Ltd, Cichester, West Sussex, UK.
- [15] Cumming, G., Fidler, G., Vaux, D. L. (2007): Error bars in experimental biology. – *Journal of Cell Biology* 177(1): 7-11. [10.1083/jcb.200611141](https://doi.org/10.1083/jcb.200611141).

- [16] Dáder, B., Fereres, A., Moreno, A., Trębicki, P. (2016): Elevated CO₂ impacts bell pepper growth with consequences to *Myzus persicae* life history, feeding behaviour and virus transmission ability. – Scientific Reports 6: 19120. doi: 10.1038/srep19120.
- [17] Epenhuijsen, V. C. W., Carpenter, A., Butler, R. (2002): Controlled atmospheres for the post-harvest control of *Myzus persicae* (Sulzer) (Homoptera: Aphididae): effects of carbon dioxide concentration. – Journal of Stored Products Research 38: 281-291.
- [18] Fiore, C. (1960): Effects of temperature and parental age on the life cycle of the dark mealworm, *Tenebrio obscurus* Fabricius. – Journal of the New York Entomological Society 68(1): 27-35.
- [19] Folmer, O., Black, M., Hoeh, W., Lutz, R., Vrijenhoek, R. (1994): DNA primers for amplification of mitochondrial cytochrome c oxidase subunit I from diverse metazoan invertebrates. – Molecular Marine Biology and Biotechnology 3: 294-299.
- [20] Goverde, M., Erhardt, A. (2003): Effects of elevated CO₂ on development and larval food-preference in the hutterfly *Coenonympha pamphius* (Lepidoptera, Satyridae). – Global Change Biology 9: 74-83.
- [21] Harmanto, H. J. T., Salokhe, V. M. (2006): Influence of insect screens with different mesh sizes on ventilation rate and microclimate of greenhouses in the humid tropics. – Agricultural Engineering International: The CIGR Ejournal. Manuscript BC 05 017. Vol. VIII. January 2006.
- [22] Harrison, J., Frazier, M. R., Henry, J. R., Kaiser, A., Klok, C. J., Rascon, B. (2006): Responses of terrestrial insects to hypoxia or hyperoxia. – Respiratory Physiology & Neurobiology 154: 4-17. <https://doi.org/10.1016/j.resp.2006.02.008>.
- [23] Hebert, P. D. N., Cywinska, A., Ball, S. L., deWaard, J. R. (2003): Biological identifications through DNA barcodes. – Proceedings of the Royal Society of London B 270: 313-321. 1098/rspb.2002.2218.
- [24] Hsia, W. T., Kao, S. S. (1987): Application of head width measurements for instar determination of corn earworm larvae. – Taiwan R. O. C. 29: 277-282.
- [25] Janse van Rensburg, L. (2006): A morphological analysis of weevils from sub-Antarctic Prince Edward Islands: an assessment of ecological influences. – PhD Thesis, Faculty of Natural & Agricultural Sciences, University of Pretoria, Pretoria.
- [26] Johns, T. C., Gregory, J. M., Ingram, W. J., Johnson, C. E., Jones, A. et al. (2003): Anthropogenic climate change for 1860 to 2100 simulated with the HadCM3 model under updated emission scenarios. – Climate Dynamics 20: 583-612.
- [27] Junior, A. C., Parra, J. R. P. (2013): Effect of Carbon dioxide (CO₂) on mortality and reproduction of *Anagasta kuehniella* (Zeller 1879), in mass rearing, aiming at the production of *Trichogramma* spp. – Anais da Academia Brasileira de Ciências 85(2): 823-831. <http://dx.doi.org/10.1590/S0001-37652013000200021>.
- [28] Kim, D. S., Lee, J. H., Yiem, M. S. (2001): Temperature-dependent development of *Carposina sasakii* (Lepidoptera: Carposinidae) and its stage emergence models. – Environmental Entomology 30(2): 298-305.
- [29] Kumar, S., Gadagkar, S. R. (2000): Efficiency of the neighbour-joining method in reconstructing deep and shallow evolutionary relationships in large phylogenies. – Journal of Molecular Evolution 51: 544-553. <https://doi.org/10.1007/s002390010118>.
- [30] Kumar, S., Tamura, K., Jacobsen, I. B., Nei, M. (2001): MEGA2: Molecular Evolutionary Genetics Analysis Software. – Arizona State University, Tempe, AZ. <https://doi.org/10.1093/bioinformatics/17.12.1244>.
- [31] Long, S. P., Ainsworth, E. A., Leakey, A. D. B., Nosberger, J., Ort, D. R. (2006): Food for thought: lower-than-expected crop yield stimulation with rising CO₂ stimulation. – Science 312: 1918.
- [32] Loudon, C. (1988): Development in low of *Tenebrio molitor* oxygen levels. – Insect Physiology 34(2): 97-103. [https://doi.org/10.1016/0022-1910\(88\)90160-6](https://doi.org/10.1016/0022-1910(88)90160-6).
- [33] Loudon, C. (1989): Tracheal hypertrophy in mealworms: design and plasticity in oxygen supply systems. – Journal of Experimental Biology 147: 217-235.

- [34] Macherey-Nagel (2016): Genomic DNA from Insect: User Manual Nucleospin DNA[®] Insect. – Macherey-Nagel, Dürer, Germany.
- [35] McLeod, A. R., Long, S. P. (1999): Free-air carbon dioxide enrichment (FACE) in global change research; a review. – *Advances in Ecological Research* 28: 1-56.
- [36] Mestrovic, N., Mravinac, B., Plohl, M., Ugarkovic, D., Bruvo-Madaric, B. (2006): Preliminary phylogeny of *Tribolium* beetles (Coleoptera: Tenebrionidae) resolved by combined analysis of mitochondrial genes. – *European Journal of Entomology* 103: 709-715.
- [37] Miglietta, F., Peressotti, A., Vaccari, F. P., Zaldei, A., deAngelis, P., Scarascia-Mugnozza, G. (2001): Free-air CO₂ enrichment (FACE) of a poplar plantation: the POPFACE fumigation system. – *New Phytologist* 150: 465-476. 10.1046/j.1469-8137.2001.00115.x.
- [38] Morales-Ramos, J. A., Rojas, M. G., Shapiro-Ilan, D. I., Tedders, W. L. (2011): Nutrient regulation in *Tenebrio molitor* (Coleoptera: Tenebrionidae): self-selection of two diet components by larvae and impact on fitness. – *Environmental Entomology* 40: 1285-1294.
- [39] Nederhoff, E. M. (1994): Effects of CO₂ Concentration on Photosynthesis, Transpiration and Production of Greenhouse Fruit Vegetable Crops. – PhD Thesis. Wageningen, The Netherlands.
- [40] Norby, R. J., Zak, D. R. (2011): Ecological lessons from free-air CO₂ enrichment (FACE) experiments. – *Annual Review of Ecology, Evolution, and Systematics* 42: 181-203. <https://doi.org/10.1146/annurev-ecolsys-102209-144647>.
- [41] Oehme, V., Högy, P., Franzaring, J., Zebitz, C. P. W., Fangmeier, A. (2011): Response of spring crops and associated aphids to elevated atmospheric CO₂ concentrations. – *Journal of Applied Botany and Food Quality* 84: 151-157.
- [42] Okada, M., Lieffering, M., Nakamura, H., Yoshimoto, M., Kim, H. Y., Kobayashi, K. (2001): Free-air CO₂ enrichment (FACE) using pure CO₂ injection: system description. – *New Phytologist* 150: 251-260.
- [43] Panzavolta, T. (2007): Instar determination for *Pissodes castaneus* (Coleoptera: Curculionidae) using head capsule widths and lengths. – *Environmental Entomology* 36(5): 1054-8. [https://doi.org/10.1603/0046-225X\(2007\)36\[1054:IDFPCC\]2.0.CO;2](https://doi.org/10.1603/0046-225X(2007)36[1054:IDFPCC]2.0.CO;2).
- [44] Park, Y. K., Choi, Y. C., Lee, S. H., Lee, J. S., Kang, S. H. (2012): Fecundity, life span, developmental periods and pupal weight of *Tenebrio molitor* L. (Coleoptera: Tenebrionidae). – *J. Seric. Entomol. Sci.* 50(2): 126-132.
- [45] Peltonen, P. A., Julkunen-Tiitto, R., Vapaavuori, E., Holopainen, J. K. (2006): Effects of elevated carbon dioxide and ozone on aphid oviposition preference and birch bud exudate phenolics. – *Global Change Biology* 12(9): 1670-1679.
- [46] Punzo, F., Mutchmor, J. A. (1980): Effects of temperature, relative humidity and period of exposure on the survival capacity of *Tenebrio molitor* (Coleoptera: Tenebrionidae). – *Journal of the Kansas Entomological Society* 53(2): 260-270. 10.2307/25084029.
- [47] Kittas, C., Katsoulas, N., Bartzanas, T. (2005): Effect of vents' opening and insect screen on greenhouse ventilation. – International Conference "Passive and Low Energy Cooling for the Built Environment", May 2005, Santorini, Greece, pp. 59-64.
- [48] Ren, Y. L., O'Brien, I. G., Whittle, C. P. (1994): Studies on the Effect of Carbon Dioxide in Insect Treatment with Phosphine. – In: Highley, E., Wright, E. J., Banks, H. J., Champ, B. R. (eds.) *Stored Product Protection, Proceedings of the 6th International Working Conference on Stored-Product Protection, 17-23 April 1994, Canberra, Australia*, pp.173-177. CAB International, Wallingford, UK.
- [49] Rizzo, J., Rouchka, E. C. (2007): Review of Phylogenetic Tree Construction (pp. 1-7, Rep.). – University of Louisville Bioinformatics Laboratory Technical Report Series. Report Number TR-ULBL-2007-01. University of Louisville Bioinformatics Laboratory, Louisville, KY, USA.

- [50] Roth, S. K., Lindroth, R. L. (1995): Elevated atmospheric CO₂: effects on phytochemistry, insect performance and insect parasitoid interactions. – *Global Change Biology* 1: 173-182.
- [51] Ryan, G. D., Rasmussen, S., Xue, H., Parsons, A. J., Newman J. A. (2014): Metabolite analysis of the effects of elevated CO₂ and nitrogen fertilization on the association between tall fescue (*Schedonorus arundinaceus*) and its fungal symbiont *Neotyphodium coenophialum*. – *Plant Cell Environment* 37: 204-212.
- [52] Sanchez-Guerrero, M. C., Lorenzo, P., Medrano, E., Castilla, N., Soriano, T., Baille, A. (2005): Effect of variable CO₂ enrichment on greenhouse production in mild winter climates. – *Agricultural and Forest Meteorology* 132: 244-252.
- [53] Scherber, C., Gladbach, D. J., Stevnbak, K., Karsten, R. J., Schmidt, I. K., Michelsen, A., Albert, K. R., Larsen, K. S., Mikkelsen, T. N., Beier, C., Christensen, S. (2013): Multi-factor climate change effects on insect herbivore performance. – *Ecology and Evolution* 3(6): 1449-1460. [10.1002/ece3.564](https://doi.org/10.1002/ece3.564).
- [54] Siemianowska, E., Kosewska, A., Aljewicz, M., Skibniewska, K. A., Polak-Juszczak, L., Jarocki, A., Jedras, M., (2013): Larvae of mealworm (*Tenebrio molitor* L.) as European novel food. – *Agricultural Science* 4(6): 287-291. <http://dx.doi.org/10.4236/as.2013.46041>.
- [55] Singh, P. (1982): The rearing beneficial insects. – *New Zealand Entomologist* 7(3): 304-310. <http://dx.doi.org/10.1080/00779962.1982.9722404>.
- [56] Stiling, P., Cornelissen, T. (2007): How does elevated carbon dioxide (CO₂) affect plant–herbivore interactions? A field experiment and meta-analysis of CO₂-mediated changes on plant chemistry and herbivore performance. – *Global Change Biology* 13: 1823-1842.
- [57] Stiling, P., Moon, D. C., Hunter, M. D., Colson, J., Rossi, A. M., Hymus, G. J., Drake, B. (2003): Elevated CO₂ lowers relative and absolute herbivore density across all species of a scrub-oak forest. – *Oecologia* 134: 82-87.
- [58] Tang, Q., Dai, Y., Zhou, B. (2012): Regulatory effects of *Tenebrio molitor* Linnaeus on immunological function in mice. – *African Journal of Biotechnology* 11(33): 8348-8352.
- [59] Thompson, J. D., Higgins, D. G., Gibson, T. J. (1994): CLUSTAL W: Improving the sensitivity of progressive multiple sequence alignment through sequence weighting, positions-specific gap penalties and weight matrix choice. – *Nucleic Acids Research* 22: 4673-4680. <https://doi.org/10.1093/nar/22.22.4673>.
- [60] Werner, R. A., Holsten, E. H., Matsuoaka, S. M., Burnside, R. E. (2006): Spruce beetles and forest ecosystems in south-central Alaska: A review of 30 years of research. – *Forest Ecology and Management* 227: 195-206.
- [61] Williams, R. S., Lincoln, D. E., Norby, R. J. (2003): Development of gypsy moth larvae feeding on red maple saplings at elevated CO₂ and temperature. – *Oecologia* 137(1): 114-122.
- [62] Yamada, Y., Ikeda, T. (2000): Development, maturation, brood size and generation length of the mesopelagic amphipod *Cyphocaris challengerii* (Gammaridea: Lysianassidae) of Southwest Hokkaido, Japan. – *Marine Biology* 137: 933-942. <https://doi.org/10.1007/s002270000397>.
- [63] Ye, X. Q., Liu, D. H., Hu, C. (2001): Some factors' effects on the solubility of protein from yellow mealworm (*Tenebrio molitor* L) larvae – *Journal of Zhejiang University Science* 2(4): 436-438. <https://doi.org/10.1007/BF02840562>.
- [64] Yin, J., Sun, Y., Wu, G., Ge, F. (2010): Effects of elevated CO₂ associated with maize on multiple generations of the cotton bollworm, *Helicoverpa armigera*. – *Entomologia Experimentalis et Applicata* 136: 12-20.
- [65] Zalucki, M. P., Clarke, A. R., Malcolm, S. B. (2002): Ecology and behavior of first instar larval Lepidoptera. – *Annual Review of Entomology* 47: 361-393.
- [66] Zhou, S., Criddle, R. S., Mitcham, E. J. (2001): Metabolic response of *Platynota stultana* pupae during and after extended exposure to elevated CO₂ and reduced O₂ atmospheres. – *Journal of Insect Physiology* 47: 401-409.

A QUICK COMPARISON OF PATROL EFFORTS FOR SUPPORTIVE PROTECTION: A CASE STUDY OF TWO STATIONS IN VIETNAM

DONG, L. K.^{1,2,3*} – SUTINEE, S.^{1,4} – HOA, A. X.¹ – DONG, N. P.³ – ALI, S.¹ – MANOP, P.⁵ – KUAANAN, T.^{1*}

¹*Faculty of Environmental Management, Princes of Songkla University
Hat Yai 90110, Thailand*

²*People's Committee of Thanh Hoa Province, 440000, Vietnam*

³*Department of Agricultural and Rural Development, Thanh Hoa Province 440000, Vietnam*

⁴*Coastal Oceanography and Climate Change Cluster, Princes of Songkla University
Hat Yai 90110, Thailand*

⁵*Faculty of Law, Princes of Songkla University, Hat Yai 90110, Thailand*

**Corresponding authors*

*e-mail: Ledongthph@gmail.com (L. K. Dong); uhugua@hotmail.com (T. Kuaanan)
phone: +84-985-517-789*

(Received 16th Dec 2017; accepted 27th Feb 2018)

Abstract. Law enforcement efforts related to patrol routes may be sufficiently supporting forest protection around the world. However, the adequacy of patrol efforts of stable patrol routes, with regard to illegal activities on conservation at the local level, has infrequently been explored in the past time. This study is to compare the highest qualification of current threats to conservation in protected areas (PAs) of both Nam Tien and Hon Can forest stations (FSs) which belongs to Pu Hu and Xuan Lien Nature Reserves (NRs). A total of eleven-track was explored using a conventional patrol performance. Typically, forest rangers have established the permanent GPS-tracks through the areas with the highest potential of negative effects of conservation in the sub-area forest because of recording and preventing effective illegal activities. As a result, patrol-hours of patrolling routes in both sides were correlated to illegal activity encounters and the number of staff. In contrast, the number of illegal activity in Nam Tien FS was correlated with patrol-distance. It is concluded that forest management should not only consider on the number of staff, but also patrol-hours could be one of a specific indicator of working field in the short-term period of adaptive patrol in the sustainable conservation.

Keywords: *law enforcement effort, conservation, forest, illegal activity, patrol routes*

Introduction

Forest, as the largest natural benefit, plays an essential role in the activities of global conservation (Kusters and Belcher, 2004; Bach et al., 2005; Queiroz et al., 2013; Zhou, 2015; Patarkalashvili, 2016a). Due to cattle grazing, logging, and poaching, that have been declining biodiversity (Struhsaker, 1997; He et al., 2009; Critchlow et al., 2016) by strengthened human preferences and human inefficiencies of collecting resources acquisition. Usually, there are several stakeholders in local areas with often have the conflict of interests in forest management. It should be noted that residents commonly gather fuelwood and timber illegally, as well as other NTFPs (Allendorf et al., 2007a). And the protective function hugely depends on the small-scale local situation (Teich and Bebi, 2009). Consequently, it has been affecting forest protection, especially in the

protected forest where the NRs resides (Araújo, 2003; Liang et al., 2011; Fuentes, 2011). These issues get more complex when disturbances to forest functioning and management have been shown off (Rist and Moen, 2013; Zhou, 2015).

The key to conservation and protection of species and their natural habitat is to reduce human activities in such PAs that significantly play an outstanding role in biodiversity conservation (Stoll-Kleemann, 2010; Patarkalashvili, 2016) and request the observation and prevention of its (Young, 2017). To protect biodiversity effectively, PAs, as nature reserves and national parks in Vietnam, have been established (Bleher et al., 2006; Isbell et al., 2011; Ciccacese et al., 2012; Clark et al., 2013; Geldmann et al., 2013). Conservation strategy in the PAs has been improving protection which involves stakeholders like local communities, the government authorities, and international organizations (Thi et al., 2017). And, noncompliance with regulations is often the rule from government or location areas, rather than reality, illegal activity and others of forest resource requirement grow continues (Arias, 2015). Particularly, to enhance management protection, a simple instrument is required for an assessment of human activity (Bleher et al., 2006).

In all sub-stations from NRs, as special-use forest areas, forest rangers are greatly responsible for the protective action of a certain area where local people frequently have to change their behavior, as natural resources they were formerly using maybe come off-limits (Stevens, 1997). Local managers of NRs may apply for specific regulations of inside core-zone more strictly than outside forest protection. For example, whilst no activity extraction is allowed by law (Albers and Grinspoon, 1997; No 24/10/2010/ND-CP, 2010). Regular on foot patrols focus on recording the extraction of timber, reduce poaching, avoid encroachment and restrict livestock grazing (Allendorf et al., 2007b), sometimes requires controlling illegal activity encounters. Thus, law enforcement practices by foot patrolling are commonly the approach to prohibit illegitimate activities in NRs, although the efficiency of such patrolling actions has often been questioned (Mukul et al., 2014). The following patrolling activity, the conventional styles of stable patrol routes on foot is applied and recorded by Global Positioning System (GPS)-based monitoring (Jachmann, 2008a, c; Gandiwa et al., 2014; Wiafe, 2016).

Few studies have informed increased law enforcement performance in response to a decline in illegal activities in the level of forest station in Asia and Vietnam protected areas (Jachmann, 2008a, c), due to stable patrol routes which have been typically applying for PAs. In addition to this, Gandiwa et al. (2014): and Wiafe (2016) presented the proportion of all illegal activity encounter were relatively high in man-days and distance covered in one PAs. Further, with respects to illegal activity distribution, lack of law enforcement patrolling have been combined to sink in biodiversity conservation as a result of the growth of illicit activities (Bassett, 2005; Ogutu et al., 2011). Even although, there are some forest stations which support and implement the regular patrol actions. However, relatively rare research on stable patrol efforts of forest station level have been conducted in effective conservation, thus it is still unknown or lacks sufficient law enforcement effort of permanent patrol routes to address the threats to conservation (Bleher et al., 2006). Equivocally, various inquiries of information on patrol effort are still blind under forest management without evaluation on sustainable forest management. Regularly, information on patrol routes is conducted and recorded in a productive manner and normal law enforcement performance on foot (Jachmann, 2008a, c; Gandiwa et al., 2014; Wiafe, 2016). Crucially, almost of information on dangerous conservation derive from patrolling routes have been commonly recorded by

forest rangers (Jachmann, 2008a, c) or a supportive group of forest protection. It is openly significant for look into conservation activity based on two forest stations in the different nature reserves. Particularly, almost study have considered on patrolling in the long-term such as each quarter and year. Thus, in the short-term, there have not explored as filling as this research.

Due to analysis the overall effect of patrolling exercises (distance and/or hour) and illegal activity encounters between Hon Can and Nam Tien FSs during the research period, that are independent and dependent variables (Gandiwa et al., 2013). Hence, the purpose of the study is to (1) compare law enforcement ranger in both forest stations by getting to explore the circumstances if patrol performance commonly show-off, (2) compare overall relative illegal activity richness and diversity amongst two forest stations (Werner and Raffa, 2000), (3) analyze efficient patrol efforts for effective conservation on stable patrol system of both stations in NRs if rangers have been frequently implementing their patrolling routes. It is crucial to recognize the areas where illegal activities were presented and focused in the short-term period because of concentrated conservation and management efforts (Rica et al., 2017). Addition to this, there is different patrol ranger efforts in both sides if rangers have been continually patrolling in this way.

Material and methods

Site description

This study was conducted in both forest stations likely Hon Can and Nam Tien FSs in Xuan Lien and Pu Hu NRs respectively. Both forest stations are the closest to each town and the most crowded fringe population in buffer zone. Moreover, both nature reserves are the biggest in PAs in Thanh Hoa province. In local and national level, it is well-known patrol ranger effort amongst nature reserves. The description of two study areas, including foresters and effective patrol time, have been summarily presented (*Table 1*).

Table 1. Summary of basic information on both study areas

Name of stations	Name of NRs	Number of sub-areas	Total areas (ha)	Forest officers	Effective patrol staff/times	Distance from station (km)	Average Elevation (m)
Nam Tien	Pu Hu	6	2,900	2	8	0.9-10	165-1,240
Hon Can	Xuan Lien	4	2,400	4	6	0.1-6	90-1,549

Specifically, Hon Can FS belongs to Xuan Lien NR located in Thuong Xuan district in Thanh Hoa province, in the northeast Vietnam, near the border with Nam Xuan biodiversity conservation area in neighboring Laos. And Xuan Lien NR covers an area of approximately 24,000 ha and is lied between latitude 19°52' to 20°02'N, longitude 104°58' to 105°15'E. Hon Can FS, among 5 forest stations, is the only one station controlling and patrolling 2,900 ha of the core-zone of the NRs (*Table 1*) and responsible for the law enforcement. The fully protected core-zone of Hon Can FS (the South of border NRs) is to consider on 355 households and 1,612 inhabitants in three adjacent villages in the buffer zones. Due to the high density in the buffer-zone, there is

constant pressure on the protected area with illegal activities like logging, encroachment, poaching etc.

Pu Hu NR is located in two districts, such as Quan Hoa and Muong Lat in Thanh Hoa province, in the northeast Vietnam. It has a mountainous area of around 22,688 ha (latitude 20°30' to 20°40'N and longitude 104°40' to 105°05'E). There are separately seven protected areas of which Nam Tien FS is one station controlling and patrolling 3,000 ha of the core-zone of the nature reserve. In the protected buffer zones, there have around 12 villages in Nam Tien and Thien Phu communities with 450 families and 1,200 habitats. Particularly, the local citizen living in and around NRs often influence the ability of the PA to meet conservation commission (Ormsby and Kaplin, 2005). Similar to the issue of Hon Can FS area, there have been hunting, cutting, and grazing.

Data collection

The study focused on research in the Hon Can and Nam Tien protection areas and data collected from May to August 2017 (*Fig. 1*). The survey following the main track was conducted by author and rangers which forest stations have been frequently patrolling as law enforcement practice, and noting any observations indicating non-permitted activities caused by humans or livestock (Ormsby and Kaplin, 2005). The observation was once of both forest stations how to patrol and what to explore. A comparison of these patrol activities was pointed out the estimation of patrolling efficiency in both sides. During the working field, the location of illegal activity was left marks in the land, tree, stone, etc. Addition to this, an observation of hearing, feeling, and directed observation the landscape was recorded by using GPS device and standardized data sheet (Gray and Kalpers, 2005; Jachmann, 2008c; Wiafe, 2016). Such indicator of illegal activities could be location and direction marks by humans made with stones, sticks or marks on trees. Additionally, slip or drag-marks on the ground caused by tree trunks, bamboo, branches or hunted animals.

The primary observations of distinguishing marks and indicators of illegal activities were collected on such field trips and filed by local forest officers from both forest stations, sometimes Department of Science and International Cooperation and the Department of Law Enforcement of the Head-Office of both NRs as well as the Nature Protection Groups of the adjoining villages. The patrol tracks and coordinate-points (the longitude and latitude points of appearance of illegal activity (Jachmann, 2008a) from the GPS were tabulated with Microsoft Excel and transferred into MapInfo Software. Data for pressure and threat facing both forest stations were derived from an evaluation of protected areas patrol efforts effectiveness (Ayivor et al., 2013) which mainly carried out the forest rangers regularly. In order to avoid bias, author and the same rangers patrolled during the research. Even through, rangers have not been working the permanent location.

Data analysis

After collecting the data, descriptive statistics were designed to the summary of the characteristic of illegal activity found, and a Spearman's rank correlation among variables such as illegal activity found, patrol-hours, patrol's distance and man-patrol-day (Jachmann, 2008c; Wiafe, 2016). The number of illegal activity found, and protection given by the government rangers between Hon Can and Nam Tien FSs were distinct among the patrolling tracks. Law enforcement efforts were simply analyzed the

effective patrol-distance and man-day derived (Jachmann, 2008a, b) or special patrol-hour as well (Wiafe, 2016). A non-parametric Mann-Whitney (U) test was used to compare the relative abundance of illegal activity found and other variable law enforcement efforts between the two forest station areas.

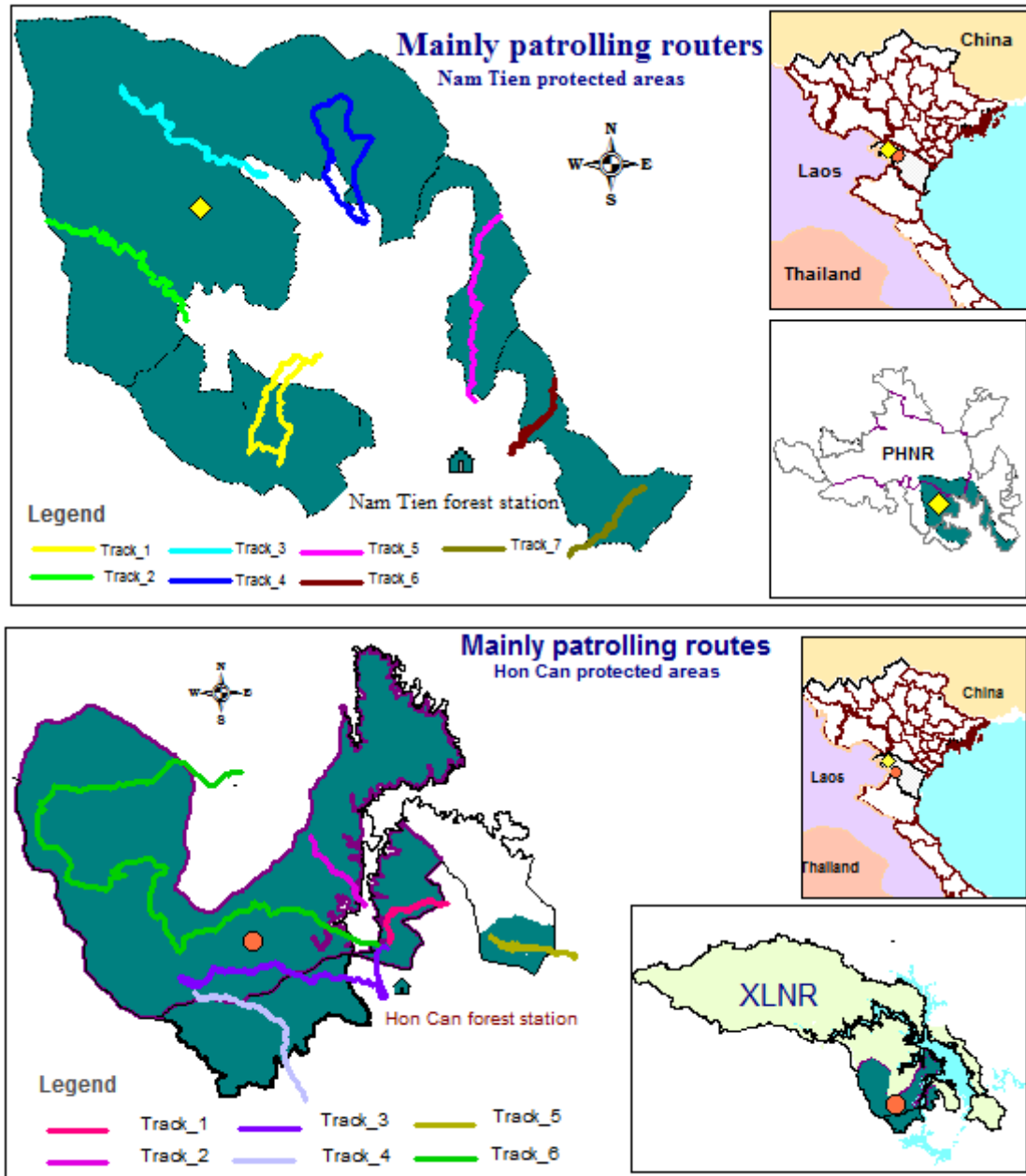


Figure 1. The location of both case study areas (2017)

Results

Totally, the findings from this study, following selected seven and six patrol-tracks, were normally patrolled on foot by forest officers of Hon Can and Nam Tien FSs respectively. Due to stable patrol-routes, almost patrolling tracks were thoroughly cross at least sub-areas of forest protection except for one track in Hon Can FS. These tracks

were presented with different priorities, like distance, time consumption, foresters and illegal activity found in protected areas. As all patrol-routes in both forest stations can be displayed (*Fig. 1*).

Staff's performance of patrolling

The mean number of distance of patrol efforts was not significantly lower for Nam Tien FS (5.89 ± 1.71) compared to Hon Can FS (6.17 ± 3.02) ($U = 23.5$, $p = 0.898$). Similarly, the mean number of patrol-hours Nam Tien (3.43 ± 1.46) and Hon Can (4.84 ± 4.09) ($U = 22.0$, $p = 0.749$) as well. Furthermore, the trend of the proportion of illegal activity encounter and staffs in Nam Tien is slightly high to distance patrolled, in opposite to Hon Can. Due patrol-hour in both case studies, the trend of illegal activity found/staff improved more exponentially in Nam Tien than in Hon Can FSs (*Fig. 2*).

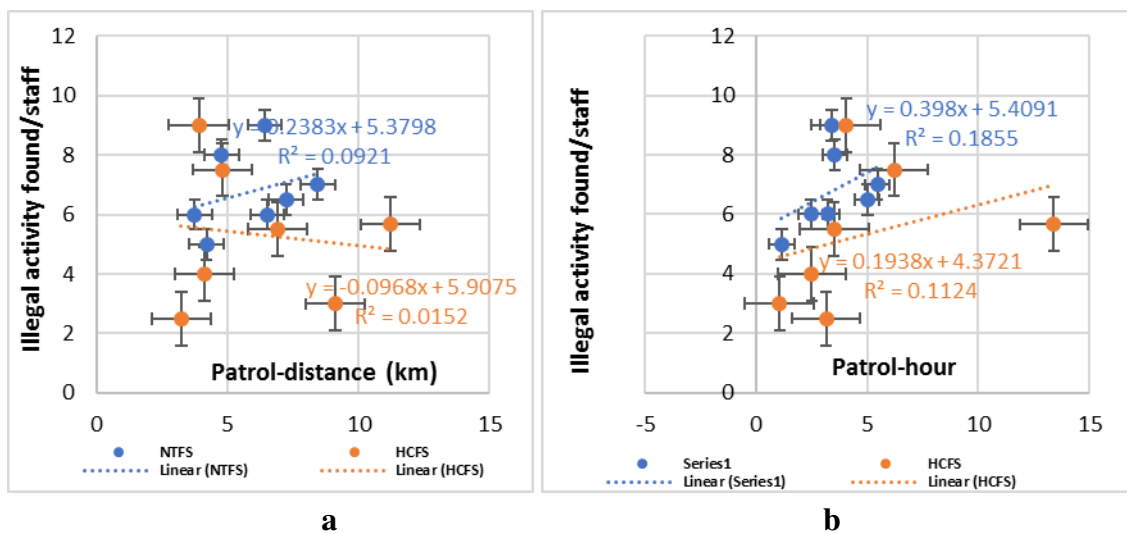


Figure 2. Trends of proportion of illegal activity encounter/staff in term of (a) patrol-distance and (b) patrol-hour

The number of forest officers were correlated with long routes in Nam Tien FS ($r_s = 0.791$, $p = 0.034$), whilst Hon Can FS had different aspect ($r_s = 0.134$, $p = 0.775$). However, our results of patrol-hour was opposite to Wiafe (2016) report when the number of staffs were correlated in both sides [Nam Tien, $r_s = 0.791$, $p = 0.034$; Hon Can ($r_s = 0.802$, $p = 0.03$)]. According to Jachmann (2008a), the relation between the number of staffs and illegal activity encounter was significantly correlated, and there was the similarity of Nam Tien ($r_s = 0.679$, $p = 0.034$) and of Hon Can ($r_s = 0.802$, $p = 0.03$).

Differential illegal activity found

A total of 61 and 71 illegal activity encounters were simultaneously captured in Nam Tien and Hon Can FSs respectively. The average illegal activity found was 8.71 (± 3.546) Nam Tien and 10.14 (± 4.488) Hon Can (*Fig. 3*). The number of livestock grazing was the most popular amongst illegal activity found arounds coordinated points in Nam Tien and Hon Can FSs (19 and 17 respectively). Some examples for illegal activity founds are presented (*Fig. 4*). Bird's nares (2 recording points) and transport

timber (2 recording points) were only found in Hon Can FS. Gunshot's heard were higher in Hon Can FS (11 points) compared to Nam Tien FS (4 points). The number of illegal activity found in both stations were not significant ($U = 59.5, p = 0.974$).

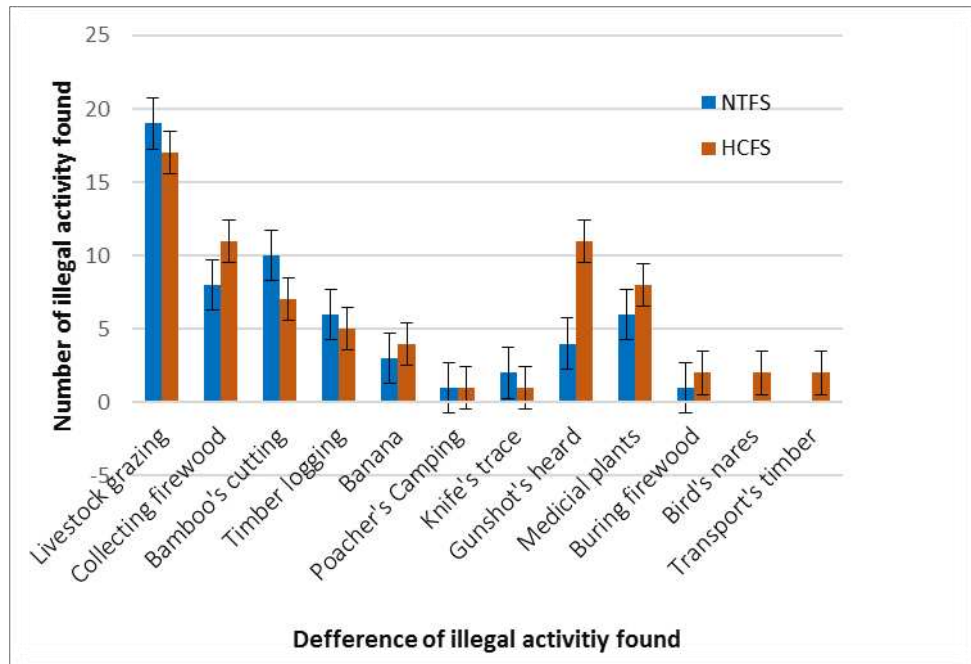


Figure 3. The diversity of encountered illegal activity

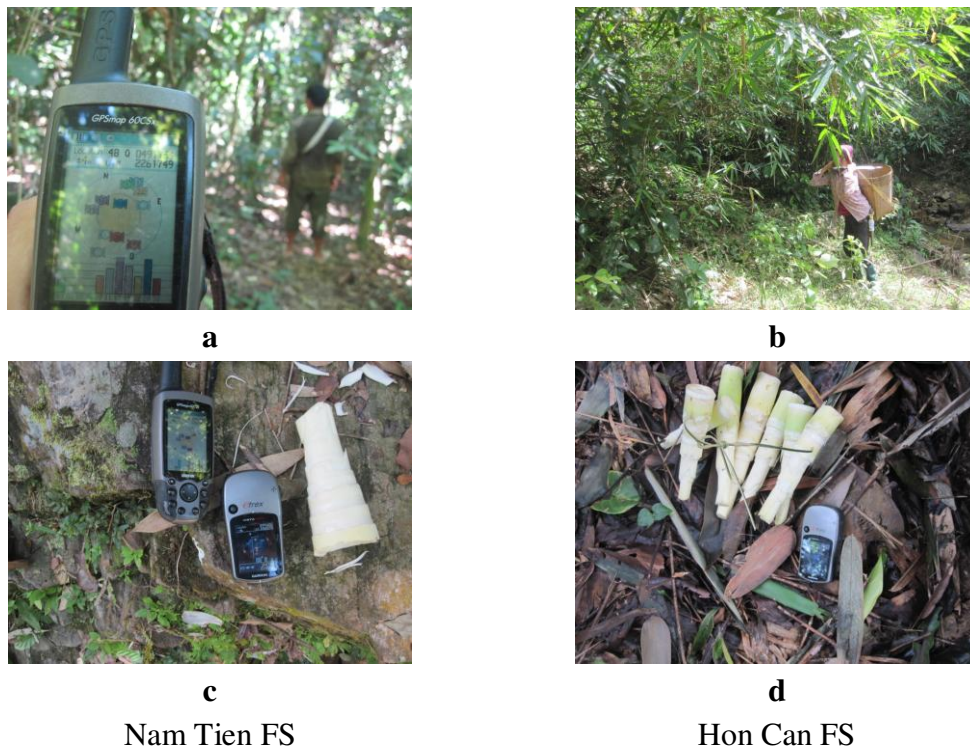


Figure 4. Human's illegal activity found both sides: (a, b) Firewood collection; (c, d) Bamboo collection, 2017 (by author, 2013)

Fluctuation of illegal activity found from law enforcement efforts

This study showed that the longer patrol-distance and patrol-hour by forest officer in both stations have led to higher number of illegal activity found (Fig. 5). Seemly, law enforcement efforts were increased, and illegal activity found was increasing too. Specifically, the relationship between patrol-hour and illegal activity encounters was statistically significant [Nam Tien ($r_s = 0.955$, $p = 0.001$); Hon Can ($r_s = 0.857$; $p = 0.014$)]. Contrast to patrol-distance, it was correlated with illegal activity found in Nam Tien ($r_s = 0.793$, $p = 0.033$) while it was opposite to Hon Can ($r_s = 0.571$; $p = 0.18$). In this case of encountered illegal activity, it was evident that the patrol hour is more important than the distance of patrol routes.

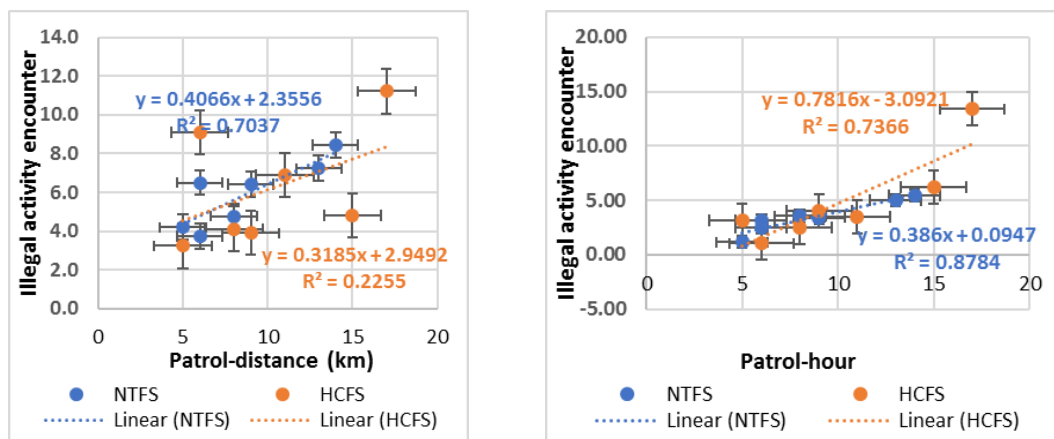


Figure 5. The tendency of illegal activity found in term of patrol-distance and patrol-hour

Interestingly, ratio of illegal activity found/patrol-distance, each case study, was not correlated to rate of illegal activity found/patrol-hour [Nam Tien FS ($r_s = -0.214$, $p = 0.645$); Hon Can FS ($r_s = -0.36$; $p = 0.939$)]. Furthermore, the relation of illegal activity found/patrol-distance and illegal activity found/patrol-hour, were not significant in both sides ($U = 19$, $p = 0.482$; $U = 22$, $p = 0.749$ respectively). However, the trend of illegal activity found/patrol-distance was directly increased in Hon Can FS, compared to contrary to Nam Tien FS situation with slight decline (Fig. 6). Particularly, there was not different in both forest stations for illegal activity found in term of distance ($p = 0.52$) and patrol-hour ($p = 0.482$).

Discussion

Patrol performance

An understanding of the law enforcement that influence patrol effort can improve the forest management of natural resource (Abbot and Mace, 1999). Base on frequently patrolling routes of observation and prohibition of illegal activities sufficiently, the patrol effort by local rangers significantly depends on both distances and on the time-consuming of each track. As a result, similarity to Jachmann (2008a) and Wiafe (2016) research, across all the patrol routes, due to distance patrolled and forest officers that were correlated in Nam Tien FS, in opposite to Hon Can FS as Risdianto et al. (2016) reported. Quite surprisingly, however, the patrol-hour in both was statically correlated

with number staffs. It was undoubted that the number of staff in Hon Can is higher 100% than that is in Nam Tien, and implied that the few protection staff like Nam Tien FS lead to less opportunity to decline illegal activity (Jachmann, 2008c; Wiafe, 2016). According to Jachmann (2008a) and Wiafe (2016), they enabled to patrol for a long period. That was possible that manager might focus on the number of staff in Nam Tien FS instead of Hon Can FS somehow.

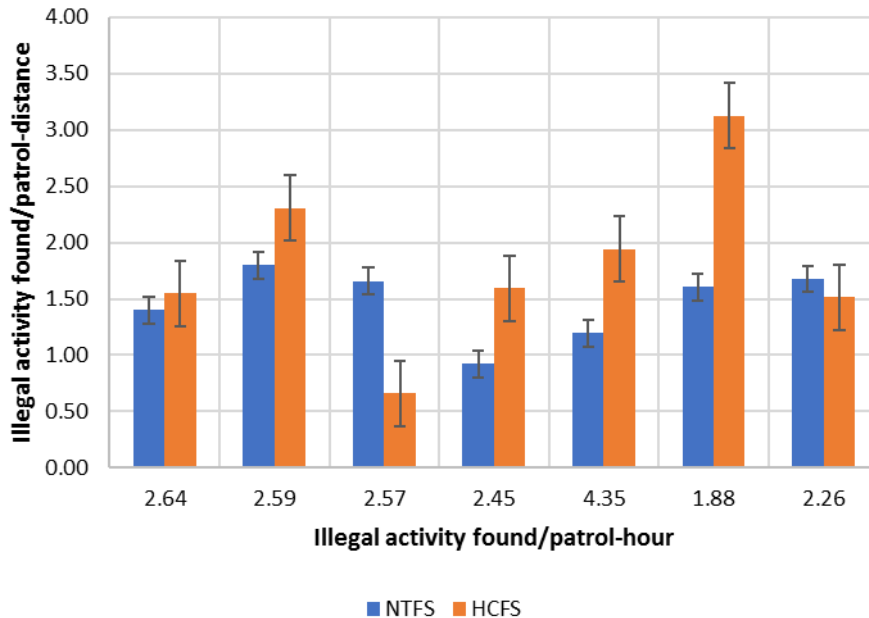


Figure 6. Trend of encounter rate of illegal activity found/patrolling distance and patrol-hour

Commonly, when the increasing number of staffs are similar to illegal activity found. Even though, there were certainly many influences of staffs to show off variable patrol (regarding distances and hours) or illegal activity found, however, it might hint that the protection staffs were the available indicator of patrol-hour and illegal activity explored. Actually, the patrol-hours from local rangers was depended on topography and several factors such as strict discipline of management characteristics, habit, serious issue of illegal activity found and senior staff efforts (Jachmann, 2008b). Based on buffer zone areas aspect, the cause given for illegal activities suggests that the economic, culture and unemployment should be accounted for the high consideration on patrolling in the richness of resources. Clearly, law enforcement may influence patterns of illegal activities in a comparison of two forest stations in different protected areas (Abbot and Mace, 1999).

Illegal trend and patrol efforts

It is undoubted that ecologic grazing always guaranteed adjacent community maintenance and it may lead to biodiversity conservation issues (Tichit et al., 2007) and influence to plant diversity (O'Connor et al., 2010). When comparing illegal activity encountered on stable patrol routes from both sides, mainly due to differences in visibility, there has been needed to distinguish between both FSs (Jachmann, 2008b). This is no surprise because this study showed that the longer patrol-distance and patrol-hour by forest officer in both stations have led to higher number of illegal activity found

in the long-term period (*Fig. 5*) (Jachmann, 2008a, c; Ayivor et al., 2013; Gandiwa et al., 2014; Wiafe, 2016). It denoted average trends of illegal activity encounters both in terms of patrol-distance and patrol-hour used for patrolling in the different tracks respectively. In both areas, upward trends of the ratio of illegal activity found in term of patrol-distance and patrol-hour in both sides were increasingly observed (Wiafe, 2016) (*Fig. 5*). As Plumptre et al (2014) represented that the current patrol effort based on distance did not deter illegal activities beyond in short-term evaluation.

Wiafe (2016) presented that there were many factors, e.g. the political plan, economy, and people's knowledge that converted the trend of contribution to illegal activity and law enforcement efforts to bring it down. Additionally, there are internal factors such as leadership styles, political management, logistics provide that might have an impact on field patrolling and other related operations (Jachmann, 2008c). External factors, e.g. topography, social, motivation, and educational level should also be considered. However, this research did not consider it because of the time constraint.

Conclusion

Effective law enforcement is crucial for conservation of our case study (Holmern et al., 2007). Overall, the finding from this study found out that the index of staff and patrol-time was an important part of law enforcement in conservation areas as for example of analysis of two forest stations above. The way of monitoring system presented in this research quickly provided useful feedback the local level of forest protection management (Jachmann, 2008b) without time-consuming of fieldwork in the large area. Further, during patrol effort implied to patrol-hour as the important quality of law enforcement performance of patrolling and it correlated with patrol-distance.

In the future, it is essential for the local level of management of the forest protection apply and compare the law enforcement practice among forest stations, due to the specific solution for excluding or at least minimizing these pressures and threat illegal activities (Mohseni, 2018) regarding the objectives of conservation. This research could be useful in the conventional law enforcement for observing the current situation and beginning the patrol planning strategy. However, it needs more thorough research about the law enforcement situation in the long-time period on both sides. The fluctuation of the amount of encountered illegal activity, in the similarity of patrolling routes, will be the subject of the forthcoming study. Addition to this, the strategies and planning from patrol staffs were freely altered, at any time, with regard to attaining patrol focuses but it relies on what the patrol forest officers have experienced and how the performance of patrol have been shown (Wiafe, 2016). Improving conservation is therefore essential for the conduct of law enforcement action from forest ranger that could be affected and supported protected areas.

Acknowledgements. We thank the Faculty of Environmental Management of Princes of Songkla University – Thailand for financing and supporting this research. Also, I appreciate the support of the forest rangers in Nam Tien and Hon Can forest stations as well as the Department of Law Enforcement and Department of Science and International Cooperation in both nature reserves for providing their technical services and cooperating to carry out the field research, being relevant advisers and sharing their experiences. Special thanks to supporting from Nature Protection Groups in adjacent villages for assistance during the field trips.

Conflict of interest. The authors definitely confirm that this article content has no conflict of interest.

REFERENCES

- [1] Abbot, J. I. O., Mace, R. (1999): Managing protected woodlands: Fuelwood collection and law enforcement in Lake Malawi National Park. – *Conservation Biology* 13(2): 418–421. <https://doi.org/10.1046/j.1523-1739.1999.013002418.x>.
- [2] Albers, H. J., Grinspoon, E. (1997): A comparison of the enforcement of access restrictions between Xishuangbanna Nature Reserve (China) and Khao Yai National Park (Thailand). – *Environmental Conservation* 24(4): 351–362. <https://doi.org/10.1017/S0376892997000465>.
- [3] Allendorf, T. D., Smith, J. L. D., Anderson, D. H. (2007): Residents' perceptions of Royal Bardia National Park, Nepal. – *Landscape and Urban Planning* 82(1–2): 33–40. <https://doi.org/10.1016/j.landurbplan.2007.01.015>.
- [4] Araújo, M. B. (2003): The coincidence of people and biodiversity in Europe. – *Global Ecology and Biogeography* 12(1): 5–12. <https://doi.org/10.1046/j.1466-822X.2003.00314.x>.
- [5] Arias, A. (2015): Understanding and managing compliance in the nature conservation context. – *Journal of Environmental Management* 153: 134–143. <https://doi.org/10.1016/j.jenvman.2015.02.013>.
- [6] Ayivor, J. S., Gordon, C., Ntiama-Baidu, Y. (2013): Protected area management and livelihood conflicts in Ghana: A case study of Digya national park. – *PARKS The International Journal of Protected Areas and Conservation* 19(1): 37–47.
- [7] Bach, C. E., Kelly, D., Hazlett, B. A. (2005): Forest edges benefit adults, but not seedlings, of the mistletoe *Alepis flavida* (Loranthaceae). – *Journal of Ecology* 93(1): 79–86. <https://doi.org/10.1111/j.1365-2745.2004.00961.x>.
- [8] Bassett, T. J. (2005): Card-carrying hunters, rural poverty, and wildlife decline in northern Côte d'Ivoire. – *Geographical Journal* 171(1): 24–35. <https://doi.org/10.1111/j.1475-4959.2005.00147.x>.
- [9] Bleher, B., Uster, D., Bergsdorf, T. (2006): Assessment of threat status and management effectiveness in Kakamega Forest, Kenya. – *Biodiversity and Conservation* 15(4): 1159–1177. <https://doi.org/10.1007/s10531-004-3509-3>.
- [10] Ciccacese, L., Mattsson, A., Pettenella, D. (2012): Ecosystem services from forest restoration: Thinking ahead. – *New Forests* 43(5–6): 543–560. <https://doi.org/10.1007/s11056-012-9350-8>.
- [11] Clark, N. E., Boakes, E. H., McGowan, P. J. K., Mace, G. M., Fuller, R. A. (2013): Protected areas in South Asia have not prevented habitat loss: a study using historical models of land-use change. – *PLoS ONE* 8(5). <https://doi.org/10.1371/journal.pone.0065298>.
- [12] Critchlow, R., Plumptre, A. J., Alidria, B., Nsubuga, M., Driciru, M., Rwetsiba, A., et al. (2016): Improving law-enforcement effectiveness and efficiency in protected areas using ranger-collected monitoring data. – *Conservation Letters* 0(0): 1–9. <https://doi.org/10.1111/conl.12288>.
- [13] Fuentes, M. (2011): Economic growth and biodiversity. – *Biodiversity and Conservation* 20(14): 3453–3458. <https://doi.org/10.1007/s10531-011-0132-y>.
- [14] Gandiwa, E., Heitkönig, I. M. A., Lokhorst, A. M., Prins, H. H. T., Leeuwis, C. (2013): Illegal hunting and law enforcement during a period of economic decline in Zimbabwe: A case study of northern Gonarezhou National Park and adjacent areas. – *Journal for Nature Conservation* 21(3): 133–142. <https://doi.org/10.1016/j.jnc.2012.11.009>.
- [15] Gandiwa, E., Zisadza-Gandiwa, P., Mango, L., Jakarasi, J. (2014): Law enforcement staff perceptions of illegal hunting and wildlife conservation in Gonarezhou National Park, southeastern Zimbabwe. – *Tropical Ecology* 55(1): 119–127.
- [16] Geldmann, J., M. Barnes, L. Coad, I. D. Craigie, M. Hockings, Burgess, N. D. (2013): Effectiveness of terrestrial protected areas in reducing habitat loss and population

- declines. – *Biological Conservation* 161: 230–238. <https://doi.org/10.1016/j.biocon.2013.02.018>.
- [17] Gray, M., Kalpers, J. (2005): Ranger based monitoring in the Virunga-Bwindi region of East-Central Africa: A simple data collection tool for park management. – *Biodiversity and Conservation* 14(11): 2723–2741. <https://doi.org/10.1007/s10531-005-8406-x>.
- [18] He, G., Chen, X., Beaer, S., Colunga, M., Mertig, A., An, L., et al. (2009): Spatial and temporal patterns of fuelwood collection in Wolong Nature Reserve: Implications for panda conservation. – *Landscape and Urban Planning* 92(1): 1–9. <https://doi.org/10.1016/j.landurbplan.2009.01.010>.
- [19] Holmern, T., Muya, J., Røskft, E. (2007): Local law enforcement and illegal bushmeat hunting outside the Serengeti National Park, Tanzania. – *Environmental Conservation* 34(1): 55. <https://doi.org/10.1017/S0376892907003712>.
- [20] Isbell, F., Calcagno, V., Hector, A., Connolly, J., Harpole, W. S., Reich, P. B., et al. (2011): High plant diversity is needed to maintain ecosystem services. – *Nature* 477(7363): 199–202. <https://doi.org/10.1038/nature10282>.
- [21] Jachmann, H. (2008a). Illegal wildlife use and protected area management in Ghana. – *Biological Conservation* 141(7): 1906–1918. <https://doi.org/10.1016/j.biocon.2008.05.009>.
- [22] Jachmann, H. (2008b). Monitoring law-enforcement performance in nine protected areas in Ghana. – *Biological Conservation* 141(1): 89–99. <https://doi.org/10.1016/j.biocon.2007.09.012>.
- [23] Kusters, K., Belcher, B. (eds.) (2004): – *Forest Products, Livelihoods and Conservation. Case Studies of Non-Timber Forest Product Systems (Vol. 1 – Asia)*. – CIFOR, Jakarta, Indonesia.
- [24] Liang, J., Zhou, M., Verbyla, D. L., Zhang, L., Springsteen, A. L., Malone, T. (2011): Mapping forest dynamics under climate change: A matrix model. – *Forest Ecology and Management* 262(12): 2250–2262. <https://doi.org/10.1016/j.foreco.2011.08.017>.
- [25] Mohseni, F. (2018): Identification of threat and pressure factors on protected areas using RAPPAM methodology (case study: Khuzestan Province, Iran) *Applied Ecology and Environmental Research* 16(1): 591–603.
- [26] Mukul, S. A., Herbohn, J., Rashid, A. Z. M. M., Uddin, M. B. (2014): Comparing the effectiveness of forest law enforcement and economic incentives to prevent illegal logging in Bangladesh. – *International Forestry Review* 16(3): 363–375. <https://doi.org/10.1505/146554814812572485>.
- [27] No 24/10/2010/ND-CP, C. Administration and management of special-use forest, Vietnam Government § (2010): Hanoi, Vietnam. – http://moj.gov.vn/vbqp/lists/vn%20bn%20php%20lut/view_detail.aspx?itemid=26113.
- [28] O'Connor, T. G., Kuyler, P., Kirkman, K. P., Corcoran, B. (2010): Which grazing management practices are most appropriate for maintaining biodiversity in South African grassland? – *African Journal of Range and Forage Science* 27(2): 67–76. <https://doi.org/10.2989/10220119.2010.502646>.
- [29] Ogutu, J. O., Owen-Smith, N., Piepho, H. P., Said, M. Y. (2011): Continuing wildlife population declines and range contraction in the Mara region of Kenya during 1977-2009. – *Journal of Zoology* 285(2): 99–109. <https://doi.org/10.1111/j.1469-7998.2011.00818.x>.
- [30] Ormsby, A., Kaplin, B. A. (2005): A framework for understanding community resident perceptions of Masoala National Park, Madagascar. – *Environmental Conservation* 32(2): 156. <https://doi.org/10.1017/S0376892905002146>.
- [31] Patarkalashvili, T. (2016): Some problems of forest management of Georgia. – *Annals of Agrarian Science* 14(2): 108–113. <https://doi.org/10.1016/j.aasci.2016.04.002>.
- [32] Plumptre, A. J., Fuller, R. A., Rwetsiba, A., Wanyama, F., Kujirakwinja, D., Driciru, M., et al. (2014): Efficiently targeting resources to deter illegal activities in protected areas. – *Journal of Applied Ecology* 51(3): 714–725. <https://doi.org/10.1111/1365-2664.12227>.

- [33] Queiroz, J. S. de, Griswold, D., Tu, N. D., Hall, P. (2013): Vietnam Tropical Forest and Biodiversity Assessment. US Foreign Assistance Act, Section 118/119 Report August, 2013. – Sun Mountain International and the Cadmus Group, Inc., Quito, Ecuador.
- [34] Rica, C., Gil-fernández, M., Sáenz, J., Carrillo-Jiménez, E., Wong, G. (2017): Distribution and hotspots of the feeding areas of jaguars on sea turtles at a national park in Costa Rica [Distribuição e pontos de concentração de áreas de predação de tartarugas]. – *Neotropical Biology and Conservation* 12(96): 2–11. <https://doi.org/10.4013/nbc.2017.121.01>.
- [35] Risdianto, D., Martyr, D. J., Nugraha, R. T., Harihar, A., Wibisono, H. T., Haidir, I. A., et al. (2016): Examining the shifting patterns of poaching from a long-term law enforcement intervention in Sumatra. – *Biological Conservation*. <https://doi.org/10.1016/j.biocon.2016.10.029>.
- [36] Rist, L., Moen, J. (2013): Sustainability in forest management and a new role for resilience thinking. – *Forest Ecology and Management* 310: 416–427. <https://doi.org/10.1016/j.foreco.2013.08.033>.
- [37] Stevens, S. (1997): – *Conservation through Cultural Survival: Indigenous Peoples and Protected Areas*. – Island Press, Washington, DC.
- [38] Stoll-Kleemann, S. (2010): Evaluation of management effectiveness in protected areas: Methodologies and results. – *Basic and Applied Ecology* 11(5): 377–382. <https://doi.org/10.1016/j.baae.2010.06.004>.
- [39] Struhsaker, T. T. (1997): *Ecology of an African Rain Forest: Logging in Kibale and the Conflict between Conservation and Exploitation*. – University Press of Florida, Gainesville.
- [40] Teich, M., Bebi, P. (2009): Evaluating the benefit of avalanche protection forest with GIS-based risk analyses-A case study in Switzerland. – *Forest Ecology and Management* 257(9): 1910–1919. <https://doi.org/10.1016/j.foreco.2009.01.046>.
- [41] Thi, H. Do, Krott, M., Böcher, M. (2017): The success of scientific support for biodiversity conservation policy: The case of Ngoc Son Ngo Luong nature reserve in Vietnam. – *Journal for Nature Conservation* 38: 3–10. <https://doi.org/10.1016/j.jnc.2017.05.002>.
- [42] Tichit, M., Doyen, L., Lemel, J. Y., Renault, O., Durant, D. (2007): A co-viability model of grazing and bird community management in farmland. – *Ecological Modelling* 206(3–4): 277–293. <https://doi.org/10.1016/j.ecolmodel.2007.03.043>.
- [43] Werner, S. M., Raffa, K. F. (2000): Effects of forest management practices on the diversity of ground-occurring beetles in mixed northern hardwood forests of the Great Lakes Region. – *Forest Ecology and Management* 139(1–3): 135–155. [https://doi.org/10.1016/S0378-1127\(99\)00341-2](https://doi.org/10.1016/S0378-1127(99)00341-2).
- [44] Wiafe, E. D. (2016): Wildlife laws monitoring as an adaptive management tool in protected area management in Ghana: a case of Kakum Conservation Area. – *Springer Plus* 5(1): 1440. <https://doi.org/10.1186/s40064-016-3129-x>.
- [45] Young, K. R. (2017): National park protection in relation to the ecological zonation of a neighboring human community: an example from northern Peru. – *Mountain Research and Development* 13: 267–280. <http://dx.doi.org/10.2307/3673656>.
- [46] Zhou, M. (2015): Adapting sustainable forest management to climate policy uncertainty: A conceptual framework. – *Forest Policy and Economics* 59: 66–74. <https://doi.org/10.1016/j.forpol.2015.05.013>.

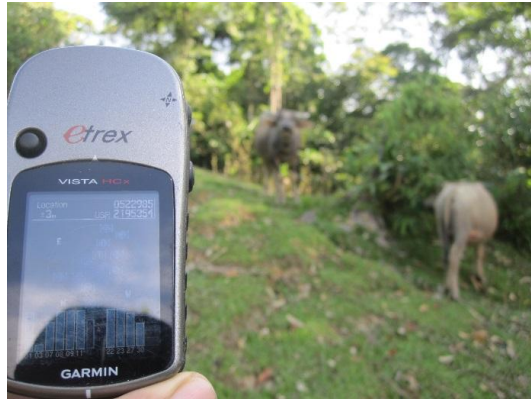
APPENDIX

In Hon Can station

Firewood collection by local people



Cattle grazing in nature reserve



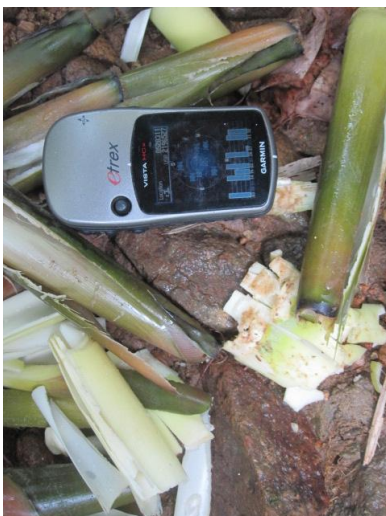
Collecting non-timber forest product



Banana leaf harvesting



Bamboo's shoot harvesting



Bamboo harvesting



In Nam Tien station

Bamboo harvesting



Basket of Bamboo shoot harvesting



Bamboo shoot harvesting



Thatch harvesting



Camping hunter



Bamboo harvesting



LOW LIGHT PHYTOPLANKTON GENERA OBSERVED IN THE COASTAL AND ESTUARINE WATERS OF GOA, INDIA

RAMAKRISHNAN, R.* – THAYAPURATH, S. – MANGUESH, U. G. – DIAS, A. B.

*National Institute of Oceanography, Goa 403004, India
(e-mail: suresh@nio.org; phone: +91-83-2245-0365)*

**Corresponding author
e-mail: reshmitharamakrishnan@gmail.com*

(Received 20th Jul 2017; accepted 6th Dec 2017)

Abstract. This is the first study carried-out to understand the phytoplankton genera in the low light (less than 50 $\mu\text{mol}/\text{m}^2/\text{s}$ of photosynthetically available radiation) for the estuarine and coastal waters of Goa, India. There were 93 phytoplankton genera observed of which the most abundant were *Skeletonema* spp., *Leptocylindrus* spp., *Thalassiosira* spp., *Cerataulina* sp., and *Fragilariopsis* sp. The centric diatom *Skeletonema* spp. was the most abundant phytoplankton genera observed during all the seasons. Similarly, other abundant genera observed all through the year in low light in the coastal and estuarine waters were *Cerataulina* sp., *Chaetoceros* spp., *Coscinodiscus* spp., *Leptocylindrus* spp., *Navicula* spp., *Nitzschia* spp., *Pleurosigma* spp., *Pseudo-nitzschia* spp., and *Thalassiosira* spp. Phytoplankton observed only in estuarine waters were *Bacillaria* sp., *Planktoniella* sp., *Biddulphia* sp., and *Asterionellopsis* spp., while *Enotia* sp., *Oxytoxum* sp., were observed only in the coastal waters during the summer season. Contributions of chlorophyll a and fucoxanthin were relatively higher in low light regions, while the photoprotective pigment β -carotene was lower than observed at the surface. The maximum spectral light available at the low light region varied for water types, and was 537 to 581 nm in the coastal waters, while it shifted to longer wavelengths 561 to 648 in the estuarine waters.

Keywords: *coastal waters, estuaries, low light, photoacclimation, umbrophillic phytoplankton*

Introduction

Light is the source of life on planet Earth. However, unlike the terrestrial environment where there is no dearth of solar light required for photosynthesis, the aquatic regions are not blessed to have sufficient light at all depths. Phytoplankton are planktons or ‘wanderers’ and have to survive wherever they are taken and hence phytoplankton have the abilities to survive at extreme light levels. The acclimation of phytoplankton under extreme light conditions are labeled related to light adaptations such as high light or sun or ‘heliophilic’ and adapted to low light or shade or ‘umbrophillic’ (Ryther and Menzel, 1959). Photoacclimation is their way of life (Dubinsky et al., 2010). Though it has been shown in laboratory studies that the minimum light level required by phytoplankton is about 2 $\mu\text{mol}/\text{m}^2/\text{s}$ (Overmann and Garcia-Pichel, 2005), the actually observed light levels are reported to be even lower (Raven and Cockell, 2006). They are very efficient at utilizing the energy and it has been observed that at the very low light respiration rates are much lower. Most of the microscopic O_2 evolving organism of cyanobacteria and eukaryotes can have photolithotrophic growth, i.e. using photons as the sole energy to compensate irradiance as low as about 0.35 $\mu\text{mol}/\text{m}^2/\text{s}$ (Raven et al., 2000).

The light is spectral in nature with varying levels of energy inversely proportional to the wavelengths. Hence these phytoplankton in low light regions need to be studied for their photoacclimation and ‘chromatic acclimation’. Though it has been argued that the spectral light was inconsequential and was believed earlier that photosynthesis required

light in the PAR region (Dring, 1981), which however proved wrong with recent studies. Recent studies revealed that spectral light does play an important role in photosynthesis (Gorai et al., 2014).

The light harvesting capabilities can be appreciated when it is observed that there are extensive deep chlorophyll maxima observed just near the 1% of light levels (Moore et al., 2006; Dubinsky, 2010). The global primary productivity estimations do consider light levels only till 1% and it has been evident from various studies and observations that there were plenty of phytoplankton even below this light levels whose contributions were significant and cannot be ignored. There also seems to hold some relations with regards to their light utilization for photosynthesis between the taxonomic groups of phytoplankton and cell sizes observed in low light (Richardson et al., 1983; Geider et al., 1986; Cullen and Macintyre, 1998; Finkel, 2001; Boyd et al., 2010).

One of the earliest studies on phytoplankton community in the coastal and estuarine waters of Goa were from Devassy and Goes (1988) which provided information on the seasonal variations of phytoplankton communities in the coastal and estuarine waters. These drowned river valley type estuaries are known as ‘monsoonal estuaries’ and the monsoon has an influence on the phytoplankton community (Patil and Anil, 2011). Detailed studies of the phytoplankton in these estuaries exhibited the large diversities of the phytoplankton communities, with blooms and harmful algae (Matondkar et al., 2007; Patil and Anil, 2011; Pednekar et al., 2012, 2014).

Presently there is no information available of the phytoplankton composition in the low light regions of the waters of Goa. The availability of light at the benthic regions of the estuarine and coastal waters of Goa show spatial and temporal variations and there were regions in the water column that were under very low light. This is the first study that reports the phytoplankton genera at low light in these coastal and estuarine waters of Goa and the variations of physical, biological and optical parameters at these low light regions.

Materials and methods

Study area

The field measurements were carried out in the coastal and estuarine waters of Goa, a site located between latitude 15.3° to 15.73°N and longitude 73.6 to 74.1°E at the central west coast of India (*Fig. 1*). The study areas included coastal waters and the two estuaries Mandovi and Zuari. One of the main factors that influence these waters are the rains during the southwest monsoon in the months of June to September hence they are often called as “monsoonal estuaries”. Tides are the sole driving force for circulation and mixing in the estuaries during the non-monsoon season (Shetye et al., 2007; Vijith et al., 2009). There are much fewer discharges during the non-monsoon seasons and the waters are vertically well mixed. Monsoonal upwelling is the common feature observed during the south-west monsoon in the coastal waters of Goa, which plays an important role in the biogeochemistry of these waters. Seasonal hypoxia has been observed in the sub-surface waters during the post-monsoon period of September to October (Naqvi et al., 2000, 2006). The coastal waters have algal blooms of varied species, some of which are seasonal such as *Trichodesmium* blooms which were often observed during the summer season (Naqvi et al., 1998; Desa et al., 2005; Parab et al., 2006; Gomes et al., 2008). Temperature inversions were also reported in these waters (Thadathil and Gosh, 1992). Large variations in the colored dissolved organic matter

(CDOM) were observed in these waters with contrasting features in the estuarine and coastal waters (Dias et al., 2017).

The depth of the stations in the coastal waters varied between 2.5 to 26 m and 2 to 8 m in the estuaries. The optical studies indicate that Secchi depth varies from 2.1 to 3.1 m in the coastal waters and 1.2 to 2.4 m in the estuaries.

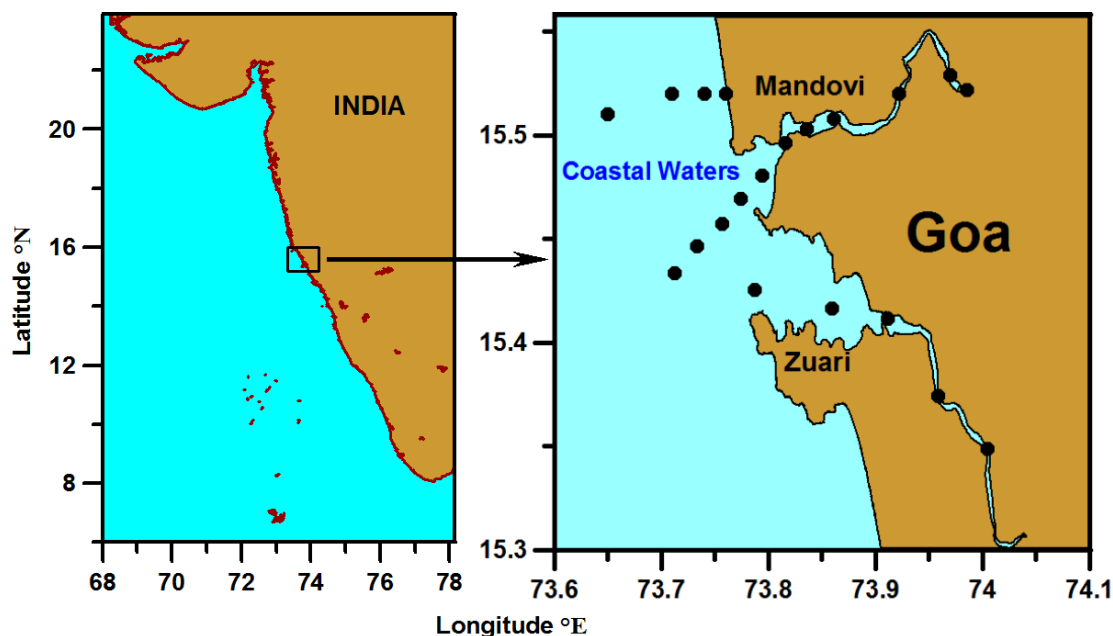


Figure 1. Study area showing water sample collections sites in the coastal and estuarine waters of Goa, India

Environmental data and sample collection

There were two types of data used for the study, the one that was available from the measurements using in-situ profiling instrument and the other available from the water samples collected at the same stations as in-situ measurements. The measurements and water samples were collected during field measurement campaigns on a boat in the coastal and estuarine waters every month during fair weather conditions at pre-identified stations (*Fig. 1*). No measurements were carried out in the coastal waters during the monsoon period. The data include from the period 2013 to 2016 covering 50 stations of which 37 were in the estuaries and 13 in the coastal waters.

Most of the earlier studies related to low light and photoacclimation were restricted in the lower region of PAR about $30 \mu\text{mol}/\text{m}^2/\text{s}$ (Fisher et al., 1996; Anning et al., 2000; Zastrow, 2001; Staehr et al., 2002; Rodriguez et al., 2006; Finkel et al., 2006; Dubinsky and Stambler, 2009) the data used for this study included only data at depths with PAR values less than $50 \mu\text{mol}/\text{m}^2/\text{s}$, which is equivalent to about $12.5 \text{ W}/\text{m}^2$ of solar irradiance in PAR region (Suresh et al., 1996). Though the minimum value of PAR measured was about $0.22 \mu\text{mol}/\text{m}^2/\text{s}$ this could be within small error considering the detection limit of the radiometer. The mean of the spectral dark readings taken in the laboratory was about $0.2 \mu\text{W}/\text{cm}^2/\text{nm}$ and dark current readings were taken care during processing. All optical, physical, biological and ancillary parameters were obtained at the same depths of low light observations (*Fig. 2*).

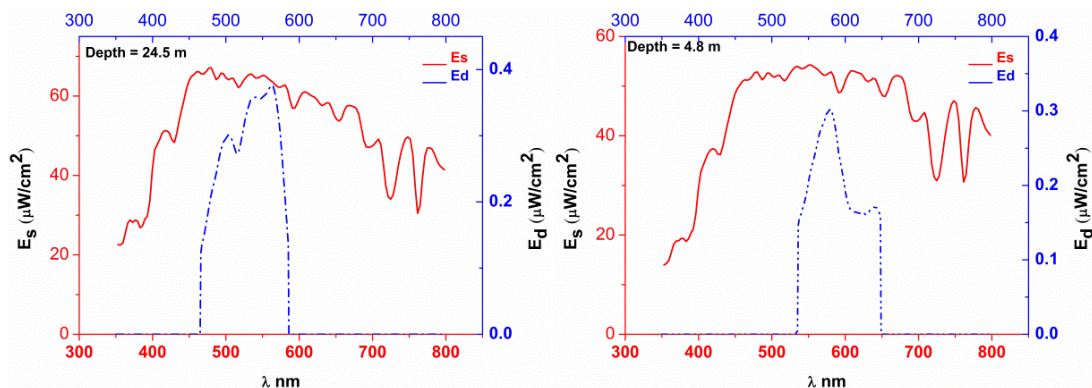


Figure 2. Solar irradiance at the surface of the water (straight line) and at low light region (dashed line) for the two stations in the coastal waters of Goa (left) and Mandovi estuary (right). Depth at low light is indicated in the top left corner of each diagram

The water samples were collected either by Niskin water sampler or automated water sampler using silicon transparent pipe with the pump. The water samples were used for analysis in the laboratory for phytoplankton taxonomy with light microscope (Olympus BX 51) and scanning electron microscope (Hitachi TM3030), and the same water sample were used for deriving chlorophyll using fluorometric method (Trilogy-Turner), total suspended matter using the gravimetric method, CDOM using spectrophotometer (Shimadzu UV-2600) and pigments using HPLC (Agilent 1100 series).

The water samples (250 ml) were collected in amber colored plastic bottles and preserved following the method described by Santhanam et al. (1987) using 2 ml of Lugol's iodine solution. For microscopic analysis, samples were concentrated to 5-10 ml by siphoning the top layer with a tube covered with a 10 μm nytex filter on one end. Sample concentrates were transferred to a 1 ml capacity Sedgwick-Rafter and counted using a light microscope (Olympus BX 50) at 20x and 40x magnification. Phytoplankton cell identifications were based on standard taxonomic keys (Tomas, 1997). The results were expressed as numbers of cells L^{-1} .

The water samples collected at discrete depths were preserved and analyzed in the laboratory following the standard protocols. The biological parameter included colored dissolved organic matter (CDOM), chlorophyll (Chl), total suspended matter (TSM). The phytoplankton pigments were measured using HPLC. Apart from the biological parameters derived from the water sample analysis, the depth profiles of parameters such as CDOM, chlorophyll fluorescence were available from the optical sensors available with the hyper-spectral radiometer.

The optical properties were measured in-situ using profiling optical instruments. The apparent optical properties were derived from the measurements using a hyper-spectral profiling radiometer Hyper-OCR (Satlantic, Canada), which provided profiles of downwelling irradiance, upwelling radiance, diffuse attenuation coefficients, PAR (photosynthetically available radiation (400-700 nm)) and surface solar irradiance in the spectral range of 350-800 nm. The mean of the spectral dark readings taken in the laboratory was about $0.2 \mu\text{W}/\text{cm}^2/\text{nm}$. This was considered as the detection limit. The surface irradiance data were available from a reference sensor mounted at a clear site on the boat. The inherent optical properties were measured using an AC-9 instrument (Wet Labs) which provided profiles of absorption and beam attenuation coefficient (without the contributions from pure water) at nine wavelengths. The instrument AC-9 was

calibrated in the laboratory prior to every field measurement using optically clean water, whereas hyperspectral radiometer was periodically factory calibrated. The optical data were processed following the standard protocols (Mueller 2003, Mueller et al., 2003). The radiometer data were processed using the latest software Prosoft provided by the manufacturer of the radiometer.

The ancillary parameters such as temperature, salinity, and density were available from the profiling radiometer. Secchi depth was also measured.

Results

There were 93 phytoplankton genera observed in the low light regions of coastal and estuarine waters of the study area and listed here are the 20 phytoplankton genera and their abundance (Table 1). The abundance of phytoplankton genera is given as the percent of the total counts of all genera. Most of these genera listed here have also been reported earlier to reside in low light conditions such as *Asterionella* sp. (Zastrow, 2001), *Chaetoceros* spp. (Finkel et al., 2006), *Coscinodiscus* spp. (Key et al., 2010), *Cyclotella* sp. (Fisher et al., 1996), *Ditylum* sp. (Staehr et al., 2002), *Fragilaria* sp. (Karst-Riddoch et al., 2009), *Prorocentrum* sp. (Rodriguez et al., 2006), *Skeletonema* spp. (Anning et al., 2000), *Synechococcus* spp. (Barlow and Alberte, 1987), and *Thalassiosira* sp. (Dubinsky and Stambler, 2009). Most of the genera observed here were diatoms and diatoms can adapt to all light levels (Richardson et al., 1983).

Table 1. The physical environmental parameter for low light phytoplankton genera observed in coastal and estuarine waters of Goa

Low light phytoplankton genera	Mean percentage occurrence	Minimum temp (°C)	Maximum temp (°C)	Minimum salinity	Maximum salinity	Minimum density (kg/m ³)	Maximum density (kg/m ³)
<i>Skeletonema</i> spp.	13.03	25.038	32.39	0.14	35.42	4.66	22.61
<i>Leptocylindrus</i> spp.	7.65	25.038	32.09	0.14	35.42	4.66	22.76
<i>Thalassiosira</i> spp.	7.46	25.038	31.18	2.81	35.31	4.66	22.61
<i>Cerataulina</i> sp.	6.93	27.485	32.33	2.81	35.74	4.66	22.58
<i>Fragilariopsis</i> sp.	6.70	32.346	32.35	31.88	31.88	18.61	18.61
<i>Chaetoceros</i> spp.	5.56	25.038	32.33	0.39	35.74	4.66	22.61
<i>Asterionellopsis</i> spp.	5.38	25.038	29.33	11.05	35.31	4.66	22.61
<i>Licmophora</i> sp.	4.76	25.038	31.19	11.96	35.42	4.79	22.61
<i>Navicula</i> spp.	4.70	25.038	32.35	0.14	35.74	4.66	22.76
<i>Oxytoxum</i> sp.	4.70	32.284	32.28	26.67	26.67	14.75	14.75
<i>Coscinodiscs</i> spp.	4.19	25.038	32.33	11.05	35.74	4.66	22.61
<i>Pseudo-nitzschia</i> spp.	4.07	27.111	32.28	0.14	35.42	4.66	22.43
<i>Nitzschia</i> spp.	3.76	25.038	32.35	0.14	35.74	4.66	22.76
<i>Heterocapsa</i> sp.	3.50	32.284	32.28	26.67	26.67	14.75	14.75
<i>Prorocentrum</i> spp.	3.22	27.275	32.33	0.39	35.74	10.69	22.58
<i>Cochlodinium</i> sp.	3.20	27.275	32.33	11.05	35.09	4.66	22.52
<i>Pleurosigma</i> spp.	3.08	25.038	32.35	0.14	35.31	4.66	22.61
<i>Bacillaria</i> sp.	2.95	26.641	30.33	0.14	34.89	19.28	21.54
<i>Cyclotellas</i> pp.	2.89	25.038	32.35	11.05	35.74	4.66	22.61
<i>Dactyliosolen</i> sp.	2.53	25.038	32.09	0.39	34.81	4.66	22.61

There were about 80 genera observed in the “very” low light regions (less than $5 \mu\text{mol}/\text{m}^2/\text{s}$ of PAR). The leading twenty phytoplankton in these very low light regions as per their abundance were *Skeletonema* spp., *Leptocylindrus* spp., *Thalassionema* spp., *Chaetoceros* spp., *Cerataulina* sp., *Bacillaria* sp., *Navicula* spp., *Nitzschia* spp., *Pseudo-nitzschia* spp., *Proboscia* sp., *Coscinodiscus* spp., *Prorocentrum* spp., *Dactyliosolen* sp., *Cylindrotheca* sp., *Lauderia* sp., *Pleurosigma* spp., *Licmophora* sp., *Thalassiosira* spp., *Eucampia* sp. and *Cyclotella* spp. The images of ten most occurring low light phytoplankton are shown in *Figure 3*.



Figure 3. Microscopic images of A) *Asterionellopsis* sp., B) *Navicula* sp., C) *Nitzschia* sp., D) *Thalassiosira* sp., E) *Cerataulina* sp., F) *Pseudo-nitzschia* sp., G) *Cyclotella* sp., and SEM (Scanning electron microscope) images of H) *Chaetoceros* sp., I) *Coscinodiscus* sp., and J) *Skeletonema* sp.

Physical parameters

The measurements on physical characteristics of the waters were taken during all seasons in estuarine and coastal (except monsoon) waters which showed large variations in salinity, temperature, and density over the period of study which were consistent with

the earlier observations by others for these waters. The range of physical environmental parameters observed at the occurrences of these twenty genera in low light are given in *Table 1*. The temperature varied between 25.0 and 32.9 °C, the salinity from 0.14 to 35.7 and density from 4.6 to 22.7(kg/m³).

Morphology

The shapes of phytoplankton genera observed in low light were mostly cylindrical, rectangular box, a prism on parallelogram base and spherical.

Spatial and temporal variations

To study the temporal pattern the seasons were labeled as summer (March-May), monsoon (June-September), post-monsoon (October-November) and winter (December-February) season. The phytoplankton genera were selective in their adaptations to the seasons and water types. There were distinct patterns of adaption of phytoplankton genera observed with those noticed only on coastal waters or estuaries and during a particular season and while others inhabiting in all waters at all times.

Skeletonema spp., is a type of cylindrical, non-flagellated centric diatom group with cosmopolitan distribution and was the most frequently and abundantly observed genera in these waters during all season (Matondkar et al., 2007; Patil and Anil, 2011; Pednekar et al., 2014). Similarly, other genera observed all through the year in the coastal and estuarine waters were *Cerataulina* spp., *Chaetoceros* spp., *Coscinodiscus* spp., *Leptocylindrus* spp., *Navicula* spp., *Nitzschia* spp., *Pleurosigma* spp., *Pseudonitzschia* spp., and *Thalassiosira* spp.

Bacillaria sp., *Planktoniella* sp., *Biddulphia* sp., *Isthmia* sp., and *Asterionellopsis* spp., were only observed in estuarine waters (Matondkar et al., 2007). *Enotia* sp. and *Oxytoxum* sp., were observed only in the coastal waters during the summer season.

Optical parameters

There were two types of optical parameters, one that provided information on the amount of light available and the second that described the optical properties of water.

The optical parameters observed at these low light regions that quantified the amount of light available were photosynthetically available radiation (PAR) 400-700 nm, the percentage of PAR (%PAR) and downwelling spectral solar irradiance (Ed) which were observed at depth and the spectral solar irradiance measured above the surface of the water.

There were also optical properties of water that described the light in these water. These included apparent and inherent optical properties. The inherent optical properties were absorption, beam attenuation, and backscattering coefficients. These parameters characterized the light conditions and suggested the reasons for the low light conditions. The apparent optical properties included the downwelling irradiance (Ed), PAR and diffuse attenuation coefficient (Kd). The optical parameters that were indicators of the penetration of light were the transparency of water (Secchi depth) and first optical depth Z90.

The statistics of the observed optical parameters are listed in *Table 2*, and these parameters were observed at the water column depths where the PAR values were less than 50 $\mu\text{mol}/\text{m}^2/\text{s}$, which is equivalent to about 12.5 W/m^2 (Suresh et al., 1996). The %PAR were less than 10 in these waters.

Table 2. Optical parameter observed during low light environmental condition at coastal and estuarine waters off Goa

Parameters	Minimum	Maximum	Mean	SD
PAR ($\mu\text{mol}/\text{m}^2/\text{s}$)	0.21	50.86	13.45	15.79
%PAR	0.01	8.21	1.33	1.70
Wavelength of maximum solar irradiance at low light depth (nm)	534	648	577	21.90
Maximum spectral irradiance of light at low light depth ($\mu\text{W}/\text{cm}^2$)	0.14	9.26	2.90	2.88
Wavelength of maximum surface solar irradiance (nm)	460	551	494	30
Maximum of surface spectral irradiance ($\mu\text{W}/\text{cm}^2$)	23.18	178.97	102	38.3
Absorption at 412 nm (m^{-1}) (without water)	0.29	12.74	2.33	2.46
Absorption at 676 nm (m^{-1}) (without water)	0.03	0.65	0.16	0.11
Beam attenuation at 412 nm (m^{-1}) (without water)	2.40	126.17	13.29	19.7
Beam attenuation at 676 nm (m^{-1}) (without water)	1.66	141.61	10.44	20.6
Back scattering coefficient at 676 nm	0.02	0.90	0.16	0.18
Diffuse attenuation coefficient at 490 nm	0.009	4.26	1.1	0.88
Wavelength at maximum Z_{90} (nm)	481	582	561	24
Maximum Z_{90} (m)	0.55	8.15	2.38	2.0

Biological parameters

The pigment data from HPLC analysis were available only for few stations in the low light region are reported here. From these limited data of phytoplankton pigments, apart from chlorophyll, the most abundant pigments were fucoxanthin, zeaxanthin, and β -carotene (Fig. 4). The contribution of the individual pigment to the total pigment was derived by normalizing the pigment values with the total pigments. Contributions of chlorophyll a and fucoxanthin were relatively higher in low light regions, while β -carotene was lower than observed at the surface. One of the noteworthy observations was the contribution of chlorophyll a to be above 60% at the low light region, while at the surface it was about 50%.

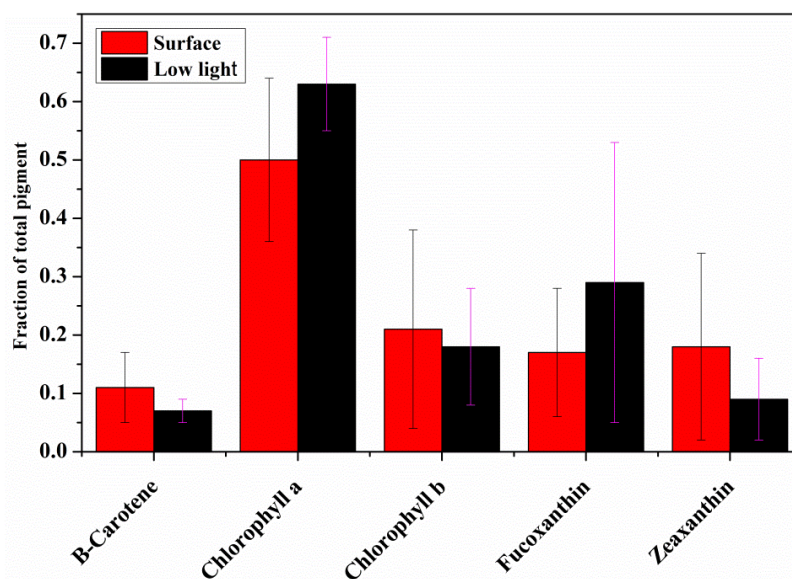


Figure 4. Phytoplankton pigments at the surface and low light region

Apart from the information on the phytoplankton pigments, the other parameters available from waters samples analysis were chlorophyll, CDOM, and total suspended matter and supporting biological parameters measured with optical sensors available on profiling radiometer were CDOM and chlorophyll fluorescence. pH was determined with a hand held pH meter (*Table 3*). The values of chlorophyll, CDOM, and TSM were appreciable to the mean value of these parameters observed in the water column.

The presence of optically active substances that attenuate light and create low light conditions were evident from the high values of the optical properties such as absorption due to CDOM, absorption in the blue region at 412 nm, beam attenuation coefficients (attenuation and scattering), high backscattering coefficient and diffuse attenuation coefficient. The biological parameters like CDOM and TSM were also found to be higher at the bottom. CDOM absorb light particularly in the blue and green region, leaving less light in the PAR region, while particles scatter and attenuate light. The high TSM could be due to the river transport and resuspension from the bottom.

Table 3. Biological parameters observed during low light environmental condition at coastal and estuarine waters of Goa

Parameter	Minimum	Maximum	Mean	SD
Chlorophyll <i>a</i> (mg/m ³)	0.4	12.83	3.9	2.9
Total suspended matter (TSM) (g/m ³)	3.06	110	20.74	21.45
CDOM absorption at 412 nm, a_g (412) (m ⁻¹)	0.08	0.86	0.34	0.22
CDOM fluorescence	0.02	15.91	2.38	2.43
Fluorescence	0.3	3.74	1.32	0.83
pH	7.12	8.18	7.63	0.31

Discussion

The low light regions are close to the bottom and the phytoplankton will require an adequate supply of nutrients for their sustenance. There is no dearth of nutrients in these estuaries (Verlencar, 1987). Mandovi and Zuari estuaries are also sources of nutrients to the coastal waters, though their concentrations are comparatively lower than estuaries. These help in the sustenance of the efficient light harvesting umbrophillic phytoplankton and seem to be the reason for the relatively higher chlorophyll found in these low light waters.

Photoacclimation by phytoplankton to extreme levels of light affects pigment ratios of these phytoplankton. Our observations on the distributions of pigments at high and low light show that chlorophyll and fucoxanthin were higher at low light levels, which agree with earlier studies that show light-harvesting pigments increase under low light and particularly chlorophylls, phycobilins, fucoxanthin and peridinin under low light (Dubinsky and Stambler, 2009; Pinchasov-Grinblat et al., 2011). β -carotene help in photoprotective mechanism under high light conditions and in low light conditions they are inconsequential so β -carotene were relatively lower (Krinsky, 1989; Fan et al., 1995; Choudhury and Behera, 2001; Wang et al., 2003; Schagerl and Muller, 2006). Fucoxanthin is associated with diatoms and used to indicate its abundance and its level was higher at low light regions than the surface. Most of the species observed here were diatoms and they can adapt to all light conditions (Richardson et al., 1983).

Most of these species listed here have also been reported earlier by others reside in low light conditions such as *Asterionella* sp. (Zastrow, 2001), *Chaetoceros* spp. (Finkel et al., 2006), *Coscinodiscus* spp. (Key et al., 2010), *Cyclotella* sp. (Fisher et al., 1996), *Ditylum* sp. (Staehr et al., 2002), *Fragilaria* sp. (Karst-Riddoch et al., 2009), *Prorocentrum* sp. (Rodriguez et al., 2006), *Skeletonema* spp. (Anning et al., 2000), *Synechococcus* spp. (Barlow and Alberte, 1987), and *Thalassiosira* sp. (Dubinsky and Stambler, 2009).

Apart from the metabolic rate (growth, photosynthesis, respiration) light utilization by phytoplankton is also influenced by their size and shape (Raven, 1984; Kirk, 1994; Finkel, 2001). Morphometric and allometric parameters of phytoplankton are important indicators of the phytoplankton ecology and are related to the nutrient uptake, light utilization for photosynthesis (Vadrucci et al., 2013). Phytoplankton such as *Thalassiosira* spp., and *Skeletonema* spp., are filamentous types. The filamentous shape has better light antennae and therefore can photosynthesize with high capacity at low ambient light (Reynolds, 1997). Phytoplankton genera have been categorized according to their shapes (Sun and Liu, 2003) and the phytoplankton shapes observed here in low light were mostly cylindrical, rectangular box, a prism on parallelogram base and spherical, suggesting these shapes could be of advantage in efficient light harvesting.

The maximum solar light available was within the spectral range of 537 to 648 nm and the range varied for water types, and was 537 to 581 nm in the coastal waters, while it shifted to longer wavelengths 561 to 648 in the estuarine waters. The chromatic requirements can also be justified from the light absorbing properties by pigments in phytoplankton. The ubiquitous pigment present in all the phytoplankton is the chlorophyll a with major absorption occurring around 440 nm. The absorptions of other pigments chlorophyll b (Chlb), chlorophyll c (Chlc), fucoxanthin (Fuco), β -carotene (β -caro), and peridinin (Peri), have absorption peaks in the blue-green regions. Thus, it is evident that for photosynthesis blue-green light is essential. The phytoplankton surviving at low lights have a high efficient mechanism of light harvesting and utilizing every photon available (Stambler and Dubinsky, 2007; Dubinsky and Stambler, 2009; Halsey and Jones, 2015). The spectral light availability could change in future due to anthropogenic activities and climate change affecting the river run-off that will affect the optically active parameters such as the concentrations of CDOM, particle load (algal and non-algal), which could alter the underwater light field and spectral light in water. Hence, there is a need to understand the chromatic acclimation of these phytoplankton species observed in the low light.

Most of the primary production evaluated through models and measurements were limited to a lower limit of 1% light levels (Dubinsky, 2010) however it is noticed there were considerable amount of umbrophillic phytoplanktons below this 1% light levels and hence neglecting the contribution of these phytoplankton could underestimate the primary production and carbon related budgeting.

Monsoon plays an important role in the variations of turbidity and nutrient levels in these waters.

Conclusion

The study focused on the phytoplankton species of the estuaries and coastal waters of Goa in low light regions, which has been attempted for the first time for these waters. The results of the studies, even with this limited data, provided sufficient evidence of

the various phytoplankton species, pigment variations, spectral light and the environmental conditions in the low light regions.

Though this study has been limited and preliminary in only reporting the phytoplankton communities and bio-optical conditions at low light levels, this could lay a foundation for the further studies related to phytoplankton acclimation in these waters. There are lots to understand of phytoplankton in the extreme light levels (Dubinsky, 2009). The light levels and nutrients in these estuaries and coastal waters could be affected by anthropogenic influence, monsoon and climatic changes and hence a continuous monitoring of the umbrophillic species of phytoplankton with regards to changes in these parameters will need to be studied to understand the phytoplankton acclimations in low light levels. There is also a gap in the present study without the information on the nutrients and this could have supplemented to understand the role of nutrients in the photoacclimation and light utilization efficiencies of these phytoplankton listed in the low light (Dubinsky and Schofield, 2010). Hence there is a scope to study the nutrient availability and the phytoplankton growth and related topics such as the limiting nutrient levels for the survival of various species of phytoplankton in low light depending on their size and characteristics, role of micro and macro nutrients, since the watershed of the estuaries of Goa include iron ore and manganese mines, the role micronutrients such as iron (Fe) need to be studied.

Acknowledgements. The authors are grateful to the Director, CSIR-National Institute of Oceanography, Goa, India for the kind support. Authors are also indebted to the colleagues for the field measurements, discussions, and assistance in preparing the manuscript. This work was funded by ESSO-Indian National Centre for Ocean Observing System (INCOIS) under SATCORE program, Space Application Centre (ISRO) under MOP3 and NRSC (National Remote sensing centre) under NISCES programme.

REFERENCES

- [1] Anning, T., MacIntyre, H. L., Pratt, S. M., Sammes, P. J., Gibb, S., Geider, R. J. (2000): Photoacclimation in the marine diatom *Skeletonema costatum*. – *Limnol Oceanogr* 45: 1807-1817.
- [2] Barlow, G., Alberte, R. S. (1987): Photosynthetic characteristics of phycoerythrin containing marine *Synechococcus* spp. 11. Time course responses of photosynthesis to photoinhibition. – *Marine Ecology-Progress Series* 39: 191-196.
- [3] Boyd, P. W., Strzepek, R., Fu, F., Hutchins, D. A. (2010): Environmental control of open-ocean phytoplankton groups: now and in the future. – *Limnol Oceanogr* 55: 1353-1376.
- [4] Choudhury, N. K., Behera, R. (2001): Photoinhibition of photosynthesis: Role of carotenoids in photoprotection of chloroplast constituents. – *Photosynthetica* 39: 481-488.
- [5] Cullen, J. J., Macintyre, J. G. (1998): Behavior, Physiology and the Niche of Depth-Regulating Phytoplankton. – In: Anderson, D. M., Cembella, A. D., Hallegraeff, G. M. (eds.) *Physiological Ecology of Harmful Algal Blooms*. Springer-Verlag, Heidelberg.
- [6] Desa, E., Suresh, T., Matondkar, S. G. P., Goes, J., Mascarenhas, A. A. M. Q., Parab, S. G., Shaikh, N., Fernandes, C. E. G. (2005): Detection of *Trichodesmium* bloom patches along the eastern Arabian Sea by IRS-P4/OCM ocean color sensor and by in-situ measurements. – *Indian Journal of Marine Sciences* 34: 374-386.
- [7] Devassy, V. P., Goes, J. I. (1988): Phytoplankton community structure and succession in a tropical estuarine complex (Central West Coast of India). – *Estuarine, Coastal and Shelf Science* 27: 671-685.

- [8] Dias, A. B., Suresh, T., Sahay, A., Chauhan, P. (2017): Contrasting characteristics of colored dissolved organic matter of the coastal and estuarine waters of Goa during summer. – *Indian Journal of Geo-Marine Science* 46: 860-870.
- [9] Dring, M. J. (1981): Chromatic adaptation of photosynthesis in benthic marine-algae-an examination of its ecological significance using a theoretical model. – *Limnol Oceanogr* 26: 271-284.
- [10] Dubinsky, Z., Schofield, O. (2010): From the light to the darkness: Thriving at the light extremes in the oceans. – *Hydrobiologia* 639: 153-171.
- [11] Dubinsky, Z., Stamble, N. (2009): Photoacclimation processes in phytoplankton: mechanisms, consequences, and applications. – *Aquatic Microbial Ecology* 56: 163-176.
- [12] Fan, L., Vonshak, A., Gabbay, R., Hirshberg, J., Cohen, Z., Boussiba, S. (1995): The biosynthetic pathway of astaxanthin in a green algae *Haematococcus pluvialis* as indicated by inhibition with diphenylamine. – *Plant Cell Physiol* 36: 1519-1524.
- [13] Finkel, Z. V. (2001): Light absorption and size scaling of light-limited metabolism in marine diatoms. – *Limnol Oceanogr* 46: 86-94.
- [14] Finkel, Z. V. (2006): Irradiance and the elemental stoichiometry of marine phytoplankton. – *Limnol Oceanogr* 51: 2690-2701.
- [15] Fisher, T., Minnaard, J., Dubinsky, Z. (1996): Photoacclimation in the marine algae *Nannochloropsis* sp. (Eustigmatophyte): a kinetic study. – *Journal of Plankton Research* 18: 1797-1818.
- [16] Geider, R. J., Platt, T., Raven, J. A. (1986): Size dependence of growth and photosynthesis in diatoms: a synthesis. – *Marine Ecology-Progress Series* 30: 93-104.
- [17] Gomes, H. D. R., Goes, J. I., Matondkar, S. G. P., Parab, S. G., Al-Azri, A. R. N., Thoppil, P. G. (2008): Blooms of *Noctiluca miliaris* in the Arabian Sea – an in situ and satellite study. *Deep Sea Research Part I. – Oceanographic Research Papers* 55: 751-765.
- [18] Gorai, T., Katayama, T., Obata, M., Murata, A., Taguchi, S. (2014): Low blue light enhances growth rate, light absorption, and photosynthetic characteristics of four marine phytoplankton species. – *Journal of Experimental Marine Biology and Ecology* 459: 87-95.
- [19] Halsey, K. H., Jones, B. M. (2015): Phytoplankton strategies for photosynthetic energy allocation. – *Annual Review of Marine Science* 7: 265-297.
- [20] Karst-Riddoch, T. L., Malmquist, H. J., Smol, J. P. (2009): Relationships between freshwater sedimentary diatoms and environmental variables in Subarctic Icelandic lakes. – *Fundamental and Applied Limnology* 175: 1-28.
- [21] Key, T., McCarthy, A., Campbell, D. A., Six, C., Roy, S., Finkel, Z. V. (2010): Cell size trade-offs govern light exploitation strategies in marine phytoplankton. – *Environ Microbiol* 2: 95-104.
- [22] Kirk, J. T. O. (1994): *Light and Photosynthesis in Aquatic Ecosystems*. – Cambridge University Press, Cambridge, UK.
- [23] Krinsky, N. I. (1989): Antioxidant functions of carotenoids. – *Free Radical Biology and Medicine* 7: 617-635.
- [24] Matondkar, P. S. G., Gomes, H. D., Parab, S. G., Pednekar, S., Goes, J. I. (2007): Phytoplankton Diversity, Biomass and Production. – In: Shetye, S. R., Kumar, D., Shankar, D. (eds.) *The Mandovi and Zuari Estuaries*. National Institute of Oceanography, Dona Paula, India.
- [25] Moore, M. C., Suggett, D. J., Hickman, A. E., Kim, Y. N., Tweddle, J. F., Sharples, J., Geider, R. J., Holligan, P. M. (2006): Phytoplankton photoacclimation and photoadaptation in response to environmental gradients in a shelf sea. – *Limnol Oceanogr* 51: 936-949. doi: 10.4319/lo.2006.51.2.0936.
- [26] Mueller, J. L. (2003): In-water Radiometric Profile Measurements and Data Analysis Protocols. – In: Mueller, J. L., G. S. Fargion, C. R. McClain (eds.) *Ocean Optics Protocols for Satellite Ocean Color Sensor Validation, Revision 4, Volume III*, pp. 7-20. NASA Goddard Space Flight Center, Greenbelt, Maryland.

- [27] Mueller, J. L., Fargion, G. S., McClain, C. R., Pegau, S., Zaneveld, J. R. V., Mitchell, B. G., Kahru, M., Wieland, J., Stramska, M. (2003): Ocean Optics Protocols for Satellite Ocean Color Sensor Validation. Volume IV: Inherent Optical Properties: Instruments, Characterizations, Field Measurements and Data Analysis Protocols. – NASA Goddard Space Flight Center, Greenbelt, Maryland.
- [28] Naqvi, S. W. A., George, M. D., Narvekar, P. V., Jayakumar, D. A., Shailaja, M. S., Sardesai, S., Sarma, V. V. S., Shenoy, D. M., Naik, H., Maheswaran, P. A., KrishnaKumari, L., Rajesh, G., Sudhir, A. K., Binu, M. S. (1998): Severe fish mortality associated with red tide observed in the sea off Cochin. – *Current Science* 75: 543-544.
- [29] Naqvi, S. W. A., Jayakumar, D. A., Narvekar, P. V., Naik, H., Sarma, V. V. S. S., D'souza, W., Joseph, S., George, M. D. (2000): Increased marine production of N₂O due to intensifying anoxia on the Indian continental shelf. – *Nature* 408: 346-349.
- [30] Naqvi, S. W. A., Naik, H., Jayakumar, D. A., Shailaja, M. S., Narvekar, P. V. (2006): Seasonal Oxygen Deficiency over the Western Continental Shelf of India. – In: Neretin, L. N. (ed.) *Handbook of Past and Present Water Column Anoxia*. Springer, Dordrecht.
- [31] Overmann, J., Garcia-Pichel, F. (2005): The Phototrophic Way of Life. – In: Dworkin, M. (ed.) *The Prokaryotes: An Evolving Electronic Resource for the Microbiological Community*. Springer, New York.
- [32] Parab, S. G., Matondkar, S. G. P., Gomes, H. D. R., Goes, J. I. (2006): Monsoon-driven changes in phytoplankton populations in the eastern Arabian Sea as revealed by microscopy and HPLC pigment analysis. – *Continental Shelf Research* 26: 2538-2558.
- [33] Patil, S., Anil, A. C. (2011): Variations in phytoplankton community in a monsoon-influenced tropical estuary. – *Environ Monit Assess* 182: 291-300.
- [34] Pednekar, S. M., Prabhu Matondkar, S. G., VijayaKerker. (2012): Spatiotemporal distribution of harmful algal flora in the tropical estuarine complex of Goa, India. – *The Scientific World Journal* 2012: 1-11.
- [35] Pednekar, S. M., Kerker, V., Matondkar, S. G. P. (2014): Spatiotemporal distribution in phytoplankton community with distinct salinity regimes along the Mandovi estuary, Goa, India. – *Turk J Bot* 3: 800-818.
- [36] Pinchasov-Grinblat, Y., Hoffman, R., Dubinsky, Z. (2011): The effect of photoacclimation on photosynthetic energy storage efficiency, determined by photoacoustics. – *Open Journal of Marine Science* 1: 43-49.
- [37] Raven, J. A. (1984): A cost-benefit analysis of photon absorption by photosynthetic unicells. – *New Phytologist* 98: 593-625.
- [38] Raven, J. A., Cockell, C. S. (2006): Influence on photosynthesis of starlight, moonlight, planet light, and light pollution (reflections on photosynthetically active radiation in the universe). – *Astrobiology* 6: 668-675.
- [39] Raven, J. A., Kübler, J. E., Beardall, J. (2000): Put out the light, and then put out the light. – *J. Mar. Biol. Assoc.* 80: 1-25.
- [40] Reynolds, C. S. (1997): *Vegetation Processes in the Pelagic. A Model for Ecosystem Theory*. – ECI, Oldendorf.
- [41] Richardson, K., Beardall, J., Raven, J. A. (1983): Adaptation of unicellular algae to irradiance: an analysis of strategies. – *New Phytol* 93: 157-191.
- [42] Rodriguez, F., Chauton, M., Johnsen, G., Andresen, K., Olsen, L. M., Zapata, M. (2006): Photoacclimation in phytoplankton: implications for biomass estimates, pigment functionality and chemotaxonomy. – *Marine Biology* 148: 963-972.
- [43] Ryther, J. H., Menzel, D. W. (1959): Light adaptation by marine phytoplankton. – *Limnol Oceanogr* 4: 492-497.
- [44] Santhanam, R. N., Ramanathan, Venkataramanujan, K., Jegatheesun, G. (1987): *Phytoplankton of the Indian seas*. – Daya Publication House, Delhi. <http://www.nal.usda.gov>.
- [45] Schagerl, M., Muller, B. (2006): Acclimation of chlorophyll a and carotenoid levels to different irradiances in four freshwater cyanobacteria. – *J Plant Physiol* 163: 709-716.

- [46] Shetye, S. R., Shankar, D., Neetu, S., Suprit, K., Michael, G. S., Chandramohan, P. (2007): The Environment That Conditions the Mandovi and Zuari Estuaries. – In: Shetye, S. R., Kumar, D., Shankar, D., (eds.) The Mandovi and Zuari Estuaries. National Institute of Oceanography, Dona Paula, India.
- [47] Staehr, P. A., Henriksen, P., Markager, S. (2002): Photoacclimation of four marine phytoplankton species to irradiance and nutrient availability. – Aquatic Microbial Ecology 238: 47-59.
- [48] Stambler, N., Dubinsky, Z. (2007): Marine Phototrophs in the Twilight Zone. – In: Seckbach, J. (ed.) Algae and Cyanobacteria in Extreme Environments. Series: Cellular Origin, Life in Extreme Habitats and Astrobiology. Springer, Dordrecht.
- [49] Sun, J., Liu, D. (2003): Geometric models for calculating cell bio volume and surface area for phytoplankton. – J Plankton Res 25: 1331-1346.
- [50] Suresh, T., Desa, E., Desai, R. G. P., Jayaraman, A., Mehra, P. (1996): Photosynthetically available radiation in the central and eastern Arabian sea. – Current Science 71: 883-887.
- [51] Thadathil, P., Gosh, A. K. (1992): Surface layer temperature inversion in the Arabian Sea during winter. – Journal of Oceanography 48: 293-304.
- [52] Tomas, C. R. (1997): Identifying Marine Phytoplankton. – Academic Press, San Diego, CA.
- [53] Vadrucci, M. R., Mazziott, C., Fiocca, A. (2013): Cell biovolume and surface area in phytoplankton of Mediterranean transitional water ecosystems: methodological aspects. – Transitional Waters Bulletin 7: 100-123.
- [54] Verlençar, X. N. (1987): Distribution of nutrient in the coastal and estuarine waters of Goa. – Mahasagar Bulletin of the National Institute of Oceanography 20: 205-215.
- [55] Vijith, V., Sundar, D., Shetye, S. R. (2009): Time-dependence of salinity in monsoonal estuaries. – Estuarine, Coastal and Shelf Science 85: 601-608.
- [56] Wang, M. C., Bohmann, D., Jasper, H. (2003): JNK signaling confers tolerance to oxidative stress and extends lifespan in drosophila. – Developmental Cell 5: 811-816.
- [57] Zastrow, J. C. (2001): Photoacclimation of the Diatom *Asterionellaformosa* in a Simulated Vertically Mixed Water Column. – The University of Wisconsin, Milwaukee.

TASOS1 AND TATM20 GENES EXPRESSION AND NUTRIENT UPTAKE IN WHEAT SEEDLINGS MAY BE ALTERED VIA EXCESS CADMIUM EXPOSURE AND INOCULATION WITH AZOSPIRILLUM BRASILENSE SP7 UNDER SALINE CONDITION

GHASSEMI, H. R.¹ – MOSTAJERAN, A.^{2*}

¹*Department of Biology, University of Isfahan, Isfahan, Iran*

²*Plant Science Division, Biology Department, University of Isfahan, Isfahan, Iran*
(phone: +98-91-8335-0785; fax: +98-31-3793-2456)

**Corresponding author*

e-mail: mostajerana@yahoo.com; phone: +98-31-3793-2471; fax: +98-31-3793-2456

(Received 19th Oct 2017; accepted 27th Feb 2018)

Abstract. Excess of salt and cadmium (Cd) damage the plant's growth; however, Cd toxicity is more severe under saline condition. *Triticum aestivum* transmembrane 20 (*TaTM20*) and salt overly sensitive (*SOS*) respond to salinity. Moreover, wheat-*Azospirillum* association system leads to an increase in wheat tolerance to abiotic stresses. Less information exists related to the effect of salinity and Cd under wheat-*Azospirillum* associated system. Therefore, this experiment was conducted to evaluate the effect of *Azospirillum*-wheat association under salinity and/or Cd stresses. Wheat seedlings (Sardari cultivar) inoculated with *Azospirillum brasilense* Sp7 and grown for five days, and then transferred into hydroponic media for five more days with and without 200 mmol NaCl and/or 50 mg L⁻¹ Cd, respectively. Root and shoot samples were separated and then dry weight, proline, photosynthetic pigments, catalase (CAT) and ascorbate peroxidase (APX) activities, Cd, Fe, Ca, Na, K were measured. Simultaneously, relative expression of *TaSOS1* and *TaTM20* in the root were measured. The results show salinity and/or Cd have increased root's *TaSOS1* expression and higher upregulation was seen in inoculated seedlings. Meanwhile *TaTM20* gene expression upregulated only under Cd and Cd plus salinity conditions. Salinity and/or Cd were increased root and shoot proline, CAT, APX, Na⁺ and Cd whereas dry weight, pigments, Fe, Ca, K were decreased. *A. brasilense* could improve salinity and Cd adverse effects by more upregulation of *TaSOS1* transcript level, lower Na/K ratio and less Fe and Ca deficiency, higher pigments, proline and APX and CAT activities to produce more dry weight.

Keywords: *chlorophyll, carotenoid, Fe, Na, K, dry weight*

Introduction

A considerably large portion of arable land (estimated 20% of total cultivated and 33% of irrigated lands) in the world is affected by salinity (Nellemann, 2009). Furthermore, the salt affected lands are increasing 10% annually due to the low precipitation, high surface evaporation, weathering of rocks, irrigation with saline water, and poor cultivation. It has been estimated that more than 50% of the arable land would be salinized by the year 2050 (Jamil, 2011). Salinity has inhibitory effects on crop production (such as wheat) by altering phenological indexes through root growth (Neumann, 1995), root/shoot ratio (El-Hendawy, 2005), osmoticum components (Hamdia, 2004), ions imbalance (Wakeel, 2013) and total dry matter (Pessaraki and Huber, 1991).

Cadmium (Cd) is a heavy metal, considered harmful to plants, animals and also human beings (Yamaguchi et al., 2009). It occurs naturally in the earth's crust and can be added to the environment via water and soil through natural weathering and human

activities such as adding fertilizers, pesticides and industrial and/or domestic effluents (Alloway and Steinnes, 1999; Nriagu and Sprague, 1987; Sheppard et al., 2009). Its values range 0.2-1.0 mg Kg⁻¹ of dry soil to 50 mg Kg⁻¹ of agricultural soil. The maximum permissible addition (MPA) of the heavy metal/metalloid content in the soil is the key idea upon the standardization of the soil contamination (Vodyanitskii, 2016).

Although Cd is not essential for plant and biological systems, different crops will take up and accumulate Cd differently depending on its availability in the environment (Grant and Sheppard, 2008). However, Cd induces oxidative stress, which damages cellular organelles in many plants (Yadav and Chandra, 2013). In addition, Cd could interfere with the uptake of some mineral nutrition such as iron and calcium (Astolfi, 2012; Roth, 2006) and causes mineral concentration imbalance (Chang et al., 2012; Dražić et al., 2004; Lux et al., 2011).

Salinity and heavy metals impose adverse effects on plant growth and its productivity especially in arid and semi-arid regions (Leblebici et al., 2011). Several researchers have reported higher toxic effects of Cd in saline condition (Khoshgoftar et al., 2004). Although the addition of NaCl causes higher sodium absorption by a plant which decreases plant production (Dražić et al., 2004). Chloride of NaCl forms CdCl₂ in the present of Cd and therefore leads to more Cd absorption due to the much higher solubility of CdCl₂ among its Cd components. CdCl₂ has solubility limit of 1,680,000 mg L⁻¹ at 20°C in water (National Research Council, 1997). This condition causes more Cd toxicity for plant growth (Smolders et al., 1998).

Plant growth promotion rhizobacteria (PGPRs) help the plant to grow better by different mechanisms. It has been reported that PGPRs act in favor of plant mineral uptake (Askary et al., 2009), more phytohormones production (Kang et al., 2014) as well as modification in some gene expression (Vargas-Garcia et al., 2012). Creus et al. (1997) also confirmed the reduction of adverse effects of salinity and osmotic stresses on the length and dry weight of wheat plants when inoculated by *Azospirillum brasilense*.

Concerning inoculation and heavy metal, there are two consequences of using PGPRs in environments polluted by heavy metals. Some researchers believe that PGPRs can absorb and accumulate heavy metals and reduce soil and water pollution level (Belimov et al., 2005; Ma et al., 2009; Prapagdee and Khonsue, 2015), while some others believe PGPRs are able to reduce the availability of heavy metals in the soil and water which in turn lead to more growth and yield production (Belimov et al., 2005; Belimov and Dietz, 2000; Dell'Amico et al., 2008; Gao et al., 2012). In any way, one of the safe approaches to revert the detrimental effects of Cd and salinity on crop production is establishing an associated system between crops and soil microorganisms such as *Azospirillum* species with wheat cultivars. *Azospirillum* spp. not only can improve wheat productivity through higher root and shoot development (Amooaghaie et al., 2002), more nutrient uptake (Askary et al., 2009) and improvement of phytohormones but also can reduce adverse effects of salinity and Cd under saline (Upadhyay et al., 2011) and Cd-stressed conditions (Belimov and Dietz, 2000).

Kim et al. (2008) showed *Triticum aestivum* transmembrane 20 (*TaTM20*) gene expression in wheat plant upregulated due to the excess of Cd. They also showed that this gene confers Cd tolerance to yeast transgenic containing *TaTM20* gene. Ramezani et al. (2013) and Kim et al., (2008) The upregulation of salt overly sensitive 1 (*TaSOS1*) and *TaTM20* under saline condition (Ramezani et al., 2013) and *TaTM20* upregulation under Cd polluted conditions (Kim et al., 2008) are also reported. Xu et al. (2008) demonstrated *SOS1* upregulation at both roots and shoots of wheat plants under saline condition. They

also showed that yeast transgenic containing *TaSOS1* gene has higher salt tolerance as compared to non-transgenic ones. In addition, Taherinia et al. (2015) revealed that salinization was affected *SOS1* transcript level positively in kallar grass (*Leptochloa fusca* L.) a halophyte plant which is highly tolerant to saline and sodic soil and water.

Accordingly, it can be proposed that *Azospirillum* species may contribute to the upregulation of *TaSOS1* and *TaTM20* gene expression in wheat plants under saline and Cd polluted condition and improve salinity and Cd tolerance. Not only that, *Azospirillum* may help to limit Cd absorption by plant root. Therefore, this research was conducted to evaluate *TaSOS1* and *TaTM20* gene expression in the roots and also chlorophyll (a and b) and carotenoid of the shoots. Simultaneously other indexes such as Fe, Ca, K, Na, Cd, proline, antioxidant enzymes (CAT and APX) of the roots and shoots of wheat seedlings (Sardari cultivar) were measured under excess of salinity, Cd and inoculated conditions.

Materials and methods

Preparation of inoculants and seeds

Azospirillum brasilense Sp7 (standard strain) was obtained from NCIMB Ltd, Germany. Then cultured in an NFB liquid medium supplemented with NH_4Cl (0.25 g L^{-1}) at 30°C (Brenner et al., 2005) in Erlenmeyer flasks for 48 h and used a rotary shaker at 200 rpm (logarithmic phase). The growth was harvested by centrifuging (1000 g , 10 min), washed with sterile saline phosphate buffer and then re-suspended in phosphate buffer at concentration of 10^7 CFU ml^{-1} of *A. brasilense* Sp7 (Askary et al., 2009).

Wheat (*Triticum aestivum* L., Sardari cv.) seeds obtained from Institute of Agricultural and Research, Isfahan, Iran. The seeds were surface sterilized by dipping in 95% ethanol for 2 min and then in 1% sodium hypochlorite (NaOCl) for 1 min followed by six washes in sterile distilled water (Sauer and Burroughs, 1986). The sterilized wheat seeds were vernalized at 4°C for one night.

For germination, sterilized seeds were kept in dark on water agar in autoclaved petridishes held at 25°C temperature. After 24 hours, uniform seedlings were divided into two groups. The first group was inoculated by 10^7 CFU ml^{-1} *A. brasilense* Sp7 and the second group transferred into free bacteria phosphate buffer (Bashan, 1990) as control (non-inoculated). After 3 hours, all plants (inoculated and none inoculated) were transferred into pots containing sterile perlite and irrigated with 1/4 strength of Hoagland's nutrient solution (Hoagland and Arnon, 1950). The plants kept in a glasshouse under 16/8 h (Light/Dark) photoperiod using white light (photon density $650 \mu\text{mol m}^{-2} \text{ s}^{-1}$) at $25 \pm 2^\circ\text{C}$ for 5 days. Then, besides control pots, both groups were treated with 200 mM of NaCl and/or 50 mg L^{-1} of cadmium as CdCl_2 as treatment for five more days. This experiment conducted in a completely randomized design with three replicates. At day-10 of the experiment (five days after salt and Cd stresses applied), roots and shoots of plant samples were separated and washed with distilled water. Some of the separated plant samples immediately frozen in liquid nitrogen for real-time quantitative PCR and the remaining samples were used for different analysis.

Real-time quantitative PCR

Real-time PCR was performed using RB SYBR master mix (RNA Biotech, Iran). The total RNA was isolated from frozen roots using Itraizol reagent (RNA biotech, Iran)

and the first strand cDNA was synthesized using the M-MLV reverse transcriptase (Fermatas). Gene-specific primers were used for *TaSOS1* (Gen Bank Accession No. AY326952), *TaTM20* (Gen Bank Accession No. DQ323065) and *G3PDH* (Gen Bank Accession No. EU022331). The sequences of the primers designed to amplify *TaTM20* were as follows: 5'-CCGATCCTCTTGCACA ACTA-3' and 5'-ATGGACAGCATGAAGCTCAC-3'; (Kim et al., 2008) the primers for *G3PDH* were as follows: 5-TCACCACCGAGTACATGACC-3' and 5'-TCGTCCTTGAGCTTGATGT-3' (Kim et al., 2008); and the primers for *TaSOS1* were as follows: 5'-GGGATGATGAGGA ACTTGGG-3' in sense direction and 5'-CTTGTCAGGAACATCGTGGG-3' in anti-sense direction (Xu et al., 2008). The PCR conditions were 94 °C for 4 min followed by 40 cycles of 94 °C for 10 s, 62 °C for 40 s, 72 °C for 60 s, followed by 7 min at 72 °C. Serial dilutions of cDNA were used to obtain optimized standard curve amplification efficiency and the best cDNA concentration for real-time PCR. The relative expression of each gene as the fold expression was calculated through Livak and Schmittgen's method (2001).

Plant pigment determination

Chlorophyll a and b and carotenoid were performed according to Arnon (1967) with some modifications. 100 mg fresh leaves were homogenized in 2 ml 80% acetone with mortar. Homogenates were centrifuged at 4°C for 10 min (3500 rpm). Supernatants were used for the analysis of pigments. Absorbance of plant sample was determined at 645, 663 and 470 nm, respectively and then the following equations (Eq. 1-3) were used for calculation of different pigments.

$$\text{Chlorophyll } a = \frac{(19.3 \times A_{663} - 0.86 \times A_{645})V}{100W} \quad (\text{Eq.1})$$

$$\text{Chlorophyll } b = \frac{(19.3 \times A_{645} - 3.6 \times A_{663})V}{100W} \quad (\text{Eq.2})$$

$$\text{Carotenoids} = \frac{100(A_{470}) - 3.27(\text{mg Chl } a) - 104(\text{mg Chl } b)}{227} \quad (\text{Eq.3})$$

Determination of sodium and potassium content

Sodium and potassium content of shoot and root were measured based on the method described by Skoog et al. (2005). To do so, 100 mg powder of dry sample (70 °C for 72 hours) was digested with 10 ml 3 % (w/v) aqueous sulfosalicylic acid for 24 h at 4 °C, then sample extract was purified using Whatman No. 1 filter paper. Na⁺ and K⁺ concentration were measured using flame photometry method (Gallenkamp flame analyzer, England).

Determination of Ca, Cd, and Fe

100 mg dry weight of each sample (roots and shoots separately) was digested in 3 ml of a 1- 4 (v/v) mixture of 37% (v/v) HCl and 65% (v/v) HNO₃ in Teflon cylinders for 7 h at 140 °C. After adjustment of volume to 10 ml with deionized water, Ca, Cd, and Fe was determined using an atomic absorption spectrophotometer (AAS, Shimadzu model 6200).

Determination of proline content

Proline content of roots and shoots were determined using Bates et al. (1973) method. The fresh plant samples (100 mg) was homogenized with 4 mL sulfosalicylic acid (3.0%) in a mortar. The suspension was centrifuged at room temperature at 3000 rpm for 5 min. The supernatant was mixed well with 4 mL acidic ninhydrin reagent. The reaction mixture was vortexed and the content of the tubes was placed in a boiling water bath for 60 min. Then, the content was cooled in the ice bath and the mixture was extracted with 4 mL of toluene. The absorbance of toluene layer was recorded at 520 nm using Shimadzu spectrophotometer (Shimadzu UV-160, Japan). The concentration of the unknown samples was calculated using standard curve.

Enzyme extract and antioxidant assay

Plant's shoot samples were extracted for enzymes assay by homogenizing in an ice-cold 50-mM sodium phosphate buffer of pH 7.4 along with 1% (w/v) polyvinyl poly pyrrolidone (PVP) by a pre-chilled mortar and pestle. Homogenized mixture was centrifuged at 13000 g for 20 min at 4°C. The supernatant was directly used for various enzymatic assay as crude enzyme extract. The quantification of soluble protein present in the extract was done by Bradford's method (Bradford, 1976) using bovine serum albumin (BSA) as standard. Catalase (CAT) activity (EC.1.11.1.6) was measured by estimating the breakdown of H₂O₂, which was determined at 240 nm as described by Beers and Sizer (1952). The enzyme activity was expressed as $\mu\text{mol decomposition of H}_2\text{O}_2 \text{ min}^{-1} \text{ mg}^{-1} \text{ protein}$. Ascorbate peroxidase (EC.1.11.1.11) activity was done by using the method described by Nakano and Asada (1981) and the enzyme activity was expressed as $\mu\text{mol decomposition of ascorbate min}^{-1} \text{ mg}^{-1} \text{ protein}$.

Statistical analysis

MSTAT-C software was used for ANOVA calculation and Duncan's multiple range tests were used to compare the mean values using 95% confidence interval. Excel was used to draw the necessary graphs. The experiment was a completely randomized design.

Results

Root and shoot dry weight

The maximum amount of root (7.44 mg plant⁻¹) and shoot (21.91 mg plant⁻¹) dry weight was observed in inoculated plants not exposed to any salinity and/or Cd. At non-inoculated condition, adding Cd to the nutrient media has caused a significant reduction in dry weight of root (24.1) and shoot (18.1%) as compared to their control ($P \leq 0.05$), while dry weight of shoot and root wheat seedlings unaffected under 200 mmol NaCl (*Fig. 1*). The dual stresses of salinity and Cd lead to more reduction of roots (14.8%) and shoots (9.0%) dry weight when compared with the Cd stress alone.

In inoculated plants not exposed to Cd and/or salinity, root and shoot dry weight significantly were increased by 22.97 and 9.7%, respectively in comparison to their control. At Cd stress condition, inoculation significantly alleviated harmful effects of Cd on shoot dry weight as compared to non-inoculated plants. Root and shoot dry weight of inoculated seedlings and also the seedling plants were grown under saline condition showed significant difference when compared with control seedlings.

Although in dual stresses a reduction in root and shoot dry weight of inoculated plants were observed, but inoculation significantly improved the root and shoot dry weight by 12.8 and 16.67%, respectively when compared to non-inoculated ones.

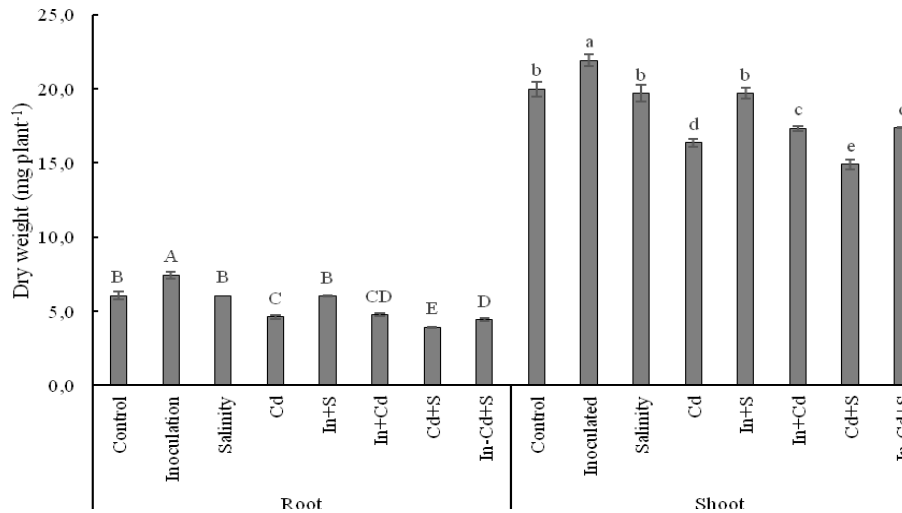


Figure 1. Effect of inoculation, salinity and Cd on average ($n = 3 \pm SD$) dry weight of roots and shoots of wheat seedlings. Differences in lower and upper case letters on the bar graph indicated significant difference ($P < 0.05$) in their mean values based on Duncan's multiple range tests.

Root and shoot proline content

Inoculated seedlings had lower proline in the root and the shoot when compared to control plants. Salinity didn't have a significant effect on shoot proline, meanwhile, proline of root was increased from 0.7 to 1.14 $\mu\text{mol g}^{-1}$ FW ($P < 0.05$, Fig. 2). Cd also showed a significantly ($P < 0.05$) increase in proline of root and shoot by 60 and 44%, respectively. Dual effect of Cd and salinity causes an addition of proline in the root (21.4%) and shoot (13.0%) of non-inoculated plants compared to control seedlings.

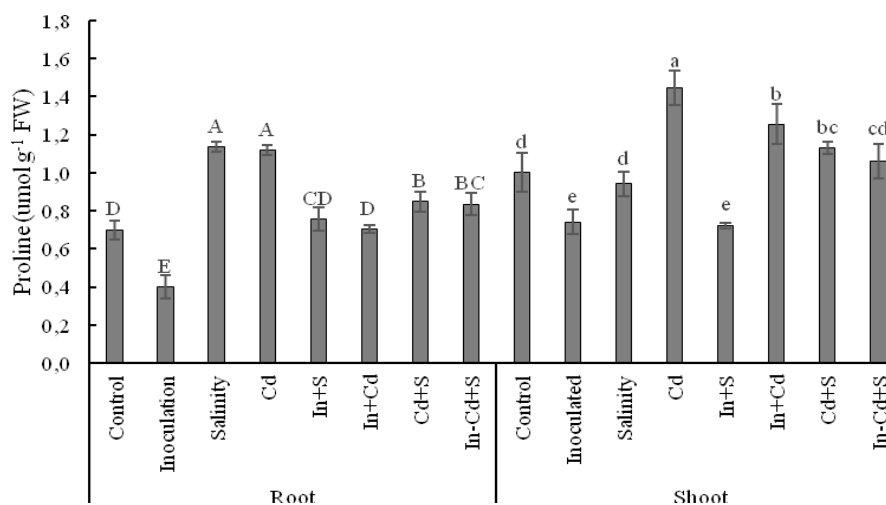


Figure 2. Effect of inoculation, salinity and Cd on average ($n = 3 \pm SD$) proline content of roots and shoots of wheat seedlings ($n = 3 \pm SD$). Differences in small and cap letters on the bar graph indicated difference in their mean values based on Duncan's multiple range tests.

The lowest amount of proline was measured in the root and the shoot of inoculated plants not exposed to Cd and/or salinity. However, the higher values of proline in the root was measured under excess of salinity and Cd and in the shoot belonged to Cd treatment. When seedlings were inoculated with *Azospirillum brasilense* then the high proline accumulation under Cd excess and/or salinity significantly has been reduced to lower amounts which were still higher than in control plants.

Shoot pigments

Inoculation caused addition (22%) of chlorophyll a when compared to control seedlings. In comparison to control plants, significantly less chlorophyll ($P < 0.05$, Table 1) was seen in the shoot of seedlings exposed to Cd or Cd+salinity (56.10 and 51.22%, respectively). However, inoculation was increased chlorophyll a of seedlings exposed to Cd or Cd+salinity as much as control plants. The amount of chlorophyll b was reduced more under Cd than salinity in non-inoculated plants. In contrast, chlorophyll b was increased in inoculated plants under salinity and/or Cd, but it was still lower than control plants. Total chlorophyll (a and b) showed a positive relation with inoculation while a negative relation was observed in excess of Cd and/or salinity conditions with total chlorophyll. Cd (55.36%) and Cd+salinity (53.56%) significantly decreased total chlorophyll of non-inoculated seedlings as compared to control plants.

Maximum total chlorophyll ($0.65 \text{ mg Plant}^{-1}$) was observed in inoculated not exposed to any treatment. The maximum reduction of total chlorophyll was seen under excess Cd and Cd+salinity in non-inoculated seedlings when compared to control plants.

Table 1. Effect of inoculation, salinity and Cd on the mean values ($n = 3$) of chlorophylls (a, b, total) and Carotenoids in the shoot of wheat seedlings. Differences in the letters on the mean values indicated the significant difference in their means based on Duncan's multiple range tests.

Treatments	Chlorophyll a	Chlorophyll b	Total chlorophyll	Carotenoids
Control	0.41 ^B	0.15 ^A	0.56 ^B	1.35 ^D
Inoculation (In)	0.50 ^A	0.16 ^A	0.65 ^A	1.36 ^{CD}
Salinity (Sal)	0.40 ^B	0.12 ^C	0.52 ^B	1.56 ^B
Cadmium (Cd)	0.18 ^C	0.06 ^D	0.25 ^C	0.70 ^E
In + S	0.43 ^B	0.13 ^B	0.56 ^B	1.70 ^A
In + Cd	0.41 ^B	0.14 ^B	0.54 ^B	1.48 ^{BC}
Cd + Sal	0.20 ^C	0.06 ^D	0.26 ^C	0.72 ^E
In + Sal + Cd	0.40 ^B	0.14 ^B	0.54 ^B	1.40 ^{CD}

Antioxidant assays

In most cases, the amount of APX and CAT activities were higher in the shoot than root seedlings and also the amount of CAT activity was higher than APX. The lowest and the highest activities of APX were observed in root and shoot of control and treated seedlings expose to Cd+salinity. Their amounts in the roots were 0.41 and $1.22 \mu\text{mol min}^{-1} \text{mg}^{-1} \text{protein}$ ($P < 0.05$, Fig. 3) and for shoot were 0.29 and $1.42 \mu\text{mol min}^{-1} \text{mg}^{-1} \text{protein}$, respectively. This is almost 197.5% addition in roots and 389.6% for shoots. Inoculation did not have any effect on APX activity of seedlings compared to control.

However, inoculation caused reduction of APX activities of the seedlings exposed to Cd and/or salinity but their amounts still were more than control seedlings.

Change in CAT activities under different conditions was approximately similar to APX activities of the roots and shoots. The lowest and the highest activities of CAT were observed in root and shoot of control and treated seedlings expose to Cd+salinity. Their amounts in the roots were 0.5 and 1.35 $\mu\text{mol min}^{-1} \text{mg}^{-1}$ protein ($P < 0.05$, Fig. 3) and for shoot were 0.25 and 1.17 $\mu\text{mol min}^{-1} \text{mg}^{-1}$ protein, respectively. This is almost 170.0% addition in roots and 368% for shoots. Inoculation did not have any effect on CAT activity of seedlings compared to control. However, inoculation also showed no changes in CAT activities of the seedlings exposed to Cd or salinity but their amounts still were more than control seedlings.

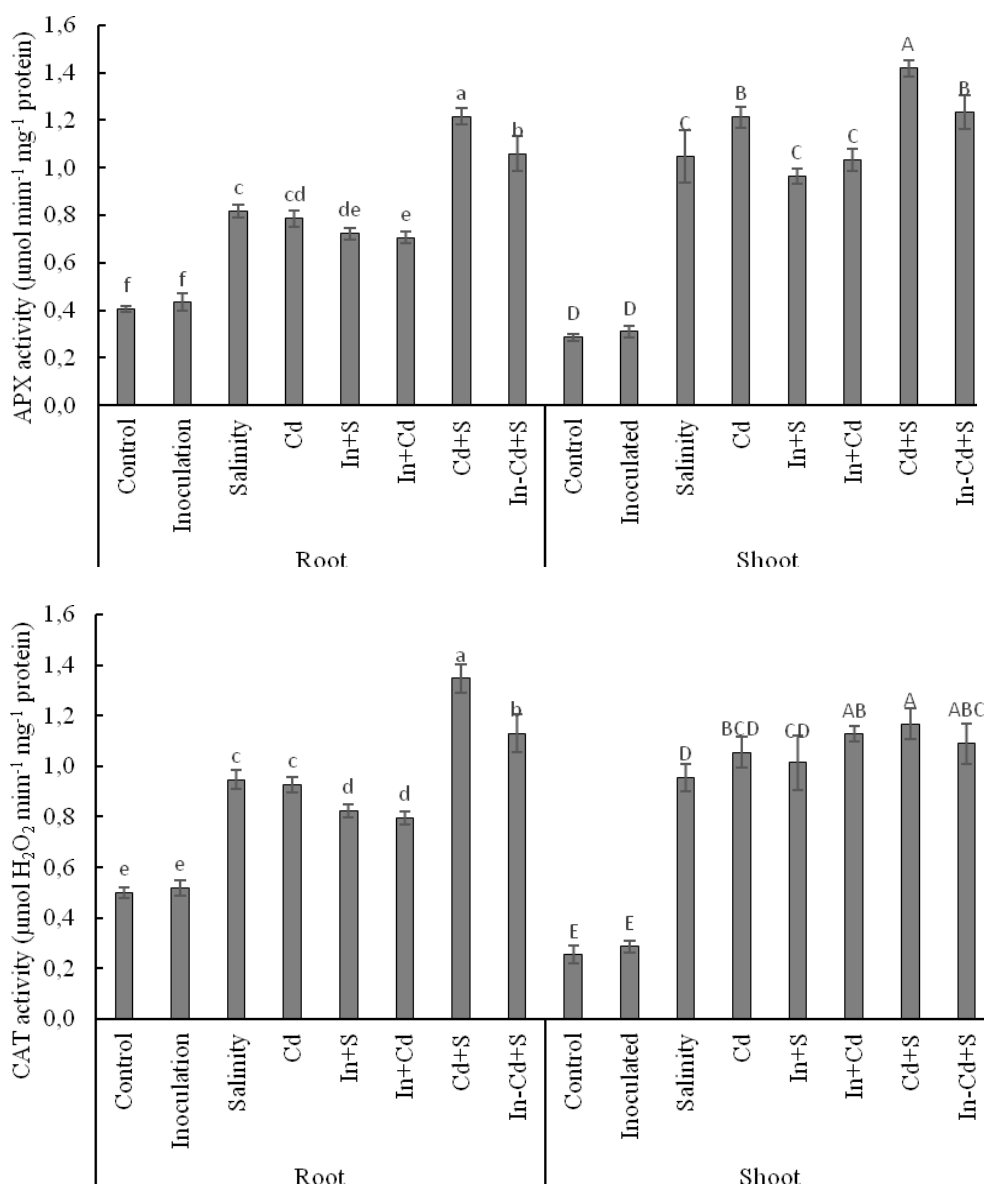


Figure 3. Effect of Salinity (Sal) and Cd, inoculation (In) and their interactions on the activities of APX and CAT in the shoot of wheat seedlings in inoculated and non-inoculated condition. Mean values ($n = 3$) with the same letter are not significantly different at $P < 0.05$.

Cadmium, sodium, potassium, calcium and iron of root and shoot

There was not any Cd in the root of seedlings of non-inoculated or inoculated plants under control and salinity conditions. While its amount in the root of treated seedlings was increased to 32.18 mg g⁻¹ (Cd-treated), 28.27 (Cd and inoculated), 38.49 (Cd and salinity) and 33.29 mg g⁻¹ DW for inoculated+Cd+salinity treated seedlings. It was found that the amount of Cd in Cd+salinity treated of non-inoculated plants was the highest and significantly ($P < 0.05$) higher than the other treatments. Also, inoculation reduced the Cd concentration of plant exposed to Cd. It is interesting that Cd in the shoot of inoculated seedlings (7.52 mg g⁻¹ DW) did not show significant reduction compared to non-inoculated plants exposed to Cd (7.01 mg g⁻¹ DW). At non-inoculation condition, the Cd of roots and shoots raised due to the combined effect of Cd+salinity.

In non-inoculated seedlings, the amount of Fe in the roots and shoots (Table 2) was the highest (0.38 and 0.16 mg g⁻¹ DW, respectively) and a significant reduction was observed in roots treated with Cd (21.05) and salinity (23.68%) stress, but inoculation couldn't help the Fe uptake by the roots under Cd and/or salinity conditions. However, *Azospirillum* helped to increase the amount of Fe in unstresses seedlings to more than control plants and reached to 0.51 mg g⁻¹ DW (the highest amount). Fe in the shoots and roots of inoculated and non-inoculated seedlings followed a similar trend.

Table 2. Effect of various tested treatments on roots and shoots nutrients of seedlings wheat plants. Values with the same letter are not significantly different at $P < 0.05$.

Treatments	Root (mg g ⁻¹ DW)					Shoot (mg g ⁻¹ DW)				
	Cd	Fe	Ca	Na	K	Cd	Fe	Ca	Na	K
Non-inoculated	0.00 ^D	0.38 ^B	1.88 ^B	1.32 ^E	6.30 ^B	0.00 ^C	0.16 ^B	2.22 ^B	0.49 ^B	18.28 ^B
Inoculated (In)	0.00 ^D	0.51 ^A	2.14 ^A	0.80 ^F	9.87 ^A	0.00 ^C	0.22 ^A	2.46 ^A	0.20 ^E	22.50 ^A
Salinity (Sal)	0.00 ^D	0.29 ^D	1.15 ^D	1.83 ^A	4.81 ^D	0.00 ^C	0.11 ^C	1.53 ^D	0.60 ^A	15.70 ^{DE}
Cadmium (Cd)	32.18 ^B	0.30 ^{CD}	1.07 ^D	1.76 ^{AB}	4.83 ^D	7.01 ^B	0.12 ^C	1.57 ^D	0.58 ^A	15.50 ^{DE}
In + Sal	0.00 ^D	0.32 ^C	1.52 ^C	1.59 ^D	5.35 ^C	0.00 ^C	0.13 ^C	2.04 ^{BC}	0.30 ^D	17.08 ^{BC}
In + Cd	28.27 ^C	0.31 ^{CD}	1.55 ^C	1.62 ^{CD}	5.34 ^C	7.52 ^{AB}	0.13 ^C	1.95 ^C	0.33 ^{CD}	16.67 ^{CD}
Cd + Sal	38.49 ^A	0.30 ^{CD}	1.13 ^D	1.71 ^{BC}	4.72 ^D	7.66 ^A	0.11 ^C	1.60 ^D	0.56 ^A	15.30 ^E
In + Sal+ Cd	33.22 ^B	0.31 ^{CD}	1.56 ^C	1.55 ^D	5.26 ^C	7.71 ^A	0.12 ^C	1.92 ^C	0.37 ^C	16.18 ^{CDE}

Calcium concentration in the roots and shoots of inoculated plants not exposed to salinity and/or Cd increased by 13.83 and 10.81%, respectively when compared to control plants. Cd, or salinity and also salinity+Cd in both roots and shoots of seedlings caused a significant reduction in Ca content. However, inoculation was improved its amount in the root and shoot but their amount was still less than the control ones.

In non-inoculated condition, the amount of Na in the root and shoot was 1.32 and 0.49 mg g⁻¹ DW. While application of salinity increased Na of the roots (38.63%) and shoots (22.45%) in non-inoculated plants. Dual effect of Cd and salinity show the highest amount of Na in the roots and shoots; however, its amount was less in inoculated plants exposed to Cd and/or salinity. When plants were inoculated then the amount of Na in the roots and shoots decreased by 39.4% and 59.2%, respectively. Simultaneously K of the roots and shoots increased by 56.6 and 23%, respectively. Inoculation decreased harmful effects of Cd and/or salinity via less Na and increase in K uptake and its accumulation in the roots and shoots of inoculated plants. In whole plant (root and shoot), the best and the

worst conditions for Na content were measured in inoculated (0.28 mg g⁻¹ DW) and salinity (2.43 mg g⁻¹ DW) seedlings, respectively. However, the worst and the best conditions for K were seen in seedlings treated with Cd+salinity (20.1 mg g⁻¹ DW) and inoculated but not exposed to any treatment (32.3 mg g⁻¹ DW), respectively.

TaSOS1 and *TaTM20* genes expression

In non-inoculated condition, there was not any significant expression and difference for *TaSOS1* of roots in control and inoculated seedlings (Fig. 4) while Cd (14.13 fold change) and salinity (32.43 fold change) significantly caused addition of expression of *TaSOS1*. In inoculated seedlings, the *TaSOS1* expression significantly was decreased in Cd-treated seedlings as equal as control seedlings, but there was higher expression of *TaSOS1* under saline condition (61.03). In dual effects of Cd and salinity, the *TaSOS1* expression was the highest (72.89 fold changes) and inoculation cause addition of its upregulation under salinity but no effect under other treatments.

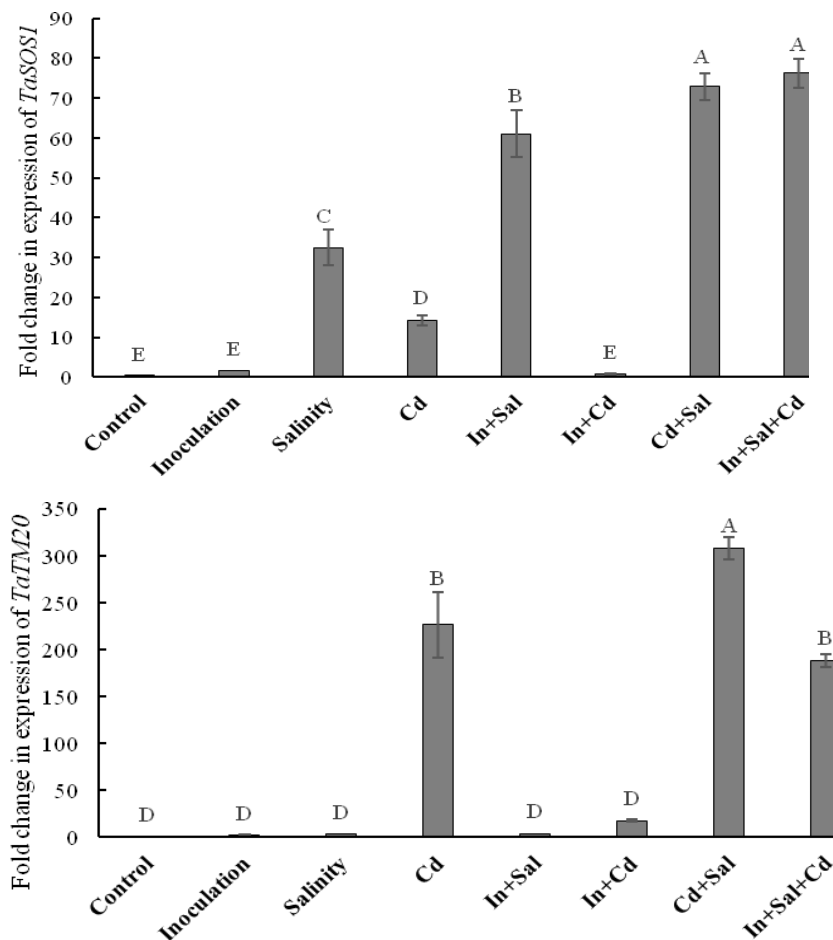


Figure 4. Fold change expression of *TaSOS1* and *TaTM20* genes in the root of inoculated (*A. brasilense*, 10⁷ CFU ml⁻¹) and non-inoculated wheat seedlings grown under saline and non-saline (200 mmol NaCl) condition. The plant samples were obtained five days after salt application. The growth conditions were light density of 650 μmol m⁻²S⁻¹ and temperature of 25 °C. Each value represents mean of three individual measurements ± SE. Different letters represent significant differences at the 95% confidence interval.

There were no significant differences in *TaTM20* gene expression in non-inoculated and inoculated seedlings when seedlings were not exposed to Cd or salinity. Simultaneously, salinity had no significant effect on *TaTM20* expression either in inoculated or non-inoculated seedlings not exposed to Cd. However, Cd by itself could increase *TaTM20* expression significantly (226.3 fold change) in non-inoculated seedlings but when inoculated with *A. brasilense* there was significantly less *TaTM20* expression when compared to control seedlings. The highest effect in *TaTM20* expression was seen in combined treatments of Cd and salinity (308.3 fold change). While this effect was lower (188.3 fold change) in dual effects under inoculated with *A. brasilense*.

Discussion

A large portion of agricultural land suffers from salinity, which causes a reduction in agricultural production (Siadat, 1998). Simultaneously, the deficiency of plant nutrients causes fertilizer application to increase crop yields (Adams, 1991; Dobermann, 2000). Most chemical fertilizers especially phosphorous and also manure mainly contains unwanted elements such as Cd and nickel (He and Singh, 1994). This is because of the waste application and industrial activities. Many researchers have pointed out that crops are affected by the excess of salinity and heavy metals (Corwin and Ahmad, 2015; Leblebici et al., 2011; Shah et al., 2011). Cd and NaCl have been identified as important abiotic stresses in crop production (Corwin and Ahmad, 2015; Mahajan and Tuteja, 2005).

Our results indicated that root and shoot dry weight decreased under excess of Cd and salinity+Cd. This result is similar to that of Leblebici et al., (2011) who showed the relative growth rate of *Lemnaceae* plants (*Spirodela polyrrhiza*) was decreased under salinity+Cd condition. Excess Cd in the soil can reduce the growth of plants by direct or indirect effect on photosynthesis pigments, gas exchange parameters as well as plant nutrient imbalance (Gohar et al., 2003; Parida et al., 2003; Shah et al., 2011). Moreover, it is possible that shoot and root dry weight affected by the toxic effects of Cd due to mainly the chlorocomplexes formation (Weggler-Beaton et al., 2000). In contrast, plant growth promotion rhizobacteria (PGPRs) can reduce the harmful effects of salinity and Cd stress (El-Dengawy et al., 2011; Stout et al., 2010). Our results show *Azospirillum brasilense* improved salinity and/or Cd adverse effects on root and shoot dry weight. These results are accordance with the result obtained by Giller et al., (1998) who showed that bacteria can reduce the phytotoxicity of the contaminated soil by heavy metals. In addition, Stout et al., (2010) indicated that bacteria could serve as a phytoprotective factor in their relationship with *Lemna minor*, preventing uptake of toxic Cd. Also, El-Dengawy et al., (2011) reported that inoculation of Carob seedlings (*Ceratonia siliqua* L.) with *A. lipoferum* under saline condition could improve the reduction of seedling growth rate, K^+/Na^+ content and root characters. PGPRs can help the plant to grow better by different mechanisms such as efficient mineral uptake (Askary et al., 2009), more phytohormones production (Kang et al., 2014) and better tolerant to abiotic stresses (Vargas-Garcia et al., 2012).

Salinity could lead to osmotic stress (Carillo et al., 2008), disruption of homeostasis and ion distribution (Zhang, 2008) as well as formation of reactive oxygen species (Matysik, 2002) in plant cell that has harmful effects on plant growth and its productivity. Proline production is one of the mechanisms that enable the plant to tolerate adverse effect of environmental stresses. Proline is thought to contribute to

osmotic adjustment, detoxification of ROS, and protection of membrane integrity (Heuer, 2010). Addition of proline in our experiment is similar to Tavakoli et al., (2016) who showed saline condition could accumulate the proline content of three Iranian wheat cultivars. In addition, Sharmila et al., (2017) also demonstrated that Cd-induced iron deficiency and promotes proline accumulation in *Brassica juncea* plants. Although there are numerous reports related to accumulation of proline in plant cells after inoculation with some *Azospirillum* Spp.. Our result showed a negative correlation between proline content of non-inoculated wheat seedlings and inoculation ones with *A. brasilense* Sp7. This result may be due to the fact that *Azospirillum* Spp. may facilitate its beneficial effects in different ways on the host plant.

Many studies have shown a reduction in photosynthetic pigments in saline soil (Leblebici et al., 2011; Shafi et al., 2009; Tiwari, 2010 ; Jamil et al., 2007). Our result also showed a reduction in photosynthesis pigments of shoots under saline condition which is similar to the result of El-Dengawy et al., (2011) who demonstrated chlorophyll content decreased in response to salinity in leaves of carob seedlings. It seems that reduction in chlorophyll could be due to less number of chloroplast and disorganization of thylakoid's membrane structure in leaves under salt stress. In addition, our results are consistent with Cheng et al., (2013) who showed an increase in carotenoids of shoot as a way to cope with the saline condition, especially in glycophyte plants. Photosynthetic pigments may be negatively affected by Cd stress in different ways. For example, Cd prevented the chlorophyll production by affecting the synthesis of 5-aminolaevulinic acid, disabling the protochlorophyllide reductase (Stobart et al., 1985) and Fe deficiency (Fodor et al., 2005; Wallace et al., 1992). In addition, the increase in Cd concentration caused loss of chlorophyll and damage to membrane in two maize cultivars (Ekmekçi, et al., 2008). The result of this experiment showed a reduction of shoot chlorophyll due to excess of salinity and/or Cd, meanwhile, *A. brasilense* was able to prevent further reduction of shoot chlorophyll under dual treatments (Table 1). This result in some way is similar to Zhang et al., (2008b) who indicated *B. subtilis* GB03 increases photosynthetic efficiency by increasing chlorophyll content in *Arabidopsis*. In addition, Wani and Khan (2010) showed that photosynthetic pigments of chickpea (*Cicer arietinum* L.) improved by *Bacillus* species under different Cd concentration. Reduction of chlorophyll in our experiment under Cd or salinity conditions should be one of the reasons for dry weight reduction and the higher reduction of dry weight in Cd+salinity could be due to more solubility of Cd under higher NaCl of the media.

Antioxidant enzymes activity have been studied specially under stress conditions (Asada, 2006; Shafi et al., 2009). It has been reported that antioxidant enzymes activity could be increase due to stressful condition. Our result clearly demonstrated that salt and/or Cd significantly have increased APX and CAT activity, but their amounts were decreased when seedlings were inoculated with *A. brasilense* under stress condition. Similar results are reported by different researches. Shafi et al., (2009) showed salinity and Cd stress caused an increase in enzymatic antioxidants such as CAT in three wheat cultivars. In addition, Asada (2006) indicated that APX plays an important role in plant defense against oxidative stress by scavenging H₂O₂. Salinity and Cd generate oxidative stress in plants, leading to a limited growth and even plant death. Oxidative stress is one of the main causes of cellular damage in all organisms exposed to a wide variety of stress conditions (Lin and Kao, 2001; Liu, 2006). It is well known that some of PGPRs such as *Azospirillum* Spp. could help and improve the adverse effect of oxidative stress.

For instance, Bashan et al., (2005) showed inoculation of wheat plants with *Azospirillum* could increase auxiliary photoprotective pigments in shoot of plant which may protect chlorophyll from oxidation during exposure to salt stress. Furthermore, Othman (2015) showed the ability of *A. brasilense* Sp7 in production of ACC deaminase which may be responsible for better growth of rice seedlings. Under stress condition, excess ROS production leads to an increase in plant hormone such as ethylene to prevent the ROS induced damage to reduce the enzymatic antioxidants production (Cho and Seo, 2005). Afterward, degradation of the ethylene precursor ACC by bacterial ACC deaminase releases plant from ethylene induced stress (Figueiredo et al., 2008). In this experiment, inoculation could have alleviated the negative effects of salinity and/or Cd stress (Fig. 3). It appears that reduction in the activity of antioxidant enzymes may be due to the reduction of severity of stress experienced by inoculated seedlings. Omar et al., (2009) and Othman (2015) indicated that antioxidant enzyme activity significantly decreased in barely plants inoculated with *A. brasilense*.

Uptake of mineral by plant's root and its distribution was affected by a variety of factors such as heavy metals and salinity (Daneshbakhsh et al., 2013; Dražić et al., 2004; Khoshgoftar et al., 2004; Khoshgoftarmanesh, 2009). Concerning the concentration of Cd of the roots (32.18) and the shoots (7.01 mg g⁻¹DW) of non-inoculated seedlings, a higher portion of the Cd taken up by wheat seedlings would remain in the roots rather than moving into shoots. This may be because of the cell wall polyanions and also accumulation of Cd in the vacuole of the root cells (Stolt, 2003). Liu et al., (2009) reported similar conclusion. They show that the accumulation of toxic heavy metals in winter wheat roots was significantly higher than in the aerial parts. Addition of Cd was most seen in the roots (19.61%) and then in shoots (9.27%) in non-inoculated seedlings under salinity+Cd condition when compared to Cd-treated seedlings. Sodium chloride can increase the adverse effect of Cd via more mobilization of Cd in the soil solution and consequently more uptake of Cd by plant roots can happen (Khoshgoftar et al., 2004). In addition, Fe, Ca and K of root in non-inoculated seedlings significantly decreased due to the excess of salinity and/or Cd in the root media. Therefore excessive Cd and/or salinity affects the rate of uptake and distribution of certain essential nutrients in plants, and consequently, this phenomena may be responsible for mineral deficiency/imbalance which causes limited plant growth. Uptake of Cd occurs via the same transmembrane carriers used to uptake Ca²⁺ and Fe²⁺, so addition of Cd can decrease the concentration of calcium and iron in plant (Dražić et al., 2004; Roth et al., 2006). Same conclusion reported by different researchers. Chang et al., (2012) found Fe²⁺ and K⁺ content of root and shoot significantly decreased in Cd-treated rice seedlings. Also, Astolfi et al., (2012) showed that Fe deficiency enhanced in barley plants under excess of Cd availability.

Under saline condition, the competition between uptake of sodium and potassium by non-inoculated plants favored sodium ions, but potassium uptake was increased in the wheat seedlings inoculated with *Azospirillum* (Table 2). Inoculation improved harmful effects of Cd and/or salinity via less Na and high K uptake and accumulation in the roots and shoots of inoculated plants. At the same time, less sodium entry into the cell and less potassium leakage out of the cell maybe happen. Reduction of sodium in the roots of inoculated seedlings may be the result of higher expression of *TaSOS1* under excess of sodium.

PGPRs can affect the uptake of nutrient by changing root-uptake characteristics (Martinez-Toledo, 1991), and consequently change in relative growth rate (Rodelas et

al., 1999; Tinker, 1984). We observed that *A. brasilense* could help to prevent sodium uptake by plant in inoculated wheat seedlings. It has been reported that production and secretion of bacterial exopolysaccharides to the root environment and in turn reducing the availability of Na^+ in the media is the cause of less Na uptake. This conclusion can be made on the basis of the result obtained by Upadhyay et al., (2011). They indicated that some of the native strains of bacteria which separated from the wheat rhizosphere of the soils were able to establish salt tolerance by bacterial secretion such as exopolysaccharides.

Lin et al., (1983) reported that inoculation of Zea and Sorghum bicolor roots with *A. brasilense* increased the uptake of several mineral ions such as NO_3^- , K^+ , and H_2PO_4^- . Also, Chang et al., (2012) showed that Cd could decrease Fe and K^+ concentration, increase APX and CAT activity antioxidant enzymes and also improve Fe status which is able to reduce the toxicity of rice seedlings. Furthermore, the low iron content of plants that are grown under the high level of heavy metals generally shows chlorosis, since iron deficiency inhibits both chloroplast development and chlorophyll biosynthesis (Imsande, 1998).

The cell membrane plays an important role in metal homeostasis, via preventing or stimulation of nutrient passage into cell. Cd could alter the plasma membrane permeability by lipid peroxidation, reduction of ATPase activity (Fodor et al., 1995) and altering the activities of genes related to Na homeostasis. Our data showed Cd enhanced sodium of plant tissue (almost 24%) and eventually, the *TaSOS1* gene expression significantly increased to 14.3 fold change in Cd-treated seedlings compared to control plants. Our result show under saline condition, the competition between uptake of sodium and potassium by non-inoculated plants favored sodium ions (Wakeel, 2013; Tester and Davenport, 2003). Thus, antiporters of plant cell plasma membrane (*SOS1*) should be involved to maintain the plant cell ion homeostasis. Our results are consistent with Taherinia (2015), Ramezani et al., (2013) and Xu et al., (2008) who demonstrated salt stress could increase the relative *TaSOS1* gene expression. In addition, we observed inoculation of seedlings with *A. brasilense* Sp7 can contribute to salt tolerate via overexpression of *TaSOS1* gene. Although there is not any report related to the effects of *A. brasilense* on the upregulation of *TaSOS1* in wheat seedlings, Vargas-Garcia et al. (2012) showed ethylene receptors genes expression in rice plants upregulated due to the inoculation with *A. brasilense* Sp245. There are some other reports relate to an increase in transcripts of some other genes involved in nutrient uptake in response to *A. brasilense* (Cavalcante, 2007; Kim, 2015; Nogueira, 2001).

Plant cell reduces the adverse effects of Cd through different mechanisms like secretion of organic acids (Nigam, 2001), using Casparian strip of the root plant cell (Lux, 2004), ABC transporters (Bovet et al., 2005; Verbruggen et al., 2009), antioxidant enzymes (Mishra, 2006) and expression of some genes which *TaTM20* gene is one of them (Kim et al., 2008). So it is predictable that the *TaTM20* gene expression for inhibition and detrimental effects to plant would be increased. *Figure 4b* shows not only Cd increased the relative *TaTM20* gene expression to 226.32 fold change but also an additive effect was observed in its expression under combined Cd+salinity (308.14 fold change). When we use manure containing Cd in agricultural land, especially under saline condition, potassium content of the root reduces because of chloride complexation of Cd (Ciećko, 2004; Smolders et al., 1998). Also, Kim et al., (2008) demonstrated Cd stress could increase the relative *TaTM20* gene expression as well as Cd tolerance through the stimulation of Cd efflux from the cell.

Under Cd+salinity stress, the relative *TaTM20* gene expression in inoculated seedlings (188.36) was less than non-inoculated ones (308.14 fold change). Simultaneously we obtained better growth and less Na and higher potassium in the shoots and roots which indicated that inoculation provides a better condition for plant to grow. This result is in some ways similar to the result of Belimove and Dietz (2000) who showed that associative bacteria were capable of decreasing partially the toxicity of Cd for the barley plants through the improvement of nutrient uptake. Since the *TaTM20* gene is known recently, so there is not enough information to present a good conclusion. However, it is possible that *Azospirillum* contributed to plants to tolerate the stress condition through the extension of the root system, secretion of exopolysaccharides and alteration of *TaTM20* expression, which in turn decreasing the Cd uptake and its accumulation in the cytosol of a cell.

Conclusion

In non-inoculated condition, a reduction of Fe, Ca, K content and addition of Na, Cd, proline, antioxidant enzyme (CAT and APX), chlorophyll (a and b) and carotenoid in the root and shoot were observed under excess of Cd. However, the changes in the measured indexes were higher for the excess of Cd under salinity. Losing of dry weight of roots and shoots was significantly correlated to measured indices. In excess of salinity or Cd, *TaSOS1* expression was upregulated in the root of seedlings, and reached its maximum under dual effect of Cd and salinity (72.89 fold change). However, *TaTM20* upregulation was more Cd dependent than salinity or inoculation but Cd had higher effect on *TaTM20* upregulation under saline condition which might be because of more Cd solubility in the media.

Inoculation with *A. brasilense* improved root and shoot dry weight, caused more accumulation of Fe, Ca and potassium but less uptake of Cd and Na in seedlings not exposed to Cd and salinity. Simultaneously, in inoculated seedlings there were less adverse effects on shoot's pigments such as chlorophyll a and carotenoid under excess of salinity and Cd. These events coincided with upregulation of *TaSOS1* under saline and/or Cd stress conditions.

Acknowledgements. Thanks to the University of Isfahan for financial support, and also thanks to the Department of Biology for cooperation and providing space and facilities. We also thank Dr. Manoochehr Tavassoli and Dr. Abolghasem Esmaeili for some gene expression explanation. Authors' contribution: Concept and design of study and finalizing the manuscript belongs to Akbar Mostajeran, layout and laboratory work as well as preparation of manuscript draft were obtained by Hamid-Reza Ghassemi and finally analysis and/or interpretation of data were made by all authors.

REFERENCES

- [1] Adams, P. (1991): Effects of increasing the salinity of the nutrient solution with major nutrients or sodium chloride on the yield, quality and composition of tomatoes grown in rockwool. - *Journal of Horticultural Science* 66(2): 201-207.
- [2] Alloway, B.J., Steinnes, E. (1999): Cadmium in Soils and Plants, eds. McLaughlin, M.J., Singh, B.R. Springer Netherlands, pp. 97-123.

- [3] Amooaghaie, R., Mostajeran, A., Emtiazi, G. (2002): The effect of compatible and incompatible *Azospirillum brasilense* strains on proton efflux of intact wheat roots. - *Plant and Soil* 243(2): 155-160.
- [4] Arnon, A. (1967): Method of extraction of chlorophyll in the plants. - *Agron. J* 23(112-121).
- [5] Asada, K. (2006): Production and scavenging of reactive oxygen species in chloroplasts and their functions. - *Plant Physiology* 141(2): 391-396.
- [6] Askary, M., Mostajeran, A., Amooaghaei, R., Mostajeran, M. (2009): Influence of the co-inoculation *Azospirillum brasilense* and *Rhizobium meliloti* plus 2, 4-D on grain yield and N, P, K content of *Triticum aestivum* (cv. Baccros and Mahdavi). - *American-Eurasian Journal Agric. & Environ. Sci* 5(296-307).
- [7] Astolfi, S., Zuchi, S., Neumann, G., Cesco, S., di Toppi, L., Pinton, R. (2012): Response of barley plants to Fe deficiency and Cd contamination as affected by S starvation. - *Journal of Experimental Botany* 63(3): 1241-1250.
- [8] Bashan, Y. (1990): Short exposure to *Azospirillum brasilense* Cd inoculation enhanced proton efflux of intact wheat roots. - *Canadian Journal of Microbiology* 36(6): 419-425.
- [9] Bashan, Y., Bustillos, J.J., Leyva, L.A., Hernandez, J.-P., Bacilio, M. (2005): Increase in auxiliary photoprotective photosynthetic pigments in wheat seedlings induced by *Azospirillum brasilense*. - *Biology and Fertility of Soils* 42(4): 279-285.
- [10] Bates, L., Waldren, R., Teare, I. (1973): Rapid determination of free proline for water-stress studies. - *Plant and Soil* 39(1): 205-207.
- [11] Beers, R.F., Sizer, I.W. (1952): A spectrophotometric method for measuring the breakdown of hydrogen peroxide by catalase. - *Journal of Biological Chemistry* 195(1): 133-140.
- [12] Belimov, A., Hontzeas, N., Safronova, V., Demchinskaya, S., Piluzza, G., Bullitta, S., Glick, B. (2005): Cadmium-tolerant plant growth-promoting bacteria associated with the roots of Indian mustard (*Brassica juncea* L. Czern.). - *Soil Biology and Biochemistry* 37(2): 241-250.
- [13] Belimov, A.A., Dietz, K.-J. (2000): Effect of associative bacteria on element composition of barley seedlings grown in solution culture at toxic cadmium concentrations. - *Microbiological Research* 155(2): 113-121.
- [14] Bovet, L., Feller, U., Martinoia, E. (2005): Possible involvement of plant ABC transporters in cadmium detoxification: a cDNA sub-microarray approach. - *Environment International* 31(2): 263-267.
- [15] Bradford, M.M. (1976): A rapid and sensitive method for the quantitation of microgram quantities of protein utilizing the principle of protein-dye binding. - *Analytical Biochemistry* 72(1-2): 248-254.
- [16] Carillo, P., Mastrodonato, G., Nacca, F., Parisi, D., Verlotta, A., Fuggi, A. (2008): Nitrogen metabolism in durum wheat under salinity: accumulation of proline and glycine betaine. - *Functional Plant Biology* 35(5): 412-426.
- [17] Cavalcante, J., Vargas, C., Nogueira, E., Vinagre, F., Schwarcz, K., Baldani, J., Ferreira, P., Hemery, A. (2007): Members of the ethylene signalling pathway are regulated in sugarcane during the association with nitrogen-fixing endophytic bacteria. - *Journal of Experimental Botany* 58(3): 673-686.
- [18] Chang, Y.C., Chao, Y.-Y., Kao, C.H. (2012): The role of iron in stress response to cadmium in rice seedlings. - *Crop, Environment and Bioinformatics* 9: 175-183.
- [19] Cheng, Y.J., Kim, M.D., Deng, X.P., Kwak, S.S., Chen, W. (2013): Enhanced salt stress tolerance in transgenic potato plants expressing IbMYB1, a sweet potato transcription factor. - *J. Microbiol. Biotechnol* 23(12): 1737-1746.
- [20] Cho, U.H., Seo, N.-H. (2005): Oxidative stress in *Arabidopsis thaliana* exposed to cadmium is due to hydrogen peroxide accumulation. - *Plant Science* 168(1): 113-120.

- [21] Ciec ko, Z., Kalembasa, S., Wyszowski, M., Rolka, E. (2004): Effect of soil contamination by cadmium on potassium uptake by plants. - *Journal of Environmental Studies* 13(3): 333-337.
- [22] Corwin, D.L., Ahmad, H.R. (2015): Spatio-temporal impacts of dairy lagoon water reuse on soil: heavy metals and salinity. - *Environ Sci Process Impacts* 17(10): 1731-48.
- [23] National Research Council (1997): Toxicologic Assessment of the Army's Zinc Cadmium Sulfide Dispersion Tests. The National Academies Press, Washington, DC.
- [24] Creus, C.M., Sueldo, R.J., Barassi, C.A. (1997): Shoot growth and water status in *Azospirillum*-inoculated wheat seedlings grown under osmotic and salt stresses. - *PLANT Physiology and Biochemistry-Paris*- 35: 939-944.
- [25] Daneshbakhsh, B., Khoshgoftarmansh, A.H., Shariatmadari, H., Cakmak, I. (2013): Phytosiderophore release by wheat genotypes differing in zinc deficiency tolerance grown with Zn-free nutrient solution as affected by salinity. - *Journal of Plant Physiology* 170(1): 41-46.
- [26] Dell'Amico, E., Cavalca, L., Andreoni, V. (2008): Improvement of *Brassica napus* growth under cadmium stress by cadmium-resistant rhizobacteria. - *Soil Biology and Biochemistry* 40(1): 74-84.
- [27] Dobermann, A. (2000): Rice: Nutrient disorders & nutrient management. *Int. Rice Res. Inst.*
- [28] Drazi c, G., Mihailovi c, N., Stojanovi c, Z. (2004): Cadmium toxicity: The effect on macro-and micro-nutrient contents in soybean seedlings. - *Biologia Plantarum* 48(4): 605-607.
- [29] Ekmek ci, Y., Tanyola c, D., Ayhan, B. (2008): Effects of cadmium on antioxidant enzyme and photosynthetic activities in leaves of two maize cultivars. - *Journal of Plant Physiology* 165(6): 600-611.
- [30] El-Dengaway, E., Hussein, A.A., Alamri, S.A. (2011): Improving growth and salinity tolerance of carob seedlings (*Ceratonia siliqua* L.) by *Azospirillum* inoculation. - *Am.-Eurasian J. Agric. Environ. Sci.* 11(3): 371-384.
- [31] El-Hendawy, S.E., Hu, Y., Yakout, G.M., Awad, A.M., Hafiz, S.E., Schmidhalter, U. (2005): Evaluating salt tolerance of wheat genotypes using multiple parameters. - *European Journal of Agronomy* 22(3): 243-253.
- [32] Figueiredo, A.C., Barroso, J.G., Pedro, L.G., Scheffer, J.J. (2008): Factors affecting secondary metabolite production in plants: volatile components and essential oils. - *Flavour and Fragrance Journal* 23(4): 213-226.
- [33] Fodor, E., Szab -Nagy, A., Erdei, L. (1995): The effects of cadmium on the fluidity and H⁺-ATPase activity of plasma membrane from sunflower and wheat roots. - *Journal of Plant Physiology* 147(1): 87-92.
- [34] Fodor, F., G sp r, L., Morales, F., Gogorcena, Y., Lucena, J.J., Cseh, E., Kr pfl, K., Abad a, J., S rvari,  . (2005): Effects of two iron sources on iron and cadmium allocation in poplar (*Populus alba*) plants exposed to cadmium. - *Tree Physiology* 25(9): 1173-1180.
- [35] Gao, Y., Miao, C., Wang, Y., Xia, J., Zhou, P. (2012): Metal-resistant microorganisms and metal chelators synergistically enhance the phytoremediation efficiency of *Solanum nigrum* L. in Cd-and Pb-contaminated soil. - *Environmental Technology* 33(12): 1383-1389.
- [36] Giller, K.E., Witter, E., Mcgrath, S.P. (1998): Toxicity of heavy metals to microorganisms and microbial processes in agricultural soils: a review. - *Soil Biology and Biochemistry* 30(10): 1389-1414.
- [37] Gohar, Z., Ahmad, R., Gul, H. (2003): Growth and development of cotton roots at various soil texture undersaline conditions. - *Pakistan Journal of Botany* 2(1): 12-19.
- [38] Grant, C., Sheppard, S. (2008): Fertilizer impacts on cadmium availability in agricultural soils and crops. - *Human and Ecological Risk Assessment* 14(2): 210-228.

- [39] Hamdia, M.A.E.-S., Shaddad, M., Doaa, M.M. (2004): Mechanisms of salt tolerance and interactive effects of *Azospirillum brasilense* inoculation on maize cultivars grown under salt stress conditions. - *Plant Growth Regulation* 44(2): 165-174.
- [40] He, Q.B., Singh, B.R. (1994): Crop uptake of cadmium from phosphorus fertilizers: I. Yield and cadmium content. - *Water, Air, and Soil Pollution* 74(3): 251-265.
- [41] Heuer, B. (2010): Role of proline in plant response to drought and salinity. - *Handbook of plant and crop stress*. CRC Press, Boca Raton 213-238.
- [42] Hoagland, D.R., Arnon, D.I. (1950): The water-culture method for the growing plants without soil. 347. - *California Agricultural Experimental Station* 347
- [43] Imsande, J. (1998): Iron, sulfur, and chlorophyll deficiencies: a need for an integrative approach in plant physiology. - *Physiologia Plantarum* 103(1): 139-144.
- [44] Jamil, A., Riaz, S., Ashraf, M., Foolad, M.R. (2011): Gene expression profiling of plants under salt stress. - *Critical Reviews in Plant Sciences* 30(5): 435-458.
- [45] Kang, S.-M., Khan, A.L., Waqas, M., You, Y.-H., Kim, J.-H., Kim, J.-G., Hamayun, M., Lee, I.-J. (2014): Plant growth-promoting rhizobacteria reduce adverse effects of salinity and osmotic stress by regulating phytohormones and antioxidants in *Cucumis sativus*. - *Journal of Plant Interactions* 9(1): 673-682.
- [46] Khoshgoftar, A.H., Shariatmadari, H., Karimian, N., Kalbasi, M., van der Zee, S.E.A.T.M., Parker, D.R. (2004): Salinity and Zinc Application Effects on Phytoavailability of Cadmium and Zinc. - *Soil Science Society of America Journal* 68(6): 1885-1889.
- [47] Khoshgoftarmanesh, A.H., Aghili, F., Sanaeiostovar, A. (2009): Daily intake of heavy metals and nitrate through greenhouse cucumber and bell pepper consumption and potential health risks for human. - *International Journal of Food Sciences and Nutrition* 60 Suppl 1:199-208.
- [48] Kim, J.S., Lee, J., Seo, S.G., Lee, C., Woo, S.Y., Kim, S.H. (2015): Gene expression profile affected by volatiles of new plant growth promoting rhizobacteria, *Bacillus subtilis* strain JS, in tobacco. - *Genes & Genomics* 37(4): 387-397.
- [49] Kim, Y.Y., Kim, D.Y., Shim, D., Song, W.Y., Lee, J., Schroeder, J.I., Kim, S., Moran, N., Lee, Y. (2008): Expression of the novel wheat gene *TM20* confers enhanced cadmium tolerance to bakers' yeast. - *Journal of Biological Chemistry* 283(23): 15893-15902.
- [50] Brenner, D.J., Krieg N. R., Stanley, J.T., (2005): Genus *Azospirillum*. - *Bergey's manual of systematic bacteriology*, 2th edition, volume two, 1:94-104.
- [51] Leblebici, Z., Aksoy, A., Duman, F. (2011): Influence of salinity on the growth and heavy metal accumulation capacity of *Spirodela polyrrhiza* (*Lemnaceae*). - *Turkish journal of biology* 35(2): 215-220.
- [52] Lin, C.C., Kao, C.H. (2001): Cell wall peroxidase activity, hydrogen peroxide level and NaCl-inhibited root growth of rice seedlings. - *Plant and Soil* 230(1): 135-143.
- [53] Lin, W., Okon, Y., Hardy, R.W. (1983): Enhanced mineral uptake by *Zea mays* and *Sorghum bicolor* roots inoculated with *Azospirillum brasilense*. - *Applied and Environmental Microbiology* 45(6): 1775-1779.
- [54] Liu, D., Wang, M., Zou, J., Jiang, W. (2006): Uptake and accumulation of cadmium and some nutrient ions by roots and shoots of maize (*Zea mays* L.). - *Pakistan Journal of Botany* 38(3): 701.
- [55] Liu, W.X., Liu, J.W., Wu, M.Z., Li, Y., Zhao, Y., Li, S.R. (2009): Accumulation and translocation of toxic heavy metals in winter wheat (*Triticum aestivum* L.) growing in agricultural soil of Zhengzhou, China. - *Bulletin of Environmental Contamination and Toxicology* 82(3): 343-347.
- [56] Livak, K.J., Schmittgen, T.D. (2001): Analysis of relative gene expression data using real-time quantitative PCR and the $2^{-\Delta\Delta CT}$ method. - *Methods* 25(4): 402-408.
- [57] Lux, A., Martinka, M., Vaculik, M., White, P.J. (2011): Root responses to cadmium in the rhizosphere: a review. - *Journal of Experimental Botany* 62(1): 21-37.

- [58] Lux, A., Šottníková, A., Opatrná, J., Greger, M. (2004): Differences in structure of adventitious roots in *Salix* clones with contrasting characteristics of cadmium accumulation and sensitivity. - *Physiologia Plantarum* 120(4): 537-545.
- [59] Ma, Y., Rajkumar, M., Freitas, H. (2009): Inoculation of plant growth promoting bacterium *Achromobacter xylosoxidans* strain Ax10 for the improvement of copper phytoextraction by *Brassica juncea*. - *Journal of Environmental Management* 90(2): 831-837.
- [60] Mahajan, S., Tuteja, N. (2005): Cold, salinity and drought stresses: an overview. - *Archives of Biochemistry and Biophysics* 444(2): 139-58.
- [61] Martínez-Toledo, M., Salmerón, V., González-López, J. (1991): Biological characteristics of *Azotobacter* spp. in natural environments. - *Trends Soil Sci* 1: 15-23.
- [62] Matysik, J., Alia, Bhalu, B., Mohanty, P. (2002): Molecular mechanisms of quenching of reactive oxygen species by proline under stress in plants. - *Current Science* 525-532.
- [63] Mishra, S., Srivastava, S., Tripathi, R., Govindarajan, R., Kuriakose, S., Prasad, M. (2006): Phytochelatin synthesis and response of antioxidants during cadmium stress in *Bacopa monnieri* L. - *Plant Physiology and Biochemistry* 44(1): 25-37.
- [64] Nakano, Y., Asada, K. (1981): Hydrogen peroxide is scavenged by ascorbate-specific peroxidase in spinach chloroplasts. - *Plant and Cell Physiology* 22(5): 867-880.
- [65] Nellesmann, C. (2009): The environmental food crisis: the environment's role in averting future food crises: a UNEP rapid response assessment. UNEP/Earthprint.
- [66] Neumann, P.M. (1995): The role of cell wall adjustments in plant resistance to water deficits. - *Crop Science* 35(5): 1258-1266.
- [67] Nigam, R., Srivastava, S., Prakash, S., Srivastava, M. (2001): Cadmium mobilisation and plant availability—the impact of organic acids commonly exuded from roots. - *Plant and Soil* 230(1): 107-113.
- [68] Nogueira, E.d.M., Vinagre, F., Masuda, H.P., Vargas, C., Pádua, V.L.M.d., Silva, F.R.d., Santos, R.V.d., Baldani, J.I., Ferreira, P.C.G., Hemery, A.S. (2001): Expression of sugarcane genes induced by inoculation with *Gluconacetobacter diazotrophicus* and *Herbaspirillum rubrisubalbicans*. - *Genetics and Molecular Biology* 24(1-4): 199-206.
- [69] Nriagu, J.O., Sprague, J.B. (1987): Cadmium in the aquatic environment. -
- [70] Omar, M.N.A., Osman, M.E.H., Kasim, W.A., Abd El-Daim, I.A. (2009): Salinity and water Stress: Improving Crop Efficiency, eds. Ashraf, M., Ozturk, M., Athar, H.R. Springer Netherlands, Dordrecht, pp. 133-147.
- [71] Othman, N.F.H. (2015): Effects of ACC deaminase activity of *Azospirillum Brasilense* (Sp7) and *Escherichia Coli* (L2) on growth of rice seedlings. Pp 152
- [72] Pakdaman, N., Ghaderian, S.M., Ghasemi, R., Asemaneh, T. (2013): Effects of calcium/magnesium quotients and nickel in the growth medium on growth and nickel accumulation in *Pistacia atlantica*. - *Journal of Plant Nutrition* 36(11): 1708-1718.
- [73] Parida, A., Das, A., Mitra, B. (2003): Effects of NaCl stress on the structure, pigment complex composition, and photosynthetic activity of mangrove *Bruguiera parviflora* chloroplasts. - *Photosynthetica* 41(2): 191-200.
- [74] Pessarakli, M., Huber, J. (1991): Biomass production and protein synthesis by alfalfa under salt stress. - *Journal of Plant Nutrition* 14(3): 283-293.
- [75] Prapagdee, B., Khonsue, N. (2015): Bacterial-assisted cadmium phytoremediation by *Ocimum gratissimum* L. in polluted agricultural soil: a field trial experiment. - *International Journal of Environmental Science and Technology* 12(12): 3843-3852.
- [76] Ramezani, A., Niazi, A., Abolmoghadam, A.A., Babgohari, M.Z., Deihimi, T., Ebrahimi, M., Akhtardanesh, H., Ebrahimie, E. (2013): Quantitative expression analysis of *TaSOS1* and *TaSOS4* genes in cultivated and wild wheat plants under salt stress. - *Molecular Biotechnology* 53(2): 189-197.
- [77] Rodelas, B., González-López, J., Pozo, C., Salmerón, V., Martínez-Toledo, M.V. (1999): Response of Faba bean (*Vicia faba* L.) to combined inoculation with *Azotobacter* and *Rhizobium leguminosarum* bv. viceae. - *Applied Soil Ecology* 12(1): 51-59.

- [78] Roth, U., von Roepenack-Lahaye, E., Clemens, S. (2006): Proteome changes in *Arabidopsis thaliana* roots upon exposure to Cd²⁺. - Journal of Experimental Botany 57(15): 4003-4013.
- [79] Sauer, D., Burroughs, R. (1986): Disinfection of seed surfaces with sodium hypochlorite. - Phytopathology 76(7): 745-749.
- [80] Shafi, M., Bakht, J., Hassan, M.J., Raziuddin, M., Zhang, G. (2009): Effect of cadmium and salinity stresses on growth and antioxidant enzyme activities of wheat (*Triticum aestivum* L.). - Bulletin of Environmental Contamination and Toxicology 82(6): 772-776.
- [81] Shah, S.S., Mohammad, F., Shafi, M., Bakht, J., Zhou, W. (2011): Effects of cadmium and salinity on growth and photosynthesis parameters of *Brassica* species. - Pakistan Journal of Botany 43(1): 333-340.
- [82] Sharmila, P., Kumari, P.K., Singh, K., Prasad, N.V.S.R.K., Pardha-Saradhi, P. (2017): Cadmium toxicity-induced proline accumulation is coupled to iron depletion. - Protoplasma 254(2): 763-770.
- [83] Sheppard, S., Grant, C., Sheppard, M., De Jong, R., Long, J. (2009): Risk indicator for agricultural inputs of trace elements to canadian soils all rights reserved. No part of this periodical may be reproduced or transmitted in any form or by any means, electronic or mechanical, including photocopying, recording, or any information storage and retrieval system, without permission in writing from the publisher. - Journal of Environmental Quality 38(3): 919-932.
- [84] Siadat, H. (1998): Proceeding of the Conference on New Technologies to Combat Desertification. pp. 12-15.
- [85] Skoog, D., West, D., Holler, F., Crouch, S. (2005): Flame photometric determination of sodium. - Analytic Chemistry: An Introduction. Edition 7:594-631.
- [86] Smolders, E., Lambregts, R.M., McLaughlin, M.J., Tiller, K.G. (1998): Effect of soil solution chloride on cadmium availability to Swiss chard. - Journal of Environmental Quality 27(2): 426-431.
- [87] Stobart, A.K., Griffiths, W.T., Ameen-Bukhari, I., Sherwood, R.P. (1985): The effect of Cd²⁺ on the biosynthesis of chlorophyll in leaves of barley. - Physiologia Plantarum 63(3): 293-298.
- [88] Stolt, J.P., Sneller, F.E.C., Bryngelsson, T., Lundborg, T., Schat, H. (2003): Phytochelatin and cadmium accumulation in wheat. - Environmental and Experimental Botany 49(1): 21-28.
- [89] Stout, L.M., Dodova, E.N., Tyson, J.F., Nüsslein, K. (2010): Phytoprotective influence of bacteria on growth and cadmium accumulation in the aquatic plant *Lemna minor*. - Water Research 44(17): 4970-4979.
- [90] Taherinia, B., Kavousi, H.R., Dehghan, S. (2015): Isolation and characterization of plasma membrane Na⁺/H⁺ antiporter (*SOS1*) gene during salinity stress in kallar grass (*Leptochloa fusca*). - EurAsian Journal of BioSciences 9:12-20.
- [91] Tavakoli, M., Poustini, K., Alizadeh, H. (2016): Proline accumulation and related genes in wheat leaves under salinity stress. - Journal of Agricultural Science and Technology 18(3): 707-716.
- [92] Tester, M., Davenport, R. (2003): Na⁺ tolerance and Na⁺ transport in higher plants. - Ann Bot. 91(5):503-27.
- [93] Tinker, P. (1984): The role of microorganisms in mediating and facilitating the uptake of plant nutrients from soil. - Plant and Soil 76(1-3): 77-91.
- [94] Tiwari, J.K., Munshi, A.D., Kumar, R., Pandey, R.N., Arora, A., Bhat, J.S., Sureja, A.K. (2010): Effect of salt stress on cucumber: Na⁺/K⁺ ratio, osmolyte concentration, phenols and chlorophyll content. - Acta Physiologiae Plantarum 32(1): 103-114.
- [95] Upadhyay, S.K., Singh, J.S., Singh, D.P. (2011): Exopolysaccharide-producing plant growth-promoting rhizobacteria under salinity condition. - Pedosphere 21(2): 214-222.

- [96] Vargas-Garcia Mdel, C., Lopez, M.J., Suarez-Estrella, F., Moreno, J. (2012): Compost as a source of microbial isolates for the bioremediation of heavy metals: in vitro selection. - *Science of the Total Environment* 431: 62-67.
- [97] Vargas, L., de Carvalho, T.L.G., Ferreira, P.C.G., Baldani, V.L.D., Baldani, J.I., Hemerly, A.S. (2012): Early responses of rice (*Oryza sativa* L.) seedlings to inoculation with beneficial diazotrophic bacteria are dependent on plant and bacterial genotypes. - *Plant and Soil* 356(1): 127-137.
- [98] Verbruggen, N., Hermans, C., Schat, H. (2009): Mechanisms to cope with arsenic or cadmium excess in plants. - *Current Opinion in Plant Biology* 12(3): 364-372.
- [99] Vodyanitskii, Y.N. (2016): Standards for the contents of heavy metals in soils of some states. - *Annals of Agrarian Science* 14(3): 257-263.
- [100] Wakeel, A. (2013): Potassium–sodium interactions in soil and plant under saline-sodic conditions. - *Journal of Plant Nutrition and Soil Science* 176(3): 344-354.
- [101] Wallace, A., Wallace, G., Cha, J. (1992): Some modifications in trace metal toxicities and deficiencies in plants resulting from interactions with other elements and chelating agents-the special case of iron. - *Journal of Plant Nutrition* 15(10): 1589-1598.
- [102] Wani, P.A., Khan, M.S. (2010): *Bacillus* species enhance growth parameters of chickpea (*Cicer arietinum* L.) in chromium stressed soils. - *Food and Chemical Toxicology* 48(11): 3262-3267.
- [103] Weggler-Beaton, K., McLaughlin, M.J., Graham, R. (2000): Salinity increases cadmium uptake by wheat and Swiss chard from soil amended with biosolids. - *Soil Research* 38(1): 37-46.
- [104] Xu, H., Jiang, X., Zhan, K., Cheng, X., Chen, X., Pardo, J.M., Cui, D. (2008): Functional characterization of a wheat plasma membrane Na⁺/H⁺ antiporter in yeast. - *Archives of Biochemistry and Biophysics* 473(1): 8-15.
- [105] Yadav, S., Chandra, R. (2013): Effect of heavy metals and phenol on bacterial decolourisation and COD reduction of sucrose-aspartic acid Maillard product. - *Journal of Environmental Sciences (China)* 25(1): 172-80.
- [106] Yamaguchi, H., Fukuoka, H., Arao, T., Ohyama, A., Nunome, T., Miyatake, K., Negoro, S. (2009): Gene expression analysis in cadmium-stressed roots of a low cadmium-accumulating solanaceous plant, *Solanum torvum*. - *Journal of Experimental Botany* 61(2): 423-437.
- [107] Zhang, H., Kim, M.-S., Sun, Y., Dowd, S.E., Shi, H., Paré, P.W. (2008a): Soil bacteria confer plant salt tolerance by tissue-specific regulation of the sodium transporter HKT1. - *Molecular Plant-Microbe Interactions* 21(6): 737-744.
- [108] Zhang, H., Xie, X., Kim, M.-S., Korniyev, D.A., Holaday, S., Paré, P.W. (2008b): Soil bacteria augment *Arabidopsis* photosynthesis by decreasing glucose sensing and abscisic acid levels in planta. - *The Plant Journal* 56(2): 264-273.

ABSENCE OF *WOLBACHIA* IN RED PALM WEEVIL, *RYNCHOPHORUS FERRUGINEUS* OLIVIER (COLEOPTERA: CURCULIONIDAE): A PCR-BASED APPROACH

ALI, H.^{1,2} – MUHAMMAD, A.^{1,2} – HOU, Y.^{1,2*}

¹State Key Laboratory of Ecological Pest Control for Fujian and Taiwan Crops, Fujian Agriculture and Forestry University, Fuzhou 350002, China

²Fujian Provincial Key Laboratory of Insect Ecology, College of Plant Protection, Fujian Agriculture and Forestry University, Fuzhou 350002, Fujian, China

*Corresponding author

e-mail: ymhou@fafu.edu.cn; phone/fax: +86-591-8376-8654

(Received 8th Nov 2017; accepted 27th Feb 2018)

Abstract. Among the intracellular bacterial symbionts, the genus *Wolbachia* (Rickettsiaceae: Rickettsiales) is one of the most abundant taxa associated with reproductive systems of various insects. It is cytoplasmic inherited endosymbiont that induce various reproductive alterations. Characterization analysis has revealed that a number of arthropods harbour *Wolbachia* sp. estimates from 20-80%, with emphasize on Coleopterous insects (41 species have been reported so far). Therefore, in the context of broad existence and unique phenotypic actions to alter reproductive systems of various insect, we aimed to determine the intriguing possibility of this endosymbiont from one of the deadliest palm pest, i.e. red palm weevil (RPW), *Rynchophorus ferrugineus* (Curculionidae) from different geographical locations using polymerase chain reactions (PCR) with four sets of *Wolbachia*-specific primers (SPs) along with one pair of universal bacterial primer (BP). Parallel analysis was also carried out with *Wolbachia* strain isolated from whitebacked plant hopper, *Sogatella furcifera* (Homoptera: Delphacidae), as a positive control. Our analysis confirmed the absence of *Wolbachia* sp. across the various life stages of RPW reared in laboratory or captured from the field. Moreover, the phylogenetic analysis of all closely related *Wolbachia*-mediated weevils were compiled and retrieved from NCBI database indicates the extent of transfection of this bacterium into RPW for the future work on biological control of RPW. This study may facilitate to understand further evolutionary consequences of *Wolbachia* infection in weevils.

Keywords: RPW, biological control, endosymbiotic bacteria, *Wolbachia*, PCR

Introduction

A number of symbiotic bacteria associated with insects profoundly influence their host physiology. Among these endosymbionts, *Wolbachia* sp. belongs to order Rickettsiales, is widely distributed in invertebrates (Arthropods). The evidences are mounting that *Wolbachia* can infect a number of insect species (20-80%) (Werren and Windsor, 2000; Jiggins et al., 2001; Tagami and Miura, 2004; Hilgenboecker et al., 2008; Zug and Hammerstein, 2012) from different orders including Diptera, Hymenoptera, Coleoptera, Lepidoptera, Orthoptera, and Hemiptera/Homopter (Werren and Windsor, 2000). Extrapolations of this percentage among the total number of insects and nematode species make *Wolbachia* one of the most abundant endosymbiont. This genus has also been reported from filarial nematodes, the causative agents of river blindness and elephantiasis in human (Fenn et al., 2006). *Wolbachia* has the potential to distort the host reproductive system by various phenotypic effects (Blagrove et al., 2012; Ali et al., 2016) such as cytoplasmic incompatibility (Poinsot et al., 2003) (CI), parthenogenesis induction (Stouthamer et al., 1999) (PI), male killing (MK) (Jiggins et

al., 2001) and feminization (Negri et al., 2006). Among these phenotypes, MK, PI, and feminization are highly selective advantageous to female-biased sex ratio while the CI is related to decreasing the number of offspring by reducing the egg hatchability. Phylogenetic analysis has revealed that a total of 8-11 distant *Wolbachia* supergroups designated as A-K has been proposed so far (Lo et al., 2002; Casiraghi et al., 2005). Among these supergroups, A and B are high presumably distributed in arthropods while supergroup C and D belong to terrestrial nematodes with the exception of endosymbionts from *Mansonella* spp., which are recognized in supergroup F. Anyhow, new supergroups with the range of novel *Wolbachia*-mediated hosts has not yet been completely investigated, although new phylogenetic lineages along with novel host are progressively discovered (Casiraghi et al., 2005).

Moreover, breeding behavior, (Gazla and Carracedo, 2009; Miller et al., 2010), sex determination, (Rigaud, 1997), eusociality (Stouthamer et al., 1999) and speciation (Bordenstein, 2003) of the host may also be profoundly affected or altered by *Wolbachia* sp. It is also known to play roles both protective or antagonistic in some RNA viral infections in *Drosophila* (Osborne et al., 2012) and establishes obligate associations as observed in all infected nematodes (Fenn and Blaxter, 2004; Fenn et al., 2006) and rarely in some arthropods (Dedeine et al., 2005; Hosokawa et al., 2010). Remarkable biology, and diverse phenotypic effects of *Wolbachia* and its potential application for the control of vector-borne diseases such as dengue fever, malaria or filariasis (Kambris et al., 2009) offers promising tools to control various economically important invasive species of agriculture and medical importance.

The beetle superfamily Curculionoidea (Insecta: Coleoptera) is one of the most plenteous, diverse, dominant and successful animal group containing more than 60,000 described and likely to contain further 220,000 undescribed species (Oberprieler et al., 2007). Among the Curculionoidea family, red palm weevil (RPW), *Rynchophorus ferrugineus* (Olivier) is one of most invasive pest of almost 26 palm species (Malumphy and Moran, 2009) including date palm, *Phoenix dactylifera* L., oil palm, *Elaeis guineensis* (Murphy and Briscoe, 1999), coconut palm, *Cocos Nucifera*, and Canary Island date palm, *Phoenix canariensis*. The RPW is a concealed tissue borer which undergoes complete metamorphosis (life cycle going through egg, larvae, pupae and adult stages as shown in Fig. 1) and the greater part of its life stages are found inside the palm tree.

Damage manifestations are showed by the presence of tunnels in the trunk, oozing of thick yellow to brown fluid from the tree, the presence of chewed up plant tissue in and around openings in the trunk, the occurrence of a fermented smell from the fluid inside infested tunnels in the trunk, and/or breaking of the trunk or toppling of the palm crown (Kaakeh et al., 2001). In China, damages of RPW initially reported in Guangdong during 1997 and spread rapidly to other parts (Chongqing, Fujian, Hainan Island, Hong Kong, Guangdong, Guangxi, Guizhou, Jiangsu, Jiangxi, Shanghai, Sichuan, Taiwan, Tibet, Yunnan and Zhejiang) (Li et al., 2009). Nowadays, this pest is widely distributed, found in Oceania, Asia, Africa, Europe (several countries around the mediterranean basin) and the Middle East (Howard et al., 2001).

Symbiotic association between beetles and microbial consortia have been broadly investigated. From last few decades, more than thirty weevils have been investigated to harbor *Wolbachia* (Lachowska et al., 2010), with number increasing gradually (41 beetles as shown in Table 1). Many of which belong to supergroup A or B, except the one discovered in *Rhinocyllus conicus* (Froehlich) that belongs supergroup F (Lo et al.,

2002). In view of the widespread distribution as well as the manipulation of host mating and reproduction, *Wolbachia* has attracted the interest of biologists because they maybe used as a novel environmentally friendly tool for insect pest control. Bearing in mind the importance of *Wolbachia*, first, we investigate the presence of *Wolbachia* infection in RPW with the aim to explore the potential use of this endosymbiont as biological control agent against it. This is the first novel study to interrogate the existence of *Wolbachia* in RPW using PCR-based approach. Secondly, according to our best knowledge we compiled all weevils which have been proven to *Wolbachia* positive from previous literatures (*Table 1*) and finally, we constructed a phylogenetic relationship between previously identified *Wolbachia* strains in closely related coleopterans species with RPW for further understanding the evolutionary consequences of *Wolbachia* infection in weevils.

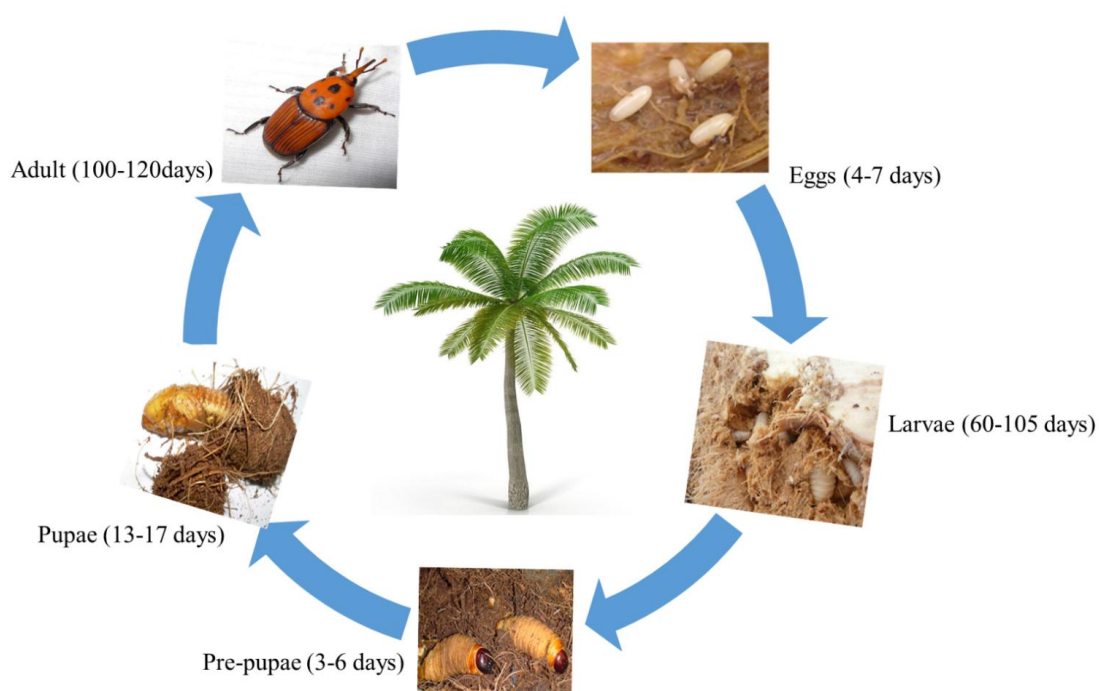


Figure 1. Life cycle (egg to adult stage) of red palm weevil (RPW), *Rynchophorus ferrugineus* (Curculionidae). Number of days may vary according to environmental conditions

Material and methods

Insect collections and rearing

The present study was conducted at the Key Laboratory of Insect Ecology, Department of Plant Protection, Fujian Agriculture and Forestry University, Fuzhou-China. Specimens of RPW were collected from different geographical locations (*Table 2* and *Fig. 2*) during 2014-2017 from infested palm trees. From every location at least 10 specimens were captured. Collected adults and larvae were placed in perforated plastic boxes with host plant tissues and transported to the laboratory for further rearing and DNA extraction. Laboratory population was maintained under control conditions (Temp 25-28 °C, RH 65-70%, 12:12 light-dark cycle) (Hou and Weng, 2010) and provided with sugarcane (*Saccharum officinarum*) for feeding and oviposition.

Table 1. *Wolbachia* infection on the basis of *Wolbachia* outer surface protein (*wsp*) and filamenting temperature sensitive mutant *Z* protein (*FtsZ*) in all known Coleopteran species reported so far

Coleopteran hosts		Accession no. of <i>Wolbachia</i>		References
Scientific name	Family	<i>wsp</i> gene	<i>ftsZ</i> gene	
<i>Sitophilus zeamais</i>	Curculionidae	AB469362	-	Kageyama et al., 2010
<i>Otiorrhynchus sulcatus</i>	Curculionidae	-	-	Son et al., 2008
<i>Adalia bipunctata</i>	Curculionidae	AJ130714	-	Hurst et al., 1999
<i>Naupactus cervinus</i>	Curculionidae	GQ402145	-	Rodriguero et al., 2010
<i>Xylosandrus germanus</i>	Curculionidae	AB359039	-	Kawasaki et al., 2010
<i>Ceutorhynchus obstructus</i>	Curculionidae	-	HM012590	Floate et al., 2011
<i>Hypera postica</i>	Curculionidae	-	-	Iwase et al., 2015
<i>Sitophilus oryzae</i>	Curculionidae	-	KP762388	Li et al., 2015
<i>Lissorhoptrus oryzophilus</i>	Curculionidae	-	GU478334	Chen et al., 2012
<i>Rhinocyllus conicus</i>	Curculionidae	-	-	Campbell et al., 1992
<i>Conotrachelus nenuphar</i>	Curculionidae	GU013552	-	Zhang et al., 2010
<i>Tribolium madens</i>	Tenebrionidae	AF275546	-	Fialho and Stevens, 2000
<i>Tribolium confusum</i>	Tenebrionidae	AF020083	-	Ming et al., 2015
<i>Aulacophora nigripennis</i>	Chrysomelidae	GU236978	-	Jeong et al., 2009
<i>Chelymorpha alternans</i>	Chrysomelidae	DQ842458	-	Baldo et al., 2006
<i>Altica lythri</i>	Chrysomelidae	KF163375	-	Jackel et al., 2013
<i>Aphthona nigricutis</i>	Chrysomelidae	-	AY136550	Roehrdanz et al., 2006
<i>Hermaphysa mercurialis</i>	Chrysomelidae	-	KF163372	Jackel et al., 2013
<i>Callosobruchus latealbus</i>	Chrysomelidae	AB545610	-	Kondo et al., 2011
<i>Diabrotica virgifera zaeae</i>	Chrysomelidae	DQ091305	-	Giordano et al., 1997
<i>Oreina liturata</i>	Chrysomelidae	HG970634	-	Montagna et al., 2014
<i>Oreina cacaliae</i>	Chrysomelidae	HG325863	-	Montagna et al., 2014
<i>Diabrotica virgifera virgifera</i>	Chrysomelidae	-	AY136551	Roehrdanz and Levine, 2007
<i>Diabrotica cristata</i>	Chrysomelidae	-	AY007556	Clark et al., 2001
<i>Callosobruchus chinensis</i>	Chrysomelidae	AB038339	-	Kondo et al., 2011
<i>Diabrotica barberi</i>	Chrysomelidae	-	AY136552	Roehrdanz and Levine, 2007
<i>Brontispa longissima</i>	Chrysomelidae	MG345108	-	Ali et al., 2018
<i>Octodonta nipae</i>	Chrysomelidae	MG551861	-	Unpublished data
<i>Harmonia axyridis</i>	Coccinellidae	-	KM288833	Goryacheva et al., 2015
<i>Pityogenes chalcographus</i>	Scolytinae	DQ993183	-	Avtzis et al., 2008
<i>Hypothenemus hampei</i>	Scolytidae	AF389084	-	Vega et al., 2002
<i>Byturus tomentosus</i>	Byturidae	AJ585376	-	Malloch et al., 2005
<i>Megabruchidius sophorae</i>	Bruchidae	AB545607	-	Kondo et al., 2011
<i>Callosobruchus analis</i>	Bruchidae	AB469357	-	Kageyama et al., 2010
<i>Oryzaephilus mercator</i>	Silvanidae	KJ152808	-	Li et al., 2015
<i>Oryzaephilus surinamensis</i>	Silvanidae	AB469190	-	Kageyama et al., 2010
<i>Luciola unmunsana</i>	Lampyridae	FJ156729	-	Jeong et al., 2009
<i>Lasioderma serricorne</i>	Anobiidae	AB469359	-	Kageyama et al., 2010
<i>Stegobium paniceum</i>	Anobiidae	AB469917	-	Kageyama et al., 2010
<i>Byctiscus venustus</i>	Rhynchitidae	GU236986	-	Jeong et al., 2009
<i>Anthrenus verbasci</i>	Dermestidae	AB469915	-	Kageyama et al., 2010

Note: Scientific names, families and their accession numbers are given. Blank boxes indicates either not available or not known accession numbers from NCBI database

Table 2. Tested specimens of red palm weevil (RPW), *Rynchophorus ferrugineus* (Curculionidae), their collection year and place of collection

S. No	Date of collections	Collected samples	Strain name	Host plant	Original place of collections
1	16/10/2015	Egg (lab collected)	LE	<i>S. officinarum</i>	Fuqing, Fujian, China
2	16/10/2015	Lab larvae	LL	<i>S. officinarum</i>	Fuqing, Fujian, China
3	16/10/2015	Lab pupa	LP	<i>S. officinarum</i>	Fuqing, Fujian, China
4	16/10/2015	Lab adult male	LM	<i>S. officinarum</i>	Fuqing, Fujian, China
5	16/10/2015	Lab adult female	LF	<i>S. officinarum</i>	Fuqing, Fujian, China
6	12/5/2014	Hainan adult male	HM	<i>P. canariensis</i>	Hainan province, China
7	12/5/2014	Hainan adult female	HF	<i>P. canariensis</i>	Hainan province, China
8	10/7/2014	Guanxi adult male	GM	<i>P. canariensis</i>	Guanxi province, China
9	10/7/2014	Guanxi adult female	GF	<i>P. canariensis</i>	Guanxi province, China
10	2/3/2015	Shangai adult male	SM	<i>P. canariensis</i>	Shangai, China
11	2/3/2015	Shangai adult female	SF	<i>P. canariensis</i>	Shangai, China
12	2/4/2015	Longyan adult male	LogM	<i>P. canariensis</i>	Longyan, Fujian, China
13	2/4/2015	Longyan adult female	Logf	<i>P. canariensis</i>	Longyan, Fujian, China
14	11/7/2015	Xiamen adult male	XM	<i>P. canariensis</i>	Xiamen, Fujian, China
15	11/7/2015	Xiamen adult female	XF	<i>P. canariensis</i>	Xiamen, Fujian, China
16	15/8/2015	Fuqing adult male	FM	<i>P. canariensis</i>	Fuqing, Fujian, China
17	15/8/2015	Fuqing adult female	FF	<i>P. canariensis</i>	Fuqing, Fujian, China
18	25/8/2016	Zhangzhou adult male	ZM	<i>P. canariensis</i>	Zhangzhou, Fujian, China
19	25/8/2016	Zhangzhou adult female	ZF	<i>P. canariensis</i>	Zhangzhou, Fujian, China
20	3/9/2017	Ningde adult male	NM	<i>P. canariensis</i>	Ningde, Fujian, China
21	3/9/2017	Ningde adult female	NF	<i>P. canariensis</i>	Ningde, Fujian, China

DNA extraction

For DNA extraction all samples (Table 2 and Fig. 2) were sterilized with 75% alcohol and rinsed three times with autoclaved double distilled water. Total genomic DNA extraction was performed from various life stages (egg, larvae, pupa, male and female) of lab-reared specimens, while only field caught adult stage (male or female) from different geographical locations using DNeasy Blood and Tissue Kit (Qiagen, Valencia, USA) in accordance with the manufacturer's protocol with final elution step repeated twice in 100 µl of buffer AE. The concentration and purity of the extracted DNA was quantified using a NanoDrop 2000 spectrophotometer (Thermo Scientific, Wilmington, DE).

PCR amplification for *Wolbachia* detection

The presence of *Wolbachia* in extracted DNA of RPW specimens was screened using PCR amplification with four *Wolbachia* SPs and a universal bacterial primer (Pu et al., 2016) (Table 3). PCR reactions contained a total volume of 25 µl comprised of 2 µl of template DNA, 12.5 µl of 2X Taq PCR Master-mix (Tiangen Biotechnology Beijing, China), 1 µl of each primer, and 8.5 µl double distilled water. Each reaction run with a positive control (*Wolbachia* DNA from *Sogatella furcifera* (Horvath) and negative control (without DNA). Amplified PCR products were run on 1% agarose gel (0.5 µg/ml ethidium bromide, TRIS-EDTA-Buffer; Fisher, Waltham, MA) and visualized using UV illuminator.

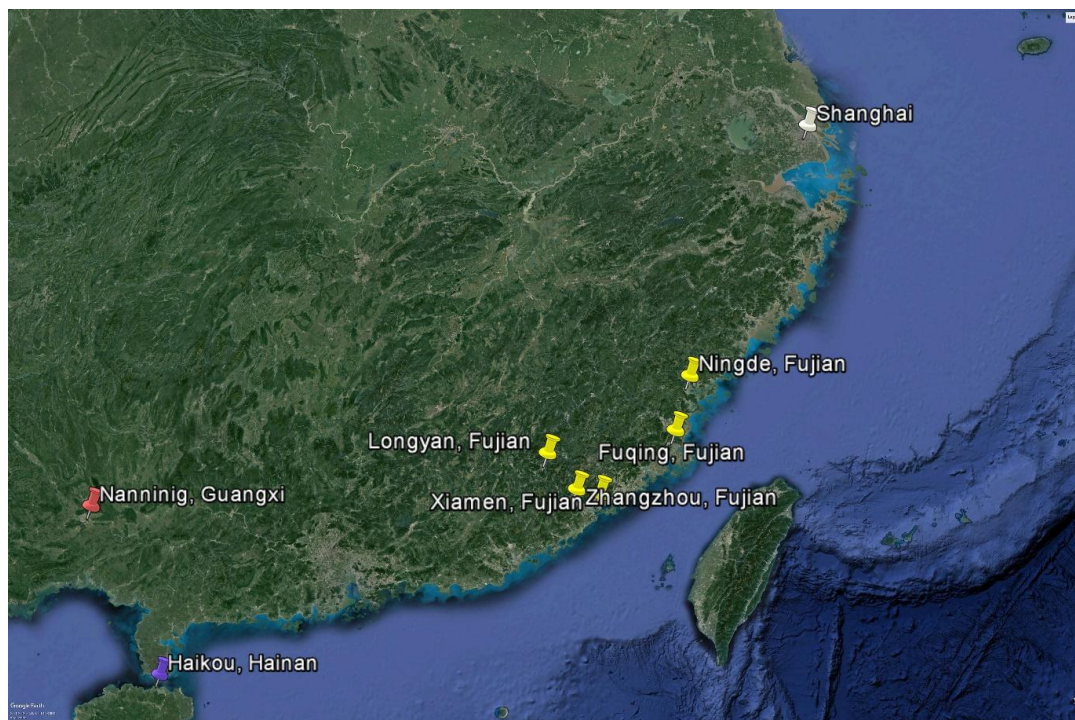


Figure 2. Map of sampling sites from different geographic locations (Fujian, Guangxi, Shanghai and Hainan province) of China. Red palm weevil (RPW), *Rynchophorus ferrugineus* (Curculionidae) specimens collected from same locations represent same color, while different colors represent variable provinces of China. The map was obtained from Google Earth (<https://www.google.com/earth/desktop/>)

Table 3. Four sets of *Wolbachia* specific primers (SPs) along with universal bacterial primer (BP) with PCR thermal cycling conditions used in this study

Primer	Primer sequence	PCR cycling conditions	FL	Reference
<i>Wolbachia</i> SPs	1) wsp81F: 5'-TGG TCC AAT AAG TGA TGA AGA AAC-3' wsp691R: 5'-AAA AAT TAA ACG CTA CTC CA-3'	94 °C for 4 min, 40 s at 94 °C, 40 s at 55 °C, 1 min at 72 °C, Extension step of 10 min at 72 °C	≈600bp	Zhou et al., 1998
	2) wsp1: 5'-GGATCCGGGTCCAATAAGTGATGAAGAAAC-3' wsp2: 5'-GGATCCTTAAAACGCTACTCCAGCTTCTGC-3'	-do-	-do-	Baldo et al., 2006
	3) wspF: 5'-GGGTCCAATAAGTGATGAAGAAAC-3' wspR: 5'-TAAAACGCTACTCCAGCTTCTGC-3'	-do-	-do-	Ming et al., 2015
4)	FtsF: 5'-GTA TGC CGA TTG CAG AGC TTG-3' FtsR: 5'-GCC ATG AGT ATT CAC TTG GCT-3'	95 °C for 10 min, 1 min at 95 °C, 1 min at 55 °C, 2 min at 70 °C, Extension step of 5 min at 72 °C	≈750bp	Kondo et al., 2011
Universal BP	1) 27F: 5'-TCG ACATCGTTTACGGCGTG-3' 1492R: 5'-CTA CGGCTACCTTGTTACGA-3'	94 °C for 3 min, 40 s at 94 °C, 40 s at 55 °C, 1 min at 72 °C, Extension 5 min at 72 °C	≈1400bp	Pu and Hou, 2016

SPs: specific primers; BP: bacterial primer; FL: fragment length; PCR: polymerase chain reactions

***Wolbachia* positive strain**

Wolbachia strain used in this study as a positive control was originally isolated from a lab-reared adult of *S. furcifera* (Horvath) (Homoptera, Delphacidae) known to be infected by *Wolbachia* under the accession number of FJ713766.1 retrieved from National Center for Biotechnology Information (NCBI) database (<https://www.ncbi.nlm.nih.gov/nucleotide/224797910>). PCRs were carried with total volume of 50 µl comprised of 4 µl of template DNA, 50 µl of 2X Taq PCR Master mix (Tiangen Biotechnology Beijing, China), 2 µl of each primer, and 17 µl double distilled water to amplify the targeted genes. The PCR products, after evaluation of positive amplification verified through gel electrophoresis, were subjected to cloning and transformations. A 2 µl of purified amplification product from 1% agarose gel extracted using MiniElute Gel Extraction Kit (Qiagen) was directly ligated into the pGEM T-Easy Cloning Vector (Promega, Madison, WI) in accordance with the protocol. Ligation products were transformed into T1 Competent Cells (Qiagen), which were plated on 0.5% ampicillin Luria-Bertani broth (LB) selection plates (S-Gal LB Agar Blend, Sigma-Aldrich, St Louis, MO) and incubated overnight at 37 °C. At least three positive clones were picked and labeled according to sample and incubated in 1000 µl LB broth (0.5% ampicillin) for 10 h at 37 °C and 300 rpm. After shaking, 2 µl finally confirmed sample via diagnostic PCR were sent to sequencing company (life science Company).

Phylogenetic analysis

We retrieved the sequences of previously identified *Wolbachia* strains (41 species) from closely related weevils to RPW by running search on NCBI GeneBank database (<http://www.ncbi.nlm.nih.gov/BLAST>). All *Wolbachia* strains retrieved from the NCBI GeneBank were aligned using ClustalW and tree was constructed with MEGA5.05 software (Tamura et al., 2011). The aligned sequences were corrected manually if necessary and best fit model was chosen for cladogram analysis.

Results

Detection of *Wolbachia* in RPW

According to our PCR results, all four *Wolbachia* SPs (*wsp*81F-*wsp*691R, *wsp*F-*wsp*R, *wsp*1-*wsp*2 and *fts*F-*fts*R) yielded negative results except for the positive control as shown in *Table 4*. Based on these results, we comprehensively rejected the hypothesis of the presence of this endosymbiont in field-collected, or lab-reared RPW samples (egg, larvae, pupa, and adult) and concluded that RPW is not naturally infected by *Wolbachia* sp. (*Table 4*). On the other hand, bacterial universal primer (27F, 1492R) showed visible bands (≈1400 bp) on agarose gel across the all tested life stages (*Table 4*) except for the negative control which shows the purity of DNA isolated from all targeted specimens. Contrary with above assumptions, all four *Wolbachia* SPs including *Wolbachia* outer surface protein (*wsp*) and filamenting temperature sensitive mutant Z protein (*ftsZ*) genes were used against positive control (*S. furcifera*) yielded ≈600 bp and ≈750 bp respectively after running on 1% agarose gel electrophoresis (*Table 4*). To ensure the authenticity of targeted regions of *wsp* and *ftsZ* genes from positive control were blasted against NCBI database and the results demonstrated the same sequence fragments under the accession numbers of FJ713766 and JN560721 respectively. Visible fragments only in positive control indicates the integrity of DNA.

Table 4. *Wolbachia* infected (+) or uninfected (-) diagnostic PCR results against laboratory reared and field collected specimens of red palm weevil (RPW), *Rynchophorus ferrugineus* (Curculionidae) with four pairs of *Wolbachia* SPs and one pair of universal BP

	Sample	Universal BP	<i>Wolbachia</i> SPs			
		27F 1492R	wsp81 F wsp691R	wspF wspR	wsp1 wsp2	ftsF ftsR
Laboratory reared	LE	+	-	-	-	-
	LL	+	-	-	-	-
	LP	+	-	-	-	-
	LM	+	-	-	-	-
	LF	+	-	-	-	-
Field collected	HM	+	-	-	-	-
	HF	+	-	-	-	-
	GM	+	-	-	-	-
	GF	+	-	-	-	-
	SM	+	-	-	-	-
	SF	+	-	-	-	-
	LogM	+	-	-	-	-
	Logf	+	-	-	-	-
	XM	+	-	-	-	-
	XF	+	-	-	-	-
	FF	+	-	-	-	-
	ZM	+	-	-	-	-
	ZF	+	-	-	-	-
	NM	+	-	-	-	-
	NF	+	-	-	-	-
NC	-	N/A	N/A	N/A	N/A	
PC	N/A	+	+	+	+	

SPs: specific primers; BP: bacterial primer; N/A: not applied; NC: negative control; PC: positive control

Phylogenetic relationship of previously described Wolbachia strains from order Coleoptera

Wolbachia is widely distributed in Coleopteran insects and majority of weevil species have been reported *Wolbachia* infected which are taxonomically closely related to RPW. However, in our PCR assay, we were unable to detect the presence of *Wolbachia* sp. in RPW. Total length of alignments were ≈ 600 bp for 26 *wsp* and ≈ 750 bp for 10 *ftsZ* gene sequences were used to construct phylogenetic tree, while 3 weevils (*Otiorhynchus sulcatus*, *Hypera postica*, *Rhinocyllus conicus*) (Table 1), we were unable to find their *Wolbachia* sequence from NCBI database. We construct a phylogenetic relationship between previously identified *Wolbachia* strains in closely related coleopterans species with RPW in order to understand the future of *Wolbachia* transfection into RPW and exploit it in pest management. *Wolbachia* strains were named after the host insect species, and the GeneBank accession number are listed as well (Fig. 3).

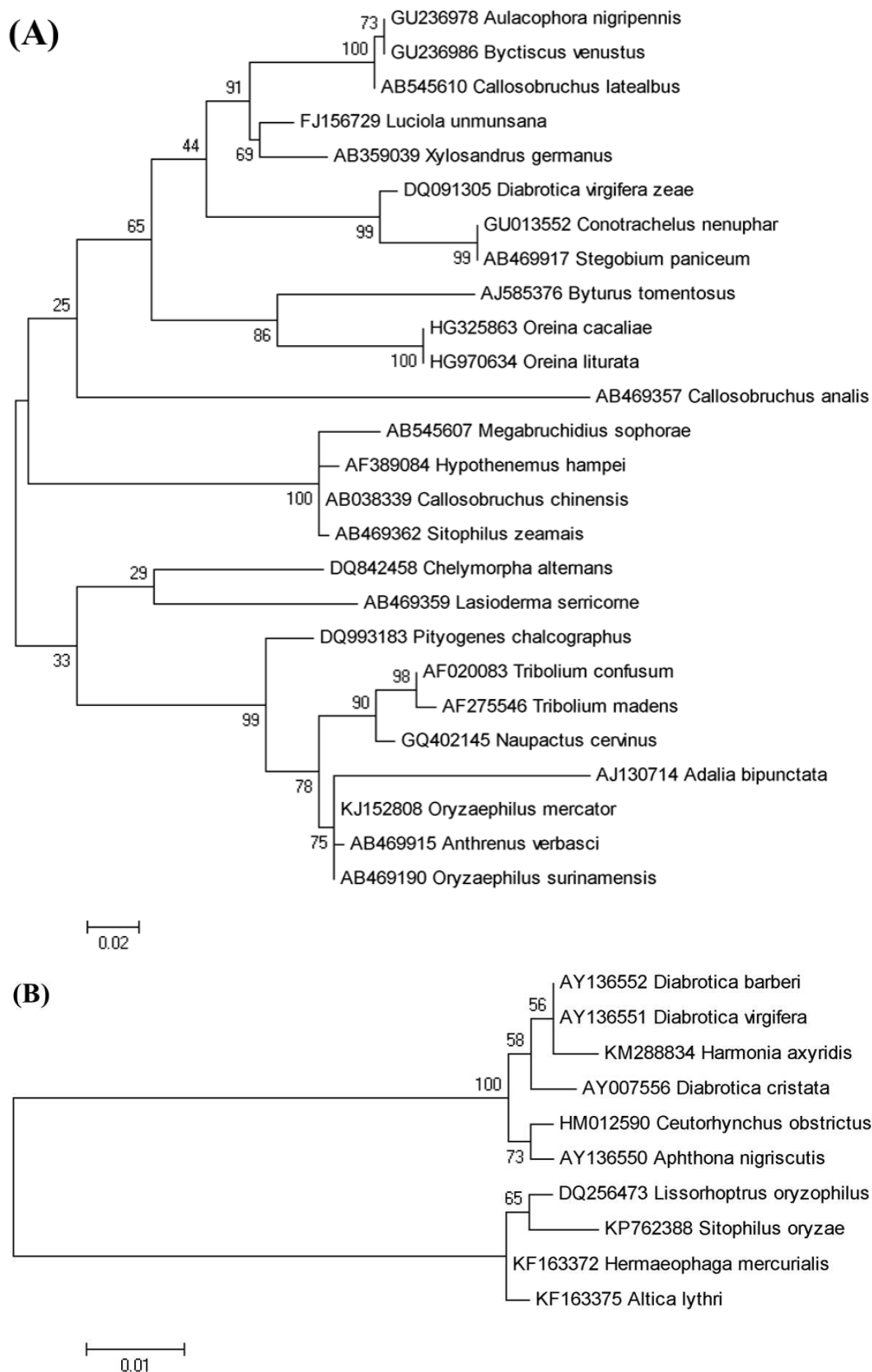


Figure 3. Maximum likelihood (ML) phylogenetic tree of previously reported *Wolbachia* positive individuals in coleopteran insects based on *wsp* (A) and *ftsZ* (B) gene sequences. Bootstrap values shown next to nodes are based on 1000 replicates

Discussion

Numerous invertebrates harbor endosymbiotic microorganisms, including terrestrial isopods (Rigaud et al., 2001), mites (Breeuwer and Jacobs, 1996), and all major orders of insects (Werren et al., 2000). Every insect species has its own set of endosymbiotic species that can vary greatly, even within the same insect species. The variation depends on factors such as sex, life stage, biotype, and geographic location (Pan et al., 2012). *Wolbachia* is one of the widespread ubiquitous intracellular bacterial symbionts that have evolved several phenotypic strategies (male killing, parthenogenesis, feminization and cytoplasmic incompatibility) to manipulate the reproductive system of the various insect, nematodes, crustacean etc.

In various weevils, these endosymbionts are broadly investigated and reported to have extremely interdependent associations like in *Nardonella* and many members of Dryophthoridae. For example, West Indian sweet potato weevil, *Euscepes postfasciatus* (Fairmaire), when endosymbionts were removed through the utilization of antibiotics, its structure, size, body weight, and developmental rate was significantly reduced (Kuriwada et al., 2010). *Wolbachia* were reported from ≈ 30 weevils (Lachowska et al., 2010) so far which is quite a large number as its abundance. However, as a whole, current knowledge of the bacterial communities and their associations with natural hosts are still limited. In the context of *Wolbachia* importance as a bio-control agent and broad existence in all arthropods especially in Coleopteran insects, we planned a study to unravel the question about the presence of *Wolbachia* sp. in RPW. Furthermore, to improve our previous knowledge about the existence of *Wolbachia* in weevils, we compiled up to date known *Wolbachia*-inherited weevils in this study. Based on our results, we confirmed that *Wolbachia* is not present in both laboratory reared and field collected specimens of RPW in any developmental stage. A PCR assay based study was conducted by Bordenstein et al. (2003) in a diverse set of nonfilariid species and the results demonstrated the absence of *Wolbachia* in Nonfilariid Nematodes which is quite similar to our study conclusion. Other studies such as Voronin et al. (2015), McNulty et al. (2012) are also in line with our results. There could be several possible reasons such as co-evolution, stochasticity (Jansen et al., 2008), fitness costs incurred by infection (Sarakatsanou et al., 2011; Suh et al., 2013; Dykstra et al., 2014), high temperature, (Clancy et al., 1998), imperfect maternal transmission and/or agricultural application of bactericide (McManus et al., 2002), high host specificity all are behind the absence of *Wolbachia* in RPW but without any authentic surveys all explanation remains possibilities which still need to be determined.

The congruence of *Wolbachia* sp. with filariid dated back to about 100 million years suggesting that *Wolbachia* sp. has coevolved with the host organism and became an integral organ of the host (Casiraghi et al., 2001). Lo et al. (2002) has suggested that *Wolbachia* sp. are highly host specific. However, recent studies have shown that this can be cultured in vitro as well as can be injected and manipulated in other non-host organisms which not only infects host soma but also infects somatic tissue and maintain this infection into various generation (stock populations of *Drosophila melanogaster*) after initial injections of *Wolbachia* sp. Transfection of *Wolbachia* sp. from naturally infected host to non-host organism such as RPW would open new avenues for developing an effective bio-control strategy against this devastating pest of palm trees.

Conclusion and future prospects

Wolbachia species are widely distributed in arthropods, mites, terrestrial isopods and all major insect orders particularly in Coleopteran insects. However, in this study, there is no evidence of *Wolbachia* presence in all tested developmental stages either laboratory reared or field collected specimens of RPW at any geographical locations of China. Therefore, on the basis of our results we concluded that *Wolbachia* sp. is not present in the population of RPW. Greater awareness, in combination with rapidly expanding knowledge base of *Wolbachia* (particularly in the areas of genomics, cell biology and molecular biology) and comparable endosymbionts, offers new directions for incorporating them in bio-control programs. The capacity of *Wolbachia* that cause CI in arthropod species has created interest in their use as a mechanism to drive desirable traits (for example resistance to disease) into insect vector populations. The use of *Wolbachia* infected males is also being developed as a mechanism to decrease pest populations by inducing elevated CI, similar to the use of sterile male programs to control pest insects. However, incorporation of *Wolbachia* in biocontrol research strategies may be restricted by technical challenges. For example, infections can be manipulated by elimination, transfection or genetic modification. The former has been achieved in many cases, transfection has been accounted less frequently, and genetic modification has yet to be achieved. However, given advances in recent years, we are optimistic that results of ongoing and future research will expand opportunities to use *Wolbachia* and similar endosymbiotic bacteria in bio-control programs.

Acknowledgements. We are very grateful to the grant from the National Key R & D Program of China (2017YFC1200605) and Fujian Science and Technology Special Project (2017NZ0003-1-6).

Conflict of interest. The authors declare to have no potential conflicts of interests.

REFERENCES

- [1] Ali, H., Hou, Y., Tang, B., Shi, Z., Huang, B., Muhammad, A., Sanda, N. B. (2016): A way of reproductive manipulation and biology of *Wolbachia pipientis*. – Journal of Experimental Biology and Agricultural Sciences 4: 156-168.
- [2] Ali, H., Muhammad, A., Hou, Y. (2018): Infection density dynamics and phylogeny of *Wolbachia* associated with coconut hispine beetle, *Brontispa longissima* (Gestro) (Coleoptera: Chrysomelidae) by multilocus sequence type (MLST) genotyping. – Journal of Microbiology and Biotechnology (In press).
- [3] Avtzis, D. N., Arthofer, W., Stauffer, C. (2008): Sympatric occurrence of diverged mtDNA lineages of *Pityogenes chalcographus* (Coleoptera, Scolytinae) in Europe. – Biological Journal of the Linnean Society 94: 331-340.
- [4] Baldo, L., Hotopp, J. C. D., Jolley, K. A., Bordenstein, S. R., Biber, S. A., Choudhury, R. R., Hayashi, C., Maiden, M. C., Tettelin, H., Werren, J. H. (2006): Multilocus sequence typing system for the endosymbiont *Wolbachia pipientis*. – Applied and Environmental Microbiology 72: 7098-7110.
- [5] Blagrove, M. S., Arias-Goeta, C., Failloux, A. B., Sinkins, S. P. (2012): *Wolbachia* strain wMel induces cytoplasmic incompatibility and blocks dengue transmission in *Aedes albopictus*. – Proceedings of the National Academy of Sciences 109: 255-260.
- [6] Bordenstein, S. R. (2003): Symbiosis and the origin of species. – Insect Symbiosis 1: 347.
- [7] Bordenstein, S. R., Fitch, D. H., Werren, J. H. (2003): Absence of *Wolbachia* in nonfilariid nematodes. – Journal of Nematology 35: 266.

- [8] Breeuwer, J., Jacobs, G. (1996): *Wolbachia*: intracellular manipulators of mite reproduction. – *Experimental and Applied Acarology* 20: 421-434.
- [9] Campbell, B. C., Bragg, T. S., Turner, C. E. (1992): Phylogeny of symbiotic bacteria of four weevil species (Coleoptera: Curculionidae) based on analysis of 16S ribosomal DNA. – *Insect Biochemistry and Molecular Biology* 22: 415-421.
- [10] Casiraghi, M., Favia, G., Cancrini, G., Bartoloni, A., Bandi, C. (2001): Molecular identification of *Wolbachia* from the filarial nematode *Mansonella ozzardi*. – *Parasitology Research* 87: 417-420.
- [11] Chen, S. J., Lu, F., Cheng, J. A., Jiang, M. X., Way, M. O. (2012): Identification and biological role of the endosymbionts *Wolbachia* in rice water weevil (Coleoptera: Curculionidae). – *Environmental Entomology* 41: 469-477.
- [12] Clancy, D. J., Hoffmann, A. A. (1998): Environmental effects on cytoplasmic incompatibility and bacterial load in *Wolbachia*-infected *Drosophila simulans*. – *Entomologia Experimentalis et Applicata* 86: 13-24.
- [13] Clark, T. L., Meinke, L. J., Skoda, S. R., Foster, J. E. (2001): Occurrence of *Wolbachia* in selected diabroticite (Coleoptera: Chrysomelidae) beetles. – *Annual Entomological Society of America* 94: 877-885.
- [14] Dedeine, F., Bouletreau, M., Vavre, F. (2005): *Wolbachia* requirement for oogenesis: occurrence within the genus *Asobara* (Hymenoptera, Braconidae) and evidence for intraspecific variation in *A. tabida*. – *Heredity* 95: 394-400.
- [15] Dykstra, H. R., Weldon, S. R., Martinez, A. J., White, J. A., Hopper, K. R., Heimpel, G. E., Asplen, M. K., Oliver, K. M. (2014): Factors limiting the spread of the protective symbiont *Hamiltonella defensa* in *Aphis craccivora* aphids. – *Applied and Environmental Microbiology* 80: 5818-5827.
- [16] Fenn, K., Blaxter, M. (2004): Are filarial nematode *Wolbachia* obligate mutualist symbionts?. – *Trends in Ecology and Evolution* 19: 163-166.
- [17] Fenn, K., Conlon, C., Jones, M., Quail, M. A., Holroyd, N. E., Parkhill, J., Blaxter, M. (2006): Phylogenetic relationships of the *Wolbachia* of nematodes and arthropods. – *PLoS Pathogens* 2: e94.
- [18] Fialho, R. F., Stevens, L. (2000): Male-killing *Wolbachia* in a flour beetle. – *Proceedings of the Royal Society of London. Series B* 267: 1469-1473.
- [19] Floate, K. D., Coghlin, P. C., Dossdall, L. (2011): A test using *Wolbachia* bacteria to identify Eurasian source populations of cabbage seedpod weevil, *Ceutorhynchus obstrictus* (Marsham), in North America. – *Environmental Entomology* 40: 818-823.
- [20] Gazla, I., Carracedo, M. (2009): Effect of intracellular *Wolbachia* on interspecific crosses between *Drosophila melanogaster* and *Drosophila simulans*. – *Genetics and Molecular Research* 8: 861-869.
- [21] Giordano, R., Jackson, J. J., Robertson, H. M. (1997): The role of *Wolbachia* bacteria in reproductive incompatibilities and hybrid zones of *Diabrotica* beetles and *Gryllus* crickets. – *Proceedings of the National Academy of Sciences* 94: 11439-11444.
- [22] Goryacheva, I., Blekhman, A., Andrianov, B., Gorelova, T., Zakharov, I. (2015): Genotypic diversity of *Wolbachia pipientis* in native and invasive *Harmonia axyridis* Pall., 1773 (Coleoptera, Coccinellidae) populations. – *Russian Journal of Genetics* 51: 731-736.
- [23] Hilgenboecker, K., Hammerstein, P., Schlattmann, P., Telschow, A., Werren, J. H. (2008): How many species are infected with *Wolbachia*? A statistical analysis of current data. – *FEMS Microbiology Letters* 281: 215-220.
- [24] Hosokawa, T., Koga, R., Kikuchi, Y., Meng, X. Y., Fukatsu, T. (2010): *Wolbachia* as a bacteriocyte-associated nutritional mutualist. – *Proceedings of the National Academy of Sciences* 107: 769-774.
- [25] Howard, F. W., Giblin-Davis, R., Moore, D., Abad, R. G. (2001): *Insects on Palms*. – CABI, Wallingford, UK.

- [26] Hurst, G. D., Jiggins, F. M., von der Schulenburg, J. H. G., Bertrand, D., West, S. A., Goriacheva, I. I., Zakharov, I. A., Werren, J. H., Stouthamer, R., Majerus, M. E. (1999): Male-killing *Wolbachia* in two species of insect. – Proceedings of the Royal Society of London. Series B 266: 735-740.
- [27] Iwase, S., Tani, S., Saeki, Y., Tuda, M., Haran, J., Skuhrovec, J., Takagi, M. (2015): Dynamics of infection with *Wolbachia* in *Hypera postica* (Coleoptera: Curculionidae) during invasion and establishment. – Biological Invasions 17: 3639-3648.
- [28] Jackel, R., Mora, D., Dobler, S. (2013): Evidence for selective sweeps by *Wolbachia* infections: phylogeny of *Altica* leaf beetles and their reproductive parasites. – Molecular Ecology 22: 4241-55.
- [29] Jansen, V. A. A., Turelli, M., Godfray, H. C. J. (2008): Stochastic spread of *Wolbachia*. – Proceedings of the Royal Society of London. Series B 275: 2769-2776.
- [30] Jeong, G., Kang, T., Park, H., Choi, J., Hwang, S., Kim, W., Choi, Y., Lee, K., Park, I., Sim, H. (2009): *Wolbachia* infection in the Korean endemic firefly, *Luciola unimunsana* (Coleoptera: Lampyridae). – Journal of Asia-Pacific Entomology 12: 33-36.
- [31] Jiggins, F. M., Hurst, G. D., Schulenburg, J. H. G., Majerus, M. E. (2001): Two male-killing *Wolbachia* strains coexist within a population of the butterfly *Acraea encedon*. – Heredity 86: 161-166.
- [32] Kaakeh, W., Khamis, A., Aboul-Nour, M. M. (2001): The Red Palm Weevil: the Most Dangerous Agricultural Pest, pp. 90-165. – United Arab Emirates University Press, Dubai.
- [33] Kageyama, D., Narita, S., Imamura, T., Miyanoshita, A. (2010): Detection and identification of *Wolbachia* endosymbionts from laboratory stocks of stored-product insect pests and their parasitoids. – Journal of Stored Products Research 46: 13-19.
- [34] Kambris, Z., Cook, P. E., Phuc, H. K., Sinkins, S. P. (2009): Immune activation by life-shortening *Wolbachia* and reduced filarial competence in mosquitoes. – Science 326: 134-136.
- [35] Kawasaki, Y., Ito, M., Miura, K., Kajimura, H. (2010): Superinfection of five *Wolbachia* in the alnus ambrosia beetle, *Xylosandrus germanus* (Blandford) (Coleoptera: Curculionidae). – Bulletin of Entomological Research 100: 231-239.
- [36] Kondo, N. I., Tuda, M., Toquenaga, Y., Lan, Y. C., Buranapanichpan, S., Horng, S. B., Shimada, M., Fukatsu, T. (2011): *Wolbachia* infections in world populations of bean beetles (Coleoptera: Chrysomelidae: Bruchinae) infesting cultivated and wild legumes. – Zoological Science 28: 501-508.
- [37] Kuriwada, T., Hosokawa, T., Kumano, N., Shiromoto, K., Haraguchi, D., Fukatsu, T. (2010): Biological role of *Nardonella* endosymbiont in its weevil host. – PloS One 5: e13101.
- [38] Lachowska, D., Kajtoch, L., Knutelski, S. (2010): Occurrence of *Wolbachia* in central European weevils: correlations with host systematics, ecology, and biology. – Entomologia Experimentalis et Applicata 135: 105-118.
- [39] Li, Y., Zeng-Rong, Z., Ruiting, J., Lian-Sheng, W. (2009): The red palm weevil, *Rynchophorus ferrugineus* (Coleoptera: Curculionidae), newly reported from Zhejiang, China and update of geographical distribution. – Florida Entomologist 92: 386-387.
- [40] Li, Y. Y., Fields, P., Pang, B. P., Coghlin, P., Floate, K. (2015): Prevalence and diversity of *Wolbachia* bacteria infecting insect pests of stored products. – Journal of Stored Products Research 62: 93-100.
- [41] Lo, N., Casiraghi, M., Salati, E., Bazzocchi, C., Bandi, C. (2002): How many *Wolbachia* supergroups exist? – Molecular Biology and Evolution 19: 341-346.
- [42] Malloch, G., Fenton, B. (2005): Super-infections of *Wolbachia* in byturid beetles and evidence for genetic transfer between A and B super-groups of *Wolbachia*. – Molecular Ecology 2: 627-637.

- [43] Malumphy, C., Moran, H. (2009): Red palm weevil, *Rhynchophorus ferrugineus*. Plant pest factsheet. – www.fera.defra.gov.uk/plants/publications/documents/factsheets/redPalmWeevil.pdf (accessed 7 June 2011).
- [44] McManus, P. S., Stockwell, V. O., Sundin, G. W., Jones, A. L. (2002): Antibiotic use in plant agriculture. – *Annual Review Phytopathology* 40: 443-465.
- [45] McNulty, S. N., Fischer, K., Mehus, J. O., Vaughan, J. A., Tkach, V. V., Weil, G. J., Fischer, P. U. (2012): Absence of *Wolbachia* endobacteria in *Chandlerella quiscalii*, an avian filarial parasite. – *Journal of Parasitology*: 98(2): 382-387.
- [46] Miller, W. J., Ehrman, L., Schneider, D. (2010): Infectious speciation revisited: impact of symbiont-depletion on female fitness and mating behavior of *Drosophila paulistorum*. *PLoS Pathogens*. – 6: e1001214.
- [47] Ming, Q. L., Shen, J. F., Cheng, C., Liu, C. M., Feng, Z. J. (2015): *Wolbachia* infection dynamics in *Tribolium confusum* (Coleoptera: Tenebrionidae) and their effects on host mating behavior and reproduction. – *Journal of Economic Entomology* 108: 1408-1415.
- [48] Montagna, M., Chouaia, B., Sacchi, L., Porretta, D., Martin, E., Giorgi, A., Lozzia, G. C., Epis, S. (2014): A new strain of *Wolbachia* in an Alpine population of the viviparous *Oreina cacaliae* (Coleoptera: Chrysomelidae). – *Environmental Entomology* 43: 913-922.
- [49] Murphy, S., Briscoe, B. (1999): The red palm weevil as an alien invasive: biology and the prospects for biological control as a component of IPM. – *Biocontrol News and Information* 20: 35-46.
- [50] Negri, I., Pellicchia, M., Mazzoglio, P., Patetta, A., Alma, A. (2006): Feminizing *Wolbachia* in *Zyginidia pullula* (Insecta, Hemiptera), a leafhopper with an XX/X0 sex-determination system. – *Proceedings of the Royal Society of London. Series B* 273: 2409-2416.
- [51] Oberprieler, R. G., Marvaldi, A. E., Anderson, R. S. (2007): Weevils, weevils, weevils everywhere. – *Zootaxa* 1668: 491-520.
- [52] Osborne, S. E., Iturbe-Ormaetxe, I., Brownlie, J. C., O'Neill, S. L., Johnson, K. N. (2012): Antiviral protection and the importance of *Wolbachia* density and tissue tropism in *Drosophila simulans*. – *Applied and Environmental Microbiology* 78: 6922-6929.
- [53] Pan, H., Li, X., Ge, D., Wang, S., Wu, Q., Xie, W., Jiao, X., Chu, D., Liu, B., Xu, B. (2012): Factors affecting population dynamics of maternally transmitted endosymbionts in *Bemisia tabaci*. – *PloS One* 7: e30760.
- [54] Poinot, D., Charlat, S., Mercot, H. (2003): On the mechanism of *Wolbachia*-induced cytoplasmic incompatibility: Confronting the models with the facts. – *Bioessays* 25: 259-265.
- [55] Hou, Y., Weng, Z. (2010): Temperature-dependent development and life table parameters of *Octodonta nipae* (Coleoptera: Chrysomelidae). – *Environmental Entomology* 39: 1676-1684.
- [56] Pu, Y. C., Hou, Y. M. (2016): Isolation and identification of bacterial strains with insecticidal activities from *Rhynchophorus ferrugineus* Oliver (Coleoptera: Curculionidae). – *Journal of Applied Entomology* 140: 617-626.
- [57] Rigaud, T. (1997): Inherited Microorganisms and Sex Determination of Arthropod Hosts. – In: O'Neill, S. L., Hoffmann, A. A., Werren, J. H. (eds.) *Influential Passengers: Inherited Microorganisms and Arthropod Reproduction*, pp. 81-102. – Oxford University Press, Oxford.
- [58] Rigaud, T., Pennings, P., Juchault, P. (2001): *Wolbachia* bacteria effects after experimental interspecific transfers in terrestrial isopods. – *Journal of Invertebrate Pathology* 77: 251-257.
- [59] Rodriguero, M., Confalonieri, V., Guedes, J., Lanteri, A. (2010): *Wolbachia* infection in the tribe Naupactini (Coleoptera, Curculionidae): association between thelytokous parthenogenesis and infection status. – *Insect Molecular Biology* 19: 631-640.

- [60] Roehrdanz, R., Levine, E. (2007): *Wolbachia* bacterial infections linked to mitochondrial DNA reproductive isolation among populations of northern corn rootworm (Coleoptera: Chrysomelidae). – Annual Entomological Society of America 100: 522-531.
- [61] Roehrdanz, R., Olson, D., Bouchier, R., Sears, S., Cortilet, A., Fauske, G. (2006): Mitochondrial DNA diversity and *Wolbachia* infection in the flea beetle *Aphthona nigriscutis* (Coleoptera: Chrysomelidae): an introduced biocontrol agent for leafy spurge. – Biological Control 37: 1-8.
- [62] Sarakatsanou, A., Diamantidis, A. D., Papanastasiou, S. A., Bourtzis, K., Papadopoulos, N. T. (2011): Effects of *Wolbachia* on fitness of the Mediterranean fruit fly (Diptera: Tephritidae). – Journal of Applied Entomology 135: 554-563.
- [63] Son, Y., Luckhart, S., Zhang, X., Lieber, M. J., Lewis, E. E. (2008): Effects and implications of antibiotic treatment on *Wolbachia*-infected vine weevil (Coleoptera: Curculionidae). – Agricultural and Forest Entomology 10: 147-155.
- [64] Stouthamer, R., Breeuwer, J. A., Hurst, G. D. (1999): *Wolbachia pipientis*: microbial manipulator of arthropod reproduction. – Annual Reviews in Microbiology 53: 71-102.
- [65] Suh, E., Dobson, S. L. (2013): Reduced competitiveness of *Wolbachia* infected *Aedes aegypti* larvae in intra- and interspecific immature interactions. – Journal of Invertebrate Pathology 114: 173-177.
- [66] Tagami, Y., Miura, K. (2004): Distribution and prevalence of *Wolbachia* in Japanese populations of Lepidoptera. – Insect Molecular Biology 13: 359-364.
- [67] Tamura, K., Peterson, D., Peterson, N., Stecher, G., Nei, M., Kumar, S. (2011): MEGA5: molecular evolutionary genetics analysis using maximum likelihood, evolutionary distance, and maximum parsimony methods. – Molecular Biology and Evolution 28: 2731-2739.
- [68] Vega, F. E., Benavides, P., Stuart, J. A., O'Neill, S. L. (2002): *Wolbachia* infection in the coffee berry borer (Coleoptera: Scolytidae). – Annual Entomological Society of America 95: 374-378.
- [69] Voronin, D., Abeykoon, A. M., Gunawardene, Y. S., Dassanayake, R. S. (2015): Absence of *Wolbachia* endobacteria in Sri Lankan isolates of the nematode parasite of animals *Setaria digitata*. – Veterinary Parasitology 207(3-4): 350-354.
- [70] Werren, J. H., Windsor, D. M. (2000): *Wolbachia* infection frequencies in insects: evidence of a global equilibrium?. – Proceedings of the Royal Society of London. Series B 267: 1277-1285.
- [71] Zhang, X., Luckhart, S., Tu, Z., Pfeiffer, D. G. (2010): Analysis of *Wolbachia* strains associated with *Conotrachelus nenuphar* (Coleoptera: Curculionidae) in the eastern United States. – Environmental Microbiology 39: 396-405.
- [72] Zhou, W., Rousset, F., O'Neill, S. (1998): Phylogeny and PCR-based classification of *Wolbachia* strains using *wsp* gene sequences. – Proceedings of the Royal Society of London. Series B 265: 509-515.
- [73] Zug, R., Hammerstein, P. (2012): Still a host of hosts for *Wolbachia*: analysis of recent data suggests that 40% of terrestrial arthropod species are infected. – PloS one 7: e38544.

PLANT TRAITS AND BIOMASS ALLOCATION OF *GENTIANA HEXAPHYLLA* ON DIFFERENT SLOPE ASPECTS AT THE EASTERN MARGIN OF QINGHAI-TIBET PLATEAU

XUE, J.^{1,2} – HE, J.^{1,2} – WANG, L.^{1,3} – GAO, J.^{1,4} – WU, Y.^{1*}

¹Chengdu Institute of Biology, Chinese Academy of Sciences, Chengdu 610041, China

²University of Chinese Academy of Sciences, Beijing 100049, China

³ABA Teachers University, Wenchuan 623002, China

⁴East China Normal University, Shanghai 200241, China

*Corresponding author

e-mail: wuyan@cib.ac.cn; phone: +86-28-8289-0511; fax: +86-28-8289-0511

(Received 14th Nov 2017; accepted 7th Mar 2018)

Abstract. The growth, biomass partitioning and reproduction of alpine *Gentiana hexaphylla* species in local microclimates have important ecological significance in the study of the adaptation strategies of alpine plants. At the eastern edge of the Qinghai-Tibet Plateau in China we set up eight sample positions surrounded by mountains at an altitude of 4000 m and subsequently transplanted and measured the indices of growth, biomass allocation and reproduction of *Gentiana hexaphylla* to investigate the adaptation strategies in different slope aspects. Our results showed that slope aspects significantly affected the survival and reproduction strategies of *Gentiana hexaphylla*. Plants growing on sunny slopes tend to reproduce sexually, and those growing on shady slope are inclined to reproduce asexually. Along the circumference of the mountain, from slope S to slope SW, the growth of plant height from the early vegetation stage to the full bloom stage showed a wave shape and biomass accumulation showed a “W”-like pattern. The adaption strategy of *Gentiana hexaphylla* has a stronger correlation with soil organic carbon, soil total nitrogen and phosphorus than with light intensity, soil annual temperature and soil water content. Our results will help to understand the physiological adaptation of *Gentiana hexaphylla* in different slope aspects and explore the rule of plant functions and character responses to various habitats, so as to reveal the life cycle strategy.

Keywords: *Gentiana hexaphylla*, slope aspect, adaption strategy, growth, biomass allocation, reproduction

Introduction

Alpine ecosystems, owing to their high altitude, high temperature differences around the clock, and highly varying and major abiotic factors, greatly affect the adaptation and evolution of plants. Ontogenetic modifications and modulation respond to the harsh alpine environment with a high degree of specialization through evolutionary adaptation (Körner, 2003). Embedded in different floras of the world, high mountains often bear greater biodiversity than those in their surrounding lowlands (Körner, 2003; Barthlott et al., 1996). Alpine plants can survive in extreme environments with different reproduction strategies to maintain the stabilization of populations (Stöcklin, 1992; Körner, 2003). Due to their extreme environmental conditions and high biodiversity, high mountain ecosystems are an ideal region for studying plant adaptations (Sun et al., 2014). Studying the growth traits, biomass allocation and reproduction of plants in severe environments is conducive to understanding the reasons for the biodiversity of high mountain ecosystems. As a typical fragile and sensitive ecosystem, plant structure

and functional trait responses to different habitats were helpful for understanding the mechanisms of plant adaptation to extreme environments and predicting vegetation change under the background of climate change (Schneider, 1993; IPCC, 2001).

Topography is a comprehensive indicator of habitat conditions that can create local microclimates (Cantón et al., 2004). As a vital topographic factor, slope aspect affects the daily cycle of solar radiation and has a strong influence on aspects of the microclimate, especially air and soil temperature, soil moisture and soil nutrition (Rosenberg et al., 1983; Fekedulegn et al., 2003; Auslander et al., 2003). Soil temperature and moisture significantly influence soil nutrient mineralization in different slope aspects (Sternberg and Shoshany, 2001; Ai et al., 2017). Previous studies found that the spatial variation in slope aspect was a determinant element for community structure, species diversity, ecosystem processes and plant functional traits (De Bello et al., 2006; Bennie et al., 2008; Carletti et al., 2009). Along the circumference of the mountain, the spatial variation in slope aspect displays a natural habitat gradient. Due to the complexity of the ecological environment and the specialization of alpine plants, it is important to conduct research on different slope aspects in alpine ecosystems.

Plants inhabiting harsh environments have evolved highly specialized phenological, morphological and physiological mechanisms and structures (Caldwell, 1968, 1979; Nagy and Grabherr, 2009). Plant height (PH) and leaf number are indicators of plant interactions with their environment (Grassein et al., 2010), and biomass partitioning of plants drives carbon assimilation and nutrient absorption (Poorter et al., 2012). Specific leaf area (SLA) can show large variability in response to irradiance, temperature, and water availability (Pigliucci and Kolodynska, 2002; Poorter et al., 2009). Numerous studies have explored plant ecological adaptations and reproductive mechanisms (Ohba, 1988; He et al., 2005; Yang and Sun, 2006; Peng et al., 2012). Flower structure traits indicate the ability of sexual reproduction (Mcintosh, 2002), while the branch numbers of plants indicate the ability for asexual reproduction (He, 2017). Allometric theory has been used increasingly in the relationship between plant plasticity response and plant functional traits (Weiner, 2004; Bonser and Aarssen, 2009). The change in habitat conditions caused by slope aspect deeply affects plant growth rhythm; to understand how plant functional traits respond to the topographic environment, the important ecological factors must be identified by researching the allometric growth relationships among plant traits for plants growing in different slope aspects. There are many studies on the effects of elevation on plant adaptation, and several slope orientation studies have discussed the different effects of sunny vs shady slope position on alpine plant growth, but there is very little research concerning the effect of slope aspect along a continuous mountain level-curve ring. *Gentiana hexaphylla*, a perennial herbaceous species, grows well in the harsh alpine environment and distributed in all slope aspects around the mountains, but its growth differs. These plants reproduce both sexually and vegetatively from rhizomes (Bynum, 2001). At the same time, the flower of *Gentiana hexaphylla* was larger than that of other herbs at the sample sites, which was easy to observe. Different slope aspects are due mainly to the distribution of hydrothermal condition. There is a lack of research on the growth traits, biomass partitioning and reproduction of this taxon, and we have studied the effect of elevation (He et al., 2017) and now discuss the influence of slope aspects to make the research more systematic. We set 8 sites to investigate the different survival strategies on different slope aspects on a relatively isolated mountain. We proposed several hypotheses: (1) slope aspects significantly affected plant growth, biomass allocation and reproduction strategies; (2) along the

circumference of the mountain, the increasing of plant height and the increment of biomass from vegetation stage to full bloom stage were significantly affected by slope aspects; and (3) *Gentiana hexaphylla* grew on different slope aspects using different reproduction strategies to ensure the survival of individuals and the continuation of populations. Proposing these hypotheses will further our understanding of the physiological adaptive ability of *Gentiana hexaphylla* in different slope aspects and will clarify the patterns of responses to different habitats among plant traits.

Materials and methods

Site characteristics

The study area was located in Snow Ridge ($32^{\circ}44'42''\sim 32^{\circ}44'46''$ N, $103^{\circ}43'44''\sim 103^{\circ}43'49''$ E) in Songpan County, Sichuan Province, at the eastern edge of the Qinghai-Tibet Plateau in China (Figs. 1 and 2). The average altitude of the study area is 4,005~4,074 m. Snow Ridge belongs to the Minshan mountain system. The climate of the study area is characterized by a long winter and a short summer. This region has the typical humid and semi-humid continental monsoon climate of the plateau cold temperate zone. It has a warm rainy season, and the air temperature varies significantly from day to night. The zone has a mean annual temperature of 2.8°C and a mean month temperature from -7.6°C in January to 9.7°C in July, and there is no absolutely frost-free period. The mean annual solar radiation hours are 1827.5 h, and the average annual precipitation is 634.8 mm. The yearly accumulated temperature above 10°C is 428.6°C (Chen, 2011). The soil belongs to the mountain brown meadow group. Vegetation is the alpine meadow type (Chen, 2008).

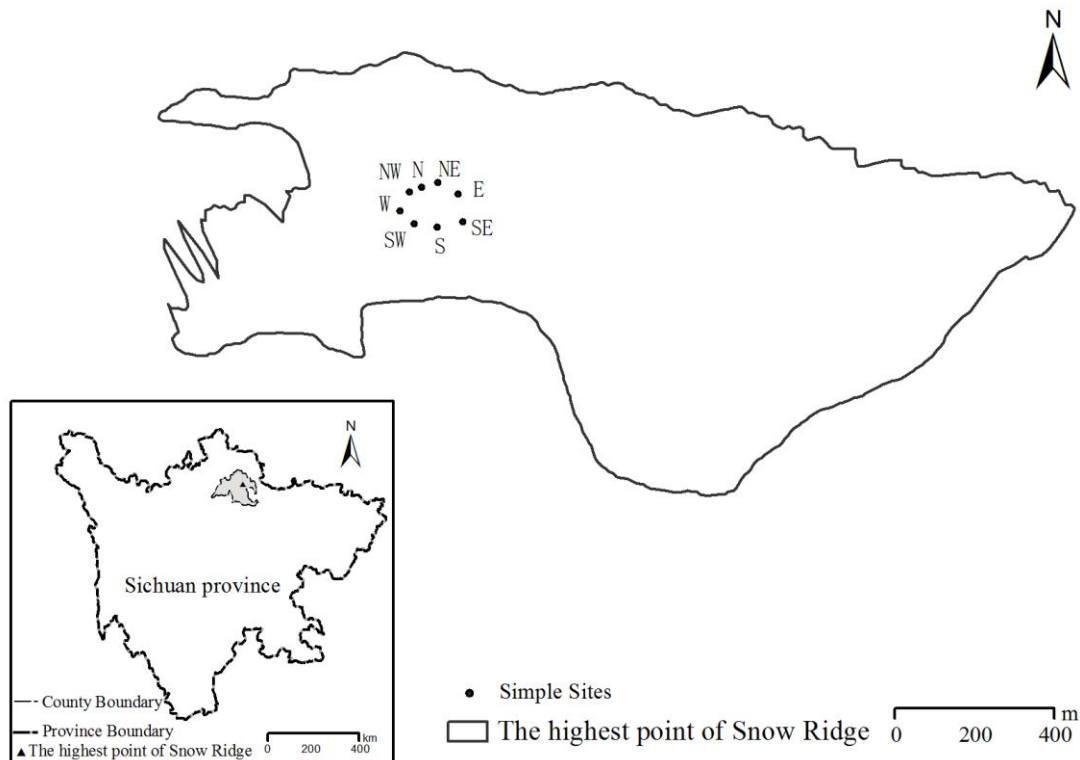


Figure 1. Map of the location of sample sites



Figure 2. Habitat photos

Materials

Gentiana hexaphylla, distributed in alpine meadows, grassland and roadside slopes (2700-4400 m), is a perennial herbaceous species that develops two or three flowering shoots and a single terminal flower on each flowering shoot. Roots are mostly slightly fleshy and fibrous. Stems are clustered, diffuse, obliquely ascending, and papillate. Basal rosette leaves are absent or poorly developed. The calyx tube is narrowly obconic and the corolla is blue with a pale yellow-white base and dark blue streaks. Stamens are inserted at the basal part of the corolla tube, and anthers are narrowly ellipsoid. Stigma lobes are oblong, and capsules are ovoid-ellipsoid. Seeds are light brown and ellipsoid to ovoid. The flowering and fruiting period lasts from July to September.

Experimental design

One relatively isolated mountain was selected as the area of study. We set up 8 sample positions as sites on the southern (S), southeast (SE), east (E), northeast (NE), northern (N), northwest (NW), west (W), and southwest (SW) slopes along the circumference of mountain. The target plants were selected and fixed beginning in May 2016 after the snow melt. We dug up the whole plant (complete with roots) along with the original soil (10 cm × 10 cm) to ensure that the target plant was located in the centre position. We chose 800 plants with similar heights that were growing well, and then moved and fixed them to the 8 sites (100 plants per transplant site). Plants were then placed in a ditch that was dug before the experiment. The surrounding soil was used to ensure that the sample plants were flush with the ground. The plant samples were fixed at 50 cm intervals for the follow-up experiment. The plants (*Gentiana hexaphylla*) were transplanted to each of the 8 sites according to the above method.

Sample collection and treatment in the laboratory

At the full bloom stage in 2017, 30 individual flowering plants were randomly selected from each of the 8 sites along the slope. Fresh leaf samples were scanned by a flatbed scanner (CanoScan5600F, Canon, Tokyo, Japan), and then Photoshop CS4 and Matlab 7.9 were used to calculate the leaf area (Vile et al., 2005). Each sample was placed in an oven at 65 °C and dried to constant weight, and dried samples were weighed with an electrical balance of 1/10000 g resolution. At each sample position, three transplantable original soil samples were taken and sieved (< 2 mm); roots and visible organic debris were removed by hand. Light intensity was measured by a digital illuminance meter (TES-1332A) at 10: 00 every day during the flower stage. The surface soil temperature (10 cm) was measured by an RTE (iButton-TMEX). Soil water

content was measured by the oven drying method. Approximately 100 g of each soil sample was air-dried for analysis of soil properties (e.g., C, N, and P). Soil organic carbon was determined by potassium dichromate oxidation (Allen, 1989). The total nitrogen was determined by the Kjeldahl method (Allen, 1989), and the vanadium molybdenum yellow colorimetric method was used for the determination of total phosphorus (Bao, 2000).

Statistical analysis

One-way ANOVA was used to compare the differences in soil water content, soil organic carbon, total nitrogen, total phosphorus, plant height, branch number, leaf number, specific leaf area and biomass of different plant structures among sample positions. Principal component analysis (PCA) was conducted to demonstrate the effects of abiotic factors on plant traits and biomass allocation. Figures were drawn using Origin 9.0. All statistical analyses were conducted using SPSS 19.0 (SPSS Inc., Chicago, IL, USA). Differences were considered significant when $P < 0.05$.

The relationships between aboveground biomass and belowground biomass, reproductive biomass and vegetative biomass, and photosynthetic biomass and non-photosynthetic biomass were analysed using the allometric model $y = ax^b$. The formula is expressed logarithmically as $\log y = \log a + b \log x$ (x and y represent biomass, a is a standardized constant, and b is the allometric growth index) (Niklas, 2005). Standardized major axis (SMA) slope-fitting techniques were used to calculate the slope (b) and intercept ($\log a$) of the allometric growth equation (Wright et al., 2001; Warton et al., 2006). The above analysis was conducted in SMART Version 2.

Results

Environmental factors of different slope aspects

The daily average temperature of increasing and decreasing temperature was higher on slopes S, SE, and SW than on slopes NW, NE, and N during the four stages of plant growth. Meanwhile, slopes E and W also showed a higher temperature than that on slopes NW, NE, and N (Fig. 3). There was no significant difference in light intensity among sites ($F = 0.776$, $p = 0.616$). The differences in mean annual temperature were significant ($F = 34.886$, $p < 0.001$). The mean annual temperature of slope E was significantly greater than those of the sunny slopes and slope W, while the temperatures of the sunny slopes and slope W were significantly greater than the temperatures of the shady slopes. There was a significant difference in soil water content among sites ($F = 4.445$, $p = 0.006$). Slope N had the highest soil water content (43.54%), but slope NW had the lowest (34.38%), and the difference was significant. At the same time, the soil water content of slope N was significantly higher than that of slopes S and E. There were significant differences in soil organic carbon (SOC), soil total nitrogen (STN), and soil total phosphorus (STP) among sites ($F = 4.919$, $p = 0.004$; $F = 4.826$, $p = 0.004$; $F = 8.859$, $p < 0.001$, respectively). Overall, the soil organic carbon, total nitrogen and phosphorus of slope W were the highest, and those of slope S were lowest (Table 1).

Morphological traits at the full bloom stage under different slope aspects

Plant height ($F = 4.909$, $P < 0.001$), branch number ($F = 2.231$, $P = 0.033$), specific leaf area ($F = 9.958$, $P < 0.001$) and leaf number ($F = 2.601$, $P = 0.013$) were

significantly different among sites. The plant heights on slopes S and E were remarkably higher than those on the other five slope aspects, except for slope NW. Branch number on slope N was the largest and significantly larger than those on slopes NW, NE, E and W. The specific leaf area on slope SW was significantly higher than those on the other slope aspects. The leaf number on slopes SW and NE were significantly greater than those on slopes NW and W (Fig. 4, Table 2).

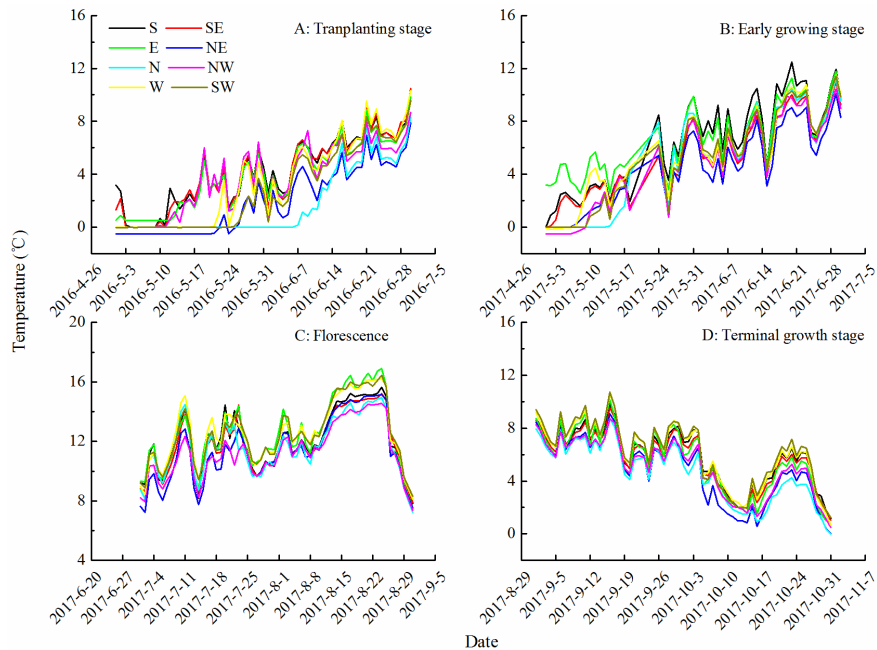


Figure 3. Daily mean soil temperature at sample position. A, B, C, and D represent the different stages of plant growth. S, SE, E, NE, N, NW, W, and SW represent the eight different slope aspects

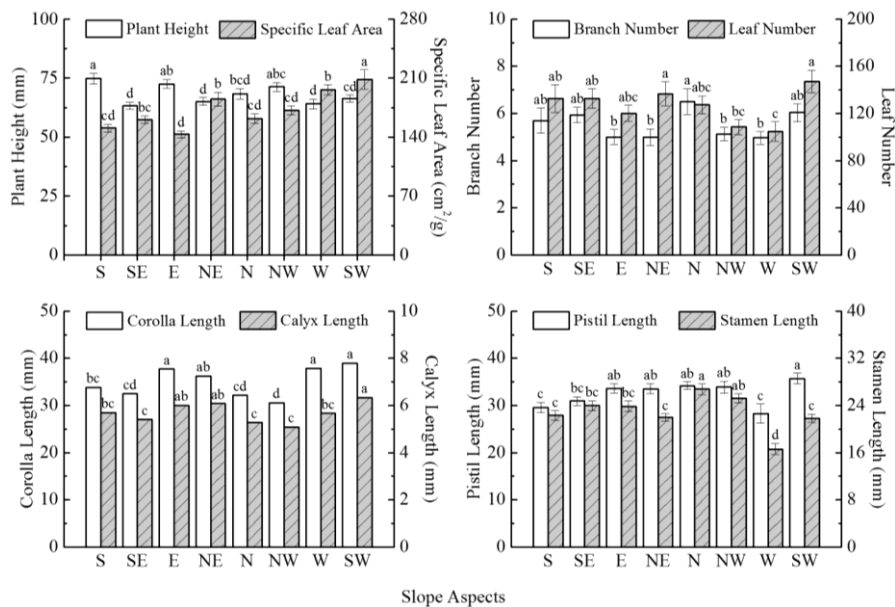


Figure 4. Plant height, specific leaf area, branch number, leaf number and flower traits on different slope aspects. The data were represent the mean \pm SE ($n = 30$)

Table 1. Comparison of environmental traits among different sampling sites

Sample position	Latitude and longitude	Altitude (m)	Light intensity (20 000 lux)	Mean annual temperature (°C)	Soil water content (%)	Soil organic carbon (g/kg)	Soil total nitrogen (g/kg)	Soil total phosphorus (g/kg)
S	N 32°44'42" E 103°43'47"	4074	975.00 ± 36.66	3.24 ± 0.04 ^b	38.81 ± 0.23 ^b	29.57 ± 0.46 ^d	2.69 ± 0.06 ^d	0.61 ± 0.01 ^d
SE	N 32°44'43" E 103°43'49"	4070	954.33 ± 46.00	3.06 ± 0.13 ^b	39.16 ± 3.02 ^{ab}	31.95 ± 2.94 ^{cd}	2.80 ± 0.22 ^{cd}	0.68 ± 0.04 ^{cd}
E	N 32°44'45" E 103°43'48"	4063	900.00 ± 84.66	3.59 ± 0.32 ^a	38.37 ± 1.39 ^{bc}	31.21 ± 1.08 ^{cd}	2.86 ± 0.11 ^{cd}	0.72 ± 0.02 ^{bc}
NE	N 32°44'46" E 103°43'47"	4050	894.33 ± 95.63	1.81 ± 0.00 ^d	40.48 ± 0.52 ^{ab}	33.66 ± 0.45 ^a	2.93 ± 0.07 ^{bcd}	0.66 ± 0.01 ^{cd}
N	N 32°44'46" E 103°43'45"	4005	884.00 ± 86.12	2.20 ± 0.24 ^c	43.54 ± 0.68 ^a	37.03 ± 0.90 ^{ab}	3.30 ± 0.07 ^{ab}	0.79 ± 0.02 ^{ab}
NW	N 32°44'45" E 103°43'44"	4010	848.00 ± 123.44	2.32 ± 0.01 ^c	34.38 ± 0.83 ^c	34.33 ± 1.08 ^{bc}	2.79 ± 0.12 ^{cd}	0.68 ± 0.04 ^{cd}
W	N 32°44'44" E 103°43'44"	4055	874.00 ± 126.48	3.00 ± 0.00 ^b	40.63 ± 0.59 ^{ab}	38.92 ± 0.67 ^a	3.38 ± 0.06 ^a	0.83 ± 0.02 ^a
SW	N 32°44'43" E 103°43'45"	4061	951.67 ± 62.01	3.09 ± 0.28 ^b	40.56 ± 1.14 ^{ab}	33.37 ± 1.57 ^{bcd}	3.16 ± 0.14 ^{abc}	0.82 ± 0.03 ^a
F			0.776	34.886	3.853	4.919	4.826	8.859
<i>p</i>			0.616	< 0.001	0.012	0.004	0.004	< 0.001

The data represent the mean ± SE (n = 3). Data with the same letters within the same column indicate no significant difference at the *p* < 0.05 level. The same below.

Table 2. Effects of slope aspect on plant height, branch number, specific leaf area, leaf number and flower traits

Slope aspect	Plant height (mm)	Branch number	Specific leaf area (cm ² g ⁻¹)	Leaf number	Corolla length (mm)	Calyx length (mm)	Pistil length (mm)	Stamen length (mm)
S	74.77 ± 2.30 ^c	5.70 ± 0.54 ^{ab}	150.72 ± 4.66 ^a	132.50 ± 11.77 ^a	33.87 ± 0.10 ^{bc}	5.70 ± 0.02 ^{bc}	29.59 ± 1.07 ^c	22.31 ± 0.81 ^c
SE	63.23 ± 1.58 ^{ab}	5.93 ± 0.33 ^{ab}	160.83 ± 4.23 ^{bc}	132.63 ± 8.29 ^b	32.46 ± 0.10 ^{cd}	5.40 ± 0.02 ^c	30.93 ± 0.96 ^{bc}	23.98 ± 0.84 ^{bc}
E	72.50 ± 1.90 ^{abc}	5.00 ± 0.31 ^b	143.35 ± 3.96 ^{bc}	120.17 ± 6.59 ^c	37.76 ± 0.09 ^a	6.01 ± 0.02 ^d	33.61 ± 0.98 ^{ab}	23.83 ± 0.91 ^{bc}
NE	65.03 ± 1.65 ^{bc}	5.00 ± 0.35 ^b	184.92 ± 8.38 ^c	136.67 ± 10.23 ^c	36.26 ± 0.09 ^{ab}	6.09 ± 0.01 ^{ab}	33.53 ± 1.06 ^{ab}	21.99 ± 0.58 ^c
N	68.30 ± 2.18 ^{abc}	6.50 ± 0.55 ^a	162.01 ± 5.38 ^{bc}	127.20 ± 7.78 ^c	32.16 ± 0.06 ^{cd}	5.28 ± 0.02 ^c	34.18 ± 0.84 ^{ab}	26.75 ± 0.91 ^a
NW	71.27 ± 1.84 ^a	5.13 ± 0.29 ^b	171.93 ± 5.13 ^{abc}	108.47 ± 6.21 ^c	30.55 ± 0.10 ^d	5.09 ± 0.02 ^c	33.87 ± 1.30 ^{ab}	25.19 ± 0.79 ^{ab}
W	64.04 ± 2.12 ^c	4.96 ± 0.27 ^b	196.09 ± 5.94 ^{ab}	104.67 ± 8.22 ^c	37.89 ± 0.09 ^a	5.67 ± 0.02 ^{bc}	28.28 ± 2.01 ^c	16.61 ± 0.94 ^d
SW	66.27 ± 1.57 ^{bc}	6.03 ± 0.38 ^{ab}	208.07 ± 11.64 ^a	147.17 ± 9.57 ^b	38.96 ± 0.10 ^a	6.33 ± 0.02 ^a	35.71 ± 1.13 ^a	21.83 ± 0.71 ^c
F	4.909	2.231	9.958	2.601	11.685	4.735	4.367	12.803
<i>p</i>	< 0.001	0.033	< 0.001	0.013	< 0.001	< 0.001	< 0.001	< 0.001

The data represent the mean ± SE (n = 30). Data with the same letters within the same column indicate no significant difference at the *p* < 0.05 level.

Corolla length ($F = 11.685$, $P < 0.001$), calyx length ($F = 4.735$, $P < 0.001$), pistil length ($F = 4.367$, $P < 0.001$) and stamen length ($F = 12.803$, $P < 0.001$) were significantly different among the eight slope aspects. The corolla length of plants grown on slope SW was the largest and was significantly greater than that of plants grown on slopes NE, S, SE, N and NW, the calyx length on slope SW was the largest and was significantly greater than that of that on slopes S, W, SE, N and NW; the pistil length on slope SW was significantly greater than that on slopes SE, S and W; and the stamen length on slopes N and NW were significantly greater than those on the other slopes (Table 2).

Biomass allocation of organs and allometric relationships on different slope aspects

Root biomass allocation was significantly different among the eight slope aspects ($F = 10.511$, $p < 0.001$); root biomass allocation on slopes W and N were significantly larger than that on other slope aspects. Stem biomass allocation was significantly different among the eight slope aspects ($F = 9.228$, $p < 0.001$); the stem biomass allocation on slopes S, SW and E were significantly greater than that on slopes NW, SE, N and W, and that on slope W was remarkably lower than those on the other slope aspects. Leaf biomass allocation did not remarkably among slope aspects ($F = 1.295$, $p = 0.254$). Flower biomass allocation was not significantly different among the eight slope aspects ($F = 1.390$, $p = 0.211$). The ratio of belowground biomass/aboveground biomass was significantly different among the eight slope aspects ($F = 16.165$, $p < 0.001$); the ratio on slope W was significantly larger than that on the other slope aspects, and the ratio on slope N was remarkably greater than that on slope S (Fig. 5, Table 3).

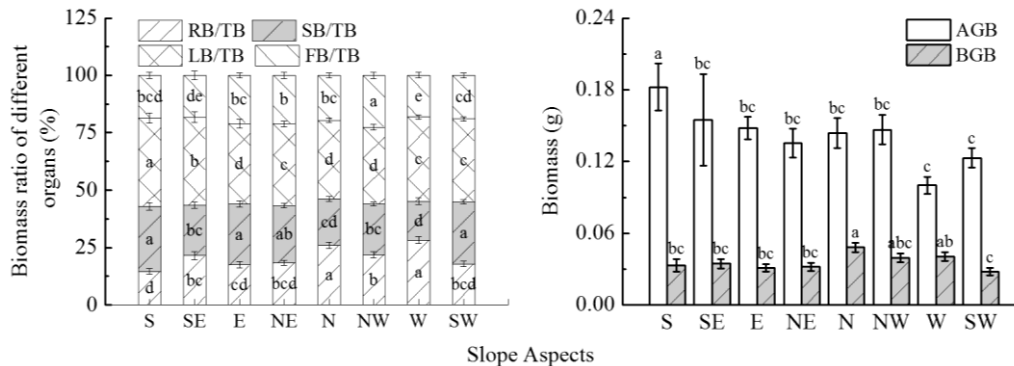


Figure 5. Biomass allocation on different slope aspects. RB/TB represents root biomass allocation, SB/TB represents stem biomass allocation, LB/TB represents leaf biomass allocation, FB/TB represents flower biomass allocation, AGB represents aboveground biomass, and BGB represents belowground biomass. The data represent the mean \pm SE ($n = 30$)

There was a significant difference in the belowground/aboveground biomass relationships among different slope aspects (WALD = 18.672, $p = 0.009$). The relationship between belowground and aboveground growth was allometric. There were no significant differences between reproductive/vegetative biomass relationships among different slope aspects (WALD = 8.564, $p = 0.267$). The allometric relationship among the 8 sites had a common slope of 1.007, which was not significantly different from 1 (chi square test: $\chi^2 = 0.015$, $p = 0.903$). The relationship between reproductive and vegetative growth was isometric. Further examination showed that the intercepts of

reproductive and vegetative biomass in different slopes were not significantly different, and there was no significant coaxial drift. There was a significant difference between photosynthetic/non-photosynthetic biomass relationships among the different slope aspects (WALD = 17.394, $p = 0.019$). The relationship between photosynthetic and non-photosynthetic growth was allometric (Table 4).

Table 3. Biomass allocation and root/shoot ratio of plants on different slope aspects

Sample	RB/TB	SB/TB	LB/TB	FB/TB	BGB/AGB
S	0.15 ± 0.01 ^d	0.28 ± 0.02 ^a	0.38 ± 0.02	0.19 ± 0.01	0.75 ± 0.07 ^e
SE	0.22 ± 0.02 ^{bc}	0.22 ± 0.01 ^{bc}	0.38 ± 0.02	0.18 ± 0.02	1.09 ± 0.11 ^{bc}
E	0.17 ± 0.01 ^{cd}	0.27 ± 0.01 ^a	0.35 ± 0.02	0.21 ± 0.01	0.69 ± 0.04 ^{de}
NE	0.18 ± 0.01 ^{bcd}	0.25 ± 0.01 ^{ab}	0.36 ± 0.01	0.21 ± 0.01	0.70 ± 0.11 ^{cde}
N	0.26 ± 0.01 ^a	0.20 ± 0.01 ^{cd}	0.34 ± 0.01	0.20 ± 0.01	1.38 ± 0.11 ^b
NW	0.22 ± 0.01 ^b	0.22 ± 0.01 ^{bc}	0.33 ± 0.01	0.23 ± 0.01	0.95 ± 0.13 ^{bcd}
W	0.28 ± 0.01 ^a	0.17 ± 0.02 ^d	0.37 ± 0.01	0.18 ± 0.01	1.49 ± 0.18 ^a
SW	0.18 ± 0.01 ^{bcd}	0.27 ± 0.01 ^a	0.36 ± 0.01	0.19 ± 0.01	0.65 ± 0.04 ^{de}
F	10.511	9.228	1.295	1.390	16.165
<i>p</i>	< 0.001	< 0.001	0.254	0.211	< 0.001

RB/TB, SB/TB, LB/TB, and FB/TB represent root, stem, leaf, and flower biomass partitioning, respectively. BGB/AGB represents aboveground/belowground biomass. The data represent the mean ± SE (n = 30). Data with the same letters within the same column indicate a not significant difference at the $p < 0.05$ level.

Table 4. Allometric scaling exponents and the test of isometry between plant functional traits on different slope aspects

Sample position	R^2	<i>p</i>	Slope (95% confidence interval)	Intercept (95% confidence interval)	Test of isometry		
					F	<i>p</i>	
BGB-AGB	S	0.529	<0.001	1.568 (1.206, 2.040) ^a	-0.358 (-0.705, -0.011)	12.865	0.001
	SE	0.217	0.010	1.085 (0.776, 1.519) ^a	-0.533 (-0.899, -0.166)	0.241	0.628
	E	0.121	0.060	1.805 (1.265, 2.576) ^{ab}	-0.034 (-0.607, 0.540)	12.458	0.001
	NE	0.617	<0.001	1.693 (1.335, 2.147) ^{ab}	-0.046 (-0.426, 0.334)	22.195	<0.001
	N	0.389	<0.001	0.902 (0.670, 1.215) ^{ab}	-0.553 (-0.803, -0.303)	0.488	0.491
	NW	0.273	0.003	1.179 (0.852, 1.630) ^{abc}	-0.426 (-0.782, -0.070)	1.048	0.315
	W	0.377	0.001	1.651 (1.199, 2.723) ^{bc}	0.245 (-0.312, 0.803)	10.955	0.003
	SW	0.431	<0.001	1.653 (1.240, 2.205) ^c	-0.080 (-0.544, 0.385)	13.536	0.001
FB-VB	S	0.174	0.022	0.715 (0.507, 1.010)	-0.913 (-1.132, -0.693) ^a	3.951	0.057
	SE	0.155	0.031	1.030 (0.727, 1.450)	-0.688 (-1.044, -0.332) ^{ab}	0.029	0.867
	E	0.263	0.004	1.154 (0.833, 1.600)	-0.459 (-0.801, -0.117) ^{ab}	0.788	0.382
	NE	0.353	0.001	0.819 (0.603, 1.113)	-0.764 (-1.010, -0.519) ^a	1.753	0.196
	N	0.406	<0.001	1.156 (0.862, 1.552)	-0.499 (-0.800, -0.197) ^{abc}	1.002	0.325
	NW	0.459	<0.001	1.130 (0.853, 1.497)	-0.439 (-0.733, -0.146) ^{bc}	0.781	0.384
	W	0.241	0.009	1.148 (1.807, 1.631)	-0.535 (-0.940, 0.129) ^c	0.627	0.436
	SW	0.312	0.001	0.939 (0.685, 1.288)	-0.710 (-1.004, -0.416) ^c	0.160	0.693

PB-NPB	S	0.312	<0.001	1.748 (1.275, 2.398) ^A	0.472 (-0.076, 1.019)	14.079	0.001
	SE	0.340	0.001	1.518 (1.114, 2.069) ^{AB}	0.328 (-0.186, 0.841)	7.824	0.009
	E	0.024	0.413	1.238 (0.852, 1.799) ^{ABC}	-0.059 (-0.528, 0.409)	1.331	0.258
	NE	0.542	<0.001	1.471 (1.135, 1.906) ^{AB}	0.204 (-0.196, 0.605)	9.568	0.004
	N	0.723	<0.001	0.975 (0.796, 1.194) ^C	-0.312 (-0.503, -0.122)	0.064	0.802
	NW	0.740	<0.001	1.278 (1.050, 1.554) ^{ABC}	-0.041 (-0.286, 0.203)	6.603	0.016
	W	0.705	<0.001	1.034 (0.828, 1.291) ^C	-0.202 (-0.455, 0.050)	0.094	0.761
	SW	0.719	<0.001	1.078 (0.879, 1.321) ^{BC}	-0.170 (-0.407, 0.067)	1.556	0.462

BGB-AGB represents above- and below-ground biomass, FB-VB represents reproduction- and vegetation- growth biomass, PB-NPB represents photosynthesis- and non photosynthesis- growth biomass. The data represent the mean \pm SE ($n = 30$). Data with the same letters within the same column indicate a not significant difference at $p < 0.05$ level.

Growth mass and biomass increment from early vegetation stage to full bloom stage

There were significant differences in plant height increase ($F = 3.574$, $p = 0.001$), stem biomass increment ($F = 5.421$, $p < 0.001$), and belowground biomass increment ($F = 2.682$, $p = 0.011$). Δ PN on slope S was significantly greater than those on slopes SW, NE, W and SE. Δ SB on slope S was significantly greater than those on other slope aspects, except slope E. Δ LB was not significantly different among the eight slope aspects. Δ TB on slope S was remarkably greater than those on slopes SW and W. Along the circumference of the mountain, from slope S to slope SW, the increment in stem biomass, leaf biomass, total biomass, and the increase in leaf numbers showed a “W”-like trend, while the increase in plant height and the increment in belowground biomass showed a wave shape. The increasing of plant height and the increment of belowground biomass showed different trends. From slope S to slope SW, Δ PH had two spikes and three troughs of the wave. Δ BGB on slope N was significantly greater than those on other slopes, except slope W and NW (Fig. 6, Table 5).

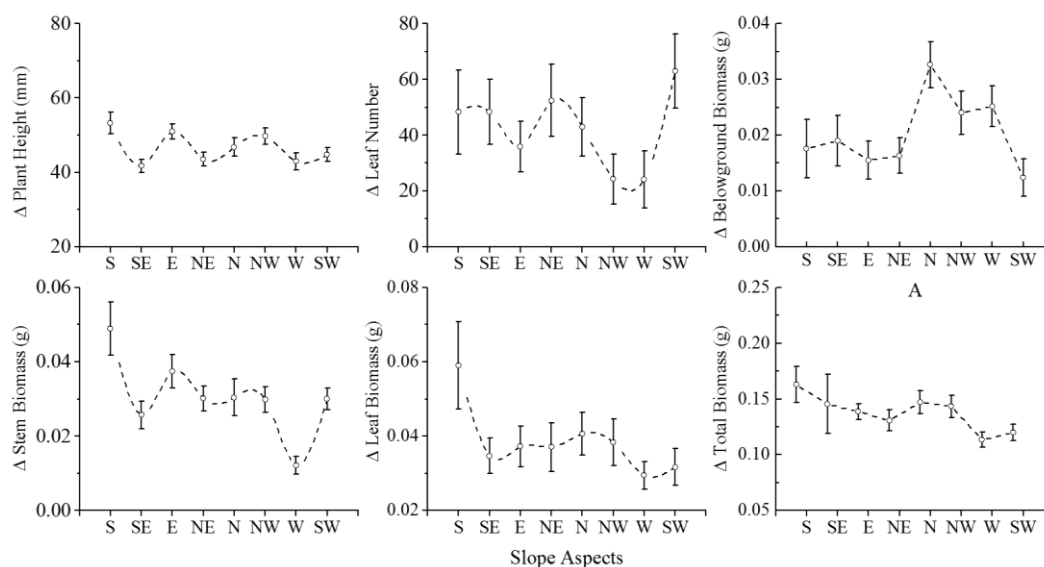


Figure 6. The growth mass and biomass increment from vegetation stage to full bloom stage on different slope aspects

Table 5. Increase in plant height and biomass from the early vegetation stage to the full bloom stage among slope aspects

Slope aspects	Δ PH (mm)	Δ LN	Δ SB (g)	Δ LB (g)	Δ BGB (g)	Δ TB (g)
S	53.27 ± 2.86 ^a	48.27 ± 15.11 ^{ab}	0.05 ± 0.01 ^a	0.06 ± 0.01	0.02 ± 0.01 ^b	0.17 ± 0.02 ^a
SE	41.73 ± 1.77 ^d	48.40 ± 11.63 ^{ab}	0.03 ± 0.00 ^b	0.07 ± 0.04	0.02 ± 0.00 ^b	0.14 ± 0.04 ^{ab}
E	51.00 ± 2.07 ^{ab}	35.93 ± 9.02 ^{ab}	0.04 ± 0.00 ^{ab}	0.04 ± 0.01	0.02 ± 0.00 ^b	0.13 ± 0.01 ^{ab}
NE	43.53 ± 1.93 ^{cd}	52.43 ± 12.90 ^{ab}	0.03 ± 0.00 ^b	0.04 ± 0.01	0.02 ± 0.00 ^b	0.12 ± 0.01 ^{ab}
N	46.80 ± 2.46 ^{abcd}	42.97 ± 10.56 ^{ab}	0.03 ± 0.00 ^b	0.04 ± 0.01	0.03 ± 0.00 ^a	0.15 ± 0.02 ^{ab}
NW	49.77 ± 2.20 ^{abc}	24.23 ± 8.97 ^b	0.03 ± 0.00 ^b	0.04 ± 0.01	0.02 ± 0.00 ^{ab}	0.14 ± 0.02 ^{ab}
W	42.96 ± 2.32 ^{cd}	24.11 ± 10.31 ^b	0.01 ± 0.00 ^c	0.03 ± 0.00	0.03 ± 0.00 ^{ab}	0.10 ± 0.01 ^b
SW	44.77 ± 1.86 ^{bcd}	62.93 ± 13.36 ^a	0.03 ± 0.00 ^b	0.03 ± 0.01	0.01 ± 0.00 ^b	0.10 ± 0.01 ^b
F	3.547	1.325	5.421	0.846	2.682	1.706
<i>p</i>	0.001	0.239	< 0.001	0.55	0.011	0.108

Δ PH represent the increase in plant height, Δ LN represent the increase in leaf number, Δ SB represent the increase in stem biomass, Δ LB represent the increase in leaf biomass, Δ BGB represent the increase in belowground biomass and Δ TB represent the increase in total biomass. The data represent the mean ± SE (n = 30). Data with the same letters within the same column indicate a not significant difference at the $p < 0.05$ level.

Effect of environmental factors on plant characters and growth

There were two principal components that were composed of environmental factors and had remarkable eigenvalues. The cumulative variance proportion explained by the first two principal components was 81.92%. The first principal component (z1, 56.03%) mainly consisted of soil organic carbon, soil total nitrogen and soil total phosphorus. The second principal component (z2, 25.89%) was composed of light intensity, mean annual temperature and soil water content (Fig. 7). As interpreted in Table 6, F/V was significantly correlated with the second component ($R^2 = 0.717$, $p = 0.008$), Δ SB was significantly correlated with the first principal component ($R^2 = 0.537$, $p = 0.039$), R/S and Δ LB were significantly marginally correlated with the first principal component ($R^2 = 0.464$, $p = 0.063$; $R^2 = 0.464$, $p = 0.063$), and Δ BGB and Δ TB were not significantly correlated with the principal component ($R^2 = 0.350$, $p = 0.122$; $R^2 = 0.420$, $p = 0.082$) (Fig. 7, Table 6).

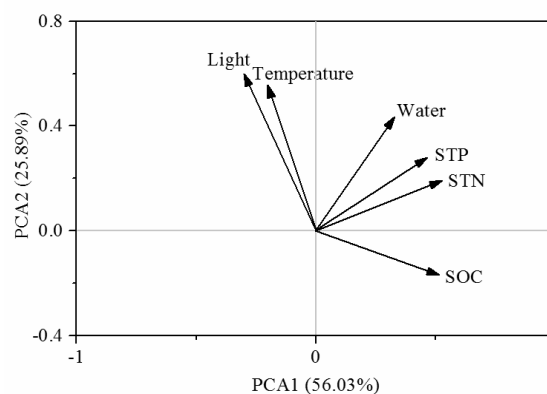


Figure 7. PCA ordination diagram of environmental factors. Light represents light intensity, Water represents soil water content, Temperature represents mean annual temperature of soil, STP represents soil total phosphorus, STN represents soil total nitrogen and SOC represents soil organic carbon

Table 6. Stepwise regression analysis of plant traits and biomass with principal components

Dependent variable	Independent variable (Partial R-Square)		Intercept	R ²	p
	Z1	Z2			
PH	-	-	68.175	-	-
R/S	0.122 (0.464)	-	0.961	0.464	0.063
F/V	-	-0.016 (0.717)	0.259	0.717	0.008
ΔPH	-	-	-	-	-
ΔSB	-0.004(0.537)	-	0.031	0.537	0.039
ΔLB	-0.005(0.450)	-	0.043	0.450	0.069
ΔBGB	0.002 (0.350)	-	0.020	0.350	0.122
ΔTB	-0.008(0.420)	-	0.132	0.420	0.082

Discussion

Effect of slope aspects on plant height, branch number, specific leaf area, leaf number and flower structure traits at full bloom stage

Plant height, branch number, specific leaf area and leaf number were significantly affected by slope aspect. Alpine plants change their survival strategy to adapt to different environmental conditions. Plant height is a sign of the ability of plants to compete for space resources (Westoby, 1998, 2002). This ability can be understood as a race upwards for the light. The plant height was highest on slope S, and was significantly higher than plant that on shady and partially sunny slopes. Plants in harsh locations tend to decrease their height to adapt to strong wind environments (Kudo, 1992; Chen, 2011). Studies have shown that decreasing plant height plays an important role in avoiding the risk of shady slope with less light radiation, low temperature and strong wind (Körner and Neumayer, 1989; Méndez and Traveset, 2003). Plants prefer to grow shorter to reduce energy loss (Körner, 2003; Fabbro, 2004). At the same time, a reduction in plant size along elevational gradients can explain this question from other aspects (Körner et al., 1989; Fabbro, 2004; Fan, 2009). Leaf number is critical for the development of plants to enhance photosynthetic efficiency (Li et al., 2015), but light intensity among the eight slope aspects was not significantly different, so there was no significant difference between sunny slope and shady slope in leaf number. Increasing branch number is a way for asexual reproduction, which would be important for alpine plants as an adaptation to harsh environments (He et al., 2017). In our results, the branch number of the plants on slope N was remarkably greater than that on the partial shady slope, slope E and slope W, which indicated that the shady slope was conducive to asexual reproduction. Bonser et al. (1994) reported that plants tend to increase branch number when solar radiation is strong, which is opposite to our results. There were more diverse communities of pollinators visiting low elevation populations than high elevation populations (Bingham and Orthner, 1998; Arroyo, 1982). The climatic conditions of the shady slope were severe compared to those of the sunny slope, which was similar to the comparison of high elevation to low elevation, as plants prefer to

increase investment to the propagules of asexual reproduction for population stability. The reasons may be that specific leaf area (SLA) can have large variability in response to irradiance, temperature, and water availability (Pigliucci and Kolodynska, 2002; Poorter et al., 2009). Specific leaf area is related to photosynthetic capacity and refers to the ability to acquire resources (Reich et al., 1997, 1999; Wright et al., 2004), which is associated with plant survival strategy. Many studies have shown that the lower SLA tends to be related more to lower leaf water content than to higher leaf thickness for herbaceous leaves with sclerophyllous leaves growing in a low temperature environment (Dijkstra and Lambers, 2010; Garnier and Laurent, 1994; Arendonk and Poorter, 1994; Shipley, 1995; Ryser and Aeschlimann, 1999). In our experiment, soil total nitrogen was higher on slopes W and SW, so SLA of *Gentiana hexaphylla* on slopes SW and W was larger than on other slope aspects. For this reason, this finding was consistent with the research that species with tender leaves have few cell walls per unit leaf area and a high proportion of their volume is occupied by nitrogen-rich protoplasts (Reich, 1993; Garnier and Laurent, 1994; Vendramini et al., 2002). The carbon assimilation ability of these species was strong.

Slope aspect significantly affects flower structure traits including corolla length, calyx length, pistil length and stamen length. As the reproductive organs of plants, flowers play an indispensable role in protecting the genes of continuity and supporting genetic diversity. Flower size was closely related to pollinator visitation (Fenster et al., 2004). The vast majority of plants receive a variety of different species as visitors (Fenster et al., 2004). Meanwhile, flowers are the key factor affecting the evolution of plants and the guarantee of sexual reproduction (Goodwillie et al., 2010). The greater the flower number, the better is the possibility of producing offspring. Bynum (2001) says that *Gentiana hexaphylla* shows a low probability of autogamy because of the temporal and spatial separation of male and female reproduction traits, indicating the importance of pollinators for outcrossing. The experiments of Nilsson (1988) and Johnson and Steiner (1997) suggested that the reduction in corolla tube reduces reproductive success. In our study, corolla and calyx length were greater on slope SW than on slopes S and SE, and the lowest on slopes N and NW. Slope SW had a high rate of reproductive success. Above all, *Gentiana hexaphylla* grows in shady slopes, increasing asexual reproduction and investment of male organs to compensate for the influence of harsh environments of sexual reproduction in alpine ecosystems.

Effect of abiotic environmental factors on resource allocation patterns and allometric relationships in alpine plants on different slope aspects

Leaf biomass partitioning and flower biomass partitioning on different slope aspects did not significantly differ, but there were significant effects on other organ biomass partitioning. Plants adjusted their functional traits and biomass allocation to adapt to a harsh habitat when subjected to environmental stress or resource constraints to improve competitiveness and survival fitness (Sultan, 1992). Niklas and Enquist (2001) reported an isometric relationship between belowground and aboveground biomass across non-woody plants. The resulting, belowground /aboveground biomass, had an allometric relationship, which means that the accumulating rate of underground biomass was greater than the rate of aboveground biomass. This result was opposite to that of Niklas and Enquist. Most allocation issues were triggered by allometric growth, which can also be used to quantify the relationships between growth and partitioning (Weiner, 2004). To adapt to the harsh ecological environment in alpine ecosystems, more biomass is

allocated to the underground to produce fleshy roots. In this study, photosynthetic /non-photosynthetic biomass growth showed that an allometric relationship expressed photosynthetic biomass accumulation faster than that of non-photosynthetic biomass. At the same time, photosynthetic biomass on the sunny slopes was significantly greater than those on the shady slopes and slope W, and there was no significant difference in leaf biomass allocation among the different slopes. Plants were prone to make full use of light conditions and increased area of photosynthesis for increasing plant adaptability to the environment (Körner, 2003). Leaf biomass partitioning was a rather conserved trait in cold high elevation climate regions. However, alpine plants tend to invest more biomass in photosynthetic tissue for growth and persistence than do herbaceous species in cold habitats (Körner, 2003; Patty et al., 2010). There was a significant correlation between R/S and soil nutrients. Soil organic carbon, total nitrogen and phosphorus on slope W were highest and these on slope S were lowest. The root biomass and proportion of biomass allocation among different slopes had the same trend as soil nutrients. In the experimental area, site E was the windward slope and site W was the leeward slope. Long-term operating soil weathering and erosion processes accelerated lower soil nutrients in shady slopes and slope E (Rech et al., 2001). Northern slopes exhibited a higher productivity and water content was an important limiting factor for plant growth (Gong et al., 2008), which was opposite to our results. The annual direct radiation on slope S was higher than on slopes SW, W and N (McCune and Keon, 2002). Higher radiation resulted in higher soil temperature (McCune and Keon, 2002), which led to faster decomposition of soil organic matter, meaning that slope S accumulated less soil organic carbon than did slopes SW, N and W. Thus, plants growing on slope west-facing slope and shady slopes inclined to increase belowground biomass, while plants growing on sunny slopes were more conducive to increase aboveground biomass.

The relationship between plant growth from the early vegetation stage to the full bloom stage and environmental factors on different slope aspects

Slope aspect was an important topographic variable that substantially modified light radiation, soil temperature and soil water content, influencing the ecological processes and creating microclimates that differ significantly from the regional climatic conditions (Buffo et al., 1972; Flint and Childs, 1987; Nikolov and Zeller, 1992; McCune and Keon, 2002; Bennie et al., 2008; Zhang et al., 2015). The micro-environmental conditions on different aspects may have marked effects on the growth and development of the plants (Li et al., 2013). There was a significant relationship between growth and environmental factors composed of light intensity, mean annual temperature and soil water content. The sunny slopes had a larger light intensity and higher mean annual temperature, which was more beneficial for herbs to grow higher and increase biomass (Poorter et al., 2012). The reason why plants grown on slope N were larger than those grown on partially shady slopes may be associated with soil water content. Gong et al. (2008) showed that water was an important factor for plant growth. *Gentiana hexaphylla* adopted a different growth strategy. Soil organic carbon, soil total nitrogen and soil total phosphorus were the primary factors influencing the increment from the early vegetation stage to the full bloom stage. Soil nutrients are restrictive factors for plant growth, affecting the material circulation of plants (Sterner and Elser, 2002). The herbs growing on the slope contained more nutrients and were prone to

increase root biomass, and those growing in lower nutrient places tend to increase aboveground biomass.

Conclusion

Slope aspect had marked effects on the growth and reproduction of *Gentiana hexaphylla*. The plants grown on a shady slope inclined to increase belowground biomass, while plants grown on a sunny slope were more conducive to increase aboveground biomass. This phenomenon was more related to soil organic carbon, soil total nitrogen and phosphorus than to light intensity, soil temperature, and soil water content. *Gentiana hexaphylla* inclined to increase sexual reproduction investment on sunny slopes and increase male organ input and asexual reproduction on shady slope. Along the circumference of the mountain, from slope S to slope SW, the growth of plant height from the early vegetation stage to the full bloom stage showed a wave shape, and the increment in organ biomass showed a “W” shape.

Acknowledgements. We thank Chen Zukang and Zhang Baozhen for assistance in the field. This study was funded by National Key R&D Program of China (2017YFC0505005-1), the National Natural Science Foundation of China (No. 31400389, 41661144045).

REFERENCES

- [1] Ai, Z. M., He, L. R., Xin, Q., Yang, T., Liu, G. B., Xue, S. (2017): Slope aspect affects the non-structural carbohydrates and C: N: P stoichiometry of *Artemisia sacrorum* on the Loess Plateau in China. – *Catena* 152: 9-17.
- [2] Allen, S. E. (1989): *Chemical Analysis of Ecological Material*. – Blackwell Scientific Publications, Oxford.
- [3] Arendonk, J. J. C. M. van, Poorter, H. (1994): The chemical composition and anatomical structure of leaves of grass species differing in relative growth rate. – *Plant, Cell & Environment* 17(8): 963-970.
- [4] Arroyo, M. T. K., Primack, R. B., Armesto, J. J. (1982): Community studies in pollination ecology in the high temperate Andes of central Chile. I. Pollination mechanisms and altitudinal variation. – *American Journal of Botany* 69(1): 82-97.
- [5] Auslander, M., Nevo, E., Inbar, M. (2003): The effects of slope orientation on plant growth, developmental instability and susceptibility to herbivores. – *Journal of Arid Environments* 55(3): 405-416.
- [6] Bao, S. D. (2000): *Soil and Agricultural Chemistry Analysis* (in Chinese). – China Agriculture Press, Beijing.
- [7] Barthlott, W., Lauer, W., Placke, A. (1996): Species diversity in vascular plants: towards a world map of phytodiversity. – *Erdkunde* 50(4): 317-327.
- [8] Bennie, J., Huntley, B., Wiltshire, A., Hill, M. O., Baxter, R. (2008): Slope, aspect and climate: Spatially explicit and implicit models of topographic microclimate in chalk grassland. – *Ecological Modelling* 216(1): 47-59.
- [9] Bingham, R. A., Orthner, A. R. (1998): Efficient pollination of alpine plants. – *Nature* 391(6664): 238-239.
- [10] Bonser, S. P., Aarssen, L. W. (1994): Plastic allometry in young sugar maple (*Acer-Saccharum*): adaptive responses to light availability. – *American Journal of Botany* 81(4): 400-406.

- [11] Bonser, S. P., Aarssen, L. W. (2009): Interpreting reproductive allometry: Individual strategies of allocation explain size-dependent reproduction in plant populations. – *Perspectives in Plant Ecology, Evolution and Systematics* 11(1): 31-40.
- [12] Buffo, J., Fritschen, L. J., Murphy, J. L. (1972): Direct Solar Radiation on Various Slopes from 0 to 60 Degrees North Latitude. – Pacific Northwest Forest and Range Experiment Station, Portland, OR.
- [13] Bynum, M. R., Smith, W. K. (2001): Floral movements in response to thunderstorms improve reproductive effort in the alpine species *Gentiana algida* (Gentianaceae). – *American Journal of Botany* 88(6): 1088-1095.
- [14] Caldwell, M. M. (1968): Solar ultraviolet radiation as an ecological factor for alpine plants. – *Ecological Monographs* 38(3): 243-268.
- [15] Caldwell, M. M. (1979): Plant life and ultraviolet radiation: Some perspective in the history of the Earth's UV climate. – *Bioscience* 29(9): 520-525.
- [16] Cantón, Y., Del Barrio, G., Sole-Benet, A., Lazaro, R. (2004): Topographic controls on the spatial distribution of ground cover in the Tabernas badlands of SE Spain. – *Catena* 55(3): 341-365.
- [17] Carletti, P., Vendramin, E., Pizzeghello, D., Concheri, G., Zanella, A., Nardi, S., Squartini, A. (2009): Soil humic compounds and microbial communities in six spruce forests as function of parent material, slope aspect and stand age. – *Plant and Soil* 315(1-2): 47-65.
- [18] Chen, W. N., Wu, Y., Wu, N., Luo, P. (2008): Effect of snow-cover duration on plant species diversity of alpine meadows on the eastern Qinghai-Tibetan Plateau. – *Journal of Mountain Science* 5(4): 327-339.
- [19] Chen, W. N., Wu, Y., Wu, N., Wang, Q. (2011): Effect of snowmelt time on growth and reproduction of *Pedicularis davidii* var. *pentodon* in the eastern Tibetan Plateau. – *Plant Biosystems - An International Journal Dealing with all Aspects of Plant Biology* 145(4): 802-808.
- [20] De Bello, F., Leps, J., Sebastia, M. T. (2006): Variations in species and functional plant diversity along climatic and grazing gradients. – *Ecography* 29(6): 801-810.
- [21] Dijkstra, P., Lambers, H. (2010): Analysis of specific leaf area and photosynthesis of two inbred lines of *Plantago mayor* differing in relative growth rate. – *New Phytologist* 113(3): 283-290.
- [22] Fabbro, T., Körner, C. (2004): Altitudinal differences in flower traits and reproductive allocation. – *Flora* 199(1): 70-81.
- [23] Fan, D. M., Yang, Y. P. (2009): Altitudinal variations in flower and bulbil production of an alpine perennial, *Polygonum viviparum* L. (Polygonaceae). – *Plant Biology* 11(3): 493-497.
- [24] Fekedulegn, D., Hicks, R. R., Colbert, J. J. (2003): Influence of topographic aspect, precipitation and drought on radial growth of four major tree species in an Appalachian watershed. – *Forest Ecology and Management* 177(1): 409-425.
- [25] Fenster, C. B., Armbruster, W. S., Wilson, P., Dudash, M. R., Thomson, J. D. (2004): Pollination syndromes and floral specialization. – *Annual Review of Ecology Evolution and Systematics* 35(35): 375-403.
- [26] Flint, A. L., Childs, S. W. (1987): Calculation of solar radiation in mountainous terrain. – *Agricultural and Forest Meteorology* 40(3): 233-249.
- [27] Garnier, E., Laurent, G. (1994): Leaf anatomy, specific mass and water content in congeneric annual and perennial grass species. – *New Phytologist* 128(4): 725-736.
- [28] Gong, X., Brueck, H., Giese, K. M., Zhang, L., Sattelmacher, B., Lin, S. (2008): Slope aspect has effects on productivity and species composition of hilly grassland in the Xilin River Basin, Inner Mongolia, China. – *Journal of Arid Environments* 72(4): 483-493.
- [29] Goodwillie, C., Sargent, R. D., Eckert, C. G., Elle, E., Geber, M. A., Johnston, M. O., Kalisz, S., Moeller, D. A., Ree, R. H., Vallejo-Marin, M., Winn, A. A. (2010): Correlated evolution of mating system and floral display traits in flowering plants and its

- implications for the distribution of mating system variation. – *New Phytologist* 185(1): 311-321.
- [30] Grassein, F., Till-Bottraud, I., Lavorel, S. (2010): Plant resource-use strategies: the importance of phenotypic plasticity in response to a productivity gradient for two subalpine species. – *Annals of Botany* 106(4): 637-645.
- [31] He, J. D., Xue, J. Y., Gao, J., Wang, J. N., Wu, Y. (2017): Adaptations of the floral characteristics and biomass allocation patterns of *Gentiana hexaphylla* to the altitudinal gradient of the eastern Qinghai-Tibet Plateau. – *Journal of Mountain Science* 14(8): 1563-1576.
- [32] He, Y. P., Duan, Y. W., Liu, J. Q., Smith, W. K. (2005): Floral closure in response to temperature and pollination in *Gentiana straminea* Maxim. (Gentianaceae), an alpine perennial in the Qinghai-Tibetan Plateau. – *Plant Systematics and Evolution* 256(1-4): 17-33.
- [33] IPCC (2001): Third Assessment Report of Working Group II. – *Climate Change 2001: Impacts, Adaptation and Vulnerability*. – Cambridge University Press, Cambridge.
- [34] Johnson, S. D., Steiner, K. E. (1997): Long-tongued fly pollination and evolution of floral spur length in the *Disa draconis* complex (*Orchidaceae*). – *Evolution* 51(1): 45-53.
- [35] Kareiva, P. M., Kingsolver, J. G., Huey, R. B. (1993): *Biotic Interactions and Global Change. Patterns and Determinants of Climate and Landscape Change: Scenarios of Global Warming*. – Sinsuer Associates Inc., Sunderland, MA.
- [36] Körner, C. (2003): *Alpine Plant Life: Functional Plant Ecology of High Mountain Ecosystems*. – Springer-Verlag, Heidelberg.
- [37] Körner, C., Neumayer, M., Menendez-Riedl, S. P., Smeets-Scheel, A. (1989): Functional morphology of mountain plants. – *Flora* 182: 353-383.
- [38] Kudo, G. (1992): Performance and phenology of alpine herbs along a snow-melting gradient. – *Ecological Research* 7(3): 297-304.
- [39] Li, D., Wang, X. F., Zhang, X. B., Chen, Q. Y., Xu, G. H., Xu, D. Y., Wang, C. L., Liang, Y. M., Wu, L. S., Huang, C., Tian, J. G., Wu, Y. Y., Tian, F. (2016): The genetic architecture of leaf number and its genetic relationship to flowering time in maize. – *New Phytologist* 210(1): 256-268.
- [40] Li, Q. H., Xu, J., Li, H. Q., Wang, S. X., Yan, X., Xin, Z. M., Jiang, Z. P., Wang, L. L., Jia, Z. Q. (2013): Effects of aspect on clonal reproduction and biomass allocation of layering modules of *Nitraria tangutorum* in nebkha dunes. – *PLoS One* 8(10): e79927.
- [41] McCune, B., Keon, D. (2002): Equations for potential annual direct incident radiation and heat load. – *Journal of Vegetation Science* 13(4): 603-606.
- [42] Mcintosh, M. (2002): Plant size, breeding system, and limits to reproductive success in two sister species of *Ferocactus* (Cactaceae). – *Plant Ecology* 162(2): 273-288.
- [43] Nagy, L., Grabherr, G. (2009): *The Biology of Alpine Habitats*. – Oxford University Press, UK.
- [44] Niklas, K. J. (2005): Modelling below- and above-ground biomass for non-woody and woody plants. – *Annals of Botany* 95(2): 315-321.
- [45] Niklas, K. J., Enquist, B. J. (2001): Invariant scaling relationships for interspecific plant biomass production rates and body size. – *Proceedings of the National Academy of Sciences of the United States of America* 98(5): 2922-2927.
- [46] Nikolov, N. T., Zeller, K. F. (1992): A solar radiation algorithm for ecosystem dynamic models. – *Ecological Modeling* 61(3-4): 149-168.
- [47] Nilsson, L. A. (1988): The evolution of flowers with deep corolla tubes. – *Nature* 334(6178): 147-149.
- [48] Ohba, H. (1988): *The Alpine Flora of the Nepal Himalayas: An Introductory Note. The Himalayan Plants*. – University of Tokyo Press, Tokyo.
- [49] Patty, L., Halloy, S. R. P., Hiltbrunner, E., Körner, C. (2010): Biomass allocation in herbaceous plants under grazing impact in the high semi-arid Andes. – *Flora* 205(10): 695-703.

- [50] Peng, D. L., Zhang, Z. Q., Xu, B., Li, Z. M., Sun, H. (2012): Patterns of flower morphology and sexual systems in the subnival belt of the Hengduan Mountains, SW China. – *Alpine Botany* 122(2): 65-73.
- [51] Pigliucci, M., Kolodynska, A. (2002): Phenotypic plasticity and integration in response to flooded conditions in natural accessions of *Arabidopsis thaliana*. – *Annals of Botany* 90(2): 199-207.
- [52] Poorter, H., Niinemets, U., Poorter, L., Wright, I. J., Villar, R. (2009): Causes and consequences of variation in leaf mass per area (LMA): a meta-analysis. – *New Phytologist* 182(3): 565-588.
- [53] Poorter, H., Niklas, K. J., Reich, P. B., Oleksyn, J., Poot, P., Mommer, L. (2012): Biomass allocation to leaves, stems and roots: meta-analyses of interspecific variation and environmental control. – *New Phytologist* 193(1): 30-50.
- [54] Rech, J. A., Reeces, R. W., Hendricks, D. M. (2001): The influence of slope aspect on soil weathering processes in the Springerville volcanic field, Arizona. – *Catena* 43(1): 49-62.
- [55] Reich, P. B. (1993): Reconciling apparent discrepancies among studies relating life span, structure and function of leaves in contrasting plant life forms and climates: 'The blind men and the elephant retold'. – *Functional Ecology* 7(6): 721-725.
- [56] Reich, P. B., Walters, M. B., Ellsworth, D. S. (1997): From tropics to tundra: global convergence in plant functioning. – *Proceedings of the National Academy of Sciences* 94(25): 13730-13734.
- [57] Reich, P. B., Ellsworth, D. S., Walters, M. B., Vose, J. M., Gresham, C., Volin, J. C., Bowman, W. D. (1999): Generality of leaf trait relationships: a test across six biomes. – *Ecology* 80(6): 1955-1969.
- [58] Rosenberg Rosenberg, N. J., Blad, B. L., Verma, S. B. (1983): *Microclimate—The Biological Environment*. – Wiley, Chichester.
- [59] Ryser, P., Aeschlimann, U. (1999): Proportional dry-mass content as an underlying trait for the variation in relative growth rate among 22 Eurasian populations of *Dactylis glomeratas* L. – *Functional Ecology* 13(4): 473-482.
- [60] Shipley, B. (1995): Structured interspecific determinants of specific leaf area in 34 species of herbaceous angiosperms. – *Functional Ecology* 9(2): 312-319.
- [61] Sternberg, M., Shoshany, M. (2001): Influence of slope aspect on Mediterranean woody formations: comparison of a semiarid and an arid site in Israel. – *Ecological Research* 16(2): 335-345.
- [62] Sterner, R. W., Elser, J. J. (2002): *Ecological stoichiometry: The biology of elements from molecules to the biosphere*, pp. 167-196. – Princeton University Press, Princeton.
- [63] Stöcklin, J. (1992): Umwelt, Morphologie und Wachstumsmuster klonaler Pflanzen: eine Übersicht. – *Botanica Helvetica* 102: 3-21.
- [64] Sultan, S. E. (1992): Phenotypic plasticity and the neo-Darwinian legacy. – *Evolutionary Trends in Plants* 6(2): 61-71.
- [65] Sun, H., Niu, Y., Chen, Y. S., Song, B., Liu, C. Q., Peng, D. L., Chen, J. G., Yang, Y. (2014): Survival and reproduction of plant species in the Qinghai-Tibet Plateau. – *Journal of Systematics and Evolution* 52(3): 378-396.
- [66] Vendramini, F., Diaz, S., Gurvich, D. E., Wilson, P. J., Thompson, K., Hodgson, J. G. (2002): Leaf traits as indicators of resource-use strategy in floras with succulent species. – *New Phytologist* 154(1): 147-157.
- [67] Vile, D., Garnier, E., Shipley, B., Laurent, G., Navas, M. L., Roumet, C., Lavorel, S., Diaz, S., Hodgson, J. G., Lloret, F., Midgley, G. F., Poorter, H., Rutherford, M. C., Wilson, P. J., Wright, I. J. (2005): Specific leaf area and dry matter content estimate thickness in laminar leaves. – *Annals of Botany* 96(6): 1129-1136.
- [68] Warton, D. I., Wright, I. J., Falster, D. S., Westoby, M. (2006): Bivariate line-fitting methods for allometry. – *Biological Reviews of the Cambridge Philosophical Society* 81(2): 259-291.

- [69] Weiner, J. (2004): Allocation, plasticity and allometry in plants. – *Perspectives in Plant Ecology, Evolution and Systematics* 6(4): 207-215.
- [70] Westoby, M. (1998): A leaf-height-seed (LHS) plant ecology strategy scheme. – *Plant and Soil* 199(2): 213-227.
- [71] Westoby, M., Falster, D. S., Moles, A. T., Vesk, P. A., Wright, I. J. (2002): Plant ecological strategies: Some leading dimensions of variation between species. – *Annual Review of Ecology and Systematics* 33(1): 125-159.
- [72] Wright, I. J., Reich, P. B., Westoby, M. (2001): Strategy shifts in leaf physiology, structure and nutrient content between species of high- and low-rainfall and high- and low-nutrient habitats. – *Functional Ecology* 15(4): 423-434.
- [73] Wright, I. J., Reich, P. B., Westoby, M., Ackerly, D. D., Baruch, Z., Bongers, F., Cavender-Bares, J., Chapin, T., Cornelissen, J. H., Diemer, M., Flexas, J., Garnier, E., Groom, P. K., Gulias, J., Hikosaka, K., Lamont, B. B., Lee, T., Lee, W., Lusk, C., Midgley, J. J., Navas, M. L., Niinemets, U., Oleksyn, J., Osada, N., Poorter, H., Poot, P., Prior, L., Pyankov, V. I., Roumet, C., Thomas, S. C., Tjoelker, M. G., Veneklaas, E. J., Villar, R. (2004): The worldwide leaf economics spectrum. – *Nature* 428(6985): 821-827.
- [74] Yang, Y., Sun, H. (2006): Advances in the functional ecology of alpine and arctic plants. – *Acta Botanica Yunnanica* 28(1): 43-53.
- [75] Zhang, Y. L., Li, X., Bai, Y. L. (2015): An integrated approach to estimate shortwave solar radiation on clear-sky days in rugged terrain using modis atmospheric products. – *Solar Energy* 113: 347-357.

EVALUATION OF CHEMICAL COMPOSITION OF LENTIL SEEDS IN SOLE CROP AND ROW INTERCROPPED WITH NAKED OATS IN AN ORGANIC FARM

KRASKA, P.¹ – ANDRUSZCZAK, S.^{1*} – STANIAK, M.² – KWIECIŃSKA-POPPE, E.¹ – RÓŻYŁO, K.¹ – RUSECKI, H.¹

¹*Institute of Agricultural Ecology, Department of Herbology and Plant Cultivation Techniques, University of Life Sciences in Lublin, Akademicka 13, 20-950 Lublin, Poland*

²*Department of Forage Crop Production, Institute of Soil Science and Plant Cultivation, State Research Institute, Czartoryskich 8, Puławy, Poland*

*Corresponding author

e-mail: sylwia.andruszczak@up.lublin.pl; phone: +48-81-445-66-87

(Received 22nd Nov 2017; accepted 7th Mar 2018)

Abstract. The field experiment was conducted to evaluate how row intercropping of the lentil with naked oats as a supporting plant impacts macro- and micronutrient content of two lentil varieties ‘Tina’ and ‘Anita’ as well as a mixture of these two varieties. Additionally, amino acid content and fatty acid composition of lentil seeds were determined. Lentil was sown at a row spacing of 20 and 25 cm. In var. ‘Tina’ seeds, a higher content of K, Ca, Mg, Mn and B was determined than in var. ‘Anita’. ‘Anita’ seeds, in turn, were characterized by a higher content of fat, N, P, Cu, Zn and Fe. Lentil seeds sown at a spacing of 20 cm had a higher content of P, K, Ca, Cu, Zn and B compared to a spacing of 25 cm, but they contained less nitrogen. The presence of oats as a supporting crop deteriorated the quality of lentil seeds by contributing to a reduced content of N, P, K, Cu, Zn, Mn, Fe and B compared to sole cropped lentil. A higher content of C18:0, C18:2, C18:3, C20:0, OMEGA 3, and OMEGA 6 acids was determined in ‘Anita’ seeds. Var. ‘Tina’, in turn, contained more C16:0, C18:1 acids. In ‘Anita’ seeds, the content of most evaluated amino acids was determined to be significantly higher than in ‘Tina’ seeds.

Keywords: *nutritional components, Lens culinaris, cultivation with supporting plant, lodging degree, organic farming*

Introduction

Legume seeds are a valuable high-protein dietary component of high biological value (Kowalczyk et al., 2007; Grusak, 2010; Kahraman, 2016). The lentil (*Lens culinaris* Medic.) is one of the oldest cultivated plants (Alghamdi et al., 2014; Kahraman, 2016). The chemical composition of lentil seeds meets the “ideal diet” requirements because they contain little fat (about 0.7-3.4%) and a lot of protein (21-29%) of high nutritional value (Ionescu and Roman, 2013; Alghamdi et al., 2014). Apart from that, lentil seeds and sprouts are a rich source of phytoestrogens, folic acid, vitamins E and C, micronutrients as well as substances with antioxidant properties (Szwejkowska, 2012; Świeca, 2015). In Poland traces of lentil cultivation date back to the early Middle Ages. Seeds of this species are a valuable protein food of high biological value. Registration of the first native lentil varieties has been a great success of Polish plant breeding. This species has low soil, fertilizer and water requirements. It is a valuable component of crop rotation that improves the stand for the succeeding crop (Zawieja, 2006; Żabiński, 2008; Alghamdi et al., 2014). It is worth mentioning that *Fabaceae* plants have the ability to live in symbiosis with rhizobia that fix free atmospheric nitrogen. The use of lentil in an organic farm is justified by its natural ability to fix atmospheric nitrogen. An additional source of nitrogen can

reduce competition between crops in nitrogen uptake and increase the amount of nitrogen available to the succeeding crop (Duchene et al., 2017). Especially in organic farms, lentil plays an extremely important role in crop rotation. It contributes to an increase the yield of succeeding plants by improving soil structure as well as reducing diseases and pests.

Lentil is characterized by high susceptibility to lodging, which adversely affects seed yield and significantly impedes harvesting with a combine harvester (Peñaloza et al., 1992; Zawieja, 2006). Intercropping can effectively reduce lodging of crops susceptible to it. A condition for using this type of cropping is to select a supporting crop and its proportion in the mixture that will help reduce crop lodging, while in the case of a low lentil yield, the supporting component largely decreases the risk of total yield loss (Zawieja, 2006; Duchene et al., 2017). However, it is important to select an appropriate crop species performing the supporting function because mutual shading of the component crops can reduce biological nitrogen fixation and consequently decrease yields (Fujita et al., 1992).

The study hypothesized that row intercropping of lentil with a supporting crop would effectively reduce crop lodging and in consequence improve seed quality. In the case of low lentil yield, the supporting component would also perform the role of a yield producing crop. Sowing a mixture of lentil varieties may contribute to better use of crop space, reduce the spread of fungal pathogens and increase yield stability when adverse conditions occur during the growing season.

The aim of this study was to evaluate the chemical composition of seeds of lentil grown in pure stand and in a variety mixture (50% + 50%) as well as row intercropped with naked oats as a supporting crop at a row spacing of 20 and 25 cm under organic farming system.

Materials and methods

Field experiment and cultivation management

During the period from 2014 to 2016, a controlled field experiment was conducted at the Model Organic Farm in Chwałowice (Municipality of Iłża, Radom County, Masovian Voivodeship) belonging to the Agricultural Advisory Center in Brwinów, Radom Branch, Poland (51°18'N, 21°30'E) (Fig. 1). The experiment was established on brown soil, with an organic carbon content of 14.11 g kg⁻¹ and a pH of 6.15 in 1 M KCl. The soil was characterized by the following nutrient content: P – 73.9 mg kg⁻¹; K – 1430 mg kg⁻¹; Mg – 1765 mg kg⁻¹; B – 1.98 mg kg⁻¹; Mn 494 mg kg⁻¹; Cu – 5.67 mg kg⁻¹; Zn – 47 50 mg kg⁻¹; Fe – 1125 mg kg⁻¹.

The experimental factors were as follows:

A) Lentil (*Lens culinaris* Medic.) variety

- Tina
- Anita
- mixture of varieties: Tina (50%) + Anita (50%)

B) Row spacing

- 20 cm
- 25 cm

C) Lentil cropping method

- sole cropping (without a supporting crop)
- row intercropping with naked oats (*Avena nuda* L.) var. 'Polar'.

The varieties ‘Tina’ and ‘Anita’ are the only Polish lentil varieties. ‘Tina’ was registered in the National List of Varieties in 1998. It was created as a spontaneous mutant with LGR – 2, while var. ‘Anita’, in turn, was registered in the National List of Varieties in 1999. This is a local population from the Lublin region, introduced by inbreeding and individual selection. These varieties are medium high (40-60 cm) and have a medium number of nodes per stem. They produce green leaves consisting of a large number (more than 11) leaflets. Their flowers are white colored, with three flowers per node. The pods are short, medium wide, and sharp pointed. These varieties differ in seed color – ‘Tina’ produces green seeds, whereas ‘Anita’ yellow ones. The seeds germinate at a temperature of 4-5 °C. This plant requires lighter and permeable soils with a pH close to neutral (COBORU, 2000).



Figure 1. Localization of the study site (Public Domain, <https://commons.wikimedia.org/w/index.php?curid=89531>)

The experiment was set up as a split-block design with three replicates. The area of a single plot was 8 m². Each year the total number of plots in the experiment was 36. A legume/cereal mixture was the previous crop for the experimental stand. Before sowing, 15 t ha⁻¹ of manure based compost was applied and ploughed in. Lentil seeds at a rate of 90 kg ha⁻¹ and oat seeds at a rate of 50 kg ha⁻¹ were sown in the second 10 days of April. Naked oats were sown separately in the interrows of the lentil crop (Fig. 2). Sowing was carried out using self-propelled plot drill Øyjord Wintersteiger (Austria).

Lodging index of lentil plants was determined according to the formula (Szpryngiel et al., 1998):

$$K = \frac{H}{L}$$

K – lodging index

H – height of lentil plants in the field [cm]

L – length of lentil stem measured in laboratory conditions [cm]

Lentil was harvested when the lower pods were brown and the seeds were hard. Anita and Tina varieties intercropped with oat as supporting crop as well as in sole crop mature at a similar rate, which resulted in the fact that the harvest could be done at the same time. Before harvest, plants of lentil and oat have been cut by hand from 2 m² sampling areas in each plot. Collected samples were threshed using laboratory thresher Wintersteiger LD 180. The remaining plants were harvested using Winterstiger combine.



Figure 2. Canopy of lentil cultivated with naked oat as a supporting crop

Weather conditions

Weather conditions during the study period varied substantially. The growing season in 2014 was wettest, with a particularly high rainfall recorded in the months of May and July. In 2015 the air temperature was at a similar level as in the first year of the study, but the amount of rainfall was much lower (by 40% on average). The year 2016 should be characterized as hot and dry, since the air temperature was higher by almost 6 °C than in the previous years, whereas the total rainfall was three times lower compared to 2014 (*Table 1*).

Chemical analysis of lentil seeds

Each year, material for analysis was collected at commercial maturity. The following were determined in seed samples taken from each plot: total protein (mineralization in sulfuric acid; determination by the Kjeldahl distillation method; titration detection), N (mineralization in sulfuric acid and oxygenated water; determination by the Kjeldahl distillation method; titration detection), P (mineralization in sulfuric acid and oxygenated water; determination by the vanadium-molybdate spectrophotometric method; Spekol spectrophotometer, Carl Zeiss Jena, Germany), K and Ca (mineralization in sulfuric acid and oxygenated water; determination by flame

photometry; Jenway PEP7 photometer, UK), Mg (mineralization in sulfuric acid and oxygenated water; determination by atomic absorption spectrometry; Perkin-Elmer spectrometer, USA), Cu, Zn, Mn, Fe (mineralization in perchloric and nitric acid (1:4); determination by atomic absorption spectrometry; Avanta spectrometer, GBC Scientific Equipment, Australia), B (oven mineralization with Ca(OH)₂; determination by the spectrophotometric curcumin method; Spekol spectrophotometer). Moreover, the following were determined in 'Tina' and 'Anita' seeds: fat content (Soxhlet method), fatty acid composition by gas chromatography (according to standard PN-ISO 5509), and amino acid content by ion-exchange chromatography (INGOS amino acid analyzer, Czech Republic).

Table 1. Rainfalls and temperature in the vegetation seasons of the years 2014-2016 according to the Meteorological Station at Model Organic Farm in Chwałowice

Years	Months					Sum/Mean
	IV	V	VI	VII	VIII	
Rainfalls (mm)						
2014	56.9	181.4	46.7	157.7	30.0	472.5
2015	49.5	142.0	46.0	31.7	13.5	282.7
2016	17.8	41.7	37.8	26.9	30.7	154.9
Temperature (°C)						
2014	10.2	14.0	14.7	20.7	21.6	16.2
2015	8.6	13.0	17.3	20.1	22.4	16.3
2016	14.9	21.1	25.6	24.6	24.1	22.1

Statistical analysis

The obtained results were statistically analyzed by analysis of variance. The means were compared using least significant differences based on the Tukey's test ($P \leq 0.05$). Calculations were made using the ARSTAT statistical program, developed at the Faculty of Applied Mathematics and Information Technology of the University of Life Sciences in Lublin.

Results and discussion

Naked oats intercropped with lentil performed well its function, preventing lodging of the lentil crop. In the plots with oats used as the supporting crop, the varieties 'Tina' and 'Anita' as well as their mixture were less prone to lodging, which is evidenced by the significantly higher value of the lodging index compared to lentil cultivation without the supporting crop (Fig. 3).

The content of macro and micronutrients in lentil seeds significantly depended on weather conditions during plant growth (Figs. 4 and 5). The highest content of Fe and the lowest content of N, P, Ca, Cu, Mn and B was found in the year 2014 which was characterized by the highest rainfall compared to the growing season of 2015 and 2016. In the second year of the study, lentil seeds contained the highest amount of K and Ca but the content of Mg, Zn and Fe was the lowest. In turn, the lowest K content and the highest Zn and B content was found in the last year of the study which was hot and dry.

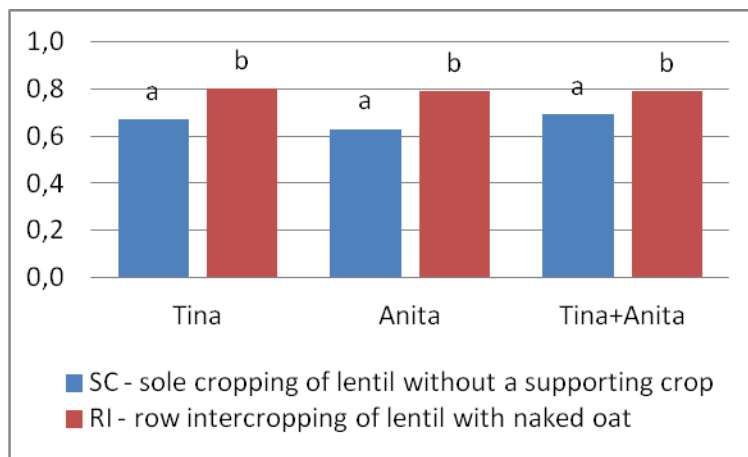


Figure 3. The effect of cultivar and lentil cropping method on lodging index of lentil crop (mean for 2014-2016) (different letters indicate significant difference at $P \leq 0.05$)

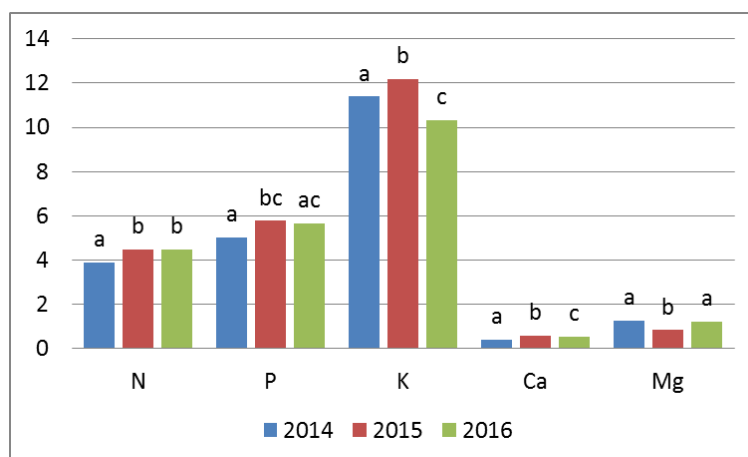


Figure 4. Macroelements content (g kg^{-1}) of lentil seeds during the study years (independent on experimental factors) (different letters indicate significant difference at $P \leq 0.05$)

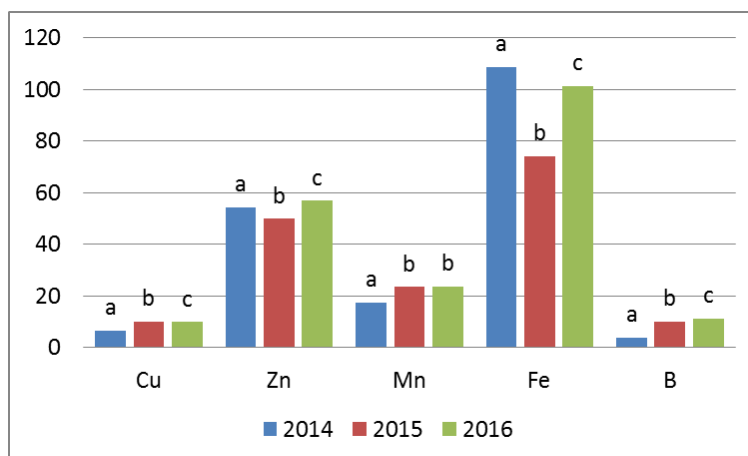


Figure 5. Microelements content (mg kg^{-1}) of lentil seeds during the study years (independent on experimental factors) (different letters indicate significant difference at $P \leq 0.05$)

The highest content of N, P, Cu, Zn and Fe was determined in var. ‘Anita’ seeds while, in turn, the ‘Tina’ variety was characterized by the highest content of K, Ca, Mg, Mn and B (Tables 2 and 3). Lentil sown in wider rows (25 cm) produced a higher amount of nitrogen in its seeds, whereas a higher seed content of P, K, Ca, Cu, Zn and B was determined for lentil sown at a spacing of 20 cm. Seed Mg, Mn and Fe content was not dependent on row spacing. Sowing lentil with oats as a supporting crop significantly reduced the seed content of N, P and K as well as of all micronutrients (Cu, Zn, Mn, Fe, B) compared to sole cropped lentil. This could have been due to the competition for nutrients between the intercropped components.

Table 2. The effect of cultivar, row spacing and lentil cropping method on macroelements content (g kg^{-1}) in lentil seeds (mean for 2014-2016) (T^1 – Tina; A^2 – Anita; SC^3 – sole cropping of lentil without a supporting crop; RI^4 – row intercropping of lentil with naked oats; ns^5 – not significant at $P \leq 0.05$)

Treatment		N	P	K	Ca	Mg
Cultivar	T^1	4.14	5.35	11.47	0.631	1.178
	A^2	4.39	5.58	11.30	0.423	1.127
	T+A	4.33	5.53	11.14	0.461	1.040
	LSD _{0.05}	0.028	0.035	0.157	0.0130	0.0338
Row spacing	20 cm	4.28	5.52	11.38	0.529	1.112
	25 cm	4.30	5.45	11.23	0.481	1.118
	LSD _{0.05}	0.019	0.024	0.106	0.0091	ns ⁵
Lentil cropping method	SC^3	4.31	5.55	11.44	0.502	1.114
	RI^4	4.27	5.42	11.17	0.509	1.116
	LSD _{0.05}	0.019	0.024	0.106	ns	ns
Cultivar x row spacing	$T \times 20 \text{ cm}$	4.15	5.37	11.25	0.649	1.185
	$T \times 25 \text{ cm}$	4.14	5.33	11.69	0.613	1.170
	$A \times 20 \text{ cm}$	4.33	5.59	11.36	0.429	1.124
	$A \times 25 \text{ cm}$	4.44	5.56	11.25	0.417	1.130
	$T+A \times 20 \text{ cm}$	4.35	5.59	11.54	0.509	1.028
	$T+A \times 25 \text{ cm}$	4.32	5.47	10.74	0.414	1.052
	LSD _{0.05}	0.049	0.061	0.271	0.0232	ns
Cultivar x lentil cropping method	$T \times SC$	4.17	5.44	11.65	0.626	1.157
	$T \times RI$	4.12	5.26	11.29	0.637	1.199
	$A \times SC$	4.41	5.63	11.32	0.433	1.131
	$A \times RI$	4.37	5.52	11.28	0.413	1.124
	$T+A \times SC$	4.35	5.58	11.32	0.446	1.054
	$T+A \times RI$	4.32	5.49	10.96	0.476	1.026
	LSD _{0.05}	ns	0.061	0.271	0.0232	0.0585

In the study by Özer and Kaya (2010), the seed K content in different lentil varieties ranged from 2.85 to 4.63 g kg^{-1} , P 0.57-1.35 g kg^{-1} , Mg 0.46-0.73 g kg^{-1} , while Zn 12.8-38.9 g kg^{-1} . These values are markedly lower than in the present study. At the same time, these authors showed a higher content of Ca (0.54 to 2.17 mg kg^{-1}) and Fe (72.4 to 310.3 mg kg^{-1}). Analyzing the mineral composition of 35 lentil genotypes, Alghamdi et al. (2014) found K and P content to be significantly dependent on the genotype, and this

content was from 6.74 to 10.61 g kg⁻¹ and from 2.87 to 5.47 g kg⁻¹, respectively. Zia-Ul-Haq et al. (2011), in turn, found a lower content of K, P, Fe, Zn and Mn, and a higher content of Ca and Cu in seeds of four lentil varieties compared to the present study.

Table 3. The effect of cultivar, row spacing and lentil cropping method on microelements content (mg kg⁻¹) in lentil seeds (mean for 2014-2016) (T¹ – Tina; A² – Anita; SC³ – sole cropping of lentil without a supporting crop; RI⁴ – row intercropping of lentil with naked oats; ns⁵ – not significant at P ≤ 0.05)

Treatment		Cu	Zn	Mn	Fe	B
Cultivar	T ¹	8.55	51.76	23.13	91.76	8.67
	A ²	9.58	57.10	20.54	98.58	8.28
	T+A	8.42	52.12	20.98	93.70	8.02
	LSD _{0.05}	0.091	0.664	0.388	1.057	0.066
Row spacing	20 cm	8.94	54.09	21.57	94.55	8.99
	25 cm	8.76	53.22	21.53	94.81	7.65
	LSD _{0.05}	0.062	0.451	⁵ ns	ns	0.045
Lentil cropping method	SC ³	9.42	55.27	21.92	97.55	8.69
	RI ⁴	8.28	52.04	21.17	91.82	7.96
	LSD _{0.05}	0.062	0.451	0.264	0.718	0.045
Cultivar x row spacing	T × 20 cm	8.27	52.71	23.00	89.99	9.73
	T × 25 cm	8.83	50.82	23.26	93.53	7.60
	A × 20 cm	9.68	56.99	20.92	98.31	9.61
	A × 25 cm	9.48	57.21	20.16	98.86	6.95
	T+A × 20 cm	8.89	52.59	20.79	95.35	7.65
	T+A × 25 cm	7.97	51.65	21.17	92.06	8.39
	LSD _{0.05}	0.157	1.148	0.671	1.829	0.115
Cultivar x lentil cropping method	T × SC	9.96	53.55	23.06	91.61	8.91
	T × RI	7.14	49.97	23.20	91.92	8.43
	A × SC	9.76	59.26	20.23	102.96	9.19
	A × RI	9.40	54.94	20.85	94.20	7.37
	T+A × SC	8.53	53.01	22.48	98.07	7.98
	T+A × RI	8.31	51.22	19.48	89.33	8.07
	LSD _{0.05}	0.157	1.148	0.671	1.829	0.115

A statistically proven interaction between lentil varieties and row spacing revealed that var. ‘Tina’ sown at a spacing of 25 cm, compared to a 20 cm spacing, was characterized by a significantly higher content of K, Cu and Fe and, at the same time, a lower content of Ca, Zn and B. In the case of var. ‘Anita’, the use of a wider row spacing significantly increased the seed content of protein, N and B, whereas the Cu and Mn content decreased.

The effect of row intercropping on macro- and micronutrient content in lentil seeds was dependent on the variety. Compared to sole cropping, the ‘Tina’ variety intercropped with oats as a supporting crop showed a significantly lower content of P, K, Cu, Zn and B. The presence of oats in the ‘Anita’ crop significantly reduced the P, Cu, Zn, Fe and B content in lentil seeds while, in turn, row intercropping of the variety mixture with a supporting crop brought about a decrease in the content of elements such as P, K, Cu, Zn, Mn and Fe. At the same time, the Ca and B content was found to significantly increase. It is worth noting that, as regards the sole cropping treatments

and the treatment with the mixture of varieties, the seed content of protein and nitrogen in lentil row intercropped with oats was lower than in lentil grown in pure stand. Nevertheless, the revealed relationship only had a trend character and was not statistically significant.

In the opinion of Szwejkowska (2012) as well as Stępniaak-Sołyga and Wojtasik (2003), a limited amount of rainfall during the growing season in combination with elevated air temperature promotes the accumulation of total protein in legume seeds. This was confirmed to a certain extent by this study. In the years 2015 and 2016, when the total rainfall was lowest and the average air temperatures highest, the total protein content in lentil seeds was significantly higher than in the wet and slightly colder year of 2014 (Table 1 and Fig. 6). At the same time, in 2016 the highest fat content in lentil seeds was determined. On the other hand, the low fat content found in 2015 is probably attributable to the fact that the highest seed yield was obtained this year, which in turn resulted from favorable rainfall conditions, in particular in the months of May and June.

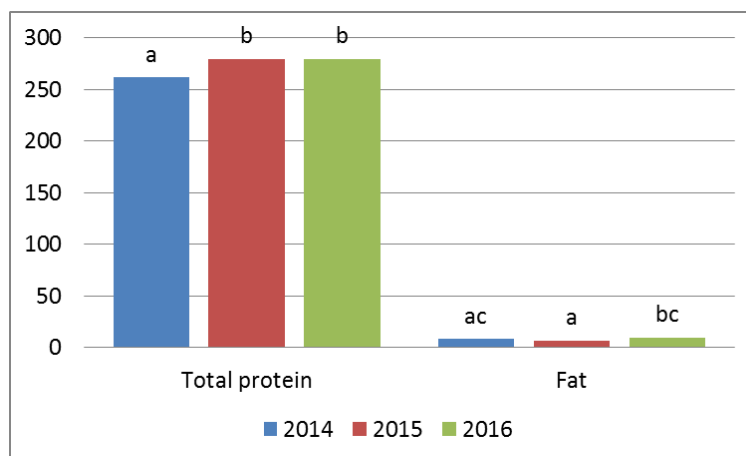


Figure 6. Total protein and fat content (g kg^{-1}) of lentil seeds during the study years (independent on experimental factors) (different letters indicate significant difference at $P \leq 0.05$)

Higher content of total protein was determined in var. ‘Anita’ seeds than the ‘Tina’ variety (Table 4). In a study by Wang et al. (2009), the seed protein content in different lentil varieties was at a similar level as in the present study (251.5 to 290.5 g kg^{-1}). In studying 10 lentil varieties, Özer and Kaya (2010) determined the seed protein content at a level of 266.6 to 278.5 g kg^{-1} , whereas Hamdi et al. (2012) found this content to range from 241.8 g kg^{-1} to 315.2 g kg^{-1} . Costa et al. (2006) showed a slightly lower content of this component (206 g kg^{-1}), whereas Ionescu and Roman (2013), in evaluating the chemical composition of 7 organically grown lentil varieties, determined the protein content at a level from 211.4 g kg^{-1} to 228.5 g kg^{-1} . In the opinion of Karadavut and Genc (2010), lentil varieties exhibit distinct variation in terms of their ability to accumulate total protein in seed. Similar conclusions arise from a study by Szwejkowska (2012).

A significantly higher fat content was determined in var. ‘Anita’ seeds. Compared to ‘Tina’, this variety also exhibited a higher content of C18:0, C18:2, C18:3, PUFA, OMEGA 3 and OMEGA 6 acids. However, it contained less C16:0, C18:1, SFA and MUFA acids (Table 4). Evaluating several lentil varieties originating from organic

farming, Ionescu and Roman (2013) found the seed fat content to range from 2.95 to 3.40%. In a study by Karadavut and Genc (2010), the fat content in lentil seeds was several times higher than in this study, from 25.3 g kg⁻¹ to 30.6 g kg⁻¹. Alghamdi et al. (2014) determined the fat content in lentil seeds at a level of 9.9 g kg⁻¹, while in the study by Özer and Kaya (2010) it ranged between 7.6 to 14.4 g kg⁻¹, thus at a similar level to that found in the present study.

Table 4. Total protein, fat content (g kg⁻¹) and fatty acids profile (%) in lentil seeds (mean for 2014-2016) (T¹ – Tina; A² – Anita; SFA³ – Saturated fatty acid; MUFA⁴ – Mono unsaturated fatty acid; PUFA⁵ – Poli unsaturated fatty acid; ns⁶ – not significant at P ≤ 0.05)

Chemical composition	Cultivar		LSD _{0.05}
	T ¹	A ²	
Total protein	265.2	281.1	1.76
Fat	7.9	8.3	0.17
C14:0	0.71	0.75	ns ⁶
C16:0	15.15	12.76	1.318
C18:0	2.01	2.71	0.695
C18:1	27.78	22.61	1.494
C18:2	35.66	42.17	1.035
C18:3	13.11	15.28	0.350
C20:0	1.01	1.17	ns
Others	4.57	2.55	0.242
SFA ³	21.10	18.29	0.054
MUFA ⁴	29.71	23.91	0.062
PUFA ⁵	49.19	57.99	0.089
OMEGA 3	13.43	15.53	0.055
OMEGA 6	35.66	42.17	0.073

Taking into account the amino acid content in lentil seeds, the least favorable weather conditions occurred in 2016. The highest air temperature during growing season and insufficient amount of rainfall noted in this year significantly decreased the content of Thr, Met, Asp, Glu, Pro, Ser and Gly, compared to 2014 and 2015 (Figs. 7 and 8). At the same time, the content of Arg in 2016 was the highest.

In the opinion of Alghamdi et al. (2014), different lentil genotypes show large variation in seed amino acid content, which was confirmed in the present study. The ‘Anita’ variety was characterized by a significantly higher content of most of the amino acids evaluated. Only the Cys, Met and Tyr content was higher in var. ‘Tina’ seeds. In turn, the Phe content was the same in seeds of both varieties (Tables 5 and 6). Among the amino acids evaluated, the highest content was found for glutamine (from 44.5 to 45.7 mg g⁻¹). Hefnawy (2011) also determined the highest content of glutamine in lentil seeds. Alghamdi et al. (2014) drew special attention to arginine content, which was quite high in all lentil genotypes evaluated, ranging from 6.6 to 10 g kg⁻¹. In turn, Kahraman (2016) determined the isoleucine content in six lentil genotypes at a level from 4.57 to 4.76%, leucine from 5.21 to 5.68%, methionine from 0.92 to 1.49%, phenylalanine from 3.85 to 4.30%, threonine from 2.47 to 3.37%, tryptophan from 0.56 to 1.37%, and valine from 4.35 to 5.01%.

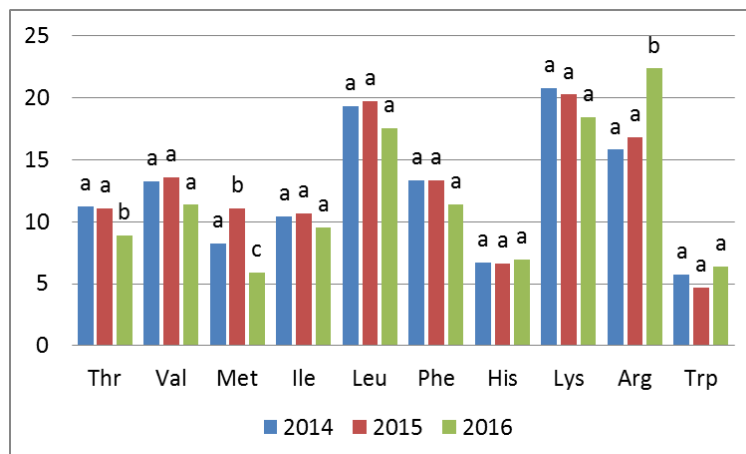


Figure 7. Essential amino acids content (mg g^{-1}) of lentil seeds during the study years (independent on experimental factors) (different letters indicate significant difference at $P \leq 0.05$)

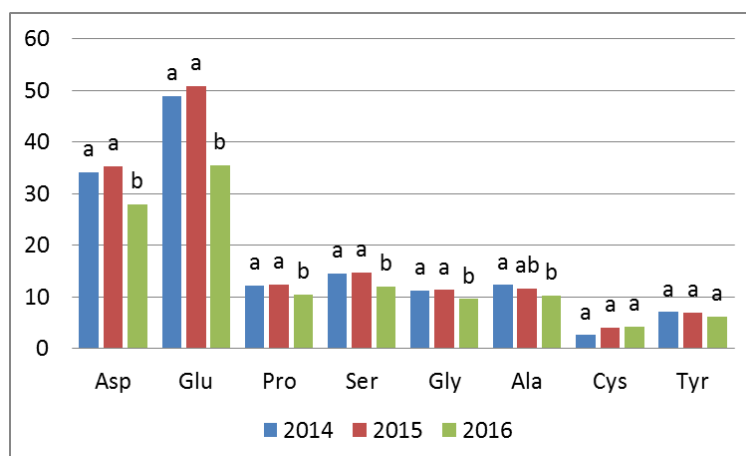


Figure 8. Nonessential amino acids content (mg g^{-1}) of lentil seeds during the study years (independent on experimental factors) (different letters indicate significant difference at $P \leq 0.05$)

Table 5. Essential amino acids content (mg g^{-1}) in lentil seeds (mean for 2014-2016) (T^1 – Tina; A^2 – Anita; ns^3 – not significant at $P \leq 0.05$)

Amino acid	Cultivar		LSD _{0.05}
	T^1	A^2	
Thr	10.17	10.60	0.035
Val	12.47	13.00	0.035
Met	8.56	8.24	0.040
Ile	10.08	10.37	0.042
Leu	18.70	19.00	0.051
Phe	12.70	12.70	ns^3
His	6.49	7.00	0.043
Lys	19.57	20.03	0.242
Arg	17.97	18.67	0.069
Trp	5.48	5.68	0.043

Table 6. Nonessential amino acids content (mg g⁻¹) in lentil seeds (mean for 2014-2016) (T¹ – Tina; A² – Anita)

Amino acid	Cultivar		LSD _{0.05}
	T ¹	A ²	
Asp	32.33	32.50	0.056
Glu	44.50	45.70	0.127
Pro	11.29	12.00	0.028
Ser	13.57	13.97	0.039
Gly	10.55	10.94	0.040
Ala	11.23	11.57	0.060
Cys	3.82	3.44	0.035
Tyr	6.83	6.72	0.021

Conclusions

The results of this study reveal that the organically grown ‘Anita’ variety was characterized by a higher content of N, P, Cu, Zn and Fe in grain as well as most of evaluated amino acids than the ‘Tina’ variety. At the same time, a higher content of total protein, fat and Omega 3 and Omega 6 polyunsaturated fatty acids was determined in var. ‘Anita’ seeds. Lentil sown in wider rows produced a higher total protein content in its seeds. The presence of oat as a supporting crop in the lentil crop decreased the accumulation of total protein, N, P, K and all micronutrients evaluated (Cu, Zn, Mn, Fe, B) compared to the treatment with sole cropped lentil.

In organic farming, there is a constant need to seek new, more effective solutions for control of agricultural pests. Due to the high nutritional value of lentil and its suitability for cultivation under organic farming conditions, in the future it seems necessary to undertake research on the possibility of reducing the incidence of fungal pathogens, taking into account intercropping, sowing varietal mixtures, and different crop densities. Testing other plant species that could be used as supporting crops in lentil cultivation seems an interesting aspect. At the same time, it is worth to include more varieties of lentil in the study to draw more general conclusions.

Acknowledgements. This research was supported by the Ministry of Agriculture and Rural Development, Ministry of Science and Higher Education in Poland.

REFERENCES

- [1] Alghamdi, S., Khan, A. M., Ammar, M. H., El-Harty, E. H., Migdadi, H. M., El-Khalik, S. M. A., Al-Shameri, A. M., Javed, M. M., Al-Faifi, S. A. (2014): Phenological, nutritional and molecular diversity assessment among 35 introduced lentil (*Lens culinaris* Medik.) genotypes grown in Saudi Arabia. – International Journal of Molecular Sciences 15: 277-295.
- [2] COBORU (2000): The List of Vegetable Plant Varieties / Lista odmian roślin warzywnych. – The Research Centre for Cultivar Testing, Słupia Wielka.
- [3] Costa, G. E. A., Queiroz-Monici, K. S., Reis, S. M. P. M., Oliveira, A. C. (2006): Chemical composition, dietary fibre and resistant starch contents of raw cooked pea, common bean, chickpea, and lentil legumes. – Food Chemistry 94: 327-330.

- [4] Duchene, O., Vian, J. F., Celette, F. (2017): Intercropping with legume for agroecological cropping systems: Complementarity and facilitation processes and the importance of soil microorganisms. A review. – *Agriculture, Ecosystems and Environment* 240: 148-161.
- [5] Fujite, K., Ofosu-Budu, K. G., Ogata, S. (1992): Biological nitrogen fixation in mixed legume-cereal cropping systems. – *Plant and Soil* 141(1-2): 155-175.
- [6] Grusak, M. A. (2010): Nutritional and Health Beneficial Quality of Lentil. – In: Erksine, W., Muehlbauer, F. J., Sarker, A., Sharma, B. (eds.) *The Lentil: Botany, Production and Uses*, pp. 368-390. CABI, Oxfordshire.
- [7] Hamdi, A., Mona, M. A. A., Shaaban, M., Ezzat, Z. M. (2012): Agronomic, seed protein and quality characters of the most promising lentil genotypes in Egypt. – *World Applied Sciences Journal* 20(1): 70-79.
- [8] Hefnawy, T. H. (2011): Effect of processing methods on nutritional composition and anti-nutritional factors in lentils (*Lens culinaris*). – *Annals of Agricultural Science* 56(2): 57-61.
- [9] Ionescu, A. M., Roman, G. V. (2013): Research regarding chemical composition and nutritional value of *Lens Culinaris* Medik. Species (lentil) in organic agriculture. – *Scientific Works. Series C. Veterinary Medicine* 59(1): 98-101.
- [10] Kahraman, A. (2016): Nutritional components and amino acids in lentil varieties. – *Selcuk Journal of Agriculture and Food Sciences* 30(1): 34-38.
- [11] Karadavut, U., Genc, A. (2010): Relationships between chemical composition and seed yield of some lentil (*Lens culinaris*) cultivars. – *International Journal of Agriculture and Biology* 12: 625-628.
- [12] Kowalczyk, D., Stryjecka, M., Baraniak, B. (2007): The profile of functional properties of native and acylated lentil protein concentrates and their trypsin hydrolysates. – *Żywność. Nauka. Technologia. Jakość* 5(54): 102-112.
- [13] Özer, M. S., Kaya, F. (2010): Physical, chemical and physicochemical properties of some lentil varieties grown in Turkey. – *Journal of Food, Agriculture and Environment* 8(3-4): 610-613.
- [14] Peñaloza, H. E., Levío, C. J., Guerrero, C. J. (1992): Seed yield losses caused by lodging in lentil (*Lens culinaris* Medik.), cv. Araueana-INLA. – *Agricultura Técnica* 52(3): 294-300.
- [15] Stępniaak-Sołyga, P., Wojtasik, J. (2003): Zawartość składników pokarmowych i mineralnych w nasionach grochu (*Pisum sativum*), lędźwianu (*Lathyrus sativus*), soczewicy jadalnej (*Lens culinaris*) i soi (*Glycine max*). – *Annales Universitatis Mariae Curie-Skłodowska Sectio EE Zootechnica* 21(2): 175-185.
- [16] Świeca, M. (2015): Production of ready-to-eat sprouts with improved antioxidant capacity: Optimization of elicitation conditions with hydrogen peroxide. – *Food Chemistry* 180: 219-226.
- [17] Szpryngiel, M., Siwiło, R., Szymański, W., Zając, M. (1998): *Technologia i technika zbioru mieszanek zbożowo-strączkowych. Instrukcja wdrożeniowa.* – AR, Lublin.
- [18] Szwejkowska, B. (2012): The effect of cultivation technology on protein content of lentil (*Lens culinaris* Medic.) seeds. – *Annales Universitatis Mariae Curie-Skłodowska Sectio E Agricultura* 67(2): 20-27.
- [19] Wang, N., Hatcher, D. W., Toews, R., Gawalko, E. J. (2009): Influence of cooking and dehulling on nutritional composition of several varieties of lentils (*Lens culinaris*). – *Food Science and Technology* 42(4): 842-848.
- [20] Żabiński, A. (2008): The impact of intercropping of lentil with supporting plant on cropping and characteristics of plants belonging to this species, which are important during combine harvest. – *Inżynieria Rolnicza* 10(108): 283-290.
- [21] Zawieja, J. (2006): Response of lentil (*Lens culinaris* Medic.) on intercropping with cereals as affected by rates and sowing dates. Part I. Biometrical traits and weed infestation. – *Zeszyty Naukowe Uniwersytetu Przyrodniczego we Wrocławiu. Rolnictwo* 89(546): 377-386.
- [22] Zia-Ul-Haq, M., Ahmad, S., Aslam-Shad, M., Iqbal, S., Qayum, M., Ahmad, A., Luthria, D. L., Amarowicz, R. (2011): Compositional studies of lentil (*Lens culinaris* Medik.) cultivars commonly grown in Pakistan. – *Pakistan Journal of Botany* 43(3): 1563-1567.

EFFECT OF CARBON EMISSION CAP ON EQUILIBRIUM OUTPUT BASED ON IS-LM-EE MODEL

ZHANG, M. R.^{1*} – YANG, W. K.¹ – LEE, C. M.² – FAN, Q. B.¹

¹*School of Economics, Yangtze University, Jingzhou 434020, China*

²*Institute of Natural Resources Management, National Taipei University
New Taipei City 23741, Taiwan*

**Corresponding author
e-mail: zhmr88@163.com*

(Received 23rd Nov 2017; accepted 7th Mar 2018)

Abstract. Human society must strive to reduce the greenhouse gas emissions in order to control the global climate warming, but the carbon emission reduction behavior will affect the investment and consumption demand. This paper has modified the IS-LM-EE models in the existing literature. Using the new IS-LM-EE models of carbon tax system and of carbon emission cap-and-trade system, the paper analyzes the effect of the carbon emissions cap on the equilibrium output. The research results show that the carbon tax system has less impact on equilibrium output than the carbon cap-and-trade system if other conditions are the same. The carbon emissions cap and the carbon abatement investment will bring out the crowding-out effects and decrease the equilibrium output.

Keywords: *cap-and-trade, carbon tax system, IS-LM-EE model, environmental macroeconomic policy, crowding-out effects*

Introduction

Under the support of the world's two biggest polluters, the United States and China, the Paris Global Climate Agreement had come into force legally on the November 4, 2016 (the threshold of agreement entering into effect is that more than 55 countries of producing at least 55% of global emissions have ratified the Paris Agreement). It is a major stride to keep global warming at a maximum of 2 °C and to pursue efforts to limit it to 1.5 °C (UNFCCC, 2015). The objective of the Paris Agreement is to put forward the urgency of enhanced and immediate mitigation action of the climate change. In order to meet the Paris Global Climate Agreement target of staying well below 2 °C and pursuing a 1.5 °C target, the United Nations Environment Programme (UNEP) pointed out that countries of the Intergovernmental Panel on Climate Change (IPCC) need to cut down about 12~14 billion tons of greenhouse gas emissions before 2030 based on the intended nationally determined contributions (INDCs) (UNEP, 2016).

Natural resources are limited, and the carrying capacity of the environment ultimately limits the scale of economic growth (Rezai and Stigl, 2016). In order to maintain sustained economic growth and environmental quality, we need to adopt positive environmental policies to reduce exhaustible resources consumption, waste discard and greenhouse gas emissions. The macroeconomic policy tools will promote the sustainable economic growth (Fontana and Sawyer, 2016; Halkos and Paizanos, 2015; Jackson and Victor, 2016; Rezai et al., 2013; Taylor et al., 2016; Zhang and Lee, 2017).

The mitigation action of the greenhouse gas emissions requires that environmental policy tools, financial policy tools and monetary policy tools should match and coordinate each other. Therefore, Daly (1991) constructed the theory of environmental

macroeconomics with the environmental constraint, Heyes (2000), Lawn (2003), Sim (2006), Decker and Wohar (2012) researched the financial policy tools and monetary policy tools matching and coordinating to realize the sustainable development with the limited environmental resources by using the IS-LM-EE model. Lawn (2007) and Razmi (2016) analyzed the main role of the environmental macroeconomics policy tools in open economy. IS-LM-EE model mainly studies the decision issues of the equilibrium output and equilibrium interest rate among the equilibrium product market, equilibrium money market and equilibrium environmental market. IS curve and LM curve respectively represents the combination of different output and interest rate in the equilibrium product market and the equilibrium money market. The environment equilibrium curve (EE) serves as of all interest–output combinations when the consumed natural capital (such non-renewable resources as oil, coal, etc., or such renewable resources as lumber, river flow for hydropower, etc., or such waste discard as waste gas, waste water, waste residue discharge.) in production process exactly offsets the natural environment’s ability to regenerate (or absorb) them. The relation of complementariness or substitution between the natural capital and physical capital (or manmade capital) will affect the slope of EE schedule. The environmental quality will become better (worst) when the intersection point of IS and LM curve is on the left (right) of EE curve. The economy can achieve sustainable development when the intersection point of IS and LM curve is on the EE curve. As a result, the economy achieves sustainable development.

The difference between IS-LM-EE models is that the same combination of fiscal policy and monetary policy has different effects on economic growth. For instance, the tight fiscal and expansionary monetary policy will promote economic growth on the Heyes (2000) and Sim (2006) IS-LM-EE models, but the same policy combination will lead to economic recession on Decker and Wohar (2012) IS-LM-EE model. Meanwhile, IS-LM-EE models of Heyes (2000), Lawn (2003), Decker and Wohar (2012) lack further automatic adjustment mechanism, although Sim (2006) model analyzes the automatic adjustment mechanism by using the conception of the “output gap”, but the lag of adjustment mechanism will bring great threat to environmental quality.

Considering that the global warming will affect the economic sustainable development, therefore, the motive of government constraining carbon emissions cap is to promote the sustainable development of human society and economy. The government or manufacturers will invest the equipment of clean energy or technology of carbon capture and storage in order to realize the targets of carbon abatement. Assumed the fund of the government abatement investment come from carbon tax revenue and the fund of the manufacturers abatement investment come from a part of productive funds. So, the traditional analytical framework of the IS-LM-EE models have neglected the influence of manufacturers or government carbon abatement investment on IS curve.

Natural capital will provide renewable or nonrenewable resources and ecological services (such as, absorption of wastes, basic life-support functions, and amenity services) in production process (Ekins et al., 2003; Fontana and Sawyer, 2016). But the concept of natural capital is also controversial (Burkett, 2003). This paper will modify the EE curve. We use total carbon allowance to substitute the amount of natural capital in EE curve and introduce the investment of carbon abatement into EE Curve. The carbon abatement investment behavior of manufacturers or government will affect on the aggregate demand; therefore, this paper also modify the IS curve by introducing the

investment of carbon abatement. This paper builds up the new IS-LM-EE model by using adjusted IS and EE curve and traditional LM curve and analyzes the effect of the carbon emission cap on equilibrium output.

Equilibrium output of new IS-LM-EE model

Constructing new IS-LM-EE model

The new IS-LM-EE framework includes the following variables:

Y = real total output

r = real interest rate

I_{car} = investment of carbon abatement

\bar{E}_{car} = given carbon emissions cap

C = consumption expenditures

C_0 = autonomous consumption expenditures

G = autonomous government expenditures (assumed to be exogenous)

I = investment expenditures

I_0 = autonomous investment expenditures

T = total tax

TR = government transfer expenditure

T_{car} = total carbon tax

$\frac{M}{P}$ = real money supply

M = nominal money supply

P = price level (assumed to be constant)

P_{car} = carbon tax rate or carbon price

E = natural capital

Λ = institutional parameters of environmental regulation

a) Adjusted environment equilibrium curve (EE)

The Heyes's (2000) and Sim's environment equilibrium curve (EE) equation is as follows: $EE(Y, r, E, \Lambda) = 0$. It is very difficult to solve the equilibrium solution of IS-LM-EE Model when EE curve is parabolic. For the convenience of analysis, We use \bar{E}_{car} and I_{car} respectively to substitute for E and Λ and obtain the adjusted EE curve equation: $EE(Y, r, \bar{E}_{car}, I_{car}) = 0$. We expand the left side of the adjusted EE curve equation by using the first order Taylor expansion; therefore, we will obtain adjusted linear EE curve equation:

$$\mu Y + \theta r - \zeta I_{carbon} = \bar{E}_{carbon} \quad (\text{Eq.1})$$

Equation 1 is the adjusted linear equilibrium curve (EE) with the fixed carbon emission target. Where, μ is the carbon emission intensity to the total output with given technical level, θ is the interest rate sensitivity coefficient to the carbon emissions, according to the Heyes's (2000) hypothesis of the substitute between natural capital and man-made capital, there is $\theta > 0$. ζ is the emissions reduction investment

coefficient. Following Heyes's (2000) opinion, we assume that the EE curve of the negative slope is steeper than the IS curve.

The position of EE curve will be determined by the investment scale of the carbon abatement and the carbon emissions cap on the *Equation 1*. It will increase the more space of economic growth when the investment scale of the carbon abatement or the carbon emissions cap increases. Therefore, adjusted EE curve will move towards right, and vice versa. In order to carry out the international obligations of the reducing greenhouse gases (GHGs), some governments determine their carbon emission cap based on the intended nationally determined contributions (INDCs), but the stringent carbon abatement control goals will affect the economic growth, which is perhaps one of the reasons for the Trump administration's decision to pull out of the Paris Global Climate Agreement on June 1st 2017.

b) Adjusted IS curve

Following view of Keynes's macroeconomics, we assume that the aggregate demand consists of consumer demand, investment demand and government demand in the closed economy. Without consideration the carbon abatement investment, we can assume that the function of consumer demand, of investment demand and of government demand are respectively as follows:

Function of consumer demand (*Eq. 2*):

$$C = C_0 + c(Y - T + TR) \quad (\text{Eq.2})$$

Function of investment demand (*Eq. 3*):

$$I = I_0 - br \quad (\text{Eq.3})$$

Function of government demand (*Eq. 4*):

$$G = G \quad (\text{Eq.4})$$

Here, $c(0 \leq c < 1)$ stands for the marginal propensity to consume, $b(b > 0)$ stands for sensitivity coefficient of investment to interest rates. Therefore, the traditional aggregate demand function is as follows (*Eq. 5*):

$$Y = C_0 + c(Y - T + TR) + (I_0 - br) + G \quad (\text{Eq.5})$$

Case one:

If we assume that the government takes on the carbon abatement investment responsibility by levied carbon tax with the manufacturers according to the polluter paying principle, and the total carbon tax revenue are used in the activity of government carbon abatement investment and the manufacturers do not invest the carbon abatement activity. Namely, $I_{car} = T_{car}$. Meanwhile, the function of investment demand and of government demand will be unchanged.

So, the adjusted function of consumer demand is as follows (*Eq. 2a*):

$$C = C_0 + c(Y - T - T_{car} + TR) \quad (\text{Eq.2a})$$

Equation 5 will change as follows (Eq. 5a):

$$Y = C_0 + c(Y - T - I_{car} + TR) + (I_0 - br) + G \quad (\text{Eq.5a})$$

Namely, adjusted IS curve equation is as follows (Eq. 6a):

$$(1 - c)Y + br + cI_{car} = C_0 + I_0 + cTR + G - cT \quad (\text{Eq.6a})$$

Case two:

If we assume that the government encourage the manufacturers to invest carbon abatement activity by the carbon cap-and-trade system, and the manufacturer investment will be divided into productive investment and emission abatement investment. The emission abatement investment is unproductive investment, to increase the emission abatement investment increasing means the productive investment decreasing when the total capital is fixed. Meanwhile, the function of consume demand and of government demand will be unchanged.

The adjusted function of investment demand is as follows (Eq. 3a):

$$I = I_0 - br - I_{car} \quad (\text{Eq.3a})$$

Therefore, Equation 5 will change as follows (Eq. 5b):

$$Y = C_0 + c(Y - T + TR) + (I_0 - br - I_{car}) + G \quad (\text{Eq.5b})$$

Namely, adjusted IS curve equation is as follows (Eq. 6b):

$$(1 - c)Y + br + I_{car} = C_0 + I_0 + cTR + G - cT \quad (\text{Eq.6b})$$

Equation 6a or 6b is the adjusted IS curve with the investment of carbon emission reduction.

Obviously, the investment scale of the carbon abatement will determine the position of IS curve.

c) LM curve

In order to facilitate the analysis, we still adopt the traditional LM curve in the money market (Eq. 7):

$$gY - hr = \frac{M}{P} \quad (\text{Eq.7})$$

Where, $g (g > 0)$ is the sensitivity coefficient of money demand to national income, $h (h > 0)$ is the sensitivity coefficient of money demand to the real interest rate.

d) New IS-LM-EE model

Case one:

Equations 1, 6a and 7 constitute new IS-LM-EE model based on the carbon tax system. The model is as follows (Eq. 8a):

$$\begin{cases} (1-c)Y + br + cI_{car} = C_0 + I_0 + cTR + G - cT \\ gY - hr = \frac{M}{P} \\ \mu Y + \theta r - \zeta I_{car} = \bar{E}_{car} \end{cases} \quad (\text{Eq. 8a})$$

Case two:

Equations 1, 6b and 7 constitutes new IS-LM-EE model based on the carbon cap-and-trade system. The model is as follows (Eq. 8b):

$$\begin{cases} (1-c)Y + br + I_{car} = C_0 + I_0 + cTR + G - cT \\ gY - hr = \frac{M}{P} \\ \mu Y + \theta r - \zeta I_{car} = \bar{E}_{car} \end{cases} \quad (\text{Eq. 8b})$$

Equilibrium solution of the IS-LM-EE model

In the systems of equations (Eq. 8a), we obtain the equilibrium solution of output, interest rate and investment of carbon abatement (Eqs. 9a, 10a, 11a):

$$Y_{tax} = \frac{\zeta h A_0 + (\zeta b + c\theta) \frac{M}{P} + ch \bar{E}_{car}}{cg\theta + \mu ch + \zeta gb + \zeta h(1-c)} \quad (\text{Eq. 9a})$$

$$r_{tax} = \frac{\zeta g A_0 - [c\mu + \zeta(1-c)] \frac{M}{P} + cg \bar{E}_{car}}{cg\theta + \mu ch + \zeta gb + \zeta h(1-c)} \quad (\text{Eq. 10a})$$

$$I_{car}^{tax} = \frac{(g\theta + \mu h) A_0 + [\mu b - \theta(1-c)] \frac{M}{P} - [gb + h(1-c)] \bar{E}_{car}}{cg\theta + \mu ch + \zeta gb + \zeta h(1-c)} \quad (\text{Eq. 11a})$$

In order to assure the nonnegative investment of carbon abatement, we assume (Eq. 12a):

$$I_{car}^{tax} = \frac{(g\theta + \mu h) A_0 + [\mu b - \theta(1-c)] \frac{M}{P} - [gb + h(1-c)] \bar{E}_{car}}{cg\theta + \mu ch + \zeta gb + \zeta h(1-c)} \geq 0 \quad (\text{Eq. 12a})$$

In the systems of equations (Eq. 8b), we obtain the equilibrium solution of output, interest rate and investment of carbon abatement (Eqs. 9b, 10b, 11b):

$$Y_{trade} = \frac{\zeta h A_0 + (\zeta b + \theta) \frac{M}{P} + h \bar{E}_{car}}{g\theta + \mu h + \zeta gb + \zeta h(1-c)} \quad (\text{Eq.9b})$$

$$r_{trade} = \frac{\zeta g A_0 - [\mu + \zeta(1-c)] \frac{M}{P} + g \bar{E}_{car}}{g\theta + \mu h + \zeta gb + \zeta h(1-c)} \quad (\text{Eq.10b})$$

$$I_{car}^{trade} = \frac{(g\theta + \mu h) A_0 + [\mu b - \theta(1-c)] \frac{M}{P} - [gb + h(1-c)] \bar{E}_{car}}{g\theta + \mu h + \zeta gb + \zeta h(1-c)} \quad (\text{Eq.11b})$$

In order to assure the nonnegative investment of carbon abatement, we assume (Eq. 12b):

$$I_{car}^{trade} = \frac{(g\theta + \mu h) A_0 + [\mu b - \theta(1-c)] \frac{M}{P} - [gb + h(1-c)] \bar{E}_{car}}{g\theta + \mu h + \zeta gb + \zeta h(1-c)} \geq 0 \quad (\text{Eq.12b})$$

Obviously, there is $Y_{tax} \geq Y_{trade}$ and $I_{car}^{tax} \geq I_{car}^{trade}$ when $0 \leq c < 1$. This shows that it has less impact on equilibrium output when the government takes on the carbon abatement investment responsibility by levied carbon tax with the manufacturers.

We assume that the carbon tax rate is P_{car} . Based on the previous analysis, the real carbon emissions of the manufacturer is $\zeta I_{car} + \bar{E}_{car}$. So, the total carbon tax revenue is $T_{car} = I_{car} = P_{car} \times (\zeta I_{car} + \bar{E}_{car})$. Therefore, the carbon tax rate must be satisfied (Eq. 13):

$$P_{car} = \frac{1}{\zeta + \frac{[cg\theta + \mu ch + \zeta gb + \zeta h(1-c)] \bar{E}_{car}}{(g\theta + \mu h) A_0 + [\mu b - \theta(1-c)] \frac{M}{P} - [gb + h(1-c)] \bar{E}_{car}}} \quad (\text{Eq.13})$$

Equation 13 shows that the carbon tax rate will be affected by fiscal policy, or the monetary policy, or the carbon emission goal. For example, the carbon tax rate will increase when the government implements the expansionary fiscal policy, or expansionary monetary policy, or decreasing the carbon emission cap. But the carbon tax rate will be very difficult to change in the short period when the government levies the carbon tax to the manufacturer with the fixed carbon tax rate. The new IS-LM-EE model with the carbon tax system will be very difficult to realize new equilibrium with the change of the environmental macroeconomic policy tool. But the new IS-LM-EE model with the cap-and-trade system will automatically realize the new equilibrium with the change of the environmental macroeconomic policy tool. In this sense, the manufacturer

taking on the carbon abatement investment responsibility is better than the government taking on the carbon abatement investment responsibility by levied carbon tax.

Crowding-out effects of the carbon emissions cap on the new IS-LM-EE model

IS curve and LM curve will decide equilibrium output and the carbon abatement investment is null if the government does not restrain the carbon emissions cap. The equilibrium output is as follows (Eq. 14):

$$Y^* = \frac{hA_0 + b \frac{M}{P}}{(1-c)h + bg} \quad (\text{Eq.14})$$

Owing to the government restrains the carbon emissions cap and the carbon abatement investment is unproductive investment, the carbon emissions cap and the carbon abatement investment will bring out the crowding-out effects and decrease the equilibrium output.

Let, $\Delta Y_{tax} = Y^* - Y_{tax}$, $\Delta Y_{trade} = Y^* - Y_{trade}$.

Therefore (Eqs. 15 and 16):

$$\Delta Y_{tax} = \frac{(g\theta + \mu h)chA_0 + [\mu b - (1-c)\theta]ch \frac{M}{P} - [(1-c)h + bg]ch\bar{E}_{car}}{[cg\theta + \mu ch + \zeta gb + \zeta h(1-c)][(1-c)h + bg]} \quad (\text{Eq.15})$$

$$\Delta Y_{trade} = \frac{(g\theta + \mu h)hA_0 + [\mu b - (1-c)\theta]h \frac{M}{P} - [(1-c)h + bg]h\bar{E}_{car}}{[g\theta + \mu h + \zeta gb + \zeta h(1-c)][(1-c)h + bg]} \quad (\text{Eq.16})$$

Obviously, there is $\Delta Y_{tax} < \Delta Y_{trade}$ when $0 \leq c < 1$. This shows that the crowding-out effects of carbon tax system is less than of carbon cap-and-trade system.

Environmental macroeconomic policy analysis in the new IS-LM-EE model

The equilibrium solutions have the similar form in two kinds of new IS-LM-EE model. So we only analyze the effect of any environmental macroeconomic policy tools change in the new IS-LM-EE model with the carbon cap-and-trade system.

According to the hypothesis, the EE curve of the downward sloping is steeper than IS curve of, namely, $-\frac{\mu}{\theta} < -\frac{1-c}{b}$, $\theta > 0$.

Expansionary fiscal policy

The derivatives of Equations 9b and 11b on government expenditures G are as follows:

$$\frac{dY_{trade}}{dG} = \frac{\zeta h}{g\theta + \mu h + \zeta gb + \zeta h(1-c)} > 0 \quad (\text{Eq.17})$$

$$\frac{dI_{car}^{trade}}{dG} = \frac{g\theta + \mu h}{g\theta + \mu h + \zeta gb + \zeta h(1-c)} > 0 \quad (\text{Eq.18})$$

Equations 17 and 18 show that the equilibrium output and the equilibrium investment of the carbon abatement will increase when the government implements the expansionary fiscal policy by enlarging the government purchase expenditure.

As shown in Figure 1, IS₀, LM and EE₀ curve will achieve the equilibrium in point A. The IS curve will shift to the right from the IS₀ to IS₂ when the government implements the expansionary fiscal policy, so the expansionary fiscal policy will increase total output, also increases of carbon emission, so the manufacturer needs to increase the investment of carbon abatement, so, the EE curve also shift to the right, the IS curve starts to shift to left from the IS₂ to IS₁ when the manufacturers increase the investment of the carbon abatement. The IS₁, LM and EE₁ curve will achieve new equilibrium at the point B.

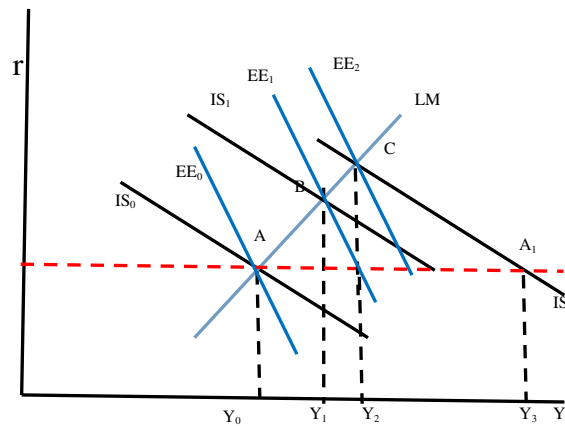


Figure 1. Expansionary fiscal policy

Expansionary monetary policy

The derivatives of Equations 9b and 11b on money supply are as follows:

$$\frac{dY_{trade}}{dM} = \frac{\zeta b + \theta}{P} \frac{1}{g\theta + \mu h + \zeta gb + \zeta h(1-c)} > 0 \quad (\text{Eq.19})$$

$$\frac{dI_{car}^{trade}}{dM} = \frac{\mu b - \theta(1-c)}{P} \frac{1}{g\theta + \mu h + \zeta gb + \zeta h(1-c)} > 0 \quad (\text{Eq.20})$$

Equations 19 and 20 show that the equilibrium total output and the equilibrium investment of the carbon abatement will increase when the government implements the expansionary monetary policy by enlarging the money supply.

As shown in Figure 2, IS₀, LM₀ and EE₀ curve will achieve the equilibrium in point A. The LM curve will shift to the right from the LM₀ to LM₁ when the government implements the expansionary monetary policy by increasing nominal money supply, the total output increasing will lead to the carbon emission increasing, so the manufacturer needs to increase the investment of carbon abatement, the EE curve also shifts to the

right, the IS curve starts to shift to left from the IS_1 to IS_0 when the manufacturers increase the investment of carbon abatement. The IS_1 , LM_1 and EE_1 curve will achieve new equilibrium at the point B.

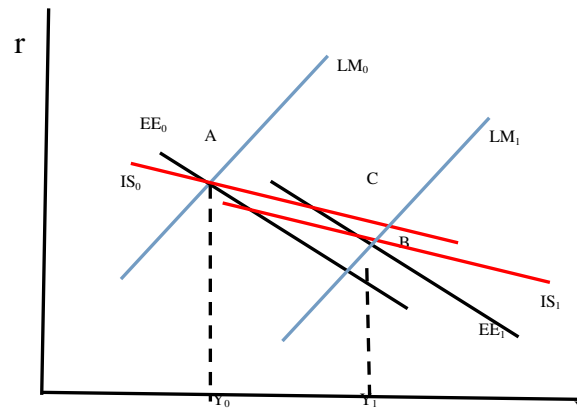


Figure 2. Expansionary monetary policy

Raising carbon emissions cap

The derivatives of *Equations 9b* and *11b* on carbon emissions cap are as follows:

$$\frac{dY_{trade}}{d\bar{E}_{car}} = \frac{h}{g\theta + \mu h + \zeta gb + \zeta h(1-c)} > 0 \quad (\text{Eq.21})$$

$$\frac{dI_{car}^{trade}}{d\bar{E}_{car}} = \frac{-[gb + h(1-c)]}{g\theta + \mu h + \zeta gb + \zeta h(1-c)} < 0 \quad (\text{Eq.22})$$

Equation 21 shows that the equilibrium output will increase when the government increases the carbon emissions cap. *Equation 22* shows that the investment of the carbon emission reduction will decrease when the government increases the carbon emissions cap.

As shown in *Figure 3*, IS_0 , LM_0 and EE_0 curve will achieve the equilibrium in point A.

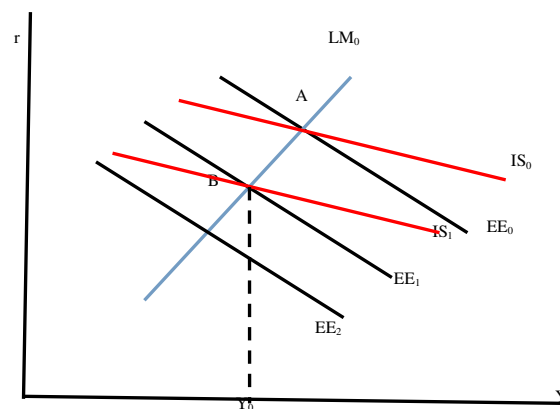


Figure 3. Decrease carbon emissions cap

The EE_0 curve will shift to the left to the position of EE_2 curve when the government decreases the carbon emissions cap. The carbon emission in production process at the intersection A of the IS_0 curve and LM_0 curve will exceed the given carbon emission cap, so the manufacturer needs to increase the investment of the carbon abatement, the EE_2 curve will shift to the right to the position of EE_1 curve. Owing to increasing the investment of the carbon emission reduction, the IS curve start to shift to left from the IS_0 to IS_1 . The IS_1 , LM_0 and EE_1 curve will achieve new equilibrium at the point B.

Macroeconomic policy tools portfolio

Next, we research the effect of the environmental macroeconomic policy portfolio on the equilibrium output with the fixed carbon emissions cap and the unchanged investment of the carbon emission reduction.

The perfect differential of Equations 9b and 11b are as follows (Eqs. 23 and 24):

$$dY_{trade} = \frac{\zeta h dA_0 + (\zeta b + \theta) \frac{dM}{P} + h d\bar{E}_{car}}{g\theta + \mu h + \zeta gb + \zeta h(1-c)} \quad (\text{Eq.23})$$

$$dI_{car}^{trade} = \frac{(g\theta + \mu h) dA_0 + [\mu b - \theta(1-c)] \frac{dM}{P} - [gb + h(1-c)] d\bar{E}_{car}}{g\theta + \mu h + \zeta gb + \zeta h(1-c)} \quad (\text{Eq.24})$$

If we assume that the fixed carbon emissions cap and the investment of the carbon emission reduction remain unchanged, and the government implements the expansionary fiscal policy by enlarging the government purchase expenditure.

Therefore, $dA_0 = dG$, $dI_{car}^{trade} = d\bar{E}_{car} = 0$, $\frac{dM}{P} = -\frac{(g\theta + \mu h)dG}{\mu b - \theta(1-c)}$, and

$$dY_{trade} = \frac{-[\zeta h(1-c) + \zeta bg + g\theta + \mu h]\theta dG}{[g\theta + \mu h + \zeta gb + \zeta h(1-c)][\mu b - \theta(1-c)]}.$$

This shows that the expansionary fiscal policy needs to collocate tight monetary policy when the fixed carbon emissions cap and the investment of the carbon emission reduction remain unchanged. The expansionary fiscal and tight monetary policy portfolio decreases the equilibrium output, vice versa. This conclusion is similar to the implication of macroeconomic policy portfolio on Heyes's IS-LM-EE model.

Conclusion

This paper revises the IS curve and EE curve under the constraint of given carbon emission cap and the investment of carbon abatement based on previous studies, and sets up two kinds of the IS-LM-EE model with carbon tax system and the IS-LM-EE model with carbon cap-and-trade system. The research results show that the equilibrium output of carbon tax system is more than of carbon emission cap-and-trade system. But the new equilibrium will be very difficult to realize with the fixed carbon tax rate in the IS-LM-EE model with carbon tax system when the environmental macroeconomic policy instruments change; however, the new equilibrium will automatic realize in the IS-LM-EE model with carbon cap-and-trade system at same condition. Thus, the carbon

cap-and-trade system is more reasonable and practicable than the carbon tax system in practice. The new IS-LM-EE models will automatically achieve new equilibrium by adjusting the investment scale of the carbon abatement when any policy tool of environmental macroeconomic policy changes. There exists the crowding-out effects of the investment of the carbon abatement in the new IS-LM-EE model. The expansionary fiscal policy needs to collocate tight monetary policy when the fixed carbon emissions cap and the investment of the carbon emission reduction remain unchanged. This policy portfolio will decrease the equilibrium output, vice versa.

The conclusion of this paper is based on Heyes's (2000) hypothesis of the substitute between natural capital and man-made capital and the EE curve of the negative slope being steeper than the IS curve. The conclusion can be changed if the hypothesis of the substitute between natural capital and man-made capital, or of the negative slope EE curve being steeper than the IS curve changes. Thus, we need to study the effect of carbon emission cap on equilibrium output with complementarity between natural capital and man-made capital in new IS-LM-EE model. We also need to study the effect of carbon emission cap on equilibrium output with new IS-LM-EE model in the open economy in the future.

Acknowledgements. The authors are deeply grateful to APPLIED ECOLOGY AND ENVIRONMENTAL RESEARCH editor and two anonymous reviewers for their valuable comments. This work was supported by the grant from research and development foundation for humanities and social sciences of Yangtze University [Project No. 2017cszb06].

REFERENCES

- [1] Burkett, P. (2003). Natural capital, ecological economics and Marxism. – *Int. Pap. Polit. Econ.* 10(3): 1-62.
- [2] Daly, H. E. (1991): Towards an environmental macroeconomics. – *Land Economics* 67(2): 255-259.
- [3] Decker, C. S., Wohar, M. E. (2012): Substitutability or complementarity? Re-visiting Heyes' IS-LM-EE model. – *Ecological Economics* 74: 3-7.
- [4] Ekins, P., Simon, S., Deutsch, L., Folke, C., De Groot, R. (2003). A framework for the practical application of the concepts of critical natural capital and strong sustainability. – *Ecological Economics* 44(2-3): 165-185.
- [5] Fontana, G., Sawyer, M. (2016): Towards post-Keynesian ecological macroeconomics. – *Ecological Economics* 121: 186-195.
- [6] Halkos, G., Paizanos, E. (2015): Environmental macroeconomics: A critical literature review and future empirical research directions. – https://mpra.ub.uni-muenchen.de/67432/1/MPRA_paper_67432.pdf.
- [7] Heyes, A. (2000): A proposal for the greening of textbook macro: "IS-LM-EE". – *Ecological Economics* 32(1): 1-7.
- [8] Jackson, T., Victor, P. A. (2016): Does slow growth lead to rising inequality? Some theoretical reflections and numerical simulations. – *Ecological Economics* 121: 206-219.
- [9] Lawn, P. (2007): Increasing Sustainable National Income by Restoring Comparative Advantage as the Principle Governing International Trade. *Frontier Issues in Ecological Economics*. – Edward Elgar Publishing, Cheltenham, UK and Northampton, MA, USA.
- [10] Lawn, P. A. (2003): On Heyes' IS-LM-EE proposal to establish an environmental macroeconomics. – *Environment and Development Economics* 8(1): 31-56.
- [11] Razmi, A. (2016): The macroeconomics of emission permits: simple stylized frameworks for short-run policy analysis. – *Eastern Economic Journal* 42(1): 29-45.

- [12] Rezai, A., Stigl, S. (2016): Ecological macroeconomics: Introduction and review. *Ecological Economics* 121: 181-185.
- [13] Rezai, A., Taylor, L., Mechler, R. (2013): Ecological macroeconomics: An application to climate change. – *Ecological Economics* 85: 69-76.
- [14] Sim, N. C. (2006): Environmental Keynesian macroeconomics: some further discussion. *Ecological Economics* 59(4): 401-405.
- [15] Taylor, L., Rezai, A., Foley, D. K. (2016): An integrated approach to climate change, income distribution, employment, and economic growth. – *Ecological Economics* 121: 196-205.
- [16] United Nations Environment Programme (UNEP) (2016): The Emissions Gap Report. A UNEP Synthesis Report, 2016. – http://uneplive.unep.org/media/docs/theme/13/Emissions_Gap_Report_2016.pdf.
- [17] UNITED NATIONS, PARIS AGREEMENT (2015): http://unfccc.int/files/essential_background/convention/pdf/english_paris_agreement.pdf application
- [18] Zhang, M., Lee, C. (2017): Economic policy of sustainable development based on IS-LM-EE model. – *Applied Ecology and Environmental Research* 15(3): 785-795.

GROWTH AND DEVELOPMENT OF COMMON BEAN (*PHASEOLUS VULGARIS* L.) VAR. PINTO SALTILLO EXPOSED TO IRON, TITANIUM, AND ZINC OXIDE NANOPARTICLES IN AN AGRICULTURAL SOIL

MEDINA-PÉREZ, G.¹ – FERNÁNDEZ-LUQUEÑO, F.^{2*} – TREJO-TÉLLEZ, L. I.³ – LÓPEZ-VALDEZ, F.⁴ –
PAMPILLÓN-GONZÁLEZ, L.⁵

¹*Transdisciplinary Doctoral Program in Scientific and Technological Development for the Society, Cinvestav, Zacatenco, Mexico City, C. P. 07360, Mexico*

²*Sustainability of Natural Resources and Energy Program, Cinvestav-Salttillo, Coahuila de Zaragoza, C. P. 25900, Mexico*

³*Colegio de Postgraduados, Campus Montecillo, Carretera Mexico-Texcoco km 36, C. P. 56230, Mexico*

⁴*Instituto Politécnico Nacional, CIBA-IPN, Tepetitla de Lardizábal, C. P. 90700, Tlaxcala, Mexico*

⁵*División Académica de Ciencias Biológicas, UJAT, Carretera Villahermosa-Cárdenas Km 0.5, C.P. 86100, Tabasco, Mexico*

**Corresponding author*

e-mail: cinves.cp.cha.luqueno@gmail.com; phone: +52-844-438-9625

(Received 29th Nov 2017; accepted 7th Mar 2018)

Abstract. Sustainable use of nanoparticles (NP) in the agriculture requires a deep understanding in order to determine their benefits potential as well as their toxicological impacts. Common bean plants were growing and irrigated with suspensions of magnetite, ferrihydrite, hematite, zinc oxide, or titanium dioxide NP at 0, 3, or 6 g L⁻¹ in a 120 days' greenhouse experiment, in order to investigate the effect of these NP on growth and development of common bean. None of the five NP modified significantly the chlorophyll content of common bean plants, while at least one concentration of hematite, ferrihydrite or magnetite increased significantly the total N of roots or shoots, the number of pods, dry weight of pods, the number of seeds, and yield of common bean. Additionally, at least one concentration of zinc oxide or titanium dioxide decreased significantly the number of pods, the fresh weight of pods and the number of seeds. These finds are an important factor to take into account with regard to the applicability of NP for long-term use in crops, but the selection of the proper NP at their adequate concentration is important for realizing higher benefits for an agrosustainable target.

Keywords: *agro-food industry, agronanotechnology, chlorophyll content, potential hazard or risk of nanoparticles, sustainable development, nanofertilizer, Phaseolus vulgaris L.*

Introduction

While nanoparticles (NP) occur naturally in the environment and have been intentionally used for centuries, the production and use of engineered NP has seen a recent spike, which makes environmental release almost certain (Maurer-Jones et al., 2013). Keller et al. (2013) estimated that 63–91% of over 260,000–309,000 metric tons of global engineered nanomaterials production in 2010 ended up in landfills, with the balance released into soils (8–28%), water bodies (0.4–7%), and atmosphere (0.1–1.5%). It is well known that hundreds of NP are being used worldwide in a wide range

of products or devices, however, at our knowledge there are not standardized techniques nor laws governing the proper management of NP during their production, distribution, use, and confinement. This implies that NP may be released into the environment despite their potential harmful effects on human and environmental health.

Among some properties that comprise the bean are their high content of iron, vital for a proper brain development, help to correct biliary disorders, rheumatic diseases, lower cholesterol level and is effective against anemia, and their consumption can prevent some types of cancer. Per 100 common bean grams, 20 g are protein, 5.8 g are fat and 3 g are fiber (Lépiz et al., 2010).

In some prior research conducted on this topic, the results were varied, some of them showed favorable aspects due to the use of nanoparticles as the case of Ma et al. (2010), whose experimental data evinced that the TiO₂ nanoparticles at concentrations of 2.5-40 g kg⁻¹ soil, improved the growth of the spinach. Other results exhibited no significant effects, as presented by Doshi et al. (2008), where aluminum nanoparticles did not show a significant effect on common bean studies performed in sand columns with concentrations up to 17 mg L⁻¹ of aluminum. In addition, some studies present negative effects on the development and growth of established crops. Canas et al. (2008) indicated that monolayer carbon nanotubes caused significant affectations in the root elongation of crops such as tomato, cabbage, carrot and lettuce.

There have been published some studies that intend to demonstrate that some metallic NP are able to increase the growth and development of some crops, i.e., the NP are used as if they were fertilizers (Burke et al., 2015; Rico et al., 2011). However, the potential effect of NP on yield and yield components has not been studied when NP are considered as a collateral consequence of the NP polluted environment. It is still a challenge assessing most of the effect of NP in natural soils. It should be noted that NP have different pathways, effects, fates and behaviors that might vary within living organisms, soils and contaminants (Cornelis et al., 2014; Rodrigues et al., 2016). In this regard, the objective of this research was to investigate the effect of different nanoparticles such as iron, titanium and zinc oxide on growth and development of common bean plants cropped in an agricultural soil under greenhouse conditions, as a contribution to the new emerging field called econanotoxicology.

Materials and methods

Experimental site

This study was carried out in a greenhouse of the 'Programa de Sustentabilidad de los Recursos Naturales y Energía del Cinvestav-Salttillo' located in Saltillo, Coahuila, Mexico. This area is located in the southeastern state of Coahuila, centered at 25° 31' N, 101° 37' W, at an altitude of 1,600 m above sea level. According to FAO/UNESCO soil classification system, the soil is a Haplic Xerosol with pH 7.3 and electrolytic conductivity 4.8 dS m⁻¹, a water holding capacity (WHC) of 865 g kg⁻¹, an organic carbon content of 1.5 g C kg⁻¹ soil, and a total N content of 0.7 g N kg⁻¹ soil.

Biological material

Common bean seeds were donated by 'INIFAP-Celaya, Mexico'. All seeds were kept in the dark at 4 °C until use. Pinto Saltillo was developed to solve the problem of

traditional varieties of ‘pinto’ type, which has a reduced postharvest life, due to the accelerated darkening of the seed coat.

Nanomaterials

Nanoparticles of magnetite, ferrihydrite and hematite were manufactured according to Pariona (2012), while nanoparticles of zinc oxide and titanium dioxide were purchased from ‘Materiales nanoestructurados S.A de C.V. (San Luis Potosí, México)’. Its crystallographic system was cubic, hexagonal or tetragonal (*Table 1*). The X-ray diffraction was conducted to verify the pure phase samples (*Fig. 1*), and the magnetic properties of the samples were measured by MicroMag™ 2900 Alternating Gradient Magnetometer (*Fig. 2*).

Table 1. Physicochemical characteristics of nanoparticles used to irrigate common bean crop (*Phaseolus vulgaris* L.) in a 120 days greenhouse experiment.

Oxide	Molecular formula	Color	Particle size	Crystallographic system	Magnetic properties
Magnetite	Fe ₃ O ₄	Black	6 a 20 nm	Cubic	Superparamagnetic
Ferrihydrite	FeOOH•xH ₂ O	Dark brown	2 a 3 nm	Hexagonal	Antiferromagnetic
Hematite	α-Fe ₂ O ₃	Red ochre	80 a 94 nm	Hexagonal	Weakly antiferromagnetic
Zinc oxide	ZnO	White	< 50 nm	Tetragonal	Weakly ferromagnetic
Titanium dioxide	TiO ₂	White	< 50 nm	Hexagonal	Weakly ferromagnetic

Cultivation of plants in the greenhouse

The full experimental setup was repeated three times. The first one was carried out from January to May, 2016, the second one, from February to June, 2016, and the third one from March to July, 2016. Sixty sub-samples of 3,500 g soil, i.e., five kinds of nanoparticles (nano-Fe₃O₄, nano-FeOOH•xH₂O, nano-α-Fe₂O₃, nano-ZnO, and nano-TiO₂) × three replicates × four concentrations, were added to square plastic pots whose length, width, and height were 17 × 15 × 17 cm, respectively. Five treatments (nanoparticles) at four concentrations (zero, one, three, and six g L⁻¹) were applied to the soil during irrigation so that we sprayed each plastic pot with 500 mL of a zero, one, three, or six g nano L⁻¹ suspension, throughout the experiment. Three seeds of common bean were planted in one hundred and eighty plastic pots, i.e., five nanoparticles × three replicates × four concentrations on three experiments. The seeds were placed at two cm depth in each plastic pot. Five days after planting, the seedlings were thinned to one plant per plastic pot. The plastic pots were placed in the greenhouse for 120 days. A plastic container was placed under each plastic pot to collect drained liquid. However, irrigation was well controlled so that no leaching was observed. Thirty, 60 and 120 days after sowing, three plastic pots were selected at random from each treatment and each concentration. The entire soil column was removed from the plastic pot and the 0-7.5 cm and 7.5-15 cm depth, where the samples were taken with care not to damage the root structure. The roots were manually separated from the shoots of the plant. Then the soil was carefully disaggregated with the hands to avoid the rupture of the roots. Subsequently, the soil was sifted gently to extract the pieces of root that may have been left in it, in order to be sure that 100% of the roots were removed, washed and weighed. After that, the root was extended and measured along with the shoots length. The roots

and shoots were dried at 70 °C, were weighed and analyzed for Ti, Fe, Zn, and total N. The soils from 0-7.5 cm and 7.5-15 cm of depth were analyzed for pH, CE, Ti, Fe, and Zn. The amount of chlorophyll was quantified every two days after sowing, beginning at day 15 (Fig. 3). The temperature and moisture content inside the greenhouse during the experiment were 24 °C and 35-45%, respectively.

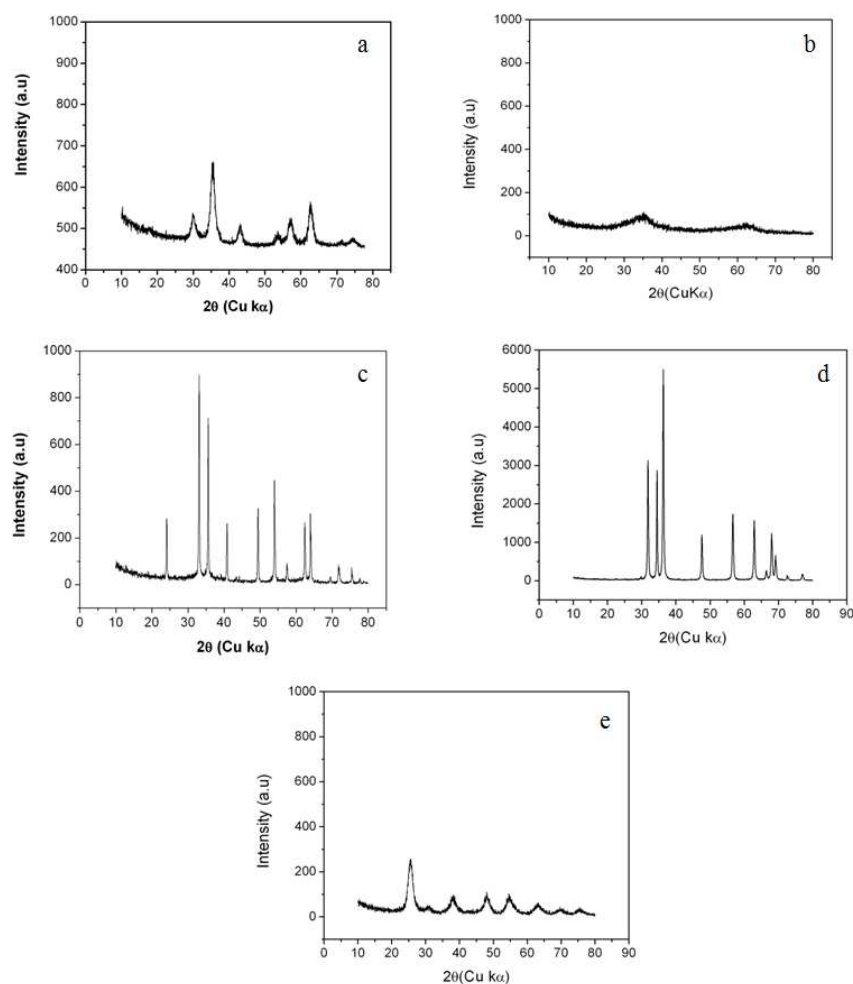


Figure 1. X-ray diffraction patterns of nanoparticles of a) Magnetite, b) Ferrihydrite, c) Hematite, d) ZnO, and e) TiO₂.

Chemical analyses

The pH was measured in 1:2.5 soil or wastewater sludge/H₂O suspension using a 716 DMS Titrino pH meter (Metrohm Ltd. CH.-901, Herisau, Switzerland) fitted with a glass electrode (Thomas, 1996). The EC was determined in a 1:5 soil/H₂O suspension as described by Rhoades et al. (1989). The organic C in soil was measured in a total organic carbon analyzer TOC-VCSN (SHIMADZU, USA). The inorganic C was determined by adding 5 mL 1 M hydrogen chloride (HCl) solution to 1 g air-dried soil and trapping CO₂ evolved in 20 mL 1 M NaOH. Total N in soil, root and shoot was measured by the Kjeldahl method using concentrated H₂SO₄, K₂SO₄ and CuSO₄ to digest the sample (Bremner, 1996). Soil particle size distribution was defined by the hydrometer method as described by Gee and Bauder (1986). Water holding capacity

was measured on 6.5 kg soil placed in a PVC tube (length 50 cm and \varnothing 16 cm), water-saturated, stoppered with a PVC ring and left to stand overnight to drain freely. The WHC is defined as (Gardner, 1986), $WHC = [(soil\ water-saturated - soil\ dried\ at\ 105\ ^\circ C) / soil\ dried\ at\ 105\ ^\circ C] * 1000$. The units of WHC are expressed in $g\ kg^{-1}$. The amount of chlorophyll was measured with a Minolta SPAD-502 Chlorophyll meter (Markwell et al., 1995). The Fe, Ti and Zn were determined by inductively coupled plasma mass spectrometry (ICP-MS).

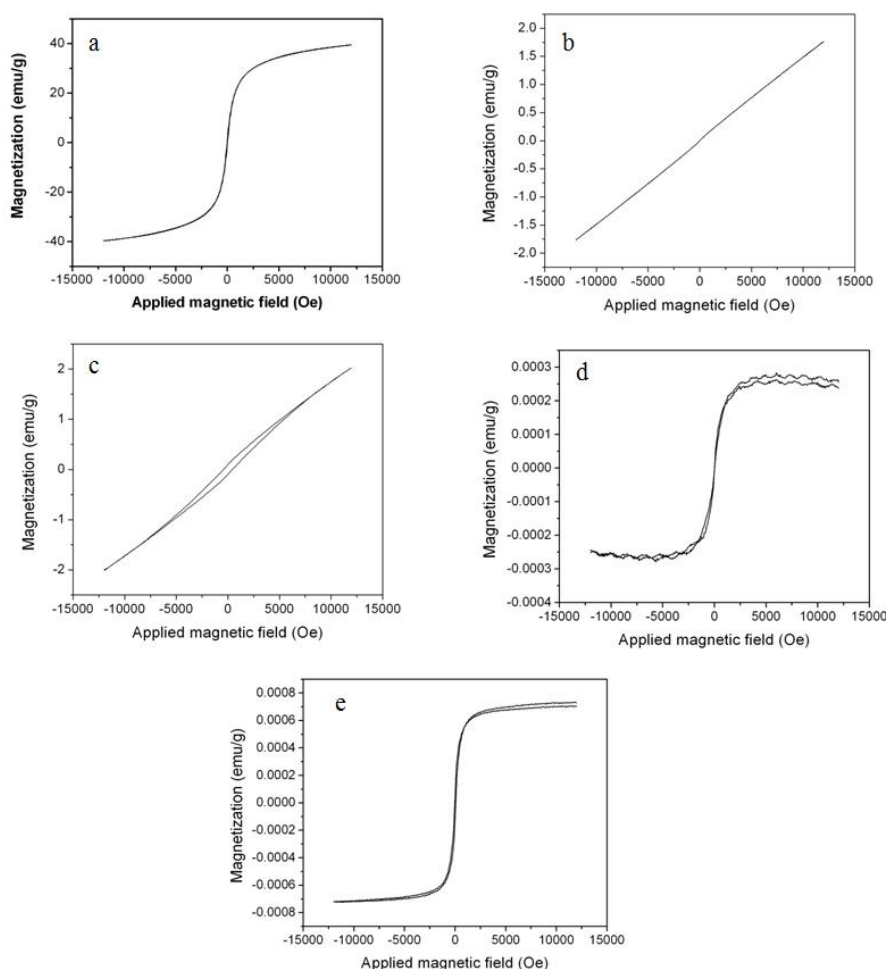


Figure 2. Magnetization curves of a) Magnetite, b) Ferrihydrite, c) Hematite, d) ZnO and e) TiO₂.

Statistical analyses

The data were subjected to an analysis of variance (ANOVA) and means compared with the Tukey test using Statistical Analysis System (SAS) software version 8.0 for Windows (SAS Institute, 1989). Soil and plant characteristics were subjected to one-way analysis of variance using a general lineal models procedure (PROC GLM) to test for significant differences between treatments ($P < 0.05$). Methodology for PCA analysis may be found in Fernández-Luqueño et al. (2016). All analyses were performed using the SAS statistical package (SAS Institute, 1989). All data presented

were the mean of three replicates in soil from three different plots, while the whole experiment was repeated three times ($n = 27$), sampled after 30, 60, and 120 days.

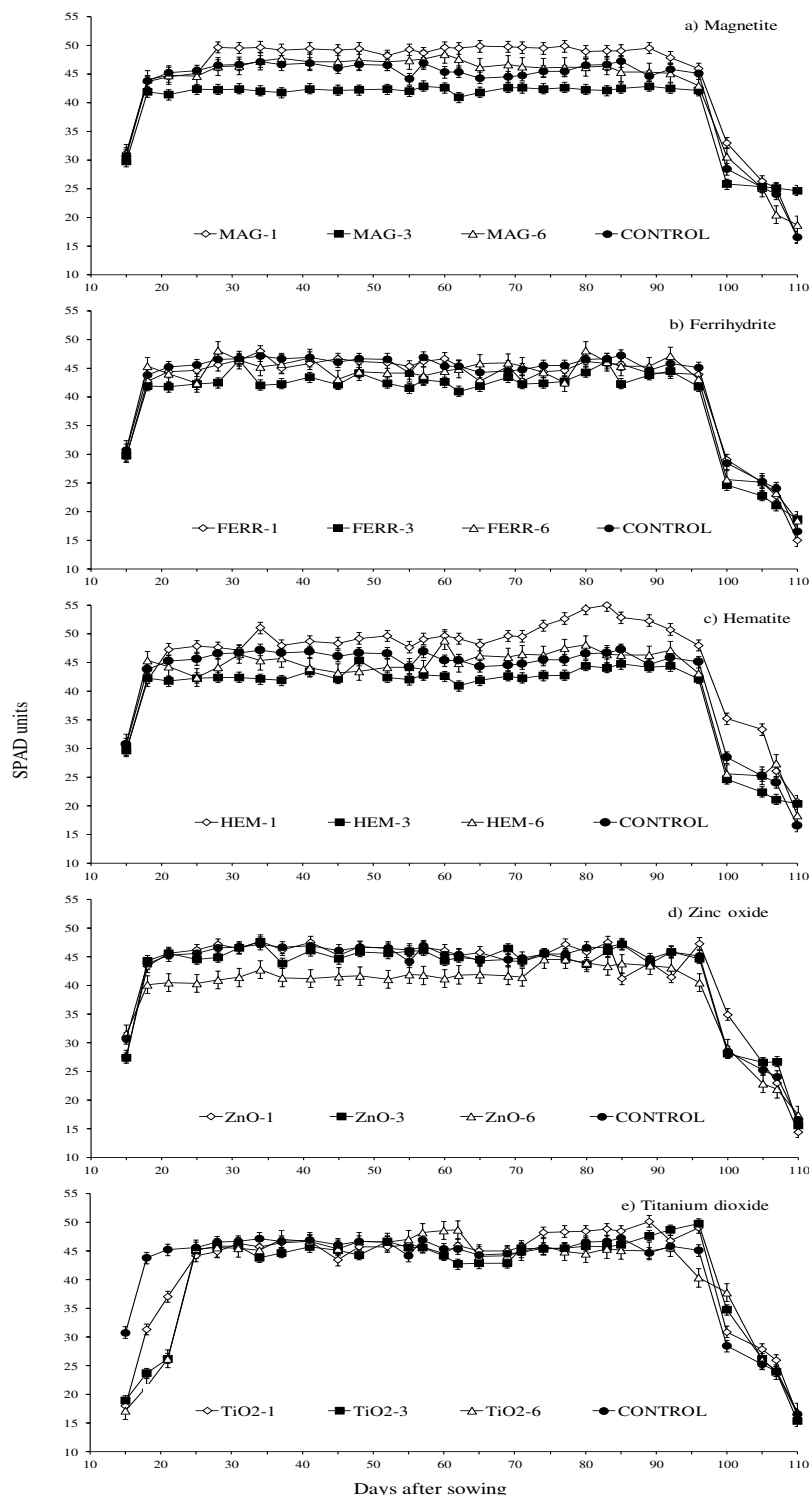


Figure 3. SPAD units of bean plants (*Phaseolus vulgaris* L.) cultivated in an agricultural soil irrigated with 500 mL of zero, one, three, or six g nanoparticle L^{-1} suspension. Nanoparticles of Fe_3O_4 , $FeOOH \cdot xH_2O$, $\alpha-Fe_2O_3$, ZnO, and TiO_2 were used. Data are the mean of three pots \times three different soils \times three experiments \times three measurements by each plant, i.e., $n = 81$. Each experiment lasted 120 days.

Results

SPAD units

The concentration of the chlorophyll quantified on leaves of common bean plants cultivated in an agricultural soil irrigated with 500 mL of zero, one, three, or six g nanoparticle L⁻¹ suspension, during 120 days after sowing is shown in *Figure 3*. SPAD Units data are related to the chlorophyll content, which maintained slightly unchanged over the time with values between 40 to 50 SPAD units in most of the experiment, excepting the HEMATITE treatment (HEM-1) which the SPAD units reached 55. The lowers chlorophyll values were presented in all the treatments during the onset of the measurements and at the end of the growing stage, i.e., at 15 and 95 days after sowing, respectively.

Plant characteristics and crop yield

Most of the plant and yield characteristics (root fresh weight, root dry weight, root length, shoot fresh weight, shoot dry weight, shoot length, and SPAD units) were not significantly different between nanoparticles treatments, compared with the CONTROL treatment ($P < 0.05$) (*Table 2*). FERRIHYDRITE treatments at 3 and 6 g L⁻¹ and HEMATITE at 1 g L⁻¹ increased significantly the concentration of total N in roots, compared with the CONTROL treatment. All FERRIHYDRITE treatments and HEMATITE at 3 and 6 g L⁻¹ increased significantly the concentration of total N in shoots, compared with the CONTROL treatment (*Table 2*).

The MAGNETITE and FERRIHYDRITE treatments at 6 g L⁻¹ increased significantly the number of pods, compared with the CONTROL treatment. However, the ZINC OXIDE and TITANIUM OXIDE treatments at 6 g L⁻¹ decreased significantly the number of pods, compared with the CONTROL treatment (*Table 2*). The fresh weight of pods decreased significantly when plants were amended with MAGNETITE or HEMATITE at 3 or 6 g L⁻¹, and when they were amended with FERRIHYDRITE or ZINC OXIDE at 6 g L⁻¹, compared with the CONTROL treatment (*Table 2*). The dry weight of pods decreased significantly when plants were amended with FERRIHYDRITE at 3 g L⁻¹, but MAGNETITE at 3 or 6 g L⁻¹ increased significantly the dry weight of pods, compared with the CONTROL treatment (*Table 2*). MAGNETITE and FERRIHYDRITE increased significantly the number of seeds when plants were amended with 6 g L⁻¹, while HEMATITE increased it significantly when plants were amended with 3 or 6 g L⁻¹. However, plants amended with ZINC OXIDE or TITANIUM DIOXIDE decreased significantly the number of seeds, compared to the CONTROL treatment. MAGNETITE or HEMATITE at 3 or 6 g L⁻¹ and FERRIHYDRITE at 6 g L⁻¹ increased significantly the yield, while ZINC OXIDE or TITANIUM DIOXIDE decreased it significantly, compared with the CONTROL treatment (*Table 2*). Nanoparticles did not affect significantly the SPAD units.

The seed number was strongly significantly correlated with fresh or dry weight of roots, length of root or shoot, total nitrogen of shoot, and with number, fresh or dry weight of pods (*Table 3*). Seed yield was strongly significantly correlated with fresh weight of root, total nitrogen of root, dry weight of shoot, total nitrogen of shoot, with number, fresh or dry weight of pods, and with seed number. In addition, SPAD units was strongly significantly correlated with total nitrogen of shoot and with yield (*Table 3*).

Table 2. Characteristics of common bean (*Phaseolus vulgaris* L.) cultivated in an agricultural soil irrigated with 500 mL at zero, one, three, or six g nanoparticle L⁻¹ suspension. The whole experiment was repeated three times (the first time, from January to May, 2016; the second one, from February to June, 2016; and the third one, from March to July, 2016). Each whole experiment lasted 120 days. Root and shoot data are the mean of values measured after 30, 60 and 120 d, i.e., n = 81. The pods and seeds data are the mean of values measured after 120 d, i.e., n = 27. SPAD unit's data are the mean of three measures twice a week during 14 weeks, i.e., n = 1,988 (3 soils × 3 replicates × 3 measures per plant × 3 sampling dates × 2 measures per week × 14 weeks).

Treatments / g NP L ⁻¹	Root ^o				Shoot				Pods			Seeds		SPAD
	Fresh weight	Dry weight	Length	Total Nitrogen	Fresh weight	Dry weight	Length	Total Nitrogen	Number	Fresh weight	Dry weight	Number	Yield	Units
Control														
0	13.6 a ^Σ	1.1 a	28.1 ab	25.8 c	17.9 a	2.8 a	21.4 ab	27.3 e	14.6 cd	20.5 de	5.5 cd	49.6 cd	3.6 fg	35.8 ab
Magnetite (Fe ₃ O ₄)														
1	10.0 a	1.0 a	24.9 ab	26.4 bc	15.6 a	1.7 a	22.0 ab	30.3 cde	15.7 bcd	20.9 cde	5.9 c	48.7 cde	3.9 defg	38.4 a
3	11.3 a	0.8 a	24.0 ab	28.9 abc	14.5 a	1.5 a	22.7 ab	29.8 cde	16.3 bc	22.5 bc	6.6 ab	49.0 cde	4.8 ab	35.8 ab
6	13.5 a	1.2 a	19.0 ab	30.4 abc	17.3 a	1.9 a	25.9 b	32.1 bcde	17.3 ab	26.0 a	7.1 a	64.3 a	4.7 bc	36.4 ab
Ferrihydrite (FeOOH·xH ₂ O)														
1	11.8 a	1.0 a	28.9 ab	30.5 abc	17.8 a	2.6 a	21.4 ab	33.8 abcd	14.7 cd	20.7 cde	5.5 cd	55.0 bc	3.6 g	36.0 ab
3	11.6 a	1.1 a	27.8 ab	32.1 a	16.7 a	2.9 a	21.9 ab	34.9 abc	15.3 bcd	20.3 cd	4.5 e	51.0 cd	3.8 efg	36.0 ab
6	12.3 a	1.3 a	27.1 ab	32.0 a	15.7 a	2.7 a	19.2 ab	35.0 abc	19.3 a	26.9 a	5.6 cd	67.0 a	4.2 cd	36.6 ab
Hematite (α-Fe ₂ O ₃)														
1	14.7 a	1.3 a	25.1 a	31.0 ab	18.3 a	3.0 a	20.2 ab	32.3 bcde	15.7 bcd	22.0 bcd	5.5 cd	53.7 bcd	4.0 def	37.6 ab
3	14.3 a	1.3 a	28.2 ab	30.0 abc	19.5 a	3.2 a	17.0 ab	37.2 ab	15.0 cd	23.6 b	5.9 c	60.0 ab	5.2 a	35.7 ab
6	14.8 a	1.4 a	31.0 ab	30.0 abc	18.1 a	2.9 a	19.4 ab	38.5 a	16.0 bcd	25.9 a	5.9 bc	60.7 ab	5.1 a	36.6 ab
Zinc Oxide (ZnO)														
1	11.1 a	0.9 a	21.2 ab	28.1 abc	15.7 a	2.4 a	17.0 ab	29.8 cde	15.0 cd	19.4 e	5.2 cde	45.3 def	4.0 defg	35.3 ab
3	11.9 a	1.0 a	19.6 ab	29.1 abc	15.5 a	2.2 a	15.7 a	30.2 cde	15.3 bcd	21.1 cde	5.5 cd	40.7 ef	3.9 defg	34.9 ab
6	13.1 a	0.8 a	21.1 ab	28.6 abc	16.8 a	2.6 a	18.2 ab	30.4 cde	12.3 e	23.8 b	5.2 cde	37.7 fg	4.1 de	36.7 ab
Titanium dioxide (TiO ₂)														
1	11.1 a	0.9 a	17.6 ab	27.7 abc	13.8 a	2.1 a	17.5 ab	28.3 e	14.0 de	19.2 e	5.0 de	31.3 gh	4.0 defg	34.7 b
3	11.9 a	1.0 a	17.1 b	30.0 abc	13.3 a	2.4 a	15.7 a	28.8 de	15.7 bcd	21.1 de	5.3 cd	23.7 h	3.9 defg	35.7 ab
6	11.5 a	1.0 a	22.0 ab	28.5 abc	18.2 a	2.0 a	16.3 a	29.5 de	12.0 e	21.9 bcd	5.0 de	26.3 h	4.1 de	34.2 b
MSD ^τ	9.05	0.64	13.5	5.0	9.4	1.7	9.2	5.4	2.0	1.9	0.7	8.5	0.4	3.5

^oFresh or dry weights are expressed in g; Length is in cm; Total nitrogen is in g N kg⁻¹ dry plant; Yield is in g per plant.

^ΣValues with the same letter within the columns are not significantly different (*P* < 0.05).

^τMinimum significant difference (*P* < 0.05).

Table 3. Correlations between characteristics of common bean crop (*Phaseolus vulgaris* L.) cultivated in an agricultural soil irrigated with 500 mL at zero, one, three, or six g NP L⁻¹ suspension. Data were pooled among five treatments, three soils and the three replicates of the whole experiment. Each experiment lasted 120 days.

Plant characteristics	Root ^o				Shoot				Pods			Seeds	
	Fresh weight	Dry weight	Length	Total Nitrogen	Fresh weight	Dry weight	Length	Total Nitrogen	Number	Fresh weight	Dry weight	Number	Yield
Root dry weight	0.867***												
Root length	0.891***	0.834***											
Root total N	-0.238***	0.005	-0.289***										
Shoot fresh weight	0.839***	0.870***	0.762***	0.142									
Shoot dry weight	0.894***	0.876***	0.852***	-0.062	0.883***								
Shoot length	0.848***	0.815***	0.809***	-0.075	0.837***	0.780***							
Shoot Total N	-0.037	0.245***	-0.041	0.839***	0.313***	0.150	0.121						
Pods number	0.279	0.428***	0.210	0.155	-0.064	-0.108	0.297***	0.166					
Pods fresh weight	0.344***	0.462***	0.155	0.332***	-0.278	-0.121	0.078	0.501***	0.292***				
Pods dry weight	0.062	0.130***	0.023	0.005	-0.218	-0.429***	0.379***	0.112	0.272	0.341***			
Seed number	0.415***	0.616***	0.647***	0.058	0.115	0.195	0.492***	0.421***	0.480***	0.400***	0.343***		
Seed yield	0.200***	0.241	0.060	0.396***	-0.183	-0.301***	-0.013	0.622***	0.276**	0.475***	0.295***	0.270***	
SPAD Units	-0.039	0.001	-0.008	0.099	-0.014	-0.017	0.023	0.186***	0.182	0.122*	0.121	0.149	0.341***

*P < 0.005; **P < 0.001; ***P < 0.0001

Principal component analysis

Loading for parameters obtained after VARIMAX rotation are given in *Table 4*. The plants characteristics had three significant PCs. The first principal component (PC1) explained 31% of variation and was related to root fresh weight, root dry weight, root length, shoot total nitrogen, number of pods, pod fresh weight, seed yield, number of seeds, and SPAD units. The second principal component (PC2) explained 20% of variation and was related to shoot fresh weight and shoot dry weight, while the third principal component (PC3) explained 14% of variation and was related to root total nitrogen but negatively related to shoot length and pod dry weight. The three principal components explained 65% of variation (*Table 4*).

On the scatter plot with PC1 and PC2, the kinds of NP or their concentrations are clearly separated from each other (*Fig. 4a*). HEMATITE and FERRIHYDRITE can be found in the upper right quadrant, while MAGNETITE, ZINC OXIDE or TITANIUM DIOXIDE lie in the two left quadrants. The CONTROL treatment lies in the lower left quadrant (*Fig. 4a*). On the scatter plot with PC1 and PC3, the treatments are visually distinct (*Fig. 4b*). The HEMATITE, FERRIHYDRITE, and CONTROL treatments lie in the two-right quadrant, while MAGNETITE, ZINC OXIDE or TITANIUM DIOXIDE lie in the two left quadrants (*Fig. 4b*).

Table 4. Rotated loading on the PC of bean plants characteristics (*Phaseolus vulgaris* L.) cultivated in an agricultural soil irrigated with 500 mL at zero, one, three, or six g NP L⁻¹ suspension. NP of Fe₃O₄, FeOOH·xH₂O, α-Fe₂O₃, ZnO, and TiO₂ were used. Data were pooled among the five treatments and three experiment repetitions. The whole experiment was repeated three times (from January to May 2015; the second one from February to June 2015; and the third one from March to July 2015). Each whole experiment lasted 120 days.

Statistical and measurements	Principal components ^a		
	PC1	PC2	PC3
Eigenvalues	4.27	2.83	1.94
Proportions	0.31	0.20	0.14
Rotated loading on three retained components			
Root fresh weight	65 ^{*,b}	14	30
Root dry weight	80 [*]	32	5
Root length	67 [*]	61	-9
Shoot fresh weight	20	74 [*]	10
Shoot dry weight	24	79 [*]	42
Shoot length	35	12	-80 [*]
Root total nitrogen	33	-50	59 [*]
Shoot total nitrogen	70 [*]	-31	44
Number of pods	57 [*]	-10	-26
Pod fresh weight	64 [*]	-40	6
Pod dry weight	36	-37	-54 [*]
Seed yield	52 [*]	-60	12
Number of seeds	80 [*]	17	-29
SPAD units	43 [*]	-31	-9

^aOnly principal components with Eigenvalues > 1 and that explain > 10% the total variance were retained

^bParameters with significant loading (> 0.4) on the within column principal component.

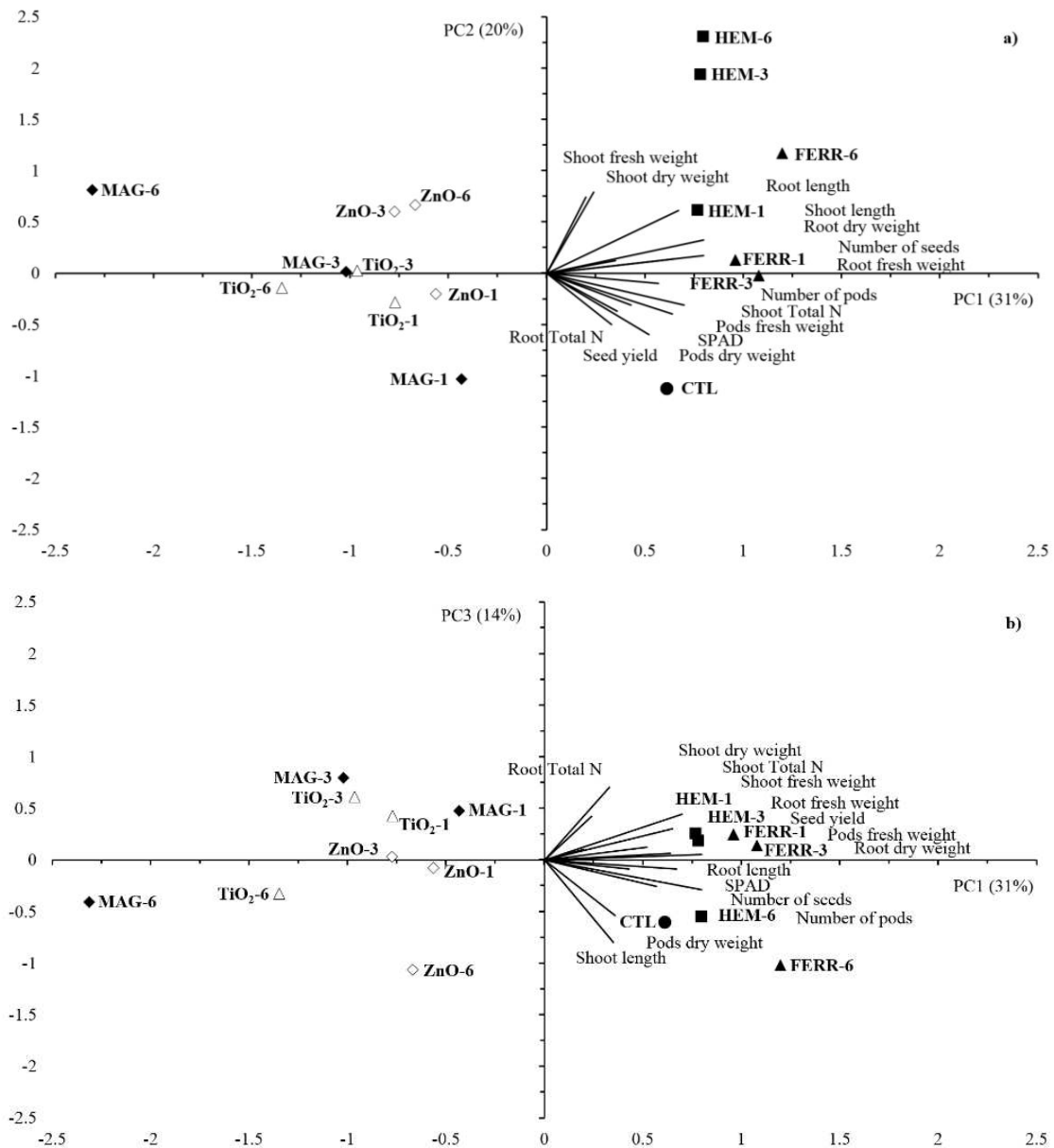


Figure 4. Principal component analysis performed on characteristics of bean plants (*Phaseolus vulgaris* L.) cultivated in an agricultural soil irrigated with 500 mL of zero, one, three, or six g nanoparticle L⁻¹ suspension. Nanoparticles of Fe₃O₄, FeOOH·xH₂O, α-Fe₂O₃, ZnO, and TiO₂ were used. Data are the mean of three square plastic pots with 3.5 kg dry soil each one, for three different soils and three experiments, i.e., n = 27. Each whole experiment lasted 120 days. The first two factors explain 51% of the variation. MAG-1 (500 mL of 1 g NP-Fe₃O₄ suspension), MAG-3 (500 mL of 3 g NP-Fe₃O₄ suspension), MAG-6 (500 mL of 6 g NP-Fe₃O₄ suspension); FERR-1 (500 mL of 1 g NP-FeOOH·xH₂O suspension), FERR-3 (500 mL of 3 g NP-FeOOH·xH₂O suspension), FERR-6 (500 mL of 6 g NP-FeOOH·xH₂O suspension); HEM-1 (500 mL of 1 g NP-α-Fe₂O₃ suspension), HEM-3 (500 mL of 3 g NP-α-Fe₂O₃ suspension), HEM-6 (500 mL of 6 g NP-α-Fe₂O₃ suspension); ZnO-1 (500 mL of 1 g NP-ZnO suspension), ZnO-3 (500 mL of 3 g NP-ZnO suspension), ZnO-6 (500 mL of 6 g NP-ZnO suspension); TiO₂-1 (500 mL of 1 g NP-TiO₂ suspension), TiO₂-3 (500 mL of 3 g NP-TiO₂ suspension), and TiO₂-6 (500 mL of 6 g NP-TiO₂ suspension).

Discussion

All treatments showed a lower chlorophyll content during the onset of the measurement at 15 days after sowing. This behavior suggests that the common bean plants were not in the fullness of the photosynthetic process. SPADS curves commonly show a decreasing trend due to the measurement was done leaf by leaf at the beginning of vegetative growth (Ribeiro de Cunha et al., 2015). About the SPAD units, Gómez et al. (2011) reported values near to 40 – 45 SPAD units. Anderson and Ryser (2015). However, measured leaves chlorophyll concentration in common bean reported range between 30 and 40 SPAD units. In this study, none of the treatments increased the chlorophyll content of bean plants, nevertheless the SPAD units' values are consistent with the values reported by other authors. Fernández-Luqueño et al. (2008, 2010) stated that the SPAD units decreased abrupt and significantly as soon as onset the plant senescence processes. Additionally, Hong et al. (2005) reported that leaves of spinach (*Spinacia oleracea* L.) treated with TiO₂ nanoparticles had higher levels of photosynthesis compared to untreated leaves.

Several studies on the application of nanoparticles in a relatively broad range of species have attempted to understand the effect on plant growth. For instance, Lin and Xing (2007) reported that ZnO nanoparticles can inhibited seed germination of ryegrass. On the other hand, Stampoulis et al. (2009) did not found a cause-effect on seed germination, root elongation and biomass of zucchini (*Cucurbita pepo* L.) amended with nanoparticles in hydroponic solutions. In this study root fresh weight, root dry weight, root length, shoot fresh weight, shoot dry weight, shoot length, and SPAD units were not significantly different between nanoparticles treatments, compared to the CONTROL treatment ($P < 0.05$), i.e., NP did not change significantly some biomass parameters such as root or shoot dry weight. NP did not affect significantly the growing processes, but whether some characteristics related to yield components such as those linked to pods or seeds. It is assumed that in this study the NP-induced toxicity might not affect the plant growth. However, it has to be noted that other modes of actions as photo-induced toxicity and NP-dissolved ion effects might elicit toxicity (Fernández-Luqueño et al., 2014).

In this research, we found that at least one concentration of HEMATITE, FERRIHYDRITE or MAGNETITE increased significantly the total N of roots or shoots, the number of pods, dry weight of pods, the number of seeds, and yield of common bean. Burke et al. (2015) reported that Fe₃O₄ nanoparticles can affect the root system as wells as leaf phosphorous content from soybean plants (*Glycine max* (L.) Merr.), but Quoc et al. (2014) found that iron NP increased up 16% the yield of soybean in comparison with the control sample. In addition, Martinez-Fernandez et al. (2016) found reduction of the root functionality from sunflower plants (*Helianthus annuus* L.) by iron oxide nanoparticles. On the other hand, at least one concentration of HEMATITE, FERRIHYDRITE or MAGNETITE decreased significantly the fresh or dry weight of pods. Jeyasubramanian et al. (2016) stated that Fe₂O₃ nanoparticles increased the stem and root lengths and biomass production of spinach plant (*Spinacia oleracea* L.), while the effects were dependent of time and dose.

At least one concentration of ZINC OXIDE or TITANIUM DIOXIDE decreased significantly the number of pods, the fresh weight of pods and the number of seeds. Jacob et al. (2013) found that TiO₂ NP did not affect biomass production in common bean plants grown in nutrient solutions at 0, 6, and 18 mmol Ti L⁻¹. However, Adhikari et al. (2016) stated that application of nano-zinc oxide particles enhanced the auxin

indole-3-acetic acid (IAA) production in plant roots of maize (*Zea mays* L.), soybean (*Glycine max* L.), pigeon pea (*Cajanas cajan* L.), and ladies finger (*Abelmoschus esculentus* L.), which subsequently improved the overall growth. In addition, it has been reported that independent of NP type, a concentration of 250 mg kg⁻¹ of TiO₂ and ZnO NP promoted the highest plant height, root length, and biomass (Raliya et al., 2015). These authors stated that zinc oxide NP had a twin role of being an essential nutrient and a co-factor for nutrient mobilizing enzymes.

It is well known that NP are up taken by the vascular network but the accumulation rate in tissue is different for root and shoot systems from each plant species, while each NP type might have a differential interaction ship with cells as effect of the growing stage, NP size, time exposition, and biotic and abiotic factors. These considerations could be the main reason for the wide variability of results when attempting know the effects of NP on plants. Additionally, it has to be highlighted that some plants NP-treated do not show any observable phenotypic changes in overall growth indicating that environmental NP pollution could be dangerously unnoticed.

Conclusions

None of the five kinds of NP used in this experiment (magnetite, ferrihydrite, hematite, zinc oxide or titanium dioxide) modified significantly the chlorophyll content of common bean plants as witnessed by the SPAD units' values. However, nanoparticles of magnetite, ferrihydrite, hematite, zinc oxide or titanium dioxide modified significantly at least one plant characteristic or one yield component of common bean, such as SPAD units, root length, root total N, shoot length, shoot total nitrogen, pod number, pod fresh weight, pod dry weight, seed number or yield. The nanoparticles with Fe such as magnetite, ferrihydrite, or hematite were those that increased significantly more crops characteristics such as total N of roots or shoots, the number of pods, dry weight of pods, the number of seeds, and yield of common bean. These finds are an important factor to take into account with regard to the applicability of NP for long-term use in crops but, the selection of the proper NP at their adequate concentration is important for realizing higher benefits for an agrosustainable target. Additionally, there is the need of generating more data on chronic effects from long terms and concentration exposure of nanoparticles in plants, which is important for a better understanding of the potential hazard or risk of these nanoparticles, while more studies are also necessities in order to identify the highest potential of NP in the rural sector and in the agro-food industry worldwide.

Acknowledgements. This research was founded by 'Ciencia Básica SEP-CONACyT' projects 151881 and 287225, the Sustainability of Natural Resources and Energy Program (Cinvestav-Saltillo), and Cinvestav Zacatenco. M-P G. received grant-aided support from 'Becas Conacyt'. F-L F, T-T LI, L-V F, and P-G L received grant-aided support from 'Sistema Nacional de Investigadores (SNI)', Mexico.

REFERENCES

- [1] Adhikari, T., Kundu, S., Rao, A. S. (2016): Zinc delivery to plants through seed coating with nano-zinc oxide particles. – *Journal of Plant Nutrition* 39(1): 139-149.
- [2] Anderson, R., Ryser, P. (2015): Early autumn senescence in red maple (*Acer rubrum* L.) is associated with high leaf anthocyanin content. – *Plants* 4(3): 505-522.

- [3] Bremner, J. M. (1996): Total Nitrogen. – In: Sparks, D. L. (ed.) *Methods of Soil Analysis Chemical Methods, Part 3*. Soil Science Society of America Inc., American Society of Agronomy, Madison, WI, USA.
- [4] Burke, D. J., Pietrasiak, N., Situ, S. F., Abenojar, E. C., Porche, M., Kraj, P., Lakliang, Y., Samia, A. C. S. (2015): Iron oxide and titanium oxide nanoparticle effect on plant performance and root associated microbes. – *International Journal of Molecular Science* 16: 23630-23650.
- [5] Canas, J. E., Long, M. Q., Nations, S., Vadan, R., Dai, L., Luo, M. X., Ambikapathi, R., Lee, E. H., Olsyk, D. (2008): Effects of functionalized and nonfunctionalized single-walled carbon nanotubes on root elongation of select crop species. – *Environmental Toxicology and Chemistry* 27(9): 1922-1931.
- [6] Cornelis, G., Hund-Rinke, K., Kuhlbusch, T., Van den Brink, N., Nickel, C. (2014): Fate and bioavailability of engineered nanoparticles in soil: a review. – *Critical Reviews in Environmental Science and Technology* 44(24): 2720-2764.
- [7] Doshi, R., Braida, W., Christodoulatos, C., Wazne, M., O'Connor, G. (2008): Nano-aluminum: transport through sand columns and environmental effects on plants and soil communities. – *Environmental Research* 106(3): 296-303.
- [8] Fernández-Luqueño, F., Dendooven, L., Munive, A., Corlay-Chee, L., Serrano-Covarrubias, L. M., Espinosa-Victoria, D. (2008): Micro-morphology of common bean (*Phaseolus vulgaris* L.) nodules undergoing senescence. – *Acta Physiologiae Plantarum* 30(4): 545-552.
- [9] Fernández-Luqueño, F., Reyes-Varela, V., Martínez-Suárez, C., Salomon-Hernández, G., Yañez-Meneses, J., Ceballos-Ramirez, J. M., Dendooven, L. (2010): Effect of different nitrogen sources on plant characteristics and yield of common bean (*Phaseolus vulgaris* L.). – *Bioresource Technology* 101(1): 396-403.
- [10] Fernández-Luqueño, F., López-Valdez, F., Valerio-Rodríguez, M. F., Pariona, N., Hernández-López, J. L., García-Ortíz, I., López-Baltazar, J., Vega-Sánchez, M. C., Espinosa-Zapata, R., Acosta-Gallegos, J. A. (2014): Effects of Nanofertilizers on Plant Growth and Development, and Their Interrelationship with the Environment, pp. 211-224. – In: López-Valdez, F., Fernández-Luqueño, F. (eds.). *Fertilizers: Components, Uses in Agriculture and Environmental Impact*. NOVA Science, New York, USA.
- [11] Fernández-Luqueño, F., López-Valdez, F., Dendooven, L., Luna-Suarez, S., Ceballos-Ramirez, J. M. (2016): Why wastewater sludge stimulates and accelerates removal of PAHs in polluted soils? – *Applied Soil Ecology* 101: 1-4.
- [12] Gardner, W. H. (1986): Water Content. – In: Klute, A. (ed.) *Methods of Soil Analysis. Physical and Mineralogical Methods, Part 1*. Soil Science Society of America Inc., American Society of Agronomy, Madison, WI, USA.
- [13] Gee, G. W., Bauder, J. W. (1986): Particle Size Analysis. – In: Klute, A. (ed.) *Methods of Soil Analysis, Part 1. Physical and Mineralogical Methods*. Soil Science Society of America Inc., American Society of Agronomy, Madison, WI, USA.
- [14] Gomez, E. J. B., Castaneda, C. L., Shibata, J. K., Gallegos, J. A. A., Colin, S. M., Perez, N. M. (2011): Advances in Mexico on bean breeding for tolerance to high temperature and drought. – *Revista Fitotecnia Mexicana* 34(4): 247-255.
- [15] Hong, F., Zhou, J., Liu, C., Yang, F., Wu, C., Zheng, L. (2005): Effect of nano-TiO₂ on photochemical reaction of chloroplast of spinach. – *Biological Trace Element Research* 105: 269-279.
- [16] Jacob, D. L., Borchardt, J. D., Navaratnam, L., Otte, M. L., Bezbaruah, A. N. (2013): Uptake and translocation of Ti from nanoparticles in crops and wetland plants. – *International Journal of Phytoremediation* 15(2): 142-153.
- [17] Jeyasubramanian, K., Thoppey, U. U. G., Hikku, G. S., Selvakumar, N., Subramania, A., Krishnamoorthy, K. (2016): Enhancement in growth rate and productivity of spinach grown in hydroponics with iron oxide nanoparticles. – *RSC Advances* 6(19): 15451-15459.

- [18] Keller, A. A., McFerran, S., Lazareva, A., Suh, S. (2013): Global life cycle releases of engineered nanomaterials. – *Journal of Nanoparticle Research* 15(6), UNSP 1692.
- [19] Lépiz, I. R., López, J. J., Sánchez, J. J., Santacruz, R. F., Nuño, R. R., Rodríguez, G. E. (2010): Características morfológicas de formas cultivadas, silvestres e intermedias de frijol común de hábito trepador. – *Revista Fitotecnia Mexicana* 33(1): 21-28.
- [20] Lin, D. H., Xing, B. S. (2007): Phytotoxicity of nanoparticles: inhibition of seed germination and root growth. – *Environmental Pollution* 150(2): 243-250.
- [21] Ma, X. M., Geiser-Lee, J., Deng, Y., Kolmakov, A. (2010): Interactions between engineered nanoparticles (ENPs) and plants: Phytotoxicity, uptake and accumulation. – *Science of the Total Environment* 408(16): 3053-3061.
- [22] Markwell, J., Osterman, J. C., Mitchell, J. L. (1995): Calibration of the Minolta SPAD-502 leaf chlorophyll meter. – *Photosynthesis Research* 46: 467-472.
- [23] Martínez-Fernández, D., Barroso, D., Komarek, M. (2016): Root water transport of *Helianthus annuus* L. under iron oxide nanoparticles exposure. – *Environmental Science and Pollution Research* 23(2): 1732-1741.
- [24] Maurer-Jones, M. A., Gunsolus, I. L., Murphy, C. J., Haynes, C. L. (2013): Toxicity of engineered nanoparticles in the environment. – *Analytical Chemistry* 85(6): 3036-3049.
- [25] Pariona, M. N. (2012): Efecto de nanoparticulas de óxido de hierro en la germinación y crecimiento de tres especies forestales. – M. Sc. Thesis. Universidad de la Sierra Juárez Oaxaca, Mexico.
- [26] Quoc, B. N., Trong, H. D., Hoai, C. N., Xuan, T. T., Tuong, V. N., Thuy, D. K., Thi, H. H. (2014): Effects of nanocrystalline powders (Fe, Co and Cu) on the germination, growth, crop yield and product quality of soybean (Vietnamese species DT-51). – *Advances in Natural Sciences: Nanosciences & Nanotechnology* 5(1): 015016.
- [27] Raliya, R., Nair, R., Chavalmane, S., Wang, W. N., Biswas, P. (2015): Mechanistic evaluation of translocation and physiological impact of titanium dioxide and zinc oxide nanoparticles on the tomato (*Solanum lycopersicum* L.) plant. – *Metallomics* 7(12): 1584-1594.
- [28] Rhoades, J. D., Mantghi, N. A., Shauser, P. J., Alves, W. (1989): Estimating soil salinity from saturated soil-paste electrical conductivity. – *Soil Science Society of America Journal* 53: 428-433.
- [29] Rico, C. M., Majumdar, S., Duarte-Gardea, M., Peralta-Videa, J. R., Gardea-Torresdey, J. L. (2011): Interaction of nanoparticles with edible plants and their possible implications in the food chain. – *Journal of Agricultural Food and Chemistry* 59: 3485-3498.
- [30] Ribeiro de Cunha, A., Katz, I., de Pádua Sousa, A., Martínez Uribe, R. A. (2015): Índice SPAD en el crecimiento y desarrollo de plantas de lisianthus en función de diferentes dosis de nitrógeno en ambiente protegido. – *Idesia* (33)2: 97-195.
- [31] Rodrigues, S. M., Trindade, T., Duarte, A. C., Pereira, E., Koopmans, G. F., Römkens, P. F. A. M. (2016): A framework to measure the availability of engineered nanoparticles in soils: Trends in soil tests and analytical tools. – *Trends in Analytical Chemistry* 75: 129-140.
- [32] SAS Institute (1989): *Statistic Guide for Personal Computers*. Version 6.04. – SAS Institute, Cary, NC.
- [33] Stampoulis, D., Sinha, S. K., White, J. C. (2009): Assay-dependent phytotoxicity of nanoparticles to plants. – *Environmental Science & Technology* 43(24): 9473-9479.
- [34] Thomas, G. W. (1996): Soil pH and Soil Acidity. – In: Sparks, D. L. (ed.) *Methods of Soil Analysis: Chemical Methods Part 3*. Soil Science Society of America Inc., American Society of Agronomy Inc., Madison, WI, USA.

GENETIC VARIATION IN *CYPRINION MACROSTOMUS* HECKEL, 1843 POPULATIONS AS REVEALED BY PARTIAL COI SEQUENCES OF MITOCHONDRIAL DNA

PARMAKSIZ, A.

*Department of Biology, Faculty of Science-Literature, Harran University, Şanlıurfa, Turkey
(e-mail: aprmksz@gmail.com; phone: +90-414-318-3562; fax: +90-414-318-3541)*

(Received 23rd Dec 2017; accepted 13th Mar 2018)

Abstract. *Cyprinion macrostomus* Heckel, 1843 naturally thriving in river systems of Euphrates and Tigris is a species with economic importance. In this study genetic diversity of *C. macrostomus* populations was determined based on gene sequencing analysis of mitochondrial DNA cytochrome c oxidase subunit I (mtDNA COI) locus. Seven polymorphic sites and eight haplotypes were detected taking 41 samples from two populations. Mean haplotype diversity (h) and nucleotide diversity (π) were calculated to be $h = 0.529$ and $\pi = 0.00158$; respectively. All values obtained from two populations after neutrality tests were calculated to be negative and were statistically insignificant ($p > 0.05$). Results obtained with this research are the data noted for the first time for *C. macrostomus* species thriving in Turkey. Certain haplotypes (H3, H5, H6, H7 and H8) determined for mtDNA COI locus are the new results to the literature and created a novel data set for genetic diversity of this species.

Keywords: *Cyprinidae*, genetic diversity, polymorphism, Euphrates River, Tigris River

Introduction

Euphrates and Tigris River Systems have a great deal of important capacity and potential for fish biodiversity and fishery for Turkey. Euphrates and Tigris Rivers undergo considerable change as the result of human activities. Numerous dams were built on these rivers in order to provide water for production of energy, agricultural fields and neighboring cities. Thus, differences occurring in riverbed have led to significant variation in physical, chemical, and biological composition of the river. Furthermore, environmental factors such as industrial factors, intensive fishery, and destruction of habitats will lead to extinction of several species or decrease of populations (Kuru, 1986; Ünlü et al., 1997).

Consumption of freshwater fish which are an alternative to meet protein needs of the population that has been elevating especially because Syrian immigrants have been moving to Southeastern Anatolia in recent years, has increased. The fish species preferred most by people with economically low level of income was identified to be *C. macrostomus*. Body of this fish, that is maximum 20 cm long, is covered by scales and laterally flattened. The mouth is large, flat, and located ventrally. Caudal fin is forked, free edges of dorsal and anal fins are concave. This omnivorous species feeds on phytoplanktons and zooplanktons (Bilici, 2009).

C. macrostomus species belonging to Cyprinidae family has distribution in Iraq, Iran, Syria, and Turkey (Kelle, 1978; Kuru, 1980). This species inhabits in Euphrates and Tigris River Systems and Orontes (Asi) River in Turkey (Kuru, 1975; Kelle, 1978; Balık, 1988; Timur et al., 1983; Taysı, 2014).

Some studies conducted on this species include; karyotype analysis in Malatya Karakaya Dam Lake by Gaffaroğlu and Yüksel (2004); hematology in Sivas Topardıç Stream and Balıklı Çermik localities by Duman and Şahan (2014); phylogenetic and phylogeographical relationship of *C. macrostomus*, *C. kais*, *Carasobarbus chantrei* in Euphrates and Tigris

Rivers studied by Durna et al. (2012) via nuclear DNA-ISSR (microsatellite) and mtDNA (PZR-RFLP) methods; histological characteristics of pancreas, liver, intestines in Sivas Balıklı Hot spring by Taysı (2014); morphological differences between *C. macrostomus* populations in Euphrates River by Bilici et al. (2015).

C. macrostomus is caught by fishermen and has economic importance because it is consumed by local people. Genetic diversity and population structure of that species need to be known in order to manage and protect the species possessing economic importance. There is only one study (Durna et al., 2012) about genetic diversity of this fish species amongst the studies which have been carried out on *C. macrostomus* up to the present time, that study did not included any DNA sequencing analysis. The goal of this research is to determine genetic diversity of *C. macrostomus* populations in Euphrates and Tigris Rivers by practicing sequence analysis for mtDNA COI locus. mtDNA is generally considered to be an ideal indicator for studies of population genetics because it is maternally inherited and has rapid mutation rate (Avise, 1987). Besides its use for distinguishing similar species, mtDNA COI locus is one of the most used molecular markers for determination of the differences between populations of the same species (Croos and Palsson, 2010; Keskin and Atar, 2012).

Materials and methods

Study area, sample collection, DNA extraction and amplification of mtDNA COI

The localities of Euphrates River (Adiyaman) and Tigris River (Diyarbakır) System were found to be appropriate for sampling because of the number of populations, the availability of land conditions, the availability of sufficient number of fishermen and the proximity to the city center. 18 individuals from the Adiyaman, 23 individuals from Diyarbakır (Fig. 1), 41 in total, were caught by fishing method, transferred in to laboratory alive preserving within chambers with ice. 2 g specimen were dissected from muscle tissues at the base of pectoral or dorsal fins of samples caught, kept in refrigerator at +4 °C until DNA isolation process by placing inside 1.5 ml centrifuge tube containing 95% ethanol.

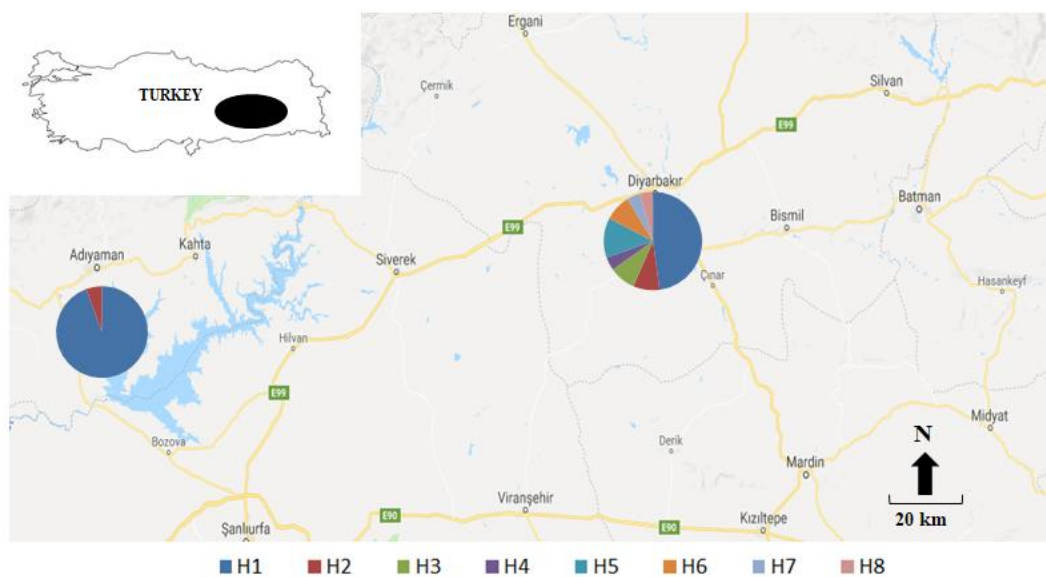


Figure 1. Location of study area and geographic distribution of haplotypes

In this study, total DNA isolation from muscle tissue was practiced using GeneJET Genomic DNA Purification Kit (Thermo Scientific). Total DNAs were obtained by applying the protocol for this kit. In order to control the existence of DNA, 2 µl was taken from DNA samples of each individual, placed in to tank including 0.8% agarose gel, 0.5xTBE (Tris/Boric acid/EDTA Buffer) solution with the addition of 2 µl stain (3x Loading dye) and SYBR Green, run in electrophoresis at 120 V for 30 min, then viewed in device giving off ultraviolet (UV) light. The 5-end of the mtDNA COI region was amplified using the following primers: COI-625F (5'-CAACCAACCACAAAGACATTGGCAC-3'), COI-625R (5'-GACTTCTGGGTGGCCAAAGAATCA-3') (Darabi et al., 2014).

The PCR process was carried out by using BIO-RAD T100™ Thermal Cycler device. Protocols of PCR were completed in totally 35 cycles including; initial denaturation at 95 °C for 3 min, denaturation for 30 s at 95 °C, 30 s at 61 °C for annealing, and 45 s at 72 °C for extension, and finally terminated keeping specimens at 72 °C for 5 min. PCR mixture used in order to amplify this locus is as follows; totally 25 µl consisting of 13.9 µl dH₂O, 2.5 µl 1x PCR buffer, 2 µl MgCl₂, 0.5 µl dNTPs, 1 µl primer (F + R), 0.1 µl Taq polimeraz and 50 ng template DNA. 2% agarose gel was used in order to check resulting products of PCR process. Sequence analysis was carried out in 3500 XL Genetic Analyzer (Thermo Fisher Scientific) by sending obtained PCR products to a commercial company.

Sequence analysis of mtDNA COI

Raw data of mtDNA sequences, which were delivered by commercial company, were evaluated and converted in to FASTA format by using ChromasPro v 2.0.1 (Technelysium Pty Ltd). Resulting sequences of all individuals in FASTA format were aligned utilizing BioEdit software version 7.2.5 program.

The number of polymorphic sites and haplotypes, diversity of haplotypes and nucleotides, Tajima D and Fu's Fs statistics were calculated for populations by using DnaSP5.10.01 program. The phylogenetic relationship between haplotypes was identified by Network version 5.0 software. Phylogenetic analyses were performed in MEGA 7 program with respect to Neighbor joining tree model using K2 parameter and phylogenetic tree was built. Bootstrap test (1000 repeats) was used for testing reliability of nodes (branches) on the tree. Sequences obtained from the present study were compared to sequences found in GenBank and phylogenetic tree was established.

Results

Genetic variation

Seven variable sites and eight haplotypes were identified by sequencing an average of 600 bp fragments of mtDNA COI 625 locus in totally 41 *C. macrostomus* samples from Euphrates and Tigris Rivers. Nucleotide variations of this region are shown in *Table 1*. Haplotype diversity (h), the nucleotide diversity (π) and the neutrality tests for each population were given in *Table 2*.

As seen in *Table 3*, totally 2 (H1-H2) haplotypes in Euphrates population and all of the 8 haplotypes in Tigris population were indentified. Haplotype which is common in both populations and represented with the highest number of individuals is H1 (*Fig. 2*).

Table 1. Nucleotide variations and haplotypes of mtDNA COI 625

Haplotypes	190	316	334	421	436	508	550
H1	A	G	C	C	C	C	C
H2	.	A
H3	.	A	.	T	.	.	.
H4	T	.
H5	G	.	.	.	T	.	.
H6	T	.	.
H7	.	A	T
H8	.	A	.	T	.	.	T

Table 2. Genetic diversity and neutrality tests of *C. macrostomus* populations (n = number of individuals, N_h : number of haplotypes, h : haplotype diversity, π : nucleotide diversity)

Locality	n	N_h	h	π	Tajima's D	Fu's Fs
Euphrates River	18	2	0.111	0.00018	-1.16467	-0.794
Tigris River	23	8	0.759	0.00252	-0.67096	-2.925
Total	41	8	0.529	0.00158	-1.18176	-3.637

Mean haplotype diversity was calculated as ($h = 0.529$); mean nucleotide diversity as ($\pi = 0.00158$). Population of Tigris was the one to have both higher haplotype diversity ($h = 0.759$) and higher nucleotide diversity ($\pi = 0.00252$).

Table 3. The haplotypes distribution according to populations

Haplotypes	Euphrates River	Tigris River	Total
H1	17	11	28
H2	1	2	3
H3	-	2	2
H4	-	1	1
H5	-	3	3
H6	-	2	2
H7	-	1	1
H8	-	1	1

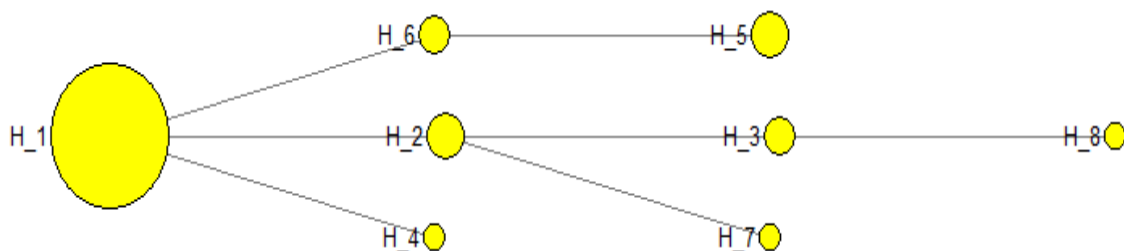


Figure 2. Haplotype network of *C. macrostomus* haplotypes

Eight haplotypes in total were determined in Median-Joining Network of haplotypes created for 41 *C. macrostomus* samples analyzed, resulting network shows the existence of a haplotype (H1) indicating an evolutionary connection. This haplotype was detected to be the most abundant one in both of the populations (Fig. 2).

As seen in Table 4, similarities were compared by blasting H1 haplotype sequence, which was obtained in our study and is an ancestry one in GenBank (available at <http://blast.ncbi.nlm.nih.gov>).

Table 4. Information about sequences of H1 haplotype obtained in our study showing the maximum ident in GenBank

Species	Country	Accession	Maximum ident %
<i>Cyprinion sp.</i>	Iranian	KM590431.1	100
<i>Cyprinion sp.</i>	Iranian	KM590430.1	99
<i>Cyprinion macrostomus</i>	Iranian	KM590433.1	99
<i>Cyprinion sp.</i>	Iranian	KM590432.1	99
<i>Cyprinion sp.</i>	Iranian	KM590429.1	98
<i>Cyprinion watsoni</i>	Iranian	KM590434.1	99
<i>Cyprinion watsoni</i>	Iranian	KM590435.1	99
<i>Cyprinion semiplotum</i>	Japan	AP011253.1	90
<i>Cyprinion semiplotum</i>	India	KF511536.1	90
<i>Cyprinion semiplotum</i>	India	KJ957768.1	90

Phylogenetic tree drawn based on 8 haplotypes of mtDNA COI locus from populations Euphrates and Tigris and sequences of species from genus *Cyprinion* in GenBank are seen in Figure 3.

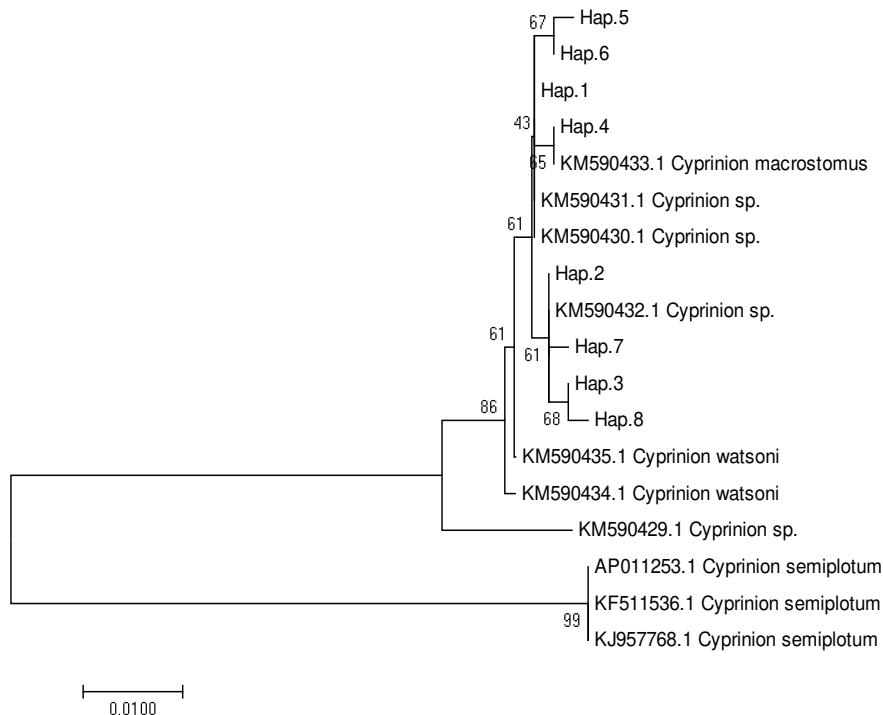


Figure 3. Neighbor-joining tree based on haplotypes of *Cyprinion* genus

Two major branches are seen on the tree in *Figure 3* and samples of this study and samples from Iran are placed on one branch, *Cyprinion semiplotum* species from India and Japan is on the other branch. Samples of Iran, *Cyprinion* sp (KM590430.1 and KM590431.1) have haplotype H1, *Cyprinion macrostomus* (KM590433.1) H4, *Cyprinion* sp. (KM590432.1) H2; these are similar with haplotypes in our research.

Neutrality tests

Neutrality tests are used broadly to reveal the past population history. In present study Tajima's D (1996) and Fu's Fs (1997) tests were applied for the deviation of populations from the standard neutral mode. Tajima's D value; was negative in both Euphrates (-1.16467) and Tigris (-0.67096) populations, and it was also negative in sum (-1.18176) which was found to be statistically insignificant ($p > 0.05$). Fu's Fs tests were negative in Euphrates (-0.794) and Tigris (-2.925) populations as well, it was also negative in sum (-3.637) and found to be statistically insignificant ($p > 0.05$).

Discussion

Genetic diversity of populations were researched in this study via sequencing mtDNA COI 625 of totally 41 *C. macrostomus* individuals including 18 samples from Adıyaman 23 individuals from Diyarbakır. Seven polymorphic and eight haplotypes were identified on this locus. While only 2 haplotypes (H1-H2) were found in population of Adıyaman, all haplotypes were observed in population of Diyarbakır. Different haplotype diversity of both populations results from the fact that the habitat where samples were taken was either stream or dam lake. Because, all of the individuals representing Adıyaman population were obtained from Atatürk Dam Lake, all of the individuals representing Diyarbakır population were collected from river. Since rivers have richer habitats than lakes, it is expected for Diyarbakır population to have greater genetic diversity. In addition, it is also expected for geographical isolation resulting from dams built on these rivers to lead to genetic variations between populations of fish. Haplotype H1 was seen in totally 28 individuals and it is possible to declare that haplotype H1 is ancestry because it is the most abundant haplotype in both populations. It was estimated that occurrence of ancestral haplotype in both populations was associated with geological localization of both rivers in the past. Upper parts of Euphrates and Tigris in Pleistosen were flowing to fresh water lakes located behind the sea retreating in late Miocene, lower parts were flowing to inland lake, then to Persian Gulf (Demirsoy, 1999).

With the same primer, Parmaksız and Ekşi (2017) determined 6 polymorphic sites and 7 haplotypes from populations of *Capoeta trutta* and Parmaksız et al. (2017) 2 polymorphic sites and 3 haplotypes from populations of *Barbus grypus*. The number of polymorphic sites and haplotypes in our study were higher compared to these two studies.

Data obtained as the result of analyzing mtDNA COI 625 sequences of certain fish species inhabiting in Euphrates and Tigris Rivers Systems in Turkey and data of this study were given in *Table 5*.

According to *Table 5*, both the number of haplotypes (8) and nucleotide diversity (0.00158) in this study are higher compared to other species. Nucleotide diversity is a precise method used for genetic analysis of populations (Nei and Li, 1979). Genetic diversity could be influenced by life period, characteristic of populations, environmental

conditions and population size (Nei, 1987; Avise, 2000). *Barbus grypus* is the species with the lowest nucleotide variety. The reason for this is supposed to result from decreased number of individuals because it is the most fished species.

Table 5. Data of fish species studied by using mtDNA COI 625 in Turkey

Species	n	Nh	h	π	Tajima's D	Fu's Fs
<i>Capoeta trutta</i>	47	7	0.642	0.00138	-1.08945	-2.946
<i>Barbus grypus</i>	36	3	0.246	0.00045	-0.91306	-1.098
<i>Cyprinion macrostomus</i>	41	8	0.529	0.00158	-1.18176	-3.637

In Median joining network analysis, we can see that haplotype H1 is located in the center of network and dominant, also all haplotypes are consisted of haplotype H1 (Fig. 2). We can also report that haplotype H1 is connected with other haplotypes on Neighbor joining tree and therefore haplotype H1 is ancestry haplotype (Fig. 3). In addition, mtDNA COI 625 primer distinguishes species resplendently. It placed *Cyprinion watsoni* and *Cyprinion semiplotum* species on a branch separated from *Cyprinion macrostomus* species.

Tajima's D ve Fu's Fs values were negative in populations of Euphrates and Tigris, all of the resulting values were not statistically significant ($p > 0.05$). These values predict that populations are in neutral balance.

All of the results obtained by this study are the data extracted for the first time for *C. macrostomus* species thriving in Turkey. Despite the fact that haplotypes H1, H2 and H4 for mtDNA COI 625 locus were determined in studies conducted in Iran, haplotypes H3, H5, H6, H7 and H8 identified in this research are new results for the literature, created a new data set for genetic diversity of this species.

Conclusions

Since the number of individuals and populations used in the present study was low, it is likely for variations by chance to occur. Therefore, it will be useful for genetic diversity of this fish species to study on greater number of individuals and more populations in further research.

Acknowledgements. This study was funded by Harran University Research Fund (HÜBAK Project No: 17219).

REFERENCES

- [1] Avise, J. C. (2000): Phylogeography. – Harvard University Press, London.
- [2] Avise, J. C., Arnold, J., Ball, R. M., Bermingham, E., Lamb, T., Neigel, J. E., Reeband, C. A. Saunders, N. (1987): Intraspecific phylogeography: the mitochondrial DNA bridge between population genetics and systematics. – *Annu Rev Ecol Syst* 18: 489-522.
- [3] Balık, S. (1988): Systematic and Zoogeographical Investigation of Freshwater Fish Living in the Inland Waters of the South Anatolian Region. – Ass. Prof. Thesis, Ege University, İzmir.

- [4] Bilici, S. (2009): Variation Belonging to Morphometric and Meristic, the Study of *Cyprinion macrostomus* (Heckel, 1843) and *Cyprinion kais* (Heckel, 1843) Living in the Different Zones of Tigris River. – Master Thesis, Kafkas University, Kars.
- [5] Bilici, S., Cicek, T., Baysal, A., Unlu, E., Alp, A. (2015): Morphological differences among the *Cyprinion macrostomus* (Cyprinidae) populations in the Tigris River. – Journal of Survey in Fisheries Sciences 2(1): 67.
- [6] Croos, D. M., Palsson, S. (2010): Mitochondrial DNA variation and population genetic structure of white shrimp *Fenneropenaeus indicus* along the coastal belt of Sri Lanka. – Aquat Living Resour 23: 315-32.
- [7] Darabi, A. R., Kashan, N., Fayazi, J., Aminafshar, M., Chamani, M. (2014): Investigation of phylogenetic relationship among two *Barbus* species (Cyprinidae) populations with mitochondrial DNA using PCR sequencing. – IJBPAS 4(2): 302-311.
- [8] Demirsoy, A. (1999): General and Turkey Zoogeography “Animal Geography”, 2nd edn. – Metaksan, Ankara.
- [9] Duman, S., Şahan, A. (2014): The identification of some parameters and non-specific immune respond in *Cyprinion macrostomus* (Heckel, 1843) living in Kangal (Sivas) Balıklı Çermik thermal hot spring and Topardıç Stream (Sivas). – Yunus Research Bulletin 4: 21-28.
- [10] Durna, S., Bardakçı, F., Deger, N. (2012): Genetic diversity of *Cyprinion macrostomus* Heckel, 1843 (Teleostei: Cyprinidae) in Anatolia. – Turkish Journal of Fisheries and Aquatic Sciences 12: 651-659.
- [11] Fu, Y. X. (1997): Statistical tests of neutrality against population growth, hitchhiking and background selection. – Genetics 147: 915-925.
- [12] Gaffaroğlu, M., Yüksel, E. (2004): Karyotype analysis of *Cyprinion macrostomus* Heckel, 1843 (Pisces: Cyprinidae). – GÜ Kırşehir Eğitim Fak. Derg. 5: 235-239.
- [13] Kelle, A. (1978): Taxonomic and Ecological Investigations on Fishes Living in the Tigris River. – PhD Thesis, Dicle University, Diyarbakır.
- [14] Keskin, E., Atar, H. H. (2012): Determination of genetic variation among blue crab (*Callinectes sapidus*) populations along Mediterranean coast of Turkey using COI sequences. – Journal of FisheriesSciences.com 6(2): 125-131.
- [15] Kuru, M. (1975): Systematic investigations on fishes (Pisces) living in Euphrates and Tigris systems. – TÜBİTAK V. Science Congress Publications 430: 329-338.
- [16] Kuru, M. (1980): Key to the inland water fishes of Turkey, Part III. – Hacettepe Bull. Nat. Sci. Eng. 9: 123-133.
- [17] Kuru, M. (1986): Tigris and Euphrates Rivers will be established on the dams and threaten to fish species. – VIII. National Biology Congress, İzmir, Microbiology, Hydrobiology and Zoology Bulletin 2: 589-597.
- [18] Kuru, M. (1999): Vertebrate Animals, 5th ed. – Palme Press, Ankara.
- [19] Nei, M. (1987): Molecular evolutionary genetics. – Columbia University Press, New York.
- [20] Nei, M., Li, W. H. (1979): Mathematical model for studying genetic variation in terms of restriction endonucleases. – Proc Natl Acad Sci 76: 5269-5273.
- [21] Parmaksız, A., Ekşi, E. (2017): Genetic diversity of the cyprinid fish *Capoeta trutta* (Heckel, 1843) populations from Euphrates and Tigris rivers in Turkey based on mtDNA COI sequences. – Indian J. Fish. 64(1): 18-22.
- [22] Parmaksız, A., Şeker, Ö., Aslan, N., Oymak, A. (2017): Determination of genetic diversity in *Barbus grypus* Heckel, 1843 populations by mtDNA COI gene sequences. – Yunus Research Bulletin 1: 103-107.
- [23] Tajima, F. (1996): The amount of DNA polymorphism maintained in a finite population when the neutral mutation rate varies among sites. – Genetics 143: 1457-1465.
- [24] Timur, M., Çolak, A., Marufi, M. (1983): Identification of fish species in Sivas and investigation of the effect of skin diseases treatment. – Ankara Üniversitesi Vet. Fak. Dergisi 30(2): 276-282.

- [25] Taysı, M. R. (2014): Investigation of the properties of histological and histochemical in the spotted carp's (*Cyprinion macrostomum* Heckel, 1843) intestines, liver and pancreas. – Master Thesis, Fırat University, Elazığ.
- [26] Ünlü, E., Özbay, C., Kilic, A., Coskun, Y., Şeşen, R. (1997): The effects of GAP on fauna. – Turkey Environment Foundation Publications 125: 79-102.

TRANSFERABILITY OF SSR MARKERS FROM RELATED *FICUS* SPECIES TO *FICUS CARICA* L. AND ASSESSMENT OF EFFECTIVENESS OF THE MARKERS

IKTEN, H.* – SOLAK, S. S. – YILMAZ, Y.

Department of Agricultural Biotechnology, Faculty of Agriculture, Akdeniz University
07070 Antalya, Turkey

*Corresponding author
e-mail: haticeikten@akdeniz.edu.tr

(Received 12th Jan 2018; accepted 13th Mar 2018)

Abstract. The objective of the study was to test the transferability of previously developed SSR markers for different *Ficus* species to *Ficus carica*. A total of 54 SSR simple sequence repeats (SSRs) primers previously developed for *Ficus montana*, *F. septica*, *F. sycomorus*, *F. (sycomorus) racemosa*, *F. (urostigma) rubiginosa*, and *F. insipida* were tested on 32 fig (*Ficus carica* L.) genotypes. Out of 54, 38 primers amplified the genomic DNA of *Ficus carica* genotypes, while the remaining 16 primers showed either no amplification or unreadable gel images. Out of 38, 17 primers were polymorphic and produced 62 alleles with an average of 3.64 bands per locus. The transferability rate from different *Ficus* species to *Ficus carica* varied from 90.9% (*F. rubiginosa* and *F. racemosa*) to 33.3% (*F. septica*). Some of the primers from donor species namely Frac13, Frac83, Frac241, Fsyc07, FinsA1, FM4-15, and FM4-70 resulted in similar banding patterns in the *Ficus carica* genome, suggesting that they were developed from the same loci and primer binding sites are conserved. Three loci (Fsyc11, FinsQ5 and FinsN3) produced more alleles in *Ficus carica* than donor species. Sixty-two SSR alleles, could distinguish all fig genotypes thoroughly, and UPGMA cluster analysis grouped them into two groups. As a conclusion, 17 primers developed for related *Ficus* species successfully amplified polymorphic bands in *Ficus carica* and distinguished all fig genotypes thoroughly. The transferability of SSRs to *Ficus carica* from related species affirmed the possibility of being used of these markers for genetic diversity, mapping and comparative genetic analysis.

Keywords: fig, microsatellite markers, molecular characterization, genetic diversity, genetic relationship

Introduction

Fig (*Ficus carica* L.), one of the oldest fruit crops in the world, belongs to the family of Moraceae which includes 60 genera and more than 2000 species of trees, shrubs and herbs. The genus *Ficus* includes over 1000 species classified into about 48 subgenera (Condit, 1969; Storey, 1975). There are two basic types of figs: caprifig and edible figs. Caprifig bear both male and female flowers whereas edible figs bear only female flowers. The only *Ficus* species cultivated for their fruits are the *F. carica* and *F. sycomorus*. *Ficus carica* L. is cross-pollinated and has a diploid ($2n = 26$) genome (Darlington and Wylie, 1955).

There are limited numbers of researches in *Ficus carica* aiming to understand the genome structure and determine the genetic character of genetic sources. Molecular markers are useful tools for genetic diversity, population structure and genetic mapping studies. There are also morphological and biochemical methods for detection of genetic variations, however being limitless and not affected by growing stage of the plant and environmental conditions makes molecular markers preferable (Rahnavard, 2016). There are different molecular marker systems such as random amplified polymorphic DNA (RAPD), sequence-related amplified polymorphism (SRAP), amplified fragment

length polymorphism (AFLP) and simple sequence repeat (SSR) used for determination of genetic variation among the plant genotypes. Microsatellite markers (simple sequence repeats- SSR) are widely used marker systems since they are reliable, codominant, highly polymorphic and suitable for automation. However microsatellite markers are species-specific and developing SSR markers is time consuming and expensive. SSR primers developed for one species could be transferred into related species. There have been several reports on the transferability of SSR markers among the related crops (Pierantoni et al., 2004; Gasic et al., 2009; Mnejja et al., 2010; Fan et al., 2013). Transferability of SSR markers among the *Ficus* species is significant in the previous studies. Giraldo et al. (2005) evaluated 26 SSR markers in 13 different *Ficus* species. Nazareno et al. (2009) tested 15 microsatellite loci, previously developed for *Ficus* (*Pharmacosycea*) *insipida*, *Ficus* (*Sycomorus*) *racemosa* and *Ficus* (*Urostigma*) *rubiginosa* for cross amplification in specimens of *F. citrifolia* and *F. eximia*. Heer et al. (2012) developed seven primers from Expressed sequence tag (EST) libraries of *F. citrifolia* and *F. popenoei* (subgen. *Urostigma* sect. *Americana*) and successfully transferred these markers along with five previously developed anonymous loci to basal subgenus *Pharmacosycea* sect. *Pharmacosycea* and seven species of the derived subgenus *Urostigma* (*F. citrifolia*, *F. colubrinae*, *F. costaricana*, *F. nymphaeifolia*, *F. obtusifolia*, *F. pertusa*, and *F. popenoei*).

The usefulness of the transferred markers was also tested for estimating the genetic diversity and relationships of the population in the above mentioned studies and current study. The choice of the effective marker is very important for phylogenetic, genetic mapping and evolutionary genetic studies for achieving effective and reliable results. The amplification performance of the marker is measured by producing reliable, repeatable and polymorphic fragments.

The objective of the current study was to examine the transferability of 54 SSR markers previously developed for *F. montana*, *F. septica* (Zavodna et al., 2005), *F. sycomorus* (Ahmed et al., 2007), *F. (Sycomorus) racemosa*, *F. (Urostigma) rubiginosa* (Crozier et al., 2007) and *F. insipida* (Vignes et al., 2006) to *Ficus carica*. To ensure the effectiveness of the markers, all successfully transferred microsatellites have been evaluated for determining genetic diversity and relationship among the 32 fig genotypes (*Ficus carica* L.).

Material and method

Plant material and DNA extraction

Total genomic DNA was extracted from young, frozen leaves of 32 genotypes (16 male, 16 female) previously collected from trees located at Fig Research Center, Aydin, Turkey and kept at -20 °C. DNA extraction was performed based on the modified cetyltrimethylammonium bromide (CTAB) method (Doyle and Doyle, 1990). DNA samples were electrophoresed on 1% agarose gels stained with ethidium bromide and adjusted to 30 ng/μl final concentrations.

Amplification conditions

Initially 54 SSR markers were screened using four genotypes to see the amplification performance. The PCR with the non- amplified primers was repeated. Then based on amplification performance 38 primers across all 32 genotypes were selected to be used.

Polymerase chain reactions (PCRs) were performed in a total volume of 15 µl containing 30 ng/µl genomic DNA template, 1 µl of 10×PCR buffer, 1 µl of 2.5 mM dNTP mixture, 1 µl of 25 mM MgCl₂, 0.5 µl each of forward and reverse primer (10 pmol/µl), and 0.1 µl of 5 U/µl Taq polymerase. Labeled primers were used (IRD700 and IRD800) following the protocol described by Schuelke (2000). Forward primers were labeled with a adaptor sequences (GGAAACAGCTATGACCAT) at its 5' end. The reactions were performed with the following conditions: 94 °C for 3 min, then 35 cycles of 94 °C for 40 s, 53-65 °C for 50 s, and 72 °C for 1 min, and a final step at 72 °C for 10 min. PCR products (15 µl) were mixed with 50 µl formamide loading buffer (98% formamide, 10 mM EDTA, 0.25% bromophenol blue, 0.25% xylene cyanol, pH 8.0) and denatured for 3 min at 95 °C, and cooled on ice. Separation was performed on a Li-Cor - IR² 4200 Genetic Analyzer (Li-Cor Biosciences) using 5.5% denaturing polyacrylamide gel on 25 cm plate.

Data analysis

Only reproducible bands with high intensity were scored as present (1) or absent (0). The genetic similarity matrix was calculated using Numerical Taxonomy Multivariate Analysis System (NTSYS-pc) version 2, 1 software package (Exeter Software, Setauket, NY, USA) (Rohlf, 2000). Based on the similarity matrix, a dendrogram showing the genetic relationships between genotypes was constructed by the unweighted pair group method with arithmetic average (UPGMA) using SAHN module of the software NTSYS-pc. In addition, principal component analysis (PCA) was performed using the EIGEN and PROJ modules based on Jaccard's similarity coefficient.

The transferability (amplification rate) of SSR marker developed for each donor species were calculated by counting the amplified markers in *Ficus carica* regardless of polymorphism according to formula by Kuleung et al.(2004) (Eq. 1):

$$\text{Amplification (\%)} = \text{number of amplified markers} \times 100 / \text{total number of markers} \quad (\text{Eq.1})$$

Results

A total of 54 SSR markers were screened with four genotypes for amplification performance and 38 microsatellites were successfully amplified. Thirty-eight SSR loci were then employed to detect genetic diversity and relationship among the 32 *Ficus carica* genotypes and a total of 89 alleles were produced with the 2.34 average alleles per locus. In the present study, of the 38 loci transferred, 21 of which were monomorphic and 17 were polymorphic for *Ficus carica* and produced 62 alleles. The number of polymorphic bands per SSR locus ranged from 2 to 14 with a mean of 3.64 alleles per locus. The sizes of the fragments ranged from 110 to 310 bp. The primer FM4-15 produced highest number of band (14) in *Ficus carica* comparing the other primers, indicating amplification of more than two loci (Table 1).

Similarity matrix was used to study genetic diversity among 32 genotypes. The highest value of similarity was 0.80 found between the genotypes 'Noire de Caromb' and 'Kavak' and genotypes 'Armut ilek' and 'Bostancı'. Minimum similarity value was 0.47 between genotypes 'Buyukkonkur' and 'Morözer'. To test the usefulness of the transferred primers for analysis of genetic diversity on *Ficus carica* population the clustering pattern of the genotypes was assessed.

Table 1. Transferability and characterization of *Ficus racemosa* and *Ficus rubiginosa* (Crozier et al., 2007), *Ficus sycomorus* (Ahmed et al., 2007), *Ficus insipida* (Vignes et al., 2006), *F. montana* and *F. septica* ((Zavodna et al., 2005) SSR loci in 32 *Ficus carica* genotypes

Microsatellite marker	Species	Primer sequence (5'–3')	TA	PA	Product length
Frac13	<i>F. racemose</i>	F: CACGTTACGCTGCAA R: GATAGAGAAGGCATATCCAGAG	4	4	127-141
Frac29	<i>F. racemose</i>	F: CCAGGCATATGCATCTTGTGTA R: CTCGCAGCTTTCCTCGCA	1	M	200
Frac83	<i>F. racemose</i>	F: TGAACCTTCAATAACATCGGGTT R: CTCATGCAATCATAGCACTCA	3	3	175-225
Frac86	<i>F. racemose</i>	F: TGTCACTGTTCTGTTTGTGC R: CAGCCAACCTCAAGTATAAGA	1	M	180
Frac110	<i>F. racemose</i>	F: CCAGAACAGTTGGACGTAAC R: GGATTACCCGCGCTATGAAGT	1	M	240
Frac113	<i>F. racemose</i>	F: CTGGGTCTCTCTATTACCAAC R: GCTGATCTTCTCGGATGCT	3	3	231-233
Frac154	<i>F. racemose</i>	F: ACCCAAGAGCCCAAACCTCGT R: TCAACCCTTGCTCCTTGC	NA		—
Frac202	<i>F. racemose</i>	F: AGAGATATGATGTTCTAGTGCA R: CTCGCTCCCACTTAAATACAAG	1	M	200
Frac222	<i>F. racemose</i>	F: ACCCATATAGCAGTCTTCAGA R: GCTTGTTGACTCCGCAACTA	1	M	215
Frac241	<i>F. racemose</i>	F: GGCTCAAGCAAGGGATGGA R: CGAGCTCATTGTTTATCGACC	3	3	280-294
Frac244	<i>F. racemose</i>	F: ACCTAGAATCATAACCCTTCA R: CCCATAAACTACGATACATAAGA	1	M	310
Frub29	<i>F. rubiginosa</i>	F: CCACTTTGGAATGTCACCTGGA R: TGAACACGCCAACTGAGAATG	1	M	225
Frub38	<i>F. rubiginosa</i>	F: TGAACACGCCAACTGAGAATG R: ACAGCTGCCAAATTCCTTGA	2	2	205-215
Frub61	<i>F. rubiginosa</i>	F: GTACACTCTCTTAGCTGCC R: TACCTTTCTCTGGACATTC	1	M	160
Frub93	<i>F. rubiginosa</i>	F: GATATTTCAATAACATCTCCTCAAC R: TACGTTTGTATGGACTTTGGC	NA		—
Frub391	<i>F. rubiginosa</i>	F: AGATGTCAAATAAGGTCAGCT R: AGATGCAGTTCATACAATTC	1	M	164
Frub398	<i>F. rubiginosa</i>	F: GTACCTTAGATTCTAGTGTGAG R: TGGGATCTCATGAACTATTTAC	1	M	204
Frub412	<i>F. rubiginosa</i>	F: ACATCAAATTTCTTAGATCGGTTG R: ATCCAGAGCGGCAAACACACAAG	1	M	220
Frub415	<i>F. rubiginosa</i>	F: GCACGTAGTCGGTGTAAAGC	1	M	162

Frub416	<i>F. rubiginosa</i>	R: CTGTGCGGAATAAAAAGCTAGC F: CAGCAATGATCTTGACCT	5	2	240-280
Frub422	<i>F. rubiginosa</i>	R: GTACTCATCAATATCTCTAAACAAC F: GCGTGAAATTTATGCTATGA	1	M	196
Frub436	<i>F. rubiginosa</i>	R: GCGTGAAATTTATGCTATGA F: GTACTGTGATTAGTATCTTTGA	2	2	175-180
Fsyc01	<i>F. sycomorus</i>	R: CTAGCAATAACTCACTGATATTG F: CAAATGAAAAACACAAATTTGCCAAC	NA		—
Fsyc02	<i>F. sycomorus</i>	R: TGCAAGTACTAATTCCTCTGCCGTG F: CAGCAGCAGATTATCATTATGGC	NA		—
Fsyc04	<i>F. sycomorus</i>	R: GTTTCTTCGTAAACTATATTCTCTGCCAGCC F: CAAACTACGCCTTCATTTCTTCCAC	1	M	200
Fsyc05	<i>F. sycomorus</i>	R: CGCAAGCAAGCTGCTCCTC F: CCGGAGGCTCGAAAGACAAG	1	M	260
Fsyc06	<i>F. sycomorus</i>	R: TCAAATTTCCAATCCCAAACCC F: GGGCTTCGAATTGCTTCCAG	1	M	197
Fsyc07	<i>F. sycomorus</i>	R: GTTTCTT-TTCGTCTTCGTTTGCGATG F: TCTACAAGACACTTAACAATTTTAGCACC	2	2	140-160
Fsyc08	<i>F. sycomorus</i>	R: TCACATCGAGTTGTGCTTGC F: TCTCTTTGTGGTTGATGCCA	3	3	211-215
Fsyc09	<i>F. sycomorus</i>	R: CGCCAATTGGAGAGACTACATT F: GCTTACTCCCAGCCGTTATG	2	2	110-113
Fsyc11	<i>F. sycomorus</i>	R: AATTGAACAAATTGTCTGTATGC F: CACAAGGTGGAGAGTGCTCG	3	3	280-310
Fsyc12	<i>F. sycomorus</i>	R: TTCCCTACTCATTTACCTTCTCCTTC F: ACACATGATATTTGAATAGCACTCTTTC	NA		—
Fsyc13	<i>F. sycomorus</i>	R: CCACGATGGTTAGAAAACCG F: TGGAGATGTGAATATCATTGGACGTG	NA		—
FinsI12 F	<i>F. insipida</i>	R: CGACGAACAGTTAGTATCGGTAACAGC F: GAACCTTCAACCTCAATCAA	NA		—
Finsj10	<i>F. insipida</i>	R: CTCCCCTTTCCTAGTCCTTA F: AGGTGGAATGAGGAGAGAGT	1	M	180
Finsk9	<i>F. insipida</i>	R: AAACATCCTTTCTGGACTTG F: ACGCACTTAACCCCTTTCAG	NA		—
FinsM5	<i>F. insipida</i>	R: TTCGAGTCAACGAAACAAA F: ATGAATGGTGAAATCCTGAA	NA		—
FinsN1	<i>F. insipida</i>	R: CATGGCCTCAACTTAGAAAC F: AGGGCTGAGATAGGTTGATT	NA		—
FinsN3	<i>F. insipida</i>	R: TAAGTTGGTGTGTGGCATC F: AAAACTTCTCCTCTGCTATTTT	3	2	185-198
FinsP8	<i>F. insipida</i>	R: TTTGCTTCTTCTGTGTTGAC F: TGAAGAAAACGGAGCTTG	1	M	180
		R: CTAAATCTGACGGTTCAAAA			

FinsQ5	<i>F. insipida</i>	F: CATGTCAGGAGGTGTCTAGG R: CTCCAAATGGGTATGTCAAG	5	4	164-178
FinsQ6	<i>F. insipida</i>	F: TTCTCCAATTAACCTCCAA R: CATGAAATCACCTTCCTCAT	1	M	120
FinsT7	<i>F. insipida</i>	F: GAATCTGGAGGTGGAATAAAC R: AAAGATCGCTCGTCAACC	NA		—
FinsU7	<i>F. insipida</i>	F: CGTGTATTGATGTGTGTGTG R: TCACCTCCTCCTTCTTTTG	NA		—
FinsA1	<i>F. insipida</i>	F: AATCCCCGTA CTTC ACTTG R: AGAACTTATTGCACGGACAG	5	5	194-222
FinsH5	<i>F. insipida</i>	F: GACCGTATAGATGATTTGGG R: CATCCTGTGAACGACACTT	1	M	270
FM4-15	<i>F. montana</i>	F: ATCTTCGTCGGTATTGCTTTCACT R: GGAAGAGAACCCTTTTTGTATTGG	14	14	200-285
FM4-18	<i>F. montana</i>	F: CGTATGGCCCATGCTTGACTCAC R: CTCGGATTGCCACGTGTAGGTTG	1	M	185
FM1-27	<i>F. montana</i>	F: GTGATTTGCGATGGCGTGTTTA R: TCTTCGCTTGCTCGTCAGTGTCC	NA		—
FM3-64	<i>F. montana</i>	F: GATGGTGTGTTGTTCGATGGTCAT R: GCGGCTCGGTGGA ACTTGAG	NA		—
FM4-70	<i>F. montana</i>	F: CAGATGAGGTTGACGATGTTATTG R: TAAACCCTCTTCAAATTC ACTCTC	7	6	202-232
FS4-11	<i>F. septica</i>	F: AAGGCAACGGGGATAAAGTATTCA R: CTCCGAGAGCAACTCCATCACG	NA		—
FS3-31	<i>F. septica</i>	F: CATCATCCCCGTCAGAAAGTGAGG R: TGAGGCGGTGATGGTGATTGAAT	2	2	240-242
FS3-37	<i>F. septica</i>	F: CAAACGAGGAACAACACATACAGC R: GATGCACAGGAGTTAACGGGAATG	NA		—
Total			89	62	

Seventeen SSR loci could distinguish the 32 fig genotypes with 62 alleles and UPGMA cluster analysis grouped these individuals into two main clusters with genetic similarity ranging from 0.63 to 0.80. Cluster I is divided to two subclusters (1-A and 1-B) at the similarity level of 0.65 and included 29 genotypes, while Cluster 2 consisted of 3 genotypes. ‘Noire de Caromb’ and ‘Kavak’ stayed on close to and grouped into Cluster I along with ‘Beyaz Orak’. Two genotypes ‘Armut İlek’ and ‘Bostancı’ were appeared to very close (80%) on the dendrogram. Three genotypes, ‘Sarilop’, ‘Sarikilis’ and ‘Turnaboyu’ separated from the majority of the genotypes and placed on the Cluster 2 (Fig. 1). The male and female genotypes were randomly placed on the dendrogram. Although a few female genotypes namely ‘Noire de Cromb’, ‘Kavak’, ‘Beyaz Orak’ and ‘Mor özer’ and male genotypes namely ‘Derviş Ali’, ‘Kızılay’, ‘Bostancı’ and ‘Armut İlek’ placed on together in a small cluster the rest of the genotypes clustered regardless of the gender (Fig. 1) The male and female genotypes were partly grouped in the two dimensional graph as well, a few male genotypes placed on the upper part and

some female genotypes on the bottom of the matrix. But most of the male and female genotypes scattered randomly on the two dimensional graph as expected (Fig. 2).

Discussion

In current study overall, 70.37% (38/54) of the tested SSRs successfully amplified at least one PCR product in *Ficus carica* (Table 1). Mnejja et al. (2010) obtained similar results with *Prunus* and successfully transferred 63.9% of SSRs to other *Prunus* species. Dirlwanger et al. (2002) transferred 41 primers developed in peach successfully to sweet cherry (80.5%). In the present study, the highest transferability rate (90.9%) was observed with SSRs developed for *F. rubiginosa* (Frub) and for *F. racemosa* (Frac). The transferability rate of Fsync (*F. sycomorus*), FM (*Ficus montana*) and Fins (*Ficus insipida*) primers were 63.6%, 60% and 53.84%, respectively. The lowest transferability rate (33.3%) was obtained with SSRs developed for *F. septica* (FS). Nazareno et al. (2009) reported high transferability (80%) of microsatellite markers developed from *Ficus insipida* (Fins), *Ficus racemosa* (Frac) and *Ficus rubiginosa* (Frub) to *Ficus citrifolia* and *Ficus eximia*. In present study, Frub loci developed for *F. rubiginosa* and Frac loci developed for *F. racemose* showed a high transferability rate. However, these two SSRs are monomorphic in both loci in the current studied population. They may produce polymorphic loci in different population.

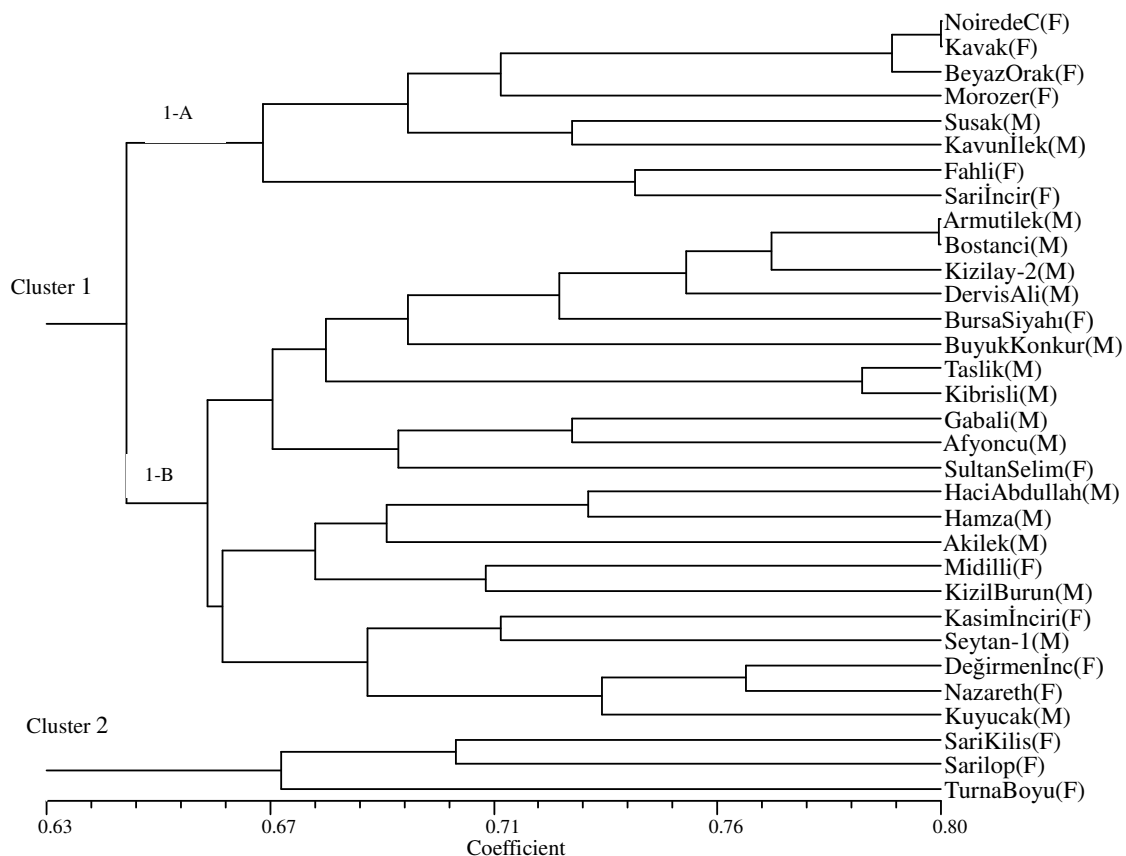


Figure 1. The dendrogram based on average distance coefficients among 32 individuals (16 female 16 male) with 62 SSR markers

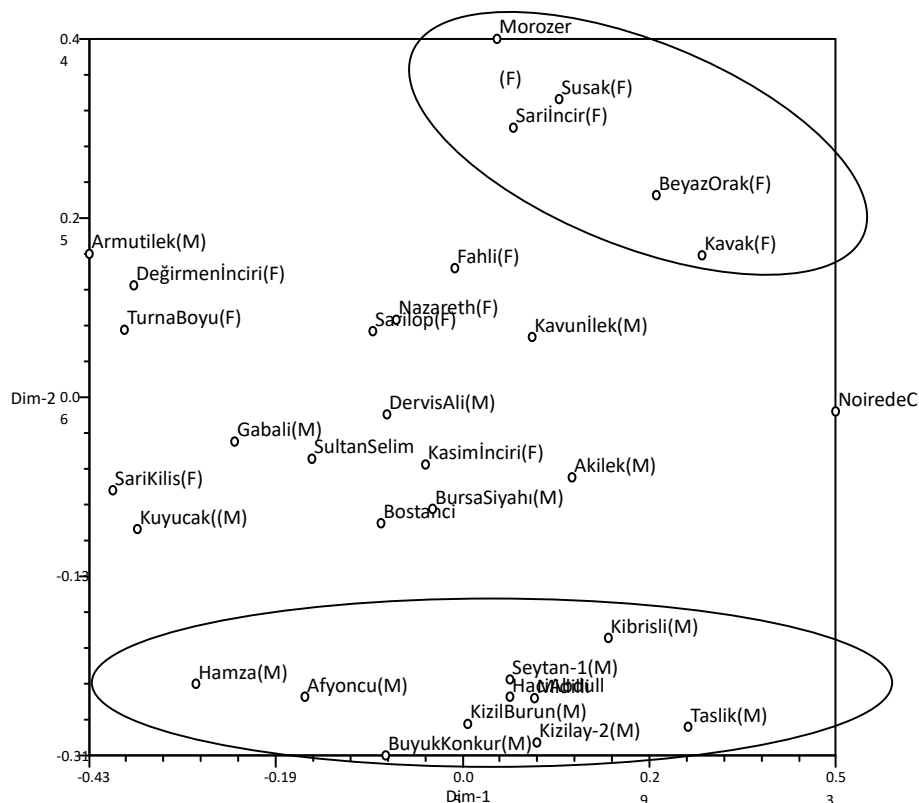


Figure 2. Two-dimensional plot from PCA of 32 fig genotypes (16 female, 16 male) analyzed with SSR markers

In current study 38 SSR loci produced 89 alleles with the 2.34 average alleles per locus. Comparing this results with previous studies; Giraldo et al. (2005) developed and tested 26 SSR loci on 15 *Ficus carica* cultivars and obtained 79 total bands with the average of 3 bands per SSR. The amplification pattern of the FM4-15 in our study was similar that of Zavodna et al. (2005) in which they obtained 14 alleles in donor species, *Ficus montana*. This may indicate that some of the region on *Ficus carica* and *Ficus montana* genome may be conserved. Of the 54 primers tested 16 did not amplify on *Ficus carica*. Similar result was reported by Giraldo et al. (2005). They tested 26 microsatellite SSR primers developed for *Ficus carica* on 13 different *Ficus* species and eight primers did not give amplification on *Ficus* species and they did give amplification on two *Morus* species.

Amplified markers from related species generally resulted in similar banding patterns in the *Ficus carica* genome, suggesting that they were developed from the same loci and primer binding sites are conserved. Similar alleles and length of amplification products were obtained with Frac13 (120, 135, 196), Frac83 (175-192-225), Frac 241 (280, 285, 294), Fsync07 (140-160), FinsA1 (194-222), FM-4-15 (200-285) FM4-70 (202-232) when compared with the donor species (Crozier et al., 2007; Ahmed et al., 2007; Zavodna et al., 2005). There were some differences in a few SSR loci with the originally developed species and *Ficus carica*. Three loci (Fsync11, FinsQ5 and FinsN3) produced more alleles in *Ficus carica* than the originally developed species (Ahmed et al., 2007; Vignes et al., 2006). Nazareno et al. (2009) indicated that most of the primers (Frac86, Frub29, Frub61, Frub391, Frub415, Frub422) produced more than one band in

Ficus citrifolia and *Ficus eximia* whereas in the current study all of these primers amplified monomorphic bands in the *Ficus carica* (Table 1). This argued that the genetic diversity in *Ficus carica* may be less than *Ficus citrifolia* and *Ficus eximia*.

Conclusion

As a conclusion, 38 primers successfully transferred to *Ficus carica* of which 17 were polymorphic and produced 62 alleles. The polymorphic microsatellites are later employed to determine the genetic diversity among the *Ficus carica* genotypes. The produced 62 alleles discriminated the 32 *Ficus carica* genotypes successfully which shows the effectiveness of the markers.

Our results indicated a high level of transferability between *Ficus carica* and related *Ficus* species which provides a growing number of SSR for *Ficus carica*. This is an important benefit for species with genomic studies are limited. Transferred SSR markers can be used in the future studies for linkage and QTL mapping studies and molecular characterization of the genetic resources of *Ficus carica*. The 21 SSR primers produced monomorphic bands in the current studied population should be tested in the future studies to see the polymorphism levels in different population.

Acknowledgements. The authors thank to Erbeyli Fig Research Institute-Aydın, Turkey for research material and Akdeniz University for laboratory infrastructure and facilities.

REFERENCES

- [1] Ahmed, S., Dawson, D. A., Compton, S., Gilmartin, P. (2007): Characterization of microsatellite loci in the African fig *Ficus sycomorus* L. (Moraceae). – *Molecular Ecology Notes* 7: 1175–1177.
- [2] Condit, I. J. (1969): *Ficus: The Exotic Species*. – Division of Agricultural Sciences, University of California, California.
- [3] Crozier, Y. C., Cheng, X., Yan Yao, J., Field, A. R., Cook, J. M., Crozier, R. H. (2007): Microsatellite primers for *Ficus racemosa* and *Ficus rubiginosa*. – *Molecular Ecology Notes* 7: 57–59.
- [4] Darlington, C. D., Wylie, A. P. (1955): *Chromosome Atlas of Flowering Plants*, 2nd ed., pp. 183–185. – George Allen & Unwin Ltd., London.
- [5] Dirlwanger, E., Cosson, P., Tavaud, M., Aranzana, M. J., Poizat, C., Zanetto, A., Arús, P., Laigret, F. (2002): Development of microsatellite markers in peach [*Prunus persica* (L.) Batsch] and their use in genetic diversity analysis in peach and sweet cherry (*Prunus avium* L.). – *Theor Appl Genet* 105: 127–138.
- [6] Doyle, J. J., Doyle, J. L. (1990): Isolation of plant DNA from fresh tissue. – *Focus* 12: 13–15.
- [7] Fan, L., Zhang, M. Y., Liu, Q. Z., Li, L. T., Song, Y., Wang, L. F., Zhang, S. L., Wu, J. (2013): Transferability of newly developed pear SSR markers to other rosaceae species. – *Plant Mol Biol Rep* 31: 1271–1282. DOI: 10.1007/s11105-013-0586-z.
- [8] Gasic, K., Han, Y., Kertbundit, S., Shulaev, V., Iezzoni, A. F., Stover, E. W., Bell, R. L., Wisniewski, M. E., Korban, S. S. (2009): Characteristics and transferability of new apple EST-derived SSRs to other Rosaceae species. – *Mol Breed* 23: 397–411.
- [9] Giraldo, E., Viruel, M. A., Lopes-Corrales, M., Hormaza, J. I. (2005): Characterisation and cross-species transferability of microsatellites in the common fig (*Ficus carica* L.). – *Journal of Horticultural Science and Biotechnology* 80: 217–224.

- [10] Heer, K., Machado, C. A., Himler, A. G., Herre, E. A., Kalko, E. K. V., Dick, C. W. (2012): Anonymous and EST-based microsatellite DNA markers that transfer broadly across the fig tree genus (*Ficus*, Moraceae). – American Journal of Botany: e330–e333 2012. <http://www.amjbot.org/>.
- [11] Kuleung, C., Baenziger, P. S., Dweikat, I. (2004): Transferability of SSR markers among wheat, rye, and triticale. – Theor Appl Genet 108: 1147–1150. DOI: 10.1007/s00122-003-1532-5.
- [12] Mnejja, M., Garcia-Mas, J., Audergon, J. M., Arús, P. (2010): *Prunus* microsatellite marker transferability across rosaceous crops. – Tree Genetics & Genomes 6: 689. DOI: 10.1007/s11295-010-0284-z.
- [13] Nazareno, A. G., Pereira, R. A. S., Feres, J. M., Mestriner, M. A., Alzate-Marin, A. L. (2009): Transferability and characterization of microsatellite markers in two Neotropical *Ficus* species. – Genetics and Molecular Biology 32: 568–571.
- [14] Pierantoni, L., Cho, K. H., Shin, I. S., Chiodini, R., Tartarini, S., Dondini, L., Kang, S. J., Sansavini, S. (2004): Characterisation and transferability of apple SSRs to two European pear F1 populations. – Theor Appl Genet 109: 1519–1524.
- [15] Rahnavard, A. (2016): Genetic and biochemical diversity of *Hypericum Perforatum* L. grown in the Caspian climate of Iran. – Applied Ecology And Environmental Research 15(1): 665-675.
- [16] Rohlf, J. F. (2000): NTSYS-pc: Numerical Taxonomy and Multivariate Analysis System. – Exeter Software, Setauket, New York.
- [17] Schuelke, M. (2000): An economic method for the fluorescent labelling of PCR fragments. – Nature Biotechnology 18: 233–234.
- [18] Storey, W. B. (1975): Figs. – In: Janick, J., Moore, J. N. (eds.) Advances in Fruit Breeding, pp. 568–589. Purdue University Press, West Lafayette, Indiana.
- [19] Vignes, H., Hossa, M., Beaune, D., Fevre, D., Anstett, M. C., Borges, R. M., Kjellberg, F., Chevallier, M. H. (2006): Development and characterization of microsatellite markers for a monoecious *Ficus* species, *Ficus insipida*, and cross-species amplification among different sections of *Ficus*. – Molecular Ecology Notes 6: 792–795.
- [20] Zavodna, M., Arens, P., Van, P. J., Vosman, B. (2005): Development and characterization of microsatellite markers for two dioecious *Ficus* species. – Molecular Ecology Notes 5: 355–357.

FROM AN EMPIRICAL TO CONCEPTUAL MODELING VIEW OF ENERGY CROP PRODUCTIVITY

ŠIMKŪNAS, A.* – DENISOV, V. – VALAŠINAITĖ, S. – JANKAUSKIENĖ, R. – IVANAUSKAITĖ, A.

Marine Technology and Natural Sciences Faculty, Klaipėda University, Klaipėda, Lithuania

**Corresponding author*

e-mail: alvydas.simkunas@gmail.com; phone: + 370-861-701-993

(Received 19th Jan 2018; accepted 13th Mar 2018)

Abstract. When empirical research provides incomplete data, it is often not accepted, especially if the primary data is slightly controversial. This article investigates this situation exactly, where there is little data and quite unexpected results. A conceptual modeling approach is applied here to supplement the empirical research and to examine the yield obtained from the *Silphium perfoliatum* energy plant under certain environmental conditions in Lithuania. The designed conceptual model is based on an analysis of informational relationships within the “donor-acceptor” (“source-sink”) plant (sub)system. It was found, that the chlorophyll-*a* amount did not affect the yield, what according to the model, may be determined by the different acceptor activity. Nitrogen and potassium influenced the biomass positively, possibly through the activation of acceptor metabolism and assimilate transport, and the consequent signaling on the photosynthetic apparatus (via cytokinin and sugar). Meanwhile, the high phosphate amount in soil negatively influences the yield. A hypothesis of yield limitation by signaling through the high phosphate levels in the case of slowed down photosynthesis is proposed. In addition to determining the causality of the yield formation, the conceptual modeling enables us to make use of limited empirical data to design future experiments, aimed at testing the hypothesis and verifying the model.

Keywords: *energy plant Silphium perfoliatum; yield formation conceptual model; system dynamics methodology; donor-acceptor causal relationships; yield inhibition via phosphate*

Introduction

The list of crops grown both in Europe and in Lithuania is constantly supplemented with new, poorly investigated energy plants. These plants grow rapidly and create a large biomass, although because of economic and ecological reasons, they are grown in poorly cultivated soils (McKendry, 2002a; Jakienė et al., 2015; Allen et al., 2014). Not only is productivity important while growing such plants, but also their ecological impact, i.e. less harmful environmental impact. In seeking to obtain a sufficient yield in non-fertile soils, it is necessary to apply agricultural practices aimed at addressing the main yield-limiting factor, otherwise the yield sharply decreases. The same strategy (to affect the limiting factor) is applied while seeking to reach the proper ecological effect – to minimize any impurities that pollute the environment and complicate the technological process. So we face challenges in achieving both a higher plant yield and a positive ecological effect.

One of the less investigated energy crops, *Silphium perfoliatum* L., is suitable for biochemical conversion, i.e. methane extraction via anaerobic digestion. This is achieved because of the large biomass of this plant and its easily degraded materials, i.e. the stems are filled with a spongy core. The average yield of *S. perfoliatum* is 13-15 t/ha, and high yields may be obtained up to 15-17 t/ha (Gansberger et al., 2015). So the dry matter yield per hectare of *S. perfoliatum* may be approximately equal to that of maize, while some authors reported an approximately 20% lower yield per hectare for *S. perfoliatum* than for maize (Aurbacher et al., 2012). Meanwhile, other authors reported

(Stockmann et al., 2013) a 20-50% lower yield per hectare for *S. perfoliatum* than for maize. While growing these plants, it is also important to be aware of the ecological impact during the methane extraction process – slag formation, which depends on the biomass ash content. The following impurities could be present: particulates, tar, N, S and alkali compounds. The problem of slag formation is caused by the alkali content of the biomass (McKendry, 2002b). So while growing *S. perfoliatum*, it is important to pay attention to the yield increase along with its quality.

Up until now, plenty of empirical data has been accumulated about energy crop yield formation accomplished through the use of fertilizers, liming soils, etc. (Douglas et al., 1987; Wrobel et al., 2013; Šiaudinis et al., 2012). Many authors also suggest that further research is needed in the following directions: first year trial equipment optimization, control of weeds and pests, opportunities to use a form of different geographical origin for both economic activity and plant-breeding, and the application of energy plants (incl. *S. perfoliatum*) in medicine (Kowalski and Wolski, 2003; Gansberger et al., 2015). However, up until now, the empirical viewpoint has prevailed in the field research of energy plants, so the typical results obtained lack an explanatory nature and (eco)system level conceptualisation (Adegbidia et al., 2001; Borkowska et al., 2009; Maughan et al., 2012; Jasinskas et al., 2014; Šiaudinis et al., 2015). They are not oriented enough towards the causality of agroecosystem processes and their interconnections. Such an examination of individual processes encompasses a broad spectrum of topics and a great number of unrelated experiments and field trials.

When empirical research provides little or incomplete data, it is often not accepted, especially if the primary data is even slightly controversial. This article investigates this situation exactly, where there is little data or quite unexpected results (for example, when a significant correlation between chlorophyll concentration and biomass is absent, or when the phosphate concentration in a soil has a negative influence on biomass). A systemic conceptual approach, which is applied here to examine the yield obtained from the *S. perfoliatum* energy plant under certain environmental conditions, is based on an analysis of informational relationships that are important for photosynthesis control within the “donor-acceptor” (“source-sink”) plant (sub)system. The resulting causal model of yield formation includes both internal (donor-acceptor) and external (fertilization, illumination, etc.) factors, which enables us to analyse all the experimental field results from the chosen conceptual viewpoint. Moreover, the conceptual model itself can be further formalized and refined, constructing a simulation model, which can then be investigated in computer experiments in order to supplement weak empirical data with a new set of synthetic data. To sum up, the representation of sparse or incomplete empirical data via a conceptual model can help in identifying the origins of contradictions, to reveal their significance, to explain causality of factors, and thus, to provide more added value to the research results.

The underlying concept of “donor-acceptor” (“source-sink”) applied here takes into account that the photosynthesis and yield formation processes directly depend on the activity of a leaf, as a donor (source) of photoassimilates (Rossi et al., 2015; Yu et al., 2015). Meanwhile, it is known that the intensity of photosynthesis is also regulated via signals related with the acceptors (sink), i.e. areas involved in the metabolic activities of growing and reserving (Mokronosov, 1981; Nancy, 1994; Chikov, 2008; Paul and Foyer, 2001; Fatichi et al., 2014; Yu et al., 2015; Rossi et al., 2015). In particular, the latter is confirmed by positive correlations detected between photosynthetic activity and the acceptors’ growth indices (relative and absolute growth rate) (Mokronosov, 1981). It

is also known that some photosynthesis genes (Rubisco small subunit, plastocyanin genes, etc.) are turned off by feedback control loops when carbohydrates are not used enough in acceptors, and they accumulate in the leaves (Paul and Foyer, 2001; Tognetti et al., 2013). The main signal substances in this regulation network are soluble carbohydrates, mostly sucrose. Meanwhile, photosynthesis throughout the entire plant level is regulated from other parts of the plant system, i.e. acceptors, and the productivity of photosynthesis depends to a great extent on systemic determination.

It is important to keep in mind that photosynthesis may be limited by any component of the “donor-acceptor” system, and it depends on specific environmental conditions – the amount of light, water content in the soil, and mineral nutrition components (Mokronosov, 1981; Brown, 1988; Rossi et al., 2015). From the donor side, the limitation of photosynthesis is possible because of insufficient light, or when the CO₂ fixation becomes insufficient and limits the growth and yield. It should be mentioned that in a situation when the amount of sugar is not sufficient, growth is not reduced directly, but through regulatory mechanisms, i.e. SNrK1 kinase activation, thus, growth is suppressed and adapted to the donor potency (Lastdrager et al., 2014; Yu et al., 2015). Alternately, when the donor activity and sucrose amount increase, the amount of signal carbohydrate trehalose 6-phosphate (T6P) also increases, which indicates good donor functioning and inhibits the kinase SNrK1 activity, thus stopping the suppression of growth. Photosynthesis can be also limited through the growth limitations of acceptors, and this can be caused by different factors (for example, a phosphates deficit) (Rychter and Rao, 2005; Lawlor and Paul, 2014). In this case, a smaller amount of sugar is used, and photosynthesis slows down because of feedback control. It is also important to note that the interaction between donor and acceptor changes during ontogenesis, for example, during the later ontogenesis phases, an entirely new group of acceptors, i.e. generative structures, are formed. Then, with the assimilates more oriented towards inflorescence, root nutrition may suffer, which slows down photosynthesis and limits the yield (Mokronosov, 1981; Chikov, 2008) Thus, the systemic determination of photosynthesis is non-static, i.e. it changes through the influence of both environmental conditions and ontogenetic drift.

The study deals with the following research issue: which of the investigated system components, i.e. either donor or acceptor, limits the yield of an *S. perfoliatum* energy crop under the influence of specific environmental conditions (Lithuanian climate, *Cambisols*, different soil NPK in the experimental plots). The aim of the study is to design a conceptual model of the *S. perfoliatum* energy plant’s productivity, enabling the identification of such limiting components and to delineate further research directions for it. In particular, the study will assess the relationships of the chlorophyll content within the *S. perfoliatum* biomass and the influence of the amount of root nutrition medium indices (general amounts of nitrogen, mobile phosphorus and potassium available) to the *S. perfoliatum* biomass. It will also compare the influence of different factors (chlorophyll content in the leaves and nitrogen, phosphorus and potassium present in the soil) to *S. perfoliatum* productivity. As already mentioned, the primary data from the experimental fields is incomplete and somewhat controversial, however, at the same time, is quite interesting and provocative, inviting further interpretation. To make use of it, it is combined with known physiological assumptions to produce a conceptual model of energy plant productivity, based on the analysis of informational relations that are important for the control of photosynthetic productivity within the “donor-acceptor” (“source-sink”) plant (sub)system.

Materials and methods

The object and location of investigation

The object of investigation was the cup plant (*Silphium perfoliatum* L.), which belongs to *Asteraceae* family (Wrobel et al., 2013). It is a perennial C₃ plant, which is used as an energy crop. The possibility of using this plant in biogas production has been determined by its botanical characteristics, i.e. its large biomass, as each plant grows 10-25 stalks, having 8-12 internodes with a length of 20-30 cm (Wrobel et al., 2013). Its easy degradation is ensured by the spongy core that fills the stalks.

The experiment location – Lithuania, Šiauliai district, Bubiai eldership, Bagdoniškės village. Coordinates: 55.766919, 23.1864474.

Although native to North America, *S. perfoliatum* has also adapted to different European climates (Kowalski and Wolski, 2003; Stanford, 1990). The optimal growth temperature for these plants is about 20°C, although they survive under the temperature as low as -30°C (Stanford, 1990; Gansberger et al., 2015). These plants grow mainly in places with high air humidity and soil moisture (Stanford, 1990; Gansberger et al., 2015). Its very strong root system (30-150 cm in length) allows *S. perfoliatum* to survive during drought periods (Stanford, 1990; Grebe et al., 2012; Schoo et al., 2013). The minimum water requirement is around 400-500 mm per year and 200-250 mm per vegetation period, similar to maize (Grebe et al., 2012). This plant has also been introduced in Lithuania, where both the temperature and precipitation amounts (600-650 mm in the experimental area) are proper for its cultivation.

Currently, only seeds of a different geographical origin are available, but no approved varieties with typical characteristics (Biertümpfel et al., 2013; Grebe et al., 2012). *S. perfoliatum* has a wide genetic range. In our case, the seeds were obtained from Germany.

Plant growing and the study area selection

Seedlings were grown in cassettes with a substrate composed of peat, sand and compost soil (at a ratio 2:1:1). The cassettes were kept in a greenhouse about 60 days till the stage of three-four leaves. Then the seedlings were planted in soil (at the end of June). Plants were not applied with fertilizers, and were watered only in the greenhouse. The yield was taken in the second and third year. This paper examines the third year yield.

Two fields, named A and B, were chosen for growing *S. perfoliatum* and the same conventional cultivation process applied in each field. Two plots with plants of different size were chosen for each field to study the differences in yield. After this, the plots were named I, II (from field A) and III, IV (from field B). Each plot covered 3 m². The plots were divided into 3 parts, each part being 1 m², and samples of soil, leaves and green mass were taken from them.

Plant leaves, soil and plant biomass samples collection

S. perfoliatum leaves were taken from the investigated plots (I, II, III, IV), seeking to identify the concentrations of chlorophyll. Three leaf samples were randomly picked from each plot (one from each 1 m² plot area). The samples were taken from the same apical positions of the plants. Samplings were made 3 times during 2014: on September 18th, September 25th and October 2nd.

Soil samples were taken from investigated plots I, II and IV, seeking to identify the soil pH, granulometric composition and total nitrogen, mobile potassium and

phosphorus amounts. To form the samples, 20 cm of the upper soil layer were taken from each plot (one from each 1 m² plot area), and a common sample for each entire plot was formed. The soil samples were taken on July 1st, 2014.

The *S. perfoliatum* green mass yield from plots I, II, III and IV was estimated on October 2nd, 2014. Three green mass yields were cut from each plot and weighed (one from each 1 m² plot area).

Determination of chlorophyll a concentration, soil sample investigation and biomass weighing

The concentration of chlorophyll in the *S. perfoliatum* leaf tissues was estimated according to the protocol of Hiscox and Israelstam (1979). The chlorophyll was extracted using dimethyl sulfoxide (DMSO) and quantified by spectrophotometry at the 645nm and 663nm wavelengths. The concentration of chlorophyll a was expressed in g/l of fresh weight using the following equation: (g/l) = 0.0127 × A₆₆₃ – 0.00269 × A₆₄₅ (Arnon, 1949; Eleuch et al., 2012).

The soil pH was estimated in a 1 mol/l KCl suspension. The concentrations of total nitrogen (N), mobile phosphorus (P₂O₅) and mobile potassium (K₂O) were estimated by the acetate-lactate Egner-Riem-Doming (A-L) method, as this method is the most appropriate for potassium and phosphorus detection in sandy loam soils (Mažvila et al., 2006). The research results were obtained from air-dry soil samples at the Agrochemical Research Laboratory (Lithuanian Research Center for Agriculture and Forestry).

The plant biomass was estimated, having cut the above-ground parts of all the plants growing in each 1 m² and measuring their fresh weight with a balance. The data obtained was expressed in kg/m². As the water requirements were equally fulfilled in the investigated plots, the measured fresh weight differences should reflect the differences of dry mass as well.

Statistical analysis and the conceptual model design

The yield of the investigated plots was evaluated using the ANOVA method. The criterion *p* shows the significance of differences between the variants (plots), and the detected criteria of LSD_{0.05} and LSD_{0.01} allowed estimating the significance of the yield differences between the particular plots. The amount of chlorophyll a and amount of total nitrogen, mobile phosphorus and mobile potassium in the soil had an influence on the *S. perfoliatum* biomass, and this influence was estimated using the linear regression method.

The systemic conception of photosynthesis regulation was applied to perform the causal analysis of the yield formation process. It is based on the detailed analysis of the “donor-acceptor” relationships within the plant system (Mokronosov, 1981; Lerbs et al., 1984; Hirel et al., 2007; Paul and Foyer, 2001; Sandmann et al., 2011; Rychter and Rao, 2005; Lemoine et al., 2013). The preliminary conceptual model of the yield formation was created, in which the causal relationships were represented by the material and informational flows between the identified system components.

Results

The green matter of the *S. perfoliatum* yield in the investigated fields was estimated. The results of the ANOVA statistical method showed that the growing location influenced the yield: *p* = 0.033 (< 0.05) (*Fig. 1*). To estimate the significance of the

yield differences between the fields, the $LSD_{0.5}$ and $LSD_{0.1}$ statistical indices were calculated. Based on this criterion, the statistically significant yield differences were determined for the I and III plots (0.05 significance level) and between the I and IV plots (0.01 significance level) (see Fig. 1).

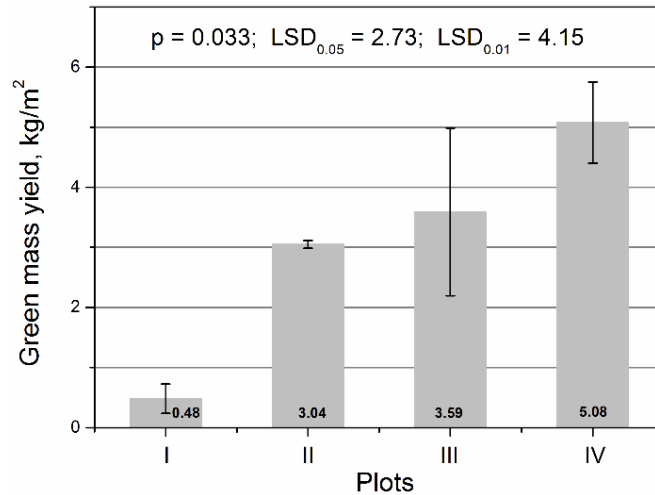


Figure 1. Green mass yield of *S. perfoliatum* in the investigated fields. The standard errors of the mean are shown

During the vegetation period, the assimilate donor (leaf) characteristic, chlorophyll a concentration, was estimated dynamically; the measurements were made 3 times (Table 1, Fig. 2). It was found that the chlorophyll a concentration had influenced the *S. perfoliatum* biomass insignificantly (the yield correlation indices from the different chlorophyll measurements: $r^2 = 0.106$, $r^2 = 0.198$, $r^2 = 0.0609$).

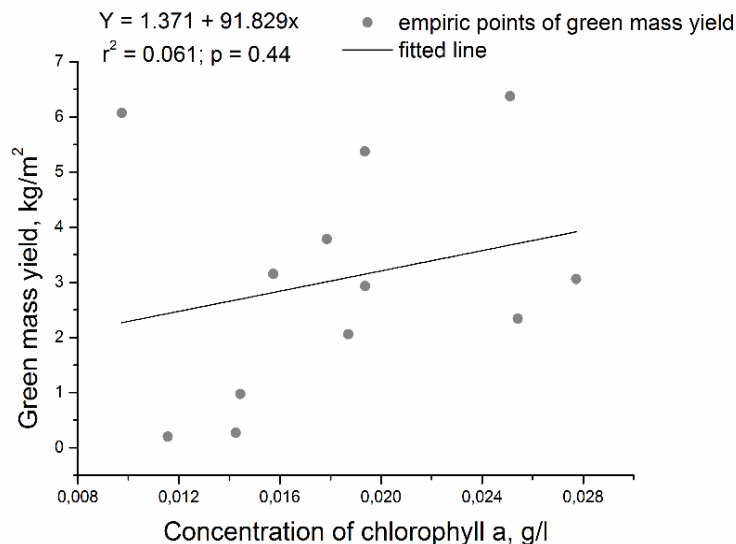


Figure 2. Green mass dependency on the chlorophyll a concentration found in the *S. perfoliatum* leaves (chlorophyll concentration on 2014 10 02)

Table 1. The statistical indices of linear regression between the chlorophyll a concentration and green mass ($Y = a + bx$)

Date of determination	r^2	Slope (b)	$P(b)$	Intercept (a)	$P(a)$
2015 09 18	0.106	228.708	233.884	-1.875	4.526
2015 09 25	0.198	237.149	150.743	-0.919	2.585
2015 10 02	0.0609	91.829	114.074	1.371	2.172

The mineral nutrition factors, such as the concentrations of total nitrogen (0.102 – 0.118%), mobile potassium (164 – 332 mg/kg) and mobile phosphorus (228 – 291 mg/kg) in the soil of the investigated field plots were estimated. It was determined that the total nitrogen concentration in the soil had positively influenced the biomass of *S. perfoliatum* ($r^2 = 0.58$), the influence of the mobile potassium to biomass was also similar ($r^2 = 0.55$) (see Figs. 3A, 3B). So the amount of the plant biomass was larger in the plots where the nitrogen and potassium concentrations in the soil were higher. Meanwhile, a higher mobile phosphorus concentration in the soil reduced the *S. perfoliatum* biomass ($r^2 = 0.54$) (see Fig. 3C).

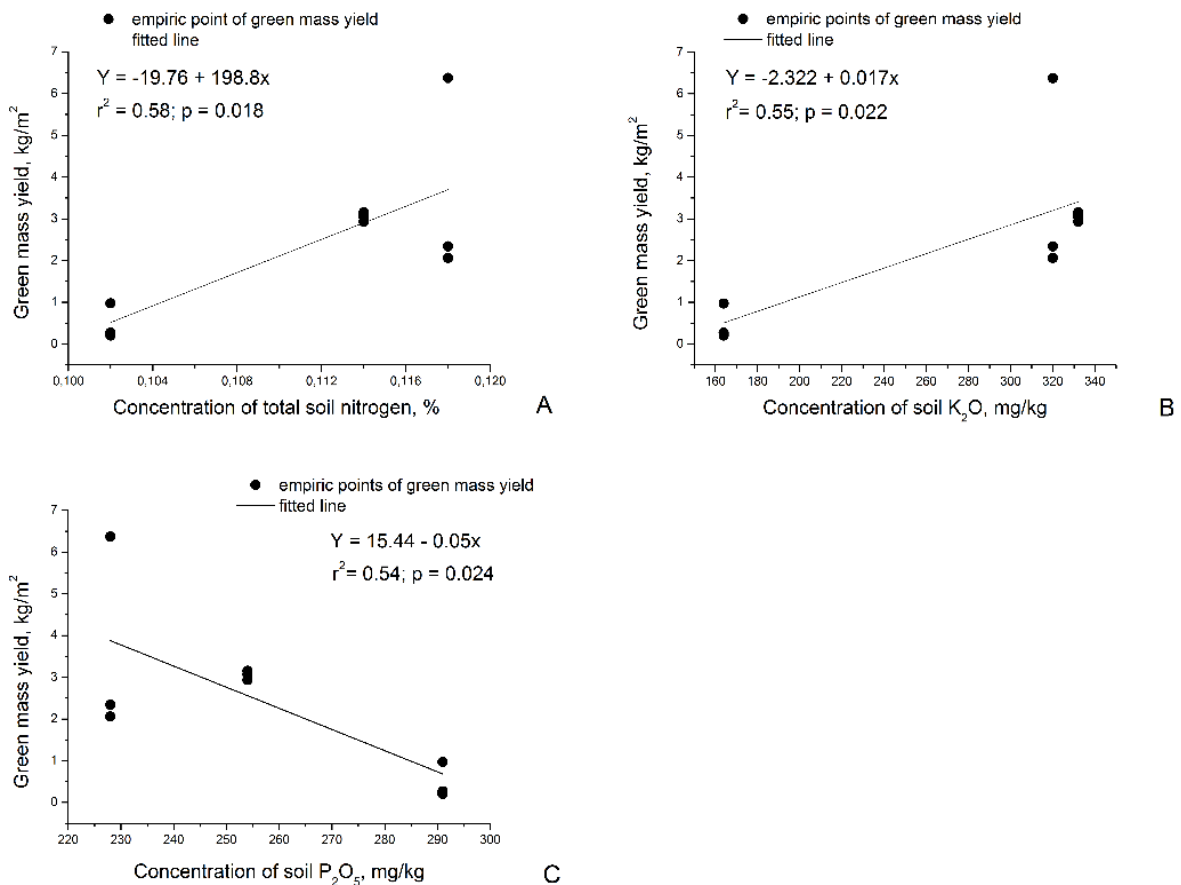


Figure 3. Green mass dependence on the nutrient concentrations in the soil: A – from the total nitrogen (%), B – from mobile potassium (mg/kg), C – from mobile phosphorus (mg/kg)

In summarizing the results, it can be stated that the concentration of the light absorption component, chlorophyll a, influenced the yield of *S. perfoliatum* insignificantly. The influence of the mineral nutrition factors on the *S. perfoliatum* biomass was also estimated: the total nitrogen and mobile potassium concentrations influenced the biomass positively, whereas the mobile phosphorus concentration had a negative influence on the biomass.

Discussion

It was found that an important donor's characteristic, the chlorophyll a concentration, insignificantly influenced the yield of *S. perfoliatum* within the described limits (the determination coefficients of the three investigation periods were as follows: $r^2 = 0.106$, $r^2 = 0.198$, $r^2 = 0.0609$) (see *Fig. 2; Table 1*). This is a little contradictory of well-known facts regarding the correlation between chlorophyll concentration and biomass (Andrianova and Tarchevskii, 2000). Meanwhile, it does not contradict with another well-known fact, that the photosynthesis of C_3 plants (such as *S. perfoliatum*) is not limited by summer illumination conditions, i.e. chlorophyll and light reactions have some reserve opportunities (Hall and Rao, 1994). The finding that the correlation between the chlorophyll a and biomass was absent and also the fact that there was no limitation by the air nutrition conditions lead to the assumption that the dispersion of the photosynthetic productivity of the *S. perfoliatum* energy plant at different chlorophyll a concentrations may be explained by other factors limiting photosynthesis and yield. This is a precondition in searching for an explanation by employing the systemic conception of photosynthesis regulation, which is based on the "donor-acceptor" relationships. The main hypothesis made by the authors is that the yield differences may be explained by the different acceptors' activity, which determines the photosynthesis through signalling (informational flows).

Thus, the conceptual modeling approach was employed by the authors for further analysis and interpretation of the yield formation process. To develop a conceptual model of the energy plant's productivity, both empirical results and physiological assumptions were used together with the known literature data available. The suggested causal conceptual model is presented in *Figure 4A*. The model causal loop diagram was created based on several sources; one of them is the conceptual scheme of A. T. Mokronosov (1981), which shows the relationships between the donor and the acceptor. To reveal the functioning of the donor and acceptor in more detail, the original scheme was expanded by including the influence of external factors (controlled and uncontrolled) previously discussed by other authors (Mokronosov, 1981; Lerbs et al., 1984; Nancy, 1994; Hirel et al., 2007; Paul and Foyer, 2001; Taiz and Zeiger, 2006; Sandmann et al., 2011; Rychter and Rao, 2005; Lemoine et al., 2013). The novelty of the proposed model is that it employs a methodology of systems dynamics modeling (Sterman, 2000) and makes a clear distinction between material and informational flows within the donor-acceptor system of the plant. Besides, comparing to the conceptual schemes mentioned above, it includes two new feedback loops, representing signalling through the levels of cytokinin and, especially, through phosphate.

An in-depth analysis of the interaction of individual components may require further refinement of the conceptual model's specifications. To accomplish this, it was proposed that very detailed diagrams of the plant's biochemical processes be summed

up at a higher abstraction level. In particular, the authors summarized the detailed biochemical pathways of the photosynthesis-phosphate interaction (presented in Heldt and Piechula, 2011; Huber and Huber, 1992; Nielsen et al., 2004; Taiz and Zeiger, 2006) and brought them to a higher conceptual level, which is more practically sound and helpful for typical agronomic research. This conceptual phosphate-photosynthesis sub-model is presented in Fig. 4B and is discussed in detail below along with the interpretation of the results of the field experiments presented in the previous section.

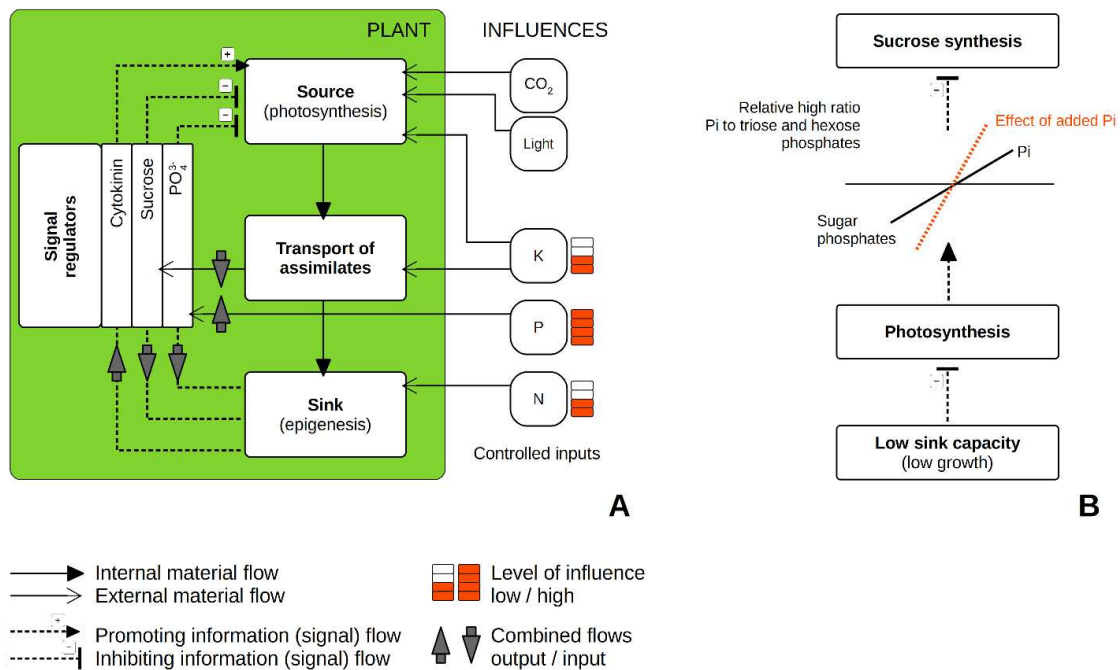


Figure 4. The causal loop diagrams for the conceptual model of photosynthesis and yield formation under specific environmental conditions (A) and for the sub-model of phosphates interaction (B)

The results of field experiments show the positive influence of the total nitrogen concentration in soil on *S. perfoliatum* biomass ($r^2 = 0.58$, see Fig. 3A). This increase in photosynthetic productivity while fertilizing with nitrogen is consistent with the fact that the CO_2 and NO_2^- reductions carried by photosynthesis do not compete in terms of reduction, even under average illumination conditions (Alekhina et al., 1996). Moreover, it is known that with better root nutrition with nitrogen and when the entire root system is functioning well, the cytokinin signal is transmitted to the shoots, informing them about the need for more photoassimilates, so photosynthetic genes (including Rubisko, carbonic anhydrase, etc.) are activated, stomata are opened and, thus, photosynthesis is intensified (Lerbs et al., 1984; Paul and Foyer, 2001) (see Fig. 4A.: Informational flow “N – sink – cytokinine – source”). Plus, nitrogen is important for cell division processes and for the metabolic activity of acceptors in sucrose utilization (Nancy, 1994; Hirel et al., 2007). In growing acceptors, sucrose utilization depends on the supply of amino acids (Paul and Foyer, 2001). Because of these reasons, better nutrition with nitrogen can lead to the increased activity and sucrose consumption of acceptors, which lessens the suppression of photosynthesis and leads to a growth in

productivity (see. *Fig. 4A*: Informational flow “N – sink (epigenesis) – sucrose – source”). To sum up, in assessing productivity, a sufficiently large dispersion of yield at various chlorophyll a concentrations may be identified by differences in the activity of the acceptors, dictated by mineral nutrition, and then following by the signal’s impact (gibberellin, sugar, etc.) on photosynthetic metabolism. The study shows that the mobile potassium concentration also influenced the *S. perfoliatum* biomass positively ($r^2 = 0.55$, see *Fig. 3B*). The mobile potassium concentration varied greatly – from 165 to 330 mg/kg in the soils of the field plots, i.e. the investigated soils ranged from medium to very high in regard to their potassium content (Mažvila et al., 2006). According to the literature, the influence of potassium on photosynthesis can occur by promoting the transport of assimilates from the leaves (Sandmann et al., 2011). Potassium promotes the removal of sucrose from leaves, and it reduces its concentration in leaves. Thus, this feedback control reduces the inhibition of photosynthesis and increases the entire plant’s productivity (see. *Figure 4A*: Informational flow: “K – transport of assimilates – sucrose – source”).

Carbon and nitrogen intake in plants takes place according to a certain ratio, while maintaining a functional balance between the above-ground part and roots (Bastow Wilson, 1988). The required carbon assimilation, while maintaining a defined C/N ratio is not only achieved by the photosynthetic intensity regulation described in the preceding paragraph, but also by the required formation of leaf surface area. It is known that the leaves of dicots have significantly longer growth zones than roots (Dale, 1982; Ivanov, 2011). It helps them to achieve the required growth rate of leaf surface area, and it also means an increase in photosynthetic productivity. The authors found that the meristem of monocots, specifically of grasses, may be about 3 times longer than now supposed (Šimkūnas et al., 2018). These observations additionally confirm the fact that carbon assimilation (either by changing the intensity of photosynthesis or the assimilating surface area) reaches its scale or level in different ways, which are affected by acceptor activity and mineral nutrition.

It should be mentioned that the limitation of photosynthesis and yield resulting from a phosphate deficiency is often encountered and almost exclusively described in the literature (see the review by Rychter and Rao, 2005). The inhibition of photosynthesis caused by a phosphate deficiency may occur especially in acidic soils, where phosphates are chemically bound and not readily available for plants. In this study, we found some unexpected negative influence on the *S. perfoliatum* biomass ($r^2 = 0.54$) (see *Fig. 3C*) attributable to the mobile phosphate concentration in the soil. The mobile phosphorus concentrations in the soils ranged from 228 to 291 mg/kg, i.e. these soils ranged from sufficient to high saturation according to the amount of phosphorus they contained (Mažvila et al., 2006).

It is known that reduced triose phosphate and glucose-6 phosphate concentrations are accompanied by an increased phosphate concentration in the cytosol, thus, a relatively high phosphate content produces a signal indicating slow photosynthesis and a low metabolic level in plant cells (Nielsen et al., 2004). Since the sucrose synthesis pathway enzymes are inhibited by this signal (fructose 1,6-bisphosphatase is inhibited through fructose-2,6 phosphate, and sucrose phosphate synthase is inhibited by phosphate allosterically and through SnRK1), the sucrose synthesis rate is “adapted” to the low energy status of cells (see *Fig. 4B*) (Huber and Huber, 1992; Nielsen et al., 2004; Heldt and Piechula, 2011; Tognetti et al., 2013). As already mentioned, photosynthesis may be slowed down by a lack of acceptors activity when there is a deficiency of N and K or

by other factors. During slowed down photosynthesis, when the external phosphate content available increases, the relative amount of phosphates increases even more in the cytosol. In such a way, it can provide a signal indicating extremely slow photosynthesis, which can lead to additional suppression of sucrose synthesis, and therefore, the plant biomass decreases (see. *Figs. 4B* and *4A*, informational flow: “P – signal PO_4^{3-} – source”). Besides this, according to the literature data, when a plant is supplied with sufficient phosphates, an increase in their quantity may precipitate zinc (Zn) in plant tissues (Fageria, 2006; Hafeez et al., 2013). A lack of Zn or its low concentration increases phosphorus transport to the shoots and its concentration in leaves, which can cause the mentioned suppression of photosynthesis in plants (Mousavi et al., 2012). The detected suppression of photosynthesis by phosphates in the background of a nitrogen and potassium deficiency shows the importance of a balance of nutrient ions for the formation of plant productivity.

The essential role of acceptors in photosynthesis and yield limitation through sucrose and gibberellin signalling is predicted by the conceptual model. The limitation of photosynthesis and yield attributable to signalling caused by high phosphate levels is also emphasized. Therefore, the informational flows, which are usually a subject of biochemical investigations, need to be incorporated in further field trial experiments as well, in order to facilitate the verification of the conceptual model. First, the specific growth characteristics of acceptors (meristemic growth on the morphometric, cytological, etc. levels) and the intensity of photosynthesis under various nutritional conditions should be evaluated, thus assessing the potential limitations of photosynthesis because of growth. In particular, it is worth estimating the change in photosynthesis intensity during the saltatory changes of the acceptors' growth under the influence of various stressors. Second, to prove that the yield limitation can be caused by the inhibition of the acceptors' growth, we propose that the hypothesis regarding the high concentration of sucrose and low concentration of cytokinin (signal compounds) in some compartments of leaves in the case of slow acceptors' growth be checked experimentally. Finally, the influence of large phosphate concentrations in a soil on photosynthetic productivity in the case of inhibited growth should be investigated in more detail.

In parallel, these regularities could be also validated under controlled conditions. In particular, an integrated climatic-hydroponic system developed by the authors provides all the necessary conditions required for such kind of validation experiments (Šimkūnas et al. 2018). The results of all these experiments should be directly used to refine the conceptual model proposed here. As the model expresses a generic conception of yield formation, it, therefore, can be used also for other energy plants and in a variety of environmental conditions. Meanwhile, the model can be refined according to a particular case, so it can reveal also a different causality for yield limitation. The energy plants are very fast growing, and the yield limitation through acceptors (i.e. the growing parts) could be more frequently met.

Conclusions

The designed conceptual model of *S. perfoliatum* productivity provides a significant methodological value while interpreting scarce and sometimes controversial empirical results. The model employs a systemic view of the concept of the “donor-acceptor” plant system and is based on the analysis of both material and informational

relationships between the system components. To develop such a model of energy plant productivity, both empirical results and physiological assumptions along with known literature data are used. The representation of the field experimental data through use of the conceptual model provides a missing link between the field experiment's results and the molecular-biochemical investigations of the informational flows that regulate photosynthesis.

The field trial (empirical) results show the absence of dependence between the donor characteristic (chlorophyll a concentration) in regard to yield. According to the designed conceptual model, the yield differences may be explained by the differences in acceptor activity, which determines photosynthesis through signalling (informational flows).

The total nitrogen and mobile potassium concentrations in the soil positively influenced the productivity of *S. perfoliatum*. The article argues that nitrogen influenced the growth of biomass positively through the metabolic activation of acceptors, signalling the photosynthetic apparatus (through the increased cytokinin and the decreased sugar concentration). Meanwhile, the positive influence of potassium on biomass growth may express itself through the activation of the transport of assimilates from leaves (i.e. signalling through the decreased sugar concentration in leaves), thus promoting photosynthesis through feedback control.

In this study, some unexpected negative influence attributable to the mobile phosphate concentration in the soil on the *S. perfoliatum* biomass was found. To interpret this observation, the hypothesis of photosynthesis and yield limitation by signalling through high phosphate levels in the case of photosynthesis that has already slowed down is proposed.

To verify the conceptual model and test the underlying novice hypothesis, further research is needed. A detailed plan for that is delineated in the Discussion section. In particular, it is proposed that the study of plant information processes (carbohydrate, gibberellin and phosphate signalling) be incorporated in field research, along with synchronous measurements of the donor's (photosynthesis) activity characteristics and acceptor's growth rates.

REFERENCES

- [1] Adegbidi, H. G., Volk, T. A., White, E. H., Abrahamson, L. P., Briggs, R. D., Bickelhaupt, D. H. (2001): Biomass and nutrient removal by willow clones in experimental bioenergy plantations in New York State. – *Biomass and Bioenergy* 20: 399-411.
- [2] Allen, B. et al. (2014): Space for energy crops – assessing the potential contribution to Europe's energy future. – Institute for European Environmental Policy. – Report produced for BirdLife Europe, European Environmental Bureau and Transport & Environment. IEEP, London.
- [3] Alekhina, N. D., Krendeleva, T. E., Polesskaya, O. G. (1996): Relationships between nitrogen assimilation and photosynthesis in leaf cells of C3-plants. – *Russian Journal of Plant Physiology* 43: 119-130.
- [4] Andrianova, I. E., Tarchevskii, I. A. (2000): Chlorophyll and productivity of plants. – Moscow, Nauka (in Russian).
- [5] Arnon, D. A. (1949): Copper enzymes in isolated chloroplasts. Polyphenoloxidase in *Beta vulgaris*. – *Plant Physiology* 24: 1-15.

- [6] Aurbacher, J., Benke, M., Formowitz, B., Glauert, T., Haiermann, M., Herrmann, C. et al. (2012): *Energienpflanzen für Biogasanlagen*. – Rostock, Fachagentur Nachwachsende Rohstoffe.
- [7] Bastow Wilson, J. (1988): A review of evidence on the control of shoot:root ratio, in relation to models. – *Annals of Botany* 61: 433-449.
- [8] Biertümpfel, A., Reinhold, G., Götz, R., Zorn, W. (2013): Leitlinie zur effizienten und umweltverträglichen Erzeugung von Durchwachsener Silphie (Leitlinie No. 1). – Leitlinien der Thüringer Landesanstalt für Landwirtschaft, Jena.
- [9] Borkowska, H., Molas, R., Kupczyk, A. (2009): Virginia Fanpetals (*Sida hermaphrodita* Rusby) Cultivated on Light Soil Height of Yield and Biomass Productivity. – *Polish Journal of Environmental Studies* 18: 563-568.
- [10] Brown, R. H. (1988): Growth of the Green Plant. – In: Tesar, M. B. (ed.) *Physiological Basis of Crop Growth and development*, Madison, American Society of Agronomy: 153-174.
- [11] Chikov, V. I. (2008): Evolution of notions about relationships between photosynthesis and plant productivity. – *Russ J of Plant Physiol.* 55: 130-143.
- [12] Dale, J. E. (1982): *The growth of leaves*. – London, Edward Arnold (Publishers) Ltd.
- [13] Douglas, J. A., Follett, J. M., Halliday, I. R., Hughes, J. W., Par, C. R. (1987): *Silphium*: preliminary research on a possible new forage crop for New Zealand. – *Proceedings Agronomy Society of New Zealand* 17: 51-53.
- [14] Eleuch, L., Rezgui, S., Daaloul, A. (2012): Induced physiological traits by NACL in Two barley cultivars. – *Biologia Tunisie* 7: 59-66.
- [15] Fageria, V. D. (2006): Nutrient interactions in crop plants. – *Journal of Plant Nutrition* 24: 1269-1290.
- [16] Fatichi, S., Leuzinger, V., Körner, Ch. (2014): Moving beyond photosynthesis: from carbon source to sink-driven vegetation modeling. – *New Phytologist* 201: 1086-1095.
- [17] Gansberger, M., Montgomery, L. F. R., Liebhard, P. (2015): Botanical characteristics, crop management and potential of *Silphium perfoliatum* L. as a renewable resource for biogas production: a review. – *Industrial Crops and Products* 63: 362-372.
- [18] Grebe, S., Beleu, T., Döhler, H., Eckel, H., Frisch, J., Fröba, N. et al. (2012): *Witzel Energiepflanzen: Daten für die Planung des Energiepflanzenanbaus*. 2nd ed. – Darmstadt, KTBL.
- [19] Hafeez, B., Khanif, Y. M., Saleem, M. (2013): Role of zinc in plant nutrition – a review. – *American Journal of Experimental Agriculture* 3: 374-391.
- [20] Hall, D. O., Rao, K. K. (1994): *Photosynthesis*. 5th ed. – Cambridge, Cambridge University Press.
- [21] Heldt, H-W., Piechula, B. (2011): *Plant biochemistry*. 4th ed. – London, Elsevier Academic Press.
- [22] Hirel, B., Le, G. J., Ney, B., Gallais, A. (2007): The challenge of improving nitrogen use efficiency in crop plants: towards a more central role for genetic variability and quantitative genetics within integrated approaches. – *Journal of Experimental Botany* 58: 2369-2387.
- [23] Hiscox, J. D., Israelstam, G. F. (1979): A method for the extraction of chlorophyll from leaf tissue without maceration. – *Canadian Journal of Botany* 57(12): 1332-1334.
- [24] Huber, S. C., Huber, L. J. (1992): Role of sucrose-phosphate synthase in sucrose metabolism in leaves. – *Plant Physiology* 99: 1275-1278.
- [25] Ivanov, V. B. (2011): *Cellular mechanisms of plant growth*. – Moscow, Nauka (in Russian).
- [26] Jakienė, E., Spruogis, V., Romaneckas, K., Dautartė, A., Avižienytė, D. (2015): The bio-organic nano fertilizer improves sugar beet photosynthesis process and productivity. – *Žemdirbyste-Agriculture* 102(2): 14-46.
- [27] Jasinskas, A., Simonavičiūtė, R., Šiaudinis, G., Liaudanskienė I., Antanaitis, Š., Arak, M., Olt, J. (2014): The assessment of common mugwort (*Artemisia vulgaris* L.) and cup plant

- (*Silphium perfoliatum* L.) productivity and technological preparation for solid biofuel. – *Žemdirbyste-Agriculture* 101: 19-26.
- [28] Kowalski, R., Wolski, T. (2003): Evaluation of phenolic acid content in *Silphium perfoliatum* L. leaves, inflorescences and rhizomes. – *Electronic Journal of Polish Agricultural Universities*. <http://ejpau.media.pl/series/volume6/issue1/horticulture/art-03.html>.
- [29] Lastdrager, J., Hanson, J., Smeekens, S. (2014): Sugar signals and the control of plant growth and development. – *Journal of Experimental Botany* 65: 799-807.
- [30] Lawlor, D. W., Paul, M. J. (2014): Source/sink interactions underpin crop yield: the case for trehalose 6-phosphate/SnRK1 in improvement of wheat. – *Frontiers in Plant Science* 5: 418
- [31] Lemoine, R., La Camera, S., Atanassova, R., Dédaldéchamp, F., Allario, T., Pourtau, N., Bonnemain, J. L., Laloi, M., Coutos-Thévenot, P., Maurousset, L., Faucher, M., Girousse, C., Lemonnier, P., Parrilla, J., Durand, M. (2013): Source-to-sink transport of sugar and regulation by environmental factors. – *Frontiers in Plant Science* 4: 1-21.
- [32] Lerbs, S., Lerbs, W., Klyachko, N. L., Romanko, E. G., Kulaeva, O. N., Wollgiehn, R., Parthier, B. (1984): Gene expression in cytokinin-and light-mediated plastogenesis of *Cucurbita cotyledons*: ribulose-1,5-bisphosphate carboxylase/oxygenase. – *Planta* 162(4): 289-298.
- [33] Maughan, M., Bollero, G., Lee, D. K., Darmody, R., Bonos, S., Cortese, L. et al. (2012): *Miscanthus* × *giganteus* productivity: the effects of management in different environments. – *GCB Bioenergy* 4: 253-265.
- [34] Mažvila, J., Antanaitis, A., Lubyte, J., Arbačiauskas, J., Adomaitis, T., Mašauskas, V., Vaišvila, Z. (2005): Different methods of potassium analysis and their suitability for lithuanian soils. – *Agronomijas vēstis Latvian Journal of Agronomy* 8: 53-57.
- [35] Mažvila, J., Vaičys, M., Buivydaite, V. (2006): Lietuvos dirvožemių makromorfologinė diagnostika. Dotnuva – Akademija, Lietuvos žemdirbystės institutas
- [36] McKendry, P. (2002a): Energy production from biomass (part 1): overview of biomass. – *Bioresource Technology* 83: 37-46.
- [37] McKendry, P. (2002b): Energy production from biomass (part 3): gasification technologies. – *Bioresource Technology* 83: 55-63.
- [38] Mokronosov, A. T. (1981): Ontogenical aspect of photosynthesis. – *Nauka, Moscow* (in Russian).
- [39] Mousavi, S. R., Galavi, M., Rezaei, M. (2012): The interaction of zinc with other elements in plants: a review. – *International Journal of Agriculture and Crop Sciences* 24: 1881-1884.
- [40] Nancy, L. (1994): Nutrient deficiencies and vegetative growth and crop productivity. – In: Amarjit, B. (ed.) *Mechanisms of Plant Growth and Improved Productivity Modern Approaches*. Ludhiana, Punjab Agricultural University.
- [41] Nielsen, T. H., Rung, J. H., Viladsen, D. (2004): Fructose-2,6-biphosphate: a traffic signal in plant metabolism. – *Trends in Plant Science* 9: 556-562.
- [42] Paul, M. J., Foyer, C. H. (2001): Sink regulation of photosynthesis. – *Journal of Experimental Botany* 52: 1383-1400.
- [43] Rossi, M., Bermudez, L., Carrari, F. (2015): Crop yield: challenges from a metabolic perspective. – *Current Opinion in Plant Biology* 25: 79-89.
- [44] Rychter, A. M., Rao, I. M. (2005): Role of phosphorus in photosynthetic carbon metabolism. – In: Pessaraki, M. (ed.) *Handbook of photosynthesis*. New York, Marcel Dekker; 123-148.
- [45] Sandmann, M., Skłodowski, K., Gajdanowicz, P., Michard, E., Rocha, M., Gomez-Porrás, J. L., González, W., Corrêa, L. G., Ramírez-Aguilar, S. J., Cuin, T. A., van Dongen, J. T., Thibaud, J. B., Dreyer, I. (2011): The K⁺ battery-regulating Arabidopsis K⁺ channel AKT2 is under the control of multiple post-translational steps. – *Plant Signaling & Behavior* 6: 558-562.

- [46] Schoo, B., Wessel-Terharn, M., Schroetter, S., Schittenhelm, A. (2013): Vergleichende Untersuchung von Wurzelmerkmalen bei Silphie und Mais. – In: Pekrun, C., Wachendorf, M., Francke-Weltmann, L. (eds.) Nachhaltige Erzeugung von Nachwachsenden Rohstoffen, Mitt. Ges. Pflanzenbauwiss. Presented at the Tagung der Gesellschaft für Pflanzenbauwissenschaften e.V., Liddy Halm, Weihenstephan, 241-242.
- [47] Stanford, G. (1990): *Silphium perfoliatum* (cup-plant) as a new forage. – In: Smith, D. D., Jacobs, C. A. (eds.) Recapturing a Vanishing Heritage. Presented at the 12th North American Prairie Conference, University of Northern Iowa, Cedar Falls, 33-38.
- [48] Serman, J. D. (2000): Business Dynamics: Systems thinking and modeling for a complex world. – McGraw Hill. ISBN 0-07-231135-5.
- [49] Stockmann, F., Fritz, M. (2013): Einfluss von Standort und Herkunft auf das Erragspotenzial der Durchwachsenen Siphie (*Silphium perfoliatum* L.) unter bayerischen Anbaubedingungen. – In: Pekrun, C., Wachendorf, M., Francke-Weltmann, L. (eds.) Nachhaltige Erzeugung von Nachwachsenden Rohstoffen, Mitt. Ges. Pflanzenbauwiss. Presented at the Tagung der Gesellschaft für Pflanzenbauwissenschaften e. V. Liddy Halm, Weihenstephan, 146-147.
- [50] Šiaudinis, G., Šlepetienė, A., Jasinskas, A., Karčauskienė, D. (2012): The evaluation of common mugwort (*Artemisia vulgaris* L.) and cup plant (*Silphium perfoliatum* L.) biomass and energetic productivity in Western Lithuania *Albeluvisols*. – *Žemdirbyste-Agriculture* 99(4): 357-362.
- [51] Šiaudinis, G., Jasinskas, A., Šarauskius, E., Steponavičius, D., Karčauskienė, D., Liaudanskienė I. (2015): The assessment of Virginia mallow (*Sida hermaphrodita* Rusby) and cup plant (*Silphium perfoliatum* L.) productivity, physico-mechanical properties and energy expenses. – *Energy* 93: 606-612.
- [52] Šimkūnas, A., Valaškaitė, S., Denisov, V. (2018): Comparative systemic analysis of the cellular growth of leaves and roots in the controlled conditions. – *Journal of Plant Physiology* 220: 128-135.
- [53] Taiz, L., Zeiger, E. (2006): Plant physiology, 4th ed. – Sunderland, Massachusetts: Sinauer Associates, Inc., Publishers.
- [54] Tognetti, J. A., Pontis, H. G., Martinez-Noel, G. M. (2013): Sucrose signaling in plants: a world yet to be explored. – *Plant Signaling & Behavior* 8(3): e23316.
- [55] Yu, S. M., Lo, S. F., Ho, H. D. (2015): Source-Sink Communication: Regulated by Hormone, Nutrient, and Stress Cross-Signaling. – *Trends in plant science* 20: 844-857.
- [56] Wrobel, M., Fraczek, J., Francik, S., Slipek, Z., Krzysztof, M. (2013): Influence of degree of fragmentation on chosen quality parameters of briquette made from biomass of cup plant *Silphium perfoliatum* L. – Proceedings of 12th International Scientific Conference Engineering for Rural Development May 23-24, 2013, Latvia University of Agriculture: 653-657.

EFFECT OF THE SEASONAL BURNING ON TREE SPECIES IN THE GUINEA SAVANNA WOODLAND, GHANA: IMPLICATIONS FOR CLIMATE CHANGE MITIGATION

AMOAKO, E. E.^{1*} – MISANA, S.² – KRANJAC-BERISAVLJEVIC, G.¹ – ZIZINGA, A.³ – BALLU DUWIEJA, A.¹

¹*Department of Ecotourism & Environmental Management University for Development Studies
P.O. Box 1882 Tamale, Ghana*

²*Department of Geography, University of Dar es Salaam, Tanzania*

³*College of Agriculture and Environment Sciences, Makerere University, Uganda*

**Corresponding author
e-mail: eamoako@uds.edu.gh*

(Received 6th Oct 2016; accepted 7th Mar 2018)

Abstract. The indiscriminate burning of vegetation is a common practice in the Guinea savanna of Ghana. Burning begins at the onset of the dry season (November) and lasts until the end (April). This study investigated the effects of time of burning on tree diversity and density in the Mole National Park, Ghana. A total of 36 (10 m x 10 m) quadrats were randomly demarcated in three treatments of early and late dry season burning and non-burning study plots. Samples were taken in March, a few weeks after the late burning period. Twenty seven different species belonging to fourteen families were recorded in all the treatments. Most of the species identified belonged to the families *Combretaceae*, *Fabaceae* and *Leguminosae*. *Vitellaria paradoxa*, *Terminalia avicennioides*, *Combretum adenogonium* and *Combretum molle* were the most common and abundant in all treatments. Late burning plots recorded the lowest diversity amongst the three treatments. Non-burning plots had higher tree density than burnt plots. Early burning treatment recorded more diverse individual species but had the lowest density. Higher tree densities would enhance carbon sequestration. However, ecosystem resilience is also dependent on the diversity of biotic communities among other factors. Sustainable land use practices including protections of trees on farms and prescribed early dry season burns could be an option to contribute to the mitigation of climate change in the region. Late dry season fires are a threat to tree species populations and should be discouraged.

Keywords: *burning frequency, species composition, Guinea savanna, Mole National Park*

Introduction

Savannas are known to support a large number of plant species with usually only one or a few kinds of grass and some common tree species (Scholes & Walker, 1993; Burgess, 1995). Anthropogenic disturbance including the use of fire is an important driver of vegetation types and diversity in the savanna (Sheuyange et al, 2005; Andersen et al, 2012). To a large extent, however, most savanna species have adapted different mechanisms to survive persistent fires, which include developing fire-resistant barks, roots that grow deeply into the ground and growing dormant buds. Thus, African savannas have been influenced by fire and have adapted to it over long periods of time. (Trollope, 1984; Beringer et al., 2007; Van Wilgen, 2009).

Fire is used by most rural dwellers in savannas to stimulate the growth of fresh forage for animals, for the tapping of honey and the hunting of animals. Fire is also used with the aim of minimising labour cost on land preparation and to increase agricultural production and productivity. It is used frequently and extensively by groups as well as

individuals for hunting, compared to the other methods of hunting. Vast areas are burnt through these activities, thus affecting the main sources of livelihood for local people (Eriksen, 2007; Adongo et al., 2012). The savanna ecological zones (Guinea, Sudan and Coastal Savanna) of Ghana, cover about two-thirds of the country (Bagamsah, 2005; Armah et al., 2011). They are characterised by scattered trees and shrubs usually interspersed with arable crops and referred to as 'agroforestry parklands' (Callo-Concha et al., 2013; Sinare and Gordon, 2015). A bulk of annual crops such as cereals, legumes, yam, as well as livestock are produced here, mainly for household consumption and for the local market and these are often the very drivers for the annual practice of bush burning in these ecoregions.

The Northern Region of Ghana contains about 50% of all the savanna areas in the country and has recorded higher occurrences of fires (40-80%) in the last 40 years, compared to all the other regions of Ghana (Korem 2005; Amanor, 2002; Kugbe et al., 2012). The frequent and uncontrolled fires may influence plant diversity and densities in the already sparsely populated tree ecosystems (Andersen and Williams, 2012). Consequently, this could exacerbate the impact of land degradation on ecosystems, which are already characterised by prolonged drought spells such as the Guinea and Sudan Savanna zones of Ghana. Some studies (Thonicke et al., 2000; Andersen et al., 2012) have shown that ecosystem degradation reduces carbon sequestration and thus may turn carbon sinks to sources thereby exacerbating the impacts of climate change in the region. Although fires rarely kill large trees, many other life forms are significantly affected. Saplings and some grass species may die as a result (Trollope, 1984).

However, fires are purported to break dormancy of some plant species source which results into enhancing the recruitment of many other species with different traits that might be adaptive in fire-prone environments (Auld and Bradstock, 1996). Fire is also reported to be effective in the elimination of competing plants and improving habitats (Denslow, 2002). However, fire has differential impacts on landscapes within savannas due to differences in factors such as ground water content, topography and plant type (Sheuyange and Weladji, 2005). Thus late season fires may be detrimental to some plant species and may cause the extinction of some plants. Slash and burn has been reported to affect the recovery and succession of species. Although fires are purported to be an indispensable tool for managing savanna ecosystems, including grassland and rangeland vegetation quality and monitoring, the influence of fire on plant species density and diversity still need to be studied further. This is because the regime of burning or non-burning has influence on tree populations and diversity, which is a major determinant of the health of terrestrial ecosystems (Brookman-Amissah et al., 1980; Kutiel, 1997).

The time of ignition of fire during the long period of drought in the savanna may have serious ecological implications on all life forms, particularly on plant species. The explicit role of the time and frequency of burning or non-burning in savanna ecosystem management is very significant in this regard. However, very few studies have been conducted on how the time of burning influences species composition in the savannas of Ghana. Some studies have shown that the frequency at which the vegetation is burnt determines the species that dominates a plant community but not the time of burning (Brookman-Amissah et al., 1980; Sackey and Hale, 2008). Sheunyang et al. (2005), argued that fires decreased shrub species richness, but positively influenced tree species richness. The study further showed that different plant species responded to fire differently. Thus, different fire regimes may favour the growth of different plant species

or gradually cause in the extinction of some plants (Myers et al., 2004; Penman, Binns and Kavanagh, 2007). The season of burning might affect different species differently.

This study, therefore, was conducted to investigate the effect of the time of burning on abundance and species diversity of trees. The assumption was that the time of burning in the dry season influences the composition of tree species in the Guinea savanna ecosystem of the Northern region of Ghana. We hypothesized that the time and frequency of burning does affect species composition. The paper also discusses the implication of tree species abundance and diversity for climate change mitigation.

Materials and methods

Study area

The study was conducted on study plots in the Mole National Park (Latitude 9°12' - 10°06' N; Longitude 1°25' - 2°17' W with an elevation of 150m). The Park is 484.4 sq km and located in the West Gonja District of Northern Region of Ghana. It contains a wide variety of ungulates (Waterbucks, Hippos, Bushbuck Duikers, Warthogs, Elephants) birds and tree species. The park has a total of 32 fringe communities.

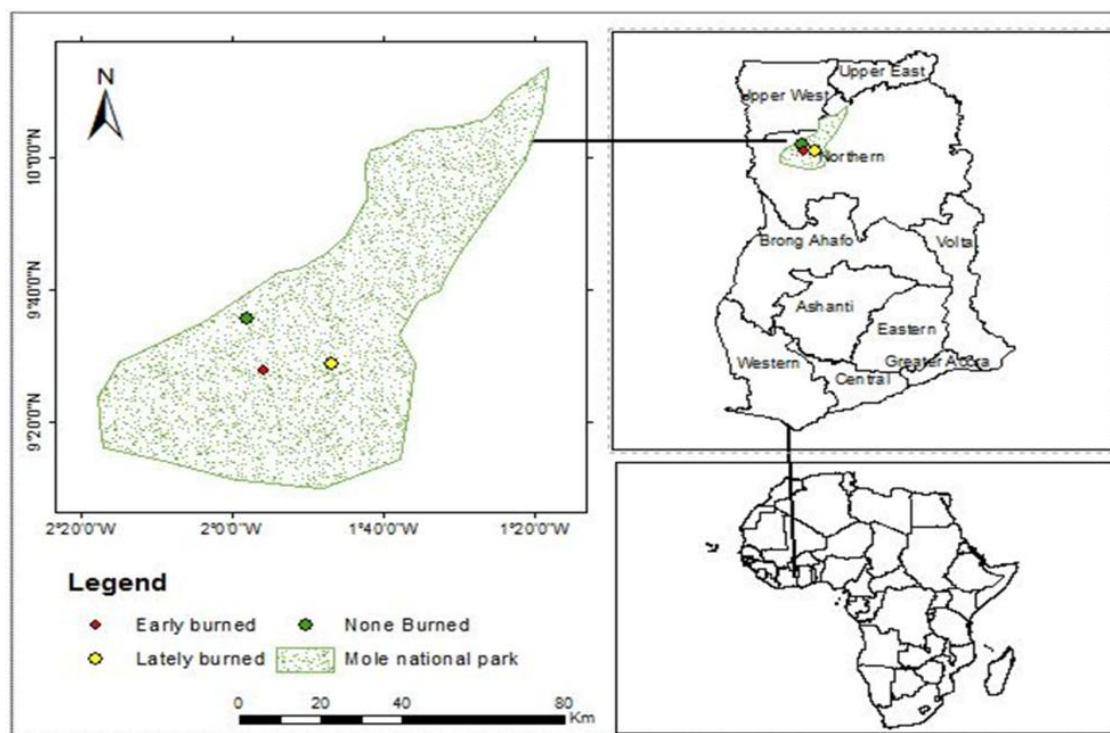


Figure 1. Location of the study: Mole National Park, Northern region, Ghana
(Created by Hadgu Hishe, 2015)

The climate is semi-arid and sub-humid with a unimodal rainfall distribution. The rainy season begins in May and ends in October with a mean monthly rainfall ranging from 900 mm to 1000 mm during the peak between July and September (Boubacar et al., 2005).

The vegetation is Guinea savanna characterized by drought resistant woody species such as *Vitellaria spp*, *Combretum spp*, *Burkea spp*, and *Isoberlinia spp*. The Guinea savanna occupies about 60 % total land area of the Northern Savanna zone.

The soils are laterite concrete formations of granite, voltaian shale and sandstones. They are comparatively low in organic matter, with low moisture content as a result of their high drainage characteristics than soils in southern Ghana (Mikkelsen and Langohr, 1998; Owusu-Bennoah et al., 1991).

The region experiences long periods of drought from November to April with little or no rainfall. Maximum temperatures typically 40 °C occur towards the end of the dry season and minimum temperatures in December and January, with a mean annual temperature of 27 °C. The Harmattan winds, which occur during the months of December to early February, have a considerable effect on the temperatures in the region, which may vary between 14 °C at night and 40 °C during the day (Siaw, 2001). These dry conditions and the strong Harmattan winds facilitate vegetation burning.

Data collection and analysis

Information on vegetation burning as obtained from the Faculty of Renewable Natural Resources, University for Development Studies and the Management of the Mole National Park indicated that smaller portions in the Park are demarcated for early burning, late burning and non-burning for study purposes for the Natural Resource Management students at the University for Development Studies and the Kwame Nkrumah University of Science and Technology in Ghana.

Burning is prescribed in the Park for both late and early dry season burn, firstly, to prevent the vegetation from transitioning into thickets or closed woodland which may not be favorable for the variety of animals that inhabit the Park and also to stimulate more grass growth for the animals so that animals in the Park do not stray into the fringe communities.

Tree sampling was carried out in plots exposed to early burning (EB), late burning (LB) - and non-burning (NB). The plots were demarcated in 1994 in areas that were already subjected to prescribed early burning and late and non-burning. An area within the Mole Park was excluded from burning for study purposes. This was made possible because the area is bounded by roads, which serve as fire breaks. The early season burns are carried out between November and December, depending on the time the rains end, whereas the late dry season burning is carried out towards the end of February up to the ending of March. The map below indicates areas that are burnt early and late within the park. The non-burning area is not indicated on the map below, because it is a relatively small portion of land located behind the Park headquarters meant for study purpose, otherwise the whole park experiences some form of burning within the year.

Sampling of tree species was conducted to examine the impact of early season (November-January) late season (February-April) and non-burning regimes on tree diversity and densities. A total of 36 quadrats were laid in the three (200 m by 200 m) plots. Three (10 m x10 m) quadrats were located randomly within 4 (50 m by 50 m) subplots in each plot, about 50 m away from the plot boundaries to reduce edge effects. Trees of diameter at breast height >3 cm and height > 0.5 m tall were identified by their scientific names in each quadrat. This was done with the assistance of Warden, who has been working in the park for over 30 years. The numbers of species identified in quadrat was also recorded.

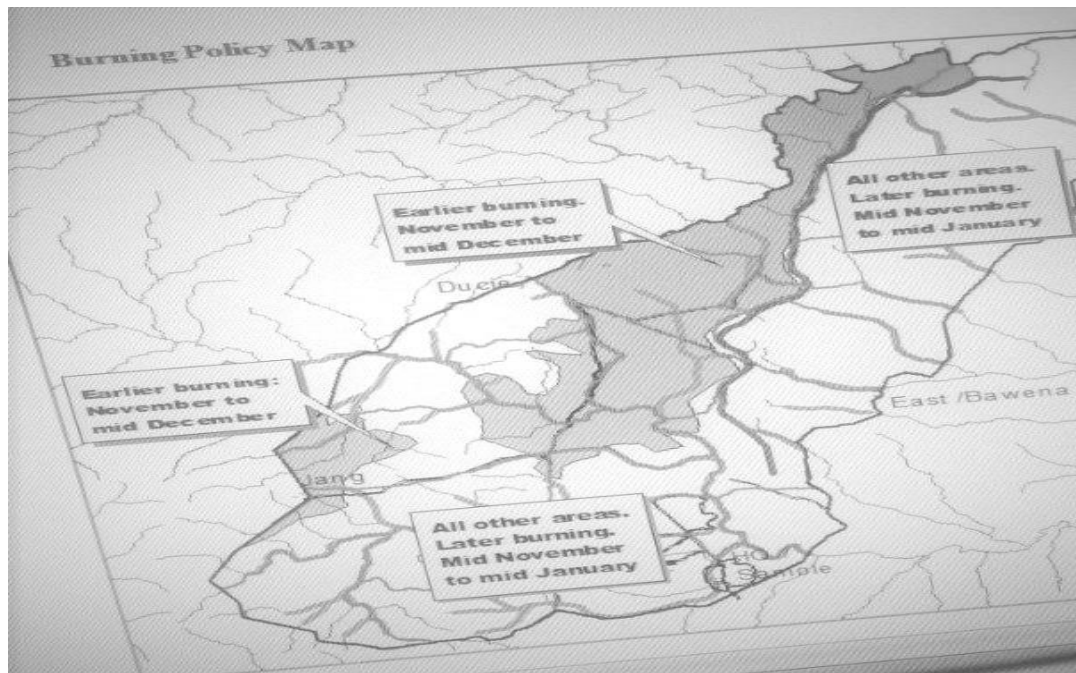


Figure 2. Fire management plan, Mole National Park
(Source: Mole National Park Management, 2017)

A Geographical Positioning System was used to obtain the coordinates of location of treatment plots. EB ($9^{\circ}16'15.30''\text{N}$, $1^{\circ}51'02.90''\text{W}$), LB ($9^{\circ}17'02.36''\text{N}$, $1^{\circ}49'08.11''\text{W}$), NB ($9^{\circ}15'40.20''\text{N}$, $1^{\circ}51'10.18''\text{W}$). Sampling was done between 27th and 28th March 2015 and 29 and 1 April 2017, a few weeks after the late season burning.

The data collected on tree census in late burning, early burning, and non-burnt plots were extrapolated to a hectare as a measure of density per treatment. This was carried out to determine the influence of fire on tree population. Data was statistically analysed using GraphPad InStat 3 which tested for normality using Kolmogorov Smirnov and analysed the significance using Kruskal-Wallis. The means, standard deviation and frequencies of species were calculated in Microsoft Excel to compare the presence, abundance and composition of species in the treatments.

Results

The result of species frequency and tree density estimates are shown in *Table 1* below. The data did not pass a normality test. A non-parametric statistics test (Kruskal Wallis) was used to compare the mean between treatments. A *post hoc* was not performed, $p=0.99$.

Twenty seven different species, belonging to 14 families were identified in all the three treatments. Seven species were found common all the treatments (EB, LB and NB). Generally, species that recorded relatively higher (pooled) frequencies belong to *Combretaceae*, *Leguminosae*, *Sapotaceae*, *Celastraceae*, *Meliaceae* and *Rubiaceae* whilest those occurring in low frequencies belonged to *Anacardiaceae*, *Olacaceae*, *Ebenaceae*, *Moraceae*, *Bixaceae*, *Phyllanthaceae*, and *Asparagaceae* (*Table 2*). *Combretaceae* had a higher occurrence of individual species (*Terminalia avicennioides*

Guill. & Perr, *Combretum molle* R.Br. ex G.Don, *Combretum adenogonium* Steud. Ex A. Rich) and were more common to all treatments (Fig. 3) than species of the other families.

Seven species, including *Diospyros mespiliformis* Hochst. ex A. DC were found to be common in early season burning and non-burning treatments. *Anogeissus leiocarpa* (DC.) Guill. & Perr. was found in non-burning and late burning treatments. *Pterocarpus erinaceus* Poir., *Combretum nigrican* Lepr. ex Guill. & Perr, *Trichilia rubescens* Oliv. were found common in early burning and late burning treatments.

Some species were exclusive to the different burning treatments. These species were, however, relatively low in frequencies (Table 2). *Ditarium microcarpum* Guill. & Perr *Detarium microcarpa* and *Isoberlinia doka* Craib & Stapf. and *Pteleopsis suberosa* Engl. & Diels were present in early burning treatment only. *Chochlospermum angolense*, *Daniellia Oliveri* and *Ficus glumosas* Delile, and *Anacardium occidentale* were in late season burning treatment only. *Dracaena* species and *Pseudocedrela kotschyi* (Schweinf.) were identified in non-burning treatments only. *Vitellaria paradoxa* C. F. Gaertn was present in all treatments, with the highest frequency in non-burning treatment. All other species identified in non-burning treatment plots were also present in early burning and late burning plots (Fig. 3).

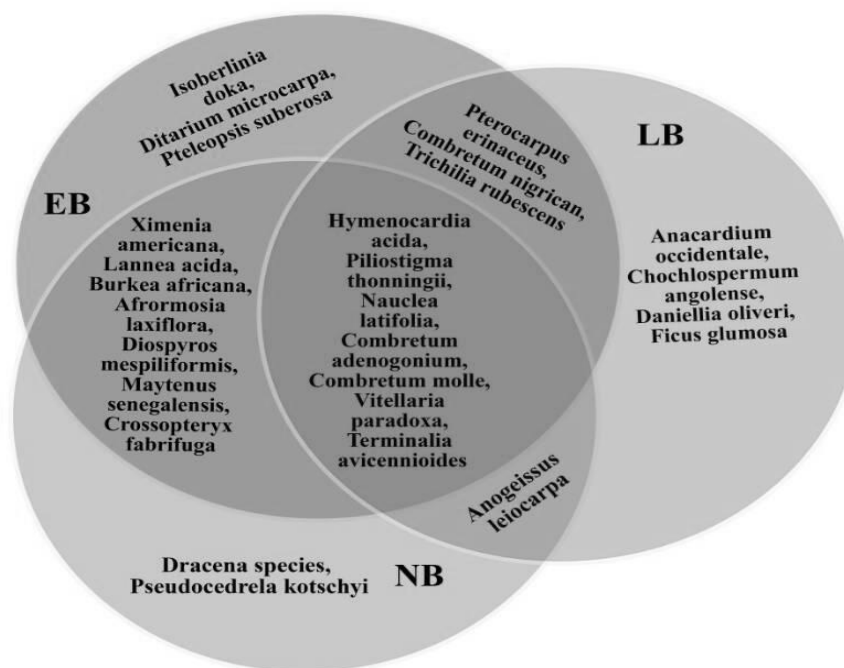


Figure 3 Species identified in early burning, late burning and non-burning treatments (Field data, 2017)

A total of 19 species were identified in early burning treatment. Two species, *Terminalia avicennioides* and *Combretum adenogonium* were found in relatively high frequencies (Table 1). The remaining 17 species including *Pteleopsis suberosa*, *Isoberlina doka*, *Combretum molle*, *Maytenus senegalensis*, *Burkea africana*, *Nauclea latifolia*, *Lannea acida*, *Detarium Microcarpa*, *Ximenia americana*, *Diospyros mespiliformis* were found in relatively low frequencies. The least occurring species were more even in frequency than the dominant species (Table 1).

Table 1. Influence of fire on species population in treatments

Species	EB		LB		NB		Pooled Freq	Family
	Freq	Mean±SD	Freq	Mean±SD	Freq	Mean±SD		
<i>Afromosia laxiflora</i>	10	2.43±0.91	15	2.30±1.25	20	2.84±1.67	45	Leguminosae
<i>Anarcadium occidentale</i>	0	0.000	1	0.29±0.08	0	0	1	Anacardiaceae
<i>Anogeissus leicarpa</i>	0	0.000	2	0.39±0.17	78	12.05±6.50	80	Combretaceae
<i>Burkea africana</i>	5	0.69± 0.46	0	0	1	0.29±0.083	6	Fabaceae
<i>Cochlospermum angolense</i>	0	0.000	6	0.68±0.5	0	0	6	Combretaceae
<i>Combretum adenogonium</i>	41	3.47±3.73	33	4.94±2.75	16	1.23±1.33	90	Combretaceae
<i>Combretum molle</i>	13	1.40±1.18	11	2.39±0.912	5	1.16±0.48	29	Combretaceae
<i>Combretum nigricans</i>	1	0.31±0.09	0	0	0	0	1	Combretaceae
<i>Crossopteryx febrifuga</i>	3	0.65±0.27	0	0	0	0	3	Rubiaceae
<i>Daniellia oliveri</i>	0	0.000	4	0.78±0.33	0	0	4	Fabaceae
<i>Detarium Microcarpum</i>	3	0.65±0.27	0	0	0	0	3	Leguminosae
<i>Diospyros mespiliformis</i>	1	0.30±0.09	0	0	3	0.45±0.25	4	Ebenaceae
<i>Dracena palm</i>	0	0.000	0	0	1	0.28±0.08	1	Asparagaceae
<i>Ficus glumosa</i>	0	0.000	6	1.24±0.5	0	0	6	Moraceae
<i>Hymenocardia acida</i>	0	0.000	9	2.30±0.75	1	0.28±0.08	10	Phyllanthaceae
<i>Isoberlinia doka</i>	10	1.14±0.91	0	0	0	0	10	Leguminosae
<i>Lannea acida</i>	3	0.65±0.27	0	0	5	0.99±0.42	8	Anacardiaceae
<i>Maytenus senegalensis</i>	8	1.56±0.72	0	0	9	1.29±0.75	16	Celastraceae
<i>Nauclea latifolia</i>	4	0.51±0.36	15	2.63±1.25	1	0.29±0.08	20	Rubiaceae
<i>Piliostigma thonningii</i>	1	0.30±0.09	2	0.39±0.17	6	0.80±0.50	9	Fabaceae
<i>Pseudocedrela kotschyi</i>	0	0.000	3	0.45±0.25	13	3.18±1.08	16	Meliaceae
<i>Pteleopsis suberosa</i>	10	2.43±0.0.91	0	0	0	0	10	Combretaceae
<i>Pterocarpus erinaceus</i>	0	0.000	2	0.39±0.167	0	0	2	Fabaceae
<i>Terminalia avicennioides</i>	55	2.72±5.0	239	14.59±19.92	89	5.567±7.416	388	Combretaceae
<i>Trichilia rubescens</i>	1	0.30±0.09	10	0.84±0.83	0	0	11	Meliaceae
<i>Vitellaria paradoxa</i>	17	1.86±1.55	11	0.99±0.92	349	19.916±29.083	377	Sapotaceae
<i>Ximenia americana</i>	1	0.302±0.91	0	0	1	0.2887±0.083	2	Olacaceae
Total number of species	187	0	369	0	598	0		
Density (hectare)	1,558		3,075		4,983			

p-value p=0.99

Kruskal-Wallis Statistic 1.929

(Field data, 2017)

A total of 15 species were identified in the late burning treatment. Of the four common dominant species, (*Terminalia avicennioides*, *Combretum adenogonium*, *Afrormosia laxiflora* and *Nauclea latifolia*), *Terminalia avicennioides* was found to be the most dominant. The least occurring species were *Piliostigma thonningii* and *Pterocarpus erinaceus* (Table 1).

Non-burning treatment recorded a total of 17 different species, Out of which *Vitellaria paradoxa* was found to be the most dominant (Table 1). *Terminalia avicennioides*, *Combretum adenogonium* and *Isoberlinia doka* also recorded relatively high frequencies. *Lannea acida*, *Anogeissus leiocarpa* and *Burkea africana*, *Afrormosia laxiflora* were amongst the least occurring species.

Species with relatively low frequencies were more even in occurrence than the dominant species in all the treatments (Table 1). *Terminalia avicennioides* was present in all treatments. However, it had the highest frequency in the late season treatment whilst *Vitellaria paradoxa* recorded highest frequency in the non-burning treatment.

Discussion

Species richness and abundance

The characteristics of trees in this ecological zone are defined by the response to regeneration after fire, thus most are fire and drought resistant (Renes, 1991; Russell-Smith et al., 2012; Sinare and Gordon, 2015). However, some of the species identified may be absent or present in an uncontrolled fire disturbed savanna which may vary with the extent of disturbance and land use type (Denslow, 2002; Chimsah et al., 2013).

With the exception of *Anacardium occidentale* which was rare in occurrence in late burning treatment, all other species are native to the Guinea savanna (Sinare and Gordon, 2015; Cardoso et al., 2016). *Anacardium occidentale* was most probably brought in by animals or some other agents of dispersal from fringe villages that grow them on their farms.

The most dominant and widespread species identified in all three treatments belonged to the *Combretaceae*, *Leguminosae* and *Fabaceae* which confirms other studies that most Sudano-Guinean savanna woodland species typically fall within these families (Aubréville, 1949). They thrive under harsh weather conditions and areas where fires are recurrent. Although the species *Parkia biglobosa*, was known to be a predominant species associated with the Leguminosae in the Guinea savanna woodland as purported by Aubréville (1949), the species was not recorded in any of the treatments in this study and confirms the IUCN listing of the tree as a vulnerable species. *Isoberlinia doka*, *Anogeissus leiocarpa* and *Combretum nigrifican* which were also predominant Combretaceae species that previously defined the Guinea savanna woodland recorded in a very low occurrence, thus may be threatened by the frequency and season of fire (Legris and Blanco, 1979). Most of the species identified in the early season and the late season burning treatments were present in the non-burning treatment (Fig. 3). This shows non-burning treatment as a replica of both the late and early season burning treatments. The species found solely in the non-burning treatment were *Dracaena* and *Pseudocedrela Kotschyi*.

Those species found exclusive to burning treatment are hardy and can withstand the frequency of burns, thus confirming findings from other studies that fire breaks seed dormancy of some savanna species ensuring natural regeneration after fire (Trollope, 1984; Higgins et al, 2000).

Practicing non-burning may suppress the growth of some savanna species, which require fire to germinate. Also, the high leaf litter observed during sampling in the non-burnt treatment may not be a desirable condition for the growth of light tolerant species, thus the lowering prevalence of such species.

The higher species richness and evenness was observed in the early season burning treatment, which had the lowest tree density (*Table 1*). This could be attributed to the fact that there was not much dryness at the time of burning. Hence the fire did not destroy sensitive seeds and saplings, but rather enhanced the germination of the seeds by breaking their dormancy, increasing the diversity in early burnt areas of the park (Gijsbers et al., 1994). This also means that early burning favours the growth of different species in the savanna, compared to late burning, as observed in this study. Thus early season burning could be prescribed to promote diversity where particular species need moderate fire for regeneration.

Late burning had a relatively adverse effect on diversity, probably because late season fires are usually so hot that plant species may not be able to survive the intensity. Late season burns, as observed, do not only kill grasses but tree species as well, depending on the intensity and duration of fire (Trollope, 1984; Cardoso et al., 2016).

The higher tree population in the non-burning treatment confirms that savannas are not climax vegetation; when disturbance is minimised, they can gradually transform into a woodland or forest (Bond and Midgley, 2001; Bassett et al. 2003). This condition will allow seeds buried in the soil to germinate and grow, and if there is no disturbance, where initially grass was abundant, eventually tree species will dominate. The relatively low tree density identified in the burning treatment compared to the non-burning indicates that higher burning frequency in general, has a negative influence on tree density as it was also revealed in study conducted in the savanna of Ghana and Cote d'Ivoire (Brookman-Amisah et al., 1980; Bassett et al., 2003).

The most common species identified regenerate from seed, but also through resprouting and this may not need a longer time lapse for regeneration after fire (Lovett and Haq, 2000; Sackey and Hale, 2008). Most *Combretaceae* species and *Leguminosae* are tolerant to fires, drought and also to fire exclusion, with a higher probability of regeneration from resprouting after fire and other disturbances (Gijsbers et al., 1994; Higgins et al., 2000; Sackey and Hale, 2008). This explains their higher presence in all the treatments. Most of the species in this family are normally dehiscent or indehiscent and need fire to enhance germination which reflected in the very low presence in non-burning treatment, which presupposes that these species are also tolerant to late season fires. *Vitellaria paradoxa*, on the other hand, does regenerate easily by seed and also by resprouting as revealed by these others (Lovett and Haq, 2000), hence the higher number of species recorded in the non-burning treatment (*Table 1*).

Although fire plays a role in the structure and function of savanna ecosystems, a report on the Park management (Mole Park Management Report, 2005) indicated that some species are associated with types of soil in the park which, implies that the species identified in the various treatments may not solely be influenced by fire but also by the soil type (Van Wilgen, 2000; Dzwonko et al., 2015).

Implications of burning and tree populations and diversity for climate change mitigation

All vegetation absorbs carbon dioxide; however trees do absorb carbon on a larger scale than other forms (Scholes and Walker, 1993; Resh et al., 2002). Trees thus play an imperative role in climate change mitigation. A few studies purported that most savanna

trees are of the C3 photosynthetic pathway and therefore has a considerably greater atmospheric carbon exchanges than savanna grasses, which are mainly of the C4 photosynthetic pathway (Downton and Tregunna, 1968; Lloyd et al., 2008). Therefore, tree populations and species diversity may be used as a valuable proxy for healthy and resilient savannas, to mitigating the impacts of climate change through stocking and sinking carbon. The United Nations Framework Convention on Climate Change (UNFCCC) envisages mitigation through creating or enhancing carbon sinks and reducing anthropogenic emissions sources of CO₂. Thus, sustainable land use practices including traditional agroforestry practices such as the maintenance of agroforestry parkland in the Guinean-Sudano savanna would enhance mitigation (Bassett et al., 2003).

Frequent anthropogenic fires in the savannas, according to Murphy and Bowman (2012) are contributing to the loss of vegetative carbon to the atmosphere accounting for about 44% of the global emission (Van Der Werf et al., 2010). Thus, more fires in the savanna may exacerbate the impact of climate change by releasing carbon into the atmosphere and destroying carbon sinks (trees and grasses). Increasing wind, and rainfall, coupled with the high transpiration during the dry season according to Hulme, (2005) and Sheuyange, (2005) are a favourable condition for dry season burns, where the grass serve a fuel for burning. With this trend, it is apparent that large wildfires can be expected to increase in frequency, intensity and severity (Bassett et al., 2003; Hulme, 2005). Studies in tropical savannas in Australia have confirmed an apparent in change in fire conditions (hot temperatures and high fuel load), which will result in extensive fires (Cary, 2002; Catchpole, 2002).

The higher tree density as observed in the non-burning treatment could enhance carbon sequestration as most savanna trees with smaller leaf sizes are drought tolerant and have high carbon intake even in the dry season. Also, Langevelde et al. (2003) indicated that soil moisture availability is one of the main factors that regulate the growth of trees and grasses in the savanna. However, during the Harmattan (windy dry season in north of Ghana), as a result of the high evapotranspiration, coupled with high evaporative cooling, all the grass species wither, thus the process of carbon sequestration is halted (Simpson, 2013). More trees guarantee an all year round carbon intake when extrapolated to a larger scale (Lugo and Brown, 1992). Growing more tree through afforestation, reforestation and good forest management practices and also non-burning should be encouraged. Early season burns, on the other hand, could enhance diversity of some tree species and should also be encouraged (*Fig. 3*). Higher tree diversity contributes to building resilient terrestrial ecosystems, which is very important with the changing climates (Elmqvist et al., 2003). A characteristic of the resilient ecosystems is their ability to withstand and adapt to extreme weather conditions. The diversity of species implies a stable and sustainable ecological function: different tree species may have different levels of sequestering carbon and providing other ecosystem services better than others (Resh et al., 2002; Mandal et al., 2016). The study confirms previous studies (Myers et al., 2004; Fernandes et al., 2013) which found that prescribed early season burning plays a in savanna ecosystems by improving on vegetation diversity. However, annual late season burning that occur even under a good management system will consequently result in reduction of species density and diversity.

In the north of Ghana, the Hamattan conditions could enhance intensive and extensive fires, thereby the lost of more species during late season burns (Brookman-Amisshah et al., 1980; Kasei et al, 2014). The heavy rains (900 mm to 1000 mm) but short rainy season (between June and October) are conditions conducive to the growth of grass

species, thus to the accumulation of more fuel load for burning during the dry season (Trollope and Trollope, 2002; Bassett et al., 2003; Kugbe et al., 2012). The continuous indiscriminate dry season burning and particularly, late dry season burning, will to a large extent affect the health and resilience of the Guinea savanna if not regulated. This could hamper mitigation efforts against rising global temperatures.

Conclusion

The study revealed that seasonal burning had a negative effect on tree density, relative to non-burning within treatments. Non-burning however promotes tree population density, rather than diversity. The annual burning had a negative effect on tree density, relative to non-burning within treatments. Species richness and evenness were higher in burning treatments than in non-burning. Burning promoted the growth of *Terminalia Avicennioides* and other *Combretum* species whereas non-burning was a desirable condition for *Vitellaria paradoxa* (*Sapotaceae*). Thus, non-burning would increase the populations of species which are not fire-dependent for recruitment. The protection of *Vitellaria Paradoxa* from fire and other disturbances would easily increase populations which would have greater benefits for communities in the north of Ghana because of the role it plays in rural livelihoods.

A balance between tree density and diversity will be most desirable; therefore the frequency and time burning play a very important role in sustaining ecosystems for climate change mitigation. Non-burning should be encouraged in fire-degraded ecosystems to restore species and habitats and also enhance carbon sequestration.

This study could serve as a baseline for scaling-up of studies on burning, species diversity and density and also for further studies on unmanaged areas with unplanned fire regimes in the Savanna and Forest Transition zones of Ghana. There is the need to monitor the annual fires in the study site (Mole Park) to see what the Park is gaining or losing in terms of animal species diversity and populations through the fires. The findings calls for the strengthening of community sensitization and collaborative stakeholder engagement on the impact of burning and non-burning on species including economic species like *Vitellaria paradoxa*.

Traditional tree-based land use practices, such as agroforestry should be encouraged to minimise the conversion of savanna woodlands into grasslands. This is because grass species wither and die as a result of the Hammattan conditions, their efficacy of all year sequestration of carbon is reduced.

Prescribed early dry season burns should be the best option against indiscriminate burning as practiced in unprotected and community managed woodlands; this can be achieved through advocacy by district assemblies and other relevant stakeholders.

Acknowledgements. This research is supported by funding from the Department for International Development (DFID) under the Climate Impact Research Capacity and Leadership Enhancement (CIRCLE) programme.

We express our sincere gratitude to the Ghana Forestry Commission, for granting Permission for the field study to be carried out in Mole National Park. The lead author is also grateful to the Center for Climate Change Studies, University of Dar es Salaam which hosted me for the CIRCLE Programme. Dr Peter Burt of NRI - Department of Agriculture, Health and Environment University of Greenwich, UK, was an advisor during the fellowship, thanks for your inputs in improving the manuscript.

REFERENCES

- [1] Adongo, R., Nkansah, D. O., Salifu, S. M. A. (2012): Social and psychological aspects of communal hunting (*pieli*) among residents of Tamale Metropolis in the Northern Region of Ghana African Journal of Hospitality. – *Tourism and Leisure* 2:1-15
- [2] Agyemang, I., McDonald, A. Carver, S. (2007): Application of the DPSIR framework to environmental degradation assessment in northern Ghana. – *Natural Resources Forum* 31(3): 212-225.
- [3] Amanor, K. S. (2002): Bushfire Management, Culture and Ecological Modernisation in Ghana. – *IDS Bulletin* 33(1): 65-74.
- [4] Andersen, A., Cook, G. Williams, D. (2012): Savanna burning: The ecology and economy of fire in tropical savannas. – *Austral Ecology* 37: 633-633.
- [5] Armah, F. A., Odoi, J. O., Yengoh, G. T., Obiri, S., Yawson, D. O., Afrifa, E. K. A. (2011): Food security and climate change in drought-sensitive savanna zones of Ghana. – *Mitigation and Adaptation Strategies for Global Change* 16: 291306.
- [6] Aubréville, A. (1958): Sudano-Guinean Forest Flora. – Geographical Publishing Company, Paris.
- [7] Auld, T. D., Bradstock, R. A. (1996): Soil temperatures after the passage of a fire: Do they influence the germination of buried seeds? – *Austral Ecology* 21: 106-109.
- [8] Bagamsah, T. T. (2005): The Impact of Bushfire on Carbon and Nutrient Stocks as Well as Albedo in the savanna of northern Ghana. – In: Vlek, P. L. G., Denich, M., Martius, C., Rogers, C. (eds) *Ecology and Development Series 25*. Cuvillier Verlag, Gottingen.
- [9] Bassett, T. J., Koli Bi, Z., Quattara, T. (2003): Fire in the savanna – In: Bassett, T., J., Crumme, D. (eds.) *African Savannas. Global Narratives and Local Knowledge of Environmental Change* Portsmouth, Heinemann Oxford, UK.
- [10] Beringer, J., Hutley, L. B., Tapper, N. J. Cernusak, L. A. (2007): Savanna fires and their impact on net ecosystem productivity in North Australia. – *Global Change Biology* 13: 990-1004.
- [11] Blench, R. (2001): Trees on the march: the dispersal of economic trees in the prehistory of West-Central Africa. – ODI, Safa Conference, 12-15 July, 2000. Cambridge, UK.
- [12] Bond, W. J. Midgley, J. J. (2001): Ecology of sprouting in woody plants: the persistence niche. – *Trends in Ecology & Evolution* 16: 45-51.
- [13] Bond, W. J., Woodward, F. I., Midgley, G. F. (2004): The global distribution of ecosystems in a world without fire. – *New Phytologist* 165: 525-538
- [14] Brookman-Amisshah, J., Hall, J. B., Swaine, M. D., Attakorah, J. Y. (1980): A re-assessment of a fire protection experiment in North-Eastern Ghana savanna. – *Journal of Applied Ecology* 17: 85-99
- [15] Brown, S. (1993): Tropical forests and the global carbon cycle: the need for sustainable land-use patterns. – *Agriculture, Ecosystems & Environment* 46: 31-44
- [16] Burgess, T. L. (1985): Desert Grassland, Mixed Shrub Savanna, Shrub Steppe, or Semi Desert Scrub: The Dilemma Of Co-Existing Growth Forms. – In: McClaran, M. P., Van Devender, T. R. (eds.) *The Desert Grassland*. – University of Arizona Press, Tucson.
- [17] Callo-Concha, D., Gaiser, T., Webber, H., Tischbein, B., Müller, M., Ewert, F. (2013): Farming in the West African Sudan savanna: Insights in the context of climate change. – *African Journal of Agricultural Research* 8: 4693-4705.
- [18] Cardoso AW, Medina-Vega JA, Malhi Y, Adu-Bredu S, Ametsitsi GKD, Djagbletey G, van Langevelde F, Veenendaal E, Oliveras I. 2016: Winners and losers: tropical forest tree seedling survival across a West- African forest–savanna transition. – *Ecology & Evolution* 6: 3417-3429.
- [19] Cary, G. J. (2002): Importance of Changing Climate for Fire Regimes. – In: Bradstock, R. A., Williams, J. E., Gill, M. A. (eds.) *Flammable Australia: The fire regimes and Biodiversity of a Continent*. Cambridge University Press, Cambridge

- [20] Catchpole, W. (2002): Fire properties and burn patterns in a heterogeneous landscape. – In: Bradstock, R. A., Williams, J. E., Gill, M. A. (eds.) *Flammable Australia: The fire regimes and Biodiversity of a Continent*. Cambridge University Press, Cambridge
- [21] Chimsah, F. A., Nyarko, G., Yidana, J. A., Abubakari, A.-H., Mahunu, G. K., Abagale, F. K., Quainoo, A. (2013): Diversity of tree species in cultivated and fallow fields within Shea Parklands of Ghana. – *Journal of Biodiversity and Environmental Sciences* 3: 2220-6663.
- [22] Denslow, J. S. (2002): Invasive alien woody species in Pacific island forests. – *Unasylva* 53: 62-63
- [23] Dzwonko, Z., Loster, S., Gawroński, S. (2015): Impact of fire severity on soil properties and the development of tree and shrub species in a Scots pine moist forest site in southern Poland. – *Forest Ecology and Management* 342: 56-63
- [24] Elmqvist, T., Folke, C., Nyström, M., Peterson, G., Bengtsson, J., Walker, B., Norberg, J. (2003): Response diversity, ecosystem change, and resilience. – *Frontiers in Ecology and the Environment* 1: 488-494.
- [25] Eriksen, C. (2007): Why do they burn? Fire, rural livelihoods, and conservation in Zambia. – *The Geographical Journal* 173: 242-256
- [26] Fernandes, P. M., Davies, G. M., Ascoli, D., Fernández, C., Moreira, F., Rigolot, E., Stoof, C. R., Vega, J. A., Molina, D. (2013): Prescribed burning in southern Europe: Developing fire management in a dynamic landscape. – *Frontiers in ecology and the Environment* 11: 1-11
- [27] Gignoux, J., Lahoreau, G., Julliard, R., Barot, S. (2009): Establishment and early persistence of tree seedlings in an annually burned savanna. – *Journal of Ecology* 97: 484-495.
- [28] Gignoux, J., Clobert, J., Menaut, J.-C. (1997): Alternative fire resistance strategies in savanna trees. – *Oecologia* 110: 576-583.
- [29] Gijbers, H. J. M., Kessler, J. J., Knevel, M. K. (1994): Dynamics and natural regeneration of woody species in farmed parklands in the Sahel region (Province of Passore, Burkina Faso). – *Forest Ecology and Management* 64: 1-12.
- [30] Higgins, S. I., Bond, W. J., Trollope, W. S. W. (2000): Fire, resprouting and variability: a recipe for grass-tree coexistence in savanna. – *Journal of Ecology* 88: 213-229.
- [31] Houghton, R. (2012): Carbon emissions and the drivers of deforestation and forest degradation in the tropics. – *Environmental Sustainability* 4: 597-603
- [32] Hulme, P. E. (2005): Adapting to climate change: Is there scope for ecological management in the face of a global threat? – *Journal of Applied Ecology* 42: 784-794.
- [33] Kasei, R. A., Ampadu, B., Yalevu, S. (2014): Impacts of climate variability on food security in Northern Ghana. – *Journal of Earth Sciences and Geotechnical Engineering* 4: 47-59
- [34] Korem, A., 1985: *Bush fire and agricultural development in Ghana*. – Ghana Publishing Corporation, Tema.
- [35] Kugbe, J. X., Vlek, P. L. G., Fosu, M., Tamene, L., Desta, M. D. (2012): Annual vegetation burms across the northern savanna region of Ghana. – *Nutr. Cycle Agroecosyst.* 93: 265-284.
- [36] Langevelde, van F., Veenendaal, E., Oliveras, I. (2016): Winners and losers: tropical forest tree seedling survival across a West African forest-savanna transition. – *Ecology and evolution* 6: 3417-3429
- [37] Legris, P., Blasco, F. (1979): Joint pilot project for tropical forest monitoring. – Unpublished report, FAO/UNESCO.
- [38] Lovett, P. N., Haq, N. (2000): Diversity of the Sheanut tree (*Vitellaria paradoxa* C. F. Gaertn.) in Ghana. – *Genetic Resources and Crop Evolution* 47: 293-304.
- [39] Lugo, A. E., Brown, S. (1992): Tropical forests as sinks of atmospheric carbon. – *Forest Ecology and Management* 54: 239-255.

- [40] Mandal, R. A., Kumar, P., Chandra Dutta, I., Thapa, U., Karmacharya, S. B. (2016): Carbon Sequestration in Tropical and Subtropical Plant Species in Collaborative and Community Forests of Nepal – *Advances in Ecology*: 1529703
- [41] Mikkelsen, J. H., Langohr, R. (2004): Indigenous knowledge about soils and a sustainable crop production a case study from the Guinea woodland savannah (Northern Region), Ghana. – *Danish Journal of Geography* 104: 13-26.
- [42] Murphy, B. P., Bowman, D. M. J. S. (2012): What controls the distribution of tropical forest and savanna? – *Ecology Letters* 15: 748-758
- [43] Myers, B., Allan, G., Bradstock, R., Dias, L., Duff, G., Jacklyn, P., Landsberg, J., Morrison, J., Russell-Smith, J., Williams, R. (2004): *Fire Management in the Rangelands tropical savanna's*. – CRC, Darwin.
- [44] Obuobie, E., Barry, B. (2005): The Volta river-basin. – In: Boubacar, B., Obuobie, E., Andreini, M., Andah, W., Pluquet, M (eds.) *International Water Management Institute Report*, 190.
- [45] Owusu-Bennoah, E., Acquaye, D. K., Abekoe, M. (1991): Efficient fertilizer use for increased crop production: Use of phosphorus fertilizers in concretionary soils of northern Ghana in alleviating soil fertility constraints to increased crop production in West Africa. – Dordrecht Springer, Netherlands.
- [46] Penman, T. D., Binns, D. L., Kavanagh, R. P. (2007): Prescribed burning: how can it work to conserve the things we value? – *Wildland Fire* 20: 721-733
- [47] Pistorius, T. (2012): From RED to REDD+: the evolution of a forest-based mitigation approach for developing countries. – *Current Opinion in Environmental Sustainability* 4: 638-645.
- [48] Kutiel, P. (1997): Spatial and Temporal Heterogeneity of Species Diversity in a Mediterranean Ecosystem Following Fire. – *Wildland Fire* 7: 307-315.
- [49] Renes, G. J. B. (1991): Regeneration capacity and productivity of natural forest in Burkina Faso. – *Forest Ecology and Management* 41: 291-308
- [50] Resh, S. C., Binkley, D., Parrotta, J. A. (2002): Greater Soil Carbon Sequestration under Nitrogen-Fixing Trees Compared with Eucalyptus Species – *Ecosystems* 5: 217-231.
- [51] Russell-Smith, J., Djoeroemana, S., Maan, J., Pandanga, P. (2007): Rural Livelihoods and Burning Practices in Savanna Landscapes of Nusa Tenggara Timur, Eastern Indonesia. – *Human Ecology* 35: 345-359.
- [52] Russell-Smith, J., Edwards, A. C., Price, O. F. (2012): Simplifying the savanna: the trajectory of fire-sensitive vegetation mosaics in northern Australia. – *Biogeography* 39: 1303-1317.
- [53] Sackey, I., Hale, W. (2008): Effects of perennial fires on the woody vegetation of mole national park, Ghana. – *Science and Technology* 28: 36-47.
- [54] Scholes, R., Walker, B. (1993): Tree-grass interactions. – In: Scholes, R., Walker, B (eds.) *An African Savanna: Synthesis of the Nylsvley Study*. Cambridge, Cambridge University Press., 215-229.
- [55] Sheuyange, A., Oba, G., Weladji, R. B. (2005): Effects of anthropogenic fire history on savanna vegetation in northeastern Namibia. – *Environmental Management* 75: 189-198.
- [56] Siaw, D. E. K. A. (2001): State of forest genetic resources in Ghana. – Sub-regional workshop on the conservation, management, sustainable utilization and enhancement of forest genetic resources in Sahelian and North-Sudanian Africa (Ouagadougou, Burkina Faso, 22-24 September 1998). Forest Genetic Resources Working Group, FAO.
- [57] Simpson S. E. (2013): *The developing world: An introduction*. – Longman Group Limited, Longman Scientific & Technical, Harlow.
- [58] Sinare, H., Gordon, L. J. (2015): Ecosystem services from woody vegetation on agricultural lands in Sudano-Sahelian West Africa. *Agriculture. – Ecosystems & Environment* 200: 186-199

- [59] Thonicke, K., Venevsky, S., Sitch, S., Cramer, W. (2001): The role of fire disturbance for global vegetation dynamics: Coupling fire into a dynamic global vegetation model. – *Global Ecology and Biogeography* 10: 661-677
- [60] Trollope, W. S. W. (1984): *Fire in Savanna*. – Springer, Berlin.
- [61] Trollope, W. S. W., Trollope, L. A. (2002): *Fire behaviour a key factor in the fire ecology of African grassland and savannas*. – Millpress, Rotterdam
- [62] Van Der Werf, G. R., Randerson, J. T., Giglio, L., Collatz, G. J., Mu, M., Kasibhatla, P. S., Morton, D. C., Defries, R. S., Jin, Y., Van Leeuwen, T. T. (2010): Global fire emissions and the contribution of deforestation, savanna, forest, agricultural, and peat fires (1997–2009). – *Atmospheric Chemistry and Physics* 10: 11707-11735.
- [63] Van Wilgen, B. W. (2009): The evolution of fire management practices in savanna protected areas in South Africa. – *South African Journal of Science* 105: 343-349.

PRINCIPLE AND APPLICABILITY OF COSMIC-RAY NEUTRON METHOD FOR MEASURING SOIL MOISTURE

ZHAO, H. – ZHAO, Y. – WANG, F. Q.* – MA, D. F.

*North China University of Water Resources and Electric Power
No.136, Jinshui Road, 450046 Zhengzhou, China*

**Corresponding author
e-mail: wangfuqiang@ncwu.edu.cn*

(Received 15th Jul 2017; accepted 19th Dec 2017)

Abstract. Regional soil moisture monitoring has always been a difficult point in many researches. The traditional point measurement and the large scale remote sensing monitoring are always unable to obtain information of medium and small scale regional soil moisture. As a new type of mesoscale soil moisture condition monitoring method, the cosmic ray neutron method can obtain the soil moisture information within 300 m radius of the source region, which covers the shortage of the point measuring method and remote sensing method. This study utilized cosmic ray neutron instrument (CRS) to constantly monitor soil moisture, and conducted the applicability research of cosmic ray neutron method in soil moisture monitoring. Results show high consistency of CRS and time domain reflectometer (TDR) measurements, the fitting degree is 0.847, the root mean square error is 0.020 kg/kg. Also, CRS is sensitive to precipitation, it can clearly show the increase of soil moisture under different conditions, while the sensitivity of TDR is relatively poor. This research can provide a reference for dynamic change monitoring of regional mesoscale soil moisture.

Keywords: *soil moisture, CRS, TDR, mesoscale, precipitation*

Introduction

At present, there are dozens of methods for measuring soil moisture, and traditional methods for measuring soil moisture include drying method, actual volumetric method, specific gravity method, ray method (Klenke et al., 1991), dielectric property method (Gong et al., 1997; Roth et al., 2004) and so on. Although these methods can accurately estimate the moisture content of soil profile, they are point measurement methods with small measurement scales, and measurement results can only represent the soil moisture status of this point, so spatial representation is small. Due to soil heterogeneity (Kim et al., 1997; Desilets et al., 2010), traditional point measurement methods can meet the requirements only by increasing to a larger area proportionally. Therefore, sufficient point measurement data are required for calculation, which greatly increases the cost and is only technically possible (Zreda et al., 2008; Hejazi et al., 2017). The use of remote sensing method for soil moisture monitoring at abroad began in the late 1960s, and in the 1970s, the study of soil moisture monitoring by remote sensing has achieved rapid and all-around development. Remote sensing technology has advantages such as fast aging, strong dynamic contrast, long-term dynamic large-area monitoring and good spatial-temporal resolution (Njoku et al., 1996), but it also has disadvantages such as shallow measuring depth, poor penetration, poor sensitivity, and short satellite flight life (Entekhabi et al., 2004; Andreasen et al., 2016; Hashemi, 2017).

In recent years, the technology of measuring regional soil moisture content using cosmic-ray neutron method has been rapidly developed. This method works based on the principle that cosmic-ray neutrons are moderated by the hydrogen atoms in soil

water (Chrisman et al., 2013; Radan et al., 2017). The soil moisture content can be calculated only by passively measuring the intensity of neutrons near the ground after moderating (Villarreyes et al., 2011; Vazdani et al., 2017). It has characteristics such as large spatial coverage, and low requirements for soil salinity, soil density, soil texture and so on, and it can meet its power needs by using solar energy as energy, with the maximum measuring range of about 670 m and measuring depth of 12~76 cm (Gong et al., 1997; Desilets et al., 2013; Xiao et al., 2017). In this paper, nearly three months of continuous monitoring of soil moisture of Hubei Water Scientific Experiment Station, the East of Henan Water Conservancy Administration using a cosmic-ray neutron probe was conducted, and the results were compared and analyzed with the measurement results of TDR (Time Domain Reflectometry) to study the application of cosmic-ray neutron method in agricultural areas in the plains.

Principle of cosmic-ray neutron method for measuring soil moisture

Technical principle

The high-energy particle streams coming from the Milky Way Galaxy are captured into the atmosphere due to the Earth's magnetic field, and interact with the nuclei in the atmosphere to produce secondary cosmic rays, which collide with the nuclei in the soil to produce fast neutrons with 1-2 MeV of energy. These fast neutrons gradually collide with various nuclei in the atmosphere and the Earth's surface and thus are moderated, then become thermal neutrons with 0.025 eV of energy and epithermal neutrons with 1-10 eV of energy. One part of the moderated fast neutrons are absorbed by the soil and the other part the moderated fast neutrons are scattered into the air (Zreda et al., 2012; Yang et al., 2017).

The intensity of underground neutron is determined by two characteristics, namely soil scattering and soil absorption. The two most important soil scattering characteristics are: 1. Scattering cross section of material. 2. Average logarithmic energy attenuation per collision, namely effective collision times (Gong et al., 1997). Studies show that because the moderating power of hydrogen atoms exist widely in the soil in the nature, and hydrogen atoms exist in water, the greater the soil moisture, the greater the number of hydrogen atoms in the soil, and the stronger the capacity of soil to moderate and absorb fast neutrons, and the fewer the number of fast neutrons measured on the Earth's surface. Measurement of high heterogeneous soil using cosmic-ray neutron method showed that the neutron intensity was inversely proportional to soil moisture content (Chrisman et al., 2013). Therefore, the measurement of intensity of the moderated neutrons on the Earth's surface can well reflect the soil moisture content.

Measuring range and depth

The size of measuring range of CRS method did not depend on soil moisture content, instead, it was inversely proportional to atmospheric pressure (Chrisman et al., 2013). In thin air, the air density was small, and there is a small number of molecules per unit volume of air, so the propagation distance of neutrons was farther. Typically, the relationship between source zone radius and atmospheric pressure can be represented by *Equation 1* (Jiao et al., 2013):

$$R = R_0 \frac{P_0}{P} \quad (\text{Eq.1})$$

where R_0 was measuring radius under reference pressure P_0 (300 m, radius under one standard atmospheric pressure, was usually used), R was radius under current pressure P . The perennial mean pressure in the study area was about 10^5 Pa, and the calculations showed that the measuring radius of the source area was about 304 m.

Measuring depth had a very strong correlation on soil moisture. Because the higher the soil moisture, the larger the number of hydrogen atoms in the soil, and the stronger the capacity of soil to moderate and absorb fast neutrons, thus, fast neutrons cannot continue to propagate downward, so the measuring depth was not very great. According to the simulative results of MCNPX (Monte Carlo N-Particle eXtended), the variant range of measuring depth was from 12 cm (simulated moisture content was 0.40 m³/m³ when soil was moist) to 76 cm (simulated moisture content was 0 when soil was dry) (Gong et al., 1997). The measuring depth can be obtained by calculation using Equation 2 proposed by Franz (Deng et al., 2007; Klenke et al., 1991):

$$Z = \frac{5.8}{\frac{\rho_{bd}}{\rho_w} \tau + \theta_m + 0.0829} \quad (\text{Eq.2})$$

where Z was effective measuring depth (cm); ρ_{bd} was soil bulk density (g/cm³); ρ_w was the density of liquid water, the default was 1 g/cm³; τ was lattice water content (0~0.05, the mass ratio of minerals in soil to bound water of soil particle, which was ignored in the calculation in this paper), and θ_m was the mass water content of soil (kg/kg).

Correction method and inversion function

Related researches showed that the propagation of fast neutrons is affected by many factors in addition to soil moisture, and factors having the most significant effect on the propagation of fast neutrons are atmospheric pressure and atmospheric vapor.

(1) Atmospheric pressure correction

For a certain source region, the higher the atmospheric pressure, the greater the density of gas molecules, the greater the chance that fast neutrons collided with atmospheric particles, and the lower the intensity of neutrons near the ground measured by neutron probe, on the contrary, the lower the atmospheric pressure, the higher the intensity of neutrons near the ground measured by neutron probe, thereby leading to error of calculated results. The effects of atmospheric pressure can be corrected by using correction coefficient f_p (Villarreyes et al., 2011) as shown in Equation 3:

$$f_p = \exp \frac{P - P_0}{L} \quad (\text{Eq.3})$$

where P was atmospheric pressure during sampling; P_0 was mean atmospheric pressure during the experiment; L was mass attenuation length of high-energy neutron, which was 128 g/cm^2 in high latitude region and 142 g/cm^2 in low latitude region, during the period it showed progressive change.

(2) Atmospheric vapor correction

Through experiment, Rosolem et al. (2013) concluded that the intensity of neutrons near the ground measured by neutron probe was completely determined by the soil moisture when the air did not contain any atmospheric vapor, while the intensity of fast neutrons near the ground measured by neutron probe was affected at different levels when the air contained different levels of atmospheric vapor. Therefore, he put forward Equation 4 of atmospheric vapor correction coefficient (CWV) to correct atmospheric vapor:

$$CWV = 1 + 0.0051(\rho - \rho_0) \quad (\text{Eq.4})$$

where ρ was the actual density of atmospheric vapor (g/m^3); ρ_0 was the absolute density of atmospheric vapor on the Earth's surface, which usually took 0.

To sum up, the intensity of fast neutrons after atmospheric pressure correction and atmospheric vapor correction was finally obtained (Eq. 5):

$$N = N_{raw} \cdot f_p \cdot CWV \quad (\text{Eq.5})$$

where N was the intensity of fast neutrons after atmospheric pressure correction and atmospheric vapor correction; N_{raw} was the original intensity of fast neutrons measured by neutron probe (Heidbüchel et al., 2015).

Introduction to the study area

In this study, Huibei Water Scientific Experiment Station, the East of Henan Water Conservancy Administration was chosen as the study area. Located in Xinglong Village, Kaifeng County, Henan Province, $114^\circ 35'$ east longitude, $34^\circ 40'$ north latitude, it is formed by alluvion of the Yellow River, featuring low and flat, mostly clay, loam and sandy soil, single underlying surface condition, suitable for crop cultivation. It has warm temperate continental monsoon climate, with an annual average temperature of $14.52 \text{ }^\circ\text{C}$, most rain falling between June and September, and an annual mean precipitation of 662.8 mm . During the experiment of April 2016~July 2016, wheat and corn were planted in the source region.

Material and methods

Sampling and determination of measuring depth

(1) During the experiment, soil samples 50 m, 100 m, 200 m, 300 m in the east, south, west, north of the cosmic-ray neutron probe were taken and treated, and the sampling depths were 0~10 cm, 10~20 cm and 20~30 cm, respectively. The location of

the cosmic-ray neutron probe and the distribution of the sampling points are shown in *Figure 1*.

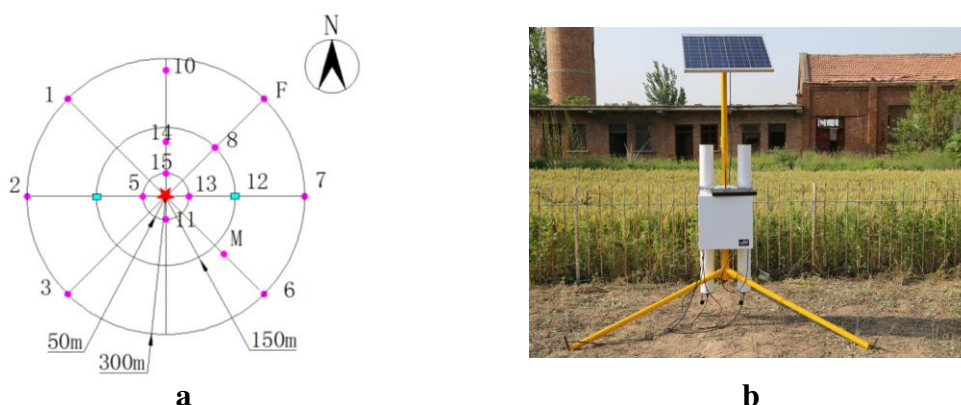


Figure 1. (a) The location of instrument and sampling points: red star denotes cosmic-ray moisture sensor; dots represent 14 locations in CRS footprint; rectangles represent time domain reflectometry. (b) The location of the cosmic-ray sensing probe

Soil moisture content (the arithmetic average of multiple sampling points within measuring range) and soil bulk density were obtained by calculation after drying and weighing, 29 cm, effective measuring depth of CRS was obtained by calculation by *Equation 2*.

(2) According to the measuring range and effective measuring depth of CRS, a sampling point 150 m in the east and west of the cosmic-ray neutron probe were chosen respectively using the existing TDR device in the study area, and moisture probes were placed in three levels, namely 0~10 cm, 10~20 cm and 20~30 cm, and the arithmetic average of data measured by TDR was conducted and then converted into mass water content.

Parameter calibration

Desilets et al. (2010) created a function relationship between the number of neutrons on a soil moisture on the basis of MCNPX (Monte Carlo N-Particle eXtended) model, as shown in *Equation 6*:

$$\theta(N) = \frac{\alpha_0}{\frac{N}{N_0} - \alpha_1} - \alpha_2 \quad (\text{Eq.6})$$

where $\theta(N)$ was the mass water content of soil (kg/kg); N was the number of fast neutrons after atmospheric pressure correction and atmospheric vapor correction; N_0 was the number of fast neutrons when the air in the same source region did not contain any atmospheric vapor, which was a constant value; $\alpha_0, \alpha_1, \alpha_2$ were parameters, and $\alpha_0 = 0.0808, \alpha_1 = 0.372, \alpha_2 = 0.115$ when the soil moisture content was greater than 0.02 kg/kg.

By using the number of fast neutrons in the source region after atmospheric pressure correction and atmospheric vapor correction and the soil moisture content after conducting arithmetic average method using weighing method, and N_0 can be obtained through inverse deduction.

Results analysis and discussion

According to N_0 after parameter calibration and *Equation 6*, changes in soil moisture of the source region per hour from April 27, 2016 to July 7, 2016 were obtained by calculation. By comparing CRS data and TDR observation results, the following conclusions can be drawn:

(1) *Figure 2* shows that the soil moisture content range measured by CRS was 0.11~0.21 kg/kg, with an average soil moisture content of the source region of 0.15 kg/kg; the soil moisture content range measured by TDR was 0.12~0.17 kg/kg, with an average soil moisture content of 0.14 kg/kg. Thus, the monitoring results of the two were consistent. Among which, the data with absolute error smaller than 0.01 kg/kg accounted for 51.42% of total data, and the data with absolute error greater than 20% accounted for 12.92% of total data, their fitting degree was 0.847 (*Fig. 3*), and root mean square error (RSME) was 0.020 kg/kg. It showed that the soil moisture content range measured by CRS was quite consistent with that measured by TDR, thereby providing real-time soil moisture conditions for farm management decisions to meet the needs of production practice.

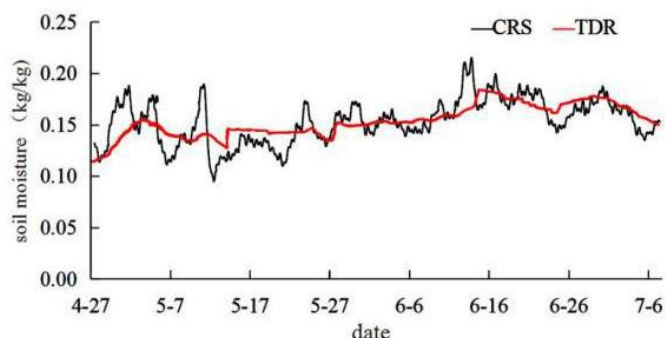


Figure 2. The comparison of CRS and TDR soil moisture in experiment period

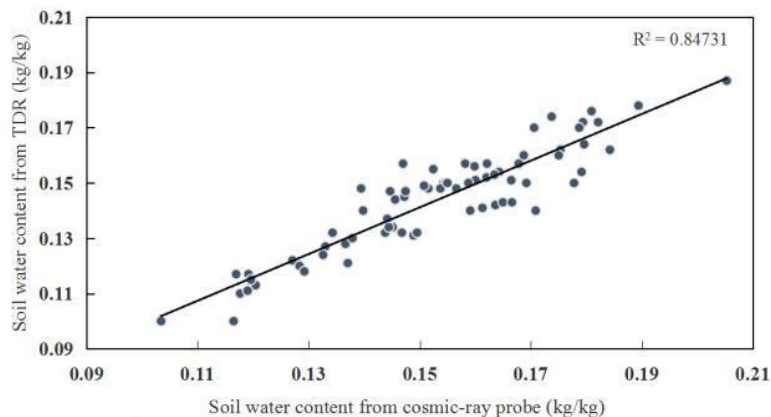


Figure 3. The comparison of CRS and TDR daily soil moisture in experiment period

(2) *Figure 4* shows that during the experiment there were 16 rainfalls, regardless of the size of rainfall, CRS had good responsiveness to each rainfall, namely, the soil moisture content immediately increased when there was a rainfall, and the response lag time was about 1 h; while TDR only responded to four large rainfalls (May 14, May 27, June 14 and June 24), with soil moisture content range of 0.01~0.02 kg/kg, and did not respond to small rainfalls. Thus, the following conclusions can be drawn: CRS had more sensitive response to different rainfall events compared with TDR, and can better reflect the changes in soil moisture corresponding to the rainfall.

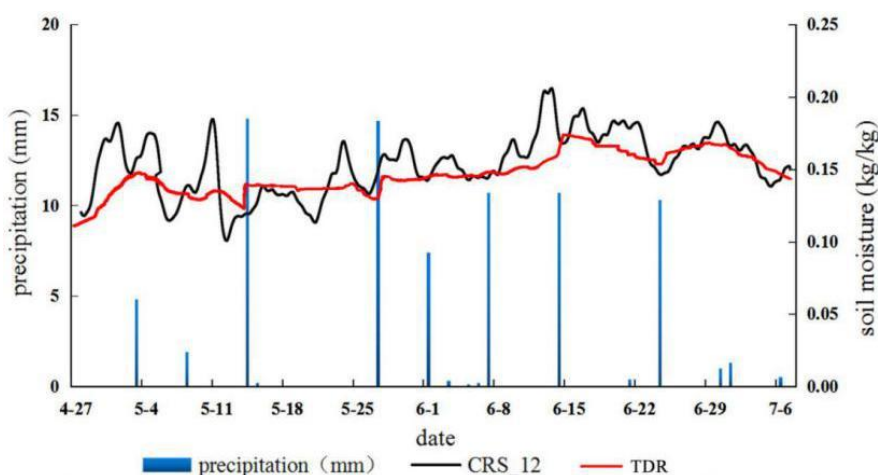


Figure 4. The response of CRS and TDR for precipitation in experiment period

Conclusion

The cosmic-ray neutron method had many advantages in determination of soil moisture: low requirements for soil type, a mesoscale, non-invasive and non-contact measurement mode, without radioactive sources, easy to be automated, and can be combined well with remote sensing technology. This technology can bridge the traditional gap between traditional point measurement and remote sensing large-scale detection.

Through nearly three months of analysis of CRS, TDR and other related meteorological factors, the following conclusions can be drawn: the cosmic-ray neutron probe had good applicability in agricultural areas in the plains. The soil moisture content range measured by CRS was quite consistent with that measured by TDR, their fitting degree was 0.847, and root mean square error (RSME) was 0.020 kg/kg; in addition, though CRS and TDR can perform automatic and continuous monitoring of soil moisture, CRS had more sensitive response to different rainfall events compared with TDR, and can better reflect the changes in soil moisture corresponding to the rainfall, while TDR only responded to large rainfalls, and did not respond to small rainfalls. The cosmic-ray soil moisture observation system can accurately measure the soil moisture of mesoscale farmland and its dynamic change, thereby providing basis for farm management decisions.

In the experiment, in addition to the influence of atmospheric pressure and atmospheric vapor on the calculated results of CRS, the plants, microorganisms and

humus on the underlying surfaces in the source region can also have an influence on the propagation of fast neutrons, and at present there is no perfect method to correct these influences. The effects caused by lattice water and water inorganic matter can be eliminated by the first field soil moisture correction (Zreda et al., 2012). For the problems in the cosmic-ray neutron method for measuring soil moisture, a more rational function formula to be created is the emphasis and difficulty for further promotion of the cosmic-ray neutron method.

Acknowledgements. The authors acknowledge the National Key Research and Development Program of China (2016YFC0401401), the Major Research Plan of the National Natural Science Foundation of China (91547209), the National Natural Science Foundation of People's Republic of China (51579101, 51709111), and the Science-tech Innovation Talents in University of Henan province (15HASTIT044). The authors would like to express their sincere gratitude to the anonymous reviewers for their constructive comments and useful suggestions that helped us improve our paper.

REFERENCES

- [1] Andreasen, M., Jensen, K. H., Zreda, M. et al. (2016): Modeling cosmic ray neutron field measurements. – *Water Resources Research* 52(8): 6451-6471.
- [2] Chrisman, B., Zreda, M. (2013): Quantifying mesoscale soil moisture with the cosmic-ray rover. – *Hydrology & Earth System Sciences Discussions* 10(6): 7127-7160.
- [3] Deng, Y. C., Xu, Y. H. (2007): Introduction to the methods of soil moisture content measuring. – *China Hydrology* 27(4): 20-24.
- [4] Desilets, D., Zreda, M. (2013): Footprint diameter for a cosmic-ray soil moisture probe: Theory and Monte Carlo simulations. – *Water Resources Research* 49(6): 3566-3575.
- [5] Desilets, D., Zreda, M., Ferré, T. P. A. (2010): Nature's neutron probe: Land surface hydrology at an elusive scale with cosmic rays. – *Water Resources Research* 46(11): W11505.
- [6] Entekhabi, D., Njoku, E. G., Houser, P. et al. (2004): The hydrosphere State (hydros) Satellite mission: an Earth system pathfinder for global mapping of soil moisture and land freeze/thaw. – *IEEE Transactions on Geoscience & Remote Sensing* 42(10): 2184-2195.
- [7] Franz, T. E., Zreda, M., Ferre, T. P. A. et al. (2012): Measurement depth of the cosmic ray soil moisture probe affected by hydrogen from various sources. – *Water Resources Research* 48(8): 9200-9200.
- [8] Franz, T. E., Wang, T., Avery, W., Finkenbiner, C., Brocca, L. (2015): Combined analysis of soil moisture measurements from roving and fixed cosmic ray neutron probes for multiscale real-time monitoring. – *Geophysical Research Letters* 42(9): 3389-3396.
- [9] Gong, Y., Li, Z., Liao, C. et al. (1997): Measurement of field soil water by using time domain reflectometry. – *Advances in Waterence* 8(4): 329-334.
- [10] Hashemi, N. (2017): Recognizing the potential of sustainable use of pasture resources in south khorasan province with approach of carrying capacity. – *Environment Ecosystem Science* 1(2): 09-12.
- [11] Heidbüchel, I., Güntner, A., Blume, T. (2015): Use of cosmic ray neutron sensors for soil moisture monitoring in forests. – *Hydrology & Earth System Sciences Discussions* 12(9): 9813-9864.
- [12] Hejazi, S. M., Lotfi, F., Fashandi, H., Alirezazadeh, A. (2017): Serishm: an eco-friendly and biodegradable flame retardant for fabrics. – *Environment Ecosystem Science* 1(2): 05-08.
- [13] Jiao, Q., Zhu, Z., Liu, S. et al. (2013): Research and application of cosmic-ray fast neutron method to measure soil moisture in the field. – *Advances in Earth Science* 28(10): 1136-1143.

- [14] Kim, C. P., Stricker, J. N. M., Feddes, R. A. (1997): Impact of soil heterogeneity on the water budget of the unsaturated zone. – *Water Resources Research* 33(5): 991-999.
- [15] Klenke, J. M., Flint, A. L. (1991): Collimated neutron probe for soil water content measurements. – *Soil Science Society of America Journal* 55(4): 916-923.
- [16] Njoku, E. G., Entekhabi, D. (1996): Passive microwave remote sensing of soil moisture. – *Journal of Hydrology* 184(1): 101-129.
- [17] Radan, A., Latifi, M., Moshtaghi, M., Ahmadi, M., Omidi, M. (2017): Determining the sensitive conservative site in Kolah Ghazi National Park, Iran, in order to management wildlife by using GIS software. – *Environment Ecosystem Science* 1(2): 13-15.
- [18] Rosolem, R., Shuttleworth, W. J., Zreda, M. et al. (2013): The Effect of atmospheric water vapor on neutron count in the cosmic-ray soil moisture observing system. – *Journal of Hydrometeorology* 14(5): 1659-1671.
- [19] Roth, K., Wollschlager, U., Cheng, Z. H., Zhang, J. B. (2004): Exploring Soil Layers and Water Tables with Ground-Penetrating Radar. – *Pedosphere* 14(3): 273-282.
- [20] Vazdani, S., Sabzghabaei, G., Dashti, S., Cheraghi, M., Alizadeh, R., Hemmati, A. (2017): FMEA techniques used in environmental risk assessment. – *Environment Ecosystem Science* 1(2): 16-18.
- [21] Villarreys, C. A. R, Baroni, G., Oswald, S. E. (2011): Integral quantification of seasonal soil moisture changes in farmland by cosmic-ray neutrons. – *Hydrology & Earth System Sciences* 15(12): 3843-3859.
- [22] Xiao, H., Wang, M., Sheng, S. (2017): Spatial evolution of URNCL and response of ecological security: a case study on Foshan City. – *Geology, Ecology, and Landscapes* 1(3): 190-196.
- [23] Yang, S., Li, J., Song, Y. (2017): Application of surfactant Tween 80 to enhance Fenton oxidation of polycyclic aromatic hydrocarbons (PAHs) in soil pre-treated with Fenton reagents. – *Geology, Ecology, and Landscapes* 1(3): 197-204.
- [24] Zreda, M. Desilets, D., Ferré, T. P. A. et al. (2008): Measuring soil moisture content non-invasively at intermediate spatial scale using cosmic-ray neutrons. – *Geophysical Research Letters* 35(21): L21402.
- [25] Zreda, M. Shuttleworth, W. J., Zeng, X. et al. (2012): COSMOS: the COsmic-ray Soil Moisture Observing System. – *Hydrology & Earth System Sciences* 16(11): 4079-4099.

GEOELECTRICAL RESISTIVITY SURVEY FOR GROUNDWATER POTENTIAL – A CASE STUDY OF NANDI RIVER BASIN, TAMIL NADU, INDIA

PRABHU, K.^{1,2*} – SIVAKUMAR, R.¹

¹*Department of Civil Engineering, SRM Institute of Science and Technology
Kattankulathur, India*

²*Department of Civil Engineering, GRT Institute of Engineering & Technology, Tiruttani, India*

**Corresponding author*

e-mail: k.prabhumtech@gmail.com; phone: +91-97-9061-4711

(Received 8th Oct 2017; accepted 27th Feb 2018)

Abstract. Ground water plays a vital role in the development of human activities. The supply of groundwater is limited and understanding the groundwater system is important to ensure sustainable use. In the present study Geoelectrical resistivity survey was carried out to assess groundwater potential zones in Nandi river basin, Tamil Nadu, India. The Vertical Electrical Soundings (VES) of Schlumberger configuration survey was conducted at 27 locations up to a depth of 150 m. The results of VES data were interpreted using IPI2WIN software. The resultant VES curves show different layers of sub-surface true resistivity and subsequent thickness are generated for understanding the lithology and hydrogeological conditions of the study area. The natural resources of groundwater potential zones are identified from the true resistivity and its thickness of sub surface layer.

Keywords: *groundwater, vertical electrical sounding, resistivity, hydrogeological, natural resources*

Introduction

Groundwater is a most valuable natural resource for irrigation, domestic and other purposes of water necessities in many parts of India. About 70% of the total amount of freshwater on Earth is contained in rivers, lakes, and glaciers. About 30% is contained in aquifers as groundwater (Salas et al., 2014). Shereif H. Mahmoud (2014) states that in water resource planning, groundwater is attracting increased attention due to the shortage of high-quality subsurface water for drinking and the increasing need of water for domestic, agricultural and industrial use. It has become crucial not only to target potential zones of groundwater but also to monitor and conserve this important resource. The scarcity of freshwater is the main problem faced by many countries exacerbated by the increasing population which creates the increasing need of the freshwater.

Groundwater is more advantageous as a source of portable water because it is free from chemical and biological contaminants, if it is properly saved it needs less or no purification before it can be used for industrial and domestic purposes. Most of the people depend upon groundwater as a source of water for all activities like drinking, agriculture and domestic use (Ahamed et al., 2016). Generally, it occurs in subsurface geological formations under hydrostatic pressure in the pores and cracks of rocks. The study area also geologically consists of crystalline rocks of various ages. In India, over two-thirds of the surface area totaling about 2.40 million sq. km. is occupied by hard rock regions and nearly 50% of the replenishable resources of groundwater occur in these rocks (Singhal, 2008). The movement and occurrence of groundwater are

extensively controlled by weathering and fractures of hard rock beneath the surface of the study area. Hydrogeologically the weathered rock has a porosity and contains a considerable quantity of water, because of its moderately high clay content, as it has a low permeability (Krishnamurthy et al., 2008). The preservation, planning, and governance of groundwater resources is the daunting challenges in the hard rock areas. Also, the groundwater potential have been affected by the rapid climate change (Shakib and Shojarastegari, 2017).

Since the quality and quantity of groundwater are associated with the subsurface conditions of the Earth, the geophysical survey plays a vital role in understanding the occurrence and distribution of groundwater in different hydrogeological circumstances. A wide range of geophysical survey methods are used in mining, in the industrial and environmental sectors. Geophysical survey methods are cost-effective and environmentally safer and there is no disturbance of subsurface materials (Reynolds, 2011). Vast areas of the surface field can be surveyed quickly at relatively less expensive, providing information to aid the location of boreholes. The principal methods used in geophysical exploration include seismic, gravity, magnetic, electrical resistivity, self- potential, induced polarization, and electromagnetic method. The use of geophysical surveys have increased tremendously over the last decades. Hence, the suitable geophysical resistivity survey methods are deployed based on the physical properties of a target being investigated.

Study area

The study area “Nandi river basin” falls within the part of two districts of Tamil Nadu namely Tiruvallur and Vellore Districts and a small adjoining part of Chittoor District of Andhra Pradesh. The study area lies between the latitudes $13^{\circ}03'28''\text{N}$ to $13^{\circ}15'59''\text{N}$ and longitudes $79^{\circ}17'30''\text{E}$ to $79^{\circ}43'25''\text{E}$ covering an area of 710 km^2 (Fig. 1).

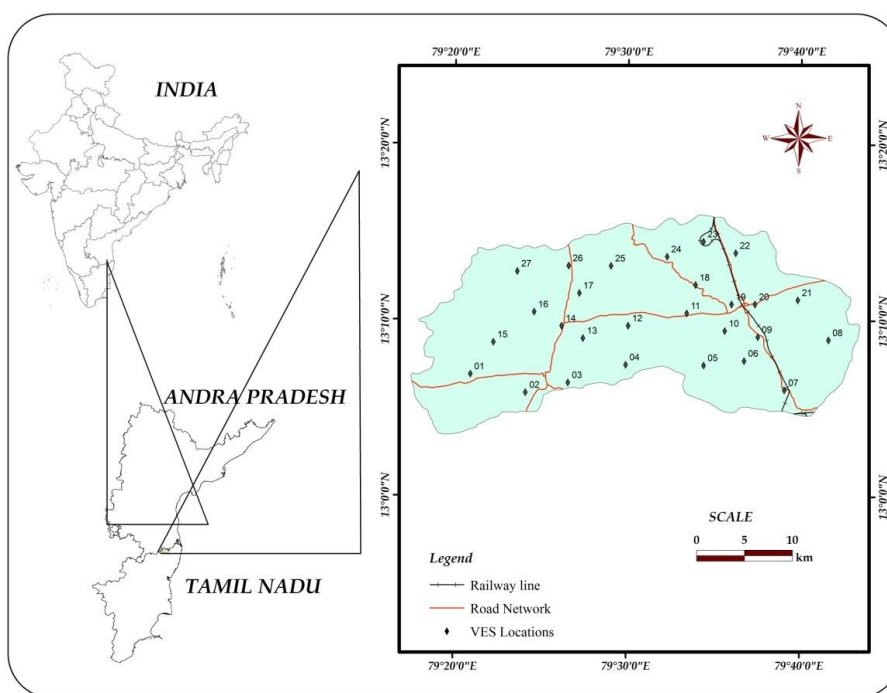


Figure 1. Base map of the study area

The Nandi river originates from Puttur hills at an altitude of 582 m near Singasamudram in Andhra Pradesh, and it enters Tamil Nadu and feeds the Sholingur tank. The surplus of this tank feeds the Viranatturu tank and from this tank, the river takes a regular course. The chief irrigation sources in the area are the tanks, wells, and tube/bore wells.

The study area receives 795 mm rainfall as an annual average, of which 535 mm is contributed by the northeast monsoon, and the rest by the southwest monsoon. Although the study area has a lack of rainfall, agriculture is not extensively practiced in the region. Crops like paddy, sugarcane and mango tree are planted in some areas, which are the main sources of income for the majority of residents.

Geology

The geology of the area is important for determining the influence of its physiographic characteristics. The main purpose of investigating the geology of a river basin is a hydrological project to determine the permeability of the substratum (Musy and Higy, 2011). The porosity and permeability of the rock formation considerably influence the flow of groundwater. Hence, the knowledge of porosity and permeability of rock formation gives an insight into the groundwater supply and its flow paths. The study area above a permeable substratum transmits considerable amount of water to the aquifers in the rainy events so that during dry periods, the water can be extracted as groundwater.

The study area is essentially composed of several crystalline rocks as well as sedimentary rocks, shown in *Figure 2*.

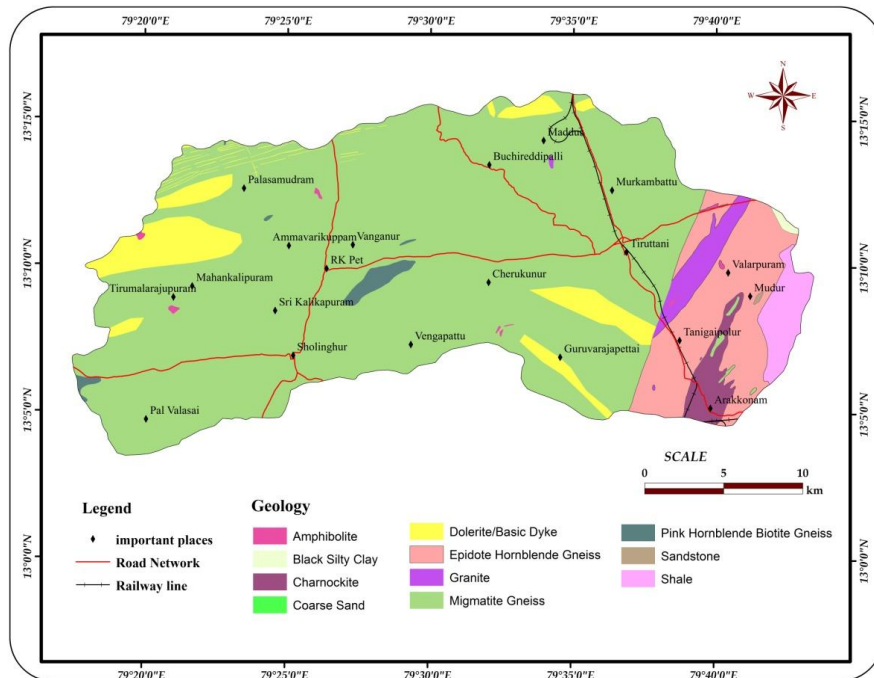


Figure 2. Geology map of the study area

Migmatite gneiss is the major rock, covering about 547.39 km² (77%) of the total study area, Followed by Epidote hornblende gneiss with a spatial extent of 68.32 km². The

younger sedimentary rocks include shale (14.78 km²), sandstone (0.20 km²), black silty clay (0.96 km²) and coarse sand (0.04 km²) covered 2.25% of the study area. Dolerite dykes are found as isolated linear bodies, reserving about 47.50 km². The remaining rock types include amphibolite, charnockite, granite, and pink hornblende-biotite gneiss, each covering small portions of the study area. The Archaen crystalline rock is underlain in the subsurface geology of the study area; hence the groundwater may infiltrate in the weathered zone and fractured rocks. So the fractures play a significant and crucial role in fluid flow, particularly for the movement and accumulation of groundwater in hard rock areas. If minor fracture interconnections are present in the rock, those give numerous supply of groundwater.

Materials and methods

In VES survey, the direct current is injected into the surface of the Earth through two current electrodes and the resultant potential variations are measured at the surface with the help of a voltmeter connecting two potential electrodes. The conductive property of rock is essential to have knowledge about the mode of conduction through various materials. At most, rocks are poor conductors, the resistivity of their rocks would be pretty large. In some cases, the fractures and pore spaces present in the rocks are filled with water which has dissolved minerals derived from weathering of rocks. The dissolved minerals tend to disintegrate into positively charged cations and negatively charged anions, moving through the water in opposite directions. This movement of ions opposite to each other initiates ionic conduction process. Thus the rocks act as electrolytic conductors where the current is carried by Total Dissolved Solids (TDS) present in the water. Hence the resistivity of a rock depends on the mobility and concentration of TDS in water, the volume and arrangement of the pore spaces.

A detailed knowledge of geology is the most important aspects for classifying the Earth's layers because the rocks exhibit a wide range of electrical resistivity. For instance, igneous rocks tend to have the highest resistivity, sedimentary rocks are the most conductive, largely due to their high pore fluid content and metamorphic rocks contain transitional but the overlapping resistivity (Reynolds, 2011). A successful result of the survey depends on meticulous planning in site selection and data acquisition. The electrical resistivity prospecting of the basic electric parameters of electric current, potential difference, resistance and apparent resistivity which is together used to derive the true resistivity of Earth's layers during data processing. Electric current is measured by the ammeter and is expressed in amps whereas the potential difference by a voltmeter, expressed in terms of volts. The Potential difference is just an electrical pressure difference required to make an electric current flow. Commonly an increase in potential difference boosts the current flow through the rocks. According to Ohm's law, the resistance of a rock is the ratio of potential difference (Δv), and the current (I), i.e. $R = \Delta v/I$, measured in ohms. The primary aim of the VES survey is to obtain the true resistivity of a rock layer for the subsurface; but the Earth is not composed of homogenous materials, and it is not possible to measure the true resistivity of the rock directly. Instead, apparent resistivity (ρ_a) is measured by multiplying the resistance (R) with the geometric factor (K) of the electrode array chosen for the investigation; the ρ_a varies with the electrode array type.

Then the true resistivity (ρ) of the rock layer is obtained through the manual curve matching technique or computer programs during data processing. There are three primary types of electrode configuration Wenner, Schlumberger, and dipole-dipole array are employed in geophysical method. For the present study the Schlumberger array has been used. When comparing the electrode configuration, Schlumberger sounding can be conducted faster, since the movement of the electrodes is mainly confined to the current electrodes only, while during the entire sounding, the potential electrodes may have to be shifted four times altogether (Ramanuja Chary, 2012).

Field procedure

In total 27 VES survey locations were selected over the study area and the electrical investigation data were collected at the specific locations using DDR-3 Resistivity Meter. The Geoelectrical resistivity survey was carried out during the month of July 2016 and at every survey location 37 observations were carried out. The investigation for each VES location was started at 2 m depth and was completed at 150 m depth which is the maximum depth of investigation. The Schlumberger configuration of VES survey carried out the maximum electrode spacing of 300 m as shown in *Figure 3*. The current electrode ($AB/2$) spacing varied from 1 to 150 m and the potential electrode ($P_1P_2/2$) spacing varied from 1 to 20 m.

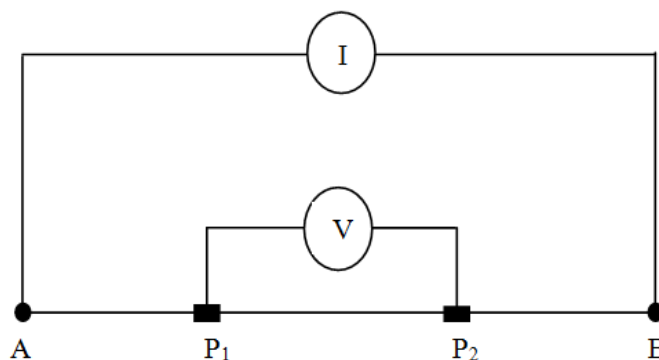


Figure 3. VES survey electrode arrangement

The measured apparent resistivity values were plotted on a logarithmic graph against the half-electrode spacing ($AB/2$) values using the software IPI2WIN. The resulting VES curves, known as sounding curves were adjusted until the minimum RMS error was achieved. Four layered curve types were generated with the aid of the software. Curve types were classified based on the relative resistivity values of layers and were used for qualitative and quantitative interpretation.

Results and discussion

The field data were interpreted and processed quantitatively and qualitatively by using curve matching techniques. The quantitative interpretation involves the determination of the number of geoelectrical layers as well as the true depth, thickness, and resistivity of each layer (Barseem, 2015). The true resistivity and thickness of layers for quantitative analysis of VES represented in *Table 1*. The qualitative interpretation

provides an insight into curve shape, curve type, and the number of layers that are represented in *Table 2*.

Table 1. Resistivity and thickness of layers for quantitative analysis of VES

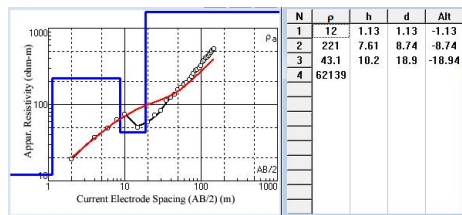
VES no.	Village name	Resistivity (ohm-m)				Layer thickness (m)		
		ρ_1	ρ_2	ρ_3	ρ_4	h_1	h_2	h_3
1	Gopalapuram	75.5	166	683	904	2.17	15.8	117
2	Misarakandapuram	12.4	248	493	558	1.6	53.5	132
3	Sholinghur	12	221	43.1	62139	1.13	7.61	10.2
4	Vangapattu	10.6	222	37.6	935	1.42	1.65	9.19
5	Guruvarajapet	63.8	772	134	901	1.43	1.22	4.02
6	Gadavarikandigai	50.2	88.3	869	214	1.18	8.82	15.2
7	Arakkonam	23.5	311	160	1710	2.08	3.89	32.5
8	Mudur	13.9	479	13	599	3.39	3.08	6.68
9	Saraswathi Nagar	103	204	754	924	3.33	9.04	37.7
10	Kannika Puram	216	956	123	3180	1.5	4.01	4.84
11	Koramangalam	11.2	535	29.1	36638	1.47	2.79	7.16
12	Beerakuppam	72.5	311	3941	8025	2.37	10.7	7.25
13	Vellathur	25.1	272	112	845	1.31	8.69	5.85
14	Ramakrishnaraja Pet	2.76	531	17.1	17724	0.697	3.6	11.4
15	Mahankalikapuram	71.4	251	77.2	325	1.14	0.69	14.2
16	Ammaiyarkuppam	94.2	41.7	978	645	4.99	8.16	5.44
17	Vanganur	36.6	268	30.9	51283	1.07	1.72	6.49
18	Thekkaloor	220	3162	113	2245	1.2	1.26	11.4
19	Tiruttani (Sai Baba Nagar)	13.9	344	61	924	1.07	3.03	15.5
20	Tiruttani (Erular Colony)	40.3	85.5	16.4	210	2.12	2.23	11.9
21	Perungalathur	11.7	41.2	12	12649	1.96	1.33	3.69
22	Ponpadi	19.7	1.66	5.92	830	1.05	1.04	3.83
23	Mathur	11.2	23	73	307	1.24	4.79	12.3
24	B.R. Palli	113	577	162	1676	1.12	0.448	8.78
25	Nochili	48.3	78.9	200	3875	1.61	10	29.8
26	Korakuppam	17.9	10.8	34.8	11836	1.7	1.82	5.94
27	Palasamudram	69	43.1	94.5	675	1.12	3.44	15.3

Table 2. Curve types for qualitative analysis of VES

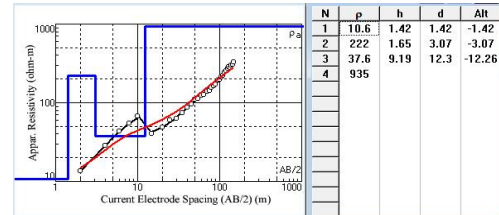
VES no's	Curve characteristics	Curve type	Layers
3, 4, 5, 7, 8, 10, 11, 13, 14, 15, 17, 18, 19, 20, 21, 24	$\rho_1 < \rho_2 > \rho_3 < \rho_4$	KH	4
1, 2, 9, 12, 23, 25	$\rho_1 < \rho_2 < \rho_3 < \rho_4$	AA	4
16	$\rho_1 > \rho_2 < \rho_3 > \rho_4$	HK	4
22, 26, 27	$\rho_1 > \rho_2 < \rho_3 < \rho_4$	HA	4
6	$\rho_1 > \rho_2 > \rho_3 < \rho_4$	QH	4

KH-type curve

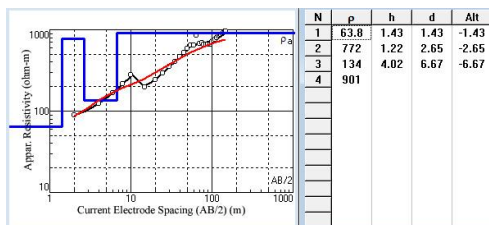
The KH curves are morphologically characterized by the resistive sequence of $\rho_1 < \rho_2 > \rho_3 < \rho_4$. In general, the VES profiles belonging to this curve type show highly conductive top soil layer, and relatively high resistance in bottom layers, indicating the possibility of water saturation in the third layer, most of which possess highly contrasting low resistivity values between the second and fourth layers. *Figure 4* shows the interpretation of VES curves (KH-Type) using the IPI2WIN software.



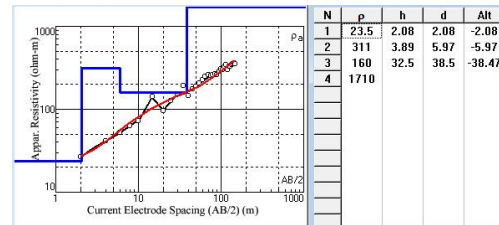
VES 3



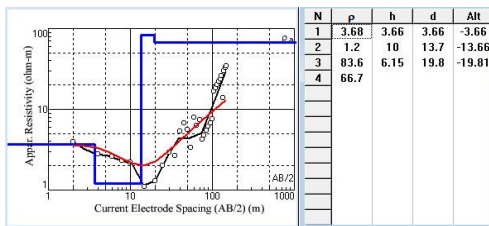
VES 4



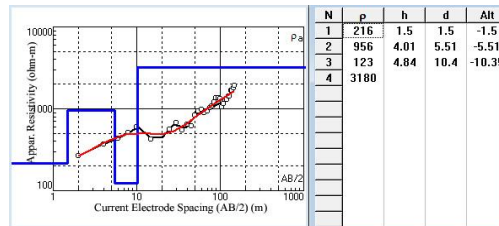
VES 5



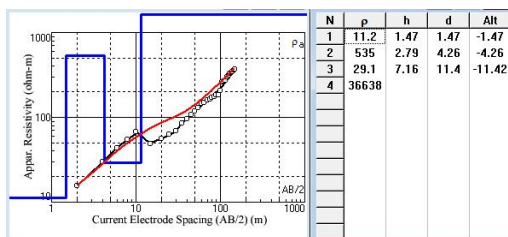
VES 7



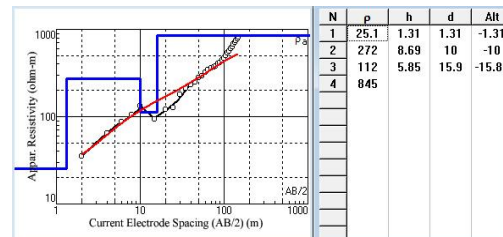
VES 8



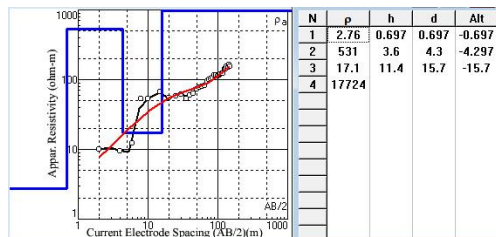
VES 10



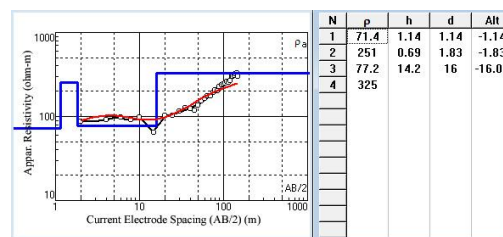
VES 11



VES 13



VES 14



VES 15

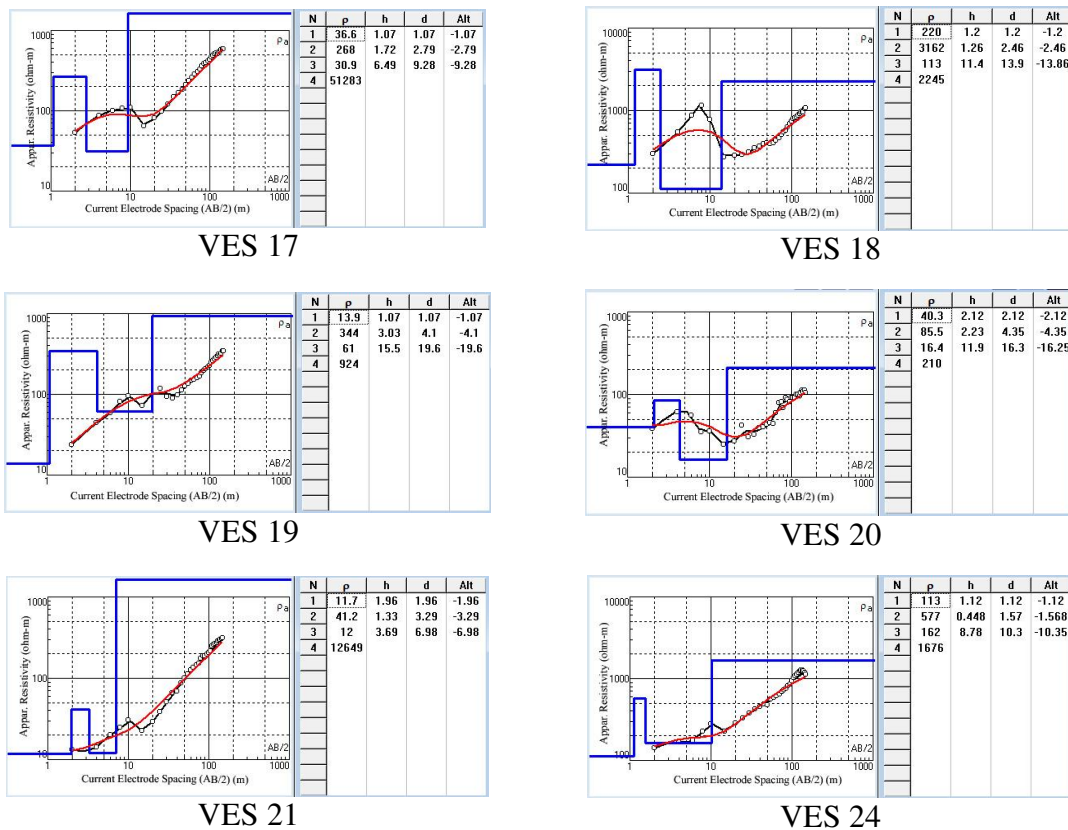


Figure 4. Interpretation of VES curves - KH-type

VES 3, 4, 7, 8, 11, 13, 14, 17, 19 and 21 show the topsoil layers with resistivity ranges from 2.76 ohm-m to 36.6 ohm-m, indicating the presence of clay constituents between 20% to 40% in soil (Reynolds, 2011) and varying in thicknesses from 0.697 m to 3.39 m; while VES 5, 10, 15, 18, 20 and 24 exhibit topsoil layers with resistivity values ranging from 40.3 ohm-m to 220 ohm-m, revealing the soil composition with lack of clay content and the thicknesses vary from 1.12 m to 2.12 m.

Commonly, all VES curves of the KH represent the third layer as the fractured layer filled with water. Hence, based on the third layer thickness, its original depth, and its resistivity contrast with its overlying and underlying layers, the degree of groundwater potential has been inferred from a VES curve. Accordingly, VES 3, 7, 10, 11, 13, 14, 17, 19, 20 and 21 can be indicative of good groundwater yield, while VES 4, 5, 8, 15, 18 and 24 display the origin of third layers at relatively shallow depth, implying the presence of clay formation or the temporary groundwater yield.

AA-type curve

The resistivity sequence of $\rho_1 < \rho_2 < \rho_3 < \rho_4$ makes the shape of AA type curve. In most cases, the first layer starts with relatively low resistivity values and the fourth layer ends with relatively high resistivity ranges, showing the steady increase in the resistivity values as a function of depth. This is the obvious fact of the AA type curve. Figure 5 shows the interpretation of VES curves - AA-Type.

In VES 1, 2, 9, 12, 23 and 25 represent the topsoil with thickness ranges from 1.24 m to 3.33 m and resistivity ranges from 11.2 ohm-m to 103 ohm-m. Hence, the low

resistivity of topsoil depends on the proportion of clay mineral constituents in soil, the grain size, and moisture content, whereas high resistivity soil exhibits lack of moisture and clay content, and coarse-grained mineral constituents present in the soil.

VES 25 denotes the second layer as a weathered layer with the resistivity of 78.9 ohm-m, followed by the third layer of 200 ohm-m, pointing to the high probability of reasonable groundwater occurrence in the third layer. The weathered zone starts at 1.60 m down the surface and extends up to 10 m. The third layer is a fracture zone of 29.8 m thickness. A rapid increase of resistivity values in the fourth layer authenticates the existence of water table confined to the third layer. Similarly, VES 12 depicts weathered zone of 10.7 m thickness with the resistivity of 311 ohm-m, starting at 2.37 m below the surface and this layer is followed by relatively high resistivity layers having 3941 ohm-m, indicating the possible occurrence of clay patches in the weathered zone. Also, the weathered zone may contain some amount of rainwater percolated through the soil. The resistivity of the fourth layer expresses the fresh rock formation where the occurrence of groundwater is the mostly doubtful. Below the topsoil layer, the resistivity ranges of the VES 1, 2, 9 and 23 expose the absence of any fractured rock layers up to the depth of maximum investigation, leading to poor groundwater potential.

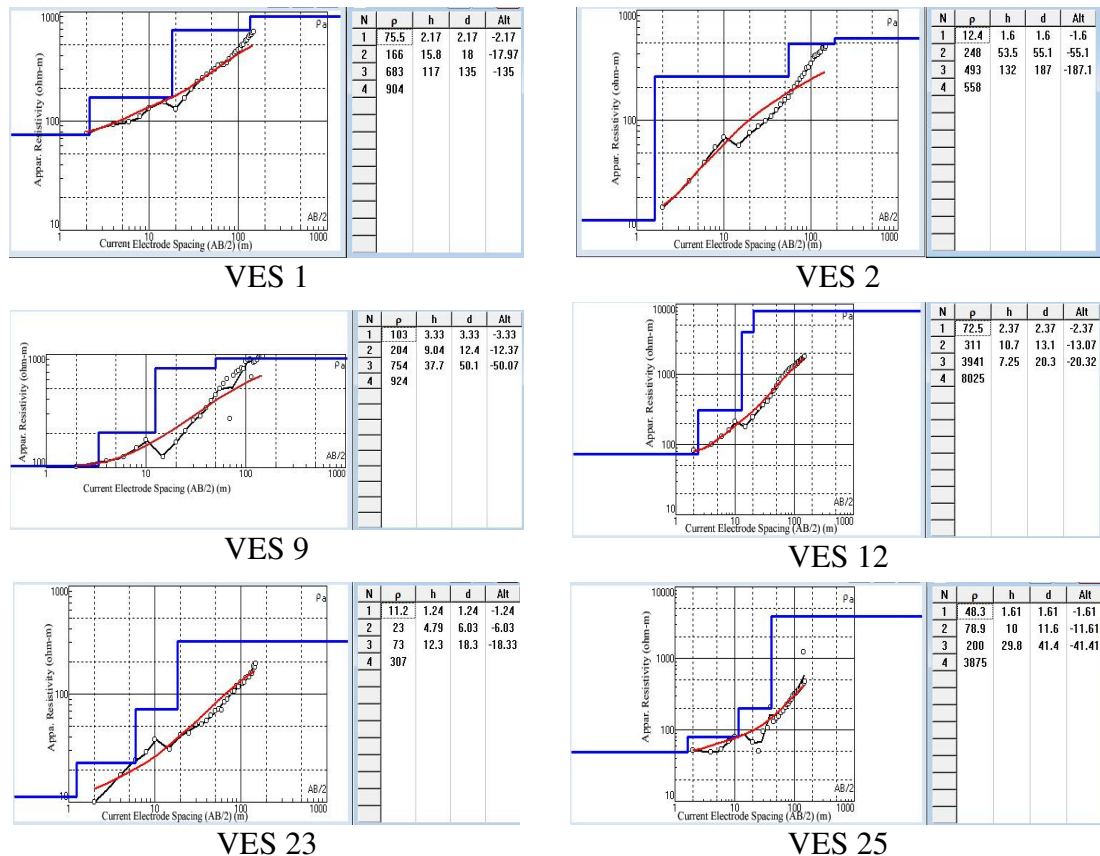


Figure 5. Interpretation of VES curves - AA-type

HK type curve

The HK type curve is defined by the resistivity sequence of $\rho_1 > \rho_2 < \rho_3 > \rho_4$. The topsoil resistivity (94.2 ohm-m) of VES 16 discloses soil composition with deficient clay constituents and reveal a second layer with relatively lower resistivity values than

the topsoil layer, ranging 41.7 ohm-m. It reveals the probable existence of a clay layer or highly altered weathered zones which can act as better conduits for groundwater movement down to deep aquifers if present. The third layer shows a sudden increase in resistivity value with the indication of the absence or lack of fractured rock layers. The fourth layer is followed by the third layer with slight reduction in the resistivity value; the slightly reduced resistivity can be due to the emergence of interconnected fractures capable of yielding moderate groundwater. The interpretation of VES curves HK-Type is shown in *Figure 6*.

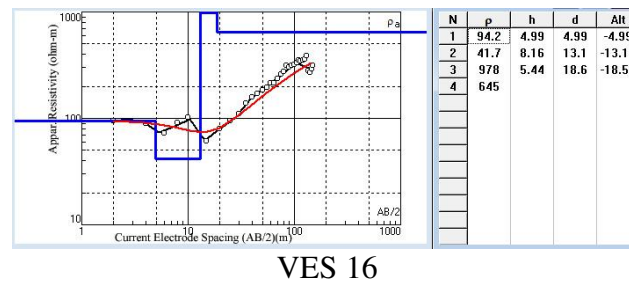


Figure 6. Interpretation of VES curves - HK-type

HA type curve

HA type curve is defined by the resistivity sequence of $\rho_1 > \rho_2 < \rho_3 > \rho_4$. In this curve type, the resistivity of the first layer always exceeds the resistance of the second layer, followed by a progressive increase in the resistivity of successive layers in terms of depth. In most cases, just beneath the third layer, an immediate increase is observed in the resistivity of the fourth layer which can be the sign of a massive hard rock formation. The interpretation of VES curves HK-Type is shown in *Figure 7*.

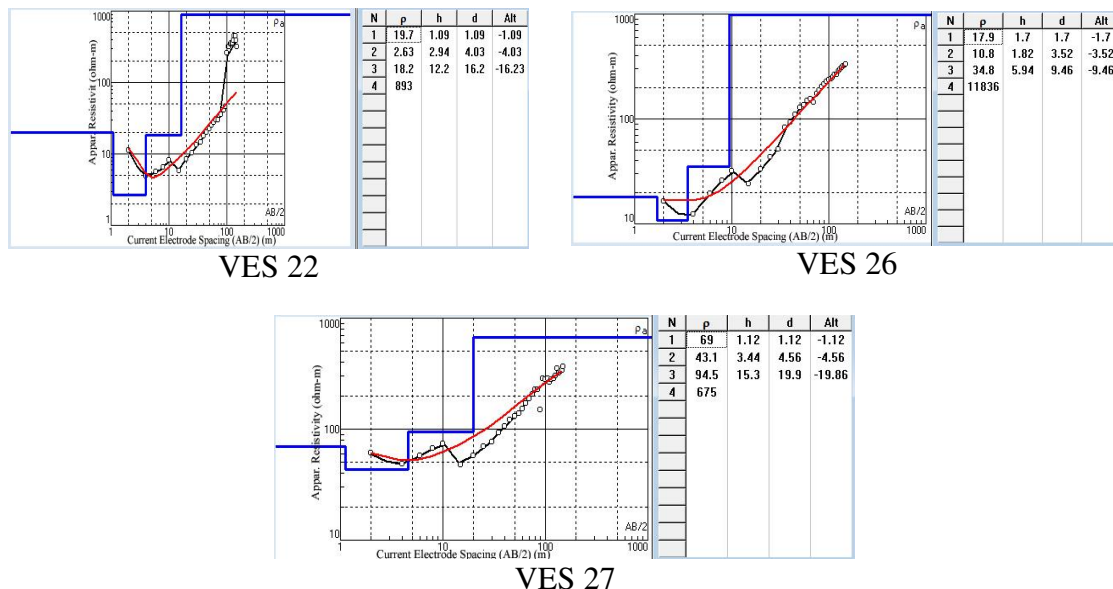


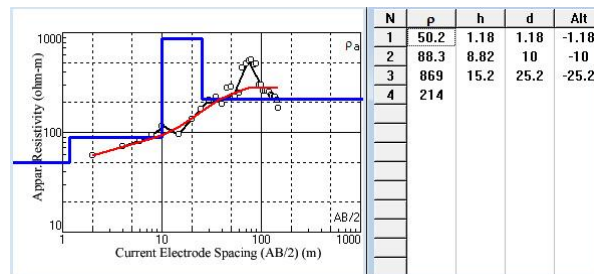
Figure 7. Interpretation of VES curves - HA-type

VES 22, 26 and 27 have the topsoil with resistivity values ranging from 17.9 ohm-m to 69 ohm-m, showing the signs of fine particles along with clay content. The minimum

and maximum thickness of the topsoil layer vary from 1.05 m to 1.70 m. The VES curves of HA type indicate a massive rock formation with highly contrasting resistivity values ranging from 675 ohm-m to 11836 ohm-m. As these HA curves show the second layer with resistivity ranges lesser than the topsoil layer and there is an increase in the resistivity of the successive layer, it is obvious that the second layer is highly weathered and cannot be expected as the groundwater potential.

QH type curve

The morphology of this type of curve is defined by the resistivity sequence of $\rho_1 < \rho_2 < \rho_3 > \rho_4$. The VES 6 consists of a QH type curve, where the resistivity of first, the second and the third layers are defined by relatively high resistivity ranges from 50.2 ohm-m, 88.3 ohm-m, and 869 ohm-m respectively. The fourth layer shows relatively fewer resistivity values 214 ohm-m, indicating highly weathered zones in association with fracture zones. In general a QH type curve indicates good groundwater potential zones. *Figure 8* shows the interpretation of VES curves - QH-Type.



VES 6

Figure 8. Interpretation of VES curves – QH-type

Conclusion

The Vertical Electrical Sounding (VES) of Schlumberger configuration survey was performed in 27 locations within the study area to find out the groundwater potential zones in Nandi river basin. From the VES survey data, the four layered KH, AA, HK, HA, and QH type curves, accounting for 59.26%, 22.22%, 3.70%, 11.11%, and 3.70%, respectively, were generated. Based on the VES survey investigation, VES of 3, 7, 10, 11, 13, 14, 17, 19, 20 and 21 belonging to KH type curve show good groundwater potential under the depths ranging from 3.69 to 32.5 m. The VES 4, 5, 8, 15, 18 and 24 display the origin of the third layers at relatively shallow depth, implying the presence of clay formation or the temporary groundwater yield. The AA type curve of VES 25 reveals the high probability of groundwater at a depth of 10 m and the occurrence of groundwater is the most doubtful in case of VES 12. In addition, VES of 1, 2, 9 and 23 of AA type unveil the absence of any fractured rock layers up to the depth of maximum investigation, leading to poor groundwater potential. The HK type curve of the VES 16 indicates moderate groundwater potential below depths of 18.6 m. With the VES 22, 26 and 27 of HA type; poor groundwater potential can be expected. The VES 6 defined by QH type infers good groundwater potential zones below the depths of 25.2 m. Hence, from the geoelectrical resistivity survey investigation, the location of groundwater potential zones were identified. Also the groundwater recharge potential zones are fully depend on the environmental factors like rainfall and climatic conditions.

Acknowledgements. The authors would like to thank SRM Institute of Science and Technology and GRT Institute of Engineering & Technology for providing all necessary facilities and constant encouragements for doing this research work.

REFERENCES

- [1] Ahamed, A. J. Loganathan, K. Ananthkrishnan, S. Ahmed, J. K. C. Ashraf, M. A. (2016): Evaluation of Graphical and multivariate statistical methods for classification and evaluation of Groundwater in Alathur block, Perambalur District, India. – *Applied Ecology and Environmental Research* 15(3): 105-116.
- [2] Amidu, S. A., Olayinka, A. I. (2006): Environmental assessment of sewage disposal systems using 2D electrical resistivity imaging and geochemical analysis: A case study from Ibadan, Southwestern Nigeria. – *Environmental Engineering, Geosciences* 7(3): 261-272.
- [3] Barseem, M. S., El Lateef, T. A. A., El Deen, H. M. E., Abdel Rahman, A. A. A. A. (2015): Geoelectrical exploration in South Qantara Shark Area for supplementary irrigation purpose-Sinai-Egypt. – *Hydrology Current Research* 6: 207. DOI: 10.4172/2157-7587.1000207.
- [4] Huang, B. B., Niu, J. T., Gui, F. L., Zhang, X. H. (2017): Water resources deployment model for Pingshui river basin. – *Applied Ecology and Environmental Research* 15(3): 985-998.
- [5] Krishnamurthy, N. S. Chandra, S., Kumar, D. (2008): Geophysical Characterization of Hard Rock Aquifers. – In: Ahmed, S., Jayakumar, R., Salih, A. (eds.) *Groundwater Dynamics in Hard Rock Aquifers*. Springer, Dordrecht.
- [6] Mahmoud, S. H. (2014): Delineation of potential sites for groundwater recharge using a GIS-based decision support system. – *Environ Earth Sci* 72: 3429-3442. DOI: 10.1007/s12665-014-3249-y.
- [7] Musy, A., Higy, C. (2011): *Hydrology - A Science of Nature*. –Taylor and Francis Group, LLC, New York.
- [8] NRSA (2008): *Groundwater Prospect Mapping Using Remote Sensing and GIS*. Rajiv Gandhi National Drinking Water Mission Project Manual. – National Remote Sensing Agency, Hyderabad.
- [9] Ramanuja Chary, K. R. (2012): *Geophysical techniques for groundwater exploration*. – Professional Books Publisher, Hyderabad. ISBN: 978-81-909728-2-6.
- [10] Reynolds, J. M. (2011): *An Introduction to Applied and Environmental Geophysics*, 2nd ed. – Wiley-Blackwell, Chichester.
- [11] Salas, J. D., Govindaraju, R. S., Anderson, M., Arabi, M., Frances, F., Suarez, W., Lavado-Casimiro, W. S., Green, T. R. (2014): *Modern Water Resources Engineering - Introduction to Hydrology*. Handbook of Environmental Engineering, Vol. 15. – Springer, New York. DOI: 10.1007/978-1-62703-595-8.
- [12] Shakib, H. S., Shojarastegari, H. (2017): Climate change impacts and water resources management. – *Applied Ecology and Environmental Research* 15(4): 741-754.
- [13] Singhal, B. B. S. (2008): Nature of Hard Rock Aquifers: Hydrogeological Uncertainties and Ambiguities. – In: Ahmed, S., Jayakumar, R., Salih, A. (eds.) *Groundwater Dynamics in Hard Rock Aquifers*. Springer, Dordrecht.
- [14] Venkateswaran, S., Ayyandurai, R. (2015): Groundwater potential zoning in upper Gadilam river basin Tamil Nadu. – *Aquatic Procedia* 4: 1275-1282.
- [15] Venkateswaran, S., Vijay Prabhu, M., Karuppanan, S. (2014): Delineation of groundwater potential zones using geophysical and GIS techniques in the Sarabanga sub basin, Cauvery River, Tamil Nadu, India. – *International Journal of Current Research* 2(1): 58-75.

STATISTICAL INFERENCE PROCEDURE BY THE INFORMATION-BASED TEST AND ITS APPLICATION IN MARINE CLIMATOLOGY

SEZER, A. – ASMA, S. – OZDEMIR, O.*

*Department of Statistics, Faculty of Science, Anadolu University, 26470 Eskisehir, Turkey
(phone: +90- 222-335-0580; fax: +90-222-320-4910)*

**Corresponding author
e-mail: ozerozdemir@anadolu.edu.tr*

(Received 9th Oct 2017; accepted 13th Mar 2018)

Abstract. Objectives of ecological studies should drive all aspects of design. These objectives must include hypothesis testing and appropriate sample size. High level of unexplained variation is typical in many ecological studies and may lead to incorrect inference about the population. Choosing appropriate sample size is one key strategy to cope with unexplained variation. In this study, we aim to determine sample size which depends upon the information-based test and show the superiority of this approach over the likelihood ratio test. Particularly, we focused on finding appropriate sample size for testing the variance of the normal distribution and Rayleigh distribution. The power curves are obtained both for information-based test and the likelihood ratio test by the Monte Carlo simulations. We used wave height data to show how the inference procedure should follow both for the likelihood test and information-based test procedure. In agreement with the theoretical results of Janssen (2014) it is found that wave height obeys the Rayleigh distribution. Sample size determination for testing the variance of the normal distribution and Rayleigh distribution with different parameters is demonstrated for the fixed effect sizes.

Keywords: *likelihood ratio test, effect size, sample size, Monte Carlo simulation, power curves*

Introduction

Sample size determination is one of the most essential parts of the statistical design in the ecological studies and it is usually a difficult one. The ecologists, first want to know how many subjects should be included in their study (sample size) and how these subjects should be selected (sampling methods). Second, they desire to attribute a *p*-value to their results to claim significance of results. In ecological point of view, choosing appropriate sample size is essential to develop statistical distributions, used for predicting the occurrence of a species at a particular location (Wood et al., 2015; Kass et al., 2016). The availability of novel and sophisticated statistical techniques means we are better equipped than ever to extract signal from noisy ecological data, but it remains challenging to know how to apply these tools, and which statistical technique(s) might be best suited to answering specific questions (Low-Decarie et al., 2014; Zuur and Ieno, 2016).

Lynch (2017) has shown the principle of minimizing the cost-plus-loss is used to simultaneously find optimal plot size and sample size for forest sampling using the Fairfield Smith relationship between plot size and the variance among cubic metre volumes per hectare. Indeed, reducing the number of animal subjects used in biomedical experiments is desirable for ethical and practical reasons. Kramer and Font (2017) discussed how the number of current control animals can be reduced, without loss of statistical power, by incorporating information from historical controls. Dziak et al. (2014) empirically addressed the question of how large a sample size is needed to avoid

underextraction when using the bootstrap likelihood ratio test to choose a number of classes in latent class analysis.

Once the basic study design and planned analysis methods are defined, there are three parameters under the control which define the power of the study. These are the sample size, the effect size defined by the alternative hypothesis and significance level. Considering these parameters and the power of the study together, fixing any of three will allow calculating the fourth. However there are several obstacles that we need to handle. For example how do we know the population parameter, given that we are only planning the experiment and so no data have been collected yet? In those cases, sometimes, there are historical data that can be used to estimate parameter(s) in the power function. However most of the time we may not have preliminary data from which to estimate population parameter, in this case a pilot study is needed.

In the frequentist inference, sample size calculations are made by the power function. Lenth (2001) made criticism for some ill-advised shortcuts relating to power and sample size. Actually, there are several approaches to determine sample size. One can specify the desired confidence interval and then determine sample size that achieves that goal. Another approach involves studying the power of a test of hypothesis. The power of a test is defined as the probability that we correctly reject the null hypothesis, given that alternative hypothesis is true.

Most of the literature about determination of sample size depends on likelihood ratio test. Recently, Kullback-Leibler information-based test have become popular as complementary approaches to classical hypothesis testing (Burnham and Anderson, 2002). Esteban et al. (2001) also gave the power comparisons of four different entropy estimators. Gupta (2007) studied testing equality of variances of observations in the different treatment groups assuming treatment effects are fixed. Akaike's information criterion based on information theory, is a common metric used by ecologist to evaluate and select among alternative ecological models (Burnham and Anderson, 2002; Richards, 2005). Applications of entropy principles to evolution and ecology are of tantamount importance given the central role spatiotemporal structuring plays in both evolution and ecological succession. Recently, Schepsmeier (2015) tested normality and introduced a new goodness-of-fit test for regular vine copula models, a flexible class of multivariate copulas based on a pair-copula construction. Vranken et al. (2015) made a review on the use of entropy in landscape ecology for heterogeneity, unpredictability, scale dependence and their links with thermodynamics. Roach et al. (2017) obtained a qualitative interpretation of the role of entropy in evolving ecological systems. Martin and Poletto (2018) showed how to apply the theory of entropy to determine sediment concentration.

It is common to test hypothesis about the population standard deviation using the likelihood ratio test (LRT). In particular, the likelihood ratio test statistic is assumed to follow a χ^2 with degrees of freedom equal to number of parameters that are tested. For the purpose of the power and sample calculation in the generalized models, two major tests have been proposed. These are the score test and the likelihood ratio statistics developed by Self and Mauritsen (1988). Lehmann (2006) pointed that the LRT agrees with tests obtained from other principles (for example it is UMP unbiased or UMP invariant). Generally LRT seems to lead to satisfactory tests. However, counter-examples are also known in which the test is quite unsatisfactory; see for example Perlman and Wu (1999) and Menéndez et al. (1992).

Self et al. (1992) described an approach for sample size/power calculations that is based on non-central chi-square approximation to the distribution of likelihood ratio statistic. Shieh (2000) has given a direct extension of the approach described in Self et al. (1992) for power and sample calculations in generalized linear models. There is also a detailed review paper of Adcock (1997) which presents key techniques on frequentist approach and several Bayesian methods.

Information-theoretic principles are commonly, used in the test literature for different purposes such as testing normality, homogeneity of variances for several populations. Unfortunately, there is not enough study about the sample size determination related with entropy based statistic. In this study, we goal to obtain appropriate sample size which depends upon the information-based test (IT) and show the superiority of this approach over the likelihood ratio test by a simulation study and real data set.

Materials and methods

Likelihood ratio test and information-based test

Likelihood ratio test

Let X_1, X_2, \dots, X_n be a random sample of n observations from a population with probability density function (pdf) $f(x|\theta)$. Let null hypothesis (H_0) specify that $\theta \in \omega_0$, where ω_0 is the subset of the set of all possible values of θ and the alternative hypothesis H_a specify that $\theta \in \omega_1$, where ω_1 is disjoint from ω_0 and parameter space $\Omega = \{\omega_0 \cup \omega_1\}$.

Assume that hypothesis are composite, each likelihood value is evaluated at that value of θ that maximizes it, yielding the generalized likelihood ratio test statistic (Eq. 1):

$$\Lambda = \frac{\sup_{\theta \in \omega_0} [L(\theta)]}{\sup_{\theta \in \Omega} [L(\theta)]}, \quad (\text{Eq.1})$$

where $L(\theta)$ denote the likelihood function of the probability distribution.

The ratio of this two maxima is small if there are parameter points in the alternative hypothesis is more likely than for any parameter point in the null hypothesis. In this case null hypothesis should be rejected and alternative hypothesis accepted as true.

Information-based test

Shannon's entropy associated with a probability density function f with respect to sigma finite measure (ν) is defined by (Eq. 2)

$$H(f) = - \int_{\mathcal{X}} f(x) \log f(x) d\nu(x) \quad (\text{Eq.2})$$

where $\chi = \{x : f(x) > 0\}$ is the support set for f . Entropy is used as an index of diversity in a population.

In the case when $f(x) = \frac{1}{\sqrt{2\pi\sigma^2}} \exp\left(-\frac{(x-\mu)^2}{2\sigma^2}\right)$ is the pdf associated with a normal distribution with mean μ and variance σ^2 , the entropy of the normal probability distribution is

$$H(N(\mu, \sigma^2)) = \log \sqrt{\sigma^2 2\pi e}. \quad (\text{Eq.3})$$

The entropy of normal distribution does not depend on the mean value, so the information-based statistic defined by Eq. 3 cannot be applied to a test concerned with the mean of the population. In the present study, we define the information-based statistic as the difference of the entropy of the distribution under the null hypothesis and alternative hypothesis (Eq. 4),

$$I = \log \sqrt{\sigma^2 2\pi e} - \log \sqrt{\hat{\sigma}^2 2\pi e}, \quad (\text{Eq.4})$$

where $\hat{\sigma}^2$ is maximum likelihood estimator of the variance of $N(\mu, \sigma^2)$.

According to central limit theorem information-based statistic I approaches 0 as the sample size increases. It should be noted that presented statistic can take both negative and positive values. This means that if this statistic takes values close to zero the null hypothesis will be accepted otherwise test will be rejected. However, it is not possible to find the asymptotic distribution of this test statistic. Bootstrap sampling method will be used in order to calculate the critical values of this distribution.

Results

Example 1: a simulation study with normal distribution

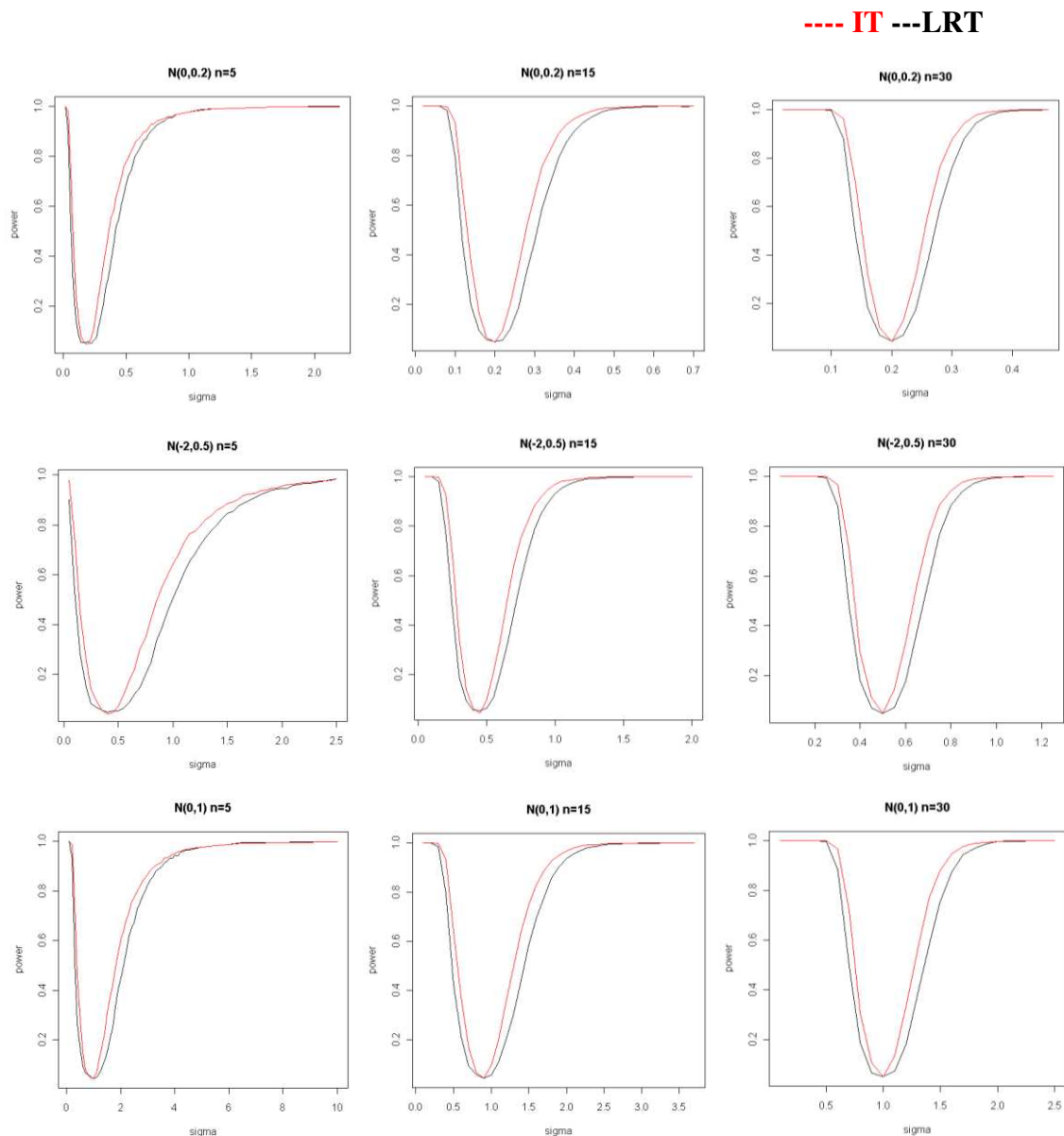
In this section, first we conduct Monte Carlo simulations to show the superiority of IT over the LRT test and after that we consider the sample size determination with respect to the power level, effect sizes and significance level. We generated 10,000 random sample of size $n \geq 5$ from several normal densities. Then the information based test values are ordered $I_{n,1}, I_{n,2}, \dots, I_{n,10000}$ and since $\alpha = 0.05$ is used, the required critical values for the two sided hypothesis are found as the 2500th and 7500th order statistics.

Since IT for the normal distribution depends only on the population standard deviation, we should state alternative hypothesis for the IT by considering effect size on standard deviation of the population. Suppose that we wish to test the hypothesis that the variance of a normal population σ^2 equals a specified value, say σ_0^2 . We state the null hypothesis $H_0 : \sigma^2 = \sigma_0^2$, and the alternative hypothesis $H_1 : \sigma^2 = \sigma_0^2 + \delta$, where δ denote the effect size. The effect size δ refers to the magnitude of the effect under the alternative hypothesis. The effect size should represent the smallest difference that would be of clinical or biological significance and is usually determined by the

scientific considerations, rather than statistical ones. Obtaining an effect size of scientific importance requires meaningful input from the researcher. For example, a treatment effect that reduces failure of a disease or a treatment by 1% might be clinically important, while a treatment effect that reduces asthma symptoms by 20% may be of little clinical interest.

Although we can obtain the asymptotic distribution of LRT for testing the standard deviation of a normal distribution, the distribution of the information based test under the normality cannot be found analytically. In particular, the likelihood ratio test statistic is assumed to follow a χ^2 with degrees of freedom equal to number of parameters that are tested. However, the critical values for IT with common significance level $\alpha = 0.05$ are calculated by the Monte Carlo method.

First, we obtained the power curves for the normal distributions with the sample sizes $n = 5, 15, 30$. These power curves are illustrated in *Figure 1*.



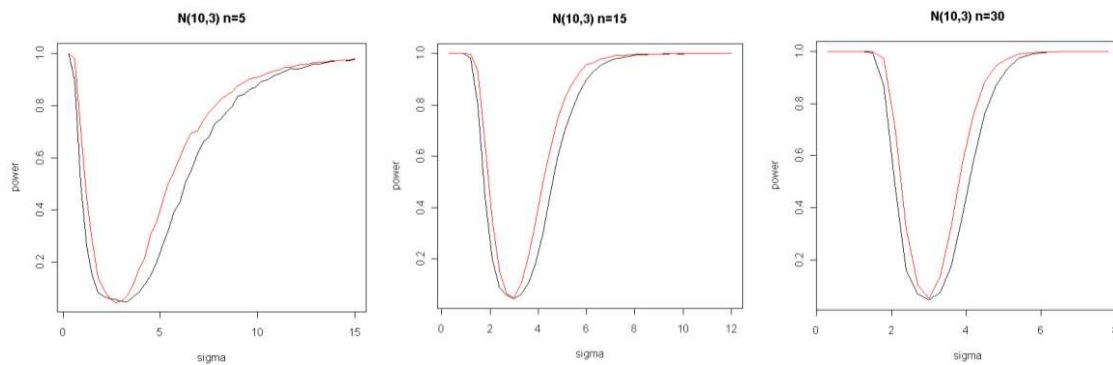
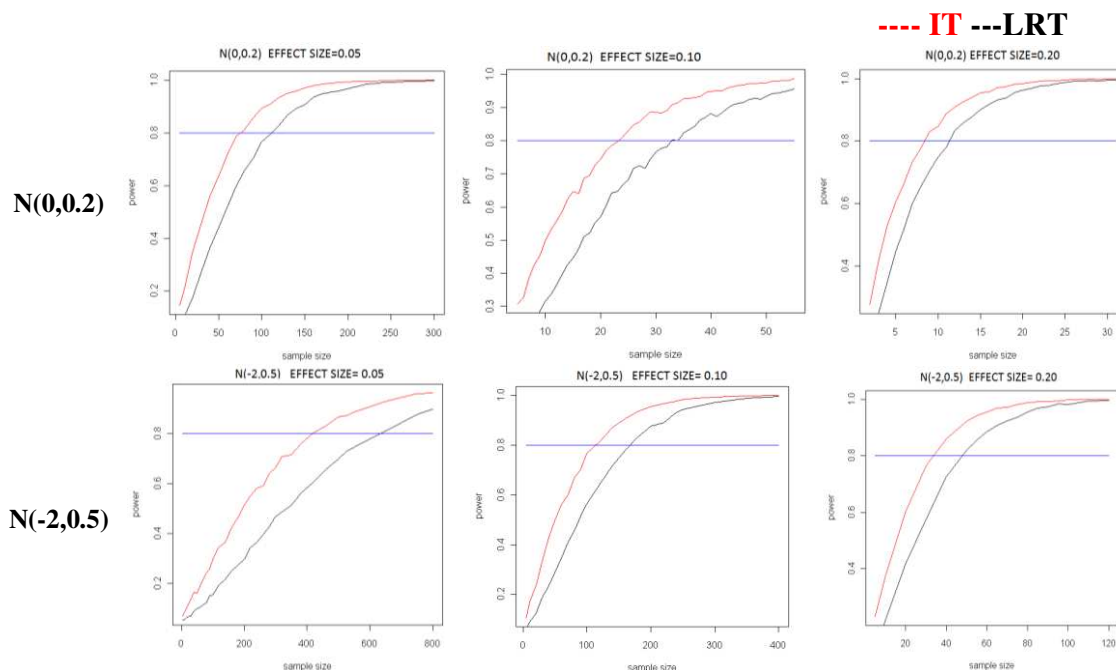


Figure 1. Power curves for the normal distributions with the sample sizes $n = 5, 15, 30$

We used these graphs to decide the appropriate effect size to obtain the required power for the design of the study. Since, it is common to choose the power between .80 and .98 in the literature, the domain of the power function corresponding to these points provide us an idea for the range of δ values. From this range, one may specify the δ values according to the ecological importance. For instance, for $N(0,1)$ with sample size 30, the δ interval that corresponds to power between .80 and .98 is [1.6-2.0]. This means that δ can be chosen from the interval [0.6-1.0] to attain the power between .80 and .98. Indeed, we take the effect size δ as 0.6, 0.7, 0.8 to demonstrate the change in the power with respect to sample size (Fig. 2).

In a similar way, we choose the effect size δ as 0.05, 0.10, 0.20 both for $N(0,0.2)$ and $N(-2,0.5)$ and as 2.6, 2.7, 2.8 for $N(10,3)$.

When we graphed the power versus sample size with different effect sizes, it can be seen that both IT and LRT curves are monotonically increasing function of the sample size. Figure 2 is also helpful for the researchers to decide the appropriate sample size for fixed power and effect size.



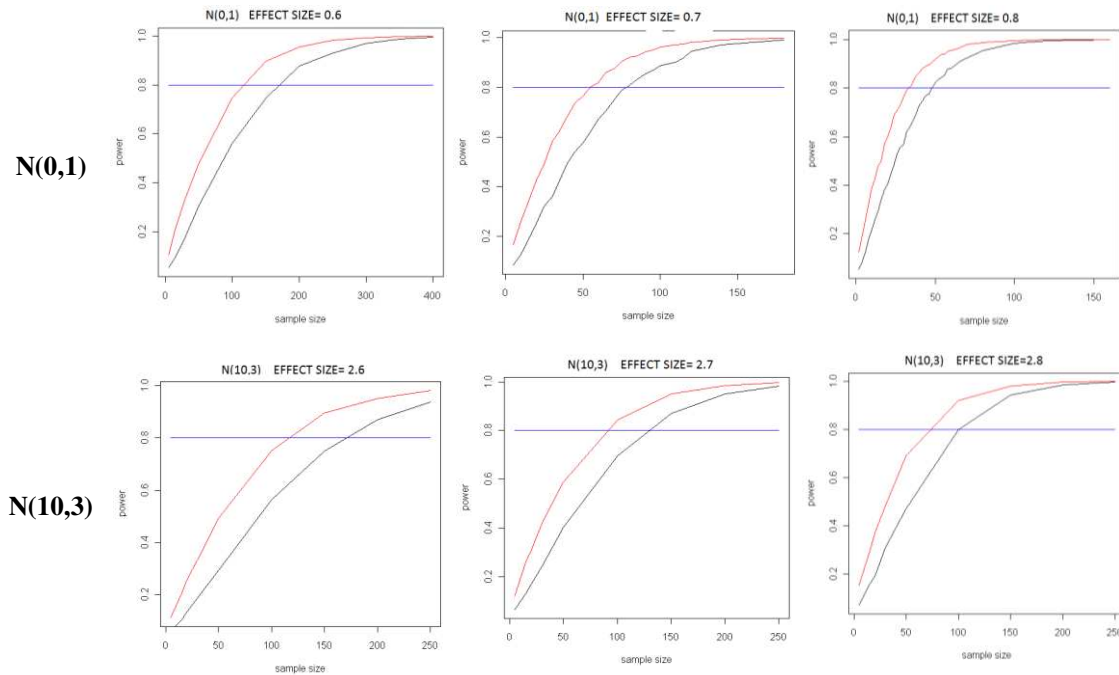


Figure 2. Power per sample of size n with different effect sizes for both IT and LRT curves

Figure 2 provides appropriate sample sizes for the data that are simulated from $N(0,0.2)$, $N(-2,0.5)$, $N(0,1)$ and $N(10,3)$ respectively. For example, for the $N(0,0.2)$ when the effect size is given 0.05, we attain 80% power for the LRT with sample size is around 100. On the other hand with same effect size, and sample size we obtain power around 90% for the IT test. However to attain 90% power with LRT test we need sample size around 150 by the likelihood ratio test.

When we increase the effect size to the 0.10, we attain 80% power for the LRT with the sample size is around 35. However, with the same effect size and same sample size we obtain power around 90% for the IT test. Clearly, for small effect sizes we need larger sample sizes to obtain the same power.

Example 2: a study with real data by Rayleigh distribution

The deep water buoy (15.5°N, 69.25°E) recorded daily significant wave height data off Goa by The National Institute of Ocean Technology, Chennai, India have also been considered for this work for a one year period January 1 to December 31, 2000.

The data consist of 2517 data points recorded in different times of a day per a year. For our analysis, since we have large data set, we assume that this data is the real population and can be modeled by using Rayleigh distribution. The distribution of significant wave height data off Goa has mean 1.5958, standard deviation is 0.9769 and the maximum likelihood estimation for the parameter of Rayleigh distribution is 1.3229. So, the following two-sided hypothesis can be constructed:

$$H_0 : \sigma = 1.3229$$

$$H_1 : \sigma \neq 1.3229$$

Then, 50 observations were randomly selected to get a random sample for the calculations. The sample arises with mean 1.4126 and standard deviation 0.8129. The maximum likelihood estimation of the Rayleigh parameter for the sample data was calculated as $\hat{\sigma}=1.1496$. LRT and IT test statistics are found as 3.6021 and 0.14048, respectively. Hence, the null hypothesis that claims the data comes from the Rayleigh distribution with parameter $\sigma = 1.3229$ accepted.

Our empirical results in Example 2 shows that test accepts the null hypothesis, as it is expected. However, for the same experiment run 100000 times the IT provides higher power than the LRT, as demonstrated by the simulation results in *Figure 3* (Sezer and Asma, 2010).

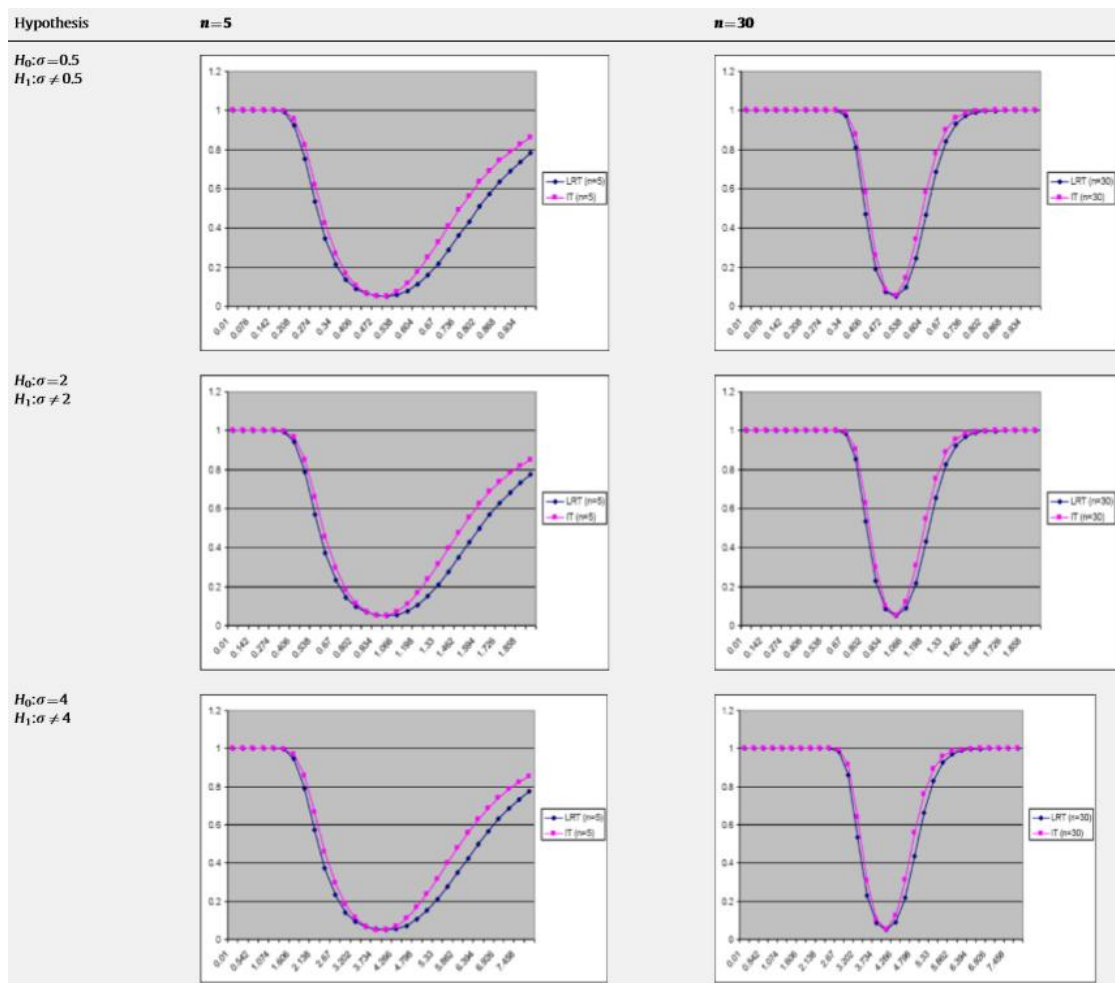


Figure 3. Power functions for $H_0 : \sigma = \sigma_0; H_1 : \sigma \neq \sigma_0$

Discussion

In this study, we focused on finding appropriate sample size for testing the variance of the normal distribution and Rayleigh distribution. The power curves are obtained both for the IT and the LRT by the Monte Carlo simulations. When we graphed the power versus sample size with different effect sizes, it can be seen that both IT and LRT curves are monotonically increasing function of the sample size. Based on the power curves, an algorithm is stated to specify an interval for the possible values of the effect

size. In order to determine sample size with the LRT and the IT, we should have the following steps:

1. Specify the null hypothesis and the alternative hypothesis.
2. Specify the significance level α .
3. Obtain the power curves for given sample size and significance level.
4. Determine the range of the appropriate effect size based upon the power curves.
5. Specify the target value of the power of the test.
6. Finally, obtain the sample size for the fixed power value.

Conclusion

As conclusion, IT gives more powerful results than LRT with the same sample size. Simulation results indicate that IT outperforms over the LRT in regarding to get smaller sample to attain the same level of the power. Wave height data is used to introduce show the inference procedure works both for the likelihood test and information-based test. In agreement with the theoretical results of Janssen (2014) it is found that wave height obeys the Rayleigh distribution.

Clearly, Rayleigh distribution can be used efficiently to calculate the associated probabilities in marine climatology. We suggest to use IT test to determine appropriate sample size at the beginning of the study. Our simulation studies will be expanded with different skewed distributions belong to other exponential family members such as Log-Normal and three-parameter Weibull distributions.

REFERENCES

- [1] Adcock, C. J. (1997): Sample size determination: a review. – *The Statistician* 46: 261-283.
- [2] Burnham, K. P., Anderson, D. R. (2002): Fitting the negative binomial distribution to biological data. – *Biometrics* 9: 176-200.
- [3] Dziak, J. J., Lanza, S. T., Tan, X. (2014): Effect size, statistical power, and sample size requirements for the bootstrap likelihood ratio test in latent class analysis. – *Structural Equation Modeling: A Multidisciplinary Journal* 21(4): 534-552.
- [4] Esteban, M. D., Castellanos, M. E., Morales, D., Vajda, I. (2001): Monte Carlo comparison of four normality tests using different entropy estimates. – *Communication in Statistics-Simulation and Computation* 30: 761-785.
- [5] Gupta, A. K., Harrar, S. W., Pardo, L. (2007): On testing homogeneity of variances for nonnormal models using entropy. – *Statistical Methodology and Application* 16: 245-261.
- [6] Janssen, P. A. E. M. (2014): On a random time series analysis valid for arbitrary spectral shape. – *Journal of Fluid Mechanics* 759: 236-256.
- [7] Kass, R. E., Caffo, B. S., Davidian, M., Meng, X. L., Yu, B., Reid, N. (2016): Ten simple rules for effective statistical practice. – *PLOS Computational Biology* 12: p.e. 1004961.
- [8] Kramer, M., Font, E. (2017): Reducing sample size in experiments with animals: historical controls and related strategies. – *Biological Reviews* 92(1): 431-445.
- [9] Lehmann, E. L. (2006): On Likelihood Ratio Tests. – In: Rojo, J., Pérez-Abreu, V. (eds.) *The Second Erich L. Lehmann Symposium Optimality. IMS Lecture Notes-Monograph Series. Vol. 49*, pp. 1-8. IMS, Beachwood, OH.
- [10] Lenth, R. V. (2001): Some practical guidelines for effective sample size determination. – *The American Statistician* 55: 187-193.

- [11] Low-Decarie, E., Chivers, C., Granados, M. (2014): Rising complexity and falling explanatory power in ecology. – *Frontiers in Ecology and the Environment* 12: 412-418.
- [12] Lynch, T. B. (2017): Optimal sample size and plot size or point sampling factor based on cost-plus-loss using the Fairfield Smith relationship for plot size. – *Forestry* 90(5): 697-709.
- [13] Martins, P. D., Poletto, C. (2018): Entropy for determination of suspended sediment concentration: parameter related to granulometry. – *Journal of Environmental Engineering* 144(3): 04017111-04017111-7.
- [14] Men'endez, J. A., Rueda, C., Salvador, B. (1992): Dominance of likelihood ratio tests under cone constraints. – *American Statistician* 20: 2087-2099.
- [15] Perlman, M. D., Wu, L. (1999): The Emperor's new tests (with discussion). – *Statistical Science* 14: 355-381.
- [16] Richards, S. A. (2005): Testing ecological theory using the information-theoretic approach: examples and cautionary results. – *Ecology* 86: 2805-2814.
- [17] Roach, T. N. F., Nulton, J., Sibani, P., Rohwer, F., Salamon, P. (2017): Entropy in the tangled nature model of evolution. – *Entropy* 19(5): 192.
- [18] Schepsmeier, U. (2015): Efficient information based goodness-of-fit tests for vine copula models with fixed margins: A comprehensive review. – *Journal of Multivariate Analysis* 138: 34-52.
- [19] Self, S., Mauritsen, R. (1988): Power/sample size calculations for generalized linear models. – *Biometrics* 44: 79-86.
- [20] Self, S., Mauritsen, R., Ohara, J. (1992): Power calculations for likelihood ratio tests in generalized linear models. – *Biometrics* 48: 31-39.
- [21] Sezer, A., Asma, S. (2010): Statistical power of an information-based test and its application to wave height data. – *Computers and Geosciences* 36: 1316-1324.
- [22] Shieh, G. (2000): On power and sample size calculations for likelihood ratio tests in generalized linear models. – *Biometrics* 56: 1192-1196.
- [23] Vranken, I., Baudry, J., Aubinet, M., Visser, M., Bogaert, J. (2015): A review on the use of entropy in landscape ecology: heterogeneity, unpredictability, scale dependence and their links with thermodynamics. – *Landscape Ecology* 30(1): 51-65.
- [24] Wood, S. N., Goude, Y., Shaw, S. (2015): Generalized additive models for large data sets. – *Journal of the Royal Statistical Society: Series C (Applied Statistics)* 64: 139-155.
- [25] Zuur, A. F., Ieno, E. N. (2016): A protocol for conducting and presenting results of regression type analyses. – *Methods in Ecology and Evolution* 7: 636-645.

INFLUENCE OF EXTERNAL RESISTANCE AND ANODIC pH ON POWER DENSITY IN MICROBIAL FUEL CELL OPERATED WITH *B. SUBTILIS* BSC-2 STRAIN

CÓRDOVA-BAUTISTA, Y.¹ – PARAGUAY-DELGADO, F.² – PÉREZ HERNÁNDEZ, B.³ – PÉREZ HERNÁNDEZ, G.¹ – MARTÍNEZ PEREYRA, G.¹ – RAMÍREZ MORALES E.^{*1}

¹Universidad Juárez Autónoma de Tabasco, Avenida Universidad S/N, Zona de la Cultura, Col. Magisterial, Centro, Villahermosa, Tabasco 86040, México
(e-mail: Yolanda.cordova@ujat.mx, cordovab@hotmail.com)

²Centro de Investigación en Materiales Avanzados, Miguel de Cervantes 120, Chihuahua, Chihuahua 31136, México

³Laboratorio de pre-secuenciación del Instituto de Ecología A. C., El Haya, CP 91070 Xalapa, Veracruz, México

*Corresponding author
e-mail: erik.ramirez@ujat.mx, eriking10@hotmail.com

(Received 25th Nov 2017; accepted 19th Mar 2018)

Abstract. Microbial fuel cells (MFCs) are bioelectrochemical devices able to convert chemical energy into electricity. The selection of anodic pH and external resistances play a significant role in the overall performance of the device. This research presents the effect of operational conditions of the MFC using *B. Subtilis* in anode. The effect of pH and external resistance were determined by 3² full factorial design. Data were analyzed statistically by ANOVA and $p \leq 0.05$ was considered statistically significant. The surface response analysis evidenced interaction and quadratic effect of the pH and external resistance on the power density generation. With a second-order polynomial model the optimum conditions of the system were determined. It maximized the power at pH of 8.6 and an external resistance of 220 Ω , delivering power density of 405 mW/m². The chemical oxygen demand (COD) removal efficiency and coulombic efficiency (CE) were 82% and 15%, respectively. The maximum specific growth (μ) and substrate uptake (k_1) rate for electrochemically active bacteria (EAB) at optimum conditions were 0.19/h and 0.019/h respectively. These experimental results show the importance of the simultaneous effect of pH and external resistance, which is even more influential than if they were studied separately.

Keywords: bioenergy, electrochemically active bacteria, 3² full factorial design, bioelectrochemical system, kinetics modelling

Introduction

The amount of research about renewable energy is increasing, due to the inadequate supply of fossil fuels and their negative effects on environment and the economy. One promising technology is MFC. It can be used to produce bioelectricity, hydrogen or to remediate contaminants. A typical MFC device has two chambers which are anode and cathode, both are separated by a proton exchange membrane (PEM) (Logan, 2008). MFC is considered sustainable for bioenergy generation, because it produces electricity from organic waste through the direct oxidation of EAB. They grow in the anode chamber where the organic matter is oxidized to produce electrons and protons, with CO₂ and biomass as final products. Electron transport to the anode is either direct, through physical contact of the microbes via cytochromes or nanowire structure, or indirect, via a soluble redox active mediator (Roy et al., 2014). To date, many EABs have been reported in MFC researches, including *Shewanella* (Ringeisen et al., 2006),

Pseudomonas (Jayapriya and Ramamurthy, 2012), *Escherichia* (Zhang et al., 2006), *Enterobacter* (Nimje et al., 2011), *Klebsiella* (Zhang et al., 2008), *Citrobacter* (Huang et al., 2015), *Desulfuromonas* (Holmes et al., 2004), *Geobacter* (Nevin et al., 2008), *Rhodospirillum rubrum* (Chaudhuri and Lovley, 2003), *Clostridium* (Park et al., 2001), *Bacillus* (Wu et al., 2014), *Tolomonas* (Lou et al., 2013), *Corynebacterium* (Liu et al., 2010) and *Kocuria* (Luo et al., 2015).

EAB plays a crucial role on the performance of MFCs. Therefore, it is important to know the EABs growth behaviour under different environmental conditions. Modelling of bacterial growth kinetics describe the behaviour of microorganism. Currently, both models Monod and Gompertz correspond to a universal model. However, the Monod model is fitted with a poorer correlation. The Gompertz model has been widely applied to describe the asymmetrical sigmoid shape of microbial growth, due to being statistically accurate and easy-to-use, when compared to other sigmoidal functions (Gil et al., 2011). The models used to describe growth may or may not be coupled with substrate uptake. The Monod model has a wide range of applications in nutrient removal kinetic for batch cultures. Although Monod kinetic in substrate uptake has been successfully applied, some research shows that this model to anaerobic processes is rather difficult. In this study complex structure models were avoided. Thus, the first order model proposed by Sarioglu and Gökçek (2016) was used.

On the other hand, the selection of suitable anodic pH could be crucial for the EAB grown and it affects the efficient proton motion through the PEM. In addition, the external resistance in MFC regulates the anode potential, enabling to the EAB the balance of the electrode reduction kinetics with the potential energy to gain available growth of the EAB (Nimje et al., 2011; González et al., 2014). To Understand the influence factors that improve the performance of MFCs mathematical modelling can be applied. The Models of MFCs are classified into two main groups, namely Mechanism-based models and Application-based models. The Mechanism-based models are based on different bioelectrochemical reactions in an MFC. Those include bulk liquid models, electrochemical models, biofilm models and special models. Although the complexity limits the practical application of these models. The Application-based models are divided into the Electrical model and the Learning and controlling model (Xia et al., 2018). The Learning and controlling aspects are mainly used to optimize the output power, which contributes to improve the development of MFCs application. These models need an experimental design approach (Martínez-Conesa et al., 2017). Then, it is necessary to study factors such as anodic pH and external resistance which maximize power output of the MFC using *B. subtilis* BSC-2 strain as EAB.

In the present research the influence of two independent variables were evaluated: anodic pH and external resistance on power density (dependent variable). Further, it was aimed to optimize independent variable using surface response methodology (RSM) to achieve adequate response of MFC. For this purpose, data were collected by mathematical and statistical techniques to build the empirical model. These values could be used to analyse the interaction of different factors on dependent variables (Jia et al., 2014; Madani et al., 2015; Myers et al., 2016).

The growth and substrate uptake kinetic parameters of *B. subtilis* were evaluated under optimal conditions, finding optimized values which could be used for future design and simulations of MFCs.

Materials and methods

Bacterial strain

The bacterial strain was isolated from the wastewater collected from a sugar factory, located in R/a Santa Rosalía Cárdenas, Tabasco, Mexico (18°05'46.5"N and 93°21'45.9"W). The wastewater samples were taken from 10 randomly selected points. For each selected point 1 L of the sample was collected in autoclaved glass bottle. Subsequently the samples were transported inside a cooler to the biotechnology laboratory, where they were kept at 4°C before use (APHA, 2012). Then ten mL of each sample were inoculated in Erlenmeyer flasks containing 90 mL of sterile distilled water. For counting viable bacteria, this suspension was serially diluted in triplicate and 0.1 mL of suspension was spread on nutrient agar plates by spread plate method (Madigan et al., 2012). The plates were incubated at 28 °C for 72 h. The bacterial isolates were then characterized at colony level (Kumar, 2015).

Bacterial strain identification

The Gram reaction was determined using violet crystal and safranin, afterwards the stained cells were observed by optical microscope (VE-BC1, VELAB Microscopes Inc). The morphology of each bacterial strain was observed through micrographs that were taken by scanning electron microscope JEOL JSM-6010LA (Hitachi, Tokyo, Japan) according to Holmes et al. (2004). The KIT API 20 E and 50 CH (BioMérieux) were used for the biochemical and physiological characterization of the strains according to the manufacturer's instructions.

Genomic DNA from each strain was isolated using the ZR Fungal / Bacterial DNA Miniprep extraction kit (D605). The V3-V5 region of the 16S rRNA gene was amplified using the primers 16sV3-V5F-TACGGRAGGCAGCAG- and 16sV3-V5R-CCGTCAATTCMTTGTGAGTTT. Each PCR reaction contained 200 uM DNTPs (Deoxyribonucleotide triphosphates), 0.2 uM of each 1 u Mytaq Pol enzyme primer (Bioline). The amplification was carried out on the Thermocycler C1000 Touch Thermal Cycler (BIORAD) using the following PCR conditions: 94 °C 3 min 1 cycle, 35 cycles of 94 °C 30 s, 55 °C 30 s and 72 °C 60 s. A final extension of 72 °C for 5 min. The PCR product was checked on a 1.5% agarose gel (sigma A9539) stained with Midori Green Advanced (Nippon Europe Genetics) and visualized by UV light. PCR products were purified using the Wizard SV Gel and PCR Clean-Up System kit (Promega). Sequencing of PCR products was performed by Macrogen Inc. in Seoul, South Korea using an automated sequencer ABI3730 XL (Applied Biosystem). The sequence (raw sequence) was analyzed in the program sequencer version 5.4. (GeneCodes). The sequences were compared to the available sequences in the nucleotide database of the National Center for Biotechnology Information (NCBI) using the local search tool (BLASTn).

Inoculum preparation

Under axenic conditions the BSC-2 isolate microbial was extracted from the agar plate with bacteriological handle, then it was placed in the Erlenmeyer flask with nutrient broth containing 8 g of meat extract per liter of water. Fermentation was maintained for two days at 37 °C. Subsequently the cell biomass was separated from the broth by centrifugation at 5000 rpm for 20 min. Then they were washed three times

with buffer solution (sodium phosphate buffer 50 mM at pH 7.0). Finally, the washed biomass was suspended in 10 mL of buffer solution (Luo et al., 2015). After, the suspension was used as inoculum to the MFC experiment.

MFC construction and operation

By triplicate, a modified double-chamber MFC was constructed from Logan method (Logan, 2008; *Fig. 1*), it was made using polypropylene (PP5) bottles with an approximate working volume of 700 mL. Both chambers were attached by a chlorinated polyvinyl chloride (CPVC) bridge connected to a union nut of the same material, which contained a 2 cm diameter nafion 117 proton exchange membrane (Fuel Cell inc., USA). To prevent leakage in both chambers, CPVC nuts were used with rubber packing of 1.3 cm in diameter. The anode was carbon felt with 8 cm diameter and 1 cm thickness. The cathode was 5 x 5 cm² (40% Pt, 0.3 mg cm², Fuel Cell Inc., USA). Before use, electrodes were treated to remove impurities as follows: the anode was immersed in 1 mol/L HCl solution for 24 h and then in 1 mol/L NaOH solution for 3 h at the end it was rinsed with distilled water for several times (Liu et al., 2010). The cathode was immersed previously in acetone for 24 h and then in distilled water by overnight (Madani et al., 2015). These two electrodes were firmly connected into an external unit by thin copper-aluminium alloy wire (0.6 mm diameter). The surface exposure of the wire was isolated with epoxy resin to prevent corrosion.

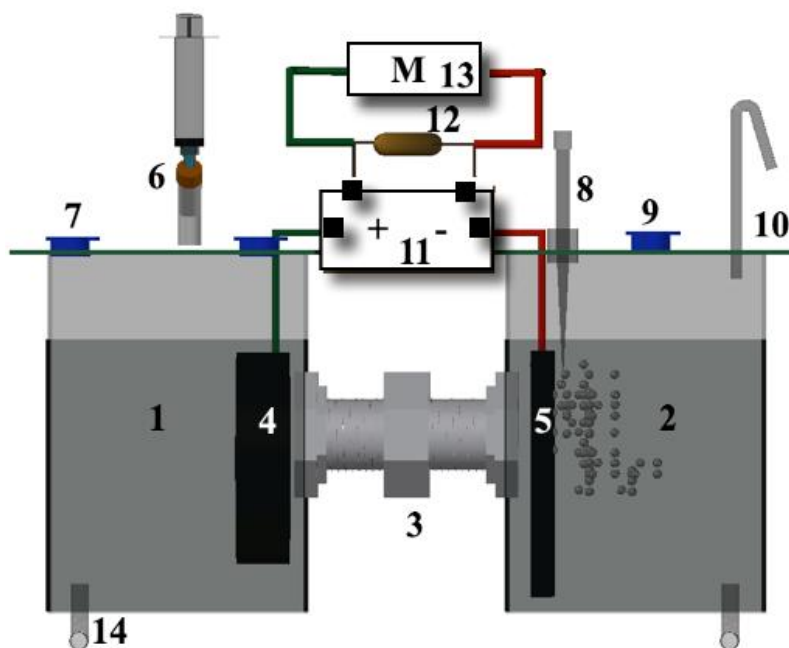


Figure 1. Schematic representation of the double chamber MFC. 1) Anodic chamber; 2) Cathodic chamber; 3) Proton exchange membrane (PEM); 4) Anode electrode; 5) Cathode electrode; 6) sample taking; 7) Influent; 8) Air inlet; 9) Buffer influent; 10) Atmospheric vent; 11) Blinker board; 12) external resistance; 13) Digital multimeter; 14) Effluent.

The anode chamber was completely sealed by gaskets to create a completely anaerobic condition. The fuel used for this chamber was synthetic sugar wastewater (Pradeed et al., 2014). The anode chamber was filled with 600 mL of synthetic sugar

wastewater, 100 mL of 52 mM phosphate buffer solution (K_2HPO_4 , 5.4 g/L and KH_2PO_4 , 2.6 g/L; pH 7) (Madani et al., 2015) and 10 mL liquid microbial inoculum. Bacterial concentration in the anolyte of anode chamber was determined by measuring its optical density at 660 nm (OD_{660}) with the GENESYS 20 model spectrophotometer (Thermo Electron corp., USA). The initial OD_{660} of the anolyte was 0.006 (37×10^3 UFC/mL). Permanently it was maintained under anaerobic conditions. The cathode chamber was aerobic and it contained phosphate buffered at 82 mM (K_2HPO_4 , 8.8 g/L and KH_2PO_4 , 4.3 g/L; pH 7) (Madani et al., 2015) and it was aired continuously by an aquarium pump. The MFC was operated in a batch mode at room temperature (25 °C).

Experimental design

The present study used a three-level factor full factorial design for optimization and to find the adequate pH and external resistance values. Response surface graphics were used to study the factor interaction between the variables. The independent variables were the anodic pH (X_1) and the external resistances (X_2). Three factorial levels were coded for low, medium and high settings (-1, 0 and +1 respectively) for two independent variables. A total of 9 experimental runs were required for analysing the interaction of each level on response variable (Table 1). The selected response investigated variable was the power density (Y) and it was analysed by multiple factorial regression analysis using the following quadratic model (Eq. 1):

$$Y_i = b_1X_1 + b_2X_2 + b_{12}X_1X_2 + b_{11}X_1^2 + b_{22}X_2^2 \quad (\text{Eq.1})$$

Where Y_i stands for the responses; b_0 is the arithmetic mean response of all trials; and b_1 is the estimated coefficient for factor X_1 . The main effects, X_1 and X_2 , represent the average value of changing factor one at a time; X_1X_2 represent the interaction terms and the polynomial terms X_{21} and X_{22} are used to assess nonlinearity. The statistical experimental design was analysed by using the software MINITAB® Release 14.12.0.

Table 1. Variables and their levels for 3^2 full factorial design

Independent variables		
Coded value	pH	Resistance (Ω)
Low (-1)	7	47
Medium (0)	8	100
High (+1)	9	220

Dependent variable: power density (mW/m^2)

Analytical measurement and calculation

Voltage was continuously measured by a multimeter (aplabvc97), the current intensity was determined using Ohm's law (Eq. 2) and power density was obtained according to Equation 3.

$$I = \frac{V}{R} \quad (\text{Eq.2})$$

$$Power\ density = \frac{V^2}{A \times R} \quad (Eq.3)$$

where, V is the potential (volts), I is the current intensity, A is electrode surface area (square meter), R is external resistance (Ω).

The concentration of the total sugar was determined by the phenol-sulfuric acid method using sucrose as the standard solution (Dubios et al., 1956). In the anode chamber, the COD (mg/L) were analysed by closed reflux colorimetric method as mentioned in Standard Methods (APHA, 1998). Liquid samples were centrifuged at 8000 rpm for 5 min and the supernatants were used for measurement. CE is defined as the fractional recovery of electrons from the substrate, it was calculated using Equation 4 (Logan et al., 2006):

$$CE = \frac{M \int_0^t I dt}{n \nu v x F (COD_0 - COD_t)} \times 100 \quad (Eq.4)$$

where M is the molecular weight of oxygen, I is the current, F is Faraday's constant (98,485 C/mol-e), n = 4 is the number of electrons exchanged per mole of oxygen, and ν is the anolyte volume, COD₀ is the influent COD, COD_t the effluent COD and t is time.

To monitor bacterial growth, samples were withdrawn aseptically at each 1 h interval and cell growth was monitored by OD₆₀₀. Which was converted to colony forming units (CFU) using a pre-established calibration curve (UFC/mL vs OD at 600 nm). The growth and substrate uptake rates were obtained by non-linear regression analysis, fitting Gompertz model (Eq. 5) and First order model (Eq. 7) to experimental data respectively (Okpokwasili and Nweke, 2005; Sarioglu and Gökçek, 2016).

$$\text{Log}N_{(t)} = A + C e^{-e^{-B(t-M)}} \quad (Eq.5)$$

where N(t) is the population density at time t [Log (CFU/mL)], A stands for the microbial counts when the time lowered indefinitely; it is equivalent to the initial bacteria level, C stands for the microbial counts when the time increased indefinitely, M is the time at which the exponential growth rate is maximal (h) and B is the relative growth rate at M time. The growth rate (μ) can be obtained using Equation 6:

$$\mu = (BxC)/e \quad (Eq.6)$$

The substrate uptake rate (k_1) that is the kinetic constant for substrate uptake, can be obtained from Equation 7:

$$S_t = S_0 e^{-k_1 t} \quad (Eq.7)$$

Results and discussion

Phenotypic and genotypic characteristics of isolates bacteria

Isolation of bacteria was carried out in nutrient agar culture medium, where macroscopic characterization at the colony level allowed to observe strains with circular and irregular shapes, whitish, round and wavy, flat and convex elevation. Cells were

Gram-positive and the micrographs show that the bacteria have an oval shape with 1.2 to 1.4 and 1.4 to 1.6 μm dimensions for BCC-1 and BSC-2 strain respectively (Fig. 2). Both BCC-1 and BSC-2 strain were positive for the catalase and nitrate reduction tests. The BSC-2 strain can ferment mannose, sorbitol, arabinose, rhamnose, ribose, glucose and sucrose. The BCC-1 strain can ferment ribose, glucose and sucrose, but it cannot ferment mannose, sorbitol arabinose and rhamnose (Table 2). Such characteristics indicate that they are genus *Bacillus* bacteria, moreover due to the difference in carbohydrates fermentation, it can be said that these are two species of *Bacillus*.

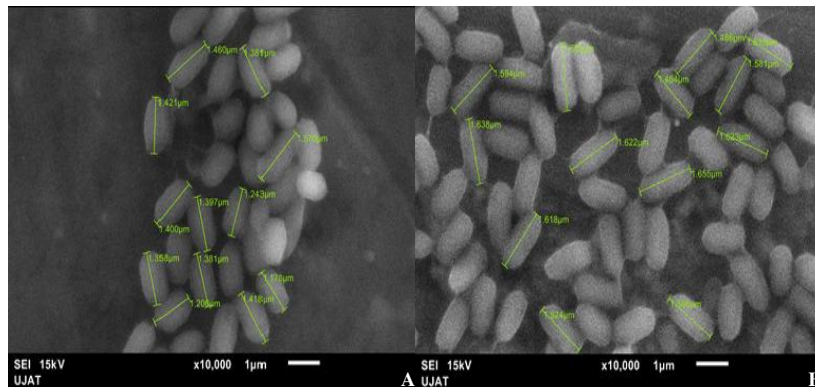


Figure 2. SEM micrographs for A) BCC-1 and B) BSC-2

Table 2. Phenotypic characteristics of bacterial strains

Characteristics	BCC-1 (<i>B. Cereus</i>)	BSC-2 (<i>B. Subtilis</i>)
Shape	Circular	Irregular
Colour	Whitish	Whitish
Edge	Round	Wavy
Elevation	Convex	Flat
Consistency	Viscose	Dry and Rough
Microscopic characteristics	1.2-1.4 μm	1.4-1.6 μm
Catalase	+	+
Oxidase	-	-
Nitrate	+	+
Mannose	-	+
Sorbitol	-	+
Arabinose	-	+
Rhamnose	-	+
Ribose	+	+
Glucose	+	+
Sucrose	+	+

After the BLAST search the sequence analysis of the 16S ribosomal gene confirmed that BCC-1 strain showed a 99% likeness with the *Bacillus cereus* sequence (KX170761.1) and BSC-2 strain a 99% similarity to *Bacillus subtilis* (GQ392049.1). Hence, BCC-1 and BSC-2 were designated as *B. cereus* and *B. Subtilis* respectively. However, because *B. cereus* is considered by the Food and Drug Administration (FDA) as a pathogenic organism (Tallent et al., 2012) its use in this work was ruled out. Thus, *B. subtilis* was selected only, since it is widely used in the food and pharmaceutical industry (Zhu et al., 2015). Additionally, the *B. subtilis* sequences were deposited on the Genebank under the accession number KY508314.

Optimization by factorial design

The factorial design was used to investigate the effect of pH and external resistance on power density. Table 3 shows the data obtained for the experimental trial and the values of power density were fitted in the design to get the model equations for the response variable.

Table 3. Full factorial design with their experimental coded level of independent variables observed response values

Batch no.	Levels of independent variables (factors)		Dependent variable (response)
	pH, X ₁	Resistance (Ω), X ₂	Power density (mW/m ²)
MFC ₁	-1	-1	059.42 ± 3.03 ^a
MFC ₂	-1	0	037.89 ± 1.09
MFC ₃	-1	1	121.39 ± 2.12
MFC ₄	0	-1	006.91 ± 0.77
MFC ₅	0	0	327.64 ± 58.85
MFC ₆	0	1	313.65 ± 19.00
MFC ₇	1	-1	002.70 ± 0.63
MFC ₈	1	0	002.21 ± 0.97
MFC ₉	1	1	416.10 ± 86.77

^aMean ± SD, n = 3. +1: higher values, 0: medium values, -1: lower values

The full model equation relating to the power density as response is:

$$\text{Power density (mW/m}^2\text{)} = 250.50 + 45.92 X_1 + 130.35 X_2 - 109.45 X_1^2 - 24.17 X_2^2 + 93.19 X_1 X_2 \quad (\text{Eq.7})$$

Statistical testing model was developed with the Fisher statistical test for ANOVA. Table 4 shows the values Prob>F of all regression model terms that were less than 0.05, which indicates, model terms are significant at a confidence interval of 95%. Also, the model F-value of 18.18 implies that the quadratic model is significant. The lack-of-fit test describes the variation of the fitted model. The model has non-significant lack-of-fit value (F-value = 4.87, p < 0.05), indicating a significant correlation between the factors and response (Myers et al., 2016).

Model simplification was carried out by eliminating non-significant terms (p > 0.05) in the above model equation (Eq. 7), now giving the following equation (Eq. 8):

$$\text{Power density (mW/m}^2\text{)} = 232.81 + 45.92 X_1 + 127.81 X_2 - 109.45 X_1^2 + 93.19 X_1 X_2 \quad (\text{Eq.8})$$

As the model was generated by taking only the significant terms from the full model, the results are deduced by interpreting the reduced model. *Table 5* shows the effect of factors and associated p values for power density, for both full model and reduced model.

The coefficients in the regression with more than one factor term represent an interaction term. A positive value represents a synergistic effect which favours optimization, while a negative sign indicates an antagonistic effect or inverse effect between the factors and the response (Sarabia and Ortiz, 2009). Thus, for the reduced model the regression equation (*Eq. 8*) and *Table 5* show that power density was significantly influenced by synergistic effect of pH, the resistance as well as interaction term X_1X_2 (pH x resistance) with p-value of 0.032, 0.000 and 0.001, respectively. While the quadratic term of pH has a negative effect on power density with p-value of 0.004. The results indicate that the increase in power density is the consequence of the strong interaction between the pH and the resistance. Furthermore, the pH values demonstrated a quadratic effect on power density which indicates that optimal levels of pH are inside of the experimental region.

Table 4. ANOVA results of quadratic model for power density

Source	df	Sum of squares	Mean square	F-value	P-value
Model	4	511072	127768	18.18	0.000 ^a
Linear	2	329622	173106	24.63	0.000
Square	1	71872	71872	10.22	0.004
Interaction	1	109578	109578	15.59	0.001
Residual Error	22	154646	7029		
Lack-of-Fit	4	131904	32976	4.87	0.056
Pure Error	5	22742	6763		
Total	26	665718			

^aSignificant terms at $p < 0.05$, R-Squared = 86% and Adj R-Squared = 84%

Table 5. The factor effects of full model and reduced model for power density

Factor	Full model			Reduced model		
	X coefficient	t	P-value	X coefficient	t	P-value
X_1	45.92	2.261	0.035 ^a	45.92	2.296	0.032
X_2	130.35	6.495	0.000 ^a	127.81	6.632	0.000
X_1X_2	93.19	3.888	0.001 ^a	93.19	3.948	0.001
X_1^2	-109.45	-3.148	0.005 ^a	-109.45	-3.198	0.004
X_2^2	-24.17	-0.573	0.573	-	-	-
Intercept	250.50	5.964	0.000 ^a	232.81	8.297	0.000

^aSignificant terms at $p < 0.05$

Response surface and contour plot

The MRS approach is a helpful tool for developing, improving and optimizing process as it allows elucidating the relationship between the dependent and independent variables (Sarabia and Ortiz, 2009; Myers et al., 2016). The response surface and

contour plot are very useful to illustrate and understand the main, interaction and quadratic effects on maximum power density. The response surface and contour graphs of the effects of pH and resistance that produced maxima power density is shown in *Figure 3A* and *3B*. It can be observed that the curvature introduced by quadratic term (pH) and that the power density presents a maximum value. *Figure 3A* also shows the tendency of the power density to increase as the resistance increases. The results presented a maximum value obtained for an intermediary value between pH 8 and pH 9 for the different resistances considered. However, the maximum value is observed between 150 and 220 Ω . It is clear that the pH value has strong effect on production power density because during microbial growth the enzymatic reaction that occurs in the microbial body has an optimum pH. Environmental changes in pH affect the active center of the enzyme and the state of ionization of substrate molecule and enzyme molecule, thus the combine of enzyme and substrate is affected. The higher or lower pH values will influence the stability of the enzyme that could be damaged irreversibly, which results in bacterial inactivation. In addition, the pH value also affects metabolism and absorption of nutrients through influencing the stability of membrane structure and solubility of nutrients, thus affecting the growth rate of microorganisms. Because any microorganisms should live in an appropriate pH value, microbial growth can be inhibited when the pH microenvironment is below or above of the appropriate pH value (Madigan et al., 2012). Furthermore, the selection of anodic pH value ensures the efficient movement of protons through PEM due to the driving force for the anode reaction increases with an increasing anolyte pH, this improves the diffusion of protons through membrane. The positive effects of alkaline pH in the power density using MFCs has been reported previously (Liu et al., 2010; Rago et al., 2016).

Moreover, the external resistance in the MFC directly influences the anode availability as an electron acceptor. In addition, it also exerts a selective pressure on the electrogenic bacterial community. Since a low external resistance (50 to 500 Ω) promotes growth and metabolic activity of the microorganisms then electron transport to the cathode is facilitated (Lyon et al., 2010). Zhang et al. (2011) mentioned that external resistance appropriate in MFC regulates the anode potential, enabling the electrogenic microorganisms to balance the reduction electrode kinetics with potential energy gain and thus reduces losses by activation. In this work, increasing the pH value from 7 to 9 with external resistance of 220 Ω the power density was enhanced nearly to 3.4 times (from 121.3 to 416.10 mW/m^2). These results revealed that the interaction effect between pH and resistance was remarkable, then the effect of pH on power density generation was highly depended on the level of the external resistance.

Figure 3B shows the contour plot, the contour areas represent constant responses, which correspond to power density from 0 to 400 mW/m^2 . It was determined from the contour that maximum power density higher to 400 mW/m^2 could be obtained with pH range between 8.5 and 8.8 with external resistance of 220 Ω . Hence, by equation (*Eq. 8*) the location of optimum was determined for pH of 8.6 and an external resistance of 220 Ω . The maximum value of power density at this point was estimated to be 405 mW/m^2 . In order to confirm the predicted results of the model, the experiment verification was made for three times under optimal conditions. The average of maximum power density was $402.55 \pm 2.63 \text{ mW/m}^2$ with small error-values of -0.6. This reveals that mathematical model obtained from the 3^2 factorial design was adequate. The optimized MFC was characterized by COD removal efficiency, coulombic efficiency, growth kinetics and substrate uptake of *B. subtilis*.

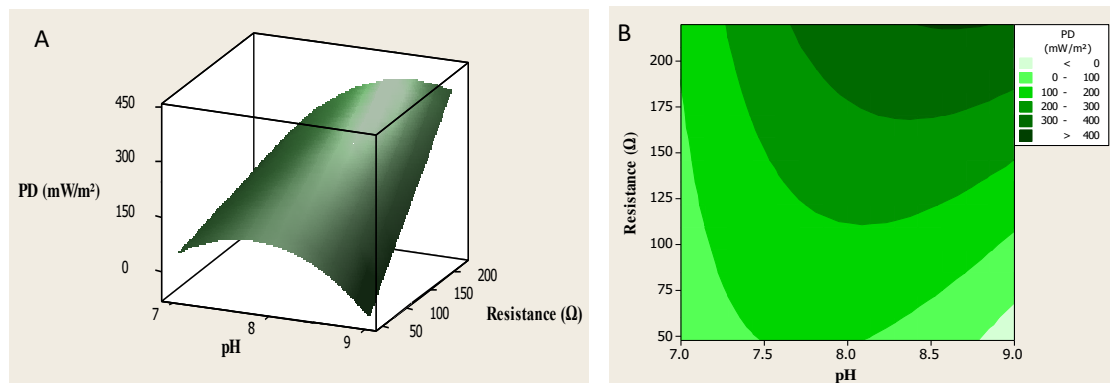


Figure 3. A: Response surface plot for power density. B: Contour plot for power density

COD removal and coulombic efficiency

In the MFC operated with anodic pH of 8.6 and resistance 220 Ω , the average COD of the synthetic wastewater effluent was 524.5 ± 10 mg/ L. Since the COD in the effluent was 3009 ± 32 mg/L, the COD removal efficiency was 82%. CE represents the conversion efficiency of organic compounds to an electric charge. In this research, the average CE was $15 \pm 1.26\%$ indicating that 15% of the available electrons in the removed substrate were used for current production. These operating conditions might be responsible for the substrate degradation by *B. subtilis* due to its growth and metabolism, which results in high COD removal efficiency. However, the low efficiency coulombic might be because of the metabolite production in the anodic chamber or also low electron transfer efficacy due to such limitations associated with electrodes as the difficulty of accessibility of electrons to anode or cathode as a deposition of interfering or insulating substances on electrodes. Similar results were obtained for *L. sphaericus*, it produced a coulombic efficiency of 12.69% in a double chamber MFC using lactate as substrate and with proteinaceous substrate the COD removal was about 74% (Nandy et al., 2013; He et al., 2014). In that regard in a MFC with *E. cloacae* to pH 8.5 in anodic chamber 65% of the COD was removed and the coulombic efficiency was 3%. Therefore, *B. subtilis* BSC-2 used in MFC is effective at COD removal as well as in current production.

Determination of μ and k_I for *B. subtilis* in optimized MFC

The kinetic parameters μ and k_I was determined by curve-fitting of date with Gompertz and First order model, respectively. The Figure 4A shows that observed date gave a reasonably good fit to the *B. subtilis* kinetic growth described by Equation 5. In addition, the high determination coefficient ($R^2 = 0.98$) value shows the ability of this model in describing the *B. subtilis* growth kinetics. The growth rate of *B. subtilis* obtained in MFC operated with anodic pH of 8.6 and resistance of 220 was 0.19/h. Figure 4B shows the sucrose consumption and the fitted model by Equation 7. The coefficient of determination $R^2 = 0.97$ shows that the model had an excellent fit to the experimental results, obtaining $k_I = 0.019$ /h. Miroliaei et al. (2015) investigated the kinetics of pure cultures of *E. coli* and *Shewanella sp.* in an air cathode MFC, the kinetics parameters were predicted using Monod and Moser models. To *E. coli* the determination coefficient R^2 was found to be 0.92 for Moser model and 0.94 for Monod model. To *Shewanella sp.* the determination coefficient R^2 was 0.90 and 0.94 for Moser

and Monod models, respectively. To *E. coli* the maximum specific growth rate with Monod model was 0.42/h. And to *Shewanella sp.* the maximum specific growth rate with Monod model was 1.54/h. Zhang et al. (2013) studied the nitrate degradation in anodic denitrification microbial fuel cell (AD-MFC). This study was supported by four degradation kinetics models, i. e. Haldane ($R^2 = 0.79$), Edwards ($R^2 = 0.83$), Luong ($R^2 = 0.97$) and Hand-Levenspiel ($R^2 = 0.99$). Hand-Levenspiel model was selected as the best model. Therefore, the selecting of suitable model in the modelling of bacterial growth and substrate uptake may depend on the kind of microorganism, anolyte characteristics and operating conditions etc. (Okpokwasili and Nweke, 2005; Sarioglu and Gökçek, 2016).

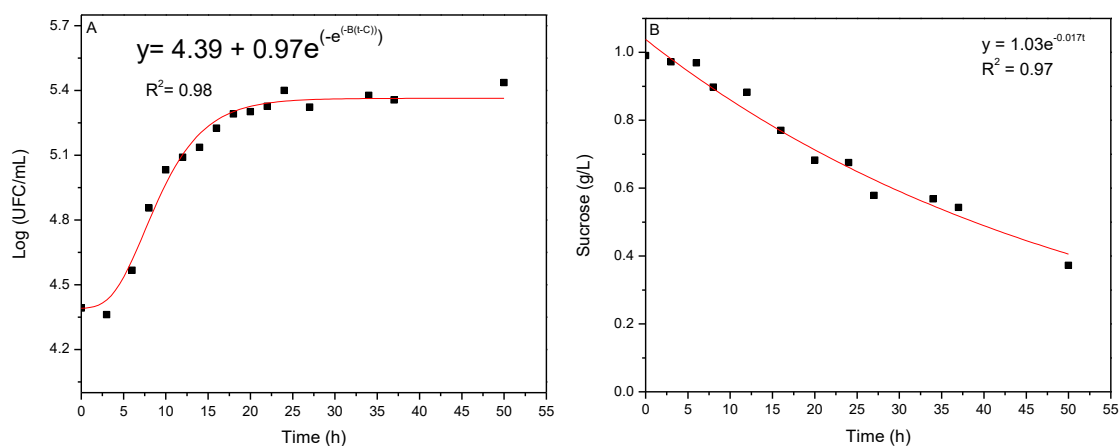


Figure 4. A: *B. subtilis* growth value and the fitted model by Equation 5. B: Sucrose concentration value and fitted model by Equation 7

Conclusion

This study examines the effects of the pH and the external resistance on the performance of dual chambered MFC in maximizing the power density. Using 3^2 full factorial design, the effects of independent variables were studied and optimized. Checking the validity of the model, the statistical indicator p-value was determined to be statistically adequate. Based on MSR a quadratic polynomial equation was developed. It is noteworthy that, in this research the maximum power density (405 mW/m^2) of the MFC was significantly influenced by the pH and the external resistance and the optimal conditions were selected: anodic pH of 8.6 and external resistance of 220Ω . The model terms for power density are significant to predict the power density based upon the pH and the external resistance. Furthermore, electrochemically active *B. subtilis* BSC-2 strain has the ability to remove the 82% of the COD synthetic sugar wastewater and produce clean energy. The Gompertz and First order kinetic models gave high determination coefficient, for growth and substrate uptake, respectively. More MFC models are expected to be developed in the future due to their great advantages for optimization, especially for the practical application of MFC technology for simultaneous production of energy and water treatment.

REFERENCES

- [1] APHA (1998): Standard Methods for the Examination of Water and Wastewater, 20th ed. – American Public Health Association/American Water Works Association/Water Environment Federation, Washington DC.
- [2] APHA/AWWA/WEF (2012): 9060 Samples. Standard Methods for the Examination of Water and Wastewater. 22nd edition. – American Public Health Association, American Water Works Association, Water Environment Federation, Washington, DC.
- [3] Chaudhuri, S. K., Lovley, D. R. (2003): Electricity generation by direct oxidation of glucose in mediatorless microbial fuel cells. – Nat. Biotechnol. 21: 1229-1232.
- [4] Dubios, M., Gilles, K. A., Hamilton, J. K., Rebers, P. A., Smith, F. (1956): Colorimetric method for determination of sugars and related substances. – Anal. Chem. 28: 350-356.
- [5] Gil, M. M., Miller, F. A., Brandão, T. R. S., Silva, C. L. M. (2011): On the use of the Gompertz model to predict microbial thermal inactivation under isothermal and non-isothermal conditions. – Food Eng. Rev. 3: 17-25.
- [6] González, C. A. del, Cañizares, P., Lobato, J., Rodrigo, M., Fernández, M. F. J. (2014): Effects of External Resistance on Microbial Fuel Cell's Performance. – Lefebvre, G., Jiménez, E., Cabañas, B. (eds.), Environment, Energy and Climate Change II, pp. 175-196. Springer International Publisher, Switzerland.
- [7] He, H., Yuan, S. J., Tong, Z. H., Huang, Y. X., Lin, Z. Q., Yu, H. Q. (2014): Characterization of a new electrochemically active bacterium, *Lysinibacillus sphaericus* D-8, isolated with a WO₃ nanocluster probe. – Process Biochem. 49: 290-294.
- [8] Holmes, D. E., Bond, D. R., Lovley, D. R. (2004): Electron transfer by *Desulfobulbus propionicus* to Fe(III) and Graphite electrodes. – Appl. Environ. Microbiol. 70(2): 1234-1237.
- [9] Huang, J., Zhu, N., Cao, Y., Peng, Y., Wu, P., Dong, W. (2015): Exoelectrogenic Bacterium phylogenetically Related to *Citrobacter freundii*, isolated from anodic biofilm of a microbial fuel cell. – Appl. Biochem. Biotechnol. 175: 1879-1891.
- [10] Jayapriya, J., Ramamurthy, V. (2012): Use of non-native phenazines to improve the performance of *Pseudomonas aeruginosa* MTCC 2474 catalysed fuel cells. – Bioresour. Technol. 124: 23-28.
- [11] Jia, Q., Wei, L., Han, H., Shen, J. (2014): Factors that influence the performance of two-chamber microbial fuel cell. – Int. J. of Hydrogen Energ. 39: 13687-13693.
- [12] Kumar, S. (2015): Textbook of Microbiology for Bsc Nursing. 1st ed. – Jaypee Brother Medical Publishers, New Delhi.
- [13] Liu, M., Yuan, Y., Zhang, X. L., Zhuang, L., Zhou, S. G., Ni, J. R. (2010): Bioelectricity generation by a Gram-positive *Corynebacterium sp.* strain MFC03 under alkaline condition in microbial fuel cells. – Bioresour. Technol. 101(6): 1807-1811.
- [14] Logan, B. E. (2008): Microbial Fuel Cells. – John Wiley & Sons Inc, New Jersey, USA.
- [15] Logan, B. E., Hamelers, B., Rozendal, R. A., Schrorder, U., Keller, J., Freguia, S., Aelterman, P., Verstraete, W., Rabaey, K. (2006): Microbial fuel cells: Methodology and technology. – Environ. Sci. Technol. 40: 5181-5192.
- [16] Luo, J., Yang, J., He, H., Jin, T., Zhou, L., Wang, M., Zhou, M. (2013): A new electrochemically active bacterium phylogenetically related to *Tolomonas osonensis* and power performance in MFCs. – Bioresour. Technol. 139: 141-148.
- [17] Luo, J., Li, M., Zhou, M., Hu, Y. (2015): Characterization of a novel strain phylogenetically related to *Kocuria rhizophila* and its chemical modification to improve performance of microbial fuel cells. – Biosens. Bioelectron. 69: 113-120.
- [18] Lyon, D. Y., Buret, F., Vogel, T. M., Monier, J. M. (2010): Is resistance futile? Changing external resistance does not improve microbial fuel cell performance. – Bioelectrochemistry. 78: 2-7.

- [19] Madani, S., Gheshlaghi, R., Mahdavi M, A., Sobhani, M., Elkamel, A. (2015): Optimization of the performance of a double-chamber microbial fuel cell through factorial design of experiments and response surface methodology. – *Fuel*. 150: 434-440.
- [20] Madigan, M. T., Martinko, M. J., Dunlap, P. V., Clark, D. P. (2012): *Brock Biology of Microorganisms*. 12 ed. – Pearson, San Francisco.
- [21] Martínez-Conesa, E. J., Ortiz-Martínez, V. M., Salar-García, M. J., Delos Rios, A. P., Hernández-Fernández, F. J., Lozano, L. J., Godínez, C. (2017): A Box-Behnken design-based model for predicting power performance in microbial fuel cells using wastewater. – *Chem. Eng. Commun.* 204: 97-104.
- [22] Miroliaei, M. R., Samimi, A., Mohebbi-Kalhari, D., Khorram, M. (2015): Kinetics investigation of diversity cultures of *E. coli* and *Shewanella* sp., and their combined effect with mediator on MFC performance. – *J. Ind. Eng. Chem.* 25: 42-50.
- [23] Myers, R. H., Montgomery, D. C., Anderson-Cook, C. (2016): *Response Surface Methodology*. 4th ed. – John Wiley & Sons, Hoboken, USA.
- [24] Nandy, A., Kumar, V., Kundu, P. P. (2013): Utilization of proteinaceous materials for power generation in a mediatorless microbial fuel cell by a new electrogenic bacteria *Lysinibacillus sphaericus* VA5. – *Enzyme Microb. Technol.* 53: 339-344.
- [25] Nevin, K. P., Richter, H., Covalla, S. F., Johnson, J. P., Woodard, T. L., Orloff, A. L., Jia, H., Zhang, M., Lovley, D. R. (2008): Power output and coulombic efficiencies from biofilms of *Geobacter sulfurreducens* comparable to mixed community microbial fuel cells. – *Environ. Microbiol.* 10: 2505-2514.
- [26] Nimje, V. R., Chen, C. Y., Chen, C. C., Tsai, J. Y., Chen, H. R., Huang, Y. M., Jean, J. S., Chang, Y. F., Shih, R. C. (2011): Microbial fuel cell of *Enterobacter cloacae*: Effect of anodic pH microenvironment on current, power density, internal resistance and electrochemical losses. – *Int. J. Hydrog. Energy* 36(17): 11093-11101.
- [27] Okpokwasili, G. C., Nweke, C. O. (2005): Microbial growth and substrate utilization kinetics. – *Afr. J. Biotechnol.* 5: 305-317.
- [28] Park, H. S., Kim, B. H., Kim, H. S., Kim, H. J., Kim, G. T., Kim, M., Chang, I. S., Park, Y. K., Chang, H. I. (2001): A novel electrochemically active and Fe (III)-reducing bacterium phylogenetically related to *Clostridium butyricum* isolated from a Microbial Fuel Cell. – *Anaerobe* 7: 297-306.
- [29] Pradeed, N. V., Vidyashree, K. G., Pooja, J., Anupama, S., Laskshmi, P., Arun Kumar, J. M., Ankitha, K. (2014): Treatment of sugar industry wastewater in anaerobic downflow stationary fixed film (DSFF) reactor. – *Sugar Tech.* 16(1): 9-14.
- [30] Rago, L., Baeza, J. A., Guisasola, A. (2016): Increase performance of hydrogen production in microbial electrolysis cells under alkaline conditions. *Bioelectrochemistry*. – 109: 57-62.
- [31] Ringeisen, B. R., Henderson, E., Wu, P. K., Pietron, J., Ray, R., Little, B., Biffinger, J. C., Meehan-Jones, J. M. (2006): High power density from a miniature microbial fuel cell using *Shewanella oneidensis* DSP10. – *Environ. Sci. Technol.* 40(8): 2629-2634.
- [32] Roy, J. N., Babanova, S., Garcia K. E., Cornejo, J., Ista, L. K., Atanassov, P. (2014): Catalytic biofilm formation by *Shewanella Oneidensis* MR.1 and anode characterization by expanded uncertainty. – *Electrochim. Acta.* 126: 3-10.
- [33] Sarabia, L. A., Ortiz, M. C. (2009): *Response Surface Methodology*. – In: Brown, S. D., Tauler, R., Walczak, B. (eds.) *Comprehensive Chemometrics. Chemical and Biochemical Data Analysis*, Section 1.12, pp. 345-390. Elsevier, Amsterdam.
- [34] Sarioglu, M. C., Gökçek. O. B. (2016): Treatment of automotive industry wastewater using anaerobic batch reactors: The influence of substrate/inoculum and molasses/wastewater. – *Process Saf. Environ. Prot.* 102: 648-654.
- [35] Tallent, S. M., Kotewicz, K. M., Strain, E. A., Bennett. R. W. (2012): Efficient isolation and identification of *Bacillus cereus* group. – *J. AOAC Int.* 95(2): 446-451.

- [36] Wu, S., Xiao, Y., Wang, L., Zheng, Y., Chang, K., Zheng, Z., Yang, Z., Varcoe, J. R., Zhao, F. (2014): Extracellular electron transfer mediated by flavins in Gram-positive *Bacillus sp.* WSXY1 and yeast *Pichia stipitis*. – *Electrochim. Acta.* 146: 564-567.
- [37] Xia, C., Zhang, D., Pedrycz, W., Zhu, Y., Guo, Y. (2018): Models for microbial fuel cells: A critical review. – *J. Power Sources* 373: 119-131.
- [38] Zhang, J., Zheng, P., Zhang, M., Chen, H., Chen, T., Xie, Z., Cai, J., Abbas, G. (2013): Kinetics of substrate degradation and electricity generation in anodic denitrification microbial fuel cell (AD-MFC). – *Bioresour. Technol.* 149: 44-50.
- [39] Zhang, L., Zhou, S., Zhuang, L., Li, W., Zhang, J., Lu, N., Deng, L. (2008): Microbial fuel cell based on *Klebsiella pneumoniae* biofilm. – *Electrochem. commun.* 10: 1641-1643.
- [40] Zhang, L., Zhu, X., Li, J., Qiang, L., Ye, D. (2011): Biofilm formation and electricity generation of a microbial fuel cell started up under different external resistances. – *J. Power Sources.* 196: 6029-6035.
- [41] Zhang, T., Cui, C., Chen, S., Ai, X., Yang, H., Shen, P., Peng, Z. (2006): A novel mediatorless microbial fuel cell based on direct biocatalysis of *Escherichia coli*. – *Chem. Commun.* 21: 2257-2259.
- [42] Zhu, Y., Liu, Y., Li, J., Shin, H-D., Du, G., Liu, L., Chen, J. (2015): An optimal glucose feeding strategy integrated with step-wise regulation of the dissolved oxygen level improves N-acetylglucosamine production in recombinant *Bacillus subtilis*. – *Bioresour. Technol.* 177: 387-392.

TEMPORAL CHANGES IN CONCENTRATION OF PM10 DUST IN POZNAŃ, MIDDLE-WEST POLAND AS DEPENDENT ON METEOROLOGICAL CONDITIONS

KALBARCZYK, R.^{1*} – KALBARCZYK, E.² – RASZKA, B.³

¹*Institute of Landscape Architecture, Wrocław University of Environmental and Life Sciences
Grunwaldzka St. 55, 50-357 Wrocław, Poland
(phone: +48-71-320-1858; fax: +48-71-320-1863)*

²*Department of Spatial Econometrics, Adam Mickiewicz University in Poznań
Krygowskiego St. 10, 61-680 Poznań, Poland
(phone: +48-61-829-6309; fax: +48-61-829-6127)*

³*Department of Spatial Management, Wrocław University of Environmental and Life Sciences
Grunwaldzka St. 55, 50-357 Wrocław, Poland
(phone: +48-71-320-5677)*

**Corresponding author
e-mail: robert.kalbarczyk@upwr.edu.pl*

(Received 15th Dec 2017; accepted 13th Mar 2018)

Abstract. The present analysis is based on hourly data of suspended dust PM10 and meteorological conditions. The aim of the study was to determine the time structure of PM10 concentration and its dependence on meteorological conditions. Hourly data from 2005-2016 were collected from the State Monitoring of Environment situated in Poznań, middle-west Poland. Analysis of the relationship between weather and concentration of PM10 was conducted using the correlation analysis and multiple regression. Time course of PM10 concentration and meteorological elements was characterized not only in the entire 2005-2016 time period but also in its successive years – in daily, monthly and seasonal time steps. In the years 2005-2016, the daily concentration of PM10 significantly depended on meteorological conditions, the strictest dependence being found for wind speed and air temperature. The most frequently recorded, 33% overall, hourly concentration of PM10 was from within the ranges 10-15 and 15-20 $\mu\text{g m}^{-3}$. A large, $> 90 \mu\text{g m}^{-3}$, pollution of the atmosphere in the three seasons of the year: winter, spring and autumn was registered mostly between 20 and 4 h. In winter, the large $> 90 \mu\text{g m}^{-3}$, hourly concentrations of suspended PM10 dust, were accompanied by below average values of air temperature, above average relative air humidity, below average wind speeds, from E direction mainly, and above average atmospheric pressure.

Keywords: *air pollution, bio-climate of town, ecological politics of the state, human health, meteorological conditions*

Introduction

One of the most common air pollutants is an airborne particle of a grain diameter of less than 10 μm (PM10). Its prevalence is a consequence of diverse and multiple emission sources. PM10 can be a mixture of organic and inorganic substances, may contain toxic substances, often multi-ring aromatic hydrocarbons, heavy metals, and also dioxins and furanes (Chwil et al., 2015; Emmanouil et al., 2017; Flores et al., 2017; Tasić et al., 2017; Cesari et al., 2018). The anthropogenic dust pollutants come mainly from combustion of fuel to derive energy and from technological processes conducted in industrial plants, and also from transport, mostly road traffic. Atmospheric dust

comes also from fires or volcanic and seismic activity (Kieseewetter et al., 2013; Gliniak et al., 2015).

Particles with a diameter less than 10 μm (PM10), enters the human organism by way of respiratory pathways or indirectly through the digestive tract, when polluted food is consumed (Gładka and Zatoński, 2016; Chiang et al., 2017). Suspended dust is adsorbed in upper stretches of the respiratory tract, whence it is expelled or is accumulated, or permeates into the lungs (D'Amato et al., 2010). The elders, children or the respiratory and circulatory duct sufferers are especially exposed to the negative interaction with the dusts (Badyda et al., 2016; Maji et al., 2017; Pannullo et al., 2017; Sosa et al., 2017; Yang et al., 2017). According to WHO there is convincing evidence that dust in the air, irrespective of its source, has detrimental effect on human health (World Health Organization, 2013).

As reported by the Government Inspectorate (NIK's Report, 2014), air pollution in Poland is the cause of 45,000 early deaths. For example, an inhabitant of a large Polish town (at least 0.5 mln) lives two and a half years less, on average. It should, however, be emphasized that estimation of the influence of suspended dust in the atmosphere on human health still remains very difficult and imperfect (Gustafsson et al., 2014; Segersson et al., 2017).

In the Poznań agglomeration, the daily norm of PM10 dust, 50 $\mu\text{g m}^{-3}$ acc. to Polish regulations, was surpassed in 42 days in 2013 on average, and in 48 days in 2016, mostly in the winter season. Poland, in recent years, was infamously 2nd or 3rd among the EU nations in regard of potential exposure of its city inhabitants to the suspended PM10 dust pollution (NIK's Report, 2014). In Poland, the informing and alarm levels for PM10 dust are as high as 200 and 300 $\mu\text{g m}^{-3}$, respectively. For example, in Italy and France it is approx. four times less than in Poland, and in Hungary and the Check Republic – approx. 3 times less (Richter and Williams, 1998; Judy-Rezler and Toczko, 2016).

In some large cities of Poland, an ecological program has been introduced in order to diminish air pollution (Resolution no. 3056 of the Great-Poland Voivodship of 29 Dec. 2016). In the ecological programs, a series of actions is stated that aim at protection against air pollution, from planting trees or replacement of coal furnaces to building cycling paths and transition from the wheel transport to public transport. To make the program of air quality improvement adequate to the specifics of a town, information concerning the timely structure of PM10 concentration is needed (Balakrishnaiah et al., 2011; Bielec-Bąkowska et al., 2011; Bigi and Ghermandi, 2016; Redington et al., 2016; Mok et al., 2017), and also its dependence on meteorological conditions (Adamek and Ziernicka-Wojtaszek, 2017; Li et al., 2017; Stafoggia et al., 2017; Tiwari et al., 2017). The aim of the study was to determine the time structure of PM10 concentration and its dependence on meteorological conditions in the fifth biggest Polish city, Poznań.

Material and methods

Study area

The initial data from the years 2005-2016 were collected from the Voivodship Inspectorate of Environment Protection called Poznań-Botnik, situated in the middle part of Poznań, in Henryk Dąbrowski street ($\lambda = 16^{\circ}52'52''$ E, $\varphi = 52^{\circ}25'08''$ N, hs = 89 m a.s.l.) (Fig. 1). The immission-meteorological station (its code: WpPoznDabrow) is installed on the grounds of the University Botanic Garden of Adam Mickiewicz

University, in close proximity to residential and recreational areas. A dominant type of development in the vicinity of the station is low, single-family housing.

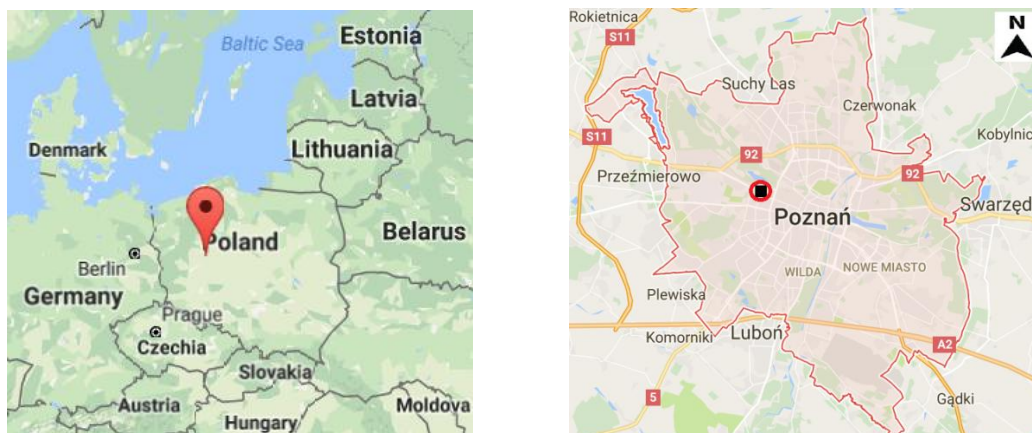


Figure 1. Location of the station of air quality assessment (■) and of meteorological station (○) in Poznań. Source: <https://www.google.pl/> (accessed on 04.10.2017)

Material

The investigation uses hourly data on concentration ($\mu\text{g m}^{-3}$) of PM10 pollution, and also hourly data on meteorological conditions: air temperature (T_a , $^{\circ}\text{C}$), relative humidity of the air (R_h , %), atmospheric pressure (P_a , hPa), speed (V , m s^{-1}) and direction of wind (WD). All parameters, i.e. the concentration of suspended PM10 dust and meteorological elements, describing so-called city background, are measured automatically with analyzers and sensors attested by the Main Inspectorate for Environment Protection.

Methods

The influence of meteorological conditions on concentration of suspended PM10 dust in the years 2005-2016 was estimated with the use of Pearson's correlation. The analysis of the dependence weather-concentration of PM10 was carried out in successive months of the year (from January to December), and also in the four seasons of year: winter (from December to February), spring (from March to May), summer (from June to August) and in autumn (from September to November). Whereas, evaluation of the collective effect of considered meteorological elements on PM10 immission level was made using the multiple regression method. Assessment of compliance of the model with empirical data was made on the basis of the value of the corrected determination coefficient (R^2 adj, %), which takes into account the number of independent variables, and the percent difference between standard deviation of PM10 concentration and the standard error of estimation of the multiple regression equation (S_d-S_y , %). The participation of a meteorological element in explaining the value of PM10 immission was determined on the basis of the partial correlation coefficient and t-Student test. Both in the analysis of correlation and in multiple regression the dependent transformed variable $f(\text{PM10})$ was calculated from the formula (Eq. 1):

$$f(\text{PM10}) = \text{Log}(\text{PM10}) \quad (\text{Eq.1})$$

where *PM10* signifies concentration of suspended dust particles smaller than 10 µm.

The structure of occurrence of PM10 concentrations within the assumed intervals has been characterized in the whole multiyear period 2005-2016 both in daily and seasonal time steps. In a similar pattern, as in the case of frequency of occurrence of PM10 concentration, the time course of PM10 concentration and meteorological elements has been described, and additionally monthly analysis in successive years were made.

For the most unfavorable, winter, aero-sanitary conditions in Poznań (in the years 2005-2016) the mean values of meteorological elements were determined. To this end, from the set of all hourly initial data two groups of data were selected on the basis of suspended PM10 dust – $< 20 \mu\text{g m}^{-3}$ and $> 90 \mu\text{g m}^{-3}$. The basis for determination of boundary values, that describe small and large values of PM10 in the air were percentile values, 30 and 90% respectively, determined on the basis of the entire set of data (ca. 25,000 hourly values). Recorded both for small ($< 20 \mu\text{g m}^{-3}$) and large ($> 90 \mu\text{g m}^{-3}$) values of PM10 the values of the meteorological elements Ta, Rh, Pa, V and WD were calculated for successive hours of 24 h day and night.

Results and discussion

Relation between PM10 concentration and meteorological conditions

The assessment of the relation, conducted in 2005-2016, between daily concentration of PM10 dust, transformed according to the formula (Eq. 1) and analyzed meteorological elements has shown a significant, negative influence of air temperature: in winter ($r = -0.36$, $P < 0.01$), spring ($r = -0.15$, $P < 0.01$) and autumn ($r = -0.31$, $P < 0.01$) and significant, positive in summer ($r = 0.49$, $P < 0.01$) (Table 1).

Table 1. Relation between daily concentration of suspended PM10 dust and meteorological elements. The years 2005-2016

Element	Season of the year			
	Winter (December-February) (n = 1034)	Spring (March-May) (n = 1089)	Summer (June-August) (n = 1032)	Autumn (September-November) (n = 997)
Ta (°C)	-0.36***	-0.15***	0.49***	-0.31***
Rh (%)	0.08***	-0.07***	-0.15***	0.13***
Pa (hPa)	0.15***	0.13***	n.s.	0.22***
V (m s ⁻¹)	-0.58***	-0.27***	-0.40***	-0.45***

Ta – air temperature (°C), Rh – air relative humidity (%), Pa – atmospheric pressure (hPa), V – wind speed (m s⁻¹), n – number of samples, *** significant with $P \leq 0.01$, n.s. – non significant at $P < 0.1$

In spring-summer season the Rh index has a significantly negative effect on PM10 concentration. Atmospheric pressure had significant positive effect on the content of suspended PM10 dust in the year, save for summer, the strongest dependence being documented for autumn ($r = 0.22$, $P < 0.01$). High pressure is recorded when the radiation cooling of the low air layers occurs and often unstable equilibrium in the atmosphere, including near-ground elevated inversions. The anemometric conditions, described by wind speed, were significantly, negatively correlated with the level of PM10 dust content in all considered seasons of the year. Correlation coefficients calculated for this dependence varied from -0.27 in spring to -0.58 in winter.

For a full description of the influence of meteorological conditions on concentration of the dust, the relation weather-PM10 was considered in successive months, hour by hour (Fig. 2). Highest positive values ($r \geq 0.4$) of correlation coefficient for the relation Ta-PM10 were found for the May-September period, at 7-11 h; whereas highest negative ($r \leq -0.4$) – in January-February at 21-17 h. Air humidity had strongest negative effect on PM10 in the March-September period at 7-11, and strongest positive – in November-December, in night, morning and afternoon hours. Low pressure was accompanied by low concentration of PM10 during April-September at 11-21 h. Wind speed favorably affected air quality, as it is apparent from Table 1. A positive relationship V-PM10 was found in April-May at 17-20 h.

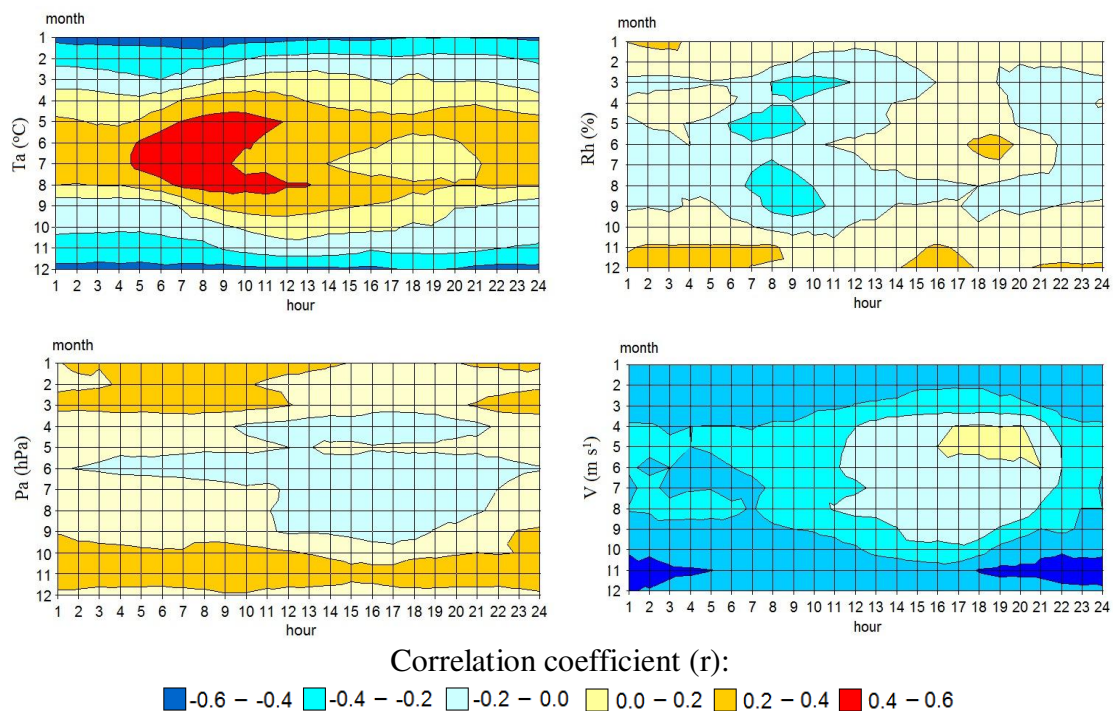


Figure 2. Monthly distribution of the relations between hourly PM10 concentrations and meteorological elements. The years 2005-2016

Meteorological elements in the system determined the value of PM10 concentration, from ca. 13 to 38%, but mostly in autumn, and then in winter (Table 2).

The strongest influence in all the seasons on air pollution had Ta and V. The partial correlation coefficients calculated for the independent variables in the multiple regression equations varied from -0.18 for winter to 0.404 for summer in the case of Ta and from -0.29 to -0.57 for autumn in the case of V. Aside of the indicators Ta and V, in spring a significant negative effect on PM10 exerted also air humidity, and in summer – atmospheric pressure.

Frequency of PM10 occurrence in seasons of the year

The measured PM10 concentration throughout the year was, most frequently, in the four assumed intervals: 10-15, 15-20, 20-25 and 25-30 $\mu\text{g m}^{-3}$, respectively, with the frequencies ca. 16, 17, 14 and 11% (Fig. 3), respectively. A bit less frequently, ca. 8%,

was recorded pollution in the range 30-35 $\mu\text{g m}^{-3}$. Large dust concentration ($> 60 \mu\text{g m}^{-3}$) was infrequent ($< 2\%$).

Table 2. Assessment of the combined effect of meteorological conditions on daily concentration of PM10 dust. The years 2005-2016

Season of the year	Coefficients of partial correlation of multiple regression				n	Evaluation of the equation quality	
	Ta (°C)	Rh (%)	Pa (hPa)	V (m s^{-1})		R ² _{adj.}	Sd-Sy (%)
Winter (December-February)	-0.18 (-6.84)*			-0.51 (-19.35)	1034	36.5	23.6
Spring (March-May)	-0.26 (-8.36)	-0.097 (-3.17)		-0.309 (-10.608)	1089	13.1	11.2
Summer (June-August)	0.404 (14.48)		-0.18 (-6.62)	-0.29 (-10.304)	1032	31.8	17.7
Autumn (September-November)	-0.34 (-13.38)			-0.57 (-22.45)	997	37.8	22.2

*In brackets are given values of t-Student's test at significance level $P < 0.01$, R²_{adj.} - adjusted determination coefficient (%), Sd-Sy (%) - percent difference between standard deviation of PM10 concentration and standard deviation in estimation of the multiple regression equation. Other explanations, see Table 1

The frequency of particular PM10 dust size occurrence in respective seasons of the year was not always the same as in the scale of the entire year. In winter, the largest dust pollution was in the two intervals - 15-20 and 20-25 $\mu\text{g m}^{-3}$, with similar frequency of ca. 11%. In autumn, as throughout the year, PM10 concentration was most often from 10 to 30 $\mu\text{g m}^{-3}$. A similar distribution of frequency was for the warmer seasons of the year. In spring, in the four successive intervals from 10 to 30 $\mu\text{g m}^{-3}$, concentration of particles less than 10 μm occurred at almost 60% frequency in total, and in summer it was 85%. In all the seasons, a small ($< 5 \mu\text{g m}^{-3}$) concentration of the pollution was rarely recorded, at frequency varying from 0.1% in summer to 1.8% in winter. In summer, there was not a result of PM10 concentration greater than 55 $\mu\text{g m}^{-3}$.

The frequency of a certain size of PM10 in the respective seasons depended on time of the day and night (Fig. 3). In winter, the air pollution in the range 0-10 $\mu\text{g m}^{-3}$ was most often from 11 to 14%, recorded at 3-10 h; whereas in the range 10-20 $\mu\text{g m}^{-3}$ it was 20% frequent at 4-16 h. In the successive ranges, from 20 to 80 $\mu\text{g m}^{-3}$, dust concentration did not exhibit a marked daily variation. Large (90-100 and $> 100 \mu\text{g m}^{-3}$) dust concentrations were most frequently recorded in evening and night hours. Smallest dust concentrations in spring and summer (0-10 $\mu\text{g m}^{-3}$) were recorded mostly at 12-19 h, and in the range 10-20 $\mu\text{g m}^{-3}$ at 11-18 h. In the two seasons the PM10 $> 50 \mu\text{g m}^{-3}$ was most frequent in late afternoon and night hours. In summer, the concentration was small ($< 10 \mu\text{g m}^{-3}$) and $> 20\%$ frequent at 10-20 h, and a medium one ($> 50 \mu\text{g m}^{-3}$) at 22-3 h.

Variation of PM10 concentration and meteorological elements

The content of PM10 in the air exhibited seasonal variation (Fig. 4). The annual variation of PM10 was around 31.5 $\mu\text{g m}^{-3}$. In Poznań, in 2005-2016, the concentration

in winter ($42.4 \mu\text{g m}^{-3}$) was over two times greater than in summer ($18.8 \mu\text{g m}^{-3}$), in autumn a little higher (by $4.1 \mu\text{g m}^{-3}$) than in spring. The highest, over $40 \mu\text{g m}^{-3}$, mean concentration of the pollution was recorded in November-March period, and it varied from $40 \mu\text{g m}^{-3}$ in December to ca. $46 \mu\text{g m}^{-3}$ in February. The highest, amounting to $39.1 \mu\text{g m}^{-3}$, annual PM10 concentration occurred in 2011, and the lowest ($27.8 \mu\text{g m}^{-3}$) – in 2007. However, in individual months, the highest concentrations of the pollution were in different years; for instance, in January 2010, February 2012, June 2008 and August 2015.

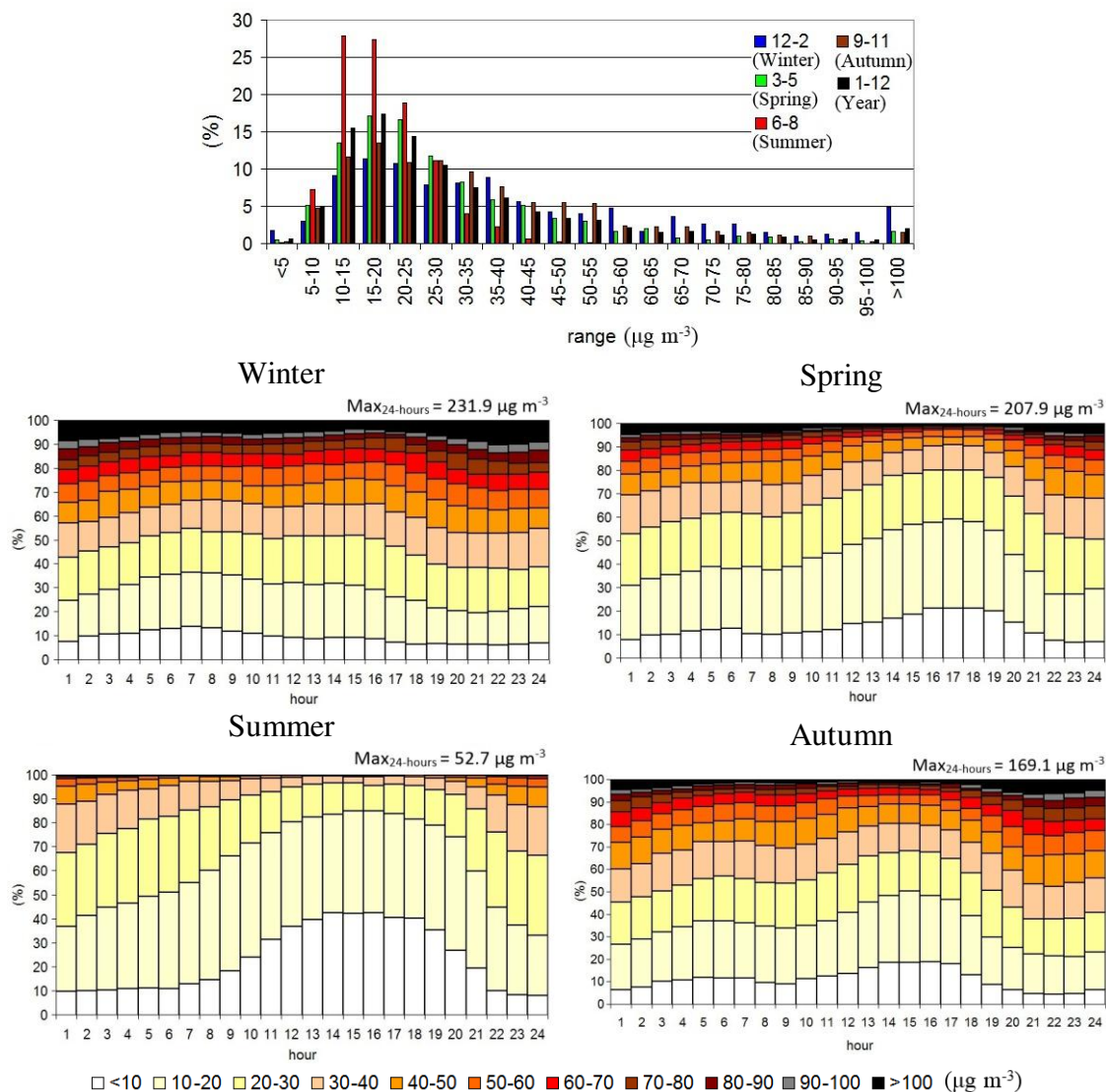
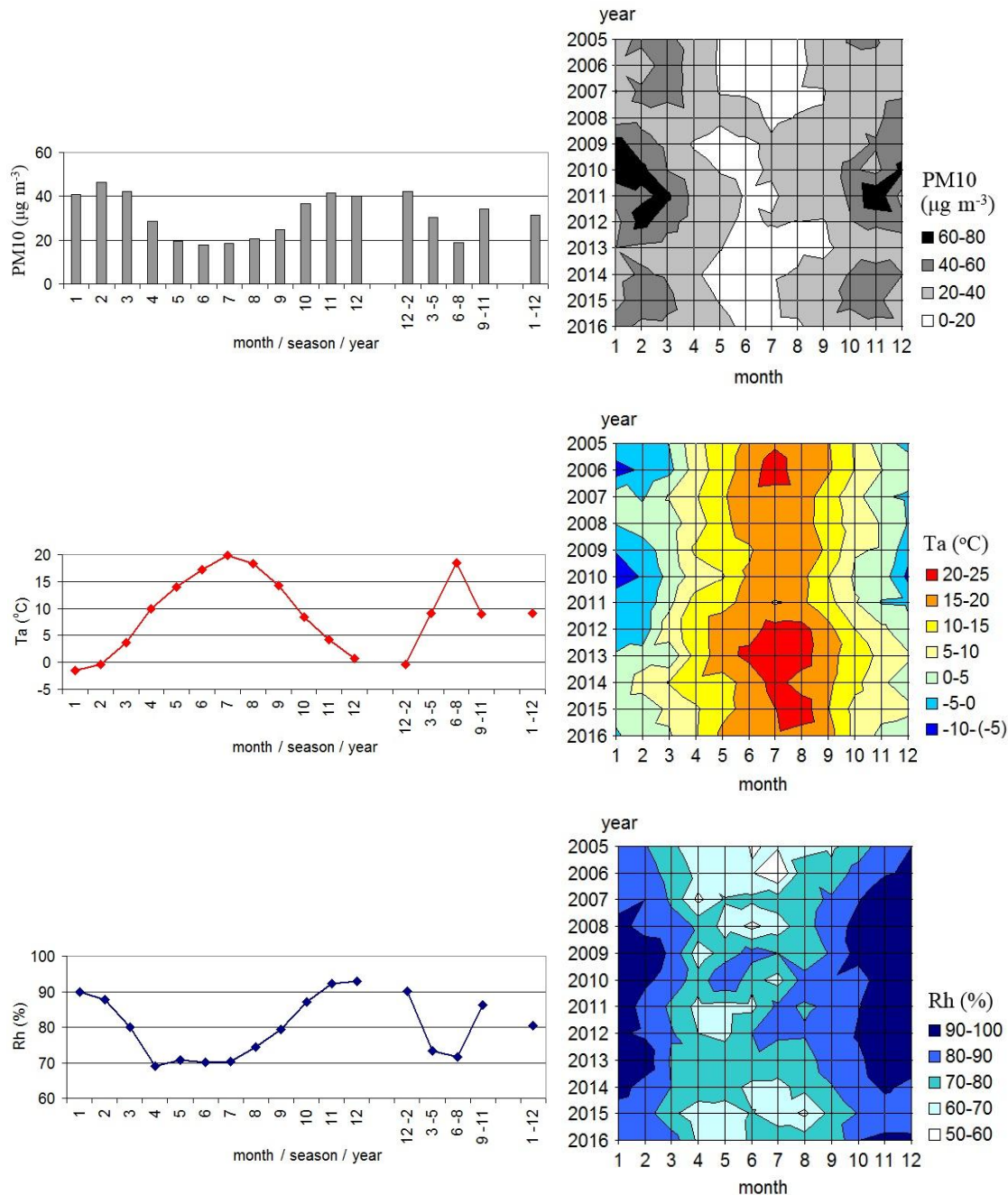


Figure 3. Frequency of occurrence of hourly PM10 concentration in the multiple-year period 2005-2016

The air temperature in the multiple-year period, in annual scale was 9.1°C , and varied depending on month from -1.5°C in January to 19.8°C in July (Fig. 4), being a little lower (by 0.2°C) from spring to autumn. In the successive years of the period the summers were found to be warmer and warmer, especially in July-August, and also winter. For example, in January 2006 T_a was only -7.5°C , and in January 2015 it was

even 2.5°C. The monthly course of Rh was a reverse of Ta. Such highest mean relative humidity of the air was recorded in December (93.0%), and then in November (92.3%). In months of the best air quality with respect to dustiness, i.e. in May-July, the Rh varied around ca. 70%. The most wet year, of the considered ones, was 2010 when Rh varied from 74.8 to 93.6% in winter. Unlike Ta and Rh, the atmospheric pressure showed a reversed time course, the highest Pa was in October (1007.5 hPa), and then in December (1006.3 hPa) and in September (1006.2 hPa). The mean multi-year values of the indicator Pa was 1005.1 hPa and varied from 1002.7 hPa in 2010 to 1009.0 hPa in 2005.



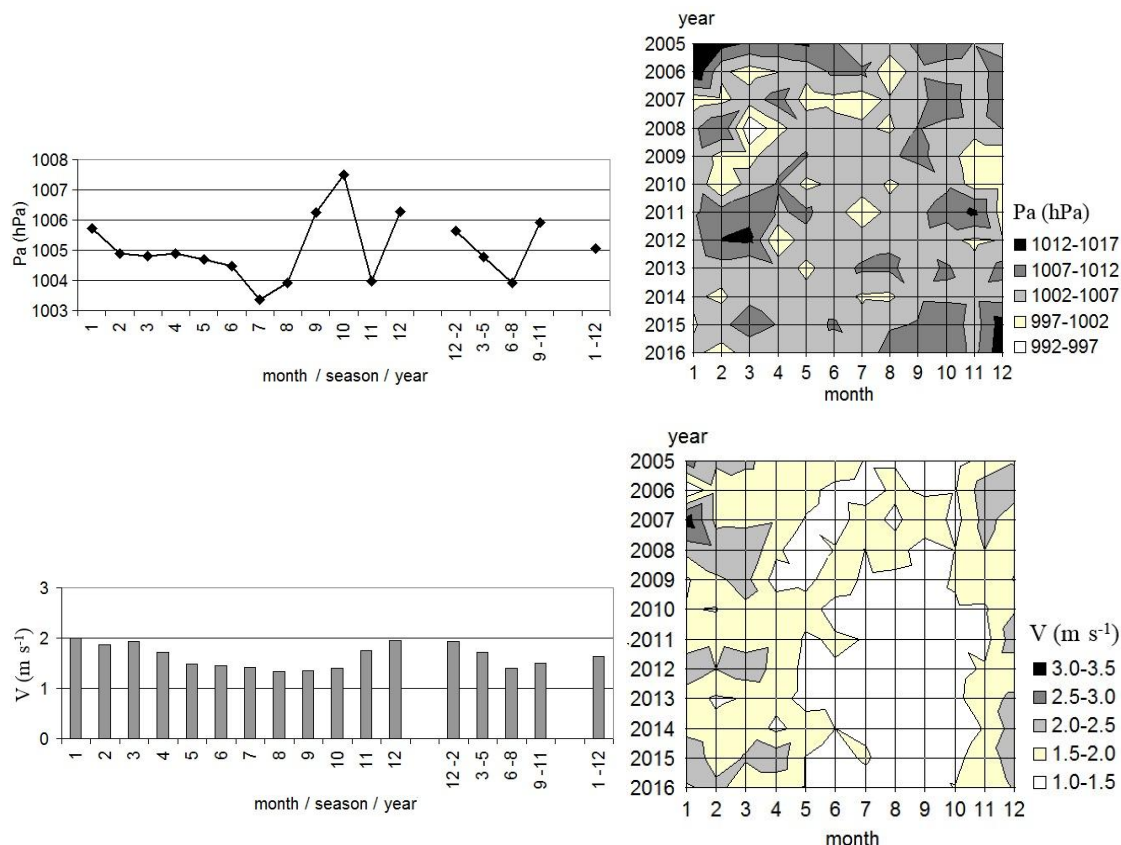


Figure 4. Course of occurrence of PM10 concentration and meteorological elements in the multiple-year period 2005-2016, and by the years

In turn, wind speed, which strongly determined PM10 content in all considered seasons, varied from 1.3 m s^{-1} in August and September to 2.0 m s^{-1} in January and December of 2005-2016. In spring wind speed was, on average, by 0.2 m s^{-1} greater than in autumn, i.e. inversely than PM10 concentration. It blew the strongest in 2007, when the mean monthly V was from 1.3 m s^{-1} in June to even 3.2 m s^{-1} in January.

At the measurement point, in 2005-2016, the wind was most often from SW (18.8%), and then from W (16.2%) (Fig. 5). Most infrequent was the wind from N and NE, 3.7 and 5.0%, respectively. In the 12-year period, windless weather was at 5.2% frequency. The content of suspended dust exhibited not only annual but also daily changes (Fig. 6). The highest, $\geq 50 \mu\text{g m}^{-3}$, PM10 concentration in 2005-2016 was recorded in the months of February and March at 21-2 h, and in November at 20-24 h. Dustiness was lowest in the period May – August at 10-20 h, and in June-July even from 6 or 7 h. When dustiness was highest, the air temperature varied, on average, from -5 to 5°C (Fig. 6). Small dust content was recorded when T_a was from 15 to 25°C , mostly at 9-20 h. The time course of R_h , like that of PM10 and T_a , was close to the latitudinal one. In the study period, the content of water vapour in the air was greatest in autumn and winter months at 18-9 h, in January and February only from 21 h. In the case of atmospheric pressure the time course was less variable. The highest Pa, varying from 1006 to 1008 hPa, occurred mostly in September-October during day and night, and in December, apart from 13-15 h.

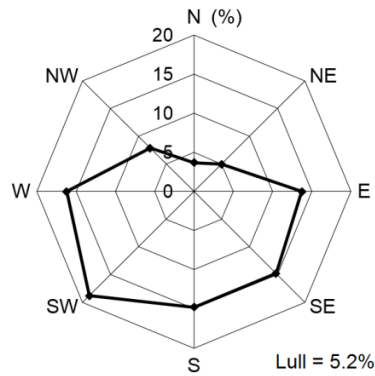


Figure 5. Annual wind directions, constructed on the basis of hourly data. The years 2005-2016

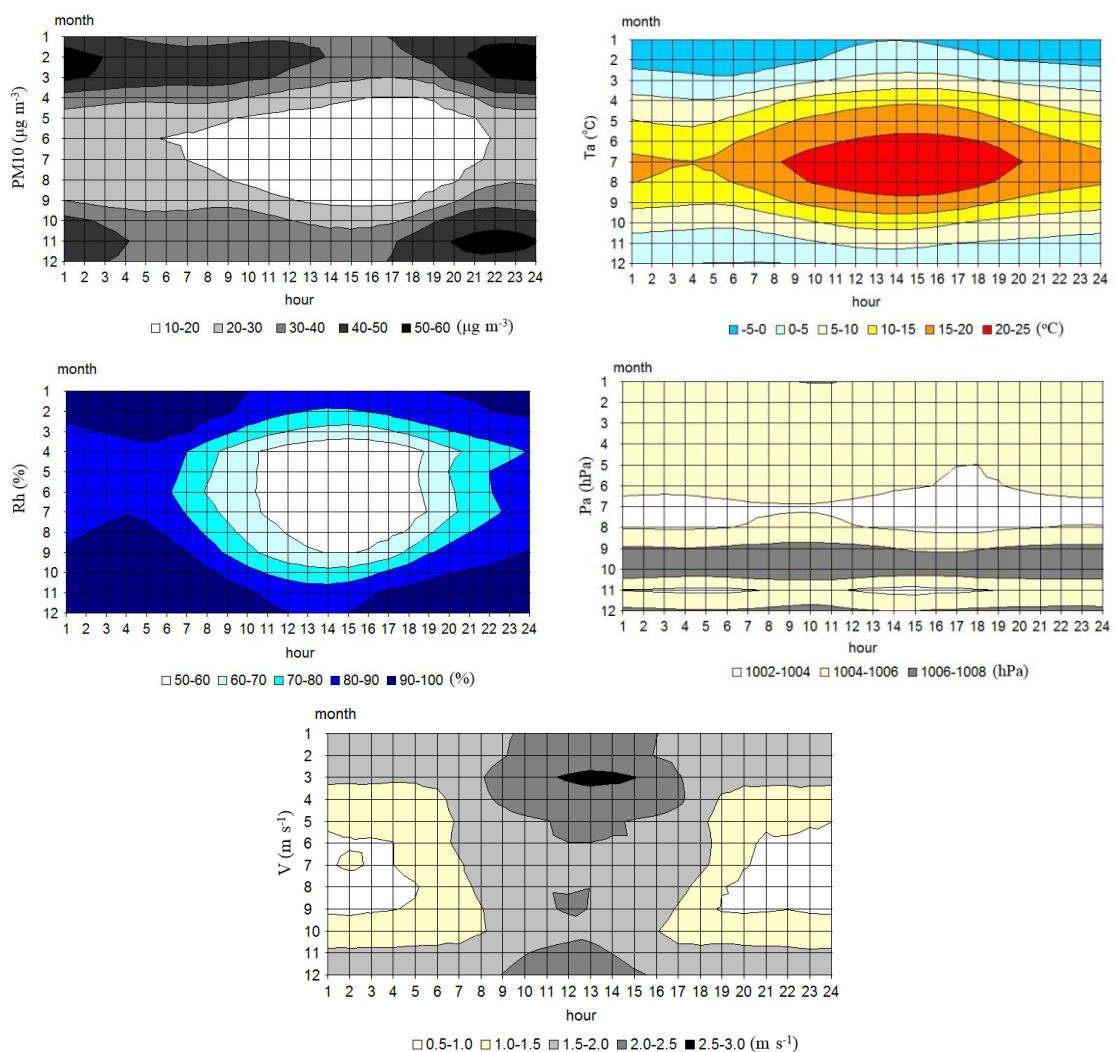


Figure 6. Timely structure of PM10 concentration and meteorological elements hour by hour in the analyzed period of 2005-2016

Pa in the range 1002-1004 hPa was most pronounced in the period June-August and in November, being so in June at 16-19 h, in July in day and night, in August at 13-21 h

and 1-6 h, in November at 1-7 h and 12-18 h. However, wind speed clearly depended not only on month but also on the hour. In the period 2005-2016, it blew the strongest (from 2.0 to 3.0 m s⁻¹) in January-April at 9-16 h and in November-December at 10-14 h; and the weakest, ≤ 1 m s⁻¹, it blew in June-September at 20-4 h.

In the years 2005-2016 (from December to February), small, ≤ 20 µg m⁻³, concentration of PM10 was not much differentiated in successive hours of the day, and varied from 11.8 µg m⁻³ at 7 h to 13.0 µg m⁻³ at 17 h (Fig. 7). A higher than average, ≥ 12.6 µg m⁻³, small PM10 concentration was calculated for 10-1 h. In winter, an opposite time course was found for large, ≥ 90 µg m⁻³, dust concentration; above average (≥ 123.6 µg m⁻³) for 22-9 h. Small, hourly concentrations of the analyzed dust pollution were accompanied by higher air temperatures – from 1.2 to 3.3°C, and large ones – by lower temperature from -7.8 to -3.5°C, which is according to the relations Ta-PM10 (Table 1).

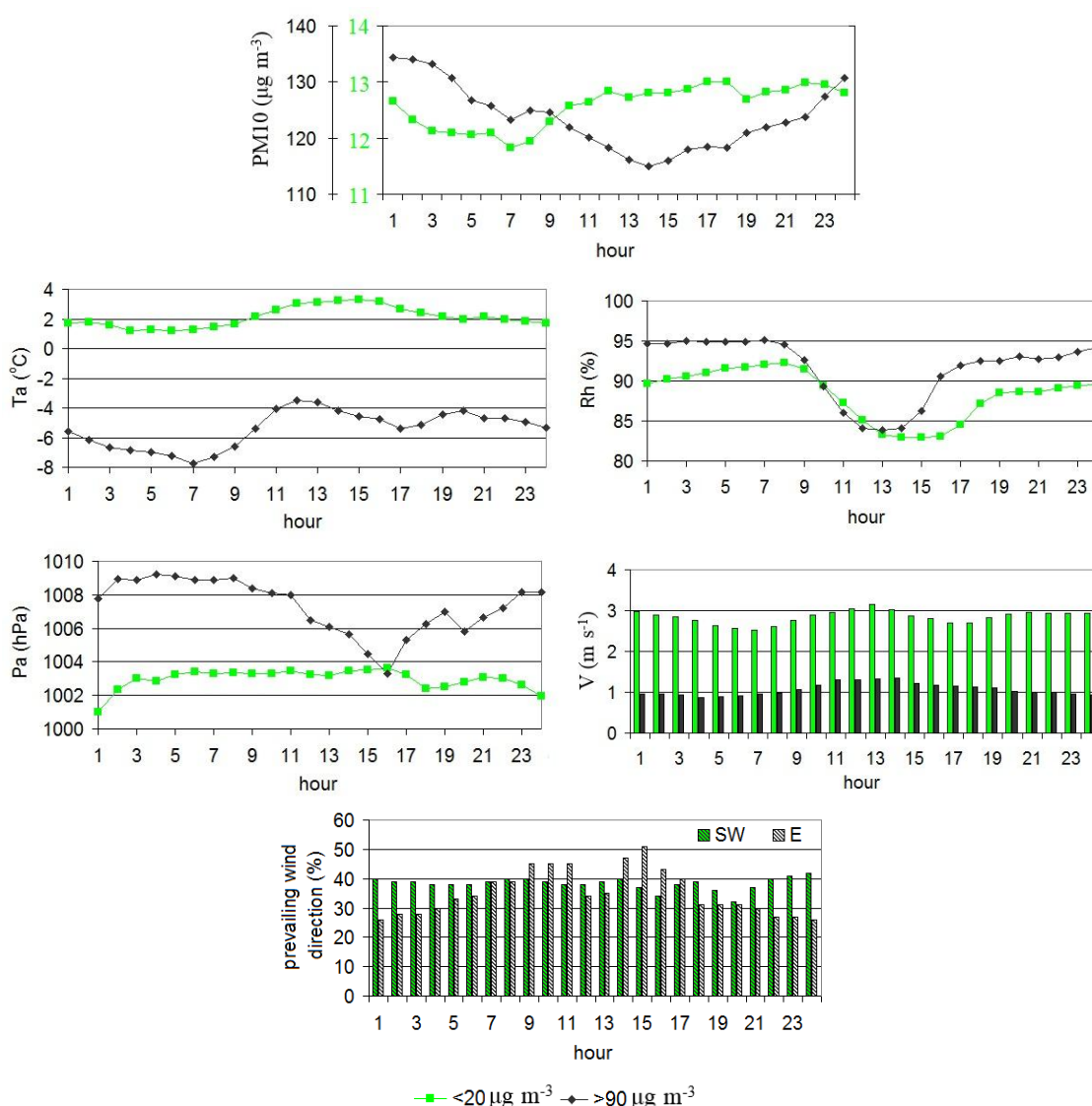


Figure 7. Winter, hourly concentrations of suspended PM10 dust, small (< 20 µg m⁻³) and large (> 90 µg m⁻³), together with meteorological conditions. The years 2005-2016

Small and large PM10 concentrations and accompanying meteorological conditions

Small dust content was accompanied by above-average wind speed, whose daily variation was from 2.5 to 3.2 m s⁻¹, the strongest wind being from 11 to 14 h. Clean air was recorded at the station when the wind was from SW, blowing at a frequency of 32 to 42%. In turn, lower than average values of Rh and Pa induced small dust concentrations. The Rh, varying from ca. 84 to 91%, were accompanied by both small and large PM10 concentrations. Unfavorable aero-sanitary conditions in December-February, when PM10 ≥ 90 µg m⁻³, were recorded in the study period under the daily meteorological conditions: Ta – from -7.8 to -3.5°C, Rh – from 84 to 95%, Pa– from 1003.3 to 1009.2 hPa, V – from 0.9 to 1.3 m s⁻¹ and wind mainly from 26 to even 51% from the E direction. The wind was most often from E at 9-11 and 14-17.

Discussion

The work has proved that PM10 concentration in Poznań increased in the periods of a temperature drop in winter, autumn and spring but also during an increase in temperature in summer. The deterioration of air quality in the autumn-winter and spring period might be connected with an increased intensity of burning solid, conventional fuels and biomass in the Poznań heat and power plants, and also in individual heating installations, in which, regrettably, also municipal waste is burned (Ćwiek and Majewski, 2015). High concentration of PM10 dust in the summer period was most likely related, among other things, to the nuisance of dusting from unsurfaced roads and construction sites. The more than average air humidity in the autumn-winter period was also conducive to high air dust levels. High air humidity without rain but with fog formation may induce an increased concentration of suspended dust whose particles may serve as condensation nuclei for water molecules (Judy-Rezler and Toczko, 2016).

The work has proved a negative effect of Rh on the level of PM 10 concentration in the spring-summer period. With an increased content of water vapor in the atmosphere, the probability of wet deposition increases. This may cause self-cleaning of the atmosphere and a decrease in the level of dust concentration. On the other hand, in the case of atmospheric pressure positive correlations with PM10 were proved in three seasons of the year, except for summer. High pressure is recorded with radiative cooling of low atmosphere layers and often with formation of stable equilibrium in the atmosphere, including ground or elevated inversions.

Correlation coefficients between PM10 concentration and wind velocity assumed significantly negative values in all the examined seasons of the year. Long-lasting weather calm and low wind velocity are conducive to concentration of dust pollutants. Similar correlations between PM10 concentration and meteorological elements were observed by Kalbarczyk and Kalbarczyk (2008) in the town of Suwałki (north-east Poland) and by Krynicka and Drzeniecka-Osiadacz (2013) in Wrocław (south-west Poland).

The complex of meteorological elements most strongly determined PM10 concentration in autumn and next in winter; in all seasons of the year the strongest influence on dust pollution was exerted by Ta and V. Meteorological elements in models describing air quality were also used by Rogalski et al. (2014), Majewski et al. (2015), Czernecki et al. (2017) and Stafoggia et al. (2017).

The PM10 content in air showed yearly, seasonal variability. PM10 concentration in winter was twice as high as in summer; however, the highest concentration of the

analyzed pollutant in particular years was recorded in various months, both in January or February and in June or August. A similar time distribution of PM10 concentration throughout the year, which was probably an effect of variable activity of emission sources in particular months, was found by Bielec-Bąkowska et al. (2011), Jędruszkiewicz et al. (2017) and Czernecki et al. (2017).

The content of suspended dust underwent changes not only in subsequent years, but also displayed daily variability. The highest PM10 concentration in 2005-2016 was recorded in the cold season of the year, at late-evening hours; the lowest concentration was observed in summer months during the day. Daily variation of the content of suspended dust against the background of time distribution was also investigated by Tiwari et al. (2017).

Unfavorable aerosanitary conditions in winter were mostly recorded with easterly winds. In the eastern part of Poznań there are heat and power plants which, aside from causing air pollution, supply heat and electrical power mainly for the city. In particular years of the analyzed multi-year period increasingly warm summers, especially in the July-August period, and also winters could be observed. The monthly course of Rh was opposite compared to Ta; the highest average relative humidity of air was recorded in November and December. In Poznań, the highest air humidity was also recorded in November and December in 1951-1990 (Farat, 1996). At the measurement point wind was predominantly from the SW direction, and next the W direction; the directions N and NE were recorded least frequently; the average frequency of weather calm amounted to approx. 5.2%. Compared to Farat's (1996) study, weather calm occurred with a similar frequency to 1951-1990. The remaining meteorological parameters (Ta, Rh, Pa and V) also did not deviate considerably from those in the research studies by Farat (1996) and Kalbarczyk (2010), which were conducted in 1966-2005. Such a high consistency of results is fairly surprising.

It occurred despite the fact that the second half of the 1990s was the period of introducing electrical sensors, marked by a greater accuracy, to weather monitoring. Also research on climate change indicates that in Poland there are ongoing changes in meteorological elements, confirmed by significant trends found during the years of the research.

Conclusions

The conducted research has shown dependence of daily PM10 concentration on meteorological conditions, mainly on air temperature variability and wind velocity. The strength and direction of the effect of the analyzed meteorological elements on PM10 concentration depended on the season of the year, the month and the time of day. The variability of dust concentration was explained by regression equations where meteorological elements were independent variables, with an accuracy from 13% (spring) to about 38% (autumn). The highest air dust levels were observed in winter, most frequently at late-evening hours and at night. In Poznań, increased air dust levels in winter occurred with low air temperatures, high relative humidity, low wind velocity, mainly from the E direction, and high atmospheric pressure. Meteorological elements which, as shown, significantly affect the level of PM10 concentration but also other air pollutants require constant observation due to changes in climatic conditions of Poland and the world.

REFERENCES

- [1] Adamek, A., Ziernicka-Wojtaszek, A. (2017): Variability of particulate matter PM10 concentration in Sosnowiec, Poland, depending on the type of atmospheric circulation. – *Applied Ecology and Environmental Research* 15(4): 1803-1813. DOI: http://dx.doi.org/10.15666/aeer/1504_18031813.
- [2] Badyda, A., Gayer, A., Czechowski, P. O., Majewski, G., Dąbrowiecki, P. (2016): Pulmonary function and incidence of selected respiratory diseases depending on the exposure to ambient PM10. – *Int. Mol. Sci.* 17(11): 1954. DOI: 10.3390/ijms17111954.
- [3] Balakrishnaiah, G., Raghavendra Kumar, K., Suresh Kumar Reddy, B., Rama Gopal, K., Reddy, R. R., Reddy, L. S. S., Narasimhulu, K., Nazeer Ahammed, Y., Balanarayana, C., Krishna Moorthy, K., Suresh Babu, S. (2011): Characterization of PM, PM10 and PM2.5 mass concentrations at a tropical semi-arid station in Anantapur, India. – *Indian J. Radio Space* 40: 95-104.
- [4] Bielec-Bąkowska, Z., Knozová, G., Leśniok, M., Matuszko, D., Piotrowicz, K. (2011): High suspended dust concentrations in Brno, Sosnowiec and Krakow (the year 2009 as an example). – *Prace Geograficzne* 126: 67-84.
- [5] Bigi, A., Ghermandi, G. (2016): Trends and variability of atmospheric PM2.5 and PM10-2.5 concentration in the Po Valley, Italy. – *Atmos. Chem. Phys.* 16: 15777-15788. DOI: 10.5194/acp-16-15777-2016.
- [6] Cesari, D., De Benedetto, G. E., Bonasoni, P., Busetto, M., Dinoi, A., Merico, E., Chirizzi, D., Cristofanelli, P., Donato, A., Grasso, F. M., Marinoni, A., Pennetta, A., Contini, D. (2018): Seasonal variability of PM2.5 and PM10 composition and sources in an urban background site in Southern Italy. – *Sci. Total Environ.* 612: 202-213. DOI: 10.1016/j.scitotenv.2017.08.230.
- [7] Chiang, Y. H., Yang, H. J., Chen, S. C., Hu, C. W., Tsai, C. T., Lai, D. J., Kuo, C. Y. (2017): Inhalation exposure of children to indoor PM10 and associated metals during river-dust episodes. – *Air Qual. Atmos. Health* 10: 381-388. <https://doi.org/10.1007/s11869-016-0426-z>.
- [8] Chwil, S., Kozłowska-Strawska, J., Tkaczyk, P., Chwil, P., Matraszek, R. (2015): Assessment of air pollutants in an urban agglomeration in Poland made by the biomonitoring of trees. – *J. Elem.* 20(4): 813-826. DOI: 10.5601/jelem.2015.20.1.742.
- [9] Ćwiek, K., Majewski, G. (2015): The influence of meteorological factors on the development of air pollutants concentration – Cracow case study. – *Sci. Rev. Eng. Env. Sci.* 67(2): 54-66 (in Polish).
- [10] Czernecki, B., Półrolniczak, M., Kolendowicz, L., Marosz, M., Kendzierski, S., Pilgaj, N. (2017): Influence of the atmospheric conditions on PM10 concentrations in Poznań, Poland. – *J. Atmos. Chem.* 74(1): 115-139. <https://doi.org/10.1007/s10874-016-9345-5>.
- [11] D'Amato, G., Cecchi, L., D'Amato, M., Liccardi, G. (2010): Urban air pollution and climate change as environmental risk factors of respiratory allergy: an update. – *Journal of Investigational Allergology and Clinical Immunology* 20(2): 95-102.
- [12] Emmanouil, C., Drositi, E., Vasilatou, V., Diapouli, E., Krikonis, K., Eleftheriadis, K., Kungolos, A. (2017): Study on particulate matter air pollution, source origin, and human health risk based of PM10 metal content in Volos City, Greece. – *Toxicol. Environ. Chem.* 99(4): 691-709. [doi.org/10.1080/02772248.2016.1242005](http://dx.doi.org/10.1080/02772248.2016.1242005).
- [13] Farat, R. (1996): Climate of Poznan. – In: Kurek, L. (ed.) *The Natural Environment of the City of Poznan*. Vol. 1., Chapter 7, pp. 69-78. Wydział Ochrony Środowiska Urzędu Miasta Poznania, Poznan (in Polish).
- [14] Flores, R. M., Kaya, N., Eşer, Ö., Saltan, Ş. (2017): The effect of mineral dust transport on PM10 concentrations and physical properties in Istanbul during 2007-2014. – *Atmos. Res.* 197: 342-355. DOI: 10.1016/j.atmosres.2017.07.009.
- [15] Gładka, A., Zatoński, T. (2016): Impact of air pollution on respiratory diseases. – *Kosmos* 65(4): 573-582. (in Polish).

- [16] Gliniak, M., Zuśka, Z., Miczyński, J. (2015): Evaluation of dust pollution level in Kraków agglomeration on the example of Al. A. Mickiewicza. – *Logistyka* 4: 8876-8881. (in Polish).
- [17] Gustafsson, M., Forsberg, B., Orru, H., Åström, S., Tekie, H., Sjöberg, K. (2014): Quantification of Population Exposure to NO₂, PM_{2.5} and PM₁₀ and Estimated Health Impacts in Sweden 2010. Report. – Swedish Environmental Research Institute, Stockholm.
- [18] Jędruskiewicz, J., Czernecki, B., Marosz, M. (2017): The variability of PM₁₀ and PM_{2.5} concentrations in selected Polish agglomerations: the role of meteorological conditions, 2006-2016. – *Int. J. Environ. Health Res.* 20: 1-22. DOI: 10.1080/09603123.2017.1379055.
- [19] Judy-Rezler, K., Toczko, B. (eds.) (2016): Dust in the atmosphere. A compendium of knowledge about dust pollution in Poland. – *Inspekcja Ochrony Środowiska. Biblioteka Monitoringu Środowiska* (in Polish).
- [20] Kalbarczyk, R. (2010): Unfavourable thermal conditions of air at the turn of the 20th and 21st centuries reducing crop productivity of pickling cucumber (*Cucumis sativus* L.) in Poland. – *Span. J. Agric. Res.* 8(4): 1163-1173. DOI: 10.5424/sjar/2010084-1406.
- [21] Kalbarczyk, R., Kalbarczyk, E. (2008): Concentration of gas and particulate air pollutants in Suwałki analysed in relation to meteorological conditions. – *Pol. J. Natur. Sci.* 23: 134-151.
- [22] Kiesewetter, G., Borcken-Kleefeld, J., Schöpp, W., Heyes, C., Bertok, I., Thunis, P., Bessagnet, B., Terrenoire, E., Amann, M. (2013): Modelling compliance with NO₂ and PM₁₀ air quality limit values in the GAINS model. – TSAP Report #9, Version 1.0.
- [23] Krynicka, J., Drzeniecka-Osiadacz, A. (2013): Analysis of variability in PM₁₀ concentration in the Wrocław agglomeration. – *Pol. J. Environ. Stud.* 22: 1091-1099.
- [24] Li, L., Wu, A. H., Cheng, I., Chen, J. C., Wu, J. (2017): Spatiotemporal estimation of historical PM_{2.5} concentrations using PM₁₀, meteorological variables, and spatial effect. – *Atmos. Environ.* 166: 182-191. <https://doi.org/10.1016/j.atmosenv.2017.07.023>.
- [25] Majewski, G., Rogula-Kozłowska, W., Czechowski, P. O., Badyda, A., Brandyk, A. (2015): The impact of selected parameters on visibility: first results from a long-term campaign in Warsaw, Poland. – *Atmosphere-Basel* 6: 1154-1174. DOI: 10.3390/atmos6081154.
- [26] Maji, K. J., Arora, M., Dikshit, A. K. (2017): Burden of disease attributed to ambient PM_{2.5} and PM₁₀ exposure in 190 cities in China. – *Environ. Sci. Pollut. Res.* 24: 11559-11572. DOI: 10.1007/s11356-017-8575-7.
- [27] Mok, K. M., Miranda, A. I., Yuen, K. V., Hoi, K. I., Monteiro, A, Ribeiro, I. (2017): Selection of bias correction models for improving the daily PM₁₀ forecasts of WRF-EURAD in Porto, Portugal. – *Atmos. Pollut. Res.* 8: 628-639. <https://doi.org/10.1016/j.apr.2016.12.010>.
- [28] NIK's Report (2014): Protection of the air against pollution. Information about control results. – Raport NIK 2014. nr ewid. 177/2014/P/14/086/LKR (in Polish).
- [29] Pannullo, F., Lee, D., Neal, L., Dalvi, M., Agnew, P., O'Connor, F. M., Mukhopadhyay, S., Sahu, S., Sarran, C. (2017): Quantifying the impact of current and future concentrations of air pollutants on respiratory disease risk in England. – *Environ. Health* 16: 29. <https://doi.org/10.1186/s12940-017-0237-1>.
- [30] Redington, A. L., Witham, C. S., Hort, M. C. (2016): Source apportionment of speciated PM₁₀ in the United Kingdom in 2008: Episodes and annual averages. – *Atmos. Environ.* 145: 251-263. <https://doi.org/10.1016/j.atmosenv.2016.09.047>.
- [31] Resolution no. 3056/2016 of Great-Polish Voivodship of 29 Dec. (2016): Resolution no. 3056/2016 of Great-Polish Voivodship Administration of Dec. 29, 2016 accepting the motion of the Regional Convention on the program for air quality protection in the Great-Polish area (in the range of PM₁₀ dust, PM_{2.5} and B(a)P). [Uchwała nr 3056/2016 Zarządu Województwa Wielkopolskiego z dnia 29 grudnia 2016 roku w sprawie

- przyjęcia projektu uchwały Sejmiku Województwa Wielkopolskiego w sprawie określenia programu ochrony powietrza dla strefy wielkopolskiej (w zakresie pyłu PM10, PM2,5 oraz B(a)P)] (in Polish).
- [32] Richter, D., Williams, W. P. (1998): Assessment and Management of Urban Air Quality in Europe. EEA monograph no. 5. – European Environment Agency, Copenhagen.
- [33] Rogalski, L., Smoczyński, L., Krzebietke, S., Lenart, L., Mackiewicz-Walec, E. (2014): Changes in sulphur dioxide concentrations in the atmospheric air assessed during short-term measurements in the vicinity of Olsztyn, Poland. – *J. Elem.* 735-748. DOI: 10.5601/jelem.2014.19.2.634.
- [34] Segersson, D., Eneroth, K., Gidhagen, L., Johansson, C., Omstedt, G., Nylén, A. E., Forsberg, B. (2017): Health impact of PM10, PM2.5 and black carbon exposure due to different source sectors in Stockholm, Gothenburg and Umea, Sweden. – *Int. J. Environ. Res. Public Health* 14: 742. DOI: 10.3390/ijerph14070742.
- [35] Sosa, B. S., Porta, A., Colman Lerner, J. E., Banda Noriega, R. B., Massolo, L. (2017): Human health risk due to variations in PM10-PM2.5 and associated PAHs levels. – *Atmos. Environ.* 160: 27-35. <https://doi.org/10.1016/j.atmosenv.2017.04.004>.
- [36] Stafoggia, M., Schwartz, J., Badaloni, Ch., Bellander, T., Alessandrini, E., Cattani, G., de' Donato, F., Gaeta, A., Leone, G., Lyapustin, A., Sorek-Hamer, M., de Hoogh, K., Di, Q., Forastiere, F., Kloog, I. (2017): Estimation of daily PM10 concentrations in Italy (2006–2012) using finely resolved satellite data, land use variables and meteorology. – *Environ. Int.* 99: 234-244. <https://doi.org/10.1016/j.envint.2016.11.024>.
- [37] Tasić, V., Kovačević, R., Maluckov, B., Apostolovski-Trujić, T., Matić, B., Cocić, M., Šteharnik, M. (2017): The content of as and heavy metals in TSP and PM10 near copper smelter in Bor, Serbia. – *Water Air Soil Pollut.* 228: 230. <https://doi.org/10.1007/s11270-017-3393-6>.
- [38] Tiwari, S., Dumka, U. C., Gautam, A. S., Kaskaoutis, D. G., Srivastava, A. K., Bisht, D. S., Chakrabarty, R. K., Sumlin, B. J., Solmon, F. (2017): Assessment of PM2.5 and PM10 over Guwahati in Brahmaputra River Valley: Temporal evolution, source apportionment and meteorological dependence. – *Atmos. Pollut. Res.* 8: 13-28. <https://doi.org/10.1016/j.apr.2016.07.008>.
- [39] World Health Organization (2013): Review of Evidence on Health Aspects of Air Pollution. REVIHAAP Project. – WHO Regional Office for Europe, Copenhagen, Denmark.
- [40] Yang, W.Y, Zhang, Z.Y, Thijs, L., Bijnsens, E. M., Janssen, B. G., Vanpoucke, C., Lefebvre, W., Cauwenberghs, N., Wei, F. F., Luttun, A., Verhamme, P., Van Hecke, E., Kuznetsova, T., D'hooge, J., Nawrot, T. S., Staessen, J. A. (2017): Left ventricular function in relation to chronic residential air pollution in a general population. – *Eur. J. Prev. Cardiol.* 24(13): 1416-1428. <https://doi.org/10.1177/2047487317715109>.

COMPARISON OF ADAPTIVE NEURO-FUZZY INFERENCE SYSTEM, ARTIFICIAL NEURAL NETWORKS AND NON-LINEAR REGRESSION FOR BARK VOLUME ESTIMATION IN BRUTIAN PINE (*PINUS BRUTIA* TEN.)

ÇATAL, Y.^{1*} – SAPLIOĞLU, K.²

¹*Forestry Faculty, Süleyman Demirel University, 32260 Isparta, Turkey*

²*Engineering Faculty, Süleyman Demirel University, 32260 Isparta, Turkey*

**Corresponding author*

e-mail: yilmazcatal@sdu.edu.tr; phone: +90-246-211-3955; fax: +90-246-211-3948

(Received 14th Dec 2017; accepted 26th Mar 2018)

Abstract. The bark is required to determine the volume of bark while identifying tree volume in forest planning. Since the bark volume of brutian pine (*Pinus brutia* Ten.) is considerably more when compared to other tree species, a real-like estimation should be made for the amount of bark. In this study, the Adaptive Neuro-Fuzzy Inference System (ANFIS) method was implemented in the bark estimation. The results obtained with the ANFIS method were compared with the results obtained with the Non-Linear Regression (NLR) and Artificial Neural Networks (ANN) methods. Among the eight models that can be used to determine the bark volume in the NLR method, the Morgan-Mercer-Flodin (MMF) model was determined to be the model giving the best results. Brutian pine bark volume model with the smallest values of the indicators used (MAE = 0.01630; RMSE = 0.02345; FI = 0.955363 and Bias = 0.00151) is the MMF nonlinear model. The amount of bark obtained with the ANFIS method provided better results when compared to ANN and to NLR. The slope graphs for the values estimated with the real value and method for the ANFIS, ANN and NLR methods were found to be 44.01°, 44.60° and 44.83°, respectively. In conclusion, the bark estimation with the ANFIS method provided better results when compared to the ANN and LNR methods.

Keywords: *bark amount, multiple regression, forest inventory, modelling, regression models*

Introduction

The bark thickness of trees is defined as the area remaining in between the cambium layer and the outer limit of the stem. It is very important to determine the amount of bark, as well as the volume of the individual trees. Because, bark appears as the biggest waste material since it does not have a wide usage area in the wood industry. Sometimes, bark constitutes 20% of the tree volume (Laasasenaho et al., 2005; Cellini et al., 2012). At times considered a bothersome waste product, bark is now widely used as an industrial fuel, in soil amelioration, and as ground cover. Bark is also a possible source of chemical feed stocks (Doruska et al., 2009). Today, most pulp and paper mills, plywood plants, and sawmills burn all their bark to produce energy to run the plant and to dry products (Adler, 2007; Bowyer et al., 2007).

The main element in even-aged forest management is growth and yield prediction. Prediction consists in predicting harvest and future growth stocks, which are essential for forest management. It is highly important to estimate in advance the amount of usable wood to be obtained from the forest during the planning stage in forest management. However, the correct determination of the bark amount in an individual tree is one of the most significant components of planning. Furthermore, the amount of

bark volume to be included in the stand simulation models as a variable is an important component for the models to be operated correctly.

The bark volume is generally expressed as a percentage according to the total tree volume. This rate varies by tree species, diameter, total height, age, height on stem, site index, genotypes and similar characteristics (Philip, 1994; Laassenaho et al., 2005). It was determined that different habitats and growing conditions in different coniferous tree species provide different results related to bark thickness (Loetsch et al., 1973; Wilhelmsson et al., 2002; Laasasenaho et al., 2005; Sönmez et al., 2007). There are also differences between the origins of the same tree species (Mc Connon et al., 2004; Kohnle et al., 2012). Thus, it is important to determine bark thickness. The bark thickness and the relationship between the bark thickness and the other tree parameters are investigated by many researchers (Malone and Liang, 2009; Stängle et al., 2017). However, there are a limited number of studies on the bark volume (Laasasenaho et al., 2005; Cellini et al., 2012). There are not a sufficient number of studies on the bark volume of tree species in Turkey (Kahrیمان et al., 2016).

Linear and non-linear regression models revealing the bark volume are tested (Kozak and Yang, 1981; Diamantopoulou, 2005; Malone and Liang, 2009; Cellini et al., 2012). Due to some prejudices resulting from the method of least squares and the fact that errors in the regression equations may be big, alternative methods are studied (Diamantopoulou, 2005). The most common ones among these methods are Artificial Neural Networks (ANN) and Adaptive Neuro-Fuzzy Inference System (ANFIS). A number of researchers have investigated the applicability of ANN models to the field of forest modelling (Zhang et al., 2000; Leduc et al., 2001; Liu et al., 2003; Corne et al., 2004; Leite et al., 2011). There are also studies on forestry with ANFIS (Bui et al., 2012; Pradhan, 2013; Jaafari et al., 2017). It was determined in the previously conducted studies that the ANN method provides better truth results for training and testing data in determining the amount of bark when compared to the regression method (Diamantopoulou, 2005).

Pinus brutia (*Pinus brutia* Ten.) is a pine native to the eastern Mediterranean region. Brutian pine in Turkey is an important tree species, which has a spreading area of 5.6 million hectares. It constitutes 25.1% of the forests in Turkey. Brutian pine stands meet an important part of the wood need in Turkey (GDF, 2015).

The aim of this study is to reveal the method by which the amount of bark in brutian pine trees in Turkey, where it has the widest spreading area in the world, can be determined correctly. Firstly, the appropriate model was determined with Non-Linear Regression (NLR) method among many models. Secondly, the bark volumes found with the ANN and ANFIS methods as an alternative to the NLR method with this model determined were compared, and the method providing the most real-like result was determined.

Materials and methods

Material

Brutian pine trees in the forests of Antalya, Isparta and Burdur regions located in the south of Turkey were measured within the scope of the study (*Fig. 1*). The study areas is situated between 37°13'49'' N, 29°23'54'' E, to 37°13'49'' N, 31°26'31'' E, average slope 10-25°, predominantly south aspect 600-1000 m altitude. The study area is found

on calcareous formations. The soil is generally shallow or medium-deep, and stony, with a predominantly clay texture.

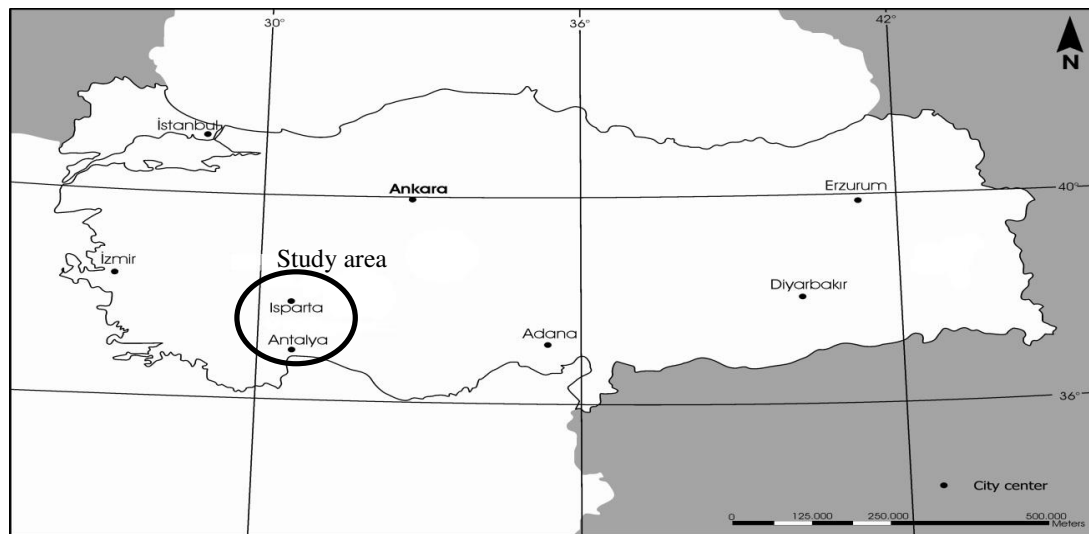


Figure 1. Location of study area in Turkey

Six stands were selected to different site quality. The stands have same aged, pure and normal canopy. A total of 338 trees enough to compare statistics were cut, and the following variables were measured: breast height diameter- $d_{1.3}$ (cm), paired data of diameters- d_i (cm) and height- h_i (m) along the stem, total height of the tree- H (m), bark thickness for each d_i and h_i , BT_i (cm). Measures were taken with metric tapes over cut faces of each log, with a precision of ± 1 mm.

The cylinder volume and log volume were provided volume by using diameter values with and without bark obtained on the stem, and the volume of each section was provided volume with the Smalian's formula, and the end part was provided volume with the cone volume formula. The total volume of the parts was obtained from the tree volume with and without bark (Eq. 1; Avery and Burkhart, 2002; West, 2009).

$$v = \frac{\pi}{4} (d_{0.3}^2) 0.3 + \frac{\pi}{4} \left(\frac{d_{0.3}^2 + d_i^2}{2} \right) l_i + \frac{\pi}{4} \left(\frac{d_i^2 + d_{i+1}^2}{2} \right) l_{i+1} + \dots + \frac{\pi}{4} \left(\frac{d_{n-1}^2 + d_n^2}{2} \right) l_{i+n} + \frac{\pi}{4} \frac{1}{3} d_k^2 l_t \quad (\text{Eq.1})$$

In the equation π is 3.14159; v_i is the i^{th} volume of the k sections of the bole; v_t is the top section volume; $d_{0.3}$, $d_{1.3}$, $d_{3.3}$, ..., d_k are diameters at different height and l_t is the length of the top bole section.

Thus, the tree volume with bark (v), tree bark volume (v_b) obtained by subtracting tree volume without bark from tree volume with bark, breast height diameter with bark ($d_{1.3}$) and breast height diameter without bark ($d_{1.3u}$) values of a tree were acquired.

Non-linear regression (NLR)

It is required to ensure some preconditions to perform the regression analysis. These conditions are the facts that data exhibit normal distribution, there is a linear relationship between dependent and independent variables, homoscedasticity is provided, there are not multi-collinearity problems, and error terms are independent of

each other (Hair et al., 2009). In this study for the NLR, whether the amount of bark, which was a dependent variable, exhibited normal distribution was tested with the Lilliefors test. It is an improvement on the Kolomogorov-Smirnov (K-S) test-correcting the K-S for small values at the tails of probability distributions-and is therefore sometimes called the K-S D test. Many statistical packages (like SPSS) combine the two tests as a “Lilliefors corrected” K-S test. Unlike the K-S test, Lilliefors can be used when you do not know the population mean or standard deviation. Essentially, the Lilliefors test is a K-S test that allows you to estimate these parameters from your sample (SPSS-Guide, 2010).

Whether variances are distributed homogeneously is tested with Levene’s test. Levene’s test is used to test if k samples have equal variances. Equal variances across samples are called homogeneity of variance. Some statistical tests, for example the analysis of variance, assume that variances are equal across groups or samples. The Levene test can be used to verify that assumption (Hair et al., 2009). The Durbin-Watson test statistic tests the null hypothesis that the residuals from an ordinary least-squares regression are not auto-correlated against the alternative that the residuals follow an AR1 process (Tabachnick and Fidell, 2014). The Durbin-Watson statistic ranges in value from 0 to 4. A value near 2 indicates non-autocorrelation (Cellini et al., 2012); a value toward 0 indicates positive autocorrelation; a value toward 4 indicates negative autocorrelation (Anderson et al., 2004). The variance inflection factor (VIF) value is a measure of the amount of multicollinearity in a set of multiple regression variables. The presence of multicollinearity within the set of independent variables can cause a number of problems in the understanding the significance of individual independent variables in the regression model. Using variance inflation factors helps to identify multicollinearity issues so that the model can be adjusted (SPSS-Guide, 2010). These preconditions have been tested in this study.

The following commonly used models in forestry were selected for NLR. The Logistic (Eq. 2); Gompertz (Eq. 3); Mitscherlich (Eq. 4); Morgan-Mercer-Flodin (Eq. 5); Verhulst (Eq. 6); Asymptotic Regression (Eq. 7); Richards (Eq. 8) models were used for the non-linear regression method to determine the bark volume (Norusis, 2000).

$$\text{Logistic Model} \quad v_b = \frac{1}{(1+e)^{-z}} \quad (\text{Eq.2})$$

$$\text{Gompertz Model} \quad v_b = \beta_0 \exp(-\beta_1 \exp(-\beta_2 Z)) \quad (\text{Eq.3})$$

$$\text{Mitscherlich Model} \quad v_b = \beta_0 + \beta_1 \exp(-\beta_2 Z) \quad (\text{Eq.4})$$

$$\text{Morgan-Mercer-Flodin Model} \quad v_b = \frac{\beta_0 \beta_1 + \beta_2 Z^{\beta_3}}{\beta_1 + Z^{\beta_3}} \quad (\text{Eq.5})$$

$$\text{Verhulst Model} \quad v_b = \frac{\beta_0}{1 + \beta_1 \exp(-\beta_2 z)^{\beta_3}} \quad (\text{Eq.6})$$

$$\text{Asymptotic Regression Model} \quad v_b = \beta_0 - (\beta_1 * \beta_0^Z) \quad (\text{Eq.7})$$

Richards Model
$$v_b = \frac{\beta_0}{1 + \beta_1 \exp(-\beta_2 Z)^{\frac{1}{\beta_3}}} \quad (\text{Eq.8})$$

β_0 , β_1 refer to the regression coefficients in the equation. *Equation 9* was used to obtain the Z value.

$$Z = \beta_0 + \beta_1 d_{1.3} + \beta_2 d_{1.3u} + \beta_3 v \quad (\text{Eq.9})$$

The final state of the equations was achieved by including *Equation 9* in the non-linear regression equations. The coefficients of the non-linear regression models were obtained with the NLR module in the SPSS statistics package program. The methods of Norusis (2000) were used for an appropriate initial value.

Artificial neural networks (ANN)

ANN were developed by inspiring from the human brain, and they are the information processing structures connected to each other with the aid of weighted connections (Hotunoğlu and Karakaya, 2011). Each cell has its own memory. The basic logic of the ANN is that it cannot learn by itself. One of the biggest disadvantages of the ANN is the memorization of the system. It can memorize by establishing a relationship between disconnected events given to it. It is required to distinguish the test data to understand whether the system is based on memorization or learning and to test the system with these data after the learning process (Chang et al., 2010). If the learning process is completed successfully, a high statistical relationship is found in the analyses conducted for the test data. However, if a model including a high statistical relationship in training cannot exhibit this relationship to the test, it is not successful. Therefore, a certain part of the data is separated for the test. The operation hierarchy of the system is presented below in a graph (*Fig. 2*).

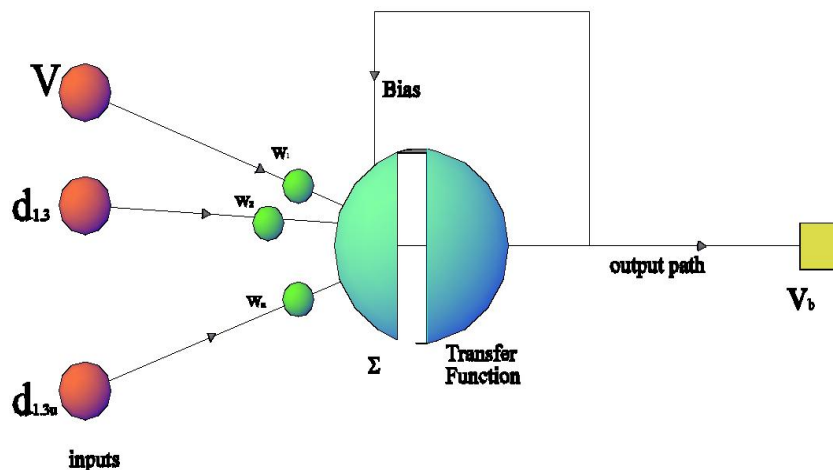


Figure 2. ANN operation sequence diagram

Inputs: They are the information sent from outside to an artificial cell. They are determined by the user. *Weights:* They are used to determine the significance level of

the incoming information. They are reassigned by being rearranged in return for each error during training. *Addition function*: This function calculates the net incoming input to a cell. This operation can be performed with many different functions. The most common one is the weighted addition. Each incoming information is found by multiplying it by its weight (Geem and Roper, 2009). *Activation Function*: It determines the output in return for the incoming input. In general, a non-linear function is selected. An easy differentiation of the function is extremely important in terms of the speed of the process due to the use of the activation function derivative, especially in feed-back networks. Sigmoid functions are the most common functions.

The feed forward back propagation learning algorithm was used in the operation of the model in question. This algorithm consists of two steps. The first one is the feed forward step that forwards the external information input in the input cells to calculate the output information in the output units. The second step is the back propagation of the differences between the values calculated in the output unit and the observation values. The hidden layer output expression in the hidden layers in artificial neural networks is calculated as in *Equation 10* (Partal et al., 2008).

$$y_j = f\left(\sum x_i W_{ij}\right) \quad (\text{Eq.10})$$

Here, each neuron is multiplied by the weights of the input signals and summed up. Here, f is the activation function used in hidden and output layers, and its expression is indicated in *Equation 11*.

$$f_j = \frac{1}{1 + e^{-x_j}} \quad (\text{Eq.11})$$

The square of the difference between the required value of the output neuron and the real value provides the E error value. The expression of the E error value is indicated in *Equation 12*.

$$E = \frac{1}{2} \sum_i (y_i - d_i)^2 \quad (\text{Eq.12})$$

The amounts of bark were determined with ANN with these sequences of actions

Adaptive neuro-fuzzy interface system (ANFIS)

ANFIS, developed by Jang (1993), only minor applications of landslide-related studies have been reported (Bui et al., 2012). ANFIS is a multilayer feed-forward network, in which each node performs a particular function on incoming signals and has a set of parameters pertaining to this node (Jang, 1993). ANFIS combines fuzzy logic and ANNs by using the mathematical properties of ANNs in tuning a rule based fuzzy inference system that approximates how the human brain processes information (Akib et al., 2014). The multiplicity and homogeneity of the data are extremely important for the results of the model to operate. The cluster types and number of the data may vary by the type and complexity of the problem (Dongkyun et al., 2018). Each input parameter is introduced to the system (*Fig. 3*).

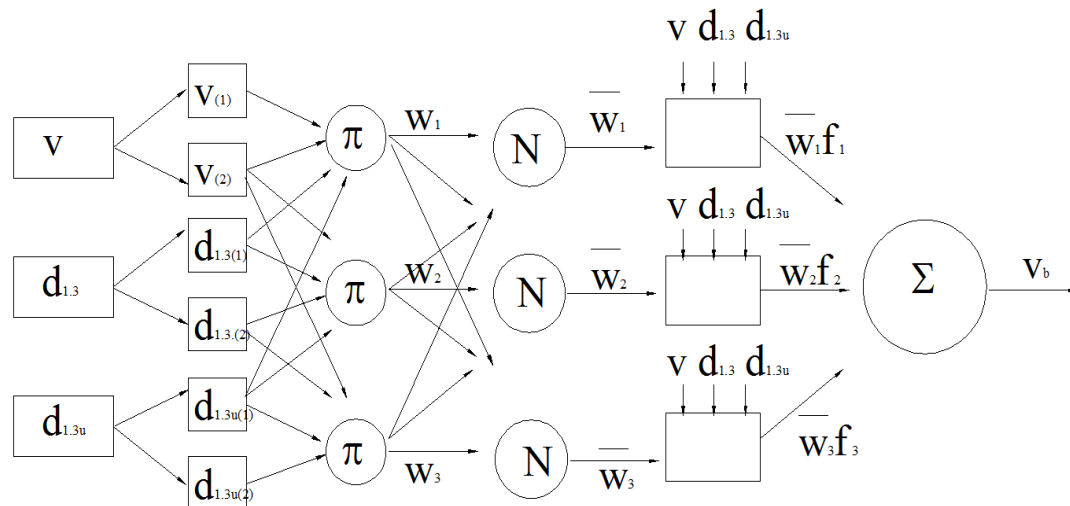


Figure 3. ANFIS operation sequence diagram

The cluster number for these parameters introduced is determined. In the next step, weight values are assigned to each input parameter, and they are multiplied. The outputs obtained are sent to the total function, and the errors are determined. These operation steps are repeated until the errors are minimized.

Comparison of methods

Comparison of estimation of methods was based on graphical and numerical analysis of residuals and five goodness of fit statistics: mean absolute error (MAE) (Eq. 13), which expresses the average of absolute errors between forecast and actual value; root mean square error (RMSE) (Eq. 14), which analyses the precision of estimations; fix index (FI) (Eq. 15), which reflect the total variability that is explained by the model considering the total number of parameters to be estimated; mean error (Bias) (Eq. 16), which average error for estimated values. The best regression yielded the smallest MAE, RMSE, Bias and the largest FI. These evaluation statistics are defined as:

$$\text{Mean absolute error} \quad MAE = \frac{\sum_{i=1}^n |v_i - \hat{v}_i|}{n} \quad (\text{Eq.13})$$

$$\text{Root mean square error} \quad RMSE = \sqrt{\frac{\sum_{i=1}^n (v_i - \hat{v}_i)^2}{n - k}} \quad (\text{Eq.14})$$

$$\text{Fit Index} \quad FI = 1 - \left[\frac{\sum_{i=1}^n (v_i - \hat{v}_i)^2}{\sum_{i=1}^n (v_i - \bar{v}_i)^2} \right] \quad (\text{Eq.15})$$

$$\text{Mean error} \quad \text{Bias} = \frac{\sum_{i=1}^n (v_i - \hat{v}_i)}{n} \quad (\text{Eq.16})$$

where v_i = observed bark volume, \hat{v}_i = predicted bark volume, \bar{v} = mean of observed bark volume, n = number of observations in dataset and k = number of estimated parameters.

Results

The data measured are randomly divided into two sets by ANN. The method application was performed with the training data, and the consistency of the results of the process applied with the testing data was determined. While training data are randomly selected, attention has been carried out for the maximum and minimum data which should be situated in these data. The training data consisted of 221 trees (65%), and the testing data consisted of 117 trees (35%). Training and testing data were compared with t-test (t value = 0.012). With use of a two-tailed t-test for independent two samples, there was not significant difference between the training and testing data ($p > 0.05$). The summary of the training and testing data is presented in *Table 1*.

Table 1. Some statistics for the training and testing data

	Training data (n = 221)				Testing data (n = 117)			
	$d_{1.3}$	$d_{1.3u}$	v	v_b	$d_{1.3}$	$d_{1.3u}$	v	v_b
Minimum	5.3	4.4	0.010	0.004	10.2	8.5	0.040	0.006
Maximum	60.9	49.7	2.795	0.553	49.0	42.5	2.291	0.422
Mean	25.7	21.0	0.680	0.136	23.4	19.5	0.580	0.113

In *Table 1*, $d_{1.3}$ = diameter of breast height diameter (cm), $d_{1.3u}$ = breast height diameter without bark (cm), v = the tree volume with bark (m^3), v_b = tree bark volume (m^3).

For the NLR, whether the amount of bark, which was a dependent variable, exhibited normal distribution was tested with the Lilliefors test. Since the variance and average of the population were not known, the Lilliefors test and the normality test were conducted. Since the test statistics were found to be 5.246 ($p < 0.001$), the data were distributed homogeneously. Whether variances were distributed homogeneously was tested with Levene's test, and it was determined that the variances of the data were distributed homogeneously (4.164; $p < 0.001$). The Durbin-Watson value was found to be 1.987 in this study. This result indicates that there is not auto-correlation between the error terms of the independent variable. The variance inflection factor (VIF) value is required to be less than 10 to be able to test the multi-collinearity problem (SPSS-Guide, 2010). The VIF values were found to be less than 10 in this study.

According to the results obtained for *Equations 2-8* with the non-linear regression analysis, the results obtained as a result of the comparison made by using real values and regression analysis values are presented in *Table 2*.

Table 2. The results obtained according to the regression equations

Eq. no	MAE	RMSE	FI	Bias
2	0.03456	0.03480	0.92541	0.00223
3	0.02856	0.03258	0.93012	0.00302
4	0.02723	0.37820	0.93125	0.00285
5	0.01630	0.02345	0.955363	0.00151
6	0.02856	0.03152	0.91021	0.00278
7	0.03256	0.04023	0.89012	0.00326
8	0.04450	0.05321	0.87202	0.00365

For the eight nonlinear equations of *Table 2*, the range of the MAE values are 0.0163-0.05125 m³, and the range of the RMSE are 0.02345-0.05562 m³, the range of the Bias values is 0.00153-0.00455 m³ with the lowest values for the nonlinear model of *Equation 5*. The range of the FI values is 0.959363-0.851251 with the highest values for the nonlinear model of *Equation 5* too.

$$v_b = \frac{\beta_0\beta_1 + \beta_2(\beta_4 + \beta_5d_{1.3} + \beta_6d_{1.3u} + \beta_7v)^{\beta_3}}{\beta_1 + (\beta_4 + \beta_5d_{1.3} + \beta_6d_{1.3u} + \beta_7v)^{\beta_3}} \quad (\text{Eq.17})$$

The coefficients for *Equation 5*, which is the most appropriate model, were found to be β_0 :30.97118; β_1 :-8.84891; β_2 :26.88242; β_3 :4.92827; β_4 :0.00635; β_5 :-0.00760; β_6 :0.08300; β_7 :1.45622.

The real bark volume values and the estimated volume values were compared with four evaluation criteria for three methods used in the determination of the amount of bark in an individual tree (*Table 3*).

The actual measured values of the brutian pine bark volume were compared to the corresponding values predicted by the all methods. Results are given in *Table 3* and also the comparisons were made with the help of paired t-test, 45° line test.

Table 3. The evaluation criterion values obtained for the NLR, ANN and ANFIS methods

Methods	MAE	RMSE	FI	Bias	Slope (°)	t-Value
NLR	0.01630	0.02345	0.955363	0.00152	44.60	1.525
ANN	0.01077	0.01537	0.971205	0.00125	44.84	1.124
ANFIS	0.00838	0.01157	0.988612	0.00046	44.91	0.852

The values of estimation errors for NLR, ANN and ANFIS in the testing data sets were 0.00152, 0.00125 and 0.00046 m³, respectively. This shows that the ANFIS model of *Table 3* gave an estimation error that was 1.2 times smaller than the ANN model and was 3.3 times smaller than the best nonlinear model (*Eq. 17*).

The brutian pine bark volume estimates by the NLR model of *Equation 17*, by the ANN model and by the ANFIS of versus measured values for the training and testing data set are shown in *Figure 4a-f*, respectively. The proximity of each point to the 45° line throughout the range of the measured bark volume (*Fig. 4a-f*) indicates that the

ANFIS model is more accurate compared to the NLR model and the ANN model for test data (Fig. 4b, d, f).

As seen from Figure 4, it was observed that the real and estimated values in the graph obtained for the model and test data provided more distributed results when compared to the NLR method. The ANFIS method provided the best result graphically. The test values of slope were also calculated and respectively were found equal to 44.01° , 44.60° and 44.83° . The training values of slope were also calculated and respectively were found equal to 44.60° , 44.84° and 44.91° .

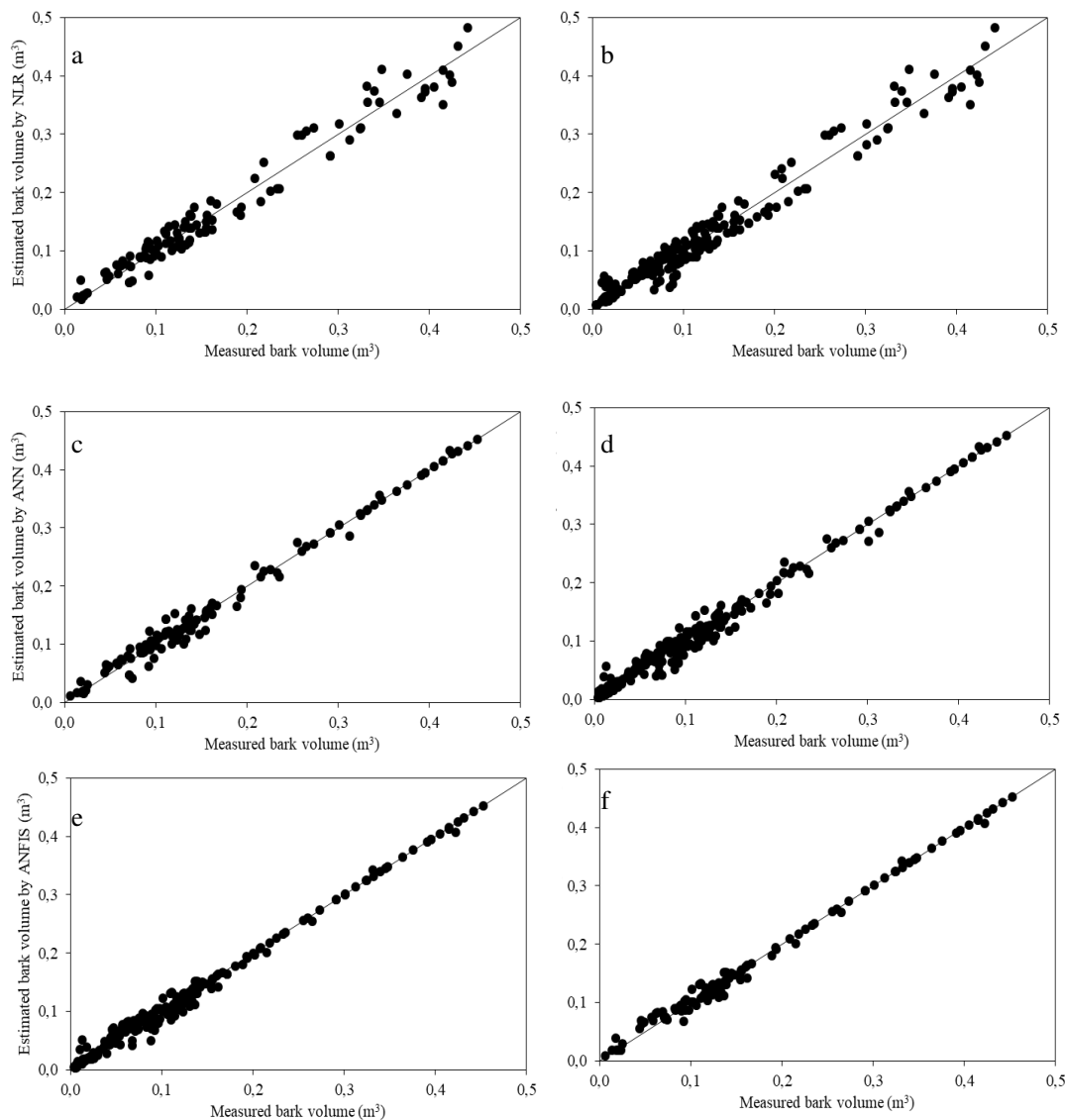


Figure 4. The amounts of bark volume obtained with the NLR (a-training, b-testing), ANFIS (c-training, d-testing) and ANN (e-training, f-testing) methods corresponding to the real volume values

The estimated volume value and actual volume values obtained with ANFIS, ANN and NLR methods were compared with the paired samples t test. The t-values were found to be 1.525, 1.124 and 0.852, respectively. The computed t-values for the NLR,

ANN and ANFIS model were less than the table t-value (1.96 for $\alpha = 0.05$). According to results difference was not found between actual values and estimated values for each of this tree methods.

Discussion

Bark volume depends on its thickness and stem diameter. These variables are being affected by tree age and stand conditions because of diameter of breast height increases (Laasasenaho et al., 2005; Sönmez et al., 2007; Kahriman et al., 2016). However, measuring the parameters of the stands is time consuming. Therefore, parameters that can be easily measured are needed. Linear and non-linear regression models with easily measured variables are used to estimate bark volume (Laasasenaho et al., 2005; Cellini et al., 2012). Due to some prejudices resulting from the method of least squares and the fact that errors in the regression equations may be big, alternative methods are studied. The most common ones among these methods are ANN and ANFIS. But, the use of these methods in forestry is limited. It was determined in the previously conducted studies that the ANN method provides better truth results for training and testing data in determining the amount of bark when compared to the regression method (Diamantopoulou, 2005).

In this study, it was determined that ANFIS method shown better results from ANN and NLR when the variables the tree volume with bark (v), breast height diameter with bark ($d_{1.3}$) and breast height diameter without bark ($d_{1.3u}$) values of a tree which are easy to measure during forest inventories were used in tree bark volume (v_b) estimation. This was followed by ANN and NLR, respectively. Although prediction of the tree bark volume with ANFIS is a complex process requiring specialized, it will be possible to obtain more accurate results by using in forestry. In additional, using the variables the tree volume with bark, breast height diameter with bark and breast height diameter without bark values of a tree measured from the tree, the tree bark volume can also be calculated with sufficient accuracy by the NLR method. For the NLR method, the nonlinear model of Morgan-Mercer-Flodin model was found as the best model. Diamantopoulou (2005) obtained the same equation as being the most appropriate regression equation among the previously conducted studies.

Conclusion

There is not a direct method of measurement for the determination of the bark volume on trees. Alternatively, the amount of bark is tried to be estimated with various methods. In this study, an appropriate regression equation (NLR method) was selected for the estimation of the tree volume with bark, double bark thickness values and the bark volume that is the tree parameter derived from these values, and the bark estimation was made with the ANN and ANFIS methods. The methods were compared as a result of this estimation.

As a result of this study, the bark volume can be obtained more correctly with the ANFIS modelling method. Together with the fact that the ANFIS method used becomes widespread in the forestry studies to be conducted, more realistic results can be obtained in the modelling of forest resources and stand developments.

REFERENCES

- [1] Adler, A. (2007): Accumulation of Elements in Salix and Other Species Used in Vegetation Filters with Focus on Wood Fuel Quality. – Doctoral Thesis. Swedish University of Agricultural Sciences, Uppsala.
- [2] Akib, S., Mohammadhassani, M., Jahangirzadeh, A. (2014): Application of ANFIS and LR in prediction of scour depth in bridges. – Computers and Fluids 91: 77-86.
- [3] Anderson, N., De Dreu, C. K. W., Nijstad, B. A. (2004): The routinization of innovation research: a constructively critical review of the state of the science. – Journal of Organizational Behaviour 25: 147-173.
- [4] Avery, T. E., Burkhart, H. E. (2002): Forest Measurements. 5th ed. – McGraw-Hill, New York.
- [5] Bowyer, J. L., Shmulsky, R., Haygreen, J. G. (2007): Forest Products and Wood Science: An Introduction. – Wiley Blackwell, Oxford.
- [6] Bui, D. T., Pradhan, B., Lofman, O., Revhaug, I., Dick, O. B. (2012): Landslide susceptibility mapping at Hoa Binh province (Vietnam) using an adaptive neuro fuzzy inference system and GIS. – Computers and Geosciences 45: 199-211.
- [7] Cellini, J. M., Galarza, M., Burns, S. L., Martinez-Pastur, G. J., Lencinas, M. V. (2012): Equations of bark thickness and volume profiles at different heights with easy-measurement variables. – Forest Systems 21(1): 23-30.
- [8] Chang, F., Kao, L., Kuo, Y., Liu, C. (2010): Artificial neural networks for estimating regional arsenic concentrations in a blackfoot disease area in Taiwan. – Journal of Hydrology (388): 65-76.
- [9] Corne, S. A., Carver, S. J., Kunin, W. E., Lennon, J. J., Van Hees, W. W. S. (2004): Predicting forest attributes in southeast Alaska using artificial neural networks. – Forest Science 50(2): 259-276.
- [10] Diamantopoulou, M. J. (2005): Artificial neural networks as an alternative tool in pine bark volume estimation. – Computers and Electronics in Agriculture 48: 234-244.
- [11] Dongkyun, I., Sung-Uk, C., Byungwoong, C. (2018): Physical habitat simulation for a fish community using the ANFIS method. – Ecological Informatics (accepted manuscript in press).
- [12] Doruska, P. F., Patterson, D., Hartley, J., Hurd, M., Hart, T. (2009): Newer technologies and bioenergy bring focus back to bark factor equations. – J. For. 107: 38-43
- [13] GDF (2015): The Presence of Forest in Turkey. – Republic of Turkey Ministry of Forestry and Water Affairs General Directorate of Forestry Publishing, Ankara.
- [14] Geem, Z., Roper, W. (2009): Energy demand estimation of South Korea using artificial neural network. – Energy Policy 37: 4049-4054.
- [15] Hair, J. F., Black, W. C., Babin, B. J., Anderson, R. E. (2009): Multivariate Data Analysis. – Prentice Hall, Upper Saddle River, NJ.
- [16] Hotunoğlu, H., Karakaya, E. (2011): Forecasting Turkey's energy demand using artificial neural networks: three scenario applications. – Ege Academic Review 2011(special issue): 87-94.
- [17] Jaafari, J., Rezaeian, J., Omrani, M. S. (2017): Spatial prediction of slope failures in support of forestry operations safety croat. – J. For. Eng. 38(1): 107-117.
- [18] Jang, J. S. (1993): ANFIS: adaptive network based fuzzy inference system. – IEEE Transactions on Systems, Man and Cybernetics 23(3): 665-685.
- [19] Kahriman, A., Sönmez, T., Şahin, A., Yavuz, M. (2016): A bark thickness model for calabrian pine in Turkey. – Proceedings of the 2nd International Conference on Science, Ecology and Technology, Barcelona, 23-25 August 2016, pp. 661-670.
- [20] Kohnle, U., Hein, S., Sorensen, F. C., Weiskittel, A. R. (2012): Effects of seed source origin on bark thickness of Douglas-fir (*Pseudotsuga menziesii*) growing in southwestern Germany. – Can. J. For. Res. 42(2): 382-399.

- [21] Kozak, A., Yang, R. C. (1981): Equations for estimating bark volume thickness at commercial trees in British Columbia. – *Forestry Chronicle* 1981: 112-115.
- [22] Laasasenaho, J., Melkas, T., Alden, S. (2005): Modelling bark thickness of *Picea abies* with taper curves. – *Forest Ecology and Management* 206(1): 35-47.
- [23] Leduc, D. J., Matney, T. G., Belli, K. L., Baldwin, V. C. (2001): Predicting diameter distributions of longleaf pine plantations: a comparison between artificial neural networks and other accepted methodologies. – *Southern Research Station RS 25*: 1-17.
- [24] Leite, H. G., da Silva, M. L. M., Binoti, D. H. B., Fardin, L., Takizawa, F. H. (2011): Estimation of inside-bark diameter and heartwood diameter for *Tectona grandis* Linn. trees using artificial neural networks. – *Eur. J. Forest Res.* 130: 263-269.
- [25] Liu, C., Zhang, L., Davis, C. J., Solomon, D. S., Brann, P. B., Caldwell, L. E. (2003): Comparison of neural networks and statistical methods in classification of ecological habitats using FIA data. – *Forest Science* 49(4): 619-631.
- [26] Loetsch, F., Zohrer, F., Haller, K. E. (1973): *Forest Inventory. Volume II.* – BLV Munich.
- [27] Malone, T., Liang, J. (2009): A bark thickness model for white spruce in Alaska northern forests. – *Int. J. For. Res.* 2009(3): 1-5.
- [28] Mc Connon, H., Knowles, R. L., Hansen, L. W. (2004): Provenance affects bark thickness in Douglas fir. – *For. Sci.* 34: 77-86.
- [29] Norusis, M. J. (2000): *SPSS for Windows.* – Prentice Hall, Englewood Cliffs.
- [30] Partal, T., Kahya, E., Cığızoğlu, K. (2008): Estimation of precipitation data using artificial neural networks and wavelet transform. – *ITU Journal of Engineering* 7(3): 73-85.
- [31] Philip, M. S. (1994): *Measuring Trees and Forests.* – CAB International, Wallingford, Oxon, UK.
- [32] Pradhan, B. (2013): A comparative study on the predictive ability of the decision tree, support vector machine and neuro-fuzzy models in landslide susceptibility mapping using GIS. – *Computers and Geosciences* 51: 350-365.
- [33] Sönmez, T., Keleş, S., Tilki, F. (2007): Effect of aspect, tree age and tree diameter on bark thickness of *Picea orientalis*. – *Scand. J. For. Res.* 22(3): 193-197.
- [34] *SPSS Guide* (2010): *SPSS Survival Manual: A Step by Step Guide to Data Analysis using SPSS for Windows, 4th ed.* – Open University Press, McGraw Hill.
- [35] Stängle, S. M., Sauter, U. H., Dormann, C. F. (2017): Comparison of models for estimating bark thickness of *Picea abies* in southwest Germany: the role of tree, stand, and environmental factors. – *Annals of Forest Science* 74: 1-10.
- [36] Tabachnick, B. G., Fidell, L. S. (2014): *Using Multivariate Statistics.* – Harlow Pearson Education Limited, Boston, USA.
- [37] West, P. W. (2009): *Tree and Forest Measurement, 2nd ed.* – Springer Verlag, Berlin.
- [38] Wilhelmsson, L., Arlinger, J., Spangberg, K., Lundqvist, S. O., Grahn, T., Hedenberg, O., Olsson, L. (2002): Models for predicting wood properties in stems of *Picea abies* and *Pinus sylvestris* in Sweden. – *Scand. J. For. Res.* 17(4): 330-350.
- [39] Zhang, Q. B., Hebda, R. I., Zhang, O. J., Alfaro, R. I. (2000): Tree-ring growth responses to climatic variables using artificial neural networks. – *Forest Science* 46(2): 229-239.

SHIFT IN THE ANNUAL GROWTH CYCLE OF GRAPEVINES (*VITIS VINIFERA* L.) IN WEST HUNGARY

KOVÁCS, E.^{1*} – PUSKÁS, J.² – POZSGAI, A.¹ – KOZMA, K.³

¹*Doctoral School of Environmental Sciences, ELTE Eötvös Loránd University
Pázmány P. sétány 1/A, H-1117 Budapest, Hungary*

²*Savaria Department of Geography, ELTE Eötvös Loránd University
Károlyi G. tér 4, H-9700 Szombathely, Hungary*

³*Department of Environmental Engineering, Széchenyi István University
Egyetem tér 1, H-9026 Győr, Hungary*

**Corresponding author
e-mail: kovacserik19@gmail.com*

(Received 2nd Jan 2018; accepted 7th Mar 2018)

Abstract. Regional climate change has noticeable influence on grape and wine production in West Hungary. Sopron and Zala wine-growing regions are among the potential winners of the climate change, previously rather unsuitable for viticulture. Over the past 30 years, the minimum and maximum temperatures significantly increased, the precipitation decreased, nevertheless, the convective precipitation increased by 14 days during the growing season. Each climate indicator has changed between 1986 and 2015 compared to the previous 30 years (1956-1985). One of the effects of climate change is a significant shift in the annual growth cycle of grapevines (phenological phases). Budbreak begins nearly 8 days earlier, flowering 7 days and the veraison 8 days, while the harvest has been shifted to a date 11 days respect to the previous period. The time between the budbreak and the flowering has shortened by 4.5 days.

Keywords: *climate change, agroclimate, growing-season, phenology, Carpathian Basin*

Introduction

Climate change is one of the most determinative challenges in the 21st century and protection against the extremities. The decreasing precipitation and the increasing temperatures have several visible signs both in Europe and in Hungary during the growing season and dormancy period (Gaál et al., 2012; Cook and Wolkowich, 2016).

Since the middle of the 20th century, the border of ideal wine-producing areas in Europe has been pushed to the North roughly by 50-100 km (Bowen et al., 2004; Mozell and Thach, 2014), which, by the middle of the 21st century, means further significant expansion to the North (Hoffmann et al., 2007). Areas where the growing of wine grape (*Vitis vinifera* L.) of good quality with high sugar content was previously unimaginable, are now becoming suitable (e.g. North Germany, Baltic countries, etc.).

Mainly, the domesticated plants react to the changed circumstances sensitively in temperate climate regions, therefore grapevine is one of the most notable indicators of climate change (Durack et al., 2014).

For the production, it is important to take into consideration the balance of soil-climate-variety in all cases (Fraga et al., 2013). As a result of the climatic change such balance may waver in the negative or positive direction (Fraga et al., 2014), therefore it is particularly important to plant such grape varieties and their clones, which are able to adapt to the changes (Grzeskowiak et al., 2013; Ignaciuk and Mason-D'Croz, 2014).

The main objective of our research was to examine the phenological response of grapevine to the climate change in West Hungary over the past 30 years.

Material and method

The study area

The research and the observation are performed in the area of the Sopron and Zala wine-growing regions situated on the western part of the Carpathian Basin.

Most parts of the area of Sopron wine region belongs to Sopron Mountains and Kőszeghegység, while most part of Zala wine-growing region belongs to Egerszeg-Letenye Hills, Zalaapáti Ridge, Lenti Hills and Kerkamente (*Fig. 1*).

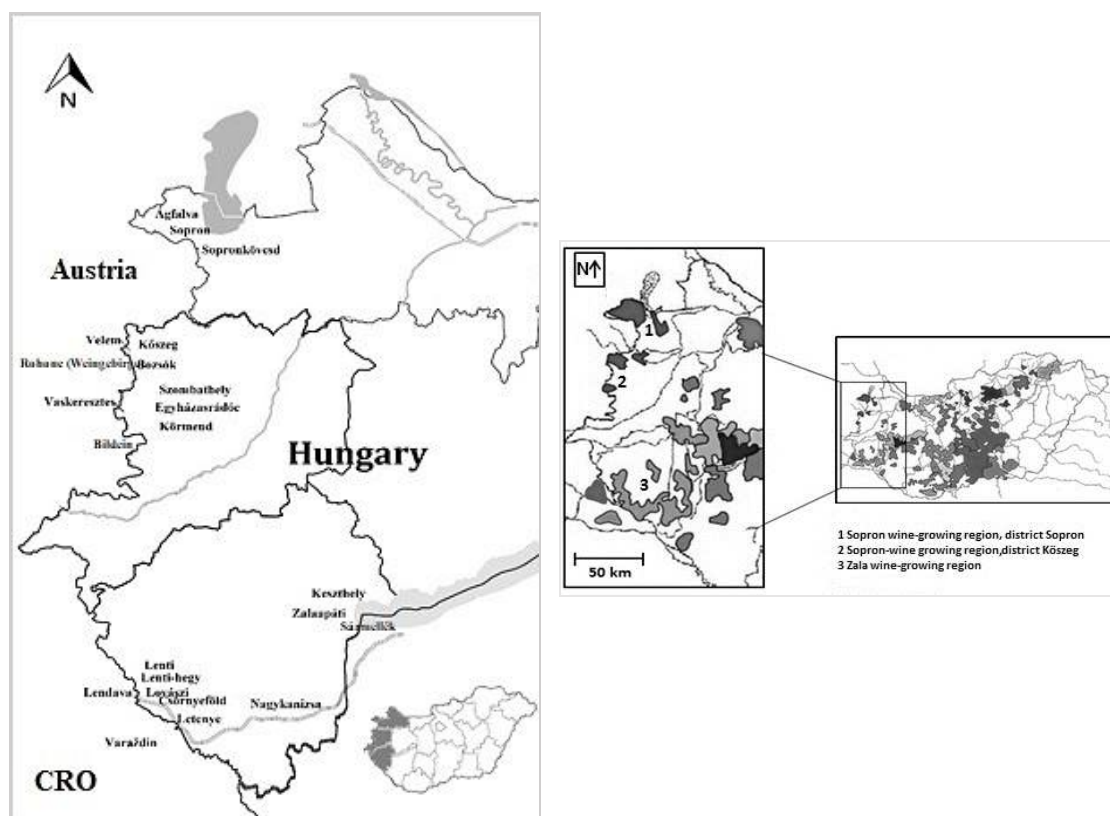


Figure 1. The used meteorological stations (left) and the studied wine-growing regions (right)

The western areas are characterised by pseudo-gley forest soil, the eastern areas by luvisol, while on the northern part of Zalaapáti Ridge we can find alluvial soil, which is rich in water supply, however its quality is not very good. (Dövényi, 2010). The soil of both wine regions is cohesive, Zala wine-growing region is characterised by slight slope grape hills, while in Kőszeghegység (and Vas Hills) steep slopes are frequent, often with eroded soil, which are free from extreme, strong frost.

The northern part of the Sopron wine-growing region belongs to the moderately cool-moderately dry climate region, while Zala wine-growing region and Kőszeghegység belong to the moderately cool-moderately humid climate category (Péczy, 2002).

The annual average temperature is 9-9.3 °C in the area of the Sopron district of the Sopron wine region, 8-9 °C in Kőszeghegyalja, 9.8-10 °C in the area of the Zala wine-growing region (Justyák, 1998).

The annual precipitation is around 750-770 mm, a bit more than the quantity suitable for the needs of the grapevine, but not so outstanding as in some French, German or Swiss wine regions.

The rainiest area is Kőszeghegyalja, the driest is Zalaapáti Ridge. The number of hours of sunshine is around 1800-2000 h, which increases from north towards south.

In the case of the wine grape, while analysing the climate data from the temperature aspect, the value of the active amount of heat (Growing Degree Days) during the growing season must be taken into consideration (the additional heat sum above 10 °C, when certain life processes of the plants are starting). The average of the GDD during the growing seasons of previous 30 years (1956-1985) amounts to 1120-1170 °C in the studied area, which according to our calculations, went up to an average of 1200 °C between 1986 and 2015 (sd = 42.31).

Huglin-index (Heliothermal Index of Huglin) has been developed for the wine-growing regions, which is a refined and modified warm bioclimatic index (Huglin, 1986), which gives the amount of the number of the days when the average temperature is higher than +10 °C between 1st of April and 30th of September, considering the changing photoperiod between 40-50° latitude (Hoppmann, 2010).

On the Northern Hemisphere the calculation of the Huglin-index is the following (Eq. 1, Huglin, 1986; Maaß and Schwab, 2011):

$$HI = K \cdot \sum_{01.04}^{30.09} \frac{(T_{med} - 10) + (T_{max} - 10)}{2} \quad (\text{Eq.1})$$

T_{med} = daily air temperature (°C)

T_{max} = daily maximum air temperature (°C)

Base temperature = 10 °C

K = length of day coefficient (varying from 40° = 1.02 to 50° = 1.06), it was calculated by 1.05

According to our calculations, during the period 1986-2015, the value of the Huglin-index fluctuates between 1950-2100 °C in the studied area. The annual data show significantly increasing trend ($p < 0.01$) (Kovács et al., 2017).

Hungary is located on the northern border of the grape productivity, because most of the grape varieties are resistant to frost only up to -15 °C. Due to such circumstance, the grape could be efficiently grown only by certain cultivation practices and in the appropriate places of production (Kriszten, 1999).

On the bases of the Huglin-index, Blaufränkisch, Müller-Thurgau, Pinot noir, Pinot Blanc, Chardonnay, Cabernet franc etc. can be grown efficiently in the area of the wine regions (Apró, 2016; Puskás and Károssy, 2013).

If the temperature continues to rise in the future during the growing season in the wine-growing regions, it will be worth cultivating more temperature sensitive wine grape varieties. On the bases of the homogenised average of 30 years (1986-2015), most of the rainfalls occur in the area from May to the end of August, nearly 350 mm. This period of the growing season starts with flowering and lasts until ripening. Thus, the proper quantity of precipitation is very important for each year, in order to ensure that

the plant can use the adequate quantity of humidity for building of the cells (Mesterházy et al., 2014).

The studied wine-growing regions belong to regions, which are not exposed to the danger of drought (Bussay et al., 1999). Drought is the long-lasting lack of precipitation combined with excessive heat that is the daily maximum temperature exceeding 25 °C and the soil moisture falling below 20 % (Keddy, 2007).

The climate conditions of the wine-growing regions suggest that the area is ideal for the northern wine grape varieties, as well as for the varieties needing more precipitation, while it is less favourable for the Mediterranean varieties or those requiring little precipitation. The latter can be efficiently cultivated where the value of the Huglin-index is at least 2150-2200 °C, the number of sunny hours is more than 2100-2200 h and the precipitation in the growing season does not exceed 300 mm (Clarke and Rand, 2001).

Owing to the climate of the wine-growing regions, the Sopron red wines have a fresh character and flavour, which recall mainly the red berries. The most growers are specialised in the production of the red wines. The white grape varieties are rare in Sopron, hardly accessible, but it is frequent in Zala. There are red wine blendings in the wine-growing region, in most cases their base is typically Blaufränkisch, which may be completed by the wines of the cabernet varieties, by Merlot, Zweigelt, recently more and more frequently by Syrah.

Tools and methods

A specifically executed phenological research has been started at the wineries in the Zala and the Sopron wine-growing regions at the beginning of the years 2000. The five most frequent wine grape varieties are examined (Zala wine region: Pinot Gris, Welschriesling, Müller-Thurgau, Zweigelt, Királyleányka; Sopron wine region: Blaufränkisch, Zweigelt, Chardonnay, Cabernet Sauvignon and Green Veltliner) on the plantation of 21 winegrowers.

For the purposes of the research, the data of the calibrated meteorological stations were used, which are located near and in the area of the Sopron and Zala wine-growing regions. Among them the ones situated in Szombathely, Körmend, Kőszeg, Nagykanizsa, Iklódbördőce, Keszthely, Zalaegerszeg, Sármellék belong to the Hungarian Meteorological Service (OMSZ).

We have our own calibrated private stations installed in districts of Zala wine-growing region, in Csörnyeföld, Letenye, Nagykanizsa, Lovászi, Lenti, Lentihegy, Zalaapáti, Keszthely, Lendva (Lendava) and Varasd (*Varaždin*), as well as in Kőszeghegyalja-Vaskeresztes in the Sopron wine-growing region, in Sopronfalva, Ágfalva, Kőszeg (Kőszegfalva), Velem, Szombathely, Vaskeresztes and Bozsok and near to the Austrian-Hungarian border in Burgenland (*Fig. 1*).

The examination of the general climate parameters (annual average temperature, monthly average temperature, annual precipitation, monthly precipitation) is not sufficient for the description of the conditions of a certain production place because they only show a superficial character. This is the reason why special parameters and indicators have been created (e.g. summer days $T_{\max} > 25$ °C, hot days $T_{\max} > 30$ °C, heat days $T_{\max} > 35$ °C, Photosynthesis Critical Point $T_{\max} > 38$ °C, etc.), many of which are used in agro-climatic researches on the whole, and some indicators are applied specifically for the examination of particular production places or wine regions.

A statistical “cleaning” was made on the received data, then homogenization and interpolation were executed.

Regarding the change of the climate parameters, the analysed period is 1986-2015 (the examination results of the phenological thread are not exact when being “laid” between 1981 and 2010). Budbreak, flowering, veraison and harvest were investigated among the phenological phases.

Since the efficient growing of the grape absolutely requires the knowledge of the soil (type, albedo, temperature), the climate, as well as the gradient, the exposure and the roughness of the slope, the examination of the phenological processes of the grape was personally executed during the budbreak 2 or 3 times a week, during the flowering day by day, from the veraison until the beginning of the harvest once a week and during the harvest several times a week by the assistance of the growers.

In the studied area, most of all in Kőszeghegyalja and in the area of Vas Hills, Kerkamente, Muramente, the formation of smaller units possessing a peculiar microclimate often occurs, even within small areas, it may happen that the risk of the spring frost is different in two respective vineyards. For the estimation of the risk of the spring frost, the most suitable indicators are the following:

$T_{\min}4i5$ = average minimum temperature in April and May, 2 m above ground

$T_{\min} + 5 4i5$ = average minimum temperature of April and May, 5 cm above ground

$T_{\min} + 50 4i5$ = average minimum temperature of April and May, 50 cm above ground

Due to the lack of data, the last two indicators have been analysed with respect of the period after 2001.

The sugar content was examined too. For this test, the winegrowers give us data and a database was created by us about the cyclonic and anticyclonic days, 60 days preceding the harvests, based on Péczely’s large-scale weather types (Makra et al., 2007).

Results

Climate parameters

In the viticulture, there are several climate indicators and their combinations, which are applied for the description of the production places and for the expression of the needs of the grape. They are used in examinations possessing series of data from several decades, on the one hand for the definition and for the demonstration of the climatic change, on the other hand for the description of the individual plots (Hlaszny, 2012).

In the course of the analysis of the indicators, as functions of the individual weather parameters, weather parameters were defined, which can be directly connected to the character of the vegetal response (Carter et al., 2007). Analysis of the climatic indicators plays a significant role in the methodology of the impact assessment of the climatic change (Hlaszny, 2012). By means of the information resulting from the change of the individual indicators, so conclusions can be drawn regarding the growing conditions in the future (Hlaszny, 2012).

The successful growing of the grape is determined also by the hours of sunshine, but most of all by the temperature and the precipitation.

Between 1956 and 2015 the annual average temperature increased by 1.1 °C in the Sopron and Zala wine-growing regions, by 1.2 °C in the Zala wine-growing region and by 0.9 °C in the Sopron wine-growing region. The acceleration of the increase of the

temperature can be observed from the second half of the years 1980. Between 1986 and 2015 the increase of the temperature is significant, it reached 1.47 °C (1.38 °C in Sopron and 1.55 °C in Zala wine-growing region) (Fig. 2). In the field of the studied regions among the ten hottest years of the period 1956-2015, seven were measured after 1990. The four years with the highest average temperature were 2015 (11.9 °C), 2014 (11.6 °C), 2012 (11.2 °C) and 2011 (11.1 °C).

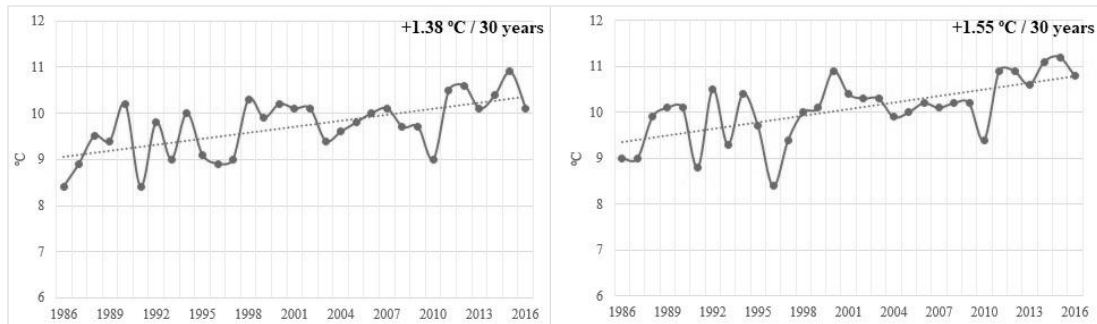


Figure 2. Change in mean temperature (avg. +1.4 °C/30 years). Sopron wine-growing region (left), Zala wine-growing region (right)

If the changes in the temperatures were analysed also by seasons, it can be seen more vigorous modifications in case of some seasonal temperature average. The average temperature has significantly increased in spring, summer and autumn.

The average temperature of the growing season (1st April - 31st October) increased by 2.8 °C, while in the dormancy period by 1.3 °C, during the 30 days preceding the budbreak (15th March – 15th April) by 1.8 °C, before the blooming from 15.1 °C to 16.4 °C, during the time of the blooming from 16.4 °C to 18.1 °C, before the veraison by 2.4 °C, to 20.8 °C (Fig. 3).

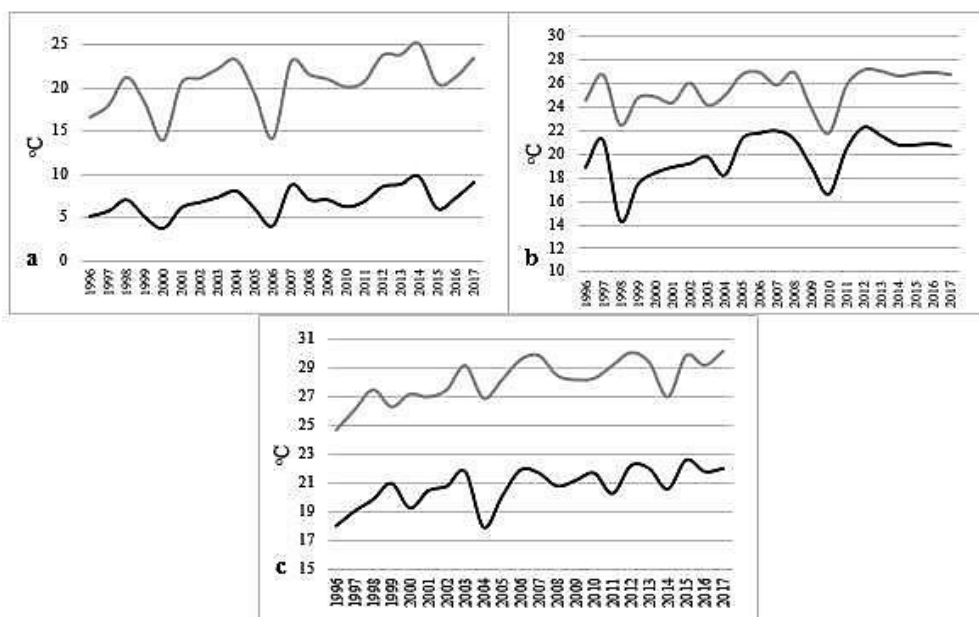


Figure 3. Mean and maximum temperature trends, 30 days preceding the budbreak (a), 20 days preceding the blooming (b) and 15 days preceding the veraison (c)

During the time of the harvest the maximum and minimum temperatures have increased considerably, the former is higher by 2.2 °C than the previous average, the latter by 2.0 °C. Although the change is not significant, but the number of late-spring frost days ($T_{\min} < 4$) has increased by 4 days, in the meantime the increase in the number of the summer days ($T_{\max} > 25$ °C) is significant.

For the smooth process of the vegetation cycle of the grape, it is necessary to summarize the temperature impacts, which affected the plant. This is the so-called active amount of heat.

It can be obtained the value of the amount of active heat, if the value of temperature is above + 10 °C (biological 0 °C) during the growing season. On the bases of the above it can be concluded, that the amount of active heat values has considerably changed in the studied wine regions since 1986. In the Sopron district of the Sopron wine-growing region from 1120 °C to 1240 °C, in the area of the district Kőszeg-Vaskeresztes from 1090 °C to 1220 °C, in the Zala wine region from 1110 °C to 1290 °C (sd = 89.12) (Fig. 4).

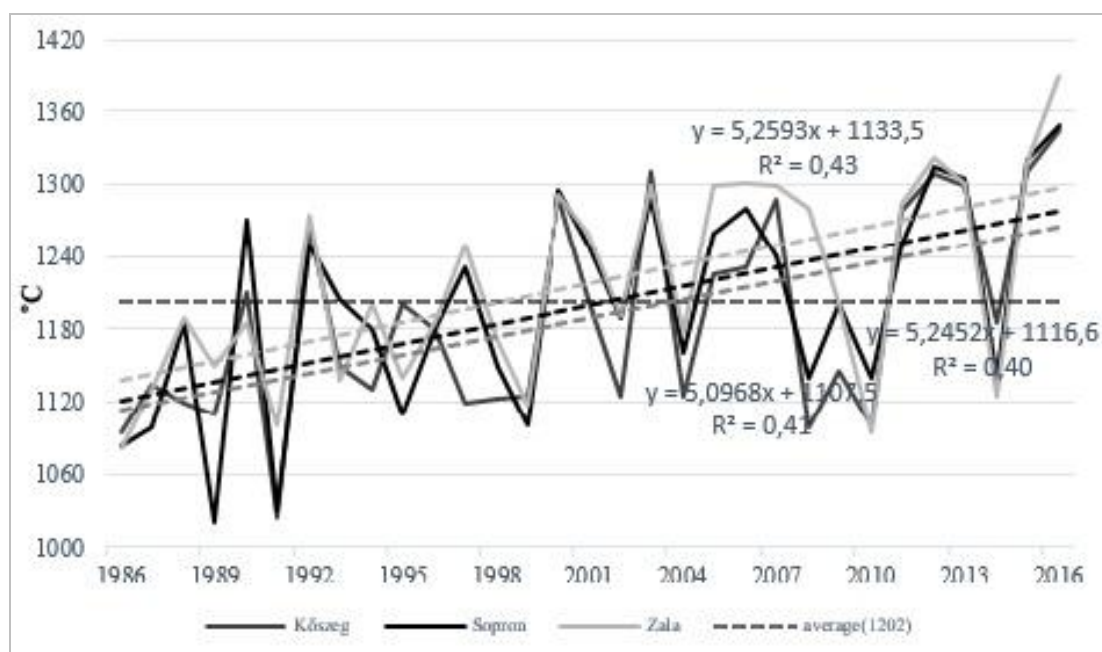


Figure 4. Value of the amount of active heat in the studied wine-growing regions since 1986

The number of intense heat days ($T_{\max} > 35$ °C) and hot days ($T_{\max} > 30$ °C) has increased significantly in the studied region, nearly by 250-300 %. The high number itself of intense heat days and hot days may not cause any problem in viticulture (in Sicily the number of the annual of intense heat days amounts to 65-70 days) (Orlandi et al., 2009).

Such condition means a danger only if suitable ways of protection are not available and the hot weather lasting for several days may result in the damage of the fresh green sprouts, the flowers, the fruit tubers and the foliage or in case the temperature is durably above 38 °C, the photosynthesis of the grapevine may slow down or may even stop

(Frankel, 2014). The average number of days with temperature above 38 °C is 1.5 day/year in the period 1986-2015.

According to the water needs, 88 % of the water and moisture absorbed during the growing season is used by the grapevine in the phases of the maturation and ripening, while only 12 % at the beginning of the growing season, from the budbreak until the end of the flowering (Currle et al., 1983), therefore the precipitation, as indicator is relevant in the second part of the growing season most of all.

The annual precipitation has not changed considerably in the studied area.

Considering the phenological researches, it is important to examine the change of the precipitation in the growing season. In the period between 1st of April until 31st of October the quantity of fallen rain has decreased by 21 % (it is most significant in August and September), while it has increased by 23 % in the dormancy period.

Between the veraison and the period preceding the harvest, the fallen rain has decreased by 25 % nearly, while the number of days with heavy precipitation ($R_{\text{day}} > 20$ mm) has increased from 5 to 11 days.

As previously was mentioned, the grapevine can be grown successfully in case the precipitation does not exceed 300 mm in the growing season. In the studied wine regions, such value is even slightly higher, 360 mm. Besides the quantity of the precipitation, its type is also important from the point of view of the productivity. This is the point where we need to mention the snowy days.

The number of days with snow cover (the ground is covered by snow) is a relevant factor, as the snow while melting, filtrates slowly into the soil, consequently the moisture reaches the deeper layers of the ground as well, which is mainly necessary for older plants with deep roots. The roots have no dormancy period (Herbst and Herbst, 2003). In case the temperature of the soil does not fall below 5-6 °C, the growth of the root is continuous both vertically and horizontally. To accomplish this, the grapevine needs moisture. The winter precipitation of solid form, by its “isolating” character, protects the young stems from the strong frost (Lobell et al., 2008). Change in each important *Vitis* indicator is shown in the *Table 1*.

The snow cover of the Sopron and Zala wine-growing region is 43 days on the bases of the average measured in the period 1956-1985, which has considerably dropped in the past 30 years, by 21 days.

Early phenological responses of grapevines

Considering the time of the budbreak begins 8 days earlier, the flowering also begins 7 days earlier (as for Királyleányka and Green Veltliner 12 days) (*Fig. 5*), the time between the budbreak and the flowering has shortened by 4 days, which is not significant. This is the time when the buds that will become next year’s crops begin to form.

The total time of the flowering has shortened by 5 days. Although the flowering happens earlier, the massive proportion (55-60 %) is reached 2-3 days later (*Fig. 6*).

The stage of fruit set follows flowering almost immediately, climate and the health of the vine play an important role with low humidity, high temperatures and water stress having the potential of severely reducing the amount of flowers that get fertilized (Mullins et al., 1992).

It is observed by us that varieties like Merlot, Syrah and Cabernet Franc react sensitively to the very high temperatures and very low precipitation. These grape varieties are prone to the abnormal fruit set, if the weather too extreme.

Table 1. Change in each important *Vitis* indicator in Sopron and Zala wine-growing regions

Indicator	1956-1985	1986-2015	Standard deviation (1986-2015)
Mean January temperature °C	-0.8	0.6	0.4
July mean temperature °C	19.4	21.2	1.8
Growing season mean temperature(01.04. – 31.10) °C	15.2	17.9	1.4
Growing season maximum temperature (01.04. – 31.10) °C	23	25.2	1.7
Growing season minimum temperature (01.04. – 31.10) °C	7.4	9.5	0.9
Harvest time maximum temperature(15.08. – 15.10) °C	22.2	25.4	1.1
Cool night index (September) °C	10.2	10.6	0.5
Summer rainfall (01.06. – 31.08) mm	271	248	64
Hot days (Tmax > 30 °C) day	14	22	5
Frost days (Tmin < 0 °C) day	103	84	21
Vitis frost days (Tmin < -8 °C) day	53	32	6.5
Extreme frost days (Tmin < -15 °C) day	16	8	4.5
Photosynthesis critical point (Tmax > 38.5 °C) day	1	2	1.5
Huglin-index (01.04. – 30.09) °C	1890-1990	1950-2100	85
Bloom period precipitation (15.05 – 30.06) mm	85	74	21.14
Ripening period precipitation (15.08 – 15.10) mm	141	115	38.59
Growing season precipitation (01.04.-31.10) mm	402	360	68.87
Precipitation before Veraison (01.07. – 15.07) mm	21	16	8.9
Snow-covered days (at least 5 cm) day	24	18	7
Dry days (Rday < 0.1 mm) (01.08 – 31.10) day	19	26	11
Gladstones frost index SFIg = [(AT _{max} + AT _{min}) / 2]minT _{min}	13.22	12.18	6.4
T _{min} 4i5 °C	3.1	2.9	0.96
T _{min} +5 4i5 °C	-	2.1	1.18
T _{min} +50 4i5 °C	-	2.4	1.25

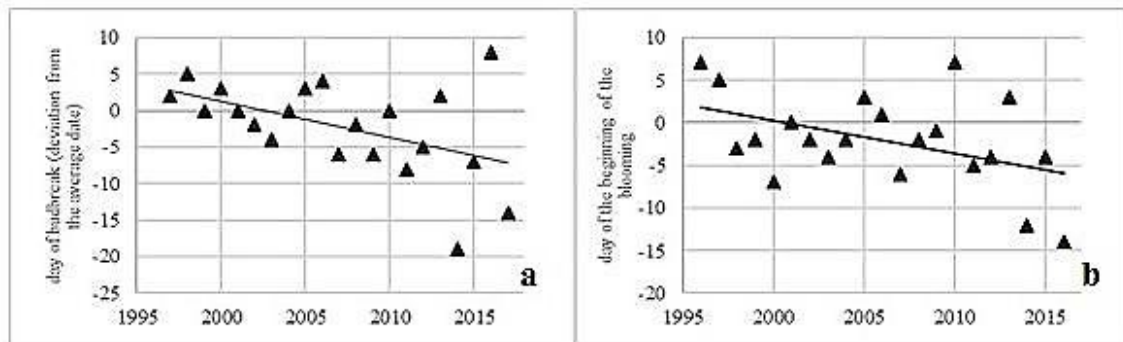


Figure 5. Day of budbreak (a) and blooming (if at least 10 % of flowers are observable) (b) since 1996

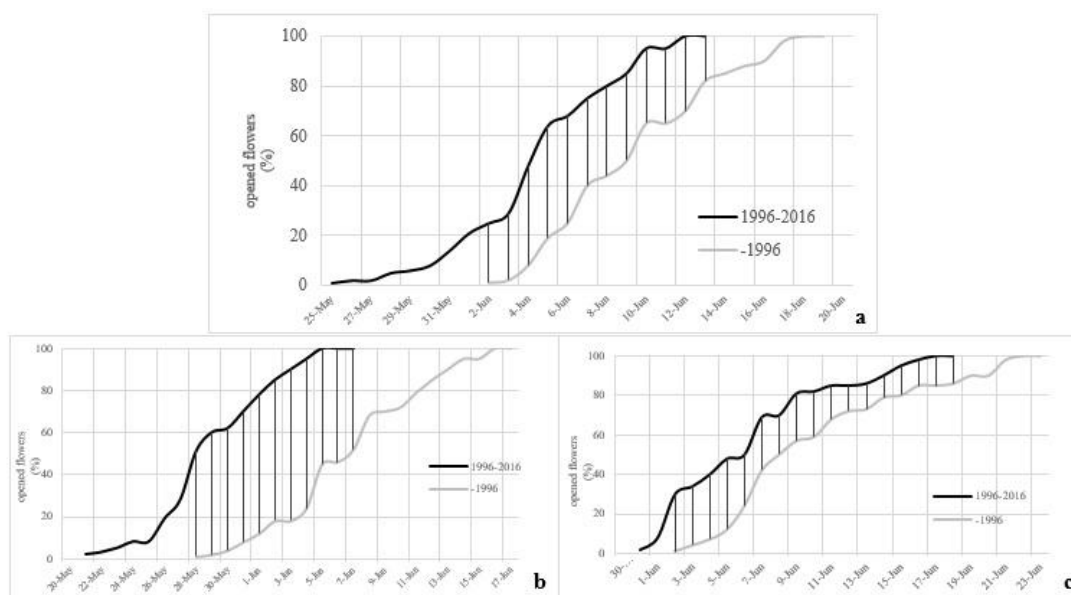


Figure 6. Change in the processes of the flowering (a: all varieties, b: Merlot, c: Pinot Gris) in Sopron and Zala

Veraison and harvest

The next phenological mainstage is the veraison. The berries are green and hard to the touch. In the middle of this stage, the building of the cells speeds up. The ripening process starts around the middle of July if the temperatures are adequate in the field of the studied region.

No considerable change has been observed concerning the maturation, however during the time of the veraison we have observed, most of all in case of the red varieties. This phenological stage is pushed 13 days earlier for Merlot and 10 days earlier for Zweigelt.

The emergence of the colours is faster than before. Harvests happens 11 days earlier respect to the previous period (1971-1995) (Fig. 7), the number of anticyclonic days has increased by 12 % during the period 1986-2015, between 1996 and 2017, such increase reached 19 % in the 60 days preceding the harvests.

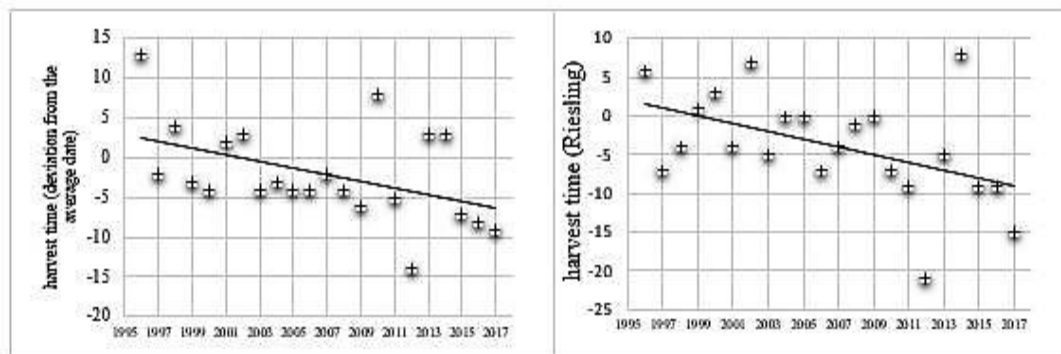


Figure 7. The mean harvest time of all varieties (left) and Riesling (one of the most sensitive varieties) (right) in Sopron and Zala since 1996 (deviation from the average date, $sd = 4.74$)

This is due mainly to the blocking anticyclones in summer. Some climatic scenarios show that in the Euro-Atlantic areas such situations will arise more frequently during the whole year, particularly in winter and in summer (Mokhov et al., 2014). As a result of the increasing anticyclonic situations, during the 60 days preceding the harvests less precipitation is falling, the cloud cover has decreased by 8 %, and as mentioned previously, the number of sunshine days, excessive heat days and hot days has increased, thus the sugar accumulation and the forced ripening became faster (Hajdu and Borbásné, 2009).

The relationship ($r = 0.88$) between the proportion of anticyclonic days in the 60 days preceding the harvests and accumulation of sugar in the must is significant ($p < 0.01$). The result of the regression calculations is $R = 0.8015$. By the increase of the proportion of the anticyclonic days, the sugar accumulation in the must at the moment of the harvest is increasing. Considering the period since 1996, the number of anticyclonic days was very high in 2003, 2006, 2011, 2012 and 2017. As far as the active heat surplus is concerned, in such years higher value was registered (1280-1310 °C), therefore the sugar accumulation and ripening were both faster, the sugar surplus (content) in the must was 55-60 g/l. In such years the precipitation during the time of the ripening (between 1st of August and 30th of September) lags behind the average by 31 %, 2012 was very dry, then the difference reached 38 %. Excluding 2006 (humidity was high, avg. 71-72 %), when the amount of sugar in the must is above 17.6 °M, or considering a scale of 1 to 6, the vintage of the red wines always scored 4 (quality) or above (high quality), on the bases of the data of Sopron and Zala winegrowers, the white varieties also score above 4 (particularly Pinot Gris (late harvest) and Riesling (dry berry selection)).

When certain wine grape varieties are investigated, it can be concluded that the anticyclonic days in the 60 days preceding the harvests had the strongest impact on the must of Blaufränkisch, Müller-Thurgau, Leányka and Zweigelt. Correlation coefficient $r = 0.87$. The correlation is also strong in case of Pinot Gris, Királyleányka (Pinot Gris $r = 0.80$ Királyleányka $r = 0.81$, Cabernet Sauvignon $r = 0.71$ (medium strong)).

Following the first frost, the leaves begin to fall as the grape plant starts to enter its winter dormancy period.

Conclusions

Climate and its changes are the key controlling factors in grape and wine production, affecting the suitability of certain grape varieties in the studied wine-growing regions. Climate data of the last 30 years has shown that the temperatures has risen with a linear warming trend of ~ 1.2 °C/30 years and this affects viticulture of the Zala and Sopron wine-growing region. The increasing temperature and the decreasing precipitation have positive and negative effects in the studied wine-producing regions.

Extremities originating from the changes of temperature and precipitation can be considered beneficial regarding wine production.

A significant shift has taken place in the annual growth cycle of grapevines, budbreak begins nearly 8 days earlier, flowering 7 days and the veraison 8 days, while the harvest has been shifted to a date 11 days respect to the previous period. The time between the budbreak and the flowering has shortened by 4.5 days. The sugar degree measured at the time of the harvest is increasing by the rate of the increase of the anticyclonic days in summer and early autumn and that from 5 years 3 are either good or excellent vintages, while previously from 5 only 1 got such qualification, are all presumably among the consequences of the climatic change.

The research will be continued, extending to all wine grape varieties and a new phenological index will be formed for the winegrowers and researchers.

Acknowledgements. Supported by the ÚNKP 17-3 New National Excellence Program of the Ministry of Human Capacities.

REFERENCES

- [1] Apró, M. (2016): Application and Development of Detection Methods of Grape Viruses in the Survey of Virus Infection of Vineyards. – Doctoral (PhD) Thesis. University of Pannonia, Keszthely.
- [2] Bowen, P. A., Bogdanoff, C. R., Estergaard, B. (2004): Impacts of using polyethylene sleeves and wavelength-selective mulch in vineyards. I. Effects on air and soil temperatures and degree day accumulation. – *Canadian Journal of Plant Science* 84(2): 545-553.
- [3] Bussay, A., Szinell, Cs., Szentimrey, T. (1999): Az aszály magyarországi előfordulásainak vizsgálata és mérhetősége. Éghajlati és agrometeorológiai tanulmányok 7. – OMSZ, Budapest (in Hungarian).
- [4] Carter, T. R., Parry, M. L., Porter, J. H. (2007): Climatic change and future agroclimatic potential in Europe – *International Journal of Climatology* 11(3): 251- 269.
- [5] Clarke, O., Rand, M. (2001): *Encyclopedia of Grapes*. – Harcourt, New York.
- [6] Cook, B. I., Wolkowich, E. M. (2016): Climate change decouples drought from early wine grape harvests in France. – *Nature Climate Change* 6: 715-719.
- [7] Curre, O., Bauer, O., Hofäcker, W., Schumann, F., Frisch, W. (1983): *Biologie der Rebe*. – Meiningen Verlag, Neustadt (in German).
- [8] Dövényi, Z. (2010): *Inventory of Microregions in Hungary*, 2nd ed. – MTA (Hungarian Academy of Sciences), Budapest.
- [9] Durack, P. J., Gleckler, P., Landerer, F. W., Taylor, K. E. (2014): Quantifying underestimates of long-term upper-ocean warming. – *Nature Climate Change* 4: 999-1005. DOI: 10.1038/nclimate2389.

- [10] Fraga, H., Malheiro, A., Moutinho-Pereira, J., Santos, J. A. (2013): Future scenarios for viticultural zoning in Europe: ensemble projections and uncertainties. – *International Journal of Biometeorology* 57(6): 909-925.
- [11] Fraga, H., Malheiro, A. C., Moutinho-Pereira, J., Santos, J. A. (2014): Climate factors driving wine production in the Portuguese Minho region. – *Agricultural and Forest Meteorology* 185: 26-36.
- [12] Frankel, C. (2014): *Land and Wine: The French Terroir*. – University of Chicago Press, Chicago.
- [13] Gaál, M., Moriondo, M., Bindi, M. (2012): Modelling the impact of climate change on the Hungarian wine regions using Random Forest. – *Applied Ecology and Environmental Research* 10(2): 121-140.
- [14] Grzeskowiak, L., Costantini, L., Lorenzi, S., Grando, M. S. (2013): Candidate loci for phenology and fruitfulness contributing to the phenotypic variability observed in grapevine. – *Theoretical and Applied Genetics* 126(11): 2736-2776.
- [15] Hajdu, E., Borbásné, S. É. (2009): *Abiotikus stresszhatások a szőlő életterében*. – Agroiinform Kiadó, Budapest (in Hungarian).
- [16] Herbst, R., Herbst, S. T. (2003): *The New Wine Lover's Companion*. 2nd ed. – Barrons, New York.
- [17] Hlaszny, E. (2012): *Early Phenological Responses of Grapevine (*Vitis vinifera* L.) in Kunság Wine-Growing Area Based on Plant Surveys, Weather Observations and Regional Climate Model*. – Doctoral (PhD) Thesis. Corvinus University of Budapest, Budapest.
- [18] Hoffmann, M., Hoppmann, D., Hannes, R. S. (2007): *Einfluss der Klimaveränderung auf die phänologische Entwicklung der Rebe sowie die Säurestruktur der Trauben*. – FA Geisenheim, DDW Geisenheim.
- [19] Hoppmann, D. (2010): *Terroir, Wetter-Klima-Boden*. – Verlag Ulmer KG, Stuttgart (in German).
- [20] Huglin, P. (1986): *Biologieetécologie de la vigne*. – Ed. Payot, Lausanne-Paris (in French).
- [21] Ignaciuk, A., Mason-D'Croz, D. (2014): *Modelling Adaptation to Climate Change in Agriculture-OECD Food, Agriculture and Fisheries Papers 70*. – OECD Publishing, Paris.
- [22] Justyák, J. (1998): *Magyarország éghajlata. Climate of Hungary* – Kossuth Egyetemi Kiadó, Debrecen (in Hungarian).
- [23] Keddy, P. A. (2007): *Plants and Vegetation: Origins, Processes, Consequences*. – Cambridge University Press, Cambridge.
- [24] Kriszten, Gy. (1999): *Tavasztól-tavaszig a szőlőben* – Mezőgazda Kiadó, Budapest (in Hungarian).
- [25] Kovács, E., Puskás, J., Pozsgai, A. (2017): Positive Effects of Climate Change on the Field of Sopron Wine-Growing Region in Hungary. – In: Karacostas, T. S. et al. (eds.), *Perspectives on Atmospheric Sciences*, pp. 607-613. Springer Atmospheric Sciences, Zürich.
- [26] Lobell, D., Burke, T., Tebaldi, C., Matarndera D. M., Falcon, P. W., Naylor, R. L. (2008): Prioritizing climate change adaptation needs for food security in 2030. – *Science* 319: 607-610.
- [27] Maaß, U., Schwab, A. (2011): *Wärmeanspruch von Rebsorten*. – *Klimawandel und Sortenwahl* 10: 29-31 (in German).
- [28] Makra, L., Mika, J., Bartzokas, A., Sümeghy, Z. (2007): Relationship between the Péczely's large-scale weather types and air pollution levels in Szeged, Southern Hungary. – *Proceedings of the 8th Hellenic Conference on Meteorology, Climatology and Atmospheric Physics C*: 135-145.
- [29] Mesterházy, I., Mészáros, R., Pongárcz, R. (2014): The Effects of Climate Change on Grape Production in Hungary. – *Időjárás* 118(3): 193-206.

- [30] Mokhov, I. I., Timazhev, A. V., Lupo, A. R. (2014): Changes in atmospheric blocking characteristics within Euro-Atlantic region and Northern Hemisphere as a whole in the 21st century from model simulations using RCP anthropogenic scenarios. – *Global and Planetary Change* 122: 265-270.
- [31] Mozell, M. R., Thach, L. (2014): The impact of climate change on the global wine industry: Challenges & solutions. – *Wine Economics and Issues* 3(2): 81-89.
- [32] Mullins, M. G., Bouquet, A., Williams, L. E. (1992): *Biology of the Grapevine*. – Cambridge University Press, Cambridge.
- [33] Orlandi, S., Di Stefano, V., Lucchesini, P., Puglisi, A., Bartolini, G. (2009): Current trends of agroclimatic indices applied to grapevine in Tuscany (Central Italy) – *Időjárás* 113(1-2): 69-78.
- [34] Péczely, Gy. (2002): *Éghajlattan [Climatology]*. – Nemzeti Tankönyvkiadó, Budapest (in Hungarian).
- [35] Puskás, J., Károssy, Cs. (2013): A bor minőség és az időjárás közötti összefüggések néhány jellemzője a Kőszeg-hegylajai borok és Szombathely 100 éves napi meteorológiai adatai alapján. – 4. Szőlő és Klíma Konferencia, Kőszeg, CD-ROM: 142-153. (in Hungarian).

EFFECT OF MANNITOL STRESS ON MORPHOLOGICAL, BIOCHEMICAL AND POLYPHENOL PARAMETERS IN BROCCOLI SPROUTS (*BRASSICA OLERACEA* VAR. *ITALICA*)

KIANI, S. – BABAIEANJELODAR, N.* – BAGHERI, N. – NAJAFIZARRINI, H.

*Department of Plant Breeding, Sari Agricultural Sciences and Natural Resources University
Sari, Mazandaran, Iran*

**Corresponding author
e-mail: n.babaeiyan@umz.ac.ir*

(Received 29th Oct 2017; accepted 13th Mar 2018)

Abstract. To assess the effect of drought stress induced by mannitol at three levels (0, 88 and 176 mM) on biochemical and polyphenolic traits of six F₁ broccoli hybrids, a factorial experiment based on completely randomized design in three replications was implemented at research station of Agricultural Sciences and Natural Resources University, Sari, Mazandaran, Iran in 2016. The results showed that mannitol stress reduced dry weight and shoot length significantly for all varieties but with a different rate. Total phenolic, flavonoid, and anthocyanin contents, the activity of enzymatic antioxidants, and DPPH activity were significantly higher under 176 Mm mannitol application condition than control. In addition, results showed that mannitol stress increased the content of sulforaphane. Marathon genotype showed the highest content of sulforaphane among all varieties under both normal (6.139) and under stress (14.122) conditions. Marathon and Heraklion genotypes could be suggestively used for breeding program to increase content of sulforaphane coupled with other traits. Since the content of sulforaphane along with phenolic compounds and antioxidant activities were higher under both severe and moderate stress conditions, using moderate mannitol stress treatment can be implemented for increasing the content of these suitable compounds in broccoli.

Keywords: *sulforaphane, DPPH, principal component, flavonoid, malondialdehyde*

Abbreviations

ROS	Reactive oxygen species
H ₂ O ₂	Hydrogen peroxide
O ₂	Superoxide radicals
MDA	Malondialdehyde
SOD	Superoxide dismutase
APX	Ascorbic peroxidase
POX	Guaiacul peroxidase
CAT	Catalase
DPPH	2, 2-diphenyl-1-picrylhydrazyl

Introduction

Broccoli (*Brassica oleracea* var. *Italica*) is a member of the Brassicaceae family and its wild form is found throughout the Mediterranean region and is widely cultivated in many countries of Europe and America along with Asian countries (Abou El-Magd et al., 2013). Broccoli is one of the highly valuable vegetable that is rich in nutrients content and it has many benefits for human health. Broccoli sprouts contain a substance called sulforaphane which intensely reduces the number, size, and proliferation of cancerous tumors; and moreover the sprout is rich in fiber, carotenoids, vitamin A, vitamin C and vitamin K (Beecher 1994,

Pereira et al., 2002). This plant is grown as an either spring or autumn crop, but it is sensitive to cold and dry condition especially at early stages. Worldwide, water shortages and drought stress is among the most important abiotic stresses limiting crop production (Lemoine et al., 2010). Due to the uniformity of the soil environment and lack of environmental control in the field, laboratory investigations have a special importance to assess the tolerance of plants against drought stress. To create an artificial environment controlling water potential, substances with high molecular weight are used. Mannitol, as a high molecular weight substance, owing to inducing a condition with osmotic solution identical to natural environment, is often used to control water potential in drought stress studies and controlled environments (Guo et al., 2011).

Drought stress increases the accumulation of reactive oxygen species (ROS) such as hydrogen peroxide (H_2O_2), superoxide radicals (O_2^-), and hydroxyl (OH^\cdot) leading to oxidative stress (Saed-Moucheshi et al., 2014b). Production of reactive oxygen species causes lipid peroxidation along with protein and nucleic acid degradation. Plants are able to reduce the damaging effect of reactive oxygen species by different mechanisms. One of these mechanisms is involved in enzymatic or non-enzymatic antioxidant defense system. Antioxidant enzymes such as catalase (CAT), superoxide dismutase (SOD), and peroxidase (POX) are involved in detoxifying oxygen free radicals in plants' cells (Saed-Moucheshi et al., 2014a). In response to increased production of reactive oxygen species, the capacity of antioxidant defense systems and the activity of antioxidant enzymes are increased. The first enzymatic barrier against produced oxidants is SOD, which converts O_2^- to H_2O_2 , a molecule with relatively lower radical activity. H_2O_2 could be detoxified into water and oxygen by the CAT and ascorbate peroxidase (APX) enzymes. Peroxidase has an important role in detoxification of H_2O_2 which can swept away this compound by using ascorbic acid as an electron donor for the reduction of H_2O_2 to H_2O (Saed-Moucheshi et al., 2014b). During this reaction, ascorbic acid is transformed to monodehydroascorbate. POX are glycoproteins that are able to use phenols similar to hydrogen donors to cope with high content of oxygen free radicals. Furthermore, involvement of POX in plant development processes, lignin production, ethylene biosynthesis, plant defenses against stresses, and wound restoration have been proved (Hossain et al., 2015). Changes in the activity of antioxidant enzymes under NaCl stress (Tian et al., 2016) and heat stress (Lin et al., 2010) have been also reported in broccoli sprouts. Additionally, damages to the proteins along with accumulation of some free amino acids such as proline in order to maintain osmotic pressure leading to regulate protein synthesis in cells has been observed under abiotic stresses (Osakabe et al., 2014). Some researchers claimed that the reduction in synthesis of some types of proteins is attributed to decrease in their polysome numbers (Han and Wagner, 2014, Suzuki et al., 2014). In addition to changes in the content of proteins, lipids are affected by induced abiotic stresses. Membrane lipid peroxidation normally results in production of some aldehyde namely malondialdehyde (MDA) which is a quick responsive compound to oxidative stress (Berger et al., 2016). Furthermore, ethylene and salicylic acid are two phytohormones composed of polyphenols which are important in stress responses of the plants which have direct, indirect, and cascading effects on some vital activities of the plants such as photosynthesis and plant developments under stress conditions (Gupta and Huang, 2014).

The current study tends to find out about the responses of the different genotypes of the broccoli to water shortage stress caused by mannitol under laboratory and controlled environment through considering different morphological, biochemical, and polyphenols parameters. In addition, to screen the most useful F₁ hybrids for being used in plant breeding and human nutritional programs. In addition, evaluate the relationship between measured parameters by using advanced and multivariate statistical techniques in order to help breeders to use them as screening criteria for indirect selection of genotypes with higher nutritional qualities.

Materials and methods

Experimental procedure

Seeds of the six F₁ broccoli genotypes (Castle Dome, Green Magic, Heraklion, Marathon, Matsuri and Sacora) prepared from PS America, Inc and TOKITA SEED CO. LTD (Japan) companies were used in a factorial experiment with two factors (Mannitol levels and genotypes) on the bases of completely randomized design (CRD) with three replication and in each replication with 10 petri dishes. The seeds were soaked in ethanol 70% for 2 minutes and then were in undated with Bleach (sodium hypochlorite) 20% for 10 minutes; after that, the seeds were washed 4 times with deionized water. Five seeds were transferred to each sterile petri dish containing wet filter papers. The periods of 16 hours of light and 8 hours of darkness in a growth chamber at 23 °C (day)/ 20 °C (night) temperature with average humidity of 70% were applied and continued during the experiment. The five-day small sprouts of broccoli were treated with 88 and 176 mM mannitol for 48 hours (two days). Therefore, the samples were taken from the seven days old sprout to assess the biochemical and growth-related traits.

Measurements of the traits

Shoot length, root length, and dry weight were measured as growth related traits. Shoot and root lengths were measured using a precise measure on the bases of centimeter. For measurement dry weight, fresh shoots were placed in aluminum foils and kept in an oven for 48 h under 70 °C, and then were weighed with a precise scale on the bases of gram. The mean of the five used sprout in each petri dish was used for each replication.

Total protein content was measured by the method of Bradford (1976) at 595 nm spectrophotometric wave length. MDA and H₂O₂ contents were estimated by the methods of Heath and Packer (1968) and Velikova et al. (2000), respectively. Enzymatic antioxidants consist of SOD, APX, POX, and CAT were measured using the methods of Giannopolitis and Ries (1977), Nakano and Asada (1981), Dazy et al., (2008), and Aebi (1984), respectively. The methods described by Ainsworth and Gillespie (2007), Oomah and Mazza (1996), and Yuan et al. (2009) were used for the measurement of phenol, flavonoid, and anthocyanin contents in broccoli sprouts, respectively. DPPH as the total activities of the sprout to scavenge reactive oxygen species were estimated using Brand-Williams et al. (1995) method. Using HPLC standard, sulforaphane content in the broccoli sprout was measured for each variety under each treatment after determining the peaks based on the method of Brader et al. (2006).

Statistical analyses

Data were analysed by one-way ANOVA in SAS 9.3, followed by Duncan's multiple range test (DMRT) comparison test. PROC CORR of SAS 9.3 was used for assess Pearson's correlation coefficient between all pairs of measured traits. The graphs for mean comparison were drawn by Excel 2016 software. Multivariate analyses namely principal component analysis (PCA) and biplot graph were assessed by Minitab v. 16.

Results

Analysis of variance and mean comparison

Table 1 is presenting the results of analysis of variance for all measured traits. The main effect of genotype was significant ($p < 0.01$) for all traits. In addition, the effect of mannitol showed significant effect on all measured traits ($p < 0.01$) except for root length. The interaction between genotypes and mannitol was significant for all parameters. Since the interaction effect between genotypes and mannitol showed high significant in the ANOVA table.

The results of multiple mean comparison based on Duncan's multiple range test subjected to growth related traits, shoot length and root length, along with some polyphenols consist of total phenol content, flavonoid content, and anthocyanin content are prepared in *Table 2*. In all genotypes, control treatment showed higher shoot length than two other levels of mannitol application. In Heraklion, Marathon, Green Magic, and Matsuri genotypes, application of 176 mM mannitol resulted in the lowest shoot length, but in other genotypes application of 88 mM mannitol obtained the lowest shoot length with no significant difference from 176 mM. Castle Dome and Matsuri genotypes showed higher shoot length in comparison with other ones. The highest shoot length was achieved in Matsuri genotype under no application of mannitol (6.87 cm), while the lowest shoot length was obtained in Sacora under the application of 88 mM mannitol (3.33 cm). Similar to the shoot length, the response of different genotypes to different levels of mannitol were different for root length. In Sacora, Heraklion and Matsuri genotypes, the control treatment showed higher root length than the two other levels of mannitol application. On the contrary, in Marathon, Green magic, and Castle Dome genotypes no application of mannitol resulted in lower root length in compare to other levels. The highest and the lowest root length were obtained in Marathon genotype under the application of 176 mM mannitol (13.53 cm) and Sacora genotypes under 176 mM mannitol (6.83 cm), respectively. Response of dry weight of different broccoli sprouts to different levels of mannitol application is depicted in *Table 2*. Dry weight of all F_1 hybrids were reduced by application of mannitol in compare to control. Excluding the Castle Dome genotype, higher level of mannitol application (176 mM) resulted in lower dry weight. Matsuri and Castle Dome genotypes showed higher dry weigh than the other genotypes.

Highest total phenol content was obtained in Marathon genotype under 176 mM ($112.29 \text{ mg g}^{-1} \text{ FW}$) while the lowest content was obtained in Sacora genotype under no application of mannitol ($39.52 \text{ mg g}^{-1} \text{ FW}$). Flavonoid of all genotypes except for Marathon reached a higher content with application of higher mannitol concentration. The highest flavonoid content ($123.4 \text{ mg g}^{-1} \text{ FW}$) was achieved in Heraklion under highest concentration of mannitol (176 mM), while the lowest

content achieved in Matsuri under no application of mannitol (28.73 mg g⁻¹ FW). Anthocyanin content of genotype Matsuri decreased in response to higher application of mannitol. However, the response of all other genotypes to higher concentration of mannitol was to increase the anthocyanin content. Marathon under application of 176 mM mannitol obtained the highest anthocyanin content (0.623 mg g⁻¹ FW) among all treated plots, while castle Dome genotype under no application of mannitol showed the lowest anthocyanin content (0.14 mg g⁻¹ FW).

MDA and H₂O₂ as two important markers indicating the severity of the stresses in plant were measured in all genotypes under all mannitol treatments, which their results are presented in *Table 2*. In all genotypes, higher mannitol content resulted in higher content of both MDA and H₂O₂. Heraklion and Marathon showed highest ratio for increase in the content of MDA in response to mannitol application. Similarly, Marathon and Green Magic genotypes showed the highest difference between control and mannitol application among all genotypes regarding H₂O₂. Green Magic (3.96 μmol mg⁻¹ FW) and Sacora genotype (0.77 μmol mg⁻¹ FW) both under 176 mM mannitol application resulted in the highest content of MDA and H₂O₂, respectively. In contrast, the lowest content of both MDA and H₂O₂ were observed in Castle Dome genotype under no application of mannitol.

SOD, CAT, POX, and APX as the enzymatic ROS scavengers were measured using spectrophotometric tool. The response of all enzymatic antioxidants to higher concentration of mannitol were to increase their activities in all genotypes. The rate of increase in Matsuri genotype regarding SOD was higher than other genotypes (104 and 166% increase in 88 and 176 mM mannitol in relation to control). Similar results regarding other measured enzymatic antioxidant were observed for this variety (*Table 2*). Excluding CAT, Marathon genotype showed the highest enzymatic activities among all genotypes under 176 mM mannitol application. Heraklion genotype under highest application mannitol showed the highest activity for CAT. The lowest activity of SOD, CAT, POX, and APX were observed in Sacora, Matsuri, Green Magic and Sacora under control treatment, respectively. The activity of DPPH which is an abbreviation for 2, 2-diphenyl-1-picrylhydrazyl was also measured as a free radical scavenger (*Table 2*). In genotype Marathon, the antioxidant activity by DPPH under no application of mannitol showed a high significant difference with application of 88 mM mannitol, but application of 176 mM showed a lower significant activity in compare to control. Similarly, in all other genotypes, the higher concentration of mannitol resulted in higher activity of DPPH. The highest activity of DPPH achieved in Heraklion genotype under the application of 176 mM mannitol (85.46 mmol kg⁻¹), but the lowest activity was resulted from control treatment in var. Matsuri (64.71 mmol kg⁻¹).

Sulfurphane as an important compound in broccoli was also measured in all genotypes under all treatments, which its results are presented in *Fig. 1*. The response of all genotypes to application of mannitol were to increase the content of sulforaphane but the rate of increase in some genotypes consist of Sacora and Castle Dome were low. The rate of increase in the content of sulforaphane in Masuri and Heraklion was higher in response to increase the concentration of mannitol with a high positive trend. Marathon and Green Magic showed a great increase from no application to 88 mM application of mannitol, but the difference between 88 and 176 mM mannitol remained insignificant. Under all mannitol levels and in total, the content of sulforaphane was highest in Marathonin comparison to other genotypes.

Table 1. Analysis of variance for measured traits in six F1 hybrids broccoli under mannitol treatment

Source	DF	Mean Square													
		DW	Shoot length	Root length	Sulfo-raphane	MDA	H ₂ O ₂	Phenol	Flavonoid	Antho-cyanin	SOD	CAT	POX	APX	DPPH
Variety	5	0.17**	5.64**	40.3**	46.58**	4.18**	0.32**	3465.78**	1314.91**	0.24**	5910.37**	1220.73**	764.16**	4187.53**	57.45**
Mannitol	2	0.06**	11.42**	1.05ns	139.3**	0.3**	0.07**	1338.42**	1985.89**	0.05**	5891.76**	2493.38**	999.84**	11596.67**	169.84**
Interaction	10	0.02**	1.56**	2.97**	15.17**	0.6**	0.14**	106.31**	999.98**	0.005**	446.94**	135.99**	89.54**	363.52**	58.15**
Error	36	0.001	0.05	0.33	0.27	0.001	0.0004	4.68	2.03	0.0003	2.46	1.04	0.47	0.86	0.57
Coefficient of Variation		3.51	4.59	5.71	6.47	1.23	6.46	3.7	2.06	4.16	2.39	2.98	3.61	1.96	0.92

** , * , and ns: significant at 0.01, 0.05 level, and non-significant at 0.05 level.

DW: Dry wight, MDA: Malondialdehyde, H₂O₂: hydrogen peroxide, SOD: Super Oxide Dismutase, CAT:Catalase, POX: Guaiacul Peroxidase, APX:Ascorbic Peroxidase, DPPH:1,1-diphenyl-2-picrylhydrazyl

Table 2. Multiple mean comparison of measured traits for interaction between broccoli varieties and mannitol treatment

Variety	Mannitol (mM)	Dry weight (g)	Shoot length (cm)	Root length (cm)	Phenol (mg/g FW)	Flavonoid (mg/g FW)	Antho-cyanin (mg/g FW)	MDA (μmol mg ⁻¹ FW)	H ₂ O ₂ (μmol mg ⁻¹ FW)	SOD (μmol mm ⁻¹ mg ⁻¹ p)	CAT (μmol mm ⁻¹ mg ⁻¹ p)	POX (μmol mm ⁻¹ mg ⁻¹ p)	APX (μmol mm ⁻¹ mg ⁻¹ p)	DPPH (mmol kg ⁻¹)
Sacora	0	0.36H	6.367B	7.833I	39.524L	63.667G	0.451E	2.551H	0.23J1	24.011L	26.472I	10.939J	14.976N	82.323F
	88	0.32I	3.333K	7.667IJ	47.476HIJ	83.067C	0.505D	2.722G	0.35G	37.553J	32.672FG	11.222J	40.422I	84.091BCDE
	176	0.314I	4.467FG	6.833J	66.333D	83.933C	0.582B	2.935F	0.77A	31.146K	35.637E	13.043I	55.255G	84.495ABC
Heraklion	0	0.41G	5.567CD	13.033AB	45.238JK	51.733J	0.487D	2.373I	0.2H	66.522F	33.413F	26.287E	27.013K	82.02FG
	88	0.344H	4.7F	11.1D	52.317EFG	72E	0.534C	3.223D	0.44F	76.005E	48.789C	30.866D	71.515E	85.152AB
	176	0.35H	3.567JK	12.5BC	51.619EFG	123.4A	0.543C	3.869B	0.52E	82.162D	64.764A	37.062B	95.819B	85.455A

Marathon	0	0.355H	4.3GH	12.067C	85.143C	58.333HI	0.423E	2.049K	0.16G	82.394D	32.415FG	15.002H	45.985H	75.96H
	88	0.314I	4.033HI	13.167AB	97.952B	72.133E	0.543C	2.223J	0.3J	101.629B	45.854D	26.929E	84.076C	85.404A
	176	0.293IJ	3.8IJ	13.533A	112.286A	91.133B	0.623A	3.055E	0.53D	126.464A	55.502B	42.997A	110.646A	83.737CDE
Green Magic	0	0.46F	5.1E	8.933GH	45.667IJK	57.086I	0.369F	3.21D	0.18HI	55.538H	21.558J	5.477M	16.437N	82.273FG
	88	0.39G	4.4FGH	8.5GHI	50.571FGH	71.467E	0.482D	3.619C	0.64C	76.06E	31.465G	21.666F	23.257L	83.232DEF
	176	0.35H	3.267K	10.667DE	54.952E	75.533D	0.535C	3.958A	0.71B	96.427C	44.827D	33.826C	34.731J	84.394ABCD
Matsuri	0	0.89A	6.867A	9.933FE	40.952L	28.733K	0.214G	1.695M	0.09JK	18.845M	11.419L	5.334M	18.729M	64.717I
	88	0.83B	5.7C	8.1HI	48.952GHI	53.133J	0.195GH	1.957L	0.06KL	40.68I	29.054H	11.405J	44.655H	82.929EF
	176	0.65E	4.333FGH	7.667IJ	67.238D	60.333H	0.199GH	2.051K	0.16J	74.025E	55.548B	16.032GH	80.11D	84.293ABCD
Castle Dome	0	0.9A	6.6AB	9.333FG	42.667KL	53J	0.14I	1.701M	0.01M	35.627J	10.782L	6.883L	9.382O	81.061G
	88	0.72D	5.233DE	10.667DE	53.524EF	81.267C	0.179H	1.938L	0.05L	59.043G	15.741K	9.733K	18.207M	83.586CDE
	176	0.79C	5.933B	10.833DE	50.238FGH	67.067F	0.219G	2.05K	0.15j	95.877C	20.97J	16.338G	60.532F	84.04BCDE

Means with the same letter(s) in each column are not significantly different (Duncan 1%).

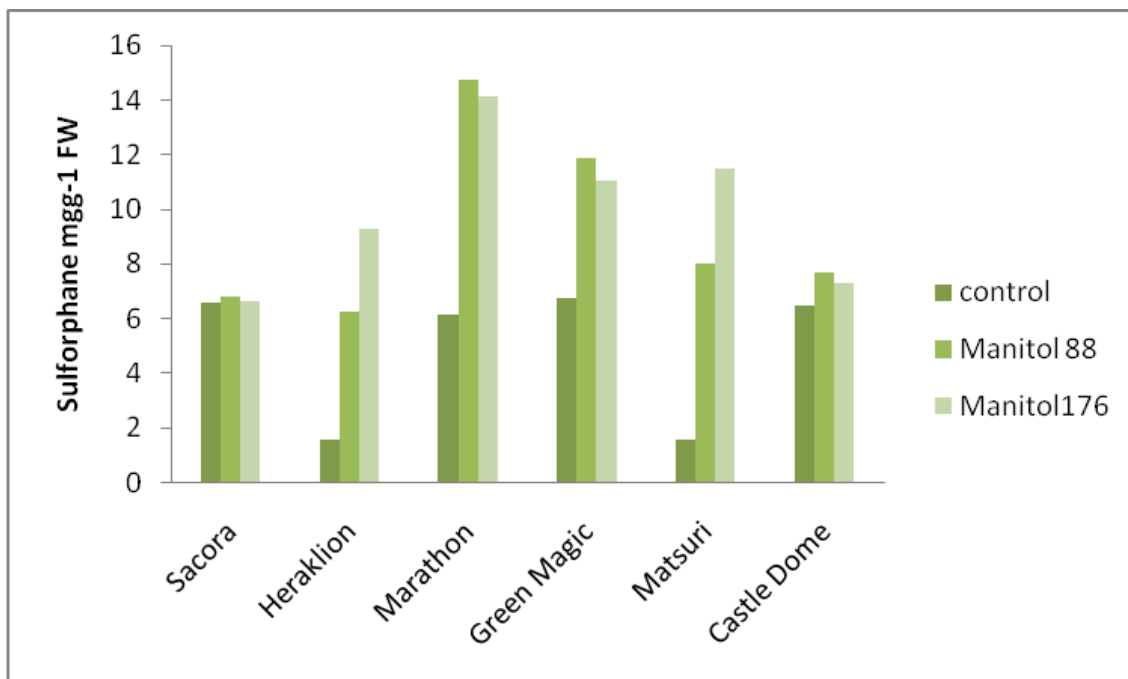


Figure 1. Response of sulfonaphan content of different broccoli genotypes to mannitol treatment

Correlation between measured traits

The pairwise correlations between all pairs of measured traits based on Pearson method is presented in *Table 3*. Except for shoot length (0.74), dry weight showed negative correlations with all other traits. Similar to dry weight, all pairwise correlations of shoot length, excluding dry weight, were negative. The only insignificant correlation of shoot length was related to root length (-0.19). Root length showed negative correlation with shoot length and dry weight but these correlations were not statistically significant. Excluding dry weight and shoot length, all other correlations of root length were positive, but its correlation only with phenol content (0.5), SOD (0.7), and POX (0.67) were significant. Sulfonaphane showed significant correlations with shoot length (-0.61), phenol content (0.65), SOD (0.66), CAT (0.58), POX (0.52), APX (0.58), and DPPH (0.47). The content of sulfonaphane showed no significant correlations with flavonoid (0.29) and anthocyanin (0.31). MDA revealed negative significant correlations with dry weight (-0.67) and shoot length (-0.57). Also, the correlations of MDA with H₂O₂ (0.79), flavonoid (0.61), anthocyanin (0.61), CAT (-0.54), and POX (-0.51) were significant. Similar to MDA, the correlations of H₂O₂ with dry weight (-0.66) and shoot length (-0.63) were negatively significant. Furthermore, H₂O₂ showed significant correlations with MDA (0.79), flavonoid (0.59), anthocyanin (0.63), SOD (-0.43), CAT (-0.64), POX (-0.47). Phenol content showed significant positive correlations with all enzymatic antioxidant. The correlation of flavonoid with CAT was positively significant (0.51), but its correlations with other enzymatic antioxidant were not significant. Anthocyanin showed positive significant correlations with CAT (0.63) and POX (0.69). All internal correlations of enzymatic antioxidants were positively significant. DPPH as a stable compound with antioxidant ability showed positive significant correlation with SOD (0.48), Cat (0.53) and POX (0.49) but its correlations with APX were not significant.

Table 3. Pearson correlation coefficients for all pairs of the traits measured in different varieties of broccoli under mannitol treatment

	DW	SL	RL	DPPH	MDA	H ₂ O ₂	Phenol	Flavonoid	Antho- cyanin	SOD	CAT	POX	APX	Sulfo- raphane
DW	1													
SL	0.74**	1												
RL	-	-	1											
DPPH	0.23ns	0.19ns	0.41n s	1										
MDA	-0.52*	-0.53*	0.04n s	0.22ns	1									
H ₂ O ₂	-	-	0.06n s	-	0.79**	1								
Phenol	0.66**	0.63**	0.46ns	0.16ns	0.12ns	0.18ns	1							
Flavonoid	-	-0.5*	0.5*	0.35ns	0.61**	0.59**	0.16ns	1						
Anthocyanin	-0.53*	-	0.17n s	0.34ns	0.61**	0.63**	0.42ns	0.44ns	1					
SOD	-	-	0.31n s	0.48*	-	-0.43*	0.69**	0.26ns	0.39ns	1				
CAT	0.38ns	-0.52*	0.7**	0.53*	0.22ns	-	0.52*	0.51*	0.63**	0.6**	1			
POX	0.63**	0.75**	0.34n s	0.49*	-0.54*	0.64**	0.51*	0.38ns	0.69**	0.79**	0.82**	1		
APX	-0.58*	-0.6**	0.67**	0.3ns	-0.51*	-0.47*	0.7**	0.38ns	0.69**	0.79**	0.82**	0.72**	1	
Sulforaphane	-	-0.54*	0.44n s	0.24ns	-	-	0.65**	0.29ns	0.44ns	0.67**	0.84**	0.72**	0.58*	1
	0.34ns	-	0.16n s	0.47*	0.18ns	-	0.19ns	0.31ns	0.66**	0.58*	0.52*	0.58*	0.58*	1

** , * , and ns: significant at 0.01, 0.05 level, and not-significant at 0.05.

To achieve more sophisticated results without the effect of other correlated variables on sulforaphane, the direct effect of all variables by holding all the effect of all other variable fixed using path coefficient analysis were implemented (*Table 4*). The path analysis showed that dry weight, H₂O₂ content, and then phenol content were the most influential variables positively affecting the content of sulforaphane, respectively. On the other hand, shoot length showed a negative coefficient in the path analysis. The coefficient of all other variables in the path analysis were negligible.

Principal component

Principal component analysis was carried out to assess the inter relationship among 14 measured traits in this study. The results showed that the first two PCs accounted for about 81 percent of total variability. Therefore, the biplot for the first two PCs in which both genotypes and parameters can be depicted in a same plot was prepared (*Table 5*). Dry weight and shoot length showed negative association with all other traits because they placed in a revers proximity to all other traits in the two dimensional graph of first two components. Matsuri and Castle Dome as two close genotypes were placed in the area near to the dry weigh and shoot length. Root length, sulforaphane content, phenol content, APX, SOD, POX, and CAT showed acute angles one another and also had positive high coefficients with both first and second components. Marathon was fixed solely in adjacent to these traits nearer to sulforaphane than all other genotypes. H₂O₂, MDA, DPPH, flavonoid content, and anthocyanin content showed positive high coefficients with first component but negative high coefficient regarding the second component. Genotypes Heraklion and Green Magic placed in near to these parameters, while Green Magic showed closest distance with DPPH and Heraklion with flavonoid content. Genotype Sacora showed a revers trend to all other genotypes considered in this study. Sacora obtained negative high coefficient with both components and was solely placed in a separate group (*Fig. 2*).

Table 4. Direct effect of each variable through sulforaphane content

Variable	Coefficient
DW	0.850992
Shoot length	-0.52174
Root length	0.041577
MDA	0.266981
H ₂ O ₂	0.848199
Phenol	0.771737
Flavonoeid antocyanin	-0.04394
SOD	-0.16695
CAT	-0.03846
POD	-0.32892
APX	-0.37341
DPPH	0.407253
	0.458507

Table 5. Proportion of each principal component and the related score of each trait

	PC1	PC2
Eigenvalue	7.9454	3.3633
Proportion	0.567529	0.240236
Cumulative	0.567529	0.807764
DW	-0.323	-0.186
Shoot length	-0.333	-0.062
Root length	0.228	-0.322
sulforaphane	0.172	-0.266
MDA	0.242	0.351
H ₂ O ₂	0.311	0.212
Phenol	0.204	-0.404
Flavonoid	0.262	0.23
Aantocyanin	0.328	0.173
SOD	0.247	-0.305
CAT	0.291	-0.085
POD	0.322	-0.109
APX	0.215	-0.364
DPPH	0.186	0.358

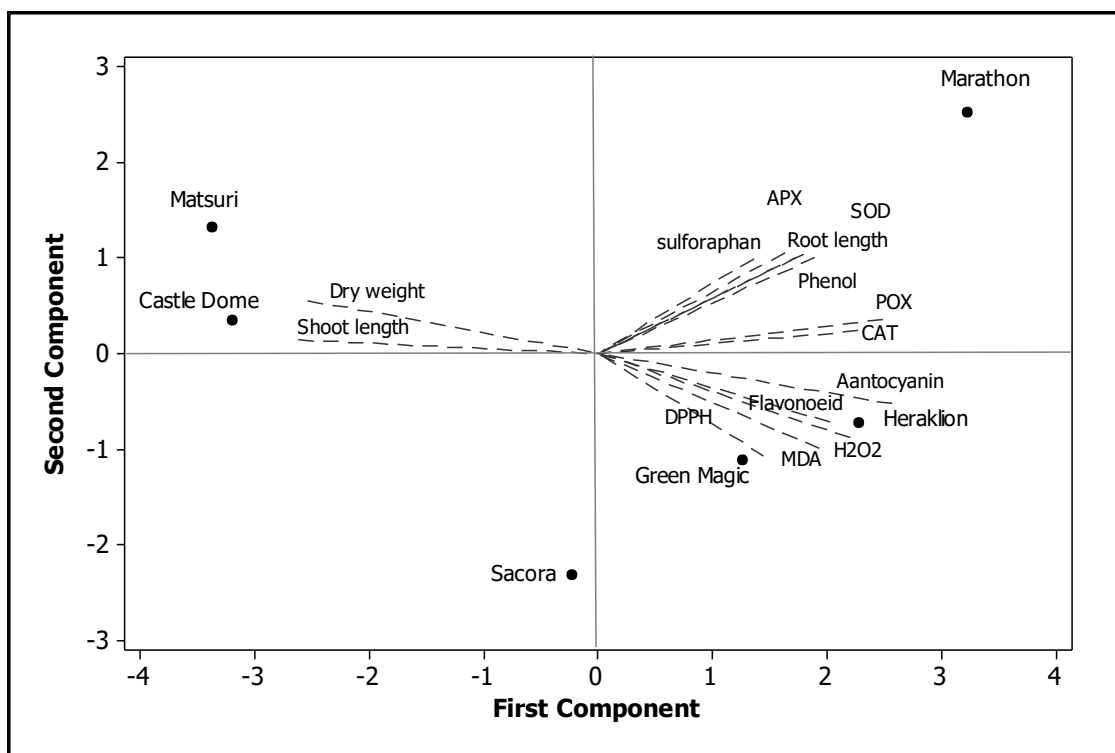


Figure 2. Biplot genotypes and traits using first two components of principal component analysis

Discussion

The results of the current study indicated that application of mannitol significantly decreased shoot dry weight and shoot length in all genotypes. Some genotypes had lower decrease rate in comparison with other genotypes regarding shoot length (Marathon genotype) and shoot dry weight (Marathon and Heraklion genotypes), however they might not show the highest values for these traits. Root length response to mannitol application in different genotypes was varied. Most of the genotypes showed increase in root length in response to mannitol application but some genotypes (Sacora and Heraklion) showed decrease. However, the rate of decrease in Heraklion was not significant. The reduction of shoot length and dry weight might be due to the falling off in the rate of photosynthesis under osmotic stress caused by mannitol application as a representative of drought stress. Chaves et al. (2009) reported that under drought stress the closure of stomata occurs to maintain the water content in the plant cells, which directly affects the growth rate of the plant's shoot. Also, the decline in the leaf area and other photosynthetic part of the plant is doubled with the stomatal closure and make photosynthesis rate to be even more reduced (Berger et al., 2016). On the other hand, the reaction of the root to drought stress might be different from what is predictable in shoot. It is well established that the root of the plants is seeking for water storage by increase its length and number of lateral roots and hairy roots (Chaves et al., 2009). The subject of root system architecture (RSA) under drought stress is revealing that under drought stress, the growth of the root can be increased, maintained at determined level, or even decreased; but the rate of growth in the shoot would normally decrease, and so that the overall growth of the root under drought stress would be always higher than the shoot (Uga et al., 2013). Furthermore, it has been stated by some researchers that tolerant genotypes are normally responding to drought in different ways which is one of the most effective way is to enlarge the root growth, while the susceptible genotypes are not able to manage this growth as properly as the tolerant genotypes (De Dorlodot et al., 2007).

In all genotypes, the content of total phenols, flavonoid, and anthocyanin increased. Marathon and Heraklion genotype showed relatively higher content of these three traits than other genotypes, while the Marathon genotype could be stand out as the highest responsive variety. Based on the study of Gawlik-Dziki (2008) phenolic compounds in vegetables, herb, and other edible plants can make them act as reducing agents and respond to oxidant compounds. In this situation, phenolic compounds can be used as hydrogen donators leading to quench the free radicals. Phenolic acids and flavonoids reportedly have shown strong antioxidant properties. They are able to react to radicals and catalyze oxidative reactions resulted in scavenging free radicals and stabilizing them in plants (Saed-Moucheshi et al., 2014b). Under drought stress, the content of free radicals or ROS in plant's cells is arisen which normally causes damages to cell apparatus; therefore, higher content of phenolic compounds indicates higher tolerance of genotype and plants to drought stress. Moreover, it has been reported that antioxidant activity of edible parts of the plants is linked with anti-mutagenic and anticancer genic properties. Subsequently, genotypes with higher content of natural antioxidants as phenolic compounds can be suggested for being used in nutritional programs and food content of human. In addition to broccoli, the extracts of varies fruits and vegetables have showed higher phenolic compounds in response to drought stress (Gawlik-Dziki, 2008).

MDA and H₂O₂ content are two important markers of oxidative stress induced in plants (Vosough et al., 2015). The lower the content of these two compounds under stress condition, the lower the damages to the plants under this situation (Saed-Moucheshi et al., 2014b). Genotypes and cultivars with lower content of MDA and H₂O₂ under stress condition would reveal higher tolerant to stress. In this study the content of both MDA and H₂O₂ increased under drought stress; however, the response rates of genotypes were varied. Castle Dome showed lower content of these compounds than other genotypes under all mannitol levels. In addition, the difference between mannitol levels in Marathon and Heraklion were relatively lower in compare to other genotypes. Under drought stress, the generation of ROS is increased from the steady level in the plant result in oxidative stress. H₂O₂ and other high reactive oxygen compounds can directly react with lipids and other apparatuses of cell membrane leading to lipid peroxidation and higher content of MDA (Hossain et al., 2015).

The activity of all assessed enzymatic antioxidant in this study increased in all genotypes in response to the increase of mannitol levels. Among all genotypes, Marathon showed relatively higher activity for this antioxidant under mannitol applications. In addition, Heraklion showed higher activity of this antioxidant under drought stress. Additionally, DPPH antioxidant activity indicated that the antioxidant activity of broccoli sprout is higher under drought stress condition. Marathon variety showed a high increase in the DPPH antioxidant activity in response to mannitol levels. The induced response of drought stress is to heighten the generation of ROS, which in turn induces the activity of antioxidant compounds and specially the enzymatic ones. In varies studies, higher activity for enzymatic antioxidant under stress condition indicates higher ability of the plants in response to stress condition (Gupta and Huang, 2014; Hossain et al., 2015; Nakano and Asada, 1981). Based on this viewpoint, genotypes with higher activity of enzymatic antioxidant can be considered as higher tolerant genotypes to drought stress. Changes in the activity of antioxidant enzymes under various environmental stresses have been also reported (Baxter et al., 2014). In addition to phenolic compounds and enzymatic antioxidant, DPPH which itself is a radical compound normally acts as a scavenger for other dangerous radicals and therefore its content is a marker for higher antioxidant activity in plants.

The response of all genotypes to application of mannitol were to increase the content of sulforaphane but the rate of increase in some genotypes consist of Sacora and Castle Dome genotypes were low. Marathon and Green magic showed a great increase from zero to 88mM application of mannitol, but the difference between 88 and 176 mM mannitol remained non-significant. Under all mannitol levels and in total, the content of sulforaphane was highest in Marathon in comparison to other genotypes. Owing to the anticarcinogenic and anticancer functions, sulforaphane is an important compound in broccoli sprout. Since sulforaphane is a naturally available inducer of phase II enzymes in human and animal bodies that is able to detoxify cancer-causing chemicals, it would be appropriate to use such foods and plants part as broccoli, which are containing this compound to use its anti-cancerous properties. Additionally, sulforaphane has a cytoprotective effect against oxidative stress (Gu et al., 2011). Considering the relationship among measured parameters, it is turned out that the shoot dry weight along with shoot length showed negative correlation with other measured traits. There were positive correlations among sulforaphane content, root length, total phenol content, SOD, APX, CAT, and POX. In addition, there were significant correlations among flavonoid content, anthocyanin content, MDA, H₂O₂. Gu et al.

(2011) investigated the effect of sucrose on the sulforaphane content in broccoli sprouts and stated that there was a significant correlation between glucosinolate, sulforaphane and antioxidant activity with phenol contents (137). Baczek-Kwinta et al. (2006) stated that SOD activity was different in different genotypes of cabbage under drought treatment. Similar results were reported by Joon-Ho and Sang (2015) and Dominguez-Perles et al. (2010) and indicated that there was no significant correlation between the sulforaphane content and the antioxidant activity of DPPH in Broccoli and other plants in the *Brassicaceae* family.

Furthermore, grouping of the varieties according to the measured parameters resulted in cluster Marathon genotype as separate group. In this study, Marathon showed relatively high values for the most of the measured traits, while the content of MDA and H₂O₂ were roughly lower than the other varieties.

Conclusion

The overall results of this study showed that the application of mannitol as a compound that decreases the osmotic potential of cells and simulates the drought stress in the *in vitro* condition, is a suitable compound for being used to induce the simulated drought stress in laboratory experiment. In addition, induced stress changed the content of measured traits and activities of enzymatic antioxidant. Mannitol stress reduced shoot dry weight and shoot length significantly for all genotypes but with the different rate. Marathon and Heraklion genotypes showed higher growth related traits under relatively all conditions. The response of marathon to mannitol application related to total phenolic content, flavonoid content, anthocyanin content, the activity of all enzymatic antioxidant, and the activity of DPPH was higher than the other genotypes. H₂O₂ and MDA content as the negative markers of oxidative stress were higher under mannitol stress condition. Results showed that sulforaphane content of the different genotypes under different stress levels was different. Mannitol stress increased the content of sulforaphane. Marathon showed the highest content of sulforaphane among all genotypes under both normal and stress conditions. Considering all these results together put us in touch with a suggestion that Marathon is the most proper genotypes for both cultivation and breeding aims among all studied genotypes. Heraklion genotype showed to be in second order regarding the content of measured traits after marathon with a high significant content of sulforaphane comparing other genotypes. Therefore, Heraklion might be a useful genotype being considered in line with marathon in breeding programs. Furthermore, both severe and moderate stresses increased sulforaphane amount along with phenolic compounds and antioxidant actives; therefore, it could be elucidated that moderate drought stress condition (88 mM concentration of Mannitol) which led to relatively low decreases in growth parameters comparing control condition, might be applicable for inducing higher content of sulforaphane and phenolic compounds in broccoli. More studies are needed to assess whether bioactive molecular accumulation really improve the biological / functional properties of these bioactive molecule enriched-sprouts.

Acknowledgements. The authors are grateful to the Agricultural and Natural Resources University, Sari, Mazandaran, Iran for providing the facilities for the investigations.

REFERENCES

- [1] Abou El-Magd, M., Mahmoud, A. R., Hafiz, M. M. and Ali, A. H. (2013): Effect of different levels of mineral phosphorus fertilizer and bio-phosphorus on vegetative growth, head yield and quality of broccoli. – *Research Journal of Agriculture and Biological Sciences* 9(5): 164-169.
- [2] Aebi, H. (1984): [13] catalase in vitro. – *Methods in enzymology* 105: 121-126.
- [3] Ainsworth, E. A., Gillespie, K. M. (2007): Estimation of total phenolic content and other oxidation substrates in plant tissues using folin–ciocalteu reagent. – *Nature protocols* 2(4): 875-877.
- [4] Baczek-Kwinta, R., Filek, W., Grzesiak, S., Hura, T. (2006): The effect of soil drought and rehydration on growth and antioxidative activity in flag leaves of triticale. – *Biologia plantarum* 50: 55-60.
- [5] Baxter, A., Mittler, R. Suzuki, N. (2014): Ros as key players in plant stress signalling. – *Journal of experimental botany* 65(5): 1229-1240.
- [6] Beecher, C. W. (1994): Cancer preventive properties of varieties of *brassica oleracea*: A review. – *The American journal of clinical nutrition* 59(5): 1166S-1170S.
- [7] Berger, J., Palta, J., Vadez, V. (2016): Review: An integrated framework for crop adaptation to dry environments: Responses to transient and terminal drought. – *Plant Science* 253: 58-67.
- [8] Brader, G., Mikkelsen, M. D., Halkier, B. A., Tapio Palva, E. (2006): Altering glucosinolate profiles modulates disease resistance in plants. – *The Plant Journal* 46(5): 758-767.
- [9] Bradford, M. M. (1976): A rapid and sensitive method for the quantitation of microgram quantities of protein utilizing the principle of protein-dye binding. – *Analytical biochemistry* 72(1-2): 248-254.
- [10] Brand-Williams, W., Cuvelier, M.-E., Berset, C. (1995): Use of a free radical method to evaluate antioxidant activity. – *LWT-Food Science and Technology* 28(1): 25-30.
- [11] Chaves, M. M., Flexas, J., Pinheiro, C. (2009): Photosynthesis under drought and salt stress: Regulation mechanisms from whole plant to cell. – *Annals of botany* 103(4): 551-560.
- [12] Dazy, M., Jung, V., Féraud, J.-F., Masfarau, J.-F. (2008): Ecological recovery of vegetation on a coke-factory soil: Role of plant antioxidant enzymes and possible implications in site restoration. – *Chemosphere* 74(1): 57-63.
- [13] De Dorlodot, S., Forster, B., Pagès, L., Price, A., Tuberosa, R., Draye, X. (2007): Root system architecture: Opportunities and constraints for genetic improvement of crops. – *Trends in plant science* 12(10): 474-481.
- [14] Dominguez-Perles, R., Martinez-Ballesta, M. C., Carvajal, M., Garcia-Viguera, C., Moreno, D. A. (2010): Broccoli-derived by-products—a promising source of bioactive ingredients. – *Journal of Food Science* 75: 383-392.
- [15] Gawlik-Dziki, U. (2008): Effect of hydrothermal treatment on the antioxidant properties of broccoli (*brassica oleracea* var. *Botrytis italica*) florets. – *Food chemistry* 109(2): 393-401.
- [16] Giannopolitis, C. N., Ries, S. K. (1977): Superoxide dismutases i. Occurrence in higher plants. – *Plant physiology* 59(2): 309-314.
- [17] Gu, Y., Guo, Q., Zhang, L., Chen, Z., Han, Y., Gu, Z. (2011): Physiological and biochemical metabolism of germinating broccoli seeds and sprouts. – *Journal of Agricultural and Food Chemistry* 60: 209-213.
- [18] Guo, R., Yuan, G., Wang, Q. (2011): Effect of sucrose and mannitol on the accumulation of health-promoting compounds and the activity of metabolic enzymes in broccoli sprouts. – *Scientia Horticulturae* 128(3): 159-165.
- [19] Gupta, B., Huang, B. (2014): Mechanism of salinity tolerance in plants: Physiological, biochemical, and molecular characterization. – *International journal of genomics* 2014.

- [20] Han, S.-K., Wagner, D. (2014): Role of chromatin in water stress responses in plants. – *Journal of experimental botany* 65(10): 2785-2799.
- [21] Heath, R. L., Packer, L. (1968): Photoperoxidation in isolated chloroplasts: I. Kinetics and stoichiometry of fatty acid peroxidation. – *Archives of biochemistry and biophysics* 125(1): 189-198.
- [22] Hossain, M. A., Bhattacharjee, S., Armin, S.-M., Qian, P., Xin, W., Li, H.-Y., Burritt, D. J., Fujita, M., Tran, L.-S. P. (2015): Hydrogen peroxide priming modulates abiotic oxidative stress tolerance: Insights from ros detoxification and scavenging. – *Frontiers in plant science* 6.
- [23] Hwang, J. H., Lim, S. B. (2015): Antioxidant and anticancer activities of broccoli by-products from different cultivars and maturity stages at harvest. – *Preventive Nutrition and Food Science* 20(1): 8-14
- [24] Lemoine, M. L., Chaves, A. R. , Martínez, G. A. (2010): Influence of combined hot air and uv-c treatment on the antioxidant system of minimally processed broccoli (*brassica oleracea* l. Var. *Italica*). – *LWT-Food Science and Technology* 43(9): 1313-1319.
- [25] Nakano, Y., Asada, K. (1981): Hydrogen peroxide is scavenged by ascorbate-specific peroxidase in spinach chloroplasts. – *Plant and cell physiology* 22(5): 867-880.
- [26] Oomah, B. D., Mazza, G. (1996): Flavonoids and antioxidative activities in buckwheat. – *Journal of Agricultural and Food Chemistry* 44(7): 1746-1750.
- [27] Osakabe, Y., Yamaguchi-Shinozaki, K., Shinozaki, K., Tran, L. S. P. (2014): Aba control of plant macroelement membrane transport systems in response to water deficit and high salinity. – *New Phytologist* 202(1): 35-49.
- [28] Pereira, F. M. V., Rosa, E., Fahey, J. W., Stephenson, K. K., Carvalho, R., Aires, A. (2002): Influence of temperature and ontogeny on the levels of glucosinolates in broccoli (*brassica oleracea* var. *Italica*) sprouts and their effect on the induction of mammalian phase 2 enzymes. – *Journal of Agricultural and Food Chemistry* 50(21): 6239-6244.
- [29] Saed-Moucheshi, A., Pakniyat, H., Pirasteh-Anosheh, H., Azooz, M. (2014a): Role of ROS as signaling molecules in plants. – In: p, Ahmad (ed.) *Reactive Oxygen Species, Antioxidant Network and Signaling in Plants*. Springer Publication, New York, USA: 585-626.
- [30] Saed-Moucheshi, A., Shekoofa, A., Pessarakli, M. (2014b): Reactive oxygen species (ROS) generation and detoxifying in plants. – *Journal of Plant Nutrition* 37(10): 1573-1585.
- [31] Suzuki, N., Rivero, R. M., Shulaev, V., Blumwald, E., Mittler, R. (2014): Abiotic and biotic stress combinations. – *New Phytologist* 203(1): 32-43.
- [32] Uga, Y., Sugimoto, K., Ogawa, S., Rane, J., Ishitani, M., Hara, N., Kitomi, Y., Inukai, Y., Ono, K., Kanno, N. (2013): Control of root system architecture by deeper rooting 1 increases rice yield under drought conditions. – *Nature Genetics* 45(9): 1097-1102.
- [33] Velikova, V., Yordanov, I. and Edreva, A. (2000): Oxidative stress and some antioxidant systems in acid rain-treated bean plants: Protective role of exogenous polyamines. – *Plant Science* 151(1): 59-66.
- [34] Vosough, A., Ghouchani, R., Saed-Moucheshi, A. (2015): Genotypic variation and heritability of antioxidant related traits in wheat landraces of iran. – *Biological Forum* 7(2): 43-47
- [35] Yuan, Y., Chiu, L.-W., Li, L. (2009): Transcriptional regulation of anthocyanin biosynthesis in red cabbage. – *Planta* 230(6): 1141.

EVALUATION OF PHYSIOLOGICAL INDICES OF WATERLOGGING TOLERANCE OF DIFFERENT MAIZE VARIETIES IN SOUTH CHINA

LI, W.^{1#} – MO, W.^{1,2#} – ASHRAF, U.^{3#} – LI, G.¹ – WEN, T.¹ – ABRAR, M.⁴ – GAO, L.¹ – LIU, J.^{1*} – HU, J.^{1*}

¹*Crops Research Institute, Guangdong Academy of Agricultural Sciences, Guangdong Provincial Key Laboratory of Crop Genetic Improvement, Guangzhou, China*

²*Department of Crop science and Technology, College of Agriculture, South China Agricultural University, Guangzhou, 510640, Guangdong, China*

³*Department of Agronomy, University of Agriculture, Faisalabad, Pakistan*

⁴*State Key Laboratory of Grassland Agro-Ecosystems, School of Life Sciences, Lanzhou University, Lanzhou, China*

**Corresponding authors*

e-mails: liu_jhxs@163.com (J. Liu); Jghu2003@263.net (J. Hu)

#Equal contributors

(Received 11th Jan 2018; accepted 13th Mar 2018)

Abstract. Maize is extremely sensitive to waterlogging stress. A pot experiment was conducted to study the morpho-physiological characteristics of 18 different maize cultivars (widely grown in South China) under waterlogging stress at seedling stage. Results showed that maize shoot growth was inhibited in terms of plant height and dry weight whilst leaf chlorophyll contents were also decreased under waterlogging stress. Root length, root hairs, root surface area and root volume were also declined under waterlogged conditions. Furthermore, activity of antioxidants i.e., superoxide dismutase (SOD), peroxidase (POD), and catalase (CAT) were increased considerably under waterlogging stress compared to control. The soluble protein content also increased in some maize cultivars whereas malondialdehyde (MDA) contents were found to be decreased in some cultivars that may be due to higher antioxidant enzyme activities. Furthermore, the principal component analysis (PCA) showed that the coefficients of comprehensive indices (Z) for protein contents, SOD, POD and CAT were higher in Z1, the soluble protein content and MDA content in Z2 while the SPAD and F_v/F_m values in Z3 were remained higher than other parameters.

Keywords: *antioxidant enzymes, chlorophyll, maize, root, waterlogging stress*

Introduction

Maize is an important food crop in the world (Ashraf et al., 2016), whereas China is ranked first with respect to area under maize cultivation and yield (Qi et al., 2012). Maize is more susceptible to water logging stress, especially at seedling stage thus resulting in poor stand establishment (Ren et al., 2016a). Anaerobic conditions due to waterlogging, inhibit the growth of plant roots, causing decline in root/shoot ratio and root dry weight thus indirectly affect the aboveground growth (Grzesiak et al., 2014; McDaniel et al., 2016; Yu et al., 2017). In response to waterlogging stress, maize root cells cleave to form aeration tissue for maintaining oxygen diffusion and high absorption efficiency (Zaidi et al., 2003). Most of the previous studies which are related to aboveground response of maize to waterlogging showed that plant height, dry weight

and leaf photosynthesis severely got affected by waterlogging (Ren et al., 2016b; Shin et al., 2016; Wang et al., 2012). Lipid peroxidation caused chloroplastic membrane destruction is one of the responses of plants to waterlogged conditions. It results in chlorophyll destruction causing reduction in the efficiency of PSII (F_v/F_m) (Mielke and Schaffer, 2010; Yordanova and Popova, 2007).

Plants produce reactive oxygen species (ROS), such as hydrogen peroxide (H_2O_2), superoxide anions (O_2^-), hydroxyl radical ($\cdot OH$) and singlet oxygen (1O_2) in the absence of oxygen (Cheng et al., 2015; Pucciariello and Perata, 2016). Excessive ROS induce damage to proteins, lipids, carbohydrates and DNA, thus causing cell lipid peroxidation, which is harmful to plant (Gill and Tuteja, 2010). Malondialdehyde (MDA) is the final product of lipid peroxidation so its content can reflect the degree of membrane lipid peroxidation. Plants have developed an antioxidant system including superoxide dismutase (SOD), peroxidase (POD), catalase (CAT) and other antioxidant enzymes to control ROS levels and regulate various physiological processes which play an important role in plant adaptation and tolerance to abiotic stress (Hossain et al., 2009; Wang et al., 2016a). Previous studies showed that the trend of antioxidant enzymes activity increase transiently and then decrease sharply with the increase of waterlogging (Gill and Tuteja, 2010; Liu et al., 2015a). Furthermore, plants regulate the cell osmotic potential and protect the function of various enzymes through the biosynthesis and accumulation of osmotic adjustment (Wu et al., 2015; Yordanova and Popova, 2007).

Membership function is often used for comprehensive evaluation of crop waterlogging stress (Zhou et al., 2003). However, there is a certain limitation on the comprehensive evaluation of crop waterlogging tolerance by the membership function because of the correlation between indicators. The principal component analysis can convert the original indexes into new comprehensive and independent indicators (Liu et al., 2015b). The comprehensive evaluation value of each variety can be obtained by weighing the value of each comprehensive index and the corresponding membership function value of varieties. This study was aimed to explore the morphological and physiological responses of 18 different Chinese maize varieties to waterlogging stress.

Materials and methods

Experimental material and growing conditions

A pot experiment was conducted by using 18 maize varieties, i.e., Guangtian 2 (GT2), Xinmeixiazhen (XMXZ), Huameitian 8 (HMT8), Guangnuo 1 (GN1), Xinmeixiangnuo (XMXN), Zhengtian 68 (ZT68), Yuexiannuo 2 (YXN2), Yuetian 13 (YT13), Yuebainuo 3 (YBN33), Yuetian 27 (YT27), Yuetian 28 (YT28), Yuebainuo 6 (YBN6), Zhengtian 89 (ZT89), Yuecainuo 2 (YCN2), Yuehuanuo 1 (YHN1), Yuezinuo 5 (YZN5), Yuetian 16 (YT16), Yuetian 22 (YT22) provided by Crop Research Institute, Guangdong Academy of Agricultural Sciences, Guangzhou, China. 30 seeds were evenly planted in each plastic pot (10 cm in height and 6 cm in diameter) containing 500 g soil with $22.87 \text{ g}\cdot\text{kg}^{-1}$ organic matter, available nitrogen $10.03 \text{ mg}\cdot\text{kg}^{-1}$, available phosphorus $70.21 \text{ mg}\cdot\text{kg}^{-1}$, available potassium $100.41 \text{ mg}\cdot\text{kg}^{-1}$ and pH 6.8. The pots were placed at Agricultural Meteorological Observatory in South China Agricultural University and covered with a transparent plastic shed from the top.

Treatments

Each variety included control (no waterlogging) and waterlogging treatments having three replications. All pots were filled with water to 3 cm above the soil surface at three leaves stage except control and waterlogged conditions were maintained for two days. The samples were taken and the related morphological indexes were determined within 12 h after draining the water.

Observations

Morphological characters

The plant height was measured from soil surface to the highest tip of leaves. The fresh sample of plant shoots was placed in the oven at 75°C and dried to a constant weight for measurement of the shoot dry weight. The shoot dry weight of the plant was weighed by the electronic analytical balance (BSA224S, Sartorius, Taiwan).

Root morphological index determination

The root was scanned with Epson Expression 10000XL (Epson America Inc., Long Beach, US). After scanning, the root morphological indexes i.e., root length, root mean diameter, root surface area and root volume were analyzed by WinRHIZO image analysis system (Regent Instruments Inc., CA).

SPAD value and chlorophyll fluorescence determination

The relative chlorophyll content of leaves was measured by a SPAD meter (SPAD-502, Konica-Minolta, Japan), a precise and rapid method of leaf chlorophyll determination. 10 leaves were determined for each treatment and the SPAD values were measured at the upper, middle and lower parts in each leaf. The chlorophyll fluorescence was measured with a modulated chlorophyll fluorometer (FMS-2, Hansatech Instruments, Norfolk, UK) according to Wang et al. (2012): Minimal fluorescence (F_0) was measured after leaves adapted to dark for 30 min, and maximal fluorescence (F_m) was induced by strong saturation pulsed light after leaves adapted to dark for 30 min. The maximum efficiency of PSII (F_v/F_m) was calculated as $(F_m - F_0)/F_m$.

Physiological parameters

To determine physiological parameters, the second and third leaves of plant sample were collected and stored in refrigerator at -80 °C till biochemical analyses.

Enzyme was extracted by adding 0.30 g fresh sample to 4 mL of 0.05 mol·L⁻¹ phosphate buffer (pH = 7.8) in an ice bath, and then solution was transferred into 5 mL centrifuge tube for centrifugation at 8000 rpm at 4 °C for 15 min. The supernatant is the enzyme solution.

The superoxide dismutase (SOD, EC 1.15.1.1) activity was measured by using nitro blue tetrazolium (NBT) method (Li, 2000). The reaction mixture contained 1.5 mL of 0.5 mmol·L⁻¹ phosphate buffer (pH = 7.8), 0.3 mL of 130 mmol·L⁻¹ methionine, 0.3 mL of 0.75 mmol·L⁻¹ of nitro-tetrazolium chloride Blue, 0.3 mL of 0.02 mmol·L⁻¹ riboflavin, 0.3 mL of 0.1 mmol·L⁻¹ EDTA-Na₂, 0.05 mL enzyme solution and 0.25 mL distilled water. Phosphoric buffer (pH = 7.8) was used as control. After mixing, the light was irradiated under 4000 lx for 20 min, and the reaction was stopped by covering with black cloth. Then, the color changed was measured at 560 nm and one unit of SOD

activity equaled the volume of extract needed to cause 50% inhibition of the color reaction and expressed as $U \cdot g^{-1}$.

The peroxidase (POD, EC1.11.1.7) activity was measured by using guaiacol method (Li, 2000). One cuvette was added with 1 mL of 0.3% H_2O_2 , 0.95 mL of 0.2% guaiacol, 1 mL of phosphate buffer (pH = 7.0) and 0.05 mL of 0.05 $mol \cdot L^{-1}$ phosphate buffer (pH = 7.8) as a zero tube. The other one was added with 1 mL of 0.3% H_2O_2 , 0.95 mL of 0.2% guaiacol, 1 mL phosphate buffer (pH = 7.0) and 0.05 mL enzyme solution. The color changed was measured at 470 nm immediately, and an absorbance value was recorded after every 30 s for 2 min. One POD unit of enzyme activity was defined as the absorbance increase because of guaiacol oxidation by 0.01 ($U \cdot g^{-1}$).

The catalase (CAT, EC 1.11.1.6) activity was measured by ultraviolet spectrophotometry (Wang et al., 2016b). One quartz cuvette (3 mL) was added with 1.95 mL of distilled water, 1.00 mL of 0.3% H_2O_2 solution and 0.05 mL of PBS buffer (pH = 7.8). The other one was added with sodium phosphate buffer instead of the enzyme solution. The other one was added with the enzyme solution instead of PBS buffer. After rapid mixing, the color change was measured at 240 nm, and an absorbance value was recorded after every 30 s for 2 min. The absorbance changed by 0.01 per minute is a relative activity of the CAT unit ($U \cdot g^{-1}$).

The malondialdehyde (MDA) content was determined by thiobarbituric acid method (Li, 2000). One test tube was added with 1.5 mL supernatant, 2 mL of 0.5% thiobarbituric acid (TBA) solution and phosphate solution. The other one was added with 1.5 mL of 0.05 $mol \cdot L^{-1}$ phosphate buffer (pH = 7.8) and 2 mL of 0.5% thiobarbituric acid solution as control. Test tubes were heated at 100 °C for 30 min and then cooled in an ice bath immediately. After centrifugation at 3000 rpm for 15 min, the supernatant was taken and the absorbance was measured at 450, 532 and 600 nm. The MDA content ($\mu mol \cdot L^{-1}$) was calculated as: $MDA \text{ content} = 6.45 (OD_{532} - OD_{600}) - 0.56OD_{450}$.

Soluble protein content was determined by Coomassie brilliant blue G-250 method (Bradford, 1976). The supernatant was mixed with the Coomassie brilliant blue G-250 solution and the absorbance of the reaction mixture was read at 595 nm with a spectrophotometer. Solution protein content was determined from a standard curve (bovine serum albumin) and expressed as $\mu g \cdot g^{-1}$.

Statistical analysis

Analyses of variances (ANOVA) were performed by the Linear Model Procedure of Statistix version 8 (Statistix 8, Analytical, Tallahassee, Florida, USA). Comparisons of means among different treatments were made according to the least significant difference (LSD) at the 5% probability level. The figures were made by using the Graph Pad Prism 6 for Windows (Graph Pad Software Inc., CA, USA).

Comprehensive evaluation

The evaluation system of different maize varieties to waterlogging was established by waterlogging tolerance coefficient, principal component analysis, membership function and cluster analysis based on the response mechanism of maize to waterlogging.

Waterlogging tolerance coefficient (WTC) was used to measure waterlogging tolerance of varieties. WTC could eliminate difference between varieties and treatments.

The WTC was calculated as: $WTC = \text{Mean value of treatment} / \text{Mean value of control}$ (Liu et al., 2010b).

Principal component analysis (PCA) was used to analyze the WTC of investigated parameters, and the original investigated parameters were converted into new independent comprehensive indexes.

Membership function (MF) was further used to assess the comprehensive indexes. The membership function value of the comprehensive index is obtained by the following formula (Eq. 1) according to (Zhou et al., 2003):

$$U(X_j) = (X_j - X_{\min}) / (X_{\max} - X_{\min}) \quad (\text{Eq.1})$$

where X_j is the j th comprehensive index, X_{\min} is the minimum of j th comprehensive index, and X_{\max} is the maximum of j th comprehensive index.

The weight of each comprehensive index is calculated by the contribution rate (Eq. 2):

$$W_j = \frac{P_j}{\sum_{j=1}^n P_j} \quad (\text{Eq.2})$$

where W_j is the weight of j th comprehensive index in all comprehensive indicators, and P_j is the contribution rate of the j th comprehensive index.

The following formula (Eq. 3) was used to estimate the waterlogging tolerance of different maize varieties:

$$D = \sum_{j=1}^n [U(X_j) \times W_j]. \quad (\text{Eq.3})$$

Results

Analysis of variance of the investigated parameters

All maize varieties differed significantly regarding most of the investigated parameters except for F_v/F_m value in leaves. Waterlogging also affected most of the investigated parameters; however, no significant effect was noted for SPAD value in leaves and root volume. For variety and waterlogging interaction, the significant effects were observed for most of the investigated parameters, except for F_v/F_m value in leaves (Table 1).

Morphological characters

Waterlogging significantly reduced the plant height of XMXZ, GN1, YT13, TBN3, YT27, YT28, YHN1, YZN5 and YT22 by 18.62%-43.33%, compared with the control (Fig. 1A). After waterlogging, the shoot dry weight was significantly reduced by 60.00%, 39.13%, 33.33% and 57.14% for HMT8, YBN3, TBN 6, YHN1 respectively, while other varieties did not have significant difference (Fig. 1B).

Root morphological characters

Waterlogging treated seedlings significantly decreased root length of XMXN, YBN3, YCN2, YHN1, YZN5, YT16 and YT22 by 23.52%-61.56%, compared to the control

(Fig. 2A). As for root surface area, there is a significant decrease in XMXN, YBN3, YCN2, YHN1 and YZN5, while a notable increase in shoot was observed for GT2 (Fig. 2B). In addition, a significant improvement in root mean diameter was recorded for XMXZ, HMT8, XMXN, ZT68, YBN3, YT27, YHN1 and YT16 (Fig. 2C). After waterlogging, the root volume was significantly improved for GT2, XMXZ, HMT8, ZT68 and YT27 in different degrees, whereas an obvious decline is observed in YT 13, ZT89, YCN 2, YHN1 and YZN5 (Fig. 2 D).

Furthermore, the results of variance analysis showed that there was no significant change in the root volume of maize seedling after waterlogging, this change was due to the difference of genotype (Table 1).

Table 1. Analysis of variance of the investigated parameters (F value)

Index	V	T	V × T
Plant Height	14.21**	98.02**	3.02**
Shoot dry weight	11.1**	33.82**	5.07**
SPAD value in leaves	7.03**	3.00ns	2.11*
F _v /F _m value	1.67ns	16.57**	1.91ns
CAT activity in leaves	106.42**	275.81**	7.41**
POD activity in leaves	110.69**	273.39**	7.35**
SOD activity in leaves	110.29**	273.94**	7.37**
MDA content in leaves	79.64**	20.37**	30.15**
Soluble protein	43.52**	254.69**	23.72**
Root length	23.13**	188.25**	9.11**
Root surface area	19.56**	34.17**	8.78**
Root mean diameter	6.97**	123.24**	7.29**
Root volume	39.11**	2.94ns	20.95**

V, variety; T, treatment; V×T, variety and treatment interaction; ns, non-significant at P < 0.05 level; *, significant at P < 0.05 level; **, significant at P < 0.01 levels

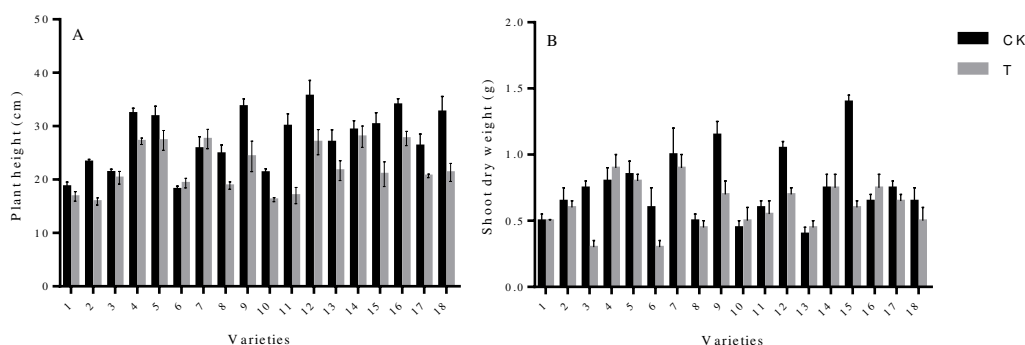


Figure 1. Plant height and shoot dry weight of maize (A and B, respectively). Capped bars represent standard error. Variety 1-18 represents GT2, XMXZ, HMT8, GN1, XMXN, ZT68, YXN2, YT13, YBN33, YT27, YT28, YBN6, ZT89, YCN2, YHN1, YZN5YT16 and YT22, respectively

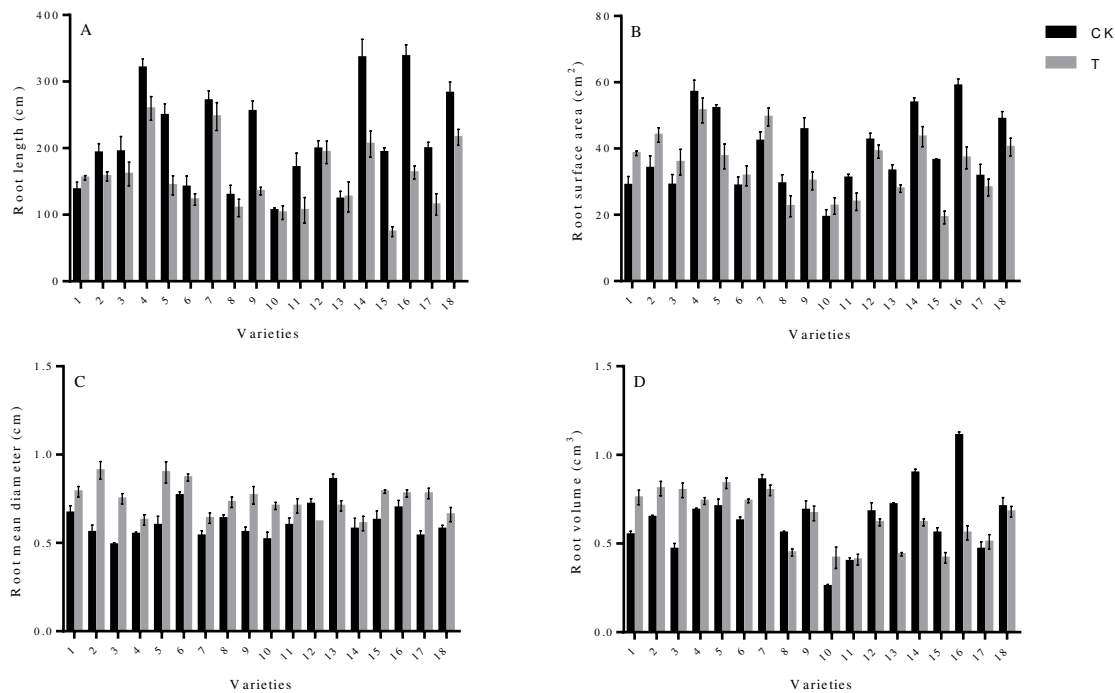


Figure 2. Root length, root surface area, root mean diameter and root volume of maize (A, B, C, D, respectively). Capped bars represent standard error. Variety 1-18 represents GT2, XMXZ, HMT8, GN1, XMXN, ZT68, YXN2, YT13, YBN33, YT27, YT28, YBN6, ZT89, YCN2, YHN1, YZN5YT16 and YT22, respectively

SPAD value and chlorophyll fluorescence

There was no significant effect of waterlogging on chlorophyll content in maize, and the difference of SPAD value was due to the difference among varieties. The SPAD value was significantly reduced in YT28, YBN6 and YHN1. Nevertheless, non-significant effect of waterlogging treatment was observed for SPAD value in other varieties (Fig. 3A). For F_v/F_m value, significant decline was recorded for YBN3, ZT89 and YT22 up to 7.35%, 11.09% and 14.36%, respectively. Additionally, no significant changes were observed in remaining varieties (Fig. 3B).

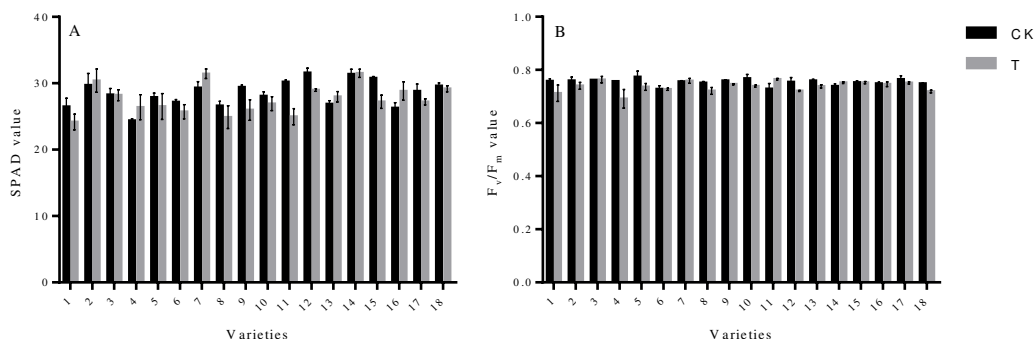


Figure 3. SPAD value and F_v/F_m value in leaves of maize (A and B). Capped bars represent standard error. Variety 1-18 represents GT2, XMXZ, HMT8, GN1, XMXN, ZT68, YXN2, YT13, YBN33, YT27, YT28, YBN6, ZT89, YCN2, YHN1, YZN5YT16 and YT22, respectively

Antioxidant enzymatic activities

Waterlogging treated maize seedlings significantly increased SOD activity of XMXZ, HMT8, GN 1, XMXN, YT 13, YBN3, YT28, TBN 6, ZT 89, YCN 2, YZN5 and YT22. This increase in SOD activity ranged from 19.16% to 56.89% (Fig. 4A). The POD activity was also induced by waterlogging treatment, and significant increase in XMXZ, HMT8, GN1, XMXN, ZT68, YT13, YBN3, YT28, TBN 6, ZT 89, YCN2, YZN5 and YT22 was observed ranging from 19.16% to 106.96% (Fig. 4B). Significant increment of CAT activity was recorded for HMT8, GN1, XMXN, YT13, YT28, TBN 6, YCN2, YZN5 and YT22 ranging from 26.08% to 57.29% (Fig. 4C).

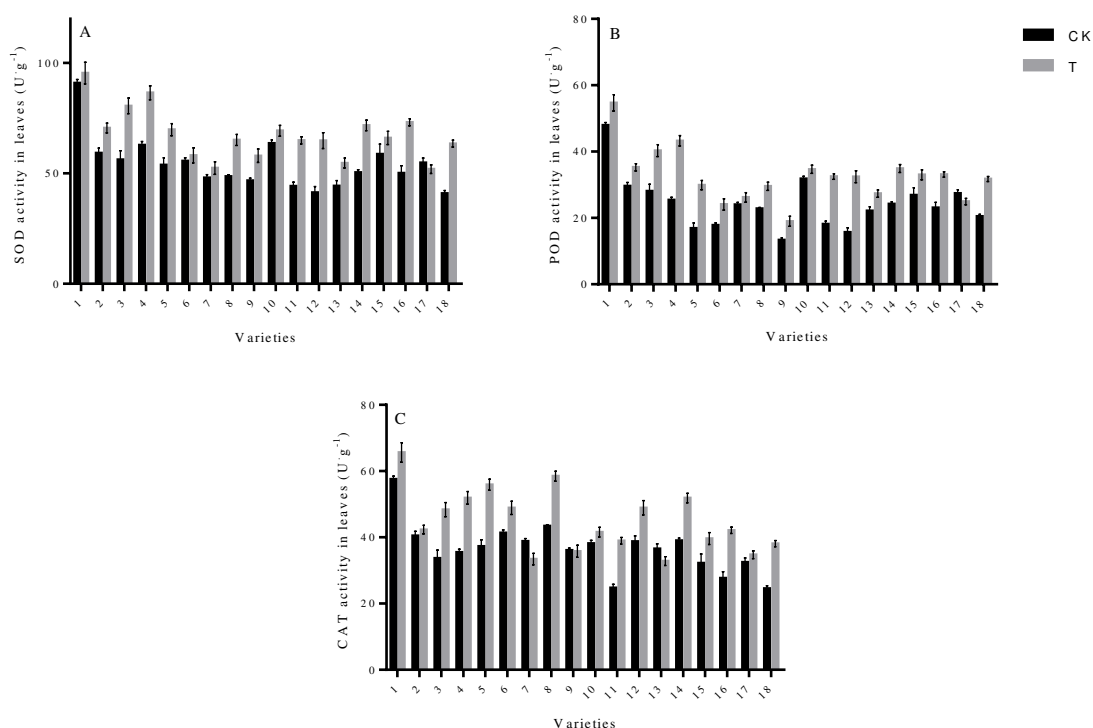


Figure 4. SOD, POD, CAT activity in leaves of maize (A, B, C respectively). Capped bars represent standard error. Variety 1-18 represents GT2, XMXZ, HMT8, GN1, XMXN, ZT68, YXN2, YT13, YBN3, YT27, YT28, YBN6, ZT89, YCN2, YHN1, YZN5, YT16 and YT22, respectively

Protein content and MDA content

For protein content, waterlogging treatment significantly improved protein content of GT2, XMXZ, HMT8, GN1, YXN2, YT13, YHN1, YZN5 and YT16 by 136.22%, 15.45%, 72.34%, 27.49%, 21.02%, 16.59%, 37.32%, 37.39% and 21.23%, respectively (Fig. 5B). Apart from GT2, HMT8, YT13 and TBN6, the MDA contents of remaining varieties were reduced. Especially, waterlogging reduced MDA contents of XMXZ, XMXN and YXN2 significantly by 24.49%, 33.68% and 24.67%, respectively (Fig. 5A).

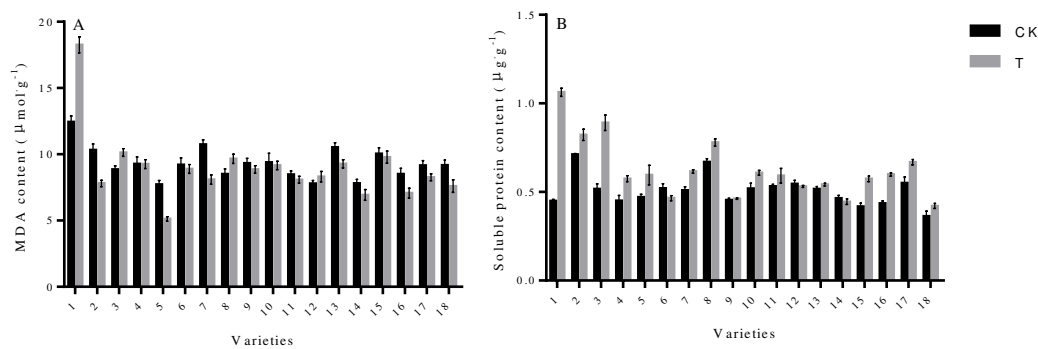


Figure 5. MDA content and soluble protein content in leaves of maize (A and B). Capped bars represent standard error. Variety 1-18 represents GT2, XMxz, HMT8, GN1, XMxN, ZT68, YXN2, YT13, YBN33, YT27, YT28, YBN6, ZT89, YCN2, YHN1, YZN5YT16 and YT22, respectively

Comprehensive evaluation

The original investigated parameters were converted into three comprehensive indexes to analyze the WTC of physiological parameters using PCA (Table 2).

Table 2. Coefficients of comprehensive indexes (Z) and proportion

	SOD activity	POD activity	CAT activity	Soluble protein	F _v /F _m value	SPAD value	MDA content	Proportion
Z1	0.582	0.559	0.477	-0.230	0.030	0.188	-0.178	0.364
Z2	0.124	0.135	0.292	0.609	-0.308	-0.134	0.630	0.251
Z3	0.004	0.003	0.246	-0.013	0.663	-0.703	0.071	0.192

From Table 2, it can be noted that the coefficient of protein content, SOD, POD and CAT activity in Z1 is larger, the soluble protein content and MDA content in Z2 is larger, while the SPAD and F_v/F_m value in Z3 is larger. The contribution rates of the three comprehensive indexes (Z1, Z2, Z3) were 36.46%, 25.12% and 19.20% respectively, and the cumulative contribution rate was 80.78%. It can be used to evaluate the tolerance of maize.

The membership function analysis of all the comprehensive indexes of maize varieties showed that there was more resistance of the cultivar to waterlogging at larger U value on the same comprehensive index. Took Z1 as example, under waterlogging, the U(1) value of YBN6 was the largest, indicating that YBN6 had the best waterlogging resistance compared with GT2 having minimum U(1) value which indicated that GT2 had less resistance against waterlogging. D value is a comprehensive index reflecting the waterlogging resistance of maize varieties. The higher D value indicated better resistance against waterlogging. Using K-means clustering using D values, the varieties can be divided into three categories. The varieties can be divided into three categories using D values. The first category being the waterlogging tolerant variety, included YT28, TBN6, YT22 and HMT8. The second category being the moderately waterlogging tolerant varieties includes XMxN, YZN5, GN1, YCN2, YT13, YCN1, GT2, YBN3 and ZT68, while the third category indicated waterlogging sensitive variety i.e., YT27, XMxz, ZT 89, YT16 and YXN2 (Table 3).

Table 3. The value of each variety's comprehensive index (Z), index weight (IW), U(x), D

Varieties	Comprehensive index			Membership function value			D	Waterlogging tolerance
	Z1	Z2	Z3	U(1)	U(2)	U(3)		
GT2	-2.87	3.89	-0.12	0.00	1.00	0.37	0.40	11
XMZX	-0.74	-1.25	-0.83	0.39	0.11	0.23	0.27	15
HMT8	0.49	1.62	0.51	0.62	0.61	0.49	0.59	4
GN1	1.47	1.16	-2.04	0.80	0.53	0.00	0.53	7
XMXX	1.5	-0.15	-0.15	0.81	0.30	0.36	0.55	5
ZT68	-0.74	-1	0.65	0.39	0.15	0.52	0.35	13
YXN2	-1.5	-1.89	-0.88	0.25	0.00	0.22	0.17	18
YT 13	-0.05	0.89	0.26	0.52	0.48	0.44	0.49	9
YBN33	-0.68	-0.61	0.66	0.41	0.22	0.52	0.38	12
YT 27	-1.51	-0.34	-0.36	0.25	0.27	0.32	0.27	14
YT28	1.83	0.04	3.16	0.87	0.33	1.00	0.73	1
YBN 6	2.53	0.5	-1.48	1.00	0.41	0.11	0.61	2
ZT 89	-0.83	-1.19	-1.11	0.38	0.12	0.18	0.25	16
YCN 2	1.05	-0.95	0.74	0.73	0.16	0.53	0.51	8
YHN1	-1.15	0.05	1.31	0.32	0.34	0.64	0.40	10
YZN 5	1.56	-0.13	-0.4	0.82	0.30	0.32	0.54	6
YT16	-2.31	-0.86	0.17	0.10	0.18	0.43	0.20	17
YT22	1.94	0.23	-0.09	0.89	0.37	0.38	0.61	3
IW				0.45	0.31	0.24		

Discussion

Root is an important plant part that absorbs water and nutrients from soil. The well-growing roots ensure higher photosynthetic efficiency, higher yield and stability (Hayashi et al., 2013). Previous studies showed that the morphological parameters of winter wheat roots were significantly reduced after waterlogging, especially the root number and root length, thus inhibited the absorption of water and nutrients (Dickin and Wright, 2008). Waterlogging led to root hypoxia, inhibiting mitochondrial respiration and ATP synthesis (Liu et al., 2014). Due to energy constraints, the ability of roots to absorb water and nutrients is reduced, that results in the reduction of root growth rate and dry matter accumulation (Wang et al., 2012). Root/shoot ratio reflects the correlation between plant shoots and roots, so the reduction in root/shoot ratio indicates maize growth inhibition (Grzesiak et al., 2014). In this study, waterlogging inhibited maize root and lateral root growth. Overall, root length, root surface area and root volume of most maize varieties were lower than non-waterlogging conditions, however, the root morphological changes were as follows: the roots became shorter and thicker, the root hair and their bifurcation also suffered decline. The order of inhibition for root morphological indexes was: root length > root surface area > root volume > root mean diameter. These results corroborate with the findings of Liang et al. (2009). Waterlogging causes root hypoxia, thus indirectly affecting the growth and development of shoots (Qi et al., 2012). Waterlogging inhibited the growth of plant shoots which resulted in the reduction of plant height (Shin et al., 2016). Waterlogging at seedling stage inhibits seedling growth whereas reduction in plant height is directly related to flooding duration (Liu et al., 2013). The results of this study showed that the plant

height of different maize seedlings decreased varying from different degree of waterlogging.

Previous studies showed that waterlogging caused decline in stomatal conductance and chlorophyll content of maize seedlings that resulted in reduced net photosynthetic rate and destruction of photosynthetic electron transport system (Ahmed et al., 2002; Wang et al., 2012). In this study, waterlogging caused a decline in SPAD value and F_v/F_m value. Chlorophyll is an important photosynthetic pigment and its content affects the plant's ability to assimilate photosynthetic products. The reduction in chlorophyll content is a sensitive indicator for abiotic stress (Candan and Tarhan, 2012). Waterlogging led to the leaf senescence and chlorophyll degradation thus affecting the accumulation of photosynthetic products, leading to biomass reduction (Ren et al., 2016b; Wang et al., 2016a). A decline in F_v/F_m values under water logged conditions, showed the destruction of PSII photochemical reaction (Baker, 2008; Liu et al., 2010a).

Soluble proteins participate in the osmotic regulation of plant cells. Accumulation of soluble proteins maintains plant cell osmotic potential, and increases plant tolerance to waterlogging stress (Yu et al., 2017). In this study, the soluble protein content in most of maize varieties was improved compared with the control, especially in the GT2, having significance increase of 136.22%. While in a previous study, the content of soluble protein in DH605 and ZD958 leaves decreased by 12.5% and 8.4% respectively, after 6 days of flooding at three-leaf stage (Wu et al., 2014). Combined with these results, the soluble protein content showed inverse relation with the flooding duration.

Waterlogging induced regulations of antioxidant enzymes i.e., SOD, POD and CAT and lipid peroxidation (in terms of MDA content) (Figures 4). Activity of antioxidant enzymes (SOD, POD and CAT) was found higher in most seedlings under waterlogged conditions, however waterlogging stress lowered MDA content in most of maize varieties (Fig. 5A). Antioxidant enzymes effectively scavenged the ROS generated by biological or non-biological stress in plant, thereby protecting the cell membrane and improving plant resistance (Gill and Tuteja, 2010; Wang et al., 2016a). Antioxidant enzymes removed excessive free radicals such as superoxide-radical ($O_2^{\cdot-}$) and hydrogen peroxide (H_2O_2) from cells thus maintaining ROS at a low level and allowing intracellular ROS production and scavenging to be in a dynamic equilibrium state (Hao et al., 2003; Liu et al., 2014). Waterlogging induced antioxidant enzyme activity in plants to reduce the damage caused by ROS. This activity of antioxidant enzyme was positively correlated with waterlogging resistance (Yin et al., 2010). MDA is the final product of lipid peroxidation. It acts in combination with the cell membrane to inhibit functional proteins from destructing cell structure and function thus ultimately affecting cell metabolism (Liu and Jiang, 2015). Previous studies showed that MDA content in wheat increased significantly after 7 days of flooding. It accelerated the degree of lipid peroxidation by causing severe damage to the cell membrane (Yu et al., 2017). In this study, the results differed from previous studies due to differences in flooding time and decline in MDA content may be due to the scavenging of antioxidant enzyme. In this case of prolonged flooding time, there may be a significant increase in MDA content because waterlogging may resulted in the destruction of the antioxidant enzymes (Liu et al., 2015a). ROS stimulated the protection mechanism of antioxidant enzymes to prevent maize from short-term flooding. But the activity of antioxidant enzymes declined sharply with the increase in flooding duration (Wu et al., 2014).

Evaluation of the waterlogging resistance of maize is a complex problem and it is difficult to evaluate comprehensively with single index. The basic aim of screening and

breeding waterlogged resistant varieties of maize is to establish an evaluation system which contains varieties, treatments and indicators (Wang et al., 2007; Zhou et al., 2003). Principal component analysis can transform the individual indicators into comprehensive indicators and then calculate the weight according to the contribution rate of each comprehensive index (Liu et al., 2015b). Membership function is used to calculate the membership function value of each comprehensive index. Through the weight calculation, we can get the comprehensive evaluation value (D value) of maize waterlogging tolerance. In this study, the waterlogging tolerance of maize varieties was evaluated by principal component analysis, membership function and cluster analysis as: YT28>TBN6>YT22>HMT8>XMXN>YZN5>GN1>YCN2>YT13>YHN1>GT2>YBN3>ZT68>YT27>XMXZ>ZT89>YT16>YXN2.

Conclusion

In this experiment, the morphological characteristics and physicochemical properties of different maize varieties under seedling waterlogging were studied. Overall, water logging conditions at early stages hampered the morphological and physiological traits of maize. The results may have some limitations requiring further conformational experiments. In addition, waterlogging evaluation system of different maize varieties was established according to their response mechanism. This evaluation system provided a theoretical basis for exploring the physiological basis of maize waterlogging.

Author contributions. W. L., T. W., J. L. and J. H. designed the research, W. L., W. M. and G. L. performed the experiments and collected the data, W. L., A. U., W. M., J. L. and J. H. analyzed the data and wrote the manuscript, W. L., A. U., and M. A. edited the manuscript and provided guidance during experimentation.

Acknowledgments. This research was supported by the Project of the Guangdong Province Science and Technology Program (2015B020202006, 2016B020233004, 2016A030303030, 2016A020210030, 2017B020203003, 2017A030303045, 2017B090907023), and the Team Project of Guangdong Agricultural Department (2017LM2148), and the President Fund project of the Guangdong Academy of Agricultural Sciences (201509,201510).

REFERENCES

- [1] Ahmed, S., Nawata, E., Hosokawa, M., Domae, Y., Sakuratani, T. (2002): Alterations in photosynthesis and some antioxidant enzymatic activities of mungbean subjected to waterlogging. – *Plant Sci.* 163: 117–123.
- [2] Ashraf, U., Salim, M. N., Sher, A., Sabir, S. U. R., Khan, A., Pan, S. G., Tang, X. (2016): Maize growth, yield formation and water-nitrogen usage in response to varied irrigation and nitrogen supply under semi-arid climate. – *Turk. J. Field Crops* 21: 88–96.
- [3] Baker, N. R. (2008): Chlorophyll fluorescence: a probe of photosynthesis in vivo. – *Annu. Rev. Plant Biol.* 59: 89–113.
- [4] Bradford, M. M. (1976): A rapid and sensitive method for the quantitation of microgram quantities of protein utilizing the principle of protein-dye binding. – *Anal. Biochem.* 72: 248–254.
- [5] Candan, N., Tarhan, L. (2012): Tolerance or sensitivity responses of *Mentha pulegium* to osmotic and waterlogging stress in terms of antioxidant defense systems and membrane lipid peroxidation. – *Environ. Exp. Bot.* 75: 83–88.

- [6] Cheng, X.-X., Yu, M., Zhang, N., Zhou, Z.-Q., Xu, Q.-T., Mei, F.-Z., Qu, L.-H. (2015): Reactive oxygen species regulate programmed cell death progress of endosperm in winter wheat (*Triticum aestivum* L.) under waterlogging. – *Protoplasma* 253: 311–327.
- [7] Dickin, E., Wright, D. (2008): The effects of winter waterlogging and summer drought on the growth and yield of winter wheat (*Triticum aestivum* L.). – *Eur. J. Agron.* 28: 234–244.
- [8] Gill, S. S., Tuteja, N. (2010): Reactive oxygen species and antioxidant machinery in abiotic stress tolerance in crop plants. – *Plant Physiol. Biochem. PPB Soc. Francaise Physiol. Veg.* 48: 909–930.
- [9] Grzesiak, M. T., Szczyrek, P., Rut, G., Ostrowska, a., Hura, K., Rzepka, a., Hura, T., Grzesiak, S. (2014): Interspecific differences in tolerance to soil compaction, drought and waterlogging stresses among maize and triticale genotypes. – *J. Agron. Crop Sci.* 201: 330–343.
- [10] Hao, Y. L., Pan, J. B., Zhang, Q. Z., Yang, J. (2003): Effect of waterlogging on growth and generation at different stages in maize. – *Chin. Agric. Sci. Bull.* 2003(6): 58–60+63.
- [11] Hayashi, T., Yoshida, T., Fujii, K., Mitsuya, S., Tsuji, T., Okada, Y., Hayashi, E., Yamauchi, A. (2013): Maintained root length density contributes to the waterlogging tolerance in common wheat (*Triticum aestivum* L.). – *Field Crops Res.* 152: 27–35.
- [12] Hossain, Z., López-Climent, M. F., Arbona, V., Pérez-Clemente, R. M., Gómez-Cadenas, A. (2009): Modulation of the antioxidant system in citrus under waterlogging and subsequent drainage. – *J. Plant Physiol.* 166: 1391–1404.
- [13] Li, H. S. (2000): Principle and Technology of Plant Physiological and Biochemical Experiment. – Higher Education Press, Beijing.
- [14] Liang, Z. J., Tao, H. B., Wang, P. (2009): Recovery effects of morphology and photosynthetic characteristics of maize seedlings after waterlogging. – *Acta Ecol. Sin.* 29: 3977–3986.
- [15] Liu, M., Jiang, Y. (2015): Genotypic variation in growth and metabolic responses of perennial ryegrass exposed to short-term waterlogging and submergence stress. – *Plant Physiol. Biochem.* 95: 57–64.
- [16] Liu, M., Li, Y., Guo, G. H., Liu, H. Y., Li, G. H., Wang, S. H., Liu, Z. H., Ding, Y. F. (2015a): Comparison on submergence tolerance of different type rice at tillering stage in lower reaches of Yangtze River. – *Chin. J. Appl. Ecol.* (26)5: 1373–1381.
- [17] Liu, M. Y., Sun, J., Wang, K. Y., Liu, D., Li, Z. Y., Zhang, J. (2014): Spermidine enhances waterlogging tolerance via regulation of antioxidant defence, heat shock protein expression and plasma membrane H⁺-ATPase activity in *Zea mays*. – *J. Agron. Crop Sci.* 200: 199–211.
- [18] Liu, R. X., Jing, Y. X., Xiao, L., Li, G. L., Yang, D. J., Nie, K. Y. (2010a): Effects of flooding depth on gas exchange, chlorophyll fluorescence and growth of *Melaleuca alternifolia* seedlings. – *Acta Ecol. Sin.* 30(19): 5113–5120.
- [19] Liu, Y. Z., Tang, B., Zhang, Y. L., Ma, K. J., Xu, S. Z., Qiu, F.Z. (2010b): Screening methods for waterlogging tolerance at maize (*Zea mays* L.) seedling stage. – *Agr Sci China* 3: 362–369.
- [20] Liu, Z., Zhou, W., Lv, J., He, P., Liang, G., Jin, H. (2015b): A simple evaluation of soil quality of waterlogged purple paddy soils with different productivities. – *PloS One* 10: 1–16.
- [21] Liu, Z. G., Liu, Z. D., Xiao, J. F., Nan, J. Q., Gong, W. J. (2013): Waterlogging at seedling and jointing stages inhibits growth and development, reduces yield in summer maize. – *Trans. Chin. Soc. Agric. Eng.* 29(5): 44–52.
- [22] McDaniel, V., Skaggs, R. W., Negm, L. M. (2016): Injury and recovery of maize roots affected by flooding. – *Appl. Eng. Agric.* 32: 627–638.
- [23] Mielke, M. S., Schaffer, B. (2010): Leaf gas exchange, chlorophyll fluorescence and pigment indexes of *Eugenia uniflora* L. in response to changes in light intensity and soil flooding. – *Tree Physiol.* 30: 45–55.

- [24] Pucciariello, C., Perata, P. (2016): New insights into reactive oxygen species and nitric oxide signalling under low oxygen in plants. – *Plant Cell Environ.* 40(4): 473–482.
- [25] Qi, W.-Z., Liu, H.-H., Liu, P., Dong, S.-T., Zhao, B.-Q., So, H. B., Li, G., Liu, H.-D., Zhang, J.-W., Zhao, B. (2012): Morphological and physiological characteristics of corn (*Zea mays* L.) roots from cultivars with different yield potentials. – *Eur. J. Agron.* 38: 54–63.
- [26] Ren, B., Zhang, J., Dong, S., Liu, P., Zhao, B. (2016a): Root and shoot responses of summer maize to waterlogging at different stages. – *Agron. J.* 108: 1060–1069.
- [27] Ren, B., Zhang, J., Dong, S., Liu, P., Zhao, B. (2016b): Effects of duration of waterlogging at different growth stages on grain growth of summer Maize (*Zea mays* L.) under field conditions. – *J. Agron. Crop Sci.* 202: 564–575.
- [28] Shin, S., Kim, S.-G., Jung, G.-H., Kim, C.-G., Son, B.-Y., Kim, J. T., Kim, S. G., Yang, W., Kwon, Y., Shim, K.-B., et al. (2016): Evaluation of waterlogging tolerance with the degree of foliar senescence at early vegetative stage of maize (*Zea mays* L.). – *J. Crop Sci. Biotechnol.* 19: 393–399.
- [29] Wang, F., Liu, J., Zhou, L., Pan, G., Li, Z., Zaidi, S. H.R., Cheng, F. (2016a): Senescence-specific change in ROS scavenging enzyme activities and regulation of various SOD isozymes to ROS levels in psf mutant rice leaves. – *Plant Physiol. Biochem.* 109: 248–261.
- [30] Wang, J., Zhou, M. X., Xu, R. G., Lu, C., Huang, Z. L. (2007): Studies on selecting indices and evaluation methods for barley's (*Hordeum vulgare* L.) waterlogging tolerance. – *Sci. Agric. Sin.* 40: 2145–2152.
- [31] Wang, Q., Liu, Z. W., Xu, W. J. (2016b): Ultraviolet spectrophotometry measurement of catalase activity in maize. – *Chin. Agric. Sci. Bull.* 32(15): 159–165.
- [32] Wang, X., Liu, T., Li, C., Chen, H. (2012): Effects of soil flooding on photosynthesis and growth of *Zea mays* L. seedlings under different light intensities. – *Afr. J. Biotechnol.* 11: 7676–7683.
- [33] Wu, B. C., Zhang, J. W., Li, X., Fan, X., Dong, S. T., Zhao, B., Liu, P. (2014): Effect of waterlogging on leaf senescence characteristics of summer maize in the field. – *Chin. J. Appl. Ecol.* 25(4): 1022–1028.
- [34] Wu, S., Hu, C., Tan, Q., Li, L., Shi, K., Zheng, Y., Sun, X. (2015): Drought stress tolerance mediated by zinc-induced antioxidative defense and osmotic adjustment in cotton (*Gossypium Hirsutum*). – *Acta Physiol. Plant.* 37: 167.
- [35] Yin, D., Chen, S., Chen, F., Guan, Z., Fang, W. (2010): Morpho-anatomical and physiological responses of two *Dendranthema* species to waterlogging. – *Environ. Exp. Bot.* 68: 122–130.
- [36] Yordanova, R. Y., Popova, L. P. (2007): Flooding-induced changes in photosynthesis and oxidative status in maize plants. – *Acta Physiol. Plant.* 29: 535–541.
- [37] Yu, M., Zhou, Z., Deng, X., Li, J., Mei, F., Qi, Y. (2017): Physiological mechanism of programmed cell death aggravation and acceleration in wheat endosperm cells caused by waterlogging. – *Acta Physiol. Plant.* 39: 23.
- [38] Zaidi, P. H., Rafique, S., Singh, N. N. (2003): Response of maize (*Zea mays* L.) genotypes to excess soil moisture stress: Morpho-physiological effects and basis of tolerance. – *Eur. J. Agron.* 19: 383–399.
- [39] Zhou, G. S., Mei, F. Z., Zhou, Z. Q., Zhu, X. B. (2003): Comprehensive evaluation and forecast on physiological indices of waterlogging resistance of different wheat varieties. – *Sci. Agric. Sin.* 36(11): 1378–1382.

ANALYSIS OF LAND USE/LAND COVER CHANGES FOLLOWING POPULATION MOVEMENTS AND AGRICULTURAL ACTIVITIES: A CASE STUDY IN NORTHERN TURKEY

ŞEN, G.^{1*} – GÜNGÖR, E.²

¹*Faculty of Forestry, Kastamonu University, 37200 Kastamonu, Turkey
(phone: +90-532-562-5998; fax: +90-366-215-2316)*

²*Faculty of Forestry, Bartın University, 74100 Bartın, Turkey
(phone: +90-532-628-3318; fax: +90-378-223-5069)*

**Corresponding author*

e-mail: gsen@kastamonu.edu.tr; phone: +90-532-562-5998; fax: +90-366-215-2316

(Received 15th Jan 2018; accepted 26th Mar 2018)

Abstract. This study analyzes the changes in spatial and temporal patterns of land use/cover from 1999 to 2014 in the city of Kastamonu, which is located at the center of the western Black Sea Region of Turkey. In this study, Kastamonu constitutes the study area, which is 65% covered with forests. Remote sensing, geographical information systems, and economic and demographic variables have been used for the analysis. The results showed that 0.2% of forested areas have been converted to settlement areas, and 8.5% have been converted to agricultural lands during this period. On the other hand, 12.5% of settlement areas and 30.4% of agricultural lands were transformed into forested area in the same period. A net increase of 15.1% (108768.2 ha) happened in forest areas between 1999 and 2014. The annual percentage of forestation for forest areas within the study period was 0.94% in Kastamonu. In Kastamonu, the most important factor in the increase of forested areas is demographic movement, which decreased agriculture and animal husbandry due to declining populations in rural areas between 1999–2017. The abandoned agricultural areas have turned into forest areas. Grazing pressure on forests has decreased with the decrease in animal husbandry. This has been effective in structural improvements and spatial increase of forest areas. However, the development of substitute products in wood, widespread use of solar energy systems in rural areas, and the construction of more insulated buildings are other factors that are effective in increasing forest areas.

Keywords: *spatiotemporal analysis, land use/cover change, socio-economic impact on forest, Kastamonu, Turkey*

Introduction

The importance of forest ecosystems is ever increasing, as forested ecosystems maintain the Earth's ecological balance. Pollution and destructive effects from rapid increases in population coupled with rapid industrial development require us to be more sensitive about forests (Seçkin, 1995). In fact, forest areas simultaneously fulfill many ecological, economic, social, and esthetic functions. Forested areas provide many important functions such as reducing all types of air pollution (Yigit et al., 2016; Sevik et al., 2016), reduce noise (Aricak et al., 2016), have a psychologically positive effect (Cetin and Sevik, 2016a), help save energy (Cetin and Sevik, 2016b), and are an important economic resource (Tunçtaner et al., 2007; Sevik, 2012); further, they prevent erosion (Özel et al., 2015; Sevik et al., 2017), reduce wind speed, hold soil through their roots and prevent rain and streams from carrying the soil away, and protect wild life and hunting sources (URL1, 2004; Güneş Şen and Aydın, 2017). Furthermore, open green

areas with plants are important for human activity (Ertekin and Özel, 2010; Cetin et al., 2017; Özel and Ertekin, 2012). These functions, therefore, play a greater role, particularly in highly populated areas. However, when the amount and structure of forested area change, there may be problems in completely fulfilling these functions.

The history of permanent forest destruction dates back to the Neolithic period (Kaplan et al., 2009; Ostlund et al., 2015). However, destruction started to occur during the Industrial Revolution at the end of the eighteenth century (Simpson et al., 2003). According to research by the Food and Agriculture Organization, 16 million ha of forested area were lost between 1990 and 2000, and 13 million ha of forested area were lost between 2000 and 2010 (FAO, 2010). In fact, forest destruction occurs because of the effect of various factors such as ecological (tree species, composition, etc.), natural regeneration capacity, productivity and natural disasters (Ostlund et al., 2015; Trbojevic et al., 2012).

The effects of forest destruction do not remain at a regional level and may have a global impact. According to previous studies, deforestation is the second-largest source of anthropogenic carbon dioxide emissions and causes a net reduction of carbon storage in terrestrial ecosystems (De Sy, et al., 2015). Moreover, forest destruction leads to various effects, such as a decrease in biological diversity, endemics of rare living creatures, and even loss of generations (De Sy et al., 2015; Ochoa-Quintero et al., 2015; Barlow et al., 2016). According to the results of a study conducted in South America, the total deforested area and related gross carbon losses from 1990 to 2005 reached 57.7 million ha and 6.460 gigatonnes of carbon, respectively (De Sy, et al., 2015). In other studies, the deforestation rate was reported to be 3.74–4.09 million ha per year in 1990s and 3.28–4.87 million ha per year in 2000s (Hansen et al., 2010; Harris et al., 2012; Eva et al., 2012; Achard et al., 2014). Carbon loss related to deforestation was calculated as 306–698 petagrams per year in 1990s and 322–845 petagrams of carbon per year in 2000s (Baccini et al., 2012; Harris et al., 2012; Eva et al., 2012; Achard et al., 2014; Houghton, 2012; Tyukavina et al., 2015). Therefore, the loss in forested area is not only a loss of the ecosystem but also has numerous consequences, some of which occur on the global scale and may directly or indirectly affect people, plants, and animals.

Outstanding factors among the causes of forest destruction are as follows: changes in land use; turning forested areas into agricultural or settlement areas; climate changes; and forest fires (Chauchard et al., 2010; Schweizer et al., 2017; Kucuk et al., 2017; Cabral and Costa, 2017). Previous studies have suggested that each of these three factors are fundamentally human-derived. Forested areas are destroyed and used for different purposes to fulfill the demands of the increasing population, and the change in the global climate arising from the destruction of the ecosystem caused by human activities damages the forested areas at a significant level. In addition, > 90% of forest fires break out as a result of human activities (Harvey, 2016; Šturm and Podobnikar, 2017).

However, human activities (i.e., anthropogenic factors) are the biggest factor that contributes to forest destruction. At this point, economic activities, population sizes, and people's beliefs emerge as the main factors determining the impact of human activities in a forest (Ostlund et al., 2015; Bayramoğlu and Kadioğulları, 2018). High-quality forested areas are intensely exposed to the human effect because of plank timber production. Pressure from rural and urban populations cause legal and illegal increases in these utilizations. With respect to changes in population and movements, forests are positively affected on the one hand and negatively affected on the other. To maintain

and manage the biodiversity, it is important to understand the dynamics of forest losses and consequences of human effects, which are the leading cause for such losses (Puyravaud, 2003; Lele and Joshi, 2009; Sen et al., 2015). In this context, such areas should be continuously monitored, and solutions should be developed to avoid current inconveniences and pressures on forests. This monitoring is particularly crucial for biologically rich areas. In this manner, contemporary data would be obtained for sustainable forest management, which would allow decision makers to perform more accurate analyses.

In this study, we analyzed the spatial and temporal changes in land use and land cover during 1999–2014 in Kastamonu City, which is in the Black Sea Region in northwest Turkey. In addition, some socio-economic variables have been examined in relation to changes in the land use/cover. This study fills the gap through a large-scale analysis of land use/cover change using stand-type maps occurring in air photo data, particularly focusing on the Kastamonu forests during the 1999–2017 period.

Study area

Kastamonu Province is located in the western part of the Black Sea Region in Turkey between the north latitudes of 41–42 and east longitudes of 33–46 (*Fig. 1*). Its surface area is 13108 km² (Öztürk and Özdemir, 2013).



Figure 1. Geographic location of the Kastamonu Province

There are two national parks in the study area: The Küre Mountains National Park, which that Protected Areas Network parks certification, and the Ilgaz Mountain National Park (Anonymous, 2014; Öztürk and Ayan, 2015). Moreover, the Küre Mountains are home to five distinct habitat types, which are categorized as endangered habitats, as per the Bern Conventions (BERN) (KMNP, 2017).

Ilgaz Mountain National Park (IMNP) contains approximately 10% of plant species in Turkey; 64 of these plant species are endemic. IMNP has been identified as one of Turkey's most important plant areas by WWF. The protected natural forests in the IMNP create suitable habitats for many mammal species. Grizzly bear, deer, wolf, fox, wild boar, roe deer, rabbit and otter are some of the mammals in this area (URL2, 2016). At the same time, IMNP is recognized as one of the "97 Important Bird Areas" in Turkey due to predatory birds (URL3, 2017). Another important point in terms of species diversity is the Küre Mountains National Park. In this national park, 1050 plant species, including 158 endemic species, have been identified (URL2, 2016); 59 of these plant taxa are endangered (URL3, 2017).

More than 65% of Kastamonu is covered with forest; 48% of the general area is productive productive woodland; 17% is degraded forest; and 35% is forestless (URL4, 2017; Güneş Şen, 2015).

In Kastamonu, economically the most important sector is agriculture. Agricultural activity depends on vegetative production and forestry because the country is located on a rich forest belt. The agricultural area covers only 28% of the total land of the province. There are some agricultural products in this area, e.g., wheat, barley, and potatoes. Sugar beets, cannabis, and garlic are also produced as industrial crops (URL5, 2014; URL6, 2006). According to 2017 data, the population of Kastamonu is around 360366 persons. The population makes up approximately 0.5% of the country's population. Forty-eight percent of the population live in the city center, and the remaining population live in districts and villages (TUIK, 2017). The population status of Kastamonu Province according to the years is shown in *Table 1*. There are 21 municipalities, including the city center and 1071 villages in the Kastamonu Province.

Table 1. Urban and rural population of Kastamonu Province (2000–2015)

Years	Urban population	Rural population	Total population
2000	174020	201456	375476
2007	184685	175681	360366
2010	196162	165060	361222
2015	226868	145765	372633

As shown in *Table 1*, the total population decreased by 2843 persons (0.8%) in Kastamonu. When we look at the rural population, it can be seen that the decline in the population is almost 28%.

Materials and methods

There are various methods for collecting, analyzing, and presenting natural resources data to explain forest dynamics. In particular, the use of remote sensing and geographic information systems (GIS) can greatly shorten and simplify the analysis process

(Gautam et al., 2003). Analysis of temporal changes in area use and covers in Kastamonu Province was performed in two steps. In the first step, stand-type maps for 1999, 2009, and 2014 were quantified and rectified using Arc/Info GIS, and a data set was created for temporal change analysis. In the second step, temporal changes and transitions in the land cover were analyzed.

This study used data-gathered stand-type maps produced by the General Directorate of Forestry for years 1999, 2009, and 2014. These maps were then scanned and registered at the 1:25000 scale using first-order nearest-neighbor rules with UTM projection. We then used ArcGIS® software to overlay the maps and compute changes in land area over time as well as changes between classes of land cover and/or land use (Cakir et al., 2008).

A rough-level classification approach was employed in the study area. Classification refers to a broad simplification of large land-use types and land covers defined by type composition and nonforested areas (Karahalil et al., 2009). Eleven land cover classes were included in the analysis (Table 2).

Table 2. Land use/land cover classes description

Land use/cover classes	AL	Agricultural land
	SA	Settlement areas
	W	Areas covered with standing water
	PM	Productive mixed wood
	PPC	Productive * pure stands composed of coniferous trees
	PPB	Productive pure stands composed of broad-leaved trees
	DPC	Degraded ** pure stands composed of coniferous trees
	DPB	Degraded pure stands composed of broad-leaved trees
	DM	Degraded mixed wood
	OA	Forest land, meadow, and mining field
	AF	Areas for forestation

*Productive forest (PF): Productive forest with a > 10% estimated tree crown cover

**Degraded forest (DF): Degraded forest with a < 10% estimated tree crown cover

In addition, forest management plans and information about demographic change, economic conditions, and living standards of local people were obtained and evaluated to determine socio-economic factors and administrative intervention influencing changes in land use.

After that, the data were analyzed to identify changes in land use and land cover over time; the study supplemented these findings by examining forest management plans and socio-demographic data to understand potential contributors to the changes of land use and land cover.

The annual rate of decrease or increase should be also revealed to the impact of a decrease in forest sources on the protection of biodiversity. For this purpose, the annual rate of forestation was calculated using Equation 1 (Puyravaud, 2003).

$$P = \left(\frac{1}{t_2 - t_1} \ln \frac{A_2}{A_1} \right) \times 100 \quad (\text{Eq.1})$$

where P is the percentage of forestation/deforestation per year, and A_1 and A_2 are the amount of forest cover at time points t_1 and t_2 , respectively.

In addition to those listed above, changes that have occurred in forested areas and population movements, which are considered to have the greatest impact on this change, as well as the number of large and small cattle, amount of arable land, and yield of farming activities were comparatively evaluated and interpreted.

Results

Spatial and temporal changes in land use/cover

The land use/cover status of Kastamonu Province for the years 1999, 2009, and 2014 were determined as a result of analyses. The results are shown in *Table 3* and *Figures 2, 3, and 4*.

Table 3. Evolution of selected landscape variables in the study area from 1999 to 2014

Year	1999		2009		2014	
	ha	%	ha	%	ha	%
OA	23560.2	1.85	312.4	0.02	6040.3	0.48
AF	8624.3	0.68	2721.7	0.21	2745.9	0.22
DPC	49423.6	3.89	79833.5	6.28	78315.7	6.17
DM	85434.1	6.73	10315.7	0.81	10621.9	0.84
DPB	111002.2	8.74	89508.0	7.05	88627.9	6.98
SA	21059.2	1.66	23152.4	1.82	23489.8	1.85
W	454.0	0.04	1020.8	0.08	1000.7	0.08
PPC	222055.4	17.48	360646.5	28.39	360529.6	28.38
PM	112648.2	8.87	127449.8	10.03	125227.2	9.86
PPB	139947.2	11.02	163217.5	12.85	165956.6	13.06
AL	496053.6	39.05	412083.9	32.44	407706.4	32.10
Grand total	1270262.1	100.00	1270262.1	100.00	1270262.1	100.00

The forested area in Kastamonu Province is 832024.8 ha, according to the stand-type maps from forest management plans. This area constitutes 63.5% of the Kastamonu Province. On the basis of analysis performed in 1999, approximately 39.05%, 1.66%, 19.36%, 37.37%, and 56.72% of the total area subject to analysis was calculated as the agricultural area, settlement area, degraded area, productive land, and forested area, respectively; whereas, in 2009, approximately 32.44%, 1.82%, 14.14%, 51.27%, and 65.42% of the total area were calculated as the agricultural area, settlement area, degraded area, productive land, and forested area, respectively. In 2014, the ratio of the settlement area in Kastamonu increased to 1.85%, while the ratio of the agricultural area decreased to 32.10%, but there was no significant change in the forested area, and the ratio of forested to total area was 65.28%.

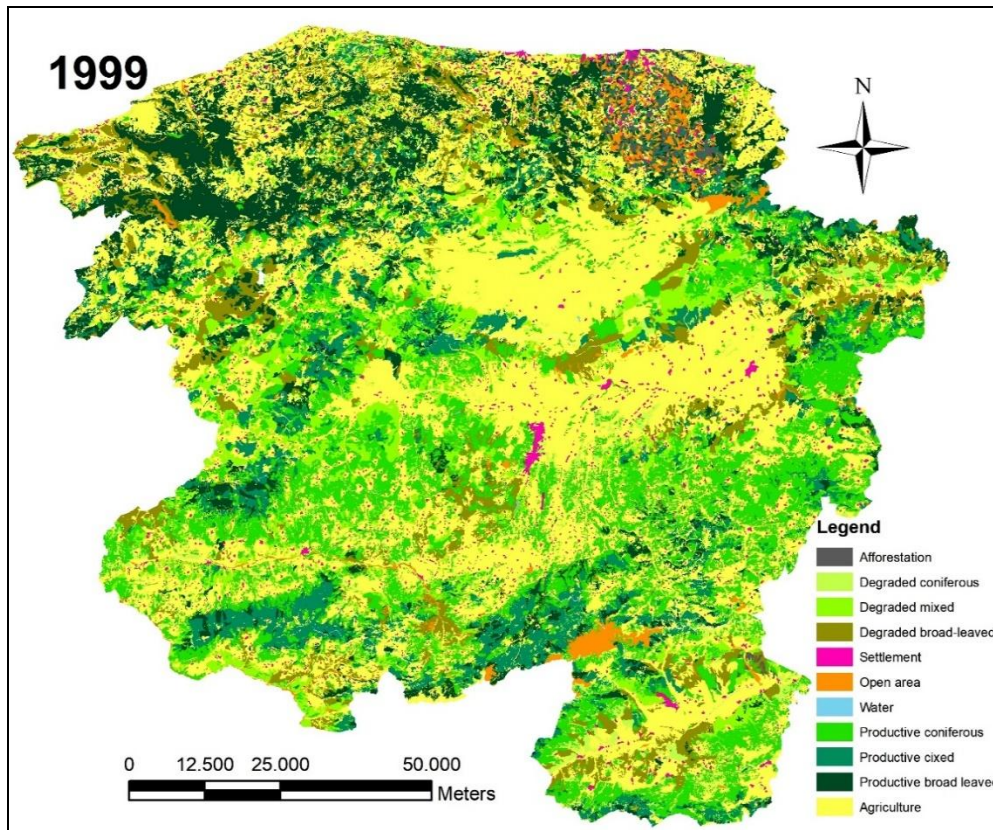


Figure 2. Land use/cover status of Kastamonu Province in 1999

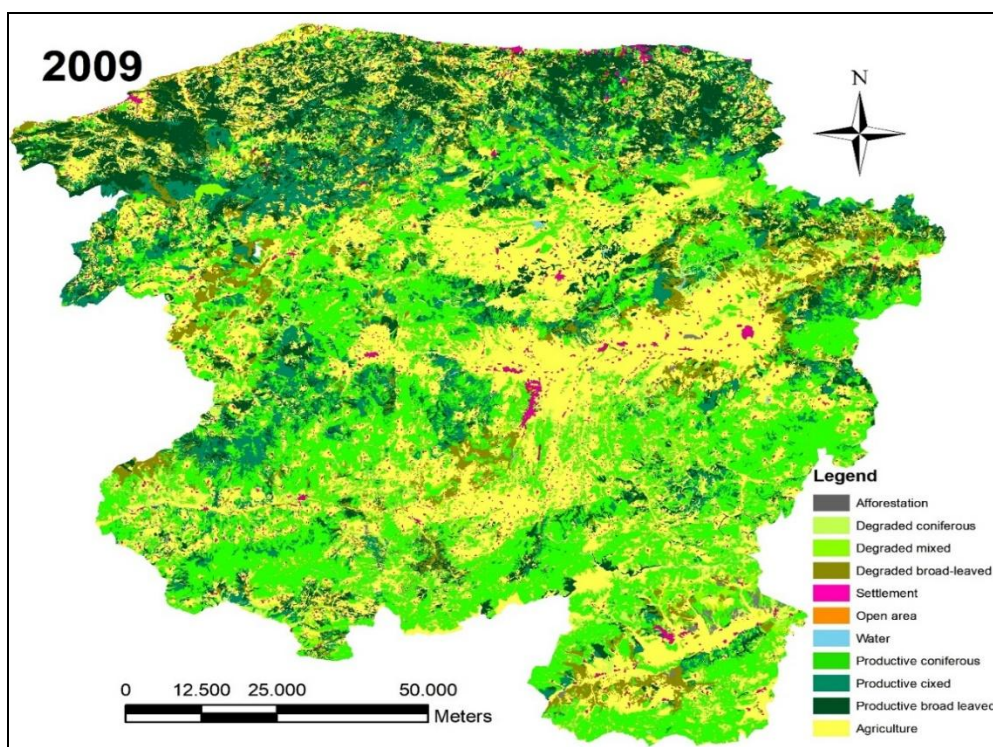


Figure 3. Land use/cover status of Kastamonu Province in 2009

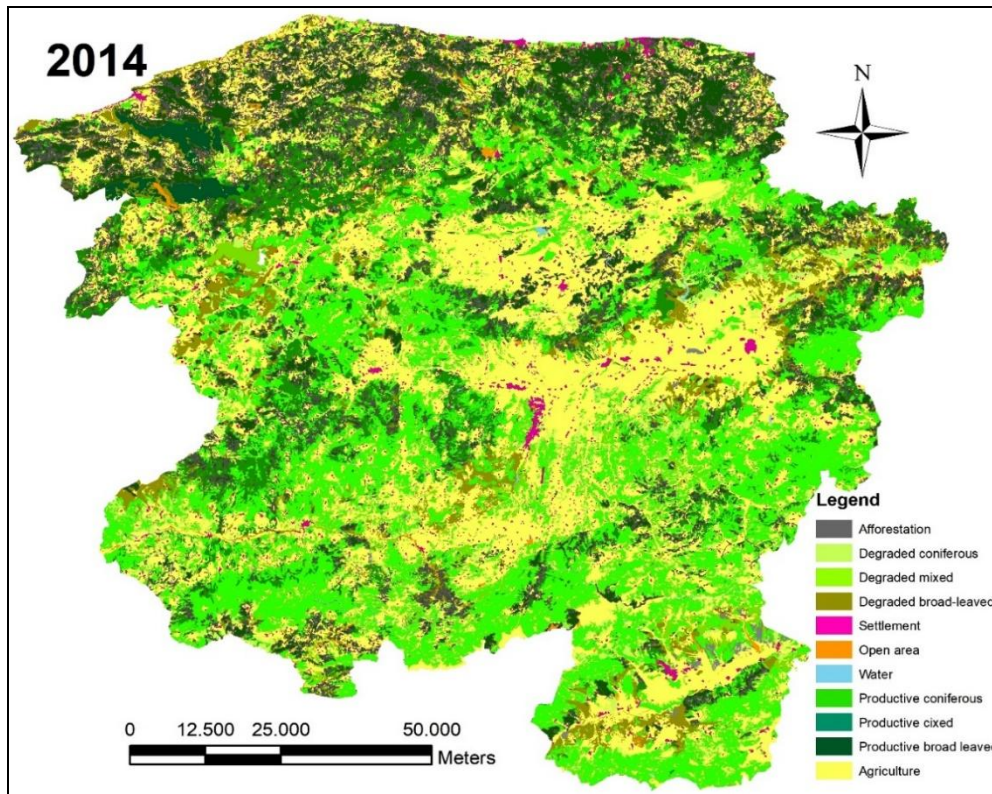


Figure 4. Land use/cover status of Kastamonu Province in 2014

Transition among land use/land cover types

The results of analyses regarding the use of land use/cover in Kastamonu are shown in Tables 4, 5, and 6.

Table 4. Transition matrix of land use/cover changes in Kastamonu Province from 1999 to 2009

1999–2009											
Changed from	OA	AF	DPC	DM	DPB	SA	W	PPC	PM	PPB	AL
OA	39.9	2.9	1491	21.4	2183.1	132.3	88.7	2099.9	1313.2	6496.4	9691.6
AF	0	314.6	204.5	30.4	327.6	31.1	0	1532.7	1449.9	4378.5	355
DPC	3.7	111.2	18514.5	805.9	3628.7	115.5	12	17396.8	2700.3	1304.9	4830
DM	12.6	241.3	14625	5356.2	8526.9	87.8	24.3	20690.4	18556.4	11880.4	5432.7
DPB	27	345.2	6791.7	1592.2	40408.3	123.5	41	11173.7	11406.9	28983.1	10109.6
SA	25.9	11	226.8	28.2	280.7	12467.2	5.7	393.9	183.6	619.9	6816.2
W	1.5	0	14.5	0	3.9	3.5	203.3	4.1	12.1	24.9	186.2
PPC	51.1	652.2	8955	690.5	2652.8	189.4	22.7	175744.8	20511.3	5182.9	7402.8
PM	0.1	40.3	3873.6	133	5583.7	43.3	72.9	65018.5	22932.4	11041.4	3909.2
PPB	0.5	0.9	1726.5	77.1	4406.7	72.2	8.4	26157.8	35480.4	68194.3	3822.3
AL	150	1002.3	23410.4	1580.6	21505.6	9886.7	541.8	40434	12903.1	25110.7	359528.4

Table 5. Transition matrix of land use/cover changes in Kastamonu Province from 2009 to 2014

2009–2014											
Changed from	OA	AF	DPC	DM	DPB	SA	W	PPC	PM	PPB	AL
OA	117.1	0	6.9	0.5	6.7	14.5	1	33.4	28.6	24.3	79.3
AF	3.6	2124.8	53.5	49.4	42	4.1	1.4	228.2	2.2	14.2	198.3
DPC	191.3	50.3	44784.9	87.2	2311	239.5	25.7	17789.7	2509	2061.4	9783.5
DM	29.5	29.6	254.8	6755.3	135.6	25.6	1.3	1354.8	272	267	1190.3
DPB	379.3	60.1	1444.1	229.5	61181.9	297.3	59.5	4978.7	3266.7	7629.1	9981.7
SA	66.7	14.3	345	28.4	383	13750.2	8.1	521.1	190.4	389.3	7456.1
W	31.4	0	47.8	0.9	66.2	8.1	604.2	24.9	8.4	24.6	204.4
PPC	306.9	193.5	16898.5	1358	4704.2	534.6	19.8	289959.6	12679	7720.1	26272.3
PM	111.6	6.4	2559	272.6	3372.1	200.3	12.7	11646.5	92376.8	9754.9	7136.8
PPB	415.5	8.2	2026.5	344.9	7995	490	50.3	7280.2	8289.9	120952.3	15364.7
AL	3829.2	254.7	10013.1	1100.8	11305.6	7909.7	213.3	26325.4	6818.4	15185.3	329128.3

Table 6. Transition matrix of land use/cover changes in Kastamonu Province from 1999 to 2014

1999–2014											
Changed from	OA	AF	DPC	DM	DPB	SA	W	PPC	PM	PPB	AL
OA	1771.1	5.5	1429.7	21.5	1819.4	167.2	51.2	2714	1363.7	6300.3	7916.6
AF	16.1	287.8	214.4	41.2	388.8	77.1	0	1468.2	1367.9	4200.9	561.9
DPC	107.2	116.9	13233	723.6	3403.4	226.7	13.2	20399.5	2290.5	1609.4	7300.1
DM	277.2	249.4	12939.7	4186.2	8166.6	170	24.5	22646.1	17705.8	11600.2	7468.6
DPB	877	354.5	5876.1	1730.4	34279.9	267.1	69.9	12741.7	11572.5	29290	13943.3
SA	70.8	18.2	396.1	46.1	470.4	9323.5	8.2	675.1	280.4	771.4	8998.9
W	28.8	0	28.8	0.9	26.1	4.8	126.3	15.9	20.2	29.8	172.4
PPC	227.8	615.2	13211.2	1360.5	3891.3	403.5	45.4	157223.9	21131.3	6845.4	17099.9
PM	86.2	38.7	4883.1	237.6	5715	123.6	81	62788.5	21239.5	10773.7	6681.3
PPB	214.8	5.5	2373.8	251.9	6267.5	213.2	12.1	25655.7	32878.8	63401.3	8672.7
AL	2363.3	1054.2	23729.8	2022.2	24199.6	12513.2	568.9	54201	15376.7	31134.2	328890.6

Areal and qualitative improvements in forested areas have attracted increasing attention. An increase of approximately 35% in total productive forested areas from 1999 to 2014 has drawn attention, while 65.56% of degraded forests in 1999 maintained their degraded forest quality in 2014. Approximately 42% of degraded coniferous forests turned into productive coniferous forests, and 8% of these forests turned into productive leaved or mixed forest, while 26% of degraded broad-leaved forests turned

into productive broad-leaved forest; 22% of these forests turned into productive mixed or productive coniferous forest, and > 60% of degraded mixed forests turned into productive forest. Approximately 24% of productive forest also turned into degraded forested area from 1999–2014. Apart from that, > 30% of agricultural areas turned into forested areas, and 2.52% of these areas turned into settlement areas; whereas 66.3% of these areas maintained their agricultural area quality. This ratio indicates that the agricultural area was the highest-rated area that turned into settlement areas.

Analysis of the forestation/deforestation rate

Forestation/deforestation ratios of Kastamonu were determined for 1999–2009, 2009–2014, and 1999–2014. Ratios obtained from this analysis are shown in *Table 7*.

Table 7. *Forestation/deforestation ratios of Kastamonu Province*

	1999–2009	2009–2014	1999–2014
Productive forest	3.16	0.01	2.11
Degraded forest	–3.14	–0.23	–2.17
Total forest	1.43	–0.04	0.94

As shown in *Table 7*, productive forests have a positive forestation rate, while degraded forests have a negative value, that is, degraded forests generally decrease. The annual forestation ratio from 1999 to 2009 decreased to 3.16% for productive forests and to –3.14% for degraded forests. The annual forestation ratio from 2009 to 2014 decreased to 0.01% for productive forests. The deforestation ratio for degraded forests decreased and regressed to –0.23%. When the study period is evaluated in general, the annual forestation ratio for the general forestation area was 0.94%. The forestation ratio for degraded forests was negative, while this ratio was positive for productive forests.

Discussion

This study particularly indicates that significant changes have occurred in the forest structure, and the changes show similar results of other studies conducted in Turkey. Previous studies showed that the current forested area increased by 15% during 1999–2014 (107768.2 ha). However, despite the decrease of 28% (68294.4 ha) in the degraded forest areas, the productive forest areas increased from 37% (177062.6 ha). In a study covering the period from 1987 to 2000 in the Kastamonu Province, it was determined that 111466 ha of forest area have increased, while open areas of 112888 ha have decreased. In this period, forested areas increased by 8.43% in total (Turan et al., 2010). Similar results were obtained in a study conducted in the Daday District of Kastamonu. In the study, it was determined that the productive forest areas in the Daday region increased by 92.4% between 1970 and 2010. On the other hand, corrupt forested areas decreased by 57.7% (Zengin et al., 2018). These results show that forested areas in Kastamonu are steadily increasing. In 1987, 32.1% of Kastamonu was covered with forest (Turan et al., 2010), while it increased to 63.5% in 2017.

Similar results were obtained by studies in Turkey. In a study conducted in Gümüşhane Province, it was determined that forested areas increased by 6.54% (6928 ha), and the annual forestation ratio increased to 0.50% during 1987–2000 (Kadioğulları and Başkent, 2008). In a study conducted in Macka, located in the northeast of Turkey, it was determined that high mountain forests showed an increase of 200.6 ha during 1973–2008 (Sen et al., 2015). In a study conducted in Koprulu Canyon, Karahalil et al. (2009) found that the percentage of stands decreased by 5.6% during 1965–1984 and increased by 8.04% during 1984–2008. The cumulative forest accretion accounted for 1.9% (548.7 ha) of the whole area of NP. This rate translates to an annual amount of 12.7 ha forest improvement (Karahalil et al., 2009).

It could be thought that two important factors are effective in changing the land use/cover in Kastamonu. The first effective factor is population movement, especially immigration from rural areas to city centers and other cities, which is important for land use/cover changes in the area (Table 1). The change in Kastamonu's urban population during 1990–2015 is shown in Table 1. According to the results presented in this table, the urban population of Kastamonu decreased to 372633 persons as of 2015, whereas the total urban population was 423611 persons in 1990. The rural population decreased from 274901 persons in 1990 to 145765 persons in 2015, whereas the urban population increased from 148710 persons in 1990 to 226868 persons in 2015. When these figures are evaluated in general, it is observed that the urban population in 2015 is approximately 1.5 times more than the urban population in 1990. The rural population decreased by approximately 47% from 1990 to 2015. This is an indicator of mass migration from village to town. Along with urban–suburban migration, there is also population migration from the province to the other provinces. The total population, which was 423611 in 1990, declined by 12% in 2015 to 372633. These migratory movements could have different effects on land use and cover. Conversion of agricultural land to forest as a result of a decrease in rural population has been the main factor for increase in forests (Fig. 5). It was determined that agricultural areas were converted to forested and settlement areas. Although the decrease in rural population has a positive impact on forests, population increase in city centers leads to conversion of forested areas into settlement areas. In total, 1404.1 ha of forested area was converted to settlement areas during 1990–2014.

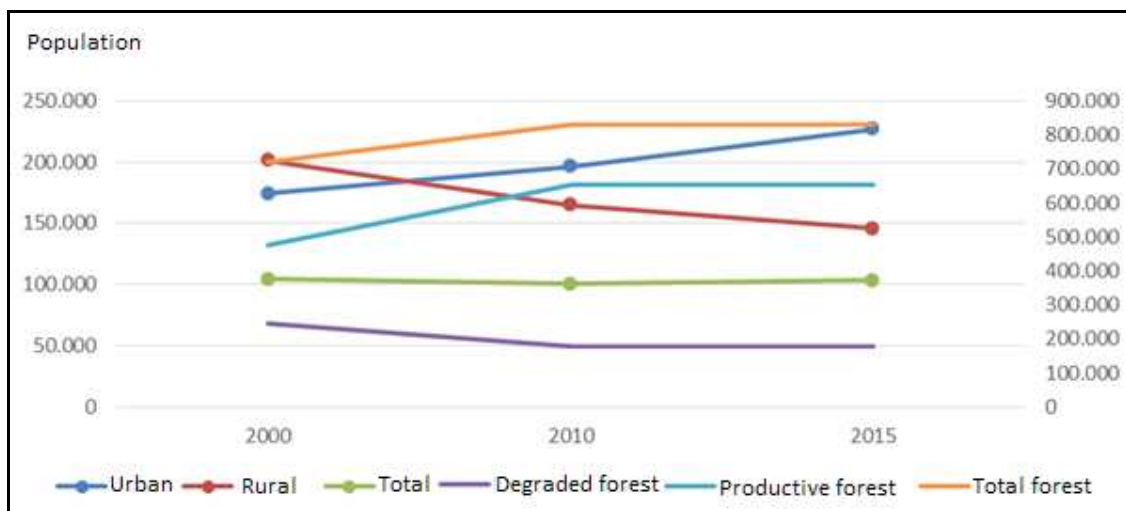


Figure 5. Population of Kastamonu Province and changes in forested areas

When sectoral distribution of gross value added was reviewed, it was observed that the share of the agricultural sector in the developmental zone, including Kastamonu (Sinop, Cankırı, and Kastamonu), is 22.6%; it is well above Turkey's average, which is 9.5%. This study showed that the poverty ratio in the region is high. Agricultural lands in the region are small because of forested areas and their topography. The grains and feed crops have the highest share in plant production. The most significant agricultural activity in conformity with the regional structure is the husbandry activities. The husbandry activities are generally performed by small-scale family enterprises (URL5, 2014). *Figure 6* shows the changes in livestock numbers, amount of arable land, and grain and vegetable production.

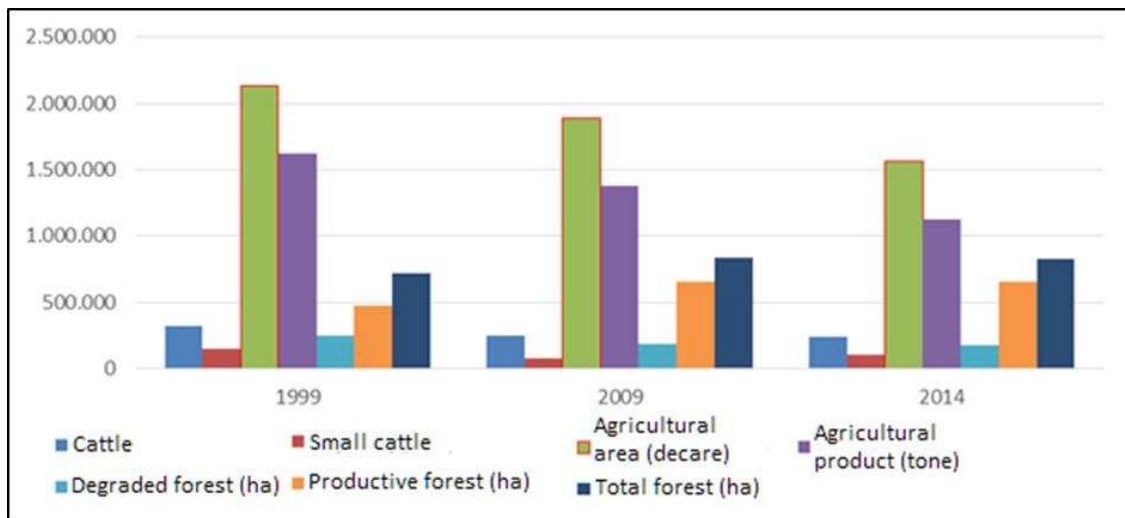


Figure 6. Agricultural variables and changes in forested areas in Kastamonu Province (1999–2014)

The decrease in agricultural activities along with changes in rural population also affect forests. In parallel with the decline in animal numbers, grazing pressure on the forest areas of the animals has decreased. In addition, the use of forests for fuel, lumber, and animal feed by the rural population has decreased. The decrease in all these pressures could have a positive impact on forest growth.

Between 1970 and 2010, in the study conducted in the Daday region of Kastamonu, it was determined that agricultural areas decreased by 57% in parallel with the decrease of the rural population. Particularly, it has stated that the young population leaving the villages is effective in this decrease. This study also found that population movements were concentrated in the city center (Zengin et al., 2018). Another study conducted for Kastamonu Province stated that the main reason for the increase of forest area between 1987–2000 was the population increase (Turan et al., 2010). However, the Kastamonu Forest Regional Directorate found that land use/change is also affected by afforestation activities. The afforestation contributed to the increase of forest areas and the transformation of degraded forest areas into productive forest areas.

Conclusions

This study investigated the spatial changes in land use/cover in Kastamonu in detail. The effects of changes in population and agriculture on forested areas were also revealed. Between 1999 and 2014, forested areas in Kastamonu increased by 15.1% in total. In this period, productive forest areas increased by 37.3% while degraded forested areas decreased by 27.8%. In the same period, the SAs increased by 11.5%, and the ALs decreased by 17.8%. During this change, 42.1% of open areas and 69.6% of agriculture areas have turned into forest areas; 47.2% of degraded forest areas have turned into productive forest areas. At the same time, 0.2% of forest areas and 2.5% of agricultural areas have been converted into settlement areas. The most important factor influencing this change is the migration from rural to urban, particularly after the 1980s. Societies are dynamic, and this dynamism affects the Earth's surface. Therefore, understanding the spatiotemporal changes in land use/cover and associated factors and the dynamics in change are important for sustainable planning of natural resources. However, all those factors should be studied in more detail on the human factor, which has the most influence on this change.

Monitoring and evaluation remain important. These analyses are particularly important for the sustainable management of ecosystems and efficient use of natural resources. For this reason, this monitoring must be elaborated upon and give weight to studies, particularly those in which socio-economic variables and human influence effects on land use are identified.

Acknowledgements. This research did not receive any specific grant from funding agencies in the public, commercial, or nonprofit sectors. Gökhan Şen and Ersin Güngör designed the research, coordinated the data analysis, and wrote the paper. Thanks to Burak Arıca and Hakan Şevik at Kastamonu University for all the help. The authors declare no conflict of interest.

REFERENCES

- [1] Achard, F., Beuchle, R., Mayaux, P., Stibig, H. J., Bodart, C., Brink, A., et al. (2014): Determination of tropical deforestation rates and related carbon losses from 1990 to 2010. – *Global Change Biology* 20(8): 2540-2554.
- [2] Anonymous (2014): Kastamonu province state of the environment report 2014. – T. C. Kastamonu Valiliği Çevre ve Şehircilik İl Müdürlüğü: 174. Kastamonu, Turkey. <http://webdosya.csb.gov.tr/db/ced/editedosya/Kastamonu%202014.pdf> (accessed on 13.06.2017).
- [3] Arıca B, Enez K, Özer Genc, C, Sevik, H. (2016): A method study to determine buffering effect of the forest cover on particulate matter and noise isolation. – 1st International Symposium of Forest Engineering and Technologies (FETEC 2016), pp. 177-185.
- [4] Baccini, A., Goetz, S. J., Walker, W. S., Laporte, N. T., Sun, M., Sulla-Menashe, D., et al. (2012): Estimated carbon dioxide emissions from tropical deforestation improved by carbon-density maps. – *Nature Climate Change* 2: 182-185.
- [5] Barlow, J., Lennox, G. D., Ferreira, J., Berenguer, E., Lees, A. C., Mac Nally, R., et al. (2016): Anthropogenic disturbance in tropical forests can double biodiversity loss from deforestation. – *Nature* 535(7610): 144-147.
- [6] Bayramoğlu, M. M., Kadioğulları, A. (2018): Analysis of land use change and forestation in response to demographic movement and reduction of forest crime. – *EURASIA*

- Journal of Mathematics, Science and Technology Education 14(1): 225-238: DOI: 10.12973/ejmste/79640.
- [7] Cabral, A. I. R., Costa, F. L. (2017): Land cover changes and landscape pattern dynamics in Senegal and Guinea Bissau borderland. – *Applied Geography* 82: 115-128.
- [8] Cakir, G., Sivrikaya, F., Keleş, S. (2008): Forest cover change and fragmentation using Landsat data in Maçka State Forest Enterprise in Turkey. – *Environmental Monitoring and Assessment* 137: 51-66.
- [9] Cetin, M., Sevik, H. (2016a): Evaluating the recreation potential of Ilgaz Mountain National Park in Turkey. – *Environmental Monitoring and Assessment* 188(1): 1-10.
- [10] Cetin, M., Sevik, H. (2016b): Measuring the Impact of Selected Plants on Indoor CO2 Concentrations. – *Polish Journal Environmental Studies*. 25(3): 973-979.
- [11] Cetin, M., Sevik, H., Isinkaralar, K. (2017): Changes in the particulate matter and CO2 concentrations based on the time and weather conditions: The case of Kastamonu. – *Oxidation Communications* 40(1-2): 477-485.
- [12] Chauchard, S., Beilhe, F., Denis, N., Carcaillet, C. (2010): An increase in the upper tree-limit of silver fir (*Abies alba* Mill.) in the Alps since the mid-20th century: A land-use change phenomenon. – *Forest Ecology and Management* 259(8): 1406-1415.
- [13] De Sy, V., Herold, M., Achard, F., Beuchle, R., Clevers, J. G. P. W., Lindquist, E. et al. (2015): Land use patterns and related carbon losses following deforestation in South America. – *Environmental Research Letters* 10(12): 124004.1-15. DOI: 10.1088/1748-9326/10/12/124004.
- [14] Ertekin, M., Özel, H. B. (2010): Black Pine (*Pinus nigra* Arnold.) and Lebanon Cedar (*Cedrus libani* A. Rich.) Plantations for Erosion Control in Çorum Region. – *International Journal of Bartın Forestry Faculty* 12(18): 77-85.
- [15] Eva, H. D., Achard, F., Beuchle, R., de Miranda, E. E., Carboni, S., Seliger, R., et al. (2012): Forest cover changes in tropical South and Central America from 1990 to 2005 and related carbon emissions removals. – *Remote Sensing* 4(5): 1369-1391.
- [16] FAO (2010): Global Forest Resources Assessment 2010. Main Report. – FAO Forestry Paper #163.244 Rome, Italy. <http://www.fao.org/docrep/013/i1757e/i1757e00.htm> (accessed on 19.10.2017).
- [17] Gautam, A. P., Webb, E. L., Shivakoti, G., Zoebisch, M. (2003): Land use dynamics and landscape change pattern in a mountain watershed in Nepal. – *Agriculture, Ecosystems & Environment* 9(1-3): 83-96.
- [18] Güneş Şen, S. (2015): The disposition and characteristics of precipitation at different stand structures in Kastamonu-Daday region. – Msc. Thesis, Kastamonu University, Graduate School of Natural and Applied Sciences, Kastamonu.
- [19] Güneş Şen, S., Aydın, M. (2017): Evaluation of land use conditions of ponds at Taşköprü. – *International Taşköprü Pompeiopolis Science Cultural Arts Research Symposium*, April 10-12: Taşköprü-Kastamonu, Turkey. <https://yadi.sk/d/soS-JxsS3RMM6v>.
- [20] Hansen, M. C., Stehman, S. V., Potapov, P. V. (2010): Quantification of global gross forest cover loss. – *Proceedings of the National Academy of Sciences of the United States* 107(19): 8650-8655.
- [21] Harris, N., Brown, S., Hagen, S., Saatchi, S., Pertova, S., Salas, W., et al. (2012): Baseline map of carbon emissions from deforestation in tropical regions. – *Science* 336(6088): 1573-1576.
- [22] Harvey, B. J. (2016): Human-caused climate change is now a key driver of forest fire activity in the western United States. – *Proceedings of the National Academy of Sciences* 113(42): 11649-11650.
- [23] Houghton, R. (2012): Carbon emissions and the drivers of deforestation and forest degradation in the tropics. – *Current Opinion in Environmental Sustainability* 4(6): 597-603.

- [24] Kadioğulları, A. İ., Başkent, E. Z. (2008): Spatial and temporal dynamics of land use pattern in Turkey: a case study in Gümüşhane. – *Environmental Monitoring and Assessment* 138: 289-303.
- [25] Kaplan, J. O., Krumhardt, K. M., Zimmermann, N. (2009): The prehistoric and preindustrial deforestation of Europe. – *Quaternary Science Reviews* 28 (27-28): 3016-3034.
- [26] Karahalil, U., Kadioğulları, A. İ., Başkent, E. Z., Köse, S. (2009): The spatiotemporal forest cover changes in Köprülü Canyon National Park (1965–2008). – *African Journal of Biotechnology* 8(18): 4495-4507.
- [27] Kucuk, O., Topaloglu, O., Altunel, A. O., Cetin, M. (2017): Visibility analysis of fire lookout towers in the Boyabat State Forest Enterprise in Turkey. – *Environmental Monitoring and Assessment* 189(7): 329.
- [28] Küre Mountains National Park (KMNP) (2017): Küre Mountains. – <http://www.kdmp.gov.tr/sayfa/kure-daglari> (accessed on 23.02.2018).
- [29] Lele, N., Joshi, P. K. (2009): Analyzing deforestation rates, spatial forest cover changes and identifying critical areas of forest cover changes in North-East India during 1972–1999. – *Environmental Monitoring and Assessment* 156(1-4): 159-70. DOI: 10.1007/s10661-008-0472-6.
- [30] Ochoa-Quintero, J. M., Gardner, T. A., Rosa, I., Barros Ferraz, S. F., Sutherland, W. J. (2015): Thresholds of species loss in Amazonian deforestation frontier landscapes. – *Conservation Biology* 29(2): 440-451.
- [31] Ostlund, L., Hörnberg, G., DeLuca, T. H., Liedgren, L., Wikström, P., Zackrisson, O. et al. (2015): Intensive land use in the Swedish mountains between AD 800 and 1200 led to deforestation and ecosystem transformation with long-lasting effects. – *Ambio* 44(6): 508-520.
- [32] Özel, H. B., Ertekin, M. (2012): The change of stand structure in Uludağ fir (*Abies nordmanniana* subsp. *bornmuelleriana* Mattf.) forests along an altitudinal gradient. – *Kastamonu University Journal of Forestry Faculty* 12(3): 96-104.
- [33] Özel, H. B., Kırdar, E., Bilir, N. (2015): The effects of magnetic field on germination of the seeds of oriental beech (*Fagus orientalis* Lipsky.) and growth of seedlings. – *Agriculture & Forestry/Poljoprivreda i Sumarstvo* 61(3): 195-206.
- [34] Öztürk, S., Ayan, S. (2015): Management alternatives in national park areas: The case of Ilgaz Mountain National Park. – *eco.mont - Journal on Protected Mountain Areas Research* 7: 37-44.
- [35] Öztürk, S., Özdemir, Z. (2013): The effects of urban open and green spaces on life quality: a case study of Kastamonu. – *Journal of Kastamonu University Faculty of Forestry* 13(1): 109-116.
- [36] Puyravaud, J. P. (2003): Standardizing the calculation of the annual rate of deforestation. – *Forest Ecology and Management* 177: 593-596.
- [37] Schweizer, D. W., Cisneros, R. (2017): Forest fire policy: change conventional thinking of smoke management to prioritize long-term air quality and public health. – *Air Quality, Atmosphere & Health* 10(1): 33-36.
- [38] Seçkin, B. (1995): Amenajman ve silvikültür ilişkisi, ekonomi-ekoloji ilkesine uygun orman işletmeciliği özlemim. – *Orman Mühendisliği Dergisi* 2: 25-27.
- [39] Sen, G., Bayramoglu, M. M., Toksoy, D. (2015): Spatiotemporal changes of land use patterns in high mountain areas of Northeast Turkey: a case study in Maçka. – *Environmental Monitoring and Assessment* 187(8): 515. DOI 10.1007/s10661-015-4727-8.
- [40] Sevik, H. (2012): Variation in seedling morphology of Turkish fir (*Abies nordmanniana* subsp. *bornmulleriana* Mattf.). – *African Journal of Biotechnology* 11(23): 6389-6395.
- [41] Sevik, H., Cetin, M., Kapucu, Ö. (2016): Effect of light on young structures of Turkish Fir (*Abies nordmanniana* subsp. *bornmulleriana*). – *Oxidation Communications* 39 (I–II): 485-492.

- [42] Sevik, H., Cetin, M., Kapucu, O., Aricak, B., Canturk, U. (2017): Effects of light on morphologic and stomatal characteristics of Turkish Fir needles (*Abies nordmanniana* subsp. *Bornmulleriana* Mattf.). – *Fresenius Environmental Bulletin* 26(11): 6579-6587.
- [43] Simpson, I. A., Vésteinsson, O., Adderley, W. P., Mc Govern, T. H. (2003): Fuel resource utilization in landscapes of settlement. – *Journal of Archaeological Science* 30(11): 1401-1420.
- [44] Šturm, T., Podobnikar, T. (2017): A probability model for long-term forest fire occurrence in the Karst forest management area of Slovenia. – *International Journal of Wildland Fire* 26(5): 399-412.
- [45] Trbojevic, N., Mooney, D. E., Bell, A. J. (2012): A firewood experiment at Eiríksstaðir: A step towards quantifying the use of firewood for daily household needs in Viking Age Iceland. – *Archaeologia Islandica* 9: 29-40.
- [46] Tunçtaner, K., Özel, H. B., Ertekin, M. (2007): According to urban landscape design, the determination of legislation and regulation for conservation of historical environment. – *International Journal of Bartın Forestry Faculty* 9(11): 11-225.
- [47] Turan, S. Ö., Günlü, A. (2010): Spatial and temporal dynamics of land use pattern response to urbanization in Kastamonu. – *African Journal of Biotechnology* 9(5): 640-647.
- [48] Turkish Statistical Institute (TUIK) (2017): Population of Kastamonu City. – www.tuik.gov.tr (accessed on 23.08.2017).
- [49] Tyukavina, A., Baccini, A., Hansen, M. C., Potapov, P. V., Stehman, S. V., Houghton, R. A., et al. (2015): Aboveground carbon loss in natural and managed tropical forests from 2000 to 2012. – *Environmental Research Letters* 10074002. DOI: 10.1088/1748-9326/10/7/074002.
- [50] URL1 (2004): Natural Resources. – <https://www.ugc.ac.in/oldpdf/modelcurriculum/Chapter2.pdf> (accessed on 01.11.2017).
- [51] URL2 TC Kastamonu Valiliği (2016): Kastamonu doğal güzellikleri ve eko turizm merkezi. – <http://www.kastamonu.gov.tr/doga-turizm> (accessed on 03.10.2017).
- [52] URL3 (2017): Sözcü newspaper. Kastamonu Haberi: Küre Dağları'nda yeni endemik tür belirlendi. – <http://www.sozcu.com.tr/2017/gundem/son-dakika-haberi/kure-daglarinda-yeni-endemik-tur-belirlendi-1721562/> (accessed on 23.11.2017).
- [53] URL4 Forestry General Directorate (2017): İllere göre orman varlığı. – <https://www.ogm.gov.tr/Sayfalar/Ormanlarimiz/Ilere-Gore-Orman-varligi.aspx> (accessed on 18.12.2017).
- [54] URL5 T. C. Kuzey Anadolu Kalkınma Ajansı (2014): TR82 Düzey 2 bölgesi bölge planı 2014-2023 Kastamonu - Çankırı - Sinop İlleri. – [https://www.kuzka.gov.tr/paylasim/20160401_tr82_bolge_plani_\(WEB\).pdf](https://www.kuzka.gov.tr/paylasim/20160401_tr82_bolge_plani_(WEB).pdf) (accessed on 23.11.2017).
- [55] URL6 TEB Kobi Akademi (2006): İller için gelecek stratejileri Kastamonu Gelecek Stratejisi Sonuç Raporu. – <https://www.teb.com.tr/document/kastamonu.pdf> (accessed on 09.12.2017).
- [56] Yigit, N., Sevik, H., Cetin, M., Kaya, N. (2016): Determination of the Effect of Drought Stress on the Seed Germination in Some Plant Species. – In: Rahman, I. M., Begum, Z. A., Hasegawa, H. (eds.) *Water Stress in Plants*, Chapter 3, pp. 43/62. INTECH Open Book Publisher, Vienna.
- [57] Zengin, H., Değermenci, A. S., Bettinger, P. (2018): Analysis of temporal changes in land cover and landscape metrics of a managed forest in the West Black Sea region of northern Turkey: 1970–2010. – *Journal of Forestry Research* 29(1): 139-150.

THE EFFECT OF MULCHING ON SOIL TEMPERATURE, WINTER POTATO (*SOLANUM TUBEROSUM* L.) GROWTH AND YIELD IN FIELD EXPERIMENT, SOUTH CHINA

LI, X. B.^{1,2†} – SUO, H. C.^{1,2†} – AN, K.^{1,2} – FANG, Z. W.^{1,2} – WANG, L.^{1,2} – ZHANG, X. L.^{1,2} – LIU, X. J.^{1,2*}

¹*The Crop Research Institute, Guangdong Academy of Agriculture
18 Jinying West 2nd Street, 510640 Guangzhou, Guangdong, China*

²*Key Laboratory of Crop Genetics and Improvement of Guangdong Province
20 Jinying, 510640 Guangzhou, Guangdong, China*

**Corresponding author*

e-mail: 13609741790@163.com; phone: +86-20-3703-8559; fax: +86-20-8551-4269

†These authors have contributed equally to this work.

(Received 8th Aug 2017; accepted 11th Jan 2018)

Abstract. The growth of winter potato, which is mainly planted in South China, is negatively affected by low temperatures. However, mulching is an effective method to increase soil temperatures. Here, the effects of black plastic, white plastic and rice straw mulch were assessed on soil temperatures, as well as on potato growth and yield through field experiment. The daily mean temperatures increased by up to 7.5°C and 6.5°C under black and white plastic mulch, respectively, compared with no mulch. Furthermore, the emergence rates and dates were accelerated by mulching, with the greatest tuber yields being observed under the black mulch treatment in two growing seasons. Additionally, mulching altered the soil's fertility properties and soil microorganism composition. Taken together, mulching with black plastic film is an effective method that benefits winter potato production in Typical Pearl River Delta Plain in south China.

Key words: *plastic mulch, soil fertility, potato yield, emergence rate, soil temperature*

Introduction

Potato (*Solanum tuberosum* L.) is an important crop worldwide; ranking fourth after rice, wheat and maize, and it has a significant economic role. Currently, China is the largest potato producer in the world (FAO, 2014). In China, the North China Plain and Loess Plateau are major potato production regions because of their environmental conditions, including high altitudes, large diurnal air temperature fluctuations and abundant sunlight. However, these areas have typical arid and semiarid climates in which water scarcity is a substantial threat to crop yields (Wang et al., 2005). Thus, water-saving becomes the most critical factor in enhancing potato yield and quality. Mulching improves water conservation by reducing soil evaporation rates and increasing the water-use efficiency. Plastic mulch combined with drip irrigation has been used as an effective water-saving measure for the cultivation of potato in North China (Wang et al., 2011a; Liu et al., 2017; Zhang et al., 2017a).

In addition to saving water, plastic mulching also decreases nitrate leaching (Johnie and Josiah, 1998; Pat and Brenda, 2002; Romić et al., 2003), suppresses weed populations (Ghosh et al., 2006; Ramakrishna et al., 2006), kills pathogens (Vos et al., 1995; Triki et al., 2001), decreases soil bulk densities (Anikwe et al., 2007) and regulates soil temperature (Baghour et al., 2002; Ramakrishna et al., 2006; Wang et al., 2009; Hou et al., 2010; Ibarra-Jiménez et al., 2011; Dvořák et al., 2012; Zhao et al.,

2012). Reports on potato yield when plastic mulch is used are controversial, with some studies describing yield reductions (Baghour et al., 2002; Wang et al., 2009, 2011b), while others yield increases (Mahmood et al., 2002; Wang et al., 2005, 2009; Hou et al., 2010; Zhao et al., 2012, 2014; Ruízmachuca et al., 2014; Zhang et al., 2017b). These discrepancies may be attributed to differences in weather conditions among locations and study years, as well as soil temperature differences between mulched and non-mulched soil (Hou et al., 2010). Soil temperature is a main factor that regulates biomass accumulation, potato canopy development and potato tuber growth (Wolf et al., 1990; Delden et al., 2000). The optimum temperature for potato growth ranges from 15°C to 18°C. Tuberization occurs at low temperatures below 21°C and is delayed, or even inhibited, at temperatures above 30°C (Hay and Allen, 1978).

The South China provinces of Guangdong, Guangxi, Hainan and Fujian form a major winter potato production region. It has a typical sub-tropical and tropical monsoon climate, with plentiful annual rainfall, but the daily mean temperature is higher than 25°C from May to October. Thus, potato growth is restricted in the winter (November to March) in fallow paddy fields. Winter potato production is a significant component in meeting the market demand for potatoes in the spring and in realizing all-year production and a year-round supply. However, temperatures below 15°C often occur during the potato growing season, especially in the early growing period, and sometimes the temperature falls below 0°C, which threatens the winter potato yield. Fortunately, increased soil temperatures caused by mulching were noticed by farmers, and plastic mulch, as well as rice straw mulch, has been widely employed in winter potato production. While there is plenty of information regarding the plastic mulch and spring potato production in North China (Wang et al., 2005, 2009, 2011a; Zhao et al., 2012, 2014), there is little information concerning winter potato production under mulch in South China. In this study, the effects of plastic and rice straw mulch on winter potato growth were explored. The objectives of this study were to (1) evaluate the effects of mulch on soil temperature during the winter growing season; (2) assess the influence of mulch on the emergence rate and date, and the tuber size and yield of winter potato; and (3) explore the changes in soil fertility properties and microorganisms under mulch.

Materials and methods

Experimental site

Field experiments were carried out in 2013 to 2014 and 2014 to 2015 at Baiyun Experimental Station of Guangdong Academy of Agricultural Sciences in Guangzhou. It has a typical sub-tropical monsoon climate and has two or three harvests per year. *Table 1* is the brief description of this experimental site. The Global Position System (GPS) coordinates of the experimental site was shown in *Figure 1*.

Experimental design

The experiment was designed as a randomized complete block with three replications and the following four treatments: (1) Black plastic mulch, (2) White plastic mulch, (3) Rice straw mulch, and (4) Bare soil. The plastic was 135 cm wide and 0.02 mm thick polyethylene film. The main agronomic management practises are shown in *Table 2*.

Temperature measurements

Weather data were obtained from the weather station located near the experimental site. Soil temperatures for each treatment were measured with HOBO® 12-Bit Temperature Smart Sensor Manual connecting with HOBO® Micro Station Quick Start (Onset Computer Corporation, Pocasset, United States), which were placed in the centre of the middle bed at soil depths of 5 cm, 10 cm, 15 cm, 20 cm and 25 cm.

Table 1. Brief description of experimental site

Items	Value	Annotation
Location	113°17E', 23°8N'	Lies in Baiyun Experimental Station of Guangdong Academy of Agricultural Sciences in Guangzhou, Guangdong province, South China
Altitude (m)	27	
Air temperature (°C)		The average of 1951-2008
Average	20.8	
Maximum	39.0	In July
Minimum	0	In January
Precipitation (mm)	1738	
Evaporation (mm)	1700	Annual pan evaporation
Sunshine hours (h)	>1800	
Groundwater table (m)	<10	
Average bulk density (cm ⁻³)	1.33	
Frost-free period, day(d)	320	
Major crops	Rice	
Pre-crop	Rice	
Land surface	Typical Pearl River Delta Plain, the main land-use type is paddy field	

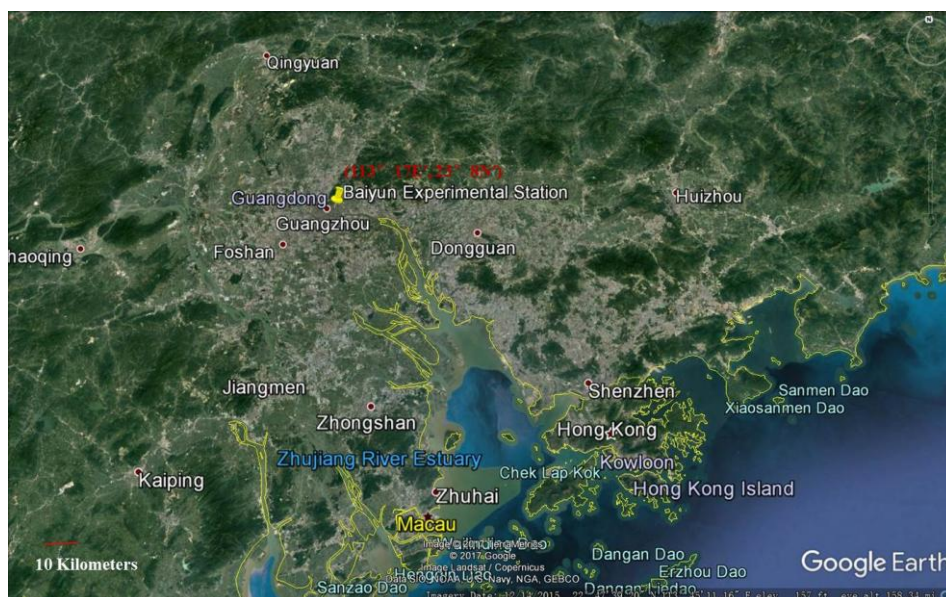


Figure 1. GPS coordinates of the experimental site. The image is generated by the software of Google Earth

Table 2. The key information of planting seeds and the management of potato in the experiment

Items	2013 to 2014	2014 to 2015
Potato cultivar	Yueyin85-38	
Farmyard manure	75t ha ⁻¹	
Fertilizer	One-time application, fertilizer containing nitrogen (285 kg ha ⁻¹), P ₂ O ₅ (225 kg ha ⁻¹) and potassium (450 kg ha ⁻¹)	
Planting mode	Ridges with two rows	
Sowing depth	10 cm	
Sowing date	Nov. 20, 2013	Nov. 27, 2014
plant protection	Spray 600 times dilution INFINITO (BAYER®, GERMAN) solution at 50 days and 60 days after emergence	
Hilling	Hilling twice, after emergence and at tillering stage	
Irrigation frequencies	Furrow irrigation once a month	
Weed control	Removing weeds before tillering stage	

Plant sampling

The emergence rate, emergence date and duration were recorded when 75% plants had acquired the characteristics of the stage under each treatment. The roots and shoots of three plants per treatment were measured to determine the fresh weight and were then oven-dried at 105°C for 48 h to determine the dry weight (Wang et al., 2005). After harvesting, ten plants in each treatment were randomly sampled for the indoor test, and the tubers were divided manually into two grades, greater than and less than 50 g fresh weight.

Soil properties analysis

In two growing seasons, three soil samples were taken randomly from the surface to a soil depth of 5 cm in each treatment before sowing and after harvesting. The soil's available nitrogen, phosphorus and potassium were detected. Soil available nitrogen includes ammonium and nitrate forms of nitrogen. In diffusion dishes containing ferrous sulphate, the soil was hydrolysed and reduced under a strong alkaline environment. Nitrogen in the soil was converted into ammonia and then absorbed by a boric acid solution. The absorbed liquid ammonia was titrated with sulfuric acid, and the available nitrogen content was calculated based on the amount of the sulfuric acid (Duan et al., 2007). Soil available potassium was extracted by 1 mol/L acetic acid ammonium and then measured by a flame photometer (Du et al., 2004). Soil available phosphorus was extracted by a solution of 0.05 mol/L HCl and 0.025 mol/L H₂SO₄ and then measured by a spectrophotometer (Jiao et al., 2015).

Soil microorganism analysis

In two growing seasons, three soil samples were taken randomly from the surface to a soil depth of 5 cm in each treatment before sowing and after harvesting. Counts of total bacteria were measured on 10⁻⁵ and 10⁻⁴ nutrient agar medium (5 gL⁻¹ peptone, 3 gL⁻¹ beef extract, 1 gL⁻¹ yeast extract, 15 gL⁻¹ agar, 5 gL⁻¹ glucose) (Wollum, 1982) counts of total actinomycetes were measured on 10⁻⁴ and 10⁻³ Gausserime synthetic agar medium (20 gL⁻¹ Soluble Starch, 0.5 gL⁻¹ NaCl, 1 gL⁻¹ KNO₃, 0.5 gL⁻¹ K₂HPO₄·3H₂O,

0.5 gL⁻¹ MgSO₄·7H₂O, 0.01 gL⁻¹ FeSO₄·7H₂O, 15 gL⁻¹ agar, pH7.4), and total fungi were measured on Martin's Rose Bengal agar medium (5 gL⁻¹ peptone, 10 gL⁻¹ glucose, 1 gL⁻¹ KH₂SO₄, 0.5 gL⁻¹ MgSO₄, 0.01 gL⁻¹ rose bengal sodium, 14 gL⁻¹ agar, pH 6.0) (Martin, 1950). The plates were incubated in darkness at 25°C for 3 to 4 d for the bacteria, 10 d for the fungi and 7 d for the actinomycetes.

Statistical analysis

The One-Way ANOVA procedure in SPSS Statistics 17.0 was used to conduct analysis of variance. Mean values of the treatments were compared using the Duncan test at $p \leq 0.05$. Mean values are reported in *Tables 3, 5, 6, 7, 8* and *Figure 5*.

Results

Air and soil temperature

In the growing season from October 2013 to April 2014, the mean monthly air temperature ranged from 13.0°C to 24.0°C, averaging 17.3°C, monthly maximum air temperature was in the range of 18.0°C~29.0°C and the monthly minimum air temperature was in the range of 8.0°C~19.0°C. There were 60 days had a daily minimum temperature lower than 15.0°C, mainly concentrated in the December to February, and extreme low temperature was 3.0°C (*Fig. 2a*). In the growing season from October 2014 to April 2015, the mean monthly air temperature ranged from 13.0°C to 25.0°C, averaging 18.3°C, monthly maximum air temperature was in the range of 17.0°C to 30.0°C and the minimum air temperature was in the range of 9.0°C to 20.0°C. There were 63 days had a daily minimum temperature lower than 15.0°C, mainly concentrated in the December to February, and extreme low temperature was 4.0°C (*Fig. 2b*).

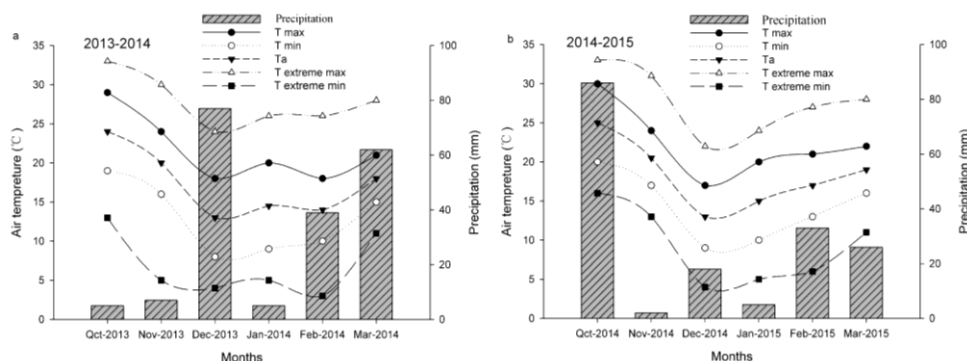


Figure 2. Average monthly air temperature and precipitation during the potato growing season in 2013~2014 and 2014~2015. *T max*: maximum average monthly air temperature; *T min*: minimum average monthly air temperature; *Ta*: average monthly air temperature. *T extreme max*: extreme maximum average monthly air temperature; *T extreme min*: extreme minimum average monthly air temperature

During the growing season from October 2014 to February 2015, the daily mean soil temperature in different depths under black and white plastic mulch were higher 0°C~7.5°C, 0°C~6.5°C compared with that in bare soil, respectively (*Fig. 3a, 3b*).

However, rice straw mulch mainly decreased soil temperature, the temperature differences in different depths between rice straw mulch and bare soil was $-2.5^{\circ}\text{C}\sim 1.0^{\circ}\text{C}$ (Fig. 3c). At the early growing season, daily mean soil temperature under black and white plastic mulch were higher $1.0\sim 7.5^{\circ}\text{C}$, $1.0\sim 6.5^{\circ}\text{C}$ than that in bare soil (Fig. 3a, 3b), but the soil temperature under rice straw was close to or even lower than bare soil, the temperature differences in different depths between rice straw mulch and bare soil was $-2.5^{\circ}\text{C}\sim 1.0^{\circ}\text{C}$ (Fig. 3c). In the middle growing season, as the plant canopy enlarged, the soil surface was shaded, the soil temperature differences between mulch and non-mulch became smaller, $0\sim 4.3^{\circ}\text{C}$ for black plastic mulch, $0\sim 3.5^{\circ}\text{C}$ for white plastic mulch, $-1\sim 0.67^{\circ}\text{C}$ for rice straw mulch (Fig. 3a-c). In the late growing days, the plant leaves senescent and dropped, the soil temperature increasing again, black and white plastic mulch also showed small soil temperature differences compared with that in bare soil, $0.8\sim 2.0^{\circ}\text{C}$ and $0\sim 2.2^{\circ}\text{C}$, respectively (Fig. 3a, 3b). And the differences between rice straw mulch and bare soil was even more smaller, $-0.83^{\circ}\text{C}\sim 0.83^{\circ}\text{C}$ (Fig. 3c).

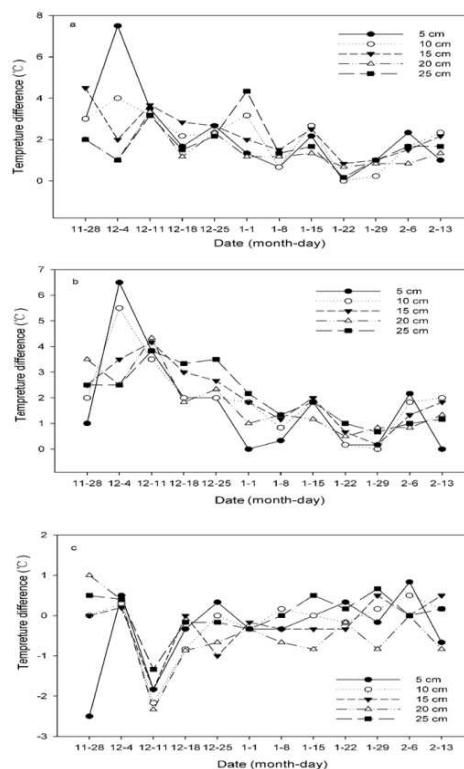


Figure 3. Differences in daily mean soil temperature at different soil depths under mulch and no-mulch conditions. a: black plastic mulch; b: white plastic mulch; c: rice straw mulch

Emergence rate and growth stages duration

Due to the favourable changes in soil temperature by mulching, the emergence rate was increased by 16.2%, 14.9% and 11.0% under black, white and rice straw mulch, respectively in the winter of 2013. Similarly, in 2014 winter, the emergence rate was improved by 14.0%, 14.2% and 10.4% under black, white and rice straw mulch, respectively (Table 3).

Table 3. Emergence rate of potato under different mulching conditions in 2013~2014 and 2014~2015

Treatments	Emergence rate (%)		Increasing in emergence rate (%)	
	2013-2014	2014-2015	2013-2014	2014-2015
Black plastic mulch	88.7a	90.1a	16.2	14.0
White plastic mulch	87.1a	90.4a	14.9	14.2
Rice straw mulch	83.4a	86.5b	11.0	10.4
Bare soil	72.2b	75.6c	--	--

Means within columns followed by different lower-case letters (a, b, c) stand for significance different at $p \leq 0.05$

Besides increasing the emergence rate, the emergence also been accelerated by mulch. Compared to bare soil, emergence was 10 d, 8 d and 1 d earlier in 2013 growing season and 7 d, 4 d and 1 d earlier in 2014 growing season under black, white and rice straw mulch, respectively (Table 4). And due to the early emergence, the corresponding maturation periods were less 4 d, 9 d and 1 d in 2013 growing season and 4 d, 11 d and 1 d in 2014 growing season under black, white and rice straw mulch, respectively (Table 4, Fig. 4).

Table 4. The date of sowing, emergence and maturing under different mulch conditions in 2013 to 2014 and 2014 to 2015 growing seasons

	2013-2014			2014-2015		
	Sowing 2013	Emergence 2013	Maturing 2014	Sowing 2014	Emergence 2014	Maturing
Black plastic mulch	Nov.26	Dec.18 (22b)	Mar.29 (123b)	Nov.20	Dec.6 (16b)	Mar.16 (116b)
White plastic mulch	Nov.26	Dec.20 (24b)	Mar.23 (117c)	Nov.20	Dec.9 (19b)	Mar.9 (109c)
Rice straw mulch	Nov.26	Dec.26 (30a)	Apr.1 (126a)	Nov.20	Dec.15 (25a)	Mar.19 (119a)
Bare soil	Nov.26	Dec.28 (32a)	Apr.2 (127a)	Nov.20	Dec.13 (23a)	Mar.20 (120a)

The numbers in parentheses indicate the duration days, and means within columns followed by different lower-case letters (a, b, c) stand for significance different at $p \leq 0.05$

Biomass accumulation

Aboveground fresh and dry weight increased gradually during the growing season in 2014. At the 30 d after sowing, the plants under black and white plastic mulch showed significantly higher accumulation ($p < 0.05$) both in fresh and dry weight compared with rice straw treatment and bare soil. At the 45 d after sowing, the plants under only black plastic mulch showed significantly higher accumulation of fresh and dry weight. During the middle growing period, no difference was observed among the treatments. And at the late growing days, the black plastic treatment showed much higher above-ground fresh and dry weight (Fig. 5a, 5b). Under-ground fresh and dry weight increased rapidly during the growing season in 2014. At the early growing days, there was no significant difference among the treatments. However, the black plastic mulch showed highest fresh and dry weight from 75 d to 105 d after sowing, and significant difference

were found for dry weight at 90 and 105 d after sowing (Fig. 5c, 5d). Tuber biomass showed the same tendency with under-ground biomass, which the black plastic treatment have the highest fresh and dry weight in the later growing period, and significant differences were found for tuber dry weight at 90 and 105 d after sowing (Fig. 5e, 5f).



Figure 4. Potato field performance in 2014 to 2015 growing seasons. a: the photo was taken on 16 December, 2014; b: the photo was taken on 26 January, 2015

Tuber size and yield

Based on weight, tubers were divided into two grades: small tubers (< 50 g) and large tubers (≥ 50 g). In 2013~2014, the black plastic mulch treatments had the greatest weight and number of large tubers, and then followed by the rice straw mulch and bare soil; the white plastic mulch is the lowest. While, with respect to small tubers, the white plastic mulch treatment showed significantly heavier and much more number of small tubers than other mulch treatments and bare soil ($p \leq 0.05$). Thus, the tuber numbers and weight were significantly higher in the black mulch than other treatment and bare soil ($p \leq 0.05$) (Table 5).

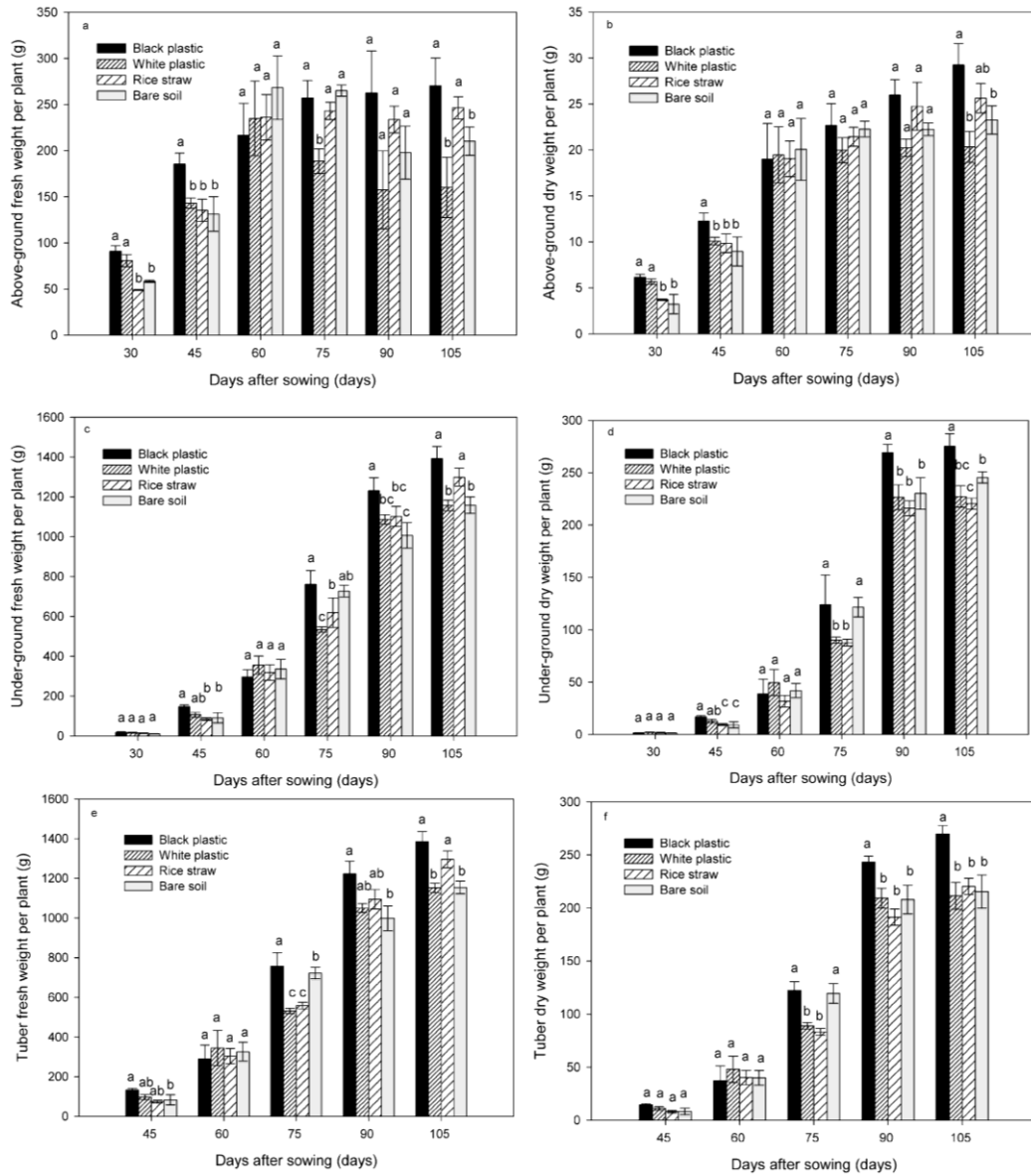


Figure 5. Above-ground and under-ground biomass under different mulch conditions. a: above-ground fresh weight per plant; b: above-ground dry weight per plant; c: under-ground fresh weight per plant; d: under-ground dry weight per plant; e: tuber fresh weight per plant; f: tuber dry weight per plant. Means within columns followed by different lower-case letters (a, b, c) stand for significance different at $p \leq 0.05$

In 2014~2015, the rice straw mulch treatment had the greatest number of large tubers, which was significant different with white plastic mulch ($p \leq 0.05$), but no significant difference with black plastic mulch and bare soil. The black plastic mulch had the greatest weight of large tubers, which was significant different with white plastic mulch ($p \leq 0.05$), but no significant difference between black plastic mulch and bare soil. Although, the white plastic mulch treatment showed the greatest weight and number of small tubers, there were no significant difference among the three mulch treatments and bare soil. In total tuber number and weight, there were no significant differences among all the treatments ($p \leq 0.05$) (Table 5).

Table 5. Potato tuber grades and weight of ten sample plants under different mulching conditions in 2013~2014 and 2014~2015 growing seasons

	Tuber numbers of ten plants			Tuber weight of ten plants		
	W \geq 50 g	W<50 g	Total	W \geq 50 g	W<50 g	Total
2013-2014						
Black plastic mulch	42.67 \pm 2.86a	22.32 \pm 1.01ab	64.17 \pm 2.21a	5.57 \pm 0.29a	0.63 \pm 0.12ab	6.20 \pm 0.24a
White plastic mulch	29.33 \pm 3.63c	25.33 \pm 2.67a	50.83 \pm 1.67b	3.83 \pm 1.11c	0.71 \pm 0.11a	3.87 \pm 0.58b
Rice straw mulch	39.33 \pm 5.76ab	15.00 \pm 2.89b	50.83 \pm 5.46b	4.60 \pm 0.27ab	0.33 \pm 0.06b	4.93 \pm 0.31b
Bare soil	33.67 \pm 2.86bc	17.67 \pm 1.45ab	50.83 \pm 3.00b	4.20 \pm 0.16bc	0.67 \pm 0.09a	4.87 \pm 0.15b
2014-2015						
Black plastic mulch	42.67 \pm 2.27ab	7.33 \pm 2.33a	50.00 \pm 3.78a	8.32 \pm 0.59a	0.24 \pm 0.10a	8.47 \pm 0.57a
White plastic mulch	39.02 \pm 3.67b	10.00 \pm 3.06a	49.00 \pm 5.51a	6.91 \pm 0.39b	0.34 \pm 0.17a	7.31 \pm 0.51a
Rice straw mulch	48.33 \pm 2.86a	7.33 \pm 2.09a	55.67 \pm 3.84a	7.96 \pm 0.17ab	0.22 \pm 0.10a	8.21 \pm 0.23a
Bare soil	48.21 \pm 3.74ab	5.00 \pm 2.64a	54.67 \pm 3.28a	8.08 \pm 0.39ab	0.12 \pm 0.09a	7.87 \pm 0.05a

W: weight per tuber

The values indicate means \pm standard deviation of ten biological replicates, and means within same columns followed by different lower-case letters (a, b, c) stand for significance different at $p \leq 0.05$

The highest tuber yields for the two growing season were observed in the black mulch treatment, which was 21.5% and 12.0% higher than bare soil in 2013~2014 and 2014~2015 respectively. And then followed by rice straw mulch, 9.4% and 8.0% higher than bare soil in 2013~2014 and 2014~2015 respectively, the lowest tuber yield was obtained in the white plastic mulch treatment, 7.5% and 4.0% lower than bare soil in 2013~2014 and 2014~2015, respectively (*Table 6*).

Table 6. Yields of potato under different mulch conditions in 2013~2014 and 2014~2015 growing seasons

Treatments	2013~2014				2014~2015			
	Black plastic	White plastic	Rice straw	Bare soil	Black plastic	White plastic	Rice straw	Bare soil
Yield (kg ha ⁻¹)	2790.3a	2043.6b	2418.5b	2191.5b	3852.2a	3262.5b	3681.8a	3390.2b
Increasing in yield (%)	21.5	-7.2	9.4	-	12.0	-4.0	8.0	-

The increasing in yield (%) was compared with the bare soil treatment

Means within columns followed by different lower-case letters (a, b, c) stand for significance different at $p \leq 0.05$

Soil fertility properties

The soil fertility properties were measured before sowing and after harvest in each season. Higher contents of available nitrogen, potassium and phosphorus were recorded after harvest both in mulch and non-mulch treatments compared with before sowing. In both growing seasons, the content of available nitrogen (N) was increased significantly ($p \leq 0.05$) higher in rice straw mulch compared with that in bare soil, increased by 1.14% and 1.10%, respectively, and lowest content of available N were found in black and white plastic mulch treatments. In 2013~2014 growing season, the content of available phosphorus (P) was increased most in black and white mulch, then in rice straw mulch, bare soil was the lowest. However, in 2014~2015 growing season the content of available P was increased most in white mulch and bare soil, then in black plastic mulch, rice straw mulch was the lowest. With respect to content of available potassium (K), in 2013~2014 growing season, black plastic, white plastic and rice straw mulch showed significantly higher content of available K compared with that in bare soil. While in 2014~2015 growing season, black plastic mulch, rice straw mulch and bare soil showed significantly higher content of available K compared with that in bare soil (Table 7).

Table 7. The contents of available N, P, K under different mulch conditions in 2013~2014 and 2014~2015 growing seasons

Treatments	Available N (mg/kg)			Available P (mg/kg)			Available K (mg/kg)		
	Before sowing	After harvest	Increase in yield (%)	Before sowing	After harvest	Increase in yield (%)	Before sowing	After harvest	Increase in yield (%)
2013~2014									
Black plastic	83.95	124.95	0.49c	25.11	38.15	0.52a	60.00	101.50	0.7a
White plastic	88.37	117.48	0.33c	27.95	43.12	0.54a	64.00	102.50	0.60b
Rice straw	79.53	170.09	1.14b	24.29	34.34	0.41ab	58.00	93.00	0.60b
Bare soil	89.47	143.60	0.60b	25.51	33.85	0.33b	66.00	88.00	0.33b
2014~2015									
Black plastic	66.37	92.27	0.39c	55.61	76.78	0.38a	95.00	140.00	0.47a
White plastic	64.52	92.27	0.43c	59.67	87.81	0.47a	93.50	122.50	0.31b
Rice straw	67.11	141.10	1.10a	64.17	81.73	0.27b	90.00	142.50	0.58a
Bare soil	63.41	108.17	0.71b	51.33	76.33	0.49a	90.00	135.00	0.50a

The numbers in parentheses indicate the duration days, and means within columns followed by different lower-case letters (a, b, c) stand for significance different at $p \leq 0.05$

Soil microorganism

Total bacteria

Counts of total bacteria were increased after harvest both in mulch and non-mulch treatments in two growing season. In 2013, the rice straw mulch showed highest growth of total bacteria amount, and the white plastic mulch is the lowest. But no such difference was apparent in 2014, the highest growth of total bacteria amount was found in black plastic mulch, and lowest was in bare soil plot (Table 8).

Total fungi

Counts of total fungi were reduced after harvest both in mulch and non-mulch treatments in two growing seasons and showed same tendency. The largest reduction of total fungi amount was observed in white plastic mulch and smallest reduction was found in rice straw mulch (Table 8).

Total actinomycetes

Counts of total actinomycetes were also reduced after harvest both in mulch and non-mulch treatments in two growing seasons. Significantly reduction was obtained in bare soil in 2013~2014 and in white plastic mulch in 2014~2015, no significantly difference in counts of total actinomycetes was found in other treatments (Table 8).

Table 8. Soil microorganisms evaluated under different mulch conditions in 2013~2014 and 2014~2015 growing seasons

	2013~2014			2014~2015		
	Before sowing	After harvest	Increased by (%)	Before sowing	After harvest	Increased by (%)
	Total bacteria (*10 ⁵ CFU g ⁻¹ dry soil)			Total bacteria (*10 ⁵ CFU g ⁻¹ dry soil)		
Black plastic	164	196	0.20b	123	458	2.72a
White plastic	372	423	0.14b	137	426	2.11b
Rice straw	358	632	0.77a	135	381	1.82b
Bare soil	275	348	0.27b	105	237	1.26c
	Total fungi (*10 ³ CFU g ⁻¹ dry soil)			Total fungi (*10 ³ CFU g ⁻¹ dry soil)		
Black plastic	133	41	0.69ab	119	63	0.47ab
White plastic	321	40	0.88a	120	34	0.72a
Rice straw	230	164	0.28b	125	84	0.328b
Bare soil	258	121	0.53ab	110	44	0.6ab
	Total actinomycetes (*10 ⁵ CFU g ⁻¹ dry soil)			Total actinomycetes (*10 ⁵ CFU g ⁻¹ dry soil)		
Black plastic	22	12	0.45ab	132	101	0.23b
White plastic	55	40	0.27b	109	63	0.42a
Rice straw	31	22	0.29b	88	60	0.32ab
Bare soil	39	16	0.59a	124	82	0.34ab

CFU: colony-forming unit. Data represents three replicates, and means within columns followed by different lower-case letters (a, b, c) stand for significance different at $p \leq 0.05$

Discussion

Unlike in northern China, where potato is planted in June and harvested in October, in southern China, the potato growing season is from November to next year's April, and the limiting factor is low temperatures below 15°C, especially in the early growing days of December and January. There were more than 40 d with mean temperatures below 15°C (Fig. 2). According to our research, the daily mean temperature was 0°C to 7.5°C and 0°C to 6.5°C higher under black and white plastic mulch than under non-mulch conditions (Fig. 3). Thus, mulching is an effective method to increase the top-soil's temperature. Because of the favourable changes in soil temperature caused by mulching, the emergence rate increased and the emergence date was accelerated (Tables 3, 4). Above-ground fresh and dry weights increased gradually during the growing season in 2014. At 30 d after sowing, the plants under black and white plastic mulch

showed significantly higher accumulations both in fresh and dry weights compared with those of the rice straw treatment and bare soil. At 45 d after sowing, only the plants under black plastic mulch showed significantly higher accumulations of fresh and dry weights (Fig. 5a, 5b). Under-ground fresh and dry weights increased rapidly during the growing season in 2014, the black plastic mulch showed the greatest fresh and dry weights from 75 d to 105 d after sowing, and significant differences were found for dry weights at 90 d and 105 d after sowing (Fig. 5c, 5d). The tuber biomass showed the same tendency as the under-ground biomass, with the black plastic treatment having the greatest fresh and dry weights in the later growing period, and significant differences were found among tuber dry weights at 90 and 105 d after sowing (Fig. 5e, 5f). The tuber numbers and weights were significantly greater under the black mulch than under the other treatments and bare soil (Table 5), the greatest tuber yields for the two growing seasons were observed under the black mulch treatment, and they were 21.5% and 12.0% greater than in bare soil in 2013 to 2014 and 2014 to 2015, respectively (Table 6). Higher soil temperatures with the plastic mulch were also observed in other reports (Baghour et al., 2002; Ramakrishna et al., 2006; Wang et al., 2009; Hou et al., 2010; Ibarra-Jiménez et al., 2011; Dvořák et al., 2012; Zhao et al., 2012), and for other crops, such as maize (Liu et al., 2009; Zhou et al., 2012), tomatillo (Díaz-Pérez et al., 2005), broccoli (Díaz-Pérez, 2009), tomato (Díaz, 2002), and spring wheat (Li et al., 1999; 2004). However, increasing the soil temperature can harm potato production, especially in regions with enough or excess heat. For instance, the highest daily soil temperatures at 5 cm and 10 cm depths were above 30°C during the period from early May to late June, which is detrimental to potato tuber initiation and bulking (Wang et al., 2009). Thus, the excessive heat generated by the plastic film is mostly responsible for the lower yields, and similar results have been demonstrated (Baghour et al., 2002; Wang et al., 2009; Hou et al., 2010; Zhao et al., 2012).

Rice straw mulch has also been widely employed because it is convenient and cost efficient. The soil temperature under rice straw was close to or even lower than bare soil only, and the temperature differences at different depths between rice straw mulch and bare soil were -2.5°C to 1.0°C (Fig. 3). Similar results were also found in other reports. Wang (2011a) found that the maximum soil temperatures in the soil surface layer were 4°C to 6°C lower in straw mulched plots than in non-mulched plots. Kar (2003) showed that the soil temperature was 3°C to 4°C less in rice straw-mulched plots than in non-mulched plots. Samad (2014) confirmed that *Arachis pintoii* and rice straw mulch effectively decreased soil temperatures. Plastic mulch produces a greater temperature effect than rice straw mulch, because plastic mulch has no pores for water movement and the black-coloured plastic absorbs more light from the sun (Samad, 2014). In our research, the tuber yield in rice straw mulch was 9.4% and 8.0% greater than that of bare soil in 2013 to 2014 and 2014 to 2015, respectively (Table 6). Higher yields were observed in other reports (Kar and Kumar, 2007; Samad et al., 2014), which might be due to the conservation of soil moisture and favourable soil temperatures.

In both natural and agricultural ecosystems, soil microorganisms play key roles in the recycling of elements, and they are essential for biological processes. Because microorganisms respond to stressful conditions, soil microorganism counts and activity level assessments are useful for estimating the soil's fertility. Here, the total amount of bacteria increased, while the fungi and actinomycetes decreased after harvesting compared with before sowing (Table 8). In addition, there was no consistency trend in the microorganismal changes, except the significant decline in total fungal counts under

the white plastic mulch (Table 8). On the contrary, ordinary plastic mulch increased yields led to no significant decreases in the total microbial diversity compared with non-mulched soil (Kapanen et al., 2008; Liu et al., 2012; Chen et al., 2014). However, Continuous plastic-film mulching sowed increasing in microbial activity (Wang et al., 2017). Additional, plastic mulch in asparagus crops induce changes on the incidence and distribution of the mycotoxin deoxynivalenol in soil, and also on the mycobiome abundance and diversity, with a positive selection of *Fusarium* species at the root zone (Muñoz et al., 2015). However, mulching changed other soil fertility associated properties. The content of available nitrogen was significantly increased by rice straw mulch in both growing seasons, and no tillage was beneficial to releasing straw nitrogen. The contents of available phosphorus and potassium significantly increased under mulching compared with non-mulching in the 2013 to 2014 growing season, while in the 2014 to 2015 growing season, the contents of the available phosphorus and potassium decreased significantly under rice straw and white plastic mulch, respectively (Table 7). The two year experimental period was too short to determine any well-regulated changes. To understand the environmental and agronomic effects of mulching, comparative and long-term agronomic assessments need to be conducted (Steinmetz et al., 2016).

Conclusion

In our study, black plastic mulch increased the soil temperature and was more suitable for potato emergence and tuber bulk in winter potato production in South China. Furthermore, the emergence rate, and above- and under-ground biomass, also increased. Finally, potato yields were significantly increased. Therefore, mulching with black plastic film is an effective farming practice for winter potato production in the Typical Pearl River Delta Plain of south China, or other typical sub-tropical monsoon regions with similar climate.

Acknowledgements. We thank Dr. Jing Lǚ for comments and revisions on an earlier version of the manuscript. The experiments comply with the current laws of the China. This study was funded by the Science and Technology Planning Project of Guangdong Province (2017B020203002 , 2016A020207002, 2017A020208021); the Technology Research and Development Subsidies Project of Department of Finance of Guangdong Province (639) to YueCaiGong in 2015; and the Scientific Research Special Fund of Public Welfare Industry (Agriculture) (201503123-03), the Develop Grain Production Project of Guangdong Province (27) to YueNongJi in 2017.

REFERENCES

- [1] Anikwe, M. A. N., Mbah, C. N., Ezeaku, P. I., Onyia, V. N. (2007): Tillage and plastic mulch effects on soil properties and growth and yield of cocoyam (*Colocasia esculenta*) on an ultisol in southeastern Nigeria. – Soil & Tillage Research 93: 264-272.
- [2] Baghour, M., Moreno, D. A., Hernández, J., Castilla, N., Romero, L. (2002): Influence of root temperature on uptake and accumulation of Ni and Co in potato. – Journal of Plant Physiology 159: 1113-1122.
- [3] Chen, Y., Wen, X., Sun, Y., Zhang, J., Wu, W., Liao, Y. (2014): Mulching practices altered soil bacterial community structure and improved orchard productivity and apple quality after five growing seasons. – Scientia Horticulturae 172: 248-257.

- [4] Delden, A. V., Pecio, A., Haverkort, A. J. (2000): Temperature response of early foliar expansion of potato and wheat. – *Annals of Botany-London* 86: 355-369.
- [5] Díaz, J. C. (2002): Colored plastic film mulches affect tomato growth and yield via changes in root-zone temperature. – *Journal of the American Society for Horticultural Science* 127: 127-135.
- [6] Díaz-Pérez, J. C. (2009): Root zone temperature, plant growth and yield of broccoli [*Brassica oleracea* (Plenck) var. *italica*] as affected by plastic film mulches. – *Scientia Horticulturae* 123: 156-163.
- [7] Díaz-Pérez, J. C., Phatak, S. C., Giddings, D., Bertrand, D., Mills, H. A. (2005): Root zone temperature, plant growth, and fruit yield of tomatillo as affected by plastic film mulch. – *Hortscience* 40: 1312-1319.
- [8] Du, S., Gao, X. Z., Li, H. F., Lu, R. H., Jiang, Q. Q. (2004): Determination of exchangeable potassium and no-exchangeable potassium content in soil. – *NY/T889-2004*:1-3.
- [9] Duan, X. Y., Yang, R. R., Lv, Y. H., Zhang, X. F., Xie, H., Liu, X. L., Zhao, L. (2007): Determination of soil available nitrogen. – *DB13/T 843-2007*:1-3.
- [10] Dvořák, P., Tomášek, J., Kuchtová, P., Hamouz, K., Hajšlová, J., Schulzová, V. (2012): Effect of mulching materials on potato production in different soil-climatic conditions. – *Romanian Agricultural Research* 29: 201-209.
- [11] Ghosh, P. K., Dayal, D., Bandyopadhyay, K. K., Mohanty, M. (2006): Evaluation of straw and polythene mulch for enhancing productivity of irrigated summer groundnut. – *Field Crops Research* 99: 76-86.
- [12] Hay, R. K. M., Allen, E. J. (1978): Tuber initiation and bulking in the potato under tropical conditions: the importance of soil and air temperature. – *Tropical Agriculture, Trinidad* 55: 289-296.
- [13] Hou, X. Y., Wang, F. X., Han, J. J., Kang, S. Z., Feng, S. Y. (2010): Duration of plastic mulch for potato growth under drip irrigation in an arid region of Northwest China. – *Agricultural and Forest Meteorology* 150: 115-121.
- [14] Ibarra-Jiménez, L., Lira-Saldivar, R. H., Valdez-Aguilar, L. A., Río, J. L. D. (2011): Colored plastic mulches affect soil temperature and tuber production of potato. – *Acta Agriculturae Scandinavica Section B-Soil and Plant Science* 61: 365-371.
- [15] Jiao, R. Z., Dong, Y. H., Sun, Q. W. (2015): Phosphorus determination methods of restsoils. – *LY/T 1232-2015*:6-12.
- [16] Johnie, R. S., Josiah, W. W. (1998): Modifying heat unit accumulation with contrasting colors of polyethylene mulch. – *Hortscience A Publication of the American Society for Horticultural Science* 33: 210-214.
- [17] Kapanen, A., Schettini, E., Vox, G., Itävaara, M. (2008): Performance and environmental impact of biodegradable films in agriculture: A field study on protected cultivation. – *Journal of Polymers and the Environment* 16: 109-122.
- [18] Kar, G. (2003): Tuber yield of potato as influenced by planting dates and mulches. – *Journal of Agrometeorology* 5: 60-67.
- [19] Kar, G., Kumar, A. (2007): Effects of irrigation and straw mulch on water use and tuber yield of potato in eastern India. – *Agricultural Water Management* 94: 109-116.
- [20] Li, F. M., Guo, A. H., Hong, W. (1999): Effects of clear plastic film mulch on yield of spring wheat. – *Field Crops Research* 63: 79-86.
- [21] Li, F. M., Wang, J., Xu, J. Z., Xu, H. L. (2004): Productivity and soil response to plastic film mulching durations for spring wheat on entisols in the semiarid Loess Plateau of China. – *Soil & Tillage Research* 78: 9-20.
- [22] Liu, C. A., Jin, S. L., Zhou, L. M., Jia, Y., Li, F. M., Xiong, Y. C., Li, X. G. (2009): Effects of plastic film mulch and tillage on maize productivity and soil parameters. – *European Journal of Agronomy* 31: 241-249.

- [23] Liu, Y., Lin, M., He, X., Gang, C., Ma, X., An, L., Feng, H. (2012): Rapid change of AM fungal community in a rain-fed wheat field with short-term plastic film mulching practice. – *Mycorrhiza* 22: 31-39.
- [24] Liu, Y., Yang, H. S., Li, Y. F., Yan, H. J., Li, J. S. (2017): Modeling effects of plastic film mulching on irrigated maize yield and water use efficiency in sub-humid Northeast China. – *International Journal of Agricultural & Biological Engineering* 10(5): 69-84.
- [25] Mahmood, M. M., Farooq, K., Hussain, A., Sher, R. (2002): Effect of mulching on growth and yield of potato crop. – *Asian Journal of Plant Sciences* 1:132-133.
- [26] Martin, J. P. (1950): Use of acid, rose bengal and streptomycin in the plate method for estimating soil fungi. – *Soil Science* 69: 215-232.
- [27] Muñoz, K., Schmidt-Heydt, M., Stoll, D., Diehl, D., Ziegler, J., Geisen, R., Schaumann, G. E. (2015): Effect of plastic mulching on mycotoxin occurrence and mycobiome abundance in soil samples from asparagus crops. – *Mycotoxin Research* 31: 191-201.
- [28] Pat, B., Brenda, F. (2002): Response of plasticultured bell pepper to staking, irrigation frequency, and fertigated nitrogen rate. – *Horticultural Science* 37: 95-100.
- [29] Ramakrishna, A., Tam, H. M., Wani, S. P., Long, T. D. (2006): Effect of mulch on soil temperature, moisture, weed infestation and yield of groundnut in northern Vietnam. – *Field Crops Research* 95: 115-125.
- [30] Romic, D., Romic, M., Borosic, J., Poljak, M. (2003): Mulching decreases nitrate leaching in bell pepper (*Capsicum annuum* L.) cultivation. – *Agricultural Water Management* 60: 87-97.
- [31] Ruízmachuca, L. M., Ibarrajiménez, L., Valdezaguilar, L. A., Robledotorres, V., Benavidesmendoza, A., Fuente, C. D. L. (2014): Cultivation of potato – use of plastic mulch and row covers on soil temperature, growth, nutrient status, and yield. – *Acta Agriculturae Scandinavica Section B-Soil and Plant Science* 65: 30-35.
- [32] Samad, S., Mustafa, M., Baharuddin, Rampisela, D. A. (2014): The effect of mulch and fertilizer on soil temperature of a potato growth. – *International Journal of Agriculture Systems* 1: 91-102.
- [33] Steinmetz, Z., Wollmann, C., Schaefer, M., Buchmann, C., David, J., Tröger, J., Muñoz, K., Frör, O., Schaumann, G. E. (2016): Plastic mulching in agriculture. Trading short-term agronomic benefits for long-term soil degradation? – *Science of the Total Environment* 550: 690-705.
- [34] Triki, M. A., Priou, S., Mahjoub, M. E. (2001): Effects of soil solarization on soil-borne populations of *Pythium aphanidermatum* and *Fusarium solani* and on the potato crop in Tunisia. – *Potato Research* 44: 271-279.
- [35] Vos, J. G. M., Uhan, T. S., Sutarya, R. (1995): Integrated crop management of hot pepper (*Capsicum spp.*) under tropical lowland conditions: Effects of rice straw and plastic mulches on crop health. – *Crop Protection* 14: 445-452.
- [36] Wang, F. X., Feng, S. Y., Hou, X. Y., Kang, S. Z., Han, J. J. (2009): Potato growth with and without plastic mulch in two typical regions of Northern China. – *Field Crops Research* 110: 123-129.
- [37] Wang, F. X., Wu, X. X., Shock, C. C., Chu, L. Y., Gu, X. X., Xue, X. (2011a): Effects of drip irrigation regimes on potato tuber yield and quality under plastic mulch in arid Northwestern China. – *Fuel & Energy Abstracts* 122: 78-84.
- [38] Wang, F. X., Xiu, X. W., Clinton, C. S., Chu, L. Y., Gu, X. X., Xue, X. (2011b): Effects of drip irrigation regimes on potato tuber yield and quality under plastic mulch in arid Northwestern China. – *Field Crops Research* 122: 78-84.
- [39] Wang, L., Li, X. G., Lv, J., Fu, T. T., Ma, Q. J., Song, W. Y., Wang, Y. P., Li, F. M. (2017): Continuous plastic-film mulching increases soil aggregation but decreases soil pH in semiarid areas of China. – *Soil & Tillage Research* 167:46-53.
- [40] Wang, X. L., Li, F. M., Jia, Y., Shi, W. Q. (2005): Increasing potato yields with additional water and increased soil temperature. – *Agricultural Water Management* 78: 181-194.

- [41] Wolf, S., Marani, A., Rudich, J. (1990): Effects of temperature and photoperiod on assimilate partitioning in potato plants. – *Annals of Botany-London* 66: 513-520.
- [42] Wollum, A. G. (1982): Cultural Methods for Soil Microorganisms. – In: Page, A. L., Miller, R. H., Keeney, D. R. (eds.) *Methods of Soil Analysis. Part 2. Chemical and Microbiological Properties*. American Society of Agronomy, Madison, WI.
- [43] Zhang, F., Zhang, W., Qi, J., Li, F. M. (2017b): A regional evaluation of plastic film mulching for improving crop yields on the loess plateau of china. – *Agricultural & Forest Meteorology* 248: 458-468.
- [44] Zhang, Y. L., Wang, F. X., Shock, C. C., Yang, K. J., Kang, S. Z., Qin, J. T., Li, S. E. (2017a): Influence of different plastic film mulches and wetted soil percentages on potato grown under drip irrigation. – *Agricultural Water Management* 180:160-171.
- [45] Zhao, H., Xiong, Y. C., Li, F. M., Wang, R. Y., Qiang, S. C., Yao, T. F., Mo, F. (2012): Plastic film mulch for half growing-season maximized WUE and yield of potato via moisture-temperature improvement in a semi-arid agroecosystem. – *Agricultural Water Management* 104: 68-78.
- [46] Zhao, H., Wang, R. Y., Ma, B. L., Xiong, Y. C., Qiang, S. C., Wang, C. L., Liu, C. A., Li, F. M. (2014): Ridge-furrow with full plastic film mulching improves water use efficiency and tuber yields of potato in a semiarid rainfed ecosystem. – *Field Crops Research* 161: 137-148.
- [47] Zhou, L. M., Jin, S. L., Liu, C. A., Xiong, Y. C., Si, J. T., Li, X. G., Gan, Y. T., Li, F. M. (2012): Ridge-furrow and plastic-mulching tillage enhances maize–soil interactions: Opportunities and challenges in a semiarid agroecosystem. – *Field Crops Research* 126: 181-188.

BIO-CONTROL OF *MICROCYSTIS AERUGINOSA* BLOOM USING VARIOUS AQUATIC ORGANISMS BY DUAL STABLE ISOTOPE (^{13}C AND ^{15}N) TRACERS

KIM, M. S.¹ – KWON, J. T.² – LEE, Y.³ – HA, S. Y.⁴ – HONG, S.⁵ – YOON, S. H.¹ – SHIN, K. H.^{6*}

¹*Department of Fundamental Environment Research, Environmental Measurement & Analysis Center, National Institute of Environmental Research, Incheon 22689, Republic of Korea*

²*Monitoring and Analysis Division, Geum River Basin Environmental Office, Ministry of Environment, Republic of Korea*

³*Marine Ecosystem and Biological Research Center, Korea Institute of Ocean Science and Technology, Busan 49111, Republic of Korea*

⁴*Division of Polar Ocean Science, Korea Polar Research Institute Incheon 21990, Republic of Korea*

⁵*Department of Ocean Environmental Sciences, Chungnam National University, Daejeon 34134, Republic of Korea*

⁶*Department of Marine Sciences and Convergent Technology, Hanyang University Ansan 15588, Republic of Korea*

**Corresponding author*

e-mail: shinkh@hanyang.ac.kr; phone: +82-31-400-5536; fax: +82-31-416-6173

(Received 7th Aug 2017; accepted 15th Jan 2018)

Abstract. The application of ^{13}C and ^{15}N labeled phytoplankton makes it possible to directly follow the pathway and transfer of food source (cyanobacteria) into consumers (aquatic organisms), in contrast to past studies where only changes in compositions of chlorophyll-*a*, clarity, and nutrients were taken as the evidence for these processes. To evaluate the effect of biocontrol by aquatic organisms (aquatic plants; *Iris pseudoacorus*, filter feeder bivalve; *Sinanodonta arcaeformis*, and *Unio douglasiae*, macroinvertebrate; *Caridina denticulate*, carnivore fish; *Pseudobagrus fulvidraco*, *Odontobutis platycephala*, planktivore fish; *Pseudorasbora parv*, and omnivore fish; *Misgurnus anguillicaudatus*) on large toxigenic cyanobacteria bloom (*Microcystis aeruginosa*) in the freshwater ecosystem, we conducted a biomanipulation test on *in situ* ponds using dual stable isotope tracers (^{13}C and ^{15}N). As a filter feeding bivalve, *S. arcaeformis* could incorporate more toxic cyanobacteria cells than *U. douglasiae*, demonstrating its larger detoxification capacity. Also, macroinvertebrate (*C. denticulate*) continuously assimilated to cyanobacteria species in combination with zooplankton and detritus, probably due to detoxification capacity. Indeed, the aquatic plants (*I. pseudoacorus*) seem to be nutrient uptakes in water column and inhibit to light attenuation, comparing to cyanobacteria species. As a primary consumer of phytoplankton, zooplankton (Copepoda) consumed to small and edible particles which is changed from inedible toxic filamentous cyanobacteria species through the grazing efficiency by aquatic organisms. However, various kinds of fishes hardly feed on toxic cyanobacteria directly. Our result suggests that the native species, like *Sinanodonta sp.* and *C. denticulate*, are very useful bio-control organisms on toxic cyanobacteria bloom rather than carnivore, omnivore and planktivore fish. Furthermore, if an aquatic plant that can not only remove nutrients but also provide habitats to aquatic organisms (zooplankton, bivalves and shrimps) is developed, it can help control toxic cyanobacteria blooms. Therefore, it is considered that the development and establishment of habitat of useful organisms is very necessary for water quality improvement. Our biomanipulation technique may provide a key tool for efficient management and restoration of eutrophied reservoirs.

Keywords: *bio-control, toxic cyanobacteria, Microcystis aeruginosa, stable isotope tracer, water management*

Introduction

Eutrophication in freshwater environment is a worldwide problem resulting in extensive blooms of blue-green algae including freshwater cyanobacteria (Beklioglu, 1999). It is well known that some freshwater cyanobacteria (i.e. *Microcystis*, *Anabaena* and *Oscillatoria*) may produce a wide range of toxins (cyanotoxins) as well as secondary metabolites under certain conditions of growth and environment factors (Figueiredo et al., 2004). Its potential toxicity including microcystins (Watanabe et al., 1992), cause a harmful effect to aquatic ecosystem, and decrease the biodiversity by eliminating other phytoplankton species (Bouvy et al., 2000), and can be harmful to many kinds of aquatic organisms including cladocerans (Boon et al., 1994; Matveev et al., 1994), copepods (Koski et al., 1999), shrimps (Engstrom et al., 2001; Kim et al., 2017a), bivalves (Bontes et al., 2007; Kim et al., 2017b) and fishes (Mohamed et al., 2003). To prevent toxic effect of cyanobacteria bloom in freshwater ecosystem, many countries have investigated for a long time (Perrow et al., 1997; Mehner et al., 2004). There are two accepted strategies for the control of water quality in nutrient-rich freshwater ecosystems (Wium-Anderson et al., 1982), which are to reduce the external nutrient load and to manipulate phytoplankton biomass through biological treatment in large water body, such as lakes and reservoirs (Carpenter et al., 1995). To control the external nutrient load is often expensive, it is difficult to obtain the positive results (Braband et al., 1990), while biomanipulation techniques which increase biomass of zooplankton through reduction of planktivorous fishes by 'top-down' cascade showed significant effect (Shapiro et al., 1975). However, many researchers dispute to control of algal biomass with grazing by zooplankton, especially under toxic cyanobacteria blooms (Bernardi and Giussani, 1990; Degans and Meester, 2002). In such circumstances, and progressive biomanipulation approach, based on the direct control of phytoplankton by filter feeding planktivorous fish appears to be more effective (Smith, 1985; Miura, 1990; Drenner et al., 1987). It has proved that filter-feeding fish, such as silver carp (*Hypophthalmichthys molitrix*), bighead carp (*Artocarpus nobilis*) and tilapia (*Oreochromis niloticus*), are effective candidates for bio-control of plankton communities to eliminate cyanobacteria, through suppress to phytoplankton for prey as well as zooplankton (Starling, 1993; Xie and Yang, 2000; Lu et al., 2002; Lu et al., 2006). However, these filter-feeding fishes are not common fishes in many countries, such as Korea and Japan, even though most intensively cultured fish species in Asia and comprise much of the production of Chinese and America aquaculture (Liang et al., 1981). On the contrary, An et al. (2009) and Kim et al. (2017a) argued that filter-feeding macroinvertebrate (*Caridina denticulate*) as native species can easily reduce to blue-green algae than planktivore fishes, as a result, cyanobacteria accumulations might constitute up to 69% of biomass carbon in freshwater atyid shrimp (*Peristemia australiensis*) (Piloa et al., 2008). In addition, the use of bivalve species (Unionids) which contribute to bio-control of eutrophication through bio-filter effectiveness by reducing algal biomass (Reeders et al., 1990; Soto et al., 1999; Kim et al., 2017b) are probably more suitable for shallow lake which mainly consist of soft substrate (mixture of mud and sand) instead of zebra mussel which requires hard substrate for settlement, with their high filtration rates on phytoplankton have been promoted as a tool in biomanipulation of lakes (Reeders et al., 1990). Also, aquatic plants are themselves part of the food web, and could be control massive algae bloom through competing for nutrients and other resources with phytoplankton and periphyton (Ozimek et al., 1990; van Donk et al., 1993).

Here, we compared assimilation efficiency of newly candidates aquatic organism as a bio-control, such as macroinvertebrate filter feeder (*C. denticulate*), bio-filter bivalve (*Unio douglasiae*, *Sinanodonta arcaiformis*) and aquatic plant (*Iris pseudoacorus*), instead of famously bio-control planktivore fish (*H. molitrix*, *A. nobilis* and *O. niloticus*) under massive toxic cyanobacteria (mostly *Microcystis aeruginosa* and *Anabena spirodides*) bloom using dual stable isotope tracers (^{13}C and ^{15}N). Also, we investigated other planktivore fish (*Pseudorasbora parva*) as a bio-control, omnivore fish (*Misgurnus anguillicaudatus*) as a benthic scavenger, carnivore fish (*Pseudobagrus fulvidraco*, *Odontobutis platycephala*) as a regulating of other fish and macroinvertebrate biomass. The labeling isotope technique could be a possible method for tracking their fates in the natural biota, with involving energy sources and pathways (Peterson and Fry, 1987; Parker et al., 1989). The applications of ^{13}C - and ^{15}N -labeled phytoplankton make it possible to directly follow the assimilation pathways of carbon and nitrogen in aquatic organisms, in contrast to previous studies which only monitored changes in environmental conditions such as Chl. *a*, nutrients, turbidity and MC concentration (Benndorf et al., 1990; Jeppesen et al., 1997; An et al., 2010). This is the first study, to evaluate the bio-control efficiency through various candidate organisms under massive toxic cyanobacteria blooms in artificial pond using dual stable isotope tracers (^{13}C and ^{15}N).

Materials and methods

Experimental design for artificial pond

An artificial small pond is located in Sukmoon wetland (36°57'4"N, 126°37'5"E) at mid western region of South Korea (Fig. 1). The enclosure small ponds including muddy sediment consisted of two series of individual capacity 100 ton (size 10 × 5 × 2 m), having a reference and manipulated ponds (Fig. 1):

1. Reference pond (RP, in situ water containing massive biomass of *M. aeruginosa* and *A. spirodides*)
2. Manipulated pond (MP, in situ water containing massive biomass of *M. aeruginosa* and *A. spirodides* and aquatic organisms (bivalve ; *U. douglasiae*, *S. arcaiformis*, macroinvertebrate filter feeder; *C. denticulate*, carnivore fish ; *P. fulvidraco*, *O. platycephala*, planktivore fish; *P. parva*, omnivore fish ; *M. anguillicaudatus*, floating aquatic plant; *I. pseudoacorus*)

The candidate organisms were captured from agricultural reservoirs using hand nets (mesh size < 2 × 2 mm), kept for 2 weeks in water tanks and maintained at temperature of 25 ± 1°C, Dissolved Oxygen (DO) levels of 6±1 mg L⁻¹, pH levels of 7~8, and a photoperiod of around 16L:8D. Individuals were starved for 48 h prior to the beginning of experiment. The bivalves were collected by trawling in agricultural reservoir. They were kept in aquaria filled with reservoir water in a layer of sand, and kept at 17~20°C temperature under a 16L:8D regime. Individuals were fasted for 48 h prior to the experiment.

For the in situ pond experiment, the individual numbers of candidate organisms were determined through the preliminary experiments; bivalve *U. douglasiae* and *S. arcaiformis* (5 ind. m⁻²), macroinvertebrate filter feeder *C. denticulate* (3 ind. m⁻²) and carnivore fish *P. fulvidraco* (0.24 ind. m⁻²). The carnivore fish (*O. platycephala*), planktivore fish (*P. parva*) and omnivore fish (*M. anguillicaudatus*) were lived originally in artificial pond.

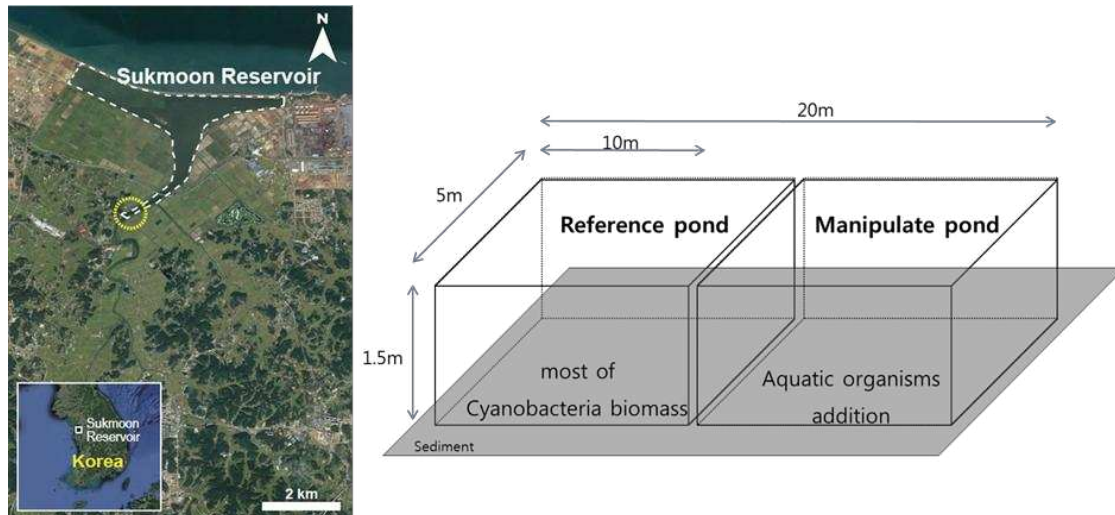


Figure 1. The map shows to small pond experimental station in Sukmoon wetland. The filled circle represents to study site. The experiments were designed as reference pond (most of cyanobacteria biomass) and manipulated pond (aquatic organisms addition ; bivalve (*U. douglasiae*, and *S. arcaiformi*), macroinvertebrate filter feeder (*C. denticulate*), carnivore fish (*P. fulvidraco* and *O. platycephala*), planktivore fish (*P. parva*) and omnivore fish (*M. anguillicaudatus*))

***In situ* artificial pond experiment**

The artificial pond experiment was conducted while the massive toxic cyanobacteria bloom occurred, contributing to around 89% of cyanobacteria biomass during experimental period. The enclosures were filled by pumping the lakes water which mostly contained toxic cyanobacteria species. Each enclosure was maintained for two days to stabilize the water condition. As isotope tracers, NaHCO_3 (Isotech; $^{13}\text{C} > 99\%$) and $(\text{NH}_4)_2\text{SO}_4$ (Isotech; $^{15}\text{N} > 99\%$) were added to each pond, and maintain for a day. ^{13}C content of the dissolved inorganic carbon (DIC) pool was increased up to about 5% and ^{15}N content of the ammonium pool was also enriched up to about 10%. The aquatic organisms (*I. pseudoacorus*, *C. denticulate*, *P. fulvidraco*, *U. douglasiae* and *S. arcaiformis*) were added into manipulate pond. The samples of water and aquatic organisms were collected at the 1st, 2nd, 3rd, 4th, 5th, 6th, 8th, 10th, 13th, 16th and 21nd day after addition.

Analysis of water quality parameters

Two replicate of water samples were collected to determine the concentrations of dissolved inorganic nitrogen (DIN : NH_4^+ , $\text{NO}_3^- + \text{NO}_2^-$) and phosphate (PO_4^{3-}) in each pond. The concentrations of DIN and phosphate were measured by standard colorimetric techniques following the methods of Strickland and Parsons (1964) using UV-spectrophotometer (Cary 50). Chl-*a* concentration was determined by using a fluorescence spectrophotometer (Turner Design, 10R) after extraction with 90% acetone for 24 h. Water temperatures were measured using a multi-parameter water quality sensor (YSI Environmental Monitoring System 660, USA). All environmental parameters including nutrients, chlorophyll-*a* (Chl-*a*) and water temperature were monitored during the experimental period.

Enumeration and biomass determination of phytoplankton and zooplankton

Water samples for enumeration of phytoplankton cells were sedimented for 24 h, and a known volume of the concentrated sample was placed in a Sedgewich-Rafter counting chamber, where at least 300 cells were counted under 200-400× magnification. It is difficult to count some taxa (e.g., *Microcystis sp.*) as individual cell bases; thus, they were enumerated only as larger units. Phytoplankton cell density was determined on the basis of geometric solids that closely approximated each cell or colony shape (Wetzel and Likens, 1991). In addition, we selected to specific zooplankton taxa (copepoda) under microscope using micro-pipette, and placed on combusted 25 mm GF/F filter, and kept at -20°C refrigerator.

Analysis of stable isotope ratio

For analyzing C and N stable isotope ratio of particulate organic matter (mostly phytoplankton), water samples were passed into 20 µm size mesh to remove zooplankton, and remaining water samples filtered through pre-combusted (450°C, 24 h) glass fiber filters (GF/F Whatman) using gentle vacuum filtration. Zooplankton were collected with micropipette under a microscope, and filtered on pre-combusted (450°C, 5 h) glass fiber filters (GF/F Whatman) before freezing. All filters were fumed for 24 h with saturated hydrochloric acid (HCl) to remove inorganic carbon and dried completely using freeze drier. The biota sampling was carried out using hand nets (mesh size 2 × 2 mm) in manipulate pond. The bivalve samples were dissected in order to separate the digestive gland, stomach, muscle (abductor), gill and mantle. The macroinvertebrate and fish samples were divided into muscle and digestive gland. The plant samples were separated into leaf and root. All tissue samples were freeze-dried and then ground to a fine powder using grinder (FRITSCH-planetary mono mill, Pulverisette 6, Germany). The freezing and storage processes do not affect δ¹³C and δ¹⁵N values of biota tissue (Kim et al., 2013). Homogenized powder samples were decalcified with 1N HCl for at least 24 h to remove possible carbonates. But subsamples for δ¹⁵N analysis did not be treated as it has been reported that HCl treatment affect δ¹⁵N values (Kim et al., 2016). After the samples were re-dried using freeze drier, and ground to fine powder which was thoroughly mixed before analysis. Measurements of carbon and nitrogen stable isotopic ratios were performed with a continuous flow isotope ratio mass spectrometer (Isoprime 100; GV Instrument, U.K.) which coupled to an elemental analyzer (Vario Microcube, U.K.). Isotopic ratios were presented as δ values (‰) expressed relative to the Vienna PeeDee Belemnite (VPDB) standard and to atmospheric N₂ for carbon and nitrogen, respectively. Reference materials were IAEA-CH6 (δ¹³C = -10.45 ± 0.04‰) and IAEA-N1 (δ¹⁵N = 0.4 ± 0.2‰). The analytical precision was within 0.2‰ and 0.5‰ for carbon and nitrogen respectively. Isotope ratios were reported in per mil (‰) using standard delta notation (*Eq. 1*):

$$\delta X = \left\{ \left(R_{\text{sample}} - R_{\text{std}} \right) / R_{\text{std}} \right\} \times 1000 (\text{‰}) \quad (\text{Eq. 1})$$

where X = ¹³C or ¹⁵N, R = ¹³C/¹²C or ¹⁵N/¹⁴N, and std (standard) = Vienna Peedee Belemnite (VPDB) for carbon or air N₂ for nitrogen, respectively.

For this study, the δ -values were converted to atom %, which is more appropriate for labelled samples. Conversion was done according to *Equation 2*:

$$A \text{ (atom \%)} = 100 / \left[1 / \left\{ (\delta \text{ sample} / 1000 + 1) \times a_{\text{ns}} \right\} + 1 \right] \quad (\text{Eq. 2})$$

a_{ns} for carbon is 0.011180, for nitrogen is 0.0036765.

Determination of MCs concentration

The purification and analysis of MCs were carried out using the methods developed by Harada et al. (1988). For analyzing MCs concentration of the particulate organic matter (mostly phytoplankton, POM), water samples were passed into 20 μm size mesh to remove zooplankton, and remaining water samples filtered through pre-combusted (450°C, 24 h) glass fiber filters (GF/F Whatman) using gentle vacuum filtration. From a sample of freeze-dried *Microcystis* cell material, the MCs were extracted twice with 20 mL of 5% (v/v) acetic acid for 1 h while shaking at 140 rpm. The extract was centrifuged at $12,000 \times g$, and then the supernatant was applied to a C18 cartridge (Sep-Pak; Waters Association, Milford, MA, USA). The cartridge was rinsed with water and 20% methanol in water. The eluate from the cartridge with 90% methanol in water was evaporated to dryness, and the residue was dissolved in 100% methanol. The sample solution was analyzed on an HPLC (Agilent Technologies 1200 series, Santa Clara, CA, USA). The separation was performed on an ODS column (Cosmosil 5C18-AR, 4.6 mm \times 150 mm) reverse-phase column and the mobile phase was a 0.1% formic acid:water solution with constant flow at 1 mL min^{-1} . The MCs were identified by their UV spectra and retention times, and by spiking the sample with purified standards of MC-LR (Sigma, Sigma-Aldrich, Yong In, Korea), MC-YR (Sigma, Sigma-Aldrich, Yong In, Korea) and MC-RR (Sigma, Sigma-Aldrich, Yong In, Korea). MCs concentrations were determined by comparing the peak areas of the test samples with those of the standards available (MC-LR, MC-YR and MC-RR, Sigma, Sigma-Aldrich, Yong In, Korea).

Results

Environmental conditions in artificial pond

Total nitrogen (TN) concentration in reference pond showed higher value than manipulated pond on 3rd day after beginning the experiment, ranging from 1.5 to 1.8 mg/L, because floating aquatic plant continuously take up DIN in water column (*Table 1*). Total phosphorus (TP) concentration in reference pond showed a higher value until 5 days after beginning experiment, but it showed fluctuation since 5 days to end of the experimental period, probably due to resuspension of the phosphorus from sediment through windy turbulence and organisms movement (*Table 1*). Chl-*a* concentration in manipulated pond was dramatically decreased than that in the reference pond after beginning 2nd day, ranging from 257.6 to 15.6 $\mu\text{g/L}$ (*Table 1*). It is indicated that toxic cyanobacteria bloom inhibited by aquatic organisms as their prey. Water temperature showed same pattern both in reference and manipulated pond, with slightly decrease after 23 October (*Table 1*).

Table 1. Analysis of environmental factors and MC concentration (-LR, -RR, -YR) between manipulate pond and reference pond (n = 5, Mean ± S.D.)

Date	Chl.a (µg/L)		Water column DIN (mg/L)		Water column DIP (mg/L)		MC concentration (ug/L)	
	Manipulate pond	Reference pond	Manipulate pond	Reference pond	Manipulate pond	Reference pond	Manipulate pond	Reference pond
Sep. 13	257.6±5.2	217.9±8.1	1.01±0.13	0.83±0.06	0.09±0.004	0.08±0.003	11.29± 2.15	11.21±0.19
Sep. 14	217.5±3.0	218.9±5.0	0.61±0.08	0.91±0.08	0.01±0.000	0.01±0.002	8.87±3.81	13.00± 0.87
Sep. 15	107.8±6.4	223.4±5.2	0.79±0.06	1.59±0.08	0.07±0.002	0.18±0.002	1.41±0.18	24.65±2.97
Sep. 16	115.7±5.0	227.2±5.2	0.76±0.23	1.25±0.26	0.09±0.007	0.12±0.004	3.41±0.33	14.07±1.41
Sep. 17	113.6±5.1	248.8±5.5	0.38±0.07	1.12±0.17	0.01±0.002	0.09±0.000	7.27±0.18	20.30±2.30
Sep. 18	87.2±6.2	166.0±6.4	0.62±0.00	1.08±0.06	0.07±0.007	0.05±0.000	4.92±0.23	13.56±2.53
Sep. 19	46.5 ±7.1	213.2±7.8	0.64±0.13	1.27±0.09	0.08±0.001	0.11±0.001	5.67±0.11	17.54±0.93
Sep. 21	47.8±8.8	213.9±8.2	0.80±0.08	1.45±0.08	0.10±0.001	0.08±0.006	4.65±0.62	13.77±0.58
Sep. 23	23.6±5.6	215.5±5.7	0.84±0.20	1.46±0.06	0.11±0.004	0.07±0.003	5.83±0.05	11.83±1.14
Sep. 26	22.8±5.0	155.7±5.0	0.71±0.17	1.76±0.17	0.09±0.000	0.09±0.002	18.77±1.89	21.27±3.15
Sep. 29	19.0±3.4	189.5±3.8	0.73±0.06	1.67±0.05	0.10±0.000	0.07±0.000	10.48±1.21	24.15±1.38
Oct. 3	15.6±2.1	156.1±2.9	0.93±0.09	1.87±0.21	0.09±0.001	0.10±0.000	5.88±0.53	9.14±0.46

MC concentration of POM

The MC concentrations of the POM in the reference pond and manipulated pond showed remarkable variation (Table 1). Within two days of beginning the experiment, the MC concentration showed a remarkable decrease of the POM in the manipulated pond while the reference pond maintained a relatively constant MC concentration through the end of the experiment. However, those values did increase slightly, possibly due to release from filter feeders as fecal pellets or expelled cyanobacteria cells in water column at last 7 days.

Enumeration and biomass determination of phytoplankton and zooplankton

The relative proportions of phytoplankton species at the beginning of manipulation experiment showed that the most dominant species was cyanophyceae (88.7%), next was bacillariophyceae (7.5%), chlorophyceae (2.6%), cryptophyceae (0.6%), and dinophyceae (0.4%) were followed (Table 2). The cyanophyceae algae (*M. aeruginosa*, *A. spiroides*, *Synechocystis pevalekii*, *Aphanocapsa elachista* and *Chroococcus* sp.) were usually pre-dominant (89% of total phytoplankton biomass) in both pond at the beginning of experiment (Table 2). The cell density of phytoplankton in reference pond maintained similar biomass with small fluctuation during the entire experiment, but those in manipulated pond dramatically decreased (Fig. 2). When the experiment was ended, relative proportion cyanophyceae species in reference pond slightly changed from 88% to 82%, but those in manipulate pond was remarkably decreased from 88% to 21% during the study period (Fig. 2). It might be caused by biomanipulation effects that

the aquatic organisms (zooplankton, bivalve, macroinvertebrate and fishes) reduce to cyanophyceae biomass as a prey, and prevent to decrease the biodiversity by eliminating cyanophyceae species. These results supported that aquatic organisms feeding on the ^{13}C and ^{15}N labeled phytoplankton, resulted in apparently enriched ^{13}C and ^{15}N atom % which was defined as dietary assimilation in their body during study period (Figs. 3, 4 and 5). The rotifer was usually pre-dominant (93% of total zooplankton biomass) in all ponds, next was copepoda (4.6%) and cladocera (2.4%) were followed (Table 3). The cell density of zooplankton dramatically decreased from 12,594 to 795 cells mL^{-1} in manipulated pond than reference pond, ranging from 12,667 to 2,769 cells mL^{-1} , due to aquatic organisms fed on those cells (Fig. 2).

Table 2. Major species and relative proportions (%) of phytoplankton taxa in the initial artificial pond in Sukmoon wetland at the beginning of mesocosm

Class	Species	Cell density (cells mL^{-1})	Relative proportion (%)
Cyanophyceae	<i>Microcystis aeruginosa</i>	53,200	88.72
	<i>Anabena spirodides</i>	9,160	
	<i>Synechocystis pevalekii</i>	2,640	
	<i>Aphanocapsa elachista</i>	1,740	
	<i>Chroococcus sp</i>	1,410	
Chlorophyceae	<i>Secenedemus sp</i>	1,380	2.68
	<i>Staurastrum sp</i>	310	
	<i>Monoraphidium contortum</i>	370	
Cryptophyceae	<i>Cryptomonas erosa</i>	480	0.62
Dinophyceae	<i>Ceratium hirundinella</i>	340	0.44
Bacillariophyceae	<i>Synedra acuse</i>	480	7.53
	<i>Synedra sp</i>	260	
	<i>Navicula sp</i>	300	
	<i>Awlucoseira granulata</i>	2,560	
	<i>Awlucoseira sp</i>	220	
	<i>Nitzschia holsatica</i>	420	
	<i>Cyclotella comta</i>	1,540	

Table 3. Major species and relative proportions (%) of zooplankton taxa in the initial artificial pond in Sukmoon wetland at the beginning of mesocosm

Class	Species	Cell density (cells mL ⁻¹)	Relative proportion (%)
Cladocera	<i>Bosmina longispina</i>	156	2.43
	<i>Diaphanosoma brachyurum</i>	148	
Copepoda	<i>Cyclops strenuous</i>	140	4.66
	<i>Daphnia retrocurva</i>	142	
	<i>Nauplius</i>	301	
Rotifera	<i>Ascomorpha ecaudis</i>	2,621	92.91
	<i>Asplanchna herricki</i>	284	
	<i>Brachionus calyciflorus</i>	128	
	<i>Brachionus diversicornis</i>	346	
	<i>Filinia longiseta</i>	801	
	<i>Filinia terminalis</i>	124	
	<i>Keratella cochlearis</i>	5,014	
	<i>Keratella valga</i>	1,521	
	<i>Polyathra dolichoptera</i>	112	
	<i>Trichocerca birostris</i>	542	
	<i>Trichocerca branchyura</i>	0	
	<i>Trichocerca capucina</i>	38	

¹³C and ¹⁵N atom (%) of POM, Copepoda and aquatic organisms

The ¹³C and ¹⁵N atom % of particulate organic carbon (POC) and particulate organic nitrogen (PON) in POM (mostly phytoplankton) in reference and manipulated ponds showed similar variation trends (Fig. 3). Within one day after addition of the tracers, ¹³C and ¹⁵N atom % were remarkably enriched in the POM through active phytoplankton assimilation, but manipulated pond showed, mostly a little bit, lower atom% value rather than reference pond after 3rd day. However, those values were saturated and declined slightly at the end of time. The incorporated ¹³C and ¹⁵N atom % of copepod after 2nd day in both ponds showed a clear enrichment, demonstrating that copepoda fed the ¹³C and ¹⁵N labeled POM as a diet (Fig. 3). ¹³C and ¹⁵N atom % value in copepod were higher in manipulated than reference pond after 3rd day in beginning experiment, indicating copepoda grazing was larger in manipulated pond.

The incorporation rates of carbon and nitrogen into muscle and digestive gland of the aquatic organisms were calculated based on the increased ¹³C and ¹⁵N atom % through dietary assimilation. Most aquatic organisms showed continuously apparent enrichment of ¹³C and ¹⁵N tracers in their tissues during the experiment period (Figs. 4, 5 and 6). According to different bivalve species, *U. douglasiae* showed 1.08~1.11 ¹³C and 0.36~0.61 ¹⁵N atom % respectively, *S. arcaiformis* showed a 1.08~1.20 ¹³C and 0.36~1.28 ¹⁵N atom % respectively during experimental period in manipulated pond (Figs. 4, 5 and 6). The different atom % might be on account of different

assimilation capacity between two freshwater bivalve species. As a macroinvertebrate, *C. denticulate* showed apparently enrichment of ^{13}C and ^{15}N tracers rather than other species, 1.08~1.24 for ^{13}C atom % and 0.36~1.27 for ^{15}N atom %, demonstrating that those organisms has higher assimilation efficiency to toxic cyanobacteria cells through feeding activity (Figs. 4, 5 and 6). Among the fish species, incorporated ^{13}C and ^{15}N atom % in *M. anguillicaudatus* species showed 1.08~1.12% and 0.36~0.59% respectively, *P. parva* showed 1.08~1.12% and 0.36~0.72% respectively, *P. fulvidraco* showed 1.08~1.12% and 0.36~0.58% respectively, and *O. platycephala* showed 1.08~1.13% and 0.36~0.60% respectively, during study period in manipulated pond (Figs. 4, 5 and 6). The incorporated ^{13}C and ^{15}N atom % among the fishes were various probably due to differential feeding type such as carnivore, planktivore and omnivore. As a floating aquatic plant, *I. pseudoacorus* showed 1.08~1.08 ^{13}C and 0.37~2.13 ^{15}N atom % respectively, during experimental period in manipulated pond (Figs. 4, 5 and 6). *I. pseudoacorus* showed significantly enriched ^{15}N atom %, due to assimilating inorganic nitrogen in water column through its root, however it was hardly enriched ^{13}C atom % because it uptakes carbon dioxide from the atmosphere through its leaf rather than root.

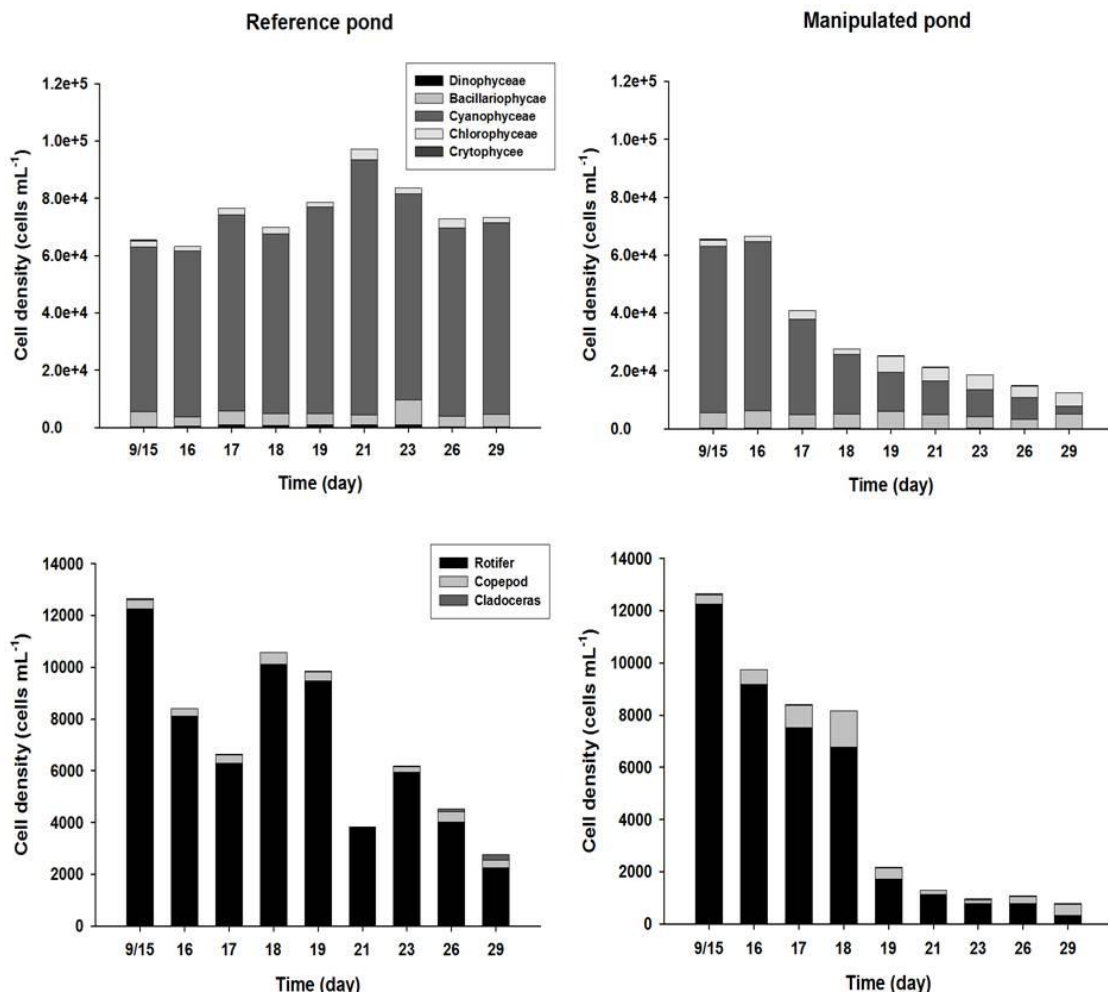


Figure 2. Temporal variation of phytoplankton and zooplankton groups to the each total biomass in the two kinds of ponds (reference and manipulated ponds) during study period

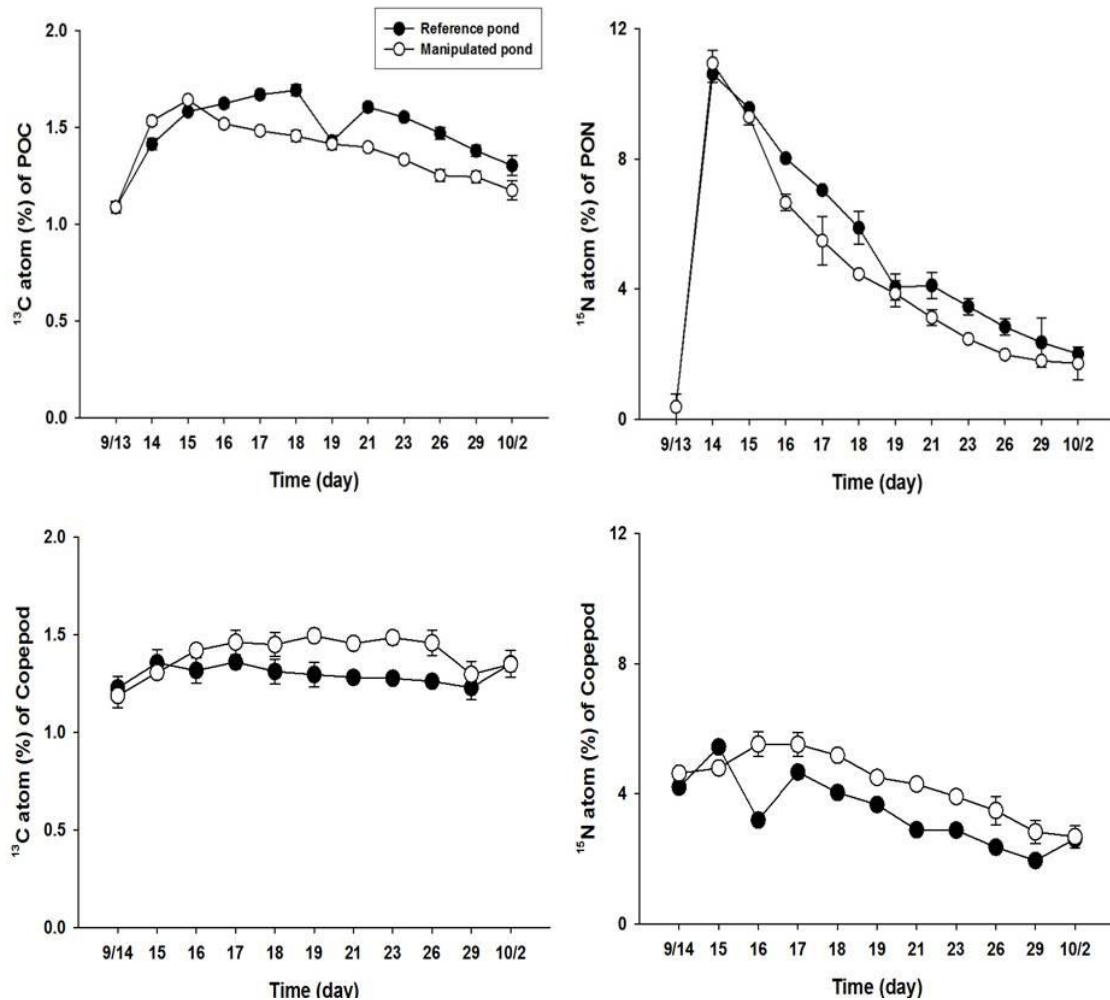


Figure 3. The ^{13}C and ^{15}N atom (%) of POM and Copepod in reference and manipulated ponds during study period

Discussion

Comparing grazing by differential *Sinanodonta bivalve* species

In this study, the incorporated ^{13}C and ^{15}N atom % of aquatic organisms means that newly photosynthesized phytoplankton cells were assimilated into those cells. Even though similar *Sinanodonta* freshwater bivalve species were used, the incorporated ^{13}C and ^{15}N atom % of *U. douglasiae* bivalve showed lower value rather than other bivalves during entire experiment period (Fig. 4).

This result reflects that *U. douglasiae* has smaller capacity to assimilate toxic cyanobacteria derived diet, and affected by the occurrence of toxic-producing cyanobacteria bloom. In this study, we did not determine cyanotoxic compound like microcystin (MC) in aquatic organisms. However, it is well known that cyanobacteria, especially members of the genera *Mycrocystis*, *Anabaena*, *Aphanizomenon* and *Oscillatoria*, produce MC as a common toxic and potentially harmful compound in the freshwater environments (Figueiredo et al., 2004). Relative proportion percent of phytoplankton taxa in this study, *Mycrocystis* and *Anabaena* species consist of 88%. Indeed, hepatoxins like MC are produced by *M. aeruginosa* (Rinehart et al., 1994).

Therefore, two kinds of bivalves as well as aquatic organisms should be influenced by toxic stress through harmful MC compounds in our study. For that reason, we assumed that *U. douglasiae* species could not assimilate any more and excreted their prey in the form of feces and pseudofeces into the water column, demonstrating its limited ability to incorporate toxic-producing cyanobacteria cells, while we found that *S. arcaefomis* bivalves continuously assimilated toxic-producing cyanobacteriacells into their body as a prey, demonstrating its ingestion of those cells (Fig. 4). To explain differential incorporated atom % between each bivalves, toxic cyanobacteria bioaccumulation and tolerance need to be considered (Fig. 4), because toxic cyanobacteria species, likes a *Myrocystis* and *Anabaena*, impact on prey ingestion rate of bivalve (Bontes et al., 2007). Bioaccumulation pattern of cyanobacterial toxins was different according to bivalve species. Yokoyama and Park (2002) reported that MC concentration in *U. douglasiae* was higher than *S. woodiana* and *C. plicata* bivalve, indicating that some kinds of bivalves are quite tolerant to cyanobacterial toxins and are able to depurate these cyanotoxins efficiently. It is known that MC can conjugate with glutathione (GSH) and ultimately degrades to MC-Cys and increase water solubility, consequently reducing the toxicity and enhancing excretion of MC (Kondo et al., 1992). In this study, *S. arcaefomis* bivalves showed higher assimilation rate, comparing to *U. douglasiae* species, it means that they tend to depurate these cyanotoxins efficiently, or excrete to out-interior as a form of feces and pseudofeces rather than *U. douglasiae* species. However, we did not consider excretion without digestion and assimilation because incorporated C and N atom % was continuously enriched in *S. arcaefomis* which means to assimilate toxic cyanobacteria cells as a their prey (Fig. 4). Therefore, it seems that *U. douglasiae* slowly expel the toxic cyanobacteria cells that are not ingested and digested in stomach and digestive gland. Therefore, our results demonstrate that *S. arcaefomis* bivalves would ingest newly photosynthesized toxic cyanobacteria cells into its body, but that it may have an immunological system to depurate toxic microcystin, in contrast to *U. douglasiae*.

In this study, ^{13}C and ^{15}N atom % of five different organs (muscle, digestive gland, mantle, gill and stomach) among the three bivalves were determined during the experimental period. The incorporation rate which means synthesized newly tissue through the isotopically enriched new diet reflects the metabolic breakdown of old tissue synthesized during feeding on a previous diet and its subsequent replacement by tissue synthesized from the new diet. It is widely accepted that enrichment processes are tissue-specific. Raikow and Hamilton (2001) demonstrated that stable isotope enrichment of tissues (gland and muscels) in unionid bivalves reflected short-term and long-term assimilation of nutrients. Furthermore, differences in isotopic ratios for each tissues and turnover rates have been observed in mussel *Pecten maximus* (Lorrain et al., 2002) and *Mytilus galloprovincialis* (Deudero, 2009). In this study, bivalves showed a different isotopic enrichment among the tissues, showing more enriched in the digestive gland and stomach organ during entire experiment period because those organs have relatively faster turnover rate and reflects short-term assimilation records (Raikow and Hamilton, 2001) (Figs. 5 and 6).

Indeed, muscle organ of bivalves showed lower enriched atom % than digestive gland organ because of slower turnover and relatively long-term integration of energy source (Raikow and Hamilton, 2001). The mantle and gills tissues indicated relatively low incorporation rate because these organs have slow turnover rates integrating diet isotopic signatures over a longer time period than other tissues such as digestive gland

which has faster turnover rates (Lorrain et al, 2002). Also, Hill et al. (2009) reported that mantle tissue replaced its carbon isotopes faster than gill parts, while gill tissue was faster than adductor muscle in the mussel *Perna perna* because mantle is the main energy source for sustaining gonadal development.

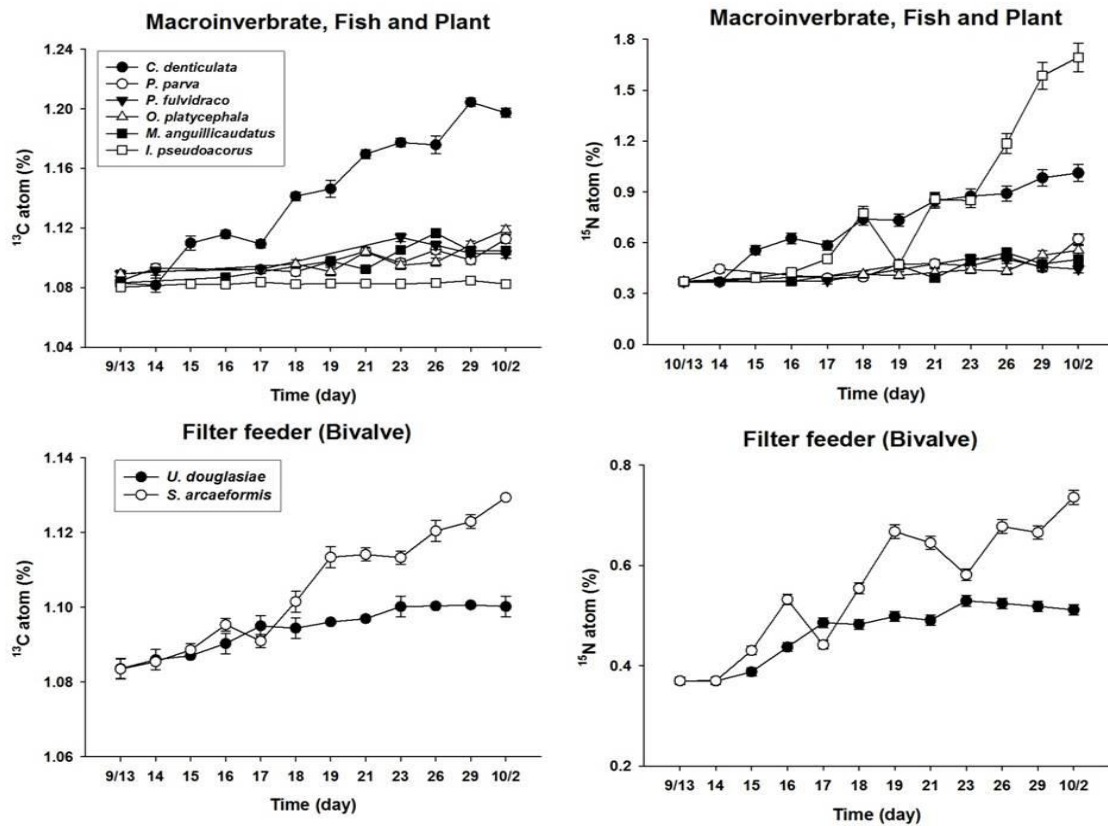


Figure 4. Incorporation of ^{13}C and ^{15}N atom (%) into predator (fish and macroinvertebrate) and plant in manipulated pond during study period

From a management perspective, freshwater bivalves are efficiently filter feeders capable of depleting suspended particles in water column (Kim et al., 2011), so it may be a feasible method for water quality control (Reeders and Bij de Vaate, 1990; Soto and Mena, 1999). Among the freshwater bivalves, the zebra mussels (*D. polymorpha*) showed higher clearance rate in single cells of the *Microcystis* (Baker et al., 1998), a reverse gradient exists between those mussel densities and the cyanobacterial biomass (Ibelings et al., 2003), so those mussels could be used as a potential tool in the biomanipulation of shallow lakes, suffering from harmful cyanobacterial blooms (Reeders and Bij de Vaate, 1990). However non-native mussel species (*D. polymorpha*) threaten native mussel because invasive species often differ greatly from native species in resource use and trophic interactions, they have great potential to negatively affect ecosystems (Naddafi et al., 2007). Therefore, we are sure that for shallow lakes or reservoirs with soft substrates, unionids are better adapted to these habitats than zebra mussels that hard substrate for settlement. For that reason, we recommend the native bivalve species, like unionids, than famously invasion species (*D. polymorpha*) for biomanipulation on harmful cyanobacteria bloom in lakes or reservoirs. Unionid

mussels can filter large amounts of the water column, as long as their biomass is large (Vaughn et al., 2004). However, the research of common native freshwater bivalve (unionid mussels, like *Sinanodonta* sp. and *Unio* sp.), especially toxic cyanobacteria bloom conditions, was very unique except below citation. Therefore, our result is very important information to evaluate bio-control effects. Yokoyama and Park (2002) revealed that *Sinanodonta* bivalves persisted to toxic cyanobacteria bloom and showed lower bioaccumulation patterns of MC, and *Sinanodonta*'s grazing capacity, per individual, is equal or higher than *D. polymorpha* (Bontes et al., 2007). For example, *Sinanodontabivalves* showed $\times 12$ higher efficiencies of clear unit per square meter per unit of water volume than *Dreissena* mussels (Pires et al., 2005; Bontes et al., 2007). *Sinanodonta* bivalves had a larger effect on the primary productivity of toxic cyanobacteria, demonstrating a more realistic achievement for biomanipulation. Also, *Sinanodonta* (*S. arcaefomis* and *S. woodiana*) should incorporate more toxic cyanobacteria cells than *U. douglasiae*, probably due to its larger detoxification capacity (Kim et al., 2017b). As a result, *S. arcaefomis* and *S. woodiana* could be useful organisms to reduce massive toxic cyanobacteria blooms in eutrophic agricultural reservoirs and lakes.

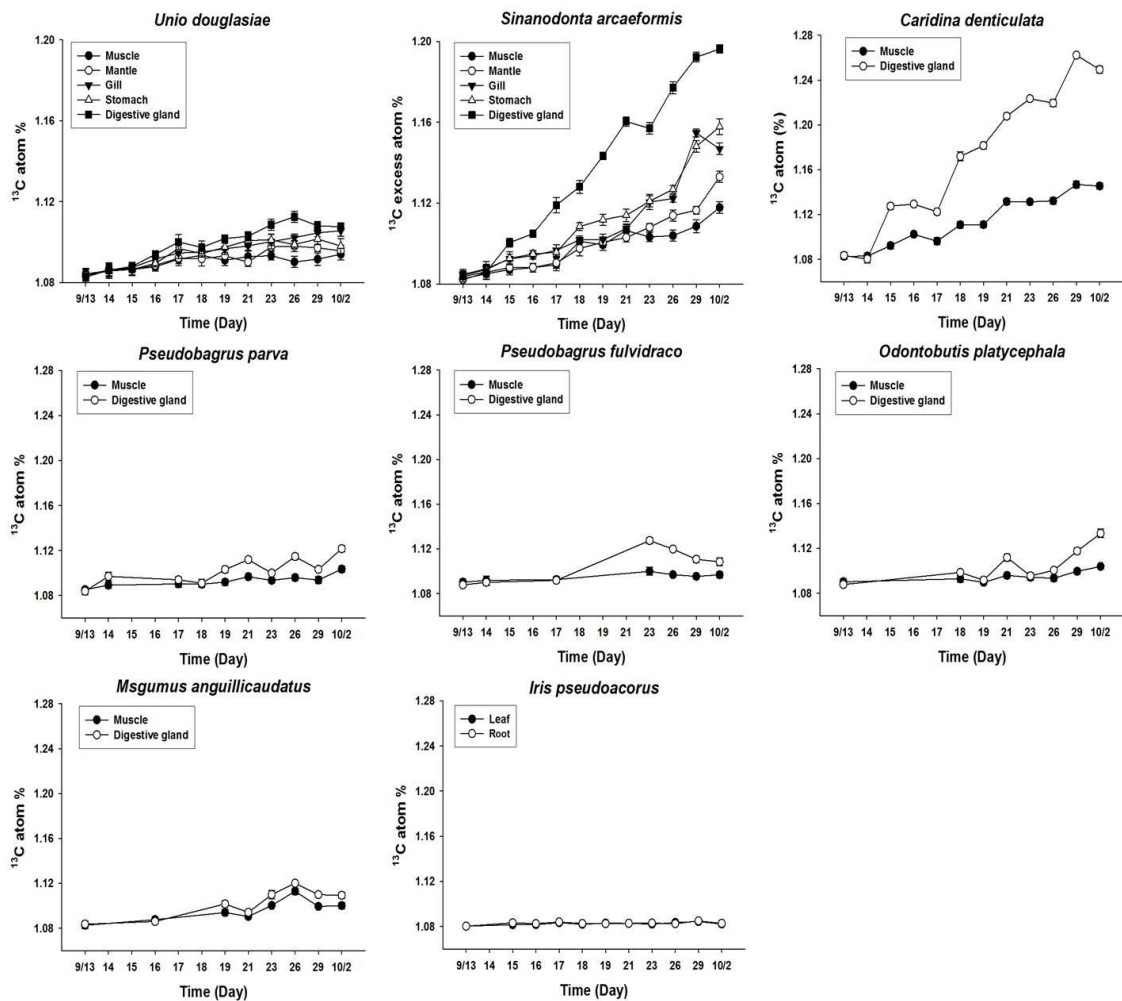


Figure 5. Incorporation of ^{13}C atom (%) into part of aquatic organisms tissue in manipulated pond during study period

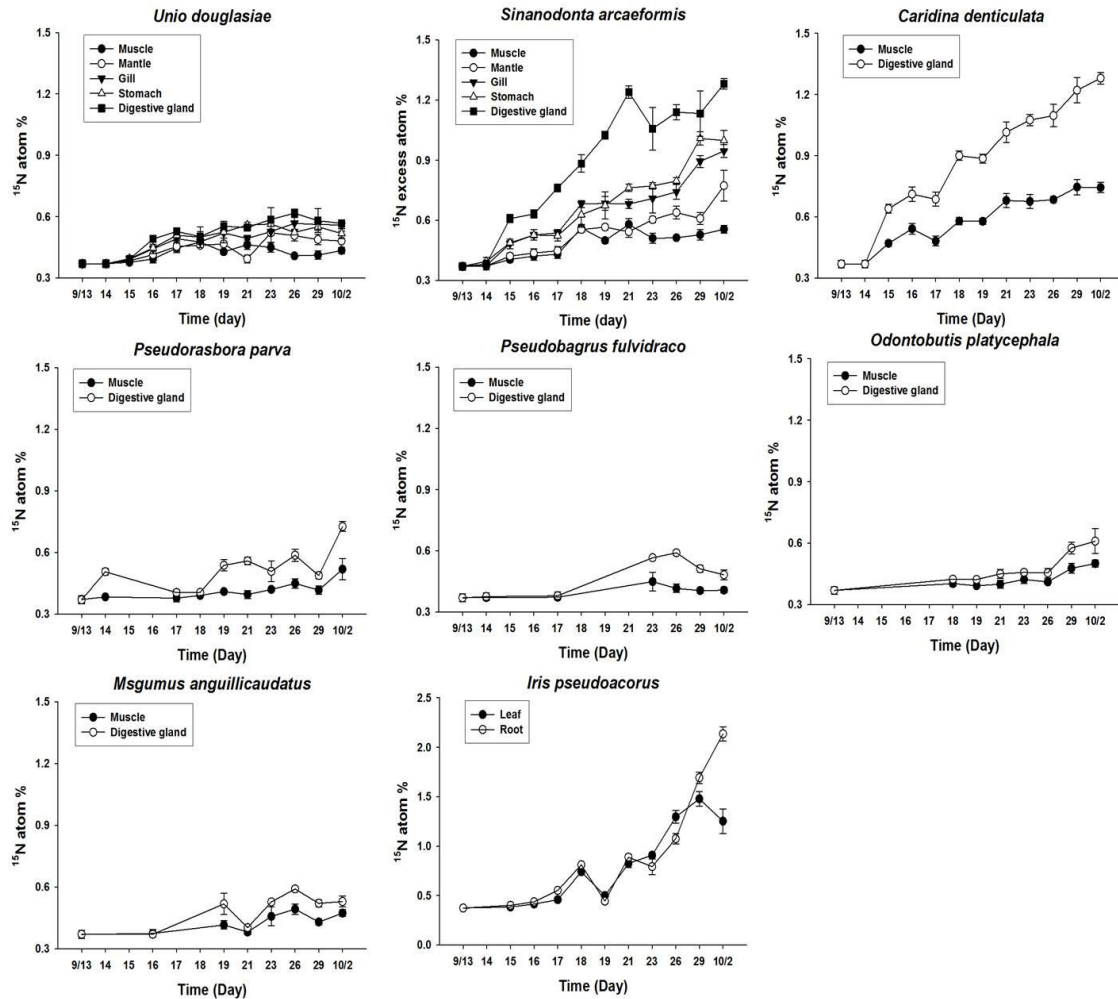


Figure 6. Incorporation of ¹⁵N atom (%) into individually part of aquatic organisms tissue in manipulated pond in Sukmoon wetland during study period

Assimilation correlation between macroinvertebrate and various fish species

In the past study, *C. denticulate* did not easily uptake cyanobacteria as a prey because it contained poor nutrition and toxicity for aquatic invertebrates (Proter and Orcutt, 1980). However, our data appears that *C. denticulate* accumulated large amounts of isotopically enriched ¹³C and ¹⁵N prey cell, comparing to planktivore, omnivore, carnivore fishes and other bivalve species (Fig. 4). The enriched ¹³C and ¹⁵N of *C. denticulate* in our study, we could assume that *C. denticulate* also continuously assimilated enriched cyanobacteria species as a diet. However, we couldn't convince that *C. denticulate* uptake to *M. aeruginosa*, because *C. denticulate* may be to expel the toxic cyanobacteria cells that are not ingested and digested in stomach and digestive gland, in the form of feces and pseudofeces, which is released into the water column. If so be that the *C. denticulate* undigested foods and released into the water column, the ¹³C and ¹⁵N atom % probably highly enriched in digestive gland tissue and slightly enriched in their muscle tissue, due to hardly transport energy from digestive gland to muscle tissue. However, the ¹³C and ¹⁵N atom % of both digestive gland and muscle tissue in *C. denticulate* always clearly enriched until ending of experiment (Fig. 4), it is

indicate that *C. denticulate* fed upon their enriched *M. aeruginosa* through digestion and assimilated energy in their body.

As a food source, cyanobacteria accumulations in *C. denticulate* may not only include the transfer of C and N, but also the transfer of cyanobacteria hepatotoxins or related compounds. Despite toxic cyanobacteria blooms influence aquatic organisms in manipulated pond during the study period, how *C. denticulate* could show the highest ^{13}C and ^{15}N values except aquatic plant for ^{15}N atom % value (Fig. 4). Some reports introduced detoxification that the organism enzymatically can form a conjugate of the hepatotoxin, which helps the organism to survive under cyanobacterial stress (Pflugmacher et al., 1998). This detoxification occurs in various aquatic organisms such as macrophytes, bivalves and fishes (Wiegand et al., 1999). However, toxic inhibition enzyme is still unclear in the macroinvertebrate. Our results may offers new possibility that *C. denticulate* have an immunological system to depurate toxic microcystin, due to actively assimilate toxic cyanobacteria as shown higher ^{13}C and ^{15}N atom % values. Therefore, *C. denticulate* is key-stone taxa that are capable of removing cyanobacteria algal populations. Many research supported our hypothesis that macroinvertebrate was possible for bio-control on massive toxic cyanobacterial bloom through laboratory and field study. An et al. (2010) supported that macroinvertebrates, *C. denticulate* as a same species of our study and *P. paucidens*, were effective candidates for phytoplankton control, compared to fishes in *M. aeruginosa* bloom condition through mesocosm experiment, and Kim et al. (2017a) reported that *C. denticulate* actively assimilated toxic *M. aeruginosa* through stable isotope tracer experiments. Moreover, mysid shrimps (*M. relicta*) showed high survival in the presence of toxic cyanobacteria through laboratory experiment (Engstrom et al., 2002), *M. mixta* didn't showed to increase mortality during experiment period where mysids were exposed to high concentrations of toxic *N. spumigena*, which suggests that they may be tolerant against cyanobacterial toxins (Engstrom et al., 2001). Therefore, we suggest that *C. denticulate* is very effective candidates for inhibiting of toxic cyanobacteria blooms, may be achieve favorable responses, such as a reduction in algal biomass and attainment of clear water.

As a management perspective, it is very important to control cyanobacterial blooms to reduce their harmful effects on aquatic ecosystems. In previously, it has proved that filter-feeding fish, such as silver carp (*H. molitrix*), bighead carp (*A. nobilis*) and tilapia (*O. niloticus*), are effective candidates for bio-control of plankton communities to eliminate cyanobacteria, but it is consider that amount of feces by various fishes were also excreted into water column which leads to excessive nutrient loading problem. Indeed, it has a problem about invasion species and it is difficult to sustain and stabilize fish and zooplankton community through feeding mechanism by biomanipulation, probably owing to the complexity of natural ecosystems. Therefore, we recommend that *C. denticulate*, which is native species, can apply to control toxic cyanobacteria blooms as a newly candidate bio-control species. The *C. denticulate* species could be a useful aquatic organism for bio-control through feeding activity, and are efficient filter feeders capable of depleting suspended particles, including phytoplankton, zooplankton, detritus and other abiotic particles in water column.

Freshwater fishes including *O. platycephla*, *P. fulvidraco* (carnivore fish), *P. parva* (planktivore fish) and *M. anguillicaudatus* (omnivore fish) had a lower atom % value rather than bivalves and macroinvertebrate species (Fig. 5). *P. fulvidraco* and *O. platycephla* species is a carnivore fish in stream in Korea, feeding mainly on insect, invertebrate and small fishes (Han et al., 2001; Iwata et al., 1988). ^{13}C and ^{15}N atom %

of *P. fulvidraco* slightly enriched owing to those consuming ^{13}C and ^{15}N incorporated invertebrate such as *C. denticulate* and zooplankton, but had a lower values than their prey during the entire experimental period. Furthermore, ^{13}C and ^{15}N atom % in *P. fulvidraco* were decreased distinctly after 26th October, while those in *O. platycephala* increased (Fig. 6). *M. anguillicaudatus* as a omnivorous fish is a bottom-dwelling scavenger, feeding mainly on organic material, tubifex worms and other small aquatic organisms (Kim et al., 2002). *P. parva* is a widely distributed planktivore in the littoral zones of freshwater ecosystem in China, Japan and Korea (Masuda et al., 1988). We expected that ^{13}C and ^{15}N atom % of *P. parva* and *M. anguillicaudatus* might be increased during the study period because their prey is mainly enriched phytoplankton or deposition organic matter, but ^{13}C and ^{15}N atom % in *P. parva* slightly increased while it was decreased after 29th October in *M. anguillicaudatus*. These results demonstrate that it slowly assimilate their prey, because toxic microcystins in cyanobacteria may to influence on feeding capacity in fishes. Bioaccumulation of microcystins in fish has been well documented (Malbrouck et al., 2006). Therefore, ^{13}C and ^{15}N atom % of all fishes showed lower assimilation rate, compared to those in bivalve, zooplankton and macroinvertebrate during the entire experimental period. Xie et al. (2005) found that the large amount of microcystins in *H. molitrix* a phytoplanktivorous fish was detected in the intestines, also Specziár et al. (1997) reported that cyanobacteria *M. aeruginosa* was more abundant in phytoplanktivorous than omnivorous fish, since omnivorous fish normally consume zooplankton and detritus. Among the fishes in our study, planktivore and omnivore fishes consumed mainly phytoplankton or organic matter, so they may be affected directly by toxic cyanobacteria. Therefore, we suggest that these fishes couldn't directly control massive algal bloom, even though some filter feeding silver carp and bighead carp (*Aristichthys nobilis*) fishes drastically reduced cyanobacteria (*M. aeruginosa*) bloom (Miura, 1990). In this study, we proposed that in applied biomanipulation, fish reductions may have positive effects on phytoplankton reduction and increased water clarity in dependent of their effects on zooplankton grazing, because they may influence on cyanobacteria bloom through P-supply, due to either by excretion or by sediment bioturbation.

Impact of floating macrophytes on cyanobacteria community

Here, as a floating aquatic plant *I. pseudoacorus* which is a part of the freshwater ecosystem, was added in manipulation pond to reduce cyanobacteria bloom. In this study, *I. pseudoacorus* species showed 1.07~1.08 ^{13}C and 0.37~2.13 ^{15}N atom % respectively, in manipulated pond (Figs. 5 and 6). It was hardly enriched ^{13}C atom % because plant used carbon dioxide from the atmosphere through their leaf. However, it showed higher ^{15}N atom % value (Fig. 4) and decreased TN concentration in manipulated pond because of absorbing the nutrients by *I. pseudoacorus* in water column, thus continuously inorganic nitrogen is accumulated in their leaf and root (Table 1). Macrophytes can assimilate preferential nutrients, like nitrate and phosphate, from the water column, because floating macrophytes maintain a competitive advantage over microalgae through increased nitrogen uptake (Barko and James, 1998). However, nutrient availability in macrophyte beds may depend on both the macrophyte species and density (Sondergaard and Moss, 1998). In this study, the floating *I. pseudoacorus* covered about 10% of the water surface area. So, we consider self-shading effects, especially floating macrophytes, that has been shown to significantly reduce phytoplankton abundance in vegetated areas because of lower light irradiation to the

water column under the floating macrophytes (Ozimek et al., 1990). Also, the chemical substances excreted from macrophytes have long been suspected to suppress phytoplankton growth (Hutchinson, 1975). Some studies have reported that the production and excretion of alleochemicals by aquatic macrophytes may be an effective defense strategy against other photosynthetic organisms, like epiphyton and phytoplankton, in the competition for light and nutrients (Gopal and Goel, 1993). For the above reason, our results assumed that the growth of phytoplankton could be regulated by aquatic plants, which is likely to play an important role in the suppression of phytoplankton biomass, so floating plant (*I. pseudoacorus*) should be possible manipulation to control massive cyanobacteria blooms.

Influence on zooplankton (copepod) feeding process through bio-control

Our data showed that cell density of zooplankton decreased from 12,667 to 2,769 cells mL⁻¹ and from 13,001 to 795 cells mL⁻¹ in reference and manipulated pond, respectively during study period (Fig. 2). The reason for decreasing cell density of zooplankton in reference pond might be toxic cyanobacteria effects which reduce grazing pressure by zooplankton (DeMott et al., 1991), while aquatic organisms such as fishes can influence zooplankton biomass as a prey in manipulated pond. Although the cell density of zooplankton dramatically decreased was in manipulated pond, the ¹³C and ¹⁵N atom (%) of copepoda showed higher value than reference pond (Fig. 3). Why dietary assimilation rate of copepoda in manipulated pond was increased than reference pond even though zooplankton had a pressure by aquatic organisms? The cyanobacteria are inedible prey size, mostly colonial or filamentous, for most species of zooplankton, and only small colonies or dispersed cells of cyanobacteria can be ingested (Jarvis et al., 1987). For this reason, it is generally assumed that aquatic organisms may induce shortened breakage cells of larger filaments of cyanobacteria species through the feeding process, allowing the later consumption of cyanobacteria by zooplankton species. It is well known that each zooplankton species differs in its selective feeding patterns depending mainly on prey size (Pagano et al., 1999). Eventually, there is the possibility of breakage of filaments by some aquatic organisms (e.g., bivalve, macroinvertebrate, various fishes) in this study, which suggests that inedible cyanobacterial filaments may be changed efficiently grazing small size and edible particles by zooplankton species (e.g., copepod). In this study, zooplankton species consumed breaking down of cyanobacteria aggregate even though cyanobacteria has a toxic effect to zooplankton, demonstrating enriched ¹³C and ¹⁵N atom (%) of zooplankton species in manipulated pond. Therefore, bio-control using aquatic organisms could be change shape and size of cyanobacteria aggregates through their feeding activity, thus could change grazing efficiency of zooplankton.

Ecosystemic effects

Methods for the purification of contaminated water using various kinds of organisms are within the category of ecological engineering water quality improvement techniques, including aquatic vascular plants, algae, zooplankton, and fish and shellfish. From the viewpoint of the living organism, the technology of improving the water quality by using organisms is to grow by absorbing the nutrients. However, from the viewpoint of the user, it is possible to expect a more economical, long-term and environmentally friendly effect as compared with the engineering technique. Especially,

development of submerged plants can contribute to the improvement of water quality by not only eliminating nutrients but also by providing habitat useful for zooplankton and invertebrates through feeding on algae. In addition, the installation of the artificial plant island can partially inhibit the light, thereby contributing to the suppression of the occurrence of algae, and has various indirect effects such as an aesthetic point of view. Therefore, it is considered that the development and establishment of habitat of useful organisms is very necessary for water quality improvement. Also water quality improvement through the use of biological food webs is to inhibit algae growth by increasing algae feeding rates using organisms with higher rates of algae feeding (such as bivalves, shrimps, etc.). This will be more effective in connection with the development and installation of the useful biological habitat described above.

Conclusion

As a filter feeding bivalve groups, *S. arcaeformis* has a larger feeding capacity rather than *U. douglasiae* on cyanobacteria bloom condition. Also, macroinvertebrate (*C. denticulate*) continuously assimilated their diet through detoxification for toxic prey quality. Furthermore, aquatic plants (*I. pseudoacorus*) compete nutrients uptakes and light availability with cyanobacteria in the water column. This study assumed that zooplankton (Copepoda) consumed small particles of cyanobacteria which is induced by shortened breakage cells of longer filamentous cyanobacteria by aquatic organism through the grazing behavior. However, various kind of fishes (carnivore; *P. fulvidraco*, *O. platycephala*, planktivore; *P. parva*, omnivore; *M. anguillicaudatus*) hardly feed on toxic cyanobacteria directly. Especially, development of submerged plants can contribute to the improvement of water quality by not only eliminating nutrients but also by providing habitat useful for zooplankton and invertebrates through feeding on algae. Furthermore, if an aquatic plant that can not only remove nutrients but also provide habitats to aquatic organisms (zooplankton, bivalves and shrimps) is developed, it can help control toxic cyanobacteria blooms. Therefore, it is considered that the development and establishment of habitat of useful organisms is very necessary for water quality improvement. Our biomanipulation technique may provide a key tool for efficient management and restoration of eutrophied reservoirs.

Acknowledgements. This work was supported by the National Institute of Environment Research R&D of Korea government (NIER) and National Research Foundation of Korea (NRF) grant funded by the Korea government (MSIP) (NRF-2016R1E1A1A01943004).

REFERENCES

- [1] An, K. G., Lee, J. Y., Kumar, H. K., Lee, S. J., Hwang, S. J., Kim, B. H., Park, S. K., Um, H. Y. (2010): Control of algal scum using top-down biomanipulation approach and ecosystem health assessments for efficient reservoir management. – *Water, Air, and Soil Pollution* 205: 3-24.
- [2] Baker, S. M., Levinton, J. S., Kurdziel, J. P., Shumway, S. E. (1998): Selective feeding and biodeposition by zebra mussels and their relation to changes in phytoplankton composition and seston load. – *Journal of Shellfish Research* 17: 1207-1213.
- [3] Barko, J. W., James, W. F. (1998): Effects of Submerged Aquatic Macrophytes on Nutrient Dynamics, Sedimentation, and Resuspension. – In: Jeppesen, E., Søndergaard,

- M., Christoffersen, K. (eds.) The Structuring Role of Submerged Macrophytes in Lakes. Springer, New York.
- [4] Kozłowski-Suzuki, B., Karjalainen, M., Lehtiniemi, M., Engstrom-Ost, J., Koski, M., Carlsson, P. (2003): Feeding, reproduction and toxin accumulation by the copepods *Acartia bifilosa* and *Eurytemora affinis* in the presence of the toxic cyanobacterium *Nodularia spumigena*. – *Marine Ecology Progress Series* 249: 237-249.
- [5] Bontes, B. M., Verschoor, A. M., DionisioPires, L. M., Van Donk, E., Ibelings, B. W. (2007): Functional response of *Anodonta anatina* feeding on a green algal and four strains of cyanobacteria, differing in shape, size and toxicity. – *Hydrobiologia* 584: 191-204.
- [6] Bouvy, M., Falcao, D., Marinho, M., Pagano, M., Moura, A. (2000): Occurrence of *Cylindrospermopsis* (Cyanobacteria) in 39 Brazilian tropical reservoirs during the 1998 drought. – *Aquatic Microbial Ecology* 23: 13-27.
- [7] Braband, A., Faafeng, B. A., Nilssen J. P. M. (1990): Relative importance of phosphorus supply to phytoplankton production: fish excretion versus external loading. – *Canadian Journal of Fisheries and Aquatic Sciences* 47: 364-372.
- [8] Carpenter, S. R., Christensen, D. L., Cole, J. J., Cottingham, K. L., He, Xi., Hodgson, J. R., Kitchell, J. F., Knight, S. E., Pace, M. L., Post, D. M., Schindler, D. E., Voichick, V. (1995): Biological control of eutrophication in lakes. – *Environmental Science and Technology* 29: 784-786.
- [9] Degans, H., De Meester, L. (2002): Top-down control of natural phyto- and bacterioplankton prey communities by *Daphnia magna* and by the natural zooplankton community of the hypertrophic Lake Blankaart. – *Hydrobiologia* 439: 39-49.
- [10] DeMott, W. R., Moxter, F. (1991): Foraging on cyanobacteria by copepods: responses to chemical defenses and resource abundance. – *Ecology* 72: 1820-1834.
- [11] Deudero, S., Box, A., Tintore, J. (2009): Stable isotopes and metal contamination in caged marine mussel *Mytilus galloprovincialis*. – *Marine Pollution Bulletin* 58: 1025-1031.
- [12] Dionisio Pires, L. M., Bontes, B. M., Van Donk, E., Ibelings, B. W. (2005): Grazing on colonial and filamentous, toxic and non-toxic cyanobacteria by the zebra mussel *Dreissena polymorpha*. – *Journal of Plankton Research* 27: 331-339.
- [13] Engstrom, J., Viherluoto, M., Viitasalo, M. (2001): Effects of toxic and non-toxic cyanobacteria on grazing, zooplanktivory and survival of the mysid shrimp *Mysis mixta*. – *Journal of Experimental Marine Biology and Ecology* 257: 269-280.
- [14] Engstrom, J., Lehtiniemi, M., Green, K., Kozłowski-Suzuki, B., Viitasalo, M. (2002): Does cyanobacterial toxin accumulate in mysid shrimps and fish via copepods? – *Journal of Experimental Marine Biology and Ecology* 276: 95-107.
- [15] Figueiredo, D. R., Azeiteiro, U. M., Esteves, S. M., Goncalves, F. J. M., Pereira, M. J. (2004): Microcystin-producing blooms-a serious global public health issue. *Ecotoxicology and Environmental Safety* 59: 151-163.
- [16] Gopal, B., Goel, U. (1993): Competition and allelopathy in aquatic plant communities. – *Botanical Review* 59: 155-210.
- [17] Han, K. N. (2001): Feeding habits of larva and juvenile of the Korean bullhead, *Pseudobagrus fulvidraco* (Richardson). – *Journal of Aquaculture* 14: 35-42 (in Korean).
- [18] Harada, K. I., Matsuura, K., Suzuki, M., Oka, H., Watanabe, M. F., Oishi, S., Dahlem, A. M., Beasley, V. R., Carmichael, W. W. (1988) Analysis and purification of toxic peptides from cyanobacteria by reversed-phase high-performance liquid chromatography. – *J Chromatogr* 448:275-283.
- [19] Hill, J., McQuaid, C. (2009): Effects of food quality on tissue-specific isotope ratios in the mussel *Perna perna*. – *Hydrobiologia* 635: 81-94.
- [20] Hutchinson, G. E. (1975): *A Treatise on Limnology*. Vol. III. *Limnological Botany*. – Wiley, New York.

- [21] Ibelings B. W., Vonk M., Los H. F. J., van der Molen, D. T., Mooij, W. M. (2003): Fuzzy modeling of cyanobacterial surface waterblooms: validation with NOAA-AVHRR satellite images. – *Ecological Applications* 13: 1456-1472.
- [22] Iwata, A., Jeon, S. R., Miguro, N., Choi, K. C. (1988): Embryonic development of a gobiid fish, *Odontobutis platycephala*. – *Korean Journal of Ecology and Environments* 21: 25-32.
- [23] Jarvis, A. C., Hart, R. C., Combrink, S. (1987): Zooplankton feeding on size fractionated *Microcystis* colonies and *Chlorella* in a hypereutrophic lake (Hartbeespoort Dam, South Africa): implications to resource utilization and zooplankton succession. – *Journal of Plankton Research* 9: 1231-1249.
- [24] Kim, B. H., Lee, J. H., Hwang, S. J. (2011) Inter- and intra-specific differences in filtering activities between two unionids, *Anodonta woodiana* and *Unio douglasiae*, in ambient eutrophic lake waters. – *Ecological Engineering* 37: 1957-1967.
- [25] Kim I. S., Park, J. Y. (2002): *Freshwater Fishes of Korea*. – Kyo-Hak Publishing, Seoul.
- [26] Kim, M. S., Hwang, J. Y., Kwon, O. S., Lee, W. S. (2013): Analytical methodology of stable isotopes ratios: Sample pretreatment, analysis and application. – *Korean Journal of Ecology and Environments* 46: 471-487.
- [27] Kim, M. S., Lee, W. W., Suresh Kumar, S., Shin, S. H., Robarge, W., Kim, M. S., Lee, S. R. (2016): Effects of HCl pretreatment, drying, and storage on the stable isotope ratios of soil and sediment samples. – *Rapid Communications in Mass Spectrometry* 30: 1567-1575.
- [28] Kim, M. S., Lee, Y., Hong, S., Hwang, S. J., Kim, B. H., An, K. G., Park, Y. S., Park, S. G., Um, H. Y., Shin, S. H. (2017a): Effects of biocontrol with an atyid shrimp (*Caridina deniculata*) and a bagrid catfish (*Pseudobagrus fulvidraco*) on toxic cyanobacteria bloom (*Microcystis aeruginosa*) in a eutrophic agricultural reservoir. – *Paddy and Water Environments* 15: 483-497.
- [29] Kim, M. S., Lee, Y., Ha, S. Y., Kim, B. H., Hwang, S. J., Kwon, J. T., Choi, J. W. and Shin, K. H. (2017b): Accumulation of microcystin (LR, RR and YR) in three freshwater bivalves in *Microcystis aeruginosa* bloom using dual isotope tracer. – *Marine Drugs* 15: 226.
- [30] Kirk, K. L., Gilbert, J. J. (1992): Variation in herbivore response to chemical defenses: zooplankton foraging on toxic cyanobacteria. – *Ecology* 73: 2208-2217.
- [31] Kondo, F., Ikai, Y., Oka, H., Okumura, M., Ishikawa, N., Harada, K., Matsuura, K., Murata, H., Suzuki, M. (1992): Formation, Characterization, and toxicity of the glutathione and cysteine conjugates of toxic heptapeptide microcystins. – *Chemical Research in Toxicology* 5: 591-596.
- [32] Koski, M., Rosenberg, M., Viitasalo, M. (1999): Reproduction and survival of the calanoid copepod *Eurytemora affinis* fed with toxic and non-toxic cyanobacteria. – *Marine Ecology Progress Series* 186: 187-197.
- [33] Liang, Y., Melack, J. M., Wang, J. (1981): Primary production and fish yields in Chinese ponds and lakes. – *Transactions of the American Fisheries Society* 110: 346-350.
- [34] Lorrain, A., Paulet, Y. M., Chauvaud, L., Savoye, N., Donval, A., Saout, C. (2002): Differential $\delta^{13}\text{C}$ and $\delta^{15}\text{N}$ signatures among scallop tissues: implications for ecology and physiology. – *Journal of Experimental Marine Biology and Ecology* 275: 47-61.
- [35] Lu, K., Jin, C., Dong, C., Gu, B., Bowen, S. H. (2006): Feeding and control of blue-green algal blooms by tilapia (*Oreochromis niloticus*). – *Hydrobiologia* 568: 111-120.
- [36] Lu, M., Xie, P., Tang, H. J., Shao, Z. J., Xie, L. Q. (2002): Experimental study of trophic cascade effect of silver carp (*Hypophthalmichthys molitrix*) in a subtropical lake, Lake Donghu: on plankton community and underlying mechanisms of changes of crustacean community. – *Hydrobiologia* 487: 19-31.
- [37] Malbrouck, C., Kestemont, P. (2006): Effects of microcystins on fish. – *Environmental Toxicology and Chemistry* 25: 72-86.

- [38] Masuda, H., Amakoa, K., Araga, C., Uyeno, T., Yoshino, T. (1988): The fishes of the Japanese Archipelago. – Tokai University Press, Tokyo (in Japanese).
- [39] Matveev, V., Matveeva, L. A., Jones, G. J. (1994): Study of the ability of (*Daphnia carinata*) King to control phytoplankton and resist cyanobacterial toxicity: implications for biomanipulation in Australia. – Australian Journal of Marine and Freshwater Research 45: 889-904.
- [40] Miura, T. (1990): The effects of planktivorous fishes on the plankton community in a eutrophic lake. – Hydrobiologia 200: 567-579.
- [41] Naddafi, R., Pettersson, K., Eklov, P. (2007): The effect of seasonal variation in selective feeding by zebra mussels (*Dreissena polymorpha*) on phytoplankton community composition. – Freshwater Biology 52: 823-842.
- [42] Ozimek, T., Gulati, R. D., van Donk, E. (1990): Can macrophytes be useful in biomanipulation of lakes? The lake Zwemlust example. – Hydrobiologia 200/201: 399-407.
- [43] Pagano, M., Saint-Jean, L., Arfi, R., Bouvy, M., Guiral, D. (1999): Zooplankton food limitation and grazing impact in a eutrophic brackish-water tropical pond (Cote D'Ivoire, West Africa). – Hydrobiologia 390: 83-98.
- [44] Parker, P. L., Anderson, R. K., Lawrence, A. (1989): A d13C and d15N Tracer Study of Nutrition in Aquaculture: *Penaeus Vannamei* in a Pond Grow-Out System. – In: Rundel, P. W., Ehleringer, J. R., Nagy, K. A. (eds.), Stable Isotopes in Ecological Research. Springer-Verlag, New York.
- [45] Pflugmacher, S., Wiegand, C., Oberemm, A., Beattie, K. A., Krause, E., Codd, G. A., Steinberg, C. E. W. (1998): Identification of an enzymatically formed glutathione conjugate of the cyanobacterial hepatotoxin microcystin-LR: the first step of detoxication. – Biochimica et Biophysica Acta 1425: 527-533.
- [46] Piola, R. F., Suthers, I. M., Rissik, D. (2008): Carbon and nitrogen stable isotope analysis indicates freshwater shrimp *Paratya australiensis* Kemp, 1917 (Atyidae) assimilate cyanobacterial accumulations. – Hydrobiologia 608: 121-132.
- [47] Pires, L. D., Bontes, B. M., Van Donk, E., Ibelings, B. W. (2005): Grazing on colonial and filamentous, toxic and non-toxic cyanobacteria by the zebra mussel *Dreissena polymorpha*. – Journal of Plankton Research 27: 331-339.
- [48] Porter, K. G., Orcutt, J. D. (1980): Nutritional Adequacy, Manageability, and Toxicity as Factors that Determine the Food Quality of Green and Blue-Green Algae for *Daphnia*. – In: Kerfoot, W. C. (ed.) Evolution and Ecology of Zooplankton Communities. New England University Press, Hanover.
- [49] Raikow, D. F., Hamilton, S. K. (2001): Bivalve diets in a midwestern US stream: A stableisotope enrichment study. – Limnology and Oceanography 46: 514-522.
- [50] Reeders, H. H., Bij de Vaate, A. (1990): Zebra mussel (*Dreissenapolymorpha*): a new perspective for water quality management. – Hydrobiologia 200/201: 437-450.
- [51] Rinehart, K. I., Namikoshi, M., Choie, B. W. (1994): Structure and biosynthesis of toxins from blue-green algae (cyanobacteria). – Journal of Applied Psychology 6: 159-176.
- [52] Shapiro, J., Lamarra, V., Lynch, M. (1975): Biomanipulation: an Ecosystem Approach to Lake Restoration. – In: Brezonik, P. L., Fox, J. L. (eds.) Proceeding of a Symposium on Water Quality Management through Biological Control. University of Florida, Gainesville.
- [53] Søndergaard, M., Moss, B. (1998): Impact of Submerged Macrophytes on Phytoplankton in Shallow Freshwater Lakes. – In: Jeppesen, E., Søndergaard, M., Christoffersen, K. (eds.) The structuring Role of Submerged Macrophytes in Lakes. Springer, New York.
- [54] Soto, D., Mena, G. (1999): Filter feeding by the freshwater mussel, *Diplodonchilensis*, as a biocontrol of salmon farming eutrophication. – Aquaculture 171: 65-81.
- [55] Specziár, A., Tölg, L., Biró, P. (1997): Feeding strategy and growth of cyprinids in the littoral zone of Lake Balaton. – Journal of Fish Biology 51: 1109-1124.

- [56] Strickland, J. D. H., Parsons, T. R. (1972): A Practical Handbook of Seawater Analysis. – Fisheries Research Board of Canada, Ottawa.
- [57] Vanderploeg H. A., Liebig J. R., Carmichael, W. W., Agy, M. A., Johengen, T. H., Fahnenstiel, G. L., Nalepa, T. F. (2001): Zebra mussel (*Dreissena polymorpha*) selective filtration promoted toxic *Microcystis* blooms in Saginaw Bay and Lake Erie. – Canadian Journal of Fisheries and Aquatic Science 58: 1208-1221.
- [58] Vaughn, C. C., Gido, K. B., Spooner, D. E. (2004): Ecosystem processes performed by unionid mussels in stream mesocosm: species role and effects of abundance. – Hydrobiologia 527: 35-47.
- [59] Wiegand, C., Pflugmacher, S., Oberemm, A., Meems, N., Beattie, K. A., Steinberg, C. E. W., Codd, G. A. (1999): Uptake and effects of microcystin-LR on detoxication enzymes of early life stages of the zebra fish (*Daniorerio*). – Environmental Toxicology 14: 89-95.
- [60] Wium-Andersen, S., Christophersen, C., Houen, G. (1982): Allelopathic effects on phytoplankton by substances isolated from aquatic macrophytes (Charales). – Oikos 39: 187-190.
- [61] Xie, L. Q., Xie, P., Guo, L. G., Li, L., Miyabara, Y., Park, H. D. (2005): Organ distribution and bioaccumulation of microcystinsin freshwater fish at different trophic levels from the eutrophic lake Chaohu, China. – Environmental Toxicology 20: 293-300.
- [62] Xie, P., Yang, Y. (2000): Long-term changes of Copepoda community (1957–1996) in a subtropical Chinese lake stocked densely with planktivorous filter-feeding silver and bighead carp. – Journal of Plankton Research 22: 1757-1778.
- [63] Yokoyama, A., Park, H. D. (2002): Mechanism and prediction for contamination of freshwater bivalve (Unionidae) with the cyanobacterial toxin, microcystin, in the hypereutrophic Lake Suwa, Japan. – Environmental Toxicology 17: 424-433.

AN INTRODUCTION TO SELECTED INNATE IMMUNE-RELEVANT GENES IN FISH

ABO-AL-ELA, HAITHAM G.

*Animal Health Research Institute, Shibin Al-Kom Branch, Agriculture Research Centre
El-Minufiya, Egypt
e-mail: haithamgamal2@gmail.com; aboalela@ahri.gov.eg; phone: +20-12-2469-5931*

(Received 6th Aug 2017; accepted 5th Dec 2017)

Abstract. Aquaculture (aquafarming) especially that related to fish receives a great deal of attention because of its importance to science and economy. To illustrate, aquaculture is a fast growing sector of industry, and a source of many materials, as well as fish act as a good model for scientific research. The immune system has two main arms: innate (non-specific) and adaptive (specific). Innate immunity acts as a firewall not only against pathogens, but also against any foreign bodies, chemical agents or even environmental changes. However, there are many members of such system; but everyone has a particular function, like players in an orchestra. Fish rely mainly on their innate immunity; many studies were done to characterise, determine or understand the behaviour of immune-related genes in normal and disease conditions. To harness the real power beyond natural or innate immunity, we should understand the function of their members or genes. Herein, this review summarises and focuses on some genes related to innate immunity in different fish species.

Keywords: *aquaculture, fish immunity, gene expression, immune-related genes, innate immunity*

Abbreviations: CAS – cellular apoptosis susceptibility; dph – days post-hatching; GST – glutathione S-transferase; IFN – interferon; Ig – immunoglobulin; IL – interleukin; IL1ra –IL1 receptor antagonist; MT – 17 α -methyltestosterone; Mx – myxovirus resistance; NCCs – non-specific cytotoxic cells; NK – nature killer; PAMP – pathogen associated molecular pattern; PRRs – pattern recognition receptors; Th1 – T-helper1; TLR – toll-like receptor; TNF – tumour necrosis factor; VTG – vitellogenin

Introduction

The immune response is a cascade of diverse reactions and proceedings that aims to eliminate the recognised foreign agent. Although specific or non-specific immunity are both important ways of the immune response, the non-specific immune response is the first step and the ready weapon for fighting pathogens. The immune system is very sensitive and they can be affected by exogenous treatment or change. Thus, for instance, it can be inferred that a set of genes related to immunity were greatly disrupted during and after stopping the 17 α -methyltestosterone (MT; commonly used hormone in monosex production) treatment in the Nile tilapia, *Oreochromis niloticus* (Abo-Al-Ela et al., 2017a; Abo-Al-Ela, 2018).

Identification of genes that related to immunity in fish and determination of their expression patterns receive a great attention. Mostly, the increase in the expression of immune genes is usually considered as a sign for immune stimulation or enhanced immune response; however, recently, Nile tilapia received MT for a short period showed an up-regulation in the expression of innate immune genes, but with a marked decrease in the phagocytic activity and index, and genotoxicity. On the other hand, those exposed to vitamin C alone or plus MT showed somewhat normal expression of the same genes with a significant enhancement in several immune parameters (Abo-Al-Ela et al., 2017b).

There are many genes involved in the immune response either via direct or indirect way. This review looks at some of the key elements or genes of innate immunity. It focuses on the potential function of these genes and the change in its gene expression in normal and abnormal cases.

Selected innate immunity-relevant genes

Toll-like receptors (tlr)

The main difference between innate and adaptive immunity is the type of receptors used to recognise pathogens (Medzhitov, 2007). Innate immune recognition depends on number of receptors, including pattern recognition receptors (PRRs) with a broad specificity that have evolved to sense the pathogen associated molecular pattern (PAMPs) (Janeway and Medzhitov, 2002; Medzhitov and Janeway, 2002). There are many functionally distinct classes of PRRs; however, the best characterised are toll-like receptors (TLRs) (reviewed in Alvarez-Pellitero, 2008).

PRRs are classified into two groups: cytosolic and membrane bound receptors. The membrane bound receptors, including the TLRs, detect viral nucleic PAMPs inside the endosomal compartment where numerous viruses lose their coat and expose their genome for replication and transcription. TLR7 and TLR8 sense the single stranded RNA PAMPs and cytosine-phosphate-guanosine motifs of DNA (Kawai et al., 2004; Liu et al., 2011b; Zou and Secombes, 2011; Zhang and Gui, 2012). TLRs found on phagocytic and epithelial cells recognise different pathogen (Akira et al., 2001; Takeda and Akira, 2001; Alvarez-Pellitero, 2008). For example, Tlr7 can recognise viruses (Lee et al., 2013) and initiate an IFN (interferon) response against viruses (Baum and Garcia-Sastre, 2010), bacteria (Kumar et al., 2011) and parasites (Zhao et al., 2013).

The constitutive gene expression of *tlr7* was found in several organs and tissues in zebrafish at different stages of development (Jault et al., 2004), and in other fish species (Tanekhy et al., 2010). Salmon *tlr7* gene expression was sensitive to Ifn and Il (interleukin) 1 β (Lee et al., 2013).

TLR signalling cascades lead to the enhanced production of pro-inflammatory cytokines, such as IL1 β , TNF (tumour necrosis factor), IL8 (Rauta et al., 2014) and IFN molecules, which alert adaptive immune cells to an existing pathogen and mediate direct defence responses (Iwasaki and Medzhitov, 2004; Kawai and Akira, 2010). In addition, triggering TLRs can result in apoptosis (Salaun et al., 2007).

Exogenous IFN α up-regulated *TLR7* mRNA expression in macrophages (Miettinen et al., 2001). It was found that a TLR7 ligands stimulator triggered the expression of *ifna* and *mx*; thus, it potentiated the antiviral activity in Atlantic salmon, *Salmo salar* L. (Kileng et al., 2008; Sun et al., 2009), induced the IFN response in salmonid leukocytes (Palti et al., 2010; Svingerud et al., 2012) and stimulated IFN and TNF secretions from peripheral blood mononuclear cells in rat (Hammerbeck et al., 2007).

Similarly, activation of TLR7 is required to produce imidazoquinoline-inducible IFN by macrophages (Hemmi et al., 2002). In addition, the TLR7/TLR8 agonist stimulated the production of Ifn, Il1 β and Il8 in rainbow trout leukocytes (Palti et al., 2010). These lead to T-helper1 (Th1) immune response and CD4+ T-cell activation, which is vital for the host's antiviral defence (Jault et al., 2004).

Cytokines and chemokines

The immune system of fish contains both non-specific and specific mechanisms, and has cellular and humoral mechanisms to fight pathogens. Mononuclear phagocytes and T-lymphocytes from the non-specific and specific immunity pathways, respectively, are typically the major cell sources of the immune modulators, cytokines. Cytokines, are generally defined as interleukins, lymphokines, members of the TNF family and chemokines, based on the cells from which they are secreted, their functions and their targets (Alejo and Tafalla, 2011); they have a significant function in complement activation, chemotaxis, and pathogen opsonisation in the process of phagocytosis (Secombes et al., 2001; Salaun et al., 2007).

The earliest immune mediators released following virus infection are cytokines, which regulate the induction and maintenance of innate and acquired antiviral responses (Tortorella et al., 2000) and allow the clearance of viral infection (He et al., 2006). The pro-inflammatory cytokines produced by Th1 cells, IFN γ and TNF α/β , induce innate and cell-mediated responses against bacteria, fungi and viruses, resulting in their clearance, as well as having anti-tumour effects (Davidson et al., 1996; Micallef et al., 1996; Wan and Flavell, 2009; Choi et al., 2013; Gerber et al., 2013; Assani et al., 2014; Lai et al., 2014).

Many fish cytokines are identified, such as IL1 β (Zou et al., 1999), IL2 (Bird et al., 2005a), IL4 (Li et al., 2007), IL6 (Bird et al., 2005b), IL8 (Lee et al., 2001), IL10 (Savan et al., 2003), IL11 (Wang et al., 2005), IL12 (Yoshiura et al., 2003), IL15 (Bei et al., 2006), IL17 (Gunimaladevi et al., 2006), IL18 (Zou et al., 2004a), Tnf α (Savan and Sakai, 2004), Ifn γ (Zou et al., 2004b) and myxovirus resistance (Mx) (Staeheli et al., 1989).

Interleukin 1 (il1)

The IL1 family, one of the major IL families in fish and mammals, has four main members: IL1 α , IL1 β , IL18 (interferon-gamma inducing factor) and IL1 receptor antagonist (IL1ra) (Dinarello, 1997; 1999; Mulero et al., 1999; Busfield et al., 2000; Smith et al., 2000; Pan et al., 2001). However, il1 β is the most studied in relation to innate immunity in fish.

Interleukin 1 β (il1 β)

IL1 β is well-characterized cytokine, plays an important role in cellular responses to immunological challenges, infection and inflammation. Macrophages are the primary source of IL1 β , although it is secreted by various other cell types including nature killer (NK) cells, B-cells, Langerhans cells of the skin, peripheral neutrophilic granulocytes, endothelial cells, fibroblasts and microglia cells (Huisling et al., 2004; Tassakka and Sakai, 2004). IL1 β is a key player in the defence against microorganism invasion and tissue injury and is able to induce immune responses by stimulating lymphocytes or by enhancing the release of other cytokines that can activate NK cells, macrophages and lymphocytes (Low et al., 2003).

In fish, *il1 β* is constitutively expressed in several tissues, such as spleen, head kidney and liver, and higher expression has been detected in the spleen (Tafalla et al., 2005; Lu et al., 2008). Moreover, upon administration with recombinant IL1 β , the systemic gene expression of *il1 β* was induced in rainbow trout, *Oncorhynchus mykiss* (Hong et al., 2003), yellowfin sea bream, *Acanthopagrus latus* (Jiang et al., 2008), orange-spotted grouper, *Epinephelus coioides* (Lu et al., 2008) and grass carp, *Ctenopharyngodon idella* (Bo et al., 2015).

The mRNA level of *il1 β* significantly increased in response to bacterial (Mohanty and Sahoo, 2010), viral (Tafalla et al., 2005) and parasitic (Bridle et al., 2006; Mladineo and Block, 2010) infections, indicating its main role as a member in immune system. Furthermore, in chronically stressed fish (Bermejo-Nogales et al., 2007), during the smolting of Atlantic salmon (Ingerslev et al., 2006), as well as in acute stress in common carp, *Cyprinus carpio* L. (Metz et al., 2006) there was an increase in the expression of pro-inflammatory cytokines (*il1 β* , *tnfa*).

Even a change in the dietary components in hybrid tilapia (Zhang et al., 2014b) or the addition of oxytetracycline, formic and propionic acid/salt mixture to the feed of Nile tilapia (Reda et al., 2016) changed the expression of *il1 β* and disease resistance. Intraperitoneal injection of the common carp with the toxic material carbon tetrachloride (CCl₄) up-regulated the gene expressions of inflammatory cytokines, including *il1 β* and *tnfa* (Jia et al., 2014).

Tumour necrosis factor alpha (tnfa)

TNF α was first identified in fish as a single copy gene in the stimulated leukocytes of the Japanese flounder, *Paralichthys olivaceus* (Hirono et al., 2000). TNF α is a central regulatory cytokine in antimicrobial and inflammatory responses (Grayfer et al., 2008). The treatment of *Rhodococcus equi* infected mice with antibodies against IFN γ and TNF α increased the tissue colony counts. Thus, IFN γ and TNF α are involved in cell-mediated immunity against bacterial infection (Nordmann et al., 1993). Furthermore, *Tnfa* has the ability to induce the gene expression of *il1 β* and *il8* (Zou et al., 2003).

TNF α is involved in viral (Purcell et al., 2004) and ectoparasitic (Saurabh et al., 2011) invasions. Moreover, the expression of *tnf* could be considered for the assessment of fry-rearing environment (Lam et al., 2011).

TNF α stimulates the proliferation of trout leucocytes. TNF α and macrophage activating factor synergistically act on rainbow trout macrophages. This synergy causes elevation in respiratory burst activity in trout macrophages and this action is ablated after pre-incubation with neutralising mouse anti-TNF α IgG antibody (Hardie et al., 1994). TNF α can enhance chemotactic responses and phagocytosis in a dose-dependent manner, induce nitric oxide production in primary macrophages, and prime respiratory burst in monocytes (Grayfer et al., 2008).

Tnfa is predominantly expressed in non-specific cytotoxic cells (NCCs) of tilapia (Praveen et al., 2006a). The pro-apoptotic effects of TNF α are mainly responsible for macrophage-mediated cytotoxicity (Goetz et al., 2004). Recombinant tilapia *Tnfa* is highly cytotoxic to mammalian cells (Praveen et al., 2006a), and the trout *Tnfa* markedly stimulated cytotoxicity in murine L929 cells (Qin et al., 2001). In other words, this cytotoxic effect may be because TNF α has the ability to decrease telomerase activity and cause telomeric disturbances (shortening, fusions, and losses) and additional chromosomal aberrations (Beyne-Rauzy et al., 2004).

TNF α plays an important role in regulation of the biosynthesis of steroid hormones (Yan et al., 1993; Zhao et al., 1996). There is possible reciprocal feedback among IL1 β , TNF α and testosterone. The basal secretion of testosterone in purified leydig cells and whole testis cells was stimulated by TNF and IL1 β (Warren et al., 1990). In Nile tilapia, *tnfa* expression showed an early up-regulation and late down-regulation upon treatment with MT (Abo-Al-Ela et al., 2017a). These give us an indication about the interaction between cytokines and sex hormones in fish, which may result in positive or negative action.

Chemokines

Chemokines are a large multifunctional family of cytokines (**Chemotactic cytokines**) (Laing and Secombes, 2004a). They are a diverse group of small cytokines that can be divided into numerous families. Chemokines are structurally related and contain four invariant cysteine residues. Based on the arrangement of these cysteine residues, they are classified into four subfamilies: CXC (α), CC (β), C (γ) and CX3C (δ) (Baggiolini, 1998; Murphy et al., 2000; Alejo and Tafalla, 2011). Furthermore, a new family of chemokines called CX, which includes five members, has been determined in zebrafish, *Danio rerio* (Nomiyama et al., 2008). Interestingly, some microorganisms (especially viruses) appear to have copies of chemokine genes, probably to confuse the immune system of the host (Laing and Secombes, 2004a), which in this way may protect themselves.

CXC-chemokines

The Cys-Xaa-Cys (CXC)-chemokines are a superfamily of the chemotactic cytokines that play a vital role in leucocyte chemotaxis; they are able to recruit various immune cells to infection sites (Kim et al., 2007; Liu et al., 2007), and they are substantial and selective mediators in leukocyte migration to secondary lymphoid organs and inflammatory sites (Vandercappellen et al., 2008). They have been categorized as key regulators of the immune defence, acting as a link between innate and adaptive responses (Alejo and Tafalla, 2011).

In vitro, an CXC-chemokine significantly induces leukocyte recruitment, including granulocytes, lymphocytes, monocytes/macrophages and neutrophils; they have distinct effects on phagocyte activation; they increase respiratory burst activity; they induce a moderate increase in $IL1\beta$; and they up-regulate the expression of a wide range of immune relevant genes, including *il1\beta*, *il8*, *tnfa* and *mx* (Li et al., 2012; van der Aa et al., 2012).

Additionally, CXC-chemokines play an essential role in hepatic injury, recovery and regeneration (Clarke et al., 2009). Macrophage-derived chemokines are capable of inducing both respiratory burst and the release of lysosomal enzyme from macrophages in mouse and enhancing the killing and phagocytic activities of macrophages against *E. coli* (Matsukawa et al., 2000).

CXC-chemokine is expressed in a basal manner and is found most noticeably in immune organs, such as the tissue and phagocytes of the anterior kidney and the spleen (Huising et al., 2003; Baoprasertkul et al., 2004). CXC-chemokine transcripts and proteins can show a marked increase and play vital roles in the immune response against bacterial (Baoprasertkul et al., 2004), viral (Li et al., 2012) and parasitic (Huising et al., 2003) infections. During the early stages of turbot embryo development after fertilization, a low expression level of CXC-chemokine was first detected at the somite stage. Interestingly, turbot chemokine expression was markedly and rapidly induced in the spleen, liver and head kidney as well as in turbot embryonic cells after challenge with *Vibrio anguillarum* (Liu et al., 2007).

Interleukin 8 (il8)

The first CXC-chemokine reported in fish was I18 (Najakshin et al., 1999). The role of ELR^+ CXC-chemokines including I18 (CXCL8) is to enhance the adherence of neutrophils to endothelial cells, followed by migration along a gradient of chemokines

conjoined with matrix proteins and cell surfaces towards the inflammatory site (Laing and Secombes, 2004a). I18 is a powerful chemoattractant to neutrophils, cytokine-stimulated eosinophils, basophils and peripheral blood T-lymphocytes (White et al., 1989; Warringa et al., 1991; Baggiolini et al., 1994).

The recombinant I18 induced migration of head kidney lymphocytes and peripheral blood leukocytes, promoted the proliferation of these cells in a dose-dependent manner, and up-regulated the expression of *il1 β* and *il8* in head kidney lymphocyte culture (Hu et al., 2011; Sun et al., 2011). Fish *il8* is expressed in many tissues under normal condition and it is clearly up-regulated after bacteria, viral and external parasitic challenges (Tafalla et al., 2005; Covello et al., 2009; Ming et al., 2013).

CC-chemokine

CC-chemokines are a major subfamily of chemokines, and are essential members of the innate immune system (Hu and Zhang, 2015); they provoke chemotaxis (recruitment, activation and adhesion) of various types of leukocytes under normal physiological and inflammatory conditions (He et al., 2004; Colobran et al., 2007; Peatman and Liu, 2007; Borza et al., 2010). They are also involved in normal developmental processes as well as the maintenance and organization of lymphoid organ architecture (He et al., 2004). They primarily target mononuclear cells rather than the neutrophils that mediate either homeostatic or pro-inflammatory mechanisms (Laing and Secombes, 2004a). CC-chemokines are involved in antibacterial and antiviral immune responses in fish (Su et al., 2012; Kim et al., 2013).

Nakharuthai et al. (2016) isolated a CC-chemokine in Nile tilapia that participate in early immune defences against pathogens such as bacteria, in which many tissues especially the spleen, liver and peripheral blood leukocytes express significantly higher transcript levels than controls. *In vitro*, recombinant CC-chemokine proteins efficiently stimulated phagocytic activity in Nile tilapia (Nakharuthai et al., 2016) and Japanese flounder (Kono et al., 2003).

The chemotactic activity of peripheral blood leucocytes was markedly evoked in response to stimulation by recombinant CC-chemokine protein (Khattiya et al., 2007; Zhang et al., 2008; Li et al., 2011). Moreover, in humans, CC-chemokines can activate macrophages to kill parasites by means of nitric oxide (Villalta et al., 1998). Interestingly, CC-chemokines were secreted following the stimulation of trout macrophage-like cells by recombinant TNF α (Laing and Secombes, 2004b), which indicates an interaction between several cytokines.

CC-chemokines are constitutively expressed in lymphoid-rich tissues, such as liver, head kidney, spleen, gill and peripheral blood leucocytes (Laing and Secombes, 2004b; Khattiya et al., 2007; Li et al., 2011; Su et al., 2012). Their expression was detected during the early developmental stages of the blunt snout bream, before hatching and at 62 h post fertilization, and were strongly induced and quickly up-regulated upon nitrite stress, supporting the possible existence of pro-inflammatory function (Zhang et al., 2014a). More recently, a set of CC-chemokine ligand genes have been identified and characterized from the channel catfish. Many of the identified CC-chemokines were significantly up-regulated following bacterial infection and hypoxia (Fu et al., 2017), supporting the possible effect of external environmental stress as hypoxia on immune-related gene expression.

Interferon (ifn)

Viral diseases are a serious pathogenic threat, and they have an important concern in the fish aquaculture industry (Langevin et al., 2013); thus, fish antiviral responses are the focus of research, especially on species that have commercial value. Innate defences can play a central role in fish resistance to viral infections (Ellis, 2001). The IFN family is a key component of innate and adaptive immunity (Schroder et al., 2004; Collet, 2014). The IFN system is a powerful and a rapid defence mechanism and a hallmark against viral (Samuel, 1991; Verrier et al., 2011) as well as bacterial (Schultz et al., 2004; Chen et al., 2010) and parasitic infections (Stolte et al., 2008) in vertebrates and fish; it is also involved in tumour control (Schroder et al., 2004).

IFN has the ability to inhibit the cellular replication and propagation of different viruses (Sadler and Williams, 2008; Collet, 2014). IFNs are divided into three subfamilies, type I, type II and type III, based on the relevant receptors they interact with and the immune responses initiated by them (Sadler and Williams, 2008; Zou and Secombes, 2011). Homologues of type I and type II *Ifn* have been found in many teleost fish species, including sea bass, *Dicentrarchus labrax* (Casani et al., 2009). IFNs recognise viral PAMPs via an array of PRRs (Pichlmair and Sousa, 2007; Kawai and Akira, 2009).

In mammals, IFN induces the pro-apoptotic genes that result in the destruction of infected cells (Chawla-Sarkar et al., 2003). The recombinant *Ifn γ* of goldfish have been found to stimulate the respiratory burst responses of macrophages and neutrophils, and increase the nitric oxide production and the phagocytic responses of the macrophages (Grayfer and Belosevic, 2009).

Myxovirus resistance (mx)

The *Mx* gene was discovered for the first time in a strain of mice (A2G) that is resistant to influenza viruses type A and type B (Lindenmann, 1962). The first isolated fish *Mx* was in perch (Staeheli et al., 1989).

The *Mx* protein is rapidly accumulated in the cytoplasm or nucleus, and it self-assembles to form oligomers that interfere with virus replication (Lee and Vidal, 2002; Haller et al., 2007). Lin et al. (2005) found that, in Japanese flounder, the *Mx* protein is concentrated in the cell cytoplasm; however, in mouse, *Mx* accumulates in the cell nucleus and inhibits viruses that are known to replicate in that part of the cell (Haller et al., 2007). The possible antiviral mechanisms of *Mx* include blocking the transport of viral nucleocapsids, inhibition of viral RNA transcription or translation and targeting of viral elements, such as viral polymerase complex (Stranden et al., 1993; Kochs and Haller, 1999; Haller et al., 2007).

Constitutive expression of *mx* was found in blood leukocytes, as well as the kidney, liver, spleen, heart, intestine, gills, muscle, brain and peritoneal cavity fluid of many fish species (Lee et al., 2000; Bergan and Robertsen, 2004; Tafalla et al., 2004). The IFN antiviral state is established by the up-regulation of antiviral proteins gene expression, including *mx* (Jensen and Robertsen, 2002). Viral infection clearly induces *ill β* , *tnfa* and *mx* expression in a variety of immune tissues found in fish (Lee et al., 2000; Poisa-Beiro et al., 2008; Kim et al., 2009). On its own, the over-expression of the IFN-induced *Mx* protein can provide complete viral resistance against various viruses in fish (Larsen et al., 2004; Lester et al., 2012).

Disruption of the *Mx* gene caused a repression of innate immunity against viruses and rapid death (Haller et al., 1998). Moreover, in Atlantic salmon, the stress that accompanies the smolting process alerted the basal transcript levels of *mx* (Das et al., 2007).

Immunoglobulin M (IgM)

Immunoglobulin (Ig) genes encode a family of defence proteins known as antibodies. Antibodies are synthesised by B-cells, which undergo a complex series of somatic mutations and chromosomal rearrangements to generate antibodies with high specificity. IgM has a low molecular weight. Ig consists of two heavy chains and two light chains, linked together by disulphide bonds (Warr, 1995). The immune system in fish reported to contain four types of Ig: IgM, IgZ, IgD and IgT (Randelli et al., 2008).

IgM antibodies comprise the major component of the body antibodies, and it is the first category of antibodies generated during a primary antibody response. The IgM antibodies vary from other categories of antibodies in that they are mainly produced by B1 cells, with the apparent lack of stimulation by specific antigens. Most pathogens trigger a humoral immune response that results in an early increase in antigen-specific IgM, followed by a more specific response of antigen-specific antibodies: IgA, IgG and IgE (such as IgT/Z and IgD in fish) (Boes, 2000).

The first appearance of IgM in lymphocytes differs considerably among fish species. In channel catfish and rainbow trout, the first appearance of surface IgM occurs about one week after hatching. The maternal antibody that is transmitted to eggs and embryos has been detected in several species, including tilapia, carp, plaice, sea bass and salmon (Magnadottir et al., 2005). The IgM-like protein levels decreased gradually as yolk was absorbed (12 days post-hatching, dph) during pre-larval stages of tilapia. After yolk utilisation, the feeding and free swimming begins. About this time, the IgM-like protein drops to its lowest levels, but it increases rapidly during the post-larval stages (Takemura, 1993). *IgM* transcripts were also detectable at 5 dph in the striped trumpeters, *Latris lineata* (Covello et al., 2013). However, in chum salmon (*Oncorhynchus keta*), the serum IgM concentrations remained at a low level until 40 dph, and then they increased rapidly at 48 dph (Nagae et al., 1993).

In teleost fishes, IgM is the only member of the specific humoral defence system that is modulated by aquatic environment factors, such as water temperature, salinity and suspended solids (Dominguez et al., 2004). In particular, the levels of plasma IgM were decreased in cold-treated and stressed tilapia (Chen et al., 2002). Hypoxia significantly suppressed *IgM*, *il1 β* gene expression, and it also delayed antibody production in infected Nile tilapia (Gallage et al., 2016).

IgM secretion and expression can be altered in response to chemicals or hormones. In Nile tilapia, the organochlorine insecticide, endosulfan, led to a significant increase in the secretion of IgM; consequently, it may encourage the production of autoantibodies and the development of autoimmune problems after exposure to infection (Tellez-Banuelos et al., 2010), and after short treatment with MT (Abo-Al-Ela et al., 2017b). Furthermore, common carp, exposed to chlorpyrifos (an organophosphate pesticide that is widely used in agricultural) for 7 days, showed an augmentation in *IgM* expression at the earlier stage of exposure, but it was reduced at the later stage (Li et al., 2013).

Vitellogenin (vtg)

The egg-yolk precursor, vitellogenin (Vtg), acts as a nutrient source for developing embryos, and it also participates in innate immunity (Zhang et al., 2011; Lu et al., 2012). Vtg is a multivalent pattern recognition receptor that has the ability to recognise pathogens via interaction with PAMPs (Li et al., 2008; Li et al., 2009), and it has hemagglutinating and antimicrobial activities (Zhang et al., 2005; Liu et al., 2009). It is able to bind virus, lipopolysaccharide, peptidoglycan, lipoteichoic acid and glucan. It can also act as a bactericidal molecule capable of binding to bacteria, inhibiting bacterial activities and damaging bacterial cell walls (Zhang et al., 2011). Vtg is an opsonin that is able to enhance phagocytosis; it significantly up-regulates the expression of pro-inflammatory cytokine genes, *il1 β* and *tnfa* (Liu et al., 2011a). It has been reported that Atlantic salmon serum Vtg can neutralise the action of the infectious pancreatic necrosis virus (Garcia et al., 2010). All of these elucidate that Vtg is an immune-relevant protein involved in the host defence process against microbes, including bacteria and viruses (Zhang et al., 2011).

In zebrafish larvae, *vtg* gene transcription was detected during the early stages of development, 7 days after fertilisation (Wang et al., 2011). The treatment of mature female Nile tilapia with high levels of MT resulted in a pronounced decrease in the plasma Vtg levels (Lazier et al., 1996). Hepatic Vtg levels were significantly decreased in female medaka (*Oryzias latipes*) treated with MT at concentrations of 380 ng/L and 188 ng/L for 3 weeks (Kang et al., 2008).

Cellular apoptosis susceptibility (cas)

Apoptosis is the process of cellular death; it is considerably different from necrosis, which is recognised as the classic system of cell death (Cotter et al., 1990). Apoptosis is an important biological process that destroys virus-infected cells, and it is presumed to be an innate response to counteract viral infection (Wrzesien-Kus et al., 2004). Replicating viruses may directly induce suicide of the host cell or promote recognition by natural killer cells and cytolytic T-cells, and these immune effector cells induce apoptosis (Tortorella et al., 2000).

Several genes control the apoptosis process; for example, cellular apoptosis susceptibility (*cas*). CAS is a microtubule-associated protein that links with microtubules and mitotic spindles (Brinkmann et al., 1995; Scherf et al., 1996). Mitotic spindles are cellular organelles, which play a role in chromosome segregation during cell division (Kuriyama and Nislow, 1992). CAS is associated with cell proliferation and apoptosis (Brinkmann, 1998) and in protection against apoptotic cell death (Praveen et al., 2006b). The Cas protein is important in the regulation of teleost immune functions. NCCs are one of the cellular sources for *cas* transcription in tilapia fish. The up-regulated expression of *cas*, following exposure to stress-activated serum, indicates the involvement of *cas* as a protector against apoptotic cell death (Praveen et al., 2006b). Furthermore, NCCs in tilapia treated with recombinant tilapia *Tnfa* revealed an up-regulation of *cas* expression, indicating that *cas* may act as a mediator for protective effects of *Tnfa* on NCC (Praveen et al., 2006b).

In many cases, apoptosis can harm virus replication. Therefore, viruses may protect themselves through the inhibition of proteins implicated in the apoptotic process (He et al., 2006).

Glutathione S-transferase (gst)

The glutathione *S*-transferases (GSTs), a multifunctional family of enzymes, are a natural defence system that catalyse the conjugation of many harmful electrophiles with reduced glutathione through formation of a thioether bond (Scott et al., 1992). GST, a main player in the detoxification system and in antioxidant defence (Frova, 2006; Puerto et al., 2011), plays a vital role in immune responses (Wang et al., 2013). Its expression is greatly changed in response to bacterial challenges in the Mediterranean mussel, *Mytilus galloprovincialis* (Wang et al., 2013), and also was in line with the expression of immune-related genes in Nile tilapia (Abo-Al-Ela et al., 2017a).

Interestingly, the treatment of sertoli cells with TNF α induced a decrease in basal GST α transcription levels in a dose-dependent manner. TNF α also inhibited the hormone testosterone-stimulated *GST α* expression (Benbrahim-Tallaa et al., 2002), which give another example for the cross-link between GST α and immune members.

Some GSTs possess peroxidase activity against organic peroxides, thus they can protect from lipid peroxidation, while other specific enzymes can reduce peroxidised DNA, so they may be involved in DNA repair (Scott et al., 1992). In a previous study, tilapia were subjected to cadmium chloride. Significant increases were evident in the detoxification enzymes of liver and kidney, including Gst from the seventh day continuously until the fifteenth day, and then reduced slightly on the thirtieth day of cadmium stress (Basha and Rani, 2003). To this end, oxidative stress could badly affect the immune parameters.

Conclusive remarks

The synergism of the immune system is finely tuned in such a way that each player in this orchestra cooperates to protect the living body. In the last few years, there have been great advances in the field of fish immunology, although diseases continue to cause economic losses to industry's aquaculture sector. This field of study has prompted researchers to investigate the role, function and molecular characterization of other genes that may participate in the immune system. Many of the mentioned references support the theory of the powerful link and interaction between the immune system and body status (hormones, treatment, environment, etc.). However, it will be necessary to gain a deep understanding of the mechanism underlying gene-gene interactions and the molecular bases of immune functions.

REFERENCES

- [1] Abo-Al-Ela, H. G. (2018): Hormones and fish monosex farming: A spotlight on immunity. – *Fish & Shellfish Immunology* 72: 23-30.
- [2] Abo-Al-Ela, H. G., El-Nahas, A. F., Mahmoud, S., Ibrahim, E. M. (2017a): The extent to which immunity, apoptosis and detoxification gene expression interact with 17 alpha-methyltestosterone. – *Fish & Shellfish Immunology* 60: 289-298.
- [3] Abo-Al-Ela, H. G., El-Nahas, A. F., Mahmoud, S., Ibrahim, E. M. (2017b): Vitamin C modulates the immunotoxic effect of 17 α -methyltestosterone in Nile tilapia. – *Biochemistry* 56(14): 2042-2050.
- [4] Akira, S., Takeda, K., Kaisho, T. (2001): Toll-like receptors: critical proteins linking innate and acquired immunity. – *Nature Immunology* 2(8): 675-680.

- [5] Alejo, A., Tafalla, C. (2011): Chemokines in teleost fish species. – *Developmental and Comparative Immunology* 35(12): 1215-1222.
- [6] Alvarez-Pellitero, P. (2008): Fish immunity and parasite infections: from innate immunity to immunoprophylactic prospects. – *Veterinary Immunology and Immunopathology* 126(3–4): 171-198.
- [7] Assani, K., Tazi, M. F., Amer, A. O., Kopp, B. T. (2014): IFN- γ stimulates autophagy-mediated clearance of *Burkholderia cenocepacia* in human cystic fibrosis macrophages. – *Plos One* 9(5): e96681.
- [8] Baggiolini, M. (1998): Chemokines and leukocyte traffic. – *Nature* 392(6676): 565-568.
- [9] Baggiolini, M., Dewald, B., Moser, B. (1994): Interleukin-8 and related chemotactic cytokines - Cxc and Cc chemokines. – *Advances in Immunology* 55: 97-179.
- [10] Baoprasertkul, P., Peatman, E., Chen, L. Q., He, C. B., Kucuktas, H., Li, P., Simmons, M., Liu, Z. J. (2004): Sequence analysis and expression of a CXC chemokine in resistant and susceptible catfish after infection of *Edwardsiella ictaluri*. – *Developmental and Comparative Immunology* 28(7-8): 769-780.
- [11] Basha, P. S., Rani, A. U. (2003): Cadmium-induced antioxidant defense mechanism in freshwater teleost *Oreochromis mossambicus* (Tilapia). – *Ecotoxicology and Environmental Safety* 56(2): 218-221.
- [12] Baum, A., Garcia-Sastre, A. (2010): Induction of type I interferon by RNA viruses: cellular receptors and their substrates. – *Amino Acids* 38(5): 1283-1299.
- [13] Bei, J. X., Suetake, H., Araki, K., Kikuchi, K., Yoshiura, Y., Lin, H. R., Suzuki, Y. (2006): Two interleukin (IL)-15 homologues in fish from two distinct origins. – *Molecular Immunology* 43(7): 860-869.
- [14] Benbrahim-Tallaa, L., Boussouar, F., Rey, C., Benahmed, M. (2002): Tumor necrosis factor-alpha inhibits glutathione S-transferase-alpha expression in cultured porcine Sertoli cells. – *Journal of Endocrinology* 175(3): 803-812.
- [15] Bergan, V., Robertsen, B. (2004): Characterization of Atlantic halibut (*Hippoglossus hippoglossus*) Mx protein expression. – *Developmental and Comparative Immunology* 28(10): 1037-1047.
- [16] Bermejo-Nogales, A., Saera-Vila, A., Calduch-Giner, J. A., Navarro, J. C., Sitja-Bobadilla, A., Perez-Sanchez, J. (2007): Differential metabolic and gene expression profile of juvenile common dentex (*Dentex dentex* L.) and gilthead sea bream (*Sparus aurata* L.) in relation to redox homeostasis. – *Aquaculture* 267(1-4): 213-224.
- [17] Beyne-Rauzy, O., Recher, C., Dastugue, N., Demur, C., Pottier, G., Laurent, G., Sabatier, L., Mansat-De Mas, V. (2004): Tumor necrosis factor alpha induces senescence and chromosomal instability in human leukemic cells. – *Oncogene* 23(45): 7507-7516.
- [18] Bird, S., Zou, J., Kono, T., Sakai, M., Dijkstra, J. M., Secombes, C. (2005a): Characterisation and expression analysis of interleukin 2 (*IL-2*) and *IL-21* homologues in the Japanese pufferfish, *Fugu rubripes*, following their discovery by synteny. – *Immunogenetics* 56(12): 909-923.
- [19] Bird, S., Zou, J., Savan, R., Kono, T., Sakai, M., Woo, J., Secombes, C. (2005b): Characterisation and expression analysis of an interleukin 6 homologue in the Japanese pufferfish, *Fugu rubripes*. – *Developmental and Comparative Immunology* 29(9): 775-789.
- [20] Bo, Y. X., Song, X. H., Wu, K., Hu, B., Sun, B. Y., Liu, Z. J., Fu, J. G. (2015): Characterization of interleukin-1 beta as a proinflammatory cytokine in grass carp (*Ctenopharyngodon idella*). – *Fish & Shellfish Immunology* 46(2): 584-595.
- [21] Boes, M. (2000): Role of natural and immune IgM antibodies in immune responses. – *Molecular Immunology* 37(18): 1141-1149.
- [22] Borza, T., Stone, C., Rise, M. L., Bowman, S., Johnson, S. C. (2010): Atlantic cod (*Gadus morhua*) CC chemokines: Diversity and expression analysis. – *Developmental and Comparative Immunology* 34(8): 904-913.

- [23] Bridle, A. R., Morrison, R. N., Cunningham, P. M. C., Nowak, B. F. (2006): Quantitation of immune response gene expression and cellular localisation of interleukin-1 beta mRNA in Atlantic salmon, *Salmo salar* L., affected by amoebic gill disease (AGD). – *Veterinary Immunology and Immunopathology* 114(1-2): 121-134.
- [24] Brinkmann, U. (1998): CAS, the human homologue of the yeast chromosome-segregation gene CSE1, in proliferation, apoptosis, and cancer. – *American Journal of Human Genetics* 62(3): 509-513.
- [25] Brinkmann, U., Brinkmann, E., Pastan, I. (1995): Expression cloning of cDNA that render cancer-cells resistant to *Pseudomonas* and diphtheria-toxin and Immunotoxins. – *Molecular Medicine* 1(2): 206-216.
- [26] Busfield, S. J., Comrack, C. A., Yu, G., Chickering, T. W., Smutko, J. S., Zhou, H., Leiby, K. R., Holmgren, L. M., Gearing, D. P., Pan, Y. (2000): Identification and gene organization of three novel members of the *IL-1* family on human chromosome 2. – *Genomics* 66(2): 213-216.
- [27] Casani, D., Randelli, E., Costantini, S., Facchiano, A. M., Zou, J., Martin, S., Secombes, C. J., Scapigliati, G., Buonocore, F. (2009): Molecular characterisation and structural analysis of an interferon homologue in sea bass (*Dicentrarchus labrax* L.). – *Molecular Immunology* 46(5): 943-952.
- [28] Chawla-Sarkar, M., Lindner, D. J., Liu, Y. F., Williams, B., Sen, G. C., Silverman, R. H., Borden, E. C. (2003): Apoptosis and interferons: Role of interferon-stimulated genes as mediators of apoptosis. – *Apoptosis* 8(3): 237-249.
- [29] Chen, W. H., Sun, L. T., Tsai, C. L., Song, Y. L., Chang, C. F. (2002): Cold-stress induced the modulation of catecholamines, cortisol, immunoglobulin M, and leukocyte phagocytosis in tilapia. – *General and Comparative Endocrinology* 126(1): 90-100.
- [30] Chen, W. Q., Xu, Q. Q., Chang, M. X., Zou, J., Secombes, C. J., Peng, K. M., Nie, P. (2010): Molecular characterization and expression analysis of the IFN-gamma related gene (*IFN-gamma rel*) in grass carp *Ctenopharyngodon idella*. – *Veterinary Immunology and Immunopathology* 134(3-4): 199-207.
- [31] Choi, I. K., Li, Y., Oh, E., Kim, J., Yun, C. O. (2013): Oncolytic adenovirus expressing IL-23 and p35 Elicits IFN- γ - and TNF- α -co-producing T Cell-mediated antitumor immunity. – *Plos One* 8(7).
- [32] Clarke, C. N., Kuboki, S., Tevar, A., Lentsch, A. B., Edwards, M. (2009): CXC chemokines play a critical role in liver injury, recovery, and regeneration. – *American Journal of Surgery* 198(3): 415-419.
- [33] Collet, B. (2014): Innate immune responses of salmonid fish to viral infections. – *Developmental and Comparative Immunology* 43(2): 160-173.
- [34] Colobran, R., Pujol-Borrell, R., Armengol, M. P., Juan, M. (2007): The chemokine network. I. How the genomic organization of chemokines contains clues for deciphering their functional complexity. – *Clinical and Experimental Immunology* 148(2): 208-217.
- [35] Cotter, T. G., Lennon, S. V., Glynn, J. G., Martin, S. J. (1990): Cell death via apoptosis and its relationship to growth, development and differentiation of both tumor and normal cells. – *Anticancer Research* 10(5A): 1153-1159.
- [36] Covello, J. M., Bird, S., Morrison, R. N., Battaglione, S. C., Secombes, C. J., Nowak, B. F. (2009): Cloning and expression analysis of three striped trumpeter (*Latris lineata*) pro-inflammatory cytokines, *TNF-alpha*, *IL-1 beta* and *IL-8*, in response to infection by the ectoparasitic, *Chondracanthus goldsmidi*. – *Fish & Shellfish Immunology* 26(5): 773-786.
- [37] Covello, J. M., Bird, S., Morrison, R. N., Bridle, A. R., Battaglione, S. C., Secombes, C. J., Nowak, B. F. (2013): Isolation of *RAG-1* and *IgM* transcripts from the striped trumpeter (*Latris lineata*), and their expression as markers for development of the adaptive immune response. – *Fish & Shellfish Immunology* 34(3): 778-788.

- [38] Das, B. K., Collet, B., Snow, M., Ellis, A. E. (2007): Expression of interferon type I and II, *Mx* and gamma IP genes in the kidney of Atlantic salmon, *Salmo salar*, is induced during smolting. – *Fish & Shellfish Immunology* 23(3): 514-520.
- [39] Davidson, N. J., Leach, M. W., Fort, M. M., Thompson-Snipes, L., Kuhn, R., Muller, W., Berg, D. J., Rennick, D. M. (1996): T helper cell 1-type CD4(+) T cells, but not B cells, mediate colitis in interleukin 10-deficient mice. – *Journal of Experimental Medicine* 184(1): 241-251.
- [40] Dinarello, C. A. (1997): Interleukin-1. – *Cytokine & Growth Factor Reviews* 8(4): 253-265.
- [41] Dinarello, C. A. (1999): Interleukin-18. – *Methods: A Companion to Methods in Enzymology* 19(1): 121-132.
- [42] Dominguez, M., Takemura, A., Tsuchiya, M., Nakamura, S. (2004): Impact of different environmental factors on the circulating immunoglobulin levels in the Nile tilapia, *Oreochromis niloticus*. – *Aquaculture* 241(1-4): 491-500.
- [43] Ellis, A. E. (2001): Innate host defense mechanisms of fish against viruses and bacteria. – *Developmental and Comparative Immunology* 25(8-9): 827-839.
- [44] Frova, C. (2006): Glutathione transferases in the genomics era: New insights and perspectives. – *Biomolecular Engineering* 23(4): 149-169.
- [45] Fu, Q., Yang, Y., Li, C., Zeng, Q., Zhou, T., Li, N., Liu, Y., Li, Y., Wang, X., Liu, S., Li, D., Liu, Z. (2017): The chemokine superfamily: II. The 64 CC chemokines in channel catfish and their involvement in disease and hypoxia responses. – *Developmental and Comparative Immunology* 73: 97-108.
- [46] Gallage, S., Katagiri, T., Endo, M., Futami, K., Endo, M., Maita, M. (2016): Influence of moderate hypoxia on vaccine efficacy against *Vibrio anguillarum* in *Oreochromis niloticus* (Nile tilapia). – *Fish & Shellfish Immunology* 51: 271-281.
- [47] Garcia, J., Munro, E. S., Monte, M. M., Fourrier, M. C. S., Whitelaw, J., Smail, D. A., Ellis, A. E. (2010): Atlantic salmon (*Salmo salar* L.) serum vitellogenin neutralises infectivity of infectious pancreatic necrosis virus (IPNV). – *Fish & Shellfish Immunology* 29(2): 293-297.
- [48] Gerber, S. A., Sedlacek, A. L., Cron, K. R., Murphy, S. P., Frelinger, J. G., Lord, E. M. (2013): IFN-gamma mediates the antitumor effects of radiation therapy in a murine colon tumor. – *American Journal of Pathology* 182(6): 2345-2354.
- [49] Goetz, F. W., Planas, J. V., MacKenzie, S. (2004): Tumor necrosis factors. – *Developmental and Comparative Immunology* 28(5): 487-497.
- [50] Grayfer, L., Belosevic, M. (2009): Molecular characterization, expression and functional analysis of goldfish (*Carassius auratus* L.) interferon gamma. – *Developmental and Comparative Immunology* 33(2): 235-246.
- [51] Grayfer, L., Walsh, J. G., Belosevic, M. (2008): Characterization and functional analysis of goldfish (*Carassius auratus* L.) tumor necrosis factor-alpha. – *Developmental and Comparative Immunology* 32(5): 532-543.
- [52] Gunimaladevi, I., Savan, R., Sakai, M. (2006): Identification, cloning and characterization of interleukin-17 and its family from zebrafish. – *Fish & Shellfish Immunology* 21(4): 393-403.
- [53] Haller, O., Frese, M., Kochs, G. (1998): Mx proteins: mediators of innate resistance to RNA viruses. – *Revue Scientifique Et Technique De L Office International Des Epizooties* 17(1): 220-230.
- [54] Haller, O., Staeheli, P., Kochs, G. (2007): Interferon-induced Mx proteins in antiviral host defense. – *Biochimie* 89(6-7): 812-818.
- [55] Hammerbeck, D. M., Bursleson, G. R., Schuller, C. J., Vasilakos, J. P., Tomai, M., Egging, E., Cochran, F. R., Woulfe, S., Miller, R. L. (2007): Administration of a dual toll-like receptor 7 and toll-like receptor 8 agonist protects against influenza in rats. – *Antiviral Research* 73(1): 1-11.

- [56] Hardie, L. J., Chappell, L. H., Secombes, C. J. (1994): Human tumor necrosis factor alpha influences rainbow trout *Oncorhynchus mykiss* leucocyte responses. – *Veterinary Immunology and Immunopathology* 40(1): 73-84.
- [57] He, C. B., Peatman, E., Baoprasertkul, P., Kucuktas, H., Liu, Z. J. (2004): Multiple CC chemokines in channel catfish and blue catfish as revealed by analysis of expressed sequence tags. – *Immunogenetics* 56(5): 379-387.
- [58] He, W., Yin, Z. X., Li, Y., Huo, W. L., Guan, H. J., Weng, S. P., Chan, S. M., He, J. G. (2006): Differential gene expression profile in spleen of mandarin fish *Siniperca chuatsi* infected with ISKNV, derived from suppression subtractive hybridization. – *Diseases of Aquatic Organisms* 73(2): 113-122.
- [59] Hemmi, H., Kaisho, T., Takeuchi, O., Sato, S., Sanjo, H., Hoshino, K., Horiuchi, T., Tomizawa, H., Takeda, K., Akira, S. (2002): Small anti-viral compounds activate immune cells via the TLR7 MyD88-dependent signaling pathway. – *Nature Immunology* 3(2): 196-200.
- [60] Hirono, I., Nam, B. H., Kurobe, T., Aoki, T. (2000): Molecular cloning, characterization, and expression of *TNF* cDNA and gene from Japanese flounder *Paralichthys olivaceus*. – *Journal of Immunology* 165(8): 4423-4427.
- [61] Hong, S. H., Peddie, S., Campos-Perez, J. J., Zou, J., Secombes, C. J. (2003): The effect of intraperitoneally administered recombinant IL-1 beta on immune parameters and resistance to *Aeromonas salmonicida* in the rainbow trout (*Oncorhynchus mykiss*). – *Developmental and Comparative Immunology* 27(9): 801-812.
- [62] Hu, Y. H., Chen, L., Sun, L. (2011): CXCL8 of *Scophthalmus maximus*: Expression, biological activity and immunoregulatory effect. – *Developmental and Comparative Immunology* 35(10): 1030-1037.
- [63] Hu, Y. H., Zhang, J. (2015): CsCCL17, a CC chemokine of *Cynoglossus semilaevis*, induces leukocyte trafficking and promotes immune defense against viral infection. – *Fish & Shellfish Immunology* 45(2): 771-779.
- [64] Huisling, M. O., Stolte, E., Flik, G., Savelkoul, H. F. J., Verburg-van Kemenade, B. M. L. (2003): CXC chemokines and leukocyte chemotaxis in common carp (*Cyprinus carpio* L.). – *Developmental and Comparative Immunology* 27(10): 875-888.
- [65] Huisling, M. O., Stet, R. J. M., Savelkoul, H. F. J., Verburg-van Kemenade, B. M. L. (2004): The molecular evolution of the interleukin-1 family of cytokines; IL-18 in teleost fish. – *Developmental and Comparative Immunology* 28(5): 395-413.
- [66] Ingerslev, H. C., Cunningham, C., Wergeland, H. I. (2006): Cloning and expression of *TNF-alpha*, *IL-1 beta* and *COX-2* in an anadromous and landlocked strain of Atlantic salmon (*Salmo salar* L.) during the smolting period. – *Fish & Shellfish Immunology* 20(4): 450-461.
- [67] Iwasaki, A., Medzhitov, R. (2004): Toll-like receptor control of the adaptive immune responses. – *Nature Immunology* 5(10): 987-995.
- [68] Janeway, C. A., Medzhitov, R. (2002): Innate immune recognition. – *Annual Review of Immunology* 20: 197-216.
- [69] Jault, C., Pichon, L., Chluba, J. (2004): Toll-like receptor gene family and TIR-domain adapters in *Danio rerio*. – *Molecular Immunology* 40(11): 759-771.
- [70] Jensen, I., Robertsen, B. (2002): Effect of double-stranded RNA and interferon on the antiviral activity of Atlantic salmon cells against infectious salmon anemia virus and infectious pancreatic necrosis virus. – *Fish & Shellfish Immunology* 13(3): 221-241.
- [71] Jia, R., Cao, L. P., Du, J. L., Wang, J. H., Liu, Y. J., Jeney, G., Xu, P., Yin, G. J. (2014): Effects of carbon tetrachloride on oxidative stress, inflammatory response and hepatocyte apoptosis in common carp (*Cyprinus carpio*). – *Aquatic Toxicology* 152: 11-19.
- [72] Jiang, S. G., Zhang, D. C., Li, J. Z., Liu, Z. X. (2008): Molecular characterization, recombinant expression and bioactivity analysis of the interleukin-1 beta from the yellowfin sea bream, *Acanthopagrus latus* (Houttuyn). – *Fish & Shellfish Immunology* 24(3): 323-336.

- [73] Kang, I. J., Yokota, H., Oshima, Y., Tsuruda, Y., Shimasaki, Y., Honjo, T. (2008): The effects of methyltestosterone on the sexual development and reproduction of adult medaka (*Oryzias latipes*). – *Aquatic Toxicology* 87(1): 37-46.
- [74] Kawai, T., Akira, S. (2009): The roles of TLRs, RLRs and NLRs in pathogen recognition. – *International Immunology* 21(4): 317-337.
- [75] Kawai, T., Akira, S. (2010): The role of pattern-recognition receptors in innate immunity: update on toll-like receptors. – *Nature Immunology* 11(5): 373-384.
- [76] Kawai, T., Sato, S., Ishii, K. J., Coban, C., Hemmi, H., Yamamoto, M., Terai, K., Matsuda, M., Inoue, J., Uematsu, S., Takeuchi, O., Akira, S. (2004): Interferon-alpha induction through toll-like receptors involves a direct interaction of IRF7 with MyD88 and TRAF6. – *Nature Immunology* 5(10): 1061-1068.
- [77] Khattiya, R., Kondo, H., Hirono, I., Aoki, T. (2007): Cloning, expression and functional analysis of a novel-chemokine gene of Japanese flounder, *Paralichthys olivaceus*, containing two additional cysteines and an extra fourth exon. – *Fish & Shellfish Immunology* 22(6): 651-662.
- [78] Kileng, O., Albuquerque, A., Robertsen, B. (2008): Induction of interferon system genes in Atlantic salmon by the imidazoquinoline S-27609, a ligand for toll-like receptor 7. – *Fish & Shellfish Immunology* 24(5): 514-522.
- [79] Kim, H. J., Yasuike, M., Kondo, H., Hirono, I., Aoki, T. (2007): Molecular characterization and gene expression of a CXC chemokine gene from Japanese flounder *Paralichthys olivaceus*. – *Fish & Shellfish Immunology* 23(6): 1275-1284.
- [80] Kim, J. W., Kim, E. G., Kim, D. H., Shim, S. H., Park, C. I. (2013): Molecular identification and expression analysis of the CC chemokine gene in rock bream (*Oplegnathus fasciatus*) and the biological activity of the recombinant protein. – *Fish & Shellfish Immunology* 34(3): 892-901.
- [81] Kim, Y. S., Ke, F., Zhang, Q. Y. (2009): Effect of beta-glucan on activity of antioxidant enzymes and Mx gene expression in virus infected grass carp. – *Fish & Shellfish Immunology* 27(2): 336-340.
- [82] Kochs, G., Haller, O. (1999): Interferon-induced human MxA GTPase blocks nuclear import of Thogoto virus nucleocapsids. – *Proceedings of the National Academy of Sciences of the United States of America* 96(5): 2082-2086.
- [83] Kono, T., Kusuda, R., Kawahara, E., Sakai, M. (2003): The analysis of immune responses of a novel CC-chemokine gene from Japanese flounder *Paralichthys olivaceus*. – *Vaccine* 21(5-6): 446-457.
- [84] Kumar, H., Kawai, T., Akira, S. (2011): Pathogen recognition by the innate immune system. – *International Reviews of Immunology* 30(1): 16-34.
- [85] Kuriyama, R., Nislow, C. (1992): Molecular-components of the mitotic spindle. – *Bioessays* 14(2): 81-88.
- [86] Lai, R., Jeyanathan, M., Shaler, C. R., Damjanovic, D., Khera, A., Horvath, C., Ashkar, A. A., Xing, Z. (2014): Restoration of innate immune activation accelerates Th1-cell priming and protection following pulmonary mycobacterial infection. – *European Journal of Immunology* 44(5): 1375-1386.
- [87] Laing, K. J., Secombes, C. J. (2004a): Chemokines. – *Developmental and Comparative Immunology* 28(5): 443-460.
- [88] Laing, K. J., Secombes, C. J. (2004b): Trout CC chemokines: comparison of their sequences and expression patterns. – *Molecular Immunology* 41(8): 793-808.
- [89] Lam, F. W. S., Wu, S. Y., Lin, S. J., Lin, C. C., Chen, Y. M., Wang, H. C., Chen, T. Y., Lin, H. T., Lin, J. H. Y. (2011): The expression of two novel orange-spotted grouper (*Epinephelus coioides*) TNF genes in peripheral blood leukocytes, various organs, and fish larvae. – *Fish & Shellfish Immunology* 30(2): 618-629.
- [90] Langevin, C., Aleksejeva, E., Passoni, G., Palha, N., Levraud, J. P., Boudinot, P. (2013): The antiviral innate immune response in fish: Evolution and conservation of the IFN system. – *Journal of Molecular Biology* 425(24): 4904-4920.

- [91] Larsen, R., Rokenes, T. P., Robertsen, B. (2004): Inhibition of infectious pancreatic necrosis virus replication by Atlantic salmon Mx1 protein. – *Journal of Virology* 78(15): 7938-7944.
- [92] Lazier, C. B., Langley, S., Ramsey, N. B., Wright, J. M. (1996): Androgen inhibition of vitellogenin gene expression in tilapia (*Oreochromis niloticus*). – *General and Comparative Endocrinology* 104(3): 321-329.
- [93] Lee, E. Y., Park, H. H., Kim, Y. T., Choi, T. J. (2001): Cloning and sequence analysis of the interleukin-8 gene from flounder (*Paralichthys olivaceus*). – *Gene* 274(1-2): 237-243.
- [94] Lee, J. Y., Hirono, I., Aoki, T. (2000): Cloning and analysis of expression of Mx cDNA in Japanese flounder, *Paralichthys olivaceus*. – *Developmental and Comparative Immunology* 24(4): 407-415.
- [95] Lee, P. T., Zou, J., Holland, J. W., Martin, S. A. M., Kanellos, T., Secombes, C. J. (2013): Identification and characterization of TLR7, TLR8a2, TLR8b1 and TLR8b2 genes in Atlantic salmon (*Salmo salar*). – *Developmental and Comparative Immunology* 41(2): 295-305.
- [96] Lee, S. H., Vidal, S. M. (2002): Functional diversity of Mx proteins: Variations on a theme of host resistance to infection. – *Genome Research* 12(4): 527-530.
- [97] Lester, K., Hall, M., Urquhart, K., Gahlawat, S., Collet, B. (2012): Development of an *in vitro* system to measure the sensitivity to the antiviral Mx protein of fish viruses. – *Journal of Virological Methods* 182(1-2): 1-8.
- [98] Li, J. H., Shao, J. Z., Xiang, L. X., Wen, Y. (2007): Cloning, characterization and expression analysis of pufferfish interleukin-4 cDNA: The first evidence of Th2-type cytokine in fish. – *Molecular Immunology* 44(8): 2078-2086.
- [99] Li, X. Y., Liu, L., Zhang, Y. N., Fang, Q., Li, Y. Y., Li, Y. L. (2013): Toxic effects of chlorpyrifos on lysozyme activities, the contents of complement C3 and IgM, and IgM and complement C3 expressions in common carp (*Cyprinus carpio* L.). – *Chemosphere* 93(2): 428-433.
- [100] Li, Y. X., Sun, J. S., Sun, L. (2011): An inflammatory CC chemokine of *Cynoglossus semilaevis* is involved in immune defense against bacterial infection. – *Fish & Shellfish Immunology* 31(3): 446-452.
- [101] Li, Y. X., Hu, Y. H., Sun, J. S., Sun, L. (2012): CsCXCe1: A novel *Cynoglossus semilaevis* CXC chemokine that functions as a chemoattractant and an immunomodulator for peripheral blood leukocytes. – *Developmental and Comparative Immunology* 37(1): 55-64.
- [102] Li, Z. J., Zhang, S. C., Liu, Q. H. (2008): Vitellogenin functions as a multivalent pattern recognition receptor with an opsonic activity. – *Plos One* 3(4): e1940.
- [103] Li, Z. J., Zhang, S. C., Zhang, J., Liu, M., Liu, Z. H. (2009): Vitellogenin is a cidal factor capable of killing bacteria via interaction with lipopolysaccharide and lipoteichoic acid. – *Molecular Immunology* 46(16): 3232-3239.
- [104] Lin, O. E., Ohira, T., Hirono, I., Saito-Taki, T., Aoki, T. (2005): Immunoanalysis of antiviral Mx protein expression in Japanese flounder (*Paralichthys olivaceus*) cells. – *Developmental and Comparative Immunology* 29(5): 443-455.
- [105] Lindenmann, J. (1962): Resistance of mice to mouse-adapted influenza a virus. – *Virology* 16(2): 203-204.
- [106] Liu, M., Pan, J. L., Ji, H. F., Zhao, B. S., Zhang, S. C. (2011a): Vitellogenin mediates phagocytosis through interaction with Fc gamma R. – *Molecular Immunology* 49(1-2): 211-218.
- [107] Liu, Q. H., Zhang, S. C., Li, Z. J., Gao, C. R. (2009): Characterization of a pattern recognition molecule vitellogenin from carp (*Cyprinus carpio*). – *Immunobiology* 214(4): 257-267.
- [108] Liu, S. Y., Sanchez, D. J., Cheng, G. H. (2011b): New developments in the induction and antiviral effectors of type I interferon. – *Current Opinion in Immunology* 23(1): 57-64.

- [109] Liu, Y., Chen, S. L., Meng, L., Zhang, Y. X. (2007): Cloning, characterization and expression analysis of a novel CXC chemokine from turbot (*Scophthalmus maximus*). – *Fish & Shellfish Immunology* 23(4): 711-720.
- [110] Low, C., Wadsworth, S., Burrells, C., Secombes, C. J. (2003): Expression of immune genes in turbot (*Scophthalmus maximus*) fed a nucleotide-supplemented diet. – *Aquaculture* 221(1-4): 23-40.
- [111] Lu, A. J., Hu, X. C., Xue, J., Zhu, J. R., Wang, Y., Zhou, G. Z. (2012): Gene expression profiling in the skin of zebrafish infected with *Citrobacter freundii*. – *Fish & Shellfish Immunology* 32(2): 273-283.
- [112] Lu, D.-Q., Bei, J.-X., Feng, L.-N., Zhang, Y., Liu, X.-C., Wang, L., Chen, J.-L., Lin, H.-R. (2008): Interleukin-1 beta gene in orange-spotted grouper, *Epinephelus coioides*: Molecular cloning, expression, biological activities and signal transduction. – *Molecular Immunology* 45(4): 857-867.
- [113] Magnadottir, B., Lange, S., Gudmundsdottir, S., Bogwald, J., Dalmo, R. A. (2005): Ontogeny of humoral immune parameters in fish. – *Fish & Shellfish Immunology* 19(5): 429-439.
- [114] Matsukawa, A., Hogaboam, C. M., Lukacs, N. W., Lincoln, P. M., Evanoff, H. L., Kunkel, S. L. (2000): Pivotal role of the CC chemokine, macrophage-derived chemokine, in the innate immune response. – *Journal of Immunology* 164(10): 5362-5368.
- [115] Medzhitov, R. (2007): Recognition of microorganisms and activation of the immune response. – *Nature* 449(7164): 819-826.
- [116] Medzhitov, R., Janeway, C. A. (2002): Decoding the patterns of self and nonself by the innate immune system. – *Science* 296(5566): 298-300.
- [117] Metz, J. R., Huisling, M. O., Leon, K., Verburg-van Kemenade, B. M. L., Flik, G. (2006): Central and peripheral interleukin-1 beta and interleukin-1 receptor I expression and their role in the acute stress response of common carp, *Cyprinus carpio* L. – *Journal of Endocrinology* 191(1): 25-35.
- [118] Micallef, M. J., Ohtsuki, T., Kohno, K., Tanabe, F., Ushio, S., Namba, M., Tanimoto, T., Torigoe, K., Fuji, M., Ikeda, M., Fukuda, S., Kurimoto, M. (1996): Interferon-gamma-inducing factor enhances T helper 1 cytokine production by stimulated human T cells: Synergism with interleukin-12 for interferon-gamma production. – *European Journal of Immunology* 26(7): 1647-1651.
- [119] Miettinen, M., Sareneva, T., Julkunen, I., Matikainen, S. (2001): IFNs activate toll-like receptor gene expression in viral infections. – *Genes and Immunity* 2(6): 349-355.
- [120] Ming, C., Rui, W., Liping, L., Huang, T., Weiyi, H., Jian, L., Chao, L., Aiyang, L., Honglin, L., Wanwen, L. (2013): Sequence and evolution differences of *Oreochromis niloticus* CXC contribute to the diversification of cellular immune responses in Tilapia with treatment of *Streptococcus iniae*. – *Journal of Animal and Veterinary Advances* 12(3): 303-311.
- [121] Mladineo, I., Block, B. A. (2010): Expression of cytokines IL-1 beta and TNF-alpha in tissues and cysts surrounding *Didymocystis wedli* (Digenea, Didymozoidae) in the Pacific bluefin tuna (*Thunnus orientalis*). – *Fish & Shellfish Immunology* 29(3): 487-493.
- [122] Mohanty, B. R., Sahoo, P. K. (2010): Immune responses and expression profiles of some immune-related genes in Indian major carp, *Labeo rohita* to *Edwardsiella tarda* infection. – *Fish & Shellfish Immunology* 28(4): 613-621.
- [123] Mulero, J. J., Pace, A. M., Nelken, S. T., Loeb, D. B., Correa, T. R., Drmanac, R., Ford, J. E. (1999): IL1HY1: A novel interleukin-1 receptor antagonist gene. – *Biochemical and Biophysical Research Communications* 263(3): 702-706.
- [124] Murphy, P. M., Baggiolini, M., Charo, I. F., Hebert, C. A., Horuk, R., Matsushima, K., Miller, L. H., Oppenheim, J. J., Power, C. A. (2000): International union of pharmacology. XXII. Nomenclature for chemokine receptors. – *Pharmacological Reviews* 52(1): 145-176.

- [125] Nagae, M., Fuda, H., Hara, A., Kawamura, H., Yamauchi, K. (1993): Changes in serum immunoglobulin m (IgM) concentrations during early development of chum Salmon (*Oncorhynchus keta*) as determined by sensitive ELISA technique. – *Comparative Biochemistry and Physiology - Part A* 106(1): 69-74.
- [126] Najakshin, A. M., Mechetina, L. V., Alabyev, B. Y., Taranin, A. V. (1999): Identification of an IL-8 homolog in lamprey (*Lampetra fluviatilis*): early evolutionary divergence of chemokines. – *European Journal of Immunology* 29(2): 375-382.
- [127] Nakharuthai, C., Areechon, N., Srisapoome, P. (2016): Molecular characterization, functional analysis, and defense mechanisms of two CC chemokines in Nile tilapia (*Oreochromis niloticus*) in response to severely pathogenic bacteria. – *Developmental and Comparative Immunology* 59: 207-228.
- [128] Nomiyama, H., Hieshima, K., Osada, N., Kato-Unoki, Y., Otsuka-Ono, K., Takegawa, S., Izawa, T., Yoshizawa, A., Kikuchi, Y., Tanase, S., Miura, R., Kusuda, J., Nakao, M., Yoshie, O. (2008): Extensive expansion and diversification of the chemokine gene family in zebrafish: Identification of a novel chemokine subfamily CX. – *BMC Genomics* 9(1): 222.
- [129] Nordmann, P., Ronco, E., Guenounou, M. (1993): Involvement of interferon-gamma and tumor necrosis factor-alpha in host defense against *Rhodococcus equi*. – *Journal of Infectious Diseases* 167(6): 1456-1459.
- [130] Palti, Y., Gahr, S. A., Purcell, M. K., Hadidi, S., Rexroad, C. E., Wiens, G. D. (2010): Identification, characterization and genetic mapping of TLR7, TLR8a1 and TLR8a2 genes in rainbow trout (*Oncorhynchus mykiss*). – *Developmental and Comparative Immunology* 34(2): 219-233.
- [131] Pan, G. H., Risser, P., Mao, W. G., Baldwin, D. T., Zhong, A. W., Filvaroff, E., Yansura, D., Lewis, L., Eigenbrot, C., Henzel, W. J., Vandlen, R. (2001): IL-1H, an interleukin 1-related protein that binds IL-18 receptor/IL-1Rrp. – *Cytokine* 13(1): 1-7.
- [132] Peatman, E., Liu, Z. J. (2007): Evolution of CC chemokines in teleost fish: a case study in gene duplication and implications for immune diversity. – *Immunogenetics* 59(8): 613-623.
- [133] Pichlmair, A., Sousa, C. R. E. (2007): Innate recognition of viruses. – *Immunity* 27(3): 370-383.
- [134] Poisa-Beiro, L., Dios, S., Montes, A., Aranguren, R., Figueras, A., Novoa, B. (2008): Nodavirus increases the expression of Mx and inflammatory cytokines in fish brain. – *Molecular Immunology* 45(1): 218-225.
- [135] Praveen, K., Evans, D. L., Jaso-Friedmann, L. (2006a): Constitutive expression of tumor necrosis factor-alpha in cytotoxic cells of teleosts and its role in regulation of cell-mediated cytotoxicity. – *Molecular Immunology* 43(3): 279-291.
- [136] Praveen, K., Leary, J. H., Evans, D. L., Jaso-Friedmann, L. (2006b): Molecular cloning of cellular apoptosis susceptibility (CAS) gene in *Oreochromis niloticus* and its proposed role in regulation of non-specific cytotoxic cell (NCC) functions. – *Fish & Shellfish Immunology* 20(4): 647-655.
- [137] Puerto, M., Gutierrez-Praena, D., Prieto, A., Pichardo, S., Jos, A., Miguel-Carrasco, J., Vazquez, C., Camean, A. M. (2011): Subchronic effects of cyanobacterial cells on the transcription of antioxidant enzyme genes in tilapia (*Oreochromis niloticus*). – *Ecotoxicology* 20(2): 479-490.
- [138] Purcell, M. K., Kurath, G., Garver, K. A., Herwig, R. P., Winton, J. R. (2004): Quantitative expression profiling of immune response genes in rainbow trout following infectious haematopoietic necrosis virus (IHNV) infection or DNA vaccination. – *Fish & Shellfish Immunology* 17(5): 447-462.
- [139] Qin, Q. W., Ototake, M., Noguchi, K., Soma, G. I., Yokomizo, Y., Nakanishi, T. (2001): Tumor necrosis factor alpha (TNF alpha)-like factor produced by macrophages in rainbow trout, *Oncorhynchus mykiss*. – *Fish & Shellfish Immunology* 11(3): 245-256.

- [140] Randelli, E., Buonocore, F., Scapigliati, G. (2008): Cell markers and determinants in fish immunology. – *Fish & Shellfish Immunology* 25(4): 326-340.
- [141] Rauta, P. R., Samanta, M., Dash, H. R., Nayak, B., Das, S. (2014): Toll-like receptors (TLRs) in aquatic animals: Signaling pathways, expressions and immune responses. – *Immunology Letters* 158(1-2): 14-24.
- [142] Reda, R. M., Mahmoud, R., Selim, K. M., El-Araby, I. E. (2016): Effects of dietary acidifiers on growth, hematology, immune response and disease resistance of Nile tilapia, *Oreochromis niloticus*. – *Fish & Shellfish Immunology* 50: 255-262.
- [143] Sadler, A. J., Williams, B. R. G. (2008): Interferon-inducible antiviral effectors. – *Nature Reviews Immunology* 8(7): 559-568.
- [144] Salaun, B., Romero, P., Lebecque, S. (2007): Toll-like receptors' two-edged sword: when immunity meets apoptosis. – *European Journal of Immunology* 37(12): 3311-3318.
- [145] Samuel, C. E. (1991): Antiviral actions of interferon - interferon-regulated cellular proteins and their surprisingly selective antiviral activities. – *Virology* 183(1): 1-11.
- [146] Saurabh, S., Mohanty, B. R., Sahoo, P. K. (2011): Expression of immune-related genes in rohu *Labeo rohita* (Hamilton) by experimental freshwater lice *Argulus siamensis* (Wilson) infection. – *Veterinary Parasitology* 175(1-2): 119-128.
- [147] Savan, R., Sakai, M. (2004): Presence of multiple isoforms of TNF alpha in carp (*Cyprinus carpio* L.): genomic and expression analysis. – *Fish & Shellfish Immunology* 17(1): 87-94.
- [148] Savan, R., Igawa, D., Sakai, M. (2003): Cloning, characterization and expression analysis of interleukin-10 from the common carp, *Cyprinus carpio* L. – *European Journal of Biochemistry* 270(23): 4647-4654.
- [149] Scherf, U., Pastan, I., Willingham, M. C., Brinkmann, U. (1996): The human CAS protein which is homologous to the CSE1 yeast chromosome segregation gene product is associated with microtubules and mitotic spindle. – *Proceedings of the National Academy of Sciences of the United States of America* 93(7): 2670-2674.
- [150] Schroder, K., Hertzog, P. J., Ravasi, T., Hume, D. A. (2004): Interferon-gamma: an overview of signals, mechanisms and functions. – *Journal of Leukocyte Biology* 75(2): 163-189.
- [151] Schultz, U., Kaspers, B., Staeheli, P. (2004): The interferon system of non-mammalian vertebrates. – *Developmental and Comparative Immunology* 28(5): 499-508.
- [152] Scott, K., Leaver, M. J., George, S. G. (1992): Regulation of hepatic glutathione-S-transferase expression in flounder. – *Marine Environmental Research* 34(1-4): 233-236.
- [153] Secombes, C. J., Wang, T., Hong, S., Peddie, S., Crampe, M., Laing, K. J., Cunningham, C., Zou, J. (2001): Cytokines and innate immunity of fish. – *Developmental and Comparative Immunology* 25(8-9): 713-723.
- [154] Smith, D. E., Renshaw, B. R., Ketchum, R. R., Kubin, M., Garka, K. E., Sims, J. E. (2000): Four new members expand the interleukin-1 superfamily. – *Journal of Biological Chemistry* 275(2): 1169-1175.
- [155] Staeheli, P., Yu, Y. X., Grob, R., Haller, O. (1989): A double-stranded RNA-inducible fish gene homologous to the murine influenza-virus resistance gene *Mx*. – *Molecular and Cellular Biology* 9(7): 3117-3121.
- [156] Stolte, E. H., Savelkoul, H. F. J., Wiegertjes, G., Flik, G., Verburg-van Kemenade, B. M. L. (2008): Differential expression of two interferon-gamma genes in common carp (*Cyprinus carpio* L.). – *Developmental and Comparative Immunology* 32(12): 1467-1481.
- [157] Strandén, A. M., Staeheli, P., Pavlovic, J. (1993): Function of the mouse Mx1 protein is inhibited by overexpression of the PB2 protein of influenza-virus. – *Virology* 197(2): 642-651.
- [158] Su, Y. L., Guo, Z. X., Xu, L. W., Jiang, J. Z., Wang, J. Y., Feng, J. (2012): Identification of a cobia (*Rachycentron canadum*) CC chemokine gene and its involvement in the inflammatory response. – *Fish & Shellfish Immunology* 32(1): 204-210.

- [159] Sun, B. J., Robertsen, B., Wang, Z. Q., Bin, L. (2009): Identification of an Atlantic salmon IFN multigene cluster encoding three IFN subtypes with very different expression properties. – *Developmental and Comparative Immunology* 33(4): 547-558.
- [160] Sun, J. S., Zhao, L., Sun, L. (2011): Interleukin-8 of *Cynoglossus semilaevis* is a chemoattractant with immunoregulatory property. – *Fish & Shellfish Immunology* 30(6): 1362-1367.
- [161] Svingerud, T., Solstad, T., Sun, B. J., Nyrud, M. L. J., Kileng, O., Greiner-Tollersrud, L., Robertsen, B. (2012): Atlantic salmon type I IFN subtypes show differences in antiviral activity and cell-dependent expression: Evidence for high IFN β /IFN γ -producing cells in fish lymphoid tissues. – *Journal of Immunology* 189(12): 5912-5923.
- [162] Tafalla, C., Aranguren, R., Secombes, C. J., Figueras, A., Novoa, B. (2004): Cloning and analysis of expression of a gilthead sea bream (*Sparus aurata*) Mx cDNA. – *Fish & Shellfish Immunology* 16(1): 11-24.
- [163] Tafalla, C., Coll, J., Secombes, C. J. (2005): Expression of genes related to the early immune response in rainbow trout (*Oncorhynchus mykiss*) after viral haemorrhagic septicemia virus (VHSV) infection. – *Developmental and Comparative Immunology* 29(7): 615-626.
- [164] Takeda, K., Akira, S. (2001): Roles of Toll-like receptors in innate immune responses. – *Genes to Cells* 6(9): 733-742.
- [165] Takemura, A. (1993): Changes in an immunoglobulin M (IgM)-like protein during larval stages in Tilapia, *Oreochromis mossambicus*. – *Aquaculture* 115(3-4): 233-241.
- [166] Tanekhy, M., Kono, T., Sakai, M. (2010): Cloning, characterization, and expression analysis of Toll-like receptor-7 cDNA from common carp, *Cyprinus carpio* L. – *Comparative Biochemistry and Physiology - Part D* 5(4): 245-255.
- [167] Tassakka, A. C. M. A. R., Sakai, M. (2004): Expression of immune-related genes in the common carp (*Cyprinus carpio* L.) after stimulation by CpG oligodeoxynucleotides. – *Aquaculture* 242(1-4): 1-12.
- [168] Tellez-Banuelos, M. C., Santerre, A., Casas-Solis, J., Zaitseva, G. (2010): Endosulfan increases seric interleukin-2 like (IL-2L) factor and immunoglobulin M (IgM) of Nile tilapia (*Oreochromis niloticus*) challenged with *Aeromonas hydrophila*. – *Fish & Shellfish Immunology* 28(2): 401-405.
- [169] Tortorella, D., Gewurz, B. E., Furman, M. H., Schust, D. J., Ploegh, H. L. (2000): Viral subversion of the immune system. – *Annual Review of Immunology* 18: 861-926.
- [170] Van der Aa, L. M., Chadzinska, M., Golbach, L. A., Ribeiro, C. M. S., Verburg-van Kemenade, B. M. L. (2012): Pro-inflammatory functions of carp CXCL8-like and CXCL10 chemokines. – *Developmental and Comparative Immunology* 36(4): 741-750.
- [171] Vandercappellen, J., Van Damme, J., Struyf, S. (2008): The role of CXC chemokines and their receptors in cancer. – *Cancer Letters* 267(2): 226-244.
- [172] Verrier, E. R., Langevin, C., Benmansour, A., Boudinot, P. (2011): Early antiviral response and virus-induced genes in fish. – *Developmental and Comparative Immunology* 35(12): 1204-1214.
- [173] Villalta, F., Zhang, Y., Bibb, K. E., Kappes, J. C., Lima, M. F. (1998): The cysteine-cysteine family of chemokines RANTES, MIP-1 alpha, and MIP-1 beta induce trypanocidal activity in human macrophages via nitric oxide. – *Infection and Immunity* 66(10): 4690-4695.
- [174] Wan, Y. Y., Flavell, R. A. (2009): How diverse—CD4 effector T cells and their functions. – *Journal of Molecular Cell Biology* 1(1): 20-36.
- [175] Wang, C. Y., Zhao, J. M., Mu, C. K., Wang, Q., Wu, H. F., Wang, C. L. (2013): cDNA cloning and mRNA expression of four glutathione S-transferase (*GST*) genes from *Mytilus galloprovincialis*. – *Fish & Shellfish Immunology* 34(2): 697-703.
- [176] Wang, J. X., Shi, X. J., Du, Y. B., Zhou, B. S. (2011): Effects of xenoestrogens on the expression of vitellogenin (*vltg*) and cytochrome P450 aromatase (*cyp19a* and *b*) genes in

- zebrafish (*Danio rerio*) larvae. – Journal of Environmental Science and Health - Part A 46(9): 960-967.
- [177] Wang, T. H., Holland, J. W., Bols, N., Secombes, C. J. (2005): Cloning and expression of the first nonmammalian interleukin-11 gene in rainbow trout *Oncorhynchus mykiss*. – FEBS Journal 272(5): 1136-1147.
- [178] Warr, G. W. (1995): The immunoglobulin genes of fish. – Developmental and Comparative Immunology 19(1): 1-12.
- [179] Warren, D. W., Pasupuleti, V., Lu, Y., Platler, B. W., Horton, R. (1990): Tumor necrosis factor and interleukin-1 stimulate testosterone secretion in adult male rat Leydig cells *in vitro*. – Journal of Andrology 11(4): 353-360.
- [180] Warringa, R. A. J., Koenderman, L., Kok, P. T. M., Kreukniet, J., Bruijnzeel, P. L. B. (1991): Modulation and induction of eosinophil chemotaxis by granulocyte-macrophage colony-stimulating factor and interleukin-3. – Blood 77(12): 2694-2700.
- [181] White, M. V., Yoshimura, T., Hook, W., Kaliner, M. A., Leonard, E. J. (1989): Neutrophil attractant activation protein-1 (Nap-1) causes human basophil histamine-release. – Immunology Letters 22(2): 151-154.
- [182] Wrzesien-Kus, A., Smolewski, P., Sobczak-Pluta, A., Wierzbowska, A., Robak, T. (2004): The inhibitor of apoptosis protein family and its antagonists in acute leukemias. – Apoptosis 9(6): 705-715.
- [183] Yan, Z., Hunter, V., Weed, J., Hutchison, S., Lyles, R., Terranova, P. (1993): Tumor necrosis factor-alpha alters steroidogenesis and stimulates proliferation of human ovarian granulosa cells *in vitro*. – Fertility and Sterility 59(2): 332-338.
- [184] Yoshiura, Y., Kiryu, I., Fujiwara, A., Suetake, H., Suzuki, Y., Nakanishi, T., Ootake, M. (2003): Identification and characterization of *Fugu* orthologues of mammalian interleukin-12 subunits. – Immunogenetics 55(5): 296-306.
- [185] Zhang, J., Chen, L. P., Wei, X. L., Xu, M. X., Huang, C. X., Wang, W. M., Wang, H. L. (2014a): Characterization of a novel CC chemokine *CCL4* in immune response induced by nitrite and its expression differences among three populations of *Megalobrama amblycephala*. – Fish & Shellfish Immunology 38(1): 88-95.
- [186] Zhang, J. Z., Ao, J. Q., Chen, X. H. (2008): Molecular and functional characterization of a novel CC chemokine in large yellow croaker (*Pseudosciaena crocea*). – Fish & Shellfish Immunology 25(5): 664-671.
- [187] Zhang, S. C., Sun, Y. N., Pang, Q. X., Shi, X. D. (2005): Hemagglutinating and antibacterial activities of vitellogenin. – Fish & Shellfish Immunology 19(1): 93-95.
- [188] Zhang, S. C., Wang, S. H., Li, H. Y., Li, L. (2011): Vitellogenin, a multivalent sensor and an antimicrobial effector. – International Journal of Biochemistry & Cell Biology 43(3): 303-305.
- [189] Zhang, Y. B., Gui, J. F. (2012): Molecular regulation of interferon antiviral response in fish. – Developmental and Comparative Immunology 38(2): 193-202.
- [190] Zhang, Z., Xu, L., Liu, W. S., Yang, Y. L., Du, Z. Y., Zhou, Z. G. (2014b): Effects of partially replacing dietary soybean meal or cottonseed meal with completely hydrolyzed feather meal (defatted rice bran as the carrier) on production, cytokines, adhesive gut bacteria, and disease resistance in hybrid tilapia (*Oreochromis niloticus* female x *Oreochromis aureus* male). – Fish & Shellfish Immunology 41(2): 517-525.
- [191] Zhao, F., Li, Y. W., Pan, H. J., Shi, C. B., Luo, X. C., Li, A. X., Wu, S. Q. (2013): Expression profiles of toll-like receptors in channel catfish (*Ictalurus punctatus*) after infection with *Ichthyophthirius multifiliis*. – Fish & Shellfish Immunology 35(3): 993-997.
- [192] Zhao, Y., Nichols, J. E., Valdez, R., Mendelson, C. R., Simpson, E. R. (1996): Tumor necrosis factor-alpha stimulates aromatase gene expression in human adipose stromal cells through use of an activating protein-1 binding site upstream of promoter 1.4. – Molecular Endocrinology 10(11): 1350-1357.

- [193] Zou, J., Secombes, C. J. (2011): Teleost fish interferons and their role in immunity. – *Developmental and Comparative Immunology* 35(12): 1376-1387.
- [194] Zou, J., Cunningham, C., Secombes, C. J. (1999): The rainbow trout *Oncorhynchus mykiss* interleukin-1 beta gene has a different organization to mammals and undergoes incomplete splicing. – *European Journal of Biochemistry* 259(3): 901-908.
- [195] Zou, J., Peddie, S., Scapigliati, G., Zhang, Y., Bols, N. C., Ellis, A. E., Secombes, C. J. (2003): Functional characterisation of the recombinant tumor necrosis factors in rainbow trout, *Oncorhynchus mykiss*. – *Developmental and Comparative Immunology* 27(9): 813-822.
- [196] Zou, J., Bird, S., Truckle, J., Bols, N., Horne, M., Secombes, C. (2004a): Identification and expression analysis of an IL-18 homologue and its alternatively spliced form in rainbow trout (*Oncorhynchus mykiss*). – *European Journal of Biochemistry* 271(10): 1913-1923.
- [197] Zou, J., Yasutoshi, Y. B., Dijkstra, J. M., Sakai, M., Ototake, M., Secombes, C. (2004b): Identification of an interferon gamma homologue in Fugu, *Takifugu rubripes*. – *Fish & Shellfish Immunology* 17(4): 403-409.

THE IMPACT OF ENVIRONMENTAL FACTORS ON DISTRIBUTION OF *FERULA OVINA* (BOISS.) BOISS. IN NORTHWEST IRAN

AGHAJANLOU, F.¹ – GHORBANI, A.^{1*} – ZARE CHAHOUKI, M. A.² – MOSTAFAZADEH, R.¹ –
HASHEMI MAJD, K.³

¹*Department of Natural Resources, Faculty of Agriculture and Natural Resources, University of
Mohaghegh Ardabili
Ardabil, Iran*

²*Department of Rehabilitation of Arid and Mountainous Regions, University of Tehran
Tehran, Iran*

³*Department of Soil Science, Faculty of Agriculture and Natural Resources, University of
Mohaghegh Ardabili
Ardabil, Iran*

**Corresponding author
e-mail: a_ghorbani@uma.ac.ir*

(Received 1st Aug 2017; accepted 11th Jan 2018)

Abstract. *Ferula ovina* is a forage species, and of the species that is very important in soil conservation and water protection in the rangelands. It has become an endangered species in Iran due to regular cutting and overgrazing. The focus of this study is to investigate the effect of ecological factors on distribution of *F. ovina* in the study area. Samples were collected from three habitats (sites) where *F. ovina* was present along with three sites which did not have it. Three 150 m transects were established based on random-systematically method on each site. On each transect, 10 square plots (2×2 m) were set up, and soil surface features were measured. Climatologic factors were assessed and physiographic factors were extracted for each site. Soil samples were collected from a 0–30 cm depth for each transect, and the values of soil were determined through laboratory analysis. According to the results, a significant difference was found for the parameters of elevation, slope, aspect, temperature, EC, pH, OC, phosphorus, clay, silt and sand ($P \leq 0.01$) between habitats where *F. ovina* were present and absent. Results of discriminant analysis suggested that the amount of sand and gravel on soil surface, phosphorous, clay, and EC were effective factors in the distribution of target species.

Keywords: *ecological factors, species distribution model, discriminant analysis*

Introduction

Environmental variables affect the distribution of plant species (Ashcroft et al., 2011). Therefore, identification of effective variables on spatial distributions of plant communities is an essential issue in ecology (Araujo and Guisan, 2006; Bagheri et al., 2017). Often, there are many combinations of predictor variables that can describe the species distributions, especially when environmental variables are correlated, which leads to uncertainty on the effects of each variable (Platts et al., 2008; Murray and Conner, 2009). Therefore, determining the plant habitats and effective variables on their distributions is the first step in rangeland management (Bagheri et al., 2017). The study of species distribution studies focuses on defining environmental variables that control a plant's movement into adjacent habitats (Arundel, 2005; Mirzaei Mossivand et al., 2017). These variables or controllers outline various spatial aspects of individual plant species distributions (Ghorbani et al., 2015).

The presence and distribution of plant species in rangeland ecosystems are not random, but variations of climate, soil, topography, anthropological and other attributes play a major role in their expansion (Ghorbani et al., 2015; Akbarlou and Nodehi, 2016). Determination of the variables that control the presence and distribution of rangeland species is one of the main objectives in rangeland ecosystems studies and assessment (Mirzaei Mossivand et al., 2017). However, interactions among plant species and both soil properties and other environmental variables have been well established for some plant species (Bagheri et al., 2017; Mirzaei Mossivand et al., 2017). However, understanding how a variety of plant species in native rangelands responds to soil properties and other environmental variables is not properly known (Ghorbani et al., 2015; Zare-Chahouki and Piri-Sahragard, 2016). Xian-Li et al. (2008) have studied the relationships among vegetation, soil and topography in a dry-warm river valley in south west China. Their results confirmed that plant diversity is mainly correlated with soil water content, and soil water content was mainly determined by soil texture, especially clay content. The results of Yibing (2008) achieved using principal components analysis (PCA) and correspondence analysis (CA) in China, which showed that the soil's physical and chemical properties such as nutrients, moisture, salinity, and pH were effective on the homogeneity of the habitat.

In the study of relationships between environmental variables and species diversity in Loess plateau of China, Zhang and Dong (2010) reported that elevation, soil type, slope and aspect were important factors in Loessi zone's recovery and had determining factor roles in species distribution. Zare-Chahouki and Zare-Chahouki (2010), in a study on the relationship between environmental variables and species distribution in arid and semiarid areas, concluded that soil texture, salinity, soil depth, available N, K, OM, lime and soil moisture were the major soil variables responsible for differences in the pattern of species. Ghorbani and Asghari (2014) in a study of environmental factors affecting the distribution of *Festuca ovina* in the southeastern rangelands of Sabalan, reported that this species is more compatible to higher altitudes as well as lower temperatures and does not tolerate soil salinity, and is more compatible with a pH of 7.1 to 7.3. Moreover, they concluded that OM, P, and K provide better conditions for its growth.

Studies have revealed that soil attributes are of the main parameters in distribution of plant societies, particularly in arid land (Goodal and Perry, 1979) and correlation of some soil chemical characters as well as soil humidity with vegetation cover have been documented in different studies (Dyakov, 2014; Sheikh et al., 2014; Gemedo et al., 2014). However, there are other studies, which emphasized the role of climatic and topographic parameters in addition to physical and chemical specifications in plant species distribution (Davies et al., 2006; Ghorbani et al., 2015; Mirzaei Mossivand et al., 2017).

Ferula L. is the third largest genus of the Apiaceae family (Yaqoob and Nawchoo, 2015; 2016) and includes 180–185 species (Pimenov and Leonov, 2004) that have been reported from USSR, Pakistan, India, western Himalayas, Saudi Arabia, China and Iran (Kurzyrna-Mlynik et al., 2008; Yaqoob and Nawchoo, 2016). It has large presence in Asia, particularly in Turkey, Iran and Turkmenistan compared to other genera in the family (Pimenov and Leonov, 1993). Thirty-two species of *Ferula* have been reported from Iran, where some of its species are known as Endemic (Mozaffarian, 1983; 2007; Yaqoob and Nawchoo, 2016). The popular Persian name of the most of *Ferula* species is "Koma" and *F. ovina* (Boiss.) Boiss. It is one of these species which is distributed in different regions of Iran (Mozaffarian, 1983; 2007).

Anti-spasmodic, anti-cholinergic and smooth muscle relaxant activities of the aqueous extracts of *F. ovina* have previously been reported and it can be termed a medicinal plant (Al-

Khalil et al., 1990; Ghannadi et al., 2002; Moghaddam Matin et al., 2014). Studies showed that ecological parameters (rainfall, fog and altitude) affect the quality of resins produced by *Ferula* species (Safaian and Shokri, 1993; Menglan et al., 2005). *Ferula* species can be consumed fresh or processed in several forms. Leaves and essential oils in *Ferula* spp. traditionally have been considered to have medicinal value and there is strong evidence of anti-microbial active compounds (Syed et al., 1987).

F. ovina is consumed for resins or as a grazing plant (Amooaghaie, 2009). As Amooaghaie (2009) reported that *F. ovina* is a forage species, it has become an endangered species in Iran due to regular cutting and overgrazing. Azhir and Shahmoradi (2007) conducted a preliminary descriptive study of *Ferula ovina*'s natural habitat in Tehran province, Iran. They have reported that this species is distributed over 2000 to 3200 m above sea level, in areas where mean annual precipitation is higher than 400 mm and mean annual temperature is about 8.0 °C. They also reported that the *Ferula* species is distributed in areas where EC is lower than 1 ds/m and pH 7 to 7.7, on loamy to sandy soil texture. Its distribution observed is in different aspects on the 40 to 50% slopes. The density of *Ferula* species in distributed habitats varies from 1600 to 2300 bunch per hectare. The vegetation stage starts from early May and seed ripening takes place in June. However, locals harvest it at the end of the growth stage as winter forage for their sheep and goat. *F. ovina* is distributed in the Zanzan province as a main species of rangelands (Aghajanlou et al., 2015). Therefore, regarding the importance of *F. ovina* in forage production, soil conservation and water protection in rangelands, and its status in the context of vegetation of Iran, many more studies are needed to understand the factors affecting its growth and distribution.

This study was conducted to investigate the effects of environmental variables on the distribution of *F. ovina* species in the rangelands of Zanzan province in northwest of Iran and determine the most important and effective environmental variables in its distribution. This was also done to chalk out appropriate management strategies for maintenance, restoration and development of its communities on the growing areas. To improve the management of rangelands and offer a baseline for restoration attempts, an understanding of the variables that determine the rangelands species distribution is required. For this purpose, this study was conducted to identify the roles of topography, climate and soil properties, in the distribution of *F. ovina*. Identification of these properties in a given rangeland helps one chart proper management strategies for restoration of similar rangelands.

Materials and methods

The study area

The study area was selected in the rangelands of Zanzan province, Iran (*Fig. 1*). Initially, in order to recognize the distribution of the genus *Ferula*, an overall study was conducted by literature review (Hedge et al., 1982; Mozaffarian, 2007; Aghajanlou et al., 2015). Moreover, fieldwork was conducted in Zanzan province to select the habitats for *Ferula* genus. Three habitats with the local name of Soltanieh (48° 49' 35"E; 36° 18' 20"N), Zakr-Khanchay (48° 44' 41" E; 36° 41' 30"N) and Shilander (48° 37' 54"E; 36° 50' 01"N) were selected with *F. ovina* distribution (*Figs. 1, 2 and 3*). The selected habitats' slope ranges from about 47 to 62% and geographical aspects of the three study sites are southern, southern, and southern to northern, respectively. According to recorded data of meteorological stations (a 10-year period, 2006 to 2015) within and around the selected regions, mean annual precipitation of the selected sites are 403, 347 and 327 mm, respectively. Moreover, the mean annual temperatures of the studied sites are 7.2 °C, 8.3 °C, and 6.4 °C, respectively. Maximum and

minimum precipitation occurs in February and July, respectively. Soil textures of the selected habitats are loam, loam and sandy loam, respectively. Main species of the selected habitats includes perennial herbaceous such as *Tanacetum polycephalum*, *Pimpinella tragium*, *Campanula steveni*, *Clastapus vestitus* and *Nepeta heliotropifolia*, dominant grasses such as *Agropyrum libanoticum*, *Festuca ovina*, *Bromus tomentellus* and *Poa bulbosa* and shrubs such as *Acantholimon festucaceum*, *Thymus kotschyanus*, *Astragalus baghensis*, *Astragalus gossypinus*, *Silene bupleuroides* and *Hypericum scabrum* (Aghajanlou et al., 2015).

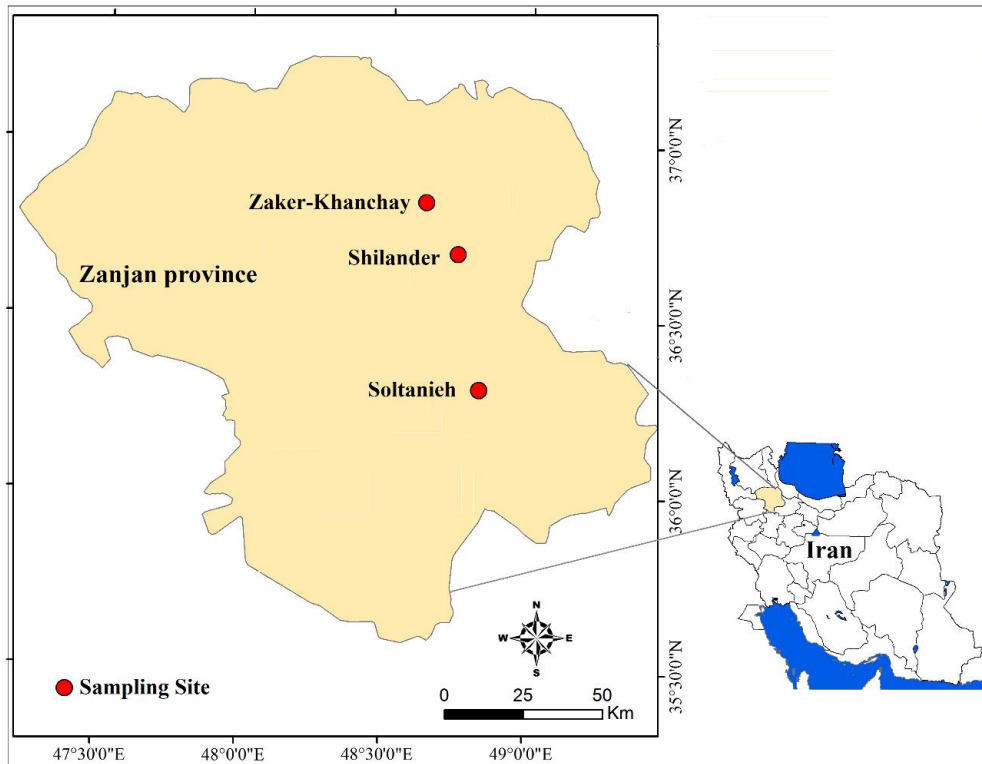


Figure 1. The location of the study area, and selected sites on Zanzan province, Iran



Figure 2. *Ferula ovina* (Boiss.) Boiss. a perennial forbs growing in Zanzan province in Iran, a) The habitat of Shilander and b) The habitat of Zaker-Khanchay and



Figure 3. Over-harvesting of *F. ovina* for providing winter forage for livestock in the study area by locals, **a)** and **b)** the habitat of Soltanieh

Sampling

In each habitat, initially one site with *F. ovina* distribution was selected as the presence of the selected species. Near to each of the selected sites, another site which did not have *F. ovina* species was selected in the same habitat. Therefore, a total of six sites (with *F. ovina* presence and absence) were selected. Three 150-m transects were established based on random-systematically method on each site. On each transect, 10 square plots (2×2 m) were set up having 15 m intervals. The total numbers of plots were 180. The established transects were parallel to each other and perpendicular to the slope. Plot size was calculated using minimal area method (Cain, 1938), and the number of plots was obtained using statistical methods. Total canopy cover (TCC), canopy cover of target species (CCTS), and percentage of stone and gravel (PSG) on the soil surface and bare soil were recorded in each site. Soil samples were collected from a 0–30 cm depth (Northup et al., 1999), in the first, middle and end of each transect in all the sites.

Soil properties such as electrical conductivity (EC), soil acidity (pH), soil organic carbon (OC), total neutralizing value (TNV), soil potassium (K), soil phosphorus (P), soil texture (percentage of sand, silt and clay) and saturation humidity (SP) (Burt, 2004; Jafarian et al., 2008), were determined in the soil lab of the Agricultural and Natural Resources Research Centre of Zanjan province. Spatial variations of soil properties were mapped using geostatistical methods including semi-variogram analysis and kriging interpolation in the same spatial resolution (pixel size $10 \text{ m} \times 10 \text{ m}$). In this regard, geostatistical analysis was done using GS⁺5 software and digital soil layers were prepared in GIS environment. Digital elevation model (DEM) was derived using 1:25000 topographic maps of the National Cartographic Centre of Iran, with 10 m resolution. Elevation, slope and aspect maps of each sampling plot were derived from the DEM. The annual precipitation, annual mean temperature (Mean T.), mean annual maximum temperature (Max T) and mean annual minimum temperature (Min T) were extracted using a derived gradient formula from meteorological data (synoptic and climatological stations) and calculated by considering the DEM for each site in GIS environment. All these variables were then extracted for the sampling plots using ArcGIS10. Sampling occurred in May and Jun 2015.

Data analysis

The normality of the recorded data was examined using the Kolmogorov-Smirnov test. The one-way ANOVA statistical test was used to analyse the significant difference between the effects of environmental variables on the presence or absence of *F. ovina*. The t-test and Tukey's test were used to evaluate the differences among the variables studied in sites with presence and absence of *F. ovina*. The importance of each measured variable in the distribution of selected species was analysed using discriminant analysis. Stepwise, discriminant analysis (DA) was employed to determine the significance of the variables studied on species distribution and for verifying the grouping of sampling locations (Savić et al., 2008; Edokpa et al., 2009). SPSS18 software was used for data analysis.

Results

Characteristics of the measured variables in three selected habitats are presented in *Table 1*. The quantity of annual precipitation, annual mean temperature (Mean. T.), acidity (pH), percentage of total neutralizing value (TNV), percentage of sand and silt, and the percentage of total canopy cover (TCC) had no significant effect ($P \leq 0.05$), the amount of other variables such as altitude, percentage of slope, aspect, annual mean minimum temperature (Min. T.), annual mean maximum temperature (Max. T.), electrical conductivity (EC), percentage of organic carbon (OC), quantity of potassium, quantity of exchangeable phosphorus, percentage of clay, percentage of stone and gravel on the soil surface and saturation humidity percentage (SP) with or without the presence of *F. ovina* were significantly different ($P \leq 0.01$) in the Zaker- Khanchay site. Meanwhile, in the Shilander site, quantity of annual precipitation, annual mean temperature, acidity, exchangeable phosphorus (p), percentage of stone and gravel on the soil surface (PSG) and percentage of total canopy cover had no significant effect ($P \leq 0.05$), other variables such as altitude, percentage of slope, aspect, annual mean minimum temperature, annual mean maximum temperature, electrical conductivity, percentage of total neutralizing value, percentage of organic carbon, quantity of potassium (K), percentage of silt, percentage of sand, percentage of clay and saturation humidity percentage had a significant differences ($P \leq 0.01$) in the sites where the target species was present and absent. According to the results, phosphorus, percentage of clay, percentage of stone and gravel on the soil surface, aspect, annual precipitation, annual mean temperature and total canopy cover was not significantly different ($P \leq 0.05$) between the sites where the target species was present and absent in Soltanieh. But other variables such as altitude, percentage of slope, annual mean minimum temperature, annual mean maximum temperature, electrical conductivity, acidity, percentage of total neutralizing value, percentage of organic carbon, quantity of potassium, percentage of sand, percentage of silt and saturation humidity percentage were significantly different ($P \leq 0.01$) between the sites where *F. ovina* was present and absent. The results showed that about 37% of species composition in Soltanieh site belonged to *F. ovina*, which was the highest amount among the studied habitats. *F. ovina* is distributed in the Soltanieh habitat with average slope of about 62%, at an average altitude of 2410 metres above sea level. Average value of the measured variables in Soltanieh habitat were as follows: Electrical conductivity 0.38 ds/m, pH 7.8, and percentage of total neutralizing value was 5.3. Moreover, the percentage of organic carbon was 2.9, potassium 373 ppm and phosphorus 12.3 ppm. The soil texture was determined as loamy, amount of precipitation 403 mm per year and annual mean temperature was 7.2 °C (*Table 1*).

Table 1. Comparison of measured attributes in the presence and absence of species *F. ovina* habitats

Habitat Variables	Zaker-Khanchay		t	Shilander		t	Soltaneh		t	F
	Presence	Absence		Presence	Absence		Presence	Absence		
	Mean± S.E	Mean± S.E		Mean± S.E	Mean± S.E		Mean± S.E	Mean± S.E		
Altitude	2420 ^c ± 4.00	2467 ^b ± 0.50	-11.70 ^{**}	2471 ^b ± 7.10	2495 ^a ± 3.80	-2.94 ^{**}	2410 ^c ± 5.50	2388 ^d ± 1.60	3.91 ^{**}	92.78 ^{**}
Slope	47.30 ^c ± 1.00	42.30 ^d ± 0.40	4.54 ^{**}	53.30 ^b ± 0.40	46.70 ^e ± 0.40	10.77 ^{**}	61.70 ^a ± 1.20	53.30 ^b ± 0.40	6.73 ^{**}	88.90 ^{**}
Aspect	285 ^a ± 3.90	75 ^c ± 3.90	37.70 ^{**}	270 ^a ± 0.00	60 ^c ± 3.90	53.30 ^{**}	150 ^b ± 15.80	150 ^b ± 4.00	0.00 ^{ns}	174.00 ^{**}
Precipitation	347 ^b ± 0.50	350 ^b ± 0.50	-11.70 ^{ns}	327 ^c ± 0.80	328.70 ^c ± 0.40	-2.95 ^{ns}	402.80 ^a ± 0.60	399.20 ^a ± 0.20	3.91 ^{ns}	92.76 ^{**}
Mean. T.	8.30 ^a ± 0.00	8.10 ^a ± 0.00	11.70 ^{ns}	6.40 ^c ± 0.03	6.20 ^c ± 0.02	2.88 ^{ns}	7.20 ^b ± 0.03	7.10 ^b ± 0.01	3.86 ^{ns}	92.45 ^{**}
Min. T.	-1.50 ^b ± 0.03	-1.50 ^a ± 0.00	11.80 ^{**}	-1.50 ^c ± 0.05	-1.70 ^c ± 0.03	2.91 ^{**}	-1.08 ^b ± 0.00	-0.92 ^a ± 0.04	-3.92 ^{**}	93.72 ^{**}
Max. T.	15.90 ^b ± 0.01	15.70 ^c ± 0.00	11.98 ^{**}	15.70 ^c ± 0.01	15.60 ^d ± 0.01	3.05 ^{**}	15.98 ^b ± 0.02	16.07 ^a ± 0.00	-3.81 ^{**}	95.31 ^{**}
EC	0.39 ^{bc} ± 0.10	0.47 ^b ± 0.10	-4.82 ^{**}	0.28 ^c ± 0.10	0.87 ^a ± 0.09	-6.66 ^{**}	0.38 ^{bc} ± 0.01	0.47 ^b ± 0.01	-6.07 ^{**}	30.15 ^{**}
pH	7.17 ^b ± 0.04	7.18 ^b ± 0.04	-0.23 ^{ns}	7.04 ^c ± 0.01	7.07 ^d ± 0.01	-3.49 ^{ns}	7.6 ^a ± 0.02	7.5 ^b ± 0.02	23.58 ^{**}	131.1 ^{**}
TNV	1.77 ^d ± 0.05	1.30 ^d ± 0.80	4.79 ^{ns}	4.30 ^b ± 0.10	2.90 ^c ± 0.30	4.20 ^{**}	5.30 ^a ± 0.01	0.20 ^e ± 0.01	37.80 ^{**}	23.70 ^{**}
OC	2.70 ^{ab} ± 0.08	1.30 ^c ± 0.06	13.6 ^{**}	3.30 ^a ± 0.2	2.20 ^b ± 0.07	4.94 ^{**}	2.90 ^a ± 0.30	1.40 ^c ± 0.07	5.08 ^{**}	26.97 ^{**}
K	346 ^{bc} ± 16.50	209 ^d ± 2.40	8.20 ^{**}	419 ^a ± 23.20	262 ^d ± 7.30	6.45 ^{**}	373 ^{ab} ± 28.30	278 ^{cd} ± 10.70	3.13 ^{**}	20.40 ^{**}
P	10.30 ^a ± 0.20	3.10 ^b ± 0.11	31.00 ^{**}	12.60 ^a ± 0.40	11.40 ^a ± 0.10	1.11 ^{ns}	12.33 ^a ± 0.70	9.87 ^a ± 1.30	1.64 ^{ns}	21.50 ^{**}
Sand	56.70 ^a ± 1.80	57.30 ^a ± 0.60	-0.34 ^{ns}	43.30 ^{bc} ± 0.50	47.30 ^b ± 0.50	-6.11 ^{**}	42.30 ^c ± 1.20	55.30 ^a ± 0.80	-9.30 ^{**}	46.59 ^{**}
Silt	32.30 ^c ± 1.40	29.70 ^{cd} ± 0.20	1.90 ^{ns}	46.70 ^a ± 0.60	37.30 ^b ± 0.50	11.7 ^{**}	40.30 ^b ± 1.06	27.00 ^d ± 0.30	12.04 ^{**}	85.38 ^{**}
Clay	11 ^{cd} ± 0.50	13 ^c ± 0.50	-2.70 ^{**}	10.00 ^d ± 0.00	15.30 ^b ± 0.10	-5.06 ^{**}	17.70 ^a ± 0.20	17.30 ^a ± 0.50	0.00 ^{ns}	34.30 ^{**}
PSG	44.80 ^{ab} ± 3.40	31.70 ^{bc} ± 2.60	3.06 ^{**}	47.90 ^a ± 3.10	45.40 ^{ab} ± 4.00	0.49 ^{ns}	36.10 ^{abc} ± 4.60	26.80 ^c ± 2.80	1.87 ^{ns}	6.38 ^{**}
SP	31.70 ^c ± 0.90	49.30 ^a ± 0.50	-16.88 ^{**}	49 ^a ± 1.20	40.70 ^a ± 0.26	5.63 ^{**}	49.30 ^a ± 2.50	36 ^{bc} ± 0.80	4.98 ^{**}	34.20 ^{**}
TCC	38.20 ^a ± 2.80	43.70 ^a ± 2.80	-1.43 ^{ns}	40.20 ^a ± 2.90	35.40 ^a ± 2.30	1.39 ^{ns}	43.90 ^a ± 2.30	39.40 ^a ± 1.90	1.54 ^{ns}	1.81 ^{ns}
CCTS	10.80 ^b ± 1.50	0.00 ^c ± 0.00	7.06 ^{**}	10.10 ^b ± 1.10	0.00 ^c ± 0.00	6.60 ^{**}	17.60 ^a ± 1.80	0.00 ^c ± 0.00	9.93 ^{**}	42.50 ^{**}

ns, ** and * are no-significant differences, significant at 1 and 5 percent probability level, respectively
Similar words indicating no difference and different letters indicate significant differences in the rows

The analysis of variance of variables in different sites under the study indicated a significant difference ($P \leq 0.01$) (Table 1). The total canopy cover had not been recognized as significant in the selected sites. According to the results of discriminant analysis (Table 2), four canonical functions were defined, in which the first function explains the 97.5% variance. Moreover, the second, third and fourth functions justified around 1.8%, 0.70% and 0.0% of variance. Eigenvalues and canonical correlation were more in the first function than in the second function. On the other hand, Wilks' Lambda values had increased from the first function to the fourth audit function and chi-square value was significant at the first, second, third and fourth functions ($P \leq 0.01$). Thus, the average value of groups was significantly different (Table 3). It can be concluded that the first function has higher discrimination power in decomposition of the groups.

Table 2. Eigenvalues and the percentage of variance explained by functions in the discriminant analysis

Function	Eigenvalue	Percent of variance	Cumulative %	Canonical correlation
1	17246.86	97.50	97.50	1.00
2	319.16	1.80	99.30	0.998
3	116.61	0.70	100.00	0.996
4	8.62	0.00	100.00	0.947

Table 3. The values of Wilks' lambda in discriminant analysis

Test of function (s)	Wilks' lambda	Chi-square	df	Sig.
1 through 4	0.00	3180.31	44	0.00
2 through 4	0.00	1804.79	30	0.00
3 through 4	0.00	991.39	18	0.00
4	0.10	319.19	8	0.00

The discriminant coefficients of the variables have shown in Table 4. These results indicated the linear correlation between environmental variables and discrimination function. Precipitation was primarily the most influential factors in the first function. While in the second function, the percentage of slope, silt, sand and percentage of stone and gravel on the soil surface (PSG) turned out to be the most effective factors. Moreover, saturation humidity (SP), mean annual temperature (mean. T.), altitude and organic carbon (OC) were determined as effective factors in the third function, and finally, phosphorus (P), potassium (K), total of neutralizing value (TNV), acidity (pH), electrical conductivity (EC) and clay in the fourth function, to identify sites and distribution of *F. ovina* species.

According to the results of stepwise discriminant analysis (Table 5), discriminant function coefficients for the studied species using canonical functions in the first function is as follows (Eq. 1):

$$Y = 0.171SP - 2.833 EC + 5.056 pH - 1.619 TNV - 1.559 OC + 0.177 Silt - 0.207 Clay + 0.008 Aspect - 0.025 Altitude + 2.967 Mean T + 4.217 Precipitation - 1544.03 \quad (\text{Eq.1})$$

where, the saturation humidity (SP), electrical conductivity (EC), acidity (pH), total of neutralizing value (TNV), organic carbon (OC), silt, clay, aspect, altitude, mean annual temperature (Mean T) and annual precipitation are parameters that determined as effective in the equation, whereas Y is the presence or absence of target species in equation.

Table 4. Discriminant coefficient of factors in canonic functions

Variable	Functions			
	1	2	3	4
Precipitation (mm)	0.958*	0.089	-0.088	-0.059
Slope (%)	0.027	-0.385*	-0.082	-0.035
Silt (%)	-0.004	0.083*	0.016	-0.040
Sand (%)	0.000	-0.064*	-0.004	0.043
PSG (%)	0.039	0.063*	0.025	0.029
Aspect (°)	-0.007	0.025	0.149*	-0.086
SP (%)	0.000	0.037	-0.070*	0.023
Mean T. (°C)	0.009	-0.019	0.065*	-0.016
Altitude (m)	-0.009	0.017	-0.061*	0.036
OC (%)	-0.002	0.039	-0.046*	0.005
P (ppm)	0.022	-0.237	-0.096	-0.560*
K (ppm)	-0.002	0.032	-0.076	-0.332*
TNV (%)	-0.002	0.228	0.019	0.325*
pH	0.010	0.052	-0.007	0.306*
EC (ds/m)	-0.004	0.020	-0.007	-0.179*
Clay (%)	0.007	0.000	-0.015	-0.022*

*Largest absolute correlation between each variable and any discriminant function

Table 5. Canonical discriminant function coefficients

Variables	Function			
	1	2	3	4
SP	0.171	-1.829	0.117	0.412
EC	-2.837	11.749	-16.538	-13.053
pH	5.056	-30.753	13.408	3.451
TNV	-1.619	12.962	-4.947	-0.114
OC	-1.559	18.309	1.298	-3.823
Silt	0.177	-1.068	1.040	0.290
Clay	-0.207	1.266	-0.404	-0.839
Aspect	0.008	0.011	0.115	-0.013
Altitude	-0.025	0.202	0.161	0.460
Mean T.	2.967	6.617	78.136	102.263
Precipitation	4.217	0.325	-0.063	-0.012
(Constant)	-1544.03	-428.691	-1182.9	-2023.9

The results of the classification of the studied habitats using discriminant analysis have been shown in *Table 6*. The result presented in *Table 6*, shows the frequency as well as the observed and predicted values of adjustment. Frequency percentage provided in *Table 6* represents the level of matching in observed and predicted items. Accordingly, if the data of *F. ovina* was placed in the discrimination function, the function would recognize correctly in 100% of the membership of the species in the group Zaker-Khanchay. Meanwhile, 100% membership of species was in Shilander and Soltanieh groups. Moreover, if data of the sites (without the target species) was placed in the discrimination function, the function would detect correctly, in 100% of cases, membership in the non-presence group. This indicates correct selection of factors affecting the distribution and dissemination of the studied species. In general, the value of a person's membership (100%) proves accuracy of recognizing the group function.

Table 6. The results of classification using discriminant analysis^a

	Group	Predicted group membership					Total
		1	2	3	4	5	
Original count %	1	100.0	0.0	0.0	0.0	0.0	100.0
	2	0.0	100.0	0.0	0.0	0.0	100.0
	3	0.0	0.0	100.0	0.0	0.0	100.0
	4	0.0	0.0	0.0	100.0	0.0	100.0
	5	0.0	0.0	0.0	0.0	100.0	100.0

^a100.0% of original grouped cases correctly classified

Group1, The Zaker.Khanchay habitat (with presence of *F. ovina*). Group2, Adjacent Zaker-Khanchay and Shilander habitat (with absence of *F. ovina*). Group3, The Shilander habitat (with presence of *F. ovina*). Group4, The Soltanieh habitat (with presence of *F. ovina*). Group5, Adjacent Soltanieh habitat (with absence *F. ovina*)

Discussion and conclusion

The presence, absence and plant species distribution in natural ecosystems depend on factors such as climate, edaphic, available resources, competition among species, natural and non-natural stress, and plant biological zone. In a large scale, the distribution of plant communities is more influenced by the climate and secondly by the edaphic factors, while in local scale, edaphic factors and available sources are the most important factors and other factors are the next critical ones (Fridley, 2001; Mirzaei Mossivand et al., 2017).

The results of the analysis of variance for the parameters of the studied sites showed that from the 20 evaluated parameters (*Table 1*), except for the canopy cover of species, other variables have a significant difference ($P \leq 0.01$). Thus, according to the results, it can be concluded that the ecological conditions of each habitat are different. On the other hand, the results of the Canonical Discriminant Function Coefficients (*Table 5*) indicated that in the presence or absence of the *Ferula ovina* species in the studied habitats, the percentage of saturation humidity (SP), the percentage of electrical conductivity (EC), acidity (pH), percentage of total neutralizing value (TNV), percentage of organic carbon (OC), percentage of silt, aspect, altitude, mean annual temperature (mean T.), and the annual precipitation were effective factors.

Although the *F. ovina* species was one of the dominant species of vegetation in the southern regions of the study area, in other geographic areas it was also distributed in

a sporadic manner. Indubitably, the geographical aspect affects the amount of soil humidity, soil temperature, and light intensity received by the plant. The difference in the light intensity in different aspects of hillside and crests affect the local climate and plant communities (Gonzales-Alcaraz et al., 2014). It seems that alterations in the local climate conditions are among the main factors influencing the distribution and presence or absence of the target species. Based on field observations, it has been proved that *F. ovina* mainly dominated the hillsides that had a greater light intensity. Investigations conducted on the descriptive autecology study of *F. ovina* in Iran are in agreement with our findings. Azhir and Shahmoradi (2007) concluded that the distribution and presence or absence of the *F. ovina* species depend on the geographical aspect and percentage of slope.

Precipitation, mean annual temperature, and altitude not only affected the presence or absence of the species, but the impact of precipitation on the distribution of the studied species in the locations was the most effective factor. These results are in agreement with the findings of Davies et al. (2007) which state that topographic characteristics (e.g., elevation, slope and aspect) are closely associated with the local climate (e.g. precipitation, evaporation and temperature) that greatly impacts plants. This is also in conformity with Xu et al. (2013), who stated that precipitation and temperature are consistently highlighted as influential in the distribution of plants (Xu et al., 2013).

The percentage of silt in the soil in the habitat of *F. ovina* was higher than habitats where it was absent and the clay and sand percentage of soil in sites where the target species was present was lower than the habitats where it was absent. In other words, it seems that the studied species prefer soils that have a medium texture, as the soil texture was an effective factor in the distribution and presence or absence of the *F. ovina*. Soil texture due to the influence of moisture amount and available nutrients in plants, water holding capacity in the soil, food cycle, ventilation, depth of plant rooting, and the amount of runoff flowing after rainfall on the soil surface as well as the distribution of plants plays a role (EL-Sheikh and Youssef, 1981; EL-Ghani, 2003). Accordingly, previous reports have mentioned that soil texture is a key factor in the presence or absence of the plant in the studied locations (Taghipour et al., 2008; Ghorbani and Asghari, 2014).

The quantity of the total of neutralizing value (TNV) in the habitats of *F. ovina* is significantly higher than the places without the species. It seems that the TNV has been identified as an effective factor in discriminating locations. However, it has had less effect on the distribution of species in locations with the presence of the *F. ovina* species. Previous studies on *F. ovina* have also emphasized that this species had a significant percentage of canopy cover on a relatively calcareous geological formation in comparison to other places. Likewise, it was the dominant species in many areas of Iran (Azahir and Shahmoradi, 2007).

The electrical conductivity (EC) represents the amount of conductive solute contained in the soil solution, one of the main ones being salt (sodium chloride). Although the studied sites were not saline areas, the amount of electrical conductivity in the presence of the species was between 0.28 to 0.39 ds/m, in mutuality, and in the absence of the species it was between 0.47 to 0.87 ds/m. Salinity and soil salinity are commonly found on agricultural land, and the lands on which they are located (mountainous lands) are considered as saline soils in non-saline soils, but it seems that even this difference has caused electrical conductivity (EC) to be among the factors influencing the presence or absence of the species in the studied locations.

Another important factor in the distribution of the species in the habitats was the percentage of slope. The highest percentage of canopy cover of the target species was observed in the habitat that had a higher slope percentage among all the habitats. Usually, slope is considered a limiting factor in the distribution and establishment of plants. As the slope increases, the depth of soil and soil moisture decreases, and as a result, the plants' establishment is restrained. Our results are in conflict with this issue.

This species, although in the growth stages due to the presence of the volatile compounds, is not heavily grazed, but after the end of the growing period and when the branches and leaves become yellow, they play a major role in grazing in the late summer and early autumn. Of course, it plays a more important role in fodder forage in local livestock feeders (Fig.3). Thus, the slope as a natural factor in this case has led to a reduction in overgrazing and the inappropriate use of rangelands, and it has been a limiting factor in the studied locations. However, it did not affect the distribution of the target species.

This rangeland species has an extensive canopy cover and is important not only in forage production, but due to the wide canopy cover and the extent of the root system, it increases the humus and soil organic matter. It can also be considered as one of the most important species in decreasing soil erosion.

Though organic carbon had a relatively small effect on the distribution of the species in the studied locations, it was one of the factors influencing the presence or absence of the species studied. The results of many studies showed that organic carbon was one of the soil characteristics affecting the distribution and presence or absence of vegetation in the evaluated areas. These findings were in agreement with the results of Ayyad (1976), Mahdavi et al. (2009), Kooch et al. (2007). A study of the ecological distribution of some indicator species and their effective soil factors showed that the distribution and presence or absence of vegetation in those areas correlated with the soil properties such as soil texture, quantity of phosphorus, percentage of organic carbon, and acidity.

The increased uses of fossil fuels, land use change and degradation of vegetation have led to the release of a huge amount of greenhouse gases into the atmosphere (Hamburg et al., 1997). Carbon dioxide is the most important greenhouse gas and increasing its density in the atmosphere has increased global warming and climate change. Moreover, climate change is one of the most important challenges that have very adverse effects on the environment and human life on the planet (Hamburg et al., 1997; IPCC, 2007; UNDP, 2000). The global estimate of carbon in rangeland soils is about 30% of its total amount in the planet (Sarapatka and Cizkova, 2013). One of the most effective ways to reduce greenhouse gases is to sequester them in soil or plant organs (Rossi et al., 2009). Plant biomass is one of the factors affecting the storage of organic carbon in soil and the species studied is one of the species that has a high biomass in rangelands. The high organic carbon content of the soil and its significant difference in sites with the presence of target species relative to sites without its presence indicates the important role of this species in the accumulation of organic carbon in these areas. In this regard, Ghoreyshi et al. (2013) also indicated that with increasing the organic matter, more carbon was stored in the soil of the studied sites.

In other studies, the percentage of stone and gravel on the soil surface (PSG) was another factor affecting the distribution of the studied species in the locations, which was in agreement with the results of Assadian et al. (2017). In many ecological studies, the percentage of stone and gravel on the soil surface is not very noticeable. Its amount plays an important role in maintaining soil moisture, water penetration in the soil, and

soil conservation in sloping lands. Especially in arid regions like Iran, PSG is important for maintaining the moisture in the under soil, and can play an important role in the survival of plants.

Although many similar results from other studies were cited to support our above-mentioned discussion, there still existed some different aspects between our studies and other ones. For example, Xu et al. (2013) documented precipitation and temperature are consistently highlighted as influential in the distribution of plants, while the percentage of slope, silt, sand and the percentage of stone and gravel on the soil surface were more important than temperature in our study. However, it is very difficult to really discern the differences in the results from different studies, because the vegetation, soil, and topography relationship is very complicated per se; the aims of the other studies and the associated measures taken were very different and the local conditions also varied from one study to another. In this regard, Amooaghaie (2009) has reported that the *F. ovina* species is among the endangered ones distributed in many areas in Iran. On the other hand, it seems in view of different reasons including habitat degradation due to inappropriate and unsuitable usage such as over grazing and even excessive harvesting for winter forage of livestock in areas by local people, it is certain that some characteristics of environmental factors such as topography, climate, soil texture, the amount of gypsum and lime, and some other characteristics of the soil are in compatible, and are the nature of the ecosystems.

However, how human activities and exploitation of rangeland ecosystems will cause some of the factors such as soil organic matter, potassium and phosphorus in this study to be affected by this process, and the distribution, presence and absence of species will affect in the locations. This is an important theory or framework to direct the practice of ecosystem restoration and management. It is difficult to directly restore the original species in the degraded dry lands; hence, several steps following a natural succession sequence would be necessary. In addition, plant degradation is not only an ecological but also an economic and social problem; some relevant conservation policies are needed to reduce human disturbance on the ecosystem. Thus, in the restoration and management of species habitats, not only vegetation and environmental factors but also human activities should be considered.

This study has tried to provide some useful information on the distribution of *F. ovina*. Results will be useful in developing future *F. ovina* management guidelines, which can be used to rehabilitate and develop the habitats of this rangelands species in the regions, and this can play an important role in the issue of carbon sequestration, soil erosion and soil conservation in the rangelands. Other factors influencing the distribution of the species such as biotic interactions, genetic adaptation, and the species' dispersal abilities should be taken into account in order to draw relevant conclusions to have a better conservation, as well as oriented decisions.

REFERENCES

- [1] Aghajanlou, F., Fayaz, M., Mussavi, A., Abdinejad, P. (2015): Ecological Regions of Iran: Vegetation Types of Zanzan Province. – Research Institute of Forest and Rangelands of Iran, Tehran.
- [2] Akbarlou, M., Nodehi, N. (2016): Relationship between some environmental factors with distribution of medicinal plants in Ghorkhud protected region. – Journal of Rangeland Science 6(1): 63-72.

- [3] Al-Khalil, S., Aqel, M., Afifi, F. (1990): Effects of an aqueous extract of *Ferula ovina* on rabbit and guinea pig smooth muscle. – *Journal of Ethnopharmacology* 30(1): 35-42.
- [4] Amooaghaie, R. (2009): The effect mechanism of moist-chilling and GA3 on seed germination and subsequent seedling growth of *Ferula ovina* Boiss. – *The Open Plant Science Journal* 3: 22-28.
- [5] Araujo, M. B., Guisan, A. (2006): Five (or so) challenges for species distribution modeling. – *Journal of Biogeography* 33: 1677-1688.
- [6] Arundel, S. T. (2005): Using spatial models to establish climatic limiters of plant species distributions. – *Ecological Modelling* 182: 159-181.
- [7] Ashcroft, M. B., French, K. O., Chisholm, L. A. (2011): An evaluation of environmental factors affecting species distributions. – *Ecological Modeling* 222(3): 524-531.
- [8] Assadian, G., Javadi, S. A., Jafary, M., Arzani, H., Akbarzadeh, M. (2017): Relationship between environmental factors and plant communities in enclosure rangelands. – *Journal of Rangeland Science* 7(1): 20-34.
- [9] Ayyad, M. (1976): The vegetation and environment of the western Mediterranean coastal land of Egypt. IV. The habitat of non-saline depressions. – *Journal of Ecology* 64: 713-722.
- [10] Azhir, F., Shahmoradi, A. A. (2007): Autecological study of *Ferula ovina* in rangelands of Tehran province. – *Iranian Journal of Range and Desert Research* 21(3): 359-367.
- [11] Bagheri, H., Ghorbani, A., Zare Chahouki, M. A., Jafari, A.A. Sefidi, K. (2017): Halophyte species distribution modeling with MaxEnt model in the surrounding rangelands of Meighan playa, Iran, – *Applied Ecology and Environmental Research* 15(3): 1473-1484. DOI: http://dx.doi.org/10.15666/aeer/1503_14731484.
- [12] Burt, R. (2004): Soil Survey Laboratory methods. Soil Survey Investigations Rep. 42, vs. 4.0. USDA. – Natural Resources Conserv. Serv., Washington, DC.
- [13] Cain, S. A. (1938): The species-area curve. – *American Midland Naturalist* 21: 81-146.
- [14] Davies, K. W., Bates, J. D., Miller, R. F. (2006): Vegetation characteristics across part of the Wyoming big sagebrush alliance. – *Rangeland Ecology and Management* 59: 567-575.
- [15] Davies, K. W., Bates, J. D., Miller, R. F. (2007): Environmental and vegetation relationships of the *Artemisia tridentata* Spp. Wyomingensis alliance. – *Journal of Arid Environments* 70: 478-494.
- [16] Dyakov, N. R. (2014): Gradient analysis of vegetation on the south slope of Vitosh Mountain, Southwest Bulgaria. – *Applied Ecology and Environmental Research* 12(4): 1003-1025.
- [17] Edokpa, I. W., Erimafa, J. T., Iduseri, A. (2009): Application of discriminant analysis to predict the class of degree for graduating students in a university system. – *International Journal of Physical Sciences* 4(1): 016-021.
- [18] EL-Ghani Monier, M. (2003): Soil-vegetation relationships in a coastal desert plain of southern Sinai, Egypt. – *Journal of Arid Environment* 55: 607-628.
- [19] El-Sheikh, A. M., Youssef, M. M. (1981): Halophytic and Xerophytic vegetation near Al-Kharj springs. – *Jour. College of Science* 12: 5-21.
- [20] Fridley, J. D. (2001): The influence of species diversity on ecosystem productivity: how, where and why? – *Oikos* 93: 514-526.
- [21] Gemedo, D., Brigitte, L. M., Johannes, I. (2014): Relationships between vegetation composition and environmental variables in the Borana rangelands, Southern Oromia, Ethiopia Sinet, Ethiopia. – *Journal of Science* 37(1): 1-12.
- [22] Ghannadi, A., Sajjadi, S. E., Beigihasan, A. (2002): Composition of the essential oil of *Ferula ovina* (Boiss.) Boiss. from Iran. – *Iranian DARU Journal of Pharmaceutical Sciences* 10(4): 165-167.
- [23] Ghorbani, A., Asghari, A. (2014): Study the influence of ecological factors on *Festuca ovina* distribution in southeast rangelands of Sabalan. – *Iranian Journal of Range and Desert Research* 21(2): 368-381.

- [24] Ghorbani, A., Abbassi Khalaki, M., Omidi, A., Zare hesari, B. (2015): Compare some ecological factors affecting the distribution of plants species *Artemisia austriaca* and *Artemisia fragrans* Wild. Jacq. in southeastern rangelands of Sabalan. – Iranian Journal of Rangeland 9(2): 129-141.
- [25] Ghoreyshi, R., Goly, E., Motamedi, J., Keivan Behjou, F. (2013): Carbon sequestration capacity in rangeland ecosystems and its relation with soil physical and chemical characteristics in rangelands of Khoy. – Iranian Journal of Applied Soil Research 1(2): 34-44.
- [26] Gonzales-Alcaraz, M. N., Jimenez-Carceles, F. J., Alvarez Y., Alvarez-Rogel, J. (2014): Gradient of soil salinity and moisture and plant distribution in a Mediterranean Semi-Arid Saline watershed: A model of soil- plant relationships for contributing to the management. – Catena 115: 150-158.
- [27] Goodal, D. W., Perry, R. A. (1979): Arid-Land Ecosystem. – Syndics of the Cambridge University Press, Cambridge.
- [28] Hamburg, S. P., Harris, N., Jaeger, J., Karl, T. R., McFarland, M., Mitchell, J. F. B., Oppenheimer, M., Santer, S., Schneider, S., Trenberth, K. E., Wigley T. M. L. (1997): Common Questions about Climate Change. United Nation Environment Program. – World Meteorology Organization, Geneva.
- [29] Hedge, I. C., Lamond, J. M., Rechinger, K. H. (1982): *Ferula* (Flora Iranica Umbelliferae series no. 162). – Akademische Druck- u. Verlagsanstalt, Graz.
- [30] IPCC (2007): Climate Change. The Scientific Basis. IPCC Fourth Assessment Report. – Cambridge University Press, Cambridge.
- [31] Jafarian, Z., Arzani, H., Jafari, M. (2008): Analyzing the relationship between distribution or plant communities and climatic and physiographic factors using classification and ordination methods in Rineh Rangelands. – Iranian Journal of Rangeland 6:125-141.
- [32] Khatibi, R., Ghasemi Arian, Y., Jahantab, E., Haji Hashemi, M. R. (2012): Investigation on relationships between soil properties and vegetative. – Iranian Journal of Range and Desert Research 19(1): 72-81.
- [33] Kooch, Y., Bahmanyar, H. J. M. A., Pormajidian, M. R. (2007): Ecological distribution of indicator species and effective edaphical factors on the Northern Iran lowland forests. – Journal of Applied Science 7: 1475-1483 (in Persian).
- [34] Kurzyna-Mlynik R., Oskolaski, A. A., Downie, S. R., Kopacz, R., Dzka, A. W., Spalik, K. (2008): Phylogenetic position of the genus *Ferula* (Apiaceae) and its placement in tribe Scandiceae as inferred from nr DNA ITS sequence variation. – Plant Systematics and Evolution 274: 47-66.
- [35] Mahdavi, A., Heidari, M., Bastam, R., Abdollah, H. I. (2009): Study of vegetation cover on the soil condition and physiographic of habitat (Case Study: Kabir kuhe Ilam protected area). – Journal of Forest Research and Poplar 17(4): 581-593 (in Persian).
- [36] Menglan, S., Watson, M. F. (2005): Flora of China, Vol. 14, pp. 174-180. – Science Press and Missouri Botanical Garden Press, Beijing and St. Louis. <http://flora.huh.harvard.edu/china/index.html>.
- [37] Mirzaei Mossivand, A., Ghorbani, A. Keivan Behjou, F. (2017): Effects of some ecological factors on distribution of *Prangos uloptera* and *Prangos pabularia* in rangelands of Ardabil province, Iran, – Applied Ecology and Environmental Research 15(4): 957-968. DOI: http://dx.doi.org/10.15666/aeer/1504_957968.
- [38] Moghaddam Matin, M., Nakhaeizadeh, H., Bahrami, A. R. (2014): Ferutinin, an apoptosis inducing terpenoid from *Ferula ovina*. – Asian Pacific Journal of Cancer Prevention 15(5): 2123-2128.
- [39] Mozaffarian, V. (1983): The Family of Umbelliferae in Iran - Keys and Distribution. – Research Institute of Forests and Rangelands of Iran, Tehran.
- [40] Mozaffarian, V. (2007): Flora of Iran (Umbelliferae), Vol. 54. – Research Institute of Forest and Rangelands of Iran, Tehran.

- [41] Murray, K., Conner, M. M. (2009): Methods to quantify variable importance: implications for the analysis of noisy ecological data. – *Ecology* 90: 348-355.
- [42] Northup, B. K., Brown, J. R., Holt, J. A. (1999): Grazing impact on the spatial distribution of soil microbial biomass around tussock grasses in a tropical grassland. – *Journal of Applied Soil Ecology* 13: 259-270.
- [43] Pimenov, M., Leonov, M. (1993): *The Genera of Umbelliferae*. – Royal Botanic Gardens, Kew.
- [44] Pimenov, M., Leonov, M. (2004): The Asian Umbelliferae biodiversity database (ASIUM) with particular reference to South-West Asian taxa. – *Turkish Journal of Botany* 28: 139-145.
- [45] Platts, P. J., McClean, C. J., Lovett, J. C. (2008): Predicting tree distributions in an East African biodiversity hotspot: model selection, data bias and envelope uncertainty. – *Ecological Modelling* 218: 121-134.
- [46] Rossi, J., Govaerts, A., De Vos, B., Verbist, B., Vervoort, A., Poesen, J., Muys, B., Deckers, J. (2009): Spatial structures of soil organic carbon in tropical forests—a case study of Southeastern Tanzania. – *Catena* 77: 19-27.
- [47] Safaian, N., Shokri, M. (1993): Botanical and ecological study of species of the genus *Ferula* (medicinal plants) in Mazandaran province. – *Acta Horticulture* 333: 79-81.
- [48] Sarapatka, B., Cizkova, S. (2013): The influence of different types of grassland on soil quality in upland areas of Czech Republic. – *Journal of Environmental Biology* 35: 453-459.
- [49] Savić, M., Brcanov, D., Dakić, S. (2008): Discriminant Analysis – Applications and Software Support. – *Management Information Systems* 3(1): 029-033.
- [50] Sheikh, S. A., Rabia, M., Rabia, S. (2014): Environmental diversification and spatial variations in riparian vegetation. – *Pakistan Journal of Botany* 46(4): 1203-1210.
- [51] Syed, M., Hanif, M., Chaudhary, F. M. (1987): Antimicrobial activity of the essential oils of Umbelliferae family: Part IV. *Ferula narthex*, *Ferula ovina* and *Ferula oopoda*. – *Pakistan Journal of Scientific and Industrial Research* 30: 19-23.
- [52] Taghipour, A., Mesdaghi, M., Heshmati, G. A. (2008): The effect of on distribution of range species at Hazar Jarib area of Behshahr. – *Iranian Journal of Agriculture Science and Natural Resources* 15(4): 195-205.
- [53] UNDP (2000): Carbon sequestration in the decertified rangelands of Hossein Abad, through community-based management. – Program Coordination, pp. 1-7.
- [54] Xian-Li, X., Ke-Ming, M., Bo-Jie, F. (2008): Relationships between vegetation, soil, and topography in a dry warm river valley, SW China. – *Catena* 75: 138-145.
- [55] Xu, Z. Z., Shimizu, H., Yagasaki, Y., Ito, S., Zheng, Y. R., Zhou, G. S. (2013): Interactive effects of elevated CO₂, drought, and warming on plants. – *Journal of Plant Growth Regulation* 32: 692-707. DOI: 10.1007/s00344-013-9337-5.
- [56] Yaqoob, U., Nawchoo, I. A. (2015): Phytochemical screening of the root tuber extracts of *Ferula jaeschkeana* Vatke. – *Journal of Essential Oil Bearing Plants* 19(1): 208-211. DOI: <https://doi.org/10.1080/0972060X.2014.908149>.
- [57] Yaqoob, U., Nawchoo, I. A. (2016): Distribution and taxonomy of *Ferula L.*: A Review, Research & Reviews. – *Journal of Botany* 5(3): 15-23.
- [58] Yibing, Q. (2008): Impact of habitat heterogeneity on plant community pattern in Gurbantunggut Desert. – *Geographical Science* 14(4): 447-45.
- [59] Zare-Chahouki, M. A. (2010): *Data Analysis in Natural Resources Research Using SPSS Software*. – University of Tehran Press, Tehran.
- [60] Zare-Chahouki, M. A., Piri-Sahragard, H. (2016): Maxent modelling for distribution of plant species habitats of rangelands (Iran). – *Polish Journal of Ecology* 64(4): 453-467.
- [61] Zare-Chahouki, M. A., Zare Chahouki, A. (2010): Predicting the distribution of plant species using logistic regression. – *Desert* 15: 151-158.
- [62] Zhang, J. T., Dong, Y. (2010): Factors affecting species diversity of plant communities and the restoration process in the loess area of China. – *Ecological Engineering Special Issue: Vegetation and Slope Stability* 36: 345-350.

NEW BIOSTRATIGRAPHICAL FINDINGS ON THE PADEHA FORMATION BASED ON CONODONT ACCUMULATION IN YAZDANSHAHR, KERMAN, CENTRAL IRAN

NASEHI, E.

*Department of Geology, Faculty of Science, Islamic Azad University, Natanz Branch
Natanz, Iran*

e-mail: nasehehsan@gmail.com

(Received 9th Jun 2017; accepted 27th Oct 2017)

Abstract. The aim of the study was the biostratigraphical evaluation of Padeha Formation based on conodont accumulation in Yazdanshahr. The section under study is located north of Yazdanshahr in northwestern Zarand County in Kerman, central Iran. After investigating several sections of the Padeha formation in the Kerman area, one fossiliferous section was chosen for study. In terms of lithology, the section is composed mainly of red-colored clastic and evaporative rock with carbonate intercalations. The conodont accumulations indicate two local biozones: the *Zieglerodina remscheidensis* and *Pandorinellina steinhornensis* assemblage zones and the Eugenathodontidae-Icriodus assemblage zone. Based on the abundance of Spathognathodontidae and similarities to global biozones, these biozones were found to be of the Late Silurian (Early Pridoli) age. No evidence of the *Icriodus* genus (especially *woschmidti* or post-*woschmidti* species) was observed in this assemblage. The latter biozones manifest the appearance of Eugenathodontidae in the Early Devonian; therefore, a sedimentary hiatus exists within the Late Silurian to the start of Early Devonian (Late Pridoli to Pragian). The sediment was deposited in a depositional environment ranging from lagoons to shallow waters (inner carbonate platform). The Yazdanshahr section was the most complete of the Padeha formation because conodonts were found in the lower, middle and upper parts of the section. This function will allow researchers to correlate their sections with these findings based on stratigraphic principles.

Keywords: *Icriodus, sedimentary environment, Silurian, Kerman, biozones*

Introduction

Devonian deposits in Iran were first reported on a geological map prepared by the National Iranian Oil Company. Located near Gush-Kamar in the Ozbak-Kuh mountains, the type section was studied by Ruttner et al. (1968), Stocklin (1971) and Stocklin et al. (1965, 1991). Late Silurian-Early Devonian sediment has been studied in Kerman province in Iran and reported according to stratigraphic principles (Huckriede et al., 1962). Most recent studies have been based on conodonts, fish remnants, brachiopods, corals and palynomorphs. The following authors have recently worked on conodonts: Ahmadi et al., 2012; Bahrami, 2011, 2013, 2014, 2015; Boncheva et al., 2007; Adhamian, 2003; Ashuri, 2004, 2006; Gholamalian, 2007; Gholamalian and Kebriaei, 2008; Gholamalian et al., 2009; Yazdi, 1999; Weddige, 1984.

Geologically speaking, Iran is divided into five structural units: the Zagros, Alborz, Sanandaj-Sirjan, Eastern Iran and Central Iran (Stocklin et al., 1965; Stocklin, 1968; Stocklin and Nabavi, 1971; Stocklin and Setudehnia, 1991; Heydari et al., 2008). In terms of structure, Central Iran is composed of five blocks: the Lut, Tabas, Kalmard, Posht-Badam, Anar and Dehshir (Alavi, 1991; Heydari et al., 2008; *Fig. 1*). Devonian sediment has been described in the Jeirud Formation in the Central Alborz (Assereto, 1963), the Khoshyeilagh formation in the northeastern Alborz (Bozorgnia, 1973), the Moli and Ilanqareh Formation (unofficial name) in West Azerbaijan and Maku (western

Alborz) (Alavi-Naini and Bolourchi, 1973) and the Pedeha, Sibzar, Bahram and Shisto formations in Central Iran (Ruttner et al., 1968).

The type section of the Padeha formation is named after the village of Padeha in the Ozbak-Kuh mountains (Eastern Iran). Lithologically characterized by red sandstone, dolomite and gypsum at Ozbak-Kuh (eastern Central Iran), the Padeha formation overlies the fossiliferous carbonates of the Niur formation and underlies the Sibzar dolomites. This formation formed in the Early Devonian and exhibits shallow facies related to the Caledonian orogeny (Ruttner et al., 1968; Stocklin, 1971). The Padeha formation was deposited in an inner platform and extends across all of the Central Iran basin. Based on its stratigraphic position, this formation has been aged back to the Early Devonian.

Devonian deposits in Iran (Pedeha, Sibzar, etc.) are not well known and a large deal of uncertainty is associated with them. In general, Early Paleozoic Devonian deposits in Iran precipitated in separate geological units. Few studies have been done on the effect of sea level at the time the Late Silurian and Early Devonian rock formed. Evidence indicates the effect of Caledonian movement (Ruttner et al., 1968; Stocklin, 1971). Sea transgression covered most of Iran in the Middle and Late Devonian. In the present research, an attempt is made to determine the age of the sediment based on conodont accumulation.

Methodology and study area

The structural units of Iran were investigated and the Kalmard block was selected for study. The study area is located about 18 km from Zarand and 70 km to the northeast of Kerman. The measured section was delimited as 31°3'55"N and 30°2'40"N latitude and 56°17' 5"E and 56°15'10"E longitude (Fig. 1).

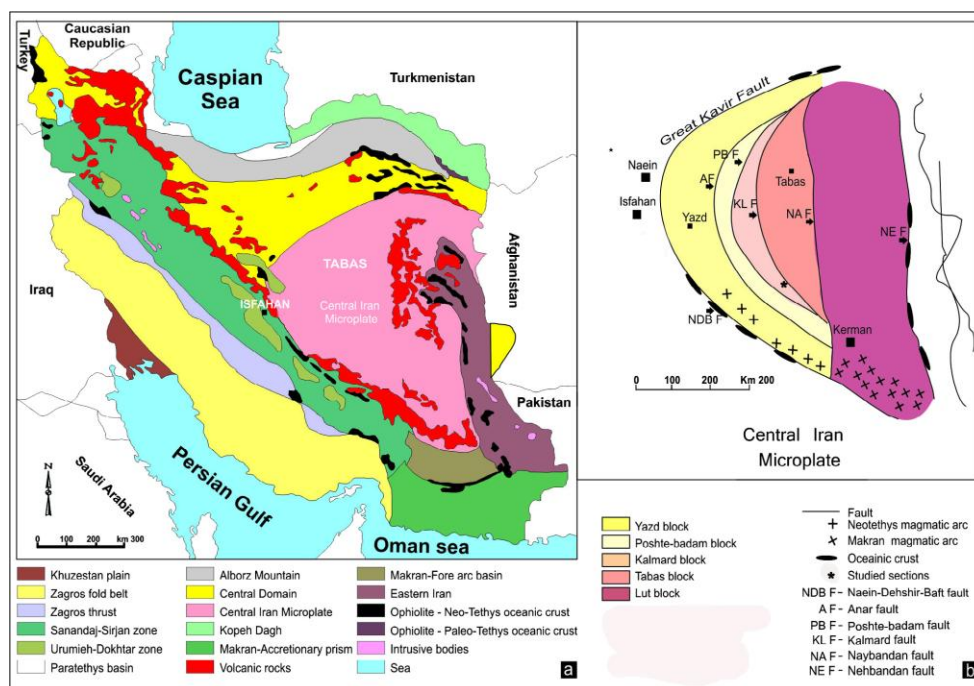


Figure 1. Structural units of Iran located in the studied section

Field sampling and length measurements were undertaken systematically wherever a change in the lithology was identified to carefully investigate the biostratigraphy of the study area. If needed, more than one sample (+4 kg) was taken from the corresponding bedding. The samples were studied carefully after undergoing the following preparation steps: crushing (to dimensions of 3 cm), acid treatment (10% acetic acid), washing, sieving (75, 125, 250 and 710 mesh), picking (with a needle) and photography.

Discussion

An investigation on Late Silurian and Devonian deposits (Padeha, Sibzar, and Bahram) in the Central Iran microplate indicates that, during the Late Silurian, most of Central Iran was exposed out of water. The Devonian deposits in Central Iran formed in separate basins. Evidence indicates a radical variation in thickness even at short distances. For instance, the Hur section is 280 m thick (Ahmadi et al., 2012), the Varkamar section is 210 m thick and the Neqeleh section is about 200 m thick. The Nachf section is about 120 m thick and the Shomal-Tar section is about 200 m (near Isfahan) (Bahrami et al., 2015). The Shahmirzad section is 450 m thick (Heydari et al., 2008) and the Soh section is 88 m thick (Adhamian, 2003).

These radical changes in thickness can be attributed to horst and graben basins from the Caledonian and Hercynian epirogenic phases in Central Iran (Soffel and Forster, 1980; Weddige, 1984). The presence of gypsum as evaporative facies in the section base along with carbonate intercalations containing Spathognathodontidae indicate a lagoon on an inner carbonate platform (*Table 1*) (Sweet, 1988; Flugel, 2010). The presence of evaporative facies in the Late Silurian can be attributed to the Ardenian orogeny. The Early Devonian red-colored clastic facies with carbonate intercalations can be attributed to the Earian orogeny.

Lithostratigraphy of Yazdanshahr section

The study area is located in the northern Shabjereh mountains near Khorramabad (northeastern Kerman, Central Iran; *Fig. 2*). The local sedimentary rock were different types of clastic, colloidal carbonate and evaporative rock. The lower boundary is covered by alluvial deposits. The two local members were identified as follows:

Lower boundary (base): talus and fluvial (covered)

Member I

Lithozone I

1. 20 m of grey, reddish and white gypsum with clay or gypsum-bearing clay intercalations.
2. 6.8 m of olive green lime and the fresh grayish green colour (argillaceous micrite or sandy mudstone becoming pelmicrite or wackestone in the upper layers).
3. 58 m of white to red gypsum with grey-coloured shaley limestone intercalations.
4. 32.8 m of brick-coloured sandstone in alternation with limestone in fresh red color with layering thickness of 0.5-1 m. The penetration of ferrous compounds into the rocks caused their red appearance (sample 3).
5. 4.5 m of light grey and creamy light-grey limestone. This limestone encompasses gypsum beddings in the form of two 1-m thick hard beddings (sample 5).

Table 1. Distribution of conodont species in Yazdanshahr column

Yazdan shahr	18	19	20	21	22	23	24	25	40	42	49	50	51	53	61	62	67	69	70	73	74	76	80	89	90	91	###	Total
<i>Bipennatus</i> Philip, 1965									3	4	2	3	2	3	1	3	2	1	2	3								29
<i>Bipennatus bipennatus</i> Bischoff and Ziegler, 1957										2								3	21	2								28
<i>B.bipennatus bipennatus</i> Bischoff and Ziegler, 1957																												0
<i>Distomodius</i> sp.Branson and Mehl 1947		1	1																									2
<i>Hindeodlla compressa</i> Huddle, 1934								1														1				1	3	
<i>Hindeodella equidentata</i> Rhodes, 1953								2																				2
<i>Icriodus</i> sp Branson and Mehl 1934									2	4												5	1					12
<i>Icriodus brevis</i> , Stauffer, 1940,									2		2														2	1		7
<i>Icriodus brevis brevis</i> Stauffer, 1940																									1		1	
<i>I. brevis spicatus</i> Youngquist and Pelerson, 1947																									3	1		4
<i>Icriodus.regularicresens</i> Bultynck, 1970											1											2	1	1	2			7
<i>I. struvei</i> Weddig, 1977																						2	1					3
<i>Ligonodina</i> Ulrich and Bassler 1926			1		2	2	2	1																				8
<i>Ligonodina elegans</i> Walliser 1964																												0
<i>Lonchodina</i> Bassler, 1925		1	3	1	4	6	6	1																				22
<i>Neopripiodus</i> Rhodes and Muller , 1956		1	1	2	1	2	3	5																				15
<i>Neopripiodus bicurvatus</i> Branson and Mehl, 1933		1	3	2	2	1																						9
<i>Ozarkodina</i> Branson and Mehl, 1933		2	3	4	4	3	2																					18
<i>Ozarkodina confluens</i> Branson and Mehl, 1933		2	6	5	4	2	1																					20
<i>Ozarkodina denckmanni</i> Ziegler, 1956		2	1		2	1																						6
<i>Ozarkodina media</i> Walliser, 1957				1																								1
<i>Ozarkodina typical</i> Branson and Mehl, 1933			4	4	3	3	1																					15
<i>Ozarkodina Ziegleri</i> Walliser, 1964		1	2	3	3		1																					10
<i>Panderodus simplex</i> Branson and Mehl, 1933		1	2	2																								5
<i>Pandorinellina exigua</i> Philip, 1966		3	5	6	5	4	2																					25
<i>Pandorinellina steinhornensis</i> Ziegler, 1956		2	1	5	4	4	2																					18
<i>Plectospathodus</i> Branson and Mehl, 1933		2	3	3	1																							9
<i>Trichonodella symetrica</i> Branson and Mehl, 1933		1	3	4	6	5	2																					21
<i>Wurmiella excavata</i> Branson and Mehl, 1933			1	2	2																							5
<i>Zieglerodina remscheidensis</i> Ziegler, 1960		2	5	3	6	4	1																					21
Total	22	45	47	49	37	23	9	8	11	4	3	2	3	1	3	2	4	23	5	4	8	2	7	3	0	1	###	

Yazdanshahr

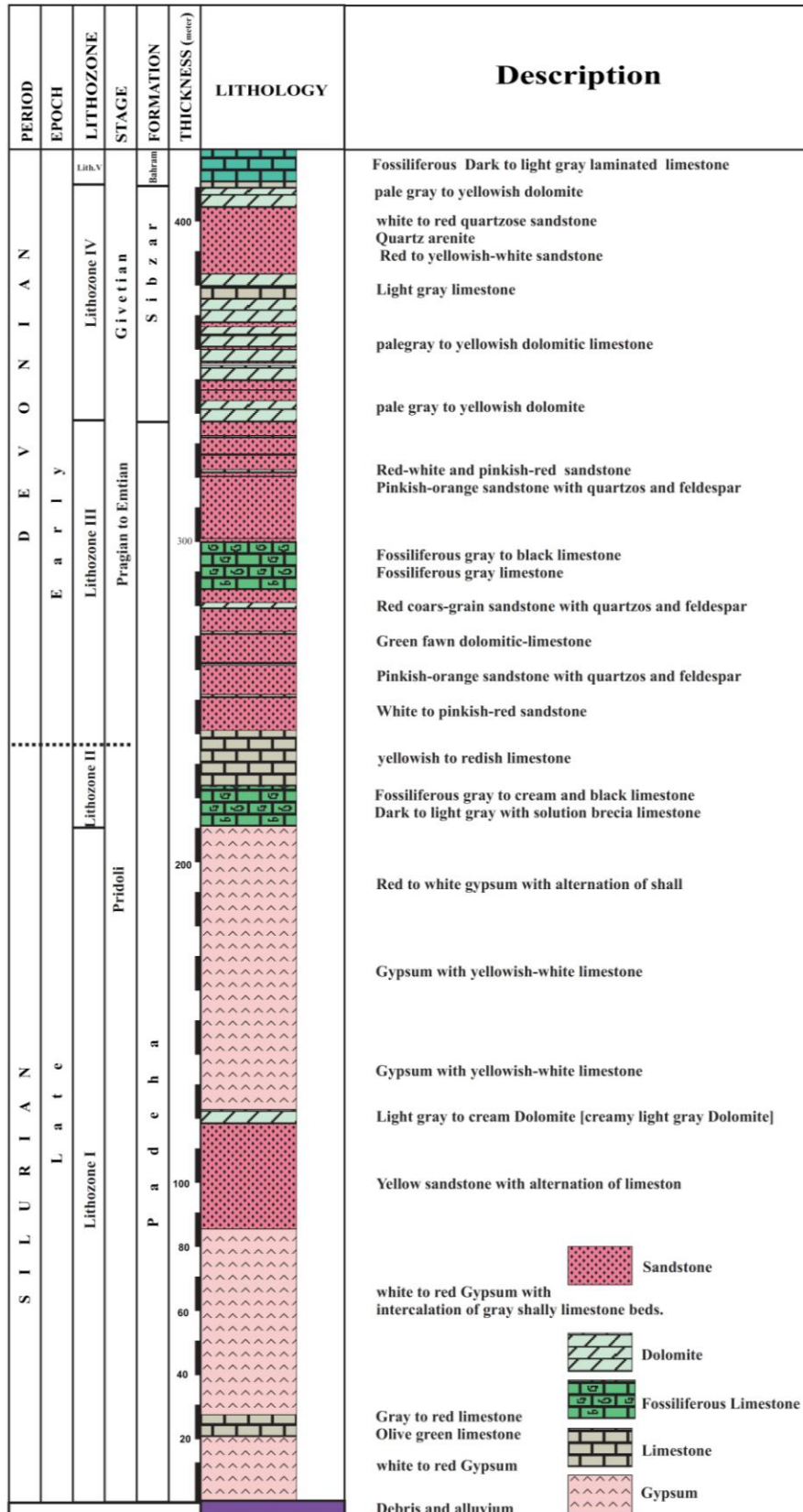


Figure 2. Lithostratigraphic section of Yadanshahr, Iran

6. 88.4 m of soft gypsum with thinly-bedded intercalations of pease-coloured limestone.

Lithozone II

7. 13 m of light- to dark-grey limestone together with shell fragments (sandy bioclast lime wackestone/pelbioclast lime wackestone or sandy biomicrite/pelbiomicrite (light- to dark-grey limestone)). Solution breccia from the dissolution of gypsum can be observed in the base of this rock unit. The identified conodonts include:
 - a. *Ozarkodina confluens* (Branson and Mehl, 1933)
 - b. *Spatognathodus primus* (Branson and Mehl, 1933)
 - c. *Pandorinellina steinhornensis* (Ziegler, 1956)
 - d. *O. confluens* (Branson and Mehl, 1933)
 - e. *P. exigua* (Philip, 1966)
 - f. *Zieglerodina remscheidensis* (Ziegler, 1960)
 - g. *Distomodus* (Branson and Mehl, 1947)
 - h. *Hindeodella equidentata* (Rhodes, 1953)
 - i. *Ligonodina* (Ulrich and Bassler, 1926)
 - j. *L. elegans* (Walliser, 1964)
 - k. *Lonchodina* (Bassler, 1925)
 - l. *Neopripiodus bicurvatus* (Branson and Mehl, 1933)
 - m. *O. denckmanni* (Ziegler, 1956)
 - n. *O. ziegleri* (Walliser, 1964)
 - o. *Panderodus simplex* (Branson and Mehl, 1933)
 - p. *Trichonodella symetrica* (Branson and Mehl, 1933)
8. 17.4 m of yellow to grey limestone, creamy with no fossil which gradually turns to red.

Member II

Lithozone III

9. 10.2 m of red-white-brick-coloured sandstone containing siliceous cement with quartz and feldspar.
10. 1 m of thinly-bedded red to white dolomitic sandy limestone (dolograinstone or sandy dolosparite).
11. 10 m of red sandstone with siliceous cement and abundant quartz and feldspar grains. It turns gradually to micrite and microsparite. The identified conodonts include:
 - a. *I. struvie* (Weddige, 1977)
 - b. *I. regularicresens* (Bultynck, 1970)
 - c. *I. brevis* (Staulfer, 1940)
 - d. *I. brivis spicatus* (Youngquist and Peterson, 1947)
 - e. *Bipennatus bipennatus* (Bischoff and Ziegler, 1957)
12. 8.7 m of thinly bedded clay-bearing red sandstone containing trace fossils.
13. 1 m of gray marl limestone (micrite to microcrystalline matrix, laterally becoming bioclastic lime wackestone or biomicrite)
14. 7 m of coarse-grained red lime sandstone with weak carbonate cement and abundant clastic grains of quartz and feldspar
15. 2 m of light green dolomitic limestone (packstone-dolosparite) with sparicalcite cement and abundant rhombohedral calcite

16. 4 m of red to white sandstone with medium to coarse grains of quartz and feldspar and siliceous cement
Lithozone IV (Sibzar formation)
17. 15 m of grey to dark limestone to dolostone with sparicalcite cement and abundant rhombohedra of dolomite. Organic remnants of crinoid debris, fish teeth and conodonts are as follows:
 - a. *I. brevis* (Stauffer, 1940)
 - b. *B. bipennatus sub sp.*
18. 20.2 m of red sandstone (quartz arenite), medium- to coarse-grained quartz along with nodules of iron oxide (opaque minerals, feldspar and siliceous cement)
19. 0.2 m of dark gray limestone (biosparite-grainstone) with sparicalsite cement and calcite rhombohedra. The only conodont is *Ozarkodina* sp.
20. 17 m of red sand with argillaceous matrix together with three light-grey dolostone beddings
21. 6.7 m of yellowish grey dolostone (dolograinstone-dolosparite). The identified conodonts include:
 - a. *Icriodus* sp., *I. struvei* (Weddige, 1977)
 - b. *I. brevis* (Stauffer, 1940)
 - c. *I. brevis brevis* (Stauffer, 1940)
 - d. *Bipennatus* sp., *B. bipennatus* (Bischol and Ziegler, 1957)
 - e. *Ozarkodina* sp.
22. 4.5 m of white to red quartzose sandstone
23. 20.4 m of light-grey to yellow dolomite (dolosparite dolograinstone) with three layers of red sandstone.
24. 8 m of light grey to yellow dolostone with quartzose grains and sparit calcite cement. Identified conodonts include:
 - a. *Icriodus* sp., *I. aff. regularicresens* (Bultynck, 1970)
 - b. *Bipennatus sp 2.*
25. 20.63 m of white to red quartzose sandstone
26. 6 m of light-gray dolomite (dolograinstone dolosparite)
27. 2 m of marl containing trilobite, ostracoda, Ecinid spine and bryozoan
Bahram grey brachiopoda limestone (Bahram Formation)

Biozonation of Yazdanshahr section

The conodont collections in this section contain 15 genus, 20 species and 5 subspecies were identified (*Fig. 3*). Together, these identify two biozones as follows:

1. Zieglerodina remscheidensis, Pandorinellina steinhornensis assemblage zone. The elements collected in this part relate to *Spathognathodontidae* and include the following:
 - *O. confluence* (Branson and Mehl, 1933) (*Spathognathodus primus*; Branson and Mehl, 1933)
 - *Zieglerodina remscheidensis* (Ziegler, 1960) (*S. remscheidensis*; Ziegler, 1960)
 - *Pandorinellina steinhornensis* (Ziegler, 1966) (*S. steinhornensis*, Ziegler, 1956)
 - *P. exiguus philipi* (Klapper, 1969)

Yazdanshahr

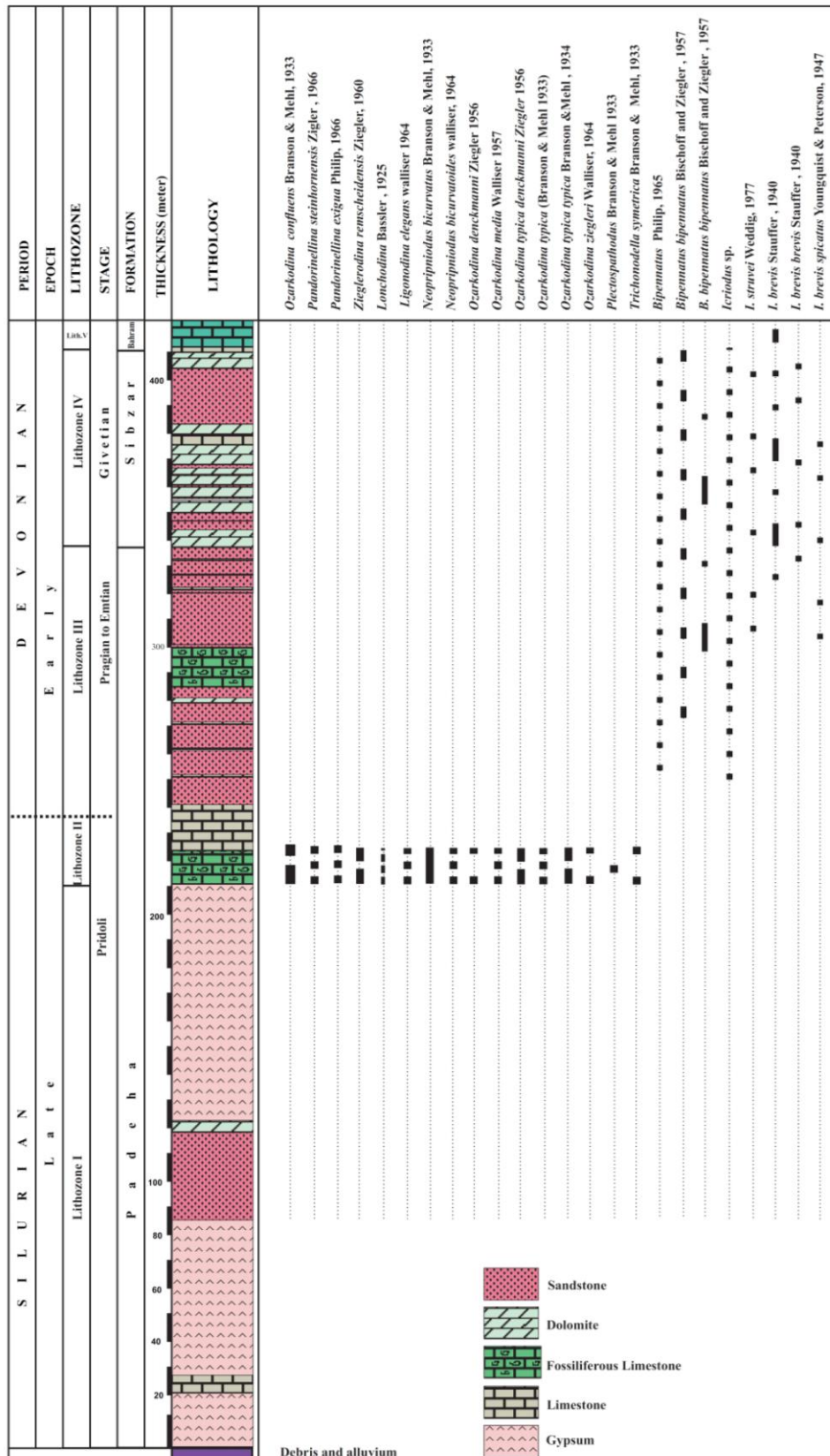


Figure 3. Biostratigraphic section of Yadanshahr, Iran

The collected elements were comparable to the following:

- Murphy et al. (2004) (from Nevada, Spain, Germany and Czech Republic)
- Farrel (2004) (from Camelford limestone, Australia)
- Corradini et al. (2014) (from Cellon section)
- Corriga et al. (2011) (from Malinfier section, Italy)
- Mathieson et al. (2016) (from Cobra Supergroup in Western New South Wales, Australia)
- Drygant and Szaniawski (2012) (from Podolia, Ukraine)
- Corriga et al. (2014) (from Tafilalt, southeastern Morocco)
- Ziegler (1975, 1991)

As such, the age of this biozones is Pridoli.

2. *Eugenathodontidae-Icriodus* assemblage zone

The elements collected in this part are related to *Eugenathodontidae* and include the followings genus:

- *Bipennatus* (Philip, 1965)
- *B. bipennatus* (Bischoff and Ziegler, 1957)
- *B. bipennatus bipennatus* (Bischoff and Ziegler, 1957)
- *Icriodus* sp.
- *I. struvei* (Weddige, 1977)
- *I. brevis* (Stauffer, 1940)
- *I. brevis brevis* (Stauffer, 1940)
- *I. brevis spicatus* (Youngquist and Peterson, 1947)

As such, the age of this biozone is Pragian to Emsian with the collected elements being comparable to those in the following work:

- Mathieson et al. (2016) (from Cobra Supergroup in Western New South Wales, Australia); Murphy (2005) (from Nevada)
- Murphy (2005) (from Nevada)
- Corriga et al. (2014) (from Podolia, Ukraine)
- Clark et al. (1966) (from Nevada)
- Nasehi (1996) (from Central Iran)
- Ziegler (1975, 1991)

It is difficult to identify the contact between the Silurian and Devonian. The studied section exhibit a stratigraphic hiatus between the Late Pridoli and Early Pragian. Lochkovian deposits have not been observed in Iran; therefore, Central Iran was exposed out of water.

Conclusion

The studied section indicates that the Padeha Formation has two members across this area. The lower part (evaporative deposits with carbonate intercalations) has been aged back to the Late Silurian, while the upper part of Padeha Formation (clastic deposits

with carbonate intercalations) is reported to be formed in the Early Devonian. The contact between the lower and upper parts exhibits a sedimentary hiatus (Late Pridoli to Late Emsian). Stratigraphists and geologists can correlate the stratigraphic column with this section. Using stratigraphic principles, it will be possible to solve the problem of age determination in Central Iran.

Within this time window, present-day Iran formed on the northern margin of the Gondwana Supercontinent, which later divided into separate structural units under the effect of Caledonian epirogenic movement (from faulting and formation of horst and graben basins). In the Late Silurian and Early Devonian, sea transgression and regression occurred, respectively. Note that the transgression at this time extended to limited parts of Iran. The evidence presented herein confirms the hypothesis of a horst and graben basin along the paleo faults in Central Iran in the Early Paleozoic.

REFERENCES

- [1] Adhamian, A. (2003): Middle Devonian (Givetian) conodont biostratigraphy in the Soh area, north of Esfahan, Iran. – *Courier Forschungsinstitut Senckenberg* 245:183–193.
- [2] Ahmadi, T., Dastanpour, M., Vaziri, M. (2012): Upper Frasnian (upper Devonian) *Polygnathus* and *Icriodus* conodonts from the Bahram formation, Hur section, Kerman province, Southeastern Iran. – *Rivista Italiana di Paleontologia e Stratigrafia* 118(2):203–213.
- [3] Alavi, M. (1991): Tectonic Map of the Middle East. – Geological Survey of Iran. 60 pp.
- [4] Alavi-Naini, M., Bolourchi, M.H. (1973): Explanatory Text of the Maku Quadrangle Map. – Geological Survey of Iran. A1 44P.
- [5] Ashouri, A.R. (2004): Late Devonian and Middle-Late Devonian conodonts from eastern and northern Iran. – *Revista Española Micropaleontología* 3: 355–365.
- [6] Ashouri, A.R. (2006): Middle Devonian–Early Carboniferous conodont faunas from the Khoshyeilagh Formation, Alborz Mountains, north Iran. – *Journal of Sciences* 17: 53–65.
- [7] Assereto, R. (1963): The Paleozoic formations in central Elburz (Iran). – *Rivista Italiana di Paleontologia e Stratigrafia* 69:503–543.
- [8] Bahrami, A., Corradini, C., Over, D. J., Yazdi, M. (2013): Conodont biostratigraphy of the upper Frasnian–lower Famennian transitional deposits in the Shotori Range, Tabas area, Central-East Iran Microplate. – *Bulletin of Geosciences* 88(2):369–388.
- [9] Bahrami, A., Corradini, C., Yazdi, M. (2011): Upper Devonian–Lower Carboniferous conodont biostratigraphy in the Shotori Range, Tabas area, Central-East Iran Microplate. – *Bollettino della Società Paleontologica Italiana* 50(1):35–53.
- [10] Bahrami, A., Königshof, P., Boncheva, I., Tabatabaei, M.S., Yazdi, M., Safari, Z. (2015): Middle Devonian (Givetian) conodonts from the northern margin of Gondwana (Soh and Natanz regions, North-West Isfahan, Central Iran): biostratigraphy and palaeoenvironmental implications. – *Palaeobiodiversity and Palaeoenvironments* 95(4): 555–577.
- [11] Bahrami, A., Zamani, F., Corradini, C., Yazdi, M., Ameri, H. (2014): Late Devonian (Frasnian) conodonts from the Bahram Formation in the Sar-e-Ashk Section, Kerman Province, Central-East Iran Microplate. – *Bollettino della Società Paleontologica Italiana* 53(3): 179–188.
- [12] Bassler, R. S. (1925): Classification and stratigraphic use of the conodonts. – *Bulletin of the Geological Society of America* 36:218–220.
- [13] Bichoff, G., Ziegler, W. (1957): Die Conodontenchronologie des Mittel – devons und des tiefsten Oberdevons. – *Abh. Hess. Landesamt Bodenforsch.* 22: 1–136, 16 text-figs., 5 tables, 21 pls., Wiesbaden.

- [14] Boncheva, I., Bahrami, A., Yazdi, M., Toraby, H. (2007): Carboniferous Conodont biostratigraphy and Late Paleozoic Platform Evolution in South Central Iran (Asadabad Section in Ramsheh area - SE Isfahan). – *Rivista Italiana di Paleontologia e Stratigrafia* 113 (3): 329-356.
- [15] Bozorgnia, F. (1973): Paleozoic foraminifera biostratigraphy of central and east Alborz Mountain, Iran. – National Iranian oil company, Tehran. Geological Laboratories, Publ. no. 4.
- [16] Branson, E. B., Mehl, M. G. (1933): Conodonts from the Bainbridge Formation (Silurian) of Missouri. – *University of Missouri Studies* 8:39-52.
- [17] Branson, E. B., Mehl, M. G. (1934): Conodonts from the Bushberg Sandstone and equivalent formation of Missouri. – *Univ. Missouri Stud.* 8:265-299, pls. 22-24, Columbia/Mo.
- [18] Branson, E. B., Mehl, M. G. (1941): New and little known Carboniferous conodont genera. – *Journal of Paleontology* 15:97-106.
- [19] Bultynck, P. (1970): Revision stratigraphique et paleontologique (Brachiopodes et Conodontes) de la coupe du Couvinien. – *Mem. Inst. Geol. Univ. Louvain* 26:1-152, 16 text-figs., 39 pls., Louvain.
- [20] Clark, D. L., Ethington, R. L. (1966): Conodonts and biostratigraphy of the lower and middle Devonian of Nevada and Utah. – *Journal of Paleontology* 40(3): 659-689.
- [21] Corradini, C., Corrigan, M. G., Mannik, P., Schonlaub, H. P. (2014): Revised conodont stratigraphy of the Cellon section (Silurian, Carnic Alps). – *Lethaia* 48(1):56-71. DOI: 10.1111/let.12087.
- [22] Corrigan, M. G., Corradini, C., Pondrelli, C. M., Simonetto, L. (2011): Lochkovian (Lower Devonian) conodonts from Rio Malinfier section (Carnic Alps, Italy). – *Gortania. Geologia, Paleontologia, Paleontologia* 33: 31-38.
- [23] Corrigan, M. G., Corradini, C., Walliser, O. H. (2014): Upper Silurian and Lower Devonian conodonts from Tafilalt, southeastern Morocco. – *Bulletin of Geosciences* 89(1): 183200.
- [24] Drygant, D., Szaniawski, H. (2012): Lochkovian conodonts from Podolia, Ukraine and their stratigraphic significance. – *Acta Palaeontologica Polonica* 57(4):833–861.
- [25] Farrell, J. R. (2004): Silurian-Devonian conodonts from the Camelford Limestone, Wellington, New South Wales, Australia. – *Journal of Paleontology* 47(4): 937-982.
- [26] Flügel, E. (2010): *Microfacies of Carbonate Rocks, Analysis, Interpretation and Application.* – Springer-Verlag, Berlin.
- [27] Gholamalian, H. (2007): Conodont biostratigraphy of the Frasnian-Famennian boundary in the Esfahan and Tabas areas, central Iran. – *Geol. Quart.* 51:453-476.
- [28] Gholamalian, H., Ghorbani, M., Sajadi, S. H. (2009): Famennian conodonts from Kale-Sardar section, Eastern Tabas, Central Iran. – *Riv. Ital. Paleontol. Stratigr.* 115:141–158.
- [29] Gholamalian, H., Kebriaei, M. R. (2008): Late Devonian conodonts from the Hojedk section, Kerman Province, southeastern Iran. – *Rivista Italiana di Paleontologia e Stratigrafia*, Milan 114(2):171-181.
- [30] Heydari, E., Arzani, N., Hassanzadeh, J. (2008): Mantle plume: the invisible serial killer-application to the Permian–Triassic boundary mass extinction. – *Palaeogeogr Palaeoclimatol Palaeoecol* 264:147–162.
- [31] Huckriede, R., Kursten, M., Venzlaff, H. (1962): *Zur Geologie des gebietes Zwischen Kerman und Saghand (Iran).* – *Beih. Geol. Jb.* 51:197 S., 10 Taf., Hannover
- [32] Huddle, J. W. (1934): Conodonts from the new Albany Shale of Indiana. – *Bull. Amer. Paleont.* 21 (72): 1-136, 3 text-figs., 12 pls., Ithaca/N. Y.
- [33] Klapper, G. (1969): Lower Devonian conodont sequence, Royal Creek, Yukon, Territory, and Devon Island, Canada. – *Journal of Paleontology* 43(1):1-27.
- [34] Mathieson, D., Mawson, R., Simpson, A. J., Talent, J. A. (2016): Late Silurian (Ludlow) and Early Devonian (Pragian) conodonts from the Cobar Supergroup, western New South Wales, Australia. – *Bulletin of Geosciences* 91(3):583-652.

- [35] Murphy, M. A. (2005): Pragian conodont zonal classification in Nevada, western North America. [Zonación de conodontos praguenses en Nevada, oeste de Norteamérica.] – *Revista Española de Paleontología* 20(2): 177-206.
- [36] Murphy, M. A., Valenzuela-Ríos, J. L., Carls, P. (2004): On classification of Pridoli (Silurian)-Lochkovian (Devonian) Spathognathodontidae (Conodonts). – University of California, Riverside, Campus Museum Contribution 6:1-25.
- [37] Nasehi, E. (1996): Early to Middle Devonian conodont from central Iran. – *Geo. Sci. Quart.* 6(21-22): 78-87. (In Persian with English abstract).
- [38] Philip, G. M. (1965): Lower Devonian conodonts from the Tyers area, Gippsland, Victoria. – *Proceedings of the Royal Society of Victoria* 79:95-117.
- [39] Philip, G. M. (1966): Lower Devonian conodonts from the Buchan Group, eastern Victoria. – *Micropaleontology* 12:441-460.
- [40] Rhodes, F. H. T. (1953): Some British Lower Paleozoic conodont faunas. – *Phil. Trans. Roy. Soc. London, ser. B*, 237: 261-334, 20 text-figs., 4 tables, pls. 20-23, London.
- [41] Rhodes, F. H. T., Muller, K. J. (1956): The conodonts genus *Prioniodus* and related forms. – *J. Paleont.* 30: 695-699, 1 table, Tulsa/Okla.
- [42] Ruttner, A., Nabavi, M., Hajian, J. (1968): Geology of the Shirgesht area (Tabas Area, East Iran). – *Geol. Surv. Iran Rep.* 4:1-133.
- [43] Soffel, H. C., Forster, H. G. (1980): Apparent polar wander path of central Iran and its geotectonic interpretation. – *J. Geomag. Geoelectr.* 32(Suppl. II): 117-135.
- [44] Stocklin, J. (1968): Structural history and tectonics of Iran: A review. – *Amer. Assoc. Petrol. Geologists Bull.* 52 (7). DOI: 10.1306/5D25C4A5-16C1-11D7-8645000102C1865D
- [45] Stocklin, J., (1971): Stratigraphic Lexicon of Iran. Part 1: Central, North, and East Iran. – Geological Survey of Iran, Reports 18:1-338.
- [46] Stocklin, J., Eftekhari-Nezhad, J., Hushmand-Zadeh, A. (1965, reprinted 1991): Geology of the Sotori range (Tabas area, east Iran). – Geological Survey of Iran, Reports 3: 1-69.
- [47] Stocklin, J., Nabavi, M. H. (1971): Explanatory text of the Boshruyeh Quadrangle map 1:250,000. – Geological Survey of Iran, Geological Quadrangle J7: 1-50.
- [48] Stocklin, J., Setudehnia, A. (1991): Stratigraphic Lexicon of Iran. – Geological Survey of Iran, Reports 18: 1-376.
- [49] Stuffer, C.R. (1940): Conodonts from the Devonian and associated clays of Minnesota. – *Journal of Paleontology* 14:417-435.
- [50] Sweet, W. C. (1988): *The Conodonts: Morphology, Taxonomy, Paleoecology and Evolutionary History of Long-Extinct Animal Phylum*. – Oxford University Press, New York.
- [51] Ulrich, E. O., Bassler, R. S. (1926): A classification of the toothlike fossils, conodonts. – *Proc. U. S. Nat. Mus.* 68, art. 12: 1-63, 4 text-figs., 11 pls., Washington/ D. C.
- [52] Walliser, O. H. (1957): Conodonten aus dem oberen Gotlandium Deutschlands und der Karnischen Alpen. – *Notizblatt des hessischen Landesamtes für Bodenforschung* 85:28-52. Pls 1-3. 3 figs.
- [53] Walliser, O.H. (1964): Conodonten des Silurs. – *Abhandlungen des Hessischen Landesamtes für Bodenforschung zu Wiesbaden* 41:1-106.
- [54] Weddige, K. (1984): Zur Stratigraphie und Paläogeographie des Devons und Karbons von N.E., Iran. – *Senckenbergiana lethaea* 65(1-3):179-223.
- [55] Weddige, K. (1977): Die Conodonten der Eifel-Stufe im Typusgebiet und in benachbarten Faziesgebieten. – *Senckenbergiana Lethaea* 58(4-5): 271-419. 9 fig., 20 tab.6 pl., Frankfurt/Main.
- [56] Yazdi, M. (1999): Late devonian-carboniferous conodonts from Eastern Iran. – *Riv. Ital. Paleontol. Ratigr.* 105:167-200.
- [57] Youngquist, W., Peterson, R. F. (1947): Conodonts from the Sheffield Formation of north-central Iowa. – *J. Paleont.* 14: 417-435, pls. 58-60, TTulsa/Okla.

- [58] Ziegler, W. (1956): Unterdevonischen Conodonten, insbesondere aus dem Schönauer und dem Zоргensis-Kalk. – Notizblatt des hessischen Landesamtes für Bodenforschung 84: 93-106.
- [59] Ziegler, W. (1960): Conodonten aus dem Rheinischen Unterdevon (Gedinnium) des Remscheider Sattels (Rheinisches Schiefergebirge). – Palaont. Z. 34:169-201, 2 text-figs., 3 tables, pls. 13-15, Stuttgart.
- [60] Ziegler, W. (1966): Eine Verfeinerung der Conodontengliederung an der Grenze Mittel-/Oberdevon. – Fortschr. Geol. Rheinld. Westf. 9: 647-676, 4 text-figs., 5 tables, 6 pls., Krefeld.
- [61] Ziegler, W. (ed.) (1975): Catalogue of conodonts II. 404 pp. – E. Schweizerbart'sche Verlagsbuchhandlung, Stuttgart.
- [62] Ziegler, W. (ed.) (1991): Catalogue of Conodonts V. – E. Schweizerbart'sche Verlagsbuchhandlung, Stuttgart.

APPENDIX

Plate 1

1. *Bipennatus* Philip, 1965
2. *B. bipennatus bipennatus* Bischoff and Ziegler, 1957
3. *B. bipennatus bipennatus* Bischoff and Ziegler, 1957
4. *B. bipennatus bipennatus* Bischoff and Ziegler, 1957
5. *B. bipennatus bipennatus* Bischoff and Ziegler, 1957
6. *Bipennatus bipennatus* Bischoff and Ziegler, 1957
7. *Bipennatus bipennatus* Bischoff and Ziegler, 1957
8. *Bipennatus bipennatus* Bischoff and Ziegler, 1957
9. *Bipennatus* sp.aff *B. palethorpei* Telfond, 1975 (Plate 2: 4, 8)
10. *Bipennatus* Philip, 1965
11. *Bipennatus* Philip, 1965
12. *Bipennatus bipennatus* Bischoff and Ziegler, 1957
13. *Bipennatus bipennatus* Bischoff and Ziegler, 1957

Plate 1

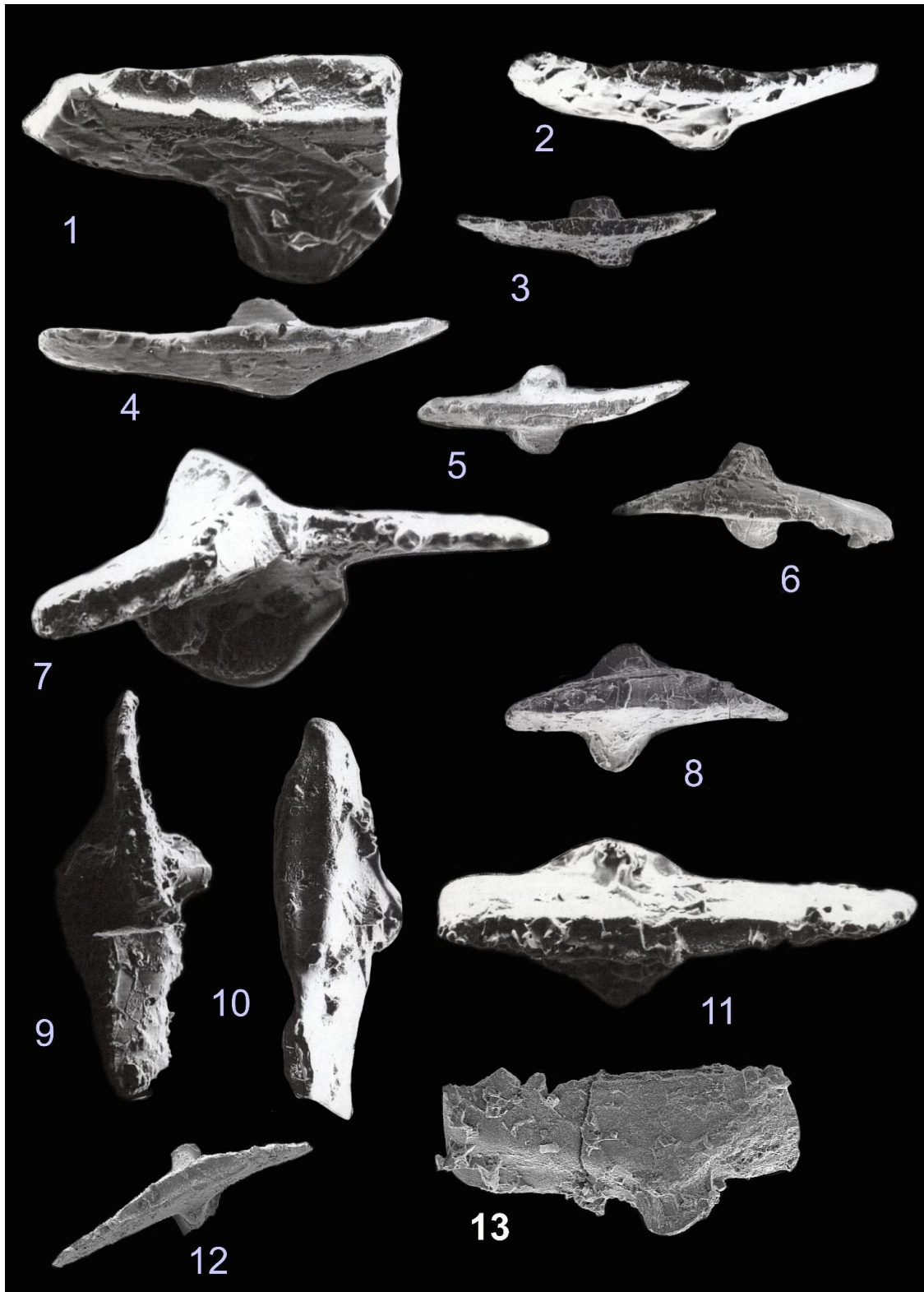


Plate 2

1. *Ozarkodina ziegleri* Walliser, 1964
2. *Ozarkodina ziegleri* Walliser, 1964
3. *Trichonodella symetrica* Branson and Mehl, 1933
4. *Ozarkodina ziegleri* Walliser, 1964
5. *Ozarkodina ziegleri* Walliser, 1964
6. *Ozarkodina* Branson and Mehl, 1933
7. *Ozarkodina ziegleri* Walliser, 1964
8. *Trichonodella symetrica* Branson and Mehl, 1933
9. *Ozarkodina* Branson and Mehl, 1933
10. *Trichonodella symetrica* Branson and Mehl, 1933
11. *Trichonodella symetrica* Branson and Mehl, 1933
12. *Trichonodella symetrica* Branson and Mehl, 1933
13. *Trichonodella symetrica pinnula* Philip, 1966
14. S element of ? *Ozarkodina* Branson and Mehl, 1933

Plate 2

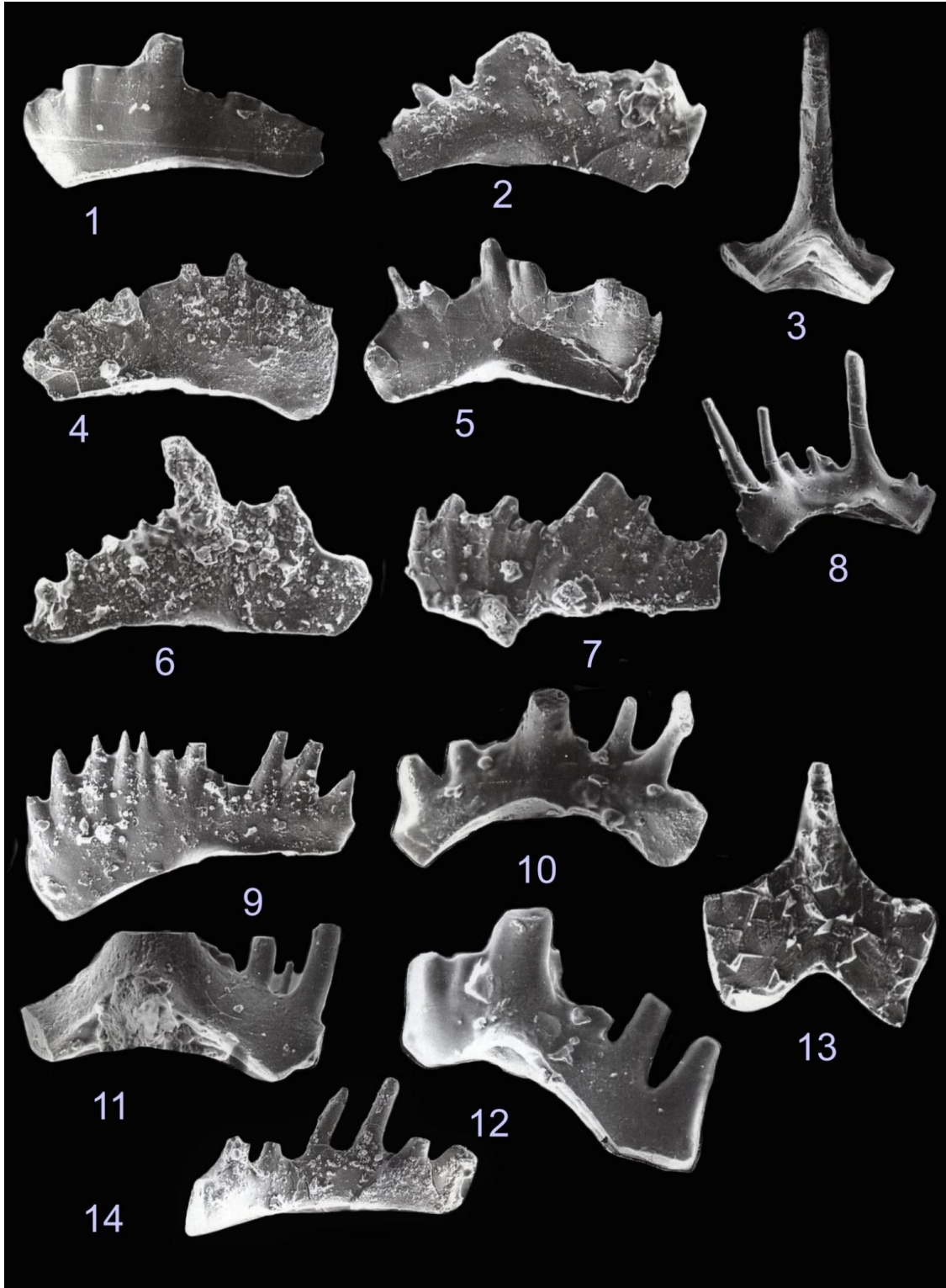


Plate 3

1. *Ligonodina elegans* Walliser 1964
2. *Ligonodina* Bassler, 1925
3. *Distomodus* Branson and Mehl 1947
4. *Lonchodina* Bassler, 1925
5. *Hindeodella equidentata* Rhodes, 1953
6. *Ozarkodina typica denckmanni* Ziegler, 1956
7. *Ozarkodina denckmanni* Ziegler, 1956
8. *Ozarkodina denckmanni* Ziegler, 1956
9. *Lonchodina* Bassler, 1925
10. *Ozarkodina typica denckmanni* Ziegler, 1956
11. *Ozarkodina typica denckmanni* Ziegler, 1956
12. *Ozarkodina typica denckmanni* Ziegler, 1956
13. *Ozarkodina typica denckmanni* Ziegler, 1956
14. *Ozarkodina ziegleri* Walliser, 1964
15. *Ozarkodina typica denckmanni* Ziegler, 1956
16. *Ozarkodina typica denckmanni* Ziegler, 1956

Plate 3

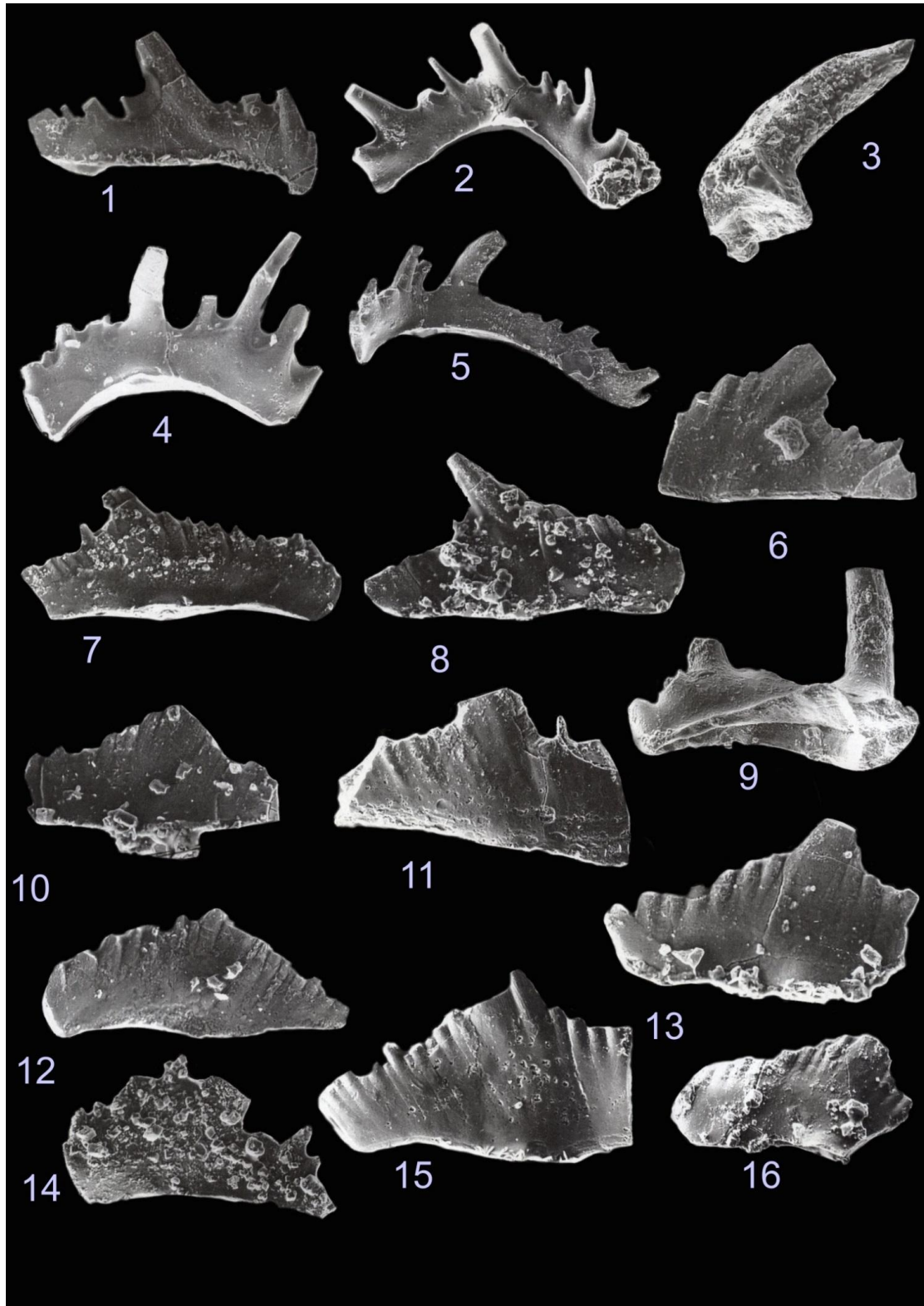


Plate 4

1. *Hindeodella* *subtillis* N166
2. *Hindeodella* *equidentata* Rhodes, 1953 N22
3. *Wurmiella* *excavata* Branson and Mehl, 1933; *Neopripiodus* *excavatus* Branson and Mehl, 1933 N30
4. *Lonchodina* Bassler, 1925 N20
5. *Ligonodina* *salopina* Rhodes, 1953, N24
6. *Ligonodina* *salopina* Rhodes, 1953, N25
7. *Neopripiodus* *bicurvatus* Branson and Mehl, 1933 N30
8. *Wurmiella* *excavata* Branson and Mehl, 1933 *Neopripiodus* *excavatus* (Branson and Mehl)
9. *Wurmiella* *excavata* Branson and Mehl, 1933 *Neopripiodus* *excavatus* (Branson and Mehl) N
10. *Neopripiodus* *bicurvatoides* Walliser, 1964 N30
11. *Lonchodina* Bassler, 1925 N21
12. *Wurmiella* *excavata* Branson and Mehl, 1933; *Neopripiodus* *excavatus* (Branson and Mehl) N20
13. *Lonchodina* Bassler, 1925 N20
14. *Lonchodina* Bassler, 1925 N
15. *Wurmiella* *excavata* Branson and Mehl, 1933 *Neopripiodus* *excavatus* (Branson and Mehl) N20

Plate 4

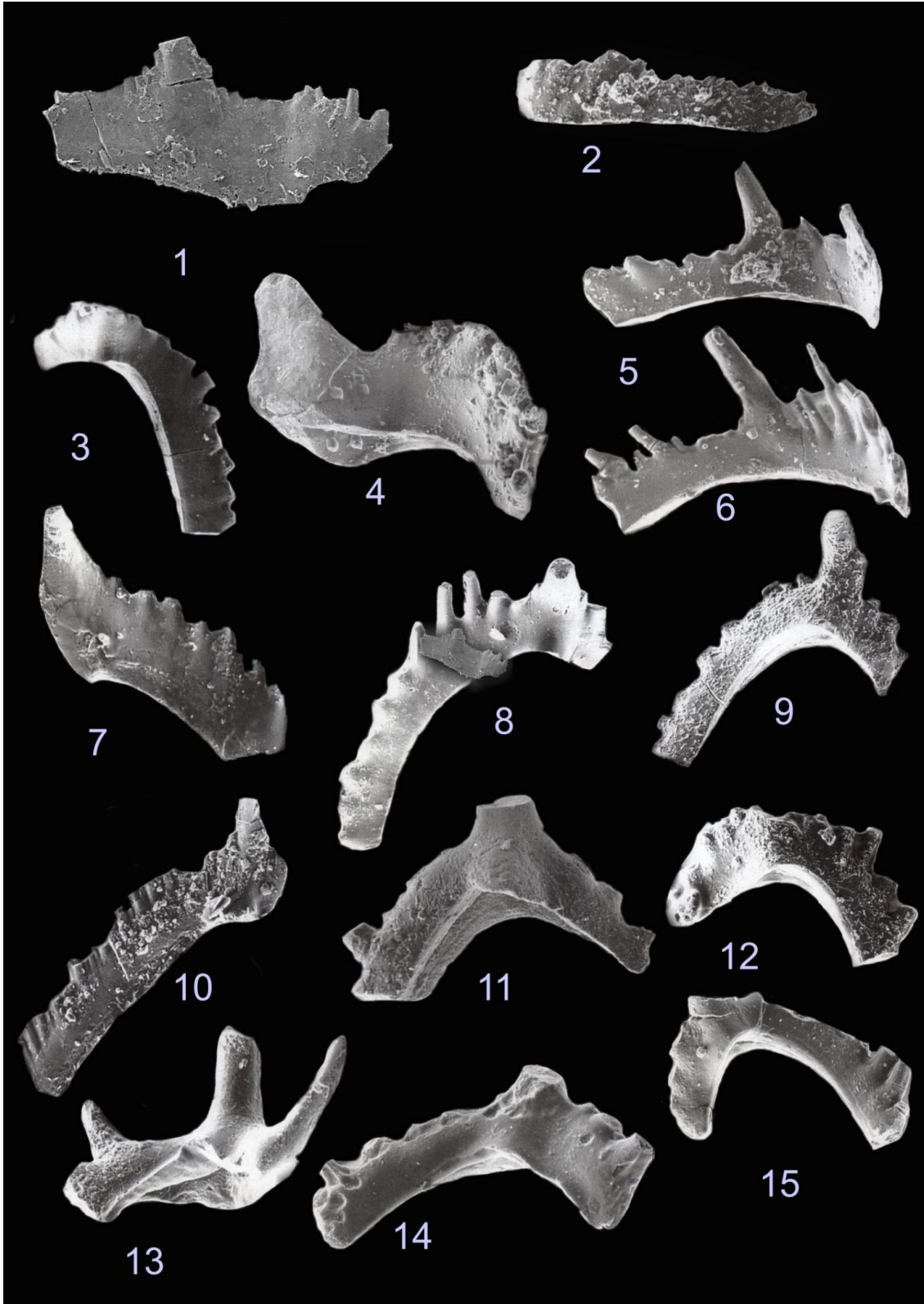


Plate 5

1. *Ozarkodina confluens* Branson and Mehl, 1933 (*Spatognathodus primus primus* Branson and Mehl, 1933) N21
2. *Ozarkodina confluens* Branson and Mehl, 1933 (*Spatognathodus primus primus* Branson and Mehl, 1933) N19
3. *Zieglerodina remscheidensis* Ziegler, 1960 (*Spathognathodus remscheidensis* Ziegler, 1960) N 22
4. *Zieglerodina remscheidensis* Ziegler, 1960 (*Spathognathodus remscheidensis* Ziegler, 1960) N25
5. *Zieglerodina remscheidensis* Ziegler, 1960 (*Spathognathodus remscheidensis* Ziegler, 1960) N19
6. *Zieglerodina remscheidensis* Ziegler, 1960 (*Spathognathodus remscheidensis* Ziegler, 1960) N25
7. *Ozarkodina confluens* Branson and Mehl, 1933 (*Spatognathodus primus* Branson and Mehl, 1933) N19
8. *Ozarkodina confluens* Branson and Mehl, 1933 (*Spatognathodus primus* Branson and Mehl, 1933) N24
9. *Pandorinellina exigua* Philip, 1966 (*Spathognathodus exiguous* Philip, 1966) N21
10. *Pandorinellina exigua* Philip, 1966 (*Spathognathodus exiguous* Philip, 1966) N21
11. *Pandorinellina exigua* Philip, 1966 (*Spathognathodus exiguous* Philip, 1966) N22
12. *Pandorinellina exigua* Philip, 1966 (*Spathognathodus exiguous* Philip, 1966) N21
13. *Pandorinellina exigua* Philip, 1966 (*Spathognathodus exiguous* Philip, 1966) N20
14. *Zieglerodina remscheidensis* Ziegler, 1960 (*Spathognathodus remscheidensis* Ziegler, 1960) N19
15. *Pandorinellina exigua* Philip, 1966 (*Spathognathodus exiguous* Philip, 1966) N21
16. *Pandorinellina cf exigua* Philip, 1966 (*Spathognathodus exiguous* Philip, 1966) N19
17. *Pandorinellina sp* Muller & Muller 1957
18. *Pandorinellina steinhornensis* Ziegler, 1966 (*Spathognathodus steinhornensis* Ziegler, 1956) N23
19. *Ozarkodina cf confluens* Branson and Mehl, 1933 (*Spatognathodus primus* Branson and Mehl, 1933) N25
20. *Zieglerodina cf remscheidensis* Ziegler, 1960 (*Spathognathodus remscheidensis* Ziegler, 1960) N21
21. *Pandorinellina cf steinhornensis* Ziegler, 1966 (*Spathognathodus steinhornensis* Ziegler, 1956) N19

Plate 5

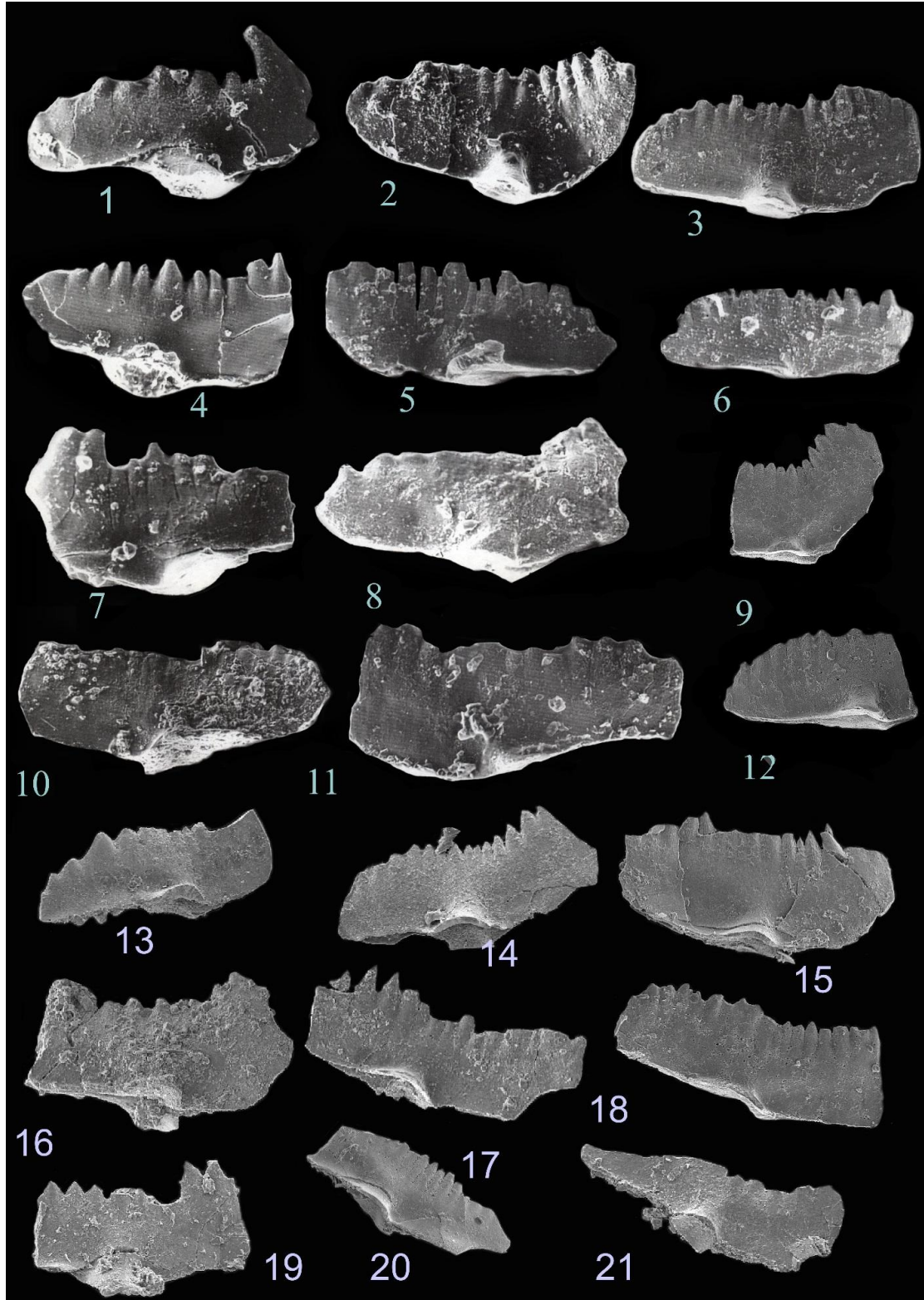


Plate 6

1. *Zieglerodina remscheidensis* Ziegler, 1960 (*Spathognathodus remscheidensis* Ziegler, 1960) N26
2. *Ozarkodina confluens* Branson and Mehl, 1933 (*Spatognathodus primus* Branson and Mehl, 1933) N25
3. ?*Pandorinellina exigua* Philip, 1966 (*Spathognathodus exiguous* Philip, 1966)
4. *Zieglerodina remscheidensis* Ziegler, 1960 (*Spathognathodus remscheidensis* Ziegler, 1960) N24
5. *Ozarkodina confluens* Branson and Mehl, 1933 (*Spatognathodus primus primus* Branson and Mehl, 1933) N26
6. *Pandorinellina steinhornensis* Ziegler, 1966 (*Spathognathodus steinhornensis* Ziegler, 1956) N18
7. *Pandorinellina steinhornensis* Ziegler, 1966 (*Spathognathodus steinhornensis* Ziegler, 1956) N24
8. *Ozarkodina confluens* Branson and Mehl, 1933 (*Spatognathodus primus primus* Branson and Mehl, 1933) N20
9. *Zieglerodina remscheidensis* Ziegler, 1960 (*Spathognathodus remscheidensis* Ziegler, 1960)
10. *Pandorinellina steinhornensis* Ziegler, 1966 (*Spathognathodus steinhornensis*, Ziegler, 1956) N20
11. *Pandorinellina exigua* Philip, 1966 (*Spathognathodus exiguous* Philip, 1966) N22
12. *Pandorinellina exigua* Philip, 1966 (*Spathognathodus exiguous* Philip, 1966) N22
13. *Pandorinellina steinhornensis* Ziegler, 1966 (*Spathognathodus steinhornensis* Ziegler, 1956) N26
14. *Pandorinellina exigua* Philip, 1966 (*Spathognathodus exiguous* Philip, 1966) N20
15. *Pandorinellina exigua* Philip, 1966 (*Spathognathodus exiguous* Philip, 1966) N22
16. *Pandorinellina steinhornensis* Ziegler, 1966 (*Spathognathodus steinhornensis* Ziegler, 1956) N19
17. *Pandorinellina steinhornensis* Ziegler, 1966 (*Spathognathodus steinhornensis* Ziegler, 1956) N26
18. *Ozarkodina confluens* Branson and Mehl, 1933 (*Spatognathodus primus* Branson and Mehl, 1933) N19
19. *Pandorinellina exigua* Philip, 1966 (*Spathognathodus exiguous* Philip, 1966) N20
20. *Pandorinellina steinhornensis* Ziegler, 1966 (*Spathognathodus steinhornensis* Ziegler, 1956) N21
21. *Ozarkodina confluens* Branson and Mehl, 1933 (*Spatognathodus primus* Branson and Mehl, 1933) N24
22. *Pandorinellina steinhornensis* Ziegler, 1966 (*Spathognathodus steinhornensis* Ziegler, 1956) N19

Plate 6

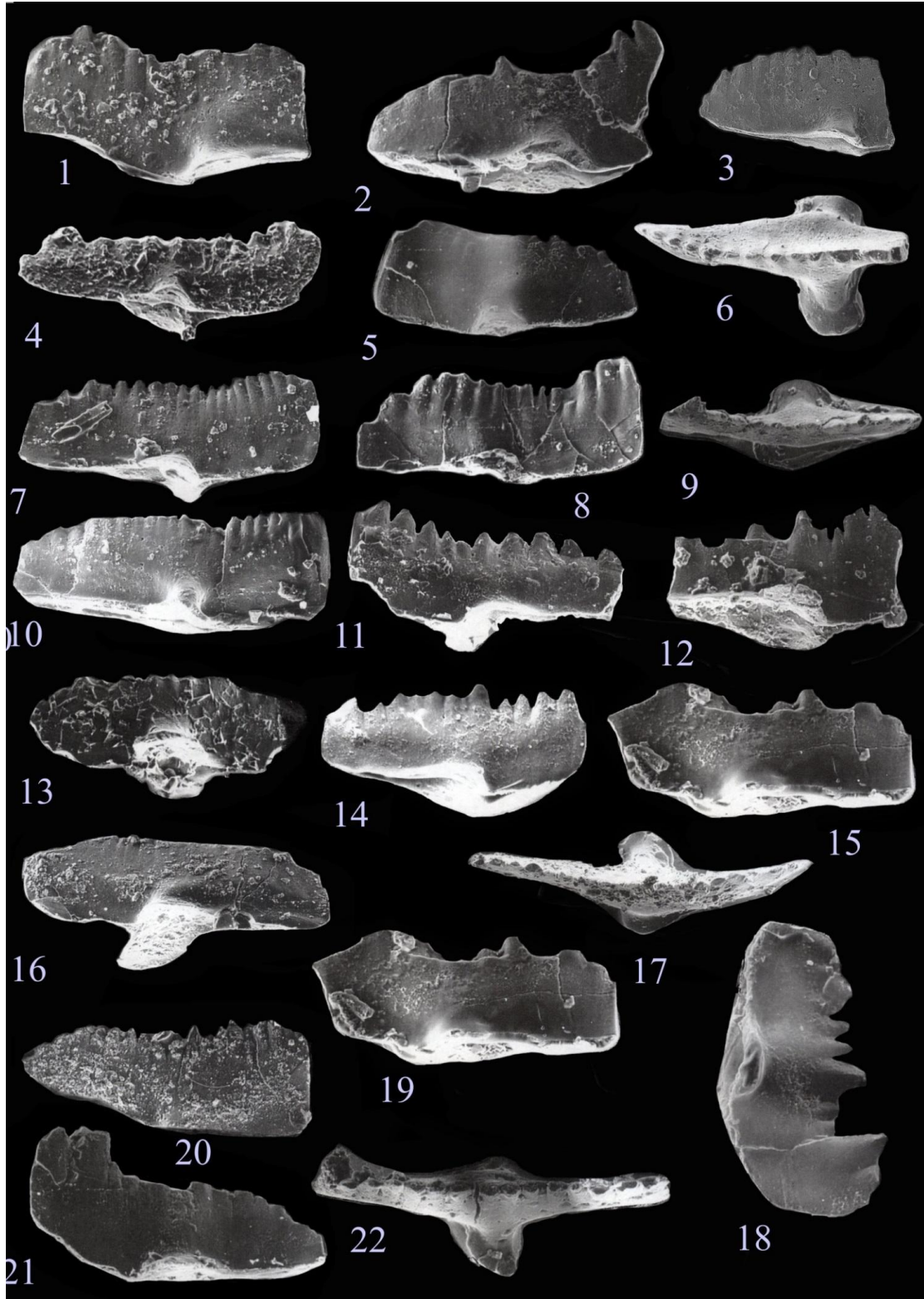


Plate 7

1. *Icriodus brivis spicatus* Youngquist and Peterson, 1947 no. 65
2. *Icriodus brevis brevis* Stauffer, 1940
3. *Icriodus regularicresens* Bultynck, 1970
4. *Icriodus regularicresens* Bultynck, 1970
5. *Icriodus sp* Branson and Mehl, 1934
6. *Icriodus regularicresens* Bultynck, 1970
7. *Icriodus regularicresens* Bultynck, 1970
8. *Icriodus struvei* Weddige, 1977
9. *Icriodus.regularicresens* Bultynck, 1970
10. *Icriodus struvei* Weddige, 1977
11. *Icriodus regularicresens* Bultynck, 1970
12. *Icriodus struvei* Weddige, 1977
13. *Icriodus regularicresens* Bultynck, 1970
14. *Icriodus sp*
15. *Icriodus brivis spicatus* Youngquist and Peterson, 1947
16. *Icriodu brivis spicatus* Youngquist and Peterson, 1947

Plate 7

